TRANSACTIONS
OF THE GEOLOGICAL INSTITUTE

V.B. Kurnosov, B.P. Zolotarev, A.V. Artamonov,
S.M. Lyapunov, G.L. Kashinzev, O.V. Chudaev,
A.L. Sokolova, and S.A. Garanina

ALTERATION EFFECTS IN THE UPPER OCEANIC CRUST - DATA AND COMMENTS

Technical Note

Volume Contents

Preliminary pages

Russian Academy of Sciences
Geological Institute

TRANSACTIONS OF THE GEOLOGICAL INSTITUTE
Founded in 1932
Volume 581

ALTERATION EFFECTS IN THE UPPER OCEANIC CRUST - DATA AND COMMENTS
(Technical Note)

AUTHORS
Victor B. Kurnosov, Boris P. Zolotarev, Andrey V. Artamonov, Sergey M. Lyapunov, Georgii L. Kashinzev, Oleg V. Chudaev, Alla L. Sokolova, and Svetlana A. Garanina

REVIEWERS FOR THIS VOLUME
Ivar O. Murdmaa
Igor M. Simanovich

EDITOR-IN-CHIEF
Mikhail G. Leonov

Moscow
2008

The authors ask anyone who references our publication properly credit the source of the information.

Reference to this volume should be made as follows:

Printed booklet citation:
Kurnosov, V.B., Zolotarev, B.P., Artamonov, A.V., Lyapunov, S.M., Kashinzev, G.L., Chudaev, O.V., Sokolova, A.L., and Garanina, S.A., 2008. Technical Note: Alteration effects in the upper oceanic crust - data and comments. *Proc. GIN*, issue 581[Booklet]: Moscow, GEOS.

CD-ROM volume citation:
Kurnosov, V.B., Zolotarev, B.P., Artamonov, A.V., Lyapunov, S.M., Kashinzev, G.L., Chudaev, O.V., Sokolova, A.L., and Garanina, S.A., 2008. Technical Note: Alteration effects in the upper oceanic crust - data and comments. *Proc. GIN*, issue 581[CD-ROM]. Available from: Geological Institute, Moscow 119017, Pyzhevsky Lane 7, Russian Federation.

WWW PDF volume citation:
Kurnosov, V.B., Zolotarev, B.P., Artamonov, A.V., Lyapunov, S.M., Kashinzev, G.L., Chudaev, O.V., Sokolova, A.L., and Garanina, S.A., 2008. Technical Note: Alteration effects in the upper oceanic crust - data and comments. *Proc. GIN*, issue 581[Online]. Available from World Wide Web:
< **http://www.ginras.ru/files/docs/publications/TechNote_ AlterationEffects.pdf** >. [Cited YYY-MM-DD]

Copies of this publication may be obtained from Publications Distribution Center, Geological Institute, Pyzhevsky Lane 7, Moscow 119017, Russian Federation.
The address for information: vic-kurnosov@rambler.ru

ISSN and ISBN
Printed booklet: ISSN 0002-3272; ISBN 978-5-89118-404-6
CD-ROM volume: ISSN 0002-3272; ISBN 978-5-89118-407-7
World Wide Web volume: ISSN 0002-3272; ISBN 978-5-89118-408-4

Editorial Board:
Mikhail G. Leonov (Editor-in-Chief), Mikhail A. Akhmetiev,
Yurii O. Gavrilov (Deputy Editor-in-Chief), Kiril E. Degtyarev,
Yurii V. Kariakin (Executive Secretary), Yurii G. Leonov, Mikhail A. Semikhatov,
Sergey D. Sokolov, and Mikhail D. Khutorskoy

Transactions of the Geological Institute / Geological Inst. – Moscow: Publisher Academy of Sciences of USSR, 1932-1964. Moscow: Nauka, 1964. - . - ISSN 0002-3272

Vol. 581: Alteration effects in the upper oceanic crust – data and comments (Technical Note) / V.B. Kurnosov, B.P. Zolotarev, A.V. Artamonov, S.M. Lyapunov, G.L. Kashinzev, O.V. Chudaev, A.L. Sokolova, and S.A. Garanina – Moscow: GEOS, 2008. – 33 p. (Booklet) + full version (CD-ROM volume or WWW PDF volume) – 1046 p.; il. 139.

ALTERATION EFFECTS IN THE UPPER OCEANIC CRUST: DATA AND COMMENTS

Technical Note

Victor B. Kurnosov, Boris P. Zolotarev, Andrey V. Artamonov, Sergey M. Lyapunov, Georgii L. Kashinzev, Oleg V. Chudaev, Alla L. Sokolova, and Svetlana A. Garanina

Prepared by the Geological Institute, Russian Academy of Sciences, Moscow, Russian Federation

TABLE OF CONTENTS

Supplementary Material:

TABLE OF CONTENTS

Supplementary Material:

ALTERATION EFFECTS IN THE UPPER OCEANIC CRUST—DATA AND COMMENTS

Victor B. Kurnosov[1], Boris P. Zolotarev[1], Andrey V. Artamonov[1], Sergey M. Lyapunov[1], George L. Kashinzev[2], Oleg V. Chudaev[3], Alla L. Sokolova[1], and Svetlana A. Garanina[1]

ABSTRACT

This report presents new data on chemical and mineralogical composition and density of altered and fresh igneous rocks from key Deep Sea Drilling Project (DSDP)/Ocean Drilling Program (ODP) holes drilled on the following main tectonomagmatic structures of the ocean floor:

1. Mid-ocean ridges and abyssal plains and basins (DSDP Legs 37, 61, 63, 64, 65, 69, 70, 83, and 91 and ODP Legs 106, 111, 123, 129, 137, 139, 140, 148, and 169);
2. Seamounts and guyots (DSDP Legs 19, 55, and 62 and ODP Legs 143 and 144);
3. Intraplate rises (DSDP Legs 26, 33, 51, 52, 53, 72, and 74 and ODP Legs 104, 115, 120, 121, and 183); and
4. Marginal seas (DSDP Legs 19, 59, and 60 and ODP Legs 124, 125, 126, 127, 128, and 135).

Study results of altered gabbro from the Southwest Indian Ridge (ODP Leg 118) and serpentinized ultramafic rocks from the Galicia margin (ODP Leg 103) are also presented. Samples were collected by the authors from the DSDP/ODP repositories, as well as during some *Glomar Challenger* and *JOIDES Resolution* legs.

This report also includes descriptions of thin sections, geochemical diagrams, data on secondary mineral assemblages, and recalculated results of chemical analyses with corrections for rock density. The atomic content of each element can be quantified in grams per standard volume (g/1000 cm^3).

The suite of results can be used to estimate mass balance, but parts of the data need additional work, which depends on locating fresh analogs of the altered rocks studied here. Results of quantitative estimation of element mobility in recovered sections of the upper oceanic crust as a whole are shown for certain cases: Hole 504B (Costa Rica Rift) and Holes 856H, 857C, and 857D (Middle Valley, Juan de Fuca Ridge).

[1]Geological Institute, Russian Academy of Sciences, Pyzhevsky Lane 7, Moscow 109017, Russian Federation. Correspondence author: **kurnosov@ginras.ru**

[2]Institute of Oceanology, Russian Academy of Sciences, Nakhimov Str. 36, Moscow 117218, Russian Federation.

[3]Far East Geological Institute, Far East Branch of Russian Academy of Sciences, Prospect 100-letiya of Vladivostok, Vladivostok 690022, Russian Federation.

INTRODUCTION

Water-rock interaction in the oceanic crust is of great importance in controlling global geochemical fluxes. Chemical exchange between seawater and igneous basement largely controls concentrations of some elements in the ocean and precipitation of metallic sulfides both under and on the seafloor. The process of water-rock interaction involves geochemical exchange between oceanic lithosphere and hydrosphere through convective hydrothermal systems within the global spreading system (mid-ocean ridges and marginal spreading

seas), as well as within intraplate volcanic zones (seamounts) and, possibly, in transform fracture zones.

The concept of oceanic crust alteration includes changes in mineral and chemical composition of primary igneous rocks within Layers 2 and 3 by water-rock interaction in hydrothermal convection cells above magma chambers in mid-ocean ridges under conditions of zeolite, greenschist, and amphibolite facies metamorphism. Water-rock interaction significantly affects seawater and provides a source of metals for ore accumulation (e.g., Edmond et al., 1982; Edmond and Von Damm, 1983; Kurnosov, 1986; Hannington et al., 1995; Elderfield and Schultz, 1996). Mineralization of solutions circulating in the oceanic crust is believed to principally result from extraction of chemical elements from the host rocks. Bischoff and Dickson (1975) were the first to support this concept using laboratory experiments. This process affects physical properties of rocks (Harrison, 1981; Ewing and Houtz, 1979) and magma generation in volcanic arcs when altered oceanic crust enters subduction zones (Hofman and White, 1982). It also supports biological activity. The study of this process sheds light on the relation between crustal and mantle sources of the matter for formation of chemical composition of solutions that circulate in the oceanic crust and discharge on the ocean floor as hot and cold submarine springs, so-called black and white smokers, respectively.

Alteration of the oceanic crust is being investigated by many scientists (e.g., Alt et al., 1985, 1986; Bass, 1976; Corliss et al., 1979; Edmond, 1992; Edmond et al., 1979, 1982; Hart, 1973; Honnorez, 1981; Honnorez et al., 1983; Humphris and Thompson, 1978; Kawahata, 1983; Kurnosov et al., 1983, 1986, 1992, 1995; Kurnosov and Murdmaa, 1996; Lyle, 1976; Rona et al., 1983; Rona, 1988; Thompson, 1973). The authors have made significant contributions in this field, particularly in understanding the real zonality and succession of alteration conditions in mid-ocean ridges. The oceanic crust alteration facies are already known, including zeolite/smectite, greenschist, and amphibolite facies metamorphism, as well as oxidative and nonoxidative types of alteration at low through high temperatures. The problem is to more precisely determine the actual position of these facies within the oceanic crust and both the global spreading system and intraplate rises, including guyots.

Quantitative evaluation of geochemical effects resulting from hydrothermal metasomatosis within the upper oceanic lithosphere is among the least understood subjects today. Metasomatosis takes place in the oceanic crust from intermediate magma chambers to the ocean floor throughout open hydrothermal systems, which include moderate- to high-temperature areas with extremely strong rock alteration and enormous areas with weak low-temperature alteration. In summary, the weak geochemical processes in the low-temperature parts of hydrothermal systems, hardly detectable by analyses, may substantially contribute to mass redistribution of elements in the hydrothermal metasomatic systems as a whole. Because of this, we included in this study key holes from which rocks, weakly altered at low temperatures, were recovered, as well as rocks with well-expressed medium- to high-temperature alteration containing thick massive sulfide deposits in the upper oceanic crust.

This report provides basic data for a quantitative estimate of geochemical effects of hydrothermal metasomatosis within the upper oceanic lithosphere. We accompany these data with necessary comments and note essential gaps in this study for future research. Moreover, we try to demonstrate with several examples that it is possible to estimate the complete element gain/loss during rock alteration in certain key Deep Sea Drilling Project (DSDP)/Ocean Drilling Program (ODP) holes best prepared for such analysis.

This report also contains data on the complex study of chemical and mineralogical compositions and density of both altered and fresh igneous rocks recovered from key DSDP/ODP holes drilled in the main tectonomagmatic structures of the ocean floor. Detailed descriptions of thin sections (see **“Appendix A”**) and geochemical diagrams are shown to distinguish

petrographically and geochemically uniform rock groups within which element gain/loss can only be estimated. Moreover, we present recalculated results of chemical analyses for all individual samples of fresh and altered magmatic rocks studied with correction for rock density. The results are presented in grams per 1000 cubic centimeters for each element (see **"Appendix B"**). These data serve as a basis for quantitative estimation of element gain/loss in each altered rock sample studied.

The results of element gain/loss determination for individual samples were used to estimate the mass balance of elements in water-rock interactions in the entire section recovered in a hole. These estimates include all varieties of altered and unaltered rocks constituting a complete section of the crust penetrated by a hole. The mass balance estimation procedure requires compiling element distribution curves in cores and/or tables for altered rocks compared to their fresh analogs.

This report contains examples of such cores from Hole 504B (Costa Rica Rift) and Holes 856H, 857C, and 857D drilled in the Middle Valley, Juan de Fuca Ridge. An example of a table with showing numerical data (in g/1000 cm^3) on gain/loss of elements in nonoxidative and oxidative environments of basalt alteration from the Kerguelen Plateau (Holes 1137A and 1140A) can be found in Kurnosov et al. (2003; table T14). Later, when insufficient data are supplemented, such core records and tables of comparisons of element contents in altered and unaltered rocks of the same type will be compiled for other studied holes.

We encourage all scientists to investigate this complicated and time-consuming process. Interested scientists are free to apply and/or extend the basic data presented in this *Report* in any reasonable scientific direction, including statistical approaches. These fresh analyses will be especially important if new deep-sea holes encounter structures that promote further steps toward quantitative evaluation of geochemical effects of the hydrothermal metasomatosis in the oceanic crust. The data obtained by different researchers may considerably advance our understanding of the contribution of water-rock interaction to the chemical composition of solutions that circulate in the crust over intermediate magma chambers and discharge onto the ocean floor and/or into the sedimentary cover. These data, in turn, lead to the evaluation of global material masses that migrate because of geochemical interactions between internal and external geospheres (oceanic lithosphere and the ocean) through subaqueous hydrothermal systems within hydrothermally active ocean floor structures during the Mesozoic–Cenozoic history of the Earth (i.e., spreading zones, seamounts, intraplate rises, zones of volcanic and hydrothermal reactivation, and transform faults). The research of material redistribution by hydrothermal metasomatosis of oceanic crustal rocks also involves ophiolites. The famous Troodos ophiolite section recovered in boreholes in Cyprus (Robinson, 1992) is an especially suitable prospect for such a study.

METHODS

Each altered and fresh sample chosen for mass balance calculation of alteration in the oceanic upper crust must be studied in detail, including petrographic description, estimation of vesicularity, whole-rock chemistry, and primary and secondary mineralogy, as well density.

Often, analytical data obtained by different researchers were not suitable for our report, as they did not correspond to the demands of the sampling procedure or to the methods of study. These data, with rare exceptions, do not contain several of the necessary components for the complex analysis (e.g., abundance of H_2O^+, Fe_2O_3, FeO, and CO_2; petrographic description; determination of secondary mineral assemblages; and density determination) of each rock sample included in the study. Therefore, in spite of abundant diverse

data obtained from the altered and fresh rocks and published in the *Proceedings of the Ocean Drilling Program* volumes, we could not use these data in most cases.

We studied DSDP/ODP samples of magmatic rocks in detail and obtained some interesting analyses results to add to the results available in *Proceedings of the Ocean Drilling Program*. Our investigations comprised the following:

1. Study both petrographic and chemical compositions of unaltered and altered rocks.
2. Study secondary mineral assemblages.
3. Determine the densities of fresh and altered rocks.
4. Calculate the number of atoms of each element in a standard volume of both fresh and altered rocks on the basis of the atomic-volumetric method of recalculation of chemical analyses with correction for porosity.

All analyses were conducted at the Geological Institute of Russian Academy of Sciences (Moscow). Some samples were analyzed at the Far East Geological Institute, Far East Branch of Russian Academy of Sciences (Vladivostok), Oceanological Institute of Russian Academy of Sciences (Moscow), and Moscow State University.

Sampling Ideology

First, we chose samples for the study of secondary mineral assemblages and chemical composition of altered rocks, including oxidative and nonoxidative types of alteration. To study the redistribution of chemical elements in rocks during alteration, we paid close attention to the direct distribution of elements in altered rocks (i.e., groundmass minerals and matrix and phenocrysts). This resulted in preferential sampling of massive rocks. Also, for completely vesicular rock samples, we sampled vesicular basalts. In both cases, we tried to avoid sampling rocks with veins, since the composition of such rocks often indicates hydrothermal circulation in large blocks of the oceanic crust and may not reflect redistribution of chemical elements in individual samples of host rocks. Also, vein minerals have already been well studied during other DSDP/ODP legs, as well as by other researchers. We did not neglect, however, the study of veinlets in the samples. In summary, our study of alteration mineralogy was concentrated mainly on secondary minerals instead of groundmass minerals and matrix and phenocryst minerals; however, we did occasionally sample whole-rock alteration halos around fractures.

To avoid serious errors in estimation of chemical element mobility in the oceanic crust due to alteration of basalts, we analyzed various petrochemical rock types separately. These types are represented by tholeiitic, subalkaline, and alkaline basalts; andesites, dacites, and rhyolites; high-magnesium basalts and andesites; and gabbros, dunites, and harzburgites. These main types are divided into subtypes. We analyzed petrochemical variations separately for each subdivision. Thus, to differentiate data on redistribution of elements due to alteration of basalts from data on element variations in their original composition, we analyzed data from samples, for example, with different TiO_2, MgO, minor element, and rare earth element (REE) contents. Within recognized types and subtypes, we determined massive and vesicular, glassy and aphyric, phyric igneous, and brecciated rocks, as well as their oxidized and nonoxidized varieties. We assigned the sparsely phyric varieties, containing <5% phenocrysts, to the aphyric rock group and placed the conventional boundary between oxidized and nonoxidized bulk rocks based on $Fe_2O_3/FeO = 1.60$.

Petrography, X-Ray Diffraction, Electronography, and Electron Microscopy

Altered and fresh basalts were studied in thin section in order to determine mineralogy. Secondary minerals from igneous rocks were studied in thin section and examined by X-ray diffraction (XRD) on oriented specimens. Prior to XRD analyses, any specimens with clay minerals were prepared by grinding the basalt pieces to 1–2 mm in an agate mortar and mixing with distilled water to concentrate the clay minerals in suspension. Each specimen was air-dried, treated with glycerol and, in part, ethylene glycol, and heated at 550°C for 1 hr. DRON-3 and DRON-4 X-ray diffractometers with CuKα emission, Ni filters, and slit widths of 1 and 0.5 mm were used to analyze the specimens.

An electron micrograph and a Tesla BS-540 electron microscope were used to determine clay minerals and their parameter *b* (Far East Geological Institute).

Density Analysis

We determined the density of igneous rocks by weighing the samples using an analytical balance with a precision of 0.001 g. The routine method included (1) weighing the sample after drying at temperatures from 105° to110°C for 8 hr to as long as 36 hr and (2) weighing the sample in both air and water. The densities of many samples, primarily vesicular, were determined without weighing in water. We shaped the rock samples to a geometrically regular form using a diamond saw or disk with diamond powder, measured the size and volume and determined the constant weight of the dried sample, arithmetically divided it by volume, and obtained its density in grams per cubic centimeter. Samples of rocks that could be crumbled were dipped in melted paraffin at 60°C before weighing in water.

Wet Chemical Analysis

Major elements in bulk samples of igneous rocks were analyzed by the classical wet chemistry methods (Zolotarev and Choporov, 1978). This included the determination of H_2O^+, H_2O^-, Fe_2O_3, FeO, and CO_2, and, for several samples, S_{total}.

X-Ray Fluorescence Analysis

Analyses for Y, Nb, Rb, Sr, Ba, Cr, Ni, Co, V, Cu, Pb, and Zn were performed by X-ray fluorescence (XRF) on a MagiXpro wave-sequential X-ray spectrometer.

Rare Earth Element Analysis

REEs, Sc, Hf, Ta, and Th in igneous rocks were determined by radiochemical neutron activation analysis (NAA). Samples (100 mg) were irradiated together with a standard with a thermal neutron flux of 1.2×10^{13} $n/cm^2 \cdot s$ for 20 hr. REE fractions were separated radiochemically. Gamma spectrometry determination of REEs was performed on an ORTEC gamma spectrometer with a GEM-20-P4 coaxial Ge (Li) detector.

The accuracy of the results was checked against U.S. Geological Survey BCR-1, AGV-1, and DNC-1 standards (Govindaraju, 1989). Precision and accuracy of major and minor element data are shown in Table **T1.**

T1. Precision and accuracy of major and trace elements, p.356.

Atomic Volume Method of Recalculation of Chemical Data and Mass Balance Calculation

We used the atomic volume system for recalculation of chemical data as the preferred method for determination of matter gain/loss during alteration of igneous rocks (Kurnosov, 1986, 1992). The procedures for these calculations

are described by Kazizyn and Rudnik (1968).

This method shows the atomic form of rock components in a standard volume and requires recalculation of chemical analyses corrected for porosity to reflect real packing of atoms in minerals. The atomic content of each element can be quantified in grams per standard volume.

To estimate the mass balance resulting from metasomatic processes, calculations must be based on geometric volumes (i.e., with regard to porosity). A greater composition percentage (in weight percent) of matter does not necessarily correspond to greater absolute content in the rock.

We recalculated the chemical data using the following formula (Kazitzyn and Rudnik, 1968):

$$P_i = 0.166 \times a_i \times P_o^i \times d_v \times R_o, \quad (1)$$

where

P_i = content of element (g) in 1000 cm³ of rock,
a_i = atomic weight of element,
P_o^i = value of element in the oxidized form (wt%),
d_v = density of the sample (g/cm³), and
R_o = transitional coefficient for each oxide (Table **T2**).

T2. Values of transitional coefficient, p.357.

We excluded H_2O^- from chemical analyses data and recalculated results to 100%.

We simplified these calculations for oxides by replacing the constant ($0.166 \times a_i \times R_o$) for each oxide with coefficient K (Table **T3**). Therefore,

T3. Values of coefficient K, p.358.

$$P_i = K \times P_o^i \times d_v. \quad (2)$$

To calculate the abundance of a trace elements in weight percent per 1000 cm³ of rock, one can use Equation **E1** or **E2.** The transitional coefficient R can be calculated as

$$R = (1000:16.6):a_i \text{ or} \quad (3)$$

$$R = 60.241:a_i, \quad (4)$$

where a_i = atomic weight of an element.

The content of a trace element is shown in parts per million (grams per ton of rock) using the following equation:

$$P_i = P_a^i \times d_v \times 10^{-3}, \quad (5)$$

where

P_i = content of a chemical element (grams in 1000 cm³) of rock,
P_a^i = value of trace element (grams per ton of rock or ppm), and
d_v = density of the sample (grams per cubic centimeter).

We used Equation **E5** in our recalculations of data on contents of trace elements.

To avoid gross errors during the determination of matter gain/loss, it is necessary to ensure that the protolith has been accurately identified. Collection of such samples is very complex.

Comparison of massive and vesicular basalt samples within one group may result in a gross error. Vesicular basalts are widespread in seamounts.

Altered vesicular and highly vesicular basalts have less element per unit volume before alteration than massive basalts.

Significant errors are inevitable during determination of element gain/loss, as well as when the rocks with different vesicularity are included in the same comparison group. So, in this estimation with the use of the atomic volume system for recalculation of chemical data, it is necessary that the analyzed rocks were grouped by vesicularity. The exception to this rule is the study of bulk-rock chemical changes through lava flows, which show strongly varying vesicularity from top to bottom. In this case, the atomic volume method can not be used; therefore, the rock chemical compositions are directly compared. The results of such comparison, however, may not correspond to the real element gain/loss. If for some reason it was difficult to correctly estimate the mass balance, we compared the data of the chemical analyses that were not recalculated in grams per 1000 cm^3 using the rock densities, as was the case with basalts showing wide variation of vesicularity. In these cases, we always noted that the results obtained in this way may not correspond to the element real gain/loss through rock alteration.

ALTERATION OF IGNEOUS ROCKS FROM MID-OCEAN RIDGES

Mid-ocean ridges stretch for >60,000 km in the Earth's oceans. They are characterized by the presence of hydrothermal systems. Water-rock interaction in these hydrothermal systems results in hot springs ("black smokers") on the floor of axial valleys. Our present knowledge of igneous rock alteration in these giant structures needs further improvement. We have continued the study of alteration of young and ancient basalts from the axis and flanks of mid-ocean ridges in the Pacific and Atlantic Oceans.

Costa Rica Rift

Hole 504B

Site 504 is located in the eastern equatorial Pacific near the Costa Rica Rift axis (Fig. **F1**). Hole 504B was drilled during seven DSDP/ODP legs (Table **T4**). The recovered basalts are 5.9 Ma (Becker, Sakai, et al., 1988). Hole 504B penetrated 2111.0 m of rock. Below 274.5 m of sediment, the hole penetrated 571.5 m of volcanic rock (pillow lavas and flows) from 274.5 to 846 meters below seafloor (mbsf), a 209-m-thick transition zone (846–1055 mbsf), and a 1050-m-thick sheeted dike complex (upper dikes from 1055 to 1500 mbsf and lower dikes from 1500 to 2111 mbsf). Drilling stopped in the lowermost sheeted dike complex near the upper third layer of the oceanic crust.

Alteration of igneous rocks, mineralogy, chemical composition, distribution and zonation of secondary minerals, replacement of phenocrysts, minerals of groundmass and interstitial glass, formation of veins and filling of vesicles, and conditions and sequences of secondary mineral formation in Hole 504B were studied in great detail by Adamson (1983), Alt and Emmerman (1985), Alt and Chaussidon (1989), Alt et al. (1983, 1985a, 1985b, 1986, 1989, 1995, 1996a, 1996b), Autio et al., 1989; Becker et al. (1988), Honnorez (1981), Honnorez et al. (1983, 1985), Ishizuka (1989), Laverne (1983), Laverne et al. (1995), Noack et al. (1983), Pertsev and Boronikhin (1983a, 1983b), Pertsev and Kurdyukov (1996), Schandl and Gorton (1995), Sharaskin et al. (1983), Shimizu et al. (1989), Sparks (1995), Vanko et al. (1996), Zuleger et al. (1995, 1996), and others. We participated in the study of alteration mineralogy of the volcanic section in Hole 504B during Legs 69 and 70 (Kurnosov et al., 1983).

We studied additional samples of basalts and dolerites recovered during DSDP Legs 69, 70, and 83 and ODP Legs 111, 137, 140, and 148. Samples were taken from slightly, moderately, and highly altered and fresh

F1. Site 504 in the eastern Pacific, p.173.

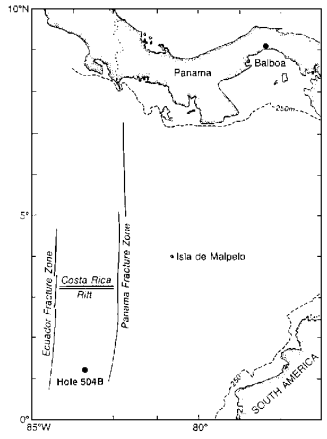

T4. Basement hole in Costa Rica Rift, p.359.

rocks in massive, fractured, and brecciated zones, as well as oxidized basalts. In igneous rocks, we examined the secondary minerals that replace phenocrysts, groundmass minerals, and interstitial glass and occur in veins and vesicles. We also studied mobility of elements in relation to alteration under different conditions (smectitization, chloritization, and amphibolization) and in nonoxidative and oxidative environments.

Petrography and Bulk-Rock Chemical Composition

The basement cored in Hole 504B was divided into 294 lithologic units. The rocks are aphyric or sparsely to highly phyric (plagioclase-olivine, occasionally with clinopyroxene) fine- to medium grained basalts and dolerites and are geochemically typical mid-ocean-ridge basalts (MORB) (see *Proceedings of the Ocean Drilling Program, Scientific Results*, Volumes 69, 83, 111, 137/140, and 148).

Petrographic descriptions of thin sections of the selected igneous rocks are shown in **"Appendix A,"** p.1. They are divided into aphyric (from pillow lavas) and phyric (from sheeted dike complex) varieties with various amounts of plagioclase, clinopyroxene, and olivine phenocrysts. Basalts and dolerites are essentially undifferentiated in silicity, Al_2O_3, Fe, Mg, and Ti and belong to the low-alkaline type of the tholeiitic MORB series (Fig. **F2;** Tables **T5, T6, T7, T8, T9, T10, T11**). These igneous rocks are similar to normal tholeiitic MORB with abundant siderophile and chalcophile minor elements, but they are somewhat depleted in Nb, Zr, Rb, and Sr (Fig. **F3**). Normalized REEs indicate that igneous rocks in Hole 504B are depleted in large-ion lanthanides and Eu and are related to a homogeneous group of rocks (Fig. **F4**).

Alteration Mineralogy

Secondary Minerals in Igneous Rocks. The total distribution of secondary minerals in basement recovered from Hole 504B was presented by Alt et al. (1996a) (Fig. **F5**).

We examined secondary minerals that replace groundmass and phenocryst minerals (without veinlet minerals) in basalts (Table **T12**). Petrographic observations of alteration mineralogy, as well as identification of secondary minerals by XRD, are shown in **"Appendix A,"** p.1. See Kurnosov et al. (1983) for a detailed description of secondary minerals from the volcanic section and olivine replaced with secondary minerals, interstitial glass, pyroxene, and plagioclase.

Table **T12** shows that basalts from the upper 580 m of Hole 504B (to a depth of ~850 mbsf) are smectitized. Trioctahedral smectites (saponite type) are the principal secondary minerals in basalts from the volcanic section. The lower boundary of smectitization is located in the uppermost part of the transition zone, whereas in the upper part of the section (274.5–751 mbsf), smectites with Na-K-interlayer cations were identified as well (**"Appendix A,"** p.1). Chloritic minerals (mixed-layer chlorite-smectite with ~20% smectite layers and mixed-layer chlorite-swelling chlorite) were found in the smectite zone of the volcanic section (560–580 mbsf). Below 850 mbsf, clay minerals are represented by chloritic minerals.

In the transition zone (846–1055 mbsf), chlorites contain low amounts of swelling layers (5%–10%). Several samples from this zone contain corrensite. In the lowermost part of the transition zone, swelling chlorite was found.

In the dike complex as a whole (1055–2111 mbsf), stable-structure chlorite formation is typical. Chlorite persists in dikes, but distribution of chlorite minerals in the upper (1055–1500 mbsf) and lower (1500–2111 mbsf) dikes is different. In the upper dikes, the swelling chlorite and mixed-layer chlorite-smectite minerals, including a corrensite-like mineral, are common. The mixed-layer chlorite-smectite group of minerals contains fewer smectite layers (~40%) than corrensite from the transition zone. In contrast to the upper dikes,

F2. AFM diagram for basalts, Hole 504B, p.174.

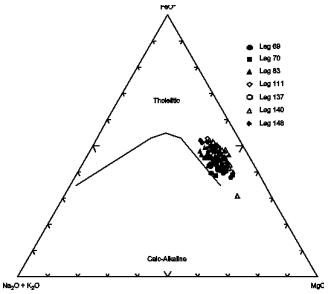

T5. Basalts, Hole 504B (Leg 69), p.360.

T6. Basalts, Hole 504B (Leg 70), p.365.

T7. Basalts, Hole 504B (Leg 83), p.372.

T8. Basalts, Hole 594B, p.377.

T9. Basalts, Hole 504B (Leg 137), p.380.

T10. Basalts, Hole 504B (Leg 140), p.381.

T11. Basalts, Hole 504B (Leg 148), p.385.

F3. Nb-Zr-Y diagram for basalts, Hole 504B, p.175.

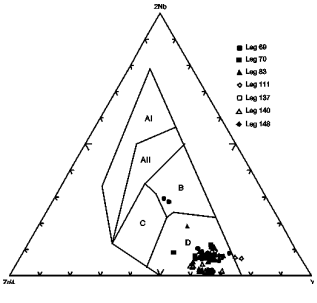

swelling chlorite and mixed-layer chlorite-smectite minerals are an insignificant admixture in the lower dikes.

It is clearly seen that in both the transition zone and the dike section, against a background of ubiquitous chlorite formation, the amount of swelling layers in the mixed-layer chlorite-smectite minerals decreases with depth. Below 1815 mbsf, minerals with swelling interlayers are not formed, and the number of swelling interlayers in chlorite also tends to decrease with depth. In the transition zone, swelling layers in chlorite usually make up ~5%–10%. In the dike section, the swelling interlayers are rarely found in chlorite from the rocks of the upper dikes.

Amphiboles and chlorite are widespread in both the transition zone and the sheeted dike complex; however, they are most common in the lower dike section, especially from 1630 mbsf to the bottom of the hole. Zones of alteration, mainly chloritization and amphibolization of dolerites, are located in this interval. In the upper dikes, a sharp increase in amphibole was observed twice, at ~1081 and 1482 mbsf. In thin sections from the dike zone, uralite and tremolite were optically identified (see "Appendix A," p.1). Amphiboles partly or completely replace pyroxene. There are small grains of titanite in the centers of tremolite grains. Titanite was also found in chlorite aggregates. Alt et al. (1996a) showed that titanite replaces titanomagnetite. Chlorites are found in the interstices between plagioclase laths replacing olivine, clinopyroxene, and plagioclase. Albite was found from 1000 mbsf to the bottom of the hole. It replaces plagioclases and is sometimes found among vein minerals. The highest amount of talc was found in the lower dikes (1712–1731 mbsf). Quartz in trace amounts was determined by XRD throughout Hole 504B.

Thin section studies show that uralitic amphibole was partly replaced with chlorite at 1781.03 and 1992.14 mbsf. At 1813.16 mbsf, chlorites are replaced with amphiboles (see **"Appendix A,"** p.1).

Vein Minerals. Vein minerals from the volcanic section (274.5–846 mbsf) are trioctahedral and dioctachedral smectites, Fe-Mg and Fe chlorite, talk, hematite, phillipsite, natrolite, aragonite, calcite, Mn minerals, analcime, okenite, gyrolite, thomsonite (identified by N.N. Pertsev), anhydrite, quartz, cristobalite, apophylite, actinolite, pyrite, chalcocite, bismutite(?), foujasite, Fe hydrosilicate, magnesite, and undetermined minerals 12.9 Å and 3.20 Å (Kurnosov et al., 1983). Below 846 mbsf in the transition zone and dike section, we studied only a few samples with thin veins (Table **T13**).

Comparison of clay minerals from veins and salbands of veins (Table **T13**) with those from host rocks (Table **T12**) shows that their composition differs in some cases.

In the volcanic section at 518.14 and 527.18 mbsf, basalt contains smectite with ~10% mica layers and small admixtures of chlorite. In veins, smectites (dominant), mixed-layer smectite-swelling chlorite minerals, and chlorite were determined in trace amounts. Clay minerals from veins contain a higher chlorite component than the interior basalts surrounding the veins.

At 536.14 mbsf, trace amounts of smectite (principal mineral) and chlorite were identified in the host rock (brecciated basalt). In the cemented matter of the breccia, only mixed-layer smectite-chlorite minerals were found. At 561.57 mbsf, basalt contains smectite, but in the vein, mixed-layer smectite-chlorite minerals were recognized as well as smectites. At 588.46 mbsf, chlorite is present in trace amounts in veins, in contrast to the host basalt.

At 810.07 mbsf, basalt contains smectites with ~20% mica layers. In veins, mixed-layer chlorite-smectite minerals with ~20% swelling layers occur in trace amounts, as well as smectites with ~10% mica layers. Host basalt at 828.70 mbsf contains mixed chlorite and smectite, with smectite prevailing, and veins contain chlorite and smectite.

In the uppermost part of the transition section (908 mbsf), basalt

F4. Chondrite-normalized REEs for basalts, Hole 504B, p.176.

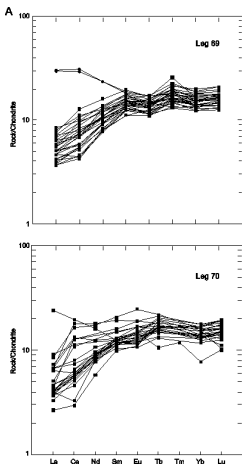

F5. Lithostratigraphy, Hole 504B, p.180.

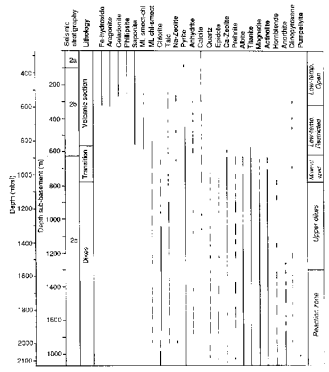

T12. XRD basalts, Hole 504B, p.386.

T13. Veins, Hole 504B, p.389.

contains corrensite and mixed-layer chlorite-smectite minerals with ~10% swelling interlayers. In veins, only chlorite with ~5% swelling interlayers was found.

In basalts beneath the top of the basement, hematite, celadonite, phillipsite, smectites of predominantly light green and reddish brown colors, calcite, anhydrite, and K-feldspar (identified by Pertsev and Boronikhin, 1983b) were found mainly in cracks and along the fractured zones to a depth of ~300 m. These zones are oxidized and do not contain sulfides, which are widespread in deeper parts of the section recovered from Hole 504B.

Bulk-Rock Chemical Changes

Studies of the mobility of chemical elements have been made, and the alteration mass balance of igneous rocks from different parts of the basaltic layer section in the cores of Hole 504B have been calculated by Alt and Emmermann (1985), Alt et al. (1996b), Bach et al. (1996), Honnorez et al. (1983), Kepezhinskas et al. (1995), Pertsev and Boronikhin (1983a), Sparks (1995), and Zuleger et al. (1995). Synthesis of these results (Alt et al., 1996a) showed that the altered rocks from the upper volcanic section (274.5–846 mbsf) contain high amounts of K, Rb, B, CO_2, and H_2O^+ (note: see Alt et al., 1996a, for isotopic changes). Red and black halos around veins and small patches are more chemically altered than the host rocks. Some elements in these rocks show primary features, such as P and Ti contents. The same chemical changes as those seen in the upper volcation zone are observed in the lower volcanic section, but they are much less intense. The bulk rocks of the upper sheeted dikes and transition section exhibit striking chemical changes compared to the lower part of the effusive section. In the transition zone, H_2O^+ and Li contents increase and CO_2 content is sporadically high, though it decreases downhole in the sheeted dike complex. Al_2O_3 and TiO_2 contents are slightly increased. K_2O and Fe_2O_3/FeO ratios decrease downhole. CaO and Na_2O are depleted or enriched. In the altered rocks, La/Sm ratios increase. Increases in MgO contents were not observed in the altered bulk rocks. In the lower sheeted dikes, sharp loss of Cu, Zn, and S occurs. In some samples, CaO content is low, Na_2O content is elevated, and slight positive Eu anomalies are observed. H_2O^+ and CO_2 contents are slightly increased, and loss of K and Li takes place. TiO_2 and P_2O_5 show limited mobility. Neither the lower nor upper dikes are enriched in Mg.

The most accurate data on the redistribution of chemical elements through rock alteration can be obtained by using the atomic volume system for recalculation of chemical data with correction for density (Kazizyn and Rudnik, 1968). Using this method, we calculated the content of each element in the study samples in grams per 1000 cm^3 (see "Appendix B", Table AT1). The distribution of elements in fresh and altered igneous rocks in Hole 504B is shown in Figure **F6**. Increases and decreases of elements in altered rocks were considered in comparison to the concentrations of elements in fresh analogs for each part of the section (upper and lower volcanic sections, transition zone, upper dikes, and lower dikes). Comparisons were made for aphyric and glassy basalts, phyric basalts, oxidized basalts, dolerites, and brecciated/fractured rocks.

In the upper volcanic section, decreases in Si, Fe_{total}, Ca, and Ce contents in the altered basalts from all rock groups were recognized. Decreases in content were also seen for Na, Mg, P, V, Zr, La, Sm, Yb, Y, Nd, and Eu, with exceptions for Na in oxidized rocks, P in aphyric basalts, and La, Sm, Yb, Y, Nd, and Eu in dolerites. Nd content increases in one sample of oxidized basalt. Ti is depleted in several samples of altered phyric and oxidized basalts. Al is depleted or enriched in all rock groups except dolerites. In the uppermost part of the upper volcanic section, Mn contents decrease in the altered phyric and oxidized basalts. Below this section, Mn contents increase in several samples of phyric and aphyric basalts and dolerites. Mg is either depleted, as seen in several samples of altered aphyric and phyric basalts and fractured rocks, or enriched,

AT1. Major and trace elements, Hole 504B, p.1.

F6. Whole-rock chemical compositions, Hole 504B, p.181

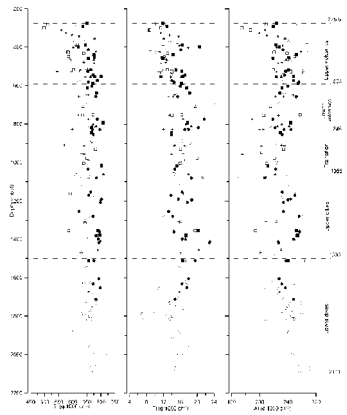

as seen in one sample of altered dolerite. K contents increase in altered basalts from all rock groups. It should be emphasized that K contents have a wide range of values in fresh rocks from the upper volcanic section. In the upper part of the section, Cu is depleted in altered phyric and oxidized basalts. In one sample of phyric basalt from the lower part of the section, increases in Cu contents were observed. In other samples of the fractured rock, losses of Tb and Lu take place. Contents of Ni decrease slightly in several samples of altered phyric and aphyric basalts and fractured rocks. Co decreases or increases in aphyric and oxidized basalt. Rb is enriched or depleted, Sr increases in oxidized basalt, and Ba is enriched in altered phyric and aphyric basalts and several samples of brecciated rock.

In the lower volcanic section, chemical changes caused by alteration were similar but less intense to nonexistent.

In the transition zone, chemical changes are mainly similar to changes seen in the volcanic sections with some differences in behavior of elements. Several samples of altered rocks record alteration leading to increases in Na, Cu, Zn, Ni, Co, Ba, Sm, and Eu. It should be noted that K contents in fresh rocks of the transition zone and dike section are very low; therefore, low K contents in the altered rocks from those sections are not associated with alteration.

The least mobile elements during alteration are those from the upper dikes, but, in several samples, some mobility of Si, Al, Mg, Ca, Cu, Ni, Co, and Sr was observed.

Study of element mobility through alteration of igneous rocks shows that in the reaction zone (the lower sheeted dike complex—zone of amphibolization and chloritization of rocks), the greatest loss of Si, Ti, Fe_{total}, Mn, Mg, Zn, La, Sm, Yb, Y, Eu, and Lu occurs, whereas the concentrations of Cr, Ni, Co, V, Nb, and Sr increase. In the altered dolerites, K and Rb from the lower part of the section increase (K increases slightly). Al, Ca, Na, P, Cu, Zr, Ce, Nd, and Tb are depleted or enriched and loss of Ca, Cu, Zr, Ce, Nd, and Tb predominates in the reaction zone.

Oxidative alteration (upper volcanics) reflects whole-rock increases in H_2O^+, K, Fe_2O_3, Sr, and Rb and decreases in Si and Ca. In the extreme oxidative zones, rocks lose Ti, Al, Fe_{total}, Mn, P, Cu, Co, V, Zr, La, Sm, Yb, Nd, Eu, Y, and Ce (Fig. **F6**).

Brief Comments

The study of secondary minerals in basalts recovered from Hole 504B shows that amphibolization, chloritization, and smectitization zones (the change of greenschist facies to smectite facies) demonstrate vertical zonation of temperatures in the upper part of the oceanic crust. This zonation is complicated with alternation of chloritization and amphibolization zones in the petrographically and geochemically homogeneous lower part of the section in Hole 504B (dike complex). In the smectite zone of the volcanic section (560–580 mbsf), chloritic minerals (mixed-layer chlorite-smectite and mixed-layer chlorite-swelling chlorite) were found. Against a background of general temperature decrease upward in the section and fixed in the greenschist alteration (through the transition zone) by basalt smectitization in the section of the ocean crust basaltic layer (Layer 2) recovered from Hole 504B for its total thickness, we can interpret these observations as a heterogeneous environment of vulcanite hydrothermal alteration. It is known that such an environment occurs in the peripheral parts of the hydrothermal convective systems characterized by subhorizontal water flows moving along the fractured and brecciated zones. This phenomenon was best studied in Iceland.

Study of clay minerals from veins and comparison with clay minerals from igneous rocks showed that conditions of clay mineral formation in host rocks and fractures in the volcanic section and upper part of the transition zone

were not identical. Veins often contain chloritic components, whereas the host rocks are only smectitized. Solutions in the fractures were hotter than those altering the basalts. This phenomenon was not observed below 908 mbsf. At great depths, the temperatures of the solutions from fractures and host rocks are probably equalized. Compositions of the fluids were likely similar as well. Sources supplying the elements for the chemical composition of solutions decrease with depth to the minimum.

The temperature of the convective cell was probably not uniform through time. Evidence for this can be signs of both retrograde metamorphism (uralitic amphibole partly replaced by chlorite at 1781.3 and 1992.14 mbsf) and prograde metamorphism (chlorites replaced by amphiboles in the sample from 1813.16 mbsf).

Alt et al. (1996a) proposed the model of alteration of the crust in Hole 504B. Alteration of the transition zone and upper dikes (to 1500 mbsf) occurred in a series of stages:

1. Chlorite, actinolite, albite-oligoclase, and titanite;
2. Quartz, epidote, and sulfides;
3. Anhydrite; and
4. Zeolites and calcite.

Mineral assemblages of two early stages are typical of the greenschist facies (maximum temperature = 350°–380°C). The lower dikes (1500–2111 mbsf) are related to an early high-temperature (>380°C) alteration stage with formation of hornblende and anorthite. Their content is similar to that of the upper dike greenschist assemblages (~300°–400°C) but with rare epidote-quartz veins. The pillow section was altered at temperatures <150°C. In the upper 310 m, alteration occurred with oxidizing seawater. Stages 3 and 4 took place as the crust moved off axis. Cold seawater discharged downcrust with the formation of anhydrite (Stage 3). Stage 4 led to calcic zeolites and calcite formation at temperatures of 100°–250°C.

In the context of the history of manifestation of oxidative alteration in the upper part of the oceanic crust basaltic layer recovered from Hole 504B, two main stages of alteration can be distinguished (Kurnosov et al., 1983; Kurnosov, 1986):

1. The first stage takes place in the axial spreading zone. It is characterized by hydrothermal nonoxidative alteration. The first stage of alteration may occur in a broad range of temperatures (from high temperatures in the sheeted dike complex to low temperatures in the upper part of the pillow section, in accordance with vertical temperature zonation observed above a magmatic chamber). It should be noted that the rocks drilled in Hole 504B, at the first stage of alteration, were not in the discharge zone of hot solutions. Otherwise, the effusive part of the section would have been altered under the greenschist facies conditions, as observed during Leg 139 in the axial valley of the Juan de Fuca Ridge (Kurnosov et al., 1994). High-temperature alteration of igneous rocks from the lower part of the hole is connected with vertical temperature zonation above a magmatic chamber. We propose that the most significant alteration of basalts comes to an end at the first stage.
2. The second stage of alteration is related to migration of basalts off the spreading axis toward the zone of mass inflow of cold seawater to the fractured and brecciated zones as a result of tectonic movement of the oceanic crust. Oxidative alteration dominates at this stage. It is expressed along the fractured zones to a depth of ~300 m in basalts. The secondary mineral assemblages (hematite, celadonite, phillipsite, calcite, anhydrite, and K-feldspar) demonstrate a mineral formation temperature interval of ~80° and less. Anhydrite in its turn may be an

indicator of sharp cooling of hot solutions through their mixing with seawater penetrating basalts (i.e., it may fix the existence of the zones where hydrotherms boil up). The highest content of anhydrite in the lower part of the volcanic section is within the 751- to 810-mbsf interval (Kurnosov et al., 1983). The hydrothermal mineral formation temperatures in the zones of boil-up, studied in the hydrothermal systems of Kamchatka (Russia), range from 300°–250°C to 200°–170°C and lower (Rychagov, 2003). Precipitation of anhydrite at deeper horizons can be of another origin. First, it concerns the anhydrite formation immediately in the rock and not in veins. A wide interval of depths of the anhydrite occurrence in veins may reflect a gradual subsidence of the boundary of the hot solutions and seawater mixing as the oceanic upper crustal section, recovered from Hole 504B, moves away from the spreading axial zone (i.e., from the highest temperature part of the hydrothermal system). So, increase of depth of the seawater penetration into the oceanic crust under the spreading conditions can be fixed. The oxidative environment is superimposed on the nonoxidative one. This stage is important for alteration of the uppermost part of basaltic crust, but it is incomparable in its scale with alteration of the entire basaltic layer. It is important to note that oxidative alteration in axial zones of mid-ocean ridges is unknown (ODP Legs 106, 109, 142, 139, and 169).

The next stage of alteration takes place after formation of the sedimentary cover above the basement rocks. The present-day temperature of 165°C in Hole 504B, which was measured at 1280 mbsf (Becker, Sakai, et al., 1988; Gable et al., 1989), has probably no significant influence on further alteration of basalts in this section, as a 274.5-m-thick sediment cover prevents seawater penetration to the basalt layer. The only seawater present is that which was accumulated by basalts during previous stages of alteration. This process is probably less expressive and, in the absence of seawater, restricted in time because of the limited quantity of water. At the same time, the process of basalt alteration can be active under the screening sediment cover if subhorizontal flows of seawater run along the fractured and brecciated zones, possibly at great distances from the places where it penetrates the oceanic crust.

Results on the mobility of elements due to alteration of igneous rocks revealed that the most significant mobility of elements occurred in the “reaction zone” (lower dikes) and upper volcanics. In the uppermost and lowermost parts of the section, behavior tendencies of many elements are similar (Fig. F6). In the lower volcanic section, chemical changes caused by alteration were similar to those in the upper volcanic section but less intense or nonexistent. In the transition zone, chemical changes are chiefly similar to those in the volcanic section. Several samples of altered rocks record that alteration causes increases in Na, Cu, Zn, Ni, Co, and Ba, the least mobile elements during alteration of igneous rocks from the upper dikes, but in several samples, some mobility of Si, Al, Mg, Ca, Cu, Ni, Co, and Sr was recognized. At the same time, mobility of Si, Al, Mg, Ca, Cu, Ni, Co, and Sr was established to be comparable with the mobility level of these elements in other sections. Oxidative alteration is, for the most part, reflected in the whole-rock increase of H_2O^+, K, Fe_2O_3, Sr, and Rb and decrease of Si and Ca. In the most oxidized rock samples, loss of Ti, Al, Fe_{total}, Mn, P, Cu, Co, V, Zr, La, Sm, Yb, Nd, Eu, Y, and Ce was fixed.

As a whole, in the upper oceanic crust (~1900 m thick), many elements are mobile in igneous rock alteration under nonoxidative and oxidative conditions.

Middle Valley, Juan de Fuca Ridge, and Escanaba Trough, Gorda Ridge

In the upper part of the oceanic crust, water-rock interaction in the spreading zones is realized most intensively in hydrothermal uplift zones

(discharge of hot solutions with a temperature of ~300°C and interactions of water with basalts at temperatures as high as 400°C). The most representative areas were drilled in the Middle Valley of the Juan de Fuca Ridge during Legs 139 and 169 (Davis, Mottl, Fisher, et al., 1992; Fouquet, Zierenberg, Miller, et al., 1998). The Middle Valley is located near the southwestern extremity of Canada (Fig. **F7**). This tectonomagmatic structure is a medium-rate spreading center (58 mm/yr) that is developing at a triple junction with the Sovanco Fracture Zone and the Nootka fault (Davis and Villinger, 1992).

The axial valley of Escanaba Trough at the southern end of the Gorda Ridge near the Mendocino Fracture Zone was drilled during Leg 169 (Fig. F7). In contrast to the Middle Valley, Escanaba Trough has a low spreading rate (24 mm/yr) and lower temperatures at the sediment/basalt interface (~80°C for Escanaba and ~270°C for the Middle Valley) (Davis and Becker, 1994; Davis and Villinger, 1992). The hydrothermal vents at Escanaba Trough are also lower in temperature than those at the Middle Valley (from 13.5° to 217°C vs. 285°C) (Campbell et al., 1994; Fouquet, Zierenberg, Miller, et al., 1998; Zierenberg and Miller, 2000).

We have studied samples of basalts and dolerites in Holes 855A, 855D, 856A, 856B, 856H, 857C, 857D, 858F, and 858G in the Middle Valley and Holes 1037B and 1038I in Escanaba Trough (Table **T14**). The samples were taken from altered and fresh massive rocks. Petrographic descriptions of thin sections, XRD data, and electron microscopy and micrography results from clay minerals are shown in **"Appendix A,"** p.27. Some of the samples of igneous rocks from Holes 856A, 857C, and 857D, as well all samples from Holes 858F and 858G, were studied earlier (Kurnosov et al., 1994). Abundances of major and minor elements in the altered and fresh igneous rocks were calculated for all samples (see "Appendix B", Tables **AT2, AT3, AT4, AT5, AT6, AT7, AT8**). Densities are shown in the chemical composition tables. The density data are very similar to those for basalts in Holes 856H, 1037B, and 1038I (Groschel-Becker, 2000).

During Legs 139 and 169, the most highly altered igneous rocks were recovered from Hole 856H (Bent Hill area of the Middle Valley). Alteration is as much as 70%–100% of the rock volume, H_2O^+ contents are ~8.58 wt%, and densities are from ~3 g/cm^3 in fresh basalt to 2.36 g/cm^3 in highly altered rock. Element mobility, therefore, was studied in the altered igneous rocks in Hole 856H. Element mobility was also studied in the altered igneous rocks in Holes 857C and 857D, which are less altered than the basalts and dolerites in Hole 856H.

Holes 855A and 855D

Site 855 is located near the eastern boundary of the fault scarp (Fig. **F8**) in an area with low heat flow and where basalts were encountered at 74 mbsf (Davis, Mottl, Fisher, et al., 1992). Petrographic descriptions of thin sections of the selected igneous rocks in Holes 855A and 855D are shown in **"Appendix A,"** p.27. These igneous rocks are represented by phyric and aphyric basalts. Phyric basalts contain various amounts of plagioclase and clinopyroxene phenocrysts, as much as 20%. The basalts are slightly differentiated MORB (Figs. **F9, F10, F11**). Additional samples of basalts are very slightly altered or fresh. H_2O^+ contents vary from 0.28 to 0.32 wt% and densities from 2.87 to 2.94 g/cm^3 (Table **T15**) and show low-temperature alteration. The principal secondary mineral is smectite with ~20% mica layers (Table **T16; "Appendix A,"** p.27). Stakes and Franklin (1994) determined low-temperature ranges of the secondary minerals smectite, celadonite, and carbonate. These basalts were used as fresh analogs (see "Appendix B", Table **AT2**) of altered igneous rocks from zones of hydrothermal activity when estimating element mobility in Holes 856H, 857C, and 857D.

F7. Sites in Middle Valley, Juan de Fuca Ridge, and Escanaba Trough, Gorda Ridge, p.192.

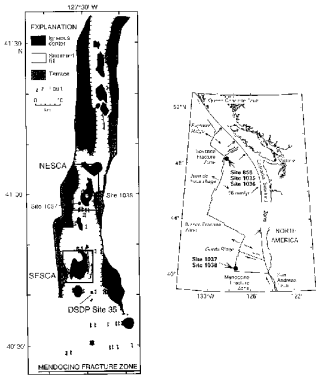

T14. Additional basement holes, Legs 139 and 169, p.392.

AT2. Major and trace elements, Holes 855A and 855D, p.25.

AT3. Major and trace elements, Holes 856A and 856B, p.26.

AT4. Major and trace elements, Hole 856H, p.27.

AT5. Major and trace elements, Holes 857C and 857D, p.29.

AT6. Major and trace elements, Holes 858F and 858G, p.35.

AT7. Major and trace elements, Hole 1037B, p.36.

AT8. Major and trace elements, Hole 1038I, p.38.

Holes 856A and 856B

Site 856 is located on Bent Hill in the eastern part of the Middle Valley, ~3 km west of the fault scarp eastern boundary and 4 km east of the present-day rift axis (Fig. **F8**). The Bent Hill area was formerly the site of high-temperature hydrothermal discharge (Fouquet, Zierenberg, Miller, et al., 1998; Zierenberg and Miller, 2000). In the area, two mounds of massive sulfide were investigated; the Bent Hill massive sulfide and ODP Mound massive sulfide (Davis, Mottl, Fisher, et al., 1992).

Holes 856A and 856B are located at the center and on the southern edge of Bent Hill, respectively. In these holes, among the Pleistocene turbidites, sills were recovered at 112 mbsf and lower in Hole 856A and at 63 and 120 mbsf in Hole 856B. Temperatures at the bottoms of the holes were 60°C in Hole 856A and 160°C in Hole 856B (Davis, Mottl, Fischer, et al., 1992).

The studied rocks are phyric olivine basalt. Olivine phenocrysts range from 5% to 15% (see **"Appendix A,"** p.28) of the rock volume. Geochemically, the basalts are MORB (Figs. **F9, F10, F11;** Table **T17**). The igneous rocks in Holes 856A and 856B are similar to the most primitive rocks of the northern Juan de Fuca Ridge MORBs (Davis, Mottl, Fisher, et al., 1992; Van Wagoner and Leybourne, 1991).

For the most part, the basalts are slightly to moderately altered or fresh. H_2O^+ contents are from 0.58 to 2.32 wt% and rock densities are from 2.88 to 3.03 g/cm^3 (Table **T17**). The principal secondary mineral in Hole 855A is smectite with ~10%–30% mica layers. Basalt in Hole 855B is very slightly altered and contains XRD reflexes similar to chlorite, smectite, mixed-layer smectite-chlorite minerals, and talc (Table **T16; "Appendix A,"** p.28).

Element contents of basalts in Holes 856A and 856B are shown in "Appendix B", Table **AT3**.

Hole 856H

Hole 856H is in the central part of the Bent Hill massive sulfide deposit (height = 35 m) located 100 m south of Bent Hill. At a distance of 200 m from Site 856, there is a single hydrothermal vent with a temperature of 264°C (Zierenberg and Miller, 2000). Hole 856H was drilled to 500 mbsf. The hole penetrated the massive sulfide from 0 to 103.6 mbsf, and samples contained pyrrhotite and pyrite sulfides with trace amounts of sphalerite/wurtzite, isocubanite, and chalcopyrite. A sulfide feeder zone is at 103.6–210.6 mbsf. The uppermost unit is siltstone and mudstone with subvertical sulfide veins of isocubanite, chalcopyrite, and pyrrhotite. Below this interval, sediments contain disseminated sulfides with copper-enriched sandstone (Deep Cooper Zone) (Lawrie and Miller, 2000; Marquez and Nehlig, 2000). In the interval from 210.6 to 431.7 mbsf, the interbedded turbidite and hemipelagic sediments of the Pleistocene were recovered. Below this interval, igneous rocks were drilled (431.7–500 mbsf), revealing a complex of five 1- to >5-m-thick basaltic sills, 39.6 m of sediments (431.7–471.3 mbsf), and 28.9 m of basaltic flows (Fouquet, Zierenberg, Miller, et al., 1998; Zierenberg and Miller, 2000).

Petrography and Bulk-Rock Chemical Composition

Petrographic descriptions of thin sections from Hole 856H show that the igneous rocks are represented by aphyric, sparsely phyric, and phyric basalts with varying amounts of plagioclase, clinopyroxene, olivine phenocrysts, and dolerites (see **"Appendix A,"** p.28).

Basalts and dolerites are slightly differentiated in alkaline elements, FeO*, and MgO (Figs. **F12, F13;** Table **T18**). Variation diagrams of normalized REEs demonstrate that basalts in Hole 856H are tholeiitic MORB (Fig. **F14**). Low REE contents in several samples of basalts are caused by alteration. The

F8. Sites in Middle Valley, Juan de Fuca Ridge, p.193.

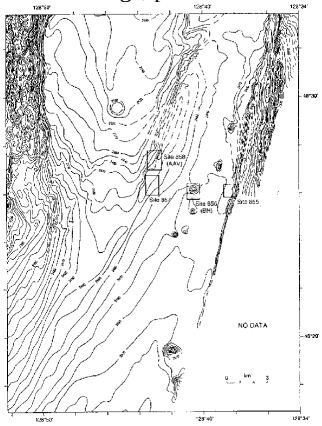

F9. AFM diagram for basalts, Sites 855, 856, 857, 858, p.194.

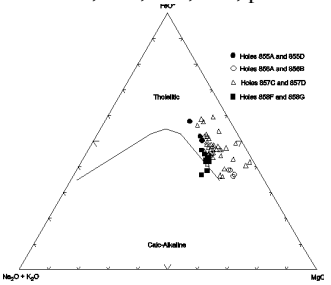

F10. Nb-Zr-Y diagram for basalts, Sites 855, 856, 857, 858, p.195.

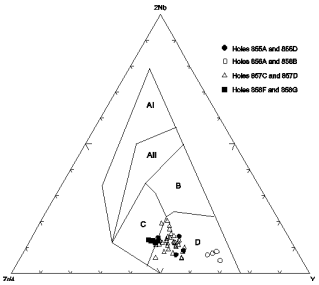

F11. Chondrite-normalized REEs for basalts, Sites 855, 856, 857, 858, p.196.

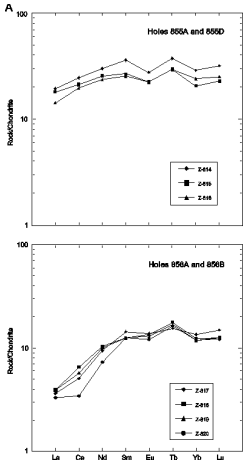

REE spectrum is slightly enriched in small ions of elements (particularly Tb) and highly depleted in Eu. The igneous rocks in Hole 856H are low-alkaline tholeiitic MORB (Fouquet, Zierenberg, Miller, et al., 1998).

Alteration Mineralogy

Highly altered igneous rocks are lighted. Phenocrysts, as well as primary minerals and interstitial glass in the groundmass, are often completely replaced with secondary minerals. Plagioclase is replaced by albite, zeolite, and chlorite; olivine is replaced with chlorite and magnetite; clinopyroxene is replaced with uralite (amphibole) and chlorite; and interstitial glass is replaced by chlorite, albite, and ore minerals. Epidote may be present, but because of the very small grains, it is difficult to determine. There are small grains of titanite in the rocks. In several thin sections, thin veins (0.1–0.2 mm) were found containing aggregates of albite and chlorite (see **"Appendix A,"** p.28). In basalts, numerous veins containing chlorite, quartz, chalcopyrite, pyrrhotite, sphalerite, calcite, and epidote were found (Fouquet, Zierenberg, Miller, et al., 1998; Zierenberg and Miller, 2000).

XRD studies of the fine fraction removed from the igneous rocks showed mineralogically uniform alteration. The principal secondary mineral is chlorite (Table **T16; "Appendix A,"** p.28). There is quartz in all samples. Poor evidence of vertical zonation is shown by the appearance of trace amounts of amphibole and talc downhole in Hole 856H.

Amphibole was determined from 466 mbsf to the bottom of the hole (500 mbsf). Talc was found below 490 mbsf (Table **T16**). The white veinlets at 434.4, 494.2, and 496.12 mbsf contain quartz. The secondary mineral assemblages demonstrate greenschist facies alteration conditions at temperatures of ~300°–350°C.

Bulk-Rock Chemical Changes

In the basaltic sill complex and basaltic flows in Hole 856H, extremely sharp decreases in Ca, Na, K, Cu, Zn, Rb, Sr, and S_{total} contents in the highly altered igneous rocks of all groups were identified (Fig. **F15;** "Appendix B", Table **AT4**). Si and Al contents decrease in the altered phyric and aphyric basalts and dolerites. Cr and Ni contents have a wide range of values in the altered rocks; however, several altered aphyric basalts and dolerites contain less Cr and Ni than their fresh analogs. In the samples of the most highly altered aphyric and phyric basalts, Eu, Ce, and Nd contents are decreased. La and Nb contents decrease in the highly altered aphyric basalts, but La and Nb are immobile in phyric basalts and dolerites.

Alteration leads to an increase of H_2O^+, Ti, Fe_{total}, Mn, and Mg, as well as Tb, Yb, and Lu, in several highly altered rocks (Fig. **F15**). There is a marked increase in P content in several samples of the highly altered igneous rocks of all groups. Co and V contents increase in altered aphyric and phyric basalts and dolerites; however, in the lowermost part of Hole 856H (the unit of basaltic flows), Co and V contents decrease in altered aphyric basalts and dolerites. The behavior of Y is similar to that of Co but is less pronounced. Sm contents often increase in dolerites. In altered aphyric basalts, Sm contents are depleted or enriched. Zr is an immobile element in the alteration (chloritization) of all igneous rock groups.

The study of element mobility at extremely high alteration of igneous rocks in Hole 856H and the results obtained by the Shipboard Scientific Party (Fouquet, Zierenberg, Miller, et al., 1998) showed similar behavior of Si, Al, Fe, K, Ca, Na, Ce, Cu, Zn, and Sr. Other elements, mainly Mn, Mg, Ti, Cr, and Nb, behave inversely.

Holes 857C and 857D

Site 857 is 5.2 km west of the fault scarp eastern boundary (Fig. **F8**) on

T15. Basalts, Holes 855A and 855D, p.393.

T16. Fine fraction, Legs 139 and 169, p.394.

T17. Basalts, Holes 856A and 856B, p.397.

F12. AFM diagram for basalts, Holes 856H, 1037B, and 1038I, p.198.

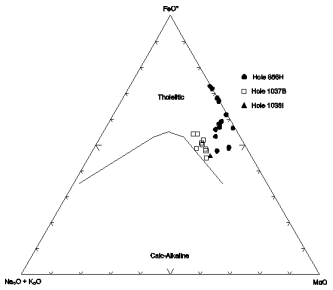

F13. Nb-Zr-Y diagram for basalts, Holes 856H, 1037B, and 1038I, p.199.

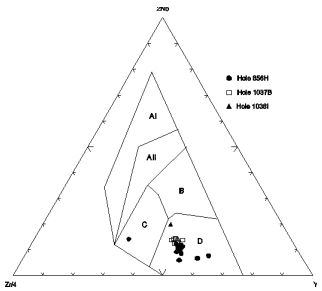

T18. Basalts, Hole 856H, p.398.

F14. Chondrite-normalized REEs for basalts, Holes 856H, 1037B, and 1038I, p.200.

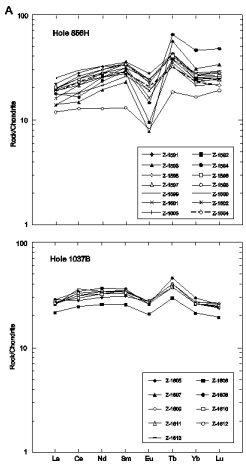

a major thermal anomaly, where the seafloor heat flow exceeds 0.8 W/m^2. Heat flow increases north of the site toward a hydrothermal vent field 1.6 km away. Heat flow is 4 W/m^2 and vents have a temperature of ~276°C (Shipboard Scientific Party, 1992). Hole 857C was drilled to 567.7 mbsf, where a temperature of ~260°C was estimated. Basaltic sills interlayering with sediments were encountered between 471.1 and 567.7 mbsf. Hole 857D, a deep reentry hole, was drilled 50 m north of Hole 857C to a total depth of 936.2 mbsf. Sills and interlayering sediments were cored between 581.1 and 936.2 mbsf (Table **T14**).

Petrography and Bulk-Rock Chemical Composition

The igneous rocks at Site 857 are phyric, sparsely phyric, and aphyric basalts, but for the most part they are dolerites (aphyric, sparsely phyric, and phyric dolerites, aphyric gabbro-dolerites, and congo-dolerites). Phenocrysts are plagioclase and pyroxene, with dominant plagioclase phenocrysts (from 2%–3% to 50%) (see **"Appendix A,"** p.31). The igneous rocks are slightly differentiated MORB tholeiites (Figs. **F9, F10, F11;** Table **T19**). Basalts in Holes 857C and 857D are decreased in Eu. The igneous rocks in Hole 857C and 857D were most likely derived from a normal MORB [N-MORB] parent melt (Shipboard Scientific Party, 1992).

Alteration Mineralogy

The igneous rocks recovered from Holes 857C and 857D are often 15%–30% altered (see **"Appendix A,"** p.31) and mainly chloritized (Table **T16**). H_2O^+ content is 1.27–4.22 wt% and densities are 2.45–2.88 g/cm^3 (Table **T19**). Several samples from Site 857 have H_2O^+ contents as high as 8.45 wt% and densities as low as 2.26 g/cm^3, in contrast to the highly altered igneous rocks from Hole 856H.

Plagioclase is partially albitized and replaced by chlorite, epidote, and zeolite. Clinopyroxene is partially or completely chloritized and uralitized with formation of fine-grained aggregates of leucoxene and titanite. Olivine is replaced with chlorite and leucoxene. Groundmass glass is chloritized with very small grains of leucoxene and titanite. The aggregates of very small grains (<0.01 mm) of opaque minerals (~15% of the rock volume) often occur as spots in the rock. Parts of interstices are filled with chlorite, uralite, quartz, and small grains of opaque minerals, leucoxene, and titanite. Ti magnetite is partly replaced with small grains of leucoxene and titanite. Veinlet minerals are represented by chlorite, leucoxene, chalcedony, sulfides, epidote, quartz, albite, orthoclase, sanidine, and opaque minerals. Chlorite, epidote, quartz, and sulfide minerals fill large vesicles (Kurnosov et al., 1994) (see **"Appendix A,"** p.31).

XRD study of the fine fraction removed from the igneous rocks show that the principal secondary mineral is chlorite for the whole section of basalts recovered from Holes 857C and 857D (Kurnosov et al., 1994). Quartz and amphibole were found in trace amounts. In the upper part of the section, this monotony in distribution of secondary minerals was violated by the formation of mixed-layer clay minerals. In the interval at ~500–502 mbsf, there is chlorite as well as the mixed-layer chlorite-swelling chlorite mineral. At 482 and 472 mbsf, a corrensite-like mineral and smectite were identified, respectively (Table **T16; "Appendix A,"** p.31). XRD study of samples of the bulk rock showed that the principal minerals are quartz and chlorite.

The igneous rocks from Site 857 are chloritized and silicified, and epidote, albite, and uralite also occur. They have undergone alteration under the greenschist facies, similar to basalts and dolerites from Hole 856H, but at Site 857 the volume of altered rocks is less than in Hole 856H. This depends, most likely, on their lower permeability (massive dolerites predominate) with other similar conditions of alteration and high temperature (300°C). The presence of mixed-layer clay minerals and smectites ~502 mbsf in the form of bands against a background of total chloritization and the order of their distribution (from the bottom upward, chloritic swelling layers, chloritic swelling layers with smectite

F15. Whole-rock chemical compositions, Hole 856H, p.202.

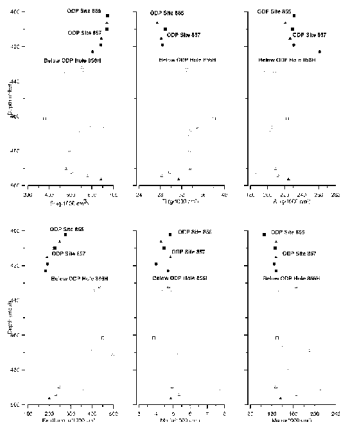

T19. Basalts, Holes 857C and 857D, p.400.

layers, and then smectite as an independent mineral) show poor zonation in rock alteration and irregularity in the distribution water-rock interaction conditions in the upper part of the recovered section at Site 857.

Bulk-Rock Chemical Changes

Element mobility through alteration of the igneous rocks at Site 857 is less pronounced than that of the rocks in Hole 856H (Fig. **F16;** "Appendix B", Table **AT5**). Tendencies in behavior of some elements, however, are analogous. Ca, Na, K, Rb, Sr, S_{total}, Si, Al, Cr, Ce, and Nd contents decrease; Ti, Fe_{total}, Mn, Mg, and Lu contents increase; and Co, V, and Sm contents are depleted or enriched. Behavior of other elements is not fully coincident with behavior established for the intense alteration of the magmatic rocks in Hole 856H. In addition, it is shown that Sn contents decrease in the altered dolerites at Site 857, and Ba contents increase in several samples.

F16. Whole-rock chemical compositions, Site 857, p.208.

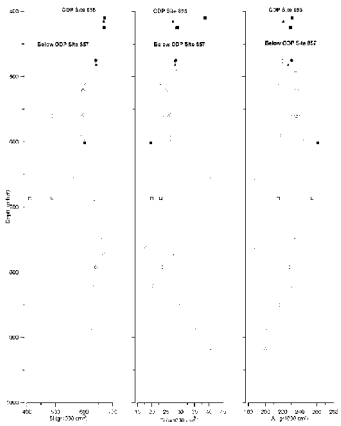

Holes 858F and 858G

Site 858 is located 1.6 km north of Site 857 (Fig. **F8**) at an active hydrothermal vent field where numerous vents with temperatures ranging from 255° to 276°C have been observed (Davis, Mottl, Fischer, et al., 1992). The area, Dead Dog vent field, is the principal center of hydrothermal activity in the Middle Valley. At Site 858, six holes were drilled to penetrate the zone of uplifting hydrotherms (Davis, Mottl, Fischer, et al., 1992). Only Holes 858F and 858G reached the basalts (Table **T14**). Holes 858F and 858G are located 30–50 m from the underwater hot spring and 75 m from Hole 858B, which is only a few meters away from a 276°C hydrothermal vent where sediments altered under the greenschist facies were sampled almost up to the oceanic bottom (Kurnosov et al., 1994). Hole 858F, from which basalts were recovered in the 248.9- to 296.9-mbsf interval, and deep-reentry Hole 858G (432.6 mbsf) were drilled approximately in the center of the field (Davis, Mottl, Fischer, et al., 1992).

Petrography and Bulk-Rock Chemical Composition

The studied basalts in Holes 858F and 858G are sparsely phyric and phyric basalts with olivine and plagioclase phenocrysts (<1%–15%) and hyalopilitic, vitrophyric, and microlitic groundmass textures (see **"Appendix A,"** p.37). In some parts, the basalts are slightly vesicular (as much as 5%). Geochemical data and show that these basalts are slightly differentiated and belong to tholeiitic MORB (Figs. **F9, F10;** Table **T20**). The differentiation is in the slight accumulation of alkaline elements and FeO*. Normalized REEs also indicate that the igneous rocks in Holes 858F and 858G are tholeiitic MORB (Fig. **F11**).

T20. Basalts, Holes 858F and 858G, p.406.

Alteration Mineralogy and Bulk-Rock Chemical Changes

Thin sections demonstrate that the igneous rocks are slightly altered basalts and make up ~10% of the rock volume (see "Appendix A," p.37). H_2O^+ content is 1.50–2.89 wt% (Table **T20**). Phenocrysts and minerals and interstitial glass of groundmass are partly replaced with chlorite (see **"Appendix A,"** p.37). Plagioclase is sometimes replaced by albite. Groundmass glass is replaced with chlorite and there are small, rare grains of leucoxene and titanite. Vesicles in all basalts of the section are filled with chlorite. In the bottom of the section (423.65 mbsf), the central parts of vesicles are filled with chlorite, and an aggregate of epidote was found. One vesicle is filled with an aggregate of quartz. In the lowermost sample studied, plagioclase is mainly replaced with albite and epidote, with some plagioclase replaced with opal and chalcedony (Kurnosov et al., 1994). Pyroxene is replaced with chlorite and leucoxene, and groundmass glass is chloritized and epidotized.

XRD study of the fine fraction removed from basalts showed that chlorite and mixed-layer chlorite-swelling chlorite mineral are the principal secondary minerals in the altered basalts (Table **T16; "Appendix A,"** p.37).

Chemical analysis showed that chlorites from the basalts are enriched in Mg and Fe (Kurnosov et al., 1994). Trace amounts of quartz and amphibole were found in several samples. In the bottom of the section, below ~403 mbsf in Hole 858G, the principal secondary mineral is chlorite. XRD study of bulk rock showed that, besides chlorite, the principal secondary mineral is quartz; the rocks for the most part are chloritized and silicified. Silicification took place largely in the upper part of the section in Hole 858F to ~278 mbsf.

The secondary mineral assemblages (mixed-layer chlorite-swelling chlorite minerals and slightly albitized plagioclase) indicate that the basalts in Holes 858F and 858G were altered under the upper part of the greenschist facies at temperatures <300°C. In the lowermost part of the basalt sequence in Hole 858G, the water-rock interaction temperature was higher, and the principal secondary minerals are epidote, albite, chlorite, and quartz.

Influence of ascending hot solutions on alteration is evident in the alteration of the igneous rocks under the greenschist facies conditions; however, mineral and chemical alteration of basalts in the area around Holes 858F and 858G affects only a small part of their volume (~10%). Permeability of those basalts is most likely not sufficient for significant alteration, in contrast to Hole 856H, whose rocks are almost completely altered.

Element contents of basalts in Holes 858F and 858G are shown in "Appendix B", Table **AT6**.

Hole 1037B

Hole 1037B was drilled to obtain an unaltered section of the oceanic crust for comparison with the hydrothermally altered Central Hill area, Site 1038 (Fouquet, Zierenberg, Miller, et al., 1998). The hole is near the spreading axis 5 km south of the hydrothermal venting area (Fig. **F7**). From Hole 1037B, sediments (0–507.8 mbsf) and igneous rocks (507.8–546 mbsf) were recovered (Table **T14**).

Petrography and Bulk-Rock Chemical Composition

Olivine-plagioclase phyric basalts have microlitic and hyalopilitic textures with 15%–25% phenocrysts. Aphyric dolerites are found with ophitic, intersertal-ophitic, and ophitic-poikilophitic groundmass textures (see **"Appendix A,"** p.39). In the geochemical diagrams, all studied basalts and dolerites fall in the MORB field (Figs. **F12, F13, F14;** Table **T21**) and are slightly enriched in $Na_2O + K_2O$, compared with the basalts from Hole 856H.

T21. Basalts, Hole 1037B, p.407.

Alteration Mineralogy

The igneous rocks are slightly altered or fresh. H_2O^+ contents are 0.18–0.75 wt% and densities are 2.85–2.95 g/cm³, the same as those of fresh basalts (Table **T21**).

Olivine is fresh or replaced by biotite with opaque minerals. Clinopyroxene is replaced with an aggregate of uralite (amphibole) and clay minerals. Groundmass glass is partly replaced by uralite or biotite and clay minerals, sometimes in association with opaque minerals. Vesicles and veinlets are filled with uralite (see **"Appendix A,"** p.39). Leg 169 scientists identified Mg-smectite, chlorite, and calcite in vesicles (Fouquet, Zierenberg, Miller, et al., 1998). In veins, they also found Mg-hornblende that precipitated from a high-temperature (>350°C) solution.

XRD study of the fine fraction removed from basalts showed that the principal secondary minerals are Ca-Mg and Na-K smectites with ~10%–30% mica layers with quartz, amphibole, talc, chlorite, and illite in trace amounts (Table **T16; "Appendix A,"** p.39). Na-K smectite and smectite correlates with Ca-Mg cations filling the interlayers and varies along the section. Na-K smectite increases in the uppermost part of the hole (508 mbsf). Downhole in the section, from ~518 to 527 mbsf, Ca-Mg smectite predominates. Below 527 mbsf, the

Na-smectite amount decreases and completely disappears at the bottom of the hole (**"Appendix A,"** p.39). Illite was found as a persistent mineral only in Hole 1037B.

The secondary minerals, dominated by smectites, indicate low-temperature alteration of the magmatic rocks in Hole 1037B under smectite facies. Vertical zonation in secondary mineral formation is shown in the gradual change of Ca-Mg smectite to Na-K smectite from the bottom of Hole 1037B upward. Veinlets composed of chlorite, amphibole, and quartz represent channels circulating the hydrothermal solutions that caused the alteration of enclosing rocks. The temperature of the solutions circulating in the fractures in the rock was >200°C. Mg-hornblende precipitation showed a higher temperature of fluids (>350°C).

Element contents of basalts in Hole1037B are shown in "Appendix B", Table **AT7**.

Hole 1038I

Hole 1038I was located near the top of the Central Hill in Escanaba Trough (Fig. **F7**) and penetrated a 1.5-m basalt sill at 161 mbsf. A basalt flow was encountered at 403.3 mbsf and only 67 cm of pillow basalt was penetrated (two pieces were recovered). The hole is located near the center of the hydrothermal uplift zone, but at 85.5 mbsf, the temperature was 15.2°C. A temperature of ~87°C was calculated for the bottom of the hole (Fouquet, Zierenberg, Miller, et al., 1998).

We studied one sample of basalt from Hole 1038I. The basalt is sparsely olivine-plagioclase phyric (5% phenocrysts) with hyalopilitic texture of the groundmass (see **"Appendix A,"** p.40). Geochemically, the rock is typical MORB (Table **T22;** Figs. **F12, F13, F14**).

T22. Basalts, Hole 1038I, p.409.

The principal secondary mineral is smectite with chlorite and quartz in trace amounts (Table **T16; "Appendix A,"** p.40). Leg 169 scientists identified calcite filling small vesicles and thin subvertical fractures (Fouquet, Zierenberg, Miller, et al., 1998). The basalts were altered under low-temperature conditions.

Element contents of the basalts in Hole 1038I are shown in "Appendix B", Table **AT8.**

Brief Comments

Smectitization is the most common type of igneous rock alteration in the uppermost part of the oceanic crust and occurs at temperatures <150°–200°C. This type of alteration was named smectite facies instead of zeolite facies (Kurnosov, 1986, 1992). Alteration of the igneous rocks from the volcanic section (Layer 2A of the oceanic crust) under the smectite facies was recognized in holes that are located beyond the areas of hot solution discharge (Site 855 and Hole 856A in the Middle Valley and Holes 1037B and 1038I at Escanaba Trough). Solutions in the fractures were often hotter than those altering the basalts. For example, in Hole 1037B, the veinlets are composed of chlorite, amphibole, and quartz. The temperature of the solutions in fractures was >200°C and sometimes even >350°C, as indicated by Mg-hornblende in the veins, whereas the host rocks were altered at temperatures <200°C.

Ubiquitous smectitization of basalts in the uppermost part of the oceanic crust is disrupted in zones of hot fluid ascent in areas of hydrothermal activity (i.e., the upper boundary of the greenschist facies is significantly uplifted, like a diapir, as compared to its typical location at the boundary of the volcanic section and the sheeted dike complex) (see **"Hole 504B"**). These areas were drilled during Legs 139 and 169 in the Middle Valley, Juan de Fuca Ridge; at Bent Hill sulfide mound (Hole 856H); a major thermal anomaly (Site 857); and Dead Dog vent field (Holes 858G and 858F). A set of secondary minerals reflects alteration of igneous rocks in these holes under greenschist facies at

temperatures of ~300°–350°C. Principal clay minerals are chlorite and often chlorite and quartz. Chloritization of igneous rocks from the uppermost part of the oceanic crust (volcanic section) is an indicator of rock alteration in the hot fluid discharge environment.

A lower rock volume was altered in Holes 857C, 857D, 858G, and 858F than in Hole 856H, probably because of their lower permeability with other similar conditions of alteration. Zonation in the secondary mineral formation through alteration, recognized during Legs 139 and 169, manifested itself poorly.

Data on the mobility of elements caused by high alteration of igneous rocks in Hole 856H revealed that under greenschist facies, elements are significantly mobile.

Comparison of mobility of elements from igneous rocks of the volcanic section (Layer 2A of the oceanic crust) through alteration in the zone of solution ascent under conditions of chloritization in Hole 856H (Middle Valley, Juan de Fuca Ridge) and under conditions of chloritization and amphibolization in Hole 504B (Costa Rica Ridge) for the dike complex (Layer 2B of the oceanic crust), especially for the lower dikes (reaction zone), showed that both dolerites from the reaction zone (lower dikes) and basalts from the effusive section lose Si, Zn, La, and Eu under conditions of greenschist facies alteration. In the reaction zone, loss and supply of Ca, Na, K, Cu, Al, Ce, and Nd occur, but in the effusive section, basalts lose these elements.

Ti, Fe, Mn, and Mg are removed from dikes in the reaction zone, but in the effusive section, the altered basalts gain these elements, most likely because of supply from solutions ascending from the reaction zone. The same tendency is characteristic of P and Tb through alteration of rocks in the dike complex. In the effusive complex, these elements enrich the altered basalts. Dikes often lose Zr, some samples gained Zr, but in the effusive section Zr is immobile.

Through alteration, dikes become enriched in Ni, Co, V, Nb, Sr, and, probably, Rb and depleted in Sm, Yb, Y, and Lu. Concurrently, the effusive basalts lose Rb and Sr through alteration. Behavior of Ni, Co, V, Nb, Sm, Yb, Y, and Lu is less definite. Both their evacuation from and supply to the basalts occur. In some samples, they are immobile.

In the future, when the hole penetrates the lower parts of the reaction zone localized in the gabbro layer of the oceanic crust, we will be able to obtain a fuller picture of the redistribution of elements in the upper part of the oceanic crust that takes place in the high-temperature part of the hydrothermal system, including the zone of uplift and discharge of hot solutions.

Gulf of California, Offshore Southern California, and Baja California

We studied igneous rocks recovered from the spreading axis (Guaymas Basin; Leg 64, Hole 477) and from the flanks of the northern part of the East Pacific Rise (Leg 63, Holes 469 and 473 and Leg 65, Holes 483B and 485A) in the Gulf of California and off Southern California, as well as from off-ridge igneous activity (Leg 63, Hole 471; offshore Baja California). Location of the holes is shown in Figures **F17** and **F18** and in Table **T23**. The igneous rocks in the holes were studied in comparison with the altered basalts and dolerites recovered from Hole 504B (flank of the Costa Rica Rift) and during Legs 139 and 169 in hydrothermally active areas (Middle Valley, Juan de Fuca Ridge and Escanaba Trough, Gorda Ridge).

Hole 477

Hole 477 is located in the center of the southern rift in the Guaymas Basin with high heat flow (20 heat flow units [HFU]) on “zero-age” crust

T23. Additional basement holes, Legs 63–65, p.410.

F17. Sites in the Gulf of California, p.220.

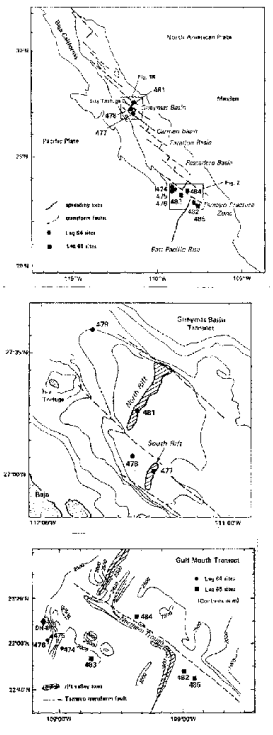

(Curray, Moore, et al., 1982). This rift is located on the land as a system of the San Andreas faults. The hole was drilled to 191 m. A dolerite sill was encountered between 58.0 and 105.5 mbsf (Table **T23**). Sediments below the sill in Holes 477 and 477A are hydrothermally altered with resulting dolomite, pyrite, pyrrhotite, anhydrite, zeolites, possibly K-feldspar, quartz, sphene, zoisite, epidote, chlorite, and albite. A reading from the core on deck was 40°C (Curray, Moore, et al., 1982). Temperature measurements taken in sediments in Hole 477 were 50°C at 49 mbsf (above the sill) and 87°C at 168 mbsf (below the sill) (Curray, Moore, et al., 1982). In Hole 477A, located 165 m northwest of Hole 477, temperature measurements were 87°–78°C at 173 mbsf.

Petrography and Bulk-Rock Chemical Composition

Dolerites in Hole 477 are aphyric to plagioclase-phyric (Curray, Moore, et al., 1982). Petrographic descriptions of thin sections of the selected igneous rocks are shown in **"Appendix A,"** p.41. Dolerites are represented by aphyric, sparsely phyric, and phyric varieties with varying amounts of plagioclase phenocrysts (10%–50%). The dolerite is medium to coarse grained with ophitic, poikilophitic, microlitic, and doleritic groundmass textures.

Dolerites do not essentially differ in silicity, Al_2O_3, Mg, and Ti (Table **T24**) and belong to the low-alkaline type of the tholeiitic MORB series with a poorly manifested Fenner trend of differentiation with accumulation of iron (Fig. **F19**). In the Zr/4-2Nb-Y diagram (Fig. **F20**), the basalts are located in the transition zone between fields D and C, which are basalts of N-MORB type such as volcanic arc tholeiites or intraplate tholeiites. The basalts are slightly enriched in Zr. Chondrite-normalized REEs also indicate that igneous rocks in Hole 477 are N-MORB (Fig. **F21**). Only sample z-1254 is enriched (E)-MORB. The studied dolerites are related to a homogeneous group of rocks. Geochemistry of the igneous rocks at Site 477 was studied in detail by Saunders et al. (1982).

Alteration Mineralogy and Bulk-Rock Chemical Changes

Petrographic study revealed that the igneous rocks are mainly fresh. Several samples are slightly altered (5%–10%) (see **"Appendix A,"** p.41). H_2O^+ contents in dolerites are low at 0.1–0.79 wt% (Table **T24**).

XRD study of the fine fraction removed from dolerites showed that all studied samples of the rocks were determined by secondary minerals, even though they were absent or in very small amounts in interstices shown thin sections (Table **T25; "Appendix A,"** p.41). Principal secondary minerals are smectites with ~10%–20% mica layers. Smectites contain different cations in interlayers (Na-K and Ca-Mg cations, Mg > Ca). Different cation smectites are found together. Smectites with Na-K cations are dominant in the interlayers. From 92.76 mbsf to the basement of the dolerite unit, only smectites with Na-K cation interlayers have been identified. Such distribution of different cation smectites is opposite to that recognized in Hole 1037B. In the upper part of the sill, chlorite, amphibole, and talc, in minor amounts, have been found together with smectites. Chlorite and talc disappear completely or almost completely in the lower part of the dolerite unit from 92.76 to 98.81 mbsf. Amphibole disappears downhole in the section from 90.86 mbsf. Thus "inverted" distribution of secondary minerals in the dolerite unit reflects somewhat different alteration conditions in the upper and lower parts of the sill. The mixed-layer chlorite-smectite minerals (with ~15% swelling interlayers), amphibole, and quartz were determined in trace amounts (Table **T25; "Appendix A,"** p.41).

Dominance of smectites among the secondary minerals (Hole 477) indicates alteration of magmatic rocks at relatively low temperatures (<150°–200°C) under smectite facies conditions. Chlorite, amphibole, and talc, found in the upper part of the dolerite unit, most likely reflect a higher temperature of rock alteration. In spite of the position of Holes 477 and 477A in the axial zone of spreading (Guaymas Basin) with a high heat flow (20 HFU), alteration of

F18. Sites off Baja California, p.221.

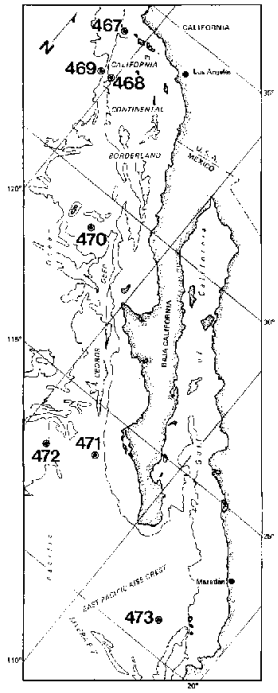

T24. Basalts, Hole 477, p.411.

F19. AFM diagram for basalts, Hole 477, p.222.

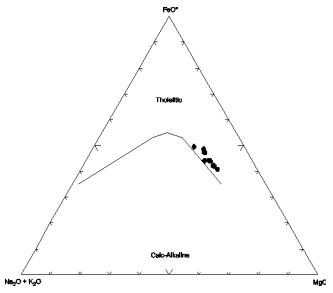

F20. Nb-Zr-Y diagram for basalts, Hole 477, p.223.

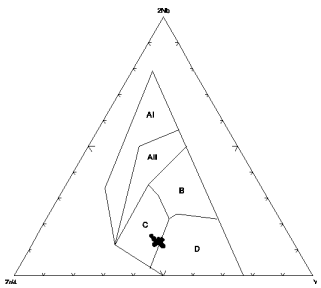

igneous rocks did not occur in the extreme hydrothermal environment under greenschist facies as it had in the Middle Valley, Juan de Fuca Ridge (Sites 856, 857, and 858).

Weak alteration of dolerites at Site 477 has little effect on their initial composition, so it would be possible to detect any mobility of the elements (Table **T24;** "Appendix B", Table **AT9**).

Holes 483B and 485A

Holes 483B and 485A are located not far from the axis of the East Pacific Rise. Site 483 is ~52 km west of the rise crest and Site 485 is ~20 km east of the rise crest (Fig. **F17**). The topmost part of the basement in Hole 483B contains massive basalts with interlayered sediments. Below 160.5 mbsf, the basement consists of pillow lavas, massive basalts, and sediments (Lewis, Robinson, et al., 1983). In Hole 485A, the lower 178 m consist of sediments (56%) and massive basalts (44%) of acoustic basement (Lewis, Robinson, et al., 1983).

Petrography and Bulk-Rock Chemical Composition

Leg 65 scientists (Lewis, Robinson, et al., 1983) reported that in Hole 483B both phyric and aphyric basalts were recovered. Plagioclase and olivine are the most common phenocrysts in the phyric varieties. The massive basalts in Hole 485A are thicker and coarser grained than massive basalts in Hole 483B. The basalts are fine grained near the margins of the basalt units, coarse grained in the centers, and gabbroic in the thickest unit and sparsely to moderately phyric with plagioclase and olivine phenocrysts.

Petrographic descriptions of thin sections from the selected igneous rocks are shown in **"Appendix A,"** p.42**.** In Hole 483B (Unit 10), the igneous rocks are represented by olivine-plagioclase phyric basalt with varying amounts of phenocrysts (10%–40%) and are sparsely vesicular (<1%–3%; from 0.05–0.4 to 0.6–1.2 mm). The basalts are crystallized or fine grained with vitrophyric, microlitic, hyalopilitic-microlitic, hyalopilitic, microdoleritic, and pilotaxitic groundmass textures. In Hole 485A, the studied igneous rocks are represented by basalts and dolerites with dolerites dominating. They are olivine-plagioclase, olivine-clinopyroxene-plagioclase, and olivine phyric varieties with varying amounts of phenocrysts (10%–20%). The basalts have microlitic, vitrophyric, and hyalopilitic groundmass textures. Dolerites are represented by aphyric, plagioclase, and olivine-plagioclase phyric varieties with varying amounts of phenocrysts (5%–15%). They are fine and medium grained to coarse grained with doleritic, microdoleritic, ophitic, and intersertal-poikilophitic groundmass textures. Sample 65-485A-30R-3, 139–140 cm, represents coarse-grained gabbro-dolerite.

In chemical composition, basalts from Holes 483B (Unit 10) and 485A and dolerites are abyssal oceanic tholeiites with a poorly manifested Fenner trend of differentiation with accumulation of iron (Fig. **F22;** Tables **T26, T27**). The Zr/4-2Nb-Y diagram (Fig. **F23**) and the pattern of distribution of REEs (Fig. **F24**) in the studied igneous rocks agree with these conclusions (Zolotarev and Margolin, 1983).

Alteration Mineralogy

The basalts in Hole 483B (Unit 10) are, for the most part, slightly altered (~5%–10%). Several samples were altered more strongly, as much as 15%–20% of the rock volume (see **"Appendix A,"** p.42). H_2O^+ contents in the basalts are 0.10–0.48 wt% and densities are 2.90–3.06 g/cm^3 (Table **T26**), showing that the basalts are fresh. Olivine is completely replaced with brownish green clay minerals and sometimes by clay minerals with carbonate and iron hydroxides. Glass is partly replaced with clay minerals and opaque dust. Vesicles are filled with brownish green clay minerals and sometimes with opaque dust.

F21. Chondrite-normalized REEs for basalts, Hole 477, p.224.

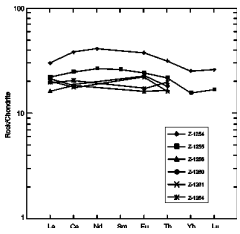

T25. Fine fraction, Legs 63–65, p.413.

AT9. Major and trace elements, Hole 477, p.39.

F22. AFM diagram for basalts, Holes 483B and 485A, p.225.

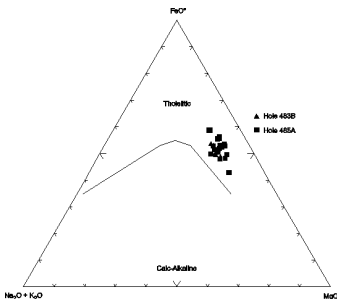

T26. Basalts, Hole 483B, p.415.

T27. Basalts, Hole 483B, p.416.

XRD study of the fine fraction extracted from the basalts in the interval 262.51–265.35 mbsf (Hole 483B; Unit 10) was performed for two thin lava flows, 0.95 and 0.50 m thick, with glassy chilling crusts in the uppermost and lowermost areas. From the first flow (Section 65-483B-32R-1; 262.51–263.45 mbsf), we took five samples from the uppermost to lowermost part of the section. From the second flow (Section 65-483B-32R-2; 264.95–265.45 mbsf), three samples from the upper, lower, and central part of the flow were taken. There is no difference in the composition of secondary minerals from different parts of the flows. In all samples, the principal secondary minerals are smectites with ~10%–30% mica layers. Smectites with Ca-Mg and Na-K cations filling the interlayers were found. Ca-Mg or Na-K smectite formation does not depend on sample position either in the upper, lower, or central part of the flow. Quartz and chlorite are ubiquitous in trace amounts (Table **T25; "Appendix A,"** p.42). Smectite predominance among secondary minerals reflects low-temperature alteration environment for basalts in the lowermost part of the magmatic rock section (Hole 483B; Unit 10).

Morrison and Thompson (1983) showed that basalts in Hole 483B contain mixed precipitates of iron hydroxides and silica locally in the groundmass and in vesicles, indicating strong oxidation. They also showed that smectites are often highly enriched in iron and K_2O.

In the igneous rocks in Hole 485A, H_2O^+ content is 0.42–1.71 wt% and densities are 2.81–3.12 g/cm³ (Table **T27**), similar to those in fresh basalts. As a whole, the igneous rocks are slightly altered. Only one sample of basalt with hyalopilitic groundmass texture (Sample 65-485A-38R-2, 36–37 cm) contains 2.75 wt% H_2O^+ and has a density of 2.75 g/cm³. Olivine is fresh or completely or partially replaced by iddingsite and opaque minerals and sometimes completely replaced by limonite. Interstices contain clay minerals and small grains of opaque minerals, quartz, and very small grains (<1 mm) of albite.

XRD study of the fine fraction removed from petrographic fresh and altered dolerites and basalts in Hole 485A showed that all samples contain secondary minerals (Table **T25; "Appendix A,"** p.42). The secondary minerals were studied earlier in detail (Kurnosov, 1986). Principal secondary minerals are trioctahedral smectites (b = 9.18–9.20 Å). Study of the fine fraction removed from the rocks shows the smectites to be Fe Mg in composition with cations in interlayers. In Sample 65-485A-17R-1, 114–115 cm, MgO = 10.00 wt%, Fe_2O_3 = 6.01 wt%, FeO = 6.62 wt%, CaO = 5.35 wt%, Na_2O = 2.02 wt%, and K_2O = 0.17 wt%. In Sample 65-485A-26R-1, 16–18 cm, MgO = 8.48 wt%, Fe_2O_3 = 4.88 wt%, FeO = 6.71 wt%, CaO = 6.20 wt%, Na_2O = 2.31 wt%, and K_2O = 0.16 wt%. At 223.60 and 224.12 mbsf, saponite and swelling chlorite were determined. Chlorite, serpentine, mixed-layer chlorite-smectite minerals, illite, talc, amphibole, cristobalite, quartz, and carbonate were found in trace amounts.

Comparison of the slowly and quickly chilled basaltic bodies shows that in the well-crystallized beds of basalts (Units 2, 4, 5, and 8) reaching 30 m in thickness and classified with sills, minerals with a chlorite structure are common among the secondary minerals. In the central part of Bed 4, they prevail over smectite. Among the secondary minerals, talc, actinolite, more rarely serpentine(?), carbonate, and illite are, as a rule, found in as admixtures. A close regularity in the secondary mineral formation in the center of Unit 5 was recognized during Leg 65 (Lewis, Robinson, et al., 1983). In contrast to the sills, Unit 1, which is considered a surface flow with chilling crusts, bears a simpler complex of the secondary minerals and is dominated by smectite. Talc, chlorite, and carbonates were found as a very poor admixtures. Therefore, study of the secondary minerals of the fine fraction removed from the igneous rocks recovered from Hole 485A showed that the variations in composition against the monotonous predominance of smectite formation along the section are related with the individual conditions of development in each magmatic body and not with the downward zonation. The participants of Leg 65 did not observe any regular increase of alteration grade with depth (Lewis, Robinson, et al., 1983).

F23. Nb-Zr-Y diagram for basalts, Holes 483B and 485A, p.226.

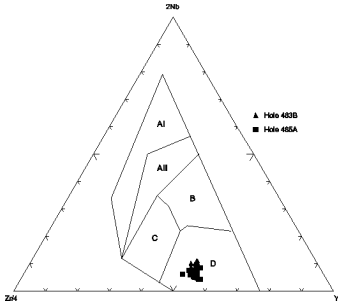

F24. Chondrite-normalized REEs for basalts, Holes 483B and 485A, p.227.

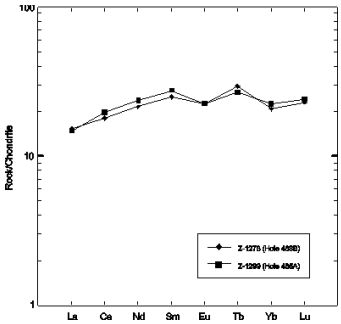

The igneous rocks in Hole 485A are massive with a minor amount of fractures. The vein complex is poorly developed. Two types of low-temperature veins are predominant: smectite-carbonate-pyrite and smectite. The smectite veins were formed at a later time and cut through the smectite-carbonate-pyrite veins. Diagnostics of vein minerals was obtained mainly by XRD. In veins and altered areas, smectite, illite, chlorite, serpentine, an undetermined 9.5 Å mineral, quartz, aragonite, calcite, sphene, fairchildite(?), and pyrite were found (Kurnosov, 1986). Smectites from veins and highly altered areas are also classified with saponites (b = 9.20–9.22 Å), and chemical analysis shows that they are Fe-Mg varieties (Kurnosov, 1986). Vein pyrites contain ~510 ppm Cu, 500 ppm Ni, and 2500 ppm Zn. Au and Ag were not found.

Secondary minerals found in the igneous rocks from the Gulf of California reflect alteration conditions when the oxidative influence of water does not appear in igneous rocks of zero age (Site 477) and 0.85 Ma (Hole 485A). In basalts from 2.4 Ma (Hole 483B), secondary minerals characteristic of an oxidizing environment were recognized. Under moderate-rate spreading (~6 cm/yr), the oxidizing environment manifests itself ~1–2 m.y. after basalt eruption.

Bulk-Rock Chemical Changes

Basalts in Hole 483B are very weakly altered. Alteration of igneous rocks in Hole 485A is slightly stronger but poor as a whole (Table **T27**). Well-crystallized basalts and dolerites, predominant in the section of Hole 485A, are fresh or very poorly altered, so they were not used in the estimation of element gain/loss through alteration. For this purpose, only glassy, strongly altered basalts from the marginal parts of the basalt units were chosen. In contrast to the well-crystallized basalts and dolerites, they compose an insignificant portion of the basement section drilled in Hole 485A. In the total redistribution of matter through rock alteration, these marginal basalts do not play any role.

Of all studied samples of glassy basalts, only one sample of altered basalt (Sample 65-485A-38R-2, 36–37 cm) can be effectively used for estimation of element mobility. This sample contains 2.75 wt% H_2O^+ and has a density of 2.75 g/cm^3 (Table **T27**). Comparison of major and minor element contents in fresh and altered glassy basalt showed that with this extent of basalt alteration, only Si and Ca loss from basalt are confidently determined. A weak tendency of loss of Mn, Fe, Zn, and Cu is also observed.

Element contents of basalts in Holes 483B and 485A are shown in "Appendix B", Tables **AT10** and **AT11**.

AT10. Major and trace elements, Hole 483B, p.41.

AT11. Major and trace elements, Hole 485A, p.42.

Hole 473

Hole 473 is located on the Rivera plate at the mouth of the Gulf of California east of the East Pacific Rise crest (Fig. **F18**). Igneous rocks below the sediments (248.1 mbsf) to the base (287.5 mbsf) of the igneous section (Table **T23**) are mainly massive diabase with a density of 2.7 g/cm^3 (Yeats, Hag, et al., 1981).

Petrography and Bulk-Rock Chemical Composition

During shipboard investigation (Yeats, Hag, et al., 1981) it was determined that the diabase is fine to medium grained, aphyric and massive, compositionally and texturally uniform, and composed mainly of plagioclase, clinopyroxene, and minor opaque minerals. Grain size increases gradually away from each contact. The texture of the diabase is intersertal to subophitic and ophitic (Grechin et al., 1981).

Petrographic descriptions of thin sections from the selected igneous rocks are shown in **"Appendix A,"** p.46. The igneous rocks in Hole 473 are represented by dolerite. Dolerites are mostly aphyric with plagioclase phyric varieties and ~10% phenocrysts, fine to medium grained with intersertal-

doleritic texture of the groundmass.

Dolerites in Hole 473 are tholeiites with a poorly manifested Fenner trend of differentiation with accumulation of iron (Fig. **F25;** Table **T28**). In the Zr/4-2Nb-Y diagrams and REEs, dolerites are plotted as N-MORB (Fig. **F26**). Geochemical study of the igneous rocks in Hole 473 indicates that they are large-ion-lithophile element depleted tholeiites similar to typical abyssal tholeiites (Shibata et al., 1981).

Alteration Mineralogy and Bulk-Rock Chemical Changes

Petrographic study of basalts in Hole 473 showed that they are either fresh or very slightly altered, with alteration as much as 5%–7% of the rock volume. H_2O^+ contents in basalts is low at 0.36–0.61 wt% and densities are 2.72–2.93 g/cm^3 (Table **T28**). In vesicular rocks, the vesicles are 0.5–1.2 mm across and make up ~20% of the rock. Vesicles are filled completely with clay minerals (Sample 63-473-32R-2, 133–140 cm) (see **"Appendix A,"** p.46). The vesicular rock has 2.14 wt% H_2O^+ and a density of 2.47 g/cm^3 (Table **T28**). Interstitial glass, olivine, and partial pyroxene are replaced with smectites. Vesicles are filled with clay minerals (Grechin et al., 1981). During shipboard investigation, it was determined (Yeats, Hag, et al., 1981) that greenish brown smectite is the common alteration mineral, filling vesicles as well as interstices between plagioclase laths and clinopyroxenes. Clay minerals and calcite pseudomorphs on olivine occur occasionally. Calcite and clay minerals also fill fractures.

XRD study of the fine fraction removed from dolerites showed that principal secondary mineral is smectite with ~20% mica layers (Table **T25; "Appendix A,"** p.46). In smectite interlayers, cations are Na-K. Quartz is present in trace amounts. Smectite formation indicates a low-temperature alteration environment in Hole 473 (smectite facies). A veinlet in Sample 63-473-29R-1, 90–95 cm, contains Na-K smectite and aragonite. A veinlet in Sample 63-473-32R-2, 133–140 cm, contains Ca-Mg smectite, chlorite, quartz, and calcite(?). Celadonite from vesicles was identified in the thin sections but was not found by XRD analysis. Vesicles are filled with smectites.

Grechin et al. (1981) determined an iron-rich nontronite-like mineral among the smectites. K-feldspar was found by Verma (1981). These minerals are indicators of oxidizing environments; however, the scientists did not report iron hydroxides (Yeats, Hag, et al., 1981). Thus, the expected development of the superimposed oxidizing environment in dolerites in Hole 473, which is at a greater distance from the rift axis than Hole 483B, is expressed in the formation of only the iron-rich nontronite-like mineral and, probably, K-feldspar. This set of secondary minerals is scarce in contrast to that of the oxidation zone in Hole 504B, in spite of the fact that the age of magmatic rocks and thickness of overlapping sediments in Holes 504B and 473 are similar (5.9 m.y., 274 m and 6–6.5 m.y., 248 m, respectively). In the oxidation zone in Hole 504B, observed to ~300 m beneath the upper part of the basement, iron hydroxides, limonite, phillipsite, celadonite, Fe smectite, and K-feldspar were found in fractures, halos, and oxidized patches. It may be suggested that the intense development of the oxidation process did not occur at Site 483 because of the predominance of well-crystallized massive rocks (dolerites) in the basement section and their poor permeability and weak jointing.

Dolerites in Hole 473 are very slightly altered. H_2O^+ content in basalts is low at 0.36–0.61 wt% and densities are 2.72–2.93 g/cm^3 (Table **T28**). These data show the basalts are fresh or very slightly altered. Disparity in element content in fresh and slightly altered dolerites is small ("Appendix B", Table **AT12**) and within the limit of analytical error.

Hole 469

Hole 469 is located on the foot of Patton escarpment (Fig. **F18**). The

F25. AFM diagram for basalts, Holes 469, 471, and 473, p.228.

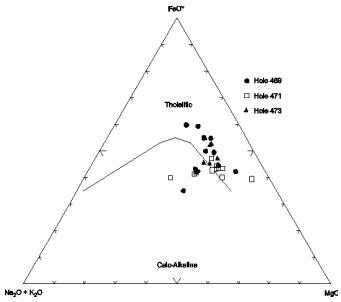

T28. Basalts, Hole 473, p.419.

F26. Nb-Zr-Y diagram for basalts, Holes 469, 471, and 473, p.229.

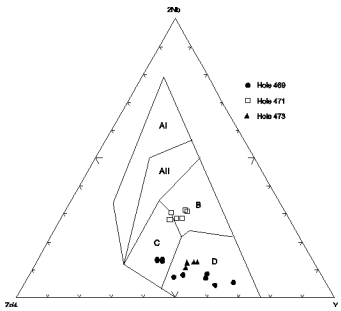

AT12. Major and trace elements, Hole 473, p.45.

hole was drilled to 453.5 mbsf. The lower 85 m is igneous rocks. Metalliferous sediments overlying pillow basalt characterize this site as the west flank of the East Pacific Rise. The igneous sequence includes an 18.5-m-thick sill separated from underlying pillow basalt by 5 m of chalk and metalliferous clay (Yeats, Hag, et al., 1981).

Petrography and Bulk-Rock Chemical Composition

Petrographic descriptions of thin sections from igneous rocks selected for study are shown in **"Appendix A,"** p.46**.** All studied samples from the sill and basement (pillow lavas) are represented by basalt. The basalts are aphyric and sparsely phyric. Phenocrysts are clinopyroxene and plagioclase (a single segregate) or only plagioclase (<1%). Aphyric basalts are with intersertal, intersertal-microdoleritic, pilotaxitic, and vitrophyric groundmass textures. Sometimes basalts are sparsely vesicular (~5% vesicles; 0.1–0.6 mm). Petrographic study indicates that these basalts are mostly aphyric. We studied two samples of the altered glassy crusts from the chilled margin of basalt. Results of petrographical study of the basalts as a whole are similar to the results obtained by Shibata and DeLong (1981) and Grechin et al. (1981).

The basalts are mainly located in the MORB field with a poorly manifested Fenner trend of differentiation with accumulation of iron. Three samples are in the calc-alkaline basalts field (Fig. **F25;** Table **T29**). In the Zr/4-2Nb-Y diagram, many basalts are located in the N-MORB field (Fig. **F26**). These results, as well as REE data (Fig. **F27**), agree with the data from Hole 469 that were obtained earlier by Grechin et al. (1981), Shibata and DeLong (1981), and Shibata et al. (1981).

T29. Basalts, Hole 469, p.420.

F27. Chondrite-normalized REEs for basalts, Holes 469, 471, and 473, p.230.

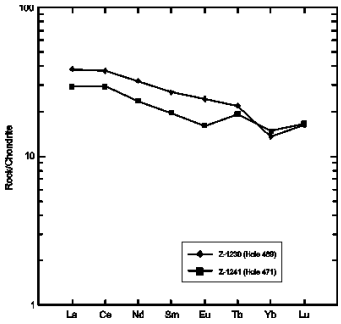

Alteration Mineralogy and Bulk-Rock Chemical Changes

Petrographic study of basalts in Hole 469 showed that they are slightly altered or fresh (see **"Appendix A,"** p.46). H_2O^+ content is 0.29–1.59 wt% (Table **T29**). Slight alteration of basalts is evident from their chemical composition (Grechin et al., 1981). H_2O^+ content in basalts is mainly <1 wt%, with the exception of the glassy crusts from pillow lavas. Sample 63-469-48R-1, 22–28 cm, is ~60%–70% altered (see **"Appendix A,"** p.46) with a H_2O^+ content of 4.22 wt% (Table **T29**).

Petrographic descriptions demonstrate that interstitial glass is replaced with clay minerals and calcite. The vesicles are filled with clay minerals and glass.

Shibata et al. (1981) found olivine completely replaced by talc, smectite, and magnetite. They also report that veinlets are filled with clay minerals and calcite. Calcite, talc, mica, amphibole, quartz, and an unidentified zeolite were found in trace amounts (Yeats, Hag, et al., 1981).

Fe_2O_3/FeO ratios as high as 3.15 and 4.01 (Table **T29**) show that many basalts and glassy crusts oxidized differently. Shibata et al. (1981) observed a brownish gray color in basaltic pillow lavas along fractures and veinlets and along the chilled rims. Grechin et al. (1981) found iron colloform structure hydroxides that frequently comprise the peripheral parts of vesicles. Some vesicles contain accumulations of reddish brown ore material at their centers. Reddish brown ore minerals are also arranged along selvage veins. The oxidation process that took place in the basalts recovered from Hole 469 is analogous to the basalt oxidation in Hole 504B.

XRD study of the fine fraction removed from basalts and glass showed that the principal secondary minerals are smectites with ~10%–20% mica layers (Table **T25; "Appendix A,"** p.46). The same results were obtained earlier by Grechin et al. (1981). In smectites, interlayers contain Na-K cations. Rarely there is quartz and amphibole in trace amounts. Chilling glass (Samples 63-469-48R-1, 49–53 cm) is replaced by different smectite cations (Na-K and Ca-Mg are in interlayers). The veinlets (Samples 63-469-44R-1, 3–8 cm, and 50R-2, 27–32 cm) contain Na-K smectite and calcite with illite. The smectite and

calcite assemblage indicates a low-temperature alteration environment (~150°–200°C) in Hole 469 (smectite facies).

Basalts in Hole 469 are slightly altered. Differences in element contents between fresh and slightly altered basalts are small (Table **T29;** "Appendix B", Table **AT13**). Elements are immobile or weakly mobile.

AT13. Major and trace elements, Hole 469, p.46.

Hole 471

Hole 471 is located on the foot of the continental slope of Baja California (Fig. **F18**) on the Franciscan-like terrain of the California continental borderland. Site 471 has a high geothermal gradient (24°C at 142.5 mbsf) and high heat flow (3.9 HFU) based on heat probes (Yeats, Hag, et al., 1981). The hole was drilled to 823 mbsf. The sediments are 81.5 m thick (Table **T23**). Between the overlying pelagic sediment and underlying igneous rocks, there is a deposit of pyrite, chalcopyrite, and Zn sulfide (~35 cm) and a 5-cm-thick metalliferous sediment layer (Yeats, Hag, et al., 1981; Devine and Leinen, 1981). The igneous rocks are represented by extensively altered diabase with common brecciated structures and slickenslides resulting from faulting after consolidation (Yeats, Hag, et al., 1981). Shibata and DeLong (1981) showed that the diabasic rocks in Hole 471 are possibly the products of off-ridge igneous activity.

Petrography and Bulk-Rock Chemical Composition

Petrographic descriptions of thin sections of igneous rocks selected for our study are shown in **"Appendix A,"** p.47. All studied samples are represented by aphyric medium- to coarse-grained dolerites with intersertal-ophitic, intersertal-doleritic, and intersertal-poikilophitic groundmass textures. As a whole, the results of petrographic study of the basalts are similar to the data obtained by Shibata and DeLong (1981) and Grechin et al. (1981).

Many dolerites studied in Hole 471 were located in the MORB field with a poorly manifested Fenner trend of differentiation with accumulation of iron. Three samples (Samples 63-471-80R-2, 98–102 cm; 82R-1, 127–132 cm; and 82R-2, 15–18 cm) are located in the calc-alkaline basalts field (Fig. **F25;** Table **T30**). In the Zr/4-2Nb-Y diagram (Fig. **F26**), dolerites are located in the E-MORB and transitional (T)-MORB fields. The REE data are in Fig. **F27.** The results are similar to those from earlier study of igneous rocks in Hole 471 (Grechin et al., 1981; Shibata and DeLong, 1981).

T30. Basalts, Hole 471, p.422.

Alteration Mineralogy

Petrographically, dolerites studied in Hole 471 are moderately to strongly altered (~40%–50%) (see **"Appendix A,"** p.47). H_2O^+ content in the altered dolerites is 2.32–5.48 wt% and densities are 2.3–2.5 g/cm^3 (Table **T30**).

Petrographic descriptions (see **"Appendix A,"** p.47) showed that the central parts of many plagioclase grains were filled with an aggregate of chlorite, which replaces glass in grains of plagioclase. For the most part, the laths of plagioclase are replaced with albite and chlorite. A portion of the Ti-augite grains is chloritized along the margins. Interstitial glass is completely replaced by chlorite. From 787 mbsf (Sample 63-471-84R-1, 9–16 cm) to basement, plagioclase is not albitized, and interstitial glass, in contrast to the overlying dolerites, is replaced with brownish green clay mineral and sometimes with chlorite admixture. In some interstices, fine isomorphic grains of albite and orthoclase and abundant needles of apatite were found. Shibata and DeLong (1981) found biotite, lesser amphibole, and quartz in some samples from Cores 84R–88R. Shibata and DeLong (1981) also found brownish green clay mineral throughout the diabase unit in association with calcite, talc, and occasionally zeolites. Dark-colored minerals are replaced with calcite that fills pores and fissures in plagioclase. Clay minerals are developed on dark-colored minerals and in interstices (Grechin et al., 1981). The secondary minerals, typical of the oxidation environment, were not found in dolerites in Hole 471.

Fe_2O_3/FeO ratios (0.44–1.43) also show that dolerites were not affected by the oxidation process, in spite of their high permeability. This is probably connected with the position of Site 471 in the area of the ridge's eruptive and hydrothermal activity, where ascending solutions without oxidative effect predominated.

XRD study of the fine fraction removed from dolerites (Table **T25; "Appendix A,"** p.47) showed that in the upper part of the dolerite unit (751.85–770.65 mbsf) the principal secondary mineral is corrensite. Quartz, calcite, and mixed-layer chlorite-smectite minerals with domination of chlorite layers were determined in trace amounts. In the upper part of the dolerite unit, corrensite, minor quartz, and a very slight admixture of calcite and mixed-layer chlorite-smectite minerals occur at 751.85 mbsf, and the amount of mixed-layer chlorite-smectite mineral increases downhole to 770.65 mbsf at the background of dominating corrensite. At the bottom of this part of the section, their amounts are approximately equal (quartz and calcite are found in trace amounts). The black veinlet (Sample 63-471-82R-1, 127–132 cm; 770.27 mbsf) contains corrensite, chlorite, and calcite.

In the lower part of the dolerite unit (787.09–808.69 mbsf), the principal secondary minerals are smectites with 10%–20% mica layers. Chlorite, which is present in all studied samples as an easily determined admixture, and occasionally quartz are found as a very small admixture. The interlayers in smectites are filled predominantly with Mg cation. The brown veinlet (Sample 63-471-87R-2, 19–26 cm; 808.69 mbsf) contains smectite and trace amounts of chlorite, quartz, and illite(?).

XRD study of clay minerals agree with those obtained by Grechin et al. (1981). Moreover, these scientists studied the uppermost section of the dolerite unit (Samples 63-471-79-1, 130–137 cm; 742.80 mbsf and 80-1, 78–84 cm; 751.28 mbsf), where they found chlorite with a faintly distinct admixture of mixed-layer chlorite-smectite minerals. Below 751.28 mbsf, smectite and mixed-layer chlorite-smectite minerals were found with smectite being dominant. Study of a sample from the lowermost part of the dolerite unit (Sample 63-471-88-2, 0–6 cm; 815.5 mbsf) showed that the principal secondary mineral here is smectite. In Sample 63-471-83R-2, 61–67 cm (780.11 mbsf), corrensite was recognized as the main secondary mineral with chlorite admixture also present.

Taking into account the results of Grechin et al. (1981), two alteration zones can be distinguished in the dolerite unit. The lower zone (781–823 mbsf) is smectite. The upper zone (741.5–781 mbsf) is composed of three subzones. The lower subzone (~751.5–781 mbsf) is corrensite. Downhole from this interval, the amount of the mixed-layer smectite-chlorite minerals increases from an admixture to a content almost equal to that of corrensite, and albite replacing plagioclase was petrographically determined in this subzone. The middle subzone (~745–751.5 mbsf) is smectite with a subordinate amount of the mixed-layer chlorite-smectite mineral. The upper subzone (741.5–745 mbsf) is chlorite.

Thus, the higher temperature alteration under greenschist facies took place in the upper part of the dolerite unit. Lower-temperature alteration took place under the smectite facies in the lower part of the dolerite unit. The "inverted" vertical zonality of alteration of igneous rocks is probably related to the position of Site 471 on the area of off-ridge eruptive and hydrothermal activity, which could control the supply of hot solutions (~300°C) to the upper part of the dolerite unit along the subhorizontal fractures and brecciated zones from the ascending branch of the hydrothermal system thought to be near these zones. For example, these conditions were recognized in the upper part of the section recovered by Hole 856H, drilled on the massive sulfide mound of Bent Hill, the Middle Valley, Juan de Fuca Ridge, Legs 139 and 169. This suggestion can be supported by metalliferous sediment and sulfide deposits found in Hole

471 in the basement of the sedimentary section at the contact with the dolerite unit.

Bulk-Rock Chemical Changes

All the dolerites studied in Hole 471 are moderately to strongly altered (~50%) (see **"Appendix A,"** p.47). H_2O^+ content is 2.32–5.48 wt% and densities are low at 2.3–2.5 g/cm^3 (Table **T30**). Bulk-rock chemical changes of dolerites in Hole 471 are similar to those recognized at Site 857, the Middle Valley, Juan de Fuca Ridge (Tables **T19, T30;** "Appendix B", Table **AT14**). Fresh analogs of the altered E-MORB and T-MORB dolerites were not found in Hole 471 to calculate the matter balance. Therefore, to estimate the element gain/loss through alteration, fresh, initially identical dolerites from other DSDP and ODP holes can be used.

AT14. Major and trace elements, Hole 471, p.48.

Brief Comments

Smectites predominance among secondary minerals in igneous rocks from the spreading axis (Site 477) and flanks (Holes 469, 485A, 483B, and 473) of the northern part of the East Pacific Rise indicates low-temperature alteration of rocks (<150°–200°C) under smectite facies conditions. In spite of the position of Site 477 in the axial zone of spreading (Guaymas Basin) with a high heat flow (20 HFU), alteration of igneous rocks did not take place in the extreme hydrothermal environment under greenschist facies conditions, as was the case in the Middle Valley, Juan de Fuca Ridge (Sites 856 and 858). As a whole, igneous rocks from the holes we studied are poorly altered, particularly the dolerites. Dolerites from the uppermost section of the oceanic crust under smectite facies conditions are stable to alteration at the limited fracturing and absence of rock brecciation (at low water/rock ratio).

Wide distribution of dolerites in the basement drilled during Legs 63, 64, and 65 also influenced the formation of an oxidative alteration environment under spreading conditions (i.e., during displacement of newly formed crust onto the flanks of the mid-oceanic ridge). In Hole 473, igneous rocks 6–6.5 Ma with 248-m-thick sediments overlapping the basement (similar to those of Hole 504B) show only poor evidence of this process and the development of an iron-rich nontronite-like mineral (Grechin et al., 1981) and K-feldspar (Verma, 1981). Intense development of an oxidizing process (by analogy with Hole 504B) did not happen in Hole 473 because of the predominance of well-crystallized, poorly fractured rocks (dolerites) in the basement section. Oxidation alteration occurred in Hole 483B, located 52 km off the axis of spreading and from which basalts of 2.4 Ma were recovered, and in Hole 469, where basalts are 16.5–17.5 Ma.

Weak alteration of the igneous rocks recovered from Holes drilled during Legs 63, 64, and 65 does not influence their initial chemical composition to the extent that element mobility can be estimated with confidence. Estimation of mass balance, made on several samples of poorly to moderately altered glassy basalts from the marginal parts of the basalt units (Hole 485A), showed that with this extent of alteration, only loss of Si and Ca from the rock is determined with relative confidence. A weak tendency of loss of Mn, Zn, and Cu from the rock is also observed.

Distinct from the holes drilled during Legs 63, 64, and 65, Hole 471 is in the area of the off-ridge igneous and hydrothermal activity. Dolerites from Hole 471 are strongly fractured and brecciated. They are moderately to strongly altered under greenschist and smectite facies conditions. The "inverted" vertical zonation of the igneous rock alteration recognized at Site 471 could originate from the supply of hot solutions (~300°C) to the upper part of the dolerite unit along the fractured and brecciated subhorizontal zones. Dolerites in Hole 471 do not show mineral traces of the oxidizing process, which is characteristic of zones of ascending hot solutions.

Mid-Atlantic Ridge, Deep Drill Valley, FAMOUS Area

Hole 332B

Hole 332B (36°52.72′N, 33°38.46′W; water depth = 1806 m) is located in Deep Drill Valley ~30 km west of the Mid-Atlantic Ridge axis in the French-American Mid-Ocean Undersea Study (FAMOUS) area (Fig. **F28**). Penetration to the acoustic basement is 583 m (basement recovery = 121.70 m) with a hole depth of 721.5 mbsf. The oldest sediment cored in Hole 332B is from the Late Pliocene (3.6 Ma). The hole penetrated young basalts of 3.6 Ma (Mitchell and Aumento, 1977). Heat flow is very low (0.5 HFU), much lower than theoretical values, and two sediment temperatures were measured in the hole: 6.0°C at 69 mbsf and 6.52°C at 94.5 mbsf. Bottom water temperature is 4.5°C (Hyndman et al., 1977).

F28. FAMOUS area in the northern Atlantic Ocean, p.231.

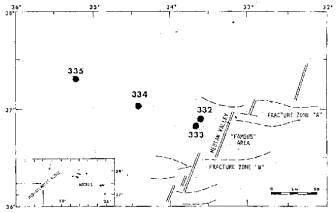

Petrography and Bulk-Rock Chemical Composition

The basement drilled in Hole 332B consists mainly of extrusive basalts and intrusive or massive flow units present in Cores 9, 10, 11, and 26 (Flower et al., 1977). Numerous layers of chalk and limestone are intercalated with basalts in the upper part of the hole. Eleven major lithologic units and 45 subunits have been defined on the basis of phenocryst composition (Aumento, Melson, et al., 1977). Major lithologic units include moderately to highly plagioclase and olivine phyric basalts as well as less abundant aphyric basalts. Groundmass textures are aphanitic or intersertal in most rocks. The units were divided into 45 subunits based on cooling breaks as evidenced by glassy rinds, breccia zones, sedimentary interbeds, and vesicular zones (Flower et al., 1977).

We have studied chemistry, petrography, alteration, and densities in 27 additional samples of basalts from Unit 1 (Subunits 1 and 2), Unit 2 (Subunit 3), Unit 3A (Subunit 7), Unit 3B (Subunit 8), Unit 4 (Subunits 12 and 13), Unit 5 (Subunits 14 and 15), Unit 6 (Subunits 19, 20, and 21), Unit 7 (Subunit 23), Unit 8 (Subunit 25), Unit 9 (Subunits 26, 32, 36, and 38), Unit 10 (Subunits 41 and 44), and Unit 11 (Subunit 45). Petrographic descriptions performed by shipboard scientists (Aumento, Melson, et al., 1977), by Flower et al. (1977) are similar to those performed by our team.

Petrographic descriptions of thin sections of igneous rocks selected for our study are shown in **"Appendix A,"** p.48. All studied samples from Units 1–11 are represented by coarse-, medium-, and fine grained plagioclase, olivine-plagioclase, clinopyroxene-plagioclase, olivine-clinopyroxene and olivine phyric basalts, and aphyric basalts. Petrographic study indicates that these basalts are mostly phyric. The amount of phenocrysts varies from 5% to 50% and sizes are from 0.2 to 4–6 mm. The phyric basalts have doleritic, intersertal, intersertal-microdoleritic, microlitic, pilotaxitic, vitrophyric-pilotaxitic, variolitic, subvariolitic, and hyalopilitic groundmass textures. The aphyric basalts have intersertal, intersertal-microdoleritic, vitrophyric-pilotaxitic, and vague-subvariolitic groundmass textures. The basalts are vesicular (3%–30%) and vesicles are 0.1–1.5 mm across.

All of the basalts are typical oceanic tholeiites that are found for midocean ridge basalts (Strong and Jamieson, 1977). They are the varieties of relatively fresh, chemically primitive, low-titanium olivine or olivine-plagioclase phyric tholeiitic basalts (Hodges and Papike, 1977). Dmitriev (1977) determined two main magma types for basalts in Hole 332B. Magma Group 1 is characterized by high MgO, relatively high Fe_{total}, and low SiO_2 and CaO. Petrographically, these basalts range from coarsely phyric to aphyric. Magma Group 2 has relatively high contents of SiO_2 and CaO and low MgO and Fe_{total}. Broad variations in Al_2O_3, CaO, and especially Fe_{total} and TiO_2 characterize this group. Dmitriev (1977) also determined two subgroups (2a and 2b) on the basis of chemistry and mineralogy. Subgroup 2a has higher contents of SiO_2, Fe_{total}, and TiO_2, but lower Al_2O_3 and CaO than those of Subgroup 2b. Subgroup 2a

consists of aphyric or sparsely phyric basalts with phenocrysts of plagioclase, olivine, and clinopyroxene.

All studied samples are practically nondifferentiated in silicity (Table **T31**). Basalts are slightly differentiated in Mg. In general, these rocks represent typical tholeiitic MORB with low Ti, Zr, alkaline, and alkaline earth elements. Cr and Ni vary in abundance (Table **T31**). As a rule, these elements are more abundant in olivine and clinopyroxene-olivine varieties. All classification diagrams (Figs. **F29, F30, F31**) provide evidence that these studied basalts belong to the tholeiitic MORB series (N-MORB and E-MORB). Some variations in normalized REE ratios (Fig. **F31**), as well as in contents of minor elements (Table **T31**), are due to fractionation of rock-forming minerals (plagioclase, olivine, and clinopyroxene).

T31. Basalts, Hole 332B, p.424.

F29. AFM diagram for basalts, Hole 332B, p.232.

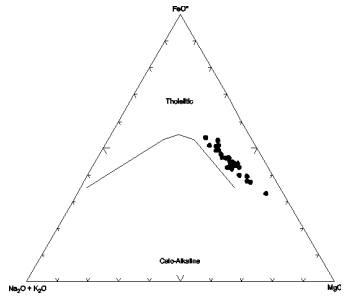

F30. Nb-Zr-Y diagram for basalts, Hole 332B, p.233.

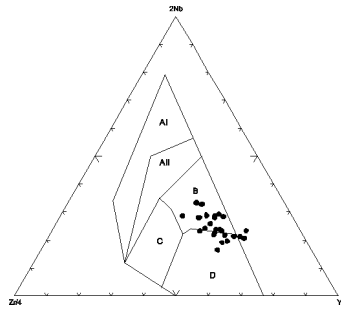

F31. Chondrite-normalized REEs for basalts, Hole 332B, p.234.

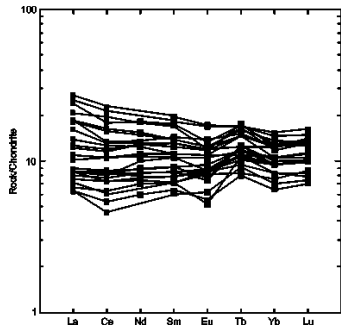

Alteration Mineralogy

Leg 37 scientists (Aumento, Melson, et al., 1977) revealed that basalts in Hole 332B are slightly to moderately altered at low-temperature seawater-rock interaction. Many rocks exhibit a lower grade of alteration. Robinson et al. (1977) reported the replacement of olivine and interstitial groundmass material by smectite. Olivine is often partly or completely replaced with smectite, carbonate, iron hydroxide, and silica. Plagioclase is invariably fresh or slightly altered and cut by veinlets of carbonate and phillipsite. Pyroxene is fresh. Veins contain smectites and carbonate. Vesicles are open or partly to completely filled with secondary minerals. As a whole, secondary minerals in vesicles are represented by smectites, carbonates (calcite, aragonite, dolomite, and magnesite), phillipsite, pyrite, leucoxene, manganese coatings, hematite, iron hydroxides, opal, and magnesium-aluminum sulfate mineral (Robinson et al., 1977; Andrews et al., 1977). Smectites have a basal spacing of 14 Å (e.g., smectites have Mg-cation interlayers). Color, chemical composition, and distribution of smectites in Hole 332B were studied in detail by Robinson et al. (1977). They showed that the brownish to bluish smectites are high-Mg and low-K varieties. The yellow and red smectites are high-Fe and high-K varieties. The most intense alteration occurs in Cores 40–47 and is characterized by carbonate (Flower et al., 1977).

Iron oxides occur along fractures and vesicle walls in oxidation halos. Hematite is formed later than smectite. Most of the hematite appears to have been formed by the breakdown of olivine (Robinson et al., 1977). Hydroxides are found as veins and patches in the more altered basalts (Hall and Fischer, 1977).

Robinson et al. (1977) showed that nonoxidative alteration in the holes of Leg 37 is the most widespread and involves the growth of blue or brown smectites and minor carbonate. The second type of alteration (oxidative), superimposed on the first, involved oxidation in halos or bands along fractures and veinlets and results in the formation of iron hydroxides, yellow or red smectites, phillipsite, and abundant carbonate. Alteration halos are commonly 10–20× the width of the associated fractures.

All samples of basalts from our collection are slightly to moderately altered. H_2O^+ content varies from 0.33 to 2.05 wt%. Basalts with H_2O^+ contents of <1–1.5 wt% predominate (Table **T31**). Densities of the rocks are 2.80–2.90 g/cm^3 (Table **T31**), similar to those for fresh rocks. The low densities result from vesicularity (see **"Appendix A,"** p.48). The basalts reflect nonoxidative alteration with Fe_2O_3/FeO ratios of 0.34–1.67 (Table **T31**).

Petrographic study showed that smectites replace olivine and groundmass glass. Carbonate sporadically replaces olivine. Plagioclase and clinopyroxene groundmass are partly replaced with smectites. Clinopyroxene is replaced by smectite, but often it is fresh. Vesicles are hollow or filled with volcanic glass or zeolite and carbonate. Smectites often cover walls in vesicles and fill thin cracks. Some of the cracks are connected with vesicles (see **"Appendix A,"** p.48). Glass is palagonized in the hyaloclastite breccia from

Sample 37-332B-48R-1, 73–76 cm. It contains veinlets with siliceous minerals. Basalts are fresh or slightly altered (5%–10%). Only isolated samples of basalts with greater vesicularity (15%–30%) are replaced by clay minerals from vesicles (see **"Appendix A,"** p.48). Studied basalts are slightly altered at low water/rock ratios.

XRD study of the fine fraction removed from basalts showed that the principal secondary mineral is smectite with ~10%–40% mica layers (see **"Appendix A,"** p.48) and contain Na-K and Mg-Ca interlayer cations. We have not determined any regularity in distribution of smectites throughout the hole. Illite with ~20% swelling interlayers, chlorite, and talc rarely occur with smectite as an admixture.

Major secondary phases in basalts in Hole 332B are represented by smectites and calcite, which are indicative of low-temperature alteration.

Bulk-Rock Chemical Changes

Using direct comparison of chemical compositions of variously altered rocks, Robinson et al. (1977) showed that nonoxidative alteration produces an increase in whole-rock H_2O^+ without notable changes in K_2O, CO_2, and Fe_2O_3/FeO ratio. The oxidative alteration is indicated by the whole-rock increases in H_2O^+, K_2O, and Fe_2O_3/FeO ratio and slight decreases in CO_2 and SiO_2. Whole-rock values of Al_2O_3, TiO_2, and P_2O_5 are relatively unaffected by alteration. The presence of secondary leucoxene indicates that TiO_2 is not completely immobile during alteration, but there is no evidence of any outside source (Robinson et al., 1977). Basing on the study of oxidized basalts in Hole 332B, Andrews et al. (1977) supposed that with possible exception of Mn, the distributions of Ti, Ni, Co, Cu, Zn, and Sr are not much affected by low-temperature oxidative alteration.

Weak alteration of basalts in Hole 332B that took place mainly in a nonoxidative environment cause elements to be immobile, or the level of mobility is so slight that it is impossible to detect any redistribution of elements with certainty. The element contents for the studied basalts are shown in "Appendix B", Table **AT15**.

AT15. Major and trace elements, Hole 332B, p.50.

Brief Comments

As recognized by Robinson et al. (1977), two types of alteration of 3.6 Ma basalts from Hole 332B are identical to two types of alteration of 5.9 Ma igneous rocks from Hole 504B (Costa Rica Rift). The first type resulted from the earliest nonoxidative alteration and the second type, superimposed on the first one, originated from oxidative alteration. Two types of alteration of magmatic rocks have also been established on the flanks of the East Pacific Rise in Hole 483B, the Gulf of California (2.4 Ma basalts) and in Hole 469 off Southern California (~17 Ma basalts). This allows the conclusion that under the spreading conditions on the flanks of mid-oceanic ridges, the superimposed oxidative alteration of the basement rocks is permanently developing.

As a whole, basalts in Hole 332B are poorly altered, and at the most common nonoxidative stage of alteration, any appreciable redistribution of elements through water-rock interaction did not occur.

Oxidative alteration is reflected in whole-rock increases of H_2O^+, K_2O, and Fe_2O_3/FeO ratios and slight decreased of CO_2 and SiO_2 (Robinson et al., 1977).

Mid-Atlantic Ridge Rift Valley, Serocki Volcano

Hole 648B

Hole 648B (22°55.320′N, 44°56.825′W; water depth = 3326 m) is located at the smooth rim of the summit plateau of a small axial volcano

(Serocki Volcano) in the Mid-Atlantic Ridge rift valley, ~70 km south of the Kane Fracture Zone (Fig. **F32**). Hole 648B was drilled during Legs 106 and 109. During Leg 106, drilling was stopped at 33.3 mbsf (basement recovered = 6.2 m). Hole 648B reached 50.5 mbsf during Leg 109. Hole 648B penetrated young Quaternary basalts (Detrick, Honnorez, Bryan, Juteau, et al., 1988).

Petrography and Bulk-Rock Chemical Composition

Leg 106 and 109 scientists (Detrick, Honnorez, Bryan, Juteau, et al., 1988) found that the uppermost 30 m of the recovered basalt section consists of pillow lavas, which built the volcanic edifice. The pillow lavas contain aphyric to sparsely olivine-plagioclase phyric basalt with a fine grained groundmass and <1% vesicles. The lower lithologic units consist of a vesicular, sparsely olivine-plagioclase phyric basalt with as much as 10% hollow vesicles underlain by massive holocrystalline basalt. The vesicular basalt ~3 m thick and probably represents the top of a massive flow or ponded lava. The holocrystalline, sparsely olivine-plagioclase phyric basalt probably makes up the lower 17.5 m of the hole. These lower units probably represent massive flows that ponded inside Serocki Volcano. The basalts in Hole 648B petrographically and geochemically represent typical MORB, which are similar to basalts from the 22°–25°N region (Detrick, Honnorez, Bryan, Juteau, et al., 1988; Di Donato et al., 1990).

We have studied 8 additional samples of basalts in Hole 648B from Units 3, 9, 14, 20, 21, and 23–25 (see **"Appendix A,"** p.52). All of them are represented by poorly crystallized (glassy) hyalobasalt varieties with phenocrysts and microphenocrysts of plagioclase (1%–7%) and olivine (from single crystals to 1%). Rocks are mainly massive with occasional isolated vesicles. Basalts are nondifferentiated in silicity, Fe, and Mg. According to the abundance of Ti, these rocks are high-Ti tholeiites (Table **T32**). Geochemical diagrams classify them as normal tholeiitic MORB (Figs. **F33, F34**). The variation diagram of normalized REE ratios (Fig. **F35**) is in agreement with the classical trend of normal (typical) tholeiitic MORB. Contents of minor (Cr, Ni, Co, V, and Zr) and alkaline (Rb and Sr) earth elements show low variability and contents that are characteristic of normal tholeiitic MORB (Table **T32**). The freshness of basalts and their geochemical characteristics make them useful for geochemical references of basalts from the Atlantic Ocean.

Alteration Mineralogy and Bulk-Rock Chemical Changes

Shipboard scientists (Detrick, Honnorez, Bryan, Juteau, et al., 1988) showed that all basalts from Hole 648B are fresh. Incipient alteration occurs along fractures. Also, fresh basalts were recognized during Leg 109 in Hole 648B. XRD analysis was used to determine weak reflexes of smectites, which replace interstitial glass.

Di Donato et al. (1990) and Park and Staudigel (1990) demonstrated that although basalts in Hole 648B are fresh, some samples with black halos (low-temperature alteration) are slightly enriched in K, Rb, and U. They show increased loss on ignition (LOI) and $^{87}Sr/^{86}Sr$ ratios. Dark bands consist of protoceladonites, iron oxyhydroxides, and rare manganese oxides (Adamson, and Richards, 1990).

All additionally studied basalts are fresh (H_2O^+ = 0.25–0.53 wt%) and nonoxidized (Fe_2O_3/FeO = 0.25–0.56) (Table **T32**). XRD analysis shows very slight traces of smectite and quartz (see **"Appendix A,"** p.52). These study results, including calculated quantity of major and trace elements ("Appendix B", Table **AT16**) can serve as reference data on fresh unaltered rocks for mass balance calculations of genetically similar but altered rocks in cases when fresh N-MORBs are absent in the recovered section.

Brief Comments

Study of basalts in Hole 648B showed that immediately after eruption

F32. Site in the Kane Fracture Zone, p.235.

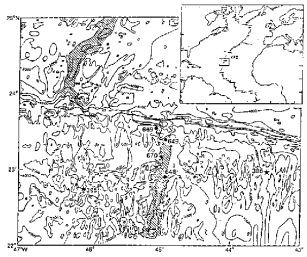

T32. Basalts, Hole 648B, p.428.

F33. AFM diagram for basalts, Hole 848B, p.236.

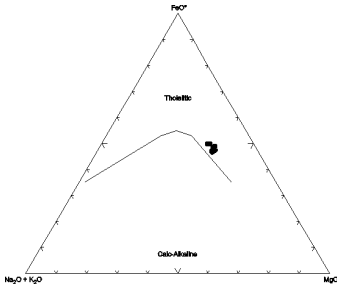

F34. Nb-Zr-Y diagram for basalts, Hole 848B, p.237.

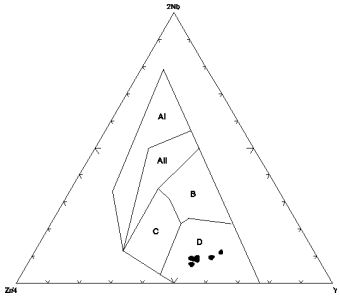

in the axial zone of the spreading ridge, basalts were preserved fresh, especially if they are poorly permeable and not localized in the zone of high heat flow and ascending hot solutions. The mineral products of autometamorphism were not found.

ALTERATION OF IGNEOUS ROCKS FROM ABYSSAL BASINS AND PLAINS

The upper part of the oceanic crust of abyssal basins and plains consists of mainly typical tholeiitic basalts (MORB) and is overlapped by the sedimentary cover. Mesozoic igneous rocks are interesting for study of alteration effects in the upper part of the oceanic crust through time. We have continued the study of alteration of the igneous rocks from abyssal basins and plains in Nauru Basin (DSDP Leg 61), Southwest Pacific Basin (DSDP Leg 91), Argo Abyssal Plain (ODP Leg 123), and Pigafetta Basin (ODP Leg 129).

Nauru Basin

Holes 462 and 462A

The Nauru Basin is located in the southwest Pacific. This area formed at fast-spreading (4.7 cm/yr) Mesozoic crust (Larson, Schlanger, et al., 1981). In the northern part of the basin, west of the Ralik Chain of the Marshall Islands, Holes 462 and 462A were drilled at ocean depths of 5181 m and 5177 m, respectively, at Site 462 during Leg 61 (Fig. **F36**). Coring in Hole 462 (7°14.25′N, 165°01.83′E; depth = 617 mbsf) recovered 558.6 m of sediments, the oldest being Cenomanian brown clay and chert, and 58.4 m of six basalt sills 0.5–9 m thick and one sill at least 30 m thick. Coring in Hole 462A (7°14.50′N; 165°01.90′E) penetrated to 1068.5 mbsf and recovered 564.3 m of sediments, the oldest being Barremian brown-red clay, volcaniclastic sandstone, and siltstone, and 504.2 m of basement that contains a complex of single and multiple diabase sills and extrusions. A total of 300 m of basement cores were recovered (recovery = ~60%). The upper 617 m of Hole 462A duplicated Hole 462 (Larson, Schlanger, et al., 1981). The temperature gradient in the basalts is low; ~3.5°C/100 m. This value was obtained from estimation of temperature in Hole 462 at 133.5 mbsf (8.4°C), 181 mbsf (10.7°C), 219 mbsf (12.3°C), and 608 mbsf (22.4°C) (Boyce, 1981).

In the Nauru Basin, two large cycles of tholeiitic magmatism were distinguished (Shcheka, 1981). The very ancient complex consists of pillowlike basalts 0.2–1.5 m thick located below 730 mbsf. They are separated by ~30-m-thick dolerite sills. This part of the section contains hyaloclastites in the 994–998 mbsf interval. The younger cycle is located at 730 mbsf and above and consists of a series of dolerite sills and hyaloclastites.

Igneous rocks contain: (1) individual sills (Units 6, 12, 13, 21, and 25) with thicknesses from tens of centimeters to >50 m, (2) multiple sills (Units 1–5, 31, and 33), (3) basaltic flows and groups of flows (Units 23, 26, and 29), (4) hyaloclastites or hyaloclastic breccias, and possibly (5) pillow lavas (Unit 34) (Larson, Schlanger, et al., 1981).

Petrography and Bulk-Rock Chemical Composition

In the Nauru Basin, fine- to coarse grained basalts were found. Groundmass textures are from variolitic to doleritic. Downhole in the section to 700 mbsf, there are augite and labradorite/bitovnite phenocrysts. From 700 to ~800 mbsf, there are olivine and bitovnite phenocrysts. From ~800 mbsf to the bottom, there are augite, olivine, and labradorite/bitovnite phenocrysts. Petrographic composition of the igneous rocks was described in detail by Leg 61 scientists (Larson, Schlanger, et al., 1981).

Petrographic descriptions of thin sections from the selected igneous

F35. Chondrite-normalized REEs for basalts, Hole 848B, p.238.

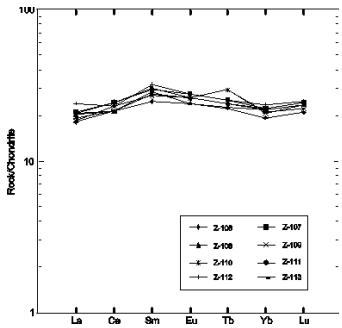

AT16. Major and trace elements, Hole 648E, p.53.

F36. Site in the Nauru Basin, western Pacific Ocean, p.239.

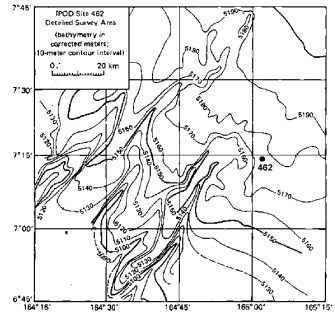

rocks are given in **"Appendix A,"** p.52. The rocks are represented by phyric and aphyric varieties of dolerites and basalts with varying amounts of plagioclase, clinopyroxene, and olivine phenocrysts (total phenocrysts = 1%–20%) and widely varying groundmass textures.

Batiza (1981), Tokuyama and Batiza (1981), Seifert (1981), and Shcheka (1981) determined that basalts in Holes 462 and 462A are tholeiitic MORB. Shcheka (1981) distinguished, based on chemical composition, two complexes of igneous rocks. Low-K tholeiitic basalts from the lower complex (below 730 mbsf) are related to primitive tholeiites. Basalts of the upper complex (above 730 mbsf) with higher TiO_2 content (1.3 –2.2 wt%), are related to differentiated tholeiites. The igneous rocks of the upper complex are more ferruginous than basalts from the lower complex.

The igneous rocks from the samples are nondifferentiated in silicity, Fe, and Mg. Petrochemical and geochemical diagrams classify them as normal low-alkaline tholeiitic MORB (Figs. **F37, F38;** Table **T33**). Variation diagrams of normalized REE ratios (Fig. **F39**) are in agreement with the classical trend of normal (typical) tholeiitic MORB. Batiza (1981) showed that the sills were more enriched in all REEs than the flows. Therefore, when estimating mass balance, it is impossible to compare samples of rocks from sills to those from flows.

Alteration Mineralogy and Bulk-Rock Chemical Changes

Leg 61 scientists (Larson, Schlanger, et al., 1981) revealed that the igneous rocks in Holes 462 and 462A are altered at low-temperature seawater-rock interaction (<150°C). Olivine is replaced with iddingsite and volcanic glasses are palagonitized. Veins contain clay minerals, pyrite, calcite, opal-quartz, and zeolites. In these rocks, higher temperature secondary minerals such as epidote, albite, and actinolite are absent, and any rocks exhibit a lower grade alteration. The igneous rocks have low contents of H_2O^+ and LOI (Larson, Schlanger, et al., 1981; Tokuyama and Batiza, 1981; Shcheka, 1981). Only a few samples of glassy basalts are moderately altered.

Additionally studied samples of basalts are, for the most part, slightly altered. H_2O^+ contents rarely reach 2 wt% and only in one sample is it 2.65 wt% (Table **T33**). Densities of the fresh and very slightly altered basalts are predominantly 2.80–2.95 g/cm^3 (Table **T33**). During Leg 61, density of numerous samples from the igneous rocks in Hole 462A was estimated (Larson, Schlanger, et al., 1981). Predominant densities are 2.90–3.00 g/cm^3 show that in the Nauru Basin, fresh and very slightly altered basalts and dolerites dominate. Basalts have low Fe_2O_3/FeO ratios of 0.29–1.01 (Table **T33**) that reflect nonoxidative alteration. Thin section examination showed that fresh rocks predominate and some are slightly altered (5%–10%). Only olivine is completely replaced with green and brown iddingsite. Rarely, interstitial glass is replaced with clay minerals and opaque minerals. Plagioclase and clinopyroxene are not altered (see **"Appendix A,"** p.53).

XRD study of the fine fraction removed from the basalts showed that the principal secondary mineral in all sections is smectite (saponite). Chlorite and illite are rare and found in trace amounts (see **"Appendix A,"** p.53). Secondary minerals from basalt groundmass and vein minerals were studied in detail (Kurnosov et al., 1981; Windom and Book, 1981). Vein minerals occur in the seven types of associations: (1) saponite, (2) saponite with talc, (3) saponite with magnetite, (4) saponite with Ca-minerals (okenite, calcite, gyrolite-truscotite, heulandite, wairakite, and apophyllite), (5) saponite with pyrite, (6) actinolite-tremolite, and (7) celadonite-glauconite with swelling minerals, calcite, and iron hydroxides (Kurnosov et al., 1981). Chlorite, phillipsite, magnetite, quartz, and chabazite were also identified in veins. In Sample 61-462A-32R-1, 10–14 cm, the 0.4-mm-thick veinlet consists of 70% clinopyroxene replaced by green uralite. Vein minerals reflect a wide temperature range for the solution that circulated in the igneous rocks, from

F37. AFM diagram for basalts, Holes 462 and 462A, p.240.

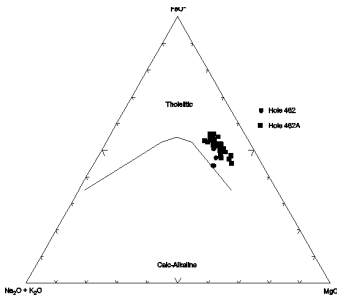

F38. Nb-Zr-Y diagram for basalts, Holes 462 and 462A, p.241.

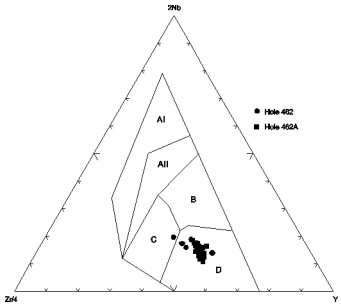

T33. Basalts, Holes 462 and 462A, p.429.

F39. Chondrite-normalized REEs for basalts, Holes 462 and 462A, p.242.

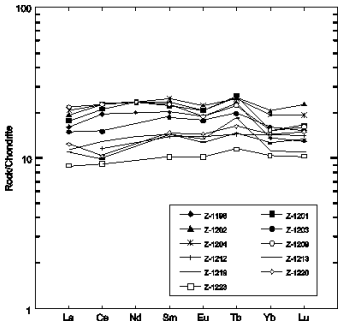

100° to 300°–400°C, in contrast to the monotonous low-temperature alteration conditions of host-rocks, on which the vein minerals had weak influence. Oxidative alteration minerals (iron hydroxides, celadonite-glauconite, calcite, and mixed-layer smectite-illite mineral) occur in veins, vesicles, and, in some samples, in basalt groundmass in the uppermost part of the basement (10–11 m). In this interval, pyrite disappears and moderate- to high-temperature vein minerals are not found (Kurnosov et al., 1981; Windom and Book, 1981). Thus, the superimposed oxidative alteration of Cretaceous basalts in the Nauru Basin was weakly manifested.

As a whole, weak alteration of magmatic rocks in Holes 462 and 462A, having taken place in a nonoxidative environment, causes the elements to be practically immobile. Poor loss of Si, Ca, Fe_{total}, Al, Cu, Zn, Co, and Ni was observed in some samples of the altered glassy basalts from marginal parts of extrusions. Element contents for the studied basalts are given in "Appendix B", Table **AT17**.

AT17. Major and trace elements, Holes 462 and 462A, p.54.

Brief Comments

The Cretaceous igneous rocks from the Nauru Basin are weakly altered, as shown by their high degree of crystallization and poor permeability (low water-rock ratio). Alteration occurred in a nonoxidative environment and at low-temperature (<150°C) under smectite facies conditions analogous to those of the first stage of basalt alteration typical of mid-oceanic axial zone areas, which are beyond the zones of high hydrothermal activity. Vein minerals demonstrate that solutions of different temperatures (<100°C to 300–400°C) circulated on fractures. The second stage of basalt alteration (oxidative), common on the flanks of mid-oceanic ridges, did not occur in the Nauru Basin except for a thin oxidative zone in the uppermost part of the basement. Absence of the intensive second stage of alteration is probably related to a specificity of the intraplate development of the Nauru Basin. Jurassic basement in the Central Pacific was intruded in the Nauru Basin by a sill complex of Cretaceous mid-plate volcanism (Larson and Schlanger, 1981).

Slight alteration of the Cretaceous igneous rocks of the Nauru Basin is analogous to that of the Quaternary basalts from the Gulf of California (Legs 63, 64, and 65) or young 3.6 Ma igneous rocks from the FAMOUS area, Mid-Atlantic Ridge (Leg 37, Hole 332B). This comparison shows that there is no noticeable influence of time on alteration of basalts in the oceanic crust.

Southwest Pacific Basin

Hole 595B

Hole 595B (23°49.34′S, 165°31.61′W; water depth = 5615 m) is located in the Southwest Pacific Basin ~1000 km east of the Tonga Trench (Fig. **F40**). The hole penetrated the ancient Mesozoic Pacific crust (basement penetration = 54 m; 69.8–123.8 mbsf; basement recovery = 15.28 m). The igneous rocks are represented by typical tholeiites of mid-ocean ridges (Menard, Natland, Jordan, Orcutt, et al., 1987).

F40. Southwestern Pacific Ocean site, p.243.

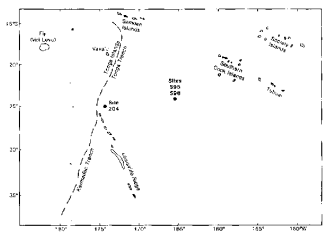

Petrography and Bulk-Rock Chemical Composition

Three lithologic units were recognized in the sequence (Menard, Natland, Jordan, Orcutt et al., 1987). Unit 1 (Core 1) consists of gray to brownish, fine- to medium grained, slightly vesicular aphyric basalts. Unit 2 (Cores 2–6) consists of dark gray, fine grained to glassy aphyric basalt with ferrobasalt attributes. Unit 3 (Core 7) consists of dark gray, aphyric, fine grained and variolitic basalts.

We studied 11 additional samples of basalts from Units 2 and 3 (see **"Appendix A,"** p.56). All basalts are aphyric and fine grained with variolitic, subvariolitic, intergranular, and intersertal groundmass textures. Several

samples are represented by vesicular basalt (~3% vesicles, 0.2–0.4 mm across). Basalt from Sample 91-595B-6R-2, 129–131 cm, is phyric with doleritic texture.

Drilling in Hole 595B recovered light REE–depleted olivine-bearing tholeiites and ferrobasalts with trace element ratios identical to N-MORBs from elsewhere in the Pacific Ocean (Saunders, 1987).

Most of studied samples represent aphyric high-Ti varieties (Table **T34**). They are somewhat enriched in alkaline elements, especially in K. The only exclusion is Sample 91-595B-6R-2, 129–131 cm. It is probable that this sample was taken from a dike. Basalts are poorly differentiated in silicity. Three-component (AFM) diagrams characterize these rocks as normal tholeiitic MORB with a calc-alkaline trend (Figs. **F41, F42**). Cr, Ni, and Co contents are lower, whereas V, Sr, and Zr contents are somewhat higher than in typical MORBs (Table **T34**). The spectrum of normalized ratios of REEs is similar to that of normal MORB (Fig. **F43**), with differences in Eu minimum and some higher general level of REE content.

Alteration Mineralogy and Bulk-Rock Chemical Changes

Leg 91 scientists (Menard, Natland, Jordan, Orcutt, et al., 1987) and Saunders (1987) showed that basalts in Hole 595B are hydrothermally altered. They determined that glass and olivine are completely replaced with clay minerals and clinopyroxene is partly replaced with clay minerals. Units 1 and 2 and some Unit 3 basalts contain fractures lined with iron oxyhydroxides, carbonates, and green clays. We adopt the point of view of these scientists: main alteration processes occur at or near the spreading ridge from which these basalts erupted.

Additionally studied samples of basalts are slightly to moderately altered. H_2O^+ content varies from 1.04 to 1.7 wt%, and several samples contain 1.8–1.9 wt%. Only one sample with 2.18 wt% H_2O^+ was determined (Table **T34**). The studied basalts represent two types of alteration: nonoxidative, in which the Fe_2O_3/FeO ratio is 0.98–1.53, and oxidative, in which the Fe_2O_3/FeO ratio is 1.91–3.67 and secondary minerals typical of oxidative alteration are present. Basalt samples are oxidized in variable degrees (Table **T34**). Smectite is a predominant secondary mineral (see **"Appendix A,"** p.56) and contain Na-K interlayer cations. Smectites replace olivine and groundmass glass and fill vesicles. Occasionally, smectites replace plagioclase.

The increase of H_2O^+, as much as 2.18 wt% in the oxidized basalts in Hole 595B, is accompanied by decreases in Si, Mg, Ca, Ni, Co, and Cu and by increases in K, Al, Fe_{total}, P, REE, Rb, Sr, and Ba ("Appendix B", Table **AT18**).

Brief Comments

The secondary mineral assemblage in basalts in Hole 595B is characteristic of low-temperature alteration under smectite facies conditions. The degree of alteration of basalts from Mesozoic crust corresponds to that of most basalts of mid-ocean ridges, from which these basalts erupted. This suggests that main alteration events occur in basalts in the spreading ridges. Ancient fragments of the basaltic crust preserve this degree of alteration.

Oxidative alteration was determined in basalts in Hole 595B as well as in young basalts on the flanks of mid-ocean ridges in the Pacific and Atlantic Oceans. Most of the studied samples of basalts are oxidized.

Argo Abyssal Plain

Hole 765D

Hole 765D (15°58.54′S, 117°34.49′W; water depth = 5713.8 m) is located in the southern Argo Abyssal Plain on the oldest oceanic crust in the

T34. Basalts, Hole 595B, p.434.

F41. AFM diagram for basalts, Hole 595B, p.244.

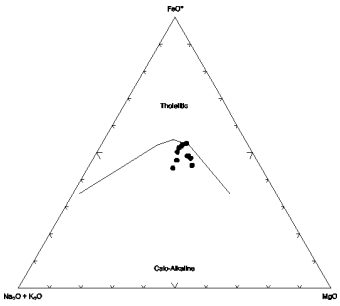

F42. Nb-Zr-Y diagram for basalts, Hole 595B, p.245.

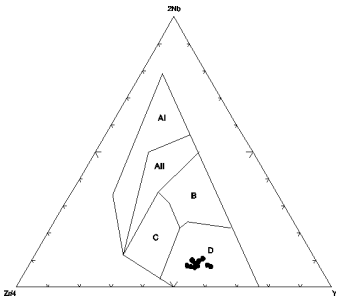

F43. Chondrite-normalized REEs for basalts, Hole 595B, p.246.

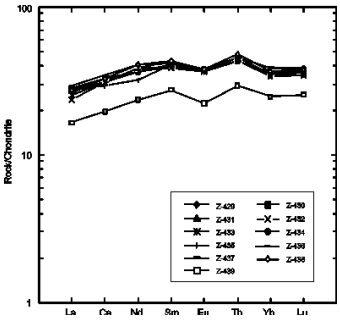

AT18. Major and trace elements, Hole 595B, p.59.

northeast Indian Ocean off the northwest margin of Australia (Fig. **F44**). The Argo Abyssal Plain is extremely flat and located north of the Exmouth Plateau. On the north it is bounded by the Java Trench. Hole 765D penetrated the lowermost Cretaceous and upper Berriasian to Valanginian Indian Ocean crust to 1194.9 mbsf (Gradstein, Ludden, et al., 1992). Basement penetration is 247 m, from 947.9 to 1194.9 mbsf, and basement recovery is 76.6 m.

Petrography and Bulk-Rock Chemical Composition

Drilling in Hole 765D recovered mostly iron-rich normal tholeiitic N-MORB (Ishiwatari, 1992; Ludden, and Dionne, 1992). REE distribution shows uniform concentration of heavy rare earth elements (HREE) and depletion in light rare earth elements (LREE) typical of N-MORB (Ishiwatari, 1992; Ludden, and Dionne, 1992). The chemical composition of the basalts is homogeneous throughout the whole basement section. Geochemical characteristics for Site 765 show that basalts were formed at the onset of spreading (Ludden, and Dionne, 1992). The entire volcanic section comprises pillow basalts (54%), massive basalts (28%), brecciated pillow basalts (8%), autoclastic breccia (6%), and diabase (4%). A total of 22 lithologic units were recognized in the volcanic sequence (Gradstein, Ludden, et al., 1992). They consist mainly of aphyric basalts or, rarely, sparsely to moderately phyric basalts (Gradstein, Ludden, et al., 1992; Ishiwatari, 1992).

We have studied 11 additional samples of basalts from lithologic Units 1, 3, 6, 7, 13, 14, 16, 17, and 22 (Table **T35**). Most selected samples are represented by aphyric fine- to medium grained basalts with intergranular, subvariolitic, microlitic, and poikilophitic groundmass texture (see **"Appendix A,"** p.58). Basalts are mainly vesicular (1%–10% vesicles, 0.1–0.5 mm across). All of them are practically nondifferentiated in silicity, intermediate-Ti, low-alkaline tholeiitic N-MORB (Figs. **F45, F46;** Table **T35**). Cr, Ni, Co, Sr, and Zr are typically low in abundance (Table **T35**). The spectrum of REE distribution is similar to that of tholeiitic MORB but differs in some depletion of light lanthanides and Eu (Fig. **F47**).

Alteration Mineralogy and Bulk-Rock Chemical Changes

Leg 123 scientists (Gradstein, Ludden, et al., 1992) showed that, in general, basalts in Hole 765D are altered under low-temperature brownstone facies conditions of ocean-floor metamorphism. Bass (1976) classified such conditions as oxidative alteration. Much of the basaltic section is slightly altered. Hyaloclastite breccias are completely replaced by clay minerals. The scientists also showed that green clay, calcite, zeolite, and iron hydroxides replace plagioclase, olivine, and glass and fill both vesicles and fractures. The percentage of secondary minerals increases in alteration halos along fractures. Oxidation halos, as well as calcite, zeolite, and smectite, occur throughout the 247-m-thick basement. Celadonite is known only in the upper half of the penetrated section of basalts (142 m); however, later it was shown that celadonite occurs throughout the core (Gillis et al., 1992). Gillis at al. (1992) showed that pillow margins and the interior of the lava units are variably altered. They contain celadonite, iron oxyhydroxides, zeolites, calcite, and saponite. Orange and green halos are located in parallel fractures and extend for several centimeters into the host-rock. Clay minerals from halos are enriched in K_2O and Fe_2O_3. Plagioclase is partly replaced by Ca-Na zeolites and/or albite in altered basalts. This led Gillis et al. (1992) to suppose that albitization of plagioclase indicates that basalts were initially altered at low temperatures and then reheated off-axis by conductive heat flow in a closed environment, but reheating did not result in significant bulk-rock chemical changes.

Additionally studied samples of basalts are slightly altered. H_2O^+ contents vary from 0.35 to 1.16 wt% and densities are 2.75 to 3.00 g/cm^3 (Table T35). Brereton (1992) obtained similar data for numerous samples of basalts in Hole 765D with densities from 2.76 to 2.96 g/cm^3. All studied basalts show nonoxidative alteration in which Fe_2O_3/FeO ratios vary from 0.38 to 1.30 (Table

F44. Site in the Argo abyssal plain, p.247.

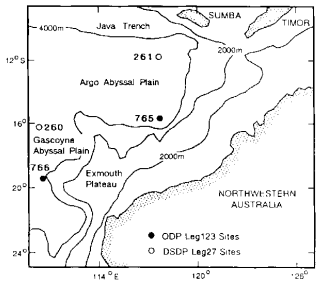

T35. Basalts, Hole 765D, p.436

F45. AFM diagram for basalts, Hole 765D, p.248.

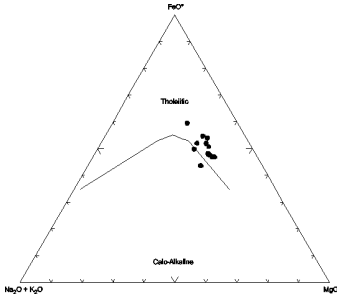

F46. Nb-Zr-Y diagram for basalts, Hole 765D, p.249.

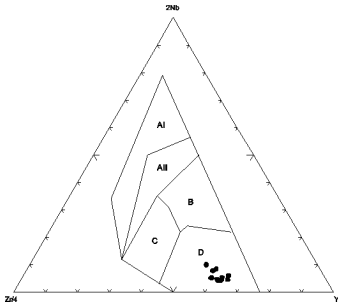

F47. Chondrite-normalized REEs for basalts, Hole 765D, p.250.

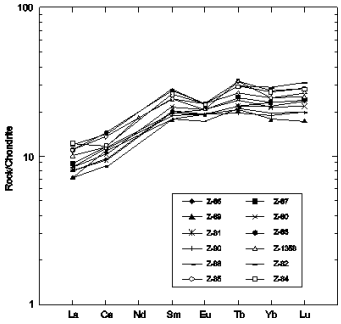

T35). In the thin sections from selected samples of basalts there no indications of oxidative alteration (see **"Appendix A,"** p.58).

Smectites predominate among secondary minerals in basalts (see **"Appendix A,"** p.58) and contain Na-K and Mg-Ca interlayer cations. Hydromica occurs in several samples in trace amounts. Hydromica predominates in association with smectite only in the lower part of the section (Samples 123-765D-27R-2, 31–33 cm, and 27R-3, 4–6 cm). Smectites replace olivine and groundmass glass, fill vesicles, and occasionally associate with carbonate. In large vesicles, carbonate tends to occur in the central parts, whereas smectites are restricted to the peripheries.

As a whole, elements are practically immobile, as shown by the slight alteration of selected basalts in Hole 765D in a nonoxidative environment. Concentrations of elements for the studied basalts are given in "Appendix B", Table **AT19.**

AT19. Major and trace elements, Hole 765D, p.61.

Brief Comments

The secondary mineral assemblages in basalts in Hole 765D provide evidence of low-temperature alteration under smectite facies conditions. Alteration of the basalts from the lower Cretaceous crust and mid-ocean ridges is similar. The lowermost Cretaceous fragments of basaltic crust preserve a low degree of alteration under nonoxidative conditions at low water/rock ratios. Oxidative alteration (Gradstein, Ludden, et al., 1992; Gillis et al., 1992) is common throughout the basalt section recovered from Hole 765D (247 m) and is similar to the oxidation of basalts on the flanks of the Costa Rica Rift (Hole 504B) and the Mid-Atlantic Ridge (Hole 332B).

Gillis et al. (1992) proposed another model for alteration evolution of basalts in Hole 765D. The first stage involves low-temperature oxidative alteration, and the second stage involves off-axis conductive reheating of the crust. Oxidized rocks are enriched in K_2O, Rb, Fe_2O_3, and MnO, and MgO and CaO contents are decreased.

Pigafetta Basin

Holes 801B and 801C

Site 801 is located in the southern Pigafetta Basin, west Pacific Ocean (Fig. **F48**). Hole 801B (18°38.52′N, 156°21.582′E; water depth = 5673.8 m) penetrated to a total depth of 511.20 mbsf. The sedimentary section is 461.6 m thick and the oldest sediment, calcareous silicified tuff and radiolarian metasiltstone, is of Callovian–Bathonian age (~165 Ma). Hole 801C (18°38.538′N, 156°21.588′E; water depth = 5674.0 m), located 20 m from Hole 801B, was drilled to a total depth of 594.3 mbsf. A total penetration into the oldest oceanic crust (132.7 m; 461.6–594.3 mbsf) was in Holes 801B and 801C. The basement section is represented by basaltic thin flows and thin sills. Pillow basalts begin at 495 mbsf. Site 801 first reached the Jurassic basement in the Pacific. Middle to late Jurassic basement may be the oldest in the world ocean (Lancelot, Larson, et al., 1990). It is suggested that the basalts at Site 801 represent a piece of the Pacific oceanic crust that was formed in the Jurassic.

F48. Site in Pigafetta Basin, p.251.

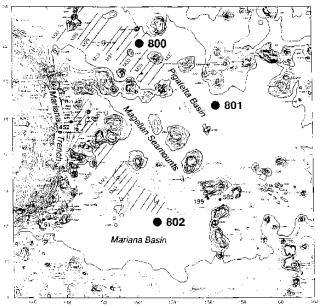

Petrography and Bulk-Rock Chemical Composition

The rock units in Holes 801B and 801C are mostly lava flows (Lancelot, Larson, et al., 1990). The igneous rocks at Site 801 range texture from glassy basalt to medium grained aphyric to phyric dolerite. A majority of the lava flows are fine grained aphyric basalts (Lancelot, Larson, et al., 1990; Floyd, and Castillo, 1992). Sparsely to moderately phyric basalts display spinel-olivine, plagioclase-olivine, and olivine-plagioclase-clinopyroxene phenocrysts (Floyd, and Castillo, 1992). The textures of aphyric basalts demonstrate glassy variolitic margins to holocrystalline intersertal and subophitic flow interiors

(Floyd, and Castillo, 1992). Phenocrysts in the alkaline rocks are plagioclases with variable olivine. Phyric tholeiites contain olivine-plagioclase phenocrysts and variable spinel.

Petrographic descriptions of thin sections of the igneous rocks in Holes 801B and 801C are given in **"Appendix A,"** p.59. The igneous rocks are aphyric massive basalts, rare phyric basalts, and aphyric and phyric dolerites (a single sample is phyric dolerite). Aphyric basalts have microintersertal and microlitic groundmass textures. Plagioclase and olivine(?)-plagioclase phyric basalts show hyaline, vitrophyric, microintersertal, and pilotaxitic textures. The basalts from Unit 23 are slightly vesicular (3%–4% vesicles, 0.2–0.3 mm across). Aphyric dolerites are fine- to medium- or coarse grained with ophitic and occasionally doleritic and doleritic-intersertal groundmass textures. Two samples from the hydrothermal deposit (Unit 8) are oolites of iron oxyhydroxides.

Floyd and Castillo (1992) and Rowbotham and Floyd (1992) showed that the basement recovered from Holes 801B and 801C is represented by an upper alkaline basalt sequence with ocean island basalt (OIB) chemical composition (commonly hawaiites) and a lower tholeiitic basalt sequence with typical N-MORB. These sequences are separated by a hydrothermal deposit. The basement was generated at an active Jurassic spreading center that was overlain after ~10 Ma, when the ocean crust would have migrated 400 km away from the active axis, by an off-axis alkaline volcanism with characteristic OIB features. The alkaline and tholeiitic sequences contain both primitive and evolved chemical groups. The primitive group of alkaline basalts, with high MgO, Ni, and Cr contents, are represented by lithologic Units B6, B7, and C1. The primitive tholeiitic group, with the highest Mg* values (Mg* = Mg/[Mg + Fe^{2+}] × 100 in atomic proportions) represented by Units C9–C20 (Floyd, and Castillo, 1992).

The selected samples of igneous rocks at Site 801 are tholeiitic N-MORB and alkaline rocks (Figs. **F49, F50;** Table **T36**). The spectrum of REE distribution also show that the studied basalts and dolerites form two geochemical groups: tholeiitic MORB and alkaline type (Fig. **F51**). The hydrothermal deposit, Unit C8 (Table **T36**), contains high SiO_2 (87.34–88.06 wt%) and Fe_2O_3 (9.26–9.50 wt%). Contents of trace elements, including REE, are very low, except Zn. Contents of Zn in the hydrothermal deposit and under basalts is approximately equal.

Alteration Mineralogy and Bulk-Rock Chemical Changes

Leg 129 scientists (Lancelot, Larson, et al., 1990) revealed that most igneous rocks are variably altered (10%–75%) in a low-temperature nonoxidative environment under zeolite facies conditions. Oxidative alteration is very minor and largely associated with the hydrothermal deposit. For nonoxidative environments, the principal secondary mineral is smectite. Carbonate, zeolites, chlorite, chlorite-smectite mixed-layer mineral, and biotite are in trace amounts, and pyrite and talc(?) were found in several samples. Interstitial glass is completely replaced with smectite or occasionally zeolite. Olivine is completely replaced by smectite or calcite patches within smectite. Plagioclase is replaced by smectites, carbonate, zeolite, and prehnite, with smectites predominant. Clinopyroxene is often fresh. The veinlets (1%–5% of the rock volume) contain calcite, quartz, green clay, and pyrite, and vesicles are filled with smectite or carbonate and sometimes pyrite. Oxidative alteration with limonite and hematite in interflow zones is post-clay production. Brecciated zones (lithologic Units 9, 13, and 24) consist of basaltic pieces with cement represented by smectite and carbonate. The hydrothermal deposit in Unit 8, at 525 mbsf in Hole 801C (Sections 129-801C-4R-1 and 4R-2), is a yellow iron-silica-rich material >3 m thick. The deposit is interpreted as a hydrothermal precipitation from seawater enriched by hydrothermal solutions derived from the Jurassic underwater hot springs in or near an active axial zone of the ridge-crest system or near silica-rich "white smokers" on the ridge flanks (Lancelot,

F49. AFM diagram for basalts, Holes 801B and 801C, p.252.

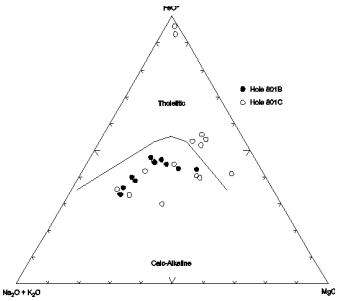

F50. Nb-Zr-Y diagram for basalts, Holes 801B and 801C, p.253.

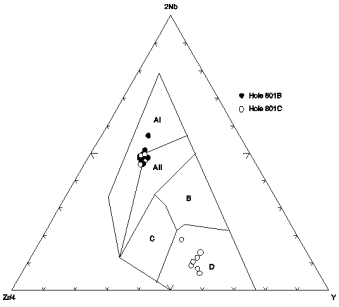

T36. Basalts, Holes 801B and 801C, p.438.

Larson, et al., 1990).

The secondary minerals of tholeiitic and alkaline basalts were studied in detail (Alt et al., 1992; Rowbotham, and Floyd, 1992). Alt et al. (1992) recognized four alteration types at Site 801: (1) saponite-type (Mg-smectite) basalts, generally slightly altered, which occur throughout the tholeiite and alkaline section at low seawater/rock ratios; (2) celadonite-type basalts, which are slightly altered and exhibit increases of alkalis, hydration, and oxidation degree, reflecting higher seawater/rock ratios and occurring locally in both the tholeiitic and alkaline sections; (3) Al-saponite-type basalts resulting in oxidation, hydration, and alkali uptake and decrease of Ca and Na, which occurs only in the alkaline basalts above the hydrothermal deposit; and (4) blue-green basalts exhibiting the greatest chemical changes (oxidation, hydration, alkali uptake, and loss of Ca, Na, and Mg), which are located in a 5-m interval beneath the deposit. Saponite- and celadonite-type alteration of the tholeiitic section takes place at temperatures <20°C. The Fe-Si-enriched hydrothermal deposit was formed from cool (<60°C) distal hydrothermal fluids. The blue-green basalts are formed in extensive alteration environments at similar temperatures. Al-saponite alteration of the alkaline basalts occurs in the low-temperature circulation system that formed the deposit (Alt et al., 1992).

Petrographic study of the igneous rocks showed that they are fresh to moderately altered (see **"Appendix A,"** p.59). H_2O^+ contents are 0.55–4.0 wt% and densities are 2.94–2.42 g/cm^3 (Table **T36**). Oxidized rocks are located beneath the hydrothermal deposit in lithologic Units C9 and C10, where Fe_2O_3/FeO ratios are 2.16–5.03, and above the deposit in Unit C7, where Fe_2O_3/FeO ratio is 5.09. Oxidized basalt predominates from the upper part of the alkaline rock sequence (Unit B4), where Fe_2O_3/FeO ratio is 7.19 (Table **T36**). In highly altered rocks, plagioclase is completely replaced by smectite or by smectite and chlorite. Sometimes plagioclase is partly replaced with albite or almost completely replaced by carbonate. Interstitial glass is completely replaced by smectite and rarely by chlorite. Clinopyroxene is partly to sometimes almost completely replaced with clay minerals. Olivine is often completely replaced by polycrystalline aggregates of iddingsite and olivine from glassy cracks is completely replaced with carbonate. The veinlets contain carbonate or clay minerals, and vesicles are filled with carbonate.

XRD study of the fine fraction removed from the igneous rocks showed that the principal secondary mineral in the tholeiitic sequence is smectite, with ~5%–30% mica-type layers (see **"Appendix A,"** p.59). The hydrothermal deposit, which separates the tholeiitic and alkaline sequences, consists of quartz and hematite. In the alkaline section, besides smectite, mixed-layer smectite-swelling chlorite minerals, mixed-layer smectite-chlorite, and chlorite were determined in trace amounts. Oxidized and nonoxidized basalts from this section contain the same clay mineral assemblage.

Secondary minerals show alteration of the igneous rocks of both tholeiitic and alkaline sequences under the smectite facies at low temperature. Slight alteration in the tholeiitic sequence was mostly at low water/rock ratios. Formation of chloritic minerals, together with smectite in the igneous rocks from the alkaline sequence, shows a higher temperature of alteration, possibly >100°C.

When nonoxidative alteration of the evolved tholeiitic basalts (tholeiitic sequence) in Hole 801C is weak, the elements are immobile or very poorly mobile. In the upper part of the tholeiitic sequence, immediately underlying the hydrothermal deposit (blue-green alteration zone distinguished by Alt et al., 1992), oxidized primitive tholeiitic basalts (lithologic Units C9 and C10) are more strongly altered, with H_2O^+ values ranging from 2.02 to 2.53 wt% and densities from 2.65 to 2.42 g/cm, (Table **T36**). Sample 129-801C-5R-5, 55–58 cm, from fresh nonoxidized rock, has a H_2O^+ content of 0.59 wt% and a density of 2.91 g/cm^3. Sample 129-801C-5R-1, 45–52 cm, from altered oxidized rock, has a H_2O^+ content of 2.02 wt% and a density of 2.65 g/cm^3. Comparison

F51. Chondrite-normalized REEs for basalts, Holes 801B and 801C, p.254.

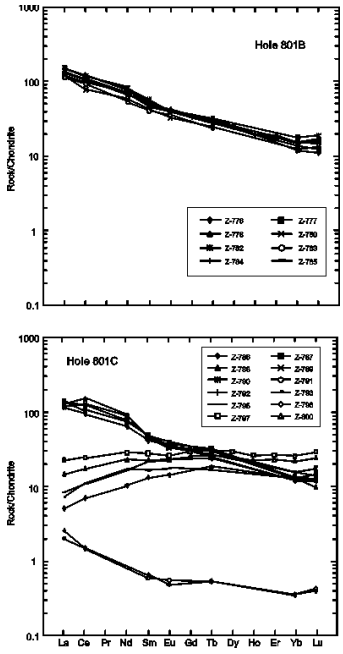

of these two samples of magmatic rocks, very similar in petrographic composition from a single geochemical group (the primitive tholeiitic basalts), showed that in the altered oxidized sample there is less Si, Fe_{total}, Mn, Mg, P, and Ni. Contents of H_2O^+, Ti, Al, Ca, Na, K, Fe_2O_3/FeO, La, Ce, Nd, Sm, Eu, Rb, Sr, Ba, and V in the altered sample increase to a different degree as compared with contents in the sample of fresh rock. Contents of the elements for the studied selected basalts are given in "Appendix B", Table **AT20**.

AT20. Major and trace elements, Holes 801B and 801C, p.62.

We were not successful in estimating the element gain/loss for the primitive alkaline rock group (lithologic Units B6 and C1) in the moderately altered igneous rocks from the alkaline sequence (Holes 801B and 801C) because there are no fresh rocks among the studied basalts. For the evolved alkaline rock group, the strongly altered rocks (Sample 129-801B-40R-1, 29–33 cm; Fe_2O_3/FeO = 7.19; H_2O^+ = 3.77 wt%; density = 2.48 g/cm^3; and Sample 129-801C-3R-1, 42–48 cm; Fe_2O_3/FeO = 5.99; H_2O^+ = 4.00 wt%, density = 2.04 g/cm^3) (Table **T36**) were compared with nonoxidized basalt (Sample 129-801B-41R-1, 130–136 cm; Fe_2O_3/FeO = 0.74; H_2O^+ = 1.55 wt%; density = 2.65 g/cm^3), which is less altered. In the oxidized rocks, Fe_{total}, Mn, Mg, Ca, Na, and Sr contents decrease and H_2O^+, Si, Ti, Al, K, Fe_2O_3/FeO, Rb, Cr, and Ni contents increase ("Appendix B", Table **AT20**). For some elements, the results obtained from the oxidized alkaline rocks do not agree with results obtained from the oxidized tholeiitic basalts, and data on behavior of Si, Ca, Na, and Ni through oxidative alteration obtained for these rock groups are contradictive.

Two samples (Sample 129-801B-41R-1, 130–136 cm; H_2O^+ = 1.55 wt%; Fe_2O_3/FeO = 0.74; density = 2.65 g/cm^3; and 43R-4, 32–40 cm; H_2O^+ = 3.26 wt%; Fe_2O_3/FeO = 1.00; density = 2.52 g/cm^3) (Table **T36**) were chosen to estimate the element behavior through alteration of the evolved alkaline rocks in the nonoxidative environment. As both samples are altered (difference in H_2O^+ content = 1.7 wt%), the element mobility was only relatively estimated. The more strongly altered sample contains less Si, Mg, Ca, K, Rb, Sr, and Rb and more H_2O^+, Al, Mn, Na, Ba, Cr, Ni, and Zn than the more weakly altered sample ("Appendix B", Table **AT20**).

Results obtained for element mobility through alteration of alkaline and tholeiitic basalts from Site 801 in oxidative and nonoxidative environments need improvement in the future, and for this, fresh analogs of the altered rocks are required.

Brief Comments

The secondary mineral assemblages reflect alteration of the igneous rocks of both tholeiitic and alkaline sequences under the smectite facies at low temperatures.

Slight alteration in the tholeiitic sequence occurred mostly at low water/rock ratios similar to alteration of young igneous rocks that are poorly permeable and located at the spreading center areas beyond the zones of ascending hot solutions. Oxidative alteration (a later alteration superimposed on the nonoxidative type) probably reflects displacement of newly formed Jurassic volcanic rocks from the spreading center to the flanks, because in the Cenozoic mid-oceanic ridges, the oxidative type of alteration in the igneous rocks was recognized on their flanks (Hole 504B, Costa Rica; Hole 332B, Mid-Atlantic Ridge; Holes 483B and 469, Gulf of California). Further overlapping of the tholeiitic basement by the igneous rocks, belonging to OIB based on composition, sealed up the alterations of basement igneous rocks in that form as they occurred in the middle Jurassic. Thus, the alteration processes and pattern of igneous rocks under the spreading conditions were preserved unchanged for ~165 m.y.

In the alkaline volcanite complex overlaying the tholeiitic basement, rock alteration probably took place at higher temperatures, which may have exceeded 100°C. This is evidenced by the formation of chlorite components,

with smectite, such as chlorite, defective chlorite, and mixed-layer minerals with chlorite layers. Oxidative alteration, similar to that in the tholeiitic basement, is developed not only directly above the hydrothermal deposit, but also in the upper part of the alkaline rock sequence. It is possible that oxidative alteration in the alkaline rock sequence (a complex of OIB) is related to penetration of seawater along the subhorizontal highly permeable zones common in the underwater volcanic edifices.

In the nonoxidative environment and poorly altered evolved tholeiitic basalts of the tholeiitic sequence, elements are immobile or very weakly mobile. In the upper part of the sequence (blue-green alteration zone distinguished by Alt et al., 1992), the oxidized primitive tholeiitic basalts (lithologic Units C9 and C10) are somewhat more strongly altered. The oxidative alteration is accompanied by decreases of Si, Fe_{total}, Mn, Mg, P, and Ni and increases, to a different degree, of H_2O^+, Ti, Al, Ca, Na, K, Fe_2O/Fe, La, Ce, Nd, Sm, Eu, Rb, Sr, Ba, and V.

In the oxidized, evolved alkaline rocks, contents of Fe_{total}, Mn, Mg, Ca, Na, and Sr decrease and those of H_2O^+, Si, Ti, Al, K, Fe_2O_3/FeO, Rb, Cr, and Ni increase. We have estimated only a tendency in the element behavior under the nonoxidative alteration of the evolved alkaline rocks: decreases in Si, Mg, Ca, K, Rb, Sr, and Pb and increases in H_2O^+, Al, Mn, Na, Ba, Cr, Ni, and Zn in the altered rock.

ALTERATION OF IGNEOUS ROCKS FROM SEAMOUNTS AND GUYOTS

Active volcanic seamounts are suitable to represent open hydrothermal systems. Conditions necessary for the development of a hydrothermal system within a seamount include heat source, high vesicularity of subhorizontal basalt flows, and a large surface area of volcanic edifice contacting with seawater, which can readily penetrate into the seamount. In extinct submarine volcanoes, we can expect “frozen” hydrothermal systems expressed as extensively altered basalts with vesicle infills and veins composed of alteration products. Redistribution of elements at water-rock interaction in open hydrothermal systems of volcanic edifices influences the chemical composition of solutions circulating within the edifices and ultimately discharging into the ocean. Therefore, seamounts contribute to the global geochemical interaction of oceanic lithosphere and hydrosphere together with axial zones of mid-ocean ridges and zones of off-ridge volcanism and hydrothermal activity. Volcanic seamounts and guyots are especially widespread in the Pacific Ocean. For example, the Emperor-Hawaiian Seamount chain extends ~6000 km.

We studied altered and fresh basalts recovered during DSDP Legs 19 and 55 on the Meiji, Ojin, Nintoku, and Suiko Seamounts and during ODP Legs 143 and 144 on the Allison, Resolution, Lo-En, Wodejebato, and Massachusetts Institute of Technology (MIT) Guyots as examples of basalt alteration in the intraplate volcanoes. This chapter also contains the study results of altered trachytes from the Southern Hess Rise (DSDP Leg 62), although this structure is not a seamount. Alkaline composition of the Hess Rise rocks is typical for volcanic rocks from the upper parts of seamounts.

Emperor Seamount Chain

The Emperor Seamount chain is a part of the Hawaiian-Emperor chain that consists of 107 central-type volcanoes. Their total volume exceeds 740×10^3 km^3 of lava (Bargar and Jackson, 1974). The chain formed during the last 70 m.y. and Wilson (1963) suggested that the Hawaiian Islands were formed because of the Pacific lithosphere’s plate motion relative to the Hawaiian hot spot. The Hawaiian Ridge extends to the northwest at a distance of ~3500 km.

After a sharp bend to the north, it continues as the 2300-km-long Emperor Seamount chain until the intersection of the Kurile and Aleutian trenches (Fig. **F52**). Water depth over the seamount summits is >1000 m and reaches 3000 m at the northern end of the chain (Meiji Seamount).

F52. Sites on the Emperor Seamount chain, p.255.

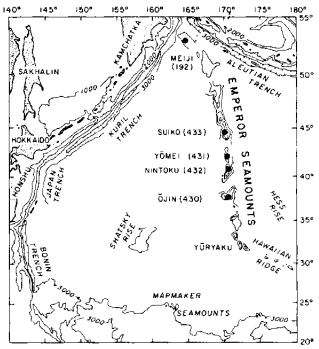

Peculiarities in composition and alteration environment of basalts from the Emperor Seamount chain are reflected by their altered varieties. In general, igneous rocks of the Hawaiian-Emperor chain are represented by tholeiitic basalts differing from both the mid-ocean ridge and abyssal basin floor tholeiites in higher alkalinity and Ti content. Moreover, alkaline blanket basalts occur elsewhere in the upper volcanic complex of seamounts (MacDonald, 1968). The stratified "flaky pie" structure of volcanic seamounts, built up of subhorizontal, highly vesicular subaerial basalt flows, provides free penetration of seawater into the volcanic edifices. The seawater likely penetrates into the upper part of the edifice roots. Seamounts possibly provide more favorable conditions for seawater penetration than the mid-ocean ridges, because they have a much wider specific area of water-rock contact, as well as numerous highly permeable interbeds, mainly represented by highly vesicular and brecciated flow tops. Each submarine volcano essentially represents a hydrothermal system, where water-rock interaction takes place under low-temperature conditions in edifice margins and under high-temperature conditions within the central hot zone, as well as in sites of hot solutions discharge. Subaerial volcanic flows have undergone laterite weathering resulting in the formation of red oxidized soil.

We studied selected samples of basalts from Ojin (Hole 430A), Nintoku (Hole 432A), Suiko (Holes 433A and 433C), and Meiji (Hole 192A) Seamounts (Fig. F52). Volcanic rocks recovered from these seamounts are petrographically and geochemically similar to Hawaiian lavas. They include hawaiite, mugearite, alkaline basalt, and tholeiitic basalt (Jackson et al., 1980).

Hole 430A

Hole 430A (37°59.29′N, 170°35.86′E; water depth = 1478.8 m) is located on Ojin Seamount at the southern part of the Emperor Seamounts chain (Fig. **F52**). Ojin Seamount is capped by lagoonal sediments. The hole penetrated 47.5 m of calcareous ooze and sand interbedded with 11.8 m of volcaniclastic sediments at the base. The oldest sediment is of upper Paleocene age. Basalts were cored to a total depth of 85.5 m (Jackson, Koisumi, et al., 1980). Drilling in Hole 430A recovered five subaerial basalt flow units. The upper four flow units are represented by hawaiite, coarsely vesicular and partly oxidized in places and massive in flow interiors. The lower flow unit is composed of tholeiites (Jackson, Koisumi, et al., 1980). The third and fourth units are separated by a red oxidized soil. K-Ar age of the basalts from Ojin Seamount is ~55.2 Ma (Dalrymple et al., 1980a).

Petrography and Bulk-Rock Chemical Composition

During Leg 55, Jackson, Koisumi, et al. (1980) ascertained that basalts of the upper four flow units in Hole 430A are petrographically and chemically uniform. The units are aphyric to sparsely olivine and plagioclase phyric basalts with subtrachytic texture and vary from intergranular (flow margins) to subophitic (flow centers). The groundmass is fine grained, consisting of olivine, clinopyroxene, plagioclase, titanomagnetite, apatite, and glass (Kirkpatrick et al., 1980). The rocks belong to the alkaline series and may be classified as hawaiite. They contain Na-rich plagioclase ($An_{30–35}$), fayalitic olivine (Fo_{65}), and apatite. The chemical composition is characterized by high contents of K_2O (1.57–1.95 wt%), Na_2O (4.08–4.61 wt%), SiO_2 (50–51 wt%), and P_2O_5 (~1.20 wt%,), whereas CaO content is low, ranging from 6.75 to 7.43 wt% (Kirkpatrick et al., 1980; Bence et al., 1980). The hawaiites in Hole 430A are very similar in their mineral chemistry (Clague et al., 1980). Both the petrography and chemistry of the four basalt flows show that Ojin Seamount is a volcano of the Hawaiian type (Jackson, Koisumi, et al., 1980). Two small rock pieces were

recovered from flow Unit 5. The rock is phyric basalt with intergranular groundmass texture. Phenocrysts are represented by olivine, augitic clinopyroxene, and plagioclase. The groundmass consists of olivine, clinopyroxene, plagioclase, titanomagnetite, ilmenite, and glass (Kirkpatrick et al., 1980). The low K_2O and P_2O_5 contents show that the basalt is an island-type tholeiite (Jackson, Koisumi, et al., 1980; Kirkpatrick et al., 1980). Concentration of Cr and Ni in the tholeiite is higher than that in the hawaiites, and concentrations of Ba, Sr, Zn, Zr, and Y are lower (Kirkpatrick et al., 1980). The hawaiite is enriched in both LREE and HREE. The tholeiitic basalt contains much less REE than the hawaiite (Bence et al., 1980; Jackson, Koisumi, et al., 1980).

We have studied 6 additional samples from flow Units 2 and 3 (hawaiites). Aphyric rocks with subtrachytic and trachytic groundmass textures predominate. Vesicularities vary from slight to 25% of the rock volume (see **"Appendix A,"** p.62). Vesicles vary from 1.2 to 5 mm. The groundmass contains plagioclase (andesine [An_{48-35}]; 40%–75%), clinopyroxene (5%–15%), glass (15%–25%), and opaque minerals (5%–15%). Orthoclase (~5%) occurs in some samples. At the bottom of flow Unit 2 (Samples 55-430A-6-1, 6–11cm, and 98–103 cm), hawaiites are clinopyroxene-phyric and aphyric with microdoleritic and intersertal-doleritic groundmass textures, respectively. Phenocrysts constitute 35% of the rock volume.

Hawaiites are enriched in alkaline elements, particularly in K, as well as in P and Ti (Table **T37**). Geochemical diagrams provide evidence that these rocks belong to the intraplate alkaline group (Figs. **F53, F54, F55**).

Alteration Mineralogy

Kirkpatrick et al. (1980) and Clague et al. (1980) showed that hawaiites in Hole 430A are slightly altered. Alteration degree of the rock in a thin section is ~10%–20% of the rock volume (see **"Appendix A,"** p.62). Low contents of H_2O^+ (0.94–1.53 wt%) indicate slight alteration of the rocks. Chemical composition of hawaiites by Cambon et al. (1980) also confirm their slight alteration, as H_2O^+ contents vary from 0.89 to 1.67 wt%. Interstitial glass is replaced with smectite. Olivine is often completely replaced with iddingsite and smectite and rarely with calcite. Smectites contain Na-K cations in interlayers in the upper part of flow Unit 1 and Ca-Mg cations in the rest of Unit 1, as well as in Units 2, 3, and 4. Plagioclase and clinopyroxene, as well some of the olivine, are fresh. Rims of magnetite are replaced with hematite. The plagioclase tholeiite is very slightly altered (~5%), whereas olivine is completely replaced with iddingsite and smectite. Smectite contains Mg-Ca cations in interlayers. Plagioclase, clinopyroxene, and iron-titanium oxides are fresh (Kirkpatrick et al., 1980; Clague et al., 1980).

According to our study, selected samples of hawaiite are slightly to moderately altered, as H_2O^+ contents vary from 0.45 to 1.96 wt% of the rock volume (Table **T37**). The studied samples are mainly altered under an oxidizing environment. Oxidation degree is variable and Fe_2O_3/FeO ratio values range from 1.68 to 5.66. Sample 55-430A-5R-4, 105–108 cm, is strongly oxidized. Petrographic study on selected samples show that the hawaiites in Hole 430A are slightly to moderately altered, from 5%–10% to 15%–20% of the rock and rarely as much as 30% (see **"Appendix A,"** p.62). The interstitial glass is completely replaced with clay minerals and several grains of opaque minerals are oxidized to brownish red. Plagioclase is replaced with clay minerals along thin fissures by 15%–20% and rarely as much as 40%. Clinopyroxene is altered in different degrees: both fresh grains and grains replaced by smectite, chlorite, hydrobiotite occur. Olivine is completely replaced with golden-brown smectite.

XRD and electron diffraction studies of the fine fraction extracted from hawaiites show that groundmass is mainly replaced with trioctahedral saponite-type smectite (b = 9.19 Å) (Tables **T38, T39**). Microprobe chemical composition data of smectites from interstitial glass in hawaiites indicate that

T37. Hawaiites, Hole 430A, p.442.

F53. AFM diagram for igneous rocks, Holes 430A, 432A, 433C, and 192A, p.256.

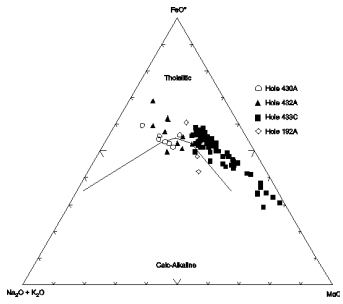

F54. Nb-Zr-Y diagram for igneous rocks, Holes 430A, 432A, and 433C, p.257

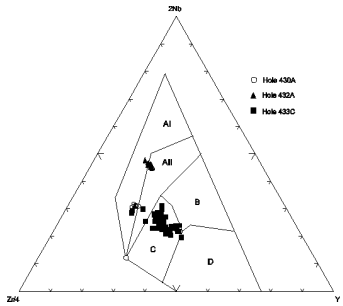

F55. Chondrite-normalized REEs for igneous rocks, Holes 430A, 432A, and 433C, p.258.

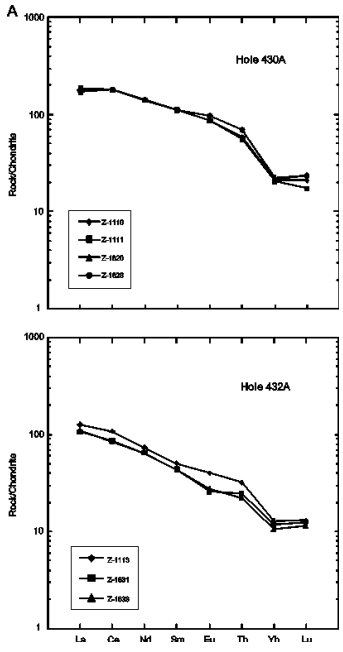

T38. Fine fraction, Leg 55, p.443.

they belong to Fe-Mg-smectites (Fe_{total} = 14.0%–22.2%, MgO = 14.1%–17.2%). Concentration of K_2O ranges from 0.07% to 0.67% and Na_2O content is ~1.2% (Dalrymple et al., 1980a). Wet chemical analysis of the <0.001-mm fraction extracted from the hawaiite (Sample 55-430A-6R-1, 6–11 cm), shows the following contents of major oxides: Fe_2O_3 = 12.15 wt%, FeO = 1.83 wt%, MgO = 7.84 wt%, Na_2O = 2.14 wt%, and K_2O = 1.32 wt% (Table **T40**). Distribution of secondary minerals was studied in flow Unit 2 (~6–7 m thick) from the uppermost to lowermost intervals and are represented by highly vesicular hawaiite from the top (Samples 55-430A-5R-4, 39–43 cm, and 5R-5, 33–37 cm), center (Samples 55-430A-5R-5, 96–101 cm, and 6R-1, 6–11 cm), and bottom (Samples 6R-1, 96–98 cm, and 6R-1, 98–103 cm) of the flow. We did not find any differences in composition of secondary minerals within the section of flow Unit 2 (Table **T38**). Principal secondary mineral is smectite throughout. Along with smectites, mixed-layer smectite-swelling chlorite mineral is detected in trace amounts in many hawaiite samples. Trace amounts of illite are found only in samples from the top and bottom of the flow. In a thin section from the bottom of the flow (Sample 55-430A-6R-1, 98–103 cm), we observed several areas of probably albitizited plagioclase.

Vesicles in the hawaiites in Hole 430A are hollow, with walls covered by a dark green clay mineral or infilled with greenish gray clay. The greenish gray clay consists of trioctahedral smectite (*b* = 9.19 Å) (Tables **T41, T42**). Contents of K_2O and Na_2O in the smectite are 0.60 and 2.11 wt%, respectively (Table **T43**). Microprobe study of the greenish gray clay from the same sample showed the following concentrations of elements: Fe_{total} = 17.74%, MgO = 16.72%, Na_2O = 1.76%, and K_2O = 0.26% (Table **T44**). Besides smectite, the greenish gray clay from several vesicles contains a mixed-layer smectite-chlorite mineral and calcite (Sample 55-430A-5R-5, 96–101 cm) (Table **T41**). An undetermined mineral with XRD reflections of 2.99, 2.70, and 2.46 Å was also detected in the greenish gray clay from Sample 55-430A-6R-1, 6–11 cm. A similar XRD pattern characterizes the synthetic cadmium carbonate. In the upper, highly vesicular part of flow Unit 2, walls of large vesicles are covered by yellow clay (Sample 55-430A-5R-4, 39–43 cm) (Table **T41**). The yellow clay consists of smectite. The electron diffraction pattern demonstrates two parameter *b* values, 8.99 and 9.21 Å, approximately of equal intensity (Table **T42**). The yellow smectite is possibly dioctahedral. We could not select a pure sample of yellow clay pellicle without contamination by basalt. Because of this, the parameter *b* = 9.21 Å likely belongs to trioctahedral smectite from the groundmass. Some vesicles are completely infilled with carbonate commonly dominated by calcite. Aragonite occurs in several large vesicles. In Sample 55-430A-6R-1, 98–103 cm, we observed transparent radial axial aragonite crystals infilling a vesicle (Table **T41**). Minor amounts of calcite occur together with aragonite. Walls of the vesicle are covered by greenish gray clay, whereas carbonate infills its central part. The clay consists of smectite. Rare veinlets contain black smectite. In Sample 55-430A-6R-1, 6–11 cm, we found a trace amount of calcite. In some veinlets, an admixture of mixed-layer smectite-chlorite mineral and illite occurs together with smectite (Sample 55-430A-6R–3, 19–24 cm) (Table **T41**).

The secondary mineral assemblage (smectites and carbonates) detected in whole rocks, vesicles, and veinlets in Hole 430A shows that alteration of hawaiites from the upper part of the Ojin Seamount took place at low temperatures under the smectite facies. A higher temperature possibly existed in lower parts of the lava flows, as indicated by the appearance of albite replacing primary plagioclase. The hawaiite, as a whole, is slightly altered. Yellow smectites from vesicular zones in the uppermost parts of the subaerial lava flows, oxidized interstitial glass, and high ratios of Fe_2O_3/FeO in the hawaiites reflect a high seawater/rock ratio and oxidative environment at the water-rock interaction.

Bulk-Rock Chemical Changes

T39. Parameter *b* of clay minerals, Leg 55, p.444.

T40. Fraction <0.001 mm, Leg 55, p.445.

T41. Vesicles and veins, Leg 55, p.446.

T42. Parameter *b* of clay minerals, Leg 55, p.447.

T43. Clay minerals from vesicles and veins, Leg 55, p.448.

T44. Microprobe analyses, Leg 55, p.449.

Element content in hawaiites in Hole 430A is given in "Appendix B", Table **AT21**. As a whole, the hawaiites in Hole 430A are not suitable for the estimation of element gain/loss at their alteration level, as most of the rocks are only slightly altered. Variations in vesicularity hamper the comparative analysis of the chemical composition of altered and fresh rocks in terms of rock density. For a correct comparison, we need rock samples with similar vesicularity. Fresh rock samples from the Hawaiian Islands should likely be used for this analysis.

AT21. Major and trace elements, Hole 430A, p.66.

The available samples only allow us to reveal the difference in bulk-rock chemical composition of altered and relatively fresh hawaiites; however, it should be taken into account that this difference may not correspond to the real element gain/loss at water-rock interaction. We compared the most altered, slightly oxidized aphyric massive hawaiite (Sample 55-430A-6R-3, 19–24 cm; H_2O^+ = 1.96 wt%; Fe_2O_3/FeO = 1.70) (Table **T37**) with the less altered, nonoxidized aphyric massive hawaiite (Sample 55-430A-6R-1, 98–103 cm; H_2O^+ = 0.94 wt%; Fe_2O_3/FeO = 0.75). The more altered hawaiite sample is characterized by higher contents of H_2O^+, Fe_{total}, Na_2O, K_2O, P_2O_5, Zr, Y, Sr, and Ba and lower contents of TiO_2, Nb, Co, and V. In the most oxidized, highly vesicular hawaiite (Sample 55-430A-5R-4, 105–108 cm; H_2O^+ = 0.45 wt%; Fe_2O_3/FeO = 5.66) (Table **T37**), the difference in element contents is more significant. In this sample, contents of Fe_{total}, MnO, Na_2O, K_2O, P_2O_5, Zr, Y, Nb, Rb, Sr, and Ba are higher and contents of SiO_2, MgO, Cr, Ni, Co, V, and Cu are lower than in Sample 55-430A-6R-1, 98–103 cm.

Hole 432A

Hole 432A (41°20.03′N, 170°22.74′E; water depth = 1309.8 m) is located on the Nintoku Seamount to the north of Ojin Seamount within the Emperor Seamounts chain (Fig. **F52**). The hole penetrated 74 m (42.1 m of sediments and 31.9 m of basalts). The lowermost sediment represented by conglomerate and sandstone is of Paleocene age. It is underlain by a thin red clay bed above basalt (Jackson, Koisumi, et al., 1980). The conglomerate contains fragments of alkaline basalt, hawaiite, and mugearite as erosion products of a high basaltic island. Three flow units of subaerial alkaline basalt were cored in Hole 432A. The two upper units, flow Units 1 and 2, are represented by alkaline basalt (0.6 and 2 m thick, respectively). Flow Unit 3 is transitional between alkaline basalt and hawaiite (the flow bottom was not reached). The top of flow Unit 1 has been eroded. At the boundary between flow Units 2 and 3, there is a 10-cm-thick red to reddish brown clay soil (Jackson, Koisumi, et al., 1980). K-Ar age of the basalts from the Nintoku Seamount is ~56.2 Ma (Dalrymple et al., 1980a).

Petrography and Bulk-Rock Chemical Composition

Petrographic composition of basalts in Hole 432A was studied in detail during Leg 55 (Jackson, Koisumi, et al., 1980), as well as by Kirkpatrick et al. (1980). Flow Units 1 and 2 are petrographically similar. The alkaline basalts are plagioclase phyric with intersertal to diabasic groundmass textures. Large-zoned plagioclase phenocrysts, as much as 1 cm, comprise 5%–15% of the rock. The groundmass consists of plagioclase laths (~50%), titanaugite (20%–25%), olivine (4%–8%), titanomagnetite (4%–6%), glass (20%), and apatite in trace amounts. Textures of the alkaline basalt are subophitic, subtrachytic, glomerophyric, microlitic, and intergranular. The tops of flow Units 1 and 2 are vesicular. Vesicles at the flow tops are 2–5 mm in diameter, but the largest ones reach a diameter of as much as 20 mm. At the bottom of the flows, vesicles are 2–3 mm in diameter. Flow Unit 3 is massive throughout, except the upper and lower part of the unit and a few local rows of vesicles in the central part. Vesicles are 1–5 mm in diameter. The top of the unit contains as much as 20% vesicles. Flow Unit 3 is sparsely phyric basalt. Phenocrysts, ~1% of the rock, are represented by plagioclase and olivine. Groundmass is fine grained, with grain sizes of ~0.05 mm. The groundmass contains plagioclase laths (~50%), clinopyroxene (24%–29%), titanomagnetite (~10%), olivine (1%–13%), and

traces of biotite and apatite. The groundmass texture is intergranular, microlitic, subtrachytic, and ophitic.

Flow Units 1 and 2 in Hole 432A are chemically similar to Hawaiian-type alkaline basalt. Flow Unit 3 is transitional between alkaline basalt and hawaiite (Jackson, Koisumi, et al., 1980; Kirkpatrick et al., 1980). Avdeiko et al. (1980) suggest that the chemical composition of flow Unit 3 is close to the average hawaiite from the Hawaiian Islands. The REE patterns are more linear and more depleted in HREE than those of the Ojin alkali basalts. The large ion lithophile (LIL) trace-element abundances for the Nintoku basalts are similar to those of the Hawaiian alkaline basalts and of the alkaline basalt from the Ojin Seamount, whereas the Zr/Nb ratio is lower in the Nintoku basalts (Bence et al., 1980).

Fourteen samples from flow Units 1, 2, and 3 in Hole 432A were subjected to analyses. Petrographic study (see **"Appendix A,"** p.63) showed that the rocks from flow Units 1 and 2 are represented by plagioclase phyric medium grained basalt with microdoleritic to microdoleritic-intersertal and doleritic groundmass textures. The phenocrysts consist of plagioclase (~30%–40%; andesine-labradorite [$An_{50–52}$]). The groundmass is composed of plagioclase (labradorite [An_{54}] and andesine [$An_{40–46}$]) (25%–30%), clinopyroxene (10%–25%), olivine (10%), glass (5%), and opaque minerals (5%–10%). Samples 55-432A-2R-2, 102–107 cm and 2R-3, 43–48 cm, from flow Unit 2 are vesicular (~2%–3%) and slightly oxidized (5%–10%). Basalts from flow Unit 3 were studied throughout the unit. All selected samples are without vesicles. Two samples (Sample 55-432A-3R-3, 70–75 cm, and 4R-3, 140–145 cm) are sparsely vesicular (~5%) with vesicles as much as 0.7 mm in diameter. The basalts are phyric and aphyric with microlitic groundmass texture. Basalt from the uppermost part of flow Unit 3 (Sample 55-432A-3R-1, 9–12 cm) has hyalopilitic texture. Phenocrysts consist of olivine (10%), olivine and clinopyroxene (20%), olivine and plagioclase (~30%). The groundmass contains plagioclase (labradorite [An_{66}] and andesine [$An_{40–45}$ and $An_{30–38}$]) comprising 30%–50% of the rock, clinopyroxene (10%–25%), olivine (5%–20%), glass (<5%–15%), and opaques (5%–10%). Orthoclase (10%) and apatite occur sporadically. Flow Unit 3 contains both nonoxidized and oxidized basalts (see **"Appendix A,"** p.63).

Chemical composition (Table **T45**) and geochemical diagrams (Figs. **F53, F54, F55**) provide evidence that these rocks belong to the intraplate alkaline group.

T45. Alkali basalts, Hole 432A, p.450.

Alteration Mineralogy

The chemical composition determined by Avdeiko et al. (1980), Cambon et al. (1980), Kirkpatrick et al. (1980), shipboard analyses (Jackson, Koisumi, et al., 1980), and our data (Table **T45**) reveals that the alteration degree of alkaline basalts recovered from Hole 432A varies from slight to strong, whereas H_2O^+ content ranges from 1.30 to 4.50 wt%. Petrographic study of the basalts from flow Units 1, 2, and 3 shows that altered basalts constitute from 5%–10% to 25% of the rock (Kirkpatrick et al., 1980) (see **"Appendix A,"** p.63). The data by Kirkpatrick et al. (1980) and shipboard thin section examination (Jackson, Koisumi, et al., 1980), as well our thin section descriptions (see **"Appendix A,"** p.63), show that olivine is commonly replaced with iddingsite and smectite and, in some cases, with iddingsite, smectite, and calcite. Olivine from basalts of flow Unit 3 is replaced with olive-green smectite and chlorite(?) and rarely with phillipsite, whereas some of the olivine grains are fresh. Plagioclase from the flow interiors is fresh, but glass inclusions are altered to clay minerals. Clinopyroxene is commonly fresh or slightly altered in oxidized parts of the flows. Plagioclase and olivine from the oxidized flow tops and bottoms are more altered. The interstitial glass is replaced with clay, occasionally associated with carbonate. Rare phillipsite occurs in the groundmass. XRD data by Kirkpatrick et al. (1980) show that smectites contain Ca-Mg cations in interlayers. Some magnetite grains are partly replaced by

hematite. Most vesicles are filled or lined with calcite, dark gray or light green clay, or yellow or brown smectite. Calcite veins occur in the central part of flow Unit 2. Vesicular tops and bottoms of the flows are more altered and oxidized, whereas massive gray basalts from the flow centers are fresh or slightly altered. Partially oxidized flow interiors occur in flow Units 2 and 3. The reddish brown top of flow Unit 3 is strongly altered and oxidized (Kirkpatrick et al., 1980). In Sample 55-432A-3R-1, 9–12 cm, from this part of the flow, a high Fe_2O_3/FeO ratio of 12 is fixed (Table **T45**). The basalt from this unit is dusky brown. Along fissures, the brown rock is strongly altered and oxidized. Oxidized zones along fissures are as much as 2–3 cm thick (Jackson, Koisumi, et al., 1980).

XRD study of the fine fraction extracted from selected samples of the basalts in Hole 432A (Table **T38**) show that the rocks are mainly replaced with smectite. The alkaline rocks from flow Unit 2 somewhat differ from the transitional rocks between alkaline basalt and hawaiite (flow Unit 3). We detected only smectite in the alkaline basalts, whereas the transitional rock contains, besides smectite, a mixed-layer smectite-swelling chlorite mineral in trace amounts. The smectite, which replaces interstitial glass, belongs to the Fe-Mg smectites. Microprobe study of smectites in Samples 55-432A-3R-2, 120–126 cm, and 5R-2, 57–66 cm, shows that they contain, respectively, FeO^* (18.1% and 21.0%), MgO (14.2% and 15.6%), K_2O (0.65% and 0.18%), and Na_2O (1.1% and 1.2%) (Dalrymple et al., 1980a). All samples, except for the uppermost and lowermost ones, contain illite in trace amounts (Table **T38**). The same results were noted in hawaiites in Hole 430A (Ojin Seamount). Trace amounts of kaolinite, as a product of subaerial weathering, is identified at the top of flow Unit 3 (Sample 55-432A-3R-1, 0–3 cm) (Table **T38**). In this sample, glassy basalt is oxidized and replaced by dioctahedral Al-smectite (montmorillonite; b = 9.01 Å) (Table **T39**). Contents of K_2O and Na_2O in the fine fraction extracted from this sample are 2.06 and 1.92 wt%, respectively (Table **T40**). Olivine in the basalt from the interior of flow Unit 3 (Samples 55-432A-3R-3, 70–75 cm, and 4R-3, 140–145 cm) is replaced by smectite (Table **T46**).

T46. Secondary minerals replaced by olivine, Leg 55, p.452.

Vesicles in the rocks in Hole 432A are commonly infilled by greenish gray clay rarely associated with carbonates (Table **T41**). The greenish gray clay was studied in Samples 55-432A-2R-2, 69–74 cm (alkaline basalt), 3R-3, 70–75 cm, and 5R-1, 100–105 cm (transitional rock between alkaline basalt and hawaiite). The clay extracted from vesicles consists of smectite (Table **T41**). Besides smectite, mixed-layer smectite-chlorite mineral and calcite occur in more alkaline basalts of flow Unit 3 within the greenish gray clay (Table **T41**). In the upper part of flow Unit 2, vesicles in alkaline basalt contain red clay (Sample 55-432A-2R-2, 6–11 cm). The red clay extracted from vesicles consists of dioctahedral Fe smectite (b = 9.05 Å) (Tables **T41, T42**). Content of K_2O in the red clays is 1.75 wt% (Table **T43**). Some vesicles are infilled with calcite (Table **T41**). In Sample 55-432A-5R-1, 100–105 cm, aragonite occurs among carbonates infilling a large vesicle. A minor amount of calcite is detected together with aragonite. An unidentified mineral with XRD reflections of 9.3 and 3.11 Å is found in the same vesicle (Table **T41**). Dark brown Mn crust, 1–2 mm thick, is fixed under calcite crystals in a large vesicle within the vesicular alkaline basalt from the lowermost sample of flow Unit 2 (Sample 55-432A-2CC, 0–3 cm) (Table **T41**). The crust has a botryoidal surface. XRD pattern displays two reflections at 9.47 and 4.72 Å. According to analytical electron microscopy, the crust consists of todorokite in triple intergrowth and individual crystals. Microelectronography revealed that besides todorokite, the crust contains bernesite and vernadite. Microprobe data show that the Mn crust consists of Mn (54.5%), Mg (9.8%), Al (7.7%), and Ni, Cu, and Zn (as much as 0.1%). Rare veinlets contain black smectite (Sample 55-432A-3R-2, 15–20 cm) (Table **T41**).

The assemblage of secondary minerals dominated by smectites and carbonates in groundmass, vesicles, and veins shows that the alkaline series of basalts recovered from Hole 432A from the upper part of the Nintoku Seamount

have been altered at the low temperatures of the smectite facies within relatively cold parts of the volcanic edifice remote from the hot solutions ascension zone. Major alteration of basalts occurred within oxidation zones, which were mainly located at the top and bottom of flow units. Interiors of the partially oxidized or nonoxidized flow units are slightly altered. The studied rocks were altered at high water/rock ratio values in conditions of sublateral seawater flows. The oxidative type of rock alteration was not distinctly separated in time from the nonoxidative type, as in the mid-ocean ridges. In mid-ocean ridges, alteration of igneous rocks develops through two successive stages. The first stage occurs within the axial spreading zone, where the entire volume of variously permeable rocks is altered under nonoxidative conditions. Later on, when basalts are displaced to ridge flanks during plate motion, oxidative alteration is superimposed on nonoxidative alteration.

In cases where there is laterite weathering, alteration of basalts begins in oxidizing conditions (i.e., before underwater nonoxidative and oxidative alteration).

Bulk-Rock Chemical Changes

Element content in basalts in Hole 432A is given in "Appendix B", Table **AT22**. Three selected samples of alkaline basalt in Hole 432A, flow Units 1 and 2 (Table **T45**), appeared to be unfavorable for estimation of element gain/loss during rock alteration. They are slightly altered at almost the same level. H_2O^+ ranges from 0.93 to 1.51 wt% (Table **T45**). Low H_2O^+ content, 1.47–1.97 wt%, in other samples (Avdeiko et al., 1980; Cambon et al., 1980; Kirkpatrick et al., 1980) also reflects a slight alteration of alkaline basalts in Hole 432A. Petrographic studies show that only ~5%–10% of the rock has undergone alteration (see **"Appendix A,"** p.63).

AT22. Major and trace elements, Hole 432A, p.67.

The alteration degree of the rock transitional between alkaline basalt and hawaiite in Hole 432A (flow Unit 3) varies from slight to moderate (as much as 25%) (see **"Appendix A,"** p.63). The content of H_2O^+ is as much as 4.59 wt% in Sample 55-432A-3R-1, 9–12 cm (Avdeiko et al., 1980) (Table **T45**). Comparing the chemical composition of this highly oxidized vesicular basalt sample (Fe_2O_3/FeO = 12; density = 2.10 g/cm^3) (Table **T45**) with that of the least altered nonoxidized massive basalt (Sample 55-432A-3R-2, 15–20 cm; Fe_2O_3/FeO = 0.87; density = 2.86 g/cm^3; H_2O^+ = 1.27 wt%), we revealed that the oxidized altered basalt contains less SiO_2, MgO, CaO, Na_2O, Sr, Ba, V, and more H_2O^+, Fe_{total} (with higher Fe_2O_3/FeO ratio), MnO, TiO_2, Al_2O_3, K_2O, P_2O_5, Zr, Nb, Rb, Zn, and REE, except for Lu. Changes in major element content during alteration of igneous rocks in flow Unit 3 were described earlier by Avdeiko et al. (1980) based on the study of their distribution throughout the flow.

Holes 433A and 433C

Holes 433A (44°46.60′N, 170°01.26′E) and 433C (44°46.63′N, 170°01.23′E) were drilled at the northwestern side of the Suiko Seamount within the Emperor Seamounts chain at a water depth of 1861.8 m (Fig. **F52**). Hole 433A penetrated 174 m (163.5 m of sediments and 10.5 m of alkaline basalt of the Hawaiian type from a single flow). Hole 433C penetrated 550.5 m (163.0 m of sediments and 387.5 m of subaerial basalts; recovery = 50.9%). The lowest sediment is represented by reef limestone (Hole 433A) and sand intercalated within the basaltic basement (Hole 433C) and is of Paleocene age (Jackson, Koisumi, et al., 1980). Three flows of alkaline basalt and numerous tholeiitic basalt flows were cored in Hole 433C. The scientists of Leg 55 (Jackson, Koisumi, et al., 1980) divided the basalt sequence at Site 433C into 67 volcanic units and 114 lava flows. Many of the flow units are separated by vesicular, oxidized, brecciated tops and less oxidized bottoms (Jackson, Koisumi, et al., 1980). K-Ar age of the basalts from the Suiko Seamount is ~64.7 Ma (Dalrymple et al., 1980a).

Petrography and Bulk-Rock Chemical Composition

Alkaline basalts in Hole 433A contain olivine (~1%), clinopyroxene (as much as 4%), and plagioclase (4%–12%) phenocrysts. The groundmass has microlitic, intergranular, and subtrachytic textures and contains olivine, clinopyroxene, plagioclase, magnetite, ilmenite, rare apatite, and some clay after glass (Avdeiko et al., 1980; Kirkpatrick et al., 1980). Chemical composition shows that these rocks belong to the alkaline basalts (Cambon et al., 1980; Kirkpatrick et al., 1980).

The scientists of Leg 55 (Jackson, Koisumi, et al., 1980), as well as Avdeiko et al. (1980), Kirkpatrick et al. (1980), and ourselves (see **"Appendix A,"** p.64), studied petrographic composition of basalts belonging to the tholeiitic series, including olivine tholeiites and tholeiitic picrites, in Hole 433C. They have olivine or olivine, clinopyroxene, and plagioclase phenocrysts, as well as olivine-plagioclase, olivine-clinopyroxene, clinopyroxene-plagioclase, or plagioclase phenocrysts. Aphyric basalts also occur. The groundmass minerals include olivine, clinopyroxene, plagioclase, titanomagnetite, ilmenite, sulfide blebs, and glass. Samples 433C-24R-7, 133–139 cm; 37R-3, 79–87 cm; and 39R-5, 87–94 cm, contain pigeonite (Kirkpatrick et al., 1980). The textures are intersertal, microlitic, doleritic, doleritic-vitrophyric, vitrophyric, hyalopilitic, pilotaxitic, micropoikilophitic, and trachytic. Groundmass textures are mainly microlitic (see **"Appendix A,"** p.64). The flow tops and bottoms are almost totally composed of glass (Kirkpatrick et al., 1980). Samples are mainly vesicular with vesicles of different size (0.1–10 mm), which comprise from 1% to as much as 50%–55% of the rocks (see **"Appendix A,"** p.64). The tholeiitic sequence is divided into 25 chemical and mineralogical groups (Kirkpatrick et al., 1980). These include two types of tholeiitic basalt: high-Zr type, with relatively high TiO_2/MgO and Zr/Ni values, and low-Zr type, with relatively low TiO_2/MgO and Zr/Ni values. These two types are interbedded throughout the section (Kirkpatrick et al., 1980). Tholeiitic basalts have chondrite-normalized REE patterns with uniform relative LREE enrichment and some HREE depletion. The pattern is typical for tholeiites from the Hawaiian-Emperor Seamounts and Hawaiian Islands (Bence et al., 1980; Clauge et al., 1980).

Our geochemical results for the studied samples of basalts in Hole 433C (Suiko Seamount) are similar to the results obtained by Kirkpatrick et al. (1980) and Clague et al. (1980). In the AFM diagram, almost all data plot in the field of tholeiitic basalts with a poorly manifested Fenner trend of differentiation with accumulation of iron (Fig. **F53**). Olivine basalts and tholeiitic picrites are located in the field of basalts with high MgO content. Diagrams of Zr/4-2Nb-Y (Fig. **F54**) provide evidence that the rocks in Hole 433C belong to intraplate tholeiites with an enrichment trend in Nb and decrease in concentrations of Y as compared to MORB. The chondrite-normalized REE data also show an enrichment in REE content relative to MORB (Fig. **F55**). All classification diagrams provide evidence that the tholeiites in Hole 433C belong to the same group of intraplate tholeiites. Several samples of the tholeiites have higher content of Zr (Fig. **F54**).

Alteration Mineralogy

Alkaline basalts in Hole 433A are slightly altered (10%–14%). Olivine is completely replaced with smectite with traces of chlorite(?) or calcite and smectite. Vesicles are filled with olive-green smectite (Kirkpatrick et al., 1980). Contents of H_2O^+ in two samples of alkaline basalts from the hole studied by Kirkpatrick et al. (1980) are low (0.77 and 1.06 wt%).

Thin section examination of selected samples showed that interstitial glass is replaced with smectite and olivine is replaced by smectite with a trace amount of chlorite. Plagioclase is fresh, or in some cases, slightly altered. XRD analyses of the fine fraction extracted from alkaline basalts shows that the rocks are mainly replaced with smectites with a trace of mixed-layer smectite-swelling

chlorite (Table **T38**). In Sample 55-433A-21R-3, 128–134 cm, from the interior of flow Unit 1, alkaline basalt is replaced with smectite and swelling chlorite (Table **T38**). Swelling chlorite is fixed in this part of the flow, whereas Avdeiko et al. (1980) determined plagioclase with the maximum length of crystals. Olivine is replaced by trioctahedral smectite (b = 9.18 Å) (Table **T47**). Vesicles are filled with calcite and greenish gray clay (Table **T41**) consisting of trioctahedral smectite (b = 9.19 Å) (Table **T42**).

T47. Parameter *b* of clay minerals replaced by olivine, Leg 55, p.453.

The chemical composition data by Avdeiko et al. (1980), Cambon et al. (1980), Kirkpatrick et al. (1980), shipboard analyses (Jackson, Koisumi, et al., 1980), as well as our results (Table **T48**), show that the basalts in Hole 433C vary from fresh to extensively altered. H_2O^+ content ranges from 0.33 to 6.01 wt%. Thin section examination of the basalts shows that alteration degree varies from 2%–4% to 78% of the rock. The alteration degree of alkaline basalts is 7%–15%. Alteration degree of tholeiites and plagioclase tholeiites ranges from 2%–4% to 35%–40%. Olivine tholeiites alteration degree varies from 18% to 67%, and that of tholeiitic picrites ranges from 36%–38% to 78% (Kirkpatrick et al., 1980). Alteration degree of our selected samples varies from 5% to 85% of the rock, with most samples showing alteration from 15%–20% to 30%–40% (see **"Appendix A,"** p.64). These basalts are mainly nonoxidized, but oxidized varieties with Fe_2O_3/FeO ratios of 1.62–7.8 (Table **T48**) also occur. The data by Kirkpatrick et al. (1980), shipboard analyses (Jackson, Koisumi, et al., 1980), Avdeiko et al. (1980), and our results of thin section examination (see **"Appendix A,"** p.64) show that plagioclase and clinopyroxene are unaltered, but in some cases we noted a partial alteration of these minerals. Some plagioclase crystals are replaced by smectite, in some cases by phillipsite and K-feldspar. Clinopyroxene is altered to amphibole and/or phillipsite. Most olivine grains are completely or partly replaced with iddingsite and green or yellow smectite. Calcite or chlorite occurs besides smectite, and some olivine grains are fresh. Interstitial glass is replaced by clay minerals, and magnetite is partly replaced with hematite. Most vesicles are filled or lined with yellow to olive-green smectite, but some of them contain yellowish green celadonite or calcite. Several vesicles are filled with phillipsite and rare smectite. Sparse veinlets consist of calcite.

T48. Tholeiitic basalts, Hole 433C, p.454.

Secondary Minerals in Igneous Rocks. XRD study of the fine fraction extracted from selected samples of the basalts of tholeiitic series in Hole 433C (Table **T49**) shows that tholeiites are replaced by smectite, in some cases associating with minor chlorite and/or mixed-layer smectite-chlorite mineral. Secondary minerals replacing olivine tholeiites include smectite, mixed-layer chlorite-swelling chlorite, and smectite-chlorite minerals. Chlorite occurs only in trace amounts. Traces of serpentine are also fixed. Secondary mineral assemblage of tholeiitic picrites is that of olivine tholeiite; however, chlorite and mixed-layer chlorite-swelling chlorite mineral often occur as dominant minerals or are equal to smectite. Phillipsite also occurs in trace amounts. Comparison of altered rocks shows that the composition of secondary minerals reflects the rock type. In the succession from tholeiite through olivine tholeiite to tholeiitic picrite, the assemblage of secondary minerals changes from smectite through mixed-layer minerals with chloritic component to chlorite, respectively.

T49. Fine fraction, Leg 55, p.464.

Tholeiites. Smectites from nonoxidized tholeiites belong to the trioctahedral smectites (b = 9.19 and 9.24 Å) **(**Table **T39**). Smectites from tholeiites of the highly oxidized tops of flows consist of smectite with parameter b = 9.18 Å and containing higher Fe. A parameter b of 9.18 Å marks the boundary between nontronite and saponite. Oxidized tholeiite also contains Al-smectite (montmorillonite, b = 8.98 Å) (Table **T39**). Chemical composition of smectites from nonoxidized tholeiites provides evidence that they belong to Fe-Mg saponites. Microprobe composition of smectites from interstitial glass in Samples 55-433C-15R-6, 16–31 cm, and 28R-2, 73–80 cm, is characterized by the following values: SiO_2 = 45.1% and 45.9%, TiO_2 = 0.17% and 0.34%, Al_2O_3 = 6.3% and 4.3%, FeO^* = 15.5% and 15.4%, MgO = 14.2% and 15.3%,

CaO = 0.29% and 0.48%, Na_2O = 2.24% and 1.73%, K_2O = 0.09% and 0.14%, respectively (Dalrymple et al., 1980a). Wet chemical analysis of the fine fraction extracted from tholeiite (Sample 55-433C-48R-3, 10–15 cm) shows the following concentrations: Fe_2O_3 = 11.41 wt%, FeO = 2.66 wt%, MgO = 9.14 wt%, Na_2O = 1.57 wt%, and K_2O = 0.36 wt% (Table **T40**). Olivine is replaced with smectites (Table **T46**). Smectites within olivine grains in the tholeiite Sample 55-433C-45R-6, 129–133 cm, are possibly trioctahedral smectites (*b* = 9.18 Å) (Table **T47**).

Secondary minerals from the tholeiites dominated by smectites demonstrate monotonous distribution throughout the 350-m-thick basement section recovered from Hole 433C (Table **T49**). Vertical zonation of alteration is absent in the rocks from the upper part of the Suiko Seamount.

Distribution of secondary minerals was studied in the sections of individual tholeiite flows from top to bottom (flow Units 9, 11a, 11c, 13, 25, and 60). Composition and distribution of secondary minerals dominated by smectites are monotonous in the flows (Table **T49**). In oxidized parts of the flows, we determined two types of smectites: Al-smectite of dioctahedral type (montmorillonite) and smectite similar to nontronite, the latter reflecting the boundary between dioctahedral and trioctahedral smectites. Fe-Mg saponites (trioctahedral) are common for interior nonoxidized parts of the flows (Table **T39**).

Olivine Tholeiites. Smectites from nonoxidized olivine tholeiites are represented by saponite (trioctahedral; *b* = 9.24 Å) (Table **T39**). Smectites from oxidized olivine tholeiites have parameter *b* value of 9.19 Å. This reflects a higher iron content in their lamellar structure. Chemical composition of smectites from nonoxidized olivine tholeiites suggests that they belong to Fe-Mg saponites. Wet chemical analysis of the fine fraction showed that this smectite contains more MgO than smectites from tholeiite (Table **T40**). Olivine in the olivine tholeiites is replaced by smectite with an admixture of chlorite (Table **T46**). This smectite is trioctahedral (*b* = 9.20 Å) (Table **T47**). Illite also occurs among secondary minerals replacing olivine in the oxidized olivine tholeiites (Table **T46**).

We found that smectites occur in the top and bottom of the 7.5-m-thick section of flow Unit 48, but mixed-layer minerals with chloritic components dominate in its interior (Table **T49**).

Tholeiitic Picrites. Distribution of secondary minerals in tholeiitic picrites is studied in ~10-m-thick flow Unit 19b (Table **T49**). Smectites and a mixed-layer smectite-chlorite mineral dominate at the top of the flow, whereas below to the flow bottom, smectites and chlorite prevail among the secondary minerals. In Sample 55-433C-24R-7, 108–114 cm, trioctahedral chlorite (*b* = 9.24 Å) is the main secondary mineral (Table **T39**). Smectites from tholeiitic picrite contain 0.75 wt% K_2O (Table **T40**). Olivines in tholeiitic picrites are replaced by smectites with chlorite in trace amounts. Serpentine and calcite were also determined in trace amounts (Table **T46**). Smectites from olivine are trioctahedral (*b* = 9.22 and 9.25 Å; Samples 55-433C-27R-2, 138–144 cm, and 32R-1, 82–88 cm) (Table **T47**).

The study of secondary minerals from basalts of the tholeiitic series recovered from Hole 433C showed that mineral and chemical compositions of clay minerals are controlled by the igneous rock type. Tholeiites are consistently replaced by smectites. In olivine tholeiites, mixed-layer chlorite-swelling chlorite and smectite-chlorite minerals may constitute a considerable proportion among secondary minerals, besides smectites. The smectites contain more MgO than those from tholeiites. In tholeiitic picrites, besides secondary minerals characteristic for olivine tholeiites, chlorite occurs in interiors of the flows as a major secondary mineral. In oxidized parts of the tholeiitic series of basalt flows, smectites are higher in iron than trioctahedral Fe-Mg smectites from the internal parts; moreover, oxidized tholeiites contain dioctahedral Al-smectites

(montmorillonite). Olivine is mainly replaced by trioctahedral smectite in all rock varieties of the tholeiitic basalt series. Besides smectite, a chlorite phase is formed in altered olivines from olivine tholeiites, whereas serpentine occurs in olivines from the tholeiitic picrite. An admixture of illite is fixed in the oxidized olivine tholeiite.

Minerals from Vesicles. In highly vesicular, tholeiitic series basalts in Hole 433C, vesicles are filled with smectites, chloritic minerals, serpentine, hydromica, calcite, aragonite, phillipsite, talc(?), and unidentified minerals (Table **T50**). In all samples of tholeiitic series basalts, vesicles are filled with greenish gray clay. In tholeiites, widespread walled vesicles are lined with black budlike clay. Green and blue clay minerals are rare in studied samples.

T50. Vesicles and veins, Leg 55, p.466.

Black Clay. Black clay is widespread in large vesicles of basalts both from nonoxidized and oxidized zones. In all cases, a fibrous clay film, ~1 mm thick, occurs beneath the black clay. XRD patterns of the black clay and fibrous clay film are identical, and we identified them as smectites. These smectites belong to the trioctahedral type (b = 9.21–9.22 Å) (Table **T42**). In the black clay from Sample 55-433C-12R-2, 32–37 cm, an admixture of unidentified minerals showed XRD reflections at 9.4 and 4.90 Å and at 3.22 and 3.18 Å. The latter two reflections are close to those of laubmannite, which mainly consists of iron and phosphorus. The 9.4 Å mineral is also identified in black clay from Sample 55-433C-45R-3, 61–66 cm (Table **T50**). Phillipsite occurs in the black clay from oxidized zones of flow Units 11a, 25, 33, 48, and 60. Individual phillipsite crystals are directly attached to the oxidized surface of vesicles. Smectitic incrustations and films envelope the base of phillipsite crystals, but never underlay them.

Greenish Gray Clay. The greenish gray clay infilling vesicles in all of the tholeiitic series basalt varieties is identical to the black clay, according to XRD, and consists mainly of smectites. The smectites contain Na-K cations and K cations in interlayers (12.4 and 10.8–11.5 Å reflections) and are trioctahedral (b = 9.20–9.22 Å) (Table **T42**). Greenish gray clay from several vesicles contains calcite. Wet chemical analyses and microprobe data of the greenish gray clay from vesicles in tholeiitic series basalts (Tables **T43, T44**) show that the clay from olivine tholeiite, and especially from tholeiitic picrite, is higher in magnesium than that from tholeiite.

Unlike the greenish gray clay in tholeiites, the greenish gray clay from large vesicles in olivine tholeiites contains, besides smectites, chlorite-group minerals. Greenish gray clay from vesicles of tholeiitic picrites contains mixed-layer smectite-chlorite mineral and serpentine as well as trioctahedral smectites. In Sample 55-433C-32R-1, 82–87 cm, it consists totally of serpentine (Table **T50**).

Comparison of microprobe data on the greenish gray clay composition from tholeiite vesicles (Sample 55-433C-41R-1, 66–71 cm), olivine tholeiite (Sample 55-433C-10R-1, 25–31 cm), and tholeiitic picrite (Sample 55-433C-27R-2, 138–144 cm) (Table **T44**) revealed an increasing trend of MgO and K_2O contents in the clay for the succession tholeiite → olivine tholeiite → tholeiitic picrite. MgO content increases from 18.97%–24.77% to 32.21%, and K_2O content increases from 0.06%–0.20% to 0.26%. Contents of FeO* and Na_2O decrease from 14.84%–4.70% to 5.41% and from 3.26%–2.06% to 0.68%, respectively. This result reflects a dependence of chemical composition of the greenish gray clay from vesicles on the vesicular rock composition. The difference in MgO and FeO* content indicates that smectites from tholeiite vesicles are higher in iron, whereas those from olivine tholeiite and tholeiitic picrite belong to higher magnesian varieties.

The greenish gray clay is, in many cases, underlain by a ~1-mm-thick green clay veneer. As a result, the greenish gray clay occurs as if within a shell composed of the green clay. The green clay was studied in Samples 55-433C-10R-1, 25–31 cm, and 23R-2, 12–17 cm (Table T50). It consists of trioctahedral

smectite (*b* = 9.21 Å) (Table **T42**) and contains an admixture of mixed-layer smectite-swelling chlorite mineral. In Sample 55-433C-10R-1, 25–31 cm, we studied the chemical composition of the green clay film that covers the wall of a vesicle and of the greenish gray clay infilling its core (Table **T44**). The green clay contains more Al_2O_3, FeO*, MnO, and CaO and less MgO and Na_2O than the greenish gray clay.

Green Clay. Green clay with illite infills small vesicles in tholeiites and olivine tholeiites. This clay is studied in Samples 55-433C-28R-4, 30–37 cm; 39R-6, 114–118 cm; 45R-4, 109–114 cm; and 45R-6, 97–102 cm. XRD data show that the green clay consists of hydromica and smectite (Table **T50**). Parameter *b* of hydromica is 9.12 Å (Sample 55-433C-45R-4, 109–114 cm) (Table **T42**). The electron diffraction data indicate Polytype 1M hydromica. Thin section study revealed a zonation of vesicles infilled with green clay. Walls of the vesicles are lined by a pellicle of brown smectite that is replaced by green smectite inward. The next zone inward is represented by green smectite, and the centers of the vesicles are infilled by illite.

Blue Clay. In the bottom of flow Unit 48, walls of large vesicles in the olivine basalt are lined by budlike blue clay with transparent phillipsite crystals at its surface (Sample 55-433C-39R-6, 114–118 cm) (Table **T50**). The blue clay consists of smectite and illite with an admixture of mixed-layer smectite-chlorite mineral. Parameter *b* is 9.19 and 9.04 Å (Table **T42**).

Several vesicles in the tholeiitic series basalts are infilled with calcite (Samples 55-433C-10R-6, 57–62 cm; 27R-2, 138–144 cm; 34R-3, 41–46 cm; 34R-4, 97–101 cm; and 45R-6, 129–133 cm) (Table **T50**). Aragonite was found in a large vesicle in the tholeiitic picrite (Sample 55-433C-10R-1, 25–31 cm).

Vein Minerals. Veins are rare in studied samples. They are thin (several millimeters thick) and occur within contact zones of lava flows. In Samples 55-433C-23R-2, 12–17 cm; 32R-2, 126–132 cm; and 39R-2, 35–40 cm, the veins contain smectites (Table **T50**). A brownish red vein (Sample 55-433C-43R-1, 118–123 cm) consists of nontronite (*b* = 9.12 Å) (Tables **T42, T50**). Wet chemical analysis of the brownish red smectite shows increased K_2O content (1.46 wt%). The clay also contains more Al_2O_3 and is strongly depleted in MgO compared to the greenish gray clay from vesicles (Tables **T43, T44**). In oxidized zones of the lava flows, veins contain phillipsite, as in Sample 55-433C-14R-1, 2–7 cm, or calcite, as in Samples 55-433C-33RR-2, 126–134 cm, and 34R-1, 108–114 cm (Table **T50**). Carbonates from veins and vesicles in the basalts in Hole 433C were studied in detail by McKenzie (1980).

Composition of secondary minerals infilling vesicles and veins and replacing the rock itself depends on the rock type and on the type of its alteration (oxidative or nonoxidative). Mineralogy of the greenish gray clay from vesicles changes in the succession of tholeiite to olivine tholeiite to tholeiitic picrite as follows: smectite to smectite and chloritic minerals to smectite, chloritic minerals, and serpentine or only serpentine. In the greenish gray clay within the rock succession, we noted an increasing trend of MgO (18.97% to 24.77% to 32.21%) and K_2O (0.06% to 0.20% to 0.26%) contents and a decreasing trend of FeO^* (14.84% to 4.70% to 5.41%) and Na_2O (3.26% to 2.06% to 0.68%) content. Smectites from vesicles in the tholeiite are higher in iron, whereas those in the olivine tholeiite and tholeiitic picrite are higher in magnesium. In the green and blue clays infilling vesicles of oxidized basalts, smectites approach the nontronite type, being accompanied by illite and phillipsite. Brownish red veins from oxidized rims of the flows consist of nontronite, phillipsite, and calcite. The brownish red clay contains more K_2O, Fe_2O_3, and Al_2O_3 and is strongly depleted in MgO, compared to the greenish gray clay.

The assemblages of secondary minerals in the tholeiitic series basalts, as well as in their vesicles and veins, shows that alteration of the subaerial volcanic rocks from the upper part of the Suiko Seamount took place under the

smectite facies within relatively cold parts of the volcanic edifice. The studied rocks were altered at high water/rock ratios under conditions of sublateral oxic seawater flows. The oxidative effect on rock alteration was strongest in vesicular basalts from the flow tops throughout the 350-m-thick basalt section recovered from Hole 433C.

Bulk-Rock Chemical Changes

Element content in the tholeiitic series basalts in Hole 433C are presented in "Appendix B", Table **AT23.** The quantitative estimate of the element gain/loss, expressed as an element mass per a rock volume unit, is calculated from chemical analyses, taking into account the rock density. This estimation, however, met difficulties related to the wide variations in vesicularity of the selected basalt samples (from 1% to as much as 55% of the rock) and thus in primary rock densities. In order to escape estimation errors, it is necessary to discriminate between the effects of density changes caused by rock alteration and density variations in the primary volcanic rock. For this we have to separately compare massive and vesicular varieties of petrographically and chemically uniform rocks at their various alteration degrees. Altered vesicular rocks should be compared to their fresh analogs with the same vesicularity. Fresh vesicular rocks were not recovered from Hole 433C, but volcanic rocks from the Hawaiian Islands may be used as fresh analogs of the altered vesicular rocks in future studies.

AT23. Major and trace elements, Hole 433C, p.68.

Therefore, we can only compare the chemical composition of basalts with wide vesicularity variations from the top of the flow through the interior to the bottom without considering their densities to estimate bulk-rock chemical changes during alteration throughout flows. We have to emphasize that the results obtained may not coincide with actual bulk-rock chemical changes during rock alteration, especially in the case of strong alteration.

Distribution of major elements was earlier analyzed throughout several flow units by Avdeiko et al. (1980): in the 19.4-m-thick flow Unit 19b (tholeiitic picrites), in the ~7-m-thick flow Unit 48 (olivine tholeiites), and in several flows of tholeiites (flow Unit 9, 3.5 m thick; flow Unit 11a, 7.5 m thick; flow Unit 13, 12.2 m thick; flow Unit 25, 8.2 m thick; flow Unit 48, 7 m thick; flow Unit 54, 7.5 m thick; and flow Unit 60, 4.6 m thick). We used these results and added the data on minor elements (Table **T48**). Alteration of rocks from the top and interior of the flows appeared to be the most contrasting. The basalts from the bottom of the flows are less vesicular, often nonoxidized, and less altered than basalts from the flow top.

Tholeiitic Picrites. Tholeiitic picrite from the highly vesicular top of flow Unit 19b is oxidized and extensively altered. Fe_2O_3/FeO ratio is 2.18 and H_2O^+ content is 5.70 wt% (Table **T48**). In this uppermost part of the flow, MgO and CaO contents are minimal at 12.28 and 2.59 wt%, respectively. In contrast, contents of TiO_2, Al_2O_3, and Na_2O, 1.82, 12.94, and 1.90 wt%, respectively, are higher than in the interior of the flow where the contents of TiO_2, Al_2O_3, and Na_2O are 0.84–1.32, 7.60–8.45, and 1.53–1.66 wt%, respectively. In the altered nonoxidized bottom of the flow, H_2O^+ content is as much as 4.59 wt% and Fe_2O_3/FeO ratio is 0.38. The difference in element contents in the tholeiitic picrites between those from the flow bottom and flow interior is considerably less contrasting than that between the top of the flow and the interior. Only MgO content is lower in the bottom than in the interior (~21 vs. 23.87 wt%). K_2O content is higher at the top and bottom of the flow at 0.74 and as much as 1.24 wt%, respectively, whereas the interior is characterized by a low K_2O content of 0.13 wt%. The chemical variations throughout the flow depend on two factors: olivine formation and alteration of tholeiitic picrites (Avdeiko et al., 1980). As a whole, the tholeiitic picrites from flow Unit 19b, including the flow interior, are moderately to strongly altered (see **"Appendix A,"** p.64) with H_2O^+ contents ranging from 2.64 to as much as 5.70 wt% (Table **T48**). It is difficult to discriminate between the influence of primary minerals formation during their

crystallization from the melt in different parts of the cooling basalt flow and postvolcanic alteration on the content of most elements in tholeiitic picrites from the top, bottom, and interior of the flow. The same difficulty concerns minor elements; however, increases in Fe_2O_3, K_2O, and H_2O^+ contents and Fe_2O_3/FeO ratio values, as well as the behavior of Na_2O, CaO, and MgO at the flow top, is apparently controlled by the rock alteration. Fresh analogs of the massive tholeiitic picrites from flow Units 4h and 19b, as well as of vesicular rocks necessary for the comparison, are absent among the studied samples.

Olivine Tholeiites. The distribution of major elements in the olivine tholeiites was most completely studied throughout flow Unit 48 (Avdeiko et al., 1980). Chemical composition of the olivine tholeiites from the top and interior of the flow have been compared. Olivine tholeiite from the top is highly vesicular (55%), altered (H_2O^+ = 4.04 wt%), and oxidized (Fe_2O_3/FeO = 2.50) (see **"Appendix A,"** p.64**;** Table **T48**). It contains less SiO_2, TiO_2, Al_2O_3, MnO, CaO, P_2O_5, Cu, Zn, and Sr and more H_2O^+, Fe_{total} (with higher Fe_2O_3/FeO ratio), MgO, Na_2O, and K_2O than the tholeiite from the flow interior (Table **T48**).

We also compared two samples of identical tholeiites with similar vesicularity (~1%–3%) and microlitic texture from different flow units: the altered (H_2O^+ = 3.18 wt%) oxidized (Fe_2O_3/FeO = 3.19) olivine tholeiite (Sample 55-433C-34R-2, 41–46 cm, from flow Unit 33) and relatively fresh (H_2O^+ = 0.80 wt%) nonoxidized (Fe_2O_3/FeO = 1.31) olivine tholeiite (Sample 55-433C-35R-6, 59–64 cm, from flow Unit 35). The more altered olivine tholeiite contains less SiO_2, TiO_2, MnO, CaO, Na_2O, K_2O, P_2O_5, Cu, Y, Nb, Rb, Sr, and Ba and more H_2O^+, Al_2O_3, MgO, Fe_2O_3/FeO ratio, and V (REE were not determined in these samples). The rest of the samples of olivine tholeiites from other flows are moderately to strongly altered, and their fresh analogs are absent for comparison (Table **T48**).

Tholeiites. In all six tholeiite flows studied in detail (flow Units 9, 11a, 13, 25, 54, and 60), the tops are highly vesicular, intensely altered, and oxidized (see **"Appendix A,"** p.64**;** Table **T48**). These characteristics are less expressed in the flow bottoms. The tholeiites from the interiors are slightly vesicular or massive, less altered, and commonly nonoxidized. The alteration mode at the top and bottom of the flows is analogous to that of the flows described in flow Units 19b and 48. Comparison of chemical compositions of the tholeiites from the top and interior of the flows shows that a higher content of H_2O^+, K_2O, Fe_{total}, Fe_2O_3/FeO ratio, and Rb and a lower content of CaO, SiO_2, Al_2O_3, P_2O_5, Sr, and Zn in the basalts from the tops vs. basalts from the interiors is a common chemical pattern for all flows. The contents of TiO_2, MnO, MgO, Na_2O, V, Cu, Zr, Y, Nb, and Ba in some flows are higher in the tops than in the interiors and lower sections in other flows. Contents of Cr, Ni, and Co increase at the flow top or do not change. The comparison of REE contents in the tholeiites from the top and interior of flow Unit 9 shows that at the top (Sample 55-433C-12R-1, 75–80 cm; H_2O^+ = 4.26 wt%; Fe_2O_3/FeO = 4.16), contents of La, Ce, Nd, Sm, Eu, Tb, Yb, and Lu are higher than in the interior (Sample 55-433C-12R-2, 136–141 cm; H_2O^+ = 1.80 wt%; Fe_2O_3/FeO = 0.84) (Table **T48**).

Besides the comparison of chemical compositions of tholeiites from the top and interior of several lava flows recovered from Hole 433C, we also compared chemical compositions of tholeiites from different parts of the recovered section. The altered and fresh massive tholeiites are considered separately from the vesicular rocks. The vesicular tholeiites were divided into groups with vesicularities of 40%–50%, 30%–35%, 15%–20%, 5%–10%, and <5% of the rock, as determined in the thin sections (see **"Appendix A,"** p.64).

The massive tholeiites (Samples 55-433C-12R-2, 136–141 cm; 13R-2, 69–72 cm; 14R-4, 26–31 cm; 14R-4, 47–52 cm; 15R-5, 88–92 cm; 17R-1, 64–69 cm; 21R-3, 20–23 cm; 22R-5, 48–52 cm; 28R-5, 77–81 cm; 28R-5, 107–109 cm; 42R-1, 2–6 cm; 45R-5, 119–122 cm; 46R-3, 78–83 cm; and 47R-1, 8–13 cm), described in the thin sections (see **"Appendix A,"** p.64), are mainly fresh

or slightly altered and nonoxidized. Contents of H_2O^+ range from 0.33 to 1.06 wt% and Fe_2O_3/FeO ratio is <1.60 (Table **T48**). Several samples of the tholeiites are more altered (H_2O^+ = 1.60–2.67 wt%), and some samples are oxidized (Fe_2O_3/FeO = 1.85–2.67). Two samples were selected from different parts of the section recovered from Hole 433C (Sample 55-433C-21R-3, 20–23 cm; H_2O^+ = 2.67 wt%, and 17R-1, 64–69 cm; H_2O^+ = 0.33 wt%) for chemical composition comparison of altered and fresh nonoxidized massive tholeiites. Altered tholeiite is characterized by lower contents of SiO_2, TiO_2, MnO, CaO, K_2O, Zn, Rb, and Ba and higher contents of Al_2O_3, MgO, Na_2O, P_2O_5, Cr, Ni, and Fe_2O_3/FeO ratio. The samples are rather uniform in their REE content. The oxidized unaltered massive tholeiite (Sample 55-433C-15R-5, 88–92 cm; H_2O^+ = 0.50 wt%; Fe_2O_3/FeO = 2.61), as compared to the fresh nonoxidized tholeiite (Sample 55-433C-28R-5, 77–81 cm; H_2O^+ = 0.52 wt%; Fe_2O_3/FeO = 0.64), contains less SiO_2, MnO, CaO, Cr, Co, Rb, and Ba, as well as La, Ce, Nd, and Sm, but more Fe_{total}, MgO, Na_2O, K_2O, and V.

Among the five groups of vesicular rocks listed above, we selected the tholeiites with maximum vesicularity (40%–50%) for comparison. This group includes Samples 55-433C-12R-1, 75–78 cm; 14R-1, 2–7 cm; 27R-6, 38–43 cm; 42R-3, 83–88 cm; 45R-3, 61–66 cm; and 45R-6, 24–31 cm (see **"Appendix A,"** p.64). The tholeiites of this group mainly underwent an intense alteration (H_2O^+ = 5.68 wt%) (Table **T48**) and are highly oxidized (Fe_2O_3/FeO = 6.20–7.80). The intensely altered, highly oxidized tholeiite (Sample 55-433C-27R-6, 38–43 cm; H_2O^+ = 5.68 wt%; Fe_2O_3/FeO = 6.20) contains less SiO_2, MnO, CaO, Na_2O, P_2O_5, Cr, and Zn, but more TiO_2, Fe_{total}, K_2O, Ni, V, and Cu, than the fresh nonoxidized tholeiite (Sample 55-433C-45R-6, 24–31 cm; H_2O^+ = 0.51 wt%; Fe_2O_3/FeO = 0.65). In the more strongly altered tholeiite (Sample 55-433C-12R-1, 75–80 cm) (Table **T48**), contents of SiO_2, MnO, CaO, Na_2O, V, Zn, Sr, and Ba are lower than in the fresh tholeiite (Sample 55-433C-45R-6, 24–31 cm), but contents of Fe_{total}, MgO, K_2O, P_2O_5, Cr, Ni, Cu, Y, Nb, Sr, as well as REE (La, Ce, Nd, Sm, Eu, Tb, Yb, and Lu) are higher. The oxidized slightly altered tholeiite (Sample 55-433C-45R-3, 61–65 cm; H_2O^+ = 1.73 wt%; Fe_2O_3/FeO = 5.36) contains less SiO_2, Al_2O_3, MnO, MgO, CaO, P_2O_5, Cu, Zn, Y, La, Sm, Yb, and Lu and more Fe_{total}, Na_2O, K_2O, Cr, Ni, Co, V, Nb, Rb, and Ba, as compared to the fresh tholeiite in Sample 55-433C-45R-6, 24–31 cm (Table **T48**).

Hole 192A

Hole 192A (53°00.57′N, 164°42.81′E; water depth = 3014 m) is located on the Meiji Seamount at the northwest end of the Emperor Seamounts chain (Fig. **F52**) and penetrated 1057 m. The sediment and sedimentary rock sequence (0–1044 mbsf) consists of Holocene through Cretaceous (middle Maastrichtian) beds of diatomaceous sediments, chalk and calcareous claystone, and minor size-graded sand and silt beds. At 1044 mbsf, the sedimentary sequence overlies an alkaline basalt and trachybasalt (1044–1057 mbsf) (Creager, Scholl, et al., 1973). Five alkaline basalt pillow lava units were cored in Hole 192A. The units have an upper chilled glassy margin and variolitic to subdiabasic textures from the margins to the interiors of the flows (Creager, Scholl, et al., 1973).

Petrography and Bulk-Rock Chemical Composition

Petrographic composition of the basalts in Hole 192A was studied by Stewart et al. (1973) and the scientists of DSDP Leg 19 (Creager, Scholl, et al., 1973). They showed that in glassy rims, clinopyroxenes, minor altered olivine, and labradorite or andesine crystals form phenocrysts (as much as 15% of the rock) that float in basal glass darkened by iron oxides. Toward the interior of the flows, the rock is variolitic texture. In the flow interiors, textures range from diabasic to subgabbroic. In the diabasic portions, phenocrysts are of the same size as those in the glassy rims of the flows, but olivine is absent. There are large phenocrysts of sanidine, as much as 0.5 cm, in the interiors, and they

replace calcic plagioclase cores. Sanidine is not found in the glassy and variolitic parts of the flows. The basalts in Hole 192A have a mineralogy typical of alkaline basalts, but their chemistry is more typical for tholeiites (Stewart et al., 1973).

The samples of basalts in Hole 192A are represented by tholeiite and alkaline basalts (Table **T51;** Fig. **F53**).

T51. Basalts, Hole 192A, p.471.

Alteration Mineralogy

Pyroxene-plagioclase basalts in Hole 192A are intensely altered with clay and calcite. Vesicles and fractures are filled with montmorillonite, nontronite, nontronite and celadonite, iron oxides (usually goethite), and calcite (Creager, Scholl, et al., 1973; Stewart et al., 1973). In the diabasic portions, plagioclases are replaced by secondary K-feldspar (sanidine).

We studied seven additional samples of basalts in Hole 192A from 1044.93 to 1056.45 mbsf. XRD study of the fine fraction extracted from selected samples showed that the rocks are replaced with trioctahedral smectite (b = 9.19–9.20 Å) (Tables **T52, T53**). In most samples, mixed-layer smectite-swelling chlorite and an admixture of celadonite are fixed along with smectite, and trace amounts of chlorite are found in several samples (Table **T52**). In Sample 19-192A-5R-2, 43–53 cm, celadonite and smectite occur in almost equal proportion. Celadonite belongs to dioctahedral 1M polytype (b = 9.06 Å) (Table **T53**). XRD pattern with a slight reflection (002) identifies it as Fe hydromica. Parameter b of celadonites from basalts ranges from 9.04 to 9.08 Å (Table **T53**). Chemical composition of the fine fraction extracted from three selected samples shows high K_2O contents of 1.20, 2.50, and 3.30 wt% (Table **T54**). The fine fraction with high concentration of celadonite from Sample 19-192A-5R-2, 43–53 cm, contains 3.30 wt% K_2O and 16 wt% Fe_{total} (Table **T54**). High concentrations of celadonite are noted at the flow tops, mainly in vesicles and veinlets. Contents of H_2O^+ in altered basalts varies from 1.30 to 2.4 wt% (Table **T51**), indicating low to moderate alteration level.

T52. Fine fraction, Leg 19, p.472.

T53. Clay minerals from fine fraction, Leg 19, p.473.

T54. Fraction <0.001 mm, Leg 19, p.474.

Brief Comments

The assemblages of secondary minerals (dominated by smectites and carbonates) in subaerial basalts of both alkaline and tholeiitic series, as well as in vesicles and veins within those rocks (Holes 430A, 432A, 433A, 433C, and 192A), point to alteration of studied volcanic rocks from the upper part of the Emperor Seamounts at low temperatures, under the smectite facies, in relatively cold parts of the volcanic edifices remote from zones of ascending hot solutions. McKenzie (1980) ascertained a low temperature (<50°C) of carbonate formation in vesicles and veins within basalts in Hole 433C based on oxygen and carbon isotope composition. The studied rocks have been altered at high water/rock ratios in the environment of sublateral seawater flows mainly at the tops of lava flows throughout the 350-m-thick basalt section recovered from Hole 433C on the Suiko Seamount. In the mid-oceanic ridges, evidence of oxidative environment are fixed at a maximum depth of ~300 m, mainly along vertical fissures (Hole 504B, Costa Rica Rift). The strongest alteration of basalts from seamounts occurs in oxidation zones mainly located at the tops of flow units. Interiors of the flow units, partially oxidized or nonoxidized, are less altered. The oxidative alteration was not separated in time from the nonoxidative type as much as in mid-ocean ridges. Therefore, the mechanism of oxidative basalt alteration in volcanic seamounts differs noticeably from that in mid-ocean ridges.

The low-temperature alteration produces a restricted set of secondary minerals. This is mainly represented by trioctahedral smectites or smectites with carbonates. Vertical zonality is commonly absent in the studied basalt sections that build up the seamounts. The monotonous pattern of secondary mineral distribution in tholeiites (tholeiites constitute 99% of the volcanic rock volume in seamounts) is disturbed by alkaline basalts and hawaiites, as well as by

olivine tholeiites and tholeiitic picrites. The mineralogy and chemistry of secondary mineral assemblages that replace these rocks and fill their vesicles and fissures depends on rock type, as well as on alteration environment (nonoxidative or oxidative).

In the rock series tholeiite → alkaline basalt → hawaiite → olivine tholeiite → tholeiitic picrite, the following secondary minerals are formed: smectites; smectites + mixed-layer smectite-swelling chlorite minerals in trace amounts; smectites + mixed-layer smectite-swelling chlorite minerals in trace amounts + illite in trace amounts (illite occurs at the flow top and bottom only); smectites + mixed-layer chlorite-swelling chlorite and smectite-chlorite minerals; and smectites + mixed-layer chlorite-swelling chlorite and smectite-chlorite minerals (sometimes with serpentine in trace amount) + chlorite, or only chlorite, respectively. Tholeiite, alkaline basalt, and hawaiite are replaced by Fe-Mg smectites with MgO content of ~9 wt% (Table **T40**). Smectites replacing olivine tholeiite and tholeiitic picrite are higher in magnesium, with MgO contents as much as 15–21 wt% (Table **T40**). Smectites replacing hawaiite and alkaline basalt contain more K_2O (1.32 and 1.18 wt%, respectively) than smectites from tholeiite (K_2O = 0.36 wt%) and olivine tholeiite, which contains 0.25–0.52 wt% K_2O (Table **T40**). In the oxidized parts of the flows, smectites are higher in iron than smectites from internal parts of the flows. Dioctahedral Al-smectite of montmorillonite type with high K_2O content (2.06 wt%) is detected in the oxidized zone (Table **T40**). The difference between FeO_3 + FeO/MgO ratio values, as well as K_2O content in basalts of alkaline and tholeiitic series from the greenish gray and red clay of vesicles and veins in these rocks, are demonstrated in Table **T55.**

T55. Fe_2O_3 + FeO/MgO and K_2O (wt%), Emperor Seamounts, p.475.

Composition of secondary minerals which replace olivines also depend on the rock type and on the type of rock alteration. Olivines in all varieties of tholeiitic basalts are mainly replaced by trioctahedral smectite. Chlorite phase is formed along with smectite in altered olivines from olivine tholeiite, whereas serpentine is also fixed in olivines from tholeiitic picrite. An admixture of illite is found among secondary minerals replacing olivine from oxidized olivine tholeiite.

An internal zonality exists in individual lava flows. Variations in secondary minerals through tholeiite flows are minimal (flow Units 9, 11a, 11c, 13, 25, and 60 in Hole 433C). Besides the dominating trioctahedral smectite, an admixture of chlorite appears in interiors of the flows. In the olivine tholeiite flow (flow Unit 48; ~7.5 m thick), smectite dominates at the top and bottom, but mixed-layer chlorite-swelling chlorite mineral becomes dominating towards the flow interior. Chlorite is widespread in the tholeiitic picrite flow beneath its top (flow Unit 19b; ~10 m of the thickness in Hole 433C). Oxidized margins of flows contain more ferruginous smectites, as well as dioctahedral Al-smectite (montmorillonite).

Composition of secondary minerals infilling vesicles and veins also depends on the enclosing rock type and alteration type (oxidative or nonoxidative). In the rock series tholeiite → hawaiite → olivine tholeiite → tholeiitic picrite, the greenish gray clay from vesicles has the following assemblages of secondary minerals: smectites; smectites + occasionally mixed-layer smectite-chlorite mineral in trace amounts; smectites + chloritic minerals; and smectites + chloritic minerals + serpentine or only serpentine, respectively. Carbonates are found in vesicles from all rock types. In the greenish gray clay from this succession of rocks, MgO content increases (18.97% → 16.72% → 24.77% → 32.21%) and K_2O content varies (0.06% → 0.26% → 0.20% → 0.26%). In the succession of rock types tholeiite → olivine tholeiite → tholeiitic picrite, contents of FeO* (14.84% → 4.70% → 5.41%) and Na_2O (3.26% → 2.06% → 0.68%) in the greenish gray clay decrease (Table **T44**). Smectites from vesicles of tholeiite and hawaiite are more ferruginous, whereas smectites from vesicles of olivine tholeiite and tholeiitic picrite are higher in magnesium. The lowest content of K_2O in greenish gray clay from vesicles (0.06%) is fixed

in tholeiite (Table **T44**). Smectites are close to the nontronite type in green and blue clay from vesicles of oxidized basalts. These clays also contain illite and phillipsite. Brownish red veins in oxidized rims of the flows consist of nontronite, phillipsite, and calcite. Brownish red clay contains more K_2O, Fe_2O_3, and Al_2O_3 and is strongly decreased in MgO, as compared to the greenish gray clay.

Alteration is the most contrasting in rocks from the top and interior of the flows. Higher values of H_2O^+, K_2O, Fe_{total}, Fe_2O_3/FeO ratio, and Rb and lower contents of CaO, SiO_2, Al_2O_3, P_2O_5, and Sr in basalts from the tops vs. those from the interiors is a common feature for many basalt flows. Behavior of other elements does not show any certain relationship to the position of rock in different parts of the flow.

West Pacific Guyots

After the Emperor Seamounts, similar guyots from the West Pacific Cretaceous seamounts were studied. During ODP Legs 143 and 144, seven guyots of the Mid-Pacific Mountains, Marshall Islands, Marcus-Wake Guyots, and Japanese Guyots were drilled (Fig. **F56**). We studied alteration of basalts from the Allison Guyot (Hole 865A), Resolution Guyot (Hole 866A), Limalok Guyot (Hole 871C), Lo-En Guyot (Hole 872B), Wodejebato Guyot (Holes 874B, 875C, and 876A), and MIT Guyot (Hole 878A).

F56. Sites on guyots in the northwestern Pacific Ocean, p.260

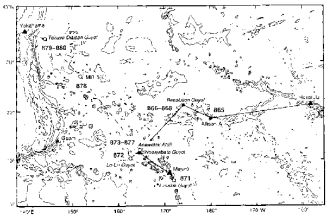

Hole 865A

Allison Guyot is located in the central part of the Mid-Pacific Mountains (Sager, Winterer, Firth, et al., 1993) (Fig. **F56**). Hole 865A (18°26.410′N, 179°33.339′W; water depth = 1518.4 m) penetrated 139 m of pelagic sediments ranging from mid-Paleocene to Quaternary in age, 698 m of upper Albian shallow-water limestone, and 33 m of alkaline basalt. Basalts (multiple sill) alternating with limestone were recovered below 831.8 mbsf. The sills represent a late pulse of igneous activity at Allison and the volcanic basement is below the sills. The oldest sill has an $^{40}Ar/^{39}Ar$ radiometric date of 111.1 Ma (Pringle and Duncan, 1995a).

Petrography and Bulk-Rock Chemical Composition

Leg 143 scientists (Sager, Winterer, Firth, et al., 1993) determined that the basalts in all units in Hole 865A are identical. Chemical variations of the basalts mainly result from alteration. Basalts in Hole 865A are alkaline (Baker et al., 1995; Kurnosov et al., 1995).

We studied 13 additional samples from Units 1, 3, and 4 (Table **T56**). They are presented by aphyric basalts with hyalopilitic and pilotaxitic groundmass textures, as well as olivine or olivine-plagioclase phyric basalts (5%–25% phenocrysts) with hyalopilitic, vitrophyric, pilotaxitic, intersertal-microlitic (microdoleritic), and microlitic textures (Kurnosov et al., 1995) (see **"Appendix A,"** p.75). The basalts are vesicular (1%–2% to 40%; 1.5–2.5 to 10 mm in diameter) and massive (see **"Appendix A,"** p.75). Groundmass consists of olivine (from ~2%–3% to 5%; 0.1–1.5 mm), plagioclase (labradorite [$An_{55–56}$] and andesine [An_{45}]; 30%–60%), clinopyroxene (5%–35%), glass (from 5%–10% to 50%), and opaque minerals (5%–15%).

T56. Alkaline basalts, Hole 865A, p.476.

Geochemical results of the study of additional basalt samples from Hole 865A confirmed the previous results (Baker et al., 1995; Kurnosov et al., 1995). In the AFM diagram, almost all samples plot in the field of tholeiites showing a Fenner trend with accumulation of iron (Fig. **F57**). The position of some samples results from extensive alteration. The Zr/4-2Nb-Y diagram (Fig. **F58**) indicates that basalts in Hole 865A belong to intraplate alkaline rocks and tholeiites enriched in Nb and depleted in Y. The chondrite-normalized REE pattern demonstrates an enrichment of basalts in large-ion components relative to small-ion ones, as is typical for intraplate basalts (Fig. **F59**). Concentration of

F57. AFM diagram for basalts, Holes 865A and 866A, p.261.

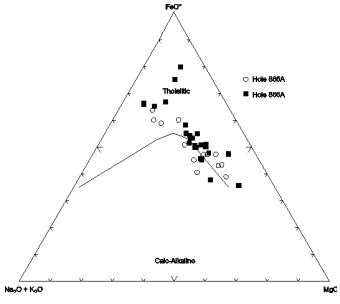

REE is similar to that in alkaline basalts of the Hawaiian Islands. Diagrams show that all studied samples of basalts from Hole 865A represent volcanic rocks an identical geochemical group.

Alteration Mineralogy

Leg 143 scientists (Sager, Winterer, Firth, et al., 1993), Baker et al. (1995), and Kurnosov et al. (1995) showed that most basalts in Hole 865A are extensively to completely altered. Petrographic study of the alteration of basalts from Units 1, 3, and 4 shows a wide range of alteration degree, from 15%–20% to as much as 100% of the rock (see **"Appendix A,"** p.75). These variations are reflected by variations in H_2O^+ content (1.52–7.59 wt%) (Table **T56**). Shipboard thin section examination (Sager, Winterer, Firth, et al., 1993) and the data by Baker et al. (1995) and Kurnosov et al. (1995), as well our thin section description of additional samples (see **"Appendix A,"** p.75), show that ferromagnesian minerals are completely replaced by clay minerals, Fe oxyhydroxides, and calcite. In the better preserved rocks, about half of the clinopyroxene phenocrysts are fresh. Plagioclase microphenocrysts are replaced by an admixture of smectite and carbonate or zeolite and smectite. Some of the plagioclase microphenocrysts are sossuritized. In Sample 143-865A-94R-1, 97–102 cm, plagioclase is fresh. Some of the interstitial K-feldspar is secondary. Glass is completely replaced by clay. Vesicles are infilled with carbonate, smectites and carbonate, or smectites.

In the fine fraction extracted from selected samples of alkaline basalts recovered from Hole 865A, XRD analyses revealed many secondary minerals (Table **T57**), such as smectites, swelling chlorite, mixed-layer smectite-chlorite and swelling chlorite-smectite minerals, illite, chlorite, serpentine(?), kaolinite, gypsum, hematite, calcite, quartz, and siderite. The smectite group comprises both pure smectite and smectite with 10%–40% mica layers with different dominating interlayer cations (Na-K and Ca-Mg). Smectite is the dominant mineral. Only in Samples 143-865A-94R-2, 102–105 cm, and 93R-2, 0–8 cm, was smectite not found. Mixed-layer smectite-chlorite or swelling chlorite is dominant secondary minerals in these samples, respectively. Illite occurs in trace amounts in almost all samples, as well as chlorite group minerals (chlorite, mixed-layer swelling chlorite-smectite and smectite-chlorite minerals, and swelling chlorite). K-feldspar is detected in several samples, as well as calcite, and quartz in trace amounts. Kaolinite, gypsum, and hematite indicate an environment of lateritic weathering. This mineral assemblage can possibly be used for correction of unit boundaries established during the leg. In Hole 865A, boundary lines were often drawn rather conditionally.

Fissures and vesicles are infilled with smectites and calcite (Table **T58**). Chlorite, serpentine, and quartz occur sporadically in trace amounts. Apatite is found in basalt (Sample 143-865A-92R-3, 80–86 cm) and in a vein within the basalt (Sample 143-865A-93R-2, 0–8 cm). The matrix from Sample 143-865A-90R-5, 52–58, cm contains siderite.

Bulk-Rock Chemical Changes

Element content in basalts from Hole 865A is given in "Appendix B", Table **AT24.**

The basalts from Unit 1 have a different vesicularity, from ~1% to as much as 20% (see **"Appendix A,"** p.75). These basalts are highly altered with H_2O^+ contents varying from ~3 to 5 wt% (Table **T56**). Because of this variable vesicularity and absence of fresh analogs, the studied basalt samples are not suitable for estimation of chemical changes at their alteration. Fresh analogs of these rocks with the same vesicularity are needed to estimate the mass balance.

Comparing the chemical composition of the most altered nonoxidized basalt from Unit 1 (Sample 143-865A-91R-3, 22–28 cm) (Table **T56**) with slightly altered nonoxidized basalt from Unit 4 (Sample 143-865A-94R-4, 133–143 cm), not taking into account rock density, we revealed that the strongly

F58. Nb-Zr-Y diagram for basalts, Holes 865A and 866A, p.262.

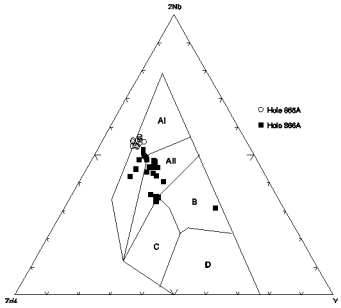

F59. Chondrite-normalized REEs for basalts, Holes 865A and 866A, p.263.

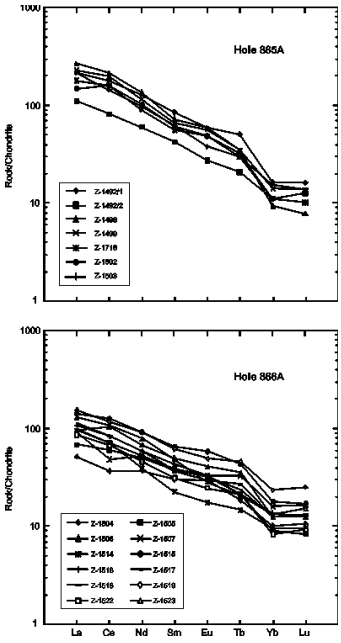

T57. Fine fraction, Legs 143 and 144, p.478.

T58. Vesicles and veins, Legs 143 and 144, p.481.

AT24. Major and trace elements, Hole 865A, p.76.

altered basalt contains less SiO_2, Fe_{total}, CaO, Na_2O, K_2O, Rb, Sr, and Ba (REE are not determined) and more Al_2O_3, TiO_2, MnO, MgO, Cr, Ni, V, Cu, Co, and Nb. Oxidized altered basalt from the upper part of Unit 1 (Sample 143-865A-90R-5, 52–58 cm) contains less SiO_2, MnO, MgO, Na_2O, P_2O_5, Co, Zr, Sr, and Ba and more Fe_{total}, (with higher Fe_2O_3/FeO ratio), K_2O, TiO_2, REE (Ce, Nd, Sm, Eu, Tb, Yb, and Lu), Cr, Ni, V, Cu, Zn, Y, Nb, and Rb than slightly altered nonoxidized basalt from Unit 4 (Sample 143-865A-94R-4, 133–143 cm). The difference in chemical composition may be caused either by primary variations in basalt composition related to fractionation of erupted melt, or by alteration. The increase in K_2O and Fe_{total} content, as well as Fe_2O_3/FeO ratio, in oxidized altered basalt likely results from alteration. Alteration affects SiO_2 and CaO contents in extensively altered nonoxidized basalt. The behavior of Sr and Ba is also significantly controlled by the alteration. Variations in other element concentrations depend on both of these factors. The relative contribution of each of these elements to the composition is difficult to evaluate.

Similar changes in chemical composition of basalts during alteration are noted in Unit 3. Intensely altered and highly oxidized basalt from Unit 3 (Sample 143-865A-92R-4, 45–47 cm) contains less SiO_2, MgO, CaO, Na_2O, P_2O_5, Cr, Ni, Zn, Sr, Ba, Yb, Lu, and more Fe_{total}, (with higher Fe_2O_3/FeO ratio), K_2O, MnO, TiO_2, Al_2O_3, V, Cu, Zr, Y, Nb, La, Ce, Nd, Sm, Eu, and Tb, as compared to slightly altered nonoxidized basalt from Unit 4 (Sample 143-865A-94R-4, 133–143 cm) (Table **T56**). In the case of slightly oxidized but highly altered basalt (Sample 143-865A-93R-3, 47–49 cm), the rock composition does not show any increase in Al_2O_3 and Nb or decrease in Na_2O. Behavior of some elements is opposite to that in nonoxidized basalt. For example, K_2O, La, Nd, Sm, Eu, Zr, and Nb content is lower, whereas content of MgO, Cr, and Ni is higher than in the slightly altered rock. As in basalts from Unit 1, variations in chemical composition of basalts from Unit 3 are caused by both primary rock composition and alteration.

Hole 866A

Resolution Guyot is located 716 km northwest of Site 865 (Leg 143) in the western Mid-Pacific Mountains (Sager, Winterer, Firth, et al., 1993) (Fig. **F56**). Igneous rocks were recovered from Hole 866A (21°19.953′N, 174°18.844′E; water depth = 1346 m) on the north edge of the guyot. The hole penetrated 1620 m of Barremian–Albian shallow-water limestone overlying 123.6 m of basalt. The basalts (lavas of intraplate tholeiitic to alkaline compositions) are subaerial and moderately to very strongly altered. The average thickness of the flows is ~10 m (ranging from 4 to 26 m). The three oldest lava flows have $^{40}Ar/^{39}Ar$ radiometric dates averaging 127.6 Ma (Pringle and Duncan, 1995a). Subaerial weathering of basalts leads to development of lateritic soils.

Petrography and Bulk-Rock Chemical Composition

As shown by shipboard descriptions (Sager, Winterer, Firth, et al., 1993), geochemical study by Baker et al. (1995), and our results (Kurnosov et al., 1995), the volcanic rocks of Resolution Guyot are undifferentiated alkaline basalts. The chemical composition of the basalts was transformed by strong alteration.

We have studied 24 additional samples from Units 2, 4, 6, 8, 9, 10, 11, and 12 (Table **T59**). All samples are represented by olivine, plagioclase-olivine, and, rarely, pyroxene-olivine-plagioclase basalts (see **"Appendix A,"** p.77) with 1%–35% phenocrysts. The groundmass of phyric basalts is mainly microlitic texture, as well as pilotaxitic, hyalopilitic, and vitrophyric textures. Aphyric basalt is determined only in Sample 143-866A-182R-4, 26–30 cm. The groundmass contains olivine (5%–15%; from 0.1–0.3 to 0.9 mm), plagioclase (labradorite [An_{54}] and andesine [$An_{32–47}$]; 10%–60% of the rock), clinopyroxene (15%–35%; <0.1 mm), glass (4%–60%), and opaque minerals

T59. Alkaline basalts, Hole 866A, p.486.

(5%–20%). Baker et al. (1995) showed that some interstitial areas contain albite and K-feldspar. The basalts are mainly massive (see **"Appendix A,"** p.77). In vesicular basalts (~30% of the rocks), vesicles are from 1%–3% to 35% of the rock and vary in size from 0.1–0.7 mm and 0.9–2 mm to 5–10 mm (see **"Appendix A,"** p.77). Part of the basalt is brecciated.

Our geochemical studies of additional basalt samples from Hole 866A confirm the results obtained earlier (Baker et al., 1995; Kurnosov et al., 1995). In the AFM diagram, almost all points plot in the tholeiites differentiation field with a Fenner trend and accumulation of iron (Fig. **F57**). The location of some points in the diagram is related to extensive alteration. The Zr/4-2Nb-Y diagram (Fig. **F58**) indicates that basalts in Hole 866A belong to intraplate alkaline rocks and tholeiites. The chondrite-normalized REE pattern demonstrates these rocks are intraplate basalts (Fig. **F59**). Concentration of REEs is similar to that in alkaline basalts of the Hawaiian Islands. The diagrams show that all studied samples of basalts from Hole 866A belong to a single geochemical group of volcanic rocks.

Alteration Mineralogy

Leg 143 scientists (Sager, Winterer, Firth, et al., 1993) showed that basalts in Hole 866A are moderately to very strongly altered. The strongly altered and oxidized basalts have undergone subaerial weathering. The red interbasaltic intervals reflect periods of exposure to tropical or subtropical weathering and are represented by laterite soil, in situ weathering of the rubble tops of lava flows, or redeposit rubble.

Petrographic study of selected samples of the basalts in Hole 866A (see **"Appendix A,"** p.77) shows that alteration varies from slight to moderate (10%–25%). Basalts that have undergone tropical weathering are very strongly altered (as much as 100%). The different alteration degrees are reflected by wide variations in H_2O^+ content (1.00–7.10 wt%) and significant changes in densities (from 2.91 to 2.15 g/cm^3) in massive basalts (Table **T59**). Shipboard thin section examination (Sager, Winterer, Firth, et al., 1993) and data by Baker et al. (1995) and Kurnosov et al. (1995), as well as our thin section descriptions of additional samples (see **"Appendix A,"** p.77), show that olivine and glass are completely replaced by clay minerals, iron oxides, and calcite. Small crystals are replaced by iddingsite, whereas large crystals are slightly replaced by secondary minerals. Baker et al. (1995) found that serpentines occur among secondary minerals after olivine. Clinopyroxene is replaced by smectite and iddingsite. Plagioclase is replaced with a mixture of smectite and hematite, and some plagioclase crystals are sericitized. Vesicles and thin fissures are infilled with smectites and/or carbonate. Several vesicles are encrusted by smectite and iron oxides. Traces of zeolites are found among alteration products in basalts and vesicles.

In the fine fraction extracted from selected samples of basalts from Hole 866A, XRD analyses (Table T57) determined smectites, mixed-layer swelling chlorite-smectite and smectite-chlorite minerals, chlorite, swelling chlorite, illite, kaolinite, gypsum, hematite, calcite, and quartz. Smectite predominates among the alteration products throughout the basalt sequence. Smectites are represented by different varieties, from pure to those containing ~10% mica layers. Smectite with Na and K interlayer cations predominates (Kurnosov et al., 1995). Electron microprobe analysis of smectites from Sample 143-866A-181R-3, 91–96 cm, show that FeO and MgO composition is similar to Fe saponite (21% FeO and 15% MgO) (Baker et al., 1995). As a whole, alkaline basalts in Hole 866A are replaced mainly by smectites. Chloritic minerals were found in several samples. Illite and particularity K-feldspar are more rare than in alkaline basalts from Hole 865A. Calcite and quartz occur in trace amounts. Kaolinite, gypsum, and hematite were found in several samples and exhibit a laterite weathering environment.

Fissures and vesicles are infilled with smectite or calcite. In Sample

143-866A-180R-3, 67–72 cm (Table **T58**), the vesicles are infilled with mixed-layer swelling chlorite-smectite and swelling chlorite minerals. Calcite and ankerite infill a large vesicle in Sample143-866A-171R-3, 121–123 cm.

Bulk-Rock Chemical Changes

Concentration of elements in basalts from Hole 866A is presented in "Appendix B", Table **AT25**. In order to estimate element gain/loss at alteration, the basalts are divided into four groups:

AT25. Major and trace elements, Hole 866A, p.78.

1. Very slightly altered nonoxidized basalts (Samples 143-866A-180R-4, 12–17 cm; 182R-1, 3–8 cm; and 182R-2, 58–63 cm).
2. Slightly to moderately altered nonoxidized basalts (Samples 143-866A-180R-1, 27–32 cm; 180R-3, 67–72 cm; 185R-3, 41–46 cm; and 189R-1, 65–69 cm).
3. Slightly altered oxidized basalts (Samples 143-866A-179R-5, 40–45 cm; 187R-1, 99–104 cm; and 188R-1, 82–89 cm).
4. Strongly oxidized basalts that were highly altered by tropical or subtropical weathering (Samples 143-866A-171R-2, 109–111 cm; 171R-4, 131–134 cm; 178W-1, 37–38 cm; and 178W-1, 79–81 cm).

Vesicular basalts are distinguished as a separate group. They are most intensely altered and especially interesting for estimation of element gain/loss. Fresh analogs of the altered rocks are required for a correct estimation of mass-balance in the future. Fresh rock samples from the Hawaiian Islands are most likely for this analysis.

Hole 871C

Limalok Guyot (Leg 144 Hole 871C) is located in the Ratak Chain of the southern Marshall Islands (Premoli Silva, Haggerty, Rack, et al., 1993) (Fig. **F56**). Limalok Guyot is the youngest of the guyots in the Marshall Islands. Hole 871C (5°33.438′N, 172°20.658′E; water depth = 1254.6 m) is located at the top of the guyot. The hole was washed to 133.7 mbsf and cores were recovered from 133.7 to 500 mbsf. The recovered material includes limestones of middle Eocene to early late Paleocene age (133.7–422.9 mbsf), clay (422.9–451.5 mbsf), and altered basalt (451.5–500 mbsf). The uppermost 6 m of "basement" consists of volcanogenic breccias.

Petrography and Bulk-Rock Chemical Composition

The volcanic rocks in Hole 871C are highly magnesian basanites. The massive lava flows range from 1 to >7 m in thickness near the end of the eruptive events of the Limalok Guyot (Christie et al., 1995; Dieu, 1995). All basalts have a similar mineralogy and minor variations textures and mineral proportions and are enriched by olivine microphenocrysts (~15%) (Christie et al., 1995).

T60. Basanites, Hole 871C, p.490.

We have studied 15 additional samples from Units 6, 7B, 8, 13, 17, 20, 21A, 21E, 21F, 22A, 22D, and 22G (Table **T60**). All samples are phyric basalt with most of the selected samples containing olivine phenocrysts (as much as 30%). Rare samples have minor plagioclase or pyroxene phenocrysts (see **"Appendix A,"** p.80). The groundmass is mainly microlitic texture, occasionally with vitrophyric and hyalopilitic textures. The groundmass consists of clinopyroxene (30%–85%; <0.1 mm and rarely 0.1–0.2 mm in size), olivine (2%–10%; 0.1–0.2 mm in size), glass (5%–90%), and opaque minerals (2%–10%). The basalts are massive and vesicular (see **"Appendix A,"** p.80). Vesicles are from 2% to 40% of the rock and vary in size from 0.2 to 3 mm. Basalts from Units 6 and 7 are brecciated.

F60. AFM diagram for igneous rocks, Holes 871C, 872B, 874B, and 878A, p.264.

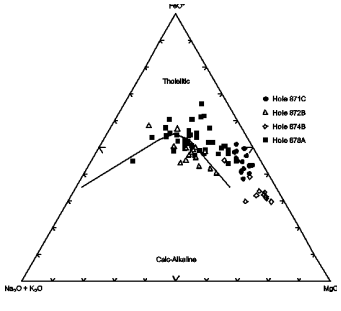

Results of our geochemical studies of additional basalt samples from Hole 871C (Figs. **F60, F61**) indicate the basalts belong to the intraplate alkaline rocks. The chondrite-normalized REE pattern also demonstrates that they are intraplate basalts (Fig. **F62**). The diagrams show that all studied samples of

basalts from Hole 871C belong to a single geochemical group of volcanic rocks.

Alteration Mineralogy

Low-temperature hydrothermal alteration was determined throughout the lava sequence (Christie et al., 1995). Basalt is patchily altered to a deep purplish brown with zones of continuous brownish alteration surrounding isolated, less altered gray parts of rock (Christie et al., 1995). Vesicles are filled with calcite, clay, and zeolite and thin veins include light green clay (Christie et al., 1995).

Petrographic study of selected samples of the basalts from Hole 871C (see **"Appendix A,"** p.80) shows that alteration varies widely. Basalts mainly are moderately altered (20%–30%). H_2O^+ contents from 2.10 to 6.13 wt% (Table **T60**) correlates with moderate to strong alteration. Densities vary from 2.94 to 2.44 g/cm^3 (Table **T60; "Appendix A,"** p.80) and correlate with the level of alteration of massive basalts. Thin section examination of additional samples of basalts (see **"Appendix A,"** p.80) showed that olivine is completely replaced by clay minerals and iddingsite or carbonate and clay minerals. Several grains of olivine are completely oxidized. Occasionally, olivine phenocrysts are fresh (Sample 144-871C-38R-1, 117–120 cm). Glass is replaced by clay minerals. Clinopyroxene is replaced with smectite and iddingsite. Plagioclase is replaced by smectite and carbonate or smectite and iddingsite.

Vesicles and thin fissures are infilled with smectites and/or carbonate. Several vesicles are infilled with chalcedony(?) (Sample 144-871C-38R-1, 117–120 cm) or zeolites(?) (Sample 144-871C-38R-3, 83–87 cm).

XRD analyses of the fine fraction extracted from basalts from Hole 871C show that secondary minerals (Table **T57**) contain smectites, mixed-layer swelling chlorite-smectite and smectite-chlorite minerals, chlorite, swelling chlorite, serpentine, illite, hematite, calcite, quartz, and analcime. Smectites predominate throughout the basalt sequence and are represented by different varieties, from pure to those containing ~10% mica layers. Smectites with interlayer Na and K cations predominate (Kurnosov et al., 1995). Electron microprobe analysis of smectites from Sample 143-866A-181R-3, 91–96 cm, shows composition (21% FeO and 15% MgO) is similar to Fe saponite (Baker et al., 1995). Chloritic minerals occur together with smectites. Several samples contain serpentine and analcime in trace amounts, as well as illite, hematite, calcite, and quartz.

Thin veins contain smectite as the principal mineral (Table **T58**). In Sample 144-871C-36R-1, 79–86 cm, the thin vein consists of smectite and mixed-layer swelling chlorite-smectite mineral. The thin vein in Sample 144-871C-40R-2, 70–75 cm, contains smectite and hematite, as well as swelling chlorite and calcite in trace amounts. Large olivine crystals are replaced by smectite, mixed-layer smectite-chlorite and swelling chlorite-smectite minerals, and chlorite.

Bulk-Rock Chemical Changes

The chemical composition of the basalts from Hole 871C was transformed by alteration. Christie et al. (1995) suggested that the alteration effects in the major element data are low Na_2O and K_2O values for Limalok basanites (Hole 871C). It is also possible that some redistribution of MgO is a result of alteration. The Limalok basanites also have low K and Rb values and variable contents of Ba, Sr, and P (Christie et al., 1995).

Element content in basalts from Hole 871C is given in "Appendix B", Table **AT26**. Altered massive basalts were divided into five groups:

1. Slightly altered nonoxidized basalts (Samples 144-871C-38R-1, 117–120 cm; 38R-3, 83–87 cm; and 39R-1, 6–10 cm).
2. Moderately altered and slightly oxidized basalt (Sample 144-871C-38R-7, 0–5 cm).

F61. Nb-Zr-Y diagram for igneous rocks, Holes 871C, 872B, 874B, and 878A, p.265.

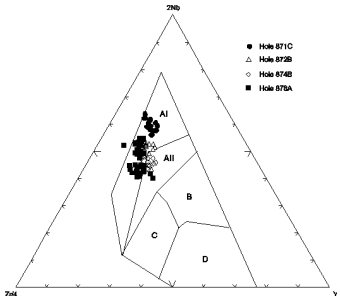

F62. Chondrite-normalized REEs for igneous rocks, Holes 871C, 872B, 874B, and 878A, p.266.

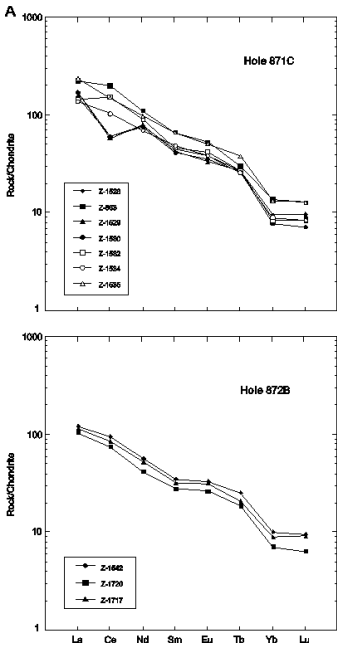

AT26. Major and trace elements, Hole 871C, p.81.

3. Moderately altered and strongly oxidized basalt (Sample 144-871C-35R-3, 76–78 cm).
4. Strongly altered and moderately oxidized basalt (Sample 144-871C-36R-1, 2–5 cm).
5. Strongly altered and strongly oxidized basalt (Sample 144-871C-39R-4, 0–5 cm).

Fresh analogs of the massive basalts, as well as vesicular rocks necessary for comparison, are absent among the studied samples. Fresh rock samples from the Hawaiian Islands should be used for this analysis.

Hole 872B

Lo-En Guyot (Leg 144, Site 872) is located in the northern Marshall Islands (Premoli Silva, Haggerty, Rack, et al., 1993) (Fig. **F56**). Hole 872B (10°05.808′N, 162°51.996′E; water depth = 1083.6 m) is located on the central portion of the guyot. The hole penetrated 192.5 mbsf and was washed to 77 mbsf and from 106 to 135 mbsf. The recovered material includes nannofossil-foraminifer ooze (middle to early Miocene) from 77.3 to 106.3 mbsf; fragments of phosphatized chalk and limestone, manganese crust, and volcaniclastic sandstone (age was not determined) from 135.2 to 135.36 mbsf; phosphatic pebbles underlain by limestone with basalt clasts (late Santonian) from 135.36 to 135.41 mbsf; and basalt (early Santonian or older) from 135.4 5 to 192.5 mbsf (~57 m). The basalt has a $^{40}Ar/^{39}Ar$ radiometric date of 112.8 Ma (Pringle and Duncan, 1995b). Igneous rocks are represented by alkaline olivine basalt. Lava flows erupted subaerally in a short space of time, which precluded soil development on the top of the flows. Some flows include brecciated flow tops and horizontal vesicle bands. Flow Units 6–9 and 11–13 are flows with thicknesses between 0.25 and 2.5 m. Thicknesses of Units 10 and 14–18 are between 1.5 and 6 m.

Petrography and Bulk-Rock Chemical Composition

The igneous sequence of the Lo-En Guyot is divided into 19 flow units (Premoli Silva, Haggerty, Rack, et al., 1993). The basalts are aphyric to sparsely clinopyroxene- and olivine-phyric. Groundmasses are microcrystalline and characterized by abundant plagioclase and titanomagnetite microphenocrysts and low abundances of olivine and clinopyroxene. The lavas recovered from Hole 872B are alkaline basalts and hawaiites. They originated during the late stage of the long-lived volcanism of the Lo-En volcano (Christie et al., 1995). The alkali-silica relationships confirm the petrographic observation that the rocks are alkaline basalts (Christie et al., 1995). Dieu (1995) suggests that the Lo-En Guyot lavas are transitional, between tholeiitic and alkalitic, and that these lavas were derived from identical parental liquids.

We studied 15 additional samples from Units 6, 9, 10, 13, 14, 16, 17, and 18 (Table **T61**). Samples are represented by phyric and aphyric basalts, olivine-plagioclase basalts, and plagioclase-olivine-pyroxene and plagioclase basalts (see **"Appendix A,"** p.82). Phenocrysts are from 5% to 10% of the rock. Phenocryst plagioclase is andesine-labradorite (An_{50}) and labradorite (An_{55}). Sample 144-872B-9R-5, 38–40 cm, is ankaramite with 48% olivine phenocrysts. The groundmass of phyric basalts is mainly microlitic texture, as well as pilotaxitic and vitrophyric textures. Aphyric basalts are hyalopilitic texture. Groundmass consists of olivine (1%–10%; <0.1 mm in size; Sample 144-872B-9R-4, 73–78 cm groundmass olivine is 15% - ankaramite?), plagioclase (labradorite [An_{56}] and andesine [An_{46} and An_{34}]; 20%–50%; 0.1–0.8 mm in size), clinopyroxene (20%–35%; from <0.1 mm to 0.1–0.3 mm in size), glass (5%–15%, in aphyric basalts as much as 75%), and opaque minerals (5%–10%). The studied basalts are mainly vesicular (see **"Appendix A,"** p.82) with vesicles varying from 2%–3% to 50% of the rock and from 0.1 to 1 mm in size, occasionally as much as 2.5–5 mm. Several samples of basalts are brecciated.

T61. Alkaline basalts and hawaiites, Hole 872B, p.492.

Our geochemical studies of additional basalt samples from Hole 872B support the previous results (Christie et al., 1995; Kurnosov et al., 1995). Almost all points in the AFM diagram fall into the field of alkaline basalts (Fig. **F60**). The Zr/4-2Nb-Y diagram (Fig. **F61**) shows the basalts in Hole 872B are intraplate alkaline rocks. The chondrite-normalized REE pattern demonstrates that these rocks belong to intraplate basalts enriched in large-ion elements (Fig. **F62**). The diagrams show that the studied samples of basalts from Hole 872B belong to a common geochemical group of volcanic rocks.

Alteration Mineralogy

All basalts from Hole 872B are strongly altered (Premoli Silva, Haggerty, Rack, et al., 1993; Christie et al., 1995). The groundmass and phenocrysts are altered to clay minerals. Groundmass colors range from yellowish brown (oxidation) to shades of gray (little or no oxidation). Units 9 and 13 contain mottled red and gray basalts. Clast colors in the breccias vary from dark red to dark gray. Vesicles are abundant in all flows (5%–40%; 0.25–1 cm in size) and are concentrated in subhorizontal bands distributed throughout the flows (Premoli Silva, Haggerty, Rack, et al., 1993). The clasts in flow-top breccias from Unit 18 are nonvesicular. The clasts in breccias from Units 10 and 14–17 are as much as 50% vesicular. The vesicles, thin veins, and matrix of the breccias contain calcite, brown clay, and white or pinkish orange zeolite (chabazite). Sometimes vesicles are lined with blue and green clays and a few are infilled with dark green clay (Premoli Silva, Haggerty, Rack, et al., 1993; Christie et al., 1995).

Petrographic study (see **"Appendix A,"** p.82) showed that the alteration varies from slight to moderate (10%–35%). Volcanic breccia and several aphyric basalts with hyalopilitic texture are 50%–100% altered. H_2O^+ content (1.08–6.15 wt%) (Table **T61**) correlates with variations of basalt alteration. Shipboard thin section examination (Premoli Silva, Haggerty, Rack, et al., 1993) and our thin section descriptions of additional samples (see **"Appendix A,"** p.82) showed that olivine is completely replaced by clay minerals, iron oxides, iddingsite, and calcite. The rims of olivine grains are oxidized and occasionally olivine phenocrysts are unaltered. Clinopyroxene is replaced by smectite and is occasionally fresh. Plagioclase is replaced with smectite and rarely by carbonate. Occasionally plagioclase is albitized. Glass is replaced by clay minerals, and opaque minerals are often oxidized. Vesicles are infilled with smectites and/or carbonate and zeolite, carbonate, and chalcedony. Thin veins contain carbonate and occasionally chalcedony and quartz. Basalt fragments with hyalopilitic groundmass texture from breccias are completely smectitized, carbonatized, and zeolitized. The matrix around the clasts is replaced by calcite, chabazite, and clay minerals.

XRD studies of the fine fraction extracted from the alkaline basalts (Table **T57**) show that secondary minerals contain smectite, mixed-layer smectite-chlorite mineral, chlorite, swelling chlorite, serpentine, illite, hematite, calcite, chabazite, analcime, and talc(?). The dominating secondary mineral is smectite with interlayer Ca-Mg cations. The assemblages of secondary minerals in alkaline basalts in Holes 872B, 865A, and 866A are similar. In contrast, basalts in Hole 872B do not contain kaolinite, gypsum, K-feldspar, or quartz.

Thin veins in alkaline basalts contain smectite and calcite as the as principal mineral (Table **T58**). The veinlet from Sample 144-872B-5R-3, 104–108 cm consists of smectite and illite. In Samples 144-872B-5R-3, 104–108 cm, and 9R-5, 38–40 cm, the fissures are infilled with smectite, dolomite, and analcime.

Bulk-Rock Chemical Changes

Concentrations of elements in basalts in Hole 872B are presented in "Appendix B", Table **AT27**. Because most selected basalts in Hole 872B are vesicular, we could not estimate element gain/loss using density data

AT27. Major and trace elements, Hole 872B, p.83.

recalculated from chemical analyses to determine absolute content. Several samples of nonvesicular basalts are also inapplicable for such calculation, as the altered basalt is aphyric, whereas other samples are represented by phyric basalts. Aphyric and phyric basalts should be analyzed in separate rock groups. Moreover, this group of rocks includes brecciated basalts with very low density values as a result of the primary character of the rocks. Because of this, we compared chemical compositions of basalts without recalculation to absolute content by using rock density. Results of this comparison may not coincide to the real element gain/loss at alteration.

Aphyric and phyric basalts have been considered separately. For aphyric basalts, variously altered rocks are compared with almost fresh nonoxidized basalt from Sample 144-872B-5R-1, 56–58 cm (H_2O^+ = 1.49 wt%; Fe_2O_3/FeO = 1.03) (Table **T61**). The most altered and oxidized basalt (Sample 144-872B-8R-2, 9-12 cm; H_2O^+ = 6.15 wt%; Fe_2O_3/FeO = 18.63) contains more Fe_{total}, K_2O, P_2O_5, Cr, Ni, Co, and Sr and less SiO_2, TiO_2, Al_2O_3, MnO, MgO, CaO, Na_2O, V, Zn, Zr, Nb, Y, and Rb. Element content trends are generally the same in less altered and oxidized basalts (Samples 144-872B-8R-1, 50–54 cm, and 63–68 cm; H_2O^+ = 4.17 and 3.37 wt%; Fe_2O_3/FeO = 15.81 and 13.05, respectively) with the exception of MnO, Na_2O, P_2O_5, and Sr content. The comparison of these element contents in three basalt samples shows increase in both alteration degree (H_2O^+ contents from 3.37–4.17 to 6.15 wt%) and oxidation degree (Fe_2O_3/FeO ratio from 13.05–15.81 to 18.63), compared to the relatively fresh basalt (H_2O^+ = 1.49 wt%; Fe_2O_3/FeO = 1.03), first leads to a strong rise in MnO content. Subsequently, MnO content does not change and even decreases in the most altered and oxidized rock. Content of Na_2O increases, but then decreases with increasing alteration and oxidation degree of the rock. Contents of P_2O_5 and Sr decrease and rise again only in the most altered and oxidized rock.

In the phyric basalts group, altered rocks are compared with almost unaltered nonoxidized basalt (Sample 144-872B-7R-6, 10–15 cm; H_2O^+ = 1.45 wt%; Fe_2O_3/FeO = 1.11) (Table **T61**). Moderately oxidized and slightly altered basalt (Sample 144-872B-7R-4, 102–107 cm; H_2O^+ = 1.17 wt%; Fe_2O_3/FeO = 4.08) contains somewhat greater amounts of Fe_{total}, Na_2O, and K_2O and less SiO_2, MgO, CaO, and Ba. Sample 144-872B-8R-4, 24–29 cm (moderately altered basalt; H_2O^+ = 2.07 wt%), without any influence of oxidation (Fe_2O_3/FeO = 1.48) and unlike the previous sample, contains less MnO, MgO, K_2O, P_2O_5, Nb, and Rb and more Sr compared to Sample 144-872B-7R-6, 10–15 cm. This result demonstrates the difference in element content in the alteration of basalts with formation of mainly water-containing minerals and at oxidative alteration.

Influence of bulk-rock chemical changes under oxidative conditions (Fe_2O_3/FeO ratio from 3.74–16.07 to 59.09) and at a moderate level of alteration (H_2O^+ content from 3.02 to 4.35 wt%) is considered in Samples 144-872B-5R-4, 65–68 cm; 7R-3, 32–37 cm; and 7R-1, 8–12 cm (Table T61). The most oxidized basalt (Sample 144-872B-7R-1, 8–12 cm) contains more Fe_{total}, Na_2O, K_2O, and Zn and less SiO_2, Al_2O_3, MgO, CaO, Sr, and Ba, as compared to Sample 144-872B-7R-6, 10–15 cm.

Therefore, all oxidized altered basalts, which prevail in Hole 872B, contain more Fe_{total} and K_2O and often Na_2O and less SiO_2, CaO, MgO, Sr, and Ba and often Al_2O_3, as compared to unaltered rocks. Content of other elements is variable. Nonoxidized altered basalt is characterized by lower K_2O, MnO, and P_2O_5 content and higher Sr content than oxidized basalts.

Holes 874B, 875C, and 876A

Wodejebato Guyot (Leg 144, Site 874) is located 44 km northwest of Pikinni Atoll in the Ralik Chain in the northern Marshall Islands (Premoli Silva, Haggerty, Rack, et al., 1993) (Fig. **F56**). Hole 874B (12°00.228′N,

164°56.388′E; water depth = 1374.9 m) is located on the inner perimeter ridge and penetrated 193.5 mbsf. The recovered material includes 0.11 m of manganese crust and manganese-phosphate coated limestone conglomerate (Maastrichtian–middle Eocene); 162.7 m of rudist-algal-foraminiferal limestone (Maastrichtian–late Campanian?); 14.9 m of ferruginous clay, claystone, and extensively altered vesicular basalt (Campanian–?); and 15.8 m of basalt. The basaltic lava samples appear to be from a single ankaramite flow. Basalt has a $^{40}Ar/^{39}Ar$ radiometric date of 83 Ma (Pringle and Duncan, 1995b).

Petrography and Bulk-Rock Chemical Composition

The basaltic lava in Hole 874B is presented by a single ankaramite flow (Premoli Silva, Haggerty, Rack, et al., 1993). Leg 144 scientists showed that ankaramites are highly phyric (25% olivine, 15% clinopyroxene, and 5%–10% plagioclase phenocrysts). The groundmass is intersertal to pilotaxitic texture and consists of 25%–40% titanaugite, 10% titanomagnetite, 5% olivine, and 40% plagioclase.

We have studied 10 additional samples from flow Unit 1 (Table **T62**). Ankaramites are pyroxene-olivine phyric with vitrophyric and microlitic groundmass textures (see **"Appendix A,"** p.84). Phenocrysts make up 50%–60% of the rock, olivine 40%–55% (0.4–5.0 mm in size), clinopyroxene 5%–20% (as much as 5.5 mm in size), and rare plagioclase. The groundmass contains glass, olivine (2%–3%), clinopyroxene microlites (as much as 15%), opaque minerals (5%–10%), and occasionally plagioclase microlites (2%–3%; <0.1 mm in size). The lower part of the flow (Samples 144-874B-24R-3, 125–130 cm, and 24R-4, 54–72 cm) is represented by plagioclase-clinopyroxene-olivine phyric rocks with 50%–70% phenocrysts that are 25%–30% olivine, 20%–25% clinopyroxene, and as much as 20% plagioclase (labradorite [$An_{59–60}$]). The selected basalts are mainly vesicular (see **"Appendix A,"** p.84). Vesicles are from 5% to 20% of the rock and vary in size from 0.1 to 2 mm and occasionally as much as 5 mm. Thin veins (from 0.01–0.1 to 0.5 mm in thickness) are 2%–5% of the rock. Samples 144-874B-22R-4, 48–53 cm, and 24R-2, 70–76 cm, represent brecciated basalts (see **"Appendix A,"** p.84).

T62. Ankaramites, Hole 874B, p.494.

Our geochemical studies of additional samples of basalts from Hole 874B confirm the results obtained earlier (Christie et al., 1995; Kurnosov et al., 1995). Almost all points in the AFM diagram plot to the field of basalts enriched in MgO (Fig. **F60**). The Zr/4-2Nb-Y diagram (Fig. **F61**) indicates that the basalts belong to the intraplate alkaline series, and the chondrite-normalized REE pattern demonstrates that they belong to intraplate basalts enriched in large-ion elements (Fig. **F62**), as also shown in the chondrite-normalized REE pattern by Christie et al. (1995) and Kurnosov et al. (1995). The diagrams indicate that the studied samples of ankaramites in Hole 874B belong to a single geochemical group of volcanic rocks.

Alteration Mineralogy

Shipboard thin section examination (Premoli Silva, Haggerty, Rack, et al., 1993) showed that alteration of ankaramites in Hole 874B decreases from the top to the bottom of the flow. Near the top of the flow, olivine phenocrysts are completely replaced with iddingsite and green clay minerals. In the bottom of the flow, olivine is replaced by clay. Clinopyroxene is mainly unaltered throughout the flow. Alteration of plagioclase phenocrysts throughout the flow is similar to the alteration of olivine. Groundmass olivine is replaced by orange clay. Plagioclase is replaced with green clay and zeolites. Groundmass throughout the flow is replaced with green and brown clay minerals. The upper part of the flow contains a subvertical, low-temperature hydrothermal vein with an alteration halo extending 3–5 cm on either side (Premoli Silva, Haggerty, Rack, et al., 1993; Christie et al., 1995). The vein contains calcite and greenish yellow clay mineral.

Petrographic study of ankaramites (see **"Appendix A,"** p.84) showed that alteration is from slight and moderate (from 5%–10% to 20%–30%) to

strong (50%–60%), with strongly altered rocks predominant. H_2O^+ contents in altered ankaramites are from 2.69 to 6.14 wt% (Table T62) and correlate with the level of alteration. Thin section examination (see **"Appendix A,"** p.84) show that olivine is replaced by clay minerals, iron oxides, iddingsite, and carbonate. The rims of olivine grains are oxidized. There are unaltered olivine phenocrysts with oxidized matter in fissures, and occasionally fissures in olivine grains are infilled with hydrobiotite(?). Clinopyroxene is fresh. Thin cracks in clinopyroxene grains are infilled with calcite. Glass is replaced by smectites. Vesicles are infilled with smectites and/or chalcedony or cristobalite and occasionally with Fe hydroxides. Thin veins consist of smectites, carbonate, and carbonate and biotite-like mineral.

XRD studies of the fine fraction extracted from ankaramites show that secondary minerals (Table **T57**) contain smectite with Ca-Mg interlayer cations, mixed-layer swelling chlorite-smectite and smectite-chlorite minerals, chlorite, swelling chlorite, serpentine, illite, hematite, calcite, quartz, and analcime (Kurnosov et al., 1995; **"Appendix A,"** p.84). Mixed-layer swelling chlorite-smectite and smectite-chlorite minerals, chlorite, swelling chlorite, as well as serpentine with smectite, replace ankaramites with a high primary magnesium content (MgO = 19%–22 wt%) (Tables **T57, T62**). In the lowermost part of Unit 1 (Sample 144-874B-24R-4, 54–72 cm), the basalt has a lower MgO content (11.5 wt%) and contains mainly smectite. Chlorite and mixed-layer smectite-chlorite occur only in trace amounts, and serpentine is absent. In this case, chlorite phases and serpentine reflect very high magnesium content of the rocks rather than higher temperature. Cracks and vesicles are infilled with smectite or calcite. Large crystals of olivine are replaced by smectites, swelling chlorite, or mixed-layer swelling chlorite-smectite mineral + swelling chlorite (Table **T58**). The ankaramite flow on Wodejebato Guyot is mainly strongly altered at low-temperature.

XRD studies of the fine fraction extracted from alkaline basalts from Holes 875C and 876A show that secondary minerals (Table **T57**) contain smectite and mixed-layer smectite-chlorite mineral, as well as trace amounts of chlorite and illite. This assemblage of secondary minerals is typical for alkaline basalts. The thin veins contain calcite (Sample 144-876A-16R-1, 6–8 cm) or smectite + calcite + chabazite (Sample 144-876A-15R-1, 32–34 cm) (Table **T58**).

Bulk-Rock Chemical Changes

Element content in basalts from Hole 874B is given in "Appendix B", Table **AT28**. Most of selected ankaramites from Hole 874B are vesicular. All rocks are altered, and their fresh vesicular analogs are absent. Because of this, we used the chemical compositions of the rocks for direct estimation of bulk-rock chemical changes (Table **T62**). It should be taken into account, however, that the obtained results may not coincide with the real gain/loss of elements.

AT28. Major and trace elements, Hole 874B, p.85.

We could compare only the most altered varieties with the least altered ankaramite sample (Sample 144-874B-24R-1, 30–35 cm; density = 2.88 g/cm^3; H_2O^+ = 2.69 wt%; Fe_2O_3/FeO = 1.21). For comparison with this weakly altered ankaramite, we chose two samples: (1) extensively altered and strongly oxidized Sample 144-874B-23R-1, 100–105 cm, with H_2O^+ content of 5.78 wt% and Fe_2O_3/FeO ratio of 14.27, and (2) extensively altered and moderately oxidized Sample 144-874B-24R-1, 100–105 cm, with H_2O^+ content of 5.30 wt% and Fe_2O_3/FeO ratio of 3.33.

The most altered and strongly oxidized ankaramite (Sample 144-874B-23R-1, 100–105 cm) is higher in Fe_{total}, Al_2O_3, Na_2O, and Co content and lower in CaO, SiO_2, K_2O, Rb, Sr, and Ba content than Sample 144-874B-24R-1, 30–35 cm. The difference in REE content is negligible. The more altered sample of ankaramite has somewhat higher La, Sm, Eu and Tb contents, whereas Ce, Nd and Lu contents are lower. Yb content is equal in the compared samples.

The least oxidized but intensely altered ankaramite (Sample 144-874B-

24R-1, 100–105 cm) contains more Al_2O_3, Na_2O, and Sr, whereas CaO, MgO, and Ba contents are lower. The difference in REE contents relative to the least altered sample are similar to those noted for the previous ankaramite sample, except for Nd, Yb, and Lu. Nd and Lu contents are the same in Sample 144-874B-24R-1, 100–105 cm, and in the least altered sample, but Yb content is somewhat higher. Besides the alteration, primary composition also contributes to variations in the chemical composition of the altered rock.

Hole 878A

MIT Guyot is an isolated feature close to the Wake Group in the 18°–28°N guyot band (Premoli Silva, Haggerty, Rack, et al., 1993) (Fig. **F56**). Hole 878A (27°19.143′N, 151°53.028′E; water depth = 1323.2 m) is located on the south edge of the guyot. The hole ended at 910 mbsf after penetrating 3.2 m of pelagic sediment (early Pleistocene–late Albian), 719.34 m of carbonates and polymictic breccia (late Aptian?–early Aptian), and 187.46 m of basalt flows and flow-top breccias. Basalts have $^{40}Ar/^{39}Ar$ radiometric dates averaging 123 Ma (Pringle and Duncan, 1995b). This section is divided into 35 igneous units including 24 lava flows and 3 volcaniclastic units. They represent at least three distinct periods of volcanism separated by two periods of weathering. The igneous units are hawaiite, basanite, and alkaline olivine basalts.

Petrography and Bulk-Rock Chemical Composition

Leg 144 scientists (Premoli Silva, Haggerty, Rack, et al., 1993) showed that the upper volcanic interval consists of two hawaiite flows. The middle volcanic interval consists of 7 basanitoid flows and breccia deposits. The lower volcanic interval contains 15 flows and 1 breccia deposit (upper 3 flows are basanitoides, and lower flows are alkaline olivine basalts).

The igneous flows and breccias were divided into 7 petrographic types (Premoli Silva, Haggerty, Rack, et al., 1993). Type 1 contains the hawaiite of Units 1 and 2. Type 2 contains basanitoid lavas of Units 8, 10, 11, 15, and 16. Type 3 volcanic flows include Unit 12 (a basanitoid breccia) and Units 18, 20, and 21 (basanitoid lavas). Type 4 (Units 22 and 23), Type 5 (Units 25, 26, 27, and 30), and Type 6 (Units 32 and 34) are alkali olivine basalt lava flows. Type 7 is Unit 35 (alkali olivine basalt). Unit 31 is represented by highly altered vitric tuff, which is not attributed as a petrographic type).

We have studied 40 additional samples from all three volcanic intervals (upper volcanic interval from Units 1 and 2; middle volcanic interval from Units 8, 10, 11, 13, 15, and 16; and lower volcanic interval from Units 20–23, 26, 30, 34 and 35 and Subunits 31A and 31B) and all seven petrographic types (see **"Appendix A,"** p.86; Table **T63**).

T63. Hawaiites, basanites, and alkaline olivine basalts, Hole 878A, p.496.

Geochemical studies of selected basalt samples from Hole 878A confirmed the results obtained by Christie et al. (1995) and Kurnosov et al. (1995) showing that the igneous rocks in Hole 878A are intraplate alkaline basalts (Figs. **F60, F61**). The chondrite-normalized REE pattern demonstrates that these rocks belong to intraplate basalts enriched in large-ion elements (Fig. **F62**).

Alteration Mineralogy

Almost all lava flows recovered from Hole 878A on MIT Guyot have reddish vesicular and/or brecciated flow tops, indicating that the sequence is subaerial (Premoli Silva, Haggerty, Rack, et al., 1993). The vesicles are infilled with white or pale to dark clay minerals. Rare veins consist of calcite and green clay. The igneous units (mesostasis and phenocrysts) are replaced with greenish brown clay minerals at low temperature. Feldspar is replaced by clay or zeolite. Olivine is replaced with greenish brown clay or is iddingsitized. Occasionally, olivine is fresh. Serpentine slickenslides occur in Sections 144-878A-89R-2 and 89R-3, reflecting relatively high alteration temperature (Premoli Silva, Haggerty, Rack, et al., 1993). Alteration decreases progressively downhole, and

the lowermost section appears to be very fresh except in areas along fractures and in iron-stained patches. The vitric tuff from Unit 31 (15.5 m thick) is represented by highly vesicular glassy clasts. The upper part of the unit (Subunit 31A; 7.5 m thick) is bleached (hydrothermally altered to light clay). The remainder (Subunit 31B) is red (highly oxidized tuff) and more lithified (Premoli Silva, Haggerty, Rack, et al., 1993).

Petrographic study of selected samples of basalts from Hole 878A (see **"Appendix A,"** p.86) showed that their alteration is different (from 2%–3% to 35%–40% of the rock). H_2O^+ content is mainly from 0.72 to 3.47 wt% and rarely as much as 4–5 wt% (Table **T63**). Basalts mainly are oxidized. Volcanic tuffs from the upper part of Unit 31 are maximally altered and oxidized with H_2O^+ content at ~6 wt% and almost all iron oxidized. The nonvesicular basalts from the lowermost part of the lava flow sequences (Units 34 and 35) are fresh or almost fresh and nonoxidized. In addition to Leg 144 shipboard secondary mineral study results from thin sections (Premoli Silva, Haggerty, Rack, et al., 1993), thin section examination (see **"Appendix A,"** p.86) showed that plagioclase is occasionally and partly replaced by sossurite, albite, and possibly zeolite (e.g., Sample 144-878A-94R-1, 0–4 cm). Glass is replaced by smectite and, rarely, by smectite and chalcedony or partly by albite and zeolite. Vesicles are infilled with carbonate and/or clay minerals and zeolite. In Sample 144-878A-93R-1, 7–11 cm, the vesicles contain celadonite(?). Thin veins consist of clay minerals and carbonate.

Bulk-Rock Chemical Changes

Concentration of elements in basalts in Hole 878A is presented in "Appendix B", Table **AT29**. Selected basalts in Hole 878A are slightly vesicular (mainly from 1% to 10%) and nonvesicular. Nonvesicular basalts, however, are best for estimation of element gain/loss (i.e., using density data in recalculation of chemical analyses to obtain absolute elements content) and are slightly altered or unaltered (see **"Appendix A,"** p.86). Vesicular basalts are most altered and oxidized and especially represented by basalt breccia. Variations in primary densities are related to varying vesicularity and brecciation degrees, which are hard to take into account and make the estimation of element gain/loss unreliable. Because of this, we directly compared the primary data on chemical composition of basalts in weight percent, and therefore results of this comparison may not coincide with the real element gain/loss at alteration. The comparative analysis of chemical composition was performed for some of the most contrasting basalt samples. Separate analyses were performed for hawaiites, basanites, alkaline olivine basalts, and basalt breccia.

AT29. Major and trace elements, Hole 878A, p.87.

Hawaiites. The hawaiites (upper volcanic interval; Units 1 and 2; petrographic Type 1) differ slightly from each other in alteration and oxidation degree. Minimum content of H_2O^+ is 1.06 wt%, and maximum content is 2.08 wt%. Oxidation degree of hawaiites is characterized by Fe_2O_3/FeO ratios of 2.16–4.24 (Table **T63**). Within this range of alteration, the most altered and oxidized hawaiite contains higher contents of MnO, K_2O, V, and Ba and lower contents of MgO, CaO, Na_2O, Zn, and Sr.

Basanites. Alteration of basanites from the middle (Units 8, 10, 11 15, and 16; petrographic Type 2) and lower (Units 20 and 21; petrographic Type 3) volcanic intervals is slight to moderate (H_2O^+ = 1.51–4.17 wt%). The basanites are mainly nonoxidized or slightly oxidized. Several basanite samples are moderately oxidized, with Fe_2O_3/FeO ratios of 3.5 and 8.4 (Table **T63**).

Among Type 2 basanites, the most altered nonoxidized sample (Sample 144-878A-84R-3, 116–120 cm; H_2O^+ = 4.17 wt%; Fe_2O_3/FeO = 1.02) is characterized by lower SiO_2, Al_2O_3, Fe_{total}, MnO, CaO, Na_2O, K_2O, Cu, and Sr contents and higher MgO and Co contents, as compared to the least altered nonoxidized sample (Sample 144-878A-85R-2, 110–114 cm; H_2O^+ = 1.84 wt%; Fe_2O_3/FeO = 1.38) (Table **T63**). Higher MgO, Cr, and Ni contents, in this case,

possibly reflect primary variations in chemical composition of the rock. In more oxidized Sample 144-878A-81R-2, 10–15 cm (H_2O^+ = 2.01 wt%; Fe_2O_3/FeO = 3.50), Fe_{total} and MgO contents are higher, whereas Al_2O_3, MnO, Na_2O, K_2O, Rb, Sr, and Ba contents are lower, as compared to the least altered nonoxidized Sample 144-878A-85R-2, 110–114 cm (Table **T63**).

Type 3 altered basanites are similarly altered (H_2O^+ = 2.04–2.28 wt%). The most oxidized rock (Sample 144-878A-88R-3, 88–92 cm; H_2O^+ = 2.23 wt%; Fe_2O_3/FeO = 8.41) contains more Fe_{total}, Al_2O_3, and K_2O and less SiO_2, MnO, MgO, CaO, Na_2O, Sr, and Ba than the fresh rock (Sample 144-878A-90R-1, 90–95 cm; H_2O^+ = 0.72 wt%; Fe_2O_3/FeO = 2.22) (Table **T63**).

Alkaline Olivine Basalts. Among the studied alkaline olivine basalts (Units 22, 23, 26, 28, and 30; petrographic Types 4 and 5), strongly altered samples (H_2O^+ = <2.82 wt%) are absent (Table **T63**). The most oxidized and altered basalt (Sample 144-878A-90R-4, 115–120 cm; H_2O^+ = 2.82 wt%; Fe_2O_3/FeO = 17.37) has higher Fe_{total}, Al_2O_3, MnO, Na_2O, K_2O, P_2O_5, V, and Rb contents and lower SiO_2, MgO, CaO, Zn, Sr, and Ba contents than the slightly altered nonoxidized basalt (Sample 144-878A-91R-4, 120–125 cm; H_2O^+ = 1.16 wt%; Fe_2O_3/FeO = 0.73). It also contains more La, Ce, Nd, Sm, Yb, and Lu and less Eu and Tb. The alkaline olivine basalts from the lowermost part of the sequence (Units 34 and 35; petrographic Types 6 and 7) are fresh, slightly altered, and nonoxidized (Table **T63**).

The intensely altered and very strongly oxidized hyalobasalt breccia (Sample 144-878A-94R-3, 124–129 cm; H_2O^+ = 5.95 wt%; practically all iron is oxidized) (Table **T63**) contains less SiO_2, Al_2O_3, MgO, CaO, Na_2O, K_2O, P_2O_5, V, Rb, Sr, and Ba and more MnO, Fe_{total}, and Ni than the almost fresh, nonoxidized hyalobasalt (Sample 144-878A-97R-2, 28–31 cm; H_2O^+ = 1.47 wt%; Fe_2O_3/FeO = 0.77). Therefore, basalt breccias, as well as the vesicular tops of lava flows, are most likely involved in the redistribution of elements during water-rock interaction in guyots.

Brief Comments

As a whole, the conditions and products of the alteration of alkaline basalt, basanite, ankaramite, and hawaiite from the West Pacific guyots studied during ODP Legs 143 and 144 correspond to the results obtained by detailed study of altered basalts from the Emperor Seamounts drilled during DSDP Legs 55 and 19. Domination of smectites among the alteration products suggests the smectite facies of basalt alteration in the oceanic crust (Kurnosov, 1986, 1992).

Two processes of basalt alteration have been suggested from the study results: low-temperature hydrothermal alteration and weathering. Low-temperature hydrothermal alteration is indicated by smectite, swelling chlorite, and mixed-layer smectite-chlorite minerals, as well as serpentine, chlorite, and illite associated with carbonates (mainly calcite, with rare ankerite), chabazite, gypsum, and rare quartz. Laterite weathering led to the formation of kaolinite-gypsum-smectite associations with hematite.

Differences in low-temperature hydrothermal mineral assemblages depend on the chemical composition of the primary basalt, rather than on differing temperatures of alteration. Increasing magnesium content in basalts is accompanied by the appearance, along with smectite, of mixed-layer smectite-chlorite minerals, chlorite, and even of serpentine. Higher alkaline element contents in primary basalts possibly lead to formation of illite and K-feldspar. Similar dependence on primary basalt composition was found in the Emperor Seamount chain.

Alteration contrasts the most in rocks from the top and interior of the flows, and bulk-rock chemical changes are therefore especially expressive here. Higher values of H_2O^+, Fe_{total}, Fe_2O_3/FeO ratio, K_2O, and MnO and lower contents of CaO, SiO_2, MgO, Sr, and Zn and often of Na_2O, Rb, and Ba in the

vesicular and/or brecciated extremely altered and highly oxidized basalts from the tops vs. basalts from the interiors is a common feature of basalt flows. Contents of other elements increase in one set of samples, and decrease or do not change in another. The variability of bulk-rock chemical changes is caused by different contributions of alteration and variations in primary chemical composition throughout the flows. Highly altered nonoxidized basalts, on the contrary, commonly contain less K_2O, and more MgO than fresh rocks. CaO content decreases in extremely altered and highly oxidized basalts.

Complete and objective estimation of element gain/loss will be possible if fresh analogs of vesicular rocks are found. Such fresh rocks are likely to be found on the Hawaiian Islands.

Trachytes from Southern Hess Rise

Hole 465A

Hole 465A (33°49.23′N, 178°55.14′E; water depth = 2161 m) is located at the end of Hess Rise (central North Pacific) near the junction of the northwest–southeast ridge and the east–northeast to west–southwest ridge (Fig. **F63**). The hole penetrated 64.3 m of Cretaceous trachyte breccia and flows (basement recovery = 23.9 m). The oldest sediment cored in the hole is early Maastrichtian.

F63. Site on southern Hess Rise, p.268.

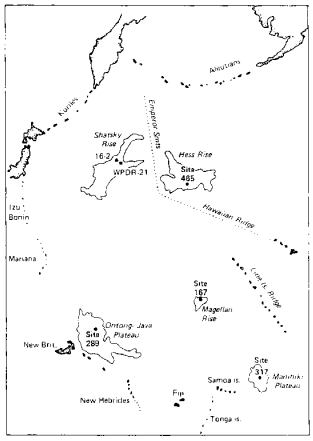

Hess Rise is a large structure formed before late Albian time probably along a mid-ocean ridge or a triple junction (the junction of the Kula, Farallon, and Pacific plates). The formation of the structure started from the extrusion of tholeiitic basalts to the south of the equator between 116 and 95 Ma. Later, the structure moved northward with the motion of the Pacific Plate and subsided (Thiede, Vallier, et al., 1981; Vallier et al., 1981; Thiede et al., 1981). Volcanic rocks recovered at Hess Rise indicate off-ridge volcanism. The volcanic archipelago is built of normal MORB basement extruded at a diverging ridge during Aptian or early Albian time. The younger volcanism began after the MORB basement had migrated off the ridge and was superimposed on normal MORB basement (Seifert et al., 1981).

Petrography and Bulk-Rock Chemical Composition

Leg 62 scientists (Thiede, Vallier, et al., 1981) and Seifert et al. (1981) determined that the cores in Hole 465A consist of strongly altered, dominantly fine grained, vesicular trachyte. All samples demonstrate trachytic texture. Studied basalts contain at least one microphenocryst phase with feldspar as the dominant phase. Plagioclase, possibly pyroxene, and iron-ore microphenocrysts, set in a groundmass of glass, iron-ore minerals, and feldspar microlites, represent original minerals. Present groundmass minerals include altered glass and feldspar microlites, which are secondary K-feldspar (Lee-Wong, 1981). Glass is the dominant phase (60%–75%). Feldspar microlites occupy from 12% to 30% of the rock. Two generations of feldspars are found in trachytes in Hole 465A. These are potassium-poor plagioclase and nearly pure K-feldspar (Lee-Wong, 1981). Leg 62 trachytes were divided into 30 layers, which were then grouped into five units. Unit 1 (411.7–429.0 m) is brecciated trachyte, Unit 2 (429.0–447.5 m) is medium grained vesicular trachyte, Unit 3 (447.5–462.5 m) is fine grained highly vesicular trachyte, Unit 4 (462.5–466.5 m) is coarse grained trachyte, and Unit 5 (466.5–476.0 m) is fine grained amygdaloidal trachyte. The vesicle abundance and size, red oxide staining, and lack of any glassy flow margins indicate shallow subaqueous or subaerial volcanism. This implies that at least parts of Hess Rise were near or above sea level prior to late Albian time (Thiede, Vallier, et al., 1981).

Chemical variations in trachytes correlate with H_2O^+ content. Hence, variations result from alteration and not from differentiation (Thiede, Vallier, et al., 1981; Seifert et al., 1981; Scott, 1981). The least altered sample is chemically similar to trachytes from many oceanic islands (Tristan da Cunha,

Gough, Fernando de Noronha, Hawaii, and St. Helena). The REE pattern of the Hawaiian trachyte is similar to that of Hole 465A rocks, but with consistently less-abundant LREE (Seifert et al., 1981). Leg 62 scientists (Thiede, Vallier, et al., 1981) and Seifert et al. (1981) interpreted trachytes in Hole 465A to be late-stage differentiates of alkaline basalt magma.

We have studied 12 additional samples of trachytes from flow Units 1, 2, 3, and 5 (Table **T64**). The studied rocks are aphyric trachy-andesite, glassy and fine grained, with hyalotaxitic, trachydoic, and pilotaxitic groundmass textures and have a fluidal structure (see **"Appendix A,"** p.91). All samples are vesicular, with vesicles (from 0.1–0.8 to 1.5–3 mm in size) comprising 5%–20% of the rock and oriented according to fluidal structure. Three samples of trachy-andesite breccia are present (Samples 62-465A-40R-3, 17–25 cm; 40R-3, 27–35 cm; and 41R-1, 113–120 cm).

All selected samples in Hole 465A belong to the trachy-andesitic series of alkaline rocks, which is not typical for initial (spreading) tectonomagmatic structures. This group of rocks is characterized by low Ti, Fe, Mg, and Ca contents and high alkaline element contents, in total ~10% or greater (Table **T64**). Alkalinity in some samples is represented by K-varieties (Samples 62-465A-44R-3, 118–123 cm; 45R-1, 81–85 cm; and 46R-1, 82–86 cm). The samples also demonstrate high Nb, Zr, and alkaline earth element contents but low abundances of siderophile and chalcophile elements (Table **T64**). Such geochemical specialization results from rock-forming mineral composition (see **"Appendix A,"** p.91). Fe-Mn silicates are practically absent in the rocks. The samples contain relatively silicic glass filled with sanidine, small amounts of opaque minerals, and single microphenocrysts of plagioclase.

Geochemical diagrams provide evidence that these rocks belong to the alkaline group (Fig. **F64**). The Zr/4-2Nb-Y diagram (Fig. **F65**) indicates that the rock composition appears outside of the AI field, which is characteristic of the intraplate alkaline basalts. This points to higher alkalinity and somewhat lower concentration of Y than the latter. This geochemical peculiarity is also evidence of the rocks belonging to the group of superalkaline rocks, such as trachytes and trachy-andesites. A special trachyte series field (e.g., alkaline-trachyte field AT) can be distinguished in this diagram. Normalized REE ratios are characterized by significant enrichment in large-ion lanthanides (Fig. **F66**). It is probable that these rocks were formed because of the differentiation of deep alkaline-olivine melts generated in nondepleted layers of the upper mantle.

Alteration Mineralogy

Leg 62 scientists (Thiede, Vallier, et al., 1981) and Seifert et al. (1981) showed that trachytes in Hole 465A are highly altered throughout the sequence. We find that the samples studied by these scientists are slightly to moderately altered, as H_2O^+ content is only 0.68–2.58 wt% (Seifert et al., 1981). All of the groundmass phases and some feldspar laths have been altered to smectites and mixed-layer clay minerals. Leg 62 scientists determined that many vesicles are filled with smectites and calcite at the centers. Pyrite occurs both as disseminated crystals and thin veins. Barite was observed in one vein. Secondary K-feldspar was recognized in trachytes (Lee-Wong, 1981). Seifert et al. (1981) supposed that trachytes recovered from Hole 465A were altered at temperatures of >150°C.

According to our study, additional samples of trachy-andesite and breccia are slightly to moderately altered (H_2O^+ = 0.77–2.07 wt%) with breccia contents of as much as 2.35 wt% (Table **T64**). All studied samples were altered under an oxidizing environment (Fe_2O_3/FeO = 2.07–13.76). Petrographic study of selected samples showed that the igneous rocks in Hole 465A are slightly to moderately altered (10%–20%) and oxidized. Glass in interstices and from vesicles is cream and yellow-brown in color. The rims of trachy-andesite fragments from breccia are highly oxidized (see **"Appendix A,"** p.91). Vesicles are completely or partially filled with greenish yellow smectites and

T64. Trachy-andesites, Hole 465A, p.502.

F64. AFM diagram for trachyandesites, Hole 465A, p.269.

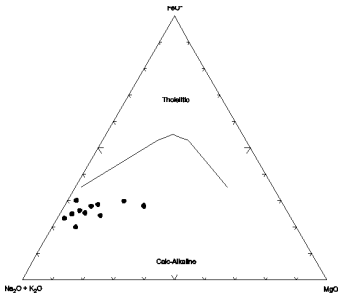

F65. Nb-Zr-Y diagram for trachyandesites, Hole 465A, p.270.

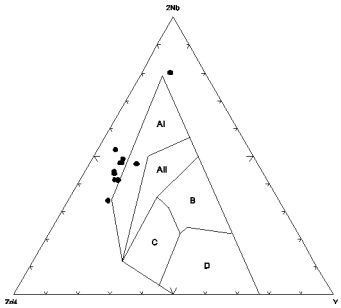

F66. Chondrite-normalized REEs for trachyandesites, Hole 465A, p.271.

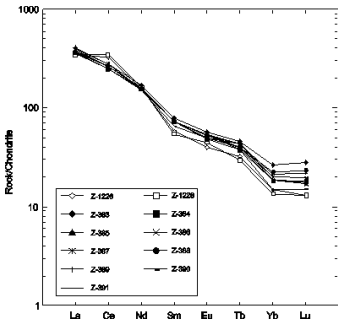

occasionally with an admixture of zeolite. Large vesicles are filled with greenish yellow smectite or calcite. Occasionally, vesicles are hollow or lined by zeolite and smectite. Plagioclase is almost completely replaced by albite and orthoclase (K-feldspar). Primary K-feldspar is partly replaced by clay mineral. The cement in breccia consists of carbonate.

XRD study of the fine fraction removed from the trachy-andesites showed that smectites dominate among the secondary minerals (see **"Appendix A,"** p.91) and have various compositions of Na-K and Mg-Ca interlayer cations. Smectites with Mg-Ca interlayer cations were found in Samples 62-465A-44R-1, 112–116 cm; 44R-3, 118–123 cm; and 45R-1, 81–85 cm, in spite of their high K_2O contents (5.14–6.42 wt%) (Table **T64**). With the exception of Sample 62-465A-46R-1, 82–86 cm (K_2O = 6.74 wt%), rocks with high concentrations of K_2O and Na_2O do not contain hydromica among the secondary minerals. Hydromica was found together smectite in this sample (see **"Appendix A,"** p.91). Mixed-layer clay minerals are absent among the secondary minerals. Breccia matrixes (Sample 62-465A-40R-3, 17–25 cm, and 41R-1, 113–120 cm) consist of mainly calcite with siderite and quartz (see **"Appendix A,"** p.91). Fragments of basalts from breccia are replaced by smectites only.

Bulk-Rock Chemical Changes

Comparison of the chemical compositions of trachytes led Leg 62 scientists (Thiede, Vallier, et al., 1981) and Seifert et al. (1981) to conclude that variations in amounts of SiO_2, K_2O, MgO, and Rb correlate well with H_2O^+ content. Trace elements do not appear to be affected by alteration, however the trachytes did demonstrate a correlation between Lu and H_2O^+. It was shown that the decrease in SiO_2, K_2O, and Lu and the increase in MgO occur against a background of increased H_2O^+ and may result from a more intense alteration of the HREE-rich mafic minerals instead of the LREE-rich feldspar.

We compared two of the most oxidized samples of trachy-andesites (Samples 62-465A-41R-2, 90–93 cm, and 42R-3, 98–103 cm; H_2O^+ = 2.07 and 1.49 wt%; Fe_2O_3/FeO = 10.03 and 13.76, respectively) with slightly oxidized rock (Sample 62-465A-46R-1, 82–86 cm; H_2O^+ = 1.12 wt%; Fe_2O_3/FeO = 2.07) (Table **T64**). Our determination of absolute contents of elements in the studied oxidized trachy-andesites ("Appendix B", Table **AT30**) also demonstrate that, in spite of slight alteration, rocks demonstrate slight tendencies both to lose K, Na, Mn, Cu, Zn, Zr, and Rb and to gain H_2O^+, Mg, Fe_{total}, Fe_2O_3/FeO ratio, Ti, P, La, Ce, Nd, Sm, Eu, Tb, Co, Nb, Sr, and Ba. It is possible that small changes in contents of many elements (besides H_2O^+, Fe_2O_3/FeO ratio, Mn, Mg, P, Zn, Rb, Sr, and Ba) in moderately oxidized but slightly altered rocks is related not to their alteration, but to differences in chemical composition of primary fresh trachy-andesites. This result requires verification, as determination of element mobility is complicated, in our case, because of variations in vesicularity, which can not be taken into account. These samples were appropriate, however, for determination of element gain/loss in an oxidative environment, as alteration of rocks with formation of water containing minerals (primarily clay minerals) is slightly expressed. In future, comparison of oxidized trachy-andesites in Hole 465A with their fresh nonoxidized analogs, possibly from other locations (e.g., Hawaiian-Emperor Seamounts or Hawaiian Islands), will allow the determination of real values of element behavior in oxidative environments.

AT30. Major and trace elements, Hole 465A, p.93.

Brief Comments

Alteration of the upper Cretaceous (early Maastrichtian) vesicular trachy-andesites resulting from off-ridge volcanism (Seifert et al., 1981) from Hess Rise (DSDP Leg 62, Hole 465A) occurs under the smectite facies (smectite as the principal secondary mineral) throughout the 64-m-thick section. The rocks are generally slightly altered at low temperature. All studied samples of trachy-andesites and breccia are oxidized. Oxidative alteration of the rocks is identified by the formation of iron oxyhydroxides, K-feldspar, greenish yellow

smectites, and calcite. This alteration type is mainly developed in highly vesicular tops and bottoms of numerous subaerial flows.

Oxidative alteration demonstrates trends both to lose Mn, Zn, and Rb and to gain H_2O^+, Mg, Fe_2O_3/FeO ratio, P, Sr, and Ba. Variations in contents of other elements are possibly related not to the oxidative alteration of trachy-andesites, but instead, to initial differences in chemical composition of fresh rocks.

ALTERATION OF IGNEOUS ROCKS FROM INTRAPLATE RISES

Intraplate rises, ridges and plateaus, as well as chains of guyots, are giant structures of the oceanic floor. These often linear structures stretch as far as 6000 km (e.g., Ninetyeast Ridge) and demonstrate characteristic morphology, composition of igneous rocks, and lava extrusion in various environments from shallow-water and subaerial to deep-water. These structures form in variable tectonic settings: (1) along mid-ocean spreading ridges; (2) during intraplate volcanism, caused perhaps by passage over a mantle hot spot; (3) as island arcs along convergent margins; (4) as a result of tectonic uplift of older oceanic crust, perhaps with synchronous volcanism; or (5) as a combination of two or more of the above (Vallier et al., 1981). Such variability of tectonic settings causes fluctuations in chemical composition of lava flows and pillow units. Combinations of these peculiarities for intraplate rises has some specificity in comparison with mid-oceanic ridges. As a result, alteration of basalts in these structures has its own characteristic features to be studied. The study of alteration of the basalts in these structures is attractive, in that this process is of a global nature in the Phanerozoic history of the Earth as in the mid-ocean ridges.

As a rule, altered basalts recovered from intraplate rises, ridges and plateaus penetrated by drilling have not been studied in much detail, which has been necessary to complete the various leg objectives. This lack of detailed data became the reason to study some additional samples of basalts from the cores of key holes. Additionally, we have studied alteration of basalts from intraplate rises, ridges and plateaus in the eastern parts of the Indian Ocean from Ninetyeast Ridge (DSDP Leg 26, Hole 254, and ODP Leg 121, Holes 756D, 757C, and 758A) and Kerguelen Plateau (ODP Leg 120, Hole 747C and ODP Leg 183, Holes 1136A, 1137A, 1138A, and 1140A); in the central Indian Ocean during ODP Leg 115 from Mascarene Plateau (Holes 706C and 707C), Chagos Ridge (Hole 713A), and Maldives Ridge (Hole 715A); in Atlantic Ocean from Vøring Plateau (ODP Leg 104, Hole 642E), Bermuda Rise (DSDP Legs 51, 52, and 53, Holes 417A and 418A), Walvis Ridge (DSDP Leg 74, Holes 525A, 527, and 528), and Rio Grande Rise (Leg 72 DSDP, Hole 516F); and in the Pacific Ocean from Manihiki Plateau (DSDP Leg 33, Hole 317A). Alteration of the studied basalts resulted from water-rock interaction through time.

F67. Site on the Vøring Plateau, p.272.

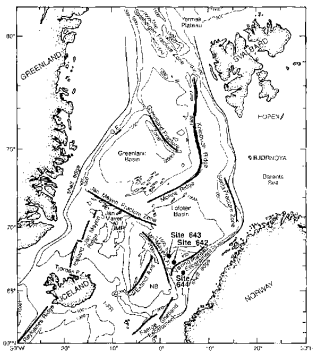

Vøring Plateau

Hole 642E

The initial opening of the Norwegian-Greenland Sea was accompanied by formation of the extrusive complex of Vøring Plateau in the rift zone (Eldholm, Thiede, Taylor, et al., 1987; Eldhom et al., 1989a, 1989b). The Vøring Plateau marginal high and other similar features in the North Atlantic are an integrated part of the North Atlantic Volcanic Province. Hole 642E (67°13.2′N, 02°55.8′E; water depth = 1289 m) is located at the outer Vøring Plateau (Fig. **F67**). The hole (depth = 1229 m) penetrated 914.4 m of basalt flows with interlayered volcaniclastic sediments and, probably, dikes. The age of oldest sediment cored is middle(?)–early Eocene (Eldholm, Thiede, Taylor, et

al., 1987).

Petrography and Bulk-Rock Chemical Composition

The penetrated volcanic section was divided into the upper series (324–1090 mbsf) and the lower series (1090–1229 mbsf) (Eldholm, Thiede, Taylor, et al., 1987). The upper series consists of 122 lava flows of aphyric to moderately plagioclase-, olivine- and, rarely, clinopyroxene-phyric oceanic tholeiite basalts of N-MORB type composition, which do not exhibit significant geochemical differences, and 3 dikes (Viereck et al., 1989; Eldholm et al., 1989a). The 55 separate interlayered volcaniclastic sediments represent ~4% of the series. The lower series is separated from the upper series by a 13.2-m-thick sediment layer. The lower series is characterized by 16 glassy, variolitic, and microcrystalline basaltic andesite flows. Six layers of interbedded volcaniclastic sedimentary rocks make up ~29% of the sections, which also contain 4 dikes (Eldholm et al., 1989a). Chemically, the flows were divided into three groups: a dacitic type, a mixture of this melt and the tholeiites, and an intermediate type. Two of the four dikes are chemically similar to their bounding flows, and the others are feeders of the upper series (Eldholm et al., 1989a; Parson et al., 1989).

We have studied 26 selected additional samples of basalts from Hole 642E (Table **T65**). All studied samples, except Sample 104-642E-102R-2, 45–47 cm (a bleached andesite), belong to tholeiitic MORB that is poorly differentiated in silicity. Basalts are represented by all varieties from aphyric through plagioclase-phyric and olivine-plagioclase-phyric basalts with intersertal, intersertal and patches with subvariolitic or subophitic, hyalopilitic, and intergranular groundmass textures, from massive to highly vesicular (see **"Appendix A,"** p.93). Naturally, this predetermines some variability in Ti (from average-Ti to high-Ti varieties), Mg, Fe, Al_2O_3, and alkaline element contents (Table **T65**). Nevertheless, these basalts are similar to normal MORB according to geochemical diagrams (Figs. **F68, F69**). Minor elements such as Cr, Ni, V, Cu, and Zr show significant variability in abundance (Table **T65**). REE distribution (Fig. **F70**) demonstrates a trend similar to that in MORB. Sample 104-642E-102R-2, 45–47 cm, is unique in geochemical characteristics, as it is andesitic in composition. The sample shows high alkalinity (especially in K), low Cr, Ni, Co, V, Cu contents, and high contents of REE, Nb, Rb, Sr, and Zr (Table **T65**).

Alteration Mineralogy

Leg 104 scientists (Eldholm, Thiede, Taylor, et al., 1987) and Viereck et al. (1989) showed that basalts in Hole 642E are slightly altered, except the uppermost 35 m where subaerial weathering has caused extensive alteration of all minerals. Olivine is completely replaced with smectite, plagioclase has suffered minor alteration to smectite in some flow units below, and clinopyroxene is generally fresh. Vesicle and vein fillings suggest the paragenesis of smectite-celadonite-calcite with or without zeolite. The secondary mineral assemblages consist of smectite, calcite, celadonite, nontronite, analcime, and heulandite in the upper part of the section. Fe smectite predominates among secondary minerals. Native Cu occurs in vesicles, fractures, and groundmass in tholeiites and associates with celadonite in flows with reddened flow tops (LeHuray, 1989). Surface weathering is located in the upper 40 m of the lava pile evidenced by the reddening of flow-top breccias and replacement of primary minerals (Viereck et al., 1989). Subaerial weathering is marked by iron oxyhydrates, halloysite, and kaolinite formation (Desprairies et al., 1989).

According to associations of secondary minerals, two types of alteration were determined. The first type of alteration is interpreted to occur at low temperature while the second was accompanied by higher temperature. The second type of alteration was superimposed on the first and is expressed in the lower 40 m of the upper series and throughout the entire lower series (Desprairies et al., 1989). The low-temperature secondary minerals consist of

T65. Basalts, Hole 642E, p.504.

F68. AFM diagram for basalts, Hole 642E, p.273.

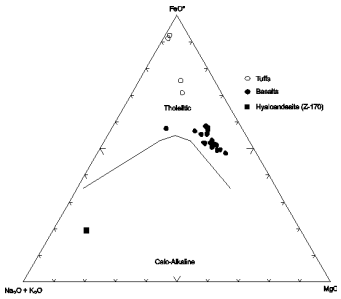

F69. Nb-Zr-Y diagram for basalts, Hole 642E, p.274.

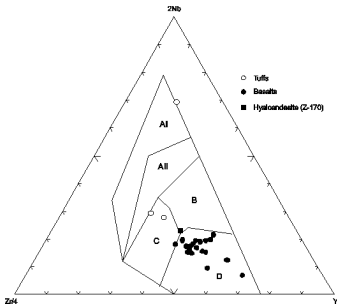

F70. Chondrite-normalized REEs for basalts, Hole 642E, p.275.

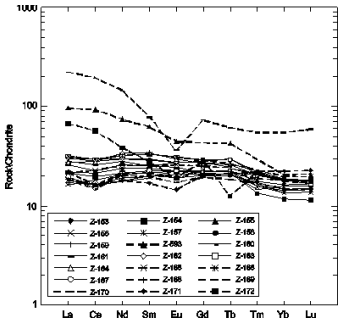

smectite, minor calcite, and celadonite, with celadonite + calcite forming later than smectite (LeHuray, and Johnson, 1989). The high-temperature alteration becomes distinct below 1044 mbsf. Below this point, discoloration increases downhole. Ankerite, quartz, and zeolites are recognized in this zone. One piece of basalt in Section 104-642E-90R-01 is bleached, possibly indicating higher alteration temperatures. The bleached zones contain SiO_2-minerals, calcite, ankerite, illite, pyrite, and clinoptilolite/heulandite. The presence of clinoptilolite suggests temperatures of 100°–130°C. Love et al. (1989) calculated temperatures of carbonate formation ranging from ~23°C near the top of the section to ~103°C at the bottom of the section.

Additionally studied selected samples of the basalts are slightly to moderately altered and demonstrate H_2O^+ variations from 0.45 to 1.85 wt% and Fe_2O_3/FeO ratios from 0.45 to 1.45 (nonoxidative type) (Table **T65**). Smectites dominate among secondary minerals (see **"Appendix A,"** p.93) and have various compositions of interlayer cations (Na-K and Ca-Mg). Smectites with Na-K interlayer cations are most abundant, as determined from XRD data. Chlorite, illite, and mixed-layer smectite-chlorite mineral sporadically occur with smectites as an admixture (see **"Appendix A,"** p.93). Smectites with carbonate fill vesicles and sporadically with carbonate replace olivine and interstitial glass and form rims around plagioclase crystals. Olivine is sometimes completely replaced by iddingsite. Clinopyroxene is fresh. Plagioclase is both fresh and replaced with smectites in the inner parts of crystals and at the contact with groundmass. Carbonate veins are present (see **"Appendix A,"** p.93). We have determined the secondary mineral assemblage that is characteristic of low-temperature alteration. Predomination of smectites among the secondary minerals shows that alteration of the basalts from Hole 642E was under the smectite facies.

The oxidative type of alteration is distributed sporadically (in a brecciated highly vesicular flow top and a basal breccia, and in an upper and a lower vesicular zones of flows) throughout the basalt section recovered from Hole 642E. The oxidized basalts (Fe_2O_3/FeO = 1.61–78.76) are more altered, with H_2O^+ contents from 1.01 to 9.14 wt% and densities decreasing to 1.80–1.48 g/cm^3 (Table **T65**). Olivine and interstitial glass is replaced by clay minerals and carbonate, vesicles are infilled with clay minerals, and veinlets contain carbonate (see **"Appendix A,"** p.93). XRD analyses show that the principal secondary mineral in oxidized basalts is smectite with Na-K-cations in interlayers (see **"Appendix A,"** p.93). The zone of subaerial weathering is reddish brown and consists of smectite with Na-K-cations in interlayers and goethite (Samples 104-642E-23R-2, 28–31 cm, and 54R-2, 83–88 cm). In Sample 104-642E-23R-2, 28–31 cm, kaolinite is principal mineral.

Bulk-Rock Chemical Changes

Based on the direct comparison of chemical composition of basalts, the Leg 104 scientists (Eldholm, Thiede, Taylor, et al., 1987) concluded that altered basalts are enriched in K_2O, Fe_{total}, Rb, and Ba; slightly enriched in Na_2O and MgO; and depleted in CaO. The high-temperature overprint did not cause significant chemical changes except in zones of discoloration, where basalts are depleted in Si, Fe, and Mg and enriched in Mn, Ca, and K.

Nonoxidized basalts in Hole 642E are slightly altered (H_2O^+ = 0.45–1.85 wt%). H_2O^+ contents from 0.84 to 1.41 wt% predominate (Table **T65**). Variation in H_2O^+ content is ~0.6 wt%; therefore, determination of element mobility is impossible, as the interval of nonoxidative alteration of basalts is very narrow.

In the lower series, a comparison of two samples, Sample 104-642E-105R-1, 64–66 cm, a fresh nonoxidized basalt (H_2O^+ = 0.86 wt%; Fe_2O_3/FeO = 0.65; density =s 2.98 g/cm^3), and Sample 104-642E-110R-1, 39–41 cm, a highly oxidized basalt (H_2O^+ = 1.64 wt%; Fe_2O_3/FeO = 10.09; density = 2.34 g/cm^3), demonstrates higher contents of H_2O^+, Fe_2O_3/FeO ratio, K, Na, La, Ce, Nd, Sm,

Zr(?), Nb, Rb, Sr, and Ba and lower contents of Si, Mg, Ca, Tb, Ni, V, Cu, and Zn in oxidized basalt than in nonoxidized fresh basalt ("Appendix B", Table **AT31**).

AT31. Major and trace elements, Hole 642E, p.95.

Brief Comments

The studied samples of basalts in Hole 642E were altered mostly in a nonoxidative environment, which is the first type of alteration. Predomination of smectites among the secondary minerals shows that alteration was under the smectite facies at mainly low temperature. Nonoxidized basalts are slightly altered, with H_2O^+ contents from 0.84 to 1.41 wt% predominate. Elements, therefore, are immobile or very slightly mobile at water-rock interaction.

Oxidative alteration is widespread throughout the basaltic section of Hole 642E (the upper and lower series) and was superimposed on nonoxidative alteration. This second type of alteration is evident in a brecciated highly vesicular flow top (average = 0.75 m), a basalt breccia (0.25 m), and in upper and lower vesicular zones, 2.5 and 0.5 m of the thickness, respectively (Desprairies et al., 1989). Active subhorizontal seawater flows were present on all levels of the basaltic section (914 m of the thickness) recovered in Hole 642E. Oxidative alteration in the basaltic section of Hole 642E is distributed differently than in Holes 504B and 332B, with oxidation occurring mainly along vertical fractures at depths of less than ~300 m into the basement (Hole 504B). Many elements in basalts are mobile during oxidative alteration. The basalts are also extremely oxidized in the subaerial weathering zone. In this case alteration of basalts begins in oxidizing conditions.

In conditions of subhorizontal seawater flows (e.g., Hole 642E), oxidized basalts show increases in H_2O^+, Fe^{+3}, K, Na, La, Ce, Nd, Sm, Zr(?), Nb, Rb, Sr, and Ba contents and decreases in Si, Mg, Ca, Tb, Ni, V, Cu, and Zn contents. Extremely oxidized breccia is depleted in Si, Ti, Mg, Ca, Na, Zr(?), Y, Sr, and Ba and enriched in H_2O^+, Fe_2O_3/FeO ratio, Al, Fe_{total}, Mn, K, Co, V, Cu, Nb, and Rb. In the extremely oxidized (iron oxyhydroxides) sample from the subaerial weathering zone, increases in H_2O^+, Fe^{+3}, Ti, Al, Fe_{total}, Mn, P, and V contents and decreases in Si, Mg, Ca, Na, Co, and Cu contents are seen. Other samples (iron oxyhydroxides) are enriched in H_2O^+, Fe_2O_3/FeO ratio, Fe_{total}, Ti, K, P(?), Zr, Y, Nb, and Rb and depleted in Si, Mn, Mg, Ca, Na, Cr, Ni, and Co. The behavior of Al, V, Zn, Sr, and Ba is different in these samples, either increasing or decreasing.

Bermuda Rise

Holes 417A and 418A

The Bermuda Rise in the West Atlantic Ocean is a broad, elliptical topographic high, 2000 km × 1000 km, with a relief of ~1.3 km. Holes 417A (25°06.63′N, 68°02.48′W; water depth = 5468 m) and 418A (25°02.10′N, 68°03.44′W; water depth = 5511 m) are located in the southern region of the Bermuda Rise (Fig. **F71**) and penetrated Cretaceous basalts. The oldest sediment cored in Hole 417A is upper Cretaceous in age (417 mbsf), and the oldest sediment cored in Hole 418A is lower Aptian (868 mbsf). Basement was penetrated to a depth of 206 m in Hole 417A, with 128.5 m recovered, and 544 m in Hole 418A, with 228.48 m recovered (Donnelly, Francheteau, Bryan, Robinson, Flower, Salisbury, et al., 1980).

F71. Sites on the Bermuda Rise, p.276.

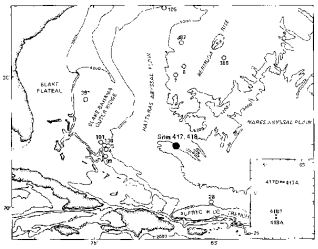

Petrography and Bulk-Rock Chemical Composition

During Leg 51 (Donnelly, Francheteau, Bryan, Robinson, Flower, Salisbury, et al., 1980) it was shown that the basement drilled in Hole 417A is represented by 15 pillow units separated by hyaloclastic pillow breccia (13%) with a thin massive basalt unit comprising 9% (~10 m thick) located near the base of the hole. The basalt is plagioclase-phyric with minor olivine and variable amounts of clinopyroxene. The massive basalts contain plagioclase,

clinopyroxene, and rare olivine. The chemical composition of the basalt represents typical MORB.

Leg 52 and 53 scientists (Donnelly, Francheteau, Bryan, Robinson, Flower, Salisbury, et al., 1980) showed that the basement drilled in Hole 418A consists of pillow basalts and pillow breccia (~80%). Massive basalt units occupy 20% and are interpreted as flows. Minor thin sedimentary layers occur throughout the section. Basalts were divided into 16 units, which vary in thickness from 7 to 113 m. The pillows have an average diameter of between 0.5 and 1.1 m. The thickness of individual units is between 2.1 and 38 m. Basalts in Hole 418A are mainly sparse to moderate plagioclase-phyric (5%–10% phenocrysts). Olivine is commonly <1% of the rock and locally as much as ~3%. Clinopyroxene is low in abundance and spinel is minor. The groundmass of phyric basalts is generally fine grained with glassy quench textures. Aphyric basalts occur in rims of pillows (few centimeters). All of the basalts are low-K tholeiites with low to moderate TiO_2 contents. Three main chemical groups were determined according to TiO_2 content: (1) low-TiO_2 (1.0–1.15 wt%), (2) moderate-TiO_2 (1.2–1.4 wt%), and (3) high-TiO_2 (1.5–1.7 wt%) groups (Donnelly, Francheteau, Bryan, Robinson, Flower, Salisbury, et al., 1980). All studied samples represent the two latter groups. On the basis of geochemical analysis of basaltic glass, Byerly and Sinton (1979) revealed that Hole 418A basalts are similar to those produced at the Mid-Atlantic Ridge and are classified as low-K tholeiites with low contents of LIL elements and strong LREE depletion (Emmermann and Puchelt, 1979; Staudigel et al., 1979).

We have studied three additional samples from Hole 417A (Units 8 and 12 [pillow lava and massive basalt units] and Unit 18) (Table **T66**). The rocks from Units 8 and 12 are represented by olivine-plagioclase-phyric basalts with hyalopilitic and pilotaxitic groundmass texture. Phenocrysts consist of olivine (2%–5%) and plagioclase (20%–25%). Basalts are sparsely vesicular (vesicles 0.3–0.8 mm in size). Dolerite from Unit 18 is plagioclase-phyric (0.7–0.8 mm plagioclase phenocrysts, ~10% of the rock) and medium grained, with ophitic-poikilophitic groundmass texture (see **"Appendix A,"** p.96). All studied basalts are tholeiitic MORB (Table **T66**).

T66. Basalts, Hole 417A, p.508.

A total of 21 additional samples were studied in Hole 418A (pillow basalts and breccia from Units 1, 5, 6B, and 13 and massive basalts from Units 2C, 14B, and 14C) (Table **T67; "Appendix A,"** p.96). Only two of the samples are doleritic texture and represent aphyric varieties. Other samples are plagioclase-phyric, occasionally with some admixture of clinopyroxene and olivine, with subvariolitic, hyalopilitic, vitrophyric, intersertal, intergranular, trachytic-subvariolitic, microlitic, and poikilophitic groundmass textures. Phenocryst abundances vary from 10% to 30%. Varieties with 20%–30% phenocrysts predominate. The rocks are sometimes slightly vesicular with 0.1–0.5 mm vesicles comprising 1%–5% of the rock. Differentiation in silicity and Fe and Mg content is poorly expressed and contents of these elements, as well as of Ca and Ti and low alkalinity, in the rocks are similar to typical MORB with relatively low contents of alkaline-earth elements and Zr (Table **T67**). The rocks also demonstrate relatively low contents and slight variability of the minor elements Cr, Ni, Co, V, and Cu (Table **T66**). Petrochemical diagrams (Figs. **F72, F73**) characterize the studied basalts as depleted tholeiitic N-MORB. This is especially apparent on REE variation diagrams, which reflect depletion in large-ion lanthanides (Figs. **F74, F75**).

T67. Basalts, Hole 418A, p.509.

F72. AFM diagram for basalts in Holes 417A and 418A, p.277.

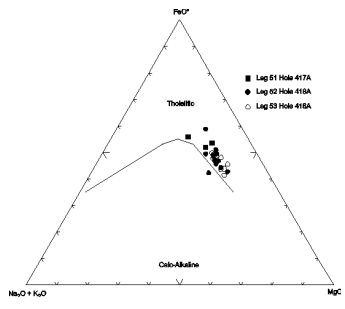

Alteration Mineralogy

Leg 52 and 53 scientists (Donnelly, Francheteau, Bryan, Robinson, Flower, Salisbury, et al., 1980) showed that basalts in Hole 418A are relatively fresh, particularly toward the base of the hole as alteration decreases downhole. The alteration is interpreted as a result of low-temperature interaction of basalts and seawater. Olivine and interstitial glass demonstrate strongest alteration and are replaced with smectite and carbonate. Downhole, olivine is often fresh. Plagioclase is commonly replaced with smectite along cleavage planes, and

vesicles are filled with calcite and/or smectite. Traces of secondary sulfides are present in some veins and in groundmass. Pink phillipsite(?) is present in the groundmass of some breccias. Humphris et al. (1979) also determined quartz, chalcedony, and opal in veins where calcite is present.

During Leg 51, it was shown (Donnelly, Francheteau, Bryan, Robinson, Flower, Salisbury, et al., 1980) that the basalts in Hole 417A were extensively altered. The basalts contain smectite, celadonite, K-feldspar, hematite, calcite, and zeolites. Fractures and interpillow voids are completely infilled with smectite, calcite, analcime, natrolite, hematite, and iron oxyhydroxides. The hyaloclastic breccias contain brownish basalt fragments. Glassy basalt debris is highly altered and surrounded with green cemented matter.

Oxygen isotope study of basalts and secondary minerals indicate that the basalts in Holes 417A and 418A were altered by seawater at low temperatures (Muehlenbachs, 1979) no higher than 50°C (Humphris et al., 1979).

Oxidative alteration is widespread in basalts in Holes 417A and 418A (Donnelly, Francheteau, Bryan, Robinson, Flower, Salisbury, et al., 1980; Humphris et al., 1979; Pertsev and Rusinov, 1979; Pritchard, 1979). The oxidation is localized along fractured and brecciated zones on the contacts of pillow lavas (i.e., oxidative alteration is distributed sporadically throughout the basalt sections) and appears to postdate most of the alteration. Light and dark brown and yellow colors, as well as secondary minerals (celadonite, limonite, hematite, iron oxyhydroxides, smectites with high Fe and K, K-feldspar, and phillipsite) indicate oxidative alteration in basalts from Holes 417A and 418A. The upper part of the basalt sequence in Hole 417A is highly oxidized (Humphris et al., 1979). Leg 52 and 53 scientists showed that in Hole 418A, iron oxyhydroxides sporadically occur in the basalt sequence down to ~400 m beneath of the top of the basement.

All samples that we studied from Hole 418A are represented by slightly altered basalts with H_2O^+ content variations of 0.13–1.43 wt%. We determined these basalts are nonoxidized, as Fe_2O_3/FeO ratio varies from 0.28 to 1.32 (Table **T66**). The only exception is Sample 52-418A-27R-2, 91–93 cm, which characterized by a slightly oxidized type of alteration (Fe_2O_3/FeO = 2.59). Two samples of hyaloclastite (Samples 52-418A-31R-2, 47–51 cm, and 134–139 cm) are oxidized with Fe_2O_3/FeO ratios of 5.94 and 4.51, respectively (Table **T66**). Smectites dominate among secondary minerals (see **"Appendix A,"** p.96) and are represented by different varieties, from pure smectite to varieties containing ~10%–30% mica layers with Na-K and Mg-Ca interlayer cations. Pure smectites dominate and smectites with Na-K interlayer cations are rare. In contrast, smectites with Mg-Ca interlayer cations are widespread in altered basalts. We have not revealed any regularity in distribution of pure smectite and smectite containing mica layers throughout the hole. Calcite, hydromica, chlorite, and talc occur as admixtures with smectite. Talc and chlorite occur in the massive basalts of the lower part of the hole (Units 14B and 14C) (see **"Appendix A,"** p.96). The sample from the massive basalt of Unit 2C contains traces of chlorite. Smectites completely replace olivine and groundmass glass. Occasionally, olivine is replaced with smectites and carbonate. Plagioclase is partly replaced by green smectites. Often, groundmass clinopyroxene is replaced with smectites. Smectites with admixtures of calcite fill vesicles and fractures. Also, vesicles and thin fractures are filled only with smectites, carbonate, or celadonite (see **"Appendix A,"** p.96).

Smectites and calcite, which represent major secondary phases in Hole 418A, provide evidence of low-temperature alteration. The presence of talc and chlorite, however, in the lower part of the section may have resulted from higher temperatures. Muehlenbachs (1979) determined the isotopic temperature for calcite in Hole 418A basalts to be between 30° and 40°C. This became grounds to stress low-temperature alteration in Cretaceous basalts in this area. All basalts

F73. Nb-Zr-Y diagram for basalts, Holes 417A and 418A, p.278.

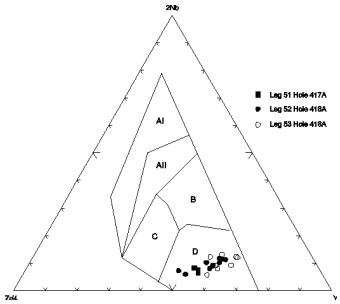

F74. Chondrite-normalized REEs for basalts, Hole 417A, p.279.

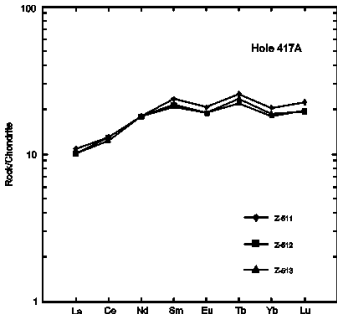

F75. Chondrite-normalized REEs for basalts, Hole 418A, p.280.

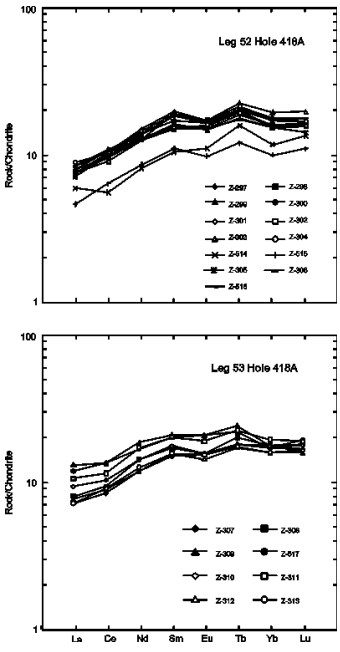

have interacted with seawater at low temperature (Friedrichsen and Hoernes, 1979; Mevel, 1979; Muehlenbachs, 1979). Calcite and smectite formed at the first stage of alteration of basalts, which was after their extrusion at ~90–110 Ma (Hart and Staugel, 1979; Rusinov et al., 1979).

It is probable that a dominant portion of calcite formed at the second stage of alteration (oxidative alteration), as shown by Robinson et al. (1977) on the example of alteration of basalts from Hole 332B, Leg 37 (Mid-Atlantic Ridge). That is why we do not exclude that temperature of vein calcite formation may reflect the second stage of alteration, which took place at significantly lower temperatures and in an oxidizing environment. This stage results from seawater descending into the crust, which migrated off the mid-oceanic ridge axis due to spreading. We suppose (Kurnosov, 1986, 1992), as have many scientists, that at the flanks of mid-oceanic ridges, this process is superimposed on the nonoxidative one. Nonoxidized alteration dominates at axial zones of mid-ocean ridges because of ascending flows of hydrothermal systems. The first stage of alteration (nonoxidative) may occur in a broad temperature range that depends on the distance of basalts from vents of hot water discharge in the center of the hydrothermal cell. To illustrate this phenomenon, one must compare alteration of basalts from axial zones of mid-ocean ridges drilled in Legs 64, 106, 139, and 169. Basalts from Legs 139 and 169 (axial valley of the Juan de Fuca Ridge) were recovered directly from the hydrothermal field. These basalts are strongly altered under the high-temperature greenschist facies. Basalts recovered during Legs 64 and 106 were altered under the lower temperature smectite facies. It is probable that varying distances from hot ascending branches of hydrothermal cells resulted in varying alteration degrees of basalts in adjacent Holes 418A and 417A.

Thus, the determined talc, chlorite, and secondary sulfides in association with smectites probably indicate that the first stage of basalt alteration in Hole 418A occurred at ~100°–150°C and at some distance from the center of ascending flows in the convective cell. Pertsev and Rusinov (1979) suppose that the temperature was relatively high during some periods of basalt alteration in Hole 418A. Temperatures of the superimposed oxidative alteration were similar to those of vein calcite formation (30°–40°C).

Three samples from Hole 417A are represented by slightly to moderately altered basalts with H_2O^+ contents varying from 0.38 to 2.38 wt% (Table **T66**). Samples 51-417A-29R-5, 58–61 cm, and 32R-2, 5–8 cm, are slightly oxidized basalts with Fe_2O_3/FeO ratios of 2.11 and 3.22, respectively, and H_2O^+ contents of 2.09 and 2.38 wt%, respectively. Basalts in Hole 417A were altered at higher temperatures than basalts in Hole 418A. Plagioclase is almost completely albitized and chloritized in Sample 51-417A-2R9-5, 58–61 cm (see **"Appendix A,"** p.96). In the fine fraction extracted from samples of basalts in Hole 417A, the XRD analyses determined smectite and mixed-layer smectite-chlorite mineral and chlorite, talc(?), hydromica, and quartz in trace amounts (see **"Appendix A,"** p.96). Muehlenbachs (1979) studied carbonates and showed that the geothermal gradient in Hole 417A is greater than that in Hole 418A: ~10°C/100 m and ~3°–5°C/100 m, respectively.

Bulk-Rock Chemical Changes

Chemical changes during alteration of basalts in Hole 418A were studied by Humphris et al. (1979). They revealed that CaO generally decreases in altered basalts, and MgO, MnO, and Fe_{total} show minor variations. Contents of K_2O and Rb increase during low-temperature alteration, whereas Na_2O contents are uniform. TiO_2, P_2O_5, and Al_2O_3 contents appear to be little affected by low-temperature alteration. Mevel (1979) recognized mobilization of Na_2O, CaO, SiO_2, MgO, Fe_{total}, and Al_2O_3 from basalts. Rice et al. (1979) showed that SiO_2, MgO, K_2O, H_2O^+, and Fe_2O_3 increased at alteration, and Al and Ti were immobile. The REEs from Ce to Yb are unfractionated relative to the fresh rocks. Ba and U contents are increased and V content is decreased. The other elements are unaffected.

We have analyzed the redistribution of chemical elements at alteration of basalts in Hole 418A. All samples are characteristic of nonoxidative alteration except Sample 52-418A-27R-2, 91–93 cm, which represents slightly oxidized basalt. Slight alteration of basalts makes determination of element mobility uncertain. The sample of slightly oxidized basalt from Hole 417A, Sample 51-417A-32R-2, 5–8 cm, contains less Si, Ca, Mg, Ni, Co, V, and Cu and more K, P, Rb, Sr, and Ba. The other elements, including REEs, are immobile at this level of alteration.

Element content of basalts in Holes 417A and 418A is given in "Appendix B", Tables **AT32** and **AT33.**

AT32. Major and trace elements, Hole 417A, p.98.

AT33. Major and trace elements, Hole 418A, p.99.

Brief Comments

Cretaceous basalts of tholeiitic N-MORB type from the Bermuda Rise are mainly altered in nonoxidative environments at low-temperature interaction with seawater under the smectite facies. Basalts in Hole 418A are relatively fresh. Basalts in Hole 417A show a stronger alteration at higher temperature than those from Hole 418A. The estimated alteration temperatures in various holes range from 10° to 80°C, and possibly to 100°–120°C. It is possible that basalts in Hole 417A were located closer to a high-temperature area of the hydrothermal system than basalts in Hole 418A. Muehlenbachs (1979) showed that the geothermal gradient in Hole 417A was greater than that in Hole 418A: ~10°C/100 m and ~3°–5°C/100 m, respectively. As a whole, the nonoxidative alteration of Cretaceous basalts in the Bermuda Rise and young basalts in the mid-ocean ridges is similar.

Oxidation of basalts spreads along subhorizontal fractured and brecciated zones and occurs sporadically in the basalt sequence to ~400 m beneath of the top of the basement (Hole 418A).

Elements are slightly mobile or unaffected at alteration in nonoxidative environments. In the oxidized basalts, contents of H_2O^+, K, Rb, Sr, and Ba and Fe_2O_3/FeO ratios are increased, while contents of Si, Ca, and Mg are decreased. Other elements, including REEs, are immobile at this level of alteration.

Manihiki Plateau

Hole 317A

Hole 317A (11°00.09′S, 162°15.78′W; water depth = 2622 m) is located near the center of the Manihiki Plateau in the Central Pacific Ocean (Fig. **F76**). The plateau is an anomalously high area surrounded by deep oceanic basins (Jackson and Schlanger, 1976). The hole penetrated 33.5 m (910–943.5 mbsf) of Cretaceous basalts, and 24.9 m of igneous rocks was recovered. The oldest sediment cored in the hole is older than Aptian–Barremian(?) age. The history of the Manihiki Plateau dates back to the extrusion of very vesicular tholeiitic basalts, probably from a spreading ridge and trapped on the Pacific plate rather than those of oceanic island type (Jackson and Schlanger, 1976; Jackson et al., 1976; Schlanger, Jackson, et al., 1976; Winterer, 1976). After the eruptive phase in the Aptian–Barremian(?), the plateau appears to have been eroded (Jenkyns and Hardy, 1976) and subsided to depths of 3000–3500 m during the last 110–120 m.y. (Lanphere and Dalrymple, 1976; Jackson, et al., 1976). The vesicular nature of basalts suggests a relatively shallow environment. Jackson et al. (1976) suggest that the Manihiki flows were erupted at water depths of <400 m (i.e., formed in a subaerial environment). Compositionally, basalts resemble those cored below the Ontong-Java Plateau (Jackson and Schlanger, 1976).

F76. Site on the Manihiki Plateau, p.281.

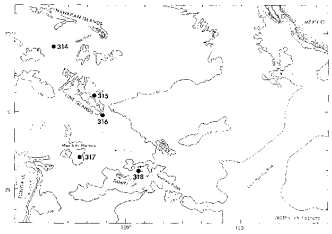

Petrography and Bulk-Rock Chemical Composition

Hole 317A penetrated the basement, which consists of thin basalt flows. Sediments occur throughout the section, including sediments of

volcanogenic origin (three intervals). As many as 10 units with thicknesses from 0.35 to 7.7 m were determined in this section (Schlanger, Jackson, at el., 1976).

Leg 33 scientists (Schlanger, Jackson at el., 1976) and Jackson et al. (1976) described the recovered basalts in detail. Basalts on Hole 317A mainly are very vesicular with "swiss cheese" tops on the lower flows, with vesicularity reaching as much as 40% of the rock and vesicles 5 cm long. The basalts contain vesicle tubes as much as 1 cm wide and 5 cm long. All 10 flow units are similar but texturally distinct. Olivine was recognized in some samples. Flow Units 1–6 contain small amounts of microphenocrysts of plagioclase, augite, and pyroxene. Groundmass from these units is very fine grained. The upper parts of flow Units 7–10 contain variable amounts of small plagioclase phenocrysts and glomeroporphyric clots of plagioclase and pyroxene in a very fine grained glassy groundmass. The lower parts of these flow units are aphyric and have coarser groundmass material. Basalts in Hole 317A are oceanic ridge tholeiites with chemical and mineral compositions that show minor variations. H_2O^+ contents are 0.72–1.80 wt%. In one sample, H_2O^+ content is 2.14 wt% (Jackson et al., 1976).

We have studied 19 additional samples of basalts from flow Units 2–7, 9, and 10 (Table **T68;** see **"Appendix A,"** p.99). Results of our description of thin sections are principally identical to those obtained the Leg 33 scientists. The studied rocks are clinopyroxene-phyric (3%–60% phenocrysts), plagioclase-clinopyroxene-phyric, plagioclase-phyric (8%–10% phenocrysts) basalts, aphyric basalts with intersertal, intergranular, microlitic, ophitic-intersertal groundmass textures, and microdoleritic basalts with patches of poikilophitic, or occasionally ophitic, groundmass texture. All samples are vesicular (0.2–5.0 mm vesicles, 5%–30% of the rock). The samples represent nondifferentiated silicity, low-Ti, and low-alkaline tholeiitic MORB (Table **T68**). Geochemical diagrams classify these basalts as tholeiites of N-MORB type (Figs. **F77, F78**) with, mainly because of Mg, a poorly expressed Fenner trend of differentiation. Judging from the content of most minor elements (Cr, Ni, Co, and V), basalts in Hole 317A are similar to typical tholeiitic MORB, though some differences, such as higher Cu and lower Zr contents (Table **T68**). The spectrum of normalized REE ratio distribution is characteristic of normal tholeiitic MORB (Fig. **F79**).

Alteration Mineralogy and Bulk-Rock Chemical Changes

Leg 33 scientists (Schlanger, Jackson et al., 1976) and Jackson et al. (1976) demonstrated that basalts in Hole 317A are moderately to highly altered, as H_2O^+ varies from 2.69 to 7 wt%. The scientists determined smectite, calcite, heulandite, celadonite, and quartz as secondary minerals. Groundmass glass is completely replaced with smectites, which are often brown smectites. Plagioclase is almost entirely replaced with smectites. Pyroxene is fresh or slightly replaced with smectites. All vesicles are partially or completely filled with brown and/or green smectite. Some calcite and zeolite with trace amounts of quartz occurs in the centers of vesicles. Celadonite is present in vesicles and replaces groundmass in Units 9 and 10.

According to our study, additional samples of basalts are fresh or slightly altered, as H_2O^+ varies from 0.10 to 1.07 wt%. They represent two types of alteration: the nonoxidative type with Fe_2O_3/FeO ratios from 0.86 to 1.57, and oxidative type with Fe_2O_3/FeO ratios from 1.62 to 2.42 (Table **T68**). Smectites predominate among secondary minerals through all basalt sections recovered from Hole 317A (see **"Appendix A,"** p.99). Smectites are represented by different varieties, from pure to those containing as much as 10% mica layers and with different compositions of Na-K and Mg-Ca interlayer cations. Pure smectite with Na-K interlayer cations dominates. Hydromica rarely occurs with smectites as an admixture. Smectites completely replace olivine and groundmass glass. Plagioclase in the central part of the basalt section is replaced with green smectites and is almost completely replaced by albite and sossurite in the lower part of the section (Sample 33-317A-34R-4,

T68. Basalts, Hole 317A, p.512.

F77. AFM diagram for basalts, Hole 317A, p.282.

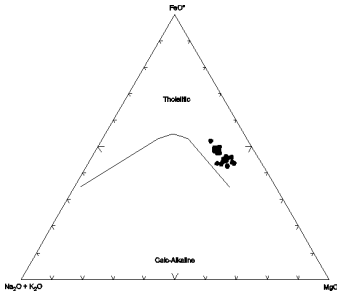

F78. Nb-Zr-Y diagram for basalts, Hole 317A, p.283.

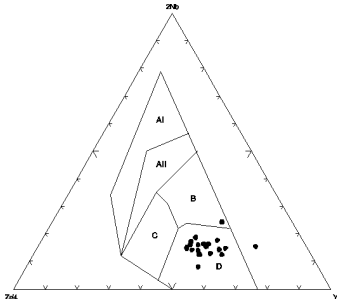

F79. Chondrite-normalized REEs for basalts, Hole 317A, p.284.

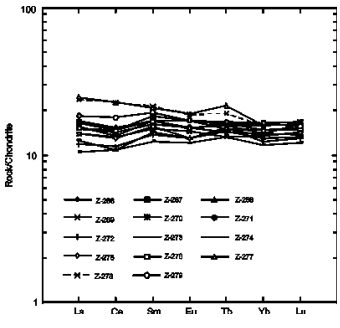

18–21 cm, and Sample 136–140 cm). Smectites or smectites with admixtures of calcite fill vesicles and fractures. The vesicles often completely or partly infill with celadonite through all basalt sections (see **"Appendix A,"** p.99). The major secondary phase, represented by smectites and calcite, is characteristic of low-temperature smectite facies alteration. Albitization of plagioclase indicates a increase of temperature in the lower part of the sequence. Celadonite and brown smectites in vesicles and groundmass show existence of oxidative alteration along highly vesicular zones of lava flows through all sequences of basalts recovered from Hole 317A. The studied samples of basalts have a weak brownish tint.

The studied samples in Hole 317A are unfavorable for determination of chemical element mobility because of very slight alteration of rocks. Maximum variation of H_2O^+ is only 0.85 wt% (Table **T68**). Element content of basalts in Hole 317A is given in "Appendix B", Table **AT34.**

AT34. Major and trace elements, Hole 317A, p.102.

Brief Comments

Cretaceous basalts of tholeiitic N-MORB type from the Manihiki Plateau are slightly altered in a nonoxidative environment at low-temperature interactions with seawater under the smectite facies. It is possible that basalts from the lowermost part of the hole are altered at higher temperature, as suggested by albitization of plagioclase.

Oxidative alteration is widespread throughout the basaltic section of Hole 317A. Basalts altered in an oxidizing environment demonstrate the association such secondary minerals as brown smectites, celadonite, and Fe hydroxides. This swiss cheese type of alteration is formed in the highly vesicular tops of the lava flow, indicating active subhorizontal seawater flows on all levels of the basaltic section (33.5 m of the thickness) recovered from Hole 317A.

As a whole, elements are slightly mobile or unaffected at slight alteration of basalts in Hole 317A.

Ninetyeast Ridge and Kerguelen Plateau

Ninetyeast Ridge is an aseismic structure stretching longitudinally along ~90°E for ~5000 km in the eastern part of the Indian Ocean. About 1000 km of its northern flank are covered with deposits of the Bengal Fan. In the south, the Ninetyeast Ridge join with the Broken Ridge, oriented along latitude 30°S. The Kerguelen Plateau is located southward from the spreading southeast Indian Ridge in the remote Antarctic sector of the Indian Ocean. It stretches for 2300 km between 46°S and 64°S (Schlich, 1975). These structures were studied during DSDP/ODP Legs 22, 26, and 121 (Ninetyeast Ridge) and Legs 119, 120, and 183 (Kerguelen Plateau). Basement rocks were recovered during these legs.

There is a widely accepted hypothesis that the Ninetyeast Ridge, the Broken Ridge, the Kerguelen Plateau, and the Rajmahal Traps (eastern India) represent volcanic products of the long-existing (during the last 120 m.y.) hotspot located near the Kerguelen-Heard Islands (Luyendyck and Rennick, 1977; Peirce, 1978; Duncan, 1978, 1981, 1991; Morgan, 1981; Royer and Sandwell, 1989; Storey et al., 1988, 1992; Weis et al., 1989; Klootwijk et al., 1991; Royer et al., 1991). The Kerguelen hotspot sources have produced a total of ~2.5×10^7 km^3 of mafic crust (Frey et al., 2003).

Cretaceous basalts exceeding Albian age drilled during Legs 119 and 120 from the transition zone and southern part of the Kerguelen Plateau possibly conjugate with Rajmahal flood basalt (Rampino and Stothers, 1988; Barron, Larsen, et al., 1989; Davies et al., 1989; Schlich, Wise, et al., 1989). The basement of the plateau was formed between 120 and 110 Ma, according to K-Ar dating (Leclaire et al., 1987; Schlich and Wise, 1992; Whitechurch et al., 1992). The Rajmahal Traps have an age of 117 Ma (Baksi, 1986). Until the

middle Eocene, the Broken Ridge was the northern part of the Kerguelen-Broken Plateau, which formed between 120 and 110 Ma at or near the axis of the spreading ridge that separated the Antarctica-Australia plate from the India plate (Munschy et al., 1992; Schlich and Wise, 1992; Royer and Coffin, 1992; Whitechurch et al., 1992). During the middle Eocene, this structure uplifted to 2500 m as a result of the intraplate rifting event (Pospichal et al., 1991; Rea et al., 1990) and was split at 45–42 Ma by the forming Southeast Indian Ridge. Later, the Broken Ridge drifted northward from 55°S to 31°S (Le Pichon and Heirtzler, 1968; Rea et al., 1990; Royer and Coffin, 1992; Munschy et al., 1992; Schlich and Wise, 1992).

At ~84 Ma, India started its motion off Australia/Antarctica. The hotspot formed the Ninetyeast Ridge in the interval between the Late Cretaceous and early Oligocene, during the northward shift of the Indian plate. This model is corroborated by the fact that elder basalts are present to the north along the Ninetyeast Ridge. Basalts vary in age from ~38 Ma (Sites 254 and 756) through 58 Ma (Site 757) to slightly >82 Ma at Site 758 (von der Borch, Sclater, et al., 1974; Duncan, 1978, 1991). The model is also confirmed by similar composition of basalts (Frey et al., 1977, 1991; Whitford and Duncan, 1978; Mahoney et al., 1983), paleomagnetic data, and geometry of the ridge (Royer et al., 1991).

The recovered basalts that cap the Ninetyeast Ridge and the Kerguelen Plateau are mainly tholeiitic and enriched in LREEs. Ferrobasalts were recognized at Sites 214, 216, and 253. Basalts at the Ninetyeast Ridge are from aphyric olivine tholeiites (Site 756) to strongly plagioclase-phyric basalts (Site 757). Basalts at Site 758 are sparsely to strongly plagioclase-phyric and have relatively high (from 8 to 10 wt%) MgO (Frey et al., 1991). Basalt flows at the Kerguelen Plateau (Site 747) are composed of aphyric to sparsely phyric plagioclase-pyroxene and olivine-plagioclase basalts (Schlich and Wise, 1992). Lavas at Sites 747, 756, and 757 formed in shallow-water to subaerial environments, whereas those at Site 758 formed in submarine environments. The studied basalts demonstrate significant fluctuations in isotope ratios from site to site. This most probably reflects varied compositions in the mantle source, which is not unusual for ridge systems (Frey et al., 1991; Saunders et al., 1991). The Ninetyeast Ridge basalts are typical OIB, which are associated with plumes on or near mid-ocean ridges. They do not contain alkaline suites and thus are inconsistent with intraplate settings, such as the Hawaiian-Emperor Chain. Basalts from the Kerguelen Plateau are transitional in composition between Indian Ocean MORB and Kerguelen-Heard islands OIB lavas. Ocean-island alkaline basalts were erupted at Site 748, the central part of the plateau. These basalts denote the existence of an uncontaminated hotspot source beneath the plateau (Shipboard Scientific Party, 1989). Formation of basalts could occur in the Kerguelen-Heard plume system, but they do not represent a simple two-component mixing of the Kerguelen plume and mid-ocean basalt mantle. A more complex model is needed to explain the formation of basalts at the Ninetyeast Ridge and Kerguelen Plateau (Storey et al., 1989, 1992; Frey et al., 1991; Saunders et al., 1991).

Researchers who studied basalts from the Ninetyeast Ridge and Kerguelen Plateau noted that all the lavas have been affected by postmagmatic alteration under low-temperature conditions. The tholeiites have been variably affected by hydrothermal alteration, as indicated by their large range of volatile contents and the nonsystematic behavior of the mobile elements with magmatic fractionation indexes (Kempe, 1974; Schlich, Wise, et al., 1989; Peirce, Weissel, et al., 1989; Frey and Sung, 1974; Storey et al., 1992; Schlich and Wise, 1992).

We have studied samples of basalts from the Kerguelen-Ninetyeast lineament recovered from Holes 254, 747C, 756D, 757C, 758A, 1136A, 1137A, 1138A, and 1140A (Fig. **F80;** Table **T69**). Holes 254 and 756D are located in the southern region of the Ninetyeast Ridge. Holes 757C and 758A are located

F80. Sites on the Ninetyeast Ridge and Kerguelen Plateau, p.285.

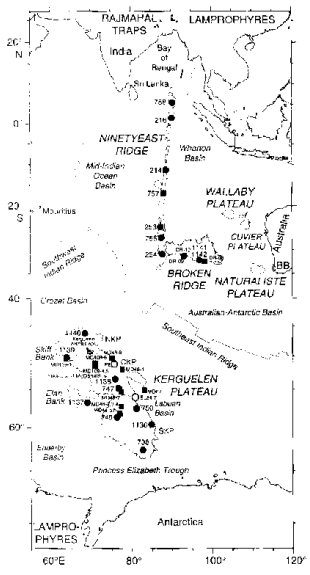

T69. Additional basement holes, Legs 26 and 120, 121, and 183, p.515.

in the central and northern regions of the Ninetyeast Ridge, respectively. Basalts were recovered from the southern, central, and northernmost parts of the Kerguelen Plateau (Holes 747C, 1136A, 1138A, and 1140A), as well as those from the eastern part of the crest of Elan Bank (Hole 1137A).

Hole 254

Petrography and Bulk-Rock Chemical Composition

About 4 m of cores were recovered from the total 42.5 m penetrated by drilling. All basalts were described as Unit 5. Magmatic rocks of Hole 254 are represented by olivine basalts, which formed in a shallow-water environment. Three types of basalts were recognized in this hole: coarse phyric basalts, altered amygdaloidal and non-amygdaloidal lavas, and completely altered fine grained autobrecciated basalts. Samples of basalts were studied by Kempe (1974) from Sections 26-254-36R-3 and 38R-1. Geochemical data obtained on two samples (Samples 26-254-36R-3, 95–97 cm, and 38R-1, 115–117 cm) indicate that volcanic rocks in Hole 254 are iron-rich tholeiitic basalts (Frey and Sung, 1974). In comparison with the second sample, the first one demonstrates higher concentrations of REE, Hf, and Ta and some enrichment in LREE.

We have studied six additional samples of basalts from Sections 26-254-35R-1, -2, and -3 and 26-254-36R-1 and -2 (Table **T70;** see **"Appendix A,"** p.102). Volcanic rocks in Hole 254 are represented in our set as follows: (1) sparsely olivine-microphyric basalts from massive (Samples 26-254-35R-1, 123–125 cm, and 35R-2, 105–107 cm) to sparsely vesicular (Sample 26-254-35R-3, 72–75 cm), and (2) aphyric olivine basalts from sparsely vesicular (Sample 26-254-36R-1, 140–143 cm) to vesicular (Samples 26-254-36R-2, 2–4 cm, and 114–118 cm). All studied samples are moderately altered (see **"Appendix A,"** p.102).

T70. Basalts, Hole 254, p.516.

According to our data (Table **T70**), the studied rocks represent a practically nondifferentiated, slightly unsaturated by silica iron-titanium series of basalts. The series is characterized by some fractionation of olivine that results in the formation of sparsely olivine-microporphyric and aphyric basalts. In general, these basalts demonstrate a low abundance in alumina but are slightly enriched in Ti and Mg in comparison with normal MORB. In the AFM diagram, data plot in the field of the tholeiitic series, which starts the Fenner trend of differentiation of Fe-Ti basalts (Fig. **F81**), as is known for basalts of the islandite series from the Galapagos Islands and Iceland. Nevertheless, the studied basalts demonstrate lower SiO_2 and partial Al_2O_3 in comparison to the latter ones (McBirney and Williams, 1969; Perfiljev et al., 1991).

F81. AFM diagram for basalts, Holes 254, 756D, 757C, and 758A, p.286.

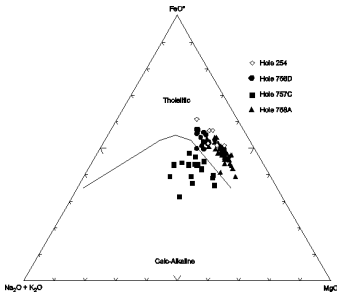

In the Zr-Nb-Y diagram, data plot mainly in the B field, which characterizes E-MORB (Fig. **F82**). Compact distribution of REE on the diagram (Fig. **F83**) is in good accordance with the petrographic homogeneity of rocks. According to this diagram, olivine basalts in Hole 254 are slightly enriched in large-ion lanthanides and their general geochemical trends occupy an intermediate position between trends of E-MORB tholeiites and intraplate basalts of oceanic islands.

F82. Nb-Zr-Y diagram for basalts, Holes 254, 756D, 757C, and 758A, p.287.

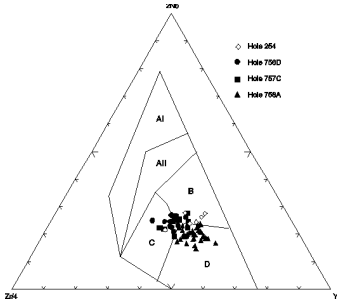

Contents of Cr, Ni, V, and Co in the studied rocks are slightly higher than contents of these elements in normal MORB (Table **T70**). This is possibly due to higher contents of Fe and Ti (geochemical affinity) in the studied basalts. Possibly these basalts represent products of the depleted mantle from the deeper source of initial melts in comparison with normal MORB. In general, contents of principal rock-forming and rare earth elements of basalts in Hole 254 are similar to data from other samples that were described during Leg 26 (Kempe, 1974; Frey et al., 1991).

Alteration Mineralogy

All studied samples from Cores 35 and 36 are moderately altered with H_2O^+ contents from 2.2 to 4.08 wt% (Table **T70;** see **"Appendix A,"** p.102).

The predominant secondary mineral is smectite (Table **T71**).

Smectite completely replaces olivine and groundmass glass. Plagioclase is partly replaced with smectite. Smectite with an admixture of carbonate fills vesicles (see **"Appendix A,"** p.102). Other clay minerals include traces chlorite and rare swelling chlorite.

Two samples from the lower portion of the section of recovered basalts (Samples 26-254-36-3, 95–97 cm [amygdaloidal basalt], and 26-254-38-1, 115–117 cm [autobrecciated basalt]) are also moderately altered with H_2O^+ contents of 1.72 and 4.09 wt%, respectively (Kempe, 1974). The lowest sample of autobrecciated basalt from Hole 254 is the most altered, containing 75% smectite. Plagioclase and pyroxene are considerably less altered (Kempe, 1974). The amygdules are filled with green spherulitic bowlingite, chlorite, or calcite. The calcite occupies the center. Olivine in this rock is replaced by iddingsite. Nonamygdaloidal laves are similarly altered in this group of rocks. Amygdules are filled with chlorite and some admixture of carbonate (Kempe, 1974). Our data provide evidence that amygdules are filled with smectite instead of chlorite.

Secondary mineral assemblages in basalts from Hole 254 are characteristic of low-temperature alteration. Rocks in Cores 35R and 36R were described during the shipboard study as dark basalt. Iron oxide occurred in amygdaloidal basalt which was sampled in the uppermost part of Core 36R (Kempe, 1974).

Bulk-Rock Chemical Changes

Basalts in Hole 254 are relatively similar in both petrographic and petrochemical composition. We have determined three groups as follows: (1) nonoxidized massive and sparsely vesicular (as much as 1%), (2) oxidized and sparsely vesicular (as much as 1%), and (3) oxidized and vesicular (5%–10%) basalts. Element content in basalts from Hole 254 in g/1000 cm^3 is given in "Appendix B", Table **AT35.**

During nonoxidative alteration, basalts in Hole 254 (H_2O^+ = 2.26–4.03 wt%, Fe_2O_3/FeO = 0.92–1.32) (Table **T70**) accumulate Mg, Mn, and REE (except Ce), as well as Sc, Cr, Ni, and Co. Simultaneously, basalts lose Ca, Na, and possibly Ti, as well as Sr, Zr, and Ba.

During oxidative alteration, the slightly oxidized basalt (H_2O^+ = 3.07 wt%, Fe_2O_3/FeO = 1.7) (Table **T70**) shows gains of various intensity of K, Na, Mn, and possibly Ti and Al, as well as REE, Sc, V, Y, Nb, Ba, and especially Rb. Oxidized basalts lose Si, Ca, Mg, Cr, Ni, and Co.

Most oxidized altered vesicular basalts, with Fe_2O_3/FeO ratios as much as 6.79 and H_2O^+ contents of 3.80 and 4.35 wt%, accumulate K, Na, Mn, and possibly Fe, P, Ti, and Al, as well as REE, V, Cu, Nb, Rb, Sr, and Zr.

The mobility data of Ti, Al, Cr and Zr are unclear. This may be because of primary variations of their contents in the rock. At the same time, Fisk and Howard (1990) have determined high contents of TiO_2 (from 5.12 to 14.96 wt%) in smectites from veins and vesicles (Leg 115 Hole 706C, Mascarene Plateau). Moreover, they determined high contents of Al_2O_3 (as much as 11.97 wt%) and an admixture of Cr_2O_3 (0.04 wt%) in these smectites. This may provide evidence of mobility of Ti, Al, and Cr during low-temperature alteration of seamount basalts.

REE mobility is not a surprise, as some highly altered MORB show mobilization of all elements, including REE and Th (Bienvenu et al., 1990).

The simultaneous gain of REE, Mn, and Sc in both nonoxidized and oxidized basalts most probably results from similarity of Fe_2O_3/FeO ratios in these varieties.

At this time, the obtained mass balance data do not provide a single answer about the real mobility of chemical elements due to alteration of basalts

F83. Chondrite-normalized REEs for basalts, Holes 254, 756D, 757C, and 758A, p.288.

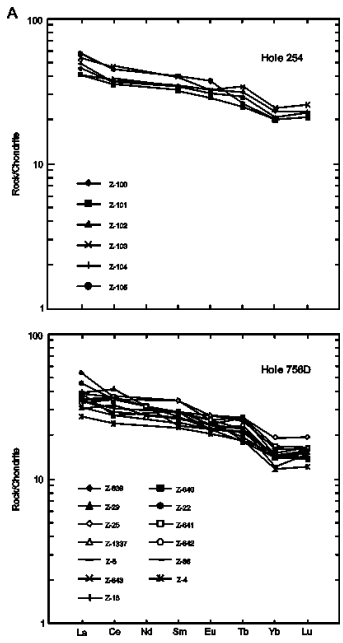

T71. Altered basalts, Hole 254, p.517.

AT35. Major and trace elements, Hole 254, p.104.

in Hole 254. Fresh or relatively fresh basalts are absent among studied samples, so we have no reference data to compare altered basalts. Moreover, each of the three studied groups of basalts contain samples of rocks altered in a narrow interval with H_2O^+. Each of the three groups of basalts is represented by an insufficient number of samples that hampers valid statistical analysis of element mobility. Thus, the obtained results permit us to discuss only probable trends in gain-loss of matter due to alteration.

Hole 756D

Petrography and Bulk-rock Chemical Composition

In Hole 756D, 26.92 m of basement was recovered from a penetration of 82 mbsf. The units represent subaerial lava flows with thicknesses of 2–6 m (Peirce, Weissel, et al., 1989).

Frey et al. (1991) studied 15 samples in great detail from 10 of the 14 flow units (1, 2, 4, 5, 6, 7, 9, 12, 13, and 14). It was recognized that the basalts are predominantly aphyric or sparsely plagioclase-phyric, massive, vesicular, and sparsely amygdaloidal. Lavas in Hole 756D are tholeiitic (Peirce, Weissel, et al., 1989; Frey et al., 1991; Saunders et al., 1991).

We studied 13 additional samples from seven flow units (5, 6, 7, 8, 9, 13, and 14) in Hole 756D (Table **T72;** see **"Appendix A,"** p.104). Eight of them are represented by aphyric basalts. Others samples represent sparsely plagioclase-phyric basalts. In all cases, the groundmass texture is similar (intergranular-microdoleritic). The basalts are vesicular and massive (see **"Appendix A,"** p.104). The degree of vesicularity is low (as much as 5%) vesicle sizes are 0.2–2 mm.

T72. Basalts, Hole 756D, p.518.

Judging from SiO_2, Al_2O_3, Mg, and alkaline contents, element contents characterize these basalts as normal tholeiitic MORB that demonstrate slight variations in Ti contents and some enlarged contents of Fe (Table **T72**). In the AFM diagram, they plot in the tholeiitic field with poorly exposed Fenner's trend that is indicative of poor differentiation of the magmatic melt and its enrichment in Fe (Fig. **F81**). The Zr-Nb-Y diagram shows that data plot in two fields, B and C, which correspond to enriched MORB and tholeiites of intraplate oceanic islands (Fig. **F82**). These characteristics (total alkalinity and relationships of Zr, Ti, Nb, and Y) indicate that basalts in Holes 254 and 756D are similar and practically nondifferentiated.

The distribution of chondrite-normalized REE in basalts in Hole 756D is characterized by the broader spectrum of contents in comparison with basalts in Hole 254 (Fig. **F83**). In the studied basalts, these parameters are slightly higher than in MORB and show similarity with tholeiites from the Hawaiian Islands. The difference is that in our case, we determined slight enrichment in large-ion lanthanides.

Contents of Cr, Ni, V, and Co in basalts in Hole 756D are lower than in basalts in Hole 254 (Table **T72**) and are similar to that in MORB. This is due to the various contents of Fe, Mg, and Ti in compared basalts, and in general our geochemical data on studied samples is similar to that obtained by Frey et al. (1991).

Alteration Mineralogy

All studied samples of basalts demonstrate relatively slight alteration (see **"Appendix A,"** p.104). H_2O^+ ranges from 0.24 to 1.89 wt% (Table **T72**). The predominant secondary mineral is smectite (Table **T73**). A mixed-layer smectite-chlorite is present together with smectite in two samples. Chlorite, mixed-layer smectite-chlorite, and hydromica are present as an admixture together with smectite in some samples (Table **T73**). Often smectite completely replaces olivine and groundmass glass (see **"Appendix A,"** p.104). Replacing olivine smectites either are brownish red and brown (or iddingsite) or are

T73. Altered basalts, Hole 756D, p.520.

grassy-green in color. In some olivines inner parts are replaced with brown or red smectite (iddingsite), whereas marginal parts are replaced with grassy-green smectite. Plagioclase phenocrysts show minor replacement by pale green smectite, and pyroxenes are partly replaced by smectite. The grassy-green smectite fills microcracks. Individual microcracks are filled by brownish red smectite. Carbonates are recognized in central parts of microcracks. Fe hydroxides occurs with smectites and carbonate in cracks. Walls of vesicles are covered by radial zonal aggregates of grassy-green smectite impregnated with Fe hydroxides. Small vesicles are completely filled with smectite (see **"Appendix A,"** p.104). Opaque minerals are partly oxidized. Neither shipboard party of Leg 121 and Saunders et al. (1991) nor we have determined zeolites in basalts in Hole 756D.

Other samples of basalts from Hole 756D (Peirce, Weissel, et al., 1989; Frey et al., 1991) contain smectite, zeolite, calcite, and goethite in vesicles and veins (Table **T73**).

According to the terminology of Bass et al. (1973, 1976), two types of alteration, oxidative and nonoxidative, are recognized in Hole 756D. Oxidative alteration is determined in all units. The margins of flow units are oxidized, and the alteration penetrates as much as tens of centimeters into the flow unit. This oxidative alteration is also expressed as haloes around veins with calcite (Peirce, Weissel, et al., 1989; Saunders et al., 1991). Iron oxides and hydroxides occur in many of the studied samples (Table **T73**). The central parts of several flow units have a dark gray color. According to Frey et al. (1991) and Saunders et al. (1991), petrographic study provides evidence that the oxidative alteration postdates the nonoxidative alteration.

Bulk-Rock Chemical Changes

Slightly altered basalts in Hole 756D do not show significant variations in content of chemical elements. Rb represents an exception as its content in altered basalts increases to several times. The shipboard study (Peirce, Weissel et al., 1989), Frey et al. (1991), and Saunders et al. (1991) have shown that oxidized basalts from Hole 756D demonstrate increases in K, Rb, and Fe_2O_3 and some decreases in CaO and MgO. Similar abundances of REE, P, Y, Zr, Hf, Nb, Ta, and Th were determined in both oxidized and nonoxidized sections of basalts in Hole 756D (Frey et al., 1991).

Basalts in Hole 756D are slightly altered in both oxidizing and nonoxidizing environments (H_2O^+ = 0.69–1.15 wt% and 0.24–1.42 wt%, respectively) (Table **T72**). Oxidized basalts contain more Fe, K, and Rb but less Ca than nonoxidized basalts. Most trace elements are immobile or very slightly mobile with this slight level of alteration ("Appendix B", Table **AT36**).

AT36. Major and trace elements, Hole 756D, p.105.

Hole 757C

Petrography and Geochemistry of Basalts

A total of 19 flow units representing 24.95 m of recovered core from a total penetration of 48.3 mbsf were recognized in Hole 757C. The units represent subaerial lava flows, and all of the rocks are moderately to highly plagioclase-phyric basalts. Aphyric basalts are absent, which is in marked contrast to basalts in Hole 756D. Most of the basalts are vesicular (as much as 25%). Several flow units demonstrate cavities >10 mm in diameter. The proportion of vesicles is higher than in basalts in Hole 756D. The degree of basalt alteration varies from slight to strong (Peirce, Weissel, et al., 1989).

Frey et al. (1991) have studied in great detail 19 samples from 12 flow units (1–14 and 16–19) in this hole. Most basalts are plagioclase-phyric with 40%–50% of plagioclase megacrysts and glomerocrysts and rare clinopyroxene phenocrysts in altered groundmass. Much of the basalts are highly altered. Lavas in Hole 757C are tholeiitic basalt (Peirce, Weissel, et al., 1989; Frey et al., 1991; Saunders et al., 1991).

We studied 18 additional samples from flow Units 2, 3, 5, 7, 9, 10, 12, and 18 (Table **T74;** see **"Appendix A,"** p.106). In our set of samples, igneous rocks in Hole 757C are represented by poorly differentiated plagioclase-phyric basalts that are massive and sparsely to highly vesicular. Vesicular basalts predominate. Vesicles are 30%–40% of the rock and between 0.2–1.5 and 2.5–8 mm in diameter. The basalts demonstrate significant variation in plagioclase phenocrysts (from 5%–7% to 60%). Groundmass has mainly intergranular/microlitic texture, and some basalts have pilotaxitic or vitrophyric texture. Rock from flow Unit 18 (Sample 121-757C-12R-1, 84–86 cm) is clinopyroxene-plagioclase-phyric basalt. Phenocrysts of clinopyroxene are as much as 1%. Sample 121-757C-9R-4, 38–42 cm, is olivine-plagioclase phyric basalt (olivine phenocryst = 5%).

T74. Basalts, Hole 757C, p.521.

According to chemical composition, these basalts represent normally silicic low-Ti and low-Fe varieties. MgO broadly varies from 3.58 to 7.49 wt%. Al_2O_3 also varies significantly from 15.78 to 23.54 wt% (Table **T74**). Thus, these basalts show affinity to high-alumina basalts. Such peculiarities in distribution of major elements may be explained by plagioclase fractionation in magmatic melt.

In the AFM diagram, data plot in the calc-alkaline field with typical Bouen's trend, which reflects low-Fe composition of magmatic melt (Fig. **F81**). In the Zr-Nb-Y diagram, data plot in the B, C, and D fields, which characterize normal and enriched MORB as well as tholeiites of intraplate oceanic islands (Fig. **F82**).

The distribution of normalized ratios of REE is notable. On one hand, there is some enrichment in large-ion lanthanides in this group of elements, as observed in basalts in Holes 254 and 756D. On the other hand, they demonstrate broader variations in their contents, lower total contents in highly plagioclase-phyric basalts, and significantly high contents in clinopyroxene varieties of flow Unit 18 (Samples 121-757C-12R-1, 84–86 cm, and 12R-2, 8–10 cm). Basalts from flow Unit 18 demonstrate some deficit in Eu (Fig. **F83**) that may have resulted from both plagioclase fractionating and similarity of their trends to those of alkaline basalts.

Thus, Hole 757C penetrated some geochemical variability of basalts that probably reflect slight differentiation during crystallization (fractionation of plagioclase).

Alteration Mineralogy

All studied samples of basalts from Hole 757C demonstrate various degrees of alteration (see **"Appendix A,"** p.106). H_2O^+ contents vary from 0.89 to 6.66 wt% (Table **T74**). The dominant secondary mineral in the basalt section in Hole 757C is represented by smectite. In some samples from the interiors of the flows, minerals of chloritic phases (mixed-layer smectite-chlorite mineral and swelling chlorite) are widespread or dominant. Analcime, natrolite, heulandite, and calcite were also determined (see **"Appendix A,"** p.106; Table **T75**). Smectite, chlorite, Na and Na-Ca zeolites, calcite, opal, and Fe-Mn oxides and hydroxides in vesicles and veins are recognized in other samples from Hole 757C (Peirce, Weissel, et al., 1989; Frey et al., 1991). K-feldspar occurs mainly in plagioclase phenocrysts (Table **T75**).

T75. Altered basalts, Hole 757C, p.524.

Olivine is completely replaced with smectite and aggregate of smectite and chlorite. In some cases, carbonate replaces central parts of olivine (see **"Appendix A,"** p.106). Volcanic glass around phenocrysts of plagioclase or included in plagioclases is completely replaced with smectite. Phenocrysts of plagioclase are significantly replaced with chlorite-smectite and occasionally carbonatized, albitized, or zeolitized. Some groundmass plagioclases are oxidized. Zeolite occurs along margins and in microcracks of plagioclase. Cracks in plagioclases and clinopyroxenes are filled with smectite. Opaque minerals are partly oxidized. Volcanic glass occurs in vesicles and is mostly

replaced with smectite-chlorite aggregate, Fe and Mn(?) oxides, radial aggregates of smectite and chlorite, and calcite. Small vesicles are completely filled with smectite-chlorite aggregate. Larger vesicles are filled with carbonate, chalcedony and cristobalite-tridymite, or zeolite. Veins of smectite are present.

As in Hole 756D, oxidative and nonoxidative alteration is recognized in Hole 757C. The oxidative zones are restricted to the uppermost flow units (Peirce, Weissel, 1989; Frey et al., 1991; Saunders et al., 1991). Iron oxides and hydroxides are recognized in basalts (Table **T75**).

Bulk-Rock Chemical Changes

Nonoxidized altered basalts (Fe_2O_3/FeO = 0.98–1.24) in Hole 757C are all slightly altered (H_2O^+ = 1.00–1.17 wt%) (Table **T74**). This results in immobile elements at this interval of alteration. Slightly oxidized more altered basalts (H_2O^+ = 0.91–2.63 wt%, Fe_2O_3/FeO = 1.77–2.41) demonstrate gains of K, Fe, Mn, P, and probably Mg, as well as REE, Zn, Y, Nb, Rb, Zr, and Ba against the background of loss of Ca (Table **T74**). More altered oxidized basalts (H_2O^+ = 4–6.66 wt%, Fe_2O_3/FeO = 4.2–7.8) are highly vesicular (30%–40%) and the most interesting for study of bulk-rock chemical changes at their alteration. Fresh analogs of these rocks with the same vesicularity were needed to estimate the mass-balance. Fresh vesicular rocks were not recovered from Hole 757C, and because of this, we used the direct chemical compositions of the rock for estimation of bulk-rock chemical changes. It should be taken into account, however, that the obtained results may not coincide with the real element gain/loss. Comparing the chemical composition of the strongly altered, oxidized, highly vesicular basalt (Sample 121-757C-12R-2, 75–79 cm; H_2O^+ = 5.12 wt%, Fe_2O_3/FeO = 7.88) with slightly altered, nonoxidized nonvesicular basalt (Sample 121-757C-12R-1, 84–86 cm; H_2O^+ = 1.39 wt%, Fe_2O_3/FeO = 0.73), shows that the highly altered basalt contains less CaO, Sr, SiO_2, and Al_2O_3, whereas the contents of most elements in this sample are higher, including REE. At the same time, an increase of Fe_{total}, MnO, K_2O, MgO, Na_2O, P_2O_5, and Rb occurs often in highly altered oxidized basalts in intraplate rises.

Element contents of basalts in Hole 757C are given in "Appendix B", Table **AT37.**

AT37. Major and trace elements, Hole 757C, p.107.

Hole 758A

Petrography and Bulk-Rock Chemical Composition

There are 29 basaltic units representing 118.54 m of recovered core from a total penetration of 177.9 mbsf in Hole 758A. Flows vary in thickness from <2 m to >20 m. Basalt units in Hole 758A are divided into three categories: (1) Massive basalt Units 1, 2, 3, 7, 10, 11, and 17, (2) thin sheet flow Units 4, 5, 6, 8, 9, 12–16, 18, 20, 22, 24, 26, and 27, and (3) pillow basalts Units 19, 21, 23, and 25. These flows were erupted in a deepwater environment. The units are phyric, sparsely plagioclase-phyric, or clinopyroxene- and plagioclase-phyric basalts. Olivine is a rare phenocryst phase and does not occur in the massive flows. All basalts are altered (Pierce, Weasel, et al., 1989).

Frey et al. (1991) studied 37 samples of basalts from 24 flow units in Hole 758A (Units 1–5, 7, 10, 11, 13–15, and 17–29). Most basalts are aphyric and sparsely plagioclase-phyric or plagioclase-clinopyroxene-glomerophyric. Lavas in Hole 758A represent tholeiitic basalts (Peirce, Weissel, et al., 1989; Frey et al., 1991; Saunders et al., 1991).

We studied 46 additional samples from flow Units 1–4, 5, 7, 10, 11, 14, 17, 19, 21, 22, 25, 27, and 29 (Table **T76;** see **"Appendix A,"** p.110). Igneous rocks in Hole 757C are represented in our set of samples by aphyric and sparsely plagioclase- and clinopyroxene-plagioclase phyric (massive, sparsely vesicular, and vesicular). There is no obvious trend in distribution of aphyric and phyric basalts along the section. Basalts demonstrate intersertal to intergranular, microlitic, pilotaxitic, intersertal, intersertal-microdoleritic,

T76. Basalts, Hole 758A, p.526.

vitrophyric, and hyalopilitic groundmass textures.

Judging from silicity, basalts represent normal MORB type, high Mg, ferruginous, and low alumina, with typical MORB content of Ti. Plagioclase-phyric basalts from flow Unit 4 (Samples 121-758A-62R-1, 57–59 cm, and 62R-3, 27–29 cm) represent an exception, as they are enriched in Al_2O_3 but low in Ti and relatively low in Fe (Table **T76**). This is probably due to fractionation of plagioclase.

In general and according to petrographic and petrochemical characteristics, the studied rocks represent practically nondifferentiated basalts of oceanic tholeiitic series. In the AFM diagram, all data plot in the tholeiitic field with distinct Fenner's trend of differentiation (Fig. **F81**). In the Zr-Nb-Y diagrams, all data plot in the D field, which is characteristic of the genetic group of normal MORB (Fig. **F82**).

The variation diagram of normalized ratios of REE indicates that the majority of samples have trends that are characteristic of normal tholeiitic MORB with very slight expressions of accumulation of large-ion lanthanides in comparison with MORB basalts (Fig. **F83**). The comparison of these data with data from Holes 254, 756D, and 757C shows some slight difference in the character of REE distribution, in that REE contents of the above mentioned holes are higher than those in basalts in Hole 758A. Also, they demonstrate some greater degree of enrichment in large-ion lanthanides.

Concentrations of Cr, Ni, V, and Co are near to those in MORB but demonstrate significant variations, especially in contents of Cr and V (Table **T76**).

In general, any systematic variations in composition of major or minor elements are absent in the section of Hole 758A.

Alteration Mineralogy

Basalts in Hole 758A show various degrees of postmagmatic alteration (5%–90%) (see **"Appendix A,"** p.110). H_2O^+ varies from 0.88 to 3.6 wt%, but predominantly with H_2O^+ contents of 1.1–2.0 wt% (Table **T76**). On the whole, these contents of H_2O^+ demonstrate predomination of low level alteration of basalts in Hole 758A.

Smectites dominate in altered basalts in Hole 758A (Table **T77**). Pseudomorphs of olive-green smectite upon olivine are present. Interstitial volcanic glass is completely replaced with olive-green or green clay minerals, sometimes with zeolite. Phenocrysts of plagioclase are replaced in their central parts with smectite. Clinopyroxenes are partly replaced with olive-green smectite along marginal parts of crystals. Microcracks in plagioclases and clinopyroxenes are filled with smectite. Vesicles are completely filled with clay minerals and inner parts are represented by radial aggregates, whereas peripheral rims are built of brownish green aggregate. Several vesicles are infilled with carbonate, and veins of smectite are present (see **"Appendix A,"** p.110).

Smectite predominates in other samples of altered basalts from Hole 758A (Peirce, Weissel, et al., 1989; Frey et al., 1991). All basalts are pervasively altered, with replacement of groundmass mesostasis and filling of vesicles and fractures with smectites. Chlorite(?), ankerite, and opal in vesicles and veins are very rare. K-feldspar was recognized in plagioclase phenocrysts in a single sample of basalt (Sample 121-758A-54R-2, 70–74 cm). Secondary sulfides are present along the section of basalts in Hole 758A (Table **T77**). Sulfides are represented by pyrite and chalcopyrite. The latter contains 2%–3% of both Ni and Co (Frey et al., 1991). Zeolites were recognized by Frey et al. (1991) in all parts of the basalt section. Calcite occurs dominantly in the upper part of Hole 758A (Table **T77**). The results of our study and data obtained by Frey et al. (1991) show that smectite/chlorite and chlorite/smectite, which were determined during the shipboard study, are represented by smectites (Table

T77. Altered basalts, Hole 758A, p.533.

T77). Also, chlorite was determined by Frey et al. (1991) with some uncertainty. Results of our study show the absence of chlorite in the studied samples.

Contrary to Holes 756D and 757C, any evidence of oxidative alteration is absent in Hole 758A (Peirce, Weissel, et al., 1989; Saunders et al., 1991). Nevertheless, our results from Hole 758A have shown that the basalts are oxidized in various degrees. Fe_2O_3/FeO ratios vary from 1 to ~2 (Table **T76**). The basalts are mainly nonoxidized, but several samples are slightly oxidized. Secondary mineral assemblages are represented mainly by olive-green and green smectite. Zeolites are present. Sulfides were recognized only in Hole 758A. Sulfides have not been determined in Holes 254, 756D, and 757C.

Bulk-Rock Chemical Changes

For estimation of bulk-rock chemical changes, the basalts in Hole 758A were divided into two main groups: massive and vesicular.

The group of massive rocks includes nonvesicular and sparsely vesicular (<1%) basalts. Aphyric basalts predominate in this group. Plagioclase phyric basalts with <2%–3% phenocrysts were also included. As a whole, the basalts of the massive group are slightly altered. H_2O^+ contents are from 0.88 to ~2 wt% (Table **T76**). Determination of element mobility is uncertain, as the interval of alteration of massive basalts is narrow. Only two samples are moderately altered (Sample 121-758A-57R-3, 7–9 cm, and 68R-3, 106–108 cm; H_2O^+ = 2.69 and 2.90 wt%, respectively) and slightly oxidized (Fe_2O_3/FeO = 1.73 and 1.98, respectively) (Table **T76**).

The group of vesicular basalts includes rocks with vesicularity from 5% to 40%. Aphyric basalts predominate. As a whole, vesicular basalts, as with the massive basalts, are slightly altered (H_2O^+ = 1.19–2.27 wt%). Rare samples contain as much as 2.68-3.61 wt% H_2O^+ are nonoxidized or slightly oxidized (Fe_2O_3/FeO = 1.14–1.85) (Table **T76**). Several samples are somewhat more oxidized and have Fe_2O_3/FeO ratios from 2.15 to 2.30. For estimation of bulk-rock chemical changes of vesicular basalts, were chose three samples: (1) relatively unaltered basalt (Sample 121-758A-71R-3, 87–89 cm; H_2O^+ = 1.28 wt%, Fe_2O_3/FeO = 1.19), (2) moderately altered nonoxidized basalt (Sample 121-758A-67R-4, 78–80 cm; H_2O^+ = 2.97 wt%, Fe_2O_3/FeO = 1.58), and (3) moderately altered slightly oxidized basalt (Sample 121-758A-73R-3, 85–87 cm; H_2O^+ = 2.68 wt%, Fe_2O_3/FeO = 2.15). All of these samples are aphyric basalts with hyalopilitic groundmass texture (see **"Appendix A,"** p.110). Their fresh vesicular analogs are absent; therefore, we used direct chemical compositions of the rocks for estimation of bulk-rock chemical changes (Table **T76**).

Comparing the chemical composition of the moderately altered nonoxidized vesicular basalt (Sample 121-758A-67R-4, 78–80 cm) with relatively unaltered basalt (Samples 121-758A-71R-3, 87–89 cm) and not taking into account rock density, we found that the strongly altered basalt contains less CaO, MnO, SiO_2, Yb, Lu, and Y and more MgO, K_2O, La, Tb, Eu, Ba, and Sr than the relatively unaltered basalt. Al_2O_3 content weakly increases in Sample 121-758A-73R-3,85–87 cm.

Element contents in basalts in Hole 758A are given in "Appendix B", Table **AT38.**

AT38. Major and trace elements, Hole 758A, p.110.

Holes 747C, 1136A, 1137A, 1138A, and 1140A

The results of study of alteration of basalts and their chemical composition from Holes 747C, 1136A, 1137A, 1138A, and 1140A in the Kerguelen Plateau were published by Kurnosov et al. (2003) and Artamonov and Zolotarev (2003).

Petrography and Bulk-Rock Chemical Composition

The basalts from the Kerguelen Plateau are represented by aphyric and sparsely phyric varieties (Coffin, Frey, Wallace, et al., 2000). **"Appendix A,"** p.117, summarizes the petrographic compositions of the samples studied. Aphyric basalts dominate in most Leg 183 holes. Rare phyric basalts prevail in Holes 1140A and 1137A. Phenocrysts are represented mainly by plagioclase; phenocrysts of olivine and clinopyroxene are rare (Hole 1137A). The total quantity of phenocrysts within phyric basalts varies from single crystals to 25% of the rock volume. The degrees of both crystallinity and vesicularity of the basalts vary greatly. Massive basalts are rare but most common in the northern part of the Kerguelen Plateau (Hole 1140A). Less vesicular basalts are recognized in Holes 1136A and 1138A. Both intergranular and intersertal textures are dominant. Vitrophyric texture is present occasionally (Hole 1140A).

The igneous rocks drilled on the Kerguelen Plateau are dominantly tholeiitic basalts. The geochemical characteristics of these basalts are unlike MORB (Frey et al., 2003).

In the AFM diagram, basalts from the Kerguelen Plateau plot in both tholeiitic and alkaline fields (Fig. **F84**). In the Zr-Nb-Y diagram, the data plot in a compact field in the areas of N-MORB (Holes 1136A and 1140A), intraplate tholeiites (Holes 1137A, 1138A, and two samples from Hole 1140A), and in two fields enriched by MORB (P-MORB) and intraplate oceanic tholeiites (Hole 747C) (Fig. **F85**). Trace element and isotopic chemistry (Hole 747C) is similar to transitional MORB (Salters et al., 1992; Schlich and Wise, 1992).

In most cases, basalts from each hole (except Hole 1140A) demonstrate similar REE in both concentration and distribution patterns (Kurnosov et al., 2003; Artamonov and Zolotarev, 2003). REE distribution (Fig. **F86**) indicates that basalts in Holes 1136A, 1137A, 1138A, and 747C are enriched in LREE in comparison with normal tholeiitic basalts of mid-ocean ridges. The variation REE diagram for basalts in Hole 1140A seems to show two groups. The trend for low-Ti basalts is similar to that typical for normal oceanic tholeiites. The trend for high-Ti basalts is enriched in LREE.

Alteration Mineralogy

Thin sections show that the basalts from Hole 1136A are slightly to moderately altered (see **"Appendix A,"** p.117). According to whole-rock chemical analyses, altered basalts contain 0.90–1.58 wt% H_2O^+ (Table **T78**). The degree of rock oxidation is moderate. Both olivine and interstitial glass are completely replaced by clay mineral aggregates (see **"Appendix A,"** p.117). Plagioclase is partly replaced by clay minerals. Vesicles are filled mainly with smectite. Hydromica, calcite, and heulandite were also identified in veins and vesicles (Table **T79**). Secondary minerals identified in basalts from Hole 1136A, from vesicles and veins and from groundmass (see **"Appendix A,"** p.117), indicate a low-temperature environment for water-rock interaction.

The altered basalts in Hole 1137A contain 0.72–3.03 wt% H_2O^+ (Table **T80**). The degree of rock oxidation is different (Fe_2O_3/FeO = 0.88–10.14). Thin sections of basalts in Hole 1137A show that ferromagnesian minerals in phenocrysts, groundmass, and interstitial glass are completely replaced by clay minerals (see **"Appendix A,"** p.117). Plagioclase phenocrysts in phyric basalt (Sample 183-1137A-45R-1, 121–126 cm) are replaced with K-feldspar, clay minerals, and carbonate. Plagioclase from the matrix is also replaced with K-feldspar. In the basement recovered from Hole 1137A, smectite is the most common mineral filling vesicles (Table **T81**). Often it is present with some admixture of clinoptilolite and heulandite. An admixture of a C_7-mineral (probably dickite) and calcite is also present. In flow Subunits 7A and 8A, vesicles also contain chlorite phases. Clinoptilolite, hydromica, and quartz are also present with smectite and chlorite phases. Veinlets contain smectite, calcite, clinoptilolite, and quartz in trace amounts. The entire complex of secondary minerals in basalts in Hole 1137A indicates the low-temperature conditions of alteration and shows absence of vertical zonation of secondary minerals in the

F84. AFM diagram for basalts, Holes 747C, 1136A, 1137A, 1138A, and 1140A, p.290.

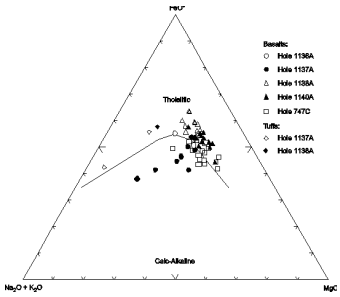

F85. Nb-Zr-Y diagram for basalts, Holes 747C, 1136A, 1137A, 1138A, and 1140A, p.291.

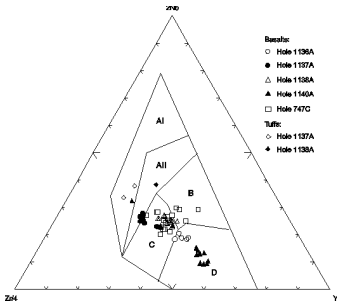

F86. Chondrite-normalized REEs for basalts, Holes 747C, 1136A, 1137A, 1138A, and 1140A, p.292.

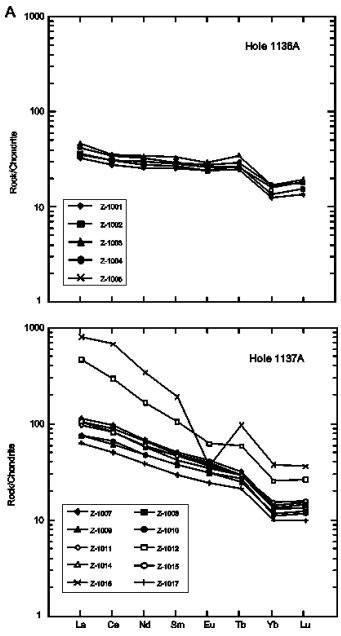

T78. Basalts, Hole 1136A, p.536.

total basalt section.

Examination of the basalts section in Hole 1138A shows that alteration varies from slight to intense (10%–50%) (see **"Appendix A,"** p.117). By chemical analysis, they contain 0.36–4.96 wt% H_2O^+ (Table **T82**). The basalts are mostly nonoxidized or only slightly oxidized, as suggested by dark gray color, study of thin sections, and Fe_2O_3/FeO ratio (from 0.40 to 3.01) (Table **T82**). In contrast, tuff (Sample 183-1138A-78R-1, 60–64 cm) is strongly oxidized (Fe_2O_3/FeO = 25.6) and altered (60% in thin section) (Table **T82;** see **"Appendix A,"** p.117).

Thin sections show that olivine is completely replaced by pale green clay mineral. Plagioclase is partly replaced by clay mineral. The interior of the plagioclase is replaced by a mica-like mineral (Sample 183-1138A-84R-5, 20–25 cm). Interstitial glass is completely replaced by clay minerals aggregate (see **"Appendix A,"** p.117).

Secondary minerals filling vesicles in basalt in Hole 1138A (Table **T83**) are characteristic and distinct from those of other Leg 183 holes in the abundance of zeolites (heulandite, clinoptilolite, mordenite, stilbite, analcime, and natrolite). Thomsonite is present occasionally. The zeolites were studied by microprobe analyses (Kurnosov et al., 2003).

All secondary minerals (clay and nonclay minerals) studied in vesicles and veins, as well as in basalt groundmass and phenocrysts, show no vertical zonation in their distribution throughout the basalt section in Hole 1138A. Within individual lava flows, there are no limitations on the presence of smectite. It fills vesicles near the top of basal flows, for example, at 4, 20, and 30 cm below the top of the lava flows (Sample 183-1138A-88R-2, 91–96 cm; 82R-2, 76–81 cm; and 81R-1, 34–39 cm, respectively), at the bottom of Unit 17 (Sample 86R-3, 72–74 cm), or at 90 cm above the bottom of Unit 10 (Sample 83R-4, 19–24 cm) (Table **T83**). Besides marginal parts of lava flows, smectite is present in the interior of basalt Units 6, 9, 11, 13, and 19 (Samples 183-1138A-81R-2, 51–57 cm; 82R-5, 19–23 cm; 83R-5, 106–109 cm; 84R-5, 20–25 cm; and 87R-2, 76–81 cm, respectively). All determinations of chlorite and serpentine(?) were made from interior and basal parts of basalt flows (Table **T83**). The data show that any vertical zonation in secondary minerals in basalt sections in total absence and the presence of zonation within individual flows.

Basalts from pillow lavas in Hole 1140A are less altered than basalts from other Leg 183 holes. Thin sections indicate alteration of basalts of 5% to 20% (see **"Appendix A,"** p.117). Only two samples had alteration of a moderate degree, from 25% to 35% (of the volume of rocks). The basalts are fresh or scarcely oxidized. The Fe_2O_3/FeO ratio is low and varies from 0.53 to 1.07 (Table **T84**). In only two samples the ratio was 2.41 and 2.31. Aggregates of clay minerals replace olivine. Plagioclase is completely replaced with clay. Interstitial glass is completely replaced by clay mineral or clay mineral and opaque minerals (see **"Appendix A,"** p.117). Vesicles are filled with smectite, and the vein is filled with calcite (Table **T85**). Joint fissures are covered, in one case, with a thin layer of smectite and chlorite and, in the other case, smectite with traces of serpentine(?) and quartz. Zeolites have not been identified, and this is the principal difference in basalt alteration from Hole 1140A (submarine extrusion) compared with those from Holes 1136A, 1137A, and, especially, Hole 1138A (subaerial extrusion).

The basalts studied in Hole 747C show varying degrees of alteration (H_2O^+ = 0.69–5.14 wt%) (Table **T86**). The massive and brecciated basalts are slightly to strongly altered (Schlich and Wise, 1992). In altered basalts, dominant secondary minerals are represented by smectite, or smectites with chlorite or swelling chlorite and chlorite (Table **T87**). Microphenocrysts of olivine are replaced with orange-red and orange-brown iddingsite or grassy-green smectite, or bluish green smectite with iddingsite rim. Coarser microphenocrysts are replaced along the margins with orange-red iddingsite,

whereas their central parts are replaced with pale green smectite. Volcanic groundmass glass is completely or partly replaced with the grassy-green or green smectite. Some phenocrysts of plagioclase are replaced in their central parts with light green smectite (see **"Appendix A,"** p.117).

Smectites and celadonite, zeolites, goethite, calcite, and quartz are determined in basalts in Hole 747C (Schlich, Wise, et al., 1989; Sevigny et al., 1992). Electron microprobe analyses of green clay in Hole 747C characterize it as Fe-Mg smectites (Sevigny et al., 1992). Zeolites were determined in amygdules, the groundmass, and altered plagioclase phenocrysts. Zeolites are represented by chabasite, natrolite, thomsonite, mesolite, stilbite, and heulandite (Sevigny et al., 1992). Calcite veins occur throughout the basalt section. The matrix of brecciated basalts contains calcite. Quartz occurs in small amounts in some vesicles.

Both oxidative and nonoxidative alteration are recognized in Hole 747C. Distinctly expressed oxidative zones occur at the tops of basalt flows. For example, tops of flows in Sections 120-747C-15R-2, 15–18 cm and 15R-3, 84–96 cm, and the brecciated basalt cemented with brownish red yellow clays in 13R-2, 35–55 cm, are red. The absence of sulfides and presence of iron hydroxide halos around veins reflect some alteration of basalts under oxidative conditions (Schlich, Wise, et al., 1989). Oxidative zones are marked by goethite, Fe hydroxides, calcite, and celadonite(?).

Bulk-Rock Chemical Changes

In Hole 747C, highly altered basalts contain less Sc, V, Cu, Y, Nb, Sr, and Ba but more Rb. Schlich, Wise, et al. (1989) have proposed that Na, K, Ba, and Rb were mobile and redistributed during the alteration process. The mobility of elements caused by alteration of basalts in Hole 747C is not absolutely distinct on the basis of the obtained data, as each of selected for the analysis rock groups (i.e., nonoxidative massive basalts, oxidative massive basalts, and oxidative vesicular basalts) is represented by only two or three samples. With relative confidence we can conclude that oxidized basalts accumulate K, Fe, and Rb.

We studied mobility of chemical elements in relation to alteration of basalts from the Kerguelen Plateau under both oxidative and nonoxidative environments (Bass, 1976; Bass et al., 1973). To estimate chemical element mobility, we used data on the amount of major and minor elements in basalts ("Appendix B", Tables **AT39, AT40, AT41, AT42, AT43**). Two examples (see Kurnosov et al., 2003, table T14) show element gain/loss in nonoxidative and oxidative environments of alteration of basalts from the Kerguelen Plateau.

Basalts in Hole 1140A have similar degrees of alteration. Nevertheless, they are favorable for analyzing the mobility of chemical elements in a "pure" nonoxidized environment, as they are neither oxidized nor vesicular. For further reference, we chose Sample 183-1140A-35R-1, 35–42 cm (H_2O^+ = 0.74 wt%, Fe_2O_3/FeO = 1.01, density = 2.93 g/cm^3) (Table **T84**). For comparison we chose nonoxidized Sample 183-1140A-34R-1, 117–121 cm (H_2O^+ = 1.40 wt%, Fe_2O_3/FeO = 0.69, and density = 2.57 g/cm^3) (Table **T84**). The trend to decrease under nonoxidative alteration in basalt is most evident in major elements, REE, Cu, Nb, Zr, Y, Rb, and Sr (Kurnosov et al., 2003, table T14). Ni, V, Co, Zn, and Ba show a weak trend to increase during slight alteration.

Sample 183-1137A-27R-1, 100–105 cm (H_2O^+ = 2.03 wt%, Fe_2O_3/FeO = 3.57), is oxidized (Table **T80**) and highly vesicular (see **"Appendix A,"** p.117). Hence, for comparison, we chose relatively fresh nonoxidized basalt with similar vesicularity (Sample 183-1137A-39R-2, 114–119 cm; H_2O^+ = 0.99 wt%). Comparison revealed that oxidizing alteration leads mostly to the accumulation of Fe, Mg, Ca, P, REE, Co, Zr, and Ba in basalts (Kurnosov et al., 2003, table T14). This is especially evident for Sr. In contrast, Si, Al, Mn, Na, K, Ni, V, Cu, Y, and Rb show a decrease.

AT39. Major and trace elements, Hole 747C, p.117.

AT40. Major and trace elements, Hole 1136A, p.120.

AT41. Major and trace elements, Hole 1137A, p.121.

AT42. Major and trace elements, Hole 1138A, p.123.

AT43. Major and trace elements, Hole 1140A, p.125.

Brief Comments

Secondary mineral assemblages (smectites, calcite, Fe oxides, and hydroxides prevailed) in basalts in Holes 254, 756D, 757C, and 758A (Ninetyeast Ridge) is typical for low-temperature alteration. Besides these secondary minerals, the rocks in Hole 757C contain Na-Ca zeolites, albite, and K-feldspar. The temperature of alteration was low but higher than in Holes 254 and 756D. The temperatures calculated at Site 757 using oxygen isotope ratios of the carbonate veins in basalts vary from 23° to 45°C (Lawrence, 1991). Replacement of plagioclase by K-feldspar from the lower portion of the oxidized zone in Costa Rica Rift (Hole 504B) occurs in the interval of 30°–80°C (Pertsev and Boronikhin, 1983b). It is logical to conclude that oxidative alteration in Hole 757C occurred in the interval of temperatures from 23° to 80°C. The presence of Na-Ca zeolites supports the suggested temperature level. Natrolite, which was determined by Saunders et al. (1991), forms in the zeolite zone with characteristic temperatures up to 100°–120°C (Kristmannsd—ttir and T—masson, 1978).

Secondary mineral assemblages indicate that the temperature of alteration in Hole 758A was somewhat higher than in Holes 756D and 757C. The temperatures calculated at Site 758A on the basis of oxygen isotope ratios of the carbonate veins in basalts and vary from 41° to 71°C (Lawrence, 1991). Sulfides and quartz may reflect higher temperatures of alteration. Sulfides from Hole 758A formed during hydrothermal alteration at low to moderate temperatures (Frey et al., 1991). Sulfate-reduction in basalts of the upper part of Hole 504B (Costa Rica Rift) occurred at ~200°C (Honnorez et al., 1983).

We have not found any vertical zonality in distribution of secondary minerals from the basalt basement recovered from Holes 254, 756D, 757C, and 758A.

It is not a surprise that mixed-layer smectite-chlorite mineral and swelling chlorite appear together with smectite among dominant secondary minerals in basalts in both Hole 757C and Hole 756D. A similar phenomenon was observed by Kurnosov (1986) by study of altered basalts throughout some flows in Hole 433C (Emperor Seamount Chain) and altered basalts from Hole 865A (Allison Guyot) (Kurnosov et al., 1995) (see **“Alteration of Igneous Rocks from Seamounts and Guyots,”** p.44).

The detailed study of 7.5-m-thick flow Unit 48 in Hole 433C revealed that smectites dominate at both top and bottom of the flow, and swelling chlorite dominates toward the center of the flow. Among clay minerals, the role of chlorite increases in central parts of the flow where clay minerals are represented by mixed-layer chlorite to swelling chlorite. Clay minerals that replace the groundmass of basalts in Unit 48 are distributed asymmetrically. Most chlorite-bearing minerals occur toward the bottom of the flow. Similar distribution was determined for plagioclases in Unit 48 (Avdeiko et al., 1980). Maximum plagioclase content and longest grains are restricted to the same portion of the flow where mixed-layer chlorite-swelling chlorite dominate and replace interstitial volcanic glass. This coincidence allows the supposition that intensive crystallization of plagioclase may have led to differences in chemical composition between the restite glass in the center of the flow and glass from marginal parts of the flow. This is primarily expressed in higher contents of Mg and Fe and lower contents of Si, Al, Ca, Na, and K. Under low-temperature alteration, glass from the inner parts of the flow was favorable for replacement with chlorite phases, whereas the glass in marginal parts was replaced with smectites.

Similar distribution of clay minerals is recognized in Hole 757C. Flow Unit 2 (~10 m thick) is most illustrative. Besides smectites, swelling chlorite dominates from 0.5 m beneath its upper boundary through the next core (Sample 121-757C-8R-2, 119–121 cm). We have recognized secondary mixed-layer

chlorite-smectite mineral from top to bottom of the unit significantly lower its central part (the central part of the unit was not recovered). Only smectites are present at the bottom of the flow (Sample 121-757C-9R-2, 24–26 cm and 9R-3, 35–37 cm), as found in basalts in Hole 433C (Emperor Seamount Chain).

In other studies, flow Units 5 and 18 (Hole 757C) show distribution of clay minerals with chlorite structures and smectite is also dependent on the position of sampling within the section of the flow. Unit 12, which is as thick as 0.29 m, represents an exception. We have determined a mixed-layer chlorite-smectite mineral as a dominant secondary mineral in the upper part of the flow. According to previous observations, one must expect smectite to prevail among clay minerals. It is probable that the top of Unit 12 was determined incorrectly and the real boundary is located above the determined one.

Oxidative alteration occurred in vesicular basalts that were erupted in a subaerial environment. The temperature of oxidative alteration was low; most probably it was similar to the temperature of calcite formation. At Site 756, temperatures were calculated on the basis of oxygen isotope ratios of carbonate veins in basalts, and they vary from 10° to 40°C (Lawrence, 1991).

We suppose that often oxidative and nonoxidative alteration in volcanic edifices results from simultaneous entering of the seawater, which is contrary to processes in spreading mid-ocean ridges. Seawater enters these edifices mainly through the most weak zones along margins of flow units, brecciated zones, and cracks where basalts suffer oxidative alteration with characteristic high seawater/rock ratio. The seawater then infiltrates flow units. Oxidative features still exist for some short distance. It is supported by the fact that oxidative alteration occurs along several tens of centimeters unto the unit and as haloes around calcite-filled veins. Within the remaining inner space of flow units where partly altered seawater infiltrates, a nonoxidative environment with low seawater/rock ratio usually predominates. The absence of vertical zonality in distribution of secondary minerals in studied holes and the appearance of mixed-layer smectite-chlorite mineral within thick units in various parts of the vertical section of basalts supports the idea of subhorizontal water filtration in this part of the basaltic edifice.

Significantly lower oxidation of basalts in Hole 758A probably because basalts effused in the deep-sea environment are mainly massive and are not favorable to formation of high seawater/rock ratios which predominates oxidizing environments. Some increase in temperature of alteration in comparison with Holes 756D and 757C and typical presence of sulfides in Hole 758A make it possible to suppose its similarity to upward migrating hydrothermal flow, in which vicinity alteration of basalts occurs in nonoxidizing environment.

Vesicular basalts from the tops of the lava flows are strongly altered. They, accordingly, bring the greatest contribution to a redistribution of elements between water and rocks at their interaction. Fresh analogs of vesicular basalts from Holes 254, 756D, 757C, and 758A are absent. We need fresh analogs of these rocks with the same vesicularity to estimate the mass-balance in gram per 1000 cm^3.

All studied samples from Holes 1136A, 1137A, 1138A, 747C (subaerial effusion), and 1140A (deep-marine environment) cored in various parts of the Kerguelen Plateau are at various degrees of alteration in low-temperature environments. Dickite(?) in trace amounts in the upper part of basalt section in Hole 1137A is indicative of subaerial weathering.

Basalts of pillow lavas recovered from Hole 1140A in the north part of the Kerguelen Plateau show minimal alteration, as they occur in the lowest temperature environment and most are not oxidized. Smectite prevails among secondary minerals, while vesicles and veins contain no zeolites, contrary to other holes of Leg 183. Circulation of hotter fluids probably occurred along cracks now filled with smectite, chlorite, serpentine(?), and quartz.

Nevertheless, these probable fluids did not play a significant role in the alteration of the basalt section of Hole 1140A.

The abundance of zeolites in basalts from Holes 1138A and 747C, in comparison with other Leg 183 holes, is probably related to their closer location to the paleoeruptive center. The presence of several varieties of zeolites and great variation in chemical composition is characteristic of rock alteration in hydrothermal systems. Comparison of zeolite and clay minerals in Leg 183 and 120 basalts and in Iceland (Kristmannsdottir and Tomasson, 1978) suggests that alteration of basalts from the central part of the Kerguelen Plateau (Holes 1138A and 747C) occurred at a temperature of 120°C and probably higher.

We have observed an absence of vertical zonation in distribution of all secondary minerals (clay minerals and zeolites) from vesicles and veins, as well as in groundmass and phenocrysts, throughout the basalt section cored during Legs 120 and 183. The presence of secondary mineral zonation was determined within individual flows. Zonation in distribution of secondary minerals within lava flows, and the absence of vertical zonation in basalt sections, were observed during a previous study of altered basalts from Suiko Guyot in the Emperor Seamount Chain (Leg 55 Hole 433C) (Kurnosov, 1986) and from Allison Guyot in the West Pacific Guyots, Hole 865A, Legs 143 and 144 (Kurnosov et al., 1995) (see **"Alteration of Igneous Rocks from Seamounts and Guyots,"** p.44).

The secondary minerals probably formed under the influence of individual basalt flows in an environment dominated by subhorizontal migration of water, primarily along contacts between lava flows. Also, band-like distribution of analcime, stilbite, and mordenite provide evidence that alteration of effusive basalts is related mostly to subhorizontal fluid flow. The influence of hot waters of interlayer-fissure circulation on the formation of subhorizontal zeolite zones in basalts is well known in Iceland (Walker, 1960; Tomasson and Kristmannsdottir, 1972; Kristmannsdottir and Tomasson, 1978).

The study of gain/loss of elements has shown that the mobility of chemical elements during alteration of basalts from the Kerguelen Plateau is different in oxidizing and nonoxidizing environments. We conclude that generally in nonoxidizing alteration environments, basalts lose most elements. In contrast, in oxidizing alteration, basalts accumulate many elements. The degree of alteration of basalts (selected for estimation of chemical element mobility) is low, so the mobility of elements seems to be at the rudiment study.

Mascarene Plateau, Chagos Bank, and Maldives Ridge

Basalts recovered during Leg 115 are genetically similar to basalts drilled during Legs 26, 120, 121, and 183 in the Kerguelen-Ninetyeast lineament and probably erupted during the motion of the Indian plate northward above the hotspot. Nevertheless, they demonstrate some variations in petrographic and geochemical composition as well in environments of their effusion on the sealer. Our major objective was to continue the study of alteration of basalts from congener volcanic lineaments of the Central and East Indian Ocean.

The Mascarene-Chagos-Maldives-Laccadive volcanic lineament is an aseismic ridge system in the central Indian Ocean basin. The basement rocks were recovered at Sites 706, 707, 713, and 715 during Leg 115 (Fig. **F87**). Volcanic activity occurred at these sites at 34, 64, 49, and 57 Ma, respectively (Duncan, and Hargraves, 1990). It is supposed (Morgan, 1981; Duncan, 1981, 1990), that the island of Mauritius, Mascarene Plateau, the Chagos Bank, the Maldive and Laccadive Ridges, and the Deccan traps (western India) were produced by the Reunion stationary hotspot and the motion of the Indian plate northward during the Tertiary time period. The main pulse of the Deccan flood basalts occurred rapidly at about the Cretaceous/Tertiary boundary (Courtillot et al., 1986). This volcanic lineament together with the Ninetyeast Ridge record

F87. Sites in the western Indian Ocean, p.295.

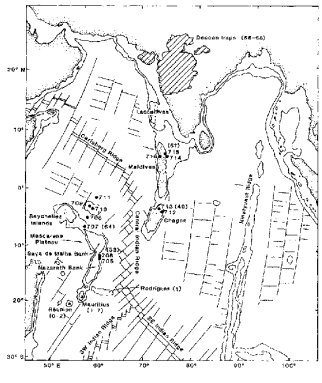

the northward motion of India during the opening of the Indian Ocean. It is supposed that the spreading of the Central Indian Ridge has been active since 35 Ma, when the Chagos Bank was rifted off the Nazareth Bank and the Ninetyeast Ridge was separated from the Kerguelen hotspot (Backman, Duncan, et al., 1988).

Alternative models suggest that the lineament is a product of volcanic activity along a transform fault associated with Tertiary seafloor spreading (Fisher et al., 1971; McKenzie and Sclater, 1977). Meyerhoff and Kamen-Kaye (1981) consider, for example, that the Mascarene Plateau is a submerged island arc.

Basalts recovered from Holes 706C, 707C, 713A, and 715A are all tholeiitic in composition (Baxter, 1990). Olivine-phyric basalts from Site 715 are similar to basalts (OIB) from Reunion, while plagioclase-phyric basalts from Sites 706, 707, and 713 show evidence of magma mixing between the hotspot and a MORB mantle. The igneous rocks from Reunion are primarily basalts that are transitional between tholeiites and alkaline basalts of Hawaii (Backman, Duncan, et al., 1988; Baxter, 1990).

We have studied samples of basalts from Holes 706C and 707C (Mascarene Plateau), 713A (Chagos Bank), and 715A (Maldives Ridge) (Table **T88**). Hole 706C is located on the northeastern margin of Nazareth Bank. Hole 707C is located in the northwestern part of the Mascarene Plateau. Hole 713A represents the northern part of the Chagos Bank. Hole 715A is located on the northeastern margin of the Maldives Ridge (Backman, Duncan, et al., 1988).

T88. Additional basement holes, Leg 115, p.551.

Hole 706C

Petrography and Bulk-Rock Chemical Composition

According to data obtained during Leg 115 (Backman, Duncan, et al., 1988), 32 lava flows in Hole 706C are built of vesicular and massive plagioclase-phyric basalts with various amounts of subordinate augite and olivine (1%–2%) phenocrysts. Basalts composing flow Units 1–30 appear to be very similar. Most of samples are fine grained. Units 31 and 32 appear to be distinct from the others as they contain large plagioclase phenocrysts (7 mm) and demonstrate abundant low pyroxene phenocrysts. Chemical data show that volcanic rocks in Hole 706C are high- and low-titanium tholeiitic basalts (upper and lower groups, respectively). The high-titanium basalts from Units 1–30 closely resemble rocks of the older alkaline group on Mauritius. The low-titanium basalts (Units 31 and 32) have compositions similar to ocean-floor basalts. All flows were erupted below the sea level (Backman, Duncan, et al., 1988; Baxter, 1990).

We have studied 11 additional samples of basalts from flow Units 12, 13, 14, 19, 20, 28, 31, and 32. Nine of eleven samples are represented by aphyric high-titanium and ferruginous practically nondifferentiated in silicity basalts (see **"Appendix A,"** p.120; Table **T89**). Samples 115-706C-9R-1, 72–74 cm, and 9R-2, 10–13 cm, are represented by plagioclase-phyric low-titanium basalt. In the AFM diagram, all samples plot in the tholeiite basalts field (Fig. **F88**). In the Zr-Nb-Y diagram, samples from Hole 706C are located in fields of intraplate tholeiites and E-MORB (Fig. **F89**). Compared to typical MORB, these basalts are depleted in siderophile elements but demonstrate some enrichment in V, Sr, and Zr (Table **T89**). Samples 115-706C-9R-1, 72–74 cm, and 9R-2, 10–13 cm, provide an exception.

T89. Basalts, Hole 706C, p.552.

F88. AFM diagram for basalts, Holes 706C, 707C, 713A, and 715A, p.296.

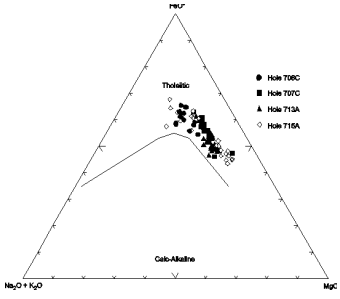

In the variation diagram, the distribution of normalized ratios of REE indicates enrichment of large-ion lanthanides (Fig. **F90**). Only in plagioclase-phyric basalt (Sample 115-706C-9R-1, 72–74 cm) is the character of REE distribution similar to that in tholeiitic MORB. Because all studied samples are practically nondifferentiated, the revealed geochemical difference could be explained by various depth of formation of initial melts.

Alteration Mineralogy

All studied samples of basalts are slightly to moderately altered with H_2O^+ contents from 0.65 to 2.12 wt% (Table **T89**), and all of them are affected with slight oxidative processes. Nevertheless, we consider these basalts to represent nonoxidized basalts, as the Fe_2O_3/FeO ratio varies from 0.75 to 1.23. We have chosen the Fe_2O_3/FeO ratio of 1.60 to mark a conditional boundary between nonoxidized and oxidized basalts. The color of all recovered basalts was determined during shipboard study as dark gray to black (Backman, Duncan, et al., 1988) (i.e., distinctly oxidized basalts are absent). Only Sample 115-706C-9R-2, 0-7 cm is very slightly oxidized (Fe_2O_3/FeO = 1.77).

Iron oxides/hydroxides are present as coatings on vesicles and in olivine together with smectite. Smectites dominate among secondary minerals (see **"Appendix A,"** p.120). Smectites replace both olivine and glass in the groundmass and completely or partly fill vesicles. Olivine has also been replaced with iddingsite, possibly with hematite. Often, plagioclase and augite are fresh and do not show signs of alteration. Smectites are represented by different varieties, from pure to those containing ~40% of mica layers (XRD data). Other identified clay minerals include hydromica and chlorite in trace amounts (see **"Appendix A,"** p.120). Blue matter from veins is hydromica.

Fisk and Howard (1990) showed that Fe beidellite is most widespread among smectites in Hole 706C. Also, Backman, Duncan, et al. (1988) demonstrated that carbonate mixture with smectite fills vesicles and sometimes replaces olivine. Pyrite was locally observed within vesicles. Secondary mineral assemblages in basalts in Hole 706C are characteristic of low-temperature alteration.

Bulk-Rock Chemical Changes

Three samples (Samples 115-706C-5R-1, 113–115 cm; 5R-3, 69–71 cm; and 6R-1, 38–40 cm) almost satisfy requirements of the mass balance calculations. These samples demonstrate little variations in their alteration (H_2O^+ = ~1 wt%). Comparison of contents of elements in these samples ("Appendix B", Table **AT44**) provide evidence that relatively slight nonoxidative alteration is accompanied by the mobility of major and minor elements including REE. Most chemical elements (Si, Ti(?), Fe, K, Na, REE, V, Cu, Zn, Y, Nb, Ba, and especially Rb) enrich rocks against the background of somewhat decreasing Mg. As it was previously shown for basalts in the Ninetyeast Ridge, the predominant element enrichment of rocks is characteristic of oxidative alteration. This contradiction roots in the basalts in Hole 706C as they are not strictly nonoxidized and demonstrate relatively high Fe_2O_3/FeO ratios.

Microprobe analyses of smectites from veins, especially from vesicles, in the Hole 706C basalts (Fisk and Howard, 1990) reflect mobility of all major elements, including Ti and Al, as well as Cr.

Greenough et al. (1990) undertook a special study of element mobility in alteration of basalts in Hole 706C. They compared the least-altered and the most-altered samples. They postulated immobility of Zr under these conditions and, hence, used element/Zr ratios. The researchers concluded that under conditions of the zeolite facies, rocks incorporate K, Rb, Cs, Li, Si, Sc, Fe, and possibly Sr, Pb, Au, Pt, and Rh. Such elements as Ca, Mg, Mn, Ni, and possibly Na, Ba, and Ir decrease in amounts. The REE as well as Zr, Nb, Y, Ti, Al, V, Th, and probably P and Hf tend to stay immobile. The behavior of Cr, Cu, Zn, Bi, Pd, and Ru remained unclear. These data do not completely correspond to our results of the analysis of element mobility.

Hole 707C

Petrography and Bulk-Rock Chemical Composition

F89. Nb-Zr-Y diagram for basalts, Holes 706C, 707C, 713A, and 715A, p.297.

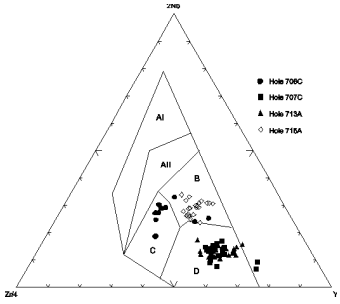

F90. Chondrite-normalized REEs for basalts, Holes 706C, 707C, 713A, and 715A, p.298.

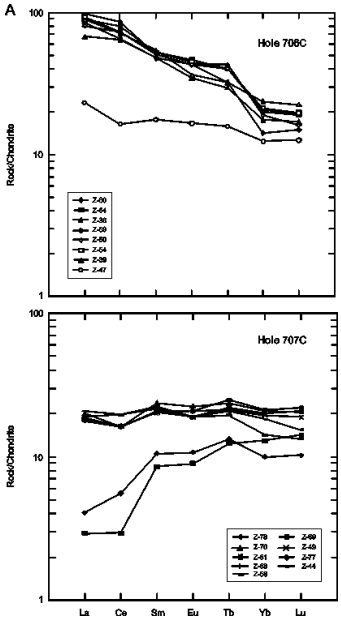

AT44. Major and trace elements, Hole 706C, p.127.

Five distinct units represent subaerial to littoral lava flows with interceded limestones of middle Paleocene age. Flows are as much as 37.6 m thick. The basalts are vesicular at the top and become massive downflow. In general they are fine to medium grained and contain plagioclase, pyroxene, and olivine phenocrysts. Hole 707C phyric basalts display no systematic intraflow petrographic variation. Tholeiitic basalts in Hole 707C show much more crystalline groundmass than Hole 706C basalts (Backman, Duncan, et al., 1988). At Site 707, as well as at Site 706, two distinct basalt types were recognized. Flow Units 4 and 5 are moderately enriched with TiO_2 (1.4%–1.5%). Units 1 and 3 are depleted in TiO_2 (0.5%–0.8%), P_2O_5, Zr, and Nb (Baxter, 1990). Basalts in Hole 707C contain significantly less TiO_2 than basalts in Hole 706C. This indicates that Hole 707C basalts are less alkaline (Backman, Duncan, et al., 1988).

We studied 22 additional samples from flow Units 1 and 3–5 (see **"Appendix A,"** p.122; Table **T90**). The results correspond with data on the thin sections study. Basalts are mainly represented by plagioclase-phyric (occasionally with admixture of clinopyroxene and olivine microphenocrysts) vesicular varieties. Phenocrysts vary from 1% to 25% in abundance (see **"Appendix A,"** p.122). All these basalts represent practically nondifferentiated and low alkaline varieties with average content of Ti. Five samples of low-titanium aphyric basalt from the upper part of the section (Samples 115-707C-22R-1, 94–98 cm, 22R-2, 49–51 cm; 23R-1, 98–100 cm; 23R-1, 32–36 cm; and 23R-4, 0–3 cm) provide an exception. These samples demonstrate some enrichment in MgO in comparison with the other samples.

T90. Basalts, Hole 707C, p.554.

The AFM diagram indicates that the basalts belong to the tholeiitic series (Fig. **F88**). As far siderophile elements, basalts in Hole 707C are slightly depleted in Cr, Ni, Co but enriched in V and Cu in comparison with typical MORB. Also, they demonstrate low concentrations of Rb, Sr, and Zr (Table **T90**). In the Zr-Nb-Y diagram, samples from Hole 707C are located in the field of N-MORB (Fig. **F89**). REE distribution demonstrates two trends (Fig. **F90**): (1) N-MORB (plagioclase-phyric basalts) and (2) basalts depleted in large-ions lanthanides (aphyric basalts; Samples 115-707C-22R-2, 49–51 cm, and 23R-1, 98–100 cm). It is probable such distribution provides evidence of various depths of melt sources as it was supposed for basalts in Hole 706C.

Alteration Mineralogy

We studied 22 additional samples of nonoxidized basalts from Hole 707C that demonstrate low degrees of alteration (see **"Appendix A,"** p.122). H_2O^+ varies from 0.39 to 1.60 wt% and Fe_2O_3/FeO ratios are low, varying from 0.47 to 1.32 (Table **T90**). All recovered basalts are dark gray to black in color. Smectites dominate among secondary minerals in altered basalts in Hole 707C. Saponite is the most abundant mineral among smectites (Fisk and Howard, 1990).

XRD data (see **"Appendix A,"** p.122) show, in general, smectites are represented by different varieties, from pure to those containing from ~20%–30% to 40% mica layers and with interlayer Na-K or Mg-Ca cations. Pure smectites dominate. A mixed-layer chlorite-swelling chlorite was recognized in one sample in trace amount. Smectites also infill microcracks and vesicles.

Smectites replace olivine and interstitial glass and fill vesicles (see **"Appendix A,"** p.122). Smectites (or iddingsite), which replace olivine, are brown in color. Plagioclase phenocrysts show minor replacement by smectites, and pyroxenes are partly replaced by smectites (see **"Appendix A,"** p.122). Secondary mineral assemblages in basalts in Hole 707C are characteristic of low-temperature alteration. Temperatures calculated at Site 707C for carbonates from basalts are from 12° to 20°C (Burns et al., 1990).

Bulk-Rock Chemical Changes

Of 22 studied samples of basalts, four (Samples 115-707C-25R-1, 108–

110 cm; 26R-3, 71–73 cm; 26R-7, 46–48 cm; and 127R-6, 29–31 cm) satisfy requirements of the mass-balance calculations. These samples are almost similar in TiO_2 content (1.60–1.75 wt%) and represent massive basalts. These samples fit the requirements of nonoxidative alteration (Fe_2O_3/FeO = 0.49–0.90). Contrary to basalts in Hole 706C, these basalts demonstrate some tendency to loose elements at their alteration. This is true for such elements as Si, Al, Fe, Mn, K, Mg(?), Ca(?), Na(?), P(?), REE (except Sm and Eu), Zn, Y, Nb, Sr, and Ba ("Appendix B", Table **AT45**).

AT45. Major and trace elements, Hole 707C, p.128.

Hole 713A

Petrography and Bulk-Rock Chemical Composition

The scientists of Leg 115 recognized 35 flow units that vary from 1 to 10 m in thickness in the core from Hole 713A. Flows are interbedded with middle Eocene chalks and volcanic ash. Hole 713A basalts have olivine tholeiitic composition. The units represent deep-water lava flows. Volcanic activity took place at ~1000 m. Highly vesicular basalts from flow Unit 1 were probably erupted at shallower depth. However, sediments between flow units were interpreted as deep-water deposits. The rocks are microporphyric to phyric basalts with phenocrysts of plagioclase, augite, and minor olivine (Backman, Duncan, et al., 1988). Two basalt types were recognized (Baxter, 1990): (1) an upper group (Units 1–5) of slightly enriched basalts and (2) a lower group (Units 6–35) of more depleted basalts. The upper group is similar to the lower group of basalts in Hole 707C.

We studied 22 additional samples from flow Units 1–6, 10–14, 18, 20, 23, 27, 31, 33, and 35 (see **"Appendix A,"** p.125; Table **T91**). All 22 studied samples are represented by phyric varieties (plagioclase-phyric or clinopyroxene-plagioclase-phyric), which usually contain individual olivine phenocrysts in groundmass. Sample 115-713A-19R-3, 9–12 cm, is olivine-plagioclase-clinopyroxene basalt. Most of the samples show the basalts are massive, but slightly vesicular varieties are also present (see **"Appendix A,"** p.125). The basalts are practically nondifferentiated in both silicity and Fe. Low-Ti varieties dominate. Basalts from the upper part of the section (from 108.67 to 133.5 mbsf) are somewhat enriched in Ti, Fe, and P compared to other samples and demonstrate high contents of Cr, Co, Cu, Nb, and Zr.

T91. Basalts, Hole 713A, p.557.

Geochemical diagrams (Figs. **F88, F89**) classify the basalts as tholeiitic N-MORB with poorly expressed Fenner's trend of differentiation. The variation diagram of normalized REE ratios (Fig. **F90**) provide evidence of two trends of distribution. Average-Ti basalts from the upper part of the section (Samples 115-713A-13R-1, 97–99 cm; 14R-3, 99–101 cm; 15R-1, 77–79 cm; and 15R-5, 85–87 cm) demonstrate normal MORB trend while the distribution of low-Ti is controlled by somewhat depletion in large-ion lanthanides. It is probable that this depletion was caused by various depths of initial melts as it was supposed for basalts in Holes 706C and 707C.

Alteration Mineralogy and Bulk-Rock Chemical Changes

The studied basalts from Hole 713A demonstrate low degrees of alteration (see **"Appendix A,"** p.125). H_2O^+ content varies from 0.15 to 1.69 wt% (Table **T91**). All of the basalts are nonoxidized and show low Fe_2O_3/FeO ratios (0.40–1.27). Basalts in Hole 713A are dark gray to black in color, as are basalts from Holes 706C and 707C.

XRD data show that smectites dominate among secondary minerals (see **"Appendix A,"** p.125). Smectites are represented by different varieties, from pure to those containing from ~10% to 40% mica layers and with Na-K and Mg-Ca interlayer cations. Pure smectites dominate. Hydromica, chlorite, calcite, and quartz occur sporadically as an admixture with smectite.

Olivine is replaced by smectites or by a mixture of smectites and calcite (see **"Appendix A,"** p.125). Volcanic groundmass and glass, either

around phenocrysts of plagioclase or included in plagioclases, are completely replaced with smectite. Phenocrysts of plagioclase are partially replaced with smectites and occasionally are carbonatized. Cracks in plagioclases and clinopyroxenes are filled with smectites. Fe and Mn(?) oxides, radial aggregates of smectites, and calcite have been recognized in vesicles. Vesicles are partly filled by smectites or carbonate. Small vesicles are completely filled with smectite aggregate. Veins of smectites are present. Secondary mineral assemblages (smectites and calcite are domination minerals) in basalts in Hole 713A are characteristic of low-temperature alteration in oceanic crust.

The low degree of alteration of basalts in Hole 713A does not clarify mass-balance calculations.

Element contents in basalts in Hole 713A are given in "Appendix B", Table **AT46.**

AT46. Major and trace elements, Hole 713A, p.131.

Hole 715A

Petrography and Bulk-Rock Chemical Composition

During Leg 115 scientists distinguished 21 subaerial flow units, 1–5 m thick, in Hole 715A. Upper parts of flow units are oxidized and weathered. Flows are vesicular (as much as 1 cm in diameter) toward the margins. Basement is overlapped by very shallow water reef limestones of early Eocene age. Two petrographically distinct groups of basalts were identified among the recovered igneous rocks. The upper group (flow Units 2, 4, 5, and 7) is plagioclase-phyric, aphanitic to fine grained basalts, which are massive to highly vesicular (as much as 20% by volume and as much as 5 mm across). All basalts appear to be somewhat oxidized, except for basalts from the lower portion of Unit 7. The lower group (Units 9 through 21) is represented by olivine-rich, phyric to aphyric fine grained basalts. The flows range from nonvesicular in the center to highly vesicular (as much as 50%) near their tops. Olivine phenocrysts (0%–15% and as much as 2 mm in length) tend to enlarge toward the top and bottom of each flow. Basalts appear to be transitional from tholeiitic to alkaline in composition. Basalts from Units 7 and 13 differ from other units in both TiO_2 and MgO contents. The high-titanium basalts are also enriched in total Fe, P, Nb, Zr, Y, Zn, Cu, and V, but are depleted in Ni and Cr (Backman, Duncan, et al., 1988; Baxter, 1990).

We studied 24 additional samples from flow Units 4, 7, 9, 10, 12, 13, 15, 16, and 19 through 21 (see **"Appendix A,"** p.128; Table **T92**). These samples are represented by both aphyric and phyric varieties. All basalts contain olivine either in groundmass or as phenocrysts. Phyric varieties are represented by plagioclase-phyric, olivine-plagioclase-phyric, and olivine-phyric basalts (see **"Appendix A,"** p.128). Most basalts are vesicular, with vesicularity varying from 1% to 3% through 50% with sizes up to 5 mm in diameter. Basalts are slightly differentiated in silicity and in contents of Mg, Ti, and Al_2O_3. All of the basalts demonstrate some deficiency in silica. Geochemical diagrams (Figs. **F88, F89**) provide evidence that the studied rocks occupy an intermediate position between tholeiitic and alkaline basalts (E-MORB). The basalts are enriched in Cr, Ni, V, Cu, and Nb and demonstrate irregular distribution of Sr and Zr (Table **T92**). The variation diagram of normalized REE (Fig. **F90**) ratios reflect slight enrichment with large-ion lanthanides. The REE spectrum is significantly broader than that in normal tholeiitic MORB.

T92. Basalts, Hole 715A, p.560.

Alteration Mineralogy

According to our study, 24 samples of basalts from Hole 715A are slightly to moderately altered (see **"Appendix A,"** p.128). H_2O^+ varies from 0.53 to 2.89 wt% (Table **T92**). Basalts vary from nonoxidized to very highly oxidized and show low to very high Fe_2O_3/FeO ratios (0.53 and 11.16, respectively). Recovered basalts are dark brown and dark gray.

XRD data show that smectites dominate in altered basalts from Hole

715A (see **"Appendix A,"** p.128). Smectites are represented by different varieties, from pure to those containing ~10%–20% mica layers and with various compositions of interlayer cations (Na-K or Ca-Mg). Mixed-layer chlorite-swelling chlorite and mixed-layer chlorite-smectite minerals, chlorite, hydromica, and calcite sporadically occur as admixtures with smectite. Mixed-layer chlorite-smectite mineral is undetermined in Sample 115-715A-23R-3, 91–95 cm, as a minor mineral with dominating smectite and hydromica as trace amounts in this sample. Vesicles and microcracks are infilled in smectites and/or calcite.

Olivine is usually altered and replaced with smectites and iddingsite (see **"Appendix A,"** p.128). Interstitial volcanic glass is completely replaced with smectite. Interstitial glass and olivine in oxidized samples are often replaced with hematite and yellowish brown smectites pigmented by limonite. Phenocrysts of plagioclase and clinopyroxene are partially replaced with smectite. Microcracks in plagioclases and clinopyroxenes are filled with smectite. Vesicles are filled with smectite and/or calcite (see **"Appendix A,"** p.128). In the oxidized tops of some units, yellowish brown smectite, limonite, and hematite replace olivine and interstitial glass and fill vesicles.

The temperature calculated at Site 715 using the oxygen isotope ratios of carbonate veins from basalts is very low and vary from 2° to 13°C (Burns et al., 1990).

Bulk-Rock Chemical Changes

Almost all studied samples represent a single group in terms of TiO_2 content. Within this group we recognized massive nonoxidized basalts (Samples 115-715A-25R-2, 80–82 cm; 25R-6, 16–18 cm; 29R-1, 64–66 cm; 29R-2, 80–82 cm; and 30R-3, 28–30 cm), variously oxidized highly vesicular (>30%) basalts (Samples 115-715A-26R-3, 17–19 cm; 30R-5, 30–32 cm; and 30R-5, 39–41 cm), and vesicular basalts (3%–10%; Samples 115-715A-31R-2, 98–100 cm, and 31R-1, 103–105 cm).

Analyses of massive nonoxidized basalts revealed near to similar absolute content of elements in these rocks, as they are very much alike in degree of alteration (H_2O^+ varies from 2.32 to 2.93 wt%). Slightly vesicular oxidized basalts are altered similar to massive nonoxidized basalts (H_2O^+ varies from 2.33 to 2.53 wt%). An oxidative alteration environment probably results in slight accumulation of REE, Si, Al, Mn, Mg, K, P, Ni, V, Cu, Zn, Nb, Rb, Sr, and Zr in basalts ("Appendix B", Table **AT47**).

AT47. Major and trace elements, Hole 715A, p.134.

Brief Comments

Slight alteration of rocks from Mascarene-Chagos-Maldives lineament (Leg 115 Holes 706C, 707C, 713A, and 715A) is probably a result of low alteration temperature and relatively low permeability to seawater in the sampled sections of basalts. The temperature of calcite formation in basalts (Hole 707C) was ~12°–20°C (Burns et al., 1990). Basalts from these holes show low permeability. They are mainly massive and sparsely vesicular, especially deep-water lava flows in Hole 713A. This became the reason to create a high water/rock ratio. The latter explain both slight alteration of basalts in Holes 706C, 707C, and 713A and the absence of oxidizing environment. All basalts from Holes 706C, 707C, and 713A are dark gray to black and demonstrate low Fe_2O_3/FeO ratios from 0.4 to 1.3.

Two types of low-grade nonoxidative and oxidative alteration were identified in Hole 715A. Oxidizing environment results from the water/rock ratio in vesicular margins of lava flows. It is primarily marked by the dark brown and brownish color of basalts. Oxidative and nonoxidative alteration occurred simultaneously, as for basalts from Ninetyeast Ridge and Kerguelen Plateau. Contrary to basalts from the Kerguelen-Ninetyeast lineament, where the highest degree of alteration was determined in oxidized basalts and especially in

highly vesicular varieties, we have not recognized this peculiarity in basalts in Hole 715A.

Secondary mineral assemblage in basalts from Leg 115 is significantly poorer than that from Kerguelen-Ninetyeast lineament. Secondary minerals are represented mainly by smectites and calcite. We have not recognized zeolites, K-feldspar, and quartz; clay minerals with chloritic structures occur very rarely. This poor association of secondary minerals corresponds with a low-temperature alteration. Burns et al. (1990) determined a low temperature of carbonate formation in these basalts: 2°–13°C in Hole 715A and 12°–20°C in Hole 707C. It is probable that all Leg 115 holes penetrated basalts from marginal parts of edifices that are most distant from the eruptive centers and uplifting of hot solutions.

The various ages of volcanic edifices of Mascarene Plateau (34 Ma in Hole 706C and 64 Ma in Hole 707C), Chagos Bank (49 Ma in Hole 713A), and Maldives Ridge (57 Ma in Hole 715A) did not significantly change the degree of basalt alteration. Basalts in all holes of Leg 115 are slightly altered.

Alteration of basalts in holes drilled during Leg 115 resulted in slight mobility of chemical elements. The main peculiarity is that oxidative alteration is accompanied mainly by accumulation of major and minor elements (including REE), whereas nonoxidative alteration is accompanied mainly by loss of elements.

Walvis Ridge

We have undertaken an additional study of alteration of basalts from seamounts of the Atlantic Ocean. Basalts recovered during Leg 74 are probably similar in genesis to basalts drilled in the Kerguelen-Ninetyeast and Mascarene-Chagos-Maldives lineaments.

We studied samples from Holes 525A, 527, and 528. These holes are located at a transect across the central province of the Walvis Ridge into the Angola Basin (Fig. **F91;** Table **T93**). Hole 525A is located near the crest of the Walvis Ridge. Holes 527 and 528 are restricted to the western slope of the Walvis Ridge. Hole 528 is located at intermediate depth between Holes 525A and 527 (Moore, Rabinowitz, et al., 1984).

F91. Sites on the Walvis Ridge, p.300.

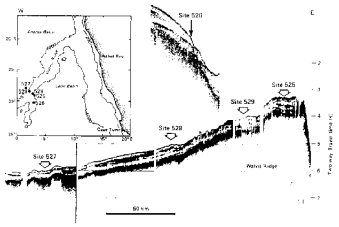

T93. Additional basement holes, Leg 74, p.563.

The Walvis Ridge is an aseismic ridge in the South Atlantic. The age of the basement basalts is ~69–71 Ma (Moore et al., 1984). This is in agreement with paleontologic age of sediments intercalated with lava flows and overlapping basement. The nature and origin of the Walvis Ridge is interpreted as a result of the African plate motion over the stationary Tristan da Cunha hot spot since 125 Ma. Parana-Etendeka flood basalts from southwest Africa that were produced by Tristan hot spot (Duncan, 1991) have the similar age.

Basalts recovered from Holes 525A, 527, and 528 are aphyric tholeiites at the ridge crest to highly plagioclase-phyric olivine tholeiites on the flank. They are also more enriched in incompatible elements than MORB (Moore, Rabinowitz, et al., 1984; Thompson, and Humphris, 1984; Moore et al., 1984). The isotopic data allow us to suppose that basalts from the Walvis Ridge generated either from mixing of depleted and enriched melts or partial melting of an unhomogeneous and variably enriched mantle source (Richardson et al., 1984).

Hole 525A

Petrography and Bulk-Rock Chemical Composition

Basalts in Hole 525A are very uniform in terms of petrography (Moore, Rabinowitz, et al., 1984). They are mainly aphyric, subophitic texture, vesicular (as much as 30%), and massive. Plagioclase is the most abundant mineral (50%–60% of the groundmass) and clinopyroxene is ~35%–45%. Olivine is

absent. Glass is present in the groundmass and dominates in glassy chilled margins. Sediments separate five flow units which are 21, 4.5, 22, 20, and 28 m thick. All units except Unit 4, which consists of pillow lavas, consist of basalt flows. Samples from Units 1 and 2 are fine- to medium grained aphyric basalt. Unit 3 consists of highly vesicular fine- to coarse grained aphyric to sparsely plagioclase and clinopyroxene phyric basalt. Textures are subophitic. Pillow basalts from Unit 4 are moderately vesicular and aphyric to sparsely plagioclase and clinopyroxene phyric with subophitic texture. Unit 5 consists of moderately vesicular glassy and fine grained basalt grading into medium- to coarse grained sparsely plagioclase phyric basalt with subophitic texture (Moore, Rabinowitz, et al., 1984).

We studied 14 additional samples of basalts from flow Units 1 and 3 through 5. These are represented by aphyric mostly vesicular basalts (see **"Appendix A,"** p.131). Basalts are poorly differentiated in silicity and contents of Ti, Fe, Mg, and alkaline elements (Table **T94**). In the AFM and Zr-Nb-Y diagrams, data plot in the fields of calc-alkaline and intraplate tholeiites (Figs. **F92, F93**). The variation diagram of normalized REE ratios reflect their enrichment in large-ion lanthanides (Fig. **F94**). They also demonstrate high variability in contents of some siderophile and chalcophile minor elements (Cr, V, and Cu). These elements are especially abundant in Samples 74-525A-53R-2, 87–90 cm, and 53R-3, 36–39 cm (Table **T94**). All samples from this hole are enriched in alkaline earth elements and Zr compared to normal tholeiites (Table **T94**). Such geochemical peculiarity may result from various depths of magmatic sources.

We determined high-Ti basalts (TiO_2 = 2.33–2.57 wt%) in flow Units 1, 3, and 5. Average-Ti basalts (TiO_2 = 0.95–1.44 wt%) dominate in Unit 3 and 4 (Table **T94**).

Alteration Mineralogy

Additionally studied samples of basalts are slightly to highly altered with H_2O^+ content from 1.12 to 5.48 wt% (Table **T94**). All basalts are oxidized at various degrees (Fe_2O_3/FeO = 0.89–4.88). We considered basalts with Fe_2O_3/FeO ratios of as much as 1.60 to be nonoxidized. Fe_2O_3/FeO ratios in oxidized basalts in Hole 525A varies from 2.01 to 4.88. Nevertheless, the color of all recovered basalts was determined during the shipboard study as gray (Moore, Rabinowitz, et al., 1984).

Smectites dominate among secondary minerals. Other identified clay minerals include hydromica in trace amounts (see **"Appendix A,"** p.131). Smectites replace clinopyroxene (augite) and glass in both groundmass and vesicles. Zeolite occurs sporadically. Clinopyroxene is altered along grain margins or is completely replaced. Plagioclase is slightly replaced with smectites and, probably, with hydromica. Calcite-smectite mixture fills vesicles and partially replaces pillow margins. Also, vesicles are filled with smectites or with calcite only. Some calcite veins are present. Secondary mineral assemblage in basalts in Hole 525A is characteristic of low-temperature alteration.

Bulk-Rock Chemical Changes

Of the 14 studied samples of aphyric basalts in Hole 525A, six samples relatively satisfy the requirements of mass balance calculations.

Group 1: Samples 74-525A-56R-1, 43–46 cm, and 61R-2, 2–5 cm, have high TiO_2 content (2.49 and 2.40 wt%, respectively). These samples are near to similar in vesicularity but sharply differ in both H_2O^+ content (1.92 and 5.48 wt%, respectively) and degree of oxidation (Fe_2O_3/FeO = 0.99 and 2.01, respectively). High alteration of vesicular basalts under oxidizing environment is accompanied mainly by increase in Si, Al, Mn, Na, K, P, REE, Cr, V, Zn, Y, Nb, Rb, Zr, and Ba, as revealed in basalts from the Ninetyeast Ridge) ("Appendix B", Table **AT48**). Such elements as Ca, Ni, Co, and Cu decrease in amounts.

T94. Basalts, Hole 525A, p.564.

F92. AFM diagram for basalts, Holes 525A, 527, and 528, p.301.

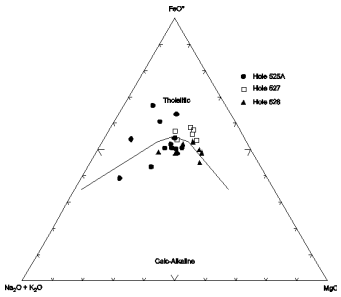

F93. Nb-Zr-Y diagram for basalts, Holes 525A, 527, and 528, p.302.

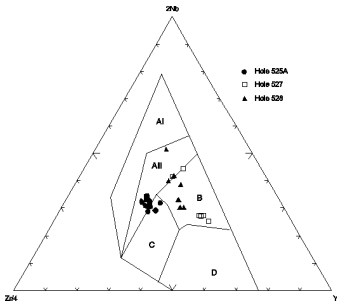

F94. Chondrite-normalized REEs for basalts, Holes 525A, 527, and 528, p.303.

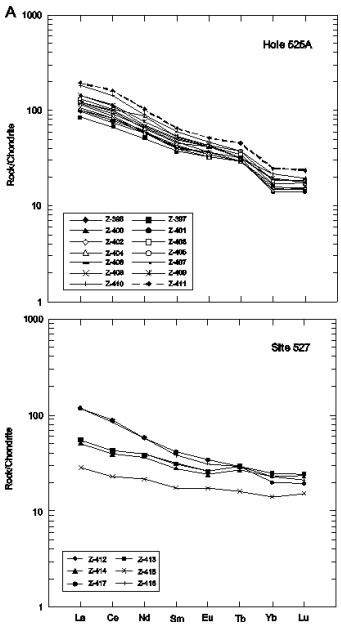

Group 2: Samples 74-525A-56R-2, 121–124 cm; 56R-3, 108–111 cm; 56R-6, 81–84 cm; 58R-4, 82–85 cm; and 59R-3, 40–42 cm, have low TiO_2 content (1.24–1.44 wt%). All of these samples are nonoxidized (Fe_2O_3/FeO = 0.89–1.30). Variation in H_2O^+ content is ~1 wt%. Within such a small interval of alteration, variations in element contents may have no relation to their mobility.

AT48. Major and trace elements, Hole 525A, p.138.

Hole 527

Petrography and Bulk-Rock Chemical Composition

The basement complex, recovered in Hole 527, consists of massive basalt flows with intercalated sediments, which are divided into five flow units. Three petrographic varieties of basalts are present in the succession from Hole 527. Units 1, 2, and 4 are composed of fine- to medium grained sparsely phyric basalt. Unit 3 consists a medium grained, highly plagioclase-phyric basalt. Unit 5 is a medium- to coarse grained aphyric basalt. Phenocrysts are represented mainly by plagioclase (80%–100%). Olivine (0%–15%) and clinopyroxene (0%–5%) are also present. Groundmass texture varies from subophitic through intergranular to "pegmatitic." Vesicles are absent throughout the basalt succession (Moore, Rabinowitz, et al., 1984).

We studied six additional samples of basalts from flow Units 1 through 3 and 5. These basalts are represented by both aphyric and phyric varieties. The phyric varieties are mainly represented by plagioclase-phyric and clinopyroxene-plagioclase-phyric basalts. All basalts are massive (see **"Appendix A,"** p.133). The studied basalts have average TiO_2 content, except Sample 74-527-42R-4, 45–48 cm (Table **T95**). Basalts are nondifferentiated in silicity. In geochemical diagrams, data plot in the Fe-rich field of tholeiitic MORB (Fenner's trend of differentiation) and E-MORB (Figs. **F92, F93**). Among siderophile elements, V demonstrates some increase in abundance. Among chalcophile elements, only Cu is increased in abundance. Contents of alkaline earth elements and Zr are characteristic of tholeiitic MORB (Table **T95**). The variation diagram of distribution of normalized REE ratios demonstrates both significant dispersion in large-ion lanthanides and their lower content in comparison with basalts in Hole 525A (Fig. **F94**)

T95. Basalts, Hole 527, p.566.

We have determined high-Ti basalt (TiO_2 = 2.53 wt%) in one sample from flow Unit 5 (Table **T95**). Other samples represent two groups of basalts, one group with TiO_2 content from 1.73 to 1.91 wt% and the other with TiO_2 content from 1.27 to 1.33 wt% (Units 1–3 and 5).

Alteration Mineralogy

All additionally studied samples from Hole 527 represent nonoxidized basalts (Fe_2O_3/FeO = 0.58–1.25) (Table **T95**). One sample from flow Unit 1 (Sample 74-527-39R-2, 131–134 cm) is oxidized and has a Fe_2O_3/FeO ratio of 2.94. All basalts show a low degree of alteration (see **"Appendix A,"** p.133). H_2O^+ ranges from 0.55 to 1.41 wt% (Table **T95**). All recovered basalts are gray (Moore, Rabinowitz, et al., 1984).

XRD data show that smectites with Na-K interlayer cations predominate among secondary minerals. Hydromica, amphibole, and chlorite occur in trace amounts (see **"Appendix A,"** p.133).

The thin sections demonstrate (see **"Appendix A,"** p.133) that smectites completely replace olivine and interstitial glass and fills thin cracks. Plagioclase and augite phenocrysts show minor replacement by smectite. Plagioclase from groundmass is essentially unaltered and clinopyroxene is altered. Secondary pyrite occurs in veins and groundmass, especially in flow Unit 5 (Moore, Rabinowitz, et al., 1984). This unit also contains chlorite in trace amounts. An assemblage of secondary minerals in basalts in Hole 527 reflects a low-temperature alteration. Possibly, temperature in Hole 527 was a higher than

in Hole 525A.

Bulk-Rock Chemical Changes

Of six studied samples of basalts only two (Samples 74-527-39R-2, 131–134 cm, and 41R-3, 39–42 cm) are appropriate for determination of element mobility caused by alteration. These samples demonstrate massive structure, low TiO_2 content (1.33 and 1.27 wt%, respectively), and slight alteration (H_2O^+ = 1.21 and 0.55 wt%, respectively) (Table **T95**). The first sample is oxidized (Fe_2O_3/FeO = 2.94), whereas the second sample is not (Fe_2O_3/FeO = 0.58). Comparison of these samples supports the conclusion made for altered basalts from the Ninetyeast Ridge; oxidative alteration is accompanied mainly by gain of matter. Oxidized basalts demonstrate higher absolute contents of Si, Al, Fe, Mn, K, REE, V, Zn, Y, Nb, Rb, Zr, and Ba, as well as lower contents of Ca, P, Cr, and probably Ni than nonoxidized basalts ("Appendix B", Table **AT49**).

AT49. Major and trace elements, Hole 527, p.140.

Other samples of basalts are near to similar in TiO_2 content (1.73–1.91 wt%) and demonstrate insufficient alteration (H_2O^+ = 0.56–0.83 wt%).

Hole 528

Petrography and Bulk-Rock Chemical Composition

Eight individual basalt flow units were recognized in the intercalation with sediments (Moore, Rabinowitz, et al., 1984). These units were grouped into two lithologic types. Type 1 is represented by Units 1 through 6 and 8. Basalts of this type are massive, gray, medium- to coarse grained, and sparsely to highly plagioclase phyric texture. Phenocrysts of olivine and clinopyroxene are very sparse. Vesicles are sparse or absent. Type 2 includes Units 2 and 7. Basalts of this type are medium gray, fine- to medium grained, and aphyric texture. Vesicles are abundant (as much as 30% of the rock volume) in the upper 40–80 cm of the units (Moore, Rabinowitz, et al., 1984).

We studied seven additional samples of basalts from flow Units 1, 2, 4, 5, and 8. The basalts are represented by aphyric, plagioclase-phyric, clinopyroxene-plagioclase-phyric, and olivine-plagioclase-phyric massive and slightly vesicular varieties (see **"Appendix A,"** p.134). All of the basalts are practically nondifferentiated. Ti and Fe are average in abundance. We determined high-Ti basalts with TiO_2 contents of 2.36 wt% in Units 2 and 8 (Table **T96**). Other samples from Units 1, 4, and 5 are represented by basalts with TiO_2 contents from 1.26 to 1.71 wt%. Judging from geochemical diagrams, these basalts can be chiefly classified as tholeiitic E-MORB with poorly expressed Bouen's trend of differentiation (Figs. **F92, F93**). Content of both siderophile and chalcophile minor elements is characteristic of normal MORB, whereas alkaline earth elements show some increase in abundance (Table **T96**). Content of Zr is similar to that in MORB. Sample 74-528-42R-1, 32–35 cm, provides an exception, as Zr content in it this sample is two times higher than in tholeiitic basalts. The variation diagram of normalized REE ratios indicate enrichment in large-ion lanthanides. The spectrum is the broadest than in any basalt in Holes 525A and 527 (Fig. **F94**).

T96. Basalts, Hole 528, p.567.

Alteration Mineralogy

According to our study, basalts in Hole 528 are slightly altered (see **"Appendix A,"** p.134). H_2O^+ content varies from 0.97 to 1.72 wt% (Table T96). We characterized all basalts as nonoxidized rocks with low Fe_2O_3/FeO ratio (0.72–1.60). As it was observed for basalts in Holes 525A and 527, basalts in Hole 528 demonstrate medium gray to gray color (Moore, Rabinowitz, et al., 1984).

Smectites dominate among secondary minerals (see **"Appendix A,"** p.134). XRD data demonstrate smectites are represented by different varieties, from pure to those containing ~10% mica layers and with Na-K and Mg-Ca

interlayer cations. Pure smectite dominates. Hydromica, chlorite, defective chlorite, calcite, heulandite(?), and quartz occur sporadically as an admixture with smectites. Smectites and mixed-layer smectite-chlorite mineral with admixtures of hydromica, talc, and defective chlorite dominate among clay minerals in Sample 74-528-40R-2, 24–27 cm.

Olivine and groundmass glass are completely replaced with smectites. Clinopyroxene is replaced with clay minerals. Phenocrysts of plagioclase are partially replaced with smectites. Vesicles are rimmed with smectites, calcite, and pyrite. Some vesicles are filled with smectites only. Secondary mineral assemblages in basalts in Hole 528 indicate a higher temperature of alteration than in Hole 525A.

Bulk-Rock Chemical Changes

The studied samples of basalts from Hole 528 are not favorable for determination of element mobility at alteration. Two samples with high TiO_2 content (2.36 and 2.37 wt%) are incomparable with each other, as one of them is highly vesicular (~30%) and the other is sparsely vesicular (<1%). One additional sample is unique in its group in TiO_2 content (1.71 wt%), and at least four other samples (TiO_2 = 1.26–1.59 wt%) are incomparable to each other as they are represented by both massive and vesicular basalts. Moreover, both degree and variations in alteration are low (H_2O^+ = 0.97–1.24 wt%).

Element contents in basalts in Hole 528 are given in "Appendix B", Table **AT50.**

AT50. Major and trace elements, Hole 528, p.141.

Brief Comments

For the most part, basalts from the Walvis Ridge (Holes 525A, 527, and 528) are slightly altered and similar in this way to basalts recovered during Leg 115. Their alteration occurred under both nonoxidizing and oxidizing environments. Some samples of oxidized basalts demonstrate variation of Fe_2O_3/FeO ratio from 2.01 to 4.88 (Holes 525A and 527).

The studied basalts contain smectites as predominant secondary minerals. In general, alteration of basalts recovered during Leg 74 occurred under low-temperature conditions. A higher temperature of alteration in these holes than in Hole 525A is inferred from the presence of pyrite and clay minerals with chloritic structures in basalts from Holes 527 and 528, as well as the presence of talc in basalts from Hole 528.

Against the background of slight alteration of basalts from the Walvis Ridge, one can see a tendency in gain of matter under oxidizing environment, as recognized in oxidized basalts from the Ninetyeast Ridge. This tendency is evident in basalts from Holes 525A and 527.

Rio Grande Rise

Hole 516F

The Rio Grande Rise is a major aseismic ridge. We studied samples of basalts from Hole 516F after Thompson et al. (1982). This hole is located on the Rio Grande Rise, western Atlantic Ocean (30°16.59′S, 35°17.10′N) (Fig. **F95**), at a water depth of 1313 m drilling penetration 1270.6 m to the subbottom of oldest sediment at 1250 m (Coniacian calcarenite). Basalt was recovered from 1252.6 to 1270.6 mbsf (Barker, Carlson, Johnson, et al., 1983). Our objective was to continue the study of basalt alteration from related volcanic structures of Atlantic Ocean.

F95. Site on the Rio Grande Rise, p.305.

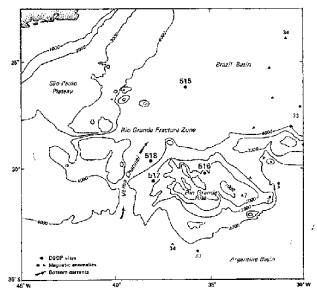

Petrography and Bulk-Rock Chemical Composition

Basalts in Hole 516F are T-MORB, similar to that found on the eastern Walvis Ridge. They are present two flow units (Thompson et al., 1982). Groundmass glass is replaced with calcite and clay minerals and both

plagioclase and pyroxene phenocrysts are partially replaced by calcite.

We studied five additional samples of basalts from Hole 516F (see **"Appendix A,"** p.135; Table **T97**), which demonstrate uniform petrography. The basalts are aphyric and sparsely plagioclase-phyric, intersertal texture, vesicular (as much as 35%), and massive (see **"Appendix A,"** p.135). Plagioclase is the most abundant mineral (45% of the groundmass), and clinopyroxene is ~35% to 40%. Olivine is present in single crystals. Glass and ore mineral (opaque) are present in the groundmass (see **"Appendix A,"** p.135).

The basalts are undersaturated in silicity and poorly differentiated. They demonstrate relatively high contents of titanium (TiO_2 = 2.45–2.63 wt%), alkaline elements, and phosphorus (Table **T97**). Judging from geochemical diagrams, one can classify these rocks as subalkaline basalts (Figs. **F96, F97**). The basalts demonstrate some decrease in some siderophile elements (Cr and Ni) and relatively high contents of Cu, Sr, Zr, and Ba (Table **T97**). The variation diagram of distribution of normalized REE ratios indicates slight enrichment of basalts in large-ion lanthanides (Fig. **F98**).

Alteration Mineralogy

Results of our study show that these basalts are slightly to moderately altered and demonstrate H_2O^+ content variations from 1.13 to 2.46 wt% (Table T97). We characterized all of the basalts as nonoxidized, as Fe_2O_3/FeO ratios vary from 0.44 to 0.95. This is in accordance with the classification of basalts as nonoxidized with Fe_2O_3/FeO ratios <1.60 and oxidized with Fe_2O_3/FeO ratios >1.60.

Thin section analyses demonstrate that smectites (sporadically with carbonate) partly or completely replace glass in the groundmass (see **"Appendix A,"** p.135). Olivine and individual phenocrysts of plagioclase are replaced completely with smectites and carbonate. Centralized vesicles have rims of smectite, zeolite, and calcite.

XRD data shows that smectites predominate among secondary minerals and hydromica occurs in trace amounts (see **"Appendix A,"** p.135).

Bulk-Rock Chemical Changes

The studied samples of basalts from Hole 516F are unfavorable for determination of element mobility as they are near to similar in degree of alteration (H_2O^+ = 1.42–2.53 wt%) and vary in vesicularity from massive to highly vesicular (see **"Appendix A,"** p.135; "Appendix B", Table **AT51**).

Brief Comments

Study results show that the basalts in Hole 516F are slightly to moderately altered and nonoxidized. Secondary mineral assemblages (smectites predominate among secondary minerals) are characteristic of low-temperature alteration.

ALTERATION OF IGNEOUS ROCKS FROM MARGINAL SEAS

The West Pacific marginal basins are of various origin. Most models are related to simple subduction processes inducing extension in the backarc area. On the contrary, the South China Sea and the Japan Sea have been interpreted as Atlantic-type basins (Rangin, Silver, von Breymann, et al., 1990). Formation of many basins is related to rifting and spreading processes. Alteration of igneous rocks in marginal basins occurs within both typical oceanic crust and in crust compositionally different from MORB. Hence, alteration of the rocks in marginal basins have specific features to be studied. Moreover, an interest in alteration processes in theses structures is promoted by

T97. Basalts, Hole 516F, p.569.

F96. AFM diagram for basalts, Hole 516F, p.306.

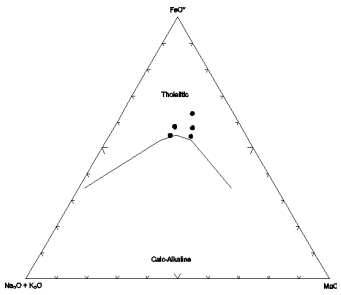

F97. Nb-Zr-Y diagram for basalts, Hole 516F, p.307.

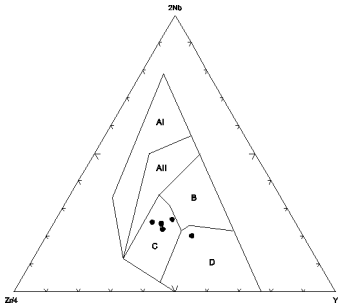

F98. Chondrite-normalized REEs for basalts, Hole 516F, p.308.

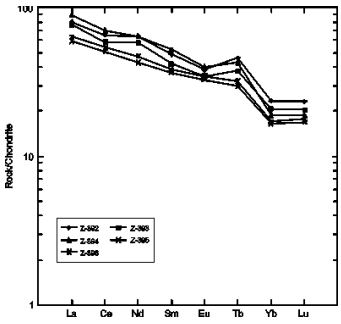

AT51. Major and trace elements, Hole 516F, p.142.

the fact that altered fragments of ancient crust from marginal sea-volcanic arc-trench systems are widespread as ophiolite terranes at continental margins and primarily at the east Asian margin.

Additionally, we have studied various igneous rocks that were altered because of seawater-rock interaction through time. Samples are from marginal basins of the West Pacific region: the Sulu Sea and the Celebes Sea (ODP Leg 124, Holes 768C and 770C), the Philippine Sea (DSDP Leg 59, Holes 447A, 448, 448A, and 449; DSDP Leg 60, Holes 453, 454A, 458, and 459B; ODP Leg 125, Holes 779A, 780C, and 786B; and ODP Leg 126, Holes 791B, 792E, and 793B), the Japan Sea (ODP Leg 127, Holes 794C, 794D, 795B, and 797C), the Lau Basin (ODP Leg 135 Hole 834B), and the Bering Sea (Leg 19 Hole 191).

Sulu and Celebes Seas

Hole 768C (8°00.04′N, 121°13.18′E; water depth = 4384.4 m; basement penetration = 221.8 m) is located in the southeast Sulu Basin, from which the oldest sediment recovered is of early Miocene age. Hole 770C (5°08.69′N, 123°40.11′E; water depth = 4504.9 m; basement penetration = 106.3 m) is located in the Celebes Sea, from which the oldest sediment recovered is of early Oligocene age (Fig. **F99**).

F99. Sites in the Sulu and Celebes Seas, p.309.

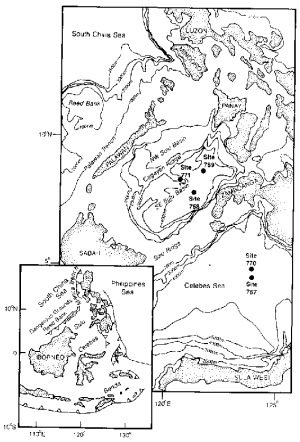

The Sulu and Celebes Seas are deep basins (4000–5000 m) located to the southeast of the South China Sea. They demonstrate complex geodynamic settings with active arc-arc or arc-continent collision zones, subduction zones, and significant strike-slip motion along major faults (Rangin, Silver, von Breymann, et al., 1990). They are near the zone of complex junction between the Pacific, Indian Ocean, and Philippine Sea plates. The Sulu Sea is a structurally complex basin, elongated in a northeast–southwest direction. It is 650 km long and 400 km wide and located between the South China Sea to the north and the Celebes Sea to the south. The Sulu Sea originated as a backarc spreading basin in the early Miocene. The Celebes Sea is 270,000 km^2 in size. The nature of the middle Eocene Celebes Sea remains unclear. It is not simply a fragment of either the Indian Ocean or the western Philippine Sea plates. Nevertheless, Silver and Rangin (1991) do not exclude that it represents a fragment of the mostly subducted Molucca Sea plate or a basin rifted from the edge of the east Asian mainland.

Hole 768C

Petrography and Bulk-Rock Chemical Composition

Rangin, Silver, von Breymann, et al. (1990) have determined that lava units in Hole 768C are petrographically similar, and that it is extremely difficult to identify their textures correctly, as well as to estimate proportions of phenocrysts and vesicles. They divided the sequence into eight units. Units 1, 4, 6, and 8 comprise sequences of pillowed and brecciated olivine-phyric basalts. Units 5 and 7 are made up of thin sheet flows of sparsely to highly olivine-phyric basalts. Units 2 and 3 are represented by olivine dolerite and microgabbro sills.

Hole 768C basalts are olivine tholeiites of primitive composition. Lava flows are characterized by high vesicularity, an uncommon feature for magma rich in MgO and erupted at early crystallization stages. Similar features have been observed in marginal and backarc basalts and are considered to be distinctive from MORB with a similar chemistry. The rocks are similar to N-MORB, but demonstrate features of transition to island-arc tholeiites (IAT) (Rangin, Silver, von Breymann, et al., 1990). Some basalts of Unit 1 have a picritic character, with MgO content ranging 14.1–9.9 wt%. Two-pyroxene microgabbro of Unit 3 also has a high MgO content, from 18.9 to 15.1 wt%, coupled with high Ni, Cr, and minimal incompatible element contents (Spadea et al., 1991). Rangin, Silver, von Breymann, et al. (1990) also determined that

the Sulu Basin backarc rocks belong to MORB/IAT transitional basalts.

We studied 43 additional samples of basalts from lava Units 1 through 7 (Table **T98**). Our petrographic and geochemical data (see **"Appendix A,"** p.136; Figs. **F100, F101**) mostly correspond to the data described above. As a rule, picritic varieties of basalts are enriched in Cr, Ni, and Co and depleted in Nb, Rb, Sr, and Zr (Table **T98**). The variation diagram of normalized REE ratios demonstrates a trend similar to that in normal tholeiitic MORB (Fig. **F102**).

Alteration Mineralogy

Spadea et al. (1991) studied altered rocks from the Sulu Basin in detail. They determined that all basement rocks from Hole 768C are, in general, strongly altered throughout, therefore, no olivine or glass is preserved. Vesicles are filled with carbonate, zeolites, and clay minerals, suggesting water-rock interaction at a low temperature. Nevertheless, the widespread occurrence of chlorite, serpentine, talc, and actinolite, together with the occasional albitization of plagioclase, indicate that the rocks also suffered hydrothermal metamorphism under low greenschist facies conditions. Olivine is replaced by clay minerals, serpentine, talc, carbonate, and iddingsite. The glassy mesostasis is replaced with smectites and, in some cases, with zeolite. Vesicles are mostly filled with zeolites, clay minerals, serpentine, Fe hydroxides, and carbonates.

All additional samples of basalts that we studied are moderately to highly altered (H_2O^+ = 1.12–6.07 wt%). These basalts represent two types of alteration: (1) nonoxidative alteration with Fe_2O_3/FeO ratios from 0.73 to 1.57 and (2) oxidative alteration with Fe_2O_3/FeO ratios from 1.61 to 5.48 (Table **T98**). Smectites and swelling chlorites, as well as different mixed-layer minerals (smectite-swelling chlorite and smectite-chlorite, including corrensite-like mineral) dominate among secondary minerals (see **"Appendix A,"** p.136). All smectites have Mg-Ca interlayer cations. Hydromica, chlorite, corrensite-like mineral or corrensite, mixed-layer smectite-swelling chlorite and smectite-chlorite minerals, calcite, analcime, and talc occur with smectites as admixtures, amphibole is sporadically present in trace amounts (see **"Appendix A,"** p.136).

Smectite and smectite-chlorite aggregate completely replace olivine and groundmass glass. Olivine is replaced with clay minerals and calcite. Glass contains patches of Fe oxides. Plagioclase is partly replaced with green smectite and very rarely with albite. The smectite-chlorite aggregate with an admixture of calcite, zeolites, and chalcedony fills vesicles. Microveins contain smectites, calcite, traces of talc, and quartz. Individual xenomorphic quartz grains and carbonate are present in the groundmass. In microgabbro, biotite is strongly chloritized and olivine is completely chloritized. Pyroxene and plagioclase are partly replaced with smectite and smectite-chlorite aggregate. Interstitial glass is replaced with smectite and smectite-chlorite aggregate with an admixture of actinolite. Hornblende is partly chloritized (see **"Appendix A,"** p.136).

Bulk-Rock Chemical Changes

Some information about mobilization of chemical elements at alteration in Hole 768C was obtained by Spadea et al. (1991). Based on the direct comparison of chemical compositions of the most-altered and least-altered samples, Spadea et al. (1991) demonstrated that alteration-related chemical changes significantly involve LOI and alkalies, and that chemical mobilization affects Cs more than Rb. Sr and Ba do not appear to be significantly affected by secondary mobilization.

We divided studied basalt samples into three groups according to MgO content (13.95–18.71, 9.63–10.92, and 6.06–8.98 wt%). These groups of samples contain oxidized, nonoxidized, massive, and vesicular basalts. The comparison of absolute element content in basalts in Hole 768C ("Appendix B", Table **AT52**) altered under oxidative conditions reveal trends in their behavior as follows. Oxidized basalts gain primarily in Rb and K, as well as in Fe^{+++}, Na,

T98. Igneous rocks, Hole 768C, p.570.

F100. AFM diagram for igneous rocks, Holes 768C and 770C, p.310.

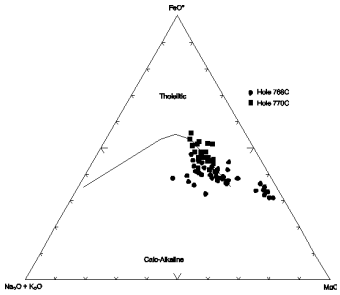

F101. Nb-Zr-Y diagram for igneous rocks, Holes 768C and 770C, p.311.

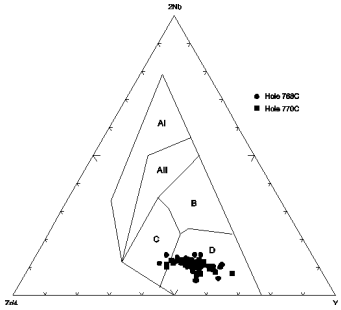

F102. Chondrite-normalized REEs for igneous rocks, Holes 768C and 770C, p.312.

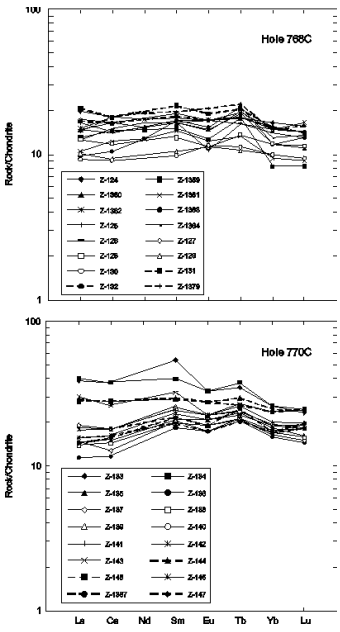

and Co. Basalts may either gain or lose Mg, Ni, Cu, Zn, Y, and Zr. In all cases, basalts demonstrate loss in Si, Ti(?), Al, total Fe, Mn, Ca, REE, Sc, V, Nb, and Sr.

AT52. Major and trace elements, Hole 768C, p.143.

The obtained data differ from the above described study results of element mobility at oxidative alteration from aseismic and mid-ocean ridges, where most mobile elements enrich basalts.

It is probable that these variations in element behavior result from combined influence of both oxidizing and nonoxidizing environments upon the studied samples at different times. Variations in each of them likely predetermine the character of elements redistribution. Presence of both oxidative and nonoxidative alteration products suggests a more complex scenario of the mixed behavior of elements. Some elements inherit the redistribution trend characteristic for the oxidative type of alteration, whereas others inherit the redistribution style that is typical for nonoxidative alteration.

Hole 770C

Petrography and Bulk-Rock Chemical Composition

Rangin, Silver, von Breymann, et al. (1990) divided the sequence into nine lava units. Units 1 and 2 are moderately and highly plagioclase-olivine-phyric pillow basalts, respectively. Unit 3 represents a pillow breccia (moderately to highly plagioclase-olivine-phyric basalts). Units 4 and 5 are represented by a brecciated, massive, amygdaloidal lava (moderately to highly plagioclase-olivine-phyric basalts). Unit 6 is a massive lava (moderately to highly plagioclase-olivine-phyric basalts). Units 7 and 8 represent dolerite sills. Unit 7 consists of a sparsely plagioclase phyric to aphyric dolerite and Unit 8 is composed of a sparsely to highly plagioclase-olivine-phyric dolerite. Unit 9 is lava with a small dike (moderately to highly olivine-plagioclase-phyric basalt). The lava units in Hole 770C are petrographically similar.

Hole 770C basalts are tholeiites with primitive to moderately fractionated MORB-type basalts (Rangin, Silver, von Breymann, et al., 1990; Serri et al., 1991). However, Sr and Nd isotopes are typical of both Indian Ocean MORBs and of some backarc basalts, such as those of Lau Basin (Serri et al., 1991).

We studied 23 additional samples of basalts from all lava units (see **"Appendix A,"** p.142; Table **T99**). In general, results correspond to data obtained by our predecessors. Most of the samples are represented by plagioclase-phyric varieties with olivine in groundmass or in phenocrysts. Some samples demonstrate doleritic texture (Samples 124-770C-5R-5, 34–38 cm; 10R-2, 110–112 cm; 12R-1, 11–13 cm; and 12R-2, 79–84 cm). Basalts are practically nondifferentiated in silica, Al_2O_3, Fe, and Mg (Table **T99**). Geochemical diagrams classify them as normal tholeiitic MORB (Figs. **F100, F101**). Siderophile, chalkophile, and alkaline earth elements, as well as Zr, are significantly variable in abundance but similar to that in normal tholeiitic MORB (Table **T99**). Moderate-Ti and high-Ti groups of basalts (TiO_2 = 1.73–2.37 wt%) occur among the studied rock varieties (Samples 124-770C-2R-3, 23–25 cm; 3R-3, 36–38 cm; 3R-4, 55–60 cm; 9R-2, 53–55 cm; 10R-2, 110–112 cm; 11R-1, 98–100 cm; and 12R-1, 11–13 cm). The remaining samples have TiO_2 contents from 1.17 to 1.57 wt% (Table **T99**). Most of samples are similar to normal tholeiitic MORB in REE distribution, whereas relatively high-Ti basalts are somewhat enriched in large-ion lanthanides and especially in Sm (Fig. **F102**).

T99. Igneous rocks, Hole 770C, p.576.

Alteration Mineralogy

Rangin, Silver, von Breymann, et al. (1990) studied altered rocks from the Celebes Sea during Leg 124. All basement rocks in Hole 770C are affected by alteration at various degrees. Vesicles are filled or partly filled with green clay minerals, calcite, and in some cases with silica. Sparse fractures are filled

with a mixture of green and brown clay, calcite, and limonite. Olivine phenocrysts are totally altered to clay, occasionally associated with calcite. Mesostasis between plagioclase and clinopyroxene crystallites and devitrified glass contain numerous tiny particles of iron oxide. Fissures are infilled with carbonate.

All studied basalt samples are slightly to moderately altered (H_2O^+ = 0.46–2.14 wt%). They represent two types of alteration: (1) nonoxidative alteration with Fe_2O_3/FeO ratios from 0.94 to 1.59 and (2) oxidative alteration with Fe_2O_3/FeO ratios from 1.67 to 2.98 (Table **T99**). Smectites dominate among secondary minerals (see **"Appendix A,"** p.142). All smectites contain Mg-Ca interlayer cations. In many cases, smectite contains as much as 20% mica layers. Samples 124-770C-4R-1, 17–19 cm, and 12R-1, 11–13 cm, contain smectite and swelling chlorite. Sample 5R-6, 106–108 cm, contains smectite and trace amounts of mixed-layer smectite-chlorite mineral. Hydromica, chlorite, amphibole, and talc associate with smectite as an admixture. Smectites completely replace olivine and groundmass glass and fills vesicles. Smectites in vesicles and interstitial glass are sporadically impregnated with Fe hydroxides. Carbonates associate with smectites in vesicles and cracks. Fe hydroxides associate with ore minerals. Smectites in Hole 770C represent the major secondary phase and provide evidence of low-temperature alteration.

Bulk-Rock Chemical Changes

Serri et al. (1991) demonstrated that MgO, CaO, and Na_2O were removed and P_2O_5 increased at the alteration of pillow basalts in Hole 770C. Moreover, amounts of Ti, Cs, Li, Rb, and K are generally high.

Redistribution of chemical elements in basalts at their alteration were analyzed for three chemical groups with TiO_2 contents of 2.20–2.37, 1.73–1.86, and 1.17–1.57 wt%. Within these groups, we recognized oxidized, nonoxidized, massive, and vesicular basalts.

The redistribution of elements at oxidative alteration of basalts in Hole 770C is similar to that in samples from Hole 786C. Basalts in Hole 770C differ in behavior of such elements as total Fe, Na, Co, V, and Cu, which demonstrates a reverse trend. Less oxidized samples of basalts in Hole 770C, with Fe_2O_3/FeO ratios of ~1.2 (samples with Fe_2O_3/FeO ratios <1.60 are determined as nonoxidized basalts), demonstrate some differences in redistribution of elements. Unlike the clearly oxidized samples (Fe_2O_3/FeO = >1.60), these samples demonstrate an increase in contents of REE, as well as Mn, Nb, and Sr against the background decrease in K and V ("Appendix B", Table **AT53**).

AT53. Major and trace elements, Hole 770C, p.149.

Brief Comments

Basalts in Holes 768C (Sulu Sea) and 770C (Celebes Sea) are altered under low-temperature smectite facies conditions in both nonoxidative and oxidative environments. The alteration and oxidation are more intense in basalts from Hole 768C.

Spadea et al. (1991) showed that basalts from the Sulu Sea are altered at a low temperature (carbonate, zeolites, and clay minerals). Spadea et al. (1991) also suggested that chlorite, serpentine, talc, and actinolite, together with the sporadic albitization of plagioclase, indicate that the rocks also suffered hydrothermal metamorphism under low greenschist facies conditions.

We believe that alteration of basalts in Hole 768C developed at low-temperature conditions. Widespread occurrence of smectites does not correspond to low greenschist mineral facies. The appearance of talc in altered basalts at the 1185–1196 mbsf interval (see **"Appendix A,"** p.136) is not an indication of high-temperature alteration. Talc is only found in picritic basalt with high contents of MgO (13.95–18.71 wt%) (Table **T98**). Occurrence of analcime in the1221–1243 mbsf interval possibly also reflects the primary basalt composition enriched in Na (Table **T98**). Formation of mixed-layer smectite-

swelling chlorite and smectite-chlorite minerals, corrensite-like mineral or corrensite, swelling chlorites and chlorite, along with smectites, is likely predestined by the primary basalt composition and its variability. Moreover, smectite also dominates at the bottom of the hole (see **"Appendix A,"** p.136), thus indicating that the alteration temperature did not increase with the subbottom depth recovered in the hole, but instead, remained low and did not exceed 100°–150°C. Rare occurrences of albite, actinolite, and amphibole(?) possibly reflect local higher temperature alteration of basalts within the section recovered in Hole 768C.

Studied samples of massive and vesicular basalts from Hole 768C represent good objects for the study of mass balance at their alteration. However, it is impossible to estimate the gain/loss of elements on the available material, because fresh analogs of the altered rocks are absent at this time. When such analogs are found, likely in other regions, the gain/loss of elements during strong alteration of the basalts recovered from Hole 768C can be estimated using the data presented in this Report.

Philippine Sea

Holes 779A and 780C are located at the southeast flank of the Conical Seamount and on its summit, respectively. The seamount is restricted to the outer arc high of the Mariana forearc at a distance of ~100 km from the trench axis. Holes 458 and 459B are located in the Mariana forearc region. Hole 458 is drilled ~85 km westward from the axis of the Mariana Trench and ~130 km eastward from the active volcanic islands. Hole 459B is located at the eastern margin of the deep sediment pond on the island-arc side of the trench slope break (Table **T100**).

T100. Additional basement holes, Legs 125, 126, 59, and 60, p.579.

Holes 791B, 453, and 454A are located in backarc basins. Hole 791B is drilled near the center of Sumisu Rift in a backarc graben westward from the Izu-Bonin island-arc volcanoes Sumisu Jima and Tori Shima. Holes 453 and 454A are restricted to the Mariana Trough ~10 km eastward from the eastern edge of the West Mariana Ridge and central portion of the Mariana Trough near the backarc axis of spreading, respectively (Table **T100**).

Holes 786B, 792E, and 793B are located in the Izu-Bonin forearc basin. Hole 786B is situated in the center of the basin ~70 km westward from the axis of the Izu-Bonin trench. Hole 792E is located on the western half of the Izu-Bonin forearc sedimentary basin. Hole 793B is positioned in the center of the Izu-Bonin forearc sedimentary basin, ~125 km westward from the axis of the Izu-Bonin Trench (Table **T100**).

Hole 447A is located on the eastern side of the West Philippine Basin between the Central Basin Ridge and the Palau-Kyushu Ridge. Hole 449 is located on the western side of the spreading Parece Vela Basin.

Hole 448 is located on the western edge of the Palau-Kyushu Ridge (remnant arc) (Table **T100**).

The scientific parties of Legs 59, 60, 125, and 126 (Scott et al., 1980; Hussong, Uyeda, et al., 1981; Fryer, Pearce, Stokking, et al., 1990; Taylor, Fujioka, et al., 1990) described in detail the geological setting of the marginal Philippine Sea. The region is made up of a complex series of arcs and basins which formed since the start of westward subduction of the Pacific lithosphere beneath the Philippine Sea Plate in the Eocene. Later, the Mesozoic Pacific oceanic lithosphere subducted to the west-northwest beneath the arcs. The tectonic configuration of the Izu-Bonin-Mariana region comprises, from east to west, the trench; the forearc terrane made up of an inner trench wall, an outer-arc high, a forearc basin, and a frontal-arc high; the active Izu-Bonin and Mariana island arcs, the Izu-Bonin backarc rifts and actively spreading Mariana backarc basin; the incipient rift basins of the Izu-Bonin backarc; the West Mariana Ridge and remnant arc; the Parece Vela and Shikoku marginal basins;

the Palau-Kyushu Ridge and westernmost remnant arc; and the inactive West Philippine Basin.

The Mariana forearc has undergone extensive uplift. A broad zone of serpentinite seamounts up to 2500 m high and 30 km in diameter, 50–120 km from the trench axis, has been identified to the west of the break in slope at the top of the inner trench wall (Fryer, Pearce, Stokking, et al., 1990). Holes 779A and 780C are located at one such diapiric serpentinite seamount (Conical Seamount). Unlike the Mariana forearc, the Izu-Bonin forearc has experienced only minor deformation since the Eocene. Holes 786B, 792E, and 793B penetrated the Izu-Bonin forearc basin floor. The backarc rifts are almost continuous along their strike. Hole 791B was drilled directly in the backarc graben (Sumisu Rift).

Holes 779A and 780C

Petrography and Bulk-Rock Chemical Composition

The section recovered in Hole 779A (Fig. **F103**) has been divided into three lithologic units (Fryer, Pearce, Stokking, et al., 1990). Unit 2 is represented in the interval from 125-779A-3R-CC to 35R-1, 133 cm. All 16 studied samples are from Unit 2. Leg 125 scientists determined that lithologic Unit 2 contains clasts of various igneous and metamorphic rocks in a clayey silt-sized serpentine matrix. The unit is divided into two subunits, but such division seems rather artificial. Subunit 2A (10.6–216.2 mbsf) is represented by blocks of serpentinized harzburgite, dunite, metabasalt, and serpentinite in a serpentine matrix. Subunit 2B (216.2–303 mbsf) is built of blocks of gabbro and serpentinized harzburgite, dunite, and metabasalt in a serpentine matrix with intercalations of detrital fine grained serpentine sediments.

Fryer, Pearce, Stokking, et al. (1990) determined that the Hole 779A section is represented by ~95% serpentinized and tectonized ultramafic and ~5% metamorphosed mafic rocks. Harzburgite (80%) dominates among ultramafic rocks; dunite (20%) is less abundant. About 60% of the mafic rocks are metabasalts, and the rest are metamicrogabbros. The primary mineralogy of serpentinized and tectonized harzburgites is represented by olivine (75%–85%), orthopyroxene (10%–25%), chromium spinel, and subordinate clinopyroxene. Dunites (preserpentinization) consist of olivine (90%– 99%), orthopyroxene (1%–9%), and spinel (as much as 1%). Metabasalt and metamicrogabbro are aphyric to microphyric the primary mineralogy contains, in subequal proportions, plagioclase and augite with considerable amounts (30%–40%) of glass. All ultramafic samples are remarkably homogeneous chemically (Fryer, Pearce, Stokking, et al., 1990). The ultramafic rocks are 40%–100% serpentinized (Sabora et al., 1992). The mafic clasts have a varied geochemical composition, reflecting MORB-like, alkaline, and IAT types (Johnson, 1992). Ishii et al. (1992) interpreted these peridotites as ultramafic rocks associated with island-arc volcanism, they are more depleted than the peridotites from the mid-ocean ridges.

We have studied 16 additional samples of igneous rocks (serpentinized and tectonized harzburgites and dunites, and metabasalt and metamicrogabbro) from Unit 2 (see **"Appendix A,"** p.146; Table **T101**). Thirteen samples are represented by apohyperbasitic serpentinites and three samples by basites.

Microgabbro cataclasite (Sample 125-779A-31R-2, 87–89 cm), olivine-clinopyroxene-plagioclase-phyric basalt (Sample 31R-CC, 10–12 cm), and metabasalt (Sample 31R-3, 30–33 cm) significantly differ major and minor element contents (Table **T101;** Figs. **F104, F105**). Apohyperbasitic serpentinites are enriched in Mg, but low in silica and alkalinity. As for minor elements, these rocks are enriched in Cr and Ni but depleted in V, Cu, Zn, Nb, Rb, Sr, Zr, and Ba (Table **T101**). They also demonstrate an unusual spectrum of normalized REE distribution (Fig. **F106**). As compared to the spectrum of basalts, they show increased content of Ce and partly La against the background of sharp

F103. Sites in the Izu-Bonin and Mariana forearcs, p.313.

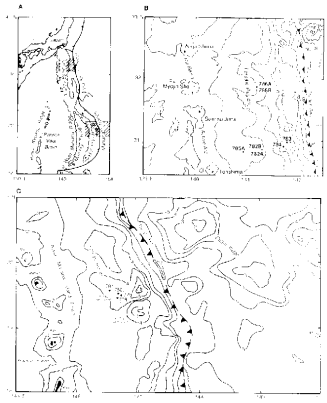

T101. Igneous rocks, 779A, p.580.

F104. AFM diagram for igneous rocks, Hole 779A, 780C, and 786B, p.314.

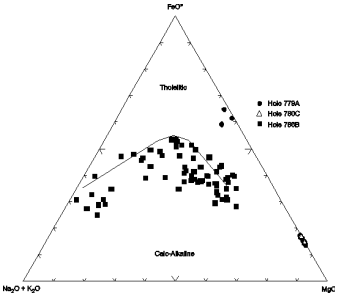

decrease in contents of Sm and Eu. The studied samples of basalts are very uniform in their chemical composition. They are common low-alkaline basalts of tholeiitic type undersaturated in silica, with middle Ti and typical REE content (Table **T101**). The spectrum of REE is similar to that in tholeiitic MORB (Fig. **F106**). The only difference is in slight depletion in large-ion lanthanides.

Alteration Mineralogy

The Mariana serpentinite seamounts provide access to the products of alteration and metamorphism of a central forearc region which have been formed by reaction with components derived from the subducting slab (Fryer, Pearce, Stokking, et al., 1990). Fryer, Pearce, Stokking, et al. (1990) determined that the degree of serpentinization of the ultramafic rocks is highly variable. In the most altered harzburgite samples, most olivine and orthopyroxene is replaced with serpentine (antigorite-rich), and chromium-spinel is probably replaced with magnetite. In partially altered spinel grains, radial arranged halos of chlorite (prehnite?) are present. The harzburgites are cut with numerous serpentine veins. Alteration of dunites is similar to that of harzburgites. Chlorite and brucite are recognized in altered dunites. Glass is intensively replaced with chlorite (prehnite) and other clay minerals. These rocks also contain carbonate, pumpellyite, sphene, and albite. They are strongly altered to prehnite/pumpellyite facies. Mineralogy of serpentinites in Holes 779A and 780A–780D was studied by Fryer and Mottl (1992). They identified lizardite, chrysotile, antigorite, greenalite, aragonite, calcite, goethite, loughlinite, sepiolite, and magnesium-rich amphibole. Lizardite, chrysotile, antigorite, greenalite, brucite, magnetite, magnesite, talc, amphibole, chlorite, calcite, and aragonite are present in the samples of metamorphosed ultramafic rocks (Sabora et al., 1992). Johnson (1992) showed that clasts of mafic rocks, both arc-derived and mid-ocean ridge–derived (most samples are represented by metabasalt, also gabbro and possibly boninite samples) are metamorphosed under a range from low-temperature zeolite facies to pumpellyite facies and perhaps lower greenschist facies. High content of CaO (as much as 25%) in one clast suggests a rodingite metamorphism.

All additionally studied samples of serpentinized ultramafic rocks from Hole 779A are strongly altered (H_2O^+ = 5.05–17.97 wt%). Most of the rocks are moderately to intensely oxidized (Fe_2O_3/FeO = 2.30–44.67). Three samples of metamorphosed mafic rocks have H_2O^+ contents ranging within 4.46–4.79 wt% and a very high content of CaO, from 19.33 to 21.87 wt% (Table **T101**). These rocks belong to non-oxidized varieties (Fe_2O_3/FeO ratio of 0.6 provides an exception).

Two additional samples of serpentinized ultramafic rocks from Hole 780C were studied: Sample 124-780C-18R-1, 31–34 cm (serpentinized verlite), and Sample 18R-1, 42–45 cm (serpentinized lherzolite) (see **"Appendix A,"** p.149; Table **T102;** Figs. **F104, F106**). These two samples have chemical compositions similar to those of serpentinized ultramafic rocks in Hole 779A.

Serpentines predominate among secondary minerals in harzburgites and dunites. Amphibole and talc occur occasionally in trace amounts with serpentine. Amphibole (actinolite?) with an admixture of chlorite occurs within serpentinized orthopyroxene. Some crystals of olivine are completely replaced with amphibole. Oxides (hematite?) are present in a serpentine vein and occur sporadically in olivine and spinel. Serpentine replaces both olivine and pyroxene in harzburgites and dunites. Serpentine is represented mainly by chrysotile. Rarely, veins are filled with an aggregate of chrysotile and antigorite. Chlorite dominates in nonoxidized samples of metamicrogabbro and metabasalt. Sample 125-779A-31R-3, 30–33 cm, contains chlorite and pumpellyite (see **"Appendix A,"** p.146).

According to electron microscopy and electron diffraction analysis, serpentine minerals in all studied samples are represented by chrysotile,

F105. Nb-Zr-Y diagram for igneous rocks, Hole 779A, 780C, and 786B, p.315.

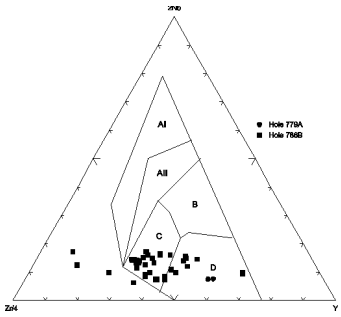

F106. Chondrite-normalized REEs for igneous rocks, Hole 779A, 780C, and 786B, p.316.

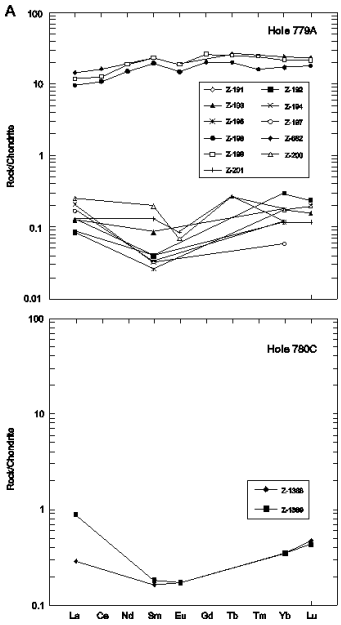

T102. Igneous rocks, Hole 780C, p.583.

lizardite, and antigorite. We have determined several polytypes of chrysotile, such as $2O_{rc1}$, $2M_{c1}$, and D_c (see **"Appendix A,"** p.146). The structural type of chrysotile is tube-in-tube. Particles of chrysotile of polytype $2O_{rc1}$ with large diameters occur in small amounts. This kind of chrysotile is named "barrel-like chrysotile" (Tokmakov et al., 1983) or "Povlen-type chrysotile" (Morandi and Felici, 1979). According to Morandi and Felici (1979), this kind of chrysotile is related to a final stage of serpentinization with hydrothermal aqueous solutions penetrating the cataclastic fracture produced by contraction of the serpentinite rocks during transition from the low-grade metamorphic environment to lower temperature conditions.

Bulk-Rock Chemical Changes

Leg 125 scientists (Fryer, Pearce, Stokking, et al., 1990) ascertained that LOI in studied samples demonstrates a positive correlation with the degree of serpentinization. In all rocks, SiO_2 and MgO inversely correlate with LOI and the degree of serpentinization, whereas Cr and Ni do not. In the metadiabase rocks, CaO content is high (18.24–21.71 wt%), and neither Na_2O or K_2O is present. This possibly results from prehnite/pumpellyite facies alteration of the rocks.

Comparison of absolute contents of elements ("Appendix B", Tables **AT54, AT55**) revealed that in both apoharzburgite serpentinite (Sample 124-779A-34R-1, 63–65 cm; H_2O^+ = 13.90 wt%, Fe_2O_3/FeO = 4.95) and serpentinized harzburgite (Sample 14R-1, 20–22 cm; H_2O^+ = 5.05 wt%, Fe_2O_3/FeO = 2.30), increase in the degree of serpentinization of harzburgite is accompanied by a loss of Si, Ti, Fe, Mn, Mg, Ce, Yb, Lu, Sc, Cr, Ni, Co, and V against a background of gain in Al, Na, La, Sm, Cu, and Zn.

The studied samples of serpentinized dunites from Hole 779A demonstrate similar degrees of alteration. To estimate mobility of elements, more samples must be obtained to expand the interval of alteration. This is also true for the studied metabasalts.

AT54. Major and trace elements, Hole 779A, p.153.

AT55. Major and trace elements, Hole 780C, p.156.

Hole 786B

Petrography and Bulk-Rock Chemical Composition

The igneous section recovered in Hole 786B (Fig. **F103**) is divided into 30 lithologic units that contain a wide variety of rock types, ranging from mafic to silicic and including basalt; high-Mg basalt; picrite; high-, intermediate-, and low-Ca boninites; intermediate- and low-Ca bronzite andesites; andesite; dacite; and rhyolite, with dispersion of Mg between 18.5 and 0 wt% MgO and silica between 48.5 and 74.5 wt% SiO_2 (Fryer, Pearce, Stokking, et al., 1990; Arculus et al., 1992).

We studied 64 additional sample of igneous rocks from lithologic Units 1 (boninite), 2 (basalt flow), 3 (andesite), 4 (andesite and andesite-basalt/boninite?), 7 (basalt flow), 9 (andesite and andesite-basalt), 11 (boninite flows), 15 (basalt, andesite, and dacite flows), 16 (andesite), 17 (basalt flow), 19 (andesite-boninite? and basalt), 20 (hyalobasalt), 22 (rhyolite flow), 24 (boninite?), 25 (andesite-basalt), 26 (rhyolite, andesite-basalt and andesite-dacite flows), 27 (basalt dike), 28 (andesite and andesite-dacite/boninite?), and 30 (andesite-basalt/boninite?). The results are given in **"Appendix A,"** p.149 (Table **T103**). The studied samples are represented by effusive rocks broadly differentiated in silicity (from basalt to rhyolite), with low Ti and variable alkaline element content (Table **T103;** Fig. **F104**), especially K. Both aphyric and phyric varieties are present (see **"Appendix A,"** p.149), with phyric varieties predominating. Phyric varieties contain plagiophyric, clinopyroxene-plagioclase-phyric, olivine-clinopyroxene, and olivine-plagioclase-phyric rocks (i.e., demonstrating practically all combinations of main rock-forming minerals). Cr, Ni, and V broadly vary in their abundance (Table **T103**). As a rule, Cr and partly Ni increase in abundance with Mg increase in the rock. Rb,

T103. Igneous rocks, Hole 786B, p.584.

Sr, and Zr broadly vary in abundance. Rb and Sr content is also generally somewhat higher than in typical tholeiitic MORB, whereas Zr content is lower (Table **T103;** Fig. **F105**). The spectrum of REE indicates poorly expressed enrichment in large-ion lanthanides (Fig. **F106**).

Alteration Mineralogy

The studied samples of igneous rocks are altered at various degrees (H_2O^+ = 0.20–4.44 wt%) and are represented by both oxidized (Fe_2O_3/FeO = 1.63–7.03; Fe_2O_3/FeO ratio for Sample 125-786B-63R-1, 118–121 cm = 18.22) and nonoxidized (Fe_2O_3/FeO = 0.48–1.47) rocks (Table **T103**).

Smectites dominate among secondary minerals (see **"Appendix A,"** p.149). They contain Mg-Ca and K-Na interlayer cations and as much as 30% mica layers. Chlorite, hydromica, cristobalite, quartz, and calcite associate with smectite as an admixture. Smectites replace olivine and groundmass glass. Olivine is replaced with carbonate and Fe oxides, in some cases an admixture of zeolite is fixed. Orthopyroxene grains are replaced with smectites around their periphery and along cracks. Smectites also fill vesicles. Occasionally vesicles are filled with carbonate or zeolites. Cracks are filled with smectites and/or zeolites. Carbonate veins are present. Matrix and vesicles in andesite breccia contain phillipsite. Tuff breccia of boninite-andesite composition is replaced with corrensite and small amounts of chlorite and quartz (Sample 125-786B-72R-2, 50–55 cm). Andesitic lava breccia contains smectites and erionite (Sample 56R-1, 20–25 cm). Andesites contain traces of phillipsite. Among secondary minerals, quartz and cristobalite are most probably inherited from the primary andesitic composition. Practically fresh rhyolites contain small amounts of quartz, chlorite, and hydromica (see **"Appendix A,"** p.149).

Bulk-Rock Chemical Changes

Alteration slightly affected contents of major elements in the igneous rocks in Hole 786B (Fryer, Pearce, Stokking, et al., 1990). Murton et al. (1992) showed that enrichment in P_2O_5, Y, and REE is a result of post-eruption fluid-rock interaction (up to greenschist facies, with development of albite-chlorite-epidote-quartz assemblages).

Comparison of absolute contents of elements in differently altered boninites (Sample 125-786B-4R-1, 142–144 cm; H_2O^+ = 1.06 wt%, Fe_2O_3/FeO = 1.04 and Sample 27R-2, 48–51 cm; H_2O^+ = 3.23 wt%, Fe_2O_3/FeO = 3.40) revealed that at oxidative alteration boninites loose Si, Ti, Al, Ca, Na, P, REE (except Ce), Sc, Cr, Co, V, Y, Sr, and Zr but gain Mg, Ce, Ni, Cu, Zn, Rb, Ba, and probably Mn ("Appendix B", Table **AT56**).

It is difficult to estimate element mobility in other rock varieties in Hole 786B. All rhyolites are practically fresh (Table **T103**).

AT56. Major and trace elements, Hole 786B, p.157.

Hole 792E

Petrography and Geochemistry of Rocks

The igneous section recovered in Hole 792E (Fig. **F107**) is divided into five units which are represented mainly by porphyritic, plagioclase-(+quartz)-orthopyroxene-clinopyroxene andesite lavas. Besides andesites, they contain andesitic hyaloclastite breccia with minor basaltic andesite and dacite (Taylor, Fujioka, et al., 1990). These lavas are similar to calc-alkaline volcanics from Japan but have lower contents of Ti, Zr, and low field strength elements (Taylor et al., 1992).

We have studied additional samples of igneous rocks from Units 1 through 5 (phyritic andesite flow). Results of our petrographic and geochemical data (see **"Appendix A,"** p.160; Table **T104;** Figs. **F108, F109, F110**) mainly correspond to the data obtained by our predecessors (Taylor, Fujioka, et al., 1990). The studied samples are represented by a broad spectrum of differentiation in silicity from andesite-basalt to andesite-dacite. The rocks

F107. Sites 791, 792, and 793 in the Sumisu Rift and Forearc Basin, Philippine Sea, p.319.

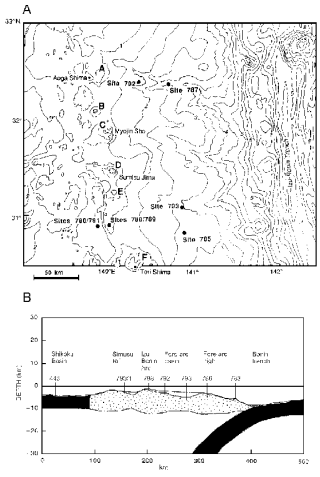

demonstrate low contents of Ti, Mg, Cr, Ni, V, Zr, Ba, and alkaline elements (Table **T104**).

Alteration Mineralogy and Bulk-Rock Chemical Changes

Leg 126 scientists (Taylor, Fujioka, et al., 1990) classified the alteration of basement rocks in Hole 792E as low-temperature alteration. They ascertained that orthopyroxene and plagioclase phenocrysts in andesites are fresh. Cracks are filled with smectites. The glassy sections of flows are replaced with smectite.

All nine additionally studied samples of igneous rocks are slightly altered (H_2O^+ = 0.67–1.53 wt%) and oxidized (Fe_2O_3/FeO = 2.87–4.76). Smectites predominate among secondary minerals (see **"Appendix A,"** p.160; Table **T104**).

Smectites with Mg-Ca interlayer cations are recognized in all samples by XRD (see **"Appendix A,"** p.160). Sample 126-792E-72R-1, 18–20 cm is, the only exception. Smectite in this sample contains K-Na interlayer cations. Cristobalite in various proportions (from trace amounts to predominance) occurs together with smectites. Quartz and hydromica sporadically occur with smectites as an admixture. Smectites replace groundmass glass and fill vesicles. Individual phenocrysts of clinopyroxene and olivine(?) or orthopyroxene(?) are completely replaced with smectite. Prismatic crystals of hornblende or orthopyroxene are replaced with an aggregate of secondary minerals including smectite, hydrotalcite(?), and possibly tremolite-actinolite (see **"Appendix A,"** p.160).

Taylor, Fujioka, et al. (1990) suggested that Y, P, Rb, K, and Sr variations within the sequence are not consistent with simple crystal fractionation.

Variations in contents of elements may not be related to their mobility, as the alteration of the studied basalt samples from Hole 792E is slight and the interval of this alteration is very narrow.

Element content in igneous rocks in Hole 792E are given in "Appendix B", Table **AT57.**

Hole 793B

Petrography and Geochemistry of Rocks

According to data obtained during Leg 126 (Taylor, Fujioka, et al., 1990) the igneous section recovered from Hole 793B (Fig. **F107**) contains breccia and massive to pillowed flows of phyric and aphyric clinopyroxene-orthopyroxene high-Mg series basaltic andesites and andesites with boninitic affinities, as well as a low-Mg series with tholeiitic affinities. The volcanic rocks in Hole 793B are exclusively andesitic, unlike the rocks with varying composition recovered from Hole 786B. The andesites are enriched in Rb, Sr, and Ba, as compared to MORB, whereas they are depleted in Ba and Sr relative to island-arc rocks. Basaltic andesites are products of synrift volcanism taking place in the forearc region and share many geochemical and petrographic characteristics of boninites. They are intermediate between low-Ti arc tholeiites from the active arc and boninites of the outer-arc high-Ti ones (Taylor et al., 1992). The basement section is divided into 17 flow units.

We studied 13 additional samples of igneous rocks from flow Units 1, 3, 9, 10, 13, 14, 15, and 17 (see **"Appendix A,"** p.161; Table **T105**). The studied samples are represented by varieties of low-Ti, low-Al, and high-Mg basalts and andesites. These rocks have boninite petrochemical specialization. They demonstrate high Cr and Ni and low Zr concentrations (Table **T105**). Geochemical diagrams (Figs. **F108, F109, F110**) provide evidence that basalts from Hole 793B belong to tholeiitic series.

T104. Igneous rocks, Hole 792E, p.593.

F108. AFM diagram for igneous rocks, Holes 791B, 792E, and 793B, p.320.

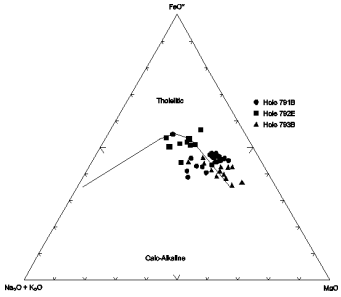

F109. Nb-Zr-Y diagram for igneous rocks, Holes 791B, 792E, and 793B, p.321.

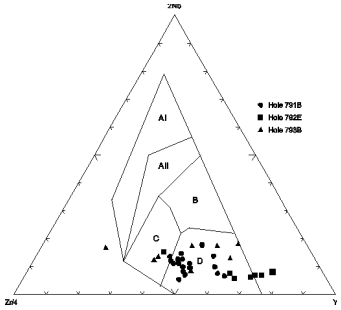

F110. Chondrite-normalized REEs for igneous rocks, Holes 791B, 792E, and 793B, p.322.

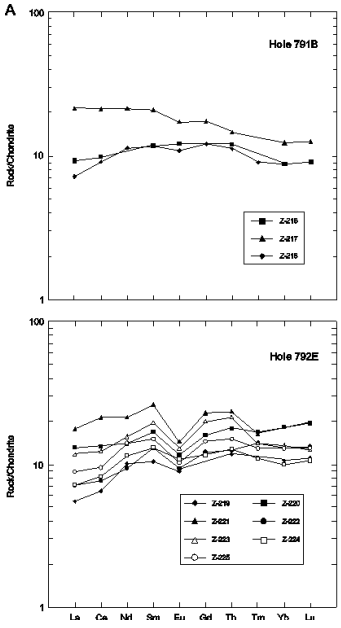

AT57. Major and trace elements, Hole 792E, p.166.

Alteration Mineralogy and Bulk-Rock Chemical Changes

Leg 126 scientists (Taylor, Fujioka, et al., 1990) ascertained that basement rocks in Hole 793B are slightly altered. Smectites and zeolites replace interstitial glass and fill fractures and vesicles. Olivine is replaced by calcite and smectite. Smectites are present along fractures in orthopyroxene crystals.

Additional samples of igneous rocks are altered at various degrees (H_2O^+ = 0.95–2.25 wt%; Sample 126-793B-86R-1, 35–40 cm, contains 3.28 wt% H_2O^+) and represent two types of alteration: (1) nonoxidized alteration with Fe_2O_3/FeO ratios from 0.66 to 1.56 and (2) oxidized alteration with Fe_2O_3/FeO ratios from 1.69 to 2.00. Sample 126-793B-86R-1, 35–40 cm, has a Fe_2O_3/FeO ratio of 6.98 (Table **T105**). Tuff (Sample 126-793B-103R-1, 37–42 cm) contains 3.73 wt% H_2O^+ and a Fe_2O_3/FeO ratio of 4.15. Breccia (Sample 126-793B-95R-2, 26–32 cm) contains 3.26 wt% H_2O^+ and a Fe_2O_3/FeO ratio of 2.77.

T105. Igneous rocks, Hole 793B, p.595.

The dominant secondary mineral is smectite with Mg-Ca and Na-K interlayer cations, as detected by XRD (see **"Appendix A,"** p.161). Hydromica associates with smectite. Quartz was recognized in the lower part of the section. The lowermost studied samples (1673.09 mbsf) contain hydromica, heulandite(?), and chlorite(?) as admixture, in association with smectite. Smectites replace olivine, sporadically with a carbonate admixture. Smectite partially replaces orthopyroxene and completely replaces interstitial glass. Smectite fills vesicles completely or partially. Domination of smectites among secondary minerals reflects low-temperature alteration. Some increase in temperature of alteration is probable in the lowermost part of the sampled section.

We have not determined the element mobility at alteration of basalts in Hole 793B, as variation of vesicularity is significant ("Appendix B", Table **AT58**).

AT58. Major and trace elements, Hole 793B, p.168.

Hole 791B

Petrography and Bulk-Rock Chemical Composition

The rift basement recovered from Hole 791B (Fig. **F107**) was divided into 29 flow units which contain basalt, basaltic "mousse," basalt breccia, diabase, and tuff (Taylor, Fujioka, et al., 1990). Our predecessors have determined that the basalts are highly vesicular, sparsely plagioclase, and olivine-plagioclase phyric. They are inferred to be of synrift origin, but are more similar to rift-wall and seamount rocks from the outer rift than to pillow basalts from the inner rift ridges. The basaltic mousse mainly consists of highly basaltic glass. Fine grained, mainly holocrystalline diabases constitute dikes or sills. They contain plagioclase, olivine, magnetite, devitrified glass, and microvesicles. Petrology and geochemistry of volcanic rocks in Hole 791B were studied in detail by Gill et al. (1992).

We studied 21 additional samples of igneous rocks from flow Units 4, 5, 6, 8, 11, 14, 15, 18, 20, 24, 26, and 28 (Table **T106**), which comprise basalt and basaltic breccia, hyalobasaltic mousse, dolerite, andesite-boninite, andesite, and tuff of andesite or andesite-basalt composition (see **"Appendix A,"** p.163). As a rule, the rocks are vesicular. The AFM and Zr-Nb-Y diagrams (Figs. **F108, F109**) and REE spectra (Fig. **F110**) of the basalts in Hole 791B are similar to that of N-MORB.

T106. Igneous rocks, Hole 791B, p.597.

Alteration Mineralogy

Additional samples of igneous rocks which we studied vary in the degree of alteration and oxidation. Content of H_2O^+ and Fe_2O_3/FeO ratio values are: (1) for basalts, 0.10–5.61 wt% and 0.62–3.40, respectively; (2) for hyalobasaltic mousse, 1.38–6.39 wt% and 0.62–2.55, respectively; (3) for dolerite, 0.89 wt% and 1.35, respectively; and (4) for andesitic tuff and breccia, 0.89–5.12 wt% and 0.51–6.22, respectively.

XRD data indicate that smectites predominate among secondary minerals in the hyalobasaltic mousse (see **"Appendix A,"** p.163). Chlorite and analcime are detected as an admixture to smectite in Sample 126-791B-73R-2, 73–75 cm. Leg 126 scientists (Taylor, Fujioka, et al., 1990) ascertained that vesicles in the basalt mousse are filled with smectite, calcite, and zeolite(?). Gill et al. (1992) showed that olivines in mousse are replaced by calcite, whereas vesicles are infilled with smectite, zeolite, and native copper. Glass is replaced by smectite. In our samples, smectites cover the walls of vesicles or partly fill them. It is probable that vesicles were primarily filled with glass, which was later replaced with grassy green smectite. Vesicles in basalt fragments are filled with palagonized glass. Plagioclase remains fresh. The glass is fresher in the matrix than in the clasts. Olivine is replaced with smectite.

XRD patterns also show that the white matrix from tuff of andesite-basalt composition (Sample 126-791B-77R-2, 0–5 cm) contains gypsum, as dominant mineral, and quartz (see **"Appendix A,"** p.163).

Secondary minerals recognized by scientists of Leg 126 and by our team reflect low-temperature alteration of igneous rocks. Nevertheless, Yuasa et al. (1992) described prehnite-pumpellyite (pumpellyite, albite, chlorite, and epidote paragenetic assemblages) facies metamorphism in the lowermost part of the basement rocks at Site 791 (Sample 126-791B-79R-1, Piece 11; tuff). They suppose that metamorphism took place during the prerifting stage of an intraoceanic arc.

Bulk-Rock Chemical Changes

The igneous rocks in Hole 791B are rather unsuitable for estimation of gain/loss of elements during rock alteration ("Appendix B", Table **AT59**), mainly owing to their variable vesicularity. Fresh analogs of the altered varieties with similar vesicularity to the studied rocks are needed for this estimation.

AT59. Major and trace elements, Hole 791B, p.170.

Direct comparison of chemical compositions of basalts and hyalobasaltic mousse provided us with the following results. Comparing two samples of basalts (Sample 126-791B-72R-2, 50–55 cm; H_2O^+ = 5.61 wt%, Fe_2O_3/FeO = 2.47, and Sample 126-791B-61R-1, 42–50 cm; H_2O^+ = 0.11 wt%, Fe_2O_3/FeO = 0.78) shows that highly altered basalt contains less SiO_2, Al_2O_3, CaO, K_2O, P_2O_5, Zn, Y, and Ba and more FeO_{total}, MnO, MgO, Na_2O, Co, V, Nb, and Rb than fresh basalt (Table **T106**). The highly altered hyalobasalt (Sample 126-791B-73R-2, 73–75 cm; H_2O^+ = 6.39 wt%, Fe_2O_3/FeO = 2.32), as compared to the slightly altered sample (126-791B-63R-1, 65–70 cm; H_2O^+ = 1.38 wt%, Fe_2O_3/FeO = 0.87) contains less SiO_2, Al_2O_3, MgO, CaO, P_2O_5, Ni, Co, Cu, Zn, Zr, Nb, Sr, Ba La, Ce, and Eu and more Na_2O, K_2O, V, and Y (Table **T106**).

Hole 447A

Petrography and Bulk-Rock Chemical Composition

F111. Sites in the Philippine Sea, p.324.

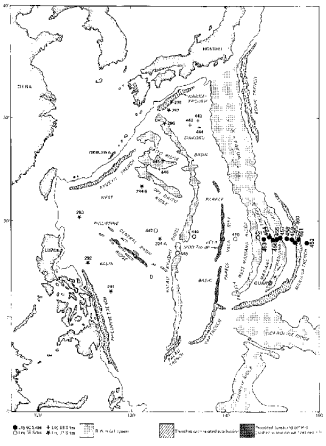

Hole 447A is located in West Philippine Sea (Fig. **F111**). Leg 59 scientists distinguished six flow units in the basalt section recovered from Hole 447A (Kroenke, Scott, et al., 1980). These units are built up of plagioclase-phyric, plagioclase-clinopyroxene-olivine-phyric, plagioclase-olivine-clinopyroxene-phyric, plagioclase-olivine-spinel-phyric, and aphyric tholeiitic basalts of massive and pillow lava flows. These basalts belong to normal tholeiitic MORB (Kroenke, Scott, et al., 1981; Wood et al, 1981; Zakariadze et al., 1981).

We studied 19 additional samples of igneous rocks from flow Units 6 through 11. These samples characterize all varieties of basalts recovered from Hole 447A (Table **T107**). Rocks are represented by aphyric, plagioclase-phyric, pyroxene-plagioclase, olivine-plagioclase, and olivine-pyroxene-plagioclase-phyric basalts (see **"Appendix A,"** p.165). Sample 59-447A-17R-3, 49–53 cm,

is andesite-basalt. As a rule, the basalts are massive or slightly vesicular (<1% of the rock volume, rarely as much as 3%–5%). The rocks belong to slightly differentiated in silicity, low-Ti basalts of tholeiitic and poorly expressed alkaline series. Concentrations of Cr, Ni, Co, V, and Sr (Table **T107**) are typical for normal tholeiitic MORB. The geochemical diagrams demonstrate that studied basalts in Hole 447A are N-MORB type (Figs. **F112, F113**). They are slightly depleted in Zr. The REE spectrum (Fig. **F114**) is similar to that in tholeiitic MORB.

Alteration Mineralogy

Leg 59 scientists (Kroenke, Scott, et al., 1981) classified alteration of basement rocks in Hole 447A as a low-temperature alteration. Olivine is mainly replaced with an aggregate of smectites and iron oxides. Interstitial and pillow margin glasses are replaced with smectites. Pyroxene remains fresh. Only rare plagioclase crystals show signs of alteration. Vesicles are partially or completely filled with smectites and carbonates and in some cases with zeolites (phillipsite). Smectites, phillipsite, and calcite are present in veins. Sulfides and rare quartz occur within the veins.

All additionally studied samples of tholeiitic basalts are slightly to moderately altered (H_2O^+ = 0.28–2.12 wt%). Slightly altered basalts are more common than moderately altered rocks. They represent both oxidative and nonoxidative alteration. Fe_2O_3/FeO ratios range from 1.63 to 2.50 in the oxidized basalts, whereas nonoxidized basalts are characterized by Fe_2O_3/FeO ratios from 0.41 to 1.57 (Table **T107**).

Smectites predominate among secondary minerals (see **"Appendix A,"** p.165). All smectites contain Mg-Ca interlayer cations. Quartz, chlorite, and hydromica as traces occur in association with smectites. Swelling chlorite is present in Samples 59-447A-14R-3, 53–58 cm, and 25R-1, 40–42 cm, and possibly in 36R-4, 31–36 cm (see **"Appendix A,"** p.165). Swelling chlorite replaces olivine and groundmass glass and fills vesicles. Often, olivine is replaced with carbonate and smectites. Phenocrysts of plagioclase are partly replaced with K-feldspar and sporadically with carbonate.

Bulk-Rock Chemical Changes

We chose two samples for comparison. Sample 59-447A-23R-1, 39–42 cm, represents fresh nonoxidized basalt (H_2O^+ = 0.65 wt%, Fe_2O_3/FeO = 0.70, density = 2.92 g/cm^3) (Table **T107**). Altered and slightly oxidized basalt is represented by Sample 59-447A-36R-4, 31–36 cm (H_2O^+ = 1.95 wt%, Fe_2O_3/FeO = 2.50, density = 2.64 g/cm^3). The comparison of absolute contents of elements in these samples ("Appendix B", Table **AT60**) revealed that altered and oxidized basalts are enriched in Al, Fe^{+3}, Na, K, Ni, Nd, Rb, and Sr but depleted in Si, Mn(?), Mg, Ca, P, Co, V, Cu, Zn, and Zr.

Holes 448 and 448A

Petrography and Bulk-Rock Chemical Composition

Leg 59 scientists divided the basement recovered from Holes 448 and 448A (Fig. **F111;** Table **T100**) into numerous units of basalt flows interbedded with 20 units of volcaniclastic sediments and 10 dikes and sills. The basalts vary from aphyric to plagioclase-clinopyroxene-orthopyroxene-pigeonite-olivine-phyric texture. The basement sequence recovered from the Palau-Kyushu Ridge consists predominantly of tholeiitic basalts, which differ from MORB in the abundance of explosive volcaniclastic debris, widespread distribution of hypersthene, and the presence of pigeonite and dikes of basaltic andesites (Kroenke, Scott, et al., 1981). The flows, dikes, and sills are all primitive island arc tholeiites with compositions similar to those of arc tholeiites from Japan (Scott, 1980; Wood et al, 1981).

We studied 37 additional samples of igneous rocks (basalt, andesite-

T107. Igneous rocks, Hole 447A, p.600.

F112. AFM diagram for igneous rocks, Sites 447, 448, and 449, p.325.

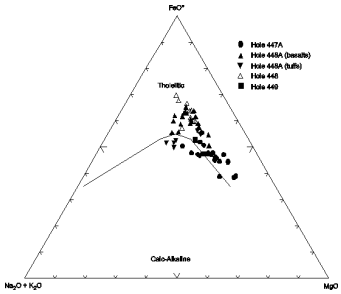

F113. Nb-Zr-Y diagram for igneous rocks, Sites 447, 448, and 449, p.326.

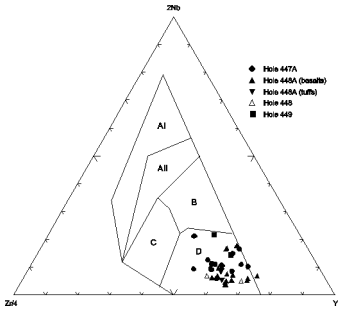

F114. Chondrite-normalized REEs for igneous rocks, Sites 447, 448, and 449, p.327.

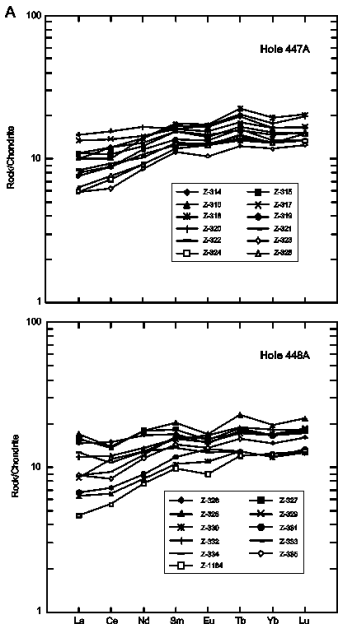

AT60. Major and trace elements, Hole 477A, p.173.

basalt, and tuff) from 21 flow units (Table **T108;** see **"Appendix A,"** p.168). Descriptions of the volcanic units are from Kroenke, Scott, et al. (1981).

T108. Igneous rocks, Holes 448 and 448A, p.603.

Unit 6: Pillowed massive flow, plagioclase-clinopyroxene-orthopyroxene-olivine phyric vesicular basalt, with 30% vesicular.
Unit 8: Pillow lava flows, plagioclase-olivine-clinopyroxene phyric basalt with 20% vesicular.
Unit 9: Pillowed massive flow, aphyric basalt, 30% vesicular.
Unit 11: Basalt flows, plagioclase-clinopyroxene-orthopyroxene-pigeonite-olivine phyric basalt, 25% vesicular.
Unit 13: Basalt flows, plagioclase-clinopyroxene-orthopyroxene-pigeonite phyric basalt, 15%–35% vesicular.
Unit 14: Pillow lavas, plagioclase-clinopyroxene-orthopyroxene-(olivine) phyric basalt, 10%–40% vesicular.
Unit 15: Volcaniclastic breccia and tuff, a clast of plagioclase-clinopyroxene phyric basalt, 20% vesicular.
Unit 17: Tuff and volcaniclastic breccia.
Unit 19: Volcaniclastic breccia.
Unit 20: Basalt flow, aphyric basalt.
Unit 23: Cognate basalt breccia, aphyric basalt, 20% vesicular.
Unit 27: Basalt dike, aphyric basalt, 10% vesicular.
Unit 31: Basalt flows, plagioclase-clinopyroxene phyric basalt, 15%–20% vesicular.
Unit 33: Flow or sill, plagioclase-clinopyroxene phyric basalt, 2%–10% vesicular.
Unit 36: Volcaniclastic breccia grading into laminated tuff.
Unit 37: Basalt dike, plagioclase-clinopyroxene phyric basalt, 2% vesicular.
Unit 40: Volcaniclastic breccia.
Unit 41: Basalt flow(?) and cognate breccia, plagioclase-clinopyroxene phyric basalt, vesicles are rare.
Unit 43: Basalt flow(?), aphyric basalt, 10% vesicular.
Unit 49: Basalt dike, plagioclase-clinopyroxene-orthopyroxene phyric basalt without vesicles.
Unit 51: Basalt dike, aphyric basalt.

All studied samples represent poorly differentiated in silicity, low-Ti tholeiitic basalts. Some samples demonstrate relatively high contents of K, especially tuff samples (Table **T108**). Cr, Ni, Co, and Zr are less abundant than in typical MORB (Table **T108**). Geochemical diagrams (Figs. **F112, F113**) demonstrate that studied igneous rocks belong to tholeiitic N-MORB. The REE spectrum is similar to that in tholeiites, but is somewhat depleted in large-ion lanthanides (Fig. **F114**).

Alteration Mineralogy

Leg 59 scientists (Kroenke, Scott, et al., 1981) have not found evidence of broad distribution of regional hydrothermal metamorphism of basalts. Nevertheless, they showed that low-grade local hydrothermal metamorphism had affected breccia below 750 mbsf, where abundant intrusions occur. Veinlets of native cooper are present within the volcaniclastic breccia (Aldrich et al., 1981). Olivine is mainly replaced with an aggregate of smectites and iron oxides. Smectites replace interstitial and pillow margin glasses. Pyroxene remains fresh. Only rare plagioclase crystals are altered. Vesicles are partially or completely filled with smectites and carbonates, occasionally with zeolites (phillipsite). Smectites, phillipsite, and calcite occur in veins. Sulfides and rare quartz are present within the veins. Oxidized basalts were recovered in the upper part of basement (84.5 m; 319.5–404 mbsf) at Site 448. Disseminated oxides were found in the 489.5–521 mbsf interval (201.5 m below basement top). In general, the igneous rocks are nonoxidized.

All additionally studied samples are slightly to moderately altered and,

in general, nonoxidized, except for tuff and breccia. Tuffs are moderately to highly altered (H_2O^+ = 2.81–6.54 wt%) (Table **T108**) and moderately to extremely oxidized (Fe_2O_3/FeO = 4.87–45.59) (Table **T108**). Breccia is moderately altered (H_2O^+ = 4.54 wt%) (Table **T108**) and highly oxidized (Fe_2O_3/FeO = 10.04) (Table **T108**). Basalts are fresh and slightly altered (H_2O^+ = 0.45–1.70 wt%) (Table **T108**) and almost all samples are nonoxidized. All andesite-basalts are fresh or almost fresh (H_2O^+ = 0.33–0.93 wt%) (Table **T108**). They are nonoxidized and slightly oxidized (Fe_2O_3/FeO = 0.59–2.44) (Table **T108**). There are slight indications of oxidation of the rocks near the bottom of the hole. In the lower part of the section (661–913 mbsf), Fe_2O_3/FeO ratios range from 2.01 to 2.44 (Table **T108**).

Petrographically, slightly oxidized rocks occur in different parts of the section (see **"Appendix A,"** p.168). Strongly oxidized tuff and breccia from the middle and lower parts of the section suggest an apparent oxidative environment, whereas signs of oxidation are visually observed in some samples from the upper part of the section up to 521 mbsf, or 201.5 m below of the top of basement (Kroenke, Scott, et al., 1981).

XRD data suggests smectites dominate among secondary minerals (see **"Appendix A,"** p.168) and completely replace groundmass glass. Smectites contain Mg-Ca and K-Na interlayer cations. Some smectites contain as much as 30%–40% mica layers. Hydromica and chlorite (as trace) sporadically occur in association with smectites. Cristobalite occurs in trace amounts together with smectites in the lowermost andesite-basalt samples from sills and dikes (flow Units 33, 37, 43, 49, and 51) (see **"Appendix A,"** p.168). Cristobalite is also recognized in the andesite basement recovered from Holes 786B and 792E in the Izu-Bonin forearc basin. Secondary minerals from Sample 59-448A-14R-2, 58–64 cm, are represented by smectite and phillipsite (see **"Appendix A,"** p.168). Vesicles are partly filled with smectites and, in some cases, with carbonate, zeolite and chalcedony. Rarely vesicles are partly filled with volcanic glass and smectites, and many vesicles are hollow. Carbonate is present in veinlets (see **"Appendix A,"** p.168).

Bulk-Rock Chemical Changes

In the volcaniclastic breccia in Hole 448A, Hajash (1980) noted an increase in total Fe, K_2O, and MgO. Moreover, he ascertained that Sample 59-448A-44R-1, 67–71 cm, is enriched in Na_2O and MgO and depleted in K_2O, CaO, and total iron. He explained these data to be a result of hydrothermal metamorphism.

We were not able to estimate element mobility in the studied samples of basalts from Holes 448 and 448A ("Appendix B", Table **AT61**), as almost all of them are vesicular varieties and slightly altered (see **"Appendix A,"** p.168; Table **T108**).

AT61. Major and trace elements, Holes 448 and 448A, p.176.

Hole 449

Petrography and Bulk-Rock Chemical Composition

Leg 59 scientists divided the basalt section recovered from Hole 449 (Fig. **F111;** Table **T100**) into two subunits (Kroenke, Scott, et al., 1981). These subunits are composed of plagioclase-olivine-spinel phyric tholeiitic basalt. Subunit 6a consists of pillow basalts, and Subunit 6b is represented by a basalt flow. These two subunits are indistinguishable from MORB (Kroenke, Scott, et al., 1981; Wood et al, 1981; Zakariadze et al., 1981).

We studied two additional samples of basalts from Subunits 6a and 6b (Table **T109;** see **"Appendix A,"** p.172). These samples are represented by aphyric, low-Ti, and low-alkaline basalts with typical tholeiitic Cr, Ni, and Co concentrations and low Zr. Judging by the geochemical diagrams (Figs. **F112, F113**), these rocks are similar to tholeiitic MORB. The REE distribution is similar to that in tholeiites (Fig. **F114**).

T109. Igneous rocks, Hole 449, p.609.

Alteration Mineralogy and Bulk-Rock Chemical Changes

Leg 59 scientists (Kroenke, Scott, et al., 1981) noted that any evidence of hydrothermal activity or metamorphism are absent in recovered basalts in Hole 449.

Two additionally studied samples of the tholeiitic basalt are slightly to moderately altered, with H_2O^+ contents ranging from 1.06 to 1.74 wt% (Table **T109**). We classified these basalts as slightly oxidized (Fe_2O_3/FeO = 1.68 and 1.88). XRD data show smectite and calcite predominate among secondary minerals (see **"Appendix A,"** p.172). Smectites contain ~30%–40% mica layers with Mg-Ca interlayer cations. Chlorite occurs as trace in association with smectites. Smectites and calcite replace groundmass glass and fill vesicles and thin veinlets (see **"Appendix A,"** p.172).

Mattey et al. (1981) detected, in general, a strong decrease in SiO_2; a slight decrease in MgO and CaO; a strong increase in K_2O, Rb, TiO_2, Fe_2O_3, and Pb; and a slight increase in Th in the element mobility during alteration of basalts recovered during Leg 59.

Element content in basalts from Hole 449 is given in "Appendix B", Table **AT62.**

Hole 453

Petrography and Bulk-Rock Chemical Composition

The basement recovered from Hole 453 (Figs. **F111, F115;** Table T100) is built up of three main parts: (1) 0–85.5 m beneath the sediments, upper igneous polymict breccia composed of diabase and basalt fragments with minor gabbro clasts cemented by a varicolored matrix; (2) 85.5–114 m, lower polymict breccia consisting mainly of metavolcanics and metabreccia (andesites and dacites) without large gabbro clasts; and (3) 114–149.5 m, sheared serpentinite and gabbro (Hussong, Uyeda, et al., 1981). All of these rocks have the geochemical characteristics of island arc magma types (Wood et al., 1982).

We studied 13 additional samples of gabbro from the interval 466–590 mbsf (Table **T110**). All studied samples are represented by tectonized (cataclastic) olivine-bearing and plagioclase-bearing gabbro (see **"Appendix A,"** p.173). The gabbro is low in Ti and alkalies (except for Sample 60-453-56R-2, 85–87 cm), undersaturated in silica, and high in Mg, except for Samples 60-453-56R-2, 33–35 cm, and 85–87 cm. Al_2O_3 content varies from 10.46 to 29.88 wt% (Table **T110**). The classification diagram (Fig. **F116**) provides evidence that they belong to the tholeiitic series, are poorly differentiated in Fe and Mg, and demonstrate the typical Fenner's trend. Two types of gabbro could be distinguished based on the content of minor elements (Table **T110**) and character of REE distribution (Fig. **F117**). The first type is characterized by a low Al. The REE spectrum is similar to that in tholeiitic basalts, but differs by depletion in large-ion lanthanides (Fig. **F117**). The second type demonstrates high Al content and low concentrations of all minor elements, except for Sr, as compared to tholeiitic basalts (Table **T110**). The REE spectrum differs from that of tholeiitic basalts in lower contents of Ce, Sm, Tb, Yb, and Lu (Fig. **F117**).

Alteration Mineralogy and Bulk-Rock Chemical Changes

During Leg 60, Hussong, Uyeda, et al. (1981) revealed that alteration of rock fragments in Hole 453 is moderate to very high. In basalt and diabase, chlorite, and stilpnomelane replace matrix and pyroxene, whereas sericite replaces plagioclase. Vesicles of metabasalts are filled with chlorite, quartz, carbonate, and prehnite. These minerals form the granoblastic groundmass together with pumpellyite, clay minerals, and iron hydroxides. Gabbro fragments contain secondary minerals of greenschist or amphibolite metamorphism facies. Major components of the matrix include clay minerals, carbonate, iron oxides, and hydroxides. Epidote, quartz, zeolite, prehnite, and

AT62. Major and trace elements, Hole 449, p.181.

F115. Generalized structure the active Mariana Arc system, p.329.

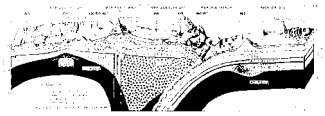

T110. Gabbros, Hole 453, p.610.

F116. AFM diagram for igneous rocks, Holes 453, 454A, 458, and 459B, p.330.

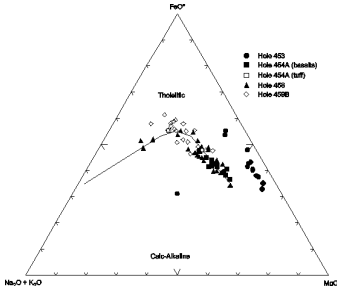

F117. Chondrite-normalized REEs in igneous rocks, Holes 453, 454A, 458, and 459B, p.331.

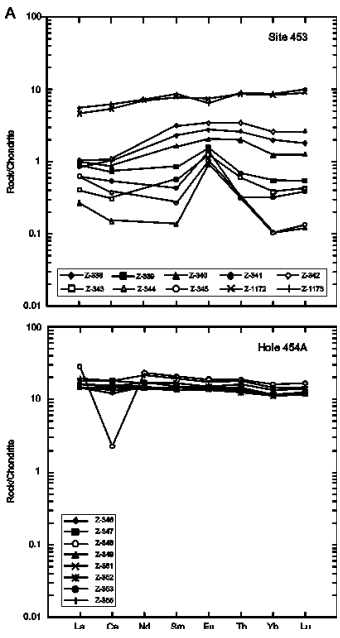

pumpellyite are also present. Hussong, Uyeda, et al. (1981) suggested that many clasts were metamorphosed before their incorporation into the breccia.

Additionally studied samples of polymict breccia are moderately to strongly altered, as H_2O^+ content ranges from 0.84 to 4.33 wt% (Table **T110**). Almost all samples represent nonoxidizing alteration (Fe_2O_3/FeO = 0.11–1.44). Sample 60-453-55R-3, 50–53 cm, is slightly oxidized with Fe_2O_3/FeO ratio of 1.85 (Table **T110**).

XRD data show that secondary minerals are represented by chlorite, serpentine, smectites, mixed-layer smectite-chlorite minerals, amphibole, analcime, talc, hydromica, and quartz in different amounts; prenite, natrolite(?), and chalcophyllite(?) are detected in trace amounts (Table **T111;** see **"Appendix A,"** p.173). Electron microscopy and electron diffraction analysis provide evidence that serpentine minerals in all studied samples are represented exceptionally by lizardite (see **"Appendix A,"** p.173). This mineral composition differs from the composition of serpentinites formed after ultramafic rocks. The latter are represented by chrysotile, lizardite, and antigorite (see **"Hole 637A"** and **"Hole 779A"**).

Numerous cracks in clinopyroxene are filled with a ferruginous chlorite-smectite aggregate or serpentine, chlorite, and ore mineral (see **"Appendix A,"** p.173). Clinopyroxene is replaced in patches with carbonate and opal. Individual grains of clinopyroxene are almost completely replaced with serpentine, whereas the grain margins are replaced with amphibole or chlorite and tremolite-actinolite. Plagioclase crystals are partly replaced with carbonate or, occasionally, with chlorite-smectite aggregate with hydromica and prehnite. Olivine is replaced with chlorite, serpentine, and smectites. Some grains of magnetite are replaced by goethite. Ore mineral is recognized in cracks within olivine.

Data on element content in the studied gabbro are presented in "Appendix B", Table **AT63.** As the breccia recovered from Hole 453 is composed of rock clasts different in chemical composition, the studied samples are not suitable for estimation of mobility of major and trace elements at alteration of the young backarc basin crust.

Hole 454A

Petrography and Bulk-Rock Chemical Composition

Hole 454A is located in the Mariana Trough (Figs. **F111, F115;** Table **T100**). Leg 60 scientists (Hussong, Uyeda, et al., 1981) divided recovered basalts into five lithologic units. Wood et al. (1982) defined three chemical types among the Hole 454A basalts. Lithologic Units 1 through 3 are similar in composition and correspond to chemical type 1. Units 4 and 5 correspond to chemical types 2 and 3, respectively. Unit 1 is represented by massive basalt flows (Core 60-454A-5R) consists of vesicular olivine-plagioclase microphyric basalt, with subophitic and intersertal texture. Unit 2 is composed of medium grained basalt (Core 6R) with aphyric, intersertal or transitional-to-spherulitic textures. Unit 3 consists of pillow basalts (Cores 8R through 10R). Unit 4 is a massive basalt flow (Cores 11R and 12R) with plagioclase and augite as major components and titanomagnetite and interstitial glass as minor components. Unit 5 consists of pillow basalts (Cores 13R through 16R). The rocks display most of characteristics of depleted interarc basin tholeiitic basalts (Wood et al., 1981).

We studied 12 additional samples of Hole 454A basalts (Table **T112**). These rocks belong to practically nondifferentiated in silicity, low-Ti tholeiitic basalts with a definite differentiation trend intermediate between the Fenner's and Bouen's trends (Fig. **F116**). The basalts are located within the field of N-MORB in the Zr-Nb-Y geochemical diagram (Fig. **F118**). Basalts in Hole 454A are similar to typical tholeiitic MORB in abundances of Cr, Ni, Co, V, and Sr,

T111. Altered gabbros, Hole 453, p.612.

AT63. Major and trace elements, Hole 453, p.182.

T112. Igneous rocks, Hole 454A, p.613.

F118. Nb-Zr-Y diagram for igneous rocks, Holes 453, 454A, 458, and 459B, p.333.

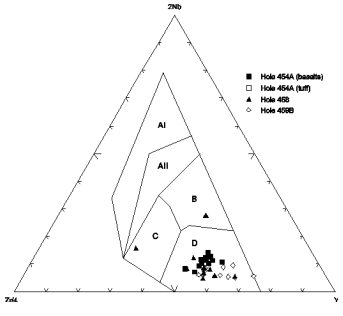

but they differ in some lower Zr concentration (Table **T112**). The spectrum of REE distribution (Fig. **F117**) is similar to that in tholeiitic basalts but differs in a generally lower content.

Alteration Mineralogy and Bulk-Rock Chemical Changes

Leg 60 scientists (Hussong, Uyeda, et al., 1981) showed that basalts recovered from Hole 454A are moderately to slightly altered. The alteration took place at typical low-temperature conditions. Clay minerals and carbonate dominate among secondary minerals.

The studied samples of basalts are fresh and slightly to moderately altered (H_2O^+ = 0.68–1.50 wt%). We classified almost all samples as nonoxidized (Fe_2O_3/FeO = 0.38–1.39). Only the uppermost Sample 60-454A-5R-1, 128–132 cm (Fe_2O_3/FeO = 1.68), is slightly oxidized (Table **T112**). XRD data indicate smectites predominate among secondary minerals (see **"Appendix A,"** p.175). Talc, hydromica, amphibole, chlorite, and quartz are present in trace amounts. Smectites inlay vesicles. Groundmass glass is replaced mainly by smectites and carbonate. Smectites replace olivine (see **"Appendix A,"** p.175).

We have not determined the mobility of elements in Hole 454 basalts, as they are slightly altered ("Appendix B", Table **AT64**). Moreover, most basalts are vesicular and vesicularity varies widely from 5% to 50% of the rock volume.

AT64. Major and trace elements, Hole 454A, p.184.

Hole 458

Petrography and Bulk-Rock Chemical Composition

Hole 458 is located in the Mariana forearc basin (Table **T100;** Figs. **F111, F115**). The rocks are divided into five lithologic units (Hussong, Uyeda, et al., 1981). Unit 1 (Cores 60-458-28R through 31R) is represented by vesicular, glassy to fine grained, two-pyroxene pillow lava resembling boninites. Unit 2 (Cores 32R through 37R) comprises two massive andesite lava flows. Unit 3 (Cores 38R through 40R) is a vesicular, glassy to fine grained andesite similar to the rocks of Unit 1. Unit 4 (Cores 41R through 46R) was divided into eight subunits built up of basalts and andesites. Unit 5 (Cores 47R through 49R) consists of massive basalts with pillow structure.

We studied 24 additional samples of basalts, andesites, and andesite-basalts from all lithologic units (Table **T113;** see **"Appendix A,"** p.177). Studied samples belong to the poorly differentiated low-Ti and low-alkaline basalt to andesite-basalt series. Fe is typically low and Mg is highly variable in abundance (Table **T113;** Fig. **F116**). In the andesite-basalt (Sample 60-458-33R-2, 127–131 cm), MgO content is as high as 11.26 wt%, which is characteristic of boninite type. The Zr-Nb-Y geochemical diagram shows that the igneous rocks belong to N-MORB (Fig. **F118**). These basalts markedly differ from tholeiitic MORB in lower minor element (Cr, Ni, Co, V, and Zr) concentration (Table **T113**). Also, the spectrum of REE distribution definitely differs from that of tholeiitic basalts (Fig. **F117**).

T113. Igneous rocks, Hole 458, p.615.

Alteration Mineralogy and Bulk-Rock Chemical Changes

Leg 60 scientists (Hussong, Uyeda, et al., 1981) recognized that almost all igneous rocks in Hole 458 suffered considerable alteration. Clay minerals, zeolite (phillipsite), and carbonate (probably calcite) are principal secondary minerals. This mineral assemblage is a product of low-grade alteration.

Additionally studied samples of igneous rocks are fresh or slightly to moderately altered (H_2O^+ = 0.40–2.84 wt%). The rock in Sample 60-458-33R-1, 32–37 cm, contains 3.65 wt% H_2O^+ (Table T113). The basalts represent nonoxidative (Fe_2O_3/FeO = 0.66–1.56) and oxidative (Fe_2O_3/FeO = 1.76–5.87) types of alteration (Table **T113**). Smectites or smectite and cristobalite association (commonly with hydromica) dominate among secondary minerals (Table **T114**). As a rule, smectites predominate in altered basalts, but andesites

T114. Altered igneous rocks, Holes 458 and 459B, p.619.

and anesite-basalts are sporadically replaced with smectites in association with cristobalite and hydromica. Smectites contain Mg-Ca and Na-K interlayer cations (see **"Appendix A,"** p.177). Amphibole, chlorite, phillipsite, analcime, and quartz occur rarely in trace amounts (Table **T114**). Cristobalite is present among secondary minerals that replace andesites and andesite-basalts in Holes 786B, 792E, and 448A. The clay from a slickenslide in Sample 60-458-33R-1, 32–37 cm, consists mainly of smectites and a mixed-layer vermiculite-mica mineral (Table **T114;** see **"Appendix A,"** p.177).

Smectites replace olivine and groundmass glass and incrust vesicles (see **"Appendix A,"** p.177). Some large vesicles are filled with carbonate. Smectites fill cracks in rocks and, in rare cases, replace clinopyroxene.

We have not determined redistribution of elements at alteration of the studied samples ("Appendix B", Table **AT65**) as they vary in composition (basalts, andesites, andesite-basalts, and boninites). Moreover, all basalts are vesicular, varying greatly from 2% to 40% of the rock volume.

AT65. Major and trace elements, Hole 458, p.186.

Hole 459B

Petrography and Bulk-Rock Chemical Composition

The rocks in Hole 459B (Table **T100;** Figs. **F111, F115**) are represented by fine- to medium grained clinopyroxene-plagioclase phyric basalts. They were divided into four lithologic units (Hussong, Uyeda, et al., 1981). Unit 1 (Cores 60-459B-60R through 62R) is a vesicular, medium grained aphyric clinopyroxene-plagioclase basalt with intersertal to subophitic textures. Unit 2 (Cores 63R through 65R) is composed of highly vesicular, fine grained sparsely phyric basalts with low degrees of crystallinity. Unit 3 (Cores 66R through 68R) consists of sparsely vesicular, medium- to coarse grained diabase. These rocks are similar to those of Unit 1. Unit 4 (Cores 68R through 73R) is represented by moderately vesicular, fine grained, sparsely clinopyroxene-plagioclase phyric basalts. This unit is similar to Unit 2. All basalts demonstrate geochemical characteristics of island-arc tholeiites with low TiO_2 and Zr and high SiO_2 (Wood et al., 1982). These basalts are divided into two major chemical types. The principal boundary is placed between Cores 64R and 65R. The first type demonstrates low TiO_2 and moderately to high Ni and Cr contents. The second chemical type has generally higher TiO_2 and considerably lower Ni and Cr.

We studied 21 additional samples of igneous rocks from all recognized units (Table **T115;** see **"Appendix A,"** p.180). The studied samples represent basalts and andesite-basalts poorly differentiated in silicity and mostly low or intermediate in Ti. They belong to the tholeiitic series with a definite trend of differentiation intermediate between the Fenner's and Bouen's trends (Fig. **F116**). The two groups can be distinguished based on the character of Ti and some minor element distribution. The first group (Samples 60-459B-60R-1, 125–127 cm, through 64R-1, 24–28 cm) is characterized by low Ti and V but relatively high Cr, Ni, and Cu (Table **T115**). The second group (Samples 60-459B-65R-1, 82–85 cm, through 73R-3, 84–88 cm) demonstrates intermediate Ti; high V; and low Cr, Ni, and Cu concentrations. Both groups are lower in Zr than typical tholeiitic MORB (Fig. **F118**). In general, basalts in Hole 459B differ from typical MORB in both the spectrum of REE distribution and in a lower level of REE content (Table **T115**).

T115. Igneous rocks, Hole 459B, p.620.

Alteration Mineralogy and Bulk-Rock Chemical Changes

Leg 60 scientists (Hussong, Uyeda, et al., 1981) revealed that Hole 459B basalts are intensely altered, especially in fractured zones. They recognized two stages of alteration: an early oxidative, probably hydrothermal, stage and a later, low-temperature, less oxidative stage (Natland and Mahoney, 1982). Low-Al, high-Fe smectites and Fe hydroxides, as well as palygorskite are characteristic of the initial alteration stage. The second stage of alteration

resulted in formation of dioctahedral and trioctahedral clay minerals and phillipsite.

Additionally studied samples of igneous rocks are slightly altered, with H_2O^+ contents from 0.37 to 1.95 wt% in the first chemical type, and from 0.72 to 2.50 wt% in the second one (Table **T115**). These basalts represent two types of alteration: nonoxidative alteration with Fe_2O_3/FeO ratios from 1.03 to 1.59, and oxidative alteration with Fe_2O_3/FeO ratios from 1.64 to 7.29 (Table **T115**). Secondary mineral assemblage is similar to that in basalts and andesites in Hole 458 (Table **T114;** see **"Appendix A,"** p.180). It is noticeable that cristobalite occurs among secondary minerals in the igneous rocks from the forearc region, as in Holes 786B, 792E, 448A, 458, and 459B. Smectites replace olivine and groundmass glass and inlay vesicles. Some olivine crystals are fresh. Carbonate with smectites occurs in vesicles and in groundmass glass. Besides smectites and carbonate, vesicles contain radial aggregates of zeolites in some cases.

We did not estimate redistribution of elements ("Appendix B", Table **AT66**) at alteration of the studied basalts and andesite-basalts, as they are slightly altered and the interval of alteration is narrow in each of the considered petrochemical groups (Table **T115**). Moreover, almost all basalts are vesicular and vary from 10% to 50% of the rock volume.

AT66. Major and trace elements, Hole 459B, p.190.

Brief Comments

Alteration of igneous rocks was studied in the following tectonomagmatic structure elements of the Philippine Sea bottom: forearc basins (Izu-Bonin and Mariana areas, Holes 786B, 792A, 793B and 458 and 459B, respectively), the Mariana Trough (Holes 453 and 454A), the Schimisu Rift (Hole 791B), the Palau-Kyushu Ridge (Holes 448 and 448A), the Parece Vela Basin (Hole 449), the West Philippine Basin (Hole 447A), and the diapir of ultramafic rocks (Conical Seamount in the forearc area, Holes 779A and 780C). They contain a wide variety of rock types ranging from mafic to silicic in composition and include basalt, high-Mg basalt, picrite, boninite, andesite, dacite, and rhyolite. Conical Seamount consists of serpentinized harzburgite, dunite, and metabasalt.

As a whole, the studied igneous rocks are altered under low-temperature conditions. Secondary mineralogy is dominated by smectites (low-temperature smectite facies of the alteration). The rocks were altered in both oxidative and nonoxidative environments. The alteration degree varies from slight to moderate. The rocks within the andesite-dacite-rhyolite series are mainly replaced by smectites with cristobalite, hydromica, and quartz.

The material-balance estimation for moderately and strongly altered rocks (i.e., applying data on rock density values for recalculation of chemical analyses) met with the following difficulties: (1) as a rule, fresh analogs of altered rocks were not found in cores from the studied holes, and the rocks themselves are similarly altered, hence providing a prohibitively narrow range of alteration degree to catch the trend in the gain/loss of elements; and (2) wide variations of vesicularity in moderately and strongly altered rocks also hampers the estimation because it is incorrect to compare the element contents for rock samples with various vesicularities. Fresh rocks with primary vesicularity similar to that in the altered rocks are required to estimate the mass-balance.

T116. Additional basement holes, Legs 127/128, p.623.

F119. Sites in the Japan Sea, p.334.

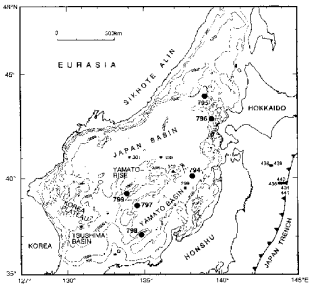

Japan Sea

We have studied samples of igneous rocks from Legs 127 and 128, Holes 794C, 794D, 795B, and 797C (Table **T116;** Fig. **F119**). Site 794 is located in the backarc northern Yamato Basin, Hole 795B was drilled in the northern Japan Sea (Japan Basin), and Hole 797C lies in the southern Yamato Basin.

In general, the Japan Sea represents a basin formed by multiaxial

backarc spreading and rifting of a continental arc during the past 30 m.y. or longer (Tamaki, 1985). Holes 794C, 794D, 795B, and 797C were drilled in two main deeps of the Japan Sea (Japan Basin and Yamato Basin). Our study is based on the review of geophysical, lithologic, and stratigraphic data by Tamaki, Pisciotto, Allan, et al. (1990) and Tamaki et al. (1992), who summarized the main ideas on tectonics, structure, and age of the basement of these deeps.

The Japan Basin is 3–3.5 km deep. It is underlain by the oceanic crust, which is ~11–12 km thick in that area. Complex pseudofault patterns similar to those generated by propagating spreading ridges are supposed to occur in the western part of the basin. Magnetic anomalies indicate that the age of this part of the basin is ~26 Ma.

The Yamato Basin is shallower (2–2.5 km) and smaller than the Japan Basin. The crust is thicker (17–19 km) and differs from the typical oceanic crust. It possibly represents a combination of laterally variable volcanic terranes. Age range for this basin is from 15 to 30 Ma. Based on Pb, Sr, and Nd isotope studies of basaltic rocks from the Sea of Japan, Cousens and Allan (1992) suggested that the major process controlling the isotope composition of basalts in Holes 794C, 795B, and 797C is mixing of subducted sediments with MORB mantle (the proportion of the sedimentary component is from 0.5% to 2.5%).

Holes 794C and 794D

Petrography and Bulk-Rock Chemical Composition

Two superimposed volcanic complexes are recovered at Site 794 (Pouclet and Bellon, 1992). The upper complex contains continental tholeiites (the rifting stage of the backarc basin). The lower complex comprises backarc basin basalts intruded during the spreading stage (mantle diapir during the rifting stage).

Hole 794C recovered aphyric to highly plagioclase phyric basaltic and doleritic sills of tholeiitic composition. Six igneous rock units have been distinguished (Tamaki, Pisciotto, Allan, et al., 1990). Unit 1 is identified in Hole 794B, whereas the other units are recovered in Hole 794C. Unit 2 (Sections 127-794C-1R-1 to 6R-1) is represented by massive, moderately to highly plagioclase phyric dolerite. Unit 3 (Sections 6R-1 to 19R-2) consists of fine- to medium grained aphyric, moderately vesicular, massive, highly fractured dolerite dominated by plagioclase. Unit 4 (Sections 10R-1 to 11R-2) is composed of massive, vesicular, medium- to fine grained aphyric dolerite dominated by plagioclase. Unit 5 (Sections 12R-1 to 13R-1) is aphyric dolerite. Unit 6 (Section 13R-2) is aphyric to moderately plagioclase phyric basalt. The rocks are similar to MORB and backarc basin basalts (Tamaki, Pisciotto, Allan, et al., 1990; Pouclet and Bellon, 1992).

We studied 10 additional samples of rocks from all recognized rock units in Hole 794C (Units 2 through 5) (Table **T117**). Most of them demonstrate doleritic texture with various amounts of plagioclase phenocrysts. The rocks are commonly vesicular, with vesicles constituting as much as 25% of the rock volume (see **"Appendix A,"** p.183). The rocks are practically nondifferentiated in silicity, contain intermediate amounts of titanium, and are slightly enriched in alkalies, mainly because of K. Judging by geochemical classification diagrams (Figs. **F120, F121**) the dolerites belong to tholeiitic MORB with significant variability in Cr, Ni, and V and higher contents of Sr relative to normal MORB (Table **T117**). The spectrum of REE distribution displays some enrichment in large-ion lanthanides (Fig. **F122**).

Thirteen additional samples were studied from rock Units 6 through 8 in Hole 794D (Table **T118**). The rocks are represented by aphyric and plagioclase phyric andesite-basalts and basalts and are commonly vesicular, with vesicles constituting as much as 25%–50% of the rock volume (see

T117. Igneous rocks, Hole 794C, p.624.

F120. AFM diagram for igneous rocks, Holes 794C, 795B, and 797C, p.335.

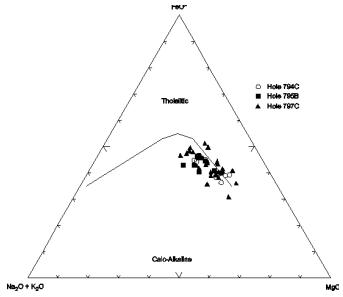

F121. Nb-Zr-Y diagram for igneous rocks, Holes 794C, 795B, and 797C, p.336.

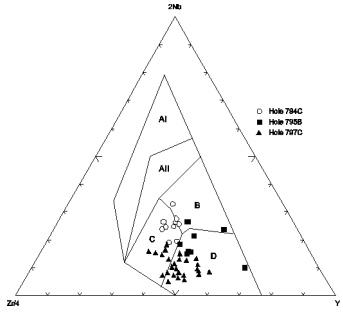

"Appendix A," p.183). Geochemical diagrams (Figs. **F123, F124**) indicate these rocks are similar to normal tholeiitic MORB.

Alteration Mineralogy and Bulk-Rock Chemical Changes

Leg 127 scientists (Tamaki, Pisciotto, Allan, et al., 1990) revealed that rocks from Hole 794C are altered. Plagioclase is slightly to highly altered to clay. Fractures are filled with green clay. Clinopyroxene, olivine, and mesostasis are also replaced with clay in strongly altered rocks (e.g., rocks from Unit 3). Besides clay minerals, trace amounts of calcite and secondary pyrite occur in mesostasis and vesicles. Proust et al. (1992) showed that primary minerals and interstices glass (Hole 794D) are replaced with clay minerals of chlorite-saponite mixed-layer composition. This mineral was also identified in veins and vesicles. Secondary veins contain calcite. Both chlorite-saponite mixed-layer and free smectites are fixed. Proust et al. (1992) estimated the temperature of secondary mineral assemblage formation to be between 150° and 180°C and lower. For example, calcite is formed at 65°C.

Additionally studied samples of rocks from Hole 794C are slightly to moderately altered (H_2O^+ = 0.91–2.34 wt%,) but rare strongly altered varieties also occur (H_2O^+ = 3.23 and 4.39 wt%) (Table **T117**). We classified the samples as products of both nonoxidative (Fe_2O_3/FeO = 1.24–1.57) and oxidative (Fe_2O_3/FeO = 1.61–3.60) alteration (Table **T117**). Smectites dominate among secondary minerals (Table **T119;** see **"Appendix A,"** p.183). They contain Mg-Ca and Na-K interlayer cations. Hydromica, chlorite, and defective chlorite occur in trace amounts. Quartz(?) is present in trace amounts in the lowest of the studied samples (see **"Appendix A,"** p.183). Smectites replace undetermined femic minerals and groundmass glass. Smectites also cover walls of vesicles or fill them (see **"Appendix A,"** p.183).

Alteration of rocks in Hole 794D is similar to that of basalts in Hole 794C (H_2O^+ = 0.80–1.91 wt%, rarely 2.61, 3.03, and 4.97 wt%) (Table **T118**). These strongly altered rocks are highly vesicular. All samples are nonoxidized, except for Samples 128-794D-11R-1, 39–43 cm, and 11R-2, 26–29 cm (Fe_2O_3/FeO = 3.45 and 2.28, respectively) (Table **T118**). As a rule, smectites predominate among secondary minerals (Table **T119;** see **"Appendix A,"** p.184). Smectites contain Mg-Ca and Na-K interlayer cations. Chlorite, calcite, quartz, and amphibole occur in trace amounts. Minerals of smectite-chlorite mixed-layer composition are either abundant or occur in trace amounts (Table **T119;** see **"Appendix A,"** p.184), unlike secondary minerals in igneous rocks from the upper part of the basement section recovered from Hole 794C. In Samples 128-794D-10R-2, 25–28 cm, and 17R-1, 87–93 cm, mixed-layer smectite-chlorite predominates. Clay minerals replace femic minerals and groundmass glass and also cover walls of vesicles or fill them (see **"Appendix A,"** p.184). Thin veinlets contain mainly smectites and minerals with chlorite component.

The secondary mineral assemblages in Holes 794C and 794D indicate low-temperature alteration with some downhole temperature increase.

Allan and Gorton (1992) estimated mobility of some elements in strongly altered rocks from Unit 5 in Hole 794C, where LOI exceeds 3.5%. MgO, K_2O, Rb, and Ba demonstrate positive correlation with LOI. On the contrary, CaO, Sc, Co, Ce, Lu, and Y show negative correlation with LOI.

We believe that the above results only demonstrate a difference between compared rock samples, but not the real mobility of elements. They cannot be considered as gain/loss of elements calculated from chemical analyses taking into account rock density. Because of the high vesicularity of basalts in Holes 794C and 794D, we are unable to estimate the mobility (gain/loss) of elements in these rocks ("Appendix B", Table **AT67**). For a correct estimation, it is necessary to use fresh analogs of these altered vesicular rocks.

F122. Chondrite-normalized REEs in igneous rocks, Holes 794C, 795B, and 797C, p.337.

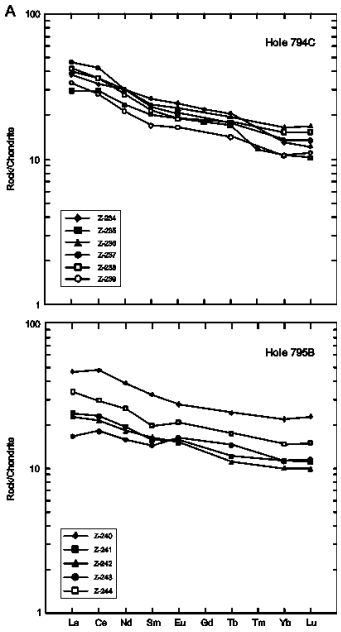

T118. Igneous rocks, Hole 794D, p.626.

F123. AFM diagram for igneous rocks, Hole 794D, p.339.

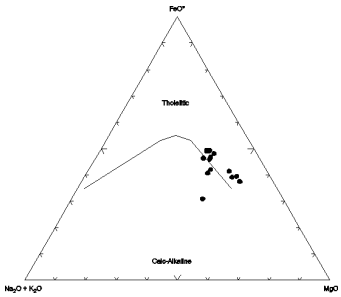

F124. Nb-Zr-Y diagram for igneous rocks, Hole 794D, p.340.

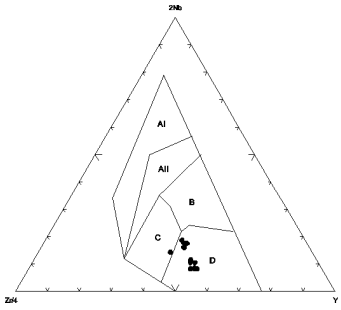

T119. Altered igneous rocks, Holes 794C and 794D, p.628.

Hole 797C

AT67. Major and trace elements, Holes 794C and 794D, p.193.

Petrography and Bulk-Rock Chemical Composition

Drilling in Hole 797C recovered high-Al basalt, alkaline basalt, and enriched tholeiitic basalt interbedded with sediments and dolerites. According to data by Tamaki, Pisciotto, Allan, et al. (1990), the igneous rocks comprise sparsely plagioclase-olivine phyric basalt (Units 1 and 2), aphyric basalt (Units 3, 4, 5, and 10 through 18), sparsely plagioclase-phyric basalt (Units 6 and 19), sparsely plagioclase-phyric dolerite (Units 7 and 9), aphyric dolerite (Units 8, 20, and 21).

T120. Igneous rocks, Hole 797C, p.629.

We studied 30 additional samples of igneous rocks from Units 1 through 5, 7 through 15, and 19, 20, and 21 (Table **T120**). The petrographic study and geochemical data allow us to recognize two rock groups. Group I (Samples 127-797C-9R-1, 43–53 cm, through 24R-6, 64–66 cm) is represented by practically nondifferentiated, mostly plagioclase phyric and olivine-plagioclase phyric basalts and low-Ti and low-alkaline dolerites. Rocks of this group are characterized by relatively high Cr and Ni and low Zr and Ba concentrations (Table **T120**). Classification diagrams (Figures **F120, F121**) indicate that these rocks are similar to tholeiitic MORB. The spectrum of REE (Fig. **F122**) is characteristic of normal tholeiitic MORB. Group II (Samples 127-797C-27R-1, 68–70 cm, through 45R-4, 8–11 cm): aphyric basalts and andesite-basalts (boninites?), which are poorly differentiated in silicity and enriched in Ti, alkaline elements, and P. These basalts are low in Cr, Ni, and Co and high in Rb, Sr, Zr and Ba (Table **T120**). In classification diagrams (Figs. **F120, F121**), these basalts plot into the fields of alkaline and calc-alkaline series with Bouen's trend of differentiation. The spectrum of REE reflect significant enrichment in large-ion lanthanides (Fig. **F122**).

Alteration Mineralogy

Leg 127 scientists (Tamaki, Pisciotto, Allan, et al., 1990) showed that rocks in Hole 797C are highly altered. Olivine is partially to totally altered to clay minerals. The plagioclase and mesostasis are slightly to strongly altered to clay. Fractures are filled with clay minerals, carbonate, and minor pyrite. Vesicles are filled with clay minerals.

Most of the additionally studied samples of igneous rocks are slightly to moderately altered (H_2O^+ = 0.80–3.84 wt%) (Table **T120**). Two samples are strongly altered (Sample 127-797C-14R-1, 88–94 cm, H_2O^+ = 4.91 wt%, brecciated basalt; and 20R-2, 104-108 cm, H_2O^+ = 6.40 wt%, basalt). All studied rocks suffered nonoxidative alteration (low Fe_2O_3/FeO ratio) (Table **T120**). Only Sample 27R-1, 68–70 cm, is believed to be a product of slightly oxidative alteration (Fe_2O_3/FeO = 2.07) (Table **T120**).

T121. Altered igneous rocks, Hole 797C, p.633.

As a rule, smectites predominate among secondary minerals (Table **T121;** see **"Appendix A,"** p.187). Chlorite, amphibole, talc, and sporadic hydromica are present in trace amounts. The smectites contain Mg-Ca and Na-K interlayer cations. In some cases, they contain as much as 20% mica layers (see **"Appendix A,"** p.187). Smectite-chlorite aggregates replace olivine and groundmass glass. Smectites occur along twin joints of plagioclase and replace plagioclase (50%–90%). Some plagioclase crystals seem to be albitized (see **"Appendix A,"** p.187). Vesicles are filled with smectites and in some samples, associated with carbonate. Rare vesicles and cracks are filled with carbonate. Some grains of amphibole occur within groundmass. The secondary mineral assemblage is characteristic of typical low-temperature alteration.

Dolerites and andesite-basalts of both petrographic and geochemical groups contain smectites and mineral sets with chlorite-smectite mixed-layer composition (swelling chlorite, mixed-layer smectite-chlorite mineral, corrensite-like mineral, corrensite, and chlorite) (Table **T121;** see **"Appendix A,"** p.187). These minerals, as well as albitized plagioclase, are evidence that

rocks suffered higher temperature alteration. Among the clay minerals, chlorite increases in abundance within the lower half of the recovered basement section. This possibly reflects a temperature increase with depth. Therefore, the Hole 797C basalts are altered at various temperatures. In Holes 797C, 794C, and 794D, minerals of chlorite-smectite mixed-layer composition occur ~90–100 m below the top of basaltic basement.

Bulk-Rock Chemical Changes

In altered rocks in Hole 797C, Allan and Gorton (1992) recognized a positive correlation of MgO, Al_2O_3, K_2O, Sr, Ce, Co, and Rb with LOI. Such elements as CaO, FeO, Lu, Yb, and Y demonstrate negative correlation with LOI.

Of studied samples from Hole 797C, two samples (127-797C-10R-2, 125–127 cm, H_2O^+ = 3.30 wt%; and 19R-2, 51–53 cm, H_2O^+ = 1.64 wt%) represent the most appropriate contrasting pair for the determination of element mobility at nonoxidative alteration of massive basalts. The comparison of absolute contents of elements in these samples ("Appendix B", Table **AT68**) have revealed that basalt at alteration loses Si, Al, Mn, Ca, Na, Ni, Cu, Zn, and Sr but gains total Fe, Mg, K, P, V, and Zr.

AT68. Major and trace elements, Hole 797C, p.196.

Hole 795B

Petrography and Bulk-Rock Chemical Composition

Basalts, basaltic andesites, and basaltic breccia were recovered from Hole 795B. These rocks have calc-alkaline and volcanic arc affinities, different from those of rocks characterizing the seafloor spreading, and represent lavas erupted within a volcanic-arc or backarc setting. The basement section in Hole 795B was divided into three igneous lithologic units (Tamaki, Pisciotto, Allan, et al., 1990). Unit 1 (683.5–703.3 mbsf) is brecciated, sparsely plagioclase pyroxene phyric basaltic andesite. Unit 2 (703.3–704 mbsf) consists of silicified brecciated moderately plagioclase phyric basalt. Unit 3 (704–762.2 mbsf); sparsely pyroxene plagioclase phyric basalt. Unit 3 is subdivided into two subunits. Subunit 3A (704–733.7 mbsf) is massive basalt, and Subunit 3B (733.7–762.2 mbsf) is brecciated basalt and basaltic andesite.

We have studied eight additional samples of igneous rocks from Unit 1 and Subunits 3A and 3B (Table **T122;** see **"Appendix A,"** p.185). All basalts are highly vesicular (from 10% to 40%, see **"Appendix A,"** p.185). The rocks are aphyric basalts practically nondifferentiated in silicity. Ti and Al vary slightly (Table **T122**). Geochemical classification diagrams (Figs. **F120, F121**) provide evidence that these rocks belong to tholeiitic MORB with poorly expressed Bouen's trend of differentiation, which is characteristic of island arc calc-alkaline series. Basalts are low in Cr, Ni, Co, Cu, and Zr and somewhat enriched in V (Table **T122**). The spectrum of REE reflects some enrichment of basalts in large-ion lanthanides (Fig. **F122**).

T122. Igneous rocks, Hole 795B, p.634.

Alteration Mineralogy and Bulk-Rock Chemical Changes

Leg 127 scientists (Tamaki, Pisciotto, Allan, et al., 1990) revealed that all rocks in Hole 795B are moderately to highly altered. Vesicles are rimmed with celadonite(?) and filled with zeolite (heulandite). Fractures are filled with clay minerals and minor zeolite. The phenocryst assemblage (plagioclase and mafic mineral) is replaced by clay minerals. Matrix comprises clay and zeolite.

Additionally studied samples of igneous rocks are slightly to moderately altered (H_2O^+ = 1.65–3.01 wt%) (Table **T122**). As a rule, the rocks are slightly to moderately oxidized (Fe_2O_3/FeO = from 1.66 to 3.05–3.99). Sample 127-795B- 38R-1, 6–8 cm, represents the nonoxidative type of alteration (Fe_2O_3/FeO = 1.44) (Table **T122**).

Smectites predominate among secondary minerals (see **"Appendix A,"** p.185) and contain Mg-Ca and Na-K interlayer cations. Hydromica, chlorite,

and heulandite(?) occur in trace amounts. Smectites replace olivine and groundmass glass and fill vesicles (see **"Appendix A,"** p.185). Cracks are filled with smectites and ore mineral. In some cases, vesicles are filled with smectites and zeolites. The secondary mineral assemblages reflect a typical low-temperature alteration.

Tamaki, Pisciotto, Allan, et al. (1990) have not revealed a correlation between content of any analyzed element and LOI in igneous rocks in Hole 795B.

We have not determined mobility of elements, as vesicularity of the studied basalts in Hole 795B is high ("Appendix B", Table **AT69**). We need fresh analogs of the altered vesicular basalts in order to evaluate the gain/loss of elements.

AT69. Major and trace elements, Hole 795B, p.201.

Brief Comments

The upper volcanic complex of Yamato Basin recovered at Sites 794 and 797 (the rifting stage of the backarc basin) is slightly to moderately altered. Strongly altered varieties are rare. Some samples are slightly to moderately oxidized. Smectites predominate among secondary minerals. The lower complex consists of backarc basin basalts and andesite-basalts extruded during the spreading stage. Their alteration is similar to that of the rocks from the upper volcanic complex. The strongly altered rocks are highly vesicular. Most samples are nonoxidized. As a rule, smectites predominate among secondary minerals. However, unlike secondary mineral assemblages from the upper complex, the rocks from the lower complex are replaced by minerals of smectite-chlorite mixed-layer composition, often abundant. Igneous rocks from the two volcanic complexes are altered under low-temperature smectite facies conditions, as indicated by the predominance of smectites among secondary minerals. The chlorite-smectite mixed-layer mineral assemblage, with albitized plagioclase and chlorite, increases to abundant amounts among secondary minerals in the lower complex, possibly evidence that rocks suffered higher temperature alteration.

The igneous rocks (lavas erupted within a volcanic arc or backarc setting) recovered from the Japan Basin (Hole 795B) are slightly to moderately altered and rarely highly altered. The samples are slightly to moderately oxidized. Smectites predominate among secondary minerals and demonstrate alteration under low-temperature smectite facies conditions, which is a typical alteration facies for the upper part of the oceanic crust.

Allan and Gorton (1992) showed that Mg, Ca, Sr, and large-ion lithophile elements were mobilized during alteration, whereas concentration of Y, Yb, and Lu decreased and Ce increased during alteration of igneous rocks at Sites 794, 795, and 797.

Lau Basin

The Lau Basin is a backarc basin that lies between the Lau Ridge remnant arc and the Tonga Ridge. Hawkins et al. (1994) described the geological setting of the Lau Basin. The Lau-Tonga system is located in a region of lithosphere convergence, and like many other arc-backarc systems, it is dominated by crustal extension. The basin evolved at two stages. The first stage involved crustal extension and rifting that developed basin structure. The second stage, involving seafloor spreading, is a response to southward-propagating rifts (Hawkins et al., 1994). The crustal extension and rifting were accompanied by eruption of MORB-like basalts. As the basin opened, numerous short-lived arc composition volcanoes formed within the basin (Hawkins et al., 1994).

Hole 834B

Hole 834B (18°34.052′S, 177°51.737′W) is located in the Lau Basin spreading center (Fig. **F125**), ~100 km eastward of the Lau Ridge (Parson et al., 1992) at a water depth of 2688.4 m. The hole ended at 435.7 mbsf. The oldest sediment (calcarenite) of late Miocene age was cored at 112.6 mbsf. Basement penetration is 272.7 m (presumed igneous basement was reached at 163 mbsf) and basement recovery is 82.67 m (Parson, Hawkins, Allan, et al., 1992).

Petrography and Bulk-Rock Chemical Composition

Participants of Leg 135 have distinguished 13 units in the basalt section recovered from Hole 834B (Parson, Hawkins, Allan, et al., 1992). The lavas are dominantly aphyric to sparsely phyric plagioclase-olivine-clinopyroxene basalts. Throughout the section, groundmass phases comprise plagioclase, clinopyroxene, and magnetite. The lavas are commonly vesicular (35%–45%) (Parson, Hawkins, Allan, et al., 1992; Hawkins and Allan, 1994). The igneous rocks in Hole 834B include relatively Mg-rich tholeiites and high Fe-Ti basaltic andesites. The igneous rocks at Site 834 are typically N-MORB with LREE depletion and high middle rare earth elements to HREEs (Ewart et al., 1994).

We studied 15 additional samples of igneous rocks from Units 2, 5, 7, and 12 (Table **T123**). The rocks are represented by aphyric and plagioclase-phyric basalts and andesite-basalts, commonly vesicular (10%–35% of rock volume) (see **"Appendix A,"** p.190). Geochemical diagrams (Figs. **F126, F127**) demonstrate that studied basalts and andesite-basalts in Hole 834B are tholeiites of N-MORB type. The REE spectrum (Fig. **F128**) is similar to that in tholeiitic MORB.

Two volcanic complexes are recovered at Site 834. The upper complex (Units 2–7) contains rocks with lower Ti, Fe, $Na_2O + K_2O$, P_2O_5, V, Zr, Y, and Ba and higher Mg, Cr, Ni, and Cu than the lower complex (Unit 12) (Table **T123**).

Alteration Mineralogy and Bulk-Rock Chemical Changes

Participants of Leg 135 scientists (Parson, Hawkins, Allan, et al., 1992) showed that basalts in Hole 834B are altered at low temperatures (<50°C). They noted palagonitization of glass and widespread zeolites (mainly phillipsite) throughout the cored section. Calcite veins occur. Low-temperature oxidative alteration is developed (celadonite, iron hydroxides often cover the walls of vesicles and infill thin veinlets). In the lower part of the section, zeolites indicate slightly higher alteration temperature. XRD revealed the presence of smectite and mixed-layer clay (Parson, Hawkins, Allan, et al., 1992).

Additionally studied rock samples from Hole 834B are slightly altered (H_2O^+ = 0.38–1.79 wt%, rarely as much as 2.38 wt%) and nonoxidized (Table **T123**).

XRD data from secondary minerals in altered rocks from the upper complex show smectites predominate among secondary minerals (see **"Appendix A,"** p.190) and contain Mg-Ca and Na-K interlayer cations. Mixed-layer smectite-swelling chlorite mineral and cristobalite occur in trace amounts in association with smectites. Smectites replace femic minerals and groundmass glass. Smectite and rarely celadonite(?) also cover walls of vesicles (see **"Appendix A,"** p.190). The secondary mineral assemblage in Hole 834B suggests low-temperature alteration of basalts and andesite-basalts from the Lau Basin.

High vesicularity and mainly slight alteration of basalts and andesite-basalts from the two volcanic complexes recovered in Hole 834B did not allow us to estimate element mobility in the rocks. Element contents in basalts in Hole 834B are given in "Appendix B", Table **AT70.**

Brief Comments

The domination of smectites among secondary minerals in Hole 834B

F125. Site in the Lau Basin, p.341.

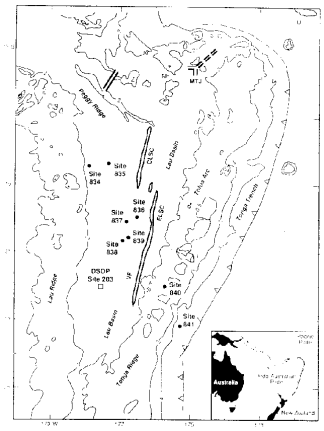

T123. Basalts, Hole 834B, p.635.

F126. AFM diagram for basalts, Hole 834B, p.342.

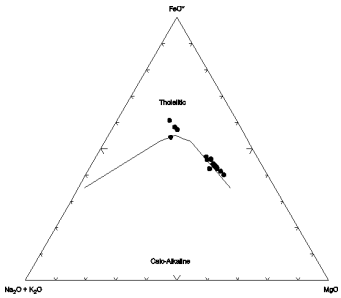

F127. Nb-Zr-Y diagram for basalts, Hole 834B, p.343.

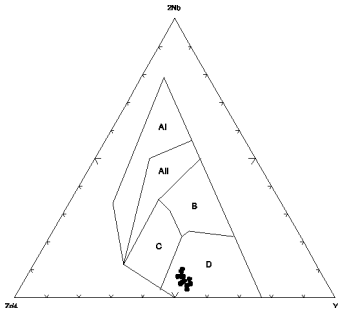

F128. Chondrite-normalized REEs for basalts, Hole 834B, p.344.

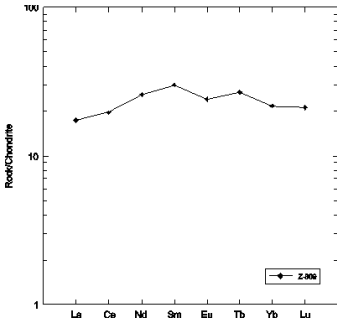

demonstrates low-temperature alteration of basalts and andesite-basalts of the Lau Basin. Cristobalite in trace amounts indicates an andesitic trend in composition of the backarc basin igneous rocks.

Bering Sea

Hole 191

Hole 191 (56°56.70′N, 168°10.72′E) is located at a water depth of 3854 m in the Kamchatka Basin (a backarc marginal basin) of the Bering Sea (Fig. **F129**). The age of oldest sediment is upper Miocene (Creager, Scholl, et al., 1973). Sediments (900 m thick) overlie tholeiitic basalt from a submarine lava flow. Hole 191 was cored to 19 m, with 1.4 m recovery (Stewart et al., 1973).

Petrography and Bulk-Rock Chemical Composition

Stewart et al. (1973) showed that the igneous rocks in Hole 191 are variolitic pyroxene-plagioclase basalts. Typical plagioclase phenocrysts compositions are An_{70}–An_{60}. Augite is subophitic and magnetite is ubiquitous. The tholeiitic basalt is characterized by low K_2O, and Ba and Sr^{87}/Sr^{86} values similar to MORB but higher Rb, Sr, and Zr concentrations, similar those in interarc basin basalts (Stewart et al., 1973).

We studied three samples of basalts from Hole 191 (Table **T124**). The rocks are represented by plagioclase-phyric and olivine-plagioclase phyric vesicular basalts with hyalopilitic or pilotaxitic groundmass texture (see **"Appendix A,"** p.192). Plagioclase phenocrysts composition is An_{52-60}. Geochemical diagrams (Figs. **F130, F131**) demonstrate that studied basalts in Hole 191 are tholeiites of N-MORB type. The REE spectrum (Tables **T124, T125;** Fig. **F132**) is similar to that in tholeiitic MORB.

Alteration Mineralogy

Stewart et al. (1973) showed that plagioclase is slightly altered. Glassy areas are replaced by nontronite and sericite(?) and also contain carbonate. Vesicles are infilled with nontronite and chlorite. The degree of alteration decreases downhole in Core 16R.

Additionally studied samples of basalts from Hole 191 (Core 16R) are slightly altered (H_2O^+ = 1.17–1.81 wt%) and nonoxidized (Fe_2O_3/FeO = 1.34–1.49) (Table **T124**). Interstitial glass is often replaced by clay mineral and vesicles are partially infilled with glass and clay mineral (see **"Appendix A,"** p.192).

XRD data indicate (see **"Appendix A,"** p.192) secondary minerals are only represented by pure smectite with Mg-Ca interlayer cations. A thin green veinlet contains smectites (dominate mineral) with Mg-Ca and Na-K interlayer cations, as well as chlorite in trace amounts.

The chemical composition of the basalts in Hole 191 is given in "Appendix B", Table **AT71.**

Brief Comments

The presence of only pure smectite among secondary minerals in Hole 191 suggests a low-temperature alteration of basalts from Kamchatka Basin, Bering Sea, which is characteristic for alteration of tholeiitic basalts from mid-ocean ridges and abyssal plains and basins.

ALTERATION OF IGNEOUS ROCKS FROM OCEANIC CRUST LAYER 3

AT70. Major and trace elements, Hole 834B, p.202.

F129. Site in the Kamchatka Basin, p.345.

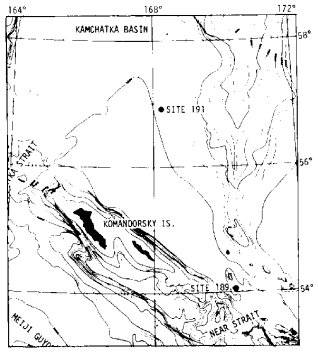

T124. Basalts, Hole 191, p.637.

F130. AFM diagram for basalts, Hole 191, p.346.

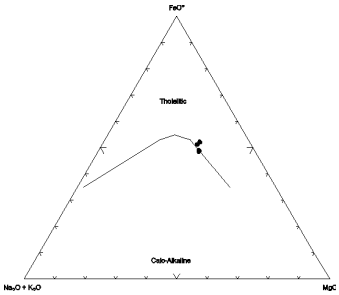

F131. Nb-Zr-Y diagram for basalts, Hole 191, p.347.

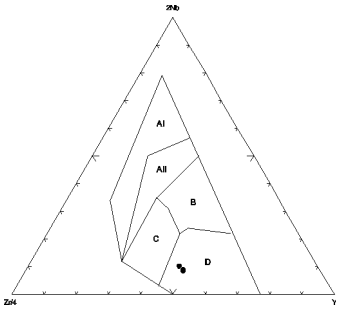

T125. Basalts, Hole 191, p.638.

Rocks from the third layer of the oceanic crust (gabbros and ultramafic rocks) outcrop at the oceanic floor or occur in its vicinity in some tectonically active segments of the oceanic crust. Often these rocks suffered metamorphism as well as relatively low temperature alteration at interaction with the seawater. The study of these processes and, especially, the estimation of mobility of chemical elements under such conditions are the most complex parts of research into alteration effects in the oceanic crust.

We analyzed samples from the southwest Indian Ocean (Leg 118 Hole 735B), Galicia Margin (Leg 103 Hole 637A), and Philippine Sea (Leg 125 Holes 779A and 780C and Leg 60 Hole 453). Results of the study of altered rocks from Holes 779A and 780C (Conical Seamount) and 453 (Mariana Trough) are given in **"Alteration of Igneous Rocks from Marginal Seas,"** p.115.

Southwest Indian Ridge

Hole 735B

We studied samples of gabbros from Hole 735B (32°43.395′N, 57°15.959′E; water depth = 719.9 m). Hole 735B is located at the eastern rim of the Atlantis II Transform (Fig. **F133**). The hole penetrated to the basement at 500.7 m and basement recovery was 434.81 m.

Leg 118 scientists (Robinson, Von Herzen, et al., 1989) described the geologic setting at Site 735. The site is restricted to a series of uplifted blocks parallel to the transform. The uplifted blocks may represent simple horsts uplifted at both the rift valley floor where the crust originates and at the adjacent ocean crust to the east. Rocks of the third oceanic layer (gabbros) outcrop at these uplifted blocks.

Petrography and Bulk-Rock Chemical Composition

Drilling in Hole 735B recovered olivine gabbro, olivine-bearing gabbro, two-pyroxene gabbro, iron-titanium oxide gabbro, troctolite, and microgabbro with rare basalt and trondhjemite. Six lithologic units were recognized in the sequence (Robinson, Von Herzen, et al., 1989). Unit I (Cores 118-735B-1D through 11D) consists of metagabbro with porphyroclastic to melonitic textures. Unit II (Cores 12R through 37R) consists of olivine and olivine-bearing gabbro. Unit III (Core 38R through interval 46R-3, 30 cm) consists of olivine gabbro with intervals of iron-titanium oxide gabbro. Unit IV (intervals 46R-3, 30 cm, through 56R-3, 90 cm) consists of Fe-Ti oxide–rich gabbro. Unit V (interval 56R-3, 90 cm, through Core 76R) consists of relatively uniform olivine gabbro characterized by a scarcity of Fe-Ti oxides and low-calcium pyroxene. Unit VI (Cores 77R through 88N) consists of olivine-rich (commonly >10%) gabbro with layers of troctolite.

We studied 18 additional samples of gabbros from all six lithologic units (Table **T126**). The studied samples are represented by variously tectonized, large-crystalline low-Ti and low-alkaline gabbros. The latter are poorly differentiated in silicity (probably because of epimagmatic quartzification) but are well enough differentiated in Mg and Al. These rocks demonstrate lower contents but higher variabilities of Cr and Ni compared to normal tholeiitic MORB (Table **T126**). These rocks are similar to normal tholeiitic MORB in content of Zr. Geochemical classification diagrams (Figs. **F134, F135**) provide evidence that gabbros are similar to typical tholeiitic MORB with poorly expressed Fenner's trend of differentiation. The REE spectrum reflects some depletion in large-ion lanthanides and some enrichment in Eu compared to normal MORB tholeiites (Fig. **F136**).

Metamorphism and Alteration

Leg 118 scientists (Robinson, Von Herzen, et al., 1989; Robinson et al., 1991; Stakes et al., 1991) demonstrated that gabbros in Hole 735B are

F132. Chondrite-normalized REEs for basalts, Hole 191, p.348.

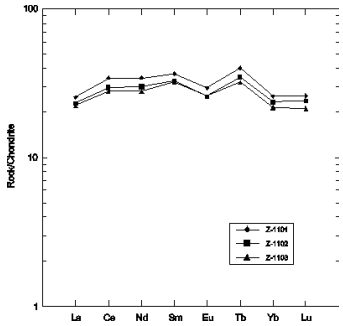

AT71. Major and trace elements, Hole 191, p.204.

F133. Hole 735B in the Atlantis II Fracture Zone, p.349.

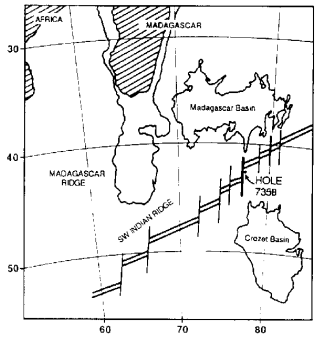

T126. Gabbros, Hole 735B, p.639.

F134. AFM diagram for gabbros, Hole 735B, p.350.

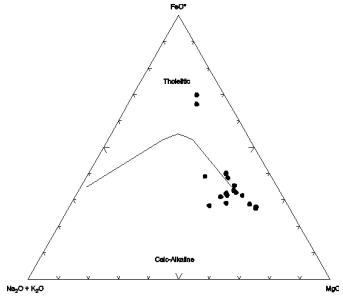

metamorphosed and altered and revealed that gabbro in Hole 735B suffered dynamothermal, cataclastic, and static alteration. Metamorphism associated with vertical cracks produced hornblende-sodic plagioclase assemblages at temperatures of ~400°–600°C. Alteration at a minimum temperature of 350°C occurred in brecciated zones under the influence of increased circulation, as well as the most intensive late oxidative overprint alteration. Carbonate veins associate with these brecciated zones and have probably resulted from the renewed circulation of cold oxygenated seawater.

Additionally studied samples of gabbros demonstrate low contents of H_2O^+ (0.15–1.27 wt%) (Table **T126**). Most of the studied rocks are characteristic of nonoxidative alteration (Fe_2O_3/FeO = 0.27–0.99) (Table **T126**). Only Sample 118-735B-12R-3, 99–101 cm, is characteristic of oxidative alteration (Fe_2O_3/FeO = 2.45). Amphibole, chlorite, and, occasionally, talc predominate among secondary minerals (see **"Appendix A,"** p.193). Talc mostly occurs in trace amounts. Besides chlorite and amphibole, the lowermost of the studied samples (118-735B-88N-1, 60–62 cm) probably contains serpentine. The secondary mineral assemblages support the conclusion of Robinson, Von Herzen, et al. (1989) that the rocks underwent high-temperature alteration. This conclusion is based mostly on the study of vein minerals.

Bulk-Rock Chemical Changes

The studied samples of gabbro from Hole 735B demonstrate low H_2O^+ content. Secondary minerals (as much as 90% of the metagabbro volume) are free of water or contain small amounts of it in the crystalline lattice. This became the reason to look for a new criterion for determining the degree of rock alteration. Absolute contents of elements in altered gabbros in Hole 735B are shown in "Appendix B", Table **AT72.**

Peridotites from the Galicia Margin

Hole 637A

Hole 637A (42°05.3′N, 12°51.8′W; water depth = 5307 m) lies on the Galicia Margin in the eastern Atlantic Ocean, off the northwest Iberian Peninsula (Fig. **F137**) The oldest sediment cored is late Miocene(?). Basement penetration was 73.6 m, with a basement recovery of 35.6 m.

The Galicia Margin is a starved passive ocean margin. Rift structures control the present-day morphology of alternation of blocks and half grabens (Boillot, Winterer, Meyer, et al., 1987). Hole 637A penetrated the peridotite ridge near the transition between oceanic and continental crust.

Petrography and Bulk-Rock Chemical Composition

Leg 103 scientists (Boillot, Winterer, Meyer, et al., 1987) described the peridotite section recovered in Hole 637A. They determined that peridotite is homogeneous in lithology and structure. Initial minerals of the peridotite are represented by olivine, orthopyroxene, and clinopyroxene, with rare plagioclase and chromium spinel. In mineral composition, these peridotites correspond to harzburgites. The penetrated section of peridotite is altered (serpentinized). Evans and Girardeau (1988) demonstrated that Hole 637A ultramafic lithologies include clinopyroxene-rich spinel harzburgite and lherzolite, as well as plagioclase-bearing peridotites.

We studied four additional samples of serpentinized harzburgites (Table **T127**). In general, petrographic and geochemical data are in agreement with data of Boillot, Winterer, Meyer, et al. (1987). All four samples represent apohyperbasite serpentinites. The precise determination of their petrographic composition is not possible, as they are 90% replaced by serpentine. We suppose that serpentinites formed after harzburgite, lherzolite, and plagioclase-bearing harzburgite. The studied serpentinites demonstrate increases in Cr and Ni but decreases in Nb, Rb, Sr, and Zr (Table **T127**). The geochemical diagram

F135. Nb-Zr-Y diagram for gabbros, Hole 735B, p.351.

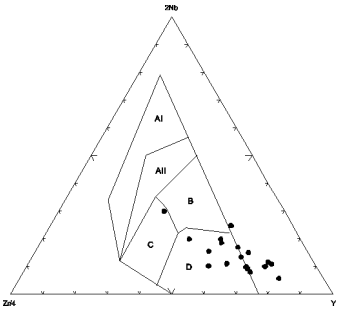

F136. Chondrite-normalized REEs for gabbros, Hole 735B, p.352.

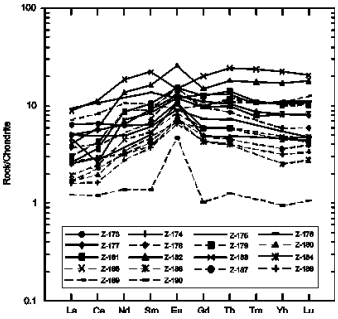

AT72. Major and trace elements, Hole 735B, p.205.

F137. Site in the Galicia margin, p.353.

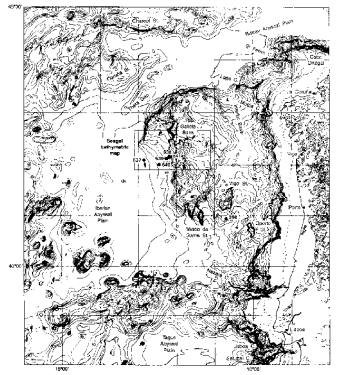

T127. Serpentinized harzburgites, Hole 637A, p.642.

(Fig. **F138**) demonstrates high-Mg content in the serpentinized harzburgites. The REE spectrum demonstrates low contents of elements and drastic deficiency in Eu (Fig. **F139**).

F138. AFM diagram for serpentinized harzburgites, Hole 637A, p.354.

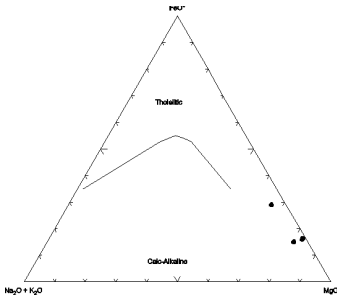

F139. Chondrite-normalized REEs for serpentinized harzburgites, Hole 637A, p.355.

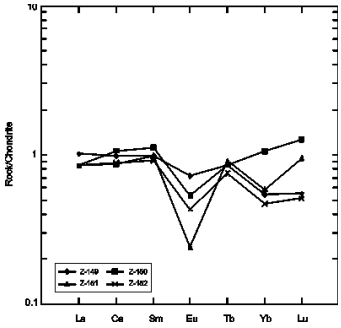

Alteration Mineralogy and Bulk-Rock Chemical Changes

All recovered peridotite from Hole 637A have high degrees of alteration; only ~5% of the primary minerals are preserved (Boillot, Winterer, Meyer, et al., 1987). Olivine is almost totally transformed into serpentine. Orthopyroxene is mainly replaced completely by serpentine or calcite and supports the formation of amphibole. Clinopyroxene is relatively fresh and in most altered samples, replaced by calcite. The secondary minerals are represented by serpentine (chrysotile and lizardite), amphibole (tremolite, hornblende is also present), and calcite. Calcite formed on the last lowest temperature stage of alteration of these rocks.

The main serpentinization of the peridotite occurred at temperatures <300°C. The formation of calcite probably occurred at temperatures of ~10°C (Agrinier et al., 1988). Stable isotope data indicate that fluid responsible for serpentinization was probably a seawater, and that water/rock ratios were high; calcite was precipitated from seawater (Evans and Baltuck, 1988).

All additionally studied samples of serpentinized peridotites are very strongly altered (H_2O^+ = 3.17–11.70 wt%) (Table **T127**). All of them are strongly oxidized (Fe_2O_3/FeO = 12.18–44.18) (Table **T127**). Serpentines and calcite predominate among secondary minerals (see **"Appendix A,"** p.195. Talc, amphibole, smectite, and goethite occur in trace amounts. Amphibole (actinolite), with some admixture of chlorite, replaces serpentinized orthopyroxene. Some crystals of olivine are completely replaced with amphibole. Oxides (hematite?) occur in the vein serpentine, occasionally in olivine, and partly in spinel. The presence of smectite supports the suggestion by Evans and Baltuck (1988) that alteration of the Hole 637A peridotites occurred at both high and low temperatures. Chlorite dominates in two nonoxidized samples of metamicrogabbro and metabasalt. In the harzburgites and dunites, serpentine replaces olivine and pyroxene. Aggregate of chrysotile and antigorite is present in veins (see **"Appendix A,"** p.195).

Serpentine is represented mostly by chrysotile (see **"Appendix A,"** p.195). In only one sample (103-637A-28R-3, 103–106 cm), electron diffraction analysis revealed antigorite, which is present in association with chrysotile and lizardite. Electron microscopy and electron diffraction analysis revealed several polytypes of chrysotile: $2O_{rc1}$, $2M_{c1}$, and D_c, as well as lizardite in trace amounts (see **"Appendix A,"** p.195). The structure type of chrysotile is tube-in-tube. Particles of large-diameter "barrel-like" (Tokmakov et al., 1983) or "Povlen-type" (Morandi and Felici, 1979) chrysotile also occur. According to Morandi and Felici (1979), this kind of chrysotile and its $2O_{rc1}$ polytype are related to a final stage of serpentinization with hydrothermal aqueous solutions penetrating the cataclastic fractures produced by contraction of the serpentinitic rocks during the changing of the low-grade metamorphic environment toward lower temperature conditions.

To estimate mobility of elements at serpentinization of ultramafic rocks, one must compare altered rocks with fresh ones (with harzburgites in our case). Element contents in serpentinized harzburgites in Hole 637A is given in "Appendix B", Table **AT73.**

AT73. Major and trace elements, Hole 637A, p.207.

ALTERATION OF IGNEOUS ROCKS FROM MAIN TECTONOMAGMATIC STRUCTURES OF THE OCEAN FLOOR: SUMMARY AND CONCLUSIONS

These study results revealed general comparative patterns of the upper oceanic crust rocks' alteration from different tectonomagmatic structures, such

as mid-ocean ridges, abyssal basins and plains, seamounts and guyots, intraplate rises, and marginal seas. Some data are also obtained on alteration and metamorphism of the lower oceanic crust rocks raised onto the bottom surface in diapirs and tectonic slabs.

Mid-Ocean Ridges (Axial Zones and Flanks)

Both fresh (Leg 106 Hole 648B; axial volcano in the Mid-Atlantic Ridge rift valley) or slightly altered (Leg 64 Site 477; Guyamas Basin in axis zone of the northern part of the East Pacific Rise) basalts and extremely altered igneous rocks (Middle Valley, Juan de Fuca Ridge, Legs 139 and 169 Sites 856, 857, and 858) occur in the axial zones of mid-ocean ridges. The rock alteration in the mid-ocean ridges takes place at various temperatures, from <150°C to as much as 350°–400°C. In general, the alteration degree of igneous rocks in the axial zones is controlled by the following main factors: (1) permeability of the rocks that depend, first of all, on their jointing and brecciation, as well as on tectonic renewal of rocks changing the water-rock ratio; (2) reactive capacity of rocks and solutions in the water-rock interaction; and (3) position of the rocks in a certain part of the hydrothermal system, either in the low-temperature (<100°–150°C) or in the medium- to high-temperature (as much as 350°–400°C) zones.

The igneous rock alteration in axial zones of mid-ocean ridges develops everywhere in the nonoxidative smectite (low-temperature alteration) and greenschist facies (high-temperature alteration in zones of hot solutions circulation) environments. Outside of the ascending hot solutions and discharge area (hydrothermal field), the lower limit of the smectite facies distribution occurs ~600 m beneath the basement surface, within the transition zone between the effusive section and upper dikes. Igneous rocks of the volcanic section (Layer 2A of the oceanic crust) are correspondingly altered under the smectite facies. Below, in the sheeted dike complex (Layer 2B), the rocks are altered under the greenschist/amphibolite facies. The change in rock alteration environment is traced within the 1900-m-thick basement section recovered and sampled in Hole 504B (Costa Rica Rift).

The vertical zonation is disturbed in areas where hot fluids ascend and discharge as submarine springs. The upper boundary of the greenschist facies is uplifted from 600 m and almost reaches the bottom surface, as at Site 858 (Middle Valley, Juan de Fuca Ridge). As a result, in areas of ascending fluids the greenschist facies occupies the space commonly belonging to the overlying smectite facies in the vertical section of the upper oceanic crust. Therefore, diapir-like uplifts of the greenschist facies boundary (up to its exposure at the ocean bottom) occur in the axial zone on the background of its general blanket-like distribution at a depth of ~600 m beneath the top of basalt layer. Such uplifts are related to ascending hot solutions and discharge at the ocean bottom. Chloritization of basalts and overlying sediments may therefore serve as an indicator of such fluid ascending zones in the uppermost oceanic crust within paleohydrothermal systems.

In spreading centers of mid-ocean ridges, the most significant alteration of igneous rocks takes place in greenschist facies conditions resulting in intense redistribution of elements because of water-rock interaction in the upper oceanic crust. Two cases are distinguished: (1) lower parts of the upper oceanic crust close to the intermediate magma chamber (the lower dike section; Hole 504B, Costa Rica Rift), and (2) strongly altered igneous rocks and sediments from zones of ascending hot solutions throughout the vertical section of oceanic crust fragments above the intermediate magma chambers (Legs 139 and 169 Sites 856, 857, and 858, Middle Valley, Juan de Fuca Ridge). In this case, we see an intensive geochemical interaction between internal and external geospheres (the oceanic lithosphere and the ocean) realized by the water-rock reactions in submarine convective hydrothermal systems.

Beyond the zones of ascending hot solutions, redistribution of elements

also takes place in the volcanic section under the smectite facies, as well as in the transition zone under the greenschist facies (Hole 504B). Redistribution of elements during low-temperature alteration under the smectite facies is mainly fixed in permeable strongly jointed and brecciated basalts with glassy groundmass structure. Massive plagioclase-phyric dolerites from the upper dike section are most resistant to alteration.

Further history of igneous rocks alteration during ocean floor spreading is related to dislocation of rock masses beyond the axial rift zone to mid-ocean ridge flanks. The alteration degree of rocks does not increase during this process, but is mainly inherited from that which is acquired in the axial zone. Robinson et al. (1977) showed that for the flank of the Mid-Atlantic Ridge (FAMOUS area), the oldest basalts drilled at Site 335 (~13 Ma) are less altered than the youngest rocks drilled at Site 332 (3.6 Ma). The latter are weakly altered, likely inheriting the alteration level within the axial spreading zone. A conservation of rock alteration is also assumed for basalts from holes drilled in the Gulf of California during Legs 65 (Holes 483B and 485A) and 63 (Hole 473). Igneous rocks from these holes are weakly altered, likely reflecting a low-temperature alteration in the axial spreading zone at the periphery of hydrothermal systems. Zones of volcanic and hydrothermal activation in off-ridges possibly represent an exception, as in Hole 471 (off Baja California). The igneous rocks from Hole 471 are moderately or even strongly altered.

Displacement of newly formed oceanic crust to mid-ocean ridge flanks results in a superposition of oxidative alteration on nonoxidative alteration (Hole 504B, Costa Rica Rift; Hole 483B, Gulf of California; Hole 469, off northern California; and Hole 332B, Mid-Atlantic Ridge). Oxidative alteration is identified by iron hydroxides, K-containing minerals (celadonite, phillipsite, and K-feldspar), as well as by green and red smectites with high contents of Fe and K. Oxidative alteration as a whole involves a much smaller rock volume than the overall nonoxidative type and only affects the uppermost part of the oceanic crust. This alteration type is fixed in vertical joints downhole to ~300 m beneath the basement surface on the flanks of mid-ocean ridges. The maximum depth of its penetration is established in Hole 504B (Costa Rica Rift). First evidence of oxidative alteration type likely appears ~1–2 m.y. after basalt extrusion in the axial spreading zone (Site 483, Gulf of California).

It is interesting to note that oxidized basalts are not found in any of the studied axial spreading zones of mid-ocean ridges. Possibly, not enough holes are drilled to date, and this may result in a false impression that cold seawater with oxidative properties for some reason does not descend into the basement at margins of hydrothermal systems located within the axial valleys. However, if this phenomenon really exists, then we may suggest that ascending nonoxidative solutions reaching the basement surface stand in the way of descending seawater and prop it up. Because of this, the oxidative environment of basalt alteration does not appear in the upper part of the basement. The seawater with oxidizing potential penetrates into the basement on flanks of mid-ocean ridges, where prop-up effect of ascending nonoxidative solutions decreases with distance from the axial valley or is completely absent.

Seawater that penetrates into the basement on flanks of mid-ocean ridges migrates as vertical fluxes or subhorizontal flows through brecciated zones, fractures, and vesicular tops of lava flows and loses its oxidizing potential. If the seawater reaches zones of ascending solutions and mixes with them, any noticeable oxidative properties are already absent.

Oxidative alteration (upper volcanic section, Hole 504B) mainly reflects an increase in bulk H_2O^+, Fe^{+3}, K, Rb, and Sr and a decrease in Si and Ca contents. A loss of Ti, Al, Fe_{total}, Mn, P, Cu, Co, V, Zr, La, Sm, Yb, Nd, Eu, Y, and Ce is fixed in most oxidized rock samples. However, we obtained different gain/loss estimates of elements for oxidation of basalts. This likely reflects a contribution of a previous nonoxidative alteration stage to bulk-rock chemical change. The most trustworthy estimates of element mobility in the

oxidized environment can be obtained in rocks which were fresh before the oxidation (i.e., not altered in the nonoxidative environment).

Abyssal Basins and Plains

Igneous rocks of Mesozoic (Jurassic–Cretaceous) oceanic crust from Nauru Basin (Leg 61), Southwest Pacific Basin (Leg 91), Argo Abyssal Plain (Leg 123), and Pigafetta Basin (Leg 129) were altered in a nonoxidative environment under relatively low-temperature smectite facies conditions (main secondary mineral is smectite). The alteration is similar to that observed in young basalts from newly formed oceanic crust within the axial zones of mid-ocean ridges, but beyond the fields of ascending hot solutions. A weak rock alteration generally predominates resulting from a low water/rock ratio. The rocks have undergone a moderate alteration only in some intervals of the drilled sections. To date, the holes drilled in Mesozoic oceanic crust have not recovered igneous rocks extremely altered at high temperatures (greenschist facies) similar those from zones of ascending hot solutions in the modern axial valley of the Juan de Fuca Ridge (Middle Valley; Legs 139 and 169 Sites 856, 857, and 858). Oxidative alteration of Mesozoic igneous rocks is superimposed on the nonoxidative type likely developed during displacement of the newly formed crust to flanks of spreading zones, as it occurs in the Cenozoic.

According to our data, alteration of Mesozoic igneous rocks is generally similar to that of basalts from the axial valleys of mid-ocean ridges beyond the hot solutions ascending and discharge fields, as well as from flanks of mid-ocean ridges. This leads to the conclusion that the rock alteration acquired in axial spreading zones and their flanks in the Jurassic and Cretaceous periods, under both nonoxidative and oxidative environments, is preserved within the abyssal areas basement during the long spreading history of the oceanic crust. Therefore, time does not considerably affect the magmatic rocks' alteration in conditions of a cold oceanic crust beneath the sedimentary cover serving as a screen. This conclusion allows us to trace the alteration history of igneous rocks in the upper oceanic crust in spreading centers and their flanks during a long period (~165 m.y.), beginning with basalts of a zero age up to Jurassic.

This typical pattern of igneous rock alteration in conditions of ocean floor spreading is complicated in the off-ridge magmatic and hydrothermal activity (ODP Leg 129 Site 801; alkaline rock section from Pigafetta Basin). In this case, the alkaline basalts show considerably stronger alteration, as compared to surrounding weakly altered tholeiites derived from spreading centers.

Igneous rocks erupted during Mesozoic intraplate volcanism have also been altered in both nonoxidative and oxidative environments of the smectite facies, but the alteration demonstrates specific features related to peculiarities of the magmatism. Cretaceous igneous rocks from Nauru Basin mainly belong to the sill complex, which intrudes on the Jurassic basement in the central Pacific (Larson and Schlanger, 1981). The igneous rocks from Nauru Basin are fresh and slightly altered at low water/rock ratio. Oxidative alteration is weakly developed here, and its evidence is only fixed within the uppermost several meters of basement. This likely results from either limited motion of newly formed igneous rocks from the center of Cretaceous volcanism or a restricted permeability of the rocks for penetration of seawater.

Mobility of elements during nonoxidative rock alteration in the Mesozoic crust does not differ from that in the Cenozoic for igneous rocks from axial zones of mid-ocean ridges. Weak and moderate alterations have taken place everywhere in the oceanic crust located beyond the zones of ascending hot solutions. Basalt samples also affected by alteration in the superimposed oxidative environment show different behaviors of elements, and even opposite analytical results are obtained for some samples. This is likely related to a time-

variable contribution of nonoxidative and superimposed oxidative alteration to the total bulk-rock chemical change in different samples. Because of this, we have to use oxidized rocks that have not undergone earlier nonoxidative alteration in order to obtain correct estimates of element behavior in an oxidative environment.

Seamounts and Guyots

Smectite or smectite with carbonate dominate among secondary minerals that replace groundmass and phenocrysts in basalts of both alkaline and tholeiite series. They also fill vesicles and joints in the subaerial lava flows from the upper part of the Emperor Seamounts chain, the West Pacific Guyots, and Hess Rise. These minerals reflect a low-temperature alteration under smectite facies conditions. The composition of secondary minerals mainly depends on the chemical composition of the igneous rocks. For example, an increase of MgO content in the rock is accompanied by formation of chlorite phases and even serpentine along with smectite. In trachy-andesite with very high K_2O content, secondary K-feldspar is formed. Such relationships are especially clear for minerals filling thin fissures and vesicles and point to water-rock interaction mainly within each individual lava flow in conditions of a sublateral water flow. Basalts from the top of lava flows with a high water/rock ratio are most intensely altered, including their oxidation, whereas strongly altered and oxidized basalts are widespread throughout the flows. Weathering under tropical or subtropical environments is noted in the uppermost parts of some flows. Kaolinite is the main indicator mineral of such weathering. The weathered basalts are also extensively oxidized; iron is totally or almost totally oxidized. Under the influence of laterite weathering, alteration of basalts begins in oxidizing conditions (e.g., before a manifestation of nonoxidative and oxidative underwater alteration).

The specific structure of the volcanic pedestals of seamounts and guyots (numerous lava flows with highly vesicular and brecciated flow tops, as well as tuff interbeds), subaerial environment of basalt lava eruptions, and absence of the basalts displacement relative to their eruption center within the volcanic edifice determined conditions for rock alteration different from those in mid-ocean ridges. First of all, oxidative and nonoxidative alteration regimes are not so strongly separated from each other in time and space, as established for the mid-ocean ridges (early nonoxidative alteration developing in axial zones and later superimposed oxidative alteration occurring in flanks). In the mid-ocean ridges, signs of basalt oxidation are fixed at a maximum depth of ~300 m below the basaltic basement top (Hole 504B, Costa Rica Rift), whereas in seamounts and guyots, oxidized basalts characterize all subaerial lava flows. Therefore, it can be assumed that oxidized basalts must occur throughout the basaltic pedestal to depths of the subaerial lava flows distribution. For example, in the Suiko seamount (Leg 55 Hole 433C), oxidized basalts occur throughout the drilled 350-m-thick basalt section. As a whole, basalts of seamounts and guyots are more strongly altered than basalts in the extrusive part of the oceanic crust (Layer 2A) from the axial zone of the mid-ocean ridges beyond the ascending hot solutions zones. Basalts from the mid-ocean ridges are commonly characterized by a patchy alteration. Weakly altered and fresh rocks constitute a considerable volume of the basement owing to a widespread occurrence of poorly permeable sills and thick lava flows. On the contrary, fresh basalts are rare in the seamounts and guyots, especially in thin flows. Moreover, extensively altered basalts characterize most flows, primarily the flow tops.

Estimation of material balance for alteration of basalts from seamounts and guyots meets some difficulties because the most altered basalts from the flow tops (and thus most interesting for this study) are vesicular and have no fresh analogues among studied core samples. Moreover, their vesicularity varies from rare vesicles to 60% of rock volume. Because of this, they cannot be compared with each other, as rock density values necessary for the recalculation

of chemical analyses to estimate the gain/loss of elements depend not only on alteration, but mainly on primary rock vesicularity. The vesicularity determined in thin sections for a single slice of the vesicular rock does not always correspond to the actual vesicularity of the rock mass. This introduces additional errors into the estimates. In order to estimate a real gain/loss of elements in this case, we need fresh analogs of the altered vesicular rocks and a precise determination of their vesicularity.

Directly comparing the entire set of chemical analyses of the rocks, we found that the vesicular and/or brecciated extremely altered and strongly oxidized basalts from the flow tops are, compared to basalts from the flow interiors, enriched in H_2O^+, Fe_{total}, Fe_2O_3/FeO ratio, K_2O, MnO and depleted in CaO, SiO_2, MgO, Sr, and Zn and often in Na_2O, Rb, and Ba. Other element contents increase in some parts of samples and decrease or stay constant in other parts. On the contrary, strongly altered nonoxidized basalts commonly contain less K_2O and more MgO compared to relatively fresh rocks. CaO content decreases, as in extremely altered and strongly oxidized basalts. Estimates of bulk-rock chemical changes during alteration may be misrepresented owing to primary differences in chemical composition of the rock within a flow.

In spite of the above noted difficulties in estimation of material balance, we can affirm that seamounts and guyots contribute considerably to the geochemical interaction between the oceanic lithosphere and the ocean itself, along with mid-ocean ridges. We need fresh rock analogues for a quantitative estimation of the mass balance, especially in the case of strongly altered vesicular rocks from DSDSP/ODP holes. The Hawaiian Islands represent a most suitable region for obtaining fresh analogs of the vesicular basalts.

Intraplate Rises

Basalts from the Vøring and Manihiki Plateaus, Bermuda Rise, Kerguelen-Ninetyeast and Mascarene-Chagos-Maldives lineaments, and Walvis and Rio Grande Ridges demonstrate a similar style of rock alteration.

Alteration of basalts varies from weak to strong in both intrasites and intersites. This patchy pattern in alteration results from varied permeability and crystallinity of basalts. Alteration of basalts occurred at various temperatures, probably depending on the distances from zones of ascending hot solutions. For example, basalts in Hole 417A show a stronger alteration at higher temperature than those from Hole 418A (Legs 51–53, Bermuda Rise). The temperature of alteration estimated in various holes ranges from 10° to 80°C and possibly to 100°–120°C.

Vesicular basalts of lava flows erupted in subaerial environments suffer alteration in both oxidizing (along vesicular and brecciated flow tops) and nonoxidizing (internal parts of lava flows and nonoxidized parts at margins of flow units) environments. Basalts from lava flows erupted in a deepwater environment have undergone nonoxidative alteration because of lack of margins on effusive bodies highly permeable for the seawater (Hole 1140A; northern part of the Kerguelen Plateau). Basalts altered in an oxidizing environment demonstrate stable associations of secondary minerals, such as brown and greenish yellow smectites, Fe oxides and hydroxides, calcite, and, sporadically, K-feldspar. Basalts altered in nonoxidizing environments demonstrate domination of trioctahedral green smectites. Clay minerals with chloritic structures (mixed-layer minerals and chlorite), hydromica, calcite, zeolites, quartz, and sulfides may occur in association with smectites.

Absence of the vertical zonation of alteration in basalt sections, zonation within lava flows, and strong alteration of basalts in vesicular and brecciated flow tops mainly under low-temperature oxidative conditions suggest that sublateral water flows dominated within the submarine volcanic edifices built up of multiple lava flows intercalated with volcaniclastics. Evidence of active subhorizontal sea water flows (oxidative alteration) are found at all levels

of the basalt sections. For example, oxidative alteration is identified in Hole 642E (Leg 104; Vøring Plateau) throughout the recovered 914-m-thick basement section composed of numerous vesicular basalt flows separated by hyaloclastites, sediments, and brecciated zones. The basalts are also intensely oxidized during subaerial weathering. In this case, the oxidizing process is the first type of basalt alteration. This is a specific realization of oxidative alteration different from that observed on flanks of mid-ocean ridges. For example, in Holes 504B (Costa Rica Rift) or 332B (Mid-Atlantic Ridge) oxidation of basalts is mainly developed in and along vertical fissures penetrating ~300 m into the basement (Hole 504B).

Such an environment characterizes marginal parts of hydrothermal systems. If the zones of ascending hot solution would have been recovered by drilling on the Vøring and Manihiki Plateaus, Bermuda Rise, Kerguelen-Ninetyeast and Mascarene-Chagos-Maldives lineaments, Walvis and Rio Grande Ridges, then they must show volcanic rock alteration similar to that in Middle Valley of Juan de Fuca Ridge (Legs 139 and 169; greenschist facies). However, such zones were not drilled on the above listed intraplate rises.

Age variations of the studied subaqueous volcanic edifices do not demonstrate any significant influence on the alteration of basalts.

Massive basalts are in most cases slightly altered. Elements are immobile or slightly mobile in these processes of water-rock interaction. Moderately altered massive basalts commonly have no fresh analogues. Because of this, studied samples demonstrate a very narrow range of alteration degree for comparison. The narrow alteration range restricts our chances to obtain real estimates of element gain/loss, and we can only detect some trends in redistribution of elements. Vesicular basalts from the tops of numerous lava flows show the strongest alteration, and thus they are especially useful for estimation of the gain/loss of chemical elements during the alteration. However, we do not have their fresh analogs with the same vesicularity. It is necessary to find such analogs to complete the estimation. The same is true for altered massive basalts, for which fresh analogs are not found in cores from the studied holes.

The preliminary results show that oxidative alteration is largely accompanied by a gain of most major and minor elements, including REE. On the contrary, nonoxidizing alteration is mainly characterized by material loss.

Marginal Seas

Igneous rocks widespread in the West Pacific region range from mafic to silicic in their composition and include tholeiitic basalts, high-magnesia basalts, picrites, boninites, andesites, dacites, and rhyolites. The analyzed material comprises rock samples from the following structures: (1) forearc basins (Izu-Bonin and Mariana areas), (2) backarc basins (Celebes and Sulu Seas, Parece Vela Basin, West Philippine Basin, Yamato Basin, Japan Basin, Lau Basin, and Kamchatka Basin in the Bering Sea), and (3) Mariana Trough, Schimisu Rift, and Palau-Kyushu Ridge within the Philippine Sea. Diapirs of serpentinized ultramafic and mafic rocks from the forearc area (e.g., Conical Seamount) are also included. As a rule, the rocks from the marginal seas of the West Pacific region are slightly to moderately altered (only some samples are strongly altered) at low-temperature smectite facies under nonoxidative and oxidative environments. Smectites mainly predominate among secondary minerals. The rocks with andesite-dacite-rhyolite composition are mainly replaced by smectites with cristobalite, hydromica, and quartz.

Most of the studied magmatic rocks have undergone a weak alteration and owing to this, elements are immobile or their mobility is within analytical error values. Fresh analogues of moderately or strongly altered massive and vesicular rocks necessary for estimation of the material balance have not been found in cores from the studied holes.

Fragments of Oceanic Crust Layer 3

Studied rocks of the third oceanic crust layer from deep-sea drilling are dominated by strongly altered varieties, likely as a result of their interaction with seawater. The water-rock interaction might considerably contribute to the chemical composition of hot solutions circulating within the lower oceanic crust in spreading zones and intraplate rises, including seamounts and guyots and perhaps in transform faults, along with the hydrothermal metasomatosis. The ascending hot solutions affect rock alteration within the upper crust and therefore contributes to the general system of geochemical interaction between external and internal geospheres (oceanic lithosphere and hydrosphere). The quantitative estimate of material redistribution during reactions of water with Layer 3 rocks will be possible only after the necessary fresh varieties are involved in the analysis. To date, we obtained contents of elements for all studied altered rocks, and these data are ready for mass-balance estimation.

Results of the Mass-Balance Estimation

Massive igneous rocks, represented by both strongly altered and fresh varieties, are the best objects for estimation of the material mass balance (i.e., using rock density data in recalculation of the chemical analyses). The most complete analysis was performed for massive basalts and dolerites of the effusive section and dike complex from Hole 504B (Costa Rica Rift) and for altered rocks from Juan de Fuca Ridge, Middle Valley (see **"Alteration of Igneous Rocks from Mid-Ocean Ridges,"** p.7).

Basalts of intraplate rises and seamounts, as well as various magmatic rocks from marginal seas, are often moderately or intensely altered, especially in highly vesicular tops of numerous lava flows. Their alteration degree is favorable for determination of element redistribution at the water-rock interaction. However, estimation of the mass balance in these rocks appear to be difficult or even impossible at the present state of study. We met with the following difficulties: (1) fresh analogues of altered rocks were not found in the same holes where the studied samples have been selected, and the rocks are altered almost at the same degree resulting in a range of alteration too narrow even for detection of element gain/loss trends; (2) wide variations in vesicularity between individual samples of moderately and strongly altered rocks does not allow us to perform this analysis, as it is incorrect to compare content of elements in rock samples with different vesicularity. In order to estimate the mass balance in these objects, we must find fresh rocks with characteristics (including vesicularity) analogous to the primary characteristics of the altered rocks.

We also applied the traditional approach to determine the mobility of elements by directly comparing chemical compositions of altered and fresh rocks (i.e., neglecting primary variations in petrography, geochemistry, and vesicularity) for several significant rock samples. The results of such comparison are given with the reservation that they may considerably differ from actual element gain/loss due to hydrothermal metasomatosis.

In spite of different methods of quantitatively estimating the material balance of igneous rock alteration, a complete set of analytical data necessary for the mass-balance estimation was obtained for each studied sample (chemical composition, description of thin sections, vesicularity, rock oxidation degree, rock density, and secondary mineral assemblages). Chemical analyses for all studied rock samples are recalculated to grams per 1000 cm^3 using the atomic-volume method and taking rock density into account. This Report contains all these data. As a result, we present here the most complete basic data for key DSDP/ODP holes drilled within main tectonomagmatic structures of the ocean floor. These data may be used for a quantitative estimation of geochemical effects of the hydrothermal metasomatosis (water-rock interaction) in the

oceanic crust. The results of mass-balance estimation inferred from a part of the data are also presented here. Other data are ready for further analysis and can be used after selection of the necessary analogues of altered rocks. The complex analytical data, including visual description of studied rock samples, will make the search for necessary analogues in other similar structures easier.

First Priority Objects for Further Investigation on the Problem

We believe that further investigations should be focused on alteration of igneous rocks in hydrothermally active areas of the oceanic crust (i.e., moderate- to high-temperature submarine hydrothermal systems). Geochemical effects of the hydrothermal metasomatosis reach their maximum only in these systems, and therefore contribute to the chemical composition of solutions that circulate within the oceanic crust and ultimately discharge onto the ocean floor, forming sulfide ore deposits both on and beneath the bottom surface and affect the composition of oceanic water.

1. It seems especially important to study cores from the middle and lower parts of the "reaction zone" when Hole 504B (Costa Rica Rift) will be drilled deeper, from 2111 to 3000 mbsf or more. At present a complete section of the upper oceanic crust, including gabbroic rocks (100.5 m), recovered in the eastern equatorial Pacific (Site 1256, Leg 206 and Expeditions 309 and 312).
2. It would be interesting to drill a hole to the maximal possible depth within the hydrothermal field in the Middle Valley, Juan de Fuca Ridge (Legs 139 and 169).
3. Attempts should be made to find sites for drilling on seamounts or guyots in order to recover paleozones of hot solution–circulation within the volcanic edifice.
4. It would be interesting to drill to maximum possible depth in order to sample paleozones of moderate- to high-temperature hydrothermal systems in different tectonomagmatic structures of marginal seas, as well as in transform faults.
5. Attempt should be made to find a zone of intense hydrothermal alteration of Cretaceous oceanic crust within the abyssal basin floor similar to that in the recent zone of greenschist facies alteration near the bottom surface described in the Middle Valley, Juan de Fuca Ridge (Legs 139 and 169).
6. It would be advisable to drill deep holes along transects within the axial valley of the mid-ocean ridge with active hydrothermal fields, which allow us to reconstruct a three-dimensional image of the hydrothermal system to estimate the mass-balance of the system as a whole and look for oxidized basalts not yet found in the axial zones of mid-ocean ridges.

ACKNOWLEDGMENTS

This research used samples and data provided by the Ocean Drilling Program (ODP). ODP is sponsored by the U.S. National Science Foundation (NSF) and participating countries under management of Joint Oceanographic Institutions (JOI), Inc. Funding for this research was provided by the Russian Foundation for Basic Research (grants N95-05-15379, N95-05-14368, N98-05-64856, N99-05-65462, N02-05-64207, and N05-05-65180) and JOI/Natural Environment Research Council (NERC) Foundation (grant 0037). We thank former Director of the Ocean Drilling Program, Philip D. Rabinowitz, and Texas A&M University for reiterated financial support of our travels to the DSDP/ODP repositories. Also, we thank Angie Miller, Gigi Delgado, and their colleagues from the ODP Publication Services Department for copyediting the manuscript and formatting the figures. We appreciate Jerry Bode's and Steve Prinz's assistance and warm welcome.

We thank the administration of Geological Institute RAS, Moscow for support of conduct of this research. We thank the chemical group from Analytical Center (Geological Institute, Moscow) for classical wet chemical analyses of rocks; Galina V. Ledneva and Vadim A. Eroshchev-Shak (Geological Institute, Moscow) for participation in description of thin sections; Nikolai Barinov and Galina A. Yudina (Far East Geological Institute, Vladivostok) for electronography and electron microscopy analyses of secondary minerals and serpentines; Gennadii Novikov (Geological Institute, Moscow) and Vladimir M. Ladygin (Moscow State University) for density analysis. Thanks to Gennadii Novikov and Tatyana Zelenova (Geological Institute, Moscow) for assistance with sample preparation for analyses and Gennadii P. Avdeiko (Institute of Volcanology, Petropavlovsk-Kamchatski) for the samples of basalts from Leg 55.

REFERENCES

Adamson, A.C., 1983. Chemistry of alteration minerals from Deep Sea Drilling Project Sites 501, 504 and 505. *In* Cann, J.R., Langseth, M.G., Honnorez, J., Von Herzen, R.P., White, S.M., et al., *Init. Repts. DSDP,* 69: Washington (U.S. Govt. Printing Office), 551–563.

Adamson, A.C., and Richards, H.G., 1990. Low-temperature alteration of very young basalts from ODP Hole 648B: Serocki volcano, Mid-Atlantic Ridge. *In* Detrick, R., Honnorez, J., Bryan, W.B., Juteau, T., et al., *Proc. ODP, Sci. Results,* 106/109: College Station, TX (Ocean Drilling Program), 181–194.

Agrinier, P., Mevel, C., and Girardeau, J., 1988. Hydrothermal alteration of the peridotites cored at the ocean/continent boundary of the Iberian Margin: petrologic and stable isotope evidence. *In* Boillot, G., Winterer, E.L., et al., *Proc. ODP, Sci. Results,* 103: College Station, TX (Ocean Drilling Program), 225–234.

Aldrich, J.B., Tieh, T.T., and Scott, R.B., 1981. Alteration of remnant arc debris, Site 448, Palau-Kyushu Ridge, Philippine Sea, Deep Sea Drilling Project Leg 59. *In* Kroenke, L., Scott, R., et al., *Init. Repts. DSDP,* 59: Washington (U.S. Govt. Printing Office), 737–742.

Allan, J.F., and Gorton, M.P., 1992. Geochemistry of igneous rocks from Legs 127 and 128, Sea of Japan. *In* Tamaki, K., Suyehiro, K., Allan, J., McWilliams, M., et al., *Proc. ODP, Sci. Results,* 127/128 (Pt. 2): College Station, TX (Ocean Drilling Program), 905–929.

Alt, J.C., Honnorez, J., Hubberten, H.-W., and Saltzman, E., 1983. Occurrence and origin of anhydrite from Deep Sea Drilling Project Leg 70, Hole 504B, Costa Rica Rift. *In* Cann, J.R., Langseth, M.G., Honnorez, J., Von Herzen, R.P., White, S.M., et al., *Init. Repts. DSDP,* 69: Washington (U.S. Govt. Printing Office), 547-550.

Alt, J.C., Anderson, T.F., Bonnell, L., and Muehlenbachs, K., 1989. Mineralogy, chemistry, and stable isotopic compositions of hydrothermally altered sheeted dikes: ODP Hole 504B, Leg 111. *In* Becker, K., Sakai, H., et al., *Proc. ODP, Sci. Results,* 111: College Station, TX (Ocean Drilling Program), 27–40.

Alt, J.C., and Chaussidon, M., 1989. Ion microprobe analyses of the sulfur isotopic composition of sulfides in hydrothermally altered rocks, DSDP/ODP Hole 504B. *In* Becker, K., Sakai, H., et al., *Proc. ODP, Sci. Results,* 111: College Station, TX (Ocean Drilling Program), 41–45.

Alt, J.C., and Emmermann, R., 1985. Geochemistry of hydrothermally altered basalts: Deep Sea Drilling Project Hole 504B. *In* Anderson, R.N., Honnorez, J., Becker, K., et al., *Init. Repts. DSDP,* 83: Washington (U.S. Govt. Printing Office), 249–262.

Alt, J.C., France-Lanord, C., Floyd, P.A., Castillo, P., and Galy, A., 1992. Low-temperature hydrothermal alteration of Jurassic ocean crust, Site 801. *In* Larson, R.L., Lancelot, Y., et al., *Proc. ODP, Sci. Results,* 129: College Station, TX (Ocean Drilling Program), 415–427.

Alt, J.C., Honnorez, J., Laverne, C., and Emmermann, R., 1986. Hydrothermal alteration of a 1 km section through the upper oceanic crust, Deep Sea Drilling Project Hole 504B: mineralogy, chemistry, and evolution of seawater-basalt interactions. *J. Geophys. Res.*, 91:10309–10335.

Alt, J.C., Kinoshita, H., Stokking, L.B., and Michael, P.J. (Eds.), 1996. *Proc. ODP, Sci. Results,* 148: College Station, TX (Ocean Drilling Program).

Alt, J.C., Laverne, C., and Muehlenbachs, K., 1985a. Alteration of the upper oceanic crust: mineralogy and processes in Deep Sea Drilling Project Hole 504B, Leg 83. *In* Anderson, R.N., Honnorez, J., Becker, K., et al., *Init. Repts. DSDP,* 83: Washington (U.S. Govt. Printing Office), 217–247.

Alt, J.C., Laverne, C., Vanko, D.A., Tartarotti, P., Teagle, D.A.H., Bach, W., Zuleger, E., Erzinger, J., Honnorez, J., Pezard, P.A., Becker, K., Salisbury, M.H., and Wilkens, R.H., 1996a. Hydrothermal alteration of a section of upper oceanic crust in the eastern equatorial Pacific: a synthesis of results from Site 504 (DSDP Legs 69, 70, and 83, and ODP Legs 111, 137, 140, and 148.) *In* Alt, J.C., Kinoshita, H., Stokking, L.B., and Michael, P.J. (Eds.), *Proc. ODP, Sci. Results,* 148: College Station, TX (Ocean Drilling Program), 417–434.

Alt, J.C., Saltzman, E.S., and Price, D.A., 1985b. Anhydrite in hydrothermally altered basalts: Deep Sea Drilling Project Hole 504B, Leg 83. *In* Anderson, R.N., Honnorez, J., Becker, K., et al., *Init. Repts. DSDP*, 83: Washington (U.S. Govt. Printing Office), 283–288.

Alt, J.C., Teagle, D.A.H., Bach, W., Halliday, A.N., and Erzinger, J., 1996b. Stable and strontium isotopic profiles through hydrothermally altered upper oceanic crust, Hole 504B. *In* Alt, J.C., Kinoshita, H., Stokking, L.B., and Michael, P.J. (Eds.), *Proc. ODP, Sci. Results*, 148: College Station, TX (Ocean Drilling Program), 57–69.

Alt, J.C., Teagle, D.A.H., Laverne, C., Vanko, D.A., Bach, W., Honnorez, J., Becker, K., Ayadi, M., and Pezard, P.A., 1996c. Ridge-flank alteration of upper ocean crust in the Eastern Pacific: synthesis of results for volcanic rocks of Holes 504B and 896A. *In* Alt, J.C., Kinoshita, H., Stokking, L.B., and Michael, P.J. (Eds.), *Proc. ODP, Sci. Results*, 148: College Station, TX (Ocean Drilling Program), 435–450.

Alt, J.C., Zuleger, E., and Erzinger, J.A., 1995. Mineralogy and stable isotopic compositions of the hydrothermally altered lower sheeted dike complex, Hole 504B, Leg 140. *In* Erzinger, J., Becker, K., Dick, H.J.B., and Stokking, L.B. (Eds.), *Proc. ODP, Sci. Results*, 137/140: College Station, TX (Ocean Drilling Program), 155–166.

Andrews, A.J., Barnett, R.L., MacClement, B.A.E., Fyfe, W.S., Morrison, G., MacRae, N.D., and Starkey, J., 1977. Zeolite facies metamorphism, geochemistry and some aspects of trace element redistribution in altered basalts of DSDP, Leg 37. *In* Aumento, F., Melson, W.G., et al., *Init. Repts. DSDP*, 37: Washington (U.S. Govt. Printing Office), 795–810.

Arculus, R.J., Pearce, J.A., Murton, B.J., and van der Laan, S.R., 1992. Igneous stratigraphy and major-element geochemistry of Holes 786A and 786B. *In* Fryer, P., Pearce, J.A., Stokking, L.B., et al., *Proc. ODP, Sci. Results*, 125: College Station, TX (Ocean Drilling Program), 143–169.

Artamonov, A.V., and Zolotarev, B.P., 2003. Volcanism of the Kerguelen Plateau (Indian Ocean): composition, evolution, and sources. *Lithol. Miner. Resour.*, 38(4):361–382.

Aumento, F., Melson, W.G., et al., 1977. *Init. Repts. DSDP*, 37: Washington (U.S. Govt. Printing Office).

Autio, L.K., Sparks, J.W., and Rhodes, J.M., 1989. Geochemistry of Leg 111 basalts: intrusive feeders for highly depleted pillows and flows. *In* Becker, K., Sakai, H., et al., *Proc. ODP, Sci. Results*, 111: College Station, TX (Ocean Drilling Program), 3–16.

Avdeiko, G.P., Khubunaja, S.A., and Vande-Kirkov, J.V., 1980. Petrography and chemical composition of the lava flows from the Emperor Seamounts, DSDP Leg 55. *Init. Repts. DSDP*, 55: Washington (U.S. Govt. Printing Office), 571–584.

Bach, W., Erzinger, J., and D.A.H. Teagle, 1996. Chemistry of the lower sheeted dike complex, Hole 504B (Leg 148): influence of magmatic differention and hydrothermal alteration. *In* Alt, J.C., Kinoshita, H., Stokking, L.B., and Michael, P.J. (Eds.). *Proc. ODP, Sci. Results*, 148: College Station, TX (Ocean Drilling Program), 39-55.

Backman, J., Duncan, R.A., et al., 1988. *Proc. ODP, Init. Repts.*, 115: College Station, TX (Ocean Drilling Program).

Baker, P.E., Castillo, P.R., and Condliffe, E., 1995. Petrology and geochemistry of igneous rocks from Allison and Resolution guyots, Sites 865 and 866. *In* Winterer, E.L., Sager, W.W., Firth, J.V., and Sinton, J.M. (Eds.), *Proc. ODP, Sci. Results*, 143: College Station, TX (Ocean Drilling Program), 245–261.

Baksi, A.K., 1986. $^{40}Ar/^{39}Ar$ incremental heating study of whole-rock samples from the Rajmahal and Bengal traps, eastern India. *Terra Cogn.*, 6:161. (Abstract)

Bargar, K.E., and Jackson, E.D., 1974. Calculated volumes of individual shield volcanoes along the Hawaiian-Emperor chain. *J. Res. U.S. Geol. Surv.*, 2:545–550.

Barker, P.F., Carlson, R.L., Johnson, D.A., et al., 1983. *Init. Repts. DSDP*, 72: Washington (U.S. Govt. Printing Office).

Barron, J., Larsen, B., et al., 1989. *Proc. ODP, Init. Repts.*, 119: College Station, TX (Ocean Drilling Program).

Bass, M.N., 1976. Secondary minerals in oceanic basalt, with special reference to Leg 34, Deep Sea Drilling Project. *In* Yeats, R.S., Hart, S.R., et al., *Init. Repts. DSDP*, 34: Washington (U.S. Govt. Printing Office), 393–432.

Bass, M.N., Moberly, R., Rhodes, J.M., Shih, C.C., and Church, S.E., 1973. Volcanic rocks cored in the central Pacific, Leg 17, Deep Sea Drilling Project. *In* Winterer, E.L., Ewing, J.I., et al., *Init. Repts. DSDP,* 17: Washington (U.S. Govt. Printing Office), 429–503.

Batiza, R., 1981. Trace-element characteristics of Leg 61 basalts. *In* Larson, R.L., Schlanger, S.O., et al., *Init. Repts. DSDP,* 61: Washington (U.S. Govt. Printing Office), 689–695.

Baxter, A.N., 1990. Major and trace element variations in basalts from Leg 115. *In* Duncan, R.A., Backman, J., Peterson, L.C., et al., *Proc. ODP, Sci. Results,* 115: College Station, TX (Ocean Drilling Program), 11–21.

Becker, K., Sakai, H., et al., 1988. *Proc. ODP, Init. Repts.,* 111: College Station, TX (Ocean Drilling Program).

Bence, A.E., Taylor, S.R., and Fisk, M., 1980. Major- and trace-element geochemistry of basalts from Ojin, Nintoku and Suiko seamounts of the Emperor seamount chain: DSDP-IPOD Leg 55. *In* Jackson, E.D., Koizumi, I., et al., *Init. Repts. DSDP,* 55: Washington (U.S. Govt. Printing Office), 599–605.

Bienvenu, P., Bougault, H., Joron, J.L., Treuil, M., and Dmitriev, L., 1990. MORB alteration: rare-earth element/non-rare-earth hygromagmaphile element fractionation. *Chem. Geol.,* 82:1–14.

Bischoff, J.L., and Dickson, F.W., 1975. Seawater-basalt interaction at 200°C and 500 bars: implications for origin of seafloor heavy metal deposits and regulation of seawater chemistry. *Earth Planet. Sci. Lett.,* 25:385–397.

Bogdanov, Y.A., Bogdanova, O.Y., Dubinin, A.V., Gorand, A., Gorshkov, A.I., Gurvich, E.G., Isaeva, A.B., Ivanov, G.V., Jansa, L.F., and Monaco, A., 1995. Composition of ferromanganese crusts and nodules at northwestern Pacific guyots and geologic and paleoceanographic considerations. *In* Haggerty, J.A., Premoli Silva, I., Rack, F., and McNutt, M.K. (Eds.), *Proc. ODP, Sci. Results*, 144: College Station, TX (Ocean Drilling Program), 745–768.

Boillot, G., Winterer, E.L., Meyer, A.W., et al., 1987. *Proc. ODP, Init. Repts.,* 103: College Station, TX (Ocean Drilling Program).

Boyce, R.E., 1981. Electrical resistivity, sound velocity, thermal conductivity, density-porosity, and temperature, obtained by laboratory techniques and well logs: Site 462 in the Nauru Basin of the Pacific Ocean. *In* Larson, R.L., Schlanger, S.O., et al., *Init. Repts. DSDP,* 61: Washington (U.S. Govt. Printing Office), 743–761.

Brereton, N.R., 1992. Physical property relationships from Sites 765–766. *In* Gradstein, F.M., Ludden, J.N., et al., *Proc. ODP, Sci. Results,* 123: College Station, TX (Ocean Drilling Program), 453–468.

Burns, S.J., Swart, P.K., and Baker, P.A., 1990. Geochemistry of secondary carbonates in Leg 115 basalts: tracers of basalt/seawater interaction. *In* Duncan, R. A., Backman, J., Peterson, L.C., et al., *Proc. ODP, Sci. Results,* 115: College Station, TX (Ocean Drilling Program), 93–101.

Byerly, G.R., and Sinton, J.M., 1979. Compositional trends in natural basaltic glasses from Deep Sea Drilling Project Holes 417D and 418A. *In* Donnelly, T., Francheteau, J., Bryan, W., Robinson, P., Flower, M., Salisbury, M., et al., *Init. Repts. DSDP,* 51, 52, 53 (Pt. 2): Washington (U.S. Govt. Printing Office), 957–972.

Cambon, P., Joron, J.L., Bougault, H., and Treuil, M., 1980. Leg 55, Emperor Seamounts: trace elements in transitional tholeiites, alkali basalts and hawaiites—mantle homogeneity or heterogeneity and magmatic processes. *In* Jackson, E.D., Koizumi, I., et al., *Init. Repts. DSDP,* 55: Washington (U.S. Govt. Printing Office), 585–597.

Campbell, A.C., German, C.R., Palmer, M.R., Gamo, T., and Edmond, J.M., 1994. Chemistry of hydrothermal fluids from the Escanaba Trough, Gorda Ridge. *In* Morton, J.L., Zierenberg, R.A., Reiss, C.A. (Eds.), *Geologic, Hydrothermal, and Biologic Studies at Escanaba Trough, Gorda Ridge, Offshore Northern California.* U.S. Geol. Surv. Bull., 2022:201–221.

Christie, D.M., Dieu, J.J., and Gee, J.S., 1995. Petrologic studies of basement lavas from northwest Pacific guyot. *In* Haggerty, J.A., Premoli Silva, I., Rack, F., and McNutt, M.K. (Eds.), *Proc. ODP, Sci. Results,* 144: College Station, TX (Ocean Drilling Program), 495–512.

Clague, D.A., Fisk, M.R., and Bence, A.E., 1980. Mineral chemistry of basalts from Ojin, Nintoku, and Suiko Seamounts Leg 55 DSDP. *In* Jackson, E.D., Koizumi, I., et al., *Init. Repts. DSDP,* 55: Washington (U.S. Govt. Printing Office), 607–637.

Coffin, M.F., Frey, F.A., Wallace, P.J., et al., 2000. *Proc. ODP, Init. Repts.*, 183 [CD-ROM]. Available from: Ocean Drilling Program, Texas A&M University, College Station, TX 77845-9547, U.S.A.

Corliss, J.B., Dymond, J., Gordon, L.I., Edmond, J.M., Von Herzen, R.P., Ballard, R.D., Green, K., Williams, D., Bainbridge, A., Crane, K., and Van Andel, T.H., 1979. Submarine thermal springs on the Galapagos Rift. *Science,* 203:1073–1083.

Courtillot, V., Besse, J., Vandamme, D., Montigny, R., Jaeger, J.-J., and Capetta, H., 1986. Deccan flood basalts at the Cretaceous/Tertiary boundary? *Earth Planet. Sci. Lett.*, 80:361–374.

Cousens, B.L., and Allan, J.F., 1992. A Pb, Sr, and Nd isotopic study of basaltic rocks from the Sea of Japan, Legs 127/128. *In* Tamaki, K., Suyehiro, K., Allan, J., McWilliams, M., et al., *Proc. ODP, Sci. Results,* 127/128 (Pt. 2): College Station, TX (Ocean Drilling Program), 805–817.

Creager, J.S., Scholl, D.W., et al., 1973. *Init. Repts. DSDP,* 19: Washington (U.S. Govt. Printing Office).

Curray, J.R., Moore, D.G., et al., 1982. *Init. Repts. DSDP,* 64 (Pts. 1 and 2): Washington (U.S. Govt. Printing Office).

Dalrymple, G.B., Lanphere, M.A., and Clague, D.A., 1980a. Conventional and $^{40}Ar/^{39}Ar$ K-Ar ages of volcanic rocks from Ojin (Site 430), Nintoku (Site 432) and Suiko (Site 433) seamounts and the chronology of volcanic propagation along the Hawaiian-Emperor Chain. *In* Jackson, E.D., Koizumi, I., et al., *Init. Repts. DSDP,* 55: Washington (U.S. Govt. Printing Office), 659–676.

Dalrymple, G.B., Lanphere, M.A., and Natland, J.H., 1980b. K-Ar minimum age for Meiji Guyot, Emperor seamount chain. *In* Jackson, E.D., Koizumi, I., et al., *Init. Repts. DSDP,* 55: Washington (U.S. Govt. Printing Office), 677–683.

Davies, H.L., Sun S-S., Frey, F.A. et al., 1989. Basalts basement from Kerguelen Plateau and trail of the Dupal plume. *Contrib. Mineral. Petrol*., 103: 457-469.

Davis, E.E., and Becker, K., 1994. Formation temperatures and pressures in a sedimented rift hydrothermal system: ten months of CORK observations, Holes 857D and 858G. *In* Mottl, M.J., Davis, E.E., Fisher, A.T., and Slack, J.F. (Eds.), *Proc. ODP, Sci. Results,* 139: College Station, TX (Ocean Drilling Program), 649–666.

Davis, E.E., Mottl, M.J., Fisher, A.T., et al., 1992. *Proc. ODP, Init. Repts.*, 139: College Station, TX (Ocean Drilling Program).

Davis, E.E., and Villinger, H., 1992. Tectonic and thermal structure of the Middle Valley sedimented rift, northern Juan de Fuca Ridge. *In* Davis, E.E., Mottl, M.J., Fisher, A.T., et al., *Proc. ODP, Init. Repts.*, 139: College Station, TX (Ocean Drilling Program), 9–41.

Desprairies, A., Tremblay, P., and Laloy, C., 1989. Secondary mineral assemblages in a volcanic sequence drilled during ODP Leg 104 in the Norwegian Sea. *In* Eldholm, O., Thiede, J., Taylor, E., et al., *Proc. ODP, Sci. Results,* 104: College Station, TX (Ocean Drilling Program), 397–409.

Detrick, R., Honnorez, J., Bryan, W.B., Juteau, T., et al., 1988. *Proc. ODP, Init. Repts.*, 106/109: College Station, TX (Ocean Drilling Program).

Devine, J.D., and Leinen, M., 1981. Chemistry of the massive sulfide deposit cored at Site 471. *In* Yeats, R.S., Hag, B.U., et al., *Init. Repts. DSDP,* 3: Washington (U.S. Govt. Printing Office), 679–686.

Di Donato, G., Joron, J.L., Treuil, M., and Loubet, M., 1990. Geochemistry of zero-age N-MORB from Hole 648B, ODP Legs 106–109, M.A.R., 22°N. *In* Detrick, R., Honnorez, J., Bryan, W.B., Juteau, T., et al., *Proc. ODP, Sci. Results,* 106/109: College Station, TX (Ocean Drilling Program), 57–65.

Dieu, J.J., 1995. Mineral compositions in Leg 144 lavas and ultramafic xenoliths: the roles of cumulates and carbonatite metasomatism in magma petrogenesis. *In* Haggerty, J.A., Premoli Silva, I., Rack, F., and McNutt, M.K. (Eds.), *Proc. ODP, Sci. Results,* 144: College Station, TX (Ocean Drilling Program), 513–533.

Dmitriev, L.V., 1977. Petrochemistry of basalts and plutonic rocks, Leg 37, Deep Sea Drilling Project. *In* Aumento, F., Melson, W.G. et al., *Init. Repts. DSDP,* 37: Washington (U.S. Govt. Printing Office), 681–693.

Donnelly, T., Francheteau, J., Bryan, W., Robinson, P., Flower, M., Salisbury, M., et al., 1979. *Init. Repts. DSDP*, 51, 52, 53 (Pts. 1 and 2): Washington (U.S. Govt. Printing Office).

Duennebier, F.K., Stephen, R., Gettrust, J.F., et al., 1987. *Init. Repts. DSDP*, 88: Washington (U.S. Govt. Printing Office).

Duncan, R.A., 1978. Geochronology of basalts from the Ninetyeast Ridge and continental dispersion in the eastern Indian Ocean. *J. Volcanol. Geotherm. Res.*, 4:283–305.

Duncan, R.A., 1981. Hotspots in the southern oceans: an absolute frame of reference for motion of the Gondwana continents. *In* Solomon, S.C., Van der Voo, R., and Chinnery, M.A. (Eds.), *Quantitative Methods of Assessing Plate Motions.* Tectonophysics, 74:29–42.

Duncan, R.A., 1990. The volcanic record of the Reunion hotspot. *In* Duncan, R.A., Backman, J., Peterson, L.C., et al., *Proc. ODP, Sci. Results*, 115: College Station, TX (Ocean Drilling Program), 3–10.

Duncan, R.A., 1991. Age distribution of volcanism along aseismic ridges in the eastern Indian Ocean. *In* Weissel, J., Peirce, J., Taylor, E., Alt, J., et al., *Proc. ODP, Sci. Results*, 121: College Station, TX (Ocean Drilling Program), 507–517.

Duncan, R.A., and Hargraves, R.B., 1990. $^{40}Ar/^{39}Ar$ geochronology of basement rocks from the Mascarene Plateau, the Chagos Bank, and the Maldives Ridge. *In* Duncan, R. A., Backman, J., Peterson, L.C., et al., *Proc. ODP, Sci. Results*, 115: College Station, TX (Ocean Drilling Program), 43–51.

Edmond, J.M., 1992. Results of water rock interactions in mid-ocean ridges. *In* Kharaka, Y.K., and Maest, A.S. (Eds.), *Proc. 7th Int. Symp. On Water-Rock Interaction* (Vol. 2): *Moderate and High Temperature Environments*, 7:885–889.

Edmond, J.M., Measures, C., McDuff, R.E., Chan, L.H., Collier, R., and Grant, B., 1979. Ridge crest hydrothermal activity and the balances of the major and minor elements in the ocean: the Galapagos data. *Earth Planet. Sci. Lett.*, 46:1–18.

Edmond, J.M., and Von Damm, K., 1983. Hot springs on the ocean floor. *Sci. Am.*, 248:78–84.

Edmond, J.M., von Damm, K.L., McDuff, R.E., and Measures, C.I., 1982. Chemistry of hot springs on the East Pacific Rise and their effluent dispersal. *Nature (London, U. K.)*, 297:187–191.

Elderfield, H., and Schultz, A., 1996. Mid-ocean ridge hydrothermal fluxes and the chemical composition of the ocean. *Annu. Rev. Earth Planet. Sci.*, 24(1):191–224. **doi:10.1146/annurev.earth.24.1.191**

Eldholm, O., Thiede, J., Taylor, E., et al., 1987. *Proc. ODP, Init. Repts.*, 104: College Station, TX (Ocean Drilling Program).

Eldholm, O., Thiede, J., and Taylor, E., 1989a. The Norwegian continental margin: tectonic, volcanic, and paleoenvironmental framework. *In* Eldholm, O., Thiede, J., Taylor, E., et al., *Proc. ODP, Sci. Results*, 104: College Station, TX (Ocean Drilling Program), 5–26.

Eldholm, O., Thiede, J., and Taylor, E., 1989b. Evolution of the Vøring volcanic margin. *In* Eldholm, O., Thiede, J., Taylor, E., et al., *Proc. ODP, Sci. Results*, 104: College Station, TX (Ocean Drilling Program), 1033–1065.

Emmermann, R., and Puchelt, H., 1979. Major and trace element chemistry of basalts from Holes 417D and 418A, Deep Sea Drilling Project Legs 51–53. *In* Donelly, T., Francheteau, J., Bryan, W., Robinson, P., Flower, M., Salisbury, M., et al., *Init. Repts. DSDP*, 51, 52, 53 (Pt. 2): Washington (U.S. Govt. Printing Office), 987–1000.

Evans, C.A., and Baltuck, M., 1988. Low-temperature alteration of peridotite, Hole 637A. *In* Boillot, G., Winterer, E.L., et al., *Proc. ODP, Sci. Results*, 103: College Station, TX (Ocean Drilling Program), 235–239.

Evans, C.A., and Girardeau, J., 1988. Galicia Margin peridotites: undepleted abyssal peridotites from the North Atlantic. *In* Boillot, G., Winterer, E.L., et al., *Proc. ODP, Sci. Results*, 103: College Station, TX (Ocean Drilling Program), 195–207.

Ewart, A., Bryan, W.B., Chappell, B.W., and Rudnick, R.L., 1994. Regional geochemistry of the Lau-Tonga arc and backarc systems. *In* Hawkins, J., Parson, L., Allan, J., et al., *Proc. ODP, Sci. Results*, 135: College Station, TX (Ocean Drilling Program), 385–425.

Ewing, J., and Houtz, R., 1979. Acoustic stratigraphy and structure of the oceanic crust. *In* Talwani, M., Harrison, C.G., and Hayes, D.E. (Eds.), *Deep Drilling Results in the Atlantic Ocean: Ocean Crust.* Am. Geophys. Union, Maurice Ewing Ser., 1:1–14.

Fisher, R.L., Sclater, J.G., and McKenzie, D.P., 1971. Evolution of the Central Indian Ridge, Western Indian Ocean. *Geol. Soc. Am. Bull.,* 82:553–562.

Fisk, M.R., and Howard, K.J., 1990. Chemistry of basalt alteration from Leg 115. *In* Duncan, R.A., Backman, J., et al., *Proc. ODP, Sci. Results,* 115: College Station, TX (Ocean Drilling Program), 791–793.

Flower, M.F.J., Robinson, P.T., Schmincke, H.-U., and Ohnmacht, W., 1977. Petrology and geochemistry of igneous rocks, DSDP Leg 37. *In* Aumento, F., Melson, W.G. et al., *Init. Repts. DSDP,* 37: Washington (U.S. Govt. Printing Office), 653–679.

Floyd, P.A., and Castillo, P.R., 1992. Geochemistry and petrogenesis of Jurassic ocean crust basalts, Site 801. *In* Larson, R.L., Lancelot, Y., et al., *Proc. ODP, Sci. Results,* 129: College Station, TX (Ocean Drilling Program), 361–388.

Fouquet, Y., Zierenberg, R.A., Miller, D.J., et al., 1998. *Proc. ODP, Init. Repts.,* 169: College Station, TX (Ocean Drilling Program).

Frey, F.A., Coffin, M.F., Wallace, P.J., and Weis, D., 2003. Leg 183 synthesis: Kerguelen Plateau–Broken Ridge—a large igneous province. *In* Frey, F.A., Coffin, M.F., Wallace, P.J., and Quilty, P.G. (Eds.), *Proc. ODP, Sci. Results,* 183, 1–48 [CDROM]. Available from: Ocean Drilling Program, Texas A&M University, College Station TX 778459547, USA.

Frey, F.A., Dickey, J.S., Jr., Thompson, G., and Bryan, W.B., 1977. Eastern Indian Ocean DSDP sites: correlations between petrography, geochemistry and tectonic setting. *In* Heirtzler, J.R., Bolli, H.M., Davies, T.A., Saunders, J.B., and Sclater, J.G. (Eds.), *A Synthesis of Deep Sea Drilling in the Indian Ocean:* Washington (U.S. Govt. Printing Office), 189–257.

Frey, F.A., Jones, W.B., Davies, H., and Weis, D., 1991. Geochemical and petrologic data for basalts from Sites 756, 757, and 758: implications for the origin and evolution of the Ninetyeast Ridge. *In* Weissel, J., Peirce, J., Taylor, E., Alt, J., et al., *Proc. ODP, Sci. Results,* 121: College Station, TX (Ocean Drilling Program), 611–659.

Frey, F.A., and Sung, C.M., 1974. Geochemical results for basalts from sites 253 and 254. *In* Davies, T.A., Luyendyk, B.P., et al., *Init. Repts. DSDP,* 26: Washington (U.S. Govt. Printing Office), 567–572.

Friedrichsen, H., and Hoernes, S., 1979. Oxygen and hydrogen isotope exchange reactions between sea water and oceanic basalts from Legs 51 through 53. *In* Donelly, T., Francheteau, J., Bryan, W., Robinson, P., Flower, M., Salisbury, M., et al., *Init. Repts. DSDP,* 51, 52, 53 (Pt. 2): Washington (U.S. Govt. Printing Office), 1177–1182.

Fryer, P., and Mottl, M.J., 1992. Lithology, mineralogy, and origin of serpentine muds recovered from Conical and Torishima forearc seamounts: results of Leg 125 drilling. *In* Fryer, P., Pearce, J.A., Stokking, L.B., et al., *Proc. ODP, Sci. Results,* 125: College Station, TX (Ocean Drilling Program), 343–362.

Fryer, P., Pearce, J.A., Stokking, L.B., et al., 1990. *Proc. ODP, Init. Repts.,* 125: College Station, TX (Ocean Drilling Program).

Gable, R., Morin, R.H., and Becker, K., 1989. Geothermal state of Hole 504B: ODP Leg 111 overview. *In* Becker, K., Sakai, H., et al., *Proc. ODP, Sci. Results,* 111: College Station, TX (Ocean Drilling Program), 87–96.

Gill, J.B., Seales, C., Thompson, P., Hochstaedter, A.G., and Dunlap, C., 1992. Petrology and geochemistry of Pliocene-Pleistocene volcanic rocks from the Izu Arc, Leg 126. *In* Taylor, B., Fujioka, K., et al., *Proc. ODP, Sci. Results,* 126: College Station, TX (Ocean Drilling Program), 383–404.

Gillis, K.M., Ludden, J.N., Plank, T., and Hoy, L.D., 1992. Low-temperature alteration and subsequent reheating of shallow oceanic crust at Hole 765D, Argo Abyssal Plain. *In* Gradstein, F.M., Ludden, J.N., et al., *Proc. ODP, Sci. Results,* 123: College Station, TX (Ocean Drilling Program), 191–199.

Goldberg, D., Broglia, C., and Becker, K., 1991. Fracturing, alteration, and permeability: *in-situ* properties in Hole 735B. *In* Von Herzen, R.P., Robinson, P.T., et al., *Proc. ODP, Sci. Results,* 118: College Station, TX (Ocean Drilling Program), 261–269.

Goodfellow, W.D., and Peter, J.M., 1994. Geochemistry of hydrothermally altered sediment, Middle Valley, northern Juan de Fuca Ridge. *In* Mottl, M.J., Davis, E.E., Fisher, A.T., and Slack, J.F. (Eds.), *Proc. ODP, Sci. Results,* 139: College Station, TX (Ocean Drilling Program), 207–289.

Govindaraju, K., 1989. 1989 compilation of working values and sample description for 272 geostandards. *Geostand. Newsl.,* 13 (spec. iss.).

Gradstein, F.M., Ludden, J.N., et al., 1992. *Proc. ODP, Sci. Results,* 123: College Station, TX (Ocean Drilling Program).

Grechin, V.I., Eroshchev-Shak, V.A., and Zolotarev, B.P., 1981. Petrochemistry of abyssal oceanic basalts and dolerites, and their secondary alterations, Site 469, 470, 471, 472, 473. *In* Yeats, R.S., Hag, B.U., et al., *Init. Repts. DSDP,* 63: Washington (U.S. Govt. Printing Office), 711–732.

Greenough, J.D., Fryer, B.J., and Robinson, P.T., 1990. Geochemical effects of alteration on mafic rocks from Indian Ocean Site 706. *In* Duncan, R.A., Backman, J., Peterson, L.C., et al., *Proc. ODP, Sci. Results,* 115: College Station, TX (Ocean Drilling Program), 85–92.

Groschel-Becker, H.M., 2000. Data report: Physical properties of sediment, basalt, and massive sulfide samples from Holes 856H, 1035D, 1035E, 1035F, and 1035H, Middle Valley, northern Juan de Fuca Ridge, and Holes 1037B and 1038I, Escanaba Trough, Gorda Ridge. *In* Zierenberg, R.A., Fouquet, Y., Miller, D.J., and Normark, W.R. (Eds.), *Proc. ODP, Sci. Results,* 169, 1–19 [CD-ROM]. Available from: Ocean Drilling Program, Texas A&M University, College Station TX 77845-9547, USA. [**HTML**]

Hajash, A., 1980. Altered rocks from Deep Sea Drilling Project Leg 59. *In* Kroenke, L., Scott, R., et al., *Init. Repts. DSDP,* 59: Washington (U.S. Govt. Printing Office), 735–736.

Hall, J.M., and Fischer, J.F., 1977. Opaque mineralogy of basement rocks, Leg 37. *In* Aumento, F., Melson, W.G. et al., *Init. Repts. DSDP,* 37: Washington (U.S. Govt. Printing Office), 857–873.

Hannington, M.D., Jonasson, I.R., Herzig, P.M., and Petersen, S., 1995. Physical, chemical processes of seafloor mineralization at mid-ocean ridges. *In* Humphris, S.E., Zierenberg, R.A., Mullineaux, L.S., and Thomson, R.E. (Eds.), *Seafloor Hydrothermal Systems: Physical, Chemical, Biological and Geological Interactions.* Geophys. Monogr., 91:115–157.

Harrison, C.G.A., 1981. Magnetism of the oceanic crust. *In* Emiliani, C. (Ed.), *The Sea* (Vol. 7): New York (Wiley), 219–239.

Hart, S.R., 1973. A model for chemical exchange in the basalt-seawater system of ocean layer 2. *Can. J. Earth Sci.,* 10:799–816.

Hart, S.R., and Staudigel, H., 1979. Ocean crust-seawater interaction: Sites 417 and 418. *In* Donnelly, T., Francheteau, J., Bryan, W., Robinson, P., Flower, M., Salisbury, M., et al., *Init. Repts. DSDP,* 51, 52, 53 (Pt. 2): Washington (U.S. Govt. Printing Office), 1169–1176.

Hawkins, J.W., and Allan, J.F., 1994. Petrologic evolution of Lau Basin Sites 834 through 839. *In* Hawkins, J., Parson, L., Allan, J., et al., *Proc. ODP, Sci. Results,* 135: College Station, TX (Ocean Drilling Program), 427–470.

Hawkins, J.W., Parson, L.M., and Allan, J.F., 1994. Introduction to the scientific results of Leg 135: Lau Basin–Tonga Ridge drilling transect. *In* Hawkins, J., Parson, L., Allan, J., et al., *Proc. ODP, Sci. Results,* 135: College Station, TX (Ocean Drilling Program), 3–5.

Hodges, F.N., and Papike, J.J., 1977. Petrology of basalts, gabbros, and peridotites from DSDP Leg 37. *In* Aumento, F., Melson, W.G., et al., *Init. Repts. DSDP,* 37: Washington, (U.S. Govt. Printing Office), 711–719.

Hofmann, A.W., and White, W.M., 1982. Mantle plumes from ancient oceanic crust. *Earth Planet. Sci. Lett.,* 27:421–436.

Honnorez, J., 1981. The aging of the oceanic crust at low temperature. *In* Emiliani, C. (Ed.), *The Sea* (Vol. 7): *The Oceanic Lithosphere:* New York (Wiley), 525–587.

Honnorez, J., Alt, J.C., Honnorez-Guerstein, B.-M., Laverne, C., Muehlenbachs, K., Ruiz, J., and Saltzman, E., 1985. Stockwork-like sulfide mineralization in young oceanic crust: Deep Sea Drilling Project Hole 504B. *In* Anderson, R.N., Honnorez, J.,

Becker, K., et al., *Init. Repts. DSDP,* 83: Washington (U.S. Govt. Printing Office), 263–282.

Honnorez, J., Laverne, C., Hubberten, H.-W., Emmermann, R., and Muehlenbachs, K., 1983. Alteration processes in Layer 2 basalts from Deep Sea Drilling Project Hole 504B, Costa Rica Rift. *In* Cann, J.R., Langseth, M.G., Honnorez, J., Von Herzen, R.P., White, S.M., et al., *Init. Repts. DSDP,* 69: Washington (U.S. Govt. Printing Office), 509–546.

Humphris, S.E., and Thompson, G., 1978. Hydrothermal alteration of oceanic basalts by seawater. *Geochim. Cosmochim. Acta,* 42:107–125.

Humphris, S.E., Thompson, R.N., and Marriner, G.F., 1979. The mineralogy and geochemistry of basalt weathering, Holes 417A and 418A. *In* Donnelly, T., Francheteau, J., Bryan, W., Robinson, P., Flower, M., Salisbury, M., et al., *Init. Repts. DSDP,* 51, 52, 53: Washington (US Govt. Printing Office), 1201–1217.

Hussong, D.M., Uyeda, S., et al., 1982. *Init. Repts. DSDP,* 60: Washington (U.S. Govt. Printing Office).

Hyndman, R.D., Von Herzen, R.P., Erickson, A.J., and Jolivet, J., 1977. Heat-flow measurements, DSDP Leg 37. *In* Aumento, F., Melson, W.G., et al., *Init. Repts. DSDP,* 37: Washington (U.S. Govt. Printing Office), 347–362.

Irvine, T.N., and Baragar, W.R.A., 1971. A guide to the chemical classification of the common volcanic rocks. *Can. J. Earth Sci.,* 8:523–548.

Ishii, T., Robinson, P.T., Maekawa, H., and Fiske, R., 1992. Petrological studies of peridotites from diapiric serpentinite seamounts in the Izu-Ogasawara-Mariana forearc, Leg 125. *In* Fryer, P., Pearce, J.A., Stokking, L.B., et al., *Proc. ODP, Sci. Results,* 125: College Station, TX (Ocean Drilling Program), 445–485.

Ishiwatari, A., 1992. Petrology, geochemistry, and mineralogy of the Early Cretaceous evolved N-MORB from Sites 765 and 766, Eastern Indian Ocean. *In* Gradstein, F.M., Ludden, J.N., et al., *Proc. ODP, Sci. Results,* 123: College Station, TX (Ocean Drilling Program), 201–213.

Ishizuka, H., 1989. Mineral paragenesis of altered basalts from Hole 504B, ODP Leg 111. *In* Becker, K., Sakai, H., et al., *Proc. ODP, Sci. Results,* 111: College Station, TX (Ocean Drilling Program), 61–76.

Jackson, E.D., Bargar, K.E., Fabbi, B.P., and Heropoulos, C., 1976. Petrology of the basaltic rocks drilled on Leg 33 of the Deep Sea Drilling Project. *In* Schlanger, S.O., Jackson, E.D., et al., *Init. Repts. DSDP,* 33: Washington (U.S. Govt. Printing Office), 571–630.

Jackson, E.D., Koizumi, I., Dalrymple, G.D., Clague, D.A., Kirkpatrick, J., and Green, H.G., 1980. Introduction and summary of results from DSDP Leg 55, the Hawaiian-Emperor hotspot experiment. *In* Jackson, E.D., Koizumi, I., et al., *Init. Repts. DSDP,* 55: Washington (U.S. Govt. Printing Office), 5–31.

Jackson, E.D., Koizumi, I., et al., 1980. *Init. Repts. DSDP,* 55: Washington (U.S. Govt. Printing Office).

Jackson, E.D., and Schlanger, S.O., 1976. Regional syntheses, Line Islands Chain, Tuamotu Island Chain, and Manihiki Plateau, Central Pacific Ocean. *In* Schlanger, S.O., Jackson, E.D., et al., *Init. Repts. DSDP,* 33: Washington (U.S. Govt. Printing Office), 915–927.

Jenkyns, H.C., and Hardy, R.G., 1976. Basal iron-titanium-rich sediments from Hole 315A (Line Islands, Central Pacific). *In* Schlanger, S.O., Jackson, E.D., et al., *Init. Repts. DSDP,* 33: Washington (U.S. Govt. Printing Office), 833–836.

Johnson, L.E., 1992. Mafic clasts in serpentine seamounts: petrology and geochemistry of a diverse crustal suite from the outer Mariana forearc. *In* Fryer, P., Pearce, J.A., Stokking, L.B., et al., *Proc. ODP, Sci. Results,* 125: College Station, TX (Ocean Drilling Program), 401–413.

Kawahata, H., 1983. Hydrothermal systems in the Mid-Ocean Ridge. *Min. Geol. (Tokyo, 1951-1991),* 3(5):347–365.

Kazitzyn, Y., and Rudnik, V., 1968. *Guide to Estimation of Mass Balance and Inner Energy during Metasomatic Rocks Formation:* Moscow (Nedra).

Kempe, D.R.C., 1974. The petrology of the basalts, Leg 26. *In* Davies, T.A., Luyendyk, B.P., et al., *Init. Repts. DSDP,* 26: Washington (U.S. Govt. Printing Office), 465–503.

Kepezhinskas, P.K., Sorokina, N.A., Mamontova, S.A., and Savichev, A.T., 1995. Rare earth and large-ion lithophile (Sr and Ba) element geochemistry of diabase dikes,

Hole 504B, Costa Rica Rift, Leg 140. *In* Erzinger, J., Becker, K., Dick, H.J.B., and Stokking, L.B. (Eds.), *Proc. ODP, Sci. Results,* 137/140: College Station, TX (Ocean Drilling Program), 107–116.

Kirkpatrick, R.J., Clague, D.A., and Freisen, W., 1980. Petrology and geochemistry of volcanic rocks, DSDP Leg 55, Emperor Seamount Chain. Init. *In* Jackson, E.D., Koizumi, I., et al., *Init. Repts. DSDP,* 55: Washington (U.S. Govt. Printing Office), 509–557.

Klootwijk, C.T., Gee, J.S., Peirce, J.W., and Smith, G.M., 1991. Constraints on the India-Asia convergence: paleomagnetic results from Ninetyeast Ridge. *In* Weissel, J., Peirce, J., Taylor, E., Alt, J., et al., *Proc. ODP, Sci. Results,* 121: College Station, TX (Ocean Drilling Program), 777–884.

Kristmannsdottir, H., and Tomasson, J., 1978. Zeolite zones in geothermal areas in Iceland. *In* Sand, L.B., and Mumpton, F.A. (Eds.), *Natural Zeolites: Occurrences, Properties, and Use:* Oxford (Pergamon), 277–284.

Kroenke, L., Scott, R., et al., 1981. *Init. Repts. DSDP,* 59: Washington (U.S. Govt. Printing Office).

Kurnosov, V., 1995. Alteration effects in the oceanic crust: review and recommendations. *In* Kharaka, Y., and Chudaev, O. (Eds.), *Water Rock Interaction:* Rotterdam (Balkema), 575–578.

Kurnosov, V., and Murdmaa, I., 1996. Hydrothermal and cold-water circulation within the intraplate seamounts: effects on rock alteration. *In* Williams, R. and Sloan H. (Eds.). *The Oceanic Lithosphere and Scientific Drilling into the 21st Century:* Woods Hole, MA (ODP-InterRidge IAVCEI Workshop), 87–88.

Kurnosov, V., Murdmaa, I., Rosanova, T., Kashintzev, G., Eroshchev-Shak, V., and Krasnov, S., 1994. Mineralogy of hydrothermally altered sediments and igneous rocks at Sites 856-858, Middle Valley, Juan de Fuca Ridge, Leg 139. *In* Mottl, M.J., Davis, E.E., Fisher, A.T., and Slack, J.F. (Eds.), *Proc. ODP, Sci. Results,* 139: College Station, TX (Ocean Drilling Program), 113–131.

Kurnosov, V., Zolotarev, B., Artamonov, A., Garanina, S., Petrova, V., EroshchevShak, V., and Sokolva, A., 2003. Data report: Alteration of basalts from the Kerguelen Plateau. *In* Frey, F.A., Coffin, M.F., Wallace, P.J., and Quilty, P.G. (Eds.), *Proc. ODP, Sci. Results,* 183, 1–40 [CDROM]. Available from: Ocean Drilling Program, Texas A&M University, College Station TX 778459547, USA. [**HTML**]

Kurnosov, V., Zolotarev, B., Eroshchev-Shak, V., Artamonov, A., Kashinzev, and Murdmaa, I., 1995. Alteration of basalts from the West Pacific Guyots, Legs 143 and 144. *In* Haggerty, J.A., Premoli Silva, I., Rack, F., and McNutt, M.K. (Eds.), *Proc. ODP, Sci. Results,* 144: College Station, TX (Ocean Drilling Program), 475–491.

Kurnosov, V.B., Kholodkevich, I.V., Chubarov, V.M., and Shevchenko, A.Ya., 1983. Secondary minerals in basalt from the Costa Rica Rift, Holes 501 and 504B, Deep Sea Drilling Project Legs 68, 69, and 70. *In* Cann, J.R., Langseth, M.G., Honnorez, J., Von Herzen, R.P., White, S.M., et al., *Init. Repts. DSDP,* 69: Washington (U.S. Govt. Printing Office), 573-583.

Kurnosov, V.B., 1986. *Hydrothermal Alterations of Basalts in the Pacific Ocean and Metal-bearing Deposits, Using Data of Deep-sea Drilling:* Moscow (Nauka).

Kurnosov, V.B., 1992. Hydrothermal water-basalts interaction in the ocean. *In* Kharaka, Y.K., and Maest, A.S. (Eds.), *Proc. 7th Int. Symp. Water Rock Interaction* (Vol. 2): *Moderate and High Temperature Environments,* 1651–1654.

Kurnosov, V.B., Kholodkevich, I.V., Chubarov, V.M., and Shevchenko, A.Y., 1983. Secondary minerals in basalt from the Costa Rica Rift, Holes 501 and 504B, Deep Sea Drilling Project, Legs 68, 69 and 70. *In* Cann, J.R., Langseth, M.G., Honnorez, J., Von Herzen, R.P., White, S.M., et al., *Init. Repts. DSDP,* 69: Washington (U.S. Govt. Printing Office), 573–583.

Kurnosov, V.B., Kholodkevich, I.V., and Shevchenko, A.Y., 1981. Secondary minerals of basalts from the Nauru Basin, Deep Sea Drilling Project Leg 61. *In* Larson, R.L., Schlanger, S.O., et al., *Init. Repts. DSDP,* 61: Washington (U.S. Govt. Printing Office), 653–671.

Kurnosov, V.B., Zolotarev, B., Artamonov, A., Garanina, S., Petrova, V., Eroshchev-Shak, V., and Sokolova, A., 2003. Data report: Alteration of basalts from the Kerguelen Plateau. *In* Frey, F.A., Coffin, M.F., Wallace, P.J., and Quilty, P.G. (Eds.),

Proc. ODP, Sci. Results, 183, 1–40 [CD-ROM]. Available from: Ocean Drilling Program, Texas A&M University, College Station TX 77845-9547, USA

Lancelot, Y., Larson, R.L., et al., 1990. *Proc. ODP, Init. Repts.*, 129: College Station, TX (Ocean Drilling Program).

Lanphere, M.A., and Dalrymple, G.B., 1976. K-Ar ages of basalts from DSDP Leg 33: Sites 315 (Line Islands) and 317 (Manihiki Plateau). *In* Schlanger, S.O., Jackson, E.D., et al., *Init. Repts DSDP*, 33: Washington (U.S. Govt. Printing Office), 649–653.

Larson, R.L., Lancelot, Y., et al., 1992. *Proc. ODP, Sci. Results*, 129: College Station, TX (Ocean Drilling Program).

Larson, R.L., and Schlanger, S.O., 1981. Geological evolution of the Nauru Basin, and regional implications. *In* Larson, R.L., Schlanger, S.O., et al., *Init. Repts. DSDP*, 61: Washington (U.S. Govt. Printing Office), 841–862.

Larson, R.L., Schlanger, S.O., et al., 1981. *Init. Repts. DSDP*, 61: Washington (U.S. Govt. Printing Office).

Laverne, C., 1983. Occurrence of melanite and aegirine-augite in Deep Sea Drilling Project Hole 504B. *In* Cann, J.R., Langseth, M.G., Honnorez, J., Von Herzen, R.P., White, S.M., et al., *Init. Repts. DSDP*, 69: Washington (U.S. Govt. Printing Office), 593–605.

Laverne, C., Vanko, D.A., Tartarotti, P., and Alt, J.C., 1995. Chemistry and geothermometry of secondary minerals from the deep sheeted dike complex, Hole 504B. *In* Erzinger, J., Becker, K., Dick, H.J.B., and Stokking, L.B. (Eds.), *Proc. ODP, Sci. Results*, 137/140: College Station, TX (Ocean Drilling Program), 167–190.

Lawrence, J.R., 1991. Stable isotopic composition of pore waters and calcite veins. *In* Weissel, J., Peirce, J., Taylor, E., Alt, J., et al., *Proc. ODP, Sci. Results*, 121: College Station, TX (Ocean Drilling Program), 447–455.

Lawrie, D., and Miller, D.J., 2000. Data Report: Sulfide mineral chemistry and petrography from Bent Hill, ODP Mound, and TAG massive sulfide deposits. *In* Zierenberg, R.A., Fouquet, Y., Miller, D.J., and Normark, W.R. (Eds.), *Proc. ODP, Sci. Results*, 169, 1-34.

LeClaire, L., Bassias, Y., Denis-Clochiatti, M., Davies, H.L., Gautier, I., Gensous, B., Giannesini, P.-J., Patriat, P., Segoufin, J., Tesson, M., and Wannesson, J., 1987. Lower Cretaceous basalt and sediments from the Kerguelen Plateau. *Geo-Mar. Lett.*, 7:169–176.

Ledbetter, J.K., and Haggerty, J.A., 1994. Late Miocene sedimentation history of the Tonga forearc at Site 840. *In* Hawkins, J., Parson, L., Allan, J., et al., *Proc. ODP, Sci. Results*, 135: College Station, TX (Ocean Drilling Program), 163–172.

Lee-Wong, F., 1981. Feldspar compositions of volcanic flow rocks from Hess Rise, Deep Sea Drilling Project Leg 62. *In* Thiede, J., Vallier, T.L., et al., *Init. Repts. DSDP*, 62: Washington (U.S. Govt. Printing Office), 967–970.

LeHuray, A.P., 1989. Native cooper in ODP Site 642 tholeiites. *In* Eldholm, O., Thiede, J., and Taylor, E., et al. (Eds.). *Proc. ODP, Sci. Results*, 104: College Station, TX (Ocean Drilling Program), 411–417.

LeHuray, A.P., and Johnson, E.S., 1989. Rb-Sr systematics of Site 642 volcanic rocks and alteration minerals. *In* Eldholm, O., Thiede, J., Taylor, E., et al., *Proc. ODP, Sci. Results*, 104: College Station, TX (Ocean Drilling Program), 437–448.

Le Pichon, X., and Heirtzler, J.R., 1968. Magnetic anomalies in the Indian Ocean and sea-floor spreading. *J. Geophys. Res.*, 73:2101–2117.

Lewis, B.T.R., Robinson, P.T., et al., 1983. *Init. Repts. DSDP*, 65: Washington (U.S. Govt. Printing Office).

Love, D.A., Frape, S.K., Gibson, I.L., and Jones, M.G., 1989. The $\delta^{18}O$ and $\delta^{13}C$ isotopic composition of secondary carbonates from basaltic lavas cored in Hole 642E, Ocean Drilling Program Leg 104. *In* Eldholm, O., Thiede, J., Taylor, E., et al., *Proc. ODP, Sci. Results*, 104: College Station, TX (Ocean Drilling Program), 449–455.

Ludden, J.N., and Dionne, B., 1992. The geochemistry of oceanic crust at the onset of rifting in the Indian Ocean. *In* Gradstein, F.M., Ludden, J.N., et al., *Proc. ODP, Sci. Results*, 123: College Station, TX (Ocean Drilling Program), 791–799.

Luyendyk, B.P., and Rennick, W., 1977. Tectonic history of aseismic ridges in the eastern Indian Ocean. *Geol. Soc. Am. Bull.*, 88:1347–1356.

Lyle, M., 1976. Estimation of hydrothermal manganese input to the oceans. *Geology*, 4(2):733–736.

Macdonald, G.A., 1968. Composition and origin of Hawaiian lavas. *Contrib. Hawaii Inst. Geophys. Year.*, 477–552.

Mahoney, J.L., Macdougall, J.D., Lugmair, G.W., and Gopalan, K., 1983. Kerguelen hot-spot source for Rajmahal Traps and Ninetyeast Ridge? *Nature (London, U. K.)*, 303:385–389. **doi:10.1038/303385a0**

Marques, L.L., and Nehlig, P., 2000. Textural analyses of vein networks and sulfide impregnation zones: implications for the structural development of the Bent Hill massive sulfide deposit. *In* Zierenberg, R.A., Fouquet, Y., Miller, D.J., and Normark, W.R. (Eds.), *Proc. ODP, Sci. Results*, 169: 1-25.

Mattey, D.P., Marsh, N.G., and Tarney, J., 1981. The geochemistry, mineralogy, and petrology of basalts from the West Philippine and Parece Vela basins and from the Palau-Kyushu and West Mariana ridges, Deep Sea Drilling Project Leg 59. *In* Kroenke, L., Scott, R., et al., *Init. Repts. DSDP*, 59: Washington (U.S. Govt. Printing Office), 753–800.

McBirney, A.R., and Williams, H., 1969. Geology and petrology of the Galapagos Island. *Mem.—Geol. Soc. Am.*, 118:197.

McKenzie, D., and Sclater, J.G., 1971. The evolution of the Indian Ocean since the Late Cretaceous. *Geophys. J. R. Astron. Soc.*, 24:437–528.

McKenzie, J., 1980. Stable isotopic study of carbonate minerals from the basalt flows on Suiko Seamount: DSDP Leg 55, Hole 433C. *In* Jackson, E.D., Koizumi, I., et al., *Init. Repts. DSDP*, 55: Washington (U.S. Govt. Printing Office), 653–658.

Menard, H.W., Natland, J.H., Jordan, T.H., Orcutt, J.A., et al., 1987. *Init. Repts. DSDP*, 91: Washington (U.S. Govt. Printing Office).

Meschede, M., 1986. A method of discriminating between different types of mid-oceanic ridge basalts and continental tholeiites with the Nb-Zr-Y diagram. *Chem. Geol.*, 56:207–218.

Mevel, C., 1979. Mineralogy and chemistry of secondary phases in low temperature altered basalts from Deep Sea Drilling Project Legs 51, 52 and 53. *In* Donnelly, T., Francheteau, J., Bryan, W., Robinson, P., Flower, M., Salisbury, M., et al., *Init. Repts. DSDP*, 51, 52, 53: Washington (U.S. Govt. Printing Office), 1299–1317.

Meyerhoff, A.A., and Kamen-Kaye, M., 1981. Petroleum prospects of the Saya de Malha and Nazareth Banks, Indian Ocean. *AAPG Bull.*, 65:1344–1347.

Mitchell, W.S., and Aumento, F., 1977. Fission track chronology of basaltic glasses from DSDP Leg 37. *In* Aumento, F., Melson, W.G. et al., *Init. Repts. DSDP*, 37: Washington (U.S. Govt. Printing Office), 625–628.

Moore, T.C., Jr., Rabinowitz, P.D., Borella, P.E., Shackleton, N.J., and Boersma, A., 1984. History of the Walvis Ridge. *In* Moore, T.C., Rabinowitz, P.D., et al., *Init. Repts. DSDP*, 74: Washington (U.S. Govt. Printing Office), 873–894.

Moore, T.C., Jr., Rabinowitz, P.D., et al., 1984. *Init. Repts. DSDP*, 74: Washington, D.C. (U.S. Govt. Printing Office).

Morandi, N., and Felice, G., 1979. Serpentine minerals from veins in serpentine rocks. *Mineralogical Magazine*, 43, 325:135-140.

Morgan, W.J., 1981. Hotspot tracks and the opening of the Atlantic and Indian Oceans. *In* Emiliani, C. (Ed.), *The Sea* (Vol. 7): New York (Wiley), 443–487.

Morrison, M.A., and Thompson, R.N., 1983. Alteration of basalt: Deep Sea Drilling Project Legs 64 and 65. *In* Lewis, B.T.R., Robinson, P., et al., *Init. Repts. DSDP*, 65: Washington (U.S. Govt. Printing Office), 643–660.

Muehlenbachs, K., 1979. The alteration and aging of the basaltic layer of the sea floor: oxygen isotope evidence from DSDP/IPOD Leg 51, 52, and 53. *In* Donnelly, T., Francheteau, J., Bryan, W., Robinson, P., Flower, M., Salisbury, M., et al., *Init. Repts. DSDP*, 51, 52, 53: Washington (U.S. Govt. Printing Office), 1159–1167.

Munschy, M., Fritsch, B., Schlich, R., Fezga, F., Rotstein, Y., and Coffin, M.F., 1992. Structure and evolution of the central Kerguelen Plateau deduced from seismic stratigraphic studies and drilling at Site 747. *In* Wise, S.W., Jr., Schlich, R., et al., *Proc. ODP, Sci. Results*, 120: College Station, TX (Ocean Drilling Program), 881–893.

Murton, B.J., Peate, D.W., Arculus, R.J., Pearce, J.A., and van der Laan, S., 1992. Trace-element geochemistry of volcanic rocks from Site 786: the Izu-Bonin forearc. *In* Fryer, P., Pearce, J.A., Stokking, L.B., et al., *Proc. ODP, Sci. Results*, 125: College Station, TX (Ocean Drilling Program), 211–235.

Natland, J.H., and Mahoney, J.J., 1982. Alteration in igneous rocks at DSDP sites 458 and 459, Mariana fore arc region relationship to basement structures. *In* Hussong, D.M., Uyeda, S., et al., *Init. Repts. DSDP,* 60: Washington (U.S. Govt. Printing Office), 769–788.

Noack, Y., Emmermann, R., and Hubberten, H.-W., 1983. Alteration in Site 501 (Leg 68) and Site 504 (Leg 69) basalts: preliminary results. *In* Cann, J.R., Langseth, M.G., Honnorez, J., Von Herzen, R.P., White, S.M., et al., *Init. Repts. DSDP,* 69: Washington (U.S. Govt. Printing Office), 497–508.

Park, K.-H., and Staudigel, H., 1990. Radiogenic isotope ratios and initial seafloor alteration in submarine Serocki volcano basalts. *In* Detrick, R., Honnorez, J., Bryan, W.B., Juteau, T., et al. *Proc. ODP, Sci. Results,* 106/109: College Station, TX (Ocean Drilling Program), 117–121.

Parson, L., Hawkins, J., Allan, J., et al., 1992. *Proc. ODP, Init. Repts.,* 135: College Station, TX (Ocean Drilling Program).

Parson, L., Viereck, L., Love, D., Gibson, I., Morton, A., and Hertogen, J., 1989. The petrology of the lower series volcanics, ODP Site 642. *In* Eldholm, O., Thiede, J., Taylor, E., et al., *Proc. ODP, Sci. Results,* 104: College Station, TX (Ocean Drilling Program), 419–428.

Peirce, J., Weissel, J., et al., 1989. *Proc. ODP, Init. Repts.,* 121: College Station, TX (Ocean Drilling Program).

Peirce, J.W., 1978. The northward motion of India since the Late Cretaceous. *Geophys. J. R. Astron. Soc.,* 52:277–311.

Perfiljev, A.S., Achmetjev, M.A., Geptner, A.R., Dmitriev, Y.I., Zolotarev, B.P., and Samygin, S.G., 1991. *Miocene Basalts of Iceland and Problems of Spreading:* Moscow (Nauka).

Pertsev, N.N., and Boronikhin, V.A., 1983a. Alteration zones near veins in basalts from Deep Sea Drilling Project Sites 501/504 and 505, Costa Rica Rift. *In* Cann, J.R., Langseth, M.G., Honnorez, J., Von Herzen, R.P., White, S.M., et al., *Init. Repts. DSDP,* 69: Washington (U.S. Govt. Printing Office), 565–572.

Pertsev, N.N., and Boronikkin, V.A., 1983b. Secondary K-feldspar in basalts at DSDP Hole 504B and the problem of K-feldsparization in oceanic basalts. *In* Cann, J.R., Langseth, M.G., Honnorez, J., Von Herzen, R.P., White, S.M., et al., *Init. Repts. DSDP,* 69: Washington (U.S. Govt. Printing Office), 589–591.

Pertsev, N.N., and Kurdyukov, E.B., 1996. Metasomatic and metamorphic peculiarities of the diabase dike alteration in Hole 504B, Leg 140. *In* Alt, J.C., Kinoshita, H., Stokking, L.B., and Michael, P.J. (Eds.). *Proc. ODP, Sci. Results,* 148: College Station, TX (Ocean Drilling Program), 97–110

Pertsev, N.N., and Rusinov, V.L., 1979. Mineral assemblages and processes of alteration in basalts at Deep Sea Drilling Project Sites 417 and 418. *In* Donelly, T., Francheteau, J., Bryan, W., Robinson, P., Flower, M., Salisbury, M., et al., *Init. Repts. DSDP,* 51, 52, 53 (Pt. 2): Washington (U.S. Govt. Printing Office), 1219–1232.

Pospichal, J.J., Dehn, J., Driscoll, N.W., van Eijden, A.J.M., Farrell, J.W., Fourtanier, E., Gamson, P., Gee, J., Janecek, T.R., Jenkins, D.G., Klootwijk, C., Nomura, R., Owen, R.M., Rea, D.K., Resiwati, P., Smit, J., and Smith, G., 1991. Cretaceous-Paleogene biomagnetostratigraphy of Sites 752–755, Broken Ridge: a synthesis. *In* Weissel, J., Peirce, J., Taylor, E., Alt, J., et al., *Proc. ODP, Sci. Results,* 121: College Station, TX (Ocean Drilling Program), 721–742.

Pouclet, A., and Bellon, H., 1992. Geochemistry and isotopic composition of volcanic rocks from the Yamato Basin: Hole 794D, Sea of Japan. *In* Tamaki, K., Suyehiro, K., Allan, J., McWilliams, M., et al., *Proc. ODP, Sci. Results,* 127/128 (Pt. 2): College Station, TX (Ocean Drilling Program), 779–789.

Premoli Silva, I., Haggerty, J., Rack, F., et al., 1993. *Proc. ODP, Init. Repts.,* 144: College Station, TX (Ocean Drilling Program).

Pringle, M.S., and Duncan, R.A., 1995a. Radiometric ages of basaltic lavas recovered at Sites 865, 866, and 869. *In* Winterer, E.L., Sager, W.W., Firth, J.V., and Sinton, J.M. (Eds.), *Proc. ODP, Sci. Results,* 143: College Station, TX (Ocean Drilling Program), 277–283.

Pringle, M.S., and Duncan, R.A., 1995b. Radiometric ages of basement lavas recorded at Loen, Wodejebato, MIT, and Takuyo-Daisan. *In* Haggerty, J.A., Premoli Silva, I.,

Rack, F., and McNutt, M.K. (Eds.), *Proc. ODP, Sci. Results,* 144: College Station, TX (Ocean Drilling Program), 547–557.

Pritchard, R.G., 1979. Alteration of basalts from Deep Sea Drilling Project Legs 51, 52, and 53, Holes 417A and 418A. *In* Donelly, T., Francheteau, J., Bryan, W., Robinson, P., Flower, M., Salisbury, M., et al., *Init. Repts. DSDP,* 51, 52, 53 (Pt. 2): Washington (U.S. Govt. Printing Office), 1185–1192.

Proust, D., Meunier, A., Fouillac, A.M., Dudoignon, P., Sturz, A., Charvet, J., and Scott, S.D., 1992. Preliminary results on the mineralogy and geochemistry of basalt alteration, Hole 794D. *In* Tamaki, K., Suyehiro, K., Allan, J., McWilliams, M., et al., *Proc. ODP, Sci. Results,* 127/128 (Pt. 2): College Station, TX (Ocean Drilling Program), 883–889.

Quinterno, P.J., 1994. Calcareous nannofossil biostratigraphy: Sites 840 (Tonga Ridge) and 841 (Tonga Trench). *In* Hawkins, J., Parson, L., Allan, J., et al., *Proc. ODP, Sci. Results,* 135: College Station, TX (Ocean Drilling Program), 267–283.

Rangin, C., Silver, E.A., von Breymann, M.T., et al., 1990. *Proc. ODP, Init. Repts.,* 124: College Station, TX (Ocean Drilling Program).

Rampino, M.R., and Stothers, R.B., 1988. Flood basalt volcanism during the past 250 million years. *Science,* 241:663–668.

Rea, D.K., Dehn, J., Driscoll, N., Farrell, J., Janecek, T., Owen, R.M., Pospichal, J.J., Resiwati, P., and the ODP Leg 121 Scientific Party, 1990. Paleoceanography of the Eastern Indian Ocean from ODP Leg 121 drilling on Broken Ridge. *Geol. Soc. Am. Bull.,* 102:679–690. **doi:10.1130/0016-7606(1990)102<0679:POTEIO>2.3.CO;2**

Rice, S., Langmuir, C.H., Bender, J.F., Hanson, G.N., Bence, A.E., and Taylor, S.R., 1979. Basalts from Deep Sea Drilling Project Holes 417A and 417D, fractionated melts of a light rare-earth depleted source. *In* Donelly, T., Francheteau, J., Bryan, W., Robinson, P., Flower, M., Salisbury, M., et al., *Init. Repts. DSDP,* 51, 52, 53 (Pt. 2): Washington (U.S. Govt. Printing Office), 1099–1111.

Richardson, S.H., Erlank, A.J., Reid, D.L., and Duncan, A.R., 1984. Major and trace elements and Nd and Sr isotope geochemistry of basalts from the Deep Sea Drilling Project Leg 74 Walvis Ridge transect. *In* Moore, T.C., Jr., Rabinowitz, P.D., et al., *Init. Repts. DSDP,* 74: Washington (U.S. Govt. Printing Office), 739–754.

Robinson, P.T., 1992. Holes CY-1 and 1a of the Cyprus Crustal Study Project: background and objectives. *In* Gibson, I.L., Mapas, J., Robinson, P.T., and Xenophontos, C. (Eds.), *Cyprus Crustal Study Project: Initial Report, Holes CY-1 and 1a.* Pap.—Geol. Surv. Can., 1–4.

Robinson, P.T., Dick, H.J.B., and Von Herzen, R.P., 1991. Metamorphism and alteration in oceanic layer 3: Hole 735B. *In* Von Herzen, R.P., Robinson, P.T., et al., *Proc. ODP, Sci. Results,* 118: College Station, TX (Ocean Drilling Program), 541–552.

Robinson, P.T., Flower, M.F.J., Schmincke, H.-U., and Ohnmacht, W., 1977. Low temperature alteration of oceanic basalts, DSDP Leg 37. *In* Aumento, F., Melson, W.G., et al., *Init. Repts. DSDP,* 37: Washington (U.S. Govt. Printing Office), 775–793.

Robinson, P.T., Von Herzen, R., et al., 1989. *Proc. ODP, Init. Repts.,* 118: College Station, TX (Ocean Drilling Program).

Rona, P.A., 1988. Hydrothermal mineralization at oceanic ridges. *Can. Mineral.,* 26:431–465.

Rona, P.A., Bostrom, K., Laubier, L., and Smith, K.L., Jr. (Eds.), 1983. *Hydrothermal Processes at Seafloor Spreading Centers:* New York (Plenum).

Rowbotham, G., and Floyd, P.A., 1992. Mineral chemistry of primary and secondary phases in basaltic rocks, Leg 129. *In* Larson, R.L., Lancelot, Y., et al., *Proc. ODP, Sci. Results,* 129: College Station, TX (Ocean Drilling Program), 305–343.

Royer, J.-Y., and Coffin, M.F., 1992. Jurassic to Eocene plate tectonic reconstructions in the Kerguelen Plateau region. *In* Wise, S.W., Jr., Schlich, R., et al., *Proc. ODP, Sci. Results,* 120: College Station, TX (Ocean Drilling Program), 917–928.

Royer, J.-Y., Peirce, J.W., and Weissel, J.K., 1991. Tectonic constraints on the hotspot formation of the Ninetyeast Ridge. *In* Weissel, J., Peirce, J., Taylor, E., Alt, J., et al., *Proc. ODP, Sci. Results,* 121: College Station, TX (Ocean Drilling Program), 763–776.

Royer, J.-Y., and Sandwell, D.T., 1989. Evolution of the eastern Indian Ocean since the Late Cretaceous: constraints from GEOSAT altimetry. *J. Geophys. Res.,* 94:13755–13782.

Rusinov, V.L., Pertsev, N.N., Arakeljanz, M.M., and Nosik, L.P., 1979. Some isotope relations in basalts from Deep Sea Drilling Project Holes 417A, 417D, and 418A. *In* Donelly, T., Francheteau, J., Bryan, W., Robinson, P., Flower, M., Salisbury, M., et al., *Init. Repts. DSDP,* 51, 52, 53 (Pt. 2): Washington (U.S. Govt. Printing Office), 1149–1151.

Rychagov, S.N., 2003. Evolution of hydrothermal-magmatic system of island arcs [Ph.D. dissert]. Institute of Volcanology, Moscow.

Sabora, K.L., Fryer, P., and Mackawa, H., 1992. Metamorphism of ultramafic clasts from Conical Seamount: Sites 778, 779, and 780. *In* Fryer, P., Coleman, P., Pearce, J.A., and Stokking, L.B. (Eds.). *ODP, Sci. Results,* 125: College Station, TX (Ocean Drilling Program), 431–443.

Sager, W.W., Winterer, E.L., Firth, J.V., et al., 1993. *Proc. ODP, Init. Repts.,* 143: College Station, TX (Ocean Drilling Program).

Salters, V.J.M., Storey, M., Sevigny, J.H., and Whitechurch, H., 1992. Trace element and isotopic characteristics of Kerguelen-Heard Plateau basalts. *In* Wise, S.W., Jr., Schlich, R., et al., *Proc. ODP, Sci. Results,* 120: College Station, TX (Ocean Drilling Program), 55–62.

Saunders, A.D., 1987. Geochemistry of basalts from Mesozoic Pacific Ocean crust: Deep Sea Drilling Project Leg 91. *In* Menard, H.W., Natland, J., Jordan, T.H., Orcutt, J.A., et al., *Init. Repts. DSDP,* 91: Washington (U.S. Govt. Printing Office), 483–494.

Saunders, A.D., Fornari, D.J., Joron, J.-L., Tarney, J., and Treuil, M., 1982. Geochemistry of basic igneous rocks, Gulf of California, Deep Sea Drilling Project Leg 64. *In* Curray, J.R., Moore, D.G., et al. (Eds.), *Init. Repts. DSDP,* 64: Washington (U.S. Govt. Printing Office), 595–642.

Saunders, A.D., Storey, M., Gibson, I.L., Leat, P., Hergt, J., and Thompson, R.N., 1991. Chemical and isotopic constraints on the origin of basalts from Ninetyeast Ridge, Indian Ocean: results from DSDP Legs 22 and 26 and ODP Leg 121. *In* Weissel, J., Peirce, J., Taylor, E., Alt, J., et al., *Proc. ODP, Sci. Results,* 121: College Station, TX (Ocean Drilling Program), 559–590.

Schandl, E.S., and Gorton, M.P., 1995. Phyllosilicate alteration of olivine in the lower sheeted dike complex, Leg 140, Hole 504B. *In* Erzinger, J., Becker, K., Dick, H.J.B., and Stokking, L.B. (Eds.), *Proc. ODP, Sci. Results,* 137/140: College Station, TX (Ocean Drilling Program), 207–216.

Schlanger, S.O., Jackson, E.D., et al., 1976. *Init. Repts. DSDP,* 33: Washington (U.S. Govt. Printing Office).

Schlich, R., 1975. Structure et ‰ge de l’ocŽan Indien occidental. *Mem. Hors-Ser. Soc. Geol. Fr.,* 6:1–103.

Schlich, R., and Wise, S.W., Jr., 1992. The geologic and tectonic evolution of the Kerguelen Plateau: an introduction to the scientific results of Leg 120. *In* Wise, S.W., Jr., Schlich, R., et al., *Proc. ODP, Sci. Results,* 120: College Station, TX (Ocean Drilling Program), 5–30.

Schlich, R., Wise, S.W., Jr., et al., 1989. *Proc. ODP, Init. Repts.,* 120: College Station, TX (Ocean Drilling Program).

Scott, R.B., 1980. Petrology and geochemistry of arc tholeiites on the Palau-Kyushu Ridge, Site 448, Deep Sea Drilling Project Leg 59. *In* Kroenke, L., and Scott, R., et al., *Init. Repts. DSDP,* 59: Washington (U.S. Govt. Printing Office), 753–796.

Scott, R.B., 1981. Geochemistry of igneous rocks in Deep Sea Drilling Project Hole 465A, Hess Rise: significance to oceanic plateau petrology and evolution. *In* Thiede, J., Vallier, T.L., et al., *Init. Repts. DSDP,* 62: Washington (U.S. Govt. Printing Office), 955–960.

Scott, R.B., Kroenke, L., Zakariadze, G., and Sharaskin, A., 1980. Evolution of the south Philippine Sea: DSDP Leg 59 results. *In* Kroenke, L., Scott, R., et al., *Init. Repts. DSDP,* 59: Washington (U.S. Govt. Printing Office), 803–816.

Seifert, K.E., 1981. Geochemistry of Nauru Basin basalts from the lower portion of Hole 462A, Deep Sea Drilling Project Leg 61. *In* Larson, R.L., Schlanger, S.O., et al., *Init. Repts. DSDP,* 61: Washington (U.S. Govt. Printing Office), 705–708.

Seifert, K.E., Vallier, T.L., Windom, K.E., and Morgan, S.R., 1981. Geochemistry and petrology of igneous rocks, Deep Sea Drilling Project Leg 62. *In* Thiede, J., Vallier, T.L., et al., *Init. Repts. DSDP,* 62: Washington (U.S. Govt. Printing Office), 945–954.

Serri, G., Spadea, P., Beccaluva, L., Civetta, M., Coltorti, M., Dostal, J., Sajona, F., Vaccaro, C., and Zeda, O., 1991. Petrology of igneous rocks from the Celebes Sea basement. *In* Silver, E.A., Rangin, C., von Breymann, M.T., et al., *Proc. ODP, Sci. Results,* 124: College Station, TX (Ocean Drilling Program), 271–296.

Sevigny, J.H., Whitechurch, H., Storey, M., and Salters, V.J.M., 1992. Zeolite-facies metamorphism of central Kerguelen Plateau basalts. *In* Wise, S.W., Jr., Schlich, R., et al., *Proc. ODP, Sci. Results,* 120: College Station, TX (Ocean Drilling Program), 63–69.

Sharaskin, A.Y., Migdisov, A.A., Rostschina, I.A., and Miklishansky, A.Z., 1983. Major- and trace-element chemistry of Hole 504B basalts and their alteration products (Costa Rica Rift, Deep Sea Drilling Project Leg 70). *In* Cann, J.R., Langseth, M.G., Honnorez, J., Von Herzen, R.P., White, S.M., et al., *Init. Repts. DSDP,* 69: Washington (U.S. Govt. Printing Office), 775–789.

Shcheka, S.A., 1981. Igneous rocks of Deep Sea Drilling Project Leg 61, Nauru Basin. *In* Larson, R.L., Schlanger, S.O., et al., *Init. Repts. DSDP,* 61: Washington (U.S. Govt. Printing Office), 633–651.

Shibata, T., and De Long, S.E., 1981. Preliminary petrology of diabases from Sites 469 and 471, Deep Sea Drilling Project Leg 63. *In* Yeats, R.S., Hag, B.U., et al., *Init. Repts. DSDP,* 63: Washington (U.S. Govt. Printing Office), 701–709.

Shibata, T., DeLong, S.E., and Lyman, P., 1981. Petrographic and chemical characterisics of abyssal tholeiites from Deep Sea Drilling Project Leg 63 off Baja California. *In* Yeats, R.S., Hag, B.U., et al., *Init. Repts. DSDP,* 63: Washington (U.S. Govt. Printing Office), 687–699.

Shimizu, H., Mori, K., and Masuda, A., 1989. REE, Ba, and Sr abundances and Sr, Nd, and Ce isotopic ratios in Hole 504B basalts, ODP Leg 111, Costa Rica Rift. *In* Becker, K., Sakai, H., et al., *Proc. ODP, Sci. Results,* 111: College Station, TX (Ocean Drilling Program), 77–83.

Shipboard Scientific Party, 1989. Site 748. *In* Schlich, R., Wise, S.W., Jr., et al., *Proc. ODP, Init. Repts.,* 120: College Station, TX (Ocean Drilling Program), 157–235.

Shipboard Scientific Party, 1992. Site 857. *In* Davis, E.E., Mottl, M.J., Fisher, A.T., et al., *Proc. ODP, Init. Repts.,* 139: College Station, TX (Ocean Drilling Program), 283–429.

Silver, E.A., and Rangin, C., 1991. Leg 124 tectonic synthesis. *In* Silver, E.A., Fisk, M., Rangin, C., and von Breymann, M.T. (Eds.), *Proc. ODP, Sci. Results,* 124: College Station, TX (Ocean Drilling Program), 3–9.

Spadea, P., Beccaluva, L., Civetta, L., Coltorti, M., Dostal, J., Sajona, F., Serri, G., Vaccaro, C., and Zeda, O., 1991. Petrology of basic igneous rocks from the floor of the Sulu Sea. *In* Silver, E.A., Rangin, C., von Breymann, M.T., et al., *Proc. ODP, Sci. Results,* 124: College Station, TX (Ocean Drilling Program), 251–270.

Sparks, J.W., 1995. Geochemistry of the lower sheeted dike complex, Hole 504B, Leg 140. *In* Erzinger, J., Becker, K., Dick, H.J.B., and Stokking, L.B. (Eds.), *Proc. ODP, Sci. Results,* 137/140: College Station, TX (Ocean Drilling Program), 81–98.

Stakes, D., MŽvel, C., Cannat, M., and Chaput, T., 1991. Metamorphic stratigraphy of Hole 735B. *In* Von Herzen, R.P., Robinson, P.T., et al., *Proc. ODP, Sci. Results,* 118: College Station, TX (Ocean Drilling Program), 153–180.

Stakes, D.S., and Franklin, J.M., 1994. Petrology of igneous rocks at Middle Valley, Juan de Fuca Ridge. *In* Mottl, M.J., Davis, E.E., Fisher, A.T., and Slack, J.F. (Eds.), *Proc. ODP, Sci. Results,* 139: College Station, TX (Ocean Drilling Program), 79–102.

Staudigel, H., Frey, F.A., and Hart, S.R., 1979. Incompatible trace-element geochemistry and $^{87/86}$Sr in basalts and corresponding glasses and palagonites. *In* Donnelly, T., Francheteau, J., et al., *Init. Repts. DSDP,* 51, 52, 53 (Pt. 2): Washington (U.S. Govt. Printing Office), 1137–1144.

Stewart, R.J., Natland, J.H., and Glassley, W.R., 1973. Petrology of volcanic rocks recovered on DSDP Leg 19 from the North Pacific Ocean and the Bering Sea. *In* Creager, J.S., Scholl, D.W., et al., *Init. Repts. DSDP,* 19: Washington (U.S. Govt. Printing Office), 615–627.

Storey, M., Kent, R.W., Saunders, A.D., Salters, V.J., Hergt, J., Whitechurch, H., Sevigny, J.H., Thirlwall, M.F., Leat, P., Ghose, N.C., and Gifford, M., 1992. Lower Cretaceous volcanic rocks on continental margins and their relationship to the Kerguelen Plateau. *In* Wise, S.W., Jr., Schlich, R., et al., *Proc. ODP, Sci. Results*, 120: College Station, TX (Ocean Drilling Program), 33–53.

Storey, M., Saunders, A.D., Tarney, J., Gibson, I.L., Norry, M.J., Thirlwall, M.F., Leat, P., Thompson, R.N., and Menzies, M.A., 1989. Contamination of Indian Ocean asthenosphere by the Kerguelen-Heard mantle plume. *Nature (London, U. K.)*, 338:574–576. **doi:10.1038/338574a0**

Storey, M., Saunders, A.D., Tarney, J., Leat, P., Thirlwall, M.F., Thompson, R.N., Menzies, M.A., and Marriner, G.F., 1988. Geochemical evidence for plume-mantle interactions beneath Kerguelen and Heard Islands, Indian Ocean. *Nature (London, U. K.)*, 336:371–374. **doi:10.1038/336371a0**

Strong, D.F., and Jamieson, R., 1977. Whole-rock chemistry of igneous rocks from DSDP Leg 37. *In* Aumento, F., Melson, W.G. et al., *Init. Repts. DSDP*, 37: Washington (U.S. Govt. Printing Office), 725–728.

Sun, S.-S., and McDonough, W.F., 1989. Chemical and isotopic systematics of oceanic basalts: implications for mantle composition and processes. *In* Saunders, A.D., and Norry, M.J. (Eds.), *Magmatism in the Ocean Basins.* Geol. Soc. Spec. Publ., 42:313–345.

Tamaki, K., 1985. Two modes of back-arc spreading. *Geology*, 13:475–478. **doi:10.1130/0091-7613(1985)13<475:TMOBS>2.0.CO;2**

Tamaki, K., Pisciotto, K., Allan, J., et al., 1990. *Proc. ODP, Init. Repts.*, 127: College Station, TX (Ocean Drilling Program).

Tamaki, K., Suyehiro, K., Allan, J., Ingle, J.C., Jr., and Pisciotto, K.A., 1992. Tectonic synthesis and implications of Japan Sea ODP drilling. *In* Tamaki, K., Suyehiro, K., Allan, J., McWilliams, M., et al., *Proc. ODP, Sci. Results*, 127/128 (Pt. 2): College Station, TX (Ocean Drilling Program), 1333–1348.

Taylor, B., Fujioka, K., et al., 1990. *Proc. ODP, Init. Repts.*, 126: College Station, TX (Ocean Drilling Program).

Taylor, B., Lapierre, H., Vidal, P., Nesbitt, R.W., and Croudace, I.W., 1992. Igneous geochemistry and petrogenesis of the Izu-Bonin forearc basin. *In* Taylor, B., Fujioka, K., Janecek, T., and Langmur, Ch. (Eds.). *Proc. ODP, Sci. Results*, 126: College Station, TX (Ocean Drilling Program), 405–430.

Thiede, J., Dean, W.E., Rea, D.K., Vallier, T.L., and Adelseck, C.G., 1981. The geologic history of the Mid-Pacific Mountains in the central North Pacific Ocean—a synthesis of deep-sea drilling studies. *In* Thiede, J., and Dinkelman, M.G., 1977. Occurrence of *Inoceramus* remains in late Mesozoic pelagic and hemipelagic sediments. *In* Perch-Nielsen, K., Supko, P.R., et al., *Init. Repts. DSDP*, 39: Washington (U.S. Govt. Printing Office), 899–910.

Thiede, J., Vallier, T.L., et al., 1981. *Init. Repts. DSDP*, 62: Washington (U.S. Govt. Printing Office).

Thompson, G., 1973. A geochemical study of the low-temperature interaction of seawater and oceanic igneous rocks . *Trans. Am. Geophys. Union*, 54:1015-1019.

Thompson, G., Humphris, S.E., and Schlling, J-G., 1982. Petrology and geochemistry of basaltic rocks from Rio Grande Rise: South Atlantic: Deep See Drilling Project Leg 72, Hole 516F. *In* Barker, P.F., Carlson, R.L., Johnson, D.A., et al., *Init. Repts. DSDP*, 72: Washington (U.S. Govt. Printing Office), 457–466.

Thompson, G., and Humphris, S.E., 1984. Petrology and geochemistry of rocks from the Walvis Ridge: Deep See Drilling Project Leg 74, Sites 525, 527, and 528. *In* Moore, T.C., Jr., Rabinowitz, P.D., et al., *Init. Repts. DSDP*, 74: Washington (U.S. Govt. Printing Office), 755–764.

Tokmakov, P.P., Gorshkov, A.I., and Yarovaja, V.S., 1983. About serpentine with unusual barrel-like morphology. *Geology and origin major endogene nonmetallic deposits:* Moscow (Nauka), 87-98.

Tokuyama, H., and Batiza, R., 1981. Chemical composition of igneous rocks and origin of the sill and pillow-basalt complex of Nauru Basin, Southwest Pacific. *In* Larson, R.L., Schlanger, S.O., et al., *Init. Repts. DSDP*, 61: Washington (U.S. Govt. Printing Office), 673–687.

Tomasson, J. and Kristmannsdottir, 1972. High temperature alteration minerals and geothermal brine, Reykjanes, Iceland. *Contrib. Mineral. Petrol.*, 36:123–134.

Vallier, T.L., Rea, D.K., Dean, W.E., Thiede, J., and Adelseck, Ch.G., 1981. The geology of Hess Rise, Central North Pacific Ocean. *In* Thiede, J., Vallier, T.L., et al., *Init. Repts. DSDP*, 62: Washington (U.S. Govt. Printing Office), 1031–1072.

Van Wagoner, N.A., and Leybourne, M.I., 1991. Evidence for magma mixing and a heterogeneous mantle on the West Valley segment of the Juan de Fuca ridge. *J. Geophys. Res.*, 96:16295–16318.

Vanko, D.A., Laverne, C., Tartarotti, P., and Alt, J.C., 1996. Chemistry and origin of secondary minerals from the deep sheeted dikes cored during Leg 148 (Hole 504B). *In* Alt, J.C., Kinoshita, H., Stokking, L.B., and Michael, P.J. (Eds.), *Proc. ODP, Sci. Results*, 148: College Station, TX (Ocean Drilling Program), 71–86.

Verma, J.P., 1981. K, Rb, Cs, Ba, and Sr contents and Sr isotope rations of igneous rocks from Deep Sea Drilling Project Leg 63. *In* Yeats, R.S., Hag, B.U., et al., *Init. Repts. DSDP*, 63: Washington (U.S. Govt. Printing Office), 733–738.

Viereck, L.G., Hertogen, J., Parson, L.M., Morton, A.C., Love, D., and Gibson, I.L., 1989. Chemical stratigraphy and petrology of the Vøring Plateau tholeiitic lavas and interlayered volcaniclastic sediments at ODP Hole 642E. *In* Eldholm, O., Thiede, J., Taylor, E., et al., *Proc. ODP, Sci. Results*, 104: College Station, TX (Ocean Drilling Program), 367–396.

von der Borch, C.C., Sclater, J.G., et al., 1974. *Init. Repts. DSDP*, 22: Washington (U.S. Govt. Printing Office).

Walker, G.P.L., 1960. Zeolite zones and dike distribution in relation to the structure of the basalts in eastern Iceland. *J. Geol.*, 68:515–528.

Weis, D., Bassias, Y., Gautier, I., and Mennessier, J.-P., 1989. DUPAL anomaly in existence 115 Ma ago: evidence from isotopic study of the Kerguelen Plateau (South Indian Ocean). *Geochim. Cosmochim. Acta*, 53:2125–2131.

Whitechurch, H., Montigny, R., Sevigny, J., Storey, M., and Salters, V.J.M., 1992. K-Ar and ^{40}Ar ages of central Kerguelen Plateau basalts. *In* Wise, S.W., Jr., Schlich, R., et al., *Proc. ODP, Sci. Results*, 120: College Station, TX (Ocean Drilling Program), 71–77.

Whitford, D.J., and Duncan, R.A., 1978. Origin of the Ninetyeast Ridge—Sr isotope and trace element evidence. *In* Zartman, R.E. (Ed.), *Short Papers of the Fourth International Conference, Geochronology, Cosmochronology, Isotope Geology*. Open-File Rep. U.S. Geol. Surv., 78-701:451–453.

Wilson, J.T., 1963. Evidence from islands on the spreading of the of the ocean floor. *Nature (London, U. K.)*, 197:536–538.

Windom, K.E., and Book, P., 1981. Vein minerals in basalt, Hole 462A, Leg 61 of the Deep Sea Drilling Project. *In* Larson, R.L., Schlanger, S.O., et al., *Init. Repts. DSDP*, 61: Washington (U.S. Govt. Printing Office), 647–651.

Winterer, E.L., 1976. Bathymetry and regional tectonic setting of the Line Islands Chain. *In* Schlanger, S.O., Jackson, E.D., et al., *Init. Repts., DSDP*, 33: Washington (U.S. Govt. Printing Office), 731–747.

Wood, D.A., Marsh, N.G., Tarney, J., Joron, J.-L., Fryer, P., and Treuil, M., 1982. Geochemistry of igneous rocks recovered from a transect across the Mariana Trough, arc, fore-arc, and trench, Sites 453 through 461, Deep Sea Drilling Project Leg 60. *In* Hussong, D.M., Uyeda, S., et al., *Init. Repts. DSDP*, Vol. 60, Washington (U.S. Govt. Printing Office), 611–645.

Wood, D.A., Mattey, D.P., Joron, J.L., Marsh, N.G., Tarney, J., and Treuil, M., 1981. A geochemical study of 17 selected samples from basement cores recovered at Sites 447, 448, 449, 450, and 451, Deep Sea Drilling Project Leg 59. *In* Kroenke, L., Scott, R., et al., *Init. Repts. DSDP*, 59: Washington (U.S. Govt. Printing Office), 743–752.

Yeats, R.S., Hag, B.U., et al., 1981. *Init. Repts. DSDP*, 63: Washington (U.S. Govt. Printing Office).

Yuasa, M., Watanabe, T., Kuwajima, T., Hirama, T., and Fujioka, K., 1992. Prehnite-Pumpellyite facies metamorphism in oceanic arc basement from Site 791 in the Sumisu Rift, western Pacific. *In* Taylor, B., Fujioka, K., et al., *Proc. ODP, Sci. Results*, 126: College Station, TX (Ocean Drilling Program), 185–193.

Zakariadze, G.S., Dmitriev, L.V., Sobolev, A.V., and Suschevskaya, N.M., 1981. Petrology of basalts of Holes 447A, 449, and 450, south Philippine Sea transect, Deep

Sea Drilling Project Leg 59. *In* Kroenke L., Scott R., et al., *Init. Repts. DSDP*, 59: Washington (U.S. Govt. Printing Office), 669–680.

Zierenberg, R.A., Fouquet, Y., Miller, D.J., and Normark, W.R. (Eds.), 2000. *Proc. ODP, Sci. Results*, 169 [CD-ROM]. Available from: Ocean Drilling Program, Texas A&M University, College Station TX 77845-9547, USA. [**HTML**]

Zierenberg, R.A., and Miller, D.J., 2000. Overview of Ocean Drilling Program Leg 169: sedimented ridges II. *In* Zierenberg, R.A., Fouquet, Y., Miller, D.J., and Normark, W.R. (Eds.), *Proc. ODP, Sci. Results*, 169, 1–39 [CD-ROM]. Available from: Ocean Drilling Program, Texas A&M University, College Station TX 77845-9547, USA. [**HTML**]

Zolotarev, B.P., and Choporov, D.Y., 1978. Petrochemistry of basalts r/v *Glomar Challenger*, Leg 45 Holes 395, 395A, and 396. *In* Melson, W.G., Rabinowitz, P.D., et al., *Init. Repts. DSDP*, 45: Washington (U.S. Govt. Printing Office), 479–492.

Zolotarev, B.P., and Margolin, E.M., 1983. Geochemistry and rare-earth element abundances of basalts from Sites 482, 483, and 485 in the Gulf of California. *In* Lewis, B.T.R., Robinson, P., et al., *Init. Repts. DSDP*, 65: Washington (U.S. Govt. Printing Office), 579–590.

Zuleger, E., Alt, J.C., and Erzinger, J., 1996. Data report: Trace-element geochemistry of the lower sheeted dike complex, Hole 504B, Leg 140. *In* Alt, J.C., Kinoshita, H., Stokking, L.B., and Michael, P.J. (Eds.), *Proc. ODP, Sci. Results*, 148: College Station, TX (Ocean Drilling Program), 455–466.

Zuleger, E., Alt, J.C., and Erzinger, J.A., 1995. Primary and secondary variations in major and trace element geochemistry of the lower sheeted dike complex: Hole 504B, Leg 140. *In* Erzinger, J., Becker, K., Dick, H.J.B., and Stokking, L.B. (Eds.), *Proc. ODP, Sci. Results*, 137/140: College Station, TX (Ocean Drilling Program), 65–80.

Figure F1. Location of Site 504 in the eastern Pacific (from Alt, Kinoshita, et al., 1996).

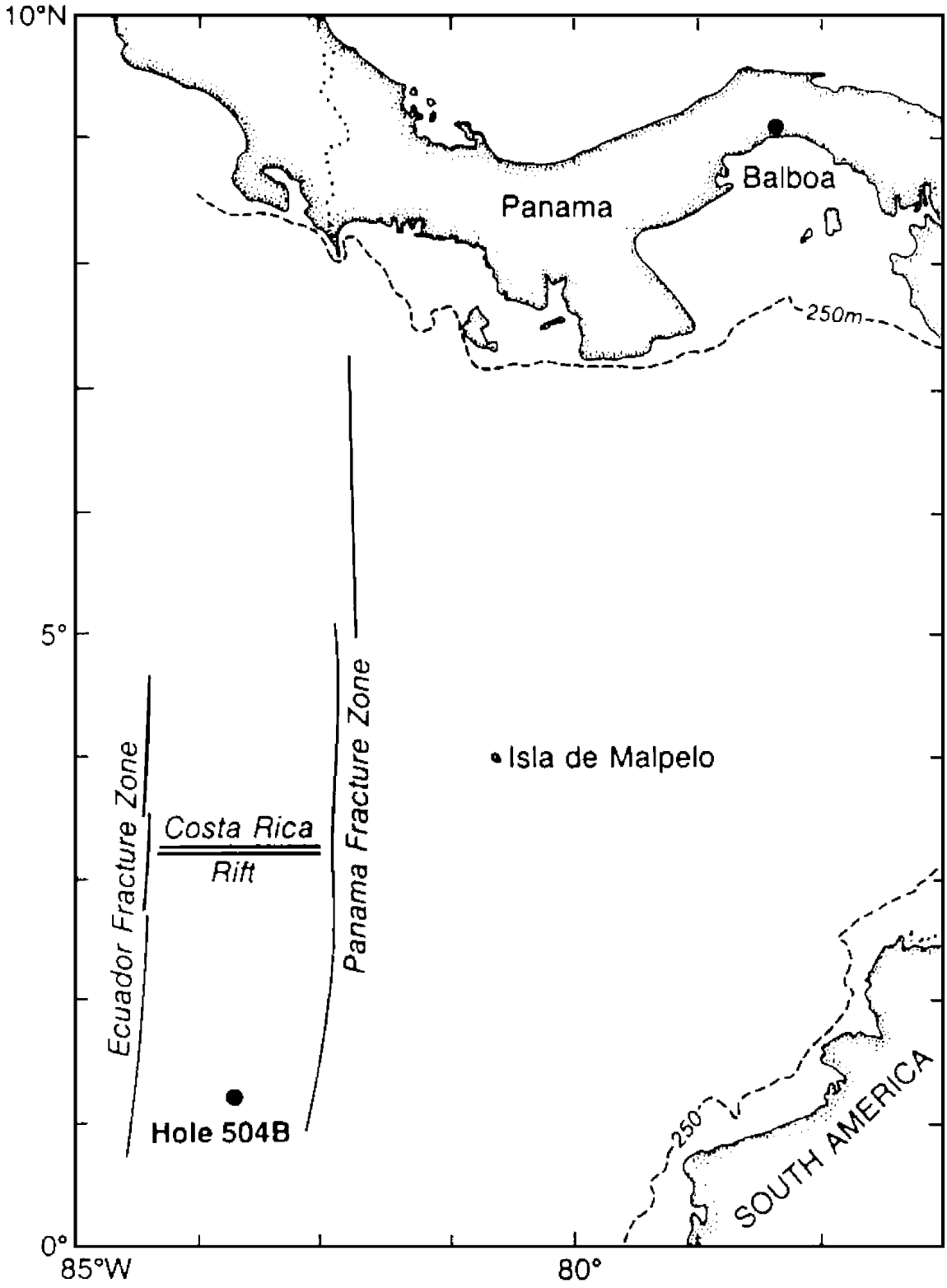

Figure F2. AFM diagram (Irvine and Baragar, 1971) for basalts in Hole 504B.

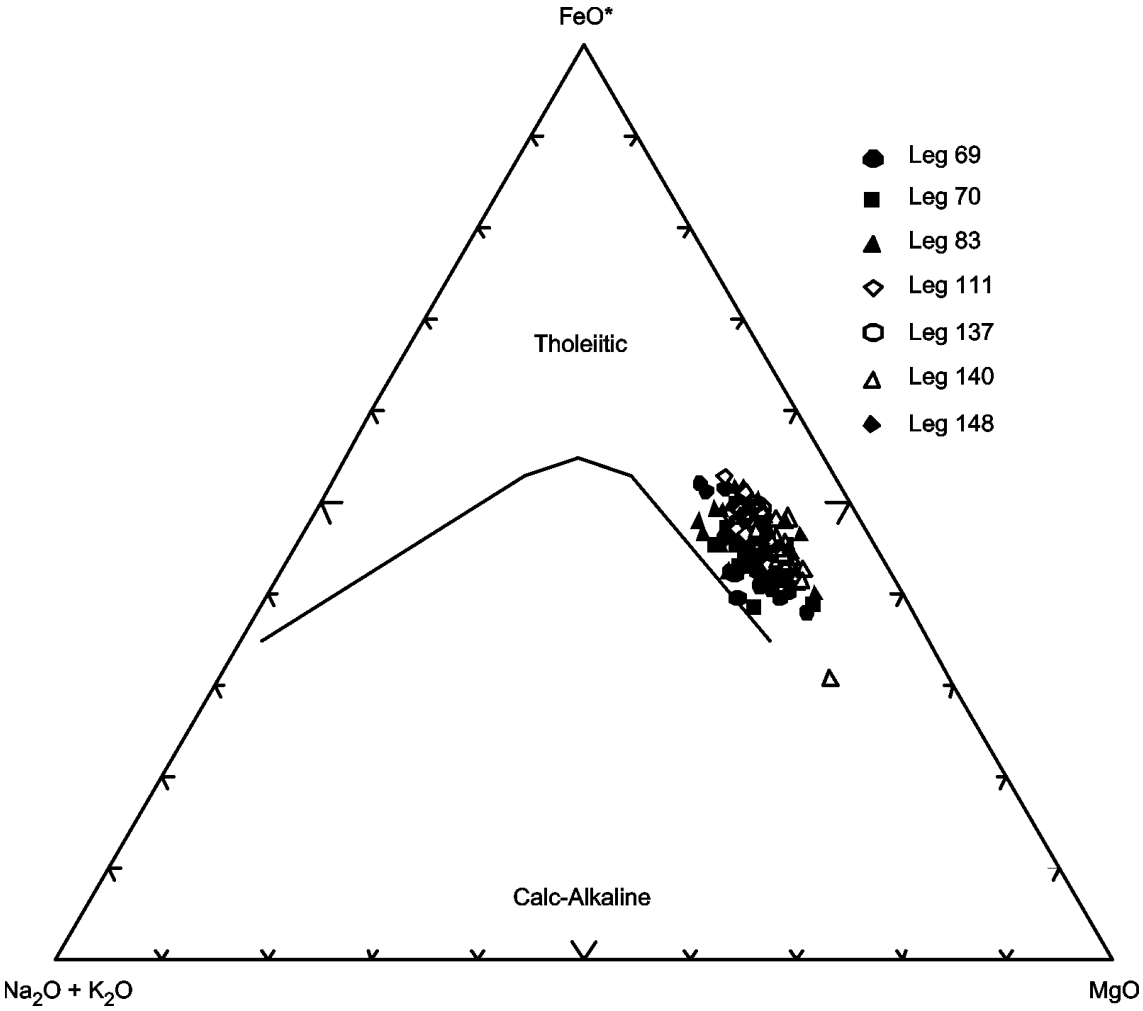

Figure F3. Discrimination Nb-Zr-Y diagram (Meschede, 1986) for basalts in Hole 504B. AI, AII = fields of intraplate alkali basalts; AII, C = fields of intraplate tholeiites; B = field of P-type MORB; D = field of N-type MORB; C, D = fields of volcanic arc basalts.

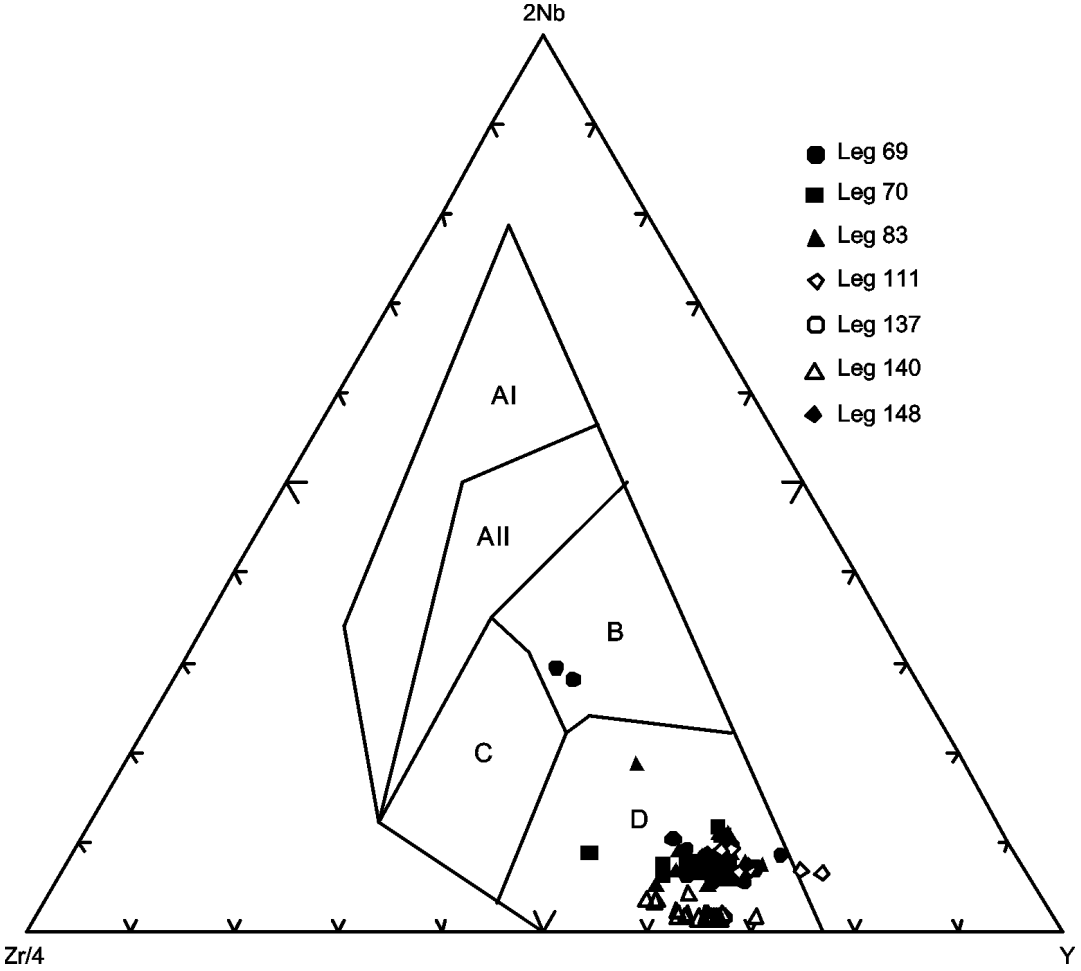

Figure F4. Chondrite-normalized rare earth element abundances for basalts in Hole 504B. Normalizing values are from Sun and McDonough (1989). (Continued on next three pages.)

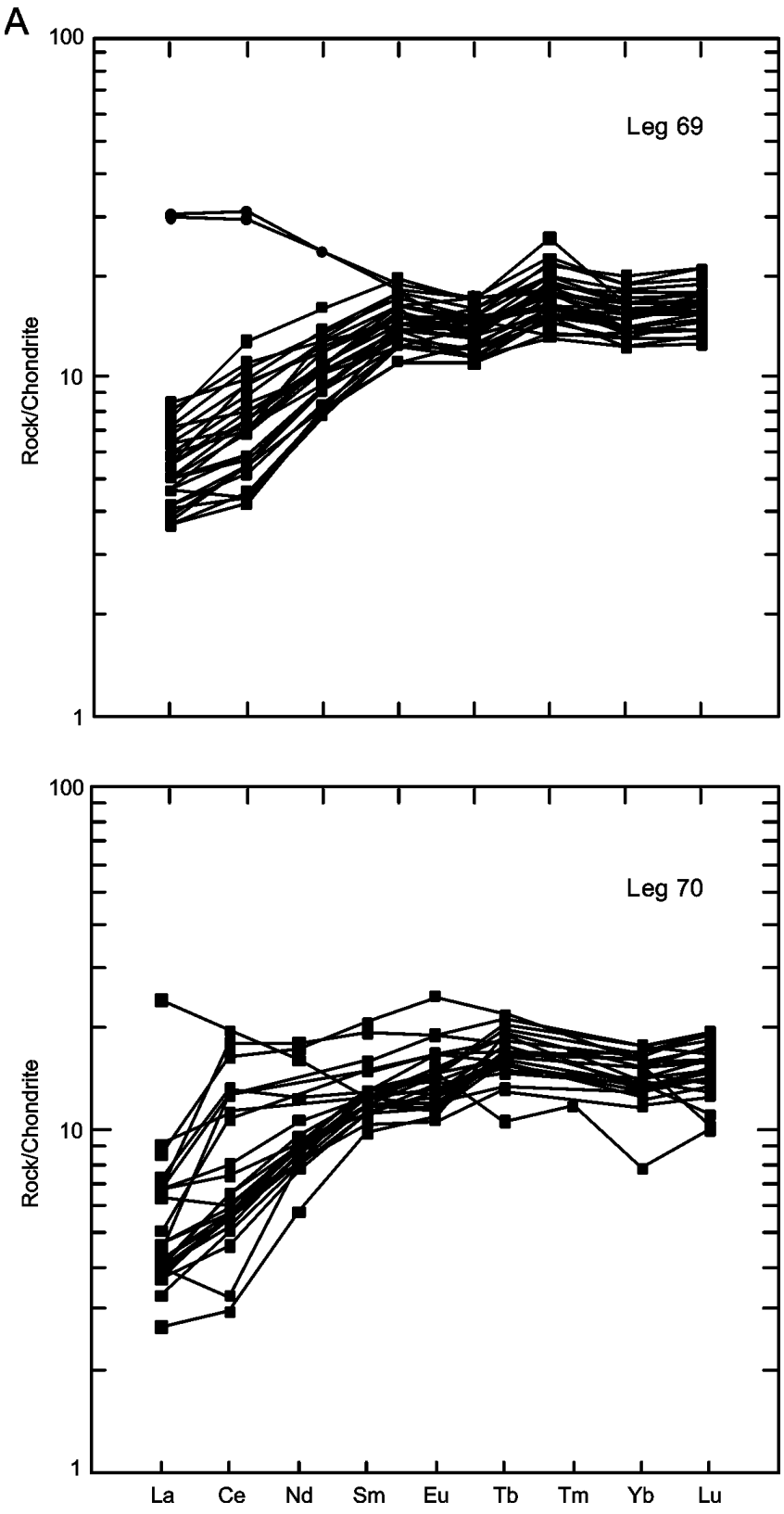

Figure F4 (continued).

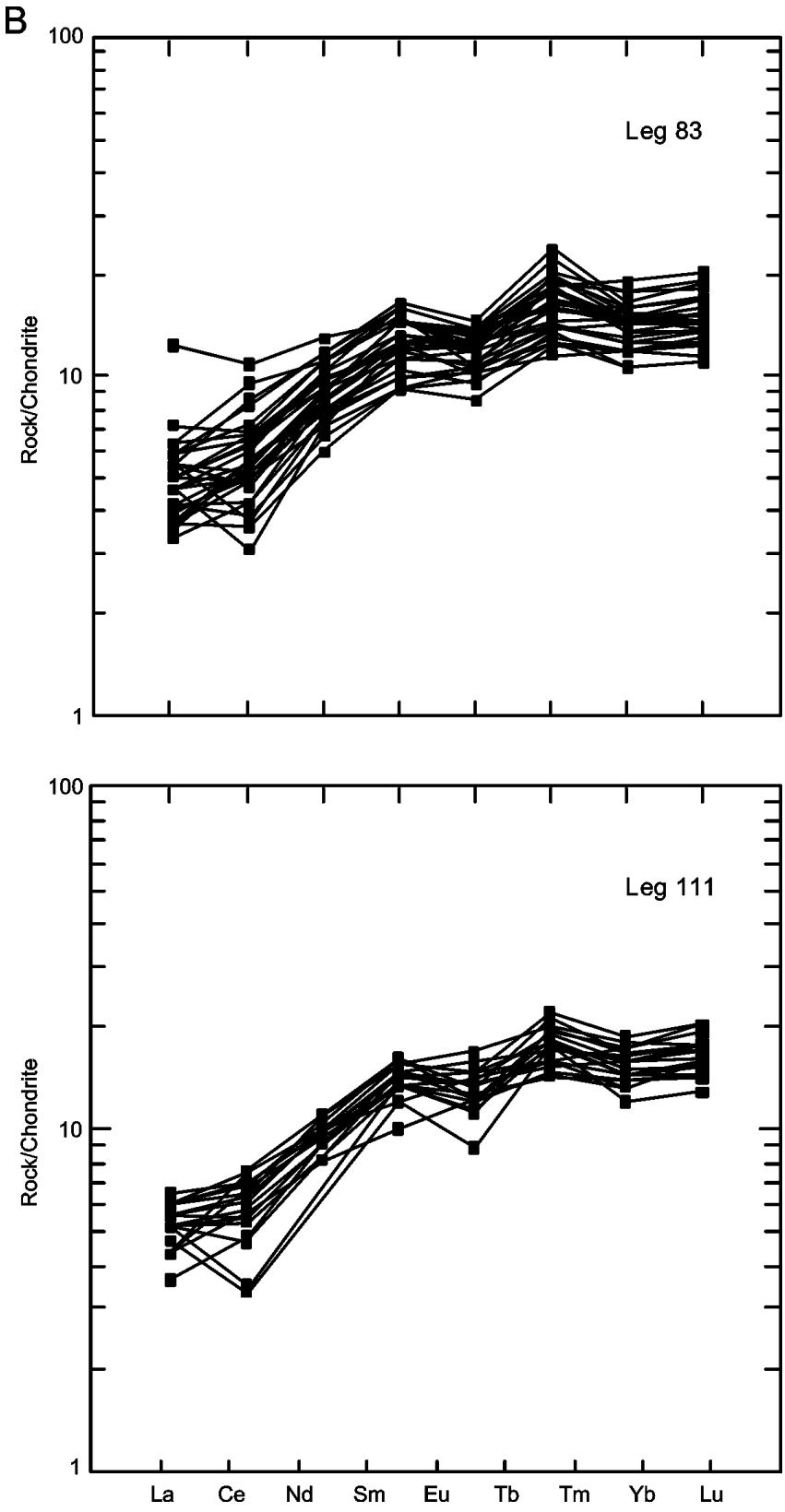

Figure F4 (continued).

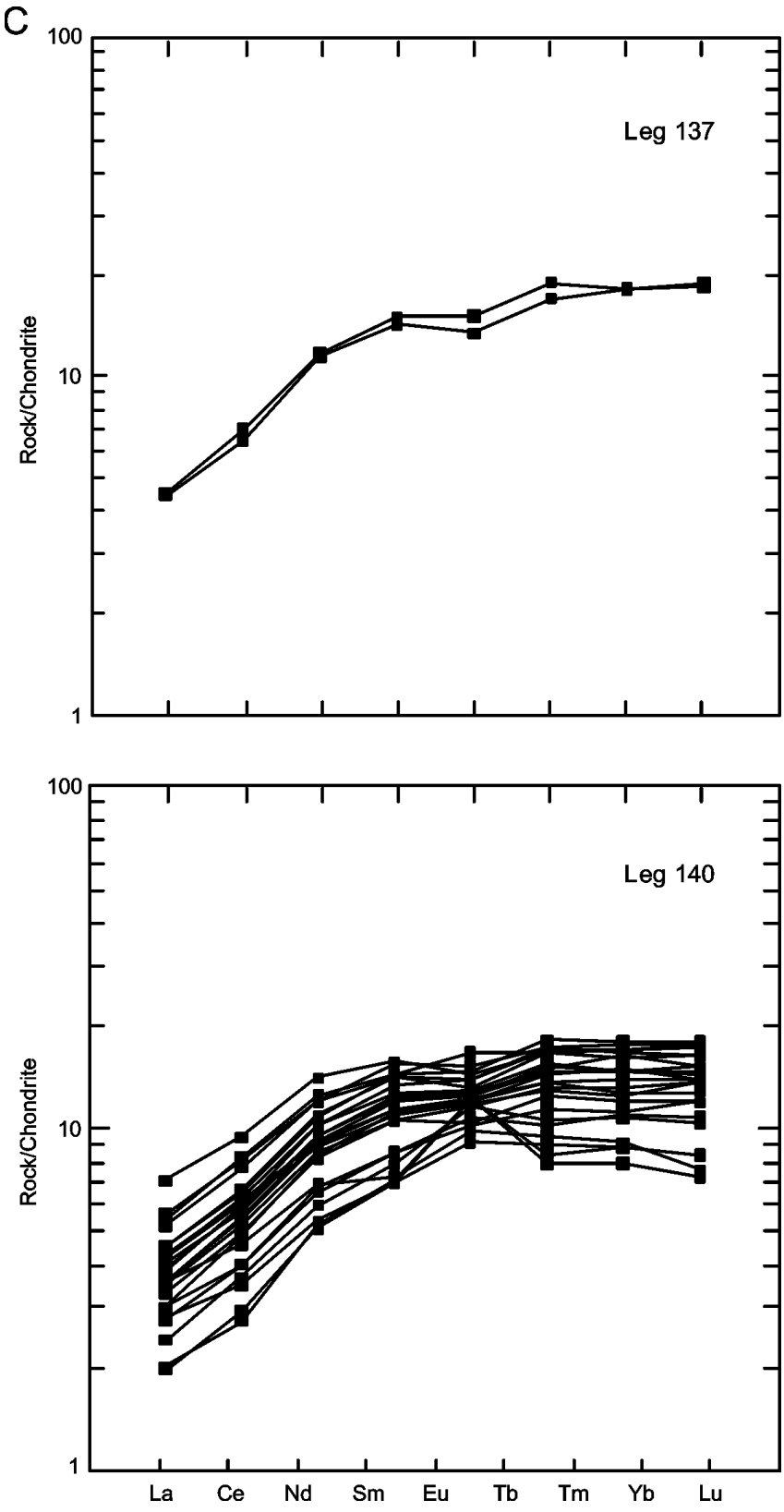

Figure F4 (continued).

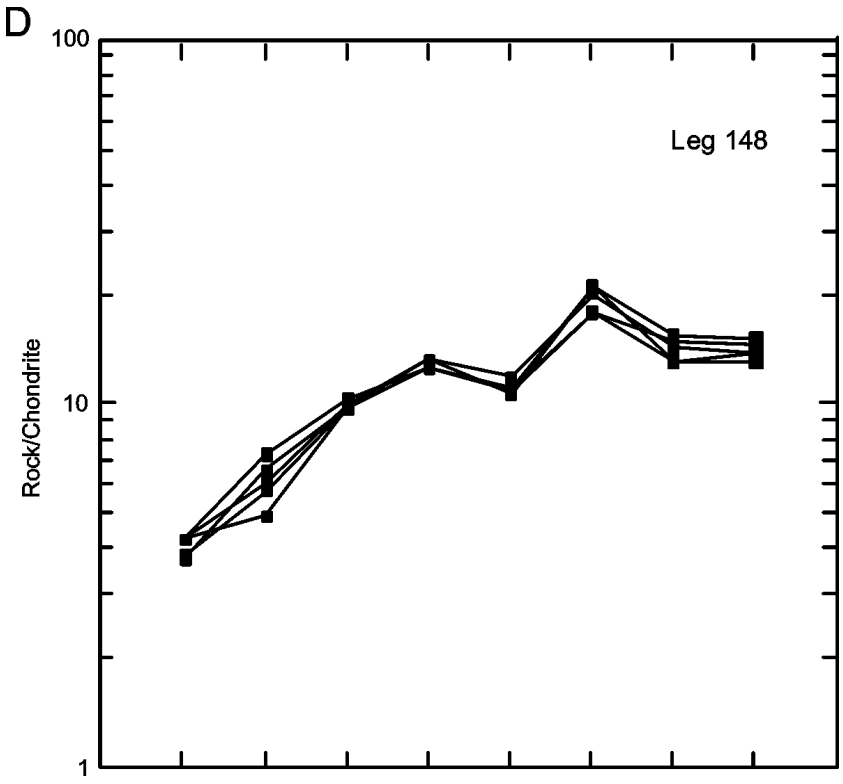

Figure F5. Lithostratigraphy of Hole 504B, showing the distribution of secondary minerals with depth (from Alt et al., 1996c).

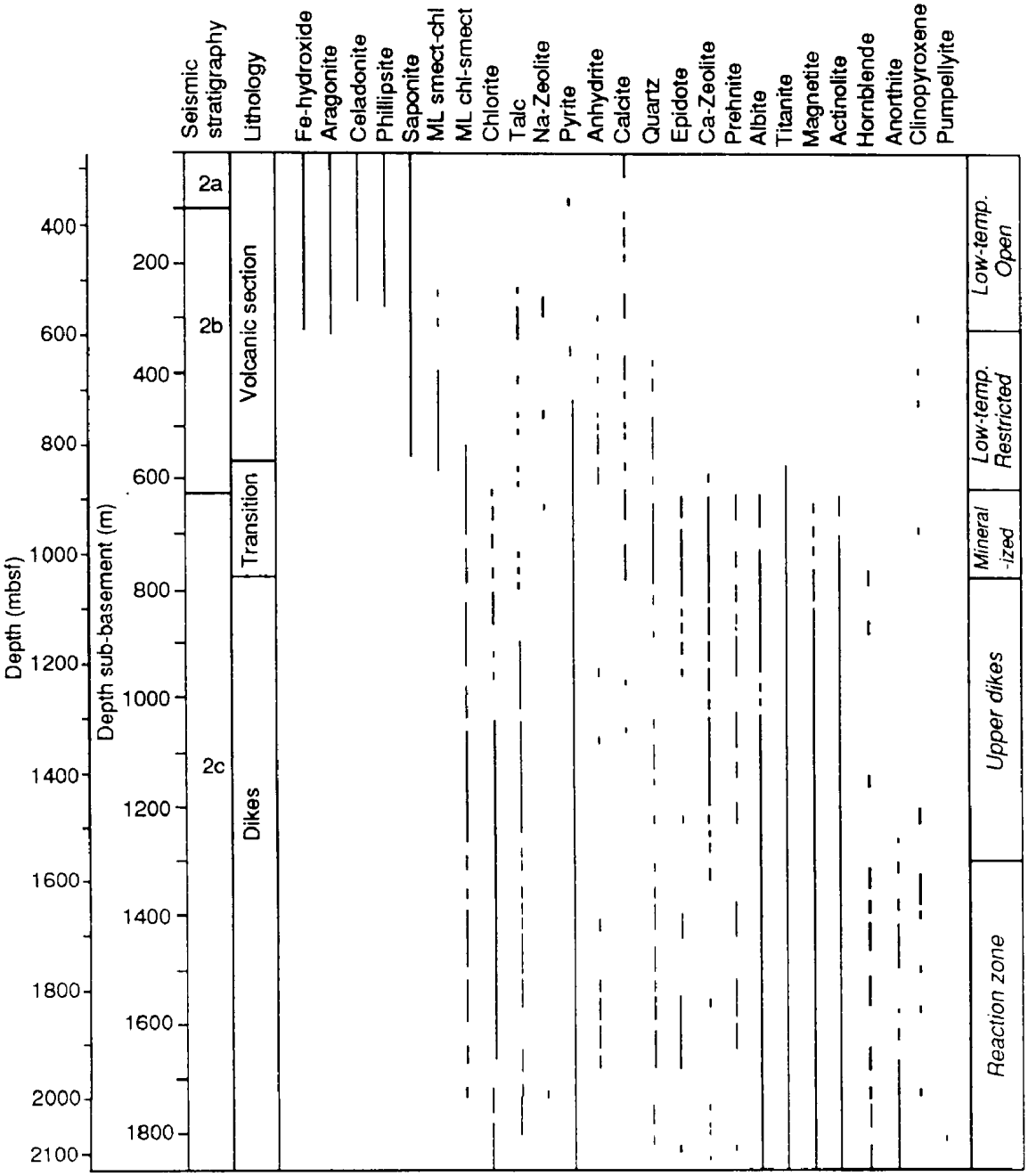

Figure F6. Whole-rock chemical compositions in Hole 504B. Triangles = aphyric and glassy basalts, squares = phyric basalts, circles = dolerites, stars = oxidized rocks, crosses = brecciated rocks and fractured rocks with fissures. Open symbols = altered rocks, closed symbols = fresh rocks. (Continued on next ten pages.)

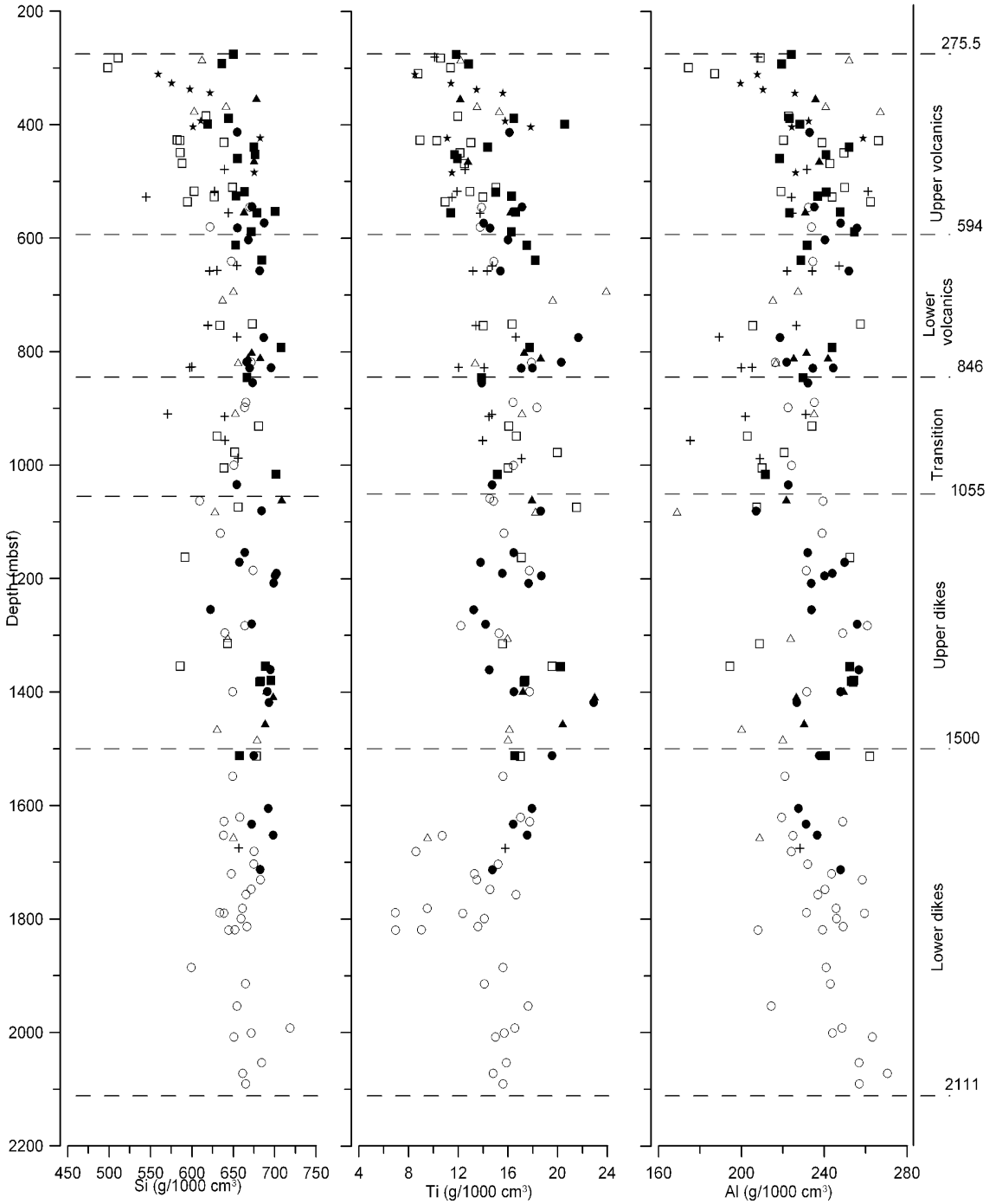

Figure F6 (continued).

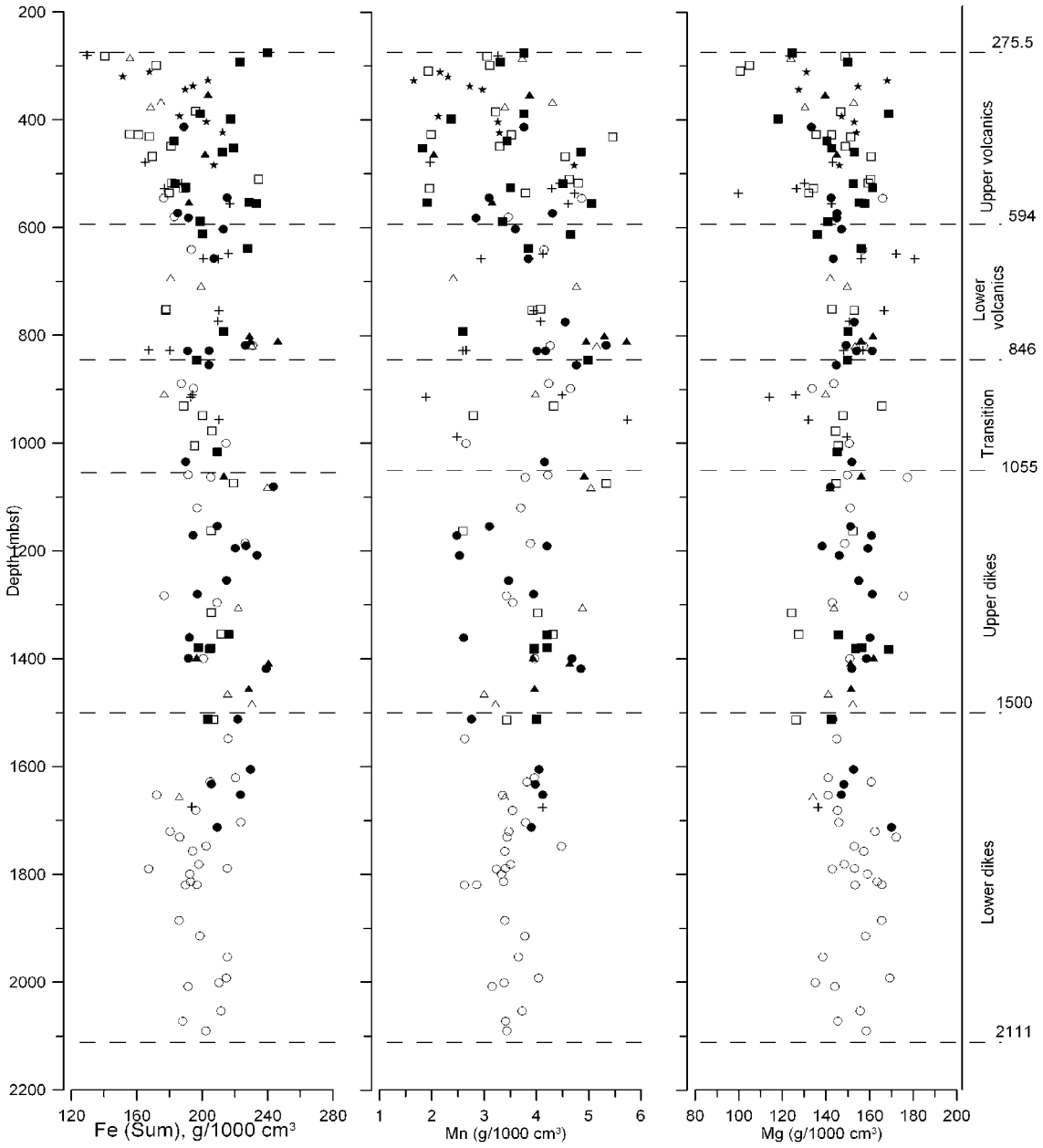

Figure F6 (continued).

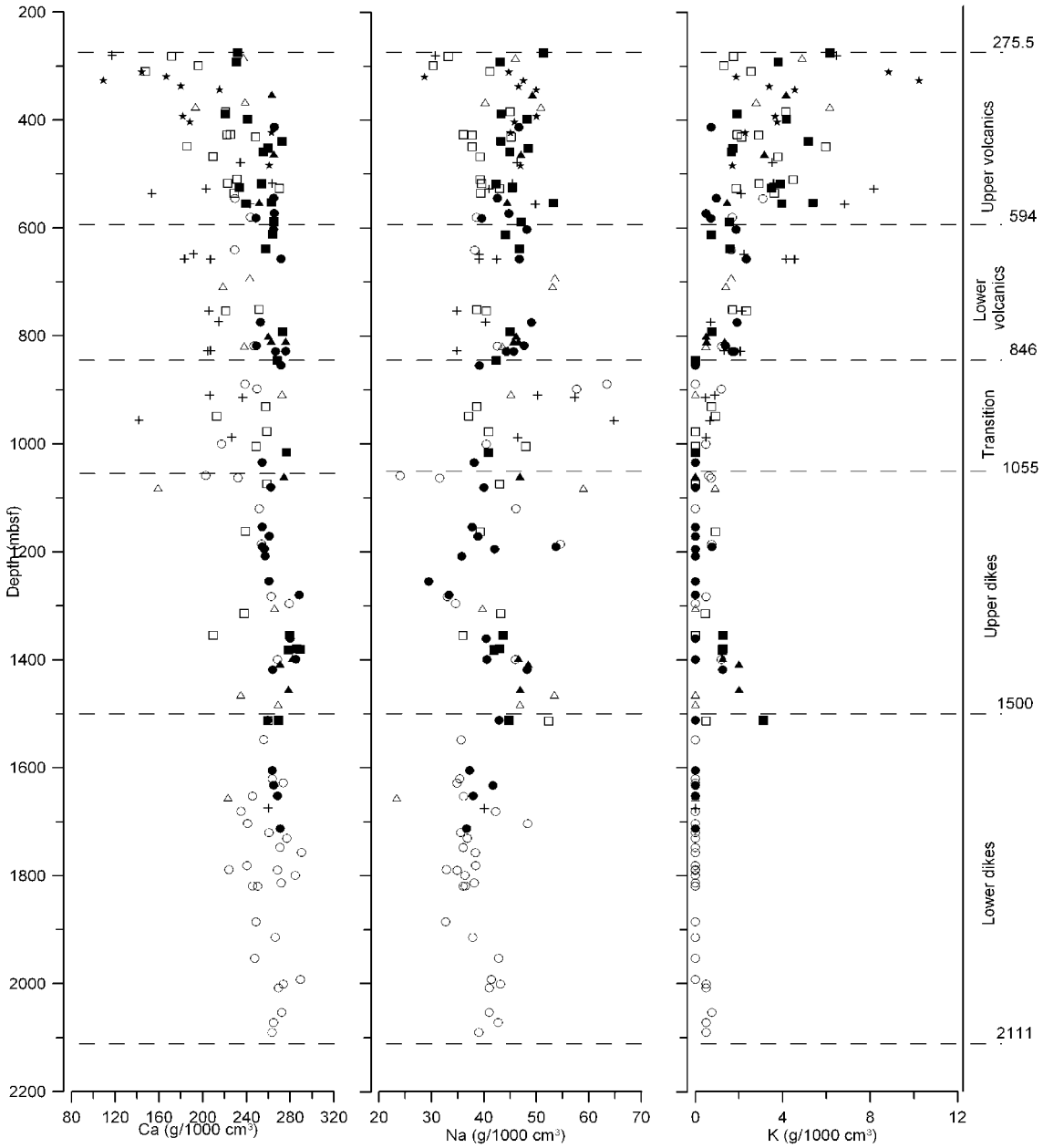

Figure F6 (continued).

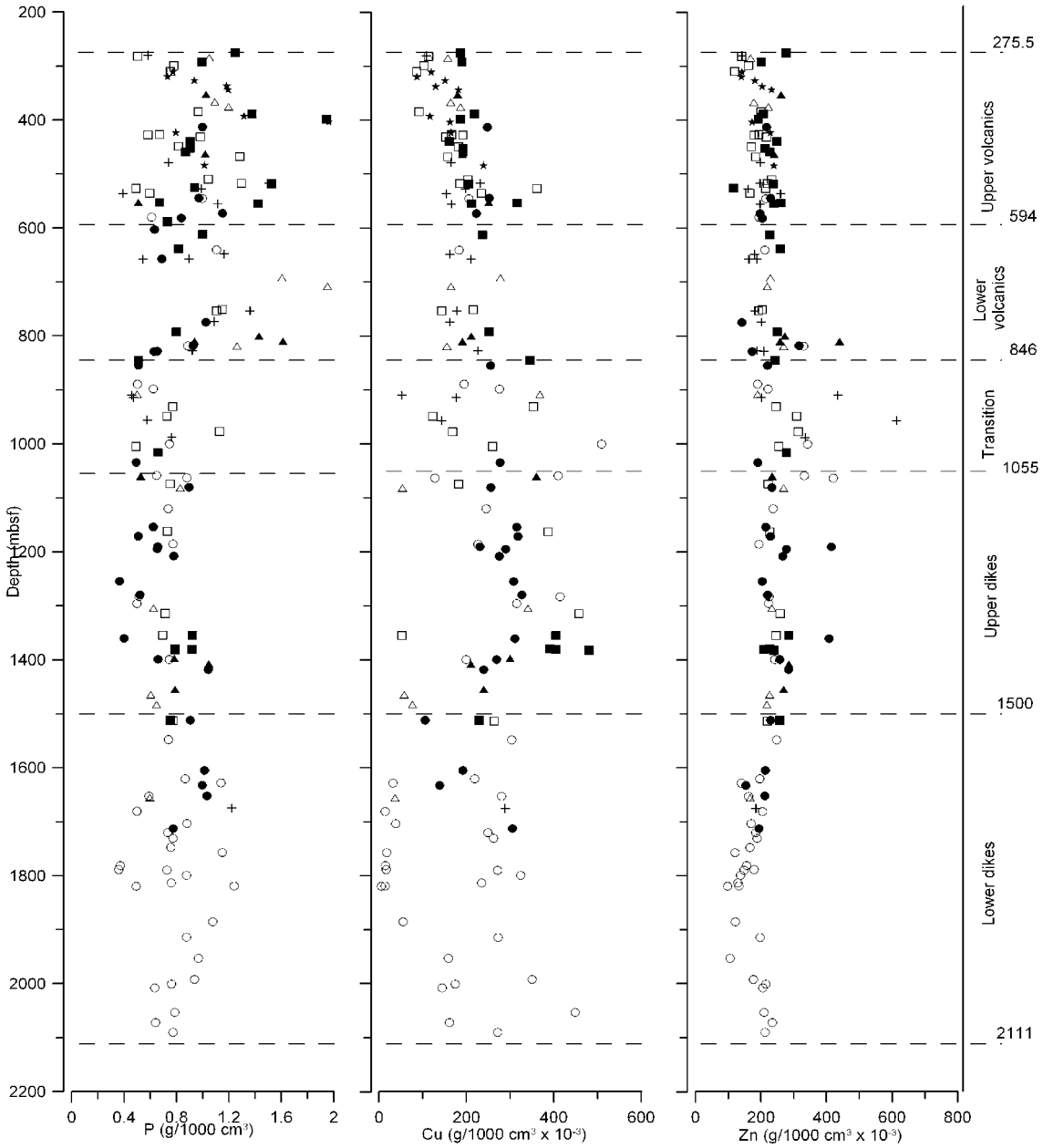

Figure F6 (continued).

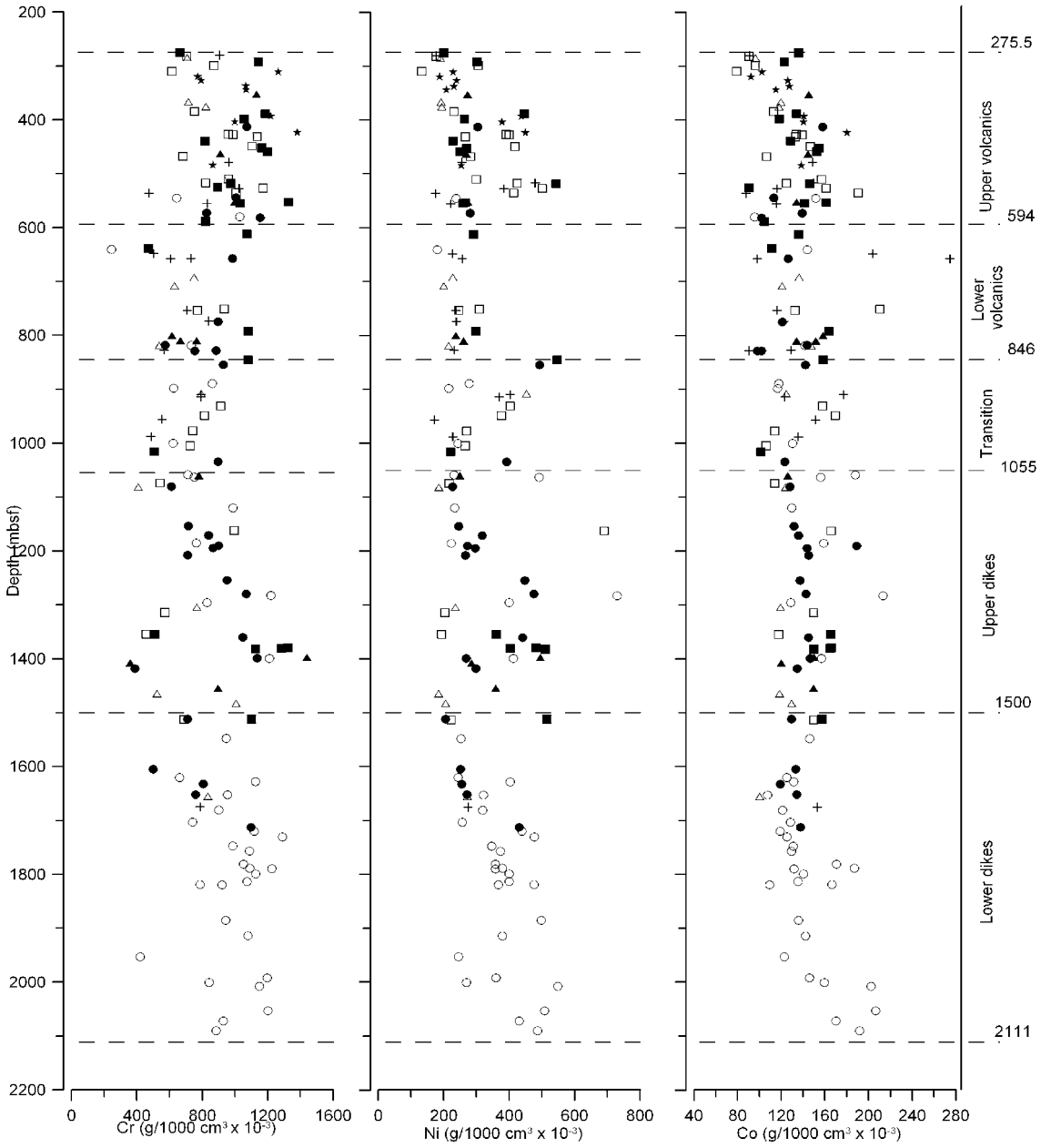

Figure F6 (continued).

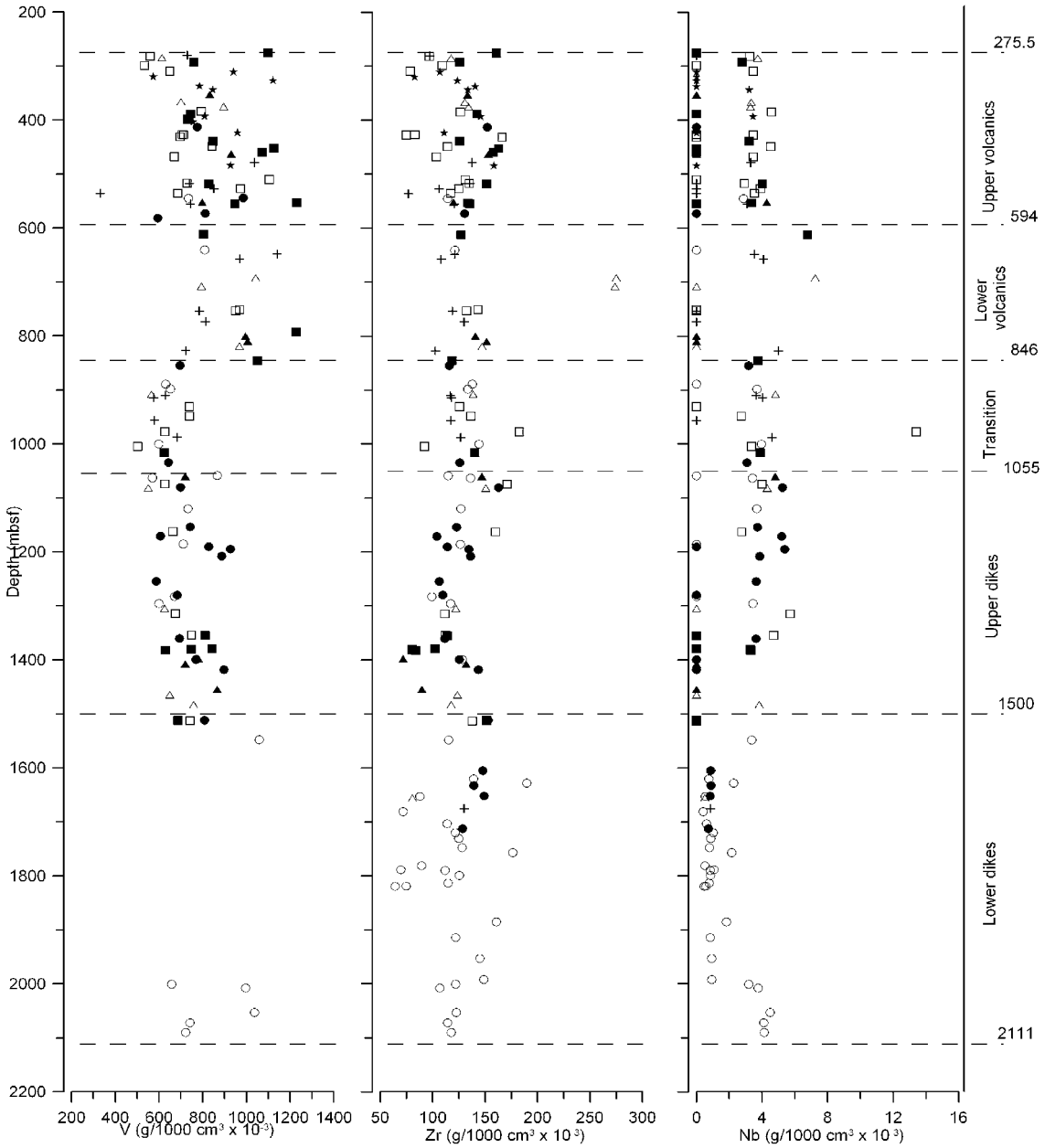

Figure F6 (continued).

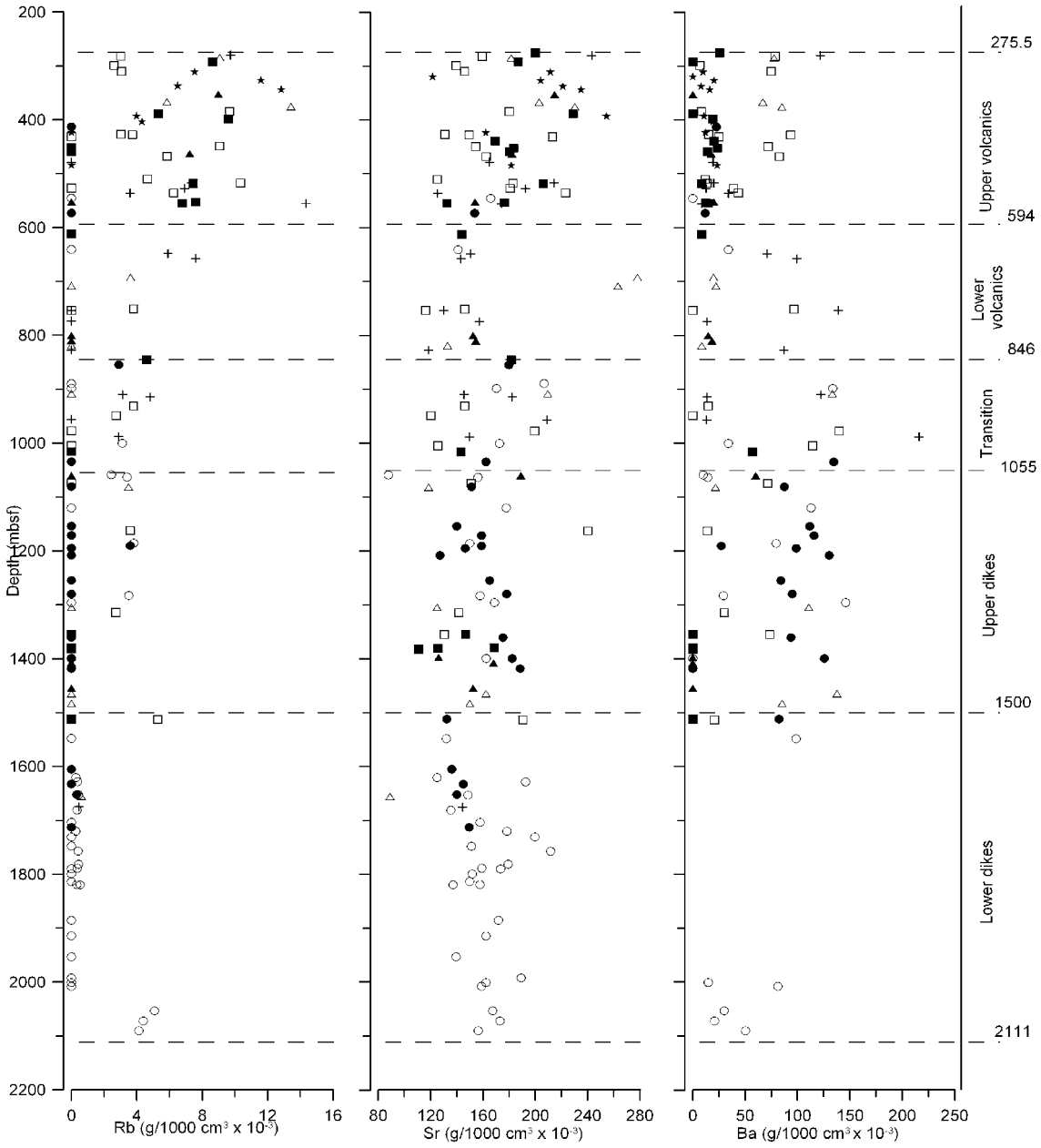

Figure F6 (continued).

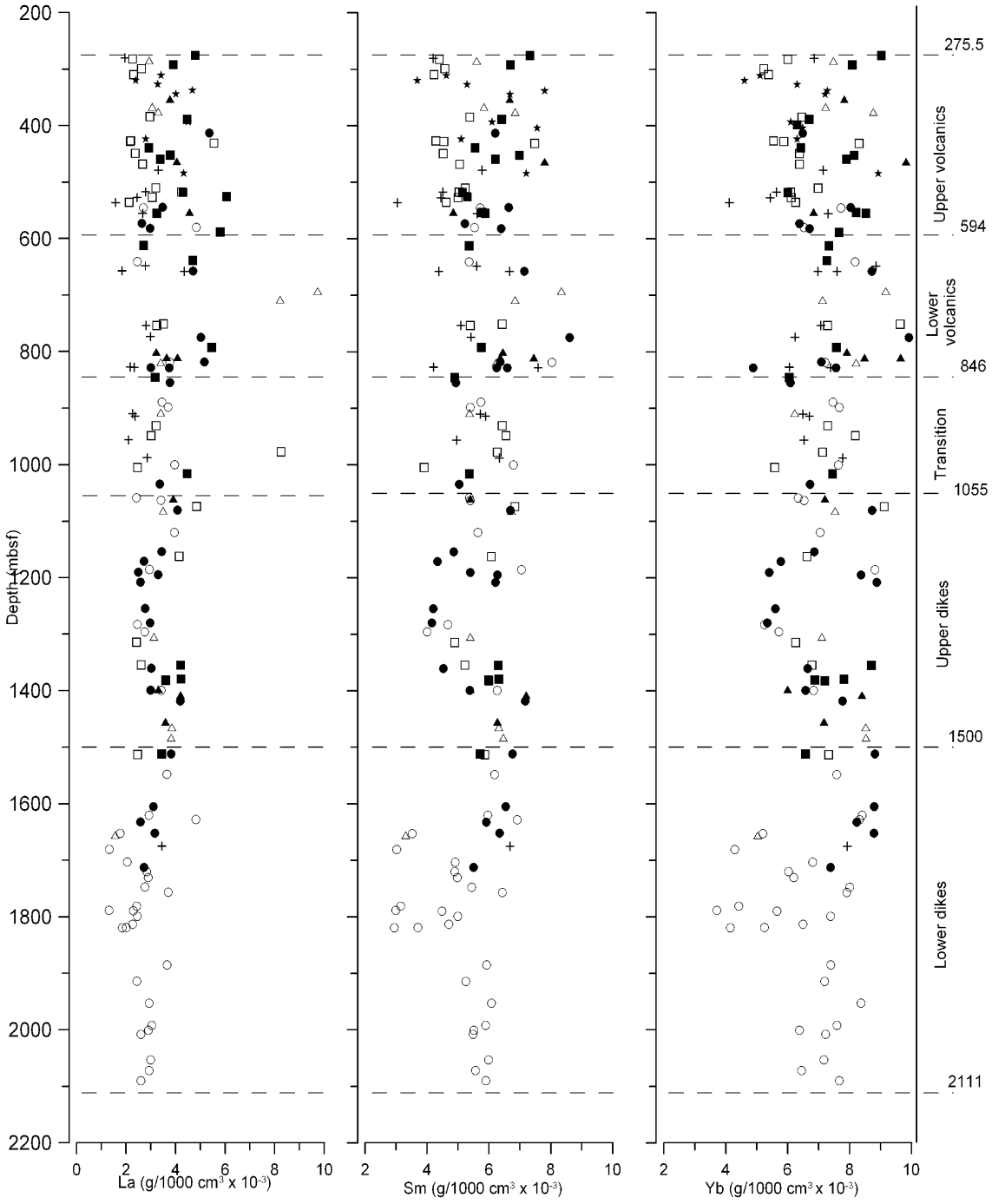

Figure F6 (continued).

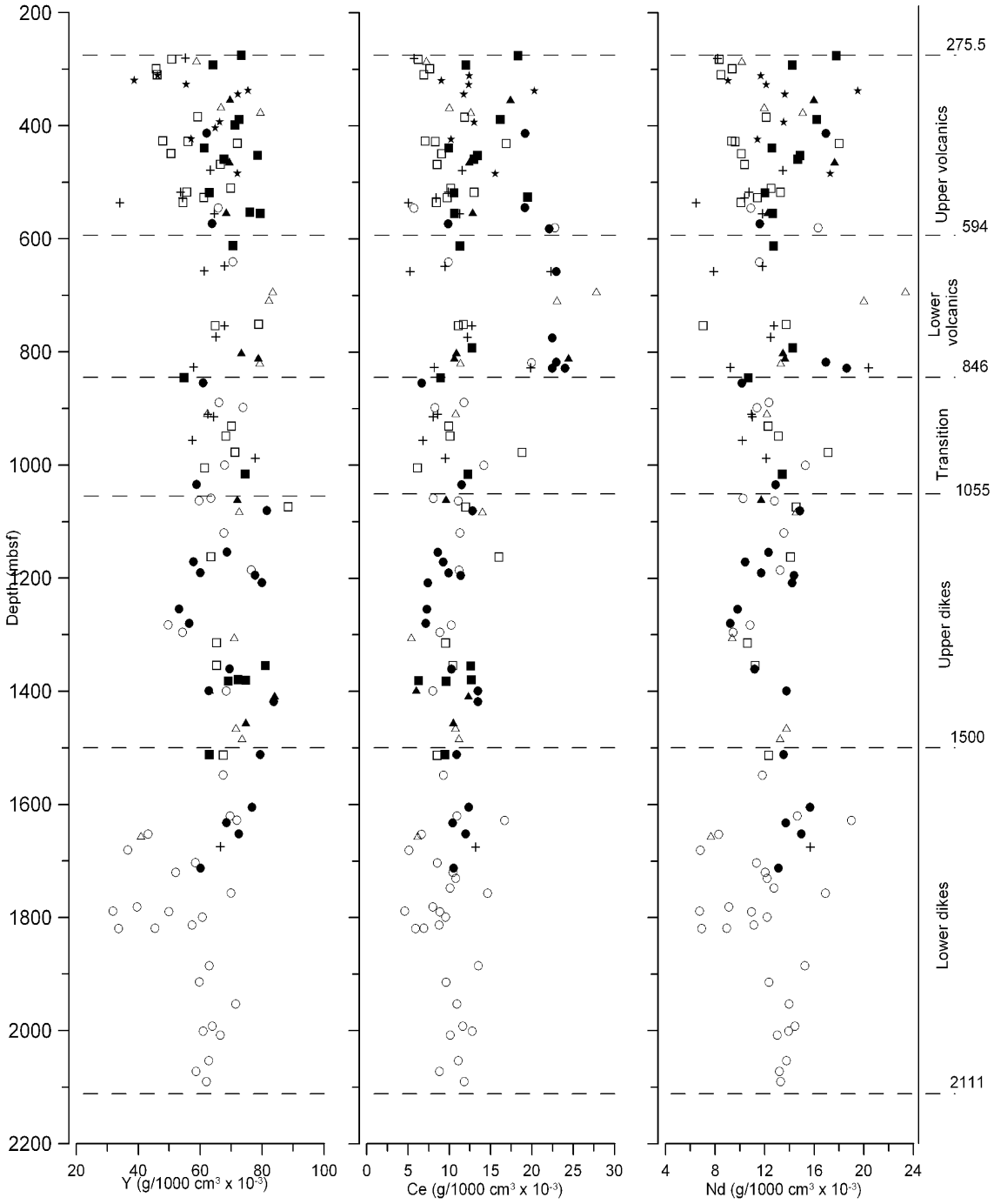

Figure F6 (continued).

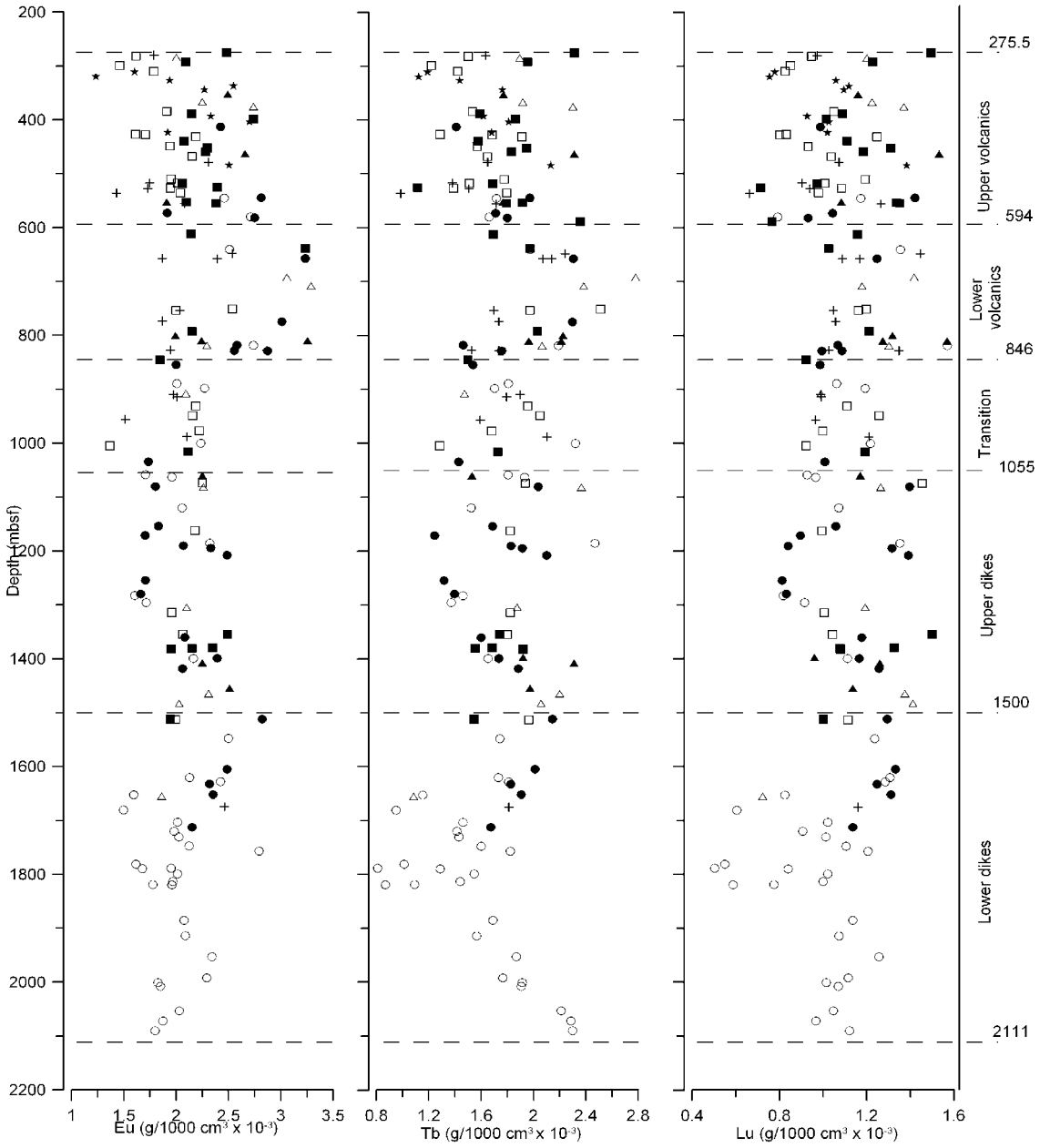

Figure F6 (continued).

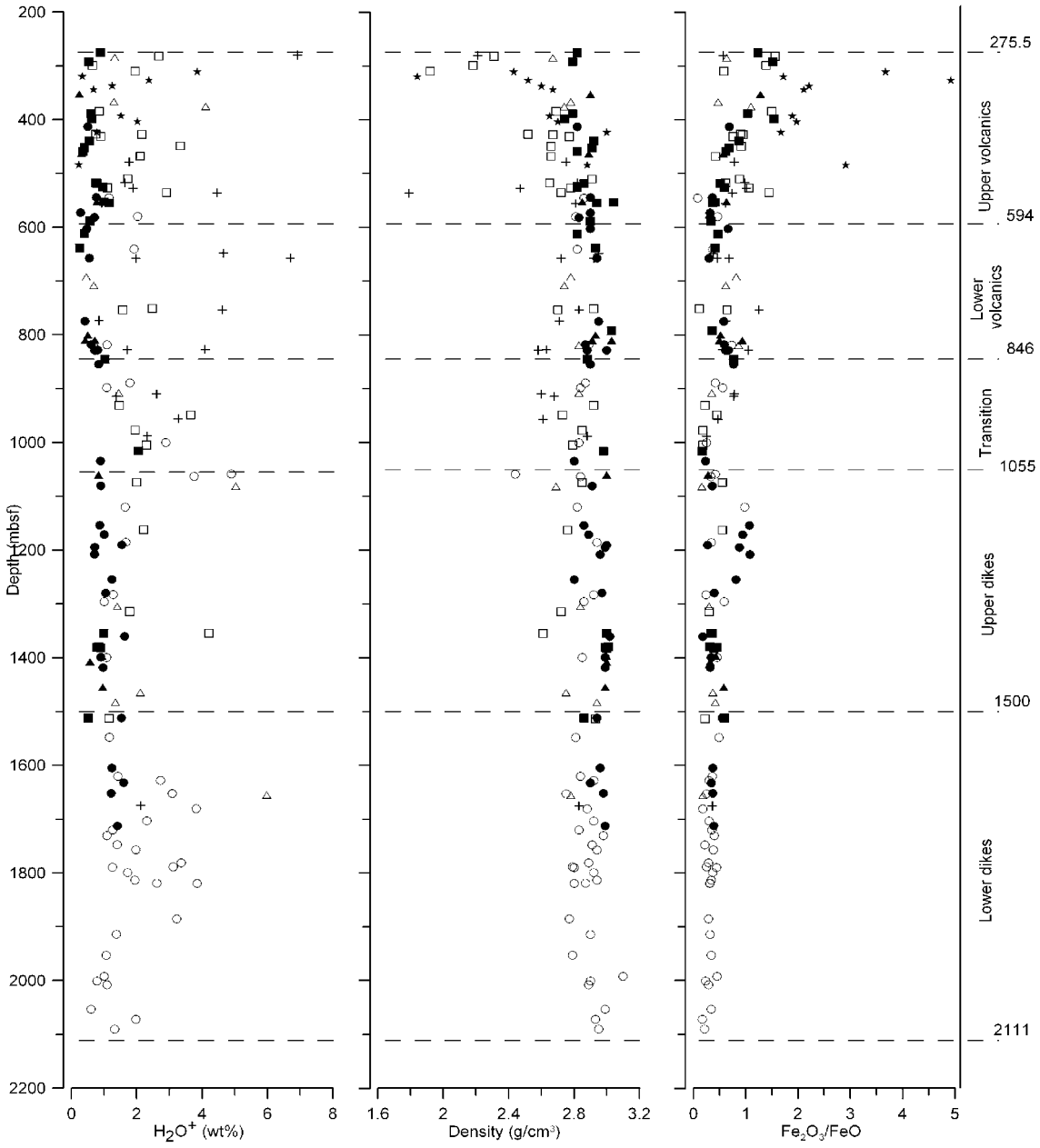

Figure F7. Drill sites for Legs 139 and 169 in the northeastern Pacific, Middle Valley of the Juan de Fuca Ridge and Escanaba Trough of the Gorda Ridge (from Zierenberg, Fouquet, Miller, and Normark, 2000). NESCA = northern Escanaba Trough study area, SESCA = southern Escanaba Trough study area.

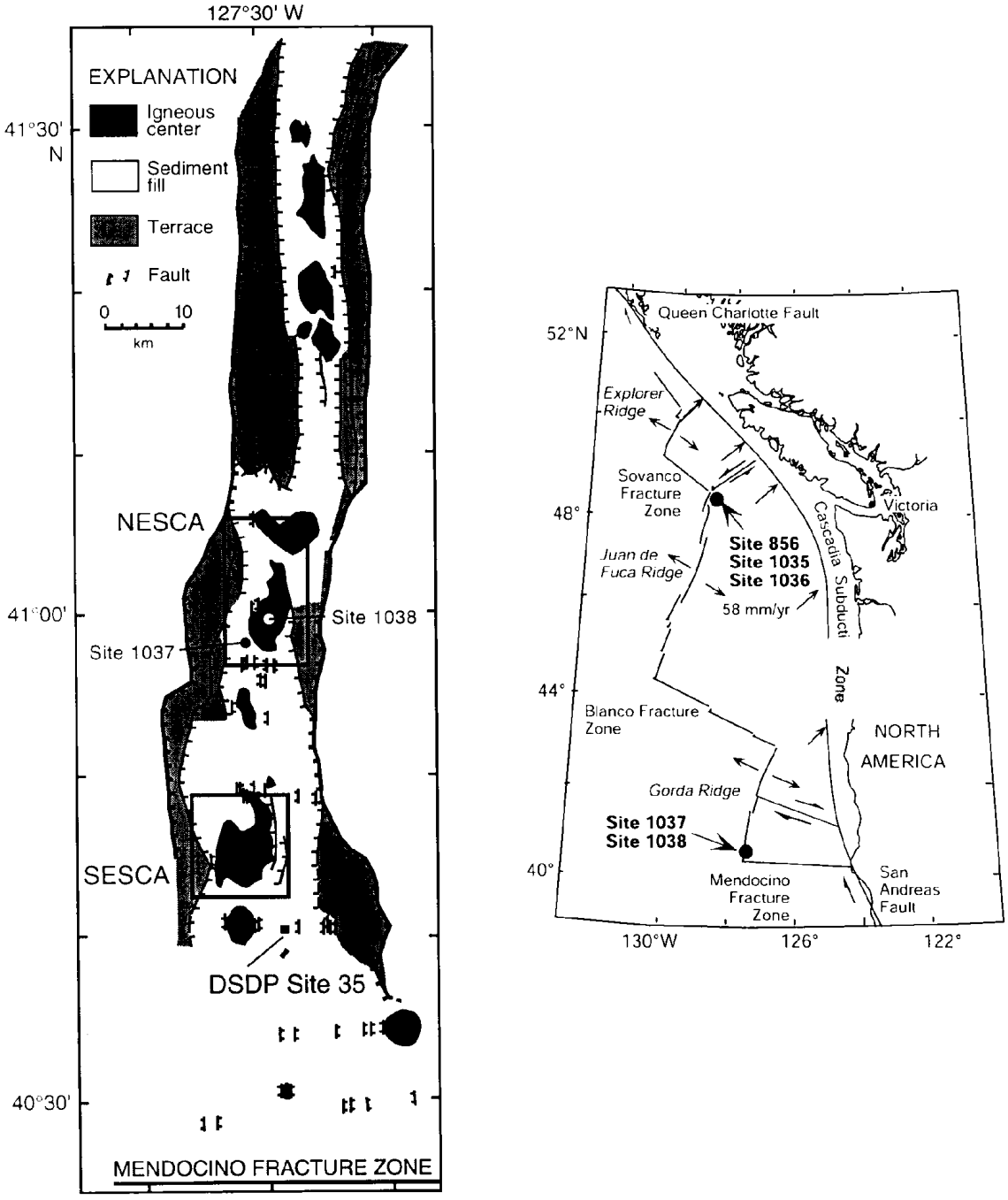

Figure F8. Sites 855–858, Middle Valley of the Juan de Fuca Ridge in the northeastern Pacific (from Goodfellow and Peter, 1994). AAV = area of active venting, BH = Bent Hill.

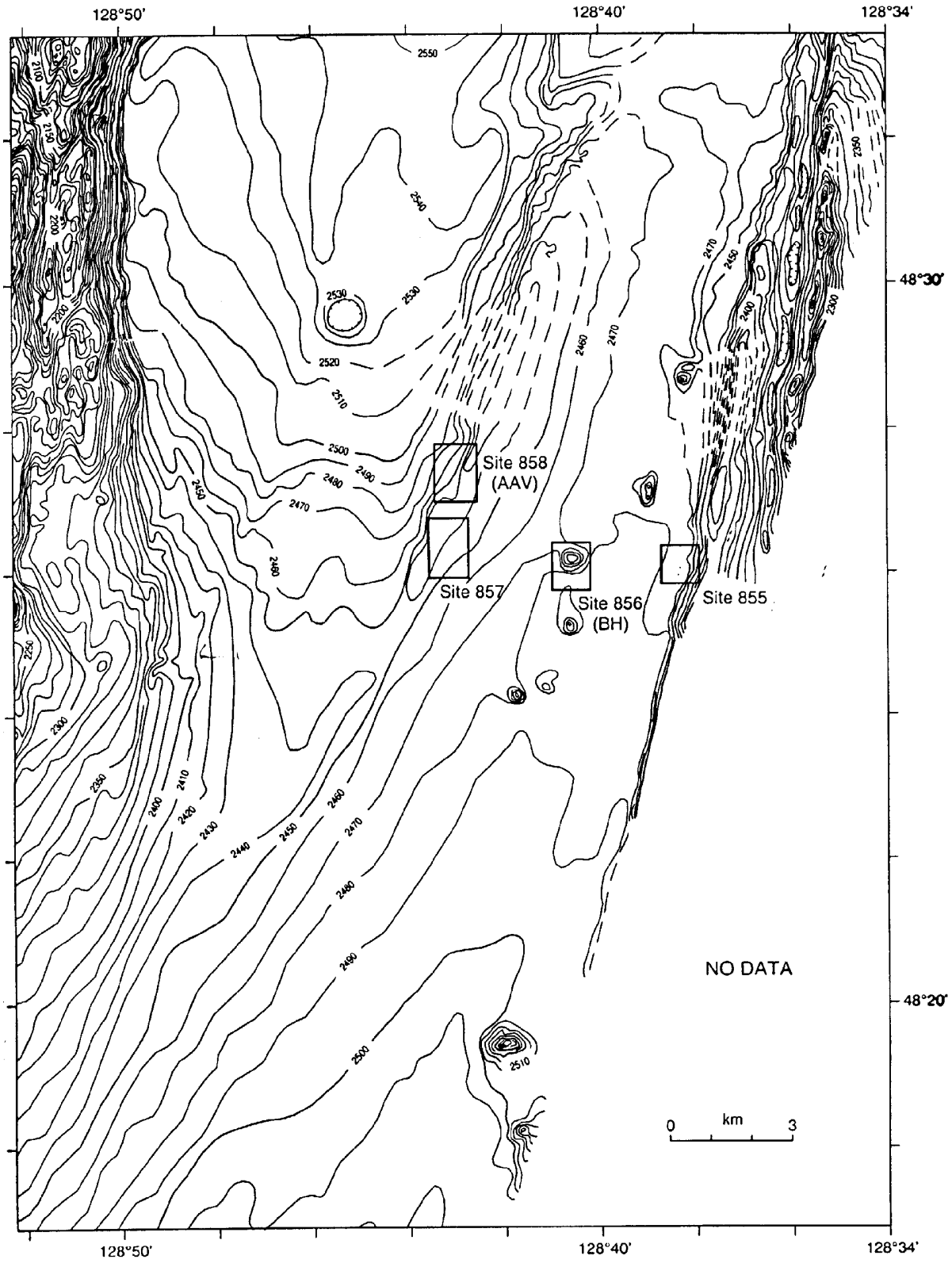

Figure F9. AFM diagram (Irvine and Baragar, 1971) for basalts in Holes 855A, 855D, 856A, 856B, 857C, 857D, 858F, and 858G.

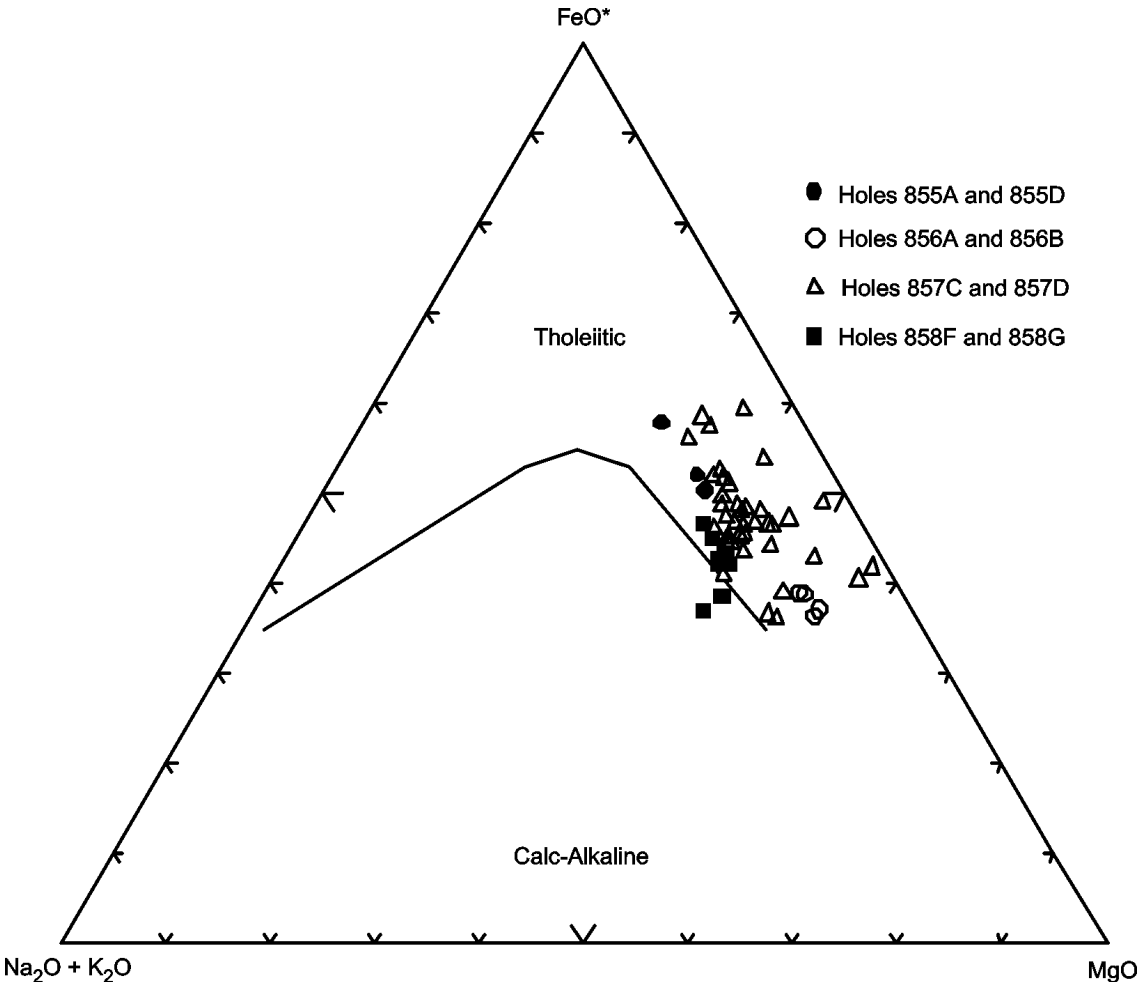

Figure F10. Discrimination Nb-Zr-Y diagram (Meschede, 1986) for basalts in Holes 855A, 855D, 856A, 856B, 857C, 857D, 858F, and 858G. AI, AII = fields of intraplate alkali basalts; AII, C = fields of intraplate tholeiites; B = field of P-type MORB; D = field of N-type MORB; C, D = fields of volcanic arc basalts.

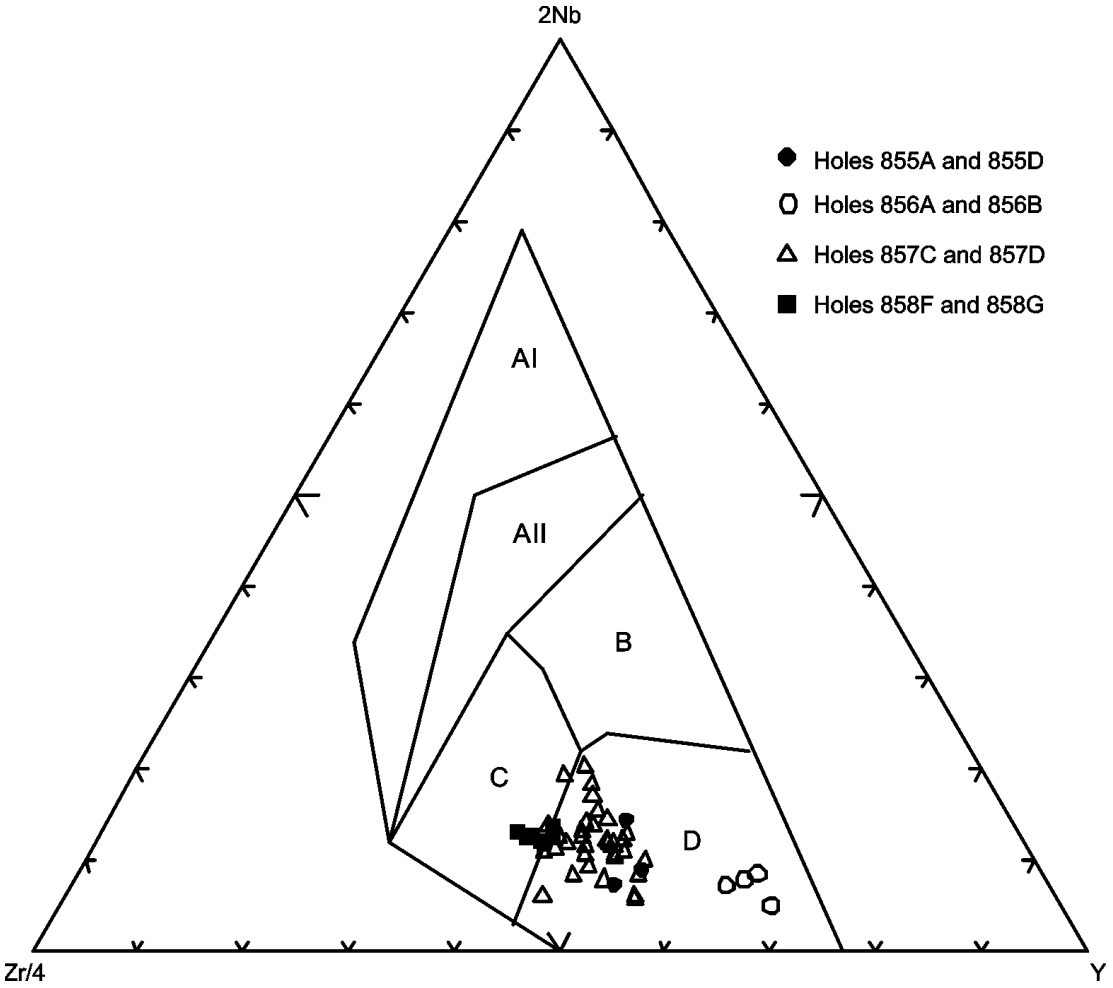

Figure F11. Chondrite-normalized rare earth element abundances for basalts in Holes 855A, 855D, 856A, 856B, 857C, 857D, 858F, and 858G. Normalizing values are from Sun and McDonough (1989). (Continued on next page.)

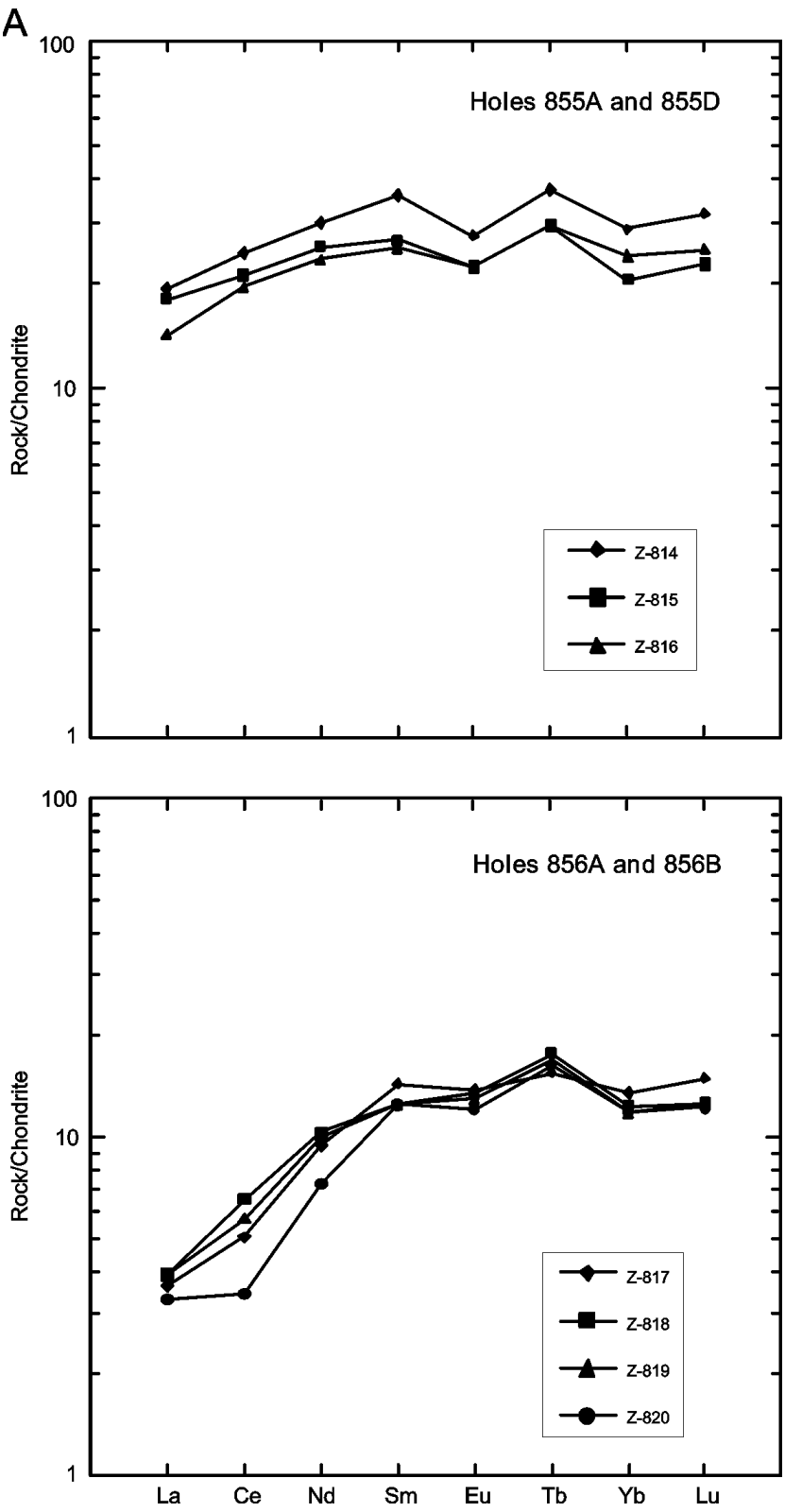

Figure F11 (continued).

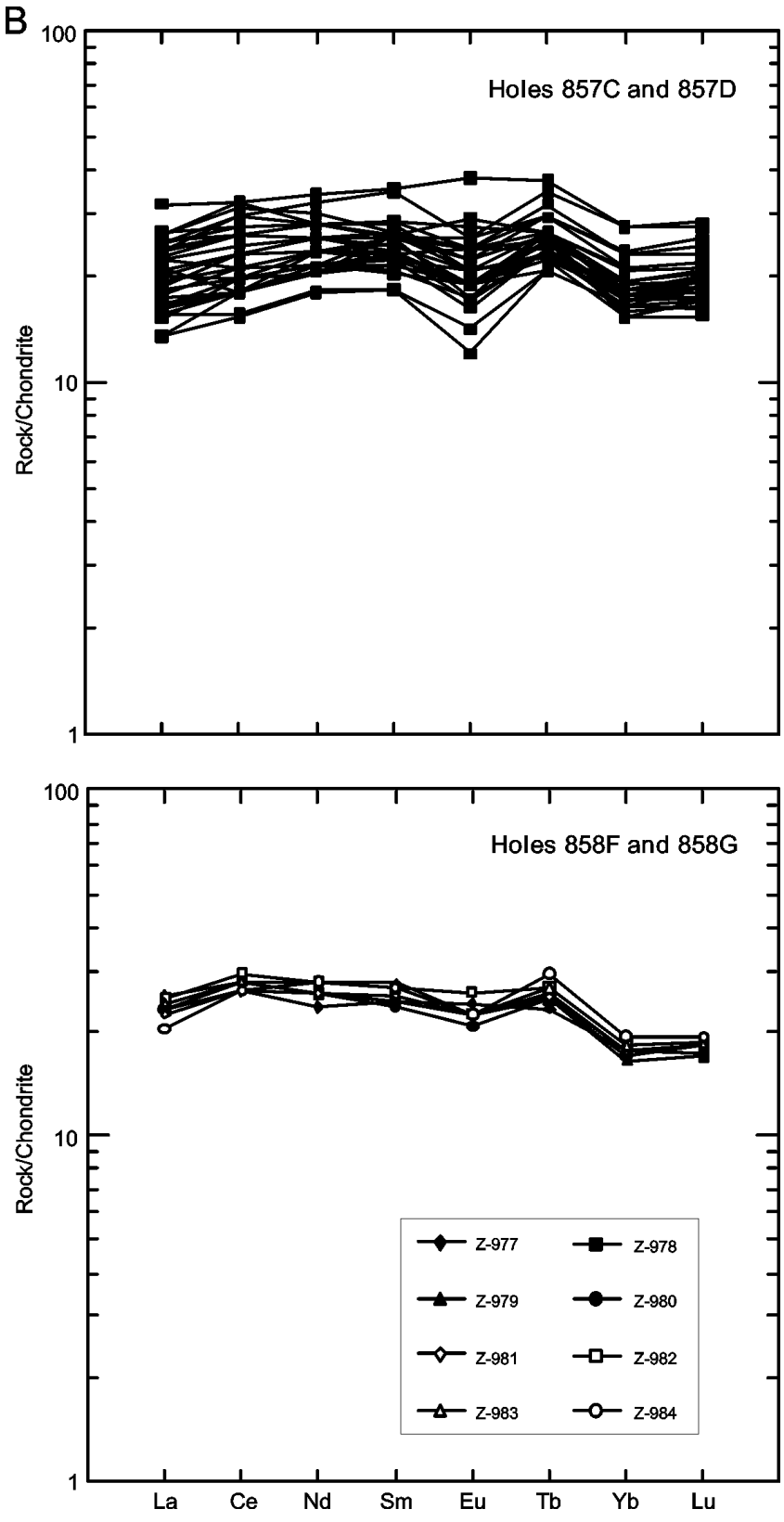

Figure F12. AFM diagram (Irvine and Baragar, 1971) for basalts in Holes 856H, 1037B, and 1038I.

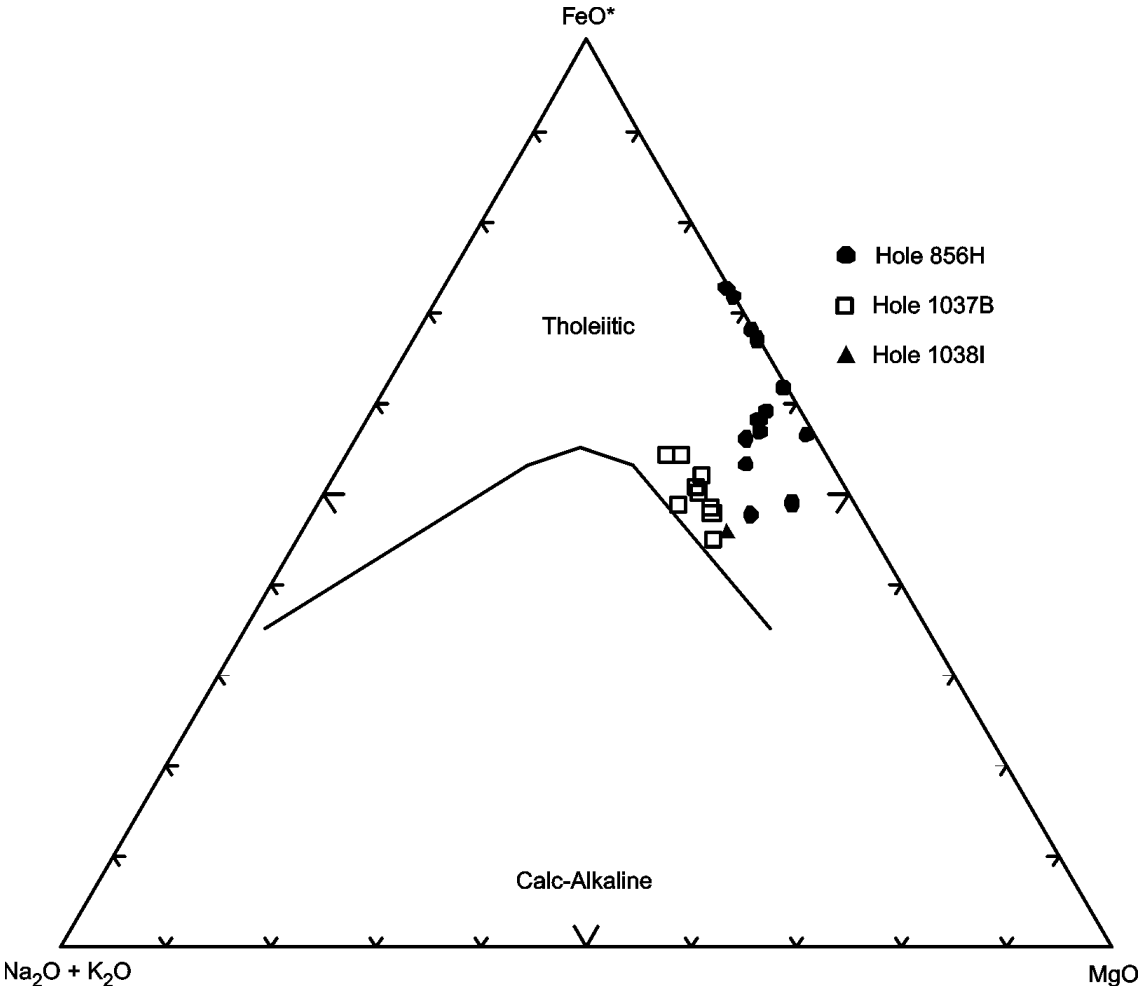

Figure F13. Discrimination Nb-Zr-Y diagram (Meschede, 1986) for basalts in Holes 856H, 1037B, and 1038I. AI, AII = fields of intraplate alkali basalts; AII, C = fields of intraplate tholeiites; B = field of P-type MORB; D = field of N-type MORB; C, D = fields of volcanic arc basalts.

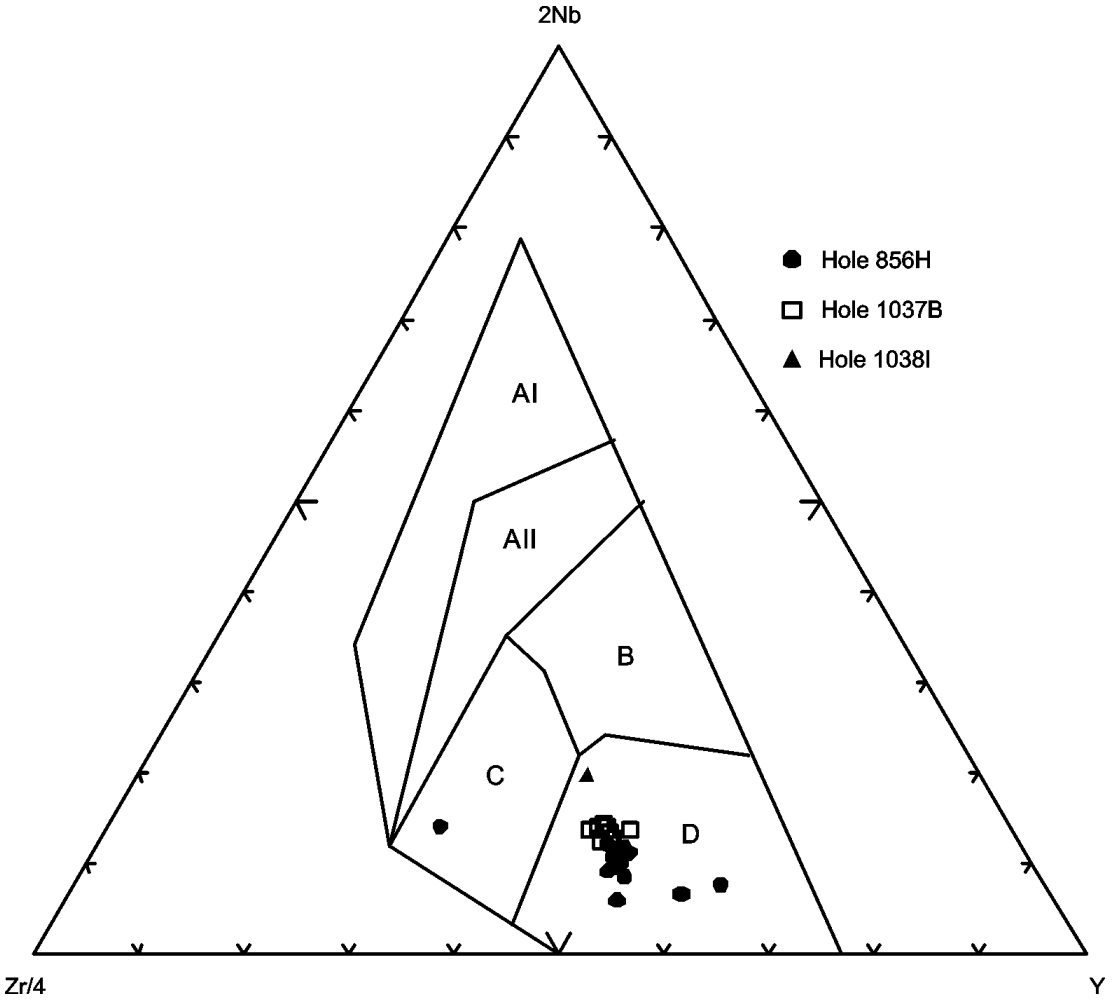

Figure F14. Chondrite-normalized rare earth element abundances for basalts in Holes 856H, 1037B, and 1038I. Normalizing values are from Sun and McDonough (1989). (Continued on next page.)

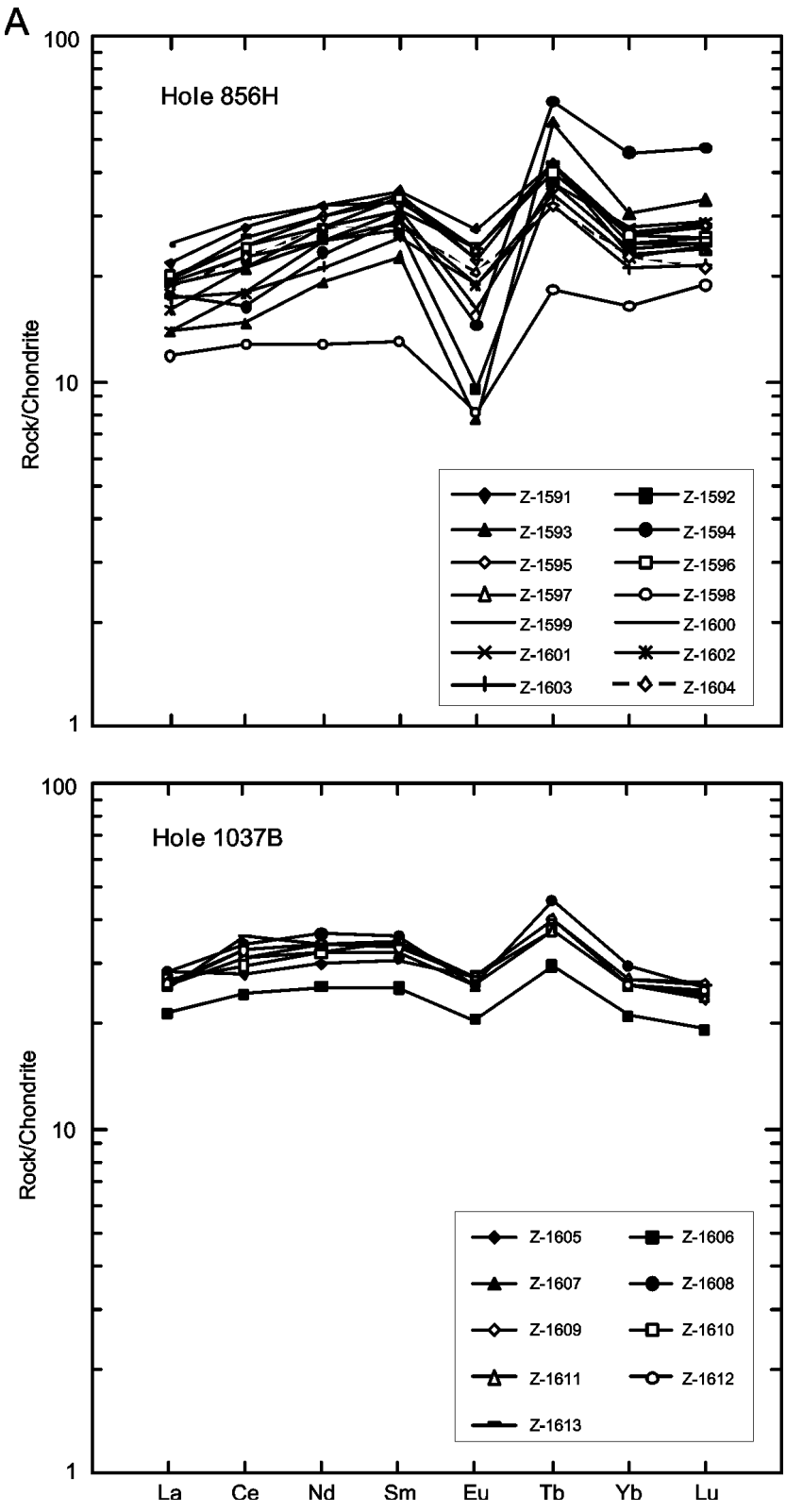

Figure F14 (continued).

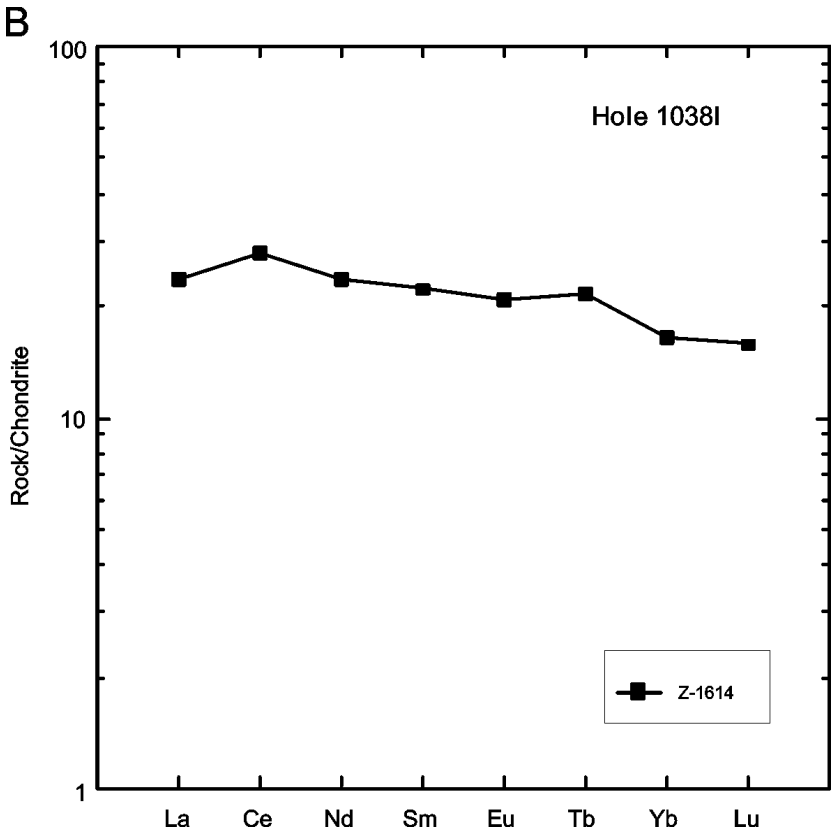

Figure F15. Whole-rock chemical compositions in Hole 856H. Triangles = aphyric basalts, squares = phyric basalts, circles = dolerites. Open symbols = altered rocks, closed symbols = fresh rocks. (Continued on next five pages.)

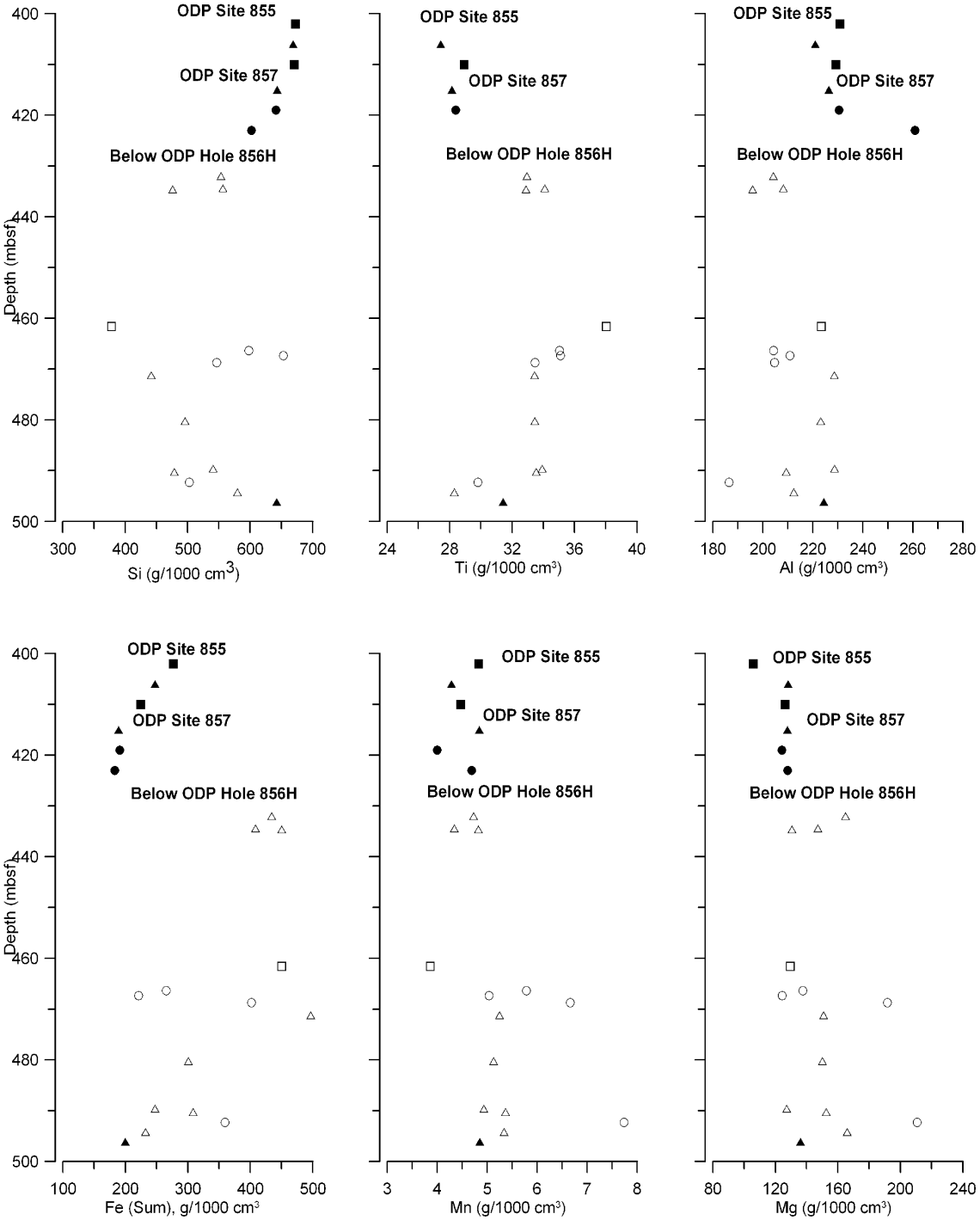

Figure F15 (continued).

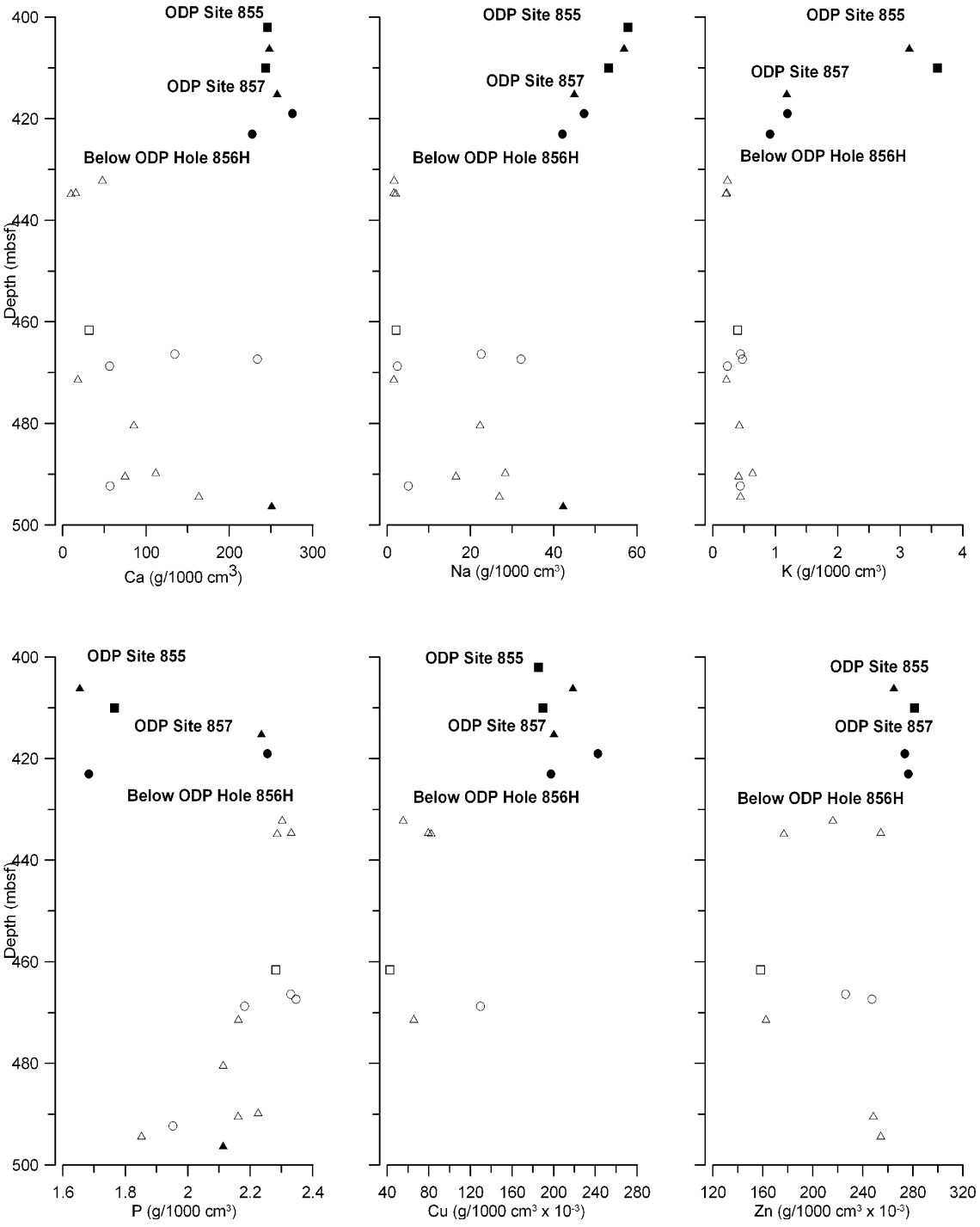

Figure F15 (continued).

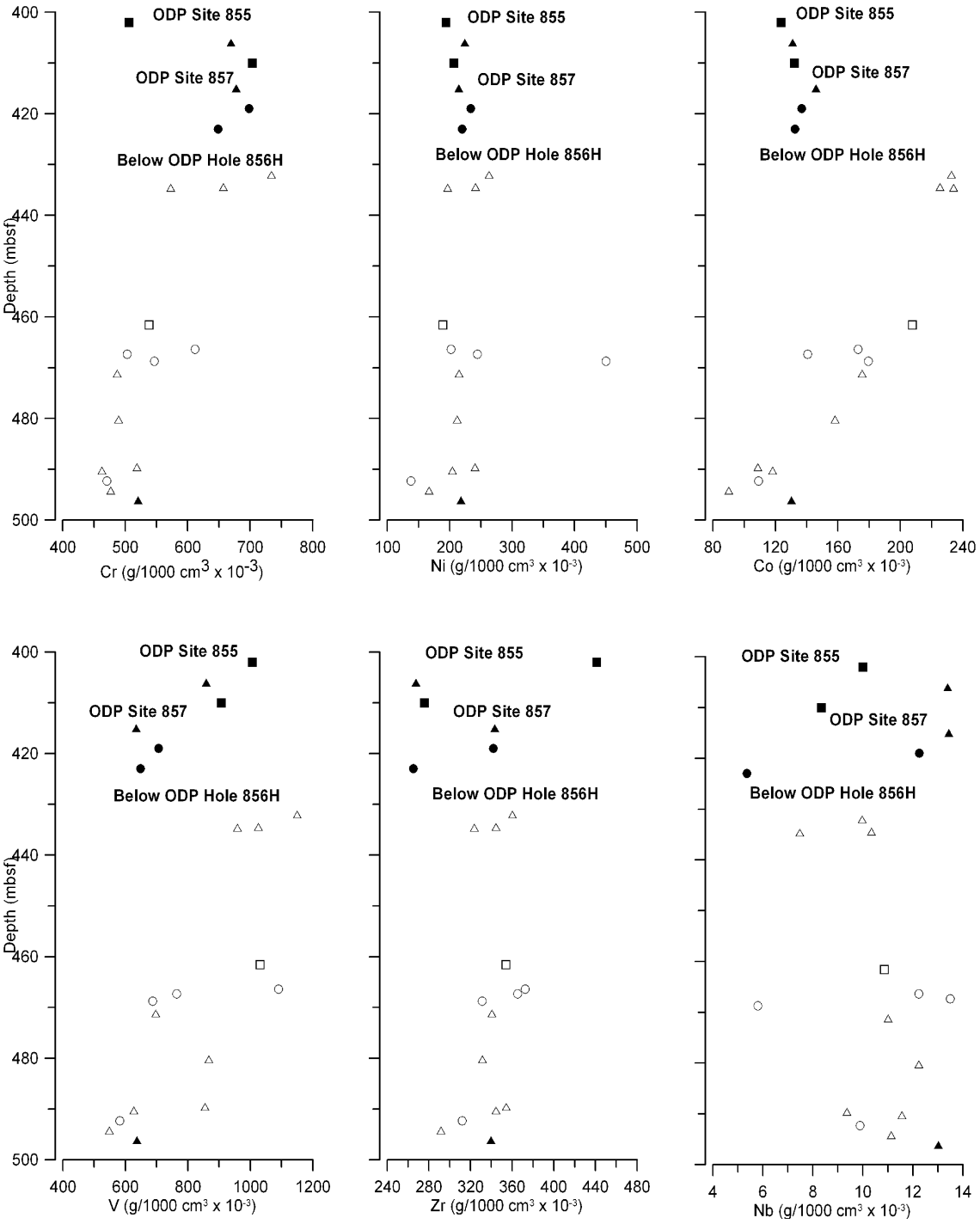

Figure F15 (continued).

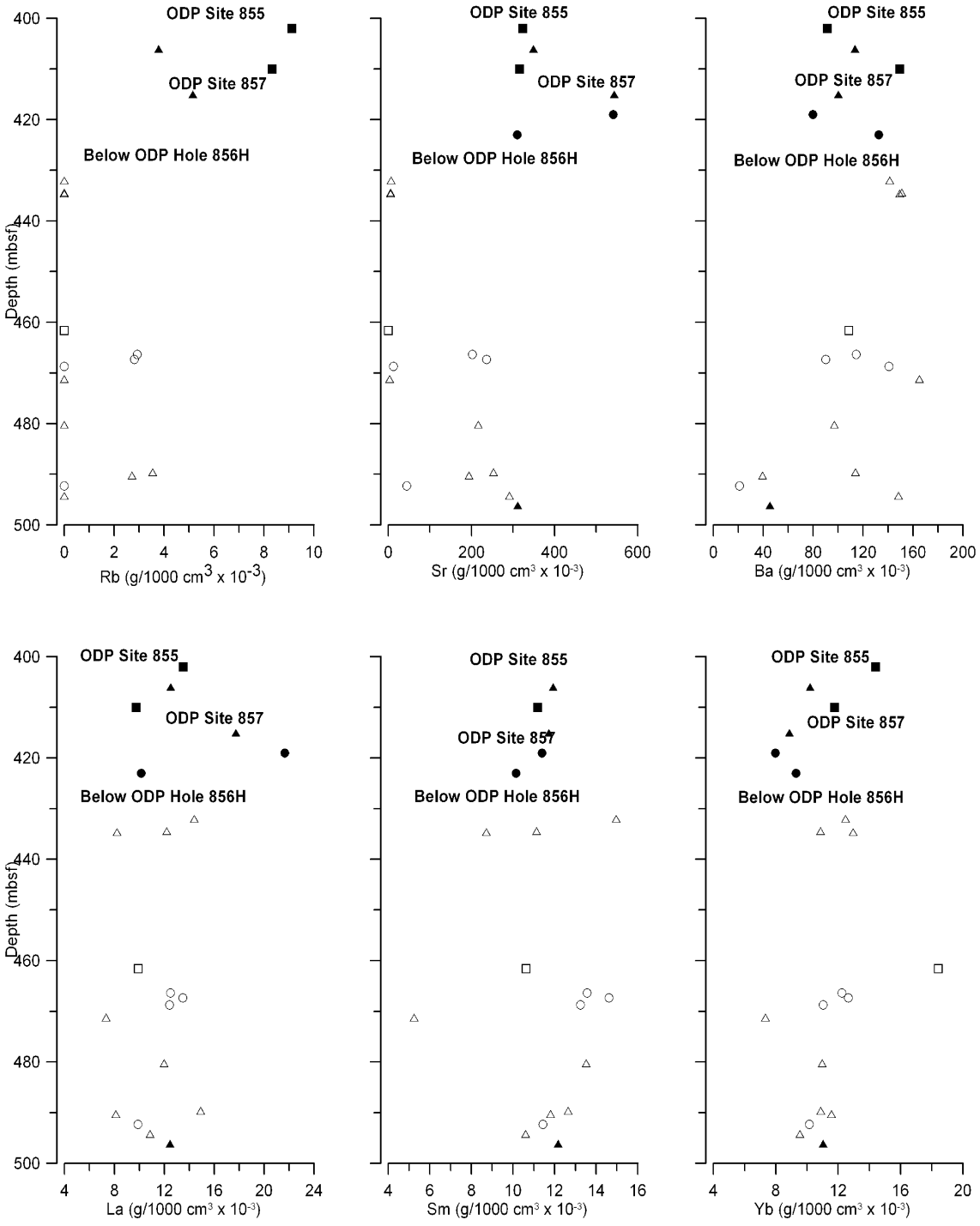

Figure F15 (continued).

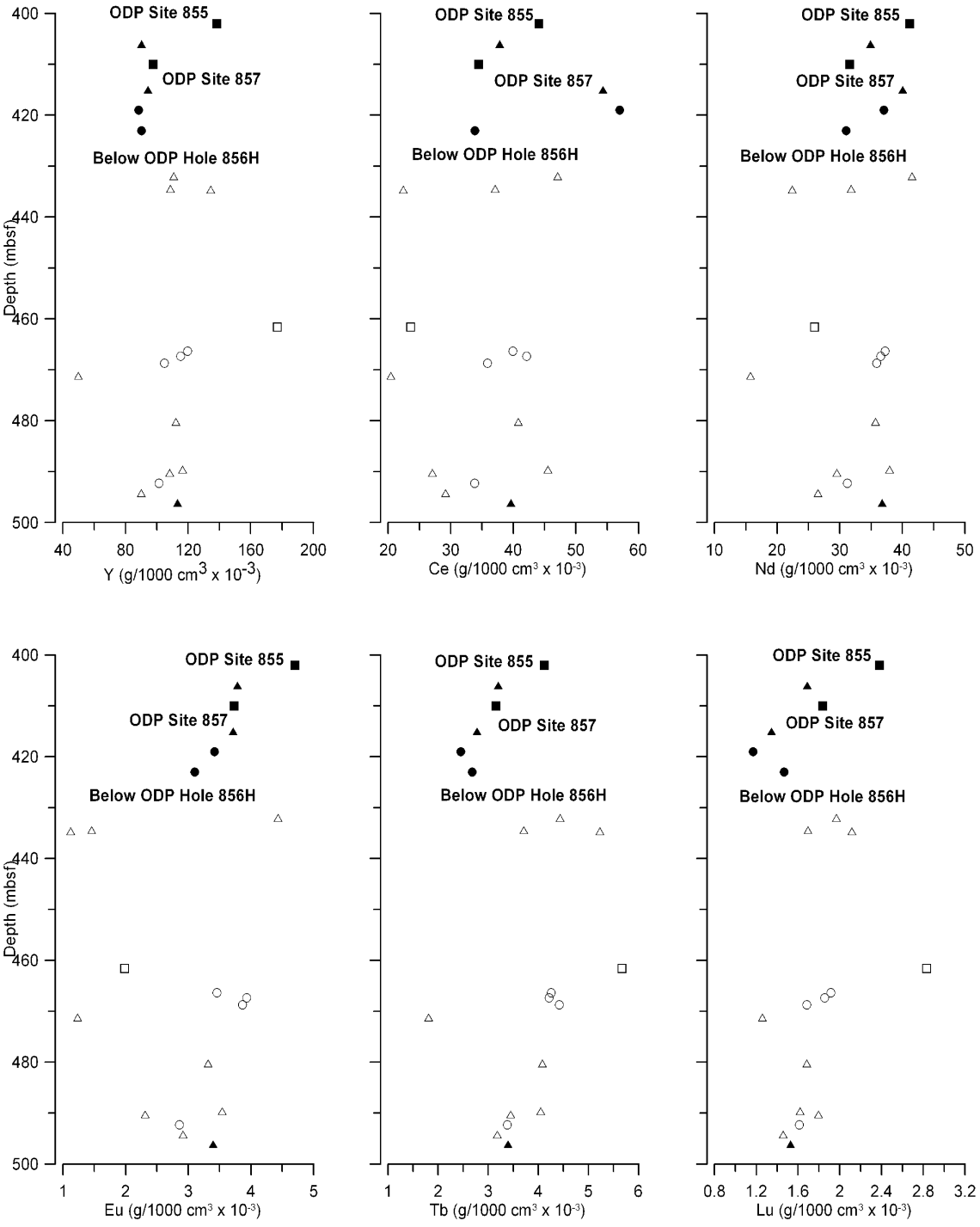

Figure F15 (continued).

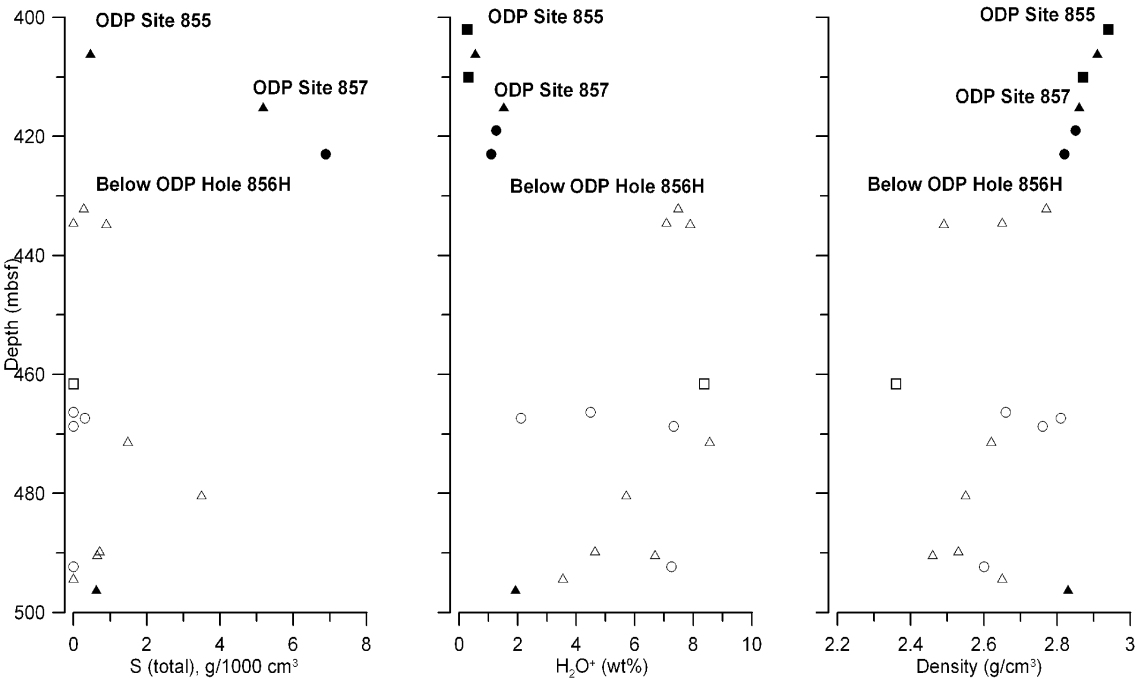

Figure F16. Whole-rock chemical compositions at Site 857. Triangles = aphyric basalts, squares = phyric basalts, circles = dolerites. Open symbols = altered rocks, closed symbols = fresh rocks. (Continued on next eleven pages.)

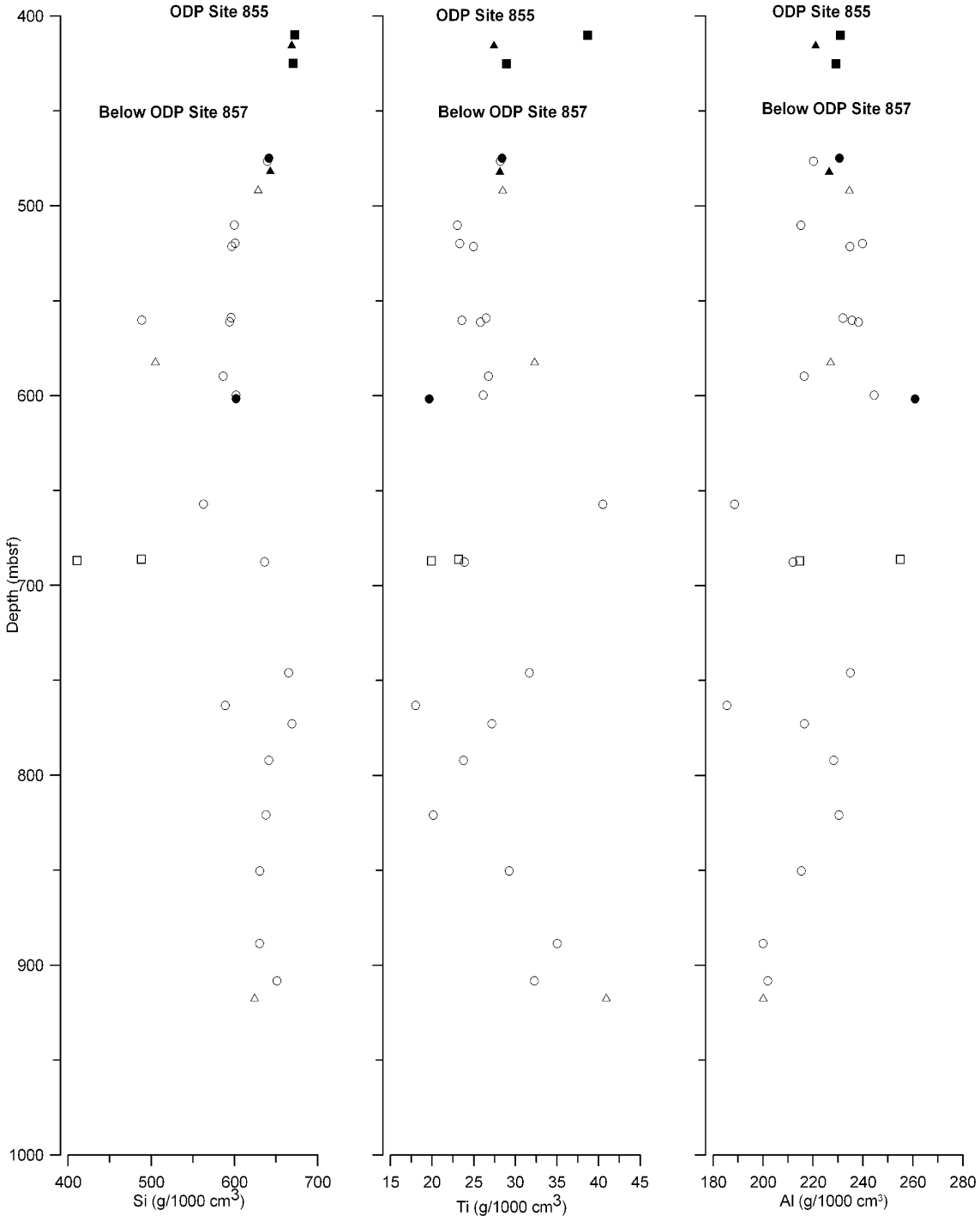

Figure F16 (continued).

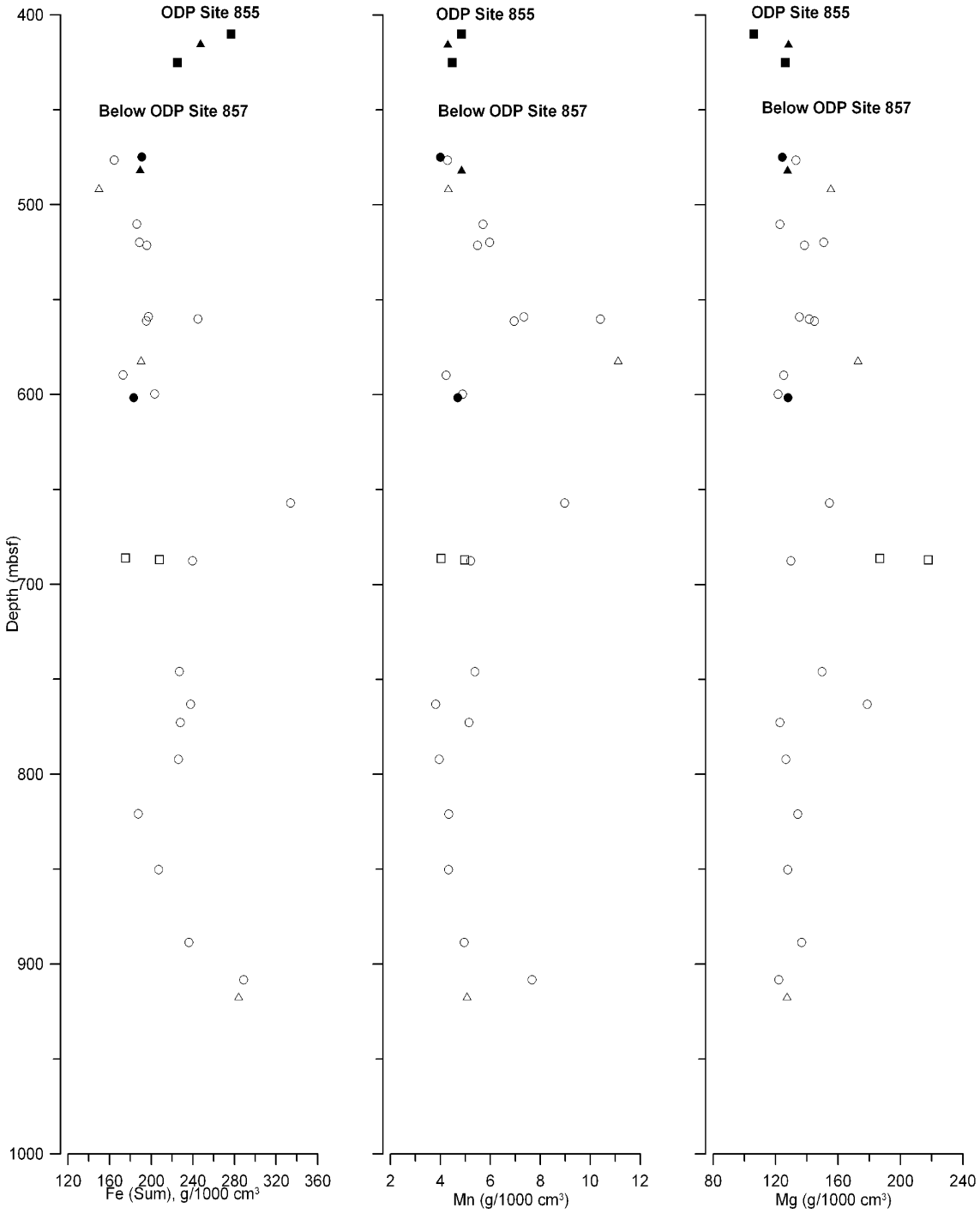

Figure F16 (continued).

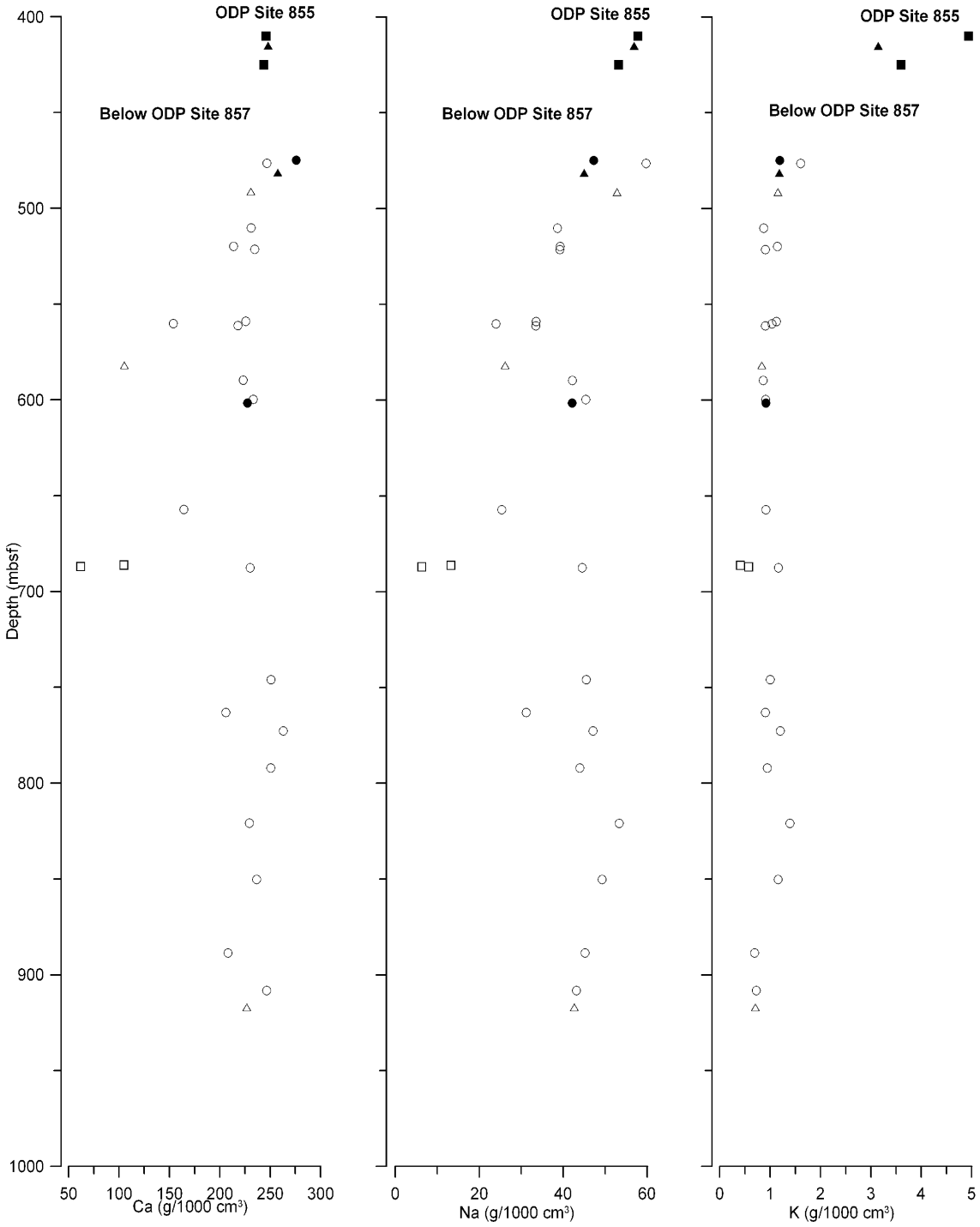

Figure F16 (continued).

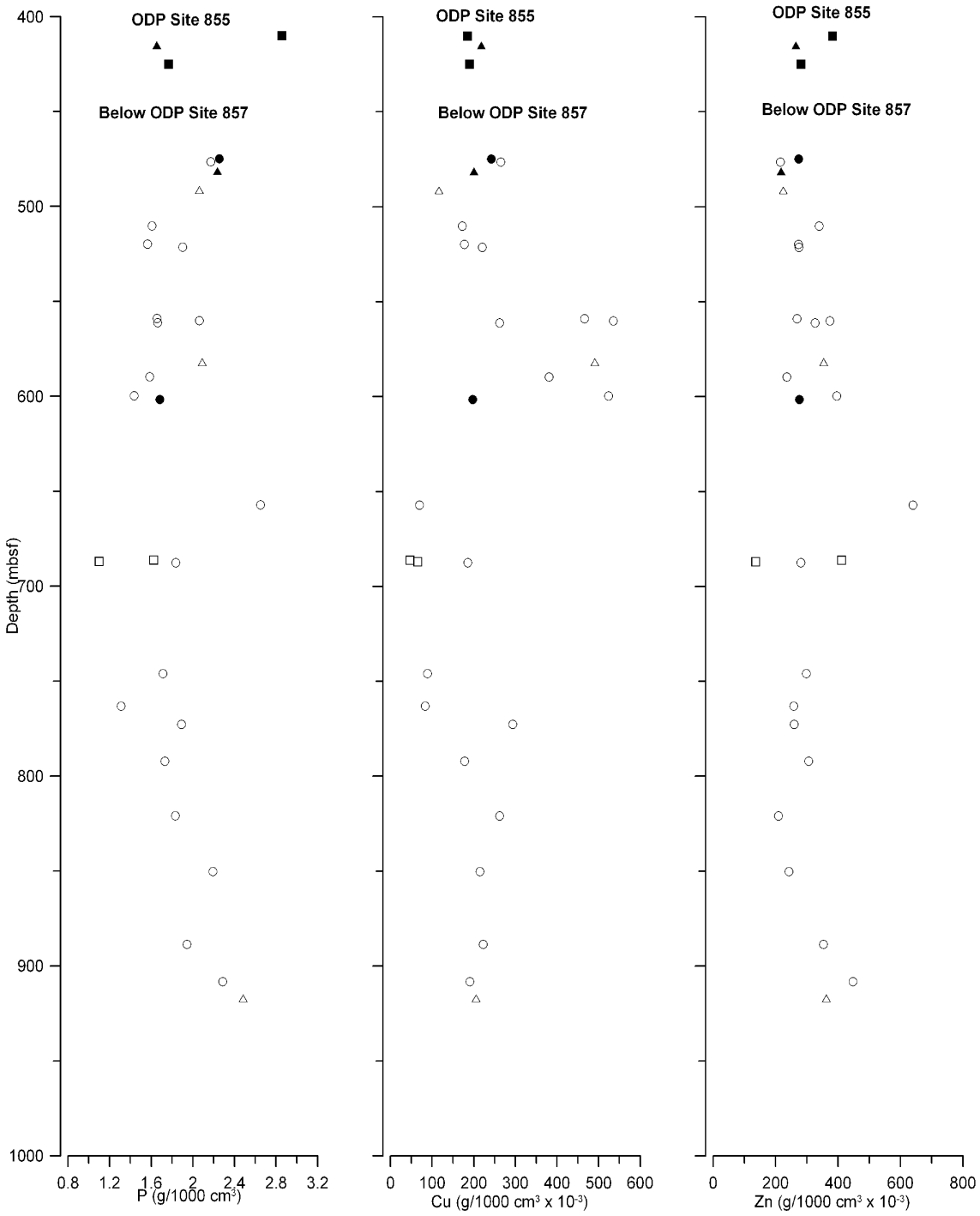

Figure F16 (continued).

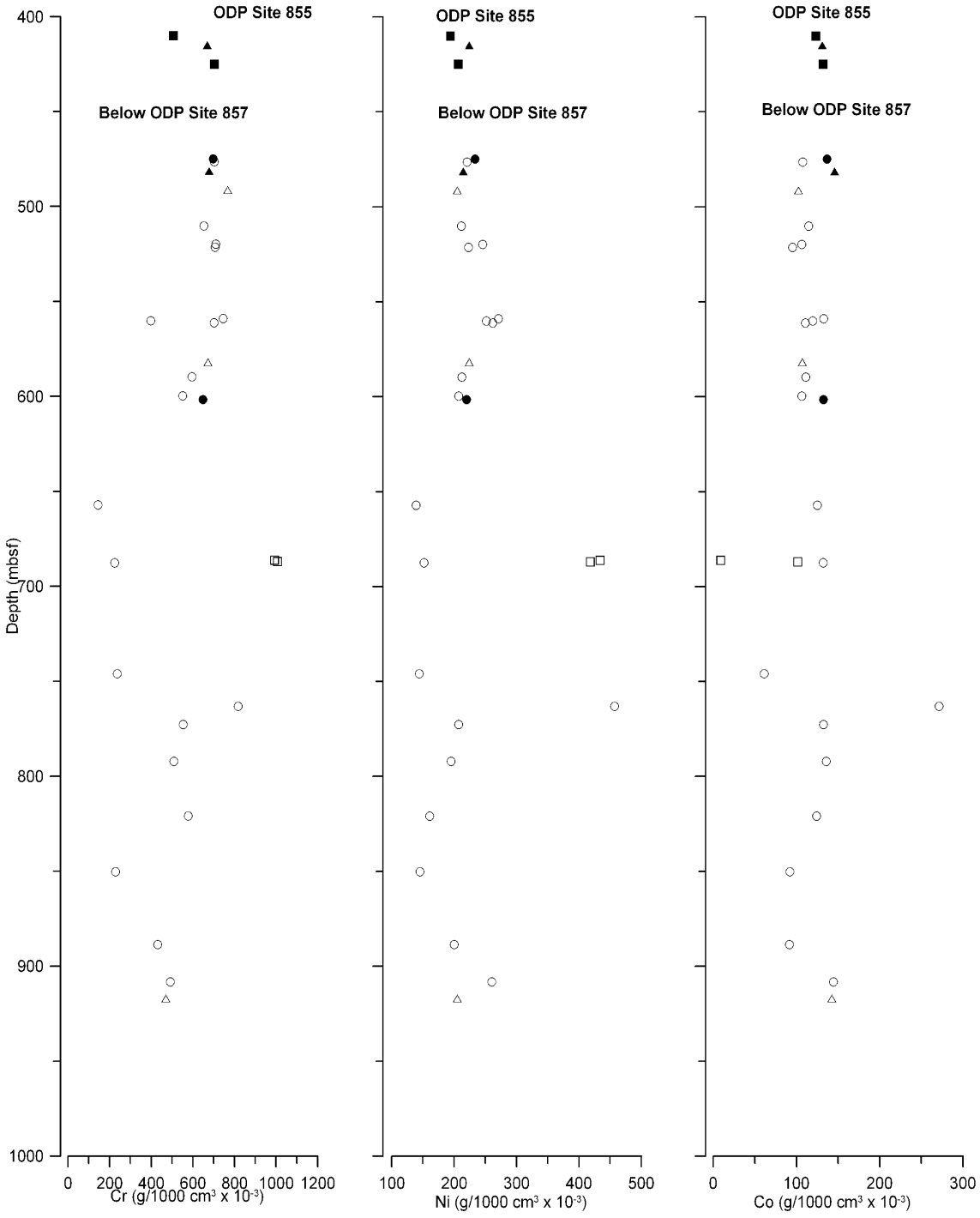

Figure F16 (continued).

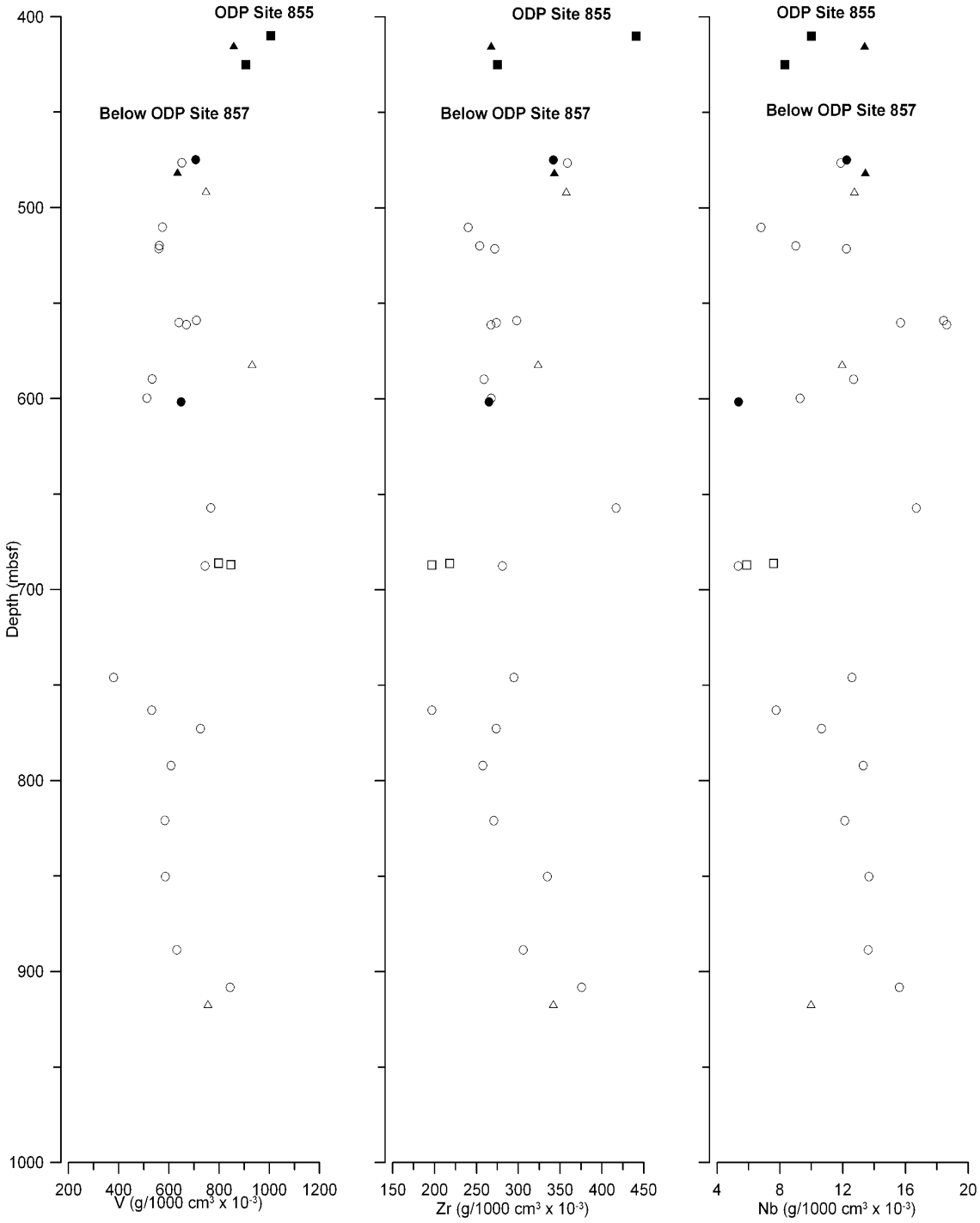

Figure F16 (continued).

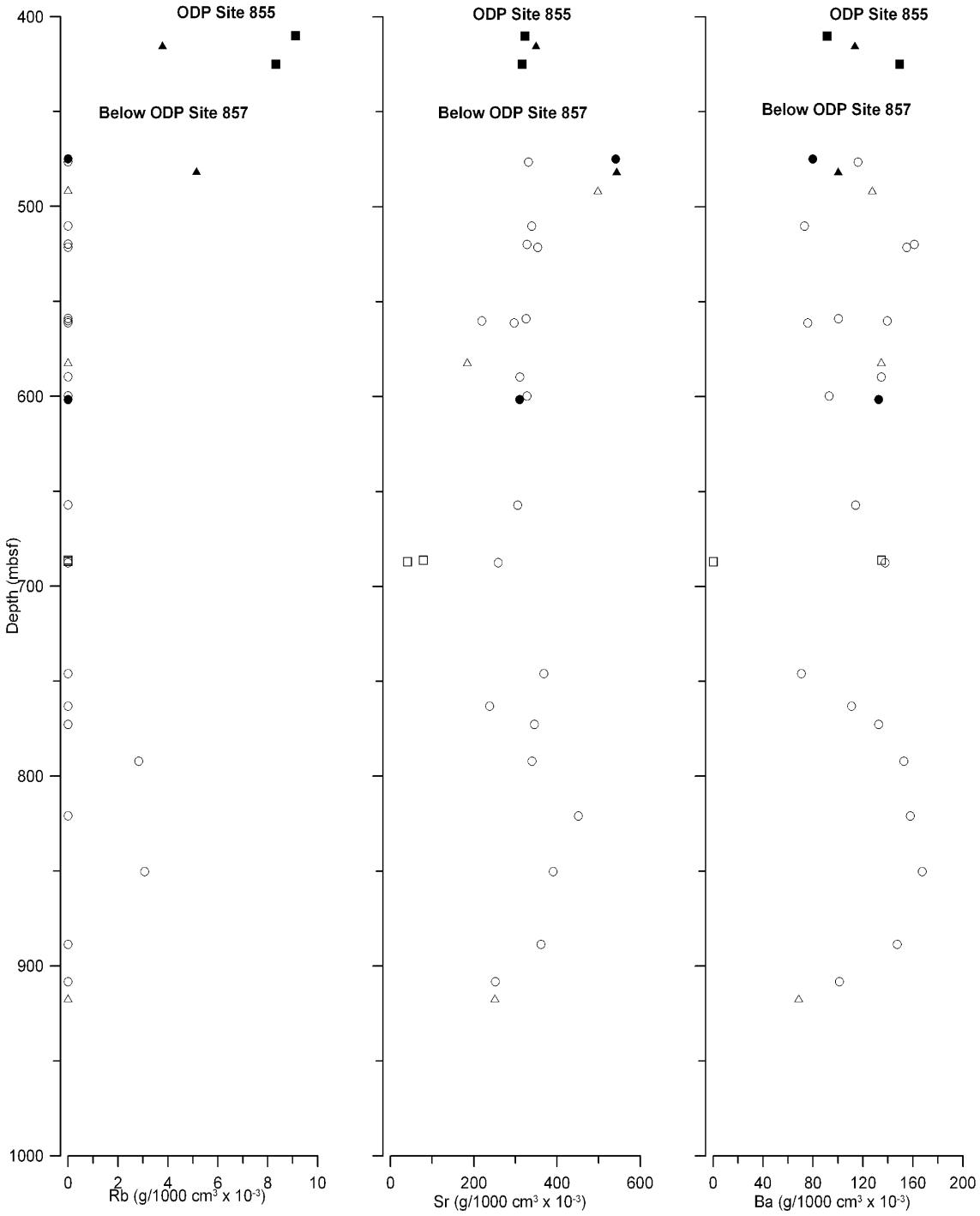

Figure F16 (continued).

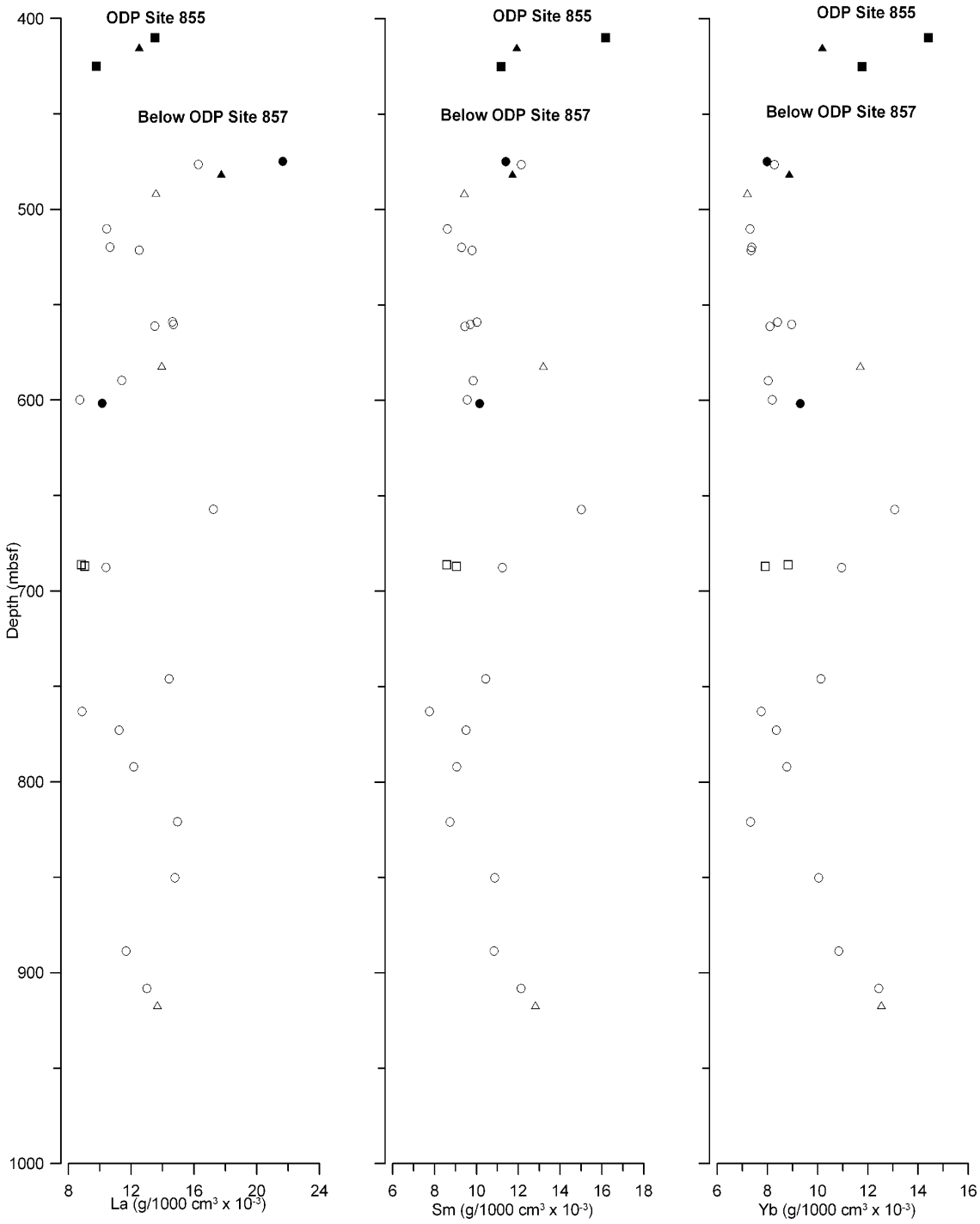

Figure F16 (continued).

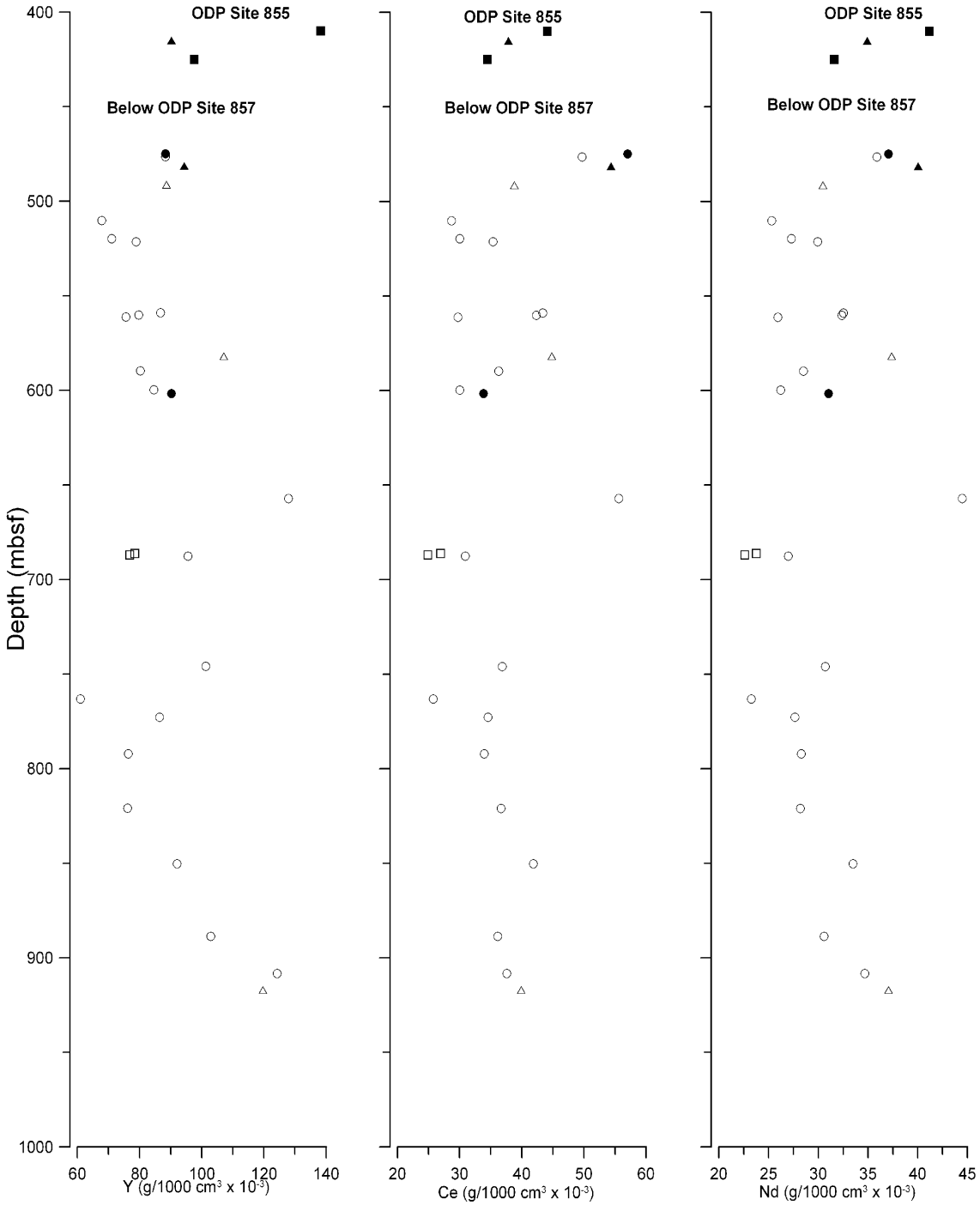

Figure F16 (continued).

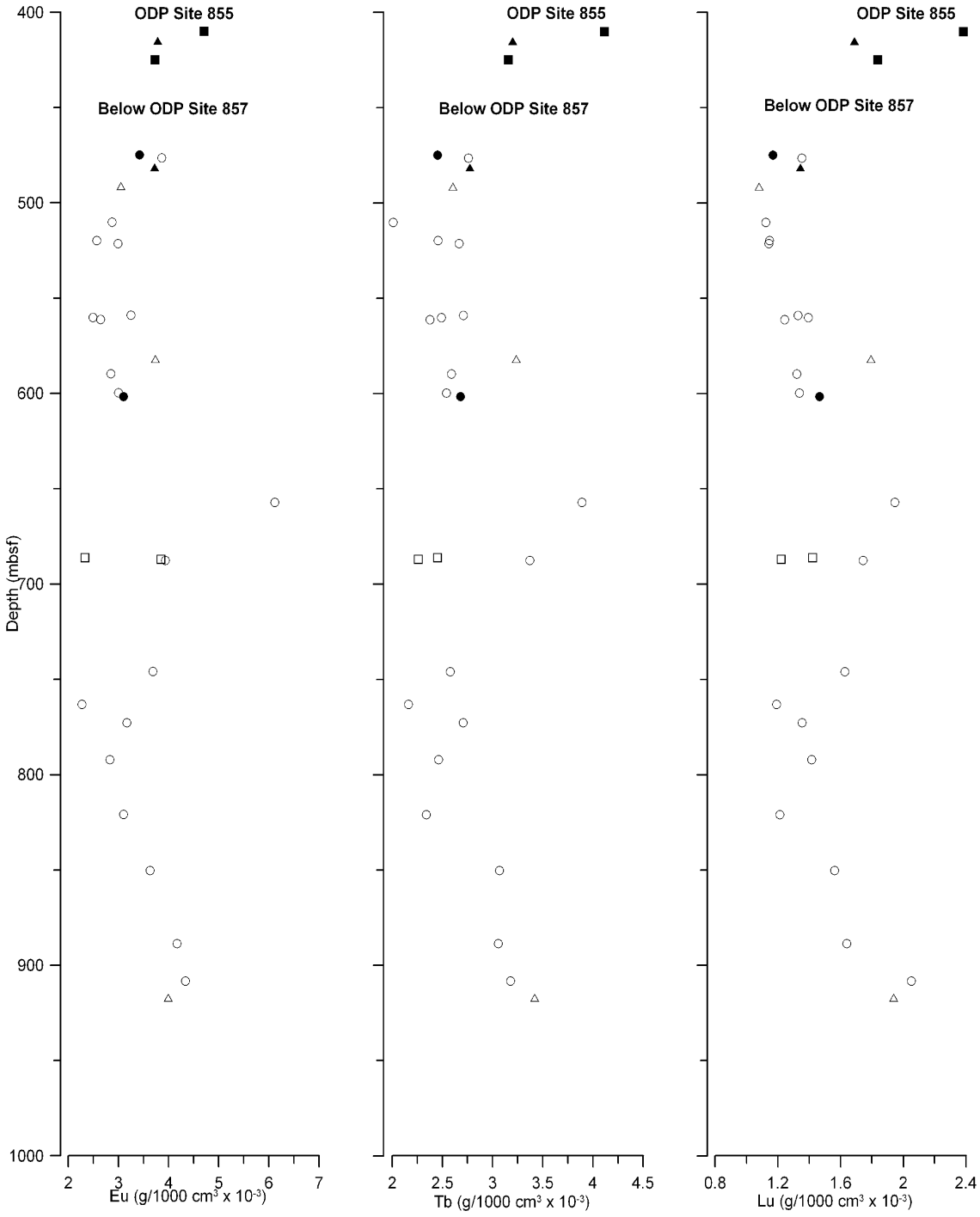

Figure F16 (continued).

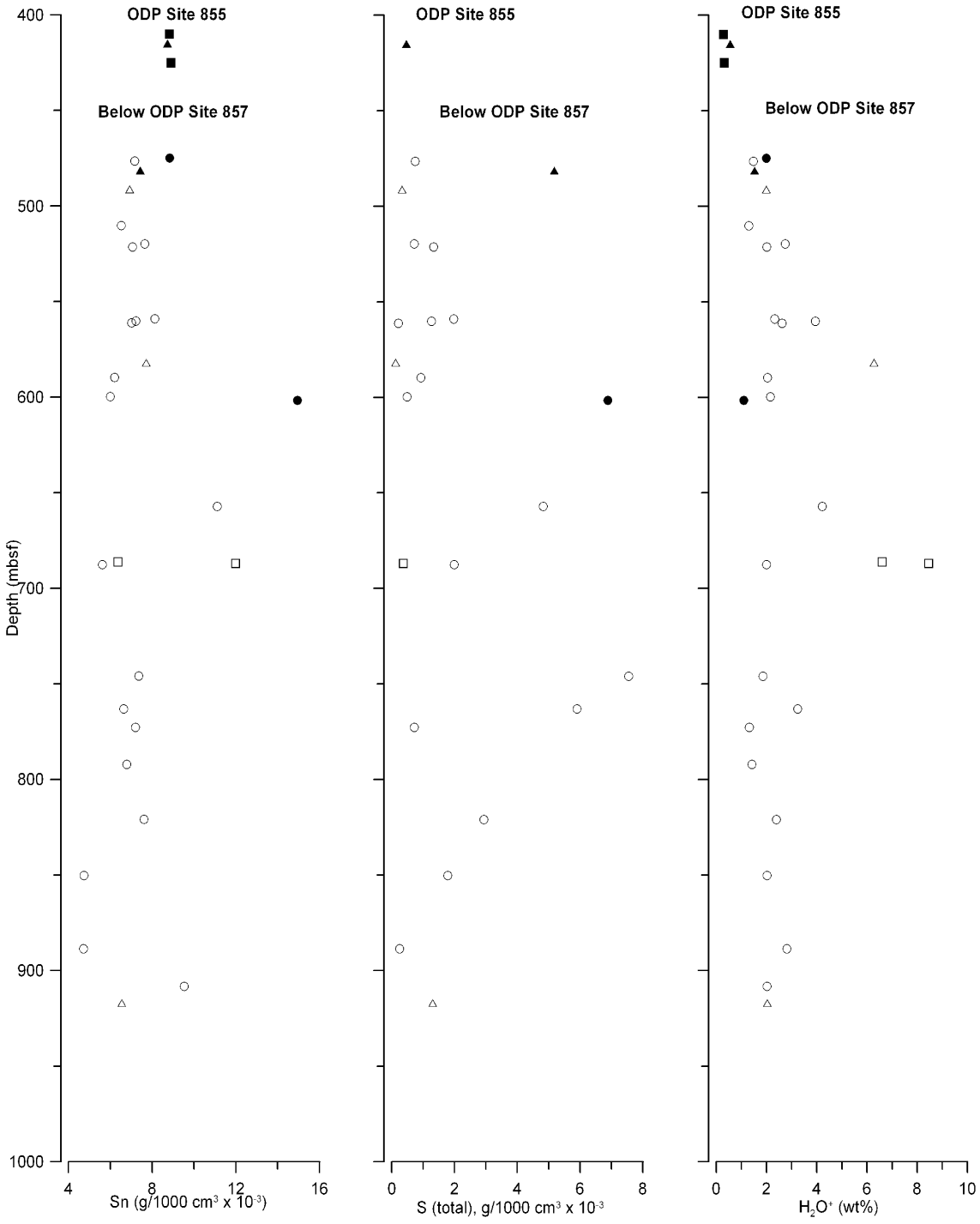

Figure F16 (continued).

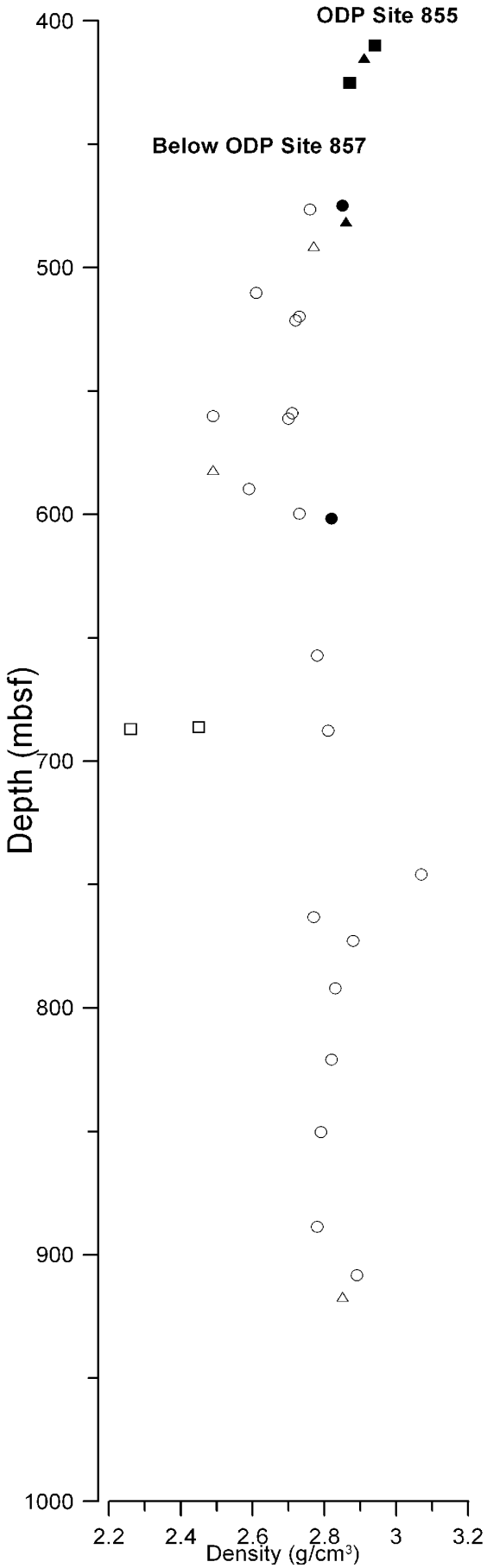

Figure F17. Drill sites for Legs 64 and 65 in the Gulf of California (from Saunders et al., 1982).

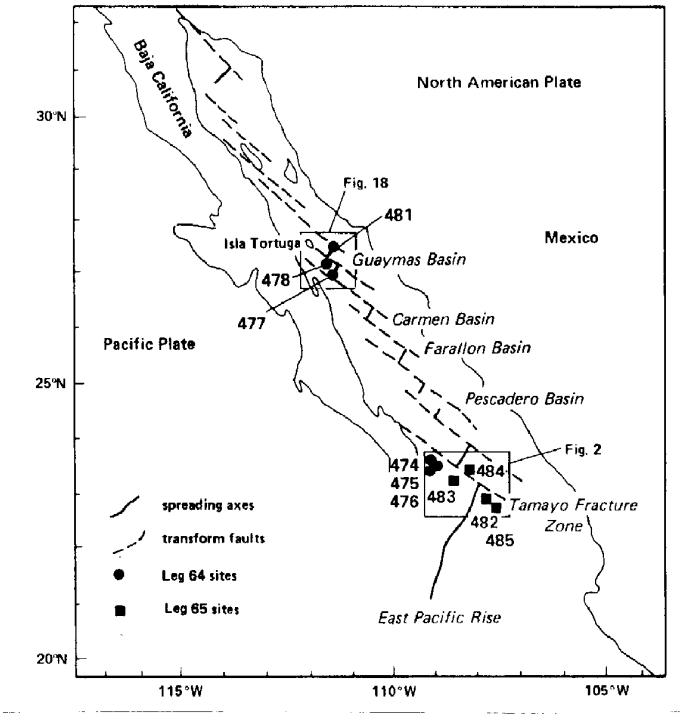

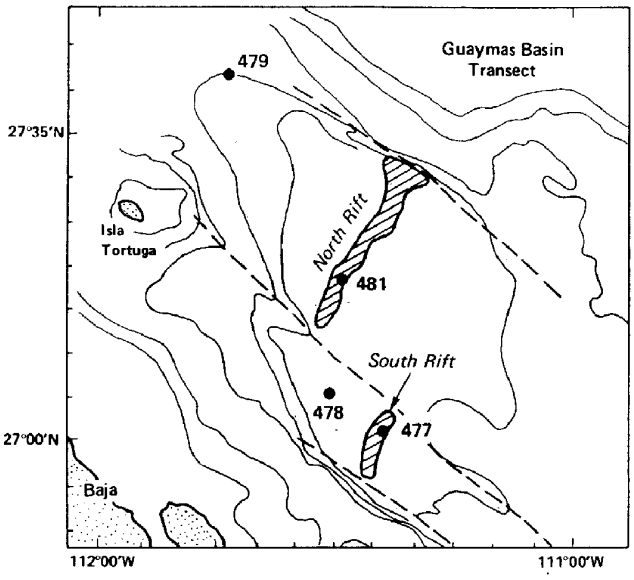

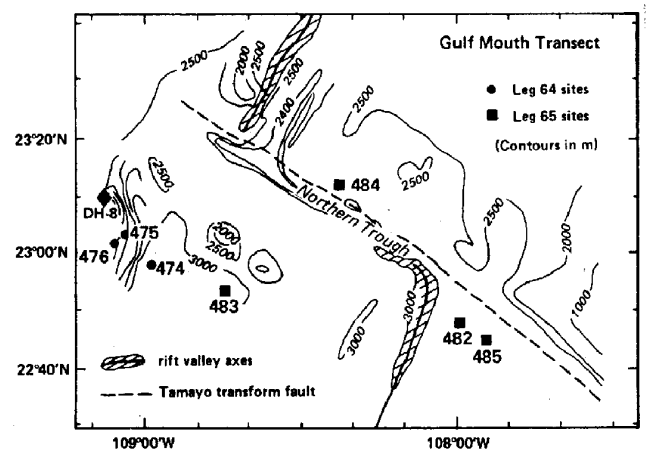

Figure F18. Drill sites for Leg 63, off Baja California (from Yeats, Hag, et al., 1981).

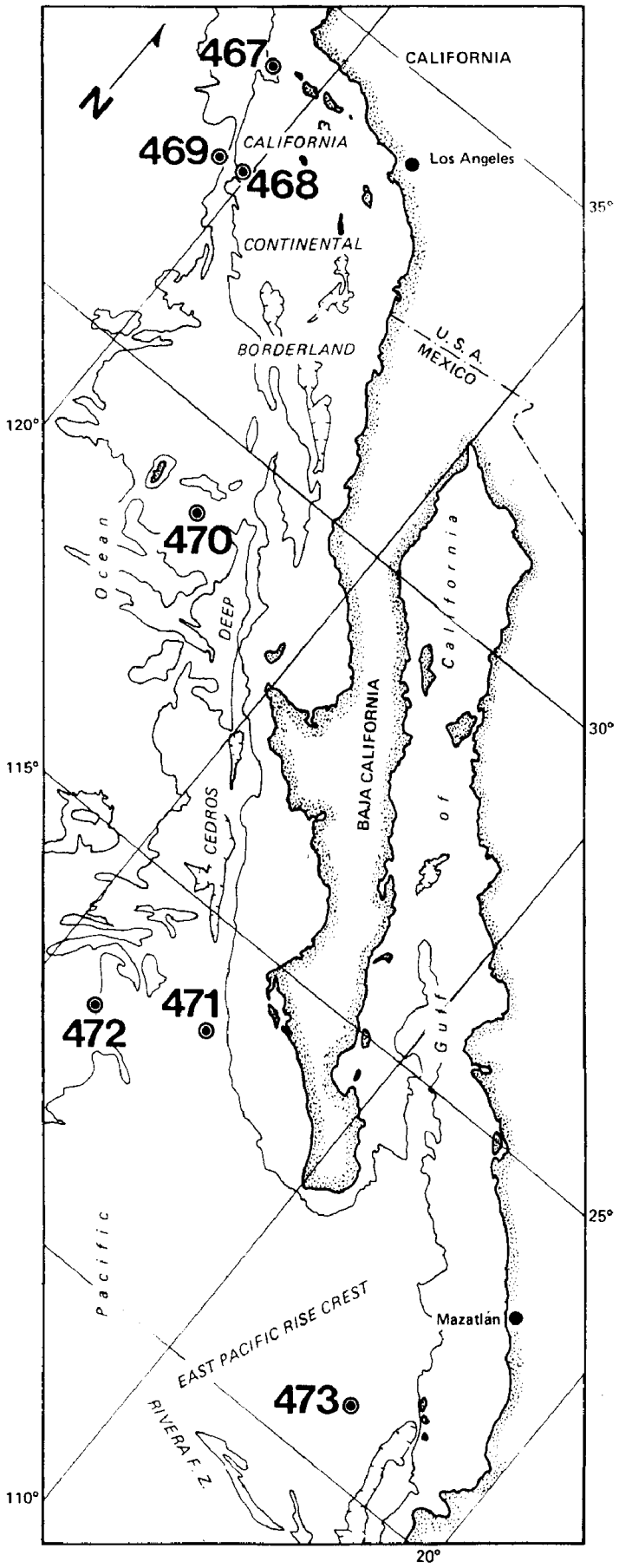

Figure F19. AFM diagram (Irvine and Baragar, 1971) for basalts in Hole 477.

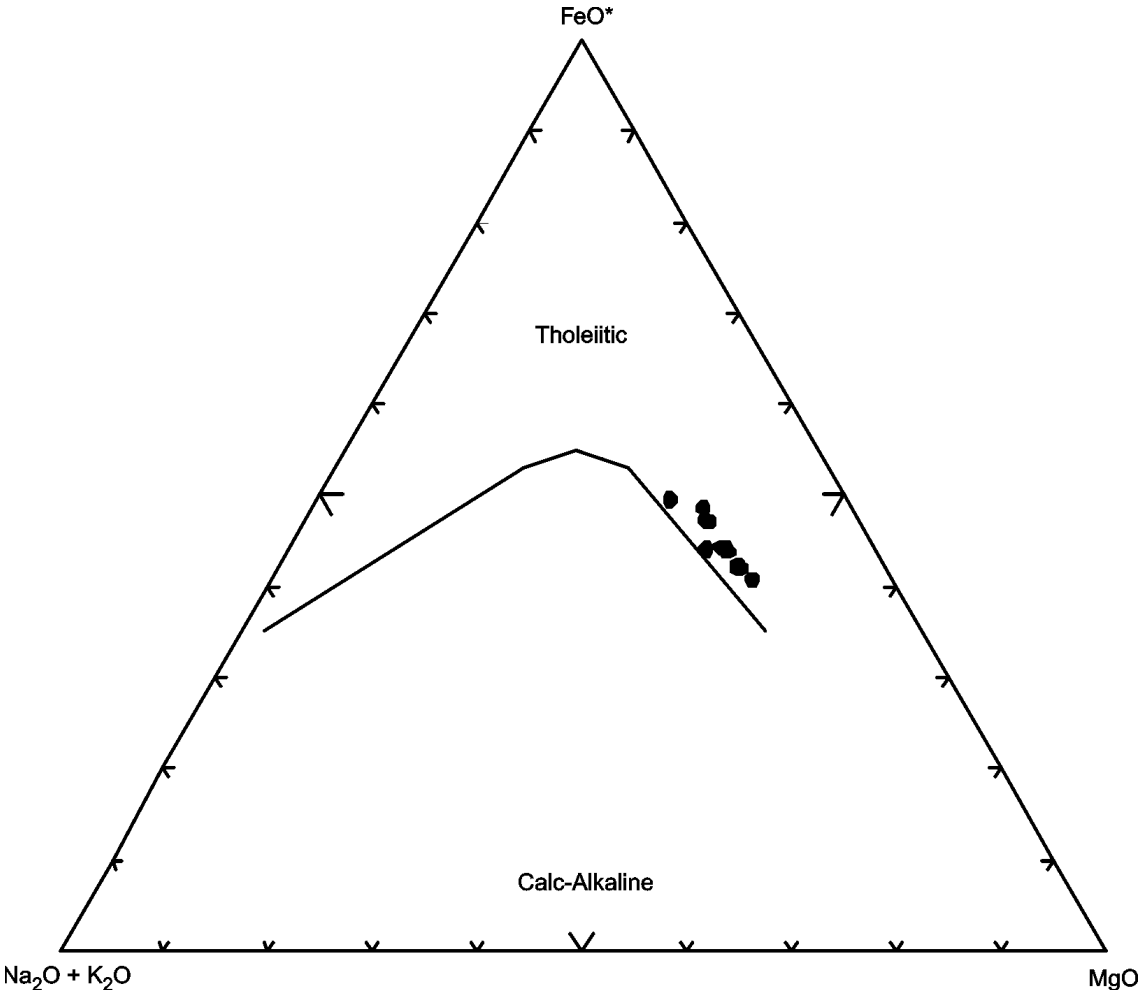

Figure F20. Discrimination Nb-Zr-Y diagram (Meschede, 1986) for basalts in Hole 477. AI, AII = fields of intraplate alkali basalts; AII, C = fields of intraplate tholeiites; B = field of P-type MORB; D = field of N-type MORB; C, D = fields of volcanic arc basalts.

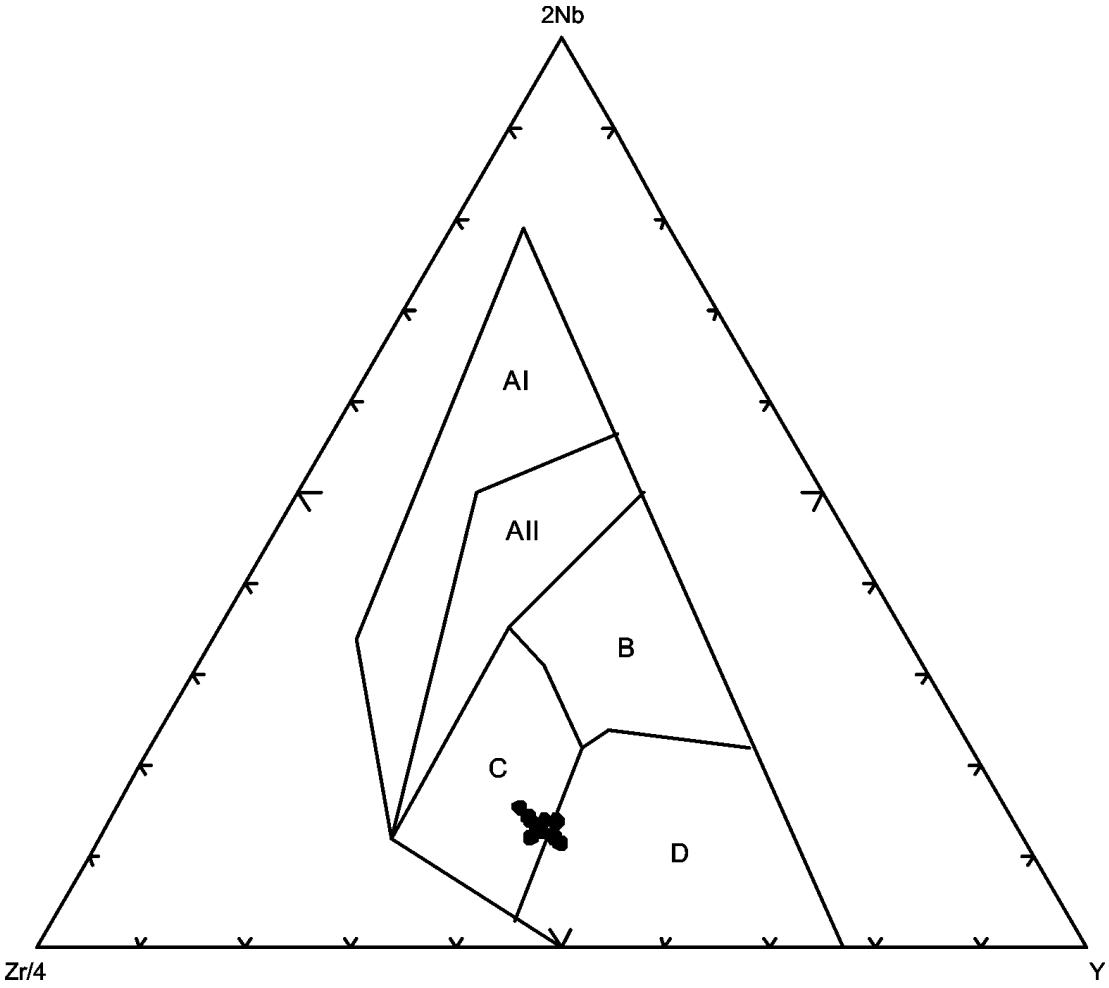

Figure F21. Chondrite-normalized rare earth element abundances for basalts in Hole 477. Normalizing values are from Sun and McDonough (1989).

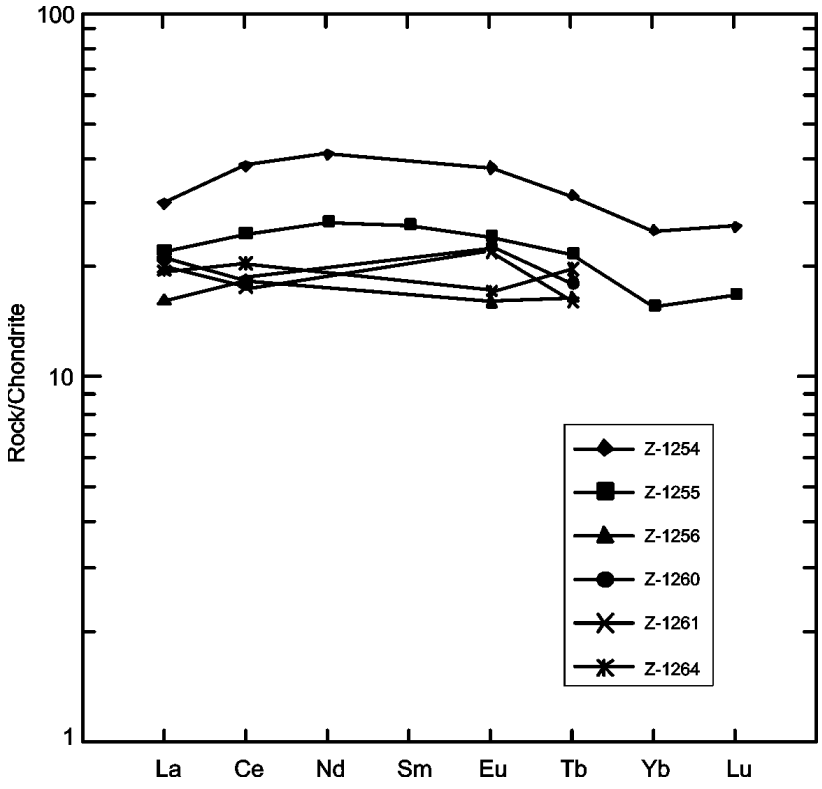

Figure F22. AFM diagram (Irvine and Baragar, 1971) for basalts in Holes 483B and 485A.

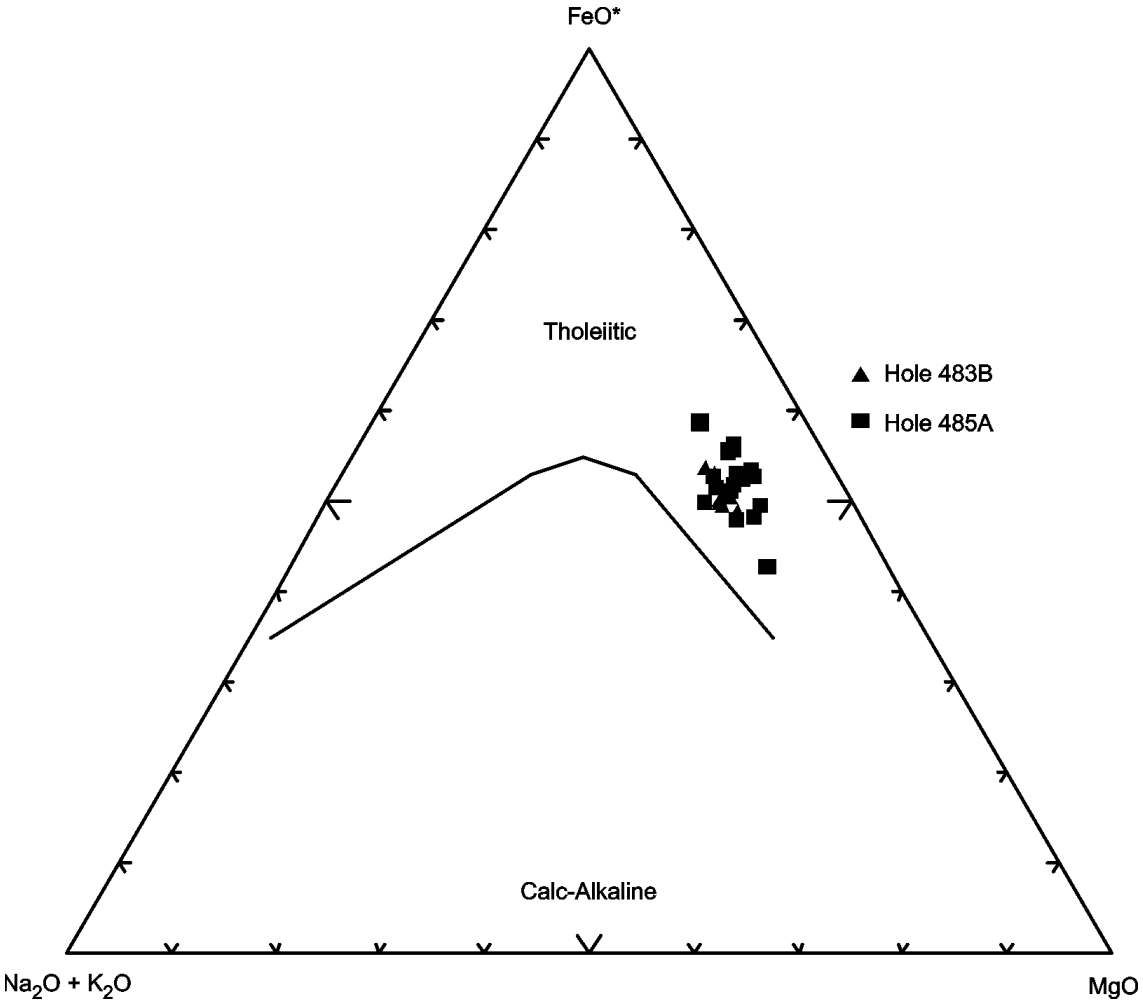

Figure F23. Discrimination Nb-Zr-Y diagram (Meschede, 1986) for basalts in Holes 483B and 485A. AI, AII = fields of intraplate alkali basalts; AII, C = fields of intraplate tholeiites; B = field of P-type MORB; D = field of N-type MORB; C, D = fields of volcanic arc basalts.

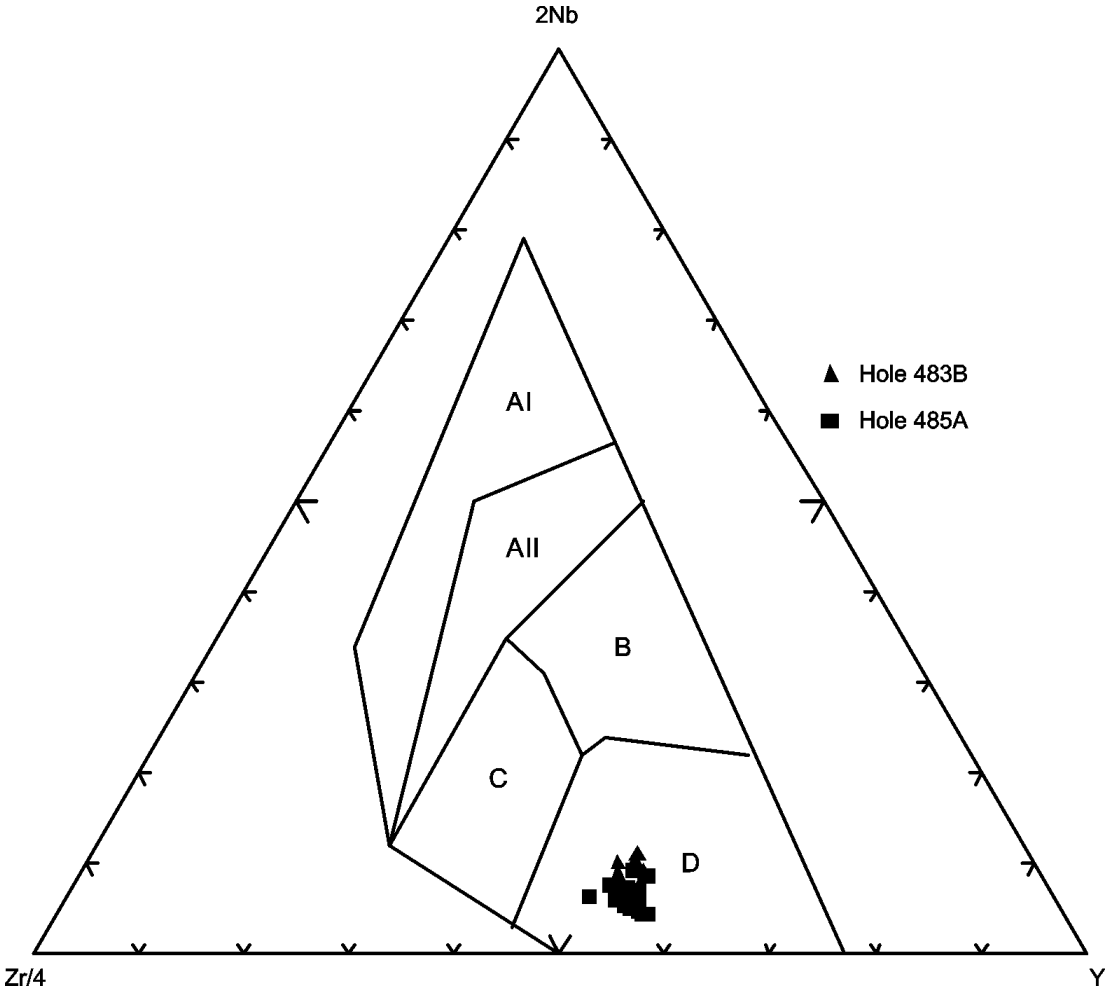

Figure F24. Chondrite-normalized rare earth element abundances for basalts in Holes 483B and 485A. Normalizing values are from Sun and McDonough (1989).

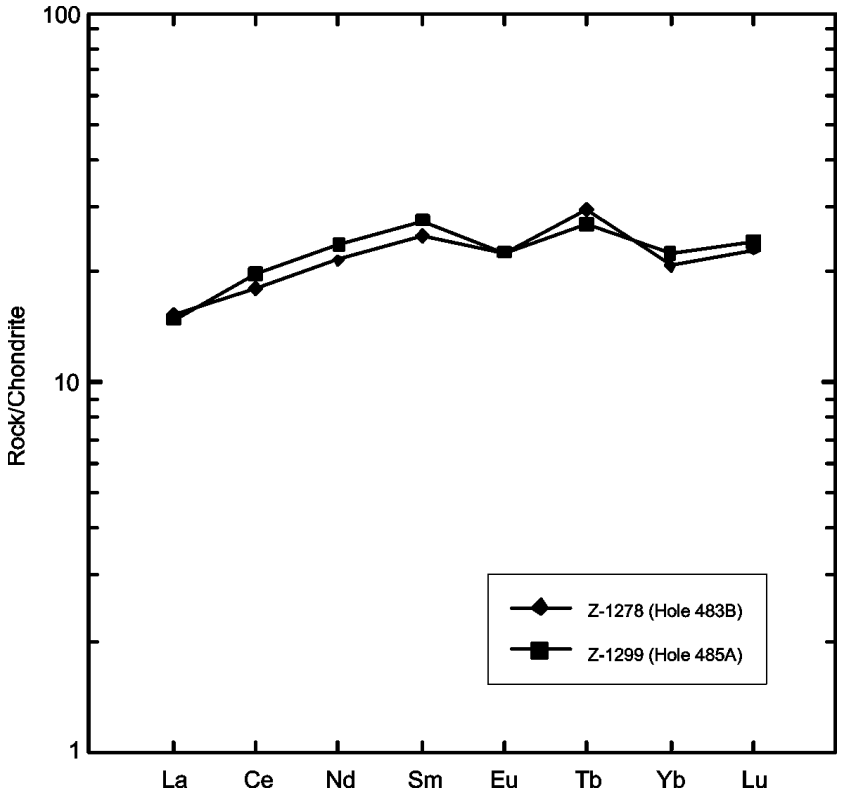

Figure F25. AFM diagram (Irvine and Baragar, 1971) for basalts in Holes 469, 471, and 473.

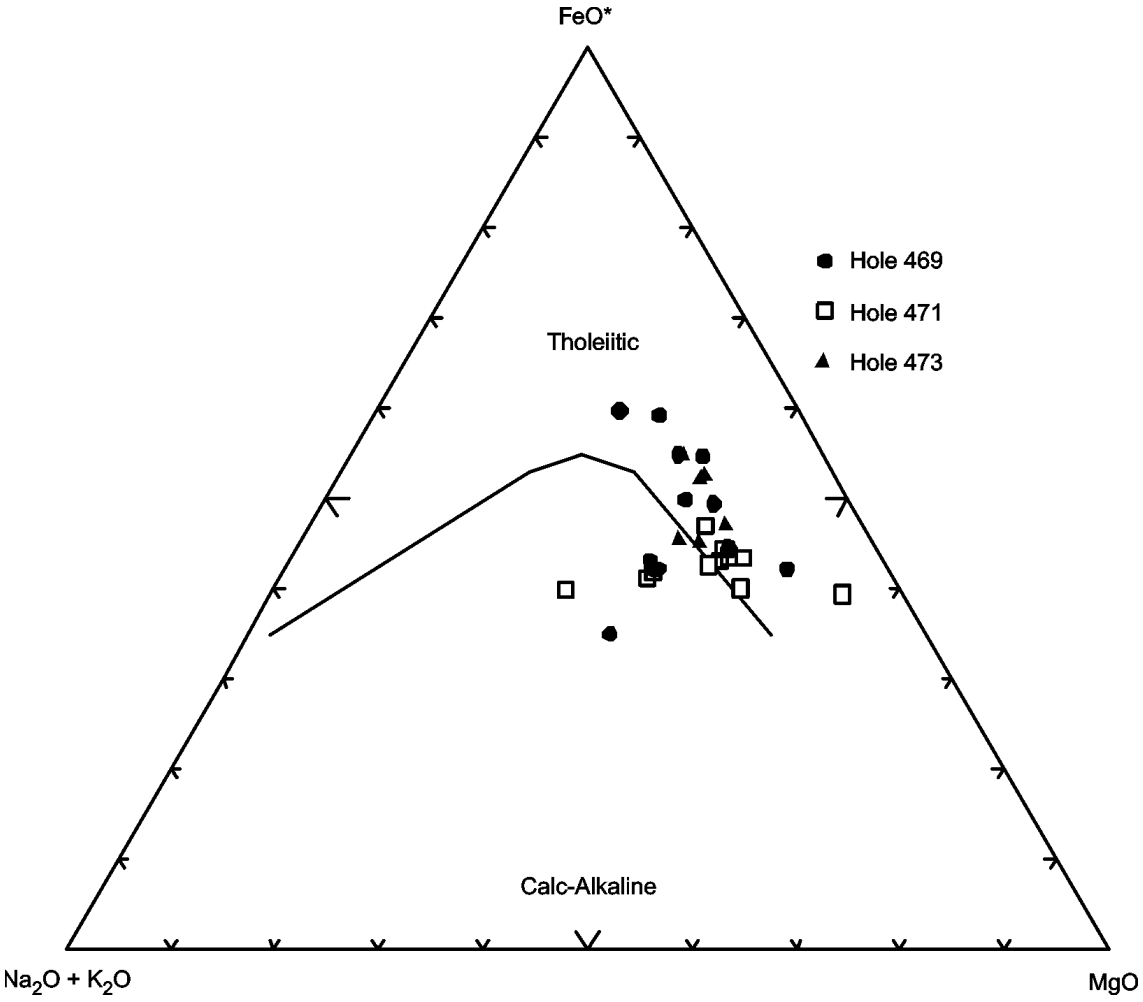

Figure F26. Discrimination Nb-Zr-Y diagram (Meschede, 1986) for basalts in Holes 469, 471, and 473. AI, AII = fields of intraplate alkali basalts; AII, C = fields of intraplate tholeiites; B = field of P-type MORB; D = field of N-type MORB; C, D = fields of volcanic arc basalts.

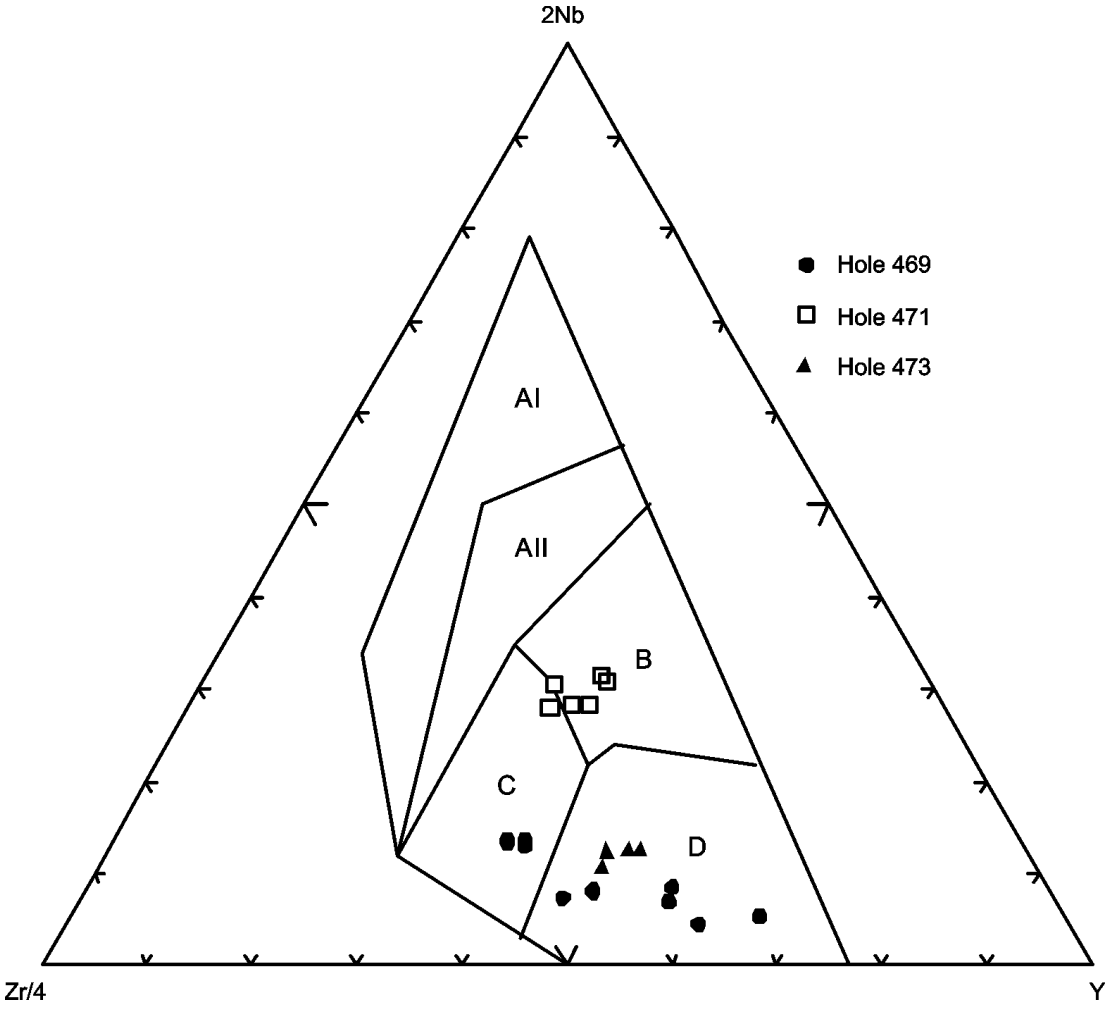

Figure F27. Chondrite-normalized rare earth element abundances for basalts in Holes 469, 471, and 473. Normalizing values are from Sun and McDonough (1989).

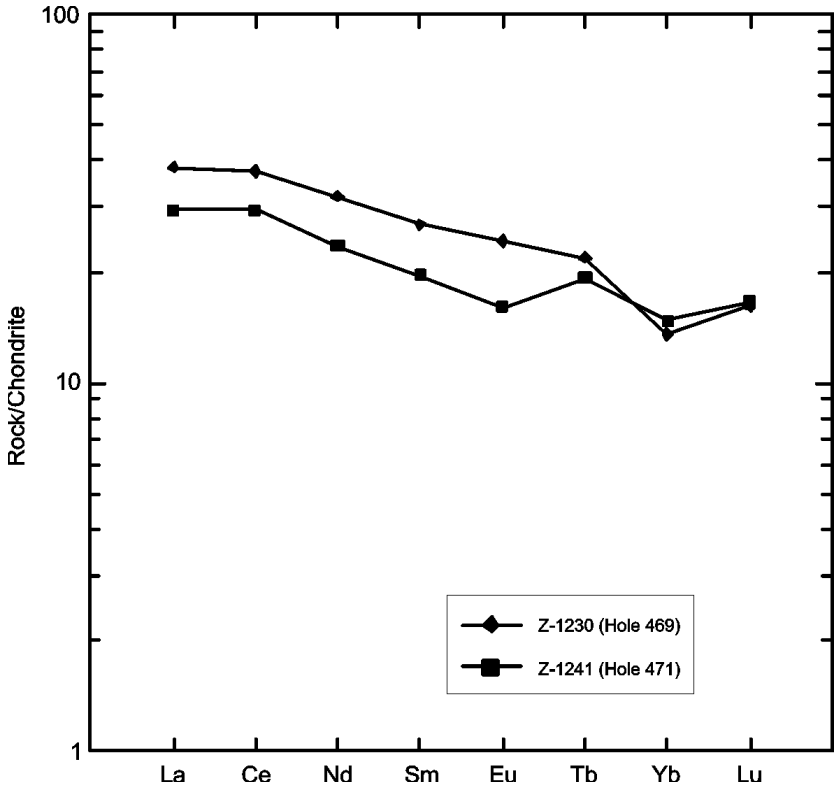

Figure F28. Leg 37 FAMOUS area in the northern Atlantic Ocean (from Aumento, Melson, et al., 1977).

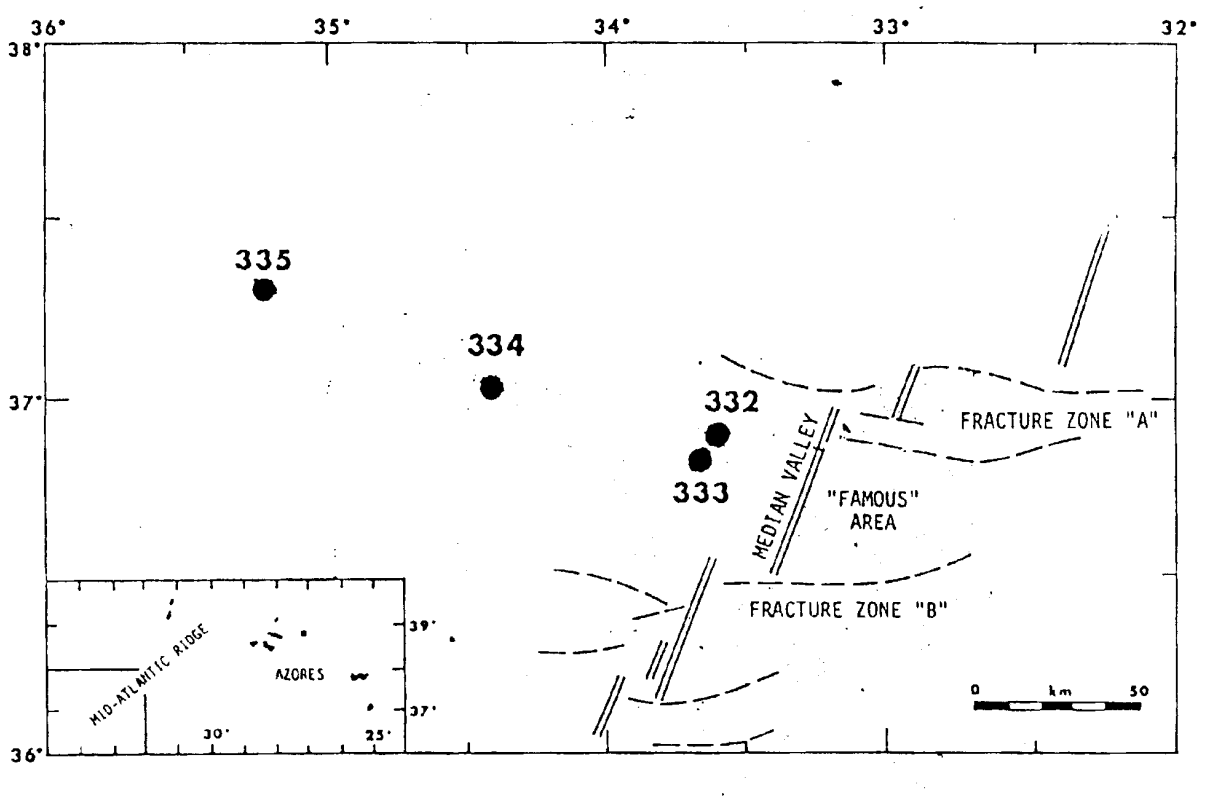

Figure F29. AFM diagram (Irvine and Baragar, 1971) for basalts in Hole 332B.

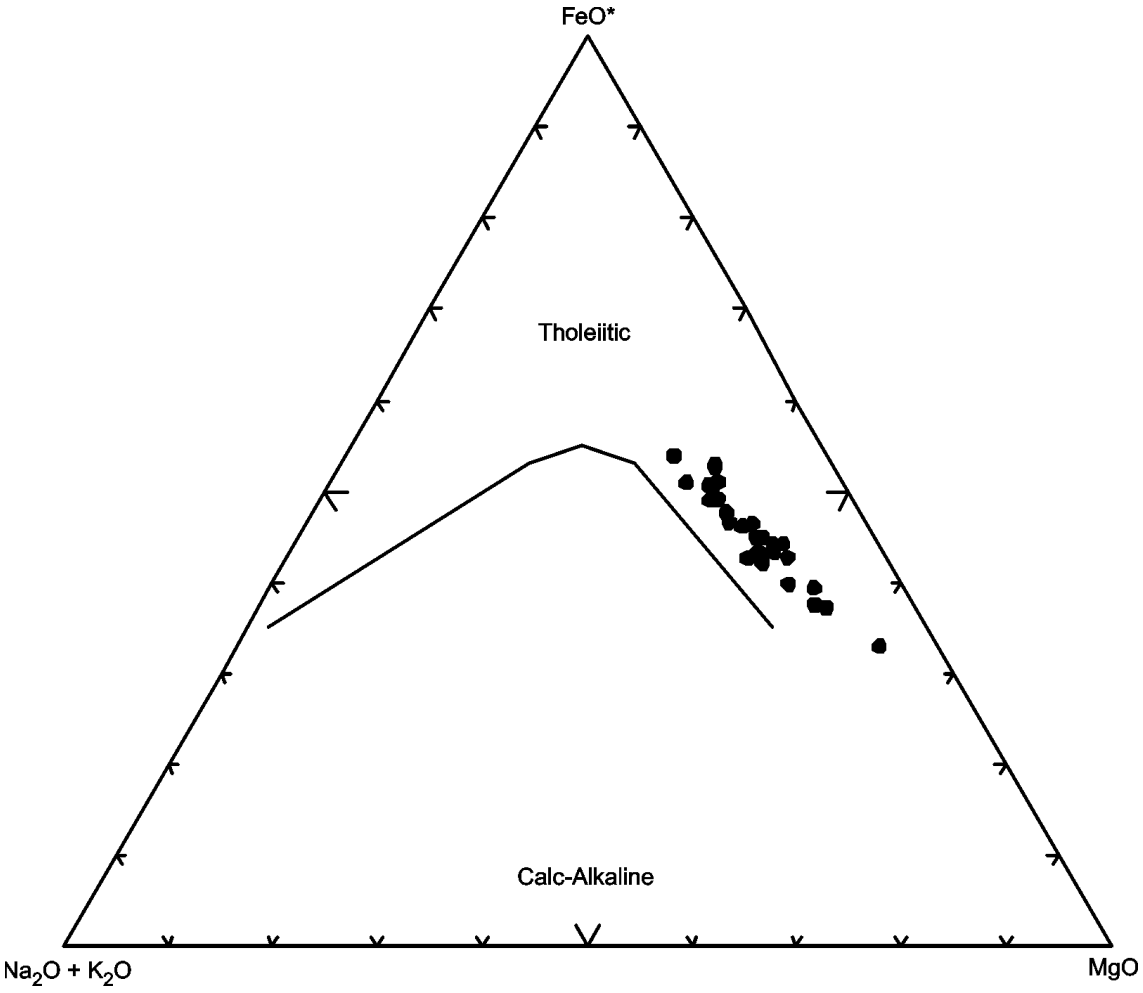

Figure F30. Discrimination Nb-Zr-Y diagram (Meschede, 1986) for basalts in Hole 332B. AI, AII = fields of intraplate alkali basalts; AII, C = fields of intraplate tholeiites; B = field of P-type MORB; D = field of N-type MORB; C, D = fields of volcanic arc basalts.

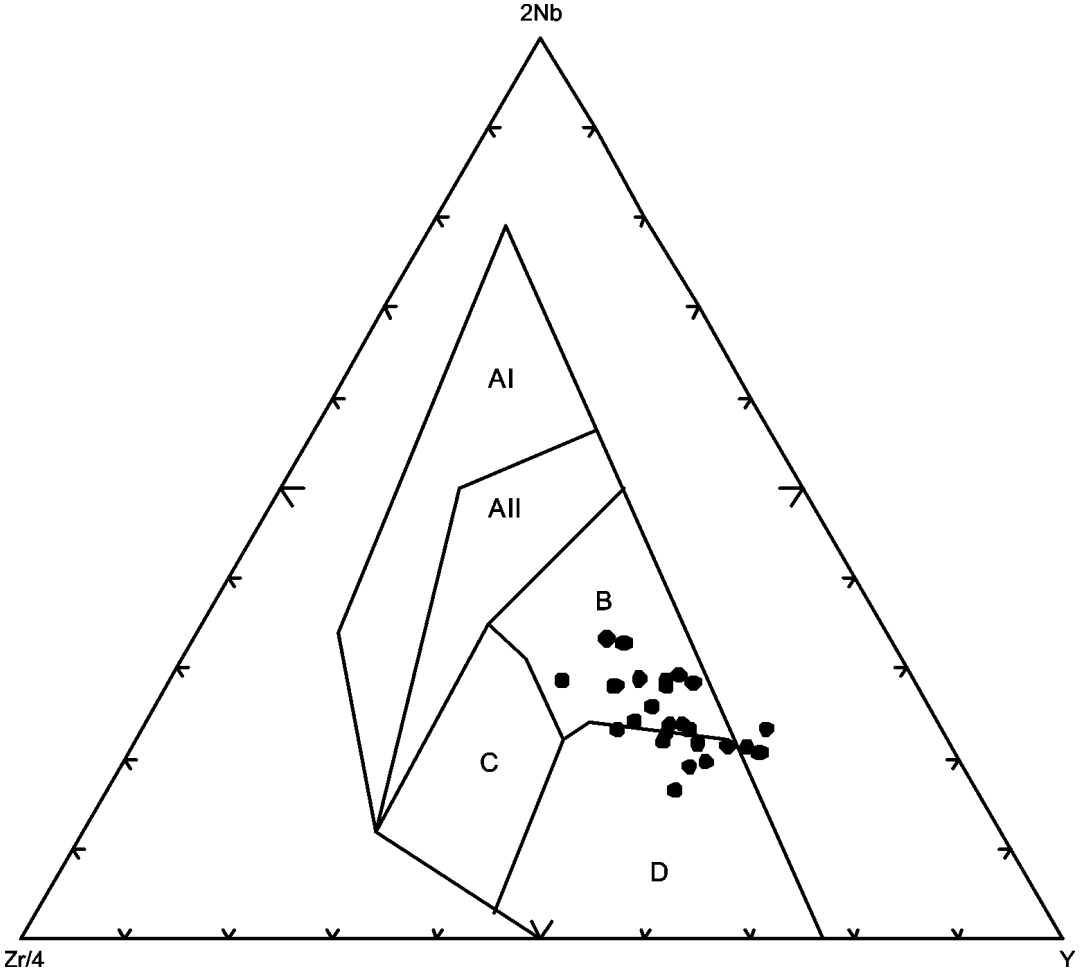

Figure F31. Chondrite-normalized rare earth element abundances for basalts in Hole 332B. Normalizing values are from Sun and McDonough (1989).

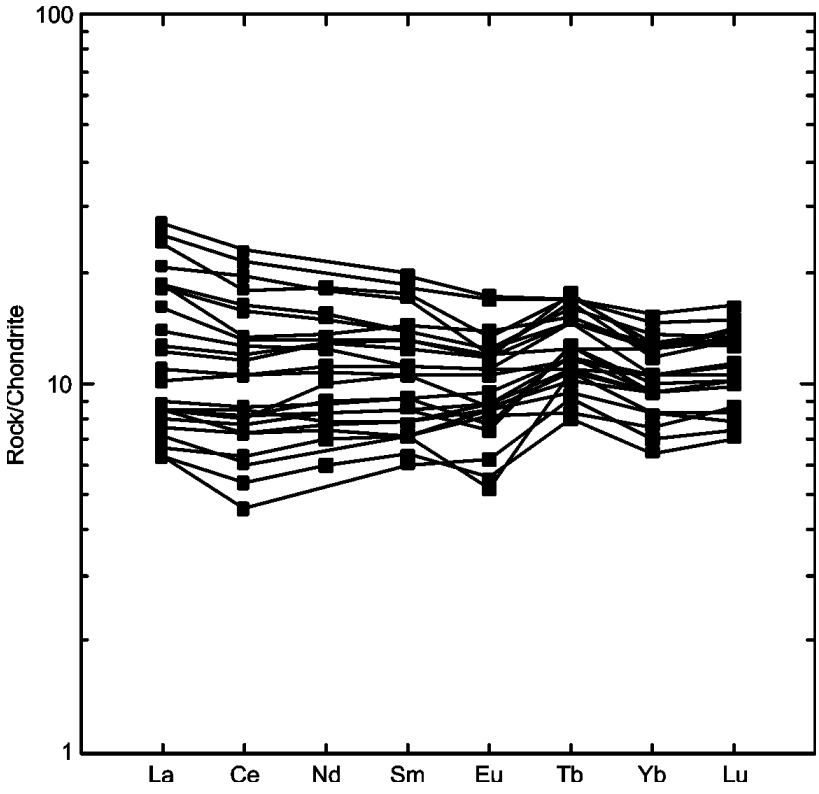

Figure F32. Site 648 drilled during Leg 106 in the Kane Fracture Zone, Atlantic Ocean (from Detrick, Honnorez, et al., 1988).

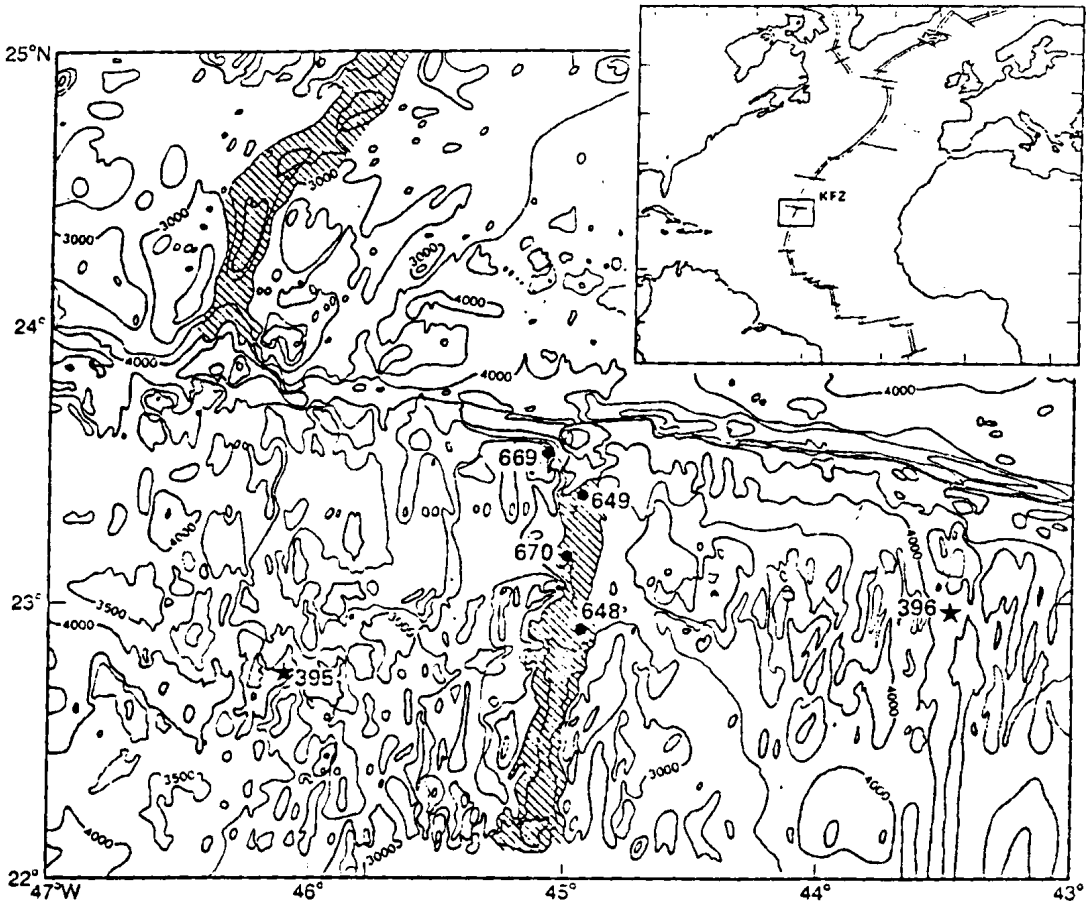

Figure F33. AFM diagram (Irvine and Baragar, 1971) for basalts in Hole 848B.

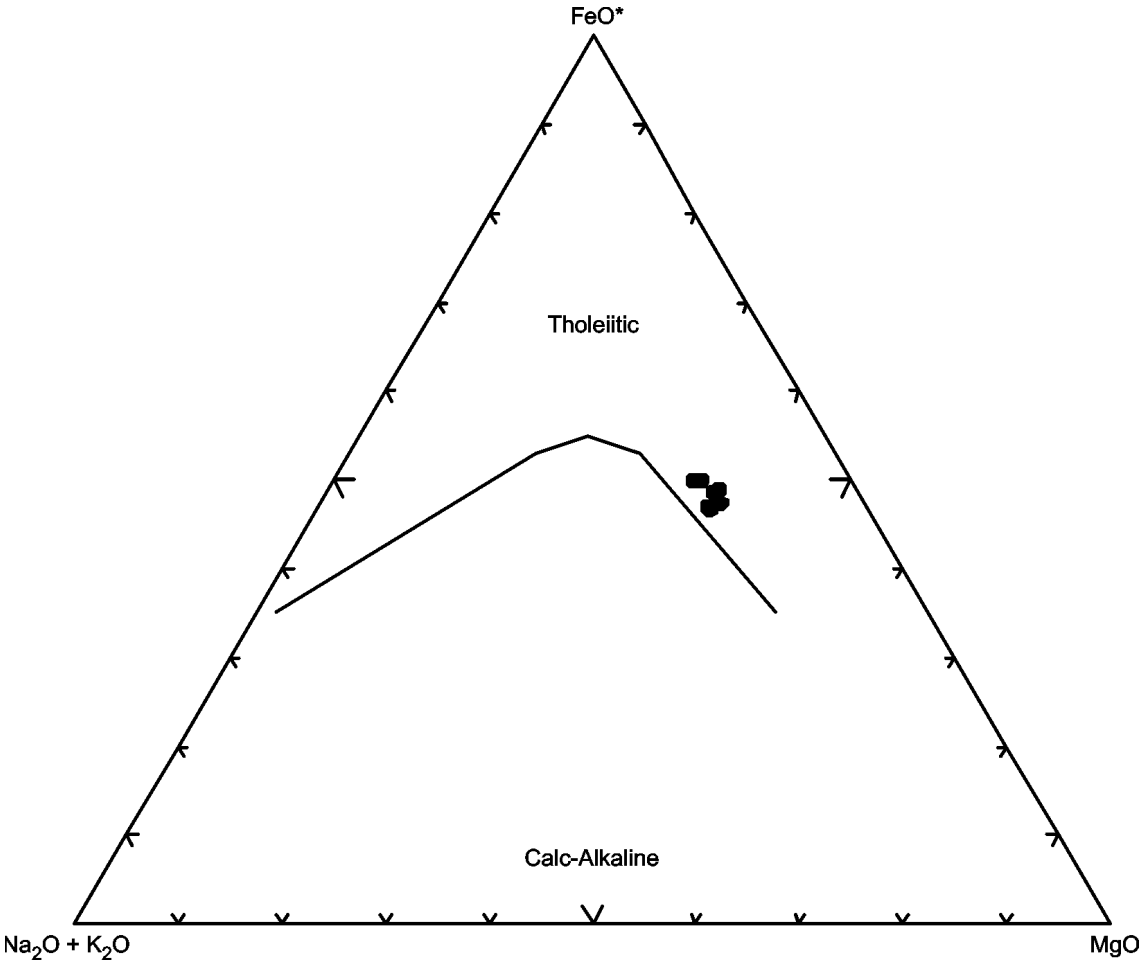

Figure F34. Discrimination Nb-Zr-Y diagram (Meschede, 1986) for basalts in Hole 848B. AI, AII = fields of intraplate alkali basalts; AII, C = fields of intraplate tholeiites; B = field of P-type MORB; D = field of N-type MORB; C, D = fields of volcanic arc basalts.

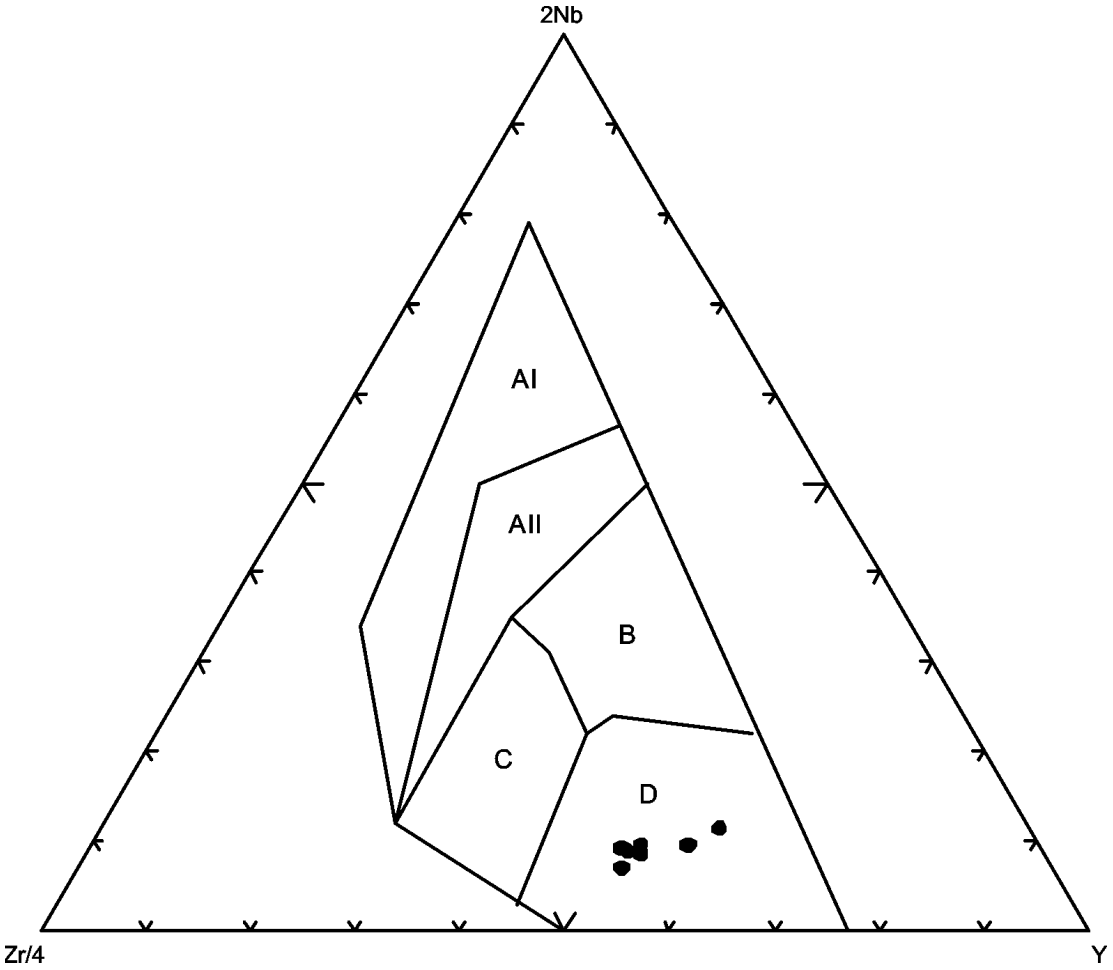

Figure F35. Chondrite-normalized rare earth element abundances for basalts in Hole 848B. Normalizing values are from Sun and McDonough (1989).

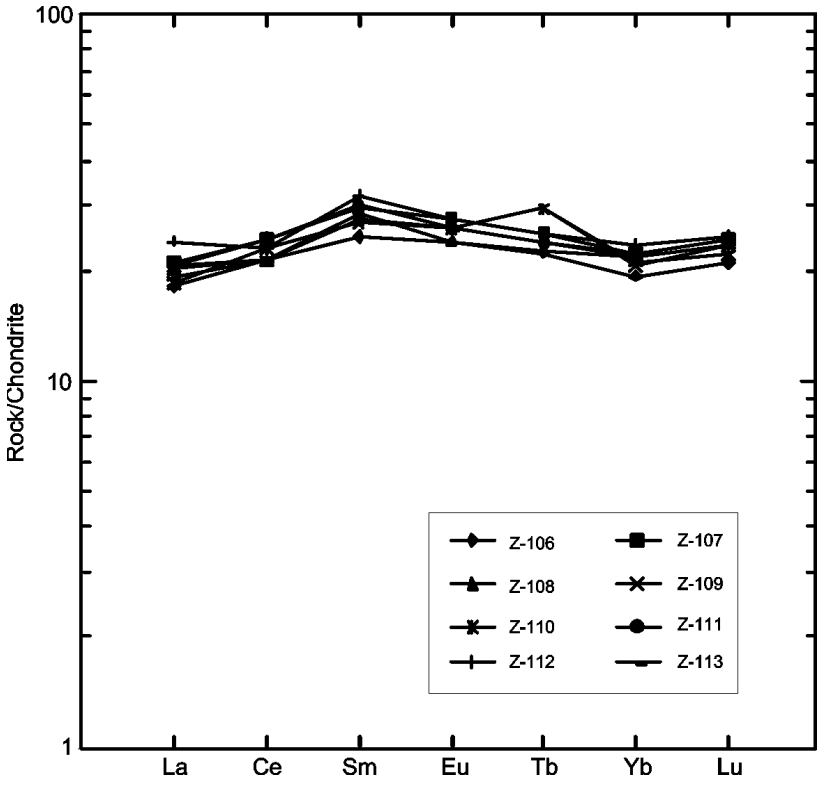

Figure F36. Site 462 drilled during Leg 61 in the Nauru Basin, western Pacific Ocean (from Larson, Schlanger, et al., 1981). IPOD = International Phase of Ocean Drilling.

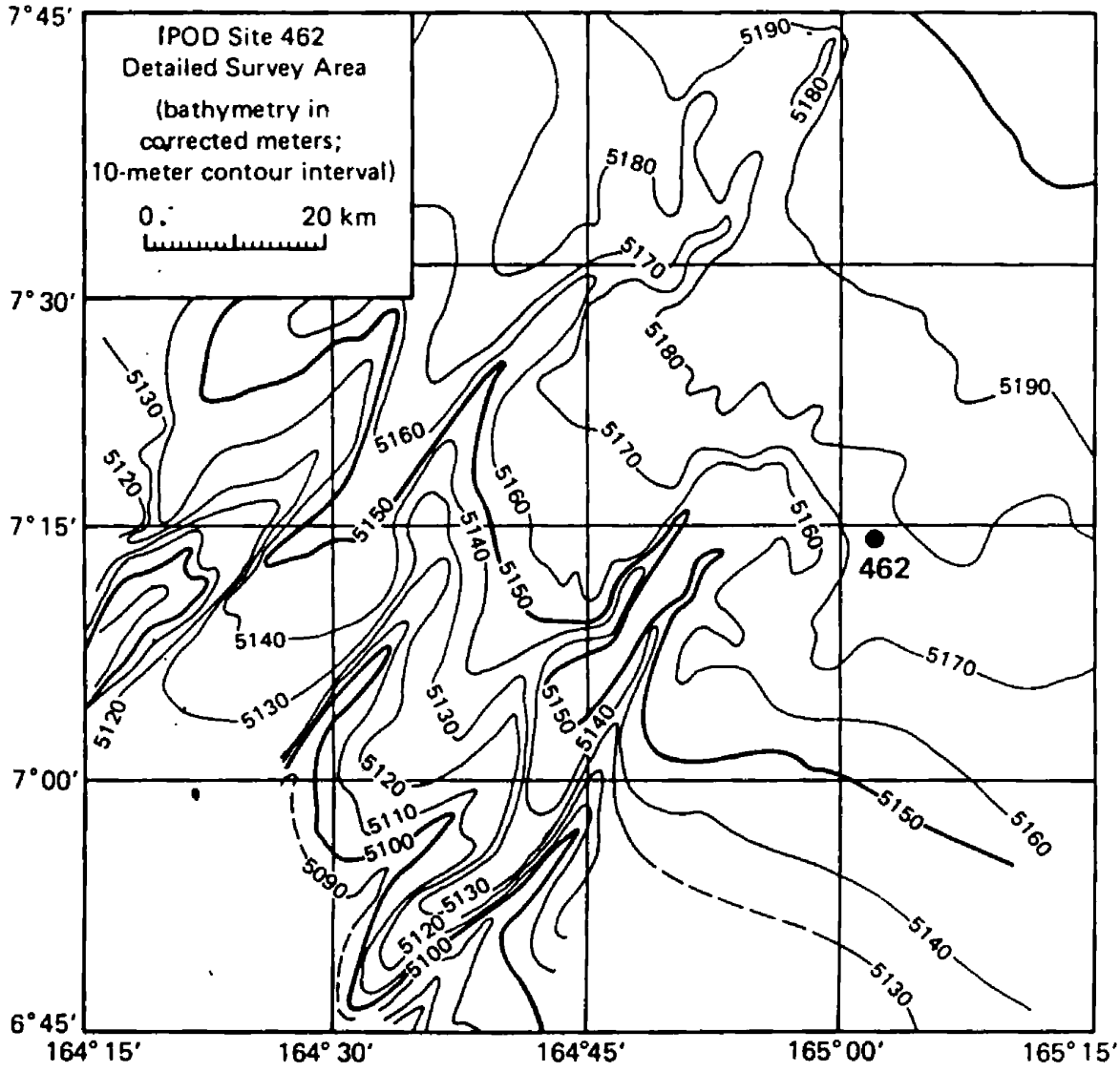

Figure F37. AFM diagram (Irvine and Baragar, 1971) for basalts in Holes 462 and 462A.

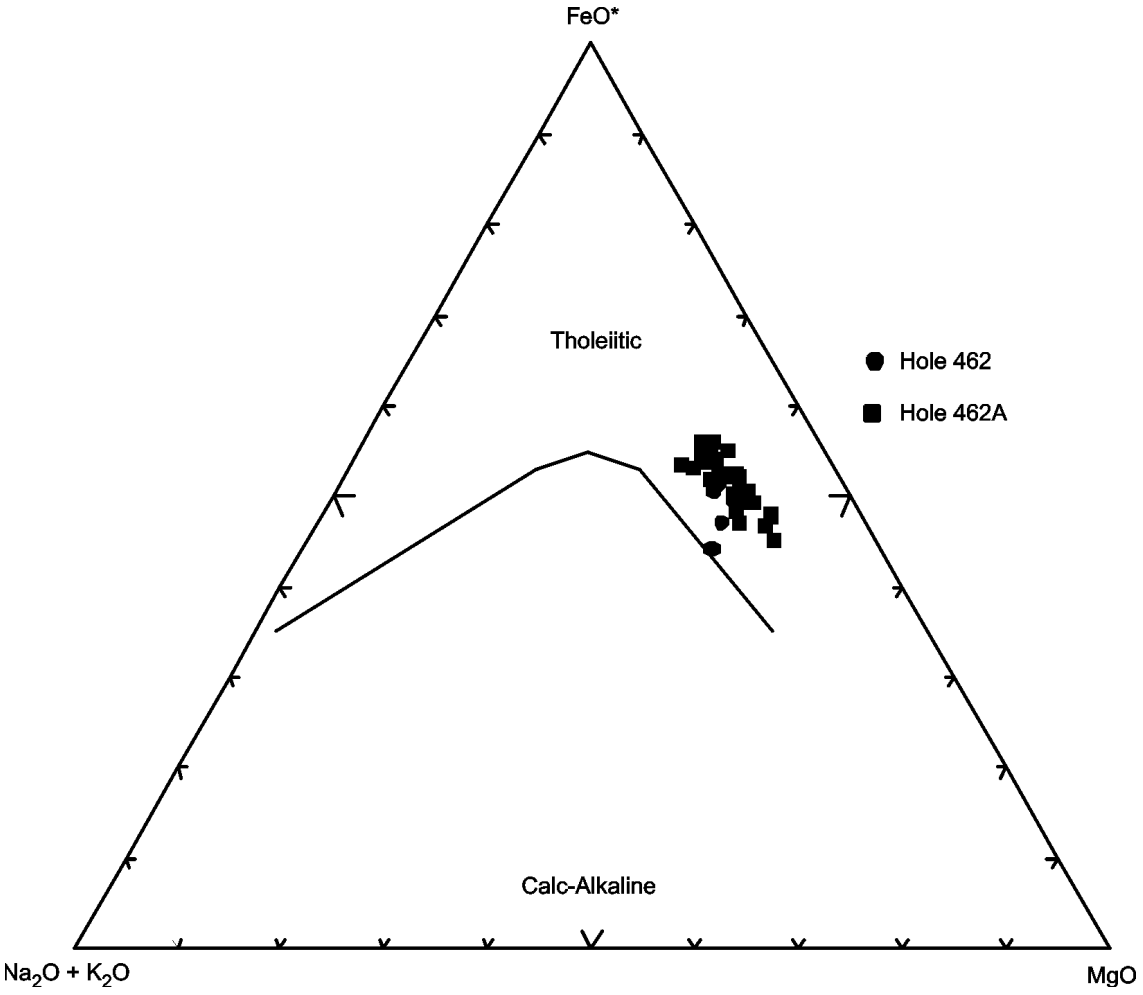

Figure F38. Discrimination Nb-Zr-Y diagram (Meschede, 1986) for basalts in Holes 462 and 462A. AI, AII = fields of intraplate alkali basalts; AII, C = fields of intraplate tholeiites; B = field of P-type MORB; D = field of N-type MORB; C, D = fields of volcanic arc basalts.

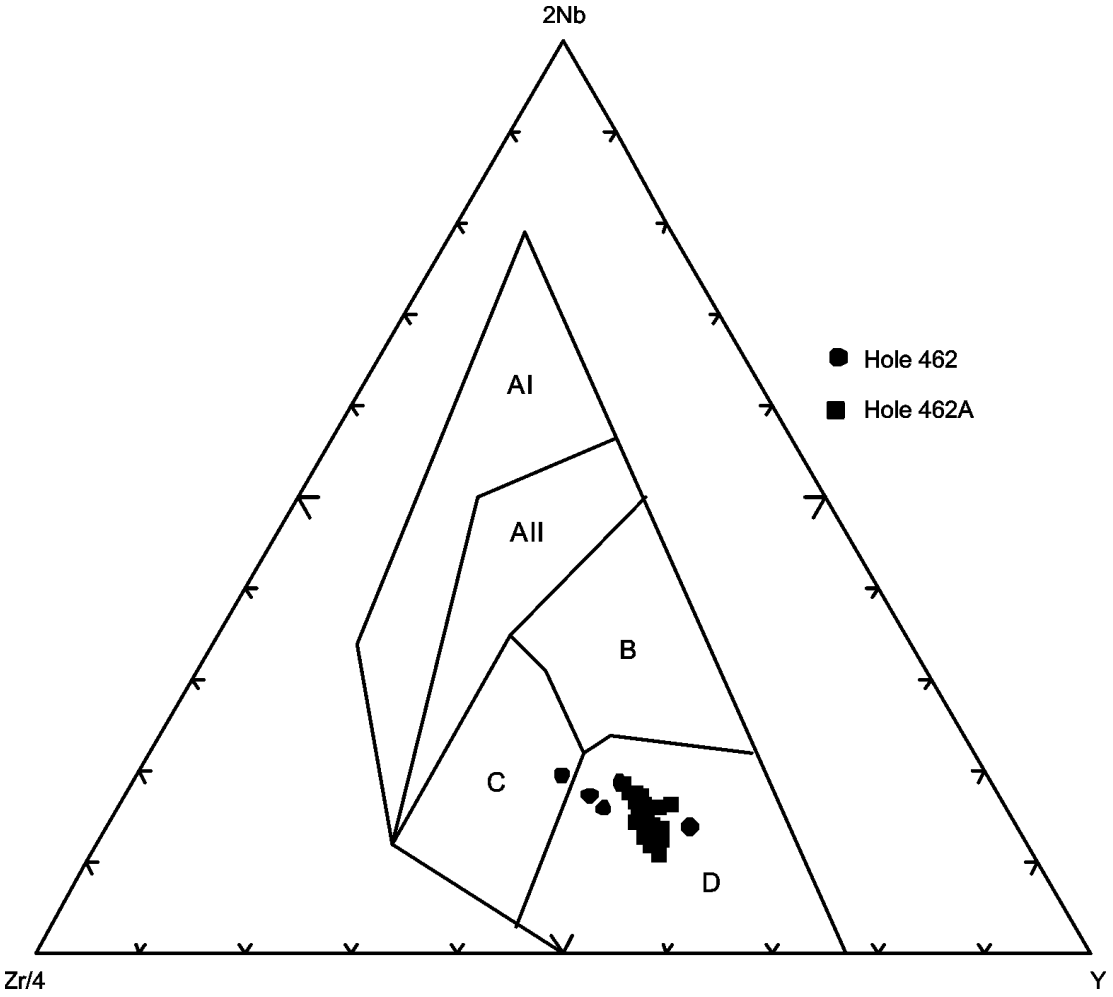

Figure F39. Chondrite-normalized rare earth element abundances for basalts in Holes 462 and 462A. Normalizing values are from Sun and McDonough (1989).

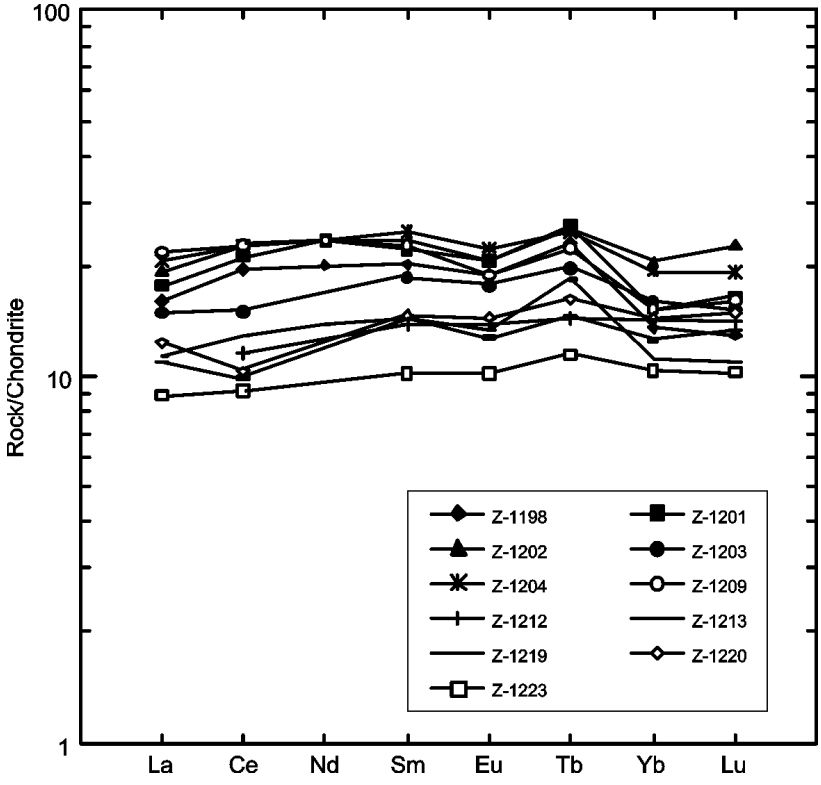

Figure F40. Southwestern Pacific Ocean and location of Site 595 drilled during Leg 91 (from Duennebier, Stephen, Gettrust, et al., 1987).

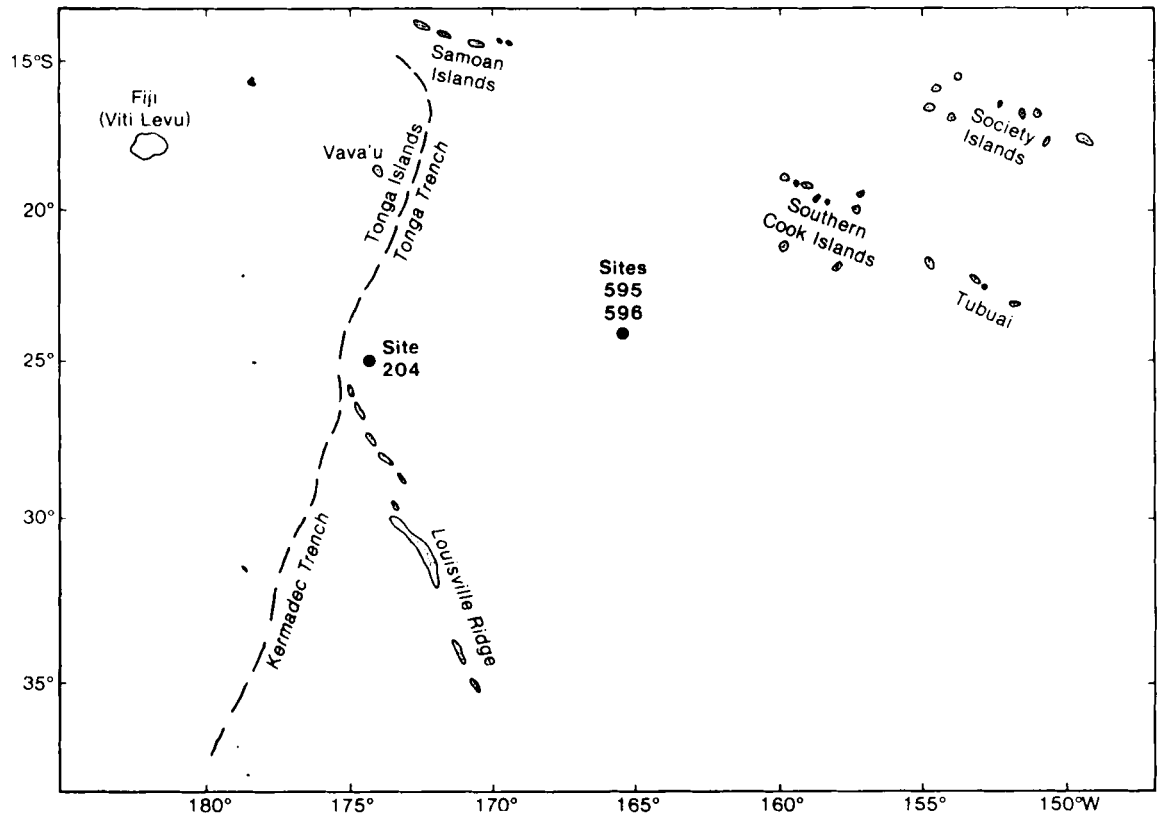

Figure F41. AFM diagram (Irvine and Baragar, 1971) for basalts in Hole 595B.

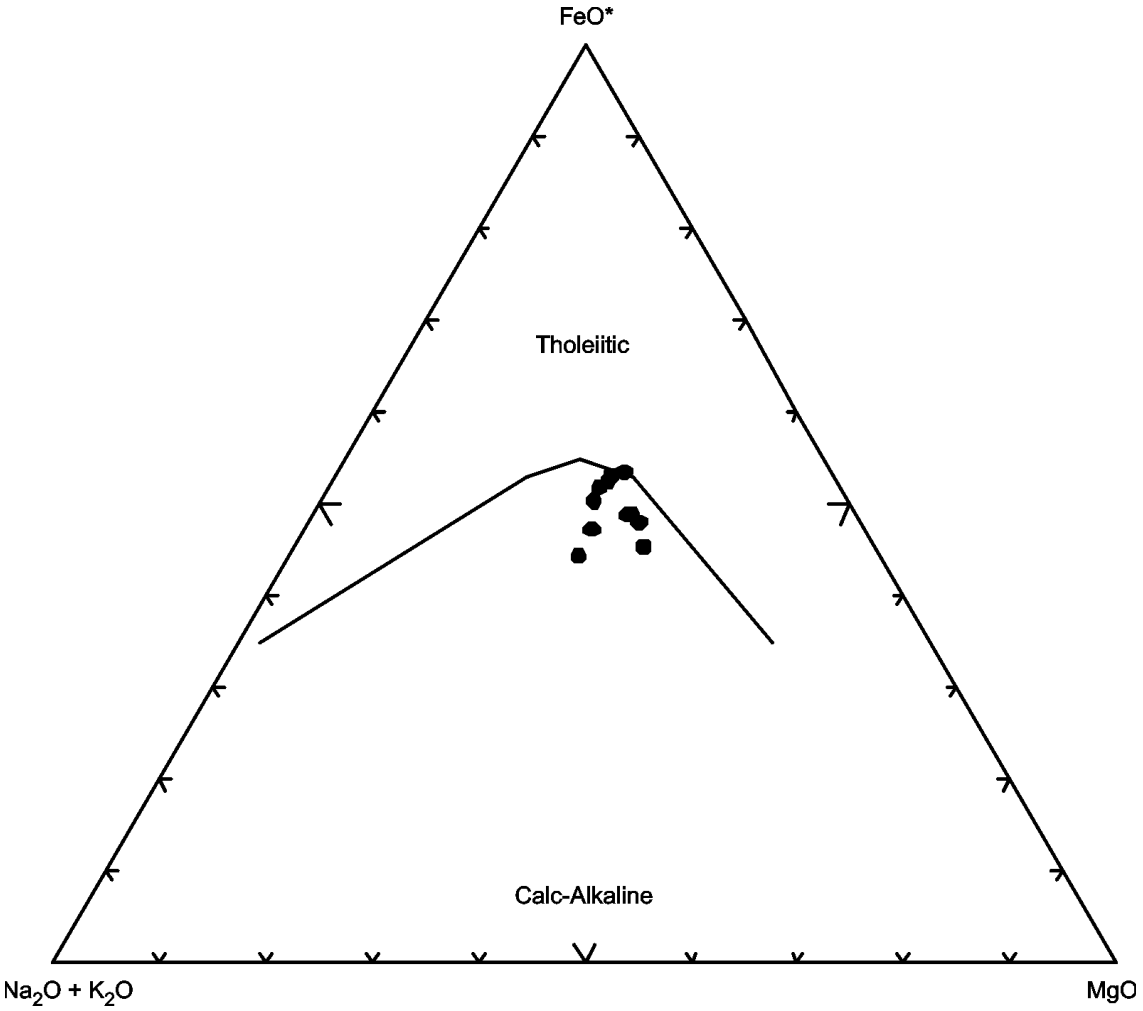

Figure F42. Discrimination Nb-Zr-Y diagram (Meschede, 1986) for basalts in Hole 595B. AI, AII = fields of intraplate alkali basalts; AII, C = fields of intraplate tholeiites; B = field of P-type MORB; D = field of N-type MORB; C, D = fields of volcanic arc basalts.

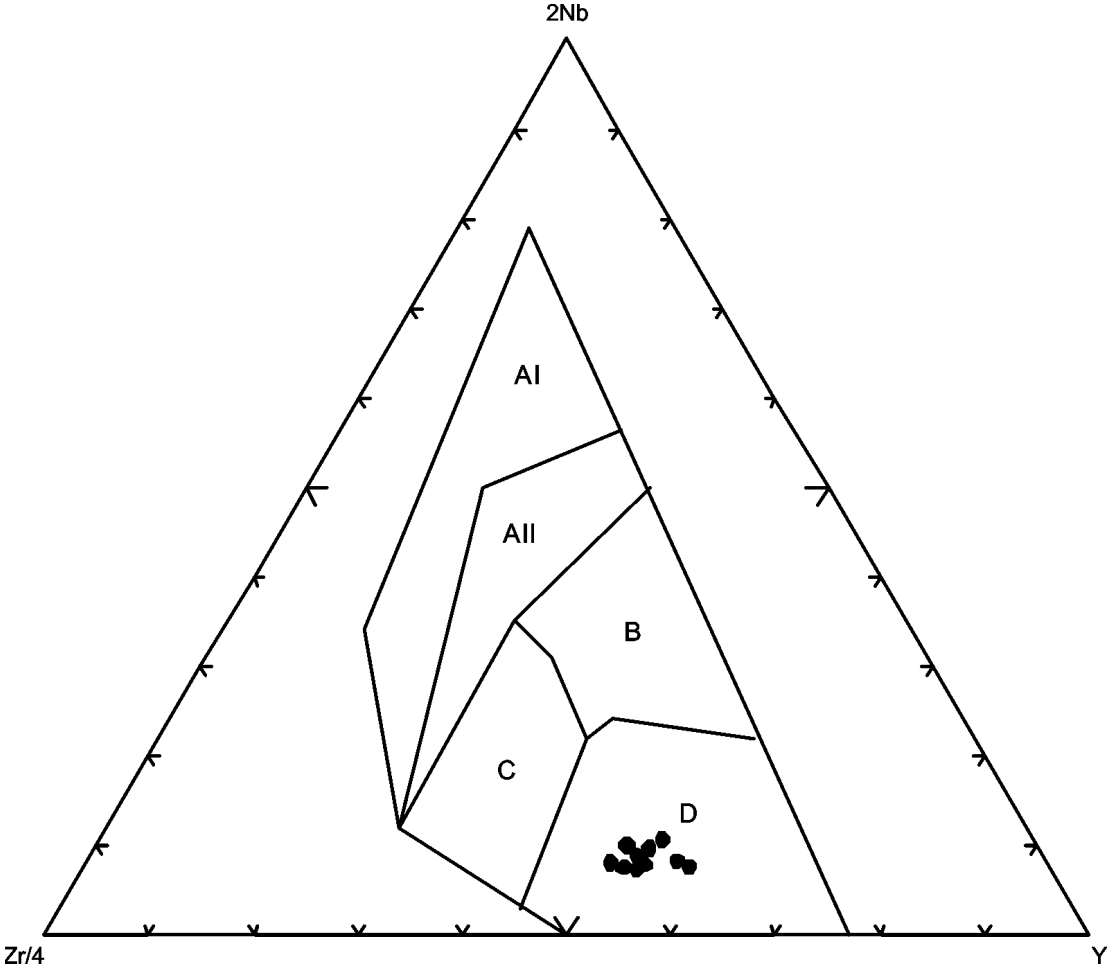

Figure F43. Chondrite-normalized rare earth element abundances for basalts in Hole 595B. Normalizing values are from Sun and McDonough (1989).

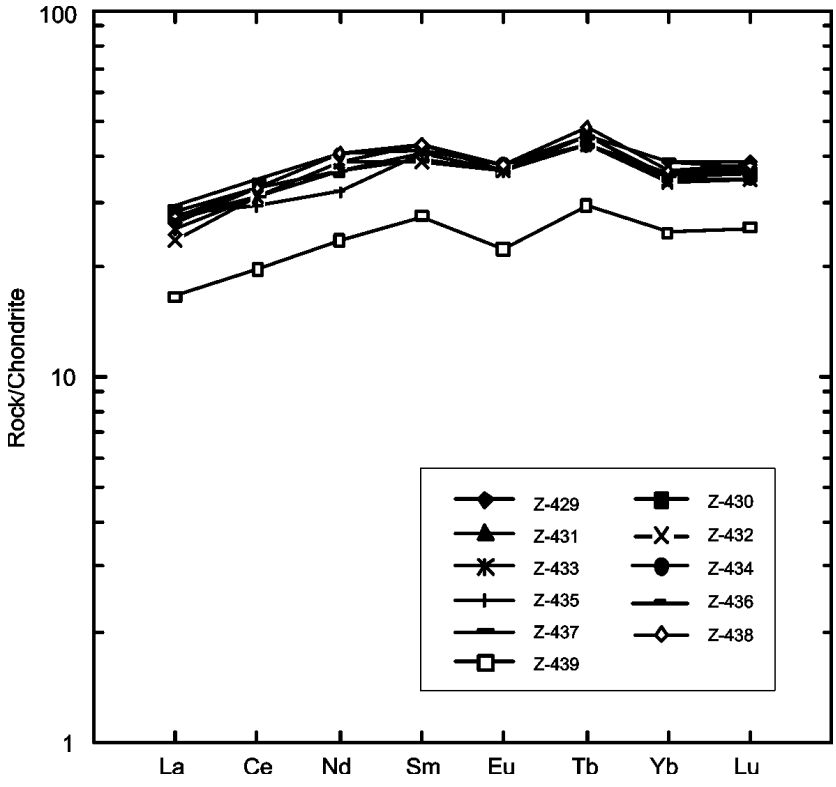

Figure F44. Site 765 drilled during Leg 123 in the Argo abyssal plain off northwestern Australia (from Gradstein, Ludden, et al., 1992).

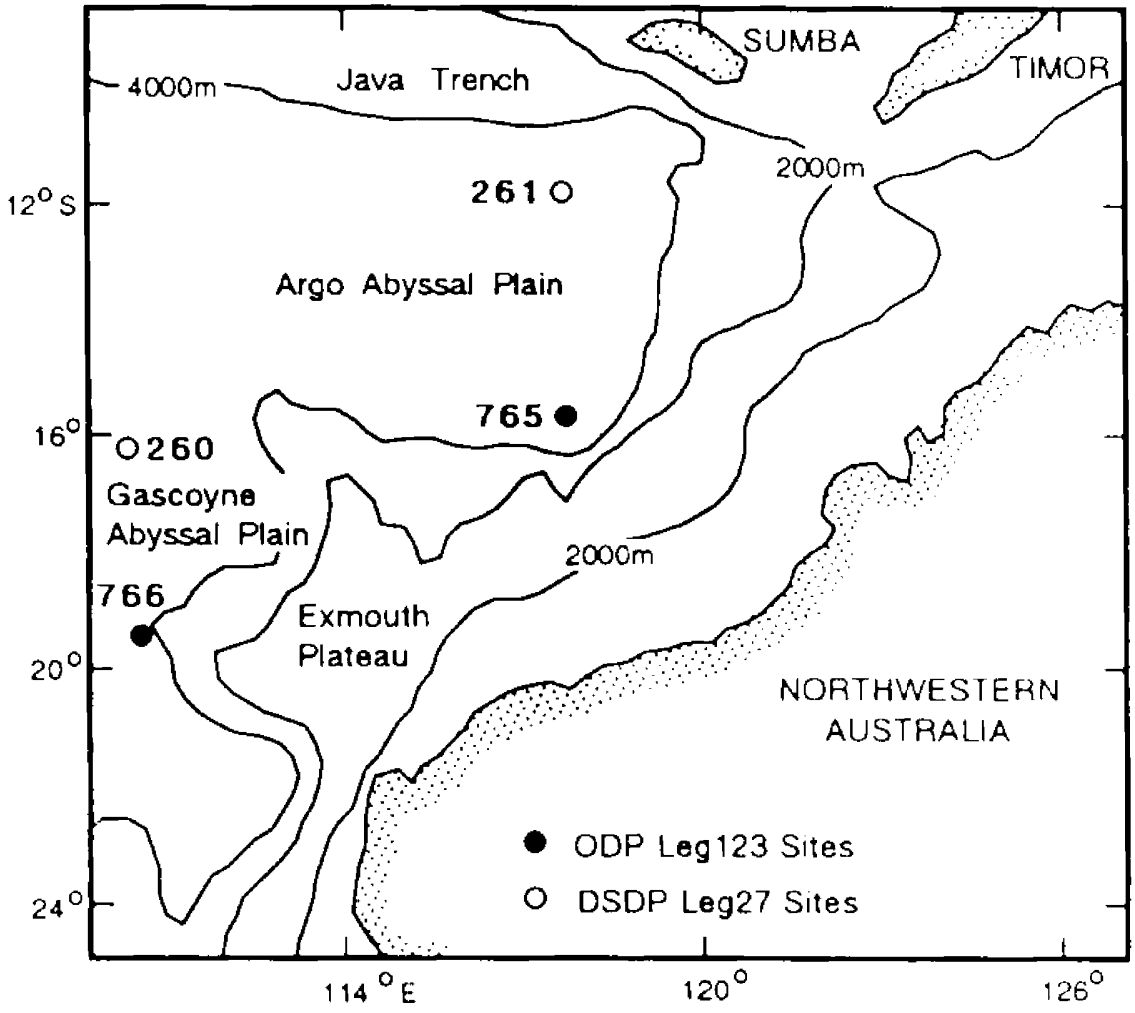

Figure F45. AFM diagram (Irvine and Baragar, 1971) for basalts in Hole 765D.

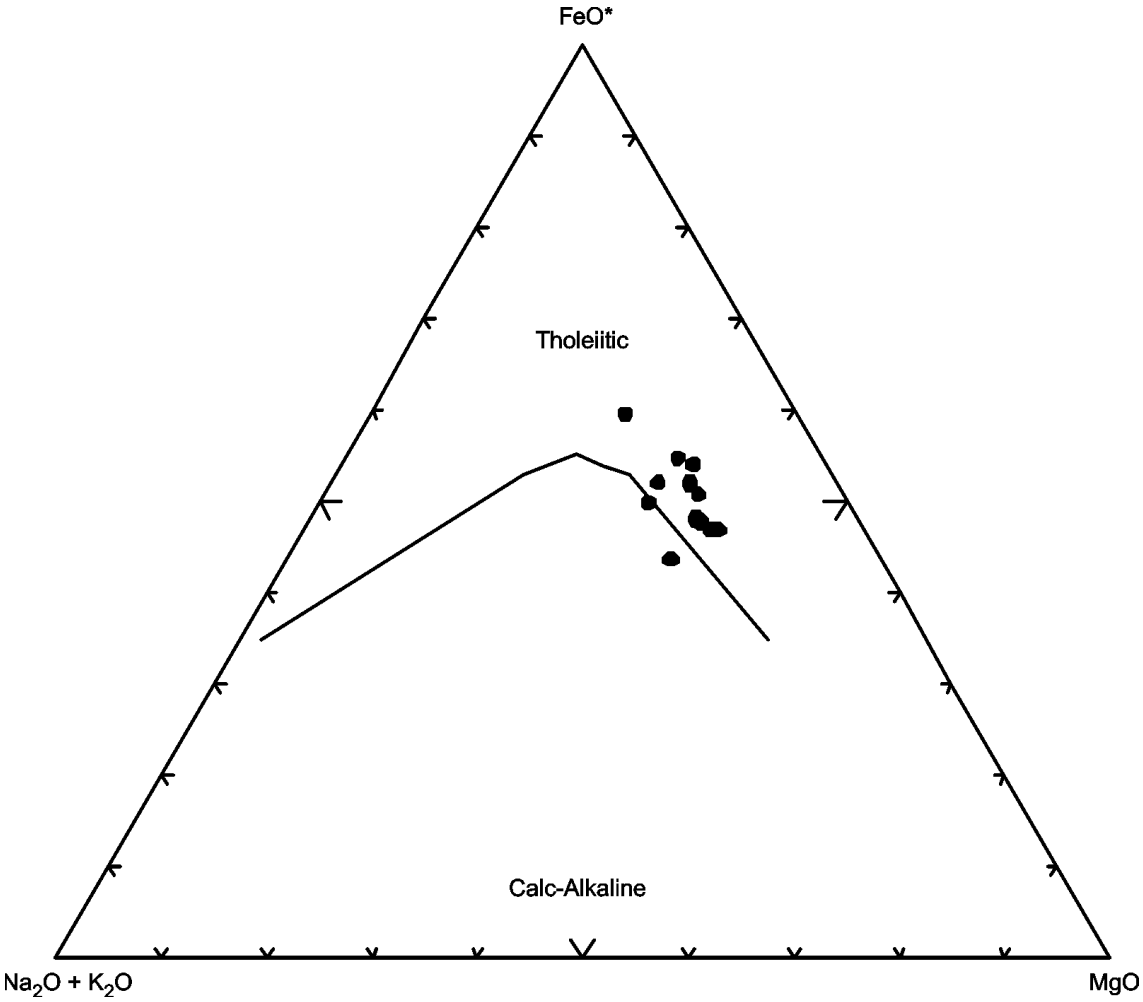

Figure F46. Discrimination Nb-Zr-Y diagram (Meschede, 1986) for basalts in Hole 765D. AI, AII = fields of intraplate alkali basalts; AII, C = fields of intraplate tholeiites; B = field of P-type MORB; D = field of N-type MORB; C, D = fields of volcanic arc basalts.

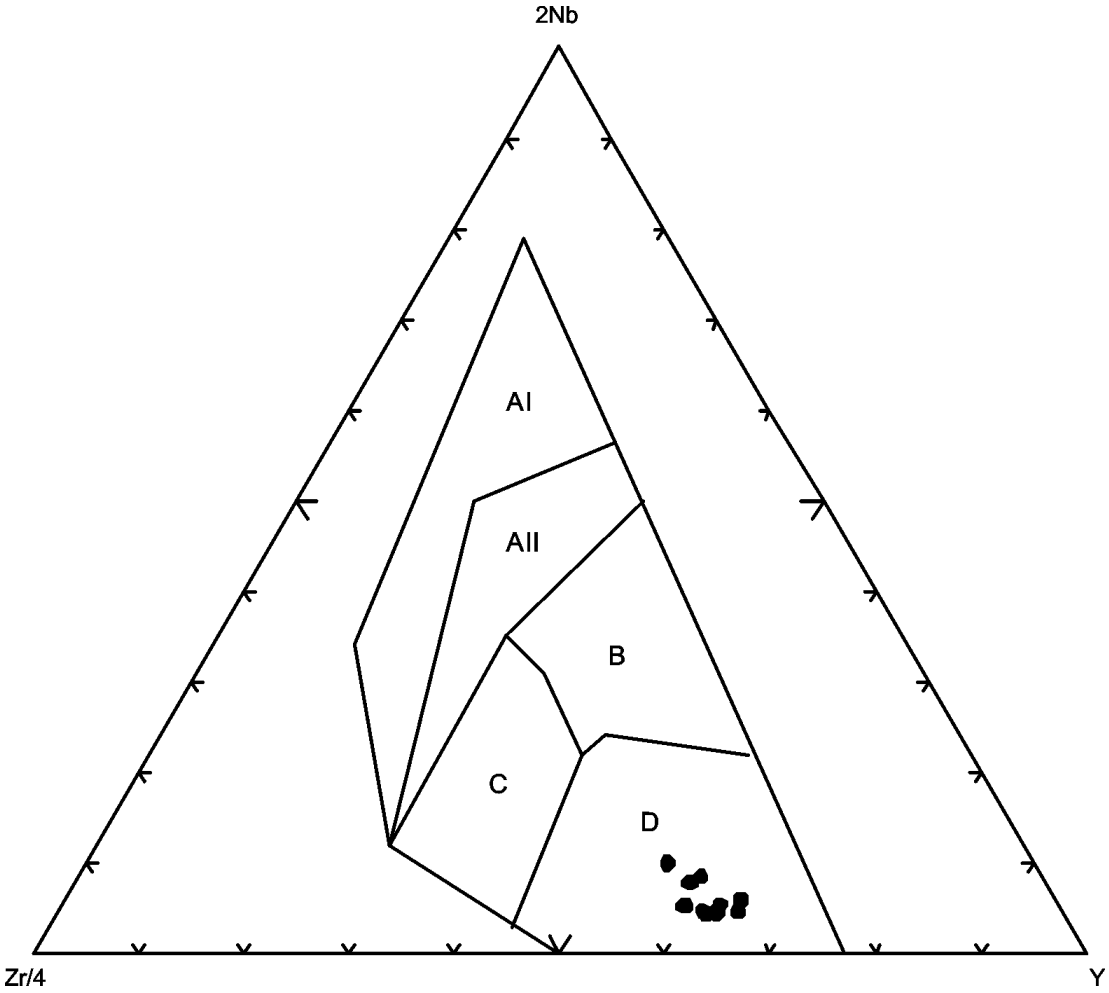

Figure F47. Chondrite-normalized rare earth element abundances for basalts in Hole 765D. Normalizing values are from Sun and McDonough (1989).

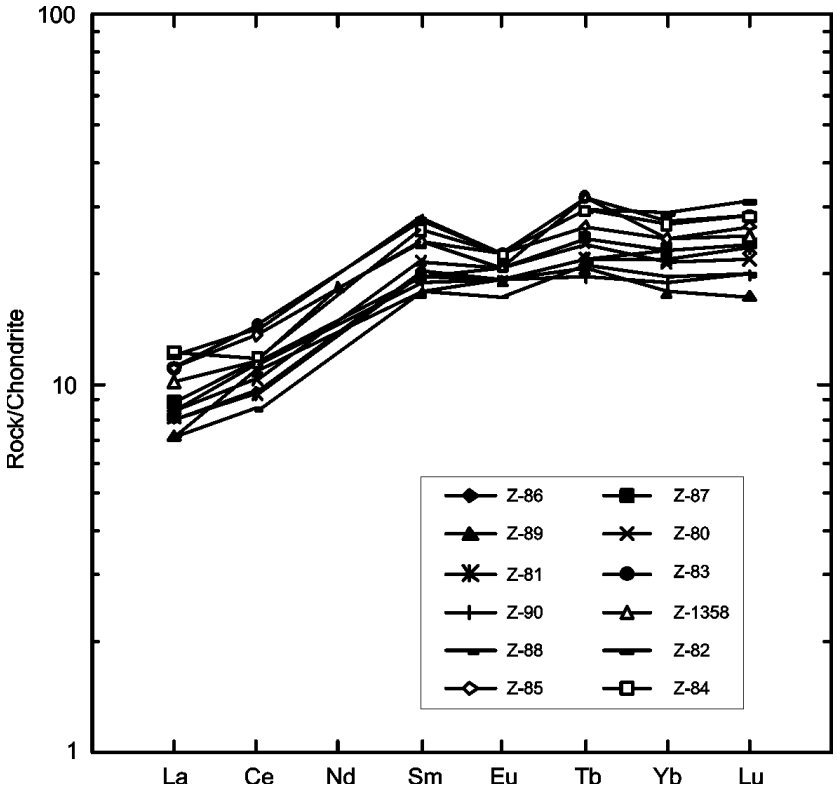

Figure F48. Site 801 drilled during Leg 129 in Pigafetta Basin, western Pacific Ocean (from Larson, Lancelot, et al., 1992).

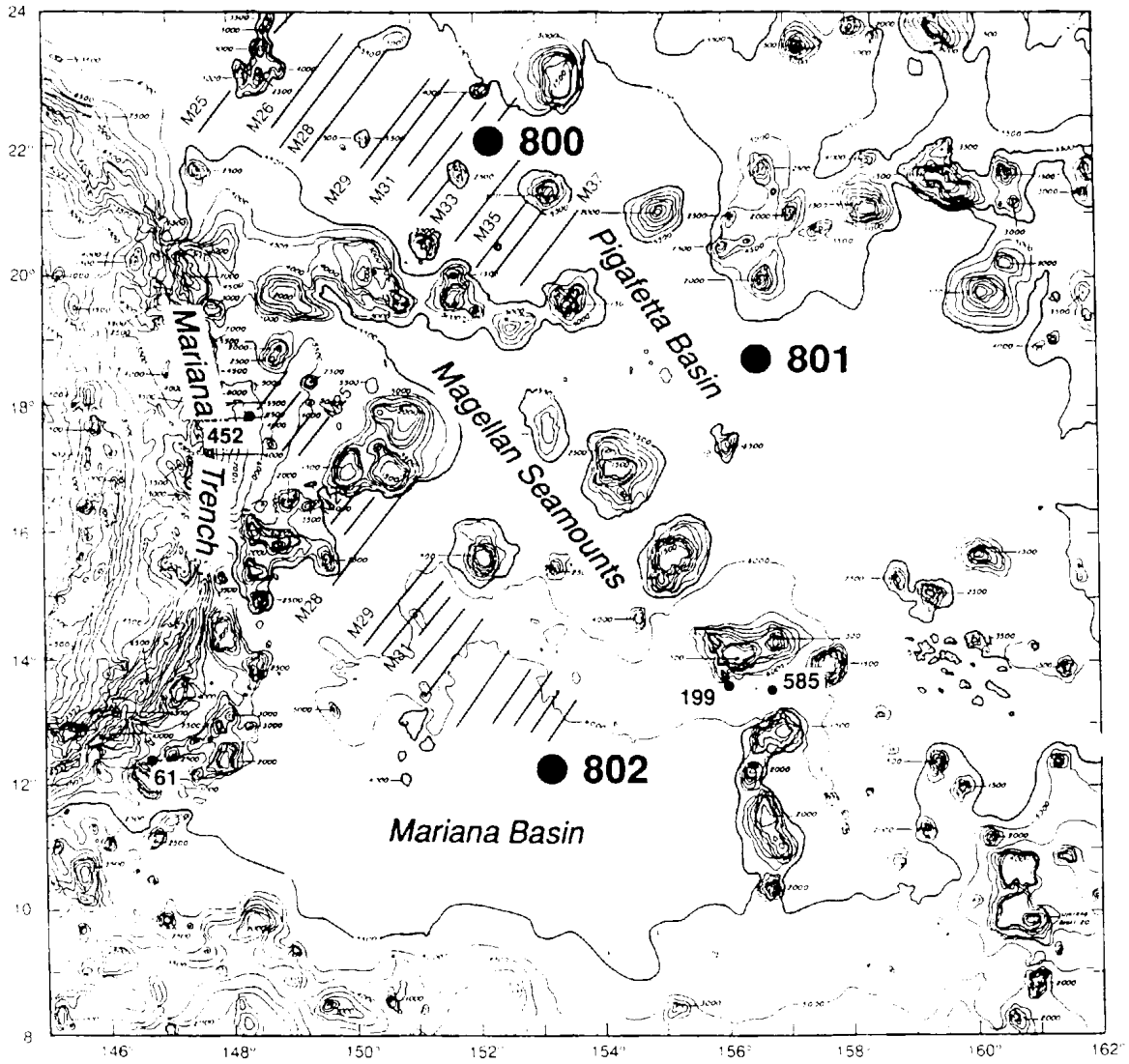

Figure F49. AFM diagram (Irvine and Baragar, 1971) for basalts in Holes 801B and 801C.

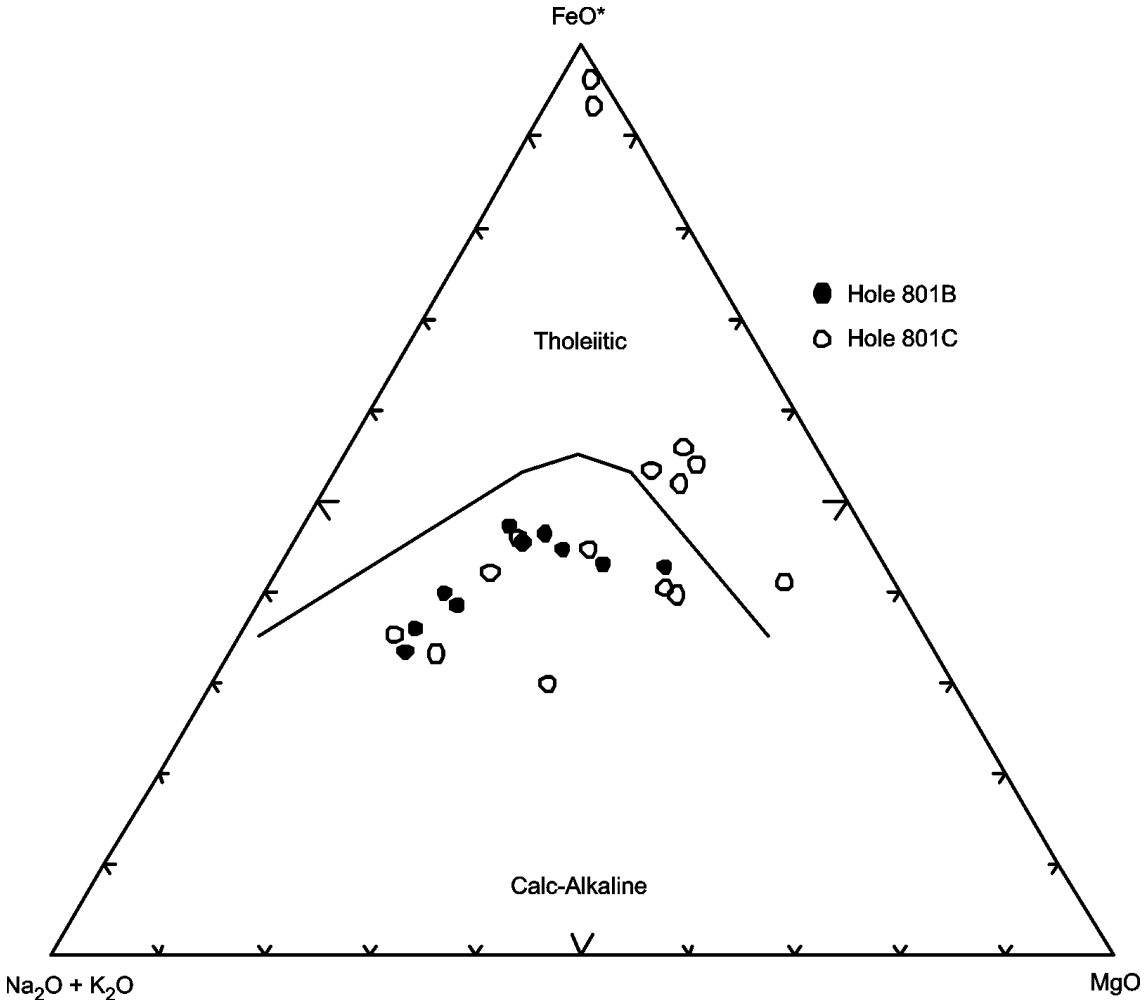

Figure F50. Discrimination Nb-Zr-Y diagram (Meschede, 1986) for basalts in Holes 801B and 801C. AI, AII = fields of intraplate alkali basalts; AII, C = fields of intraplate tholeiites; B = field of P-type MORB; D = field of N-type MORB; C, D = fields of volcanic arc basalts.

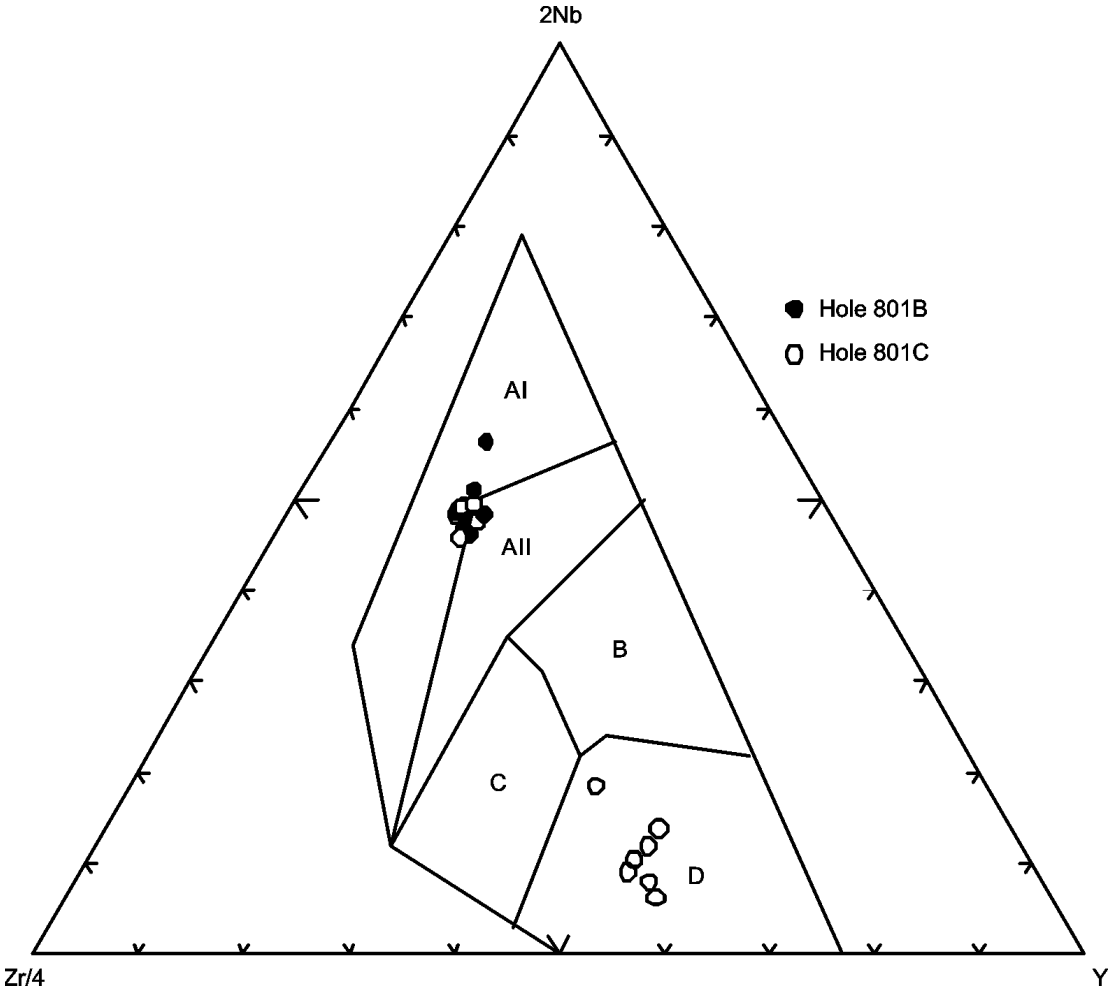

Figure F51. Chondrite-normalized rare earth element abundances for basalts in Holes 801B and 801C. Normalizing values are from Sun and McDonough (1989).

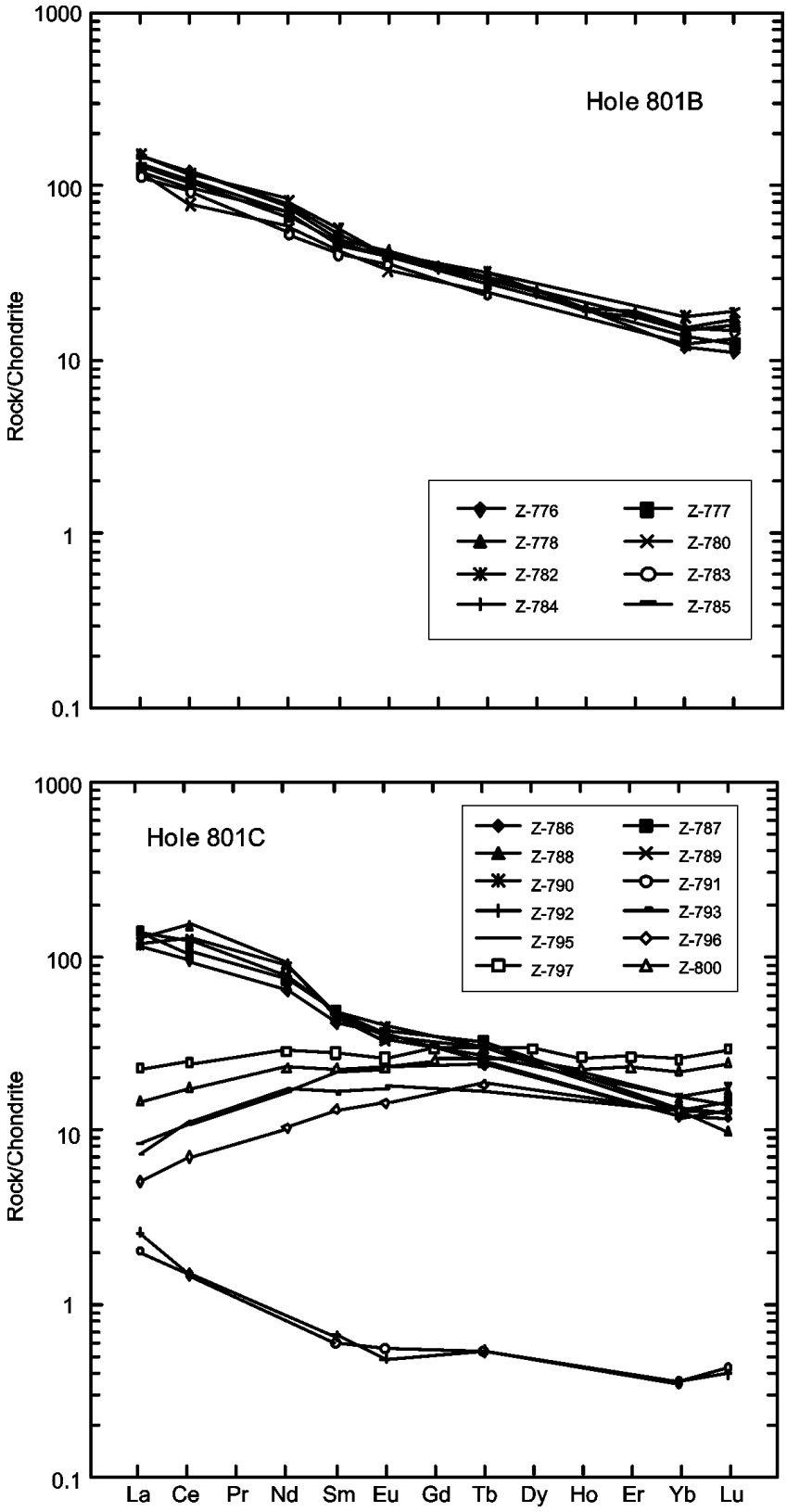

Figure F52. Leg 19 Site 192 and Leg 55 Sites 430–433 on the Emperor Seamount chain. Ages of basalts (Ma) are given in parentheses (from Dalrymple et al., 1980b).

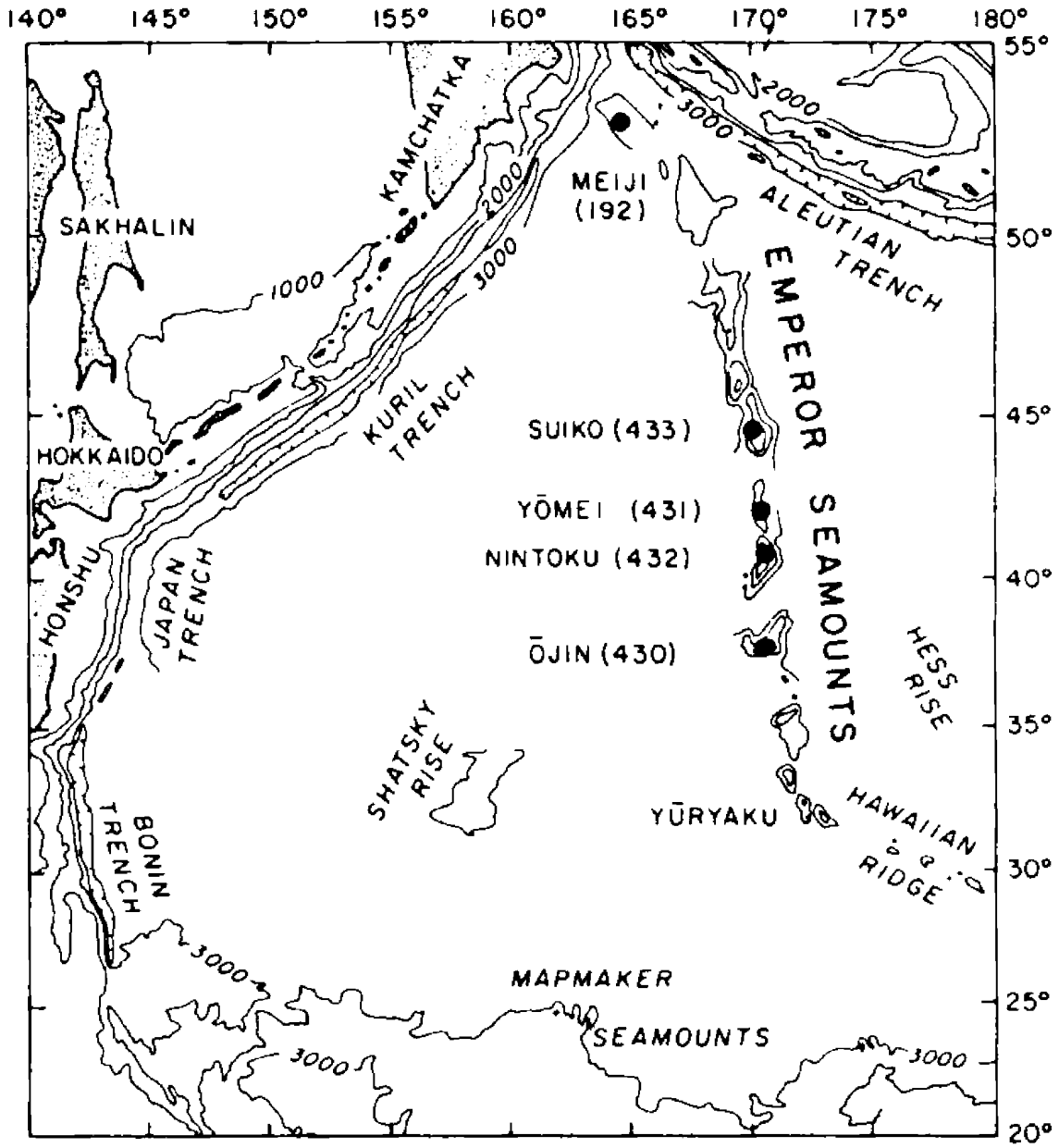

Figure F53. AFM diagram (Irvine and Baragar, 1971) for igneous rocks in Holes 430A, 432A, 433C, and 192A.

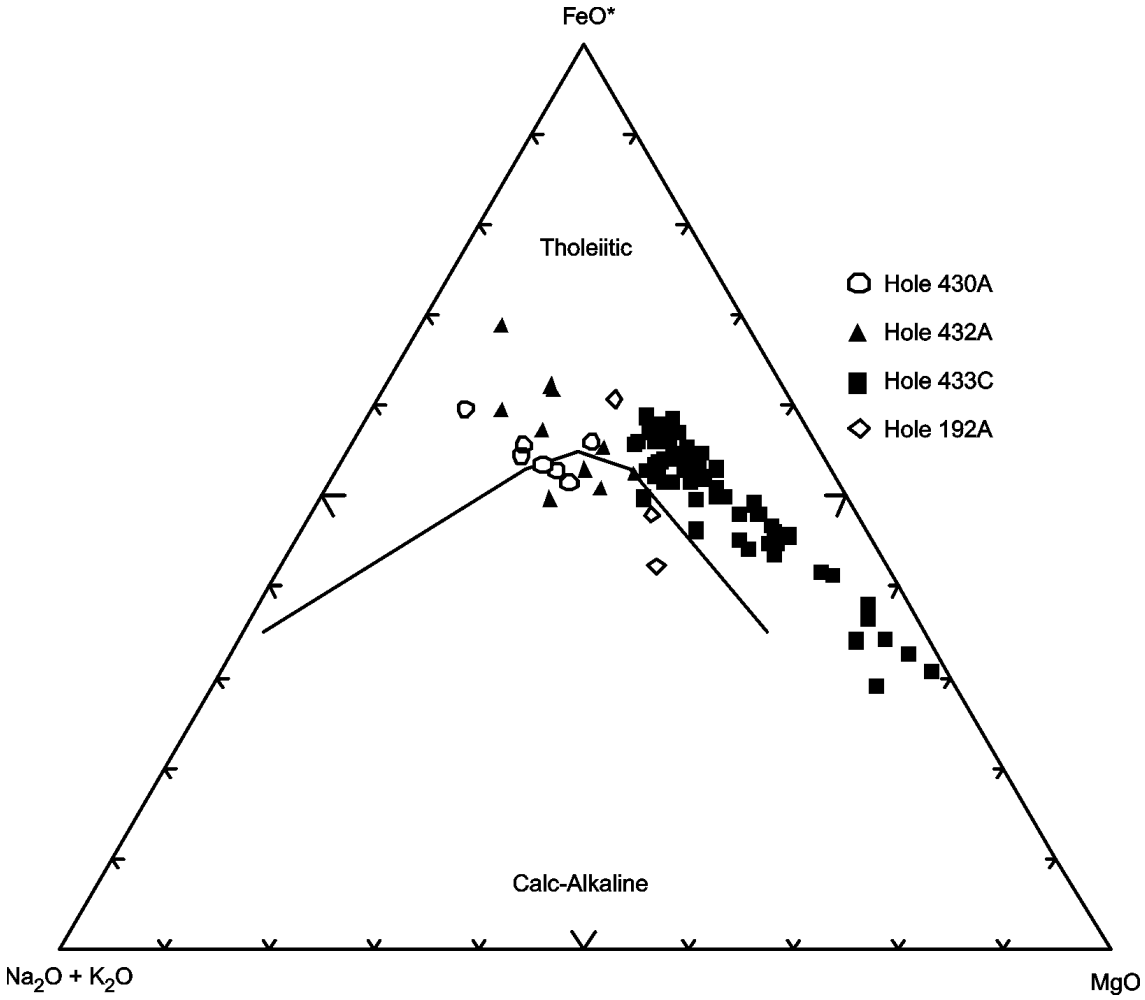

Figure F54. Discrimination Nb-Zr-Y diagram (Meschede, 1986) for igneous rocks in Holes 430A, 432A, and 433C). AI, AII = fields of intraplate alkali basalts; AII, C = fields of intraplate tholeiites; B = field of P-type MORB; D = field of N-type MORB; C, D = fields of volcanic arc basalts.

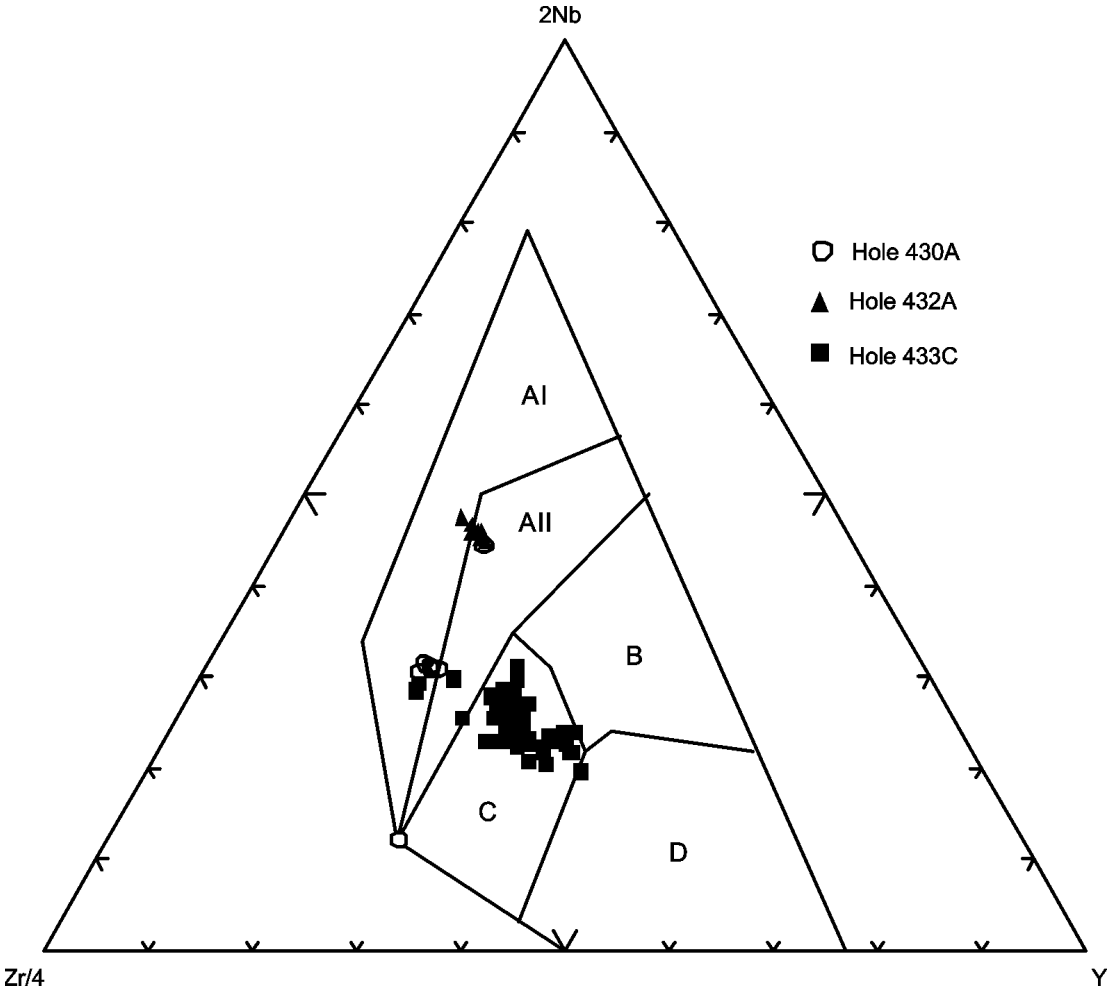

Figure F55. Chondrite-normalized rare earth element abundances for igneous rocks in Holes 430A, 432A, and 433C. Normalizing values are from Sun and McDonough (1989). (Continued on next page.)

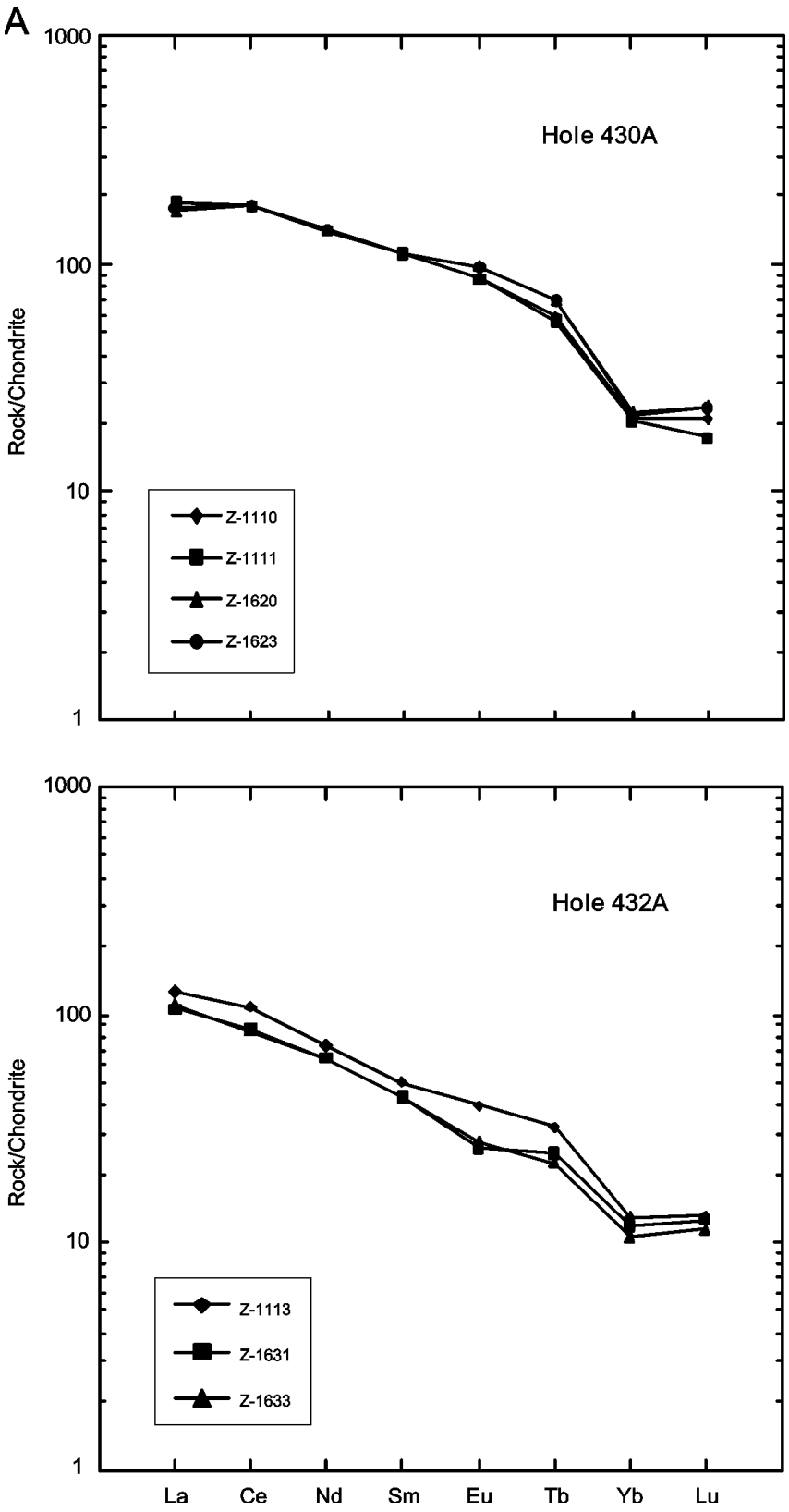

Figure F55 (continued).

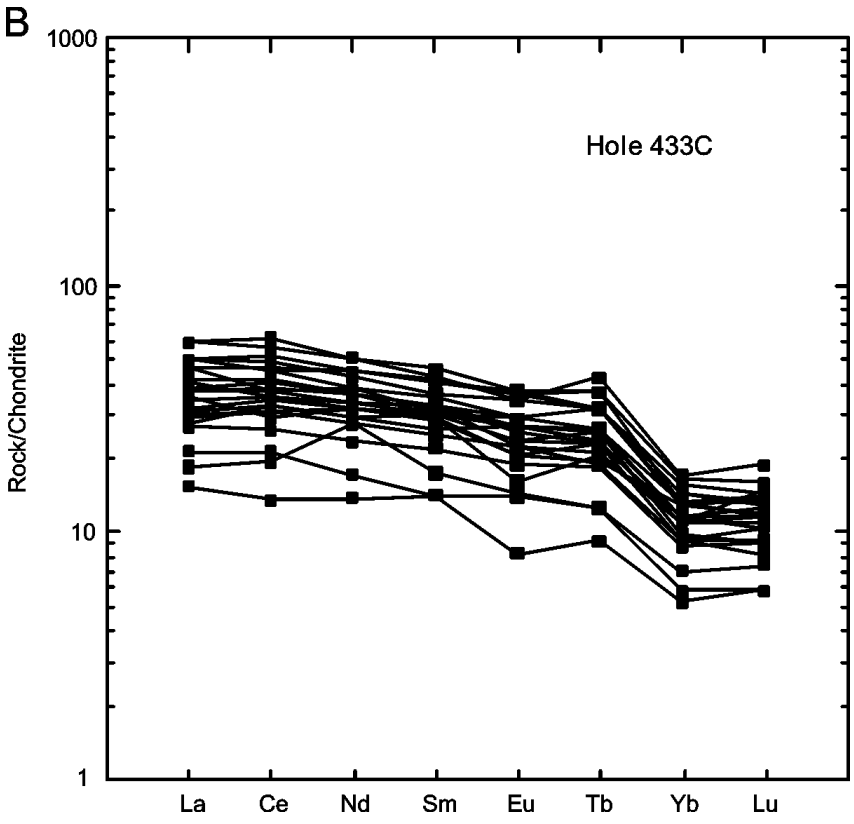

Figure F56. Leg 143 and 144 sites on guyots in the northwestern Pacific Ocean (from Bogdanov et al., 1995).

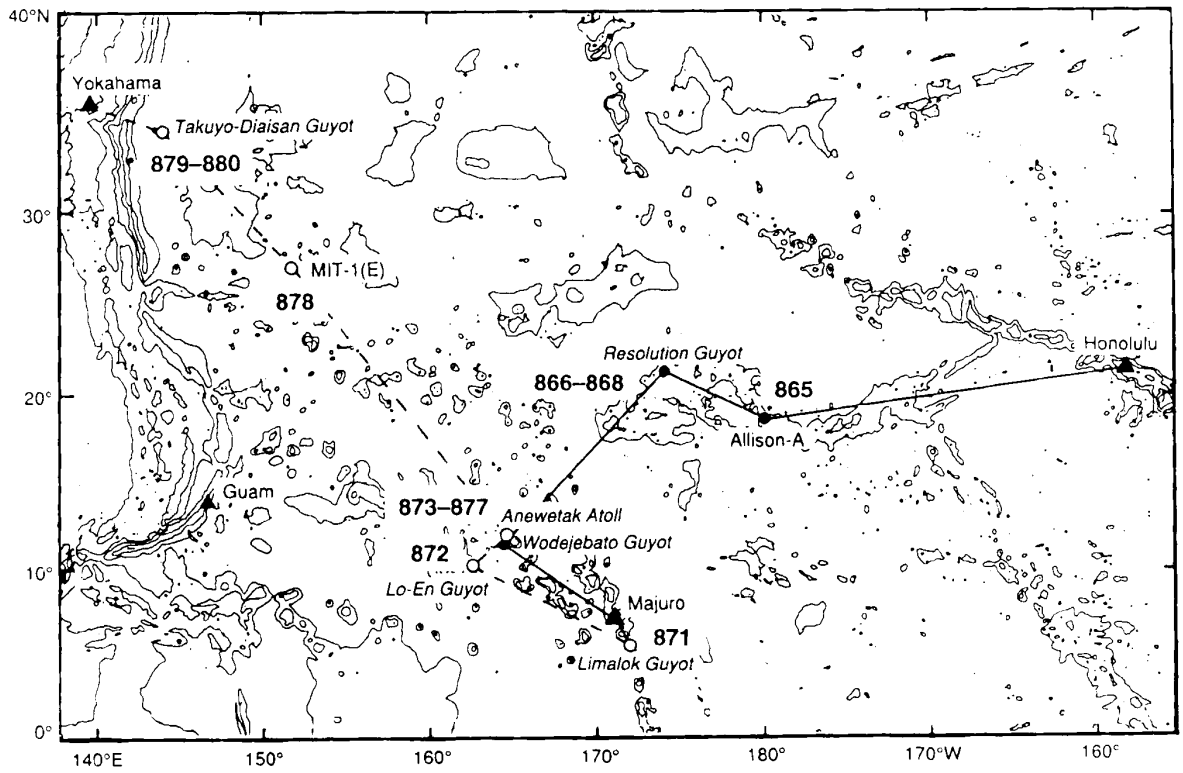

Figure F57. AFM diagram (Irvine and Baragar, 1971) for basalts in Holes 865A and 866A.

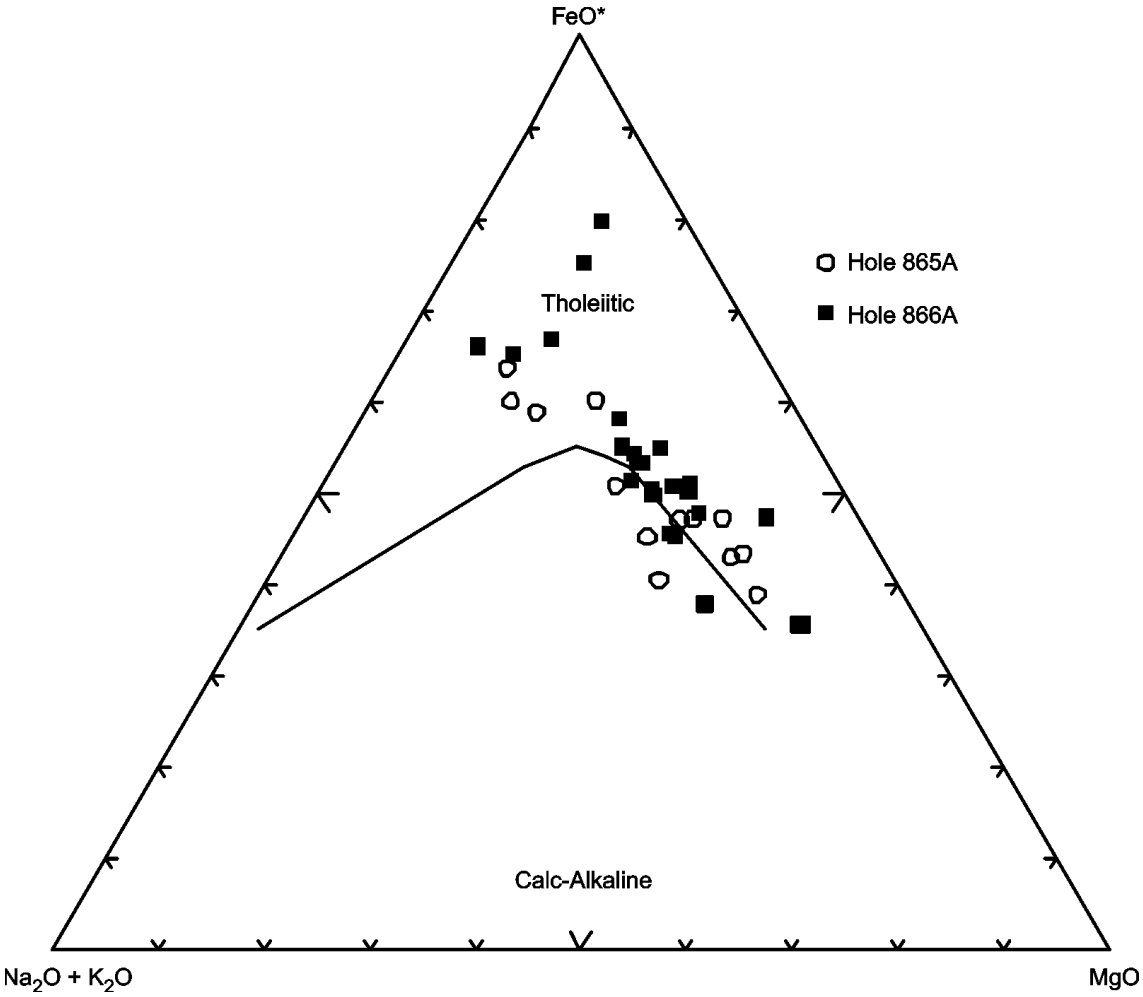

Figure F58. Discrimination Nb-Zr-Y diagram (Meschede, 1986) for basalts in Holes 865A and 866A. AI, AII = fields of intraplate alkali basalts; AII, C = fields of intraplate tholeiites; B = field of P-type MORB; D = field of N-type MORB; C, D = fields of volcanic arc basalts.

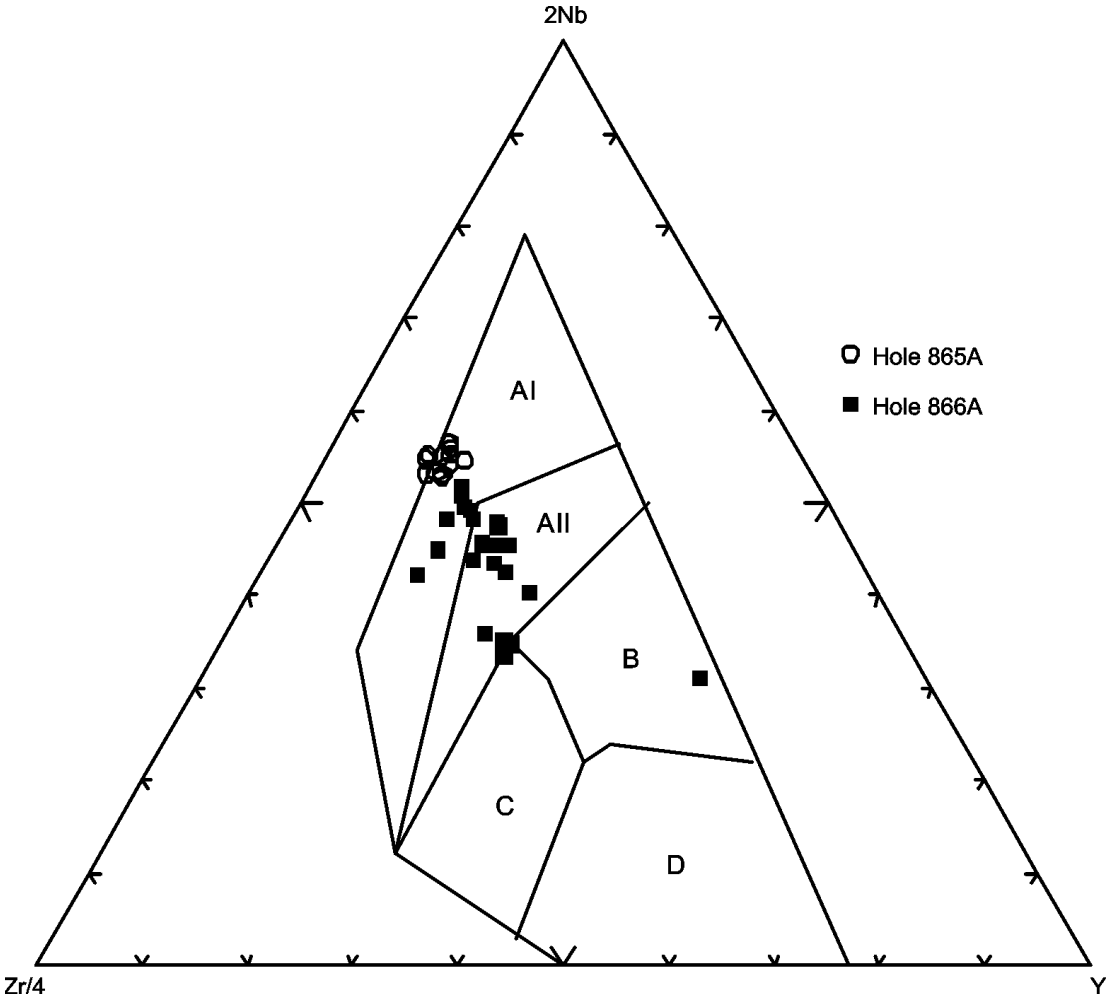

Figure F59. Chondrite-normalized rare earth element abundances for basalts in Holes 865A and 866A. Normalizing values are from Sun and McDonough (1989).

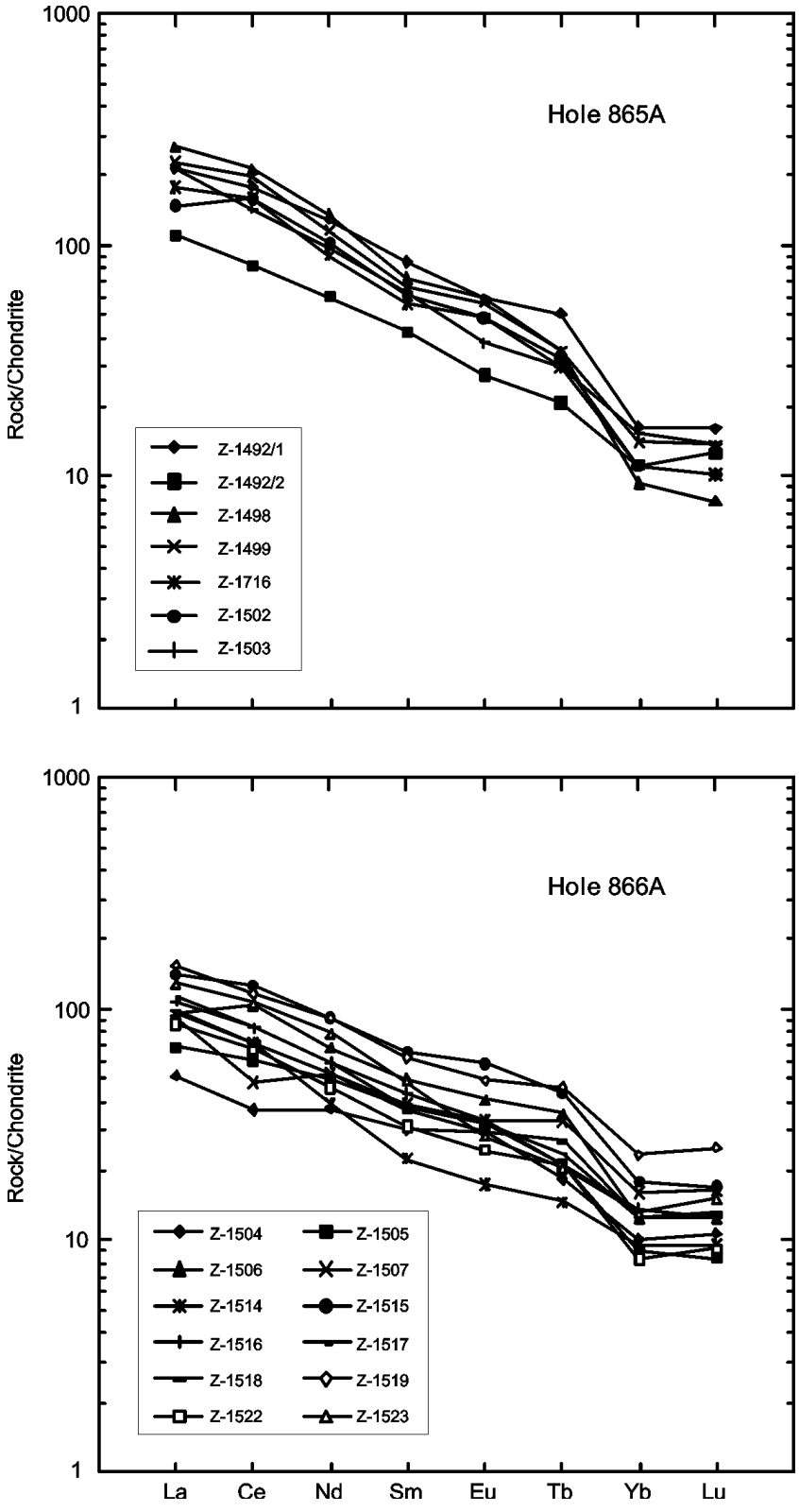

Figure F60. AFM diagram (Irvine and Baragar, 1971) for igneous rocks in Holes 871C, 872B, 874B, and 878A.

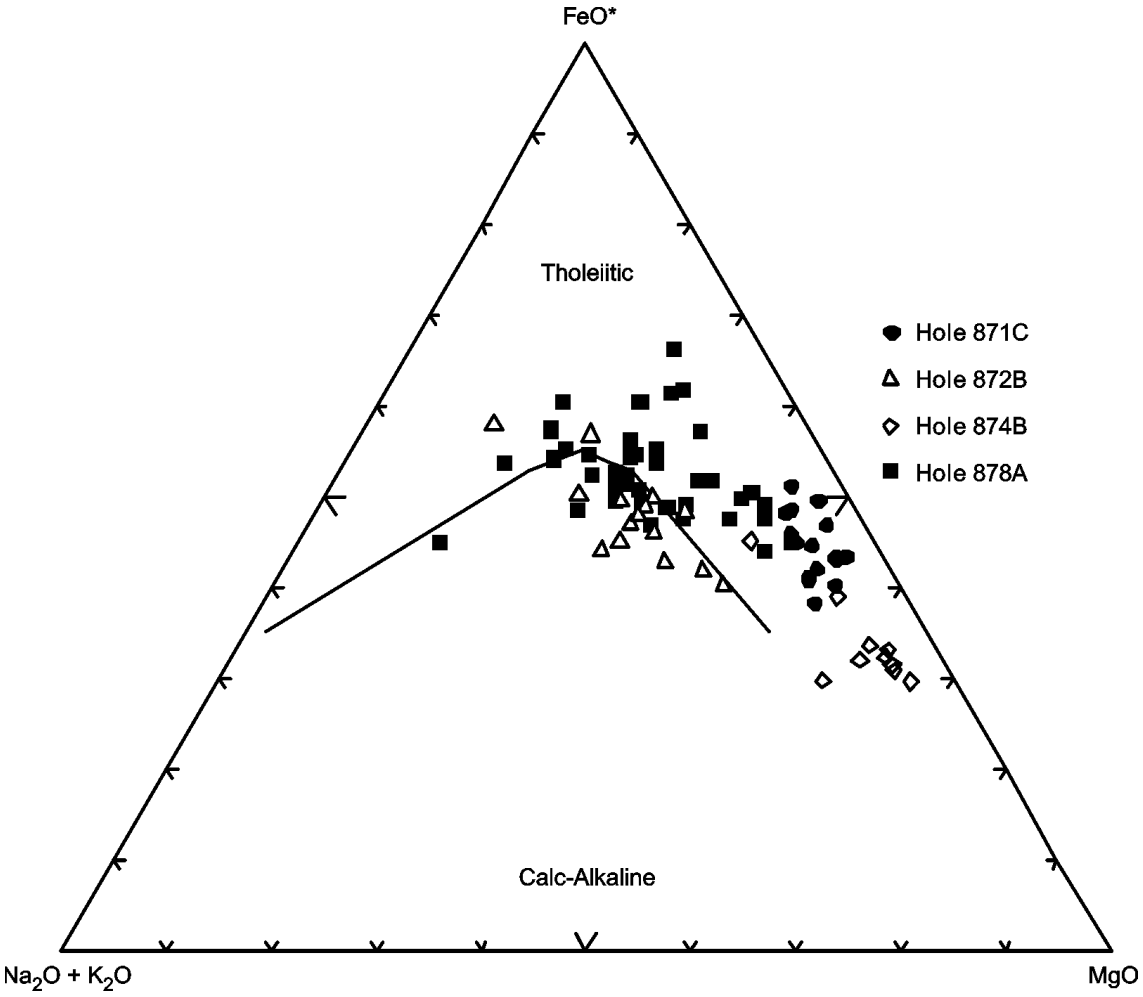

Figure F61. Discrimination Nb-Zr-Y diagram (Meschede, 1986) for igneous rocks in Holes 871C, 872B, 874B, and 878A. AI, AII = fields of intraplate alkali basalts; AII, C = fields of intraplate tholeiites; B = field of P-type MORB; D = field of N-type MORB; C, D = fields of volcanic arc basalts.

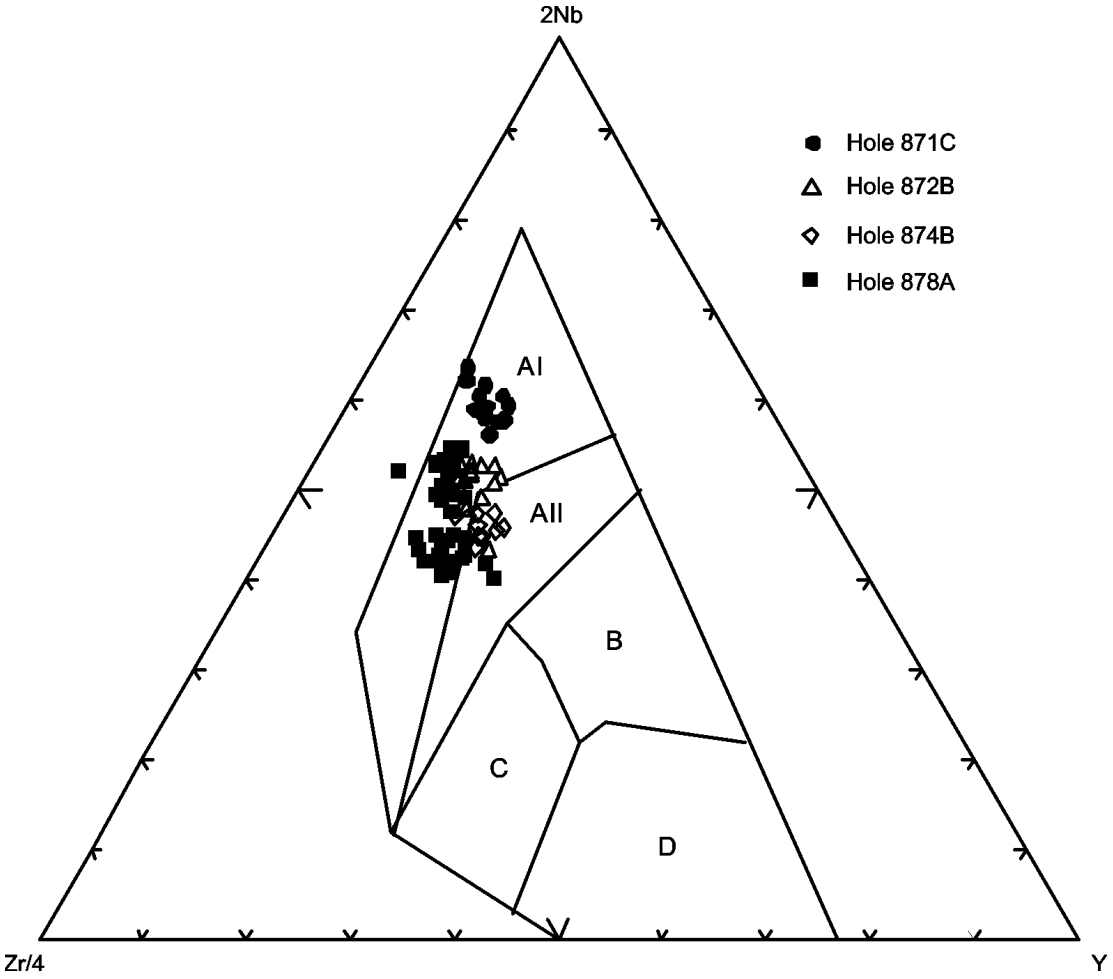

Figure F62. Chondrite-normalized rare earth element abundances for igneous rocks in Holes 871C, 872B, 874B, and 878A. Normalizing values are from Sun and McDonough (1989). (Continued on next page.)

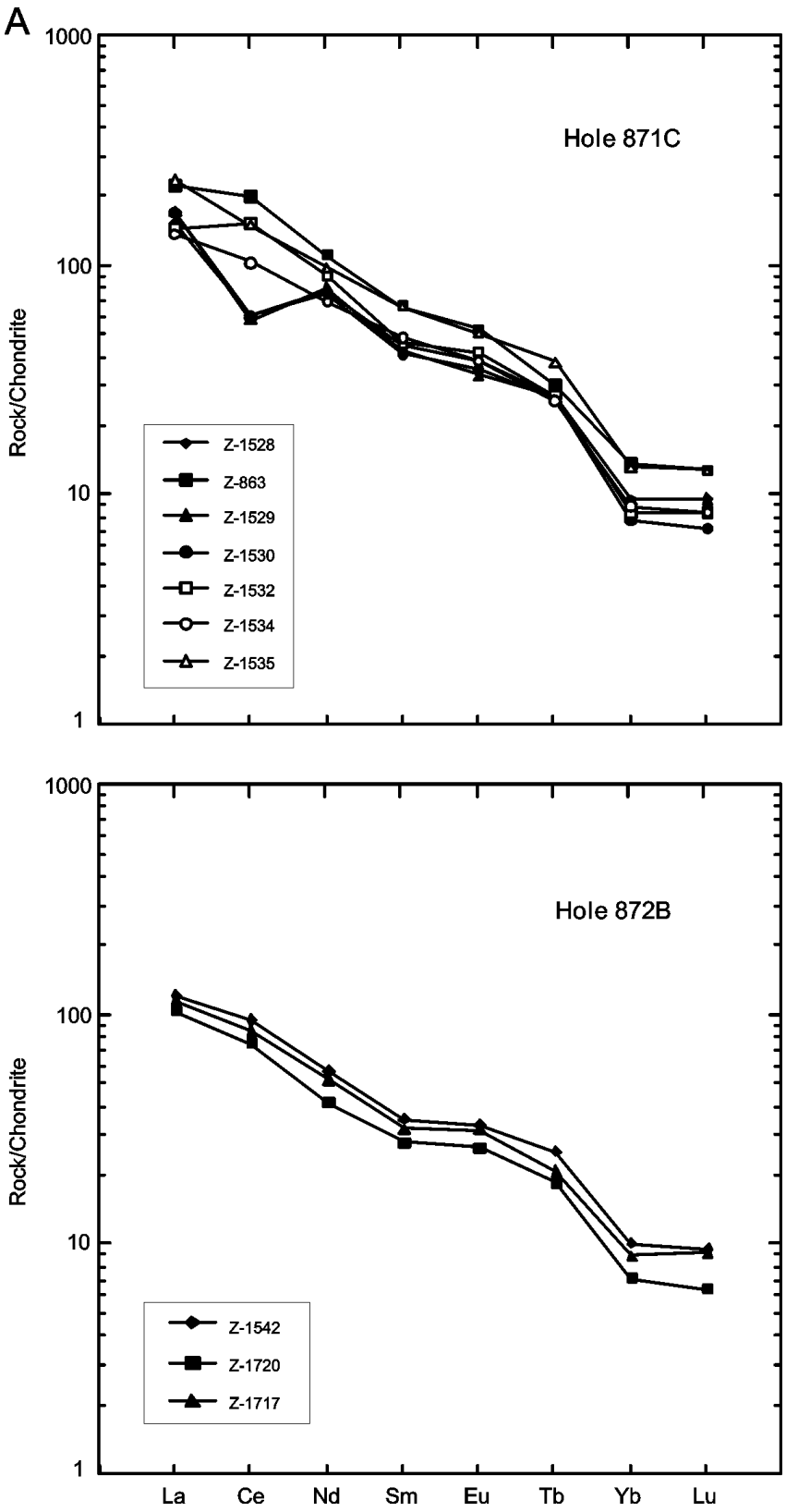

Figure F62 (continued).

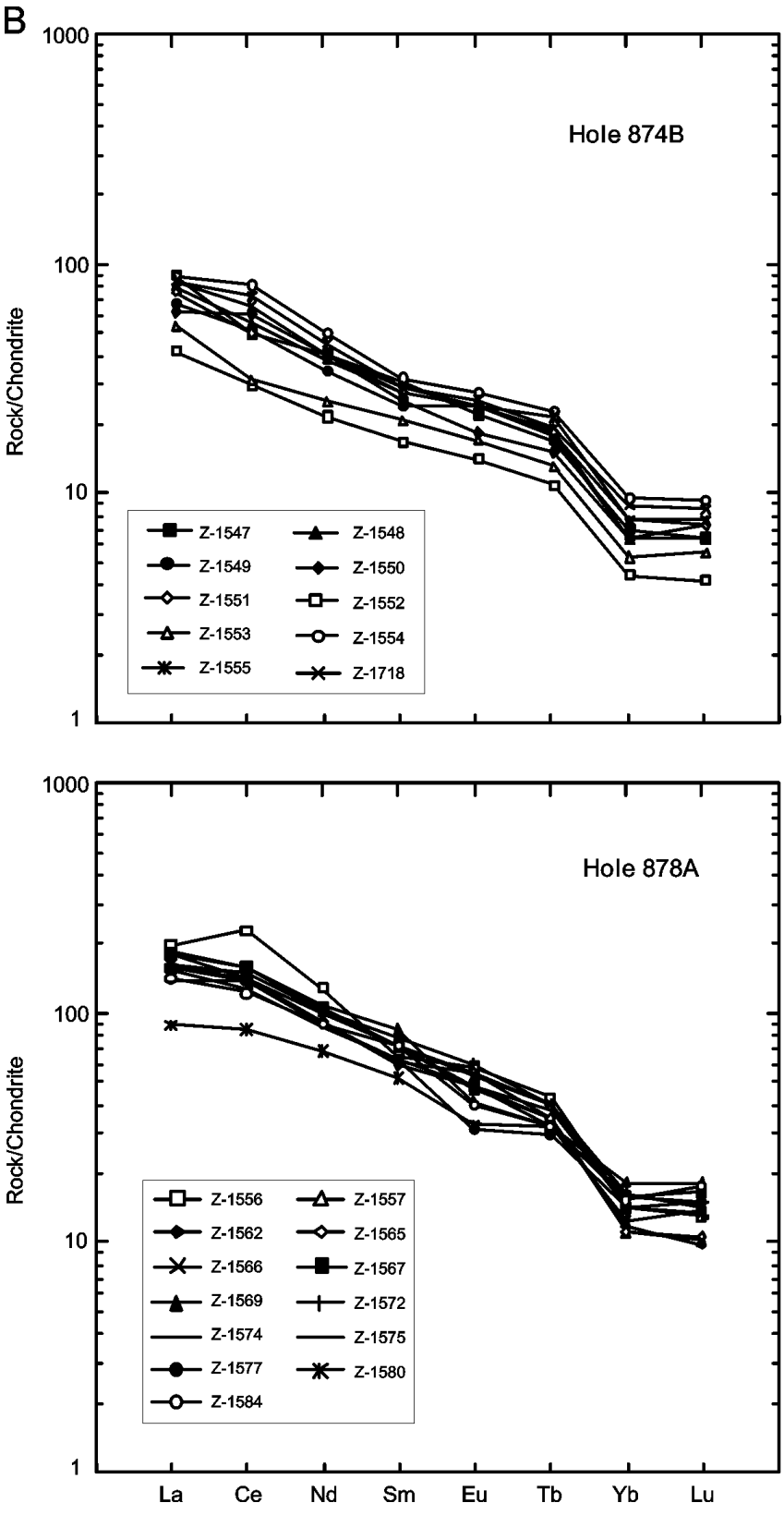

Figure F63. Leg 62 Site 465 on the southern Hess Rise (from Scott, 1981).

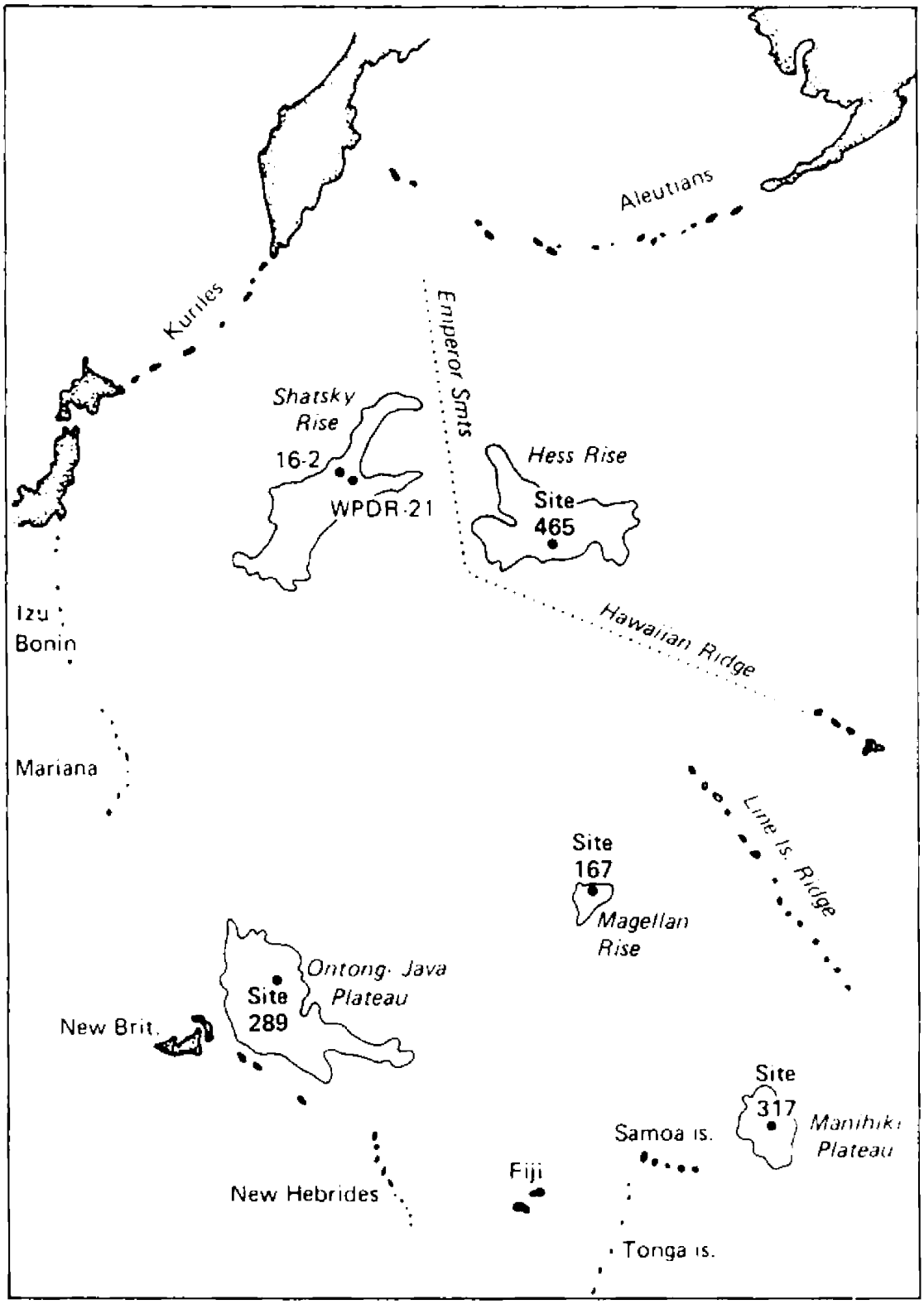

Figure F64. AFM diagram (Irvine and Baragar, 1971) for trachyandesites in Hole 465A.

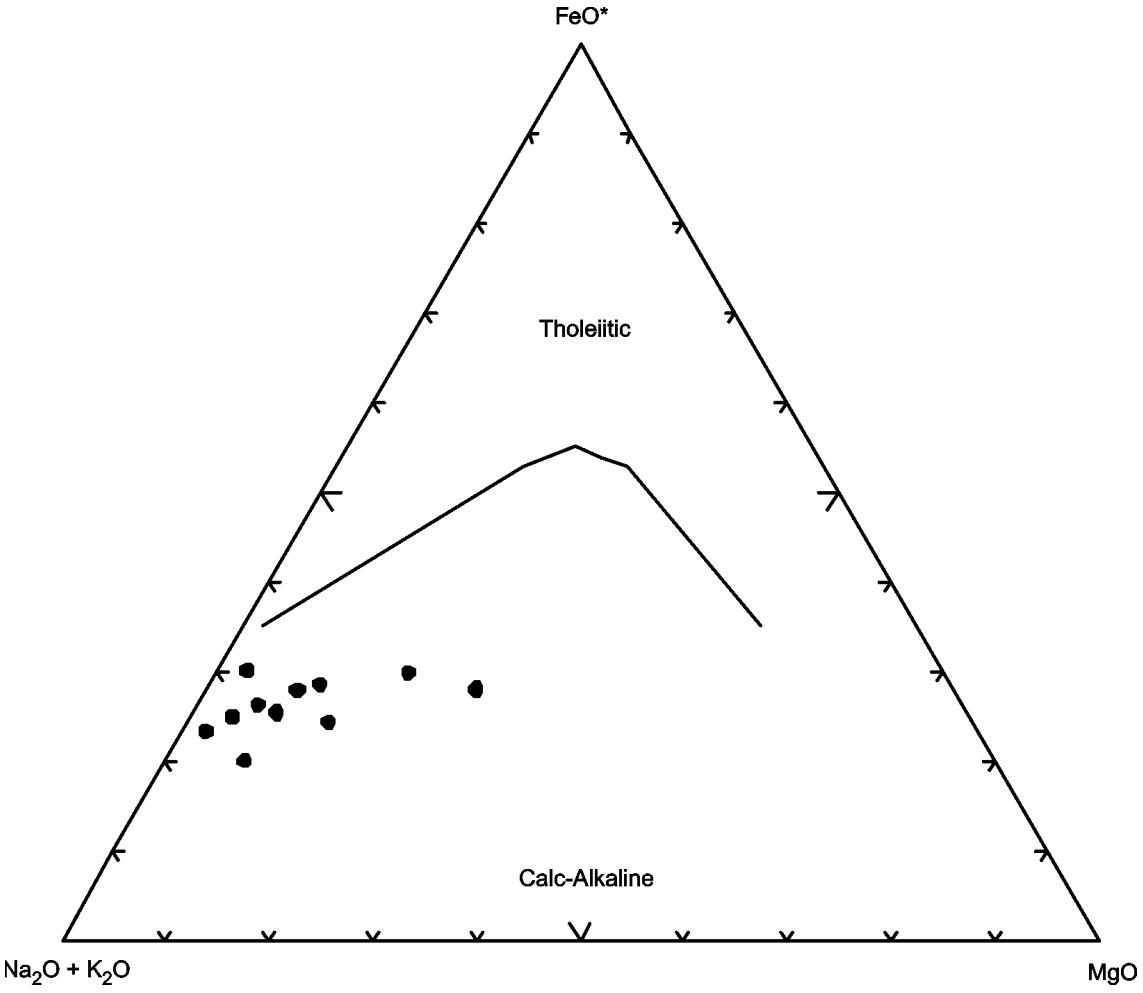

Figure F65. Discrimination Nb-Zr-Y diagram (Meschede, 1986) for trachyandesites in Hole 465A. AI, AII = fields of intraplate alkali basalts; AII, C = fields of intraplate tholeiites; B = field of P-type MORB; D = field of N-type MORB; C, D = fields of volcanic arc basalts.

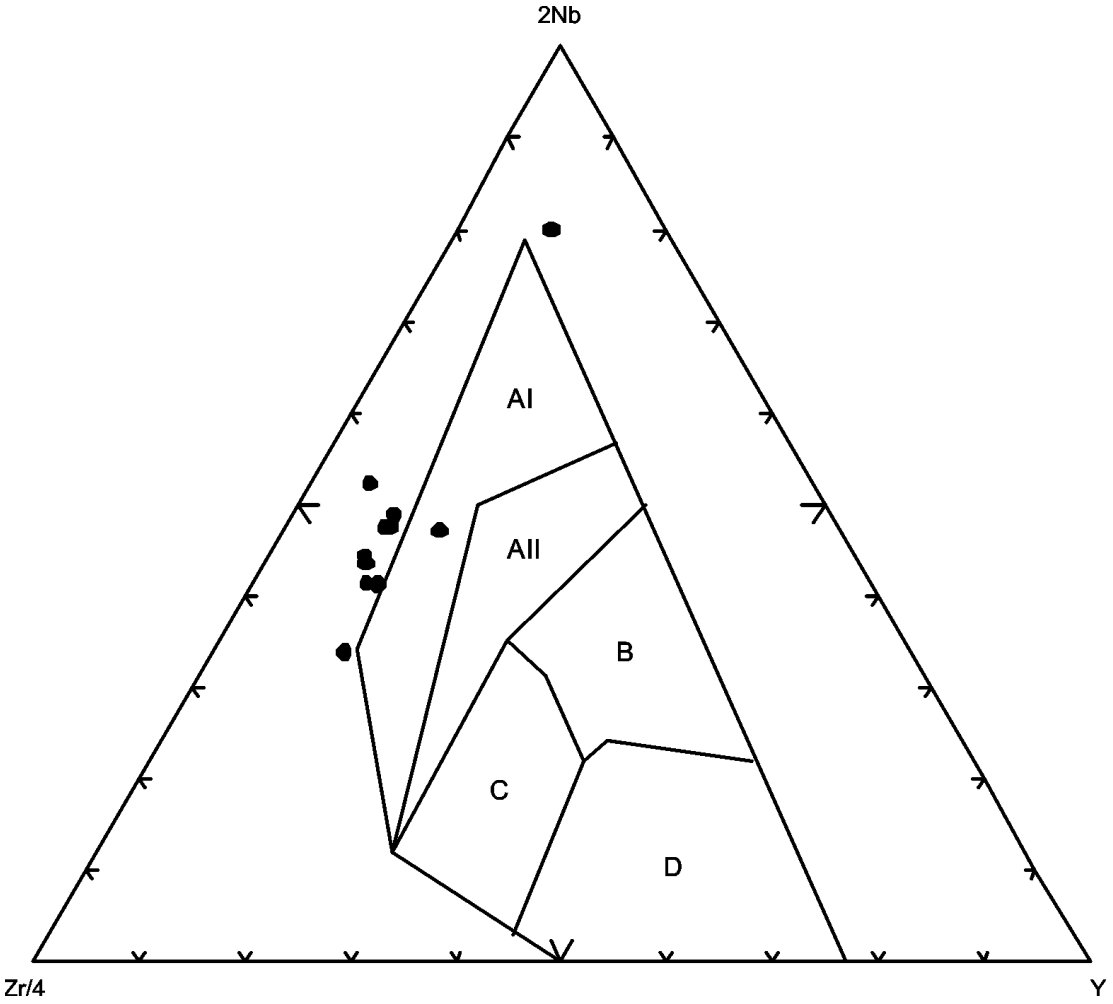

Figure F66. Chondrite-normalized rare earth element abundances for trachyandesites in Hole 465A. Normalizing values are from Sun and McDonough (1989).

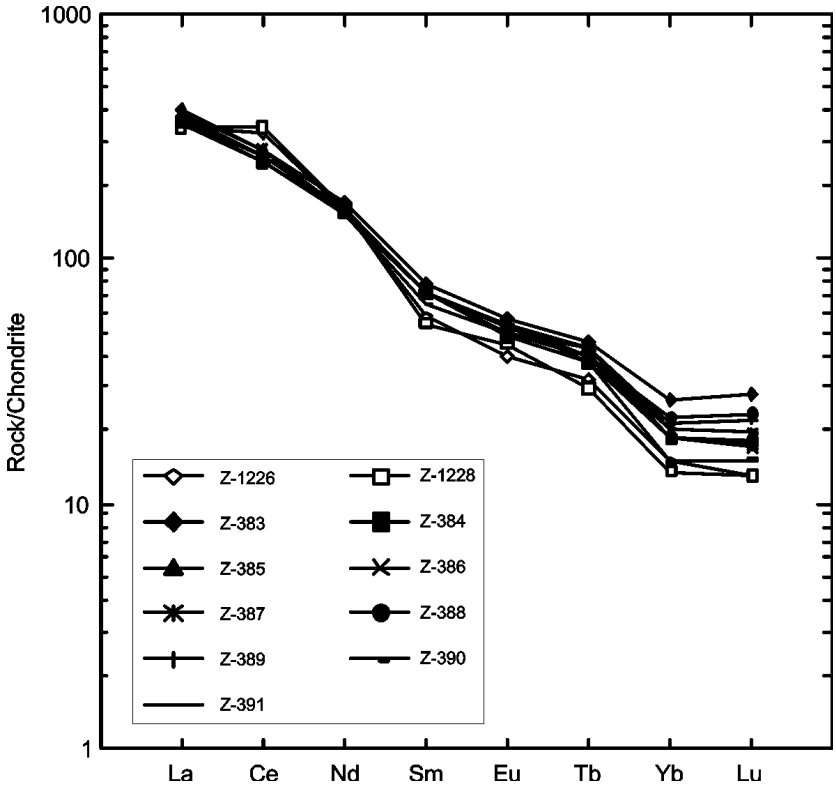

Figure F67. Site 642 drilled during Leg 104 on the Vøring Plateau (from Eldholm, Thiede, et al., 1987).

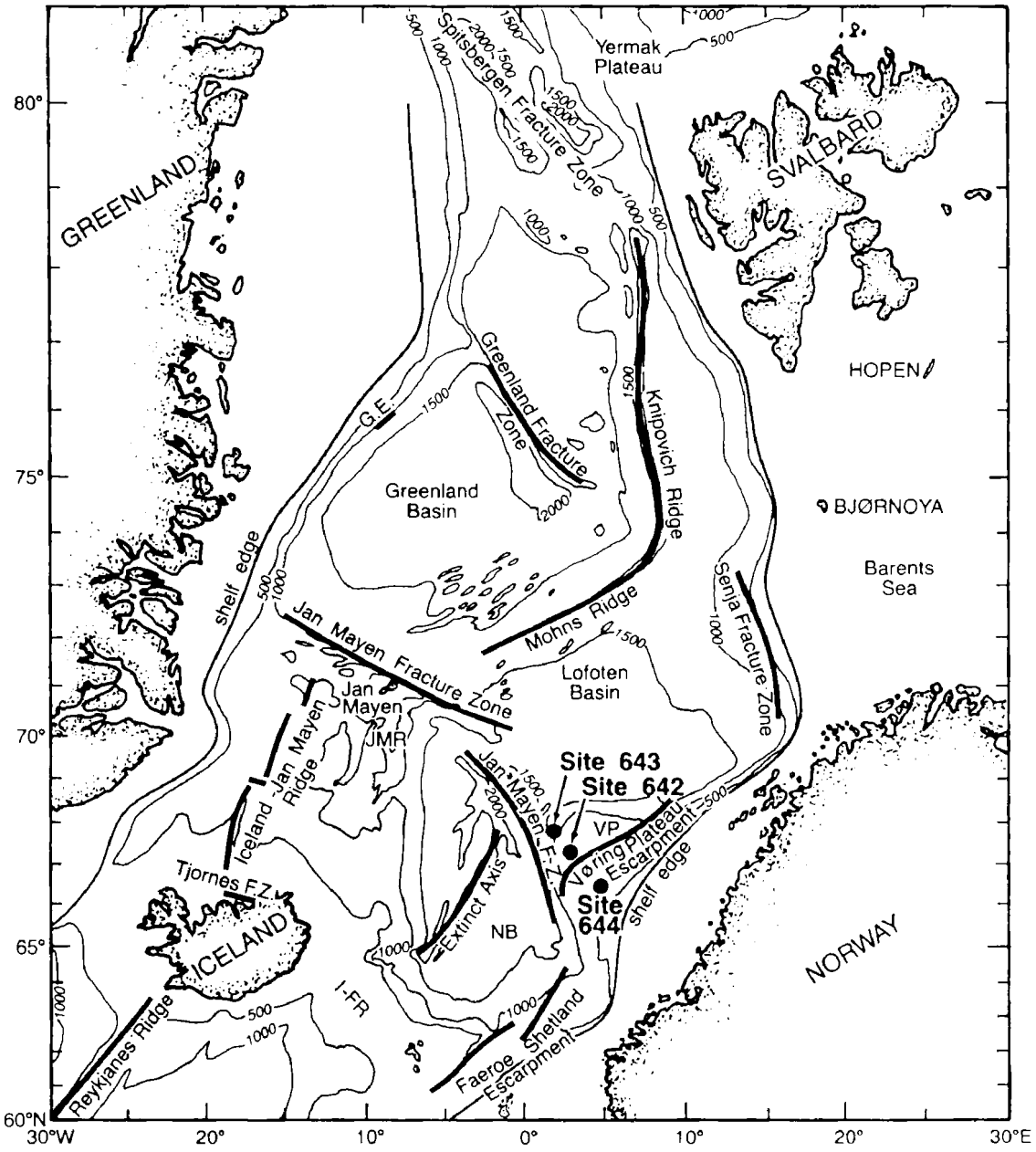

Figure F68. AFM diagram (Irvine and Baragar, 1971) for basalts in Hole 642E.

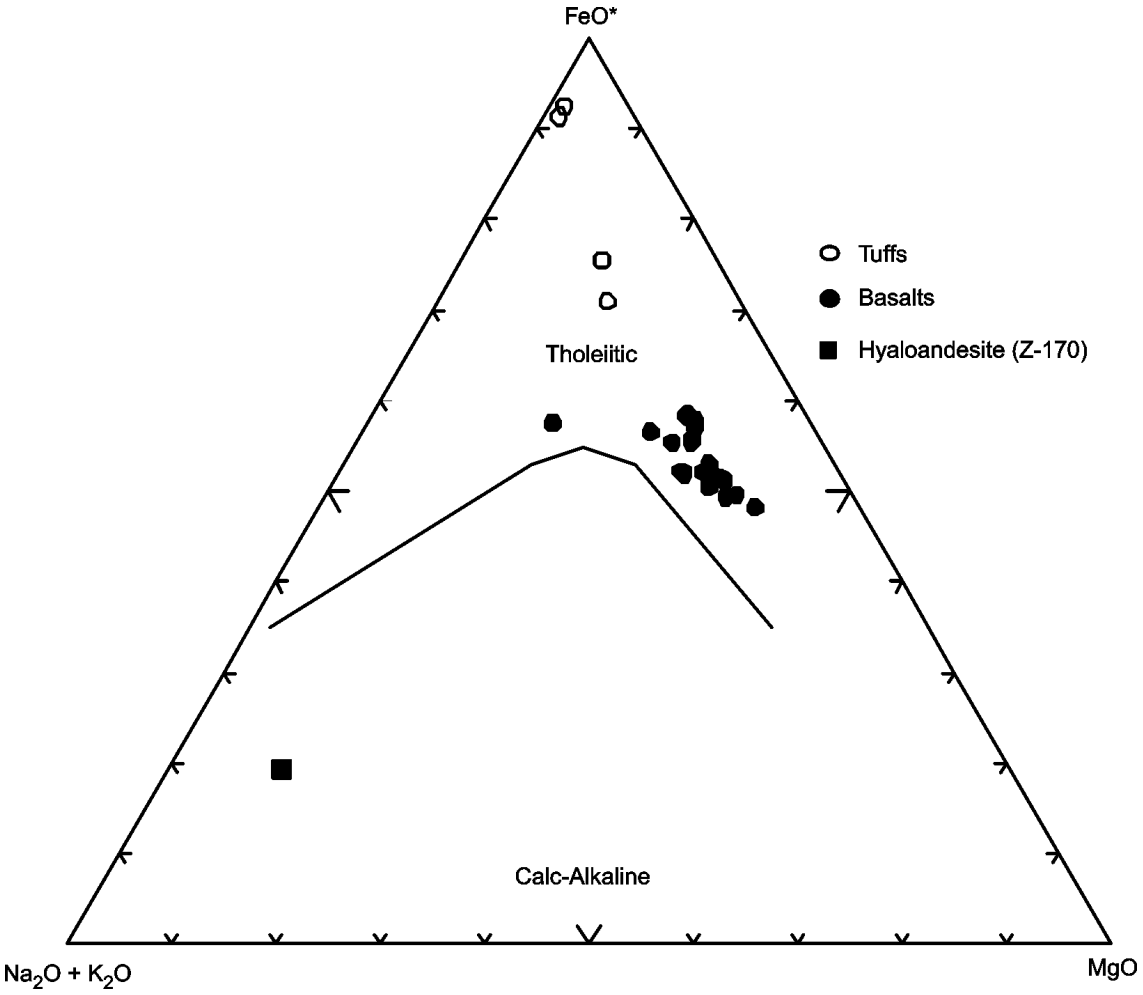

Figure F69. Discrimination Nb-Zr-Y diagram (Meschede, 1986) for basalts in Hole 642E. AI, AII = fields of intraplate alkali basalts; AII, C = fields of intraplate tholeiites; B = field of P-type MORB; D = field of N-type MORB; C, D = fields of volcanic arc basalts.

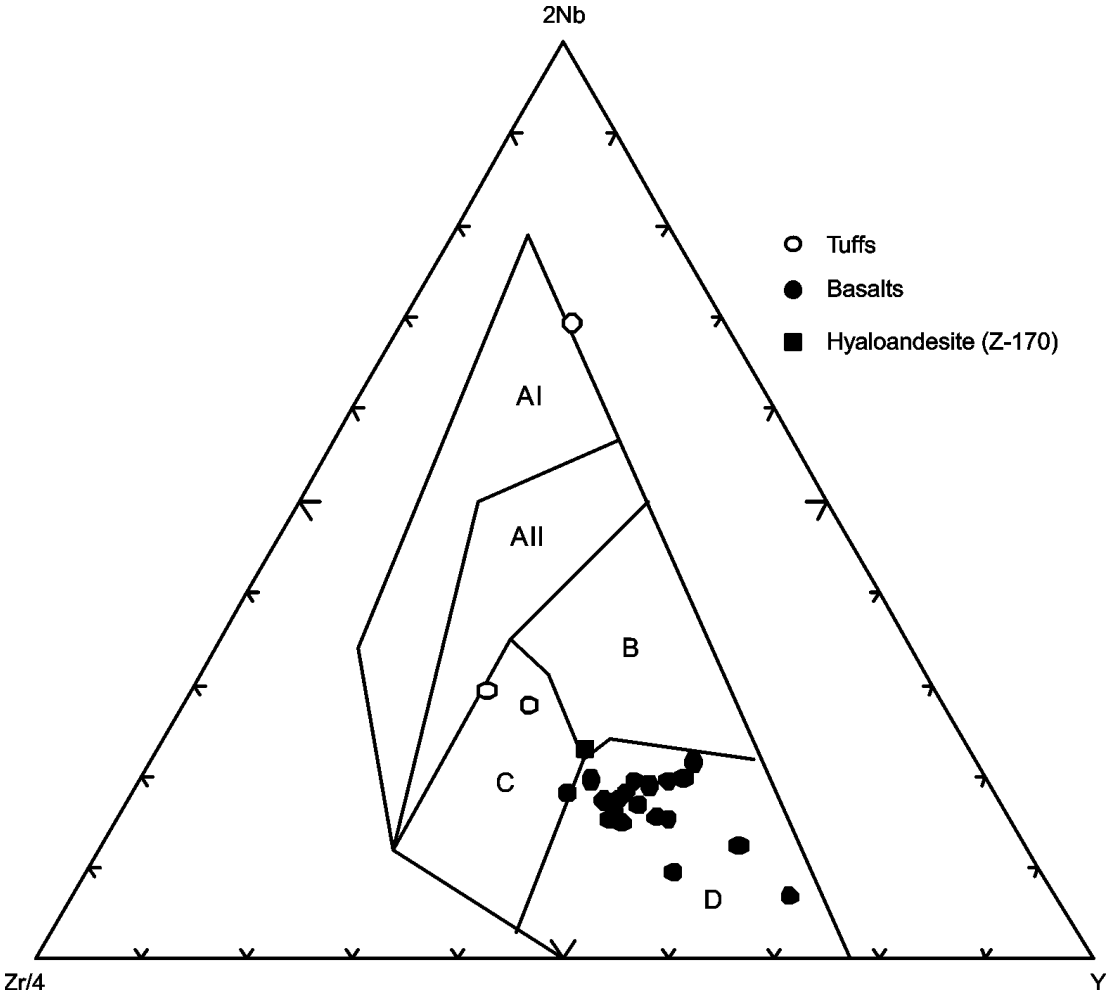

Figure F70. Chondrite-normalized rare earth element abundances for basalts in Hole 642E. Normalizing values are from Sun and McDonough (1989).

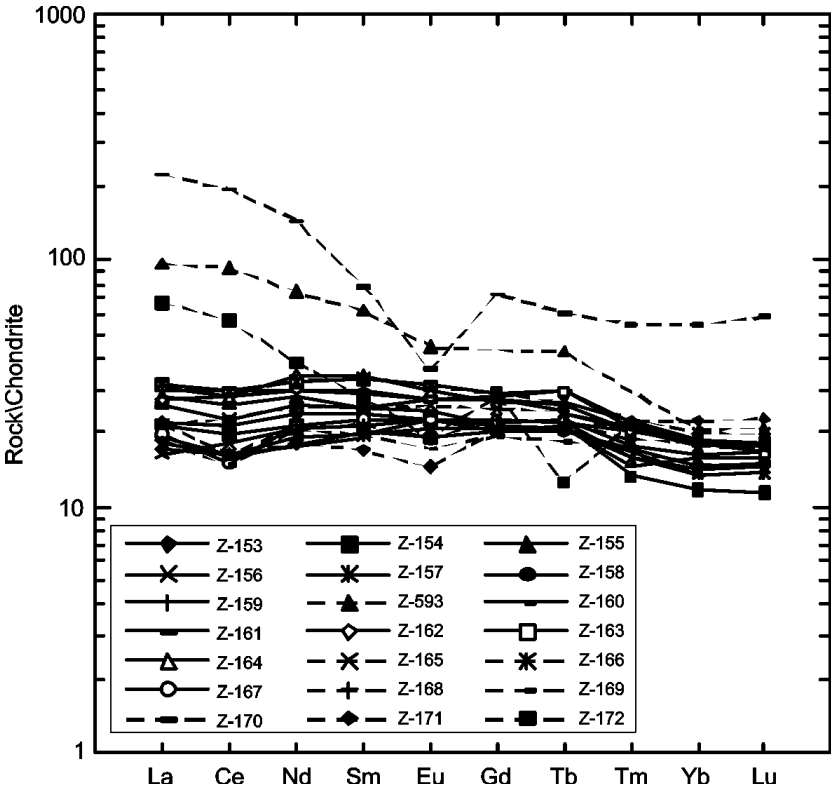

Figure F71. Sites 417 and 418 drilled during Legs 51–53 on the Bermuda Rise (from Donnelly et al., 1979).

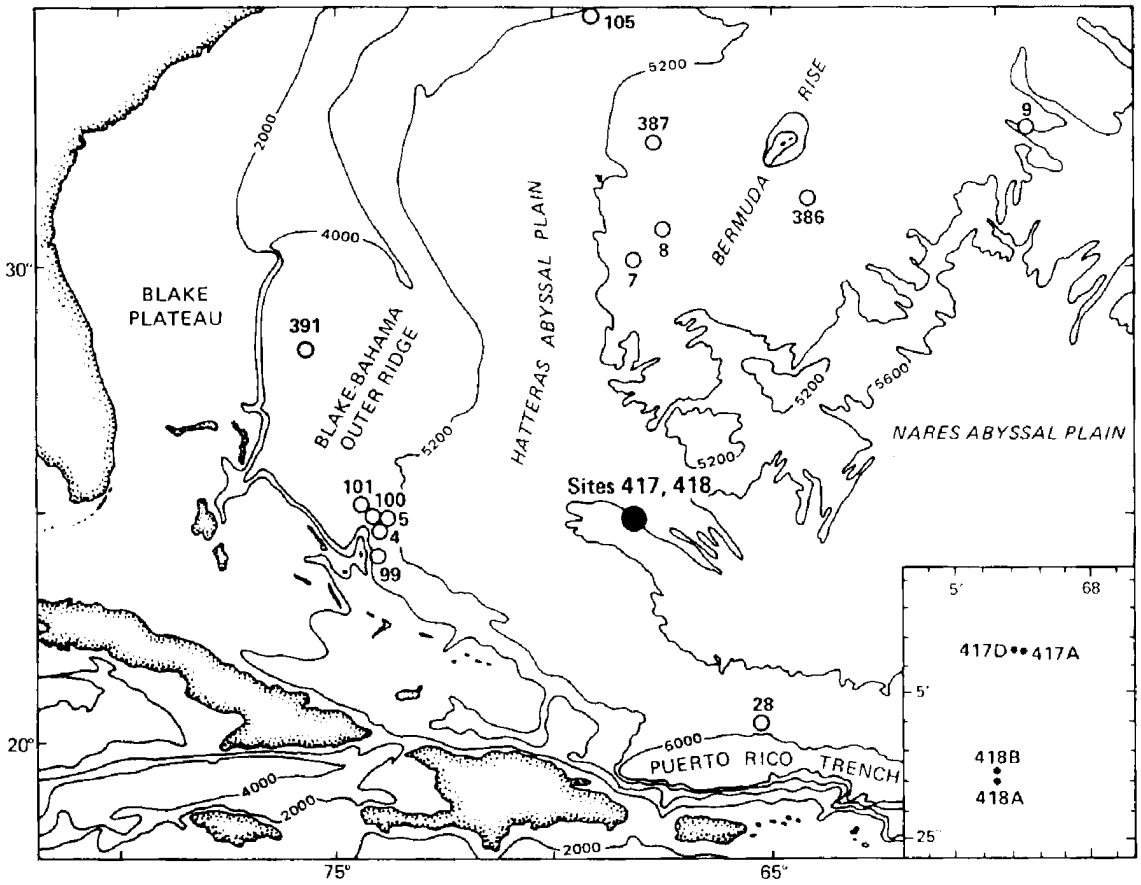

Figure F72. AFM diagram (Irvine and Baragar, 1971) for basalts in Holes 417A and 418A.

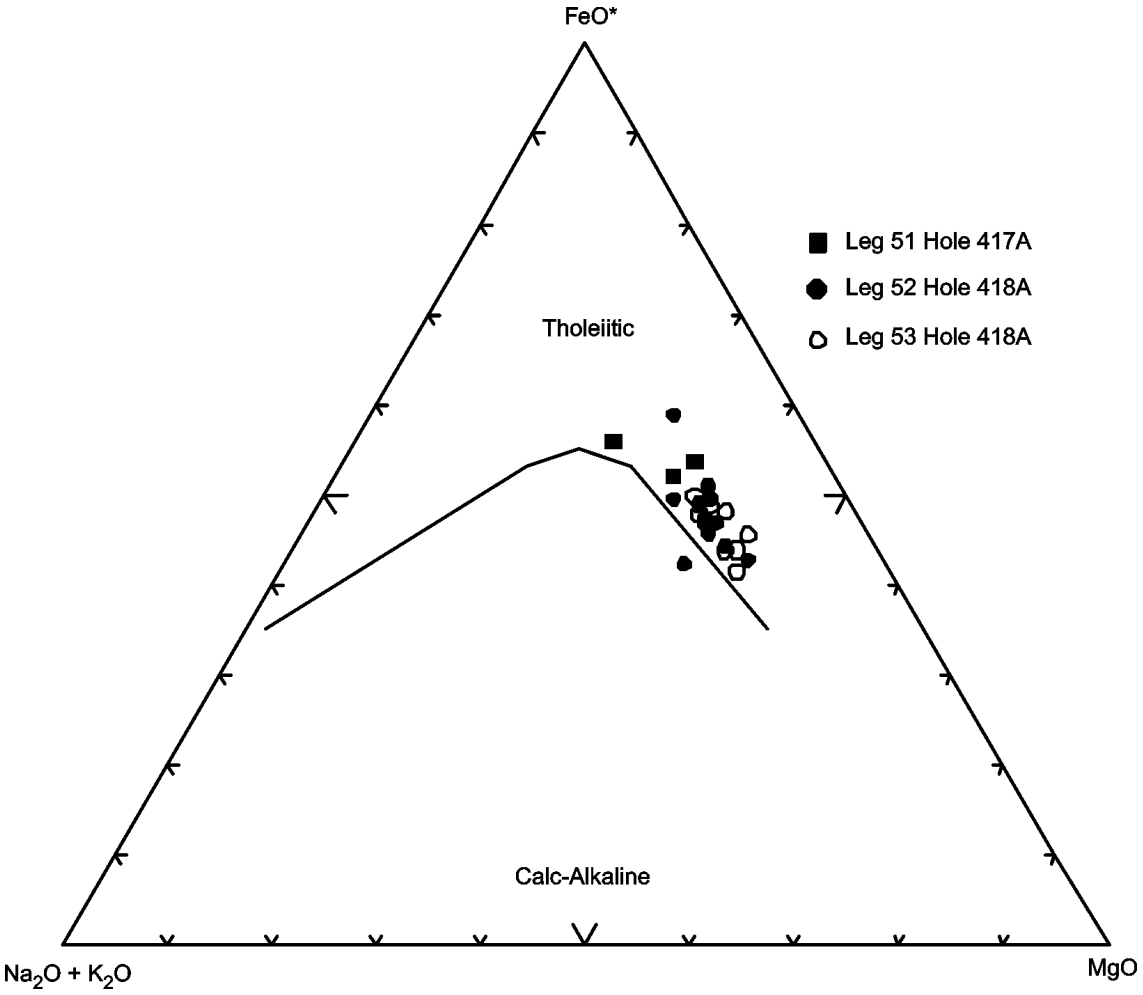

Figure F73. Discrimination Nb-Zr-Y diagram (Meschede, 1986) for basalts in Holes 417A and 418A. AI, AII = fields of intraplate alkali basalts; AII, C = fields of intraplate tholeiites; B = field of P-type MORB; D = field of N-type MORB; C, D = fields of volcanic arc basalts.

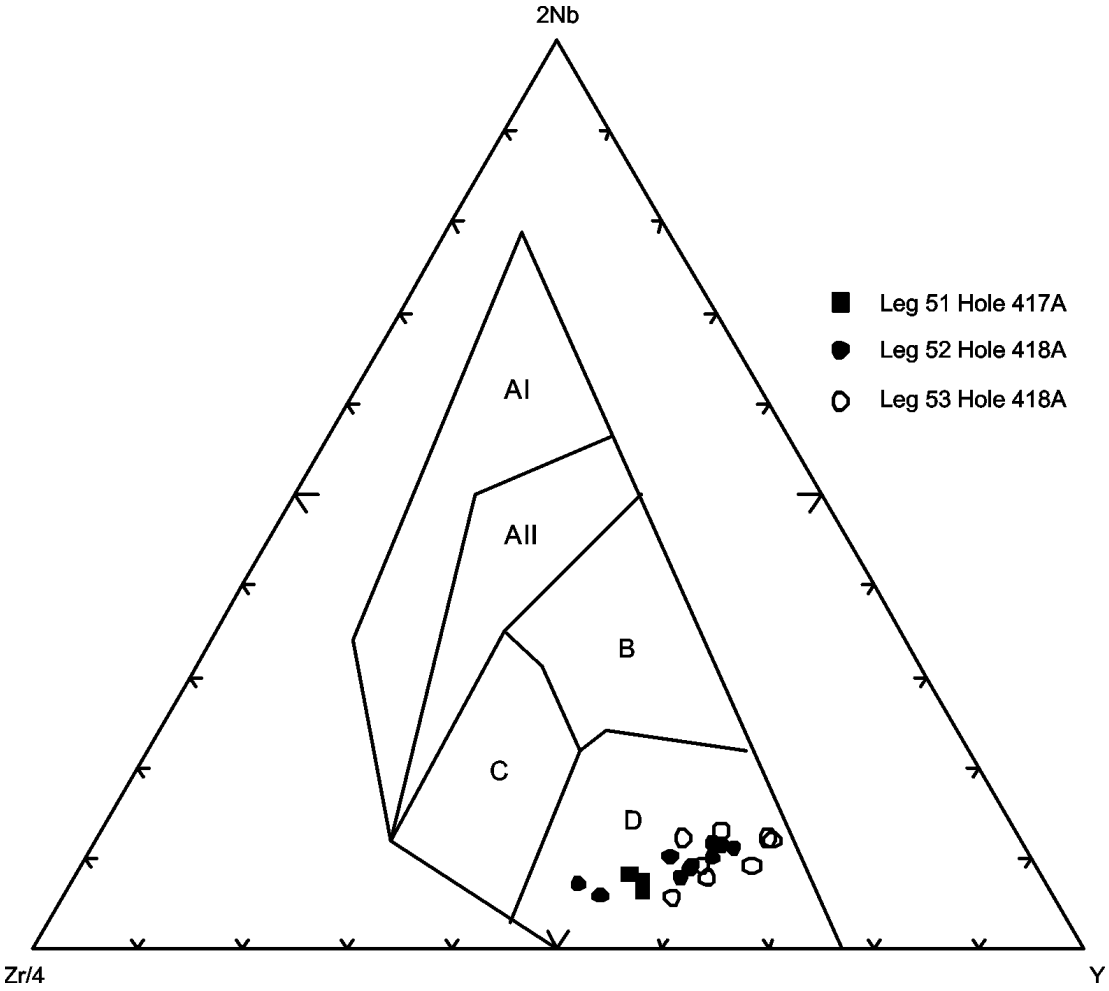

Figure F74. Chondrite-normalized rare earth element abundances for basalts in Hole 417A. Normalizing values are from Sun and McDonough (1989).

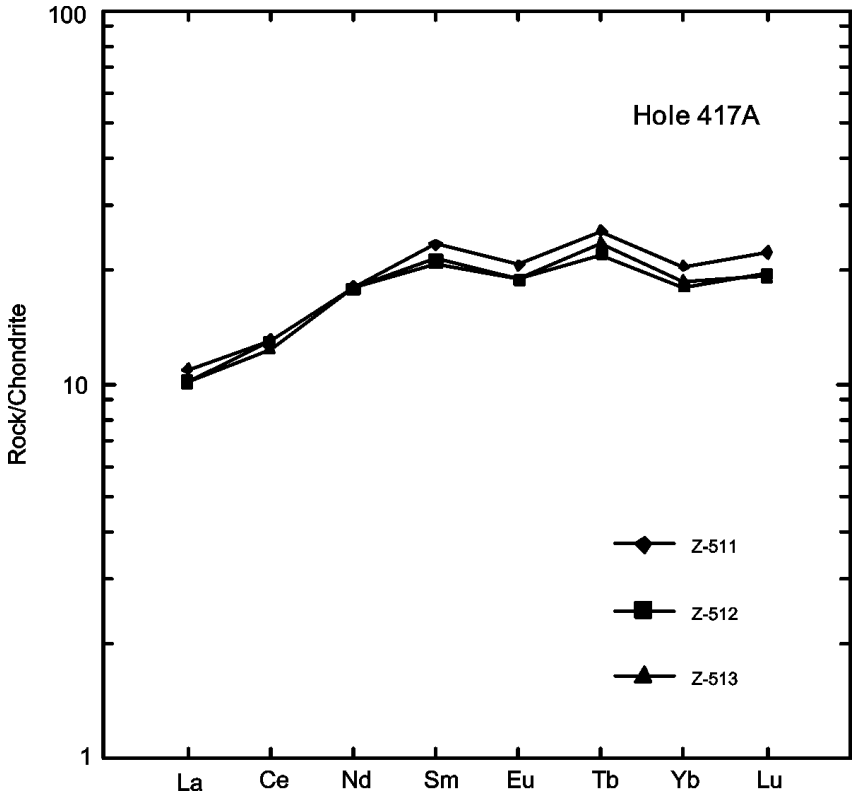

Figure F75. Chondrite-normalized rare earth element abundances for basalts in Hole 418A. Normalizing values are from Sun and McDonough (1989).

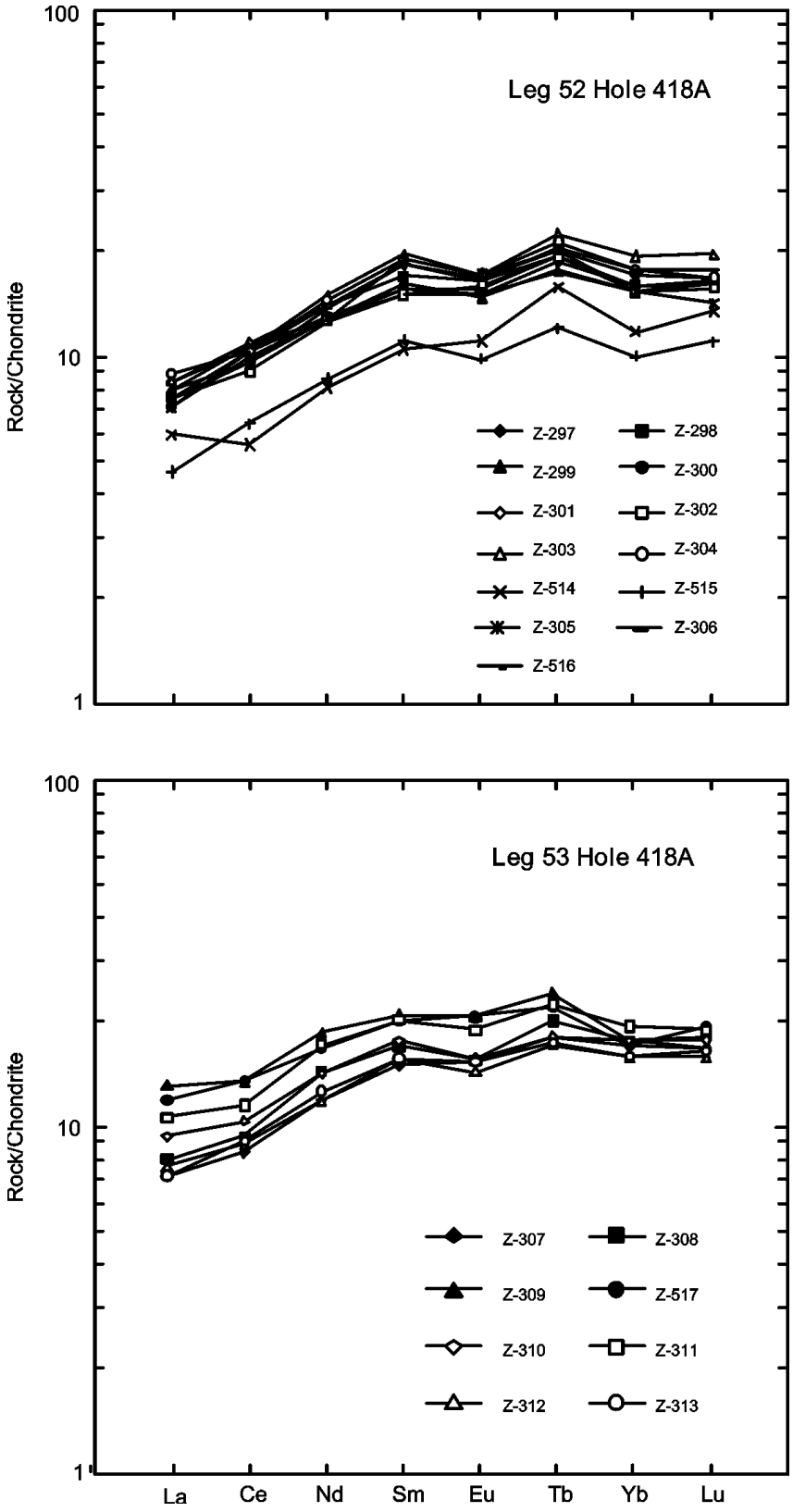

Figure F76. Site 317 drilled during Leg 33 on the Manihiki Plateau (from Schlanger, Jackson, et al., 1976).

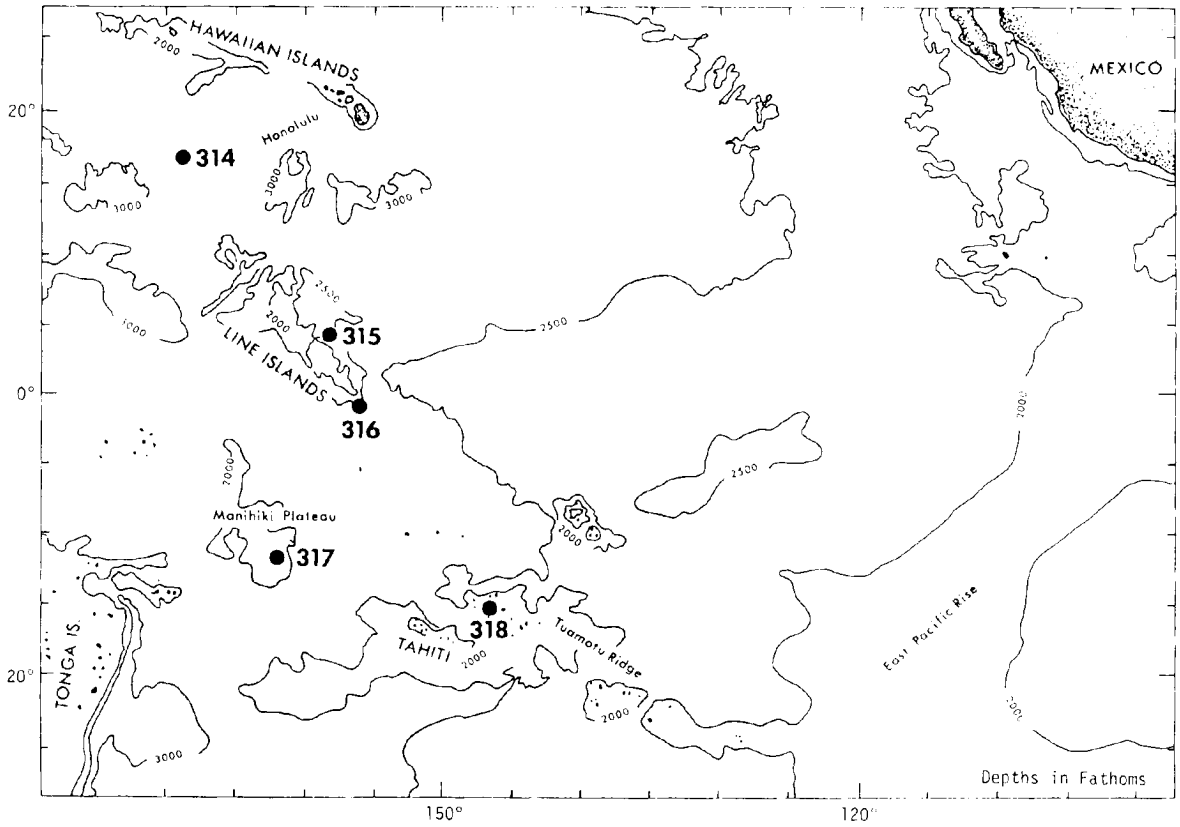

Figure F77. AFM diagram (Irvine and Baragar, 1971) for basalts in Hole 317A.

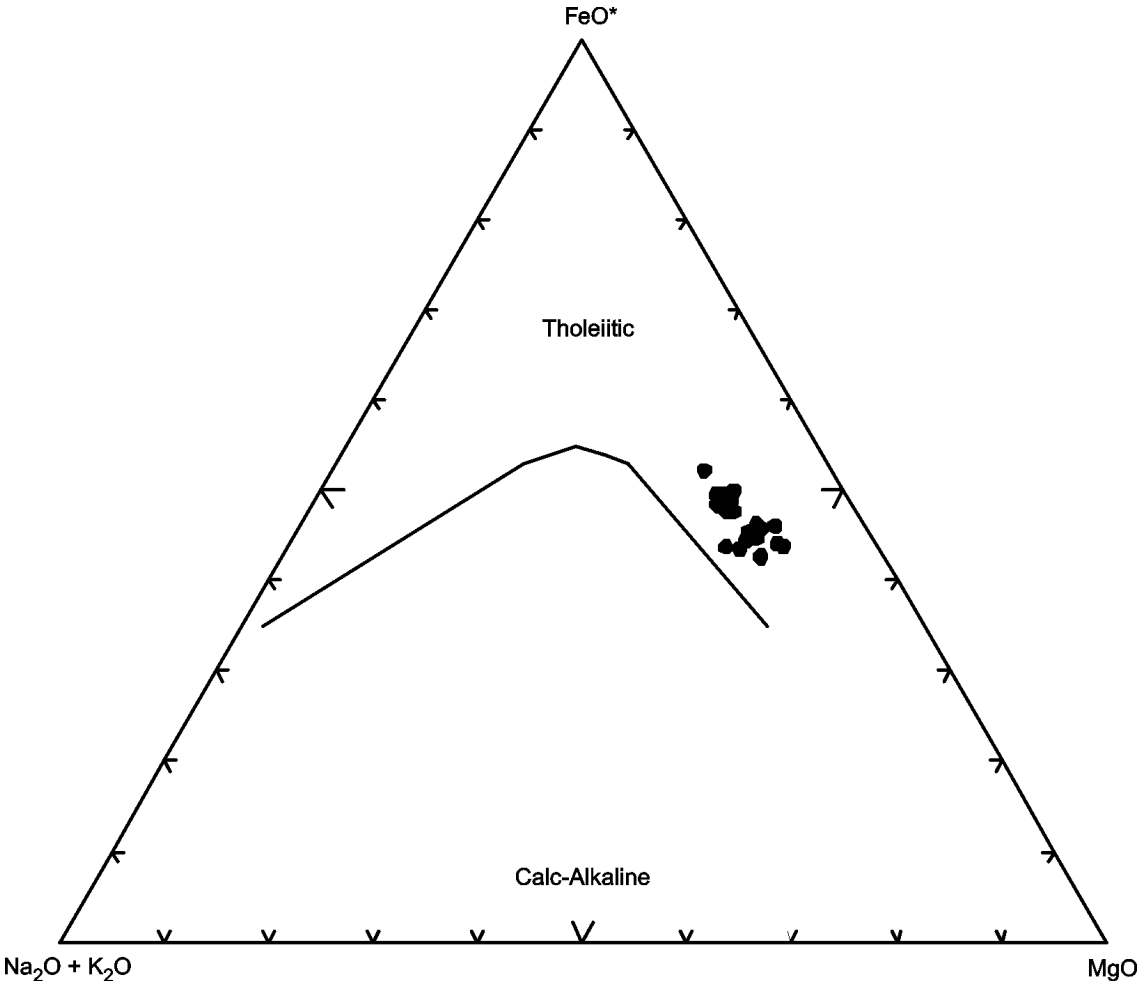

Figure F78. Discrimination Nb-Zr-Y diagram (Meschede, 1986) for basalts in Hole 317A. AI, AII = fields of intraplate alkali basalts; AII, C = fields of intraplate tholeiites; B = field of P-type MORB; D = field of N-type MORB; C, D = fields of volcanic arc basalts.

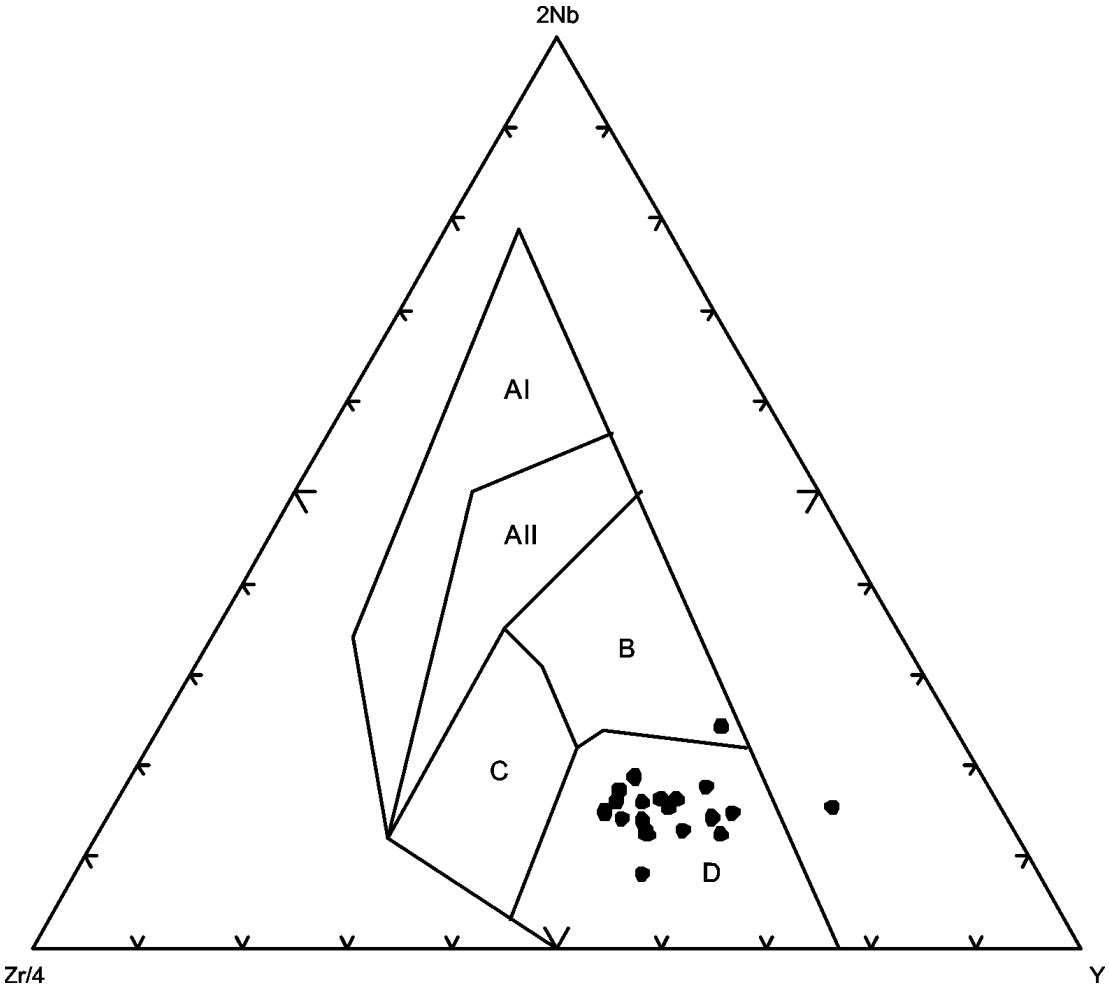

Figure F79. Chondrite-normalized rare earth element abundances for basalts in Hole 317A. Normalizing values are from Sun and McDonough (1989).

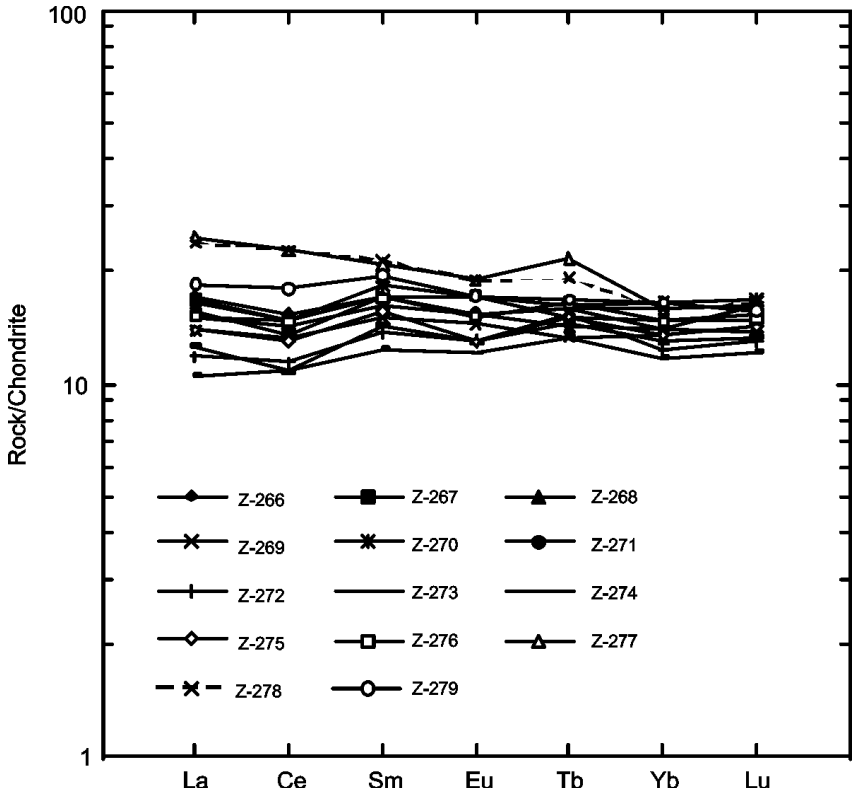

Figure F80. Leg 26, 120, 121, and 183 sites on the Ninetyeast Ridge and Kerguelen Plateau, eastern Indian Ocean (from Frey et al., 2003).

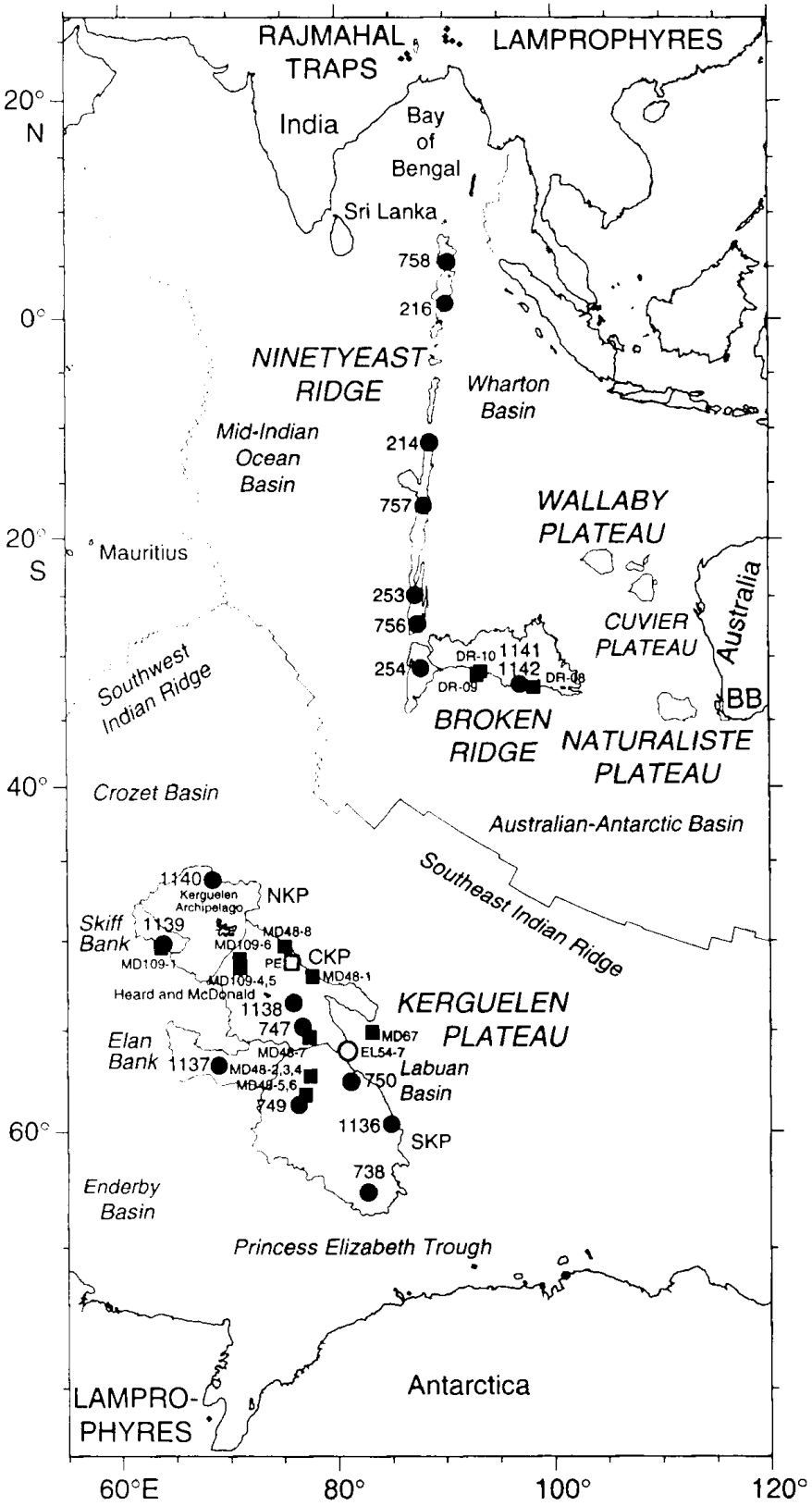

Figure F81. AFM diagram (Irvine and Baragar, 1971) for basalts in Holes 254, 756D, 757C, and 758A.

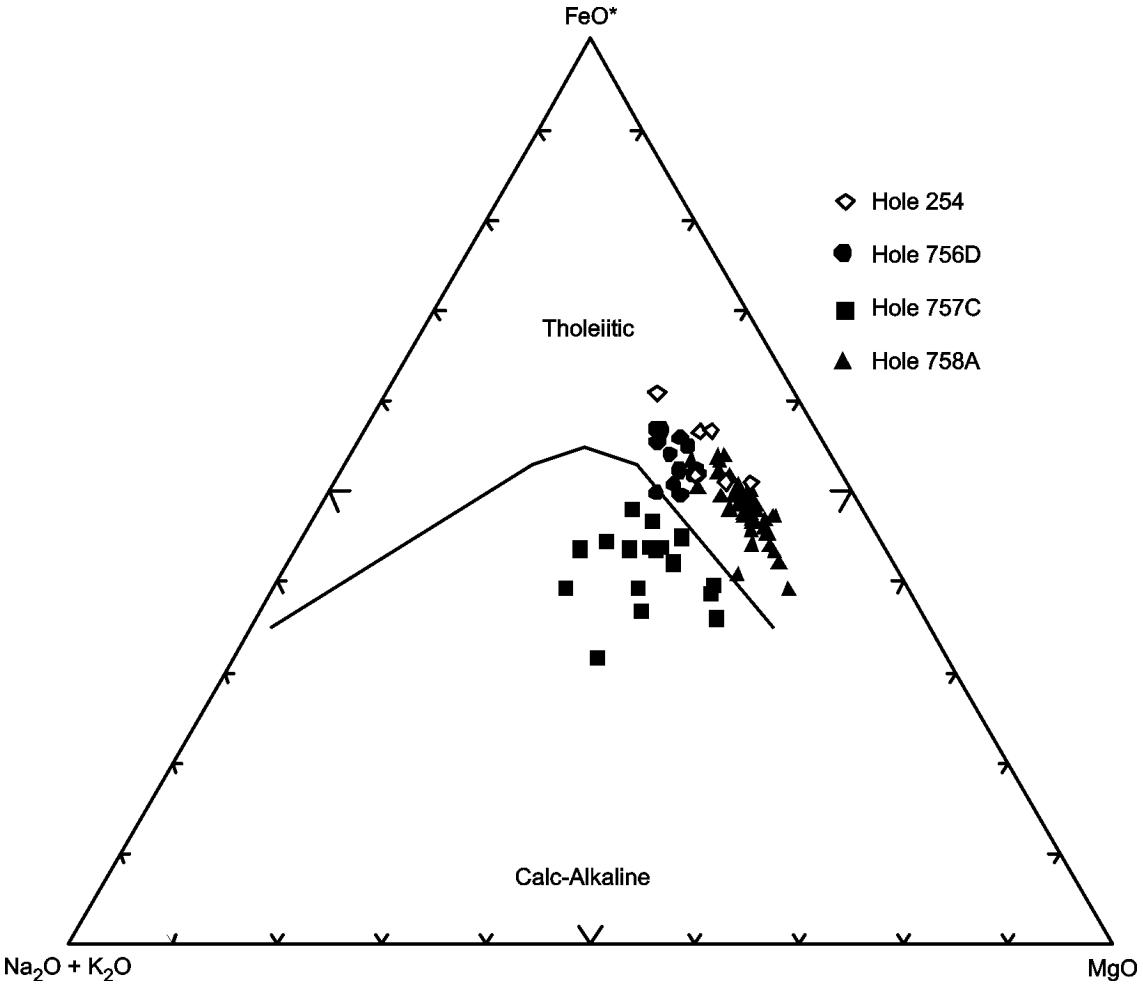

Figure F82. Discrimination Nb-Zr-Y diagram (Meschede, 1986) for basalts in Holes 254, 756D, 757C, and 758A. AI, AII = fields of intraplate alkali basalts; AII, C = fields of intraplate tholeiites; B = field of P-type MORB; D = field of N-type MORB; C, D = fields of volcanic arc basalts.

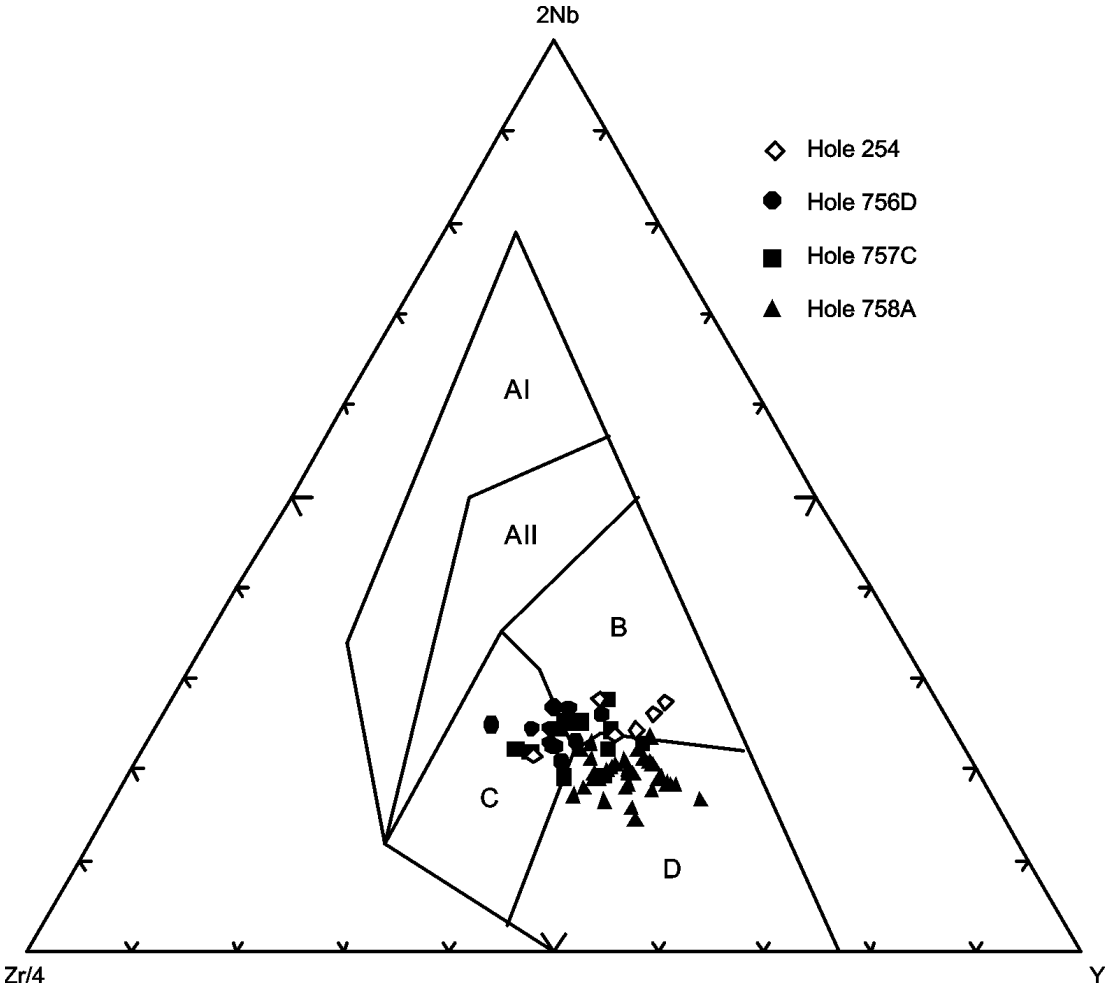

Figure F83. Chondrite-normalized rare earth element abundances for basalts in Holes 254, 756D, 757C, and 758A. Normalizing values are from Sun and McDonough (1989). (Continued on next page.)

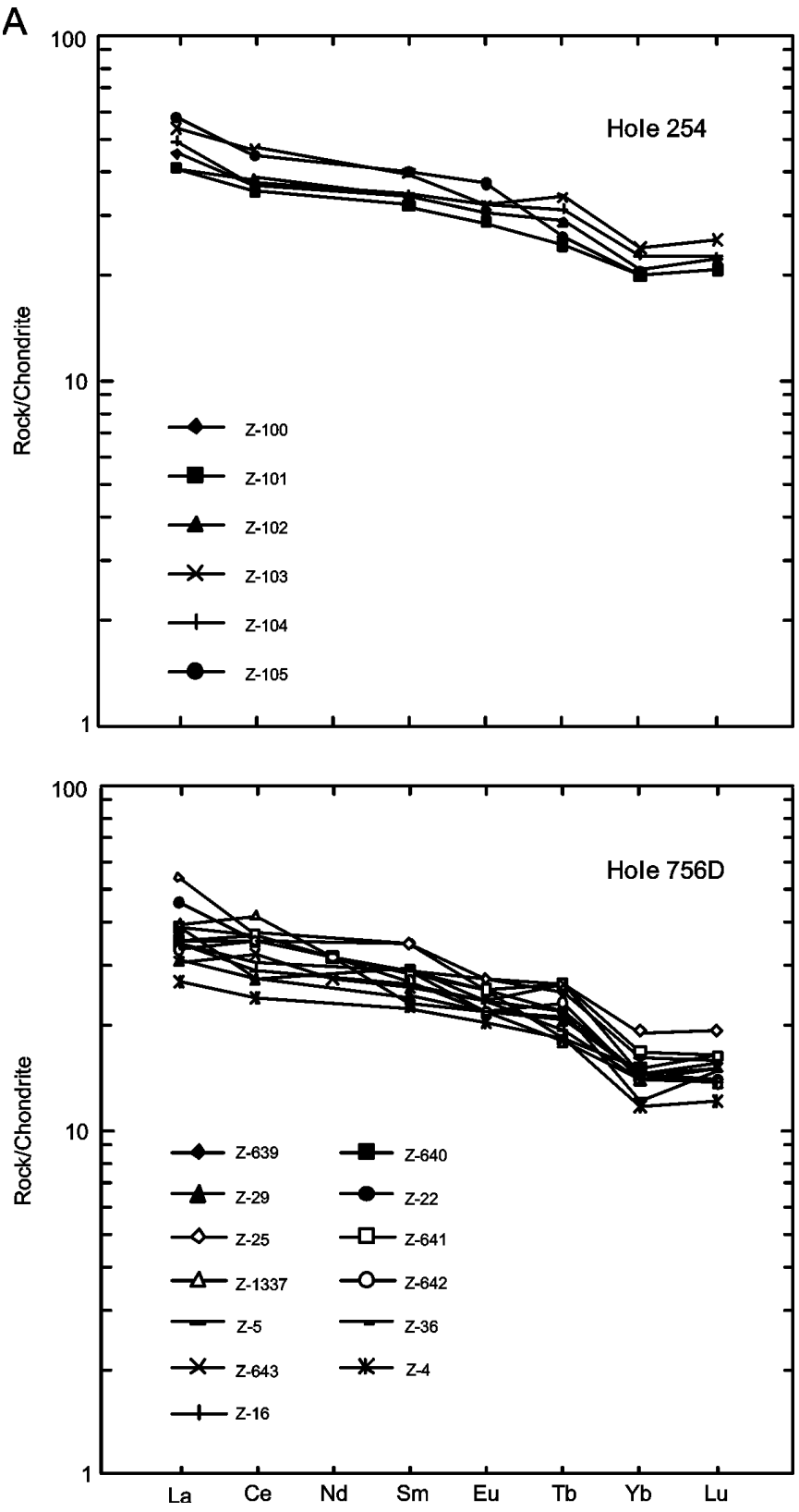

Figure F83 (continued).

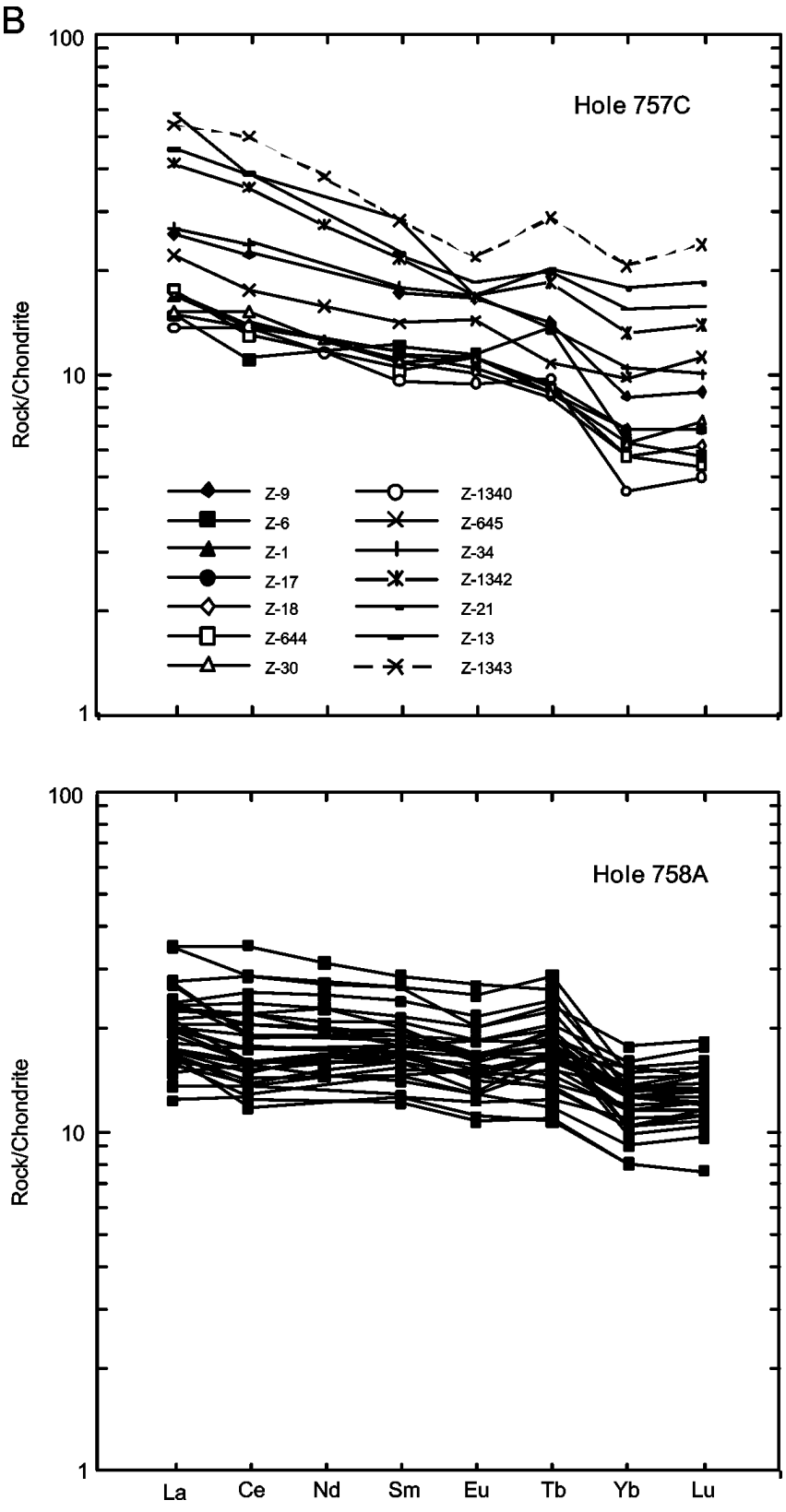

Figure F84. AFM diagram (Irvine and Baragar, 1971) for basalts in Holes 747C, 1136A, 1137A, 1138A, and 1140A.

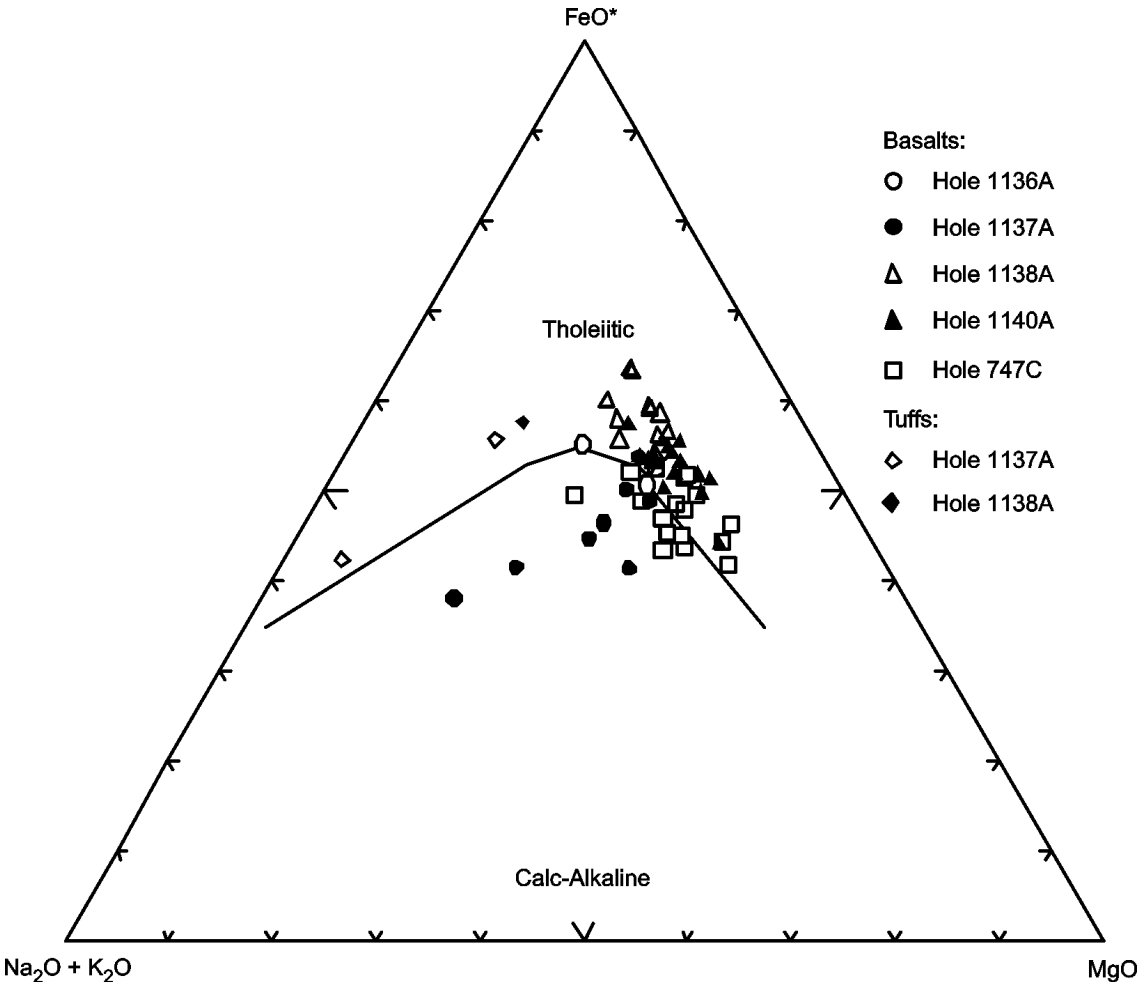

Figure F85. Discrimination Nb-Zr-Y diagram (Meschede, 1986) for basalts in Holes 747C, 1136A, 1137A, 1138A, and 1140A. AI, AII = fields of intraplate alkali basalts; AII, C = fields of intraplate tholeiites; B = field of P-type MORB; D = field of N-type MORB; C, D = fields of volcanic arc basalts.

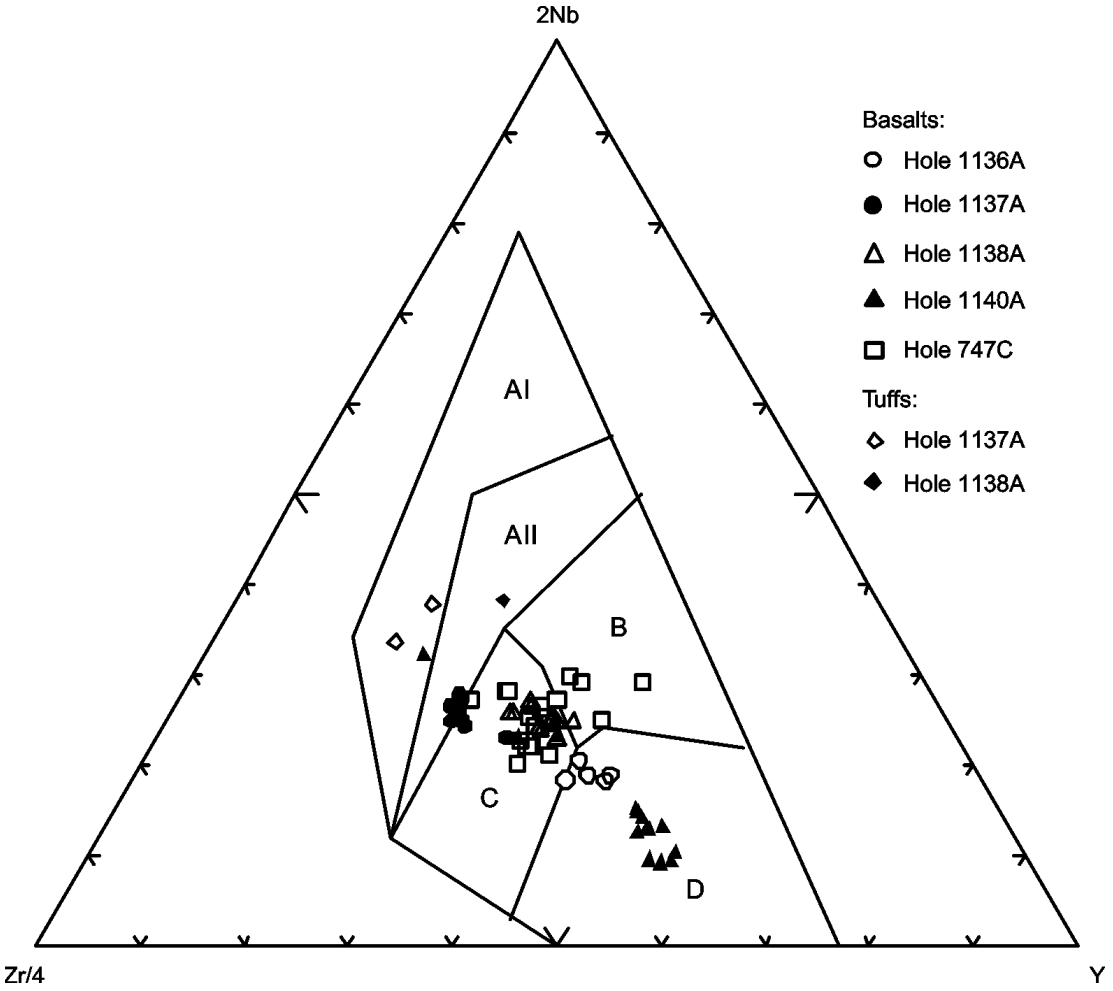

Figure F86. Chondrite-normalized rare earth element abundances for basalts in Holes 747C, 1136A, 1137A, 1138A, and 1140A. Normalizing values are from Sun and McDonough (1989). (Continued on next two pages.)

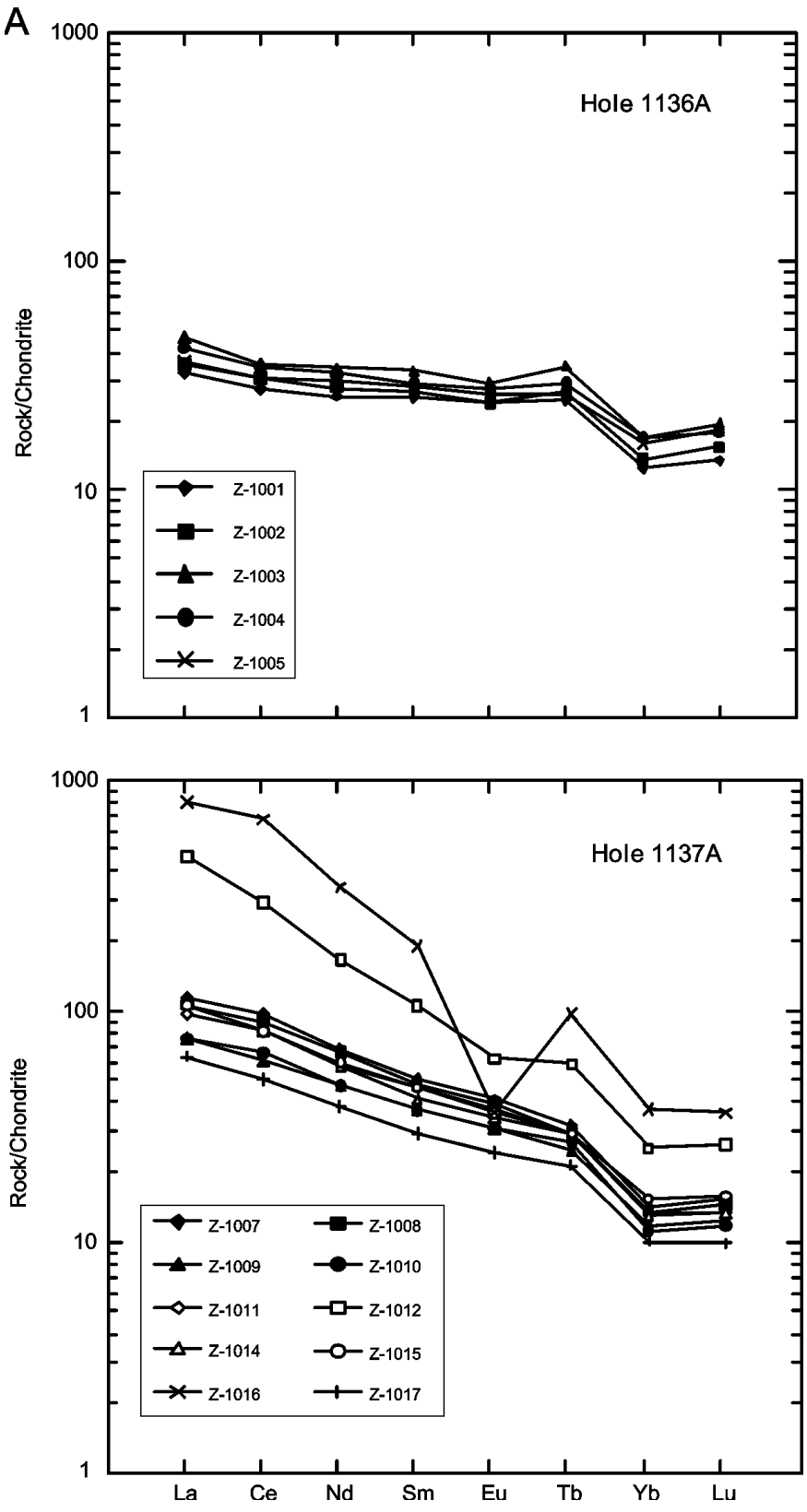

Figure F86 (continued).

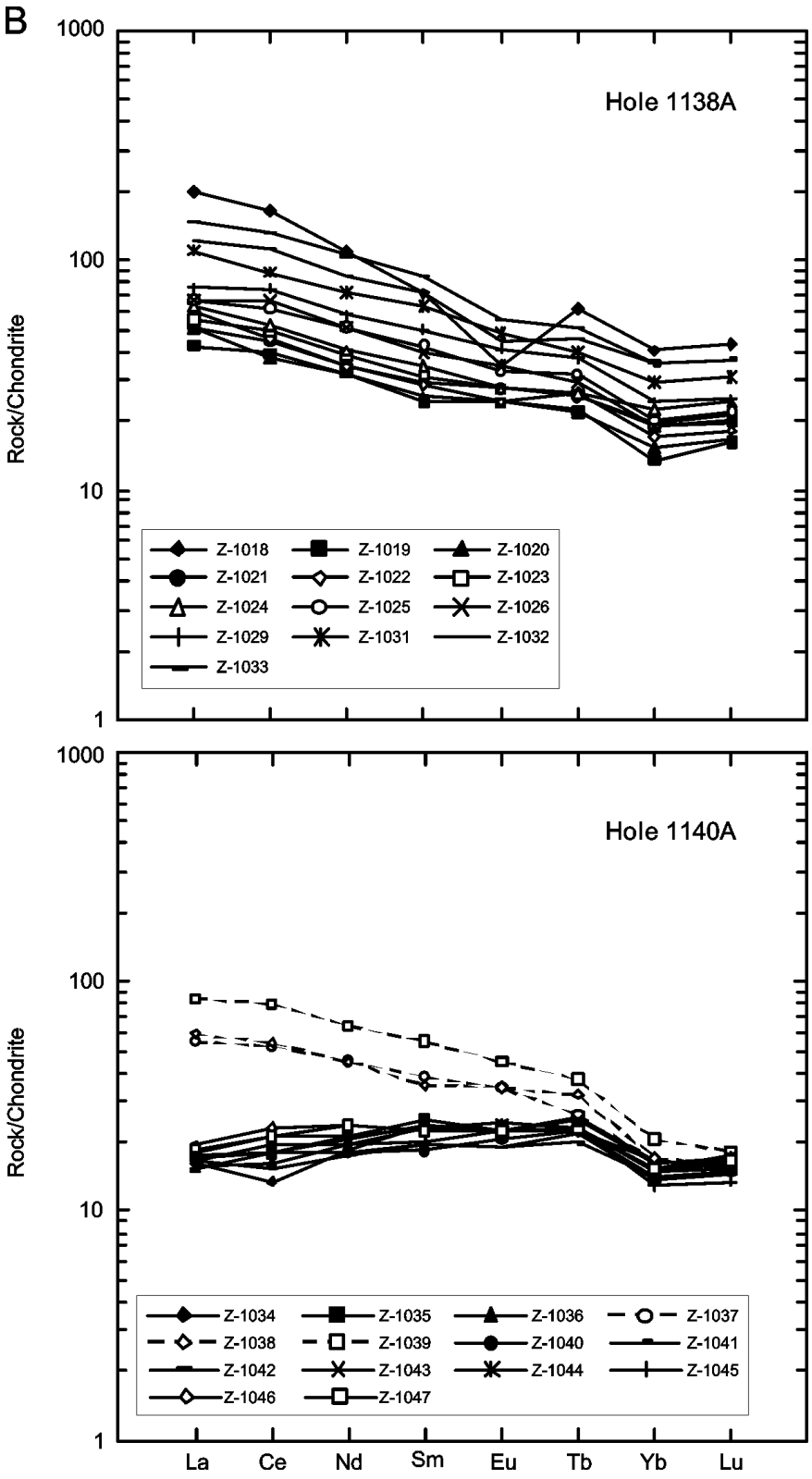

Figure F86 (continued).

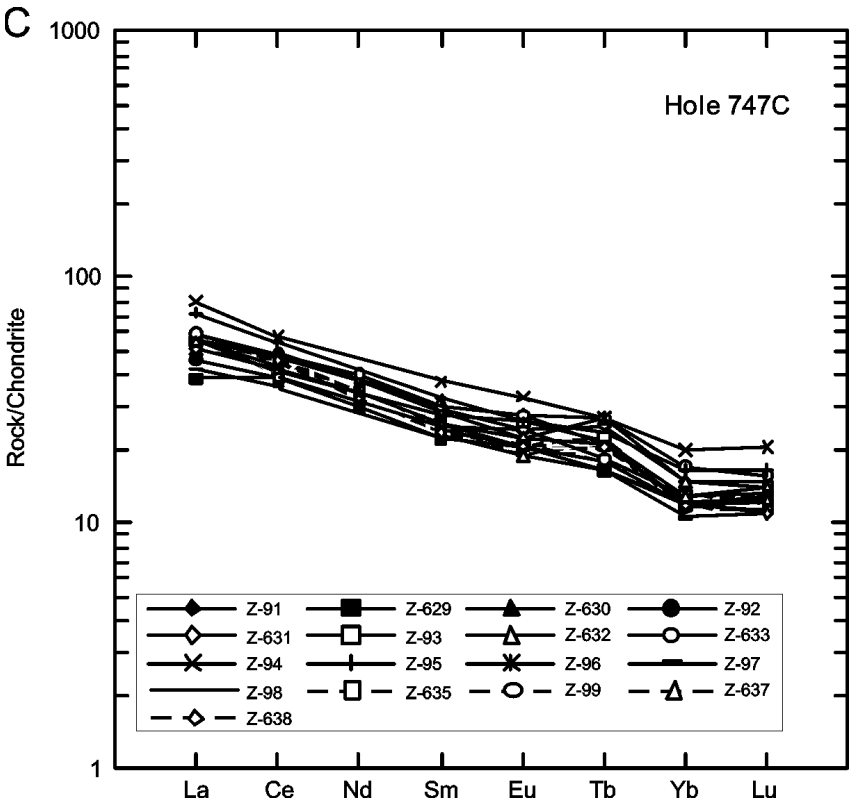

Figure F87. Leg 115 sites in the western Indian Ocean. Ages of basalts (Ma) are given in parentheses (from Baxter, 1990).

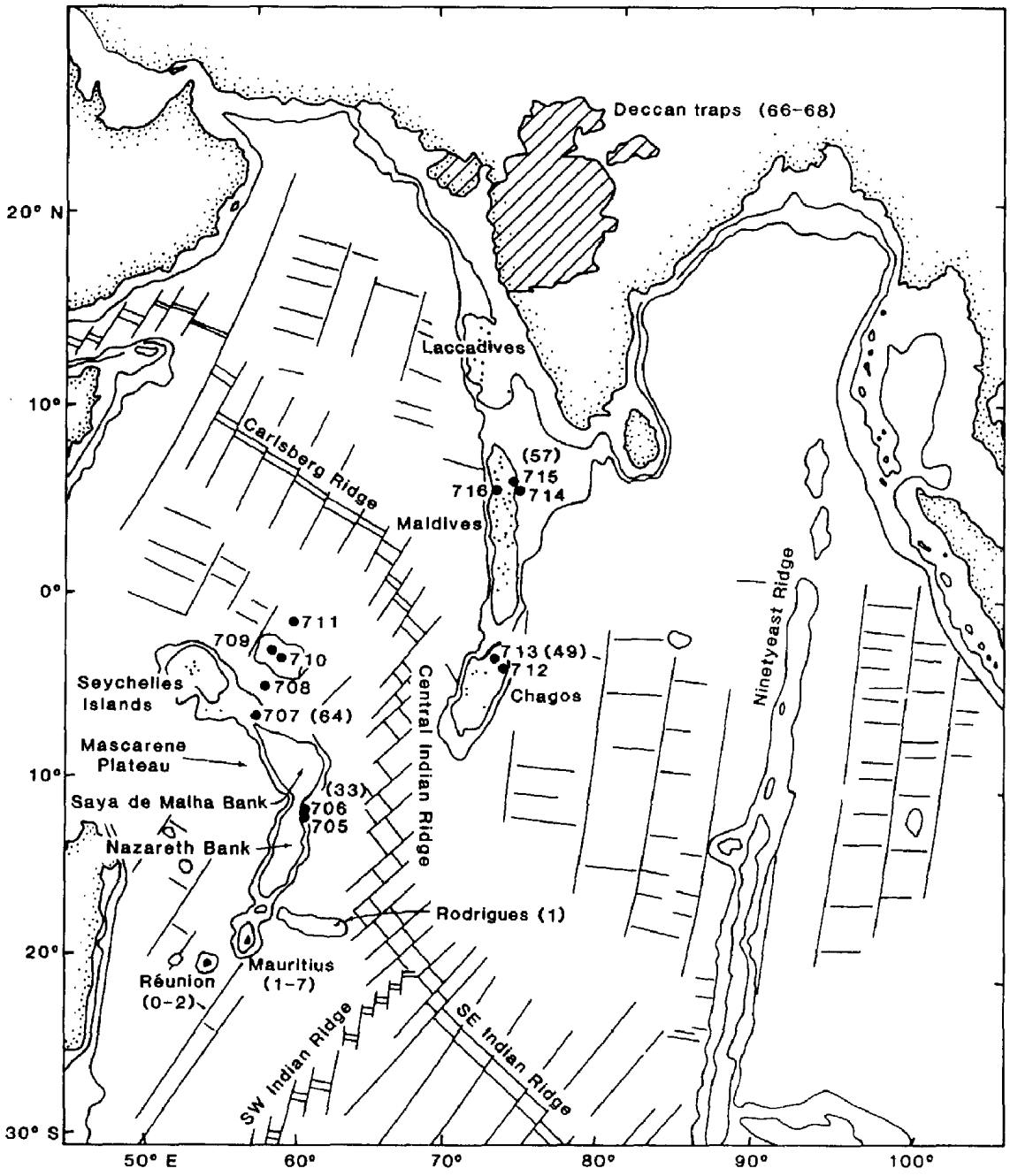

Figure F88. AFM diagram (Irvine and Baragar, 1971) for basalts in Holes 706C, 707C, 713A, and 715A.

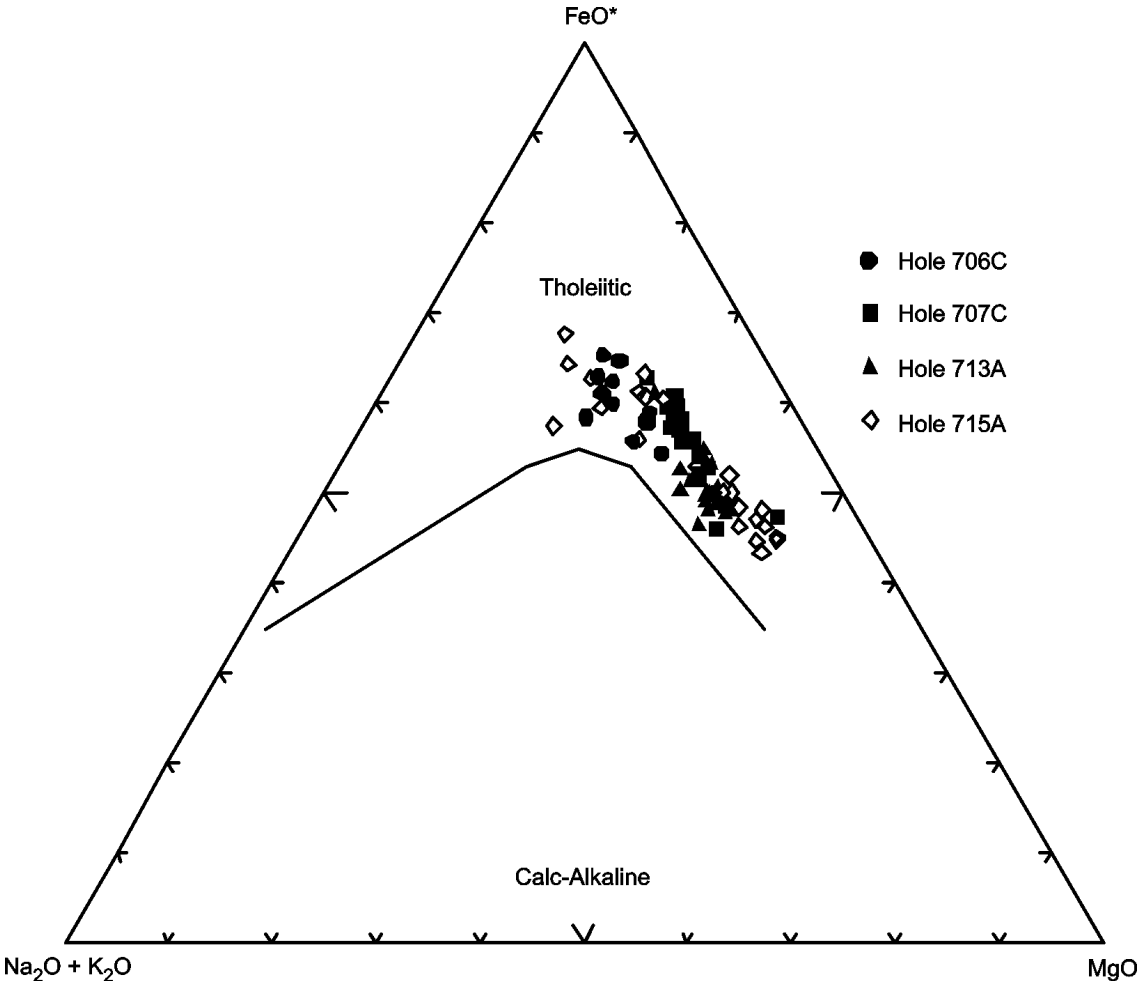

Figure F89. Discrimination Nb-Zr-Y diagram (Meschede, 1986) for basalts in Holes 706C, 707C, 713A, and 715A. AI, AII = fields of intraplate alkali basalts; AII, C = fields of intraplate tholeiites; B = field of P-type MORB; D = field of N-type MORB; C, D = fields of volcanic arc basalts.

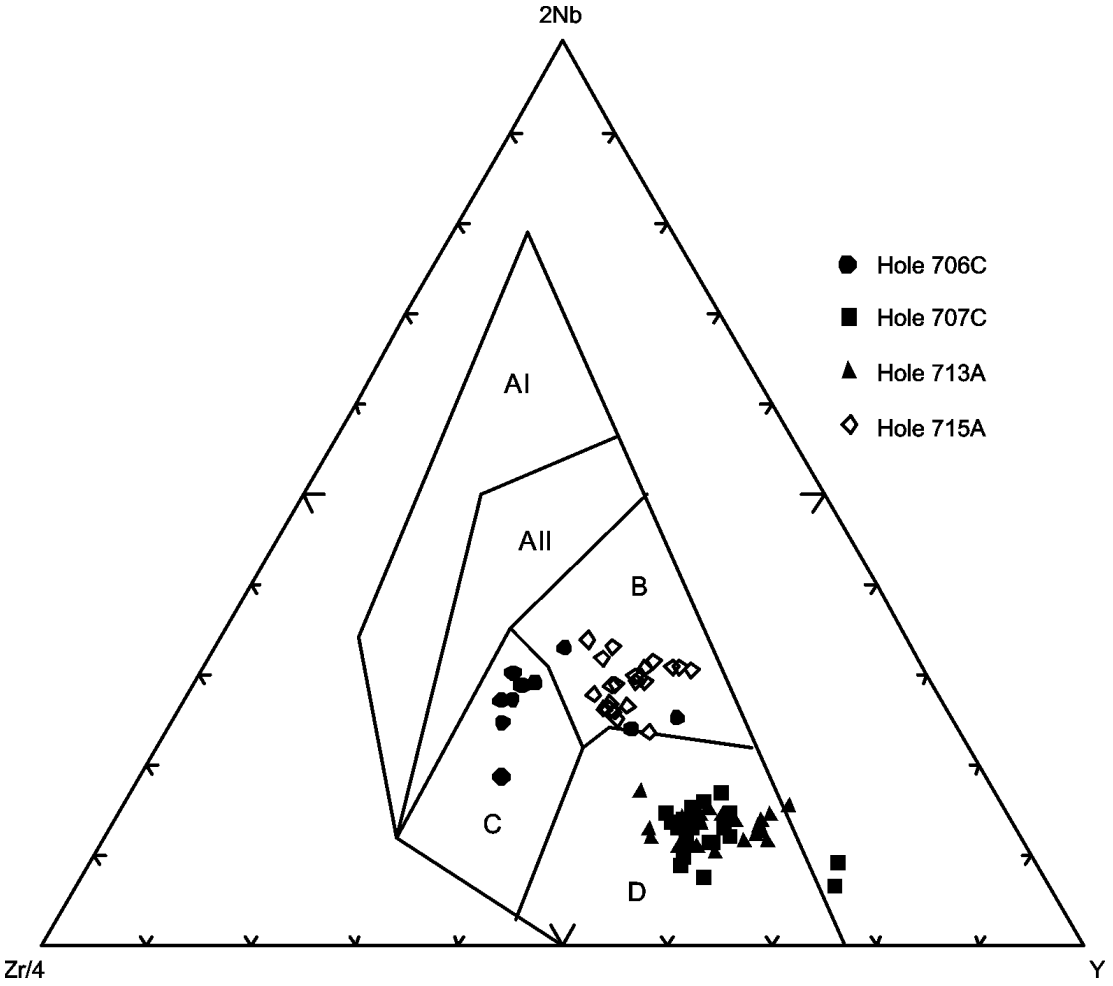

Figure F90. Chondrite-normalized rare earth element abundances for basalts in Holes 706C, 707C, 713A, and 715A. Normalizing values are from Sun and McDonough (1989). (Continued on next page.)

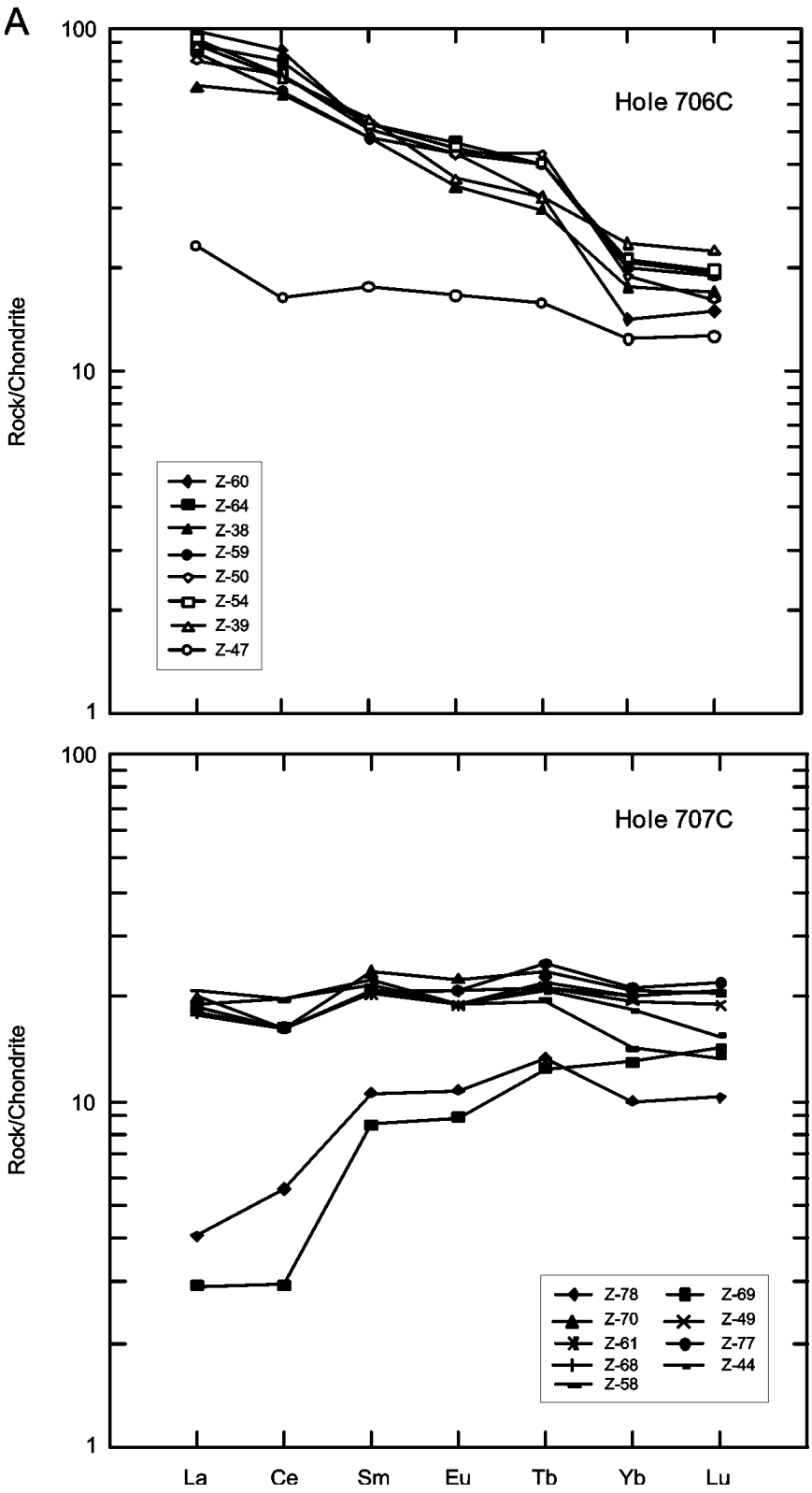

Figure F90 (continued).

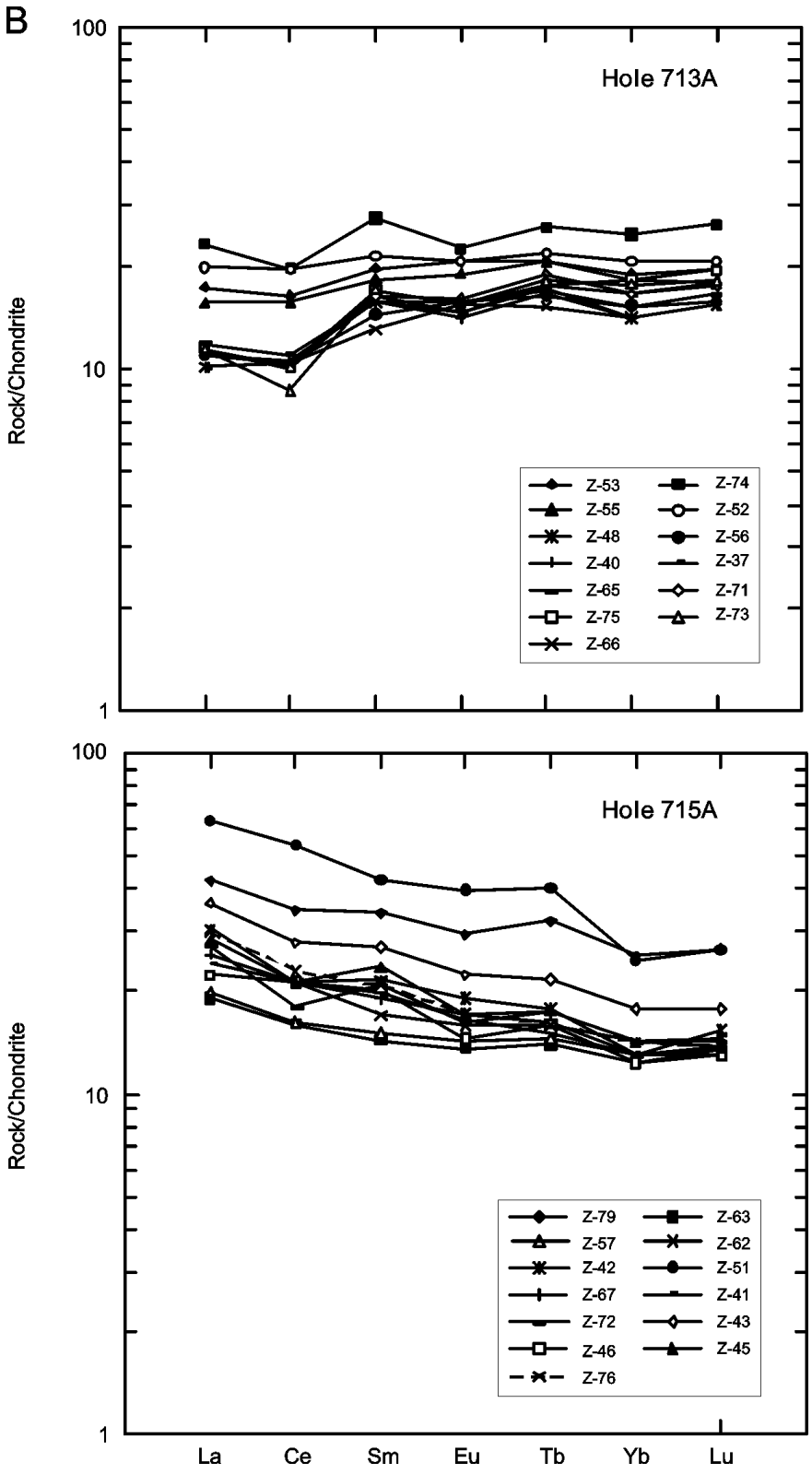

Figure F91. Leg 74 sites on the Walvis Ridge in the eastern Atlantic Ocean (from Moore, Rabinowitz, et al., 1984).

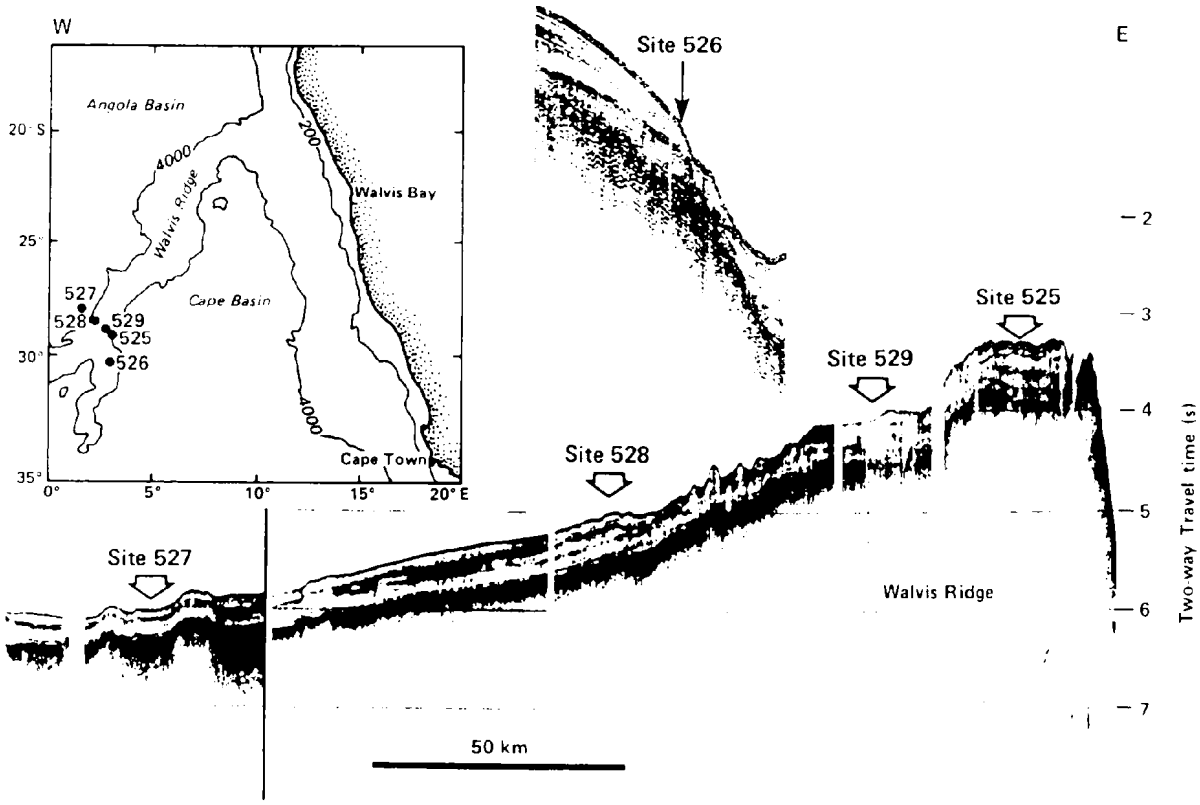

Figure F92. AFM diagram (Irvine and Baragar, 1971) for basalts in Holes 525A, 527, and 528.

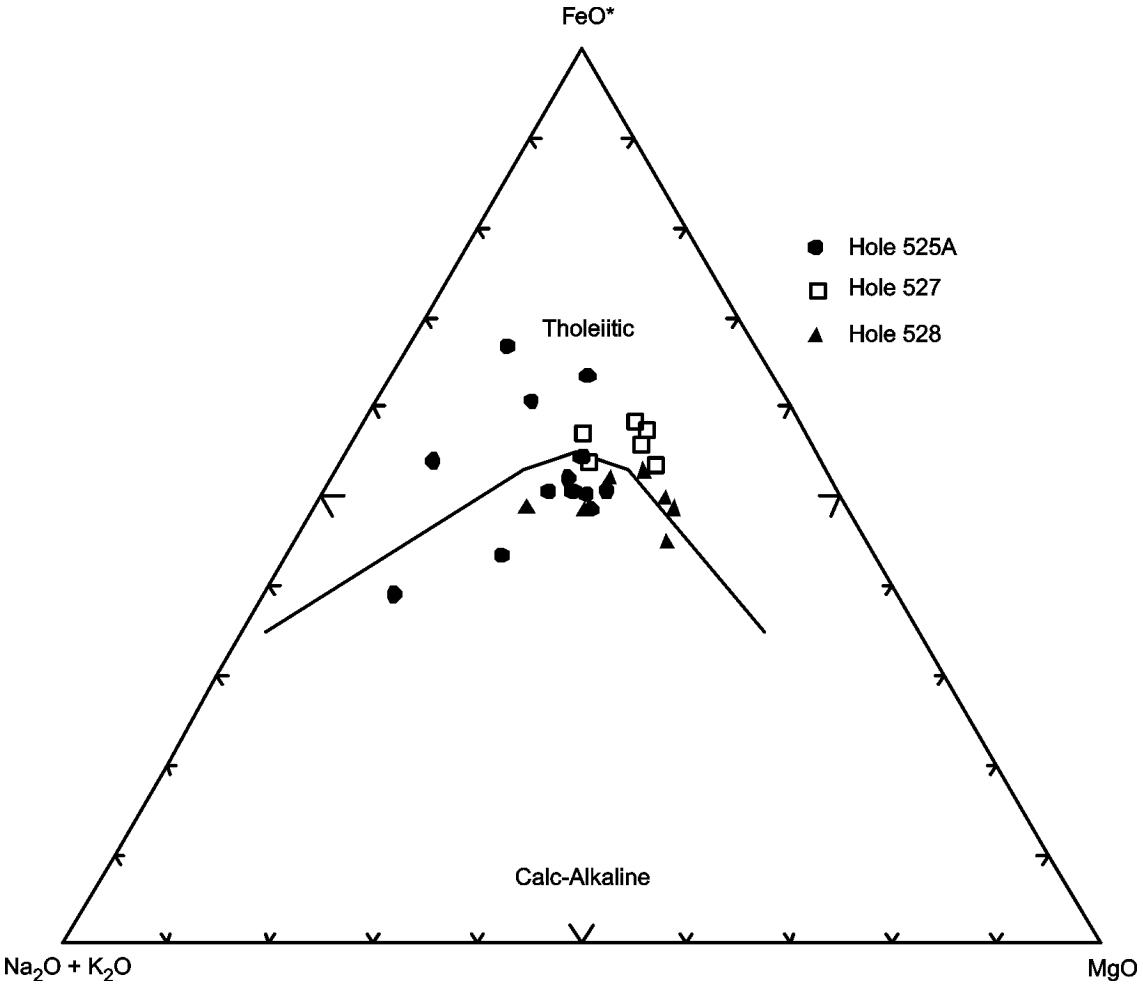

Figure F93. Discrimination Nb-Zr-Y diagram (Meschede, 1986) for basalts in Holes 525A, 527, and 528. AI, AII = fields of intraplate alkali basalts; AII, C = fields of intraplate tholeiites; B = field of P-type MORB; D = field of N-type MORB; C, D = fields of volcanic arc basalts.

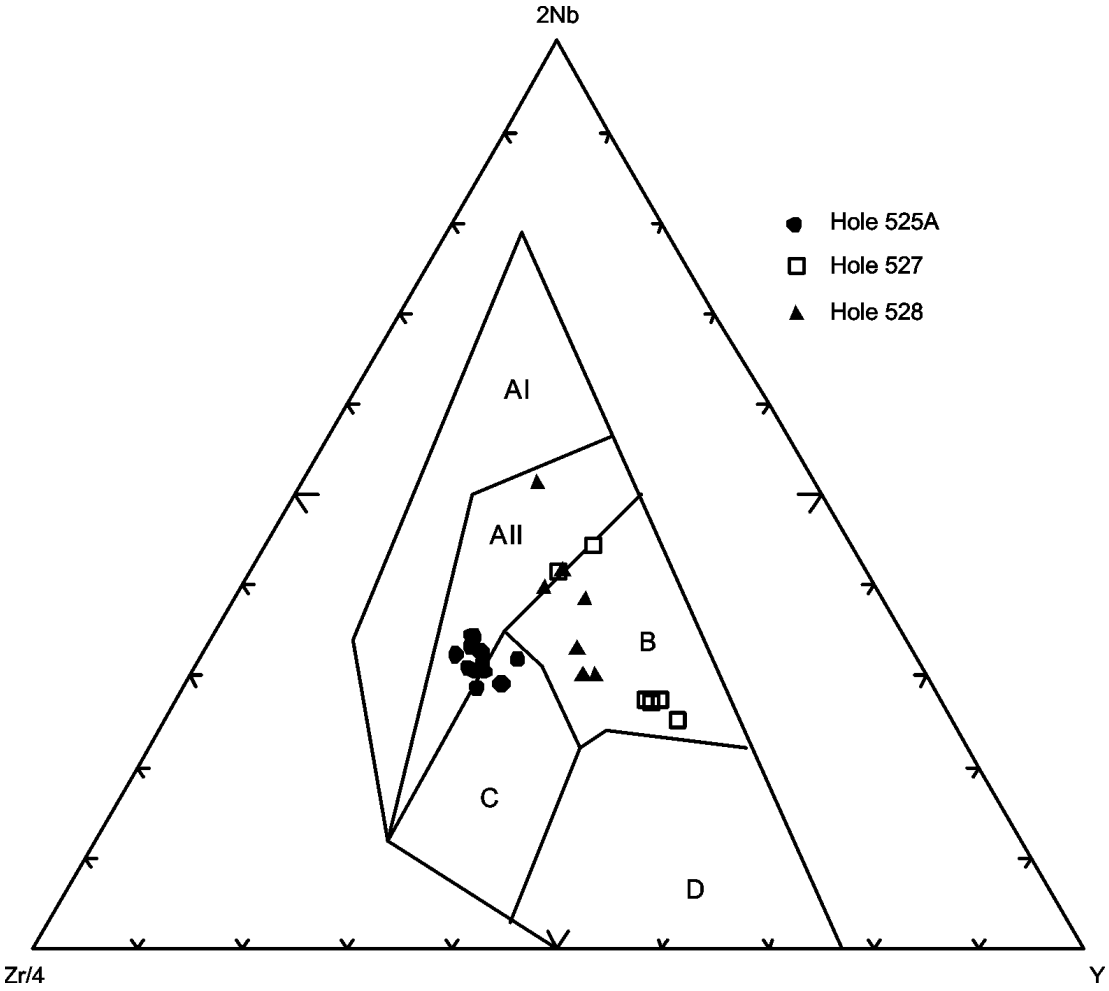

Figure F94. Chondrite-normalized rare earth element abundances for basalts in Holes 525A, 527, and 528. Normalizing values are from Sun and McDonough (1989). (Continued on next page.)

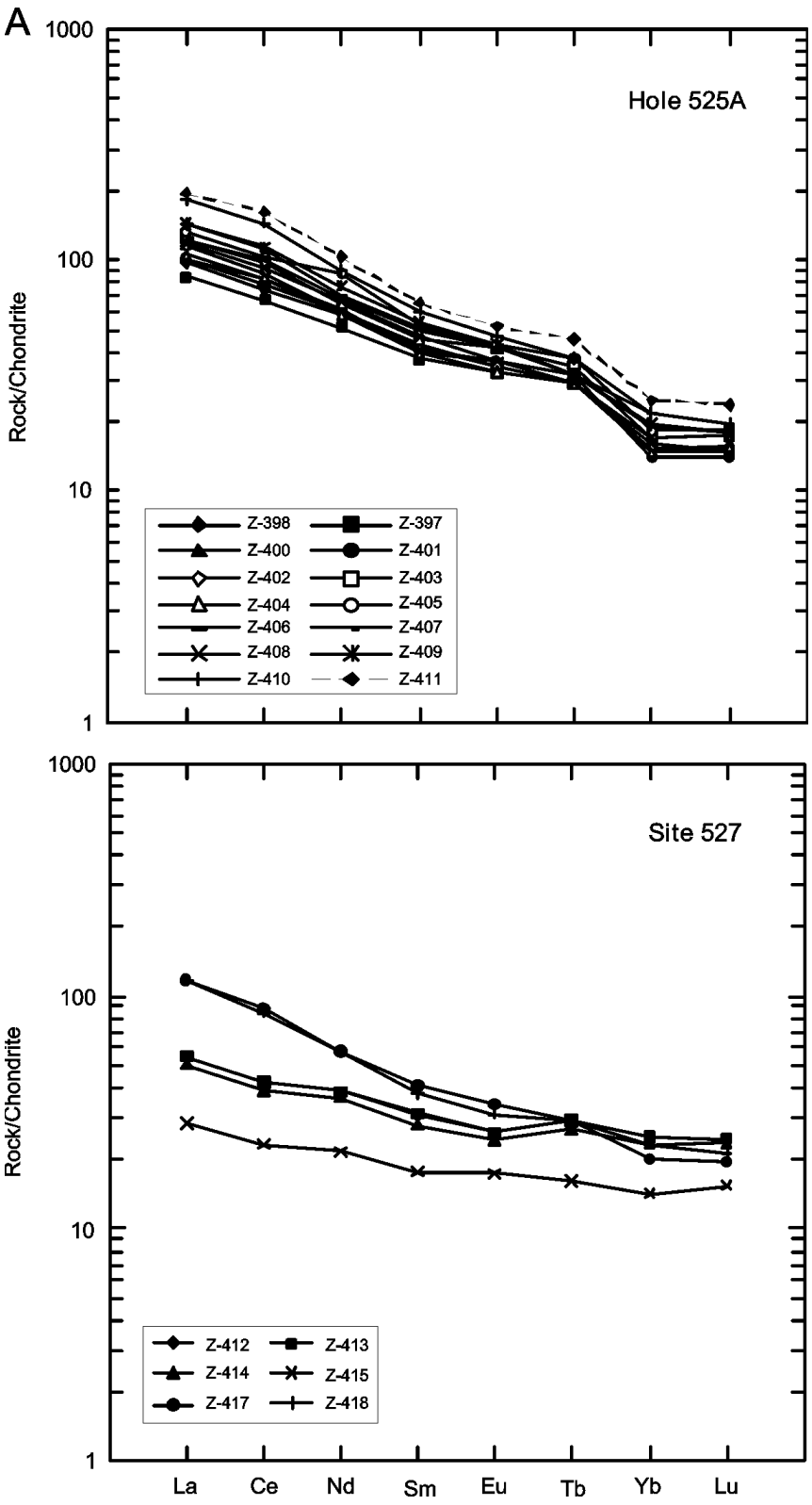

Figure F94 (continued).

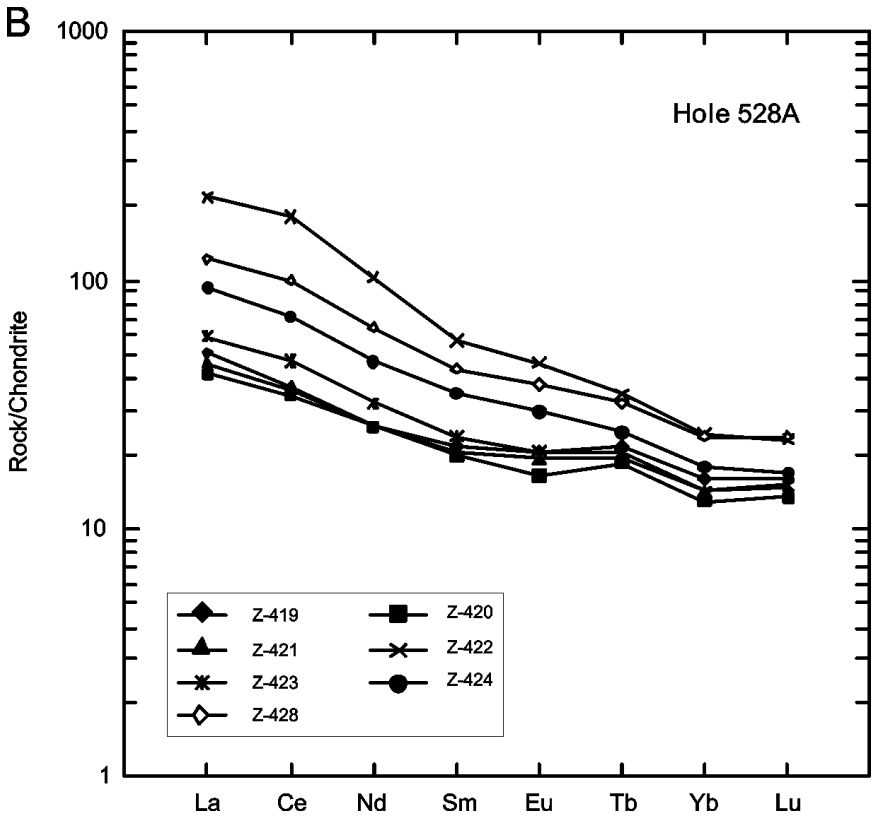

Figure F95. Site 516 drilled during Leg 72 on the Rio Grande Rise in the western Atlantic Ocean (from Barker, Carlson, et al., 1983).

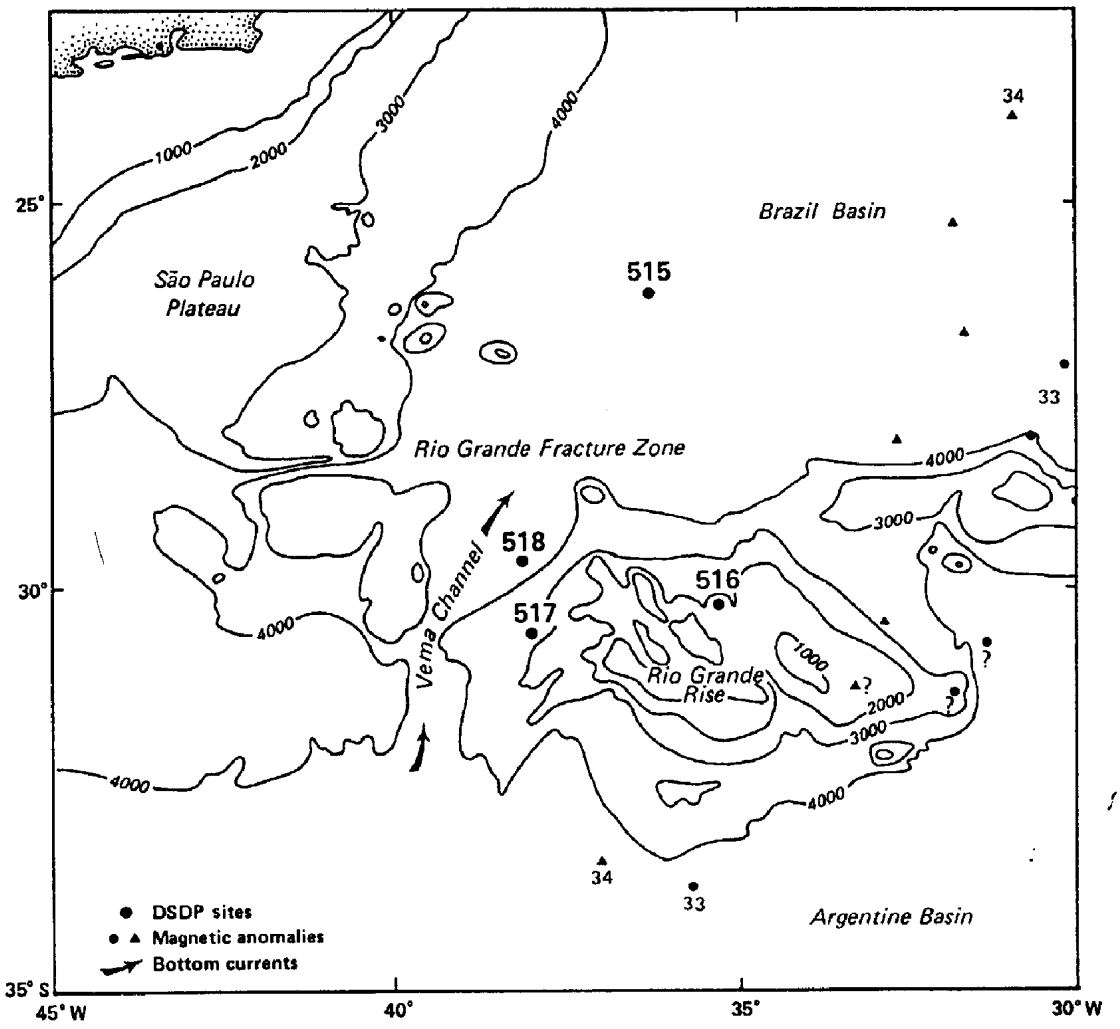

Figure F96. AFM diagram (Irvine and Baragar, 1971) for basalts in Hole 516F.

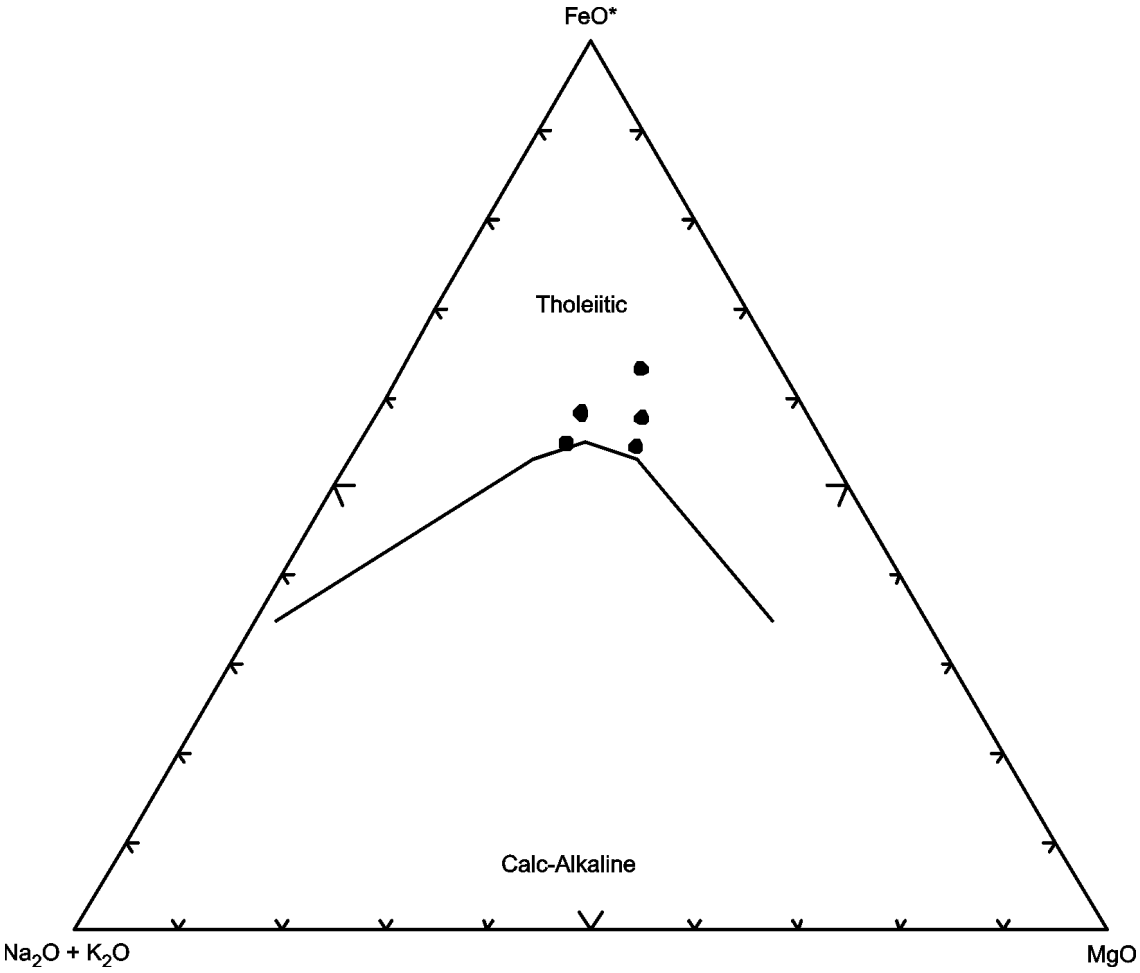

Figure F97. Discrimination Nb-Zr-Y diagram (Meschede, 1986) for basalts in Hole 516F. AI, AII = fields of intraplate alkali basalts; AII, C = fields of intraplate tholeiites; B = field of P-type MORB; D = field of N-type MORB; C, D = fields of volcanic arc basalts.

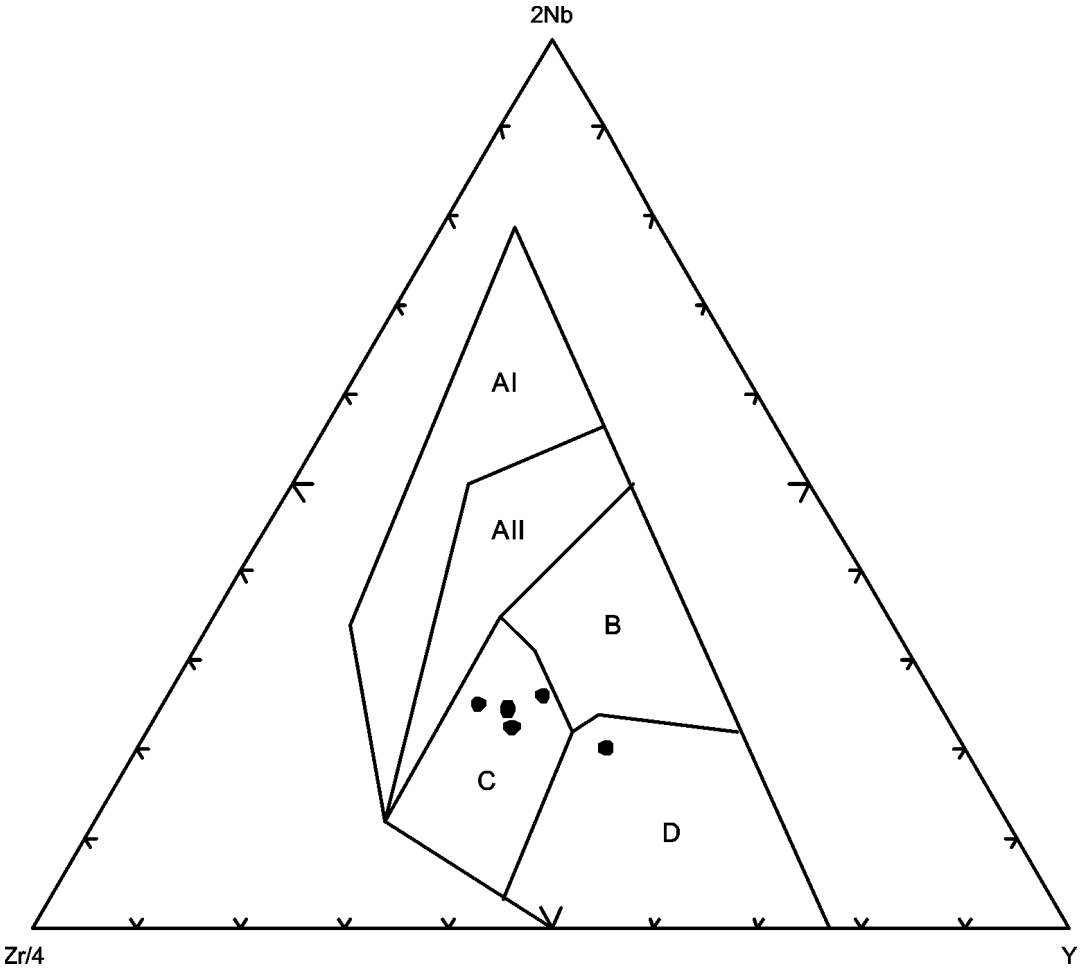

Figure F98. Chondrite-normalized rare earth element abundances for basalts in Hole 516F. Normalizing values are from Sun and McDonough (1989).

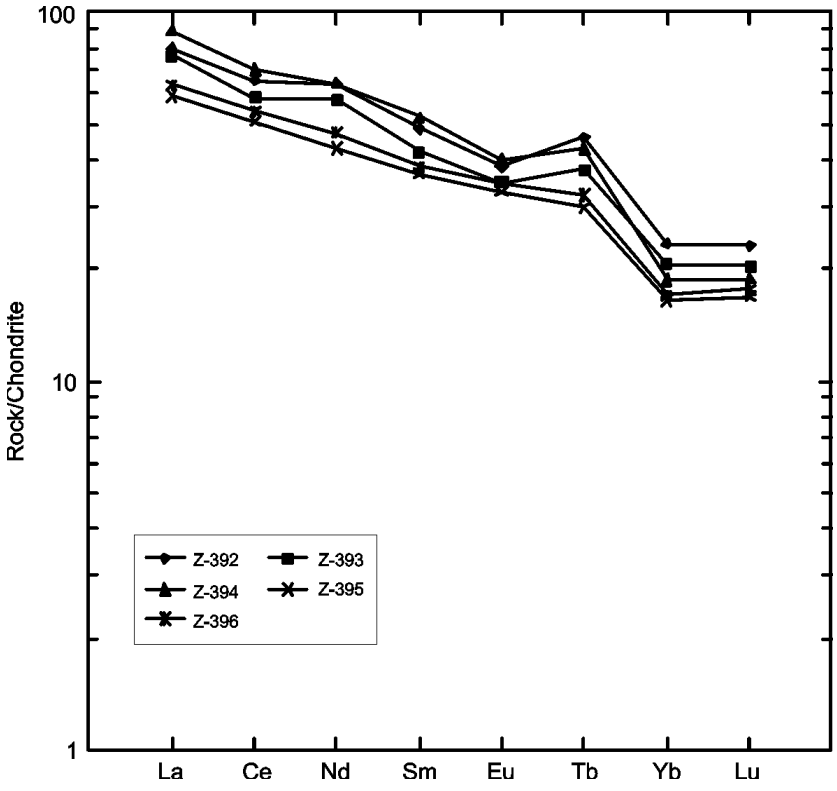

Figure F99. Sites 768 and 770 drilled during Leg 124 in the Sulu and Celebes Seas (from Rangin, Silver, et al., 1990).

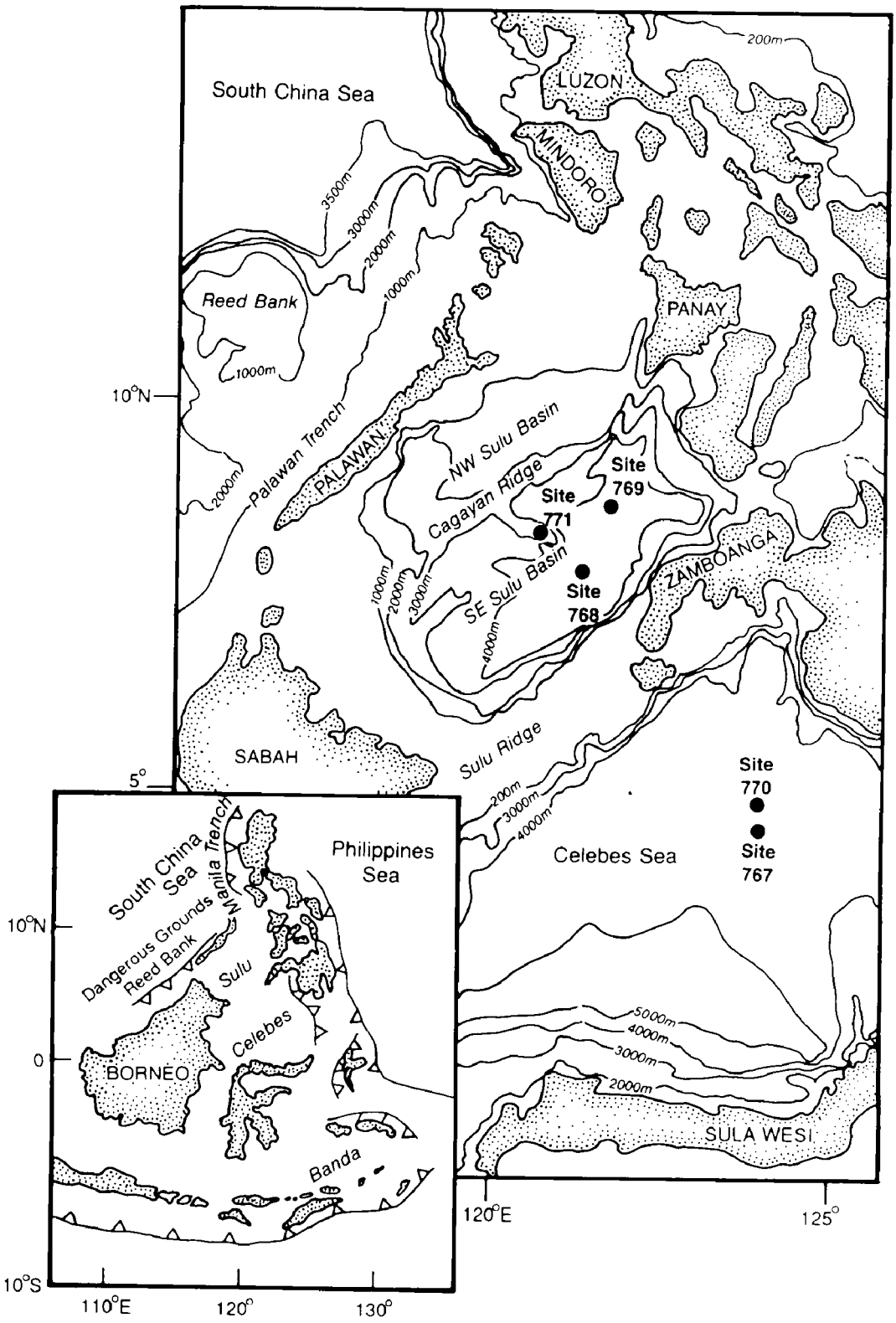

Figure F100. AFM diagram (Irvine and Baragar, 1971) for igneous rocks in Holes 768C and 770C.

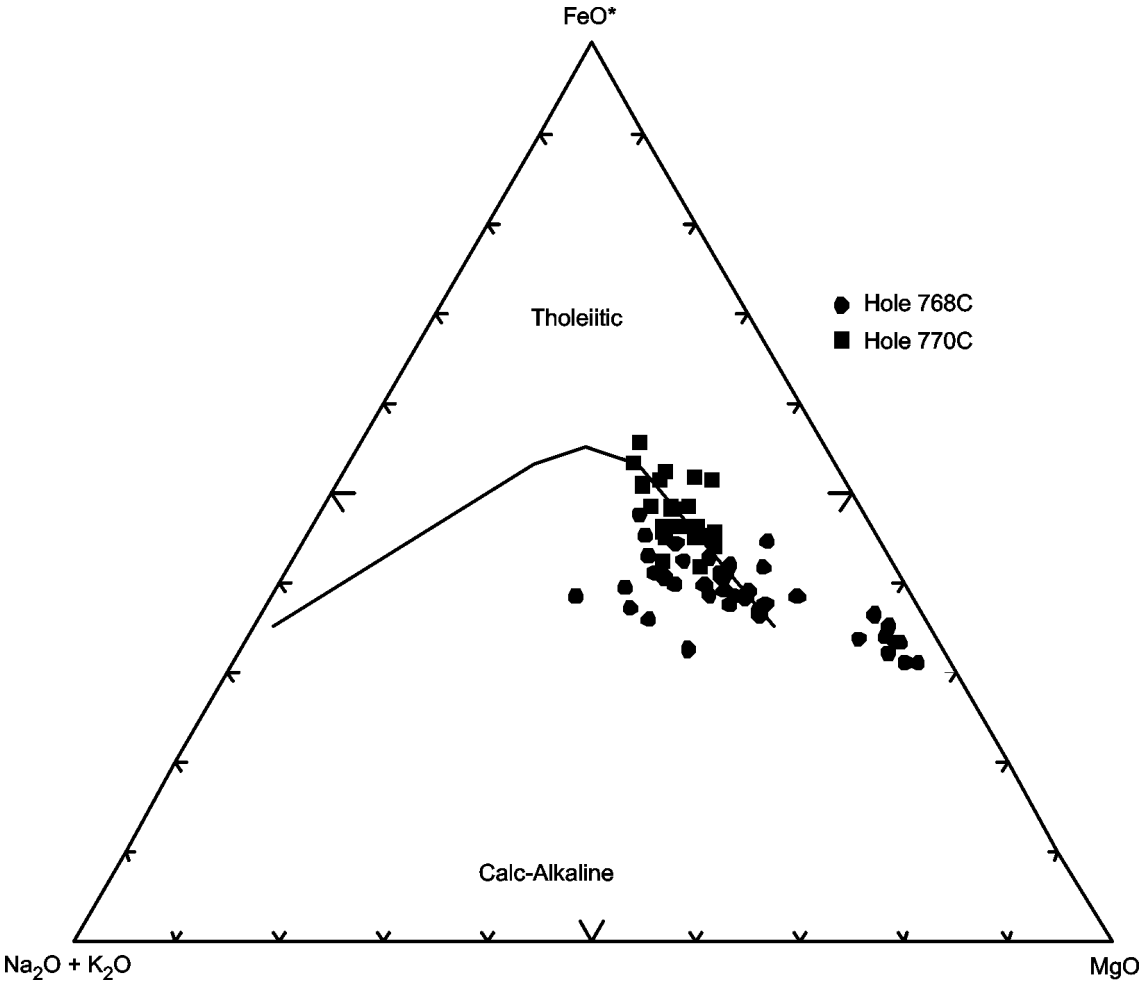

Figure F101. Discrimination Nb-Zr-Y diagram (Meschede, 1986) for igneous rocks in Holes 768C and 770C. AI, AII = fields of intraplate alkali basalts; AII, C = fields of intraplate tholeiites; B = field of P-type MORB; D = field of N-type MORB; C, D = fields of volcanic arc basalts.

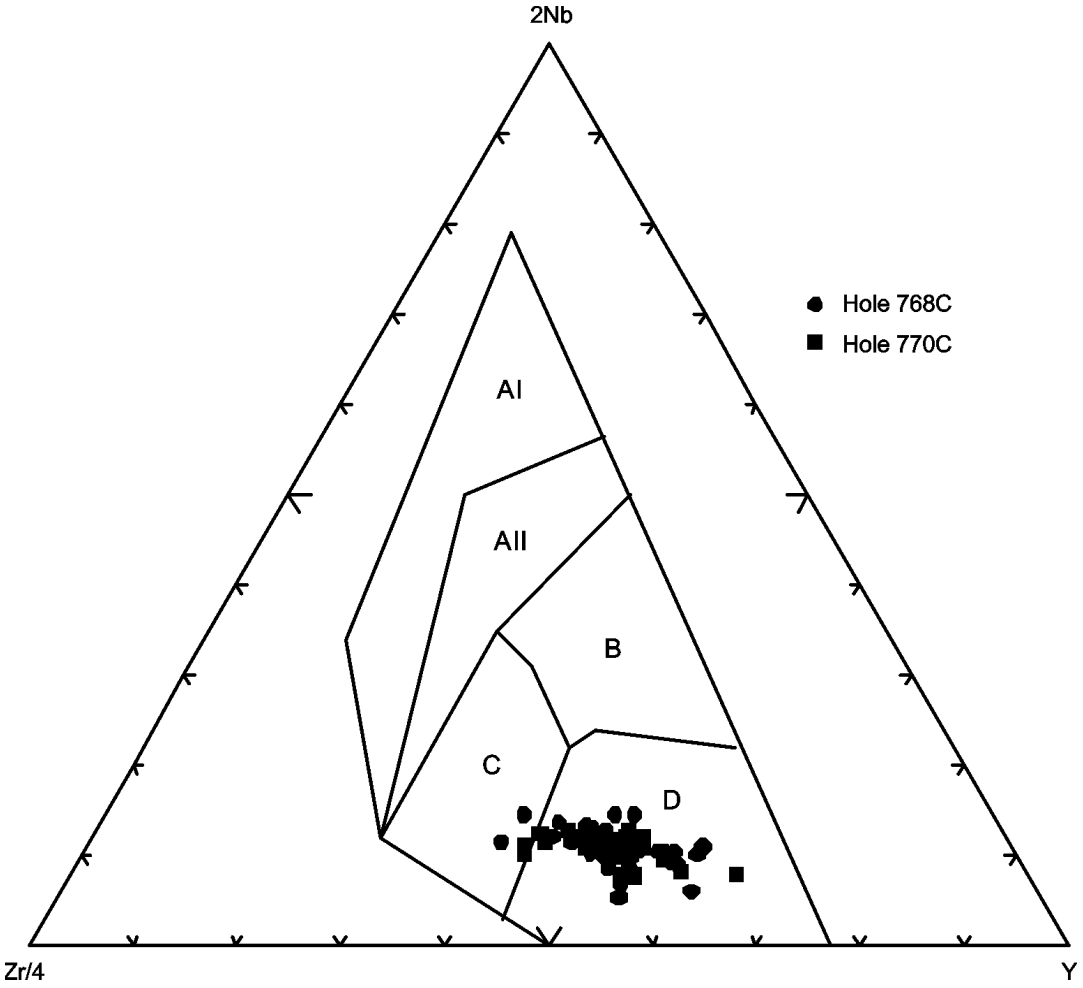

Figure F102. Chondrite-normalized rare earth element abundances for igneous rocks in Holes 768C and 770C. Normalizing values are from Sun and McDonough (1989).

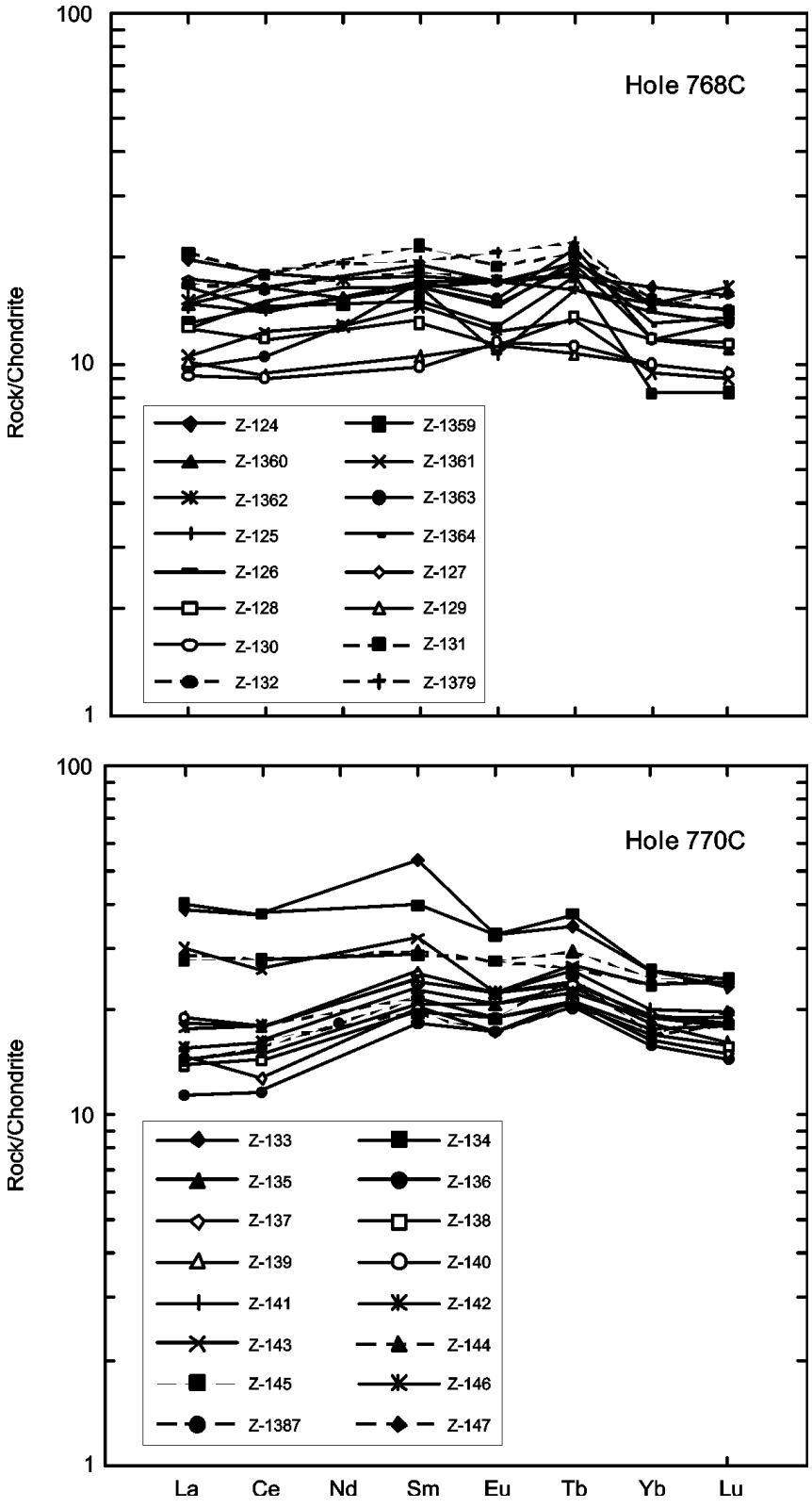

Figure F103. Sites 779, 780, and 786 drilled during Leg 125 in the Izu-Bonin and Mariana forearcs, Philippine Sea (from Fryer, Pearce, et al., 1990).

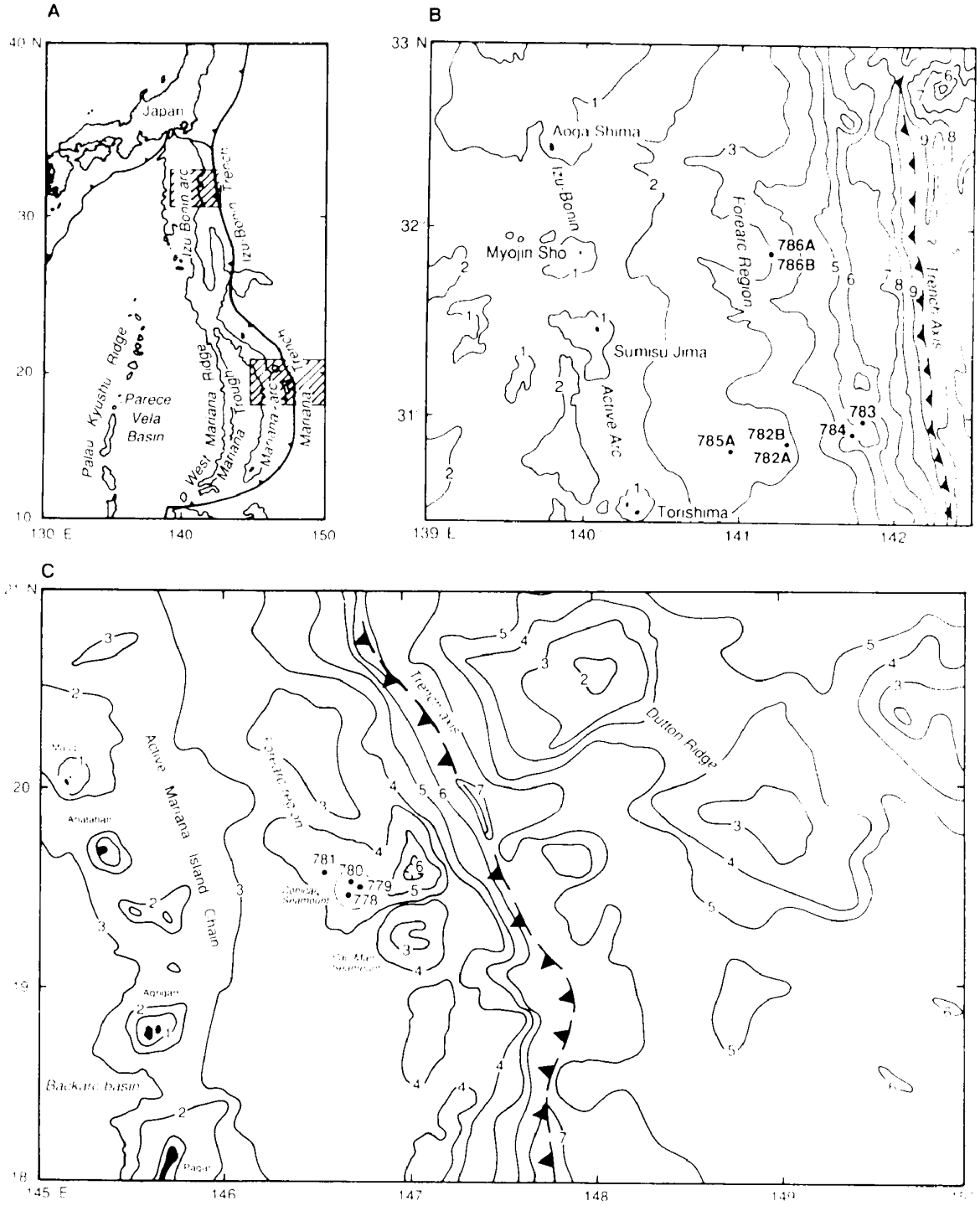

Figure F104. AFM diagram (Irvine and Baragar, 1971) for igneous rocks in Hole 779A, 780C, and 786B (Leg 125 ODP).

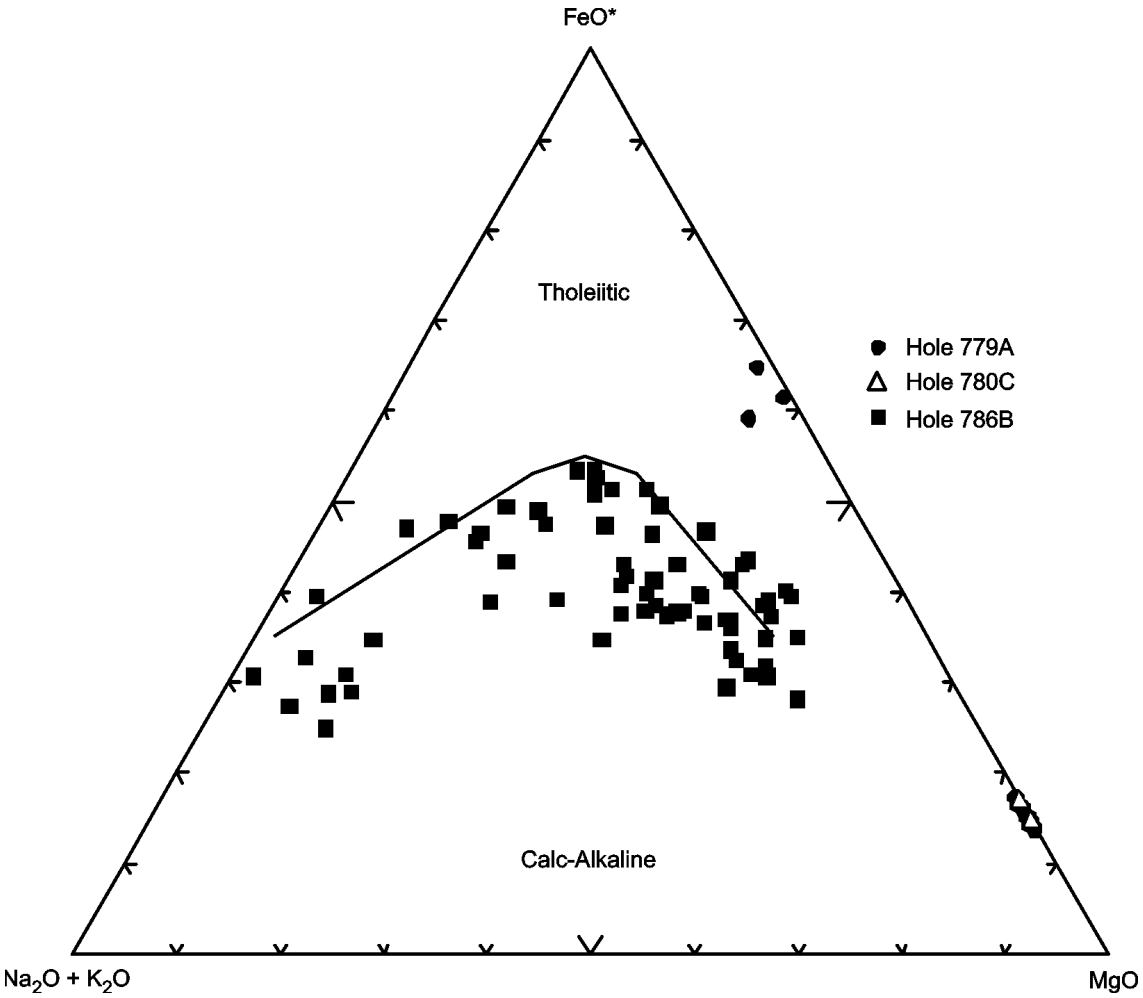

Figure F105. Discrimination Nb-Zr-Y diagram (Meschede, 1986) for igneous rocks in Hole 779A, 780C, and 786B). AI, AII = fields of intraplate alkali basalts; AII, C = fields of intraplate tholeiites; B = field of P-type MORB; D = field of N-type MORB; C, D = fields of volcanic arc basalts.

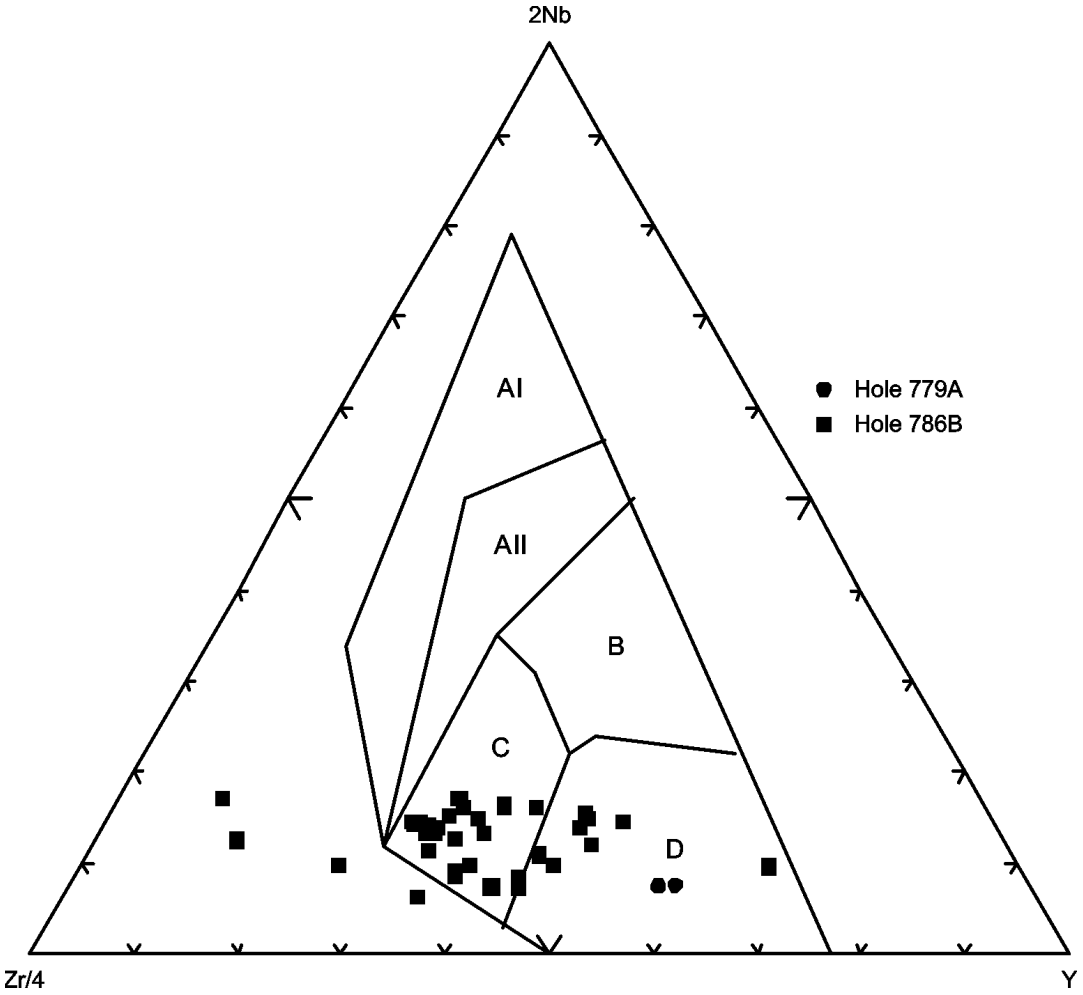

Figure F106. Chondrite-normalized rare earth element abundances for igneous rocks in Hole 779A, 780C, and 786B. Normalizing values are from Sun and McDonough (1989). (Continued on next two pages.)

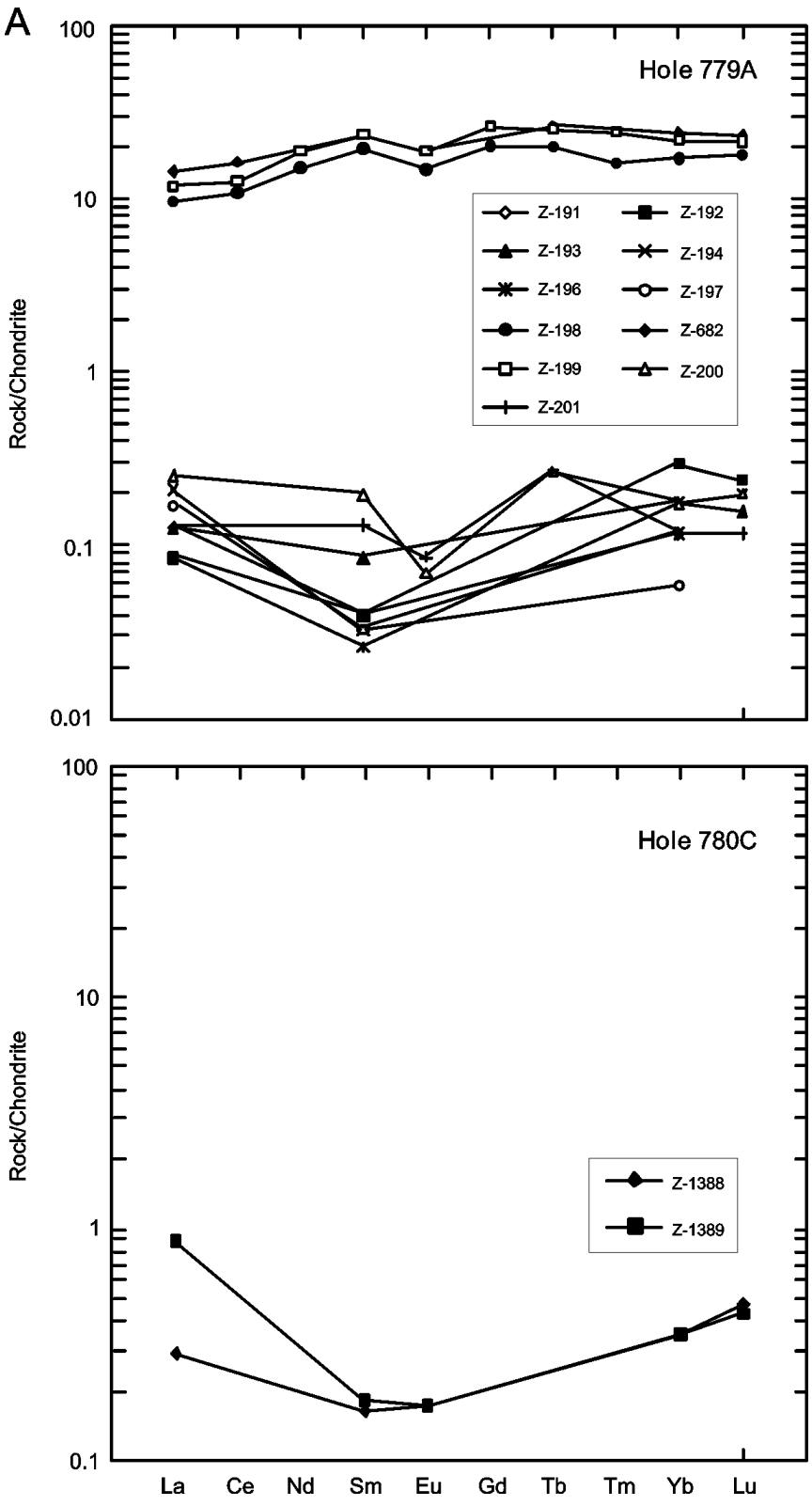

Figure F106 (continued).

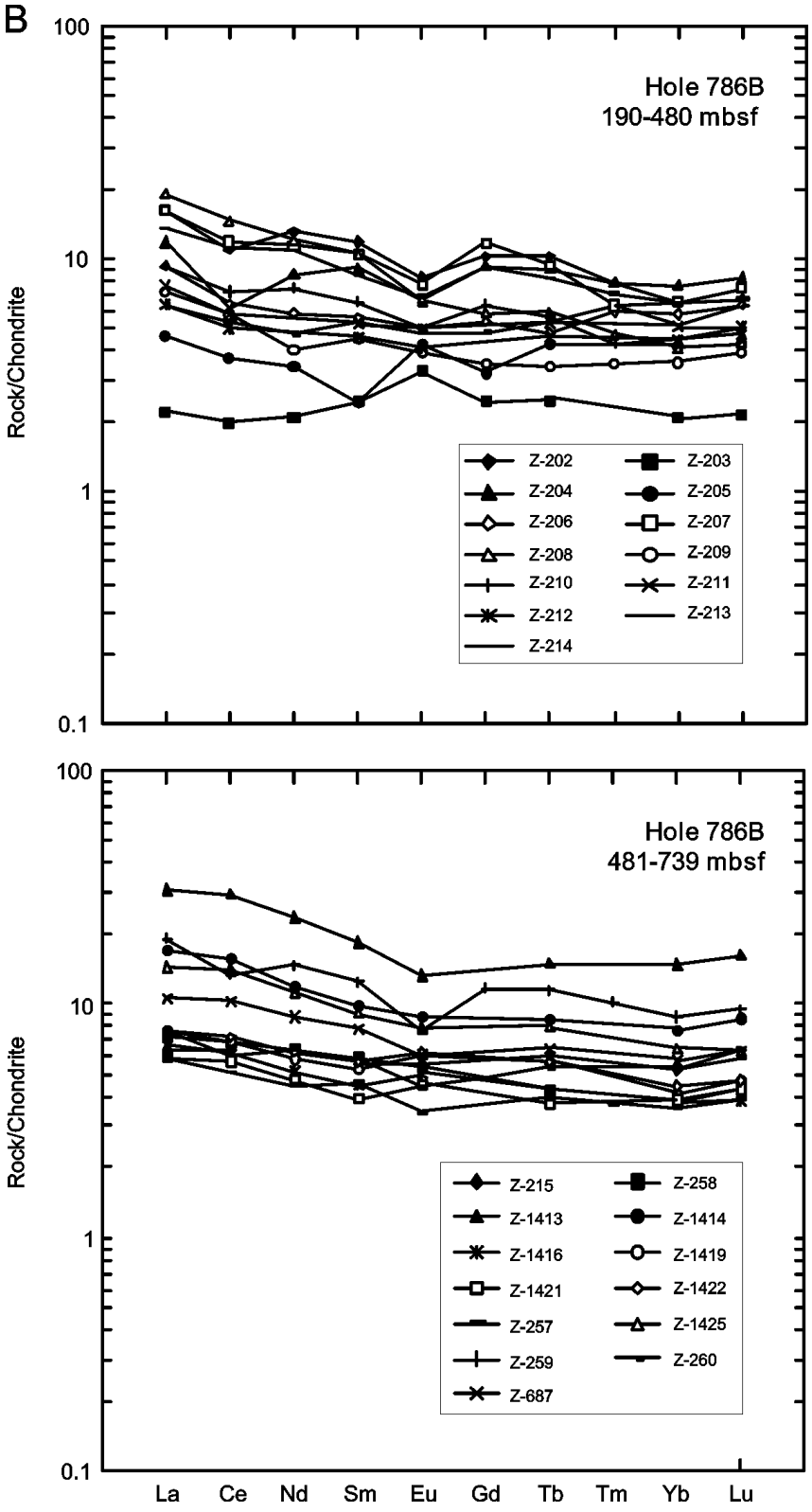

Figure F106 (continued).

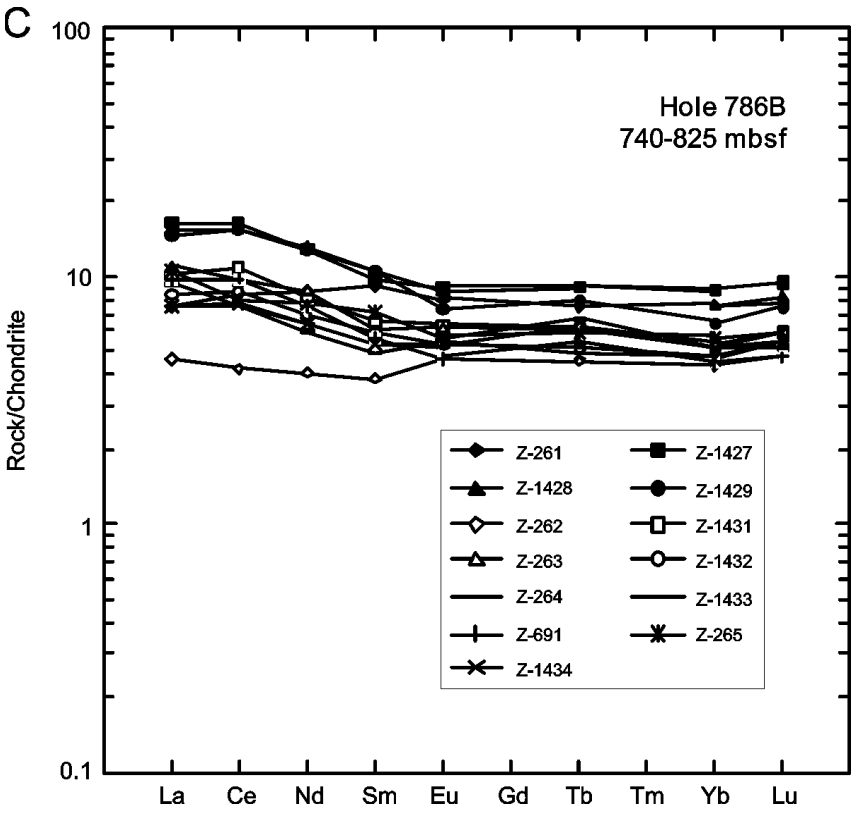

Figure F107. Sites 791, 792, and 793 drilled during Leg 126 in the Sumisu Rift and Forearc Basin, Philippine Sea (from Taylor et al., 1992).

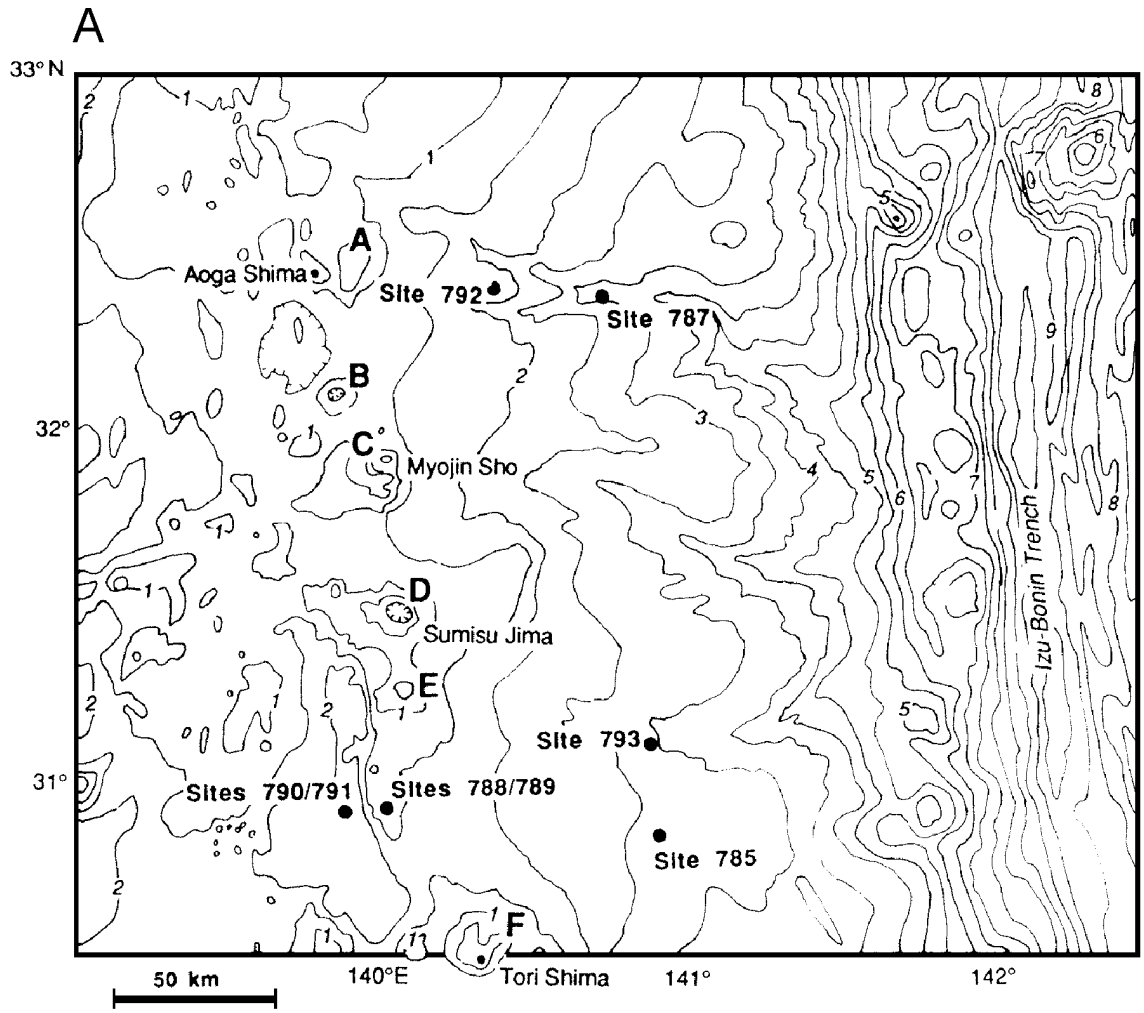

Figure F108. AFM diagram (Irvine and Baragar, 1971) for igneous rocks in Holes 791B, 792E, and 793B.

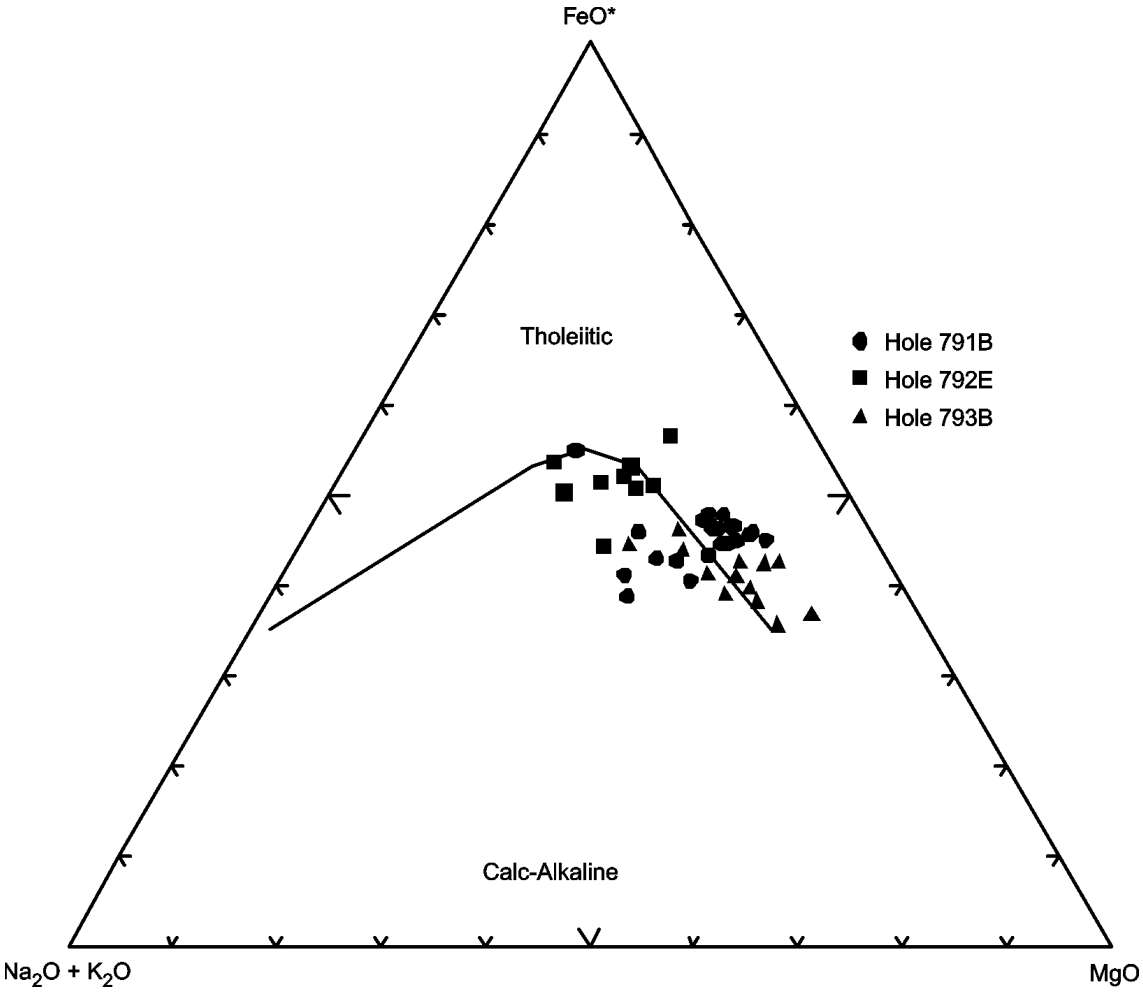

Figure F109. Discrimination Nb-Zr-Y diagram (Meschede, 1986) for igneous rocks in Holes 791B, 792E, and 793B. AI, AII = fields of intraplate alkali basalts; AII, C = fields of intraplate tholeiites; B = field of P-type MORB; D = field of N-type MORB; C, D = fields of volcanic arc basalts.

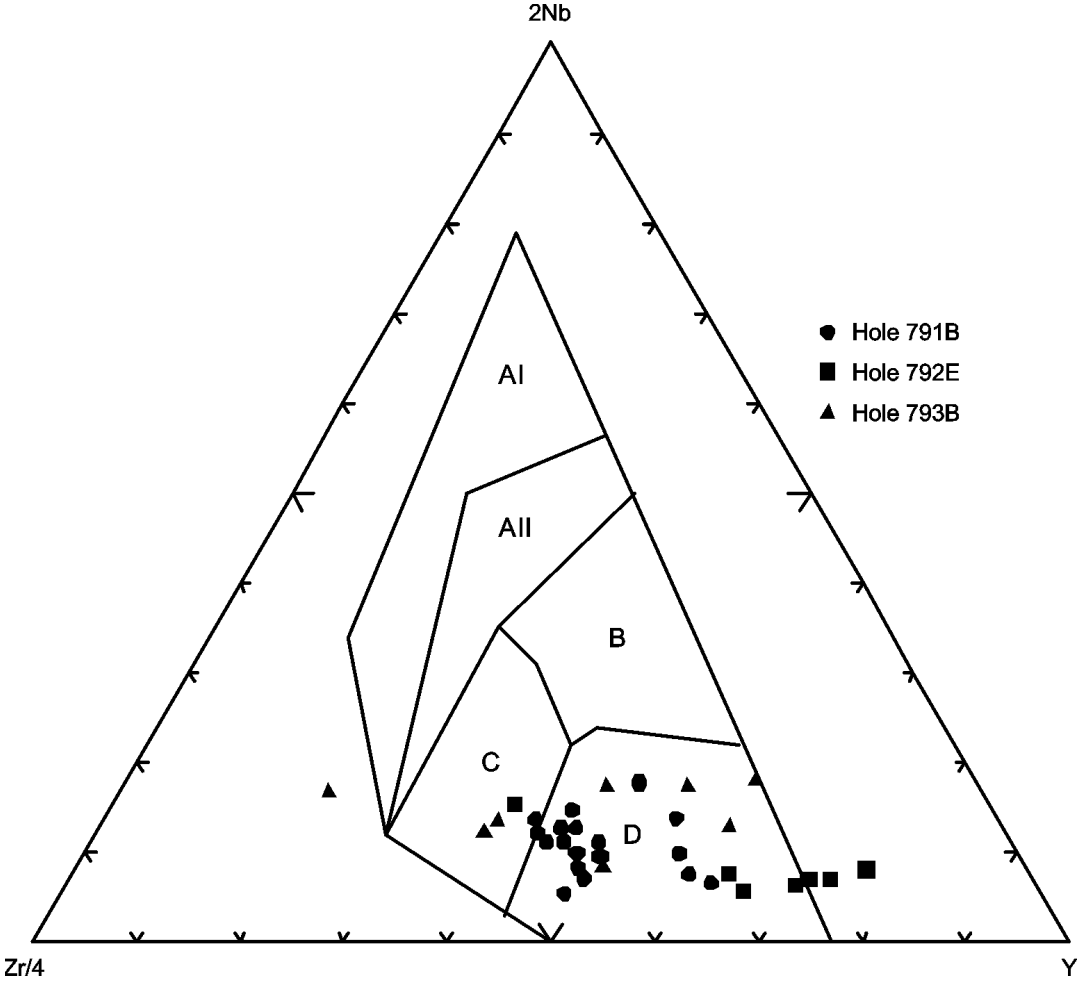

Figure F110. Chondrite-normalized rare earth element abundances for igneous rocks in Holes 791B, 792E, and 793B. Normalizing values are from Sun and McDonough (1989). (Continued on next page.)

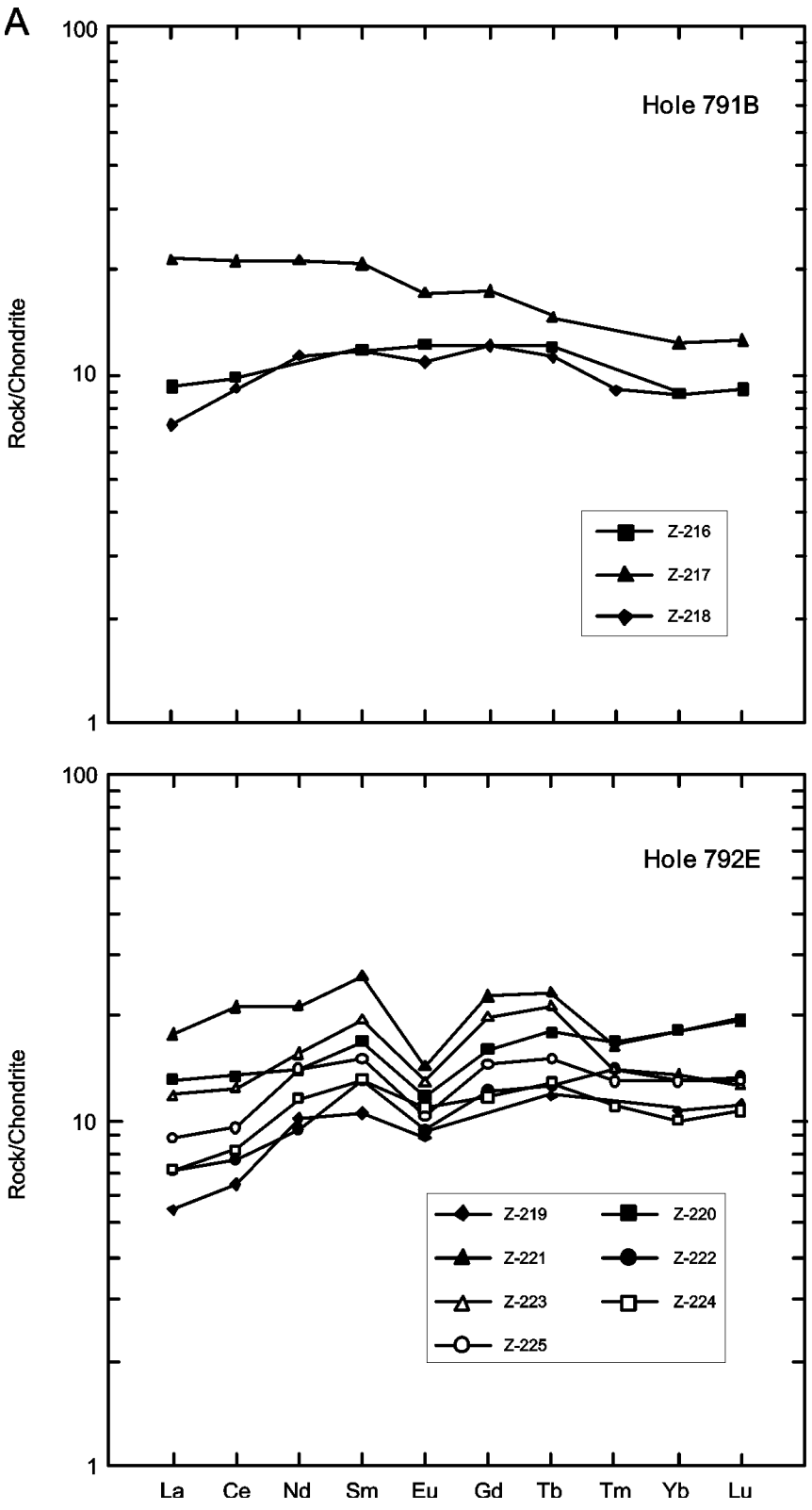

Figure F110 (continued).

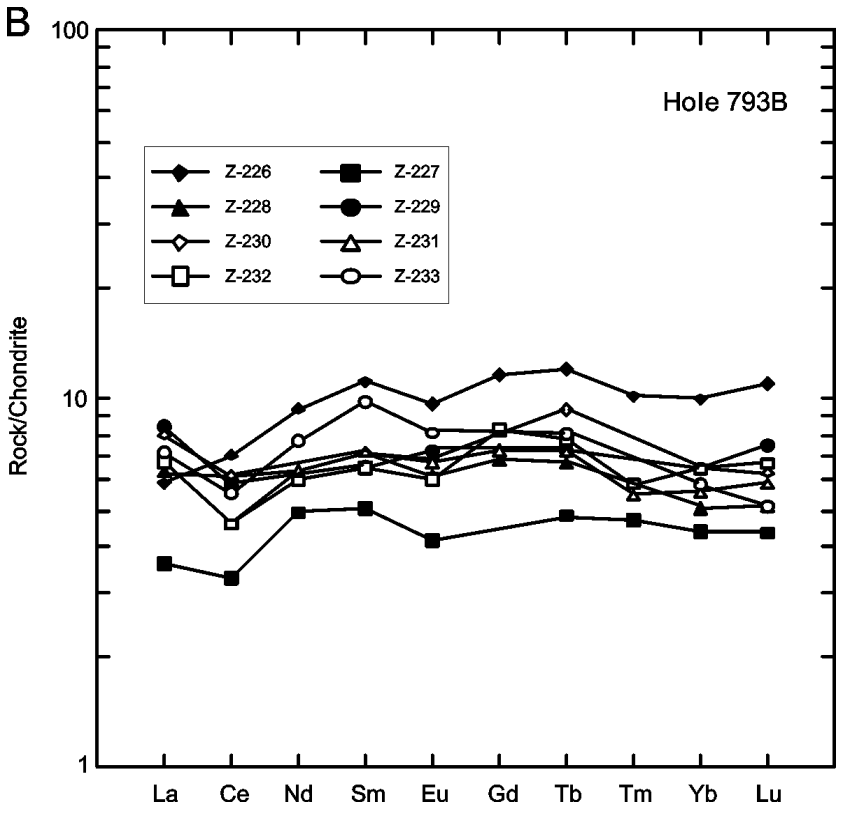

Figure F111. Sites 447, 448, 449, 453, 454, 458, and 459 drilled during Legs 59 and 60 in the Philippine Sea (from Hussong, Uyeda, et al., 1982).

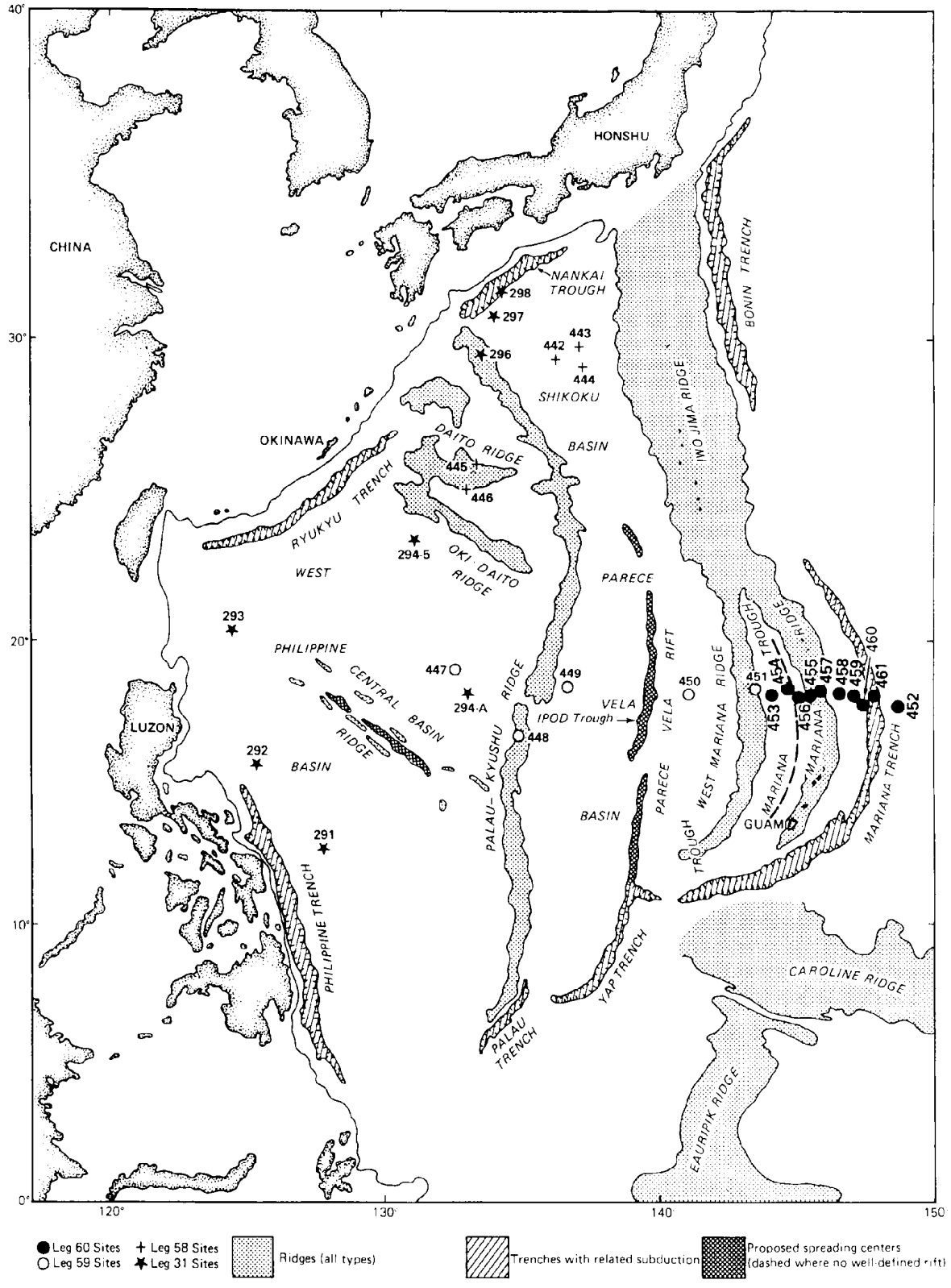

Figure F112. AFM diagram (Irvine and Baragar, 1971) for igneous rocks in Holes 447A, 448, 448A, and 449.

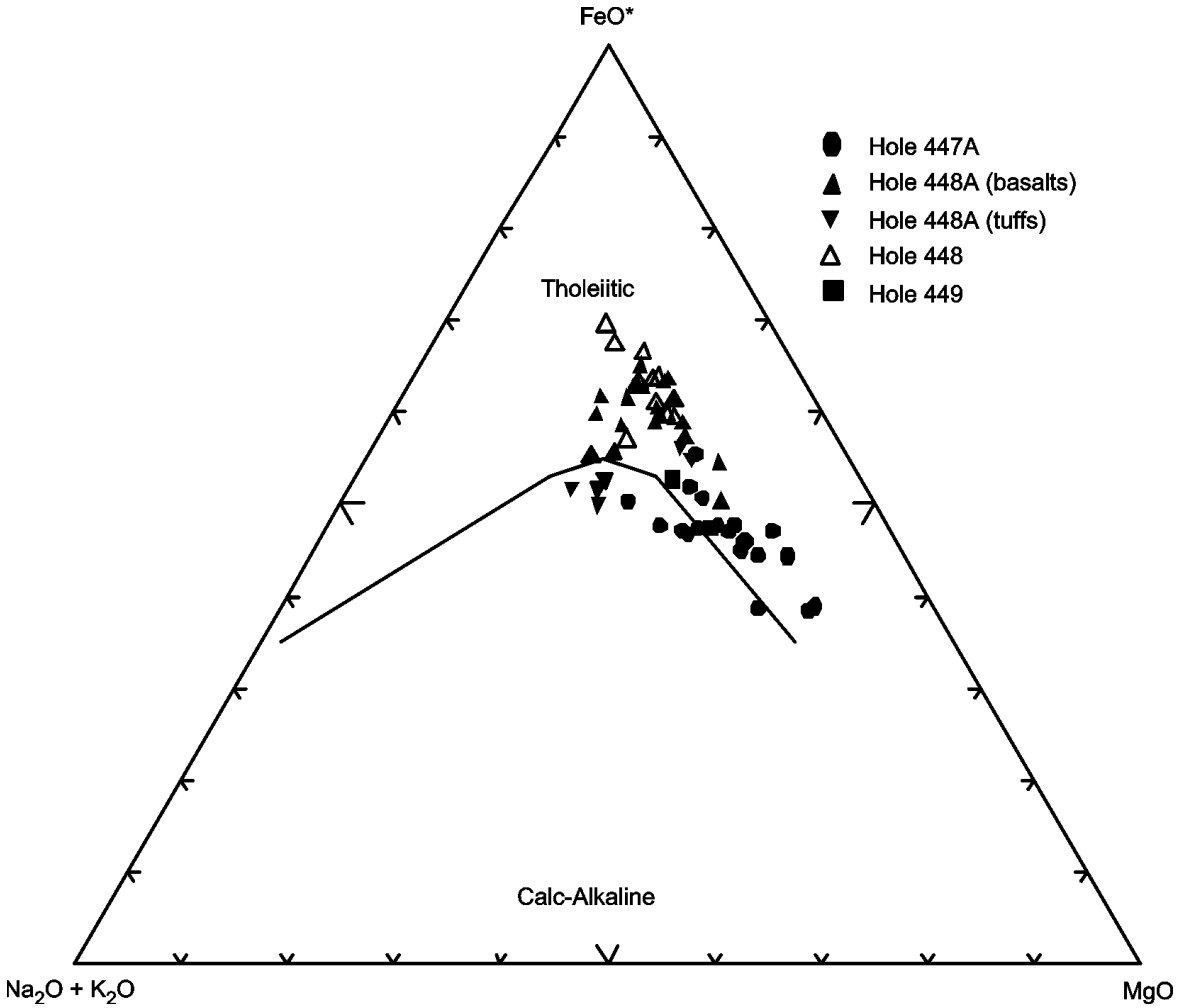

Figure F113. Discrimination Nb-Zr-Y diagram (Meschede, 1986) for igneous rocks in Holes 447A, 448, 448A, and 449. AI, AII = fields of intraplate alkali basalts; AII, C = fields of intraplate tholeiites; B = field of P-type MORB; D = field of N-type MORB; C, D = fields of volcanic arc basalts.

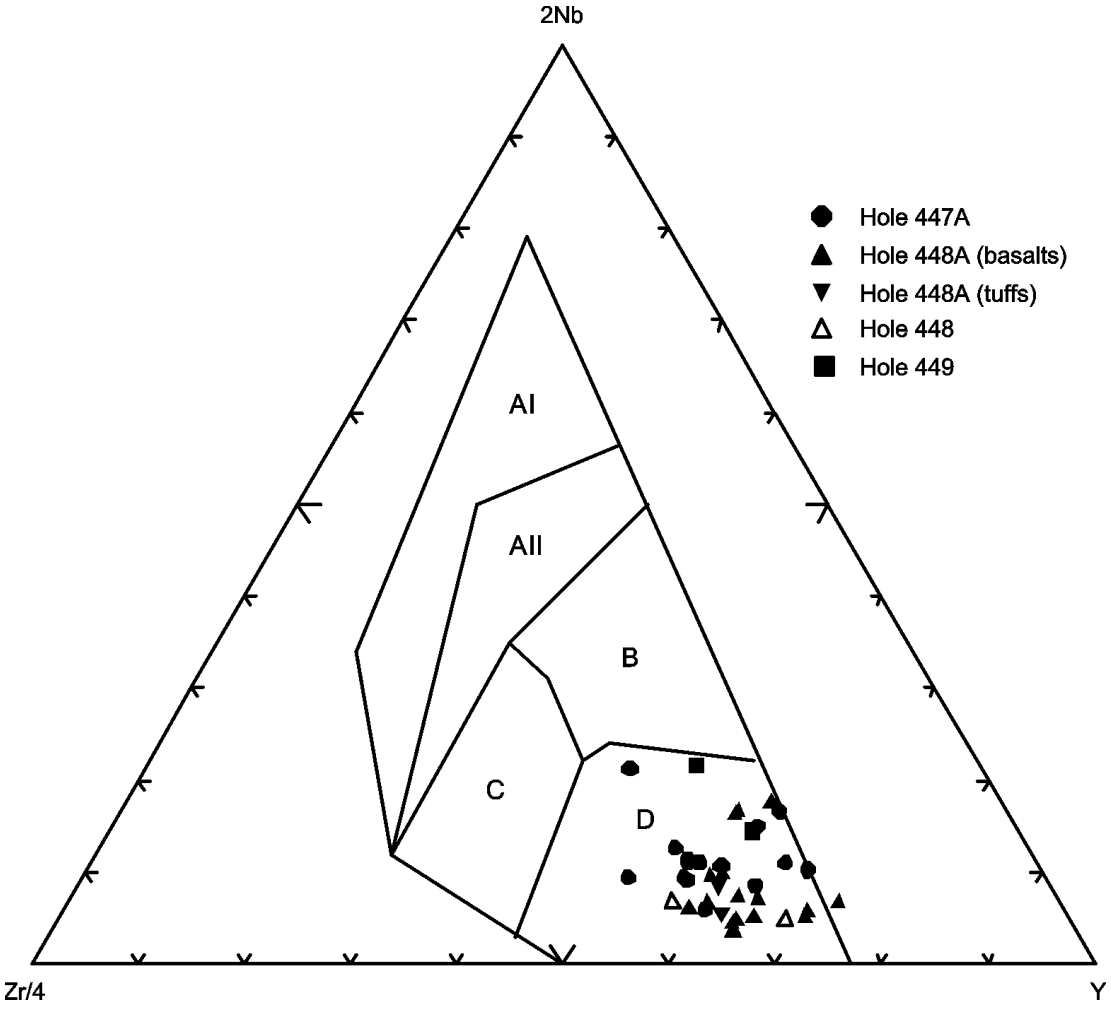

Figure F114. Chondrite-normalized rare earth element abundances for igneous rocks in Holes 447A, 448, 448A, and 449. Normalizing values are from Sun and McDonough (1989). (Continued on next page.)

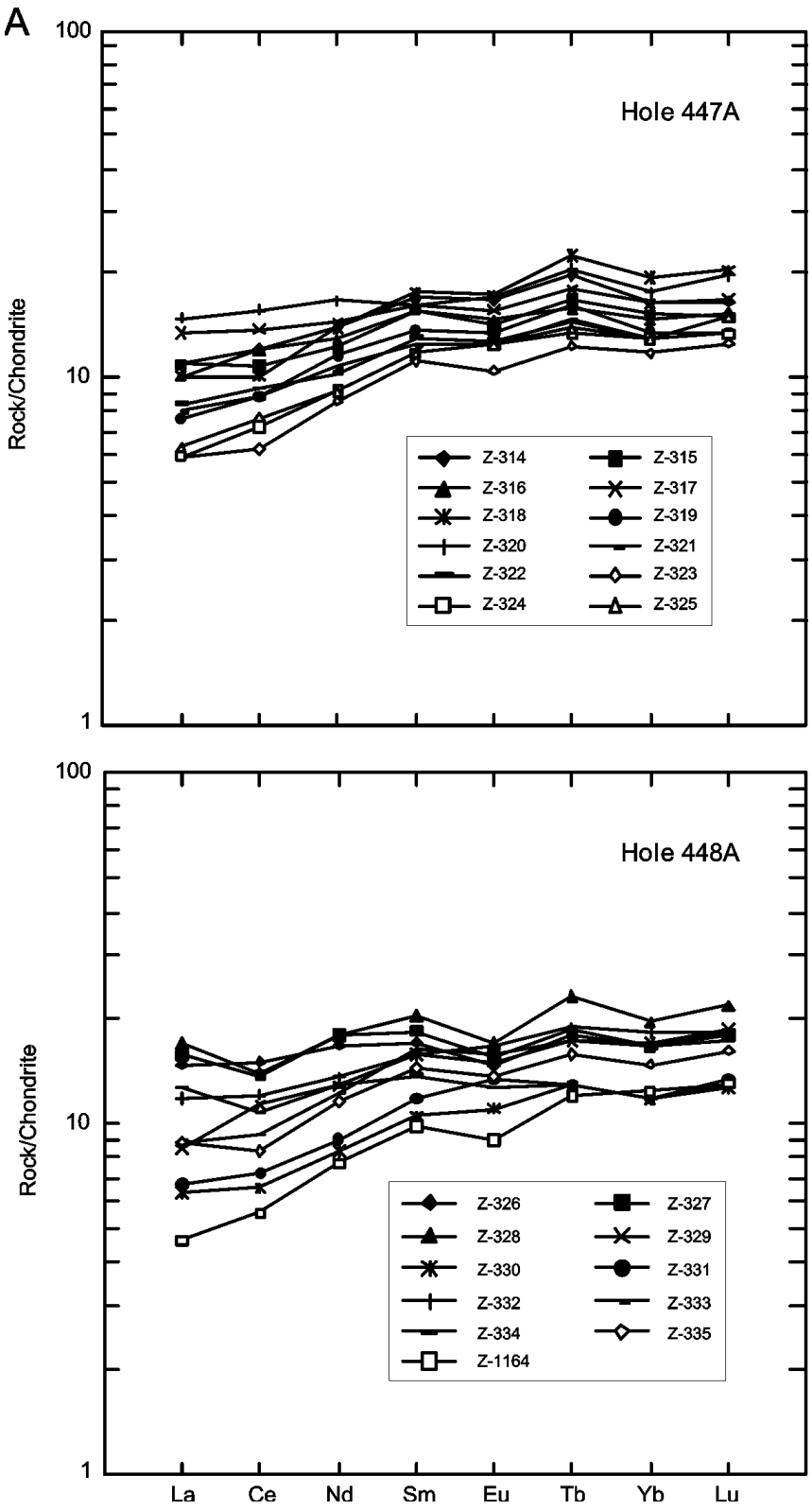

Figure F114 (continued).

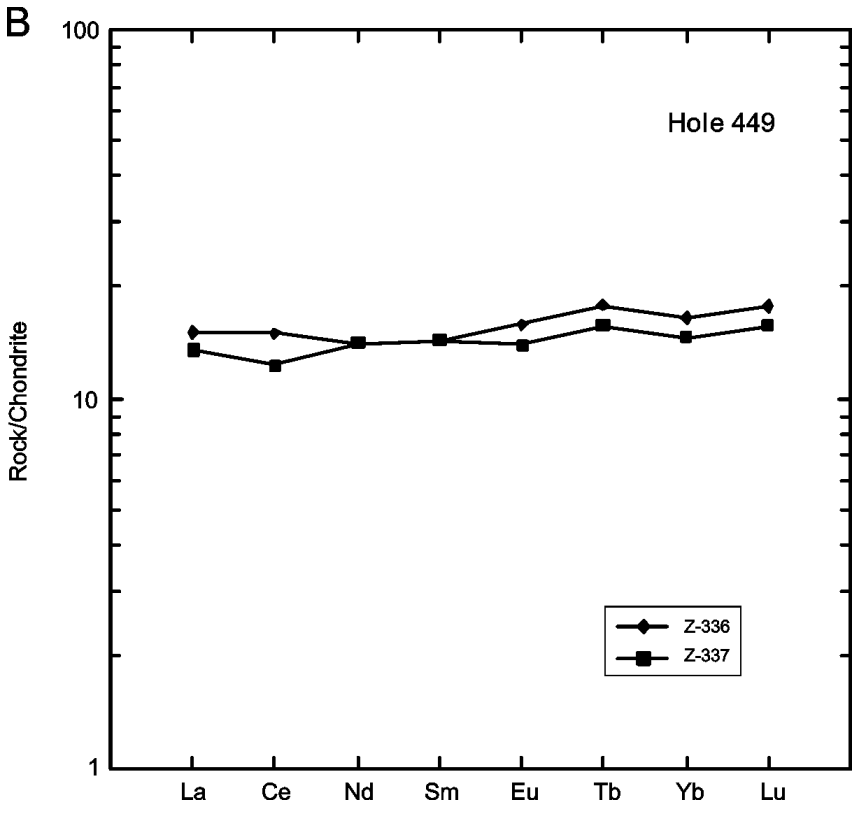

Figure F115. Generalized structure of the portion of the active Mariana Arc system drilled during Leg 60 (from Hussong, Uyeda, et al., 1982).

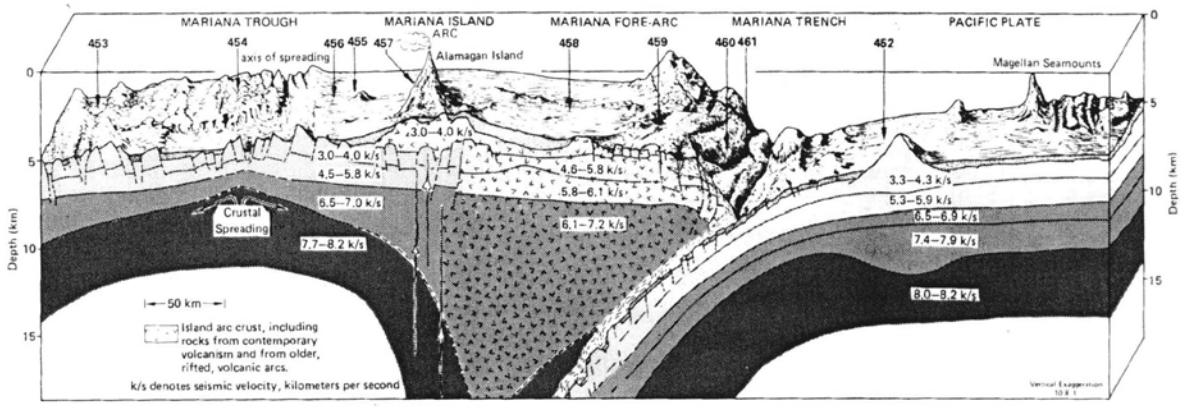

Figure F116. AFM diagram (Irvine and Baragar, 1971) for igneous rocks in Holes 453, 454A, 458, and 459B.

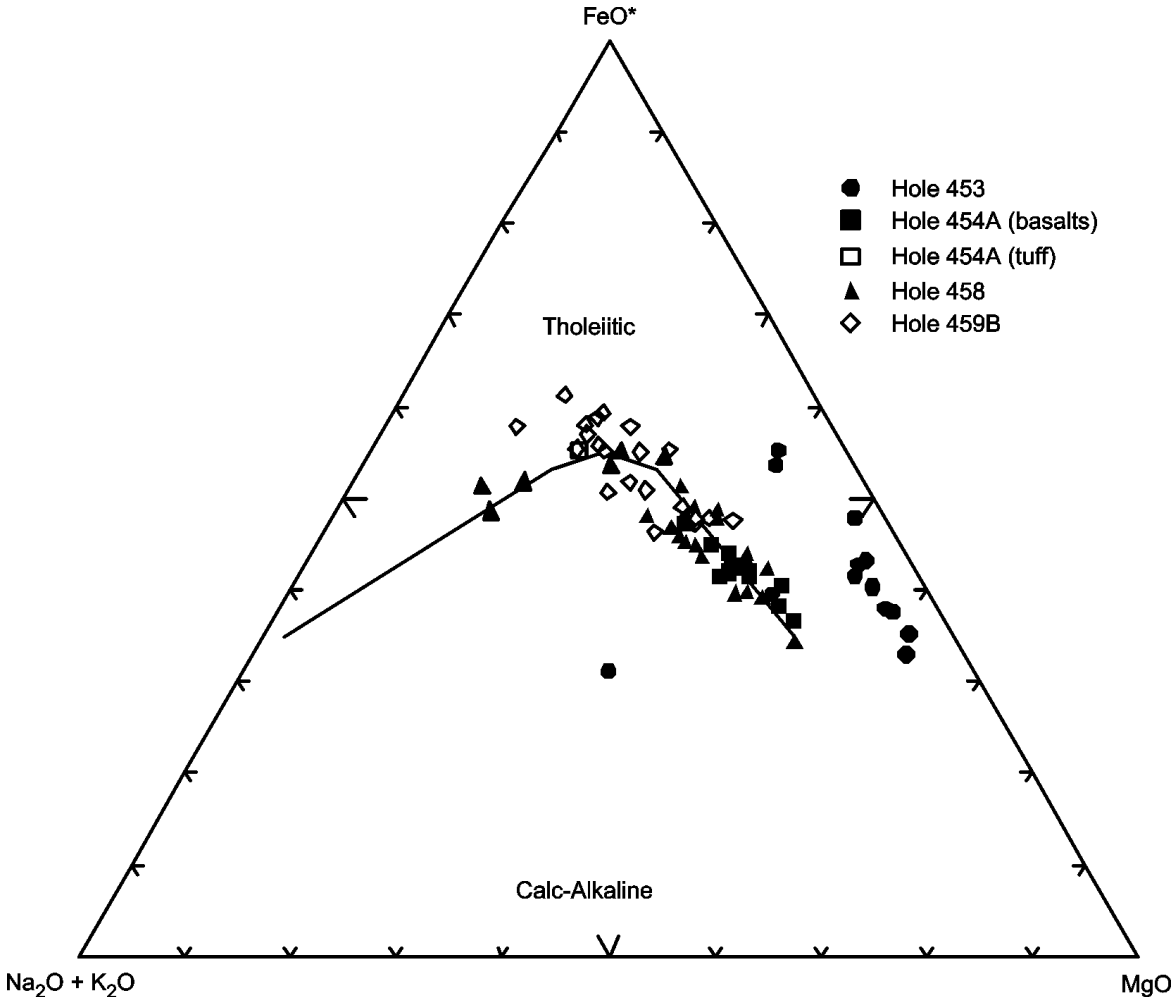

Figure F117. Chondrite-normalized rare earth element abundances in igneous rocks from Holes 453, 454A, 458, and 459B. Normalizing values are from Sun and McDonough (1989). (Continued on next page.)

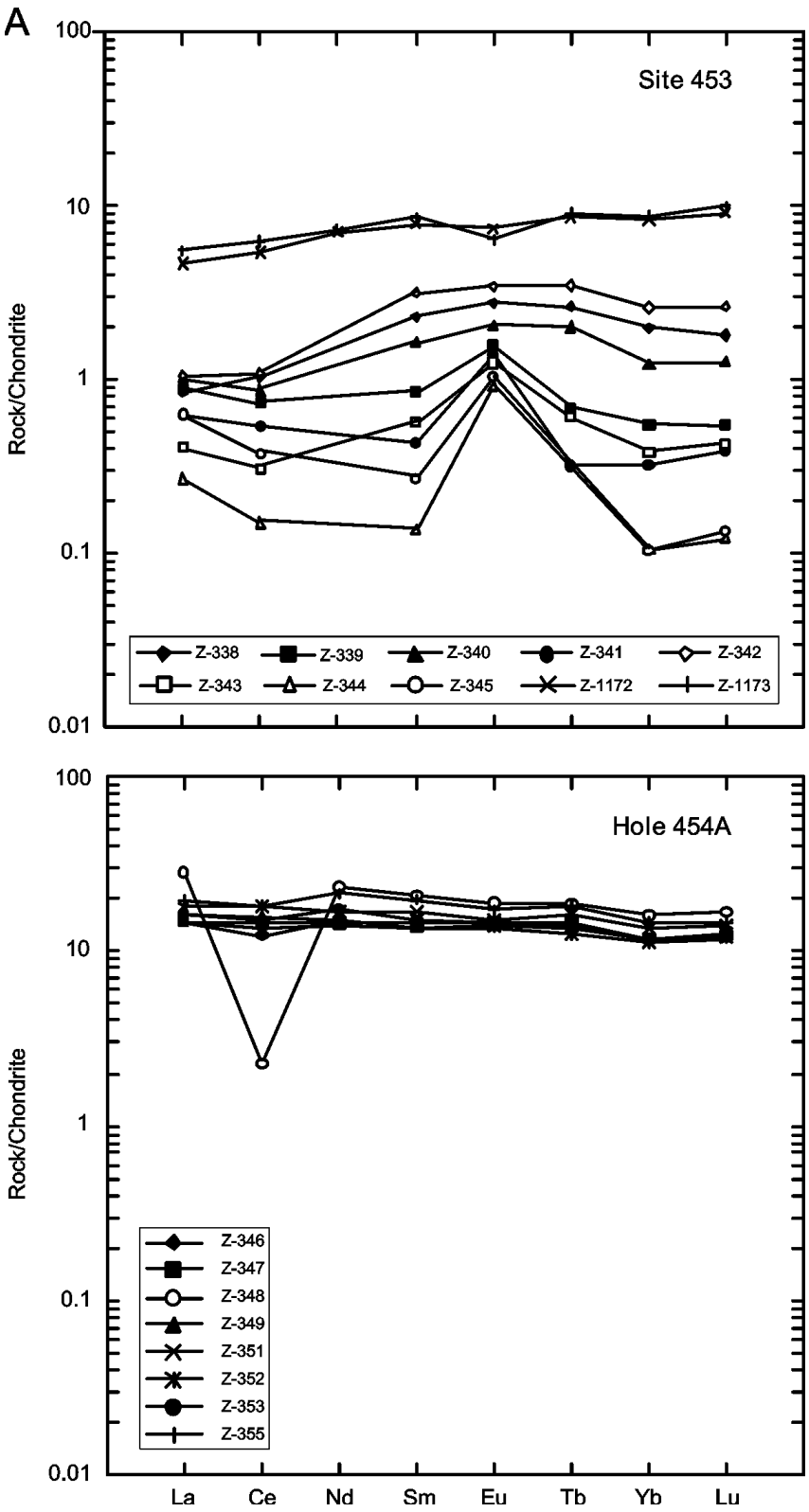

Figure F117 (continued).

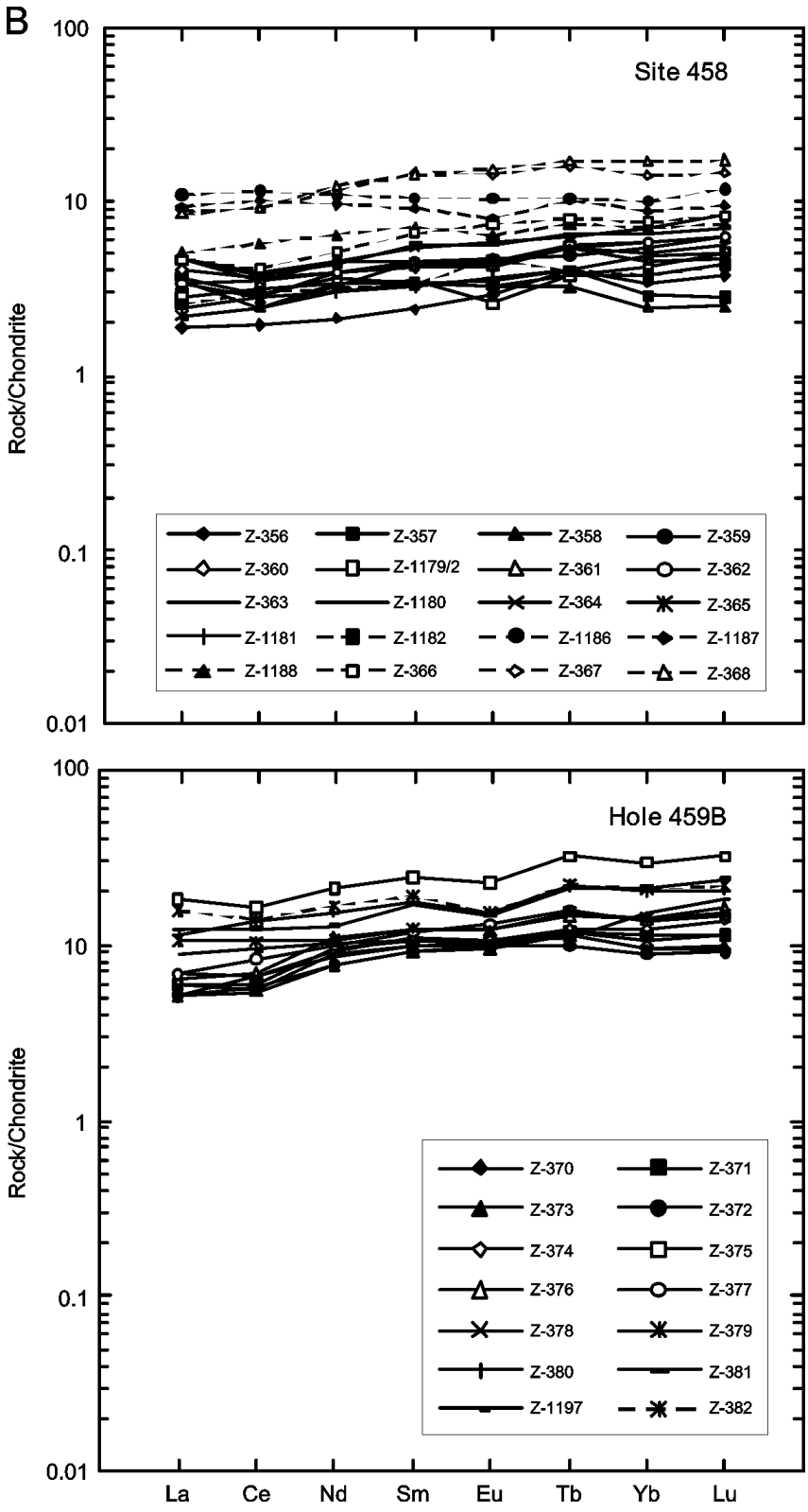

Figure F118. Discrimination Nb-Zr-Y diagram (Meschede, 1986) for igneous rocks from Holes 454A, 458, and 459B. AI, AII = fields of intraplate alkali basalts; AII, C = fields of intraplate tholeiites; B = field of P-type MORB; D = field of N-type MORB; C, D = fields of volcanic arc basalts.

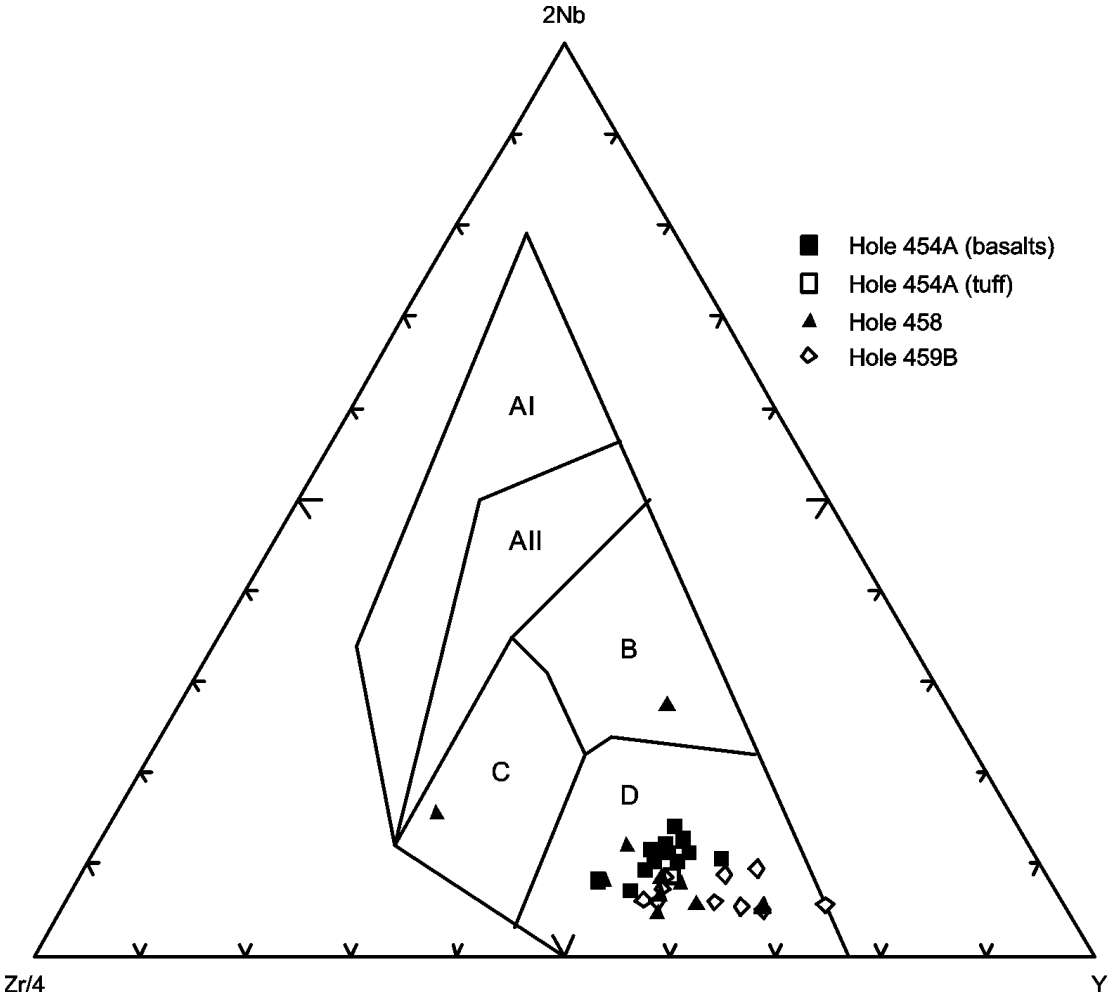

Figure F119. Sites 794, 795, and 797 drilled during Legs 127 and 128 in the Japan Sea (from Tamaki et al., 1992).

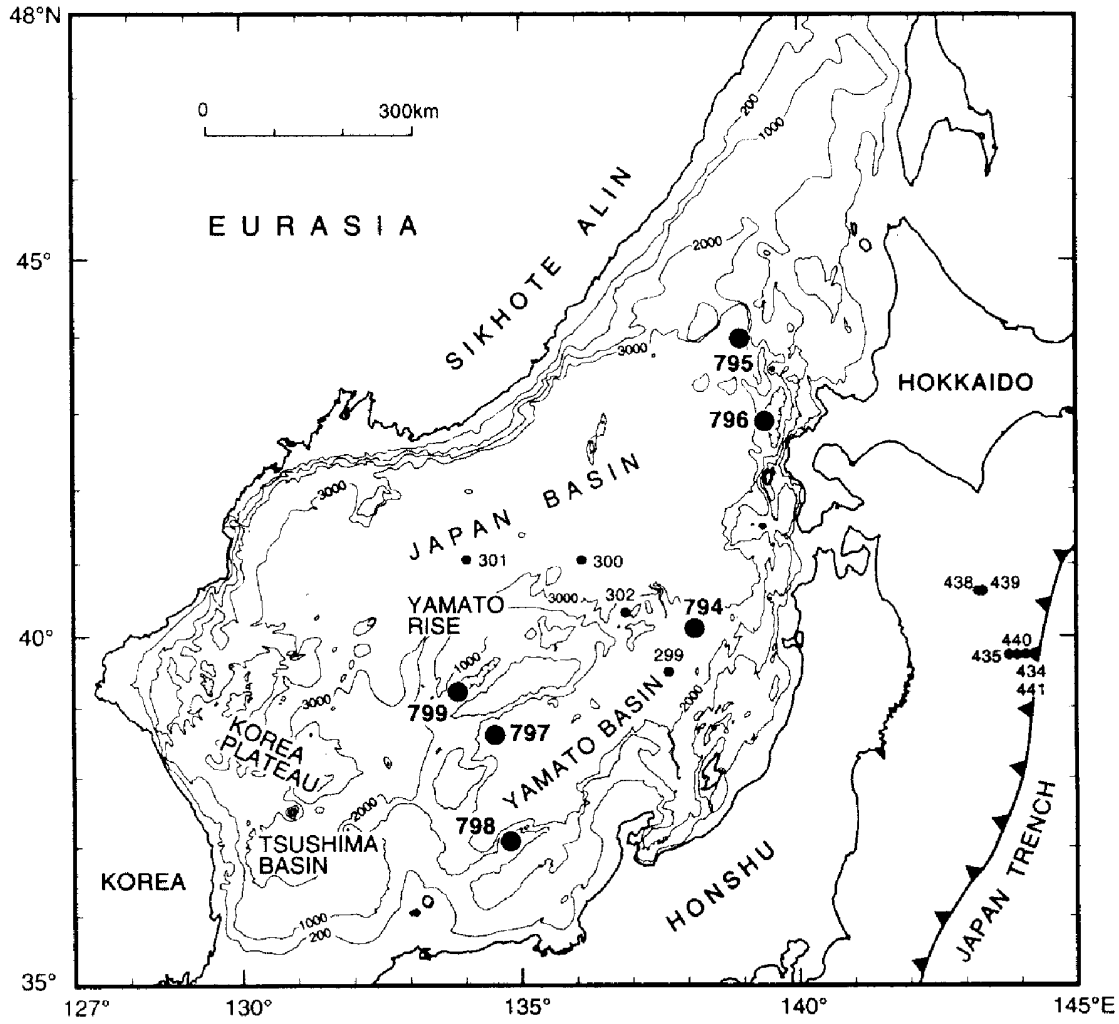

Figure F120. AFM diagram (Irvine and Baragar, 1971) for igneous rocks in Holes 794C, 795B, and 797C.

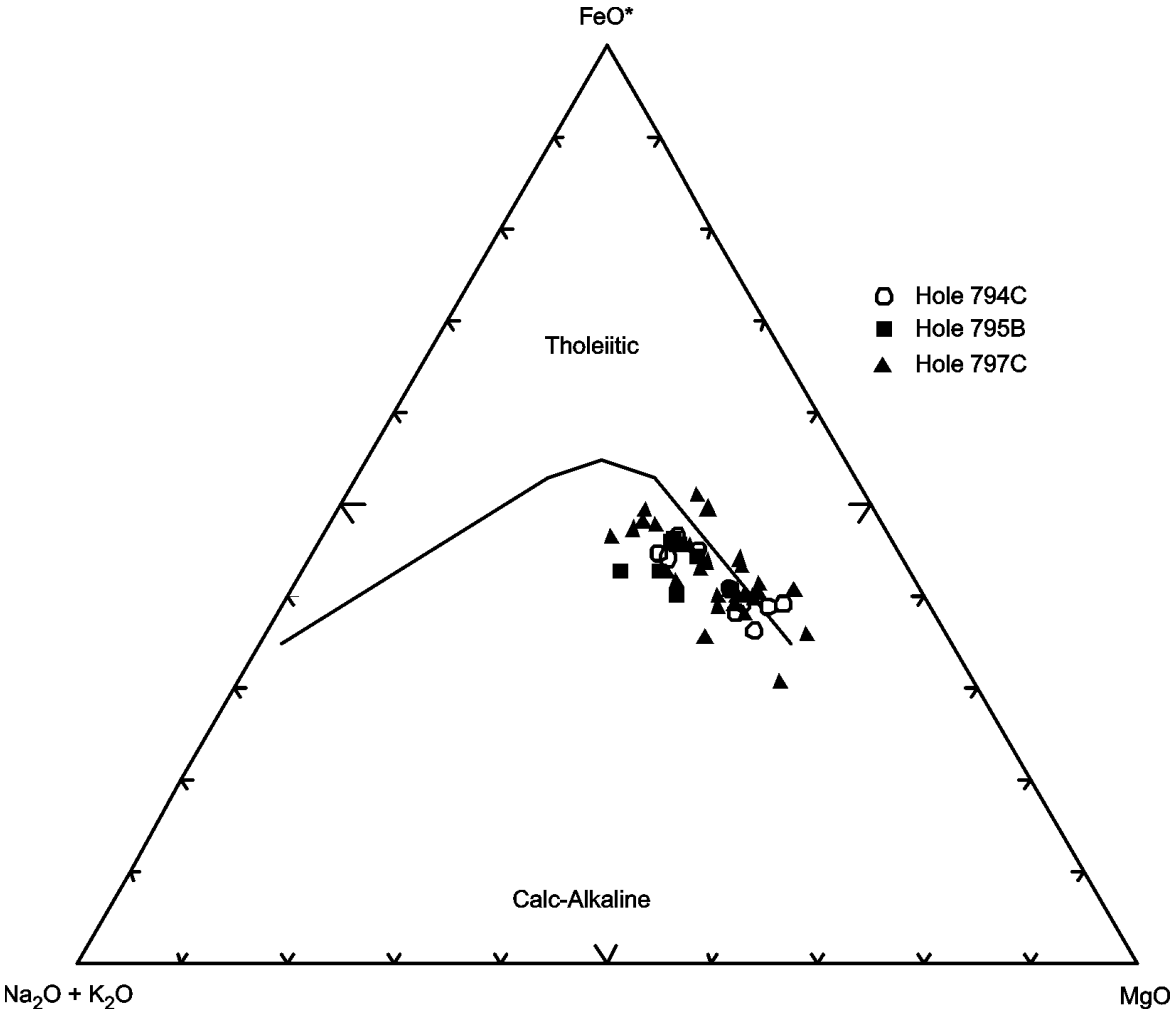

Figure F121. Discrimination Nb-Zr-Y diagram (Meschede, 1986) for igneous rocks in Holes 794C, 795B, and 797C. AI, AII = fields of intraplate alkali basalts; AII, C = fields of intraplate tholeiites; B = field of P-type MORB; D = field of N-type MORB; C, D = fields of volcanic arc basalts.

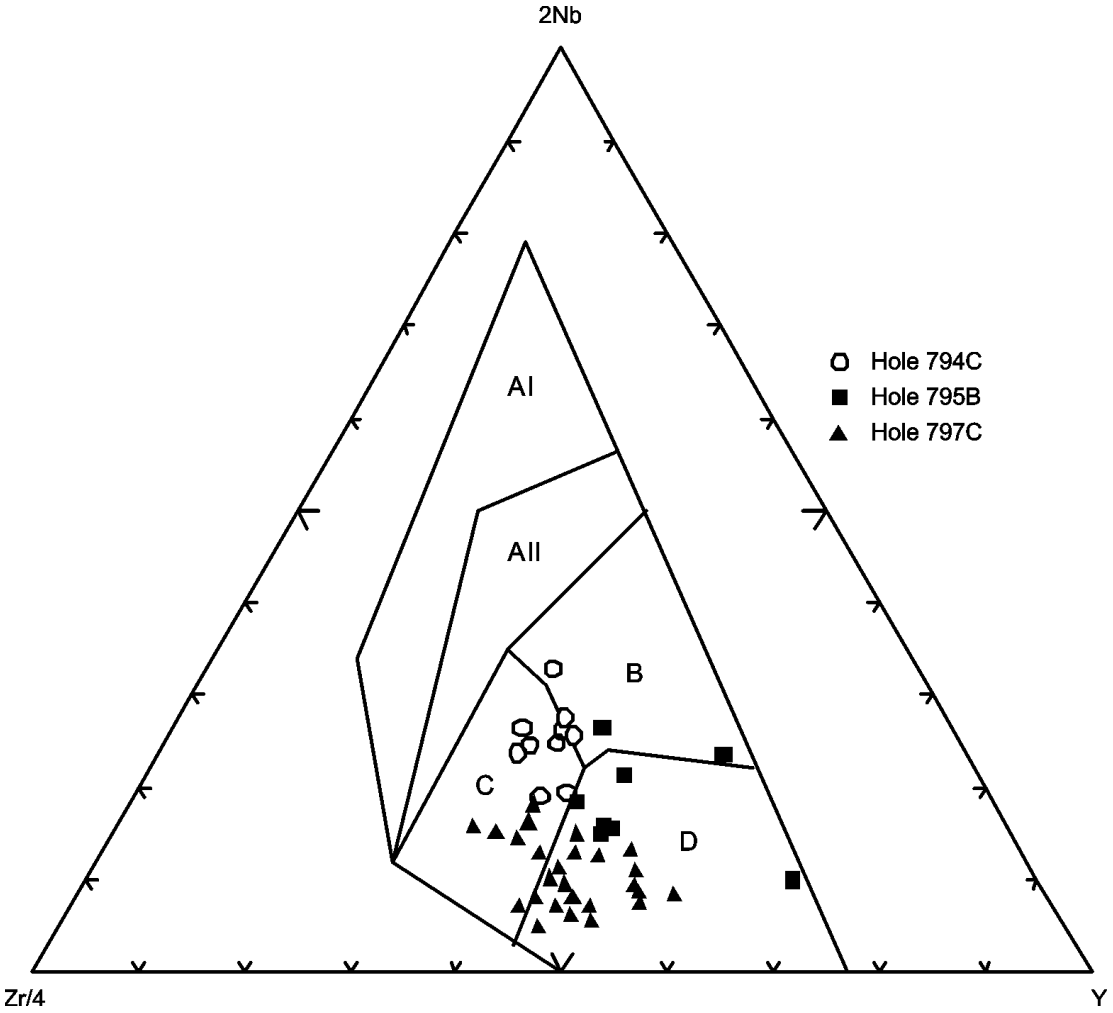

Figure F122. Chondrite-normalized rare earth element abundances in igneous rocks from Holes 794C, 795B, and 797C. Normalizing values are from Sun and McDonough (1989). (Continued on next page.)

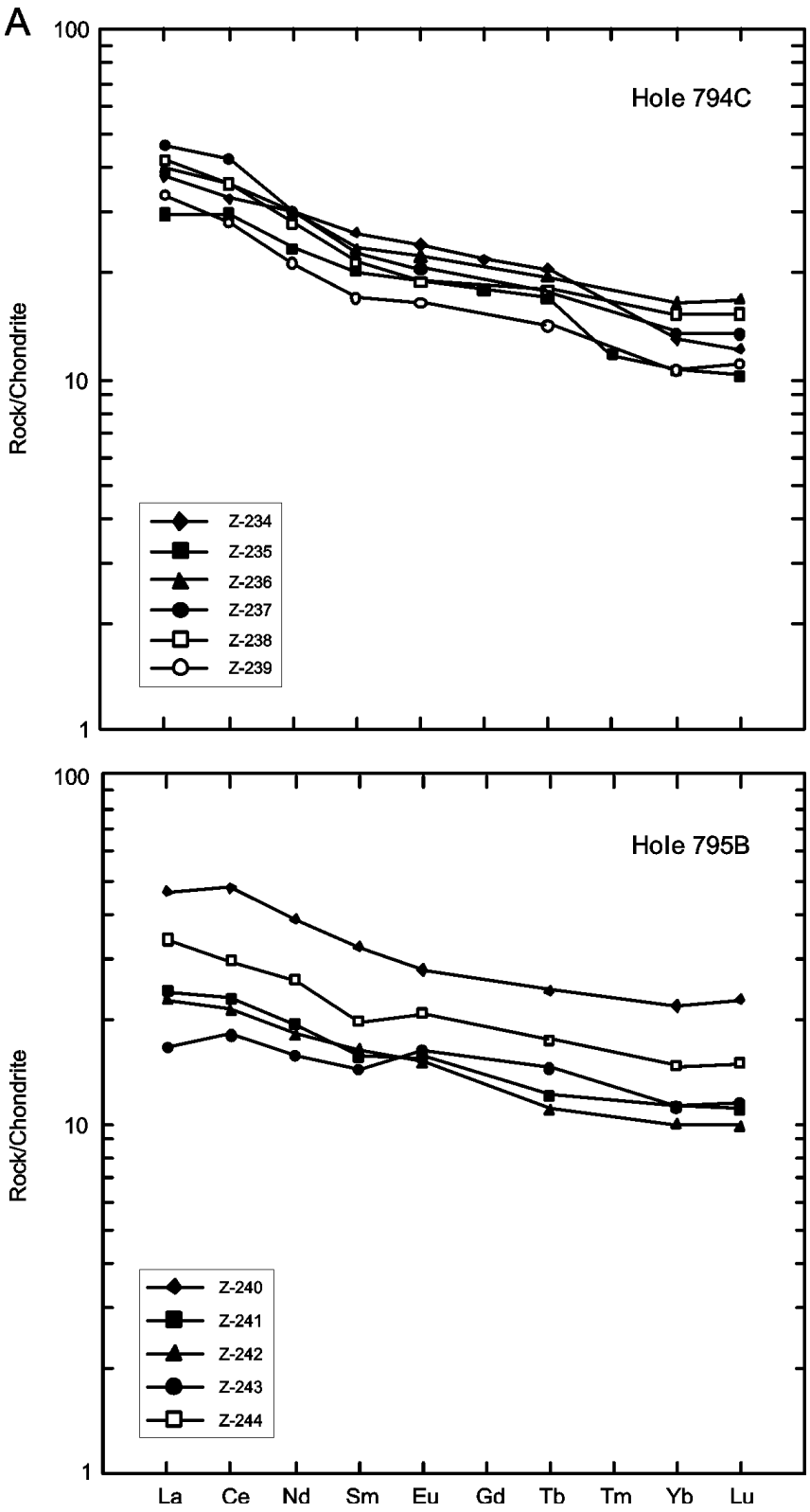

Figure F122 (continued).

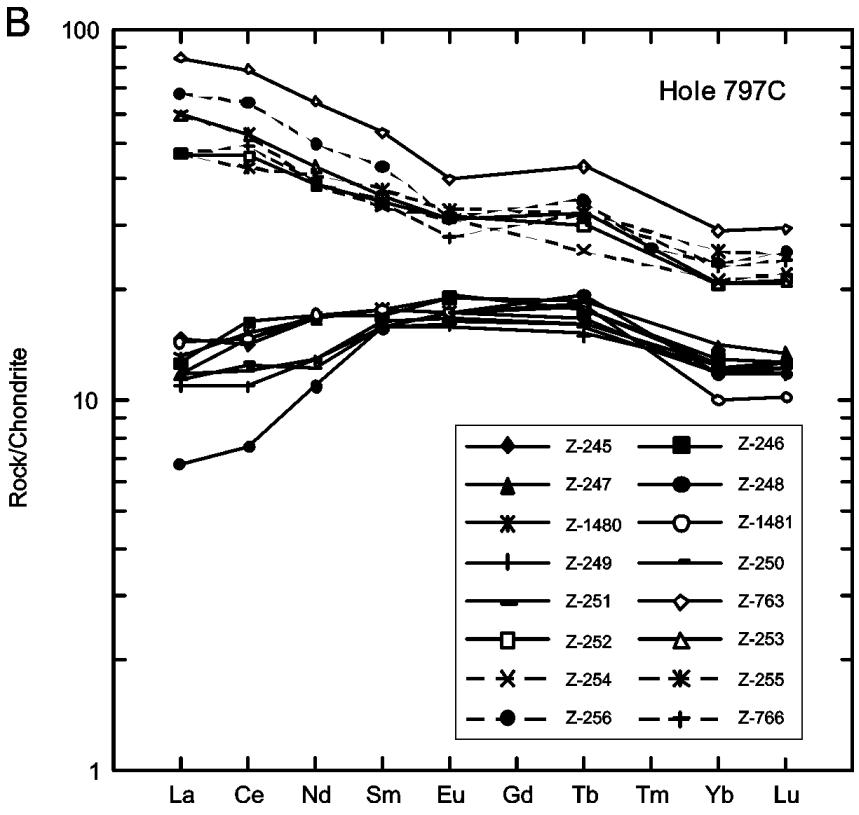

Figure F123. AFM diagram (Irvine and Baragar, 1971) for igneous rocks in Hole 794D.

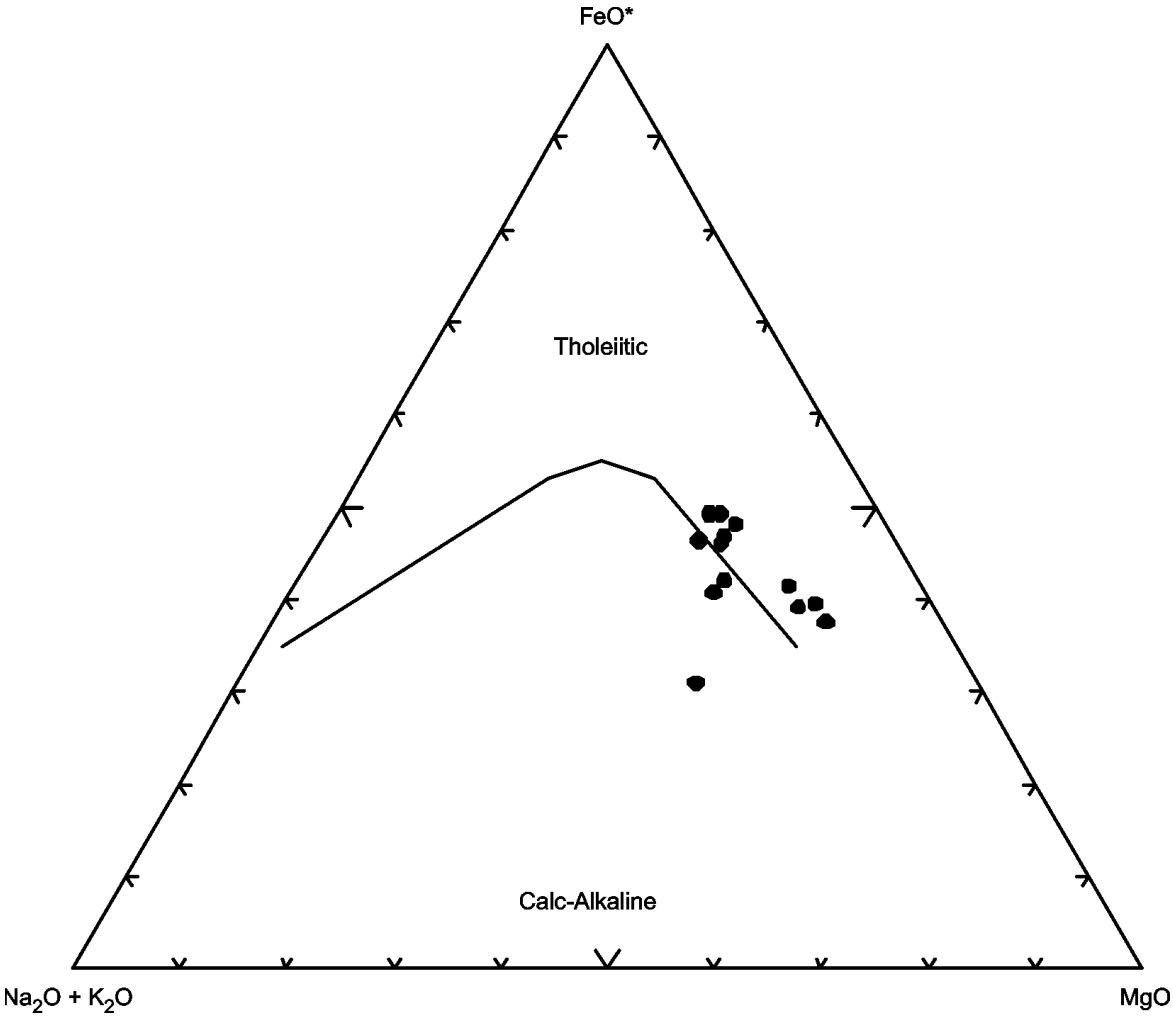

Figure F124. Discrimination Nb-Zr-Y diagram (Meschede, 1986) for igneous rocks in Hole 794D. AI, AII = fields of intraplate alkali basalts; AII, C = fields of intraplate tholeiites; B = field of P-type MORB; D = field of N-type MORB; C, D = fields of volcanic arc basalts.

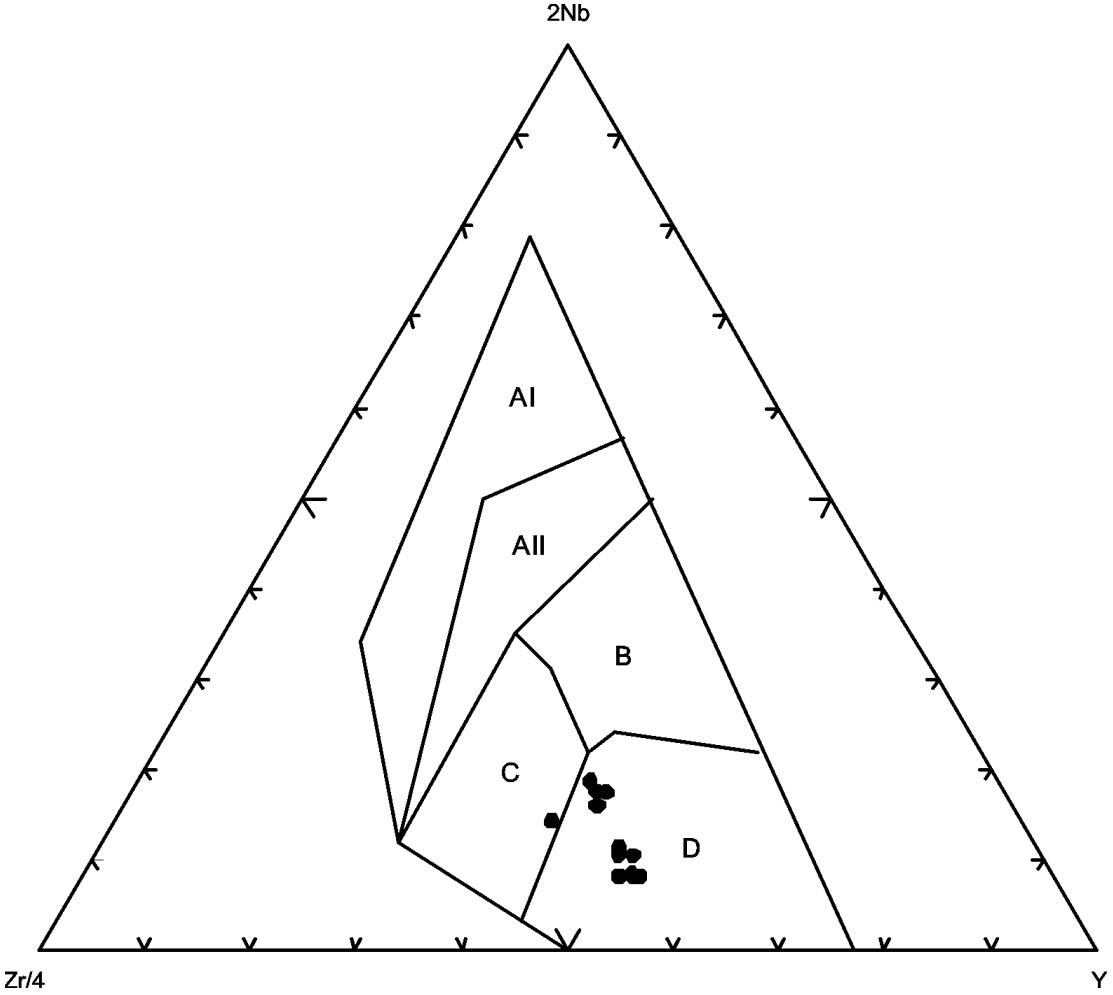

Figure F125. Site 834 drilled during Leg 135 in the Lau Basin. T = Tongpatu, E = ‘Eua, V = Vava’u, A = ‘Ata, NF = Niuafo’ou, U = Upolu. CLSC = Central Lau spreading center, ELSC = Eastern Lau spreading center. VF = Valu Fa Ridge, MTJ = Mangatolu Triple Junction (from Quinterno, 1994; Ledbetter and Haggerty, 1994).

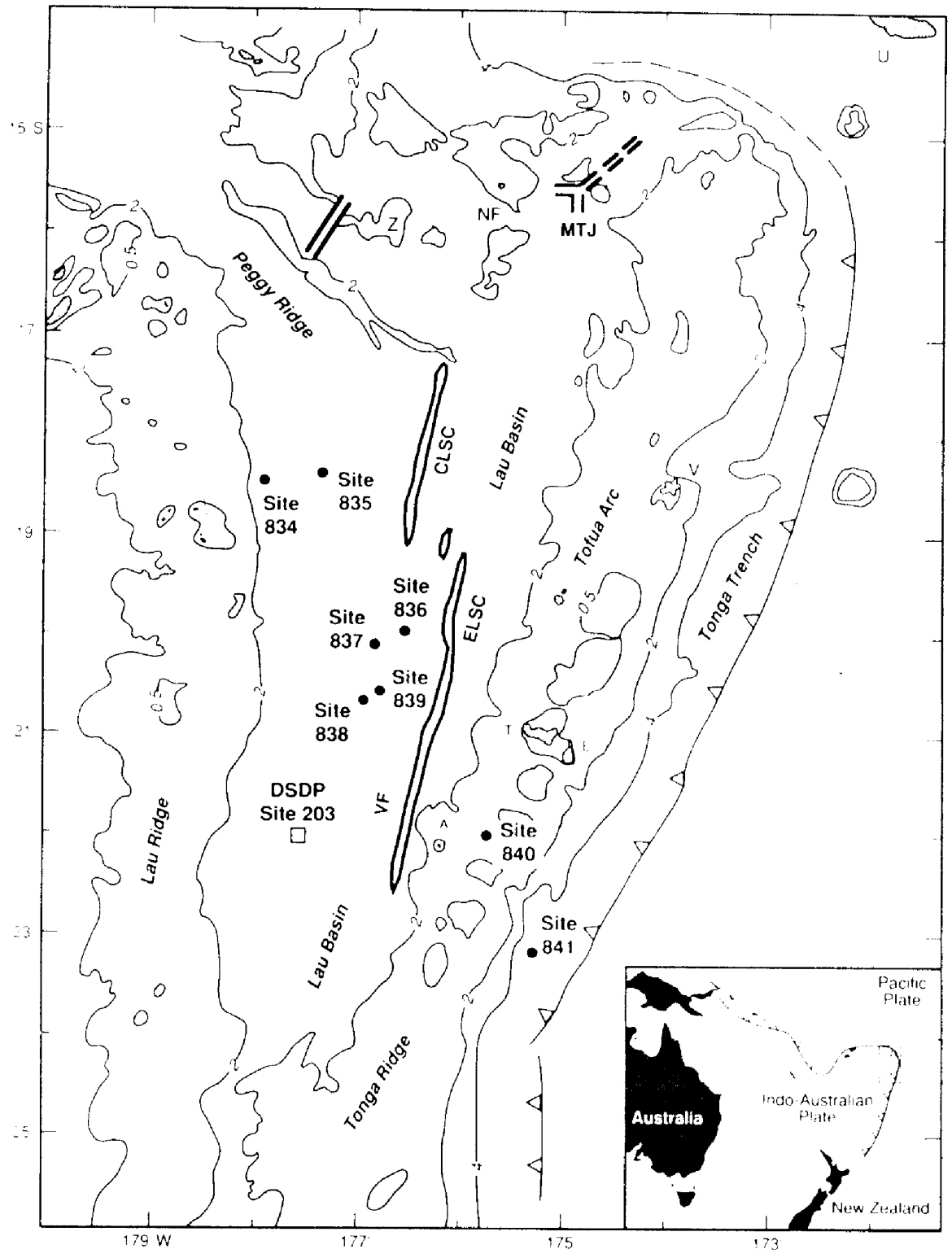

Figure F126. AFM diagram (Irvine and Baragar, 1971) for basalts in Hole 834B.

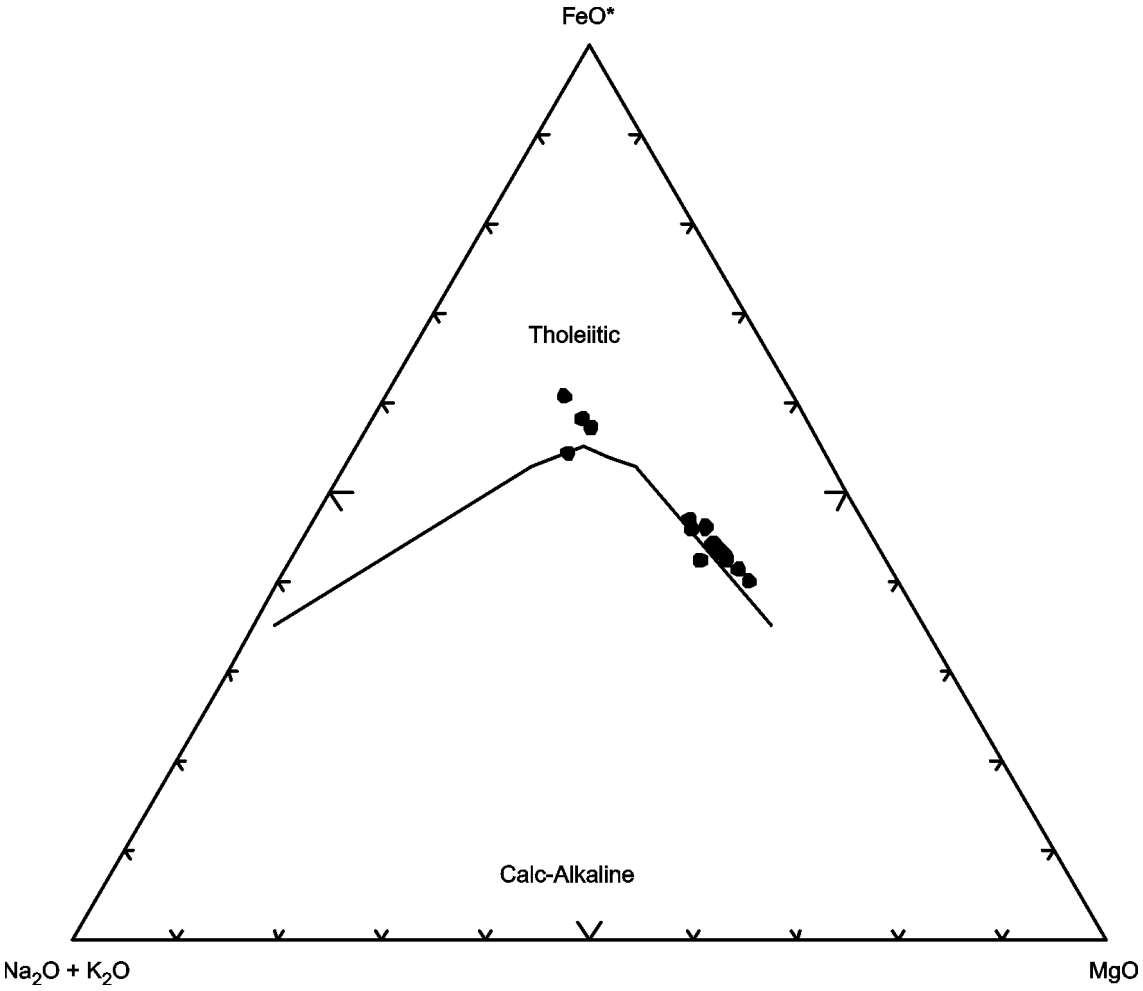

Figure F127. Discrimination Nb-Zr-Y diagram (Meschede, 1986) for basalts in Hole 834B. AI, AII = fields of intraplate alkali basalts; AII, C = fields of intraplate tholeiites; B = field of P-type MORB; D = field of N-type MORB; C, D = fields of volcanic arc basalts.

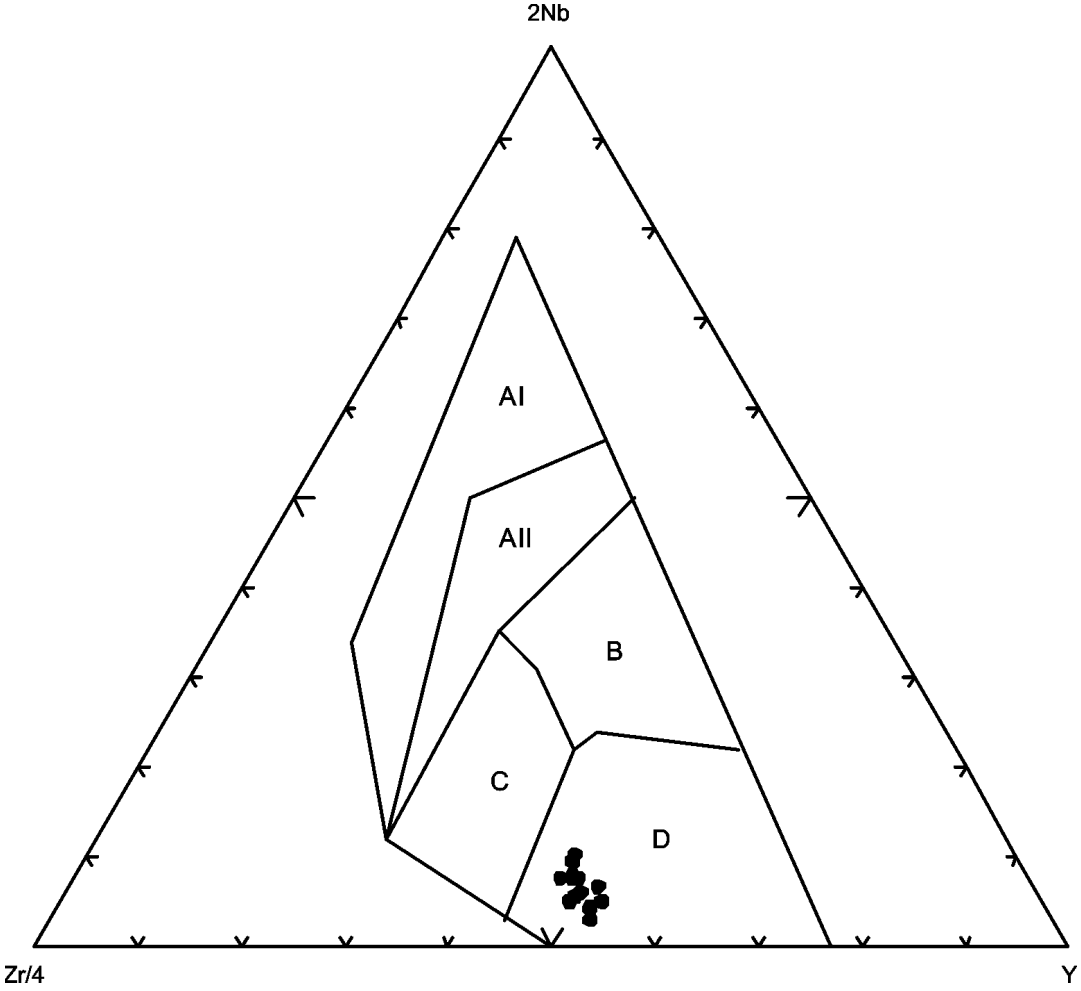

Figure F128. Chondrite-normalized rare earth element abundances for basalts in Hole 834B. Normalizing values are from Sun and McDonough (1989).

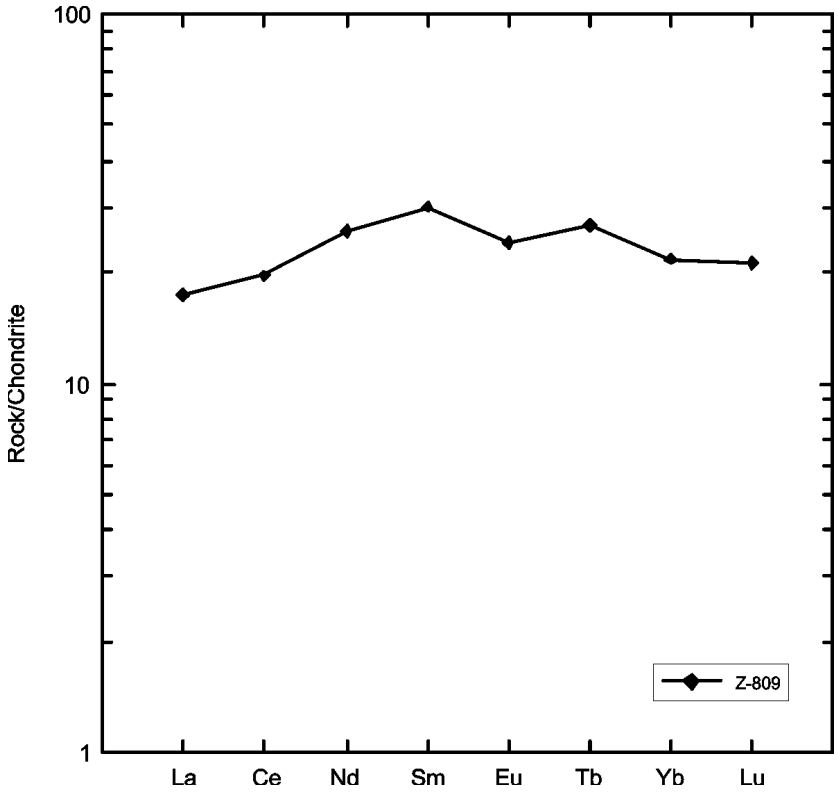

Figure F129. Site 191 drilled during Leg 19 in the Kamchatka Basin, Bering Sea (from Creager, Scholl, et al., 1973).

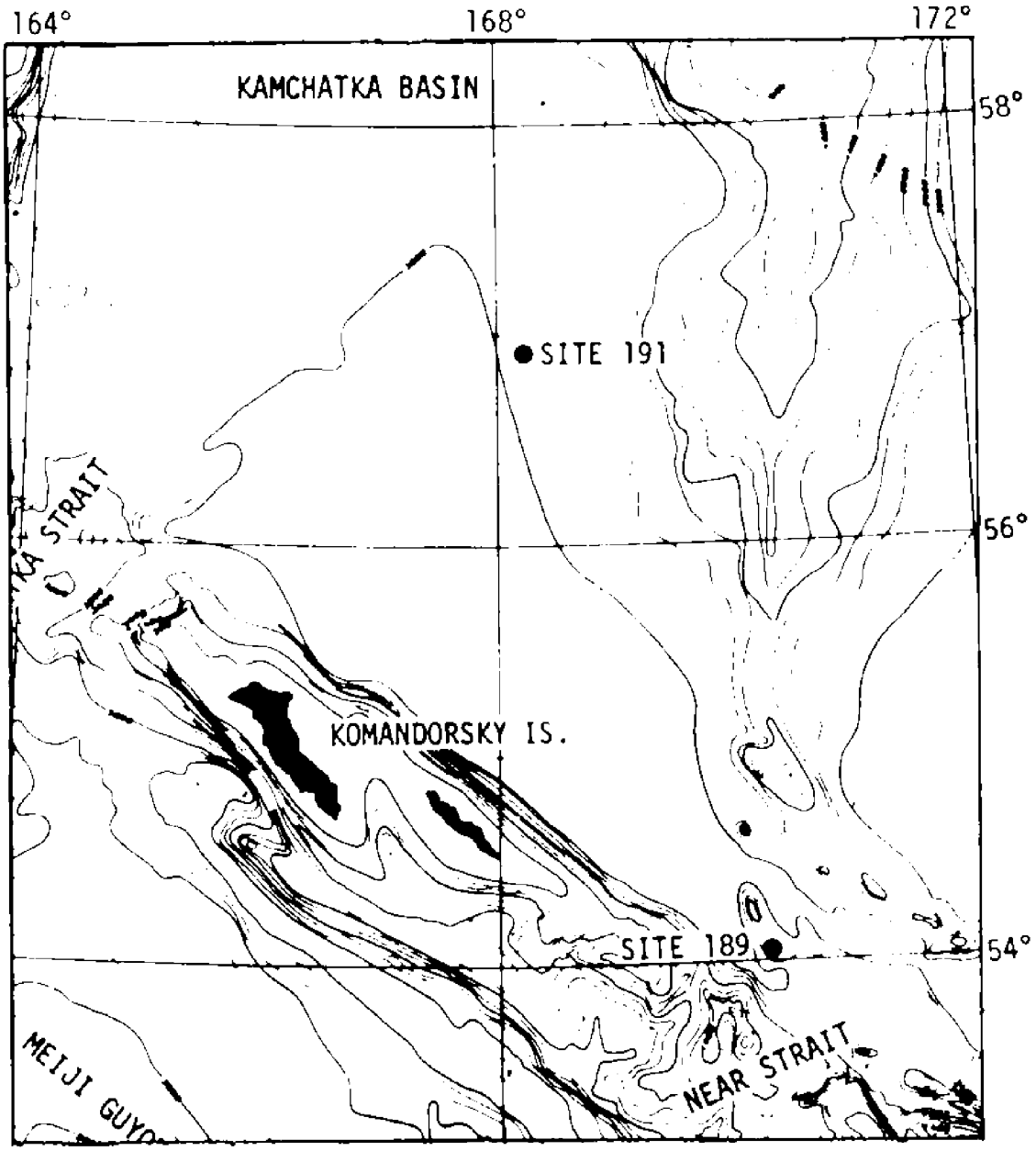

Figure F130. AFM diagram (Irvine and Baragar, 1971) for basalts in Hole 191.

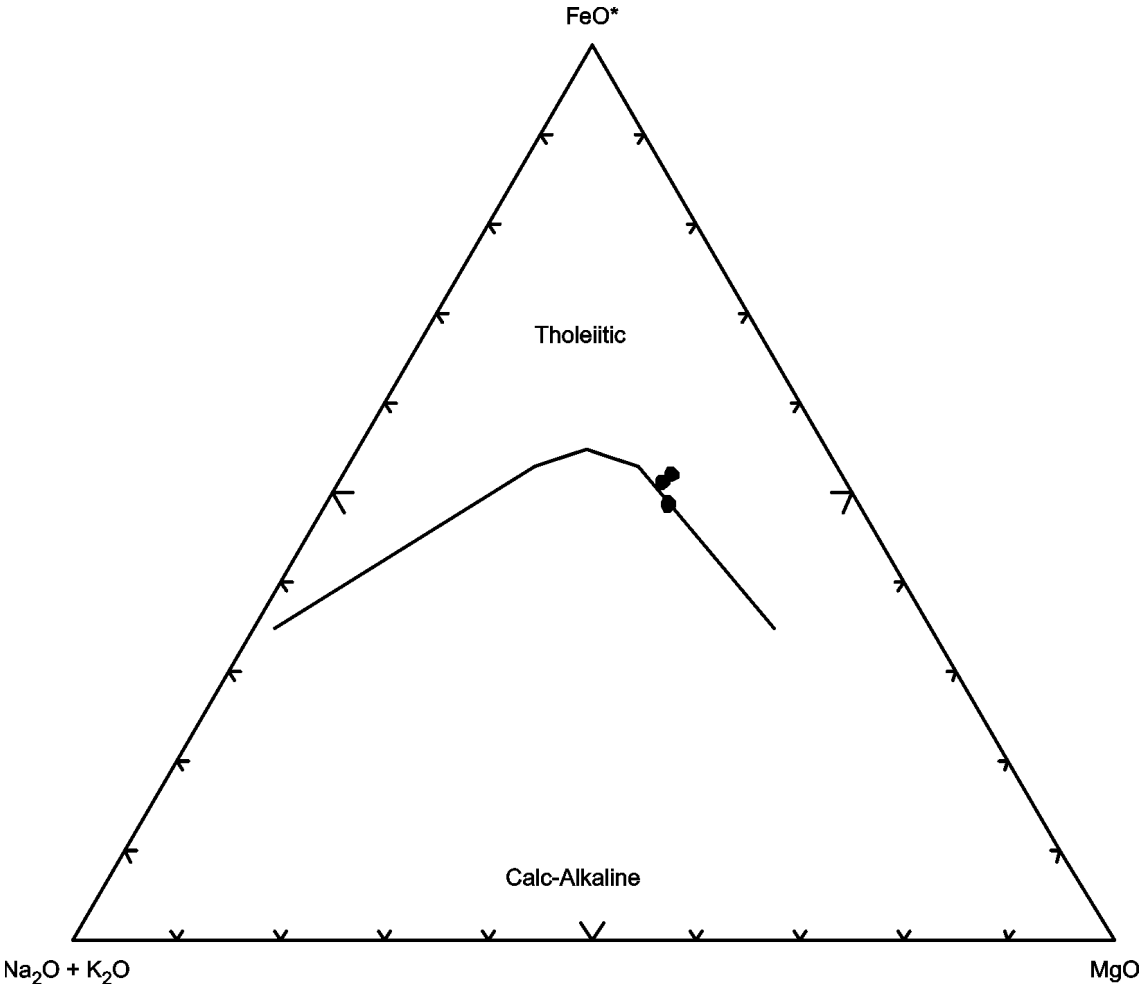

Figure F131. Discrimination Nb-Zr-Y diagram (Meschede, 1986) for basalts in Hole 191. AI, AII = fields of intraplate alkali basalts; AII, C = fields of intraplate tholeiites; B = field of P-type MORB; D = field of N-type MORB; C, D = fields of volcanic arc basalts.

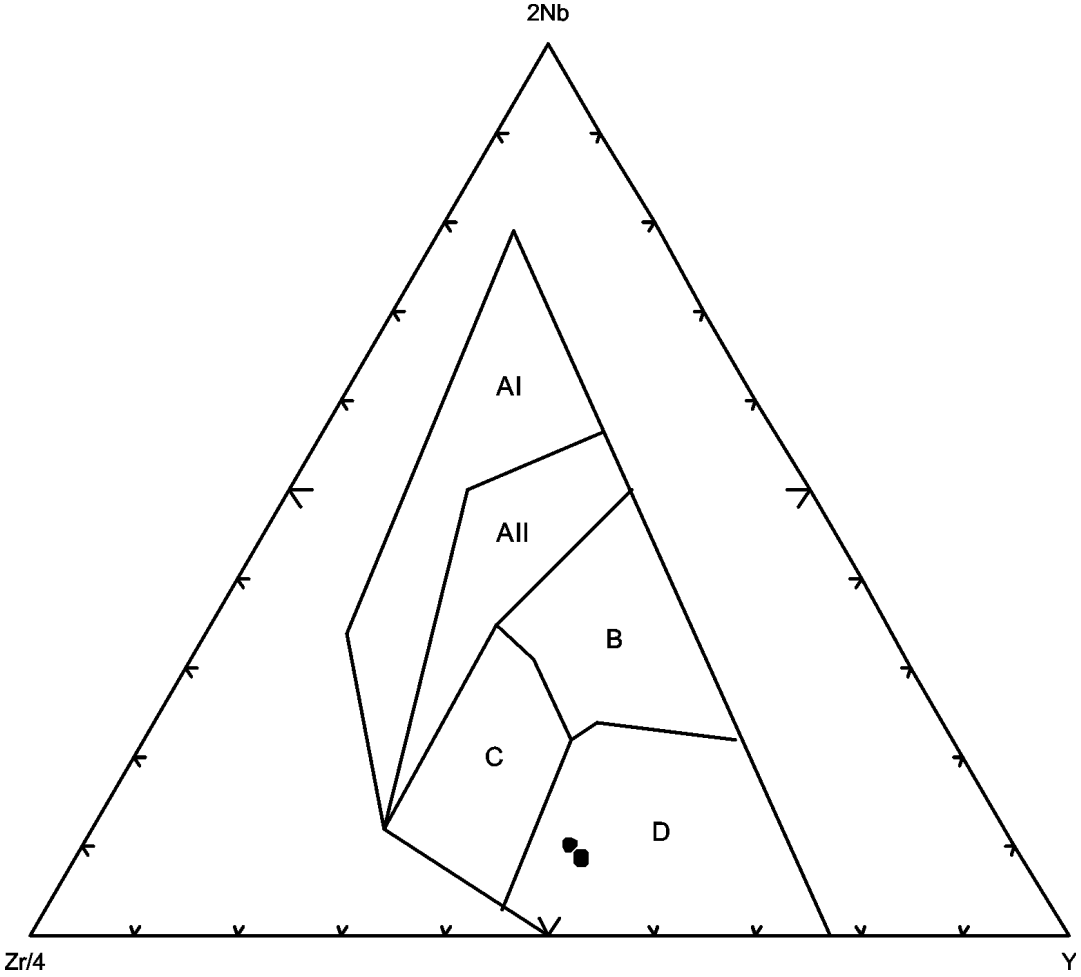

Figure F132. Chondrite-normalized rare earth element abundances for basalts in Hole 191. Normalizing values are from Sun and McDonough (1989).

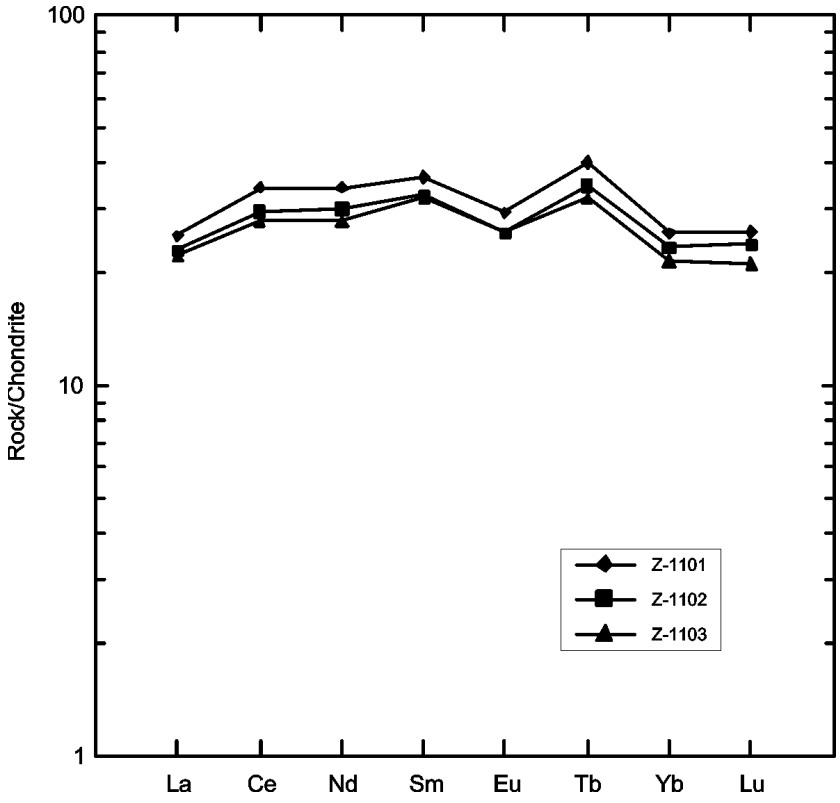

Figure F133. Hole 735B drilled during Leg 118 in the Atlantis II Fracture Zone (from Goldberg et al., 1991).

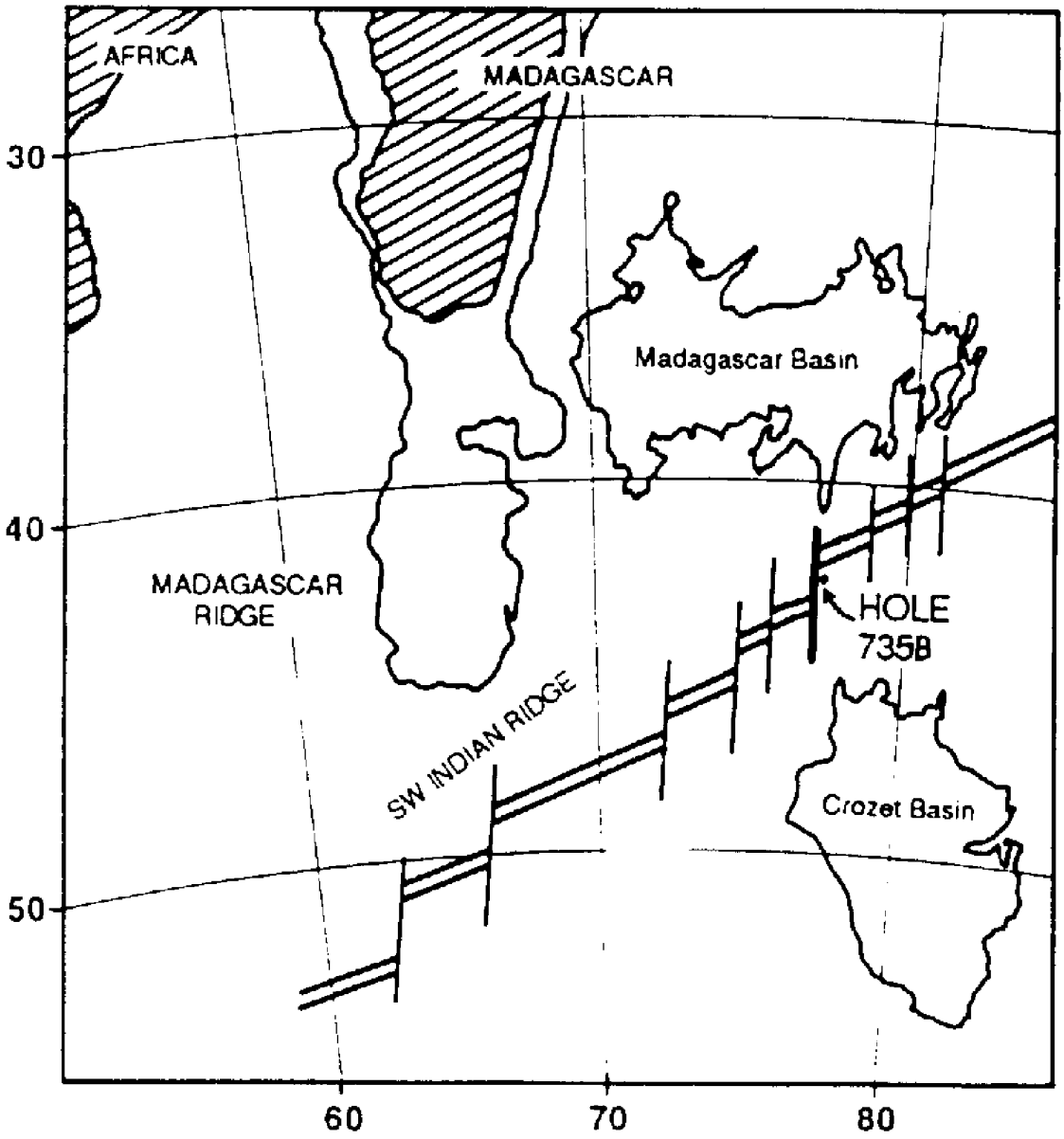

Figure F134. AFM diagram (Irvine and Baragar, 1971) for gabbros in Hole 735B.

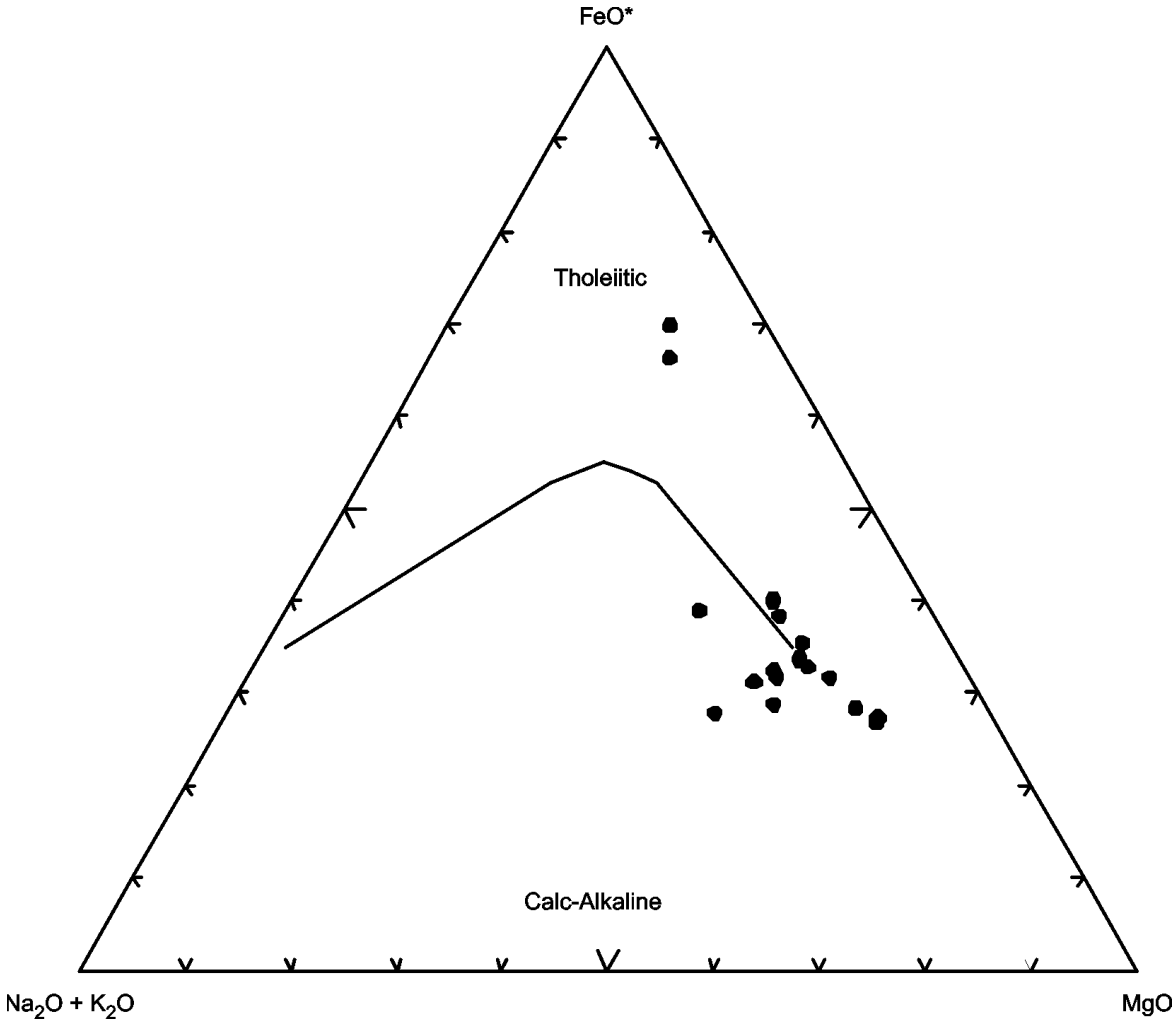

Figure F135. Discrimination Nb-Zr-Y diagram (Meschede, 1986) for gabbros in Hole 735B. AI, AII = fields of intraplate alkali basalts; AII, C = fields of intraplate tholeiites; B = field of P-type MORB; D = field of N-type MORB; C, D = fields of volcanic arc basalts.

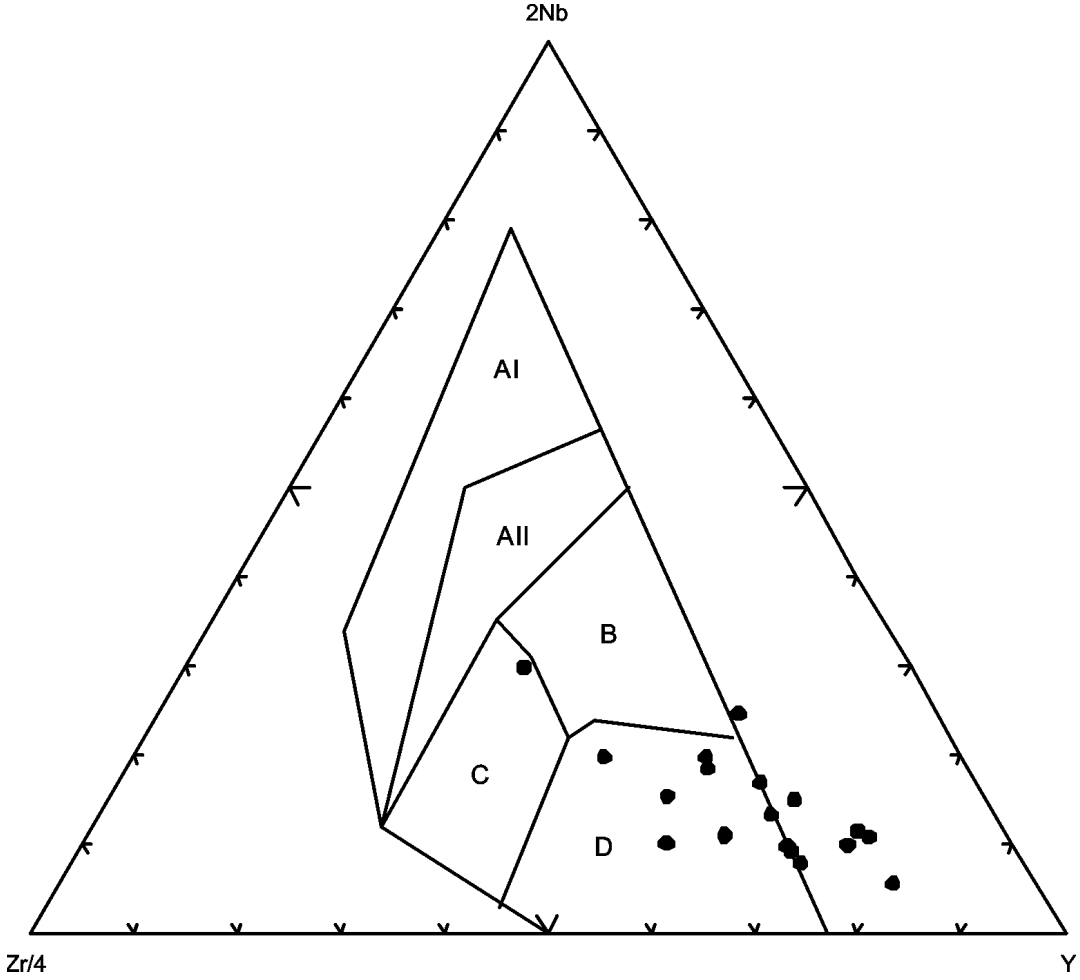

Figure F136. Chondrite-normalized rare earth element abundances for gabbros in Hole 735B. Normalizing values are from Sun and McDonough (1989).

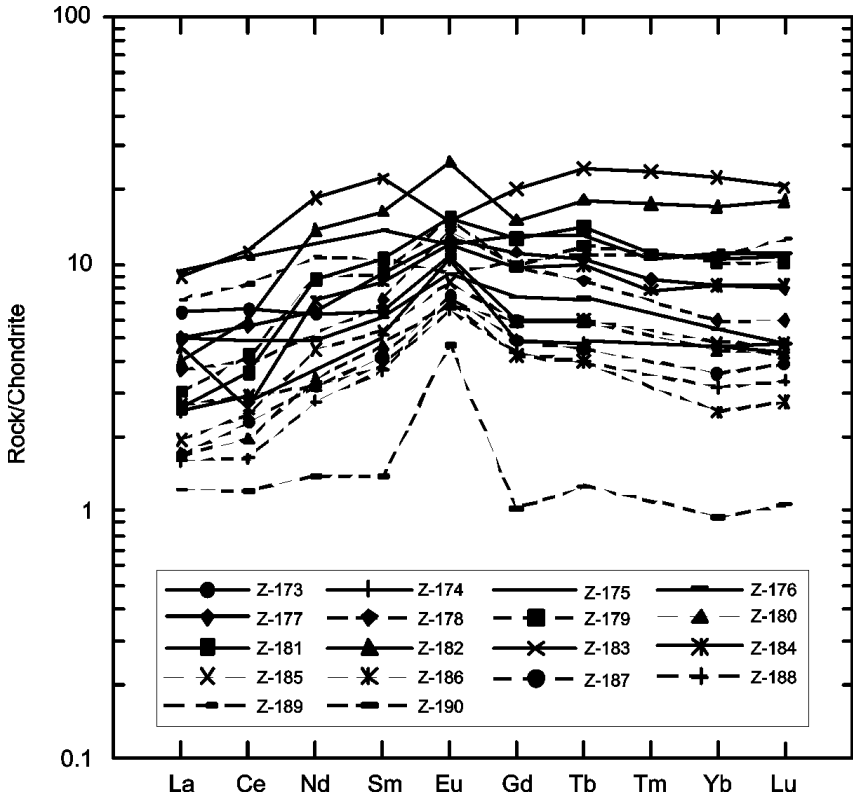

Figure F137. Site 637 drilled during Leg 103 in the Galicia Margin (from Boillot, Winterer, et al., 1987).

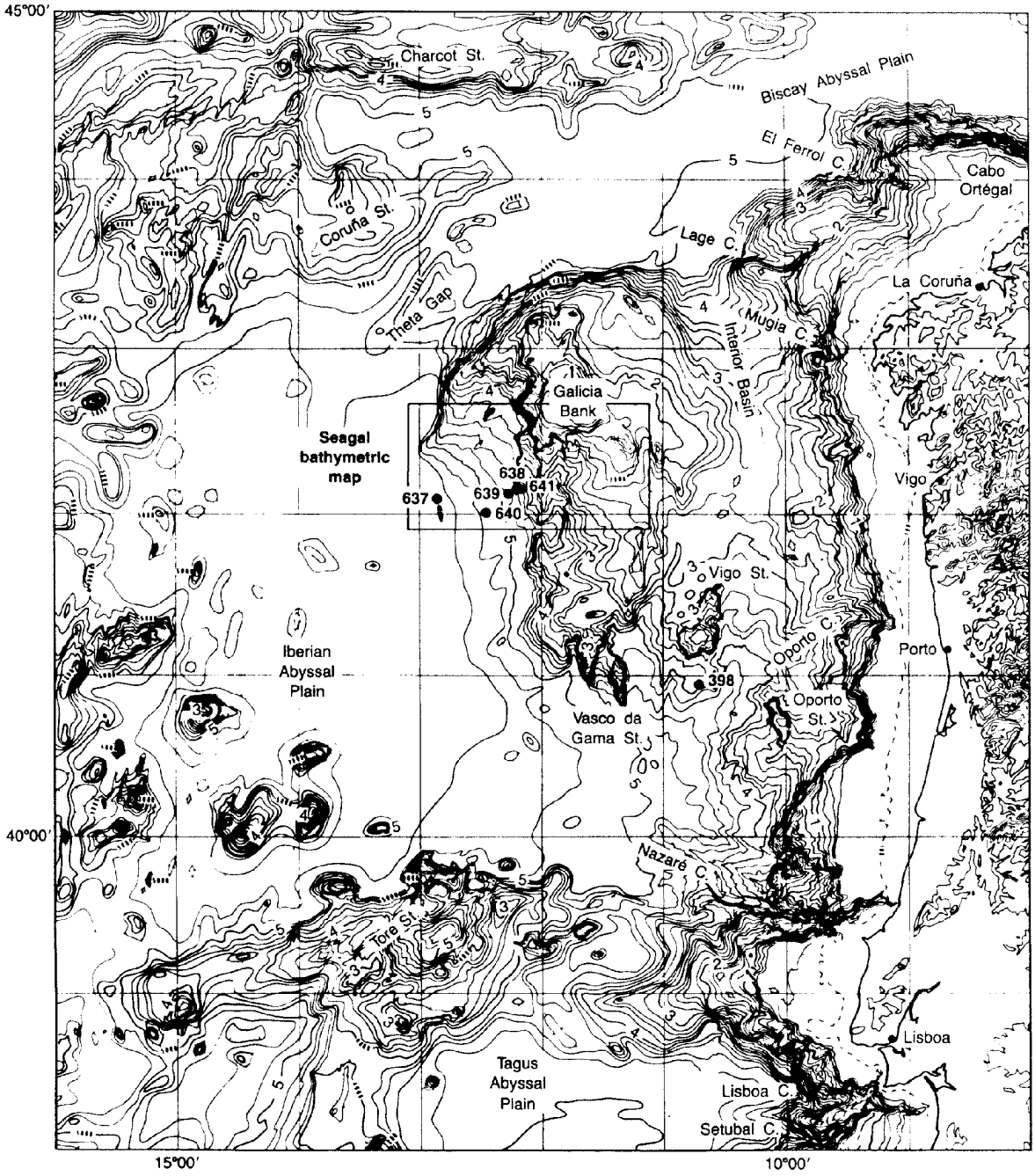

Figure F138. AFM diagram (Irvine and Baragar, 1971) for serpentinized harzburgites in Hole 637A.

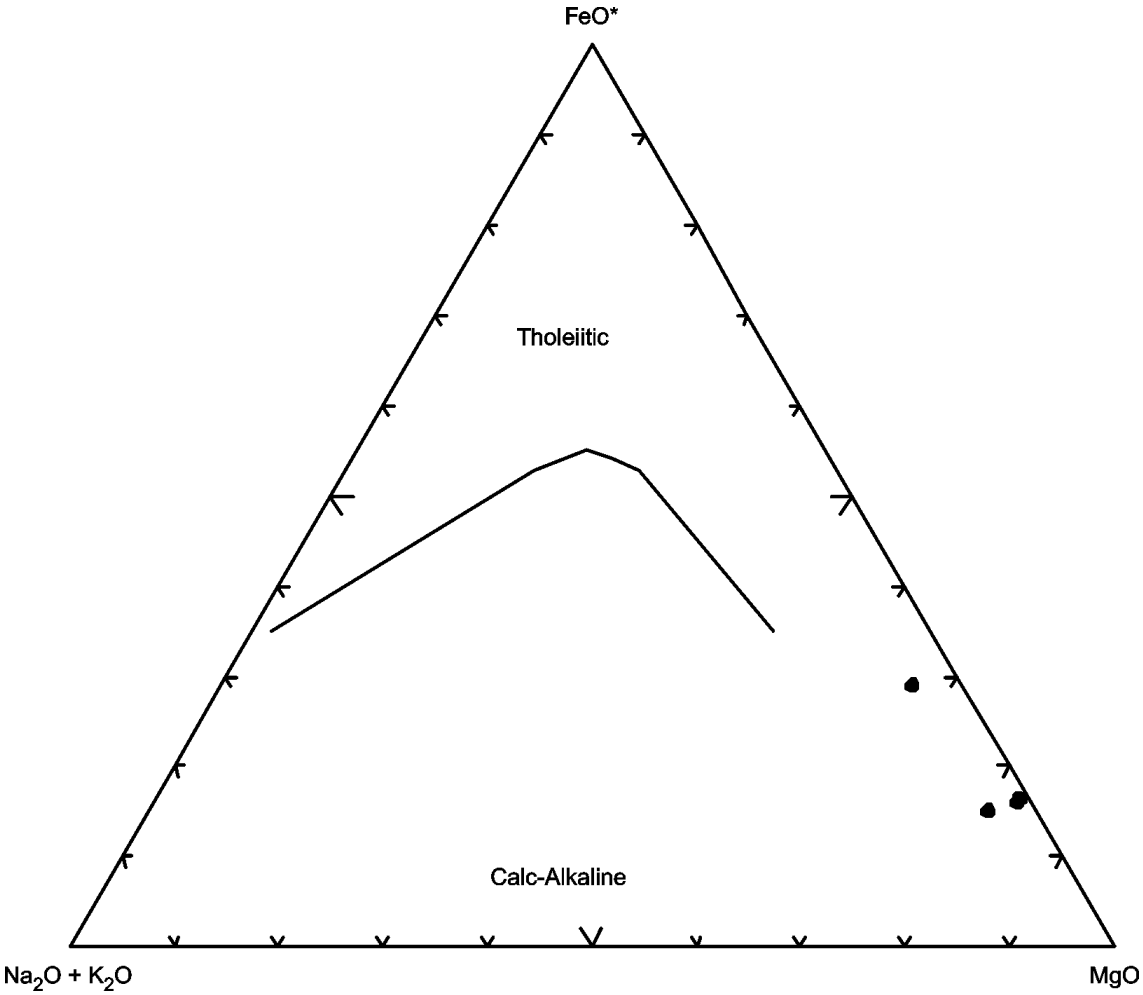

Figure F139. Chondrite-normalized rare earth element abundances for serpentinized harzburgites in Hole 637A. Normalizing values are from Sun and McDonough (1989).

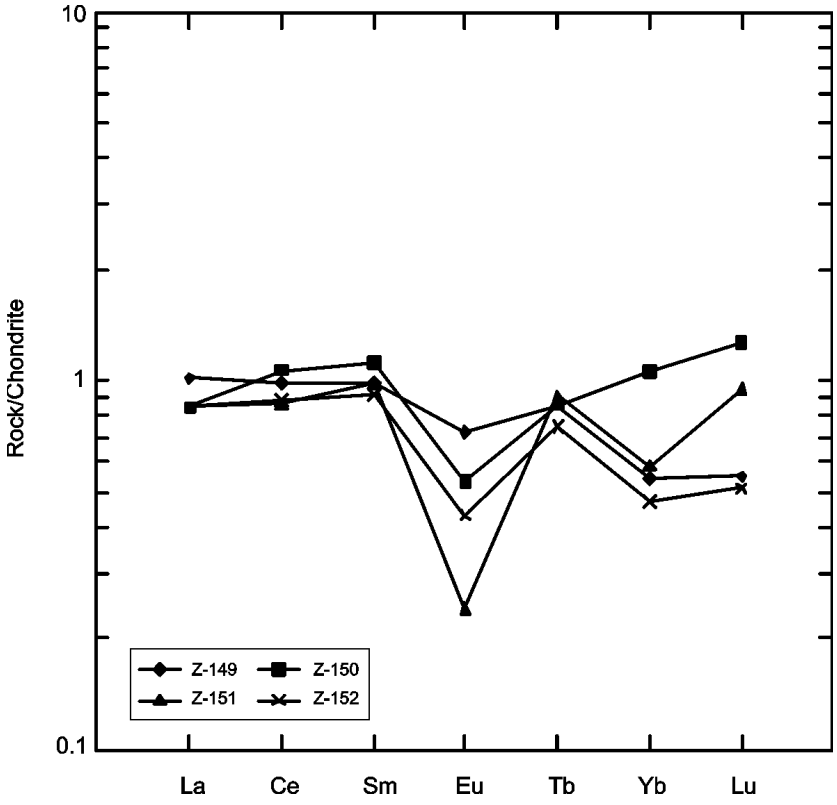

Table T1. Precision and accuracy of data of major and trace elements of international reference rocks BCR-1, AGV-1, DNC-1.

	BCR-1		AGV-1		DNC-1	
	Rec. value[1]	This work[2] (mean ± SD, N=5)	Rec. value[1]	This work[2] (mean ± SD, N=6)	Rec. value[1]	This work[2] (mean ± SD, N=4)
Major elements (wt %)						
SiO_2	54.06	53.74 ± 0.55	58.79	58.52 ± 0.60	47.04	46.80 ± 0.50
TiO_2	2.24	2.26 ± 0.12	1.05	1.10 ± 0.08	0.48	0.50 ± 0.045
Al_2O_3	13.64	13.79 ± 0.45	17.14	17.42 ± 0.60	18.30	18.53 ± 0.65
Fe_2O_3	13.41	13.57 ± 0.28	6.76	6.70 ± 0.30	9.93	10.27 ± 0.44
MnO	0.18	0.17 ± 0.015	0.09	0.09 ± 0.015	0.15	0.15 ± 0.017
MgO	3.48	3.64 ± 0.24	1.53	1.62 ± 0.15	10.05	10.20 ± 0.35
CaO	6.95	6.84 ± 0.34	4.94	4.82 ± 0.33	11.27	10.86 ± 0.35
Na_2O	3.27	3.26 ± 0.26	4.26	4.25 ± 0.29	1.87	1.85 ± 0.19
K_2O	1.69	1.66 ± 0.17	2.91	2.83 ± 0.23	0.23	0.23 ± 0.037
P_2O_5	0.36	0.36 ± 0.030	0.49	0.51 ± 0.031	0.08	0.08 ± 0.01
Trace elements (ppm)						
Cr	16	15 ± 2.0	10.1	10 ± 1.5	285	290 ± 30
Ni	13	12 ± 1.8	16	14 ± 2.5	247	240 ± 25
Co	37	35 ± 3.5	15.3	14 ± 2.5	54.7	55 ± 5.5
V	407	400 ± 35	121	120 ± 12	148	140 ± 15
Rb	47.2	45 ± 5.0	67.3	60 ± 15	4.5	4.0 ± 1.0
Sr	330	310 ± 30	667	650 ± 60	145	150 ± 15
Y	38	35 ± 5.0	20	18 ± 3	18	17 ± 3.0
Zr	190	170 ± 20	227	210 ± 25	41	40 ± 5.0
Nb	14	13 ± 2.0	15	15 ± 2.0	3.0	2.0 ± 1.0
Ba	681	670 ± 60	1226	1300 ± 100	114	110 ± 10
La	24.9	25 ± 2.0	38	36 ± 3.0	3.8	3.5 ± 0.35
Ce	53.7	54 ± 5.0	67	65 ± 5.0	10.6	10 ± 1.5
Nd	28.8	28 ± 3.0	33	32 ± 3.0	4.9	5.0 ± 0.5
Sm	6.59	6.4 ± 0.5	5.9	5.6 ± 0.5	1.38	1.4 ± 0.3
Eu	1.95	1.9 ± 0.2	1.64	1.6 ± 0.2	0.59	0.60 ± 0.1
Tb	1.05	1.0 ± 0.1	0.70	0.7 ± 0.1	0.41	0.4 ± 0.05
Yb	3.38	3.4 ± 0.3	1.72	1.7 ± 0.2	2.01	2.0 ± 0.2
Lu	0.51	0.48 ± 0.04	0.27	0.25 ± 0.03	0.32	0.31 ± 0.03
Th	5.98	5.7 ± 0.6	6.5	6.3 ± 0.6	ND	ND

Notes: [1] = recommended values from Govindaraju, 1989; [2] = data are average ± standard deviation (SD) of N analyses; ND = not determined.

Table T2. Values of transitional coefficient R_o (Kazitzyn and Rudnik, 1968).

Oxide	R_o
SiO_2	1.002
TiO_2	0.754
Al_2O_3	1.182
Fe_2O_3	0.754
FeO	0.838
MnO	0.849
MgO	1.494
CaO	1.074
Na_2O	1.944
K_2O	1.279
P_2O_5	0.849
H_2O	6.688
CO_2	1.369

Notes: Kazitzyn and Rudnik, 1968. R_o = transitional coefficient.

Table T3. Values of coefficient K.

Oxide	K
SiO_2	4.672
TiO_2	5.995
Al_2O_3	5.294
Fe_2O_3	6.990
FeO	7.769
MnO	7.743
MgO	6.030
CaO	7.146
Na_2O	7.419
K_2O	8.302
P_2O_5	4.365
H_2O	1.119
CO_2	2.730

Note: $K = 0.166 \times a_i \times R_o$.

Table T4. Characteristics of Hole 504B drilled at the Costa Rica Rift.

Hole, Leg	Latitude	Longitude	Water depth (m)	Oldest sediment cored	Basement penetration (m)	Basement recovery (m)
504B	01°13.63'N	83°43.81'W	3460	Depth sub-bottom (m): 274.5 Nature: Chert and siliceous limestone Age (estimated from magnetic anomalies): 5.9 m.y.		
69/70					574.5	168.15
83					514	106.9
111					209.1	26.42
137/140					378.9	47.69
148					110.6	9.58

Table T5. Composition of basalts from Hole 504B, Leg 69 (Costa Rica Rift, Pacific Ocean). (Continued on next four pages.)

Hole	504B	504B	504B	504B	504B	504B	504B
Core, section	2R-1	4R-1	4R-3	4R-4	5R-2	6R-1	7R-2
Interval (cm)	108-110	62-64	108-111	42-45	142-146	65-69	64-68
Piece	233	274	322	330	387	404	459
Lab number	Z-883	Z-884	Z-885	Z-886	Z-887	Z-888	Z-889
Depth (mbsf)	275.58	280.62	282.08	284.92	292.42	299.15	309.64
Unit/Subunit	1	2A	2A	2A	2A	2A	2C
Major element oxides (wt%):							
SiO_2	48.66	45.83	47.14	48.99	47.80	47.80	47.78
TiO_2	0.69	0.76	0.76	0.76	0.75	0.85	0.76
Al_2O_3	14.80	17.71	17.03	17.80	14.55	14.76	18.39
Fe_2O_3	6.29	2.83	5.06	3.01	6.45	6.13	2.94
FeO	5.13	4.98	3.24	4.79	4.27	4.40	5.07
MnO	0.17	0.19	0.17	0.18	0.15	0.18	0.13
MgO	7.22	9.23	10.63	7.68	8.73	7.79	8.69
CaO	11.35	7.39	10.34	12.42	11.35	12.28	10.76
Na_2O	2.42	1.87	1.93	2.32	2.04	1.83	2.89
K_2O	0.26	0.35	0.09	0.22	0.16	0.07	0.16
P_2O_5	0.10	0.06	0.05	0.09	0.08	0.08	0.09
LOI	2.98	8.44	3.13	1.58	3.61	3.66	2.31
Total	100.07	99.64	99.57	99.84	99.94	99.83	99.97
H_2O^+	0.89	6.92	2.68	1.33	0.53	0.65	1.95
H_2O^-	1.46				1.99	2.13	
CO_2	<0.2	0.92	0.45	0.25	<0.2	<0.2	0.36
Fe_2O_3/FeO	1.23	0.57	1.56	0.63	1.51	1.39	0.58
Density (g/cm^3)	2.82	2.21	2.31	2.67	2.79	2.18	1.92
Trace elements (ppm):							
La	1.7	0.88	0.98	1.1	1.4	1.2	1.2
Ce	6.5	2.6	2.7	2.7	4.3	3.5	3.6
Nd	6.3	3.7	3.6	3.8	5.1	4.3	4.4
Sm	2.6	1.9	1.9	2.1	2.4	2.1	2.2
Eu	0.88	0.81	0.7	0.75	0.75	0.67	0.93
Tb	0.82	0.74	0.65	0.71	0.7	0.56	0.74
Yb	3.2	3.1	2.6	2.8	2.9	2.4	2.8
Lu	0.53	0.44	0.41	0.45	0.44	0.39	0.43
Sc	ND	28	32	34	ND	ND	32
Cr	235	410	305	265	410	400	320
Ni	71	80	77	71	108	140	69
Co	48	41	39	36	44	44	41
V	390	330	242	230	272	245	338
Cu	66	49	49	59	68	47	45
Pb	<5	<5	<5	<5	<5	<5	<5
Zn	98	64	61	63	72	74	62
Sn	2.1	2.7	2.4	2.4	1.5	1.5	2.5
Zr	57	44	42	44	45	50	41
Y	26	25	22	22	23	21	24
Nb	<1	<1	1.4	1.4	1	<1	1.8
Rb	4.4	4.4	1.3	3.4	3.1	1.2	1.6
Sr	71	110	69	68	67	64	76
Ba	9	55	34	29	<3	3	39
Th	<1	ND	ND	ND	<1	<1	ND
B	ND	35	20	40	ND	ND	16

Note: ND = not determined.

Table T5 (continued).

Hole	504B	504B	504B	504B	504B	504B	504B
Core, section	7R-3	8R-3	9R-1	10R-3	11R-1	12R-1	13R-4
Interval (cm)	61-65	61-66	142-147	17-20	61-64	39-43	40-42
Piece	481	538	583	643	667	714	806
Lab number	Z-890	Z-891	Z-892	Z-893	Z-894	Z-895	Z-896
Depth (mbsf)	311.11	320.11	326.92	337.67	344.11	352.89	366.40
Unit/Subunit	2C	2D	3A	3A	3A	3A	3A
Major element oxides (wt%):							
SiO_2	47.23	48.72	45.98	47.23	48.62	49.38	49.37
TiO_2	0.56	0.50	0.71	0.83	0.95	0.69	0.81
Al_2O_3	15.47	14.73	14.06	14.67	15.58	15.16	16.36
Fe_2O_3	7.27	7.06	8.86	6.83	6.49	5.31	2.66
FeO	1.98	4.10	1.80	3.09	3.07	4.14	5.70
MnO	0.11	0.16	0.08	0.13	0.14	0.17	0.20
MgO	8.57	7.60	10.40	9.47	7.72	7.88	9.11
CaO	7.97	12.51	5.70	9.30	11.01	12.54	12.02
Na_2O	2.38	2.07	2.39	2.32	2.46	2.26	1.95
K_2O	0.42	0.12	0.46	0.15	0.20	0.17	0.12
P_2O_5	0.07	0.09	0.08	0.10	0.10	0.08	0.09
LOI	8.50	2.21	9.31	5.50	3.42	2.01	1.63
Total	100.53	99.87	99.83	99.62	99.76	99.79	100.02
H_2O^+	3.85	0.33	2.37	1.25	0.68	0.24	1.30
H_2O^-	4.65	1.21	5.79	3.60	2.21	1.08	
CO_2	<0.2	<0.2	<0.2	<0.2	<0.2	<0.2	0.33
Fe_2O_3/FeO	3.67	1.72	4.92	2.21	2.11	1.28	0.47
Density (g/cm^3)	2.43	1.84	2.52	2.60	2.67	2.90	2.78
Trace elements (ppm):							
La	1.4	1.3	1.3	1.8	1.5	1.3	1.1
Ce	5.1	4.9	4.9	7.8	4.4	6	3.6
Nd	4.8	4.9	4.8	7.5	5.1	5.5	4.3
Sm	1.9	2	2.1	3	2.5	2.3	2.1
Eu	0.66	0.67	0.77	0.98	0.85	0.86	0.81
Tb	0.49	0.61	0.57	0.96	0.66	0.61	0.69
Yb	2.1	2.5	2.5	2.8	2.7	2.7	2.6
Lu	0.32	0.41	0.42	0.43	0.41	0.4	0.44
Sc	ND	ND	ND	ND	ND	ND	36
Cr	520	420	315	410	400	390	257
Ni	94	102	95	89	78	94	69
Co	42	50	50	49	43	50	43
V	387	312	445	302	317	287	252
Cu	49	47	60	50	68	62	59
Pb	<5	<5	<5	<5	<5	<5	<5
Zn	58	76	72	78	87	90	64
Sn	2.3	1.0	1.5	2.0	2.0	1.9	2.2
Zr	44	45	49	54	50	46	47
Y	19	21	22	29	27	24	24
Nb	<1	<1	<1	<1	1.2	<1	1.2
Rb	3.1	12	4.6	2.5	4.8	3.1	2.1
Sr	87	66	81	85	88	74	73
Ba	4	<3	8	3	6	<3	24
Th	<1	1	1.2	1.3	<1	1.1	ND
B	ND	ND	ND	ND	ND	ND	35

Table T5 (continued).

Hole	504B	504B	504B	504B	504B	504B	504B
Core, section	15R-1	16R-1	16R-4	17R-1	18R-1	19R-1	20R-1
Interval (cm)	24-28	45-49	22-26	30-34	45-49	84-87	110-113
Piece	872	961	1005	1036	1087	1124	1173
Lab number	Z-901	Z-897	Z-898	Z-899	Z-900	Z-902	Z-903
Depth (mbsf)	375.24	384.45	388.72	393.30	398.45	403.84	413.10
Unit/Subunit	3C	3C	4	4	5	5	9
Major element oxides (wt%):							
SiO_2	47.04	47.69	48.21	47.69	47.53	45.82	49.02
TiO_2	0.93	0.72	0.96	0.96	1.23	1.06	0.94
Al_2O_3	18.40	15.19	14.74	16.02	15.46	15.09	15.39
Fe_2O_3	4.38	5.82	4.78	6.12	6.46	6.59	3.62
FeO	3.97	3.87	4.65	3.23	4.22	3.35	5.24
MnO	0.16	0.15	0.17	0.10	0.11	0.15	0.17
MgO	7.88	8.78	9.77	8.90	7.01	9.03	7.73
CaO	9.87	11.16	10.80	9.28	12.11	9.38	12.99
Na_2O	2.50	2.19	2.04	2.46	2.33	2.20	2.20
K_2O	0.27	0.18	0.08	0.16	0.18	0.16	0.03
P_2O_5	0.10	0.08	0.11	0.11	0.16	0.16	0.08
LOI	4.42	3.76	3.72	5.18	3.34	7.03	2.29
Total	99.92	99.59	100.03	100.21	100.14	100.02	99.70
H_2O^+	4.11	0.86	0.61	1.52	0.62	2.02	0.50
H_2O^-		2.43	2.49	3.51	1.85	3.87	1.05
CO_2	0.31	<0.2	<0.2	<0.2	<0.2	<0.2	<0.2
Fe_2O_3/FeO	1.10	1.50	1.03	1.89	1.53	1.97	0.69
Density (g/cm^3)	2.74	2.69	2.79	2.65	2.74	2.70	2.82
Trace elements (ppm):							
La	1.2	1.1	1.6	1.7	7	7.2	1.9
Ce	4.6	4.4	5.8	4.9	18	19	6.8
Nd	5.5	4.5	5.8	5.1	11	11	6
Sm	2.5	2	2.3	2.3	2.9	2.8	2.2
Eu	1	0.71	0.77	0.88	1	1	0.86
Tb	0.84	0.57	0.57	0.61	0.68	0.67	0.5
Yb	3.2	2.4	2.4	2.3	2.3	2.4	2.3
Lu	0.5	0.39	0.39	0.35	0.37	0.38	0.35
Sc	47	ND	ND	ND	ND	ND	ND
Cr	300	280	425	460	385	370	380
Ni	71	86	160	165	96	140	108
Co	43	42	48	53	43	52	56
V	327	295	267	305	267	280	275
Cu	68	34	78	44	68	60	88
Pb	<5	<5	<5	<5	<5	<5	<5
Zn	81	74	74	72	70	64	77
Sn	1.8	2.0	2.5	1.5	2.8	2.0	2.3
Zr	49	47	51	55	89	90	54
Y	29	22	26	25	26	24	22
Nb	1.2	1.7	<1	1.3	9.4	9.7	<1
Rb	4.9	3.6	1.9	1.5	3.5	1.6	<1
Sr	84	67	82	96	150	150	93
Ba	31	3	<3	4	7	7	8
Th	ND	1.1	<1	<1	1.1	<1	ND
B	54	ND	ND	ND	ND	ND	ND

Table T5 (continued).

Hole	504B	504B	504B	504B	504B	504B	504B
Core, section	21R-2	21R-4	21R-5	22R-1	23R-1	24R-1	24R-3
Interval (cm)	126-130	116-120	63-66	108-109	32-35	125-128	128-129
Piece	1215	1253	1267	1280	1314	1349	1393
Lab number	Z-904	Z-905	Z-906	Z-907	Z-908	Z-909	Z-910
Depth (mbsf)	423.76	426.66	427.63	431.08	439.32	449.25	452.28
Unit/Subunit	10	14	16	16	16	16	17
Major element oxides (wt%):							
SiO_2	48.10	48.62	46.82	48.52	48.79	47.11	48.98
TiO_2	0.61	0.58	0.64	0.77	0.81	0.76	0.66
Al_2O_3	16.09	16.24	18.79	16.01	16.09	17.71	15.39
Fe_2O_3	6.00	3.89	3.93	3.47	3.88	4.37	4.04
FeO	3.60	4.32	4.20	4.54	4.46	4.82	5.91
MnO	0.14	0.10	0.17	0.25	0.15	0.16	0.08
MgO	8.41	8.77	8.83	8.90	7.87	9.27	8.00
CaO	12.12	12.32	11.61	12.33	12.90	9.76	12.30
Na_2O	2.00	1.90	1.90	2.16	1.97	1.91	2.21
K_2O	0.09	0.09	0.13	0.09	0.21	0.27	0.07
P_2O_5	0.06	0.06	0.05	0.08	0.07	0.07	0.07
LOI	3.11	2.80	2.71	2.43	2.54	3.75	1.43
Total	100.33	99.69	99.78	99.55	99.74	99.96	99.14
H_2O^+	0.78	0.75	2.16	0.90	0.55	3.34	0.40
H_2O^-	1.55	1.33		1.23	1.06		0.66
CO_2	<0.2	<0.2	0.55	<0.2	<0.2	0.41	<0.2
Fe_2O_3/FeO	1.67	0.90	0.94	0.76	0.87	0.91	0.68
Density (g/cm^3)	3.00	2.52	2.67	2.77	2.92	2.66	2.91
Trace elements (ppm):							
La	0.93	0.87	0.81	2.0	1.0	0.89	1.3
Ce	3.4	2.8	3.1	6.1	3.4	3.4	4.6
Nd	3.8	3.7	3.6	6.5	4.3	3.8	5.1
Sm	1.7	1.7	1.7	2.7	1.9	1.7	2.4
Eu	0.64	0.64	0.64	0.79	0.71	0.73	0.79
Tb	0.56	0.51	0.63	0.69	0.54	0.59	0.67
Yb	2.1	2.2	2.2	3.0	2.2	2.4	2.8
Lu	0.34	0.33	0.3	0.45	0.38	0.35	0.45
Sc	ND	ND	27	ND	ND	33	ND
Cr	460	380	370	410	280	415	400
Ni	150	155	150	96	78	157	93
Co	60	53	52	48	44	55	53
V	320	280	267	252	290	317	387
Cu	55	66	72	55	55	68	66
Pb	<5	<5	<5	<5	<5	<5	<5
Zn	76	77	67	78	85	64	73
Sn	1.5	2.1	1.7	1.7	1.7	2.0	1.9
Zr	37	33	28	60	43	43	56
Y	19	19	21	26	21	19	27
Nb	<1	<1	1.3	<1	1.1	1.7	<1
Rb	<1	1.2	1.4	<1	5	3.4	<1
Sr	54	52	56	77	58	58	63
Ba	4	6	35	9	7	27	8
Th	<1	<1	ND	<1	1.1	ND	<1
B	ND	ND	16	ND	ND	28	ND

Table T5 (continued).

Hole	504B	504B	504B	504B	504B
Core, section	25R-2	26R-1	27R-2	28R-3	29R-1
Interval (cm)	62-66	15-18	55-58	69-73	31-34
Piece	1429	1449	1484	1530	1562
Lab number	Z-911	Z-912	Z-913	Z-914	Z-915
Depth (mbsf)	459.12	463.15	468.05	478.69	484.31
Unit/Subunit	17	17	17	19	20
Major element oxides (wt%):					
SiO_2	49.33	49.43	47.12	48.49	49.78
TiO_2	0.70	0.73	0.78	0.74	0.66
Al_2O_3	14.51	15.36	17.17	15.50	14.71
Fe_2O_3	3.82	3.34	2.48	3.45	7.38
FeO	6.18	5.88	5.93	4.42	2.54
MnO	0.22	0.09	0.22	0.09	0.21
MgO	8.93	8.22	9.97	8.40	8.34
CaO	12.58	12.69	10.97	11.62	12.58
Na_2O	2.13	2.17	1.98	2.21	2.18
K_2O	0.07	0.13	0.17	0.15	0.07
P_2O_5	0.07	0.08	0.11	0.06	0.08
LOI	1.26	1.50	2.70	4.21	1.41
Total	99.80	99.62	99.60	99.34	99.94
H_2O^+	0.35	0.31	2.11	1.77	0.23
H_2O^-	0.58	0.73		1.89	0.74
CO_2	<0.2	<0.2	0.59	<0.2	<0.2
Fe_2O_3/FeO	0.62	0.57	0.42	0.78	2.91
Density (g/cm^3)	2.82	2.89	2.66	2.75	2.88
Trace elements (ppm):					
La	1.2	1.4	1.0	1.2	1.5
Ce	4.6	4.3	3.2	4.2	5.4
Nd	5.2	6.1	3.9	4.9	6
Sm	2.2	2.7	1.9	2.1	2.5
Eu	0.81	0.92	0.81	0.84	0.87
Tb	0.65	0.8	0.62	0.6	0.74
Yb	2.8	3.4	2.4	2.6	3.1
Lu	0.42	0.53	0.39	0.39	0.48
Sc	ND	ND	30	ND	ND
Cr	425	315	257	350	300
Ni	89	93	106	93	88
Co	54	50	40	54	48
V	380	322	252	377	322
Cu	68	66	59	60	83
Pb	<5	<5	<5	<5	<5
Zn	80	83	69	72	83
Sn	2.1	2.2	1.7	2.1	2.1
Zr	56	53	39	50	55
Y	24	24	25	23	25
Nb	<1	<1	1.3	1.2	<1
Rb	<1	2.5	2.2	<1	<1
Sr	64	63	61	60	63
Ba	5	6	31	7	8
Th	<1	<1	ND	<1	1
B	ND	ND	22	ND	ND

Table T6. Composition of basalts from Hole 504B, Leg 70 (Costa Rica Rift, Pacific Ocean). (Continued on next six pages.)

Hole	504B	504B	504B	504B	504B	504B	504B
Core, section	32R-2	33R-1	33R-1	33R-2	34R-1	34R-1	34R-2
Interval (cm)	137-140	70-72	86-88	14-16	19-24	140-142	18-21
Piece	177	191	193	202	220	235	240
Lab number	Z-919	Z-916	Z-917	Z-918	Z-550	Z-920	Z-921
Depth (mbsf)	510.37	517.2	517.36	518.14	525.69	526.9	527.18
Unit/Subunit	22	22	22	22	22	23B	23B
Major element oxides (wt%):							
SiO_2	46.51	46.70	47.88	48.82	49.40*	47.75	46.25
TiO_2	0.84	0.69	0.80	0.86	0.96	0.83	0.76
Al_2O_3	15.80	17.16	15.36	15.64	15.80	16.38	16.79
Fe_2O_3	4.96	4.38	3.46	2.83	3.33	4.69	4.77
FeO	5.64	4.45	5.55	5.56	5.64	4.42	4.74
MnO	0.20	0.20	0.23	0.20	0.16	0.09	0.22
MgO	8.91	7.50	9.81	8.69	9.45	7.92	8.31
CaO	10.83	12.83	11.56	12.22	11.55	13.45	11.28
Na_2O	1.77	2.13	1.98	1.96	2.16	2.06	2.19
K_2O	0.18	0.15	0.13	0.16	0.15	0.08	0.39
P_2O_5	0.08	0.12	0.11	0.12	0.08	0.04	0.09
LOI	4.51	3.60	3.22	2.58	0.97	2.62	4.37
Total	100.23	99.91	100.09	99.64	99.64	100.33	100.16
H_2O^+	1.72	1.64	0.75	0.78	0.97	1.11	1.89
H_2O^-	2.78	1.82	1.73	1.34		1.41	2.18
CO_2	<0.2	<0.2	<0.2	<0.2	ND	0.10	0.19
Fe_2O_3/FeO	0.88	0.98	0.62	0.51	0.59	1.06	1.01
Density (g/cm^3)	2.91	2.82	2.65	2.86	2.82	2.78	2.47
Trace elements (ppm):							
La	1.1	0.99	1.6	1.5	2.15	1.1	0.99
Ce	3.5	3.5	4.9	3.7	6.9	3.5	3.4
Nd	4.3	3.8	5	4.2	ND	4.1	4.2
Sm	1.8	1.6	1.9	1.8	1.88	1.8	1.8
Eu	0.67	0.62	0.76	0.72	0.85	0.7	0.7
Tb	0.61	0.49	0.57	0.59	0.395	0.5	0.61
Tm	ND	ND	ND	ND	0.3	ND	ND
Yb	2.4	2	2.3	2.1	1.318	2.2	2.2
Lu	0.41	0.32	0.38	0.34	0.253	0.39	0.38
Sc	ND	ND	ND	ND	34	ND	ND
Cr	330	340	310	340	317	422	415
Ni	103	170	160	190	ND	180	155
Co	54	53	47	51	32	58	47
V	380	262	275	290	ND	350	345
Cu	70	82	70	72	ND	130	80
Pb	<5	<5	<5	<5	ND	<5	<5
Zn	80	70	83	83	ND	77	65
Sn	1.8	1.8	2.8	2.4	ND	2.2	2.2
Zr	45	48	51	53	ND	45	43
Y	24	19	21	22	ND	22	22
Nb	<1	<1	1.1	1.4	ND	1.4	<1
Rb	1.6	2.6	3.9	2.6	ND	<1	2.8
Sr	43	76	69	72	ND	65	78
Ba	4	7	5	3	ND	14	5
Th	<1	1	1.4	1	ND	ND	<1
B	ND	ND	ND	ND	ND	ND	ND

Note: * = major and trace element data from Sharaskin et al. (1983). ND = not determined.

Table T6 (continued).

Hole	504B	504B	504B	504B	504B	504B	504B
Core, section	35R-1	35R-2	36R-1	36R-2	37R-1	37R-1	37R-2
Interval (cm)	110-112	14-16	91-110	25-27	15-20	55-60	75-78
Piece	274	283	301A	305	344	349	373
Lab number	Z-922	Z-923	Z-551	Z-924	Z-925	Z-926	Z-927
Depth (mbsf)	535.6	536.14	544.41	545.25	552.65	553.05	554.75
Unit/Subunit	24	24	24	24	25	25	25
Major element oxides (wt%):							
SiO_2	46.79	45.09	50.40*	50.19	48.79	48.68	48.95
TiO_2	0.67	0.72	1.00	0.81	0.93	0.90	0.64
Al_2O_3	18.22	16.82	15.55	15.36	14.99	15.19	14.21
Fe_2O_3	5.33	3.60	2.62	0.60	3.40	2.88	2.81
FeO	3.71	4.86	7.34	7.41	5.43	6.96	7.59
MnO	0.18	0.34	0.14	0.22	0.14	0.08	0.22
MgO	8.05	9.22	8.26	9.63	9.00	8.36	8.82
CaO	11.77	11.96	12.99	11.24	12.11	11.95	11.28
Na_2O	1.95	1.87	2.01	2.91	2.06	2.33	3.11
K_2O	0.16	0.14	0.04	0.13	0.06	0.21	0.16
P_2O_5	0.05	0.05	0.08	0.08	0.04	0.05	0.11
LOI	3.11	5.02	1.10	1.52	3.00	2.25	1.84
Total	99.99	99.69	101.53	100.10	99.95	99.84	99.74
H_2O^+	2.91	4.46	0.76	1.15	0.78	1.00	1.15
H_2O^-					1.98	1.12	0.62
CO_2	0.20	0.56	ND	0.37	<0.1	0.13	<0.2
Fe_2O_3/FeO	1.44	0.74	0.36	0.08	0.63	0.41	0.37
Density (g/cm^3)	2.72	1.79	2.90	2.86	2.85	3.04	2.94
Trace elements (ppm):							
La	0.78	0.88	1.2	0.94	1.6	5.7	1.1
Ce	3.1	2.8	6.6	2.0	4.5	12	3.6
Nd	3.7	3.6	ND	3.8	4.3	7.5	4.3
Sm	1.7	1.7	2.29	2.0	1.7	1.9	2
Eu	0.75	0.8	0.97	0.86	0.67	0.69	0.81
Tb	0.66	0.55	ND	0.60	0.62	0.63	0.61
Tm	ND	ND	ND	ND	ND	ND	ND
Yb	2.3	2.3	2.77	2.7	2.4	2.7	2.9
Lu	0.36	0.37	0.49	0.41	0.38	0.44	0.46
Sc	20	27	46	28	ND	ND	ND
Cr	370	265	347	225	350	437	350
Ni	152	98	ND	83	96	88	88
Co	70	49	39	53	47	53	48
V	252	185	340	257	280	405	322
Cu	86	86	87	72	88	104	72
Pb	7	5		5	<5	<5	<5
Zn	61	145	79	75	84	86	81
Sn	2	2	ND	2	2.4	3.1	2.0
Zr	43	43	ND	40	42	44	46
Y	20	19	ND	23	24	25	27
Nb	1.3	<1	ND	1.0	1.5	1.1	<1
Rb	2.3	2.0	ND	<1	<1	2.5	2.3
Sr	82	70	ND	58	54	58	45
Ba	16	19	ND	<10	7	4	5
Th	ND	ND	ND	ND	ND	ND	1.3
B	54	54	ND	10	ND	ND	ND

Table T6 (continued).

Hole	504B	504B	504B	504B	504B	504B	504B
Core, section	37R-3	38R-1	39R-2	40R-1	40R-2	41R-3	43R-1
Interval (cm)	14-17	7-15	97-102	55-60	84-86	146-148	80-82
Piece	391	411	492	510	532	628	680
Lab number	Z-928	Z-929	Z-930	Z-552	Z-553	Z-554	Z-555
Depth (mbsf)	555.64	561.57	572.97	580.05	581.84	588.46	602.8
Unit/Subunit	25	25	27	27	27	27	28
Major element oxides (wt%):							
SiO_2	48.68	47.77	50.23	47.60*	49.65*	49.80*	49.30*
TiO_2	0.81	0.79	0.80	0.82	0.86	0.94	0.92
Al_2O_3	14.96	15.31	15.99	15.80	17.11	16.65	15.65
Fe_2O_3	3.89	1.56	2.01	2.74	2.16	2.24	3.90
FeO	6.35	7.84	6.32	5.95	6.79	6.85	5.94
MnO	0.21	0.24	0.19	0.16	0.13	0.15	0.16
MgO	8.34	9.43	8.21	11.23	8.51	8.09	8.41
CaO	12.02	12.03	12.69	12.20	12.33	12.84	12.78
Na_2O	2.37	2.00	2.06	1.86	1.89	2.20	2.24
K_2O	0.29	0.13	0.02	0.07	0.03	0.07	0.08
P_2O_5	0.09	0.09	0.09	0.05	0.07	0.06	0.05
LOI	1.97	2.32	1.20	2.03	0.71	0.57	0.55
Total	99.98	99.51	99.81	100.51	100.24	100.46	99.98
H_2O^+	0.93	2.16	0.28	2.03	0.71	0.57	0.47
H_2O^-	0.79		0.79				
CO_2	<0.2	0.16	0.12	ND	ND	ND	ND
Fe_2O_3/FeO	0.61	0.20	0.32	0.46	0.32	0.33	0.66
Density (g/cm^3)	2.81	ND	2.90	2.81	2.83	2.90	2.90
Trace elements (ppm):							
La	0.95	0.94	0.91	1.72	1.05	2	
Ce	4	3.4	3.4	8.1	7.8	10	
Nd	4.2	3.8	4	5.8	ND	8.1	
Sm	2	1.8	1.8	1.97	2.26	3.165	
Eu	0.74	0.84	0.66	0.965	0.972	1.424	
Tb	0.61	0.73	0.59	0.591	0.636	0.813	
Tm	ND	ND	ND	ND	0.428	ND	
Yb	2.6	3.0	2.2	2.324	2.37	2.643	
Lu	0.45	0.48	0.36	0.282	0.329	0.264	
Sc	ND	35		43	42	39	
Cr	295	330	285	366	408	282	
Ni	79	72	97	ND	ND	ND	
Co	41	90	48	34	36	36	
V	265	247	280	ND	210	ND	
Cu	59	74	77	ND	217	ND	
Pb	<5	9	<5	ND	ND	ND	
Zn	70	64	68	69	72	58	
Sn	1.7	2	1.7	ND	ND	ND	
Zr	43	42	45	ND	ND	ND	
Y	23	24	22	ND	ND	ND	
Nb	1.1	1.2	<1	ND	ND	ND	
Rb	5.1	2.7	<1	ND	ND	ND	
Sr	62	62	53	ND	ND	ND	
Ba	3	18	4	ND	ND	ND	
Th	<1	ND	1.3	ND	ND	ND	
B	ND	30	ND	ND	ND	ND	

Table T6 (continued).

Hole	504B	504B	504B	504B	504B	504B	504B
Core, section	44R-1	47R-1	47R-2	48R-1	49R-1	49R-1	49R-2
Interval (cm)	125-130	46-48	130-140	113-115	122-126	140-147	7-10
Piece	716	808	835	871	932	933	936
Lab number	Z-931	Z-556	Z-932	Z-933	Z-934	Z-559	Z-560
Depth (mbsf)	612.25	638.46	640.80	648.13	657.22	657.40	657.57
Unit/Subunit	29B	30A	30C	31	33B	33B	33B
Major element oxides (wt%):							
SiO_2	48.81	50.20*	49.24	47.33	46.00	50.00*	49.00*
TiO_2	1.02	1.04	0.88	0.83	0.75	0.88	0.88
Al_2O_3	15.29	14.80	15.73	15.77	15.08	16.30	15.45
Fe_2O_3	2.98	3.02	2.46	2.65	2.83	2.16	4.21
FeO	6.32	7.32	6.63	7.01	6.26	7.19	6.16
MnO	0.21	0.17	0.19	0.18	0.17	0.17	0.14
MgO	7.88	8.86	9.23	9.64	10.21	8.14	9.54
CaO	12.92	12.35	11.40	9.06	8.75	13.03	10.68
Na_2O	2.08	2.16	1.83	1.78	1.95	2.16	1.94
K_2O	0.03	0.07	0.07	0.09	0.17	0.10	0.20
P_2O_5	0.08	0.06	0.09	0.09	0.07	0.05	0.05
LOI	2.14	0.33	2.42	5.23	7.32	0.55	1.98
Total	99.76	100.38	100.17	99.66	99.56	100.73	100.23
H_2O^+	0.40	0.25	1.92	4.65	6.70	0.55	1.98
H_2O^-	1.26						
CO_2	0.14	ND	0.50	0.58	0.62	ND	ND
Fe_2O_3/FeO	0.47	0.41	0.37	0.38	0.45	0.30	0.68
Density (g/cm^3)	2.82	2.93	2.82	2.95	2.92	2.94	2.72
Trace elements (ppm):							
La	0.96	1.6	0.87	0.94	0.63	1.6	1.6
Ce	4	11	3.5	3.2	1.8	7.8	8.2
Nd	4.5	8.4	4.1	4	2.7	ND	ND
Sm	1.9	2.96	1.9	1.9	1.5	2.43	2.45
Eu	0.76	1.105	0.89	0.86	0.64	1.1	0.88
Tb	0.6	0.673	0.7	0.76	0.71	0.784	0.787
Tm	ND	ND	ND	ND	ND	ND	0.549
Yb	2.6	2.479	2.9	3.0	2.6	2.966	2.565
Lu	0.41	0.35	0.48	0.49	0.40	0.424	0.4
Sc	ND	43	43	47	48	42	42
Cr	380	161	87	170	250	335	223
Ni	103	ND	64	77	88	ND	ND
Co	48	38	51	69	94	43	36
V	285	ND	287	387	332	ND	ND
Cu	84	ND	65	55	72	ND	ND
Pb	<5	ND	<5	<5	<5	ND	ND
Zn	80	88	75	61	64	ND	60
Sn	3.9	ND	2.5	1.9	2.0	ND	ND
Zr	45	ND	43	41	37	ND	ND
Y	25	ND	25	23	21	ND	ND
Nb	2.4	ND	<1	1.2	1.4	ND	ND
Rb	<1	ND	<1	2.0	2.6	ND	ND
Sr	51	ND	50	51	49	ND	ND
Ba	3	ND	12	24	34	ND	ND
Th	<1	ND	ND	ND	ND	ND	ND
B	ND	ND	16	27	33	ND	ND

Table T6 (continued).

Hole	504B	504B	504B	504B	504B	504B	504B
Core, section	54R-1	56R-2	61R-1	61R-2	61R-2	64R-1	64R-2
Interval (cm)	35-38	92-95	55-60	145-149	145-149	65-68	32-35
Piece	1062	1121	1287	1314	1314	1411	1424
Lab number	Z-935	Z-936	Z-937	Z-561	Z-938	Z-939	Z-562
Depth (mbsf)	692.35	707.92	751.05	753.45	753.45	773.65	774.82
Unit/Subunit	35	36	40	40	40	42	43
Major element oxides (wt%):							
SiO_2	49.20	48.78	49.21	48.25	46.79	50.52	50.00*
TiO_2	1.41	1.17	0.93	0.83	0.79	1.00	1.23
Al_2O_3	15.18	14.54	16.62	13.80	15.10	12.89	14.05
Fe_2O_3	3.87	3.65	0.81	3.29	5.63	3.87	4.18
FeO	4.74	5.89	7.09	5.17	4.49	6.25	7.22
MnO	0.11	0.22	0.18	0.18	0.18	0.19	0.20
MgO	8.32	8.88	8.08	9.02	9.76	9.01	8.63
CaO	12.03	10.94	12.02	11.00	10.17	10.84	12.04
Na_2O	2.55	2.56	1.78	1.94	1.66	1.96	2.25
K_2O	0.07	0.06	0.07	0.10	0.09	0.03	0.08
P_2O_5	0.13	0.16	0.09	0.09	0.11	0.09	0.08
LOI	2.33	3.19	2.89	5.95	5.35	3.20	0.42
Total	99.94	100.04	99.77	99.62	99.92	99.85	100.38
H_2O^+	0.46	0.69	2.48	1.57	4.62	0.85	0.42
H_2O^-	1.64	2.02		3.62		2.11	
CO_2	0.23	<0.2	0.41	0.35	0.53	0.22	ND
Fe_2O_3/FeO	0.82	0.62	0.11	0.64	1.25	0.62	0.58
Density (g/cm^3)	2.78	2.74	2.92	2.70	2.83	2.71	2.95
Trace elements (ppm):							
La	3.5	3.0	1.2	1.2	0.99	1.1	1.7
Ce	10	8.4	4.0	4.1	4.5	4.5	7.61
Nd	8.4	7.3	4.7	2.6	4.5	4.6	ND
Sm	3.0	2.5	2.2	2.0	1.8	2	2.917
Eu	1.1	1.2	0.87	0.74	0.72	0.69	1.021
Tb	1.0	0.87	0.86	0.73	0.6	0.64	0.779
Tm	ND	ND	ND	ND	ND	ND	0.446
Yb	3.3	2.6	3.3	2.7	2.5	2.3	3.36
Lu	0.51	0.43	0.41	0.43	0.37	0.39	0.619
Sc	ND	ND	37	ND	43	ND	46
Cr	270	230	320	285	250	310	304
Ni	82	73	106	91	84	88	ND
Co	49	44	72	49	41	45	41
V	375	290	332	352	277	300	ND
Cu	100	60	74	53	63	60	ND
Pb	<5	<5	<5	<5	<5	<5	ND
Zn	82	80	70	71	64	74	48
Sn	2.4	1.6	2.5	2.4	1.8	2.2	ND
Zr	99	100	49	49	42	48	ND
Y	30	30	27	24	24	24	ND
Nb	2.6	<1	<1	<1	<1	<1	ND
Rb	1.3	<1	1.3	<1	<1	<1	ND
Sr	100	96	50	43	46	58	ND
Ba	7	8	33	<3	49	5	ND
Th	ND	<1	ND	<1	ND	1.3	ND
B	ND	ND	9	ND	15	ND	ND

Table T6 (continued).

Hole	504B	504B	504B	504B	504B	504B	504B
Core, section	66R-2	67R-1	68R-1	68R-1	69R-1	69R-1	69R-1
Interval (cm)	0-5	45-49	83-87	107-111	14-17	74-77	77-81
Piece	1506	1527	1537	1538	1540	1545	1545
Lab number	Z-940	Z-941	Z-942	Z-563	Z-564	Z-565	Z-943
Depth (mbsf)	792.5	800.45	809.83	810.07	818.14	818.74	818.77
Unit/Subunit	45	47	47	47	47	47	47
Major element oxides (wt%):							
SiO_2	49.67	48.35	47.45	49.20*	49.70*	49.60*	48.57
TiO_2	0.97	0.97	1.01	1.07	1.18	1.03	0.77
Al_2O_3	15.10	14.69	14.84	14.65	14.60	14.10	14.16
Fe_2O_3	2.39	3.50	5.22	3.51	3.93	4.51	4.98
FeO	6.84	6.75	5.60	7.01	6.62	6.20	5.78
MnO	0.11	0.23	0.24	0.22	0.24	0.19	0.23
MgO	8.16	9.00	8.42	8.89	8.62	8.99	8.79
CaO	12.53	12.23	12.55	12.66	12.16	11.92	11.52
Na_2O	1.99	2.09	2.04	2.12	2.24	1.98	2.03
K_2O	0.03	0.02	0.02	0.06	0.06	0.05	0.02
P_2O_5	0.06	0.11	0.12	0.07	0.07	0.07	0.10
LOI	1.51	1.86	2.69	0.72	0.62	1.09	2.80
Total	99.36	99.80	100.20	100.18	100.04	99.73	99.75
H_2O^+		0.50	0.43	0.72	0.61	1.09	0.74
H_2O^-		1.31	1.76				1.84
CO_2	0.13	<0.2	<0.2	ND	ND	ND	0.15
Fe_2O_3/FeO	0.35	0.52	0.93	0.50	0.59	0.73	0.86
Density (g/cm^3)	3.03	2.93	3.03	2.91	2.87	2.89	2.83
Trace elements (ppm):							
La	1.8	1.1	1.2	1.4	1.8	1.3	1.2
Ce	4.2	3.7	3.5	8.4	8	6.9	4
Nd	4.7	4.6	4.5	ND	5.9	ND	4.7
Sm	1.9	2.2	2.1	2.56	2.22	2.78	2.2
Eu	0.71	0.68	0.74	1.119	0.9	0.948	0.81
Tb	0.67	0.76	0.73	0.675	0.51	0.758	0.73
Tm	ND	ND	ND	0.538	0.417	0.499	ND
Yb	2.5	2.7	2.8	3.317	2.47	2.496	2.9
Lu	0.4	0.45	0.42	0.539	0.372	0.543	0.46
Sc	ND	ND	ND	48	45	44	ND
Cr	357	210	220	263	200	254	190
Ni	98	81	86	ND	ND	ND	76
Co	54	54	50	46	50	49	52
V	405	340	332	ND	ND	ND	342
Cu	83	72	63	ND	ND	ND	55
Pb	<5	<5	<5	ND	ND	ND	<5
Zn	82	93	85	151	110	114	95
Sn	2.5	1.8	1.9	ND	ND	ND	2.0
Zr	ND	48	50	ND	ND	ND	52
Y	ND	25	26	ND	ND	ND	28
Nb	ND	<1	<1	ND	ND	ND	<1
Rb	ND	<1	<1	ND	ND	ND	<1
Sr	ND	52	51	ND	ND	ND	47
Ba	ND	5	6	ND	ND	ND	3
Th	ND	<1	1	ND	ND	ND	1.1
B	ND	ND	ND	ND	ND	ND	ND

Table T6 (continued).

Hole	504B	504B	504B	504B
Core, section	70R-1	70R-1	70R-1	70R-2
Interval (cm)	17-20	79-82	127-130	20-23
Piece	1550	1556	1561	1564
Lab number	Z-944	Z-567	Z-568	Z-569
Depth (mbsf)	827.17	827.79	828.27	828.7
Unit/Subunit	48	48	49	49
Major element oxides (wt%):				
SiO_2	48.68	49.60*	49.70*	49.80*
TiO_2	0.76	0.91	1.00	0.99
Al_2O_3	14.69	14.65	15.40	15.40
Fe_2O_3	3.03	4.87	3.47	3.57
FeO	5.44	4.62	5.65	5.34
MnO	0.13	0.13	0.18	0.18
MgO	9.86	9.52	8.92	8.87
CaO	11.00	11.11	12.90	12.97
Na_2O	1.78	2.33	1.99	2.14
K_2O	0.06	0.10	0.07	0.07
P_2O_5	0.08	0.54	0.05	0.05
LOI	4.21	1.71	0.81	0.72
Total	99.72	100.09	100.14	100.10
H_2O^+	4.09	1.71	0.81	0.72
H_2O^-				
CO_2	0.12	ND	ND	ND
Fe_2O_3/FeO	0.56	1.05	0.61	0.67
Density (g/cm^3)	2.63	2.58	3.00	2.88
Trace elements (ppm):				
La	0.82	0.9	1	1.3
Ce	3.1	7.7	8	7.8
Nd	3.5	7.9	6.2	ND
Sm	1.6	2.94	2.2	2.17
Eu	0.74	1.11	0.852	0.998
Tb	0.58	0.673	0.586	0.609
Tm	ND	0.525	0.38	0.42
Yb	2.3	2.861	1.628	2.625
Lu	0.39	0.522	0.362	0.345
Sc	ND	42	30	27
Cr	215	343	295	262
Ni	88	ND	ND	ND
Co	49	35	34	34
V	275	ND	ND	ND
Cu	86	ND	ND	ND
Pb	<5	ND	ND	ND
Zn	71	81	25	60
Sn	1.9	ND	ND	ND
Zr	39	ND	ND	ND
Y	22	ND	ND	ND
Nb	1.9	ND	ND	ND
Rb	<1	ND	ND	ND
Sr	45	ND	ND	ND
Ba	33	ND	ND	ND
Th	ND	ND	ND	ND
B	10	ND	ND	ND

Table T7. Composition of basalts from Hole 504B, Leg 83 (Costa Rica Rift, Pacific Ocean). (Continued on next four pages.)

Hole	504B	504B	504B	504B	504B	504B	504B
Core, section	72R-2	73R-2	77R-1	78R-1	79R-3	80R-1	80R-4
Interval (cm)	60-64	56-59	78-81	60-64	50-54	5-10	3-8
Piece	5	4	4	3D	4A	1	1A
Lab number	Z-570	Z-571	Z-572	Z-573	Z-574	Z-1301	Z-1303
Depth (mbsf)	845.5	854.56	889.28	898.1	908.00	910.05	914.33
Unit	49	50	54	56	58	60	60
Major element oxides (wt%):							
SiO_2	48.70	49.16	49.47	49.67	48.88	46.36	50.51
TiO_2	0.79	0.79	0.95	1.07	1.00	0.93	0.89
Al_2O_3	14.81	14.96	15.43	14.70	15.54	16.56	14.07
Fe_2O_3	3.94	4.09	2.54	3.28	2.10	4.34	4.16
FeO	5.09	5.28	6.09	5.82	6.07	5.57	5.42
MnO	0.22	0.21	0.19	0.21	0.18	0.22	0.09
MgO	8.48	8.19	8.27	7.75	8.11	7.93	6.97
CaO	12.81	12.97	11.61	12.23	13.36	10.96	12.20
Na_2O	1.95	1.80	2.97	2.72	2.13	2.57	2.85
K_2O	<0.02	<0.02	<0.02	0.05	<0.02	0.04	0.02
P_2O_5	0.04	0.04	0.04	0.05	0.04	0.04	0.04
LOI	2.56	2.21	2.70	2.10	2.18	3.77	2.02
Total	99.39	99.70	100.26	99.65	99.59	99.29	99.24
H_2O^+	1.03	0.84	1.49	1.08	1.45	2.61	1.37
H_2O^-	1.07	0.76	0.56	0.30	0.52	0.62	0.36
CO_2	0.22	0.20	0.44	<0.20	<0.20	<0.2	<0.2
Fe_2O_3/FeO	0.77	0.77	0.42	0.56	0.35	0.78	0.77
Density (g/cm^3)	2.88	2.90	2.87	2.84	2.83	2.60	2.68
Trace elements (ppm):							
La	1.1	1.3	1.2	1.3	1.2	0.87	0.88
Ce	3.1	2.3	4.1	2.9	3.8	3.3	3
Nd	3.7	3.5	4.3	4.0	4.3	4.2	4.1
Sm	1.7	1.7	2	1.9	1.9	2.2	2.2
Eu	0.64	0.69	0.7	0.8	0.74	0.76	0.75
Tb	0.52	0.53	0.63	0.6	0.52	0.73	0.67
Yb	2.1	2.1	2.6	2.7	2.2	2.5	2.5
Lu	0.32	0.34	0.37	0.42	0.35	0.38	0.37
Cr	375	320	300	220	280	305	295
Ni	190	170	97	76	160	155	138
Co	55	49	41	41	44	68	46
V	365	240	220	230	200	242	215
Cu	120	88	68	97	130	20	66
Zn	84	76	66	78	67	167	75
Sn	ND	3.5	3	2.7	3.2	ND	ND
Zr	41	40	48	47	49	45	44
Y	19	21	23	26	22	24	24
Nb	1.3	1.1	<1	1.3	1.7	1.4	1.5
Rb	1.6	1.0	<1	<1	<1	1.2	1.8
Sr	63	62	72	60	74	56	68
Ba	54	53	64	47	36	5	5

Note: ND = not determined.

Table T7 (continued).

Hole	504B	504B	504B	504B	504B	504B	504B
Core, section	84R-2	85R-1	88R-1	89R-2	90R-4	91R-1	92R-3
Interval (cm)	48-50	58-62	68-71	74-78	112-114	115-118	38-42
Piece	7	6B	4A	9	10A	15	4
Lab number	Z-1306	Z-1307	Z-575	Z-1309	Z-1310	Z-576	Z-577
Depth (mbsf)	948.48	956.08	977.18	987.74	1000.12	1004.65	1015.88
Unit	60	60	70	71	72	75	79
Major element oxides (wt%):							
SiO_2	48.54	51.75	48.56	48.23	48.79	48.62	49.92
TiO_2	1.00	0.88	1.16	0.98	0.96	0.95	0.84
Al_2O_3	13.79	12.51	14.52	13.56	14.83	14.10	13.28
Fe_2O_3	2.91	3.38	1.40	2.35	1.98	1.40	1.29
FeO	6.65	7.19	7.97	9.42	7.89	7.68	7.80
MnO	0.13	0.28	0.31	0.11	0.12	0.32	0.26
MgO	8.81	8.26	8.34	8.52	8.75	8.58	8.00
CaO	10.72	7.50	12.61	10.90	10.64	12.38	12.86
Na_2O	1.80	3.30	1.92	2.15	1.91	2.30	1.83
K_2O	0.04	0.03	<0.02	0.02	0.02	<0.02	<0.02
P_2O_5	0.06	0.05	0.09	0.06	0.06	0.04	0.05
LOI	4.68	4.11	2.94	2.98	3.57	3.18	3.19
Total	99.13	99.24	99.82	99.28	99.52	99.55	99.32
H_2O^+	3.65	3.27	1.95	2.32	2.89	2.30	2.05
H_2O^-	0.89	0.62	0.55	0.31	0.40	0.33	0.25
CO_2	<0.2	<0.2	0.44	<0.2	<0.2	0.44	0.31
Fe_2O_3/FeO	0.44	0.47	0.18	0.25	0.25	0.18	0.17
Density (g/cm^3)	2.73	2.61	2.85	2.88	2.83	2.79	2.98
Trace elements (ppm):							
La	1.1	0.8	2.9	0.99	1.4	0.88	1.5
Ce	3.7	2.6	6.6	3.3	5	2.2	4.1
Nd	4.8	3.9	6	4.2	5.4	2.8	4.5
Sm	2.4	1.9	2.2	2.2	2.4	1.4	1.8
Eu	0.79	0.58	0.78	0.73	0.79	0.49	0.71
Tb	0.75	0.61	0.59	0.73	0.82	0.46	0.58
Yb	3	2.5	2.5	2.7	2.7	2.0	2.5
Lu	0.46	0.37	0.35	0.42	0.43	0.33	0.4
Cr	298	212	260	169	220	260	170
Ni	138	66	95	79	86	95	74
Co	62	58	40	47	46	38	34
V	271	222	220	237	212	180	210
Cu	45	55	59	382	180	93	280
Zn	113	235	110	116	121	91	93
Sn	ND	ND	3	ND	ND	3.2	2.7
Zr	50	45	64	44	51	33	47
Y	25	22	25	27	24	22	25
Nb	1	<1	4.7	1.6	1.4	1.2	1.3
Rb	1	<1	<1	1	1.1	<1	<1
Sr	44	80	70	52	61	45	48
Ba	<5	5	49	75	12	41	19

Table T7 (continued).

Hole	504B	504B	504B	504B	504B	504B	504B
Core, section	94R-3	97R-1	97R-2	98R-1	99R-2	100R-1	100R-1
Interval (cm)	91-94	88-90	108-111	80-85	93-96	19-20	83-87
Piece	10	7	10	11	11	2A	10
Lab number	Z-578	Z-1311	Z-579	Z-1312	Z-580	Z-581	Z-1313
Depth (mbsf)	1034.41	1058.38	1060.08	1062.80	1073.93	1080.69	1081.33
Unit	86	91	91	94	96	96	96
Major element oxides (wt%):							
SiO_2	49.58	47.76	50.20	45.31	48.90	49.94	49.54
TiO_2	0.87	0.98	0.99	0.86	1.25	1.06	1.12
Al_2O_3	14.89	11.47	13.86	15.71	13.64	13.34	11.76
Fe_2O_3	1.65	3.02	2.06	2.32	3.62	2.92	1.55
FeO	7.17	7.24	7.23	7.09	6.57	8.06	9.99
MnO	0.19	0.22	0.21	0.17	0.24	0.26	0.24
MgO	8.91	10.04	8.57	10.21	8.36	8.03	8.67
CaO	12.62	11.47	12.71	11.29	12.63	12.52	8.22
Na_2O	1.82	1.31	2.09	1.48	2.02	1.84	2.93
K_2O	<0.02	0.03	<0.02	0.03	<0.02	<0.02	0.04
P_2O_5	0.04	0.06	0.04	0.07	0.06	0.07	0.07
LOI	1.78	5.98	1.64	4.77	2.28	1.55	5.75
Total	99.52	99.58	99.60	99.31	99.57	99.59	99.88
H_2O^+	0.89	4.89	0.83	3.76	2.00	0.90	5.03
H_2O^-	0.36	0.93	0.29	0.64	0.27	0.34	0.69
CO_2	0.52	<0.2	0.52	<0.2	<0.20	0.31	<0.2
Fe_2O_3/FeO	0.23	0.42	0.28	0.33	0.55	0.36	0.16
Density (g/cm^3)	2.80	2.44	3.00	2.84	2.85	2.91	2.69
Trace elements (ppm):							
La	1.2	0.99	1.3	1.2	1.7	1.4	1.3
Ce	4.1	3.3	3.2	3.9	4.2	4.4	5.2
Nd	4.6	4.2	3.9	4.5	5.1	5.1	5.4
Sm	1.8	2.2	1.8	1.9	2.4	2.3	2.5
Eu	0.62	0.7	0.75	0.69	0.79	0.62	0.84
Tb	0.51	0.74	0.51	0.68	0.68	0.7	0.88
Yb	2.4	2.6	2.4	2.3	3.2	3.0	2.8
Lu	0.36	0.38	0.39	0.34	0.51	0.48	0.47
Cr	320	292	260	265	190	210	152
Ni	140	95	83	173	76	78	69
Co	44	77	42	55	40	44	46
V	230	355	240	201	220	240	205
Cu	99	168	120	45	64	88	20
Zn	68	136	78	148	78	80	100
Sn	3	ND	3	ND	3.2	3.5	ND
Zr	45	47	49	48	60	56	56
Y	21	26	24	21	31	28	27
Nb	1.1	<1	1.6	1.2	1.4	1.8	1.6
Rb	<1	1	<1	1.2	<1	<1	1.3
Sr	58	36	63	55	53	52	44
Ba	48	4	20	5	25	30	8

Table T7 (continued).

Hole	504B	504B	504B	504B	504B	504B	504B
Core, section	104R-3	109R-1	111R-1	113R-1	116R-1	117R-1	118R-1
Interval (cm)	30-33	50-54	86-89	7-10	56-60	109-113	62-66
Piece	5A	7	9	1	9	15	5
Lab number	Z-582	Z-583	Z-1314	Z-584	Z-1315	Z-1316	Z-585
Depth (mbsf)	1119.8	1154.00	1162.36	1171.07	1185.56	1190.59	1194.62
Unit	106	112	113	115	117	118	118
Major element oxides (wt%):							
SiO_2	48.27	49.68	45.36	48.36	48.83	49.82	49.98
TiO_2	0.93	0.96	1.02	0.79	1.00	0.86	1.04
Al_2O_3	16.05	15.32	17.08	16.22	14.79	15.27	15.12
Fe_2O_3	4.69	5.13	3.47	4.38	2.55	2.12	4.63
FeO	4.79	4.80	6.35	4.66	7.57	7.77	5.28
MnO	0.17	0.14	0.12	0.11	0.17	0.18	0.07
MgO	8.91	8.77	9.05	9.17	8.34	7.60	8.80
CaO	12.52	12.45	12.00	12.56	12.02	11.81	11.97
Na_2O	2.21	1.78	1.90	1.80	2.49	2.40	1.89
K_2O	<0.02	<0.02	0.04	<0.02	0.03	0.03	<0.02
P_2O_5	0.06	0.05	0.06	0.04	0.06	0.05	0.05
LOI	1.80	1.30	3.30	1.63	2.02	1.99	1.09
Total	100.40	100.38	99.75	99.72	99.87	99.90	99.92
H_2O^+	1.65	0.87	2.21	1.01	1.67	1.55	0.72
H_2O^-	0.15	0.36	0.84	0.37	0.34	0.44	0.24
CO_2	<0.20	<0.20	<0.2	<0.20	<0.2	<0.2	<0.20
Fe_2O_3/FeO	0.98	1.07	0.55	0.94	0.34	0.27	0.88
Density (g/cm^3)	2.82	2.86	2.76	2.89	2.94	3.00	2.99
Trace elements (ppm):							
La	1.4	1.2	1.5	0.94	1	0.83	1.1
Ce	4.0	3.0	5.8	3.2	3.8	3.3	3.8
Nd	4.8	4.3	5.1	3.6	4.5	3.9	4.8
Sm	2.0	1.7	2.2	1.5	2.4	1.8	2.1
Eu	0.73	0.64	0.79	0.59	0.79	0.69	0.78
Tb	0.54	0.59	0.66	0.43	0.84	0.61	0.64
Yb	2.5	2.4	2.4	2	3	1.8	2.8
Lu	0.38	0.37	0.36	0.31	0.46	0.28	0.44
Cr	350	250	360	290	260	300	290
Ni	83	86	250	110	76	91	99
Co	46	46	60	47	54	63	48
V	260	260	240	210	242	276	310
Cu	87	110	140	110	77	77	97
Zn	84	75	82	79	66	138	93
Sn	3.0	2.7	ND	3.2	ND	ND	3.3
Zr	45	43	58	36	43	38	45
Y	24	24	23	20	26	20	26
Nb	1.3	1.3	1	1.8	<1	<1	1.8
Rb	<1	<1	1.3	<1	1.3	1.2	<1
Sr	63	49	87	55	51	53	49
Ba	40	39	5	40	27	9	33

Table T7 (continued).

Hole	504B	504B	504B	504B	504B	504B	504B
Core, section	121R-1	127R-1	130R-1	130R-3	132R-1	133R-1	134R-1
Interval (cm)	32-38	97-101	88-91	78-81	76-80	46-50	147-150
Piece	5	12	8	9A	10	7	19
Lab number	Z-586	Z-587	Z-588	Z-1317	Z-589	Z-590	Z-1318
Depth (mbsf)	1207.82	1254.47	1279.88	1282.78	1295.76	1304.46	1314.47
Unit	120	131	135	135	137	138	140
Major element oxides (wt%):							
SiO_2	50.25	47.62	48.00	48.17	47.84	48.07	50.35
TiO_2	0.99	0.79	0.79	0.69	0.89	0.93	0.95
Al_2O_3	14.83	15.79	16.13	16.70	16.42	14.76	14.42
Fe_2O_3	5.52	4.62	2.49	1.52	3.63	2.33	2.28
FeO	5.13	5.73	6.22	6.34	6.13	7.88	7.63
MnO	0.11	0.16	0.17	0.15	0.16	0.22	0.19
MgO	8.14	9.19	8.92	9.87	8.27	8.32	7.53
CaO	12.10	13.04	13.47	12.46	13.65	12.98	12.19
Na_2O	1.62	1.42	1.50	1.51	1.63	1.87	2.13
K_2O	<0.02	<0.02	<0.02	0.02	<0.02	<0.02	0.02
P_2O_5	0.06	0.03	0.04	0.04	0.04	0.05	0.06
LOI	1.03	2.04	1.67	2.08	1.63	2.00	2.14
Total	99.78	100.43	99.40	99.55	100.29	99.41	99.89
H_2O^+	0.71	1.24	1.05	1.28	1.01	1.40	1.78
H_2O^-	0.32	0.32	0.28	0.57	0.40	0.25	0.36
CO_2	<0.20	0.48	<0.20	<0.2	0.22	<0.20	<0.2
Fe_2O_3/FeO	1.08	0.81	0.40	0.24	0.59	0.30	0.30
Density (g/cm^3)	2.96	2.80	2.97	2.92	2.86	2.84	2.72
Trace elements (ppm):							
La	0.87	0.99	1	0.84	0.96	1.1	0.89
Ce	2.5	2.6	2.4	3.5	3.1	1.9	3.5
Nd	4.8	3.5	3.1	3.7	3.3	3.3	3.9
Sm	2.1	1.5	1.4	1.6	1.4	1.9	1.8
Eu	0.84	0.61	0.56	0.55	0.6	0.74	0.72
Tb	0.71	0.47	0.47	0.5	0.48	0.66	0.67
Yb	3	2	1.8	1.8	2	2.5	2.3
Lu	0.47	0.29	0.28	0.28	0.32	0.42	0.37
Cr	240	340	360	418	290	270	210
Ni	90	160	160	250	140	83	75
Co	49	49	48	73	45	42	55
V	300	210	230	230	210	220	248
Cu	93	110	110	142	110	120	168
Zn	90	73	74	77	78	82	95
Sn	3.2	3	3.7	ND	3.2	3	ND
Zr	46	38	37	34	41	43	41
Y	27	19	19	17	19	25	24
Nb	1.3	1.3	<1	<1	1.2	<1	2.1
Rb	<1	<1	<1	1.2	<1	<1	1
Sr	43	59	60	54	59	44	52
Ba	44	30	32	10	51	39	11

Table T8. Composition of basalts from Hole 594B, Leg 111 (Costa Rica Rift, Pacific Ocean). (Continued on next two pages.)

Hole	504B	504B	504B	504B	504B	504B	504B
Core, section	142R-1	142R-2	143R-1	145R-1	145R-2	145R-3	147R-1
Interval (cm)	129-132	40-44	124-127	103-105	74-76	66-68	11-13
Piece	17B	6	19	13A	7F	6A	3
Lab number	Z-597	Z-114	Z-598	Z-115	Z-116	Z-117	Z-118
Depth (mbsf)	1354.09	1354.70	1360.54	1379.33	1380.54	1381.96	1397.51
Unit	153	153	155	160	160	160	163
Major element oxides (wt%):							
SiO_2	47.28	48.90	48.56	49.37	48.60	48.58	49.44
TiO_2	1.23	1.12	0.79	0.96	0.96	0.96	0.96
Al_2O_3	13.85	15.80	15.83	15.93	15.89	15.96	15.76
Fe_2O_3	2.61	2.49	1.25	2.08	2.82	2.53	2.61
FeO	7.93	6.98	6.95	6.57	6.25	6.49	6.12
MnO	0.21	0.18	0.11	0.18	0.17	0.17	0.17
MgO	7.98	8.01	8.67	8.60	8.47	9.31	8.97
CaO	11.06	12.98	12.80	13.30	13.47	12.96	13.21
Na_2O	1.83	1.95	1.78	1.92	1.88	1.88	2.10
K_2O	<0.02	0.05	<0.02	0.05	0.05	0.05	0.05
P_2O_5	0.06	0.07	0.03	0.06	0.07	0.06	0.06
LOI	4.90	1.21	2.26	1.13	0.88	1.26	1.01
Total	98.94	99.74	99.03	100.15	99.51	100.21	100.46
H_2O^+	4.21	0.98	1.63	0.84	0.78	0.90	0.94
H_2O^-	0.50	0.23	0.43	0.29	0.10	0.36	0.07
CO_2	<0.20	ND	<0.20	ND	ND	ND	ND
Fe_2O_3/FeO	0.33	0.36	0.18	0.32	0.45	0.39	0.43
Density (g/cm^3)	2.61	3.00	3.02	3.01	2.99	3.00	3.00
Trace elements (ppm):							
La	1.0	1.4	1.0	1.4	1.2	1.2	1.1
Ce	4.0	4.2	3.4	4.2	2.1	3.2	2.0
Nd	4.3	ND	3.7	ND	ND	ND	ND
Sm	2.0	2.1	1.5	2.1	2.0	2.0	1.8
Eu	0.79	0.83	0.69	0.78	0.72	0.65	0.5
Tb	0.69	0.58	0.53	0.56	0.52	0.64	0.64
Yb	2.6	2.9	2.2	2.6	2.3	2.4	2.0
Lu	0.40	0.50	0.39	0.44	0.36	0.36	0.32
Sc	ND	49	ND	46	49	47	47
Cr	175	170	347	440	430	375	480
Ni	74	120	146	160	135	170	165
Co	45	55	48	55	55	50	50
V	287	270	230	280	250	210	260
Cu	20	135	103	130	135	160	100
Pb	<5	<5	<5	<5	<5	<5	<5
Zn	94	95	135	75	70	80	85
Sn	3.4	ND	3.1	ND	ND	ND	ND
Zr	43	38	37	34	27	28	24
Y	25	27	23	24	25	23	21
Nb	1.8	<1	1.2	<1	1.1	1.1	<1
Rb	<1	<1	<1	<1	<1	<1	<1
Sr	50	49	58	56	42	37	42
Ba	28	<10	31	<10	<10	<10	<10

Note: ND = not determined.

Table T8 (continued).

Hole	504B	504B	504B	504B	504B	504B	504B
Core, section	147R-2	147R-2	148R-1	149R-1	152R-1	154R-1	156R-1
Interval (cm)	15-20	26-28	53-55	122-124	11-13	30-32	64-67
Piece	1C	1D	8	16C	2	2C	13
Lab number	Z-599	Z-119	Z-120	Z-121	Z-600	Z-122	Z-601
Depth (mbsf)	1399.05	1399.16	1407.33	1418.12	1436.01	1454.60	1464.44
Unit	163	163	164	164	169	176	178
Major element oxides (wt%):							
SiO_2	48.95	48.84	49.88	49.70	44.24	48.94	48.69
TiO_2	0.91	1.04	1.28	1.28	0.91	1.13	0.97
Al_2O_3	15.50	15.37	14.28	14.35	15.04	14.44	13.64
Fe_2O_3	2.13	2.89	2.54	2.58	3.53	3.73	2.79
FeO	6.24	6.48	8.05	7.99	9.88	6.41	7.50
MnO	0.20	0.18	0.20	0.21	0.29	0.17	0.14
MgO	8.70	8.79	8.37	8.43	9.08	8.34	8.44
CaO	13.21	13.21	12.65	12.38	7.88	12.94	11.86
Na_2O	1.81	2.18	2.18	2.18	2.55	2.10	2.60
K_2O	<0.02	0.05	0.08	0.05	<0.02	0.08	<0.02
P_2O_5	0.05	0.06	0.08	0.08	0.04	0.06	0.05
LOI	1.62	1.36	0.67	1.15	5.54	1.15	2.73
Total	99.32	100.45	100.26	100.38	98.98	99.49	99.41
H_2O^+	0.90	1.08	0.57	0.97	4.81	0.96	2.11
H_2O^-	0.35	0.28	0.10	0.18	0.50	0.19	0.16
CO_2	<0.20	ND	ND	ND	<0.20	ND	0.23
Fe_2O_3/FeO	0.34	0.45	0.32	0.32	0.36	0.58	0.37
Density (g/cm^3)	2.99	2.85	3.00	2.99	2.75	2.99	2.75
Trace elements (ppm):							
La	1.0	1.2	1.4	1.4	1.5	1.2	1.4
Ce	4.5	2.8	4.1	4.5	4.2	3.5	3.9
Nd	4.6	ND	ND	ND	4.5	ND	5.0
Sm	1.8	2.2	2.4	2.4	2.0	2.1	2.3
Eu	0.8	0.76	0.75	0.69	0.63	0.84	0.84
Tb	0.58	0.58	0.77	0.63	0.72	0.66	0.80
Yb	2.2	2.4	2.8	2.6	2.8	2.4	3.1
Lu	0.39	0.39	0.42	0.42	0.44	0.38	0.50
Sc	ND	48	52	5.2	ND	48	ND
Cr	380	425	120	130	310	300	190
Ni	90	145	95	100	95	120	67
Co	49	55	40	45	57	50	43
V	258	270	240	300	220	290	236
Cu	90	70	70	80	21	80	21
Pb	<5	<5	<5	<5	<5	<5	<5
Zn	86	85	95	95	78	90	82
Sn	3.0	ND	ND	ND	3.5	ND	2.5
Zr	42	45	44	48	38	30	45
Y	21	24	28	28	21	25	26
Nb	<1	<1	<1	<1	1.5	<1	<1
Rb	<1	<1	<1	<1	<1	<1	<1
Sr	61	57	56	63	46	51	59
Ba	42	<10	<10	<10	26	<10	50

Table T8 (continued).

Hole	504B	504B	504B	504B	504B
Core, section	158R-1	162M-1	163R-1	163R-1	169R-1
Interval (cm)	16-19	45-47	36-41	120-123	66-69
Piece	3A	5	8	24	14
Lab number	Z-602	Z-123	Z-603	Z-1319	Z-604
Depth (mbsf)	1482.66	1511.95	1511.96	1512.80	1548.26
Unit	182	187	188	189	191
Major element oxides (wt%):					
SiO_2	48.99	48.98	48.69	49.15	49.15
TiO_2	0.90	0.96	1.10	0.96	0.92
Al_2O_3	14.01	15.82	15.13	16.76	14.76
Fe_2O_3	3.07	3.52	3.54	1.68	3.34
FeO	7.24	5.95	6.44	7.51	6.82
MnO	0.14	0.18	0.12	0.15	0.12
MgO	8.51	8.22	8.00	7.09	8.50
CaO	12.69	13.14	12.25	12.33	12.66
Na_2O	2.13	2.10	1.95	2.39	1.70
K_2O	<0.02	0.13	<0.02	0.02	<0.02
P_2O_5	0.05	0.06	0.07	0.06	0.06
LOI	1.51	1.23	1.93	1.39	1.38
Total	99.24	100.29	99.22	99.49	99.41
H_2O^+	1.35	0.51	1.53	1.15	1.17
H_2O^-	0.10	0.72	0.10	0.24	0.04
CO_2	<0.20	ND	0.16	<0.2	<0.20
Fe_2O_3/FeO	0.42	0.59	0.55	0.22	0.49
Density (g/cm^3)	2.94	2.86	2.94	2.93	2.81
Trace elements (ppm):					
La	1.3	1.2	1.3	0.84	1.3
Ce	3.8	3.3	3.7	2.9	3.3
Nd	4.5	ND	4.6	4.2	4.2
Sm	2.2	2.0	2.3	2.0	2.2
Eu	0.69	0.68	0.96	0.68	0.89
Tb	0.70	0.54	0.73	0.67	0.62
Yb	2.9	2.3	3.0	2.5	2.7
Lu	0.48	0.35	0.44	0.38	0.44
Sc	ND	48	ND	ND	ND
Cr	342	385	242	235	337
Ni	70	180	70	76	90
Co	44	55	44	51	52
V	258	240	275	253	377
Cu	26	80	36	90	108
Pb	<5	<5	<5	ND	<5
Zn	74	90	78	75	88
Sn	2.5	ND	2.7	ND	3.3
Zr	40	53	52	47	41
Y	25	22	27	23	24
Nb	1.3	<1	<1	<1	1.2
Rb	<1	<1	<1	1.8	<1
Sr	51	89	45	65	47
Ba	29	<10	28	7	35

Table T9. Composition of basalts from Hole 504B, Leg 137 (Costa Rica Rift, Pacific Ocean).

Hole	504B	504B
Core, section	177R-1	181M-1
Interval (cm)	48-49	6-8
Piece	13	1
Lab number	Z-812	Z-813
Depth (mbsf)	1604.98	1620.46
Unit	206	206
Major element oxides (wt%):		
SiO_2	51.00	49.60
TiO_2	1.03	1.00
Al_2O_3	14.80	14.60
Fe_2O_3	2.81	2.72
FeO	7.64	7.54
MnO	0.18	0.18
MgO	8.71	8.23
CaO	12.70	13.00
Na_2O	1.73	1.68
K_2O	<0.05	<0.05
P_2O_5	0.08	0.07
H_2O^+	1.24	1.43
CO_2	<0.1	<0.1
Total	101.92	100.05
Fe_2O_3/FeO	0.37	0.36
Density (g/cm^3)	2.96	2.84
Trace elements (ppm):		
La	1.05*	1.03
Ce	4.17	3.84
Nd	5.29	5.15
Sm	2.21	2.1
Eu	0.84	0.75
Tb	0.68	0.61
Yb	2.97	2.96
Lu	0.45	0.46
Cr	169	233
Ni	85	86
Co	45	44
Cu	65	77
Zn	72	69
Zr	50	49
Y	25.9	24.5
Nb	0.29	0.26
Rb	<0.1	0.10
Sr	46	44

Note: Major element data from Zuleger et al. (1995).
Minor element data from Zuleger et al. (1996).
* = rare earth element data from Zuleger et al. (1996).

Table T10. Composition of basalts from Hole 504B, Leg 140 (Costa Rica Rift, Pacific Ocean). (Continued on next three pages.)

Hole	504B	504B	504B	504B	504B	504B	504B
Core, section	186R-2	187R-1	189R-1	189R-2	190R-1	193R-1	194R-1
Interval (cm)	30-31	59-60	85-86	15-17	10-14	49-51	42-44
Piece	8	14	19	3	2	13A	8
Lab number	Z-838	Z-839	Z-840	Z-841	Z-842	Z-844	Z-845
Depth (mbsf)	1628.10	1632.59	1651.85	1652.61	1655.20	1674.99	1680.82
Unit	213	216	218	218	218	220	220
Major element oxides (wt%):							
SiO_2	47.10	50.40	50.50	50.50	50.80	50.20	50.50
TiO_2	1.02	0.96	0.99	0.66	0.58	0.94	0.50
Al_2O_3	16.20	15.30	15.10	15.70	14.40	15.40	14.80
Fe_2O_3	2.14	2.41	2.68	1.67	1.38	2.43	1.34
FeO	7.16	7.10	7.31	6.69	7.49	6.72	7.61
MnO	0.17	0.18	0.18	0.16	0.16	0.19	0.16
MgO	9.18	8.61	8.24	8.64	8.11	8.08	8.42
CaO	13.20	13.00	12.70	12.70	11.40	13.00	11.50
Na_2O	1.62	1.97	1.73	1.80	1.15	1.93	1.99
K_2O	<0.05	<0.05	<0.05	<0.05	<0.05	<0.05	<0.05
P_2O_5	0.09	0.08	0.08	0.05	0.05	0.10	0.04
H_2O^+	2.73	1.60	1.22	3.09	5.98	2.12	3.82
Total	100.61	101.61	100.73	101.66	101.50	101.11	100.68
Fe_2O_3/FeO	0.30	0.34	0.37	0.25	0.18	0.36	0.18
Density (g/cm^3)	2.92	2.90	2.98	2.75	2.78	2.83	2.88
Trace elements (ppm):							
La	1.65	0.89	1.06	0.64	0.56	1.22	0.46
Ce	5.72	3.58	4.02	2.41	2.22	4.65	1.77
Nd	6.5	4.72	5.02	3.01	2.75	5.54	2.36
Sm	2.37	2.04	2.13	1.28	1.19	2.36	1.05
Eu	0.83	0.80	0.79	0.58	0.67	0.87	0.52
Tb	0.62	0.63	0.64	0.42	0.39	0.64	0.33
Yb	2.85	2.84	2.95	1.89	1.81	2.80	1.49
Lu	0.44	0.43	0.44	0.30	0.26	0.41	0.21
Cr	385	278	255	347	300	278	313
Ni	138	88	91	117	98	97	111
Co	45	41	45	39	36	54	42
Cu	11	48	252	102	13	102	5
Zn	48	53	71	59	60	65	71
Zr	65	48	50	32	29	46	25
Y	24.6	23.6	24.3	15.7	14.7	23.5	12.7
Nb	0.78	0.3	0.28	0.19	0.18	0.3	0.14
Rb	0.13	<0.1	0.11	0.16	0.22	0.16	0.12
Sr	66	50	47	54	32	51	47

Note: Major element data from Zuleger et al. (1995). Trace element data from Zuleger et al. (1996). ND = not determined.

Table T10 (continued).

Hole	504B	504B	504B	504B	504B	504B	504B
Core, section	197R-1	198R-1	199R-1	200R-2	202R-1	204R-1	208R-3
Interval (cm)	31-33	52-54	54-57	50-52	23-25	15-19	3-5
Piece	7	14	13	7B	7	4	1
Lab number	Z-846	Z-847	Z-848	Z-849	Z-850	Z-851	Z-852
Depth (mbsf)	1703.11	1712.72	1719.94	1730.60	1747.43	1756.65	1781.03
Unit	222	223	226	227	229	232	239
Major element oxides (wt%):							
SiO_2	50.10	49.30	49.40	49.40	49.70	48.70	50.00
TiO_2	0.88	0.83	0.79	0.76	0.84	0.95	0.56
Al_2O_3	15.20	15.80	16.40	16.50	15.70	15.30	16.40
Fe_2O_3	2.34	2.61	2.20	2.37	1.67	2.43	2.09
FeO	7.88	6.74	6.30	5.97	7.50	6.36	7.12
MnO	0.17	0.17	0.16	0.15	0.20	0.15	0.16
MgO	8.39	9.51	9.60	9.65	8.77	8.92	8.69
CaO	11.70	12.80	13.00	13.10	13.10	13.90	11.90
Na_2O	2.26	1.67	1.71	1.68	1.68	1.77	1.83
K_2O	<0.05	<0.05	<0.05	<0.05	<0.05	<0.05	<0.05
P_2O_5	0.07	0.06	0.06	0.06	0.06	0.09	0.03
H_2O^+	2.31	1.41	1.27	1.09	1.40	1.98	3.36
Total	101.30	100.90	100.89	101.73	100.62	100.55	102.14
Fe_2O_3/FeO	0.30	0.39	0.35	0.40	0.22	0.38	0.29
Density (g/cm^3)	2.92	2.99	2.83	2.98	2.91	2.94	2.89
Trace elements (ppm):							
La	0.70	0.91	1.00	0.97	0.95	1.26	0.84
Ce	2.93	3.52	3.69	3.62	3.47	4.98	2.76
Nd	3.88	4.38	4.25	4.09	4.38	5.75	3.15
Sm	1.68	1.84	1.73	1.67	1.87	2.19	1.09
Eu	0.69	0.72	0.70	0.68	0.73	0.95	0.56
Tb	0.50	0.56	0.50	0.48	0.55	0.62	0.35
Yb	2.33	2.47	2.13	2.08	2.75	2.69	1.53
Lu	0.35	0.38	0.32	0.34	0.38	0.41	0.19
Cr	254	367	395	433	339	370	364
Ni	88	144	155	160	119	127	124
Co	44	46	42	42	45	44	59
Cu	13	102	88	88	522	6	5
Zn	58	65	65	63	57	41	54
Zr	39	43	43	42	44	60	31
Y	20	20.1	18.4	ND	ND	23.8	13.7
Nb	0.21	0.24	0.36	0.29	0.27	0.73	0.18
Rb	<0.1	<0.1	0.1	<0.1	<0.1	0.14	0.15
Sr	54	50	63	67	52	72	62

Table T10 (continued).

Hole	504B	504B	504B	504B	504B	504B	504B
Core, section	209R-1	209R-2	211R-1	213R-1	214R-1	214R-1	222R-1
Interval (cm)	102-103	66-68	70-72	66-68	30-32	76-77	73-74
Piece	14	10	16	19	5A	8	12A
Lab number	Z-853	Z-854	Z-855	Z-856	Z-857	Z-858	Z-859
Depth (mbsf)	1788.52	1789.60	1799.20	1813.16	1818.90	1819.36	1885.33
Unit	240	240	241	243	244	244	254
Major element oxides (wt%):							
SiO_2	49.30	49.10	49.20	49.10	49.10	48.80	46.80
TiO_2	0.42	0.74	0.82	0.78	0.53	0.41	0.95
Al_2O_3	15.90	17.60	16.20	16.20	15.90	13.90	16.60
Fe_2O_3	2.07	2.45	2.40	2.21	2.20	2.07	2.01
FeO	8.22	5.53	6.48	6.56	6.93	6.78	6.92
MnO	0.16	0.15	0.15	0.15	0.13	0.12	0.16
MgO	9.23	8.51	9.19	9.33	9.67	8.99	10.01
CaO	11.40	13.50	13.90	13.10	12.10	12.40	12.70
Na_2O	1.61	1.69	1.71	1.77	1.73	1.72	1.61
K_2O	<0.05	<0.05	<0.05	<0.05	<0.05	<0.05	<0.05
P_2O_5	0.03	0.06	0.07	0.06	0.10	0.04	0.09
H_2O^+	3.12	1.26	1.72	1.94	2.62	3.85	3.22
Total	101.46	100.59	101.84	101.20	101.01	99.08	101.07
Fe_2O_3/FeO	0.25	0.44	0.37	0.34	0.32	0.31	0.29
Density (g/cm^3)	2.79	2.80	2.92	2.94	2.87	2.80	2.77
Trace elements (ppm):							
La	0.47	0.82	0.84	0.77	0.70	0.66	1.32
Ce	1.65	3.16	3.27	2.98	2.41	2.11	4.88
Nd	2.41	3.90	4.17	3.78	3.11	2.47	5.50
Sm	1.07	1.60	1.71	1.60	1.29	1.05	2.14
Eu	0.70	0.60	0.69	0.67	0.62	0.70	0.75
Tb	0.29	0.46	0.53	0.49	0.38	0.31	0.61
Yb	1.33	2.02	2.53	2.21	1.83	1.48	2.67
Lu	0.18	0.30	0.35	0.34	0.27	0.21	0.41
Cr	391	438	386	365	274	329	341
Ni	136	128	137	136	166	131	180
Co	67	47	48	46	58	39	49
Cu	6	97	111	80	5	2	20
Zn	64	53	47	44	46	35	44
Zr	25	40	43	39	26	23	58
Y	11.4	17.8	20.8	19.5	15.8	12.0	22.7
Nb	0.38	0.3	0.29	0.26	0.20	0.17	0.66
Rb	0.13	<0.1	<0.1	<0.1	0.11	0.19	<0.1
Sr	57	62	52	51	55	49	62

Table T10 (continued).

Hole	504B	504B	504B
Core, section	225R-2	230R-1	238R-1
Interval (cm)	30-32	11-14	4-7
Piece	5	3	2
Lab number	Z-860	Z-861	Z-862
Depth (mbsf)	1914.00	1953.11	1992.14
Unit	260	265	269
Major element oxides (wt%):			
SiO_2	49.60	50.50	50.10
TiO_2	0.82	1.06	0.90
Al_2O_3	16.00	14.60	15.30
Fe_2O_3	2.22	2.59	2.90
FeO	6.91	7.66	6.39
MnO	0.17	0.17	0.17
MgO	9.14	8.28	9.14
CaO	13.00	12.50	13.20
Na_2O	1.78	2.08	1.82
K_2O	<0.05	<0.05	<0.05
P_2O_5	0.07	0.08	0.07
H_2O^+	1.38	1.07	1.01
Total	101.09	100.59	101.00
Fe_2O_3/FeO	0.32	0.34	0.45
Density (g/cm^3)	2.90	2.79	3.10
Trace elements (ppm):			
La	0.84	1.05	0.98
Ce	3.31	3.91	3.75
Nd	4.25	5.00	4.66
Sm	1.81	2.18	1.90
Eu	0.72	0.84	0.74
Tb	0.54	0.67	0.57
Yb	2.48	3.00	2.45
Lu	0.37	0.45	0.36
Cr	372	151	386
Ni	131	88	116
Co	49	44	47
Cu	94	57	113
Zn	68	38	57
Zr	42	52	48
Y	20.6	25.6	20.6
Nb	0.29	0.33	0.3
Rb	<0.1	<0.1	<0.1
Sr	56	50	61

Table T11. Composition of basalts from Hole 504B, Leg 148 (Costa Rica Rift, Pacific Ocean).

Hole	504B	504B	504B	504B	504B
Core, section	234R-1	240R-1	246R-1	249R-1	251R-1
Interval (cm)	46-50	82-88	87-90	85-89	35-40
Piece	14	21	25	27	6A
Lab number	Z-1586	Z-1587	Z-1588	Z-1589	Z-1590
Depth (mbsf)	2000.86	2007.72	2053.07	2072.05	2090.25
Unit	271	274	284	290	293
Major element oxides (wt%):					
SiO_2	49.41	47.87	48.72	48.17	48.13
TiO_2	0.90	0.86	0.88	0.84	0.88
Al_2O_3	15.84	17.09	16.14	17.39	16.41
Fe_2O_3	1.75	1.93	2.35	1.20	1.58
FeO	7.73	6.73	6.94	7.16	7.38
MnO	0.15	0.14	0.16	0.15	0.15
MgO	7.70	8.21	8.59	8.21	8.88
CaO	13.16	12.96	12.68	12.61	12.47
Na_2O	2.00	1.90	1.84	1.96	1.78
K_2O	0.02	0.02	0.03	0.02	0.02
P_2O_5	0.06	0.05	0.06	0.05	0.06
LOI	1.14	1.79	1.23	1.98	2.18
Total	99.86	99.55	99.62	99.74	99.92
H_2O^+	0.79	1.09	0.60	1.98	1.33
H_2O^-	0.19	0.19	0.15	<0.1	0.16
CO_2	<0.2	<0.2	0.2	<0.2	<0.2
Fe_2O_3/FeO	0.23	0.29	0.34	0.17	0.21
Density (g/cm^3)	2.90	2.89	2.99	2.93	2.95
Trace elements (ppm):					
La	1.0	0.90	1.0	1.0	0.88
Ce	4.4	3.5	3.7	3.0	4.0
Nd	4.8	4.5	4.6	4.5	4.5
Sm	1.9	1.9	2.0	1.9	2.0
Eu	0.63	0.64	0.68	0.64	0.61
Tb	0.66	0.66	0.74	0.78	0.78
Yb	2.2	2.5	2.4	2.2	2.6
Lu	0.35	0.37	0.35	0.33	0.38
Cr	290	398	402	317	300
Ni	93	190	170	147	165
Co	55	70	69	58	65
V	227	345	347	253	245
Cu	60	50	150	55	92
Zn	74	71	70	80	72
Zr	42	37	41	39	40
Y	21	23	21	20	21
Nb	1.1	1.3	1.5	1.4	1.4
Rb	<1	<1	1.7	1.5	1.4
Sr	56	55	56	59	53
Ba	5	28	10	7	17

Table T12. Distribution of secondary minerals in basalts from Hole 504B, Costa Rica Rift, X-ray diffraction data. (Continued on next two pages).

Core, section, interval (cm)	Depth (mbsf)	Sm	Chl	Swelling chlorite	ML chl-sm	Amph	Talc	Quartz
VOLCANICS:								
69-504B-								
4R-1, 62-64	280.62	+++						
4R-3, 108-1111	282.08	+++						
5R-2, 142-146	292.42	+++						
6R-1, 65-69	299.15	+++						
7R-2, 64-68	309.64	+++						
9R-1, 142-147	326.92	+++						
10R-3, 17-20	337.67	+++						
12R-1, 39-43	352.89	+++						
13R-4, 40-42	366.40	+++						
15R-1, 24-28	375.24	+++						
16R-1, 45-49	384.45	+++						
16R-4, 22-26	388.72	+++						
17R-1, 30-34	393.30	+++						
18R-1, 45-49	398.45	+++						
19R-1, 84-87	403.84	+++						
20R-1, 110-113	413.10	+++						
21R-2, 126-130	423.76	+++						
21R-5, 63-66	427.63	+++						
22R-1, 108-109	431.08	+++						
24R-1, 125-128	449.25	+++						+
26R-1, 15-18	463.15	+++						
27R-2, 55-58	468.05	+++	+					
28R-3, 69-73	478.69	+++	+					+
70-504B-								
32R-2, 137-140	510.37	+++						+
33R-1, 86-88	517.36	+++						+
33R-2, 14-16	518.14	+++	+					+
34R-1, 140-142	526.90	+++						
34R-2, 18-21	527.18	+++	+					
35R-1, 110-112	535.60	+++						+
35R-2, 14-16	536.14	+++	+					+
37R-1, 15-20	552.65	+++						
37R-2, 75-78	554.75	+++						+
38R-1, 7-15	561.57	+++						+
39R-2, 97-102	572.97	+++						
40R-1, 55-60	580.05	+++			++[3]			+
41R-3, 146-148	588.46	+++[1]						+
47R-2, 130-140	640.80	+++						+
49R-1, 122-126	657.22	+++						
49R-2, 7-10	657.57	+++						+
61R-1, 55-60	751.05	+++						+
61R-2, 145-149	753.45	+++						+
64R-2, 32-35	774.82	+++						+
66R-2, 0-5	792.50	+++						+
67R-1, 45-49	800.45	+++						
68R-1, 107-111	810.07	+++						+
69R-1, 74-77	818.74	+++						+
70R-1, 17-20	827.17	+++						
70R-1, 127-130	828.27	+++	+				+?	+

Table T12 (continued).

Core, section, interval (cm)	Depth (mbsf)	Sm	Chl	Swelling chlorite	ML chl-sm	Amph	Talc	Quartz
70R-2, 20-23	828.70	+++	+					+
83-504B-								
72R-2, 60-64	845.50	+++	+					+
TRANSITION:								
73R-2, 56-59	854.56	+++[1]					+?	+
77R-1, 78-81	889.28		+++[2]		+++[4]	+?		+
78R-1, 60-64	898.10		+++[2]					
79R-3, 50-54	908.00		+++[2]		+++[4]	+		+
80R-1, 5-10	910.05		+++[2]			+		+
80R-2, 143-146	912.73		+++[2]					+
80R-4, 3-8	914.33		+++[2]					+
82R-2, 92-96	930.87		+++			+		+
84R-2, 48-50	948.48		+++[2]					+
85R-1, 58-62	956.08		+++			+		+
86R-1, 15-20	964.65		+++[2]			+		+
88R-1, 68-71	977.18		+++[2]			+		+
89R-2, 74-78	987.74		+++			+		+
90R-4, 112-114	1000.12		+++[2]			+		+
91R-1, 115-118	1004.65		+++[2]					+
94R-3, 91-94	1004.41		++	+++	+++[4]	+		
UPPER DIKES:								
97R-1, 88-90	1058.38		+++[2]			+		
97R-2, 108-111	1060.08		+++	+++	+++			+
98R-1, 80-85	1062.80		+++[2]			+		
99R-2, 93-96	1073.93		+++			+		
100R-1, 19-20	1080.69		+++			+		++
100R-1, 83-87	1081.33		+++[2]			+++		
104R-3, 30-33	1119.80		+++			+		+
109R-1, 50-54	1154.00		++	+++	+[5]	+		+
111R-1, 86-89	1162.36		++[2]	+++		+		
113R-1, 7-10	1171.07		++	+++	++[5]	+	+?	+
116R-1, 56-60	1185.56		+++	+		+		+
117R-1, 109-113	1190.59		+++			+	+	+
118R-1, 62-66	1194.62		+++			+	+?	+
121R-1, 32-38	1207.82		+++	+++	++[5]	+		+
127R-1, 97-101	1254.47		+++	+++		+	++	+
130R-1, 88-91	1279.88		+++	++		+	++	+
130R-3, 78-81	1282.78		++	+++		+	++	
132R-1, 76-80	1295.76		+++[2]	+++	++	+	++	+
133R-1, 46-50	1304.46		+++			+		+
134R-1, 147-150	1314.47		+++			+	+	
111-504B-								
142R-1, 129-132	1354.09		+++			+	+?	
142R-2, 40-44	1354.70		+++	++		+	+	
143R-1, 124-127	1360.54		+++	++	+	+	+?	+
145R-1, 103-105	1379.33		+++	+++	+	+	+?	+
145R-2, 74-76	1380.54		+++	+++	++[5]	+		
145R-3, 66-68	1381.96		+++	+++	+[5]	+	+?	
147R-1, 11-13	1397.51		+++	++		+	++	+
147R-2, 15-20	1399.05		+++[2]	+++	++[5]	+	+	+
147R-2, 26-28	1399.16		++	+++		+	+?	+
148R-1, 53-55	1407.33		+++	++	++[5]	+	+?	+
149R-1, 122-124	1418.12		+++	++	++[5]	+	+?	+
152R-1, 11-13	1436.01		+++			+		
154R-1, 30-32	1454.60		+++	++		+	++	

Table T12 (continued).

Core, section, interval (cm)	Depth (mbsf)	Sm	Chl	Swelling chlorite	ML chl-sm	Amph	Talc	Quartz
156R-1, 64-67	1464.44		+++			++		+
158R-1, 16-19	1482.66		++			+++		+
LOWER DIKES:								
163R-1, 36-41	1511.96		+++			+		+
163R-1, 120-123	1512.80		+++			+		+
169R-1, 66-69	1548.26		+++			++?		+
137-504B-								
177R-1, 48-49	1604.98		+++		+	+		++
181M-1, 6-8	1620.46		+++	+	+	+		++
140-504B-								
186R-2, 30-31	1628.10		+++			++		+
187R-1, 59-60	1632.59		+			+++		
189R-1, 85-86	1651.85		+++	++		+	+	+
189R-2, 15-17	1652.61		+++		++[5]	++	+?	+
190R-1, 10-14	1655.20		+++		+?	++		+
191R-1, 26-28	1661.66		+++	+?	++[5]	++		+
194R-1, 42-44	1680.82		++	+?	+[5]	+++		
197R-1, 31-33	1703.11		++	+?	+	+++		+
198R-1, 52-54	1712.72		++	+		+	+++	
199R-1, 54-57	1719.94		+++		+	+++	+++	
200R-2, 50-52	1730.60		+++	+		+++	+++	
202R-1, 23-25	1747.43		+++	+	+[3]	++	++	+
204R-1, 15-19	1756.65		+++			+++		+
208R-3, 3-5	1781.03		+++			++		+
209R-1, 102-103	1788.52		+++			++		
209R-2, 66-68	1789.60		+++	+++	+[5]	+	+	+
211R-1, 70-72	1799.20		+++	+		+	+	+
213R-1, 66-68	1813.16		+++		+[5]	+		+
214R-1, 30-32	1818.90		+++			+++		
214R-1, 76-77	1819.36		+			+++		
222R-1, 73-74	1885.33		+++			+		+
225R-2, 30-32	1914.00		+++			+++	++	+
230R-1, 11-14	1953.11		+			+++		
238R-1, 4-7	1992.14		+++			+++		+
148-504B-								
239R-1, 46-50	2000.86		+			+++	+?	
240R-1, 82-88	2007.72		+			+++		
246R-1, 87-90	2053.07		++			+++	++	+
249R-1, 85-89	2072.05		+++			++	+?	+
251R-1, 35-40	2090.25		+++			+		+

Notes: +++ = dominant, ++ = minor, + = trace.
Sm = smectites (saponite type) or mixed-layer smectite-illite mineral with mica layers (up to 10%-20 %); Chl = chlorite; ML chl-sm = mixed-layer chlorite-smectite minerals with swelling interlayers from 10%-15% up to 50%; Amph = amphibole (hornblende).
[1] = mixed-layer illite-smectite mineral with 30%-40% of mica interlayers; [2] = chlorite with single swelling interlayers (up to 5%-10 %); [3] = mixed-layer chlorite-swelling chlorite mineral; [4] = corrensite; [5] = corrensite like mineral.

Table T13. Secondary minerals identified by X-ray diffraction (XRD) in veins of basalts from the Costa Rica Rift, Hole 504B. (Continued on next two pages.)

Core, section, interval (cm)	Depth (mbsf)	Description	XRD identification
VOLCANICS:			
70-504B-			
33R-2, 14-16	518.14	Dark green clay of crust	Smectites (dominant) and mixed-layer smectite-swelling chlorite mineral (minor); chlorite in trace amounts
34R-2, 18-21	527.18	Light mat of crust	Smectites with ~ 20% of illite interlayers and analcime; chlorite in trace amounts
		Black clay and semi-transparent crystals	Calcite, smectites with ~20% of illite interlayers, mixed-layer chlorite-smectite mineral, and natrolite; analcime and anhydrite in trace amounts
35R-1, 110-112	535.60	White crystals and clay	Smectites and mixed-layer illite-smectite mineral with up to 15% of illite interlayers, and analcime; chlorite in trace amounts
35R-2, 14-16	536.14	White-pink matter cemented small pieces of basalt (matrix)	Mixed-layer smectite-swelling chlorite mineral, illite(?), calcite, analcime, natrolite, okenite, talc(?), and chalcocite
37R-2, 75-78	554.75	Milk-white matter	Analcime and gyrolite
		Green transparent matter and clay	Analcime and smectites with ~20-30% of illite interlayers; chlorite in trace amounts
38R-1, 7-15	561.57	White crystals and clay	Analcime, gyrolite, quartz, calcite(?), and 12.8A-mineral(?)
		Black clay of crust	Smectites with ~20% of illite interlayers and mixed-layer chlorite-smectite mineral (~30% of swelling interlayers); quartz in trace amounts
40R-1, 55-60	580.05	Oxidized crust	Maghemite, lepidocrocite, and goethite
		Black clay of crust	Smectites with ~20% of illite interlayers; chlorite in trace amounts
41R-3, 146-148	588.46	Black clay of crust	Smectites with ~20% of illite interlayers, swelling chlorite; chlorite and talc in trace amounts
47R-2, 130-140	640.80	Black clay of crust	Smectites with ~15% of illite interlayers; quartz in trace amounts

Table T13 (continued).

Core, section, interval (cm)	Depth (mbsf)	Description	XRD identification
61R-1, 55-60	751.05	High altered basalt White crystals and clay	Smectites; quartz in trace amounts Anhydrite and smectites with ~10% of illite interlayers; gypsum and apophyllite in trace amounts
64R-2, 32-35	774.82	Black clay of crust	Smectites with ~20% of illite interlayers; quartz in trace amounts
66R-2, 0-5	792.50	White inclusions	Anhydrite and smectite with 20% of illite interlayers; quartz and chlorite in trace amounts
		Black clay of crust	Smectites with ~15% of illite interlayers
68R-1, 107-111	810.07	Gray clay of crust	Smectites with ~10% of illite interlayers; mixed-layer chlorite-smectite mineral with ~20% of swelling interlayers in trace amounts
69R-1, 74-77	818.74	Black clay of crust	Smectites with ~10% of illite interlayers; quartz in trace amounts
70R-1, 127-130	828.27	Black clay of crust with pyrite	Smectites; swelling chlorite in trace amounts
70R-2, 20-23	828.70	Black clay of crust	Smectites and chlorite (minor)
TRANSITION: 83-504B-			
78R-1, 60-64	898.10	Green clay of crust with pyrite	Chlorite with single swelling interlayers, epistilbite(?) or clinoptilolite/ heulandite(?)
79R-3, 50-54	908.00	Black clay of crust	Chlorite with ~10% of swelling interlayers; amphybole and quartz in trace amounts
80R-1, 5-10	910.05	Dark green clay from veins	Chlorite with single swelling interlayers; quartz, calcite, and epistilbite(?) in trace amounts
80R-2, 143-146	912.73	White matter from veins	Calcite, epistilbite(?), and laumontite
		Dark green clay with pyrite from veins	Chlorite with single swelling interlayers; quartz in trace amounts
80R-4, 3-8	914.33	Dark green clay from veins	Chlorite with ~10% of swelling interlayers; quartz and heulandite in trace amounts
81R-1, 83-86	920.33	Dark green clay from veins	Chlorite with single swelling interlayers and quartz (minor)

Table T13 (continued).

Core, section, interval (cm)	Depth (mbsf)	Description	XRD identification
92R-3, 38-42	1015.88	White matter and clay from veins	Chlorite with single swelling interlayers; amphybole and epistilbite(?) in trace amounts
84R-2, 48-50	948.48	Black clay with pyrite from vein	Chlorite with ~5% of swelling interlayers and quartz; amphybole, and zeolite in trace amounts
85R-1, 58-62	956.08	Dark green clay (matrix of breccia)	Chlorite
90R-4, 112-114	1000.12	White matter and clay from veins	Quartz and chlorite with single swelling interlayers; epistilbite and amphybole in trace amounts
91R-1, 115-118	1004.65	Black clay from vein	Chlorite with single swelling interlayers; epistilbite(?) in trace amounts
92R-3, 38-42	1015.88	White matter and clay from veins	Chlorite with single swelling interlayers; amphybole and epistilbite(?) in trace amounts
92R-3, 38-42	1015.88	White matter and clay from veins	Chlorite with single swelling interlayers; amphybole and epistilbite(?) in trace amounts
UPPER DIKES:			
97R-1, 88-90	1058.38	Inclusion of white friable matter	Laumontite
		Inclusion of white hard matter	Scolecite
100R-1, 83-87	1081.33	Black and light-gray clay from matrix	Chlorite; amphybole and epistilbite(?) in trace amounts
111R-1, 86-89	1162.36	Black clay of crust	Corrensite like mineral and chlorite
117R-1, 109-113	1190.59	Black clay and white matter of crust	Chlorite and laumontite; amphybole in trace amounts
130R-3, 78-81	1282.78	Vesicle filling (black clay)	Stivensite (dominant) and talc; chlorite with ~10% of swelling interlayers and serpentine(?) in trace amounts
111-504B-			
152R-1, 11-13	1436.01	Radial-radiant white crystals of crust	Laumontite
LOWER DIKES:			
140-504B-			
193R-1, 49-51	1674.99	White matter and clay from vein	Amphybole and laumontite; chlorite in trace amounts

Table T14. Characteristics of holes drilled at the Middle Valley and Escanaba Trough, Juan de Fuca Ridge, Legs 139 and 169.

Hole	Latitude	Longitude	Water depth (m)	Oldest sediment cored	Basement penetration (m)	Basement recovery (m)
Middle Valley						
855A	48°26.563'N	128°38.271'W	2444.8	Pleistocene	11.44	0.65
855D	48°26.542'N	128°38.317'W	2443.8	Pleistocene	1.20	1.42
856A	48°26.201'N	128°40.838'W	2395.1	Pleistocene	39.10	1.98
856B	48°26.102'N	128°40.811'W	2420.0	Pleistocene	1.32	0.40
856H	48°26.020'N	128°40.859'W	2423.8	no fossil data	68.3	13.18
857C	48°26.485'N	128°42.682'W	2421.7	Pleistocene	96.60	18.34
857D	48°26.517'N	128°42.651'W	2420.6	no fossil data	355.1	37.36
858F	48°27.369'N	128°42.527'W	2415.1	no fossil data	48.00	2.71
858G	48°27.360'N	128°42.531'W	2415.1	non	155.80	6.86
Escanaba Trough						
1037B	40°57.299'N	127°30.900'W	3300.2	Pleistocene	38.20	18.80
1038I	40°059.88'N	127°29.563'W	3215.2	no fossil data	1.50	0.65

Table T15. Composition of basalts from Holes 855A and 855D, Leg 139 (Middle Valley, Juan de Fuca Ridge, Pacific Ocean).

Leg	139	139	139
Hole	855A	855A	855D
Core, section	8R-1	9R-1	6R-1
Interval (cm)	36-39	10-14	55-58
Piece	5	2	8
Lab number	Z-814	Z-815	Z-816
Depth (mbsf)	65.16	74.40	114.45
Unit	1	2	2
Major elementt oxides (wt%):			
SiO_2	48.44	49.10	49.68
TiO_2	2.17	1.57	1.67
Al_2O_3	14.68	14.32	14.99
Fe_2O_3	4.12	4.05	2.98
FeO	8.28	7.28	7.34
MnO	0.21	0.19	0.20
MgO	5.91	7.29	7.25
CaO	11.57	11.91	11.81
Na_2O	2.62	2.63	2.48
K_2O	0.20	0.13	0.15
P_2O_5	0.22	0.13	0.14
LOI	1.16	1.86	1.01
Total	99.58	100.46	99.70
H_2O^+	0.28	0.55	0.32
H_2O^-	0.64	0.62	0.33
CO_2	<0.2	<0.2	<0.2
S (total)	ND	0.16	ND
Fe_2O_3/FeO	0.50	0.56	0.41
Density (g/cm^3)	2.94	2.91	2.87
Trace elements (ppm):			
La	4.6	4.3	3.4
Ce	15	13	12
Nd	14	12	11
Sm	5.5	4.1	3.9
Eu	1.6	1.3	1.3
Tb	1.4	1.1	1.1
Yb	4.9	3.5	4.1
Lu	0.81	0.58	0.64
Cr	172	230	245
Ni	66	77	72
Co	42	45	46
V	342	295	316
Cu	63	75	66
Pb	<5	<5	<5
Zn	130	91	98
Sn	3	3	3.1
Zr	150	92	96
Y	47	31	34
Nb	3.4	4.6	2.9
Rb	3.1	1.3	2.9
Sr	110	120	110
Ba	31	39	52

Note: ND = not determined.

Table T16. Secondary minerals in fine fraction sampled from igneous rocks: Middle Valley, Juan de Fuca Ridge and Escanaba Trough, Gorda Ridge, Legs 139 and 169, X-ray diffraction data. (Continued on next two pages.)

Core, section, interval (cm)	Depth (mbsf)	Sm	Illite	Mixed-layer chlorite-smectite	Mixed-layer chlorite-swelling chlorite	Chl	Quartz	Amphibole	Talc
139-855A-							+	+	+?
8R-1, 36-39	65.16	+++					+	+	+
9R-1, 10-14	274.40	+++							
139-855B-									
6R-1, 55-58	114.45	+				+	++		
139-856A-									
13X-CC, 22-24	113.39	+++				+	+	+	+
14X-1, 34-38	114.84	+++	+			+	+	+	+
14X-1, 61-64	115.11	+++				+	+	+	+
14X -CC, 14-18	115.92	+++				++	+		++
139-856B-									
8H-CC, 0-5	63.66	+++		+++		+++	+		++
139-857C-									
59R-1, 20-22	471.30					+++	+		
59R-1, 84-87	471.94	+				+++	+	+	
59R-2, 57-59	473.15					+++	+		
59R-3, 80-83	474.82					+++	+	+	
59R-4, 88-90	476.40					+++	+		
60R-4, 53-56	481.33					+++	+	+	
60R-1, 130-132	482.10			++[1]		+++	+	+	
60R-2, 4-6	482.34			++[1]		+++	+		
61R-1, 81-83	491.31					+++	+		
61R-2, 8-10	492.08					+++	+	+	
62R-1, 70-72	500.70				++	+++	+	+	
62R-2, 40-42	501.90				++	+++		+	
63R-1, 50-52	510.20					+++	++	+	
64R-1, 18-20	519.58					+++	+	+	
64R-1, 41-44	519.81					+++		+	
64R-2, 46-49	521.36					+++	+	+	
66R-1, 34-35	539.14					+++			
68R-1, 97-100	558.97					+++	+	+	
68R-2, 69-71	560.19					+++	+	+	
68R-3, 20-23	561.20					+++	+	+	
139-857D-									
1R-1, 34-36	581.84					+++	+		
2R-1, 10-13	589.70					+++	+	+	
3R-1, 43-46	599.73					+++	+	+	
3R-2, 86-88	601.66					+++	+		
4R-2, 53-56	610.93					+++	+	+	
4R-2, 56-58	610.96					+++	+	+	
8R-1, 5-7	647.35					+++			
9R-1, 23-25	657.13					+++	+	+	
12R-1, 25-27	686.15					+++	+		
12R-1, 106-108	686.96					+++	+		
12R-2, 17-19	687.57					+++	+	+	

Table T16 (continued).

Core, section, interval (cm)	Depth (mbsf)	Sm	Illite	Mixed-layer chlorite-smectite	Mixed-layer chlorite-swelling chlorite	Chl	Quartz	Amphibole	Talc
17R-3, 72-74	737.62					+++	+	+	
18R-2, 84-85	745.94					+++	+	+	
20R-1, 64-66	763.14					+++	+	+	
21R-1, 59-61	772.79					+++	++	+	
23R-1, 57-59	792.07					+++	+	+	
24R-2, 4-7	802.74					+++	+	+	
25R-1, 73-75	811.53					+++	+	+	
26R-1, 58-60	820.88					+++	+		
29R-2, 36-39	850.26					+++	+		
33R-1, 81-83	888.61					+++	+	+	
35R-1, 29-31	907.49					+++	+	+	
35R-1, 103-106	908.23					+++	+	+	
36R-1, 3-5	916.93					+++	+		
139-858F-									
26R-1, 93-95	259.53				++	+++	+		
27R-1, 25-27	268.05				+++	+++	+	+	
28R-1, 43-45	277.93				++	+++	+		
29R-1, 39-41	287.59				++	+++	+	+	
139-858G-									
1R-1, 14-16	276.94				+	+++	+		
4R-1, 35-37	306.15				++	+++	+		
7R-1, 32-34	335.12				++	+++	+		
14R-1, 10-12	403.70					+++	+	+	
16R-1, 75-77	423.65					+++	+	+	
169-856H-									
55R-1, 28-33	431.98					+++	+		
56R-1, 10-14	434.40					+++	+		
56R-1, 28-32	434.58					+++	+		
59R-1, 90-93	461.60					+++	+		
60R-1, 65-70	466.35					+++	+	+	
60R-2, 15-20	467.35					+++	+	+	
61R-1, 52-57	468.72					+++	+	+	
62R-1, 89-90	471.19					+++	+		
63R-1, 30-35	480.20					+++	+		
64R-1, 10-14	489.60					+++	+	+	
64R-1, 75-80	490.25					+++	+	+	+
64R-2, 132-136	492.32					+++	+	+	
65R-1, 0-5	494.20					+++	+	+	
65R-2, 54-59	496.12					+++	++	+	+
169-1037B-									
57R-1, 32-37	508.12	+++				+	+	+	+
58R-1, 100-104	518.30	+++	+			+	+	+	+
58R-2, 0-5	518.70	+++	+			+	+	+	
59R-1, 65-68	527.45	+++	+			+	+	+	
60R-1, 90-95	530.30	+++	+			+	+	+	+
61R-1, 7-10	533.97	+++				+	+		+
62R-1, 13-17	538.13	+++	+			+	+		+
62R-3, 52-56	541.24	+++	+			+	+		+

Table T16 (continued).

Core, section, interval (cm)	Depth (mbsf)	Sm	Illite	Mixed-layer chlorite-smectite	Mixed-layer chlorite-swelling chlorite	Chl	Quartz	Amphibole	Talc
169-1038I-43X-3, 3-7	403.23	+++				+	+		

Notes: +++ = dominant, ++ = minor, + = trace. [1] = corrensite like mineral, Sm = smectites, Chl = chlorite.

Table T17. Composition of basalts from Holes 856A and 856B, Leg 139 (Bent Hill, Middle Valley, Juan de Fuca Ridge, Pacific Ocean).

Leg	139	139	139	139
Hole	856A	856A	856A	856B
Core, section	13X-CC	14X-1	14X-CC	8H-CC
Interval (cm)	22-24	61-64	14-18	0-5
Piece	2A	4	2B	1
Lab number	Z-817	Z-818	Z-819	Z-820
Depth (mbsf)	113.39	115.11	115.92	63.66
Unit	1	1	1	1
Major element oxides (wt%):				
SiO_2	47.43	46.71	46.21	47.36
TiO_2	0.87	0.88	0.87	0.86
Al_2O_3	15.74	17.38	15.79	15.91
Fe_2O_3	1.72	1.70	3.02	2.99
FeO	6.51	6.76	5.36	5.27
MnO	0.16	0.16	0.15	0.1
MgO	10.52	11.04	11.74	11.76
CaO	12.44	11.62	10.42	10.64
Na_2O	2.00	1.96	1.88	2.08
K_2O	0.06	0.07	0.06	0.05
P_2O_5	0.05	0.07	0.05	0.05
LOI	1.84	1.73	4.01	3.2
Total	99.34	100.08	99.56	100.27
H_2O^+	0.85	1.03	2.35	1.87
H_2O^-	0.73	0.66	1.09	1.02
CO_2	<0.2	<0.2	<0.2	0.15
S (total)	0.16	ND	0.11	<0.1
Fe_2O_3/FeO	0.26	0.25	0.56	0.57
Density	3.03	2.91	2.88	2.92
Trace elements (ppm):				
La	0.86	0.93	0.93	0.78
Ce	3.1	4.0	3.5	2.1
Nd	4.4	4.8	4.7	3.4
Sm	2.2	1.9	1.9	1.9
Eu	0.80	0.78	0.75	0.7
Tb	0.58	0.66	0.63	0.61
Yb	2.3	2.1	2.0	2.0
Lu	0.38	0.32	0.32	0.31
Cr	555	540	575	560
Ni	202	262	260	275
Co	50	53	52	66
V	192	203	207	247
Cu	72	72	73	72
Pb	<5	<5	<5	<5
Zn	96	77	74	75
Sn	2.3	2.3	2.3	2.4
Zr	35	34	34	37
Y	21	21	19	19
Nb	1.4	0.8	1.2	1.2
Rb	1.3	<1	1.0	<1
Sr	58	57	54	55
Ba	65	61	42	5

Note: ND = not determined.

Table T18. Composition of basalts from Hole 856H, Leg 169 (Bent Hill, Middle Valley, Juan de Fuca Ridge, Pacific Ocean). (Continued on next page.)

Leg	169	169	169	169	169	169	169
Hole	856H	856H	856H	856H	856H	856H	856H
Core, section	55R-1	56R-1	56R-1	59R-1	60R-1	60R-2	61R-1
Interval (cm)	28-33	10-14	28-32	90-93	65-70	15-20	52-57
Piece	5A	3	5	13	11	3	5E
Lab number	Z-1591	Z-1592	Z-1593	Z-1594	Z-1595	Z-1596	Z-1597
Depth (mbsf)	431.98	434.40	434.58	461.60	466.35	467.35	468.72
Unit	VII	III	VII	VII	VII	VII	VII
Major element oxides (wt%):							
SiO_2	42.69	44.62	40.84	34.05	47.97	49.42	42.13
TiO_2	1.98	2.13	2.20	2.67	2.19	2.07	2.01
Al_2O_3	13.90	14.73	14.84	17.76	14.46	14.08	13.92
Fe_2O_3	5.95	3.68	5.86	3.78	3.29	3.11	2.54
FeO	14.79	16.37	17.96	20.99	9.83	7.26	16.35
MnO	0.22	0.21	0.25	0.21	0.28	0.23	0.31
MgO	9.85	9.15	8.68	9.04	8.55	7.29	11.45
CaO	2.40	0.82	0.55	1.85	7.05	11.56	2.83
Na_2O	0.08	0.08	0.11	0.12	1.14	1.53	0.12
K_2O	0.01	0.01	0.01	0.02	0.02	0.02	0.01
P_2O_5	0.19	0.20	0.21	0.22	0.20	0.19	0.18
LOI	7.90	7.60	8.35	8.90	5.02	2.65	7.79
Total	99.96	99.60	99.86	99.61	100.00	99.41	99.64
H_2O^+	7.48	7.08	7.89	8.37	4.49	2.11	7.33
H_2O^-	0.25	0.34	0.36	0.27	0.31	0.18	0.24
CO_2	<0.2	<0.2	<0.2	<0.2	0.22	0.21	0.22
S (total)	0.10	<0.1	0.36	<0.1	<0.1	0.11	<0.1
Fe_2O_3/FeO	0.4	0.23	0.33	0.18	0.34	0.43	0.16
Density (g/cm^3)	2.77	2.65	2.49	2.36	2.66	2.81	2.76
Trace elements (ppm):							
La	5.2	4.6	3.3	4.2	4.7	4.8	4.5
Ce	17	14	9.0	10	15	15	13
Nd	15	12	9.0	11	14	13	13
Sm	5.4	4.2	3.5	4.5	5.1	5.2	4.8
Eu	1.6	0.55	0.45	0.84	1.3	1.4	1.4
Tb	1.6	1.4	2.1	2.4	1.6	1.5	1.6
Yb	4.5	4.1	5.2	7.8	4.6	4.5	4.0
Lu	0.71	0.64	0.85	1.2	0.72	0.66	0.61
Cr	265	248	230	228	230	179	198
Ni	95	91	79	80	76	87	163
Co	84	85	94	88	65	50	65
V	415	387	385	437	410	272	249
Cu	20	30	33	18	135	1195	47
Zn	78	96	71	67	85	88	113
Zr	130	130	130	150	140	130	120
Y	40	41	54	75	45	41	38
Nb	3.6	3.9	3	4.6	4.6	4.8	2.1
Rb	<1	<1	<1	<1	1.1	1	<1
Sr	2.3	2	2.2	<1	76	84	4.5
Ba	51	57	60	46	43	32	51

Table T18 (continued).

Leg	169	169	169	169	169	169	169
Hole	856H	856H	856H	856H	856H	856H	856H
Core, section	62R-1	63R-1	64R-1	64R-1	64R-2	65R-1	65R-2
Interval (cm)	89-90	30-35	10-14	75-80	132-136	0-5	54-59
Piece	15A	6A	3	13	20	1A	7
Lab number	Z-1598	Z-1599	Z-1600	Z-1601	Z-1602	Z-1603	Z-1604
Depth (mbsf)	471.19	480.20	489.60	490.25	492.32	494.20	496.12
Unit	VIII	VIII	VIII	VIII	VIII	VIII	VIII
Major element oxides (wt%):							
SiO_2	36.26	41.65	45.44	41.37	40.90	46.80	48.28
TiO_2	2.14	2.19	2.22	2.26	1.89	1.78	1.84
Al_2O_3	16.57	16.55	16.95	15.97	13.39	15.13	14.88
Fe_2O_3	5.36	4.77	2.95	4.07	3.29	3.19	1.74
FeO	19.71	10.91	9.85	12.39	14.62	8.41	7.47
MnO	0.26	0.26	0.25	0.28	0.38	0.26	0.22
MgO	9.60	9.77	8.28	10.22	13.29	10.38	7.92
CaO	0.98	4.69	6.13	4.22	3.02	8.62	12.32
Na_2O	0.08	1.18	1.50	0.90	0.26	1.37	2.00
K_2O	0.01	0.02	0.03	0.02	0.02	0.02	0.02
P_2O_5	0.19	0.19	0.20	0.20	0.17	0.16	0.17
LOI	9.07	6.78	5.49	7.59	8.25	4.12	2.47
Total	100.23	98.96	99.29	99.49	99.48	100.24	99.33
H_2O^+	8.56	5.71	4.64	6.69	7.25	3.55	1.93
H_2O^-	0.28	0.23	0.29	0.39	0.65	0.31	0.19
CO_2	0.23	0.23	0.23	<0.2	0.31	0.26	0.22
S (total)	0.57	1.37	0.28	0.26	<0.1	<0.1	0.22
Fe_2O_3/FeO	0.27	0.44	0.30	0.33	0.23	0.37	0.23
Density (g/cm^3)	2.62	2.55	2.53	2.46	2.60	2.65	2.83
Trace elements (ppm):							
La	2.8	4.7	5.9	3.3	3.8	4.1	4.4
Ce	7.8	16	18	11	13	11	14
Nd	6.0	14	15	12	12	10	13
Sm	2.0	5.3	5.0	4.8	4.4	4.0	4.3
Eu	0.47	1.3	1.4	0.94	1.1	1.1	1.2
Tb	0.69	1.6	1.6	1.4	1.3	1.2	1.2
Yb	2.8	4.3	4.3	4.7	3.9	3.6	3.9
Lu	0.48	0.66	0.64	0.73	0.62	0.55	0.54
Cr	186	192	205	188	181	180	184
Ni	82	83	95	83	53	63	77
Co	67	62	43	48	42	34	46
V	266	340	338	255	224	207	225
Cu	25	>10000	2755	2065	290	310	325
Zn	62	127	121	101	195	96	76
Zr	130	130	140	140	120	110	120
Y	19	44	46	44	39	34	40
Nb	4.2	4.8	3.7	4.7	3.8	4.2	4.6
Rb	<1	<1	1.4	1.1	<1	<1	<1
Sr	1.2	85	100	79	17	110	110
Ba	63	38	45	16	8	56	16

Table T19 Composition of basalts from Holes 857C and 857D, Leg 139 (Middle Valley, Juan de Fuca Ridge, Pacific Ocean). (Continued on next five pages.)

Leg	139	139	139	139	139	139	139
Hole	857C	857C	857C	857C	857C	857C	857C
Core, section	59R-1	59R-1	59R-3	59R-4	60R-1	60R-1	61R-1
Interval (cm)	20-22	84-87	80-83	88-90	53-56	130-132	81-83
Piece	1	7	4	7	3	8	6
Lab number	Z-946	Z-821	Z-822	Z-823	Z-824	Z-948	Z-950
Depth (mbsf)	471.3	471.94	474.90	476.48	481.33	482.10	491.31
Unit/Subunit	1	1	1	1	2	2	4
Major element oxides (wt%):							
SiO_2	48.98	50.22	47.83	49.51	48.39	48.49	48.39
TiO_2	1.77	1.68	1.65	1.70	1.65	2.03	1.71
Al_2O_3	16.39	15.12	15.17	15.04	15.03	15.42	15.94
Fe_2O_3	1.55	1.81	1.46	2.17	3.60	1.95	2.32
FeO	5.13	6.33	7.25	5.70	5.32	6.39	4.85
MnO	0.21	0.21	0.18	0.20	0.22	0.26	0.20
MgO	9.05	7.40	7.18	7.97	7.44	8.04	9.27
CaO	10.83	12.83	13.45	12.49	12.66	13.09	11.62
Na_2O	2.36	2.34	2.22	2.91	2.13	2.32	2.56
K_2O	0.05	0.05	0.05	0.07	0.05	0.05	0.05
P_2O_5	0.21	0.18	0.18	0.18	0.18	0.18	0.17
LOI	3.66	1.68	3.03	1.92	2.60	2.00	2.76
Total	100.19	99.85	99.65	99.86	99.27	100.22	99.84
H_2O^+	2.82	1.27	1.99	1.48	1.53	1.36	1.99
H_2O^-	0.60	0.32	0.35	0.31	0.56	0.35	0.30
CO_2	<0.2	<0.2	0.69	<0.2	<0.2	<0.2	<0.10
S (total)	ND	ND		0.27	1.82	0.51	0.12
Fe_2O_3/FeO	0.30	0.29	0.20	0.38	0.68	0.31	0.48
Density (g/cm^3)	2.55	2.63	2.85	2.76	2.86	2.80	2.77
Trace elements (ppm):							
La	6.3	6.0	7.6	5.9	6.2	5.6	4.9
Ce	17	16	20	18	19	16	14
Nd	13	13	13	13	14	12	11
Sm	4.3	4.4	4	4.4	4.1	3.9	3.4
Eu	1.2	1.6	1.2	1.4	1.3	1.4	1.1
Tb	1	0.99	0.86	1	0.97	0.94	0.94
Yb	3.5	3.3	2.8	3	3.1	3.2	2.6
Lu	0.54	0.52	0.41	0.49	0.47	0.49	0.39
Cr	270	262	245	255	237	170	277
Ni	60	62	82	80	75	69	74
Co	26	33	48	39	51	29	37
V	222	241	248	236	222	210	270
Cu	53	55	85	96	70	92	42
Pb	5	<5	<5	<5	<5	<5	<5
Zn	87	78	96	78	76	65	81
Sn	3.0	2.5	3.1	2.6	2.6	2.5	2.5
Zr	150	130	120	130	120	120	129
Y	35	31	31	32	33	30	32
Nb	4.6	5.3	4.3	4.3	4.7	4.4	4.6
Rb	1.3	<1	<1	<1	1.8	1	<1
Sr	200	190	190	120	190	180	180
Ba	44	47	28	42	35	36	46
Th	<1	ND	ND	ND	ND	1.7	ND

Note: ND = not determined.

Table T19 (continued).

Leg	139	139	139	139	139	139	139
Hole	857C	857C	857C	857C	857C	857C	857C
Core, section	61R-2	62R-1	63R-1	64R-1	64R-1	64R-2	68R-1
Interval (cm)	8-10	70-72	50-52	18-20	41-44	46-49	97-100
Piece	1	5	4	2	3	5	16
Lab number	Z-951	Z-952	Z-954	Z-955	Z-825	Z-826	Z-827
Depth (mbsf)	492.08	500.7	510.2	519.58	519.81	521.36	558.97
Unit/Subunit	5	6	7	8	8	8	12
Major element oxides (wt%):							
SiO_2	47.18	47.53	48.80	47.71	46.68	46.90	47.07
TiO_2	1.60	1.57	1.46	1.48	1.41	1.53	1.63
Al_2O_3	15.56	14.56	15.45	16.79	16.44	16.28	16.17
Fe_2O_3	2.97	3.58	2.11	1.69	1.61	2.81	3.52
FeO	5.53	5.61	7.21	6.79	7.37	6.72	6.21
MnO	0.28	0.30	0.28	0.29	0.28	0.26	0.35
MgO	10.29	8.32	7.74	7.70	9.08	8.43	8.28
CaO	9.72	12.30	12.30	12.19	10.85	12.06	11.66
Na_2O	2.30	1.65	1.98	2.20	1.92	1.94	1.67
K_2O	0.05	0.05	0.04	0.05	0.05	0.04	0.05
P_2O_5	0.15	0.13	0.14	0.13	0.13	0.16	0.14
LOI	4.68	4.15	1.88	2.41	3.52	2.61	2.90
Total	100.31	99.75	99.39	99.43	99.34	99.74	99.65
H_2O^+	2.59	3.76	1.30	1.87	2.74	2.01	2.33
H_2O^-	0.74	0.39	0.17	0.36	0.50	0.36	0.36
CO_2	<0.2	<0.2	<0.2	<0.2	<0.2	<0.2	<0.2
S (total)	0.65	ND	ND	ND	0.26	0.49	0.73
Fe_2O_3/FeO	0.54	0.64	0.29	0.25	0.22	0.42	0.57
Density (g/cm^3)	2.45	2.32	2.61	2.59	2.73	2.72	2.71
Trace elements (ppm):							
La	3.6	3.8	4	4.1	3.9	4.6	5.4
Ce	12	11	11	11	11	13	16
Nd	10	11	9.7	10	10	11	12
Sm	3.5	3.5	3.3	3.3	3.4	3.6	3.7
Eu	1.1	1.4	1.1	1.1	0.94	1.1	1.2
Tb	0.83	0.9	0.77	0.86	0.9	0.98	1
Yb	3	3	2.8	2.9	2.7	2.7	3.1
Lu	0.47	0.46	0.43	0.44	0.42	0.42	0.49
Cr	260	185	250	350	260	260	275
Ni	67	70	81	90	90	82	100
Co	44	40	44	47	39	35	49
V	202	179	220	230	206	206	262
Cu	20	26	66	78	65	81	172
Pb	5	<5	<5	5	5	<5	<5
Zn	125	90	130	102	100	101	99
Sn	2.6	2.6	2.5	2.3	2.8	2.6	3
Zr	120	110	92	90	93	100	110
Y	28	29	26	25	26	29	32
Nb	2.0	2.7	2.6	2.9	3.3	4.5	6.8
Rb	1.3	1.3	<1	<1	<1	<1	<1
Sr	140	230	130	130	120	130	120
Ba	29	21	28	22	59	57	37
Th	<1	1.6	1.6	<1	ND	ND	ND

Table T19 (continued).

Leg	139	139	139	139	139	139	139
Hole	857C	857C	857D	857D	857D	857D	857D
Core, section	68R-2	68R-3	1R-1	1R-2	2R-1	3R-1	3R-2
Interval (cm)	69-71	20-23	35-39	62-64	10-13	43-46	86-88
Piece	7	2	5A	Sediment	3	4	10B
Lab number	Z-957	Z-828	Z-829	Z-830	Z-831	Z-832	Z-959
Depth (mbsf)	560.19	561.2	581.85	583.62	589.7	599.73	601.66
Unit/Subunit	12	12	13		14A	14B	14B
Major element oxides (wt%):							
SiO_2	42.06	46.75	42.90	72.52	48.35	46.98	46.78
TiO_2	1.58	1.58	2.14	0.57	1.72	1.59	1.19
Al_2O_3	17.89	16.53	17.02	9.59	15.75	16.84	17.89
Fe_2O_3	2.15	1.72	1.14	0.62	1.56	4.01	3.52
FeO	10.74	7.69	8.70	4.50	7.17	5.93	5.39
MnO	0.54	0.33	0.57	0.09	0.21	0.23	0.22
MgO	9.44	8.83	11.37	4.30	8.00	7.35	7.70
CaO	8.66	11.21	5.85	3.42	12.03	11.90	11.56
Na_2O	1.30	1.66	1.40	1.52	2.19	2.23	2.06
K_2O	0.05	0.04	0.04	0.04	0.04	0.04	0.04
P_2O_5	0.19	0.14	0.19	0.13	0.14	0.12	0.14
LOI	5.60	3.05	8.20	2.88	2.55	2.46	3.64
Total	100.20	99.53	99.52	100.18	99.71	99.68	100.13
H_2O^+	3.95	2.62	6.28	2.64	2.04	2.16	1.10
H_2O^-	0.58	0.38	0.71	0.24	0.28	0.30	0.25
CO_2	<0.2	<0.2	<0.2	<0.2	<0.2	<0.2	<0.2
S (total)	0.51	0.08	0.05	0.05	0.36	0.18	2.50
Fe_2O_3/FeO	0.20	0.22	0.13	0.14	0.22	0.68	0.65
Density (g/cm^3)	2.49	2.70	2.49	2.40	2.59	2.73	2.82
Trace elements (ppm):							
La	5.9	5	5.6	14	4.4	3.2	3.6
Ce	17	11	18	31	14	11	12
Nd	13	9.6	15	14	11	9.6	11
Sm	3.9	3.5	5.3	2.8	3.8	3.5	3.6
Eu	1	0.98	1.5	1.5	1.1	1.1	1.1
Tb	1	0.88	1.3	0.44	1	0.93	0.95
Yb	3.6	3	4.7	1.5	3.1	3	3.3
Lu	0.56	0.46	0.72	0.23	0.51	0.49	0.52
Cr	160	260	270	52	230	202	230
Ni	101	97	90	34	82	76	78
Co	48	41	43	20	43	39	47
V	257	248	374	130	206	188	230
Cu	215	97	197	19	147	192	70
Pb	<5	<5	<5	<5	<5	<5	<5
Zn	150	121	142	89	91	145	98
Sn	2.9	2.6	3.1	2	2.4	2.2	5.3
Zr	110	99	130	93	100	98	94
Y	32	28	43	14	31	31	32
Nb	6.3	6.9	4.8	6.2	4.9	3.4	1.9
Rb	<1	<1	<1	<1	<1	<1	<1
Sr	88	110	74	140	120	120	110
Ba	56	28	54	42	52	34	47
Th	<1	ND	ND	ND	ND	ND	2.2

Table T19 (continued).

Leg	139	139	139	139	139	139	139
Hole	857D	857D	857D	857D	857D	857D	857D
Core, section	8R-1	9R-1	12R-1	12R-1	12R-2	16R-2	17R-1
Interval (cm)	5-7	23-25	25-27	106-108	17-19	59-60	45-48
Piece	1	4	5	14	3	Sediment	Sediment
Lab number	Z-962	Z-833	Z-834	Z-963	Z-964	Z-965	Z-966
Depth (mbsf)	647.35	657.13	686.15	686.96	687.57	726.0	734.35
Unit/Subunit	16B	16C	17A	17A	17A		
Major element oxides (wt%):							
SiO_2	46.48	43.65	42.17	38.42	48.56	62.70	59.95
TiO_2	1.18	2.45	1.56	1.45	1.42	0.57	0.89
Al_2O_3	16.22	12.91	19.44	17.71	14.28	12.07	15.76
Fe_2O_3	4.63	4.86	1.48	3.15	3.44	5.08	2.42
FeO	6.75	11.21	7.77	8.85	7.90	3.41	3.92
MnO	0.13	0.42	0.21	0.28	0.24	0.16	0.09
MgO	10.74	9.28	12.50	15.77	7.68	5.70	4.69
CaO	4.71	8.34	5.92	3.79	11.48	1.88	4.29
Na_2O	0.55	1.24	0.72	0.37	2.14	2.91	3.89
K_2O	0.02	0.04	0.02	0.03	0.05	0.06	0.06
P_2O_5	0.09	0.22	0.15	0.11	0.15	0.12	0.21
LOI	8.00	4.80	7.58	9.43	2.52	4.93	3.24
Total	99.50	99.42	99.52	99.36	99.86	99.59	99.41
H_2O^+	6.91	4.22	6.60	8.45	2.00	3.61	2.69
H_2O^-	0.49	0.41	0.62	0.80	0.35	0.37	0.22
CO_2	<0.10	<0.2	<0.2	<0.10	<0.2	<0.2	<0.10
S (total)	1.00	1.75	ND	0.16	0.71	1.83	<0.1
Fe_2O_3/FeO	0.69	0.43	0.19	0.36	0.44	1.49	0.62
Density (g/cm^3)	2.43	2.78	2.45	2.26	2.81	2.82	ND
Trace elements (ppm):							
La	3.7	6.2	3.6	4	3.7	16	25
Ce	9.5	20	11	11	11	35	48
Nd	8.5	16	9.7	10	9.6	14	23
Sm	2.8	5.4	3.5	4	4	3.3	4.6
Eu	0.7	2.2	0.95	1.7	1.4	0.57	1.2
Tb	0.78	1.4	1	1	1.2	0.57	0.66
Yb	2.8	4.7	3.6	3.5	3.9	1.6	2.2
Lu	0.47	0.7	0.58	0.54	0.62	0.24	0.36
Cr	372	52	405	445	80	47	265
Ni	140	50	177	185	54	32	108
Co	59	45	3.7	45	47	30	56
V	390	276	326	375	265	128	370
Cu	42	25	19	29	66	34	35
Pb	<5	<5	<5	<5	<5	<5	<5
Zn	175	230	168	60	100	123	125
Sn	4.1	4	2.6	5.3	2.0	2.2	3.2
Zr	64	150	89	87	100	140	138
Y	24	46	32	34	34	18	24
Nb	1.6	6.0	3.1	2.6	1.9	5	8.8
Rb	<1	<1	<1	<1	<1	1.5	<1
Sr	25	110	32	18	92	180	300
Ba	6	41	55	<5	49	61	6
Th	ND	ND	ND	ND	<1	4.8	ND

Table T19 (continued).

Leg	139	139	139	139	139	139	139
Hole	857D	857D	857D	857D	857D	857D	857D
Core, section	17R-3	18R-2	20R-1	21R-1	23R-1	24R-2	26R-1
Interval (cm)	72-74	84-85	64-66	59-61	57-59	4-7	58-60
Piece	11	9	8	6	10	1	6
Lab number	Z-967	Z-968	Z-969	Z-835	Z-970	Z-836	Z-972
Depth (mbsf)	737.62	745.94	763.14	772.79	792.07	802.74	820.88
Unit/Subunit	19	19	19	20A	20D	21	21
Major element oxides (wt%):							
SiO_2	49.02	47.15	46.14	49.61	48.46	47.48	48.82
TiO_2	2.10	1.75	1.10	1.57	1.40	1.51	1.20
Al_2O_3	13.16	14.70	12.82	14.17	15.22	15.82	15.56
Fe_2O_3	6.67	5.50	5.91	2.09	5.03	1.94	4.63
FeO	4.98	4.73	5.89	8.29	5.75	6.43	4.46
MnO	0.27	0.23	0.18	0.23	0.18	0.10	0.20
MgO	9.03	8.22	10.85	7.05	7.41	7.39	7.96
CaO	7.90	11.62	10.56	12.75	12.38	13.33	11.48
Na_2O	2.38	2.03	1.54	2.20	2.09	2.37	2.57
K_2O	0.04	0.04	0.04	0.05	0.04	0.05	0.06
P_2O_5	0.16	0.13	0.11	0.15	0.14	0.15	0.15
LOI	4.56	3.28	4.72	1.56	2.00	2.55	3.00
Total	100.27	99.38	99.86	99.72	100.10	99.12	100.09
H_2O^+	3.70	1.86	3.24	1.32	1.42	1.79	2.39
H_2O^-	0.62	0.18	0.62	0.18	0.19	0.24	0.29
CO_2	<0.2	<0.10	<0.2	<0.2	<0.2	<0.2	<0.2
S (total)		2.50	2.16	0.25	ND	0.15	1.05
Fe_2O_3/FeO	1.34	1.16	1.00	0.25	0.87	0.30	1.04
Density (g/cm^3)	2.63	3.07	2.77	2.88	2.83	2.78	2.82
Trace elements (ppm):							
La	4.7	4.7	3.2	3.9	4.3	5.7	5.3
Ce	14	12	9.3	12	12	16	13
Nd	12	10	8.4	9.6	10	12	10
Sm	4.1	3.4	2.8	3.3	3.2	3.6	3.1
Eu	1.4	1.2	0.82	1.1	1	1.1	1.1
Tb	1.1	0.84	0.78	0.94	0.87	0.88	0.83
Yb	4	3.3	2.8	2.9	3.1	3	2.6
Lu	0.65	0.53	0.43	0.47	0.5	0.44	0.43
Cr	90	77	295	192	180	207	205
Ni	53	47	165	72	69	70	57
Co	25	20	98	46	48	33	44
V	183	124	192	252	215	217	207
Cu	30	29	30	102	63	192	93
Pb	<5	<5	<5	<5	<5	5	<5
Zn	145	97	93	90	108	100	74
Sn	1.8	2.4	2.4	2.5	2.4	2.7	2.7
Zr	120	96	71	95	91	98	96
Y	38	33	22	30	27	25	27
Nb	4	4.1	2.8	3.7	4.7	6.1	4.3
Rb	1.6	<1	<1	<1	1	1.3	<1
Sr	140	120	86	120	120	180	160
Ba	47	23	40	46	54	44	56
Th	<1	ND	<1	ND	1.5	ND	1.9

Table T19 (continued).

Leg	139	139	139	139	139
Hole	857D	857D	857D	857D	857D
Core, section	29R-2	33R-1	35R-1	35R-1	36R-1
Interval (cm)	36-39	81-83	29-31	103-106	3-5
Piece	4	13	5	14A	1
Lab number	Z-973	Z-974	Z-975	Z-837	Z-976
Depth (mbsf)	850.26	888.61	907.49	908.23	916.93
Unit/Subunit	23A	24	25B	25B	25B
Major element oxides (wt%):					
SiO_2	48.40	48.48	45.90	47.89	46.98
TiO_2	1.75	2.10	2.40	1.85	2.40
Al_2O_3	14.58	13.58	13.34	13.10	13.29
Fe_2O_3	3.75	5.43	7.54	2.97	4.71
FeO	6.18	6.04	5.57	10.10	8.62
MnO	0.20	0.23	0.23	0.34	0.23
MgO	7.60	8.14	7.01	6.95	7.43
CaO	11.87	10.47	12.18	11.85	11.16
Na_2O	2.38	2.19	2.57	2.00	2.02
K_2O	0.05	0.03	0.03	0.03	0.03
P_2O_5	0.18	0.16	0.21	0.18	0.20
LOI	2.68	3.23	3.04	2.30	3.00
Total	99.62	100.08	100.02	99.56	100.07
H_2O^+	2.02	2.81	2.24	2.02	2.03
H_2O^-	0.22	0.24	0.14	0.24	0.29
CO_2	<0.2	<0.2	<0.2	<0.2	<0.2
S (total)	0.64	0.09	2.23	ND	0.46
Fe_2O_3/FeO	0.61	0.90	1.35	0.29	0.55
Density (g/cm^3)	2.79	2.78	2.91	2.89	2.85
Trace elements (ppm):					
La	5.3	4.2	4.8	4.5	4.8
Ce	15	13	15	13	14
Nd	12	11	13	12	13
Sm	3.9	3.9	4.6	4.2	4.5
Eu	1.3	1.5	1.4	1.5	1.4
Tb	1.1	1.1	1.4	1.1	1.2
Yb	3.6	3.9	4.6	4.3	4.4
Lu	0.56	0.59	0.71	0.71	0.68
Cr	82	155	180	170	165
Ni	52	72	84	90	72
Co	33	33	56	50	50
V	210	227	290	292	265
Cu	77	80	60	66	72
Pb	<5	<5	<5	<5	<5
Zn	87	127	108	155	127
Sn	1.7	1.7	2.4	3.3	2.3
Zr	120	110	130	130	120
Y	33	37	39	43	42
Nb	4.9	4.9	3.2	5.4	3.5
Rb	1.1	<1	<1	<1	<1
Sr	140	130	140	87	88
Ba	60	53	21	35	24
Th	1.0	<1	<1	ND	<1

Table T20. Composition of basalts from Holes 858F and 858G, Leg 139 (Middle Valley, Juan de Fuca Ridge, Pacific Ocean).

Leg	139	139	139	139	139	139	139	139
Hole	858F	858F	858F	858F	858G	858G	858G	858G
Core, section	26R-1	27R-1	28R-1	29R-1	1R-1	4R-1	7R-1	14R-1
Interval (cm)	93-95	25-27	43-45	39-41	14-16	35-37	32-34	10-12
Piece	11	6	8	8	2	9	6	2
Lab number	Z-977	Z-978	Z-979	Z-980	Z-981	Z-982	Z-983	Z-984
Depth (mbsf)	259.53	268.05	277.93	287.59	276.94	306.15	335.12	403.7
Unit/Subunit	1B	1C	1C	1C	1C	2A	2B	6
Major element oxides (wt%):								
SiO_2	48.40	48.20	47.48	48.39	48.79	47.19	46.91	48.57
TiO_2	1.88	1.82	1.63	1.41	1.72	1.56	1.75	1.60
Al_2O_3	14.92	15.66	15.65	15.26	15.81	16.46	15.57	15.00
Fe_2O_3	4.03	4.64	4.29	3.07	0.22	2.36	2.96	1.93
FeO	4.66	3.39	4.23	5.86	6.93	6.61	5.61	6.44
MnO	0.08	0.11	0.08	0.10	0.17	0.16	0.24	0.23
MgO	7.97	7.45	7.81	8.73	8.26	7.14	7.32	9.27
CaO	11.88	11.82	12.20	11.67	10.26	13.14	13.06	10.95
Na_2O	2.73	2.82	2.92	3.03	3.82	2.78	2.73	3.60
K_2O	0.08	0.05	0.06	0.06	0.04	0.05	0.05	0.08
P_2O_5	0.17	0.17	0.15	0.17	0.18	0.19	0.18	0.18
LOI	2.87	3.39	2.96	2.48	3.40	2.59	3.77	2.39
Total	99.67	99.52	99.46	100.23	99.60	100.23	100.15	100. 24
H_2O^+	1.98	2.66	2.26	2.21	2.89	1.50	2.33	2.17
H_2O^-	0.61	0.68	0.56	0.27	0.37	0.47	0.60	0.22
CO_2	<0.2	<0.2	<0.2	<0.2	<0.1	<0.1	<0.1	<0.1
S (total)	ND	ND	0.10	0.18	ND	ND	0.13	ND
Fe_2O_3/FeO	0.86	1.37	1.01	0.52	0.03	0.36	0.53	0.30
Density g/cm^3)	1.85	1.94	2.81	2.92	2.67	2.75	2.70	2.63
Trace elements (ppm):								
La	5.5	5.5	6	5.5	5.3	5.9	5.7	4.8
Ce	16	17	17	16	16	18	17	16
Nd	11	12	12	12	12	13	13	13
Sm	3.7	3.7	3.7	3.6	3.9	4.1	4.2	4.1
Eu	1.4	1.3	1.3	1.2	1.3	1.5	1.3	1.3
Tb	0.87	0.97	0.93	0.93	0.94	1.0	1.0	1.1
Yb	3	3	2.8	2.9	3	3.1	3.1	3.3
Lu	0.46	0.44	0.43	0.46	0.46	0.47	0.47	0.49
Cr	225	230	215	210	260	250	200	235
Ni	64	65	63	54	66	70	62	64
Co	29	28	32	29	38	47	34	32
V	170	181	177	184	237	205	172	195
Cu	70	66	70	50	77	66	72	170
Pb	<5	<5	<5	<5	<5	<5	<5	<5
Zn	73	74	74	52	73	75	87	81
Sn	1.7	2.1	1.6	1.8	1.7	2.1	1.5	1.6
Zr	120	130	130	120	130	120	120	130
Y	29	28	27	29	29	29	28	30
Nb	4.7	4.3	4.5	4.6	4.5	4.2	4	4.4
Rb	1.1	1.2	1.3	<1	<1	<1	<1	<1
Sr	190	190	200	200	200	200	180	180
Ba	61	38	51	52	52	35	47	48
Th	1.1	1.0	<1	<1	1.5	1.3	1.2	<1

Note: ND = not determined.

Table T21. Composition of basalts from Hole 1037B, Leg 169 (Escanaba Trough, Gorda Ridge, Pacific Ocean). (Continued on next page.)

Leg	169	169	169	169	169	169	169
Hole	1037B	1037B	1037B	1037B	1037B	1037B	1037B
Core, section	57R-1	58R-1	58R-2	59R-1	60R-1	60R-1	61R-1
Interval (cm)	32-37	100-104	0-5	65-68	90-95	120-124	7-10
Piece	8A	7C	1	10	11A	11C	1A
Lab number	Z-1605	Z-1606	Z-1607	Z-1608	Z-1609	Z-1610	Z-1611
Depth (mbsf)	508.12	518.30	518.70	527.45	530.30	530.60	533.97
Major element oxides (wt%):							
SiO_2	48.26	47.32	48.26	48.70	48.10	48.06	48.00
TiO_2	1.94	1.62	2.03	2.20	1.93	1.99	1.96
Al_2O_3	13.68	14.41	13.52	13.10	14.26	14.37	14.59
Fe_2O_3	4.44	4.17	4.69	5.33	4.64	3.37	4.47
FeO	7.98	7.19	7.19	7.54	7.04	7.33	6.90
MnO	0.19	0.15	0.19	0.20	0.20	0.20	0.19
MgO	8.04	9.62	8.04	6.91	8.00	8.22	7.55
CaO	10.25	9.30	9.69	10.36	10.30	10.53	10.36
Na_2O	2.75	2.84	3.36	3.25	2.92	2.77	2.87
K_2O	0.24	0.93	0.58	0.21	0.26	0.30	0.17
P_2O_5	0.20	0.16	0.20	0.22	0.19	0.20	0.18
LOI	1.89	1.90	1.72	1.28	1.57	2.07	2.00
Total	99.86	99.61	99.47	99.30	99.41	99.41	99.24
H_2O^+	0.91	1.00	0.75	0.23	0.30	0.38	0.56
H_2O^-	0.68	0.53	0.51	0.73	0.97	1.24	0.88
CO_2	<0.2	0.27	0.32	0.2	0.23	0.22	0.21
S (total)	0.1	<0.1	<0.1	0.11	<0.1	<0.1	<0.1
Fe_2O_3/FeO	0.56	0.58	0.65	0.71	0.66	0.46	0.65
Density (g/cm^3)	2.91	2.88	2.92	2.95	2.85	2.86	2.91
Trace elements (ppm):							
La	6.7	5.1	6.2	6.7	6.1	6.4	6.3
Ce	17	15	19	21	19	18	20
Nd	14	12	15	17	16	15	16
Sm	4.7	3.9	4.9	5.5	5.3	5.3	5.3
Eu	1.6	1.2	1.5	1.5	1.6	1.6	1.6
Tb	1.4	1.1	1.4	1.7	1.5	1.4	1.4
Yb	4.4	3.6	4.4	5.0	4.6	4.4	4.4
Lu	0.6	0.49	0.63	0.65	0.67	0.63	0.61
Cr	205	208	228	242	242	213	217
Ni	103	163	92	72	90	94	83
Co	44	47	40	46	47	50	47
V	267	254	275	360	340	340	270
Cu	43	20	54	70	43	82	47
Zn	93	66	76	70	86	86	84
Zr	140	110	140	150	130	140	140
Y	40	34	43	45	41	44	42
Nb	5.9	4.9	6.5	6.7	5.3	6	5.5
Rb	7	27	18	4.4	6.4	6.9	3.6
Sr	110	120	120	120	120	120	120
Ba	22	110	94	42	21	35	64

Table T21 (continued).

Leg	169	169
Hole	1037B	1037B
Core, section	62R-1	62R-3
Interval (cm)	13-17	52-56
Piece	2	4
Lab number	Z-1612	Z-1613
Depth (mbsf)	538.13	541.24
Major element oxides (wt%):		
SiO_2	48.58	49.52
TiO_2	2.16	2.10
Al_2O_3	14.06	13.25
Fe_2O_3	3.41	4.82
FeO	7.62	7.14
MnO	0.21	0.19
MgO	8.24	6.72
CaO	10.70	11.63
Na_2O	2.85	2.74
K_2O	0.22	0.19
P_2O_5	0.21	0.18
LOI	1.65	1.33
Total	99.91	99.81
H_2O^+	0.50	0.18
H_2O^-	0.73	0.55
CO_2	0.22	<0.2
S (total)	0.12	0.14
Fe_2O_3/FeO	0.45	0.68
Density (g/cm^3)	2.95	2.91
Trace elements (ppm):		
La	6.2	6
Ce	20	22
Nd	16	16
Sm	5.1	5.2
Eu	1.6	1.6
Tb	1.5	1.5
Yb	4.4	4.6
Lu	0.64	0.66
Cr	242	268
Ni	64	63
Co	48	48
V	362	385
Cu	63	79
Zn	119	90
Zr	140	120
Y	45	41
Nb	5.2	5.6
Rb	4.2	6.1
Sr	120	120
Ba	38	36

Table T22. Composition of basalts from Hole 1038I, Leg 169 (Escanaba Trough, Gorda Ridge, Pacific Ocean).

Leg	169
Hole	1038I
Core, section	43X-3
Interval (cm)	3-7
Piece	2
Lab number	Z-1614
Depth (mbsf)	403.23
Major element oxides (wt%):	
SiO_2	48.52
TiO_2	1.39
Al_2O_3	15.72
Fe_2O_3	2.84
FeO	6.28
MnO	0.14
MgO	7.80
CaO	11.76
Na_2O	2.54
K_2O	0.12
P_2O_5	0.15
LOI	2.24
Total	99.50
H_2O^+	0.67
H_2O^-	0.89
CO_2	0.41
S (total)	<0.1
Fe_2O_3/FeO	0.45
Density (g/cm^3)	2.89
Trace elements (ppm):	
La	5.6
Ce	17
Nd	11
Sm	3.4
Eu	1.2
Tb	0.8
Yb	2.8
Lu	0.4
Cr	300
Ni	86
Co	44
V	245
Cu	66
Zn	77
Sn	ND
Zr	98
Y	28
Nb	6.5
Rb	2.2
Sr	170
Ba	160

Note: ND = not determined.

Table T23. Characteristics of holes drilled at Gulf of California (Leg 64, Hole 477 and Leg 65, Holes 483 and 485), off south California (Leg 63, Hole 469), and Baja California (Leg 63, Holes 471 and 473).

Hole	Latitude	Longitude	Water depth (m)	Oldest sediment cored	Basement penetration (m)	Basement recovery (m)
469	32°37.00'N	120°32.90'W	453.5	Metalliferous nannofossil chalk Upper lower Miocene (16.5-17.5 m.y.)	85.0 (368.5-453.5 mbsf)	31.5
471	23°28.93'N	112°29.78'W	3101	Metalliferous sediment Middle Miocene (14.5-15 m.y.)	81.5 (741.5-823 mbsf)	30
473	20°57.92'N	107°03.81'W	3249	Siltstone, silty sand Upper Miocene (6-6.5 m.y.)	39.4 (248.1-287.5 mbsf)	18.72
477	27°01.85'N	111°24.02'W	2003	Claystone Holocene/late Quaternary	47.5 (58.0-105.5 mbsf)	12.30
483B	22°52.99'N	108°44.84'W	3070	Clay (2.4 m.y.)	157.0 (110.0-267.0 mbsf)	84.27
485A	22°44.92'N	107°54.23'W	2981	Mudstone (0.85 m.y.)	177.5 (153.5-331.0 mbsf)	93.91

Table T24. Composition of basalts from Hole 477, Leg 64 (Guaymas Basin, Gulf of California, Pacific Ocean). (Continued on next page.)

Leg	64	64	64	64	64	64	64
Hole	477	477	477	477	477	477	477
Core, section	9R-1	11R-2	12R-1	12R-2	12R-3	12R-4	12R-4
Interval (cm)	57-59	61-63	49-52	70-73	39-42	6-9	76-80
Piece	10	5	4	3C	3C	1A	1E
Lab number	Z-1254	Z-1255	Z-1256	Z-1257	Z-1258	Z-1259	Z-1260
Depth (mbsf)	60.57	79.11	86.99	88.7	89.69	90.86	91.56
Major element oxides (wt%):							
SiO_2	49.14	47.83	47.99	47.47	47.71	47.78	47.55
TiO_2	2.03	1.42	1.44	1.48	1.43	1.53	1.49
Al_2O_3	15.33	17.65	16.98	16.90	16.82	16.24	16.54
Fe_2O_3	3.37	3.44	4.02	4.20	3.60	4.55	3.25
FeO	7.00	5.50	5.31	5.32	5.67	5.32	6.00
MnO	0.17	0.14	0.15	0.15	0.14	0.16	0.16
MgO	6.81	8.88	8.57	8.42	9.33	8.91	10.00
CaO	11.54	10.96	11.34	11.42	10.77	10.89	10.50
Na_2O	3.26	2.70	2.75	2.85	2.83	2.90	2.77
K_2O	0.17	0.12	0.14	0.14	0.14	0.15	0.15
P_2O_5	0.19	0.12	0.13	0.14	0.15	0.15	0.15
LOI	0.97	1.29	1.17	0.92	1.22	1.39	1.57
Total	99.98	100.05	99.99	99.41	99.81	99.97	100.13
H_2O^+	0.13	0.61	0.20	0.43	0.33	0.42	0.62
H_2O^-	0.35	0.38	0.38	0.47	0.60	0.49	0.48
CO_2	<0.20	<0.20	<0.20	<0.20	<0.20	<0.20	<0.20
S (total)	0.14	<0.1	<0.1	0.10	<0.1	0.11	<0.1
Fe_2O_3/FeO	0.48	0.63	0.76	0.79	0.64	0.86	0.54
Density (g/cm^3)	2.47	2.67	2.62	2.77	2.70	2.87	2.70
Trace elements (ppm):							
La	7.10*	5.28*	3.86*				5.07*
Ce	23.40	15.20	11.30				11.3
Nd	19.10	12.50	ND				ND
Sm	ND	4.01	ND				ND
Eu	2.19	1.41	0.94				1.32
Tb	1.18	0.82	0.62				0.68
Yb	4.31	2.67	ND				ND
Lu	0.66	0.43	ND				ND
Cr	242	242	270	258	280	270	249
Ni	58	137	137	137	150	139	137
Co	50	50	52	52	56	57	56
V	261	190	210	215	215	225	202
Cu	79	70	66	66	61	66	70
Zn	96	96	94	91	79	79	90
Zr	140	96	96	110	100	110	110
Y	34	21	24	25	23	24	27
Nb	4.8	3.1	3.1	4.1	3.5	4.2	4.4
Rb	<1	1.3	1	1.8	2.1	1.1	1.2
Sr	230	230	220	230	220	220	210
Ba	110	37	84	52	25	22	59

Note: * = rare earth element data from Saunders et al. (1982). ND = not determined.

Table T24 (continued).

Leg	64	64	64	64
Hole	477	477	477	477
Core, section	12R-5	13R-1	13R-2	13R-2
Interval (cm)	46-50	53-62	13-17	146-150
Piece	1H	3H	3	8
Lab number	Z-1261	Z-1262	Z-1263	Z-1264
Depth (mbsf)	92.76	96.53	97.48	98.81
Major element oxides (wt%):				
SiO_2	47.53	47.78	47.42	48.00
TiO_2	1.54	1.68	1.59	1.62
Al_2O_3	17.48	16.02	16.91	16.27
Fe_2O_3	2.95	4.55	4.23	5.30
FeO	5.56	6.47	6.18	5.46
MnO	0.15	0.16	0.15	0.15
MgO	7.41	8.08	8.00	8.36
CaO	11.36	11.20	11.31	11.24
Na_2O	2.87	2.88	2.90	2.97
K_2O	0.15	0.17	0.18	0.16
P_2O_5	0.16	0.15	0.16	0.16
LOI	2.45	1.00	0.84	0.39
Total	99.61	100.14	99.87	100.08
H_2O^+	0.79	0.10	0.10	0.10
H_2O^-	1.06	0.65	0.34	0.39
CO_2	<0.20	<0.20	0.20	<0.2
S (total)	<0.1	<0.1	<0.1	<0.1
Fe_2O_3/FeO	0.53	0.7	0.68	0.97
Density (g/cm^3)	2.69	2.92	2.92	2.93
Trace elements (ppm):				
La	4.79*			4.63*
Ce	10.8			12.6
Nd	ND			ND
Sm	ND			ND
Eu	1.28			1.00
Tb	0.60			0.74
Yb	ND			ND
Lu	ND			ND
Cr	240	285	265	272
Ni	82	90	83	77
Co	50	50	52	47
V	217	235	212	237
Cu	73	79	77	77
Zn	80	84	84	79
Zr	120	120	120	120
Y	27	28	26	25
Nb	4.4	4.7	4.7	5
Rb	1.3	<1	1.3	1.9
Sr	240	230	230	230
Ba	75	45	64	86

Table T25. Secondary minerals in fine fraction sampled from igneous rocks: off southern California and Baja California (Leg 63) and Gulf of California (Legs 64 and 65), X-ray diffraction data. (Continued on next page.)

Core, section, interval (cm)	Depth (mbsf)	Sm	Cor	Mixed-layer chlorite-smectite	Chl	Illite	Quartz	Amph	Talc	Calcite
63-469-										
40R-1, 30-32	368.80	+++			+		+			
42R-1, 117-120	379.17	+++					+	+		
42R-5, 112-115	385.12	+++								
44R-1, 3-8	396.03	+++								
46R-1, 134-138	411.34	+++								
48R-1, 22-28	423.22	+++								
48R-1, 49-53	423.49	+++					+			
50R-2, 27-32	441.77	+++								
51R-1, 34-40	450.34	+++					+			
63-471-										
80R-1, 135-140	751.85		+++	+			++			+
82R-1, 127-132	770.27		+++	++						
82R-2, 15-18	770.65		+++	+++			+			
84R-1, 9-16	787.09	+++			+		+			
84R-1, 107-114	788.07	+++			+		+			
87R-2, 19-26	808.69	+++			+		+			
63-473-										
29R-1, 85-90	248.35	+++					+			
32R-2, 133-140	266.83	+++					+			
64-477-										
9R-1, 57-59	60.57	+++			++		+	+		
11R-2, 61-63	79.11	+++			++		+	++	++	
12R-1, 49-52	86.99	+++			++		+	++	++	
12R-2, 70-73	88.70	+++			++		+	++	++	
12R-3, 39-42	89.69	+++		+	++		+	++	++	
12R-4, 6-9	90.86	+++			++		+	+	++	
12R-4, 76-80	91.56	+++			++		+	+	++	
12R-5, 46-50	92.76	+++			+		+		+	
13R-1, 53-55	96.53	+++			+		+			
13R-2, 13-17	97.48	+++			+		+		+	
13R-2, 146-150	98.81	+++			+		+		+	
65-483B-										
32R-1, 1-6	262.51	+++			+		+			
32R-1, 27-31	262.77	+++			+		+			
32R-1, 44-50	262.94	+++			+		+			
32R-1, 70-74	263.20	+++			+		+			
32R-1, 90-94	263.40	+++			+					
32R-2, 95-100	264.95	+++			+		+			
32R-2, 116-123	265.16	+++					+			
32R-2, 135-141	265.35	+++			+		+			
65-485A-										
11R-3, 56-58	149.01	+++								+
11R-3, 82-84	149.27	+++							+	+
12R-1, 62-64	155.62	+++								+

Table T25 (continued).

Core, section, interval (cm)	Depth (mbsf)	Sm	Cor	Mixed-layer chlorite-smectite	Chl	Illite	Quartz	Amph	Talc	Calcite
14R-1, 56-60	160.06	+++							+	+
17R-1, 80-83	181.30	+++								
17R-1, 114-115	181.64	+++							+	
23R-1, 55-56	212.05	+++			+			+	+	+
24R-1, 71-73	216.71	+++							+	
24R-1, 86-88	216.86	+++			+				+	
25R-2, 110-112	223.60	++			+++				+	
25R-3, 12-14	224.12	++			+++				+	
26R-1, 16-18	226.16	+++			+				+	+
29R-2, 120-122	242.20	+++		+			+	+	+	
30R-3, 55-57	253.05	+++			+				+	
30R-3, 139-140	253.89	+++			+					
31R-2, 36-37	256.29	+++				+		+		
31R-2, 85-88	256.78	+++				+		+	+	
33R-1, 135-136	269.35	+++			+	+		+	+	
33R-2, 85-87	270.35	+++			+	+		+	+	+
38R-2, 1-4	314.51	+++		+					+	
38R-2, 36-37	314.76	+++		+				+	+	+
39R-5, 2-6	328.02	+++			+				+	
39R-5, 9-11	328.07	+++			+					+

Notes: +++ = dominant, ++ = minor, + = trace.
Sm = smectites, Cor = corrensite, Chl = chlorite, Amph = amphibole.

Table T26. Composition of basalts from Hole 483B, Leg 65 (Gulf of California, Pacific Ocean).

Leg	65	65	65	65	65	65	65	65
Hole	483B	483B	483B	483B	483B	483B	483B	483B
Core, section	32R-1	32R-1	32R-1	32R-1	32R-1	32R-2	32R-2	32R-2
Interval (cm)	1-6	27-31	44-50	70-74	90-94	95-100	116-123	135-141
Piece	1	2B	2D	2F	3	4A	4C	6A
Lab number	Z-1275	Z-1276	Z-1277	Z-1278	Z-1279	Z-1280	Z-1281	Z-1282
Depth (mbsf)	262.51	262.77	262.94	263.2	263.4	264.95	265.16	265.35
Major element oxides (wt%):								
SiO_2	48.30	48.44	47.94	48.08	48.40	48.78	47.10	48.04
TiO_2	1.65	1.63	1.66	1.65	1.68	1.67	1.63	1.65
Al_2O_3	13.70	14.50	13.75	13.87	14.11	14.20	13.62	13.61
Fe_2O_3	6.80	6.21	6.27	5.50	6.41	6.09	8.77	6.15
FeO	5.60	4.96	6.29	6.11	5.46	5.57	4.89	6.04
MnO	0.21	0.17	0.18	0.23	0.21	0.21	0.19	0.20
MgO	8.69	7.88	8.00	8.97	8.44	8.44	8.16	8.73
CaO	11.17	11.48	11.76	11.46	10.89	10.89	10.75	11.42
Na_2O	2.60	2.56	2.57	2.51	2.71	2.62	2.58	2.53
K_2O	0.17	0.05	0.05	0.08	0.11	0.15	0.29	0.05
P_2O_5	0.13	0.12	0.12	0.13	0.14	0.14	0.13	0.12
LOI	1.05	2.10	1.38	1.39	1.48	1.22	1.67	1.21
Total	100.07	100.10	99.97	99.98	100.04	99.98	99.78	99.75
H_2O^+	0.30	0.45	0.30	0.29	0.28	<0.1	0.48	0.20
H_2O^-	0.75	1.45	1.08	0.80	1.00	1.02	1.15	1.01
CO_2	<0.2	0.20	<0.2	0.30	0.20	<0.2	<0.2	<0.2
Fe_2O_3/FeO	1.21	1.25	1.00	0.90	1.17	1.09	1.79	1.02
Density (g/cm^3)	2.94	2.95	2.98	3.05	2.90	3.06	2.97	3.00
Trace elements (ppm):								
La				3.6				
Ce				11				
Nd				10				
Sm				3.8				
Eu				1.3				
Tb				1.1				
Yb				3.5				
Lu				0.58				
Cr	322	320	350	328	310	288	306	248
Ni	140	92	94	99	140	85	97	145
Co	57	58	61	54	56	49	51	61
V	397	390	412	375	385	370	390	415
Cu	87	77	70	66	79	79	79	73
Zn	101	112	86	100	105	90	96	90
Zr	98	99	97	100	100	100	97	96
Y	35	34	31	32	35	35	31	33
Nb	3.1	3.4	2.8	3.3	3.3	3.8	1.9	2.3
Rb	2.9	<1	<1	1.1	1.3	2.7	6.1	<1
Sr	110	110	110	110	120	120	110	110
Ba	50	42	46	22	28	65	63	9

Table T27. Composition of basalts from Hole 485A, Leg 65 (Gulf of California, Pacific Ocean). (Continued on next two pages.)

Leg	65	65	65	65	65	65	65
Hole	485A	485A	485A	485A	485A	485A	485A
Core, section	11R-3	11R-3	12R-1	14R-1	17R-1	17R-1	23R-1
Interval (cm)	56-58	82-84	62-64	56-60	80-83	114-115	55-56
Piece	1A	1B	4A	1F	5	6C	4A
Lab number	Z-1283	Z-1284	Z-1285	Z-1286	Z-1287	Z-1288	Z-1289
Depth (mbsf)	149.01	149.27	155.62	160.06	181.30	181.64	212.05
Major element oxides (wt%):							
SiO_2	47.47	48.18	49.00	50.07	49.86	48.70	49.73
TiO_2	1.64	1.32	2.23	2.02	2.13	2.50	2.23
Al_2O_3	16.57	15.84	13.70	13.79	14.53	13.80	13.78
Fe_2O_3	5.20	2.17	3.16	2.22	4.69	4.11	4.31
FeO	3.87	7.31	9.95	9.40	6.57	7.65	7.24
MnO	0.11	0.15	0.22	0.21	0.16	0.17	0.18
MgO	6.18	9.86	8.11	8.10	8.00	7.25	7.47
CaO	11.60	11.29	10.61	10.64	9.95	10.79	11.07
Na_2O	2.30	2.38	1.78	1.98	2.19	1.76	2.32
K_2O	0.10	0.11	0.05	0.05	0.07	0.10	0.12
P_2O_5	0.32	0.27	0.42	0.45	0.34	0.40	0.36
H_2O^+	1.56	0.78	0.47	0.42	1.39	1.20	0.68
CO_2	3.12	ND	ND	ND	ND	0.81	ND
LOI							
Total	100.04	99.66	99.70	99.35	99.88	99.24	99.49
H_2O^+							
H_2O^-							
CO_2							
Fe_2O_3/FeO	1.34	0.30	0.32	0.24	0.71	0.54	0.6
Density (g/cm^3)	2.81	2.91	3.12	3.09	2.94	2.99	3.01
Trace elements (ppm):							
La							
Ce							
Nd							
Sm							
Eu							
Tb							
Yb							
Lu							
Sc	42	51	67	33	45	46	40
Cr	520	190	135	98	92	67	160
Ni	280	150	84	100	160	76	110
Co	51	37	46	50	47	30	47
V	260	230	350	320	350	210	350
Cu	91	105	117	105	120	55	105
Pb	ND	21	23	22	not	not	8
Zn	ND	120	210	240	220	170	170
Sn	3	2.5	3	3	3	2	3
Zr	94	90	130	130	150	140	140
Y	32	30	45	45	49	46	46
Nb	2.9	1.4	2.2	1.8	2.6	3.2	2.6
Rb	<1	<1	<1	<1	<1	<1	1
Sr	160	130	82	97	100	98	110
Ba	60	70	80	74	65	48	70

ND = not determined.

Table T27 (continued).

Leg	65	65	65	65	65	65	65
Hole	485A	485A	485A	485A	485A	485A	485A
Core, section	24R-1	24R-1	26R-1	29R-2	30R-3	31R-2	31R-2
Interval (cm)	71-73	86-88	16-18	120-122	139-140	36-37	85-88
Piece	1D	1E	1B	3G	1P	1P	1G
Lab number	Z-1290	Z-1291	Z-1292	Z-1293	Z-1294	Z-1295	Z-1296
Depth (mbsf)	216.71	216.86	226.16	242.20	253.89	256.29	256.78
Major element oxides (wt%):							
SiO_2	48.16	49.58	48.78	46.52	49.33	48.09	48.98
TiO_2	2.15	2.11	2.20	2.31	2.27	2.40	1.57
Al_2O_3	14.58	15.69	14.05	15.16	16.14	14.84	14.30
Fe_2O_3	5.37	5.28	5.10	6.08	4.18	7.75	4.11
FeO	6.65	5.00	7.41	6.89	6.41	6.52	8.69
MnO	0.19	0.17	0.20	0.20	0.16	0.22	0.19
MgO	8.12	8.40	7.76	9.18	7.46	7.19	8.98
CaO	10.45	10.05	10.76	10.25	9.93	9.09	9.57
Na_2O	2.59	2.00	1.73	1.73	2.00	2.10	1.72
K_2O	0.09	0.05	0.10	0.13	0.05	0.20	0.09
P_2O_5	0.19	0.28	0.39	0.35	0.39	0.35	0.40
H_2O^+		1.00	0.67	1.08	1.42	1.27	1.06
CO_2		ND	ND	ND	ND	ND	ND
LOI	1.40						
Total	99.94	99.61	99.15	99.88	99.74	100.02	99.66
H_2O^+	0.68						
H_2O^-	0.70						
CO_2	<0.2						
Fe_2O_3/FeO	0.81	1.06	0.69	0.88	0.65	1.19	0.47
Density (g/cm^3)	2.90	2.96	3.02	2.90	2.97	2.87	3.04
Trace elements (ppm):							
La							
Ce							
Nd							
Sm							
Eu							
Tb							
Yb							
Lu							
Sc		40	50	50	21		65
Cr	220*	120	120	124	102	250*	200
Ni	96	120	110	81	88	88	115
Co	46	57	47	40	47	46	43
V	410	320	380	220	330	380	400
Cu		74	120	105	57		125
Pb		8	8	9	34		ND
Zn		186	230	145	170		ND
Sn		4	4	2	5		5
Zr	140	130	140	140	100	110	150
Y	43	41	47	46	36	39	50
Nb	3.3	2.6	3.2	2.3	2.9	1.6	3.1
Rb	<1	<1	<1	2.5	1.8	3.1	3
Sr	110	110	100	94	91	96	94
Ba	48	73	100	78	96	120	40

Table T27 (continued).

Leg	65	65	65	65
Hole	485A	485A	485A	485A
Core, section	33R-1	33R-2	38R-2	39R-5
Interval (cm)	135-136	85-87	36-37	2-6
Piece	1K	1I	6A	1
Lab number	Z-1297	Z-1298	Z-1299	Z-1300
Depth (mbsf)	269.35	270.35	314.76	328.02
Major element oxides (wt%):				
SiO_2	48.51	47.89	49.22	48.53
TiO_2	1.51	2.04	2.11	1.72
Al_2O_3	13.84	13.82	16.13	14.54
Fe_2O_3	5.31	4.09	4.69	3.86
FeO	5.62	8.51	5.08	6.88
MnO	0.16	0.19	0.11	0.15
MgO	8.72	8.94	7.78	8.74
CaO	11.90	10.34	8.98	11.50
Na_2O	1.74	1.92	2.19	1.78
K_2O	0.13	0.20	0.10	0.07
P_2O_5	0.43	0.53	0.36	0.43
H_2O^+	1.79	1.71	2.75	1.40
CO_2	ND	ND	ND	ND
LOI				
Total	99.66	100.18	99.50	99.60
H_2O^+				
H_2O^-				
CO_2				
Fe_2O_3/FeO	0.95	0.48	0.92	0.56
Density (g/cm^3)	2.97	3.08	2.66	2.86
Trace elements (ppm):				
La			3.5	
Ce			12	
Nd			11	
Sm			4.2	
Eu			1.3	
Tb			1.0	
Yb			3.8	
Lu			0.61	
Sc		32	44	
Cr	200*	170	220	220*
Ni	78	170	130	83
Co	46	58	57	45
V	380	330	470	340
Cu		100	106	
Pb		38	8	
Zn		210	148	
Sn		4	3	
Zr	140	140	120	110
Y	48	44	34	38
Nb	2.1	2.6	2.2	2.5
Rb	4.2	3.5	3.1	<1
Sr	94	90	120	100
Ba	38	62	85	90

Table T28. Composition of basalts from Hole 473, Leg 63 (off southern California, Pacific Ocean).

Leg	63	63	63	63	63	63
Hole	473	473	473	473	473	473
Core, section	29R-1	30R-2	32R-2	32R-3	34R-1	34R-3
Interval (cm)	85-90	126-134	133-140	51-57	0-6	0-6
Piece	6D	3A	5L	1F	1A	1A
Lab number	Z-1245	Z-1246	Z-1247	Z-1248	Z-1730	Z-1731
Depth (mbsf)	248.35	254.76	268.83	269.51	284.00	287.00
Major element oxides (wt%):						
SiO_2	50.27*	50.01*	48.31*	49.53*	49.18*	49.49*
TiO_2	1.66	1.62	1.79	1.87	1.95	1.96
Al_2O_3	16.20	15.87	14.02	14.32	13.81	14.08
Fe_2O_3	3.83	3.85	5.41	3.80	3.16	3.42
FeO	5.14	5.14	6.05	7.77	8.94	8.89
MnO	0.11	0.11	0.13	0.15	0.18	0.18
MgO	6.74	7.18	9.15	7.38	7.80	6.90
CaO	11.00	11.50	7.67	11.24	11.13	11.25
Na_2O	3.30	3.00	2.85	2.58	2.58	2.70
K_2O	0.13	0.13	0.20	0.20	0.20	0.20
P_2O_5	0.09	0.11	0.05	0.15	0.17	0.23
H_2O^+	0.61	0.58	2.14	0.50	0.42	0.36
H_2O^-	1.02	0.99	2.31	0.73	0.68	0.71
CO_2	ND	ND	ND	ND	ND	ND
Total	100.10	100.09	100.08	100.22	100.20	100.37
Fe_2O_3/FeO	0.75	0.75	0.89	0.49	0.53	0.39
Density (g/cm^3)	2.717**	2.84	2.636**	2.99	2.961**	2.948**
Trace elements (ppm):						
Cr	250	238	240	226		
Ni	68	68	70	68		
Co	58	53	58	54		
V	372	350	365	350		
Cu	73	76	60	58		
Zn	90	86	81	93		
Zr	100	94	110	110		
Y	29	28	36	38		
Nb	3.3	3.7	4.6	4.8		
Rb	<1	<1	1.1	1.3		
Sr	150	140	105	105		
Ba	<5	13	26	33		

Note: * = major element data from Grechin et al. (1981). ** = density from Grechin et al. (1981). ND = not determined.

Table T29. Composition of basalts from Hole 469, Leg 63 (Baja California, Pacific Ocean). (Continued on next page.)

Leg	63	63	63	63	63	63	63
Hole	469	469	469	469	469	469	469
Core, section	40R-1	41R-1	42R-1	42R-5	44R-1	46R-1	47R-3
Interval (cm)	30-32	7-10	117-120	112-115	3-8	134-138	86-92
Piece	1A	1A	1D	1C	1B	11	4
Lab number	Z-1229	Z-1723	Z-1230	Z-1231	Z-1232	Z-1233	Z-1724
Depth (mbsf)	368.80	371.57	379.17	385.12	396.03	411.34	417.86
Major element oxides (wt%):							
SiO_2	50.56*	51.79*	52.75*	50.88*	46.86*	47.09*	47.74*
TiO_2	1.23	1.26	1.31	1.20	1.88	2.19	2.10
Al_2O_3	15.83	16.31	16.22	16.36	13.91	14.69	13.52
Fe_2O_3	5.22	4.78	5.85	5.12	9.11	12.67	9.99
FeO	2.82	3.86	2.68	4.56	4.67	3.16	5.05
MnO	0.21	0.10	0.12	0.12	0.21	0.14	0.22
MgO	7.47	6.91	6.67	7.31	7.34	5.68	6.47
CaO	5.82	8.05	8.60	6.88	9.75	6.71	9.47
Na_2O	3.38	3.72	3.89	3.72	2.87	3.20	2.70
K_2O	3.15	0.55	0.36	1.05	0.37	0.96	0.49
P_2O_5	0.11	1.14	0.18	0.17	0.18	0.26	0.14
H_2O^+	1.04	1.06	0.47	1.24	0.54	1.43	0.74
H_2O^-	1.88	1.79	0.98	1.60	1.75	2.19	1.36
CO_2	1.05	ND	ND	ND	1.10	ND	ND
Total	99.77	101.32	100.08	100.21	100.54	100.37	99.99
Fe_2O_3/FeO	1.85	1.24	2.18	1.12	1.96	4.01	1.98
Density (g/cm^3)	2.417**	2.504**	2.66	2.362**	2.703**	2.56	2.781**
Trace elements (ppm):							
La			9.1				
Ce			23				
Nd			15				
Sm			4.1				
Eu			1.4				
Tb			0.82				
Yb			2.3				
Lu			0.41				
Cr	78		65	66	102	142	
Ni	33		33	34	53	56	
Co	46		40	46	46	60	
V	245		222	220	482	547	
Cu	29		21	37	66	66	
Zn	80		85	123	135	116	
Zr	130		130	130	110	140	
Y	27		27	25	43	39	
Nb	4.5		4.7	4.5	3.3	3.3	
Rb	26		7.3	18	7.5	14	
Sr	170		230	220	110	110	
Ba	330		270	280	110	92	

Note: * = major element data from Grechin et al. (1981). ** = density from Grechin et al. (1981). ND = not determined.

Table T29 (continued).

Leg	63	63	63	63	63
Hole	469	469	469	469	469
Core, section	48R-1	48R-1	49R-1	50R-2	51R-1
Interval (cm)	22-28	49-53	84-88	27-32	34-40
Piece	Glass 1D	Glass 5A	8A	3A	3
Lab number	Z-1234	Z-1235	Z-1236	Z-1237	Z-1238
Depth (mbsf)	423.22	423.49	432.84	441.77	450.34
Major element oxides (wt%):					
SiO_2	46.10*	44.60*	48.34*	47.26*	47.53*
TiO_2	1.88	1.66	1.92	1.77	1.42
Al_2O_3	9.24	13.06	15.61	13.61	12.91
Fe_2O_3	9.58	9.99	7.63	6.37	7.86
FeO	3.58	3.17	4.03	7.18	4.49
MnO	0.03	0.07	0.20	0.21	0.16
MgO	13.84	9.20	7.53	7.96	10.67
CaO	1.16	1.31	9.20	9.45	4.79
Na_2O	2.20	2.37	3.04	2.34	3.15
K_2O	0.61	0.87	0.37	0.41	0.54
P_2O_5	0.03	0.08	0.16	0.16	0.18
H_2O^+	4.22	4.13	0.29	1.00	1.59
H_2O^-	7.49	9.24	1.72	2.29	4.41
CO_2	ND	ND	ND	ND	ND
Total	99.96	99.75	100.04	100.01	99.60
Fe_2O_3/FeO	0.16	3.15	1.89	0.89	1.75
Density (g/cm^3)	ND	2.82	2.89	2.74	2.17
Trace elements (ppm):					
La					
Ce					
Nd					
Sm					
Eu					
Tb					
Yb					
Lu					
Cr	150		142	52	56
Ni	30		54	50	52
Co	30		48	51	53
V	377		377	365	370
Cu	49		62	53	45
Zn	58		112	121	79
Zr	110		110	105	83
Y	27		42	45	47
Nb	2.2		2.6	1.7	1.9
Rb	5.2		1.9	5.9	1.8
Sr	67		98	100	91
Ba	95		35	71	10

Table T30. Composition of basalts from Hole 471, Leg 63 (Baja California, Pacific Ocean). (Continued on next page.)

Leg	63	63	63	63	63	63	63
Hole	471	471	471	471	471	471	471
Core, section	80R-1	80R-1	80R-2	81R-3	82R-1	82R-2	84R-1
Interval (cm)	78-84	135-140	98-102	59-65	127-132	15-18	9-16
Piece	6B	9A	6G	5	9	1B	2A
Lab number	Z-1725	Z-1239	Z-1726	Z-1727	Z-1240	Z-1241	Z-1242
Depth (mbsf)	751.28	751.85	752.98	763.59	770.27	770.65	787.09
Major element oxides (wt%):							
SiO_2	46.13*	49.13	44.58*	51.05*	49.30*	49.53*	47.73*
TiO_2	2.30	2.08	2.13	1.87	1.27	1.28	1.71
Al_2O_3	14.03	13.91	13.61	14.72	14.11	14.12	13.60
Fe_2O_3	5.52	5.54	5.44	3.79	3.47	3.28	5.02
FeO	5.53	3.88	6.39	5.38	7.19	7.38	5.37
MnO	0.43	0.38	0.43	0.22	0.23	0.21	0.11
MgO	10.07	8.44	12.57	6.12	8.78	8.72	9.32
CaO	7.17	5.81	3.14	6.25	6.00	5.29	8.31
Na_2O	3.04	2.62	2.54	4.63	3.44	3.15	3.44
K_2O	0.49	0.62	1.76	2.44	2.44	2.44	0.54
P_2O_5	0.09	0.27	0.11	0.22	0.15	0.13	0.15
H_2O^+	2.43		5.48	2.82	3.53	3.65	2.04
H_2O^-	2.18		2.24	0.82	1.04	0.88	2.91
CO_2	ND		ND	ND	ND	ND	ND
LOI		7.17					
Total	99.41	99.85	100.42	100.33	100.95	100.06	100.25
H_2O^+		2.68					
H_2O^-		2.75					
CO_2		1.22					
Fe_2O_3/FeO	1.00	1.43	0.85	0.70	0.48	0.44	0.93
Density (g/cm^3)	2.618**	2.44	2.316**	2.368**	2.619**	2.54	2.62
Trace elements (ppm):							
La						7.0	
Ce						18	
Nd						11	
Sm						3.0	
Eu						0.93	
Tb						0.72	
Yb						2.5	
Lu						0.42	
Cr		175			245	195	225
Ni		60			84	71	74
Co		42			59	40	63
V		242			267	228	362
Cu		69			69	78	76
Zn		85			88	83	82
Zr		150			76	74	140
Y		35			23	23	36
Nb		16			9.7	9.3	14
Rb		7.4			19	23	2.4
Sr		250			210	200	240
Ba		195			196	220	220

Note: * = major element from Grechin et al. (1981). ** = density from Grechin et al. (1981). ND = not determined.

Table T30 (continued).

Leg	63	63	63	63
Hole	471	471	471	471
Core, section	84R-1	86R-1	87R-2	88R-2
Interval (cm)	107-114	63-69	19-26	0-6
Piece	6G	6D	1B	1A
Lab number	Z-1243	Z-1728	Z-1244	Z-1729
Depth (mbsf)	788.07	805.63	808.69	815.5
Major element oxides (wt%):				
SiO_2	47.45*	47.81*	47.25*	42.93*
TiO_2	1.79	1.28	1.23	1.02
Al_2O_3	13.38	16.42	15.62	11.99
Fe_2O_3	5.15	3.27	3.44	4.83
FeO	6.16	5.84	5.94	6.51
MnO	0.20	0.18	0.17	0.21
MgO	8.65	8.13	8.95	15.11
CaO	8.78	11.06	10.86	8.35
Na_2O	2.86	2.58	2.46	1.22
K_2O	0.61	0.31	0.31	0.38
P_2O_5	0.28	0.08	0.03	0.11
H_2O^+	2.60	2.02	2.36	4.96
H_2O^-	2.88	1.55	1.68	3.01
CO_2	ND	ND	ND	ND
LOI				
Total	100.79	100.53	100.30	100.63
H_2O^+				
H_2O^-				
CO_2				
Fe_2O_3/FeO	0.84	0.56	0.58	0.74
Density (g/cm^3)	2.65	2.743**	2.74	2.648**
Trace elements (ppm):				
La				
Ce				
Nd				
Sm				
Eu				
Tb				
Yb				
Lu				
Cr	205		237	
Ni	64		148	
Co	50		51	
V	350		232	
Cu	64		49	
Zn	77		55	
Zr	140		85	
Y	32		24	
Nb	13		8.9	
Rb	5.4		2.3	
Sr	220		190	
Ba	140		140	

Table T31. Composition of basalts from Hole 332B, Leg 37 (FAMOUS area, Deep Drill Valley, Mid-Atlantic Ridge). (Continued on next three pages.)

Leg	37	37	37	37	37	37	37
Hole	332B	332B	332B	332B	332B	332B	332B
Core, section	1R-5	2R-2	2R-3	6R-1	11R-1	14R-2	16R-2
Interval (cm)	121-124	100-103	91-94	94-96	58-60	23-26	37-40
Piece	11	11	8	10	3D	2	5
Lab number	Z-280	Z-501	Z-502	Z-281	Z-282	Z-503	Z-283
Depth (mbsf)	149.21	154.0	155.41	285.44	361.08	390.73	409.87
Unit-Subunit	1-1	1-1	1-2	2-3	3A-7	3B-8	4-12
Major element oxides (wt%):							
SiO_2	47.47	46.30	47.19	49.64	49.82	48.86	46.76
TiO_2	0.70	0.37	0.40	1.24	1.18	1.06	0.91
Al_2O_3	19.08	20.90	20.97	13.27	13.92	15.63	14.04
Fe_2O_3	3.90	3.23	3.66	4.72	3.89	5.22	4.33
FeO	3.07	2.82	3.20	6.27	6.30	4.07	5.88
MnO	0.06	0.12	0.11	0.15	0.04	0.13	0.07
MgO	6.79	6.20	6.31	7.56	7.56	7.25	8.97
CaO	16.21	16.42	15.52	12.49	12.90	13.03	13.74
Na_2O	1.69	1.54	1.57	2.25	2.20	2.13	2.14
K_2O	0.16	0.12	0.08	0.46	0.38	0.26	0.20
P_2O_5	0.02	0.04	0.03	0.10	0.08	0.11	0.05
LOI	0.95	1.87	1.00	1.32	1.25	2.00	2.36
Total	100.10	99.93	100.04	99.47	99.52	99.75	99.45
H_2O^+	0.33	0.25	0.27	0.67	0.52	0.41	0.86
H_2O^-	0.62	0.43	0.50	0.65	0.73	0.67	1.50
CO_2	ND	1.19	0.23	ND	ND	0.83	ND
Fe_2O_3/FeO	1.27	1.15	1.14	0.75	0.62	1.28	0.74
Density (g/cm^3)	2.79	2.71	2.78	2.85	2.76	2.65	2.79
Trace elements (ppm):							
La	1.7	1.5	1.5	6.4	6.0	5.7	3.8
Ce	3.7	3.3	2.8	14	13	11	8.0
Nd	ND	2.8	2.7	ND	ND	8.50	ND
Sm	1.1	0.98	0.92	3.0	2.8	2.7	2.0
Eu	0.49	0.32	0.36	1.0	0.98	0.77	0.69
Tb	0.35	0.30	0.34	0.63	0.63	0.64	0.46
Yb	1.4	1.1	1.2	2.6	2.5	2.2	2.1
Lu	0.21	0.18	0.19	0.41	0.38	0.32	0.36
Cr	255	340	240	53	145	160	435
Ni	155	85	72	68	100	71	260
Co	41	43	39	35	40	43	54
V	155	187	162	125	205	235	220
Cu	105	79	72	60	48	49	60
Pb	<5	<5	<5	<5	<5	<5	<5
Zn	55	56	52	90	100	70	70
Sn	ND	1.9	1.5	ND	ND	2.5	ND
Zr	17	19	19	56	52	61	ND
Y	9.3	10.0	9.3	24	19	17	18
Nb	2.8	2.3	2.2	7.7	8.0	6.5	1.3
Rb	1.1	2.2	1.7	6.6	3.7	9.0	1.1
Sr	74	170	93	110	100	110	ND
Ba	<10	34	30	38	49	91	ND
Th	ND	1.3	1.3	ND	ND	1.4	ND

Note: ND = not determined.

Table T31 (continued).

Leg	37	37	37	37	37	37	37
Hole	332B	332B	332B	332B	332B	332B	332B
Core, section	17R-1	21R-1	22R-1	22R-2	22R-4	24R-1	29R-1
Interval (cm)	97-103	12-15	105-108	106-108	21-25	71-75	94-98
Piece	13	1A	9	12	2	8	5D
Lab number	Z-284	Z-285	Z-286	Z-504	Z-505	Z-287	Z-288
Depth (mbsf)	418.47	455.62	466.05	467.56	469.71	484.71	532.44
Unit-Subunit	4-12	4-13	5-14	5-14	5-14	5-15	6-19
Major element oxides (wt%):							
SiO_2	47.31	45.62	47.17	46.80	48.86	47.39	45.57
TiO_2	0.92	0.85	0.93	0.96	0.86	0.92	0.84
Al_2O_3	13.83	13.48	16.48	16.56	15.72	16.12	14.59
Fe_2O_3	3.95	2.31	2.71	6.21	4.64	2.60	3.22
FeO	6.66	6.73	6.75	4.42	5.06	6.70	5.55
MnO	0.12	0.11	0.12	0.11	0.13	0.12	0.12
MgO	10.56	12.80	9.48	5.83	8.37	6.87	11.93
CaO	12.07	13.43	11.92	12.47	11.40	14.69	11.84
Na_2O	2.09	1.86	2.37	2.49	2.28	2.37	1.92
K_2O	0.27	0.18	0.18	0.26	0.15	0.18	0.23
P_2O_5	0.02	0.01	0.02	0.10	0.06	0.02	0.04
LOI	2.06	2.08	1.92	3.20	2.30	1.71	3.80
Total	99.86	99.46	100.05	99.41	99.83	99.69	99.65
H_2O^+	0.82	1.25	0.63	0.97	0.75	0.55	1.58
H_2O^-	1.24	0.83	1.29	1.36	1.03	1.16	1.17
CO_2	ND	ND	ND	0.77	0.38	ND	1.05
Fe_2O_3/FeO	0.59	0.34	0.40	1.40	0.92	0.39	0.58
Density (g/cm^3)	2.85	2.90	2.78	2.55	2.90	2.84	2.87
Trace elements (ppm):							
La	3.3	2.0	2.4	3.0	2.6	2.9	2.0
Ce	7.7	4.9	6.5	7.4	6.4	7.0	5.2
Nd	5.8	4.7	5.0	6.0	5.2	6.0	3.7
Sm	1.7	1.6	1.6	2.0	1.7	1.9	1.2
Eu	0.63	0.50	0.61	0.68	0.63	0.68	0.49
Tb	0.41	0.38	0.43	0.66	0.55	0.55	0.40
Yb	1.8	1.6	1.8	2.1	1.8	2.1	1.6
Lu	0.29	0.26	0.28	0.34	0.27	0.33	0.25
Cr	560	415	280	290	390	280	740
Ni	275	420	195	84	150	160	320
Co	55	53	45	45	47	42	54
V	230	115	190	217	232	190	155
Cu	90	50	50	63	93	56	85
Pb	<5	<5	<5	<5	<5	<5	<5
Zn	75	45	70	67	80	80	60
Sn	ND	ND	ND	3.0	1.8	ND	ND
Zr	32	23	34	41	42	35	21
Y	16	12	16	19	17	19	17
Nb	4.8	2.1	3.6	4.1	4.4	4.2	2.9
Rb	1.8	1.8	1.5	4.1	3.7	1.5	2.5
Sr	84	62	84	92	93	84	77
Ba	<10	<10	<10	50	31	25	<10
Th	ND	ND	ND	1.2	<1	ND	ND

Table 31 (continued).

Leg	37	37	37	37	37	37	37
Hole	332B	332B	332B	332B	332B	332B	332B
Core, section	33R-1	33R-2	35R-1	37R-1	37R-3	41R-1	42R-1
Interval (cm)	96-99	30-33	131-134	100-104	17-20	65-69	63-66
Piece	10E	2	6J	13	2	6A	3D
Lab number	Z-506	Z-289	Z-507	Z-508	Z-290	Z-291	Z-509
Depth (mbsf)	570.46	571.3	589.81	608.5	610.67	646.15	655.63
Unit-Subunit	6-20	6-21	7-23	8-25	9-26	9-32	9-36
Major element oxides (wt%):							
SiO_2	46.94	46.51	44.69	46.87	46.98	46.99	47.42
TiO_2	1.01	0.86	0.49	0.61	0.85	0.85	0.69
Al_2O_3	14.17	13.62	11.34	18.44	14.75	13.84	15.38
Fe_2O_3	4.36	3.76	4.63	4.71	3.84	2.60	5.01
FeO	5.97	6.06	5.59	2.82	5.37	7.15	4.65
MnO	0.06	0.08	0.10	0.04	0.11	0.12	0.15
MgO	7.17	10.09	18.25	7.30	10.92	12.54	9.67
CaO	12.52	12.88	8.98	12.35	11.47	11.22	11.71
Na_2O	2.15	2.09	1.54	1.95	2.14	1.97	1.86
K_2O	0.21	0.20	0.15	0.26	0.27	0.13	0.06
P_2O_5	0.09	0.02	0.04	0.05	0.02	0.03	0.05
LOI	4.85	3.37	3.97	4.10	3.03	2.04	2.90
Total	99.50	99.54	99.77	99.50	99.75	99.48	99.55
H_2O^+	0.75	0.85	1.03	1.79	1.72	0.78	1.00
H_2O^-	0.64	1.02	0.69	1.40	1.31	1.26	1.30
CO_2	3.41	1.50	2.25	0.68	ND	ND	0.52
Fe_2O_3/FeO	0.73	0.62	0.83	1.67	0.72	0.36	1.08
Density (g/cm^3)	2.62	2.95	2.99	2.83	2.84	2.91	2.69
Trace elements (ppm):							
La	4.9	1.9	1.6	2.0	2.0	1.8	2.1
Ce	12	4.7	3.9	5.0	5.0	4.5	5.3
Nd	8.4	3.9	3.3	3.9	4.2	3.5	4.1
Sm	2.6	1.3	1.1	1.3	1.4	1.1	1.4
Eu	0.70	0.51	0.30	0.43	0.55	0.47	0.45
Tb	0.62	0.41	0.40	0.47	0.44	0.31	0.47
Yb	2.0	1.6	1.4	1.6	1.8	1.3	1.7
Lu	0.33	0.26	0.20	0.26	0.28	0.22	0.26
Cr	76	795	640	570	835	790	610
Ni	66	320	475	152	275	395	250
Co	53	53	73	57	53	67	66
V	267	125	195	262	185	150	227
Cu	79	70	68	108	90	85	93
Pb	<5	<5	<5	<5	<5	<5	<5
Zn	86	60	71	68	65	55	79
Sn	2.1	ND	2.1	1.8	ND	ND	2.2
Zr	51	24	21	30	19	20	28
Y	19	16	9.9	11	17	15	16
Nb	6.2	3.0	1.5	2.8	3.3	2.7	2.8
Rb	4.5	2.9	2.6	3.7	1.3	<0.5	<1
Sr	130	120	79	94	59	67	80
Ba	35	22	29	34	30	<10	24
Th	<1	ND	<1	1.1	ND	ND	1.0

Table 31 (continued).

Leg	37	37	37	37	37	37
Hole	332B	332B	332B	332B	332B	332B
Core, section	42R-2	43R-1	43R-2	43R-3	46R-2	48R-1
Interval (cm)	22-25	132-136	28-31	47-50	60-63	73-76
Piece	1C	8C	1C	Breccia 2D	3B	Breccia 6
Lab number	Z-292	Z-293	Z-294	Z-510	Z-295	Z-296
Depth (mbsf)	656.72	665.82	666.28	667.97	695.1	712.73
Unit-Subunit	9-38	10-41	10-41	10-41	10-44	11-45
Major element oxides (wt%):						
SiO_2	46.86	47.32	47.53	46.46	49.16	47.00
TiO_2	0.85	1.11	1.10	0.87	1.24	0.96
Al_2O_3	14.05	16.65	17.70	16.82	13.35	13.34
Fe_2O_3	4.39	3.94	2.95	6.13	4.65	4.68
FeO	5.54	5.53	5.61	3.88	7.09	5.22
MnO	0.04	0.11	0.11	0.07	0.14	0.14
MgO	10.60	6.62	7.16	6.29	7.65	9.30
CaO	12.26	13.82	13.16	11.59	11.35	11.65
Na_2O	1.97	2.14	2.14	2.44	2.14	1.92
K_2O	0.15	0.18	0.20	0.34	0.31	0.35
P_2O_5	0.01	0.05	0.03	0.11	0.03	0.05
LOI	2.75	2.27	2.35	4.49	2.60	5.25
Total	99.47	99.74	100.04	99.49	99.71	99.86
H_2O^+	1.28	1.00	1.01	1.88	0.80	2.05
H_2O^-	1.47	1.27	1.34	2.05	1.80	3.20
CO_2	ND	ND	ND	0.56	ND	ND
Fe_2O_3/FeO	0.79	0.71	0.53	1.58	0.66	0.90
Density (g/cm^3)	2.90	2.75	2.73	2.66	2.85	2.39
Trace elements (ppm):						
La	2.0	4.4	4.3	4.4	6.2	6.0
Ce	4.5	10	9.6	8.2	14	13
Nd	3.6	7.2	7.0	6.3	11	9.0
Sm	1.2	2.1	2.1	2.2	3.0	2.4
Eu	0.51	0.72	0.72	0.80	1.0	0.85
Tb	0.44	0.55	0.60	0.57	0.73	0.6
Yb	1.6	2.2	2.3	2.1	2.6	2.1
Lu	0.25	0.35	0.34	0.35	0.42	0.31
Cr	465	170	155	195	65	335
Ni	240	80	100	64	65	150
Co	50	42	47	45	46	38
V	135	180	230	300	250	230
Cu	75	60	70	55	70	56
Pb	<5	<5	<5	<5	<5	<5
Zn	50	70	55	80	90	75
Sn	ND	ND	ND	2.0	ND	ND
Zr	25	37	42	49	60	47
Y	14	22	21	18	27	19
Nb	2.8	6.2	6.1	5.9	7.3	7.5
Rb	0.6	0.9	0.7	4.8	2.1	1.5
Sr	120	100	110	91	110	94
Ba	<10	31	35	50	59	40
Th	ND	ND	ND	1.4	ND	ND

Table T32. Composition of basalts from Hole 648B, Leg 106 (Serocki Volcano, Mid-Atlantic Ridge Rift Valley).

Leg	106	106	106	106	106	106	106	106
Hole	648B	648B	648B	648B	648B	648B	648B	648B
Core, section	1R-1	1R-2	1R-3	3R-1	4R-1	4R-1	5R-1	6R-1
Interval (cm)	67-70	85-88	60-65	85-87	15-18	61-64	15-22	1-3
Piece	12	15	12	14	4	12	4	1
Lab number	Z-106	Z-107	Z-108	Z-109	Z-110	Z-111	Z-112	Z-113
Depth (mbsf)	7.27	8.95	10.20	15.15	21.25	21.71	14.75	25.71
Unit	3	9	14	20	21	23	24	25
Major element oxides (wt%):								
SiO_2	48.61	48.75	47.62	48.58	48.44	48.43	48.27	46.95
TiO_2	1.87	1.91	1.85	2.05	1.85	1.78	2.14	2.07
Al_2O_3	13.65	15.14	13.31	12.76	13.65	13.52	12.62	14.66
Fe_2O_3	3.96	2.21	4.41	4.24	3.12	2.32	4.19	3.97
FeO	8.28	8.12	8.37	8.24	8.51	9.13	8.16	7.09
MnO	0.17	0.05	0.05	0.11	0.05	0.08	0.06	0.17
MgO	8.26	8.24	8.77	9.32	9.23	8.63	9.20	8.54
CaO	11.49	12.21	11.16	11.30	11.55	12.03	11.79	12.17
Na_2O	3.22	3.01	3.22	3.01	3.01	3.01	3.16	3.19
K_2O	0.41	0.31	0.34	0.24	0.31	0.22	0.13	0.32
P_2O_5	0.09	0.08	0.15	0.05	0.12	0.10	0.14	0.16
LOI	0.49	0.44	0.64	0.51	0.49	0.55	0.58	0.52
Total	100.50	100.47	99.89	100.41	100.33	99.80	100.44	99.81
H_2O^+	0.31	0.25	0.53	0.32	0.32	0.36	0.27	0.32
H_2O^-	0.18	0.19	0.11	0.19	0.17	0.19	0.31	0.20
CO_2	ND	ND	ND	ND	ND	ND	ND	ND
Fe_2O_3/FeO	0.48	0.27	0.53	0.52	0.37	0.25	0.51	0.56
Density (g/cm^3)	2.93	2.92	2.90	2.89	2.88	2.92	2.89	2.94
Trace elements (ppm):								
La	4.3	5.0	4.8	4.4	4.6	4.9	5.7	4.9
Ce	13	15	13	14	13	15	14	13
Sm	3.8	4.5	4.4	4.1	4.2	4.6	4.9	4.2
Eu	1.4	1.6	1.4	1.5	1.5	1.5	1.6	1.5
Tb	0.84	0.95	0.85	1.1	1.1	0.89	0.95	0.89
Yb	3.3	3.8	3.7	3.5	3.6	3.8	4.0	3.7
Lu	0.53	0.62	0.60	0.59	0.56	0.62	0.63	0.60
Sc	43	41	41	42	42	42	43	42
Cr	290	275	285	295	290	280	320	310
Ni	125	120	120	120	125	145	135	140
Co	50	40	45	40	40	55	45	55
V	320	290	340	350	320	320	340	310
Cu	60	55	65	55	60	75	80	75
Pb	<5	<5	<5	<5	<5	<5	<5	<5
Zn	95	90	90	95	95	120	100	125
Zr	74	87	82	110	110	110	110	120
Y	37	37	35	35	36	38	38	38
Nb	3.6	3.1	3.0	3.2	3.1	3.1	3.5	2.6
Rb	1.2	1.1	<1	1.0	<1	<1	<1	1.2
Sr	84	110	99	140	140	140	120	140
Ba	<10	<10	<10	<10	<10	<10	<10	<10

Note: ND = note determined.

Table T33. Composition of basalts from Holes 462 and 462A, Leg 61 (Nauru Basin, Pacific Ocean). (Continued on next four pages.)

Leg	61	61	61	61	61	61	61
Hole	462	462	462	462	462	462	462A
Core, section	60R-1	60R-2	61R-1	62R-2	63R-2	64R-1	17R-2
Interval (cm)	65-69	135-138	48-51	135-137	18-22	12-14	84-86
Piece	1A	9	3B	9	1	2	4B
Lab number	Z-1721	Z-1198	Z-1199	Z-1200	Z-1201	Z-1202	Z-1203
Depth (mbsf)	559.15	561.35	567.98	579.35	581.03	585.62	576.19
Unit	1	1	6	8	10	10	2
Major element oxides (wt%):							
SiO_2	48.44	48.04	48.22	47.02	48.90	47.91	47.9*
TiO_2	1.31	1.32	1.28	1.62	1.68	1.67	1.39
Al_2O_3	16.19	14.68	15.69	15.13	14.75	15.62	14.76
Fe_2O_3	4.48	10.77	2.59	3.82	4.51	4.51	3.78
FeO	4.45		7.29	7.87	6.96	6.48	7.96
MnO	0.16	0.22	0.24	0.24	0.21	0.24	0.25
MgO	7.56	7.97	7.59	7.86	7.82	7.57	7.33
CaO	11.10	11.24	12.45	10.56	10.03	10.28	11.77
Na_2O	2.44	2.34	2.14	2.57	2.44	2.59	2.27
K_2O	0.69	0.52	0.08	0.10	0.18	0.08	0.05
P_2O_5	0.12	not	0.10	0.14	0.28	0.14	0.15
H_2O^+	2.19	2.09	1.79	1.85	2.24	2.25	1.09
H_2O^-							1.12
CO_2	0.40	0.51	0.30	0.76	not	0.63	ND
LOI							
Total	99.53	99.70	99.76	99.54	100.00	99.97	99.82
H_2O^+							
H_2O^-							
CO_2							
Fe_2O_3/FeO	1.01		0.36	0.49	0.65	0.48	0.48
Density (g/cm^3)	2.76	2.69	2.80	2.70	2.71	2.60	2.88
Trace elements (ppm):							
La		3.8			4.2	4.6	3.55**
Ce		12			13	14	9.24
Nd		9.4			11	11	ND
Sm		3.1			3.4	3.6	2.87
Eu		1.1			1.2	1.2	1.03
Tb		0.87			0.97	0.94	0.74
Yb		2.3			2.6	3.5	2.74
Lu		0.33			0.42	0.58	0.39
Sc	40	46	48	43	48	40	48
Cr	220	227	233	196	191	205	176
Ni	150	72	87	90	90	91	78
Co	100	44	64	61	73	65	62
V	330	345	377	427	465	450	407
Cu	52	305	116	190	200	207	97
Zn	300	122	96	125	118	125	92
Sn	4	3	4	3	3	3	ND
Zr	95	83	76	96	93	95	78
Y	ND	37	25	24	28	27	26
Nb	ND	4.7	5.1	5.9	4.9	5.4	5.2
Rb	ND	8.7	<1	1.3	<1	<1	<1
Sr	ND	160	150	130	135	140	130
Ba	ND	6	16	100	130	86	52

Note: * = major element data from Tokuyama and Batiza (1981). ** = rare earth element data from Batiza (1981). *** = rare earth element data from Seifert (1981). ND = not determined.

Table T33 (continued).

Leg	61	61	61	61	61	61	61
Hole	462A	462A	462A	462A	462A	462A	462A
Core, section	24R-1	27R-2	28R-1	29R-2	30R-3	32R-1	44R-2
Interval (cm)	12-14	71-76	92-94	105-108	14-17	10-14	12-14
Piece	2B	6	4	1G	1	2A	2
Lab number	Z-1204	Z-1205	Z-1206	Z-1207	Z-1208	Z-1209	Z-1210
Depth (mbsf)	606.12	628.03	630.92	638.3	648.14	655.6	730.62
Unit	12	12	12	12	12	12	22
Major element oxides (wt%):							
SiO_2	46.61	50.26	49.97	49.92	50.25	47.48	49.72
TiO_2	1.46	1.51	1.53	1.48	1.47	1.48	0.87
Al_2O_3	15.65	13.67	13.87	13.47	13.90	14.20	14.83
Fe_2O_3	4.26	3.54	4.10	3.14	3.32	3.05	2.04
FeO	8.12	8.99	8.38	9.00	8.99	9.70	8.88
MnO	0.22	0.23	0.23	0.21	0.21	0.24	0.24
MgO	7.61	7.36	7.08	7.44	7.52	7.42	8.42
CaO	10.86	10.70	11.00	10.37	10.19	10.43	12.20
Na_2O	2.47	2.08	2.34	2.31	2.32	2.62	2.11
K_2O	0.19	0.17	0.11	0.21	0.75	0.76	0.20
P_2O_5	0.16	0.25	0.13	0.25	0.25	0.14	0.12
H_2O^+	1.94	0.75	1.11	1.73	0.42	2.00	trace
H_2O^-							
CO_2	0.40	not	0.30	not	not	0.46	ND
LOI							
Total	99.95	99.51	100.15	99.53	99.59	99.98	99.63
H_2O^+							
H_2O^-							
CO_2							
Fe_2O_3/FeO	0.53	0.39	0.48	0.35	0.37	0.31	0.23
Density (g/cm^3)	2.78	2.95	3.01	2.96	2.97	2.86	2.97
Trace elements (ppm):							
La	4.9					5.2	
Ce	14					14	
Nd	11					11	
Sm	3.8					3.5	
Eu	1.3					1.1	
Tb	0.92					0.84	
Yb	3.3					2.6	
Lu	0.49					0.41	
Sc	22	28	25	43	32	34	34
Cr	205	205	183	207	209	215	352
Ni	92	84	83	88	88	88	137
Co	65	61	57	63	53	55	56
V	450	407	380	405	430	447	372
Cu	200	185	185	175	190	180	145
Zn	113	116	113	114	135	74	113
Sn	3	7	3	3	3	4	4
Zr	93	86	88	82	80	88	51
Y	33	30	31	30	30	30	21
Nb	5.3	5.3	5.3	4.9	4.8	5.6	3.3
Rb	<1	<1	<1	<1	3	3.7	1.8
Sr	130	120	120	110	110	86	89
Ba	72	91	84	76	69	73	15

Table T33 (continued).

Leg	61	61	61	61	61	61	61
Hole	462A	462A	462A	462A	462A	462A	462A
Core, section	44R-2	47R-1	50R-3	51R-4	52R-4	53R-1	55R-2
Interval (cm)	13-14	95-96	130-134	27-30	33-36	143-146	50-52
Piece	2	9	1E	1F	1	7B	4
Lab number	Z-1722	Z-1211	Z-1212	Z-1213	Z-1214	Z-1215	Z-1216
Depth (mbsf)	730.63	747.95	777.75	783.17	792.43	793.43	803.00
Unit	22	23	24	24	25	26	26
Major element oxides (wt%):							
SiO_2	48.04	48.32	48.75*	48.27	48.34	50.23	47.90
TiO_2	0.88	0.92	0.91	1.08	0.97	0.89	0.79
Al_2O_3	14.52	15.27	15.2	14.01	14.70	14.75	14.57
Fe_2O_3	3.31	1.74	3.63	4.56	3.22	3.00	2.42
FeO	8.12	8.91	6.85	7.07	7.55	6.58	8.37
MnO	0.24	0.24	0.19	0.17	0.21	0.21	0.13
MgO	8.67	8.67	8.39	6.78	8.56	9.24	9.50
CaO	12.12	12.18	12.02	10.04	12.29	11.47	12.20
Na_2O	1.96	1.97	1.94	2.12	2.37	1.93	1.90
K_2O	0.19	0.11	0.04	0.31	0.19	0.12	0.06
P_2O_5	not	0.08	0.12	0.07	0.08	0.15	0.10
H_2O^+	1.37	1.05	1.00		1.20	0.92	1.36
H_2O^-			0.79				
CO_2	0.46	0.42	ND		0.40	not	0.60
LOI				5.30			
Total	99.88	99.88	99.83	99.78	100.08	99.49	99.90
H_2O^+				2.28			
H_2O^-				2.93			
CO_2				<0.2			
Fe_2O_3/FeO	0.41	0.20	0.53	0.65	0.43	0.46	0.29
Density (g/cm^3)	ND	2.90	2.84	2.80	2.95	2.95	2.95
Trace elements (ppm):							
La			ND**	2.7			
Ce			7.08	7.9			
Nd			ND	6.5			
Sm			2.11	2.2			
Eu			0.81	0.78			
Tb			0.54	0.69			
Yb			ND	1.9			
Lu			0.36	0.28			
Sc	58	43	47	ND	35	32	46
Cr	480	470	150	415	320	322	320
Ni	190	190	80	140	137	137	131
Co	71	63	57	66	54	52	52
V	300	300	417	467	350	362	345
Cu	260	230	118	180	135	150	140
Zn	170	167	86	90	94	88	93
Sn	4	4	ND	ND	3	3	3
Zr	71	71	57	57	54	54	54
Y	ND	ND	22	20	21	21	19
Nb	ND	ND	2.6	2.9	2.8	3.3	3.5
Rb	ND	ND	1.7	5	<1	<1	<1
Sr	ND	ND	91	88	85	88	88
Ba	ND	ND	8	47	6	31	11

Table 33 (continued).

Leg	61	61	61	61	61	61	61
Hole	462A	462A	462A	462A	462A	462A	462A
Core, section	57R-1	62R-2	65R-1	74R-4	79R-5	80R-2	88R-3
Interval (cm)	145-147	148-150	59-61	25-31	140-146	122-124	9-11
Piece	13	2F	3	1A	1J	3	Breccia 1A
Lab number	Z-1217	Z-1218	Z-1219	Z-1220	Z-1221	Z-1222	Z-1223
Depth (mbsf)	816.95	863.46	877.09	950.41	992.35	996.49	1035.49
Unit	26	30	32	35	38	40	43
Major element oxides (wt%):							
SiO_2	48.85	49.75	48.87*	48.83*	47.81	49.04	49.99
TiO_2	0.91	0.94	0.99	1.15	1.08	1.12	1.23
Al_2O_3	14.68	15.17	15.58	15.36	14.97	14.04	14.21
Fe_2O_3	4.41	3.51	3.29	3.89	4.28	2.88	4.92
FeO	5.89	6.66	7.70	7.56	6.53	8.64	6.48
MnO	0.22	0.20	0.19	0.19	0.23	0.26	0.18
MgO	8.50	9.05	7.83	7.59	8.02	8.09	7.03
CaO	12.11	11.20	11.47	11.05	12.24	11.05	11.17
Na_2O	2.28	1.96	1.96	2.05	2.21	1.92	2.22
K_2O	0.25	0.12	0.03	0.63	0.10	0.23	0.09
P_2O_5	0.18	0.21	0.11	0.12	0.10	0.23	0.10
H_2O^+	1.20	1.01	1.00	1.15	1.47	1.89	
H_2O^-			0.77	0.85			
CO_2	not	not	ND	ND	0.58	not	
LOI							1.99
Total	99.48	99.78	99.79	100.42	99.62	99.39	99.61
H_2O^+							0.25
H_2O^-							1.25
CO_2							<0.20
Fe_2O_3/FeO	0.75	0.53	0.43	0.52	0.66	0.33	0.76
Density (g/cm^3)	2.88	2.89	2.94	2.93	2.88	2.92	2.77
Trace elements (ppm):							
La			2.6**	2.93**			2.1***
Ce			6.06	6.31			5.61
Nd			ND	ND			ND
Sm			2.2	2.24			1.56
Eu			0.74	0.84			0.59
Tb			0.55	0.61			0.43
Yb			2.14	2.45			1.76
Lu			0.34	0.38			0.26
Sc	35	47	43	49	57	43	42.7
Cr	307	285	310	85	275	185	195
Ni	131	97	95	76	97	86	79
Co	55	48	52	56	54	56	58
V	348	335	348	392	362	390	407
Cu	150	150	150	160	150	170	175
Zn	92	113	92	100	98	133	118
Sn	2	2	ND	ND	3	2	ND
Zr	56	57	56	65	59	69	68
Y	20	22	21	24	22	24	26
Nb	2.5	2.7	2.7	2.7	3	3.5	2.7
Rb	1.1	<1	<1	2.6	<1	<1	1.2
Sr	89	90	95	96	97	95	97
Ba	8	7	6	115	16	46	50

Table 33 (continued).

Leg	61	61
Hole	462A	462A
Core, section	89R-2	90R-3
Interval (cm)	15-16	88-90
Piece	1	1H
Lab number	Z-1224	Z-1225
Depth (mbsf)	1038.1	1045.38
Unit	43	44
Major element oxides (wt%):		
SiO_2	49.10	47.40
TiO_2	1.15	1.18
Al_2O_3	13.88	14.31
Fe_2O_3	5.25	4.64
FeO	6.95	8.06
MnO	0.22	0.24
MgO	7.99	7.85
CaO	11.14	12.19
Na_2O	2.27	2.01
K_2O	0.25	0.07
P_2O_5	0.19	0.11
H_2O^+	1.31	1.35
H_2O^-		
CO_2	not	0.34
LOI		
Total	99.70	99.75
H_2O^+		
H_2O^-		
CO_2		
Fe_2O_3/FeO	0.76	0.58
Density (g/cm^3)	2.91	2.89
Trace elements (ppm):		
La		
Ce		
Nd		
Sm		
Eu		
Tb		
Yb		
Lu		
Sc	53	49
Cr	195	196
Ni	81	79
Co	56	55
V	397	390
Cu	180	175
Zn	121	115
Sn	3	4
Zr	68	72
Y	25	26
Nb	3.6	4.6
Rb	<1	<1
Sr	97	95
Ba	31	7

Table T34. Composition of basalts from Hole 595B, Leg 91 (South Pacific). (Continued on next page.)

Leg	91	91	91	91	91	91	91
Hole	595B	595B	595B	595B	595B	595B	595B
Core, section	2R-1	3R-1	3R-2	4R-1	4R-2	4R-3	5R-1
Interval (cm)	30-35	119-124	68-72	17-22	8-13	145-147	90-95
Piece	3	5B	3B	1B	1A	4C	6
Lab number	Z-429	Z-430	Z-431	Z-432	Z-433	Z-434	Z-435
Depth (mbsf)	73.3	82.69	83.68	87.57	88.98	91.85	97.4
Unit	2	2	2	2	2	2	2
Major element oxides (wt%):							
SiO_2	48.48	47.23	46.07	47.70	47.31	46.76	46.42
TiO_2	3.16	3.16	3.09	2.78	3.30	3.05	3.09
Al_2O_3	15.25	14.69	15.42	14.34	15.28	16.01	15.07
Fe_2O_3	4.76	7.94	9.69	8.05	7.22	7.22	8.79
FeO	4.86	3.40	2.64	4.21	3.73	3.62	3.44
MnO	0.14	0.14	0.14	0.18	0.17	0.17	0.18
MgO	5.92	6.47	5.57	5.77	6.18	5.79	5.60
CaO	9.67	7.88	6.87	8.71	7.86	7.62	8.05
Na_2O	3.18	3.65	3.65	3.41	3.65	4.36	3.59
K_2O	0.79	0.90	1.36	0.77	0.86	1.15	1.04
P_2O_5	0.22	0.31	0.31	0.22	0.26	0.24	0.35
LOI	3.14	3.75	4.71	3.49	3.88	4.37	4.01
Total	99.57	99.52	99.52	99.63	99.70	100.36	99.63
H_2O^+	1.55	1.50	2.18	1.46	1.42	1.91	1.70
H_2O^-	1.59	2.25	2.53	2.03	2.46	2.46	2.31
CO_2	ND	ND	ND	ND	ND	ND	ND
Fe_2O_3/FeO	0.98	2.34	3.67	1.91	1.94	1.99	2.56
Density (g/cm^3)	2.61	2.56	2.57	2.62	2.58	2.52	2.57
Trace elements (ppm):							
La	6.2	6.7	6.5	5.6	6.0	6.3	6.6
Ce	20	20	19	19	19	20	18
Nd	19	17	18	18	17	19	15
Sm	6.6	6.3	6.6	5.9	6.3	6.4	6.3
Eu	2.1	2.1	2.1	2.1	2.1	2.2	2.1
Tb	1.7	1.7	1.6	1.6	1.7	1.6	1.6
Yb	6.5	6.0	6.1	5.8	5.9	5.9	6.0
Lu	0.98	0.92	0.95	0.88	0.93	0.88	0.92
Cr	44	44	38	44	48	38	45
Ni	60	52	52	56	63	56	54
Co	58	48	33	42	52	48	46
V	415	392	360	450	600	575	430
Cu	60	60	47	100	54	78	46
Pb	<5	<5	<5	<5	<5	<5	<5
Zn	140	125	110	130	115	115	125
Zr	160	150	170	170	170	170	170
Y	57	57	58	54	51	57	57
Nb	5.2	5.6	4.4	3.9	4.1	4.9	3.9
Rb	16	12	10	11	12	9.1	14
Sr	110	110	120	120	120	120	130
Ba	17	<10	19	<10	<10	<10	<10

Note: ND = not determined.

Table T34 (continued).

Leg	91	91	91	91
Hole	595B	595B	595B	595B
Core, section	5R-2	6R-1	6R-2	7R-3
Interval (cm)	87-91	136-142	129-131	18-22
Piece	7A	14	15	4
Lab number	Z-436	Z-437	Z-438	Z-439
Depth (mbsf)	98.87	106.96	108.39	117.88
Unit	2	2	2	3
Major element oxides (wt%):				
SiO_2	46.89	45.99	47.37	48.30
TiO_2	2.95	3.13	3.31	2.27
Al_2O_3	14.79	19.91	16.40	15.23
Fe_2O_3	8.53	5.00	6.24	5.03
FeO	3.93	3.54	4.08	4.62
MnO	0.21	0.21	0.21	0.20
MgO	5.65	4.93	4.94	6.61
CaO	7.81	7.80	8.43	10.68
Na_2O	3.56	3.53	3.29	3.71
K_2O	1.04	1.62	1.32	0.68
P_2O_5	0.28	0.39	0.29	0.13
LOI	3.93	4.17	3.66	2.52
Total	99.57	100.22	99.54	99.98
H_2O^+	1.70	1.83	1.76	1.04
H_2O^-	2.23	2.34	1.90	1.48
CO_2	ND	ND	ND	ND
Fe_2O_3/FeO	2.17	1.41	1.53	1.09
Density (g/cm^3)	2.63	2.59	2.66	2.79
Trace elements (ppm):				
La	6.4	6.9	6.5	3.9
Ce	19	21	20	12
Nd	17	19	19	11
Sm	6.0	6.6	6.6	4.2
Eu	2.1	2.2	2.2	1.3
Tb	1.6	1.7	1.8	1.1
Yb	6.0	6.6	6.2	4.2
Lu	0.91	0.94	0.96	0.65
Cr	47	44	40	134
Ni	56	58	50	84
Co	58	48	43	43
V	420	345	390	290
Cu	50	46	60	63
Pb	<5	<5	<5	<5
Zn	110	115	115	75
Zr	170	150	170	95
Y	55	63	59	38
Nb	5.4	4.2	4.3	2.8
Rb	10	14	8.8	7.8
Sr	110	110	120	110
Ba	<10	<10	<10	<10

Table T35. Composition of basalts from Hole 765D, Leg 123 (Argo Abyssal Plain, Indian Ocean). (Continued on next page.)

Leg	123	123	123	123	123	123	123
Hole	765D	765D	765D	765D	765D	765D	765D
Core, section	1R-2	5R-1	5R-5	7R-2	9R-1	17R-2	18R-1
Inteval (cm)	8-10	130-132	143-145	135-137	17-21	49-52	82-84
Piece	1A	8E	3B	6B	1A	6	1E
Lab number	Z-86	Z-87	Z-89	Z-80	Z-81	Z-83	Z-90
Depth (mbsf)	949.48	984.5	990.63	1004.85	1021.07	1093.69	1101.92
Unit	1	3	3	6	7	13	14
Major element oxides (wt%):							
SiO_2	48.29	47.62	47.88	49.59	47.94	48.82	48.14
TiO_2	1.76	1.75	1.31	1.76	1.60	1.77	1.56
Al_2O_3	14.39	14.23	14.98	15.16	15.17	14.35	14.88
Fe_2O_3	4.39	3.16	4.21	3.35	4.15	3.36	6.70
FeO	6.41	8.21	5.46	5.16	5.48	6.42	5.17
MnO	0.20	0.23	0.08	0.16	0.16	0.19	0.13
MgO	7.26	6.85	7.79	6.83	7.59	7.20	6.71
CaO	12.19	12.11	12.31	12.27	12.36	12.21	12.07
Na_2O	2.66	2.41	2.61	2.92	2.70	2.70	2.81
K_2O	0.14	0.14	0.10	0.81	0.14	0.31	0.81
P_2O_5	0.10	0.09	0.08	0.09	0.10	0.13	0.08
Loi	2.41	2.69	3.07	1.76	2.56	2.26	1.56
Total	100.20	99.49	99.88	99.86	99.95	99.72	100.62
H_2O^+	0.37	0.42	1.16	0.47	0.35	0.60	0.78
H_2O^-	1.55	1.66	1.91	0.85	1.73	1.39	0.78
CO_2	ND	ND	ND	ND	ND	ND	ND
Fe_2O_3/FeO	0.68	0.38	0.77	0.65	0.76	0.52	1.30
Density (g/cm^3)	ND	ND	2.82	2.80	2.85	2.82	3.00
Trace elements (ppm):							
La	1.9	2.1	1.7	2.0	1.9	2.6	2.0
Ce	5.8	7.0	6.6	6.3	5.7	8.8	6.9
Nd	ND	ND	ND	ND	ND	ND	ND
Sm	3.1	3.0	2.7	3.3	3.0	4.2	2.9
Eu	1.1	1.2	1.1	1.2	1.1	1.3	1.1
Tb	0.82	0.93	0.77	0.9	0.81	1.2	0.73
Yb	3.9	3.9	3.0	3.6	3.7	4.7	3.2
Lu	0.6	0.61	0.44	0.55	0.59	0.72	0.5
Sc	53	53	51	53	51	52	48
Cr	170	143	185	275	220	200	265
Ni	66	80	75	90	110	76	100
Co	57	50	40	50	48	50	55
V	335	335	240	290	315	275	320
Cu	92	74	60	32	81	46	75
Pb	<5	<5	<5	<5	<5	<5	<5
Zn	84	95	80	80	96	87	90
Zr	59	79	69	65	77	85	78
Y	31	36	30	31	32	41	31
Nb	1.1	1.3	2.0	1.1	1.4	1.6	2.8
Rb	<1	<1	<1	11	<1	4	17
Sr	77	82	98	81	100	81	89
Ba	<10	<10	<10	63	42	40	10

Note: ND = not determined.

Table T35 (continued).

Leg	123	123	123	123	123
Hole	765D	765D	765D	765D	765D
Core, section	19R-1	22R-1	24R-1	27R-2	27R-3
Inteval (cm)	78-84	2-4	7-9	31-33	4-6
Piece	4B	1A	1A	1C	1
Lab number	Z-1358	Z-88	Z-82	Z-85	Z-84
Depth (mbsf)	1111.08	1138.62	1157.17	1187.21	1188.44
Unit	15	16	17	22	22
Major element oxides (wt%):					
SiO_2	49.85	46.79	48.43	49.98	46.83
TiO_2	1.74	1.45	1.75	1.83	1.75
Al_2O_3	15.03	14.94	14.30	14.23	13.63
Fe_2O_3	5.38	4.17	4.25	5.08	7.64
FeO	4.78	6.78	6.62	5.71	6.79
MnO	0.19	0.29	0.18	0.17	0.24
MgO	7.51	6.09	6.88	6.46	5.55
CaO	11.01	13.90	11.75	11.38	11.63
Na_2O	2.87	2.22	2.66	3.13	2.87
K_2O	0.15	0.41	0.13	0.77	0.86
P_2O_5	0.12	0.10	0.13	0.13	0.13
Loi	1.41	3.38	3.00	1.65	2.38
Total	100.04	100.52	100.08	100.52	100.30
H_2O^+	0.17	0.42	0.74	0.59	0.93
H_2O^-	0.81	1.49	1.42	0.53	0.55
CO_2	<0.20	0.90	ND	ND	ND
Fe_2O_3/FeO	1.13	0.62	0.64	0.89	1.12
Density (g/cm^3)	2.78	2.96	ND	2.86	2.75
Trace elements (ppm):					
La	2.4	1.7	2.8	2.6	2.9
Ce	7.0	5.2	8.6	8.3	7.2
Nd	8.5	ND	ND	ND	ND
Sm	3.7	2.7	4.3	3.7	4.0
Eu	1.2	1.0	1.3	1.3	1.3
Tb	1.2	0.79	1.1	1.0	1.1
Yb	4.2	3.3	4.9	4.2	4.6
Lu	0.64	0.5	0.79	0.68	0.72
Sc		50	52	53	42
Cr	210	170	160	135	155
Ni	77	90	80	58	66
Co	74	53	50	41	38
V	445	285	395	302	307
Cu	110	85	74	25	38
Pb	ND	<5	<5	<5	<5
Zn	132	86	105	120	91
Zr	92	52	98	87	76
Y	42	28	41	39	37
Nb	3.0	1.3	1.8	1.5	1.6
Rb	1.6	8.8	<1	18	20
Sr	83	75	89	76	79
Ba	8	10	64	<10	<10

Table T36. Composition of basalts from Holes 801B and 801C, Leg 129 (Pigafetta Basin, Pacific Ocean). (Continued on next three pages.)

Leg	129	129	129	129	129	129	129
Hole	801B	801B	801B	801B	801B	801B	801B
Core, section	40R-1	41R-1	41R-1	42R-1	43R-2	43R-3	43R-4
Interval (cm)	29-33	26-31	130-136	87-91	10-15	126-129	32-40
Piece	5	3	3	5B	1B	17	4A
Lab number	Z-776	Z-777	Z-778	Z-779	Z-780	Z-781	Z-782
Depth (mbsf)	477.19	483.26	484.30	488.47	493.67	496.24	496.80
Unit	B4	B5	B5	B6	B7	B9	B11
Major element oxides (wt%):							
SiO_2	53.20	45.77	46.08	46.50	44.88	42.82	45.22
TiO_2	3.58	3.31	3.24	3.01	2.68	2.85	3.38
Al_2O_3	18.96	16.03	15.80	17.23	14.46	15.40	17.32
Fe_2O_3	5.54	4.76	4.28	5.04	4.86	3.20	5.20
FeO	0.77	4.72	5.79	4.31	6.20	3.84	5.20
MnO	0.08	0.14	0.15	0.14	0.16	0.49	0.20
MgO	2.87	5.20	4.86	6.26	9.01	3.31	4.09
CaO	1.88	8.25	7.64	8.26	6.74	9.01	6.24
Na_2O	2.76	3.81	3.71	3.49	3.35	2.89	4.61
K_2O	5.84	2.14	2.61	1.97	1.79	4.55	2.34
P_2O_5	0.67	0.62	0.61	0.56	0.50	0.52	0.68
LOI	4.11	5.08	4.71	3.34	5.22	11.63	3.84
Total	100.26	99.83	99.48	100.11	99.85	100.51	100.32
H_2O^+	3.77	2.00	1.55	2.32	2.91	2.30	3.26
H_2O^-	ND	ND	ND	ND	ND	ND	ND
CO_2	0.24	2.83	3.00	0.97	2.02	8.69	2.36
Fe_2O_3/FeO	7.19	1.01	0.74	1.17	0.78	0.83	1.00
Density (g/cm^3)	2.48	2.62	2.65	2.67	2.60	2.45	2.52
Trace elements (ppm):							
La	36*	30.5	36.3		29*		36*
Ce	74*	63.8	74.16		48*		72*
Pr	ND	ND	ND		ND		ND
Nd	36*	31	35.47		27*		38*
Sm	7.9*	7.28	7.41		6.6*		8.8*
Eu	2.3*	2.32	2.47		1.9*		2.3*
Gd	ND	ND	7.23		ND		ND
Tb	1.20*	1.03	ND		0.92*		1.2*
Dy	ND	ND	6.4		ND		ND
Ho	ND	ND	1.14		ND		ND
Er	ND	ND	3.11		ND		ND
Yb	2.0*	2.31	2.6		2.1*		3.0*
Lu	0.28*	0.315	0.44		0.34*		0.48*
Cr	89	73	61	134	244	78	102
Ni	66	46	45	72	241	64	67
Co	ND	ND	ND	ND	ND	ND	ND
V	198	267	275	230	202	212	258
Cu	20	44	44	42	33	36	40
Pb	1	3	10	2	8	9	5
Zn	74	90	90	79	93	72	146
Sn	ND	ND	ND	ND	ND	ND	ND
Zr	208	272	285	246	227	218	246
Y	27	32	32	29	27	31	32
Nb	51	48	49	44	40	40	40
Rb	88	39	52	40	39	58	44
Sr	134	518	512	548	413	243	404
Ba	406	414	422	365	483	413	547
Th	ND	ND	ND	ND	ND	ND	ND

Note: * = rare earth element contents were determined in Geological Institute, Moscow. ** = major element contents were determined in Geological Institute, Moscow. *** = trace element contents were determined in Geological Institute, Moscow. The rest of chemical analyses data from Floyd and Castillo (1992). ND = not determined. [1] = hydrothermal deposit.

Table T36 (continued).

Leg	129	129	129	129	129	129	129
Hole	801B	801B	801B	801C	801C	801C	801C
Core, section	44R-1	44R-2	44R-3	1R-1	1R-2	2R-1	2R-5
Interval (cm)	107-113	27-32	28-33	109-114	11-17	1-6	101-106
Piece	2E	4A	2	2G	1A	1A	2
Lab number	Z-783	Z-784	Z-785	Z-786	Z-787	Z-788	Z-789
Depth (mbsf)	502.77	503.42	504.91	494.79	495.06	503.01	509.5
Unit	B12	B13	B14	C1	C1	C3	C6
Major element oxides (wt%):							
SiO_2	48.13	51.42	47.65	44.92	45.17	51.99	46.00
TiO_2	3.26	3.27	3.16	2.80	2.81	3.34	3.13
Al_2O_3	17.72	17.70	17.22	14.72	14.87	17.94	16.81
Fe_2O_3	4.32	3.75	4.18	3.62	4.10	3.63	3.99
FeO	3.22	3.27	5.04	6.40	6.30	3.01	6.08
MnO	0.18	0.13	0.14	0.15	0.15	0.13	0.16
MgO	3.05	3.03	4.21	9.58	9.34	2.62	6.16
CaO	4.35	3.56	7.24	6.46	6.34	2.35	6.78
Na_2O	3.12	3.20	4.08	3.45	3.63	2.53	3.67
K_2O	4.57	5.67	2.31	1.75	1.82	6.40	2.20
P_2O_5	0.57	0.55	0.57	0.60	0.53	0.60	0.53
LOI	6.96	4.40	3.63	5.30	5.03	4.75	4.62
Total	99.45	99.95	99.43	99.75	100.09	99.29	100.13
H_2O^+	3.34	2.06	1.40	3.77	3.44	2.92	1.77
H_2O^-	ND	ND	ND	ND	ND	ND	ND
CO_2	3.24	2.20	2.05	1.15	1.37	1.72	2.70
Fe_2O_3/FeO	1.34	1.15	0.83	0.57	0.65	1.21	0.66
Density (g/cm^3)	2.48	2.56	2.43	2.52	2.67	2.43	2.62
Trace elements (ppm):							
La	27	31.84	28.9	27.4	33*	30	28
Ce	56.6	66.47	60.6	57.5	64*	92	77
Pr	ND	7.68	ND	ND	ND	ND	ND
Nd	25	32.4	33	30	34*	42	41
Sm	6.18	6.97	7.09	6.37	7.4*	7.0	6.8
Eu	2.06	2.31	2.33	2.05	2.1*	2.0	1.9
Gd	ND	6.96	ND	ND	ND	ND	ND
Tb	0.882	ND	1.09	0.9	1.2*	1.1	0.99
Dy	ND	6.14	ND	ND	ND	ND	ND
Ho	ND	1.08	ND	ND	ND	ND	ND
Er	ND	2.99	ND	ND	ND	ND	ND
Yb	ND	2.52	2.6	2.05	2.2*	2.2	2.6
Lu	ND	0.4	0.382	0.299	0.37*	0.25	0.35
Cr	123	130	92	154	160	131	84
Ni	107	93	59	197	212	119	56
Co	ND	ND	ND	ND	ND	ND	ND
V	284	253	243	241	205	254	241
Cu	35	42	36	40	40	37	44
Pb	1	8	10	1	3	2	1
Zn	87	69	83	86	85	54	78
Sn	ND	ND	ND	ND	ND	ND	ND
Zr	214	254	268	242	239	258	255
Y	27	31	33	27	28	35	31
Nb	42	44	44	41	42	45	40
Rb	63	67	46	40	41	66	42
Sr	250	311	528	363	360	160	499
Ba	437	531	396	427	493	500	412
Th	ND	ND	ND	ND	ND	ND	ND

Table T36 (continued).

Leg	129	129	129	129	129	129	129
Hole	801C	801C	801C	801C	801C	801C	801C
Core, section	3R-1	4R-1	4R-2	5R-1	5R-2	5R-3	5R-5
Interval (cm)	42-48	18-21	111-114	45-52	12-17	98-100	55-58
Piece	2C	4	13	2C	1A	4B	3C
Lab number	Z-790	Z-791[1]	Z-792[1]	Z-793	Z-794	Z-795	Z-796
Depth (mbsf)	512.63	521.88	524.18	531.65	532.58	534.75	537.24
Unit	C7	C8	C8	C9	C9	C10	C13
Major element oxides (wt%):							
SiO_2	52.83	88.06**	87.34**	42.69	48.10	51.30**	47.51**
TiO_2	3.53	0.03	0.02	1.17	1.02	1.25	0.80
Al_2O_3	18.77	0.14	0.66	20.43	15.75	21.00	15.34
Fe_2O_3	5.09	9.26	9.50	2.27	6.49	4.40	2.19
FeO	1.00	0.29	0.22	1.05	1.29	0.93	6.40
MnO	0.05	0.02	0.02	0.10	0.18	0.04	0.17
MgO	3.32	0.40	0.24	3.31	3.45	2.22	9.96
CaO	1.94	<0.1	0.11	15.86	9.31	9.66	11.60
Na_2O	2.28	0.11	0.06	3.09	1.99	2.72	2.10
K_2O	5.68	0.10	0.04	0.89	4.39	0.81	0.04
P_2O_5	0.62	0.02	0.02	0.02	0.01	0.12	0.05
LOI	4.58	1.64	1.86	9.15	8.44	6.59	3.44
Total	99.69	100.07	100.09	100.03	100.42	101.04	99.60
H_2O^+	4.00	1.24	1.58	2.02	2.53	2.32	0.59
H_2O^-	ND	<0.1	<0.1	ND	ND	1.40	0.83
CO_2	0.41	<0.2	<0.2	6.45	5.17	2.87	1.98
Fe_2O_3/FeO	5.09	31.93	43.18	2.16	5.03	4.73	0.34
Density (g/cm^3)	2.04	2.36	2.46	2.65	2.51	2.42	2.91
Trace elements (ppm):							
La	33*	0.47*	0.61*	1.73		2.0*	1.2*
Ce	75*	0.90*	0.90*	6.8		6.6*	4.3*
Pr	ND	ND	ND	ND		ND	ND
Nd	36*	<0.5*	<0.5*	8		7.8*	4.8*
Sm	7.4*	0.09*	0.10*	2.52		3.3*	2.00*
Eu	2.3*	0.032*	0.028*	1.02		1.3*	0.83*
Gd	ND	ND	ND	ND		ND	ND
Tb	1.1*	0.02*	0.02*	0.62		0.88*	0.68*
Dy	ND	ND	ND	ND		ND	ND
Ho	ND	ND	ND	ND		ND	ND
Er	ND	ND	ND	ND		ND	ND
Yb	2.6*	0.06*	0.06*	2.24		2.0*	2.2*
Lu	0.44*	0.011*	0.01*	0.322		0.33*	0.32*
Cr	155	19***	20***	334	288	307***	510***
Ni	99	24***	25***	96	73	49***	170***
Co	ND	14***	14***	ND	ND	20***	59***
V	284	65***	55***	276	145	252***	210***
Cu	55	26***	26***	81	87	135***	82***
Pb	1	ND	ND	1	2	ND	<5***
Zn	85	71***	52***	52	64	66***	78***
Sn	ND	ND	ND	ND	ND	ND	2.1***
Zr	248	3.7***	5.4***	74	64	72***	48***
Y	32	1.0***	1.5***	27	19	24***	21***
Nb	46	<1***	<1***	2	4	2.1***	<1***
Rb	71	1.7***	2.0***	13	77	7.3***	1.2***
Sr	112	3.5***	3.4***	160	123	210***	100***
Ba	427	5***	4***	22	47	3***	13***
Th	ND	ND	ND	ND	ND	ND	ND

Table T36 (continued).

Leg	129	129	129	129
Hole	801C	801C	801C	801C
Core, section	7R-1	7R-3	8R-1	10R-1
Interval (cm)	53-58	38-41	9-12	55-60
Piece	4C	1E	2C	1G
Lab number	Z-797	Z-798	Z-799	Z-800
Depth (mbsf)	550.63	553.36	559.59	569.55
Unit	C21	C23	C23	C25
Major element oxides (wt%):				
SiO_2	48.26	46.65**	45.91**	49.44
TiO_2	1.93	2.02	1.98	1.62
Al_2O_3	13.23	13.97	13.24	14.02
Fe_2O_3	3.50	4.40	2.20	3.82
FeO	9.12	6.15	7.54	8.15
MnO	0.20	0.15	0.22	0.18
MgO	6.96	6.49	5.34	7.28
CaO	11.16	11.39	12.28	11.95
Na_2O	2.68	2.86	2.81	2.56
K_2O	0.08	0.06	0.19	0.06
P_2O_5	0.16	0.15	0.18	0.06
LOI	2.58	5.45	7.98	1.09
Total	99.86	99.74	99.87	100.23
H_2O^+	0.59	0.76	1.61	0.55
H_2O^-	ND	1.52	1.08	ND
CO_2	1.31	2.82	5.24	0.28
Fe_2O_3/FeO	0.38	0.72	0.29	0.47
Density (g/cm^3)	2.81	2.71	2.80	2.94
Trace elements (ppm):				
La	5.37			3.48
Ce	15.13			10.78
Pr	2.36			2.06
Nd	13.36			10.65
Sm	4.24			3.44
Eu	1.49			1.33
Gd	6.03			5.2
Tb	ND			ND
Dy	7.48			6.38
Ho	1.48			1.27
Er	4.39			3.83
Yb	4.36			3.69
Lu	0.74			0.62
Cr	140	170***	170***	175
Ni	71	66***	62***	70
Co	ND	57***	50***	ND
V	416	520***	442***	365
Cu	81	66***	47***	75
Pb	5	<5***	<5***	6
Zn	98	120***	150***	85
Sn	ND	2.5***	2.5***	ND
Zr	119	110***	110***	97
Y	44	38***	41***	38
Nb	5	3.8***	2.3***	5
Rb	1	<1***	3.1***	1
Sr	114	130***	120***	113
Ba	32	13***	<3***	14
Th	ND	<1***	<1***	ND

Table T37. Composition of hawaiites from Hole 430A, Leg 55 (Ojin seamount, Emperor Seamount chain).

Leg	55	55	55	55	55	55	55
Hole	430A	430A	430A	430A	430A	430A	430A
Core, section	5R-4	5R-5	5R-5	6R-1	6R-1	6R-2	6R-3
Interval (cm)	105-108	33-37	96-101	6-11	98-103	24-30	19-24
Piece	12	5	10	1	7B	4	2
Lab number	Z-1110	Z-1111	Z-1619	Z-1620	Z-1622	Z-1112	Z-1623
Depth (mbsf)	72.05	72.83	73.76	76.06	76.98	77.74	79.19
Flow Unit	2	2	2	2	2	3	3
Major element oxides (wt%):							
SiO_2	44.82	48.11	47.85	48.84	46.29	46.80	47.06
TiO_2	3.12	3.08	3.12	3.10	3.07	2.91	2.81
Al_2O_3	14.94	15.14	15.58	15.52	15.43	14.85	15.63
Fe_2O_3	11.61	9.88	8.01	9.10	5.44	7.98	8.00
FeO	2.05	3.22	4.18	3.00	7.26	4.76	4.71
MnO	0.23	0.10	0.09	0.08	0.13	0.13	0.14
MgO	1.85	3.57	4.12	3.43	4.94	5.29	4.73
CaO	9.07	6.69	6.55	6.82	8.32	6.09	6.07
Na_2O	4.12	4.40	4.24	4.31	3.61	4.27	4.37
K_2O	2.48	1.68	1.55	1.59	1.02	1.68	1.54
P_2O_5	1.55	1.55	1.51	1.55	0.54	1.62	1.25
LOI	4.04	2.64	2.66	2.40	3.21	3.12	3.36
Total	99.88	100.06	99.46	99.74	99.26	99.50	99.67
H_2O^+	0.45	1.38	0.95	0.54	0.94	1.43	1.96
H_2O^-	0.52	1.26	1.36	1.34	1.29	1.37	1.20
CO_2	2.75	<0.2	<0.2	<0.2	0.36	<0.2	0.20
Fe_2O_3/FeO	5.66	3.07	1.92	3.03	0.75	1.68	1.70
Density (g/cm^3)	2.17	1.93	2.56	2.69	2.80	2.22	2.71
Trace elements (ppm):							
La	44	44		41			42
Ce	110	110		110			110
Nd	66	65		65			66
Sm	17	17		17			17
Eu	5.1	5.0		5.7			5.6
Tb	2.2	2.1		2.6			2.6
Yb	3.6	3.5		3.8			3.7
Lu	0.53	0.44		0.60			0.59
Cr	<10	<10	<10	20	90	<10	85
Ni	21	28	24	28	53	21	50
Co	30	36	32	36	45	30	33
V	182	188	178	176	216	125	191
Cu	27	47	49	28	56	27	63
Zn	104	161	142	119	112	160	150
Zr	465	460	460	470	185	470	470
Y	53	52	55	50	26	51	55
Nb	38	38	38	37	29	39	12
Rb	24	20	23	23	15	17	15
Sr	640	680	590	640	485	580	610
Ba	300	280	200	250	220	225	310

Table T38. Secondary minerals in fine fraction sampled from alkaline series of basalts, Emperor Seamount chain, Leg 55: Hole 430A (Ojin seamount), Hole 432A (Nintoku seamount), and Holes 433A and 433C (Suiko seamount) (X-ray diffraction data).

Core, section, interval (cm)	Flow Unit	Depth (mbsf)	Smectites	Mixed-layer smectite-swelling chlorite	Swelling chlorite	Illite	Kaolinite	Rock type
55-430A-								
5R-4, 39-43	2	71.39	X	+?		+		Hawaiite
5R-5, 33-37	2	72.83	X	+?				Hawaiite
5R-5, 96-101	2	73.76	X	+		+		Hawaiite
6R-1, 6-11	2	76.06	X					Hawaiite
6R-1, 96-98	2	76.98	X	+				Hawaiite
6R-1, 98-103	2	76.99	X	+		+		Hawaiite
55-432A-								
2R-1, 99-104	2	42.49	X					Alkaline basalt
2R-2, 6-11	2	43.06	+					Alkaline basalt
2R-2, 69-74	2	43.69	X					Alkaline basalt
2R-2, 102-107	2	43.52	+					Alkaline basalt
2R-3, 43-48	2	44.93	+					Alkaline basalt
2CC, 0-3	2	46.00	+					Alkaline basalt
3R-1, 0-3	3	55.03	X	+			+	Transitional between alkaline basalt and hawaiite
3R-1, 9-12	3	55.09	X					- " -
3R-2, 15-20	3	55.15	X	+		+		- " -
3R-3, 70-75	3	58.70	X	+		+		- " -
4R-3, 140-145	3	68.90	X	+		+		- " -
4R-4, 80-83	3	69.70	X	+		+		- " -
4R-5, 56-61	3	71.06	X	+		+		- " -
5R-1, 100-105	3	72.00	X	+		+		- " -
55-433A-								
20R-1, 83-89	1	164.35	X					Alkaline basalt
20R-2, 42-47	1	165.42	X	+				Alkaline basalt
21R-1, 116-122	1	167.66	X	+				Alkaline basalt
21R-3, 128-134	1	170.78	X		X			Alkaline basalt
Hole 433C								
4R-1, 39-41	2	181.89	X	+				Alkaline basalt

Note: X = dominant, + = minor or trace.

Table T39. Parameter *b* of clay minerals sampled from basalts of alkaline and tholeiitic series, Emperor Seamount chain, Leg 55: Hole 430A (Ojin seamount), Hole 432A (Nintoku seamount), and Hole 433C (Suiko seamount) (Electron diffraction data).

Core, section, interval (cm)	Flow Unit	Depth (mbsf)	Parameter *b* (Å)	Rock type
55-430A-				
6R-1, 6-11	2	76.06	9.19	Hawaiite
55-432A-				
3R-1, 0-3	3	55.03	9.01	Oxidized alkaline basalt
55-433C-				
14R-1, 2-7	11a	233.02	9.18; 8.98	Oxidized tholeiite
17R-1, 64-69	13	256.14	9.19	Tholeiite
24R-7, 108-114	19d	317.28	9.24	Tholeiitic picrite
39R-1, 119-122	48	451.19	9.19	Oxidized olivine tholeiite
39R-2, 35-40	48	451.85	9.24	Olivine tholeiite
45R-3, 61-66	60	510.61	9.18; 8.98	Oxidized tholeiite
48R-3, 10-15	64	538.60	9.24	Tholeiite

Table T40. Chemical composition (wt%) of fraction less than 0.001 mm sampled from basalts of alkaline and tholeiitic series, Emperor Seamount chain, Leg 55: Hole 430A (Ojin seamount), Hole 432A (Nintoku seamount), and Hole 433C (Suiko seamount).

Hole, core, section, interval (cm)	430A 6R-1, 6-11	432A 3R-1, 0-3	433C 4R-1, 39-41	433C 48R-3, 10-15	433C 34R-2, 41-46	433C 34R-4, 97-101	433C 39R-2, 35-40	433C 24R-7, 108-114
Rock type	Hawaiite	Oxidized alkaline basalt	Alkaline basalt	Tholeiite	Olivine tholeiite	Olivine tholeiite	Olivine tholeiite	Tholeiitic picrite
SiO_2	48.70			44.77	44.48	45.76	44.44	
TiO_2	0.98			0.90	1.94	0.32	0.85	
Al_2O_3	10.59			10.31	13.35	8.46	9.62	
Fe_2O_3	12.15			11.41	8.96	5.80	10.09	
FeO	1.83			2.66	2.66	2.33	1.37	
MnO	0.07			0.07	0.19	0.25	0.07	
MgO	7.84			9.14	11.16	21.44	15.12	
CaO	2.58			3.83	7.58	1.14	1.20	
Na_2O	2.14	1.92	3.10	1.57	2.34	0.61	0.86	3.40
K_2O	1.32	2.06	1.18	0.36	0.25	0.26	0.52	0.75
LOI	9.74						12.81	
H_2O^-	1.62						2.70	
Total	99.56						99.65	

Table T41. Minerals from vesicles and veins in alkaline series of basalts, Emperor Seamount chain, Leg 55: Hole 430A (Ojin seamount), Hole 432A (Nintoku seamount), and Hole 433A (Suiko seamount) (X-ray diffraction data).

Core, section, interval (cm)	Flow Unit	Depth (mbsf)	Smectites	Mixed-layer smectite-chlorite	Illite	Calcite	Aragonite	9.3Å-mineral	Mn-mineral	Matter of vesicles or veins	Rock type
55-430A-											
5R-4, 39-43	2	71.39	X							Yellow clay from vesicles	Hawaiite
5R-5, 96-101	2	73.76	X							Greenish-gray clay from vesicles	Hawaiite
5R-5, 96-101	2	73.76	X	+		+				Greenish-gray clay and carbonate from vesicles	Hawaiite
6R-1, 6-11	2	76.06	X			+				Greenish-gray clay from vesicles	Hawaiite
6R-1, 6-11	2	76.06	X			+				Black clay from vein	Hawaiite
6R-1, 98-103	2	76.99	X							Greenish-gray clay from vesicles	Hawaiite
6R-1, 98-103	2	76.99	X			+	X			Carbonate from vesicle	Hawaiite
6R-3, 19-24	3	79.19	X	+	+					Black clay from vein	Hawaiite
55-432A-											
2R-2, 6-11	2	43.06	X							Red clay from vesicles	Alkaline basalt
2R-2, 69-74	2	43.69	X							Greenish-gray clay from vesicles	Alkaline basalt
2R-2, 69-74	2	43.69				X				Carbonate from vesicle	Alkaline basalt
2CC, 0-3	2	46.00				X				Grey crystals from vesicle	Alkaline basalt
2CC, 0-3	2	46.00							X	Dark-brown crust from vesicle	Alkaline basalt
3R-2, 15-20	3	55.15	X							Black clay from vein	Transitional between alkaline basalt and hawaiite
3R-3, 70-75	3	58.70	+	+		X				Carbonate with clay from vesicles	- " -
4R-3, 140-145	3	68.90	X	+						Greenish-gray clay from vesicles	- " -
5R-1, 100-105	3	72.00	+	+		+	X	+		Carbonate with clay from vesicles	- " -
55-433A-											
20R-2, 42-47	1	165.42	+			X				Carbonate with clay from vesicles	Alkaline basalt
21R-1, 116-122	1	167.66				X				Carbonate from vesicle	Alkaline basalt
21R-1, 116-122	1	167.66	X							Green-gray clay from vesicles	Alkaline basalt

Note: X = dominant, + = minor or trace.

Table T42. Parameter *b* of clay minerals from vesicles and veins in basalts of alkaline and tholeiitic series, Emperor Seamount chain, Leg 55: Hole 430A (Ojin seamount), Hole 432A (Nintoku seamount), and Holes 433A and 433C (Suiko seamount) (Electron diffraction data).

Core, section, interval (cm)	Flow Unit	Depth (mbsf)	Parameter *b* (Å)	Matter from vesicles	Rock type
55-430A-					
5R-4, 39-43	2	71.39	9.21; 8.99	Yellow clay	Hawaiite
5R-5, 96-101	2	73.46	9.19	Greenish-gray clay	Hawaiite
55-432A-					
2R-2, 6-11	2	43.06	9.05	Red clay	Alkaline basalt
55-433A-					
21R-3, 128-134	1	170.78	9.19	Dark-green clay	Alkaline basalt
55-433C-					
10R-1, 25-31	4a	204.75	9.21	Green clay covering walls of vesicles	Olivine tholeiite
10R-1, 25-31	4a	204.75	9.21	Greenish-gray clay from central part of vesicles	Olivine tholeiite
12R-2, 136-141	9	226.36	9.21	Black clay	Tholeiite
14R-1, 2-7	11a	233.02	9.22; 9.00	Black clay	Oxidized tholeiite
15R-1, 0-4	11c	242.50	9.20	Clay pellicle	Tholeiite
23R-2, 12-17	19b	299.62	9.20	Greenish-gray clay	Olivine tholeiite
27R-2, 138-144	24a	338.88	9.22	Greenish-gray clay	Tholeiitic picrite
32R-1, 82-88	28c	384.32	9.22	Greenish-gray glassy matter	Tholeiitic picrite
32R-5, 50-55	29	390.00	9.21	Clay	Olivine tholeiite
34R-1, 108-114	32b	403.58	9.21	Clay pellicle	Oxidized tholeiite
34R-2, 41-46	33	404.41	9.21	Greenish-gray clay	Olivine tholeiite
38R-1, 81-86	45b	441.31	9.19	Clay	Olivine tholeiite
39R-6, 114-118	48	458.64	9.19; 9.04	Blue clay	Oxidized olivine tholeiite
43R-1, 118-123	54	489.18	9.12	Brownish-red clay from vein	Tholeiite
45R-3, 119-124	60	511.19	9.22	Black clay	Tholeiite
45R-3, 119-124	60	511.19	9.22	Greenish-gray clay	Tholeiite
45R-4, 109-114	60	512.59	9.12	Green clay	Tholeiite
45R-5, 39-44	60	513.39	9.18	Greenish-gray clay	Tholeiite

Table T43. Chemical composition (wt%) of clay minerals from vesicles and veins in basalts of alkaline and tholeiitic series, Emperor Seamount chain, Leg 55: Hole 430A (Ojin seamount), Hole 432A (Nintoku seamount), and Hole 433C (Suiko seamount).

Hole, core, section, interval (cm)	430A 5R-5, 96-101	432A 2R-2, 6-11	433C 23R-2, 12-17	433C 34R-2, 41-46	433C 38R-1, 81-86	433C 43R-1, 118-123	433C 45R-3, 119-124	433C 45R-3, 119-124
Rock type	Hawaiite	Alkaline basalt	Olivine tholeiite	Olivine tholeiite	Olivine tholeiite	Tholeiite	Tholeiite	Tholeiite
Clay type	Greenish-gray clay from vesicles	Red clay from vesicles	Greenish-gray clay from vesicles	Greenish-gray clay from vesicles	Clay from vesicles	Brownish-red clay from vein	Black clay from vesicles	Greenish-gray clay from vesicles
SiO_2			41.97	41.71	44.37	45.74		
TiO_2			0.86	0.42	0.25	2.02		
Al_2O_3			12.74	6.58	9.08	14.99		
Fe_2O_3			3.44	6.13	2.02	9.01		
FeO	6.49		8.32	2.64	3.25	1.66		
MnO			0.16	0.11	0.20	0.23		
MgO			17.27	21.15	27.12	7.29		
CaO			1.68	2.54	0.68	4.99		
Na_2O	2.11	1.28	2.45	1.99	1.00	2.04	2.77	2.93
K_2O	0.60	1.75	0.42	0.10	0.29	1.46	0.31	0.47
LOI						7.60		
H_2O^-						2.72		
Total						99.75		

Table T44. Microprobe analyses of greenish-gray and green clay from vesicles in basalts of alkaline and tholeiitic series, Emperor Seamount chain, Leg 55: Hole 430A (Ojin seamount) and 433C (Suiko seamount).

Hole, core, section, interval (cm)	430A 5R-5, 96-101	433C 10R-1, 25-31	433C 10R-1, 25-31	433C 27R-2, 138-144	433C 41R-1, 66-71
Rock type	Hawaiite	Olivine tholeiite	Olivine tholeiite	Tholeiitic picrite	Tholeiite
Clay type	Greenish-gray clay filling of vesicles	Green clay covering walls of vesicles	Greenish-gray clay from center of vesicles	Greenish-gray clay filling of vesicles	Greenish-gray clay filling of vesicles
SiO_2	40.59	44.55	45.30	45.80	44.08
TiO_2	0.005	0.005	0.005	0.01	0.01
Al_2O_3	6.54	16.48	7.97	2.36	5.93
FeO	17.74	6.77	4.70	5.41	14.84
MnO	0.12	0.15	0.10	0.02	0.01
MgO	16.72	16.63	24.77	32.21	18.97
CaO	0.07	0.17	0.08	0.13	0.05
Na_2O	1.76	1.26	2.06	0.68	3.26
K_2O	0.26	0.20	0.20	0.26	0.06

Table T45. Composition of basalts of alkaline series from Hole 432A, Leg 55 (Nintoku seamount, Emperor Seamount chain). (Continued on next page.)

Leg	55	55	55	55	55	55	55
Hole	432A	432A	432A	432A	432A	432A	432A
Core, section	2R-1	2R-2	2R-3	3R-1	3R-2	3R-3	4R-3
Interval (cm)	99-104	102-107	43-48	9-12	15-20	70-75	140-145
Piece	8E	11E	1E	1	2	7	14
Lab number	Z-1624	Z-1627	Z-1629	Z-1113	Z-1631	Z-1632	Z-1633
Depth (mbsf)	42.49	43.52	44.93	55.09	55.15	58.70	68.90
Flow Unit	1	2	2	3	3	3	3
Major element oxides (wt%):							
SiO_2	45.90	46.72	45.94	43.35*	47.48*	46.88*	44.88*
TiO_2	2.65	2.59	2.15	3.40	3.10	3.10	3.17
Al_2O_3	16.26	18.19	20.04	18.52	15.48	15.76	16.52
Fe_2O_3	5.11	8.09	9.78	14.59	5.42	5.36	10.02
FeO	6.08	3.38	1.45	1.21	6.21	5.65	4.60
MnO	0.09	0.10	0.05	0.20	0.16	0.20	0.23
MgO	5.77	3.24	2.13	1.60	4.92	5.36	3.42
CaO	9.11	9.51	9.23	2.90	9.21	9.43	5.87
Na_2O	3.01	3.60	3.65	2.64	3.62	3.55	3.34
K_2O	0.83	1.12	1.21	2.23	1.30	1.20	1.47
P_2O_5	0.59	0.67	0.46	0.65	0.57	0.50	0.53
H_2O^+				4.50	1.27	1.52	3.10
H_2O^-				3.78	0.99	1.24	2.82
CO_2				ND	ND	ND	ND
LOI	3.83	2.70	3.28				
Total	99.23	99.91	99.37	99.57	99.73	99.75	99.97
H_2O^+	1.51	0.98	0.93				
H_2O^-	1.21	0.86	0.96				
CO_2	0.21	0.37	0.80				
Fe_2O_3/FeO	0.84	2.39	6.75	12.05	0.87	0.95	2.18
Density (g/cm^3)	2.75	2.69	2.50	2.10	2.86	2.82	2.61
Trace elements (ppm):							
La				30	25		26
Ce				66	53		52
Nd				34	30		30
Sm				7.7	6.7		6.7
Eu				2.3	1.50		1.6
Tb				1.2	0.92		0.83
Yb				2.2	2.0		1.8
Lu				0.33	0.32		0.29
Cr	98	79	74	85	75		88
Ni	74	64	66	50	48		62
Co	60	44	39	33	37		44
V	248	217	220	191	210		218
Cu	88	64	50	63	60		56
Zn	115	92	92	150	120		124
Zr	160	170	140	230	200		200
Y	21	21	19	26	27		25
Nb	26	28	23	38	32		32
Rb	13	17	18	28	19		20
Sr	554	670	740	260	490		420
Ba	250	280	225	91	190		165

Notes: * = major element data from Avdeiko et al. (1980). ND = not determined.

Table T45 (continued).

Leg	55	55	55
Hole	432A	432A	432A
Core, section	4R-4	4R-5	5R-1
Interval (cm)	80-83	56-61	100-105
Piece	6B	4	2B
Lab number	Z-1114	Z-1634	Z-1635
Depth (mbsf)	69.70	71.06	72.00
Flow Unit	3	3	3
Major element oxides (wt%):			
SiO_2	45.46	46.16*	48.26*
TiO_2	3.42	3.00	3.10
Al_2O_3	15.97	14.80	15.48
Fe_2O_3	10.80	5.00	5.15
FeO	3.92	7.64	5.52
MnO	0.25	0.20	0.12
MgO	3.56	5.29	4.43
CaO	5.42	8.91	7.95
Na_2O	3.56	3.34	4.05
K_2O	1.31	1.16	1.73
P_2O_5	0.63	0.50	0.68
H_2O^+		1.88	1.42
H_2O^-		1.62	1.46
CO_2		ND	ND
LOI	5.25		
Total	99.55	99.50	99.35
H_2O^+	2.71		
H_2O^-	2.07		
CO_2	<0.2		
Fe_2O_3/FeO	2.76	0.65	0.93
Density (g/cm^3)	2.57	2.80	2.69
Trace elements (ppm):			
La			
Ce			
Nd			
Sm			
Eu			
Tb			
Yb			
Lu			
Cr	90		20
Ni	54		24
Co	48		32
V	228		168
Cu	63		30
Zn	148		122
Zr	200		460
Y	28		51
Nb	32		38
Rb	20		20
Sr	410		600
Ba	180		220

Table T46. Secondary minerals replace olivines in basalts of alkaline and tholeiitic series, Emperor Seamount chain, Leg 55: Hole 432A (Nintoku seamount) and Hole 433C (Suiko seamount) (X-ray diffraction data).

Core, section, interval (cm)	Flow Unit	Depth (mbsf)	Sm	Chl phases	Serp	Illite	Calcite	Rock type
55-432A-								
3R-3, 70-75	3	58.70	X					Transitional between alkaline basalt and hawaiite
4R-3, 140-145	3	68.90	X					- " -
55-433C-								
10R-1, 25-31	4a	204.75	X	+				Olivine tholeiite
23R-2, 12-17	19b	299.62	X					Olivine tholeiite
26R-5, 89-94	22	333.39	X	+				Olivine tholeiite
27R-2, 138-144	24a	338.88	X	+	+			Tholeiitic picrite
32R-1, 82-88	28c	384.32	X		+			Tholeiitic picrite
32R-5, 50-55	29	390.00	X	+?			+	Olivine tholeiite
34R-1, 108-114	32b	403.58	X					Oxidized tholeiite
34R-2, 41-46	33	404.41	X	+?				Oxidized olivine tholeiite
34R-4, 97-101	34a	407.97	X	+				Olivine tholeiite
39R-5, 2-8	48	456.02	X	+				Olivine tholeiite
39R-6, 38-43	48	457.88	X	+				Olivine tholeiite
39R-6, 114-118	48	458.64	X	+		+		Oxidized olivine tholeiite
48R-3, 10-15	64	538.60	X					Tholeiite

Notes: X = dominant, + = minor or trace.
Sm = smectites, Chl phases = chloritic phases, Serp = serpentine.

Table T47. Parameter *b* of clay minerals replace olivines in basalts of alkaline and tholeiitic series, Emperor Seamount chain, Leg 55: Holes 433A and 433C (Suiko seamount) (Electron diffraction data).

Core, section, interval (cm)	Flow Unit	Depth (mbsf)	Parameter *b* (Å)	Rock type
55-433A-				
21R-3, 138-134	1	170.78	9.18	Alkaline basalt
55-433C-				
10R-1, 25-31	4a	204.75	9.20	Olivine tholeiite
27R-2, 138-144	24a	338.88	9.22	Tholeiitic picrite
32R-1, 82-88	28c	384.32	9.25	Tholeiitic picrite
34R-1, 108-114	32b	403.58	9.18	Oxidized olivine tholeiite
34R-7, 103-109	35	412.53	9.20	Olivine tholeiite
39R-6, 38-43	48	457.88	9.19	Olivine tholeiite
45R-6, 129-133	60	515.54	9.18	Tholeiite

Table T48. Composition of basalts of tholeiitic series from Hole 433C, Leg 55 (Suiko seamount, Emperor Seamount chain). (Continued on next nine pages.)

Leg	55	55	55	55	55	55	55
Hole	433C	433C	433C	433C	433C	433C	433C
Core, section	10R-2	10R-4	12R-1	12R-2	12R-2	12R-3	13R-2
Interval (cm)	127-133	118-121	75-80	32-37	136-141	54-57	69-72
Piece	19	8B	8A	2E	3C	1D	1J
Lab number	Z-1640	Z-1115	Z-1116	Z-1644	Z-1645	Z-1117	Z-518
Depth (mbsf)	207.27	210.21	224.25	225.32	226.36	227.04	232.19
Unit/Subunit	4a	4h	9	9	9	9	10
Major element oxides (wt%):							
SiO_2	43.32	45.94*	42.94**	43.96**	45.38**	47.33	47.14
TiO_2	2.10	1.15	2.28	2.60	2.45	2.40	2.31
Al_2O_3	14.40	8.81	13.46	14.21	14.35	14.00	12.87
Fe_2O_3	11.83	14.10	12.78	8.49	5.90	4.85	6.06
FeO	3.78		3.07	5.58	7.04	7.16	6.40
MnO	0.18	0.19	0.07	0.11	0.07	0.12	0.22
MgO	8.98	20.39	8.25	9.00	9.48	7.57	7.70
CaO	7.22	6.70	4.15	8.09	8.99	9.56	10.57
Na_2O	3.00	1.40	2.46	2.51	2.58	2.74	2.41
K_2O	0.79	0.28	1.64	0.69	0.30	0.32	0.46
P_2O_5	0.24	0.15	0.26	0.30	0.27	0.25	0.27
H_2O^+			4.26	2.15	1.80		
H_2O^-			3.98	1.98	1.66		
CO_2			ND	ND	ND		
LOI	3.97					3.46	3.03
Total	99.81	99.11	99.60	99.67	100.27	99.76	99.44
LOI		14.00					
H_2O^+	3.97	5.52				1.22	1.60
H_2O^-	ND	ND				1.37	1.36
CO_2	ND	1.76				0.29	<0.2
Fe_2O_3/FeO	3.13		4.16	1.52	0.84	0.68	0.95
Density (g/cm^3)	ND	2.38	1.62	2.46	2.62	2.51	2.85
Trace elements (ppm):							
La		5.1	14		10		12
Ce		13	38		26		28
Nd		8.1	24		17		18
Sm		2.2	6.6		5.1		4.8
Eu		0.48	2.0		1.3		1.6
Tb		0.35	1.6		0.80		1.0
Yb		0.90	2.9		1.9		2.0
Lu		0.15	0.48		0.38		0.27
Cr	525	865	255		270	245	150
Ni	340	760	141		139	144	77
Co	80	115	51		62	55	48
V	355	201	250		362	358	275
Cu	150	57	129		93	114	73
Zn	86	100	92		96	103	90
Zr	115	64	140		140	130	140
Y	22	11	35		25	27	27
Nb	10	5.2	11		12	11	13
Rb	7.2	4.5	24		1.0	3.7	3.6
Sr	170	89	180		270	275	270
Ba	90	41	35		63	110	71

Notes: * = major element data from Cambon et al. (1980). ** = major element data from Avdeiko et al. (1980). *** = major element data from Kirkpatrick et al. (1980). ND = not determined.

Table T48 (continued).

Leg	55	55	55	55	55	55	55
Hole	433C	433C	433C	433C	433C	433C	433C
Core, section	14R-1	14R-1	14R-2	14R-4	14R-4	15R-1	15R-5
Interval (cm)	2-7	33-38	115-120	26-31	47-52	0-4	82-87
Piece	1A	1G	3C	2A	2B	1	4B
Lab number	Z-1658	Z-1656	Z-1657	Z-1648	Z-1649	Z-1650	Z-1118
Depth (mbsf)	233.02	233.33	235.65	237.76	237.97	242.50	249.32
Unit/Subunit	11a	11a	11a	11c	11c	11c	13
Major element oxides (wt%):							
SiO_2	42.84**	44.02**	45.52**	46.80	49.43	45.56	46.04
TiO_2	2.45	3.00	2.90	2.58	2.44	2.19	2.83
Al_2O_3	13.78	14.47	14.37	13.38	14.52	12.69	14.97
Fe_2O_3	14.82	8.78	8.24	7.86	5.20	12.54	9.99
FeO	1.90	5.58	5.89	6.00	7.49	3.23	4.76
MnO	0.16	0.09	0.11	0.14	0.14	0.12	0.12
MgO	6.89	7.61	7.71	7.43	6.47	7.43	6.67
CaO	5.52	7.61	8.30	9.07	9.61	8.74	7.89
Na_2O	2.56	3.22	2.88	3.12	2.44	2.99	3.25
K_2O	1.23	0.76	0.61	0.23	0.27	0.87	0.90
P_2O_5	0.12	0.29	0.22	0.26	0.31	0.26	0.31
H_2O^+	2.41	2.36	1.15				
H_2O^-	4.89	2.14	1.54				
CO_2	ND	ND	ND				
LOI				2.66	1.06	2.94	1.79
Total	99.57	99.93	99.44	99.53	99.38	99.56	99.52
LOI							
H_2O^+				0.49	1.06	0.69	0.56
H_2O^-				1.69	ND	1.74	1.01
CO_2				<0.2	ND	<0.2	0.21
Fe_2O_3/FeO	7.80	1.57	1.40	1.31	0.69	3.88	2.10
Density (g/cm^3)	ND	ND	ND	2.64	2.69	ND	2.56
Trace elements (ppm):							
La							
Ce							
Nd							
Sm							
Eu							
Tb							
Yb							
Lu							
Cr	84	70	74	64	83	280	58
Ni	82	57	59	53	57	91	52
Co	77	63	72	54	76	55	38
V	388	412	415	344	425	370	272
Cu	57	120	56	93	91	205	83
Zn	63	95	102	98	100	90	126
Zr	135	160	160	150	140	130	160
Y	18	30	27	28	27	25	27
Nb	11	12	13	11	11	13	10
Rb	13	10	5.6	1.4	<1	8.7	4.7
Sr	93	255	260	280	280	280	280
Ba	73	73	7	56	120	190	37

Table T48 (continued).

Leg	55	55	55	55	55	55	55
Hole	433C	433C	433C	433C	433C	433C	433C
Core, section	15R-5	15R-6	17R-1	19R-1	21R-3	22R-5	23R-1
Interval (cm)	88-92	31-32	64-69	48-54	20-23	48-52	100-104
Piece	4B	1C	5A	4C	2	3	5D
Lab number	Z-519	Z-1119	Z-1120	Z-1655	Z-520	Z-521	Z-1121
Depth (mbsf)	249.38	250.06	256.14	261.98	282.20	294.98	299.00
Unit/Subunit	13	13	13	13	17	18	19a
Major element oxides (wt%):							
SiO_2	47.22	47.91*	49.56**	46.70**	46.18	46.31***	48.45*
TiO_2	2.77	2.57	2.60	2.82	2.16	2.79	2.32
Al_2O_3	13.56	13.87	13.42	13.85	14.53	15.49	13.27
Fe_2O_3	10.66	14.50	2.23	7.84	7.02	4.95	16.00
FeO	4.08		10.32	4.80	5.33	7.59	
MnO	0.12	0.18	0.19	0.15	0.05	0.15	0.08
MgO	6.79	6.50	6.10	7.31	7.82	6.78	9.61
CaO	9.25	10.77	11.25	8.46	8.84	9.45	5.01
Na_2O	2.88	2.50	2.47	2.84	2.67	3.22	2.60
K_2O	0.62	0.24	0.44	0.98	0.34	0.47	1.08
P_2O_5	0.31	0.28	0.24	0.31	0.30	0.31	0.06
H_2O^+			0.33	1.86		1.79	
H_2O^-			0.34	1.86		1.39	
CO_2			ND	ND		0.02	
LOI	2.02				4.20		
Total	100.28	99.32	99.49	99.78	99.44	100.71	99.48
LOI		1.33					8.54
H_2O^+	0.50	0.42			2.67		3.28
H_2O^-	1.52	ND			1.37		ND
CO_2	<0.2	0.09			<0.2		0.25
Fe_2O_3/FeO	2.61		0.22	1.63	1.32	0.65	
Density (g/cm^3)	2.69	2.95	2.99	2.48	2.69	2.90	2.23
Trace elements (ppm):							
La	12		11	8.2	12		10
Ce	28		29	22	30		26
Nd	21		21	15	20		17
Sm	6.3		6.3	4.5	5.7		4.7
Eu	2.2		2.1	1.2	2		1.4
Tb	1.2		1.4	0.87	1.2		0.86
Yb	2.7		2.3	2.0	2.2		1.6
Lu	0.37		0.36	0.32	0.31		0.24
Cr	80	61	75	78	197		263
Ni	55	51	53	63	108		225
Co	46	42	46	60	48		60
V	302	218	252	341	250		266
Cu	78	70	58	88	53		78
Zn	135	125	131	88	107		98
Zr	160	150	160	130	150		130
Y	32	30	30	24	29		14
Nb	13	11	11	11	12		9.6
Rb	2.3	1.3	3.1	5.9	1.1		18
Sr	290	295	280	230	290		200
Ba	72	82	105	79	71		52

Table T48 (continued).

Leg	55	55	55	55	55	55	55
Hole	433C	433C	433C	433C	433C	433C	433C
Core, section	23R-2	24R-1	24R-7	24R-7	24R-7	24R-7	26R-1
Interval (cm)	12-17	12-15	104-108	108-114	133-139	141-144	87-92
Piece	1C	2	3B	3C	3F	3G	2F
Lab number	Z-1661	Z-1122	Z-522	Z-1662	Z-1123	Z-1124	Z-1663
Depth (mbsf)	299.62	307.62	317.24	317.28	317.53	317.61	327.37
Unit/Subunit	19b	19b	19b	19b	19b	19b	21
Major element oxides (wt%):							
SiO_2	43.48**	46.10*	43.93	42.96**	43.30***	44.73*	46.60
TiO_2	1.82	1.33	0.84	1.32	1.23	1.24	2.17
Al_2O_3	12.94	9.76	8.45	7.60	9.00	8.88	12.51
Fe_2O_3	8.51	14.24	5.48	1.73	3.36	14.04	7.94
FeO	3.91		7.22	9.37	8.76		6.54
MnO	0.14	0.18	0.08	0.14	0.16	0.17	0.15
MgO	12.28	19.60	20.91	23.87	21.21	22.00	8.48
CaO	2.59	6.25	4.35	5.12	5.00	5.33	9.91
Na_2O	1.90	1.20	1.53	1.66	1.24	1.60	2.64
K_2O	0.74	0.13	0.98	1.24	0.21	1.08	0.21
P_2O_5	0.09	0.13	0.10	0.11	0.11	0.14	0.21
H_2O^+	5.70			3.17	4.59		
H_2O^-	5.75			1.70	1.40		
CO_2	ND			ND	0.05		
LOI			5.33				2.11
Total	99.85	98.92	99.20	99.99	99.62	99.21	99.47
LOI		6.10				4.31	
H_2O^+		4.89	2.64			3.36	0.45
H_2O^-		ND	2.11			ND	1.34
CO_2		0.52	0.45			0.24	<0.2
Fe_2O_3/FeO	2.18		0.76	0.19	0.38		1.21
Density (g/cm^3)	ND	2.78	2.87	2.90	2.90	2.92	2.84
Trace elements (ppm):							
La			3.7		4.4		
Ce			8.4		12		
Nd			6.5		13		
Sm			2.2		2.7		
Eu			0.82		0.84		
Tb			0.47		0.48		
Yb			1.0		1.2		
Lu			0.15		0.19		
Cr	675	715	630	705	850	830	276
Ni	478	640	820	680	570	590	90
Co	79	96	90	83	102	90	63
V	330	226	171	128	222	206	340
Cu	55	60	31	53	71	53	80
Zn	92	118	86	81	118	116	94
Zr	90	70	52	62	67	68	120
Y	13	16	14	14	14	14	24
Nb	6.1	4.3	3.3	4.1	4.0	4.7	8.9
Rb	8.9	2.1	12	14	3.1	15	<1
Sr	105	110	300	110	91	120	28
Ba	72	77	77	84	54	58	ND

Table T48 (continued).

Leg	55	55	55	55	55	55	55
Hole	433C	433C	433C	433C	433C	433C	433C
Core, section	26R-2	27R-2	27R-6	27R-6	28R-1	28R-2	28R-2
Interval (cm)	65-68	131-134	38-43	135-140	42-47	19-21	66-73
Piece	1G	6B	1H	5	2E	1D	4B
Lab number	Z-523	Z-1125	Z-1126	Z-1667	Z-1668	Z-1127	Z-1128
Depth (mbsf)	328.65	338.81	343.88	344.84	345.92	347.19	347.66
Unit/Subunit	21	24a	25	25	25	25	25
Major element oxides (wt%):							
SiO_2	47.82	44.00*	43.30**	46.30**	46.84	49.00*	48.70**
TiO_2	2.07	1.08	2.42	2.75	2.66	2.57	2.50
Al_2O_3	13.95	8.04	14.22	15.61	13.85	13.97	14.21
Fe_2O_3	7.14	14.67	12.27	7.57	7.55	13.24	5.00
FeO	5.04		1.98	4.20	5.21		7.64
MnO	0.06	0.18	0.08	0.13	0.14	0.16	0.15
MgO	7.35	26.02	7.28	6.80	7.94	6.89	7.14
CaO	10.64	4.29	2.60	7.80	9.41	10.29	9.73
Na_2O	2.43	1.00	2.07	2.80	2.91	2.50	2.63
K_2O	0.19	0.13	2.27	1.48	0.37	0.19	0.29
P_2O_5	0.20	0.11	0.07	0.22	0.27	0.25	0.26
H_2O^+			5.68	2.26			0.77
H_2O^-			5.07	2.06			0.67
CO_2			ND	ND			ND
LOI	2.56				2.06		
Total	99.45	99.52	99.31	99.98	99.21	99.06	99.69
LOI		5.89				1.11	
H_2O^+	0.99	4.46			0.52	0.59	
H_2O^-	1.22	ND			0.89	ND	
CO_2	0.34	0.34			0.49	0.17	
Fe_2O_3/FeO	1.42		6.20	1.80	1.45		0.65
Density (g/cm^3)	2.80	2.79	1.71	2.39	2.69	2.73	2.73
Trace elements (ppm):							
La	9						
Ce	23						
Nd	16						
Sm	4.7						
Eu	1.7						
Tb	1.0						
Yb	2.0						
Lu	0.30						
Cr	265	960	188		166	150	156
Ni	90	690	218		70	62	63
Co	48	120	58		56	46	44
V	242	206	365		340	230	233
Cu	85	73	130		76	88	83
Zn	120	122	118		105	135	130
Zr	120	67	ND		160	150	150
Y	23	12	ND		31	27	28
Nb	9.4	4.9	ND		12	11	11
Rb	<1	3.6	ND		2.6	1.9	1.3
Sr	270	71	ND		280	270	270
Ba	50	35	ND		44	72	105

Table T48 (continued).

Leg	55	55	55	55	55	55	55
Hole	433C	433C	433C	433C	433C	433C	433C
Core, section	28R-4	28R-4	28R-5	28R-5	31R-1	32R-1	34R-2
Interval (cm)	30-37	57-65	77-81	107-109	86-90	82-88	41-46
Piece	2C	5A	7B	6E	1L	3C	1K
Lab number	Z-1129	Z-1672	Z-524	Z-1130	Z-525	Z-1674	Z-1131
Depth (mbsf)	350.30	350.57	352.27	352.57	374.86	384.32	404.41
Unit/Subunit	25	25	26a	26a	27	28c	33
Major element oxides (wt%):							
SiO_2	48.30**		49.09	49.35*	46.03	39.22	44.57
TiO_2	2.37		2.67	2.78	2.57	0.93	2.13
Al_2O_3	14.19		14.25	14.11	14.56	5.93	14.66
Fe_2O_3	5.75		4.86	13.71	5.92	7.90	9.67
FeO	5.66		7.54		7.80	5.89	3.03
MnO	0.15		0.18	0.16	0.08	0.16	0.15
MgO	8.79		5.75	6.52	7.76	28.60	11.79
CaO	7.87		10.29	10.61	9.78	2.78	7.85
Na_2O	2.63		2.56	2.60	2.64	0.58	2.38
K_2O	1.16		0.38	0.21	0.40	0.08	0.24
P_2O_5	0.27		0.33	0.33	0.29	0.09	0.22
H_2O^+	1.32						
H_2O^-	1.44						
CO_2	ND						
LOI			1.89		1.89	7.01	3.18
Total	99.90		99.79	100.38	99.72	99.17	99.87
LOI				1.44			
H_2O^+			0.52	0.59	1.24	5.06	3.18
H_2O^-			1.03	ND	0.54	1.12	ND
CO_2			0.34	0.10	<0.2	<0.2	ND
Fe_2O_3/FeO	1.02		0.64		0.76	1.34	3.19
Density (g/cm^3)	2.71	2.39	2.89	2.83	2.82	2.94	2.55
Trace elements (ppm):							
La			14		12		
Ce			35		32		
Nd			24		21		
Sm			7.1		6.4		
Eu			2.2		2.1		
Tb			1.4		1.2		
Yb			2.8		2.5		
Lu			0.41		0.33		
Cr	174	168	107	168	205	760	515
Ni	72	67	59	71	150	840	330
Co	50	40	43	52	45	120	60
V	352	348	252	340	225	182	330
Cu	63	91	78	85	125	49	93
Zn	135	96	130	124	108	82	115
Zr	150	160	180	170	170	56	110
Y	28	41	31	33	31	11	22
Nb	11	11	13	13	13	3.8	8.7
Rb	14	39	8.9	1.5	4.6	1.4	<1
Sr	260	220	300	290	320	53	220
Ba	81	67	82	120	90	20	81

Table T48 (continued).

Leg	55	55	55	55	55	55	55
Hole	433C	433C	433C	433C	433C	433C	433C
Core, section	34R-3	34R-7	35R-6	36R-3	38R-5	39R-1	39R-2
Interval (cm)	60-64	103-109	59-64	90-95	90-94	119-122	35-40
Piece	1F	3L	1E	1K	1M	39	1H
Lab number	Z-526	Z-1681	Z-1682	Z-1683	Z-527	Z-1132	Z-1133
Depth (mbsf)	406.00	412.53	420.09	425.40	447.40	451.19	451.85
Unit/Subunit	33	35	35	38	47a	48	48
Major element oxides (wt%):							
SiO_2	44.56	46.64	46.92	45.00	45.36	43.00**	43.72**
TiO_2	1.82	2.27	2.37	2.17	1.98	1.93	2.30
Al_2O_3	11.90	12.64	12.83	10.84	14.35	12.49	15.25
Fe_2O_3	6.10	7.51	7.42	9.26	5.44	10.14	8.76
FeO	5.92	5.10	5.68	5.46	7.24	4.05	3.94
MnO	0.20	0.20	0.18	0.17	0.18	0.13	0.15
MgO	14.22	10.02	9.05	11.64	8.28	13.02	11.13
CaO	7.86	9.52	9.30	7.73	9.33	1.83	3.73
Na_2O	1.75	2.55	2.52	2.31	2.33	2.39	2.59
K_2O	0.12	0.23	0.37	0.32	0.17	1.29	0.73
P_2O_5	0.16	0.27	0.29	0.23	0.24	0.16	0.16
H_2O^+						4.04	3.22
H_2O^-						5.20	4.14
CO_2						ND	ND
LOI	5.92	2.94	2.37	4.63	4.70		
Total	100.53	99.89	99.30	99.76	99.60	99.67	99.82
LOI							
H_2O^+	3.97	1.07	0.80	1.99	2.08		
H_2O^-	1.38	1.12	0.75	1.50	1.90		
CO_2	0.57	0.62	<0.2	<0.2	0.70		
Fe_2O_3/FeO	1.03	1.47	1.31	1.70	0.75	2.50	2.22
Density (g/cm^3)	2.82	2.72	2.91	2.68	2.74	1.62	2.17
Trace elements (ppm):							
La	6.4				11	9.0	7.2
Ce	16				23	24	19
Nd	11				18	17	13
Sm	3.4				5.4	5.0	3.8
Eu	1.1				1.7	1.5	1.3
Tb	0.7				1.2	0.87	0.72
Yb	1.5				2.3	1.6	1.6
Lu	0.23				0.30	0.21	0.27
Cr	460	350	353	440	265	435	485
Ni	515	220	195	330	150	270	315
Co	63	67	62	80	53	59	60
V	202	260	262	321	252	272	358
Cu	70	76	116	96	73	53	60
Zn	102	96	102	92	107	83	125
Zr	97	150	160	130	140	120	140
Y	19	28	28	24	27	23	15
Nb	7	11	12	10	11	9.7	10
Rb	1.9	1.3	2.9	2.2	<1	12	11
Sr	200	250	250	200	270	130	190
Ba	66	71	94	100	59	62	49

Table T48 (continued).

Leg	55	55	55	55	55	55	55
Hole	433C	433C	433C	433C	433C	433C	433C
Core, section	39R-3	39R-5	39R-5	39R-6	41R-1	42R-1	42R-3
Interval (cm)	88-93	2-8	87-94	38-43	20-23	2-6	83-88
Piece	1F	1A	1D	1B	1C	1G	6B
Lab number	Z-1134	Z-1135	Z-1136	Z-1137	Z-528	Z-1138	Z-1695
Depth (mbsf)	453.88	456.02	456.87	457.88	469.20	478.52	482.33
Unit/Subunit	48	48	48	48	51	52	54
Major element oxides (wt%):							
SiO_2	45.28**	45.68**	48.16*	46.62**	47.92	49.26*	44.46**
TiO_2	2.10	2.12	2.22	2.10	2.27	2.37	2.22
Al_2O_3	13.03	13.49	13.20	13.41	14.41	13.89	14.75
Fe_2O_3	4.67	4.24	13.15	3.76	4.96	12.91	9.49
FeO	7.82	8.13		8.47	6.75		4.41
MnO	0.16	0.22	0.16	0.21	0.06	0.13	0.08
MgO	12.36	11.72	10.50	11.30	6.77	7.68	8.14
CaO	7.20	8.46	9.71	8.78	9.39	10.14	6.54
Na_2O	2.19	1.91	2.10	1.93	2.58	2.70	2.77
K_2O	0.26	0.38	0.22	0.31	0.25	0.25	1.20
P_2O_5	0.21	0.23	0.25	0.21	0.24	0.26	0.27
H_2O^+	2.21	1.46		2.34			3.04
H_2O^-	2.34	2.32		0.98			2.18
CO_2	ND	ND		ND			ND
LOI					3.66		
Total	99.83	100.36	99.67	100.42	99.26	99.59	99.55
LOI			2.16			2.89	
H_2O^+			1.58		0.42	1.02	
H_2O^-			ND		1.81	ND	
CO_2			0.18		0.61	0.22	
Fe_2O_3/FeO	0.60	0.52		0.44	0.74		2.15
Density (g/cm^3)	2.65	2.82	2.92	2.84	2.81	2.67	ND
Trace elements (ppm):							
La			9.1		9.8		
Ce			25		22		
Nd			17		16		
Sm			5.1		5.1		
Eu			1.6		1.7		
Tb			0.88		1.2		
Yb			1.9		2.5		
Lu			0.28		0.34		
Cr	480	410	425	355	225	240	216
Ni	300	248	265	250	82	83	66
Co	60	55	62	54	48	59	50
V	338	226	252	218	285	390	348
Cu	73	73	78	92	78	85	70
Zn	122	118	121	124	108	126	82
Zr	130	120	120	120	130	130	115
Y	23	23	23	24	30	25	30
Nb	9.5	9.5	9.3	9.6	9.6	9.3	9.2
Rb	1.2	1.1	1.4	2.2	1.2	1.6	6.6
Sr	220	225	240	230	260	250	200
Ba	100	56	77	63	74	80	56

Table T48 (continued).

Leg	55	55	55	55	55	55	55
Hole	433C	433C	433C	433C	433C	433C	433C
Core, section	43R-1	45R-3	45R-3	45R-4	45R-5	45R-5	45R-6
Interval (cm)	118-123	61-65	119-124	109-114	39-44	119-122	24-31
Piece	4B	3B	4D	4J	1C	3D	1A
Lab number	Z-1698	Z-1139	Z-1140	Z-1704	Z-1141	Z-529	Z-1142
Depth (mbsf)	489.18	510.61	511.19	512.59	513.29	514.09	514.74
Unit/Subunit	54	60	60	60	60	60	60
Major element oxides (wt%):							
SiO_2	46.44**	46.88	46.64**	47.22**	48.14**	48.85	48.79
TiO_2	2.27	2.39	2.38	2.25	2.38	2.35	2.22
Al_2O_3	16.54	13.45	15.03	14.84	14.95	13.11	14.49
Fe_2O_3	8.18	12.28	9.12	7.60	4.20	4.79	4.42
FeO	4.23	2.29	4.38	6.05	8.04	7.30	6.76
MnO	0.12	0.07	0.12	0.15	0.19	0.10	0.19
MgO	6.80	6.45	7.54	6.20	6.37	8.73	6.74
CaO	7.78	5.79	8.48	9.93	11.04	10.46	10.05
Na_2O	2.96	2.94	2.75	2.50	2.50	2.50	2.70
K_2O	0.78	1.21	0.43	0.96	0.43	0.37	0.17
P_2O_5	0.24	0.13	0.25	0.25	0.22	0.24	0.20
H_2O^+	2.52		1.51	1.73	1.00		
H_2O^-	1.36		1.16	0.50	0.50		
CO_2	ND		ND	ND	ND		
LOI		6.01				1.47	2.69
Total	100.22	99.89	99.79	100.18	99.96	100.27	99.42
LOI							
H_2O^+		1.73				0.78	0.51
H_2O^-		3.21				0.69	1.45
CO_2		<0.2				<0.2	<0.2
Fe_2O_3/FeO	1.93	5.36	2.08	1.26	0.52	0.66	0.65
Density (g/cm^3)	ND	ND	2.20	2.75	2.86	2.87	2.74
Trace elements (ppm):							
La	7.7	6.6		7.0		8.5	7.4
Ce	21	20		19		18	20
Nd	15	14		15		15	14
Sm	4.5	4.1		4.4		4.6	4.7
Eu	0.94	1.6		1.2		1.6	1.4
Tb	0.77	0.96		0.74		1.0	0.94
Yb	1.9	1.7		2.2		2.3	2.0
Lu	0.30	0.23		0.35		0.34	0.30
Cr	208	230	192	207	240	205	218
Ni	81	150	74	84	86	65	80
Co	49	65	57	70	63	44	55
V	355	392	388	375	375	265	338
Cu	73	77	53	93	125	125	119
Zn	126	99	124	89	122	125	138
Zr	130	130	130	120	120	120	120
Y	24	24	26	25	25	28	27
Nb	8.4	9.0	8.5	8.4	8.4	8.7	8.2
Rb	5.9	12	3.5	11	3.9	5.8	<1
Sr	250	190	250	250	260	270	265
Ba	77	61	54	74	87	74	54

Table T48 (continued).

Leg	55	55	55	55
Hole	433C	433C	433C	433C
Core, section	45R-6	46R-3	47R-1	49R-2
Interval (cm)	97-102	78-83	8-13	62-68
Piece	1G	2D	2A	1J
Lab number	Z-1707	Z-1709	Z-1710	Z-1712
Depth (mbsf)	515.47	520.28	526.08	547.12
Unit/Subunit	60	62a	63a	66
Major element oxides (wt%):				
SiO_2	47.70**	45.82	47.46	44.26
TiO_2	2.19	2.22	2.34	2.78
Al_2O_3	15.53	13.58	12.69	13.66
Fe_2O_3	4.94	9.18	7.74	9.50
FeO	6.11	4.96	6.40	5.24
MnO	0.19	0.13	0.15	0.19
MgO	7.59	7.72	6.99	7.35
CaO	9.70	8.99	9.63	8.96
Na_2O	2.61	2.87	2.82	2.95
K_2O	0.48	0.50	0.30	0.36
P_2O_5	0.21	0.24	0.28	0.31
H_2O^+	1.42			
H_2O^-	0.89			
CO_2	ND			
LOI		3.05	2.47	3.98
Total	99.56	99.26	99.27	99.54
LOI				
H_2O^+		0.56	0.41	1.82
H_2O^-		1.33	1.31	1.50
CO_2		<0.2	<0.2	<0.2
Fe_2O_3/FeO	0.81	1.85	1.21	1.81
Density (g/cm^3)	2.66	2.69	2.77	2.72
Trace elements (ppm):				
La				
Ce				
Nd				
Sm				
Eu				
Tb				
Yb				
Lu				
Cr	219	199	181	160
Ni	81	76	71	97
Co	77	68	60	44
V	262	356	270	188
Cu	80	96	84	125
Zn	116	98	116	98
Zr	120	140	150	170
Y	24	29	31	30
Nb	9.0	9.5	10	13
Rb	6.6	3.7	1.8	2.1
Sr	250	240	250	270
Ba	82	85	76	84

Table T49. Secondary minerals in fine fraction sampled from basalts of tholeiitic series, Emperor Seamount chain, Leg 55: Hole 433C (Suiko seamount), X-ray diffraction data. (Continued on next page.)

Core, section, interval (cm)	Flow Unit	Depth (mbsf)	Sm	Mixed-layer chlorite-swelling chlorite	Chl	Mixed-layer smectite-chlorite	Serp	Phill	Rock type
55-433C-									
10R-1, 25-31	4a	204.75	+	X	+				Olivine tholeiite
10R-2, 127-132	4d	207.27	X		+	X			-" -
10R-4, 121-123	4h	210.21	X			+	+		Tholeetic picrite
10R-6, 57-62	5	212.57	X	X	+				Olivine tholeiite
12R-1, 75-80	9	224.25	X						Tholeiite
12R-2, 32-37	9	225.32	X						Tholeiite
12R-2, 136-141	9	226.36	X		+	+			Tholeiite
12R-3, 54-57	9	227.04	X						Tholeiite
13R-2, 69-72	10	232.19	X			+			Tholeiite
14R-1, 2-7	11a	233.02	X						Tholeiite
14R-1, 33-39	11a	233.33	X						Tholeiite
14R-2, 115-120	11a	235.65	X						Tholeiite
14R-4, 26-31	11c	237.76	X						Tholeiite
14R-4, 47-52	11c	237.97	X						Tholeiite
15R-1, 0-4	11c	242.50	X						Tholeiite
15R-5, 58-63	13	249.08	X						Tholeiite
15R-5, 82-87	13	249.32	X						Tholeiite
15R-5, 88-92	13	249.38	X						Tholeiite
15R-6, 31-32	13	250.06	X						Tholeiite
16R-1, 32-38	13	252.32	X						Tholeiite
19R-1, 48-64	13	261.98	X						Tholeiite
21R-3, 20-23	17	282.20	X			+			Tholeiite
22R-5, 48-52	16	294.98	X			+			Tholeiite
23R-1, 100-104	19a	299.00	X						Tholeiite
23R-2, 12-17	19b	299.62	X	+	+				Tholeiitic picrite
24R-1, 12-15	19d	307.62	X			X	+?		Tholeiitic picrite
24R-7, 104-108	19d	317.24	X		X				Tholeiitic picrite
24R-7, 108-114	19d	317.28	+	+?	X				Tholeiitic picrite
24R-7, 133-139	19d	317.53	X	X					Tholeiitic picrite
24R-7, 141-144	19d	317.61	X		X			+?	Tholeiitic picrite
26R-1, 87-92	21	327.37	X	+	+				Tholeiite
26R-2, 65-68	21	328.65	X			+			Tholeiite
26R-5, 89-94	22	333.39	+	X	+				Olivine tholeiite
27R-2, 138-144	24a	338.88	+		X				Tholeiitic picrite
27R-6, 38-43	25	343.88	X						Tholeiite
27R-6, 134-140	25	344.84	X						Tholeiite
27R-6, 134-140	25	344.84	X						Tholeiite
28R-1, 42-47	25	345.92	X						Tholeiite
28R-2, 19-21	25	347.19	X		+				Tholeiite
28R-2, 66-73	25	347.66	X						Tholeiite
28R-4, 30-37	25	350.30	X						Tholeiite
28R-4, 57-65	25	350.57	X		+				Tholeiite
28R-5, 107-109	26a	352.57	X						Tholeiite
30R-3, 47-53	27	367.97	+	X	+				Olivine tholeiite
31R-1, 86-90	27	374.86	+		+				Olivine tholeiite
32R-1, 82-88	28c	384.32	+		X				Tholeiitic picrite
32R-5, 50-55	29	390.00	+	X					Olivine tholeiite

Table T49 (continued).

Core, section, interval (cm)	Flow Unit	Depth (mbsf)	Sm	Mixed-layer chlorite-swelling chlorite	Chl	Mixed-layer smectite-chlorite	Serp	Phill	Rock type
34R-1, 108-114	32b	403.58	X						Tholeiite
34R-2, 41-46	33	404.41	X	X	+				Olivine tholeiite
34R-3, 60-64	33	406.00	X		X				Tholeiitic picrite
34R-3, 64-68	33	406.13	+	X	+				Tholeiitic picrite
34R-4, 97-101	34a	407.97	+	X	+				Tholeiitic picrite
34R-7, 103-109	35	412.53	X						Olivine tholeiite
35R-6, 59-64	35	420.09	X						Olivine tholeiite
36R-3, 90-95	38	425.40	X	X	+				Olivine tholeiite
37R-4, 44-50	44	435.94	X	X	+				Olivine tholeiite
38R-1, 81-86	45b	441.31	X	X	+				Olivine tholeiite
38R-5, 90-94	47a	447.40	X			X	+?		Olivine tholeiite
39R-1, 115-119	48	451.15	X						Olivine tholeiite
39R-1, 119-122	48	451.19	X						Olivine tholeiite
39R-2, 35-40	48	451.85	X				+?		Olivine tholeiite
39R-3, 88-93	48	453.88	+	X	+				Olivine tholeiite
39R-5, 2-8	48	456.02	+	X					Tholeiitic picrite
39R-5, 87-94	48	456.87	+	X					Tholeiitic picrite
39R-6, 38-43	48	457.88	+	X	+	+			Olivine tholeiite
39R-6, 114-118	48	458.64	X	X					Olivine tholeiite
41R-1, 20-23	51	469.20	X						Tholeiite
41R-1, 66-71	51	469.66	X						Tholeiite
42R-1, 2-6	52	478.52	X						Tholeiite
42R-1, 36-41	52	478.86	X						Tholeiite
42R-3, 83-88	53	482.33	X		+				Tholeiite
43R-1, 118-123	54	489.18	X						Tholeiite
44R-1, 26-31	56	497.76	X						Tholeiite
44R-4, 135-140	58	503.35	X						Tholeiite
45R-2, 66-71	59	509.16	X						Tholeiite
45R-3, 61-66	60	510.61	X						Tholeiite
45R-3, 119-124	60	511.19	X						Tholeiite
45R-4, 109-114	60	512.59	X						Tholeiite
45R-5, 39-44	60	513.39	X						Tholeiite
45R-5, 119-122	60	514.09	X						Tholeiite
45R-6, 2-7	60	514.27	X						Tholeiite
45R-6, 24-31	60	514.49	X						Tholeiite
45R-6, 97-102	60	515.47	X						Tholeiite
45R-6, 129-133	60	515.54	X						Tholeiite
46R-3, 78-83	62a	520.28	X						Tholeiite
47R-1, 8-13	63a	526.08	X						Tholeiite
48R-3, 10-15	64	538.60	X						Tholeiite
49R-2, 62-68	66	547.12	X		+	+			Tholeiite

Notes: X = dominant, + = minor or trace.
Sm = smectites, Chl = chlorite, Serp = serpentine, Phill = phillipsite.

Table T50. Minerals from vesicles and veins in basalts of tholeiitic series, Emperor Seamount chain, Leg 55: Hole 433C (Suiko seamount), X-ray diffraction data. (Continued on next four pages.)

Core, section, interval (cm)	Flow Unit	Depth (mbsf)	Sm	Mixed-layer smectite-chlorite	Mixed-layer chlorite-swelling chlorite	Chl	Serp	Illite	Calcite	Arag	Phill	9.4A-mineral	Laub (?)	Matter of vesicles or veins	Rock type
55-433C-															
10R-1, 25-31	4a	204.75	X											Greenish-gray clay from center of vesicles	Olivine tholeiite
10R-1, 25-31	4a	204.75	X	X										Green clay covering walls of vesicles	Olivine tholeiite
10R-1, 25-31	4a	204.75	+							X				White crystals with green clay from vesicles	Olivine tholeiite
10R-4, 118-121	4h	210.21	+				X		+					Light-green clay from vesicles	Tholeiitic picrite
10R-6, 57-62	5	212.57	X	+?					+					Greenish-gray clay from vesicles	Olivine tholeiite
10R-6, 57-62	5	212.57	+						X					Carbonates and clay from vesicles	Olivine tholeiite
11R-3, 128-134	7	218.28	X									+		Greenish-gray clay from vesicles	Tholeiite
12R-2, 32-37	9	225.32	X									+	+	Black clay from vesicles	Tholeiite
12R-2, 136-141	9	226.36	X											Greenish-gray clay from vesicles	Tholeiite
14R-1, 2-7	11a	233.02	X								+			Black clay from vesicles	Oxidized tholeiite
14R-1, 2-7	11a	233.02	+								X			Vein	Oxidized tholeiite
14R-1, 33-39	11a	233.33	X											Black clay from vesicles	Tholeiite
14R-2, 115-120	11a	235.65	X											Greenish-gray clay from vesicles	Tholeiite
14R-4, 47-52	11c	237.97	X											Greenish-gray clay from vesicles	Tholeiite
15R-1, 0-4	11c	242.50	X											Clay covering walls of vesicles	Tholeiite

Table T50 (continued).

Core, section, interval (cm)	Flow Unit	Depth (mbsf)	Sm	Mixed-layer smectite-chlorite	Mixed-layer chlorite-swelling chlorite	Chl	Serp	Illite	Calcite	Arag	Phill	9.4A-mineral	Laub (?)	Matter of vesicles or veins	Rock type
15R-1, 0-4	11c	242.50	X											Brown clay from vesicles	Tholeiite
15R-5, 58-63	13	249.08	X											Black clay from vesicles	Tholeiite
23R-2, 12-17	19b	299.62	X											Green-gray clay from center of vesicles	Olivine tholeiite
23R-2, 12-17	19b	299.62	X	+										Green clay covering walls of vesicles	Olivine tholeiite
23R-2, 12-17	19b	299.62	X	+										Vein	Olivine tholeiite
27R-2, 138-144	24a	338.88	X	+			+							Green-gray clay from vesicles	Tholeiitic picrite
27R-2, 138-144	24a	338.88							X					Carbonates from vesicles	Tholeiitic picrite
27R-6, 38-43	25	343.88	X								X			Black clay and transparent crystals from vesicles	Tholeiite
28R-4, 30-37	25	350.30	X											Black clay from vesicles	Tholeiite
28R-4, 30-37	25	350.30	X	+				+			+	+		Clay covering walls of vesicles	Tholeiite
32R-1, 82-88	28c	384.32					X							Green-gray glassy matter from center of vesicles	Tholeiitic picrite
32R-1, 82-88	28c	384.32					X							Dark-green covering walls of vesicles	Tholeiitic picrite
32R-5, 50-55	29	390.00	+	+	X									Clay from vesicles	Olivine tholeiite
33R-2, 126-132	31	395.76	+						X					Carbonates and yellow-gray clay from vein	Olivine tholeiite
34R-1, 108-114	32b	403.58	X											Black clay from vesicles	Tholeiite
34R-1, 108-114	32b	403.58	X	+										Clay covering walls of vesicles and black clay from center of vesicles	Oxidized tholeiite
34R-1, 108-114	32b	403.58	X											Dark-green clay from center of vesicles	Oxidized tholeiite

Table T50 (continued).

Core, section, interval (cm)	Flow Unit	Depth (mbsf)	Sm	Mixed-layer smectite-chlorite	Mixed-layer chlorite-swelling chlorite	Chl	Serp	Illite	Calcite	Arag	Phill	9.4A-mineral	Laub (?)	Matter of vesicles or veins	Rock type
34R-1, 108-114	32b	403.58							X					Yellowish-white crystals from vesicles	Oxidized tholeiite
34R-1, 108-114	32b	403.58									X			Transparent crystals from vesicles	Oxidized tholeiite
34R-1, 108-114	32b	403.58	+						X					Vein	Oxidized tholeiite
34R-2, 41-46	33	404.41	X						+					Green-gray clay from vesicles	Oxidized olivine tholeiite
34R-2, 41-46	33	404.41	+						X					Carbonates and clay from vesicles	Oxidized olivine tholeiite
34R-3, 63-68	33	406.03	+?	+		X								Dark-green clay covering walls of vesicles	Tholeiitic picrite
34R-4, 97-101	34a	407.97	X											Green-gray clay from vesicles	Olivine tholeiite
34R-4, 97-101	34a	407.97	+						X					Carbonates and clay covering walls of vesicles	Olivine tholeiite
34R-7, 103-109	35	412.53	X						+					Green-gray clay from vesicles	Olivine tholeiite
36R-3, 90-95	38	425.40	X	+										Green-gray clay from vesicles	Olivine tholeiite
38R-1, 81-86	45b	444.31	+	+	X									Clay from vesicles	Olivine tholeiite
39R-1, 119-122	48	451.19	X								X			Black clay and transparent crystals from vesicles	Oxidized olivine tholeiite
39R-2, 35-40	48	451.85	X											Vein	Olivine tholeiite
39R-3, 88-93	48	453.88	X											Green-gray clay from vesicles	Olivine tholeiite
39R-5, 2-8	48	456.02	X											Green-gray clay from vesicles	Olivine tholeiite

Table T50 (continued).

Core, section, interval (cm)	Flow Unit	Depth (mbsf)	Sm	Mixed-layer smectite-chlorite	Mixed-layer chlorite-swelling chlorite	Chl	Serp	Illite	Calcite	Arag	Phill	9.4A-mineral	Laub (?)	Matter of vesicles or veins	Rock type
39R-5, 2-8	48	456.02	+		X									Gray clay from vesicles	Olivine tholeiite
39R-5, 2-8	48	456.02			+						X			White matter and clay covering walls of	Olivine tholeiite
39R-6, 38-43	48	457.88	X	+										Green-gray clay from vesicles	Olivine tholeiite
39R-6, 114-118	48	458.64	X	+				X			X			Blue clay and transparent crystals from	Oxidized olivine tholeiite
39R-6, 114-118	48	458.64	X	+				+			X			Blue clay and transparent crystals from	Olivine tholeiite
39R-6, 114-118	48	458.64	X	+				+						Green clay from vesicles	Olivine tholeiite
39R-6, 114-118	48	458.64	X	+				+						Dark-green clay from vesicles	Olivine tholeiite
41R-1, 66-71	51	469.66	X											Green-gray clay from vesicles	Tholeiite
43R-1, 118-123	54	489.18	X								+			Black clay from vesicles	Tholeiite
43R-1, 118-123	54	489.18	X											Brown-red clay from	Tholeiite
44R-4, 135-140	58	503.35	X											Black clay from vesicles	Tholeiite
45R-3, 61-66	60	510.61	X								X	+		Black clay from vesicles	Oxidized tholeiite
45R-3, 61-66	60	510.61	X								+			Green-gray clay from vesicles	Oxidized tholeiite
45R-3, 119-124	60	511.19	X											Black clay from vesicles	Tholeiite
45R-3, 119-124	60	511.19	X						+					Green-gray clay from vesicles	Tholeiite
45R-4, 109-114	60	512.59	+					X						Green clay from vesicles	Tholeiite
45R-5, 39-44	60	513.39	X											Green-gray clay from vesicles	Tholeiite
45R-6, 97-102	60	515.47	X					+						Green clay from vesicles	Tholeiite
45R-6, 129-133	60	515.54	X	+										Black clay from vesicles	Tholeiite
45R-6, 129-133	60	515.54	X	+										Green-gray clay from vesicles	Tholeiite
45R-6, 129-133	60	515.54	X						+					Gray clay from vesicles	Tholeiite

Table T50 (continued).

Core, section, interval (cm)	Flow Unit	Depth (mbsf)	Sm	Mixed-layer smectite-chlorite	Mixed-layer chlorite-swelling chlorite	Chl	Serp	Illite	Calcite	Arag	Phill	9.4A-mineral	Laub (?)	Matter of vesicles or veins	Rock type
45R-6, 129-133	60	515.54	+						X					Carbonate and clay pellicle from vesicles	Tholeiite
48R-3, 10-15	64	538.60	X											Green-gray clay from vesicles	Tholeiite

Notes: X = dominant, + = minor or trace.
Sm = smectites, Chl = chlorite, Serp = serpentine, Arag = aragonite, Phill = phillipsite, Laub = laubmannite.

Table T51. Composition of basalts* from Hole 192A, Leg 19 (Meiji seamount, Emperor Seamount chain).

Leg	19	19	19
Hole	192A	192A	192A
Core, section	5R-3	5R-4	6R-2
Interval (cm)	23-33	75-85	41-51
Depth (mbsf)	1046.23	1048.25	1054.91
Major element oxides (wt%):			
SiO_2	47.20	47.48	43.16
TiO_2	2.03	2.03	2.17
Al_2O_3	14.21	15.01	13.52
Fe_2O_3	7.30	5.97	12.74
FeO	2.96	2.61	2.44
MnO	0.15	0.15	0.16
MgO	6.45	6.75	5.17
CaO	10.45	10.31	9.49
Na_2O	2.40	2.35	2.13
K_2O	1.50	1.80	1.70
P_2O_5	0.37	0.34	0.43
H_2O^+	1.30	0.34	2.14
H_2O^-	2.90	3.44	2.98
CO_2	1.20	1.39	1.84
Total	100.42	99.97	100.07
Fe_2O_3/FeO	2.47	2.29	5.22

Note: * = all major element data were obtained from V.G. Sakhno (Far East Geological Institute, Far East Branch of Russian Academy of Sciences, Vladivostok).

Table T52. Secondary minerals in fine fraction sampled from alkaline basalts, Emperor Seamount chain, Leg 19: Hole 192A (Meiji seamount) (X-ray diffraction data).

Core, section, interval (cm)	Depth (mbsf)	Smectites	Mixed-layer smectite-swelling chlorite	Chlorite	Celadonite	Rock type
19-192A-						
5R-2, 43-53	1044.93	XX			XX	Alkaline basalt
5R-3, 23-33	1046.23	XX	X		+	Alkaline basalt
5R-4, 73-83	1048.23	X	X	+	+	Alkaline basalt
5R-6, 45-49	1050.95	X	X	+	+	Alkaline basalt
5R-6, 112-116	1051.62	X	X		X	Alkaline basalt
6R-2, 41-51	1054.91	XX	X		+	Alkaline basalt
6R-3, 45-56	1056.45	X	X	+	X	Alkaline basalt

Note: XX = dominant, X = minor, + = trace.

Table T53. Parameter *b* of clay minerals in fine fraction sampled from alkaline basalts, Emperor Seamount chain, Leg 19: Hole 192A (Meiji seamount) (Electron diffraction data).

Core, section, interval (cm)	Depth (mbsf)	Parameter *b* (Å)	Polytype of hydromica	Rock type
19-192A-				
5R-2, 43-53	1044.93	9.20; 9.06	1M	Alkaline basalt
5R-3, 23-33	1046.23	9.20		Alkaline basalt
5R-4, 73-83	1048.23	9.20; >9.06		Alkaline basalt
5R-6, 45-49	1050.95	9.20; >9.08		Alkaline basalt
5R-6, 112-116	1051.62	9.19; >9.04		Alkaline basalt
6R-2, 41-51	1054.91	9.20; >9.04		Alkaline basalt
6R-3, 45-56	1056.45	9.20; >9.06	1M	Alkaline basalt

Table T54. Chemical composition (wt%) of fraction less than 0.001 mm sampled from alkaline basalts, Emperor Seamount chain, Leg 19: Hole 192A (Meiji seamount).

Hole, core, section, interval (cm)	192A 5R-2, 43-53	192A 5R-3, 23-33	192A 6R-2, 41-51
SiO_2	42.70	41.30	42.60
TiO_2	0.66	2.56	0.95
Al_2O_3	7.29	12.10	11.14
Fe_2O_3	13.99	10.42	10.42
FeO	2.06	2.67	2.67
MnO	0.10	0.17	0.10
MgO	4.49	10.15	9.47
CaO	3.40	4.90	4.08
Na_2O	1.22	1.50	1.80
K_2O	3.30	1.20	2.50

Table T55. Average values of Fe_2O_3 + FeO/MgO ratios and contents of K_2O (wt%) in igneous rocks from Emperor Seamount chain (Kirkpatrick et al., 1980), in greenish-gray clay from vesicles, and in red clay from vesicles and veins.

Rock, clay	Igneous rock	Greenish-gray clay	Red clay	Igneous rock	Greenish-gray clay	Red clay
Elements	Fe_2O_3 + FeO/MgO	Fe_2O_3 + FeO/MgO	Fe_2O_3 + FeO/MgO	K_2O	K_2O	K_2O
Hawaiite	3.18	1.06		1.7	0.60	
Alkaline basalt	2.4			1.2		1.75
Tholeiite	1.95	0.78	1.46	0.45	0.47	1.46
Olivine tholeiite	1.17	0.30		0.30	0.27	
Tholeiitic picrite	0.58	0.16		0.21	0.38	

Table T56. Composition of alkaline basalts from Hole 865A, Leg 143 (Allison Guyot, West Pacific Guyots). (Continued on next page.)

Leg	143	143	143	143	143	143	143
Hole	865A	865A	865A	865A	865A	865A	865A
Core, section	90R-5	90R-5	90R-6	91R-1	91R-2	91R-3	92R-3
Interval (cm)	52-58	52-58	45-50	112-118	20-25	22-28	80-86
Piece	5B	5B	2	13B	2	2	1
Lab number	Z-1492-1	Z-1492-2	Z-1493	Z-1494	Z-1495	Z-1496	Z-1497
Depth (mbsf)	837.24	837.24	838.58	842.22	842.64	844.03	850.27
Unit	1	1	1	1	1	1	3
Major element oxides (wt%):							
SiO_2	39.37	18.42	43.60	42.22	40.91	40.73	42.40
TiO_2	3.64	0.77	3.34	3.54	3.74	3.68	5.40
Al_2O_3	15.71	7.41	14.50	15.43	16.99	17.19	21.61
Fe_2O_3	11.64	7.58	6.80	6.73	6.59	5.55	8.65
FeO	2.28	5.65	5.18	4.51	3.71	3.83	0.75
MnO	0.07	0.17	0.09	0.17	0.14	0.15	0.07
MgO	3.53	3.17	8.61	8.86	9.67	10.69	3.02
CaO	5.79	24.15	7.42	7.00	5.90	4.90	0.98
Na_2O	1.38	0.63	2.10	2.08	2.08	1.77	1.32
K_2O	4.01	0.87	2.01	0.81	0.78	1.38	1.31
P_2O_5	0.61	0.49	0.78	0.75	0.75	0.87	0.25
LOI	11.96	30.70	5.61	7.81	8.31	9.06	13.80
Total	99.99	100.01	100.04	99.91	99.57	99.80	99.56
H_2O^+	4.41	4.14	2.93	3.85	4.21	5.04	7.20
H_2O^-	3.41	2.75	2.15	3.00	3.42	3.17	5.65
CO_2	3.94	23.81	0.39	0.72	0.52	0.69	0.31
Fe_2O_3/FeO	5.11	1.34	1.32	1.49	1.78	1.45	11.53
Density (g/cm^3)	2.09	2.24	2.63	2.39	2.33	2.35	1.77
Trace elements (ppm):							
La	51	26					
Ce	110	50					
Nd	60	28					
Sm	13	6.5					
Eu	3.4	1.6					
Tb	1.9	0.78					
Yb	2.8	1.9					
Lu	0.41	0.32					
Cr	270	60	265	265	302	260	310
Ni	101	55	187	167	182	160	72
Co	30	30	66	67	68	45	36
V	410	131	427	498	540	462	542
Cu	61	92	61	59	73	66	41
Zn	95	<30	79	82	85	91	52
Zr	340	98	310	340	360	350	520
Y	35	24	26	30	31	29	35
Nb	72	16	67	71	77	76	100
Rb	53	20	39	7.9	7.2	11	38
Sr	200	150	570	720	530	620	330
Ba	325	240	550	580	ND	560	650

Notes: ND = not determined; z-1492-1 = basalt piece from breccia; z-1492-2 = matrix from breccia.

Table T56 (continued).

Leg	143	143	143	143	143	143	143
Hole	865A	865A	865A	865A	865A	865A	865A
Core, section	92R-4	93R-1	93R-2	93R-3	94R-1	94R-2	94R-4
Interval (cm)	45-47	30-36	0-8	47-49	97-102	102-105	133-143
Piece		4	1	2B	17D	16	9
Lab number	Z-1498	Z-1499	Z-1500	Z-1716	Z-1501	Z-1502	Z-1503
Depth (mbsf)	850.90	853.70	854.9	856.87	864.07	865.59	868.73
Unit	3	3	3	3	3	3	4
Major element oxides (wt%):							
SiO_2	42.90	41.83	42.31	40.19	44.21	39.75	45.30
TiO_2	5.44	4.20	4.12	4.26	3.70	4.10	3.40
Al_2O_3	20.11	18.58	16.03	15.09	15.07	14.90	15.90
Fe_2O_3	9.94	12.68	10.68	7.05	4.98	6.88	4.27
FeO	1.28	1.86	2.39	4.20	5.66	2.58	5.75
MnO	0.16	0.12	0.05	0.21	0.16	0.14	0.12
MgO	2.28	2.31	6.58	10.46	7.97	8.05	7.15
CaO	0.38	1.84	2.61	7.41	10.13	5.45	8.54
Na_2O	1.24	1.73	1.64	2.05	2.32	1.06	2.41
K_2O	3.29	3.50	3.38	1.47	1.09	3.78	2.08
P_2O_5	0.21	1.00	1.00	0.22	0.93	0.95	0.80
LOI	12.30	9.84	8.74	7.44	3.72	12.49	3.79
Total	99.53	99.49	99.53	100.05	99.94	100.13	99.51
H_2O^+	7.59	5.38	4.45	4.62	1.94	5.59	1.52
H_2O^-	4.55	3.82	3.15	2.31	1.37	3.73	1.23
CO_2	<0.2	0.29	0.25	ND	0.21	2.94	0.54
Fe_2O_3/FeO	7.77	6.82	4.47	1.68	0.88	2.67	0.74
Density (g/cm^3)	1.70	1.91	2.36	2.69	2.74	2.15	2.75
Trace elements (ppm):							
La	63	54		42		35	51
Ce	130	120		98		96	88
Nd	63	54		42		48	45
Sm	11	10		8.5		9.3	9.7
Eu	3.4	3.3		2.8		2.8	2.2
Tb	1.3	1.3		1.1		1.2	1.1
Yb	1.6	2.4		1.9		1.9	2.6
Lu	0.20	0.35		0.26		0.26	0.35
Cr	88	230	220	184	220	258	94
Ni	70	130	101	95	147	90	80
Co	35	50	56	40	57	60	35
V	370	263	408	265	392	485	193
Cu	59	40	44	51	59	73	47
Zn	58	98	82	79	80	182	87
Zr	510	430	360	325	350	380	370
Y	35	37	29	28	28	34	27
Nb	100	81	73	62	66	76	68
Rb	40	42	57	20	14	30	39
Sr	390	280	420	570	810	205	710
Ba	340	380	370	470	580	570	800

Table T57. Secondary minerals in fine fraction sampled from igneous rocks, West Pacific Guyots, Legs 143 and 144: Hole 865A (Allison Guyot), Hole 866A (Resolution Guyot), Hole 871C (Limalok Guyot), Hole 872B (Lo-En Guyot), Holes 874B, 875C, and 876A (Wodejebato Guyot), and Hole 878A (MIT Guyot), X-ray diffraction data. (Continued on next two pages.)

Core, section, interval (cm)	Flow Unit	Depth (mbsf)	Sm	ML SwCh-Sm	ML Sm-Ch	Chl	Sw Chl	Serp	Illite	Kaol	Gyps	Hem	K-fspar	Cal	Q	An	Talc	Rock type
143-865A-																		
90R-5, 18-21	1	836.90	X						+	++		+		+	+			Alkaline basalt
90R-5, 52-58	1	837.24	X						+					+				-" -
90R-6, 45-50	1	838.58	X	+		+			+									-" -
90R-6, 75-77	1	838.88	X			+	++		+	+	+	+		+				-" -
91R-1, 29-32	1	841.39	X			+				+	+		+	+	+			-" -
91R-1, 112-118	1	842.22	X	+?		+			+					+				-" -
91R-2, 20-25	1	842.64	X			+	++											-" -
91R-3, 22-28	1	844.03	X			+	+		+									-" -
92R-3, 80-86	3	850.27	X			+			+	+?								-" -
92R-4, 45-47	3	850.90	X						+	++	+	+	+					-" -
93R-1, 35-37	3	853.75	X			+			+	++	+	++	+	++				-" -
93R-2, 0-8	3	854.90	+				X	+?	+?									-" -
94R-1, 97-102	3	864.07	++	++		+			+			++						-" -
94R-2, 102-105	3	865.59			X	+	X		+	+	+	++						-" -
94R-4, 133-143	4	868.73	++	++			+		+									-" -
143-866A-																		
171R-2, 109-111	1	1620.80	X							X		++	+					Alkaline basalt (highly altered)
171R-3, 121-123	2	1623.21	X			+				++	+	+		+				Alkaline basalt
171R-4, 131-134	2	1623.86	X							+								-" -
178W-1, 37-38	4	1659.77	X						+	++		++						Brecciated glassy rim of basalt
178W-1, 79-81	4	1660.19	X							++					+			-" -
179R-5, 40-45	6	1664.36	X		+		+											Alkaline basalt
180R-1, 27-32	6	1667.67	++		++				+									-" -
180R-3, 67-72	6	1670.65	++		++				+									- " -
180R-4, 12-17	6	1671.60	++				++		+									-" -
182R-1, 3-8	8	1682.83	+		+	+	+											-" -
182R-2, 58-63	8	1684.85	X		+				+?									-" -
182R-4, 26-30	8	1687.17	X															-" -

Table T57 (continued).

Core, section, interval (cm)	Flow Unit	Depth (mbsf)	Sm	ML SwCh-Sm	ML Sm-Ch	Chl	Sw Chl	Serp	Illite	Kaol	Gyps	Hem	K-fspar	Cal	Q	An	Talc	Rock type
182R-4, 38-40	8	1687.29	X									+		+				Alkaline basalt
182R-4, 72-74	8	1687.63	X									+						Brecciated glassy rim of basalt
183R-1, 125-131	9	1688.55	X			+												Alkaline basalt
184R-1, 27-28	9	1692.53	X							+					+			-" -
184R-1, 137-139	9	1693.67	X									+			+			Tuffobreccia
184R-2, 23-26	9	1694.03	X									++						Alkaline basalt
185R-3, 41-46	10	1700.07	X															-" -
185R-4, 26-32	11	1701.11	X															-" -
186R-1, 39-41	11	1707.39	X								+	+						-" -
186R-2, 20-24	11	1708.70	X															-" -
187R-1, 99-104	11	1716.79	X															-" -
188R-1, 82-89	11	1727.12	X	+														-" -
189R-1, 65-69	12	1735.55	++	+	X				+?									-" -
189R-2, 115-120	12	1737.48	X	++														Tuff
144-871C-																		
35R-4, 96-98	7B	456.83	X		++				+					+				Basanite
36R-1, 79-86	8	461.89	X		++			+							+			-" -
38R-3, 83-87	17	475.49	X		++	+			+							+		-" -
38R-7, 0-5	20	479.75	X		++	+		+?										-" -
39R-4, 0-5	21E	484.48	X		+	+						+						-" -
39R-5, 120-124	21G	487.18	X		++			+?										-" -
40R-1, 126-130	22A	490.96					++		++							+		-" -
40R-2, 70-75	22D	491.90	X	++			++					+?		+				-" -
144-872B-																		
5R-1, 56-58	6	145.36	X		+		X		+									Alkaline basalt
5R-3, 104-108	9	148.66	X		X			+	+									-" -
7R-3, 32-37	14	166.24	++		++									+		+	+?	Lava breccia
7R-4, 102-107	14	168.44	X			+												Alkaline basalt
7R-6, 10-15	14	170.30	X			+											+?	-" -
8R-1, 50-54	16A	173.60	X									+					+?	Lava breccia
8R-1, 63-68	16A	173.73	X									+		+		+	+?	Tuffobreccia

Table T57 (continued).

Core, section, interval (cm)	Flow Unit	Depth (mbsf)	Sm	ML SwCh-Sm	ML Sm-Ch	Chl	Sw Chl	Serp	Illite	Kaol	Gyps	Hem	K-fspar	Cal	Q	An	Talc	Rock type
8R-2, 9-12	16A	174.69	X											++				Alkaline basalt
8R-2, 91-94	16B	175.51	X											X				-" -
9R-3, 28-33	17B	185.76	X						+?									Brecciated alkali basalt
9R-4, 73-78	18B	187.31	X											+		+		Lava breccia
9R-5, 38-40	18B	188.36	X													+		Alkaline basalt (lava breccia)
144-874B-																		
22R-4, 48-53	1	177.15	++	X					+					+		+		Brecciated ankaramite
23R-1, 100-105	1	178.70	+	X				+				+						Ankaramite
23R-2, 112-117	1	180.31		X				+				+		+				-" -
24R-1, 30-35	1	184.30	+		+	++								+	+			-" -
24R-1, 108-110	1	185.08	X		++	+								++				-" -
24R-1, 115-118	1	185.15	++		++			++						++				-" -
24R-2, 74-77	1	186.18	+		+			+						+	+			Brecciated ankaramite
24R-2, 120-124	1	186.64				+	X							+				Ankaramite
24R-4, 54-72	1	189.04	X		+	+			+									Alkaline basalt
144-875C-																		
15M-1, 35-37	1	12.95	X		++	+			+									Alkaline basalt
144-876A-																		
15R-1, 32-34	1A	139.72	X		X	+			+									Alkaline olivine basalt
16R-1, 6-8	1B	147.14	X		+				+									-" -
144-878A-																		
80R-1, 95-98	5	742.35	X															Sediment
84R-3, 112-115	15	783.98	X		+	+			+									Basanite

Notes: X = dominant, ++ = minor, + = trace;
Sm = smectite, ML SwCh-Sm = mixed-layer swelling chlorite-smectite mineral, ML Sm-Ch = mixed-layer smectite-chlorite mineral, Chl = chlorite, Sw Chl = swelling chlorite,
Serp =serpentine, Kaol = kaolinite, Gyps = gypsum, Hem = hematite, K-fspar = K-feldspar, Cal = calcite, Q = quartz, An = analcime.
Chabazite in minor amount in Sample 144-872B-8R-2, 9-12 cm. Siderite in trace amount in Sample 143-865A-90R-5, 18-21 cm.

Table T58. Minerals from vesicles and veins in igneous rocks, West Pacific Guyots, Legs 143 and 144: Hole 865A (Allison Guyot), Hole 866A (Resolution Guyot), Hole 871C (Limalok Guyot), Hole 872B (Lo-En Guyot), Holes 874B and 876A (Wodejebato Guyot), and Hole 878A (MIT Guyot), X-ray diffraction data. (Continued on next four pages.)

Core, section, interval (cm)	Flow Unit	Depth (mbsf)	Sm	ML Sm-Chl	ML SwChl-Sm	Chl	SwChl	Serp	Illite	Cal	Q	Ap	Dol	Anal	Description	Rock type
143-865A-																
90R-5, 52-58	1	837.24	X							X					White matter	Sill intruded into clayey bioclastical limestone
90R-5, 52-58	1	837.24								X					Transparent crystals in altered basalt	Alkaline basalt
90R-6, 45-50	1	838.58	X			tr?				tr					Large vesicle filling (grey-green clay)	- " -
90R-6, 45-50	1	838.58								X					Vesicle filling (white matter)	- " -
90R-6, 45-50	1	838.58								X					White veinlet	- " -
90R-6, 75-77	1	838.88								X	tr				Vesicle filling (white matter)	- " -
91R-1, 112-118	1	842.22	X							tr					Large vesicle filling (grey-green clay)	- " -
91R-2, 20-25	1	842.64	X			tr				tr					Black vein	- " -
91R-3, 22-28	1	844.03	X			tr				tr					Black vein	- " -
91R-3, 22-28	1	844.03	X												Large vesicle filling (grey-green clay)	- " -
92R-3, 80-86	3	850.27										X			Pink matter from basalt	- " -
93R-2, 0-8	3	854.90	X							tr					Vein (green-grey clay)	- " -
93R-2, 0-8	3	854.90										X?			Pink vein	- " -
94R-2, 103-104	3	865.60	X					tr							Vesicle filling	- " -

Table T58 (continued).

Core, section, interval (cm)	Flow Unit	Depth (mbsf)	Sm	ML Sm-Chl	ML SwChl-Sm	Chl	SwChl	Serp	Illite	Cal	Q	Ap	Dol	Anal	Description	Rock type
143-866A-																
171R-3, 121-123	2	1623.21								X	tr				Large vesicle filling (white matter)	Alkali basalt
171R-4, 131-134	2	1623.86	X												Veinlet	- " -
180R-1, 27-32	6	1667.67	X												Large vesicle filling (grey-green clay)	- " -
180R-3, 67-72	6	1670.65			X		X								Vesicle filling	- " -
183R-1, 125-131	9	1688.55	X												Vein	- " -
184R-1, 27-28	9	1692.53	X												Veinlet	- " -
184R-1, 137-139	9	1693.67	X												Matrix	Tuffobreccia
185R-3, 41-46	10	1700.07	X							tr					Vein (grey-green matter)	Alkali basalt
185R-4, 26-32	11	1701.11	X							tr					Large vesicle filling (grey-green clay)	- " -
186R-1, 39-41	11	1707.39	X							tr					Large vesicle filling (grey-blue clay)	- " -
187R-1, 99-104	11	1716.79	X												Vein	- " -
188R-1, 82-89	11	1727.12	X							tr					Green veinlet	- " -
189R-2, 115-120	12	1737.48	X												Grey-green matter	Tuff

Table T58 (continued).

Core, section, interval (cm)	Flow Unit	Depth (mbsf)	Sm	ML Sm-Chl	ML SwChl-Sm	Chl	SwChl	Serp	Illite	Cal	Q	Ap	Dol	Anal	Description	Rock type
144-871C-																
36R-1, 79-86	8	461.89	X		X				tr						Vein	Basanite
38R-7, 0-5	20	479.75	X			tr				tr					Veinlet (grey-green matter)	- " -
40R-1, 126-130	22A	490.96	X	X	X	X									Altered olivine crystal	- " -
40R-2, 70-75	22D	491.90	X				tr			tr					Vein	- " -
144-872B-																
5R-1, 56-58	6	145.36								X					Vein	Alkaline basalt
5R-3, 104-108	9	148.66	X						X						Vein (green-blue matter)	- " -
7R-1, 8-12	13	164.08								X					White vein	- " -
7R-4, 102-107	14	168.44	X							X					Veinlet	- " -
7R-6, 10-15	14	170.30	tr							X					Veinlet	- " -
9R-3, 28-33	17	185.76								X					Veinlet	Brecciated alkali basalt
9R-4, 73-78	18B	187.31	X							tr			X	tr	Veinlet	Lava breccia
9R-5, 38-40	18B	188.36	X							tr	tr		tr	X	Veinlet	Alkali basalt (lava breccia)

Table T58 (continued).

Core, section, interval (cm)	Flow Unit	Depth (mbsf)	Sm	ML Sm-Chl	ML SwChl-Sm	Chl	SwChl	Serp	Illite	Cal	Q	Ap	Dol	Anal	Description	Rock type
144-874B-																
22R-4, 48-53	1	177.15	X		tr					tr					Altered olivine crystal	Brecciated ankaramite
22R-4, 48-53	1	177.15	X	tr	X					tr					White matter	Brecciated ankaramite
23R-1, 100-105	1	178.70					X	tr			tr				Altered olivine crystal	Ankaramite
23R-2, 112-117	1	180.31					X	tr							Altered olivine crystal	- " -
24R-1, 30-35	1	184.30	X	tr						tr					Altered olivine crystal	- " -
24R-2, 120-124	1	186.64	tr				X								Altered olivine crystal	- " -
24R-2, 120-124	1	186.64			X		X								Altered olivine crystal	- " -
24R-2, 120-124	1	186.64			X		X								Altered olivine crystal	- " -
24R-3, 125-130	1	188.19													White-grey vein	Alkali basalt
24R-4, 54-72	1	189.04								X					Vesicle filling	- " -
24R-4, 54-72	1	189.04	X												Veinlet	- " -
144-876A																
15R-1, 32-34	1A	139.72	X							X					Veinlet	Alkali olivine basalt

Table T58 (continued).

Core, section, interval (cm)	Flow Unit	Depth (mbsf)	Sm	ML Sm-Chl	ML SwChl-Sm	Chl	SwChl	Serp	Illite	Cal	Q	Ap	Dol	Anal	Description	Rock type
16R-1, 6-8	1B	147.14								X					Veinlet	Alkali olivine basalt
144-878A																
84R-3, 112-115	15	783.98	X			tr									Veinlet	Basanite

Notes: X = dominant, tr = trace.
Sm = smectite, ML Sm-Chl = mixed-layer smectite-chlorite mineral, ML SwChl-Sm = mixed-layer swelling chlorite-smectite mineral, Chl = chlorite, Sw Chl = swelling chlorite, Serp = serpentine, Cal = calcite, Q = quartz, Ap = apatite, Dol = dolomite, Anal = analcime.
Chabazite in Sample 144-876A-15R-1, 32-34 cm. Ankerite in Sample 143-866A-171R-3, 121-123 cm. Siderite in Sample 143-865A-90R-5, 52-58 cm. Hematite in Sample 144-871C-40R-2, 70-75 cm and Sample 144-874B-22R-4, 48-53 cm.

Table T59. Composition of alkaline basalts from Hole 866A, Leg 143 (Resolution Guyot, West Pacific Guyots). (Continued on next three pages.)

Leg	143	143	143	143	143	143	143
Hole	866A	866A	866A	866A	866A	866A	866A
Core, section	171R-2	171R-4	178W-1	178W-1	179R-5	180R-1	180R-3
Interval (cm)	109-111	131-134	37-38	79-81	40-45	27-32	67-72
Piece	3		Glass	Glass		3A	1D
Lab number	Z-1504	Z-1505	Z-1506	Z-1507	Z-1508	Z-1509	Z-1510
Depth (mbsf)	1620.8	1623.86	1659.77	1660.19	1664.36	1667.67	1670.65
Unit	1	2	4	4	6	6	6
Major element oxides (wt%):							
SiO_2	41.03	41.18	40.04	36.59	45.57	45.87	45.89
TiO_2	3.38	3.67	3.47	3.11	2.72	2.70	2.66
Al_2O_3	20.13	18.83	16.08	18.47	16.69	15.97	15.98
Fe_2O_3	14.56	16.13	18.53	20.66	8.24	5.23	4.70
FeO	0.88	0.63	0.12	0.16	3.54	6.28	7.18
MnO	0.03	0.11	0.03	0.06	0.19	0.12	0.14
MgO	1.54	2.52	2.85	2.83	5.90	7.62	7.80
CaO	1.43	1.80	2.04	1.48	9.14	9.13	9.35
Na_2O	1.14	1.35	1.40	1.19	3.11	2.87	2.78
K_2O	4.50	4.17	1.31	0.77	0.55	0.39	0.36
P_2O_5	0.07	0.13	0.20	0.04	0.23	0.25	0.24
LOI	11.47	9.87	13.58	15.09	3.65	2.91	2.60
Total	100.16	100.39	99.65	100.45	99.53	99.34	99.68
H_2O^+	7.10	5.43	5.63	6.23	1.29	1.41	1.67
H_2O^-	3.55	4.26	7.95	6.54	1.33	0.95	0.70
CO_2	ND	ND	ND	ND	0.43	<0.2	0.20
Fe_2O_3/FeO	16.55	25.60	154.42	129.12	2.33	0.83	0.66
Density (g/cm^3)	2.15	2.20	2.25	2.19	2.74	2.88	2.88
Trace elements (ppm):							
La	12	16	22	21			
Ce	22	36	62	29			
Nd	17	23	31	24			
Sm	4.5	5.6	7.5	5.8			
Eu	1.7	1.8	2.3	1.9			
Tb	0.68	0.79	1.3	1.2			
Yb	1.7	1.5	2.1	2.7			
Lu	0.27	0.21	0.31	0.41			
Cr	560	ND	315	740	172	200	195
Ni	330	ND	166	278	84	104	145
Co	54	ND	44	53	35	50	62
V	255	ND	215	728	218	340	245
Cu	51	ND	41	47	66	73	75
Zn	118	ND	98	67	90	95	92
Zr	170	ND	280	140	140	130	130
Nb	21	ND	40	16	15	15	15
Y	15	ND	28	22	25	24	24
Rb	36	ND	20	15	6.9	5.9	5.0
Sr	39	ND	100	97	470	440	430
Ba	47	ND	41	6	48	160	430

Note: ND = not determined.

Table T59 (continued).

Leg	143	143	143	143	143	143	143
Hole	866A	866A	866A	866A	866A	866A	866A
Core, section	180R-4	182R-1	182R-2	182R-4	182R-4	183R-1	184R-1
Interval (cm)	12-17	3-8	58-63	26-30	72-74	125-131	27-28
Piece	1B	2	3C	4B	Breccia 8	18B	4
Lab number	Z-1511	Z-1512	Z-1513	Z-1514	Z-1515	Z-1516	Z-1517
Depth (mbsf)	1671.6	1682.83	1684.85	1687.17	1687.63	1688.55	1692.53
Unit	6	8	8	8	8	9	9
Major element oxides (wt%):							
SiO_2	45.94	46.64	47.44	42.41	43.01	45.47	45.80
TiO_2	2.64	2.28	2.30	2.00	3.59	3.30	3.36
Al_2O_3	16.12	15.09	16.31	12.67	15.54	14.55	15.00
Fe_2O_3	5.32	5.17	6.34	11.59	15.65	11.22	7.74
FeO	6.62	6.42	3.98	0.14	1.73	3.29	5.49
MnO	0.14	0.13	0.13	0.06	0.06	0.17	0.25
MgO	8.01	8.62	6.20	5.82	3.25	7.28	6.41
CaO	9.48	8.81	10.24	5.45	4.68	5.77	7.76
Na_2O	2.94	2.96	3.06	1.63	2.86	3.64	3.48
K_2O	0.38	0.49	0.47	1.26	1.71	0.75	0.61
P_2O_5	0.23	0.30	0.31	3.50	0.04	0.39	0.36
LOI	2.10	2.36	2.86	13.00	8.08	3.87	3.05
Total	99.92	99.27	99.64	99.53	100.20	99.70	99.31
H_2O^+	1.22	1.19	1.07	3.48	2.85	1.00	1.00
H_2O^-	0.64	0.71	1.11	7.83	4.50	1.90	1.33
CO_2	<0.2	<0.2	0.36	0.64	ND	0.30	<0.2
Fe_2O_3/FeO	0.80	0.81	1.59	82.79	9.05	3.41	1.41
Density (g/cm^3)	2.90	2.91	2.90	ND	1.98	2.52	2.70
Trace elements (ppm):							
La				22	33	25	26
Ce				43	76	50	50
Nd				18	42	27	27
Sm				3.4	9.7	6.5	5.7
Eu				1.0	3.3	1.9	1.8
Tb				0.54	1.60	0.79	0.87
Yb				1.6	3.0	2.3	2.1
Lu				0.24	0.43	0.31	0.33
Cr	190	232	305	79	170	170	166
Ni	150	160	172	90	133	136	85
Co	56	48	50	49	49	50	49
V	238	188	220	170	240	358	342
Cu	74	74	83	91	67	89	50
Zn	89	90	94	54	90	120	100
Zr	130	160	165	200	235	220	210
Nb	15	28	28	36	42	36	39
Y	23	27	26	110	27	31	32
Rb	6.1	13	11	24	21	7.9	12
Sr	450	330	380	220	180	400	390
Ba	150	350	410	290	170	240	120

Table T59 (continued).

Leg	143	143	143	143	143	143	143
Hole	866A	866A	866A	866A	866A	866A	866A
Core, section	184R-1	184R-2	185R-3	185R-4	186R-1	186R-2	187R-1
Interval (cm)	137-139	23-26	41-46	26-32	39-41	20-24	99-104
Piece	Tuff 7	3	1D	6B	6	5	17
Lab number	Z-1518	Z-1519	Z-1520	Z-1521	Z-1522	Z-1523	Z-1524
Depth (mbsf)	1693.67	1694.03	1700.07	1701.11	1707.39	1708.70	1716.79
Unit	9	9	10	11	11	11	11
Major element oxides (wt%):							
SiO_2	43.35	43.67	46.21	45.07	45.40	43.51	44.45
TiO_2	2.99	1.95	2.80	2.97	2.57	3.18	3.30
Al_2O_3	13.76	13.78	14.49	14.76	11.03	15.70	16.76
Fe_2O_3	12.90	12.90	7.17	10.01	9.06	11.54	10.38
FeO	2.34	0.43	5.41	2.27	2.78	2.37	2.71
MnO	0.07	0.05	0.15	0.10	0.04	0.08	0.11
MgO	6.68	5.12	7.83	8.82	12.35	7.98	6.84
CaO	4.55	4.17	8.65	4.09	2.77	4.70	5.68
Na_2O	2.78	2.16	3.18	3.39	2.70	3.03	3.45
K_2O	1.90	1.42	0.52	1.32	2.84	1.56	1.11
P_2O_5	0.24	0.26	0.37	0.39	0.13	0.40	0.44
LOI	8.52	13.62	3.05	6.10	8.22	5.20	4.31
Total	100.08	99.53	99.83	99.29	99.89	99.25	99.54
H_2O^+	2.50	4.54	1.45	1.89	3.20	1.34	1.34
H_2O^-	5.07	7.98	1.24	3.11	5.02	2.86	2.37
CO_2	0.35	1.10	0.34	0.48	ND	0.38	0.32
Fe_2O_3/FeO	5.51	30.00	1.33	4.41	3.26	4.87	3.83
Density (g/cm^3)	ND	2.10	2.75	2.26	2.02	2.41	2.42
Trace elements (ppm):							
La	23	36			20	30	
Ce	43	70			40	64	
Nd	24	42			21	36	
Sm	5.5	9.3			4.7	7.3	
Eu	1.7	2.8			1.4	1.6	
Tb	0.99	1.70			0.77	0.76	
Yb	2.1	3.9			1.4	2.2	
Lu	0.32	0.63			0.23	0.38	
Cr	159	218	178	211	187	222	184
Ni	145	129	130	98	133	130	95
Co	56	50	44	46	46	52	38
V	248	198	208	258	239	346	247
Cu	91	58	74	78	69	83	83
Zn	88	78	118	125	74	80	90
Zr	180	210	200	240	200	250	265
Nb	33	32	30	43	35	41	49
Y	28	42	27	29	25	25	29
Rb	12	15	8.7	12	13	5.4	6.6
Sr	230	305	380	370	200	410	480
Ba	280	250	150	400	250	290	440

Table T59 (continued).

Leg	143	143	143
Hole	866A	866A	866A
Core, section	188R-1	189R-1	189R-2
Interval (cm)	82-89	65-69	115-120
Piece	16A	5C	Tuff 7C
Lab number	Z-1525	Z-1526	Z-1527
Depth (mbsf)	1727.12	1735.55	1737.48
Unit	11	12	12
Major element oxides (wt%):			
SiO_2	44.70	44.96	43.63
TiO_2	2.87	2.10	1.78
Al_2O_3	14.08	12.31	11.57
Fe_2O_3	11.08	6.40	8.04
FeO	2.45	7.56	3.39
MnO	0.09	0.18	0.17
MgO	9.93	12.31	15.85
CaO	3.73	8.19	2.38
Na_2O	2.71	2.14	2.34
K_2O	2.30	0.33	1.07
P_2O_5	0.39	0.25	0.17
LOI	5.30	3.00	9.15
Total	99.63	99.73	99.54
H_2O^+	1.33	2.11	3.43
H_2O^-	2.86	0.68	4.69
CO_2	0.59	<0.2	0.46
Fe_2O_3/FeO	4.52	0.85	2.37
Density (g/cm^3)	2.32	2.90	2.18
Trace elements (ppm):			
La			
Ce			
Nd			
Sm			
Eu			
Tb			
Yb			
Lu			
Cr	256	402	345
Ni	145	232	235
Co	51	64	65
V	253	221	268
Cu	74	67	74
Zn	84	92	86
Zr	240	135	115
Nb	46	21	18
Y	26	23	18
Rb	11	6.7	5.7
Sr	330	260	180
Ba	290	190	210

Table T60. Composition of basanites from Hole 871C, Leg 144 (Limalok Guyot, West Pacific Guyots). (Continued on next page.)

Leg	144	144	144	144	144	144	144
Hole	871C	871C	871C	871C	871C	871C	871C
Core, section	35R-3	35R-3	35R-4	36R-1	36R-2	36R-3	38R-1
Interval (cm)	76-78	143-145	96-98	2-5	107-109	32-35	117-120
Piece	Breccia 3C	5B	12	7B	11	3	10
Lab number	Z-1528	Z-863	Z-1529	Z-1530	Z-864	Z-865	Z-866
Depth (mbsf)	455.07	455.80	456.83	461.89	463.58	464.26	472.97
Unit/Subunit	6	7B	7B	8	13	13	17
Major element oxides (wt%):							
SiO_2	36.78	38.04	36.16	36.53	40.19	40.04	40.55
TiO_2	3.37	3.55	3.34	3.73	2.87	2.92	2.55
Al_2O_3	12.40	12.64	11.28	12.39	12.33	11.48	11.60
Fe_2O_3	13.32	10.07	11.57	12.87	5.67	6.86	6.16
FeO	1.55	2.70	2.84	3.23	4.08	5.21	5.83
MnO	0.17	0.49	0.20	0.29	0.11	0.11	0.19
MgO	13.76	10.98	14.06	13.85	12.27	13.76	15.64
CaO	2.85	8.47	3.69	2.98	11.17	10.06	9.35
Na_2O	1.65	1.16	1.52	1.31	1.12	0.97	2.10
K_2O	0.60	0.49	0.71	0.53	0.27	0.22	0.57
P_2O_5	0.50	0.62	0.46	0.65	0.59	0.60	0.57
LOI	12.39	10.90	13.65	11.51	9.20	7.86	4.90
Total	99.34	100.11	99.48	99.87	99.87	100.09	100.01
H_2O^+	4.57	4.91	5.47	6.13	3.22	4.29	2.95
H_2O^-	5.73	4.56	5.38	4.75	3.38	2.50	0.94
CO_2	1.48	1.23	2.73	0.60	1.13	<0.2	<0.2
Fe_2O_3/FeO	8.59	3.73	4.07	3.99	1.39	1.32	1.06
Density (g/cm^3)	2.19	2.47	ND	2.44	2.47	2.69	2.86
Trace elements (ppm):							
La	36	52	40	40			
Ce	36	120	35	36			
Nd	36	51	37	35			
Sm	6.8	10	6.4	6.2			
Eu	2.2	3.0	1.9	2.0			
Tb	1.0	1.1	1.0	0.96			
Yb	1.6	2.3	1.6	1.3			
Lu	0.24	0.32	0.24	0.18			
Cr	490	540	460	520	465	480	515
Ni	240	250	225	265	290	330	340
Co	80	57	74	84	68	68	61
V	235	347	270	278	232	257	242
Cu	78	45	58	58	72	72	65
Zn	90	99	82	122	98	105	89
Zr	230	250	225	250	230	220	210
Nb	64	64	66	73	61	57	54
Y	21	31	20	29	27	25	23
Rb	22	13	27	18	5.1	7.1	8.6
Sr	230	360	300	270	555	505	780
Ba	290	400	480	560	400	340	1050

Note: ND = not determined.

Table T60 (continued).

Leg	144	144	144	144	144	144	144	144
Hole	871C	871C	871C	871C	871C	871C	871C	871C
Core, section	38R-3	38R-7	39R-1	39R-4	39R-5	40R-1	40R-2	40R-4
Interval (cm)	83-87	0-5	6-10	0-5	120-124	126-130	70-75	98-101
Piece	4	1A	2	1	10C	10A	3	3D
Lab number	Z-867	Z-1531	Z-868	Z-1532	Z-1533	Z-1534	Z-1535	Z-869
Depth (mbsf)	475.49	479.75	480.46	484.48	487.18	490.96	491.90	495.18
Unit/Subunit	17	20	21A	21E	21G	22A	22D	22G
Major element oxides (wt%):								
SiO_2	40.00	37.78	39.31	35.88	37.62	40.34	34.78	38.33
TiO_2	2.57	3.28	3.20	2.96	3.14	2.99	3.46	3.23
Al_2O_3	11.22	10.35	11.86	9.60	9.91	9.95	10.74	10.27
Fe_2O_3	6.46	10.52	6.48	14.64	11.02	8.00	16.87	7.63
FeO	6.08	5.59	5.84	2.37	5.03	6.83	1.51	5.21
MnO	0.21	0.18	0.20	0.18	0.21	0.21	0.19	0.21
MgO	14.74	14.40	12.93	18.91	15.84	17.05	14.36	14.80
CaO	9.74	8.78	11.71	1.23	9.42	9.00	3.03	11.23
Na_2O	1.92	0.68	1.20	1.29	0.74	1.94	1.25	0.81
K_2O	0.50	0.24	0.41	0.34	0.40	0.37	0.32	0.17
P_2O_5	0.53	0.62	0.62	0.43	0.49	0.50	0.74	0.53
LOI	6.24	7.20	6.09	11.30	6.08	3.24	12.78	7.29
Total	100.21	99.62	99.85	99.13	99.90	100.42	100.03	99.71
H_2O^+	3.53	4.08	3.16	5.47	3.68	2.10	4.87	3.86
H_2O^-	1.08	2.35	1.81	4.69	1.69	0.81	5.27	2.38
CO_2	<0.2	0.76	<0.2	0.55	<0.2	0.33	1.95	0.57
Fe_2O_3/FeO	1.06	1.88	1.11	6.18	2.19	1.17	11.17	1.46
Density (g/cm^3)	2.94	2.61	2.88	2.28	2.86	3.03	ND	2.83
Trace elements (ppm):								
La				34		32	55	
Ce				92		62	90	
Nd				42		32	45	
Sm				6.9		7.3	10	
Eu				2.4		2.2	2.9	
Tb				1.0		0.95	1.4	
Yb				1.4		1.5	2.2	
Lu				0.21		0.21	0.32	
Cr	500	475	455	610	660	548	655	600
Ni	340	270	305	420	427	322	398	560
Co	62	84	68	95	85	77	103	93
V	225	360	285	241	283	226	270	255
Cu	62	63	65	63	63	69	63	65
Zn	92	94	98	93	120	102	84	93
Zr	220	180	190	170	170	165	220	200
Nb	57	53	52	46	45	45	66	49
Y	27	28	21	21	24	25	32	27
Rb	11	7.3	14	12	10	15	20	9.8
Sr	590	210	540	100	290	450	230	320
Ba	970	310	320	120	210	280	100	255

Table T61. Composition of alkaline basalts and hawaiites from Hole 872B, Leg 144 (Lo-En Guyot, West Pacific Guyots). (Continued on next page.)

Leg	144	144	144	144	144	144	144	144
Hole	872B	872B	872B	872B	872B	872B	872B	872B
Core, section	5R-1	5R-3	5R-4	7R-1	7R-3	7R-4	7R-6	8R-1
Interval (cm)	56-58	104-108	65-68	8-12	32-37	102-107	10-15	50-54
Piece	6	10	10	1	Breccia 1	3	3	Breccia 7
Lab number	Z-870	Z-1536	Z-1537	Z-1538	Z-1539	Z-1540	Z-1541	Z-1542
Depth (mbsf)	145.36	148.66	149.77	164.08	166.24	168.44	170.30	173.60
Unit	6	9	10B	13	14	14	14	16A
Major element oxides (wt%):								
SiO_2	47.20	46.44	43.92	43.62	45.04	46.16	46.90	42.46
TiO_2	2.40	2.16	2.16	2.39	2.30	2.32	2.36	2.36
Al_2O_3	16.15	13.85	15.40	14.53	13.34	15.51	15.85	14.14
Fe_2O_3	4.75	7.59	9.54	13.00	11.57	9.09	5.12	13.12
FeO	4.63	5.03	2.55	0.22	0.72	2.23	4.60	0.83
MnO	0.12	0.14	0.13	0.13	0.14	0.13	0.13	0.12
MgO	7.45	8.56	7.19	7.52	7.35	7.50	8.79	4.85
CaO	9.58	8.20	6.16	4.80	6.06	7.30	9.33	4.48
Na_2O	3.10	2.89	4.34	3.09	3.37	3.28	2.94	2.67
K_2O	1.22	1.04	0.85	1.68	3.20	1.31	0.98	1.97
P_2O_5	0.38	0.29	0.22	0.35	0.36	0.33	0.38	0.32
LOI	3.09	3.68	7.16	8.86	6.48	4.80	2.63	12.5
Total	100.07	99.87	99.62	100.19	99.93	99.96	100.01	99.82
H_2O^+	1.49	1.88	4.35	3.74	3.02	1.17	1.45	4.17
H_2O^-	1.12	1.66	2.60	3.76	1.87	2.08	1.18	5.56
CO_2	<0.2	<0.2	<0.2	1.15	1.17	0.79	<0.2	2.38
Fe_2O_3/FeO	1.03	1.51	3.74	59.09	16.07	4.08	1.11	15.81
Density (g/cm^3)	2.79	2.67	2.44	2.24	2.26	2.50	2.79	2.18
Trace elements (ppm):								
La								28
Ce								57
Nd								26
Sm								5.3
Eu								1.9
Tb								0.93
Yb								1.7
Lu								0.24
Cr	65	165	198	204	207	208	175	184
Ni	45	89	81	81	67	67	63	73
Co	37	53	42	36	35	42	37	53
V	210	220	207	229	178	195	171	231
Cu	48	63	63	63	56	60	58	58
Zn	98	96	89	122	80	80	89	77
Zr	190	150	140	170	150	160	160	165
Nb	36	30	30	34	33	33	34	33
Y	21	18	22	18	22	19	21	18
Rb	22	22	9.5	25	24	22	20	18
Sr	320	350	380	270	190	430	430	190
Ba	280	360	210	280	400	280	370	200

Table T61 (continued).

Leg	144	144	144	144	144	144	144
Hole	872B	872B	872B	872B	872B	872B	872B
Core, section	8R-1	8R-2	8R-2	8R-4	9R-2	9R-3	9R-5
Interval (cm)	63-68	9-12	91-94	24-29	19-21	28-33	38-40
Piece	Tuff 7	1	3	2	1	Breccia 3	Breccia 1A
Lab number	Z-1543	Z-1720	Z-1717	Z-871	Z-872	Z-1544	Z-1546
Depth (mbsf)	173.73	174.69	175.51	177.66	184.17	185.76	188.36
Unit	16A	16A	16B	16B	17A	17B	18B
Major element oxides (wt%):							
SiO_2	42.34	41.90	45.58	43.99	45.73	48.83	48.80
TiO_2	2.29	2.02	2.49	2.18	2.82	2.5	1.67
Al_2O_3	12.85	14.93	13.98	16.13	16.95	14.89	11.51
Fe_2O_3	10.18	10.99	7.77	6.83	8.96	6.73	6.43
FeO	0.78	0.59	3.91	4.60	1.86	3.99	3.1
MnO	0.16	0.03	0.07	0.04	0.14	0.13	0.09
MgO	6.68	4.99	6.20	6.73	2.08	6.45	9.38
CaO	7.34	6.28	10.47	10.31	6.67	8.82	5.84
Na_2O	3.29	2.86	3.42	3.11	3.59	3.27	3.21
K_2O	1.98	2.40	1.33	0.87	1.48	1.1	0.44
P_2O_5	0.26	0.54	0.30	0.28	0.36	0.34	0.09
LOI	11.94	12.95	5.15	4.35	9.21	2.47	8.86
Total	100.09	100.48	100.67	99.42	99.85	99.52	99.42
H_2O^+	3.37	6.15	2.02	2.07	3.32	1.08	4.25
H_2O^-	3.78	5.00	1.73	1.37	3.48	1.06	3.8
CO_2	4.79	1.80	1.40	<0.2	2.34	<0.2	0.41
Fe_2O_3/FeO	13.05	18.63	1.99	1.48	4.82	1.69	2.07
Density (g/cm^3)	2.28	2.29	2.70	2.84	2.25	2.73	2.25
Trace elements (ppm):							
La		24	27				
Ce		45	51				
Nd		19	24				
Sm		4.2	4.8				
Eu		1.5	1.8				
Tb		0.69	0.77				
Yb		1.2	1.5				
Lu		0.16	0.23				
Cr	178	160	91	230	102	47	610
Ni	68	62	59	82	55	48	272
Co	47	45	39	47	40	34	52
V	225	166	208	212	357	180	235
Cu	54	50	56	55	65	56	63
Zn	74	72	83	97	79	88	70
Zr	160	140	190	170	200	160	97
Nb	30	28	36	29	36	33	15
Y	22	17	22	21	23	24	15
Rb	17	19	23	14	23	24	8.0
Sr	190	360	380	510	430	395	66
Ba	190	260	290	200	250	380	120

Table T62. Composition of ankaramites from Hole 874B, Leg 144 (Wodejebato Guyot, West Pacific Guyots). (Continued on next page.)

Leg	144	144	144	144	144	144	144
Hole	874B	874B	874B	874B	874B	874B	874B
Core, section	22R-4	23R-1	23R-2	24R-1	24R-1	24R-1	24R-2
Interval (cm)	48-53	100-105	112-117	30-35	100-105	120-127	70-76
Piece	Breccia 1	13	23	2	7	8	Breccia 9
Lab.number	Z-1547	Z-1548	Z-1549	Z-1550	Z-1551	Z-1552	Z-1553
Depth (mbsf)	177.15	178.70	180.31	184.30	185.00	185.20	186.14
Unit	1	1	1	1	1	1	1
Major element oxides (wt%):							
SiO_2	37.54	40.29	40.47	43.42	43.35	30.51	38.00
TiO_2	1.62	1.33	1.27	1.38	1.47	1.01	1.36
Al_2O_3	8.54	7.65	7.33	7.02	7.35	4.6	5.70
Fe_2O_3	12.08	11.27	10.65	6.35	8.99	8.07	10.38
FeO	0.81	0.79	0.42	5.23	2.7	2.31	1.66
MnO	0.21	0.18	0.17	0.17	0.16	0.07	0.07
MgO	16.34	20.53	22.27	22.06	19.35	19.79	21.20
CaO	6.45	3.92	3.77	7.07	5.2	12.84	7.05
Na_2O	1.59	1.27	1.29	1.09	1.27	1.45	1.56
K_2O	0.35	0.21	0.14	0.66	0.71	0.15	0.21
P_2O_5	0.22	0.13	0.14	0.15	0.18	0.08	0.14
LOI	13.79	11.81	11.57	4.62	8.62	19.09	12.54
Total	99.54	99.38	99.49	99.22	99.35	99.97	99.87
H_2O^+	5.05	5.78	4.47	2.69	5.3	6.02	6.14
H_2O^-	4.83	4.34	4.53	1.02	2.29	3.66	5.10
CO_2	2.97	0.67	0.23	0.38	0.43	9.05	1.30
Fe_2O_3/FeO	14.91	14.27	25.36	1.21	3.33	3.33	6.51
Density (g/cm^3)	1.96	2.34	2.33	2.88	2.53	2.63	2.34
Trace elements (ppm):							
La	20	18	15	14	17	9.3	1
Ce	29	32	30	35	29	17	18
Nd	18	17	15	18	18	9.5	11
Sm	4.4	3.9	3.5	3.6	4.0	2.4	3.0
Eu	1.2	1.3	1.3	1.0	1.3	0.77	0.93
Tb	0.60	0.66	0.63	0.53	0.65	0.38	0.46
Yb	1.1	1.0	1.0	1.0	1.2	0.69	0.83
Lu	0.15	0.15	0.15	0.17	0.17	0.098	0.13
Cr	905	940	670	1000	920	880	750
Ni	405	423	384	390	418	350	325
V	174	172	138	185	206	204	144
Co	157	113	97	81	88	71	80
Cu	29	35	39	31	33	25	13
Zn	154	118	106	108	108	53	28
Zr	110	99	87	100	100	46	75
Nb	19	17	14	15	17	8.4	12
Y	15	12	10	14	16	7.2	11
Rb	4.0	2.7	1.6	7.4	11	1.6	3.2
Sr	35	35	27	180	270	40	28
Ba	32	44	33	160	58	70	8

Table T62 (continued).

Leg	144	144	144
Hole	874B	874B	874B
Core, section	24R-2	24R-3	24R-4
Interval (cm)	120-124	125-130	54-72
Piece	18	18	3
Lab.number	Z-1554	Z-1555	Z-1718
Depth (mbsf)	186.64	188.19	189.04
Unit	1	1	1
Major element oxides (wt%):			
SiO_2	41.38	46.88	42.86
TiO_2	1.64	1.68	2.06
Al_2O_3	9.50	11.81	10.73
Fe_2O_3	10.48	5.20	8.57
FeO	0.59	2.42	4.32
MnO	0.17	0.11	0.07
MgO	18.78	13.79	11.53
CaO	4.89	7.56	10.34
Na_2O	1.38	2.04	2.28
K_2O	1.07	0.97	0.84
P_2O_5	0.21	0.20	0.19
LOI	9.20	6.66	5.95
Total	99.29	99.32	99.74
H_2O^+	4.01	3.42	3.61
H_2O^-	3.83	2.18	1.84
CO_2	<0.2	<0.2	0.50
Fe_2O_3/FeO	17.76	2.15	1.98
Density (g/cm^3)	2.33	2.39	2.78
Trace elements (ppm):			
La	20	19	19
Ce	47	42	38
Nd	22	20	18
Sm	4.6	4.2	4.2
Eu	1.5	1.3	1.4
Tb	0.80	0.76	0.67
Yb	1.5	1.2	1.4
Lu	0.22	0.18	0.2
Cr	575	690	575
Ni	308	320	215
V	122	262	202
Co	79	72	60
Cu	46	46	38
Zn	106	110	112
Zr	115	120	125
Nb	19	19	22
Y	16	17	21
Rb	11	21	15
Sr	37	340	275
Ba	88	140	320

Table T63. Composition of hawaiites, basanites, and alkaline olivine basalts from Hole 878A, Leg 144 (MIT Guyot, West Pacific Guyots). (Continued on next five pages.)

Leg	144	144	144	144	144	144	144
Hole	878A	878A	878A	878A	878A	878A	878A
Core, section	78R-2	79R-2	79R-4	80R-1	80R-5	80R-5	81R-2
Interval (cm)	64-70	9-12	24-27	95-98	20-24	106-109	10-15
Piece	3B	1	1	14	1G	4B	1
Lab number	Z-1556	Z-873	Z-874	Z-875	Z-1557	Z-876	Z-1558
Depth (mbsf)	724.12	733.22	736.07	742.35	747.16	748.02	752.55
Petrographic type	1	1	1	Sandstone	2	2	2
Unit/Subunit	1	2	2	5	8	8	10
Major element oxides (wt%):							
SiO_2	46.53	45.59	49.27	43.24	40.83	41.09	40.89
TiO_2	3.24	3.10	3.15	3.25	3.66	3.37	3.72
Al_2O_3	17.35	16.47	18.25	13.59	12.42	11.81	12.80
Fe_2O_3	8.33	10.42	7.07	12.88	7.27	7.69	10.93
FeO	3.85	2.46	2.32	0.46	5.57	5.06	3.12
MnO	0.13	0.17	0.36	0.08	0.21	0.13	0.13
MgO	4.17	3.39	2.64	3.49	10.50	10.90	10.42
CaO	7.95	5.68	4.66	3.09	12.25	11.51	10.89
Na_2O	3.5	3.16	3.25	1.86	1.55	1.65	1.56
K_2O	1.92	3.68	4.77	2.50	0.57	0.64	0.74
P_2O_5	0.79	0.71	0.83	1.71	0.67	0.62	0.66
LOI	2.56	4.95	3.87	14.15	4.41	5.08	4.37
Total	100.32	99.78	100.44	100.30	99.91	99.55	100.23
H_2O^+	1.06	2.08	1.86	4.30	2.48	3.08	2.01
H_2O^-	1.01	1.77	1.61	8.22	1.47	1.57	1.77
CO_2	0.49	1.10	<0.2	<0.2	0.46	0.43	0.24
Fe_2O_3/FeO	2.16	4.24	3.05	28.00	1.31	1.52	3.50
Density (g/cm^3)	2.73	2.65	2.64	ND	2.87	2.78	2.85
Trace elements (ppm):							
La	47				44		
Ce	140				97		
Nd	60				48		
Sm	10				11		
Eu	3.4				2.7		
Tb	1.6				1.3		
Yb	2.4				1.9		
Lu	0.33				0.26		
Cr	32	31	34	275	500	440	395
Ni	39	40	88	170	205	260	185
V	126	192	220	200	345	242	219
Co	34	37	64	49	68	65	56
Cu	36	33	155	37	52	65	50
Zn	134	98	126	80	107	93	102
Zr	280	280	320	ND	290	310	290
Nb	59	54	61	ND	56	53	54
Y	29	28	32	ND	26	30	24
Rb	38	50	49	ND	6.8	50	8.0
Sr	700	370	490	ND	560	510	550
Ba	170	360	730	ND	460	255	84

Note: ND = not determined.

Table T63 (continued).

Leg	144	144	144	144	144	144	144
Hole	878A	878A	878A	878A	878A	878A	878A
Core, section	81R-4	81R-5	83R-3	84R-2	84R-3	84R-3	84R-5
Interval (cm)	120-124	42-45	84-87	119-123	18-22	116-120	114-118
Piece	12	3A	4	6C	2A	8C	9B
Lab number	Z-1559	Z-1560	Z-877	Z-878	Z-1561	Z-1562	Z-879
Depth (mbsf)	756.35	756.94	774.00	782.55	783.04	784.02	786.95
Petrographic type	2	2	NA	2	2	2	2
Unit/Subunit	11	11	13	15	15	15	15
Major element oxides (wt%):							
SiO_2	42.50	41.97	38.36	42.53	41.83	40.59	42.42
TiO_2	3.82	3.80	3.58	2.90	3.36	3.16	2.87
Al_2O_3	14.71	14.40	16.10	13.28	13.28	13.26	13.12
Fe_2O_3	10.06	8.91	14.56	8.13	8.49	6.39	5.60
FeO	3.48	4.83	0.86	3.67	4.71	6.29	6.27
MnO	0.17	0.32	0.17	0.19	0.17	0.17	0.14
MgO	6.56	8.69	5.79	9.26	9.88	12.68	11.50
CaO	10.06	9.07	3.44	9.86	10.95	8.49	10.13
Na_2O	2.04	1.95	1.75	1.61	1.43	1.06	1.71
K_2O	1.50	1.39	1.64	1.29	1.07	1.01	1.11
P_2O_5	0.75	0.73	0.94	0.59	0.62	0.66	0.56
LOI	4.11	3.76	12.78	5.93	4.04	6.08	3.86
Total	99.76	99.82	99.97	99.24	99.83	99.84	99.29
H_2O^+	1.51	2.26	5.47	2.65	3.71	4.17	2.54
H_2O^-	1.65	1.50	5.99	2.69	0.33	1.63	0.74
CO_2	0.51	<0.2	<0.2	0.29	<0.2	<0.2	<0.2
Fe_2O_3/FeO	2.89	1.85	16.93	2.22	1.80	1.02	0.89
Density (g/cm^3)	2.78	2.78	2.29	2.66	2.76	2.82	2.76
Trace elements (ppm):							
La						43	
Ce						87	
Nd						43	
Sm						9.1	
Eu						2.8	
Tb						1.3	
Yb						2	
Lu						0.25	
Cr	220	216	270	330	367	347	195
Ni	152	148	90	235	218	212	102
V	242	222	255	215	252	246	205
Co	53	50	66	55	64	77	44
Cu	43	50	47	55	52	47	45
Zn	116	135	135	93	126	129	100
Zr	320	310	490	320	280	290	300
Nb	55	55	81	56	55	57	52
Y	31	31	27	33	27	28	28
Rb	29	28	7.2	28	23	22	25
Sr	620	610	590	310	600	430	565
Ba	120	85	140	260	330	99	320

Table T63 (continued).

Leg	144	144	144	144	144	144	144
Hole	878A	878A	878A	878A	878A	878A	878A
Core, section	85R-2	88R-3	89R-2	89R-4	90R-1	90R-2	90R-4
Interval (cm)	110-114	88-92	0-5	31-35	90-95	32-36	115-120
Piece	8	7	1A	3	6C	Breccia 1B	8
Lab number	Z-1563	Z-1564	Z-1565	Z-1566	Z-1567	Z-1568	Z-1569
Depth (mbsf)	791.90	821.59	828.82	831.83	838.10	838.78	842.61
Petrographic type	2	3	3	3	3	3	4
Unit/Subunit	16	20	21	21	21	21	22
Major element oxides (wt%):							
SiO_2	41.93	45.23	43.45	46.06	48.03	47.07	45.50
TiO_2	3.38	3.76	3.44	3.16	3.06	3.18	3.88
Al_2O_3	13.87	16.46	13.78	14.61	12.79	13.88	15.17
Fe_2O_3	7.75	12.53	10.03	6.53	8.80	12.52	12.85
FeO	5.63	1.49	3.95	5.61	3.96	0.92	0.74
MnO	0.29	0.22	0.14	0.17	0.32	0.24	0.22
MgO	8.80	4.01	7.20	7.06	6.75	4.50	5.73
CaO	11.00	5.23	8.47	8.40	8.11	3.95	3.42
Na_2O	1.78	3.13	2.71	3.14	3.60	3.30	3.19
K_2O	1.18	2.35	1.24	1.47	1.77	2.06	2.24
P_2O_5	0.70	0.75	0.63	0.70	0.78	0.81	0.88
LOI	3.45	4.83	4.39	3.37	2.20	7.64	6.61
Total	99.76	99.99	99.43	100.28	100.17	100.07	100.43
H_2O^+	1.84	2.23	2.04	2.28	0.72	2.77	2.82
H_2O^-	1.61	2.60	1.81	0.84	1.02	4.06	3.69
CO_2	<0.2	<0.2	<0.2	0.25	0.43	0.59	<0.2
Fe_2O_3/FeO	1.38	8.41	2.54	1.16	2.22	13.61	17.37
Density (g/cm^3)	2.83	2.33	2.77	2.93	2.77	2.25	2.39
Trace elements (ppm):							
La			33	39	43		44
Ce			85	91	98		97
Nd			43	48	49		50
Sm			9.4	11	11		13
Eu			3.2	3.1	2.8		2.4
Tb			1.3	1.5	1.2		1.2
Yb			1.9	2.4	2.7		3.1
Lu			0.27	0.34	0.42		0.46
Cr	250	240	257	183	160	199	188
Ni	175	170	190	134	87	148	92
V	228	206	216	122	172	188	348
Co	57	46	48	34	30	38	44
Cu	57	44	38	37	39	45	43
Zn	124	135	135	152	159	145	155
Zr	310	300	235	290	340	350	410
Nb	64	56	42	50	56	58	53
Y	29	29	28	30	33	32	37
Rb	26	35	24	35	40	45	40
Sr	660	580	520	620	670	430	430
Ba	95	100	90	670	620	240	480

Table T63 (continued).

Leg	144	144	144	144	144	144	144
Hole	878A	878A	878A	878A	878A	878A	878A
Core, section	90R-6	91R-2	91R-4	92R-4	93R-1	93R-2	93R-3
Interval (cm)	0-5	80-84	120-125	50-54	7-11	118-122	120-124
Piece	1	4B	13A	1C	3A	22	14
Lab number	Z-1570	Z-1571	Z-1572	Z-1573	Z-1574	Z-1575	Z-1576
Depth (mbsf)	844.36	848.80	852.14	860.62	865.77	868.37	869.83
Petrographic type	4	4	4	5	5	5	5
Unit/Subunit	23	23	23	26	28	30	30
Major element oxides (wt%):							
SiO_2	46.60	48.20	46.70	45.40	45.74	46.30	45.58
TiO_2	3.32	3.52	3.58	3.36	3.34	3.36	3.34
Al_2O_3	12.76	14.32	13.44	14.52	13.35	13.68	14.04
Fe_2O_3	8.69	5.76	5.41	8.08	9.74	9.03	10.68
FeO	4.84	5.79	7.40	4.26	2.47	3.58	1.95
MnO	0.18	0.17	0.19	0.20	0.22	0.43	0.13
MgO	6.70	5.59	8.36	6.70	7.09	6.25	5.82
CaO	7.03	8.03	8.12	8.35	6.10	8.55	6.74
Na_2O	3.18	3.36	3.09	3.09	3.09	3.53	3.16
K_2O	1.58	1.63	1.39	1.35	1.45	1.43	1.43
P_2O_5	0.75	0.77	0.77	0.62	0.65	0.71	0.67
LOI	4.00	2.64	1.80	3.60	6.80	3.07	5.94
Total	99.63	99.78	100.25	99.53	100.04	99.92	99.48
H_2O^+	1.60	1.14	1.16	1.91	2.66	1.23	2.04
H_2O^-	1.83	1.07	0.61	1.44	3.38	1.49	2.66
CO_2	<0.2	<0.2	<0.2	<0.2	0.24	0.32	<0.2
Fe_2O_3/FeO	1.80	1.00	0.73	1.90	3.94	2.52	5.48
Density (g/cm^3)	2.75	2.81	2.88	2.76	2.39	2.66	2.56
Trace elements (ppm):							
La			38		36	38	
Ce			92		79	88	
Nd			48		41	47	
Sm			12		9.7	11	
Eu			3.5		2.8	3.2	
Tb			1.5		1.4	1.5	
Yb			2.8		2.4	2.7	
Lu			0.36		0.33	0.38	
Cr	162	172	178	216	195	174	170
Ni	81	78	80	175	160	92	99
V	210	208	210	228	240	200	215
Co	39	38	40	48	52	35	41
Cu	36	52	43	65	52	52	45
Zn	150	170	132	90	95	96	92
Zr	350	355	335	280	300	300	290
Nb	44	47	43	40	43	44	44
Y	34	38	35	31	32	35	37
Rb	33	33	29	31	31	31	32
Sr	520	620	600	520	390	575	440
Ba	240	240	600	180	230	230	210

Table T63 (continued).

Leg	144	144	144	144	144	144	144
Hole	878A	878A	878A	878A	878A	878A	878A
Core, section	94R-1	94R-2	94R-3	94R-5	94R-7	95R-2	95R-3
Interval (cm)	0-4	0-5	124-129	102-107	70-74	0-5	125-128
Piece	1A	1A	1	Breccia 1	Breccia 1	Breccia 1	Breccia 9
Lab number	Z-880	Z-1577	Z-1578	Z-1579	Z-1580	Z-1581	Z-1582
Depth (mbsf)	875.40	876.89	879.32	881.64	883.82	886.11	888.75
Petrographic type	5	NA	NA	NA	NA	NA	NA
Unit/Subunit	30	31A	31A	31A	31B	31B	31B
Major element oxides (wt%):							
SiO_2	45.47	44.26	45.24	41.75	42.62	43.58	44.49
TiO_2	2.91	3.08	3.20	3.90	3.48	3.16	3.20
Al_2O_3	14.28	13.05	12.85	12.29	14.76	13.18	14.19
Fe_2O_3	6.89	11.85	12.54	15.37	12.76	12.08	12.39
FeO	3.87	<0.15	<0.15	<0.15	<0.15	0.45	<0.15
MnO	0.23	0.07	0.20	0.26	0.30	0.10	0.19
MgO	7.02	6.00	5.02	5.29	5.31	4.80	5.22
CaO	7.43	1.98	2.51	2.78	2.16	4.58	3.42
Na_2O	2.97	1.55	1.62	1.52	1.55	1.72	1.62
K_2O	1.41	0.39	0.43	0.25	0.29	2.91	1.90
P_2O_5	0.61	0.38	0.37	0.80	0.15	2.06	1.04
LOI	6.20	17.22	16.26	15.80	16.90	11.03	12.60
Total	99.29	99.83	100.24	100.01	100.28	99.65	100.26
H_2O^+	2.50	6.09	5.95	5.61	6.02	3.44	4.21
H_2O^-	3.22	10.31	10.07	9.75	9.79	6.47	7.45
CO_2	0.48	0.25	0.24	0.32	0.34	0.69	0.56
Fe_2O_3/FeO	1.78					26.84	
Density (g/cm^3)	2.69	1.84	1.93	1.82	1.67	1.73	1.73
Trace elements (ppm):							
La		37			21		
Ce		85			52		
Nd		42			32		
Sm		9.6			8.0		
Eu		1.8			1.9		
Tb		1.1			1.2		
Yb		2.4			2.1		
Lu		0.38			0.35		
Cr	375	168	171	194	184	182	169
Ni	255	99	133	152	95	81	88
V	217	80	105	185	82	119	175
Co	59	53	51	73	50	48	52
Cu	68	40	40	61	35	43	55
Zn	99	74	72	129	78	76	92
Zr	290	230	250	300	260	260	260
Nb	40	32	36	40	35	37	36
Y	31	38	38	35	22	34	33
Rb	21	15	15	3.6	5.6	28	29
Sr	610	130	130	150	150	230	190
Ba	305	310	130	95	165	180	450

Table T63 (continued).

Leg	144	144	144	144	144
Hole	878A	878A	878A	878A	878A
Core, section	95R-5	97R-1	97R-2	98R-2	98R-3
Interval (cm)	0-5	20-24	28-31	93-96	8-12
Piece	Breccia 1	7B	3D	5D	1B
Lab number	Z-1583	Z-1584	Z-881	Z-882	Z-1585
Depth (mbsf)	890.22	894.60	896.18	906.28	906.87
Petrographic type	NA	6	6	7	7
Unit/Subunit	31B	34	34	35	35
Major element oxides (wt%):					
SiO_2	44.75	46.83	47.35	45.94	45.76
TiO_2	3.24	3.42	3.13	2.94	3.34
Al_2O_3	13.87	13.69	15.21	13.66	13.43
Fe_2O_3	12.44	5.77	5.22	5.68	5.89
FeO	<0.15	7.98	6.81	6.73	6.89
MnO	0.08	0.16	0.14	0.17	0.16
MgO	5.66	6.59	6.27	8.83	8.59
CaO	3.38	8.68	8.40	8.95	8.73
Na_2O	1.63	3.20	3.20	2.86	2.69
K_2O	2.05	1.30	1.32	1.38	1.25
P_2O_5	1.10	0.65	0.61	0.54	0.61
LOI	11.60	1.65	1.89	1.87	2.39
Total	99.80	99.92	99.55	99.55	99.73
H_2O^+	3.47	0.79	1.47	1.26	1.38
H_2O^-	7.52	0.57	0.22	0.34	0.73
CO_2	0.44	0.27	<0.2	0.20	<0.2
Fe_2O_3/FeO		0.72	0.77	0.84	0.86
Density (g/cm^3)	1.64	2.94	2.58	2.88	2.93
Trace elements (ppm):					
La		34			
Ce		75			
Nd		42			
Sm		11			
Eu		2.3			
Tb		1.2			
Yb		2.6			
Lu		0.45			
Cr	170	92	165	260	200
Ni	82	78	90	260	195
V	192	190	227	217	176
Co	48	36	39	47	38
Cu	49	49	62	135	114
Zn	88	124	140	130	114
Zr	260	300	310	290	260
Nb	37	38	38	38	42
Y	34	36	35	31	28
Rb	24	27	31	25	27
Sr	200	560	390	560	550
Ba	380	450	280	270	190

Table T64. Composition of trachy-andesites from Hole 465A, Leg 62 (Southern Hess Rise, Pacific Ocean). (Continued on next page.)

Leg	62	62	62	62	62	62	62
Hole	465A	465A	465A	465A	465A	465A	465A
Core, section	40R-3	41R-1	41R-2	42R-1	42R-3	43R-2	44R-1
Interval (cm)	17-25	113-120	90-93	128-132	98-103	130-135	112-116
Piece	1B	9	11A	8A	9	14A	13B
Lab number	Z-1226	Z-1228	Z-383	Z-384	Z-385	Z-386	Z-387
Depth (mbsf)	412.67	420.13	421.4	429.78	432.48	440.8	448.62
Unit	1	1	1	2	2	2	3
Major element oxides (wt%):							
SiO_2	53.76	55.79	57.48	58.00	57.97	59.35	59.87
TiO_2	0.93	0.97	1.29	1.28	1.36	1.43	1.28
Al_2O_3	16.55	17.00	17.55	16.66	16.83	19.01	17.14
Fe_2O_3	3.71	4.44	3.81	4.40	4.68	2.41	4.09
FeO	0.40	0.46	0.38	0.85	0.34	0.51	0.55
MnO	0.02	0.03	0.01	0.01	0.01	0.01	0.01
MgO	3.47	2.74	2.10	1.51	1.68	1.01	0.93
CaO	1.79	2.35	2.74	2.93	2.89	2.93	2.71
Na_2O	3.54	4.61	5.55	5.79	4.98	5.33	5.72
K_2O	2.58	3.06	4.08	5.08	4.67	4.27	5.14
P_2O_5	0.18	0.26	0.29	0.26	0.20	0.22	0.16
LOI	12.59	8.13	5.21	3.67	4.01	3.09	2.18
Total	99.52	99.84	100.49	100.44	99.62	99.57	99.78
H_2O^+	2.35	1.75	2.07	1.53	1.49	1.06	0.99
H_2O^-	7.67	4.98	3.14	2.14	2.52	2.03	1.19
CO_2	0.36	0.34	ND	ND	ND	ND	ND
Fe_2O_3/FeO	9.28	9.65	10.03	5.18	13.76	4.72	7.44
Density (g/cm^3)	2.16	2.01	1.98	1.93	1.97	2.11	2.11
Trace elements (ppm):							
La	81	80	97	84	92	92	91
Ce	200	210	170	150	170	170	160
Nd	72	75	79	72	72	71	75
Sm	8.8	8.3	12	11	11	11	11
Eu	2.3	2.6	3.3	2.8	3.0	3.1	3.1
Tb	1.2	1.1	1.7	1.4	1.6	1.5	1.6
Yb	2.5	2.3	4.5	3.1	3.1	3.1	3.4
Lu	0.33	0.33	0.71	0.45	0.44	0.43	0.49
Cr	~10	~10	<5	<5	<5	<5	<5
Ni	30	17	5	<5	5	<5	5
Co	19	18	10	6	7	6	5
V	71	72	50	50	45	45	50
Cu	~5	~5	<5	5	5	<5	<5
Pb	ND	ND	5	5	<5	<5	7
Zn	57	50	30	35	20	65	175
Zr	120	710	570	750	610	680	770
Y	25	24	56	39	34	40	44
Nb	110	110	88	87	84	100	83
Rb	15	19	16	24	23	25	31
Sr	240	290	240	210	210	280	260
Ba	580	640	650	590	610	690	680

Note: ND = not determined.

Table T64 (continued).

Leg	62	62	62	62
Hole	465A	465A	465A	465A
Core, section	44R-3	45R-1	46R-1	46R-3
Interval (cm)	118-123	81-85	82-86	57-61
Piece	7A	5D	6G	8
Lab number	Z-388	Z-389	Z-390	Z-391
Depth (mbsf)	457.68	457.81	467.32	470.07
Unit	3	3	5	5
Major element oxides (wt%):				
SiO_2	58.69	58.94	57.59	55.34
TiO_2	1.21	1.10	1.15	1.07
Al_2O_3	17.28	16.88	16.78	16.90
Fe_2O_3	3.38	4.48	2.65	3.18
FeO	0.95	1.15	1.28	0.75
MnO	0.01	0.03	0.04	0.03
MgO	0.64	0.50	0.34	1.13
CaO	3.35	2.54	4.92	5.97
Na_2O	4.90	5.07	4.90	5.46
K_2O	6.42	6.42	6.74	3.96
P_2O_5	0.12	0.10	0.11	0.27
LOI	2.91	2.33	3.03	5.66
Total	99.86	99.54	99.53	99.72
H_2O^+	0.77	0.80	1.12	1.21
H_2O^-	0.69	0.58	0.26	1.65
CO_2	1.45	0.95	1.65	2.80
Fe_2O_3/FeO	3.56	3.90	2.07	4.24
Density (g/cm^3)	2.16	2.18	2.19	2.23
Trace elements (ppm):				
La	88	87	85	86
Ce	160	160	150	160
Nd	73	73	71	72
Sm	11	11	10	11
Eu	3.0	2.9	2.9	3.1
Tb	1.5	1.6	1.5	1.4
Yb	3.8	3.6	3.4	2.5
Lu	0.59	0.56	0.49	0.38
Cr	<5	<5	<5	<5
Ni	<5	<5	<5	5
Co	5	5	5	5
V	45	45	45	45
Cu	5	5	7	<5
Pb	5	5	5	5
Zn	110	125	145	65
Zr	810	710	700	680
Y	52	42	41	34
Nb	89	99	55	81
Rb	58	60	60	22
Sr	190	180	190	310
Ba	610	630	560	640

Table T65. Composition of basalts from Hole 642E, Leg 104 (Vøring Plateau, Norwegian Sea). (Continued on next three pages.)

Leg	104	104	104	104	104	104	104
Hole	642E	642E	642E	642E	642E	642E	642E
Core, section	4R-1	9R-1	10R-1	10R-2	15R-1	15R-3	18R-4
Interval (cm)	32-35	59-62	133-135	87-90	120-123	77-80	13-16
Piece	Tuff 2	4E	20	12	22	4	1
Lab number	Z-591	Z-153	Z-592	Z-154	Z-155	Z-156	Z-157
Depth (mbsf)	326.82	366.49	374.83	375.87	406.5	409.07	437.33
Unit	S4	D1	D2	D3	F11	F11	F17
Major element oxides (wt%):							
SiO_2	30.93	45.60	46.43	45.93	45.99	45.88	47.43
TiO_2	5.24	1.68	1.44	1.98	2.08	1.94	1.53
Al_2O_3	17.99	15.15	14.35	16.03	13.73	14.30	14.58
Fe_2O_3	25.99	4.89	9.41	6.28	9.51	6.07	4.39
FeO	0.33	6.26	4.34	4.32	3.75	5.82	6.68
MnO	0.29	0.17	0.17	0.13	0.10	0.18	0.15
MgO	0.37	7.62	6.64	6.35	6.74	7.46	8.40
CaO	2.72	12.33	11.68	10.20	9.01	11.60	12.38
Na_2O	1.38	2.25	2.32	2.43	2.70	2.43	2.20
K_2O	0.17	0.15	0.16	0.43	0.46	0.13	0.15
P_2O_5	0.99	0.15	0.11	0.16	0.16	0.13	0.13
LOI	13.10	3.23	3.46	5.67	5.69	3.36	1.75
Total	99.50	99.48	100.51	99.91	99.92	99.30	99.77
H_2O^+	7.75	1.36	1.46	1.85	1.85	0.98	0.89
H_2O^-	4.84	1.87	2.00	3.68	3.74	2.26	0.86
CO_2	<0.20	ND	<0.20	ND	ND	ND	ND
Fe_2O_3/FeO	78.76	0.78	2.17	1.45	2.54	1.04	0.66
Density (g/cm^3)	1.48	2.83	2.68	2.63	ND	2.75	3.00
Trace elements (ppm):							
La		5.2		5.1	6.7	3.9	4.3
Ce		13		12	16	11	10
Nd		11		10	13	9.6	9.0
Sm		3.6		3.5	3.9	3.3	3.0
Eu		1.3		1.3	1.6	1.3	1.2
Gd		4.5		4.2	5.6	4.7	4.3
Tb		0.84		0.80	0.97	0.82	0.77
Tm		0.45		0.34	0.51	0.40	0.40
Yb		2.8		2.0	3.2	2.4	2.3
Lu		0.42		0.29	0.46	0.37	0.35
Sc	ND	45	ND	51	46	43	45
Cr	36	220	285	335	300	260	300
Ni	55	145	170	165	135	145	125
Co	35	57	57	80	60	61	56
V	650	245	350	310	450	200	215
Cu	52	118	90	92	80	120	100
Pb	11	<5	<5	<5	<5	<5	<5
Zn	125	80	86	71	71	90	68
Sn	4.7	ND	3.1	ND	ND	ND	ND
Zr	ND	56	85	86	88	69	56
Y	ND	25	26	27	31	23	21
Nb	ND	4.8	4.3	4.6	5.4	4.5	4.1
Rb	ND	<1	1.5	5.4	9.2	1.2	1.3
Sr	ND	130	140	140	140	150	150
Ba	ND	20	81	22	15	26	27
Th	ND	ND	1.6	ND	ND	ND	ND

Note: ND = not determined.

Table T65 (continued).

Leg	104	104	104	104	104	104	104
Hole	642E	642E	642E	642E	642E	642E	642E
Core, section	22R-3	22R-5	23R-2	30R-2	34R-1	40R-1	46R-3
Interval (cm)	93-96	32-35	28-31	76-79	4-7	33-36	40-43
Piece	4	2	Tuff 3	2A	1	2D	1C
Lab number	Z-158	Z-159	Z-593	Z-160	Z-594	Z-161	Z-162
Depth (mbsf)	474.43	476.82	481.74	541.76	574.44	631.43	691.5
Unit	F23	F23	S12	F36	S18A	F48	F53
Major element oxides (wt%):							
SiO_2	45.26	46.84	44.06	47.36	44.86	46.38	47.43
TiO_2	1.69	1.65	3.18	2.48	2.15	1.83	2.37
Al_2O_3	14.07	15.66	10.14	13.26	13.40	14.28	13.09
Fe_2O_3	8.52	4.46	21.34	5.20	13.50	5.48	5.23
FeO	4.38	5.63	0.65	7.69	2.64	5.36	8.17
MnO	0.10	0.15	0.14	0.16	0.10	0.14	0.20
MgO	8.34	6.93	3.56	7.16	7.23	8.00	7.12
CaO	8.98	12.71	1.59	11.65	5.64	11.83	11.76
Na_2O	2.57	2.43	1.73	2.57	2.52	2.38	2.38
K_2O	0.26	0.10	1.14	0.20	1.62	0.13	0.15
P_2O_5	0.11	0.10	0.15	0.12	0.24	0.11	0.16
LOI	5.19	3.01	12.76	2.25	5.82	3.45	1.99
Total	99.47	99.67	100.44	100.10	99.72	99.37	100.05
H_2O^+	1.01	0.88	6.09	0.67	1.47	1.41	0.45
H_2O^-	4.01	2.04	6.35	1.48	3.37	2.04	1.54
CO_2	ND	ND	0.32	ND	0.68	ND	ND
Fe_2O_3/FeO	1.94	0.79	32.83	0.68	5.11	1.02	0.64
Density (g/cm^3)	ND	2.69	1.80	2.90	1.96	2.75	2.94
Trace elements (ppm):							
La	4.6	4.1	23	7.1		6.1	6.4
Ce	9.9	10	57	18		14	17
Nd	ND	ND	35	14		12	14
Sm	3.1	3.0	9.6	4.4		3.9	4.5
Eu	1.1	1.3	2.6	1.6		1.4	1.6
Gd	4.2	4.4		5.7		4.4	5.6
Tb	0.76	0.78	1.60	1.1		0.78	0.91
Tm	ND	ND	ND	0.56		0.37	ND
Yb	2.5	2.3	3.5	3.0		2.7	3.1
Lu	0.38	0.35	0.53	0.46		0.40	0.46
Sc	45	46	ND	47	ND	ND	46
Cr	200	165	56	230	235	315	140
Ni	100	90	44	90	70	110	100
Co	64	56	36	51	48	56	56
V	300	210	440	280	355	260	340
Cu	110	190	118	100	55	56	100
Pb	<5	<5	ND	<5	<5	<5	<5
Zn	60	75	148	78	92	75	78
Sn	ND	ND	ND	ND	3.1	ND	ND
Zr	46	44	255	99	110	81	94
Y	19	21	42	32	42	23	29
Nb	3.7	4.4	22	6.1	6.4	5.3	5.5
Rb	1.5	<1	44	1.0	21	<1	<1
Sr	120	130	51	180	140	170	160
Ba	23	19	62	41	26	30	35
Th	ND	ND	ND	ND	1.2	ND	ND

Table T65 (continued).

Leg	104	104	104	104	104	104	104
Hole	642E	642E	642E	642E	642E	642E	642E
Core, section	54R-2	60R-1	60R-2	69R-2	78R-2	88R-2	91R-1
Interval (cm)	83-88	68-71	25-27	59-61	46-48	70-72	18-20
Piece	Tuff 5C	14	1C	1D	5A	7B	3
Lab number	Z-595	Z-163	Z-164	Z-165	Z-166	Z-167	Z-168
Depth (mbsf)	741.03	785.58	786.65	865.29	942.36	1037.00	1063.48
Unit	S26	F63	F63	F78	F90	F102	F104A
Major element oxides (wt%):							
SiO_2	43.61	44.13	45.11	46.30	46.48	46.98	46.94
TiO_2	3.61	2.52	2.52	1.78	2.23	1.51	1.41
Al_2O_3	13.39	12.94	12.37	14.99	13.84	14.02	14.29
Fe_2O_3	16.88	9.56	8.04	5.94	6.60	6.80	8.25
FeO	0.83	4.15	4.99	5.39	6.10	4.77	2.91
MnO	0.16	0.18	0.18	0.06	0.17	0.18	0.10
MgO	3.69	8.93	8.94	7.21	6.91	7.36	7.13
CaO	3.29	7.22	8.68	11.22	11.59	12.10	9.41
Na_2O	1.84	2.47	2.38	2.47	2.47	2.20	2.20
K_2O	1.03	0.74	0.33	0.18	0.13	0.42	1.04
P_2O_5	0.08	0.16	0.15	0.13	0.15	0.11	0.15
LOI	11.08	7.09	5.98	3.83	3.06	3.57	6.04
Total	99.49	100.09	99.67	99.50	99.73	100.02	99.87
H_2O^+	2.98	1.63	1.35	0.91	0.52	0.84	1.33
H_2O^-	7.04	5.46	4.59	2.74	2.36	2.64	4.63
CO_2	0.28	ND	ND	ND	ND	ND	ND
Fe_2O_3/FeO	20.34	2.30	1.61	1.10	1.08	1.42	2.84
Density (g/cm^3)	2.35	2.42	2.60	2.70	2.77	2.67	2.36
Trace elements (ppm):							
La		7.4	7.3	5.1	7.5	4.7	5.1
Ce		18	17	14	18	9.2	10
Nd		15	16	12	15	10	10
Sm		5	5.2	3.9	5.1	3.5	3.3
Eu		1.8	1.7	1.5	1.8	1.3	1.1
Gd		5.9	5.5	5.1	ND	4.6	4.6
Tb		1.1	1.0	0.91	0.99	0.83	0.82
Tm		0.53	ND	ND	ND	0.52	0.48
Yb		3.1	3.1	3.0	3.4	3.1	3.1
Lu		0.42	0.46	0.44	0.50	0.45	0.46
Sc	ND	45	43	44	48	48	53
Cr	85	290	295	295	190	380	255
Ni	64	115	125	110	80	125	85
Co	37	63	62	60	57	62	48
V	272	450	450	310	290	290	450
Cu	185	300	110	76	100	110	37
Pb	<5	<5	<5	<5	<5	<5	<5
Zn	99	78	90	86	93	70	68
Sn	3.7	ND	ND	ND	ND	ND	ND
Zr	250	100	110	77	96	62	54
Y	52	30	28	25	29	25	30
Nb	22	5.8	6.2	3.9	5.5	3.7	3.1
Rb	15	2.9	1.3	<1	<1	19	41
Sr	130	150	160	150	180	140	100
Ba	32	24	29	19	34	30	<5
Th	1.2	ND	ND	ND	ND	ND	ND

Table T65 (continued).

Leg	104	104	104	104	104
Hole	642E	642E	642E	642E	642E
Core, section	94R-1	94R-4	102R-2	105R-1	110R-1
Interval (cm)	32-34	67-72	45-47	64-66	39-41
Piece	1B	Tuff 2B	6	7A	5B
Lab number	Z-169	Z-596	Z-170	Z-171	Z-172
Depth (mbsf)	1085.32	1090.17	1155.45	1173.14	1220.29
Unit	F105	S43	F115	D5	D7
Major element oxides (wt%):					
SiO_2	46.90	39.20	58.72	49.36	48.91
TiO_2	1.30	0.68	1.52	1.27	1.31
Al_2O_3	14.66	23.78	16.92	11.97	13.35
Fe_2O_3	3.23	17.70	2.81	5.80	11.50
FeO	7.14	0.27	0.42	8.91	1.14
MnO	0.22	0.28	0.05	0.21	0.19
MgO	8.70	0.27	1.66	7.62	3.55
CaO	12.42	1.13	4.34	10.35	8.71
Na_2O	1.93	0.88	2.34	2.47	3.74
K_2O	0.13	0.39	8.25	0.20	1.18
P_2O_5	0.11	0.08	0.27	0.10	0.13
LOI	2.67	14.91	3.19	2.20	6.80
Total	99.41	99.57	100.49	100.46	100.51
H_2O^+	1.33	9.14	1.36	0.86	1.64
H_2O^-	1.27	5.17	1.83	1.21	5.06
CO_2	ND	<0.20	ND	ND	ND
Fe_2O_3/FeO	0.45	65.56	6.69	0.65	10.09
Density (g/cm^3)	2.86	2.27	1.75	2.88	2.34
Trace elements (ppm):					
La	4.4		53	4.4	16
Ce	9		120	10	35
Nd	9.6		68	8.4	18
Sm	3.0		12	2.6	4.3
Eu	1.0		2.1	0.84	1.1
Gd	4.0		15	4.2	5.8
Tb	0.69		2.3	0.78	0.47
Tm	ND		1.4	0.57	0.55
Yb	2.5		9.3	3.8	3.1
Lu	0.38		1.5	0.58	0.46
Sc	49	ND	32	60	54
Cr	330	205	77	190	165
Ni	145	180	25	140	17
Co	54	140	14	70	55
V	225	670	165	340	270
Cu	120	185	27	66	22
Pb	<5	7	30	<5	<5
Zn	58	123	130	130	90
Sn	ND	3.5	ND	ND	ND
Zr	55	9.4	290	49	100
Y	22	2.6	81	33	35
Nb	1.9	5.6	23	1.7	7.3
Rb	2.2	21	170	6	37
Sr	110	29	150	65	120
Ba	450	31	150	56	180
Th	ND	1.1	ND	ND	ND

Table T66. Composition of basalts from Hole 417A, Leg 51 (Bermuda Rise, Atlantic Ocean).

Leg	51	51	51
Hole	417A	417A	417A
Core, section	29R-5	32R-2	44R-3
Interval (cm)	58-61	5-8	31-34
Piece	5	1	1A
Lab number	Z-511	Z-512	Z-513
Depth (mbsf)	271.58	295.05	397.81
Unit/Subunit	8	12	18B
Major element oxides (wt%):			
SiO_2	46.20	44.93	49.15
TiO_2	1.57	1.46	1.47
Al_2O_3	16.50	17.86	16.67
Fe_2O_3	7.11	8.40	4.17
FeO	3.37	2.61	6.09
MnO	0.06	0.03	0.06
MgO	6.12	4.50	6.20
CaO	10.53	10.88	11.66
Na_2O	2.20	2.04	2.24
K_2O	0.76	1.46	0.09
P_2O_5	0.15	0.25	0.13
LOI	4.60	5.68	1.45
Total	99.17	100.10	99.38
H_2O^+	2.09	2.38	0.38
H_2O^-	1.70	1.50	0.69
CO_2	0.70	1.79	0.32
Fe_2O_3/FeO	2.11	3.22	0.68
Density (g/cm^3)	2.70	2.65	2.92
Trace elements (ppm):			
La	2.6	2.4	2.4
Ce	8.0	7.9	7.6
Nd	8.5	8.4	8.4
Sm	3.6	3.3	3.2
Eu	1.2	1.1	1.1
Tb	0.96	0.83	0.89
Yb	3.5	3.1	3.2
Lu	0.57	0.5	0.49
Cr	290	257	305
Ni	71	47	88
Co	41	36	50
V	355	272	330
Cu	82	79	93
Pb	<5	<5	<5
Zn	110	82	87
Sn	1.8	2.4	2.4
Zr	90	86	84
Y	32	29	30
Nb	1.9	2.3	2.1
Rb	12	18	1.6
Sr	100	110	97
Ba	75	56	21
Th	<1	<1	<1

Table T67. Composition of basalts from Hole 418A, Legs 52 and 53 (Bermuda Rise, Atlantic Ocean). (Continued on next two pages.)

Leg	52	52	52	52	52	52	52
Hole	418A	418A	418A	418A	418A	418A	418A
Core, section	15R-1	15R-3	18R-1	19R-4	19R-7	20R-5	27R-1
Interval (cm)	98-101	129-132	81-84	86-89	6-9	10-13	33-35
Piece	1I	4D	2F	1I	1A	1B	1D
Lab number	Z-297	Z-298	Z-299	Z-300	Z-301	Z-302	Z-303
Depth (mbsf)	320.98	324.29	339.81	353.36	357.06	363.10	393.83
Unit/Subunit	1	1	2C	2C	2C	2C	5
Major element oxides (wt%):							
SiO_2	47.46	47.52	48.29	48.71	48.83	48.77	47.22
TiO_2	1.22	1.27	1.16	1.22	1.42	1.38	1.56
Al_2O_3	14.36	16.40	14.99	15.11	15.11	16.32	15.95
Fe_2O_3	4.47	4.61	3.61	3.15	3.41	2.67	4.71
FeO	5.71	4.51	6.97	6.92	6.47	6.46	4.67
MnO	0.12	0.10	0.12	0.15	0.15	0.15	0.21
MgO	7.34	7.41	7.30	7.27	7.11	7.44	7.09
CaO	13.62	11.50	12.94	13.08	12.94	12.55	12.47
Na_2O	2.48	2.70	2.42	2.48	2.70	2.51	2.70
K_2O	0.16	0.22	0.16	0.16	0.17	0.17	0.12
P_2O_5	0.07	0.09	0.01	0.05	0.19	0.16	0.22
LOI	2.73	3.44	1.72	1.36	1.50	1.02	3.01
Total	99.74	99.77	99.69	99.66	100.00	99.60	99.93
H_2O^+	0.81	1.06	0.69	0.61	0.51	0.13	1.08
H_2O^-	1.22	2.38	1.03	0.75	0.99	0.89	1.93
CO_2	0.70	ND	ND	ND	ND	ND	ND
Fe_2O_3/FeO	0.78	1.02	0.52	0.46	0.53	0.41	1.01
Density (g/cm^3)	2.77	2.68	2.86	2.98	2.91	2.92	2.86
Trace elements (ppm):							
La	1.8	1.8	1.9	1.7	2.0	1.8	2.0
Ce	5.9	6.3	5.9	6.3	6.7	5.5	6.4
Nd	6.0	6.6	6.0	6.1	6.6	5.9	7.0
Sm	2.4	2.6	2.5	2.4	2.8	2.3	3.0
Eu	0.88	0.95	0.86	0.90	0.97	0.93	1.0
Tb	0.70	0.73	0.66	0.72	0.75	0.72	0.84
Yb	2.7	2.7	2.6	2.7	2.9	2.6	3.3
Lu	0.42	0.42	0.42	0.41	0.43	0.40	0.50
Cr	190	195	180	195	180	180	217
Ni	87	74	80	100	77	77	115
Co	37	36	37	37	39	39	48
V	200	230	230	260	230	205	270
Cu	105	75	60	90	105	120	125
Pb	<5	<5	<5	<5	<5	<5	<5
Zn	60	72	60	84	110	72	95
Sn	ND	ND	ND	ND	ND	ND	ND
Zr	46	52	48	51	56	55	
Y	25	27	24	26	25	27	29
Nb	2.3	2.6	2.4	2.5	2.0	2.3	1.3
Rb	<0.5	0.9	0.7	<0.5	0.9	1.2	0.5
Sr	100	120	100	110	110	110	
Ba	<10	<10	<10	<10	<10	<10	
Th	ND	ND	ND	ND	ND	ND	ND

Note: ND = not determined.

Table T67 (continued).

Leg	52	52	52	52	52	52	53
Hole	418A	418A	418A	418A	418A	418A	418A
Core, section	27R-2	31R-2	31R-2	38R-1	38R-3	42R-3	52R-1
Interval (cm)	91-93	47-51	134-139	41-44	10-13	2-6	61-64
Piece	5B	3A	12	2C	1A	1A	6B
Lab number	Z-304	Z-514	Z-515	Z-305	Z-306	Z-516	Z-307
Depth (mbsf)	395.91	423.97	424.84	479.91	482.60	510.52	592.81
Unit/Subunit	5	5	5	5	5	6B	6B
Major element oxides (wt%):							
SiO_2	46.99	41.35	42.76	46.78	46.61	46.91	47.42
TiO_2	1.59	1.08	1.03	1.37	1.51	0.96	1.26
Al_2O_3	19.03	14.99	16.01	17.68	17.34	17.73	17.05
Fe_2O_3	9.65	7.96	7.62	4.56	4.09	4.97	3.30
FeO	3.72	1.34	1.69	3.45	4.70	3.23	5.64
MnO	0.15	0.10	0.09	0.13	0.19	0.15	0.20
MgO	6.14	7.95	8.82	6.86	5.73	6.35	6.67
CaO	11.89	7.21	4.64	10.43	13.61	13.28	13.34
Na_2O	2.43	1.53	1.48	2.46	2.41	2.19	2.61
K_2O	0.12	1.27	1.14	1.03	0.43	0.31	0.15
P_2O_5	0.16	0.05	0.06	0.17	0.20	0.06	0.19
LOI	4.19	15.38	14.82	5.58	3.04	3.17	2.18
Total	100.06	100.21	100.16	100.50	99.86	99.31	100.01
H_2O^+	1.33	3.94	1.84	1.43	1.24	0.42	0.55
H_2O^-	2.86	7.51	9.13	4.15	1.80	2.18	1.63
CO_2	ND	3.01	0.63	ND	ND	0.57	ND
Fe_2O_3/FeO	2.59	5.94	4.51	1.32	0.87	1.54	0.58
Density (g/cm^3)	2.62	ND	ND	2.63	2.82	2.72	2.86
Trace elements (ppm):							
La	2.1	1.4	1.1	1.7	1.8	1.9	1.7
Ce	6.3	3.4	3.9	6.1	5.9	6.5	5.1
Nd	6.8	3.8	4.0	6.0	6.4	6.0	5.5
Sm	2.9	1.6	1.7	2.9	2.8	2.3	2.3
Eu	1.0	0.6	0.57	1.0	0.96	0.87	0.88
Tb	0.80	0.59	0.45	0.76	0.77	0.65	0.67
Yb	3.0	2.0	1.7	2.6	3.0	2.6	2.9
Lu	0.43	0.34	0.28	0.36	0.45	0.41	0.43
Cr	235	345	325	235	177	415	225
Ni	110	62	69	135	74	148	155
Co	41	37	41	60	28	41	40
V	280	320	332	265	210	322	210
Cu	120	53	40	95	110	90	110
Pb	<5	<5	<5	<5	<5	<5	<5
Zn	105	56	61	115	90	64	90
Sn	ND	2.3	2.2	ND	ND	2.1	ND
Zr	64	64	59	57	62	56	49
Y	26	19	16	25	26	25	29
Nb	2.4	1.1	1.2	1.9	1.8	<1	2.1
Rb	1.5	21	19.0	3.6	8.2	4.9	<0.5
Sr	120	83	73	110	110	110	88
Ba	<10	5	4	31	<10	5	<10
Th	ND	<1	<1	ND	ND	<1	ND

Table T67 (continued).

Leg	53	53	53	53	53	53	53
Hole	418A	418A	418A	418A	418A	418A	418A
Core, section	52R-4	70R-1	70R-1	77R-2	77R-3	84R-2	85R-2
Interval (cm)	29-32	64-67	67-68	57-60	33-36	51-54	48-51
Piece	2	2A	2A	4A	2B	1D	3
Lab number	Z-308	Z-309	Z-517	Z-310	Z-311	Z-312	Z-313
Depth (mbsf)	596.99	743.74	743.77	795.17	796.43	847.51	851.98
Unit/Subunit	6B	13	13	14B	14B	14C	14C
Major element oxides (wt%):							
SiO_2	47.69	46.35	47.33	45.66	48.37	47.63	48.35
TiO_2	1.26	1.39	1.47	1.52	1.54	1.20	1.26
Al_2O_3	16.64	16.37	16.78	16.12	16.12	16.99	15.74
Fe_2O_3	3.24	4.45	6.09	2.05	2.22	1.86	2.00
FeO	5.82	3.69	3.66	5.60	6.64	6.50	7.09
MnO	0.18	0.11	0.14	0.19	0.20	0.19	0.20
MgO	7.20	8.16	6.52	7.08	6.67	7.97	8.38
CaO	13.19	9.39	10.45	14.76	13.38	12.53	12.74
Na_2O	2.22	2.41	2.41	2.41	2.32	2.44	2.17
K_2O	0.06	0.34	0.27	0.12	0.12	0.11	0.12
P_2O_5	0.17	0.18	0.14	0.21	0.14	0.13	0.13
Loi	2.15	6.81	4.52	4.31	2.15	2.04	1.86
Total	99.82	99.65	99.78	100.03	99.87	99.59	100.04
H_2O^+	0.66	2.38	0.65	0.47	0.42	0.50	1.20
H_2O^-	1.49	4.43	3.01	1.64	0.73	1.04	0.66
CO_2	ND	ND	<0.20	2.20	1.00	0.50	ND
Fe_2O_3/FeO	0.56	1.21	1.66	0.37	0.33	0.29	0.28
Density (g/cm^3)	2.87	ND	2.77	2.92	2.80	2.92	2.99
Trace elements (ppm):							
La	1.9	3.1	2.8	2.2	2.5	1.8	1.7
Ce	5.7	8.2	8.2	6.3	7.0	5.4	5.5
Nd	6.7	8.7	7.9	6.6	8.0	5.5	5.9
Sm	2.6	3.2	3.1	2.7	3.1	2.4	2.4
Eu	0.90	1.2	1.2	0.91	1.1	0.83	0.89
Tb	0.75	0.91	0.83	0.68	0.84	0.64	0.65
Yb	3.0	3.0	2.9	3.0	3.3	2.7	2.7
Lu	0.46	0.43	0.49	0.45	0.48	0.40	0.42
Cr	225	200	280	122	157	165	220
Ni	165	110	84	88	115	155	170
Co	36	37	58	38	41	42	44
V	220	330	415	230	285	180	210
Cu	85	70	74	90	105	95	150
Pb	<5	<5	<5	<5	<5	<5	<5
Zn	97	110	97	97	110	98	115
Sn	ND	ND	2.0	ND	ND	ND	ND
Zr	46	60	80	53	44	39	55
Y	20	28	32	28	30	26	26
Nb	2.2	2.2	1.6	3.1	2.8	2.5	1.7
Rb	<0.5	5.0	4.2	0.9	1.5	0.6	0.9
Sr	98	100	110	110	84	69	97
Ba	<10	<10	<3	<10	<10	<10	<10
Th	ND	ND	<1	ND	ND	ND	ND

Table T68. Composition of basalts from Hole 317A, Leg 33 (Manihiki Plateau, Pacific Ocean). (Continued on next two pages.)

Leg	33	33	33	33	33	33	33
Hole	317A	317A	317A	317A	317A	317A	317A
Core, section	31R-2	31R-2	31R-3	31R-4	31R-4	32R-1	32R-2
Interval (cm)	37-39	87-89	20-23	76-82	91-94	93-95	120-124
Piece	5		7	11	11	5	13
Lab number	Z-1104	Z-266	Z-267	Z-1105	Z-268	Z-269	Z-270
Depth (mbsf)	907.37	907.87	908.70	910.76	910.91	915.93	917.70
Unit/Subunit	2		3	5A	5A	5B	5B
Major element oxides (wt%):							
SiO_2	45.70	47.42	46.58	47.97	47.80	48.06	48.66
TiO_2	1.03	1.20	1.21	1.11	1.20	1.16	1.12
Al_2O_3	14.09	13.98	14.62	14.07	13.80	14.92	14.85
Fe_2O_3	7.64	6.62	6.17	7.50	6.94	6.09	7.00
FeO	3.16	3.32	3.82	3.60	4.00	4.60	4.16
MnO	0.25	0.02	0.30	0.27	0.12	0.09	0.12
MgO	9.94	9.21	9.14	8.17	8.71	8.22	7.11
CaO	8.11	9.80	10.96	10.23	10.70	11.80	11.96
Na_2O	2.41	2.40	2.40	2.10	2.34	2.15	2.27
K_2O	0.10	0.41	0.18	0.08	0.18	0.18	0.18
P_2O_5	0.07	0.07	0.05	0.08	0.09	0.05	0.07
LOI	7.47	5.00	3.94	4.63	3.64	3.18	2.54
Total	99.97	99.45	99.37	99.81	99.52	100.50	100.04
H_2O^+	0.95	1.51	0.95	0.56	0.58	0.78	0.23
H_2O^-	4.77	3.49	2.99	2.95	3.06	2.40	2.31
CO_2	<0.2	ND	ND	<0.2	ND	ND	ND
Fe_2O_3/FeO	2.42	1.99	1.62	2.08	1.74	1.32	1.68
Density (g/cm^3)	2.42	2.37	2.60	2.61	2.58	2.71	2.64
Trace elements (ppm):							
La		4.1	4.0		3.6	3.3	3.9
Ce		9.5	9.0		8.8	8.2	9.1
Sm		2.6	2.6		2.5	2.3	2.8
Eu		0.90	1.0		0.9	0.84	1.0
Tb		0.60	0.56		0.53	0.50	0.61
Yb		2.4	2.5		2.4	2.3	2.8
Lu		0.41	0.39		0.35	0.36	0.43
Cr	238	300	255	234	260	185	157
Ni	87	155	165	85	145	140	130
Co	63	59	64	71	66	60	60
V	422	350	380	420	350	290	300
Cu	185	70	265	130	270	125	120
Pb	ND	<5	<5	ND	<5	<5	<5
Zn	96	105	125	94	145	125	120
Zr	60	42	46	56	48	38	39
Y	20	17	17	20	20	20	20
Nb	2.9	2.7	2.7	1.5	2.9	2.1	3.2
Rb	<1	3.9	0.8	<1	0.8	0.8	1.0
Sr	110	94	110	110	110	94	92
Ba	7	<10	<10	8	19	20	17

Note: ND = not determined.

Table T68 (continued).

Leg	33	33	33	33	33	33	33
Hole	317A	317A	317A	317A	317A	317A	317A
Core, section	32R-3	32R-4	32R-5	32R-5	32R-6	32R-6	33R-2
Interval (cm)	60-65	112-117	58-63	89-93	64-66	104-107	20-25
Piece	7	7	1	2	6	8	2
Lab number	Z-271	Z-272	Z-273	Z-1106	Z-274	Z-1107	Z-275
Depth (mbsf)	918.60	920.62	921.58	921.89	923.14	923.54	926.20
Unit/Subunit	5B	6A	6A	6A	6A	6A	6B
Major element oxides (wt%):							
SiO_2	48.22	47.18	47.76	47.77	47.29	47.31	48.22
TiO_2	1.19	1.16	1.11	0.80	1.16	0.89	1.10
Al_2O_3	14.37	14.36	14.34	13.00	13.41	14.09	13.63
Fe_2O_3	5.61	7.18	5.15	6.49	6.23	6.73	4.98
FeO	5.34	3.47	3.94	3.23	3.96	3.51	5.77
MnO	0.12	0.12	0.07	0.20	0.12	0.27	0.18
MgO	8.13	9.60	9.18	9.77	10.13	9.43	9.61
CaO	12.17	12.14	12.97	11.66	12.14	11.59	12.42
Na_2O	2.34	1.97	2.15	1.74	1.84	1.68	2.03
K_2O	0.18	0.18	0.18	0.10	0.18	0.09	0.23
P_2O_5	0.07	0.06	0.05	0.07	0.05	0.07	0.07
LOI	2.45	3.03	2.77	4.90	3.91	4.69	2.25
Total	100.19	100.45	99.67	99.73	100.42	100.35	100.49
H_2O^+	0.64	0.45	0.28	0.73	0.60	0.79	0.14
H_2O^-	1.81	2.58	2.49	3.05	3.31	2.99	2.11
CO_2	ND	ND	ND	<0.2	ND	<0.2	ND
Fe_2O_3/FeO	1.05	2.07	1.31	2.01	1.57	1.92	0.86
Density (g/cm^3)	2.76	2.71	2.75	2.66	2.68	2.70	2.80
Trace elements (ppm):							
La	3.7	2.8	2.5		3.0		3.3
Ce	8.3	7.0	6.6		6.6		8.0
Sm	2.6	2.1	1.9		2.2		2.4
Eu	0.90	0.76	0.70		0.75		0.75
Tb	0.60	0.58	0.50		0.54		0.57
Yb	2.7	2.1	2.0		2.2		2.3
Lu	0.41	0.33	0.31		0.34		0.36
Cr	130	310	570	540	480	375	390
Ni	125	170	190	140	185	95	145
Co	50	54	60	67	60	61	50
V	260	265	265	390	280	380	210
Cu	95	120	150	135	120	90	180
Pb	<5	<5	<5	ND	<5	ND	<5
Zn	110	95	97	72	110	85	95
Zr	41	25	28	43	15	46	39
Y	21	15	16	16	16	17	17
Nb	2.6	3.4	2.0	1.9	1.8	2.1	2.6
Rb	1.1	1.0	0.9	<1	<0.5	<1	0.9
Sr	96	81	67	91	60	96	96
Ba	20	22	21	7	<10	6	<10

Table T68 (continued).

Leg	33	33	33	33	33	33
Hole	317A	317A	317A	317A	317A	317A
Core, section	33R-3	33R-3	34R-1	34R-2	34R-4	34R-4
Interval (cm)	46-51	92-96	32-34	136-141	18-21	136-140
Piece	1	3	1	28	1	21
Lab number	Z-276	Z-1108	Z-277	Z-278	Z-1109	Z-279
Depth (mbsf)	927.96	928.42	934.32	936.86	938.68	939.86
Unit/Subunit	6B	6B	7B	9	10	10
Major element oxides (wt%):						
SiO_2	47.52	46.93	48.55	49.59	48.48	48.94
TiO_2	1.17	0.98	1.30	1.19	1.13	1.29
Al_2O_3	14.92	15.34	14.63	15.48	15.15	15.05
Fe_2O_3	5.25	6.30	5.94	4.26	6.11	5.63
FeO	5.13	3.75	4.56	4.51	4.34	4.73
MnO	0.12	0.13	0.26	0.15	0.17	0.11
MgO	9.49	8.94	8.24	7.99	7.54	7.83
CaO	11.98	10.48	11.39	11.50	10.75	12.09
Na_2O	2.27	2.19	2.37	2.37	2.30	2.37
K_2O	0.23	0.16	0.18	0.39	0.19	0.24
P_2O_5	0.08	0.08	0.09	0.10	0.10	0.07
LOI	2.29	4.96	3.04	2.37	3.44	2.20
Total	100.45	100.24	100.55	99.90	99.70	100.55
H_2O^+	0.10	1.07	0.71	0.54	0.46	0.49
H_2O^-	2.19	3.09	2.33	1.83	1.98	1.71
CO_2	ND	<0.2	ND	ND	0.20	ND
Fe_2O_3/FeO	1.02	1.68	1.30	0.95	1.41	1.19
Density (g/cm^3)	2.77	2.63	2.67	2.59	2.35	2.68
Trace elements (ppm):						
La	3.6		5.9	5.7		4.4
Ce	9.0		14	14		11
Sm	2.6		3.2	3.3		3.0
Eu	0.88		1.1	1.1		1.0
Tb	0.62		0.81	0.72		0.63
Yb	2.5		2.7	2.7		2.8
Lu	0.38		0.41	0.42		0.40
Cr	207	290	230	290	295	290
Ni	120	88	125	135	93	150
Co	46	67	46	42	61	50
V	160	400	250	300	405	280
Cu	56	87	265	180	60	30
Pb	<5	ND	<5	<5	ND	<5
Zn	105	97	120	175	91	110
Zr	41	52	61	58	71	54
Y	18	19	20	21	22	18
Nb	2.1	2.6	3.4	4.1	3.5	3.3
Rb	<0.5	<1	0.9	4.4	<1	1.4
Sr	98	110	110	110	110	110
Ba	19	13	19	27	7	22

Table T69. Characteristics of holes drilled at the Ninetyeast Ridge and Kerguelen Plateau, Legs 26, 120, 121, and 183.

Hole	Latitude	Longitude	Water depth (m)	Oldest sediment cored	Basement penetration (m)	Basement recovery (m)
Leg 26						
254	30°58.15’S	87°53.72’E	1253	late Eocene-Oligocene	42.5	6.8
Leg 120						
747C	54°48.68’S	76°47.64’E	1695	Santonian	53.9	27.0
Leg 121						
756D	27°21.288’S	87°35.843’E	1524	upper Eocene	82.0	26.92
757C	17°1.389’S	88°1.812’E	1655	upper Paleocene	48.3	24.95
758A	5°23.049’N	90°21.673’E	2935	Campanian	177.9	118.54
Leg 183						
1136A	59°65.163’S	84°83.484’E	1942	early Albian	33.3	23.8
1137A	56°83.305’S	68°09.345’E	1016	Campanian	152.4	105.5
1138A	53°55.175’S	75°97.488’E	1153	Cretaceous(?)	144.5	69.0
1140A	46°27.665’S	68°49.164’E	2406	middle Miocene to early Oligocene	87.4	49.0

Table T70. Composition of basalts from Hole 254, Leg 26 (Ninetyeast Ridge, Indian Ocean).

Leg	26	26	26	26	26	26
Hole	254	254	254	254	254	254
Core, section	35R-1	35R-2	35R-3	36R-1	36R-2	36R-2
Interval (cm)	123-125	105-107	72-75	140-143	2-4	114-118
Piece	11	14	9	20	1	20
Lab number	Z-100	Z-101	Z-102	Z-103	Z-104	Z-105
Depth (mbsf)	311.23	312.55	313.72	316.40	316.52	317.64
Unit	5	5	5	5	5	5
Major element oxides (wt%):						
SiO_2	42.56	44.35	43.88	43.87	42.17	41.94
TiO_2	2.34	2.52	2.48	2.87	2.60	2.63
Al_2O_3	11.46	10.33	12.27	13.91	12.61	12.99
Fe_2O_3	7.01	9.44	7.69	8.13	10.16	14.66
FeO	7.61	7.15	6.61	5.34	5.00	2.16
MnO	0.16	0.05	0.15	0.17	0.25	0.05
MgO	10.91	9.13	9.92	8.34	8.04	6.55
CaO	8.79	9.31	9.42	8.26	7.56	5.32
Na_2O	2.22	2.51	2.70	2.91	2.41	2.81
K_2O	0.31	0.27	0.34	0.51	0.41	0.51
P_2O_5	0.15	0.22	0.12	0.13	0.21	0.16
LOI	6.88	5.19	4.75	5.97	8.42	10.32
Total	100.40	100.47	100.33	100.41	99.84	100.10
H_2O^+	3.93	2.55	2.21	2.99	3.61	4.08
H_2O^-	2.95	2.64	2.54	2.98	4.81	6.24
CO_2	ND	ND	ND	ND	ND	ND
Fe_2O_3/FeO	0.92	1.32	1.16	1.71	2.03	6.79
Density (g/cm^3)	2.73	2.75	2.66	2.57	2.55	2.30
Trace elements (ppm):						
La	11	10	10	13	12	14
Ce	23	22	24	29	23	28
Sm	5.3	5.0	5.3	6.2	5.4	6.3
Eu	1.8	1.7	1.8	1.9	1.9	2.2
Tb	1.1	0.94	1.1	1.3	1.2	0.99
Yb	3.6	3.5	3.6	4.2	4.0	3.5
Lu	0.58	0.54	0.58	0.66	0.59	0.54
Sc	41	40	40	43	41	45
Cr	485	450	360	335	350	350
Ni	270	250	250	165	210	200
Co	70	65	60	55	70	70
V	270	280	250	390	390	450
Cu	100	160	100	60	225	185
Zn	120	120	110	125	120	120
Zr	78	95	100	90	150	110
Y	33	36	34	41	34	35
Nb	9.3	9.6	9.2	12	9.8	12
Rb	1.5	1.6	1.6	4.4	1.9	2.6
Sr	81	130	140	120	160	120
Ba	66	87	84	110	82	76

Note: ND = not determined.

Table T71. Secondary minerals in basalts, Ninetyeast Ridge, Leg 26: Hole 254.

Core, section, interval (cm)	Depth (mbsf)	Unit	Smectite	Swelling chlorite	Chlorite	Carbonate/ Calcite
35-1. 123-125	311.23	5	X		+	
35-2, 105-107	312.55	5	X		+	
35-3, 72-75	313.72	5	X	+		
36-1, 140-143	316.40	5	X			+
36-2, 2-4	316.52	5	X			+
36-2, 114-118	317.64	5	X		+	
36-3, 95-97[1]	318.95	5	X		?	+
38-1, 115-117[1]	335.15	5	X		?	

Notes: X = dominant, + = trace. [1] = the data from Kempe (1974).

Table T72. Composition of basalts from Hole 756D, Leg 121 (Ninetyeast Ridge, Indian Ocean). (Continued on next page.)

Leg	121	121	121	121	121	121	121
Hole	756D	756D	756D	756D	756D	756D	756D
Core, section	6R-1	6R-2	6R-2	7R-1	7R-2	7R-3	8R-1
Interval (cm)	23-25	32-35	91-95	136-138	26-28	59-63	16-19
Piece	4	1B	1C	12C	1C	2C	2
Lab number	Z-639	Z-640	Z-29	Z-22	Z-25	Z-641	Z-1337
Depth (mbsf)	158.53	160.12	160.71	169.36	169.76	171.56	177.86
Unit	5	5	5	6	6	6	7
Major element oxides (wt%):							
SiO_2	48.03	47.10	45.89	46.52	47.09	47.46	46.83
TiO_2	1.84	1.79	1.87	2.60	2.30	2.08	2.06
Al_2O_3	14.75	14.58	13.01	15.94	15.14	13.93	14.93
Fe_2O_3	7.30	3.79	8.99	7.49	6.18	6.77	9.22
FeO	4.65	7.40	5.61	3.72	4.64	5.46	3.48
MnO	0.17	0.19	0.12	0.12	0.07	0.21	0.12
MgO	5.79	6.96	6.69	7.10	6.42	7.13	6.80
CaO	10.87	11.36	10.59	10.59	11.01	10.03	9.32
Na_2O	2.67	2.61	2.87	2.98	3.33	2.67	2.35
K_2O	0.54	0.22	0.80	0.50	0.50	0.72	0.46
P_2O_5	0.17	0.15	0.17	0.20	0.19	0.17	0.21
LOI	3.54	3.51	3.37	2.09	2.66	3.11	4.20
Total	100.32	99.66	99.98	99.85	99.53	99.74	99.98
H_2O^+	0.82	0.79	1.40	0.24	0.75	1.14	1.89
H_2O^-	1.44	1.17	1.50	1.85	1.49	1.40	1.92
CO_2	0.92	1.28	ND	ND	ND	0.57	0.37
Fe_2O_3/FeO	1.57	0.51	1.60	2.01	1.33	1.24	2.65
Density (g/cm^3)	2.88	2.76	2.88	2.73	2.87	2.78	2.71
Trace elements (ppm):							
La	8.5	8.5	7.5	11	13	9.3	9.5
Ce	23	22	17	22	23	23	26
Nd	15	15	ND	ND	ND	15	15
Sm	4.5	4.4	3.8	5.4	5.4	4.5	3.6
Eu	1.6	1.5	1.3	1.5	1.6	1.5	1.3
Tb	0.94	0.69	0.79	0.84	1.0	1.0	0.68
Yb	2.8	2.6	2.5	2.5	3.3	2.9	2.4
Lu	0.41	0.42	0.35	0.36	0.5	0.42	0.39
Sc	ND	ND	43	47	47	ND	ND
Cr	230	175	215	240	210	205	180
Ni	77	61	70	92	92	70	65
Co	47	43	37	50	48	45	34
V	305	272	275	400	335	267	205
Cu	73	93	240	165	310	73	90
Zn	107	87	58	86	90	95	71
Zr	120	110	97	130	120	120	120
Y	31	30	27	29	30	31	26
Nb	8.1	9.6	7.7	10	11	8.1	42
Rb	18	1.6	43	3.0	7.2	84	14
Sr	170	180	150	200	180	160	150
Ba	62	86	40	49	48	45	22

Note: ND = not determined.

Table T72 (continued).

Leg	121	121	121	121	121	121
Hole	756D	756D	756D	756D	756D	756D
Core, section	8R-1	9R-1	9R-3	11R-1	11R-2	12R-2
Interval (cm)	72-75	36-38	119-121	115-118	95-99	69-72
Piece	14	5	4E	17	11D	1C
Lab number	Z-642	Z-5	Z-36	Z-643	Z-4	Z-16
Depth (mbsf)	178.42	187.76	191.59	207.75	209.05	218.39
Unit	8	9	9	13	14	14
Major element oxides (wt%):						
SiO_2	48.02	47.00	47.27	47.70	45.61	47.00
TiO_2	1.83	2.56	1.72	2.02	2.56	2.47
Al_2O_3	13.78	13.88	13.21	14.07	14.16	14.91
Fe_2O_3	6.15	7.23	6.15	7.00	8.62	4.85
FeO	5.16	5.20	7.03	4.27	5.03	5.40
MnO	0.18	0.13	0.14	0.15	0.16	0.15
MgO	6.98	6.59	6.88	6.98	6.39	6.27
CaO	11.17	11.42	11.45	10.83	10.82	12.88
Na_2O	2.53	2.70	2.70	2.40	2.64	2.80
K_2O	0.42	0.61	0.31	0.40	0.69	0.39
P_2O_5	0.14	0.18	0.16	0.13	0.18	0.10
LOI	3.67	2.73	2.78	3.86	2.98	2.76
Total	100.03	100.23	99.80	99.81	99.84	99.98
H_2O^+	1.32	0.68	1.13	1.37	1.15	0.89
H_2O^-	1.64	1.98	1.43	1.66	1.83	1.87
CO_2	0.34	ND	ND	0.36	ND	ND
Fe_2O_3/FeO	1.19	1.39	0.88	1.64	1.71	0.90
Density (g/cm^3)	2.70	2.77	2.90	2.74	2.76	2.81
Trace elements (ppm):						
La	8.0	9.3	8.3	7.4	6.5	8.3
Ce	22	17	19	20	15	18
Nd	15	ND	ND	13	ND	ND
Sm	4.2	4.6	4.5	4.0	3.5	4.1
Eu	1.3	1.4	1.3	1.4	1.2	1.4
Tb	0.89	0.84	0.81	1.0	0.69	0.74
Yb	2.4	2.1	2.5	2.5	2.0	2.4
Lu	0.35	0.38	0.4	0.39	0.31	0.35
Sc	ND	49	45	ND	47	48
Cr	220	270	220	215	195	188
Ni	73	85	82	68	94	88
Co	46	50	48	47	60	47
V	280	340	315	277	340	310
Cu	47	100	85	63	130	75
Zn	94	80	74	90	74	70
Zr	110	100	94	100	110	110
Y	20	27	30	25	27	27
Nb	7.9	9.5	9.4	7.3	8.9	8.1
Rb	55	11	2.7	13	18	5.1
Sr	160	160	160	150	160	180
Ba	49	37	41	58	35	30

Table T73. Secondary minerals in basalts, Ninetyeast Ridge, Leg 121: Hole 756D.

Core, section, interval (cm)	Depth (mbsf)	Unit	Smectite	Mixed-layer smectite-chlorite	Chlorite	Hydro mica	Carbo-nate / Calcite	Zeolite	Fe-oxides and hydroxides
121-756D-									
4R-1, 35-39[1]	139.35	1						*	
4R-1, 125-126[2]	140.25	2	*						*
5R-1, 24-25[2]	148.84	2	*						
6R-1, 6-10[1]	158.36	4					*		
6R-1, 107-108[2]	159.37	5					*		
6R-2, 9-13[1]	159.89	5	*				*		*
6R-2, 44-45[2]	160.24	5	*						
6R-2, 91-95	160.71	5	+++	++		+			+
7R-1, 100-104[1]	169.00	6	*						
7R-1, 136-138	169.36	6	+++			+			
7R-2, 26-28	169.76	6	+++		+				+
7R-2, 66-68[2]	170.16	6					*		
7R-3, 50-54[1]	171.50	6	*				*		
8R-1, 20-23[1]	177.90	7	*				*	*	*
8R-1, 33-34[2]	178.03	7	*						*
8R-1, 51-52[2]	178.21	7					*		
9R-1, 36-38	187.76	9	+++						
9R-2, 21-24[1]	189.11	9	*						
9R-3, 25-26[2]	190.65	9					*		
9R-3, 119-121	191.59	9	+++	+					
10R-1, 99-103[1]	197.99	12	*						*
10R-2, 138-139[2]	199.88	12	*						
10R-3, 58-63[1]	200.58	12	*						*
11R-1, 36-37[2]	206.96	13					*		
11R-1, 40-41[2]	207.00	13	*						
11R-1, 102-106[1]	207.62	13	*						*
11R-2, 95-99	209.05	14	+++	++		+	+		+
12R-2, 22-27[1]	217.92	14	*					*	
12R-2, 69-72	218.39	14	+++						+
12R-3, 139-143[1]	220.59	14	*						

Notes: +++ = dominant, ++ = minor, + = trace, * = presence (without determination of quantity). [1] = data of mineral determinations from description of thin sections (Frey et al., 1991). [2] = data of mineral determinations from XRD analyses (Peirce, Weissel, et al., 1989).

Table T74. Composition of basalts from Hole 757C, Leg 121 (Ninetyeast Ridge, Indian Ocean). (Continued on next two pages.)

Leg	121	121	121	121	121	121	121
Hole	757C	757C	757C	757C	757C	757C	757C
Core, section	8R-1	8R-2	9R-1	9R-2	9R-3	9R-4	9R-5
Interval (cm)	127-129	119-121	59-61	24-26	35-37	38-42	70-73
Piece	5A	3I	3	1A	1A	1A	2
Lab number	Z-9	Z-6	Z-1	Z-17	Z-18	Z-1338	Z-1339
Depth (mbsf)	373.67	375.09	382.59	383.74	385.35	385.82	387.47
Unit	2	2	2	2	2	3	5
Major element oxides (wt%):							
SiO_2	43.56	45.86	45.32	46.18	45.92	42.95	47.57*
TiO_2	1.39	0.97	0.96	1.13	0.95	0.65	1.27
Al_2O_3	17.16	21.18	20.30	22.30	23.54	19.86	18.68
Fe_2O_3	6.61	4.29	5.26	2.82	2.70	4.47	11.25
FeO	1.57	1.78	2.50	2.58	2.17	1.13	
MnO	0.14	0.03	0.08	0.02	0.03	0.11	0.09
MgO	7.49	6.93	5.84	3.58	5.04	4.58	6.32
CaO	7.22	11.73	13.46	15.71	13.36	14.55	8.27
Na_2O	3.52	2.18	2.03	2.03	1.95	2.63	4.98
K_2O	1.94	0.93	0.99	0.25	0.33	0.74	1.775
P_2O_5	0.10	0.07	0.06	0.05	0.03	0.05	0.139
LOI	9.16	4.21	3.16	3.00	3.74	7.74	8.86
Total	99.86	100.16	99.96	99.65	99.76	99.46	100.34
H_2O^+	5.49	2.60	1.49	1.33	1.11	3.28	7.25
H_2O^-	3.47	1.23	1.18	1.41	2.30	1.30	1.11
CO_2	ND	ND	ND	ND	ND	3.16	0.5
Fe_2O_3/FeO	4.21	2.41	2.10	1.09	1.24	3.96	3.75
Density (g/cm^3)	2.27	2.70	2.66	2.73	2.64	2.58	2.16
Trace elements (ppm):							
La	6.2	3.6	4.1	3.6	4.2		
Ce	14	6.9	8.6	8.6	8.7		
Nd	ND	ND	ND	ND	ND		
Sm	2.7	1.9	1.8	1.8	1.7		
Eu	0.99	0.68	0.67	0.62	0.6		
Tb	0.54	0.52	0.36	0.34	0.33		
Yb	1.5	1.1	1.2	1.2	1.0		
Lu	0.23	0.15	0.18	0.18	0.16		
Sc	42	31	32	34	31	ND	ND
Cr	250	165	210	130	190	174	242
Ni	94	77	105	70	94	61	71
Co	37	30	37	24	40	33	42
V	280	145	150	125	270	168	225
Cu	125	63	52	36	75	62	88
Zn	45	40	56	42	46	58	66
Zr	58	42	36	36	39	41	70
Y	19	12	12	14	9.9	11	19
Nb	4.8	3.8	4.0	3.4	3.2	3.0	4.8
Rb	18	12	24	1.6	2.2	8.3	16
Sr	110	190	170	190	210	380	460
Ba	38	29	17	18	24	<5	130

Note: * = major element data from Frey et al. (1991). ND = not determined.

Table T74 (continued).

Leg	121	121	121	121	121	121	121
Hole	757C	757C	757C	757C	757C	757C	757C
Core, section	9R-7	9R-8	10R-2	10R-3	11R-1	11R-1	12R-1
Interval (cm)	71-73	57-60	66-70	79-81	54-58	135-137	5-9
Piece	1B	4A	5A	2C	8B	9E	1
Lab number	Z-30	Z-644	Z-1340	Z-1341	Z-645	Z-34	Z-1342
Depth (mbsf)	391.71	392.67	393.74	395.33	401.94	402.75	411.15
Unit	5	5	7	9	10	12	18
Major element oxides (wt%):							
SiO_2	46.82	46.78	42.65	43.02	45.20	42.61	48.82
TiO_2	0.85	0.65	0.69	0.74	0.74	1.12	1.02
Al_2O_3	19.51	21.38	20.95	20.45	16.52	17.02	17.88
Fe_2O_3	3.31	3.98	4.99	5.95	8.93	7.52	6.03
FeO	3.39	2.46	0.71	1.45	1.33	2.23	2.73
MnO	0.08	0.09	0.04	0.07	0.08	0.07	0.08
MgO	5.08	6.37	5.74	5.97	6.85	5.90	6.27
CaO	13.87	11.54	8.26	11.29	5.98	8.10	8.99
Na_2O	2.57	1.80	4.06	2.40	3.25	3.33	2.58
K_2O	0.56	1.01	1.43	0.99	1.99	1.95	1.57
P_2O_5	0.02	0.07	0.07	0.07	0.07	0.07	0.07
LOI	3.40	3.46	10.35	7.36	8.77	9.58	3.55
Total	99.46	99.59	99.94	99.76	99.71	99.50	99.59
H_2O^+	1.14	1.49	6.66	3.90	4.50	6.21	1.49
H_2O^-	1.92	1.12	2.20	1.63	2.85	3.03	1.34
CO_2	ND	0.58	0.95	1.63	1.11	ND	<0.2
Fe_2O_3/FeO	0.98	1.62	7.03	4.10	6.71	3.37	2.21
Density (g/cm^3)	2.93	2.70	2.23	2.40	2.39	2.33	2.64
Trace elements (ppm):							
La	4.3	3.7	3.3		5.4	6.5	10
Ce	8.1	9.5	8.6		11.0	15	22
Nd	ND	6.0	5.5		7.5	ND	13
Sm	1.6	1.7	1.5		2.2	2.8	3.4
Eu	0.66	0.66	0.56		0.85	1.0	1.0
Tb	0.35	0.34	0.37		0.41	0.52	0.71
Yb	1.0	1.1	0.79		1.7	1.8	2.3
Lu	0.14	0.19	0.13		0.29	0.26	0.36
Sc	34	ND	ND	ND	ND	38	ND
Cr	155	185	203	166	143	110	93
Ni	88	66	54	60	53	55	54
Co	33	37	31	33	30	30	38
V	160	185	181	198	265	260	336
Cu	86	66	47	53	57	81	44
Zn	28	64	57	58	67	44	79
Zr	37	46	40	43	60	48	130
Y	9.7	12	10	11	19	16	22
Nb	3.2	2.8	3.2	2.7	4.1	4.5	7.6
Rb	2.7	26	14	15	20	19	18
Sr	170	170	440	325	140	380	180
Ba	28	49	7	<5	27	34	65

Table T74 (continued).

Leg	121	121	121
Hole	757C	757C	757C
Core, section	12R-1	12R-2	12R-2
Interval (cm)	84-86	8-10	75-79
Piece	2	1	4
Lab number	Z-21	Z-13	Z-1343
Depth (mbsf)	411.94	412.68	413.20
Unit	18	18	18
Major element oxides (wt%):			
SiO_2	49.02	48.51	46.49
TiO_2	1.17	1.18	0.98
Al_2O_3	18.47	17.32	15.78
Fe_2O_3	3.01	6.14	8.67
FeO	4.10	3.47	1.10
MnO	0.05	0.12	0.08
MgO	5.38	5.62	6.29
CaO	12.10	10.45	4.50
Na_2O	2.40	2.63	5.44
K_2O	1.01	1.45	1.94
P_2O_5	0.06	0.05	0.10
LOI	3.09	3.15	8.24
Total	99.86	100.09	99.61
H_2O^+	1.39	0.89	5.12
H_2O^-	1.44	1.94	1.50
CO_2	ND	ND	1.41
Fe_2O_3/FeO	0.73	1.77	7.88
Density (g/cm^3)	2.82	2.73	2.17
Trace elements (ppm):			
La	14	11	13
Ce	24	24	31
Nd	ND	ND	18
Sm	4.4	3.5	4.4
Eu	1.0	1.1	1.3
Tb	0.78	0.76	1.1
Yb	3.1	2.7	3.6
Lu	0.48	0.41	0.62
Sc	34	36	ND
Cr	92	92	144
Ni	55	58	50
Co	30	33	32
V	240	260	236
Cu	50	24	66
Zn	62	65	89
Zr	130	130	180
Y	27	29	35
Nb	8.5	8.7	11
Rb	12	21	17
Sr	160	150	60
Ba	53	75	ND

Table T75. Secondary minerals in basalts, Ninetyeast Ridge, Leg 121: Hole 757C.
(Continued on next page.)

Core, section, interval (cm)	Depth (mbsf)	Unit	Sm	SChl	Mixed-layer sm-chl	Chl	Hydro-mica	Carbo-nate / Calcite	Zeolite	Fe-oxi-des and hydro-xides	K-feld-spar
121-757C-											
8R-1, 43-44[2]	372.83	1	*			*					
8R-1, 65-69[1]	373.05	1	*					*	*	*	
8R-1, 89-90[2]	373.29	2	*			*					
8R-1, 127-129	373.67	2	+++	++		+		+	+	+	
8R-2, 37-38[2]	374.27	2						*	*		*
8R-2, 50-51[2]	374.40	2	*?								
8R-2, 119-121	375.09	2	+++	++				+	+	+	
8R-2, 132-136[1]	375.22	2				*		*			*
8R-3, 15-16[2]	375.55	2	*			*					*
9R-1, 59-61	382.59	2	++	+++				+	+?	+	
9R-2, 24-26	383.74	2	+++								
9R-2, 47-51[1]	383.97	2	*								*
9R-2, 55-56[2]	384.05	2	*			*		*			*
9R-2, 61-62[2]	384.11	2	*?								
9R-3, 6-10[1]	385.06	2	*								
9R-3, 35-37	385.35	2	+++								
9R-4, 38-42[1]	385.82	3	*					*	*		
9R-4, 38-42	385.82	3	+++						+		
9R-4, 115-116[2]	387.65	4	*			*			*		
9R-5, 34-38[1]	388.34	4	*							*	
9R-5, 51-52[2]	388.51	5	*			*			*		
9R-5, 70-73[1]	388.70	5						*	*	*	
9R-5, 70-73	388.70	5	+			+		++	++		
9R-6, 102-106[1]	390.52	5	*					*			
9R-7, 71-73	391.71	5	+++		+					+	
9R-7, 78-82[1]	391.78	5						*		*	
10R-2, 33-37[1]	393.53	6	*?						*		
10R-2, 66-70[1]	393.86	6	*?					*	*		*
10R-3, 2-6[1]	394.72	8	*						*		
10R-3, 67-68[2]	395.29	9							*		*
10R-3, 79-81[2]	395.33	9	+++								
10R-3, 83-87[1]	395.53	9	*?					*	*		*
11R-1, 54-58	401.94	10	+++	++		+	+		++		
11R-1, 67-72	402.07	10	*					*	*		*
11R-1, 98-99	402.38	11		+++		+	+		++		
11R-1, 99-103[1]	402.39	11	*						*		
11R-1, 135-137	402.75	12	++		+++		+		++		
11R-1, 138-139[2]	402.78	12							*		*
11R-2, 10-14[1]	403.00	12	*?						*		
11R-2, 51-56[1]	403.41	13							*		*
11R-2, 94-97[1]	403.84	14							*		
11R-3, 49-54[1]	404.89	16	*								
11R-3, 71-72[2]	405.11	17	*			*					*
11R-3, 98-102[1]	405.38	17	*					*	*		
12R-1, 5-9	411.15	18	+++			+	+				
12R-1, 84-86	411.94	18	+++								
12R-2, 8-10	412.68	18	+++								
12R-2, 63-67[1]	413.08	18	*						*		*
12R-2, 75-79	413.20	18	+		+			+++	+++		

Table T75 (continued).

Core, section, interval (cm)	Depth (mbsf)	Unit	Sm	SChl	Mixed-layer sm-chl	Chl	Hydro-mica	Carbo-nate / Calcite	Zeolite	Fe-oxi-des and hydro-xides	K-feld-spar
12R-3, 64-68[1]	414.74	19	*					*	*		
12R-4, 24-29[1]	415.84	19	*						*		*
12R-4, 102-103[2]	416.62	19	*			*					*
12R-4, 135-139[1]	416.95	19						*	*		

Notes: +++ = dominant, ++ = minor, + = trace, * = presence (without determination of quantity). Sm = smectite, Chl = chlorite, SChl = swelling chlorite. [1] = data of mineral determinations from description of thin sections (Frey et al., 1991). [2] = data of mineral determinations from XRD analyses (Peirce, Weissel, et al., 1989).

Table T76. Composition of basalts from Hole 758A, Leg 121 (Ninetyeast Ridge, Indian Ocean). (Continued on next six pages.)

Leg	121	121	121	121	121	121	121
Hole	758A	758A	758A	758A	758A	758A	758A
Core, section	56R-1	57R-2	57R-3	57R-3	58R-1	58R-5	59R-7
Interval (cm)	21-23	110-114	7-9	37-41	41-43	55-57	52-56
Piece	2A	2	1	4	3	2A	1A
Lab number	Z-26	Z-647	Z-32	Z-648	Z-33	Z-8	Z-1344
Depth (mbsf)	508.61	520.5	520.97	520.98	527.51	533.65	544.84
Unit	1	2	2	2	2	2	2
Major element oxides (wt%):							
SiO_2	46.79	46.66	43.41	45.53	46.43	44.96	47.78
TiO_2	1.17	1.79	1.27	1.75	1.25	1.51	1.28
Al_2O_3	14.42	15.26	11.92	12.99	12.78	14.37	13.70
Fe_2O_3	5.60	8.04	9.85	8.92	7.27	6.90	7.07
FeO	5.40	4.13	5.70	4.52	5.54	4.75	4.51
MnO	0.10	0.17	0.10	0.31	0.18	0.12	0.16
MgO	7.95	7.89	8.93	10.20	7.78	7.32	9.34
CaO	11.88	6.63	5.45	6.17	10.02	11.40	9.41
Na_2O	2.57	2.67	2.98	2.47	2.98	2.10	2.26
K_2O	0.11	0.58	0.68	0.08	0.17	0.14	0.15
P_2O_5	0.06	0.18	0.04	0.17	0.08	0.05	0.10
LOI	3.69	5.99	9.16	7.00	5.44	6.76	3.83
Total	99.74	99.99	99.49	100.11	99.92	100.38	99.59
H_2O^+	0.88	2.02	2.69	1.94	1.13	1.91	1.43
H_2O^-	2.81	3.97	6.30	4.45	4.09	4.85	2.08
CO_2	ND	<0.2	ND	0.29	ND	ND	<0.2
Fe_2O_3/FeO	1.04	1.95	1.73	1.97	1.31	1.45	1.57
Density (g/cm^3)	2.80	2.43	2.36	2.41	2.58	2.62	2.62
Trace elements (ppm):							
La	4.1	8.5	6.7	6.7	6.6	3.0	
Ce	7.4	22.0	12	18	12	8.0	
Nd	ND	15.0	ND	13	ND	ND	
Sm	2.0	4.5	3.0	4.2	3.0	2.3	
Eu	0.73	1.60	0.96	1.50	1.1	0.9	
Tb	0.48	1.00	0.7	1.1	0.7	0.63	
Yb	1.9	2.3	1.7	2.6	1.8	2.2	
Lu	0.29	0.35	0.27	0.40	0.28	0.33	
Sc	47	ND	49	ND	51	50	ND
Cr	240	255	90	62	84	82	93
Ni	100	69	80	56	80	94	73
Co	42	49	69	46	71	73	71
V	325	545	385	505	370	620	445
Cu	195	140	155	125	210	275	132
Zn	56	160	82	120	62	65	84
Zr	36	89	59	94	63	52	70
Y	18	30	21	28	26	19	23
Nb	2.7	6.8	4.5	7.0	4.9	3.9	3.0
Rb	1.3	2.2	1.9	<1	1.6	<1	2.3
Sr	100	150	120	140	120	120	84
Ba	16	39	22	22	34	23	67

Note: ND = not determined.

Table T76 (continued).

Leg	121	121	121	121	121	121	121
Hole	758A	758A	758A	758A	758A	758A	758A
Core, section	60R-1	60R-2	60R-6	61R-2	61R-4	61R-7	62R-1
Interval (cm)	11-13	80-82	82-84	62-67	60-64	0-5	17-21
Piece	1B	2	1C	1A	1B	1A	2
Lab number	Z-31	Z-3	Z-27	Z-1345	Z-1346	Z-1347	Z-1348
Depth (mbsf)	546.01	548.20	554.22	556.53	559.43	562.91	564.47
Unit	3	3	3	3	3	3	3
Major element oxides (wt%):							
SiO_2	45.71	45.59	46.11	47.70	48.10	47.49	45.31
TiO_2	1.39	1.75	1.43	1.48	1.43	1.47	1.48
Al_2O_3	11.87	13.26	12.31	12.69	12.31	12.34	15.40
Fe_2O_3	7.76	7.89	6.55	7.02	7.41	7.44	7.38
FeO	6.10	5.05	6.09	5.21	4.70	4.23	4.37
MnO	0.14	0.17	0.10	0.15	0.14	0.16	0.20
MgO	8.99	8.78	8.26	8.79	9.02	9.49	8.97
CaO	9.19	8.76	11.26	10.12	10.09	9.33	6.77
Na_2O	2.70	2.37	2.57	2.25	2.04	2.37	2.69
K_2O	0.17	0.18	0.13	0.15	0.11	0.14	0.18
P_2O_5	0.10	0.11	0.08	0.11	0.10	0.11	0.13
LOI	5.63	6.14	5.10	4.22	4.35	5.2	6.87
Total	99.75	100.05	99.99	99.89	99.80	99.77	99.75
H_2O^+	1.81	1.15	1.47	1.17	1.76	1.19	2.27
H_2O^-	3.82	4.53	3.43	2.18	2.29	2.61	3.73
CO_2	ND	ND	ND	<0.2	<0.2	<0.2	<0.2
Fe_2O_3/FeO	1.27	1.56	1.08	1.35	1.58	1.76	1.69
Density (g/cm^3)	2.59	2.55	2.92	2.69	2.65	2.51	2.26
Trace elements (ppm):							
La	4.9	5.7	5.9				5.2
Ce	12	13	12				14.0
Nd	ND	ND	ND				9.50
Sm	2.9	3.0	2.9				2.8
Eu	1.0	1.0	1.0				1.1
Tb	0.72	0.61	0.68				0.76
Yb	2.7	2.3	2.4				2.2
Lu	0.38	0.38	0.34				0.33
Sc	50	49	48	ND	ND	ND	ND
Cr	75	225	175	198	200	223	250
Ni	77	110	94	81	84	79	86
Co	50	69	60	77	71	81	81
V	330	515	380	470	482	530	595
Cu	195	185	195	148	148	162	146
Zn	66	80	71	95	88	82	114
Zr	62	70	55	77	76	79	86
Y	27	23	23	26	22	23	19.00
Nb	4.8	5.2	4.4	4.5	4.3	4.1	5.0
Rb	2.3	<1	<1	2.1	1.7	1.7	<1
Sr	120	130	120	130	130	135	140
Ba	28	21	20	98	64	64	150

Table T76 (continued).

Leg	121	121	121	121	121	121	121
Hole	758A	758A	758A	758A	758A	758A	758A
Core, section	62R-1	62R-3	62R-3	63R-1	63R-2	63R-5	64R-1
Interval (cm)	57-59	27-29	88-92	3-5	46-50	48-50	76-80
Piece	4A	2	8A	1	1B	1A	1A
Lab number	Z-23	Z-24	Z-649	Z-19	Z-1349	Z-7	Z-650
Depth (mbsf)	564.87	567.57	568.09	573.83	575.58	580.28	583.96
Unit	4	4	5	7	7	7	7
Major element oxides (wt%):							
SiO_2	43.95	44.66	46.56	43.68	45.42	45.79	48.30
TiO_2	1.12	1.20	1.64	2.10	1.53	1.64	1.43
Al_2O_3	17.57	19.22	13.65	13.29	14.09	14.13	13.71
Fe_2O_3	4.27	3.50	8.35	8.50	7.43	5.85	6.69
FeO	3.73	3.45	3.63	4.90	4.84	4.85	4.84
MnO	0.07	0.11	0.22	0.18	0.16	0.15	0.16
MgO	9.47	7.02	9.14	9.82	9.24	9.05	8.25
CaO	8.73	12.12	7.04	5.66	8.22	10.85	10.20
Na_2O	1.88	2.30	2.44	2.63	2.36	2.18	2.12
K_2O	0.31	0.17	0.16	0.20	0.14	0.18	0.12
P_2O_5	0.04	0.05	0.14	0.15	0.12	0.05	0.13
LOI	8.29	5.84	7.20	8.73	5.99	5.73	4.10
Total	99.43	99.64	100.17	99.84	99.54	100.45	100.05
H_2O^+	2.74	2.08	2.25	3.61	1.39	1.25	1.35
H_2O^-	5.38	3.55	4.64	4.87	3.24	4.29	2.62
CO_2	ND	ND	0.28	ND	<0.2	ND	<0.2
Fe_2O_3/FeO	1.14	1.01	2.30	1.74	1.54	1.21	1.38
Density (g/cm^3)	2.39	2.55	2.27	2.38	2.46	2.60	2.61
Trace elements (ppm):							
La	4.1	3.9	5.7	8.5		4.8	5.6
Ce	8.5	7.9	15.0	18		11	14
Nd	ND	ND	11.0	ND		ND	10
Sm	2.0	1.9	3.4	4.2		2.8	3.3
Eu	0.66	0.64	1.20	1.2		1.0	1.1
Tb	0.41	0.42	0.86	0.9		0.65	0.79
Yb	1.4	1.4	2.2	3.1		2.2	2.8
Lu	0.2	0.2	0.34	0.48		0.35	0.46
Sc	41	42	ND	47	ND	50	ND
Cr	535	360	245	18	218	195	170
Ni	135	120	76	58	80	92	65
Co	58	51	61	58	67	69	57
V	320	240	520	360	560	440	350
Cu	113	81	106	215	132	165	130
Zn	36	46	105	76	99	62	104
Zr	40	35	81	99	82	59	89
Y	12	14	25	30	25	23	28
Nb	3.3	3.0	5.3	6.5	4.9	5.1	5.0
Rb	2.0	<1	1.0	<1	1.3	<1	1.7
Sr	130	130	140	130	130	120	140
Ba	19	19	15	19	64	17	26

Table T76 (continued).

Leg	121	121	121	121	121	121	121
Hole	758A	758A	758A	758A	758A	758A	758A
Core, section	64R-2	65R-2	65R-4	65R-5	65R-6	66R-1	66R-3
Interval (cm)	130-135	10-15	58-62	1-6	25-27	31-35	44-46
Piece	1B	1A	1B	1A	1A	5A	1B
Lab number	Z-1350	Z-1351	Z-1352	Z-651	Z-28	Z-1353	Z-14
Depth (mbsf)	585.78	594.09	597.26	598.03	600.45	602.41	605.54
Unit	7	10	10	10	10	11	11
Major element oxides (wt%):							
SiO_2	45.20	45.61	47.17	47.35	45.89	46.66	46.14
TiO_2	1.71	1.45	1.30	1.51	1.54	1.34	1.47
Al_2O_3	14.61	15.28	14.39	13.46	11.78	14.01	14.46
Fe_2O_3	7.08	6.97	5.65	5.71	7.97	6.53	5.24
FeO	4.87	4.02	4.83	4.15	5.33	5.02	4.56
MnO	0.20	0.19	0.16	0.19	0.14	0.15	0.10
MgO	8.89	8.83	8.62	8.10	8.16	8.90	8.35
CaO	8.23	9.03	10.81	11.80	11.25	10.04	11.28
Na_2O	2.40	2.42	2.07	2.02	2.43	2.12	2.10
K_2O	0.14	0.10	0.08	0.07	0.10	0.10	0.10
P_2O_5	0.16	0.11	0.10	0.08	0.08	0.11	0.07
LOI	5.68	5.82	4.54	5.56	4.75	4.84	5.77
Total	99.17	99.83	99.72	100.00	99.42	99.82	99.64
H_2O^+	1.01	1.55	1.30	1.45	1.16	1.33	1.64
H_2O^-	3.28	3.32	2.60	2.64	3.59	2.95	4.00
CO_2	<0.2	<0.2	0.64	1.24	ND	0.20	ND
Fe_2O_3/FeO	1.45	1.73	1.17	1.38	1.50	1.30	1.15
Density (g/cm^3)	2.40	2.36	2.59	2.66	2.62	2.52	2.63
Trace elements (ppm):							
La				5.0	4.8		3.9
Ce				13	10		9.5
Nd				9.8	ND		ND
Sm				3.0	2.8		2.6
Eu				1.1	1.0		0.94
Tb				0.70	0.72		0.56
Yb				2.2	2.2		2.0
Lu				0.34	0.32		0.3
Sc	ND	ND	ND	ND	53	ND	51
Cr	218	345	310	255	295	300	375
Ni	78	86	92	77	102	95	105
Co	79	77	72	58	55	78	58
V	572	548	470	335	330	480	360
Cu	148	146	148	102	185	134	150
Zn	113	85	84	91	66	95	58
Zr	89	78	68	61	62	73	47
Y	22	23	22	22	22	20	21
Nb	5.0	3.9	4.4	3.2	4.2	3.1	3.7
Rb	1.5	1.1	1.3	<1	<1	<1	1.0
Sr	140	130	130	130	120	130.0	110
Ba	89	48	6	17	21	6.0	<10

Table T76 (continued).

Leg	121	121	121	121	121	121	121
Hole	758A	758A	758A	758A	758A	758A	758A
Core, section	66R-5	66R-5	67R-4	67R-4	67R-6	68R-3	69R-2
Interval (cm)	2-7	50-55	79-83	78-80	28-30	106-108	45-47
Piece	1A	1E	3	3	1	8	1
Lab number	Z-652	Z-1354	Z-653	Z-12	Z-35	Z-20	Z-10
Depth (mbsf)	607.61	608.09	616.73	616.78	619.28	624.86	632.15
Unit	11	11	14	14	14	17	17
Major element oxides (wt%):							
SiO_2	45.37	44.66	46.43	44.11	45.95	44.46	45.92
TiO_2	1.35	1.44	1.63	1.93	1.20	1.41	1.43
Al_2O_3	14.22	15.30	14.47	13.18	14.87	15.25	12.95
Fe_2O_3	7.48	6.81	7.51	6.47	5.60	6.24	7.70
FeO	4.13	4.24	4.08	4.09	4.59	3.15	4.87
MnO	0.10	0.16	0.21	0.10	0.14	0.05	0.15
MgO	9.45	9.56	8.88	10.96	8.32	8.57	7.86
CaO	8.26	7.46	7.62	6.57	10.86	9.40	12.96
Na_2O	2.24	2.50	2.48	2.33	2.30	2.25	2.10
K_2O	0.08	0.13	0.10	0.20	0.08	0.21	0.15
P_2O_5	0.11	0.16	0.14	0.10	0.07	0.07	0.07
LOI	6.99	6.77	6.60	9.82	5.75	8.88	4.32
Total	99.78	99.19	100.15	99.86	99.73	99.94	100.48
H_2O^+	2.00	1.74	2.05	2.97	1.35	2.90	1.27
H_2O^-	4.10	3.91	4.28	6.55	4.40	5.75	3.05
CO_2	0.89	0.64	<0.2	ND	ND	ND	ND
Fe_2O_3/FeO	1.81	1.61	1.84	1.58	1.22	1.98	1.58
Density (g/cm^3)	2.40	2.37	2.51	2.21	2.52	2.31	2.77
Trace elements (ppm):							
La	4.2		5.8	5.2	4.4	4.1	3.3
Ce	9.9		16	10	11	8.9	8.5
Nd	7.9		12	ND	ND	ND	ND
Sm	2.5		3.8	2.7	2.7	2.3	2.4
Eu	0.78		1.3	0.99	0.84	0.77	0.9
Tb	0.65		0.94	0.75	0.52	0.45	0.53
Yb	2.0		2.4	1.8	1.8	1.6	2.1
Lu	0.30		0.35	0.28	0.3	0.25	0.32
Sc	ND	ND	ND	48	50	49	49
Cr	340	305	170	112	295	230	240
Ni	83	94	58	82	102	88	100
Co	54	69	44	47	53	51	55
V	415	500	505	430	330	340	280
Cu	130	138	180	195	152	165	140
Zn	88	121	140	70	59	50	58
Zr	66	78	87	67	42	55	49
Y	20	26	25	19	17	15	21
Nb	4.5	3.6	5.2	5.1	3.6	3.0	3.8
Rb	<1	<1	<1	<1	<1	<1	<1
Sr	140	140	150	130	120	130	110
Ba	11	<5	32	18	20	18	15

Table T76 (continued).

Leg	121	121	121	121	121	121	121
Hole	758A	758A	758A	758A	758A	758A	758A
Core, section	69R-5	69R-5	70R-2	71R-2	71R-3	72R-3	72R-4
Interval (cm)	18-21	120-123	47-50	104-107	87-89	0-5	90-95
Piece	1A	1C	4	8B	3B	1A	3
Lab number	Z-654	Z-1355	Z-655	Z-656	Z-2	Z-657	Z-658
Depth (mbsf)	635.77	636.79	641.37	651.14	652.47	660.92	663.15
Unit	17	17	19	21	22	25	25
Major element oxides (wt%):							
SiO_2	47.53	43.99	45.94	46.39	45.01	47.39	46.65
TiO_2	1.10	1.29	1.39	1.02	1.60	1.01	1.11
Al_2O_3	13.32	14.13	13.47	13.78	13.06	14.09	15.02
Fe_2O_3	6.00	7.59	6.90	7.59	5.78	6.27	6.10
FeO	4.96	4.44	3.74	3.40	4.85	4.72	3.30
MnO	0.20	0.16	0.10	0.17	0.31	0.18	0.23
MgO	9.61	9.99	10.16	9.64	8.49	8.90	9.22
CaO	11.24	6.88	7.00	8.49	12.07	10.13	9.59
Na_2O	1.83	2.28	2.26	2.17	2.16	2.00	2.10
K_2O	0.06	0.36	0.16	0.12	0.13	0.12	0.05
P_2O_5	0.10	0.12	0.18	0.13	0.11	0.15	0.13
LOI	4.00	7.96	8.50	7.00	6.37	5.34	6.40
Total	99.95	99.19	99.80	99.90	99.94	100.30	99.90
H_2O^+	0.52	2.27	2.41	1.91	1.28	1.48	1.51
H_2O^-	2.60	4.26	4.99	4.42	3.98	3.28	4.16
CO_2	0.44	0.66	0.58	0.42	ND	0.55	0.69
Fe_2O_3/FeO	1.21	1.71	1.84	2.23	1.19	1.33	1.85
Density (g/cm^3)	2.74	2.41	2.46	2.39	2.67	2.92	2.48
Trace elements (ppm):							
La	3.8		5.5	5.0	4.9	4.3	3.6
Ce	8.7		14	13	11	10	9.9
Nd	7.3		11	9.5	ND	7.9	7.0
Sm	2.5		3.2	3.1	2.6	2.7	2.2
Eu	0.87		0.97	1.0	0.87	0.91	0.76
Tb	0.64		0.76	0.73	0.58	0.65	0.59
Yb	2.3		2.2	2.5	2.4	2.7	2.0
Lu	0.35		0.31	0.38	0.39	0.42	0.32
Sc	ND	ND	ND	ND	49	ND	ND
Cr	215	224	253	254	240	225	245
Ni	90	90	77	74	117	71	76
Co	60	88	65	46	65	53	54
V	295	470	447	400	460	340	447
Cu	120	124	102	91	185	106	120
Zn	108	162	125	98	64	92	90
Zr	56	71	63	62	54	60	59
Y	20	22	25	22	22	21	19
Nb	3.2	3.5	4.4	4.6	5.5	4.0	4.2
Rb	<1	2.5	2.2	2.4	<1	3	<1
Sr	110	125	120	120	110	120	130
Ba	<10	54	16	15	<10	19	12

Table T76 (continued).

Leg	121	121	121	121
Hole	758A	758A	758A	758A
Core, section	73R-2	73R-3	73R-3	73R-4
Interval (cm)	71-74	85-87	136-140	105-110
Piece	1C	4F	5	8
Lab number	Z-659	Z-15	Z-1356	Z-1357
Depth (mbsf)	669.79	671.45	671.89	673.08
Unit	27	29	29	29
Major element oxides (wt%):				
SiO_2	47.45	44.38	45.61	46.71
TiO_2	1.19	1.35	1.19	1.24
Al_2O_3	14.30	14.01	13.35	14.48
Fe_2O_3	6.34	7.24	7.62	6.77
FeO	4.30	3.37	4.44	4.76
MnO	0.09	0.14	0.18	0.19
MgO	9.22	9.56	10.40	8.79
CaO	9.81	8.16	7.23	9.76
Na_2O	2.02	2.10	2.06	2.02
K_2O	0.08	0.14	0.06	0.10
P_2O_5	0.11	0.11	0.11	0.10
LOI	4.90	9.35	7.31	5.02
Total	99.81	99.91	99.56	99.94
H_2O^+	1.19	2.68	1.87	1.33
H_2O^-	3.03	6.35	3.80	2.96
CO_2	0.36	ND	0.34	<0.2
Fe_2O_3/FeO	1.47	2.15	1.72	1.42
Density (g/cm^3)	2.58	2.26	2.30	2.50
Trace elements (ppm):				
La	4.2	4.7		
Ce	9.4	10		
Nd	7.9	ND		
Sm	2.6	2.5		
Eu	0.87	0.87		
Tb	0.65	0.51		
Yb	2.4	1.8		
Lu	0.36	0.29		
Sc	ND	46	ND	ND
Cr	180	108	166	213
Ni	77	80	76	77
Co	57	46	71	65
V	415	430	520	460
Cu	135	185	142	148
Zn	86	58	82	95
Zr	60	50	67	67
Y	21	19	18	25
Nb	4.9	4.5	3.6	3.0
Rb	<1	<1	<1	1.6
Sr	110	100	100	110
Ba	15	<10	5	74

Table T77. Secondary minerals in basalts, Ninetyeast Ridge, Leg 121: Hole 758A. (Continued on next two pages.)

Core, section, interval (cm)	Depth (mbsf)	Unit	Sm	Mixed-layer sm/chl	Chl	Carbonate	Ankerite	Zeolite	Quartz	Sulfide
121-758A-										
54R-2, 70-74[1]	491.40	1	*							
55R-1, 30-34[1]	499.20	1	*							
55R-1, 72-73[2]	499.62	1	*			*			*	
55R-2, 84-88[1]	501.24	1	*							*
55R-4, 11-15[1]	503.51	1	*							
55R-5, 31-35[1]	505.21	1	*							*
55R-5, 82-86[1]	505.72	1	*							*
55R-6, 47-48[2]	506.87	1	*			*				
56R-1, 21-23	508.61	1	+++							
56R-1, 64-68[1]	509.04	1								*
57R-3, 6-7[2]	520.96	2		*						
57R-3, 7-9	520.97	2	+++							
57R-3, 18-22[1]	521.08	2	*							*
58R-1, 41-43	527.51	2	+++							
58R-1, 86-90[1]	527.96	2	*					*		*
58R-2, 48-49[2]	529.08	2		*						
58R-3, 62-66[1]	530.72	2	*							*
58R-4, 110-111[2]	532.70	2		*		*				
58R-5, 40-44[1]	533.50	2	*							
58R-5, 55-57	533.65	2	+++							
58R-6, 21-25[1]	534.81	2	*							
58R-7, 67-71[1]	536.77	2	*							*
59R-2, 58-62[1]	538.58	2	*							*
59R-4, 108-112[1]	542.08	2	*							*
59R-5, 74-75[1]	543.24	2		*					*	
59R-6, 61-65[1]	544.61	2	*							*
60R-1, 11-13	546.01	2	+++							
60R-1, 41-45[1]	546.31	2	*					*		*
60R-1, 88-89[2]	546.78	3	*			*				
60R-1, 122-126[1]	547.12	3	*							
60R-2, 80-82	548.20	3	+++							
60R-3, 18-22[1]	549.08	3	*							*
60R-5, 53-57[1]	552.43	3	*							
60R-5, 130-134[1]	553.20	3	*		*?					
60R-6, 82-84	554.22	3	+++							
61R-2, 33-36[1]	556.93	3	*					*		
61R-2, 62-67	557.22	3	+++		+?					
61R-3, 82-83[2]	558.92	3		*					*	
61R-4, 60-64	559.43	3	+++							
61R-5, 22-26[1]	561.32	3	*					*		*
61R-7, 0-5	564.10	3	+++							
61R-7, 6-10[1]	564.16	3	*							*
62R-1, 17-21	564.47	3	+++							
62R-1, 57-59	564.87	3	+++			+				
62R-1, 108-109[2]	565.38	4					*			
62R-1, 130-134[1]	565.60	4	*			*				*
62R-2, 16-17[2]	565.96	4		*						
62R-2, 53-54[2]	566.33	4		*					*	
62R-3, 27-29	567.57	4	+++			+				
63R-1, 3-5	573.83	7	+++							

Table T77 (continued).

Core, section, interval (cm)	Depth (mbsf)	Unit	Sm	Mixed -layer sm/chl	Chl	Carbonate	Ankerite	Zeolite	Quartz	Sulfide
62R-3, 80-84[1]	568.10	5	*		*?					
62R-4, 13-17[1]	568.93	6	*							
63R-1, 11-15[1]	573.91	7	*							*
63R-2, 46-50	575.58	7	+++							
63R-3, 109-113[1]	577.89	7	*					*?		*
63R-3, 114-118[1]	577.94	7	*							*
63R-5, 48-50	580.28	7	+++							
63R-7, 107-111[1]	583.87	7	*							*
64R-2, 121-125[1]	585.91	7	*							*
64R-2, 130-135	585.78	7	+++							
64R-3, 63-67[1]	586.83	8	*					*		*
64R-4, 54-58[1]	588.24	9	*							
65R-1, 51[1]	593.21	10	*					*		*
65R-2, 10-15	594.09	10	+++							
65R-4, 58-62	597.26	10	+++							
65R-4, 62-66[1]	597.82	10	*			*				*
65R-6, 25-27	600.45	10	+++							
65R-6, 30-34[1]	600.50	10	*							
66R-1, 31-35	602.41	11	+++							
66R-1, 55-59[1]	602.65	11	*							
66R-3, 44-46	605.54	11	+++							
66R-4, 29-33[1]	606.89	11	*							
66R-5, 28-32[1]	608.38	11	*							*
66R-5, 50-55	608.09	11	+++							
66R-6, 42-46[1]	610.02	12	*							
66R-6, 95-96[2]	610.55	12		*						
67R-2, 92-96[1]	613.92	13	*							*
67R-4, 31-35[1]	616.31	14	*							
67R-4, 78-80	616.78	14	+++							
67R-5, 86-90[1]	618.36	14	*							
67R-6, 28-30	619.28	14	+++							
68R-2, 8-12[1]	622.38	16	*							*
68R-3, 106-108	624.86	17	+++							
68R-3, 122-126[1]	625.02	17	*							
69R-2, 45-47	632.15	17	+++							
69R-5, 106-110[1]	636.65	17	*					*		*
69R-5, 120-123	636.79	17	+++							
70R-1, 71-75[1]	640.11	18	*							*
70R-2, 31-32[2]	641.21	19		*						
70R-2, 129-133[1]	642.19	19	*					*		*
71R-1, 127-131[1]	649.87	20	*							*
71R-2, 90-91[2]	651.00	21		*						
71R-2, 93-94[2]	651.03	21		*					*	
71R-3, 64-68[1]	652.24	22	*							*
71R-3, 87-89	652.47	22	+++							
72R-3, 95-99[1]	661.95	25	*							
72R-4, 27-29[1]	662.77	25	*							
72R-6, 18-22[1]	665.68	26	*					*		*
73R-1, 82-86[1]	668.42	27	*							
73R-3, 50-54[1]	671.10	28	*			*				*
73R-3, 85-87	671.45	29	+++							
73R-3, 136-140	671.89	29	+++							

Table T77 (continued).

Core, section, interval (cm)	Depth (mbsf)	Unit	Sm	Mixed -layer sm/chl	Chl	Carbonate	Ankerite	Zeolite	Quartz	Sulfide
73R-4, 105-109[1]	673.08	29	*							*
73R-4, 105-110	673.08	29	+++							

Notes: +++ = dominant, ++ = minor, + = trace, * = presence (determined without quantity). Sm = smectite, Chl = chlorite. [1] = data of mineral determinations from description of thin sections (Frey et al., 1991). [2] = data of mineral determinations from XRD analyses (Peirce, Weissel, et al., 1989).

Table T78. Composition of basalts from Hole 1136A, Leg 183 (Kerguelen Plateau, Indian Ocean).

Leg	183	183	183	183	183
Hole	1136A	1136A	1136A	1136A	1136A
Core, section	15R-2	16R-1	17R-2	18R-2	19R-1
Interval (cm)	30-36	113-118	84-90	62-67	27-31
Piece	1B	5A	7	4B	4
Lab number	Z-1001	Z-1002	Z-1003	Z-1004	Z-1005
Depth (mbsf)	128.50	138.73	146.22	149.30	157.17
Unit	1	1	2	2	2
Major element oxides (wt%):					
SiO_2	46.50	47.21	48.39	48.59	48.91
TiO_2	1.84	1.93	1.79	1.90	1.82
Al_2O_3	15.14	14.23	14.40	13.98	13.90
Fe_2O_3	9.47	7.87	5.98	5.96	4.48
FeO	2.70	3.81	4.83	5.28	7.27
MnO	0.02	0.03	0.10	0.17	0.17
MgO	4.54	6.12	6.18	6.19	6.26
CaO	7.18	7.65	7.82	8.02	9.39
Na_2O	3.39	3.24	3.22	3.19	2.93
K_2O	1.19	0.34	0.52	0.22	0.24
P_2O_5	0.17	0.14	0.19	0.19	0.17
LOI	7.61	6.97	6.04	5.76	3.90
Total	99.75	99.54	99.46	99.45	99.44
H_2O^+	1.58	1.28	1.25	1.19	0.90
H_2O^-	4.71	4.77	4.06	4.02	2.69
CO_2	1.32	0.65	0.43	0.21	<0.2
Fe_2O_3/FeO	3.51	2.07	1.24	1.13	0.62
Density (g/cm^3)	2.08	2.52	2.59	2.59	2.75
Trace elements (ppm):					
La	7.7	8.4	11	10	8.7
Ce	17	19	22	21	19
Nd	12	13	16	15	14
Sm	3.9	4.1	5.1	4.5	4.4
Eu	1.4	1.4	1.7	1.6	1.5
Tb	0.93	1.0	1.3	1.1	0.97
Yb	2.1	2.3	2.9	2.9	2.7
Lu	0.34	0.39	0.49	0.45	0.46
Cr	275	215	200	185	185
Ni	62	74	61	64	56
Co	39	47	40	42	35
V	497	320	317	347	282
Cu	30	135	90	120	133
Pb	6	5	6	6	5
Zn	88	83	85	93	93
Sn	3.8	3.8	3.3	3.5	3.0
Zr	96	87	108	104	100
Y	25	28	34	29	29
Nb	5.5	5.8	6.8	7.1	6.3
Rb	31	4.9	4.7	3.8	2.6
Sr	240	220	240	240	220
Ba	62	68	86	84	49
Th	1.1	<1	1.6	1.3	2.2

Table T79. Secondary minerals in basalts from Hole 1136A identified by X-ray diffraction.

Core, section, piece, interval (cm)	Unit	Lab number	Description	XRD identification
183-1136A-				
15R-2 (1B, 30-36)	1	Z-1001-2	Vesicle filling (dark blue clay)	Iron hydromica with ~5% of swelling layers and smectite with ~15% of mica-type layers
		Z-1001-3	Vein	Calcite
16R-1 (5A, 113-118)	2	Z-1002-2	Brown clay on the open joint	Smectite
17R-2 (7, 84-90)	2	Z-1003-2	Vesicle filling (light brown clay)	Smectite and heulandite
		Z-1003-3	Black clay on the open joint	Heulandite and smectite
18R-2 (4B, 62-67)	2	Z-1004-2	Vesicle filling	Smectite

Note: XRD = X-ray diffraction.

Table T80. Composition of basalts from Hole 1137A, Leg 183 (Kerguelen Plateau, Indian Ocean). (Continued on next page.)

Leg	183	183	183	183	183	183	183
Hole	1137A	1137A	1137A	1137A	1137A	1137A	1137A
Core, section	27R-1	29R-1	29R-3	32R-3	32R-7	34R-3	39R-2
Interval (cm)	100-105	38-43	5-9	71-76	46-50	18-23	114-119
Piece	15	1B	1B	1C	1C	Tuff 1	Breccia 9
Lab number	Z-1007	Z-1008	Z-1009	Z-1010	Z-1011	Z-1012	Z-1014
Depth (mbsf)	248.60	258.46	259.95	278.77	284.18	297.07	334.64
Unit/Subunit	3	4	4	4	4	6	7
Major element oxides (wt%):							
SiO_2	47.22	49.29	47.53	48.95	48.59	47.54	51.92
TiO_2	2.66	2.83	2.13	2.03	2.49	4.51	1.75
Al_2O_3	13.79	14.43	13.59	15.60	14.44	13.09	14.15
Fe_2O_3	8.45	5.12	7.52	4.35	5.92	11.51	6.48
FeO	2.37	5	2.27	4.93	5.52	3.75	3.24
MnO	0.11	0.1	0.08	0.11	0.12	0.16	0.26
MgO	6.28	5.54	7.35	5.75	5.74	3.46	4.96
CaO	3.82	8.2	4.46	8.66	8.75	4.16	2.57
Na_2O	3.07	3.22	2.9	3.02	3.08	2.78	2.48
K_2O	2.97	0.76	2.54	0.46	0.49	4.98	5.32
P_2O_5	0.36	0.35	0.28	0.28	0.33	0.74	0.32
LOI	8.36	4.55	8.71	5.36	4.39	3.06	6.46
Total	99.46	99.39	99.36	99.50	99.86	99.74	99.91
H_2O^+	2.03	0.79	3.03	1.20	0.19	0.72	0.99
H_2O^-	5.11	3.36	4.48	3.36	3.82	2.04	4.17
CO_2	0.4	<0.2	0.84	0.29	0.33	<0.2	0.41
Fe_2O_3/FeO	3.57	1.02	3.31	0.88	1.07	3.07	2.00
Density (g/cm^3)	2.11	2.75	2.33	2.63	2.65	2.49	2.28
Trace elements (ppm):							
La	27	25	18	18	23	110	25
Ce	59	55	37	40	50	180	50
Nd	32	31	22	22	27	78	27
Sm	7.8	7.3	5.7	5.7	7.1	16	6.3
Eu	2.4	2.3	1.8	1.8	2.2	3.6	2.0
Tb	1.2	1.1	0.93	1.0	1.1	2.2	1.1
Yb	2.4	2.3	2.0	1.9	2.3	4.3	2.2
Lu	0.39	0.37	0.31	0.30	0.34	0.67	0.34
Cr	73	84	160	160	150	220	98
Ni	32	40	45	50	47	67	30
Co	34	40	37	35	37	23	23
V	290	310	230	270	307	215	302
Cu	43	52	40	47	66	56	40
Pb	7	8	6	7	7	21	8
Zn	94	125	98	83	97	83	87
Sn	3.3	3.6	3.3	3.4	3.3	4.4	2.7
Zr	240	230	170	170	200	570	180
Y	36	33	24	25	30	52	35
Nb	18	15	12	13	14	49	12
Rb	35	6.2	30	7.7	3.3	91	75
Sr	440	550	510	540	550	660	250
Ba	290	240	310	220	190	360	250
Th	4.4	2.8	2.0	2.3	3.3	8.2	4.3

Table T80 (continued).

Leg	183	183	183
Hole	1137A	1137A	1137A
Core, section	39R-3	43R-2	45R-1
Interval (cm)	6-14	84-92	121-126
Piece	2	Tuff	1
Lab number	Z-1015	Z-1016	Z-1017
Depth (mbsf)	335.06	353.89	362.91
Unit/Subunit	8A	9	10A
Major element oxides (wt%):			
SiO_2	49.20	62.55	48.34
TiO_2	1.93	0.40	1.84
Al_2O_3	15.50	13.29	14.12
Fe_2O_3	6.02	5.78	5.80
FeO	4.34	0.57	2.70
MnO	0.24	0.06	0.28
MgO	6.02	0.76	3.84
CaO	5.65	0.56	5.03
Na_2O	3.22	3.10	0.80
K_2O	2.00	3.98	8.22
P_2O_5	0.31	0.07	0.23
LOI	5.44	8.85	8.89
Total	99.87	99.97	100.09
H_2O^+	0.76	2.19	2.03
H_2O^-	4.34	5.63	3.19
CO_2	0.28	0.79	3.67
Fe_2O_3/FeO	1.39	10.14	2.15
Density (g/cm^3)	2.55	1.81	2.32
Trace elements (ppm):			
La	25	190	15
Ce	50	410	31
Nd	28	160	18
Sm	7.1	29	4.5
Eu	2.1	2.1	1.4
Tb	1.1	3.6	0.80
Yb	2.6	6.4	1.7
Lu	0.40	0.92	0.25
Cr	97	30	170
Ni	37	22	43
Co	28	13	24
V	292	98	215
Cu	55	40	59
Pb	7	33	7
Zn	92	130	77
Sn	3.0	5.1	2.5
Zr	200	620	165
Y	31	69	25
Nb	13	68	11
Rb	24	83	120
Sr	410	79	580
Ba	210	24	320
Th	3.8	27	3.1

Table T81. Secondary minerals in basalts from Hole 1137A identified by X-ray diffraction.

Core, section, piece, interval (cm)	Unit/Subunit	Lab number	Description	XRD identification
183-1137A- 25R-4 (4, 100-115)	2A	Z-1006-2	Vein	Calcite and traces of clinoptilolite and quartz
27R-1 (15, 100-115)	3A	Z-1007-2	Vesicle filling	Smectite and dickite(?)
		Z-1007-3	Vesicle filling	Calcite and smectite, and dickite(?), traces of zeolite
29R-3 (1B, 5-9)	4	Z-1009-2	Vesicle filling (dark blue clay)	Smectite
		Z-1009-3	Vesicle filling	Smectite and clinoptilolite, traces of kaolinite(?)
32R-7 (1C, 46-50)	4	Z-1011-2	Vesicle filling (black clay)	Smectite and traces of heulandite
34R-3 (1, 18-23)	6	Z-1012-2	Green matter on the contact of basalt and tuff	Mixed-layer illite-smectite mineral with mica-type layers (from 20%-50%) and traces of hydromica with ~5% of swelling layers; quartz
37R-5 (1D, 73-79)	7A	Z-1013-2	Vesicle filling (dark blue clay)	Smectite and mixed-layer smectite-chlorite mineral and traces of zeolite
		Z-1013-3	Vein	Quartz, clinoptilolite, and smectite
		Z-1013-4	Grayish-yellow patches with white matter	Smectite and clinoptilolite
39R-2 (9, 114-119)	8A	Z-1014-2	Vesicle filling (black clay)	Smectite, chlorite, and defective chlorite and traces of hydromica and quartz
		Z-1014-3	Vesicle filling and veins (blue matter)	Smectite, hydromica, chlorite, and mixed-layer chlorite-smectite mineral
39R-3 (2, 6-14)	8A	Z-1015-2	Vesicle filling (black clay)	Chlorite and smectite with ~10%-15% mica-layers
		Z-1015-3	Large 1-cm vesicle (black clay)	Smectite and traces of defective chlorite

Note: XRD = X-ray diffraction.

Table T82. Composition of basalts from Hole 1138A, Leg 183 (Kerguelen Plateau, Indian Ocean). (Continued on next page.)

Leg	183	183	183	183	183	183	183
Hole	1138A	1138A	1138A	1138A	1138A	1138A	1138A
Core, section	78R-1	80R-4	81R-1	81R-2	82R-2	82R-5	83R-4
Interval (cm)	60-64	35-40	34-39	51-57	76-81	19-23	19-24
Piece	Tuff	2A	4A	2A	9	4	1
Lab number	Z-1018	Z-1019	Z-1020	Z-1021	Z-1022	Z-1023	Z-1024
Depth (mbsf)	727.6	751.05	756.24	757.82	767.86	771.73	779.7
Unit	2	5	6	6	9	9	10
Major element oxides (wt%):							
SiO_2	56.83	46.18	48.24	46.75	52.27	47.06	47.46
TiO_2	0.86	1.99	1.91	2.11	2.08	2.32	2.19
Al_2O_3	12.19	14.48	13.39	14.19	11.25	12.75	13.03
Fe_2O_3	7.18	9.88	7.83	5.54	7.57	5.19	3.89
FeO	0.28	3.28	4.30	6.70	4.43	8.53	9.65
MnO	0.05	0.19	0.13	0.26	0.12	0.25	0.24
MgO	1.79	6.39	6.28	5.99	5.26	6.28	5.84
CaO	2.52	9.15	8.73	10.70	7.77	10.31	10.38
Na_2O	2.16	2.66	2.58	2.65	2.27	2.79	2.86
K_2O	1.00	0.23	0.85	0.39	1.57	0.19	0.21
P_2O_5	0.14	0.21	0.21	0.20	0.16	0.25	0.27
LOI	14.80	5.32	5.54	4.15	5.33	3.81	3.62
Total	99.80	99.96	99.99	99.63	100.08	99.73	99.64
H_2O^+	3.95	0.36	1.30	0.95	1.52	0.64	0.52
H_2O^-	9.96	4.49	3.90	2.83	3.55	2.86	2.62
CO_2	<0.2	<0.2	0.34	0.26	0.26	0.31	0.22
Fe_2O_3/FeO	25.64	3.01	1.82	0.83	1.71	0.61	0.40
Density (g/cm^3)	1.46	2.50	2.34	2.53	2.47	2.44	2.62
Trace elements (ppm):							
La	47	10	12	12	14	13	15
Ce	100	24	23	27	28	30	32
Nd	51	15	15	16	16	18	19
Sm	11	3.7	3.9	4.5	4.4	4.8	5.3
Eu	2.0	1.4	1.4	1.6	1.4	1.6	1.6
Tb	2.3	0.83	0.81	0.95	1.0	0.97	0.99
Yb	6.9	2.3	2.6	3.2	2.9	3.3	3.8
Lu	1.1	0.41	0.42	0.50	0.46	0.54	0.61
Cr	30	98	80	98	63	73	88
Ni	30	58	62	66	38	56	53
Co	20	41	40	48	25	48	44
V	177	370	405	530	287	440	395
Cu	59	160	145	135	140	170	170
Pb	10	<5	6	6	5	7	6
Zn	88	79	88	107	83	108	122
Sn	5.0	3.8	3.0	3.8	1.9	3.9	4.2
Zr	300	120	110	120	130	150	160
Y	54	24	30	30	32	36	40
Nb	40	9.4	9.5	10	11	12	12
Rb	40	4.2	10	4.4	23	1.9	1.4
Sr	540	210	470	205	370	220	200
Ba	100	82	89	77	88	44	35
Th	7.4	1.8	<1	1.6	<1	2.1	<1

Table T82 (continued).

Leg	183	183	183	183	183	183
Hole	1138A	1138A	1138A	1138A	1138A	1138A
Core, section	83R-5	84R-5	86R-3	87R-2	88R-2	88R-2
Interval (cm)	106-109	20-25	72-74	76-81	47-53	91-96
Piece	9	1C	8	13	2A	4
Lab number	Z-1025	Z-1026	Z-1029	Z-1031	Z-1032	Z-1033
Depth (mbsf)	781.99	790.03	807.82	815.92	825.28	825.72
Unit	11	13	17	19	21	21
Major element oxides (wt%):						
SiO_2	47.74	47.82	46.73	46.10	47.16	44.91
TiO_2	1.97	1.93	2.24	2.53	2.68	2.74
Al_2O_3	13.97	13.97	12.72	12.78	11.30	12.12
Fe_2O_3	5.41	6.65	6.55	7.17	9.87	9.54
FeO	6.60	7.41	9.30	9.50	4.80	7.84
MnO	0.12	0.32	0.34	0.47	0.26	0.33
MgO	6.28	6.08	5.56	5.79	5.71	5.86
CaO	9.66	10.34	7.45	8.60	8.39	8.04
Na_2O	2.86	2.87	4.08	2.90	2.86	2.92
K_2O	0.42	0.29	0.37	0.55	1.29	0.59
P_2O_5	0.27	0.27	0.33	0.38	0.24	0.37
LOI	3.73	2.16	4.33	3.22	10.28	4.60
Total	99.03	100.11	100.00	99.99	104.84	99.86
H_2O^+	1.29	0.30	2.33	1.06	4.96	1.54
H_2O^-	2.44	1.82	1.65	2.16	5.31	2.97
CO_2	<0.2	<0.2	<0.2	<0.2	<0.2	<0.2
Fe_2O_3/FeO	0.82	0.90	0.70	0.75	2.06	1.22
Density (g/cm^3)	2.20	2.63	2.49	2.45	1.96	2.29
Trace elements (ppm):						
La	16	16	18	26	29	35
Ce	38	41	46	54	69	81
Nd	24	24	27	34	40	49
Sm	6.5	6.0	7.6	9.7	11	13
Eu	1.9	2.0	2.4	2.8	2.6	3.2
Tb	1.2	1.1	1.4	1.5	1.7	1.9
Yb	3.4	3.2	4.1	5.0	6.0	6.1
Lu	0.56	0.51	0.63	0.79	0.94	0.93
Cr	90	64	51	35	30	30
Ni	56	49	37	38	36	38
Co	50	44	41	50	34	45
V	487	415	355	487	430	497
Cu	135	150	245	190	260	245
Pb	7	6	7	6	7	8
Zn	108	123	122	145	128	170
Sn	4.4	3.4	2.7	3.5	3.0	5.1
Zr	170	170	230	230	260	250
Y	41	39	45	50	57	58
Nb	14	13	18	20	22	19
Rb	5.2	1.1	4.5	5.4	21	7.8
Sr	260	210	190	230	610	190
Ba	56	82	46	35	160	61
Th	1.2	2.3	2.2	2.3	1.7	3.4

Table T83. Secondary minerals in basalts from Hole 1138A identified by X-ray diffraction.

Core, section, piece, interval (cm)	Unit	Lab number	Description	XRD identification
183-1138A-				
80R-4 (2A, 35-40)	5	Z-1019-2	Vesicle filling (black clay)	Smectite and traces of both heulandite(?) and serpentine(?)
81R-1 (4A, 34-39)	6	Z-1020-2	Vesicle filling (white and blue matter)	Clinoptilolite and smectite and traces of hydromica
		Z-1020-3	Vesicle filling (black matter)	Heulandite, clinoptilolite, smectite, and traces of chlorite
		Z-1020-4	Vesicle filling or veins (white matter)	Mordenite, clinoptilolite, smectite, and traces of hydromica
		Z-1020-5	Vesicle filling (black clay)	Smectite, defective chlorite, and traces of clinoptilolite and hydromica
81R-2 (2A, 51-57)	6	Z-1021-2	Vesicle filling (black clay)	Smectite, traces of chlorite and defective chlorite
82R-2 (9, 76-81)	9	Z-1022-2	Vesicle filling or veins (gray and white matter)	Smectite, clinoptilolite, and traces of quartz
82R-5 (4, 19-23)	9	Z-1023-2	Vesicle filling (black clay)	Smectite and traces of hydromica
83R-4 (1, 19-24)	10	Z-1024-2	Vesicle filling (black clay)	Smectite
83R-5 (9, 106-109)	11	Z-1025-2	Large vesicles (white matter on walls)	Clinoptilolite, traces of smectite
84R-5 (1C, 20-25)	13	Z-1026-2	Vesicle filling (black clay)	Smectite
		Z-1026-4	Vesicles filling	Smectite and clinoptilolite-heulandite
86R-1 (13, 130-137)	17	Z-1027-2	Vesicle filling	Heulandite, magnetite, Fe-Zn-spinel (?)
		Z-1027-3	Vesicle filling	Smectite, heulandite, traces of clinoptilolite, magnetite, Fe-Zn-spinel (?)
		Z-1027A	Central parts of veins and vesicles	Stilbite, heulandite-clinoptilolite
		Z-1027B	Vesicle and vein	Heulandite-clinoptilolite
		Z-1027C	Vesicle filling	Smectite, heulandite, and analcime
		Z-1027D	Vesicle filling	Analcime, clinoptilolite, smectite
86R-3 (8, 72-74)	17	Z-1029-2	Vesicle filling (black clay)	Smectite, traces of defective chlorite, serpentine (?), and natrolite (?)
87R-1 (1, 4-9)	19	Z-1030-2	Vesicle and vein (dark clay)	Smectite, heulandite, traces of magnetite, Fe-Zn-spinel (?)
		Z-1030A	Central part of vein	Analcime, stilbite, clinoptilolite, or heulandite
		Z-1030B	Vesicle filling	Clinoptilolite or heulandite, and smectite
87R-2 (13, 76-81)	19	Z-1031-2	Vesicle filling (black clay)	Smectite and traces of hydromica
88R-2 (2A, 47-53)	19	Z-1032-2	Vesicle and vein filling (dark clay)	Heulandite-clinoptilolite and smectite
88R-2 (4, 91-96)	21	Z-1033-2	Vesicle filling (blak clay)	Smectite and traces of heulandite
		Z-1033A	Vesicle filling	Heulandite-clinoptilolite and smectite

Note: XRD = X-ray diffraction.

Table T84. Composition of basalts from Hole 1140A, Leg 183 (Kerguelen Plateau, Indian Ocean). (Continued on next page.)

Leg	183	183	183	183	183	183	183
Hole	1140A	1140A	1140A	1140A	1140A	1140A	1140A
Core, section	27R-1	27R-1	27R-2	31R-1	31R-1	32R-3	32R-4
Interval (cm)	17-27	63-67	78-83	9-13	76-79	5-10	17-20
Piece	1A	4	3B	1	5	2	2
Lab number	Z-1034	Z-1035	Z-1036	Z-1037	Z-1038	Z-1039	Z-1040
Depth (mbsf)	239.47	239.93	241.49	270.59	271.26	278.25	279.83
Unit	1	1	1	2	2	3	3
Major element oxides (wt%):							
SiO_2	47.39	46.83	46.68	47.67	48.69	48.30	47.38
TiO_2	1.21	1.10	1.12	2.05	2.23	3.14	1.10
Al_2O_3	14.71	14.32	14.44	15.51	14.94	13.52	15.26
Fe_2O_3	4.83	6.36	6.12	5.61	3.93	4.42	7.83
FeO	7.16	5.92	6.02	5.37	7.13	8.32	3.25
MnO	0.05	0.18	0.16	0.18	0.17	0.13	0.10
MgO	6.48	7.10	8.15	5.45	5.84	5.43	6.57
CaO	11.79	11.76	11.16	11.11	10.82	9.51	10.56
Na_2O	2.54	2.60	2.60	2.78	3.00	3.08	2.64
K_2O	0.13	0.44	0.11	0.58	0.36	0.52	0.81
P_2O_5	0.12	0.11	0.59	0.29	0.23	0.34	0.13
LOI	2.95	2.99	2.90	2.99	2.50	2.69	4.00
Total	99.36	99.71	100.05	99.59	99.84	99.40	99.63
H_2O^+	1.36	1.02	1.39	0.91	0.87	0.93	1.65
H_2O^-	1.28	1.18	1.44	1.44	1.50	1.64	1.96
CO_2	<0.2	0.38	<0.2	<0.2	<0.2	<0.2	<0.2
Fe_2O_3/FeO	0.67	1.07	1.02	1.04	0.55	0.53	2.41
Density (g/cm^3)	2.90	2.89	2.88	2.62	2.73	2.55	2.83
Trace elements (ppm):							
La	3.8	4.1	3.7	13	14	20	4.0
Ce	8.2	11	10	32	33	49	11
Nd	8.5	10	9.0	21	21	30	8.4
Sm	3.6	3.8	3.5	5.9	5.4	8.4	2.8
Eu	1.3	1.3	1.3	2.0	2.0	2.6	1.2
Tb	0.83	0.96	0.86	0.99	1.2	1.4	0.84
Yb	2.8	2.8	2.5	2.8	2.9	3.5	2.4
Lu	0.40	0.39	0.39	0.39	0.41	0.46	0.38
Cr	265	275	295	103	150	67	270
Ni	92	84	102	49	73	46	104
Co	50	37	59	36	47	42	50
V	305	297	310	350	372	397	352
Cu	170	140	160	135	145	145	210
Pb	6	5	5	6	6	6	5
Zn	93	88	93	102	160	137	92
Sn	3.4	3.4	2.5	3.4	3.0	3.8	2.5
Zr	81	78	78	76	160	170	230
Y	29	32	29	32	33	43	26
Nb	3.6	2.7	3.6	3.0	11	13	20
Rb	<1	9.2	1.5	7.9	2.5	5.7	12
Sr	130	130	120	250	260	250	110
Ba	54	29	48	93	120	150	11
Th	<1	1.0	1.1	1.4	1.9	2.3	1.6

Table T84 (continued).

Leg	183	183	183	183	183	183	183
Hole	1140A	1140A	1140A	1140A	1140A	1140A	1140A
Core, section	34R-1	34R-3	35R-1	35R-1	36R-4	37R-1	37R-2
Interval (cm)	117-121	100-105	35-42	83-87	61-67	93-99	55-60
Piece	4D	3	2A	4	2D	1D	2A
Lab number	Z-1041	Z-1042	Z-1043	Z-1044	Z-1045	Z-1046	Z-1047
Depth (mbsf)	295.27	297.78	303.85	304.33	317.52	318.23	318.97
Unit	5	5	6	6	6	6	6
Major element oxides (wt%):							
SiO_2	47.30	47.00	47.62	48.66	48.11	49.05	48.24
TiO_2	1.15	1.11	1.35	1.30	1.18	1.23	1.07
Al_2O_3	15.40	15.88	14.82	14.30	14.10	14.93	14.53
Fe_2O_3	4.55	6.77	6.41	4.75	4.23	4.39	5.65
FeO	6.62	2.93	6.34	6.50	6.72	6.11	6.19
MnO	0.16	0.09	0.14	0.14	0.13	0.14	0.17
MgO	7.23	8.27	6.74	6.07	7.64	6.32	6.51
CaO	10.55	10.18	11.85	12.24	11.66	12.05	12.34
Na_2O	2.60	2.63	2.73	2.82	2.76	2.82	2.79
K_2O	0.08	0.36	0.45	0.51	0.11	0.11	0.16
P_2O_5	0.11	0.11	0.12	0.12	0.12	0.12	0.13
LOI	3.70	4.53	1.50	2.08	2.76	2.12	1.91
Total	99.45	99.86	100.07	99.49	99.52	99.39	99.69
H_2O^+	1.40	1.99	0.74	0.68	1.00	0.42	0.55
H_2O^-	2.26	2.25	0.67	0.60	1.72	1.58	1.04
CO_2	<0.2	<0.2	<0.2	0.61	<0.2	<0.2	<0.2
Fe_2O_3/FeO	0.69	2.31	1.01	0.73	0.63	0.72	0.91
Density (g/cm^3)	2.57	2.57	2.93	2.87	2.95	2.80	2.88
Trace elements (ppm):							
La	3.9	3.6	4.0	4.3	3.9	4.6	4.4
Ce	9.4	11	11	13	12	14	13
Nd	8.2	8.4	9.6	10	9.0	11	11
Sm	3.0	3.0	3.6	3.5	3.1	3.4	3.4
Eu	1.1	1.1	1.3	1.4	1.3	1.3	1.3
Tb	0.74	0.81	0.94	0.85	0.85	0.85	0.84
Yb	2.4	2.3	2.7	2.6	2.2	2.5	2.6
Lu	0.38	0.37	0.43	0.44	0.34	0.41	0.42
Cr	275	320	170	180	200	180	200
Ni	84	96	65	46	64	66	82
Co	62	54	49	39	54	55	64
V	377	350	317	352	337	362	372
Cu	160	155	170	165	170	185	185
Pb	5	6	6	5	6	6	5
Zn	93	91	77	100	93	97	100
Sn	3.6	3.5	3.3	3.3	3.6	3.8	3.0
Zr	72	64	77	77	75	78	76
Y	26	25	29	31	28	28	28
Nb	3.9	2.1	3.6	3.9	2.5	4.3	3.9
Rb	<1	4.9	9.0	9.3	<1	<1	1.1
Sr	110	110	120	120	130	120	120
Ba	48	27	28	37	45	29	31
Th	<1	<1	<1	1.4	1.2	<1	<1

Table T85. Secondary minerals in basalts from Hole 1140A identified by X-ray diffraction.

Core, section, piece, interval (cm)	Unit	Lab number	Description	XRD identification
183-1140A-				
27R-1 (1A, 17-27)	1	Z-1034-2	Dark green clay on the open joint	Smectite and defective chlorite
27R-1 (4, 63-67)	1	Z-1035-2	White vein in glass	Calcite
32R-3 (Piece 2, 5-10)	3	Z-1039-2	Vesicle filling (gray green clay)	Smectite
36R-4 (2D, 61-67)	6	Z-1045-2	Black clay on the open joint	Smectite and traces of serpentine(?) and quartz

Note: XRD = X-ray diffraction.

Table T86. Composition of basalts from Hole 747C, Leg 120 (Kerguelen Plateau, Indian Ocean). (Continued on next two pages.)

Leg	120	120	120	120	120	120	120
Hole	747C	747C	747C	747C	747C	747C	747C
Core, section	12R-1	12R-1	12R-2	12R-2	12R-3	12R-3	13R-1
Interval (cm)	53-56	125-127	6-9	85-87	18-22	146-148	6-10
Piece	7A	18	1	10	3A	12	1A
Lab number	Z-91	Z-629	Z-630	Z-92	Z-631	Z-93	Z-632
Depth (mbsf)	303.53	304.25	304.56	305.35	306.18	307.46	312.56
Unit	8	10	10	10	10	10	10
Major element oxides (wt%):							
SiO_2	45.79	45.00	45.80	43.82	48.16	47.94	48.90
TiO_2	2.19	1.76	1.67	1.59	1.49	1.81	1.53
Al_2O_3	18.55	15.53	14.47	14.38	14.48	15.66	14.81
Fe_2O_3	8.77	8.89	5.83	7.74	6.38	4.22	4.96
FeO	1.19	2.08	3.61	4.75	5.02	4.97	5.62
MnO	0.20	0.22	0.24	0.02	0.14	0.05	0.18
MgO	4.45	5.51	6.60	8.51	7.08	7.24	6.63
CaO	4.68	5.94	9.55	8.84	9.80	11.76	11.43
Na_2O	3.08	1.80	2.03	2.70	2.44	3.42	2.40
K_2O	1.68	1.93	0.98	0.66	0.56	0.75	0.33
P_2O_5	0.18	0.11	0.19	0.17	0.17	0.16	0.20
LOI	8.82	11.27	8.41	5.95	3.70	2.38	2.95
Total	99.58	100.04	99.38	99.13	99.42	100.36	99.94
H_2O^+	3.56	3.56	2.81	2.30	1.35	0.69	0.57
H_2O^-	5.20	5.17	3.13	3.65	1.97	1.69	1.54
CO_2	ND	1.67	2.17	ND	0.25	ND	0.40
Fe_2O_3/FeO	7.37	4.27	1.61	1.63	1.27	0.85	0.88
Density (g/cm^3)	2.11	ND	2.44	2.59	2.60	2.76	2.76
Trace elements (ppm):							
La	14	9.2	12	11	13	13	13
Ce	29	24	26	24	29	25	29
Nd	ND	14	16	ND	18	ND	18
Sm	4.5	3.4	3.9	3.8	4.4	4.2	4.3
Eu	1.6	1.2	1.3	1.4	1.4	1.5	1.3
Tb	0.79	0.62	0.79	0.68	0.93	0.80	1.00
Yb	2.1	2.0	2.0	2.2	2.5	2.2	2.5
Lu	0.28	0.33	0.29	0.34	0.37	0.36	0.36
Sc	57	ND	ND	46	ND	48	ND
Cr	400	345	285	270	245	240	245
Ni	95	76	75	80	64	85	65
Co	55	52	52	50	52	50	48
V	540	425	357	320	312	250	312
Cu	55	100	90	100	107	100	125
Pb	6	<5	7	<5	<5	<5	<5
Zn	95	72	86	95	94	95	86
Sn	ND	2.5	2.7	ND	2.5	ND	2.4
Zr	100	120	120	95	120	130	110
Y	27	19	26	30	25	27	26
Nb	11	9.2	7.9	9	6.9	8.7	9.1
Rb	29	55	21	6.3	6.1	2.7	3.6
Sr	190	120	160	230	290	280	240
Ba	120	100	110	140	120	130	120
Th	ND	<1	1.6	ND	2.5	ND	1.8

Note: ND = not determined.

Table T86 (continued).

Leg	120	120	120	120	120	120	120
Hole	747C	747C	747C	747C	747C	747C	747C
Core, section	13R-1	13R-3	14R-1	15R-1	15R-2	16R-2	16R-2
Interval (cm)	98-102	97-99	49-51	22-24	97-99	51-53	101-105
Piece	2D	10B	3C	3A	13	1D	1G
Lab number	Z-633	Z-94	Z-95	Z-96	Z-97	Z-98	Z-635
Depth (mbsf)	313.48	316.47	322.49	331.72	333.97	343.01	343.51
Unit	10	18	19	23	25	29	29
Major element oxides (wt%):							
SiO_2	47.44	44.65	45.60	44.91	44.30	46.75	47.02
TiO_2	1.57	2.29	1.86	1.26	1.53	1.25	1.06
Al_2O_3	15.45	16.87	15.29	15.78	12.79	14.34	15.80
Fe_2O_3	8.99	8.33	7.73	6.92	8.62	7.58	6.63
FeO	2.44	3.12	3.86	3.01	3.44	3.10	3.21
MnO	0.13	0.02	0.15	0.08	0.08	0.05	0.17
MgO	6.12	6.71	7.71	7.98	9.91	7.79	7.54
CaO	8.14	7.68	9.99	8.57	8.89	9.96	9.30
Na_2O	2.58	3.12	2.91	2.61	2.13	2.13	2.15
K_2O	0.79	1.22	0.84	1.22	0.89	2.09	1.50
P_2O_5	0.16	0.22	0.18	0.14	0.13	0.10	0.15
LOI	5.58	5.37	3.79	6.84	7.71	5.40	5.00
Total	99.39	99.60	99.91	99.32	100.42	100.54	99.53
H_2O^+	1.57	1.65	1.23	2.93	5.14	2.56	2.61
H_2O^-	2.90	3.72	2.56	3.91	2.57	2.84	1.93
CO_2	0.46	ND	ND	ND	ND	ND	0.39
Fe_2O_3/FeO	3.68	2.67	2.00	2.30	2.51	2.44	2.07
Density (g/cm^3)	2.54	2.50	2.60	2.55	2.55	2.59	2.57
Trace elements (ppm):							
La	13	19	17	13	10	14	13
Ce	30	35	33	27	22	30	28
Nd	19	ND	ND	ND	ND	ND	16
Sm	4.6	5.8	4.9	3.7	3.5	3.9	3.8
Eu	1.6	1.9	1.5	1.2	1.1	1.2	1.2
Tb	1.00	1.0	0.87	0.61	0.62	0.67	0.84
Yb	2.9	3.4	2.8	2.1	1.8	2.0	2.0
Lu	0.40	0.52	0.42	0.32	0.28	0.31	0.29
Sc	ND	46	46	39	40	36	ND
Cr	255	60	95	405	425	430	340
Ni	62	90	100	135	135	115	105
Co	49	60	55	55	55	40	51
V	367	240	270	175	220	165	257
Cu	140	45	60	40	45	35	52
Pb	6	<5	<5	<5	<5	<5	<5
Zn	86	115	115	90	90	80	80
Sn	2.5	ND	ND	ND	ND	ND	2.6
Zr	120	150	91	87	88	52	100
Y	29	29	26	20	22	21	22
Nb	7.9	13	10	7.6	8.2	7	6.7
Rb	9.2	13	6.4	12	11	17	13
Sr	220	250	190	210	190	160	240
Ba	110	290	210	150	110	210	130
Th	<1	ND	ND	ND	ND	ND	1.6

Table T86 (continued).

Leg	120	120	120
Hole	747C	747C	747C
Core, section	16R-4	16R-5	16R-5
Interval (cm)	14-16	0-3	105-108
Piece	1A	1A	3C
Lab number	Z-99	Z-637	Z-638
Depth (mbsf)	345.64	347.00	348.05
Unit	30	30	31
Major element oxides (wt%):			
SiO_2	45.10	47.80	47.64
TiO_2	1.36	1.18	1.09
Al_2O_3	13.36	15.88	16.02
Fe_2O_3	6.17	3.89	6.81
FeO	4.47	5.06	3.39
MnO	0.17	0.10	0.13
MgO	10.33	7.93	6.90
CaO	10.69	10.87	9.10
Na_2O	2.32	2.32	1.92
K_2O	1.36	0.44	1.90
P_2O_5	0.10	0.17	0.14
LOI	5.04	3.80	4.80
Total	100.47	99.44	99.84
H_2O^+	2.66	1.38	2.59
H_2O^-	2.38	1.90	1.73
CO_2	ND	0.38	0.46
Fe_2O_3/FeO	1.38	0.77	2.01
Density (g/cm^3)	2.67	2.67	2.60
Trace elements (ppm):			
La	14	13	12
Ce	24	29	28
Nd	ND	16	15
Sm	3.7	3.9	3.6
Eu	1.2	1.1	1.2
Tb	0.68	0.78	0.76
Yb	2.0	2.2	2.0
Lu	0.31	0.32	0.28
Sc	38	ND	ND
Cr	290	320	360
Ni	115	93	74
Co	40	51	46
V	155	220	220
Cu	80	80	52
Pb	<5	<5	<5
Zn	80	77	68
Sn	ND	2.5	2.3
Zr	92	99	98
Y	20	19	22
Nb	7.3	8.6	7.5
Rb	9.6	1.7	15
Sr	250	260	220
Ba	120	130	200
Th	ND	1.2	1.4

Table T87. Secondary minerals in basalts from Hole 747C, Kerguelen Plateau.

Core, section, interval (cm)	Depth (mbsf)	Unit	Sm	SChl	Chl	Mic	Cal	Cb	Nt	Tm	Ms	St	Hl
120-747C-													
11R-2, 112-114[1]	299.22	4	**										*
12R-1, 53-56	303.53	8	+++			+							
12R-1, 125-127	304.25	10	+++			+							
12R-2, 6-9	304.56	10	+++										
12R-2, 85-87	305.35	10	+++		+								
12R-3, 18-22	306.18	10	+++										
12R-3, 146-148	307.46	10	+++										
13R-1, 6-10	312.56	10	+++										
13R-1, 98-102	313.48	10	+++										
13R-3, 97-99	316.47	18	+++										
14R-1, 49-51	322.49	19	+++		+								
14R-1, 102-104[1]	323.02	21						*			*		
15R-1, 22-24	331.72	23	+++		++								
15R-1, 68-70[1]	332.18	23	**					*					*
15R-2, 8-9[1]	333.08	23	**				*			*			
15R-2, 97-99	333.97	25	+++		++								
15R-4, 3-6[1]	336.03	27	**					*					
16R-1, 71-75[1]	341.71	29	**							*			*
16R-2, 2-5[1]	342.52	29					*				*	*	
16R-2, 11-14	342.61	29	+++				+						
16R-2, 51-53	343.01	29	+++	++									+
16R-2, 101-105	343.51	29	+++										
16R-2, 145-148	343.95	29	+++										+
16R-3, 13-14[1]	344.13	29	**									*	
16R-3, 76-78[1]	344.76	30	**					*	*	*			
16R-3, 109-112[1]	345.09	30	**					*					
16R-4, 14-16	345.64	30	+++	++	++								
16R-5, 0-3	347.00	30	+++										
16R-5, 105-108	348.05	31	+++										

Notes: +++ = dominant, ++ = minor, + = trace, * = presence (determined without quantity), ** = determined as clays. [1] = data of mineral determinations obtained by Sevigny et al. (1992). Sm = smectite, SChl = swelling chlorite, Chl = chlorite, Mic = hydromica, Cal = calcite, Cb = chabazite, Nt = natrolite, Tm = thompsonite, Ms = mesolite, St = stilbite, Hl = heulandite.

Table T88. Characteristics of holes drilled at the Mascarene Plateau, Chagos Bank, and Maldives Ridge, Leg 115.

Hole	Latitude	Longitude	Water depth (m)	Oldest sediment cored	Basement penetration (m)	Basement recovery (m)
706C	13°06.84’S	61°22.26’E	2519.0	early Oligocene	77.4	19.7
707C	07°32.72’S	59°01.01’E	1552.3	middle Paleocene	67.6	42.18
713A	04°11.58’S	73°23.65’E	2915.3	middle Eocene	84.7	42.26
715A	05°04.89’N	73°49.88’E	2266.3	early Eocene	76.6	30.09

Table T89. Composition of basalts from Holes 706C, Leg 115 (Mascarene Plateau, West Indian Ocean). (Continued on next page.)

Leg	115	115	115	115	115	115	115
Hole	706C	706C	706C	706C	706C	706C	706C
Core, section	3R-2	4R-2	4R-3	5R-1	5R-1	5R-3	6R-1
Interval (cm)	21-23	111-113	10-13	38-40	113-115	69-71	38-40
Piece	3	15	1	2C	10	9	2
Lab number	Z-60	Z-64	Z-1320	Z-38	Z-59	Z-50	Z-54
Depth (mbsf)	55.61	66.21	66.70	73.58	74.33	76.89	83.28
Unit	12	12	13	13	14	19	20
Major element oxides (wt%):							
SiO_2	45.64	45.65	46.10	45.15	45.91	45.58	45.99
TiO_2	3.44	3.77	3.10	2.94	3.27	3.43	3.82
Al_2O_3	11.65	11.50	13.29	12.20	12.55	10.77	11.19
Fe_2O_3	9.02	7.72	6.07	8.75	5.74	8.48	8.42
FeO	7.33	8.05	7.59	7.62	7.62	8.77	7.18
MnO	0.18	0.19	0.15	0.15	0.18	0.18	0.16
MgO	4.90	4.89	5.94	5.38	7.14	4.84	5.13
CaO	9.53	10.27	9.96	9.80	10.32	8.83	9.15
Na_2O	3.04	2.89	2.87	2.98	3.04	2.79	3.04
K_2O	1.17	0.41	0.26	1.02	0.56	1.11	1.24
P_2O_5	0.38	0.38	0.31	0.34	0.35	0.32	0.41
LOI	3.44	4.20	3.50	3.14	3.61	4.77	4.43
Total	99.72	99.92	99.14	99.47	100.29	99.87	100.16
H_2O^+	1.36	1.29	0.77	0.85	0.78	2.12	1.90
H_2O^-	2.08	2.54	2.32	1.93	2.39	2.65	1.87
CO_2	ND	ND	<0.2	ND	ND	ND	ND
Fe_2O_3/FeO	1.23	0.96	0.80	1.15	0.75	0.97	1.17
Density (g/cm^3)	2.27	2.30	2.61	2.59	2.27	2.49	2.47
Trace elements (ppm):							
La	23	21		16	20	19	22
Ce	53	49		39	40	45	45
Sm	7.8	8.0		7.4	7.3	7.7	8.0
Eu	2.5	2.7		2.0	2.5	2.5	2.6
Tb	1.2	1.5		1.1	1.5	1.6	1.5
Yb	2.4	3.5		3.0	3.4	3.2	3.6
Lu	0.38	0.49		0.43	0.48	0.41	0.50
Sc	36	37	ND	37	40	49	3.8
Cr	29	26	51	41	35	29	26
Ni	58	67	52	63	64	57	48
Co	42	57	70	55	60	67	48
V	410	340	400	335	300	445	377
Cu	105	132	120	91	125	112	125
Pb	<5	<5	ND	<5	<5	<5	<5
Zn	160	127	136	94	125	160	120
Zr	230	170	200	190	220	210	220
Y	44	43	36	36	41	40	44
Nb	19	21	16	18	11	20	20
Rb	30	2.2	1.5	23	2	20	29
Sr	260	160	260	260	270	190	240
Ba	60	70	100	72	69	64	80

Note: ND = not determined.

Table T89 (continued).

Leg	115	115	115	115
Hole	706C	706C	706C	706C
Core, section	6R-1	8R-2	9R-1	9R-2
Interval (cm)	45-50	26-28	72-74	0-7
Piece	2	1C	8	1
Lab number	Z-1321	Z-39	Z-47	Z-1322
Depth (mbsf)	83.35	104.06	112.72	113.40
Unit	20	28	31	32
Major element oxides (wt%):				
SiO_2	45.99	46.10	47.60	46.82
TiO_2	3.29	2.51	1.27	1.16
Al_2O_3	12.57	13.43	16.56	15.98
Fe_2O_3	9.00	7.39	5.44	8.27
FeO	6.28	6.54	5.68	4.68
MnO	0.14	0.10	0.12	0.29
MgO	5.49	4.74	5.10	5.68
CaO	9.08	10.89	11.65	10.18
Na_2O	3.01	3.40	2.57	2.37
K_2O	1.11	1.25	0.72	0.77
P_2O_5	0.42	0.36	0.09	0.11
LOI	3.20	2.81	3.28	2.90
Total	99.58	99.52	100.08	99.21
H_2O^+	0.85	0.65	1.50	0.85
H_2O^-	1.98	1.88	1.32	1.54
CO_2	<0.2	ND	ND	<0.2
Fe_2O_3/FeO	1.43	1.13	0.96	1.77
Density (g/cm^3)	2.28	2.61	2.63	2.81
Trace elements (ppm):				
La		21	5.5	
Ce		44	10	
Sm		8.3	2.7	
Eu		2.1	0.96	
Tb		1.2	0.59	
Yb		4.0	2.1	
Lu		0.57	0.32	
Sc	ND	38	39	ND
Cr	42	82	31	53
Ni	44	74	60	71
Co	46	46	35	60
V	395	350	245	395
Cu	140	86	132	145
Pb	ND	<5	<5	ND
Zn	137	94	50	90
Zr	240	200	44	62
Y	44	43	20	22
Nb	17	19	5.2	5.9
Rb	32	35	12	18
Sr	260	250	150	140
Ba	78	85	35	33

Table T90. Composition of basalts from Hole 707C, Leg 115 (Mascarene Plateau, West Indian Ocean). (Continued on next two pages.)

Leg	115	115	115	115	115	115	115	115
Hole	707C	707C	707C	707C	707C	707C	707C	707C
Core, section	22R-1	22R-2	23R-1	23R-1	23R-4	24R-1	25R-1	25R-2
Interval (cm)	94-98	49-51	32-36	98-100	0-3	138-140	108-110	38-42
Piece	11A	3A	1C	1N	1A	6	1H	1C
Lab number	Z-1323	Z-78	Z-1325	Z-69	Z-605	Z-606	Z-70	Z-607
Depth (mbsf)	376.54	377.59	385.62	386.28	389.62	396.28	405.58	406.33
Unit	1	1	3	3	3	4	4	4
Major element oxides (wt%):								
SiO_2	46.25	46.62	47.58	47.49	47.80	49.18	47.68	48.29
TiO_2	0.82	1.04	0.62	0.80	0.62	1.38	1.75	1.33
Al_2O_3	13.35	14.15	15.81	13.78	14.21	15.29	13.86	14.61
Fe_2O_3	6.64	6.72	5.64	5.68	5.29	5.98	5.81	6.77
FeO	5.52	5.36	4.26	5.23	5.01	4.61	6.43	5.69
MnO	0.30	0.07	0.12	0.10	0.11	0.07	0.14	0.19
MgO	8.91	9.21	8.89	8.67	8.49	5.68	6.66	6.10
CaO	8.34	8.30	11.00	10.91	11.72	10.49	10.88	11.29
Na_2O	2.48	2.56	1.44	2.25	2.60	2.11	2.48	2.46
K_2O	0.15	0.28	0.07	0.20	0.42	0.08	0.17	0.19
P_2O_5	0.04	0.04	0.03	0.01	0.03	0.13	0.11	0.11
LOI	6.50	5.51	4.00	4.75	3.29	4.50	3.83	2.49
Total	99.30	99.86	99.46	99.87	99.59	99.50	99.80	99.52
H_2O^+	1.04	1.16	1.20	1.46	1.19	1.60	1.15	0.92
H_2O^-	3.69	3.59	2.14	2.86	1.75	2.39	2.31	1.40
CO_2	1.46	ND	<0.2	ND	<0.2	<0.2	ND	<0.2
Fe_2O_3/FeO	1.20	1.25	1.32	1.09	1.06	1.30	0.90	1.19
Density (g/cm^3)	2.32	2.28	2.56	2.85	2.73	2.06	2.64	2.72
Trace elements (ppm):								
La		0.96		0.69			4.7	
Ce		3.4		1.8			10	
Sm		1.6		1.3			3.6	
Eu		0.62		0.52			1.3	
Tb		0.5		0.46			0.88	
Yb		1.7		2.2			3.5	
Lu		0.26		0.36			0.52	
Sc	ND	55	ND	54	ND	ND	55	ND
Cr	168	65	280	205	187	103	76	93
Ni	98	92	147	117	106	64	80	75
Co	75	52	75	48	53	47	42	50
V	500	358	410	250	297	535	360	415
Cu	185	230	150	155	155	81	220	120
Pb	ND	<5	ND	<5	<5	<5	<5	<5
Zn	110	78	92	65	80	90	76	100
Sn	ND	ND	ND	ND	2.7	2.7	ND	3.0
Zr	34	25	26	17	26	80	54	75
Y	18	22	14	16	18	35	29	33
Nb	2.0	<1	1.4	<1	<1	4.5	4.3	4.0
Rb	<1	1.0	<1	<1	1	4.8	<1	4.2
Sr	57	47	68	51	49	92	73	91
Ba	<5	<10	<5	<10	5	10	<10	<3
Th	ND	ND	ND	ND	<1	1.4	ND	<1

Note: ND = not determined.

Table T90 (continued).

Leg	115	115	115	115	115	115	115	115
Hole	707C	707C	707C	707C	707C	707C	707C	707C
Core, section	25R-3	25R-4	25R-5	26R-1	26R-2	26R-3	26R-5	26R-7
Interval (cm)	108-111	42-45	110-114	81-86	123-125	71-73	62-65	46-48
Piece	1M	1G	1P	1N	10	1H	1L	1E
Lab number	Z-608	Z-609	Z-610	Z-611	Z-1326	Z-49	Z-612	Z-61
Depth (mbsf)	408.43	409.27	411.45	415.11	416.91	418.01	420.64	423.76
Unit	4	4	4	4	4	4	4	4
Major element oxides (wt%):								
SiO_2	47.58	47.73	47.62	48.50	48.33	48.59	47.26	47.76
TiO_2	1.32	1.35	1.30	1.26	1.47	1.76	1.33	1.67
Al_2O_3	14.10	14.54	14.55	14.31	15.20	13.37	14.41	13.12
Fe_2O_3	6.80	6.23	6.27	5.42	4.66	4.48	5.28	5.93
FeO	5.84	6.07	6.01	6.95	6.63	8.18	6.75	9.34
MnO	0.10	0.07	0.10	0.11	0.15	0.16	0.20	0.20
MgO	7.51	7.29	7.36	6.83	7.28	6.59	7.71	6.85
CaO	11.01	10.24	10.24	10.95	10.30	10.91	11.08	10.54
Na_2O	2.46	2.45	2.43	2.36	2.52	2.43	2.47	2.43
K_2O	0.12	0.10	0.09	0.08	0.11	0.16	0.09	0.20
P_2O_5	0.11	0.10	0.13	0.13	0.11	0.11	0.10	0.11
LOI	2.83	2.99	2.92	2.72	3.00	3.12	2.84	2.27
Total	99.78	99.16	99.02	99.62	99.76	99.86	99.52	100.42
H_2O^+	0.80	1.09	1.18	0.93	0.57	0.90	1.00	0.75
H_2O^-	1.50	1.55	1.52	1.41	1.57	1.87	1.72	1.52
CO_2	0.41	<0.2	<0.2	<0.2	<0.2	ND	<0.2	ND
Fe_2O_3/FeO	1.16	1.03	1.04	0.78	0.70	0.55	0.78	0.63
Density (g/cm^3)	2.54	2.90	2.68	2.80	2.70	2.61	2.97	2.88
Trace elements (ppm):								
La						4.3		4.4
Ce						10		10
Sm						3.2		3.1
Eu						1.1		1.1
Tb						0.79		0.83
Yb						3.3		3.4
Lu						0.48		0.53
Sc	ND	ND	ND	ND	ND	52	ND	51
Cr	104	90	108	86	163	86	86	89
Ni	72	65	72	68	80	85	70	83
Co	51	49	54	47	70	53	50	50
V	470	440	452	410	520	490	455	407
Cu	107	143	180	190	255	330	190	300
Pb	<5	<5	<5	<5	ND	<5	<5	<5
Zn	95	94	90	94	126	86	90	105
Sn	3.1	2.7	2.7	2.7	ND	ND	3.2	ND
Zr	76	76	74	74	75	70	77	64
Y	32	38	33	32	30	32	32	31
Nb	2.8	4.2	3.8	3.2	4.2	4.4	2.5	4.4
Rb	1	<1	<1	<1	1.0	<1	<1	1.2
Sr	98	99	93	94	100	93	95	89
Ba	6	76	<3	7	76	17	<3	23
Th	1	ND	1.7	1	ND	ND	1.2	ND

Table T90 (continued).

Leg	115	115	115	115	115	115
Hole	707C	707C	707C	707C	707C	707C
Core, section	27R-4	27R-5	27R-6	27R-7	28R-2	28R-3
Interval (cm)	46-49	32-36	29-31	32-34	53-55	133-135
Piece	2B	5	2A	5	6A	12
Lab number	Z-613	Z-614	Z-77	Z-68	Z-44	Z-58
Depth (mbsf)	428.67	429.98	431.69	433.22	435.63	437.93
Unit	4	4	4	4	5	5
Major element oxides (wt%):						
SiO_2	48.20	48.47	47.74	47.91	44.15	48.12
TiO_2	1.39	1.30	1.60	1.72	1.56	1.75
Al_2O_3	14.44	14.68	14.80	13.13	12.27	12.76
Fe_2O_3	4.97	5.16	4.25	5.16	4.83	7.06
FeO	8.24	7.09	8.69	8.26	10.28	7.34
MnO	0.21	0.08	0.20	0.18	0.14	0.16
MgO	6.27	6.05	6.47	6.15	5.78	7.14
CaO	11.51	11.54	11.81	11.58	11.78	10.30
Na_2O	2.35	2.34	2.51	2.40	2.70	2.50
K_2O	0.08	0.10	0.18	0.20	0.22	0.25
P_2O_5	0.11	0.11	0.12	0.11	0.11	0.13
LOI	1.74	2.36	1.66	2.85	6.39	2.23
Total	99.51	99.28	100.03	99.65	100.21	99.74
H_2O^+	0.56	0.84	0.39	0.90	0.82	0.76
H_2O^-	1.09	1.26	1.27	1.58	1.37	1.47
CO_2	<0.2	<0.2	ND	ND	4.20	ND
Fe_2O_3/FeO	0.60	0.73	0.49	0.62	0.47	0.96
Density (g/cm^3)	2.98	2.84	2.94	ND	2.67	2.77
Trace elements (ppm):						
La			4.4	4.2	4.5	4.9
Ce			10	10	12	12
Sm			3.2	3.1	3.4	3.3
Eu			1.2	1.2	1.1	1.1
Tb			0.93	0.80	0.77	0.73
Yb			3.6	3.4	3.1	2.4
Lu			0.56	0.53	0.39	0.34
Sc	ND	ND	52	53	48	51
Cr	90	100	74	78	52	56
Ni	68	72	78	73	82	80
Co	48	50	45	43	59	50
V	352	362	327	335	340	295
Cu	180	197	280	220	360	280
Pb	<5	<5	<5	<5	<5	<5
Zn	90	94	87	75	86	80
Sn	2.5	2.9	ND	ND	ND	ND
Zr	76	79	68	66	62	66
Y	31	33	33	32	34	30
Nb	4.0	4.0	4.7	3.1	4.2	1.9
Rb	<1	1.0	<1	<1	1.9	1.2
Sr	90	97	96	98	110	98
Ba	9	6	21	19	14	16
Th	<1	1.6	ND	ND	ND	ND

Table T91. Composition of basalts from Hole 713A, Leg 115 (Chagos Bank, West Indian Ocean). (Continued on next two pages.)

Leg	115	115	115	115	115	115	115	115
Hole	713A	713A	713A	713A	713A	713A	713A	713A
Core, section	13R-1	13R-3	14R-3	15R-1	15R-3	15R-4	15R-4	15R-5
Interval (cm)	97-99	16-20	99-101	77-79	52-57	64-69	103-105	85-87
Piece	10C	3	5	4B	2B	1	4	5
Lab number	Z-53	Z-1328	Z-74	Z-55	Z-615	Z-616	Z-1329	Z-52
Depth (mbsf)	108.67	110.78	121.19	127.47	130.17	131.57	131.96	133.55
Unit	1	2	3	3	3	3	4	5
Major element oxides (wt%):								
SiO_2	47.12	48.00	47.13	47.35	48.52	48.34	46.80	47.75
TiO_2	1.60	1.36	1.76	1.43	1.10	1.39	1.56	1.75
Al_2O_3	13.41	15.11	14.62	12.72	13.92	13.17	13.20	13.14
Fe_2O_3	3.51	4.28	5.70	5.58	3.82	5.45	9.02	5.11
FeO	8.68	6.37	5.97	7.51	6.82	7.32	7.09	8.73
MnO	0.21	0.08	0.20	0.21	0.21	0.17	0.09	0.23
MgO	7.94	7.51	7.50	8.32	8.19	7.83	6.50	6.70
CaO	12.04	11.21	12.16	11.22	11.50	10.67	9.89	11.14
Na_2O	2.43	2.55	2.92	2.37	2.34	2.41	2.72	2.57
K_2O	0.25	0.16	0.47	0.33	0.16	0.18	0.39	0.22
P_2O_5	0.11	0.10	0.14	0.10	0.13	0.13	0.16	0.13
LOI	2.83	2.80	1.77	3.15	2.88	2.54	2.32	2.76
Total	100.13	99.53	100.34	100.29	99.59	99.60	99.74	100.23
H_2O^+	0.99	0.39	0.32	1.69	0.66	0.58	0.45	1.06
H_2O^-	1.19	1.59	1.23	1.10	1.76	1.64	1.37	1.32
CO_2	ND	0.22	ND	ND	<0.20	<0.20	<0.2	ND
Fe_2O_3/FeO	0.40	0.67	0.96	0.74	0.56	0.74	1.27	0.58
Density (g/cm3)	2.50	2.74	2.75	2.84	2.72	2.72	2.64	2.77
Trace elements (ppm):								
La	4.1		5.5	3.7				4.7
Ce	10		12	9.6				12
Sm	3		4.2	2.8				3.3
Eu	1.2		1.3	1.1				1.2
Tb	0.77		0.97	0.77				0.81
Yb	3.2		4.2	3.1				3.5
Lu	0.49		0.67	0.45				0.52
Sc	49	ND	51	51	ND	ND	ND	53
Cr	183	260	150	275	235	170	175	170
Ni	90	72	100	100	74	63	72	90
Co	57	73	69	53	53	49	54	64
V	307	460	350	240	275	347	470	465
Cu	235	177	260	235	190	240	360	295
Pb	<5	ND	<5	<5	<5	<5	ND	<5
Zn	95	180	96	86	97	98	129	105
Sn	ND	ND	ND	ND	2.4	2.6	ND	ND
Zr	72	81	78	57	68	79	95	77
Y	34	29	35	30	25	29	41	38
Nb	4.4	5.1	4.5	3.8	2.9	3.6	5.4	5.1
Rb	1.0	2.2	10	2.9	3.3	3.6	7.8	1.2
Sr	95	100	91	84	91	95	91	87
Ba	18	66	29	19	7	24	55	29
Th	ND	ND	ND	ND	1.4	1	ND	ND

Note: ND = not determined.

Table T91 (continued).

Leg	115	115	115	115	115	115	115	115
Hole	713A	713A	713A	713A	713A	713A	713A	713A
Core, section	18R-1	19R-1	19R-2	19R-3	20R-1	20R-2	20R-3	20R-4
Interval (cm)	93-95	132-134	49-53	9-12	70-72	104-108	40-42	57-62
Piece	9	13	3F	2A	5A	6B	2A	1
Lab number	Z-48	Z-56	Z-617	Z-618	Z-40	Z-619	Z-37	Z-620
Depth (mbsf)	156.13	165.72	166.28	167.38	174.60	176.39	177.30	178.92
Unit	6	10	10	11	12	13	14	18
Major element oxides (wt%):								
SiO_2	47.78	48.31	48.89	48.70	47.48	48.94	47.67	48.92
TiO_2	1.20	1.16	0.97	0.88	1.10	0.97	1.11	0.89
Al_2O_3	14.24	14.44	13.51	14.99	14.80	14.19	14.66	15.15
Fe_2O_3	4.66	4.40	4.51	3.62	4.20	3.92	4.54	3.60
FeO	6.75	7.51	6.82	6.54	5.40	6.90	6.50	6.14
MnO	0.13	0.17	0.17	0.16	0.14	0.17	0.15	0.15
MgO	7.31	7.14	7.53	7.67	7.43	7.69	6.61	7.69
CaO	12.92	12.60	12.50	12.02	13.63	11.98	13.22	12.94
Na_2O	2.43	1.96	2.32	2.42	2.87	2.30	2.70	2.32
K_2O	0.55	0.33	0.44	0.37	0.21	0.32	0.17	0.08
P_2O_5	0.06	0.06	0.08	0.08	0.04	0.08	0.05	0.09
LOI	2.23	1.93	1.58	2.12	2.20	2.28	2.11	1.96
Total	100.26	100.01	99.32	99.57	99.50	99.74	99.49	99.83
H_2O^+	0.76	0.76	0.28	0.41	0.60	0.79	0.58	0.34
H_2O^-	0.96	0.80	0.94	1.24	1.60	1.29	1.18	1.20
CO_2	ND	ND	0.22	0.20	ND	<0.20	ND	0.22
Fe_2O_3/FeO	0.69	0.59	0.66	0.55	0.78	0.57	0.70	0.59
Density (g/cm3)	2.93	2.91	2.85	2.98	2.85	2.77	2.83	2.71
Trace elements (ppm):								
La	2.4	2.6			2.6		2.4	
Ce	6.3	6.4			6.5		6.4	
Sm	2.4	2.2			2.4		2.5	
Eu	0.85	0.92			0.81		0.84	
Tb	0.64	0.61			0.62		0.66	
Yb	2.4	2.6			2.4		2.8	
Lu	0.39	0.40			0.39		0.45	
Sc	52	51	ND	ND	52	ND	52	ND
Cr	98	115	155	155	105	105	103	107
Ni	74	83	56	56	125	53	96	63
Co	42	46	44	45	70	44	48	48
V	320	300	280	280	300	275	335	302
Cu	120	105	140	190	195	120	175	160
Pb	<5	<5	<5	<5	<5	<5	<5	<5
Zn	60	84	74	72	64	93	60	88
Sn	ND	ND	2.2	2.3	ND	2.3	ND	2.3
Zr	39	37	50	53	36	51	36	51
Y	24	24	23	22	23	25	28	23
Nb	2.4	2.2	2.8	2.2	2.3	2.2	3.4	2.2
Rb	6.3	6.0	11	6.6	1.7	7.2	<1	<1
Sr	95	94	96	97	100	95	91	100
Ba	15	15	25	10	<10	15	15	<3
Th	ND	ND	<1	<1	ND	1.4	ND	1

Table T91 (continued).

Leg	115	115	115	115	115	115
Hole	713A	713A	713A	713A	713A	713A
Core, section	20R-5	20R-6	21R-1	21R-2	21R-3	22R-1
Interval (cm)	65-67	103-108	73-75	61-63	83-85	34-36
Piece	5B	1C	4B	4B	4A	5
Lab number	Z-65	Z-621	Z-71	Z-75	Z-73	Z-66
Depth (mbsf)	180.55	182.38	184.03	185.41	187.13	190.54
Unit	20	23	27	31	33	35
Major element oxides (wt%):						
SiO_2	48.19	48.64	48.00	47.61	47.24	48.38
TiO_2	1.12	0.99	1.20	1.12	1.12	1.17
Al_2O_3	14.25	14.59	15.65	14.39	14.88	14.40
Fe_2O_3	3.11	3.72	4.19	4.72	4.20	4.05
FeO	7.47	6.47	6.09	7.14	6.71	7.12
MnO	0.17	0.18	0.18	0.21	0.21	0.18
MgO	7.73	7.93	7.58	7.56	7.76	7.14
CaO	11.14	12.95	12.97	13.33	13.49	12.96
Na_2O	2.48	2.27	2.57	2.61	2.37	2.10
K_2O	0.36	0.08	0.07	0.28	0.07	0.14
P_2O_5	0.06	0.08	0.06	0.09	0.06	0.06
LOI	3.37	1.85	1.58	0.93	1.35	2.05
Total	99.45	99.75	100.14	99.99	99.46	99.75
H_2O^+	1.25	0.40	0.37	0.15	0.36	0.76
H_2O^-	1.70	1.10	1.21	0.70	0.99	1.29
CO_2	ND	<0.20	ND	ND	ND	ND
Fe_2O_3/FeO	0.42	0.57	0.69	0.66	0.63	0.57
Density (g/cm3)	2.66	2.96	2.86	3.00	2.92	2.82
Trace elements (ppm):						
La	2.8		2.7	2.7	2.7	2.4
Ce	6.7		6.1	6.2	5.3	6.3
Sm	2.4		2.5	2.6	2.6	2.0
Eu	0.91		0.93	0.90	0.90	0.89
Tb	0.63		0.71	0.66	0.68	0.57
Yb	2.60		2.8	3.1	3.0	2.4
Lu	0.42		0.44	0.49	0.46	0.39
Sc	39	ND	57	53	55	52
Cr	108	107	104	79	105	104
Ni	69	64	80	72	85	89
Co	40	52	48	40	51	53
V	240	297	307	220	247	280
Cu	140	195	185	120	175	175
Pb	<5	<5	<5	<5	<5	<5
Zn	60	87	84	65	78	80
Sn	ND	2.3	ND	ND	ND	ND
Zr	38	51	41	35	37	40
Y	24	24	23	24	24	23
Nb	2.6	2.9	2.7	2.8	2.7	2.2
Rb	6.2	<1	<1	4.8	<1	<1
Sr	92	97	92	90	85	93
Ba	17	15	<10	22	<10	15
Th	ND	<1	ND	ND	ND	ND

Table T92. Composition of basalts from Hole 715A, Leg 115 (Maldives Ridge, West Indian Ocean). (Continued on next two pages.)

Leg	115	115	115	115	115	115	115	115
Hole	715A	715A	715A	715A	715A	715A	715A	715A
Core, section	23R-2	23R-3	23R-3	24R-1	24R-2	24R-2	25R-2	25R-3
Interval (cm)	28-31	62-64	91-95	76-79	13-18	30-38	80-82	0-4
Piece	2A	11	14A	11	2	3	3C	1A
Lab number	Z-622	Z-79	Z-1333	Z-623	Z-624	Z-1334	Z-63	Z-625
Depth (mbsf)	212.54	214.42	214.67	221.26	222.03	222.20	232.30	232.39
Unit/Subunit	4	7a	7a	7b	7b	7b	9	9
Major element oxides (wt%):								
SiO_2	42.40	45.20	45.80	46.86	46.64	46.95	46.32	46.08
TiO_2	3.10	2.39	2.09	2.10	1.80	2.17	1.20	0.97
Al_2O_3	13.47	15.21	13.15	13.11	12.75	13.56	14.03	14.83
Fe_2O_3	7.67	9.39	12.08	9.88	8.90	6.89	4.24	5.48
FeO	5.67	4.89	4.39	6.15	7.99	8.17	6.81	4.60
MnO	0.18	0.17	0.16	0.16	0.21	0.18	0.18	0.19
MgO	3.89	6.52	6.46	6.08	6.15	6.53	10.20	9.48
CaO	12.51	9.81	9.08	9.81	8.98	9.74	10.33	10.52
Na_2O	2.88	2.92	2.64	2.53	2.45	2.61	1.89	2.03
K_2O	0.71	1.06	0.80	0.91	0.71	0.26	0.28	0.32
P_2O_5	0.57	0.29	0.24	0.26	0.23	0.24	0.11	0.14
LOI	6.33	2.38	3.06	2.01	2.75	2.34	4.20	4.84
Total	99.38	100.23	99.95	99.86	99.56	99.64	99.79	99.48
H_2O^+	1.48	0.79	0.99	0.79	1.09	0.25	2.89	2.32
H_2O^-	1.86	1.59	1.49	1.14	1.45	1.71	1.31	2.16
CO_2	2.99	ND	<0.2	<0.2	<0.2	<0.2	ND	0.20
Fe_2O_3/FeO	1.35	1.92	2.75	1.61	1.11	0.84	0.62	1.19
Density (g/cm^3)	2.29	2.80	2.79	2.85	2.90	2.81	2.85	2.62
Trace elements (ppm):								
La		10					4.5	
Ce		21					9.8	
Sm		5.2					2.2	
Eu		1.7					0.79	
Tb		1.2					0.52	
Yb		4.3					2.1	
Lu		0.68					0.34	
Sc	ND	50	ND	ND	ND	ND	42	ND
Cr	40	69	140	73	83	142	580	370
Ni	37	80	80	61	56	87	245	225
Co	43	43	70	45	43	66	55	56
V	327	345	490	337	277	492	230	242
Cu	94	74	140	245	140	132	85	78
Pb	<5	<5	ND	<5	<5	ND	<5	<5
Zn	170	120	150	130	102	131	63	92
Sn	2.9	ND	ND	2.6	3.0	ND	ND	2.4
Zr	ND	120	120	125	110	120	50	57
Y	ND	42	39	40	35	38	20	19
Nb	ND	13	12	13	11	12	6.7	5.5
Rb	ND	43	62	65	16	2.3	1.7	5.1
Sr	ND	110	120	120	110	120	75	86
Ba	ND	81	91	49	46	110	43	19
Th	ND	ND	ND	1.8	1.5	ND	ND	<1

Note: ND = not determined.

Table T92 (continued).

Leg	115	115	115	115	115	115	115	115
Hole	715A	715A	715A	715A	715A	715A	715A	715A
Core, section	25R-5	25R-6	25R-6	26R-2	26R-3	29R-1	29R-1	29R-1
Interval (cm)	108-112	2-4	16-18	14-20	17-19	38-42	64-66	95-97
Piece	15	1	1	1A	1B	2A	2B	3A
Lab number	Z-626	Z-1335	Z-57	Z-627	Z-62	Z-1336	Z-42	Z-51
Depth (mbsf)	236.36	236.60	237.66	240.76	242.67	268.08	268.34	268.65
Unit/Subunit	10	10	10	10	10	12	12	13
Major element oxides (wt%):								
SiO_2	46.62	46.09	45.80	46.92	39.23	46.59	45.49	48.22
TiO_2	0.92	1.02	1.16	0.94	1.27	1.42	1.26	2.95
Al_2O_3	13.74	14.40	12.53	14.43	15.32	14.90	13.85	12.58
Fe_2O_3	6.07	4.00	4.68	2.53	12.05	5.76	4.61	4.83
FeO	4.45	6.88	8.00	8.26	1.08	5.42	7.13	8.98
MnO	0.15	0.17	0.18	0.21	0.23	0.16	0.15	0.20
MgO	10.38	10.80	10.95	10.78	3.03	8.92	8.85	4.91
CaO	9.93	10.18	10.22	10.36	15.86	10.60	11.74	10.20
Na_2O	2.06	1.87	1.89	1.81	2.47	2.16	2.23	3.30
K_2O	0.50	0.23	0.33	0.25	1.13	0.22	0.20	0.85
P_2O_5	0.14	0.12	0.13	0.14	0.24	0.16	0.13	0.37
LOI	4.59	3.86	4.27	3.54	7.83	3.50	3.93	2.51
Total	99.55	99.62	100.14	100.17	99.74	99.81	99.57	99.90
H_2O^+	2.10	2.50	2.82	2.16	1.88	1.52	2.12	0.79
H_2O^-	1.91	1.27	1.14	1.12	0.92	1.69	1.81	1.33
CO_2	0.20	<0.20	ND	0.26	4.80	<0.2	ND	ND
Fe_2O_3/FeO	1.36	0.58	0.58	0.31	11.16	1.06	0.65	0.54
Density (g/cm^3)	2.58	2.66	2.86	2.80	2.19	2.76	2.74	2.56
Trace elements (ppm):								
La			4.7		5.3		7.2	15.0
Ce			9.9		13		13	33
Sm			2.3		2.6		3.3	6.5
Eu			0.82		0.92		1.1	2.3
Tb			0.54		0.59		0.67	1.50
Yb			2.2		2.4		2.2	4.2
Lu			0.35		0.37		0.39	0.67
Sc	ND	ND	41	ND	44	ND	41	50
Cr	400	370	590	385	555	342	440	37
Ni	238	215	350	235	200	167	194	68
Co	57	70	67	57	55	68	57	57
V	242	265	220	225	290	337	260	525
Cu	100	79	220	94	120	120	91	85
Pb	<5	ND	<5	<5	<5	ND	<5	<5
Zn	87	96	82	79	67	98	62	205
Sn	2.9	ND	ND	2.4	ND	ND	ND	ND
Zr	57	60	40	60	45	83	59	160
Y	22	20	21	21	22	27	22	50
Nb	5.6	7.1	6.8	6.6	7.4	9.6	7.8	21.0
Rb	17	3.8	3.8	4.7	7.2	2.2	1.9	12.0
Sr	78	83	89	85	110	140	140	180
Ba	26	97	49	62	67	110	47	150
Th	1.7	ND	ND	ND	ND	ND	ND	ND

Table T92 (continued).

Leg	115	115	115	115	115	115	115	115
Hole	715A	715A	715A	715A	715A	715A	715A	715A
Core, section	29R-2	30R-2	30R-3	30R-5	30R-5	30R-5	31R-1	31R-2
Interval (cm)	80-82	1-5	28-30	30-32	39-41	98-100	103-105	98-100
Piece	1F	1	1	3	4	9	8B	6A
Lab number	Z-67	Z-628	Z-41	Z-72	Z-43	Z-46	Z-45	Z-76
Depth (mbsf)	270.00	271.48	273.98	277.00	277.09	277.68	279.23	280.68
Unit/Subunit	13	15	16	19	19	20	21	21
Major element oxides (wt%):								
SiO_2	46.47	46.69	46.18	26.20	40.50	42.86	44.27	44.70
TiO_2	1.48	1.22	1.16	1.12	1.71	1.44	1.43	1.28
Al_2O_3	13.50	14.76	11.78	10.88	15.43	13.77	13.99	15.46
Fe_2O_3	5.46	3.80	5.52	7.09	11.35	7.08	8.68	7.65
FeO	6.97	7.12	7.16	1.14	3.15	4.98	3.53	3.60
MnO	0.15	0.21	0.11	0.16	0.17	0.18	0.10	0.16
MgO	8.70	9.65	9.29	2.41	2.83	7.40	8.49	9.51
CaO	10.65	10.48	11.31	29.24	15.88	13.20	10.64	9.74
Na_2O	1.95	1.90	2.37	2.43	2.77	2.23	2.37	2.27
K_2O	0.33	0.30	0.44	0.73	0.78	0.47	0.50	0.44
P_2O_5	0.13	0.15	0.12	0.21	0.22	0.11	0.18	0.16
LOI	4.04	3.42	4.18	18.85	5.49	6.43	5.37	5.46
Total	99.83	99.70	99.62	100.46	100.28	100.15	99.55	100.43
H_2O^+	2.28	1.74	2.35	1.18	0.89	2.20	2.25	2.48
H_2O^-	1.76	1.38	1.44	0.62	0.80	1.23	3.12	2.58
CO_2	ND	0.30	ND	17.05	3.80	3.00	ND	ND
Fe_2O_3/FeO	0.78	0.53	0.78	6.22	3.60	1.42	2.46	2.12
Density (g/cm^3)	2.77	2.89	2.79	2.48	2.07	2.77	2.50	2.66
Trace elements (ppm):								
La	6.1		5.7	6.4	8.6	5.3	6.7	7.1
Ce	13		13	11	17	13	13	14
Sm	2.9		3.0	3.2	4.1	3.1	3.6	3.2
Eu	1.0		0.96	0.94	1.3	0.84	1.0	1.0
Tb	0.61		0.56	0.65	0.81	0.60	0.65	0.60
Yb	2.2		2.2	2.4	3.0	2.1	2.4	2.4
Lu	0.34		0.33	0.36	0.45	0.33	0.35	0.35
Sc	42	ND	38	35	45	40	15	39
Cr	417	350	305	196	410	295	425	355
Ni	197	180	255	76	160	235	270	290
Co	54	56	53	21	46	59	53	51
V	220	237	185	150	330	235	315	222
Cu	105	70	63	100	330	120	100	105
Pb	<5	<5	<5	<5	<5	<5	<5	<5
Zn	87	90	50	27	68	58	76	79
Sn	ND	2.8	ND	ND	ND	ND	ND	ND
Zr	58	75	47	55	78	50	69	69
Y	23	22	22	21	29	21	23	20
Nb	8.3	7.8	7.5	7.3	10	7.7	9.9	9.5
Rb	3.5	4.2	3.8	5.8	5.6	4.8	5.6	6.0
Sr	130	130	130	160	190	150	130	140
Ba	54	20	86	48	67	53	37	60
Th	ND	<1	ND	ND	ND	ND	ND	ND

Table T93. Characteristics of holes drilled at the Walvis Ridge, Leg 74.

Hole	Latitude	Longitude	Water depth (m)	Oldest sediment cored	Basement penetration (m)	Basement recovery (m)
525A	29°04.24'S	02°59.12'E	2467	early Maastrichtian	103.5	56.9
527	28°02.49'S	01°45.80'E	4428	middle Maastrichtian	43.0	32.7
528	28°31.49'S	02°19.44'E	3800	middle Maastrichtian	80.5	45.1

Table T94. Composition of basalts from Hole 525A, Leg 74 (Walvis Ridge, Atlantic Ocean). (Continued on next page.)

Leg	74	74	74	74	74	74	74	74
Hole	525A	525A	525A	525A	525A	525A	525A	525A
Core, section	53R-2	53R-3	55R-1	56R-1	56R-2	56R-3	56R-6	58R-1
Interval (cm)	87-90	36-39	107-110	43-46	121-124	108-111	81-84	106-109
Piece	5B	3	Sediment	1G	1W	1R	10	4D
Lab number	Z-398	Z-397	Z-399	Z-400	Z-401	Z-402	Z-403	Z-404
Depth (mbsf)	575.97	576.96	593.67	602.53	604.81	606.18	610.41	622.16
Unit	1	1		3	3	3	3	3
Major element oxides (wt%):								
SiO_2	53.09	48.92	62.85	39.64	49.70	48.31	48.20	44.11
TiO_2	2.57	2.33	0.95	2.49	1.24	1.30	1.27	1.25
Al_2O_3	20.67	18.58	5.21	11.60	15.56	14.60	15.58	11.69
Fe_2O_3	4.25	4.88	5.77	6.69	4.51	6.20	6.03	8.31
FeO	0.87	3.19	5.81	6.75	5.06	5.04	4.64	5.20
MnO	<0.01	0.04	0.04	0.07	0.02	0.03	0.04	0.14
MgO	1.49	1.23	2.25	3.79	4.88	4.47	4.39	1.79
CaO	8.05	9.35	1.98	12.85	9.80	9.17	9.00	13.16
Na_2O	4.39	4.06	1.16	2.96	3.25	3.29	3.63	3.29
K_2O	1.45	1.17	2.23	0.61	0.76	1.17	1.26	1.22
P_2O_5	0.31	0.11	0.25	0.20	0.31	0.30	0.25	0.28
LOI	2.65	5.74	11.05	12.11	4.60	5.55	5.02	9.81
Total	99.79	99.60	99.55	99.76	99.69	99.43	99.31	100.25
H_2O^+	1.12	1.12	3.43	1.92	2.73	1.98	1.45	1.11
H_2O^-	1.53	1.62	3.22	2.19	1.87	1.99	2.06	1.06
CO_2	ND	3.00	4.40	8.00	ND	1.58	1.51	7.64
Fe_2O_3/FeO	4.88	1.53	0.99	0.99	0.89	1.23	1.30	1.60
Density (g/cm^3)	1.82	1.99	1.71	2.41	2.46	2.47	2.52	2.48
Trace elements (ppm):								
La	23	20	27	24	24	27	29	25
Ce	45	41	46	50	48	54	59	51
Nd	27	24	29	29	28	28	30	27
Sm	6.4	5.7	5.7	6.1	6.3	6.5	6.9	6.0
Eu	2.0	1.9	1.4	2.1	2.1	2.0	2.4	1.9
Tb	1.1	1.1	1.2	1.1	1.2	1.1	1.3	1.1
Yb	2.7	2.7	2.7	2.5	2.4	2.6	2.9	2.5
Lu	0.37	0.38	0.43	0.37	0.36	0.40	0.44	0.39
Sc	ND	ND	ND	ND	36	ND	35	ND
Cr	355	320	35	25	35	15	35	45
Ni	45	75	35	25	30	20	30	50
Co	45	120	10	35	35	25	35	50
V	520	430	100	230	260	120	250	290
Cu	230	120	15	40	55	15	35	45
Pb	<5	6	<5	<5	<5	<5	<5	<5
Zn	350	185	45	65	100	55	105	90
Zr	200	180	88	190	180	190	200	180
Y	30	29	37	30	27	29	30	29
Nb	18	15	11	19	19	20	20	18
Rb	20	14	74	2.9	5.2	15	11	13
Sr	390	360	120	400	410	380	360	420
Ba	330	270	700	230	130	140	290	230
Hf	ND	ND	ND	ND	5.5	ND	5.3	ND
Ta	ND	ND	ND	ND	1.0	ND	0.9	ND
Th	ND	ND	ND	ND	1.3	ND	2.8	ND

Note: ND = not determined.

Table T94 (continued).

Leg	74	74	74	74	74	74	74
Hole	525A	525A	525A	525A	525A	525A	525A
Core, section	58R-4	59R-3	60R-1	60R-3	60R-4	61R-2	63R-2
Interval (cm)	82-85	40-42	41-44	40-43	32-35	2-5	104-107
Piece	4C	1G	1D	1H	1D	1A	4A
Lab number	Z-405	Z-406	Z-407	Z-408	Z-409	Z-410	Z-411
Depth (mbsf)	626.42	634	640.51	643.5	644.92	651.12	671.14
Unit	4	4	4	4	4	5	5
Major element oxides (wt%):							
SiO_2	49.97	49.71	49.80	41.54	48.26	45.20	50.58
TiO_2	1.25	1.44	1.24	1.33	1.28	2.40	2.39
Al_2O_3	16.95	16.46	16.72	12.15	15.95	14.31	17.16
Fe_2O_3	4.45	4.84	6.72	6.95	6.54	6.70	4.38
FeO	4.26	4.37	2.34	3.30	4.33	3.34	3.78
MnO	0.09	0.03	0.02	0.14	<0.01	0.19	0.11
MgO	4.53	4.40	3.96	2.34	4.32	3.99	3.67
CaO	8.10	8.12	8.34	15.85	7.95	9.45	7.19
Na_2O	3.46	3.46	3.46	3.13	3.46	3.56	4.21
K_2O	0.76	0.76	0.76	0.71	0.81	1.59	2.19
P_2O_5	0.28	0.29	0.25	0.21	0.66	0.42	0.42
LOI	5.14	5.63	5.82	11.87	5.77	8.72	3.56
Total	99.24	99.51	99.43	99.52	99.33	99.87	99.64
H_2O^+	2.18	2.10	2.14	1.64	2.44	5.48	1.30
H_2O^-	2.96	2.83	2.88	2.03	2.68	2.74	1.45
CO_2	ND	0.70	0.80	8.20	0.65	0.50	0.81
Fe_2O_3/FeO	1.04	1.11	2.87	2.11	1.51	2.01	1.16
Density (g/cm^3)	2.36	2.33	2.29	2.27	2.35	2.27	2.30
Trace elements (ppm):							
La	31	34	29	28	34	43	46
Ce	63	68	62	57	70	88	99
Nd	41	33	32	31	36	42	48
Sm	7.9	7.8	7.6	7.1	8.2	9.2	10
Eu	2.5	2.4	2.4	2.1	2.5	2.7	3.0
Tb	1.4	1.2	1.2	1.1	1.2	1.4	1.7
Yb	3.1	3.7	3.2	2.9	3.3	3.7	4.2
Lu	0.47	0.49	0.45	0.44	0.46	0.50	0.60
Sc	ND	ND	ND	ND	ND	26	31
Cr	30	10	35	30	35	35	45
Ni	40	40	55	40	90	20	30
Co	35	35	50	35	70	30	40
V	390	350	390	270	390	280	350
Cu	65	60	60	45	70	30	30
Pb	<5	<5	<5	<5	<5	<5	<5
Zn	140	105	110	65	100	100	110
Zr	220	210	220	190	240	290	310
Y	36	42	36	35	40	40	49
Nb	21	22	21	17	22	27	28
Rb	3.7	4.5	5.0	3.5	4.4	17	13
Sr	430	420	450	420	430	400	430
Ba	270	270	230	230	330	380	500
Hf	ND	ND	ND	ND	ND	5.5	9.4
Ta	ND	ND	ND	ND	ND	1.3	1.2
Th	ND	ND	ND	ND	ND	2.2	4.4

Table T95. Composition of basalts from Hole 527, Leg 74 (Walvis Ridge, Atlantic Ocean).

Leg	74	74	74	74	74	74	74
Hole	527	527	527	527	527	527	527
Core, section	39R-2	39R-3	40R-1	41R-3	42R-2	42R-4	44R-3
Interval (cm)	131-134	64-67	82-85	39-42	69-72	45-48	10-13
Piece	1G	1G	3F	1C	Sediment	1C	1A
Lab number	Z-412	Z-413	Z-414	Z-415	Z-416	Z-417	Z-418
Depth (mbsf)	344.31	345.14	347.32	353.89	361.69	364.45	380.6
Unit	1	1	2	3		5	5
Major element oxides (wt%):							
SiO_2	47.94	48.10	48.04	48.35	26.94	46.84	48.18
TiO_2	1.33	1.73	1.77	1.27	0.88	2.53	1.91
Al_2O_3	13.77	13.54	12.91	16.49	6.16	12.95	13.09
Fe_2O_3	11.01	6.12	6.12	3.91	5.59	8.05	8.03
FeO	3.74	7.20	7.94	6.75	0.00	6.74	6.43
MnO	0.15	0.14	0.17	0.08	1.10	0.11	0.10
MgO	6.08	6.39	6.45	5.86	1.51	6.17	5.20
CaO	9.46	10.50	10.98	12.91	26.56	6.92	9.11
Na_2O	3.02	3.02	3.02	2.82	1.63	4.48	4.00
K_2O	0.66	0.71	0.54	0.26	2.40	1.30	1.13
P_2O_5	0.02	0.07	0.12	0.04	0.02	0.29	0.17
LOI	2.85	2.13	1.78	1.26	26.64	3.72	2.76
Total	100.03	99.65	99.84	100.00	99.43	100.10	100.11
H_2O^+	1.21	0.76	0.56	0.55	3.40	1.41	0.83
H_2O^-	1.64	1.37	1.22	0.71	3.14	2.31	1.93
CO_2	ND	ND	ND	ND	20.10	ND	ND
Fe_2O_3/FeO	2.94	0.85	0.77	0.58		1.19	1.25
Density (g/cm^3)	2.77	2.80	2.90	2.96	1.88	2.64	2.65
Trace elements (ppm):							
La	13	13	12	6.7	32	28	28
Ce	26	26	24	14	60	54	52
Nd	18	18	17	10	27	27	27
Sm	4.7	4.8	4.3	2.7	5.2	6.3	5.8
Eu	1.5	1.5	1.4	1.0	1.1	2.0	1.8
Tb	1.1	1.1	1.0	0.60	0.87	1.1	1.1
Yb	4.2	4.2	3.9	2.4	2.5	3.4	3.9
Lu	0.62	0.62	0.60	0.39	0.34	0.49	0.54
Sc	ND	45	ND	40	ND	34	ND
Cr	60	70	65	80	30	20	15
Ni	55	55	60	65	70	35	35
Co	50	45	50	45	20	50	45
V	300	350	310	250	55	290	230
Cu	200	200	230	180	20	70	120
Pb	<5	<5	<5	<5	20	<5	<5
Zn	135	115	115	85	40	85	140
Zr	97	97	85	53	130	110	140
Y	40	39	37	25	27	35	35
Nb	12	12	11	6.4	17	25	25
Rb	5.9	8.5	4.7	2.5	59	18	15
Sr	140	150	140	140	420	220	240
Ba	150	140	120	68	460	320	320
Hf	ND	3.8	ND	2.1	ND	4.2	ND
Ta	ND	0.4	ND	0.5	ND	1.8	ND
Th	ND	1.2	ND	0.7	ND	2.7	ND

Note: ND = not determined

Table T96. Composition of basalts from Hole 528, Leg 74 (Walvis Ridge, Atlantic Ocean). (Continued on next page.)

Leg	74	74	74	74	74	74	74
Hole	528	528	528	528	528	528	528
Core, section	39R-2	40R-2	40R-5	42R-1	43R-2	44R-3	46R-1
Interval (cm)	7-10	24-27	76-79	32-35	85-88	94-97	130-133
Piece	1A	1B	1C	1C	1F	1E	Sediment
Lab number	Z-419	Z-420	Z-421	Z-422	Z-423	Z-424	Z-425
Depth (mbsf)	475.07	484.74	489.76	501.32	512.35	522.94	538.3
Unit	1	1	1	2	4	5	
Major element oxides (wt%):							
SiO_2	47.82	47.13	47.61	48.86	47.73	47.83	23.13
TiO_2	1.42	1.26	1.43	2.36	1.59	1.71	0.87
Al_2O_3	15.18	17.05	15.57	12.99	15.34	14.81	4.82
Fe_2O_3	4.29	4.40	4.12	8.05	5.65	6.51	5.02
FeO	5.93	5.35	5.82	5.02	5.54	5.29	0.63
MnO	0.07	0.06	0.11	0.18	0.10	0.14	0.31
MgO	7.71	6.59	6.30	5.05	5.89	5.68	2.39
CaO	11.04	12.55	12.75	5.37	12.19	10.08	31.10
Na_2O	3.53	2.70	2.76	4.95	2.94	3.53	1.75
K_2O	0.63	0.48	0.48	2.74	0.58	0.98	1.63
P_2O_5	0.09	0.09	0.08	0.30	0.09	0.09	0.06
LOI	2.53	2.31	2.46	3.87	2.66	2.95	28.86
Total	100.24	99.97	99.49	99.74	100.30	99.60	100.57
H_2O^+	1.14	1.22	1.22	1.61	0.97	1.31	2.82
H_2O^-	1.39	1.09	1.24	2.26	1.69	1.64	2.74
CO_2	ND	ND	ND	ND	ND	ND	23.30
Fe_2O_3/FeO	0.72	0.82	0.71	1.60	1.02	1.23	7.97
Density (g/cm^3)	2.76	2.83	2.82	2.48	2.75	2.68	1.78
Trace elements (ppm):							
La	12	9.9	11	51	14	22	25
Ce	23	21	22	110	29	44	48
Nd	12	12	12	48	15	22	21
Sm	3.3	3.0	3.1	8.8	3.6	5.3	3.9
Eu	1.2	0.95	1.1	2.7	1.2	1.7	0.78
Tb	0.81	0.69	0.71	1.3	0.75	0.91	0.75
Yb	2.7	2.2	2.4	4.1	2.4	3.0	2.0
Lu	0.40	0.34	0.37	0.58	0.38	0.43	0.31
Sc	ND	ND	ND	19	37	ND	ND
Cr	44	38	69	5	57	86	28
Ni	56	63	77	14	77	60	65
Co	48	43	55	39	52	48	36
V	270	140	275	267	295	325	57
Cu	205	200	155	26	200	130	17
Pb	<5	<5	<5	<5	<5	<5	6
Zn	100	67	80	120	95	105	18
Zr	81	68	80	220	81	120	120
Y	25	19	23	47	24	31	28
Nb	9.8	8.9	9.4	54	14	22	20
Rb	11	11	8.5	30	5.0	10	39
Sr	260	270	240	170	250	230	500
Ba	160	120	140	650	170	330	860
Hf	ND	ND	ND	7.4	2.5	ND	ND
Ta	ND	ND	ND	2.6	0.7	ND	ND
Th	ND	ND	ND	5.5	1.3	ND	ND

Note: ND = not determined.

Table T96 (continued).

Leg	74	74	74
Hole	528	528	528
Core, section	46R-3	46R-5	47R-3
Interval (cm)	68-70	70-74	67-70
Piece	Sediment	Sediment	3B
Lab number	Z-426	Z-427	Z-428
Depth (mbsf)	540.68	543.7	549.67
Unit			8
Major element oxides (wt%):			
SiO_2	46.90	23.13	47.74
TiO_2	1.19	0.88	2.37
Al_2O_3	11.85	3.50	15.16
Fe_2O_3	6.32	5.25	6.35
FeO	1.40	0.63	4.58
MnO	0.01	0.13	0.21
MgO	3.64	1.82	5.48
CaO	7.05	31.46	8.23
Na_2O	3.53	1.58	4.12
K_2O	2.01	1.99	1.26
P_2O_5	0.07	no	0.39
LOI	15.50	29.90	3.76
Total	99.47	100.27	99.65
H_2O^+	4.68	3.35	1.72
H_2O^-	7.32	2.45	2.04
CO_2	3.50	24.10	ND
Fe_2O_3/FeO	4.51	8.34	1.39
Density (g/cm^3)	1.33	1.76	2.50
Trace elements (ppm):			
La	52	26	29
Ce	110	45	61
Nd	46	23	30
Sm	9.1	4.7	6.7
Eu	1.8	0.85	2.2
Tb	1.7	0.84	1.2
Yb	5.6	2.4	4.0
Lu	0.88	0.38	0.60
Sc	ND	ND	36
Cr	33	20	34
Ni	29	30	45
Co	17	8	51
V	155	52	355
Cu	37	27	78
Pb	5	6	<5
Zn	90	25	110
Zr	410	<10	170
Y	55	27	39
Nb	65	17	27
Rb	32	<10	16
Sr	240	35	300
Ba	290	520	420
Hf	ND	ND	5.0
Ta	ND	ND	2.1
Th	ND	ND	2.6

Table T97. Composition of basalts from Hole 516F, Leg 72 (Rio Grande Rise, Atlantic Ocean).

Leg	72	72	72	72	72
Hole	516F	516F	516F	516F	516F
Core, section	126R-1	126R-2	127R-1	127R-3	128R-2
Interval (cm)	70-73	53-56	55-58	64-67	126-129
Piece	2I	1E	18	1G	4B
Lab number	Z-392	Z-393	Z-394	Z-395	Z-396
Depth (mbsf)	1253.30	1254.63	1258.15	1261.24	1269.36
Unit	1	1	1	1	2
Major element oxides (wt%):					
SiO_2	42.22	40.75	44.24	41.87	42.89
TiO_2	2.46	2.45	2.57	2.63	2.48
Al_2O_3	13.52	13.66	14.91	13.64	12.46
Fe_2O_3	4.22	4.21	5.58	3.88	4.87
FeO	6.00	6.66	5.87	8.73	10.35
MnO	0.18	0.10	0.13	0.10	0.07
MgO	3.60	5.21	3.73	5.52	5.40
CaO	10.98	10.57	7.92	8.95	9.24
Na_2O	3.46	3.13	2.96	3.04	2.83
K_2O	1.01	0.42	1.12	0.40	0.34
P_2O_5	0.10	0.04	0.12	0.20	0.26
Loi	12.75	13.20	10.41	11.54	8.49
Total	100.50	100.40	99.56	100.50	99.68
H_2O^+	1.40	1.13	2.46	2.10	1.54
H_2O^-	2.00	2.07	2.15	2.14	1.50
CO_2	9.35	10.00	5.80	7.30	5.45
Fe_2O_3/FeO	0.70	0.63	0.95	0.44	0.47
Density (g/cm^3)	2.27	2.44	2.40	2.59	2.84
Trace elements (ppm):					
La	19	18	21	14	15
Ce	40	36	43	31	33
Nd	30	27	30	20	22
Sm	7.4	6.4	7.9	5.6	5.8
Eu	2.2	2.0	2.3	1.9	2.0
Tb	1.7	1.4	1.6	1.1	1.2
Yb	4.0	3.5	3.2	2.8	2.9
Lu	0.59	0.52	0.48	0.43	0.45
Cr	35	45	30	30	40
Ni	40	45	55	60	45
Co	40	40	45	65	45
V	320	380	400	350	310
Cu	290	190	420	210	230
Pb	<5	<5	<5	<5	<5
Zn	110	105	110	90	105
Zr	150	180	150	170	150
Y	49	37	36	29	30
Nb	11	12	13	12	11
Rb	15	3.9	14	4.1	3.7
Sr	280	290	280	320	250
Ba	67	150	92	120	130

Table T98. Composition of igneous rocks from Hole 768C, Leg 124 (Sulu Sea, Pacific Ocean). (Continued on next five pages.)

Leg	124	124	124	124	124	124	124	124
Hole	768C	768C	768C	768C	768C	768C	768C	768C
Core, section	74R-1	75R-1	77R-2	80R-1	80R-3	81R-1	82R-1	82R-2
Interval (cm)	100-104	142-146	26-30	90-92	65-71	11-16	64-69	10-15
Piece	10B	6	1D	1L	3B	2A	6	2B
Lab number	Z-660	Z-661	Z-662	Z-124	Z-1359	Z-663	Z-1360	Z-664
Depth (mbsf)	1057.30	1067.32	1082.30	1096.50	1099.10	1100.71	1106.24	1107.15
Unit	1	1	1	1	1	X	1	1
Major element oxides (wt%):								
SiO_2	45.56	43.82	44.95	44.78	44.10	44.54	43.45	44.99
TiO_2	0.83	0.74	0.94	1.12	0.87	1.03	0.97	1.01
Al_2O_3	14.73	12.90	14.44	15.42	14.74	14.22	15.19	15.22
Fe_2O_3	7.31	7.69	7.73	7.13	7.64	6.24	8.01	7.04
FeO	1.68	2.18	1.41	1.61	1.77	2.64	2.16	1.98
MnO	0.16	0.19	0.16	0.13	0.21	0.27	0.18	0.25
MgO	8.35	10.02	9.86	9.54	10.30	10.92	9.70	9.63
CaO	9.27	9.20	6.53	6.74	6.87	7.03	7.29	7.15
Na_2O	2.14	1.93	2.34	2.40	2.12	2.31	2.33	2.14
K_2O	0.97	0.84	1.10	1.44	1.50	1.25	1.43	1.55
P_2O_5	0.15	0.15	0.17	0.18	0.16	0.14	0.16	0.20
LOI	8.45	10.24	9.97	9.05	9.29	9.06	8.63	8.40
Total	99.60	99.90	99.60	99.54	99.57	99.65	99.50	99.56
H_2O^+	1.94	2.64	3.08	3.36	3.10	2.46	2.36	2.70
H_2O^-	3.97	4.80	5.60	5.69	4.43	4.67	4.03	4.69
CO_2	1.17	1.83	1.12	ND	0.57	0.90	0.58	0.25
Fe_2O_3/FeO	4.35	3.53	5.48	4.43	4.32	2.36	3.71	3.56
Density (g/cm^3)	2.25	2.05	1.93	2.05	2.06	1.98	2.07	2.27
Trace elements (ppm):								
La				4.7	3.1		3.5	
Ce				11	8.8		10	
Nd				ND	6.9		7.2	
Sm				2.5	2.3		2.5	
Eu				1.0	0.74		0.86	
Tb				0.66	0.66		0.71	
Yb				2.8	1.4		2.0	
Lu				0.4	0.21		0.28	
Sc	ND	ND	ND	39	ND	ND	ND	ND
Cr	570	690	530	450	505	670	420	510
Ni	235	295	210	230	210	285	155	195
Co	59	67	50	40	56	61	47	47
V	390	337	405	300	400	402	412	362
Cu	49	55	45	55	70	82	56	49
Pb	<5	<5	<5	<5	ND	<5	ND	<5
Zn	68	64	70	80	74	75	85	74
Sn	2.1	2.4	2.0	ND	ND	2.2	ND	1.9
Zr	52	51	58	55	57	67	60	63
Y	21	15	29	24	19	15	19	26
Nb	2.0	2.1	2.7	2.2	2.2	2.7	1.9	2.4
Rb	10	11	11	15	16	9.8	18	15
Sr	160	140	120	120	110	100	120	110
Ba	5	6	7	<10	10	7	25	6
Th	1.2	<1	<1	ND	ND	1.1	ND	<1

Note: ND = not determined.

Table T98 (continued).

Leg	124	124	124	124	124	124	124	124
Hole	768C	768C	768C	768C	768C	768C	768C	768C
Core, section	83R-3	84R-2	87R-1	88R-1	88R-2	89R-1	89R-2	89R-3
Interval (cm)	45-50	84-87	109-112	23-27	124-126	69-70	82-86	74-76
Piece	4	2A	5J	1B	7B	3B	4B	4
Lab number	Z-1361	Z-665	Z-1362	Z-1363	Z-125	Z-1364	Z-666	Z-667
Depth (mbsf)	1113.98	1117.94	1137.39	1146.23	1148.74	1156.39	1158.02	1159.24
Unit	1	1	1	1	2	2	2	2
Major element oxides (wt%):								
SiO_2	44.35	45.07	41.80	44.80	48.72	50.30	49.46	49.39
TiO_2	0.94	0.88	0.98	1.03	1.12	0.89	1.31	1.12
Al_2O_3	15.72	14.48	14.92	14.73	16.06	15.37	14.60	16.01
Fe_2O_3	6.64	6.64	8.41	6.40	5.78	3.58	6.33	4.65
FeO	1.94	2.75	2.87	2.35	2.94	2.59	3.02	3.13
MnO	0.15	0.23	0.20	0.16	0.16	0.18	0.23	0.22
MgO	10.10	10.24	10.50	10.68	7.06	7.68	9.02	6.70
CaO	7.01	6.91	9.25	6.34	9.11	10.99	7.44	10.21
Na_2O	2.39	2.10	2.08	1.81	3.77	3.69	2.92	3.18
K_2O	0.66	1.35	0.47	0.52	0.87	0.69	1.32	0.94
P_2O_5	0.08	0.14	0.23	0.10	0.14	0.11	0.16	0.16
LOI	9.78	8.96	8.03	11.05	3.84	3.39	4.71	3.94
Total	99.76	99.75	99.74	99.97	99.57	99.46	100.52	99.65
H_2O^+	2.86	2.42	2.73	3.30	1.77	1.12	2.59	1.82
H_2O^-	4.66	4.65	3.79	5.82	2.07	1.09	1.77	1.72
CO_2	0.44	0.41	0.60	0.51	ND	0.28	0.35	0.40
Fe_2O_3/FeO	3.42	2.41	2.93	2.72	1.97	1.38	2.10	1.49
Density (g/cm^3)	2.14	2.06	2.30	2.19	2.40	2.55	2.49	2.62
Trace elements (ppm):								
La	2.5		3.6	2.3	3.9	3.0		
Ce	7.5		11.0	6.4	8.7	9.2		
Nd	6.0		8.1	6.0	ND	7.7		
Sm	2.2		2.7	2.6	2.5	2.5		
Eu	0.72		1.0	0.89	0.62	0.84		
Tb	0.50		0.72	0.79	0.61	0.74		
Yb	1.6		2.5	2.0	2.5	2.2		
Lu	0.23		0.42	0.33	0.36	0.34		
Sc	ND	ND	ND	ND	40	ND	ND	ND
Cr	570	620	445	580	205	195	77	285
Ni	257	207	218	198	110	71	66	98
Co	68	56	63	62	40	36	45	44
V	440	412	447	455	200	233	370	297
Cu	59	49	77	63	60	32	68	55
Pb	ND	<5	ND	ND	<5	ND	<5	<5
Zn	85	68	85	87	85	68	87	69
Sn	ND	2.1	ND	ND	ND	ND	2.1	2.0
Zr	64	63	64	69	59	58	77	76
Y	13	16	19	18	21	21	25	21
Nb	1.9	2.2	2.7	2.8	2.2	2.4	2.8	2.6
Rb	11	14	9	10	14	26	19	11
Sr	130	100	130	110	120	140	120	140
Ba	54	9	34	33	<10	53	8	8
Th	ND	<1	ND	ND	ND	ND	1.3	<1

Table T98 (continued).

Leg	124	124	124	124	124	124	124	124
Hole	768C	768C	768C	768C	768C	768C	768C	768C
Core, section	89R-4	90R-1	90R-6	90R-7	91R-1	92R-1	92R-2	92R-3
Interval (cm)	83-87	16-18	58-62	98-103	55-57	54-56	95-100	108-111
Piece	3A	1A	1B	5	1C	4A	1H	1E
Lab number	Z-1365	Z-126	Z-668	Z-1366	Z-127	Z-128	Z-1367	Z-1368
Depth (mbsf)	1160.45	1165.46	1172.85	1174.06	1175.45	1185.04	1186.90	1188.28
Unit	2	2	2	2	2	3	3	3
Major element oxides (wt%):								
SiO_2	49.55	49.22	50.08	50.80	48.55	45.62	43.37	42.77
TiO_2	1.48	1.28	1.13	0.91	1.12	0.95	0.71	0.68
Al_2O_3	15.38	15.55	15.86	16.49	16.08	14.18	11.54	10.20
Fe_2O_3	7.34	4.78	5.17	4.40	4.83	3.84	6.83	7.43
FeO	2.76	3.85	3.37	3.20	3.49	4.52	3.17	4.04
MnO	0.29	0.20	0.13	0.23	0.20	0.14	0.19	0.21
MgO	6.06	6.45	6.50	6.87	7.31	13.95	17.48	18.69
CaO	8.46	9.72	9.48	10.05	11.78	8.74	6.45	6.53
Na_2O	3.47	3.68	2.66	2.77	2.70	1.65	1.06	1.08
K_2O	0.79	0.71	0.92	1.22	0.45	0.11	0.09	0.11
P_2O_5	0.21	0.16	0.18	0.14	0.15	0.08	0.08	0.10
LOI	3.70	3.93	3.82	2.87	3.18	5.85	8.80	8.02
Total	99.49	99.53	99.30	99.95	99.84	99.63	99.77	99.86
H_2O^+	2.04	2.39	2.00	1.61	1.76	3.25	3.87	4.19
H_2O^-	1.28	1.54	1.26	0.89	1.42	2.60	3.36	2.46
CO_2	<0.2	ND	0.45	<0.2	ND	ND	<0.2	0.47
Fe_2O_3/FeO	2.66	1.24	1.53	1.38	1.38	0.85	2.16	1.84
Density (g/cm^3)	2.53	2.54	2.66	2.65	2.75	2.69	2.62	2.69
Trace elements (ppm):								
La		3.5			4.1	3.0		
Ce		8.6			10.0	7.2		
Nd		ND			ND	ND		
Sm		2.6			2.9	2.0		
Eu		1.0			1.0	0.65		
Tb		0.61			0.68	0.51		
Yb		2.4			2.5	2.0		
Lu		0.33			0.36	0.29		
Sc	ND	46	ND	ND	45	34	ND	ND
Cr	60	50	82	89	130	800	~1050	~1085
Ni	53	60	58	66	85	550	510	488
Co	30	35	39	32	30	65	80	73
V	340	280	265	255	210	150	192	197
Cu	53	30	55	56	40	70	48	50
Pb	ND	<5	<5	ND	<5	<5	ND	ND
Zn	77	60	69	81	65	80	80	92
Sn	ND	ND	2.0	ND	ND	ND	ND	ND
Zr	98	65	74	76	59	42	37	41
Y	30	24	22	23	22	15	14	17
Nb	3.9	2.4	2.3	3.2	2.2	1.4	1.5	1.6
Rb	9	7.9	8.0	12.0	3.8	1.2	2.6	2.4
Sr	140	120	130	130	140	120	72	68
Ba	4	<10	8	63	<10	<10	29	52
Th	ND	ND	<1	ND	ND	ND	ND	ND

Table T98 (continued).

Leg	124	124	124	124	124	124	124	124
Hole	768C	768C	768C	768C	768C	768C	768C	768C
Core, section	92R-3	92R-4	93R-1	93R-2	93R-3	93R-4	95R-1	96R-1
Interval (cm)	111-115	0-5	40-42	10-14	113-117	27-29	89-91	108-111
Piece	1E	1	2B	2C	2F	3C	8	9A
Lab number	Z-669	Z-1369	Z-129	Z-670	Z-671	Z-130	Z-131	Z-1370
Depth (mbsf)	1188.31	1188.63	1191.90	1193.10	1195.58	1196.27	1211.29	1221.08
Unit	3	3	3	3	3	3	4	4
Major element oxides (wt%):								
SiO_2	42.94	42.41	41.07	44.71	40.67	40.19	44.69	50.67
TiO_2	0.69	0.62	0.91	0.70	0.56	0.97	1.12	1.11
Al_2O_3	11.73	11.15	10.92	11.28	9.18	10.23	15.67	13.88
Fe_2O_3	5.22	6.06	6.20	4.27	6.00	6.42	5.77	5.49
FeO	4.26	4.20	2.91	5.87	3.38	3.08	2.48	3.37
MnO	0.23	0.20	0.14	0.07	0.18	0.11	0.27	0.20
MgO	18.66	18.34	16.54	15.77	18.71	16.07	9.98	7.89
CaO	6.62	6.90	7.95	7.13	8.05	9.34	7.55	6.11
Na_2O	1.14	0.93	1.28	1.13	0.76	1.13	2.40	4.44
K_2O	0.12	0.12	0.16	0.10	0.12	0.13	0.88	1.78
P_2O_5	0.10	0.08	0.10	0.12	0.09	0.09	0.17	0.14
LOI	7.79	8.88	11.37	8.70	12.07	11.81	8.54	4.74
Total	99.50	99.89	99.55	99.85	99.77	99.57	99.52	99.82
H_2O^+	4.74	3.69	5.22	4.03	6.06	4.57	3.86	2.15
H_2O^-	2.56	3.02	5.30	3.11	4.17	5.14	4.68	1.59
CO_2	<0.20	0.79	0.85	1.54	0.76	2.10	ND	0.24
Fe_2O_3/FeO	1.23	1.44	2.13	0.73	1.78	2.08	2.33	1.63
Density (g/cm^3)	2.63	2.66	2.40	2.63	2.35	2.46	2.16	1.94
Trace elements (ppm):								
La			2.4			2.2	4.9	
Ce			5.7			5.6	11.0	
Nd			ND			ND	ND	
Sm			1.6			1.5	3.3	
Eu			0.65			0.67	1.1	
Tb			0.40			0.42	0.77	
Yb			1.7			1.7	2.6	
Lu			0.24			0.24	0.36	
Sc	ND	ND	30	ND	ND	33	39	ND
Cr	830	~1225	1150	910	750	850	325	225
Ni	540	568	800	640	560	650	200	84
Co	77	82	85	104	77	75	40	39
V	205	200	155	212	190	135	240	220
Cu	59	152	35	98	27	30	40	88
Pb	<5	ND	<5	<5	<5	<5	<5	ND
Zn	87	80	80	68	68	80	70	83
Sn	2.8	ND	ND	2.5	2.6	ND	ND	ND
Zr	45	38	29	ND	34	32	65	73
Y	14	14	14	ND	12	14	20	22
Nb	1.6	2.0	1.2	ND	1.4	1.1	2.4	2.5
Rb	2.1	3.1	2.7	ND	2.9	2.4	13	15
Sr	69	70	79	ND	54	93	130	150
Ba	5	38	<10	ND	3	<10	<10	120
Th	<1	ND	ND	ND	<1	ND	ND	ND

Table T98 (continued).

Leg	124	124	124	124	124	124	124	124
Hole	768C	768C	768C	768C	768C	768C	768C	768C
Core, section	96R-2	97R-2	97R-3	98R-2	98R-3	98R-4	99R-2	99R-3
Interval (cm)	0-5	9-13	89-94	60-65	77-79	0-5	16-21	106-110
Piece	1A	1B	7A	2C	3B	1A	1D	4C
Lab number	Z-1371	Z-672	Z-673	Z-1373	Z-132	Z-1374	Z-1375	Z-1376
Depth (mbsf)	1221.42	1231.11	1233.35	1241.50	1243.17	1243.51	1250.70	1250.00
Unit	4	4	4	5	5	5	6	6
Major element oxides (wt%):								
SiO_2	48.62	45.12	47.90	47.88	46.19	44.53	47.37	46.87
TiO_2	1.20	1.06	0.96	1.09	1.12	1.11	1.10	1.05
Al_2O_3	14.26	12.61	13.64	14.75	16.85	14.92	15.97	17.03
Fe_2O_3	6.12	5.86	5.50	4.78	5.44	5.77	8.08	7.15
FeO	3.34	3.63	2.71	3.46	3.13	3.68	1.75	1.90
MnO	0.19	0.10	0.16	0.20	0.17	0.20	0.14	0.16
MgO	7.54	9.10	8.50	8.16	6.14	7.96	6.52	7.39
CaO	6.37	9.20	10.60	7.07	7.23	8.18	7.52	7.94
Na_2O	4.35	3.04	2.65	4.50	5.82	4.09	3.70	3.27
K_2O	1.74	0.66	0.81	1.26	0.96	0.88	0.75	0.64
P_2O_5	0.15	0.16	0.13	0.12	0.17	0.16	0.15	0.14
LOI	5.95	8.86	6.11	6.51	6.76	8.38	6.57	6.48
Total	99.83	99.40	99.67	99.78	99.98	99.86	99.62	100.02
H_2O^+	3.19	4.01	2.64	3.34	5.62	4.32	2.70	2.29
H_2O^-	1.58	2.68	2.72	1.55	1.14	2.02	2.74	3.18
CO_2	0.51	1.01	0.75	1.41	ND	1.73	0.50	0.63
Fe_2O_3/FeO	1.83	1.61	2.03	1.38	1.74	1.57	4.62	3.76
Density (g/cm^3)	1.93	2.20	2.48	2.21	2.13	2.10	2.18	2.22
Trace elements (ppm):								
La					4.0			
Ce					10.0			
Nd					ND			
Sm					2.8			
Eu					1.0			
Tb					0.67			
Yb					2.6			
Lu					0.36			
Sc	ND	ND	ND	ND	40	ND	ND	ND
Cr	215	470	480	196	160	205	248	262
Ni	68	230	260	81	70	80	96	134
Co	34	53	55	32	20	36	31	34
V	257	317	240	217	185	228	340	350
Cu	71	35	29	73	25	32	63	66
Pb	ND	<5	<5	ND	<5	ND	ND	ND
Zn	78	67	67	74	60	75	75	77
Sn	ND	2.2	1.9	ND	ND	ND	ND	ND
Zr	78	62	62	70	65	70	70	68
Y	25	20	20	25	22	24	32	29
Nb	2.1	2.6	1.9	1.9	2.1	2.8	1.6	2.4
Rb	15	7	4.3	14.0	7.7	14	15	11
Sr	120	100	150	160	180	130	170	150
Ba	29	7	5	95	<10	23	4	7
Th	ND	<1	<1	ND	ND	ND	ND	ND

Table T98 (continued).

Leg	124	124	124
Hole	768C	768C	768C
Core, section	99R-4	100R-1	100R-2
Interval (cm)	46-52	32-36	13-19
Piece	3	3B	2
Lab number	Z-1377	Z-1378	Z-1379
Depth (mbsf)	1253.79	1259.12	1260.43
Unit	6	7	7
Major element oxides (wt%):			
SiO_2	46.09	46.97	48.41
TiO_2	1.01	0.94	1.09
Al_2O_3	16.35	15.55	15.87
Fe_2O_3	7.12	5.94	4.85
FeO	1.94	2.99	3.10
MnO	0.15	0.15	0.20
MgO	8.71	8.74	8.13
CaO	7.75	8.34	9.34
Na_2O	2.83	3.06	3.07
K_2O	0.72	0.44	0.68
P_2O_5	0.15	0.14	0.13
LOI	6.89	6.36	4.64
Total	99.71	99.62	99.51
H_2O^+	2.88	2.32	1.58
H_2O^-	3.38	3.28	2.05
CO_2	0.50	0.36	0.46
Fe_2O_3/FeO	3.67	1.99	1.57
Density (g/cm^3)	2.38	2.34	2.40
Trace elements (ppm):			
La			3.4
Ce			11.0
Nd			9.0
Sm			3.0
Eu			1.2
Tb			0.83
Yb			2.5
Lu			0.40
Sc	ND	ND	ND
Cr	310	255	270
Ni	142	155	148
Co	44	44	52
V	410	342	372
Cu	73	45	27
Pb	ND	ND	ND
Zn	89	74	92
Sn	ND	ND	ND
Zr	65	62	72
Y	22	21	24
Nb	1.4	3.1	1.2
Rb	13	9	10
Sr	130	150	170
Ba	8	8	8
Th	ND	ND	ND

Table T99. Composition of igneous rocks from Hole 770C, Leg 124 (Celebes Sea, Pacific Ocean). (Continued on next two pages.)

Leg	124	124	124	124	124	124	124	124
Hole	770C	770C	770C	770C	770C	770C	770C	770C
Core, section	2R-3	3R-3	3R-4	4R-1	4R-2	4R-3	4R-3	5R-2
Interval (cm)	23-25	36-38	55-60	17-19	134-140	23-27	86-88	11-13
Piece	2	4B	6	3A	12E	3	9A	1A
Lab number	Z-133	Z-134	Z-1380	Z-135	Z-1381	Z-674	Z-136	Z-137
Depth (mbsf)	426.43	436.26	437.95	442.77	445.44	445.83	446.46	453.81
Unit	1	1	1	2	2	2	2	3
Major element oxides (wt%):								
SiO_2	46.66	48.14	47.71	48.25	47.92	48.17	48.11	47.86
TiO_2	2.24	2.37	2.20	1.55	1.31	1.17	1.54	1.57
Al_2O_3	15.71	15.24	15.97	16.90	17.60	17.72	16.98	18.02
Fe_2O_3	6.99	5.50	5.60	5.06	5.60	6.01	5.23	5.12
FeO	4.18	4.68	4.73	4.05	3.23	2.02	3.56	2.67
MnO	0.33	0.21	0.22	0.14	0.14	0.14	0.11	0.11
MgO	5.35	5.58	5.91	6.24	5.74	5.98	5.81	6.90
CaO	11.78	11.40	11.20	12.76	11.54	12.34	13.01	12.16
Na_2O	3.44	3.44	3.23	2.70	2.75	2.43	2.63	2.76
K_2O	0.35	0.29	0.14	0.23	0.38	0.31	0.48	0.48
P_2O_5	0.25	0.30	0.25	0.18	0.11	0.10	0.16	0.17
LOI	2.43	2.61	2.37	2.31	3.00	2.91	2.31	2.65
Total	99.71	99.76	99.53	100.37	99.32	99.30	99.93	100.47
H_2O^+	0.95	1.86	0.46	0.81	0.73	0.54	0.85	1.19
H_2O^-	1.48	0.75	1.57	1.50	1.37	1.77	1.46	1.46
CO_2	ND	ND	<0.20	ND	<0.2	0.33	ND	ND
Fe_2O_3/FeO	1.67	1.18	1.18	1.25	1.73	2.98	1.47	1.92
Density (g/cm^3)	2.76	2.66	2.73	2.80	2.65	2.72	2.76	2.80
Trace elements (ppm):								
La	9.1	9.5		3.4			2.7	3.5
Ce	23	23		9.3			7.1	7.8
Nd	ND	ND		ND			ND	ND
Sm	8.2	6.1		3.2			2.8	3.1
Eu	1.9	1.9		1.2			1.0	1.0
Tb	1.3	1.4		0.86			0.76	0.8
Yb	4.4	4.4		3.1			2.7	2.8
Lu	0.59	0.62		0.41			0.37	0.38
Sc	40	44	ND	40	ND	ND	41	41
Cr	200	210	245	335	363	260	330	300
Ni	100	110	135	140	192	72	115	180
Co	40	45	53	40	76	48	40	60
V	270	280	385	220	360	197	205	195
Cu	45	50	73	50	68	46	45	65
Pb	<5	<5	ND	<5	ND	<5	<5	<5
Zn	95	105	121	80	90	73	80	95
Sn	ND	ND	ND	ND	ND	2.0	ND	ND
Zr	170	150	170	61	69	71	42	73
Y	41	41	42	27	29	24	24	26
Nb	6.0	5.8	5.6	1.9	2.4	1.8	1.5	3.2
Rb	3.5	<1	<1	3.4	2.7	3.1	4.2	5.5
Sr	210	200	180	110	110	100	74	130
Ba	<10	46	6	<10	6	10	<10	<10
Th	ND	ND	ND	ND	ND	<1	ND	ND

Note: ND = not determined.

Table T99 (continued).

Leg	124	124	124	124	124	124	124	124
Hole	770C	770C	770C	770C	770C	770C	770C	770C
Core, section	5R-3	5R-5	5R-6	6R-1	6R-1	6R-4	7R-1	7R-1
Interval (cm)	89-91	34-38	106-108	67-71	73-77	96-98	93-100	107-112
Piece	3B	2	5	1D	1D	6A	9A	9B
Lab number	Z-138	Z-675	Z-139	Z-676	Z-140	Z-141	Z-1385	Z-1386
Depth (mbsf)	456.09	457.42	460.76	462.57	462.63	467.36	472.43	472.57
Unit	3	3	3	4	4	4	4	4
Major element oxides (wt%):								
SiO_2	47.21	47.52	45.88	47.48	47.68	48.08	45.66	47.18
TiO_2	1.40	1.41	1.53	1.57	1.53	1.56	1.55	1.57
Al_2O_3	16.13	15.70	15.06	16.94	15.94	18.12	14.86	15.16
Fe_2O_3	6.02	6.27	4.92	8.10	5.11	3.52	8.27	7.67
FeO	3.05	2.56	3.91	0.76	3.37	3.38	3.05	3.30
MnO	0.11	0.16	0.14	0.15	0.14	0.11	0.15	0.13
MgO	7.69	7.04	6.99	6.33	6.14	5.50	5.09	6.06
CaO	11.80	12.22	13.22	12.13	12.57	12.96	13.44	11.65
Na_2O	2.70	2.43	2.82	2.67	3.12	3.00	2.72	2.80
K_2O	0.41	0.36	0.48	0.38	0.48	0.41	0.63	0.48
P_2O_5	0.21	0.13	0.25	0.15	0.21	0.20	0.18	0.13
LOI	2.98	3.83	4.79	3.20	3.56	2.63	4.50	3.43
Total	99.71	99.63	99.99	99.86	99.85	99.47	100.10	99.56
H_2O^+	1.34	1.25	2.14	0.95	1.93	1.05	1.54	1.05
H_2O^-	1.64	1.51	1.29	1.65	1.63	1.58	0.96	1.40
CO_2	ND	1.07	ND	0.26	ND	ND	2.00	0.87
Fe_2O_3/FeO	1.97	2.45	1.26	10.66	1.52	1.04	2.71	2.32
Density (g/cm^3)	2.78	2.62	2.75	2.71	2.73	2.75	2.62	2.65
Trace elements (ppm):								
La	3.3		4.5		4.5	4.3		
Ce	8.8		11		11	11		
Nd	ND		ND		ND	ND		
Sm	3.0		3.9		3.7	3.7		
Eu	1.1		1.3		1.3	1.3		
Tb	0.78		0.9		0.88	0.97		
Yb	2.9		3.2		3.3	3.4		
Lu	0.4		0.46		0.47	0.5		
Sc	40	ND	43	ND	41	41	ND	ND
Cr	285	265	255	230	235	280	317	315
Ni	120	155	135	102	95	105	124	122
Co	45	56	45	50	35	50	45	54
V	175	230	180	221	170	195	358	360
Cu	65	81	65	80	55	60	39	39
Pb	<5	<5	<5	<5	<5	<5	ND	ND
Zn	80	80	75	78	80	80	86	114
Sn	ND	2.5	ND	2.9	ND	ND	ND	ND
Zr	88	79	79	89	81	93	93	95
Y	26	28	28	30	31	30	32	31
Nb	3.0	2.5	3.3	2.9	3.5	3.5	3.3	3.1
Rb	4.3	8.3	4.8	8.0	5.2	5.8	9.2	8.0
Sr	140	120	110	150	150	170	120	130
Ba	<10	10	<10	10	<10	<10	6	7
Th	ND	<1	ND	1.5	ND	ND	ND	ND

Table T99 (continued).

Leg	124	124	124	124	124	124	124
Hole	770C	770C	770C	770C	770C	770C	770C
Core, section	7R-3	9R-2	10R-2	11R-1	12R-1	12R-2	12R-3
Interval (cm)	61-63	53-55	110-112	98-100	11-13	79-84	140-142
Piece	2A	5B	3D	7F	1	3C	13
Lab number	Z-142	Z-143	Z-144	Z-145	Z-146	Z-1387	Z-147
Depth (mbsf)	475.11	492.83	503.10	511.18	520.01	522.02	524.30
Unit	5	6	7	7	8	8	9
Major element oxides (wt%):							
SiO_2	47.93	48.00	48.77	49.49	46.72	46.86	47.91
TiO_2	1.58	1.85	1.86	2.20	1.73	1.37	1.54
Al_2O_3	16.34	14.85	14.90	14.88	13.83	14.31	15.93
Fe_2O_3	5.04	5.79	5.66	4.26	7.91	7.39	4.85
FeO	3.28	3.64	3.93	4.55	4.18	4.13	4.04
MnO	0.11	0.21	0.21	0.13	0.13	0.08	0.11
MgO	5.72	5.77	6.75	6.30	7.43	7.51	7.05
CaO	12.85	11.72	11.89	12.05	11.65	10.95	12.20
Na_2O	2.88	3.24	3.30	3.41	2.70	2.43	2.76
K_2O	0.51	0.46	0.41	0.33	0.43	0.26	0.43
P_2O_5	0.24	0.10	0.25	0.18	0.11	0.12	0.06
LOI	3.19	3.99	2.16	2.16	3.37	3.80	3.56
Total	99.67	99.62	100.09	99.94	100.19	99.21	100.44
H_2O^+	1.11	1.04	0.64	0.80	1.90	1.54	1.02
H_2O^-	2.08	1.65	1.52	1.36	0.97	0.87	1.74
CO_2	ND	1.30	ND	ND	0.50	0.72	0.80
Fe_2O_3/FeO	1.54	1.59	1.44	0.94	1.89	1.79	1.20
Density (g/cm^3)	2.67	2.76	2.79	2.72	2.87	2.83	2.76
Trace elements (ppm):							
La	3.7	7.1	6.8	6.6	4.2	3.4	3.7
Ce	9.9	16	17	17	11	9.5	9.9
Nd	ND	ND	ND	ND	ND	8.6	ND
Sm	3.5	4.9	4.5	4.4	3.3	3.3	3.0
Eu	1.2	1.3	1.6	1.6	1.1	1.1	1.0
Tb	0.84	1.0	1.1	0.98	0.8	0.9	0.76
Yb	3.2	4.0	4.2	4.0	3.0	2.9	2.9
Lu	0.48	0.61	0.61	0.63	0.46	0.50	0.46
Sc	43	43	44	47	43	ND	42
Cr	310	225	190	185	310	392	315
Ni	95	125	120	120	165	170	120
Co	55	50	60	60	50	60	55
V	250	230	210	280	220	312	200
Cu	60	35	25	55	45	88	55
Pb	<5	<5	<5	<5	<5	ND	<5
Zn	85	95	95	90	85	77	90
Sn	ND	ND	ND	ND	ND	ND	ND
Zr	100	160	140	160	86	78	74
Y	30	36	39	36	32	28	28
Nb	3.9	4.3	5.1	4.7	3.5	2.1	2.8
Rb	5.1	4.5	3.6	1.2	9.6	4.4	5.9
Sr	150	210	180	190	110	98	110
Ba	<10	<10	<10	<10	<10	7	<10
Th	ND	ND	ND	ND	ND	ND	ND

Table T100. Characteristics of holes drilled in the Izu-Bonin-Mariana region, Legs 59, 60, 125, and 126.

Hole	Latitude	Longitude	Water depth (m)	Oldest sediment cored	Basement penetration (m)	Basement recovery (m)
Leg 125						
779A	19°30.75'N	146°41.75'E	3947.2	early Pliocene(?) to late Miocene(?)	306.6	65.38
780C	19°32.53'N	146°39.21'E	3083.4	middle Pleistocene(?)	149.5	8.39
786B	31°52.45'N	141°13.59'E	3071.0	early Eocene	659.1	190.07
Leg 126						
791B	30°54.98'N	139°52.19'E	2268.5	Quaternary	315.4	28.4
792E	32°23.96'N	140°22.79'E	1787.7	late Oligocene	81.9	13.1
793B	31°06.33'N	140°53.27'E	2964.8	early Oligocene	278.1	91.8
Leg 59						
447A	18°00.88'N	133°17.37'E	6022	middle Oligocene	296.5	177.9
448	16°20.46'N	134°52.45'E	3483	middle Oligocene	265	68.7
448A	16°20.46'N	134°52.45'E	3483	middle Oligocene	594.5	168.3
449	18°01.84'N	136°32.19'E	4712	late Oligocene	40.5	6.9
Leg 60						
453	17°54.42'N	143°40.95'E	4693	earliest Pliocene	149.5	33.3
454A	18°00.78'N	144°31.92'E	3816	early Pleistocene	104.5	19.95
458	17°51.85'N	146°56.06'E	3453	early Oligocene	208.9	34.98
459B	17°51.75'N	147°18.09'E	4121	pre-late Eocene	132.5	23.94

Table T101. Composition of igneous rocks from Hole 779A, Leg 125 (Conical Seamounts, Mariana Trench Region). (Continued on next two pages.)

Leg	125	125	125	125	125	125	125
Hole	779A	779A	779A	779A	779A	779A	779A
Core, section	9R-2	11R-1	12R-1	14R-1	16R-2	17R-1	17R-3
Interval (cm)	39-41	82-86	45-49	20-22	109-111	106-110	70-72
Piece	4A	11	7	1B	11	14	8B
Lab number	Z-191	Z-677	Z-678	Z-192	Z-193	Z-679	Z-194
Depth (mbsf)	69.99	88.12	97.35	116.40	138.09	146.26	148.90
Unit	2	2	2	2	2	2	2
Major element oxides (wt%):							
SiO_2	35.67	36.93	35.33	40.88	38.33	39.13	38.07
TiO_2	0.10	<0.10	<0.10	0.17	0.16	<0.10	0.10
Al_2O_3	0.26	0.73	0.91	0.54	0.29	1.00	0.20
Fe_2O_3	6.14	6.26	6.38	5.76	7.76	5.23	6.33
FeO	1.62	1.57	0.69	2.51	1.07	2.11	1.44
MnO	0.16	0.16	0.17	0.18	0.16	0.20	0.16
MgO	41.84	37.10	38.20	43.32	40.72	42.20	42.15
CaO	0.64	1.40	0.89	0.71	0.64	0.98	0.57
Na_2O	0.09	0.11	0.11	0.09	0.17	0.09	0.09
K_2O	0.03	0.03	0.02	0.05	0.08	0.03	0.05
P_2O_5	0.01	<0.01	<0.01	0.01	0.01	<0.01	0.01
LOI	13.47	15.20	16.59	5.89	10.88	8.53	11.17
Total	100.03	99.49	99.29	100.11	100.27	99.50	100.34
H_2O^+	12.19	13.43	13.71	5.05	9.63	7.28	9.60
H_2O^-	1.07	1.36	1.86	0.62	1.22	0.57	1.26
CO_2	ND	<0.20	0.82	ND	ND	<0.20	ND
Fe_2O_3/FeO	3.79	3.99	9.25	2.30	7.25	2.48	4.40
Density (g/cm^3)	2.67	2.52	2.51	2.94	2.71	2.83	2.76
Trace elements (ppm):							
La	0.03			0.02	0.03		0.05
Ce	<0.3			ND	<0.3		<0.3
Nd	ND			ND	ND		ND
Sm	0.006			0.006	0.013		0.005
Eu	<0.003			<0.003	<0.007		<0.003
Gd	ND			ND	ND		ND
Tb	<0.01			<0.005	<0.01		<0.01
Tm	ND			ND	ND		ND
Yb	0.02			0.05	0.03		0.02
Lu	<0.006			0.006	0.004		<0.005
Sc	6.7	ND	ND	9.4	10.0	ND	7.0
Cr	1800	880	>1000	2050	2300	>1000	2100
Ni	1850	820	860	1800	2000	920	2300
Co	88	130	125	88	95	128	120
V	22	94	93	25	25	90	29
Cu	<5	16	15	20	11	19	<5
Pb	<5	<5	<5	<5	<5	<5	<5
Zn	26	54	55	30	22	59	25
Sn	ND	2.6	2.4	ND	ND	2.5	ND
Zr	<10	<1	<1	<10	<10	<1	<10
Y	<1	1.2	<1	<1	<1	<1	<1
Nb	<1	<1	<1	<1	<1	<1	<1
Rb	<1	1.5	<1	<1	<1	1.6	<1
Sr	10	8	19	<10	10	<1	<10
Ba	<5	<3	3	<5	<5	<3	<5
Th	ND	<1	<1	ND	ND	<1	ND

Note: ND = not determined.

Table T101 (continued).

Leg	125	125	125	125	125	125	125
Hole	779A	779A	779A	779A	779A	779A	779A
Core, section	22R-3	22R-3	24R-1	26R-2	29R-2	31R-2	31R-3
Interval (cm)	17-21	17-21	27-29	53-55	0-5	87-89	30-33
Piece	2	2	5	2A	20	11A	4
Lab number	Z-680	Z-195	Z-681	Z-196	Z-197	Z-198	Z-682
Depth (mbsf)	173.27	173.27	187.47	208.53	237.00	257.07	257.93
Unit	2	2	2	2	2	2	2
Major element oxides (wt%):							
SiO_2	25.66		36.64	39.51	33.48	37.22	37.53
TiO_2	<0.10		<0.10	0.16	0.05	1.76	1.72
Al_2O_3	1.02		1.35	0.42	0.49	13.90	13.51
Fe_2O_3	9.38		5.80	5.73	7.05	5.21	3.24
FeO	0.21		0.91	2.33	0.43	8.62	10.48
MnO	0.24		0.22	0.16	0.15	0.21	0.16
MgO	41.03		38.49	41.57	39.33	6.92	8.27
CaO	0.44		0.70	0.77	0.57	21.16	19.33
Na_2O	0.14		0.13	0.09	0.09	0.26	0.14
K_2O	0.02		0.03	0.05	0.05	0.05	0.01
P_2O_5	<0.01		<0.01	0.01	0.01	0.02	0.14
LOI	21.50		15.12	9.18	18.15	5.29	4.87
Total	99.64		99.39	99.98	99.85	100.62	99.40
H_2O^+	17.97		12.49	8.17	14.31	4.79	4.46
H_2O^-	1.91		1.79	0.78	3.11	0.50	0.27
CO_2	1.50		0.43	ND	0.50	ND	<0.20
Fe_2O_3/FeO	44.67		6.37	2.46	16.40	0.60	0.31
Density (g/cm^3)	ND	2.40	2.53	2.72	2.22	2.95	2.77
Trace elements (ppm):							
La				0.02	0.04	2.3	3.4
Ce				<0.3	<0.3	6.7	10
Nd				ND	ND	7.1	8.9
Sm				0.004	0.005	3.0	3.6
Eu				<0.003	<0.003	0.86	1.1
Gd				ND	ND	4.2	ND
Tb				<0.01	<0.01	0.75	1.0
Tm				ND	ND	0.41	ND
Yb				0.03	0.01	2.9	4.1
Lu				0.005	<0.003	0.46	0.60
Sc	ND	3.9	ND	6.2	6.6	45	ND
Cr	1000	2500	1000	2000	1750	165	240
Ni	715	2300	870	2250	2100	90	96
Co	117	140	120	100	105	220	64
V	82	14	90	29	22	45	267
Cu	15	<5	15	11	<5	50	88
Pb	<5	<5	<5	<5	<5	<5	<5
Zn	92	26	54	30	33	140	170
Sn	2.6	ND	2.5	ND	ND	ND	3.5
Zr	<1	<10	<1	<10	<10	68	95
Y	<1	<1	<1	<1	<1	29	35
Nb	<1	<1	<1	<1	<1	1.9	1.9
Rb	<1	<1	1.2	<1	<1	<1	<1
Sr	3.4	<10	14	<10	10	59	39
Ba	3	<5	4	<5	<5	38	18
Th	<1	ND	<1	ND	ND	ND	ND

Table T101 (continued).

Leg	125	125	125
Hole	779A	779A	779A
Core, section	31R-CC	34R-1	35R-1
Interval (cm)	10-12	63-65	118-122
Piece	2	5A	10
Lab number	Z-199	Z-200	Z-201
Depth (mbsf)	262.30	293.93	294.48
Unit	2	2	2
Major element oxides (wt%):			
SiO_2	38.10	33.38	35.12
TiO_2	1.89	0.19	0.13
Al_2O_3	13.11	0.79	0.14
Fe_2O_3	4.65	5.89	8.23
FeO	7.53	1.19	0.27
MnO	0.20	0.18	0.17
MgO	7.07	38.89	40.25
CaO	21.87	0.71	0.64
Na_2O	0.90	0.22	0.15
K_2O	0.12	0.05	0.02
P_2O_5	0.03	0.01	0.01
LOI	4.86	18.40	15.06
Total	100.33	99.90	100.19
H_2O^+	4.53	13.90	13.45
H_2O^-	0.33	3.38	1.61
CO_2	ND	0.75	ND
Fe_2O_3/FeO	0.62	4.95	30.48
Density (g/cm^3)	2.97	2.40	2.59
Trace elements (ppm):			
La	2.8	0.06	0.03
Ce	7.8	<0.3	<0.3
Nd	8.8	ND	ND
Sm	3.6	0.03	0.02
Eu	1.1	0.004	0.005
Gd	5.4	ND	ND
Tb	0.95	0.01	0.01
Tm	0.62	ND	ND
Yb	3.7	0.03	0.02
Lu	0.55	0.005	0.003
Sc	47	8.5	7.1
Cr	170	2000	2200
Ni	90	1500	1600
Co	220	25	30
V	30	15	15
Cu	45	125	120
Pb	<5	<5	<5
Zn	110	65	50
Sn	ND	ND	ND
Zr	73	<10	<10
Y	29	<1	<1
Nb	1.9	<1	<1
Rb	<1	<1	<1
Sr	48	17	13
Ba	33	<5	<5
Th	ND	ND	ND

Table T102. Composition of igneous rocks from Hole 780C, Leg 125.

Leg	125	125
Hole	780C	780C
Core, section	18R-1	18R-1
Interval (cm)	31-34	42-45
Piece	2A	2A
Lab number	Z-1388	Z-1389
Depth (mbsf)	154.31	154.42
Unit	2	2
Major element oxides (wt%):		
SiO_2	34.44	36.80
TiO_2	0.04	0.05
Al_2O_3	0.90	0.49
Fe_2O_3	5.27	6.95
FeO	2.59	1.94
MnO	0.11	0.12
MgO	41.85	39.93
CaO	0.11	0.56
Na_2O	0.04	0.05
K_2O	0.02	0.02
P_2O_5	<0.01	<0.01
LOI	13.94	12.55
Total	99.31	99.46
H_2O^+	12.23	10.71
H_2O^-	0.72	0.94
CO_2	0.63	0.90
Fe_2O_3/FeO	2.04	3.58
Density (g/cm^3)	2.57	2.72
Trace elements (ppm):		
La	0.069	0.21
Ce	<0.5	<0.5
Nd	<0.5	<0.5
Sm	0.025	0.028
Eu	0.01	0.01
Gd	ND	ND
Tb	<0.01	<0.01
Tm	ND	ND
Yb	0.06	0.06
Lu	0.012	0.011
Sc	ND	ND
Cr	615	1550
Ni	660	720
Co	110	120
V	47	69
Cu	6	12
Zn	25	21
Zr	2	1.8
Y	<1	<1
Nb	<1	<1
Rb	1.0	<1
Sr	3.4	3.0
Ba	5	5

Note: ND = not determined.

Table T103. Composition of igneous rocks from Hole 786B, Leg 125 (Izu-Bonin Forearc Basin). (Continued on next eight pages.)

Leg	125	125	125	125	125	125	125
Hole	786B	786B	786B	786B	786B	786B	786B
Core, section	4R-1	5R-1	6R-1	6R-2	8R-1	9R-1	15R-1
Interval (cm)	142-144	25-27	100-105	38-40	96-99	0-7	46-54
Piece	30	4A	24	8	17	1	7
Lab number	Z-202	Z-203	Z-1390	Z-204	Z-1391	Z-1392	Z-1393-1
Depth (mbsf)	190.42	198.85	209.20	210.08	228.56	237.10	295.46
Unit	1	1	2	2	3	3	3
Major element oxides (wt%):							
SiO_2	54.53	54.00	49.94	50.18	56.30	55.20	62.58
TiO_2	0.64	0.61	0.39	0.66	0.33	0.33	0.34
Al_2O_3	15.84	14.04	14.87	13.75	16.00	16.37	14.28
Fe_2O_3	3.54	5.30	7.02	6.35	4.64	3.95	3.36
FeO	3.41	2.16	2.52	1.97	3.95	3.63	3.59
MnO	0.09	0.09	0.12	0.11	0.11	0.11	0.10
MgO	4.57	5.55	7.15	6.58	4.00	4.20	2.30
CaO	8.00	6.72	9.30	10.87	7.56	7.84	5.77
Na_2O	4.59	3.17	2.65	3.11	3.29	3.27	3.73
K_2O	1.06	1.36	0.29	0.49	0.56	0.52	0.75
P_2O_5	0.03	0.01	0.04	0.01	0.06	0.06	0.08
LOI	3.19	7.17	5.00	5.80	3.10	3.90	2.92
Total	99.49	100.18	99.29	99.88	99.90	99.38	99.80
H_2O^+	1.06	2.21	1.11	1.02	1.15	1.33	1.88
H_2O^-	2.13	4.96	2.81	3.73	1.46	1.96	0.42
CO_2	ND	ND	0.62	1.05	0.43	0.35	0.22
Fe_2O_3/FeO	1.04	2.45	2.79	3.22	1.18	1.09	0.94
Density (g/cm^3)	2.02	1.99	2.02	2.39	2.37	2.34	ND
Trace elements (ppm):							
La	3.8	0.52		2.8			
Ce	6.7	1.2		3.7			
Nd	6.1	0.97		4.0			
Sm	1.8	0.37		1.4			
Eu	0.48	0.19		0.38			
Gd	2.1	0.50		1.9			
Tb	0.38	0.092		0.34			
Tm	0.20	ND		0.20			
Yb	1.1	0.35		1.3			
Lu	0.17	0.054		0.21			
Sc	32	29	ND	37	ND	ND	ND
Cr	380	395	450	450	23	23	20
Ni	80	150	200	260	50	45	24
Co	20	35	49	50	24	22	21
V	250	190	230	270	210	195	245
Cu	50	100	57	27	120	88	120
Pb	<5	<5	ND	<5	ND	ND	ND
Zn	65	70	81	70	84	74	79
Sn	ND	ND	ND	ND	ND	ND	ND
Zr	40	41	35	24	56	53	57
Y	12	3.7	10.0	15	11	16	9
Nb	<1	<1	<1	<1	1.0	2	2.1
Rb	10	17	76	6.7	7.4	6.8	8.9
Sr	210	160	150	130	120	220	210
Ba	36	20	6	18	7	6	7
Th	ND	ND	ND	ND	ND	ND	ND

Note: ND = not determined.

Table T103 (continued).

Leg	125	125	125	125	125	125	125
Hole	786B	786B	786B	786B	786B	786B	786B
Core, section	15R-1	15R-2	16R-2	18R-1	19R-1	20R-1	21R-2
Interval (cm)	46-54	126-130	8-12	8-13	6-10	85-89	47-49
Piece	Breccia 7	Breccia 18	2	2	2	14	3
Lab number	Z-1393-2	Z-1394	Z-1395	Z-1396	Z-1397	Z-205	Z-206
Depth (mbsf)	295.46	297.73	306.15	323.98	333.66	344.15	354.97
Unit	3	3	3	4	4	4	7
Major element oxides (wt%):							
SiO_2	51.94	53.47	55.99	52.06	57.03	49.43	52.95
TiO_2	0.34	0.32	0.34	0.34	0.31	0.24	0.25
Al_2O_3	15.26	15.48	14.91	16.03	14.82	12.95	13.04
Fe_2O_3	7.03	6.31	5.05	6.35	4.60	4.89	6.06
FeO	1.00	1.70	4.32	3.77	4.50	4.17	3.16
MnO	0.06	0.07	0.11	0.12	0.12	0.16	0.13
MgO	2.54	3.46	3.65	4.17	3.97	8.55	5.55
CaO	4.70	3.43	5.45	7.53	6.63	9.88	10.40
Na_2O	3.66	3.90	3.38	3.28	3.14	2.36	2.73
K_2O	2.25	2.29	0.70	0.80	0.66	0.40	0.50
P_2O_5	<0.01	<0.01	0.04	0.02	0.03	0.02	0.08
LOI	10.55	9.32	6.03	5.53	4.02	6.47	4.38
Total	99.33	99.75	99.97	100.00	99.83	99.52	99.23
H_2O^+	4.03	3.66	2.32	1.68	1.82	1.37	1.02
H_2O^-	5.91	5.30	2.93	3.04	1.82	2.45	0.99
CO_2	0.43	<0.2	<0.2	<0.2	<0.2	1.48	2.29
Fe_2O_3/FeO	7.03	3.71	1.17	1.68	1.02	1.17	1.92
Density (g/cm^3)	2.36	1.51	1.97	1.71	2.10	1.97	1.99
Trace elements (ppm):							
La						1.1	2.2
Ce						2.3	3.9
Nd						1.6	2.7
Sm						0.37	0.85
Eu						0.25	0.29
Gd						0.66	1.1
Tb						0.16	0.18
Tm						ND	0.15
Yb						0.70	0.98
Lu						0.11	0.16
Sc	ND	ND	ND	ND	ND	38	35
Cr	36	26	26	64	40	850	1100
Ni	42	40	27	43	44	235	190
Co	20	20	26	22	25	75	45
V	207	185	232	187	232	270	200
Cu	96	145	74	74	78	45	30
Pb	ND	ND	ND	ND	ND	<5	<5
Zn	67	64	83	90	85	80	65
Sn	ND	ND	ND	ND	ND	ND	ND
Zr	58	66	61	56	51	28	24
Y	2	3.1	8	8	7	5.2	8.3
Nb	1.7	1.4	2.0	1.7	1.7	<1	<1
Rb	34.0	34.0	9.1	9.5	8.0	3.8	8.9
Sr	160	160	220	230	210	130	140
Ba	21	<5	40	32	18	5	25
Th	ND	ND	ND	ND	ND	ND	ND

Table T103 (continued).

Leg	125	125	125	125	125	125	125
Hole	786B	786B	786B	786B	786B	786B	786B
Core, section	24R-1	24R-1	25R-1	26R-1	27R-2	30R-3	31R-2
Interval (cm)	133-135	135-140	82-86	50-55	48-51	31-33	30-34
Piece	12	22	11	7	6	4	3
Lab number	Z-207	Z-1400	Z-1401	Z-1402	Z-208	Z-209	Z-683
Depth (mbsf)	383.23	383.25	392.32	401.70	412.78	443.01	451.14
Unit	9	9	9	9	11	11	11
Major element oxides (wt%):							
SiO_2	58.91	56.34	67.51	68.41	51.15	58.45	59.91
TiO_2	0.58	0.38	0.34	0.34	0.57	0.58	0.20
Al_2O_3	15.08	16.06	13.45	13.50	12.36	13.93	13.24
Fe_2O_3	4.53	4.27	4.36	4.42	6.12	5.24	4.91
FeO	2.60	2.98	2.56	2.22	1.80	0.79	1.51
MnO	0.11	0.11	0.07	0.07	0.11	0.09	0.05
MgO	2.36	3.14	1.68	1.17	7.42	5.29	6.22
CaO	5.00	4.59	3.96	3.44	5.56	8.58	7.31
Na_2O	4.35	4.45	4.55	4.71	2.36	3.05	3.00
K_2O	1.27	1.31	0.84	1.12	1.25	0.71	0.59
P_2O_5	0.04	0.09	0.10	0.08	0.01	0.03	0.04
LOI	5.58	6.15	0.56	0.50	11.67	3.51	2.64
Total	100.41	99.87	99.98	99.98	100.38	100.25	99.62
H_2O^+	2.10	2.07	0.20	0.25	3.23	0.43	0.37
H_2O^-	3.23	3.31	0.34	0.24	8.02	1.96	1.10
CO_2	ND	<0.2	<0.2	<0.2	ND	0.75	0.58
Fe_2O_3/FeO	1.74	1.43	1.70	1.99	3.40	6.63	3.25
Density (g/cm^3)	1.75	1.69	2.11	1.94	1.69	2.51	2.54
Trace elements (ppm):							
La	3.8				4.5	1.7	
Ce	7.2				8.9	3.5	
Nd	5.3				5.6	1.9	
Sm	1.6				1.60	0.69	
Eu	0.45				0.39	0.23	
Gd	2.4				1.2	0.73	
Tb	0.35				0.22	0.13	
Tm	0.16				0.12	0.09	
Yb	1.1				0.70	0.61	
Lu	0.19				0.11	0.10	
Sc	22	ND	ND	ND	30	32	ND
Cr	35	26	24	<10	280	540	455
Ni	30	39	22	<5	155	145	155
Co	20	28	18	16	20	25	34
V	250	257	185	107	95	170	184
Cu	130	71	68	24	140	45	70
Pb	5	ND	ND	ND	40	<5	<5
Zn	85	86	66	65	85	60	61
Sn	ND	ND	ND	ND	ND	ND	2.0
Zr	61	84	73	75	25	29	49
Y	11	12	12	11	5.3	7.2	7.3
Nb	<1	1.1	2.2	1.9	<1	<1	1.5
Rb	15	17	84	17	17	8.8	9.5
Sr	200	230	200	200	120	160	170
Ba	55	37	61	39	130	42	9
Th	ND	ND	ND	ND	ND	ND	<1

Table T103 (continued).

Leg	125	125	125	125	125	125	125
Hole	786B	786B	786B	786B	786B	786B	786B
Core, section	32R-1	34R-2	34R-4	35R-2	37R-2	39R-1	39R-2
Interval (cm)	39-41	41-43	11-13	29-31	97-99	39-42	32-35
Piece	8	4	1B	4	12A	10	4A
Lab number	Z-210	Z-211	Z-212	Z-213	Z-214	Z-1404	Z-1406
Depth (mbsf)	459.39	480.21	482.91	489.79	509.87	527.19	528.62
Unit	11	15	15	15	15	15	16
Major element oxides (wt%):							
SiO_2	59.26	51.86	53.58	61.96	52.07	58.38	53.42
TiO_2	0.58	0.34	0.30	0.45	0.34	0.31	0.34
Al_2O_3	12.80	12.39	11.79	15.32	13.93	16.34	16.42
Fe_2O_3	5.10	4.03	4.64	3.75	5.33	5.74	4.65
FeO	1.89	2.91	3.16	1.74	2.27	1.83	4.56
MnO	0.07	0.11	0.13	0.06	0.11	0.04	0.12
MgO	5.06	8.31	8.85	2.75	6.76	2.94	4.47
CaO	7.85	11.31	8.89	5.81	10.69	6.33	6.32
Na_2O	3.11	2.93	2.93	4.62	3.93	3.90	3.29
K_2O	0.87	0.46	0.73	0.67	0.53	0.48	0.51
P_2O_5	0.02	0.03	0.02	0.06	0.04	0.10	0.05
LOI	3.58	5.90	4.95	2.77	4.55	3.22	5.66
Total	100.19	100.58	99.97	99.96	100.55	99.61	99.81
H_2O^+	1.22	1.37	2.29	1.55	1.22	0.81	2.42
H_2O^-	2.05	1.83	2.01	1.12	1.40	1.36	3.08
CO_2	ND	2.50	0.65	ND	1.70	<0.2	<0.2
Fe_2O_3/FeO	2.70	1.38	1.47	2.16	2.35	3.14	1.02
Density (g/cm^3)	2.53	2.32	2.61	2.00	2.51	1.94	1.82
Trace elements (ppm):							
La	2.2	1.8	1.5	3.2	1.5		
Ce	4.4	3.5	3.1	6.8	3.3		
Nd	3.5	ND	ND	5.1	2.2		
Sm	1.0	0.80	0.71	1.3	0.81		
Eu	0.29	0.29	0.24	0.40	0.28		
Gd	1.3	ND	ND	1.9	0.99		
Tb	0.21	0.20	0.17	0.31	0.20		
Tm	0.11	ND	ND	0.18	0.16		
Yb	0.76	0.87	0.76	1.1	0.88		
Lu	0.13	0.13	0.12	0.17	0.16		
Sc	29	ND	ND	ND	ND	ND	ND
Cr	440	1150	700	54	545	21	20
Ni	140	300	260	25	190	37	38
Co	20	55	35	8	40	30	30
V	155	220	145	120	170	265	390
Cu	50	23	27	40	15	47	86
Pb	<5	<5	<5	<5	<5	ND	ND
Zn	60	65	55	60	65	73	93
Sn	ND	ND	ND	ND	ND	ND	ND
Zr	33	23	22	50	27	55	56
Y	7.6	9.5	7.9	11	8.6	14.0	9.9
Nb	<1	<1	<1	1.1	<1	1.5	1.3
Rb	12	7.3	15	6.8	11	6.8	9.9
Sr	170	140	130	180	150	250	230
Ba	48	15	14	46	19	76	<5
Th	ND	ND	ND	ND	ND	ND	ND

Table T103 (continued).

Leg	125	125	125	125	125	125	125
Hole	786B	786B	786B	786B	786B	786B	786B
Core, section	40R-1	40R-2	40R-3	42R-3	43R-2	44R-1	49R-2
Interval (cm)	25-29	17-19	46-50	116-120	81-83	21-25	90-95
Piece	Tuff 6	15E	1C	10C	7	4	Breccia 4C
Lab number	Z-1407	Z-215	Z-684	Z-685	Z-258	Z-686	Z-1411
Depth (mbsf)	536.55	537.97	539.20	559.70	567.31	574.81	624.85
Unit	16	17	17	19	19	19	19
Major element oxides (wt%):							
SiO_2	57.81	48.03	44.26	59.76	56.73	49.83	53.55
TiO_2	0.33	0.34	0.23	0.22	0.30	0.34	0.31
Al_2O_3	15.80	12.87	11.04	13.06	14.11	11.78	13.45
Fe_2O_3	4.41	5.07	7.05	5.93	4.66	7.78	5.69
FeO	4.10	3.03	1.33	1.16	1.80	2.12	3.41
MnO	0.13	0.15	0.07	0.07	0.11	0.15	0.17
MgO	3.73	9.99	9.31	5.79	5.45	11.48	6.03
CaO	5.30	11.12	15.20	6.95	8.27	8.04	5.67
Na_2O	3.93	2.48	1.85	3.28	3.65	2.18	2.88
K_2O	1.31	0.38	0.25	0.75	0.90	0.36	0.95
P_2O_5	0.13	0.03	0.04	0.05	0.03	0.04	0.05
LOI	2.81	6.48	9.26	2.51	4.25	5.65	7.45
Total	99.79	99.97	99.89	99.53	100.26	99.75	99.61
H_2O^+	1.57	1.47	0.92	0.57	2.06	1.88	2.74
H_2O^-	0.94	1.95	1.50	1.07	1.74	2.99	4.02
CO_2	<0.2	2.75	6.64	0.21	0.45	0.25	<0.2
Fe_2O_3/FeO	1.08	1.67	5.30	5.11	2.59	3.67	1.67
Density (g/cm^3)	1.88	2.49	2.63	2.36	2.20	2.46	1.83
Trace elements (ppm):							
La		1.5			1.7		
Ce		3.9			4.2		
Nd		ND			3.0		
Sm		0.85			0.90		
Eu		0.32			0.31		
Gd		ND			ND		
Tb		0.23			0.16		
Tm		ND			ND		
Yb		0.89			0.65		
Lu		0.16			0.11		
Sc	ND	ND	ND	ND	ND	ND	ND
Cr	19	620	455	320	345	530	155
Ni	42	460	310	83	110	340	83
Co	24	65	50	31	27	58	32
V	212	220	197	187	170	250	267
Cu	185	30	25	27	15	33	155
Pb	ND	<5	<5	<5	<5	<5	ND
Zn	99	60	57	65	50	66	71
Sn	ND	ND	2.0	2.2	ND	2.3	ND
Zr	49	21	29	48	32	31	43
Y	12.0	9.1	7.6	8.0	5.1	9.3	8.7
Nb	<1	<1	<1	1.0	<1	1.5	1.9
Rb	15	5.9	5.9	10	10	7.8	16
Sr	170	120	140	180	170	120	200
Ba	<5	<10	4	9	39	5	28
Th	ND	ND	<1	1.3	ND	<1	ND

Table T103 (continued).

Leg	125	125	125	125	125	125	125
Hole	786B	786B	786B	786B	786B	786B	786B
Core, section	51R-2	52R-1	54R-1	55R-1	56R-1	56R-1	57R-1
Interval (cm)	0-5	10-13	55-60	132-138	20-25	97-102	41-43
Piece	1	Breccia 2	Breccia 6A	13C	2B	Breccia 3	1B
Lab number	Z-1413	Z-1414	Z-1416	Z-1419	Z-1421	Z-1422	Z-257
Depth (mbsf)	643.70	652.00	671.75	682.12	690.30	691.07	700.21
Unit	19	19	19	19	19	19	20
Major element oxides (wt%):							
SiO_2	52.36	55.52	52.21	56.12	53.88	53.66	51.97
TiO_2	0.24	0.23	0.24	0.28	0.28	0.27	0.25
Al_2O_3	12.36	12.79	11.45	12.33	11.38	11.86	10.06
Fe_2O_3	3.66	2.75	2.77	3.53	4.82	3.63	6.33
FeO	5.55	5.48	4.03	4.20	2.46	3.46	1.65
MnO	0.16	0.15	0.11	0.17	0.12	0.11	0.18
MgO	10.80	9.73	9.74	7.66	11.44	10.94	11.77
CaO	7.14	6.46	8.13	6.85	3.33	4.09	2.46
Na_2O	2.50	2.47	1.97	2.24	2.66	2.72	2.80
K_2O	0.52	0.45	0.38	0.60	1.25	1.41	1.15
P_2O_5	0.17	0.09	0.02	0.03	0.03	0.04	0.02
LOI	4.49	3.87	8.36	5.40	8.22	6.94	11.54
Total	99.95	99.99	99.41	99.41	99.87	99.13	100.18
H_2O^+	1.29	1.63	2.62	2.52	3.15	3.00	4.44
H_2O^-	2.42	1.74	2.01	1.75	3.83	3.23	7.10
CO_2	<0.2	<0.2	3.73	0.64	<0.2	<0.2	ND
Fe_2O_3/FeO	0.66	0.50	0.69	0.84	1.96	1.05	3.84
Density (g/cm^3)	2.09	2.45	2.18	2.26	2.30	2.42	2.33
Trace elements (ppm):							
La	7.3	4.0	1.6	1.8	1.4	1.8	1.4
Ce	18	9.6	3.8	4.2	3.5	4.4	3.1
Nd	11.0	5.5	2.4	2.7	2.2	2.9	2.1
Sm	2.8	1.5	0.69	0.80	0.60	0.86	0.71
Eu	0.77	0.51	0.29	0.35	0.26	0.36	0.20
Gd	ND	ND	ND	ND	ND	ND	ND
Tb	0.56	0.32	0.16	0.21	0.14	0.21	0.15
Tm	ND	ND	ND	ND	ND	ND	0.095
Yb	2.5	1.3	0.64	0.70	0.66	0.76	0.61
Lu	0.41	0.22	0.099	0.12	0.11	0.12	0.10
Sc	ND	ND	ND	ND	ND	ND	ND
Cr	730	555	570	570	790	700	1150
Ni	178	163	218	216	190	194	200
Co	42	32	38	41	40	40	33
V	270	220	210	220	210	222	230
Cu	ND	52	55	175	42	42	85
Pb	ND	ND	ND	ND	ND	ND	<5
Zn	82	82	66	68	72	70	55
Sn	ND	ND	ND	ND	ND	ND	ND
Zr	38	37	32	36	33	39	21
Y	26.0	13.0	5.4	6.5	5.4	7.3	5.4
Nb	1.9	1.9	1.3	<1	1.4	1.3	<1
Rb	6.9	7.9	8.0	12.0	16.0	16	11
Sr	160	150	190	150	100	120	210
Ba	<5	<5	<5	<5	6	5	27
Th	ND	ND	ND	ND	ND	ND	ND

Table T103 (continued).

Leg	125	125	125	125	125	125	125
Hole	786B	786B	786B	786B	786B	786B	786B
Core, section	61R-4	61R-5	61R-5	62R-1	63R-1	64R-2	64R-3
Interval (cm)	108-114	37-39	35-40	16-18	118-121	88-92	76-78
Piece	6B	6	6	2A	Tuff 13	12	8A
Lab number	Z-1425	Z-259	Z-1615	Z-260	Z-687	Z-1426	Z-261
Depth (mbsf)	734.09	735.07	735.05	738.56	749.18	760.02	761.46
Unit	22	22	22	24	25	26	26
Major element oxides (wt%):							
SiO_2	71.15	69.23	68.93	55.45	55.87	71.82	54.77
TiO_2	0.36	0.36	0.41	0.30	0.24	0.29	0.59
Al_2O_3	12.19	12.52	13.75	10.82	14.59	12.90	17.02
Fe_2O_3	1.74	2.72	1.81	4.07	5.83	1.84	4.48
FeO	2.43	0.71	2.13	3.43	0.32	1.48	2.75
MnO	0.05	0.07	0.06	0.11	0.02	0.05	0.15
MgO	0.39	0.22	0.71	10.49	5.41	0.84	5.02
CaO	3.13	3.97	2.58	4.81	3.62	1.42	7.46
Na_2O	4.33	5.24	5.41	2.99	2.80	3.36	3.55
K_2O	1.44	1.68	1.63	1.37	2.27	4.17	0.45
P_2O_5	0.09	0.11	0.09	0.02	0.04	0.07	0.04
LOI	2.30	1.76	2.10	5.78	8.47	1.08	3.71
Total	99.60	98.59	99.61	99.64	99.48	99.32	99.99
H_2O^+	0.96	0.89	0.67	1.90	2.79	0.38	1.14
H_2O^-	0.22	0.22	0.25	3.88	5.25	0.16	2.32
CO_2	1.08	0.65	1.13	ND	<0.20	0.27	ND
Fe_2O_3/FeO	0.72	3.83	0.85	1.19	18.22	1.24	1.63
Density (g/cm^3)	2.19	2.13	2.01	2.30	1.69	2.18	2.49
Trace elements (ppm):							
La	3.4	4.5		1.8	2.5		1.8
Ce	8.6	8.2		3.7	6.3		5.1
Nd	5.2	6.8		3.0	4.1		4.1
Sm	1.4	1.9		0.9	1.2		1.4
Eu	0.46	0.45		0.26	0.35		0.47
Gd	ND	2.4		1.0	ND		ND
Tb	0.30	0.43		0.20	0.24		0.28
Tm	ND	0.26		ND	ND		ND
Yb	1.1	1.5		0.90	0.97		1.3
Lu	0.16	0.24		0.15	0.16		0.20
Sc	ND	ND	ND	ND	ND	ND	ND
Cr	21	10	20	1450	5	26	28
Ni	19	18	18	330	32	28	
Co	17	5	16	48	24	17	23
V	72	60	72	190	207	69	260
Cu	32	65	32	100	65	32	100
Pb	ND	5	ND	<5	<5	ND	<5
Zn	75	70	72	65	64	91	70
Sn	ND	ND	ND	ND	2.2	ND	ND
Zr	78	59	93	21	70	77	32
Y	13.0	13	14	8.0	6.7	11.0	9.8
Nb	2.1	1.1	3.0	<1	1.3	2.5	<1
Rb	24	19	25	14	30	43	3.7
Sr	130	91	110	81	170	80	150
Ba	41	110	76	45	77	790	29
Th	ND	ND	ND	ND	ND	ND	ND

Table T103 (continued).

Leg	125	125	125	125	125	125	125
Hole	786B	786B	786B	786B	786B	786B	786B
Core, section	65R-1	65R-1	65R-3	65R-3	66R-2	66R-3	67R-1
Interval (cm)	40-44	102-107	39-44	48-52	0-5	51-56	77-79
Piece	3	13	6	Tuff 7	1A	7	9
Lab number	Z-688	Z-1427	Z-1428	Z-689	Z-1429	Z-1430	Z-262
Depth (mbsf)	767.80	768.42	770.76	770.85	778.54	780.55	787.47
Unit	26	26	26	26	26	26	27
Major element oxides (wt%):							
SiO_2	52.12	73.91	70.11	70.23	71.49	72.00	52.90
TiO_2	0.37	0.28	0.30	0.24	0.30	0.30	0.32
Al_2O_3	17.19	12.01	13.45	11.46	13.03	12.90	14.47
Fe_2O_3	4.13	2.21	1.26	4.13	0.99	1.97	2.14
FeO	3.24	1.20	2.32	0.87	2.08	1.92	3.51
MnO	0.07	0.03	0.07	0.05	0.06	0.06	0.20
MgO	5.99	1.15	1.50	1.54	1.43	1.31	10.78
CaO	7.20	1.59	1.42	2.14	0.92	1.09	8.00
Na_2O	2.84	3.87	3.25	3.10	3.16	3.39	2.80
K_2O	1.10	2.87	3.74	3.98	4.35	3.54	0.29
P_2O_5	0.06	0.06	0.07	0.06	0.07	0.07	0.02
LOI	5.61	0.90	2.20	2.00	1.40	1.12	4.26
Total	99.92	100.08	99.69	99.80	99.28	99.67	99.69
H_2O^+	2.60	0.29	0.94	1.04	0.74	0.71	2.07
H_2O^-	0.78	0.17	0.35	0.29	0.19	0.24	2.19
CO_2	1.88	0.25	0.26	<0.20	<0.2	<0.2	ND
Fe_2O_3/FeO	1.27	1.84	0.54	4.75	0.48	1.03	0.61
Density (g/cm^3)	2.50	2.20	2.08	2.20	2.10	2.12	2.58
Trace elements (ppm):							
La		3.9	3.7		3.5		1.1
Ce		10	9.5		9.5		2.6
Nd		6.0	6.1		6.0		1.9
Sm		1.5	1.6		1.6		0.59
Eu		0.52	0.51		0.43		0.27
Gd		ND	ND		ND		ND
Tb		0.34	0.34		0.30		0.17
Tm		ND	ND		ND		ND
Yb		1.5	1.3		1.1		0.74
Lu		0.24	0.21		0.19		0.12
Sc	ND	ND	ND	ND	ND	ND	ND
Cr	34	26	26	34	23	30	850
Ni	34	26	23	25	20	22	340
Co	26	16	17	18	17	18	45
V	215	69	69	105	67	70	200
Cu	77	27	79	83	79	68	55
Pb	ND	ND	ND	<5	ND	ND	<5
Zn	94	97	129	123	169	110	65
Sn	1.9	ND	ND	2.0	ND	ND	ND
Zr	50	74	77	78	78	82	26
Y	12	11	11	13.0	13	11.0	4.8
Nb	1.5	2.5	2.6	1.5	2.0	2.6	<1
Rb	8.8	26.0	38	39	40	36	4.4
Sr	140	92	89	86	82	96	120
Ba	110	630	430	390	670	600	19
Th	<1	ND	ND	1.8	ND	ND	ND

Table T103 (continued).

Leg	125	125	125	125	125	125	125	125
Hole	786B	786B	786B	786B	786B	786B	786B	786B
Core, section	68R-1	69R-2	69R-4	70R-2	70R-4	71R-4	72R-1	72R-2
Interval (cm)	10-16	79-81	107-110	46-48	0-5	32-36	15-17	50-55
Piece	Tuff 1A	1F	Tuff 1D	1F	1	3	3	Tuff 5
Lab number	Z-1431	Z-263	Z-1432	Z-264	Z-1433	Z-691	Z-265	Z-1434
Depth (mbsf)	796.40	799.59	802.37	808.86	811.19	820.26	823.75	825.6
Unit	28	28	28	28	28	30	30	30
Major element oxides (wt%):								
SiO_2	59.08	59.57	55.88	54.51	54.56	58.30	55.90	59.36
TiO_2	0.29	0.30	0.16	0.30	0.19	0.23	0.32	0.17
Al_2O_3	12.68	10.69	11.18	10.96	12.69	12.72	14.55	13.51
Fe_2O_3	2.40	5.13	4.93	4.11	4.19	5.98	4.14	2.98
FeO	2.96	2.15	2.99	2.36	3.04	1.14	2.49	3.78
MnO	0.08	0.11	0.11	0.18	0.08	0.10	0.10	0.11
MgO	8.42	7.01	8.67	8.43	9.64	8.00	6.58	6.71
CaO	3.39	4.20	3.72	6.06	4.57	4.07	6.92	4.9
Na_2O	3.76	4.12	4.06	3.27	3.01	2.75	3.46	2.71
K_2O	0.11	0.20	0.11	0.27	0.08	0.45	0.18	0.51
P_2O_5	0.05	0.04	0.05	0.05	0.04	0.04	0.03	0.04
LOI	5.99	6.25	7.49	9.04	7.56	5.65	5.34	5.38
Total	99.21	99.77	99.35	99.54	99.65	99.43	100.01	100.16
H_2O^+	1.32	2.20	0.93	3.32	1.37	3.55	2.22	2.53
H_2O^-	3.53	3.16	3.99	4.12	4.30	1.27	2.82	1.16
CO_2	0.23	0.80	1.52	1.60	0.72	0.70	0.30	1.69
Fe_2O_3/FeO	0.81		1.65	1.74	1.38	5.25	1.66	0.79
Density (g/cm^3)	2.30	2.17	2.25	2.26	2.29	2.24	2.44	2.41
Trace elements (ppm):								
La	2.4	2.6	2.0	2.2	1.8	2.3	2.5	1.8
Ce	6.6	5.9	5.3	4.6	4.6	6.0	4.9	4.7
Nd	3.8	4.1	3.3	2.8	3.0	3.5	3.6	3.0
Sm	1.0	0.92	0.90	0.75	0.82	0.86	1.1	0.81
Eu	0.37	0.36	0.31	0.32	0.30	0.27	0.33	0.31
Gd	ND	ND	ND	ND	ND	ND	ND	ND
Tb	0.23	0.23	0.23	0.25	0.19	0.20	0.22	0.18
Tm	ND	ND	ND	ND	ND	ND	ND	ND
Yb	0.90	0.87	0.88	0.87	0.80	0.76	0.96	0.79
Lu	0.15	0.14	0.15	0.13	0.14	0.12	0.15	0.14
Sc	ND	ND	ND	ND	ND	ND	ND	ND
Cr	740	980	650	1000	765	530	800	375
Ni	205	300	220	265	255	330	140	137
Co	46	45	55	48	73	52	40	39
V	204	160	206	170	368	240	250	185
Cu	93	100	135	50	74	125	65	79
Pb	ND	5	ND	<5	ND	<5	<5	ND
Zn	78	120	63	90	93	160	70	67
Sn	ND	ND	ND	ND	ND	2.3	ND	ND
Zr	50	34	47	30	36	45	34	38
Y	8.0	8.0	8.2	8.6	8.7	8.1	10	8.0
Nb	1.9	1.6	1.4	1.3	1.0	1.7	1.7	1.4
Rb	1.7	1.1	<1	2.2	<1	3.5	0.9	3.3
Sr	135	100	120	110	130	140	160	125
Ba	9	33	11	37	<5	24	25	<5
Th	ND	ND	ND	ND	ND	ND	ND	ND

Table T104. Composition of igneous rocks from Hole 792E, Leg 126 (Izu-Bonin Arc-Trench System). (Continued on next page.)

Leg	126	126	126	126	126	126	126
Hole	792E	792E	792E	792E	792E	792E	792E
Core, section	71R-1	72R-1	73R-2	74R-1	74R-2	75R-2	76R-1
Interval (cm)	84-86	18-20	76-78	54-58	64-66	62-64	26-32
Piece	8	2	6B	5B	6	7	3
Lab number	Z-219	Z-220	Z-221	Z-1450	Z-222	Z-223	Z-1451
Depth (mbsf)	810.74	819.68	831.46	839.34	840.94	850.32	857.96
Unit	1	1	1	2	3	3	4
Major element oxides (wt%):							
SiO_2	53.33	54.83	54.22	49.70	55.40	61.35	64.07
TiO_2	0.64	0.72	0.97	0.50	0.96	0.95	0.40
Al_2O_3	17.71	17.76	16.39	18.03	15.79	15.05	14.21
Fe_2O_3	5.95	6.10	6.11	7.91	6.20	5.28	5.05
FeO	2.07	1.93	1.99	1.93	2.11	1.55	1.06
MnO	0.13	0.11	0.07	0.10	0.03	0.01	0.04
MgO	3.84	3.67	4.50	4.72	4.42	2.34	3.70
CaO	9.42	8.83	9.70	8.73	8.95	8.52	5.00
Na_2O	2.48	3.04	2.49	2.06	2.81	2.87	2.58
K_2O	0.23	0.30	0.22	0.16	0.25	0.27	0.78
P_2O_5	0.10	0.23	0.23	0.02	0.05	0.08	0.06
LOI	3.75	2.92	3.60	6.10	3.53	2.23	2.65
Total	99.65	100.44	100.49	99.96	100.50	100.50	99.60
H_2O^+	1.49	1.01	1.12	1.53	1.14	0.83	0.95
H_2O^-	2.26	1.91	2.48	3.96	2.39	1.40	1.31
CO_2	ND	ND	ND	0.27	ND	ND	<0.2
Fe_2O_3/FeO	2.87	3.16	3.07	4.10	2.94	3.41	4.76
Density (g/cm^3)	2.35	2.24	2.34	1.94	2.14	2.35	2.48
Trace elements (ppm):							
La	1.3	3.1	4.2		1.7	2.8	
Ce	4.0	8.2	13		4.7	7.6	
Nd	4.7	6.5	10		4.4	7.3	
Sm	1.6	2.6	4.0		2.0	3.0	
Eu	0.52	0.68	0.83		0.54	0.75	
Gd	ND	3.3	4.7		2.5	4.1	
Tb	0.44	0.67	0.88		0.47	0.8	
Tm	ND	0.43	0.42		0.36	0.36	
Yb	1.8	3.1	3.1		2.2	2.3	
Lu	0.28	0.50	0.49		0.34	0.32	
Cr	16	16	25	32	10	6	21
Ni	15	15	15	27	13	11	20
Co	20	25	16	34	16	35	25
V	180	280	320	265	240	210	188
Cu	27	70	30	113	45	45	55
Pb	<5	<5	<5	ND	<5	<5	ND
Zn	75	75	80	84	75	65	100
Zr	27	33	31	43	31	29	47
Y	16	18	34	9.1	38	22	44
Nb	<1	1.1	<1.0	1.8	2.0	1.0	2.1
Rb	2.9	2.5	2.5	4.0	2.9	2.7	19
Sr	150	160	160	170	150	140	130
Ba	21	18	20	7	83	18	6

Note: ND = not determined.

Table T104 (continued).

Leg	126	126
Hole	792E	792E
Core, section	76R-1	78R-1
Interval (cm)	120-122	118-120
Piece	11	14
Lab number	Z-224	Z-225
Depth (mbsf)	858.90	877.78
Unit	5	5
Major element oxides (wt%):		
SiO_2	60.28	56.72
TiO_2	0.87	0.90
Al_2O_3	15.78	16.61
Fe_2O_3	4.98	5.99
FeO	1.48	1.98
MnO	0.03	0.06
MgO	2.67	3.88
CaO	8.49	8.64
Na_2O	3.02	2.70
K_2O	0.22	0.25
P_2O_5	0.05	0.05
LOI	2.24	2.70
Total	100.11	100.48
H_2O^+	0.67	0.78
H_2O^-	1.57	1.92
CO_2	ND	ND
Fe_2O_3/FeO	3.36	3.02
Density (g/cm^3)	2.16	2.42
Trace elements (ppm):		
La	1.7	2.1
Ce	5.0	5.8
Nd	5.4	6.6
Sm	2.0	2.3
Eu	0.63	0.6
Gd	2.4	3.0
Tb	0.48	0.56
Tm	0.28	0.33
Yb	1.7	2.2
Lu	0.27	0.33
Cr	6	10
Ni	10	12
Co	28	14
V	145	160
Cu	90	45
Pb	<5	<5
Zn	65	70
Zr	40	28
Y	23	23
Nb	1.0	1.1
Rb	1.9	2.4
Sr	150	150
Ba	28	20

Table T105. Composition of igneous rocks from Hole 793B, Leg 126 (Izu-Bonin Arc-Trench System). (Continued on next page.)

Leg	126	126	126	126	126	126	126
Hole	793B	793B	793B	793B	793B	793B	793B
Core, section	1R-2	86R-1	88R-1	92R-1	95R-2	103R-1	104R-1
Interval (cm)	82-84	35-40	62-67	0-5	28-32	37-42	96-98
Piece	5A				Breccia 1	Tuff	6B
Lab number	Z-226	Z-1452	Z-1453	Z-1454	Z-227	Z-1455	Z-228
Depth (mbsf)	588.82	1404.25	1423.52	1460.10	1490.78	1566.67	1576.86
Unit	X	1	1	1	3	9	10
Major element oxides (wt%):							
SiO_2	50.69	51.95	50.97	53.12	51.02	50.48	49.83
TiO_2	0.97	0.25	0.31	0.22	0.76	0.29	0.74
Al_2O_3	13.44	14.24	17.71	11.86	10.04	14.53	13.34
Fe_2O_3	5.16	6.84	4.25	3.30	6.03	5.72	4.47
FeO	4.95	0.98	3.23	5.04	2.18	1.38	4.31
MnO	0.14	0.18	0.12	0.14	0.13	0.09	0.10
MgO	9.71	5.07	5.41	11.44	10.68	6.41	8.93
CaO	10.53	6.10	9.19	7.94	8.67	4.45	10.13
Na_2O	2.08	2.41	2.06	1.74	1.87	2.22	1.87
K_2O	0.40	1.43	0.74	0.46	1.12	0.62	0.47
P_2O_5	0.04	<0.01	0.05	0.02	0.02	0.03	0.01
LOI	2.30	10.06	5.50	4.52	7.94	13.74	6.15
Total	100.41	99.51	99.54	99.80	100.46	99.96	100.35
H_2O^+	1.01	3.28	1.57	1.73	3.26	3.73	2.18
H_2O^-	1.29	5.44	3.14	2.53	4.68	7.85	3.97
CO_2	ND	0.24	0.30	0.21	ND	0.40	ND
Fe_2O_3/FeO	1.04	6.98	1.32	0.66	2.77	4.15	1.04
Density (g/cm^3)	2.66	2.07	2.15	2.45	2.18	1.95	2.36
Trace elements (ppm):							
La	1.4				0.85		1.5
Ce	4.3				2.0		3.8
Nd	4.4				2.3		3.0
Sm	1.7				0.77		1.1
Eu	0.56				0.24		0.36
Gd	2.4				ND		1.4
Tb	0.45				0.18		0.25
Tm	0.26				0.12		ND
Yb	1.7				0.74		0.86
Lu	0.28				0.11		0.13
Cr	305	223	155	320	1100	71	140
Ni	120	89	48	87	115	46	35
Co	40	51	32	42	35	37	30
V	260	80	220	205	200	347	230
Cu	120	432	50	50	55	78	75
Pb	<5	ND	ND	ND	<5	ND	<5
Zn	75	101	76	71	65	60	65
Zr	26	60	45	28	14	37	24
Y	15	4.8	14	9.1	6.8	7.3	5.8
Nb	1.6	2.0	1.2	1.7	1.1	1.3	<1
Rb	3.3	23	11	5.9	17	8.9	3.3
Sr	99	90	170	115	160	90	130
Ba	44	48	6	7	<10	7	<10

Note: ND = not determined.

Table T105 (continued).

Leg	126	126	126	126	126	126
Hole	793B	793B	793B	793B	793B	793B
Core, section	110R-2	110R-4	111R-1	112R-1	113R-3	114R-1
Interval (cm)	57-59	38-40	102-104	100-102	27-31	69-71
Piece	1C	1C	9A	3C	1C	1D
Lab number	Z-229	Z-230	Z-231	Z-232	Z-1456	Z-233
Depth (mbsf)	1635.87	1638.68	1644.42	1654.10	1665.82	1673.09
Unit	13	13	14	14	15	17
Major element oxides (wt%):						
SiO_2	51.60	51.75	50.06	52.41	50.15	50.29
TiO_2	0.74	0.72	0.63	0.66	0.27	0.73
Al_2O_3	10.59	11.05	11.60	11.40	14.63	15.15
Fe_2O_3	5.10	5.95	6.87	5.72	3.96	5.64
FeO	3.88	4.03	3.44	3.67	5.05	3.33
MnO	0.06	0.06	0.06	0.04	0.16	0.10
MgO	10.37	10.75	10.21	9.81	9.49	7.05
CaO	10.84	9.70	9.38	9.55	8.34	9.50
Na_2O	2.39	2.49	2.65	2.81	1.95	2.81
K_2O	0.86	0.99	0.97	1.14	0.19	0.81
P_2O_5	0.03	0.05	0.06	0.08	0.02	0.02
LOI	3.07	2.85	3.58	3.14	5.58	5.08
Total	99.53	100.39	99.51	100.43	99.79	100.51
H_2O^+	1.45	0.95	1.51	1.25	1.01	2.25
H_2O^-	1.62	1.90	2.07	1.89	2.64	2.83
CO_2	ND	ND	ND	ND	<0.2	ND
Fe_2O_3/FeO	1.31	1.48	2.00	1.56	0.78	1.69
Density (g/cm^3)	2.37	2.41	2.37	2.39	2.25	2.06
Trace elements (ppm):						
La	2.0	1.9	1.6	1.6		1.7
Ce	3.6	3.8	2.8	2.8		3.4
Nd	ND	ND	3.0	2.8		3.6
Sm	1.0	1.1	1.1	1.0		1.5
Eu	0.42	0.4	0.39	0.35		0.47
Gd	ND	ND	1.5	1.7		ND
Tb	0.27	0.35	0.27	0.29		0.3
Tm	ND	ND	0.14	0.15		ND
Yb	1.1	1.1	0.95	1.1		1.0
Lu	0.19	0.16	0.15	0.17		0.13
Cr	900	600	630	750	257	260
Ni	135	135	150	155	82	110
Co	60	55	50	55	52	50
V	270	230	230	270	230	350
Cu	27	45	27	50	50	40
Pb	<5	<5	<5	<5	ND	<5
Zn	70	65	70	70	83	75
Zr	14	19	13	20	36	25
Y	10	9.8	9.3	10	6.7	9.5
Nb	1.5	<1	<1	<1	1.1	<1
Rb	13	14	15	22	3.0	13
Sr	120	120	140	130	170	240
Ba	15	23	17	29	8	28

Table T106. Composition of igneous rocks from Hole 791B, Leg 126 (Izu-Bonin Arc-Trench System). (Continued on next two pages.)

Leg	126	126	126	126	126	126	126
Hole	791B	791B	791B	791B	791B	791B	791B
Core, section	57R-1	57R-1	59R-1	61R-1	63R-1	63R-1	64R-1
Interval (cm)	0-5	52-56	21-25	42-50	65-70	88-93	48-52
Piece	1B	6	Breccia 1	9	9	12	6
Lab number	Z-1435	Z-692	Z-1436	Z-1437	Z-1438	Z-1439	Z-216
Depth (mbsf)	925.90	926.42	945.41	964.92	984.35	984.58	993.48
Unit	4	5	6	8	11	11	11
Major element oxides (wt%):							
SiO_2	50.67	45.53	46.17	48.43	44.87	45.14	45.00
TiO_2	1.58	0.97	0.92	1.09	0.89	0.87	1.02
Al_2O_3	16.29	15.76	17.13	17.13	16.70	16.43	16.30
Fe_2O_3	4.62	6.43	5.23	4.08	4.90	3.99	5.01
FeO	7.46	4.63	4.71	5.22	5.61	6.49	5.69
MnO	0.19	0.21	0.14	0.15	0.16	0.17	0.17
MgO	9.18	8.52	8.75	7.55	8.72	9.45	8.48
CaO	4.67	9.94	9.60	11.43	8.35	8.35	8.80
Na_2O	3.56	2.43	2.59	2.62	2.34	2.23	2.70
K_2O	0.25	0.44	0.23	0.14	0.44	0.41	0.61
P_2O_5	0.27	0.16	0.16	0.17	0.08	0.08	0.07
LOI	1.59	4.90	4.25	2.15	6.26	5.73	6.36
Total	100.33	99.92	99.88	100.16	99.32	99.34	100.21
H_2O^+	0.10	1.76	0.90	0.11	1.38	1.39	2.73
H_2O^-	0.95	2.12	2.43	1.39	3.84	3.66	3.63
CO_2	0.54	0.49	0.52	0.65	0.39	0.39	ND
S (total)	ND	ND	ND	ND	ND	ND	ND
Fe_2O_3/FeO	0.62	1.39	1.11	0.78	0.87	0.62	0.88
Density (g/cm^3)	2.47	2.51	2.24	2.58	1.75	1.59	1.77
Trace elements (ppm):							
La							2.2
Ce							6.0
Nd							ND
Sm							1.80
Eu							0.71
Gd							ND
Tb							0.45
Tm							ND
Yb							1.50
Lu							0.23
Cr	<10	245	207	174	214	227	180
Ni	20	155	81	71	75	77	55
Co	32	51	40	40	50	55	38
V	367	252	195	252	212	370	270
Cu	42	43	42	75	72	78	65
Zn	114	64	78	88	81	85	70
Sn	ND	3	ND	ND	ND	ND	ND
Zr	86	68	68	75	51	49	35
Y	24	18	19	21	12	12	13
Nb	2.5	1	2.6	1.8	1.7	1.5	<1
Rb	2.8	8	3.6	1.5	6.3	6.8	5
Sr	270	250	220	240	190	175	160
Ba	28	7	48	39	26	26	15
Th	ND	<1	ND	ND	ND	ND	ND

Note: ND = not determined.

Table T106 (continued).

Leg	126	126	126	126	126	126	126
Hole	791B	791B	791B	791B	791B	791B	791B
Core, section	66R-2	67R-2	72R-2	73R-2	73R-2	75R-1	76R-2
Interval (cm)	0-5	123-125	50-55	80-84	73-75	97-105	48-52
Piece	1A	Breccia 16	6A	4B	Breccia 4B	14	Breccia 6A
Lab number	Z-693	Z-217	Z-1440	Z-1441	Z-218	Z-1442	Z-1443
Depth (mbsf)	1013.78	1024.83	1072.40	1081.90	1082.23	1100.27	1110.98
Unit	11	11	11	11	11	14	14
Major element oxides (wt%):							
SiO_2	45.37	45.46	41.57	40.51	41.35	44.76	40.97
TiO_2	0.91	1.06	0.90	0.94	1.06	0.96	0.90
Al_2O_3	16.49	15.92	15.81	16.32	16.17	14.53	14.18
Fe_2O_3	4.13	5.32	7.87	7.69	7.53	8.49	10.51
FeO	5.19	5.27	3.19	3.57	3.24	3.33	1.69
MnO	0.22	0.20	0.18	0.17	0.18	0.14	0.15
MgO	8.20	7.88	9.45	9.49	8.19	10.26	10.99
CaO	7.87	9.55	4.27	4.35	5.06	5.94	4.28
Na_2O	2.40	2.59	3.12	2.77	3.83	2.41	1.61
K_2O	0.50	0.46	0.89	0.80	1.32	0.32	1.02
P_2O_5	0.07	0.31	0.07	0.08	0.05	0.19	0.06
LOI	8.04	6.21	12.82	12.63	12.43	8.60	13.38
Total	99.39	100.23	100.14	99.32	100.41	99.93	99.74
H_2O^+	2.97	2.74	5.61	5.00	6.39	1.92	5.12
H_2O^-	4.77	3.47	6.36	6.22	6.04	4.85	5.71
CO_2	<0.20	ND	0.44	0.42	ND	0.40	1.48
S (total)	ND	ND	ND	ND	ND	ND	ND
Fe_2O_3/FeO	0.80	1.01	2.47	2.15	2.32	2.55	6.22
Density (g/cm^3)	1.77	1.76	1.91	1.91	ND	2.01	2.15
Trace elements (ppm):							
La		5.1			1.7		
Ce		13.0			5.6		
Nd		10.0			5.3		
Sm		3.20			1.80		
Eu		1.00			0.63		
Gd		3.60			2.50		
Tb		0.55			0.42		
Tm		ND			0.23		
Yb		2.10			1.50		
Lu		0.32			0.23		
Cr	215	170	243	233	170	198	188
Ni	56	55	71	62	65	58	58
Co	47	38	50	50	40	52	47
V	387	400	377	390	330	422	345
Cu	55	65	72	63	45	63	45
Zn	64	70	70	73	65	68	62
Sn	2	ND	ND	ND	ND	ND	ND
Zr	49	32	51	53	29	48	47
Y	14	28	14	14	26	21	11
Nb	1	<1	2.3	1.7	<1	1.8	1.8
Rb	4	4	6.0	6.4	6	3.3	12
Sr	160	170	150	150	140	150	110
Ba	5	16	<5	19	<10	20	56
Th	1	ND	ND	ND	ND	ND	ND

Table T106 (continued).

Leg	126	126	126	126	126	126	126
Hole	791B	791B	791B	791B	791B	791B	791B
Core, section	76R-3	77R-2	77R-2	77R-3	78R-1	79R-1	79R-1
Interval (cm)	40-45	0-5	132-137	18-23	24-30	5-8	45-50
Piece	4B	Tuff 1A	Tuff 6A	Tuff 1B	Breccia4	1	Tuff 5A
Lab number	Z-1444	Z-1445	Z-1446	Z-1447	Z-1448	Z-695	Z-1449
Depth (mbsf)	1112.40	1119.61	1120.93	1121.29	1128.54	1137.65	1138.05
Unit	15	18	20	20	24	26	28
Major element oxides (wt%):							
SiO_2	46.01	32.59	55.37	52.25	54.07	47.43	47.62
TiO_2	1.03	0.27	0.97	0.93	0.93	1.34	0.67
Al_2O_3	17.56	4.77	15.60	15.30	15.63	16.49	18.18
Fe_2O_3	5.78	2.79	3.25	3.59	4.18	7.01	3.32
FeO	4.27	0.82	4.63	5.19	4.03	6.97	6.56
MnO	0.18	0.04	0.12	0.15	0.16	0.38	0.20
MgO	8.31	2.31	6.03	7.32	7.58	5.15	8.47
CaO	8.75	17.70	2.58	3.49	3.85	5.72	1.86
Na_2O	2.58	1.58	1.90	1.82	2.98	5.14	4.09
K_2O	0.11	0.05	2.88	2.16	0.88	0.64	2.55
P_2O_5	0.12	0.06	0.24	0.23	0.27	0.18	0.07
LOI	4.96	17.66	6.05	7.40	5.04	3.32	6.29
Total	99.66	80.64	99.62	99.83	99.60	99.77	99.88
H_2O^+	0.89	0.99	3.28	3.84	2.56	2.02	4.47
H_2O^-	2.75	11.21	1.32	1.33	1.56	0.49	1.12
CO_2	0.51	0.40	0.87	2.18	0.46	0.49	0.57
S (total)	ND	10.12	ND	ND	ND	ND	ND
Fe_2O_3/FeO	1.35	3.40	0.70	0.69	1.04	1.01	0.51
Density (g/cm^3)	2.55	2.45	2.28	2.33	2.51	2.80	2.54
Trace elements (ppm):							
La							
Ce							
Nd							
Sm							
Eu							
Gd							
Tb							
Tm							
Yb							
Lu							
Cr	227	23	21	20	178	10	51
Ni	95	19	18	18	49	10	36
Co	52	18	20	20	30	28	36
V	400	57	110	114	242	253	355
Cu	55	25	47	47	73	29	49
Zn	91	230	172	122	111	103	88
Sn	ND	ND	ND	ND	ND	2	ND
Zr	52	25	95	95	65	68	27
Y	16	9.5	43	47	17	21	12
Nb	1.8	1.7	2.7	2.5	2.4	2	1.5
Rb	<1	1.2	68	57	6.2	10	23
Sr	230	77	75	87	190	330	400
Ba	38	<5	78	64	8	50	190
Th	ND	ND	ND	ND	ND	<1	ND

Table T107. Composition of igneous rocks from Hole 447A, Leg 59 (West Philippine Basin). (Continued on next two pages.)

Leg	59	59	59	59	59	59	59
Hole	447A	447A	447A	447A	447A	447A	447A
Core, section	14R-1	14R-3	15R-2	16R-2	16R-2	17R-3	19R-3
Interval (cm)	140-144	53-58	116-121	19-21	87-89	49-53	115-120
Piece	4L	3D	5D	3A	10	5A	8G
Lab number	Z-314	Z-315	Z-316	Z-317	Z-1144	Z-1145	Z-318
Depth (mbsf)	114.40	116.53	124.66	132.69	133.22	143.49	156.15
Unit/Subunit	6a	6b	6c	7	7	8a	8b
Major element oxides (wt%):							
SiO_2	44.83	46.43	46.80	44.50	47.14	48.40	47.66
TiO_2	1.26	1.24	1.23	1.06	1.04	1.29	1.37
Al_2O_3	17.95	17.12	17.95	16.65	16.90	16.50	16.30
Fe_2O_3	6.80	6.26	5.45	5.29	5.71	6.14	4.44
FeO	3.80	3.21	3.49	3.62	3.64	4.46	4.88
MnO	0.18	0.21	0.20	0.15	0.16	0.16	0.18
MgO	6.07	6.25	6.15	5.46	7.05	6.61	6.79
CaO	12.41	11.84	12.35	14.36	11.76	10.29	12.52
Na_2O	2.70	2.93	2.66	2.82	2.52	2.51	2.41
K_2O	0.43	0.71	0.49	0.92	0.29	0.59	0.55
P_2O_5	0.16	0.11	0.17	0.15	0.08	0.10	0.13
LOI	2.96	3.55	3.06	4.85	3.47	2.27	2.43
Total	99.55	99.86	100.00	99.83	99.76	99.32	99.66
H_2O^+	1.74	2.12	1.85	1.87	1.35	0.80	1.41
H_2O^-	1.22	1.43	1.21	0.38	0.73	0.86	1.02
CO_2	ND	ND	ND	2.60	0.64	0.21	ND
Fe_2O_3/FeO	1.79	1.95	1.56	1.46	1.57	1.38	0.91
Density (g/cm^3)	2.69	2.73	2.71	2.76	2.81	2.80	2.77
Trace elements (ppm):							
La	2.6	2.6	2.4	3.2			2.4
Ce	7.4	6.6	7.4	8.4			6.2
Nd	6.5	5.7	6.0	6.7			6.5
Sm	2.6	2.4	2.4	2.5			2.7
Eu	0.97	0.82	0.85	0.91			1.0
Tb	0.74	0.63	0.59	0.67			0.84
Yb	2.8	2.6	2.5	2.8			3.3
Lu	0.42	0.38	0.39	0.43			0.52
Cr	265	240	220	350	227	172	310
Ni	140	150	110	160	100	66	130
Co	41	44	36	37	46	38	45
V	220	155	135	270	126	355	260
Cu	110	105	105	83	130	88	90
Pb	<5	<5	<5	<5	ND	ND	<5
Zn	120	130	130	90	82	113	115
Zr	61	55	53	54	67	71	52
Y	25	23	24	27	22	30	30
Nb	2.9	1.9	2.3	2.4	2.0	2.4	2.0
Rb	4.1	5.9	3.6	30	6.6	15	6.5
Sr	120	110	120	120	130	82	67
Ba	<10	<10	<10	<10	7	47	<10

Note: ND = not determined.

Table T107 (continued).

Leg	59	59	59	59	59	59	59
Hole	447A	447A	447A	447A	447A	447A	447A
Core, section	23R-1	23R-1	24R-2	24R-2	25R-1	27R-1	28R-1
Interval (cm)	39-42	51-58	25-39	99-102	40-42	21-25	65-70
Piece	2B	5D	1B	2D	1C	2B	4C
Lab number	Z-1146	Z-1147	Z-1148	Z-1149	Z-319	Z-1150	Z-320
Depth (mbsf)	180.39	180.51	186.75	187.49	191.40	207.71	217.15
Unit/Subunit	8d	8d	9	9	9	10b	11a
Major element oxides (wt%):							
SiO_2	49.86	49.48	45.75	46.16	47.56	46.22	44.36
TiO_2	1.12	1.08	0.86	0.85	1.26	0.89	0.78
Al_2O_3	15.17	15.16	17.17	17.18	17.99	18.46	17.17
Fe_2O_3	3.86	3.30	2.68	2.40	4.35	5.60	5.38
FeO	5.54	6.47	5.00	5.81	5.55	3.43	3.47
MnO	0.18	0.17	0.15	0.15	0.18	0.17	0.14
MgO	9.05	8.38	9.51	10.21	5.19	7.52	9.62
CaO	11.10	11.26	11.56	11.18	12.53	11.29	12.10
Na_2O	2.18	2.16	2.25	2.23	2.32	2.46	2.27
K_2O	0.06	0.07	0.05	0.05	0.08	0.37	1.31
P_2O_5	0.08	0.08	0.04	0.05	0.08	0.05	0.21
LOI	1.70	1.85	4.64	3.10	2.45	3.55	2.92
Total	99.90	99.46	99.66	99.37	99.54	100.01	99.73
H_2O^+	0.65	0.28	1.79	1.57	1.72	1.78	1.67
H_2O^-	0.54	0.67	1.08	0.62	0.73	1.07	1.25
CO_2	<0.2	0.29	1.06	0.40	ND	0.21	ND
Fe_2O_3/FeO	0.70	0.51	0.54	0.41	0.78	1.63	1.55
Density (g/cm^3)	2.92	2.53	2.77	2.87	2.89	2.68	2.59
Trace elements (ppm):							
La					1.8		3.5
Ce					5.4		9.6
Nd					5.4		7.8
Sm					2.1		2.5
Eu					0.78		0.99
Tb					0.60		0.77
Yb					2.3		3.0
Lu					0.34		0.50
Cr	280	250	295	307	405	355	465
Ni	136	136	235	235	300	175	130
Co	64	57	63	64	59	55	35
V	382	355	210	230	185	270	265
Cu	90	87	130	88	83	120	70
Pb	ND	ND	ND	ND	<5	ND	<5
Zn	112	96	87	81	75	90	115
Zr	56	55	53	55	42	58	55
Y	25	25	21	21	18	20	19
Nb	1.2	<1	<1	<1	1.8	<1	4.4
Rb	<1	<1	1.3	1.0	0.5	5.1	12
Sr	67	68	110	110	100	110	94
Ba	5	9	<5	<5	<10	<5	19

Table T107 (continued).

Leg	59	59	59	59	59
Hole	447A	447A	447A	447A	447A
Core, section	29R-4	30R-3	32R-1	35R-3	36R-4
Interval (cm)	137-142	89-94	99-105	45-50	31-36
Piece	3B	3C	3K	2C	3A
Lab number	Z-321	Z-322	Z-323	Z-324	Z-325
Depth (mbsf)	231.37	238.39	253.49	278.45	288.81
Unit/Subunit	11b	11c	11e	11e	11f
Major element oxides (wt%):					
SiO_2	48.42	47.87	46.66	40.90	45.69
TiO_2	1.12	0.97	0.96	0.96	0.96
Al_2O_3	15.75	15.81	17.08	16.52	18.18
Fe_2O_3	4.76	4.83	4.97	6.38	7.12
FeO	4.52	4.34	4.37	3.62	2.85
MnO	0.16	0.14	0.16	0.16	0.16
MgO	7.62	8.18	7.04	6.80	4.90
CaO	13.01	12.71	13.66	12.57	12.77
Na_2O	2.22	2.22	2.13	3.15	3.15
K_2O	0.49	0.46	0.52	0.64	1.05
P_2O_5	0.02	0.02	0.02	0.04	0.03
LOI	2.11	2.62	1.99	2.56	3.54
Total	100.20	100.17	99.56	100.30	100.40
H_2O^+	0.94	1.16	1.23	1.14	1.95
H_2O^-	1.17	1.46	0.76	1.42	1.59
CO_2	ND	ND	ND	ND	ND
Fe_2O_3/FeO	1.05	1.11	1.13	1.76	2.50
Density (g/cm^3)	2.80	2.76	2.81	2.75	2.64
Trace elements (ppm):					
La	1.9	2.0	1.4	1.4	1.5
Ce	5.4	5.7	3.8	4.4	4.7
Nd	5.0	4.8	4.0	4.3	4.3
Sm	1.9	2.0	1.7	1.8	1.8
Eu	0.72	0.74	0.61	0.72	0.72
Tb	0.55	0.54	0.46	0.5	0.52
Yb	2.2	2.2	2.0	2.2	2.2
Lu	0.34	0.34	0.32	0.34	0.38
Cr	400	385	455	380	430
Ni	160	150	140	130	170
Co	47	44	41	40	44
V	220	200	220	190	265
Cu	100	74	140	90	74
Pb	<5	<5	<5	<5	<5
Zn	95	60	95	70	85
Zr	33	35	ND	31	36
Y	24	22	1.6	24	25
Nb	3.2	2.7	5.2	1.8	2.1
Rb	3.8	3.5	3.3	6.5	6.5
Sr	72	77	ND	74	83
Ba	<10	<10	ND	<10	<10

Table T108. Composition of igneous rocks from Holes 448 and 448A, Leg 59 (Palau-Kyushu Ridge). (Continued on next five pages.)

Leg	59	59	59	59	59	59	59
Hole	448	448	448	448	448	448	448
Core, section	37R-1	38R-1	38R-1	39R-1	39R-2	43R-2	48R-1
Interval (cm)	32-37	45-50	123-128	117-122	60-63	45-50	120-125
Piece	3C	1H	5B	10B	2F	5	11A
Lab number	Z-1152	Z-1153	Z-1154	Z-1155	Z-530	Z-1156	Z-1157
Depth (mbsf)	337.82	347.45	348.23	353.17	354.10	377.45	424.20
Unit	6	6	6	6	6	8	9
Major element oxides (wt%):							
SiO_2	47.10	43.15	48.05	47.33	48.51	46.40	46.65
TiO_2	1.44	1.30	1.45	1.43	1.48	1.41	1.43
Al_2O_3	13.93	13.15	14.41	14.36	15.41	16.18	16.27
Fe_2O_3	8.22	6.95	7.63	7.54	4.93	8.50	8.23
FeO	8.49	7.38	7.74	8.28	8.32	7.43	8.30
MnO	0.24	0.22	0.23	0.22	0.28	0.24	0.20
MgO	4.73	4.75	4.85	5.34	5.46	3.74	3.38
CaO	9.68	13.21	8.82	9.04	10.39	8.67	8.91
Na_2O	2.59	2.34	2.66	2.52	2.55	2.80	2.97
K_2O	0.58	0.60	0.86	0.62	0.53	0.65	0.47
P_2O_5	0.26	0.19	0.24	0.20	0.21	0.44	0.35
LOI	2.41	6.72	2.58	2.69	1.54	3.29	2.33
Total	99.67	99.96	99.52	99.57	99.61	99.75	99.49
H_2O^+	0.89	1.19	0.66	0.86	0.44	1.47	0.89
H_2O^-	1.25	1.46	1.59	1.58	0.95	1.82	1.18
CO_2	0.21	4.07	<0.2	<0.2	<0.20	<0.2	0.21
Fe_2O_3/FeO	0.97	0.94	0.99	0.91	0.59	1.14	0.99
Density (g/cm^3)	1.84	2.11	1.67	2.01	2.32	1.85	2.08
Trace elements (ppm):							
La							
Ce							
Nd							
Sm							
Eu							
Tb							
Yb							
Lu							
Cr	32	27	27	30	36	20	19
Ni	35	32	32	31	34	32	30
Co	40	36	38	40	52	32	32
V	472	410	457	480	515	410	492
Cu	160	135	114	135	150	125	145
Pb	ND	ND	ND	ND	<5	ND	ND
Zn	129	147	116	135	135	156	185
Sn	ND	ND	ND	ND	3.1	ND	ND
Zr	50	47	50	52	53	55	61
Y	29	27	60	38	34	34	40
Nb	<1	<1	<1	<1	1.2	<1	<1
Rb	10.0	9.2	15	8.4	7.9	9.9	6.1
Sr	150	150	150	150	150	170	170
Ba	26	10	78	72	8	24	86
Th	ND	ND	ND	ND	<1	ND	ND

Note: ND = not determined.

Table T108 (continued).

Leg	59	59	59	59	59	59	59
Hole	448	448	448	448A	448A	448A	448A
Core, section	53R-2	59R-2	61R-3	10R-4	12R-1	13R-2	14R-2
Interval (cm)	50-53	50-55	35-38	61-65	27-31	70-75	114-118
Piece	1H	2G	1D	4A	2C	Tuff 6A	4G
Lab number	Z-1158	Z-1159	Z-532	Z-533	Z-534	Z-1160	Z-535
Depth (mbsf)	472.50	529.50	549.70	295.11	309.27	346.15	487.14
Unit	11	13	13	5	5	6	11
Major element oxides (wt%):							
SiO_2	49.08	50.47	48.78	46.10	47.32	47.13	46.52
TiO_2	1.03	1.00	1.06	1.30	1.26	0.79	1.00
Al_2O_3	15.48	15.53	15.28	14.71	14.51	14.22	14.77
Fe_2O_3	5.45	6.06	5.54	7.67	7.39	10.81	10.14
FeO	8.13	7.09	6.26	7.76	8.44	0.26	5.32
MnO	0.20	0.18	0.17	0.23	0.22	0.12	0.19
MgO	5.73	4.90	4.56	5.45	5.66	4.01	5.98
CaO	9.57	9.17	10.01	10.86	10.08	3.96	10.08
Na_2O	2.53	2.56	2.76	2.52	2.47	2.47	2.59
K_2O	0.51	0.49	1.10	0.50	0.47	2.86	0.48
P_2O_5	0.12	0.17	0.11	0.18	0.16	0.02	0.24
LOI	1.83	2.25	3.26	2.56	1.90	13.05	2.84
Total	99.59	99.87	99.89	99.84	99.88	99.70	100.15
H_2O^+	0.60	0.92	0.45	0.33	0.45	4.95	0.93
H_2O^-	1.16	0.92	1.28	1.03	1.03	7.16	1.52
CO_2	<0.2	<0.2	<0.20	1.20	0.40	0.64	0.30
Fe_2O_3/FeO	0.67	0.86	0.88	0.99	0.88	41.58	1.91
Density (g/cm^3)	2.27	2.18	2.38	2.36	2.42	1.57	2.36
Trace elements (ppm):							
La							
Ce							
Nd							
Sm							
Eu							
Tb							
Yb							
Lu							
Cr	20	39	38	38	36	61	69
Ni	34	34	38	33	33	42	38
Co	38	35	45	42	40	31	43
V	427	402	360	535	480	187	675
Cu	180	252	165	180	180	150	130
Pb	ND	ND	<5	<5	<5	ND	<5
Zn	134	140	100	130	140	87	150
Sn	ND	ND	2.5	2.6	2.7	ND	2.8
Zr	52		69	51	50	33	56
Y	24	71	27	26	26	6	29
Nb	<1	27.0	1.6	1.0	<1	<1	<1
Rb	5.5	5.7	14.0	9.4	7.6	42.0	6.4
Sr	170	160	160	140	140	96	160
Ba	12	10	16	14	6	5	9
Th	ND	ND	1.3	<1	1	ND	1.2

Table T108 (continued).

Leg	59	59	59	59	59	59	59
Hole	448A	448A	448A	448A	448A	448A	448A
Core, section	15R-1	16R-1	20R-1	22R-1	26R-2	26R-2	26R-3
Interval (cm)	14-19	47-52	142-147	11-14	134-137	134-137	72-75
Piece	1B	4B	3B	1C	Tuff 3A	Tuff 3A	Tuff 1H
Lab number	Z-326	Z-327	Z-328	Z-536	Z-1162	Z-537	Z-538
Depth (mbsf)	527.64	537.47	566.92	584.61	615.84	615.84	616.72
Unit	13	13	14	15	17	17	17
Major element oxides (wt%):							
SiO_2	48.71	49.33	47.88	49.00	45.75	45.76	46.38
TiO_2	0.96	1.12	1.12	1.10	0.76	0.80	0.95
Al_2O_3	17.51	17.22	16.67	17.74	11.97	12.70	13.00
Fe_2O_3	5.69	5.08	7.15	8.30	12.71	12.09	12.14
FeO	5.62	6.65	5.87	3.52	0.28	0.54	0.35
MnO	0.17	0.17	0.16	0.13	0.22	0.25	0.22
MgO	4.39	4.22	3.88	4.12	5.25	5.13	5.45
CaO	9.94	10.56	9.48	8.40	2.10	2.69	2.46
Na_2O	2.86	2.78	2.93	3.53	2.62	2.62	2.72
K_2O	1.29	0.94	1.39	1.20	2.74	2.94	3.17
P_2O_5	0.04	0.03	0.06	0.21	0.01	0.07	0.10
LOI	3.12	1.84	3.83	2.63	15.19	14.14	13.16
Total	100.30	99.94	100.42	99.88	99.60	99.73	100.10
H_2O^+	1.34	0.64	1.70	0.81	6.54	4.50	5.16
H_2O^-	1.78	1.20	2.13	1.42	7.92	8.05	7.59
CO_2	ND	ND	ND	0.40	0.73	0.80	0.40
Fe_2O_3/FeO	1.01	0.76	1.22	2.36	45.39	22.39	34.69
Density (g/cm^3)	2.18	2.26	2.00	2.02	1.86	ND	1.82
Trace elements (ppm):							
La	3.5	3.7	4.0				
Ce	9.2	8.4	8.5				
Nd	7.8	8.4	8.3				
Sm	2.6	2.8	3.1				
Eu	0.85	0.90	0.98				
Tb	0.67	0.69	0.86				
Yb	2.8	2.8	3.3				
Lu	0.45	0.46	0.55				
Cr	23	30	18	22	54	54	53
Ni	34	34	29	27	32	28	30
Co	23	31	25	31	40	34	33
V	220	270	270	600	346	285	305
Cu	180	250	160	35	64	57	270
Pb	<5	<5	<5	<5	ND	<5	<5
Zn	85	100	120	98	82	66	62
Sn	ND	ND	ND	2.4	ND	2.0	2.4
Zr	52	62	64	74	32	32	33
Y	26	26	37	37	9	9.1	16
Nb	2.2	1.4	2.1	1.1	<1	<1	1.1
Rb	11	6.9	12	17	47	48	48
Sr	140	170	150	200	71	76	66
Ba	50	57	28	29	27	20	14
Th	ND	ND	ND	1.8	ND	1	1

Table T108 (continued).

Leg	59	59	59	59	59	59	59
Hole	448A	448A	448A	448A	448A	448A	448A
Core, section	30R-1	32R-1	33R-2	38R-2	41R-2	45R-1	47R-1
Interval (cm)	95-99	67-69	10-15	88-90	81-85	69-71	90-95
Piece	Tuff 4B	1G	1A	3A	5A	1D	1E
Lab number	Z-539	Z-540	Z-329	Z-330	Z-541	Z-331	Z-332
Depth (mbsf)	642.45	661.17	665.10	710.38	729.31	765.69	775.40
Unit	19	20	20	23	27	31	33
Major element oxides (wt%):							
SiO_2	44.24	48.10	50.13	47.32	47.42	50.15	52.31
TiO_2	1.05	1.45	1.28	0.96	0.90	1.12	1.20
Al_2O_3	11.20	14.75	14.26	14.54	15.54	14.76	14.51
Fe_2O_3	13.64	10.13	7.77	7.69	8.47	7.41	6.14
FeO	0.43	4.89	6.73	3.80	4.67	4.79	7.15
MnO	0.24	0.18	0.17	0.24	0.20	0.16	0.17
MgO	7.07	4.16	4.67	7.51	6.06	5.73	4.25
CaO	2.07	8.15	8.42	8.71	8.96	8.46	8.69
Na_2O	2.20	2.86	2.86	2.38	2.71	2.51	2.70
K_2O	1.24	1.61	0.98	0.63	0.26	0.25	0.41
P_2O_5	0.08	0.16	0.03	0.02	0.13	0.02	0.03
LOI	16.22	3.31	2.90	6.68	4.15	4.16	2.83
Total	99.68	99.75	100.20	100.48	99.47	99.52	100.39
H_2O^+	5.05	1.13	0.97	2.11	1.07	1.06	0.92
H_2O^-	10.31	1.88	1.93	4.57	2.78	3.10	1.91
CO_2	0.40	0.30	ND	ND	0.30	ND	ND
Fe_2O_3/FeO	31.72	2.07	1.15	2.02	1.81	1.55	0.86
Density (g/cm^3)	ND	2.34	2.54	2.23	2.38	2.57	2.71
Trace elements (ppm):							
La			2.0	1.5		1.6	2.8
Ce			6.9	4.0		4.4	7.4
Nd			6.0	3.9		4.2	6.3
Sm			2.4	1.6		1.8	2.4
Eu			0.87	0.64		0.78	0.96
Tb			0.64	0.48		0.48	0.70
Yb			2.9	2.0		2.0	3.1
Lu			0.47	0.32		0.34	0.46
Cr	38	23	8	365	42	28	10
Ni	28	28	22	105	33	32	26
Co	32	37	32	40	47	39	34
V	332	470	290	340	535	310	320
Cu	78	29	43	260	285	210	120
Pb	<5	<5	<5	<5	<5	<5	<5
Zn	74	140	125	85	92	100	95
Sn	2.2	2.5	ND	ND	2.8	ND	ND
Zr	37	50	32	30	40	24	40
Y	14	25	28	17	20	17	23
Nb	<1	<1	1.3	2.4	<1	2.5	3.3
Rb	25	25	12	6.0	3.1	1.3	3.2
Sr	57	140	130	130	160	140	120
Ba	6	9	34	15	17	29	42
Th	1.7	1.4	ND	ND	1.0	ND	ND

Table T108 (continued).

Leg	59	59	59	59	59	59	59
Hole	448A	448A	448A	448A	448A	448A	448A
Core, section	50R-3	51R-1	51R-3	53R-3	54R-3	57R-1	62R-1
Interval (cm)	116-121	98-102	49-52	0-5	124-128	33-36	98-102
Piece	Tuff 8	9D	3A	Breccia 1A	8C	1D	2
Lab number	Z-542	Z-333	Z-543	Z-1164	Z-544	Z-545	Z-334
Depth (mbsf)	796.56	802.48	804.94	819.50	832.74	846.83	887.98
Unit	36	37	37	40	41	43	49
Major element oxides (wt%):							
SiO_2	44.24	51.82	51.82	43.81	49.62	51.58	49.62
TiO_2	1.25	1.28	1.52	1.04	1.30	1.32	1.04
Al_2O_3	12.88	14.16	13.84	12.12	15.80	14.96	18.00
Fe_2O_3	12.61	8.98	8.46	11.75	9.04	8.89	5.80
FeO	2.59	4.25	5.46	1.17	3.70	4.24	5.12
MnO	0.15	0.13	0.21	0.16	0.17	0.16	0.14
MgO	7.15	4.95	4.12	7.12	5.00	4.12	4.34
CaO	4.93	6.74	7.84	2.48	7.90	7.73	10.96
Na_2O	3.34	2.64	2.61	2.26	2.76	2.89	2.51
K_2O	0.44	0.42	0.25	0.36	0.23	0.26	0.28
P_2O_5	0.17	0.05	0.15	0.04	0.16	0.18	0.02
LOI	9.66	5.06	3.42	17.65	4.40	3.24	2.40
Total	99.41	100.48	99.70	99.96	100.08	99.57	100.23
H_2O^+	2.81	1.45	0.90	4.54	1.19	0.94	0.60
H_2O^-	6.63	3.61	2.32	9.77	2.91	2.21	1.80
CO_2	0.20	ND	0.20	0.43	0.30	<0.20	ND
Fe_2O_3/FeO	4.87	2.11	1.55	10.04	2.44	2.10	1.13
Density (g/cm^3)	1.59	2.47	2.56	ND	2.40	2.49	2.65
Trace elements (ppm):							
La		2.1		1.1			3.0
Ce		5.7		3.4			6.6
Nd		5.7		3.6			6.0
Sm		2.5		1.5			2.1
Eu		0.91		0.52			0.73
Tb		0.65		0.45			0.48
Yb		2.8		2.1			2.0
Lu		0.44		0.33			0.33
Cr	62	9	10	54	26	20	21
Ni	35	27	26	30	29	23	37
Co	43	46	45	45	43	35	30
V	690	310	367	595	410	412	290
Cu	270	160	155	78	150	215	140
Pb	<5	<5	<5	ND	<5	<5	<5
Zn	130	115	145	70	127	125	90
Sn	2.4	ND	2.8		1.9	2.2	ND
Zr	48	38	54	39	55	56	36
Y	23	27	30	15	25	28	17
Nb	1.0	1.0	1.2	<1	1.4	1.0	1.4
Rb	3.1	2.6	3.2	5.4	2.3	3.7	0.6
Sr	170	130	130	86	150	160	190
Ba	15	44	14	77	5	7	39
Th	1.1	ND	<1	ND	1.3	1.1	ND

Table T108 (continued).

Leg	59	59
Hole	448A	448A
Core, section	65R-2	66R-2
Interval (cm)	10-15	78-83
Piece	1B	1D
Lab number	Z-335	Z-546
Depth (mbsf)	906.6	912.78
Unit	51	51
Major element oxides (wt%):		
SiO_2	48.85	51.30
TiO_2	1.28	1.26
Al_2O_3	14.25	14.48
Fe_2O_3	8.06	9.46
FeO	5.27	4.02
MnO	0.14	0.13
MgO	5.82	4.36
CaO	8.69	6.94
Na_2O	2.64	2.76
K_2O	0.21	0.29
P_2O_5	0.03	0.16
LOI	4.82	4.28
Total	100.06	99.44
H_2O^+	1.20	1.13
H_2O^-	3.62	2.89
CO_2	ND	<0.20
Fe_2O_3/FeO	1.53	2.35
Density (g/cm^3)	2.48	2.40
Trace elements (ppm):		
La	2.1	
Ce	5.1	
Nd	5.4	
Sm	2.2	
Eu	0.79	
Tb	0.59	
Yb	2.5	
Lu	0.41	
Cr	16	10
Ni	26	28
Co	27	40
V	270	457
Cu	200	140
Pb	<5	<5
Zn	80	126
Sn	ND	2.6
Zr	33	53
Y	24	28
Nb	<1	1.7
Rb	0.6	4.2
Sr	140	140
Ba	32	6
Th	ND	1.2

Table T109. Composition of igneous rocks from Hole 449, Leg 59 (Parece Vela Basin).

Leg	59	59
Hole	449	449
Core, section	15R-2	17R-2
Interval (cm)	17-20	2-6
Piece	1B	1A
Lab number	Z-336	Z-337
Depth (mbsf)	115.67	134.52
Unit/Subunit	6a	6b
Major element oxides (wt%):		
SiO_2	46.00	47.27
TiO_2	1.12	0.96
Al_2O_3	17.12	16.77
Fe_2O_3	6.45	5.97
FeO	3.43	3.55
MnO	0.14	0.13
MgO	5.18	6.74
CaO	13.57	12.00
Na_2O	2.64	2.64
K_2O	0.45	0.48
P_2O_5	0.02	0.02
LOI	3.65	3.54
Total	99.77	100.07
H_2O^+	1.74	1.06
H_2O^-	1.91	2.48
CO_2	ND	ND
Fe_2O_3/FeO	1.88	1.68
Density (g/cm^3)	2.45	2.51
Trace elements (ppm):		
La	3.6	3.2
Ce	9.2	7.5
Nd	6.6	6.6
Sm	2.2	2.2
Eu	0.92	0.81
Tb	0.67	0.59
Yb	2.8	2.5
Lu	0.45	0.40
Cr	210	275
Ni	115	145
Co	38	50
V	160	185
Cu	115	90
Pb	<5	<5
Zn	68	80
Zr	45	43
Y	22	26
Nb	4.6	3.1
Rb	6.2	6.4
Sr	150	130
Ba	23	22

Note: ND = not determined.

Table T110. Composition of gabbros from Hole 453, Leg 60 (West Side of the Mariana Trough, Philippine Sea). (Continued on next page.)

Leg	60	60	60	60	60	60	60
Hole	453	453	453	453	453	453	453
Core, section	50R-2	51R-1	51R-3	52R-2	53R-3	53R-5	55R-3
Interval (cm)	45-50	8-12	54-58	113-118	19-24	88-91	50-53
Piece	6	1	4B	10	3D	9B	3I
Lab number	Z-338	Z-339	Z-340	Z-341	Z-342	Z-343	Z-344
Depth (mbsf)	466.95	474.58	478.04	486.63	496.69	500.38	516.00
Major element oxides (wt%):							
SiO_2	43.76	41.72	43.18	39.04	44.32	41.84	37.82
TiO_2	0.64	0.32	0.36	0.24	0.64	0.19	0.55
Al_2O_3	15.70	21.35	18.23	21.50	14.41	24.40	21.99
Fe_2O_3	3.76	4.12	3.37	5.18	3.56	3.02	7.45
FeO	3.42	3.21	3.03	4.79	4.54	3.55	4.02
MnO	0.11	0.10	0.11	0.11	0.13	0.06	0.08
MgO	11.74	10.39	11.34	11.53	11.96	8.52	11.04
CaO	17.14	14.30	17.08	12.45	17.30	15.58	11.55
Na_2O	0.61	0.61	0.77	0.77	0.64	0.64	0.51
K_2O	0.17	0.27	0.25	0.32	0.27	0.13	0.12
P_2O_5	0.02	0.01	ND	ND	ND	ND	ND
LOI	2.79	3.24	2.52	3.66	2.30	2.43	5.16
Total	99.86	99.64	100.24	99.59	100.07	100.36	100.29
H_2O^+	1.72	2.71	2.05	3.10	1.97	2.01	4.33
H_2O^-	1.07	0.53	0.47	0.56	0.33	0.42	0.83
CO_2	ND	ND	ND	ND	ND	ND	ND
Fe_2O_3/FeO	1.10	1.28	1.11	1.08	0.78	0.85	1.85
Density (g/cm^3)	ND	2.90	2.91	2.83	3.06	2.87	2.78
Trace elements (ppm):							
La	0.20	0.21	0.24	0.15	0.25	0.097	0.064
Ce	0.63	0.45	0.53	0.33	0.67	0.19	0.093
Nd	<1.0	<1.0	<1.0	<1.0	<1.0	<1.0	<1.0
Sm	0.35	0.13	0.25	0.066	0.48	0.087	0.021
Eu	0.16	0.092	0.12	0.081	0.20	0.073	0.054
Tb	0.098	0.026	0.075	0.012	0.13	0.023	<0.01
Yb	0.34	0.094	0.21	0.055	0.44	0.065	0.018
Lu	0.046	0.014	0.032	0.0099	0.067	0.011	0.0031
Cr	245	65	202	9	160	45	157
Ni	57	65	63	70	60	55	95
Co	38	60	40	73	54	44	80
V	115	35	77	56	120	27	115
Cu	19	28	17	20	28	21	16
Pb	<5	<5	<5	<5	<5	<5	<5
Zn	25	50	25	62	25	16	54
Zr	<10	<10	<10	<10	<10	<10	<10
Y	2.0	<2	<2	<1	4.3	1.2	1.3
Nb	1.2	1.3	1.5	<1	<1	1.5	<1
Rb	1.5	3.2	2.3	4.3	3.7	2.0	1.1
Sr	180	340	250	320	200	360	310
Ba	31	45	22	110	34	<10	<10

Note: ND = not determined.

Table T110 (continued).

Leg	60	60	60	60	60	60
Hole	453	453	453	453	453	453
Core, section	55R-4	56R-2	56R-2	57R-4	63R-1	63R-1
Interval (cm)	127-131	33-35	85-87	2-7	80-83	130-135
Piece	12C	6A	12A	1	4A	5I
Lab number	Z-1167	Z-1169	Z-1170	Z-345	Z-1172	Z-1173
Depth (mbsf)	518.27	523.83	524.35	536.02	589.30	589.80
Major element oxides (wt%):						
SiO_2	40.01	42.69	48.07	40.04	46.68	48.14
TiO_2	0.03	0.07	0.07	0.16	0.57	0.63
Al_2O_3	26.21	29.88	25.99	23.02	10.46	11.04
Fe_2O_3	3.49	0.43	0.53	5.11	7.07	5.68
FeO	4.90	4.00	3.36	3.55	7.71	9.44
MnO	0.12	0.10	0.08	0.07	0.22	0.25
MgO	10.17	5.06	4.24	9.92	10.23	10.10
CaO	11.44	13.59	9.04	12.71	9.22	10.05
Na_2O	0.75	1.05	2.79	0.53	1.78	1.47
K_2O	0.41	0.59	1.45	0.25	0.16	0.21
P_2O_5	0.02	0.01	0.01	ND	0.01	0.05
LOI	2.23	2.77	3.60	4.64	5.48	3.04
Total	99.78	100.24	99.23	100.00	99.59	100.10
H_2O^+	1.56	2.26	2.56	3.87	1.55	0.84
H_2O^-	0.12	0.28	0.43	0.77	3.04	1.95
CO_2	0.22	0.23	<0.2	ND	0.31	0.25
Fe_2O_3/FeO	0.71	0.11	0.16	1.44	0.92	0.60
Density (g/cm^3)	2.98	2.72	2.74	2.81	2.91	2.91
Trace elements (ppm):						
La				0.15	1.1	1.3
Ce				0.23	3.3	3.8
Nd				<1.0	3.3	3.4
Sm				0.041	1.2	1.3
Eu				0.06	0.43	0.37
Tb				<0.02	0.32	0.34
Yb				0.018	1.4	1.5
Lu				0.0034	0.23	0.25
Cr	10	<10	10	18	42	43
Ni	60	30	28	94	32	33
Co	72	42	22	82	65	62
V	50	52	49	14	362	357
Cu	45	21	20	19	82	54
Pb	ND	ND	ND	<5	ND	ND
Zn	158	68	57	38	101	94
Zr	2.5	3.9	6	<10	14.00	15.00
Y	1.3	1.6	2.4	<1	11.0	13.0
Nb	<1	<1	<1	<1	<1	<1
Rb	4.1	5.3	18.0	1.5	<1	<1
Sr	320	490	450	350	180	210
Ba	270	390	590	54	83	93

Table T111. Secondary minerals in gabbros, Mariana Trough, Leg 60: Hole 453.

Core, section, interval (cm)	Depth (mbsf)	Sm	Chl	ML Sm-Chl	Serp	Hmica	Amph	Talc	Analc	Prenite	Quartz
60-453-											
50R-2, 45-50	466.95	X	X				++	+?			
51R-1, 8-12	474.58	X	X			+	++				
51R-3, 54-58	478.04		++		X		+				
52R-2, 113-118	486.63	+	X		++		++	+?			
53R-3, 19-24	496.69		X		++	+	++				
53R-5, 88-91	500.38[1]		X		X		+				
55R-3, 50-53	516.00	+	++		X		+	+			
55R-3, 142-147	516.92[2]	+	X	+		++	++		++	+?	
55R-4, 82-84	517.82	+	X			X			++		X
56R-1, 40-45	522.40	X	X			++	+	+	+		
57R-4, 2-7	536.02	+	X	+	X		+	++			
61R-1, 30-35	569.80			X							
63R-1, 130-135	589.80	X									

Notes: X = dominant, ++ = minor, + = trace.
Sm = smectite, Chl = chlorite. ML Sm-Chl = mixed-layer smectite-chlorite minerals, Serp = serpentine, Hmica = hydromica, Amph = amphibole, Analc = analcime.
[1] = chalcophyllite(?) in trace amount, [2] = natrolite(?) in trace amount.

Table T112. Composition of igneous rocks from Hole 454A, Leg 60 (West Side of the Mariana Trough, Philippine Sea). (Continued on next page.)

Leg	60	60	60	60	60	60	60	60
Hole	454A	454A	454A	454A	454A	454A	454A	454A
Core, section	5R-1	5R-1	5R-2	5R-3	5R-4	8R-1	10R-1	11R-1
Interval (cm)	3-7	128-132	50-55	115-118	10-15	100-106	45-49	58-62
Piece	1	17A	4	6A	2	Tuff	2	Sediment
Lab number	Z-1174	Z-346	Z-1175	Z-347	Z-1176	Z-348	Z-349	Z-350
Depth (mbsf)	67.03	68.28	69.00	71.15	71.60	96.00	113.45	122.58
Unit	1	1	1	1	1		3	
Major element oxides (wt%):								
SiO_2	47.85	47.76	48.80	48.22	48.55	47.44	48.91	80.96
TiO_2	0.97	1.04	0.97	1.04	0.86	1.19	1.00	0.64
Al_2O_3	16.80	15.24	17.13	15.46	16.54	12.93	16.34	4.86
Fe_2O_3	3.58	5.39	2.32	4.20	2.94	8.46	5.46	3.45
FeO	3.73	3.20	4.95	4.49	4.80	4.59	3.93	2.50
MnO	0.14	0.09	0.12	0.09	0.13	0.14	0.05	0.04
MgO	6.23	7.70	6.92	8.00	9.96	4.32	6.28	1.79
CaO	13.19	12.51	12.63	12.36	11.49	6.82	12.45	2.21
Na_2O	2.43	3.27	2.51	3.18	2.74	4.31	3.18	1.06
K_2O	0.23	0.34	0.16	0.27	0.16	1.24	0.39	0.13
P_2O_5	0.04	0.09	0.09	0.10	0.08	0.17	0.15	0.06
LOI	4.05	3.34	2.72	2.68	2.11	7.90	2.17	1.79
Total	99.24	99.97	99.32	100.09	100.36	99.51	100.31	99.49
H_2O^+	1.18	1.27	0.74	1.42	0.68	4.10	1.07	1.49
H_2O^-	1.60	2.07	1.22	1.26	1.06	3.80	1.10	0.30
CO_2	1.27	ND	0.50	ND	0.23	ND	ND	ND
Fe_2O_3/FeO	1.00	1.68	0.47	0.94	0.61	1.84	1.39	1.38
Density (g/cm^3)	2.35	2.35	2.15	2.34	2.50	1.11	2.00	2.53
Trace elements (ppm):								
La		3.5		3.5		6.7	3.8	3.4
Ce		7.5		8.8		1.4	9.6	5.7
Nd		7.0		6.8		11	7.0	4.7
Sm		2.1		2.2		3.2	2.1	1.3
Eu		0.82		0.84		1.1	0.82	0.43
Tb		0.51		0.54		0.69	0.51	0.29
Yb		2.0		2.0		2.7	2.0	1.2
Lu		0.31		0.31		0.43	0.31	0.20
Cr	188	295	245	280	272	28	237	8
Ni	71	190	95	125	155	31	110	25
Co	30	43	42	38	40	25	32	13
V	118	170	197	180	129	270	200	77
Cu	61	70	92	115	66	215	60	20
Pb	ND	<5	ND	<5	ND	<5	<5	<5
Zn	73	63	81	63	75	73	58	54
Zr	60	42	60	46	54	61	51	21
Y	22	21	22	20	19	24	20	13
Nb	2.1	1.9	2.4	2.0	1.7	1.9	2.3	1.1
Rb	3.9	2.8	2.2	2.3	2.0	14	5.9	2.4
Sr	170	150	160	180	150	230	220	64
Ba	27	22	46	36	14	230	79	61

Note: ND = not determined.

Table T112 (continued).

Leg	60	60	60	60	60	60	60
Hole	454A	454A	454A	454A	454A	454A	454A
Core, section	11R-1	11R-2	11R-4	12R-1	12R-2	13R-1	16R-1
Interval (cm)	102-109	125-128	92-97	116-120	30-34	11-15	25-30
Piece	11	7A	5	13	3B	Sediment	5
Lab number	Z-351	Z-1177	Z-352	Z-353	Z-1178	Z-354	Z-355
Depth (mbsf)	123.02	124.75	127.42	132.16	132.80	140.13	162.25
Unit	4	4	4	4	4		5
Major element oxides (wt%):							
SiO_2	49.83	49.14	48.72	49.67	49.75	50.59	49.60
TiO_2	1.14	0.92	0.96	1.04	0.93	0.96	1.24
Al_2O_3	16.27	17.14	16.14	16.29	15.98	14.39	15.30
Fe_2O_3	2.96	2.66	3.38	4.08	2.60	5.88	4.77
FeO	5.30	4.81	4.60	4.68	4.60	4.02	4.87
MnO	0.11	0.12	0.07	0.10	0.10	0.14	0.14
MgO	7.57	7.20	9.36	7.97	7.87	4.38	7.56
CaO	11.66	11.11	10.73	11.67	11.56	7.03	11.07
Na_2O	2.80	2.58	2.70	2.80	2.17	3.79	2.99
K_2O	0.37	0.11	0.24	0.20	0.13	1.22	0.66
P_2O_5	0.10	0.10	0.10	0.10	0.11	0.17	0.13
LOI	2.37	3.39	2.58	1.61	3.59	7.13	1.88
Total	100.48	99.28	99.58	100.21	99.39	99.70	100.21
H_2O^+	1.22	1.00	1.50	1.02	0.65	4.15	1.14
H_2O^-	1.15	1.38	1.08	0.59	0.90	2.98	0.74
CO_2	ND	0.34	ND	ND	1.23	ND	ND
Fe_2O_3/FeO	0.56	0.55	0.74	1.00	0.57	1.46	0.98
Density (g/cm^3)	2.17	2.04	2.30	2.12	2.00	1.13	2.23
Trace elements (ppm):							
La	4.2		3.5	3.9		6.6	4.6
Ce	11		8.2	9.1		14	11
Nd	7.8		6.6	8.1		12	10
Sm	2.6		2.1	2.3		3.0	3.0
Eu	0.88		0.79	0.83		0.96	1.0
Tb	0.61		0.47	0.53		0.69	0.68
Yb	2.3		1.9	2.0		2.9	2.5
Lu	0.36		0.30	0.32		0.47	0.37
Cr	187	258	240	240	250	18	280
Ni	105	135	170	145	135	23	130
Co	33	40	37	36	37	23	31
V	160	230	130	155	232	240	195
Cu	60	66	76	92	32	125	50
Pb	<5	ND	<5	<5	ND	<5	<5
Zn	50	80	60	60	64	75	70
Zr	51	64	45	56	66	63	66
Y	21	21	19	22	19	28	27
Nb	2.8	1.4	2.2	2.3	1.6	2.7	2.5
Rb	4.2	<1	2.4	1.6	<1	14	8.7
Sr	190	210	180	200	290	270	170
Ba	25	43	33	43	40	230	39

Table T113. Composition of igneous rocks from Hole 458, Leg 60 (Mariana Forearc Region). (Continued on next three pages.)

Leg	60	60	60	60	60	60	60
Hole	458	458	458	458	458	458	458
Core, section	28R-1	29R-1	30R-1	31R-1	32R-3	33R-1	33R-2
Interval (cm)	106-110	103-109	111-113	116-120	90-95	32-37	127-131
Piece	14	17	17	18	12A	4	14
Lab number	Z-356	Z-357	Z-358	Z-359	Z-360	Z-1179-2	Z-361
Depth (mbsf)	257.56	267.03	276.61	286.16	298.40	304.32	306.77
Unit-Subunit	1-1	1-1	1-1	2-1	2-1	2-2	2-3
Major element oxides (wt%):							
SiO_2	50.08	49.27	49.27	51.89	55.40	50.06	53.29
TiO_2	0.62	0.56	0.51	0.49	0.51	0.25	0.55
Al_2O_3	14.75	14.74	14.39	15.09	14.67	11.98	15.07
Fe_2O_3	3.47	5.51	5.53	6.16	3.85	5.22	4.90
FeO	5.30	2.86	2.72	3.51	4.29	2.37	3.26
MnO	0.15	0.07	0.08	0.10	0.09	0.30	0.14
MgO	8.67	8.48	8.14	6.16	5.39	8.12	11.26
CaO	11.18	9.32	9.18	11.21	10.92	8.07	6.20
Na_2O	2.34	2.48	2.48	2.70	2.45	1.99	2.45
K_2O	0.41	0.89	1.07	0.76	0.97	0.89	0.97
P_2O_5	ND	ND	0.01	0.03	0.03	0.04	0.03
LOI	3.27	6.23	6.17	2.05	1.50	10.02	1.65
Total	100.24	100.41	99.55	100.15	100.07	99.31	99.77
H_2O^+	1.23	2.31	2.19	1.03	0.79	3.65	0.40
H_2O^-	2.04	3.92	3.98	1.02	0.71	4.12	1.25
CO_2	ND	ND	ND	ND	ND	1.75	ND
Fe_2O_3/FeO	0.66	1.93	2.03	1.76	0.90	2.20	1.50
Density (g/cm^3)	1.90	1.99	1.97	2.21	2.41	1.84	2.38
Trace elements (ppm):							
La	0.45	0.87	0.84	1.1	0.96	0.67	0.79
Ce	1.2	1.8	1.5	2.4	2.2	1.9	1.7
Nd	1.0	1.7	1.6	2.1	1.8	1.6	1.8
Sm	0.37	0.51	0.52	0.69	0.63	0.53	0.66
Eu	0.17	0.20	0.19	0.27	0.24	0.15	0.25
Tb	0.15	0.15	0.12	0.18	0.2	0.14	0.2
Yb	0.58	0.49	0.42	0.93	0.78	0.70	0.98
Lu	0.096	0.071	0.063	0.16	0.12	0.13	0.16
Cr	150	300	305	115	142	218	182
Ni	80	93	93	63	58	75	70
Co	39	42	39	33	30	40	34
V	200	260	195	190	130	228	170
Cu	45	30	35	40	45	285	32
Pb	<5	<5	<5	<5	<5	ND	<5
Zn	70	80	73	75	45	60	62
Zr	23	22	24	22	18	23	19
Y	10	5.4	3.9	10	8.4	5.4	7.9
Nb	3.0	<1	<1	<1	<1	<1	<1
Rb	3.4	10	12	56	64	30	15
Sr	82	90	86	97	88	77	91
Ba	<10	<10	<10	26	20	7	25

Note: ND = not determined.

Table T113 (continued).

Leg	60	60	60	60	60	60	60
Hole	458	458	458	458	458	458	458
Core, section	34R-2	35R-2	36R-1	37R-2	39R-1	39R-2	40R-1
Interval (cm)	14-19	12-18	125-128	70-75	100-102	60-65	143-147
Piece	1B	2	18	8C	12A	6	1Q
Lab number	Z-362	Z-363	Z-1180	Z-364	Z-365	Z-1181	Z-1182
Depth (mbsf)	315.14	324.62	333.75	344.20	362.00	363.10	371.93
Unit-Subunit	2-3	2-4	2-4	2-6	3-1	3-1	3-1
Major element oxides (wt%):							
SiO_2	53.27	49.51	48.39	50.79	49.10	49.22	48.36
TiO_2	0.56	0.64	0.31	0.64	0.64	0.33	0.33
Al_2O_3	15.07	17.31	15.34	16.01	16.29	16.61	16.87
Fe_2O_3	5.09	5.21	5.63	5.46	4.69	4.08	6.03
FeO	3.30	4.02	2.92	3.50	3.41	3.79	2.43
MnO	0.13	0.11	0.14	0.11	0.12	0.14	0.09
MgO	6.00	5.35	7.61	6.19	6.48	6.94	6.22
CaO	11.10	11.53	7.35	11.59	9.36	8.97	7.24
Na_2O	2.53	2.80	2.18	2.53	2.57	2.01	2.37
K_2O	0.97	1.22	0.63	1.22	0.84	0.52	0.99
P_2O_5	0.03	0.05	0.01	0.04	0.02	0.01	0.02
LOI	1.65	2.02	8.81	2.04	6.25	6.62	8.38
Total	99.70	99.77	99.32	100.12	99.77	99.24	99.33
H_2O^+	0.40	1.01	1.34	0.83	2.12	1.73	2.84
H_2O^-	1.25	1.01	5.92	1.21	4.13	3.93	5.08
CO_2	ND	ND	<0.2	ND	ND	<0.2	<0.2
Fe_2O_3/FeO	1.54	1.30	1.93	1.56	1.38	1.08	2.48
Density (g/cm^3)	2.44	1.94	1.82	2.16	1.96	2.11	1.84
Trace elements (ppm):							
La	0.8	1.1	0.51	1.1	0.52	0.57	0.61
Ce	2.1	2.3	1.5	2.1	1.5	1.7	1.8
Nd	1.8	2.0	1.4	2.1	1.5	1.4	1.5
Sm	0.69	0.87	0.51	0.84	0.68	0.49	0.51
Eu	0.26	0.33	0.19	0.34	0.26	0.21	0.27
Tb	0.21	0.24	0.14	0.23	0.20	0.15	0.15
Yb	0.99	1.1	0.64	1.2	0.86	0.82	0.64
Lu	0.16	0.18	0.11	0.21	0.14	0.13	0.11
Cr	250	147	345	260	500	333	330
Ni	83	70	99	88	135	90	84
Co	39	36	63	39	51	52	42
V	190	215	385	270	265	390	332
Cu	32	35	355	40	45	56	49
Pb	<5	<5	ND	<5	<5	ND	ND
Zn	62	65	90	63	80	74	86
Zr	23	27	32	20	20	32	33
Y	7.2	8.9	6.7	8.9	7.8	6.1	4.6
Nb	<1	1.1	<1	<1	<1	<1	1.2
Rb	19	29	5	37	7.9	5.2	15
Sr	93	110	95	85	90	100	98
Ba	27	30	11	31	<10	8	110

Table T113 (continued).

Leg	60	60	60	60	60	60	60
Hole	458	458	458	458	458	458	458
Core, section	41R-1	41R-1	41R-1	42R-1	43R-2	44R-1	45R-1
Interval (cm)	2-7	102-107	40-45	60-65	45-50	140-145	130-135
Piece	1	1	1	6	7	11	15A
Lab number	Z-1183	Z-1184	Z-1185	Z-1186	Z-1187	Z-1188	Z-366
Depth (mbsf)	380.02	381.02	381.90	390.10	400.95	409.90	419.30
Unit-Subunit	4A-1	4A-1	4A-1	4B-1	4B-1	4B-1	4B-3
Major element oxides (wt%):							
SiO_2	51.06	53.34	51.86	48.26	48.58	48.02	49.14
TiO_2	0.96	1.03	0.97	0.51	0.51	0.51	0.72
Al_2O_3	16.90	17.57	17.00	15.41	15.32	15.41	15.16
Fe_2O_3	8.32	7.75	8.45	9.02	8.22	7.25	6.88
FeO	1.58	1.65	1.44	1.65	1.72	2.52	2.70
MnO	0.08	0.07	0.09	0.08	0.08	0.09	0.10
MgO	2.71	2.06	2.81	5.90	6.22	6.66	6.77
CaO	6.25	6.94	5.94	7.95	8.18	8.00	9.37
Na_2O	5.63	4.77	4.32	2.65	2.67	2.51	2.53
K_2O	1.23	1.29	1.27	0.66	0.55	0.35	0.42
P_2O_5	0.36	0.18	0.22	0.06	0.04	0.03	0.02
LOI	5.08	2.80	4.92	7.15	7.19	7.90	5.99
Total	100.16	99.45	99.29	99.30	99.28	99.25	99.80
H_2O^+	1.87	0.98	1.56	2.20	1.75	2.26	1.90
H_2O^-	2.73	1.42	2.80	3.83	3.87	4.21	4.09
CO_2	<0.2	<0.2	<0.2	<0.2	0.24	0.21	ND
Fe_2O_3/FeO	5.27	4.70	5.87	5.47	4.78	2.88	2.55
Density (g/cm^3)	1.66	1.85	1.68	1.88	1.93	1.86	1.93
Trace elements (ppm):							
La				2.6	2.2	1.2	1.1
Ce				7.0	6.2	3.5	2.5
Nd				5.1	4.5	3.0	2.4
Sm				1.6	1.4	1.1	1.0
Eu				0.60	0.46	0.37	0.43
Tb				0.39	0.38	0.28	0.30
Yb				1.7	1.5	1.2	1.3
Lu				0.30	0.24	0.19	0.21
Cr	<10	10	<10	235	248	218	365
Ni	30	24	28	68	68	82	125
Co	23	22	22	34	32	46	43
V	268	245	240	362	348	390	330
Cu	62	56	415	56	61	90	34
Pb	ND	ND	ND	ND	ND	ND	<5
Zn	96	87	92	88	88	98	105
Zr	86	91	85	44	43	45	31
Y	50	27	32	18	16	9.0	12
Nb	2.1	2.3	2.5	<1	1.0	<1	<1
Rb	27	26	29	16	14	7.9	6.4
Sr	160	160	150	120	130	120	100
Ba	43	49	65	6	5	26	<10

Table T113 (continued).

Leg	60	60	60
Hole	458	458	458
Core, section	46R-1	47R-1	48R-1
Interval (cm)	89-91	133-136	42-47
Piece	8	17	1
Lab number	Z-367	Z-368	Z-1189
Depth (mbsf)	428.39	438.33	446.92
Unit-Subunit	4C-1	5-1	5-2
Major element oxides (wt%):			
SiO_2	48.91	47.98	46.82
TiO_2	1.12	1.12	0.90
Al_2O_3	16.12	15.58	15.38
Fe_2O_3	8.68	8.75	10.00
FeO	2.58	3.49	2.37
MnO	0.09	0.10	0.08
MgO	4.56	4.84	5.82
CaO	6.29	7.04	5.94
Na_2O	3.84	3.74	3.14
K_2O	0.63	0.63	0.50
P_2O_5	0.07	0.09	0.08
LOI	6.95	6.20	8.44
Total	99.84	99.56	99.47
H_2O^+	1.93	1.61	2.52
H_2O^-	5.02	4.59	4.91
CO_2	ND	ND	0.23
Fe_2O_3/FeO	3.36	2.51	4.22
Density (g/cm^3)	1.95	2.09	2.01
Trace elements (ppm):			
La	2.1	2.0	
Ce	5.6	5.7	
Nd	5.4	5.8	
Sm	2.2	2.2	
Eu	0.84	0.89	
Tb	0.60	0.64	
Yb	2.4	2.9	
Lu	0.37	0.44	
Cr	8	5	20
Ni	62	45	47
Co	46	40	42
V	370	550	598
Cu	35	85	98
Pb	<5	<5	ND
Zn	105	180	116
Zr	49	63	58
Y	20	23	25
Nb	1.4	1.0	1.2
Rb	7.3	6.4	10
Sr	130	160	130
Ba	<10	<10	54

Table T114. Secondary minerals in igneous rocks, Mariana Forearc Basin, Leg 60: Holes 458 and 459B.

Core, section, interval (cm)	Depth (mbsf)	Unit	Sm	Crist	Verm	Hmica	Amph	Chl	Phill	Analc	Quartz
60-458-											
28R-1, 106-110	257.56	1-1	X				+	+			
29R-1, 103-108	267.03	1-1	X								
30R-1, 111-113	276.61	1-1	X								
31R-1, 116-120	286.16	2-1	X	X		+	+				
32R-3, 90-95	298.40	2-1	++	X		+	+				
33R-1, 32-37	304.32	2-2	X		X	++					+
33R-2, 127-131	306.77	2-3	X	++		+					
34R-2, 14-19	315.14	2-3	X	X		++					
35R-2, 12-18	324.62	2-4	X	X		++					
36R-1, 125-128	333.75	2-4	X								
37R-2, 70-75	344.20	2-6	X	+		+	+				
39R-1, 100-102	362.00	3-1	X			+					
40R-1, 143-147	371.93	3-1	X						+	+	
41R-1, 2-7	380.02	4A-1	X	+		+	+	+			
41R-2, 40-45	381.90	4A-1	X	X		+					
44R-1, 140-145	409.90	4B-1	X								
45R-1, 130-135	419.30	4B-3	X								
46R-1, 89-91	428.39	4C-1	X								
47R-1, 133-136	438.33	5-1	X				+				
48R-1, 42-47	446.92	5-2	X								
60-459B-											
60R-1, 125-127	559.75	1	X	++		+					
60R-2, 90-95	560.90	1	X	X		+					
61R-1, 19-22	568.19	1	X	++		+	+				
61R-1, 141-145	569.41	1	X	++		+					
64R-1, 24-28	596.74	2	X			+					
65R-1, 82-85	606.82	2	X			+					+
66R-1, 40-45	615.90	3	X			+		+			
67R-1, 107-112	626.07	3	X	++		++					
68R-1, 38-42	634.88	3	X	++		X					
69R-1, 84-87	644.84	4	X	X		+					
71R-1, 138-141	664.34	4	X	+		+					
72R-1, 124-128	673.74	4	X	++		+					
73R-1, 120-125	683.20	4	X					+			
73R-3, 84-88	685.84	4	X			+	+				

Notes: X = dominant, ++ = minor, + = trace.
Sm = smectite, Crist = cristobalite, Verm = mixed-layer vermiculite-hydromica mineral, Hmica = hydromica, Amph = amphibole, Chl = chlorite, Phill = phillipsite, Analc = analcime.

Table T115. Composition of igneous rocks from Hole 459B, Leg 60 (Mariana Forearc Region). (Continued on next two pages.)

Leg	60	60	60	60	60	60	60	60
Hole	459B	459B	459B	459B	459B	459B	459B	459B
Core, section	59R-2	60R-1	60R-2	61R-1	61R-1	62R-1	63R-1	64R-1
Interval (cm)	50-55	125-127	90-95	19-22	141-145	44-46	25-28	24-28
Piece	Sediment	11	8	2	14	4	3A	2B
Lab number	Z-369	Z-370	Z-371	Z-373	Z-372	Z-1190	Z-1191	Z-374
Depth (mbsf)	551.00	559.75	560.90	568.19	569.41	577.94	587.25	596.74
Unit		1	1	1	1	1	2	2
Major element oxides (wt%):								
SiO_2	50.48	52.66	51.33	51.37	51.98	50.66	48.75	48.69
TiO_2	0.87	0.96	0.95	0.96	0.96	0.62	0.71	0.96
Al_2O_3	11.61	15.18	15.13	15.54	14.49	14.82	17.51	16.50
Fe_2O_3	7.32	5.94	6.07	5.26	4.71	6.06	6.85	6.96
FeO	0.62	3.61	3.62	4.08	4.57	3.88	3.35	3.00
MnO	0.42	0.12	0.13	0.14	0.14	0.14	0.12	0.12
MgO	8.96	5.90	6.75	6.43	6.34	7.43	5.25	6.25
CaO	3.11	10.48	11.17	11.11	11.34	10.19	8.28	8.92
Na_2O	2.62	2.99	2.80	2.99	2.89	2.48	3.15	3.55
K_2O	1.65	0.38	0.38	0.46	0.42	0.37	0.77	0.94
P_2O_5	0.14	0.06	0.06	0.06	0.05	0.05	0.07	0.10
LOI	11.98	2.22	1.50	1.41	1.81	2.53	4.84	3.70
Total	99.78	100.50	99.89	99.81	99.70	99.23	99.65	99.69
H_2O^+	5.63	0.62	0.43	0.37	0.76	0.70	1.95	0.86
H_2O^-	6.35	1.60	1.07	1.04	1.05	1.24	2.49	2.84
CO_2	ND	ND	ND	ND	ND	<0.2	0.26	ND
Fe_2O_3/FeO	11.81	1.64	1.68	1.29	1.03	1.56	2.05	2.32
Density (g/cm^3)	ND	2.32	2.50	2.43	2.43	2.48	1.74	2.06
Trace elements (ppm):								
La	14	1.4	1.4	1.2	1.2			1.6
Ce	38	3.4	3.6	3.3	3.5			4.0
Nd	23	4.1	4.5	3.6	3.6			4.3
Sm	4.2	1.5	1.6	1.4	1.4			1.7
Eu	1.2	0.57	0.60	0.55	0.56			0.61
Tb	0.81	0.42	0.44	0.42	0.37			0.46
Yb	2.1	1.6	1.9	1.6	1.5			2.1
Lu	0.30	0.24	0.29	0.25	0.23			0.35
Cr	370	45	65	155	125	161	54	75
Ni	410	60	60	60	70	60	57	60
Co	50	40	45	40	50	38	42	50
V	155	290	270	310	300	197	475	360
Cu	120	80	85	270	70	55	120	35
Pb	20	<5	<5	<5	<5	ND	ND	<5
Zn	190	100	100	115	100	85	116	110
Zr	47	33	30	27	31	40	47	34
Y	25	15	15	16	15	15	18	20
Nb	6.2	<1	1.1	<1	<1	1.0	1.4	1.5
Rb	45	8.5	26	16	16	10	13	13
Sr	130	110	120	120	110	110	120	110
Ba	64	<10	<10	<10	<10	8	6	<10

Note: ND = not determined.

Table T115 (continued).

Leg	60	60	60	60	60	60	60	60
Hole	459B	459B	459B	459B	459B	459B	459B	459B
Core, section	65R-1	66R-1	67R-1	68R-1	69R-1	70R-1	70R-1	70R-2
Interval (cm)	82-85	40-45	107-112	38-42	84-87	85-90	105-110	30-35
Piece	9	4B	8B	3	12	6	7	2
Lab number	Z-375	Z-376	Z-377	Z-378	Z-379	Z-1192	Z-1193	Z-1194
Depth (mbsf)	606.82	615.90	626.07	634.88	644.84	654.35	654.55	655.30
Unit	2	3	3	3	4	4	4	4
Major element oxides (wt%):								
SiO_2	49.40	53.69	53.54	54.05	53.68	48.76	50.60	46.00
TiO_2	1.27	0.96	1.04	0.95	0.95	1.04	1.08	1.18
Al_2O_3	18.23	13.90	15.13	14.23	16.40	15.30	16.03	16.08
Fe_2O_3	8.81	8.72	7.42	7.84	5.36	9.26	8.06	9.45
FeO	3.48	3.60	3.98	3.39	3.74	4.02	4.24	3.38
MnO	0.13	0.14	0.13	0.12	0.07	0.12	0.13	0.18
MgO	2.44	3.82	3.65	3.64	4.14	4.93	3.72	6.06
CaO	8.18	8.08	8.20	7.44	9.72	6.94	7.28	7.29
Na_2O	4.79	3.27	3.18	3.08	3.55	3.53	3.82	3.18
K_2O	1.07	0.76	1.22	1.71	0.63	0.53	0.77	0.39
P_2O_5	0.19	0.08	0.15	0.07	0.04	0.14	0.16	0.10
LOI	1.75	2.48	2.32	3.68	1.83	5.00	3.32	6.22
Total	99.74	99.50	99.96	100.20	100.11	99.57	99.21	99.51
H_2O^+	0.72	0.85	0.75	1.86	0.82	1.32	1.01	1.73
H_2O^-	1.03	1.63	1.57	1.82	1.01	2.67	1.48	3.28
CO_2	ND	ND	ND	ND	ND	0.22	<0.2	<0.2
Fe_2O_3/FeO	2.53	2.42	1.86	2.31	1.43	2.30	1.90	2.80
Density (g/cm^3)	1.84	2.41	2.42	2.29	2.11	2.06	2.12	2.20
Trace elements (ppm):								
La	4.3	1.5	1.6	1.2	2.5			
Ce	10	4.2	5.1	4.0	6.4			
Nd	9.8	5.2	4.6	4.0	5.0			
Sm	3.7	1.9	1.8	1.5	1.9			
Eu	1.3	0.70	0.76	0.59	0.70			
Tb	1.20	0.55	0.59	0.44	0.57			
Yb	5.0	2.4	2.3	1.8	2.4			
Lu	0.81	0.41	0.37	0.29	0.38			
Cr	5	5	5	10	35	20	22	32
Ni	25	40	30	40	35	32	32	48
Co	15	50	40	40	35	35	37	42
V	500	370	370	280	300	358	450	478
Cu	45	35	30	10	30	49	56	73
Pb	<5	<5	<5	<5	<5	ND	ND	ND
Zn	115	105	160	85	100	101	95	99
Zr	59	41	45	41	45	64	73	60
Y	47	22	11	16	21	36	33	28
Nb	1.8	<1	<1	<1	1.0	<1	<1	<1
Rb	15	32	22	24	6.1	11.0	27	7.6
Sr	140	94	100	96	150	120	120	120
Ba	24	22	18	<10	25	21	8	18

Table T115 (continued).

Leg	60	60	60	60	60	60
Hole	459B	459B	459B	459B	459B	459B
Core, section	71R-1	72R-1	73R-1	73R-1	73R-2	73R-3
Interval (cm)	138-141	124-128	0-5	120-125	75-80	84-88
Piece	8	1				
Lab number	Z-380	Z-381	Z-1195	Z-1196	Z-1197	Z-382
Depth (mbsf)	664.38	673.74	682.00	683.20	684.25	685.84
Unit	4	4	4	4	4	4
Major element oxides (wt%):						
SiO_2	52.72	51.29	49.15	49.50	45.70	49.26
TiO_2	1.24	1.41	1.08	0.98	0.91	1.22
Al_2O_3	14.95	14.10	15.88	16.11	15.61	16.57
Fe_2O_3	6.81	8.83	7.30	10.17	10.94	7.05
FeO	4.67	5.00	4.59	2.37	1.50	4.28
MnO	0.10	0.14	0.15	0.16	0.15	0.07
MgO	4.32	3.22	4.24	3.83	5.25	5.36
CaO	7.85	9.20	8.69	7.01	6.73	8.19
Na_2O	3.74	3.98	3.49	3.73	3.39	3.93
K_2O	0.71	0.97	1.13	0.50	0.62	0.61
P_2O_5	0.02	0.01	0.11	0.12	0.06	0.06
LOI	3.01	2.08	3.65	5.41	8.65	3.77
Total	100.14	100.23	99.46	99.89	99.51	100.37
H_2O^+	1.02	1.08	1.03	2.01	2.50	1.10
H_2O^-	1.99	1.00	1.57	3.25	4.83	2.67
CO_2	ND	ND	<0.2	<0.2	<0.2	ND
Fe_2O_3/FeO	1.46	1.77	1.59	4.29	7.29	1.65
Density (g/cm^3)	2.17	2.01	2.03	1.94	2.21	2.03
Trace elements (ppm):						
La	2.7	2.9			2.1	3.7
Ce	8.2	7.6			5.7	8.5
Nd	7.2	6.0			4.7	7.8
Sm	2.7	2.6			1.6	2.9
Eu	0.89	0.85			0.61	0.89
Tb	0.81	0.79			0.41	0.83
Yb	3.4	3.6			2.6	3.5
Lu	0.52	0.60			0.46	0.55
Cr	<5	<5	32	25	22	5
Ni	20	30	37	36	39	30
Co	30	35	43	37	41	35
V	330	430	475	402	415	360
Cu	30	35	40	63	66	30
Pb	<5	<5	ND	ND	ND	<5
Zn	105	95	114	112	131	135
Zr	52	50	63	72	66	59
Y	18	29	23	33	18	31
Nb	1.0	1.1	1.2	<1	<1	1.3
Rb	9.1	10	19	8.9	9.9	7.0
Sr	120	110	120	150	120	140
Ba	26	21	50	35	44	<10

Table T116. Characteristics of holes drilled in the Japan Sea, Legs 127/128.

Hole	Latitude	Longitude	Water depth (m)	Oldest sediment cored	Basement penetration (m)	Basement recovery (m)
794C	40°11.40'N	138°13.86'E	2809.1	middle Miocene	109.4	34.5
794D	40°11.37'N	138°13.94'E	2806.9		160.5	
795B	43°59.24'N	138°57.87'E	3298.9	middle Miocene	78.7	17.58
797C	38°36.93'N	134°32.18'E	2864.5	early Miocene or older	346.6	140

Table T117. Composition of igneous rocks from Hole 794C, Leg 127 (Japan Sea). (Continued on next page.)

Leg	127	127	127	127	127	127	127
Hole	794C	794C	794C	794C	794C	794C	794C
Core, section	1R-1	1R-1	1R-1	4R-2	7R-1	7R-1	10R-1
Interval (cm)	48-50	111-113	138-139	82-84	56-61	120-122	85-87
Piece	7	9	11A	7G	5A	6D	7E
Lab number	Z-1457	Z-234	Z-1458	Z-235	Z-1459	Z-236	Z-237
Depth (mbsf)	560.28	560.91	561.18	583.82	601.46	602.10	623.65
Unit	2	2	2	2	3	3	4
Major element oxides (wt%):							
SiO_2	47.68	47.47	47.12	47.45	47.42	46.31	47.89
TiO_2	1.30	1.44	1.60	1.33	1.12	1.30	1.52
Al_2O_3	18.93	17.38	16.39	16.51	16.25	16.63	16.70
Fe_2O_3	5.14	5.48	7.15	6.13	6.42	6.13	5.39
FeO	3.89	4.43	3.17	3.74	2.62	2.96	3.43
MnO	0.14	0.14	0.16	0.07	0.11	0.10	0.05
MgO	6.19	7.13	6.89	7.42	9.46	9.34	8.31
CaO	6.65	7.44	6.94	9.89	5.02	6.52	8.09
Na_2O	3.01	3.35	3.24	3.13	3.33	3.24	2.87
K_2O	1.32	1.32	0.87	0.71	0.75	0.54	0.76
P_2O_5	0.22	0.26	0.19	0.22	0.17	0.23	0.17
LOI	5.14	4.47	5.87	3.73	7.67	6.90	4.69
Total	99.61	100.31	99.59	100.33	100.34	100.20	99.87
H_2O^+	2.34	2.14	1.33	1.17	0.91	4.39	1.51
H_2O^-	2.43	2.33	3.41	2.56	4.78	2.51	3.18
CO_2	<0.20	ND	<0.20	ND	<0.20	ND	ND
Fe_2O_3/FeO	1.32	1.24	2.26	1.64	2.45	2.07	1.57
Density (g/cm^3)	2.53	2.58	2.45	2.59	2.24	2.26	2.37
Trace elements (ppm):							
La		9.0		7.0		9.5	11
Ce		20		18		22	26
Nd		14		11		14	14
Sm		4.0		3.1		3.6	3.5
Eu		1.4		1.1		1.3	1.2
Gd		4.5		3.7		ND	ND
Tb		0.77		0.64		0.73	0.66
Tm		ND		0.3		ND	ND
Yb		2.2		1.8		2.8	2.3
Lu		0.31		0.26		0.43	0.34
Cr	64	60	73	80	282	305	260
Ni	26	17	28	27	85	130	130
Co	43	33	42	45	36	70	40
V	360	310	430	270	402	310	400
Cu	67	65	67	50	51	70	55
Pb	ND	5	ND	5	ND	<5	<5
Zn	237	200	187	90	78	80	85
Zr	93	88	90	71	93	90	84
Y	19	22	18	18	21	23	20
Nb	7.6	7.8	6.3	6.8	5.2	5.5	10
Rb	19	12	9.8	7.1	11	2.6	4.4
Sr	360	300	355	350	240	250	240
Ba	220	150	180	120	205	130	120

Note: ND = not determined.

Table T117 (continued).

Leg	127	127	127
Hole	794C	794C	794C
Core, section	12R-1	12R-3	12R-6
Interval (cm)	46-48	71-73	91-93
Piece	1A	11C	1I
Lab number	Z-238	Z-1460	Z-239
Depth (mbsf)	634.76	637.89	642.71
Unit	5	5	5
Major element oxides (wt%):			
SiO_2	47.07	46.08	44.81
TiO_2	1.41	1.16	1.35
Al_2O_3	15.24	16.09	15.34
Fe_2O_3	5.66	6.76	5.98
FeO	3.42	1.88	3.72
MnO	0.07	0.11	0.05
MgO	10.77	9.57	10.70
CaO	5.62	7.60	6.11
Na_2O	3.13	2.60	2.81
K_2O	1.08	0.19	0.76
P_2O_5	0.20	0.19	0.13
LOI	6.71	8.02	7.90
Total	100.38	100.25	99.66
H_2O^+	2.20	0.97	3.23
H_2O^-	4.51	4.65	4.67
CO_2	ND	<0.20	ND
Fe_2O_3/FeO	1.65	3.60	1.61
Density (g/cm^3)	2.28	2.28	ND
Trace elements (ppm):			
La	10		7.9
Ce	22		17
Nd	13		10
Sm	3.3		2.6
Eu	1.1		0.95
Gd	ND		ND
Tb	0.67		0.53
Tm	ND		ND
Yb	2.6		1.8
Lu	0.39		0.28
Cr	360	212	310
Ni	85	73	135
Co	33	51	40
V	425	345	300
Cu	60	54	55
Pb	5	ND	10
Zn	90	71	115
Zr	86	94	64
Y	21	20	17
Nb	7.0	7.1	5.7
Rb	7.2	1.3	6.4
Sr	230	270	210
Ba	140	140	110

Table T118. Composition of igneous rocks from Hole 794D, Leg 128 (Japan Sea). (Continued on next page.)

Leg	128	128	128	128	128	128	128
Hole	794D	794D	794D	794D	794D	794D	794D
Core, section	10R-2	11R-1	11R-1	11R-2	11R-3	12R-1	12R-3
Interval (cm)	25-28	39-43	89-95	26-29	108-112	24-26	107-111
Piece	1B	3E	3J	1B	4	2A	4C
Lab number	Z-768	Z-769	Z-1483	Z-770	Z-771	Z-772	Z-773
Depth (mbsf)	643.95	651.79	652.29	653.08	655.20	660.94	664.75
Unit	6	6	6	6	6	7	7
Major element oxides (wt%):							
SiO_2	47.46	44.94	45.55	45.18	45.52	48.19	47.78
TiO_2	1.03	1.08	1.08	1.02	1.00	1.59	1.68
Al_2O_3	15.60	14.28	14.32	15.19	15.16	15.67	15.58
Fe_2O_3	5.23	7.60	4.84	6.80	5.03	3.85	5.99
FeO	3.37	2.20	4.33	2.98	4.02	6.77	4.51
MnO	0.11	0.31	0.12	0.14	0.16	0.21	0.20
MgO	11.13	10.08	10.70	11.41	11.74	7.44	7.00
CaO	1.03	8.96	6.23	6.80	7.52	10.50	10.46
Na_2O	0.71	2.30	2.47	2.21	2.11	2.87	3.00
K_2O	6.10	0.41	0.31	0.28	0.35	0.21	0.18
P_2O_5	0.21	0.16	0.16	0.16	0.15	0.15	0.17
LOI	7.57	7.74	9.54	7.90	6.63	2.12	3.10
Total	99.55	100.06	99.65	100.07	99.39	99.57	99.65
H_2O^+	4.97	1.91	2.61	1.79	3.03	1.06	0.80
H_2O^-	2.60	3.96	5.33	4.25	3.30	0.85	1.78
CO_2	<0.20	1.87	0.55	0.35	<0.20	0.21	0.22
Fe_2O_3/FeO	1.55	3.45	1.12	2.28	1.25	0.57	1.33
Density (g/cm^3)	1.94	2.46	2.38	2.33	2.43	2.77	2.51
Trace elements (ppm):							
Cr	350	320	296	315	270	265	250
Ni	155	142	140	160	165	93	90
Co	46	38	64	46	47	47	51
V	340	255	405	290	260	230	260
Cu	54	40	54	50	43	65	54
Pb	<5	<5	ND	<5	<5	<5	<5
Zn	96	64	70	68	74	94	88
Sn	2.6	2.1	ND	2.6	2.2	2.6	2.5
Zr	40	43	49	47	42	92	97
Y	15	12	14	14	12	30	30
Nb	2.8	2.6	2.5	2.7	2.4	2.4	2.4
Rb	27	2.4	1.3	1.6	2	1.7	1.5
Sr	26	280	270	250	240	190	200
Ba	118	32	33	71	50	24	51
Th	ND	1.3	ND	<1	<1	<1	<1

Note: ND = not determined.

Table T118 (continued).

Leg	128	128	128	128	128	128
Hole	794D	794D	794D	794D	794D	794D
Core, section	13R-1	14R-1	15R-1	16R-1	17R-1	18R-1
Interval (cm)	73-76	72-76	79-85	110-117	87-93	40-47
Piece	3G	6A	10A	12	8	6
Lab number	Z-774	Z-775	Z-1617	Z-1484	Z-1485	Z-1486
Depth (mbsf)	666.73	671.22	680.69	690.40	699.47	708.3
Unit	7	7	7	8	8	8
Major element oxides (wt%):						
SiO_2	47.61	47.69	48.06	47.58	47.66	48.24
TiO_2	1.67	1.59	1.75	1.51	1.55	1.68
Al_2O_3	16.65	15.54	17.97	18.85	16.98	16.21
Fe_2O_3	4.61	4.11	3.82	4.41	3.93	4.55
FeO	4.82	6.73	4.82	3.52	5.74	3.91
MnO	0.11	0.21	0.19	0.11	0.13	0.14
MgO	7.32	8.19	6.29	7.27	7.43	7.58
CaO	9.97	10.36	10.31	8.00	10.19	9.68
Na_2O	3.00	2.83	3.15	3.35	2.96	3.27
K_2O	0.22	0.21	0.10	0.26	0.16	0.18
P_2O_5	0.15	0.14	0.18	0.21	0.16	0.18
LOI	3.14	1.78	3.40	4.90	2.97	3.90
Total	99.27	99.38	100.04	99.97	99.86	99.52
H_2O^+	1.57	0.92	0.85	0.87	1.67	0.91
H_2O^-	1.20	0.81	2.16	3.73	1.14	2.18
CO_2	0.22	<0.20	<0.2	0.24	<0.20	0.24
Fe_2O_3/FeO	0.96	0.61	0.79	1.25	0.69	1.16
Density (g/cm^3)	2.57	2.85	2.72	2.45	2.81	2.67
Trace elements (ppm):						
Cr	245	255	285	315	272	300
Ni	150	87	91	87	98	98
Co	56	44	70	55	61	67
V	215	225	395	405	358	382
Cu	60	65	82	58	74	90
Pb	<5	<5	ND	ND	ND	ND
Zn	84	33	95	96	85	95
Sn	2.2	2.6	ND	ND	ND	ND
Zr	93	89	100	120	93	100
Y	29	30	31	28	29	33
Nb	3.3	2.3	3.3	4.8	3.3	3.4
Rb	1.1	2	<1	1.8	1.7	1.2
Sr	200	180	260	250	190	200
Ba	31	29	7	47	70	125
Th	<1	<1	ND	ND	ND	ND

Table T119. Secondary minerals in igneous rocks, Yamato Basin, Japan Sea, Legs 127 and 128: Holes 794C and 794D.

Core, section, interval (cm)	Depth (mbsf)	Unit	Smectite	Swelling chlorite	ML Sm-Chl	Chlorite	Hydromica
127-794C-							
1R-1, 111-113	560.91	2	X			+	
4R-2, 82-84	583.82	2	X			+	+
7R-1, 120-122	602.10	3	X			+	+
10R-1, 85-87	623.65	4	X				+
12R-1, 46-48	634.76	5	X				+
12R-6, 91-93	642.71	5	X			+	+
128-794D-							
10R-2, 25-28	643.95	6			X	+	
11R-1, 89-95	652.29	6	X		+?	+	
11R-3, 108-112	655.20	6	X		+	+	
14R-1, 72-76	671.22	7	X				
15R-1, 79-85	680.69	7	X		+		
17R-1, 87-93	699.47	8	++	+	X		
18R-1, 40-47	708.30	8	X	+	+	+	

Notes: X = dominant, ++ = minor, + = trace.
ML Sm-Chl = mixed-layer smectite-chlorite mineral.

Table T120. Composition of igneous rocks from Hole 797C, Leg 127 (Japan Sea). (Continued on next three pages.)

Leg	127	127	127	127	127	127	127	127
Hole	797C	797C	797C	797C	797C	797C	797C	797C
Core, section	9R-1	10R-1	10R-2	12R-2	12R-4	13R-2	14R-1	16R-1
Interval (cm)	43-53	90-92	125-127	91-93	85-89	99-102	88-94	53-55
Piece	9	2J	8E	1F	4D	6C	12A	5B
Lab number	Z-1477	Z-1478	Z-245	Z-246	Z-756	Z-757	Z-1479	Z-247
Depth (mbsf)	561.03	570.90	572.75	591.71	594.42	601.29	609.18	627.83
Unit/Subunit	1	2	2	3	3	3	4	5C
Major element oxides (wt%):								
SiO_2	48.11	47.82	46.63	47.38	46.25	47.49	44.97	47.24
TiO_2	1.32	1.20	1.25	1.25	1.11	1.07	1.01	1.48
Al_2O_3	18.47	18.23	17.60	19.27	17.63	18.95	16.28	18.16
Fe_2O_3	5.78	3.69	0.89	2.36	3.13	2.49	4.45	3.35
FeO	3.15	4.18	5.03	3.67	5.28	4.38	3.86	4.21
MnO	0.16	0.15	0.35	0.24	0.26	0.28	0.14	0.34
MgO	5.08	6.47	9.66	6.76	7.63	7.54	11.09	7.28
CaO	9.18	10.25	10.53	11.45	12.01	9.48	3.88	10.61
Na_2O	3.90	3.30	3.27	3.56	2.80	3.01	2.53	3.37
K_2O	0.27	0.10	0.18	0.16	0.08	0.06	0.34	0.11
P_2O_5	0.13	0.12	0.02	0.08	0.09	0.10	0.10	0.09
LOI	4.43	4.17	4.15	3.83	3.00	4.49	11.10	3.39
Total	99.98	99.68	99.56	100.01	99.27	99.34	99.75	99.63
H_2O^+	1.50	1.75	3.30	2.22	1.10	1.66	4.91	2.24
H_2O^-	2.79	1.90	0.85	1.21	0.63	1.62	5.78	1.15
CO_2	<0.2	0.38	ND	0.40	0.31	<0.2	<0.2	ND
Fe_2O_3/FeO	1.83	0.88	0.18	0.64	0.59	0.57	1.15	0.80
Density (g/cm^3)	2.45	2.65	2.76	2.66	2.79	2.66	2.08	2.80
Trace elements (ppm):								
La			3.5	3.0				2.8
Ce			8.6	10				9.0
Nd			7.8	7.9				7.8
Sm			2.7	2.6				2.7
Eu			1.0	1.1				1.1
Tb			0.62	0.66				0.71
Tm			ND	ND				ND
Yb			2.0	2.2				2.4
Lu			0.31	0.32				0.34
Cr	310	265	255	350	215	255	285	345
Ni	150	147	160	180	155	158	93	210
Co	53	51	55	50	45	52	48	65
V	332	228	140	200	166	210	260	200
Cu	110	93	85	75	80	92	77	75
Pb	ND	ND	<5	<5	<5	<5	ND	<5
Zn	77	77	70	70	63	76	73	80
Sn	ND	ND	ND	ND	2.4	2.5	ND	ND
Zr	100	98	64	67	77	77	76	62
Y	21	22	16	17	20	16	18	21
Nb	1.8	2.1	<1	1.8	1.3	<1	<1	2.8
Rb	2.1	<1	1.1	<1	<1	<1	4.0	1.5
Sr	310	290	240	240	240	230	155	220
Ba	8	14	23	18	8	6	8	<10
Th	ND	ND	ND	ND	1.8	1.8	ND	ND

Note: ND = not determined.

Table T120 (continued).

Leg	127	127	127	127	127	127	127	127
Hole	797C	797C	797C	797C	797C	797C	797C	797C
Core, section	16R-2	19R-2	19R-4	19R-4	20R-2	21R-1	21R-1	21R-4
Interval (cm)	64-68	51-53	2-5	51-56	104-108	55-57	76-80	110-112
Piece	2C	3B	5B	7A	1D	10	10	2B
Lab number	Z-758	Z-248	Z-759	Z-1480	Z-1481	Z-249	Z-1482	Z-760
Depth (mbsf)	629.34	658.11	660.41	660.90	668.44	676.15	676.36	680.94
Unit/Subunit	5C	7	7	7	8	8	8	8
Major element oxides (wt%):								
SiO_2	47.05	48.25	48.28	45.50	39.87	46.92	47.28	47.89
TiO_2	1.28	1.24	0.96	1.07	1.03	0.76	1.00	0.86
Al_2O_3	19.42	17.92	17.67	18.71	17.59	16.13	18.01	18.17
Fe_2O_3	2.70	2.21	1.80	3.35	4.01	4.10	2.52	2.41
FeO	4.09	4.92	6.22	3.50	5.64	5.08	5.37	4.81
MnO	0.43	0.21	0.16	0.11	0.07	0.13	0.08	0.21
MgO	7.08	7.22	8.28	5.56	10.68	9.57	8.05	7.64
CaO	10.56	11.97	11.52	12.13	4.30	9.87	9.70	11.41
Na_2O	2.97	3.37	2.74	3.41	2.25	3.18	3.22	2.68
K_2O	0.08	0.16	0.08	0.08	0.44	0.18	0.13	0.12
P_2O_5	0.11	0.04	0.08	0.08	0.09	0.07	0.08	0.09
LOI	3.71	2.31	1.89	6.40	13.36	4.23	4.51	3.05
Total	99.48	99.82	99.68	99.90	99.33	100.22	99.95	99.34
H_2O^+	1.44	1.64	0.96	1.73	6.40	2.63	2.46	1.54
H_2O^-	1.71	0.67	0.43	1.99	4.16	1.60	1.42	1.06
CO_2	<0.2	ND	0.39	2.09	1.86	ND	<0.20	0.37
Fe_2O_3/FeO	0.66	0.45	0.29	0.96	0.71	0.81	0.47	0.50
Density (g/cm^3)	2.56	2.92	2.79	2.58	2.40	2.75	2.72	2.77
Trace elements (ppm):								
La		1.6		3.1	3.4	2.6		
Ce		4.6		9.3	9.0	6.7		
Nd		5.1		7.8	8.0	6.0		
Sm		2.4		2.7	2.7	2.4		
Eu		1.0		1.0	1.0	0.92		
Tb		0.72		0.66	0.67	0.56		
Tm		ND		ND	ND	ND		
Yb		2.0		2.1	1.7	2.1		
Lu		0.30		0.31	0.26	0.3		
Cr	270	320	245	298	328	250	232	220
Ni	180	140	82	91	150	185	132	158
Co	54	60	45	61	74	55	54	50
V	218	155	176	232	358	160	197	166
Cu	84	70	81	93	67	75	64	84
Pb	6	<5	<5	ND	ND	<5	ND	<5
Zn	88	83	68	82	68	75	110	69
Sn	2.5	ND	2.4	ND	ND	ND	ND	2.2
Zr	79	61	58	64	69	50	65	65
Y	18	21	20	18	17	20	22	17
Nb	1.0	<1	1.7	1.0	2.2	1.5	2.0	1.5
Rb	<1	2.1	<1	<1	11	1.6	1.1	1.5
Sr	230	180	170	210	120	170	180	200
Ba	10	14	5	<5	42	23	6	5
Th	<1	ND	<1	ND	ND	ND	ND	<1

Table T120 (continued).

Leg	127	127	127	127	127	127	127	127
Hole	797C	797C	797C	797C	797C	797C	797C	797C
Core, section	21R-6	24R-1	24R-4	24R-6	26R-1	27R-1	29R-1	31R-3
Interval (cm)	10-14	95-97	130-132	64-66	115-118	68-70	80-83	114-116
Piece	2	5D	7A	4	17	4G	2H	1E
Lab number	Z-761	Z-250	Z-762	Z-251	Z-763	Z-252	Z-764	Z-253
Depth (mbsf)	682.80	705.05	709.54	712.24	724.35	733.58	745.40	767.14
Unit/Subunit	8	9	9	9	10	11	12	13
Major element oxides (wt%):								
SiO_2	47.39	47.60	48.05	47.87	44.75	47.03	50.20	47.95
TiO_2	0.89	0.75	1.07	1.27	3.11	2.22	1.98	2.11
Al_2O_3	17.72	14.39	18.00	16.08	16.09	13.67	14.66	14.03
Fe_2O_3	3.05	4.71	2.10	1.94	5.95	8.10	6.09	5.46
FeO	5.30	5.47	5.12	6.21	7.28	3.91	4.38	4.04
MnO	0.26	0.35	0.22	0.10	0.54	0.19	0.17	0.35
MgO	7.35	8.89	7.56	8.51	7.36	7.89	6.01	7.17
CaO	11.31	11.45	11.48	12.07	2.89	6.38	6.79	9.84
Na_2O	2.67	3.18	2.60	3.18	3.92	4.12	3.59	3.93
K_2O	0.12	0.20	0.13	0.18	1.54	0.82	1.00	0.82
P_2O_5	0.08	0.07	0.10	0.09	0.45	0.23	0.29	0.24
LOI	3.14	2.83	3.16	2.81	5.79	4.85	4.23	4.64
Total	99.28	99.89	99.59	100.31	99.67	99.41	99.39	100.58
H_2O^+	1.62	2.12	1.31	1.79	3.06	1.57	0.80	0.98
H_2O^-	1.19	0.71	1.00	0.42	1.82	3.28	3.26	2.36
CO_2	<0.2	ND	<0.2	0.60	0.58	ND	<0.2	1.30
Fe_2O_3/FeO	0.58	0.86	0.41	0.31	0.82	2.07	1.39	1.35
Density (g/cm^3)	2.72	2.93	2.75	2.86	2.26	2.51	2.54	2.59
Trace elements (ppm):								
La		2.8		2.7	20	11		14
Ce		7.4		7.7	48	28		32
Nd		6.0		5.7	30	18		20
Sm		2.5		2.4	8.1	5.3		5.5
Eu		0.96		0.94	2.3	1.8		1.8
Tb		0.60		0.59	1.6	1.1		1.2
Tm		ND		ND	ND	ND		ND
Yb		2.1		2.0	4.9	3.5		3.5
Lu		0.32		0.32	0.74	0.54		0.53
Cr	247	230	245	230	40	190	50	110
Ni	158	100	93	100	18	55	29	55
Co	54	45	49	45	51	37	37	40
V	170	140	179	130	347	370	340	290
Cu	72	55	84	50	29	55	38	55
Pb	<5	<5	<5	<5	5	8	6	<5
Zn	76	75	73	80	135	125	93	110
Sn	2.4	ND	2.4	ND	3.3	ND	3.7	ND
Zr	68	64	78	58	280	150	190	140
Y	19	22	19	20	52	40	39	41
Nb	1.4	2.4	1.5	1.4	11	6.9	7.4	5.6
Rb	1.0	1.6	<1	2.5	14	6.6	8.3	6.7
Sr	180	180	220	200	190	270	270	260
Ba	10	22	10	18	86	110	230	120
Th	1.1	ND	1.2	ND	ND	ND	2.3	ND

Table T120 (continued).

Leg	127	127	127	127	127	127
Hole	797C	797C	797C	797C	797C	797C
Core, section	33R-1	34R-1	41R-1	44R-3	45R-1	45R-4
Interval (cm)	10-13	49-51	42-44	47-49	1-5	8-11
Piece	2B	3C	1A	4A	1A	1
Lab number	Z-765	Z-254	Z-255	Z-256	Z-766	Z-767
Depth (mbsf)	781.70	791.49	852.82	884.77	890.91	894.95
Unit/Subunit	14	15	19	20	21	21
Major element oxides (wt%):						
SiO_2	44.88	44.44	46.00	51.11	46.52	48.33
TiO_2	2.08	2.49	2.09	2.08	2.06	1.41
Al_2O_3	17.07	14.16	13.59	12.61	15.10	14.88
Fe_2O_3	5.87	6.12	4.77	5.01	3.32	4.90
FeO	6.18	4.60	6.69	6.62	7.13	5.75
MnO	0.43	0.60	0.42	0.10	0.20	0.18
MgO	8.80	6.48	7.68	6.48	8.66	6.56
CaO	3.24	8.93	8.12	3.26	5.98	9.53
Na_2O	3.60	3.65	3.08	5.07	2.61	2.77
K_2O	1.26	0.86	0.36	1.22	1.65	0.38
P_2O_5	0.35	0.26	0.24	0.33	0.25	0.23
LOI	6.00	7.98	7.26	6.61	5.95	4.55
Total	99.76	100.57	100.30	100.50	99.43	99.47
H_2O^+	3.13	2.08	3.57	3.84	3.34	1.03
H_2O^-	2.37	2.40	1.44	1.17	2.02	2.46
CO_2	<0.2	3.50	2.25	1.60	0.29	0.41
Fe_2O_3/FeO	0.95	1.33	0.71	0.76	0.47	0.85
Density (g/cm^3)	2.40	2.58	2.62	2.52	2.53	2.83
Trace elements (ppm):						
La		14	11	16	11	
Ce		32	26	39	30	
Nd		18	19	23	18	
Sm		5.1	5.7	6.6	5.3	
Eu		1.8	1.9	1.8	1.6	
Tb		0.95	1.2	1.3	1.2	
Tm		ND	ND	0.66	ND	
Yb		3.6	4.3	4.0	3.9	
Lu		0.56	0.63	0.64	0.61	
Cr	110	205	160	35	190	153
Ni	33	75	50	25	42	49
Co	30	40	45	32	43	45
V	340	420	330	340	330	245
Cu	38	50	60	40	54	50
Pb	7	<5	<5	8	5	<5
Zn	96	155	115	115	88	91
Sn	3.7	ND	ND	ND	3.2	3.0
Zr	240	150	140	200	160	150
Y	40	33	37	43	38	34
Nb	9.4	7.9	5.4	9.1	4.5	5.3
Rb	10.0	9.4	3.6	14	25	3.1
Sr	250	260	190	110	180	250
Ba	240	98	38	120	140	110
Th	3.8	ND	ND	ND	ND	1.4

Table T121. Secondary minerals in igneous rocks, Yamato Basin, Japan Sea, Leg 127: Hole 797C.

Core, section, interval (cm)	Depth (mbsf)	Unit	Sm	SwChl	ML Sm-Chl	Cor-like	Cor	Chl	Amph	Talc	Hmica
127-797C-											
10R-2, 125-127	572.75	2	X					+			
12R-2, 91-93	591.71	3	X					+	+?		
14R-1, 88-94	609.18	4	X					+			
16R-1, 53-55	627.83	5C	X					+			
19R-2, 51-53	658.11	7	X					+	+		
20R-2, 104-108	668.44	8	X		X		++	+			
21R-1, 55-57	676.15	8	X					+	+?		+
21R-1, 76-80	676.36	8	++		X						
21R-4, 110-112	680.94	8	++		++				+?		
21R-6, 10-14	682.80	8		X	X					+	
24R-1, 95-97	705.05	9	X					++		+	
24R-4, 130-132	709.54	9	X		++			+			
24R-6, 66-68	712.24	9	X					++	+?		
26R-1, 115-118	724.35	10				X					
27R-1, 68-70	733.58	11	X								+
29R-1, 80-83	745.40	12	X								
31R-3, 114-116	767.14	13	X								+
33R-1, 10-13	781.70	14				X					
34R-1, 49-51	791.49	15	X					+			
41R-1, 42-44	852.82	19	X			++		+			
44R-3, 47-49	884.77	20				X		++			
45R-1, 1-5	890.91	21	X		++						
45R-4, 8-11	894.95	21	X	X							

Notes: X = dominant, ++ = minor, + = trace.
Sm = smectite, SwChl = swelling chlorite, ML Sm-Chl = mixed-layer smectite-chlorite mineral, Cor-like = corrensite-like mineral, Cor = corrensite, Chl = chlorite, Amph = amphibole, Hmica = hydromica.

Table T122. Composition of igneous rocks from Hole 795B, Leg 127 (Japan Sea).

Leg	127	127	127	127	127	127	127	127
Hole	795B	795B	795B	795B	795B	795B	795B	795B
Core, section	35R-1	37R-1	38R-1	38R-2	38R-4	39R-2	40R-1	40R-2
Interval (cm)	60-62	33-35	6-8	87-92	28-30	22-24	27-29	123-125
Piece	4	3	1B	3B	2A	1B	3B	13
Lab number	Z-240	Z-696	Z-241	Z-1461	Z-242	Z-1462	Z-243	Z-244
Depth (mbsf)	693.80	712.93	722.26	724.17	726.98	733.62	741.87	744.33
Unit/Subunit	1	3A	3A	3A	3A	3A	3B	3B
Major element oxides (wt%):								
SiO_2	49.11	47.70	48.25	48.02	47.21	51.86	49.06	49.32
TiO_2	1.20	1.10	1.24	1.01	1.53	0.89	1.25	1.02
Al_2O_3	18.36	18.60	18.88	19.21	18.96	15.89	16.60	14.93
Fe_2O_3	5.18	5.05	4.05	5.90	5.74	5.46	5.24	6.31
FeO	1.70	3.04	2.81	1.48	2.76	2.72	1.80	2.51
MnO	0.05	0.23	0.21	0.19	0.11	0.14	0.13	0.14
MgO	4.44	5.42	5.89	5.30	5.88	5.49	6.59	6.75
CaO	7.30	10.04	9.40	9.47	10.32	7.87	9.05	8.27
Na_2O	3.35	2.92	3.18	3.26	2.99	3.05	2.60	3.18
K_2O	0.66	0.51	0.54	0.46	0.54	0.32	0.27	0.36
P_2O_5	0.33	0.25	0.18	0.24	0.16	0.32	0.07	0.24
LOI	8.33	4.94	5.12	5.33	4.13	5.82	6.90	6.56
Total	100.01	99.80	99.75	99.87	100.33	99.83	99.56	99.59
H_2O^+	2.20	0.91	2.40	0.47	1.65	1.13	3.01	3.00
H_2O^-	6.13	2.89	2.72	3.15	2.48	4.08	3.89	3.56
CO_2	ND	0.24	ND	<0.20	ND	<0.20	ND	ND
Fe_2O_3/FeO	3.05	1.66	1.44	3.99	2.08	2.01	2.91	2.51
Density (g/cm^3)	1.97	2.03	2.30	2.16	2.16	2.09	1.95	2.08
Trace elements (ppm):								
La	11		5.7		5.4		3.9	8.0
Ce	29		14		13		11	18
Nd	18		9.0		8.4		7.3	12
Sm	4.9		2.4		2.5		2.2	3.0
Eu	1.6		0.9		0.87		0.94	1.2
Tb	0.9		0.45		0.41		0.54	0.65
Yb	3.7		1.9		1.7		1.9	2.5
Lu	0.58		0.28		0.25		0.29	0.38
Cr	8	50	35	61	35	55	47	43
Ni	13	42	40	37	40	42	50	60
Co	17	37	33	40	30	40	37	37
V	100	405	450	472	450	400	450	340
Cu	15	54	65	64	70	70	55	65
Pb	<5	<5	<5	ND	<5	ND	5	<5
Zn	120	80	90	87	90	114	90	100
Sn	ND	2.4	ND	ND	ND	ND	ND	ND
Zr	120	67	50	76	52	67	54	43
Y	32	21	17	23	16	48	16	25
Nb	7.0	3.5	4.0	4.0	5.2	3.6	2.6	5.5
Rb	6.9	8.7	7.2	8.8	6.4	7.5	1.9	5.0
Sr	280	230	210	240	220	310	170	180
Ba	81	13	57	110	53	75	25	41
Th	ND	1.7	ND	ND	ND	ND	ND	ND

Note: ND = not determined.

Table T123. Composition of basalts from Hole 834B, Leg 135 (Lau Basin). (Continued on next page.)

Leg	135	135	135	135	135	135	135	135
Hole	834B	834B	834B	834B	834B	834B	834B	834B
Core, section	8R-2	8R-2	11R-2	11R-3	12R-4	13R-1	13R-1	22R-1
Interval (cm)	7-10	12-18	79-82	86-89	130-134	134-139	139-142	87-90
Piece	1A	1B	3A	3A	2	4	4	14A
Lab number	Z-801	Z-1487	Z-802	Z-1488	Z-803	Z-1489	Z-804	Z-805
Depth (mbsf)	127.46	127.51	152.07	153.64	160.51	162.34	162.39	224.07
Unit	2	2	5	5	5	5	5	7
Major element oxides (wt%):								
SiO_2	48.98	48.60	48.32	47.67	47.50	48.24	47.38	47.88
TiO_2	1.21	1.37	1.08	1.10	1.08	1.16	0.94	1.12
Al_2O_3	15.93	17.11	16.33	15.70	16.79	15.85	16.42	17.33
Fe_2O_3	4.26	3.47	3.93	4.45	2.83	4.00	3.34	4.29
FeO	5.22	4.94	4.79	4.36	5.04	5.02	4.46	4.08
MnO	0.12	0.38	0.12	0.13	0.12	0.45	0.11	0.12
MgO	6.98	7.51	7.63	8.26	8.03	7.77	8.46	6.41
CaO	11.11	10.14	11.42	10.07	11.44	9.71	11.28	12.28
Na_2O	3.03	3.26	2.84	2.90	2.60	2.95	2.57	2.80
K_2O	0.21	0.18	0.15	0.13	0.13	0.14	0.14	0.16
P_2O_5	0.13	0.13	0.13	0.10	0.11	0.11	0.10	0.13
LOI	2.57	2.70	2.77	4.81	3.65	4.02	4.02	2.85
Total	99.75	99.79	99.51	99.68	99.32	99.42	99.22	99.45
H_2O^+	0.99	0.75	1.40	1.74	1.22	1.24	1.79	0.90
H_2O^-	1.48	1.83	1.17	2.35	1.79	2.22	1.78	1.55
CO_2	ND	<0.20	ND	0.22	ND	<0.20	ND	ND
Fe_2O_3/FeO	0.82	0.70	0.82	1.02	0.56	0.80	0.75	1.05
Density (g/cm^3)	2.40	2.42	2.67	2.44	2.49	2.47	2.51	2.73
Trace elements (ppm):								
La								
Ce								
Nd								
Sm								
Eu								
Tb								
Yb								
Lu								
Cr	70	73	230	251	275	250	280	305
Ni	58	51	98	87	102	97	112	120
Co	47	49	47	55	47	62	51	52
V	257	368	205	260	242	335	217	225
Cu	80	82	84	90	81	113	78	72
Pb	<5	ND	<5	ND	<5	ND	<5	<5
Zn	74	82	74	136	64	88	64	74
Sn	3.0	ND	2.6	ND	2.6	ND	2.4	2.5
Zr	84	87	82	77	67	81	67	86
Y	23	24	23	21	21	21	19	26
Nb	2.3	2.6	1.8	1.7	<1	1.7	<1	1.7
Rb	1.3	1.1	1.8	1.0	2.1	1.4	2.1	2.4
Sr	180	180	160	170	160	180	160	150
Ba	9	33	10	29	5	32	6	5
Th	1.1	ND	2	ND	1.4	ND	1.3	1

Note: ND = not determined.

Table T123 (continued).

Leg	135	135	135	135	135	135	135
Hole	834B	834B	834B	834B	834B	834B	834B
Core, section	28R-2	33R-2	34R-2	47R-1	49R-1	49R-1	53R-1
Interval (cm)	76-78	103-105	10-14	71-74	97-100	131-135	60-62
Piece	4B	5I	1A	10	14B	16	5B
Lab number	Z-806	Z-807	Z-808	Z-809	Z-810	Z-1490	Z-811
Depth (mbsf)	254.56	283.07	287.77	364.21	374.17	374.51	393.10
Unit	7	7	7	12	12	12	12
Major element oxides (wt%):							
SiO_2	47.71	47.56	47.09	49.30	50.95	51.15	49.62
TiO_2	1.19	1.28	1.24	2.20	2.28	2.01	2.25
Al_2O_3	17.39	17.88	17.76	13.94	15.46	15.36	14.57
Fe_2O_3	2.71	3.57	3.06	6.95	6.35	5.31	7.32
FeO	5.46	5.46	5.20	6.26	4.43	7.05	5.20
MnO	0.11	0.14	0.12	0.21	0.15	0.35	0.18
MgO	7.40	7.18	7.68	3.56	3.88	4.43	4.11
CaO	11.85	12.02	11.82	8.57	8.17	7.34	8.09
Na_2O	2.77	2.83	2.75	3.87	4.36	4.25	3.87
K_2O	0.07	0.11	0.10	0.67	0.26	0.12	0.48
P_2O_5	0.12	0.12	0.13	0.22	0.25	0.19	0.21
LOI	2.72	2.20	2.32	3.90	3.10	2.50	3.64
Total	99.50	100.35	99.27	99.65	99.64	100.06	99.54
H_2O^+	1.36	1.32	0.99	2.38	1.47	0.38	1.55
H_2O^-	1.16	0.83	0.83	1.48	1.53	1.87	1.89
CO_2	ND	ND	ND	ND	ND	<0.20	ND
Fe_2O_3/FeO	0.50	0.65	0.59	1.11	1.43	0.75	1.41
Density (g/cm^3)	2.60	2.66	2.83	2.36	2.48	2.46	2.30
Trace elements (ppm):							
La				4.1			
Ce				12			
Nd				12			
Sm				4.6			
Eu				1.4			
Tb				1.0			
Yb				3.7			
Lu				0.54			
Cr	320	320	350	<5	<5	23	<5
Ni	100	103	156	29	27	20	28
Co	51	46	47	34	41	50	41
V	225	220	225	350	355	442	345
Cu	72	84	84	50	55	64	50
Pb	<5	<5	<5	<5	<5	ND	<5
Zn	66	64	72	125	97	116	110
Sn	2.2	3.0	2.7	3.0	2.7	ND	3.0
Zr	93	87	86	130	130	135	130
Y	25	24	24	38	38	38	40
Nb	1.3	1.4	1.9	1.1	1.6	2.3	1.9
Rb	<1	1.1	1.3	16	2.2	1.6	8.2
Sr	160	160	160	200	190	180	180
Ba	3	6	4	81	86	96	6
Th	1.4	1.3	1.2	ND	1.5	ND	<1

Table T124. Composition of basalts from Hole 191, Leg 19 (Bering Sea).

Leg	19	19	19
Hole	191	191	191
Core, section	16R-1	16R-1	16R-1
Interval (cm)	25-31	78-83	110-113
Lab number	Z-1101	Z-1102	Z-1103
Depth (mbsf)	910.25	910.78	911.1
Major element oxides (wt%):			
SiO_2	48.20	47.78	47.74
TiO_2	1.78	1.79	1.79
Al_2O_3	15.47	14.67	14.98
Fe_2O_3	5.92	6.28	6.17
FeO	3.97	4.51	4.62
MnO	0.25	0.25	0.24
MgO	6.25	6.15	6.15
CaO	9.97	10.42	11.07
Na_2O	3.11	3.27	3.11
K_2O	0.39	0.22	0.10
P_2O_5	0.20	0.19	0.20
LOI	3.79	3.95	3.54
Total	99.30	99.48	99.71
H_2O^+	1.64	1.81	1.17
H_2O^-	2.04	2.05	2.20
CO_2	<0.2	<0.2	<0.2
Fe_2O_3/FeO	1.49	1.39	1.34
Density (g/cm^3)	2.67	2.73	2.67
Trace elements (ppm):			
La	6	5.5	5.3
Ce	21	18	17
Nd	16	14	13
Sm	5.6	5	4.9
Eu	1.7	1.5	1.5
Tb	1.5	1.3	1.2
Yb	4.4	4	3.7
Lu	0.66	0.61	0.54
Cr	218	208	218
Ni	69	64	62
Co	48	45	47
V	272	260	260
Cu	97	90	87
Zn	116	88	86
Zr	140	140	140
Y	40	40	38
Nb	3.5	3.7	4.2
Rb	8.9	5.4	<1
Sr	160	160	160
Ba	88	91	76

Table T125. Trace-element composition* of basalts from Hole 191, Leg 19 (Bering Sea).

Leg	19	19
Hole	191	191
Core, section	16R-1	16R-1
Interval (cm)	25-31	78-83
Lab number	Z-1101	Z-1102
Depth (mbsf)	910.25	910.78
Trace elements (ppm):		
La	4.74	4.67
Ce	14.40	13.97
Pr	2.23	2.24
Nd	11.94	12.57
Sm	3.82	3.97
Eu	1.45	1.48
Gd	5.05	5.05
Tb	0.89	0.95
Dy	5.90	6.26
Ho	1.18	1.24
Er	3.56	3.77
Tm	0.50	0.52
Yb	3.40	3.44
Lu	0.51	0.49
Sc	33.0	32.73
Cr	218	208
Ni	59.04	56.99
Co	38.19	39.04
V	263.54	266.79
Cu	47.01	47.59
Pb	0.66	0.50
Zn	62.87	60.91
Zr	112.89	116.16
W	0.09	0.08
Mo	0.58	0.37
Y	29.91	30.98
Nb	3.20	3.09
Rb	8.86	4.15
Sr	144.54	148.47
Ba	10.99	8.45
Ga	15.62	16.28
Ge	1.5	1.31
Cs	0.29	0.15
Hf	4.01	3.99
Ta	0.32	0.32
Th	0.22	0.21
U	0.10	0.08

Note: * = determined by ISP-MS (inductively coupled plasma mass spectrometry) method in Institute of Geochemistry, Siberian Branch of Russian Academy of Sciences (Irkutsk).

Table T126. Composition of gabbros from Hole 735B, Leg 118 (Southwest Indian Ridge). (Continued on next two pages.)

Leg	118	118	118	118	118	118	118
Hole	735B	735B	735B	735B	735B	735B	735B
Core, section	7R-1	12R-3	19R-3	20R-1	24R-1	32R-4	41R-1
Interval (cm)	41-43	99-101	19-21	73-75	17-19	4-6	36-38
Piece	5	2I	2A	2E	1B	1A	2A
Lab number	Z-173	Z-174	Z-175	Z-176	Z-177	Z-178	Z-179
Depth (mbsf)	26.41	43.39	77.89	84.93	105.67	153.04	196.36
Unit	1	2	2	2	2	2	3
Major element oxides (wt%):							
SiO_2	47.45	51.16	50.45	49.83	48.98	50.09	52.39
TiO_2	0.30	0.63	0.49	0.52	0.83	0.60	0.96
Al_2O_3	19.49	20.12	16.03	15.73	14.82	18.66	15.00
Fe_2O_3	3.05	2.74	2.25	2.79	3.27	1.92	2.37
FeO	3.74	1.12	3.80	3.83	5.39	2.73	5.23
MnO	0.13	0.05	0.07	0.13	0.08	0.09	0.17
MgO	9.88	5.96	9.19	10.17	10.25	7.93	7.41
CaO	10.92	14.74	12.64	13.89	12.00	14.27	11.97
Na_2O	3.30	3.30	3.19	2.75	3.03	2.97	4.02
K_2O	0.32	0.05	0.13	0.10	0.13	0.10	0.13
P_2O_5	0.01	0.02	0.02	0.01	0.02	0.01	0.02
LOI	1.67	0.59	1.19	0.51	1.15	0.46	0.70
Total	100.26	100.48	99.45	100.26	99.95	99.83	100.37
H_2O^+	1.27	0.42	0.78	0.33	0.82	0.23	0.43
H_2O^-	0.27	0.17	0.33	0.18	0.29	0.17	0.21
CO_2	ND	ND	ND	ND	ND	ND	ND
Fe_2O_3/FeO	0.82	2.45	0.59	0.73	0.61	0.70	0.45
Density (g/cm^3)	2.92	ND	ND	3.01	2.93	3.00	2.99
Trace elements (ppm):							
La	1.5	0.60	2.2	1.2	1.2	0.88	0.72
Ce	4.0	1.8	6.5	3.0	3.4	2.5	2.6
Nd	2.9	ND	ND	2.3	3.0	ND	4.1
Sm	0.99	0.80	2.1	0.93	1.4	1.1	1.4
Eu	0.63	0.60	0.70	0.53	0.74	0.80	0.88
Gd	1.2	1.0	2.7	1.5	2.3	2.0	2.0
Tb	0.22	0.18	0.49	0.27	0.39	0.32	0.44
Tm	ND	ND	0.27	ND	0.22	ND	ND
Yb	0.79	0.78	1.9	0.93	1.4	1.0	1.7
Lu	0.12	0.11	0.28	0.12	0.20	0.15	0.26
Sc	13	37	41	43	43	38	ND
Cr	115	665	163	497	145	160	12
Ni	210	73	160	180	130	110	33
Co	38	10	44	31	51	17	28
V	25	90	120	87	125	38	120
Cu	<5	14	9	34	48	27	19
Pb	<5	<5	<5	<5	<5	<5	<5
Zn	<10	<10	30	30	30	<10	30
Zr	16	<10	22	<10	19	13	13
Y	7.0	7.4	18.0	8.9	15.0	9.7	15.0
Nb	<1	<1	<1	<1	<1	<1	<1
Rb	2.9	<1	<1	<1	<1	1.0	<1
Sr	160	180	140	140	150	160	150
Ba	<5	<5	<5	<5	<5	<5	<5

Note: ND = not determined.

Table T126 (continued).

Leg	118	118	118	118	118	118	118
Hole	735B	735B	735B	735B	735B	735B	735B
Core, section	44R-2	49R-1	55R-3	58R-3	62R-1	73R-5	79R-5
Interval (cm)	87-89	57-59	103-105	26-28	75-77	63-65	87-89
Piece	1F	3C	4C	1B	2D	3	6A
Lab number	Z-180	Z-181	Z-182	Z-183	Z-184	Z-185	Z-186
Depth (mbsf)	213.37	236.57	269.03	283.76	301.25	372.13	421.37
Unit	3	4	4	5	5	5	6
Major element oxides (wt%):							
SiO_2	48.50	41.97	40.32	51.13	50.65	51.03	47.25
TiO_2	0.54	6.69	7.00	0.72	0.58	0.55	0.54
Al_2O_3	14.22	10.10	10.61	13.31	13.33	17.99	21.34
Fe_2O_3	1.28	7.51	5.74	3.18	1.51	2.31	1.95
FeO	4.70	12.92	16.18	5.50	4.50	2.33	4.23
MnO	0.06	0.25	0.29	0.09	0.07	0.04	0.05
MgO	13.52	6.74	6.43	9.51	10.21	6.82	9.59
CaO	13.60	9.48	9.52	13.37	15.29	15.00	11.41
Na_2O	2.30	3.14	2.70	2.86	2.38	2.81	2.65
K_2O	0.15	0.15	0.13	0.13	0.05	0.10	0.05
P_2O_5	0.01	0.02	0.03	0.02	0.01	0.02	0.02
LOI	0.64	1.20	1.20	0.61	1.49	0.44	0.47
Total	99.52	100.17	100.15	100.43	100.07	99.44	99.55
H_2O^+	0.41	0.66	0.91	0.43	0.15	0.29	0.24
H_2O^-	0.19	0.22	0.14	0.18	1.34	0.08	0.18
CO_2	ND	ND	ND	ND	ND	ND	ND
Fe_2O_3/FeO	0.27	0.58	0.35	0.58	0.34	0.99	0.46
Density (g/cm^3)	ND	3.32	3.38	3.01	ND	3.12	2.85
Trace elements (ppm):							
La	0.40	0.62	0.95	2.1	1.1	0.46	0.64
Ce	1.20	2.2	3.6	6.9	1.6	1.5	1.8
Nd	1.60	4.0	6.4	8.6	3.3	2.1	1.5
Sm	0.72	1.6	2.5	3.4	1.3	0.82	0.59
Eu	0.40	0.90	1.5	0.86	0.69	0.49	0.41
Gd	1.2	2.6	3.1	4.1	2.0	1.2	0.87
Tb	0.22	0.53	0.68	0.91	0.37	0.22	0.15
Tm	ND	0.28	0.45	0.6	0.2	ND	ND
Yb	0.76	1.8	2.9	3.8	1.4	0.82	0.43
Lu	0.11	0.27	0.46	0.52	0.21	0.12	0.07
Sc	48	54	64	52	62	47	13
Cr	720	6	8	180	475	305	280
Ni	260	34	33	105	94	71	230
Co	40	77	80	28	26	12	40
V	75	700	365	100	120	60	30
Cu	62	56	76	31	37	27	37
Pb	<5	<5	<5	<5	<5	<5	<5
Zn	23	110	135	28	20	<10	22
Zr	<10	32	64	20	10	10	14
Y	7.3	18	27	29	14	13	4.6
Nb	1.6	1.6	2.4	<1	<1	<1	<1
Rb	<1	<1	<1	<1	<1	<1	<1
Sr	120	150	120	130	120	160	130
Ba	<5	<5	<5	<5	<5	<5	<5

Table T126 (continued).

Leg	118	118	118	118
Hole	735B	735B	735B	735B
Core, section	82R-6	85R-7	86R-3	88N-1
Interval (cm)	22-24	95-97	51-53	60-62
Piece	3	6	1F	2C
Lab number	Z-187	Z-188	Z-189	Z-190
Depth (mbsf)	450.72	481.45	484.51	500.60
Unit	6	6	6	6
Major element oxides (wt%):				
SiO_2	49.53	48.53	50.92	46.19
TiO_2	0.55	0.53	0.59	0.43
Al_2O_3	16.77	17.59	12.61	20.64
Fe_2O_3	2.52	1.66	2.72	1.92
FeO	4.25	4.08	4.06	4.17
MnO	0.03	0.09	0.10	0.07
MgO	9.29	11.61	9.92	13.37
CaO	13.40	13.30	13.99	10.49
Na_2O	2.47	2.30	2.86	2.30
K_2O	0.10	0.13	0.05	0.05
P_2O_5	0.02	0.01	0.01	0.01
LOI	0.59	0.55	1.59	0.70
Total	99.52	100.38	99.42	100.34
H_2O^+	0.26	0.42	0.86	0.42
H_2O^-	0.18	0.13	0.34	0.24
CO_2	ND	ND	ND	ND
Fe_2O_3/FeO	0.59	0.41	0.67	0.46
Density (g/cm^3)	2.98	3.07	2.96	3.01
Trace elements (ppm):				
La	0.4	0.38	1.7	0.29
Ce	1.4	1.0	5.1	0.74
Nd	1.5	1.3	5.0	0.65
Sm	0.64	0.57	1.6	0.21
Eu	0.43	0.38	0.53	0.27
Gd	1.0	0.9	2.1	0.21
Tb	0.17	0.15	0.41	0.047
Tm	ND	ND	ND	ND
Yb	0.61	0.54	1.8	0.16
Lu	0.1	0.086	0.32	0.027
Sc	36	34	44	6.9
Cr	720	1575	390	90
Ni	180	220	145	300
Co	42	32	30	42
V	72	55	92	20
Cu	25	31	14	62
Pb	<5	<5	<5	<5
Zn	28	20	18	<10
Zr	11	<10	18	<10
Y	6.1	5.6	14	2.2
Nb	<1	<1	<1	<1
Rb	<1	<1	<1	<1
Sr	110	130	150	160
Ba	<5	<5	<5	<5

Table T127. Composition of serpentinized harzburgites, from Hole 637A, Leg 103 (Galicia Margin, Atlantic Ocean).

Leg	103	103	103	103
Hole	637A	637A	637A	637A
Core, section	25R-1	26R-2	27R-1	28R-3
Interval (cm)	66-69	53-56	112-115	103-106
Piece	8B	1E	15C	14
Lab number	Z-149	Z-150	Z-151	Z-152
Depth (mbsf)	228.66	239.23	248.02	260.63
Major element oxides (wt%):				
SiO_2	28.84	34.18	34.08	15.71
TiO_2	0.21	0.21	0.22	0.11
Al_2O_3	0.43	1.36	1.62	1.03
Fe_2O_3	5.43	6.78	6.21	4.86
FeO	0.27	0.23	0.51	0.11
MnO	0.12	0.12	0.13	0.07
MgO	27.58	31.82	31.36	10.24
CaO	12.53	6.30	7.13	34.30
Na_2O	1.39	0.26	0.37	0.63
K_2O	0.13	0.08	0.08	0.10
P_2O_5	0.02	0.03	0.02	0.03
LOI	22.31	18.29	18.48	33.33
Total	99.26	99.66	100.21	100.52
H_2O^+	10.39	11.70	10.73	3.17
H_2O^-	2.92	2.67	2.10	2.26
CO_2	9.00	3.92	5.65	27.90
Fe_2O_3/FeO	20.11	29.48	12.18	44.18
Density (g/cm^3)	2.02	2.19	2.32	2.30
Trace elements (ppm):				
La	0.24	0.20	0.20	0.20
Ce	0.60	0.65	0.53	0.54
Sm	0.15	0.17	0.15	0.14
Eu	0.042	0.031	0.014	0.025
Tb	0.032	0.032	0.034	0.028
Yb	0.092	0.18	0.10	0.08
Lu	0.014	0.032	0.024	0.013
Sc	11	10	ND	7.7
Cr	1550	1550	1450	890
Ni	1500	2300	1650	1400
Co	84	78	58	19
V	38	35	27	38
Cu	19	25	14	<5
Pb	<5	<5	<5	<5
Zn	14	17	20	12
Zr	<10	<10	<10	<10
Y	<1	<1	<1	<1
Nb	<1	<1	<1	<1
Rb	<1	<1	<1	<1
Sr	30	15	22	43
Ba	<5	<5	<5	13

Note: ND = not determined.

APPENDIX A

Petrographic Descriptions

This appendix contains petrographic descriptions of igneous rocks and XRD and electron diffraction data of secondary minerals.

APPENDIX B

See tables AT1–AT73 for data on abundance of major and trace elements in igneous rock samples referenced in this *Report*.

APPENDIX A

Petrographic Descriptions

This appendix contains petrographic descriptions of igneous rocks and XRD and electron diffraction data of secondary minerals.

Costa Rica Rift (Legs 69, 70, 83, 111,137, 140, and 148)

Hole 504B

Sample 69-504B-2R-1, 108–110 cm (Piece 233), Unit 1 [Z-883]

Olivine-clinopyroxene-plagioclase-microphyric basalt, massive, with hyalopilitic groundmass texture. Microphenocrysts of plagioclase are represented by elongated laths 0.2–1 mm (10%). Large grains of labradorite (An_{62}). Small laths are andesine ($An_{43–45}$). Sparsely idiomorphic microphenocrysts of clinopyroxene (1%–3%) are colorless diopside (salite?). Groundmass: light brown weakly anisotropic interstitial glass at the first stage of crystallization. Panicle like plagioclase and clinopyroxene crystallites (in glass) form pseudovariolitic texture. Single rounded vesicles (<0.2 mm) infilled with brown anisotropic glass.

Alteration: rock is fresh; single idiomorphic crystals (0.2–0.4 mm) of olivine(?) completely replaced by isotropic brown matter and partly by green anisotropic chlorite.

Sample 69-504B-4R-1, 62–64 cm (Piece 274), Unit 2A [Z-884]

Olivine-plagioclase-phyric basalt, massive, with vitrophyric groundmass texture. Rock volume contains phenocrysts (20%) and volcanic glass. Phenocrysts: fresh olivine (5%) and glomerophyric segregates of plagioclase prismatic crystals (15%, labradorite [An_{52}]). Groundmass contains isotropic green-cream glass.

Alteration: rock is fresh.

XRD: smectites; smectite and chlorite veinlet.

Sample 69-504B-4R-3, 108–111 cm (Piece 322), Unit 2A [Z-885]

Olivine-plagioclase-phyric basalt, crystallized, massive, with intersertal-crystallitic groundmass texture. Phenocrysts of plagioclase are represented by elongated-prismatic laths (0.5–1.7 mm, 20%). More small grains form glomerophyric segregates (labradorite [An_{55}]). There are two grains of idiomorphic dark mineral (olivine?). Groundmass; needle-shaped laths, microlites of plagioclase (andesine [$An_{42–45}$]), and crystallized interstitial glass with plagioclase, opaque dust, and segregates of clinopyroxene. Crystallites form panicle like segregates.

Alteration: olivine(?) completely replaced by high double-refracted green or green-brown iddingsite-bowlingite; single small parts (up to 0.4 mm), maybe it is clinopyroxene, replaced by clay mineral.

XRD: smectites.

Sample 69-504B-4R-4, 42–45 cm (Piece 330), Unit 2A [Z-886]

Aphyric basalt (microdolerite), crystallized, massive, with intersertal-microdoleritic groundmass texture. Rocks contain plagioclase laths (40% labradorite [An_{55}], 40% clinopyroxene grains, 5% opaque mineral, and 15% glass).

Alteration: slight (15%); interstitial glass completely replaced by clay mineral.

XRD: veinlet; smectite, hematite, and phillipsite.

Sample 69-504B-5R-2, 142–146 cm (Piece 387), Unit 2A [Z-887]

Olivine-plagioclase-phyric basalt, irregularity crystallized, massive, with pilotaxitic groundmass texture. Phenocrysts: plagioclase tabular grains (as much as 2 mm, 15%, labradorite [$An_{56–58}$]), sometimes plagioclases are zonal with inclusions of glass. Olivine or clinopyroxene (5%–10%) forms idiomorphic grains with sizes up to 2 mm completely replaced by aggregate of iddingsite. Groundmass; needle-shaped microlites of plagioclase. Plagioclase is located in black weakly crystallized glass. Occasionally more crystallized parts demonstrate crystallites and microlites of clinopyroxene and opaque dust. These parts have transitional texture from pilotaxitic to intersertal-crystallitic.

Alteration: slight (10%); dark-brown mineral and small parts (0.5 mm–2 mm) replaced by green clay mineral.

XRD: smectites; veinlet of smectite and undetermined mineral (3.20 Å).

Sample 69-504B-6R-1, 65–69 cm (Piece 404), Unit 2A [Z-888]

Olivine-clinopyroxene-plagioclase-phyric basalt, weakly crystallized, massive, with pilotaxitic groundmass texture. Phenocrysts are plagioclase and dark-color mineral. Plagioclase (labradorite [An_{58}]) forms elongated-prismatic grains and their glomerophyric segregates; sizes from 0.5 to 2 mm (15%) are tabular grains (labradorite [$An_{56–58}$]). There are two types of dark-color minerals: single diamond-tabular grains (as much as 1 mm) completely replaced by iddingsite (olivine?) and small grains (0.2–0.3 mm). The latter (1%) forms segregates of completely chloritized clinopyroxene(?). Groundmass; unoriented laths and microlites of plagioclase (andesine [An_{40}]). Glass is brown-black and almost isotropic. In other parts of thin section, glass is crystallized with crystallites and microlites of clinopyroxene. There are single thin veinlets with clay mineral.

Alteration: slight (5%).

XRD: smectites; smectite veinlets.

Sample 69-504B-7R-2, 64–68 cm (Piece 459), Unit 2C [Z-889]

Plagioclase-phyric basalt, weakly crystallized, vesicular, with vitrophyric-hyalopilitic groundmass texture. Phenocrysts of plagioclase (labradorite [$An_{55–58}$]) are represented by plate and prismatic crystals (0.5–2 mm, 30%) and dark mineral. Single grains of plagioclase are zonal. Groundmass; unoriented laths and microlites of plagioclase (andesine [$An_{42–45}$]) and crystallized glass with opaque dust. Small rounded-isometric vesicles (0.05–0.1 mm) are present. There are empty vesicles (5%).

Alteration: vesicles infilled with brown-green clay mineral.

XRD: smectites; smectite, chlorite, and phillipsite veinlets.

Sample 69-504B-7R-3, 61–65 cm (Piece 481), Unit 2C [Z-890]

Olivine(?)-plagioclase-phyric basalt, weakly crystallized, massive, with vitrophyric-microlitic groundmass texture. Phenocrysts are elongated-prismatic and plate crystals of plagioclase (0.5–2 mm, 20%, labradorite [An_{65}]). Single grains of olivine are present. Groundmass; laths of plagioclase and glass (from completely isotropic brown-black glass to weakly anisotropic light brown glass). There are rounded microvesicles (0.01–0.05 mm, <1%).

Alteration: olivine replaced by iddingsite-bowlingite; vesicles infilled with clay mineral.

XRD: smectites, chlorite, hematite, and phillipsite veinlets.

Sample 69-504B-8R-3, 61–66 cm (Piece 538), Unit 2D [Z-891]

Dolerite, massive; groundmass is poikilitic-ophitic texture. Phenocrysts: plagioclase (50%, 0.2–2 mm, labradorite [An_{65}]) and clinopyroxene (salite; 40%, as much as 2 mm) grains. Spots of small (0.1 mm) grains of opaque mineral. Chlorite and pyroxene are present.

Alteration: slight.

XRD: smectites; smectite veinlets.

Sample 69-504B-9R-1, 142–147 cm (Piece 583), Unit 3A [Z-892]

Plagioclase-microphyric basalt, weakly crystallized, massive, groundmass is vitrophyric texture. Phenocrysts of plagioclase (labradorite [An_{55}]) are represented by sparse short-prismatic grains (10%) as much as 0.5 mm in size. Plagioclase grains contain glass. Groundmass glass is fresh and weakly anisotropic.

Alteration: glass from plagioclase completely replaced by clay mineral.

XRD: smectites; smectite and phillipsite veinlets.

Sample 69-504B-10R-3, 17–20 cm (Piece 643), Unit 3A [Z-893]

Plagioclase-clinopyroxene-phyric basalt, crystallized, massive, with microlitic, partly pilotaxitic groundmass texture. Plagioclase; single small (<0.5 mm) elongated-prismatic zonal grains. There is one large (2.5 mm) rounded-isometric (xenocryst) grain of salite with inclusions of short-prismatic, small (0.2 mm) grains of plagioclase (labradorite [An_{56}]). Microlites demonstrate andesine ($An_{38–40}$). Groundmass contains unoriented laths and microlites of plagioclase. Interstices contain microlites of clinopyroxene with opaque micrograin mass or weakly crystallized glass with opaque dust.

Alteration: slight (3%–5%); sparse spots (as much as 2 mm) with high chloritization; near these spots there are minor microvesicles (0.05 mm) infilled with clay mineral.

XRD: smectites; smectite and undetermined mineral (3.20 Å) veinlets.

Sample 69-504B-11R-1, 61–64 cm (Piece 667), Unit 3A [Z-894]

Plagioclase basalt, weakly crystallized, massive; groundmass is microlitic-pilotaxitic texture. Rock is the same as Sample 69-504B-10R-3, 17–20 cm (Z-893), but without grains of clinopyroxene. Glomerophyric segregate (0.4 mm) of clinopyroxene and plagioclase with poikilitic texture is present.

Alteration: slight (3%–5%).

XRD: smectite veinlets.

Sample 69-504B-12R-1, 39–43 cm (Piece 714), Unit 3A [Z-895]

Plagioclase-sparsely microphyric basalt, crystallized, massive, with microlitic, partly microdoleritic groundmass texture. Plagioclase; small (as much as 0.4 mm) laths and glomerophyric segregates (2%–3%, labradorite [An_{53}]). Groundmass contains laths and microlites of plagioclase. Interstices contain segregates of small grains of plagioclase (microdoleritic texture). Occasionally microlites of plagioclase are oriented (trachytoid texture). Opaque mineral (very small grains, often idiomorphic) is in paragenesis with clinopyroxene.

Alteration: slight (1%–2%); rare spots (1 mm) with chloritization of rock.

XRD: smectites; smectites, chlorite, and phillipsite veins.

Sample 69-504B-13R-4, 40–44 cm (Piece 806), Unit 3A [Z-896]

Plagioclase-sparsely microphyric basalt, crystallized, massive, groundmass is microlitic texture. Phenocrysts of plagioclase (labradorite [An_{62}]) are represented by sparsely glomerophyric segregates (2%) of short-prismatic grains. Groundmass contains laths (andesine [An_{47}]) and microlites of plagioclase. Interstices contain small rounded grains or their segregates (salite). Clinopyroxene occurs together with small isometric and partly idiomorphic grains of opaque mineral (as much as 15%).

Alteration: slight; very sparsely rounded spots (as much as 0.2 mm) with chloritization of rock (possibly olivine replaced by chlorite).

XRD: smectites; smectites and hematite veinlets.

Sample 69-504B-15R-1, 24–26 cm (Piece 872), Unit 3C [Z-901]

Plagioclase-sparsely microphyric basalt, uncrystallized, massive, with vitrophyric groundmass texture. Single small (as much as 0.4 mm) table-like grains of plagioclase (labradorite [An_{64}]) are located in weakly anisotropic brown glass with pseudovariolitic texture. Small segregates of plagioclase and pyroxene, ophitic texture (inclusion of microdolerite?).

Alteration: rock is fresh.

XRD: smectites; smectites, chlorite(?), and phillipsite(?) veinlets.

Sample 69-504B-16R-1, 45–49 cm (Piece 961), Unit 3C [Z-897]

Olivine-plagioclase-sparsely phyric basalt, uncrystallized, massive, with vitrophyric groundmass texture. Elongated-prismatic and tabular grains (0.6–0.8 mm) of plagioclase form glomerophyric segregates up to 15 grains (5%–7%, labradorite [$An_{55–57}$]). There are segregates of laths of plagioclase and small isometric grains of clinopyroxene. Olivine; idiomorphic small (0.2–0.3 mm) grains. Groundmass contains rare microlites of plagioclase and weakly anisotropic glass with panicle-like crystallites of clinopyroxene and plagioclase and grains of opaque mineral.

Alteration: slight; olivine completely replaced by clay mineral (center) and hematite (margin parts).

XRD: smectites; smectites and hematite veinlets.

Sample 69-504B-16R-4, 22–26 cm (Piece 1005), Unit 4 [Z-898]

Plagioclase-phyric basalt, uncrystallized, massive, groundmass is hyalopilitic texture. Short-prismatic grains (0.4–0.6 mm) of plagioclase (labradorite [An_{60}]) form glomerophyric segregates (20%). Groundmass contains needle-shaped, case-like microlites of plagioclase. Grains of plagioclase are located in weakly anisotropic brown glass.

Alteration: slight.

XRD: smectites; smectite veinlets.

Sample 69-504B-17R-1, 30–34 cm (Piece 1036), Unit 4 [Z-899]

Plagioclase-phyric basalt, uncrystallized, massive, groundmass is hyalopilitic texture. Rock is the same as Sample 69-504B-16R-4, 22–26 cm (Z-898).

Alteration: slight.

XRD: smectites; smectites and magnesite veinlets.

Sample 69-504B-18R-1, 45–49 cm (Piece 1087), Unit 5 [Z-900]

Plagioclase-phyric basalt, crystallized, massive, groundmass is microlitic (microdoleritic) texture. Plagioclase forms glomerophyric segregates of various sizes. Idiomorphic or rounded-prismatic grains (0.2–2 mm, 20%). Composition of plagioclases are labradorite ($An_{58–60}$). In a single case, there is weakly anisotropic completely oxidized brown mineral (olivine?). Groundmass contains unoriented laths and microlites of plagioclase.

Interstices contain accreted microlites of clinopyroxene and segregates of very small grains of this mineral. Pyroxene is diopside with hedenbergite in trace amounts. Very small grains of opaque mineral in paragenesis with clinopyroxene are present.

Alteration: rock is fresh.

XRD: smectites; smectites, chlorite(?), hematite, phillipsite, and undetermined mineral (3.20 Å) in veinlets.

Sample 69-504B-19R-1, 84–87 cm (Piece 1124), Unit 5 [Z-902]

Plagioclase-phyric basalt, uncrystallized, weakly vesicular, groundmass is hyalopilitic texture. Plagioclase (0.2–0.4 mm) forms glomerophyric segregates (15%, labradorite - [An_{58}]). There is a single diamond-shaped grain completely replaced by chlorite (clinopyroxene?). Groundmass contains needle-shaped microlites of plagioclase. Grains of plagioclase are located in brown-black weakly crystallized glass with opaque dust. There are small isometric vesicles (as much as 0.1 mm, 5%).

Alteration: rock is fresh; vesicles infilled with green clay mineral.

XRD: smectites; smectites and chlorite(?) in veinlets.

Sample 69-504B-20R-1, 110–113 cm (Piece 1173), Unit 9 [Z-903]

Plagioclase-phyric dolerite, crystallized, massive, small grains, groundmass is doleritic texture. Sparse elongated-prismatic laths of plagioclase as much as 2 mm (5%) are represented by labradorite (An_{62}). Groundmass has unoriented variously sized (0.2–2 mm) elongated laths of plagioclase (40%, labradorite [$An_{53–55}$]). Clinopyroxene (salite) forms small tabular grains (0.2–0.3 mm, often clinopyroxene forms panicle like segregates. Total of clinopyroxene in rock is 40%). Interstices contain parts of iddingsite in paragenesis with very small grains of sphene and brown matter in paragenesis with opaque mineral. Thin veins (0.2–0.4 mm) are present.

Alteration: rock is fresh.

XRD: smectites; smectites, hematite, and aragonite in veinlets.

Sample 69-504B-21R-2, 126–130 cm (Piece 1215), Unit 10 [Z-904]

Plagioclase-phyric basalt, weakly crystallized, massive, groundmass is pilotaxitic texture. Elongated-table grains of plagioclase (0.2–0.4 mm) forms glomerophyric segregates (labradorite [An_{55}]). Groundmass contains unoriented laths and microlites (andesine [An_{43}]). Glass is weakly anisotropic. Opaque dust is present.

Alteration: rock is fresh.

XRD: smectites; smectites and phillipsite in veinlets.

Sample 69-504B-21R-4, 116–120 cm (Piece 1253), Unit 14 [Z-905]

Plagioclase-phyric basalt, uncrystallized, massive, groundmass is hyalopilitic texture. Plagioclase (0.8–1 mm) forms short-prismatic idiomorphic grains (10%, labradorite [An_{55}]). Groundmass has needle-shaped and skeletal microlites of plagioclase in weakly anisotropic brown glass.

Alteration: rock is fresh.

XRD: smectites and hematite in veinlets.

Sample 69-504B-21R-5, 63–66 cm (Piece 1267), Unit 16 [Z-906]

Clinopyroxene-plagioclase-phyric basalt, uncrystallized, massive, groundmass is hyalopilitic texture. Elongated-prismatic and table-like grains of plagioclase (0.2–0.8 mm) forms glomerophyric segregates (10%, labradorite [An_{62}]). There is a single grain (0.5 mm) of clinopyroxene (diopside) in accretion with plagioclase grains. Groundmass contains unoriented needle-shaped microlites of plagioclase in black or brown glass.

Alteration: slight.

XRD: smectites; smectites in veinlets.

Sample 69-504B-22R-1, 108–109 cm (Piece 1280), Unit 16 [Z-907]

Olivine-plagioclase-microphyric basalt, uncrystallized, massive, groundmass is vitrophyric texture. Rock contains laths (20%) and groundmass (80%). Olivine (5%) occurs in small grains (0.2–0.3 mm) completely replaced by iddingsite. Plagioclase (0.2–0.8 mm, 15%) forms laths and prismatic grains (0.2–0.7 mm, labradorite [An_{55}] and andesine [An_{45}]. There is weakly anisotropic brown glass with rare crystallites of plagioclase. A single grain (0.5 mm) of clinopyroxene (diopside) is in accretion with plagioclase grains.

Alteration: slight (5%).

XRD: smectites; smectites in veinlets.

Sample 69-504B-23R-1, 32–35 cm (Piece 1314), Unit 16 [Z-908]

Clinopyroxene-plagioclase-phyric basalt, crystallized, massive, groundmass is microlitic and partly intersertal texture. Phenocrysts of plagioclase with various sizes (0.3–0.8 mm). There is a single elongated-prismatic crystal (3 mm). Grains often form glomerophyric segregates. Total plagioclase is 25% (labradorite [An_{60}]). Idiomorphic grains (0.5–0.7 mm, 5%) of clinopyroxene (diopside-salite) are present. Other areas of groundmass contain unoriented laths and microlites of plagioclase (andesine [An_{42}]). Interstices infilled with segregate of small, occasionally panicle-like microlites and grains of clinopyroxene and opaque mineral. Glass is brown-black and almost isotropic. In other parts of the thin section, glass is crystallized with crystallites and microlites of clinopyroxene. There are single thin veins contain chlorite.

Alteration: slight; small areas with green clay mineral.

XRD: smectites in veinlets.

Sample 69-504B-24R-1, 125–128 cm (Piece 1349), Unit 16 [Z-909]

Olivine(?)-clinopyroxene-plagioclase-phyric basalt, uncrystallized, massive; groundmass is vitrophyric texture. Phenocrysts of plagioclase (0.2–2 mm, 25%) with elongated-prismatic and table-like habite forms crystals and glomerophyric segregates. There is a single elongated-prismatic crystal (3 mm). Grains often form glomerophyric segregates. Composition of plagioclase is labradorite (An_{65}). There are single idiomorphic grains (as much as 0.5 mm). Many idiomorphic grains (0.2–0.4 mm) are completely altered. These grains are possibly olivine (2%–3%). Groundmass contains very black, dark-brown glass.

Alteration: some parts of glass replaced by chlorophaeite; olivine(?) replaced by iddingsite; very thin cracks infilled with chlorophaeite.

XRD: Ca-Mg and Na-K smectites (or mixed-layer illite-smectite mineral) contain mica layers (~10%); quartz in trace amounts; contact of basalt and black glass consists of smectites with 10% swelling interlayers; quartz in trace amounts.

Sample 69-504B-24R-3, 125–129 cm (Piece 1393), Unit 17 [Z-910]

Clinopyroxene-plagioclase-microphyric basalt, uncrystallized, massive, groundmass is vitrophyric-variolitic texture. Phenocrysts contain rare glomerophyric radial-radiant segregates of plagioclase and clinopyroxene with poikilitic like texture of dolerites. There are single elongated-prismatic laths of plagioclase. Total plagioclase is 20% of the rock volume. Laths in segregates and single crystals are 0.2–0.3 mm (andesine [An_{48}]). Groundmass contains black or weakly anisotropic glass with rounded, radial-radiant paths and varioles (variolitic texture).

Alteration: rock is fresh.

XRD: smectites and hematite in veinlets.

Sample 69-504B-25R-2, 62–66 cm (Piece 1429), Unit 17 [Z-911]

Rock is similar to Sample 69-504B-24R-3, 125–129 cm (Z-910).

Alteration: rock is fresh.

XRD: smectites, chlorite(?), and phillipsite in veinlets.

Sample 69-504B-26R-1, 15–18 cm (Piece 1449), Unit 17 [Z-912]

Olivine-microphyric basalt, weakly crystallized, massive, groundmass is hyalopilitic texture. Phenocrysts contain rare small (0.2 mm, <1%) idiomorphic minerals (olivine) completely replaced by chlorite and black opaque mineral (opacite?). Groundmass contains needle-shaped microlites and laths of plagioclase in weakly anisotropic glass.

Alteration: rock is fresh.

XRD: smectites; smectites and hematite in veinlets.

Sample 69-504B-27R-2, 55–58 cm (Piece 1484), Unit 17 [Z-913]

Clinopyroxene-plagioclase-microphyric basalt, partly crystallized, massive, groundmass is intersertal-pilotaxitic texture. Phenocrysts contain short-prismatic grains (0.5–0.8 mm, size single grain as much as 2 mm) of plagioclase (10%, labradorite [An_{52}]. A single grain of clinopyroxene (0.5 mm) is possibly diopside. Groundmass contains unoriented needle-shaped microlites of plagioclase. These laths are in various crystallized glass. Rock contains rounded microvesicles (0.05 mm, <1%).

Alteration: slight; vesicles infilled with chlorite.

XRD: smectite with ~10% mica layers with interlayer Ca-Mg cations; chlorite in trace amounts; smectites in veinlets.

Sample 69-504B-28R-3, 69–73 cm (Piece 1530), Unit 19 [Z-914]

Clinopyroxene-plagioclase-phyric basalt, uncrystallized, massive, groundmass is vitrophyric texture, brecciated. Phenocrysts of plagioclase form elongated-prismatic (as much as 2 mm) and tabular (0.5 mm) grains (15%–20%, labradorite [$An_{67–68}$]) and often form glomerophyric segregates. Clinopyroxene demonstrates small (0.2–0.3 mm) idiomorphic grains (1%–2%), sometimes in paragenesis with plagioclase. Groundmass contains black-brown, partly anisotropic glass. Rock (possibly glassy crust) is broken by microcracks (as much as 0.7 mm thick).

Alteration: slight (5%–7%); glass is fresh; microcracks infilled with chlorophaeite-palagonite.

XRD: smectite with ~10% mica layers with interlayer Ca-Mg cations; chlorite and quartz in trace amounts; smectites in veinlets.

Sample 69-504B-29R-1, 31–34 cm (Piece 1562), Unit 20 [Z-915]

Plagioclase-phyric basalt, uncrystallized, massive, groundmass is hyalopilitic-vitrophyric texture. Sparse (5%) phenocrysts of plagioclase (labradorite [An_{55}]) form table-like or prismatic grains (0.3–0.5 mm). Groundmass contains weakly anisotropic brown glass. Glass contains rare laths and microlites of plagioclase (labradorite [An_{52}]). Small segregates of clinopyroxene grains in paragenesis with laths of plagioclase (spotty crystallization of glass).

Alteration: rock is fresh.

XRD: smectites in veinlets.

Sample 70-504B-32R-2, 137–140 cm (Piece 177), Unit 22 [Z-919]

Clinopyroxene-olivine-plagioclase-phyric basalt, uncrystallized, massive, groundmass is vitrophyric texture. Elongated and short-prismatic grains (0.2–2 mm, 15%) of plagioclase form glomerophyric segregates. Composition of plagioclase phenocrysts varies from small grains (0.2–0.4 mm, labradorite [An_{55}]) to single large crystals that demonstrate labradorite-bitovnite (An_{70}). Olivine (elongated-prismatic skeletal grains; 2 mm, 5%) is present. Clinopyroxene (diopside-augite) demonstrates single idiomorphic grains as much as 2 mm in size and glomerophyric segregates of plagioclase small grains (5%). Total of phenocrysts is 25%. Groundmass contains weakly anisotropic brown glass in pseudovariolitic texture (glassy crust).

Alteration: slight; olivine completely replaced by iddingsite.

XRD: smectites with various swelling layers and with interlayer Ca-Mg cations; quartz in trace amounts; smectites and phillipsite in veinlets.

Sample 70-504B-33R-1, 70–72 cm (Piece 191), Unit 22 [Z-916]

Aphyric basalt with pilotaxitic groundmass texture. Rock contains needle-shaped microlites and laths (as much as 2.5 mm) of plagioclase (50%, labradorite [An_{55}] and andesine [An_{40}]). Olivine (small grains; 0.1–0.2 mm, 5%) is present. Glass (45%) is crystallized from black and almost isotropic to segregates of panicle like crystals. Microlites of clinopyroxene are present.

Alteration: slight (5%); olivine completely replaced by iddingsite.

Sample 70-504B-33R-1, 86–88 cm (Piece 193), Unit 22 [Z-917]

Olivine-plagioclase-phyric basalt, partly crystallized, massive, with intersertal groundmass texture. Elongated-prismatic and short-table grains (0.3–2 mm, 15%) of plagioclase form segregates. Composition is labradorite ($An_{60–62}$). Olivine (idiomorphic large grains as much as 0.8 mm) is present. There is olivine as segregate of small (0.2 mm) rounded grains in paragenesis with plagioclase. Total of olivine is 5%–10%. Other areas of groundmass demonstrate microlites and laths of plagioclase (andesine [An_{32}]). Interstices contain segregate of small isometric grains of clinopyroxene and opaque mineral. In weakly crystallized parts of the rock, pyroxene forms panicle like segregates of microlites. Opaque dust is present.

Alteration: slight; olivine completely replaced by iddingsite; microcracks in olivine infilled with Fe hydroxides.

XRD: smectites; smectites and hematite in veinlets.

Sample 70-504B-33R-2, 14–16 cm (Piece 202), Unit 22 [Z-918]

Olivine-plagioclase-phyric basalt similar to Sample 70-504B-33R-1, 86–88 cm (Z-917).

Alteration: rock is fresh.

XRD: smectites with ~10% mica layers with interlayer Ca-Mg cations; mixed-layer smectite-swelling chlorite mineral, chlorite, and quartz in trace amounts; Ca-Mg and Na-K smectites (Ca-Mg > Na-K) in veinlets.

Sample 70-504B-34R-1, 19–24 cm (Piece 220), Unit 22 [Z-550]

Olivine-plagioclase-phyric basalt, weakly crystallized, massive, groundmass is microlitic texture. Phenocrysts of plagioclase form rare short-prismatic idiomorphic grains (0.5–0.8 mm, 5%, labradorite [An_{52}]). Olivine (rounded

grains 0.5–0.8 mm, 5%) is present. Groundmass demonstrates unoriented microlites of plagioclase and segregate of very small grains of clinopyroxene and opaque mineral. Interstices contain chlorite (<1%). Rock on the whole contains many opaque mineral.

Alteration: slight; olivine completely replaced by iddingsite, margin parts of grains replaced by Fe hydroxides.

Sample 70-504B-34R-1, 140–142 cm (Piece 235), Unit 23B [Z-920]

Plagioclase-phyric basalt, uncrystallized, massive, groundmass is hyalopilitic texture. Phenocrysts of plagioclase form rare prismatic grains (0.3–0.5 mm, 10%). Composition of large laths is andesine (An_{46}). Groundmass demonstrates unoriented needle-shaped, skeletal microlites and microlaths of plagioclase. Plagioclase grains are located in dark-brown almost isotropic glass. Occasionally glass contains radial-radiant segregates of crystallites of plagioclase and clinopyroxene.

Alteration: rock is fresh.

XRD: smectites; smectites and hematite in veinlets.

Sample 70-504B-34R-2, 18–21 cm (Piece 240), Unit 23B [Z-921]

Olivine-plagioclase-phyric basalt, uncrystallized, massive, groundmass is vitrophyric texture. Phenocrysts of plagioclase (15%) form single short-prismatic grains (as much as 2 mm) and segregates (as much as 3 mm) of labradorite [An_{68}]. Other small grains (as much as 0.5 mm) are also labradorite [An_{55}]. Olivine (sparsely idiomorphic grains as much as 2 mm, often size is 0.4–0.5 mm, 5%–10%) is present. Groundmass contains weakly anisotropic dark brown glass with rare needle-shaped microlites of plagioclase. In some parts of the rock, isotropic glass is nonoxidized and is light green. It is glassy crust.

Alteration: slight; olivine completely replaced by iddingsite and very small calcite crystals; thin cracks in glass infilled with micrograin aggregate of clay mineral and zeolite(?); clay mineral salbands of cracks.

XRD: smectites with interlayer Ca-Mg cations; chlorite in trace amounts; smectites with interlayer Ca-Mg and Na-K cations (Ca-Mg > Na-K) in veinlets, mixed-layer chlorite-smectite mineral, chlorite, analcime, natrolite, and anhydrite.

Sample 70-504B-35R-1, 110–112 cm (Piece 274), Unit 24 [Z-922]

Olivine-clinopyroxene-plagioclase-sparsely phyric basalt, uncrystallized, massive, with vitrophyric groundmass texture. Phenocrysts of plagioclase form single large (3 mm) glomerophyric segregates of short-prismatic grains (0.3–1 mm, xenocrysts) and glomerophyric segregates of small elongated-prismatic lath-like grains (0.2–0.4 mm). Large grains are An_{58} labradorite, small grains are An_{55} labradorite. Olivine; rare (1%–2%) small (0.2–0.3 mm) idiomorphic fresh grains, occasionally in accretion with plagioclase laths. Clinopyroxene-xenomorphic grains (<1%). Glass of groundmass oxidized to varying degrees. Glass is from almost colorless isotropic to brown. Glass contains rare microlites of plagioclase.

Alteration: rock is fresh.

XRD: smectites with interlayer Ca-Mg and Na-K cations; chlorite and quartz in trace amounts; smectites with interlayer Ca-Mg and Na-K cations (Ca-Mg > Na-K), mixed-layer illite-smectite mineral with as much as 15% illite layers, and analcime in veinlets; chlorite in trace amounts.

Sample 70-504B-35R-2, 14–16 cm (Piece 283), Unit 24 [Z-923]

Olivine, sparsely phyric basalt, weakly crystallized, massive, with pilotaxitic groundmass texture. Phenocrysts are single idiomorphic crystals of olivine (1 mm). Groundmass demonstrates unoriented laths (sparse) and microlites of plagioclase, radial-radiant panicle like segregates of clinopyroxene and brown-black glass with opaque dust. Rock on the whole contains many opaque mineral.

Alteration: slight to moderate (15%–20%); olivine completely replaced by iddingsite; thin cracks (2–3 mm thick) infilled with rounded segregates of calcite with brown-green isotropic mineral and Fe hydroxides (Salinas); central parts veins contain chalcedony.

XRD: smectites with interlayer Ca-Mg and Na-K cations (Na-K > Ca-Mg); chlorite and quartz in trace amounts; mixed-layer smectite-swelling chlorite mineral, illite(?), calcite, analcime, natrolite, okenite, talc, and calcite in veinlets.

Sample 70-504B-36R-1, 91–110 cm (Piece 301A), Unit 24 [Z-551]

Clinopyroxene-plagioclase-phyric dolerite, crystallized, small grains, massive, groundmass is doleritic texture. Sparse (5%–7%) phenocrysts of plagioclase form table-shaped grains (0.5–0.6 mm), occasionally form glomerophyric segregates, composition is labradorite (An_{60}). Single phenocrysts are represented by clinopyroxene (0.8 mm), diopside. Groundmass demonstrates unoriented laths of plagioclase (andesine [An_{48}]).

Interstices contain small isometric grains (0.1–0.2 mm) of augite, very small xenomorphic segregates of opaque mineral, and single small aggregates of chlorophaeite (<1%).

Alteration: rock is fresh.

Sample 70-504B-36R-2, 25–27 cm (Piece 305), Unit 24 [Z-924]

Olivine-plagioclase-phyric dolerite, crystallized, small grains, massive, groundmass is doleritic texture. Phenocrysts of plagioclase (0.5 mm, single grains as much as 2 mm) form glomerophyric segregates. Large grains are labradorite (An_{68}), small grains are andesine (An_{47}). Single idiomorphic grain of olivine (2.3 mm) completely replaced by iddingsite. Groundmass demonstrates unoriented laths (0.2–0.5 mm) of plagioclase (andesine [$An_{45–47}$]). Interstices contain segregate of small grains of augite and opaque mineral. About 10% of rock demonstrates rounded-isometric parts mixed with small of grains augite and chlorite (chlorophaeite), dendritic opaque mineral and cubic segregates, and xenomorphic grains of opaque mineral.

Alteration: slight (5%).

XRD: smectites and hematite or smectites and pyrite in veinlets.

Sample 70-504B-37R-1, 15–20 cm (Piece 344), Unit 25 [Z-925]

Plagioclase-sparsely phyric basalt, weakly crystallized, massive, groundmass is hyalopilitic texture. Phenocrysts of plagioclase (<5%) are represented by rare elongated-prismatic (as much as 0.8 mm) and tabular phenocrysts of plagioclase. Large grains are labradorite (An_{64}), small grains are andesine (An_{58}). Groundmass demonstrates unoriented needle-shaped laths and microlites of plagioclase. Grains of plagioclase are located in weakly anisotropic glass. Glass demonstrates panicle like segregates of pyroxene and opaque dust. There are parts with higher levels of crystallized of rock and demonstrate segregates of diopside, laths of plagioclase with chlorite (trace), and opaque mineral.

Alteration: slight.

XRD: smectites; smectites in veinlets.

Sample 70-504B-37R-1, 55–60 cm (Piece 349), Unit 25 [Z-926]

Clinopyroxene-plagioclase-phyric basalt, uncrystallized, massive, groundmass is vitrophyric-variolitic texture. Phenocrysts of plagioclase are represented by laths and short-tabular grains (0.2–0.8 mm, 20%, labradorite [An_{56}]). Grains of plagioclase form glomerophyric segregates. Single xenomorphic grain of clinopyroxene (0.3 mm, diopside) is in accretion with laths of plagioclase. Groundmass demonstrates rare needle-shaped laths and microlites of plagioclase. Plagioclase grains are located in weakly anisotropic dark brown glass. Glass demonstrates rounded variolitic parts with radial-radiant segregation of clinopyroxene.

Alteration: rock is fresh.

XRD: smectites, hematite, and analcime in veinlets.

Sample 70-504B-37R-2, 75–78 cm (Piece 373), Unit 25 [Z-927]

Plagioclase-phyric basalt, uncrystallized, massive, groundmass is hyalopilitic texture. Phenocrysts of plagioclase (0.3–0.8 mm, 7%–10%) form glomerophyric segregates (tabular and laths). Grains of plagioclase are often with inclusions of glass. Groundmass demonstrates needle-shaped laths and microlites of plagioclase. They are located in dark brown weakly anisotropic glass. Glass contains panicle like segregates of crystallites of pyroxene with opaque dust. There are rare small parts (0.5 mm) of more crystallized rock demonstrating segregates of laths of plagioclase and xenomorphic grains (0.2–0.3 mm) of clinopyroxene. Level of the crystallization is very slight (1%–3%).

Alteration: rock is fresh.

XRD: smectites with ~20% mica layers and interlayer Ca-Mg cations; quartz in trace amounts; smectites with ~20%–30% mica layers and interlayer Ca-Mg cations in veinlets; trace chlorite, analcime, and gyrolite.

Sample 70-504B-37R-3, 14–17 cm (Piece 391), Unit 25 [Z-928]

Breccia of pyroxene-plagioclase-phyric basalt, weakly crystallized, massive, groundmass is hyalopilitic texture. Isometric basalt fragments (0.5–1.5 cm) are cemented by clay minerals. Basalt demonstrates elongated-prismatic grains and segregates of plagioclase. Groundmass glass is brown-black, some parts of glass are crystallized with segregates of plagioclase and pyroxene.

Alteration: fragments of basalt are slightly altered (10%–15%); plagioclase almost completely replaced by clay minerals; cement contains clay mineral, prehnite, and rounded segregates of isotropic colorless mineral (zeolite?).

XRD: smectites, hematite, and analcime in veinlets.

Sample 70-504B-38R-1, 7–15 cm (Piece 411), Unit 25 [Z-929]

Plagioclase-phyric basalt, uncrystallized, massive, groundmass is vitrophyric-variolitic texture. Phenocrysts of plagioclase (0.2–0.6 mm, 10%, labradorite [An_{68}]) form glomerophyric segregates (tabular and elongated-prismatic grains). There are small (0.1 mm) idiomorphic grains of olivine (<1%). Groundmass demonstrates sparse laths and microlites of plagioclase. Grains of plagioclase are located in dark-brown weakly anisotropic glass.

Alteration: slight; olivine completely replaced by iddingsite and Fe hydroxides.

XRD: smectites with interlayer Ca-Mg cations; quartz in trace amounts; veinlets with smectites (~20% mica layers and interlayer Ca-Mg and Na-K cations), mixed-layer chlorite-smectite mineral (30% swelling interlayers), hematite, calcite, quartz, analcime, gyrolite, and 12.9 Å-undetermined mineral.

Sample 70-504B-39R-2, 97–102 cm (Piece 492), Unit 27 [Z-930]

Plagioclase-phyric dolerite, crystallized, small grains, massive, groundmass is doleritic texture. Phenocrysts of plagioclase (0.4–2 mm, 20%) form glomerophyric segregates (elongated and short-prismatic grains). Composition of plagioclase is labradorite ($An_{68–69}$), smaller grains are An_{58}. A single idiomorphic grain of olivine (0.5 mm) is present. Groundmass demonstrates unoriented laths of plagioclase, composition varies from andesine (An_{45}) to labradorite (An_{52}). Interstices contain small (as much as 0.1 mm), xenomorphic, often rounded grains of diopside-augite and opaque mineral and chlorite (<1%).

Alteration: slight; olivine completely replaced by iddingsite; chlorite replaces glass.

XRD: smectites; smectites and pyrite in veinlets.

Sample 70-504B-40R-1, 55–60 cm (Piece 510), Unit 27 [Z-552]

Olivine-pyroxene-plagioclase-phyric dolerite, crystallized, medium grained, massive, groundmass is doleritic texture. Olivine; single, small (0.3 mm) altered grains and large (as much as 1.5 mm) fresh grains of augite (single grains) with laths of plagioclase. Phenocrysts of plagioclase (0.4–1.2 mm, labradorite [An_{58}]) form glomerophyric segregates (short-prismatic grains). Groundmass demonstrates unoriented laths and grains of plagioclase (0.2–0.5 mm), composition varies from andesine (An_{45}) to labradorite (An_{55}). Interstices contain rounded isometric grains (0.2–0.4 mm) of clinopyroxene-augite and segregates of clinopyroxene and laths of plagioclase. There are skeletal and idiomorphic cubic grains of opaque mineral and occasionally clay mineral (<1%).

Alteration: slight; olivine replaced by iddingsite; clay mineral replaces glass.

XRD: smectites with interlayer Ca-Mg cations; mixed-layer chlorite-smectite mineral and quartz in trace amounts; oxidized crust is maghemite, lepidolite, and goethite; black clay crust contains trace smectites with ~20% mica layers and with interlayer Ca-Mg cations, chlorite.

Sample 70-504B-40R-2, 84-–86 cm (Piece 532), Unit 27 [Z-553]

Olivine-plagioclase-phyric dolerite, crystallized, moderate-grains, massive, groundmass is doleritic texture. Olivine (5%) forms idiomorphic (1.2 mm) or partly unoriented xenomorphic (0.5 mm) grains. Phenocrysts of plagioclase (labradorite [An_{60}]) form glomerophyric segregates (3 mm in diameter) of elongated-prismatic and tabular (zonal) grains, 0.5–2 mm in size. Groundmass demonstrates elongated-prismatic grains and laths of plagioclase (0.2–0.3 mm), composition varies from andesine (An_{45}) to andesine (An_{47}). Interstices contain xenomorphic grains of augite (0.1–0.3 mm) and small (0.05–0.1 mm) grains of opaque mineral (3%–4%).

Alteration: slight; olivine partly replaced by iddingsite; trace clay mineral.

Sample 70-504B-41R-3, 146–148 cm (Piece 628), Unit 27 [Z-554]

Plagioclase-phyric basalt, weakly crystallized, massive, groundmass is microlitic texture. Phenocrysts of plagioclase (0.3–0.8 mm, 15%, labradorite [An_{55}]) form glomerophyric segregates of elongated and short-prismatic grains. Groundmass demonstrates unoriented microlites of plagioclase and segregate of small grains of clinopyroxene and opaque mineral. There are isometric vesicles (2%–3%, 0.05 mm).

Alteration: rock is fresh; vesicles infilled with clay mineral.

XRD: smectites with ~35% mica layers and interlayer Ca-Mg cations; quartz in trace amounts; smectites with ~20% mica layers and with interlayer Ca-Mg and Na-K cations (Ca-Mg > Na-K) in veinlets; chlorite and talc in trace amounts.

Sample 70-504B-43R-1, 80–82 cm (Piece 680), Unit 28 [Z-555]

Clinopyroxene-plagioclase-sparsely phyric dolerite, crystallized, moderate-grains, massive, groundmass is doleritic texture. Single grains (0.4 mm) of plagioclase form glomerophyric segregates with clinopyroxene. Composition of plagioclase is labradorite-bitovnite (An_{70}). Groundmass demonstrates unoriented elongated-prismatic laths of

plagioclase, composition varies from andesine (An_{47}) to labradorite (An_{52}). Interstices contain xenomorphic grains (0.1–0.2 mm) of augite and small xenomorphic, occasionally skeletal, grains of opaque mineral.

Alteration: rock is fresh.

Sample 70-504B-44R-1, 125–130 cm (Piece 716), Unit 29B [Z-931]

Olivine-plagioclase-phyric basalt, uncrystallized, massive, groundmass is hyalopilitic texture. Phenocrysts of plagioclase (0.5–0.8 mm, 10%, labradorite [An_{55}]) form elongated-prismatic grains. Olivine is completely replaced by iddingsite. Groundmass demonstrates needle-shaped microlites and laths of plagioclase. Glass is weakly anisotropic. Opaque dust is present.

Alteration: rock is fresh.

XRD: smectites and pyrite in veinlets.

Sample 70-504B-47R-1, 46–48 cm (Piece 808), Unit 30A [Z-556]

Olivine-pyroxene-plagioclase-phyric basalt, crystallized, massive, groundmass is microdoleritic texture. Microphenocrysts of idiomorphic olivine (0.1–0.3 mm, 1%–2%) are present. Clinopyroxene (diopside) forms single large (as much as 4 mm) elongated-prismatic crystals or tabular grains (5%, as much as 1 mm). Plagioclase forms glomerophyric segregates of elongated-prismatic crystals (0.5–0.8 mm, 5%–7%, labradorite [An_{68}]). Groundmass demonstrates unoriented microlites and laths of plagioclase. Interstices contain small grains of augite, often paniclelike segregates of clinopyroxene microlites. Opaque mineral is present (5%). Occasionally opaque mineral forms spots with skeletal grains.

Alteration: slight; olivine completely replaced by iddingsite.

Sample 70-504B-47R-2, 130–140 cm (Piece 835), Unit 30C [Z-932]

Olivine-plagioclase-phyric dolerite, crystallized, moderate-grains, massive, groundmass is doleritic texture. Small (0.2–0.4 mm) idiomorphic or partly xenomorphic grains of olivine (2%–3%) are present. Plagioclase forms sparse glomerophyric segregates and grains of short-prismatic habit. Composition of plagioclase is labradorite (An_{55}). Occasionally grains are zonal. Groundmass demonstrates unoriented laths of plagioclase (andesine [An_{43}]). Interstices contain segregates of small isometric grains of augite, small grains (0.05 mm) of opaque mineral, and chlorite (<1%). Occasionally augite forms panicle like segregates.

Alteration: slight; olivine completely replaced by iddingsite; clay mineral replaces glass.

XRD: smectites with ~20% mica layers and with interlayer Ca-Mg cations; trace quartz; smectites with Ca-Mg cations and pyrite in veinlets; trace quartz.

Sample 70-504B-48R-1, 113–115 cm (Piece 871), Unit 31 [Z-933]

Pyroxene-plagioclase-phyric basalt, brecciated, groundmass is hyaline texture. Rock demonstrates brecciated and partly palagonitized volcanic glass with rare small (0.2 mm) glomerophyric segregates of plagioclase (5%) and clinopyroxene (3%). Light cream glass is isotropic.

Alteration: glass fragments are cemented by clay minerals; volcanic glass partly palagonitized.

XRD: smectites and pyrite in veinlets.

Sample 70-504B-49R-1, 122–126 cm (Piece 932), Unit 33B [Z-934]

Clinopyroxene-plagioclase-phyric basalt, uncrystallized, massive, groundmass is vitrophyric texture. Single phenocrysts of plagioclase form short-prismatic grains (0.3–0.8 mm, 5%–8%, labradorite [An_{55}]). Groundmass demonstrates weakly anisotropic black-brown glass with variolitic texture (glassy crust).

Alteration: thin cracks infilled with clay mineral.

XRD: smectites; smectites and pyrite in veinlets.

Sample 70-504B-49R-1, 140–147 cm (Piece 933), Unit 33B [Z-559]

Olivine-phyric dolerite, crystallized, moderate-grains, vesicles (7%–8%), groundmass is doleritic texture. Phenocrysts: idiomorphic fresh grains of olivine (0.3–0.5 mm, 10%). Groundmass demonstrates unoriented laths of plagioclase (from labradorite [An_{52}] to andesine [An_{47}]). Rounded vesicles (0.2–0.4 mm) infilled with black-brown oxidized glass.

Alteration: rock is fresh; green glass from central part of vesicles is weakly anisotropic; some vesicles are lined with brown or green glass, central parts of vesicles infilled with carbonate.

Sample 70-504B-49R-2, 7–10 cm (Piece 936), Unit 33B [Z-560]

Pyroxene-plagioclase-phyric basalt, uncrystallized, massive, groundmass is vitrophyric texture. Phenocrysts of pyroxene-diopside forms segregates (0.5 mm) of small (0.1 mm) xenomorphic grains with laths of plagioclase

(1%). Plagioclase forms elongated-prismatic grains (2 mm, 5%, labradorite [An_{56}]). Groundmass demonstrates dark-brown weakly anisotropic glass with variolitic texture. Rock is weakly brecciated.

Alteration: rock is fresh; microcracks infilled with clay matter.

XRD: smectites with ~20% mica layers and interlayer Na-K cations; trace quartz.

Sample 70-504B-54R-1, 35–38 cm (Piece 1062), Unit 35 [Z-935]

Aphyric basalt, weakly crystallized, vesicles (15%–20%), groundmass is pilotaxitic texture. Groundmass has unoriented laths and microlites of plagioclase. Interstices are weakly crystallized glass. Glass demonstrates segregate of very small grains or paniclelike segregates of microlites and crystallites of pyroxene and opaque dust. Green glass replaced by chlorophaeite (2%–3%). Vesicles (2%–3%) are isometric (0.5–0.8 mm) and rounded (0.1–0.2 mm).

Alteration: slight (15%); small vesicles completely infilled with chlorophaeite.

XRD: smectites and pyrite in veinlets.

Sample 70-504B-56R-2, 92–95 cm (Piece 1121), Unit 36 [Z-936]

Aphyric basalt, uncrystallized, vesicles, groundmass is hyalopilitic texture. Rock is similar to Sample 70-504B-54R-1, 35–38 cm (Z-935) but contains more dark brown to black uncrystallized glass.

Alteration: slight; vesicles infilled with chlorophaeite.

XRD: smectites and pyrite in veinlets.

Sample 70-504B-61R-1, 55–60 cm (Piece 1287), Unit 40 [Z-937]

Olivine-pyroxene-plagioclase-sparsely microphyric basalt, uncrystallized, massive, groundmass is vitrophyric texture. Phenocryst are small (0.2 mm) segregates of xenomorphic grains of pyroxene, single (0.2 mm) idiomorphic grains of olivine and laths of plagioclase are present. Occasionally plagioclase forms elongated-prismatic grains up to 0.5 mm in size. Groundmass demonstrates dark brown to black oxidized glass. Glass contains sparse needle-shaped microlites of plagioclase. Occasionally glass is weakly crystallized and variolitic texture.

Alteration: slight; olivine completely replaced by iddingsite.

XRD: smectites with ~20% mica layers and interlayer Ca-Mg and Na-K cations (Ca-Mg > Na-K); trace quartz; smectites with interlayer Ca-Mg cations and anhydrite in veinlets; trace apophyllite, gypsum, and pyrite.

Sample 70-504B-61R-2, 145–149 cm (Piece 1313), Unit 40 [Z-561]

Olivine-plagioclase-phyric basalt, uncrystallized, massive, vesicles, groundmass is hyalopilitic texture. Olivine (1%–2%) forms small rounded–idiomorphic grains in segregates with plagioclase. Rock contains single vesicle (0.3 mm).

Alteration: slight; olivine completely replaced by iddingsite; vesicle infilled with brown-green chlorophaeite.

XRD: smectites with ~10% mica layers and interlayer Ca-Mg cations; trace quartz; smectites and pyrite in veinlets.

Sample 70-504B-61R-2, 145–149 cm (Piece 1314), Unit 40 [Z-938]

Plagioclase-sparsely phyric basalt, uncrystallized, massive, vesicles, groundmass is hyalopilitic (partly pilotaxitic) texture, brecciated. Single short-prismatic (0.8 mm) idiomorphic grains of plagioclase (2%–3%, labradorite [An_{60}]) and glomerophyric segregates of smaller grains (0.1–0.2 mm) of plagioclase. Groundmass has dark-brown weakly anisotropic glass. Glass contains paniclelike segregates of needle-shaped microlites of plagioclase. Fragments of basalt are cemented by green chlofaeite and small fragments of black isotropic glass.

Alteration: rock is fresh; altered cement (25%–30%).

XRD: Smectites or mixed-layer illite-smectite mineral with 10% mica layers.

Sample 70-504B-64R-1, 65–68 cm (Piece 1287), Unit 42 [Z-939]

Olivine-pyroxene-plagioclase-sparsely phyric basalt, massive, groundmass is hyalopilitic-vitrophyric texture. Olivine forms idiomorphic grains (0.1–0.5 mm, 2%–3%). There are sparse idiomorphic grains of pyroxene-diopside (0.4–0.8 mm). Often xenomorphic small (0.2 mm) grains of pyroxene are located in segregates with laths of plagioclase. Plagioclase forms single elongated-tabular grains (0.3–0.5 mm). Groundmass demonstrates black glass. Glass contains sparse microlites of plagioclase. Rock is partly brecciated.

Alteration: slight; olivine completely replaced by iddingsite; cement contains aggregate of quartz and chlorophaeite; occasionally birefringent hydromica is present; crack infilled with chalcedony.

XRD: smectites, anhydrite, quartz, and pyrite in veinlets.

Sample 70-504B-64R-2, 32–35 cm (Piece 1424), Unit 43 [Z-562]

Aphyric dolerite, crystallized, small grains, massive, groundmass is doleritic texture. Rock contains unoriented laths (0.1–0.5 mm) of plagioclase (40%, labradorite [An_{52}]). Interstices contain segregate of xenomorphic grains (0.1–0.2 mm) of augite (55%) and opaque mineral (5%).

Alteration: rock is fresh.

XRD: smectites with ~10% mica layers and interlayer Ca-Mg cations; trace quartz; black clay crust contains smectites with ~20% mica layers and interlayer Ca-Mg cations; trace quartz.

Sample 70-504B-66R-2, 0–5 cm (Piece 1506), Unit 45 [Z-940]

Olivine-pyroxene-plagioclase-phyric basalt, uncrystallized, massive, groundmass is vitrophyric texture. Phenocrysts demonstrate sparse idiomorphic grains of pyroxene-diopside (2 mm). Often xenomorphic (0.2–0.3 mm, 5%–7%) grains pyroxene are in segregates with laths of plagioclase, labradorite, (An_{67}). Groundmass demonstrates weakly anisotropic oxidized glass. Glass is paniclelike and variolitic texture.

Alteration: slight; olivine completely replaced by iddingsite.

XRD: smectites with ~20% mica layers and interlayer Ca-Mg cations; trace quartz; veinlets contain smectites with interlayer Ca-Mg and Na-K cations, anhydrite, and quartz; chlorite, anhydrite, and quartz.

Sample 70-504B-67R-1, 45–49 cm (Piece 1527), Unit 47 [Z-941]

Clinopyroxene-phyric basalt, crystallized, massive, groundmass is from microlitic to microdoleritic texture. There is a single glomerophyric segregate of rounded-isometric small (0.2 mm) grains of clinopyroxene (salite). Groundmass demonstrates elongated-prismatic grains of plagioclase (0.5 mm); plagioclases contain inclusions of altered glass; segregate of small grains of clinopyroxene; opaque mineral. On the whole rock is similar to Sample 70-504B-68R-1, 81–83 cm (Z-942).

Alteration: slight; interstitial clay mineral is 2%–3%, clay mineral replaces glass from plagioclase.

XRD: smectites.

Sample 70-504B-68R-1, 81–83 cm (Piece 1537), Unit 47 [Z-942]

Plagioclase-phyric basalt, crystallized, massive, groundmass is microdoleritic texture. There is a single glomerophyric segregate of elongated-prismatic grains of plagioclase (0.2–0.5 mm, labradorite [An_{55}]). Plagioclase contains altered glass. Groundmass demonstrates thin elongated (0.5 mm) laths of plagioclase. Interstices contain a segregate of clinopyroxene small grains, opaque mineral, and glass (5%).

Alteration: slight; glass from plagioclase replaced by green clay mineral; interstitial glass replaced by clay mineral.

XRD: smectites and anhydrite in veinlets.

Sample 70-504B-68R-1, 107–111 cm (Piece 1538), Unit 47 [Z-563]

Plagioclase-sparsely phyric basalt, massive, groundmass is microdoleritic texture. Single segregate of elongated-tabular grains of plagioclase (0.2–0.3 mm, labradorite [An_{55}]). Groundmass is melanocratic with laths and microlites of plagioclase (andesine [An_{38}?]; 30%), segregate of small isometric grains of augite or elongated segregates of microlites of this mineral (65%,) and opaque mineral (very small xenomorphic or skeletal grains; 5%). Opaque mineral occurs together with brown-green chlorophaeite (2%–3%).

Alteration: slight.

XRD: smectites with ~10% mica layers and interlayer Ca-Mg cations; trace quartz; veinlet contain smectites with ~10% mica layers and interlayer Ca-Mg cations; trace mixed-layer chlorite-smectite mineral (~20% swelling interlayers).

Sample 70-504B-69R-1, 14–17 cm (Piece 1540), Unit 47 [Z-564]

Plagioclase-phyric dolerite, massive, groundmass is doleritic texture. Plagioclase forms glomerophyric segregates of short and elongated-prismatic grains (0.2–1.0 mm, labradorite [An_{55}]). Groundmass demonstrates unoriented laths of plagioclase (0.1–0.2 mm). Interstices with accretions of plagioclase and small (0.1 mm) isometric grains of augite, xenomorphic grains of opaque mineral, and sparse glass.

Alteration: slight; interstitial glass replaced by green chlorophaeite.

XRD: smectites with ~20% mica layers; trace quartz.

Sample 70-504B-69R-1, 74–77 cm (Piece 1545), Unit 47 [Z-565]

Plagioclase-pyroxene-sparsely phyric dolerite, massive, fine grained, groundmass is doleritic texture. There are single phenocryst of pyroxene-diopside tabular grains (0.8 mm) and a glomerophyric segregate of elongated-prismatic grains of plagioclase. Groundmass demonstrates unoriented laths of plagioclase (0.2–0.4 mm, 40%) and

rounded-isometric grains (0.1–0.2 mm) of salite. There are spotty areas (0.5–1.0 mm) that contain small grains of pyroxene and green chlorophaeite with very small skeletal grains of opaque mineral.

Alteration: slight; chlorophaeite is 5%–7%.

XRD: smectites with ~15% mica layers and interlayer Ca-Mg cations; trace quartz; black clay crust contains smectites with ~10% mica layers and interlayer Ca-Mg cations; trace quartz.

Sample 70-504B-69R-1, 77–81 cm (Piece 1545), Unit 47 [Z-943]

Plagioclase-sparsely phyric basalt, massive, groundmass is microlitic (microdoleritic) texture. Phenocrysts with plagioclase (5%, labradorite [An_{60}]). Groundmass with microlites and microlaths (0.1–0.6 mm) of plagioclase (labradorite [An_{55}] and andesine [$An_{40–44}$]). Small grains of olivine (2%–3%) and opaque mineral (2%–3%) are present.

Alteration: slight (2%–3%); olivine replaced by iddingsite.

XRD: smectites and pyrite in veinlets.

Sample 70-504B-70R-1, 17–20 cm (Piece 1550), Unit 48 [Z-944]

Volcanic breccia with lithocrystaloclastic cement (50%). Fragments (2–5 mm) are aphyric dolerite and aphyric basalt. Cement contains small (0.1 mm) fragments of plagioclase crystals and pyroxene (70% of cement volume) and brown matter (30%).

Alteration: slight.

XRD: smectites; smectites and pyrite in veinlets.

Sample 70-504B-70R-1, 79–82 cm (Piece 1556), Unit 48 [Z-567]

Aphyric dolerite, massive, partly brecciated and cemented by lithocrystaloclastic cement. Possibly more large (10 mm) fragments of volcanic breccia than described in Sample 70-504B-70R-1, 17–20 cm (Z-944).

Alteration: slight.

Sample 70-504B-70R-1, 127–130 cm (Piece 1561), Unit 49 [Z-568]

Aphyric dolerite, massive, moderate-grains, groundmass is doleritic and poikilophitic texture. Rock contains olivine, clinopyroxene, plagioclase, and opaque mineral. Olivine forms idiomorphic grains and segregates (5%, 0.4–0.8 mm). Rock consist of mainly xenomorphic, large, elongated-prismatic laths (0.8–1.8 mm) of plagioclase (labradorite [An_{60}]).

Alteration: slight; olivine completely replaced by brown-green iddingsite.

XRD: smectite mineral with 20% mica interlayers and interlayer Ca-Mg cations; chlorite, quartz, and talc(?) in trace amounts; smectite mineral with interlayer Ca-Mg cations in veinlets; trace swelling chlorite.

Sample 70-504B-70R-2, 20–23 cm (Piece 1564), Unit 49 [Z-569]

Aphyric dolerite, massive, moderate grains, groundmass is doleritic and poikilophitic texture. Rock is the similar to Sample 70-504B-70R-1, 127–130 cm (Z-568).

Alteration: rock is fresh.

XRD: smectite mineral with 20% mica interlayers and interlayer Ca-Mg cations; chlorite and quartz in trace amounts; black veinlet contains smectite mineral with interlayer Ca-Mg cations; minor chlorite.

Sample 83-504B-72R-2, 60–64 cm (Piece 5), Unit 49 [Z-570]

Plagioclase-phyric basalt, crystallized, massive, groundmass is hyalopilitic texture. Phenocrysts of plagioclase (20%) are represented by prismatic crystals (0.3–1.2 mm, labradorite [An_{68}]). Groundmass; needle-shaped microlites and laths of plagioclase (andesine [An_{45}]; 60%) and brown anisotropic glass. Glass; segregate of plagioclase and clinopyroxene and oxidized brown-red opaque mineral (1%–2%).

Alteration: rock is fresh.

XRD: smectites with ~20% mica layers and interlayer Ca-Mg cations; chlorite and quartz in trace amounts.

Sample 83-504B-73R-2, 56–59 cm (Piece 4), Unit 50 [Z-571]

Olivine-plagioclase-phyric microdolerite, massive, groundmass is microdoleritic texture. Olivine forms single idiomorphic grains (0.8 mm). Phenocrysts of plagioclase (20%) form elongated-tabular grains (0.5–1.5 mm, labradorite [An_{56}]), occasionally plagioclase grains form glomerophyric segregates. Groundmass; unoriented laths (0.1–0.5 mm) of plagioclase (labradorite [An_{54}], 40%). Interstices contain segregates of small isometric or slightly stretched accreted grains of clinopyroxene (50%). Opaque mineral (5%–6%).

Alteration: slight; olivine completely replaced by iddingsite.

XRD: smectites with mica layers and interlayer Ca-Mg cations; quartz and talc(?) in trace amounts.

Sample 83-504B-77R-1, 78–81 cm (Piece 4), Unit 54 [Z-572]

Aphyric dolerite, fine grained, groundmass is intersertal-doleritic texture. Rock; laths (0.3–1.2 mm) of plagioclase (labradorite [An_{56}] and andesine [An_{43}]; 45%), clinopyroxene (40%), opaque mineral (5%), and glass (10%).

Alteration: slight (10%); glass completely replaced by clay mineral.

XRD: corrensite and chlorite with 10% swelling interlayers; amphibole(?) and quartz in trace amounts.

Sample 83-504B-78R-1, 60–64 cm (Piece 3D), Unit 56 [Z-573]

Plagioclase-microphyric dolerite, fine grained, massive, crystallized, groundmass is ophitic texture. Phenocrysts of plagioclase (5%) form tabular grains (0.5–0.8 mm, labradorite [An_{68}]). Groundmass; unoriented laths of plagioclase (40%, andesine [An_{48}] to labradorite [An_{54}]). Clinopyroxene; augite. Plagioclase/clinopyroxene ratio is 1:1. Opaque mineral (as much as 0.1 mm, 5%–7%) occurs together with pyroxene. Green chlorite (1%–2%) occurs in opaque mineral with pyroxene association.

Alteration: slight.

XRD: Fe chlorite with single swelling interlayers; thin clay crust contains Fe chlorite with single swelling interlayers and epistilbite(?) or clinoptilolite/heulandite(?).

Sample 83-504B-79R-3, 50–54 cm (Piece 4A), Unit 58 [Z-574]

Plagioclase-sparsely phyric basalt, massive, crystallized, groundmass is microdoleritic-intersertal texture. Phenocryst; single tabular xenocrystal (0.8 mm) of plagioclase. Groundmass; elongated-laths (0.3–0.8 mm) of plagioclase (labradorite [An_{62}]). Interstices are segregates of paniclelike grains and microlites of clinopyroxene. Opaque mineral (0.1 mm, 7%–8%) is present.

Alteration: slight; glass replaced by chlorite (15%).

XRD: corrensite and mixed-layer chlorite-smectite mineral (chlorite/smectite ratio = 90:10); quartz and amphibole in trace amounts; black clay from vein is Fe and Mg chlorite (Fe > Mg) with 10% swelling interlayers; amphibole and quartz in trace amounts.

Sample 83-504B-80R-1, 5–10 cm (Piece 1), Unit 60 [Z-1301]

Olivine-plagioclase-phyric basalt, weakly crystallized, groundmass is hyalopilitic texture. Phenocrysts (30%) are represented by sparse (5%) idiomorphic grains (0.5–1.5 mm) of olivine; plagioclase (25%) forms glomerophyric segregates of prismatic crystals (0.5–1.7 mm, labradorite [An_{60}]). Groundmass; needle-shaped grains of plagioclase (labradorite [An_{52}]) and black, weakly anisotropic glass. Idiomorphic grains of opaque mineral (0.4–0.8 mm, 5%) are present.

Alteration: moderate (30%); olivine completely replaced by chlorite; plagioclase replaced by albite (90% of plagioclase); microcrack (0.1 mm) infilled with carbonate.

XRD: mixed-layer chlorite-smectite mineral (5%–10% swelling interlayers); amphibole and quartz in trace amounts; dark-green matter from veins is Fe chlorite with single swelling interlayers; quartz, calcite, and zeolite (epistilbite?) in trace amounts.

Sample 83-504B-80R-2, 143–146 cm (Piece 12), Unit 60 [Z-1302]

Volcanic breccia of olivine-plagioclase-phyric basalt, groundmass is hyalopilitic texture, with chlorite cement (30%). Fragments of basalt (70%) are from 0.5 to 8 mm. Basalt is similar to Sample 83-504B-80R-1, 5–10 cm (Z-1301). Cement contains chlorite aggregate with Fe-Mn hydroxides.

Alteration: moderate (30%).

XRD: Fe chlorite with single swelling interlayers; quartz and (heulandite?) in trace amounts; white matter from veins is calcite, epistilbite(?), and lomontite; dark green clay from veins is Fe chlorite with single swelling interlayers; trace quartz.

Sample 83-504B-80R-4, 3–8 cm (Piece 1A), Unit 60 [Z-1303]

Olivine-plagioclase-phyric basalt, uncrystallized, groundmass is hyalopilitic texture, brecciated. Phenocrysts (10%) are represented by sparse (2%–3%) grains of olivine and prismatic grains of plagioclase (0.5–0.8 mm, labradorite [An_{60}]). Groundmass; needle-shaped laths and microlites of plagioclase (andesine–labradorite [An_{50}]) and brown isotropic glass. Idiomorphic cubic grains (0.1–0.3 mm, 5%) of opaque mineral are located in central parts of large (0.8 mm) prismatic grains of albitized plagioclase.

Alteration: slight to moderate (20%); plagioclase replaced by albite (90% of plagioclase); groundmass is chloritized; glassy crust is broken by thin (0.2–0.8 mm) cracks infilled with chlorite-pennine (10%); microcrack (0.1 mm) infilled with carbonate.

XRD: Fe and Mg chlorite with single swelling interlayers; quartz and stilbite(?) in trace amounts; dark green clay from veins is Fe and Mg chlorite (Fe and Mg in approximately equal amounts) with 10% swelling interlayers; quartz and heulandite in trace amounts.

Sample 83-504B-81R-1, 83–86 cm (Piece 10), Unit 60 [Z-1304]

Olivine-plagioclase-phyric basalt, uncrystallized, groundmass is vitrophyric texture, brecciated. Phenocrysts (30%)are represented by grains of olivine and plagioclase. Plagioclase (10%) forms grains 0.3–0.6 mm in size (labradorite [An_{60}]). Olivine (20%) forms large (0.5–0.7 mm) idiomorphic altered grains; small (0.3–0.5 mm) grains of olivine are fresh. Groundmass; black glass (70%).

Alteration: slight to moderate (20%); rock is chloritized; olivine completely replaced by chlorite; microcrack (0.8–1.7 mm) infilled with aggregate of small (0.1 mm) rounded grains of albite-oligoclase and quartz (salbands); center of vein; chlorite.

XRD: dark green clay from veins is Fe chlorite with single swelling interlayers; minor quartz.

Sample 83-504B-82R-2, 92–96 cm (Piece 6F), Unit 60 [Z-1305]

Olivine-plagioclase-phyric basalt, crystallized, groundmass is microlitic texture. Phenocrysts (15%) are represented by grains of olivine (5%) and plagioclase (10%). Olivine forms (0.5–0.8 mm) idiomorphic grains. Plagioclase (10%) forms tabular and prismatic crystals 0.4–1.7 mm in size (bitovnite [$An_{72–74}$]. Groundmass; needle-shaped laths (15%) of plagioclase (labradorite [An_{55}]), paniclelike segregates of microlites of pyroxene (50%), and plagioclase (5%).

Alteration: slight (15%); olivine completely replaced by chlorite; plagioclase replaced by albite (10%).

XRD: Fe chlorite; quartz and amphibole in trace amounts.

Sample 83-504B-84R-2, 48–50 cm (Piece 7), Unit 60 [Z-1306]

Olivine-plagioclase-phyric basalt, uncrystallized, groundmass is hyalopilitic texture. Phenocrysts (40%) represented by idiomorphic grains (0.5–0.9 mm) of olivine (15%) and tabular and prismatic grains (0.3-1.7 mm) of plagioclase. Groundmass represented by needle-shaped laths (5%) of altered plagioclase and brown-black isotropic glass (50%). Single xenomorphic grains of opaque mineral (0.1–0.3 mm) are present.

Alteration: moderate (30%–35%); olivine completely replaced by chlorite; plagioclase replaced by albite; sosuritized interstitial plagioclase.

XRD: Fe chlorite (~5% swelling interlayers); quartz and heulandite(?) in trace amounts; black clay from vein is Fe chlorite with 5% swelling interlayers and quartz; amphibole and zeolite in trace amounts.

Sample 83-504B-85R-1, 58–62 cm (Piece 6B), Unit 60 [Z-1307]

Volcanic breccia. Rock: one fragment of plagioclase-phyric basalt with vitrophyric groundmass texture and hyalo-breccia (fragments from 0.1 to 0.9 mm in size; from colorless to brown-black).

Alteration: rock is fresh; veinlet (0.4 mm thick) with granoblastic aggregate of quartz.

XRD: Fe chlorite; trace quartz and amphibole; dark green matrix from breccia is Fe chlorite.

Sample 83-504B-86R-1, 15–20 cm (Piece 2), Unit 62 [Z-1308]

Clinopyroxene-olivine-plagioclase-phyric basalt, slight crystallized, groundmass is hyalopilitic texture. Phenocrysts (20%) represented by grains (<1%, 0.6–1.2 mm) of clinopyroxene, sparse large (0.8–1 mm) idiomorphic grains of olivine (5%), and glomerophyric segregates of prismatic grains (0.2–0.7 mm) of plagioclase (labradorite [An_{65}]). Groundmass represented by needle-shaped microlites and microlaths (0.2–0.6 mm) of plagioclase (10%, labradorite [An_{52}]) and volcanic glass (70%).

Alteration: slight to moderate (20%); olivine completely replaced by chlorite; plagioclase replaced by albite (70%–80%); veinlet (0.1–0.2 mm thick) is chlorite and small grains of quartz.

XRD: Fe chlorite with single swelling interlayers (as much as 5%); trace quartz and amphibole.

Sample 83-504B-88R-1, 68–71 cm (Piece 4A), Unit 70 [Z-575]

Olivine-plagioclase-phyric basalt, crystallized, groundmass is microlitic texture. Phenocrysts (25%) represented by single (2%–3%) grains (0.3–0.6 mm) of olivine and glomerophyric segregates of prismatic and tabular grains (0.5–1.2 mm) of plagioclase (labradorite [An_{59}]). Groundmass represented by laths of plagioclase (30%), grains of clinopyroxene (35%), and olivine (10%). Opaque mineral (1%–2%) is present.

Alteration: slight (12%–15%); olivine completely replaced by iddingsite.

XRD: Fe chlorite; trace quartz and amphibole.

Sample 83-504B-89R-2, 74–78 cm (Piece 9), Unit 71 [Z-1309]

Aphyric basalt, crystallized, groundmass is microlitic texture. Rock contains microlites (0.1–0.5 mm) of plagioclase (45%, labradorite [An_{60}]). Pyroxene forms segregates of very small grains and accretions of microlites (55%) in interstices. Opaque mineral and chlorite (5%) are present.

Alteration: slight; veinlets (0.1–0.2 mm, 5%) are albite, quartz, and chlorite.

XRD: Fe chlorite; trace amphibole and quartz.

Sample 83-504B-90R-4, 112–114 cm (Piece 10A), Unit 72 [Z-1310]

Aphyric dolerite, fine grained, groundmass is intersertal-ophitic texture. Rock contains prismatic grains (40%) of altered plagioclase (labradorite [An_{60}]). Interstices contain xenomorphic grains (0.2–0.5 mm) of pyroxene (40%). Opaque mineral (5%) is present. Rock contains brown-black isotropic glass (15%).

Alteration: slight to moderate (15%–20%); albitized plagioclase; veinlets (0.1 mm) represented by microgranoblastic aggregate of albite; trace chlorite.

XRD: Fe chlorite; quartz, amphibole, and zeolite(?) in trace amounts; white matter and clay from vein is quartz and Fe chlorite with single swelling interlayers; trace amphibole and epistilbite.

Sample 83-504B-91R-1, 115–118 cm (Piece 15), Unit 75 [Z-576]

Clinopyroxene-plagioclase-sparsely phyric basalt, microvesicular, crystallized, groundmass is microlitic texture. Groundmass; microlites and microlaths of plagioclase. Clinopyroxene forms segregate of small grains with opaque dust. Vesicles (0.1–0.3 mm, 15%–20%) are isometric-rounded or isometric in shape.

Alteration: central parts of plagioclase replaced by sosurite and albite, occasionally by carbonate; interstitial plagioclase completely replaced by sosurite and albite; vesicles infilled with green chlorite.

XRD: Fe chlorite with 5%–10% smectite interlayers; trace quartz; black clay from vein is Fe chlorite with single swelling interlayers; trace epistilbite.

Sample 83-504B-92R-3, 38–42 cm (Piece 4), Unit 79 [Z-577]

Clinopyroxene-phyric basalt, partly crystallized, groundmass is poikilophitic-intersertal texture. Phenocrysts (60%) represented by rounded segregates (3 mm) of clinopyroxene-augite. Segregates of clinopyroxene and plagioclase are located in mesostasis of unoriented laths of plagioclase and weakly crystallized brown glass.

Alteration: chlorite is present (10%).

XRD: clay and white matter from veins is Fe chlorite with single swelling interlayers; amphibole and epistilbite(?) in trace amounts.

Sample 83-504B-94R-3, 91–94 cm (Piece 10), Unit 86 [Z-578]

Olivine-clinopyroxene-plagioclase-phyric dolerite, fine grained, massive, groundmass is doleritic texture. Phenocrysts (15%–20%) represented by single idiomorphic crystals of olivine (2.0 mm) and segregates of grains (0.5 mm); clinopyroxene-augite (0.5–2.0 mm, 2%–3%) and elongated-short-prismatic crystals of plagioclase (0.5–2.0 mm, labradorite-bitovnite [An_{58}]). Groundmass; short-prismatic laths of plagioclase (labradorite [An_{52}]). Interstices contain individual and segregates of small (0.1–0.2 mm) xenomorphic grains of augite. Opaque mineral (3%–5%) is present.

Alteration: slight; olivine completely replaced by iddingsite.

XRD: corrensite, Fe chlorite, and swelling chlorite; trace amphibole.

Sample 83-504B-97R-1, 88–90 cm (Piece 7), Unit 91 [Z-1311]

Plagioclase-phyric dolerite, fine grained, massive, groundmass is intersertal-doleritic texture. Phenocrysts (5%) represented by prismatic (4 mm) and tabular (0.8 mm) crystals of plagioclase. Groundmass represented by prismatic grains and laths (0.3–1.2 mm) of partly altered plagioclase (40%, labradorite [An_{55}]). Interstices contain xenomorphic grains of pyroxene, often their segregates, small (0.2 mm) grains of olivine (5%), and volcanic glass. Large (0.2–0.6 mm) grains of opaque mineral (10%) are present.

Alteration: slight (10%–15%); partly sosuritized plagioclase; olivine replaced by chlorite; chlorite replaces volcanic glass.

XRD: Fe chlorite with single swelling interlayers; amphibole and epistilbite in trace amounts; white matter (friable) is lomontite; white matter (hard) is scolecite.

Sample 83-504B-97R-2, 108–111 cm (Piece 10), Unit 91 [Z-579]

Plagioclase-sparsely phyric basalt, crystallized, massive, groundmass is microlitic texture. Phenocrysts are represented by single elongated-tabular grains of plagioclase (2%–3%, 0.2–0.3 mm, labradorite [An_{56}]).

Groundmass; microlites of plagioclase (andesine [An_{48}]; 40%) and segregates of small isometric grains of augite (60%). Opaque mineral (5%) is present.

Alteration: rock is fresh.

XRD: Fe chlorite, swelling chlorite, and corrensite-like mineral; trace quartz.

Sample 83-504B-98R-1, 80–85 cm (Piece 11), Unit 94 [Z-1312]

Aphyric dolerite, moderate grained, groundmass is intersertal-ophitic texture. Rock contains elongated laths (0.6–1.7 mm) of plagioclase (40%, labradorite [$An_{55–60}$]. Interstices contain xenomorphic grains (0.2–0.7 mm) of clinopyroxene (40%), small (0.3 mm) grains of olivine (5%), and brown-green glass (10%). Opaque mineral (2%–3%) is present.

Alteration: slight to moderate (10%–15%); plagioclase is albitized (5%–10%); olivine and glass replaced by chlorite.

XRD: Fe chlorite with single swelling interlayers; trace amphibole.

Sample 83-504B-99R-2, 93–96 cm (Piece 11), Unit 96 [Z-580]

Plagioclase-phyric basalt, crystallized, groundmass is massive, microlitic texture. Phenocrysts represented by glomerophyric segregates of short-prismatic and tabular grains of plagioclase (5%–7%, 0.5–1.7 mm, labradorite [An_{55}]). Groundmass; unoriented short-prismatic microlites and microlaths of plagioclase (andesine [An_{48}]). Interstices contain xenomorphic grains of augite (0.05–0.1 mm) or segregates. Skeletal grains of opaque mineral (5%–7%) are present.

Alteration: rock is fresh; microcracks (as much as 0.4 mm thick) infilled with chlorite-pennine (salbands), center parts of veins contain colorless mineral.

XRD: Fe chlorite; amphibole in trace amounts.

Sample 83-504B-100R-1, 19–20 cm (Piece 2A), Unit 96 [Z-581]

Aphyric dolerite, fine grained, groundmass is intersertal-ophitic texture. Rock contains unoriented microlaths (0.2–0.3 mm) of plagioclase (40%, labradorite [An_{55}]). Interstices contain xenomorphic grains of clinopyroxene-salite, small grains of opaque mineral (5%), and chlorite (5%). Microcracks (0.1–0.2 mm thick) infilled with chlorite-pennine.

Alteration: slight; chlorite is present.

XRD: Fe chlorite and quartz; trace amphibole.

Sample 83-504B-100R-1, 83–87 cm (Piece 10), Unit 96 [Z-1313]

Aphyric basalt, crystallized, groundmass is microlitic (microdoleritic) texture. Rock contains unoriented microlaths (0.1–0.5 mm) of plagioclase (30%). Interstices contain segregates of very small (0.1 mm) grains of clinopyroxene (25%) and opaque mineral (5%).

Alteration: strong (70%–75%); rock replaced by chlorite (25%) and tremolite (15%); plagioclase almost completely replaced by albite and sosurite; small (0.3 mm) grains of olivine (5%) replaced by chlorite and brown-green glass (10%) replaced by chlorite.

XRD: Fe chlorite with single swelling interlayers and amphibole; trace epistilbite(?); black and light gray matter from matrix is Fe chlorite; amphibole and epistilbite in trace amounts.

Sample 83-504B-104R-3, 30–33 cm (Piece 5A), Unit 106 [Z-582]

Olivine-plagioclase-sparsely phyric dolerite, medium grained, massive, groundmass is ophitic-poikilophitic texture. Phenocrysts (5%) represented by sparse (2%–3%) idiomorphic grains of olivine (0.3–0.5 mm) and single tabular crystals (0.7–0.8 mm) of zonal plagioclase. Groundmass represented by elongated-prismatic, often xenomorphic, grains of clinopyroxene (salite) with inclusions of short-prismatic laths of plagioclase. Clinopyroxene is present in interstices as small (0.1–0.2 mm) xenomorphic grains.

Alteration: olivine completely replaced by green chlorite.

XRD: Fe chlorite; quartz and amphibole in trace amounts.

Sample 83-504B-109R-1, 50–54 cm (Piece 7), Unit 112 [Z-583]

Plagioclase-phyric dolerite, fine grained, massive, groundmass is intersertal-poikilophitic texture. Phenocrysts: glomerophyric segregates of short-prismatic and tabular grains of plagioclase (10%, 0.4-1 mm), labradorite-bitovnite, An_{70}. Groundmass: microlaths of plagioclase, labradorite [An_{55}] and segregates of augite grains. Interstices: segregate of augite grains (up to 0.1 mm) with opaque dust.

Alteration: slight; plagioclase replaced by sosurite in microcracks; chlorite replaces glass.

XRD: swelling chlorite and Fe chlorite; corrensite-like mineral, quartz, and amphibole in trace amounts.

Sample 83-504B-111R-1, 86–89 cm (Piece 9), Unit 113 [Z-1314]

Plagioclase-olivine-phyric basalt, massive, groundmass is pilotaxitic texture. Phenocrysts (20%) are represented by olivine (10%) and plagioclase (10%). Olivine forms idiomorphic grains (0.6–1.7 mm). Plagioclase forms prismatic grains (0.4–0.9 mm, labradorite [An_{60}]) and glomerophyric segregates. Groundmass; needle-shaped microlites of plagioclase (40%) and weakly anisotropic brown-black glass (40%).

Alteration: slight to moderate (15%–20%); olivine completely replaced by chlorite; large grains of plagioclase replaced by albite and sosurite.

XRD: swelling chlorite and Fe chlorite with 10% swelling interlayers; trace amphibole; black clay from vein is chlorite and corrensite-like mineral.

Sample 83-504B-113R-1, 7–10 cm (Piece 1), Unit 115 [Z-584]

Olivine-plagioclase-phyric dolerite, medium grained, massive, groundmass is ophitic and poikilophitic texture. Phenocrysts of olivine (0.7–1.0 mm, 2%–3%) are present. Plagioclase (15%); short and elongated-tabular grains and their glomerophyric segregates (0.5–4.0 mm). Groundmass; elongated-prismatic grains and laths of plagioclase (40%–45%, labradorite [An_{55}]). Interstices contain isometric grains of clinopyroxene (diopside-salite; 0.5–0.8 mm) and segregates of smaller grains of pyroxene with laths of plagioclase. Opaque mineral (5%) forms segregates of skeletal isometric grains. Glass is present (5%).

Alteration: slight; olivine completely replaced by iddingsite and brown Fe hydroxides; chlorite replaces glass.

XRD: swelling chlorite, Fe chlorite, and corrensite-like mineral; quartz, amphibole, and talc(?) in trace amounts.

Sample 83-504B-116R-1, 56–60 cm (Piece 9), Unit 117 [Z-1315]

Clinopyroxene-plagioclase-phyric basalt (microdolerite), groundmass is microlitic (microdoleritic) texture. Phenocrysts (10%) represented by prismatic grains of clinopyroxene (5%) and plagioclase (5%). Clinopyroxene forms grains (1.7–2.5 mm), occasionally clinopyroxene includes laths of plagioclase. Plagioclase forms glomerophyric segregates of prismatic grains (0.5–0.8 mm). Groundmass; unoriented laths (0.1–0.7 mm) of plagioclase (45%, andesine [An_{48}]). Interstices contain small xenomorphic grains of clinopyroxene (40%) and opaque mineral (5%).

Alteration: slight (5%–10%); plagioclase replaced by albite-oligoclase (70%–80% of plagioclase volume); microvein (0.2 mm thick) contains chlorite and trace albite and epidote.

XRD: Fe chlorite; swelling chlorite, quartz, and amphibole in trace amounts.

Sample 83-504B-117R-1, 109-–113 cm (Piece 15), Unit 118 [Z-1316]

Plagioclase-phyric dolerite, groundmass is ophitic-poikilophitic texture. Phenocrysts are represented by tabular grains of plagioclase (1%–2%, labradorite [An_{62}]). Groundmass; laths (0.5–0.8 mm) of plagioclase (45%, andesine [An_{45}]). Interstices contain xenomorphic grains (0.2–0.5 mm) of clinopyroxene (45%). Opaque mineral (5%) is present.

Alteration: rock is fresh.

XRD: Fe chlorite; quartz, talc, lomontite, and amphibole in trace amounts; white and black matter from vein is Fe chlorite and lomontite; trace amphibole.

Sample 83-504B-118R-1, 62–66 cm (Piece 5), Unit 118 [Z-585]

Olivine-plagioclase-phyric dolerite, medium grained, massive, groundmass is doleritic and poikilophitic texture. Phenocrysts of olivine (1.5 mm) are present. Plagioclase (10%–15%); short-prismatic grains and their glomerophyric segregates (0.5–2.0 mm). Composition of central parts of plagioclase is labradorite (An_{68}), rims are An_{65}. Groundmass; unoriented laths and short-prismatic grains of plagioclase (40%–45%) from 0.2 to 1.5 mm in size (labradorite [An_{55}]; small laths are andesine [An_{43}]). Interstices contain isometric grains and segregates of grains (0.1–0.3 mm) of clinopyroxene (augite). Occasionally pyroxene forms xenomorphic grains 0.5–0.8 mm in size with inclusions of laths of plagioclase. Opaque mineral (2%–3%) is distributed uniformly.

Alteration: slight; olivine completely replaced by iddingsite and opaque dust; iddingsite-chlorite mineral (2%–3%) is present.

XRD: Fe chlorite; quartz, amphibole, and talc(?) in trace amounts.

Sample 83-504B-121R-1, 32–38 cm (Piece 5), Unit 120 [Z-586]

Olivine-plagioclase-phyric dolerite, fine grained, massive, groundmass is doleritic and ophitic texture. Rock is similar to Sample 83-504B-118R-1, 62–66 cm (Z-585), but the size of mineral grains is smaller than in Sample Z-585.

Alteration: rock is fresh.

XRD: swelling chlorite, Fe chlorite, and corrensite-like mineral; trace quartz and amphibole.

Sample 83-504B-127R-1, 97–101 cm (Piece 12), Unit 131 [Z-587]

Olivine-plagioclase-phyric dolerite, medium grained, massive, groundmass is poikilophitic texture. Phenocrysts of olivine (0.3–0.9 mm, 5%) completely replaced by iddingsite-chlorite and opaque dust. Plagioclase (20%); elongated-tabular grains (1.0–2.5 mm, labradorite [An_{68}]) and their segregates. Groundmass; elongated-prismatic laths (0.1–1.0 mm) of plagioclase (45%–50%, from An_{55} to An_{60}. Clinopyroxene-augite forms isometric grains as much as 2 mm in size with inclusions of laths of plagioclase. Interstices contain small (0.2 mm) grains and segregates of grains. Small xenomorphic grains of opaque mineral (2%–3%, 0.1 mm) are distributed uniformly.

Alteration: slight; iddingsite-chlorite mineral is present (2%).

XRD: swelling chlorite and Fe chlorite; talc, amphibole, and quartz in trace amounts.

Sample 83-504B-130R-1, 88–91 cm (Piece 8), Unit 135 [Z-588]

Clinopyroxene-olivine-plagioclase-phyric dolerite, medium grained, massive, groundmass is doleritic texture. Isometric grains of olivine (0.5–0.9 mm, 5%–7%) are present. Clinopyroxene-augite; single isometric grain (2.5 mm) with inclusions of plagioclase laths. Plagioclase; short-prismatic grains (1.0–2.5 mm, labradorite [An_{68}]). Groundmass represented by laths and short-prismatic grains (0.3–0.5 mm) of plagioclase (50%). Interstices contain small (0.1–0.3 mm) isometric grains of augite and segregates of grains. Small xenomorphic grains of opaque mineral (2%–3%) is distributed uniformly.

Alteration: slight; olivine completely replaced by iddingsite and opaque dust; chlorite is present.

XRD: Fe chlorite and swelling chlorite; talc, quartz, and amphibole in trace amounts.

Sample 83-504B-130R-3, 78–81 cm (Piece 9A), Unit 135 [Z-1317]

Olivine-plagioclase-phyric dolerite, medium grained, massive, groundmass is ophitic-poikilophitic texture. Idiomorphic grains of olivine (0.7–2.5 mm, 5%) are present. Plagioclase (5%); prismatic and tabular grains (1.5–1.7 mm, labradorite [$An_{60–62}$]). Groundmass; prismatic grains (0.2–0.8 mm) of plagioclase (35%). Clinopyroxene (40%) forms xenomorphic grains (0.2–0.5 mm). Olivine (0.2–0.3 mm, 5%), opaque mineral (5%), and chloritized glass are present.

Alteration: slight (10%–12%); olivine completely replaced by green iddingsite.

XRD: swelling chlorite and Fe chlorite; talc and amphibole in trace amounts; black matter from vesicles is stivensite (mixed-layer smectite-talc; Mg-trioctahedral mineral) and talc, chlorite with 10% swelling interlayers; serpentine(?) in trace amounts.

Sample 83-504B-132R-1, 76–80 cm (Piece 10), Unit 137 [Z-589]

Olivine-clinopyroxene-plagioclase-phyric dolerite, fine grained, massive, groundmass is doleritic texture. Idiomorphic grains of olivine (0.5–0.9 mm, 5%) are present. Clinopyroxene-augite (5%); tabular and elongated-prismatic grains (1–2 mm). Plagioclase (15%); elongated-tabular (1–2 mm) and elongated-prismatic (often glomerophyric segregates) grains (0.8–1 mm, labradorite [$An_{65–68}$]). Groundmass represented by unoriented laths, elongated-prismatic, and tabular grains (0.1–0.9 mm) of plagioclase (labradorite [An_{55}] and andesine [An_{47}]). Interstices contain segregates of augite in small, often paniclelike, grains. Opaque mineral (5%–6%) forms segregates small grains.

Alteration: slight; olivine completely replaced by iddingsite; chlorite (3%–4%) is present.

XRD: Fe chlorite with 5% swelling interlayers, swelling chlorite, and mixed-layer chlorite-smectite mineral (20% swelling interlayers); amphibole, quartz, and talc(?) in trace amounts.

Sample 83-504B-133R-1, 46–50 cm (Piece 7), Unit 138 [Z-590]

Clinopyroxene-phyric basalt, massive, groundmass is microlitic to microdoleritic texture. Single large (3 mm) idiomorphic phenocryst of clinopyroxene-salite is present. Groundmass; microlaths of plagioclase (50%, 0.1–0.2 mm, labradorite [An_{52}]). Interstices contain small (0.05–0.1 mm) grains of clinopyroxene, often with opaque dust.

Alteration: rock is fresh; microcracks (5%, 0.1–3.0 mm thick) infilled with chlorite and chalcedony.

XRD: Fe chlorite; quartz and amphibole in trace amounts.

Sample 83-504B-134R-1, 147–150 cm (Piece 19), Unit 140 [Z-1318]

Clinopyroxene-plagioclase-phyric basalt, crystallized, massive, groundmass is microlitic (microdoleritic) texture. Phenocrysts (10%) are represented by isomorphic grains of clinopyroxene (5%, 1.0–1.2 mm) and prismatic crystals of plagioclase (5%, labradorite [An_{60}]). Groundmass (90%); unoriented laths (0.3–0.7 mm) of

plagioclase (40%, andesine [An_{42}]). Interstices contain xenomorphic grains of pyroxene (40%). Opaque mineral (5%) and glass (5%) are present.

Alteration: slight (5%–10%); plagioclase partly replaced by albite and sosurite; chlorite replaces glass.

XRD: Fe chlorite; amphibole and talc in trace amounts.

Sample 111-504B-142R-1, 129–132 cm (Piece 17B), Unit 153 [Z-597]

Clinopyroxene-plagioclase-phyric basalt, incompletely crystallized, massive, groundmass is microlitic texture. Single elongated-prismatic crystal of clinopyroxene-salite (2 mm) is present. Phenocrysts of plagioclase (15%) form elongated-prismatic and tabular grains (0.5–1.5 mm) and glomerophyric segregates. Groundmass; weakly crystallized mesostasis: unoriented altered microlites of plagioclase and brown microlites of clinopyroxene with opaque dust.

Alteration: slight (10%); plagioclase partly replaced by albite-oligoclase and chlorite; chlorite (5%–7%) is present; microcrack (0.2 mm thick) infilled with hydrobiotite.

XRD: Fe chlorite; amphibole and talc(?) in trace amounts.

Sample 111-504B-142R-2, 40–44 cm (Piece 6), Unit 153 [Z-114]

Sparsely plagioclase-phyric basalt, fine grained, inequigranular, incompletely crystallized, massive. Phenocrysts of plagioclase (3%–5%) form glomerophyric segregates. Groundmass is intersertal, occasionally micropoikilophitic, texture; laths of plagioclase, clinopyroxene, opaque mineral, single crystal of olivine, and interstitial glass (<1%). Single vesicles are present.

Alteration: slight (<10%); clay minerals replace olivine and interstitial glass; vesicles are filled with clay mineral.

XRD: Fe and Mg chlorite (Fe and Mg approximately equal) and swelling chlorite; amphibole and talc(?) in trace amounts.

Sample 111-504B-143R-1, 124–127 cm (Piece 19), Unit 155 [Z-598]

Olivine-plagioclase-phyric dolerite, medium grained, massive, groundmass is doleritic texture. Idiomorphic grains of olivine (0.5–0.9 mm, 5%) are present. Plagioclase (5%); elongated-tabular grains (1–2 mm, labradorite [An_{68}]). Groundmass; elongated-prismatic lathlike grains (0.2–0.5 mm) of plagioclase (labradorite [An_{56}]). Interstices contain xenomorphic grains of clinopyroxene (salite to augite) or their segregates. Small xenomorphic grains of opaque mineral (5%) and glass (<1%) are present.

Alteration: slight; olivine completely replaced by iddingsite and chlorite; chlorite replaces glass.

XRD: Fe chlorite and swelling chlorite; corrensite-like mineral, amphibole, quartz, and talc(?) in trace amounts.

Sample 111-504B-145R-1, 103–105 cm (Piece 13A), Unit 160 [Z-115]

Sparsely plagioclase-clinopyroxene-phyric basalt, inequigranular, incompletely crystallized, massive. Phenocrysts of plagioclase (5%) form glomerophyric segregates, occasionally with clinopyroxene (<1%). Single phenocrysts of olivine are present. Groundmass: intersertal, partly poikilophitic, texture; laths of plagioclase, clinopyroxene, opaque minerals, and interstitial glass (<1%). Single vesicles are present.

Alteration: slight (<10%); clay minerals replace olivine and interstitial glass.

XRD: Fe chlorite and swelling chlorite; corrensite-like mineral, amphibole, quartz, and talc(?) in trace amounts.

Electron micrograph: b = 9.27 Å (trioctahedral chlorite).

Sample 111-504B-145R-2, 74–76 cm (Piece 7F), Unit 160 [Z-116]

Sparsely plagioclase-phyric basalt, inequigranular, incompletely crystallized, massive. Phenocrysts: plagioclase (1%) forms glomerophyric segregates. Single phenocrysts of olivine are present. Groundmass: intersertal or micropoikilophitic texture; laths of plagioclase, clinopyroxene, opaque minerals, single crystals of olivine, and interstitial glass (<1%–3%).

Alteration: slight (<10%); clay minerals replace olivine and interstitial glass.

XRD: Fe and Mg chlorite (Mg > Fe), swelling chlorite, and corrensite-like mineral; trace amphibole.

Electron micrograph: b = 9.28 Å (trioctahedral chlorite).

Sample 111-504B-145R-3, 66–68 cm (Piece 6A), Unit 160 [Z-117]

Plagioclase-clinopyroxene-phyric basalt, inequigranular, incompletely crystallized, massive. Phenocrysts: plagioclase (<1%), clinopyroxene (3%–5%), and single phenocrysts of olivine. Groundmass: intersertal and micropoikilophitic texture; laths of plagioclase, clinopyroxene, opaque minerals, and interstitial glass (<1%).

Alteration: slight (~5%); clay minerals replace olivine and interstitial glass.

XRD: Fe and Mg chlorite (Mg > Fe) and swelling chlorite; corrensite-like mineral, amphibole, and talc(?) in trace amounts.

Electron micrograph: b = 9.30 Å (trioctahedral chlorite).

Sample 111-504B-147R-1, 11–13 cm (Piece 3), Unit 163 [Z-118]

Very sparsely plagioclase-phyric basalt, inequigranular, incompletely crystallized, massive. Phenocrysts: plagioclase (<1%). Groundmass: intergranular to intersertal texture; laths of plagioclase, clinopyroxene, opaque minerals, and interstitial glass.

Alteration: slight (<5%).

XRD: Fe and Mg chlorite (Mg > Fe), talc, and swelling chlorite; trace quartz and amphibole.

Sample 111-504B-147R-2, 15–20 cm (Piece 1C), Unit 163 [Z-599]

Sparsely olivine-plagioclase-phyric basalt, massive. Single phenocryst (1 mm) of olivine is present. Phenocrysts: single glomerophyric segregate of grains of plagioclase (0.7–1.2 mm, labradorite [An_{56}]). Groundmass: laths of plagioclase (labradorite [$An_{65–50}$]. Interstices: xenomorphic grains (0.2–0.8 mm) of salite-augite. Small grains of opaque minerals (5%–7%, as much as 0.1 mm) are uniformly distributed.

Alteration: slight; olivine completely replaced by iddingsite; opaque minerals are located in microcracks in olivine; chlorite mineral is present.

XRD: Fe chlorite with 5% swelling interlayers and swelling chlorite; trace corrensite-like mineral (40% swelling interlayers), quartz, talc, and amphibole.

Sample 111-504B-147R-2, 26–28 cm (Pies 1D), Unit 163 [Z-119]

Aphyric basalt, almost completely crystallized, massive. Groundmass: intergranular texture; represented by laths of plagioclase, clinopyroxene, opaque minerals, single crystals of olivine, and small amounts of interstitial glass.

Alteration: slight (~1%–5%); clay minerals and carbonate replace olivine.

XRD: swelling chlorite; trace quartz, amphibole, and talc(?).

Sample 111-504B-148R-1, 53–55 cm (Piece 8), Unit 164 [Z-120]

Sparsely olivine-microphyric hyalobasalt, poorly crystallized, highly vesicular (0.05–0.1 mm, 40%–50%). Microphenocrysts of olivine (1%–3%) are present. Groundmass: vitrophyric texture; black volcanic glass with opaque dust and needle-shaped chaotically distributed microlaths of plagioclase.

Alteration: strong (50%–60%); clay minerals replace olivine; vesicles are filled with clay minerals.

XRD: Fe chlorite, swelling chlorite, and corrensite-like mineral; quartz, amphibole, and talc(?) in trace amounts.

Electron micrograph: b = 9.30 Å (trioctahedral chlorite).

Sample 111-504B-149R-1, 122–124 cm (Piece 16%), Unit 164 [Z-121]

Aphyric basalt, inequigranular, almost completely crystallized, massive. Groundmass: intergranular texture; laths of plagioclase, clinopyroxene, opaque minerals, and interstitial glass (<1%).

Alteration: slight (<5%).

XRD: Fe and Mg chlorite (Fe and Mg are approximately equal), swelling chlorite, and corrensite-like mineral; amphibole, quartz, and talc(?) in trace amounts.

Electron micrograph: b = 9.30 Å (trioctahedral chlorite).

Sample 111-504B-152R-1, 11–13 cm (Piece 2C), Unit 169 [Z-600]

Hydrothermally altered volcanic breccia. Rock: replaced by fine-grained aggregates of quartz, orthoclase, chlorite, and aggregate hydromica (muscovite?) and small grains of epidote. Thin veins contain chlorite and hydromica.

Alteration: very strong.

XRD: Fe chlorite; trace amphibole; white crystals are lomontite.

Sample 111-504B-154R-1, 30–32 cm (Piece 2C), Unit 176 [Z-122]

Very sparsely plagioclase-clinopyroxene-phyric basalt, inequigranular, almost completely crystallized, massive. Rare phenocrysts are represented by plagioclase and clinopyroxene. Single crystals of olivine are present. Groundmass: intergranular to intersertal texture; laths of plagioclase, clinopyroxene, opaque minerals, and interstitial glass (<1%).

Alteration: slight (5%–7%); clay minerals replace olivine and interstitial glass.

XRD: chlorite and swelling chlorite; amphibole and talc(?) in trace amounts.

Electron micrograph: b = 9.26 Å (trioctahedral chlorite).

Sample 111-504B-156-1, 64–67 cm (Piece 13), Unit 178 [Z-601]

Aphyric basalt, incompletely crystallized, massive, microlitic-intersertal in groundmass texture. Rock: unoriented microlites and microlaths of plagioclase (labradorite [An_{58}]). Interstices: various levels of crystallized glass, from small segregates of grains of augite to dark brown oxidized glass.

Alteration: rock is fresh.

XRD: Fe chlorite and amphibole; trace quartz.

Sample 111-504B-158-1, 16–19 cm (Piece 3A), Unit 182 [Z-602]

Aphyric basalt, uncrystallized, hyalopilitic in groundmass texture. Rock: unoriented needle-shaped microlites of plagioclase (20%), very small grains of opaque minerals (5%), and brown weakly anisotropic glass.

Alteration: rock is fresh; crack (0.3 mm thick) infilled with chlorite.

XRD: amphibole and Fe chlorite; trace quartz.

Sample 111-504B-162M-1, 45–47 cm (Piece 5), Unit 187 [Z-123]

Plagioclase-phyric basalt, inequigranular, incompletely crystallized, massive. Phenocrysts: plagioclase (0.8-2 mm, 7%–10%); single phenocrysts of olivine are present. Groundmass: intersertal to subvariolitic texture; laths of plagioclase, clinopyroxene, opaque minerals, and interstitial glass (<1%).

Alteration: slight (10%–15%); clay minerals replace olivine.

XRD: mixed-layer illite-smectite minerals with ~20% mica layers; trace defective chlorite.

Electron micrograph: b = 9.30 Å (trioctahedral chlorite).

Sample 111-504B-163-1, 36–41 cm (Piece 8), Unit 187 [Z-603]

Dolerite, massive. Groundmass: ophitic texture. Plagioclase: short-tabular (up to 0.5 mm) and needle-shaped (up to 3 mm) grains, labradorite [An_{55}] to andesine [An_{43}]. Interstices: xenomorphic grains of clinopyroxene from brown to almost colorless (diopside-augite). Opaque minerals (5%) form isometric, occasionally skeletal small (up to 0.1 mm), grains.

Alteration: slight; chlorite (3%–5%) is present; occasionally chlorite replaces plagioclase and pyroxene.

XRD: Fe chlorite; quartz and amphibole in trace amounts.

Sample 111-504B-163-1, 120–123 cm (Piece 4), Unit 187 [Z-1319]

Plagioclase-phyric basalt, crystallized, fine grained. Phenocrysts (10%): plagioclase (0.9–2 mm), labradorite [An_{60}]. Groundmass: microdoleritic texture; prismatic grains and laths of plagioclase (40%, 0.2–0.7 mm, andesine [An_{42}]). Interstices: xenomorphic grains of clinopyroxene (0.2–0.4 mm). Opaque minerals (5%) are present.

Alteration: slight (10%–17%); plagioclase replaced by albite (5%–7% of grain volume); rock partly (10%) is chloritized.

XRD: Fe chlorite; amphibole and quartz in trace amounts.

Sample 111-504B-169R-1, 66–69 cm (Piece 14), Unit 191 [Z-604]

Olivine-clinopyroxene-plagioclase-phyric dolerite, fine grained, massive. Single idiomorphic phenocrysts of olivine (0.7 mm) are present. Clinopyroxene (diopside-salite) forms idiomorphic grains (5%) 0.5–2 mm in size. Plagioclase (10%): glomerophyric segregates of tabular or prismatic grains, labradorite (An_{60}). Groundmass: doleritic texture; unoriented laths (0.2–0.3 mm) of plagioclase, andesine (An_{48}). Interstices contain segregates of small (0.1 mm) isometric grains of salite. Opaque minerals (7%–8%) form xenomorphic grains.

Alteration: slight; olivine completely replaced by chlorite; chlorite (<1%) is present.

XRD: Fe chlorite and amphibole; trace quartz.

Sample 137-504B-177R-1, 48–49 cm (Piece 13), Unit 206 [Z-812]

Olivine-clinopyroxene-plagioclase-sparsely phyric dolerite, medium grained, massive. Phenocrysts (5%): segregates of two small (0.2–0.3 mm) idiomorphic grains of olivine, single xenomorphic grains (up to 2 mm) of colorless diopside, and single tabular crystals (1–1.2 mm) of plagioclase, labradorite, (An_{68}). Groundmass: doleritic-ophitic texture; elongated-prismatic laths (0.1–0.8 mm) of plagioclase, labradorite (An_{55}). Interstices contain xenomorphic small (0.2 mm) grains of salite. Opaque minerals (5%–7%) form small xenomorphic grains (up to 0.1 mm).

Alteration: slight; olivine completely replaced by iddingsite (opaque minerals, 30%, is present in altered olivine); chlorite (<1%) is present.

XRD: Fe chlorite; quartz, corrensite-like mineral, and amphibole in trace amounts.

Sample 137-504B-181M-1, 6–8 cm (Piece 1), Unit 206 [Z-813]

Clinopyroxene-plagioclase-phyric dolerite, fine grained, massive. Phenocrysts (5%): isometric grains (0.5–1 mm) of clinopyroxene. Clinopyroxene includes laths of plagioclase (poikilophitic texture). Plagioclase forms rare tabular or short-prismatic grains. Groundmass: doleritic texture; prismatic and elongated-prismatic laths (0.1–0.5 mm) of plagioclase, labradorite (An_{56}). Interstices: segregates of small isometric grains of augite. Opaque minerals (5%) and chlorite (<1%) are present.

Alteration: slight.

XRD: Fe chlorite and quartz; swelling chlorite, corrensite-like mineral, and amphibole in trace amounts.

Sample 140-504B-186-2, 30–31 cm (Piece 8), Unit 213 [Z-838]

Aphyric dolerite, medium grained. Groundmass: poikilophitic texture. Rock: xenomorphic and elongated grains of clinopyroxene-salite (0.5–2 mm), clinopyroxene includes elongated (up to 2 mm) laths of plagioclase, labradorite (An_{55}), small grains (0.3 mm) of plagioclase-andesine-labradorite (An_{50}). Chlorite-pennine (30%) is present.

Alteration: moderate-strong; rock is chloritized.

XRD: Fe chlorite and amphibole; trace quartz.

Sample 140-504B-187R-1, 59–60 cm (Piece 14), Unit 216 [Z-839]

Olivine-clinopyroxene-phyric dolerite, fine grained, massive. Phenocrysts (5%): single idiomorphic grains (0.5–0.8 mm) of olivine and tabular and elongated-prismatic grains (1–1.5 mm) of clinopyroxene-salite. Groundmass: microdoleritic texture; short and elongated-prismatic laths (0.2–0.4 mm) of plagioclase, labradorite [An_{52}]. Interstices: xenomorphic small grains of salite, occasionally with opaque dust. Opaque minerals (10%) are located uniformly in rock.

Alteration: slight; olivine completely replaced by green iddingsite; chlorite (<1%) is present in interstices.

XRD: Amphibole; trace Fe chlorite.

Sample 140-504B-189-1, 85–86 cm (Piece 19), Unit 218 [Z-840]

Aphyric dolerite, fine grained, massive; Groundmass: doleritic texture. Rock: elongated-prismatic and rounded-isometric laths and grains of plagioclase, labradorite ($An_{52–55}$). Interstices: xenomorphic or rounded grains of salite and chlorite (1%). Opaque minerals (7%–8%) are present.

Alteration: slight.

XRD: Fe chlorite and swelling chlorite; quartz, amphibole, and talc in trace amounts.

Sample 140-504B-189R-2, 15–17 cm (Piece 3), Unit 218 [Z-841]

Olivine-phyric gabbro-dolerite, medium grained, massive. Phenocrysts (5%): olivine (0.3–1 mm). Groundmass: gabbro-doleritic texture; prismatic and rounded-prismatic grains (0.2–0.6 mm) of plagioclase, labradorite (An_{58}), and andesine (An_{45}). Interstices contain xenomorphic grains (0.1–0.4 mm) of clinopyroxene (from salite to augite). Opaque minerals (5%) and chlorite are present.

Alteration: slight; olivine completely replaced by chlorite, altered olivine contains opaque minerals; chlorite replaces glass.

XRD: Fe chlorite, corrensite-like mineral, and amphibole; quartz and talc(?) in trace amounts.

Sample 140-504B-190-1, 10–14 cm (Piece 2), Unit 218 [Z-842]

Aphyric basalt, massive. Groundmass: intersertal texture. Rock: unoriented prismatic laths of plagioclase (0.2–0.7 mm). Mesostasis demonstrates dark-brown matter with brown grains of clinopyroxene.

Alteration: moderate (30%–35%); rock is hydrothermally altered; plagioclase almost completely replaced by sosurite and albite; aggregate of chlorite contains very small grains of sphene.

XRD: Fe chlorite, lomontite, and amphibole; trace corrensite-like mineral(?) and quartz.

Sample 140-504B-191-1, 26–28 cm (Piece 9), Unit 218 [Z-843]@@

Plagioclase-phyric dolerite, fine grained. Groundmass: ophitic texture. Phenocrysts (20%): plagioclase tabular and prismatic crystals (1–5 mm), labradorite (An_{69}). Plagioclase crystals contain inclusions of glass. Interstices: xenomorphic grains of clinopyroxene-salite (0.2–0.3 up to 0.8–1 mm). Opaque minerals (2%–3%) and chlorite (1%) are present.

Alteration: slight.

XRD: Fe chlorite, corrensite-like mineral (40% swelling interlayers), and amphibole; swelling chlorite and quartz in trace amounts.

Sample 140-504B-193-1, 49–51 cm (Piece 13A), Unit 220 [Z-844]

Breccia of amphibolitized dolerite, cement is clay matter. Rock: fragments (5–7 mm diameter) of plagioclase-amphibole hydrothermally altered dolerite. Rock: unoriented prismatic laths of plagioclase (0.3–0.4 mm) almost completely replaced by albite and sosurite. Interstices contain xenomorphic grains (0.1–0.3 mm) of brown-green amphibole (from uralite to tremolite-actinolite). Occasionally actinolitic hornblende replaced by chlorite. Small isometric grains of sphene are located on contact plagioclase and amphibole.

Alteration: very strong.

XRD: white matter and clay from vein is amphibole and lomontite; trace Fe chlorite.

Sample 140-504B-194R-1, 42–44 cm (Piece 8), Unit 220 [Z-845]

Olivine-plagioclase-phyric dolerite, medium grained, massive. Phenocryst: single large (3 mm) idiomorphic; olivine. Plagioclase forms large (5 mm) prismatic grain. Groundmass: doleritic-ophitic texture; short and elongated-prismatic laths (0.2–1 mm) of plagioclase, labradorite (An_{56}). Interstices: isomorphic grains (0.2–0.8 mm) of clinopyroxene-salite.

Alteration: moderate (30%–35%); rock is partly amphibolitized; olivine grain completely replaced by chlorite and in central part of grains by iddingsite; plagioclase laths are albitized; occasionally pyroxene partly or completely replaced by amphibole; crystals of tremolite (up to 2.5 mm) replace of rock-forming minerals; small isometric grains of sphene are located in central parts of tremolite; rock contain chlorite.

XRD: amphibole and Fe chlorite; trace corrensite-like mineral(?).

Sample 140-504B-197R-1, 31–33 cm (Piece 7), Unit 222 [Z-846]

Olivine-clinopyroxene-plagioclase-phyric dolerite, fine grained, massive. Phenocrysts (10%): single grains (up to 2 mm) of olivine, clinopyroxene-salite (up to 2.5 mm), and grains (1.2–1.5 mm) of plagioclase. Groundmass: ophitic texture; laths (0.2–1 mm) of plagioclase, labradorite (An_{56}). Interstices contain xenomorphic small grains of salite and opaque minerals (5%).

Alteration: strong; rock replaced by amphibole and chlorite on 70%, olivine completely replaced by chlorite (pennine); occasionally crystals of plagioclase replaced by albite, chlorite, and sosurite; pyroxene replaced by amphibole.

XRD: amphibole and Fe chlorite; trace corrensite-like mineral, swelling chlorite, and quartz.

Sample 140-504B-198R-1, 52–54 cm (Piece 14), Unit 223 [Z-847]

Olivine-clinopyroxene-plagioclase-phyric dolerite, fine grained, massive. Phenocrysts (15%): olivine forms rare xenomorphic rounded grains (0.5–1 mm); clinopyroxene-salite forms large (up to 4 mm) prismatic doubled grains; laths of plagioclase. Plagioclase forms glomerophyric segregates of prismatic grains (1–1.2 mm), labradorite (An_{56}). Groundmass: doleritic texture; laths (0.2–0.8 mm) of plagioclase, labradorite (An_{55}). Interstices contain xenomorphic small grains of clinopyroxene (salite). They accrete with plagioclase. Opaque minerals (5%) and chlorite are present.

Alteration: slight; olivine completely replaced by chlorite, iddingsite, and opaque dust; chlorite replaces glass.

XRD: talc and Fe chlorite; swelling chlorite and amphibole in trace amounts.

Sample 140-504B-199R-1, 54–57 cm (Piece 13), Unit 226 [Z-848]

Olivine-clinopyroxene-plagioclase-phyric dolerite, medium grained, massive. groundmass is doleritic, occasionally poikilophitic, texture. Phenocrysts (20%): olivine (5%) forms idiomorphic grains (1–1.2 mm); clinopyroxene-salite forms large (up to 4 mm) elongated-prismatic crystals with laths of plagioclase. Plagioclase forms glomerophyric segregates of tabular and prismatic grains (1–1.5 mm), labradorite (An_{67}). Groundmass: doleritic, occasionally poikilophitic, texture; unoriented laths (0.2–1.5 mm) of plagioclase (labradorite [An_{57}]), small grains of plagioclase (andesine [An_{45}]). Interstices contain xenomorphic grains of clinopyroxene-salite (0.8–1 mm). They accrete with laths of plagioclase. Opaque minerals (5%) and chlorite (7%–8%) are present.

Alteration: slight; olivine completely replaced by iddingsite and opaque dust; chlorite replaces glass.

XRD: amphibole, talc, and Fe chlorite.

Sample 140-504B-200R-1, 50–52 cm (Piece 7B), Unit 227 [Z-849]

Olivine-plagioclase-phyric dolerite, medium grained, massive. groundmass is doleritic-poikilophitic texture. Phenocrysts (20%): olivine forms rare idiomorphic grains (up to 1 mm); plagioclase forms prismatic grains (0.6–1.5 mm) and glomerophyric segregates; labradorite (An_{60}). Groundmass: doleritic–poikilophitic texture;

elongated prismatic laths (0.2–0.8 mm) of plagioclase (labradorite [An_{55}]). Interstices contain xenomorphic grains of clinopyroxene-salite. They accrete with laths (up to 0.7 mm) of plagioclase. Opaque minerals (3%–4%) and green chlorophaeite (4%–5%) are present.

Alteration: slight; olivine completely replaced by iddingsite; chlorite replaces glass.

XRD: Fe chlorite, talc, and amphibole; s trace welling chlorite.

Sample 140-504B-202R-1, 23–25 cm (Piece 7), Unit 229 [Z-850]

Olivine-plagioclase-phyric dolerite, medium grained, massive. Phenocrysts (5%): olivine (1%) forms idiomorphic grains (0.5–0.6 mm); plagioclase (labradorite, [An_{67}]) forms tabular and short-prismatic grains (0.5–0.8 mm) with inclusions of glass. Groundmass is the same as Sample 140-504B-200R-1, 50–52 cm (Z-849).

Alteration: slight; olivine partly replaced by iddingsite.

XRD: Fe chlorite, talc, and amphibole; swelling chlorite and quartz in trace amounts.

Sample 140-504B-204-1, 15–19 cm (Piece 4), Unit 232 [Z-851]

Aphyric dolerite, massive, medium grained. Groundmass: doleritic-poikilophitic texture. Rock: unoriented laths of plagioclase (0.2–2 mm, labradorite [An_{56}]) and clinopyroxene. Opaque minerals (2%–3%) are present.

Alteration: strong (50%); rock replaced by amphibole; clinopyroxene replaced by needle-shaped segregate of amphibole.

XRD: Fe chlorite and amphibole; trace quartz.

Sample 140-504B-208-3, 3–5 cm (Piece 1), Unit 239 [Z-852]

Plagioclase-sparsely phyric dolerite, medium grained. Single prismatic grains (2–2.5 mm) of plagioclase (5%) broken by microcracks. Groundmass: doleritic-ophitic texture; laths of plagioclase (labradorite [An_{52}]). Interstices contain grains of clinopyroxene-augite and chlorite (10%). Pyroxene replaced by uralite (70% pyroxene).

Alteration: moderate to strong (40%); rock replaced by amphibole; microcracks in plagioclase infilled with clay minerals; chlorite replaces glass.

XRD: Fe chlorite and amphibole; trace quartz.

Sample 140-504B-209-1, 102–103 cm (Piece 14), Unit 240 [Z-853]

Plagioclase-phyric dolerite, massive. Phenocrysts (5%): plagioclase of (1%–2%) xenomorphic or prismatic grains (1.5–2 mm) and segregates of prismatic grains (1–1.2 mm, labradorite [An_{68}]). Groundmass: poikilophitic texture; small (0.1–0.3 mm) laths of plagioclase (labradorite [An_{56}]). Clinopyroxene (salite-augite) forms isomorphic, large (up to 3 mm) grains. Clinopyroxene grains contain laths of plagioclase.

Alteration: moderate (30%); rock replaced by chlorite; occasionally pyroxene almost completely replaced by segregate of chlorophaeite.

XRD: Fe chlorite and amphibole.

Sample 140-504B-209-2, 66–68 cm (Piece 10), Unit 240 [Z-854]

Plagioclase-phyric dolerite, medium grained, massive. Phenocrysts (30%): plagioclase represented by large (2.5 mm) and prismatic (0.5–1.2 mm) grains or segregates. Large grains are labradorite-bitovnite (An_{70}); small grains are labradorite (An_{62}). Groundmass: poikilophitic texture; unoriented laths and prismatic grains (0.3–0.8 mm, labradorite [An_{55}]). Interstices: xenomorphic grains (0.3–0.5 mm) of clinopyroxene-augite. Chlorite (5%) and opaque minerals (3%–4%) are present.

Alteration: slight.

XRD: Fe chlorite and swelling chlorite; trace corrensite-like mineral, talc, amphibole, and quartz.

Sample 140-504B-211-1, 70–72 cm (Piece 16), Unit 241 [Z-855]

Aphyric dolerite, massive, moderate grains. groundmass is ophitic-poikilophitic texture. Rock: unoriented laths of plagioclase (0.2–1 mm, labradorite [$An_{56–57}$]) Interstices contain xenomorphic grains of clinopyroxene-salite. Clinopyroxene forms xenomorphic grains (1–4 mm) with inclusions of laths of plagioclase.

Alteration: slight; chlorophaeite (3%–5%) and opaque minerals (2%–3%) are present.

XRD: Fe chlorite; amphibole, talc, quartz, and swelling chlorite in trace amounts.

Sample 140-504B-213-1, 66–68 cm (Piece 19), Unit 243 [Z-856]

Plagioclase-sparsely phyric dolerite, medium grained, massive. Single xenomorphic phenocryst of plagioclase (2.3 mm) broken by microcracks. Groundmass: poikilophitic texture; short and elongated-prismatic laths of

plagioclase (0.2–2 and 0.1 mm, labradorite [An_{60} and An_{50}]) Clinopyroxene (augite) forms large (0.5–2 mm) isometric grains containing plagioclase lath inclusions.

Alteration: strong; rock replaced by chlorite (7%–8%) and amphibole (~30%); microcracks in plagioclase infilled with chlorite.

XRD: Fe chlorite; amphibole, corrensite-like mineral, and quartz in trace amounts.

Sample 140-504B-214-1, 30–32 cm (Piece 5A), Unit 244 [Z-857]

Plagioclase-sparsely phyric dolerite, medium grained, massive. Groundmass: poikilophitic texture. Rock: same as Sample 140-504B-213-1, 66–68 cm (Z-856).

Alteration: strong; rock replaced by chlorite (7%–8%) and amphibole (~30%).

XRD: amphibole and Fe chlorite.

Sample 140-504B-214-1, 76–77 cm (Piece 8), Unit 244 [Z-858]

Aphyric dolerite, medium grained, massive. groundmass is poikilophitic texture. Rock: elongated and prismatic plagioclase laths (0.2–5 mm).

Alteration: very strong (90%); rock almost completely altered (amphibolitized and albitized); plagioclase almost completely replaced by sosurite and albite; clinopyroxene almost completely replaced by uralitic amphibole (0.3–5 mm); large grains of uralite contain altered plagioclase laths.

XRD: amphibole and lomontite; trace Fe chlorite.

Sample 140-504B-222-1, 73–74 cm (Piece 12A), Unit 254 [Z-859]

Aphyric dolerite, medium grained, massive. Groundmass: ophitic-intersertal-poikilophitic texture. Rock: unoriented elongated-prismatic, prismatic, and tabular laths (0.3–2.5 mm) of plagioclase (labradorite [$An_{50–54}$]). Small grains of clinopyroxene are located in interstices. Large grains form poikilophitic segregates with plagioclase.

Alteration: moderate to strong (40%); rock is altered (amphibole and chlorite); occasionally interstices infilled with chlorite (7%–8%) and opaque minerals; occasionally clinopyroxene replaced by isotropic earthy matter and needle-shaped amphibole.

XRD: Fe chlorite; amphibole and quartz in trace amounts.

Sample 140-504B-225-2, 30–32 cm (Piece 5), Unit 260 [Z-860]

Plagioclase-sparsely phyric dolerite, medium grained, massive. Phenocryst: single, xenomorphic, weakly zonal plagioclase (up to 2 mm) with inclusions of glass. Groundmass: doleritic-poikilophitic texture; laths of plagioclase (0.2–1.8 mm), prismatic grains (labradorite [An_{68}]) and elongated laths (labradorite [An_{60}]). Clinopyroxene (salite-augite) forms small and large grains (0.2–0.3 and 0.5–1.2 mm, respectively) containing inclusions of plagioclase laths.

Alteration: slight; interstices contain chlorite (2%–3%) and opaque minerals (2%–3%).

XRD: amphibole, Fe chlorite, and talc(?) or lomontite(?); quartz and corrensite-like mineral(?) in trace amounts.

Sample 140-504B-230-1, 11–14 cm (Piece 3), Unit 265 [Z-861]

Clinopyroxene-plagioclase-phyric dolerite, fine grained, massive. Phenocrysts (5%): plagioclase; glomerophyric segregates (1–1.5 mm across); grains (0.2–0.7 mm) are fresh (labradorite [An_{60}]). Groundmass: doleritic texture; plagioclase laths (0.2–0.5 mm, labradorite [An_{52}]). Interstices: small grains of clinopyroxene. Opaque minerals (5%) are present.

Alteration: strong (50%); clinopyroxene replaced by amphibole (uralite) on 90%, microcrack (0.2 mm in thickness) infilled by chlorite.

XRD: amphibole; trace Fe chlorite.

Sample 140-504B-238-1, 4–7 cm (Piece 2), Unit 269 [Z-862]

Plagioclase-phyric dolerite, medium grained, massive. Phenocrysts (5%): plagioclase; large (up to 2 mm) prismatic grains (labradorite [An_{58}]). Groundmass: ophitic texture; plagioclase laths (0.3–2.5 mm, labradorite [An_{53}]). Interstices: xenomorphic grains (up to 0.5 mm) of clinopyroxene-augite.

Alteration: moderate (25%); rock is chloritized and amphibolitized; clinopyroxene partly or completely replaced by uralite (15%); chlorite (10%) replaces groundmass minerals and margin parts of plagioclase phenocrysts.

XRD: Fe chlorite and amphibole; trace quartz.

Sample 148-504B-239-1, 46–50 cm (Piece 14), Unit 271 [Z-1586]

Plagioclase-phyric basalt (microdolerite). Phenocrysts (10%): plagioclase; glomerophyric segregates of prismatic grains (0.7–1.5 mm, labradorite [An_{60}]). Groundmass: microophitic texture; laths of plagioclase (0.4–0.7 mm, andesine [An_{47}]). Interstices: xenomorphic grains (0.1–0.5 mm) of clinopyroxene (15%). Opaque minerals (5%) are present.

Alteration: moderate (30%); rock is amphibolitized and chloritized; clinopyroxene replaced by uralitic amphibole (25%); occasionally there are chlorite spots in groundmass.

XRD: amphibole; trace Fe chlorite.

Sample 148-504B-240-1, 82–88 cm (Piece 2I), Unit 274 [Z-1587]

Plagioclase-phyric dolerite, coarse grained. Phenocrysts (50%): prismatic plagioclase grains (0.5–2 mm, labradorite [An_{55}] and laths (andesine [An_{44}]). Interstices: xenomorphic grains (20%) of clinopyroxene.

Alteration: moderate (30%); rock is amphibolitized; clinopyroxene replaced by uralite and uralitic hornblende (tremolite; 30%).

XRD: amphibole; trace Fe chlorite.

Sample 148-504B-246-1, 87–90 cm (Piece 25), Unit 284 [Z-1588]

Plagioclase-phyric dolerite, fine grained. Phenocrysts (5%): plagioclase; prismatic grains (1.5–1.7 mm). Groundmass: ophitic texture; prismatic grains and laths (0.2–0.7 mm) of plagioclase (40%, labradorite [An_{55}] and andesine [An_{40}]). Interstices: xenomorphic grains of clinopyroxene (40%). Opaque minerals (2%–3%) are present.

Alteration: slight (15%); rock is amphibolitized; clinopyroxene replaced partly by uralite.

XRD: amphibole, Fe chlorite, and talc(?); trace quartz.

Sample 148-504B-249-1, 85–89 cm (Piece 27), Unit 290 [Z-1589]

Plagioclase-phyric dolerite, medium grained. Phenocrysts (10%): plagioclase; zonal short-prismatic grains (up to 2.5 mm, labradorite [An_{68}]). Groundmass: ophitic texture; prismatic grains and laths (0.2–1 mm) of plagioclase (40%, labradorite [$An_{51–53}$] and andesine [An_{48}]). Interstices: xenomorphic grains (0.3–0.8 mm) of clinopyroxene (10%). Opaque minerals (1%–2%) are present.

Alteration: moderate to strong (40%); rock is amphibolitized; clinopyroxene replaced by uralite and uralitic hornblende (40%).

XRD: chlorite and amphibole; quartz and talc(?) in trace amounts.

Sample 148-504B-251-1, 35–40 cm (Piece 6A), Unit 293 [Z-1590]

Aphyric dolerite, medium grained. groundmass is intersertal-ophitic texture. Rock: plagioclase grains (0.5–2.5 mm, 35%, labradorite [$An_{55–57}$]). Interstices: xenomorphic grains of clinopyroxene and black-brown glass (15%). Opaque minerals (2%–3%) are present.

Alteration: slight (8%); glass partly replaced by chlorite (8%).

XRD: Fe chlorite; amphibole and quartz in trace amounts.

Middle Valley, Juan de Fuca Ridge, and Escanaba Trough, Gorda Ridge (Legs 139 and 169)

Hole 855A

Sample 139-855A-8R-1, 36–39 cm (Piece 5), Unit 1 [Z-814]

Plagioclase phyric basalt, massive. Phenocrysts (20%): plagioclase; prismatic and elongated-prismatic laths (0.5–1.5 mm); several of grains are zonal and have undulatory extinction (labradorite ([An_{62}]). Groundmass: pilotaxic texture; black isotropic glass containing microlites of plagioclase and panicle-like crystallites of pyroxene in accretion with opaque dust. Microvesicles (<1%) are infilled with chlorite.

Alteration: rock is fresh.

XRD: smectites with ~20% mica layers; trace chlorite, amphibole, and talc(?).

Sample 139-855A-9R-1, 10–14 cm (Piece 2), Unit 2 [Z-815]

Aphyric basalt (microdolerite), massive, crystallized. Groundmass: microdoleritic-intersertal texture. Rock: small rounded grains of fresh olivine (0.1–0.5 mm) and unoriented plagioclase laths (0.1–0.5 mm, labradorite [$An_{58–}$

$_{60}$]). Interstices: segregates of small grains of clinopyroxene and plagioclase; black glass (~5%). Opaque minerals in paragenesis with pyroxene (7%–8%). Microvesicles (~1%, 0.1–0.2 mm) are present.

Alteration: rock is fresh; vesicles infilled with smectites.

XRD: smectites with ~20% mica layers; chlorite, amphibole, and talc in trace amounts.

Hole 855D

Sample 139-855D-6R-1, 55–58 cm (Piece 8), Unit 2 [Z-816]

Pyroxene-plagioclase phyric basalt, massive, crystallized. Phenocrysts: plagioclase; segregates (up to 3 mm in size) of prismatic and elongated-prismatic grains (0.2–0.8 mm); labradorite (An_{58}). Groundmass: microlitic texture; segregate of plagioclase and clinopyroxene microlaths; single needle-shaped laths of plagioclase (andesine-labradorite [An_{50}]). Opaque minerals (7%–8%) are distributed evenly in rock.

Alteration: rock is fresh.

XRD: slightly reflexes of smectite, chlorite, and quartz.

Hole 856A

Sample 139-856A-13X-CC, 22–24 cm (Piece 2A), Unit 1 [Z-817]

Olivine microphyric basalt, massive, weakly crystallized. Phenocrysts: olivine (5%); rounded small (0.1–0.3 mm) grains. Groundmass: microlitic texture; plagioclase microlaths (labradorite [An_{52}]); segregates of very small grains; crystallites of clinopyroxene; opaque dust.

Alteration: rock is fresh.

XRD: smectites with ~20% mica layers; trace chlorite, talc, quartz, and amphibole.

Sample 139-856A-14X-1, 34–38 cm (Piece 3), Unit 1 [Z-945]

Olivine phyric basalt, massive, crystallized. Olivine (10%) and groundmass (90%). Groundmass: microlitic (microdoleritic) texture; microlites and laths of plagioclase (55%, labradorite [An_{52}] and andesine [An_{40}]); sparse crystals of plagioclase-andesine ($An_{35–37}$); small grains of olivine (0.1–0.2 mm, 3%–5%) and panicle-like segregates of plagioclase and pyroxene microlites (30%).

Alteration: rock is fresh.

XRD: smectites with ~20% mica layers; minor chlorite and talc; trace quartz, illite, and amphibole.

Sample 139-856A-14X-1, 61–64 cm (Piece 4), Unit 1 [Z-818]

Olivine phyric basalt, massive, crystallized. Phenocrysts: fresh olivine (0.2–0.5 mm, 15%). Groundmass: microlitic texture; plagioclase microlites and laths (0.2–0.3 mm, labradorite [An_{52}]).

Alteration: rock is fresh.

XRD: smectites with ~30% mica layers; minor chlorite and talc, trace quartz and amphibole.

Sample 139-856A-14X-CC, 14–18 cm (Piece 2B), Unit 1 [Z-819]

Identical to Sample 139-856A-14X-CC, 14–18 cm.

Alteration: slight; single grain of olivine partly replaced by secondary mineral.

XRD: smectites with ~30% mica layers; minor chlorite and talc; trace quartz.

Hole 856B

Sample 139-856B-8H-CC, 0–5 cm (Piece 1), Unit 1 [Z-820]

Olivine phyric basalt, massive, weakly crystallized. Phenocrysts: olivine (0.3–0.7 mm, 15%). Groundmass: pilotaxitic texture; unoriented microlites and laths of plagioclase (up to 0.3 mm, labradorite [An_{58}]). Interstitial glass is black isotropic, occasionally with anisotropic spots and single grains of pyroxene.

Alteration: slight; olivine replaced by secondary mineral in microcracks.

XRD: chlorite, smectites, mixed-layer smectite-chlorite mineral, and talc; trace quartz.

Hole 856H

Sample 169-856H-55R-1, 28–33 cm (Piece 5A), Unit VII [Z-1591]

Olivine sparsely phyric basalt. Single glomerophyric segregate (<1%); grains (0.2–0.3 mm) of olivine. Groundmass: hyalopilitic texture; plagioclase laths (0.3–0.8 mm, 15%–20%); glass (0.01–0.05 mm, brown-black microlites (0.01–0.05 mm, 30%) of clinopyroxene(?); opaque minerals (5%) and clay mineral (30%).

Alteration: very strong (70%–80%); olivine completely replaced by chlorite; plagioclase completely replaced by albite, zeolite, and clay minerals; glass completely replaced by albite and chlorite; possibly there is epidote (very small grains make identification difficult).

XRD: Fe chlorite; trace quartz.

Sample 169-856H-56R-1, 10–14 cm (Piece 3), Unit III [Z-1592]

Aphyric basalt, uncrystallized. Groundmass: hyalopilitic texture. Rock: needle-shaped laths (0.2–0.7 mm) of plagioclase (20%); glass (75%); opaque minerals (5%); small grains (0.05 mm) of titanite (<1%). Occasionally opaque minerals are partly oxidized with spots (0.5–1 mm) of Fe hydroxides (<1%).

Alteration: very strong (90%); plagioclase completely replaced by albite, zeolite, and clay minerals; glass completely replaced by microblastic aggregate of albite and chlorite.

XRD: Fe chlorite; trace quartz and cristobalite; veinlet: Fe chlorite and quartz.

Sample 169-856H-56R-1, 28–32 cm (Piece 5), Unit VII [Z-1593]

Plagioclase(?) sparsely phyric basalt. Single prismatic phenocryst (1.2–3 mm) of plagioclase(?). Groundmass: pilotaxitic texture; needle-shaped laths of plagioclase (20%) and glass. Occasionally rims of opaque minerals and groundmass in contact with opaque minerals are oxidized with formation of Fe hydroxides (2%–3%).

Alteration: very strong (90%); plagioclase phenocrysts completely replaced by chlorite and albite; groundmass plagioclase completely replaced by albite, zeolite, and clay minerals; glass completely replaced by granoblastic aggregate of albite, chlorite, and small (0.1–0.2 mm) xenomorphic grains of opaque minerals; veinlets (0.8–1.2 mm) contain chlorite (70%–80%), opaque minerals (20%), quartz (10%), and single grains of titanite.

XRD: Fe chlorite; trace quartz.

Sample 169-856H-59R-1, 90–93 cm (Piece 13), Unit VII [Z-1594]

Olivine-plagioclase phyric basalt. Phenocrysts (15%): idiomorphic grains of olivine (10%, 0.5–0.8 mm) and their glomerophyric segregate. Prismatic phenocrysts (0.6–1.9 mm) of plagioclase (5%) contain abundant inclusions of glass. Rock: grains and segregates of titanite (2%–3%, 0.1–0.5 mm). Groundmass: vitrophyric texture; light brown isotropic glass.

Alteration: slight (15%); olivine completely replaced by chlorite; plagioclase replaced by albite and chlorite.

XRD: Fe chlorite; trace quartz.

Sample 169-856H-60R-1, 65–70 cm (Piece 11), Unit VII [Z-1595]

Plagioclase phyric dolerite, fine grained. Phenocrysts (5%): stretch-prismatic grains of plagioclase (2.5–4 mm). Groundmass: intersertal-doleritic texture; laths of plagioclase (40%, 0.2–1 mm, labradorite [An_{55}]). Interstices: small grains of pyroxene (30%), opaque minerals (10%), and glass (15%).

Alteration: slight (15%); chloritized glass.

XRD: Fe chlorite; trace quartz and amphibole.

Sample 169-856H-60R-2, 15–20 cm (Piece 3), Unit VII [Z-1596]

Dolerite, medium grained. Groundmass: intersertal-ophitic texture. Rock: unoriented prismatic grains of plagioclase (35%, 0.5–1.5 mm, labradorite [An_{55}], andesine [An_{43}], and andesine [An_{39}]) Interstices: xenomorphic grains of pyroxene (20%); partly idiomorphic grains of olivine (0.3–0.7 mm). Glass (25%) with micrograins of brown segregate of pyroxene (0.01 mm), plagioclase, and green chlorite (5%–10%).

Alteration: moderate (20%–25%); olivine completely replaced by chlorite and magnetite; glass replaced by chlorite.

XRD: Fe chlorite; quartz and amphibole in trace amounts.

Sample 169-856H-61R-1, 52–57 cm (Piece 5E), Unit VII [Z-1597]

Olivine-plagioclase phyric dolerite, fine grained. Phenocrysts (~10%): prismatic grains of plagioclase (2–2.5 mm) and rounded-isometric grains (1.2–1.4 mm) of olivine(?). Groundmass: doleritic(?) texture; laths (0.3–0.5 mm) and prismatic grains of plagioclase and glass.

Alteration: very strong (100%); plagioclase phenocrysts completely replaced by chlorite and albite; olivine completely replaced by chlorite; groundmass plagioclase completely replaced by albite and chlorite; clinopyroxene replaced by uralite and chlorite; glass is replaced with granoblastic aggregate of small (0.1 mm) isometric grains of albite, chlorite, and abundant (10%) micrograins of opaque minerals (xenomorphic grains and opaque dust), occasionally chlorite contains small grains of titanite.

XRD: Fe chlorite; quartz and amphibole in trace amounts.

Sample 169-856H-62R-1, 89–90 cm (Piece 15A), Unit VIII [Z-1598]

Plagioclase sparsely phyric basalt. Phenocrysts (2%–3%): plagioclase (0.8–1.2 mm) completely replaced by chlorite. Several phenocrysts of opaque minerals (0.4–0.7 mm, 1%–2%), occasionally oxidized with formation of leucoxene and Fe hydroxides (<1%). Groundmass: vitrophyric texture; needle-shaped and skeletal microlites and laths of plagioclase (2%–3%). Plagioclase contains inclusions of glass, microlites of opaque minerals that replaced by leucoxene and titanite. gray-cream glass (95%) is weakly crystallized with formation of micrograins (0.01 mm) of pyroxene and albite.

Alteration: very strong (100%).

XRD: Fe chlorite; trace quartz.

Sample 169-856H-63R-1, 30–35 cm (Piece 6A), Unit VIII [Z-1599]

Plagioclase-olivine phyric basalt. Groundmass: vitrophyric texture. Rock: identical with Sample 169-856H-62R-1, 89–90 cm (Z-1598).

Alteration: slight (2%–3%).

XRD: Fe chlorite; trace quartz.

Sample 169-856H-64R-1, 10–14 cm (Piece 3), Unit VIII [Z-1600]

Olivine-plagioclase phyric basalt, weakly crystallized. Phenocrysts (5%): prismatic grains of plagioclase (0.5–1.5 mm, 3%, labradorite [An_{60}]) and idiomorphic grains (0.6 mm) of olivine (2%); olivine completely replaced by chlorite. Groundmass: pilotaxitic texture; needle-shaped laths (0.1–0.8 mm) of plagioclase (30%–35%, andesine-labradorite [An_{50}] and andesine [An_{38}]). Almost isotropic dark-brown glass contains opaque dust and crystals of pyroxene. Chloritized glass is ~1%.

Alteration: slight (2%–3%).

XRD: Fe chlorite; quartz and amphibole in trace amounts.

Sample 169-856H-64R-1, 75–80 cm (Piece 13), Unit VIII [Z-1601]

Olivine-plagioclase phyric basalt. Phenocrysts (5%): prismatic grains of plagioclase (0.4–0.7 mm, 3%, labradorite [An_{63}] and idiomorphic grains (0.3–0.7 mm) of olivine (2%); olivine completely replaced by chlorite. Groundmass: vitrophyric texture; needle-shaped laths of plagioclase (2%–3%) and grayish cream isotropic glass.

Alteration: slight (2%).

XRD: Fe chlorite; quartz, amphibole, and talc in trace amounts.

Sample 169-856H-64R-2, 132–136 cm (Piece 20), Unit VIII [Z-1602]

Olivine-plagioclase phyric dolerite fine grained. Phenocrysts: single (2%–3%) tabular grains of plagioclase (1.5–2 mm) completely replaced by chlorite and albite. Single idiomorphic grains (up to 2 mm) of olivine completely replaced by chlorite. Groundmass: ophitic texture, sparsely vesicular; laths (0.7–1.2 mm) of plagioclase completely replaced by albite and chlorite. Clinopyroxene (2%) replaced by chlorite. Glass(?) replaced by granoblastic aggregate of albite, chlorite, and opaque minerals (5%). On the whole rock is chloritized. Rounded vesicles (0.6–0.7 mm, 1%) completely are filled with chlorite (pennine).

Alteration: very strong (98%).

XRD: Fe chlorite; quartz and amphibole in trace amounts.

Sample 169-856H-65R-1, 0–5 cm (Piece 1A), Unit VIII [Z-1603]

Olivine-plagioclase phyric basalt, crystallized. Phenocrysts (3%–5%): tabular grains (1–1.2 mm) of plagioclase (labradorite [An_{60}]) and idiomorphic grains (1.2 mm) of olivine completely replaced by chlorite. Groundmass: intersertal texture; laths (0.4–2 mm in size) and prismatic grains (0.2–0.6 mm) of plagioclase (30%, labradorite [An_{55}] and labradorite [An_{51}]). Interstices: pyroxene partly replaced by uralite, isometric grains (0.05 mm) of albite, and opaque minerals. Clinopyroxene and glass completely replaced by granoblastic aggregate of albite and chlorite. Small isometric grains of opaque minerals and leucoxene are present. Veinlets (0.1–0.2 mm) contain granoblastic aggregate of albite and chlorite.

Alteration: moderate (40%).

XRD: Fe chlorite; trace quartz and amphibole; vein contains Fe chlorite, quartz, amphibole, and talc.

Sample 169-856H-65R-2, 54–59 cm (Piece 7), Unit VIII [Z-1604]

Plagioclase phyric basalt, crystallized. Microphenocrysts (5%): prismatic grains (0.4–0.8 mm) of plagioclase (labradorite [$An_{51–52}$]). Groundmass: microlitic texture; needle-shaped laths (up to 2 mm) of plagioclase. Case-like grains of plagioclase, center parts of crystals contain glass. Glass (75%): segregates of pyroxene and plagioclase microlites and opaque dust (5%).

Alteration: fresh rock.

XRD: Fe chlorite; trace quartz, amphibole, and talc; veinlet contains Fe chlorite, quartz, amphibole, and talc.

Hole 857C

Sample 139-857C-59R-1, 20–22 cm (Piece 1), Unit 1 [Z-946]

Olivine sparsely phyric basalt, crystallized, massive. Single grains of olivine completely replaced by secondary minerals. Groundmass: microlitic (microdoleritic) texture; needle-shaped laths and prismatic crystals of plagioclase (0.2–1.5 mm, 35%). Laths of plagioclase with 0.8–1.2 mm size are labradorite (An_{58}), <0.8 mm laths are andesine (An_{46} and An_{38}). Isometric or radial-radiant crystals of pyroxene (50%) are located in interstices. Opaque minerals (up to 15%): aggregates of very small grains (<0.01 mm) distributed in all rock and forms sparse skeletal stretching grains. Vein (~5 mm) contains chalcedony, chlorite, and opaque minerals. Host rock in contact with vein is altered; plagioclase replaced by secondary mineral, clinopyroxene partly replaced by chlorite.

Alteration: slight.

XRD: Mg-Fe chlorite (Fe > Mg); trace quartz.

Sample 139-857C-59R-1, 84–87 cm (Piece 7), Unit 1 [Z-821]

Aphyric microdolerite, massive. Groundmass: microophitic texture. Rock: unoriented laths of plagioclase (0.1–0.5 mm, labradorite [An_{56}]), small (0.1 mm) xenomorphic grains of augite, opaque minerals (5%–6%), and sparse chlorite (1%–2%).

Alteration: rock is fresh.

XRD: Mg-Fe chlorite (Fe > Mg) with ~5% swelling layers; smectite, quartz, and amphibole in trace amounts.

Sample 139-857C-59R-2, 57–59 cm (Piece 5), Unit 1 [Z-947]

Aphyric dolerite medium grained. Groundmass: ophitic texture. Rock: laths and prismatic crystals of plagioclase (0.2–1 mm, 35%, labradorite [An_{55}] and andesine [An_{40}]). Isometric grains of clinopyroxene-augite (up to 0.5 mm, 40%) and chlorite (15%) are located in interstices. Opaque minerals (7%–8%) are irregularly distributed.

Alteration: slight (~10%–15%).

XRD: Mg-Fe chlorite (Fe > Mg) with single swelling interlayers; trace quartz.

Sample 139-857C-59R-3, 80–83 cm (Piece 4), Unit 1 [Z-822]

Aphyric dolerite fine grained, massive. Groundmass: ophitic texture. Rock: unoriented laths of plagioclase (0.1–0.5 mm, labradorite [An_{51}]) partly replaced by chlorite. Dark cream augite (Ti-augite?; 0.1–0.2 mm) with pleochroism and chlorite (3%–4%) are located in interstices. Opaque minerals (5%–6%) are located in areas with chlorite.

Alteration: rock is fresh.

XRD: Mg-Fe chlorite (Fe > Mg); quartz and amphibole in trace amounts.

Sample 139-857C-59R-4, 88–90 cm (Piece 7), Unit 1 [Z-823]

Aphyric dolerite fine grained, massive. Groundmass: ophitic texture. Rock: identical to Sample 139-857C-59R-3, 80–83 cm (Z-822).

Alteration: slight (8%–10%).

XRD: Fe chlorite with single swelling interlayers; trace quartz.

Sample 139-857C-60R-1, 53–56 cm (Piece 3), Unit 2 [Z-824]

Aphyric basalt (microdolerite), massive. Groundmass: microdoleritic texture. Rock: unoriented laths of plagioclase (0.3–0.8 mm, labradorite [$An_{58–60}$]). Panicle-like segregates of microlites of plagioclase, clinopyroxene, opaque minerals (4%–5%), and chlorite (1%) are in interstices.

Alteration: rock is fresh.

XRD: Mg-Fe chlorite (Fe > Mg) with single swelling interlayers; trace quartz and amphibole.

Sample 139-857C-60R-1, 130–132 cm (Piece 8), Unit 2 [Z-948]

Dolerite blastophyric, fine grained. Groundmass: ophitic texture. Euhedral skeletal sulfide crystals (up to 3 mm, ~5%) are present. Rock: laths and prismatic crystals of plagioclase (35%, labradorite [An_{55}]). Interstices: isometric grains of augite (0.1–0.7 mm, 45%), chlorite (10%), and segregates and grains (0.01–0.05 mm) of opaque minerals. Opaque minerals replaced by leucoxene and titanite (5%–7%).

Alteration: slight to moderate (10%–20%).

XRD: Mg-Fe chlorite (Fe > Mg) with single swelling interlayers; corrensite-like mineral (minor); quartz and amphibole in trace amounts.

Sample 139-857C-60R-2, 14–16 cm (Piece 1), Unit 2 [Z-949]

Dolerite blastophyric, fine grained. Rock: blastophyric (0.6–3.5 mm) idiomorphic (cubic pyrite?) segregates of opaque minerals (15%) with rare small inclusions of plagioclase and pyroxene. Groundmass: intersertal-ophitic texture; laths and prismatic crystals of plagioclase (30%, labradorite [An_{54}] and andesine [An_{40}]). Interstices: xenomorphic grains of pyroxene-augite (40%) and small chloritized areas (10%). Small (<0.05 mm) grains of opaque minerals, leucoxene, and titanite (~5%–7%). Titanite replaces Ti-magnetite.

Alteration: moderate (25%).

XRD: Mg-Fe chlorite (Fe > Mg) with ~5% swelling interlayers; corrensite-like mineral (minor); trace quartz.

Sample 139-857C-61R-1, 81–83 cm (Piece 6), Unit 4 [Z-950]

Basalt sparsely blastophyric, crystallized. Single (<1%) small (0.9 mm) blastophyric sulfide crystal is present. Groundmass: microlitic texture; microlites and laths of plagioclase (35%, labradorite [$An_{52–55}$] and andesine [An_{44}]). Segregate of small (0.1–0.3 mm) grains of clinopyroxene (40%) and chlorite (15%). Interstices: small (<0.1 mm) grains of opaque minerals, leucoxene, and titanite (~10%).

Alteration: slight (15%).

XRD: Mg-Fe chlorite (Fe > Mg) with ~5% swelling interlayers; trace quartz.

Sample 139-857C-61R-2, 8–10 cm (Piece 1), Unit 5 [Z-951]

Aphyric basalt, crystallized. Groundmass: microlitic texture. Rock: unoriented microlites and needle-shaped laths (0.1–0.9 mm) of plagioclase (45%, labradorite [An_{55}]); very small grains of leucoxene and titanite (5%). Interstices: panicle-like segregates of microlites of clinopyroxene and chlorite (1%).

Alteration: slight (10%–15%).

XRD: Fe-Mg chlorite (Mg > Fe) with single swelling interlayers; trace quartz and amphibole.

Sample 139-857C-62R-1, 70–72 cm (Piece 5), Unit 6 [Z-952]

Aphyric congo-dolerite medium grained. Groundmass: intersertal-ophitic texture. Rock: laths and prismatic crystals (0.6–1.5 mm) of plagioclase (30%, labradorite [An_{55}]); isometric grains of augite (0.2–1.7 mm, 25%); segregate of small grains of quartz (0.1–0.4 mm, 5%) and chlorite (10%). Opaque minerals (~10%): small (0.2–0.3 mm) cubic and pseudocubic grains, pyrite? Titanite (<0.1 mm) occurs with chlorite. Veinlet (up to 4 mm) contains chalcedony, chlorite, and epidote. Rock in contact with vein is chloritized and silicified, opaque minerals replaced by leucoxene and titanite (titanite replaces Ti-magnetite). Clinopyroxene is chloritized and partly replaced by uralite (several grains). Often opaque minerals are replaced by leucoxene and titanite (5%–7%). Interstices: panicle-like segregates of microlites of clinopyroxene and chlorite (1%). Rock: very small grains of leucoxene and titanite (5%).

Alteration: moderate (30%), rock is chloritized.

XRD: Fe-Mg-chlorite (Fe > Mg) with single swelling interlayers; mixed-layer chlorite-swelling chlorite (minor); quartz and amphibole in trace amounts.

Sample 139-857C-62R-2, 40–42 cm (Piece 6), Unit 6 [Z-953]

Congo-dolerite, medium grained, blastophyric. Groundmass: intersertal-poikilophitic texture; single (1%) blastophyric sulfide crystal (up to 2.5 mm). Rock: prismatic crystals (0.5–1.7 mm) of plagioclase (20%, labradorite [An_{58}] and andesine [An_{39}]). Clinopyroxene grains (20%, 0.5–2 mm) often contain inclusions of plagioclase laths. Interstices: aggregate of chlorite (40%), uralite (7%–8%), and quartz (0.1 mm, 2%–3%). Plagioclase is partly replaced by albite. Opaque minerals (7%–8%) replaced by leucoxene. Leucoxene replaces Ti-magnetite. Microcracks are filled with chlorite.

Alteration: strong (50%–55%).

XRD: Fe-Mg chlorite (Mg > Fe); minor mixed-layer chlorite-swelling chlorite; trace amphibole.

Sample 139-857C-63R-1, 50–52 cm (Piece 4), Unit 7 [Z-954]

Congo-dolerite, aphyric, medium grained. Groundmass: intersertal-poikilophitic texture. Rock: laths and prismatic crystals (0.5–1.5 mm) of plagioclase (35%, labradorite [$An_{55–57}$] and andesine [An_{39}]). Clinopyroxene xenomorphic grains (0.3–1.7 mm) often contain inclusions of plagioclase laths. Interstices: clinopyroxene (30%), chlorite (15%), and small grains of quartz (1%–2%). Chlorite and epidote replace clinopyroxene. Opaque minerals (7%–8%) partly replaced by leucoxene and titanite. Veinlet (0.3 mm) contains chlorite and epidote. Host rock in contact with veinlet is strongly chloritized.

Alteration: moderate (25%), rock is chloritized.

XRD: Fe chlorite; quartz and amphibole in trace amounts.

Sample 139-857C-64R-1, 18–20 cm (Piece 2), Unit 8 [Z-955]

Dolerite, aphyric, medium grained. Groundmass: intersertal-ophitic-poikilophitic texture. Rock: laths and prismatic crystals (0.4–1.5 mm) of plagioclase (35%, labradorite [An_{55}] and andesine [An_{44}]). Clinopyroxene isometric grains (0.3–1.7 mm) often contain inclusions of plagioclase laths. Interstices: clinopyroxene (35%), chlorite (15%), and uralite. Chlorite and epidote replace clinopyroxene. Opaque minerals (7%–8%) partly replaced by leucoxene and titanite. Veinlet (0.3 mm) contains chlorite and epidote. Host rock in contact with veinlet is strongly chloritized.

Alteration: slight to moderate (20%), rock is chloritized.

XRD: Fe-Mg-chlorite (Fe > Mg); quartz and amphibole in trace amounts.

Sample 139-857C-64R-1, 41–44 cm (Piece 3), Unit 8 [Z-825]

Dolerite, aphyric, medium grained, massive. Groundmass: ophitic-poikilophitic-intersertal texture. Rock: stretch-prismatic and prismatic laths (0.3–0.8 mm) of plagioclase (labradorite [An_{55}]). Clinopyroxene forms small (0.2 mm) xenomorphic grains and stretch grains (up to 5 mm) with inclusions of microlaths of plagioclase (andesine [An_{43}]). Interstices (30%): chlorite (pennine) and very small opaque minerals grains (9%–10%). Occasionally opaque minerals form xenomorphic grains (up to 0.5 mm).

Alteration: moderate (30%), rock is chloritized.

XRD: Fe-Mg-chlorite (Fe > Mg); trace amphibole.

Sample 139-857C-64R-2, 46–49 cm (Piece 5), Unit 8 [Z-826]

Dolerite, aphyric, medium grained, massive. Groundmass: ophitic-poikilophitic-intersertal texture. Rock: identical to Sample 139-857C-64R-1, 41–44 cm (Z-825). Interstices: very small grains of titanite with chlorite and opaque minerals. Ti-magnetite replaced by ore mineral.

Alteration: moderate (30%), rock is chloritized.

XRD: Fe chlorite; quartz and amphibole in trace amounts.

Sample 139-857C-68R-1, 97–100 cm (Piece 16), Unit 12 [Z-827]

Dolerite, aphyric, medium grained, massive. Groundmass: ophitic-poikilophitic-intersertal texture. Rock: identical to Samples 139-857C-64R-1, 41–44 cm (Z-825) and 139-857C-64R-2, 46–49 cm (Z-826). Large (0.5–2 mm) skeletal-isometric grains of opaque minerals with inclusions of plagioclase and pyroxene. Interstices: very small grains of titanite with chlorite and opaque minerals.

Alteration: moderate (30%), rock is chloritized.

XRD: Fe chlorite; quartz and amphibole in trace amounts.

Sample 139-857C-68R-2, 69–71 cm (Piece 7), Unit 12 [Z-957]

Dolerite, aphyric, medium grained. Groundmass: intersertal-poikilophitic texture. Rock: laths and prismatic crystals (0.6–1.6 mm, single crystals up to 2.5 mm) of plagioclase (40%, labradorite [An_{55}] and andesine [An_{40}]). Clinopyroxene idiomorphic isometric grains (0.5–4.5 mm) are present. Large grains contain plagioclase laths. Interstices: chlorite, opaque minerals (5%), and sparse small (0.1 mm) grains of quartz. Opaque minerals partly replaced by leucoxene.

Alteration: slight to moderate (20%), rock is chloritized.

XRD: Fe-Mg-chlorite (Fe > Mg); quartz and amphibole in trace amounts.

Sample 139-857C-68R-3, 20–23 cm (Piece 2), Unit 12 [Z-828]

Dolerite, aphyric, medium grained. Groundmass: ophitic-intersertal texture. Rock: replaced by laths (0.3–0.8 mm) of plagioclase (labradorite [An_{53}]) with undulatory extinction. Interstices: xenomorphic grain of augite (25%, 0.3–0.5 mm) in association with opaque minerals (5%) and very small grains of titanite.

Alteration: moderate (25%), rock is chloritized.

XRD: Fe-chlorite; quartz and amphibole in trace amounts.

Hole 857D

Sample 139-857D-1R-1, 34–36 cm (Piece 5), Unit 13 [Z-958]

Plagioclase phyric basalt. Groundmass: hyalopilitic texture. Rock: phenocrysts (10%) and groundmass (90%). Phenocrysts: prismatic laths (0.8–1.7 mm) of plagioclase (labradorite [$An_{>50}$]). Groundmass: microlites and laths of plagioclase (20%, labradorite [An_{55}] and andesine [An_{42}]). Cracks in plagioclase filled with albite and chlorite. Glass (50%) completely replaced by chlorite, very small grains (<0.1 mm, 20%) of leucoxene, and titanite.

Alteration: very strong (70%–75%), rock is altered.

XRD: Fe-Mg-chlorite (Fe > Mg) with single swelling interlayers; trace quartz.

Sample 139-857D-1R-1, 35–39 cm (Piece 5A), Unit 13 [Z-829]

Plagioclase, sparsely phyric basalt, massive, weakly crystallized. Phenocrysts: tabular and prismatic grains (0.7–1.2 mm) of plagioclase (glomerophyric aggregates; labradorite [An_{56}]). Groundmass: pilotaxitic texture; laths of plagioclase (labradorite [An_{52}]). Cracks in plagioclase are filled with albite and chlorite. Glass is anisotropic (black glass with abundant, very small grains of opaque minerals and titanite); part of mesostasis consists of clinopyroxene and plagioclase microlites. Chloritization is ~5%–7%. Opaque minerals (10%–12%): occasionally skeletal grains from 0.3 to 1 mm.

Alteration: slight (10%–15%).

Sample 139-857D-2R-1, 10–13 cm (Piece 3), Unit 14A [Z-831]

Plagioclase, sparsely phyric dolerite, massive. Single (2%–3%) glomerophyric segregates of short-prismatic grains of plagioclase (0.5–0.8 mm, labradorite [An_{69}]). Zonal plagioclase has undulatory extinction. Groundmass: doleritic texture; laths of plagioclase (0.2–0.7 mm, labradorite [An_{52}]), ~10% filled with chlorite. Interstices: segregate of small isometric or panicled stretch-grains (up to 0.7 mm) of augite. Very small grains of opaque minerals are present (5%–6%).

Alteration: rock is fresh.

XRD: Fe chlorite; quartz and amphibole in trace amounts.

Sample 139-857D-3R-1, 43–46 cm (Piece 4), Unit 14B [Z-832]

Plagioclase, phyric dolerite, medium grained, massive. Phenocrysts (50%): plagioclase; large tabular grains (2–2.5 mm) and segregates of small crystals (1.2 mm, labradorite [An_{60}]). Groundmass: doleritic texture; laths of plagioclase (labradorite [An_{55}]) and segregate of panicle-like grains of clinopyroxene and plagioclase ("pegmatoidic" texture). Interstitial glass replaced by chlorite and very small grains of opaque minerals. Chlorite replaces plagioclase and partly pyroxene.

Alteration: slight (10%), rock is chloritized.

XRD: Fe chlorite; quartz and amphibole in trace amounts.

Sample 139-857D-3R-2, 86–88 cm (Piece 10B), Unit 14B [Z-959]

Plagioclase phyric dolerite, medium grained, massive. Phenocrysts: plagioclase (30%) and groundmass (70%); plagioclase is large tabular grains (2–5 mm, labradorite [$An_{55–60}$]), some sharply zoned (bitovnite in center and labradorite [An_{65}] in periphery). Groundmass: poikilophitic texture; various (0.2–1.2 mm) laths and tabular grains of plagioclase (30%, labradorite [An_{55}] and andesine [An_{48}]). Clinopyroxene (25%) forms xenomorphic grains (0.2–1.7 mm), occasionally panicle grains in interstices with plagioclase. Pyroxene and plagioclase are replaced by chlorite and leucoxene. Epidote and albite also occur. Interstices: chlorite (5%), opaque minerals (~7%–8%), Ti-magnetite, titanite.

Alteration: slight (5%).

XRD: Fe-Mg-chlorite (Fe > Mg); trace quartz.

Sample 139-857D-4R-2, 53–56 cm (Piece 11), Unit 15 [Z-960]

Plagioclase phyric basalt, crystallized. Rock: phenocrysts (15%) and groundmass (85%). Phenocrysts: plagioclase; prismatic and tabular grains (0.7–2.1 mm, labradorite [$An_{58–60}$]). Groundmass: microlitic texture; laths (up to 0.8 mm) and microlites (0.1–0.4 mm) of plagioclase (35%, labradorite [An_{55}] and andesine [An_{44}]). Interstices: microlite of clinopyroxene (from <0.1 to 0.2–0.3 mm, 30%) and chloritized glass (10%). Host rock in contact with veinlet is highly chloritized. Single microvesicle (0.3 mm × 0.6 mm) is filled with fine grained aggregate of quartz and chlorite. Zone (~10%) with small (0.2 mm) idiomorphic pseudocubic grains of pyrite(?).

Alteration: slight (10%).

XRD: Fe chlorite; quartz and amphibole in trace amounts.

Sample 139-857D-8R-1, 5–7 cm (Piece 1), Unit 16B [Z-962]

Plagioclase phyric basalt, sparsely vesicular. Phenocrysts (30%): plagioclase; short and stretch prismatic and tabular grains (0.8–3 mm, labradorite [An_{54}]) with inclusions of glass. Groundmass (45%): hyalopilitic texture; needle-shaped microlites and microlaths of plagioclase (10%, andesine [An_{45}]) and isotropic glass (35%) containing very small crystals of clinopyroxene and disseminated opaque minerals. Vein (3 mm) contains grains (0.3–0.9 mm) of orthoclase (sanidine?) and quartz. Large grain of sulfide (1.7 mm) is located in center of veinlets. Small skeletal grains (up to 0.9 mm) of sulfide (2%–3%) were identified in groundmass.

Alteration: slight.

XRD: Fe-Mg-chlorite (Fe > Mg) with single swelling interlayers.

Sample 139-857D-9R-1, 23–25 cm (Piece 4), Unit 16C [Z-833]

Aphyric dolerite, medium grained, massive. Groundmass: ophitic texture, highly altered. Rock: laths of plagioclase (0.3–0.8 mm) almost completely replaced by albite and chlorite. Interstices: clinopyroxene completely or partly replaced by chlorite and uralite. Opaque minerals (~10%) partly replaced by titanite in areas with chlorite and uralite.

Alteration: very strong (80%).

XRD: Fe chlorite with single swelling interlayers; quartz and amphibole in trace amounts.

Sample 139-857D-12R-1, 25–27 cm (Piece 5), Unit 17A [Z-834]

Plagioclase phyric basalt. Phenocrysts: large (1–3 mm) prismatic and stretch-prismatic plagioclase crystals (15%–20%, labradorite-bitovnite [An_{70}]); central parts of plagioclase contain abundant inclusions of glass. Groundmass: hyalopilitic texture; microlites and microlaths of plagioclase (labradorite [An_{55}]) and glass; completely replaced by chlorite and uralite. Rock is impregnated by opaque minerals (~20%) partly replaced by titanite.

Alteration: strong (60%).

XRD: Fe chlorite; quartz in trace amounts.

Sample 139-857D-12R-1, 106–108 cm (Piece 14), Unit 17A [Z-963]

Aphyric dolerite (basalt?), fine grained. Phenocrysts: prismatic grains of plagioclase (10%, labradorite [An_{60}]). Groundmass: vitrophyric texture; weakly crystallized, almost isotropic, glass with crystallites of plagioclase, clinopyroxene, and opaque minerals (3%–4%).

Alteration: moderate (20%–25%).

XRD: Fe chlorite; trace quartz.

Sample 139-857D-12R-2, 17–19 cm (Piece 3), Unit 17A [Z-964]

Aphyric dolerite, fine grained. Groundmass: intersertal-ophitic texture. Rock: laths of plagioclase (0.1–0.8 mm, 45%, labradorite [An_{60}] and andesine [An_{46}]). Interstices: xenomorphic (0.1–0.4 mm) grains of augite (40%), chlorite (10%–12%), and small (up to 0.3 mm) xenomorphic grains of opaque minerals (5%–7%). In chloritized areas opaque minerals replaced by leucoxene and titanite.

Alteration: slight (10%–15%).

XRD: Fe-Mg chlorite (Fe > Mg) with single swelling interlayers; trace quartz and amphibole.

Sample 139-857D-17R-3, 72–74 cm (Piece 11), Unit 19 [Z-967]

Aphyric basalt (microdolerite), crystallized. Groundmass (55%): microlitic (microdoleritic) texture, vesicular; microlites and laths (0.1–0.8 mm) of plagioclase (20%, labradorite [$An_{55–60}$]). Interstices: clinopyroxene (15%), plagioclase, and opaque minerals (10%); clinopyroxene partly replaced by uralite and chlorite, Ti-magnetite partly replaced by titanite. Rounded vesicles (1.2–4.5 mm, 45%) are filled completely or partially with chlorite. Several vesicles (in center, up to 0.8 mm) are filled by epidote and pyrite(?).

Alteration: moderate (30%).

XRD: Fe chlorite with single swelling interlayers; quartz and amphibole in trace amounts.

Sample 139-857D-18R-2, 84–85 cm (Piece 9), Unit 19 [Z-968]

Aphyric gabbro-dolerite, coarse grained, poikilophitic. Rock; prismatic and tabular grains (0.8–2.5 mm) of plagioclase (45%, labradorite [An_{60}] and andesine [An_{48}]). Clinopyroxene (35%) forms xenomorphic grains (0.5–2.5 mm) with inclusions of plagioclase laths. Chlorite and uralite replace pyroxene. Interstices (10%): chlorite,

orthoclase, needle-shaped apatite, epidote, uralite, opaque minerals, and sparse, small (<0.1 mm) grains of titanite and leucoxene. Opaque minerals (10%) are small (0.5 mm) skeletal grains. A single, large (up to 2.5 mm) blastophyric grain of sulfide is present.

Alteration: slight (10%).

XRD: Fe-Mg chlorite (Fe > Mg); quartz and amphibole in trace amounts.

Sample 139-857D-20R-1, 64–66 cm (Piece 8), Unit 19 [Z-969]

Olivine-orthopyroxene blastophyric gabbro-dolerite. Groundmass: intersertal-ophitic texture. Rock: prismatic and tabular grains (0.9–2.5 mm) of plagioclase (35%, labradorite [An_{54}] and andesine [$An_{34–40}$]). Clinopyroxene (35%) forms isometric grains (0.5–2.5 mm). Single grains replaced by uralite. About 25% of rock is chloritized. Single chloritized grains (2.5 mm) have relicts of olivine structure. Orthopyroxene is replaced by chlorite and uralite. Opaque minerals (5%) are sulfide.

Alteration: moderate (25%).

XRD: Fe-Mg chlorite (Mg > Fe) with ~10% swelling interlayers; mixed-layer chlorite-swelling chlorite mineral (minor); quartz and amphibole in trace amounts.

Sample 139-857D-21R-1, 59–61 cm (Piece 6), Unit 20A [Z-835]

Aphyric dolerite, medium grained. Groundmass: ophitic texture. Rock: stretch-prismatic laths of plagioclase (45%, 0.2–1.5 mm, labradorite [An_{60}, large laths] and labradorite [An_{55}, small laths]). Interstices: isometric (0.2–0.5 mm) grains of clinopyroxene (salite), augite (40%), chlorite (10%–12%), and small (up to 0.3 mm) xenomorphic grains of opaque minerals (5%–7%). In chloritized areas, opaque minerals are replaced by leucoxene and titanite.

Alteration: slight to moderate (15%–20%).

XRD: Fe chlorite; quartz and amphibole in trace amounts.

Sample 139-857D-23R-1, 57–59 cm (Piece 10), Unit 20D [Z-970]

Blastophyric dolerite, medium grained. Groundmass: intersertal-ophitic texture. Rock: tabular and prismatic grains (0.4–2.5 mm) of plagioclase (40%, labradorite [$An_{55–60}$] and andesine [An_{45}]). Interstices: xenomorphic grains (0.3–0.7 mm) of clinopyroxene (40%), augite or Ti-augite and segregate of chlorite and small grains (<0.1 mm) of titanite. Opaque minerals (5%): sparse idiomorphic small grains (0.2–0.4 mm) of Ti-magnetite and two large (2.5 mm) skeletal grains of sulfide.

Alteration: slight (15%).

XRD: Fe chlorite; quartz and amphibole in trace amounts.

Sample 139-857D-24R-2, 4–7 cm (Piece 1), Unit 21 [Z-836]

Aphyric dolerite, fine grained. Groundmass: doleritic texture, vesicular. Rock: unoriented laths of plagioclase (labradorite [An_{68}]) with undulatory extinction. Plagioclase partly replaced by chlorite (in cracks). Interstices: segregate of small xenomorphic grains (0.1–0.5 mm) of augite or chlorite (15%) with association with opaque minerals (7%–8%). Rounded, small (0.3 mm) vesicles (5%) completely filled with chlorite.

Alteration: moderate (20%).

XRD: Fe chlorite; quartz and amphibole in trace amounts.

Sample 139-857D-25R-1, 73–75 cm (Piece 10), Unit 21 [Z-971]

Plagioclase, sparsely phyric dolerite, fine grained. Two prismatic grains (2 and 2.5 mm) of plagioclase (labradorite [An_{68}]). Groundmass: intersertal-ophitic texture; prismatic grains (0.3–1.2 mm) of plagioclase (40%, labradorite [An_{55}] and andesine [An_{47}]). Interstices: xenomorphic grains of clinopyroxene (40%) and chlorite (10%). Clinopyroxene is replaced by chlorite. Plagioclase is replaced by chlorite, epidote, and albite. Opaque minerals (5%–7%): small (0.2 mm), evenly distributed skeletal grains. Sphene and Ti-magnetite are replaced with leucoxene.

Alteration: slight (10%).

XRD: Fe chlorite with single swelling interlayers; quartz and amphibole in trace amounts.

Sample 139-857D-26R-1, 58–60 cm (Piece 6), Unit 21 [Z-972]

Plagioclase, sparsely phyric dolerite, fine grained. Phenocrysts (2%): prismatic grains (1.2 and 2.5 mm) of plagioclase. Groundmass: intersertal-ophitic texture, sparsely vesicular, identical to Sample 139-857D-25R-1, 73–75 cm (Z-971). Rounded, small (0.5–0.7 mm) vesicles (1%) completely filled with light green isotropic glass.

Alteration: slight (10%).

XRD: Fe chlorite; trace quartz.

Sample 139-857D-29R-2, 36–39 cm (Piece 4), Unit 23A [Z-973]

Aphyric dolerite, fine grained. Groundmass: intersertal-ophitic texture; prismatic and tabular grains (0.3 and 0.9 mm) of plagioclase (40%, labradorite [An_{60}] and andesine [An_{42}]). Interstices: xenomorphic grains of clinopyroxene (40%), green chloritized glass with rare grains (10%) of titanite. Opaque minerals (10%) form xenomorphic grains (0.2–0.4 mm). Several skeletal grains (up to 0.8 mm) of sulfides are present.

Alteration: slight (10%).

XRD: Fe chlorite; trace quartz.

Sample 139-857D-33R-1, 81–83 cm (Piece 13), Unit 24 [Z-974]

Aphyric dolerite, fine grained. Groundmass: intersertal-ophitic texture, sparsely vesicular; prismatic and tabular grains (0.3 and 1.5 mm) of plagioclase (35%, labradorite [An_{55}] and andesine [$An_{39–40}$]). Clinopyroxene (30%) forms isometric grains (0.3 and 1.2 mm) containing inclusions of plagioclase laths. Interstices: chlorite (5%–7%), occasionally chlorite forms large (up to 3.5 mm) zones of chloritization with sparse, small grains of titanite; large areas (up to 4 mm) are replaced by fine grained segregate (0.1 mm) of clinopyroxene (second generation), chlorite, small grains of quartz and orthoclase (<1%), and small xenomorphic grains of opaque minerals. Opaque minerals (10%) are partly replaced by leucoxene. Rounded vesicle (1 mm) is filled with chlorite.

Alteration: slight (10%).

XRD: Fe chlorite; quartz and amphibole in trace amounts.

Sample 139-857D-35R-1, 29–31 cm (Piece 5), Unit 25B [Z-975]

Blastophyric basalt, crystallized. Blastophyric grains (0.3–1 mm) of sulfide (10%–12%) are present. Groundmass: microlitic texture; needle-shaped, panicle-like microlites and laths (0.1–0.9 mm) of case-like plagioclase (40%, labradorite [An_{60}] and andesine [An_{45}]). Interstices: plagioclase, panicle-like segregate of microlites of clinopyroxene (45%) and chlorite (5%).

Alteration: slight (10%).

XRD: Fe chlorite with single swelling interlayers; quartz and amphibole in trace amounts.

Sample 139-857D-35R-1, 103–106 cm (Piece 14A), Unit 25B [Z-837]

Aphyric dolerite, fine grained. Groundmass: doleritic texture, sparsely vesicular (2%). Rock: identical to Sample 139-857D-24R-2, 4–7 cm (Z-836).

Alteration: slight to moderate (20%).

XRD: Fe chlorite; quartz and amphibole in trace amounts.

Sample 139-857D-36R-1, 3–5 cm (Piece 1), Unit 25B [Z-976]

Olivine phyric (?) basalt (microdolerite), crystallized. Phenocrysts: sparse (2%–3%), small (0.7 mm) idiomorphic phenocrysts of olivine completely replaced by chlorite. Groundmass: microdoleritic texture; microlites and laths (0.1–0.9 mm) of plagioclase (40%, labradorite [An_{55}] and andesine [An_{38}]). Interstices: small (0.1–0.7 mm) xenomorphic grains of augite (45%), chlorite (5%), and opaque minerals (10%). Opaque minerals partly replaced by leucoxene and titanite. Occasionally there are skeletal grains (0.5 mm) of sulfide (2% of volume of opaque minerals). Plagioclase and pyroxene are chloritized. Plagioclase is replaced with albite.

Alteration: slight (10%–15%).

XRD: Fe chlorite; trace quartz.

Hole 858F

Sample 139-858F-26R-1, 93–95 cm (Piece 11), Unit 1B [Z-977]

Olivine-plagioclase, phyric basalt. Rock; phenocrysts, groundmass, and vesicles. Phenocrysts (10%): small (0.4–0.8 mm) idiomorphic grains of olivine and plagioclase; olivine completely replaced by chlorite (4%). Single, large (up to 5 mm) phenocryst of plagioclase is present. Microphenocrysts of plagioclase (0.6–1.7 mm, 6%, labradorite [An_{56}]) are present. Groundmass (85%): hyalopilitic texture, vesicular; sparse, needle-shaped microlites of plagioclase (5%, andesine [An_{40}]) and slightly anisotropic glass with crystals of clinopyroxene (80%). Plagioclase is partly replaced by chlorite. Rounded vesicles (5%, 0.9–1.5 mm) are completely filled with aggregate of light green chlorite.

Alteration: slight.

XRD: Mg-Fe chlorite (Mg > Fe); mixed-layer chlorite-swelling chlorite mineral (minor); trace quartz.

Sample 139-858F-27R-1, 25–27 cm (Piece 6), Unit 1C [Z-978]

Olivine-plagioclase, sparsely phyric basalt, crystallized. Rock: microphenocrysts (5%), groundmass (95%), and single vesicles. Phenocrysts: glomerophyric segregates of small (0.4–0.5 mm) idiomorphic grains of olivine (completely replaced by chlorite) and laths (0.5–0.9 mm) of plagioclase (3%, labradorite [An_{55}]). Groundmass: microlitic texture, sparsely vesicular; needle-shaped microlites and microlaths of plagioclase (30%–35%). Plagioclase often forms segregates with panicle-like microlites of clinopyroxene (~60%). Groundmass contains spots of brown glass. Rounded sparse vesicles (0.6 mm in across) completely are filled with chlorite.

Alteration: slight (~2%).

XRD: Mg-Fe chlorite (Mg > Fe) with ~10% swelling interlayers and mixed-layer chlorite-swelling chlorite mineral; quartz and amphibole in trace amounts.

Sample 139-858F-28R-1, 43–45 cm (Piece 8), Unit 1C [Z-979]

Olivine-plagioclase, phyric basalt. Phenocrysts (15%): olivine (2%) and plagioclase (13%). Olivine replaced by chlorite. Plagioclase forms prismatic crystals (0.3–0.9 mm, labradorite [An_{57}]). Groundmass (85%): hyalopilitic texture, sparsely vesicular; needle-shaped, case-like microlites and laths of plagioclase (10%) and weakly anisotropic brown glass. Glass contains segregates of plagioclase and clinopyroxene. Single blastophyric skeletal grain (0.7 mm) of sulfide is present. Rounded vesicles (0.2 mm) are filled with chlorite.

Alteration: slight (~3%).

XRD: Mg-Fe chlorite (Mg > Fe) with ~10% swelling interlayers; mixed-layer chlorite-swelling chlorite mineral and corrensite-like mineral (minor); trace quartz.

Sample 139-858F-29R-1, 39–41 cm (Piece 8), Unit 1C [Z-980]

Olivine-plagioclase sparsely phyric basalt. Phenocrysts (<1%): olivine and several prismatic grains of plagioclase (0.3–0.9 mm, labradorite [An_{51}]). Groundmass: vitrophyric texture, vesicular; brown isotropic glass. Rounded vesicles (0.2–1 mm, 10%) completely filled with chlorite.

Alteration: rock is fresh.

XRD: Mg-Fe chlorite (Fe ≈ Mg) with ~15% swelling interlayers; mixed-layer chlorite-swelling chlorite mineral (minor); trace quartz.

Hole 858G

Sample 139-858G-1R-1, 14–16 cm (Piece 2), Unit 1C [Z-981]

Olivine-plagioclase sparsely phyric basalt, crystallized. Phenocrysts (<5%): glomerophyric accretions of completely chloritized olivine and stretch-prismatic laths of plagioclase partly replaced by albite. Groundmass: microlitic texture; needle-shaped microlites and laths (0.1–2 mm) of plagioclase (50%, andesine [An_{37}]). Interstices: segregates of clinopyroxene microlites (35%) and light green partly chloritized glass (10%). Chlorite partly replaces plagioclase and pyroxene.

Alteration: slight (~5%).

XRD: Mg-Fe chlorite (Mg > Fe) with ~15% swelling interlayers; mixed-layer chlorite-swelling chlorite mineral (minor); trace quartz.

Sample 139-858G-4R-1, 35–37 cm (Piece 9), Unit 2A [Z-982]

Olivine-plagioclase phyric basalt. Phenocrysts (15%): glomerophyric accretions of completely chloritized olivine and laths of plagioclase (0.6–2 mm, andesine [An_{42}] and andesine-labradorite [An_{50}]). Two grains of sulfide (0.8–0.9 mm) are present. Groundmass (85%): hyalopilitic texture, single vesicle; needle-shaped microlites and laths of plagioclase (0.1–1.2 mm, 10%, andesine [An_{38}] and andesine [An_{42}]). Dark-brown glass partly crystallized to accretions of plagioclase and clinopyroxene (75%). Interstitial glass is chloritized. Single rounded vesicle (0.5 mm) is filled with chlorite.

Alteration: slight (7%–8%).

XRD: Mg-Fe chlorite (Mg > Fe) with ~10% swelling interlayers; mixed-layer chlorite-swelling chlorite mineral and corrensite-like mineral (minor); trace quartz.

Sample 139-858G-7R-1, 32–34 cm (Piece 6), Unit 2B [Z-983]

Olivine-plagioclase phyric basalt. Microphenocrysts (<5%): single grains of chloritized olivine and prismatic grains (0.8–2 mm) of plagioclase (andesine [An_{38}]). Groundmass: hyalopilitic (or vitrophyric) texture; needle shaped, case-like microlites of plagioclase (5%, andesine [An_{32}]) and almost isotropic glass (90%).

Alteration: slight (1%).

XRD: Mg-Fe chlorite (Fe ≈ Mg) with ~15% swelling interlayers; mixed-layer chlorite-swelling chlorite mineral and corrensite-like mineral (minor); trace quartz.

Sample 139-858G-14R-1, 10–12 cm (Piece 6), Unit 6 [Z-984]

Olivine-plagioclase phyric basalt, crystallized. Phenocrysts (12%): completely chloritized olivine (7%) and prismatic and tabular grains (0.8–1.7 mm) of plagioclase (5%, andesine [An_{38}]). Plagioclase partly replaced by albite, one grain replaced by albite and chalcedony. Groundmass: microlitic texture, sparsely vesicular; replaced by needle-shaped laths of plagioclase (30%, from andesine [An_{44}] to andesine-labradorite [An_{50}]). Glass is crystallized with a segregate of clinopyroxene microlites (40%) and light green isotropic glass (~10%). Opaque dust (5%–7%) is present. Vesicles are filled with chlorite.

Alteration: slight (7%–10%).

XRD: Mg-Fe chlorite (Fe > Mg) with single swelling interlayers; trace quartz and amphibole.

Sample 139-858G-16R-1, 75–77 cm (Piece 9), Unit 6 [Z-985]

Aphyric dolerite, fine grained. Groundmass: ophitic texture, vesicular; laths and prismatic grains (0.3–1.7 mm) of plagioclase (25%, labradorite {$An_{50–51}$]) replaced by albite, epidote, and clay minerals. Interstices: grains of clinopyroxene (20%) and segregate of small (0.1 mm) grains of clinopyroxene, green chloritized glass, and small (<0.01 mm) grains of leucoxene and titanite (15%). Glass contains epidote. About 5% of interstices are filled with chloritized glass. Chlorite and leucoxene replace pyroxene. Vesicles (30%, 1.5–4 mm in across) are rounded in shape and filled by chlorite. Occasionally, center of vesicles infilled with epidote. One vesicle is filled with quartz.

Alteration: moderate (30%).

XRD: Fe chlorite; quartz and amphibole in trace amounts.

Hole 1037B

Sample 169-1037B-57R-1, 32–37 cm (Piece 8A) [Z-1605]

Olivine-plagioclase phyric basalt, crystallized. Phenocrysts (25%): glomerophyric segregates of olivine (5%–8%) and plagioclase (17%–20%). Olivine forms idiomorphic fresh grains (0.3–0.6 mm). Tabular and prismatic phenocrysts (0.3–0.8 mm and up to 2 mm, respectively) of plagioclase (labradorite [An_{56}]). Groundmass: microlitic texture; needle-shaped microlites of plagioclase (30%, andesine [An_{44}]), microlites of clinopyroxene (40%), opaque minerals (1%–2%), and glass (1%–2%).

Alteration: fresh rock.

XRD: smectites with ~30% mica layers and with interlayer Na-K and Ca-Mg cations (Na-K > Ca-Mg); chlorite; quartz, amphibole, and talc in trace amounts.

Sample 169-1037B-58R-1, 100–104 cm (Piece 7C) [Z-1606]

Plagioclase sparsely phyric dolerite, medium grained. Phenocrysts: one (<1%) tabular phenocryst of plagioclase (2.5 mm). Groundmass: intersertal-doleritic texture; prismatic grains (0.2–1.2 mm) of plagioclase (40%, labradorite [An_{59}] and andesine [An_{38}]). Interstices: partly idiomorphic rounded grains of olivine (20%), occasionally olivine grains (one-quarter of all grains) partly or completely replaced by green biotite-like mica. Clinopyroxene (25%) almost completely replaced by aggregate of uralite. Glass (15%) replaced by uralite; crystallized part of glass contains crystallites of pyroxene and needles of opaque minerals (5%).

Alteration: strong (45%–50%).

XRD: smectites with ~30% mica layers and with interlayer Na-K and Ca-Mg cations (Ca-Mg > Na-K); illite, chlorite, quartz, amphibole, and talc in trace amounts. Brown vein: smectites with ~20% mica layers and with interlayer Na-K and Ca-Mg cations (Ca-Mg > Na-K); illite, chlorite, quartz and amphibole in trace amounts.

Sample 169-1037B-58R-2, 0–5 cm (Piece 1) [Z-1607]

Olivine-plagioclase phyric basalt. Phenocrysts (20%): glomerophyric segregates of olivine (5%) and plagioclase (15%). Rounded grains (0.2–0.5 mm) of olivine completely replaced by secondary minerals and biotite. Stretch-prismatic laths (0.5–1.7 mm) of plagioclase (labradorite [$An_{55–58}$]) are present. Groundmass: hyalopilitic texture, sparsely vesicular; case-like needles of microlites and microlaths (10%) of plagioclase and earthy-brown weakly anisotropic glass (70%). One rounded vesicle (0.6 mm) is filled with needles of uralite. Veinlet (0.4 mm) contains uralite.

Alteration: slight (5%–8%).

XRD: smectites with interlayer Na-K and Ca-Mg cations (Ca-Mg > Na-K); illite, chlorite, quartz, and amphibole in trace amounts.

Sample 169-1037B-59R-1, 65–68 cm (Piece 10) [Z-1608]

Olivine-plagioclase phyric basalt, crystallized. Phenocrysts (15%): glomerophyric segregates of olivine (7%) and plagioclase (8%). Grains (0.2–0.4 mm) of olivine are fresh. Tabular and prismatic laths (0.5–1.5 mm) of plagioclase (labradorite [An_{60}]). Groundmass: microlitic texture; microlites and microlaths of plagioclase (30%, andesine [An_{44}]), small (0.05–0.1 mm) rounded grains of pyroxene (50%), and opaque minerals (5%).

Alteration: rock is fresh.

XRD: smectites with interlayer Na-K and Ca-Mg cations (Ca-Mg > Na-K); illite, chlorite, quartz, and amphibole in trace amounts. Black vein: smectites with ~20% mica layers and with interlayer Ca-Mg cations; smectites with interlayer Na-K cations; illite, chlorite, quartz, amphibole, and talc in trace amounts.

Sample 169-1037B-60R-1, 90–95 cm (Piece 11A) [Z-1609]

Aphyric dolerite, fine grained, groundmass is ophitic texture. Rock: tabular and prismatic laths (0.5–1 mm) of plagioclase (45%, labradorite [An_{55}] and andesine [An_{46}]). Interstices: grains of olivine (0.3–0.5 mm, 10%) partly (10%) replaced by biotite, xenomorphic grains (0.5–1 mm) of clinopyroxene (40%), and opaque minerals (2%–3%).

Alteration: slight (~2%–3%).

XRD: smectites with ~20% mica layers and interlayer Mg cations; smectite with interlayer Na cations; illite, chlorite, quartz, amphibole, and talc in trace amounts.

Sample 169-1037B-60R-1, 120–124 cm (Piece 11C) [Z-1610]

Aphyric dolerite, fine grained. Groundmass: ophitic texture. Rock: identical to Sample 169-1037B-60R-1, 90–95 cm (Z-1609).

Alteration: slight (~2%–3%).

Sample 169-1037B-61R-1, 7–10 cm (Piece 1A) [Z-1611]

Aphyric dolerite, medium grained. Groundmass: ophitic-poikilophitic texture. Rock: tabular and prismatic laths (0.5–2.5 mm) of plagioclase (45%, labradorite [An_{60}] and andesine [An_{44}]). Interstices: grains of iddingsitized olivine (0.3–0.4 mm, 2%–3%) and glass (7%) replaced by biotite-like mica. Glass contains opaque minerals (5%). Main volume of rock consists of xenomorphic grains (0.5–2.5 mm) of clinopyroxene. Occasionally clinopyroxene contains abundant inclusions of plagioclase (poikilophitic texture; ~40% of rock).

Alteration: slight (10%).

XRD: smectites with ~10% mica layers and interlayer Ca-Mg cations; smectites with interlayer Na cations, chlorite, quartz, and talc in trace amounts.

Sample 169-1037B-62R-1, 13–17 cm (Piece 2) [Z-1612]

Aphyric dolerite, medium grained. Groundmass: intersertal-ophitic texture. Rock: identical to Sample 169-1037B-61R-1, 7–10 cm (Z-1611).

Alteration: slight (13%).

XRD: smectites with ~10% mica layers and interlayer Ca-Mg cations; trace illite, chlorite, quartz, smectites with interlayer Na cation, and talc.

Sample 169-1037B-62R-3, 52–56 cm (Piece 4) [Z-1613]

Aphyric dolerite, medium grained. Groundmass: ophitic texture. Rock: identical to Samples 169-1037B-61R-1, 7–10 cm (Z-1611) and 169-1037B-62R-1, 13–17 cm (Z-1612).

Alteration: slight (~2%).

XRD: smectites with ~10% mica layers and interlayer Ca-Mg cations; illite, chlorite, quartz, smectites with interlayer Na cation, and talc in trace amounts.

Hole 1038I

Sample 169-1038I-43R-3, 3–7 cm (Piece 2) [Z-1614]

Olivine-plagioclase sparsely phyric basalt. Phenocrysts (5%): glomerophyric segregates of olivine (2%) and plagioclase (3%). Olivine forms small (0.3–0.4 mm) idiomorphic fresh grains. Tabular and prismatic grains (0.2–0.6 mm) of plagioclase (labradorite [An_{56}]). Groundmass: hyalopilitic texture; needle-shaped microlaths of plagioclase (10%–15%, andesine [An_{42}]) and isotropic brown glass (80%–85%).

Alteration: fresh rock.

XRD: smectites with 20%–45% mica layers; chlorite and quartz in trace amounts. Black vein: smectites, chlorite, and quartz.

Gulf of California and off Baja California (Legs 63–65)

Guaymas Basin, Gulf of California (Hole 477)

Sample 64-477-9R-1, 57–59 cm (Piece 10), Unit 1b [Z-1254]

Aphyric dolerite, medium grained, massive. Rock: ophitic texture; various short- and elongated-prismatic laths of plagioclase (0.3–1.5 mm, 50%, labradorite [An_{60}] and andesine [An_{48}]); xenomorphic and partly idiomorphic grains of clinopyroxene (0.2–2 mm, 40%), opaque minerals (8%), and interstitial black glass (1%–2%).

Alteration: fresh; rock is nonoxidized.

XRD: smectite with ~15% mica layers and various interlayer cations of Na-K and Mg-Ca; minor chlorite; trace quartz and amphibole.

Sample 64-477-11R-2, 61–63 cm (Piece 5), Unit 1a [Z-1255]

Sparsely plagioclase-phyric dolerite, coarse grained, massive. Phenocrysts (10%): prismatic crystals of sparsely zonal plagioclase (2.5–5 mm, labradorite [An_{58}]). Small (0.2–0.3 mm), rounded grains of olivine are present. Groundmass: poikilophitic texture; various tabular and prismatic grains of plagioclase (60%, 0.3–1.7 mm, labradorite [An_{58}] and andesine [An_{40}]), xenomorphic grains of clinopyroxene (0.8–2 mm and up to 0.4 mm), rounded grains of olivine (10%, 0.1–0.4 mm), opaque minerals (1%–2%), and interstitial black glass (~5%).

Alteration: slight; rock is nonoxidized; clay mineral replaces glass.

XRD: smectite with ~10% mica layers and various interlayer cations of Na-K and Mg-Ca; minor chlorite with ~5% swelling interlayers, talc, and amphibole; trace quartz.

Sample 64-477-12R-1, 49–52 cm (Piece 4), Unit 1a [Z-1256]

Sparsely plagioclase-phyric dolerite, coarse grained, massive. Groundmass: poikilophitic texture. Rock: identical to Sample 64-477-11R-2, 61–63 cm (Z-1255).

XRD: smectite with ~20% mica layers; minor chlorite with ~5% swelling interlayers, amphibole, and talc; trace quartz.

Sample 64-477-12R-2, 70–73 cm (Piece 3C), Unit 1a [Z-1257]

Sparsely plagioclase-phyric dolerite, coarse grained, massive. Groundmass: poikilophitic texture. Rock: identical to Samples 64-477-12R-1, 49–52 cm (Z-1256), and 64-477-11R-2, 61–63 cm (Z-1255).

XRD: smectite with ~20% mica layers; minor chlorite, defective chlorite, amphibole, and talc; trace quartz.

Sample 64-477-12R-3, 39–42 cm (Piece 3C), Unit 1a [Z-1258]

Sparsely plagioclase-phyric dolerite, coarse grained, massive. Groundmass: poikilophitic texture. Rock: identical to Sample 64-477-12R-2, 70–73 cm (Z-1257).

XRD: smectite with ~10% mica layers and various interlayer cations of Na-K and Mg-Ca; minor chlorite, talc, and amphibole; trace mixed-layer chlorite-smectite mineral with ~15% swelling interlayers, quartz.

Sample 64-477-12R-4, 6–9 cm (Piece 1A), Unit 1a [Z-1259]

Plagioclase-phyric dolerite, coarse grained, massive. Phenocrysts (40%): prismatic large (2–2.7 mm) crystals of plagioclase (labradorite [$An_{62–63}$]). Rims of zonal plagioclase are andesine (An_{42}). Groundmass: poikilophitic texture; various (0.2–1.2 mm) tabular and prismatic grains of plagioclase (50%, andesine [$An_{42–44}$]), xenomorphic grains of clinopyroxene (20%, up to 1.5 mm) and their segregates (0.6–0.8 mm), rounded xenomorphic grains of olivine (10%, 0.3–0.7 mm), opaque minerals (1%–2%), and interstitial altered glass (~2%–3%).

Alteration: slight; rock is nonoxidized; clay mineral replaces glass.

XRD: smectite with ~10% mica layers; minor chlorite with ~5% swelling interlayers and talc; trace amphibole and quartz.

Sample 64-477-12R-4, 76–80 cm (Piece 1E), Unit 1a [Z-1260]

Plagioclase-phyric dolerite, massive. Phenocrysts (30%–35%): prismatic large (2–2.5 mm) tabular and prismatic grains of plagioclase (labradorite [$An_{60–62}$]). Groundmass: poikilophitic texture; prismatic grains and plagioclase laths (25%), xenomorphic grains of clinopyroxene (20%, 1.2–2 mm), almost idiomorphic grains (up to 0.3 mm) of olivine (10%), opaque minerals (1%–2%), and interstitial altered glass (10%) with orthoclase and needle-shaped grains of opaque minerals.

Alteration: slight; rock is nonoxidized; clay mineral replaces glass.

XRD: smectite with ~20% mica layers; minor chlorite and talc; trace amphibole and quartz.

Sample 64-477-12R-5, 46–50 cm (Piece 1H), Unit 1a [Z-1261]

Plagioclase-phyric dolerite, massive. Phenocrysts (40%): prismatic large (1.5–2.5 mm) grains of plagioclase (labradorite [$An_{65–68}$]). One grain of plagioclase is 4.8 mm. Groundmass: ophitic texture; laths of plagioclase (20%, 0.1–0.8 mm, andesine [An_{42}]), xenomorphic grains of clinopyroxene (30%), rounded small (up to 0.3 mm) grains of olivine (5%), opaque minerals (1%), and interstitial altered glass (5%).

Alteration: slight; rock is nonoxidized; clay mineral replaces glass.

XRD: smectite with ~10% mica layers; trace chlorite, talc, and quartz.

Sample 64-477-13R-1, 53–62 cm (Piece 3H), Unit 1a [Z-1262]

Plagioclase-phyric dolerite, fine grained, massive. Phenocrysts (40%): tabular, prismatic, and elongated-prismatic large (2.5–4 mm) grains of plagioclase (labradorite [An_{68}]). Groundmass: doleritic texture; laths of plagioclase (20%, 0.1–0.8 mm, andesine [$An_{42–46}$]), segregate of xenomorphic grains of clinopyroxene (30%), grains of olivine (5%, 0.1–0.3 mm), opaque minerals (2%–3%), and interstitial altered glass (1%–2%).

Alteration: fresh; rock is nonoxidized.

XRD: smectite with ~20% mica layers; trace chlorite and quartz.

Sample 64-477-13R-2, 13–17 cm (Piece 3), Unit 1a [Z-1263]

Plagioclase-phyric dolerite, fine grained, massive. Groundmass: doleritic texture. Rock: identical to Sample 64-477-13R-1, 53–62 cm (Z-1262). One phenocryst of plagioclase is 6 mm.

XRD: smectite with ~20% mica layers; trace chlorite, talc, and quartz; brown veinlet -smectite with ~20% mica layers.

Sample 64-477-13R-2, 146–150 cm (Piece 8), Unit 1a [Z-1264]

Plagioclase-phyric basalt (microdolerite), massive. Phenocrysts (40%): tabular, prismatic, and elongated-prismatic large (1.5–5 mm) grains of plagioclase (labradorite [An_{68}]) and sparse glomerophyric segregates of xenomorphic grains (0.3–0.5 mm) of plagioclase and olivine. Microphenocrysts of idiomorphic olivine grains (2%–3%, 0.5–0.7 mm) are present. Groundmass: microlitic (microdoleritic) texture; microlites (0.1–0.2 mm) and microlaths (0.2–0.5 mm) of plagioclase (20%, andesine [$An_{40–42}$]), segregate of xenomorphic grains (0.1–0.4 mm) of clinopyroxene (30%) and single xenomorphic (0.6–0.7 mm) grains of clinopyroxene, grains of olivine (2%–3%, 0.2–0.3 mm), opaque minerals (5%), and interstitial altered glass (<1%).

Alteration: fresh; rock is nonoxidized; clay mineral replaces glass.

XRD: smectite with ~20% mica layers; trace chlorite, talc, and quartz.

Gulf of California (Hole 483B)

Sample 65-483B-32R-1, 1–6 cm (Piece 1), Unit 10 [Z-1275]

Olivine(?)-plagioclase-phyric basalt, sparsely vesicular. Phenocrysts (20%): tabular zonal (0.7–0.8 mm) and elongated-prismatic laths (0.3–0.7 mm) of plagioclase (15%, andesine [An_{44}]) and their glomerophyric segregates. Microphenocrysts (0.2–0.3 mm) of altered olivine are present (5%). Groundmass: vitrophyric texture; black glass with sparse case-like microlites of plagioclase. Vesicles (3%, 0.1–0.4 mm) are rounded.

Alteration: slight; rock is nonoxidized; clay mineral replaces olivine and completely fills vesicles.

XRD: smectite with ~20% mica layers; trace chlorite and quartz; black veinlet - smectite with ~20% mica layers.

Sample 65-483B-32R-1, 27–31 cm (Piece 2B), Unit 10 [Z-1276]

Plagioclase-phyric basalt, fine grained, spotty structure, sparsely vesicular. Phenocrysts (20%): tabular, prismatic, and elongated-prismatic grains (0.8–2.5 mm) of plagioclase (labradorite [An_{60}]). Groundmass (80%): microlitic texture; glass with segregates of clinopyroxene and plagioclase. Vesicles (2%–3%, 0.2–0.6 mm) are rounded.

Alteration: slight (5%–7%); rock is nonoxidized; vesicles (or grains of olivine?) mainly completely infilled with clay mineral.

XRD: smectite with ~20% mica layers; trace chlorite and quartz.

Sample 65-483B-32R-1, 44–50 cm (Piece 2D), Unit 10 [Z-1277]

Olivine-plagioclase-phyric basalt, fine grained, spotty structure, sparsely vesicular. Phenocrysts (30%): prismatic grains (0.6–1.4 mm) of plagioclase (20%, labradorite [$An_{58–60}$]) and occasionally their glomerophyric segregates.

Altered olivine (0.3–0.8 mm) is present (10%). Groundmass (70%): hyalopilitic-microlitic texture; glass with segregates of clinopyroxene and plagioclase. Single vesicles (<1%, 0.1–0.4 mm) are rounded.

Alteration: slight (10%–12%); rock is nonoxidized; olivine replaced by clay mineral and carbonate; vesicles completely infilled with clay mineral.

XRD: smectite with ~20% mica layers; trace chlorite and quartz.

Sample 65-483B-32R-1, 70–74 cm (Piece 2F), Unit 10 [Z-1278]

Olivine-plagioclase-phyric basalt, sparsely vesicular. Phenocrysts (35%): prismatic grains of plagioclase (25%, labradorite [An_{60}]) and their glomerophyric segregates (0.6–2.5 mm). Altered olivine (15%) forms segregates of idiomorphic grains (0.5–0.7 mm). Groundmass (75%): hyalopilitic-microlitic texture; brownish black glass with crystals of plagioclase, clinopyroxene, and opaque dust. One vesicle (<1%) is present.

Alteration: slight (15%); rock is nonoxidized; olivine replaced by iddingsite, carbonate, and Fe hydroxides; vesicles completely infilled with clay mineral.

XRD: smectite with ~30% mica layers; trace chlorite and quartz. Black veinlet: smectite with ~15% mica layers.

Sample 65-483B-32R-1, 90–94 cm (Piece 3), Unit 10 [Z-1279]

Olivine-plagioclase-phyric basalt, sparsely vesicular. Phenocrysts (40%): tabular (0.6–0.7 mm) and elongated-prismatic (up to 1.2 mm) grains of plagioclase (20%, andesine [An_{42}]). Altered olivine (20%) forms idiomorphic grains (0.3–0.8 mm). Groundmass (60%): hyalopilitic-microlitic texture; black glass and sparse skeletal microlites of plagioclase. Vesicles (1%, 0.05–0.3 mm) are rounded.

Alteration: slight to moderate (20%); rock is nonoxidized; olivine completely replaced by iddingsite; vesicles infilled with clay mineral.

XRD: smectite with ~10% mica layers; trace chlorite; black veinlet - smectite with ~10% mica layers.

Sample 65-483B-32R-2, 95–100 cm (Piece 4A), Unit 10 [Z-1280]

Olivine-plagioclase-phyric basalt, sparsely vesicular. Groundmass: vitrophyric texture. Rock: identical to Sample 65-483B-32R-1, 90–94 cm (Z-1279).

Alteration: slight to moderate (20%); rock is nonoxidized; olivine completely replaced by iddingsite; part of vesicles with 0.3–0.6 mm infilled with clay mineral and opaque minerals.

XRD: smectite; trace chlorite and quartz; black veinlet - smectite with ~10% mica layers.

Sample 65-483B-32R-2, 116–123 cm (Piece 4C), Unit 10 [Z-1281]

Olivine-plagioclase-phyric basalt, spotty structure. Phenocrysts (10%): prismatic grains (0.3–0.9 mm) of plagioclase (5%, labradorite [An_{55}] and andesine [An_{42}]) and their segregates. Altered olivine (5%) forms idiomorphic grains (0.3–0.5 mm). Groundmass (90%): vitrophyric to microdoleritic texture; incompletely crystallized glass. Isometric grains of opaque minerals (5%) are present.

Alteration: slight (5%); olivine completely replaced by green iddingsite.

XRD: smectite with ~15% mica layers; trace quartz; black veinlet - smectite with ~10% mica layers.

Sample 65-483B-32R-2, 135–141 cm (Piece 6A), Unit 10 [Z-1282]

Olivine-plagioclase-phyric basalt. Phenocrysts (30%): prismatic (0.7–2 mm) and elongated-prismatic (0.9–1.8 mm) crystals of plagioclase (15%, labradorite [$An_{61–62}$] and andesine [An_{42}]). Occasionally, plagioclase crystals consist of inclusions of glass. Altered olivine (10%) forms idiomorphic grains (0.5–1.7 mm). Groundmass (70%): pilotaxitic texture; laths and microlites of plagioclase (90%, andesine [An_{40}]), microlites of clinopyroxene, and opaque minerals (5%).

Alteration: slight (15%); olivine completely replaced by greenish brown iddingsite and carbonate.

XRD: smectite with ~20% mica layers; trace chlorite and quartz.

Hole 485A

Sample 65-485A-11R-3, 56–58 cm (Piece 1A), Unit 1 [Z-1283]

Sparsely olivine-plagioclase-phyric basalt. Phenocrysts (~1%): one prismatic microphenocryst (0.5 mm) of plagioclase and one microphenocryst of olivine, which is a segregate of three idiomorphic grains (0.3–0.5 mm). Groundmass: microlitic texture; unoriented microlites (andesine [An_{34}]) and microlaths (labradorite [An_{55}]) of plagioclase (80%) and interstitial glass (20%) with crystallites of clinopyroxene and opaque dust.

Alteration: slight; rock is nonoxidized; clay mineral replaces olivine and completely fills vesicles.

Sample 65-485A-11R-3, 82–84 cm (Piece 1B), Unit 1 [Z-1284]

Olivine-plagioclase-phyric basalt. Phenocrysts (10%): idiomorphic grains (0.5–0.7 mm) of olivine and plagioclase. Groundmass: microlitic texture; microlites and laths (0.1–0.6 mm) of plagioclase (40%, labradorite [An_{55}] and andesine [An_{42}]). Interstices: segregate of small grains of clinopyroxene (45%) and very small grains of opaque minerals (5%).

Alteration: rock is fresh and nonoxidized.

Sample 65-485A-12R-1, 62–64 cm (Piece 4A), Unit 1 [Z-1285]

Olivine-clinopyroxene-plagioclase-phyric basalt. Phenocrysts (10%): glomerophyric segregates of idiomorphic grains (0.3–0.4 mm) of olivine (2%), partly idiomorphic grains (0.2–0.5 mm) of clinopyroxene (3%), and prismatic and elongated-prismatic grains (0.2–0.8 mm) of plagioclase (5%, labradorite [An_{60}] and mainly andesine [An_{42}]). Groundmass: vitrophyric texture; glass with needle-shaped microlites (1%–2%) of plagioclase and segregates of crystallites of clinopyroxene and plagioclase. Small (<0.1 mm) grains of opaque minerals are present (8%–10%).

Alteration: rock is fresh and nonoxidized.

Sample 65-485A-14R-1, 56–60 cm (Piece 1F), Unit 1 [Z-1286]

Plagioclase-phyric dolerite, fine grained. Phenocrysts (15%): prismatic grains (0.6–0.9 mm) of plagioclase (labradorite [An_{56}]) and their segregates. Groundmass: doleritic texture; microlaths (0.2–0.3 mm) and laths (0.3–0.5 mm) of plagioclase (andesine [$An_{40–42}$]). Interstices: segregate of small (0.1–0.3 mm) rounded grains of clinopyroxene (45%). Olivine (5%) and opaque minerals (5%) are present.

Alteration: slight (1%–2%); rock is nonoxidized; olivine partly replaced by iddingsite.

Sample 65-485A-17R-1, 80–83 cm (Piece 5), Unit 2 [Z-1287]

Aphyric dolerite, medium grained. Groundmass: doleritic texture; prismatic and elongated-prismatic grains (0.4–1 mm) of plagioclase (40%, labradorite [An_{54}] and mainly andesine [$An_{38–42}$]). Interstices: xenomorphic grains and segregates of small (0.1–0.3 mm) xenomorphic grains of clinopyroxene (45%), small rounded grains of olivine (3%), and small (0.1 mm) xenomorphic skeletal grains of opaque minerals (10%–12%).

Alteration: slight (3%); rock is nonoxidized; olivine completely replaced by iddingsite.

Sample 65-485A-17R-1, 114–115 cm (Piece 6C), Unit 2 [Z-1288]

Aphyric dolerite, medium grained. Rock: identical to Sample 65-485A-17R-1, 80–83 cm (Z-1287).

Alteration: slight (3%–5%); rock is nonoxidized; olivine completely replaced by iddingsite.

Sample 65-485A-23R-1, 55–56 cm (Piece 4A), Unit 4 [Z-1289]

Olivine-plagioclase-phyric basalt, fine grained. Phenocrysts (10%): idiomorphic grains (0.3–0.4 mm) of olivine (10%). Plagioclase (9%, labradorite [An_{55}]) forms large (up to 2 mm) prismatic crystals of plagioclase or glomerophyric segregates of small (0.5–0.8 mm) tabular crystals. Groundmass: doleritic texture; laths (0.2–0.7 mm) of plagioclase (40%, labradorite [An_{55}] and andesine [An_{42}]). Interstices: segregate of small (0.1 mm) rounded grains of clinopyroxene (45%) and very small (<0.1 mm) grains of opaque minerals (5%).

Alteration: rock is fresh and nonoxidized.

Sample 65-485A-24R-1, 71–73 cm (Piece 1D), Unit 4 [Z-1290]

Aphyric dolerite, coarse grained. Rock: intersertal-poikilophitic texture; prismatic and tabular grains (0.6–2.5 mm) of plagioclase (30%, labradorite [An_{60}] and andesine [An_{45}]). Interstices: xenomorphic grains (0.3–3 mm) of clinopyroxene (30%), small (0.3 mm) rounded grains of olivine (10%), opaque minerals (5%–7%), and altered glass (25%) with skeletal grains of opaque minerals and very small (<0.1 mm) microlites of albite.

Alteration: moderate (30%–35%); rock is nonoxidized; olivine completely replaced by iddingsite; clay mineral replaces interstitial glass.

Sample 65-485A-24R-1, 86–88 cm (Piece 1E), Unit 4 [Z-1291]

Aphyric dolerite, coarse grained. Groundmass: intersertal-poikilophitic texture. Rock: identical to Sample 65-485A-24R-1, 71–73 cm (Z-1290).

Sample 65-485A-26R-1, 16–18 cm (Piece 1B), Unit 4 [Z-1292]

Olivine-plagioclase-phyric, crystallized, basalt. Phenocrysts (10%): single idiomorphic grain of olivine and prismatic crystals (0.8–2.5 mm) of plagioclase (labradorite [An_{60}]). Groundmass: microlitic texture; needle-shaped and skeletal microlites and laths (0.1–0.6 mm) of plagioclase (30%), segregate of small (<0.1 mm) rounded grains of clinopyroxene (55%), and opaque minerals (5%).

Alteration: rock is fresh and nonoxidized; single grain of olivine replaced by iddingsite.

Sample 65-485A-29R-2, 120–122 cm (Piece 3G), Unit 5 [Z-1293]

Aphyric dolerite, medium grained. Rock: doleritic texture; prismatic grains (0.2–1.2 mm) of plagioclase (50%: labradorite [$An_{58–60}$] and andesine [$An_{42–43}$]). Interstices: isometric grains and segregates of clinopyroxene (40%, 0.2–0.6 mm), opaque minerals (5–8%), and altered glass (2%).

Alteration: slight (2%); rock is nonoxidized; interstitial glass completely replaced by clay mineral.

Sample 65-485A-30R-3, 139–140 cm (Piece 1P), Unit 5 [Z-1294]

Gabbro-dolerite, coarse grained. Rock: ophitic texture; prismatic, tabular, and rounded-isometric grains (1.2–5 mm) of plagioclase (60%, labradorite [An_{58}] and andesine [An_{42}]), xenomorphic grains (0.6–5 mm) of clinopyroxene (38%), idiomorphic skeletal grains (up to 0.7 mm) of opaque minerals (10%), and altered interstitial glass (1%–2%) with skeletal grains of opaque minerals.

Alteration: slight (1%–2%); rock is nonoxidized; clay mineral replaces interstitial glass.

Sample 65-485A-31R-2, 36–37 cm (Piece 1P), Unit 5 [Z-1295]

Dolerite, coarse grained. Rock: poikilophitic texture; prismatic and elongated-prismatic grains (0.3–3 mm) of plagioclase (50%, labradorite [$An_{60–62}$] and andesine [An_{40}]), isometric grains (0.5–4 mm) of clinopyroxene (30%) with prismatic crystals of plagioclase, partly idiomorphic grains (0.3–0.6 mm) of olivine (10%), xenomorphic skeletal grains (up to 1 mm) of opaque minerals (8%), and altered interstitial glass (2%).

Alteration: slight; olivine completely replaced by limonite; clay mineral replaces interstitial glass; microcrack (0.2 mm) is filled with clay mineral.

Sample 65-485A-31R-2, 85–88 cm (Piece 1G), Unit 5 [Z-1296]

Dolerite, coarse grained. Groundmass: poikilophitic texture. Rock: identical to Sample 65-485A-31R-2, 36–37 cm (Z-1295).

Alteration: slight; olivine completely replaced by Fe hydroxides; clay mineral replaces interstitial glass.

Sample 65-485A-33R-1, 135–136 cm (Piece 1K), Unit 5 [Z-1297]

Olivine-phyric basalt, medium grained. Phenocrysts (5%): idiomorphic grains (0.5–1.7 mm) of olivine. Groundmass: ophitic texture; prismatic and elongated-prismatic laths (0.3–1 mm) of plagioclase (40%, labradorite [An_{63}] and andesine [An_{42}]). Interstices: xenomorphic grains (0.1–0.7 mm) of clinopyroxene (40%), small (0.1–0.2 mm) grains of olivine (5%), and opaque minerals (10%).

Alteration: slight; olivine completely replaced by iddingsite and Fe hydroxides.

Sample 65-485A-33R-2, 85–87 cm (Piece 1I), Unit 5 [Z-1298]

Olivine-plagioclase-phyric, microdolerite. Phenocrysts (15%): idiomorphic grains (0.8–1.2 mm) of olivine (5%) and prismatic and tabular grains (0.9–1.7 mm) of plagioclase (10%, labradorite [An_{60}]). Groundmass: microdoleritic texture; laths (0.2–0.8 mm) of plagioclase (40%, labradorite [An_{55}] and andesine [An_{42}]), segregate of xenomorphic grains of clinopyroxene (40%), opaque minerals (7%–8%), and grains (0.2 mm) of olivine (1%–2%).

Alteration: slight; rock is nonoxidized; olivine replaced by iddingsite and carbonate.

Sample 65-485A-38R-2, 36–37 cm (Piece 6A), Unit 8 [Z-1299]

Olivine-plagioclase-phyric basalt. Phenocrysts (20%): idiomorphic grains (0.3–0.7 mm) of olivine (5%) and prismatic and elongated-prismatic laths (0.5–1.7 mm) of plagioclase (15%, labradorite [An_{55}]) and their glomerophyric segregates. Occasionally, plagioclase grains consist of inclusions of glass. Groundmass: hyalopilitic texture; needle-shaped microlites (0.1–0.2 mm) and microlaths (0.3–0.6 mm) of plagioclase (30%, andesine [$An_{42–44}$]) and black glass (50%) with crystallites of clinopyroxene.

Alteration: slight; rock is nonoxidized; olivine completely replaced by greenish brown iddingsite.

Sample 65-485A-39R-5, 2–6 cm (Piece 1), Unit 8 [Z-1300]

Aphyric dolerite, medium grained. Rock: intersertal-poikilophitic texture; large (1.5–2.5 mm) isometric grains of augite with abundant inclusions of plagioclase prismatic crystals; small (0.5–0.6 mm) rounded grains of clinopyroxene (50%); prismatic crystals and laths (0.5–1.2 mm) of plagioclase (30%, labradorite [An_{55}] and andesine [An_{42}]); rounded or partly idiomorphic grains altered olivine (10%); opaque minerals (5%–7%); and dark-brown interstitial glass with very small microlites of albite-oligoclase and opaque minerals.

Alteration: slight; olivine completely replaced by greenish brown iddingsite.

Off Southern California (Hole 473)

Sample 63-473-29R-1, 85–90 cm (Piece 6D), Unit 1 [Z-1245]

Plagioclase-phyric dolerite, fine grained. Phenocrysts (10%): elongated-prismatic and zonal tabular grains (0.8–1.5 mm) of plagioclase (labradorite [An_{55}]) and their segregates. Groundmass (90%): intersertal-doleritic texture; unoriented laths (0.1–0.4 mm) of plagioclase (50%, labradorite [An_{55}]). Interstices: segregate of small (0.1–0.2 mm) grains of clinopyroxene (35%), opaque minerals (5%), and greenish brown altered glass (some areas of glass are black).

Alteration: slight (5%–7%); rock is nonoxidized; interstitial glass replaced by clay mineral.

XRD: smectite with ~20% mica layers; trace quartz; dark-brown crust - smectite with ~10% mica layers and aragonite.

Sample 63-473-30R-2, 126–134 cm (Piece 3A), Unit 1 [Z-1246]

Aphyric dolerite, medium grained. Rock: intersertal-doleritic texture; prismatic grains (0.2–1.2 mm) of plagioclase (40%, labradorite [$An_{55–58}$]). Interstices: segregate of small (0.1–0.3 mm) xenomorphic grains of clinopyroxene (40%), opaque minerals (5%), and dark-brown glass (15%–20%).

Alteration: rock is fresh and nonoxidized.

Sample 63-473-32R-2, 133–140 cm (Piece 5L), Unit 1 [Z-1247]

Aphyric dolerite, fine grained, vesicular. Rock: intersertal-doleritic texture; unoriented laths (0.3–0.6 mm) of plagioclase (35%, labradorite [An_{65}] and labradorite [An_{54}]). Interstices: segregate of small (0.1–0.3 mm) xenomorphic grains of clinopyroxene (30%), opaque minerals (8%–10%), and glass (5%). Vesicles (20%, 0.5–1.2 mm) are rounded in shape.

Alteration: moderate (20%–25%); rock is nonoxidized; clay mineral replaces interstitial glass; vesicles are filled with celadonite(?).

XRD: smectite with ~20% mica layers; trace quartz. Dark veinlet: smectite with ~15% mica layers and trace defective chlorite. Vesicles infilled by smectite.

Sample 63-473-32R-3, 51–57 cm (Piece 1F), Unit 1 [Z-1248]

Aphyric dolerite, fine grained, vesicular. Groundmass: intersertal-doleritic texture. Rock: identical to Sample 63-473-32R-2, 133–140 cm (Z-1240).

Baja California (Hole 469)

Sample 63-469-40R-1, 30–32 cm (Piece 1A) [Z-1229]

Aphyric andesite-basalt, crystallized, fine grained. Rock: intersertal texture; unoriented microlites and microlaths (0.1–0.4 mm) of plagioclase (60%, andesine [An_{48}]). Interstices: segregate of very small grains of clinopyroxene (5%–10%), opaque minerals (5%), altered glass (25%), and carbonate (5%).

Alteration: moderate (20%–25%); rock is nonoxidized; clay mineral replaces interstitial glass.

XRD: smectite with ~20% mica layers; trace chlorite and quartz.

Sample 63-469-42R-1, 117–120 cm (Piece 1D) [Z-1230]

Aphyric andesite-basalt with intersertal groundmass texture, crystallized, fine grained. Rock: identical to Sample 63-469-40R-1, 30–32 cm (Z-1229).

Alteration: rock is fresh and nonoxidized.

XRD: smectite with ~20% mica layers; trace amphibole and quartz.

Sample 63-469-42R-5, 112–115cm (Piece 1C) [Z-1231]

Aphyric andesite-basalt with intersertal groundmass texture, crystallized, fine grained. Rock: identical to Sample 63-469-42R-1, 117–120 cm (Z-1230).

Alteration: rock is fresh and nonoxidized.

XRD: smectite with ~15%–20% mica layers.

Sample 63-469-44R-1, 3–8cm (Piece 1B) [Z-1232]

Aphyric basalt, sparsely vesicular. Rock: pilotaxitic texture; microlites of plagioclase (35%, andesine [An_{48}] and labradorite [An_{50}]). Interstices: very small microlites of clinopyroxene (50%), opaque dust (5%), and altered glass (5%). Vesicles (5%, 0.2–0.3 mm) are rounded. Several vesicles are filled with black glass.

Alteration: slight (5%–10%); rock is nonoxidized; interstitial glass partly replaced by clay mineral; vesicles mainly are filled with clay mineral.

XRD: smectite with ~10% mica layers; black veinlet: smectite with ~10% mica layers; white veinlet: calcite and smectite with interlayer Na cation.

Sample 63-469-46R-1, 134–138cm (Piece 11) [Z-1233]

Sparsely clinopyroxene-plagioclase-phyric basalt, sparsely vesicular. Phenocrysts: two glomerophyric segregates are represented by prismatic grains (0.2–0.3 mm) of plagioclase (labradorite [An_{52}]) and single grains (0.2–0.3 mm) of clinopyroxene. Groundmass: pilotaxitic texture; unoriented microlites (0.1–0.3 mm) of plagioclase (40%, andesine [An_{46}]) and interstitial glass (40%) with crystals of clinopyroxene and oval grains of opaque dust (10%). Vesicles (5%, 0.1 mm) are rounded.

Alteration: slight; rock is nonoxidized; vesicles mainly are filled with clay mineral.

XRD: smectite with ~15%–20% mica layers.

Sample 63-469-48R-1, 22–28cm (Piece 1D) [Z-1234]

Glassy crust of basalt.

Alteration: very strong (60%–70%); glass almost completely replaced by green clay mineral (80%–85%) and Fe hydroxides (15%–20%).

XRD: smectite with ~10% mica layers.

Sample 63-469-48R-1, 49–53cm (Piece 5A) [Z-1235]

Glassy crust of basalt.

Alteration: rock is fresh and nonoxidized.

XRD: smectite with ~10% mica layers and with different interlayer Na-K and Mg-Ca cations; trace quartz.

Sample 63-469-49R-1, 84–88cm (Piece 8A) [Z-1236]

Sparsely plagioclase-phyric basalt. Phenocrysts: single glomerophyric segregate; prismatic grains (0.3–1.5 mm) of plagioclase. Groundmass: vitrophyric texture; brown and light brown glass. light brown glass consists of crystallites of clinopyroxene, plagioclase, and opaque dust.

Alteration: rock is fresh and nonoxidized.

Sample 63-469-50R-2, 27–32cm (Piece 3A) [Z-1237]

Aphyric basalt, sparsely vesicular. Rock with vitrophyric texture; brownish green glass with crystallites of plagioclase and opaque dust. Several vesicles (<0.1 mm) are filled with glass.

Alteration: rock is fresh and nonoxidized.

XRD: smectite with ~10% mica layers; white inclusions from glass - calcite.

Sample 63-469-51R-1, 34–40cm (Piece 3) [Z-1238]

Aphyric basalt, sparsely vesicular. Rock: vitrophyric texture; black glass with crystals of plagioclase and clinopyroxene. Vesicles (2%–3%, 0.05–0.2mm) are filled by brownish green glass. One vesicle (0.6 mm) is empty, wall of vesicle is lined with clay mineral.

Alteration: rock is fresh and nonoxidized.

XRD: smectite with ~10% mica layers; trace quartz.

Hole 471

Sample 63-471-80R-1, 135–140 cm (Piece 9A), Unit 2 [Z-1239]

Dolerite and tuff (breccia) contact.

Aphyric dolerite, medium grained. Rock: ophitic-intersertal texture; elongated-prismatic grains (0.7–2.5 mm) of zonal plagioclase with undulatory extinction (50%, from andesine [An_{42}] to labradorite [An_{55}]). Central part of plagioclase consists of inclusions of glass. Interstices: isometric grains of Ti-augite (20%), volcanic glass (25%), and small (0.2 mm) isometric and needle-shaped grains (up to 1 mm) of opaque minerals (5%).

Tuff (breccia): fragments (10%, 0.3–2 mm) of clayey chert and angular small (0.1–0.3 mm) fragments (70%) of plagioclase grains, altered green volcanic glass, and opaque minerals. Cement: clayey chert matter.

Alteration: rock is nonoxidized; dolerite is moderately to highly altered (40%–50%). Glass from plagioclase grains and interstitial glass completely replaced by chlorite; augite partly replaced by chlorite; breccia of tuff: volcanic glass replaced by chlorite; clayey chert cement partly is chloritized.

XRD: corrensite; minor quartz; trace mixed-layer chlorite-smectite mineral and calcite.

Sample 63-471-82R-1, 127–132 cm (Piece 9), Unit 3 [Z-1240]

Aphyric dolerite, medium grained. Rock: intersertal-doleritic texture; elongated-prismatic laths (0.5–0.7 mm) of zonal plagioclase (40%). Interstices: segregate of small grains of clinopyroxene (20%), opaque minerals (10%, 0.01–0.1 mm), and altered glass (30%).

Alteration: moderate (40%–45%); rock is nonoxidized; plagioclase partly (30%–40%) replaced by albite, sosurite, and chlorite; interstitial glass completely replaced by chlorite.

XRD: corrensite; minor mixed-layer chlorite-smectite mineral; black vein - corrensite; trace calcite and chlorite.

Sample 63-471-82R-2, 15–18 cm (Piece 1B), Unit 3 [Z-1241]

Aphyric dolerite, medium grained. Rock: identical to Sample 63-471-82R-1, 127–132 cm (Z-1240).

Alteration: moderate (40%–45%); rock is nonoxidized; plagioclase partly (30%–40%) replaced by albite and chlorite; interstitial glass completely replaced by chlorite.

XRD: corrensite and mixed-layer chlorite-smectite mineral; trace quartz.

Sample 63-471-84R-1, 9–16 cm (Piece 2A), Unit 3 [Z-1242]

Aphyric dolerite, medium grained. Rock: ophitic-intersertal texture; elongated-prismatic grains (0.7–2.5 mm) of zonal plagioclase (50%, labradorite [An_{50}] and labradorite [An_{55}]) with undulatory extinction. Central parts of plagioclase grains consist of inclusions of altered glass. Interstices: xenomorphic grains of clinopyroxene (10%), idiomorphic large (0.7–0.8 mm), occasionally skeletal, grains of opaque minerals (7%–8%), and altered glass (30%–35%).

Alteration: strong (50%); rock is nonoxidized; glass from plagioclase and interstitial glass completely replaced by clay mineral.

XRD: smectite with ~15% mica layers; trace chlorite and quartz.

Sample 63-471-84R-1, 107–114 cm (Piece 6G), Unit 3 [Z-1243]

Aphyric dolerite, coarse grained. Rock: intersertal-poikilophitic texture; tabular (0.5–0.7 mm) and elongated-prismatic (up to 5 mm) grains of zonal plagioclase (40%, labradorite [$An_{58–62}$]) with undulatory extinction. Central parts of plagioclase grains consist of inclusions of altered glass. Interstices: xenomorphic grains of clinopyroxene and small segregates of clinopyroxene and plagioclase, opaque minerals (10%), and altered glass (10%).

Alteration: slight; rock is nonoxidized; glass from plagioclase and interstitial glass completely replaced by clay mineral; some areas of interstices consist of small idiomorphic grains of albite, orthoclase, chlorite, and abundant needles of apatite.

XRD: smectite with ~10% mica layers; trace chlorite, defective chlorite, and quartz.

Sample 63-471-87R-2, 19–26 cm (Piece 1B), Unit 3 [Z-1244]

Aphyric dolerite, coarse grained. Rock: intersertal-ophitic texture; tabular (0.7–0.9 mm) and elongated-prismatic (up to 4.5 mm) grains of plagioclase (50%, labradorite [An_{60}]). Interstices: xenomorphic grains (0.5–0.8 mm, up to 1.2 mm) of clinopyroxene, opaque minerals (5%), and altered glass (10%). Occasionally, several interstices consist of small idiomorphic grains of albite, orthoclase, chlorite, and abundant needles of apatite.

Alteration: slight; rock is nonoxidized; interstitial glass completely replaced by clay mineral; some areas of interstices consist of albite, clay mineral, and needles of apatite.

XRD: smectite with ~10% mica layers; trace chlorite and quartz; brown veinlet - smectite with ~5% mica layers; trace chlorite and quartz.

Mid Atlantic Ridge (Leg 37)

Hole 332B

Sample 37-332B-1R-5, 121–124 cm (Piece 11), Unit 1-1 [Z-280]

Plagioclase-phyric (phenocrysts 0.8–3 mm, 25%) basalt, incompletely crystallized, vesicular. Groundmass: subvariolitic texture; volcanic glass, microlites of clinopyroxene, laths of plagioclase, and opaque minerals. Vesicles (0.2–0.5 mm, 5%–10%) are rounded in shape.

Alteration: slight (~5%–10%); rock is poorly oxidized; vesicles partly infilled by smectites, occasionally by calcite.

XRD: smectites with interlayer Na-K and Mg-Ca cations; trace hydromica with swelling layers (~5%).

Sample 37-332B-2R-2, 100–103 cm (Piece 11), Unit 1-1 [Z-501]

Plagioclase-phyric basalt, vesicular. Phenocrysts: large idiomorphic prismatic grains of plagioclase (2–4 mm, 50%, labradorite [An_{56}]); second generation of phenocrysts include more small (0.5–0.8 mm) tabular grains of plagioclase (labradorite [An_{52}]). Groundmass: hyalopilitic texture; needle-shaped microlites of plagioclase and clinopyroxene, and black volcanic glass. Vesicles (0.3–0.5 mm, 3%–5%) are rounded.

Alteration: rock is fresh.

Sample 37-332B-2R-3, 91–94 cm (Piece 8), Unit 1-1 [Z-502]

Plagioclase-phyric basalt, vesicular (5%), groundmass is hyalopilitic texture. Rock is identical to Sample 37-332B-2R-2, 100–103 cm (Z-501). There are very large glomerophyric segregates of plagioclase (13 mm), several grains to 5 mm. One grain of olivine (0.2 mm) is present.

Alteration: rock is fresh.

Sample 37-332B-6R-1, 94–96 cm (Piece 10), Unit 2-3 [Z-281]

Aphyric basalt, massive, incompletely crystallized, sparsely vesicular. Groundmass demonstrates poorly expressed subvariolitic texture; volcanic glass, sparse microlites of clinopyroxene, laths of plagioclase, and opaque minerals. Vesicles (0.2–0.3 mm, ~3%) are often empty.

Alteration: slight (<5%); rock is slightly oxidized; single vesicles are filled with smectites.

XRD: smectite.

Electron micrograph: b = 9.21Å (trioctahedral smectite).

Sample 37-332B-11R-1, 58–60 cm (Piece 3D), Unit 3A-7 [Z-282]

Plagioclase-phyric (phenocrysts to 2 mm, 5%) basalt with doleritic texture. Groundmass: laths of plagioclase, microlites of clinopyroxene, single grains of olivine, and sparse (~3%) opaque minerals.

Alteration: slight (~5%); olivine and clinopyroxene are replaced with smectite.

XRD: smectites, mixed-layer smectite-illite mineral with ~40% mica layers; trace hydromica with swelling interlayers (~20%).

Electron micrograph: b = 9.18 Å (trioctahedral smectite).

Sample 37-332B-14R-2, 23-26 cm (Piece 2), Unit 3B-8 [Z-503]

Plagioclase-phyric basalt with microlitic texture, vesicular. Phenocrysts: small prismatic grains of plagioclase (15%, 0.5–1.5 mm, labradorite [An_{62}]) and segregates of plagioclase. Groundmass: needle-shaped microlaths and microlites of plagioclase (labradorite [An_{56}]) and microlites of clinopyroxene (panicle segregates). Vesicles are rounded (0.5–1 mm, 20%) and infilled partially and completely with glass, some vesicles are empty.

Alteration: rock is fresh.

Sample 37-332B-16R-2, 37–40 cm (Piece 5), Unit 4-12 [Z-283]

Sparsely clinopyroxene-phyric basalt, phenocrysts ~1 mm and glomerocrysts to 4 mm (15%–20%). Groundmass: subvariolitic texture; volcanic glass, microlites of clinopyroxene, laths of plagioclase, and admixture of opaque minerals. Vesicles (0.2–0.5 mm, ~5%) are present.

Alteration: slight (~10%); rock is slightly oxidized; vesicles are rimed with smectites.

XRD: smectite.

Electron micrograph: b = 9.19 Å (trioctahedral smectite).

Sample 37-332B-17R-1, 97–103 cm (Piece 13), Unit 4-12 [Z-284]

Micro-clinopyroxene-phyric (microphenocrysts 0.3–0.4 mm, ~5%) basalt, poorly crystallized, vesicular (0.2–0.5 mm, ~5%–10%). Groundmass: variolitic texture; volcanic glass, xenomorphic microlites of clinopyroxene, laths of plagioclase, and opaque minerals.

Alteration: slight (~5%); rock is slightly oxidized; vesicles are filled with smectites.

XRD: smectite.

Sample 37-332B-21R-1, 12-15 cm (Piece 1å), Unit 4-13 [Z-285]

Olivine-clinopyroxene-phyric (phenocrysts of clinopyroxene 1–2.5 mm, 15%; phenocrysts of olivine 1–2.5 mm, 5%) basalt, poorly crystallized, vesicular (0.2–0.4 mm, ~5%). Groundmass: subvariolitic texture; volcanic glass, xenomorphic microlites of clinopyroxene, laths of plagioclase, and opaque minerals. Single crystals of picotite are present.

Alteration: slight; vesicles are rimed with smectites.

XRD: smectite; chlorite in trace amounts.

Electron micrograph: b = 9.24 Å (trioctahedral smectite).

Sample 37-332B-22R-1, 105–108 cm (Piece 9), Unit 5-14 [Z-286]

Clinopyroxene-plagioclase-phyric basalt, poorly crystallized, vesicular (0.1–0.5 mm, ~5%), phenocrysts of plagioclase (~70%) and clinopyroxene (~30%) to 0.2 mm form glomerocrysts. Groundmass: subvariolitic texture; volcanic glass, xenomorphic microlites of clinopyroxene, laths of plagioclase, and opaque minerals. Some vesicles are filled with volcanic glass which contains thin opaque dust.

Alteration: slight (~5%); vesicles are rimed with smectites.

XRD: smectite.

Electron micrograph: b = 9.19 Å (trioctahedral smectite).

Sample 37-332B-22R-2, 106–108 cm (Piece 12), Unit 5-14 [Z-504]

Sparsely plagioclase-phyric basalt, vesicular. Phenocrysts: glomerophyric segregates of prismatic plagioclase grains (5%, 0.5–0.8 mm, labradorite [An_{56}]). Groundmass: pilotaxitic texture; needle-shaped microlaths and microlites of plagioclase (labradorite [An_{52}]) and black volcanic glass. Vesicles are rounded (0.4–0.6 mm, 10%).

Alteration: rock is fresh; some vesicles are empty to partially filled with zeolite or carbonate; veinlet (0.2 mm) consists of zeolite and carbonate.

Sample 37-332B-24R-2, 21–25 cm (Piece 2), Unit 5-14 [Z-505]

Olivine-plagioclase-phyric basalt, vesicular. Phenocrysts: glomerophyric segregates of prismatic plagioclase grains (7%–8%, up to 0.3–1.5 mm, labradorite [$An_{55–57}$]). Glomerophyric segregates consist of small (0.3–0.4 mm) grains of olivine (1%). Groundmass: pilotaxitic texture; needle-shaped microlaths and microlites of plagioclase (labradorite [An_{52}]) and black volcanic glass. Vesicles are rounded (0.2-0.4 mm, 8%–10%) and filled with glass.

Alteration: rock is fresh; olivine replaced by iddingsite.

Sample 37-332B-24R-1, 71–75 cm (Piece 8), Unit 5-15 [Z-287]

Clinopyroxene-plagioclase-phyric basalt, poorly crystallized, vesicular (0.2–0.5 mm, ~5%) Phenocrysts of plagioclase (~70%) and clinopyroxene (~30%) form glomerocrysts. Groundmass: subvariolitic texture; volcanic glass, xenomorphic microlites of clinopyroxene, laths of plagioclase, and opaque minerals. Some vesicles are filled with volcanic glass which contains thin opaque dust.

Alteration: slight (~5%); interstitial glass and clinopyroxene are replaced with smectite; vesicles are rimed with smectites.

XRD: smectite.

Electron micrograph: b = 9.30 Å (smectite with high content of Fe^{++}).

Sample 37-332B-29R-1, 94–98 cm (Piece 5D), Unit 6-19 [Z-288]

Olivine-clinopyroxene-plagioclase-phyric basalt, crystallized, vesicular (0.1–1.5 mm, ~10%). Phenocrysts of clinopyroxene (5%) are 1.1–1.2 mm. Small phenocrysts of olivine (0.1–0.7 mm) and plagioclase laths (to 0.8 mm) are present also. Groundmass texture is subvariolitic. Some vesicles are filled with volcanic glass.

Alteration: slight (~10%); rock is slightly oxidized; vesicles are filled with smectites, occasionally with calcite.

XRD: smectite.

Sample 37-332B-33R-1, 96–99 cm (Piece 10E), Unit 6-20 [Z-506]

Aphyric basalt (microdolerite), vesicular. Groundmass: intersertal-microdoleritic texture; laths of plagioclase (0.2–0.5 mm, labradorite [An_{55}]). Interstices: panicle like segregates of clinopyroxene. Volcanic glass with opaque dust is present also. Vesicles (0.2–0.6 mm, 15%) are rounded.

Alteration: rock is fresh; glass partly replaced by chlorite and palagonite; vesicles are filled with carbonate and palagonite.

Sample 37-332B-33R-2, 30–33 cm (Piece 2), Unit 6-21 [Z-289]

Olivine-clinopyroxene-phyric (phenocrysts to 2.5 mm, 10%) basalt, poorly crystallized, massive. Groundmass: subvariolitic texture; volcanic glass impregnated with opaque dust; laths of plagioclase often form quench-crystals.

Alteration: slight (5%–7%); olivine is replaced with smectite and carbonate; smectites replace interstitial volcanic glass and clinopyroxene.

XRD: smectite; trace talc(?).

Sample 37-332B-35R-1, 131–134 cm (Piece 6J), Unit 7-23 [Z-507]

Olivine-phyric dolerite, sparsely vesicular. Phenocrysts: large idiomorphic crystals (25%, 1.2–6 mm). Occasionally plagioclase crystals include grains of opaque minerals (0.4 mm). Groundmass: doleritic texture; laths of plagioclase (labradorite [$An_{56–58}$]). Interstices consist of small xenomorphic grains of olivine and panicle-like segregates of clinopyroxene. Glass is present (3%–5%). Vesicles (0.3–0.5 mm, 7%–8%) are rounded.

Alteration: rock is fresh; glass replaced by chlorite; vesicles infilled with carbonate and palagonite.

Sample 37-332B-37R-1, 100–104 cm (Piece 13), Unit 8-25 [Z-508]

Olivine-plagioclase-phyric basalt, vesicular. Phenocrysts: prismatic grains of plagioclase (15%, 0.5–0.8 mm, labradorite [An_{62}]). Olivine: small (0.1 mm) idiomorphic grains. Groundmass: hyalopilitic texture; needle-shaped microlaths and microlites of plagioclase and black glass. Vesicles (0.05–0.3–0.6 mm) are present.

Alteration: slight; olivine completely replaced by chlorite(?); vesicles infilled with clay mineral.

Sample 37-332B-37R-3, 17–20 cm (Piece 2), Unit 9-26 [Z-290]

Olivine-clinopyroxene-microphyric (phenocrysts to 1.2 mm, 5%) basalt, poorly crystallized, vesicular (0.5–0.8 mm, 20%). Groundmass: subvariolitic texture; volcanic glass, microlites of clinopyroxene, laths of plagioclase, and admixture of opaque minerals. Single crystals of picotite (0.8 mm) are present.

Alteration: slight to moderate (~20%); rock is oxidized through bands along zones of concentration of vesicles; some vesicles are filled palagonitized volcanic glass; some vesicles are filled with calcite; most filled vesicles demonstrate zonality in distribution of intercalating palagonite, smectite, and opaque minerals; some vesicles show rim of oxidized opaque minerals.

XRD: smectite.

Electron micrograph: b = 9.30 Å (smectite with high content of Fe^{++}).

Sample 37-332B-41R-1, 65–69 cm (Piece 6å), Unit 9-32 [Z-291]

Olivine-clinopyroxene-phyric basalt, almost completely crystallized, vesicular (0.5–0.8 mm, 15%). Groundmass: poorly expressed subvariolitic texture; microlites of clinopyroxene, small laths of plagioclase, and opaque minerals. Vesicles are rounded.

Alteration: slight (~15%); vesicles are filled with smectite; smectites replace interstitial volcanic glass, groundmass clinopyroxene, and fill cracks.

XRD: smectite.

Electron micrograph: b = 9.22 Å (trioctahedral smectite).

Sample 37-332B-42R-1, 63–66 cm (Piece 3D), Unit 9-36 [Z-509]

Aphyric basalt (dolerite), massive. Groundmass: intersertal-microdoleritic texture; laths of plagioclase (0.1–0.7 mm, labradorite [An_{56}]). Interstices: brownish-green glass with opaque dust and segregate of small pyroxene grains.

Alteration: slight; clay mineral replaces interstitial volcanic glass and clinopyroxene.

Sample 37-332B-42R-2, 22–25 cm (Piece 1C), Unit 9-38 [Z-292]

Aphyric basalt, sparsely vesicular. Groundmass: poorly expressed intersertal texture; volcanic glass with opaque dust, laths of plagioclase, microlites of clinopyroxene, and sparse olivine. Vesicles (0.2–0.3 mm, 3%) are rounded.

Alteration: slight; rock is slightly oxidized; vesicles are filled with smectite.

XRD: smectite.

Sample 37-332B-43R-1, 132–136 cm (Piece 8C), Unit 10-41 [Z-293]

Plagioclase-phyric (phenocrysts to 5 mm) basalt, glomerophyric, sparsely vesicular. Groundmass: subvariolitic texture; volcanic glass with opaque dust, microlites of clinopyroxene, and laths of plagioclase. Vesicles (up to 0.5 mm, 15%) are rounded.

Alteration: slight (~5%); smectites replace interstitial volcanic glass.

XRD: smectite.

Electron micrograph: b = 9.29 Å (trioctahedral smectite).

Sample 37-332B-43R-2, 28–31 cm (Piece 1C), Unit 10-41 [Z-294]

Plagioclase-phyric (phenocrysts to 4 mm) basalt, glomerophyric, and vesicular. Groundmass: hyalopilitic texture; volcanic glass with opaque dust, microlites of clinopyroxene, and laths of plagioclase. Vesicles (0.2–0.5 mm, 7%) are empty. Single vesicles are filled with volcanic glass which contains opaque dust.

Alteration: slight; smectites replace interstitial volcanic glass and groundmass clinopyroxene.

XRD: smectite containing ~10% of mica layers.

Electron micrograph: b = 9.18 Å (trioctahedral smectite).

Sample 37-332B-43R-3, 47–50 cm (Piece 2D), Unit 10-41 [Z-510]

Aphyric basalt, partly brecciated, highly vesicular. Groundmass: vitrophyric texture; needle-shaped microlites of plagioclase (up to 40%–50%) and black glass. Vesicles (~30%, 0.5 mm) are isometric.

Alteration: very strong (70%); vesicles are lined with chlorite; fragments (~0.1 cm) of basalt are cemented by clay mineral.

XRD: smectite; minor mixed-layer chlorite-smectite mineral.

Sample 37-332B-46R-2, 60–63 cm (Piece 3B), Unit 10-44 [Z-295]

Aphyric basalt, vesicular (0.1–0.8 mm, 20%). Groundmass: volcanic glass, laths of plagioclase, xenomorphic microlites of clinopyroxene.

Alteration: slight to moderate (~20%); vesicles are filled with smectite; smectites replace volcanic glass and clinopyroxene.

XRD: smectite containing ~10% of mica layers; trace hydromica.

Electron micrograph: b = 9.23 Å (trioctahedral smectite).

Sample 37-332B-48R-1, 73–76 cm (Piece 6), Unit 11-45 [Z-296]

Hyaloclastic breccia. Fragments (up to 2–4 mm) of chilled glass in groundmass of palagonized volcanic glass. Chilled glass contains small crystals of olivine and opaque minerals. Palagonized volcanic glass contains areas enriched in thinly dispersed opaque minerals.

Alteration: slight (~15%); rock is strongly oxidized; siliceous vein are present.

Serocki Volcano, Mid Atlantic Ridge Rift Valley (Leg 106)

Hole 648B

Sample 106-648B-1R-1, 69–70 cm (Piece 12), Unit 3 [Z-106]

Sparsely plagioclase-phyric hyalobasalt, poorly crystallized, massive. Phenocrysts: plagioclase (1–3 mm, 5%–7%). Groundmass: microsubvariolitic texture; black devitrified glass with rare radial laths of plagioclase (mostly quench crystals) and opaque dust. Olivine occurs in small amounts (<1%).

Alteration: rock is fresh.

XRD: trace smectite.

Sample 106-648B-1R-2, 85–88 cm (Piece 15), Unit 9 [Z-107]

Sparsely olivine-plagioclase-phyric hyalobasalt, poorly crystallized, massive. Phenocrysts: plagioclase (3%–5%). Groundmass: microsubvariolitic texture; black devitrified glass with rare radial laths of quench of plagioclase and opaque dust. Olivine is registered in small (1%) amounts.

Alteration: rock is fresh.

XRD: smectite and quartz in trace amounts.

Sample 106-648B-1R-3, 60–65 cm (Piece 12), Unit 14 [Z-108]

Sparsely micro-plagioclase-phyric hyalobasalt, poorly crystallized, massive. Microphenocrysts of plagioclase (<1%). Groundmass: hyalovariolitic texture; black volcanic glass with rare radial laths of plagioclase (mostly quench crystals) and opaque dust.

Alteration: rock is fresh.

XRD: smectite and quartz in trace amounts.

Sample 106-648B-3R-1, 85–87 cm (Piece 14), Unit 20 [Z-109]

Sparsely micro-plagioclase-phyric hyalobasalt, massive. Microphenocrysts of plagioclase (<1%) occasionally as quench crystals. Groundmass: hyaline to subvariolitic texture; black volcanic glass.

Alteration: rock is fresh; single vesicles are filled by opaque minerals.

XRD: trace quartz.

Sample 106-648B-4R-1, 15–18 cm (Piece 4), Unit 21 [Z-110]

Sparsely olivine-plagioclase-phyric hyalobasalt, poorly crystallized, massive. Phenocrysts of plagioclase (3%–5%) and single crystals of olivine. Groundmass: subvariolitic texture; black volcanic glass with subradial laths of quench crystals of plagioclase and opaque dust. Olivine is present in small (1%) amounts.

Alteration: rock is fresh.

XRD: trace quartz.

Sample 106-648B-4R-1, 61–64 cm (Piece 12), Unit 23 [Z-111]

Sparsely plagioclase-phyric hyalobasalt, poorly crystallized, sparsely vesicular. Phenocrysts: plagioclase (3%–5%). Groundmass: hyalotaxitic texture; black volcanic glass with quench laths of plagioclase and opaque dust. Vesicles (0.1–0.7 mm) are empty.

Alteration: rock is fresh; glass is palagonized through patches.

XRD: trace quartz.

Sample 106-648B-5R-1, 15–22 cm (Piece 4), Unit 24 [Z-112]

Sparsely micro-plagioclase-phyric hyalobasalt, poorly crystallized, massive. Groundmass: black volcanic glass with quench laths of plagioclase and opaque dust. Texture of rock is subvariolitic, pilotaxitic. Single vesicles (<0.5 mm).

Alteration: rock is fresh, nonoxidized.

XRD: smectite and quartz in trace amounts.

Sample 106-648B-6R-1, 1–3 cm (Piece 1), Unit 25 [Z-113]

Sparsely plagioclase-microphyric hyalobasalt, poorly crystallized, massive, with single microphenocrysts of olivine. Groundmass: subvariolitic texture; black devitrified glass with laths of plagioclase and opaque dust. Single vesicles (0.03 mm) are empty.

Alteration: rock is fresh, nonoxidized.

XRD: feldspars and amorphous matter.

Nauru Basin (Leg 61)

Hole 462

Sample 61-462-60R-2, 135–138 cm (Piece 9), Unit 1 [Z-1198]

Olivine-clinopyroxene-plagioclase-phyric basalt. Phenocrysts (20%): glomerophyric segregates of idiomorphic grains (0.3–0.4 mm) of olivine (2%), xenomorphic grains (0.1–0.3 mm) of clinopyroxene (3%), and laths (0.2–0.7 mm) of plagioclase (15%, andesine [An_{46}]). Groundmass (80%): vitrophyric texture; glass with crystallites of clinopyroxene, plagioclase, and opaque dust.

Alteration: slight; rock is nonoxidized; olivine completely replaced by green iddingsite.

Sample 61-462-61R-1, 48–50 cm (Piece 3B), Unit 6 [Z-1199]

Olivine-plagioclase-phyric basalt, crystallized. Phenocrysts (15%): glomerophyric segregates of idiomorphic grains (0.2–0.5 mm) of olivine (8%) and plagioclase. Plagioclase (10%, labradorite [An_{55}]) forms prismatic grains and laths (0.4–0.6 mm). Groundmass: microlitic texture; plagioclase (25%, andesine [An_{42}]), segregate of small (0.1–0.3 mm) rounded or isometric grains of clinopyroxene (50%), and opaque minerals (10%).

Alteration: slight; olivine completely replaced by brown iddingsite.

Sample 61-462-62R-2, 135–137 cm (Piece 9), Unit 8 [Z-1200]

Plagioclase-olivine-clinopyroxene-phyric basalt. Phenocrysts (20%): glomerophyric segregates of isometric grains (0.3–0.4 mm) of clinopyroxene (10%); olivine (7%, 0.1–0.3 mm); laths (0.2–0.4 mm) of plagioclase (3%). Groundmass (80%): microlitic texture; microlites of plagioclase (25%), clinopyroxene (50%), and opaque minerals (5%).

Alteration: slight; olivine completely replaced by brown iddingsite.

Sample 61-462-63R-2, 18–22 cm (Piece 1), Unit 10 [Z-1201]

Aphyric dolerite, fine grained. Rock with intersertal-ophitic texture; laths (0.1–0.6 mm) of plagioclase (40%, labradorite [An_{60}] and andesine [$An_{46–48}$]). Interstices: segregates of idiomorphic grains (0.1–0.5 mm) of clinopyroxene (35%), opaque minerals (5%), and altered brown and greenish brown glass (15%).

Alteration: slight; rock is nonoxidized; interstitial glass replaced by clay mineral.

Sample 61-462-64R-1, 12–14 cm (Piece 2), Unit 10 [Z-1202]

Aphyric dolerite with intersertal-ophitic texture, fine grained. Rock: identical to Sample 61-462-63R-2, 18–22 cm (Z-1201).

Sample 61-462A-17R-2, 84–86 cm (Piece 4B), Unit 2 [Z-1203]

Sparsely olivine-plagioclase-phyric basalt (microdolerite), crystallized. Phenocrysts (5%): glomerophyric segregates of small rounded and idiomorphic grains (0.2–0.6 mm) of olivine (2%). Central parts of olivine grains consist of opaque dust. Plagioclase (3%) forms prismatic grains (labradorite [An_{68}]). Groundmass with doleritic texture; laths (0.1–0.4 mm) of plagioclase (40%, andesine [An_{49}] and labradorite [An_{52}]). Interstices: segregate of small (0.1–0.3 mm) grains of clinopyroxene (40%); brown glass (5%); opaque minerals (5%).

Alteration: slight; olivine completely replaced by brown iddingsite.

Sample 61-462A-24R-1, 12–14 cm (Piece 2B), Unit 12 [Z-1204]

Aphyric dolerite, fine grained. Rock with intersertal-doleritic texture; unoriented prismatic crystals (0.1–0.7 mm) of plagioclase (40%, andesine [An_{44}] and labradorite [An_{55}]). Interstices are filled with aggregate of small (0.1–0.2 mm) rounded grains of clinopyroxene (40%), small (0.2 mm) rounded grains of altered and oxidized olivine (2%), black glass (15%), and opaque minerals (3%).

Alteration: slight; olivine completely replaced by brown iddingsite.

Sample 61-462A-27R-2, 71–76 cm (Piece 6), Unit 12 [Z-1205]

Aphyric dolerite, fine grained. Rock with doleritic texture; prismatic crystals and laths (0.1–0.6 mm) of plagioclase (40%, andesine [An_{42}] and labradorite [An_{55}]). Interstices are filled with isometric grains (0.1–0.5 mm) of clinopyroxene (45%), small (0.2 mm) rounded grains of altered olivine (2%), opaque minerals (8%), and greenish brown glass (5%).

Alteration: slight; olivine completely replaced by iddingsite.

Sample 61-462A-28R-1, 92–94 cm (Piece 4), Unit 12 [Z-1206]

Aphyric dolerite with doleritic texture, fine grained. Rock: identical to Sample 61-462A-27R-2, 71–76 cm (Z-1205).

Alteration: slight; olivine completely replaced by iddingsite.

Sample 61-462A-29R-2, 105–108 cm (Piece 1G), Unit 12 [Z-1207]

Aphyric dolerite, medium grained. Rock with doleritic-ophitic texture; prismatic crystals and laths (0.2–0.8 mm) of plagioclase (40%, andesine [An_{42}] and labradorite [$An_{52–54}$]). Interstices are filled with isometric grains (0.4–0.5 mm) and segregates of clinopyroxene (45%), opaque minerals (10%), and black or brownish black glass (5%).

Alteration: slight; rock is nonoxidized.

Sample 61-462A-30R-3, 14–17 cm (Piece 1G), Unit 12 [Z-1208]

Sparsely plagioclase-phyric dolerite, fine grained. Phenocrysts (<1%): single prismatic grain (1.8 mm) of plagioclase (labradorite [An_{62}]). Groundmass (80%) with microlitic texture; prismatic crystals (0.1–0.5 mm) of plagioclase (40%, labradorite [An_{55}] and andesine [An_{47}]), segregates of small (0.1–0.3 mm) xenomorphic grains of clinopyroxene (50%), and xenomorphic grains (0.3–0.8 mm) of opaque minerals (10%). Occasionally, clinopyroxene forms large (up to 0.5 mm) xenomorphic or prismatic grains (0.7–0.8 mm).

Alteration: rock is fresh and nonoxidized.

Sample 61-462A-32R-3, 10–14 cm (Piece 2A), Unit 12 [Z-1209]

Aphyric basalt, fine grained, crystallized. Rock with microlitic texture; microlites and microlaths of plagioclase (50%). Interstices are filled with small (0.1–0.3 mm) grains and microlites (0.4–0.5 mm) of clinopyroxene (45%), opaque minerals (3%), and green altered glass (2%).

Alteration: slight; rock is nonoxidized; interstitial glass completely replaced by clay mineral; microcrack (0.4 mm in thickness) is filled with prismatic crystals of clinopyroxene (clinopyroxene almost completely replaced by aggregate of green uralite).

Sample 61-462A-44R-2, 12–14 cm (Piece 2), Unit 22 [Z-1210]

Sparsely plagioclase-phyric basalt. Phenocrysts (10%): glomerophyric segregates of prismatic crystals and laths (0.1–0.6 mm) of plagioclase (labradorite [An_{55}]). Groundmass with vitrophyric texture; glass with radial-radiant segregates of clinopyroxene and plagioclase crystallites.

Alteration: rock is fresh and nonoxidized.

Sample 61-462A-47R-1, 95–98 cm (Piece 9), Unit 23 [Z-1211]

Olivine-plagioclase-phyric basalt (glassy crust of basalt). Phenocrysts (10%): small (0.1–0.3 mm) idiomorphic grains of olivine (5%) and prismatic crystals and laths (0.1–0.4 mm) of plagioclase (10%, labradorite [An_{60}]). Groundmass with vitrophyric texture; light cream glass (areas of brownish black glass with crystallites of plagioclase are present).

Alteration: slight; olivine completely replaced by green iddingsite.

Sample 61-462A-50R-3, 130–134 cm (Piece 1E), Unit 24 [Z-1212]

Aphyric dolerite, medium grained. Rock with doleritic-poikilophitic texture; unoriented elongated-prismatic laths (0.5–1.7 mm) of plagioclase (40%). Interstices are filled with large isometric grains (1–2.5 mm) and small (0.3–0.5 mm) grains of clinopyroxene (50%), opaque minerals (5%), and altered glass (5%).

Alteration: slight; rock is nonoxidized; interstitial glass replaced by clay mineral.

Sample 61-462A-51R-4, 27–30 cm (Piece 1F), Unit 24 [Z-1213]

Olivine-plagioclase-phyric basalt. Phenocrysts (5%): small (0.1–0.3 mm) idiomorphic grains of olivine (2%) and small laths (0.1–0.7 mm) of plagioclase (3%, labradorite [An_{58}]). Groundmass with vitrophyric texture; light cream glass.

Alteration: slight; olivine completely replaced by green iddingsite.

Sample 61-462A-52R-4, 33–36 cm (Piece 1), Unit 25 [Z-1214]

Plagioclase-phyric basalt. Phenocrysts (5%): glomerophyric segregates and individual laths (0.4–0.8 mm) of plagioclase (3%, labradorite [An_{58}]). Groundmass with hyalopilitic texture; needle-shaped plagioclase (10%, andesine [An_{40}]) and brownish gray glass with segregates of clinopyroxene crystals, plagioclase, and opaque dust.

Alteration: rock is fresh and nonoxidized.

Sample 61-462A-53R-1, 143–146 cm (Piece 7B), Unit 26 [Z-1215]

Plagioclase-olivine-phyric basalt. Phenocrysts (15%): glomerophyric segregates of small (0.2–0.4 mm) idiomorphic grains of olivine (10%). Small laths (0.4–0.6 mm) of zonal plagioclase (5%, labradorite [An_{55}]) with inclusions of glass are present. Groundmass with pilotaxitic-microlitic texture; needle-shaped microlites and microlaths (up to 0.5–0.6 mm) of plagioclase (10%, andesine $An_{39–41}$), crystallized glass with segregates of clinopyroxene microlites, and individual grains of clinopyroxene.

Alteration: slight; olivine completely replaced by greenish brown iddingsite.

Sample 61-462A-55R-2, 50–52 cm (Piece 4), Unit 26 [Z-1216]

Plagioclase-olivine-phyric basalt with pilotaxitic-microlitic groundmass texture. Rock: identical to Sample 61-462A-53R-1, 143–146 cm (Z-1215).

Sample 61-462A-57R-1, 145–147 cm (Piece 13), Unit 26 [Z-1217]

Aphyric basalt, fine grained. Rock with hyalopilitic texture; needle-shaped microlites and microlaths of plagioclase (10%) and glass with segregates of microlites and crystallites of clinopyroxene and plagioclase. Rock: identical to Sample 61-462A-53R-1, 143–146 cm (Z-1215).

Alteration: slight; rock is nonoxidized.

Sample 61-462A-62R-2, 148–150 cm (Piece 2F), Unit 30 [Z-1218]

Plagioclase-olivine-phyric basalt, spotty in structure. Phenocrysts (10%): glomerophyric segregates of plagioclase (3%) and olivine (7%). Plagioclase forms small (0.2–0.4 mm) prismatic crystals (labradorite [An_{55}]). Olivine forms segregates of small (0.1–0.3 mm) idiomorphic grains. Groundmass with hyalopilitic-microlitic texture; needle-shaped microlites and microlaths of plagioclase (andesine [$An_{45–46}$]), glass with crystallites of clinopyroxene microlites, and individual grains of clinopyroxene.

Alteration: slight; olivine completely replaced by green iddingsite.

Sample 61-462A-65R-1, 59–61 cm (Piece 3), Unit 32 [Z-1219]

Aphyric dolerite, fine grained. Rock with doleritic texture; unoriented prismatic crystals and laths (0.1–0.8 mm) of plagioclase (40%, labradorite [An_{65}] and andesine [An_{44}]). Interstices are filled with small (0.1–0.3 mm) xenomorphic grains of clinopyroxene (45%), olivine (5%), opaque minerals (5%), and greenish brown glass (5%).

Alteration: slight.

Sample 61-462A-74R-4, 25–31 cm (Piece 1A), Unit 35 [Z-1220]

Aphyric dolerite, medium grained. Rock with ophitic texture; prismatic crystals and laths (0.5–1.7 mm) of zonal plagioclase (50%). Plagioclase consist of inclusions of glass. Interstices are filled with segregate of xenomorphic grains (0.1–0.7 mm) of clinopyroxene (45%), opaque minerals, and glass (5%).

Alteration: slight (5%); interstitial glass completely replaced by clay mineral.

Sample 61-462A-79R-5, 140–146 cm (Piece 1J), Unit 38 [Z-1221]

Aphyric basalt, crystallized. Rock with microlitic texture; microlites (0.1–0.2 mm) of plagioclase (35%, labradorite [An_{53}] and andesine [An_{43}]). Interstices are filled with small (0.01–0.1 mm) rounded grains of clinopyroxene (45%), altered olivine (5%), opaque minerals (5%), and brownish oxidized glass (10%).

Alteration: slight; interstitial glass is oxidized; olivine completely replaced by clay minerals.

Sample 61-462A-80R-2, 122–124 cm (Piece 3), Unit 40 [Z-1222]

Aphyric basalt with microlitic texture, crystallized. Rock: identical to Sample 61-462A-79R-5, 140–146 cm (Z-1221).

Alteration: slight; interstitial glass is oxidized; olivine completely replaced by clay minerals.

Sample 61-462A-88R-3, 9–11 cm (Piece 1A), Unit 43 [Z-1223]

Breccia of aphyric basalt, fine grained. Rock: fragments (1.2–10 mm) of basalt and smectite cement. Basalt: identical to Sample 61-462A-80R-2, 122–124 cm (Z-1222).

Alteration: slight; cement is smectite.

Sample 61-462A-89R-2, 15–16 cm (Piece 1), Unit 43 [Z-1224]

Plagioclase-clinopyroxene-olivine-phyric basalt. Phenocrysts (10%): single (1%) prismatic crystals of plagioclase (labradorite [An_{55}]), segregates of xenomorphic grains (0.2–0.3 mm) of clinopyroxene, and idiomorphic grains (0.1–0.4 mm) of olivine (6%). Groundmass with hyalopilitic-microlitic texture; microlites and microlaths of plagioclase (40%, andesine [An_{42}]), small (0.05–0.2 mm) rounded grains of clinopyroxene, opaque minerals (5%), and greenish brown glass.

Alteration: slight; olivine is oxidized and completely replaced by greenish brown iddingsite.

Sample 61-462A-90R-3, 88–90 cm (Piece 1H), Unit 44 [Z-1225]

Plagioclase-clinopyroxene-olivine-phyric basalt. Rock: identical to Sample 61-462A-89R-2, 15–16 cm (Z-1224).

Alteration: slight; olivine completely replaced by clay minerals.

South Pacific (Leg 91)

Hole 595B

Sample 91-595B-2R-1, 30–35 cm (Piece 3A), Unit 2 [Z-429]

Aphyric basalt, fine grained, inequigranular, incompletely crystallized, sparsely vesicular. Rock is subvariolitic, occasionally variolitic, texture; laths of plagioclase, clinopyroxene, and devitrified volcanic glass with opaque dust. Single vesicles are 0.2–0.4 mm.

Alteration: slight (~10%); interstitial glass is replaced with smectite.

XRD: smectite.

Sample 91-595B-3R-1, 119–124 cm (Piece 5B), Unit 2 [Z-430]

Aphyric basalt, fine grained, incompletely crystallized, massive. Rock is subvariolitic texture; laths of plagioclase, clinopyroxene, devitrified volcanic glass with opaque dust, and isometric and elongated grains of opaque minerals.

Alteration: slight (~5%); interstitial glass is replaced with smectite.

XRD: smectite.

Sample 91-595B-3R-2, 68–72 cm (Piece 3B), Unit 2 [Z-431]

Aphyric basalt, fine grained, incompletely crystallized, massive. Rock is subvariolitic, occasionally variolitic, texture; laths of plagioclase, clinopyroxene, devitrified volcanic glass with opaque dust, and grains of opaque minerals.

Alteration: slight (~3%); interstitial glass partly replaced by smectite.

XRD: smectite.

Sample 91-595B-4R-1, 17–22 cm (Piece 1B), Unit 2 [Z-432]

Aphyric basalt, fine grained, incompletely crystallized, sparsely vesicular. Rock is intergranular texture; laths of plagioclase, clinopyroxene, olivine, devitrified volcanic glass with opaque dust, and isometric and elongated grains of opaque minerals. Rare vesicles are empty.

Alteration: slight (~5%); interstitial glass and olivine are replaced with smectites.

XRD: smectite.

Sample 91-595B-4R-2, 8–13 cm (Piece 1A), Unit 2 [Z-433]

Aphyric basalt, fine grained, crystallized, massive. Rock is subvariolitic texture; laths of plagioclase, clinopyroxene, devitrified volcanic glass with opaque dust, and isometric and elongated grains of opaque minerals. Single vesicles are present.

Alteration: slight (~3%); interstitial glass is replaced with smectite; vesicles are filled with smectite.

XRD: smectite.

Sample 91-595B-4R-3, 145–147 cm (Piece 4C), Unit 2 [Z-434]

Aphyric basalt, fine grained, incompletely crystallized, massive. Rock is intergranular, partly subvariolitic, texture; laths of plagioclase, clinopyroxene, devitrified volcanic glass, and opaque minerals.

Alteration: slight (~3%); interstitial glass is replaced with smectite.

XRD: smectite.

Sample 91-595B-5R-1, 90–95 cm (Piece 6), Unit 2 [Z-435]

Aphyric basalt, fine grained, incompletely crystallized, massive. Rock is intergranular texture; laths of plagioclase, clinopyroxene, olivine, devitrified volcanic glass, and opaque minerals. Single phenocrysts plagioclase, clinopyroxene, and olivine are registered.

Alteration: slight (~5%); interstitial glass and olivine are replaced with smectite.

XRD: smectite.

Sample 91-595B-5R-2, 87–91 cm (Piece 7A), Unit 2 [Z-436]

Aphyric basalt, fine grained, almost completely crystallized, massive. Rock is intergranular texture; laths of plagioclase, clinopyroxene, devitrified volcanic glass, and opaque minerals. Single vesicles (0.2 mm) are present.

Alteration: slight (~3%); interstitial glass is replaced with smectite; vesicles are filled with smectite.

XRD: smectite.

Sample 91-595B-6R-1, 136–142 cm (Piece 14), Unit 2 [Z-437]

Aphyric basalt, fine grained, incompletely crystallized, massive. Rock is intersertal texture; laths of plagioclase, clinopyroxene, devitrified volcanic glass, and opaque minerals. Single vesicles (0.2 mm) are present.

Alteration: slight (~3%); interstitial glass is replaced with smectite; vesicles are filled with smectite.

XRD: smectite contains ~10% of mica layers.

Sample 91-595B-6R-2, 129–131 cm (Piece 15), Unit 2 [Z-438]

Plagioclase-phyric basalt (dolerite?), completely crystallized, vesicular. Phenocrysts of plagioclase (0.5–6 mm, 60%), clinopyroxene (0.4–0.8 mm up to 1 mm, 20%), and olivine (0.2–0.4 mm, 5%). Groundmass is doleritic texture; laths of plagioclase, clinopyroxene, olivine, devitrified volcanic glass, and opaque minerals. Single vesicles (0.2 mm) are present.

Alteration: slight (~10%); interstitial glass and olivine are replaced with smectite; vesicles are filled with smectite.

XRD: smectite contains ~20% of mica layers.

Sample 91-595B-7R-3, 18–22 cm (Piece 4), Unit 3 [Z-439]

Aphyric basalt, fine grained, almost completely crystallized, vesicular (0.3–0.8 mm, ~8%). Rock is subvariolitic texture; laths of plagioclase, clinopyroxene, devitrified volcanic glass, and opaque minerals.

Alteration: slight (10%); interstitial glass and olivine are replaced with smectite; vesicles are filled with smectite.

XRD: smectite contains single mica layers.

Sample 123-765D-1R-2, 8–10 cm (Piece 1A), Unit 1 [Z-86]

Aphyric basalt, medium grained, almost completely crystallized, vesicular (0.3–0.5 to 1 mm, 10%). Single microphenocrysts of plagioclase and clinopyroxene. Groundmass is intergranular (occasionally subvariolitic) texture; laths of plagioclase, clinopyroxene, olivine, devitrified volcanic glass, and opaque dust.

Alteration: slight (10%); olivine and interstitial glass are replaced with smectite and carbonate; vesicles are filled with smectite or/and carbonate.

XRD: smectites with various content of interlayer cations: Na-K and Mg-Ca; smectites contain ~10% mica layers.

Sample 123-765D-5R-1, 130–132 cm (Piece 8E), Unit 3 [Z-87]

Aphyric basalt, fine grained, almost completely crystallized, vesicular (0.1–0.3 mm, 10%). Single microphenocrysts of plagioclase. Groundmass is subvariolitic texture; laths of plagioclase, clinopyroxene, olivine, devitrified volcanic glass, and opaque dust.

Alteration: slight (10%); olivine and interstitial glass are replaced with smectite; vesicles are filled with smectite.

XRD: smectite.

Sample 123-765D-5R-5, 143–145 cm (Piece 3B), Unit 3 [Z-89]

Aphyric basalt, fine grained, almost completely crystallized, vesicular (0.2–0.4 mm, 5%). Groundmass is subvariolitic (occasionally intergranular) texture; laths of plagioclase, clinopyroxene, olivine, devitrified volcanic glass, and opaque minerals.

Alteration: slight (~5%); rock is nonoxidized; olivine and interstitial glass are replaced with smectites; vesicles are filled with smectites.

XRD: smectites with various content of interlayer cations: Na-K and Mg-Ca.

Sample 123-765D-7R-2, 135–137 cm (Piece 6B), Unit 6 [Z-80]

Aphyric basalt (dolerite?), coarse grained, completely crystallized, vesicular (0.2–0.5 mm, 5%). Rock is poikilophitic texture; laths of plagioclase, clinopyroxene, olivine, devitrified volcanic glass, and opaque minerals.

Alteration: slight (~5%); olivine and interstitial glass are replaced with smectites; vesicles and cracks are filled with smectites.

XRD: smectites with various content of interlayer cations: Na-K and Mg-Ca; trace hydromica.

Sample 123-765D-9R-1, 17–21 cm (Piece 1A), Unit 7 [Z-81]

Aphyric basalt (dolerite?), coarse grained, completely crystallized, massive. Rock is poikilophitic texture; laths of plagioclase, clinopyroxene, olivine, devitrified volcanic glass, and opaque minerals.

Alteration: scarce (~1%); olivine and interstitial glass are replaced with smectites.

XRD: smectites with various content of interlayer cations: Na-K and Mg-Ca.

Sample 123-765D-17R-2, 49–52 cm (Piece 6), Unit 13 [Z-83]

Aphyric basalt, fine grained, almost completely crystallized, vesicular (0.2–0.3 mm, 3%). Groundmass is subvariolitic texture; laths of plagioclase, clinopyroxene, olivine, devitrified volcanic glass, and opaque minerals.

Alteration: slight (~5%); olivine and interstitial glass are replaced with smectites; vesicles are filled with smectites.

XRD: smectites with various content of interlayer cations: Na-K and Mg-Ca; trace hydromica.

Sample 123-765D-18R-1, 82–84 cm (Piece 1E), Unit 14 [Z-90]

Aphyric basalt, fine grained, almost completely crystallized, vesicular (0.2–0.3 mm, 3%). Groundmass is intergranular (occasionally) subvariolitic texture; laths of plagioclase, clinopyroxene, olivine, devitrified volcanic glass, and opaque minerals.

Alteration: slight (~3%–5%); olivine and interstitial glass are replaced with smectites; vesicles are filled with smectites.

XRD: smectites with various content of interlayer cations: Na-K and Mg-Ca; hydromica in trace amounts.

Sample 123-765D-19R-1, 78–84 cm (Piece 4B), Unit 15 [Z-1358]

Sparsely plagioclase-phyric basalt, crystallized, vesicular. Phenocrysts (1%): prismatic grains (0.6–0.8 mm) of plagioclase. Groundmass with microlitic (microdoleritic) texture; microlites and microlaths (0.1–0.2 mm) of

plagioclase (30%, andesine [$An_{44–46}$]). Interstices consist of panicle like segregate of clinopyroxene microlites (45%); volcanic glass (5%) and opaque minerals (10%). Vesicles (10%, 0.2–0.4 mm) are rounded in shape. They are empty and lined by brown glass.

Alteration: rock is fresh and nonoxidized.

XRD: smectite.

Sample 123-765D-22R-1, 2–4 cm (Piece 1A), Unit 16 [Z-88]

Aphyric basalt, fine grained, almost completely crystallized, vesicular (0.2 mm, 1%). Groundmass is intergranular (occasionally subvariolitic) texture; laths of plagioclase, clinopyroxene, olivine, devitrified volcanic glass, and opaque minerals.

Alteration: slight (~3%); rock is nonoxidized; olivine and interstitial glass are replaced with smectites; vesicles are filled with carbonate.

XRD: smectite.

Sample 123-765D-24R-1, 7–9 cm (Piece 1A), Unit 17 [Z-82]

Aphyric basalt (dolerite?), coarse grained, almost completely crystallized, massive. Rock is poikilophitic texture; laths of plagioclase, clinopyroxene, olivine, devitrified volcanic glass, and opaque minerals.

Alteration: slight (8%); rock is nonoxidized; olivine and interstitial glass are replaced with smectite.

XRD: smectite.

Sample 123-765D-27R-2, 31–33 cm (Piece 1C), Unit 22 [Z-85]

Aphyric basalt, medium grained, almost completely crystallized, vesicular (0.3–0.4 mm, 5%). Groundmass is intergranular (occasionally subvariolitic) texture; laths of plagioclase, clinopyroxene, olivine, devitrified volcanic glass, and opaque minerals.

Alteration: slight (~10%); olivine and interstitial glass are replaced with smectite; vesicles are filled with smectite or carbonate.

XRD: hydromica and smectite.

Sample 123-765D-27R-3, 4–6 cm (Piece 1), Unit 22 [Z-84]

Aphyric basalt, medium grained, almost completely crystallized, vesicular (0.3–1 mm, 8%). Single phenocrysts of plagioclase (0.5 mm). Groundmass is intergranular texture; laths of plagioclase, clinopyroxene, olivine, devitrified volcanic glass, and opaque minerals.

Alteration: slight (~10%); rock is nonoxidized; olivine and interstitial glass are replaced with smectite and carbonate; vesicles are filled with carbonate.

XRD: smectite and hydromica.

Pigafetta Basin (Leg 129)

Hole 801B

Sample 129-801B-40R-1, 26–28 cm (Piece 5), Unit B4 [Z-776]

Aphyric basalt, crystallized, massive. Rock with microintersertal texture; unoriented laths (0.5–2 mm) of plagioclase. Interstices are filled with glass and opaque dust, xenomorphic and needle-shaped grains of opaque minerals (20%).

Alteration: slight to moderate (20%); plagioclase grains and interstitial glass replaced by smectite.

XRD: smectite; trace hydromica and swelling chlorite.

Sample 129-801B-41R-1, 20–22 cm (Piece 3), Unit B5 [Z-777]

Aphyric dolerite, crystallized, massive. Rock: identical to Sample 129-801B-40R-1, 26–28 cm (Z-776).

Alteration: slight to moderate (20%).

XRD: smectite with ~20% mica layers; trace mixed-layer chlorite-smectite mineral with ~10% swelling interlayers, mica(?), and amphibole(?).

Sample 129-801B-41R-1, 141–143 cm (Piece 3), Unit B5 [Z-778]

Aphyric dolerite, coarse grained, massive. Rock with ophitic texture; elongated-prismatic crystals (1–3 mm) of zonal plagioclase (50%) with undulatory extinction. Interstices are filled with xenomorphic and elongated-prismatic grains (1–2.5 mm) of clinopyroxene-augite-Ti augite (40%).

Alteration: slight to moderate (20%); clinopyroxene partly replaced by clay mineral; some areas of interstices consist of albite, opaque minerals, smectites, chlorite, and carbonate.

Sample 129-801B-42R-1, 91–93 cm (Piece 5B), Unit B6 [Z-779]

Aphyric dolerite with ophitic texture, coarse grained, massive. Rock: identical to Sample 129-801B-41R-1, 141–143 cm (Z-778).

Alteration: moderate (25%–30%); clinopyroxene partly replaced by chlorite; biotite and apatite are present.

XRD: smectite with different interlayer cations: Na-K and Ca-Mg; trace chlorite and mica.

Sample 129-801B-43R-2, 8–10 cm (Piece 1B), Unit B7 [Z-780]

Aphyric dolerite with ophitic texture, coarse grained, massive. Rock: identical to Sample 129-801B-41R-1, 141–143 cm (Z-778) and Sample 129-801B-42R-1, 91–93 cm (Z-779).

Alteration: strong (50%); clinopyroxene partly (60%) replaced by clay mineral; chlorite replaces plagioclase.

XRD: smectite with different interlayer cations: Na-K and Ca-Mg; trace chlorite and mica.

Sample 129-801B-43R-3, 128–129 cm (Piece 17), Unit B9 [Z-781]

Plagioclase-phyric dolerite, medium grained, massive. Phenocrysts (10%): large (up to 3 mm) xenocrysts of plagioclase with inclusions of glass. Groundmass with ophitic texture; prismatic grains and laths (0.2–1 mm) of plagioclase (50%, labradorite [An_{60}] and andesine [An_{48}]). Interstices are filled with small (0.2–0.4 mm) rounded grains of altered olivine (10%), xenomorphic grains of clinopyroxene, and opaque minerals (5%–6%).

Alteration: slight (10%); olivine completely replaced by iddingsite.

Sample 129-801B-43R-4, 40–41 cm (Piece 4A), Unit B11 [Z-782]

Aphyric dolerite, fine grained, massive. Rock with doleritic texture; prismatic grains and laths (0.2–0.8 mm) of plagioclase (labradorite [An_{60}]) with undulatory extinction. Interstices are filled with grains (0.1–0.2 mm and up to 0.8 mm) of clinopyroxene and opaque minerals (4%–5%).

Alteration: slight; clay mineral is in interstices.

XRD: smectite with ~20% mica layers; trace mixed-layer chlorite-smectite mineral with ~10% swelling interlayers, mica(?), and calcite.

Sample 129-801B-44R-1, 105–107 cm (Piece 2E), Unit B12 [Z-783]

Aphyric basalt, massive. Rock with pilotaxitic texture; microlites of plagioclase (labradorite [An_{58}]), clinopyroxene, altered glass, and opaque minerals (10%).

Alteration: strong (60%); interstitial glass completely replaced by clay mineral.

XRD: smectite; minor hydromica and mixed-layer chlorite-smectite mineral; trace chlorite.

Sample 129-801B-44R-2, 32–33 cm (Piece 4A), Unit B13 [Z-784]

Aphyric basalt, crystallized, massive. Rock with intersertal texture; segregates of elongated laths (up to 2 mm) of plagioclase. Interstices are filled with altered glass and unoriented needle-shaped grains (0.1–0.2 mm) of opaque minerals (35%–40%).

Alteration: very strong (80%); plagioclase almost completely replaced by clay minerals; interstitial glass completely replaced by clay mineral.

XRD: smectite with ~10% mica layers; trace mica.

Sample 129-801B-44R-3, 27–28 cm (Piece 2), Unit B14 [Z-785]

Plagioclase-phyric basalt with xenolites(?) of dolerite.

Alteration: olivine completely replaced by carbonate; augite replaced by clay mineral; plagioclase partly replaced by clay mineral; abundant needle-shaped large (0.6–0.7 mm) grains of opaque minerals; microcracks (0.1–0.2 mm) are filled with carbonate.

Hole 801C

Sample 129-801C-1R-1, 107–109 cm (Piece 2G), Unit C1 [Z-786]

Aphyric dolerite, medium grained, massive. Rock with ophitic texture; prismatic and elongated-prismatic grains (1–2 mm) of zonal plagioclase (labradorite [$An_{62–64}$]) with undulatory extinction and grains (0.5–1 mm and up to 4 mm) of augite-Ti augite. Interstices are filled with panicle like microlites of clinopyroxene and plagioclase. Opaque minerals (7%–8%) forms needle-shaped grains (0.3–0.6 mm) and xenomorphic grains.

Alteration: moderate (30%–40%); plagioclase partly (30%) replaced by smectites and albite; clinopyroxene partly (15%–20%) replaced by chlorite; hydromica, biotite, and apatite replace microlites of clinopyroxene and plagioclase.

Sample 129-801C-1R-2, 10–11 cm (Piece 1A), Unit C1 [Z-787]

Aphyric dolerite with ophitic texture, medium grained, massive. Rock: identical to Sample 129-801C-1R-1, 107–109 cm (Z-786).

XRD: smectite with ~20% mica layers and mica; trace mixed-layer chlorite-smectite mineral with ~10% swelling interlayers.

Sample 129-801C-2R-1, 6–7 cm (Piece 1A), Unit C3 [Z-788]

Sparsely olivine(?)-plagioclase-phyric basalt, coarse grained. Phenocrysts: single tabular microphenocryst (0.5 mm) of plagioclase; idiomorphic and skeletal grains (0.3 mm) of altered dark-colored mineral (olivine?). Groundmass with vitrophyric texture; volcanic glass with panicle like segregates of olivine(?) crystallites; plagioclase and opaque dust.

Alteration: moderate (20%–30%); olivine completely replaced by carbonate; plagioclase almost completely replaced by smectites; microcrack (0.2 mm) is filled with carbonate.

Sample 129-801C-2R-5, 106–107 cm (Piece 2), Unit C6 [Z-789]

Aphyric dolerite with doleritic texture, fine grained, massive. Rock: identical to Sample 129-801C-1R-1, 107–109 cm (Z-786) and Sample 129-801C-1R-2, 10–11 cm (Z-787).

Alteration: moderate (30%); plagioclase partly replaced by smectites; clinopyroxene partly replaced by chlorite; interstitial minerals replaced by smectites, biotite, and apatite.

Sample 129-801C-3R-1, 44–46 cm (Piece 2C), Unit C7 [Z-790]

Aphyric dolerite, fine grained, massive. Rock is represented mainly by prismatic grains of plagioclase (90%). Relicts of dark-colored minerals are absent (plagioclasite?). Opaque minerals (10%) form small (0.1 mm) xenomorphic or needle-shaped grains and abundance opaque dust.

Alteration: very strong (80%–90%); plagioclase completely replaced by smectites.

XRD: smectite with ~10% mica layers; minor mixed-layer chlorite-smectite mineral with ~45% swelling interlayers; trace chlorite and mica.

Sample 129-801C-4R-1, 18–21 cm (Piece 4), Unit C8 [Z-791]

Fe hydroxides (hydrothermal deposit).

XRD: quartz.

Sample 129-801C-4R-2, 111–114 cm (Piece 13), Unit C8 [Z-792]

Rock: identical to Sample 129-801C-4R-1, 18–21 cm (Z-791).

XRD: quartz; trace goethite.

Sample 129-801C-5R-1, 44–45 cm (Piece 2C), Unit C9 [Z-793]

Plagioclase-phyric basalt, massive. Phenocrysts (8%–10%): prismatic and elongated-prismatic grains (1.2–2.5 mm) of zonal plagioclase. Groundmass with microintersertal texture; unoriented laths (0.2–0.5 mm) of plagioclase (labradorite [An_{55}]). Opaque minerals is present (8–10%).

Alteration: strong (60%); plagioclase almost completely (90%) replaced by carbonate; interstices are filled with smectites.

Sample 129-801C-5R-2, 17–18 cm (Piece 1A), Unit C9 [Z-794]

Sparsely plagioclase-phyric basalt, massive. Phenocrysts: one prismatic grain (1.3 mm) of zonal plagioclase (labradorite [An_{55}]). Groundmass with hyalopilitic texture; needle-shaped microlites of plagioclase and altered glass with opaque dust. Rock is brecciated (partly).

Alteration: very strong (90%); plagioclase phenocryst partly replaced by carbonate; interstitial glass completely replaced by clay mineral; microcracks (0.5–1 mm) are filled with clay mineral and carbonate.

XRD: smectite; trace mica with ~20% swelling interlayers and calcite.

Sample 129-801C-5R-3, 98–100 cm (Piece 4B), Unit C10 [Z-795]

Plagioclase-phyric basalt, massive. Phenocrysts (40%): prismatic grains (1–5 mm) of plagioclase (labradorite-bitovnite [An_{70}]) and their glomerophyric segregates. Groundmass with pilotaxitic texture; needle-shaped microlites and black glass.

Alteration: fresh; microcracks (5%–7%, 0.1–0.3 mm, up to 0.8 mm in thickness) are filled with carbonate.

XRD: smectite with ~30% mica layers.

Sample 129-801C-5R-5, 55–58 cm (Piece 3C), Unit C13 [Z-796]

Aphyric dolerite, fine grained, massive. Rock with doleritic-intersertal texture; laths (0.1–0.9 mm) of plagioclase (labradorite [$An_{64–68}$]). Interstices are filled with segregate of small (<0.1 mm) rounded grains of olivine (25%) and xenomorphic grains of clinopyroxene (diopside-pigeonite) with opaque minerals.

Alteration: fresh.

Sample 129-801C-7R-1, 51–53 cm (Piece 4C), Unit C21 [Z-797]

Aphyric dolerite, massive. Rock with intersertal-doleritic texture; laths (0.1–0.8 mm) of plagioclase (labradorite [$An_{55–57}$]). Interstices are filled with segregate of small (0.1–0.2 mm) isometric grains of clinopyroxene (pigeonite); altered glass (25%) with opaque minerals.

Alteration: interstitial glass replaced by clay mineral.

Sample 129-801C-7R-3, 38–41 cm (Piece 1E), Unit C23 [Z-798]

Aphyric dolerite, sparsely vesicular. Rock with intersertal-doleritic texture. Rock: identical to Sample 129-801C-7R-1, 51–53 cm (Z-797). Sparse vesicles (3%–4%, 0.2–0.3 mm) are present.

Alteration: vesicles are filled with carbonate.

Sample 129-801C-8R-1, 9–12 cm (Piece 2C), Unit C23 [Z-799]

Aphyric basalt, crystallized, sparsely vesicular. Rock with microlitic texture; microlites and laths (0.05–0.8 mm) of plagioclase (laths: labradorite [An_{68}]; microlites: labradorite [An_{55}] and andesine [An_{48}]), rounded-isometric grains of clinopyroxene (pigeonite), and glass with panicle like microlites of clinopyroxene and opaque minerals.

Alteration: microcracks (0.2 mm) are filled with carbonate and clay mineral.

XRD: smectite with ~5% mica layers.

Sample 129-801C-10R-1, 60–62 cm (Piece 1G), Unit C25 [Z-800]

Aphyric dolerite with intersertal-doleritic texture, fine grained, massive. Rock: identical to Sample 129-801C-7R-1, 51–53 cm (797).

Emperor Seamount Chain (Leg 55)

Ojin Seamount (Hole 430A)

Sample 55-430A-5R-4, 105–108 cm (Piece 12), Unit 2 [Z-1110]

Aphyric trachyandesite, vesicular. Rock with pilotaxitic (occasionally, with trachydoid) texture; microlaths (0.1–0.5 mm) of plagioclase (60%, from andesine [An_{48}] to andesine [An_{42}]), black glass (15%), and opaque minerals (10%). Vesicles (15%, 1.2–4 mm) are oval in shape.

Alteration: slight (5%–10%); rock is slightly oxidized (5%); vesicles are filled with carbonate.

Sample 55-430A-5R-5, 33–37 cm (Piece 5), Unit 2 [Z-1111]

Aphyric trachyandesite, vesicular. Rock with pilotaxitic (occasionally, with trachytoid) texture; microlaths (0.1–0.5 mm) of plagioclase (40%, from andesine [An_{46}] to andesine [An_{35}]), black to dark green altered glass (20%), and grains (0.01–0.3 mm) of opaque minerals (15%). Vesicles (25%, 2.5–5 mm) are oval in shape. Walls of vesicles are lined dark green altered glass.

Alteration: slight to moderate (15%–20%); interstitial glass replaced by clay mineral; clay mineral replaces glass from vesicles.

XRD: smectite with ~10% mica layers; trace mixed-layer smectite-swelling chlorite(?).

Sample 55-430A-5R-5, 96–101 cm (Piece 10), Unit 2 [Z-1619]

Aphyric trachybasalt, fine grained, sparsely vesicular. Rock with trachytoid texture; subparallel oriented microlaths (0.1–0.6 mm) of plagioclase (75%, andesine [$An_{39–40}$]). Interstices are filled with small (<0.1 mm) grains of clinopyroxene (5%), opaque minerals (5%), and altered glass (15%) with biotite (<1%) and chlorite. Single vesicle (2 mm) are oval in shape, empty.

Alteration: slight (15%); rock is nonoxidized; interstitial glass partly replaced by clay mineral.

Sample 55-430A-6R-1, 6–11 cm (Piece 1), Unit 2 [Z-1620]

Clinopyroxene-phyric basalt, crystallized, fine grained. Phenocrysts (35): isometric grains (0.8–1.7 mm) of clinopyroxene with abundant inclusions of plagioclase microlaths. Groundmass with microlitic texture; microlites and microlaths (0.1–0.4 mm) of plagioclase (30%, from andesine [An_{45}] to andesine [An_{37}]). Interstices are filled with isometric grains of orthoclase (5%), small grains of clinopyroxene (5%), altered dark green glass (15%), and abundant idiomorphic pseudocubic grains (0.1–0.2 mm) of opaque minerals.

Alteration: slight (15%–17%); rock is nonoxidized; interstitial glass partly replaced by clay mineral; orthoclase is pelletized.

Sample 55-430A-6R-1, 98–103 cm (Piece 7B), Unit 2 [Z-1622]

Aphyric basalt, crystallized, medium grained. Rock with intersertal-doleritic texture; laths (0.2–0.8 mm) of plagioclase (40%, andesine [$An_{42–45}$]). Interstices are filled with xenomorphic grains (0.1–0.3 mm) of clinopyroxene (35%), altered glass (20%), and opaque minerals (5%).

Alteration: slight to moderate (20%); rock is nonoxidized; interstitial glass partly by clay mineral, sparse biotite is present.

Sample 55-430A-6R-2, 24–30 cm (Piece 4), Unit 3 [Z-1112]

Aphyric hawaiite (trachyandesite), fine grained, vesicular. Rock with trachytic texture; laths and microlites (0.1–0.4 mm) of plagioclase (50%, andesine [An_{38}]). Interstices are filled with altered clinopyroxene (10%), altered glass (20%), and needles of opaque minerals (10%). Single idiomorphic grains (up to 0.4 mm) of opaque minerals are present. Vesicles (25%, 2 mm) are rounded in shape.

Alteration: moderate (30%); rock is nonoxidized; interstitial glass and clinopyroxene replaced by clay mineral; walls of vesicles are lined celadonite(?).

Sample 55-430A-6R-3, 19–24 cm (Piece 2), Unit 3 [Z-1623]

Aphyric trachybasalt, crystallized, fine grained. Rock with trachytoid texture; subparallel microlites and microlaths (0.1–0.6 mm) of plagioclase (65%, andesine [$An_{40–45}$]). Interstices are filled with small (<0.1 mm) grains of clinopyroxene (15%), laths of plagioclase, opaque minerals (5%–7%), and altered glass (15%).

Alteration: moderate (30%); rock is nonoxidized; interstitial glass and clinopyroxene completely replaced by clay mineral (sparse biotite is present in altered glass); plagioclase partly (40%–50%) replaced by smectites.

Nintoku Seamount (Hole 432A)

Sample 55-432A-2R-1, 99–104 cm (Piece 8E), Unit 1 [Z-1624]

Plagioclase-phyric basalt, crystallized, medium grained, massive. Phenocrysts (35%): two prismatic crystals (2.5 mm and 7 mm) of plagioclase. Groundmass with microdoleritic texture; laths (0.2–0.6 mm) of plagioclase (25%; andesine [An_{45}], andesine-labradorite [An_{50}], and andesine [An_{32}]). Interstices: isometric grains (0.1–0.3 mm) of clinopyroxene (20%), opaque minerals (10%), and altered glass (5%).

Alteration: slight (5%); rock is non oxidized; clay mineral replaces interstitial glass.

XRD: smectite and mixed-layer smectite-chlorite mineral; trace chlorite with swelling interlayers.

Sample 55-432A-2R-2, 102–107 cm (Piece 11C), Unit 2 [Z-1627]

Plagioclase-phyric basalt with microdoleritic groundmass texture, crystallized, medium grained, sparsely microvesicular. Rock is the same as Sample 55-432A-2R-1, 99–104 cm (Z-1624). Interstitial isometric “vesicles” (5%, 0.2–0.6 mm) are lined with celadonite(?).

Alteration: slight (1%–2%); rock is slightly oxidized (10%).

Sample 55-432A-2R-3, 43–48 cm (Piece 1E), Unit 2 [Z-1629]

Plagioclase-phyric basalt, crystallized, medium grained, sparsely vesicular. Phenocrysts (40%): large prismatic crystals (6–11) of plagioclase (labradorite [$An_{54–56}$]). Groundmass with microdoleritic-intersertal texture; microlites and laths (0.2–1 mm) of plagioclase (30%, andesine [An_{46}] and andesine [An_{40}]). Interstices consist of xenomorphic grains of clinopyroxene (10%), oxidized olivine (5%), opaque minerals (5%), and interstitial “microvesicles” (2%–3%, 0.2–0.7 mm). Two large (1.7 mm) vesicles are oval in shape.

Alteration: slight (5%–7%); clay mineral replaces interstitial glass; walls of vesicles are lined with clay mineral.

Sample 55-432A-3R-1, 9–12 cm (Piece 1), Unit 3 [Z-1113]

Olivine-phyric basalt, fine grained. Phenocrysts (10%): idiomorphic grains (0.2–3 mm) of oxidized olivine. Groundmass with hyalopilitic; glass which contains segregate of microlites (up to 0.1 mm) of plagioclase (50%), very small (up to 0.05 mm) grains of opaque minerals.

Alteration: rock is fresh.

XRD: smectite with ~10% mica layers.

Sample 55-432A-3R-2, 15–20 cm (Piece 2), Unit 3 [Z-1631]

Olivine-phyric basalt, crystallized, fine grained. Phenocrysts (10%): idiomorphic grains (0.2–1 mm) of olivine. Groundmass with microlitic texture; microlites (0.1–0.2 mm) of plagioclase (50%, andesine [An_{42}] and andesine [An_{33}]). Interstices consist of segregate of small (<0.05 mm) black grains of clinopyroxene (25%); small (<0.1 mm) grains of olivine (5%) and opaque minerals (10%).

Alteration: slight (12%); partly oxidized olivine is replaced with iddingsite.

Sample 55-432A-3R-3, 70–75 cm (Piece 7), Unit 3 [Z-1632]

Aphyric basalt, crystallized, fine grained, sparsely vesicular. Rock with microlitic texture; microlites and microlaths (0.1–0.3 mm) of plagioclase (50%, labradorite [An_{66}] and andesine [An_{46}]). Interstices consist of grains (0.01–0.4 mm) of clinopyroxene (25%), small (up to 0.3 mm) grains of olivine (5%), opaque minerals (10%). and altered glass (5%). Two vesicles (0.7 mm and 1.2 mm) are rounded in shape.

Alteration: slight (10%); olivine replaced by iddingsite; clay mineral replaces glass; vesicles are filled with smectites or carbonate.

Sample 55-432A-4R-3, 140–145 cm (Piece 14), Unit 3 [Z-1633]

Aphyric basalt, crystallized, medium grained, sparsely vesicular. Rock with microlitic texture (some areas demonstrate poikilophitic texture); idiomorphic grains (0.1–0.5 mm) of oxidized olivine (20%), xenomorphic grains (0.1–0.3 mm) of clinopyroxene (20%), microlites and microlaths (0.1–0.3 mm) of plagioclase (40%, andesine [An_{45}] and andesine [An_{40}]). Interstices consist of glass (10%) and opaque minerals (10%).

Alteration: slight (10%); plagioclase partly (10%) is pelletized and replaced by smectites; clay mineral replaces glass.

Sample 55-432A-4R-4, 80–83 cm (Piece 6B), Unit 3 [Z-1114]

Clinopyroxene-olivine-phyric alkali basalt, medium grained, massive. Microphenocrysts (20%): idiomorphic grains (up to 0.6 mm) of oxidized olivine (5%) and xenomorphic grains (0.5–0.7 mm) of clinopyroxene (15%) which contains inclusions of plagioclase microlites. Groundmass with microlitic texture; microlites (0.1–0.3 mm) of plagioclase (30%, andesine [$An_{36–37}$]), small (0.1–0.2 mm) idiomorphic grains of oxidized olivine (20%), altered grains of clinopyroxene (10%), idiomorphic (0.1 mm) grains of opaque minerals (10%), xenomorphic grains (up to 0.1 mm) of orthoclase(?) with small (0.05 mm) needles of apatite, and volcanic glass (<5%).

Alteration: slight to moderate (20%); olivine is oxidized; clinopyroxene and interstitial glass completely replaced by clay mineral.

XRD: smectite with ~20% mica layers; trace mixed-layer chlorite-smectite mineral with ~10% swelling interlayers and hydromica.

Sample 55-432A-4R-5, 56–61 cm (Piece 4), Unit 3 [Z-1634]

Olivine-plagioclase-phyric basalt, crystallized, medium grained, massive. Phenocrysts (30%): large (2.5–6 mm) rounded-tabular (xenocrysts) grains of plagioclase (20%, labradorite [An_{60}]) and idiomorphic grains (0.4–0.8 mm) of olivine (10%). Groundmass with microlitic texture; laths (0.2–0.6 mm) of plagioclase (35%, andesine [An_{46}] and andesine [An_{38}]). Interstices are filled with small (0.2 mm) grains of olivine (5%), segregate of small (0.05–0.2 mm) xenomorphic grains of clinopyroxene (20%), volcanic glass (5%) and opaque minerals (5%).

Alteration: slight to moderate (20%); oxidized olivine is replaced with iddingsite; interstitial glass completely replaced by clay mineral.

Sample 55-432A-5R-1, 100–105 cm (Piece 2B), Unit 3 [Z-1635]

Aphyric basalt, crystallized, fine grained. Rock with microlitic texture; microlites and microlaths (0.1–0.6 mm) of plagioclase (40%, oligoclase-andesine [An_{30}]). Interstices consist of small (0.1 mm) isometric grains of orthoclase and sanidine (10%), small (0.1–0.2 mm) grains of olivine (15%), clinopyroxene (25%), opaque minerals (5%), and glass (5%).

Alteration: slight (5%–10%); olivine is oxidized; clay mineral replaces glass.

Suiko Seamount (Hole 433C)

Sample 55-433C-10R-2, 127–133 cm (Piece 19), Unit 4a [Z-1640]

Olivine-phyric basalt, fine grained, vesicular. Phenocrysts (10%): idiomorphic grains (0.5–1.6 mm) of olivine. Groundmass with pilotaxitic texture; microlites and laths (0.1–0.7 mm) of plagioclase (15%, andesine [An_{45}]),

idiomorphic grains (0.2–0.4 mm) of clinopyroxene (5%), grains (0.1–0.3 mm) of olivine (5%), opaque minerals (5%), and glass (30%). Vesicles (30%, 0.2–1.7 mm) are isometric in shape.

Alteration: moderate (40%); olivine completely replaced by iddingsite; vesicles are filled with clay mineral.

Sample 55-433C-10R-4, 121–123 cm (Piece 8B), Unit 4h [Z-1115]

Olivine-phyric picrite, coarse grained. Rock with doleritic-vitrophyric texture; idiomorphic grains (0.5–2 mm) of olivine (65%). Interstices are filled with segregate of laths of plagioclase (10%, andesine [An_{38}] and andesine [An_{32}]), altered glass (20%) and xenomorphic grains (0.1–0.4 mm) of clinopyroxene (5%).

Alteration: very strong (85%); olivine completely replaced by iddingsite; smectites and carbonate (<1%) replace interstitial glass.

XRD: smectite with ~10% mica layers; trace mixed-layer chlorite-smectite mineral and serpentine; light green spot (altered olivine?): serpentine; trace smectite and calcite.

Sample 55-433C-12R-1, 75–80 cm (Piece 8A), Unit 9 [Z-1116]

Clinopyroxene-plagioclase-phyric basalt with hyalopilitic texture (glass: 70%–80%) of groundmass, poorly crystallized, highly vesicular (40%).

Alteration: moderate (25%–30%); plagioclase partly replaced by albite and pelite; vesicles are lined with clay mineral.

XRD: smectite with ~20% mica layers; trace hydromica.

Sample 55-433C-12R-2, 32–37 cm (Piece2E), Unit 9 [Z-1644]

Olivine-phyric basalt, crystallized, fine grained, highly vesicular. Phenocrysts (15%): idiomorphic grains (0.7–2 mm) of olivine. Groundmass with pilotaxitic texture; small grains (0.1–0.3 mm) of olivine (5%), microlaths (0.1–0.3 mm) of plagioclase (20%, andesine [An_{45}]), opaque minerals (5%), and brownish black glass (20%). Vesicles (40%, 0.6–5 mm) are oval and isometric in shape.

Alteration: moderate (30%–35%); olivine and plagioclase completely replaced by smectites; vesicles are lined with smectites.

Sample 55-433C-12R-2, 136–141 cm (Piece 3C), Unit 9 [Z-1645]

Clinopyroxene-plagioclase-phyric basalt, crystallized, medium grained. Phenocrysts (25%): glomerophyric segregates of clinopyroxene (0.4–0.6 mm, 10%) and tabular and prismatic grains (0.6–0.8 mm) of plagioclase (15%, labradorite [An_{62}]). Groundmass with pilotaxitic texture; laths (0.2–0.5 mm) of plagioclase (30%, andesine [An_{45}] and andesine [An_{39}]). Interstices are filled with segregate of xenomorphic grains (0.2–0.3 mm) of clinopyroxene (25%), glass (20%) and opaque minerals (5%–7%).

Alteration: slight to moderate (20%); clay mineral replaces interstitial glass, sparse biotite is presented.

Sample 55-433C-12R-3, 54–57 cm (Piece 1D), Unit 9 [Z-1117]

Olivine-plagioclase-phyric basalt, crystallized, fine grained, vesicular. Phenocrysts (10%): idiomorphic grains (0.8–1 mm) of olivine (5%) and short prismatic grains (0.8 mm) of plagioclase (5%, labradorite [An_{60}]). Groundmass with microlitic texture; microlites and laths (0.1–0.5 mm) of plagioclase (30%, andesine [An_{48}]), small (0.1–0.2 mm) grains of olivine (5%), and segregate of small (<0.1 mm) grains of clinopyroxene (30%). Vesicles (20%) are isometric in shape.

Alteration: moderate (25%); olivine completely replaced by smectites and carbonate; vesicles are filled with clay mineral.

XRD: smectite with ~10% mica layers.

Sample 55-433C-13R-2, 69–72 cm (Piece 1J), Unit 10 [Z-518]

Plagioclase-clinopyroxene-phyric dolerite, crystallized, massive. Phenocrysts (5%): sparse partly idiomorphic grains (0.5–0.8 mm) of clinopyroxene and prismatic grains (0.7–1 mm) of plagioclase. Groundmass with doleritic texture; prismatic and elongated-prismatic grains (0.1–0.5 mm) of plagioclase (50%, labradorite [$An_{56–58}$]). Interstices are filled with isometric grains (0.1–0.3 mm) of clinopyroxene (30%), xenomorphic grains (0.1–0.3 mm) of olivine (10%), opaque minerals (5%), and volcanic glass (5%).

Alteration: slight (10%–15%); olivine and interstitial glass completely replaced by clay mineral.

XRD: smectite with ~20% mica layers; trace mixed-layer smectite-chlorite with ~20% swelling interlayers.

Sample 55-433C-14R-1, 2–7 cm (Piece 1A), Unit 11a [Z-1658]

Plagioclase-phyric basalt, highly vesicular. Phenocrysts (15%): prismatic crystals (0.3–0.6 mm) of plagioclase (labradorite [An_{56}]) and their segregates. Groundmass with vitrophyric texture; black glass with microlites of plagioclase (5%, andesine [An_{43}]). Vesicles (50%, 1–7 mm) are isometric in shape.

Alteration: moderate (20%–25%); plagioclase replaced by smectite-celadonite(?) aggregate; walls of vesicles are lined with clay mineral, central parts of vesicles are filled with brownish glass, zeolite, and clay minerals.

Sample 55-433C-14R-1, 33–38 cm (Piece 1G), Unit 11a [Z-1656]

Plagioclase-phyric basalt, crystallized, medium grained, vesicular. Phenocrysts (15%): tabular and prismatic crystals (0.6–0.8 mm) of plagioclase (labradorite [An_{55}]). Groundmass with microlitic texture; laths (0.2–0.6 mm) of plagioclase (20%, andesine [An_{49}] and andesine [An_{42}]), sparse grains (0.1–0.2 mm) of olivine (3%–4%), opaque minerals (5%), and glass (1%–2%). Interstices are filled with segregate of small isometric grains of clinopyroxene (15%). Vesicles (30%, 2.5–5 mm and 0.5–0.6 mm) are oval in shape.

Alteration: slight to moderate (15%–20%); olivine is oxidized; clay mineral replaces glass; plagioclase partly replaced by clay mineral; walls of large vesicles are lined with clay mineral, small vesicles almost completely are filled with clay mineral.

Sample 55-433C-14R-2, 115–120 cm (Piece 3C), Unit 11a [Z-1657]

Sparsely clinopyroxene-plagioclase-phyric basalt, crystallized, medium grained, sparsely vesicular. Phenocrysts (5%): grains (0.5 mm) of clinopyroxene (1%) and prismatic crystals (0.6–1 mm) of plagioclase (4%, labradorite [An_{57}]). Groundmass with microlitic texture; laths (0.2–0.5 mm) of plagioclase (50%, andesine [An_{43}]), isometric grains of clinopyroxene (20%), small (up to 0.1 mm) grains of olivine (5%), opaque minerals (5%), and interstitial glass (10%). Two vesicles (up to 5 mm) are oval in shape.

Alteration: slight (15%); plagioclase partly (30%–40%) replaced by clay mineral (inclusions of glass in plagioclase crystals); olivine is oxidized; clay mineral replaces interstitial glass; walls of vesicles are lined with clay mineral.

Sample 55-433C-14R-4, 26–31 cm (Piece 2A), Unit 11c [Z-1648]

Clinopyroxene-plagioclase-phyric basalt, crystallized, medium grained. Rock is the same as Sample 55-433C-12R-2, 136–141 cm (Z-1645).

Alteration: slight to moderate (20%).

Sample 55-433C-14R-4, 47–52 cm (Piece 2B), Unit 11c [Z-1649]

Olivine-clinopyroxene-plagioclase-phyric basalt, crystallized, fine grained, sparsely vesicular. Phenocrysts (20%): sparse grains (0.4–0.6 mm) of olivine (3%–4%), partly idiomorphic grains of clinopyroxene (6%–7%), and tabular and prismatic crystals (0.7–1.5 mm) of plagioclase (10%, labradorite [An_{67}]). Groundmass with intersertal-microlitic texture; microlites and laths (0.1–0.5 mm) of plagioclase (25%, andesine [An_{47}] and andesine [An_{42}]). Interstices are filled with segregate of small (0.05–0.2 mm) grains of clinopyroxene (30%); opaque minerals (5%) and altered glass (20%). Two vesicles (up to 5 mm) are oval in shape.

Alteration: moderate (20%–25%); clay mineral replaces interstitial glass.

Sample 55-433C-15R-1, 0–4 cm (Piece 1), Unit 11c [Z-1650]

Clinopyroxene-plagioclase-phyric basalt, crystallized, fine grained, vesicular. Phenocrysts (15%): sparse idiomorphic grains (0.4–1.7 mm) of clinopyroxene (5%) and prismatic crystals (0.6–0.9 mm) of plagioclase (10%, labradorite [An_{60}]). Groundmass with microlitic texture; microlites and laths (0.1–0.6 mm) of plagioclase (20%, andesine [An_{47}] and andesine [An_{38}]). Interstices are filled with small (0.1–0.2 mm) grains of olivine (5%), small (0.01–0.2 mm) grains of clinopyroxene (20%), opaque minerals (5%), and altered glass (10%). Vesicles (35%, 1.2–4 mm) are oval in shape.

Alteration: slight (15%); plagioclase partly replaced by clay mineral (central parts of plagioclase grains); olivine is oxidized; walls of vesicles are lined with clay mineral.

Sample 55-433C-15R-5, 82–87 cm (Piece 4B), Unit 13 [Z-1118]

Plagioclase-phyric basalt, crystallized, fine grained, vesicular. Phenocrysts (10%): glomerophyric segregates of tabular grains (0.4–0.7 mm) of plagioclase (labradorite [An_{56}]). Groundmass with microlitic texture; microlites and laths (0.1–0.3 mm) of plagioclase (30%, andesine [An_{48}]), segregate of small (up to 0.1 mm) grains of clinopyroxene (30%); grains (0.1 mm) of opaque minerals (15%). Vesicles (15%, 0.2–0.6 mm) are oval and isometric in shape.

Alteration: slight to moderate (15%–20%); plagioclase almost completely (80%) replaced by clay mineral; olivine is oxidized; walls of vesicles are lined with clay mineral.

Sample 55-433C-15R-5, 88–92 cm (Piece 4B), Unit 13 [Z-519]

Olivine-plagioclase-phyric basalt, crystallized, massive. Phenocrysts (25%): idiomorphic grains (0.6–0.7 mm) of olivine and glomerophyric segregates of partly xenomorphic grains (0.3–0.5 mm) of olivine with plagioclase. Plagioclase forms tabular grains (up to 2.5 mm) with abundant inclusions of glass. Phenocrysts of plagioclase are mainly represented by glomerophyric segregates (0.5–1.2 mm) of small (0.1–0.3 mm) prismatic grains. Groundmass with microlitic (microdoleritic) texture; microlites and laths (0.05–0.3 mm) of plagioclase (50%, andesine [An_{48}]). Interstices are filled with segregate of small (<0.1 mm) grains of clinopyroxene (30%), altered green glass (10%), and opaque minerals (5%–8%).

Alteration: slight to moderate (20%); olivine completely replaced by iddingsite; plagioclase partly replaced by sosurite; clay mineral replaces interstitial glass.

XRD: smectite with ~10% mica layers.

Sample 55-433C-15R-6, 31–32 cm (Piece 1C), Unit 13 [Z-1119]

Clinopyroxene-plagioclase-phyric basalt, crystallized, medium grained, sparsely vesicular. Phenocrysts (15%): glomerophyric segregates of clinopyroxene and plagioclase (labradorite [An_{56}]). Groundmass with microdoleritic (microlitic) texture; microlites and laths (0.1–0.6 mm) of plagioclase (35%, andesine [An_{48}]). Interstices are filled with segregate of small (0.05–0.2 mm) grains of clinopyroxene (35%); opaque minerals (15%). Single vesicles (~1%, up to 0.4 mm) are isometric in shape.

Alteration: slight; rock is nonoxidized; vesicles are filled with celadonite(?).

XRD: smectite with ~10% mica layers.

Sample 55-433C-17R-1, 64–69 cm (Piece 5A), Unit 13 [Z-1120]

Clinopyroxene-plagioclase-phyric basalt with microdoleritic (microlitic) groundmass texture, crystallized, medium grained. Rock: identical to Sample 55-433C-15R-6, 31–32 cm [Z-1119].

Alteration: slight.

Sample 55-433C-19R-1, 48–50 cm (Piece 4C), Unit 13 [Z-1655]

Aphyric basalt, fine grained, vesicular. Rock with pilotaxitic texture; microlites (0.01–0.1 mm) and microlaths (0.1–0.5 mm) of plagioclase (25%, labradorite [An_{53}], andesine [An_{44}] and andesine [An_{32}]), sparse (~1%) small (up to 0.2 mm) oxidized grains of olivine and clinopyroxene (10%), brownish black glass (30%), and opaque minerals (5%). Vesicles (30%, 0.2–1.8 mm) are oval and isometric in shape.

Alteration: moderate (20%); vesicles are filled with clay mineral.

Sample 55-433C-21R-3, 20–23 cm (Piece 2), Unit 17 [Z-520]

Sparsely plagioclase-phyric basalt, crystallized, massive. Phenocrysts (2%–3%): elongated-prismatic grains (1.2–1.5 mm) of plagioclase (labradorite [An_{52-54}]) and glomerophyric segregates (up to 1.2 mm) of small (0.2–0.4 mm) grains of plagioclase. Groundmass with microlitic texture; microlites and laths (up to 0.5 mm) of plagioclase (50%, andesine-labradorite [An_{50}] and andesine [An_{44}]). Interstices are filled by segregate of small grains of clinopyroxene (30%); opaque minerals (10%), and green volcanic glass (10%). Small (0.1 mm) rounded grains of olivine (5%–7%) are present.

Alteration: slight (15%); clay mineral completely replaces glass and olivine.

XRD: smectite with ~10% mica layers; trace mixed-layer smectite-chlorite with ~15% swelling interlayers.

Sample 55-433C-22R-5, 48–52 cm (Piece 3), Unit 18 [Z-521]

Plagioclase-phyric basalt, massive. Phenocrysts (20%): prismatic grains (0.5–1.5 mm) of plagioclase (labradorite [An_{64}]) and their glomerophyric segregates. Groundmass with vitrophyric texture; greenish brown volcanic glass.

Alteration: rock is fresh.

XRD: smectite with ~10% mica layers; trace mixed-layer smectite-chlorite.

Sample 55-433C-23R-1, 100–104 cm (Piece 5D), Unit 19a [Z-1121]

Olivine-phyric basalt, fine grained, highly vesicular. Phenocrysts (10%): idiomorphic grains (0.3–1.6 mm) of olivine. Groundmass with micropilotaxitic texture; small grains (0.01–0.05 mm) of plagioclase and glass with rudimental grains (<0.01 mm) of clinopyroxene and opaque minerals. Vesicles (40%, 0.2–2 mm) are isometric in shape.

Alteration: moderate (35%–40%); olivine completely replaced by clay mineral; vesicles are filled with clay mineral, walls of vesicles are lined with cream glass.

XRD: smectite with ~20% mica layers.

Sample 55-433C-23R-2, 12–17 cm (Piece 1C), Unit 19b [Z-1661]

Olivine-phyric basalt (picrite-basalt), crystallized, fine grained, highly vesicular. Phenocrysts (25%): idiomorphic grains (0.2–1.8 mm) of olivine. Groundmass with microlitic texture; microlites and microlaths (0.05–0.3 mm) of plagioclase. Interstices are filled with segregate of small grains of clinopyroxene (10%), opaque minerals (2%–3%), and glass (2%–3%). Vesicles (40%, 2–3.5 mm) are oval and isometric in shape.

Alteration: very strong (80%); olivine, plagioclase, and glass completely replaced by smectites; vesicles are filled with smectites.

Sample 55-433C-24R-1, 12–15 cm (Piece 2), Unit 19b [Z-1122]

Olivine-phyric picrite-basalt, crystallized, coarse grained, vesicular. Phenocrysts (40%): idiomorphic grains (0.3–2 mm) of olivine. Groundmass with doleritic texture; laths (0.2–0.6 mm) of plagioclase (25%, labradorite [An_{58}] and andesine [An_{44}]). Interstices are filled with segregate or individual xenomorphic grains (0.1–0.3 mm) of clinopyroxene (20%), grains (0.1–0.3 mm) of olivine (1%–2%), and opaque minerals (5%–7%). Vesicles (10%, up to 0.7 mm) are isometric in shape.

Alteration: moderate (40%); olivine almost completely (80%) replaced by iddingsite; vesicles are filled with smectites.

XRD: smectite and mixed-layer smectite-chlorite with ~20% swelling interlayers; trace serpentine(?).

Sample 55-433C-24R-7, 104–108 cm (Piece 3B), Unit 19b [Z-522]

Olivine-phyric picrite-basalt, crystallized, massive. Phenocrysts (80%): idiomorphic grains (0.5–4.5 mm) of fresh olivine. Groundmass with microlitic texture; small (up to 0.1 mm) isometric and prismatic grains of clinopyroxene (90%) and glass (10%) which contains sparse rudiment laths or radiant grains of plagioclase.

Alteration: slight; oxidized rims of olivine grains.

XRD: smectite with ~20% mica layers and chlorite.

Sample 55-433C-24R-7, 108–114 cm (Piece 3C), Unit 19b [Z-1662]

Olivine-phyric picrite-basalt, crystallized, medium grained, vesicular. Phenocrysts (40%): idiomorphic grains (0.6–2 mm) of fresh olivine. Groundmass with microlitic texture; laths (0.1–0.3 mm) of plagioclase (10%, labradorite [An_{57}]). Interstices are filled with isometric grains of clinopyroxene (15%), opaque minerals (1%–2%), and altered brownish cream glass (10%). Vesicles (15%, up to 2.5 mm) are oval in shape.

Alteration: slight (15%); oxidized olivine rims; plagioclase partly replaced by albite; smectites replace glass.

Sample 55-433C-24R-7, 133–139 cm (Piece 3F), Unit 19b [Z-1123]

Olivine-phyric picrite-basalt with doleritic groundmass texture, crystallized, coarse grained, vesicular (25%). Rock: identical to Sample 55-433C-24R-1, 12–15 cm (Z-1122).

Alteration: moderate to strong (45%–50%); olivine partly (30%) replaced by iddingsite; plagioclase partly (30%–50%) replaced by pelite and clay mineral; vesicles are filled with clay mineral and chalcedony(?).

XRD: smectite with ~20% mica layers and mixed-layer chlorite-swelling chlorite with ~10% swelling interlayers.

Sample 55-433C-24R-7, 141–144 cm (Piece 3G), Unit 19b [Z-1124]

Olivine-phyric picrite-basalt with doleritic groundmass texture, crystallized, coarse grained, massive. Rock is identical to Samples 55-433C-24R-1, 12–15 cm (Z-1122) and 24R-7, 133–139 cm (Z-1123).

Alteration: slight (10%–15%); olivine partly (<5%) replaced by iddingsite; plagioclase partly (30%–40%) replaced by pelite and clay mineral.

XRD: smectite with ~30% mica layers and chlorite with ~10% swelling interlayers; trace phillipsite.

Sample 55-433C-26R-1, 87–92 cm (Piece 2F), Unit 21 [Z-1663]

Sparsely olivine-phyric basalt, fine grained, sparsely vesicular. Phenocrysts (1%): single idiomorphic grains (0.4–0.8 mm) of olivine. Groundmass with microlitic texture; laths (0.1–0.6 mm) of plagioclase (40%, labradorite [An_{55}], andesine [An_{48}] and andesine [An_{38}]). Interstices are filled with segregate of small grains of clinopyroxene (30%). Opaque minerals (5%) and chlorite (15%) are present. Vesicles (4%, 0.5–0.8 mm) are rounded in shape.

Alteration: slight to moderate (20%); olivine completely replaced by clay mineral; vesicles are filled with clay mineral.

Sample 55-433C-26R-2, 65–68 cm (Piece 1G), Unit 21 [Z-523]

Aphyric basalt (hawaiite-mugearite?), crystallized, sparsely vesicular. Rock with microlitic texture; unoriented laths (0.1–0.3 mm) of plagioclase (70%, andesine [An_{46}]). Interstices are filled with small (up to 0.1 mm) xenomorphic

grains of clinopyroxene (25%) and pseudocubic grains (<0.1 mm) of opaque minerals (5%). Single vesicles are registered.

Alteration: slight; plagioclase partly replaced by sosurite.

XRD: smectite with ~10% mica layers; trace mixed-layer smectite-chlorite with ~20% swelling interlayers.

Sample 55-433C-27R-2, 131–134 cm (Piece 6B), Unit 24a [Z-1125]

Olivine-phyric picrite-basalt with doleritic in groundmass texture, crystallized, coarse grained, vesicular (15%). Rock: identical to Sample 55-433C-24R-1, 12–15 cm (Z-1122).

Alteration: moderate (30%–35%); olivine partly (30%) replaced by iddingsite; vesicles are filled with smectites.

Sample 55-433C-27R-6, 38–43 cm (Piece 1H), Unit 25 [Z-1126]

Sparsely olivine-plagioclase-phyric basalt, fine grained, highly vesicular. Phenocrysts (3%–4%): single brownish red oxidized olivine and prismatic grain (2 mm) of plagioclase. Groundmass with hyalopilitic texture; microlites and laths (up to 0.7 mm) of plagioclase (20%), small (up to 0.2 mm) oxidized grains of olivine (5%), and black glass (30%). Vesicles (40%, 0.5–2 mm) are isometric, oval and rounded in shape.

Alteration: moderate (30%); plagioclase almost completely replaced by smectites; walls of vesicles are lined with clay mineral.

Sample 55-433C-27R-6, 134–140 cm (Piece 5), Unit 25 [Z-1667]

Sparsely olivine-plagioclase-phyric basalt, crystallized, fine grained, vesicular. Phenocrysts (1%–2%): single idiomorphic grains (0.9 mm) of olivine and their glomerophyric segregates; tabular grains (0.4–0.6 mm) of plagioclase (labradorite [An_{56}]). Groundmass with microlitic texture; microlites and microlaths (0.05–0.4 mm) of plagioclase (35%, labradorite [An_{51}], andesine [An_{43}] and andesine [An_{32}]). Interstices: segregate of small grains of clinopyroxene (30%); small (0.1–0.3 mm) idiomorphic grains of oxidized olivine (5%); abundant pseudocubic grains (0.05 mm) of opaque minerals (10%). Vesicles (20%, 0.3–0.8 mm) are isometric in shape.

Alteration: slight to moderate (15%–20%); olivine completely replaced by clay mineral; plagioclase almost completely replaced by clay mineral; vesicles are filled with clay mineral.

Sample 55-433C-28R-1, 42–47 cm (Piece 2E), Unit 25 [Z-1668]

Clinopyroxene-plagioclase-phyric basalt, crystallized, fine grained, vesicular. Phenocrysts (10%): sparse grains (0.6 mm) of clinopyroxene, prismatic crystals (0.9 mm) of plagioclase (andesine [An_{48}]), and glomerophyric segregates of clinopyroxene (3%) and plagioclase (7%). Groundmass with microlitic texture; microlites (<0.1 mm) and microlaths (0.1–0.2 mm) of plagioclase (30%, andesine [An_{38}]). Interstices: segregate of small grains of clinopyroxene (30%); idiomorphic grains (0.05 mm) of opaque minerals (10%). Vesicles (20%, 0.3–1.5 mm) are oval and isometric in shape.

Alteration: moderate (20%–25%); glass from plagioclase replaced by clay mineral; vesicles are filled with clay mineral.

XRD: smectite with ~10% mica layers.

Sample 55-433C-28R-2, 19–21 cm (Piece 1D), Unit 25 [Z-1127]

Clinopyroxene-plagioclase-phyric basalt with microlitic groundmass texture, crystallized, fine grained, sparsely vesicular (5%, 0.2–0.4 mm). Rock: identical to Sample 55-433C-28R-1, 42–47 cm (Z-1668).

Alteration: slight (5%); vesicles are filled with clay mineral.

XRD: smectite with ~20% mica layers; trace chlorite.

Sample 55-433C-28R-2, 66–73 cm (Piece 4B), Unit 25 [Z-1128]

Clinopyroxene-plagioclase-phyric basalt with microlitic groundmass texture, crystallized, medium grained, vesicular (10%, 0.3–2.5 mm). Rock: identical to Sample 55-433C-28R-2, 19–21 cm (Z-1127) and Sample 55-433C-28R-1, 42–47 cm (Z-1668).

Alteration: slight (10%); vesicles are filled with clay mineral.

XRD: smectite.

Sample 55-433C-28R-4, 30–37 cm (Piece 2C), Unit 25 [Z-1129]

Clinopyroxene-plagioclase-phyric basalt with microlitic groundmass texture, crystallized, fine grained, vesicular (30%, 0.3–2.5 mm). Rock: identical to Sample 55-433C-28R-2, 66–73 cm (Z-1128), Sample 55-433C-28R-2, 19–21 cm Z-1127, and 55-433C-28R-1, 42–47 cm (Z-1668).

Alteration: moderate (30%–35%); vesicles are filled with clay mineral.

Sample 55-433C-28R-4, 57–65 cm (Piece 5A), Unit 25 [Z-1672]

Sparsely plagioclase-phyric basalt, crystallized, fine grained, vesicular. Phenocrysts (5%): prismatic crystals (0.6–0.8 mm) of plagioclase (labradorite [An_{59}]). Groundmass with microlitic texture; microlites and laths (up to 0.4 mm) of plagioclase (35%, andesine [An_{48}] and andesine [An_{42}]). Interstices: segregate of small grains of clinopyroxene (35%); small idiomorphic grains of oxidized olivine (5%): opaque minerals (5%). Vesicles (15%, 0.3–0.8 mm) are oval in shape, empty.

Alteration: slight (5%); microcracks (5%, 0.1 mm) are filled with fragments of minerals and clay mineral.

XRD: smectite with ~10% mica layers; trace chlorite.

Sample 55-433C-28R-5, 77–81 cm (Piece 7B), Unit 26a [Z-524]

Clinopyroxene-plagioclase-phyric basalt (hawaiite-mugearite?), crystallized, massive. Phenocrysts (10%): elongated-prismatic grains (0.8–2 mm) of plagioclase (labradorite [An_{56}]) with small inclusions of glass and glomerophyric segregates of their grains (0.2–0.5 mm). Clinopyroxene forms partly idiomorphic grains and their segregates (0.5–1 mm). Groundmass with microlitic (microdoleritic) texture; laths (0.1–0.5 mm) of plagioclase (35%, andesine [$An_{44–46}$]), idiomorphic grains (0.1–0.3 mm) of clinopyroxene (50%), sparse small (0.1 mm) grains of olivine (1%), opaque minerals (5%), and brownish green glass (10%).

Alteration: slight; olivine replaced by clay mineral and iddingsite.

Sample 55-433C-28R-5, 107–109 cm (Piece 6E), Unit 26a [Z-1130]

Clinopyroxene-plagioclase-phyric basalt, crystallized, medium grained, massive. Phenocrysts (20%): small (0.4–0.7 mm) partly idiomorphic grains of clinopyroxene (5%) and prismatic grains (0.5–0.9 mm) of plagioclase (labradorite [An_{60}]), often plagioclase forms glomerophyric segregates. Clinopyroxene forms partly idiomorphic grains and their segregates (0.5–1 mm). Groundmass with microlitic texture; microlites and microlaths (0.1–0.4 mm) of plagioclase (30%, andesine [An_{44}] and [An_{38}]). Interstices: segregate small (0.05–0.2 mm) grains of clinopyroxene (25%); opaque minerals (5%); glass (20%).

Alteration: slight to moderate (20%); interstitial glass completely replaced by clay mineral.

XRD: smectite.

Sample 55-433C-31R-1, 86–90 cm (Piece 1L), Unit 27 [Z-525]

Olivine-plagioclase-phyric basalt (hawaiite-mugearite?), crystallized, sparsely vesicular. Phenocrysts (20%): glomerophyric segregates of partly idiomorphic rounded grains (0.1–0.6 mm) of olivine. Plagioclase (0.1–0.6 mm, labradorite [$An_{60–63}$]) forms glomerophyric segregates. Groundmass with microdoleritic texture; microlaths of plagioclase (40%, andesine [$An_{44–46}$]), segregate of small (<0.1 mm) grains of clinopyroxene (40%), volcanic glass (10%), and opaque minerals (8%–10%). Sparse vesicles (2%–3%, 0.6–1 mm) are oval in shape.

Alteration: slight (10%–12%); olivine partly replaced by iddingsite; clay mineral replaces glass; vesicles are filled with clay mineral.

Sample 55-433C-32R-1, 82–88 cm (Piece 3C), Unit 28c [Z-1674]

Olivine-phyric picrite, crystallized, coarse grained, vesicular. Phenocrysts (60%): idiomorphic grains (0.4–7.5 mm) of olivine. Groundmass with microdoleritic (microlitic) texture; small (0.01–0.3 mm) grains of olivine (5%) and laths (0.1–0.4 mm) of plagioclase (10%, andesine [An_{45}]). Interstices are filled with xenomorphic grains of clinopyroxene (12%) and opaque minerals (2%–3%). Vesicles (10%, 0.2–0.8 mm) are isometric in shape.

Alteration: moderate (20%–25%); olivine partly replaced by iddingsite; vesicles completely infilled by clay mineral.

Sample 55-433C-34R-2, 41–46 cm (Piece 1K), Unit 33 [Z-1131]

Plagioclase-olivine-phyric basalt, crystallized, medium grained, sparsely vesicular (2%–3%). Phenocrysts (20%): idiomorphic grains (0.3–1 mm) of olivine (15). Plagioclase (5%, labradorite [An_{60}]) forms sparse elongated-prismatic grains (up to 1.6 mm). Groundmass with microlitic texture; microlites and laths (0.1–0.4 mm) of plagioclase (25%), small (0.1–0.2 mm) grains of olivine (20%), small (0.1–0.2 mm) grains of clinopyroxene (15%), opaque minerals (5%), and black volcanic glass (10%).

Alteration: slight (10%–15%); olivine replaced by iddingsite.

Sample 55-433C-34R-3, 60–64 cm (Piece 1F), Unit 33 [Z-526]

Plagioclase-olivine-phyric picrite-basalt, crystallized, fine grained, massive. Phenocrysts (30%–35%): single elongated-prismatic grain (2.5 mm) of plagioclase with abundant inclusions of glass; idiomorphic grains (0.3–2 mm) of olivine. Groundmass with micropoikilophitic texture; xenomorphic grains (0.5–1.2 mm) of clinopyroxene (60%) with inclusions of laths of plagioclase (20%, andesine [$An_{43–48}$]); opaque minerals (5%) and glass (15%). Vesicles (40%, 2–3.5 mm) are oval and isometric in shape.

Alteration: moderate (40%); olivine almost completely replaced by iddingsite and Fe hydroxides; clay mineral replaces glass.

XRD: smectite with ~20% mica layers and chlorite with ~10% swelling interlayers.

Sample 55-433C-34R-7, 103–109 cm (Piece 3L), Unit 35 [Z-1681]

Plagioclase-olivine-phyric basalt, crystallized, fine grained, sparsely vesicular. Phenocrysts (15%): single prismatic crystals (0.7 mm) of plagioclase (<1%, labradorite [An_{63}]) and idiomorphic grains (0.3–1.7 mm) of olivine. Groundmass with microlitic texture; microlites and microlaths (0.05–0.6 mm) of plagioclase (30%, labradorite [An_{55}], andesine [An_{40}] and andesine [An_{32}]). Interstices: segregate of small grains (0.01 mm) of clinopyroxene (40%); opaque minerals (7%–8%); olivine (1%); glass (1%–2%). Vesicles (5%, 0.3–0.6 mm) are isometric in shape.

Alteration: slight to moderate (20%); olivine almost completely replaced by iddingsite and carbonate; clay mineral replaces glass.

Sample 55-433C-35R-6, 59–64 cm (Piece 1E), Unit 35 [Z-1682]

Clinopyroxene-plagioclase-olivine-phyric basalt, crystallized, sparsely vesicular. Phenocrysts (20%): single idiomorphic grains (0.9–1.2 mm) of clinopyroxene (2%), prismatic crystals (0.5–0.9 mm) of plagioclase (3%, labradorite [An_{53}]), and idiomorphic grains (0.8–3 mm) of olivine (15%). Groundmass with microlitic texture; microlites and laths (0.05–0.6 mm) of plagioclase (25%, labradorite [An_{55}], andesine [An_{38}]). Interstices: segregate of small grains (<0.1 mm) of clinopyroxene (30%); opaque minerals (10%); small grains (0.05–0.15 mm) of olivine (5%); glass (10%). Vesicles (1%, 0.5–1.7 mm) are oval in shape.

Alteration: moderate (25%); olivine almost completely replaced by iddingsite; clay mineral replaces glass; vesicles completely are filled with clay mineral.

Sample 55-433C-36R-3, 90–95 cm (Piece 1K), Unit 38 [Z-1683]

Olivine-phyric dolerite, crystallized, medium grained, vesicular. Phenocrysts (15%): idiomorphic grains (0.5–1.8 mm) of olivine. Groundmass with doleritic texture; small (0.1–0.2 mm) idiomorphic grains of olivine (5%) and laths (0.2–0.9 mm) of plagioclase (32%, labradorite [An_{57}], andesine [An_{42}], and andesine [An_{38}]). Interstices are filled with grains (0.1–0.3 mm) of clinopyroxene (30%), opaque minerals (2%–3%), and black glass (5%). Vesicles (10%, 0.3–0.8 mm) are isometric in shape.

Alteration: moderate (25%); olivine almost completely replaced by iddingsite; vesicles completely are filled with clay mineral.

Sample 55-433C-38R-5, 90–94 cm (Piece 1M), Unit 47a [Z-527]

Aphyric basalt, crystallized, massive. Rock with intersertal texture; laths (0.1–0.6 mm) of plagioclase (40%, andesine [$An_{44–46}$]). Interstices are filled with small (0.1–0.4 mm) xenomorphic grains of clinopyroxene (35%), opaque minerals (5%), and glass (20%).

Alteration: slight to moderate (20%); glass completely replaced by chlorite.

XRD: smectite with ~20% mica layers and mixed-layer smectite-chlorite with ~10% swelling interlayers; trace serpentine(?).

Sample 55-433C-39R-1, 119–122 cm (Piece 39), Unit 48 [Z-1132]

Sparsely olivine-phyric basalt, fine grained, highly vesicular. Phenocrysts (5%): idiomorphic grains (0.4–1.5 mm) of olivine. Groundmass with pilotaxitic texture; microsegregate of grains (0.05–0.1 mm) of olivine (10%); microlites (<0.1 mm) of plagioclase (20%); opaque minerals (5%); brown glass (5%). Vesicles (55%, 0.5–4 mm) are isometric in shape.

Alteration: very strong (70%); olivine completely replaced by iddingsite; plagioclase almost completely (90%) replaced by smectites; glass partly (50%) replaced by smectites; small vesicles completely infilled by clay mineral (zeolite is registered); walls of large vesicles are lined with clay mineral.

Sample 55-433C-39R-2, 35–40 cm (Piece 1H), Unit 48 [Z-1133]

Olivine-phyric basalt, fine grained with pilotaxitic groundmass texture, vesicular (10%, 0.4–0.8 mm). Rock: identical to Sample 55-433C-39R-1, 119–122 cm (Z-1132).

Alteration: very strong (70%).

Sample 55-433C-39R-3, 88–93 cm (Piece 1F), Unit 48 [Z-1134]

Olivine-phyric basalt, crystallized, fine grained, vesicular. Phenocrysts (10%): idiomorphic grains (1.5–2 mm) of olivine. Groundmass with microlitic texture; microlites (0.1–0.2 mm) of plagioclase (35%, andesine [An_{40}]).

Interstices: small (<0.1 mm) grains of clinopyroxene (25%), opaque minerals (1%–2%), and green glass (10%). Vesicles (20%, up to 3 mm) are oval in shape.

Alteration: moderate (20%–25%); olivine completely replaced by iddingsite; glass replaced by clay mineral; walls of vesicles are lined with clay mineral.

Sample 55-433C-39R-5, 2–8 cm (Piece 1A), Unit 48 [Z-1135]

Olivine-phyric basalt, crystallized with microlitic groundmass texture, moderate grained, sparsely vesicular (1%–2%, 1.5 mm). Rock: identical to Sample 55-433C-39R-3, 88–93 cm (Z-1134).

Alteration: moderate (35%); olivine completely replaced by iddingsite; glass replaced by clay mineral; vesicles are filled with clay mineral.

XRD: mixed-layer smectite-chlorite with ~10%–20% swelling interlayers; trace smectite.

Sample 55-433C-39R-5, 87–94 cm (Piece 1D), Unit 48 [Z-1136]

Olivine-phyric basalt, crystallized, medium grained, massive. Phenocrysts (25%): idiomorphic grains (0.3–1.7 mm) of olivine. Groundmass with microlitic texture; small (<0.3 mm) idiomorphic grains of olivine (5%), microlaths (0.1–0.3 mm) of plagioclase (30%, andesine [$An_{39–40}$]). Interstices: small (0.1 mm) grains of clinopyroxene (25%), opaque minerals (5%), and glass (10%).

Alteration: moderate (20%–25%); olivine completely or partly replaced by iddingsite; glass replaced by clay mineral.

XRD: mixed-layer smectite-chlorite with ~20% swelling interlayers; trace smectite.

Sample 55-433C-39R-6, 38–43 cm (Piece 1B), Unit 48 [Z-1137]

Olivine-phyric basalt, crystallized, medium grained, vesicular. Phenocrysts (10%): idiomorphic grains (1.2–3.5 mm) of olivine and their glomerophyric segregates. Groundmass with microlitic texture; small (up to 0.4 mm) idiomorphic grains of olivine (10%) and laths (0.1–0.3 mm) of plagioclase (30%, andesine [An_{40}]). Interstices: small (0.1 mm) grains of clinopyroxene (25%), opaque minerals (5%), and glass (10%). Vesicles (15%, 0.3–0.7 mm) are ideal rounded in shape.

Alteration: moderate (35%); olivine completely replaced by iddingsite; glass replaced by clay mineral; vesicles are filled with clay mineral.

Sample 55-433C-39R-6, 114–118 cm (Piece 1H), Unit 48 [Z-1692]

Olivine-phyric basalt, crystallized, fine grained, vesicular. Phenocrysts (15%): idiomorphic grains (up to 2.5 mm and 0.2–0.4 mm) of olivine. Groundmass with pilotaxitic texture; microlites (0.05–0.1 mm) of plagioclase (20%, andesine [An_{38}]), small (up to 0.1 mm) grains of olivine (2%–3%), clinopyroxene, and glass (25%) with crystallites of clinopyroxene and opaque minerals. Vesicles (30%, 0.5–1 mm) are rounded in shape.

Alteration: moderate (25%); olivine completely replaced by smectites; glass replaced by clay mineral; walls of vesicles are lined with clay mineral.

Sample 55-433C-41R-1, 20–23 cm (Piece 1C), Unit 51 [Z-528]

Aphyric basalt, crystallized, fine grained, vesicular. Rock with microlitic (microdoleritic) texture; laths (0.1–0.7 mm) of plagioclase (35%, andesine [$An_{43–46}$]). Interstices: segregates of plagioclase and grains (0.1–0.5 mm) of clinopyroxene (40%); opaque minerals (5%). Vesicles (20%, 0.2–0.6 mm) are rounded and oval-isometric in shape. Walls of vesicles are lined with volcanic glass.

Alteration: slight.

XRD: smectite.

Sample 55-433C-42R-1, 2–6 cm (Piece 1G), Unit 52 [Z-1138]

Plagioclase-phyric basalt, crystallized, medium grained, vesicular. Phenocrysts (20%): prismatic grains (0.8–1.5 mm) of plagioclase and glomerophyric segregates of elongated-prismatic grains of plagioclase (labradorite [$An_{58–59}$]). Groundmass with microdoleritic texture; laths (0.2–0.7 mm) of plagioclase (30%, andesine [An_{49}]). Interstices: segregate of grains (0.1–0.3 mm) of clinopyroxene (25%); glass (20%); opaque minerals (5%–7%). Vesicles (20%, 0.2–0.6 mm) are rounded and oval-isometric in shape. Walls of vesicles are lined with volcanic glass.

Alteration: moderate (20%–25%); glass replaced by clay mineral (occasionally, with biotite).

XRD: smectite with ~20% mica layers.

Sample 55-433C-42R-3, 83–88 cm (Piece 6B), Unit 54 [Z-1695]

Olivine-plagioclase-phyric basalt, crystallized, fine grained, highly vesicular. Phenocrysts (20%): single idiomorphic grains (0.3–0.7 mm) of olivine (5%) and prismatic grains (0.5–0.9 mm) of plagioclase (15%, labradorite [An_{52}] and andesine [An_{42}]). Groundmass with microlitic texture; microlites and microlaths (0.05–0.3 mm) of plagioclase (15%, andesine [An_{32}]). Interstices: small (<0.1 mm) grains of clinopyroxene (10%) and glass (5%). Vesicles (50%, 1.2–8 mm) are rounded and oval-isometric in shape.

Alteration: moderate (40%); olivine partly replaced by iddingsite; plagioclase partly (60%) replaced by clay mineral; glass replaced by clay mineral. Vesicles are lined or completely filled with clay mineral.

XRD: smectite; trace chlorite.

Sample 55-433C-43R-1, 118–123 cm (Piece 4B), Unit 54 [Z-1698]

Plagioclase-phyric basalt, crystallized, fine grained, vesicular. Phenocrysts (15%): tabular and prismatic grains (0.5–1 mm) of plagioclase (labradorite [An_{51}]) and their glomerophyric segregates. Groundmass with microlitic texture; microlites and laths (0.1–0.3 mm) of plagioclase (25%, andesine [An_{45}] and andesine [An_{41}]). Interstices: grains (0.1–0.3 mm) of olivine (5%), segregate of small (0.01 mm) grains of clinopyroxene (30%); glass (5%); opaque minerals (2%–3%). Vesicles (15%, 0.5–1.6 mm) are oval and isometric in shape.

Alteration: moderate (30%); glass completely replaced by clay mineral; plagioclase partly replaced by clay mineral; vesicles are filled with clay mineral.

Sample 55-433C-45R-3, 61–65 cm (Piece 3B), Unit 60 [Z-1139]

Sparsely plagioclase-phyric basalt, crystallized, medium grained, highly vesicular. Phenocrysts (1%): single prismatic grain (2.5 mm) of plagioclase. Groundmass with intersertal-microlitic texture; small (0.2–0.6 mm) grains of oxidized olivine (5%–7%), microlites and laths (0.1–0.7 mm) of plagioclase (20%, andesine [An_{47}]). Interstices: segregate of isometric grains (<0.1 mm, up to 0.3 mm) of clinopyroxene (15%); small grains of olivine (5%); green glass. Vesicles (40%, 0.6–2.5 mm) are rounded and isometric in shape.

Alteration: slight (15%); glass completely replaced by smectites; central parts of plagioclase replaced by smectites; vesicles are filled with clay mineral.

Sample 55-433C-45R-3, 119–124 cm (Piece 4D), Unit 60 [Z-1140]

Aphyric basalt, crystallized, medium grained, vesicular. Rock with microlitic texture; microlites and laths (0.1–0.8 mm) of plagioclase (30%, labradorite [An_{55}] and andesine [$An_{40–45}$]). Interstices: xenomorphic grains of oxidized olivine (10%), clinopyroxene (20%), opaque minerals (5%), and glass. Vesicles (25%, 1.2–5 mm) are oval in shape.

Alteration: moderate (30%–35%); central parts of plagioclase grains replaced by smectites; vesicles are filled with clay mineral.

Sample 55-433C-45R-4, 109–114 cm (Piece 4J), Unit 60 [Z-1704]

Plagioclase-phyric dolerite, crystallized, medium grained, vesicular. Phenocrysts (25%): prismatic crystals (0.8–1.6 mm) of plagioclase (labradorite [$An_{55–59}$] and andesine [An_{48}]). Groundmass with doleritic texture; laths and prismatic grains (0.1–0.6 mm) of plagioclase (30%, andesine [$An_{42–47}$]). Interstices: grains (0.2 mm) of oxidized olivine (2%–3%); segregate of isometric grains (0.1–0.4 mm) of clinopyroxene (25%); glass (2%–3%); opaque minerals (5%). Vesicles (10%, 0.1–0.9 mm) are isometric in shape.

Alteration: slight (10%); glass completely replaced by clay mineral; vesicles are filled with clay mineral.

Sample 55-433C-45R-5, 39–44 cm (Piece 1C), Unit 60 [Z-1141]

Clinopyroxene-olivine-plagioclase-phyric basalt, crystallized, medium grained, sparsely vesicular. Phenocrysts (20%): single idiomorphic grains (0.5–0.8 mm) of clinopyroxene (2%), glomerophyric segregates of prismatic crystals (0.4–0.8 mm) of plagioclase (12%–13%, labradorite [An_{62}] and labradorite [An_{54}]); olivine(?) 5%. Groundmass with microdoleritic texture; laths (0.2–0.8 mm) of plagioclase (35%, andesine [An_{48}]). Interstices: isometric grains (0.1–0.3 mm) of clinopyroxene and their segregates (20%); opaque minerals (2%–3%); glass (15%); biotite (2%). Vesicles (5%, 0.3–0.7 mm, single vesicle - 3 mm) are rounded in shape.

Alteration: moderate (25%); vesicles completely are filled with clay mineral.

Sample 55-433C-45R-5, 119–122 cm (Piece 3D), Unit 60 [Z-529]

Plagioclase-phyric dolerite, crystallized, massive. Phenocrysts (5%): glomerophyric segregates (up to 1.5–2 mm) of plagioclase (andesine [An_{48}]) grains (0.1–0.5 mm). Groundmass with doleritic texture; laths (0.2 –0.8 mm) of plagioclase (45%, andesine [$An_{42–45}$]). Interstices: segregate of xenomorphic grains (0.1–0.2 mm) of clinopyroxene (45%); glass (<5%); opaque minerals (5%).

Alteration: slight.

XRD: smectite.

Sample 55-433C-45R-6, 24–31 cm (Piece 1A), Unit 60 [Z-1142]

Sparsely clinopyroxene-plagioclase-phyric basalt, fine grained, highly vesicular. Phenocrysts (5%): single idiomorphic grains (0.9 mm) of clinopyroxene (2%) and prismatic crystals (0.8–1.2 mm) of plagioclase (38%, andesine [An_{40}]). Single microphenocryst of oxidized olivine is registered. Groundmass with hyalopilitic texture; microlites and laths (0.1–0.5 mm) of plagioclase (10%), rudiment grains of clinopyroxene (5%), and black glass (30%). Vesicles (50%, up to 5 mm) are isometric and oval in shape.

Alteration: strong (50%); vesicles completely are filled with carbonate, two vesicles are filled with clay mineral.

XRD: smectite with ~20% mica layers.

Sample 55-433C-45R-6, 97–102 cm (Piece 1G), Unit 60 [Z-1707]

Olivine-clinopyroxene-plagioclase-phyric dolerite, crystallized, medium grained, vesicular. Phenocrysts (15%): tabular and prismatic crystals (0.6–1.7 mm) of plagioclase (10%) and glomerophyric segregates of prismatic crystals (up to 0.6 mm) of plagioclase (labradorite [An_{53}]). Clinopyroxene (2%) forms grains and glomerophyric segregates of partly idiomorphic grains (0.6–0.8 mm). Olivine(5%) microphenocrysts (0.3–0.8 mm). Groundmass with doleritic texture; laths (0.1–0.7 mm) of plagioclase (30%, andesine-labradorite [An_{50}], andesine [An_{45}], and andesine [An_{35}]). Interstices: small grains of oxidized olivine (5%–7%); segregate of grains of clinopyroxene (20%); opaque minerals (7%–8%); glass (5%). Vesicles (15%, 0.8–1.7 mm and 0.3–0.7 mm) are rounded and isometric in shape.

Alteration: slight to moderate (20%); clay mineral replaces glass; vesicles are filled with clay mineral.

Sample 55-433C-45R-6, 129–132 cm (Piece 1N), Unit 60 [Z-1143]

Aphyric trachybasalt, crystallized, fine grained, sparsely vesicular. Rock with trachydoid texture; subparallel oriented microlites and laths (0.1–0.3 mm) of plagioclase (40%, andesine [$An_{38–42}$]), small grains (0.1 mm) of clinopyroxene (10%), opaque minerals (7%–8%), and dark green glass (30%). Vesicles (5%–7%, up to 2 mm) are rounded in shape.

Alteration: moderate (35%–40%); clay mineral replaces glass; vesicles are filled with clay mineral.

Sample 55-433C-46R-3, 78–83 cm (Piece 2D), Unit 62a [Z-1709]

Clinopyroxene-plagioclase-phyric basalt, crystallized, fine grained. Phenocrysts (15%): grains of clinopyroxene and their glomerophyric segregates (5%, 0.3–0.7 mm); prismatic crystals (0.7–1.2 mm) of plagioclase; glomerophyric segregates of smaller (0.3–0.5 mm) prismatic crystals of plagioclase (10%, labradorite [An_{55}]). Groundmass with intersertal-doleritic texture; laths (0.1–0.6 mm) of plagioclase (30%, andesine [An_{44}] and andesine [An_{41}]). Interstices: small (0.1–0.3 mm) grains of oxidized olivine (5%); segregate of small (0.05–0.2 mm) grains of clinopyroxene (20%); opaque minerals (5%); glass (20%).

Alteration: moderate (20%–25%); olivine partly replaced by clay mineral; glass completely replaced by clay mineral.

Sample 55-433C-47R-1, 8–13 cm (Piece 2A), Unit 63a [Z-1710]

Clinopyroxene-plagioclase-phyric basalt with intersertal-doleritic groundmass texture, crystallized, moderate grained. Rock: identical to Sample 55-433C-46R-3, 78–83 cm (Z-1709).

Alteration: slight (15%); glass completely replaced by clay mineral (biotite is registered).

XRD: smectite with ~10% mica layers.

Sample 55-433C-49R-2, 62–68 cm (Piece 1J), Unit 66 [Z-1712]

Aphyric dolerite, crystallized, medium grained. Rock with intersertal-doleritic texture; laths (0.2–1 mm) of plagioclase (45%, labradorite [An_{51}], andesine [An_{45}], and andesine [An_{39}]). Interstices: sparse (1%–2%) small (0.1 mm) grains of oxidized olivine (10%); segregate of xenomorphic grains (0.05–0.3 mm) of clinopyroxene (25%); opaque minerals (7%–8%); glass (20%).

Alteration: slight to moderate (20%); glass completely replaced by clay mineral (biotite is registered ~1%, 0.05 mm).

West Pacific Guyots (Legs 143 and 144)

Allison Guyot (Hole 865A)

Sample 143-865A-90R-5, 52–58 cm (Piece 5B), Unit 1 [Z-1492]

Aphyric basalt, vesicular. Rock with hyalopilitic texture; microlites and laths of plagioclase (25%) and black glass (55%). Vesicles (20%) are present.

Alteration: moderate (30%); plagioclase completely replaced by smectites and carbonate; central parts of vesicles are filled with carbonate.

XRD: smectite; trace hydromica (~10% swelling interlayers) and calcite; oxidized limestone intruded by sill: calcite, smectite, and siderite.

Sample 143-865A-90R-6, 45–50 cm (Piece 2), Unit 1 [Z-1493]

Aphyric basalt, vesicular. Rock with pilotaxitic texture; laths (0.2–1.2 mm) of plagioclase (45%, labradorite [An_{56}]). Interstices: small (<0.1 mm) grains of clinopyroxene (15%), subparallel oriented needles of opaque minerals (10%), and glass (20%). Vesicles (10%, 1.5–2.5 mm) are rounded in shape. Walls of vesicles are lined green glass.

Alteration: moderate (35%–45%); plagioclase completely replaced by smectites; glass completely replaced by smectite; central parts of vesicles are filled with smectites.

XRD: smectite with ~10% mica layers; trace mixed-layer swelling chlorite-smectite mineral, chlorite, and hydromica; gray-green clay from vesicles: smectite; trace calcite and chlorite(?); white matter from vesicles: calcite; white veinlet: calcite.

Sample 143-865A-91R-1, 112–118 cm (Piece 13B), Unit 1 [Z-1494]

Olivine-phyric basalt, sparsely vesicular. Phenocrysts (20%): idiomorphic grains (0.3–1.5 mm) of olivine (5%). Groundmass with hyalopilitic texture; laths and prismatic crystals of plagioclase (35%) and black glass (40%) with abundant crystals of opaque minerals. Single vesicles (5%, 0.9–1.8 mm) are rounded in shape.

Alteration: moderate (20%–25%); olivine partly replaced by iddingsite; vesicles are completely filled with smectites.

XRD: smectite; trace mixed-layer swelling chlorite-smectite mineral(?), chlorite, hydromica, and calcite; gray-green clay from vesicles: smectite; trace calcite.

Sample 143-865A-91R-2, 20–25 cm (Piece 2), Unit 1 [Z-1495]

Olivine-phyric basalt, sparsely vesicular. Phenocrysts (15%): idiomorphic grains of olivine (5%). Groundmass with hyalopilitic texture; microlites and laths of plagioclase (30%, labradorite [$An_{55–56}$]) and black glass (50%). Single large vesicle (4.5 mm) is oval in shape.

Alteration: slight (15%–20%); olivine completely replaced by iddingsite; vesicles are filled with brown partly chloritized glass and carbonate (in central parts).

XRD: smectite with ~10% mica layers; minor swelling chlorite; trace chlorite; black vein: smectite; trace chlorite, and calcite.

Sample 143-865A-91R-3, 22–28 cm (Piece 2), Unit 1 [Z-1496]

Olivine-plagioclase-phyric basalt, vesicular. Phenocrysts (10%): idiomorphic grains (0.5–0.6 mm) of olivine (3%) and prismatic crystals (up to 3 mm) of plagioclase (7%). Groundmass with hyalopilitic texture; microlites and laths of plagioclase (35%, labradorite [An_{55}]), small grains of olivine (5%), and black glass. Vesicles (10%, 0.7–1.5 mm) are rounded in shape. Walls of vesicles are lined with light green and brown glass.

Alteration: slight (15%–20%); olivine completely replaced by iddingsite; plagioclase replaced by clay mineral; vesicle is filled with carbonate (in central part).

XRD: smectite with ~20% mica layers; trace swelling chlorite, chlorite, and hydromica; black vein: smectite; trace chlorite and calcite; gray clay from vesicles: smectite.

Sample 143-865A-92R-3, 80–86 cm (Piece 1), Unit 3 [Z-1497]

Aphyric basalt with pilotaxitic texture.

Alteration: rock completely replaced by Fe-Mn hydroxides; plagioclase completely replaced by smectites.

XRD: smectite; trace, hydromica, and kaolinite(?); pink matter: apatite.

Sample 143-865A-92R-4, 45–47 cm, Unit 3 [Z-1498]

Sparsely olivine-phyric basalt, with intergranular-microdoleritic texture; euhedral olivine microphenocrysts (as large as 0.5 mm) compose ~1% of rock. Groundmass: unoriented plagioclase laths, small grains of pyroxene and opaque minerals.

Alteration: very strong; olivine replaced by iddingsite and smectite; plagioclase and pyroxene replaced by smectite; opaque dust partly oxidized; thin fissures infilled with smectite.

XRD: smectite with interlayer Na-K cations and with ~20% mica layers; minor kaolinite; trace hydromica, hematite, gypsum, and K-feldspar.

Sample 143-865A-93R-1, 30–36 cm, (Piece 4), Unit 3 [Z-1499]

Olivine-plagioclase-phyric basalt. Phenocrysts (15%): phenocrysts of altered olivine and plagioclase. Groundmass with pilotaxitic texture; altered plagioclase (60%), black oxidized glass (5%–10%), and needles of opaque minerals.

Alteration: very strong (100%) and oxidized (40%); all phenocrysts completely replaced by Fe hydroxides; groundmass plagioclase completely replaced by zeolite and smectites; interstitial glass is oxidized.

XRD: smectite with interlayer Na-K cations and with ~30% mica layers; minor kaolinite, calcite, and hematite; trace of hydromica, chlorite, gypsum, and K-feldspar; 2.70 Å (undetermined mineral).

Sample 143-865A-93R-2, 0–8 cm, (Piece 1), Unit 3 [Z-1500]

Olivine-plagioclase-phyric basalt, crystallized. Phenocrysts (20%): altered phenocrysts of olivine and plagioclase. Groundmass with intersertal (microdoleritic) texture; laths of altered plagioclase (30%), altered glass (25%), oxidized grains of olivine (5%), altered clinopyroxene (5%), and needles of opaque minerals (15%).

Alteration: very strong (100%) and oxidized (40%); all phenocrysts completely replaced by Fe hydroxides and smectites; groundmass plagioclase completely replaced by smectites; interstitial glass completely replaced by chlorite; olivine is oxidized; secondary opaque minerals was met.

XRD: swelling chlorite; trace serpentine(?) and hydromica(?); green-gray clay from vein: smectite; trace calcite; pink matter from vein: apatite(?).

Sample 143-865A-93R-3, 47–49 cm, (Piece 2B), Unit 3 [Z-1716]

Olivine-phyric basalt, crystallized, medium grained. Phenocrysts (25%): idiomorphic grains (0.3–1.7 mm) of altered olivine. Groundmass with microlitic texture; small (0.1–0.3 mm) grains of oxidized olivine (5%), laths of altered plagioclase (30%, andesine [An_{45}]), grains of altered clinopyroxene (20%), opaque minerals (5%), and altered glass (15%).

Alteration: very strong (60%–65%); olivine almost completely replaced by smectites; plagioclase almost completely (80%) is pelletized; clay mineral replaces glass.

Sample 143-865A-94R-1, 97–102 cm, (Piece 17D), Unit 3 [Z-1501]

Olivine-phyric basalt. Phenocrysts (15%): idiomorphic grains of altered olivine. Groundmass with microlitic texture; microlites and laths of fresh plagioclase (30%, labradorite [$An_{55–56}$]). Interstices: small grains of altered olivine (5%), segregate of very small (0.01 mm) grains of clinopyroxene (20%); opaque minerals (10%); altered glass (20%).

Alteration: moderate (40%); olivine completely replaced by iddingsite; clay mineral replaces glass.

XRD: smectite, mixed-layer swelling chlorite-smectite, and hematite; trace chlorite and hydromica.

Sample 143-865A-94R-2, 102–105 cm, (Piece 16), Unit 3 [Z-1502]

Olivine-phyric basalt, highly vesicular. Phenocrysts (20%): altered olivine. Groundmass with hyalopilitic texture; microlites and laths of altered plagioclase (10%–15%), small grains of altered olivine (2%–3%), and black glass (25%). Vesicles (40%, 1.2–10 mm) are oval in shape. Walls of vesicles (20%) are lined with glass.

Alteration: moderate (30%–35%); olivine completely replaced by iddingsite; plagioclase almost completely (50%–90%) replaced by smectites; 80% of vesicles completely are filled with carbonate, glass from vesicles is palagonitized.

Sample 143-865A-94R-4, 133–143 cm, (Piece 9), Unit 4 [Z-1503]

Sparsely olivine-phyric basalt, crystallized, sparsely vesicular. Phenocrysts (5%): altered olivine. Groundmass with microlitic texture; microlites and laths of plagioclase (30%, labradorite [An_{55}]). Interstices: segregate of small grains of clinopyroxene (35%); small grains of altered olivine (5%); opaque minerals (10%); altered glass (5%). Single vesicle (1%–2%, 1.7 mm) is rounded in shape.

Alteration: strong; olivine completely replaced by iddingsite; clay mineral replaces glass; vesicle completely are filled with clay mineral.

XRD: smectite and mixed-layer swelling chlorite-smectite; trace chlorite and hydromica.

Resolution Guyot (Hole 866A)

Sample 143-866A-171R-2, 109–111 cm (Piece 3), Unit 1 [Z-1504]

Olivine-phyric basalt, primary groundmass texture unidentifiable. Phenocrysts: olivine (0.1–1 mm) ~15% of rock. Groundmass: unoriented plagioclase laths, microlites of olivine (0.03–0.1 mm), and opaque minerals; rare unhedral K-feldspar.

Alteration: moderate (30%); olivine and groundmass completely replaced by smectites.

XRD: kaolinite and heterogeneous smectites; smectites contain ~30%–40% mica layers; minor hematite; trace K-feldspar.

Sample 143-866A-171R-4, 131–134 cm, Unit 2 [Z-1505]

Olivine-phyric basalt, pilotaxitic texture. Rock completely replaced by Fe hydroxides (80%) and smectites (20%).

Alteration: very strong (100%); rock is oxidized (80%).

XRD: smectite with ~30% mica layers; trace kaolinite; veinlet: smectite with ~20%–40% mica layers.

Sample 143-866A-178W-1, 37–38 cm, Unit 4 [Z-1506]

Plagioclase-olivine-phyric basalt, weakly crystallized, hyalopilitic texture, tectonized. Phenocrysts are represented mainly by euhedral olivine crystals (0.3–1 mm) and rare plagioclase phenocrysts; phenocrysts total ~10% of rock. Groundmass: represented by plagioclase microlites, volcanic glass, and opaque dust.

Alteration: very strong; smectitized and carbonatized olivine and plagioclase phenocrysts; groundmass, including glass, replaced by smectite, carbonate, and hematite; thin fissures infilled with smectite and carbonate.

XRD: smectite with interlayer Na-K cations; minor kaolinite and hematite; trace hydromica.

Sample 143-866A-178W-1, 79–81 cm, Unit 4 [Z-1507]

Aphyric apobasalt completely replaced by smectite and oxidized opaque matter.

Alteration: very strong.

XRD: smectite with interlayer Na-K cations and with ~10% mica layers; minor kaolinite; trace quartz and 3.51C-undetermined mineral.

Sample 143-866A-179R-5, 40–45 cm, Unit 6 [Z-1508]

Olivine-plagioclase-phyric basalt, crystallized, sparsely vesicular. Phenocrysts (30%): idiomorphic grains (0.4–0.9 mm) of olivine (5%) and prismatic and tabular crystals (1.5–5 mm, up to 6 mm) of plagioclase (25%, labradorite [An_{55}] and labradorite [An_{62}]). Groundmass with microlitic texture; microlites and laths (0.1–0.7 mm) of plagioclase (30%, andesine [An_{32-45}]); small (0.1–0.3 mm) grains of oxidized olivine (5%); segregate of clinopyroxene (25%) grains (<0.1 mm); green altered glass (4%), and grains (<0.1 mm) of opaque minerals (5%–7%). Two vesicles (1%–2%, 0.6 mm and 1.7 mm) are oval in shape.

Alteration: slight (10%) and weakly oxidized (5%–10%); olivine completely replaced by iddingsite; clay mineral replaces glass; vesicles infilled with clay minerals and carbonate.

XRD: smectite; trace mixed-layer smectite-chlorite and swelling chlorite.

Sample 143-866A-180R-1, 27–32 cm, (Piece 3A), Unit 6 [Z-1509]

Olivine-plagioclase-phyric basalt, crystallized. Phenocrysts (25%): phenocrysts (0.5–1.7 mm) of altered olivine (5%–7%) and grains (0.9–6 mm) of plagioclase (18%–20%, labradorite [An_{62}]). Groundmass with microlitic texture; microlites and laths of plagioclase (30%, labradorite [An_{54}], andesine [$An_{40–43}$], and andesine [An_{38}]). Interstices: clinopyroxene (25%), altered glass (5%), grains of altered olivine (5%), and opaque minerals (10%).

Alteration: slight to moderate (15%–20%) and nonoxidized; olivine completely replaced by iddingsite; clay mineral replaces glass.

XRD: smectite with ~20% mica layers and mixed-layer smectite-chlorite mineral; trace hydromica; gray-green clay from vesicles: smectite.

Sample 143-866A-180R-3, 67–72 cm, (Piece 1D), Unit 6 [Z-1510]

Olivine-plagioclase-phyric basalt, crystallized. Phenocrysts (35%): phenocrysts (1–4 mm) of olivine (10%) and grains (1–7 mm) of plagioclase (25%, labradorite [$An_{55–60}$], and andesine [An_{43}]). Groundmass with microlitic

texture; microlites and laths of plagioclase (25%, andesine [$An_{42–43}$] and andesine [An_{38}]), small grains (<0.1 mm) of clinopyroxene (25%), altered glass (5%), and opaque minerals (10%).

Alteration: moderate (20%–25%) and nonoxidized; olivine partly (30%–35%) replaced by iddingsite; clay mineral replaces glass.

XRD: smectite with ~10% mica layers and mixed-layer smectite-chlorite mineral with ~10% swelling interlayers; trace hydromica; vesicle filling: mixed-layer swelling chlorite-smectite mineral and swelling chlorite.

Sample 143-866A-180R-4, 12–17 cm, (Piece 1B), Unit 6 [Z-1511]

Olivine-plagioclase-phyric basalt, crystallized. Rock is identical with Sample 143-866A-180R-3, 67–72 cm (Z-1510).

Alteration: moderate (20%–25%) and nonoxidized; olivine partly (30%–35%) replaced by iddingsite; clay mineral replaces glass.

XRD: smectite and swelling chlorite; trace hydromica.

Sample 143-866A-182R-1, 3–8 cm, (Piece 2), Unit 8 [Z-1512]

Olivine-plagioclase-phyric basalt, crystallized. Phenocrysts (10%): phenocrysts of olivine (5%) and grains of plagioclase (5%). Groundmass with microlitic texture; microlites (0.1–0.3 mm) of plagioclase (30%, andesine [An_{38}] and rare laths (andesine [An_{42}]). Interstices: altered glass (10%), small grains (0.1–0.2 mm) of olivine (5%), and opaque minerals (10%).

Alteration: slight to moderate (15%–20%); rock is nonoxidized; groundmass olivine replaced by iddingsite; clay mineral replaces glass.

XRD: smectite, mixed-layer smectite-chlorite mineral, chlorite, and swelling chlorite.

Sample 143-866A-182R-2, 58–63 cm, (Piece 3C), Unit 8 [Z-1513]

Plagioclase-olivine-phyric basalt, crystallized. Phenocrysts (30%): grains (0.8–2.5 mm) of olivine (20%) and grains (2–2.5 mm) of plagioclase (10%, andesine [An_{42}]). Groundmass with microlitic texture; microlites (0.1–0.3 mm) of plagioclase (30%, andesine [An_{40}]), small grains of clinopyroxene (15%), altered glass (5%), and abundant small (0.1–0.3 mm) isometric grains of opaque minerals (20%).

Alteration: moderate (25%); olivine replaced by Fe hydroxides; clay mineral replaces glass.

XRD: smectite; trace mixed-layer smectite-chlorite mineral and hydromica(?).

Sample 143-866A-182R-4, 26–30 cm, (Piece 4B), Unit 8 [Z-1514]

Aphyric basalt, weakly crystallized, vesicular. Rock with hyalopilitic texture; microlites and microlaths of plagioclase (30%), black to brown glass (35%) with abundant brown grains of Fe hydroxides, and opaque minerals (10%). Vesicles (25%) are rounded in shape.

Alteration: strong (45%–50%); rock is oxidized (35%–40%); plagioclase completely replaced by pelite, albite, and Fe hydroxides.

XRD: smectite.

Sample 143-866A-182R-4, 72–74 cm, (Piece 8), Unit 8 [Z-1515]

Olivine-phyric basalt, crystallized, vesicular, brecciated. Phenocrysts: idiomorphic olivine (up to 0.5 mm) composes ~5% of rock. Groundmass with microlitic texture; unoriented plagioclase laths, pyroxene microlites, opaque dust, and interstitial glass.

Alteration: moderate; olivine and pyroxene replaced by smectite and iddingsite; plagioclase replaced by smectite and opaque dust; glass replaced by smectite; vesicles infilled and encrusted with smectite, some vesicles with oxidized Fe; glassy crust of basalt completely impregnated by Fe-Mn oxides.

XRD: smectite with interlayer Na-K cations and with ~10% mica layers; trace hematite and 4.87 Å (undetermined mineral).

Sample 143-866A-183R-1, 125–131 cm, (Piece 18B), Unit 9 [Z-1516]

Olivine-phyric basalt, crystallized, vesicular. Phenocrysts (15%): microphenocrysts (0.3–0.6 mm) of oxidized olivine. Groundmass with pilotaxitic texture; plagioclase (35%, andesine [An_{42-46}]) microlites and microlaths (0.1–0.4 mm) and interstitial green altered glass (25%). Vesicles (25%, 0.3–1.1 mm) are isometric and rounded in shape.

Alteration: moderate (40%); rock is oxidized (30%); olivine replaced by iddingsite; plagioclase replaced by clay minerals; glass replaced by clay minerals and black Fe hydroxides; vesicles infilled with clay minerals.

XRD: smectite; trace chlorite; gray-green and cream matter from vein: smectite.

Sample 143-866A-184R-1, 23–28 cm, (Piece 4), Unit 9 [Z-1517]

Clinopyroxene-biotite-olivine trachybasalt, microdoleritic, with trachytic texture. Microphenocrysts are represented by euhedral olivine crystals, biotite, and pyroxene; phenocrysts total ~15% of rock; biotite and olivine dominant. Groundmass: represented by subparallel oriented plagioclase (andesine [An_{40}]) laths, augite microlites, opaque minerals, and very small amount of interstitial glass; rare vesicles are present.

Alteration: slight (5%); olivine replaced by iddingsite; pyroxene replaced by smectite; sericitized plagioclase; smectitized groundmass glass; thin fissures and vesicles infilled with smectite.

XRD: smectite with interlayer Na-K cations and ~10% mica layers; trace kaolinite and quartz; thin fissure infilled by smectite with interlayer Na-K cations.

Sample 143-866A-184R-1, 137–139 cm, (Piece 7), Unit 9 [Z-1518]

Tuff (breccia). Rock; fragments (2–10 mm) of altered olivine basalt. Large fragments cemented by aggregate of angular small (0.4–0.6 mm) fragments (10%) of light green glass.

Alteration: very strong; basalt and cement replaced by clay minerals and Fe hydroxides.

XRD: smectite with different interlayer cations: Na-K and Ca-Mg; trace hematite and quartz; matrix from breccia: smectite.

Sample 143-866A-184R-2, 23–26 cm, (Piece 3), Unit 9 [Z-1519]

Olivine-pyroxene-phyric basalt, crystallized, vesicular. Phenocrysts (15%): single idiomorphic grain (1.5 mm) of oxidized olivine (8%) and tabular grains (1–1.2 mm) of orthoclase (12%). Groundmass with pilotaxitic texture; microlites (0.1–0.2 mm) of plagioclase (20%, andesine [An_{38}]), grains (0.1 mm) of oxidized olivine (10%), opaque minerals (5%), and black glass (20%). Vesicles (30%, 0.1–0.5 mm and 2.5–10 mm) are isometric in shape.

Alteration: slight (10%–15%); vesicles infilled and encrusted with clay mineral.

XRD: smectite with interlayer Na-K cations; minor hematite.

Sample 143-866A-185R-3, 41–46 cm, (Piece 1D), Unit 10 [Z-1520]

Clinopyroxene-olivine-plagioclase-phyric basalt, crystallized, sparsely vesicular. Phenocrysts (20%): single grain (3 mm) of clinopyroxene (2%), idiomorphic grains (0.8–1.2 mm) of altered olivine (8%), and prismatic crystals (1.2–2.5 mm) of plagioclase (15%, labradorite [An_{55}]). Groundmass with microlitic texture; microlites and microlaths (0.1–0.3 mm) of plagioclase (35%, andesine [An_{38}]). Interstices: small (<0.1 mm) grains of clinopyroxene (20%), green altered glass, and opaque minerals (5%). Vesicles (1%, 0.7 mm) are rounded in shape.

Alteration: slight (15%); groundmass olivine replaced by iddingsite and partly oxidized; clay mineral replaces glass; vesicles are encrusted with clay mineral and infilled with carbonate.

XRD: smectite; gray-green matter from vesicles: smectite; trace calcite.

Sample 143-866A-185R-4, 26–32 cm, (Piece 6B), Unit 11 [Z-1521]

Olivine-phyric basalt, crystallized, vesicular. Phenocrysts: idiomorphic olivine (up to 0.5 mm) composes ~20% of rock. Groundmass with microlitic texture; plagioclase laths (30%), interstitial glass (10%), and olivine grains. Vesicles (35%, 0.9–2 mm) are isometric in shape.

Alteration: moderate (40%); olivine oxidized; plagioclase and glass replaced by clay mineral and Fe hydroxides; vesicles infilled with clay mineral.

XRD: smectite; gray-green matter from vesicles: smectite; trace calcite.

Sample 143-866A-186R-1, 39–41 cm, (Piece 6), Unit 11 [Z-1522]

Olivine-phyric basalt, highly vesicular. Phenocrysts: single olivine grain. Groundmass with vitrophyric texture; black glass (35%), plagioclase needle-shaped microlites (5%–7%), and olivine grains (5%, 0.1 mm). Vesicles (60%–65%, 0.9–5 mm) are rounded in shape.

Alteration: strong; olivine replaced by smectite; small crystals replaced by iddingsite; plagioclase replaced by smectite; smectitized and oxidized glass; vesicles infilled with smectite.

XRD: smectite with interlayer Ca-Mg cations; trace hematite and gypsum; gray-blue matter from vesicles: smectite with interlayer Ca-Mg cations.

Sample 143-866A-186R-2, 20–24 cm, (Piece 5), Unit 11 [Z-1523]

Olivine-phyric basalt, vesicular. Phenocrysts (2%–3%): single olivine idiomorphic grains (0.8–1 mm). Groundmass with hyalopilitic texture; plagioclase needle-shaped microlites (10%, <0.1 mm), olivine small grains (5%–7%,

0.2 mm), and colorless glass (60%) with abundant crystals of clinopyroxene and opaque minerals (<0.01 mm). Vesicles (5%, 0.9–5 mm) are isometric in shape.

Alteration: slight (15%); olivine replaced by iddingsite, rims of olivine grains are oxidized; vesicles and fissures infilled with clay mineral.

XRD: smectite.

Sample 143-866A-187R-1, 99–104 cm, (Piece 17), Unit 11 [Z-1524]

Olivine-phyric basalt, crystallized. Phenocrysts: olivine (0.2–0.6 mm) composes ~15% of rock. Groundmass with microlitic texture; plagioclase microlaths (55%, 0.1–0.3 mm, andesine [An_{38}]), olivine small (0.1 mm) grains (15%), interstitial green glass (5%), and opaque minerals (10%).

Alteration: slight (5%); oxidized olivine; glass replaced by clay mineral.

XRD: smectite; gray-green vein: smectite.

Sample 143-866A-188R-1, 82–89 cm, (Piece 16A), Unit 11 [Z-1525]

Sparsely olivine-phyric basalt, crystallized. Phenocrysts: olivine composes ~5% of rock. Groundmass with pilotaxitic texture; plagioclase microlites (30%, 0.1–0.2 mm), black glass (45%), and opaque minerals (10%, 0.1–0.3 mm).

Alteration: moderate (45%); olivine oxidized and replaced by iddingsite; plagioclase almost completely replaced by clay mineral and Fe hydroxides; glass replaced by clay minerals.

XRD: smectite; trace mixed-layer swelling chlorite-smectite mineral; green veinlet: smectite; trace chlorite.

Sample 143-866A-189R-1, 65–69 cm, (Piece 5C), Unit 12 [Z-1526]

Clinopyroxene-plagioclase-olivine-phyric basalt, crystallized. Phenocrysts (30%): clinopyroxene idiomorphic grains (5%, 1.2–3 mm), plagioclase grains (10%, 1.2–4 mm, andesine [An_{31}]), and olivine idiomorphic grains (15%, 0.9–4 mm). Groundmass with microlitic texture; plagioclase microlites (30%, 0.1–0.3 mm, andesine [$An_{36–42}$]). Interstices: clinopyroxene small (<0.1 mm) grains (20%), olivine grains (5%, 0.1–0.2 mm), green altered glass, and opaque minerals (5%). Skeletal opaque minerals (10 mm) is present.

Alteration: slight (18%); groundmass olivine replaced by iddingsite (10%–100%); clay mineral replaces glass.

XRD: mixed-layer smectite-chlorite mineral; minor smectite; trace mixed-layer swelling chlorite: smectite mineral and hydromica(?).

Sample 143-866A-189R-2, 115–120 cm, (Piece 7C), Unit 12 [Z-1527]

Tuff (volcanic breccia). Rock; fragments (up to 7 mm) olivine-plagioclase-phyric basalt with large (up to 5 mm) vesicles (35%).

Alteration: strong (50%–60%); partly oxidized olivine replaced by clay mineral; plagioclase grains partly or completely pelletized and smectitized; glass replaced by clay mineral; vesicles infilled with clay mineral and carbonate; fissures infilled with clay mineral.

XRD: smectite; minor mixed-layer swelling chlorite: smectite mineral; gray-green matter: smectite.

Limalok Guyot (Hole 871C)

Sample 144-871C-35R-3, 70–76 cm (Piece 3C), Unit 6 [Z-1528]

Breccia. Oxidized crust from breccia (Fe-Mn hydroxides and carbonate).

Sample 144-871C-35R-3, 143–145 cm (Piece 5B), Unit 7B [Z-863]

Olivine-phyric basalt, highly vesicular. Phenocrysts (10%): olivine grains (0.1–0.5 mm). Groundmass with microlitic or intersertal texture; clinopyroxene rounded grains (80%, <0.1 mm) and green glass (20%). Vesicles (40%, 0.2–2 mm) are isometric in shape.

Alteration: moderate (30%); olivine replaced by carbonate and clay mineral, rims of olivine grains are oxidized; clay mineral replaces glass; vesicles infilled with carbonate.

Sample 144-871C-35R-4, 96–98 cm (Piece 12), Unit 7B [Z-1529]

Plagioclase-olivine-phyric basalt. Phenocrysts (20%): plagioclase and olivine strong altered microphenocrysts (0.1–1 mm). Groundmass with vitrophyric texture; brownish black to black glass with abundant very small grains of opaque minerals.

Alteration: plagioclase and olivine completely replaced by carbonate and chalcedony(?); cracks infilled with carbonate and chalcedony(?).

XRD: smectite; minor mixed-layer smectite-chlorite mineral; trace hydromica and calcite.

Sample 144-871C-36R-1, 79–86 cm (Piece 7B), Unit 8 [Z-1530]

Olivine-phyric basalt. Phenocrysts (5%): strong altered olivine phenocrysts (0.1–0.5 mm). Groundmass with vitrophyric texture; black glass with rare relicts of brown glass.

Alteration: olivine completely replaced by smectite.

XRD: smectite; minor mixed-layer smectite-chlorite mineral; trace serpentine and quartz; clay matter from vein: smectite and mixed-layer swelling chlorite-smectite mineral; trace hydromica.

Sample 144-871C-36R-2, 107–109 cm (Piece 11), Unit 13 [Z-864]

Olivine-phyric basalt, vesicular. Phenocrysts: olivine (0.3–1.4 mm) composes ~20% of rock. Groundmass with microlitic texture; clinopyroxene grains (85%, up to 0.1 mm), opaque minerals (10%), and interstitial glass (5%). There are vesicles (10%, 0.8–2 mm).

Alteration: moderate (25%); olivine completely replaced by clay mineral, rims of olivine are oxidized; clay mineral replaces glass; vesicles infilled with clay mineral and carbonate.

Sample 144-871C-36R-3, 32–35 cm (Piece 3), Unit 13 [Z-865]

Olivine-phyric basalt, vesicular. Rock: identical to Sample 144-871C-36R-2, 107–109 cm (Z-864).

Sample 144-871C-38R-1, 117–120 cm (Piece 10), Unit 17 [Z-866]

Clinopyroxene-olivine-phyric basalt, sparsely vesicular. Phenocrysts (30%): olivine grains (90%, 0.3–1.8 mm), single idiomorphic grains (0.8 mm) of clinopyroxene (10%), and plagioclase grains (10%, 1.2–4 mm, andesine [An_{31}]),. Groundmass with microlitic texture; clinopyroxene small grains (85%, <0.1 mm), opaque minerals (10%), and glass (5%). Single vesicles are rounded in shape.

Alteration: slight; olivine partly (20%) replaced by clay mineral; clay mineral replaces glass; vesicles are filled with zeolite(?).

Sample 144-871C-38R-3, 83–87 cm (Piece 4), Unit 17 [Z-867]

Rock: identical to Sample 144-871C-38R-1, 117–120 cm (Z-866).

XRD: smectite; minor mixed-layer smectite-chlorite mineral; trace chlorite, hydromica, and analcime.

Sample 144-871C-38R-7, 0–5 cm (Piece 1A), Unit 20 [Z-1531]

Olivine-phyric basalt, crystallized. Phenocrysts: olivine (0.3–2 mm) composes 30% of rock. Groundmass with microlitic texture; clinopyroxene grains (60%, <0.1 mm) segregate; interstitial colorless glass (7%–8%); and opaque minerals (5%).

Alteration: moderate (25%); olivine completely replaced by iddingsite, several olivine grains completely oxidized.

XRD: smectite; minor mixed-layer smectite-chlorite mineral; trace chlorite and serpentine(?); green-gray matter from veinlet: smectite; trace chlorite and calcite.

Sample 144-871C-39R-1, 6–9 cm (Piece 2), Unit 21A [Z-868]

Olivine-phyric basalt, sparsely vesicular. Phenocrysts: olivine composes 20% of rock. Groundmass with microlitic texture; clinopyroxene grains (85%), opaque minerals (10%), and interstitial glass (5%). Single vesicle (0.6 mm) is rounded in shape.

Alteration: moderate (25%); olivine completely replaced by clay mineral; clay mineral replaces glass; wall of vesicle is lined with clay mineral, central part of vesicle infilled with carbonate.

Sample 144-871C-39R-4, 0–5 cm (Piece 1), Unit 21E [Z-1532]

Plagioclase-olivine-phyric basalt. Phenocrysts (20%): olivine (15%) and plagioclase (5%). Groundmass with vitrophyric texture; black glass.

Alteration: slight to moderate (20%); plagioclase and olivine completely replaced by iddingsite and smectite.

XRD: smectite; trace mixed-layer smectite-chlorite mineral, chlorite and hematite.

Sample 144-871C-39R-5, 120–124 cm (Piece 10C), Unit 21G [Z-1533]

Olivine-phyric basalt, crystallized, vesicular. Phenocrysts: olivine idiomorphic grains (0.3–2 mm) compose 30% of rock. Groundmass with microlitic texture; olivine grains (10%, 0.1–0.2 mm); segregate of clinopyroxene grains (45%); interstitial colorless glass (5%). There are vesicles (10%, up to 3 mm).

Alteration: moderate (30%); olivine completely replaced by iddingsite; vesicles infilled with smectite and carbonate.

XRD: smectite with ~10% mica layers; minor mixed-layer smectite-chlorite mineral; trace serpentine(?).

Sample 144-871C-40R-1, 126–130 cm (Piece 10A), Unit 22A [Z-1534]

Olivine-orthopyroxene-phyric basalt, crystallized, vesicular. Phenocrysts (45%): olivine idiomorphic grains (15%, 0.3–1 mm) and orthopyroxene idiomorphic grains (30%, up to 2 mm). Groundmass with microlitic texture; olivine grains (2–3%, <0.12 mm); segregate of clinopyroxene grains (30%–35%); interstitial colorless glass (10%); opaque minerals (2%–3%). Vesicles (10%) are present.

Alteration: slight to moderate (20%); olivine completely replaced by iddingsite; pyroxene partly (10%–20%) replaced by iddingsite.

XRD: swelling chlorite and hydromica; trace analcime; altered olivine grain: smectite, mixed-layer smectite-chlorite mineral, mixed-layer swelling chlorite-chlorite mineral, and chlorite.

Sample 144-871C-40R-2, 70–75 cm (Piece 3), Unit 22D [Z-1535]

Olivine-phyric basalt. Phenocrysts (30%): strong altered olivine phenocrysts. Groundmass with vitrophyric texture; brownish black to black glass.

Alteration: moderate (30%); olivine completely replaced by iddingsite, carbonate, and Fe hydroxides.

XRD: smectite, mixed-layer swelling chlorite-smectite mineral, and swelling chlorite; trace hematite(?) and calcite; gray-green matter from vein: smectite; trace swelling chlorite and calcite.

Sample 144-871C-40R-4, 98–101 cm (Piece 3D), Unit 22G [Z-869]

Olivine-phyric basalt, vesicular. Phenocrysts (30%): strong altered olivine grains (0.2–1.2 mm). Groundmass with vitrophyric texture; glass. Vesicles (10%, 0.5–0.9 mm) are isometric in shape.

Alteration: moderate (30%); olivine completely replaced by iddingsite; vesicles infilled with carbonate or empty.

Lo-En Guyot (Hole 872B)

Sample 144-872B-5R-1, 56–58 cm (Piece 6), Unit 6 [Z-870]

Aphyric basalt, massive. Phenocrysts (10%): olivine grains (0.1–0.5 mm). Groundmass with hyalopilitic texture; needle-shaped microlites and microlaths of plagioclase (30%–35%, up to 0.5 mm, labradorite [An_{56}]), weakly crystallized glass, and opaque minerals.

Alteration: slight (10%); clay mineral replaces glass.

XRD: smectite and swelling chlorite; trace mixed-layer chlorite-smectite mineral and hydromica; white vein: calcite.

Sample 144-872B-5R-3, 104–108 cm (Piece 10), Unit 9 [Z-1536]

Sparsely olivine-plagioclase-phyric basalt, vesicular. Phenocrysts (3%–5%): single strong altered olivine grain (2 mm) and single plagioclase prismatic crystal (6 mm). Groundmass with microlitic (microdoleritic) texture; microlites and microlaths of plagioclase (35%, 0.1–0.8 mm, andesine [An_{45}]). Interstices: clinopyroxene grains (30%, 0.1–0.3 mm), opaque minerals (5%), and glass. Vesicles (10%, 0.8–1 mm) are rounded in shape.

Alteration: slight to moderate (15%–20%); olivine completely replaced by iddingsite, clay mineral, and carbonate; glass replaced by clay mineral (celadonite?); vesicles infilled with carbonate or clay mineral.

XRD: smectite and mixed-layer chlorite-smectite mineral; trace serpentine and hydromica; green-blue matter from vein: smectite and hydromica (~5% swelling interlayer).

Sample 144-872B-5R-4, 65–68 cm (Piece 10), Unit 10B [Z-1537]

Sparsely olivine-plagioclase-phyric basalt, crystallized, vesicular, brecciated. Phenocrysts (5%): strong altered olivine grains (2%, 0.4–0.6 mm) and plagioclase prismatic crystals (3%). Groundmass with microlitic texture; microlites and microlaths of plagioclase (35%, 0.1–0.3 mm). Interstices: clinopyroxene grains (30%, <0.1 mm), oxidized olivine (5%), opaque minerals (5%). Vesicles (10%, 0.9–1.5 mm) are isometric in shape. Thin fissures are present (10%).

Alteration: moderate (35%); olivine completely replaced by iddingsite; plagioclase replaced by smectite and albite; vesicles and thin fissures infilled with chalcedony and quartz.

Sample 144-872B-7R-1, 8–12 cm (Piece 1), Unit 13 [Z-1538]

Plagioclase-olivine-clinopyroxene-phyric basalt, weakly crystallized, vesicular, brecciated. Phenocrysts (10%): strong altered olivine idiomorphic grains (4%, 0.3–0.8 mm), clinopyroxene idiomorphic grains (5%, 0.4–1.5 mm), and plagioclase prismatic crystals (1%, 0.8–0.9 mm). Groundmass with vitrophyric texture; microlites of plagioclase (20%, 0.1–0.2 mm). Interstices: oxidized olivine grains (10%, <0.1 mm), clinopyroxene crystallites (25%), and opaque minerals (5%). Vesicles (30%, 0.3–1.5 mm) are isometric in shape. Thin fissures (0.1 mm) are present.

Alteration: moderate (35%); olivine completely replaced by iddingsite; plagioclase replaced by chalcedony or smectite; vesicles infilled with clay mineral, carbonate, and chalcedony; thin fissures infilled with carbonate, chalcedony, and quartz.

XRD: crystals from vein: calcite.

Sample 144-872B-7R-3, 32–37 cm (Piece 1), Unit 14 [Z-1539]

Lava breccia. Rock consists of rounded basalt fragments (70%, 1–7 mm) and cement (small fragments of basalt). Large fragments of basalt are represented by phenocrysts of oxidized olivine, plagioclase, and single clinopyroxene grains. Cement: fragments of basalt with microphenocrysts of oxidized olivine (1%–2%, 0.3–0.4 mm), single plagioclase prismatic crystals (1%), and groundmass. Groundmass; plagioclase microlites (40%, 0.1–0.3 mm), clinopyroxene crystals (30%), oxidized olivine grains (5%, <0.1 mm), and opaque minerals (5%).

Alteration: very strong (80%); olivine completely oxidized; plagioclase completely replaced by smectite.

XRD: smectite and mixed-layer smectite-chlorite mineral; trace calcite, analcime, and talc(?).

Sample 144-872B-7R-4, 102–107 cm (Piece 3), Unit 14 [Z-1540]

Clinopyroxene-olivine-plagioclase-phyric trachybasalt, crystallized, sparsely vesicular. Phenocrysts (7%–10%): clinopyroxene idiomorphic grains (1%, 0.5 mm), olivine grains (3%–4%, 0.3–0.5 mm), and plagioclase prismatic crystals (5%, 0.3–0.8 mm, andesine-labradorite [An_{50}]). Groundmass with microlitic (trachytoid) texture; parallel oriented microlites of plagioclase (35%, 0.1–0.3 mm, andesine [An_{43}] and andesine [An_{34}]). Interstices: clinopyroxene grains (30%, <0.1 mm), oxidized olivine grains (5%, 0.1 mm), light greenish yellow glass (5%), and opaque minerals (10%). Single vesicle (1.5 X 0.2 mm) is elongated-oval in shape. Thin fissure is present.

Alteration: moderate (35%); olivine replaced by iddingsite; plagioclase replaced by carbonate; vesicle infilled with chalcedony; thin fissures infilled with carbonate.

XRD: smectite with ~20% mica layers; trace defective chlorite; matter from vein: smectite and calcite.

Sample 144-872B-7R-6, 10–15 cm (Piece 3), Unit 14 [Z-1541]

Olivine-clinopyroxene-plagioclase-phyric basalt, crystallized, sparsely vesicular. Phenocrysts (15%): olivine grains (1%), clinopyroxene grains (7%, up to 1.5 mm), and plagioclase prismatic crystals (7%, 0.3–0.78 mm, labradorite [An_{55}]). Groundmass with microlitic texture; unoriented microlites and laths of plagioclase (30%, 0.1–0.4 mm, andesine [An_{43}] and andesine [An_{34}]). Interstices: clinopyroxene grains (35%), dark green glass (10%), and opaque minerals (5%–7%). Vesicles (10%) are elongated-oval in shape.

Alteration: slight (10%–12%); olivine replaced by iddingsite; clay mineral replaces glass.

XRD: smectite; trace defective chlorite and talc(?); matter from veinlet: calcite; trace smectite.

Sample 144-872B-8R-1, 50–54 cm (Piece 7), Unit 16A [Z-1542]

Lava breccia. Rock consists of angular or weakly rounded fragments (0.3–1.5 mm) of aphyric vesicular basalt with hyalopilitic texture.

Alteration: rock completely replaced by smectite, carbonate, and zeolite(?).

XRD: smectite with ~20% mica layers; trace hematite and talc(?).

Sample 144-872B-8R-1, 63–68 cm (Piece 7), Unit 16A [Z-1543]

Tuff (breccia). Rock consists of basalt fragments (0.1–3 mm). Aphyric basalt with hyalopilitic texture, vesicular (up to 50%). Thin fissures (20%) are present.

Alteration: very strong (50%–60%); glass partly (10%) replaced by clay mineral; vesicles infilled with carbonate and zeolite; thin fissures infilled with carbonate.

XRD: smectite; trace hematite, calcite, analcime, and talc(?).

Sample 144-872B-8R-2, 9–12 cm (Piece 1), Unit 16A [Z-1720]

Aphyric basalt, highly vesicular. Rock with vitrophyric and pilotaxitic texture; black glass with needle-shaped microlites (0.1–0.15 mm) of plagioclase; clinopyroxene grains (<0.05 mm) segregate; opaque minerals; and smectite. Vesicles (50%, 0.1–0.3 mm and up to 5 mm) are rounded, oval, and isometric-elongated in shape. Thin fissure (0.05 mm) was met.

Alteration: slight (5%–10%); plagioclase completely replaced by smectite, smectite partly replaces glass; vesicles infilled with quartz and chalcedony; thin fissure infilled with carbonate.

XRD: smectite with interlayer Ca-Mg cations and ~20% mica layer, calcite, and chabazite.

Sample 144-872B-8R-2, 91–94 cm (Piece 3), Unit 16B [Z-1717]

Aphyric basalt, crystallized, fine grained, vesicular. Rock with microlitic texture; plagioclase microlites and microlaths (0.05–0.2 mm, andesine [An_{46}] and andesine [An_{40}]). Interstices: clinopyroxene grains (25%, 0.01 mm) segregate; opaque minerals (10%); phlogopite (5%). Vesicles (25%, 0.4–0.9 mm) are isometric in shape. Thin fissure (0.05 mm) is present.

Alteration: moderate (25%); vesicles infilled with smectite and carbonate.

XRD: smectite with interlayer Ca-Mg cations and calcite.

Sample 144-872B-8R-4, 24–29 cm (Piece 2), Unit 16B [Z-871]

Sparsely olivine-plagioclase-phyric basalt, crystallized, sparsely vesicular. Phenocrysts (5%): single strong altered olivine grain (0.3 mm) and plagioclase prismatic crystals (0.5–2 mm, labradorite [An_{62}]). Groundmass with intersertal texture; laths of plagioclase (50%, 0.1–0.3 mm, labradorite [An_{52}]). Interstices: clinopyroxene grains (35%, <0.1 mm) segregate; needle-shaped grains of opaque minerals (5%); glass (10%). Vesicles (2%–3%, 0.1–0.3 mm) are rounded in shape.

Alteration: slight (15%); olivine completely replaced by clay mineral; clay mineral replaces glass; vesicles infilled with clay mineral.

Sample 144-872B-9R-2, 19–21 cm (Piece 1), Unit 17A [Z-872]

Aphyric basalt, weakly crystallized, vesicular. Rock with hyalopilitic texture; plagioclase microlites, altered olivine grains (up to 0.1 mm), and volcanic glass with opaque dust. Vesicles (15%–20%, 0.1–0.3 mm) are isometric in shape.

Alteration: very strong (80%); plagioclase almost completely replaced by clay mineral and sosurite; olivine completely replaced by Fe hydroxides; clay mineral replaces glass; vesicles infilled with clay mineral and carbonate.

Sample 144-872B-9R-3, 28–33 cm (Piece 3), Unit 17B [Z-1544]

Aphyric basalt, crystallized, sparsely vesicular. Rock with microlitic texture; plagioclase microlites and microlaths (50%, 0.1–0.4 mm, labradorite [An_{60}], andesine [An_{47}] and andesine [An_{38}]). Interstices: olivine idiomorphic grains (15%, 0.1 mm); clinopyroxene grains (20%, <0.1 mm) segregate; opaque minerals (5%); glass (5%). Vesicles (3%, up to 2.5 mm) are elongated-isometric in shape. Thin fissure (0.05 mm) was met.

Alteration: moderate (20%–25%); olivine completely replaced by iddingsite; glass completely replaced by clay mineral; vesicles infilled with clay mineral; thin fissure infilled with carbonate.

XRD: smectite with ~10% mica layers; trace hydromica(?); veinlet: calcite.

Sample 144-872B-9R-4, 73–78 cm (Piece 1C), Unit 18B [Z-1545]

Lava breccia. Rock consists of angular fragments (0.2–2 mm) of basalt. Olivine-phyric basalt, uncrystallized, with vitrophyric texture, sparsely vesicular. Rock consists of olivine large idiomorphic grains (15%, up to 2.5 mm) and black glass (75%) with rare microlites of clinopyroxene and plagioclase (~5%). Vesicles (10%) demonstrate irregular sizes (0.5–1 mm).

Alteration: slight (15%); vesicles infilled with smectite.

XRD: smectite; trace calcite and analcime; matter from veinlet: smectite and dolomite; trace calcite and analcime.

Sample 144-872B-9R-5, 38–40 cm (Piece 1A), Unit 18B [Z-1546]

Lava breccia. Clinopyroxene-olivine-phyric basalt (ankaramite), with vitrophyric texture, vesicular. Phenocrysts (50%): olivine large idiomorphic crystals (48%, 1.2–3 mm) and single microphenocryst (0.6 mm) of clinopyroxene (2%). Groundmass consists of dark gray glass (75%) with rare microlites of clinopyroxene, plagioclase, and olivine (<5%). Vesicles (10%, 0.1–0.4 mm) are isometric in shape. Thin fissures are present.

Alteration: strong (5%); olivine completely replaced by iddingsite, rims of olivine grains are oxidized; vesicles infilled with smectite and chalcedony; thin fissures infilled with carbonate.

XRD: smectite with ~10% mica layers; trace analcime.

Wodejebato Guyot (Hole 874B)

Sample 144-874B-22R-4, 48–53 cm (Piece 1), Unit 1 [Z-1547]

Clinopyroxene-olivine-phyric basalt (ankaramite), vesicular, brecciated. Phenocrysts (50%): olivine idiomorphic zonal large grains (0.5–2.5 mm). Clinopyroxene forms large phenocryst (5–7 mm, 5%–7%). Groundmass with vitrophyric texture; glass with abundant microlites of oxidized olivine, opaque minerals, and crystallites of

plagioclase and clinopyroxene. Vesicles (15%, 0.1–2 mm) are oval-isometric in shape. Thin fissures (5%, 0.01–0.05 mm) are present.

Alteration: strong (55%); rock is oxidized (20%); olivine replaced by iddingsite and Fe hydroxides; microcracks in clinopyroxene phenocryst infilled with carbonate; vesicles infilled with light yellowish green matter (chalcedony and smectite?); thin fissures are filled with carbonate.

XRD: mixed-layer swelling chlorite-smectite mineral; minor smectite with ~10% mica layers; trace hydromica, calcite, and analcime; altered olivine grain: smectite with ~10% mica layers; trace mixed-layer swelling chlorite-smectite mineral and calcite; white matter: smectite with ~10% mica layers and mixed-layer swelling chlorite-smectite mineral; trace mixed-layer smectite-chlorite mineral and calcite.

Sample 144-874B-23R-1, 100–105 cm (Piece 13), Unit 1 [Z-1548]

Clinopyroxene-olivine-phyric basalt (ankaramite), sparsely vesicular. Phenocrysts (60%): olivine idiomorphic large grains (55%, 1–4.5 mm). Clinopyroxene forms partly idiomorphic phenocryst (1–2.5 mm, 5%). Groundmass with vitrophyric texture; colorless glass with rare microlites of clinopyroxene. Vesicles (5%, 0.3–1.7 mm) are isometric in shape.

Alteration: strong; 60% of rock is oxidized: completely oxidized olivine; vesicles infilled by light brown matter.

XRD: mixed-layer swelling chlorite-smectite mineral; trace smectite, serpentine, and hematite; altered olivine grain: swelling chlorite; trace serpentine and quartz.

Sample 144-874B-23R-2, 112–117 cm (Piece 23), Unit 1 [Z-1549]

Clinopyroxene-olivine-phyric basalt (ankaramite), sparsely vesicular. Rock: identical to Sample 144-874B-23R-1, 100–105 cm (1548). Vesicles (20%, 0.3–1.7 mm) are isometric in shape.

Alteration: strong (55%); olivine completely replaced by iddingsite and smectite, central parts of olivine grains are oxidized; glass replaced by smectite; vesicles infilled with light cream matter.

XRD: mixed-layer swelling chlorite-smectite mineral; trace serpentine, hematite, and calcite; altered olivine grain: swelling chlorite; trace serpentine.

Sample 144-874B-24R-1, 30–35 cm (Piece 2), Unit 1 [Z-1550]

Clinopyroxene-olivine-phyric basalt (ankaramite), crystallized, sparsely vesicular. Phenocrysts (60%): fresh olivine idiomorphic large grains (50%, 0.4–3.5 mm). Clinopyroxene (augite) forms partly idiomorphic large phenocrysts (up to 3 mm, 10%). Groundmass with microlitic texture; (2%–3%) microlites (<0.1 mm) of plagioclase, oxidized olivine (2%–4%), green glass (5%), clinopyroxene microlites (15%), and opaque minerals (10%). Vesicles (1–3 mm) are isometric and rounded in shape.

Alteration: slight (5%); cracks in olivine phenocrysts infilled with Fe hydroxides; chlorite replaces glass; vesicles infilled with quartz or cristobalite(?).

XRD: chlorite with ~10% swelling interlayers; trace smectite, mixed-layer smectite-chlorite mineral, calcite, and quartz; altered olivine grain: smectite with ~20% mica layers; trace mixed-layer smectite-chlorite mineral and calcite.

Sample 144-874B-24R-1, 100–105 cm (Piece 7), Unit 1 [Z-1551]

Clinopyroxene-olivine-phyric basalt (ankaramite), crystallized, vesicular. Rock: identical to Sample 144-874B-24R-1, 30–35 cm (Z-1550). Vesicles (10%, up to 5 mm) are isometric and rounded in shape.

Alteration: strong (50%); olivine phenocrysts completely replaced by iddingsite and carbonate, several grains are completely oxidized; cracks in clinopyroxene phenocrysts infilled with carbonate; clay mineral replaces glass; vesicles infilled with chalcedony, quartz, and clay mineral.

Sample 144-874B-24R-1, 120–127 cm (Piece 8), Unit 1 [Z-1552]

Clinopyroxene-olivine-phyric basalt (ankaramite), crystallized. Phenocrysts (70%): olivine grains (50%, 0.5–4.5 mm) and clinopyroxene large isomorphic grain (up to 5 mm, 20%) with inclusions of glass. Groundmass with microlitic texture; clinopyroxene microlites (15%), glass (10%), and opaque minerals (5%).

Alteration: strong (50%–55%); olivine phenocrysts completely replaced by iddingsite, several grains almost completely replaced by Fe hydroxides, one grain is fresh; clay mineral replaces glass.

Sample 144-874B-24R-2, 70–76 cm (Piece 9), Unit 1 [Z-1553]

Clinopyroxene-olivine-phyric basalt (ankaramite), crystallized, brecciated. Phenocrysts (60%): olivine grains (50%, 1.3–2.5 mm) and clinopyroxene xenomorphic grains (1.5–2 mm, 10%). Groundmass with vitrophyric texture; colorless glass with crystallites of clinopyroxene and opaque minerals. Thin fissures are present (10%, 0.1 mm, up to 0.5 mm).

Alteration: strong (60%); olivine phenocrysts completely replaced by iddingsite and Fe hydroxides, several grains are fresh with microcracks (microcracks infilled with hydrobiotite?); thin fissures infilled with carbonate and biotite like mineral.

XRD: trace smectite, mixed-layer smectite-chlorite mineral, calcite, serpentine, and quartz.

Sample 144-874B-24R-2, 120–124 cm (Piece 18), Unit 1 [Z-1554]

Clinopyroxene-olivine-phyric basalt (ankaramite), highly vesicular. Phenocrysts (5%): two small (0.5–0.7 mm) phenocrysts of clinopyroxene and olivine grains (3%–4%). Groundmass with vitrophyric texture; black glass with microlites of plagioclase (<1%). Vesicles (49%, 0.1–0.5 mm) are rounded and isometric in shape.

Alteration: olivine phenocrysts completely replaced by Fe hydroxides; vesicles infilled with chalcedony and Fe hydroxides.

XRD: swelling chlorite; trace chlorite and calcite; altered olivine grain: swelling chlorite; trace smectite; altered olivine crystals: swelling chlorite and mixed-layer swelling chlorite-smectite mineral.

Sample 144-874B-24R-3, 125–130 cm (Piece 18), Unit 1 [Z-1555]

Clinopyroxene-olivine-phyric basalt (ankaramite), crystallized. Phenocrysts (70%): olivine idiomorphic grains (30%, 1–3 mm), clinopyroxene large (1%–5%) tabular crystals (20%) with inclusions of glass, and plagioclase prismatic crystals (20%, 0.5–2 mm, labradorite [$An_{59–60}$]) and their glomerophyric segregates. Groundmass with microlitic texture; plagioclase microlites and microlaths (10%) segregate; oxidized olivine grains (<0.1 mm, 5%); clinopyroxene (12%); and opaque minerals (2%–3%).

Alteration: moderate (30%); olivine phenocrysts completely replaced by iddingsite and Fe hydroxides.

Sample 144-874B-24R-4, 54–72 cm (Piece 3), Unit 1 [Z-1718]

Plagioclase-clinopyroxene-olivine-phyric basalt, crystallized, fine grained, sparsely vesicular. Phenocrysts (50%): glomerophyric segregates of plagioclase prismatic crystals (5%, 0.3–1.2 mm, labradorite [An_{68}]); clinopyroxene large (2.5–5 mm) idiomorphic crystals (25%); olivine idiomorphic grains (25%, 0.4–2.5 mm). Groundmass with microlitic texture; plagioclase microlites and microlaths (10%, 0.05–0.15 mm, andesine [An_{38}]); clinopyroxene grains (25%, <0.1 mm) segregate; opaque minerals (10%); glass (5%).

Alteration: moderate (20%–25%); oxidized olivine phenocrysts are replaced with iddingsite and carbonate; clay mineral replaces glass.

XRD: smectite; trace mixed-layer smectite-chlorite mineral, chlorite, and hydromica; vesicle: calcite; microfissures: smectite with ~20% interlayers of mica type.

MIT Guyot (Hole 878A)

Sample 144-878A-78R-2, 64–70 cm (Piece 3B), Unit 1 [Z-1556]

Olivine-phyric andesite-basalt (hawaiite), crystallized, vesicular. Phenocrysts (10%): oxidized olivine idiomorphic small grains. Groundmass with microlitic texture; plagioclase microlites and laths (up to 1 mm, 40%, andesine [$An_{41–42}$] and andesine [An_{32}]), clinopyroxene small grains (<0.1 mm), 30%), black oxidized grains (up to 0.2 mm) of olivine (10%), and opaque minerals (10%).

Alteration: oxidized olivine.

Sample 144-878A-79R-2, 9–12 cm (Piece 1), Unit 2 [Z-873]

Olivine-plagioclase-phyric basalt, weakly crystallized, sparsely vesicular. Phenocrysts (20%): idiomorphic small grains (0.1–0.4 mm, 10%) of oxidized olivine and laths and elongated-prismatic crystals (up to 0.7 mm) of plagioclase. Groundmass with hyalopilitic texture; plagioclase grains, small grains (<0.1 mm) of oxidized olivine, opaque dust, and glass. Vesicles (~5%, 0.2–0.3 mm) are empty.

Alteration: very strong (80%); plagioclase replaced by sosurite; clay mineral replaces glass.

Sample 144-878A-79R-4, 24–27 cm (Piece 1), Unit 2 [Z-874]

Olivine-plagioclase-phyric trachybasalt (trachyandesite), crystallized, massive. Phenocrysts (20%): olivine grains (0.1–0.3 mm, 10%) and plagioclase elongated-prismatic grains (0.5–1 mm). Plagioclase grains are parallel oriented. Groundmass with trachytic texture; parallel oriented albite microlites (40%), very small black grains and dust of opaque minerals, and clinopyroxene. Microcracks (0.1 mm) are present.

Alteration: slight to moderate (20%); olivine completely replaced by clay mineral; plagioclase replaced by pelite; microcracks infilled with opaque minerals.

Sample 144-878A-80R-5, 20–24 cm (Piece 1G), Unit 8 [Z-1557]

Olivine-phyric basanite, crystallized, fine grained, sparsely vesicular. Phenocrysts (30%): olivine idiomorphic grains (0.6–2.5 mm). Groundmass with microlitic texture; clinopyroxene microlites (30%, up to 0.1 mm), oxidized olivine grains (10%, 0.1–0.3 mm), plagioclase microlites (20%, andesine [An_{42-44}]), opaque minerals (7%–8%), and interstitial secondary carbonate (<1%). Vesicles (1%–2%, 1–4.5 mm) are rounded and oval in shape.

Alteration: moderate (30%–35%); oxidized olivine is replaced with iddingsite; interstitial carbonate (glass replaced by carbonate?), vesicles infilled with carbonate.

Sample 144-878A-80R-5, 106–109 cm (Piece 4B), Unit 8 [Z-876]

Olivine-phyric basanite, sparsely vesicular. Phenocrysts (15%): olivine idiomorphic grains (0.3–1.7 mm). Groundmass with microlitic texture; plagioclase microlites and microlaths (20%, andesine [$An_{46–48}$]); clinopyroxene grains (60%, 0.1–0.2 mm) segregate; oxidized olivine grains (10%, 0.1–0.2 mm); opaque minerals. Single vesicles (0.5 mm) are rounded in shape.

Alteration: slight (15%); oxidized olivine is replaced with iddingsite and clay mineral; vesicles infilled with clay mineral.

Sample 144-878A-81R-2, 10–15 cm (Piece 1), Unit 10 [Z-1558]

Olivine-phyric basanite, crystallized. Phenocrysts (35%): olivine idiomorphic grains (0.5–2 mm). Groundmass with microlitic texture; clinopyroxene grains (35%, up to 0.2 mm) segregate, oxidized olivine grains (10%, up to 0.4 mm), plagioclase microlites (10%, andesine [An_{42}]), and opaque minerals (10%). Thin fissure (0.5–0.9 mm) was met.

Alteration: moderate (25%); oxidized olivine is replaced with iddingsite; thin fissure infilled with chalcedony(?) and carbonate.

Sample 144-878A-81R-4, 120–124 cm (Piece 12), Unit 11 [Z-1559]

Olivine-phyric basanite, crystallized, vesicular. Phenocrysts (25%): olivine grains (0.5–0.9 mm). Groundmass with microlitic texture; clinopyroxene microlites (25%), plagioclase microlites (20%, andesine [An_{38}] and oligoclase-andesine [An_{30}]), oxidized olivine grains (10%, up to 0.2 mm), and opaque minerals (10%). Vesicles (10%, 0.6–1.5 mm) are present.

Alteration: oxidized olivine is replaced with iddingsite; vesicles infilled with carbonate and zeolite.

Sample 144-878A-81R-5, 42–45 cm (Piece 3A), Unit 11 [Z-1560]

Olivine-phyric basanite, crystallized, sparsely vesicular. Phenocrysts (25%): olivine grains (0.4–0.9 mm). Groundmass with microlitic texture; clinopyroxene microlites (25%), plagioclase microlites (25%, andesine [An_{32}]), oxidized olivine grains (10%), and opaque minerals (10%). Single large vesicle (3%–4%, 2 X 3.5 mm) is oval in shape.

Alteration: slight (5%); oxidized olivine is replaced with iddingsite; vesicles infilled with carbonate.

Sample 144-878A-83R-3, 84–87 cm (Piece 4), Unit 13 [Z-877]

Olivine-phyric basalt, sparsely vesicular. Phenocrysts (20%): oxidized olivine iiomorphic grains (0.1–0.7 mm). Groundmass with vitrophyric texture; glass with rare plagioclase and clinopyroxene crystallites and opaque minerals. Vesicle (5%, 0.1–0.3 mm) is rounded in shape, often empty.

Alteration: slight; oxidized olivine is replaced with iddingsite; walls of several vesicles are lined with clay mineral.

Sample 144-878A-84R-2, 119–123 cm (Piece 6C), Unit 15 [Z-878]

Olivine-phyric basalt (basanite?), vesicular. Phenocrysts (20%): olivine idiomorphic grains (0.1–0.7 mm). Groundmass with microlitic texture; plagioclase microlites (20%, 0.1–0.3 mm, andesine [$An_{42–44}$]), clinopyroxene idiomorphic grains (70%, up to 0.1 mm) segregate, opaque minerals (5%–7%), and glass (5%). Vesicles (10%, 0.5–3 mm) are oval-isometric in shape.

Alteration: moderate (20%–30%); oxidized olivine is partly replaced with clay mineral; clay mineral replaces glass; vesicles infilled with zeolite, clay mineral, and carbonate.

Sample 144-878A-84R-3, 18–22 cm (Piece 2A), Unit 15 [Z-1561]

Olivine-phyric basanite, crystallized, vesicular. Phenocrysts (30%): olivine grains (0.5–1.8 mm). Groundmass with microlitic texture; clinopyroxene (25%) and plagioclase (20%, andesine [An_{44}] and andesine [An_{36}]) microlites, opaque minerals (7%–8%), and oxidized olivine grains (5%). Vesicles (10%, 0.7–2.4 mm) are rounded in shape.

Alteration: slight (5%); oxidized olivine is partly replaced with iddingsite; vesicles infilled with smectite and carbonate.

Sample 144-878A-84R-3, 116–120 cm (Piece 8C), Unit 15 [Z-1562]

Olivine-phyric basanite, crystallized, vesicular. Rock: identical to Sample 144-878A-84R-3, 18–22 cm (Z-1561).

Alteration: moderate (30%); oxidized olivine is replaced with iddingsite; clay mineral replaces glass; vesicles infilled with clay mineral.

Sample 144-878A-84R-5, 114–118 cm (Piece 9B), Unit 15 [Z-879]

Olivine-phyric basanite, sparsely crystallized, vesicular. Rock: identical to Sample 144-878A-84R-3, 18–22 cm (Z-1561) and Sample 144-878A-84R-3, 116–120 cm (Z-1562).

Alteration: slight (10%); olivine partly replaced by iddingsite, clay mineral, and Fe hydroxides.

Sample 144-878A-85R-2, 110–114 cm (Piece 8), Unit 16 [Z-1563]

Olivine-phyric basanite, crystallized, sparsely vesicular. Phenocrysts (25%): olivine grains (0.3–0.8 mm). Groundmass with microlitic texture; clinopyroxene microlites (35%), opaque minerals (15%), plagioclase microlites (10%, andesine [An_{40}] and andesine [An_{32}]), oxidized olivine grains (5%, 0.1 mm), and altered green glass (5%). Vesicles (5%, 0.4–0.7 mm) are rounded in shape and infilled with oxidized light green and black glass.

Alteration: moderate (25%); oxidized olivine is replaced with iddingsite; clay mineral replaces glass.

Sample 144-878A-88R-3, 88–92 cm (Piece 7), Unit 20 [Z-1564]

Olivine-phyric basanite, crystallized, vesicular. Phenocrysts (25%): oxidized olivine grains (0.2–0.9 mm). Groundmass with microlitic texture; plagioclase microlites (30%, andesine [An_{42}] and andesine [An_{31}]), clinopyroxene grains (20%, 0.01 mm) segregate, oxidized olivine grains (5%, <0.1 mm), and opaque minerals (5%). Vesicles (10%, 0.7–1.5 mm) are isometric in shape. Walls of vesicles are lined yellowish glass.

Alteration: oxidized olivine.

Sample 144-878A-89R-2, 0–5 cm (Piece 1A), Unit 21 [Z-1565]

Clinopyroxene-plagioclase-olivine-phyric basanite, crystallized. Phenocrysts (40%): oxidized olivine grains (20%, 0.4–1.2 mm), clinopyroxene large (up to 3 mm) isometric and very idiomorphic crystals (10%), and plagioclase tabular and prismatic crystals (10%, 0.4–1.7 mm, andesine [An_{49}] and andesine [$An_{31–38}$]). Groundmass with microlitic texture; clinopyroxene grains (20%, <0.1 mm), plagioclase microlites and laths (15%, andesine [An_{35}]), oxidized olivine grains (15%, 0.1–0.3 mm), opaque minerals (5%), and glass (5%).

Alteration: slight; oxidized olivine is partly (5%) replaced with iddingsite; glass replaced by smectite and chalcedony.

Sample 144-878A-89R-4, 31–35 cm (Piece 3), Unit 21 [Z-1566]

Plagioclase-clinopyroxene-olivine-phyric basanite, crystallized. Phenocrysts (15%): oxidized olivine grains (10%, 0.9–2 mm), clinopyroxene idiomorphic grains (4%, 0.5–1.5mm), and plagioclase prismatic crystals (1%, 0.4–0.6 mm, labradorite [An_{55}]). Groundmass with microlitic texture; plagioclase microlites and laths (30%, 0.1–0.9 mm, andesine [An_{32-38}]), clinopyroxene grains (30%, <0.1 mm), oxidized olivine grains (5%, 0.1–0.2 mm), opaque minerals (5%), and light green glass (5%).

Alteration: slight; groundmass olivine completely replaced by Fe hydroxides.

Sample 144-878A-90R-1, 90–95 cm (Piece 6C), Unit 21 [Z-1567]

Clinopyroxene-plagioclase-olivine-phyric basanite, crystallized, sparsely vesicular. Phenocrysts (15%): single clinopyroxene grains (1%), plagioclase prismatic crystals (4%, 1.2–2 mm) with abundant inclusions of glass, and oxidized olivine grains (10%, 0.2–0.7 mm). Groundmass with microlitic texture; plagioclase microlites and laths (30%, andesine [An_{32-39}]), clinopyroxene grains (35%, <0.1 mm), oxidized olivine grains (5%), opaque minerals (5%), and glass (5%). Vesicles (5%) are present.

Alteration: slight; olivine phenocrysts partly (10%) replaced by iddingsite; groundmass olivine completely replaced by Fe hydroxides.

Sample 144-878A-90R-2, 32–36 cm (Piece 1B), Unit 21 [Z-1568]

Lava breccia. Rock consists of fragments of basanite. Phenocrysts (5%): oxidized olivine grains (3%, up to 2.5 mm) and clinopyroxene grains (2%, 0.5–1.5 mm). Groundmass of fragments is hyalopilitic to microlitic texture.

Alteration: moderate (30%–40%); plagioclase replaced by smectite.

Sample 144-878A-90R-4, 115–120 cm (Piece 8), Unit 22 [Z-1569]

Plagioclase-olivine-phyric alkali(?) basalt, crystallized. Phenocrysts (15%): plagioclase tabular and prismatic crystals (5%, 0.4–1.2 mm, andesine [An_{40}]) and oxidized olivine grains (10%, 0.5–2.5 mm). Groundmass with

microlitic texture; zonal plagioclase microlites (40%, oligoclase [An_{28}]) with inclusions of glass; clinopyroxene grains (20%, <0.1 mm); oxidized olivine grains (15%, 0.1–0.2 mm); opaque minerals (5%).

Alteration: moderate (30%); groundmass plagioclase completely replaced by pelite.

Sample 144-878A-90R-6, 0–5 cm (Piece 1), Unit 23 [Z-1570]

Clinopyroxene-olivine-plagioclase-phyric alkali basalt, crystallized. Phenocrysts (15%): oxidized olivine grains (5%, 0.5–1.7 mm), single clinopyroxene grains (1%): augite, and plagioclase tabular and prismatic crystals (9%, 0.5–1.2 mm, labradorite [An_{53}]) with inclusions of glass. Groundmass with microlitic texture; plagioclase laths and microlites (10%, andesine [An_{40}] and andesine [An_{31}]), clinopyroxene grains (35%, <0.1 mm), oxidized olivine grains (20%), opaque minerals (10%), and glass (5%). Biotite and carbonate (<1%) were met.

Alteration: slight; olivine phenocrysts partly (2%) replaced by iddingsite; groundmass olivine completely replaced by Fe hydroxides.

Sample 144-878A-91R-2, 80–84 cm (Piece 4B), Unit 23 [Z-1571]

Clinopyroxene-plagioclase-olivine-phyric alkali basalt, crystallized. Phenocrysts (20%): single augite grains (2%, 0.5–1.2 mm), oxidized olivine grains (10%, 0.4–1.5 mm), and plagioclase tabular and prismatic crystals (8%, up to 2.5 mm). Groundmass with microlitic texture; plagioclase laths and microlites (10%, oligoclase-andesine [An_{30}]), orthoclase isometric grains (20%, <0.1 mm), clinopyroxene grains (25%), oxidized olivine grains (15%), opaque minerals (10%), and biotite (<1%).

Alteration: slight.

Sample 144-878A-91R-4, 120–125 cm (Piece 13A), Unit 23 [Z-1572]

Olivine-clinopyroxene-plagioclase-phyric alkali basalt, crystallized. Phenocrysts (25%): olivine grains (2%, 0.6–0.8 mm), clinopyroxene xenomorphic grains (18%, 0.6–1.2 mm) and their segregates, plagioclase tabular and prismatic crystals (12%, 0.5–2.5 mm, andesine [An_{45}] and andesine [An_{38}], labradorite [An_{52}]), and idiomorphic grains of opaque minerals (0.4–0.7 mm). Groundmass with microlitic texture; plagioclase microlites and microlaths (30%, andesine [An_{48}] and andesine [An_{32}], oligoclase [An_{28}]), orthoclase isometric grains (10%, <0.1 mm), clinopyroxene (20%), olivine (5%), opaque minerals (5%), and glass (5%). Biotite (<1%) was met.

Alteration: slight; oxidized (5%) olivine, several olivine grains replaced by iddingsite.

Sample 144-878A-92R-4, 50–54 cm (Piece 13C), Unit 26 [Z-1573]

Clinopyroxene-olivine-phyric alkali basalt, crystallized, sparsely vesicular. Phenocrysts (20%): oxidized olivine grains (15%, 1–3 mm) and clinopyroxene isometric rounded grains (5%, 1.2–2 mm). Groundmass with microlitic texture; plagioclase microlites (40%, andesine [$An_{36–40}$]), orthoclase grains (5%), clinopyroxene (10%), oxidized olivine (20%, up to 0.2 mm), and opaque minerals (5%). Vesicle (<1%, 0.8 mm) infilled with green glass.

Alteration: slight; oxidized olivine, microcracks infilled with Fe hydroxides; central part of vesicle infilled with carbonate.

Sample 144-878A-93R-1, 7–11 cm (Piece 3A), Unit 28 [Z-1574]

Olivine-phyric basalt, crystallized, vesicular. Phenocrysts (10%): oxidized olivine. Groundmass with microlitic texture; clinopyroxene microlites (30%, <0.1 mm, albite-oligoclase), clinopyroxene (20%), opaque minerals (5%), and oxidized olivine (10%, up to 0.2 mm). Vesicles (25%, up to 2 mm) are elongated-isometric in shape. Walls of vesicles are lined light yellowish glass.

Alteration: slight; glass in vesicles partly replaced by clay mineral.

Sample 144-878A-93R-2, 118–122 cm (Piece 22), Unit 30 [Z-1575]

Olivine-clinopyroxene-plagioclase-phyric alkali basalt, crystallized, sparsely vesicular. Phenocrysts (35%): oxidized olivine (10%, 0.4–0.7 mm), large (up to 2.5 mm) prismatic and isometric grains of clinopyroxene (10%), and plagioclase (15%) tabular (2.5–2.7 mm, labradorite [An_{58}]) and prismatic (0.8–2.5 mm, andesine-labradorite [An_{50}]) crystals. Groundmass with microlitic texture; plagioclase microlites and laths (0.8 mm, andesine [$An_{43–45}$]), oxidized olivine grains (10%, 0.1–0.2 mm), clinopyroxene grains (10%, <0.1 mm) segregate, and opaque minerals (10%). Vesicles (5%, 0.7 mm) are rounded in shape. Walls of vesicles are lined glass.

Alteration: slight; central parts of vesicles infilled with carbonate.

Sample 144-878A-93R-3, 120–124 cm (Piece 14), Unit 30 [Z-1576]

Plagioclase-clinopyroxene-olivine-phyric basanite, crystallized, vesicular. Phenocrysts (30%): oxidized olivine (15%, 0.2–0.7 mm), clinopyroxene (10%, 0.6–1.5 mm), and plagioclase prismatic crystals (5%, andesine [An_{44}]). Groundmass with microlitic texture; plagioclase microlites and laths (25%, up to 0.6 mm, andesine [An_{42}]), oxidized olivine (15%, up to 0.2 mm), clinopyroxene grains (15%, <0.1 mm) segregate, and opaque minerals (5%). Vesicles (10%, 0.7–2.2 mm) are isometric-elongated in shape. They infilled with light cream glass.

Alteration: slight; oxidized olivine.

Sample 144-878A-94R-1, 0–4 cm (Piece 1A), Unit 30 [Z-880]

Olivine-clinopyroxene-phyric basalt, weakly crystallized, vesicular. Phenocrysts (20%): clinopyroxene grains (1.2–2 mm and 0.1–0.3 mm) and oxidized olivine (0.1–0.3 mm). Groundmass with pilotaxitic texture; plagioclase microlaths (andesine [An_{42}]), glass, clinopyroxene, and opaque dust. Vesicles (30%, 0.1–2 mm) are oval-isometric in shape, empty.

Alteration: moderate (30%); plagioclase almost completely replaced by sosurite, albite, and zeolite; clay mineral replaces glass; several small (0.3 mm) vesicles infilled with zeolite and carbonate.

Sample 144-878A-94R-2, 0–5 cm (Piece 1A), Unit 31A [Z-1577]

Aphyric basalt, highly vesicular. Rock with vitrophyric texture; volcanic glass (40%) and microvesicles (60%, 0.01–0.3 mm). Vesicles are rounded in shape and infilled with glass.

Alteration: rock is fresh.

Sample 144-878A-94R-2, 0–5 cm (Piece 1A), Unit 31A [Z-1578]

Hyalobasalt, microvesicular.

Alteration: rock almost completely (90%) replaced by Fe-Mn hydroxides.

Sample 144-878A-94R-5, 102–107 cm (Piece 1), Unit 31A [Z-1579]

Lava breccia of olivine-phyric basalt with vitrophyric texture, microvesicular. Rock consists of phenocrysts of oxidized olivine (3%–4%), colorless to black volcanic glass (40%), and microvesicles (56%–57%, 0.01–0.3 mm). Vesicles infilled with light cream glass.

Alteration: rock is fresh.

Sample 144-878A-94R-7, 70–74 cm (Piece 1), Unit 31B [Z-1580]

Lava breccia. Rock: identical to Sample 144-878A-94R-5, 102–107 cm (Z-1579).

Sample 144-878A-95R-2, 0–5 cm (Piece 1), Unit 31B [Z-1581]

Lava breccia of olivine-phyric basalt with vitrophyric texture, microvesicular (70%). Rock: identical to Sample 144-878A-94R-5, 102–107 cm (Z-1579).

Alteration: slight; oxidized olivine and glass; ~10% of vesicles infilled with carbonate.

Sample 144-878A-95R-3, 125–128 cm (Piece 9), Unit 31B [Z-1582]

Lava breccia of olivine-phyric basalt with vitrophyric texture, microvesicular (40%). Rock: identical to Sample 144-878A-94R-5, 102–107 cm. Vesicles infilled with colorless glass.

Alteration: rock is fresh.

Sample 144-878A-95R-5, 0–5 cm (Piece 1), Unit 31B [Z-1583]

Lava breccia of olivine-phyric basalt with vitrophyric texture, microvesicular (40%). Rock: identical to Sample 144-878A-94R-5, 102–107 cm (Z-1579).

Alteration: fresh; several vesicles infilled with carbonate.

Sample 144-878A-97R-1, 20–24 cm (Piece 7B), Unit 34 [Z-1584]

Sparsely olivine-clinopyroxene-plagioclase-phyric alkali basalt. Phenocrysts (5%): olivine (3%, 0.3–0.7 mm), single grains of clinopyroxene (1%), and plagioclase (1%, 1,7 mm, andesine [An_{32}]). Groundmass with hyalopilitic to microlitic texture; plagioclase laths (25%, 0.2–0.6 mm, andesine [An_{40}] and occasionally: labradorite [An_{54}]), clinopyroxene microlites (40%), opaque minerals (10%), olivine (10%), and biotite (3%–4%).

Alteration: slight (3%–5%); olivine replaced by iddingsite.

Sample 144-878A-97R-2, 28–31 cm (Piece 3D), Unit 34 [Z-881]

Sparsely olivine-phyric basalt, massive. Phenocrysts (5%): olivine idiomorphic grains (5%, 0.2–0.5 mm). Groundmass with hyalopilitic texture; laths and microlites of plagioclase(30%, andesine [$An_{40–42}$]), olivine (5%, 0.1 mm), and glass with abundant opaque dust.

Alteration: slight; olivine replaced by clay mineral.

Sample 144-878A-98R-2, 93–96 cm (Piece 5D), Unit 35 [Z-882]

Sparsely olivine-phyric basalt, massive. Phenocrysts (5%–7%): fresh olivine (0.3–1.2 mm). Groundmass with microlitic texture; plagioclase microlites (andesine [An_{42}]), olivine (5%, <0.1 mm), pyroxene, opaque minerals, and glass (5%).

Alteration: rock is fresh.

Sample 144-878A-98R-3, 8–12 cm (Piece 1B), Unit 35 [Z-1585]

Clinopyroxene-olivine-phyric alkali basalt, sparsely vesicular. Phenocrysts (10%): single clinopyroxene grains (1%, 0.4 mm) and olivine idiomorphic grains (9%, 0.3–0.7 mm). Groundmass with microlitic texture; plagioclase microlites (35%, 0.1–0.2 mm, andesine [An_{45}] and andesine [An_{38}]), clinopyroxene grains (25%, up to 0.1 mm) segregate, olivine (10%, up to 0.2 mm), opaque minerals (10%), light green glass (9%), and carbonate (1%). Vesicles (<1%) were met.

Alteration: slight (10%–15%); several olivine phenocrysts replaced by iddingsite; groundmass olivine completely replaced by iddingsite.

Hess Rise (Leg 62)

Hole 465A

Sample 62-465A-40R-3, 17–25 cm (Piece 1B), Unit 1 [Z-1226]

Lava (tuff?) breccia of aphyric trachyandesite. Rock demonstrates spotty-trachytic texture. Angular fragments (1–5 mm) of volcanic rock are represented by trachyandesite. Rock consists of laths (<5%) of altered plagioclase (andesine [An_{38}]) and cream glass. Often rock fragments are rimed by small (<0.1 mm) grains of opaque minerals (~5%).

Alteration: slight (~5%–10%); plagioclase mainly replaced by albite and orthoclase; matrix of breccia; carbonate.

XRD: smectite; matrix of breccia: calcite, siderite.

Sample 62-465A-40R-3, 27–35 cm (Piece 1C), Unit 1 [Z-1227]

Tuff (breccia of trachyandesite). Rock consists of isometric fragments of trachyandesite (60%, 1–5 mm) and matrix (40%). Matrix; angular-isometric fragments of volcanic glass (0.05–0.2 mm) and carbonate. Rock (in composition and texture): identical to Sample 62-465A-40R-3, 17–25 cm (Z-1226).

Alteration: slight (~5%–10%); rock is slightly oxidized (5%–7%); plagioclase mainly replaced by albite and orthoclase; matrix of breccia is represent by carbonate.

XRD: smectite and calcite, trace quartz and chlorite.

Sample 62-465A-41R-1, 113–120 cm (Piece 9), Unit 1 [Z-1228]

Aphyric trachyandesite, vesicular. Rock with trachytic texture; laths (0.1–0.4 mm) of altered plagioclase (10%, andesine [An_{38}]), needle-shaped grains of dark-colored mineral, glass (20%), opaque dust, and isometric grains of opaque minerals (3%). Vesicles (15%–20%, 0.1–0.5 mm) are empty. Vesicles with sizes 0.1–0.2 mm completely infilled with light cream glass.

Alteration: moderate (20%–25%); rock is nonoxidized; plagioclase mainly replaced by albite and orthoclase.

XRD: smectite with ~20% mica layers; matter from vein: calcite, siderite, and smectite with ~20% mica layers; trace quartz.

Sample 62-465A-41R-2, 90–93 cm (Piece 11A), Unit 1 [Z-383]

Aphyric trachyandesite, fine grained, glassy, poorly crystallized, vesicular (0.2–0.6 mm, 10%). Rock demonstrates hyalotaxitic texture and fluidal structure; light devitrified glass with crystals of feldspar; opaque dust; small and xenomorphic grains of opaque minerals; small amounts of various elongated plates of sanidine(?). Single phenocrysts of K-feldspar are present.

Alteration: slight (~15%); rock is slightly oxidized; vesicles are filled partly with green smectites.

XRD: smectite with ~15%–20% mica layer.

Sample 62-465A-42R-1, 128–132 cm (Piece 8A), Unit 2 [Z-384]

Aphyric trachyandesite, glassy, poorly crystallized, vesicular (0.2–0.3 mm, 7%–10%). Rock demonstrates hyalotaxitic texture and fluidal structure; light devitrified glass with crystals of feldspar; opaque dust; small and xenomorphic grains of opaque minerals; small amounts of various elongated plates of sanidine(?).

Alteration: slight (~10%); rock is slightly oxidized; vesicles are filled partly with green smectites.

XRD: smectite.

Sample 62-465A-42R-3, 98–103 cm (Piece 9), Unit 2 [Z-385]

Aphyric trachyandesite, glassy, poorly crystallized, vesicular. Rock demonstrates hyalotaxitic texture and fluidal structure; light devitrified glass with crystals of feldspar, opaque dust, small and xenomorphic grains of opaque

minerals, and small amounts of various elongated plates of sanidine(?). Vesicles (0.2–0.4 mm, 15%–20%) are rounded to elongated in shape.

Alteration: slight to moderate (15%–20%); vesicles are filled partly with green smectites.

Sample 62-465A-43R-2, 130–135 cm (Piece 14A), Unit 2 [Z-386]

Aphyric trachyandesite, glassy, poorly crystallized, vesicular (0.1–0.2 up to 1.5 mm, 10%). Rock demonstrates hyalotaxitic texture and fluidal structure; light devitrified glass with crystals of feldspar, opaque dust, small and xenomorphic grains of opaque minerals, and small amounts of various elongated plates of sanidine(?).

Alteration: slight (~10%–15%); small vesicles are filled with smectites, largess are filled with smectite and zeolites.

XRD: smectite.

Sample 62-465A-44R-1, 112–116 cm (Piece 13B), Unit 3 [Z-387]

Aphyric trachyandesite, glassy, poorly crystallized, vesicular. Rock is pilotaxitic texture; light glass with crystals of feldspar, clinopyroxene(?), opaque dust, small and xenomorphic grains of opaque minerals, and small amounts (5%–7%) of various elongated plates of sanidine(?), and single microphenocrysts of plagioclase. Various vesicles (10%–15%) are irregular in shape; as a rule they are empty.

Alteration: slight (~10%); rock is slightly oxidized.

XRD: smectite.

Sample 62-465A-44R-3, 118–123 cm (Piece 7A), Unit 3 [Z-388]

Aphyric trachyandesite, glassy, poorly crystallized, vesicular. Rock is hyalotaxitic texture; glass with crystals of feldspar, opaque dust, small and xenomorphic grains of opaque minerals, and small amounts (5%–10%) of elongated plates of sanidine(?). Various vesicles (up to 2.5 mm, ~10%) are irregular in shape.

Alteration: slight (10%–15%); rock is moderately oxidized; small vesicles are filled partly with smectites, large ones are filled with calcite.

XRD: smectite.

Sample 62-465A-45R-1, 81–85 cm (Piece 5D), Unit 3 [Z-389]

Aphyric trachyandesite, glassy, poorly crystallized, vesicular. Rock demonstrates hyalotaxitic or trachytic texture structure; light devitrified glass with crystals of feldspar, opaque dust, idiomorphic grains of opaque minerals, and small amounts of elongated plates of sanidine(?). Single table crystals of brownish hornblende are present. Various vesicles (0.1–0.8 mm, ~10%), are irregular in shape. Some vesicles filled with glass.

Alteration: slight (10%–15%); rock is slightly oxidized; small vesicles are empty or filled partly with smectites, large vesicles contain carbonate.

XRD: smectite.

Sample 62-465A-46R-1, 82–86 cm (Piece 6G), Unit 5 [Z-390]

Aphyric trachyandesite, glassy, poorly crystallized, vesicular. Rock is hyalotaxitic or trachytic texture; light devitrified glass with crystals of feldspar, opaque dust, small and xenomorphic grains of opaque minerals, and small amounts (5%–7%) of elongated plates of sanidine(?). Vesicles are various (1.5–2 mm, 5%–7%) and irregular in shape.

Alteration: slight (10%); rock is slightly oxidized; vesicles are filled partly with smectites and zeolites, some vesicles are filled with chalcedony.

XRD: smectite and hydromica.

Sample 62-465A-46R-3, 57–61 cm (Piece 8), Unit 5 [Z-391]

Aphyric trachyandesite, glassy, poorly crystallized, vesicular. Rock is hyalotaxitic texture; light devitrified glass with crystals of feldspar, pyroxene, opaque dust, small and xenomorphic grains of opaque minerals, and small amounts (5%–7%) of elongated plates of sanidine(?). Various (2–3 mm, 5%–7%) vesicles are irregular in shape.

Alteration: slight (10%); rock is moderately oxidized; vesicles are filled partly with carbonate; a narrow zone of smectites is located beneath carbonates on the walls of vesicles.

XRD: smectite; trace calcite.

Voring Plateau (Leg 104)

Hole 642E

Sample 104-642E-9R-1, 59–62 cm (Piece 4E), Unit D1 [Z-153]

Sparsely plagioclase-phyric basalt, fine grained, crystallized, vesicular (0.3–1 mm, 10%). Phenocrysts of plagioclase (0.5–1 mm, 3%). Single crystals of olivine are present. Groundmass is intergranular texture; laths of plagioclase, clinopyroxene, devitrified volcanic glass, and aggregated opaque dust.

Alteration: slight (~15%); rock is nonoxidized; smectites fill vesicles and replace both olivine and interstitial glass.

XRD: smectite; trace chlorite.

Sample 104-642E-10R-1, 133–136 cm (Piece 20), Unit D2 [Z-592]

Sparsely olivine-plagioclase-phyric basalt, fine grained, massive. Phenocrysts: two small (0.2–0.4 mm) idiomorphic grains of reddish brown oxidized olivine and prismatic grains (0.4–0.6 mm) and segregates of plagioclase (3%–4%, labradorite [An_{55}]). Groundmass with microdoleritic texture; unoriented microlaths of plagioclase (labradorite [An_{54}]), segregate of small (<0.1 mm) isomorphic grains of pyroxene, volcanic glass (7%–8%), and opaque minerals (3%–5%).

Alteration: slight; clay minerals replace glass.

Sample 104-642E-10R-2, 87–90 cm (Piece 12), Unit D3 [Z-154]

Olivine-plagioclase-phyric basalt, crystallized, vesicular (1%–2%). Phenocrysts of plagioclase (0.8–1 mm). Groundmass is intergranular texture; laths of plagioclase, clinopyroxene, olivine, devitrified volcanic glass, and aggregated opaque dust.

Alteration: moderate (~25%); rock is nonoxidized; smectites fill vesicles and replace both olivine and interstitial glass, as well as form rims around plagioclases.

XRD: smectite.

Sample 104-642E-15R-1, 120–123 cm (Piece 22), Unit F11 [Z-155]

Aphyric basalt, incompletely crystallized. Groundmass is intersertal, partly subvariolitic, texture; laths of plagioclase, clinopyroxene, olivine, brown interstitial glass, and opaque dust. Vesicles have sizes of 0.3–3.5 mm (30%). Large vesicles join each other.

Alteration: moderate (~35%); rock is slightly oxidized; smectites and carbonate fill vesicles; smectites replace olivine.

XRD: smectite.

Sample 104-642E-15R-3, 77–80 cm (Piece 4), Unit F11 [Z-156]

Olivine basalt, incompletely crystallized, massive. Plagioclase (0.5–0.8 mm, 50%) forms glomerophyric aggregates, olivine (0.3–0.5 mm, 20%), and clinopyroxene (0.2–0.4 mm, 15%). Texture of rock is intersertal, partly subophitic.

Alteration: moderate (~30%); rock is nonoxidized; smectites replace olivine and interstitial glass.

XRD: smectite.

Sample 104-642E-18R-4, 13–16 cm (Piece 1), Unit F17 [Z-157]

Aphyric basalt, almost completely crystallized, massive. Microphenocrysts of plagioclase (up to 0.3 mm, <1%) and olivine (0.1–0.3 mm, <1%). Groundmass is intergranular texture; laths of plagioclase, clinopyroxene, and devitrified volcanic glass with opaque dust.

Alteration: slight (~5%); rock is nonoxidized; smectites replace olivine and interstitial glass.

XRD: smectite.

Sample 104-642E-22R-3, 93–96 cm (Piece 4), Unit F23 [Z-158]

Sparsely plagioclase-phyric basalt, highly vesicular (0.5–2 mm, 10%). Phenocrysts of plagioclase (0.5–2 mm, 10%) form glomerophyric segregates. Single crystals of olivine are registered. Groundmass is intersertal texture; laths of plagioclase, clinopyroxene, olivine, and devitrified volcanic glass with opaque dust. Often large vesicles join each other.

Alteration: strong (50%); rock is nonoxidized; smectites replace olivine, interstitial glass, and plagioclase; vesicles are filled with smectites.

XRD: smectites with various composition of interlayer cations.

Sample 104-642E-22R-5, 32–35 cm (Piece 2), Unit F23 [Z-159]

Olivine-plagioclase-phyric basalt, massive. Phenocrysts of plagioclase (0.8–1.5 mm, 30%) form glomerophyric segregates and olivine (0.3–1 mm, 10%). Groundmass is intergranular texture; laths of plagioclase, clinopyroxene, interstitial glass, and opaque minerals.

Alteration: moderate (~20%); rock is nonoxidized; smectites replace olivine and interstitial glass.

XRD: smectites with various composition of interlayer cations.

Sample 104-642E-30R-2, 76–79 cm (Piece 2A), Unit F36 [Z-160]

Olivine basalt, massive. Groundmass is intersertal texture; laths of plagioclase, clinopyroxene, olivine, interstitial glass, and opaque minerals.

Alteration: slight (~15%); rock is nonoxidized; smectites replace olivine and interstitial glass.

XRD: smectites with various composition of interlayer cations.

Sample 104-642E-34R-1, 4–7 cm (Piece 1), Unit S18 [Z-594]

Plagioclase-phyric microdolerite, massive. Phenocrysts of plagioclase (8%–10%) form tabular and prismatic grains (0.5–0.6 mm) and segregates. Groundmass with doleritic texture; laths (0.1–0.3 mm) of plagioclase (labradorite [An_{55}]), segregate of small (0.1 mm) xenomorphic grains of clinopyroxene (grains with size up to 0.5 mm are present), interstitial greenish brown altered glass (10%), and opaque minerals (5%–7%).

Alteration: clay mineral replaces of glass.

Sample 104-642E-40R-1, 33–36 cm (Piece 2D), Unit F48 [Z-161]

Olivine basalt, fine grained, massive. Groundmass is intersertal texture; laths of plagioclase, clinopyroxene, olivine, interstitial glass, and opaque minerals.

Alteration: slight (~15%); rock is nonoxidized; smectites replace olivine and interstitial glass.

XRD: smectites with various composition of interlayer cations; trace chlorite.

Sample 104-642E-46R-3, 40–43 cm (Piece 1C), Unit F53 [Z-162]

Olivine basalt, fine grained, sparsely vesicular. Groundmass is intersertal texture; laths of plagioclase, clinopyroxene, olivine, interstitial glass, and opaque minerals. Single vesicles have size up to 1.25 mm.

Alteration: slight (~10%); rock is nonoxidized; smectites replace olivine and interstitial glass.

XRD: smectites with various composition of interlayer cations.

Sample 104-642E-60R-1, 68–71 cm (Piece 14), Unit F63A [Z-163]

Olivine basalt, fine grained, highly vesicular (0.2–2.5 mm, 30%). Groundmass is hyalopilitic texture; laths of plagioclase, clinopyroxene, olivine, interstitial glass, and opaque minerals.

Alteration: moderate 40%; rock is nonoxidized; smectites replace olivine and interstitial glass; vesicles are filled by smectites.

XRD: smectite.

Sample 104-642E-60R-2, 25–27 cm (Piece 1%), Unit F63A [Z-164]

Olivine basalt, fine grained, vesicular (0.8–1.2 mm, 5%). Groundmass is intersertal texture; laths of plagioclase, clinopyroxene, olivine, interstitial glass, and opaque minerals.

Alteration: moderate (~20%); rock is nonoxidized; smectites replace olivine and interstitial glass; vesicles are filled with smectites.

XRD: smectite.

Sample 104-642E-69R-2, 59–61 cm (Piece 1D), Unit F78 [Z-165]

Olivine-plagioclase-phyric basalt, medium grained, vesicular (0.1–0.4 mm, <5%). Phenocrysts of plagioclase (0.3–1 mm, 20%) form glomerophyric segregates. Microphenocrysts of olivine (0.1–0.5 mm, 15%). Groundmass is intersertal texture; laths of plagioclase, clinopyroxene, olivine, and interstitial glass.

Alteration: moderate (~20%); rock is nonoxidized; smectites replace olivine and interstitial glass; vesicles are filled with smectites.

XRD: smectite.

Sample 104-642E-78R-2, 46–48 cm (Piece 5A), Unit F90 [Z-166]

Sparsely plagioclase-phyric basalt, fine grained, vesicular (0.1–0.4 mm, <5%). Microphenocrysts of plagioclase (0.2–0.4 mm) form glomerophyric segregates. Groundmass is intergranular texture; laths of plagioclase, clinopyroxene, and interstitial glass.

Alteration: moderate (~20%); rock is nonoxidized; smectites replace olivine and intersertal glass.

XRD: smectites with various composition of interlayer cations.

Sample 104-642E-88R-2, 70–72 cm (Piece 7B), Unit F102 [Z-167]

Basalt, fine grained, vesicular (0.1–5 mm, 25%). Groundmass is hyalopilitic texture; laths of plagioclase, clinopyroxene, olivine, interstitial glass, and opaque minerals.

Alteration: rock is nonoxidized; smectites replace olivine and interstitial glass; vesicles are filled with smectites.

XRD: smectites with various composition of interlayer cations and contain ~20% of mica layers; trace hydromica.

Sample 104-642E-91R-1, 18–20 cm (Piece 3), Unit F104A [Z-168]

Basalt, fine grained, highly vesicular. Groundmass is hyalopilitic, partly subvariolitic, texture; laths of plagioclase, clinopyroxene, olivine, interstitial glass, and opaque minerals. Vesicles (0.2–5 mm, 50%) penetrate rock.

Alteration: strong (~50%); rock is nonoxidized; smectites replace olivine, interstitial glass, and plagioclase; vesicles are filled with smectites.

XRD: smectite contains single mica layers; trace hydromica (~15% swelling layers).

Sample 104-642E-94R-1, 32–34 cm (Piece 1B), Unit F105 [Z-169]

Sparsely plagioclase-phyric basalt, almost completely crystallized, massive. Phenocrysts of plagioclase (up to 1.5 mm, 5%) form glomerophyric segregates. Microphenocrysts of clinopyroxene (0.3–0.4 mm) are registered. Groundmass: laths of plagioclase, clinopyroxene, opaque minerals, and interstitial glass. Single vesicles (0.2 mm) are registered.

Alteration: slight (~3%); rock is nonoxidized; smectites replace olivine and intersertal glass.

XRD: smectite; trace chlorite.

Sample 104-642E-94R-4, 67–72 cm (Piece 2B), Unit S43 [Z-596]

Breccia. Fragments of rock are represented by isometric fragments of plagioclase (0.2–0.3 mm), brown oxidized glass, and opaque dust. Matrix of breccia consists of Fe hydroxides.

Alteration: strong; rock is oxidized; Fe hydrooxides in matrix of breccia.

XRD: smectite and kaolinite; trace goethite.

Sample 104-642E-102R-2, 45–47 cm (Piece 6), Unit F115 [Z-170]

Hyalobasalt, vesicular (1–2.5 mm, 3%). Phenocrysts of plagioclase (1.5–2.5 mm, 3%) within volcanic glass. Texture of rock is perlitic. Vesicles are empty.

Alteration: scarce (<1%); rock is nonoxidized.

XRD: smectite.

Sample 104-642E-105R-1, 64–66 cm (Piece 7A), UnitD5 [Z-171]

Basalt, large-crystalline, almost completely crystallized, massive. Rock is poikilophitic, partly doleritic, texture; plagioclase, clinopyroxene, olivine, volcanic glass, and opaque minerals.

Alteration: slight (~10%); rock is nonoxidized; smectites replace olivine and interstitial glass; present of carbonate.

XRD: smectite; trace mixed-layer smectite-chlorite mineral(?).

Sample 104-642E-110R-1, 39–41 cm (Piece 5B), Unit D7 [Z-172]

Olivine basalt, fine grained, incompletely crystallized, sparsely vesicular (0.2–0.3 mm). Microphenocrysts of plagioclase (0.2–0.4 mm, <1%). Groundmass is intersertal texture; laths of plagioclase, clinopyroxene, olivine, interstitial glass, and opaque minerals.

Alteration: slight to moderate (15%–20%); rock is nonoxidized; smectites replace olivine and intersertal glass; cracks are filled with carbonate.

XRD: smectite.

Bermuda Rise (Legs 51, 52, and 53)

Hole 417A

Sample 51-417A-29R-5, 58–61 cm (Piece 5), Unit 8 [Z-511]

Olivine-plagioclase-phyric basalt, sparsely vesicular. Phenocrysts: sparsely idiomorphic grains of olivine (0.3–0.5 mm, 2%–3%); plagioclase (20%, 0.3–2 mm, labradorite [An_{55}]) forms prismatic grains. Groundmass with hyalopilitic texture; needle-shaped microlites of plagioclase and black glass. Sparsely vesicles (0.3–0.8 mm) are rounded in shape.

Alteration: slight (10%–15%); olivine completely replaced by carbonate; albite replaces partly large grains of plagioclase, small crystals almost completely replaced by albite and chlorite; vesicles are rimed with black glass, central parts of vesicles infilled with palagonite and carbonate.

XRD: smectite and mixed-layer smectite-chlorite mineral.

Sample 51-417A-32R-2, 5–8 cm (Piece 1), Unit 12 [Z-512]

Olivine-plagioclase-phyric basalt, sparsely vesicular. Phenocrysts: idiomorphic grains of olivine (0.4–0.5 mm, 3%–5%); plagioclase (25%, 0.3–2 mm, labradorite [An_{55}]) form prismatic grains and segregates (up to 0.5–1 mm). Groundmass with pilotaxitic texture; needle-shaped microlites of plagioclase, small grains of pyroxene, and black glass. Sparsely rounded vesicles (0.3–0.5 mm) infilled with glass.

Alteration: moderate (25%); olivine replaced by carbonate and hydroxides of Fe; smectites almost completely replace plagioclase.

XRD: mixed-layer chlorite-smectite mineral with 80% smectite layers.

Sample 51-417A-44R-3, 31–34 cm (Piece 1A), Unit 18B [Z-513]

Plagioclase-phyric dolerite, medium grained, massive. Phenocrysts: prismatic grains of plagioclase (0.7–0.8 mm, 10%, labradorite [An_{68}]). Groundmass with ophitic-poikilophitic texture; laths of plagioclase (0.1–0.4 mm, labradorite [An_{56}] and andesine [An_{48}]); clinopyroxene forms isometric large grains (0.5–0.7 mm) with inclusions of laths of plagioclase and small isometric grains. Interstices consist of greenish brown glass (7%–8%) and opaque minerals (7%–8%).

Alteration: rock is fresh.

XRD: smectite with ~20% mica layers; trace chlorite, hydromica, quartz, and talc(?).

Hole 418A

Sample 52-418A-15R-1, 98–101 cm (Piece 1I), Unit 1 [Z-297]

Plagioclase-phyric (phenocrysts 0.2–0.8 mm, 20%) basalt, poorly crystallized, sparsely vesicular. Groundmass with subvariolitic texture; volcanic glass with opaque dust, microlites of clinopyroxene, and laths of plagioclase. Vesicles (0.2 mm, 5%) are empty. Single vesicles are filled with volcanic glass which contains opaque dust.

Alteration: slight (5%–10%); rock is nonoxidized; secondary minerals are represented by smectites and calcite; vesicles are filled with palagonitized volcanic glass, smectites, and calcite; carbonization effects some areas.

XRD: smectite (~10% of mica layers); calcite(?) in trace amounts.

Sample 52-418A-15R-3, 129–132 cm (Piece 4D), Unit 1 [Z-298]

Plagioclase-phyric (phenocrysts of plagioclase 0.8–3 mm, 15%) hyalobasalt, poorly crystallized, massive. Single microphenocrysts of clinopyroxene and olivine are present. Groundmass with subvariolitic texture; volcanic glass with opaque dust, microlites of clinopyroxene, and laths of plagioclase. Vesicles (0.2 mm, 5%) are empty. Single vesicles are filled with volcanic glass which contains opaque dust.

Alteration: slight (5%–7%); smectites and calcite replace olivine; single vesicles are filled with smectites.

XRD: smectite; calcite(?) in trace amounts.

Sample 52-418A-18R-1, 81–84 cm (Piece 2F), Unit 2C [Z-299]

Plagioclase-phyric (phenocrysts 0.2–0.8 mm, 20%) basalt, poorly crystallized; vesicular (0.5–1.5 mm, 3%). Single microphenocrysts of clinopyroxene (0.3 mm) are present. Groundmass with poorly subvariolitic texture; volcanic glass with opaque dust, microlites of clinopyroxene, and laths of plagioclase.

Alteration: slight (~15%); rock is slightly oxidized; vesicles are mostly filled by carbonate, or sparsely, palagonitized and smectitized volcanic glass; smectites replace clinopyroxene and interstitial glass.

XRD: smectite (~10% of mica layers); trace calcite(?).

Sample 52-418A-19R-4, 86–89 cm (Piece 1I), Unit 2C [Z-300]

Plagioclase-phyric basalt, poorly crystallized; massive. Plagioclase phenocrysts (0.8–2.5 mm, 15%–20% abundance) form glomerophyric segregates. Microphenocrysts of olivine (0.2–0.5 mm, 2%) are present. Groundmass is hyalopilitic texture; volcanic glass, microlites of clinopyroxene, and large laths of plagioclase (often quench crystals).

Alteration: slight (3%); rock is nonoxidized; smectites replace olivine and clinopyroxene.

XRD: smectite.

Sample 52-418A-19R-7, 6–9 cm (Piece 1A), Unit 2C [Z-301]

Olivine-plagioclase-phyric basalt, massive. Phenocrysts of plagioclase (0.8–2.4 mm, 25%) form glomerophyric segregates. Phenocrysts of olivine (0.3–0.5 mm, 1%) occur. Groundmass with intergranular texture; microlites of clinopyroxene, large laths of plagioclase (0.5 mm), and opaque minerals.

Alteration: slight (15%); rock is nonoxidized; smectites replace olivine and clinopyroxene.

XRD: smectite.

Sample 52-418A-20R-5, 10–13 cm (Piece 1B), Unit 2C [Z-302]

Olivine-plagioclase-phyric basalt, massive. Phenocrysts of plagioclase (up to 2.5 mm, 20%) form glomerophyric segregates. Phenocrysts of olivine (0.2–1.5 mm, 5%) occur. Groundmass with intergranular texture; laths of plagioclase, microlites of clinopyroxene, olivine, and opaque minerals.

Alteration: slight (15%); rock is nonoxidized; smectites replace of olivine, clinopyroxene, and interstitial glass.

XRD: smectite (~25%–30% of mica layers).

Sample 52-418A-27R-1, 33–35 cm (Piece 1D), Unit 5 [Z-303]

Plagioclase-phyric basalt, poorly crystallized, scarcely vesicular. Phenocrysts of plagioclase (0.5–1 mm, 10%). Phenocrysts of olivine (0.1–0.3 mm, <1%). Groundmass is hyalopilitic texture; volcanic glass, laths of plagioclase, of clinopyroxene and opaque minerals.

Alteration: slight (~10%); rock is slightly oxidized; smectites replace olivine and clinopyroxene, as well as fill vesicles.

XRD: smectite; trace calcite(?).

Sample 52-418A-27R-2, 91–93 cm (Piece 5B), Unit5 [Z-304]

Plagioclase-phyric hyalobasalt, poorly crystallized, sparsely vesicular (0.1–0.3 mm, <1%). Phenocrysts of plagioclase (0.8–2.5 mm, 15%) form glomerophyric segregates. Single grains of olivine are present. Groundmass with hyalopilitic texture; volcanic glass, laths of plagioclase, clinopyroxene, and opaque minerals.

Alteration: slight (~10%); rock is nonoxidized; smectites replace olivine and clinopyroxene; smectites and carbonate fill vesicles (carbonate is located in central part, smectite covers inner walls of vesicles).

XRD: smectite.

Sample 52-418A-31R-2, 47–51 cm (Piece 3A), Unit 5 [Z-514]

Plagioclase-phyric basalt, massive. Phenocrysts of plagioclase (0.8–2.7 mm, 30%). Phenocrysts: plagioclase forms prismatic grains (0.7–0.8 mm, labradorite [An_{56}]) and small prisms (0.1–0.2 mm). Groundmass with vitrophyric texture is represented mainly by volcanic glass.

Alteration: volcanic glass replaced with carbonate and palagonite.

XRD: smectite with ~10% mica layers; trace calcite, chlorite, and amphibole.

Sample 52-418A-31R-2, 134–139 cm (Piece 12), Unit 5 [Z-515]

Plagioclase-phyric basalt, massive. Phenocrysts of plagioclase (0.3–0.9 mm, 30%, labradorite [An_{67}]). Groundmass with vitrophyric texture; volcanic glass (70%).

Alteration: microcracks in glass unfilled with clay mineral and palagonite; volcanic glass is palagonitized (30%).

XRD: smectite; minor mixed-layer chlorite-smectite mineral with ~10%–15% smectite layers; trace calcite.

Sample 52-418A-38R-1, 41–44 cm (Piece 2C), Unit 5 [Z-305]

Plagioclase-phyric basalt, poorly crystallized and sparsely vesicular (0.2 mm). Phenocrysts of plagioclase (0.8–2.7 mm, 30%). Some phenocrysts form glomerophyric segregates. Groundmass with hyalopilitic texture; volcanic glass with opaque dust, clinopyroxene, laths of plagioclase. Laths of plagioclase are partly represented by quench crystals.

Alteration: moderate (~15%–20%); rock is nonoxidized; smectites replace clinopyroxene and plagioclase; carbonate and smectites fill vesicles (carbonate and smectites are located in central part, volcanic glass with opaque dust cover inner walls of vesicles).

XRD: smectite.

Sample 52-418A-38R-3, 10–13 cm (Piece 1A), Unit 5 [Z-306]

Plagioclase-phyric basalt, poorly crystallized, and sparsely vesicular (0.2–0.3 mm). Phenocrysts of plagioclase (0.5–2.5 mm, 30%) form glomerophyric segregates. Single xenomorphic crystals of olivine and clinopyroxene (0.1–0.2 mm) are present. Groundmass is trachytic to subvariolitic texture; volcanic glass, clinopyroxene, laths of plagioclase, and opaque dust.

Alteration: slight (~10%); rock is nonoxidized; smectites replace olivine, clinopyroxene and plagioclase; carbonate and smectites fill sparsely vesicles.

XRD: smectite; hydromica and talc(?) in trace amounts.

Sample 52-418A-42R-3, 2–6 cm (Piece 1A), Unit 6B [Z-516]

Olivine-plagioclase-phyric basalt, sparsely vesicular, tectonized. Phenocrysts: olivine (3%–4%) forms small (0.2–0.3 mm) idiomorphic fresh grains; plagioclase (15%–20%) forms large (1–3 mm) tabular or elongated prismatic grains (labradorite [An_{56}]) with microcracks. Groundmass with microlitic texture; needle-shaped microlites and segregate very small grains of pyroxene. Rounded vesicles (5%, 0.3–0.5 mm) are rimed with green and greenish brown glass (palagonite?).

Alteration: slight (~5%–10%); central parts of vesicles infilled with zeolite; microcracks in rock infilled with zeolite.

XRD: smectite with ~10% mica layers; trace quartz.

Sample 53-418A-52R-1, 61–64 cm (Piece 6B), Unit 6B [Z-307]

Plagioclase-phyric basalt, poorly crystallized, sparsely vesicular (1%–3%). Phenocrysts of plagioclase (0.3–2.5 mm, 30%) form glomerophyric segregates. Single crystals of plagioclase contain inclusions of volcanic glass filled with opaque dust. Single phenocrysts of olivine (0.2–1 mm, <1% abundance). Groundmass with hyalopilitic and, occasionally, subvariolitic texture; volcanic glass with opaque dust, clinopyroxene, laths of plagioclase.

Alteration: slight (~5%); rock is nonoxidized; smectites replace olivine, clinopyroxene, and interstitial glass; smectites and palagonitized volcanic glass fill vesicles.

XRD: smectite.

Sample 53-418A-52R-4, 29–32 cm (Piece 2), Unit 6B [Z-308]

Olivine-plagioclase-phyric basalt, sparsely vesicular (0.1–0.2 mm). Phenocrysts of plagioclase (0.5–2 mm, 20%) form glomerophyric segregates. Often, phenocrysts of olivine (0.3–1.5 mm, 15%) associate with glomerophyric segregates of plagioclase. Groundmass is hyalopilitic texture; volcanic glass with occasional accumulations of opaque minerals, clinopyroxene, and small laths of plagioclase (0.1–0.2 mm).

Alteration: moderate (~20%); rock is nonoxidized; smectites replace of olivine, clinopyroxene, and interstitial glass; smectites and volcanic glass with opaque minerals fill vesicles.

XRD: smectite.

Sample 53-418A-70R-1, 64–67 cm (Piece 2A), Unit 13 [Z-309]

Clinopyroxene-plagioclase-phyric hyalobasalt, sparsely vesicular (0.2–0.3 mm, 1%). Phenocrysts of plagioclase (0.8–2.5 mm, 20%) are relatively abundant. Often, phenocrysts of clinopyroxene (0.3–1 mm, 5%) tend to occur in association with glomerophyric segregates of plagioclase. Single xenomorphic crystals of olivine are present. Groundmass with hyalopilitic texture; volcanic glass with opaque dust, clinopyroxene, laths of plagioclase.

Alteration: slight (~15%); rock is nonoxidized; smectites replace of olivine, clinopyroxene and interstitial glass; smectites fill vesicles.

XRD: smectites with composition of Na-K and Mg-Ca interlayer cations.

Sample 53-418A-70R-1, 67–68 cm (Piece 2A), Unit 13 [Z-517]

Plagioclase-phyric hyalobasalt, sparsely vesicular. Phenocrysts: plagioclase (30%–35%) forms large prismatic grains (2.5–3 mm) and segregates of smaller (1–1.5 mm) grains, labradorite [An_{60}]; second generation; small (0.3–0.5 mm) prismatic grains of plagioclase, labradorite [An_{54}]. Groundmass with hyalopilitic texture; sparsely needle-shaped microlites and microlaths of plagioclase and volcanic glass. Vesicles (1%) are rounded, empty, single vesicles infilled with green chlorite.

Alteration: rock is fresh.

XRD: smectite with ~10% mica layers; trace quartz.

Sample 53-418A-77R-2, 57–60 cm (Piece 4A), Unit 14B [Z-310]

Sparsely clinopyroxene-plagioclase-phyric basalt, vesicular (0.4–0.8 mm). Phenocrysts of plagioclase (0.3–1 mm, 15%), large crystal form glomerophyric segregates. Phenocrysts of clinopyroxene (0.2–0.8 mm, 5%) are present. Single crystals of olivine occur also. Groundmass with intergranular-subophitic texture; clinopyroxene, laths of plagioclase, and opaque minerals. The latter local clusters which tend to occur with glass and, probably, olivine.

Alteration: slight (~10%); rock is nonoxidized; smectites and carbonate replace olivine and interstitial glass, as well as fill vesicles.

XRD: smectite; trace talc(?).

Sample 53-418A-77R-3, 33–36 cm (Piece 2B), Unit 14B [Z-311]

Plagioclase-phyric basalt, vesicular (0.4–1 mm). Phenocrysts of plagioclase (0.4–2.5 mm, 20%). Phenocrysts of clinopyroxene (0.2–0.5 mm, 5%). Single crystals of olivine. Groundmass with hyalopilitic texture; volcanic glass with opaque dust, clinopyroxene, laths of plagioclase.

Alteration: slight (~10%); rock is nonoxidized; smectites and carbonate replace olivine and fill vesicles.

XRD: smectite (~20% of mica layers).

Sample 53-418A-84R-2, 51–54 cm (Piece 1D), Unit 14C [Z-312]

Dolerite, massive, completely crystallized. Crystals of plagioclase (0.8–2.3 mm, 45%–50%), clinopyroxene (0.5–2.5 mm) and smaller xenomorphic crystals of the latter are ~50% abundance. Olivine is 5% abundance. Texture of rock is poikilophitic.

Alteration: slight (~10%); rock is nonoxidized; smectites-chlorite aggregate fills cracks in plagioclase and replaces of olivine.

XRD: smectite (~10% of mica layers); chlorite and talc in trace amounts.

Sample 53-418A-85R-2, 48–51 cm (Piece 3), Unit 14C [Z-313]

Olivine dolerite, massive, almost completely crystallized, medium grained. Rock; aggregate of xenomorphic and hypidiomorphic clinopyroxene (45%), plates and large laths of plagioclase (45%), and opaque minerals (1%). Poorly crystallized interstitial glass (5%) is present also. The texture of rock is hypidiomorphic-granular, poikilophitic.

Alteration: slight (~10%); rock is nonoxidized; smectites-chlorite aggregate replaces olivine and interstitial glass.

XRD: smectite; chlorite and talc in trace amounts.

Manihiki Plateau (Leg 33)

Hole 317A

Sample 33-317A-31R-2, 37–39 cm (Piece 5), Unit 2 [Z-1104]

Clinopyroxene-phyric (microphenocrysts 0.3–0.4 mm, 5%) basalt, fine grained, vesicular, groundmass is microlitic texture. Phenocrysts are represented by prismatic grains of clinopyroxene (0.2–0.8 mm, 10%). Groundmass; microlaths and microlites of plagioclase (0.1–0.4 mm, labradorite [An_{62}] and andesine [An_{47}]), microlites of clinopyroxene, volcanic glass, and opaque minerals (5%–7%). Vesicles demonstrate irregular in shape (0.3–2.5 mm, 30%).

Alteration: moderate to strong (~40%–45%); rock is nonoxidized; central parts of microlaths almost completely replaced with smectites; glass is replaced with smectites; vesicles are filled with clay mineral.

Sample 33-317A-31R-2, 87–89 cm (Piece 10), Unit 2 [Z-266]

Sparsely clinopyroxene-phyric (microphenocrysts 0.3–0.6 mm, 5%) basalt, medium grained, incompletely crystallized, vesicular. Single grains (0.3 mm) of olivine are present. Groundmass (70%) is intersertal texture; laths of plagioclase (up to 0.3 mm, andesine [An_{44}] 30%), microlites of clinopyroxene (<0.1 mm, 30%), volcanic glass (5%), and opaque minerals (5%). Vesicles (25%) demonstrate irregular in shape (0.2–0.4 and 1.7–2.8 mm, 20%).

Alteration: moderate (~30%–35%); rock is nonoxidized; vesicles are filled with smectites.

XRD: smectite with interlayer cations of Na-K; trace hydromica.

Sample 33-317A-31R-3, 20–23 cm (Piece7), Unit 3 [Z-267]

Sparsely clinopyroxene-phyric (microphenocrysts 0.3–0.5 mm, 3%) basalt, medium grained, almost completely crystallized, vesicular. Single microphenocrysts of olivine are present. Groundmass; laths of plagioclase, microlites of clinopyroxene, volcanic glass, and opaque dust. Vesicles are rounded and isometric in shape (0.2–3 mm, 30%).

Alteration: strong (~50%); rock is nonoxidized; vesicles partly filled with smectites, interstitial glass is replaced with smectites.

XRD: smectites with Na-K and Mg-Ca interlayer cations.

Sample 33-317A-31R-4, 76–82 cm (Piece 11), Unit 5A [Z-1105]

Clinopyroxene-phyric (phenocrysts 0.5–0.8 mm, 3%) dolerite, medium grained, vesicular. Groundmass (75%) with ophitic-intersertal texture; laths of plagioclase (0.3–0.7 mm, andesine [An_{48}] and labradorite [An_{54}]). Interstices infilled with xenomorphic grains of clinopyroxene and brownish black volcanic glass. Vesicles (0.5 up to 5 mm, 20%).

Alteration: rock is fresh and nonoxidized; several vesicles partly filled with clay mineral.

Sample 33-317A-31R-4, 91–94 cm (Piece 11), Unit 5A [Z-268]

Sparsely plagioclase-clinopyroxene-phyric (microphenocrysts of clinopyroxene 0.2–0.5 mm, 10%) basalt, medium grained, almost completely crystallized, vesicular. Single phenocrysts of olivine. Groundmass is intergranular texture; laths of plagioclase, microlites of clinopyroxene, volcanic glass, and opaque dust. Vesicles are rounded and isometric in shape (0.3–2.5 mm, 7%).

Alteration: slight (~10%); rock is nonoxidized; vesicles filled with smectites, interstitial glass and olivine are replaced with smectites.

XRD: smectites with Na-K and Mg-Ca interlayer cations.

Sample 33-317A-32R-1, 93–95 cm (Piece 5), Unit 5B [Z-269]

Aphyric basalt, medium grained, completely crystallized. Occasional microphenocrysts of clinopyroxene (0.2–0.4 mm, <3%). Clinopyroxene forms glomerophyric segregates. Groundmass is intergranular texture; laths of plagioclase, olivine(?), and dust of opaque minerals.

Alteration: slight (~3%); smectites replace of interstitial glass and olivine.

XRD: smectites with Na-K and Mg-Ca interlayer cations.

Sample 33-317A-32R-2, 120–124 cm (Piece 13), Unit 5B [Z-270]

Aphyric basalt, medium grained, almost completely crystallized, vesicular (0.5–5 mm, 20%). Single microphenocrysts of clinopyroxene (0.2–0.4 mm). Groundmass demonstrate intergranular texture; laths of plagioclase, microphenocrysts of clinopyroxene and volcanic glass with opaque dust.

Alteration: moderate (~20%); rock is nonoxidized; smectites fill vesicles.

XRD: smectites with Na-K and Mg-Ca interlayer cations.

Sample 33-317A-32R-3, 60–65 cm (Piece 7), Unit 5B [Z-271]

Clinopyroxene-phyric basalt, medium grained, completely crystallized, vesicular (5 mm, 20%). Microphenocrysts of clinopyroxene (0.2–0.5 mm, 5%). Groundmass; laths of plagioclase, clinopyroxene, and small amounts of volcanic glass.

Alteration: moderate (~20%); rock is nonoxidized.

XRD: smectites with Na-K and Mg-Ca interlayer cations.

Sample 33-317A-32R-4, 112–117 cm (Piece 7), Unit 6A [Z-272]

Aphyric basalt, medium grained, incompletely crystallized, vesicular (0.3–0.5 mm, 5%). Groundmass is intersertal, occasionally intergranular texture; laths of plagioclase (which often forms quench crystals), clinopyroxene, olivine, volcanic glass, and opaque minerals.

Alteration: moderate (~5%); rock is nonoxidized; smectites fill vesicles.

XRD: smectites with Na-K and Mg-Ca interlayer cations, may present smectite only which contains 10% of mica layers.

Sample 33-317A-32R-5, 58–63 cm (Piece 1), Unit 6A [Z-273]

Clinopyroxene-phyric basalt, medium grained, incompletely crystallized, some areas are almost completely crystallized, vesicular (0.2–2.5 mm, 20%). Phenocrysts of clinopyroxene (0.5–0.8 mm, 50%) and

microphenocrysts of olivine (0.2–0.3 mm, 5%). Groundmass is intersertal texture; some areas are intergranular texture; laths of plagioclase, microlites of clinopyroxene, volcanic glass, and opaque minerals.

Alteration: moderate (~20%); rock is nonoxidized; smectites fill vesicles and replace olivine and interstitial glass.

XRD: smectites with Na-K and Mg-Ca interlayer cations.

Sample 33-317A-32R-5, 89–93 cm (Piece 2), Unit 6A [Z-1106]

Plagioclase-clinopyroxene-phyric dolerite, medium grained, vesicular, ophitic-intersertal texture. Phenocrysts are represented by single glomerophyric segregates of prismatic grains of plagioclase (0.5–1 mm, labradorite [An_{68}]). Phenocrysts are represented mainly by xenomorphic grains of clinopyroxene (40%, 0.5–0.9 mm). Groundmass (50%); laths of plagioclase (labradorite [An_{55}]). Interstices infilled with small isometric grains of clinopyroxene and greenish black volcanic glass. Vesicles (1.2–2.5 mm, 10%) filled with brownish green glass.

Alteration: slight to moderate (15%–20%); rock is nonoxidized; large vesicles filled with clay mineral which replaces glass.

Sample 33-317A-32R-6, 64–66 cm (Pies 6), Unit 6A [Z-274]

Clinopyroxene-phyric basalt, coarse grained, completely crystallized, vesicular (0.5–2 mm, 15%). Phenocrysts of clinopyroxene (0.2–2 mm, 60%). Groundmass; laths of plagioclase, microlites of clinopyroxene, volcanic glass, olivine, and opaque minerals; some areas demonstrate doleritic texture.

Alteration: slight (~15%); rock is nonoxidized; smectites fill vesicles and replace olivine and interstitial glass; some vesicles are empty.

XRD: smectites with Na-K and Mg-Ca interlayer cations and contain ~10% of mica layers.

Sample 33-317A-32R-6, 104–107 cm (Piece 8), Unit 6A [Z-1107]

Plagioclase-clinopyroxene-phyric dolerite, medium grained, vesicular. Rock: phenocrysts (20%), groundmass (55%), and vesicles (25%). Groundmass is ophitic-intersertal texture. Rock: identical to Sample 33-317A-32R-5, 89–93 cm (Z-1106).

Alteration: vesicles filled with clay mineral which replaces glass.

Sample 33-317A-33R-2, 20–25 cm (Piece 2), Unit 6B [Z-275]

Plagioclase-clinopyroxene-phyric basalt, coarse grained (in some areas is fine grained), almost completely crystallized, vesicular (0.2–1.2 mm, less then 10%). Phenocrysts of clinopyroxene (0.4–0.8 mm and more, 10%). Groundmass is doleritic texture; laths of plagioclase, clinopyroxene, volcanic glass, olivine, and opaque minerals; some areas demonstrate poikilophitic texture.

Alteration: slight (~10%); rock is nonoxidized; smectites fill vesicles and replace olivine and interstitial glass; some vesicles are empty.

XRD: smectites with Na-K and Mg-Ca interlayer cations.

Sample 33-317A-33R-3, 46–51 cm (Piece 1), Unit 6B [Z-276]

Plagioclase-clinopyroxene-phyric basalt, medium grained, almost completely crystallized, vesicular. Phenocrysts of clinopyroxene (0.4–0.6 mm, 20%) and plagioclase (0.5–0.8 mm, 50%). Groundmass is ophitic texture; laths of plagioclase, clinopyroxene, volcanic glass, olivine, and opaque minerals. Vesicles are rounded, elongated, or isometric in shape (0.3–2 mm, 20%).

Alteration: moderate (~25%); rock is nonoxidized; smectites fill vesicles and replace olivine, interstitial glass, and partly plagioclase.

XRD: smectites with interlayer cations of Na-K and Mg-Ca.

Sample 33-317A-33R-3, 92–96 cm (Piece 3), Unit 6B [Z-1108]

Clinopyroxene-phyric dolerite, fine grained, vesicular. Rock: identical to Sample 33-317A-32R-5, 89–93 cm (Z-1106) and Sample 33-317A-32R-6, 104–107 cm (Z-1107). Phenocrysts (20%) are represented by grains of clinopyroxene (0.5–0.7 mm). Groundmass (70%) with ophitic-intersertal texture includes laths of plagioclase (0.1–0.3 mm, labradorite [$An_{55–58}$]), interstices filled with small grains of clinopyroxene, greenish black glass, and opaque minerals (5%).

Alteration: slight to moderate (15%–20%); glass and opaque minerals are slightly oxidized (<1%); vesicles (10%, 0.5–1.2 mm) completely filled with clay mineral which replaces glass.

Sample 33-317A-34R-1, 32–34 cm (Piece 1), Unit 7B [Z-277]

Sparsely plagioclase-phyric basalt, medium grained, incompletely crystallized, vesicular. Microphenocrysts of plagioclase (0.5–0.8 mm, 8%) and clinopyroxene (0.3–0.5 mm, 5%). Groundmass is intergranular texture; laths

of plagioclase, clinopyroxene, volcanic glass with opaque dust, and olivine. Vesicles are rounded and isometric in shape (0.5–2.5 mm, 30%).

Alteration: slight to moderate (~20%); rock is nonoxidized; smectites fill vesicles and replace olivine, interstitial glass, and partly plagioclase. Some vesicles are empty.

XRD: smectites with interlayer cations of Na-K and Mg-Ca.

Sample 33-317A-34R-2, 136–141 cm (Piece 28), Unit 9 [Z-278]

Aphyric basalt, medium grained, incompletely crystallized, vesicular. Microphenocrysts of plagioclase and clinopyroxene (up to 3 mm). Groundmass is intergranular texture; some areas demonstrate intersertal texture; laths of plagioclase, clinopyroxene, olivine, and volcanic glass with opaque dust. Occasionally vesicles organized chains (0.3–0.8 mm, 15%).

Alteration: slight to moderate (~15%); rock is nonoxidized; smectites fill vesicles and replace olivine and interstitial glass.

XRD: smectites with interlayer cations of Na-K and Mg-Ca; trace hydromica with swelling layers (~5%).

Sample 33-317A-34R-4, 18–21 cm (Piece 1), Unit 10 [Z-1109]

Clinopyroxene-plagioclase-phyric microdolerite, fine grained, vesicular, groundmass is microdoleritic texture. Phenocrysts (10%) are represented by isometric grains of clinopyroxene (0.5–0.6 mm) and short-prismatic and tabular grains of plagioclase (0.5–0.9 mm). Groundmass (70%) includes laths and microlites of plagioclase (30%, labradorite [$An_{55–58}$]), opaque minerals (15%), and glass (5%). Clinopyroxene (50%) forms segregate of very small (up to 0.1 mm) grains.

Alteration: slight (10%–15%); rock is nonoxidized; vesicles (20%, 0.3–2 mm): small vesicles infilled with green glass; large vesicles are encrusted with clay mineral.

Sample 33-317A-34R-4, 136–140 cm (Piece 21), Unit 10 [Z-279]

Sparsely plagioclase-phyric basalt, fine grained, almost completely crystallized, vesicular. Microphenocrysts of plagioclase (0.3–0.5 mm, 10%) form glomerophyric segregates. Clinopyroxene (up to 1 mm, 3%) is present. Groundmass; laths of plagioclase, microlites of clinopyroxene, olivine, volcanic glass, and opaque dust. Vesicles are rounded and isometric in shape (0.3–2.8 mm, 20%).

Alteration: rock is nonoxidized; smectites fill vesicles and replace of olivine and interstitial glass; mica partly replaces plagioclase.

XRD: smectites with interlayer cations of Na-K and Mg-Ca.

Ninetyeast Ridge (Legs 26 and 121)

Hole 254

Sample 26-254-35R-1, 123–125 cm (Piece 11), Unit 5 [Z-100]

Sparsely olivine-microphyric basalt, fine grained, incompletely crystallized, massive, spotty in structure. Some areas (3–7 mm or ~50%–70% of the thin section) demonstrate microdoleritic (poikilophitic) texture. These areas are separated by poorly crystallized glassy mass with laths of plagioclase. Texture is hyalocrystalline. Microphenocrysts of olivine (0.5–1.3 mm) are ~1%–2% abundance. Crystals are rhomboidal or tabular in shape. Tabular crystals demonstrate clear cleavage, distinct pleochroism from orange to reddish orange color, and parallel extinction. Pleochroism is weak or absent in rhomboidal crystals. Groundmass is combined by clinopyroxene, laths of plagioclase, and opaque minerals. Opaque minerals are located in glassy areas or in marginal parts between crystallized and poorly crystallized areas. Components: plagioclase (~30%), clinopyroxene (~30%), volcanic glass (~25%), opaque minerals (~5%), and olivine (<1%).

Alteration: moderate (~30%); olivine is completely replaced with reddish orange iddingsite; interstitial volcanic glass is replaced with grassy-green smectite; laths of plagioclase which are submerged in the glass are smectitized while those in crystallized areas of rock are almost fresh.

XRD: smectite; chlorite as trace.

Sample 26-254-35R-2, 105–107 cm (Piece 14), Unit 5 [Z-101]

Sparsely olivine-microphyric basalt, fine grained, incompletely crystallized, massive, spotty in structure. About 50% of the thin section is built of poorly crystallized glassy mass, which contains laths of plagioclase and demonstrates hyalocrystalline texture. About 50% of rock are crystallized (clinopyroxene and laths of plagioclase) and demonstrate poikilophitic texture. Hypidiomorphic microphenocrysts of olivine (0.3–1 mm) are restricted to crystallized areas, while opaque minerals tend to be located in poorly crystallized areas.

Components: plagioclase (~30%), clinopyroxene (~30%), volcanic glass (~30%), opaque minerals (~10%), and olivine (<0.5%).

Alteration: moderate to strong (40%–50%); olivine is completely replaced with reddish orange iddingsite; tabular crystals of olivine demonstrate cleavage are distinct pleochroism; within poorly crystallized areas interstitial volcanic glass is replaced with grassy-green smectite; laths of plagioclase in such areas are partly replaced with smectite.

XRD: smectite; chlorite as trace.

Sample 26-254-35R-3, 72–75 cm (Piece 9), Unit 5 [Z-102]

Sparsely olivine-microphyric basalt, fine grained, incompletely crystallized, sparsely vesicular. Microphenocrysts of olivine (0.3–1 mm) are ~1% abundance. Crystals are isometrically rhombic or occasionally tabular in shape. As a rule, tabular ones demonstrate both cleavage parallel to elongation of crystals and parallel extinction. Rock has spotty structure. Groundmass (~60%–70%); clinopyroxene-plagioclase aggregate which contains small amounts of opaque minerals and microphenocrysts of olivine. Texture is poikilophitic. Such areas are separated by glassy groundmass with laths of plagioclase, opaque minerals, and occasionally with olivine. Components: plagioclase (~35%), clinopyroxene (~30%), volcanic glass (~30%), opaque minerals (5%–7%), and olivine (~1%).

Alteration: moderate (25%–30%); olivine is replaced with pleochroic in orange to orange-red iddingsite; as a rule, iddingsitized olivine is replaced with green smectite both in marginal and in central parts of crystals; occasionally, pseudomorphs of olivine are surrounded by thin opacite rim, which is built of opaque minerals; interstitial glass is replaced with grassy-green smectite; laths of plagioclase are partly replaced with similar smectite.

XRD: smectite; swelling chlorite as trace.

Sample 26-254-36R-1, 140–143 cm (Piece 20), Unit 5 [Z-103]

Aphyric olivine basalt, fine grained, incompletely crystallized, sparsely vesicular, with single idiomorphic microphenocrysts of olivine (0.6 mm). Groundmass is intersertal texture; chaotically located laths of plagioclase, xenomorphic aggregates of clinopyroxene, small xenomorphic opaque minerals, and interstitial devitrified volcanic glass filled with opaque dust and idiomorphic crystals of olivine. Components: plagioclase (~50%), clinopyroxene (~40%), opaque minerals (from 5%–7%), and volcanic glass (~1%).

Alteration: slight (10%–15%); microphenocrysts of olivine are completely replaced with orange-red and reddish brown iddingsite; prismatic olivine demonstrates orange-red pleochroism; zonal replacement is obvious: central parts are built of iddingsite while margins are represented by dark green smectite; rounded vesicles (0.3–0.6 mm) are filled with green volcanic glass; occasionally, this glass is replaced with smectite and, sparsely, by an aggregate of smectite and carbonate; interstitial glass is replaced with smectite.

XRD: smectite.

Sample 26-254-36R-2, 2–4 cm (Piece 1), Unit 5 [Z-104]

Aphyric olivine basalt, fine grained, poorly crystallized, vesicular. Texture is intersertal up to hyalocrystalline. Groundmass; chaotically located laths of plagioclase, hypidiomorphic grains of olivine, and interstitial devitrified glass. The glass is filled with aggregates of clinopyroxene crystals, plagioclases, and opaque dust. Vesicles (~5%–10%) have irregular in shape. Components: plagioclase (from 50%–60%), clinopyroxene (~20%), volcanic glass (~20%), olivine (from 5% to7%), and opaque minerals (from 5%–7%).

Alteration: moderate (20%–35%); olivine is replaced with the pleochroic iddingsite and with brownish green smectite; laths of plagioclase are replaced with grayish green smectite. Interstitial glass is replaced with smectite; vesicles are filled with smectite; the latter contains some admixture of carbonate.

XRD: smectite.

Sample 26-254-36R-2, 114–118 cm (Piece 20), Unit 5 [Z-105]

Aphyric olivine basalt, fine grained, near to aphanitic, poorly crystallized, vesicular. Texture is hyalocrystalline. Groundmass; devitrified volcanic glass with chaotically located laths of plagioclase, hypidiomorphic grains of olivine, abundant opaque dust, and crystals of clinopyroxene. Vesicles (0.2–1.2 mm) have irregular in shape. Interstitial glass is opaque; it is overfilled with opaque dust. Components: plagioclase (~60%), volcanic glass (from 30%–35%), and olivine (~5%).

Alteration: moderate (30%–40%); olivine is replaced with iddingsite and brownish green smectite; from 50%–60% of plagioclase laths are replaced with green smectite; vesicles are partly filled with green smectite.

XRD: smectite; chlorite in trace amounts; smectite in vesicles.

Sample 121-756D-6R-1, 23–25 cm (Piece 4), Unit 5 [Z-639]

Sparsely plagioclase-phyric basalt, fine grained, crystallized, sparsely vesicular. Sparsely (2%–3%) prismatic phenocrysts of plagioclase (0.7–1.2 mm, labradorite [An_{68}]). Groundmass with microlitic texture; microlites and microlaths (0.1–0.4 mm) of plagioclase (labradorite [An_{51}]). Interstices consist of very small grains of clinopyroxene segregate, opaque minerals (7%–8%), and dark green partly altered glass (1%–2%). Inclusions of glass in laths and phenocrysts of plagioclase are present. Sparse vesicles (<5%, 0.5–2 mm) demonstrate oval in shape.

Alteration: interstitial glass partly replaced by clay mineral, vesicles are encrusted by chloritized(?) glass or completely infilled with clay mineral.

Sample 121-756D-6R-2, 32–35 cm (Piece 1B), Unit 5 [Z-640]

Sparsely plagioclase-phyric basalt, sparsely vesicular. Single large (3 mm) idiomorphic prismatic phenocryst of plagioclase (0.7–1.2 mm, labradorite [An_{68}]) is present. Groundmass with microlitic texture; microlites, laths, and prismatic grains (20%, 0.1–0.4 mm) of plagioclase (labradorite [$An_{55–57}$]). Interstices consist of very small grains (70%, <0.1 mm) of clinopyroxene (segregate), opaque minerals (5%), and dark green glass (5%). Inclusions of glass in laths and phenocrysts of plagioclase are present. Single vesicles (up to 0.70 mm) are present.

Alteration: rock is fresh; vesicles infilled with green-brown clay mineral.

Sample 121-756D-6R-2, 91–95 cm (Piece 1C), Unit 5 [Z-29]

Sparsely plagioclase-phyric basalt, fine grained, crystallized, sparsely vesicular. Sparsely (<1%) phenocrysts of plagioclase (2–3 mm) are tabular in shape, corroded, and fractured. Phenocrysts contain small inclusions of opaque minerals. Small grains of olivine are present. Single vesicles are from 0.5–2 mm in diameter. Groundmass; aggregate of plagioclase laths, xenomorphic grains of clinopyroxene with admixture of opaque minerals, and microphenocrysts of olivine. Groundmass demonstrates intergranular texture. Components: plagioclase (~40%), clinopyroxene (~45%), opaque minerals (~10%), and olivine (~1%).

Alteration: moderate (30%); brownish red iddingsite or occasionally brownish green smectite replace olivine; cracks in plagioclases, as well as microcracks cutting vesicles, are filled with smectite with Fe hydroxide; vesicles are filled with radial to spherical aggregate of smectite and with fine dispersed oxidized opaque dust.

XRD: smectite and mixed-layer smectite-chlorite mineral; trace hydromica.

Sample 121-756D-7R-1, 136–138 cm (Piece 12C), Unit 6 [Z-22]

Aphyric basalt, fine grained, near to aphanitic, crystallized, massive. Texture is intergranular. Single microphenocrysts of plagioclase (up to 0.3–0.5 mm), Slightly corroded, with small inclusions of idiomorphic opaque minerals. Single phenocrysts of olivine (up to 0.2–0.3 mm). Sparsely areas with interstitial volcanic glass. Components: plagioclase (~45%), clinopyroxene (~45%), opaque minerals (7%–10%), olivine (in single grains).

Alteration: slight (5%); olivine and volcanic glass in interstices are replaced with grassy-green smectite.

XRD: smectite; hydromica trace.

Sample 121-756D-7R-2, 26–28 cm (Piece 1C), Unit 6 [Z-25]

Aphyric basalt, fine grained (near to aphanitic), fractured, with single microphenocrysts (0.2–0.3 mm) of plagioclase, clinopyroxene, and olivine. Isometric opaque minerals are from 10% to 12% abundance. Groundmass; laths of plagioclase and small grains of clinopyroxene. Sparsely small areas are built interstitial volcanic glass. Single vesicles vary from 0.1 to 0.2 mm. Composition: plagioclase (~45%), clinopyroxene (~45%), opaque minerals (up to 10%), olivine (single grains).

Alteration: slight (10%); plagioclase is partly replaced with grassy-green smectite; olivine is completely replaced with smectite; interstitial volcanic glass is replaced with smectite; vesicles are filled with grassy-green smectite; cracks are filled with brownish red iddingsite; opaque minerals are partly oxidized along salbands.

XRD: smectite; trace chlorite.

Sample 121-756D-7R-3, 59–63 cm (Piece 2C), Unit 6 [Z-641]

Aphyric basalt, sparsely vesicular. Rock with microlitic texture; microlaths (0.1–0.5 mm) of plagioclase (50%, labradorite [An_{52}]). Interstices consist of small grains (<0.1 mm) of clinopyroxene (35%) segregates, opaque minerals (5%), and altered glass (10%). Sparse vesicles (2%–3%, 0.2–0.6 mm) demonstrate rounded-isometric in shape.

Alteration: slight; interstitial glass partly replaced by clay mineral, vesicles infilled with clay mineral.

Sample 121-756D-8R-1, 16–19 cm (Piece 2), Unit 7 [Z-1337]

Aphyric basalt, crystallized, vesicular. Rock with microlitic texture; microlites (0.05–0.1 mm) of plagioclase (20%, andesine [$An_{38–42}$]). Interstices consist of isometric partly oxidized grains (up to 0.1 mm) of clinopyroxene (70%), opaque minerals (5%–7%), and glass. Vesicles (5%, up to 2 mm) are rounded in shape.

Alteration: slight (5%–10%); 20%–25% of rock is oxidized; vesicles and microcracks completely infilled with clay mineral and Fe hydroxides.

Sample 121-756D-8R-1, 72–75 cm (Piece 14), Unit 8 [Z-642]

Plagioclase-phyric basalt, sparsely vesicular. Phenocrysts (5%): glomerophyric segregate of prismatic grains (0.3–0.5 mm) of plagioclase (labradorite [An_{60}]). Single small oxidized grains (0.1–0.2 mm) of olivine are present. Groundmass with microlitic texture; segregate of very small grains (<0.1 mm) of clinopyroxene (60%); microlites (0.1–0.4 mm) of plagioclase (30%, labradorite [An_{52-53}]); skeletal grains of opaque minerals (10%). Single large vesicles (up to 2 mm in diameter) are oval-elongate in shape.

Alteration: slight to moderate (15%–20%); microcracks in plagioclase grains infilled with albite and clay mineral; olivine is oxidized; clinopyroxene partly (30%) replaced by clay mineral and Fe hydroxides; vesicles infilled with clay mineral.

Sample 121-756D-9R-1, 36–38 cm (Piece 5), Unit 9 [Z-5]

Aphyric olivine basalt, fine grained, crystallized, massive, with single microphenocrysts (0.2–0.5 mm) of olivine. Groundmass; laths and hypidiomorphic crystals of plagioclase, grains of clinopyroxene, xenonomorphic and elongated to tabular opaque minerals, as well as by hypidiomorphic grains of olivine (5%–7% abundance). Single small areas are built of interstitial glass. Groundmass demonstrates intersertal texture and partly variolitic texture. Composition: plagioclase (~40%), clinopyroxene (~40%), opaques (~10%), and olivine (~10%).

Alteration: slight (10%–15%); inner parts of olivine crystals are replaced with brown iddingsite while marginal parts are replaced with grassy-green smectite; areas of interstitial volcanic glass are completely replaced with smectite; single relatively large laths of plagioclase are partly replaced with green smectite.

XRD: smectite.

Sample 121-756D-9R-3, 119–121 cm (Piece 4E), Unit 9 [Z-36]

Aphyric olivine basalt, fine grained, crystallized, massive, with single microphenocrysts of olivine. Groundmass demonstrates intergranular, partly microdoleritic, or taxitic (due to subparallel oriented laths of plagioclase) texture. Groundmass; laths of plagioclase, clinopyroxene, olivine grains, xenomorphic and elongated to tabular crystals of opaque minerals (magnetite) as well as by idiomorphic and xenomorphic grains of olivine. Sparsely single microphenocrysts of olivine are present. Composition: plagioclase (~45%), clinopyroxene (~35%), opaque minerals (~10%), and olivine (up to 10%).

Alteration: slight (10%–15%); microphenocrysts of olivine are replaced with red iddingsite in their central parts; along margins microphenocrysts are replaced with green smectite; relatively large laths of plagioclase are replaced with green smectite in their central parts; clinopyroxene is partly replaced with smectite.

XRD: smectite; trace mixed-layer smectite-chlorite mineral.

Sample 121-756D-11R-1, 115–118 cm (Piece 17), Unit 13 [Z-643]

Plagioclase-phyric basalt, massive. Phenocrysts (5%): tabular and prismatic grains (0.4–0.8 mm) of plagioclase (labradorite [An_{58}]). Groundmass with microlitic texture; very small grains of clinopyroxene (50%) segregate; microlites and microlaths of plagioclase (30%); and opaque minerals (5%). Altered olivine(?) is present (15%).

Alteration: slight (10%–15%); microcracks in plagioclase grains infilled with clay mineral, olivine(?) is oxidized and replaced by iddingsite; microcracks in rock are filled with clay mineral.

Sample 121-756D-11R-2, 95–99 cm (Piece 11D), Unit 14 [Z-4]

Aphyric basalt, crystallized, vesicular, fine grained, near to aphanitic with single microphenocrysts of plagioclase. Plagioclase often forms glomeroporphyric aggregates. Microphenocrysts are from 0.2 to 0.4 mm. Plagioclase is fractured. Vesicles (0.2–0.6 mm in diameter and 1%–3% abundance) are mostly empty and demonstrate irregular in shape. Groundmass demonstrates intergranular texture. Groundmass; laths of plagioclase, grains of clinopyroxene, idiomorphic grains of opaque minerals, and single grains of olivine. Composition: clinopyroxene (~50%), plagioclase (~40%), opaque minerals (up to 10%), and olivine (single grains).

Alteration: slight (10%); olivine is replaced with grassy-green smectite; walls of vesicles are covered with radial zonal aggregate of grassy-green smectite, impregnated with Fe hydroxides; small vesicles are completely filled with smectite; cracks in plagioclases are filled with light green smectite; carbonates are recognized in central parts of microcracks.

XRD: smectite and mixed-layer smectite-chlorite mineral; trace hydromica.

Sample 121-756D-12R-2, 69–72 cm (Piece 1C), Unit 14 [Z-16]

Aphyric olivine basalt, fine grained, crystallized, vesicular. Vesicles (0.2–1 mm) are <1% abundance. Groundmass is intergranular texture; plagioclase laths, small grains of clinopyroxene, xenomorphic opaque minerals, and hypidiomorphic olivine. Cracks are filled with opaque minerals. Composition: clinopyroxene (~45%), plagioclase (~40%), opaque minerals (~10%), and olivine (~5%).

Alteration: slight (5%–10%); olivine is replaced with grassy-green smectite; clinopyroxene is partly replaced with smectite; vesicles are filled with radial aggregates of grassy-green smectite; opaque minerals are partly oxidized.

XRD: smectite.

Hole 757C

Sample 121-757C-8R-1, 127–129 cm (Piece 5A), Unit 2 [Z-9]

Plagioclase-phyric basalt, fine grained, highly vesicular, fractured. Corroded phenocrysts of plagioclase (3–4 mm) are 5%–7% abundance. Vesicles (2–5 mm in diameter and ~25% abundance) are rounded and demonstrate irregular in shape. Groundmass; an aggregate of laths of plagioclase, xenomorphic clinopyroxene, and opaque minerals (7%–10%). Groundmass demonstrates intergranular texture.

Alteration: strong (>50%); phenocrysts of plagioclase are significantly replaced with chlorite and occasionally carbonatized; sparsely pseudomorphs of iddingsite and smectite upon olivine are present; groundmass is orange to brown in color due to oxidation of opaque minerals; outer parts of the inner surfaces in vesicles are asymmetrically covered by volcanic glass, mostly replaced with smectite-chlorite aggregate, while the inner parts are built of the fine grained aggregate of Fe and Mn(?) oxides; intermediate parts of some vesicles are filled by carbonate or occasionally zeolite; small vesicles are completely filled with smectite-chlorite aggregate and with Fe and Mn(?) hydroxides; microcracks which connect vesicles, are filled with smectite-chlorite aggregate and Fe hydroxides.

XRD: smectite and swelling chlorite; trace chlorite.

Sample 121-757C-8R-2, 119–121 cm (Piece 3I), Unit 2 [Z-6]

Plagioclase-phyric basalt, sparsely vesicular. Phenocrysts of plagioclase and their glomerophyric segregates (up to 6 mm) are ~50% abundance. Phenocrysts of plagioclase are corroded and demonstrate resorption borders. Single grains of olivine. Groundmass; fine grained aggregate of laths of plagioclase, grains of clinopyroxene, and xenomorphic grains of opaque minerals. Groundmass demonstrates intersertal texture. Occasionally, phenocrysts of plagioclase are surrounded by irregularly curved concentrations of volcanic glass. As a rule, phenocrysts of plagioclase contain microcracks and often contain inclusions of volcanic glass. Composition: plagioclase (~70%), clinopyroxene (~25%), opaque minerals (~3%), and olivine (single grains).

Alteration: strong (>50%); olivine is completely replaced with smectite and by an aggregate of smectite and chlorite; occasionally, grains of altered olivine are surrounded by opaque rims; volcanic glass around phenocrysts of plagioclase (or in plagioclases as inclusions) is completely replaced with green and brown smectite; plagioclases are replaced with brown smectite and occasionally by zeolite along margins and microcracks; opaque minerals are partly oxidized; inner surfaces of vesicles are lined by thin (0.01 mm) layer of radial aggregate of smectite and chlorite; intermediate part; calcite; microcracks in plagioclase are filled with brown smectite and occasionally by zeolite(?).

XRD: smectite and chlorite with hydrated interlayers.

Sample 121-757C-9R-1, 59–61 cm (Piece 3), Unit 2 [Z-1]

Plagioclase-phyric basalt, with fine grained incompletely crystallized groundmass, massive. Phenocrysts of plagioclase are tabular, corroded along margins, and fractured. Grains of plagioclase contain small inclusions of devitrified volcanic glass filled with opaque dust. Occasionally, phenocrysts of plagioclase are surrounded by narrow rim of the second generation plagioclase. Single idiomorphic phenocrysts (up to 2 mm) of olivine are present. Groundmass; chaotically located laths of plagioclase and xenomorphic crystals of clinopyroxene; single small grains of olivine are present also. Some areas demonstrate irregularly curved spots of interstitial volcanic glass. Small xenomorphic opaque minerals are ~3%–5% abundance. Groundmass demonstrates intergranular texture. Composition: plagioclase (50%–60%), clinopyroxene (~30%), opaque minerals (3%–5%), volcanic glass (1%–3%), and olivine (single grains).

Alteration: moderate (25%–35%); phenocrysts of olivine are completely replaced with green smectite and partly, in central parts, by carbonate; kelyphytic rims (0.1 mm) of opaque minerals (magnetite) are evident around altered grains of olivine; interstitial volcanic glass is completely replaced with smectite; veins of smectite are present;

opaque minerals are oxidized. Fe hydroxides partly impregnate groundmass, smectitized volcanic glass, and veins of smectite; cracks in plagioclases are filled with green smectite; occasionally, smectite is brown in color due to Fe hydroxide and contains fine grained aggregate of an oxidized brownish black opaque minerals. Zeolite (?) is restricted to boundaries between plagioclases of different generations.

XRD: mixed-layer chlorite-smectite mineral and smectite.

Sample 121-757C-9R-2, 24–26 cm (Piece 1A), Unit 2 [Z-17]

Plagioclase-phyric basalt, with fine grained groundmass, sparsely vesicular, almost completely crystallized. Rounded vesicles (0.1–0.2 mm) are <1% abundance. Phenocrysts of plagioclase and their glomeroporphyric segregates (5–8 mm) represent ~50%–55% of the thin section. Occasionally, phenocrysts are surrounded by the rim built of more acid material. Phenocrysts are corroded along margins. Also, phenocrysts contain small inclusions of devitrified volcanic glass filled with opaque dust. Occasionally, phenocrysts contain tabular inclusions of opaque minerals (magnetite?). As a rule, interstitial glass (~1% abundance) is localized around phenocrysts of plagioclase. Occasionally, large inclusions of glass are known within phenocrysts of plagioclase. Groundmass; nonoriented laths of plagioclase, xenomorphic grains of clinopyroxene, xenomorphic or sparsely tabular opaque minerals, and single subidiomorphic crystals of olivine. Groundmass demonstrates intergranular texture. Composition: plagioclase (60%–70%), clinopyroxene (~25%), opaque minerals (3%–5%), volcanic glass (<1%), and olivine (single grains).

Alteration: slight to moderate (20%); olivine is completely replaced with smectite; olive-green smectite completely replaced volcanic glass from both inclusions in plagioclases and interstices; vesicles are filled with olive-green smectite.

XRD: smectite.

Sample 121-757C-9R-3, 35–37 cm (Piece 1A), Unit 2 [Z-18]

Plagioclase-phyric basalt, fine grained, almost completely crystallized, sparsely vesicular. Phenocrysts of plagioclase and their segregates (both 3–8 mm) represent 60%–65% of the thin section. Faces of plagioclase are intensely corroded. Plagioclases are fractured and contain inclusions of volcanic glass with opaque dust. Interstitial glass (<1% abundance) demonstrate irregular in shape. Single vesicles are from 0.3 to 0.5 mm in diameter. Groundmass; laths of plagioclase, xenomorphic grains of clinopyroxene, and opaque minerals. Composition: plagioclase (~70%), clinopyroxene (~20%), opaque minerals (5%–7%), volcanic glass (<1%), and olivine (single grains).

Alteration: slight to moderate (15%–20%); olivine and interstitial glass are completely replaced with smectite. Inclusions of glass in plagioclases are partly replaced with smectite; vesicles are filled with smectite; cracks in plagioclases and clinopyroxenes are filled with smectite; marginal parts of clinopyroxenes are replaced with smectite.

XRD: smectite.

Sample 121-757C-9R-4, 38–42 cm (Piece 1A), Unit 3 [Z-1338]

Olivine-plagioclase-phyric basalt, crystallized, vesicular. Phenocrysts (50%): xenomorphic grains (0.8–1.5 mm) of altered olivine (5%) and large prismatic grains (1–10 mm) of plagioclase (45%, labradorite-bitovnite [An_{70}] and andesine [An_{48}]). Groundmass (30%) with microlitic texture; microlites (up to 0.1 mm) of plagioclase (5%, andesine [An_{32}]), small grains (up to 0.1 mm) of clinopyroxene (10%), black glass, and opaque minerals. Vesicles (20%, 0.3 mm and 3 mm in diameter) are isometric in shape.

Alteration: slight (5%); olivine replaced by iddingsite, part (50%) of clinopyroxene is oxidized, small vesicles are filled with clay mineral, part (30%) large vesicles completely infilled with carbonates.

XRD: smectite with ~10% mica layers; trace natrolite.

Sample 121-757C-9R-5, 70–73 cm (Piece 2), Unit 5 [Z-1339]

Plagioclase-phyric basalt, crystallized, vesicular. Phenocrysts (20%): prismatic grains (1.2–2 mm) of plagioclase (labradorite [An_{64}]). Groundmass (50%) with microlitic texture; microlites (up to 0.1 mm) of plagioclase (5%), small grains of clinopyroxene (25%), black glass (10%), and opaque minerals (10%). Vesicles (30%, 1.2–3 mm in diameter) are rounded and isometric in shape.

Alteration: slight (10%–15%); rock is slightly oxidized (10%–15%); plagioclase mainly (70%) replaced by clay minerals and albite, grains of clinopyroxene partly are oxidized, vesicles are filled with clay mineral, chalcedony, tridymite-cristobalite.

XRD: calcite and zeolite (analcime and natrolite-heulandite); trace smectite and chlorite.

Sample 121-757C-9R-7, 71–73 cm (Piece 1B), Unit 5 [Z-30]

Plagioclase-phyric basalt, fine grained, almost completely crystallized, massive. Phenocrysts of plagioclase (from 1 to 5–6 mm) represent ~45%–50% of the thin section. Phenocrysts are resorbed, fractured, and occasionally contain inclusions of volcanic glass both with and without opaque dust. Often, small grains of clinopyroxene are impregnated in glomeroporphyric segregates near margins of grains. Groundmass demonstrates intergranular texture; laths of plagioclase, clinopyroxene, and xenomorphic grains of opaque minerals. Occasionally, interstitial volcanic glass is present. Composition: plagioclase (~60%), clinopyroxene (~30%), opaque minerals (5%–7%), volcanic glass (<1%), olivine (single grains).

Alteration: moderate (30%); volcanic glass from inclusions in plagioclases is replaced with green smectite; interstitial glass is replaced with olive-green smectite; opaque minerals are partly replaced with Fe hydroxide; the latter is partly responsible for the rusty-brown color of clinopyroxenes.

XRD: smectite; trace mixed-layer smectite-chlorite mineral.

Sample 121-757C-9R-8, 57–60 cm (Piece 4A), Unit 5 [Z-644]

Plagioclase-phyric basalt, vesicular. Phenocrysts (60%): glomerophyric segregates of tabular and short prismatic grains (0.5–3 mm up to 7–8 mm) of plagioclase (approximately labradorite [An_{55}]) and individual small prismatic grains (0.8–1.5 mm) of plagioclase. Groundmass with microlitic texture; microlites of plagioclase (labradorite [An_{52}]), rounded isometric grains (0.1 mm) of clinopyroxene segregate, and grains (0.1 mm) of opaque minerals. Vesicles (15%, 0.2–0.5 mm in diameter) are isometric in shape.

Alteration: slight to moderate (15%–20%); inclusions of glass from small grains of plagioclase partly replaced by albite and clay mineral; vesicles completely are filled with clay mineral.

Sample 121-757C-10R-2, 66–70 cm (Piece 5A), Unit 7 [Z-1340]

Plagioclase-phyric basalt, crystallized, vesicular. Phenocrysts (55%): large prismatic crystals (1.5–8 mm of plagioclase (labradorite [An_{68}]). Plagioclase consists of inclusions of glass. Groundmass (25%) with microlitic texture; microlites of plagioclase (5%), grains of clinopyroxene (15%), and glass (5%). Vesicles (20%, 1–10 mm in diameter) are rounded in shape.

Alteration: slight (10%–15%); rock is oxidized (5%–10%); inclusions of glass from grains of plagioclase replaced by smectite and chalcedony; grains of clinopyroxene are oxidized; vesicles completely are filled with carbonate.

Sample 121-757C-10R-3, 79–81 cm (Piece 2C), Unit 9 [Z-1341]

Plagioclase-phyric basalt, crystallized, vesicular. Phenocrysts (40%): large prismatic and tabular crystals (1.5–5 mm) of plagioclase (labradorite [An_{68}]). Groundmass (40%) with microlitic texture; microlites of plagioclase (5%), grains of clinopyroxene (30%), and glass (5%). Vesicles (20%, 2–4 mm in diameter) are oval-isometric in shape.

Alteration: slight (5%); rock is oxidized (10%); cracks in grains of plagioclase are filled with smectite (10% of grain volume); grains of clinopyroxene partly (10%) are oxidized; vesicles (7%) completely are filled with carbonate; vesicles (10%) are empty and encrusted by glass; vesicles (3%) infilled with chalcedony.

XRD: smectite; trace calcite.

Sample 121-757C-11R-1, 54–58 cm (Piece 8B), Unit 10 [Z-645]

Plagioclase-phyric basalt, vesicular. Phenocrysts (30%–35%): large short prismatic and tabular crystals (1.5–5 mm) of plagioclase. Groundmass (35%–40%) with microlitic (occasionally, microintersertal) texture; microlites of plagioclase, small grains of clinopyroxene, greenish glass, and opaque minerals. Vesicles (30%, up to 5 mm and 0.3–0.5 mm in diameter) are rounded-isometric (large vesicles) and isometric (small vesicles) in shape.

Alteration: very strong (80%); plagioclase phenocrysts almost completely replaced by albite, clay mineral, and zeolite (in single grains albite completely replaced by smectite); microlites of groundmass plagioclase almost completely replaced by smectite and zeolite; clinopyroxene partly is oxidized; large vesicles completely are filled with zeolite (occasionally, single grains of carbonate are present among zeolite); small vesicles are lined by clay mineral and infilled in central parts with zeolite; microcracks consist of zeolite and Fe hydroxides.

XRD: smectite with ~20% mica layers; minor swelling chlorite and zeolite (analcime); trace chlorite and hydromica.

Sample 121-757C-11R-1, 98–99 cm (Piece 9C), Unit 10 [Z-646]

Plagioclase-phyric basalt, vesicular. Phenocrysts (30%): prismatic crystals (0.5–2 mm) of plagioclase. Groundmass (50%) with pilotaxitic texture; microlites of plagioclase, brownish black glass, and brown grains of clinopyroxene. Vesicles (20%, 1.5–2 mm in diameter) are rounded in shape.

Alteration: moderate (30%–40%); plagioclase phenocrysts almost completely replaced by albite and clay mineral; microlites of groundmass plagioclase almost completely replaced by albite and zeolite; vesicles are filled with fragments of glass, zeolite, and clay mineral.

XRD: swelling chlorite; minor analcime; trace chlorite and hydromica.

Sample 121-757C-11R-1, 135–137 cm (Piece 9E), Unit 12 [Z-34]

Plagioclase-phyric basalt, incompletely crystallized, cryptocrystalline, vesicular. Phenocrysts of plagioclase (0.8–5 mm) vary from 20%–25% abundance. Plagioclases are tabular, idiomorphic, Slightly corroded, occasionally fractured, and contain inclusions of opaque minerals. Some crystals contain single inclusions of volcanic glass. The latter contains opaque dust. Vesicles (up to 3–7 mm) represent ~20% of the thin section. Two types of vesicles are present. Vesicles of the first type are partly or completely filled with devitrified volcanic glass, while vesicles of the second type are originally empty. Groundmass; crystallized volcanic glass with microlites of plagioclase, clinopyroxene, small laths of plagioclase, single microphenocrysts of clinopyroxene, and olivine. Some spots of noncrystallized volcanic glass are present. Composition: plagioclase (~40%), clinopyroxene (~40%), opaque minerals (5%–7%), volcanic glass (5%–7%), and olivine (~1%).

Alteration: strong (50%–60%); olivine is completely replaced with smectite; some phenocrysts of plagioclase are replaced (up to 20%–80%) by zeolite; inclusions of volcanic glass in plagioclases are replaced along their margins by the grassy-green smectite, while their central parts are replaced with zeolite(?); smectite replaces volcanic glass in vesicles; inner parts of the originally empty vesicles are covered by the thin film of radial grassy-green smectite; this film demonstrates three layers in some vesicles: outer and inner layers are represented by an opaque aggregates, while intermediate layer is built of green smectite; some vesicles demonstrate radial zeolite; interstitial volcanic glass is replaced with smectite; cracks in plagioclases are filled with grassy-green smectite; secondary finely dispersed grassy-green mineral replaces olivine.

XRD: mixed-layer chlorite-smectite mineral and smectite; trace hydromica.

Sample 121-757C-12R-1, 5–9 cm (Piece 1), Unit 18 [Z-1342]

Plagioclase-phyric basalt, crystallized. Phenocrysts (30%): prismatic and tabular crystals (0.8–1.6 mm) of plagioclase (labradorite [An_{68}]). Groundmass (70%) with microlitic texture; short-prismatic laths (0.1–0.3 mm) of plagioclase (35%, andesine [An_{42}]), segregate of small (<0.1 mm) grains of clinopyroxene (25%); green glass (8%), and opaque minerals (2%–3%).

Alteration: slight (8%–10%); rock is non oxidized; clay mineral replaces interstitial glass.

XRD: smectite; trace chlorite and hydromica.

Sample 121-757C-12R-1, 84–86 cm (Piece 2), Unit 18 [Z-21]

Clinopyroxene-plagioclase-phyric basalt, almost completely crystallized, fine grained, massive. Tabular phenocrysts of plagioclase (1–5 mm) represent ~25% of the thin section. Occasionally, they form glomerophyric segregates with clinopyroxene. Clinopyroxene (1.5–3 mm) is <1% abundance. Phenocrysts of plagioclase occasionally contain elongated inclusion of devitrified volcanic glass both with or without opaque dust. Phenocrysts of plagioclase are corroded and fractured. A thin rims of the second generation plagioclase are restricted to corroded zones. Groundmass; an aggregate of laths of plagioclase, grains of clinopyroxene with an admixture (~1%–3%) of idiomorphic opaque minerals. Interstitial volcanic glass is ~1%–3% abundance. Cryptocrystalline aggregates of clinopyroxene are occasionally restricted to phenocrysts of plagioclase. Groundmass demonstrates intergranular texture. Composition: plagioclase (~50%), clinopyroxene (~45%), opaque minerals (1%–3%), volcanic glass (1%–3%), olivine (single grains).

Alteration: slight (~10%); smectite forms pseudomorphs upon olivine; also, it replaces both inclusions of the volcanic glass in plagioclases and interstitial glass; smectite fills microcracks in clinopyroxenes and plagioclases.

XRD: smectite.

Sample 121-757C-12R-2, 8–10 cm (Piece 1), Unit F18 [Z-13]

Plagioclase-phyric basalt, incompletely crystallized, fine grained, massive. Elongated to tabular phenocrysts of plagioclase (0.5–7 mm) vary from 30%–40% abundance. Phenocrysts are corroded and contain inclusions of opaque minerals and volcanic glass. Phenocrysts of clinopyroxene and single grains of olivine are present. Groundmass; an aggregate of laths of plagioclase, clinopyroxene, xenomorphic segregates of opaque minerals (~3%–5%), and spotty interstitial glass (~5%–10%). Groundmass demonstrates intergranular to intersertal texture. Composition: plagioclase (~60%), clinopyroxene (~30%), opaque minerals (~5%), volcanic glass (5%–10%), olivine (single grains).

Alteration: moderate (20%–30%); grassy-green smectite replaces volcanic glass from inclusions in plagioclases and interstitial glass; also, smectite forms pseudomorphs upon olivine; smectite fills microcracks in clinopyroxenes and plagioclases.

XRD: smectite.

Sample 121-757C-12R-2, 75–79 cm (Piece 4), Unit 18 [Z-1343]

Plagioclase-phyric basalt, vesicular. Phenocrysts (20%): prismatic crystals (1.3–2.5 mm) of plagioclase. Groundmass (40%) with vitrophyric texture; brown grain with very small vesicles (0.1 mm, 2%–3%). Vesicles (40%, 2.5–6 mm) are rounded in shape. Vesicles are located in brecciated zone.

Alteration: strong (60%); 40% of rock is oxidized; interstitial glass is oxidized; very small vesicles from interstitial glass infilled with opal; large vesicles and brecciated zone contain carbonate (70%) and zeolite (30%).

XRD: calcite and natrolite; trace smectite and mixed-layer smectite-chlorite mineral; white matter from vesicles: calcite; trace analcime and quartz.

Hole 758A

Sample 121-758A-56R-1, 21–23 cm (Piece 2A), Unit 1 [Z-26]

Sparsely plagioclase-phyric basalt, fine grained, massive. Phenocrysts (0.5–2.5 mm) vary from 1%–3% abundance. Occasionally, phenocrysts form glomerophyric segregates (up to 4 mm) from 3 to 4 grains of plagioclase. Groundmass demonstrates intersertal to intergranular texture. Groundmass; chaotically oriented laths of plagioclase, xenomorphic grains of clinopyroxene, interstitial volcanic glass, and angular grains of opaque minerals (magnetite). Composition: plagioclase (~50%), clinopyroxene (~25%), opaques (3%–5%), interstitial volcanic glass (~25%), and olivine (single grains).

Alteration: moderate (~30%); interstitial volcanic glass is completely replaced with olive-green smectite; clinopyroxene is slightly replaced with smectite along margins of grains; cracks in clinopyroxene are filled by smectite.

XRD: smectite.

Sample 121-758A-57R-2, 110–114 cm (Piece 2), Unit 2 [Z-647]

Clinopyroxene-plagioclase-phyric basalt, massive. Phenocrysts (10%): glomerophyric segregates of small (0.2–0.3 mm) grains of clinopyroxene and laths of plagioclase. Groundmass (90%) with pilotaxitic texture; needle-shaped microlites of plagioclase and glass with opaque minerals.

Alteration: very strong (90%); plagioclase phenocrysts are completely replaced by zeolite; groundmass plagioclase replaced by clay minerals and zeolite; clay mineral replaces interstitial glass.

Sample 121-758A-57R-3, 7–9 cm (Piece 1), Unit 2 [Z-32]

Aphyric basalt, aphanitic, cryptocrystalline, sparsely vesicular (<1% abundance). Sparse microphenocrysts of clinopyroxene and plagioclase (up to 0.2–0.3 mm). Groundmass demonstrates hyalopylitic texture with elements of variolitic organization. Vesicles (0.1–0.2 mm) are rounded in shape. Interstitial glass is ~10%–15% abundance. It contains up to 3% of opaque dust.

Alteration: strong to very strong (50%–70%); laths of plagioclase and its caselike crystals are replaced with smectite in their central parts; clinopyroxene is replaced with smectite up to 50% abundance; vesicles are filled with radial aggregate of smectite. Interstitial glass is completely replaced with smectite.

XRD: smectite.

Sample 121-758A-57R-3, 37–41 cm (Piece 4), Unit 2 [Z-648]

Aphyric basalt, massive. Rocks with intersertal texture; microlites and laths (0.2–0.3 mm) of plagioclase (andesine-labradorite [An_{50}]), rounded-isometric grains of clinopyroxene (20%), and completely smectitized glass with opaque minerals (5%–8%).

Alteration: strong (50%).

Sample 121-758A-58R-1, 41–43 cm (Piece 3), Unit 2 [Z-33]

Aphyric basalt, fine grained, sparsely vesicular. Groundmass demonstrates intersertal to intergranular texture. Vesicles (~0.5–0.7 mm) are <1% abundance. Groundmass; chaotically located laths of plagioclase. Interstices are filled with clinopyroxene and interstitial volcanic glass. Composition: plagioclase (~40%), clinopyroxene (~35%), volcanic glass (~25%). Volcanic glass contains opaque dust (occasionally in dendritic aggregates) and skeletal grains of magnetite (up to 0.01 mm).

Alteration: moderate (25%–30%); clinopyroxene is slightly replaced with smectite along margins of crystals; cracks in clinopyroxene are filled with smectite; volcanic glass is completely replaced with olive-green smectite; vesicles are filled with radial aggregates of olive-green smectite.

XRD: smectite.

Sample 121-758A-58R-5, 55–57 cm (Piece 2A), Unit 2 [Z-8]

Aphyric basalt, fine grained, massive. Groundmass domesticates intergranular to intersertal texture. Groundmass; chaotically oriented laths of plagioclase, clinopyroxene in interstices, and interstitial volcanic glass. Volcanic glass contains skeletal and xenomorphic magnetite and opaque dust. Composition: plagioclase (~45%), clinopyroxene (~35%), volcanic glass (~20%).

Alteration: moderate (~25%); clinopyroxene is slightly smectitized along peripheral parts of the crystals; interstitial volcanic glass is completely replaced with smectite; cracks in clinopyroxene are filled with smectite.

XRD: smectite.

Sample 121-758A-59R-7, 52–56 cm (Piece 1A), Unit 2 [Z-1344]

Aphyric basalt (microdolerite), crystallized, massive. Rocks with intersertal-microdoleritic texture; laths (0.2–0.7 mm) of plagioclase (10%, labradorite [An_{68}] and [An_{58}]), rounded grains (0.1–0.3 mm) of clinopyroxene (45%), greenish black glass (10%), and opaque minerals (5%).

Alteration: rock is fresh.

Sample 121-758A-60R-1, 11–13 cm (Piece 1B), Unit 3 [Z-31]

Aphyric basalt, fine grained, massive. Groundmass domesticates intergranular to intersertal texture. Groundmass; chaotically located laths of plagioclase and hypidiomorphic grains of clinopyroxene. The latter fills up to 75% of interstices between laths of plagioclase. The other space is filled with interstitial volcanic glass. Occasional glomerophyric segregates of clinopyroxene and plagioclase are present. Interstitial volcanic glass contains xenomorphic (sparsely skeletal) opaque minerals (magnetite). Composition: plagioclase (~40%), clinopyroxene (~40%), volcanic glass (15%–20%), opaque minerals (up to 5%).

Alteration: moderate (~20%–25%); secondary minerals are represented by smectite; interstitial volcanic glass and, partly, clinopyroxene are replaced with olive-green smectite along margins and microcracks.

XRD: smectite.

Sample 121-758A-60R-2, 80–82 cm (Piece 2), Unit 3 [Z-3]

Aphyric basalt, fine grained, massive. Groundmass demonstrates intersertal texture. Laths of plagioclase and xenomorphic grains of pyroxene are cemented by interstitial volcanic glass. Xenomorphic grains of magnetite and opaque dust are concentrated within interstitial glass. Composition: plagioclase (~35%), clinopyroxene (~30%), volcanic glass (~30%), magnetite (~5%), and olivine (single grains).

Alteration: moderate (~40%); idiomorphic pseudomorphs of smectite upon olivine are evident; interstitial volcanic glass is completely replaced with olive-gray smectite; clinopyroxene is partly replaced with smectite along peripheral parts of crystals; microcracks in clinopyroxene are filled with smectite.

XRD: smectite.

Sample 121-758A-60R-6, 82–84 cm (Piece 1C), Unit 3 [Z-27]

Sparsely plagioclase-phyric basalt, fine to medium grained, sparsely vesicular. Single phenocrysts of plagioclase and their glomerophyric segregates (~2–3 mm in diameter). Occasionally, small (0.1–0.3 mm) grains of olivine (3–4 grains) are grouped around such segregates. Single vesicles are 1–1.5 mm. Groundmass; plagioclase, xenomorphic grains of clinopyroxene, and irregularly distributed intersertal glass with inclusions of magnetite. Groundmass demonstrates intergranular texture; intersertal texture is present in isolated spotty areas. Composition: plagioclase (~50%), clinopyroxene (~25%), volcanic glass (~25%), magnetite (1%–3%), and olivine.

Alteration: slight to moderate (~20%); pseudomorphs of smectite upon olivine; interstitial volcanic glass is replaced with olive-green smectite; vesicles are filled with smectite.

XRD: smectite.

Sample 121-758A-61R-2, 62–67 cm (Piece 1A), Unit 3 [Z-1345]

Plagioclase-phyric basalt (microdolerite), crystallized. Phenocrysts (5%): plagioclase (0.9.3–1.2 mm, approximately labradorite [$An_{50–52}$]). Groundmass (95%) with intersertal-microdoleritic texture; laths (0.3–0.8 mm) of plagioclase (30%, labradorite [$An_{55–57}$] and andesine [An_{40}]), segregate of small grains (0.1–0.4 mm) of clinopyroxene (35%), glass (25%), and opaque minerals (2%–3%).

Alteration: slight (15%); brownish dark green glass replaced by clay mineral.

XRD: smectite; trace chlorite(?).

Sample 121-758A-61R-4, 60–64 cm (Piece 1B), Unit 3 [Z-1346]

Aphyric basalt (microdolerite), crystallized, vesicular. Rocks with intersertal-microdoleritic texture; laths (0.2–0.8 mm) of plagioclase (40%, labradorite [An_{55}] and andesine [An_{34}]), segregate of small xenomorphic grains of clinopyroxene (40%), greenish black glass (10%), and opaque minerals (5%). Sparse vesicles (5%, 0.6–0.9 mm) are oval in shape.

Alteration: slight (5%); rock is non oxidized; vesicles infilled with clay mineral.

XRD: smectite with ~10% mica layers.

Sample 121-758A-61R-7, 0–5 cm (Piece 1A), Unit 3 [Z-1347]

Aphyric basalt (microdolerite), crystallized, vesicular. Rock: identical to Sample 121-758A-61R-4, 60–64 cm (Z-1346).

Alteration: slight (5%–7%); rock is nonoxidized; vesicles infilled with clay mineral.

XRD: smectite.

Sample 121-758A-62R-1, 57–59 cm (Piece 4A), Unit 4 [Z-23]

Plagioclase-phyric basalt, fine grained, vesicular. Phenocrysts (up to 5 mm) of plagioclase are ~10% abundance. Occasionally, phenocrysts form glomerophyric segregates built of 3 or 4 crystals. Vesicles (1–1.5 mm) are ~10% abundance. Groundmass; chaotically oriented laths of plagioclase, small xenomorphic grains of clinopyroxene, and interstitial volcanic glass with opaque dust. Groundmass demonstrates hyalopylitic texture. Composition: plagioclase (~60%), clinopyroxene (~20%), volcanic glass (~20%). Magnetite is present in trace amounts.

Alteration: strong (50%–60%); volcanic glass is completely replaced with green smectite; clinopyroxene is significantly replaced with smectite; phenocrysts of plagioclase are partly replaced with smectite and slightly carbonatized; vesicles are filled with radial aggregate of green smectite; microcracks located near some vesicles are filled with smectite.

XRD: smectite; trace calcite.

Sample 121-758A-62R-3, 27–29 cm (Piece 2), Unit 4 [Z-24]

Plagioclase-phyric basalt, fine grained, sparsely vesicular, fractured. Phenocrysts (up to 4 mm) are ~15% abundance. Occasionally, phenocrysts form glomerophyric segregates represented by 2 to 4 grains. Vesicles (0.5–0.7 mm) are <1% abundance. Groundmass; laths of plagioclase, small xenomorphic grains of clinopyroxene, and a small amount of interstitial glass. Small xenomorphic grains of magnetite and opaque dust are present also. Groundmass demonstrates hyalopylitic texture. Composition: plagioclase (~50%), clinopyroxene (~30%), volcanic glass (~15%), and magnetite (up to 5%).

Alteration: moderate (~25%–30%); olive-green smectite replaces interstitial glass, volcanic glass from small inclusions in phenocrysts of plagioclases, and peripheral parts of crystals of clinopyroxene; microcracks in phenocrysts of plagioclase are filled by smectite and by small amount of carbonate; opaque minerals are oxidized.

XRD: smectite; trace calcite.

Sample 121-758A-62R-3, 88–92 cm (Piece 8A), Unit 5 [Z-649]

Plagioclase-phyric basalt, pseudo-variolitic structure. Phenocrysts (10%): tabular grains (1–1.5 mm) of plagioclase. Groundmass (90%) with pilotaxitic texture; laths and needle-shaped microlites of plagioclase (labradorite [An_{50}]) and glass with opaque dust. Vesicles (30%, 0.1–0.5 mm) are rounded-isometric in shape.

Alteration: strong (50%); interstitial glass replaced by chlorite; vesicles completely infilled with chlorite.

Sample 121-758A-63R-1, 3–5 cm (Piece 1), Unit 7 [Z-19]

Aphyric basalt, fine grained, vesicular. Vesicles (0.3–1.5 mm) are rounded and irregularly rounded. Both are ~15%–20% abundance. Groundmass; chaotically located laths of plagioclase, small xenomorphic grains of clinopyroxene, small amount of interstitial volcanic glass, and small xenomorphic surrogates of magnetite. Groundmass demonstrates intersertal texture. Composition: plagioclase (~40%), clinopyroxene (~30%), volcanic glass (~10%), and magnetite (up to 5%).

Alteration: strong (~50%); clinopyroxene is almost completely replaced with olive-green smectite; volcanic glass is completely replaced with smectite; vesicles and cracks in plagioclases are filled with smectite.

XRD: smectite.

Sample 121-758A-63R-2, 46–50 cm (Piece 1B), Unit 7 [Z-1349]

Aphyric basalt (microdolerite), crystallized, vesicular. Rock: identical to Sample 121-758A-61R-4, 60–64 cm (Z-1346).

Alteration: slight (5%); rock is non oxidized; vesicles infilled with celadonite(?), single vesicle consists of carbonate (besides celadonite?).

XRD: smectite.

Sample 121-758A-63R-5, 48–50 cm (Piece 1A), Unit 7 [Z-7]

Aphyric basalt, fine grained, vesicular, intergranular texture. Some areas demonstrate intersertal texture. Vesicles (0.5–1.5 mm) are ~5% through 7% abundance. Groundmass; chaotically located laths of plagioclase and xenomorphic grains of clinopyroxene. Opaque minerals are known as spots within interstitial glass and as xenomorphic and skeletal crystals in interstices between plagioclase and clinopyroxene. Interstitial volcanic glass is distributed as spots. Composition: plagioclase (~40%), clinopyroxene (~35%), volcanic glass (~15%–20%), opaque minerals (up to 5%), olivine (single grains).

Alteration: slight to moderate (~20%); pseudomorphs of smectite upon olivine; clinopyroxene is partly replaced with smectite along crystal margins; interstitial volcanic glass is replaced with smectite; cracks in clinopyroxene are filled with smectite; occasionally, smectite is present in fractures within twins of plagioclases.

XRD: smectite.

Sample 121-758A-64R-1, 76–80 cm (Piece 1A), Unit 7 [Z-650]

Aphyric microdolerite, massive. Rock with intersertal texture; laths of plagioclase (40%, labradorite [An_{60}]), isometric grains (0.1–0.3 mm) of clinopyroxene (30%), brownish green glass (30%), and opaque minerals (2%–3%).

Alteration: moderate (30%); interstitial glass replaced by clay mineral.

Sample 121-758A-64R-2, 130–135 cm (Piece 1B), Unit 7 [Z-1350]

Plagioclase-phyric basalt, crystallized. Single (3%) large (3 mm) glomerophyric segregate of xenomorphic grains of plagioclase (labradorite [An_{60}]). Groundmass with microlitic texture; microlites and microlaths of plagioclase (40%, labradorite [An_{55}] and andesine [An_{41}]), segregate of small grains (0.1–0.3 mm) of clinopyroxene (45%), greenish black glass (10%), and opaque minerals (2%).

Alteration: slight (7%–8%); rock is non oxidized; interstitial glass replaced by clay mineral.

XRD: smectite.

Sample 121-758A-65R-2, 10–15 cm (Piece 1A), Unit 10 [Z-1351]

Aphyric basalt, crystallized, vesicular. Rocks with pilotaxitic texture; microlites and laths of plagioclase (40%, labradorite [An_{54}] and andesine [An_{43}]), small xenomorphic grains of clinopyroxene (15%), glass (30%), and opaque minerals (5%). Sparse vesicles (5%) are oval in shape.

Alteration: moderate (35%); rock is non oxidized; glass completely replaced by clay mineral, vesicles completely infilled with clay mineral.

XRD: smectite; white matter from veinlet: calcite.

Sample 121-758A-65R-4, 58–62 cm (Piece 1B), Unit 10 [Z-1352]

Aphyric basalt (microdolerite), crystallized, sparsely vesicular. Rocks with intersertal-microdoleritic texture; laths of plagioclase (40%–45%, labradorite [An_{60}] and andesine [An_{48}]), small xenomorphic grains of clinopyroxene (40%), glass (30%), greenish black glass (15%), and opaque minerals (2%–3%). Sparse vesicles (5%) are present.

Alteration: slight (10%); rock is non oxidized; glass partly (5%) replaced by clay mineral, vesicles infilled with clay mineral and carbonate.

XRD: smectite; black veinlet: smectite.

Sample 121-758A-65R-5, 1–6 cm (Piece 1A), Unit 10 [Z-651]

Aphyric microdolerite, crystallized, massive. Rock: identical to Sample 121-758A-64R-1, 76–80 cm (Z-650).

Sample 121-758A-65R-6, 25–27 cm (Piece 1A), Unit 10 [Z-28]

Aphyric basalt, fine grained, vesicular, intergranular texture. Some areas demonstrate intersertal texture. Vesicles (0.5–1.2 mm) are ~5% abundance. Groundmass; chaotically located laths of plagioclase and xenomorphic grains of clinopyroxene. Also, groundmass contains some admixture (not <5%) of xenomorphic opaque minerals. The latter is distributed within interstitial glass, which contains opaque dust and dendritic segregates of opaques. Composition: plagioclase (~40%), clinopyroxene (~35%), volcanic glass (15%–20%), and opaque minerals (up to 5%).

Alteration: slight to moderate (~20%); interstitial volcanic glass is completely replaced with green smectite; occasionally, smectite is located in large laths of plagioclase along boundaries of twins; vesicles are completely filled with smectite; inner parts are represented by radial aggregates, while peripheral rims are built of brownish green aggregate which is oriented perpendicularly to the walls of vesicles.

XRD: smectite.

Sample 121-758A-66R-1, 31–35 cm (Piece 5A), Unit 11 [Z-1353]

Aphyric basalt (microdolerite), crystallized, sparsely vesicular. Rocks with intersertal-microdoleritic texture; laths of plagioclase (35%, labradorite [An_{55}] and andesine [An_{44}]), small xenomorphic grains of clinopyroxene (30%), greenish brown glass (12%), and opaque minerals (3%). Vesicles (20%, 0.4–0.7 mm) are oval in shape.

Alteration: moderate (30%–35%); rock is nonoxidized; glass replaced by clay mineral, vesicles completely infilled with clay mineral.

XRD: smectite.

Sample 121-758A-66R-3, 44–46 cm (Piece 1B), Unit 11 [Z-14]

Aphyric basalt, fine grained, sparsely vesicular, intergranular texture. Some areas demonstrate intersertal texture. Vesicles (0.3–1.2 mm) with irregularly rounded in shape are ~5% abundance. Groundmass; chaotically oriented laths of plagioclase and xenomorphic clinopyroxene. The latter fills interstices between plagioclases. Interstitial volcanic glass contains xenomorphic opaque minerals and opaque dust. Composition: plagioclase (~45%), clinopyroxene (~40%), volcanic glass (10%–15%), and opaque minerals (<5%).

Alteration: moderate (~20%–25%); interstitial glass is completely replaced with olive-green smectite; pyroxenes and, lesser, plagioclases are replaced with smectite along margins and cracks; vesicles are filled with smectite.

XRD: smectite.

Sample 121-758A-66R-5, 2–7 cm (Piece 1A), Unit 11 [Z-652]

Aphyric basalt, massive. Rocks with pilotaxitic texture; unoriented laths (0.1–0.3 mm) of plagioclase (50%, andesine-labradorite [An_{55}]), isometric small grains of clinopyroxene (10%), green glass (30%–35%) with opaque dust (5%–8%), completely chloritized glass, and opaque minerals (5%–8%).

Alteration: moderate to strong (40%–50%); glass replaced by chlorite, several laths of plagioclase in their central parts replaced by chlorite, microcrack (2 mm in thickness) consists of carbonate and clay mineral.

Sample 121-758A-66R-5, 50–55 cm (Piece 1E), Unit 11 [Z-1354]

Aphyric basalt, vesicular. Rocks with vitrophyric texture; glass (90%), sparse (5%) microlites of plagioclase, and microlites of clinopyroxene (10%). Single vesicle (2 mm) is isometric in shape.

Alteration: very strong (95%); rock is nonoxidized; glass and plagioclase almost completely replaced by smectites, vesicle completely infilled with smectites and carbonate.

XRD: smectite.

Sample 121-758A-67R-4, 79–83 cm (Piece 3), Unit 14 [Z-653]

Aphyric basalt, massive. Rocks with intersertal texture; elongated laths (0.3–0.8 mm) of plagioclase. Interstices consist of altered glass and small needle-shaped, skeletal or pseudo-cubic grains (0.1–0.2 mm) of opaque minerals (20%). Biotite is present.

Alteration: very strong (90%); plagioclase and glass almost completely replaced by clay mineral.

Sample 121-758A-67R-4, 78–80 cm (Piece 3), Unit 14 [Z-12]

Aphyric basalt, fine grained (near to aphanitic), sparsely vesicular, hyalopylitic texture. Groundmass; laths of plagioclase and devitrified interstitial glass. The latter contains grains of clinopyroxene and opaque dust. Vesicles (0.01–0.05 mm) are rounded and irregularly rounded in shape. Vesicles are up to 10% abundance. Composition: plagioclase (~35%), clinopyroxene (~30%), volcanic glass (~25%), and opaque minerals (~10%).

Alteration: moderate to strong (~50%); interstitial volcanic glass is replaced with smectite; clinopyroxenes are partly replaced with smectite; vesicles are completely filled with radial aggregates of smectite.

XRD: smectite.

Sample 121-758A-67R-6, 28–30 cm (Piece 1), Unit 14 [Z-35]

Sparsely plagioclase-phyric basalt, fine grained, sparsely vesicular, with single microphenocrysts of olivine. Groundmass demonstrates intergranular to intersertal texture. Phenocrysts of plagioclase (up to 2 mm) are <5% abundance. Single glomerophyric segregates of plagioclase, as well as aggregates of plagioclase and olivine(?) or with clinopyroxene are present. Interstitial glass contains opaque minerals and opaque dust. Single rounded

vesicles (0.2 mm) are present. Composition: plagioclase (~40%), clinopyroxene (~30%), volcanic glass (~20%), opaque minerals (1%–3%), and olivine (single grains).

Alteration: moderate (~30%–40%); pseudomorphs of olive-green smectite upon olivine; clinopyroxenes are partly replaced with smectite along marginal parts of crystals; interstitial volcanic glass is replaced with smectite; smectite is present along fractures and cleavage in plagioclases; vesicles are filled with smectite.

XRD: smectite.

Sample 121-758A-68R-3, 106–108 cm (Piece 8), Unit 17 [Z-20]

Sparsely plagioclase-phyric basalt, fine grained, sparsely vesicular. Some vesicles are <0.5 mm in diameter. Groundmass demonstrates intersertal texture; chaotically oriented laths of plagioclase, xenomorphic grains of clinopyroxene, and interstitial glass. Idiomorphic segregates of magnetite are restricted to volcanic glass. Composition: plagioclase (~45%), clinopyroxene (~20%), volcanic glass (~30%), opaque minerals (<5%), and olivine (single grains).

Alteration: strong (~50%–60%); interstitial glass is completely replaced with olive-green smectite; the latter also replaces some clinopyroxene; vesicles are filled with smectite; microphenocrysts of olivine are fresh.

XRD: smectite.

Sample 121-758A-69R-2, 45–47 cm (Piece 1), Unit 17 [Z-10]

Plagioclase-phyric basalt, fine grained, massive. Phenocrysts of plagioclase and their glomerophyric segregates (2–5 mm) are ~10% abundance. Groundmass; aggregate of laths of plagioclase, hypidiomorphic grains of clinopyroxene, interstitial volcanic glass, single grains of olivine, and xenomorphic segregates of opaque minerals (magnetite). Magnetite is restricted to interstitial glass. Groundmass demonstrates intergranular texture. Composition: plagioclase (~45%), clinopyroxene (~40%), volcanic glass (10%–15%), opaque minerals (<2%–5%), and olivine (single grains).

Alteration: slight (~10%–15%); occasionally clinopyroxene is replaced with smectite along peripheral parts of crystals; interstitial glass is completely replaced with olive-green smectite.

XRD: smectite.

Sample 121-758A-69R-5, 18–21 cm (Piece 1A), Unit 17 [Z-654]

Plagioclase-clinopyroxene-phyric microdolerite, vesicular. Phenocrysts (50%): prismatic grains (up to 2 mm) and glomerophyric segregates of small (up to 1 mm) grains of plagioclase (labradorite [An_{55}]); segregates of clinopyroxene (0.5–0.8 mm). Groundmass with intersertal-doleritic texture; unoriented laths (0.3–0.8 mm) of plagioclase (labradorite [An_{51}]). Interstices: segregate of small grains (0.1–0.2 mm) of clinopyroxene (50%); green altered glass (15%–20%); opaque minerals (5%). Microvesicles (10%–15%) are isometric in shape.

Alteration: slight to moderate (~20%); clay mineral replaces interstitial glass, vesicles infilled with clay mineral.

Sample 121-758A-69R-5, 120–123 cm (Piece 1C), Unit 17 [Z-1355]

Clinopyroxene-plagioclase-phyric basalt, vesicular. Phenocrysts (7%–8%): glomerophyric segregates and prismatic grains of plagioclase (approximately labradorite [An_{55}]); small (up to 0.7 mm) xenomorphic grains of clinopyroxene (2%–3%). Groundmass with hyalopilitic texture; microlites and crystals (<0.05 mm) of plagioclase, brown (<0.01 mm) grains of clinopyroxene, and altered glass. Vesicles (10%, 0.3–0.7 mm) is isometric in shape.

Alteration: strong to very strong (60%–70%); rock is nonoxidized; glass completely replaced by smectites; vesicles completely infilled with smectites and carbonate.

XRD: smectite.

Sample 121-758A-70R-2, 47–50 cm (Piece 4), Unit 19 [Z-655]

Aphyric basalt, vesicular. Rock with vitrophyric texture; dark brown glass and radial-radiant segregates of crystals of plagioclase and pyroxene. Vesicles (30%, 0.1–2 mm) are rounded and isometric in shape.

Alteration: vesicles infilled with clay mineral.

Sample 121-758A-71R-2, 104–107 cm (Piece 8B), Unit 21 [Z-656]

Aphyric basalt with vitrophyric texture, vesicular. Rock: identical to Sample 121-758A-70R-2, 47–50 cm (Z-655).

Alteration: vesicles infilled with clay mineral.

Sample 121-758A-71R-3, 87–89 cm (Piece 3B), Unit 22 [Z-2]

Aphyric basalt, fine grained, vesicular, hyalopilitic or, occasionally, subvariolitic texture. Vesicles (0.2–0.5 mm) are up to 10% abundance. Small (0.2 mm) and isometric vesicles are dominant. Groundmass; laths of plagioclase,

xenomorphic grains of clinopyroxene, devitrified interstitial glass, fine xenomorphic segregation of opaque minerals (near to opaque dust). Occasionally, laths of plagioclase demonstrate radial pattern. Composition: plagioclase (~55%), clinopyroxene (~35%), volcanic glass (~10%), and opaque minerals (<5%).

Alteration: slight to moderate (~15%–20%); interstitial glass is completely replaced with smectite; vesicles are filled with green smectite.

XRD: smectite.

Sample 121-758A-72R-3, 0–5 cm (Piece 1A), Unit 25 [Z-657]

Aphyric basalt, sparsely vesicular. Rock with vitrophyric texture; dark brown glass with sparse needle-shaped microlites of plagioclase. Microvesicles (20%) are isometric and rounded in shape.

Alteration: vesicles infilled with clay mineral, occasionally, they are lined by clay mineral.

Sample 121-758A-72R-4, 90–95 cm (Piece 3), Unit 25 [Z-658]

Aphyric basalt, sparsely vesicular. Rock with intersertal-microdoleritic texture; needle-shaped laths (up to 0.5 mm) of plagioclase (50%, andesine-labradorite [An_{50}]). Interstices consist of small grains of clinopyroxene, opaque minerals (5%–8%), and green altered glass. Vesicles (15%, 0.5–2 mm) are rounded, oval, and isometric in shape.

Alteration: moderate (30%); chlorite replaces glass, vesicles infilled with clay mineral and carbonate (occasionally, they are empty).

Sample 121-758A-73R-2, 71–74 cm (Piece 1C), Unit 27 [Z-659]

Sparsely plagioclase-phyric basalt, sparsely vesicular. Single phenocryst; glomerophyric segregate (2.5 mm) of prismatic grains (0.5–1 mm) of plagioclase (labradorite [An_{56}]). Groundmass with pilotaxitic texture; microlites of plagioclase (20%, andesine-labradorite [An_{50}]). Interstices consist of segregate of small grains of clinopyroxene (40%), green altered glass (30%), and opaque minerals (10%). Sparse vesicles (0.3–0.5 mm) are rounded in shape.

Alteration: moderate (30%); interstitial glass completely replaced by clay mineral.

Sample 121-758A-73R-3, 85–87 cm (Piece 4F), Unit 29 [Z-15]

Aphyric basalt, fine grained, vesicular, hyalopilitic texture. Isometric vesicles (0.3–0.7 mm) vary from 15%–20% abundance. Groundmass; chaotically located laths of plagioclase, small xenomorphic grains of clinopyroxene, devitrified interstitial glass, and opaque dust within glass. Composition: plagioclase (~50%), clinopyroxene (~25%), volcanic glass (~20%), opaque minerals (~5%).

Alteration: strong (~50%); interstitial glass is completely replaced with smectite; vesicles are filled with green smectite.

XRD: smectite.

Sample 121-758A-73R-3, 136–140 cm (Piece 5), Unit 29 [Z-1356]

Aphyric basalt, vesicular. Rock with pilotaxitic texture; microlites and laths of plagioclase (30%, labradorite [An_{50}] and andesine [An_{44}]). Interstices consist of small grains of clinopyroxene (15%) and altered glass (15%). Vesicles (40%, 0.8–5 mm) are rounded in shape.

Alteration: strong (55%); rock is nonoxidized; clay mineral replaces glass; vesicles completely infilled with clay mineral.

XRD: smectite.

Sample 121-758A-73R-4, 105–110 cm (Piece 8), Unit 29 [Z-1357]

Sparsely plagioclase-phyric basalt, crystallized, vesicular. Phenocrysts (3%); tabular grains (0.7–0.9 mm) of plagioclase (labradorite [An_{65}]). Groundmass (95%) with microlitic texture; laths of plagioclase (45%, andesine [An_{42-48}]). Interstices consist of segregate of xenomorphic grains of clinopyroxene (40%), brownish green altered glass (8%–10%), and opaque minerals (2%–3%). Sparse vesicles (2%) are present.

Alteration: slight (10%–12%); rock is nonoxidized; interstitial glass completely replaced by clay mineral, vesicles are filled with clay mineral.

XRD: smectite.

Kerguelen Plateau (Legs 120 and 183)

Hole 747C

Sample 120-747C-12R-1, 53–56 cm (Piece 7A), Unit 8 [Z-91]

Olivine microphyric basalt, fine grained (near to aphanitic), Slightly crystallized, massive. Groundmass; devitrified microcrystalline glass with hyalopilitic texture. Hypidiomorphic microphenocrysts (0.05–0.1 mm) of olivine vary from 5%–7% abundance. Components: plagioclase, clinopyroxene, and opaque minerals. Single spots of noncrystallized glass (0.3–0.5 mm) are present also.

Alteration: slight (~10%–15%); olivine is replaced by orange-red iddingsite; some microphenocrysts are replaced with grassy-green smectite along margins; glass is replaced with the grassy-green smectite.

XRD: smectite; trace hydromica.

Sample 120-747C-12R-1, 125–127 cm (Piece 18), Unit 10 [Z-629]

Aphyric basalt, fine grained, vesicular. Rock with intersertal texture is represent by laths (<0.1 mm) of plagioclase (40%), clinopyroxene, glass, and opaque minerals. Several isometric and rounded crystals of olivine are present. Large vesicles (up to 1–1.2 mm) demonstrate rounded in shape. Microcracks are present.

Alteration: slight (~10%); clay minerals and zeolite replace olivine and glass and infilled vesicles and microcracks.

XRD: smectite; trace hydromica.

Sample 120-747C-12R-2, 6–9 cm (Piece 1), Unit 10 [Z-630]

Olivine-clinopyroxene-plagioclase-phyric basalt, massive. Phenocrysts (8%–10%): elongated crystals of plagioclase (8%, up to 0.7 mm), single isometric grains of clinopyroxene (0.4 mm) and olivine. Groundmass with intersertal texture is represent by laths of plagioclase (20%), clinopyroxene (20%, up to 0.1 mm), and interstitial fresh glass (10%).

Alteration: slight (~10%); clay minerals replace olivine; phenocrysts of plagioclase replaced by clay minerals.

XRD: smectite.

Sample 120-747C-12R-2, 85–87 cm (Piece 10), Unit 10 [Z-92]

Basalt, fine grained (near to aphanitic), vesicular. Groundmass demonstrates intergranular texture. Groundmass; laths of plagioclase, xenomorphic clinopyroxene, opaque minerals, and small (<1%) amounts of microphenocrysts (up to 0.2 mm) of olivine. Vesicles (0.03–0.05 mm) demonstrate irregularly rounded in shape and vary from 5%–7% abundance. Components: pyroxene (50%–60%), laths of plagioclase (~30%), opaque minerals (5%–7%), and olivine (single grains).

Alteration: slight to moderate (~15%–20%); olivine is replaced with orange-brown iddingsite; occasionally grains of olivine are replaced along their peripheral parts with grassy-green smectite; glass in small vesicles is completely replaced with grassy-green smectite; in large vesicles smectite is only present in peripheral parts.

XRD: smectite; trace chlorite.

Sample 120-747C-12R-3, 18–22 cm (Piece 3A), Unit 10 [Z-631]

Clinopyroxene-plagioclase-olivine-phyric basalt, sparsely vesicular. Phenocrysts (15%–20%): isometric grains of olivine (10%, 0.5–1 mm), elongated crystals of plagioclase (10%, up to 1.2 mm), and grains of clinopyroxene. Groundmass with intergranular (partly intersertal) texture is represent by olivine (20%, up to 0.7–0.08 mm) segregates, clinopyroxene, plagioclase, interstitial altered glass (10%), and partly oxidized opaque minerals (~2%). Vesicles (5%, 0.1–0.5 mm) are mainly empty.

Alteration: slight (~10%–15%); clay mineral replaces olivine and glass; single large (> 0.5 mm) vesicles infilled with clay mineral; feldspar(?) rimes large grains of olivine.

XRD: smectite.

Sample 120-747C-12R-3, 146–148 cm (Piece 12), Unit 10 [Z-93]

Aphyric basalt, fine grained, massive. Groundmass demonstrates intergranular textures. Some areas represent intersertal texture. Single isomorphic and hypidiomorphic grains of olivine are present. Groundmass; chaotically located laths of plagioclase, xenomorphic grains of clinopyroxene, and hypidiomorphic grains of opaque minerals. Single tabular microphenocrysts of plagioclase and clinopyroxene are present. Components: clinopyroxene (~60%), plagioclase (30%–40%), opaque minerals (5%–7%), and olivine (<1%).

Alteration: slight to moderate (~15%–20%); both olivine and interstitial glass are completely replaced with grassy-green smectite.

XRD: smectite.

Sample 120-747C-13R-1, 6–10 cm (Piece 1A), Unit 10 [Z-632]

Clinopyroxene-olivine-plagioclase-phyric basalt, massive. Phenocrysts (15%): isometric tabular grains of olivine (5%, 0.5–0.5 mm), glomerophyric segregates of plagioclase tabular crystals (10%, up to 0.8 mm), and grains of clinopyroxene (1%, 0.1–0.2 mm). Large plagioclase phenocrysts have undulatory extinction. Groundmass with intersertal texture is represent by small grains (0.07 mm) of clinopyroxene, plagioclase, olivine, glass, and cubic crystals of opaque minerals.

Alteration: slight (~10%); clay mineral replaces olivine, glass, clinopyroxene, and plagioclase; feldspar(?) partly replaces plagioclase.

XRD: smectite.

Sample 120-747C-13R-1, 98–102 cm (Piece 2D), Unit 10 [Z-633]

Olivine-clinopyroxene-plagioclase-phyric basalt, vesicular. Phenocrysts (10%): single isometric grains of clinopyroxene (1.5 mm), altered olivine (0.8 mm), elongated-tabular crystals of plagioclase (0.5–0.7 mm). Groundmass (90%) with intergranular (partly intersertal) texture is represent by microlites of plagioclase, clinopyroxene, olivine, and glass with opaque dust. Vesicles (10%) demonstrate rounded in shape.

Alteration: slight to moderate (20%); clay mineral replaces olivine and glass, vesicles partly infilled with clay mineral (partly they are empty).

XRD: smectite.

Sample 120-747C-13R-3, 97–99 cm (Piece 10B), Unit 18 [Z-94]

Aphyric basalt, fine grained, crystallized, massive, trachytic or intergranular texture. Groundmass; subparallel oriented laths of plagioclase, xenomorphic pyroxene, and hypidiomorphic opaque minerals. Single hypidiomorphic microphenocrysts of olivine are present. Components: plagioclase (~50%), clinopyroxene (~45%), opaque minerals (5%–7%), olivine (up to 1%), and volcanic glass (<1%).

Alteration: slight (~10%); olivine is replaced with brown iddingsite or bluish green smectite with opacite-iddingsite rim.

XRD: smectite.

Sample 120-747C-14R-1, 49–51 cm (Piece 3C), Unit 19 [Z-95]

Aphyric basalt, fine grained, crystallized, massive (with single vesicles), and with single microphenocrysts of olivine. Groundmass demonstrates intergranular texture. Single rounded vesicles are ~0.2 mm in diameter. Microphenocrysts of olivine vary from 0.05–0.1 mm. Groundmass; chaotically located laths of plagioclase, xenomorphic clinopyroxene, and opaque minerals. Composition: plagioclase (~45%), clinopyroxene (~45%), opaque minerals (7%–10%), and olivine (1%–3%).

Alteration: slight (~7%–10%); vesicles are filled with grassy-green smectite; microphenocrysts of olivine are replaced with orange-red iddingsite; fine isometric grains of olivine within the groundmass are replaced with green smectite; some microphenocrysts of olivine demonstrate clathrate pattern of replacement: lattices of both brownish red iddingsite with an admixture of opaque minerals and green smectite are present; secondary opacite accumulations of opaque minerals are characteristic.

XRD: smectite; chlorite in trace amounts.

Sample 120-747C-15R-1, 22–24 cm (Piece 3A), Unit 23 [Z-96]

Aphyric olivine basalt, fine grained, incompletely crystallized, vesicular, with single microphenocrysts of plagioclase. Groundmass demonstrates intersertal texture. Some areas demonstrate poikilophitic texture. Microphenocrysts (up to 0.5 mm) of plagioclase are tabular in shape. Microphenocrysts (0.2–0.3 mm) of olivine are isometric. Vesicles (0.3–0.6 mm) have irregular in shape and vary from 20%–25% abundance. Groundmass; chaotically located laths of plagioclase, grains of clinopyroxene, and interstitial devitrified glass which is filled with opaque dust. Composition: plagioclase (~45%), clinopyroxene (~40%), volcanic glass (~10%), olivine (~5%), and opaque minerals (~1%).

Alteration: moderate (~25%–30%); tabular plagioclases in their central parts are replaced with pale green to almost colorless smectite; microphenocrysts of olivine are replaced along margins with orange-red iddingsite, while their central parts are replaced with pale green smectite; vesicles are filled with light green zonal smectite, central parts of vesicles are filled with pale green smectite.

XRD: smectite; minor chlorite.

Sample 120-747C-15R-2, 97–99 cm (Piece 13), Unit 25 [Z-97]

Sparsely olivine microphyric basalt, medium grained, incompletely crystallized, vesicular. Isometric microphenocrysts (0.2–0.7 mm) of olivine vary from 2%–5% abundance. Microphenocrysts of olivine unevenly

distributed in the groundmass; occasionally they form glomero-microphyric segregates. Single microphenocrysts of plagioclase vary from 0.2 to 0.5 mm. Groundmass; an aggregate of chaotically located laths of plagioclase, grains of clinopyroxene, fine isometric grains of olivine, and devitrified glass filled with opaque dust. Vesicles (0.1–0.8 mm) demonstrate irregular in shape and vary from 20%–25% abundance. Composition: plagioclase (~45%), clinopyroxene (~40%), volcanic glass and opaque minerals (~10%), olivine (5%–7%).

Alteration: moderate (~25%–30%); olivine is completely replaced with light green smectite; occasionally, it is replaced along peripheral parts of grains with orange-red iddingsite; some microphenocrysts are surrounded with opacite rim built of opaque minerals; isometric grains of olivine are replaced with light green smectite and with intersertal smectite; some relatively large laths of plagioclase are replaced in their central parts with light green smectite; vesicles are filled with light green smectite along peripheral parts; central parts of vesicles are filled with light green or almost colorless smectite.

XRD: smectite; minor chlorite.

Sample 120-747C-16R-2, 11–14 cm (Piece 1B), Unit 29 [Z-634]

Olivine-clinopyroxene-plagioclase-phyric basalt, massive. Phenocrysts (20%): clinopyroxene (12%, 0.8 mm), altered olivine (5%, 0.1–0.5 mm), and elongated crystals of plagioclase (3%, up to 0.7 mm). Groundmass (80%) with intersertal texture is represent by clinopyroxene and altered glass, plagioclase forms segregates.

Alteration: slight (15%); clay mineral replaces olivine and partly clinopyroxene, interstitial glass replaced by clay minerals.

XRD: smectite; trace calcite.

Sample 120-747C-16R-2, 51–53 cm (Piece 1D), Unit 29 [Z-98]

Aphyric olivine basalt, medium grained, incompletely crystallized, vesicular. Groundmass demonstrates intergranular to intersertal texture. Some areas demonstrate poikilophitic texture. Groundmass; laths of plagioclase, clinopyroxene, fine hypidiomorphic grains of olivine, interstitial glass, and opaque minerals. Large laths and sparsely microphenocrysts of plagioclase are ~0.5 mm. Devitrified interstitial glass is filled with opaque dust. Occasional grains of irregularly lamella opaque minerals are present within interstitial glass. Vesicles (0.2–1.2 mm) demonstrate irregular in shape. Composition: plagioclase (~40%), clinopyroxene (~40%), olivine (~10%), volcanic glass (~5%), and opaque minerals (~5%).

Alteration: moderate (~25%); fine olivine grains are completely replaced with orange-brown smectite, while coarser (0.2–0.3 mm) ones are replaced with light green smectite in central parts and with iddingsite along margins and fractures; occasionally, iddingsite is present in both central and peripheral parts; intermediate parts are replaced with green smectite; vesicles are filled with light green zonal smectite; intensity of light green color significantly varies.

XRD: smectite; minor swelling chlorite; trace heulandite.

Sample 120-747C-16R-2, 101–105 cm (Piece 1G), Unit 29 [Z-635]

Olivine-clinopyroxene-plagioclase-phyric basalt, vesicular. Phenocrysts (40%): altered olivine (1%, 0.5 mm), clinopyroxene (10%, up to 0.8 mm), and plagioclase (10%, from 0.1–0.2 to 0.8–0.9 mm). Partly plagioclase forms glomerophyric segregates. Groundmass (90%) with intersertal texture is represent by microlites of plagioclase, clinopyroxene, olivine, and altered glass. Vesicles (10%, 0.1–0.5 mm) demonstrate rounded and isometric in shape.

Alteration: slight (10%–15%); clay minerals completely replace olivine and glass, they partly replace plagioclase; vesicles partly infilled with clay minerals (partly they are empty).

XRD: smectite.

Sample 120-747C-16R-2, 145–148 cm (Piece 1A), Unit 29 [Z-636]

Clinopyroxene-olivine-plagioclase-phyric basalt, vesicular. Phenocrysts (60%): tabular grains of plagioclase (50%, from 0.4–2.5 mm), olivine (10%, up to 0.2 mm), and single grains of clinopyroxene (0.1 mm). Phenocrysts of plagioclase form glomerophyric segregates. Groundmass (40%) is intersertal (occasionally doleritic) texture. Vesicles (10%) demonstrate irregular in shape and vary from 0.1 to 4 mm.

Alteration: very strong (70%); clay mineral replaces olivine and clinopyroxene; vesicles infilled with clay minerals and zeolite.

XRD: smectite; trace heulandite.

Sample 120-747C-16R-4, 14–16 cm (Piece 1A), Unit 30 [Z-99]

Aphyric basalt, fine grained, almost all crystallized, sparsely vesicular. Groundmass demonstrates intergranular texture. Some areas (spots) demonstrate poikilophitic texture. Groundmass; chaotically located laths of

plagioclase, clinopyroxene, fine hypidiomorphic and coarser idiomorphic grains of olivine, some small amount of opaque minerals and volcanic glass. Grains of opaque minerals are finely lamella or xenomorphic. Interstitial volcanic glass contains opaque minerals as elongated lamellae or as opaque dust. Vesicles (0.1–0.5 mm) have irregular in shape. Composition: plagioclase, clinopyroxene, olivine and opaque minerals, and volcanic glass.

Alteration: moderate (~20%–25%); large laths of plagioclase are replaced in central parts with light green smectite; interstitial volcanic glass is partly replaced with green smectite; vesicles are filled with zonal light green smectite; zonality in smectite is underlined by changes from dark green to light green colors and by the presence of oxidized rusty-brown opaque minerals.

XRD: smectite; minor swelling chlorite and chlorite.

Sample 120-747C-16R-5, 0–3 cm (Piece 1A), Unit 30 [Z-637]

Olivine-clinopyroxene-plagioclase-phyric basalt, vesicular. Phenocrysts (50%): clinopyroxene (0.1–0.2 mm), unoriented elongated-tabular crystals of plagioclase (0.8–1 mm), and altered olivine (0.1 mm). Groundmass (50%) is intersertal (occasionally doleritic) texture. Vesicles (10%) demonstrate irregular in shape.

Alteration: slight (10%); clay mineral replaces glass, olivine, and partly clinopyroxene; vesicles completely infilled with clay mineral.

XRD: smectite.

Sample 120-747C-16R-5, 105–108 cm (Piece 3C), Unit 31 [Z-638]

Olivine-clinopyroxene-plagioclase-phyric basalt, highly vesicular. Phenocrysts (60%): plagioclase (50%, 0.6–0.8 mm), large crystals of plagioclase form glomerophyric segregates; clinopyroxene (4%, 0.1–0.2 mm); altered olivine (6%, 0.1–0.4 mm). Groundmass with intersertal (occasionally doleritic) texture is represent by unoriented laths of plagioclase, tabular and isometric grains (0.1–0.2 mm) of clinopyroxene, and glass with opaque dust. Vesicles (25%) demonstrate irregular in shape.

Alteration: slight (10%–15%); clay mineral replaces plagioclase, interstitial glass, olivine, and partly clinopyroxene; vesicles infilled with clay mineral (occasionally vesicles are empty in their central parts).

XRD: smectite.

Holes 1136A, 1137A, 1138A, and 1140A

Note: Petrographic description of analyzed basalts and XRD data of secondary minerals from Holes 1136A, 1137A, 1138A, and 1140A were published in Kurnosov et al. (2003).

Western Indian Ocean, Chagos Bank, and Maldives Ridge (Leg 115)

Hole 706C

Sample 115-706C-3R-2, 21–23 cm (Piece 3), Unit 12 [Z-60]

Aphyric basalt, inequigranular, incompletely crystallized, vesicular. Rock is intersertal-glassy texture; black devitrified glass, various laths of plagioclase, hypidiomorphic crystals of clinopyroxene, and opaque dust. Vesicles (0.3–0.6 mm, 5%–7%) are irregular in shape. As a rule vesicles are empty; some vesicles are partly or completely filled with clay minerals.

Alteration: slight (up to 15%); rock is nonoxidized; vesicles are filled with smectites.

XRD: smectite contains ~10% of mica layers; trace hydromica (~10% swelling interlayers).

Sample 115-706C-4R-2, 111–113 cm (Piece 15), Unit 12 [Z-64]

Aphyric basalt, inequigranular, incompletely crystallized, vesicular. Rock is intersertal texture; black devitrified glass, needle-shaped crystals of plagioclase, small grains of clinopyroxene, and opaque dust, with. Glass contains tabular microphenocrysts of plagioclase. Vesicles (0.1–0.7 mm, ~5%) are rounded in shape.

Alteration: slight to moderate (15%–20%); vesicles are filled with smectites.

XRD: smectite.

Sample 115-706C-4R-3, 10–13 cm (Piece 1), Unit 13 [Z-1320]

Aphyric dolerite, vesicular. Rock with intersertal-doleritic (occasionally ophitic) texture; prismatic crystals of plagioclase (30%, 0.2–0.7 mm, labradorite [An_{58}]), xenomorphic grains (0.1–0.4 mm) of clinopyroxene (30%), greenish brown volcanic glass, and opaque minerals (10%, 0.1–0.2 mm). Vesicles (15%, 0.3–1.5 mm) are rounded in shape; they are lined with palagonitized brown and dark green glass. Central parts of vesicles are empty.

Alteration: slight; palagonite replaces glass from interstices and vesicles.

Sample 115-706C-5R-1, 38–40 cm (Piece 2%), Unit 13 [Z-38]

Aphyric basalt, inequigranular, almost completely crystallized, highly vesicular. Rock is intergranular (occasionally micropoikiliophitic) texture; black devitrified glass, needle-shaped crystals of plagioclase, small grains of clinopyroxene, and opaque dust. Glass contains prismatic-tabular microphenocrysts of plagioclase. Vesicles (0.1–0.8 mm, ~10%–15%) are oval or irregular in shape.

Alteration: moderate (20%–25%); vesicles are filled with green smectites.

XRD: smectite contains ~20% of mica layers.

Sample 115-706C-5R-1, 113–115 cm (Piece 10), Unit 14 [Z-59]

Aphyric basalt, inequigranular, incompletely crystallized. Rock is intersertal texture; laths of plagioclase, clinopyroxene, opaque minerals, and devitrified glass. Vesicles (0.2–0.5 mm, ~1%–3%) are oval or irregular in shape.

Alteration: slight (1%–3%); vesicles are filled with smectites.

XRD: smectite.

Sample 115-706C-5R-3, 69–71 cm (Piece 9), Unit 19 [Z-50]

Aphyric hyalobasalt, poorly crystallized, vesicular (up to 1–1.5 mm, ~5%–10%). Rock is hyaline-vitrophyric texture; black volcanic glass with laths of plagioclase (25%) and xenomorphic crystals of clinopyroxene (5%).

Alteration: slight (5%); vesicles are filled with smectites.

XRD: smectite; trace hydromica (~10% swelling interlayers).

Sample 115-706C-6R-1, 38–40 cm (Piece 2), Unit 20 [Z-54]

Aphyric basalt, inequigranular, poorly crystallized, vesicular. Rock is intersertal texture; black devitrified glass, laths of tabular crystals of plagioclase, xenomorphic grains of clinopyroxene, needle-shaped opaque minerals and small amounts of diamond-shaped olivine. Vesicles (0.1–1 mm, ~7%–10%) are oval or irregular in shape.

Alteration: slight (10%–15%); rock is nonoxidized; vesicles are filled with smectites; smectites replace olivine.

XRD: smectite contains ~40% of mica layers; trace hydromica and amphibole.

Sample 115-706C-6R-1, 45–50 cm (Piece 2), Unit 20 [Z-1321]

Aphyric basalt, brecciated, vesicular. Rock with pilotaxitic texture; laths and microlites of plagioclase (25%, 0.1–0.7 mm, labradorite [An_{65}] and andesine [An_{48}]), black devitrified glass, glomerophyric segregates of small (0.2–0.4 mm) xenomorphic grains of clinopyroxene (20%), and glass (30%) with needle-shaped opaque minerals. Vesicles (25%, 0.1–0.2 mm and 0.5–0.9 mm) are oval or irregular in shape. Small vesicles infilled with brownish green glass, large vesicles are empty in centers and encrusted by palagonitized and chloritized glass. Matrix of breccia consists of green clay mineral, fragments of basalt, and reddish brown hematite(?).

Alteration: slight (10%–15%); secondary minerals: clay mineral, palagonite, and hematite(?).

XRD: smectite with ~30% mica layers; minor hydromica; trace chlorite; blue matter from veinlet: mica (celadonite?).

Sample 115-706C-8R-2, 26–28 cm (Piece 1%), Unit 28 [Z-39]

Aphyric basalt, inequigranular, poorly crystallized, vesicular. Rock is intersertal texture; devitrified glass, laths of tabular crystals of plagioclase, xenomorphic grains of clinopyroxene, needle-shaped opaque minerals and small amounts of hypidiomorphic crystals of olivine. Vesicles (0.08–1.5 mm, ~15%–20%) are oval or irregular in shape.

Alteration: moderate (20%); vesicles are filled with smectites; smectites replace olivine; thin cracks are filled with oxidized opaque minerals, zones of oxidation occur along salbands.

XRD: smectite contains ~40% of mica layers; trace hydromica (single swelling interlayers).

Sample 115-706C-9R-1, 72–74 cm (Piece 8), Unit 31 [Z-47]

Plagioclase-phyric basalt, poorly crystallized, vesicular. Phenocrysts of plagioclase (2–5 mm, 15%–20%). Groundmass is hyaline-vitrophyric texture; devitrified glass, laths and tabular crystals of plagioclase, xenomorphic crystals of clinopyroxene, opaque dust. Vesicles (0.08–1.8 mm, ~10%) are irregular in shape.

Alteration: slight (10%–15%); vesicles are filled with smectites and Fe hydroxides; hair-thin cracks are filled with Fe hydroxides.

XRD: smectite.

Sample 115-706C-9R-2, 0–7 cm (Piece 1), Unit 32 [Z-1322]

Clinopyroxene-plagioclase-phyric basalt, vesicular. Phenocrysts (40%): single large (up to 5 mm) prismatic crystals of plagioclase; glomerophyric segregates (80%) of small grains (0.1–0.3 mm) of clinopyroxene; prismatic grains (up to 0.3 mm) of plagioclase (labradorite [An_{60}]). Groundmass with hyalopilitic texture; glass (35%). Vesicles (25%, 0.1–0.2 up to 0.5 mm) completely infilled with chlorite.

Alteration: moderate (20%–25%); 25% of rock is oxidized; clay mineral replaces glass, vesicles are filled with clay mineral and limonite.

Hole 707C

Sample 115-707C-22R-1, 94–98 cm (Piece 11A), Unit 1 [Z-1323]

Sparsely plagioclase-phyric dolerite, massive, vesicular. Phenocrysts (2%–3%): single elongated-prismatic grains of plagioclase (0.8–1.2 mm). Groundmass with intersertal-doleritic texture; unoriented laths of plagioclase (50%, 0.–0.7 mm, labradorite [$An_{53–55}$]), xenomorphic grains of clinopyroxene (20%, 0.2–0.3 mm) and their segregates, and interstitial altered glass (30%). Rounded and oval isometric vesicles (5%, 1.5–2 mm) are present.

Alteration: moderate (30%–35%); clay mineral replaces glass and completely infills vesicles.

XRD: smectite with ~20% mica layers; red-brown matter from vesicles: smectite; clay matter from vesicles: smectite.

Sample 115-707C-22R-2, 49–51 cm (Piece 3A), Unit 1 [Z-78]

Sparsely plagioclase-phyric dolerite, incompletely crystallized, vesicular. Phenocrysts: single (1%) zonal tabular crystals of plagioclase (0.7 mm) with inclusions of glass. Groundmass (60%) with intersertal-doleritic texture; unoriented laths (0.3–0.5 mm) of plagioclase (50%, labradorite [$An_{58–60}$]), xenomorphic crystals segregate of clinopyroxene (30%), and interstitial altered glass. Vesicles (40%) have various, from 1.5 to 5 mm.

Alteration: strong (50%–60%); clay mineral replaces glass and completely infills vesicles.

XRD: smectites with various content of interlayer cations.

Sample 115-707C-23R-1, 32–36 cm (Piece 1C), Unit 3 [Z-1325]

Plagioclase-phyric dolerite, vesicular. Phenocrysts (25%): glomerophyric segregates (1.5–2 mm) of xenomorphic and prismatic grains (0.3–2 mm) of plagioclase (labradorite [An_{58}]). Single xenocrysts (up to 5 mm) of plagioclase are present. Groundmass (70%) with intersertal-doleritic texture; unoriented tabular and prismatic grains (0.3–0.8 mm) of plagioclase (60%, labradorite [$An_{59–60}$]), xenomorphic crystals and segregate of clinopyroxene (30%), and interstitial altered glass (10%). Xenomorphic and skeletal grains (0.1–0.2 mm) of opaque minerals are present (<1%). Single (<5%) large (up to 2.4 mm) vesicles infilled with clay mineral.

Alteration: slight (10%); clay mineral replaces glass and completely infills vesicles.

XRD: smectite.

Sample 115-707C-23R-1, 98–100 cm (Piece 1N), Unit 3 [Z-69]

Sparsely plagioclase-phyric basalt, almost completely crystallized, massive. Phenocrysts of plagioclase (up to 2–3 mm, 1%). Rock is intergranular to intersertal texture; laths and tabular crystals of plagioclase, xenomorphic crystals of clinopyroxene, opaque minerals, and interstitial glass (3%–5%).

Alteration: slight (10%); smectites replace interstitial glass.

XRD: smectite.

Sample 115-707C-23R-4, 0–3 cm (Piece 1A), Unit 3 [Z-605]

Clinopyroxene-plagioclase-phyric basalt, vesicular. Phenocrysts (20%): tabular grains of plagioclase (1.5–2 mm, labradorite [$An_{58–61}$]). Segregates consist of tabular and partly xenomorphic grains (0.6–1.2 mm, labradorite [$An_{52–55}$]) of plagioclase and rounded and partly idiomorphic small grains (0.2–0.3 mm, occasionally 0.5 mm) of clinopyroxene. Groundmass is microlitic texture; microlites and laths of plagioclase (labradorite [An_{55}]). Interstices consist of opaque minerals (5%) and altered glass (10%); small grains (0.1 mm) of clinopyroxene forms segregates. Rounded and isometric vesicles (1%, 0.7–0.8 mm) infilled with clay mineral.

Alteration: slight (10%); clay mineral replaces interstitial glass and infills vesicles.

Sample 115-707C-24R-1, 138–140 cm (Piece 6), Unit 4 [Z-606]

Clinopyroxene-plagioclase-phyric basalt, vesicular. Phenocrysts (10%): prismatic grains of plagioclase (0.3–0.7 mm, labradorite [$An_{58–60}$]) and their segregates; segregates of plagioclase and clinopyroxene (0.1–0.3 mm). Groundmass with intersertal texture; laths of plagioclase (50%, 0.1–0.3 mm), opaque minerals (5%–8%), and

altered glass (15%–20%); small grains of clinopyroxene (30%) form segregates. Altered (partly) small biotite crystals (0.1–0.2 mm) are present. Large vesicles (10%, up to 4 mm) infilled with clay mineral.

Alteration: moderate (20%–25%); clay mineral replaces interstitial glass and infills vesicles.

XRD: smectite.

Sample 115-707C-25R-1, 108–110 cm (Piece 1H), Unit 4 [Z-70]

Sparsely microplagioclase-phyric basalt, incompletely crystallized, vesicular. Microphenocrysts of plagioclase (up to 1.5–2 mm, <5%) occasionally form glomerophyric segregates. Rock is intergranular to intersertal texture; laths and tabular crystals of plagioclase, xenomorphic crystals of clinopyroxene, small idiomorphic crystals of olivine, opaque minerals, and interstitial glass (5%–7%). Vesicles (0.5–0.8 mm, ~1%–3%) are rounded in shape.

Alteration: slight (7%–10%); smectites replace interstitial glass and olivine; vesicles are filled with smectites.

XRD: smectite.

Sample 115-707C-25R-2, 38–42 cm (Piece 1C), Unit 4 [Z-607]

Plagioclase-phyric basalt, massive. Phenocrysts (20%): elongated-prismatic grains of plagioclase (up to 2 mm); segregates of smaller (0.3–0.7 mm) short-prismatic and xenomorphic grains of plagioclase. Groundmass with intersertal texture; laths of plagioclase (40%, 0.1–0.4 mm, labradorite [An_{60}]), xenomorphic grains (0.1–0.3 mm) of clinopyroxene (45%), opaque minerals (5%), and altered interstitial glass (10%).

Alteration: slight (10%); clay mineral replaces interstitial glass.

Sample 115-707C-25R-3, 108–111 cm (Piece 11M), Unit 4 [Z-608]

Clinopyroxene-plagioclase-phyric basalt, massive. Phenocrysts (20%): prismatic grains (0.1–0.4 mm) of plagioclase (labradorite [$An_{55–56}$]) and their segregates; glomerophyric segregates of plagioclase and xenomorphic grains (up to 0.5 mm) of clinopyroxene. Groundmass with microlitic-intersertal texture; laths (0.1–0.3 mm) of plagioclase (40%, labradorite [$An_{51–52}$]), opaque minerals (5%), altered glass (20%), and segregate of small grains of clinopyroxene. Altered (partly) small biotite crystals (0.1–0.2 mm) are present.

Alteration: moderate (20%); clay mineral replaces interstitial glass.

Sample 115-707C-25R-4, 42–45 cm (Piece 1G), Unit 4 [Z-609]

Clinopyroxene-plagioclase-phyric basalt, massive. Rock: identical to Sample 115-707C-25R-3, 108–111 cm (Z-608).

Alteration: moderate (20%); clay mineral replaces interstitial glass.

Sample 115-707C-25R-5, 110–114 cm (Piece 1P), Unit 4 [Z-610]

Clinopyroxene-plagioclase-phyric basalt, massive. Rock is the identical to Samples 115-707C-25R-3, 108–111 cm (Z-608), and 25R-4, 42–45 cm (Z-609).

Alteration: moderate (20%); clay mineral replaces interstitial glass.

Sample 115-707C-26R-1, 81–86 cm (Piece 1N), Unit 4 [Z-611]

Aphyric basalt, vesicular. Rock with microlitic texture; laths (0.1–0.7 mm) of plagioclase (50%, labradorite [An_{52}]), very small grains of clinopyroxene (40%), opaque minerals (5%), and altered interstitial glass (5%). Altered (partly) small biotite crystals (0.1–0.2 mm) are present. Single small (0.2–0.3 mm) rounded vesicles are lined with radial-radii and crystals of zeolite.

Alteration: slight (5%); clay mineral replaces interstitial glass, zeolite from vesicles.

XRD: smectite and smectite with ~30% mica layers.

Sample 115-707C-26R-2, 123–125 cm (Piece 10), Unit 4 [Z-1326]

Plagioclase-phyric basalt, fine grained. Phenocrysts (15%): glomerophyric segregates of tabular and prismatic grains (0.3–0.8 mm) of plagioclase, labradorite [An_{60}]. Single xenocrysts of zonal plagioclase are present. Groundmass (80%) with intersertal-microlitic texture; elongated-prismatic laths (0.1–0.7 mm) of plagioclase (50%, labradorite [An_{52}]), small rounded grains (up to 0.2 mm) of clinopyroxene (40%), xenomorphic small (0.1 mm) opaque minerals (5%), and altered volcanic glass (10%).

Alteration: moderate (20%); clay mineral replaces interstitial glass.

Sample 115-707C-26R-3, 71–73 cm (Piece 1H), Unit 4 [Z-49]

Sparsely plagioclase-phyric basalt, almost completely crystallized, massive. Phenocrysts of plagioclase (up to 1.5–3 mm, 3%–5%) occasionally form glomerophyric segregates. Rock is intergranular texture; laths and tabular crystals of plagioclase, xenomorphic crystals of clinopyroxene, single crystals of olivine, opaque minerals, and interstitial glass (5%–7%).

Alteration: slight (7%–10%); smectites replace interstitial glass and olivine.

XRD: smectite with ~20% mica interlayers.

Sample 115-707C-26R-5, 62–65 cm (Piece 1L), Unit 4 [Z-612]

Clinopyroxene-plagioclase-phyric basalt, massive. Rock is the identical to Samples 115-707C-25R-3, 108–111 cm (Z-608), 25R-4, 42–45 cm (Z-609), and 25R-5, 110–114 cm (Z-610).

Alteration: slight (5%); clay mineral replaces interstitial glass.

Sample 115-707C-26R-7, 46–48 cm (Piece 1E), Unit 4 [Z-61]

Plagioclase-phyric basalt, almost completely crystallized, sparsely vesicular. Phenocrysts of plagioclase (up to 1.5–4 mm, 7%–10%). Rock is intergranular texture; laths and tabular crystals of plagioclase, various xenomorphic crystals of clinopyroxene, small idiomorphic crystals of olivine, opaque minerals, and interstitial glass (5%–7%). Vesicles (up to 2 mm, <1%) are rounded in shape.

Alteration: slight (7%–10%); smectites replace interstitial glass and olivine; vesicles are filled with smectites.

XRD: smectite with ~20% mica interlayers.

Sample 115-707C-27R-1, 32–34 cm (Piece 4A), Unit 4 [Z-1327]

Plagioclase-phyric basalt, fine grained. Rock: identical to Sample 115-707C-26R-2, 123–125 cm (Z-1326).

Alteration: moderate; clay mineral replaces interstitial glass.

Sample 115-707C-27R-4, 46–49 cm (Piece 2B), Unit 4 [Z-613]

Clinopyroxene-plagioclase-phyric basalt, vesicular. Phenocrysts (15%–18%): glomerophyric segregates of grains (0.2–0.7 mm) of plagioclase (labradorite [An_{56}]). Groundmass with microlitic texture; laths of plagioclase (35%, labradorite [An_{52}]), segregate of clinopyroxene grains (55%, 0.1–0.2 mm), opaque minerals (5%), and altered glass (5%). Single vesicles (0.7 mm and 1.5 mm) infilled with clay mineral or carbonate.

Alteration: slight (5%); clay mineral replaces interstitial glass; vesicles infilled with clay mineral or carbonate.

Sample 115-707C-27R-5, 32–36 cm (Piece 5), Unit 4 [Z-614]

Clinopyroxene-plagioclase-phyric basalt, massive. Rock: identical to Sample 115-707C-27R-4, 46–49 cm (Z-613), except vesicularity.

Alteration: slight (<5%); clay mineral replaces interstitial glass.

Sample 115-707C-27R-6, 29–31 cm (Piece 2A), Unit 4 [Z-77]

Plagioclase-phyric basalt, almost completely crystallized, sparsely vesicular (0.05–0.07 up to 2 mm, <1%). Phenocrysts of plagioclase (up to 1–4 mm, 10%–15%). Rock is intergranular texture; laths and tabular crystals of plagioclase, various xenomorphic crystals of clinopyroxene, small idiomorphic crystals of olivine, opaque minerals, and interstitial glass (3%–5%).

Alteration: slight (7%–10%); smectites replace interstitial glass and olivine; small vesicles are filled with smectites, large ones are filled with carbonate.

XRD: smectite with ~30% mica interlayers.

Sample 115-707C-27R-7, 32–34 cm (Piece 5), Unit 4 [Z-68]

Plagioclase-phyric basalt, fine grained, inequigranular, almost completely crystallized, massive. Phenocrysts of plagioclase (up to 0.8–2 mm, 7%–10%). Rock is intergranular texture; laths of plagioclase, various crystals of clinopyroxene, olivine (<1%), opaque minerals, and interstitial glass.

Alteration: slight (5%–7%); smectites replace interstitial glass and olivine; single vesicles are filled with smectites.

XRD: smectite; trace mixed-layer chlorite-swelling chlorite mineral(?).

Sample 115-707C-28R-2, 53–55 cm (Piece 6A), Unit 5 [Z-44]

Plagioclase-phyric basalt, inequigranular, almost completely crystallized, vesicular (up to 2–5 mm, 5%). Phenocrysts of plagioclase (0.8–2.5 mm, 5%–7%). Rock is intergranular texture; laths of plagioclase, various crystals of clinopyroxene, single crystals of olivine, opaque minerals, and interstitial glass.

Alteration: slight (10%); smectites replace interstitial glass and olivine; walls of vesicles are lined with smectites, inner parts of vesicles are filled with carbonate which occasionally contains rounded segregates of smectites.

XRD: smectite.

Sample 115-707C-28R-3, 133–135 cm (Piece 12), Unit 5 [Z-58]

Sparsely plagioclase-phyric basalt, inequigranular, almost completely crystallized, massive. Phenocrysts of plagioclase (1–1.5 mm, 1%–3%). Single microphenocrysts of clinopyroxene and olivine are present. Groundmass is intergranular texture; laths and tabular of plagioclase, crystals of clinopyroxene, opaque minerals, and interstitial glass.

Alteration: slight (5%–7%); smectites replace interstitial glass, olivine, and clinopyroxene.

XRD: smectite.

Chagos Bank (Hole 713A)

Sample 115-713A-13R-1, 97–99 cm (Piece 10C), Unit 1 [Z-53]

Plagioclase-phyric basalt, almost completely crystallized, sparsely vesicular (1.5–3, 7%–10%). Phenocrysts of plagioclase (1.5–3 mm, 5%–7%). Groundmass is intersertal to intergranular texture; laths of plagioclase, various crystals of clinopyroxene, single crystals of olivine, opaque minerals, and scarce interstitial glass.

Alteration: slight (5%–7%); smectites replace interstitial glass and olivine; vesicles are filled with smectites for ~1/4th of their volumes.

XRD: smectite; trace calcite.

Sample 115-713A-13R-3, 16–20 cm (Piece 3), Unit 2 [Z-1328]

Plagioclase-phyric basalt, fine grained, vesicular. Phenocrysts (10%): tabular zonal xenocrysts (0.8–1.8 mm) of plagioclase; glomerophyric segregates of short-prismatic grains (0.3–0.7 mm, labradorite [An_{50}]) of plagioclase (occasionally with xenomorphic grains of clinopyroxene). Groundmass (80%) with intersertal-microlitic texture; laths (0.1 mm) of plagioclase (30%, labradorite [An_{50}]), opaque minerals (5%), altered volcanic glass (15%), and segregate of small grains (<0.1 mm) of clinopyroxene (50%). Vesicles (10%, 0.8–1.2 mm) in central parts are empty and lined with dark green altered glass.

Alteration: slight (10%–15%); clay mineral replaces glass.

Sample 115-713A-14R-3, 99–101 cm (Piece 5), Unit 3 [Z-74]

Sparsely plagioclase-phyric basalt, incompletely crystallized, massive. Phenocrysts of plagioclase (up to 2–3 mm, 10%). Groundmass is poikilophitic texture; laths of plagioclase, various crystals of clinopyroxene, single crystals of olivine, opaque minerals, and interstitial glass.

Alteration: slight (10%–15%); smectites replace interstitial glass and olivine.

XRD: smectite; trace hydromica.

Sample 115-713A-15R-1, 77–79 cm (Piece 4B), Unit 3 [Z-55]

Sparsely clinopyroxene-plagioclase-phyric basalt, incompletely crystallized, massive. Phenocrysts of plagioclase (up to 2–3 mm, <5%) and clinopyroxene (1–2 mm, <1%). Groundmass is poikilophitic texture; laths of plagioclase, various crystals of clinopyroxene, single crystals of olivine, opaque minerals, and interstitial glass (5%–7%).

Alteration: slight (7%–10%); smectites replace interstitial glass and olivine.

XRD: smectite; trace hydromica and defective chlorite(?).

Sample 115-713A-15R-3, 52–57 cm (Piece 2B), Unit 3 [Z-615]

Clinopyroxene-plagioclase-phyric dolerite, massive. Phenocrysts (15%): single idiomorphic grain (2.5 mm) of clinopyroxene; short-prismatic grains (1.5–2 mm) of plagioclase (labradorite [An_{60}]) and their single glomerophyric segregates. Groundmass with doleritic texture; laths of plagioclase (50%, 0.2–0.5 mm). Interstices: grains (0.1–0.3 mm) and segregates of clinopyroxene (30%), opaque minerals (5%), and altered glass (10%–15%). Single vesicles (0.7 mm and 1.5 mm) infilled with clay mineral or carbonate.

Alteration: slight (10%–15%); clay mineral replaces interstitial glass.

Sample 115-713A-15R-4, 64–69 cm (Piece 1), Unit 3 [Z-616]

Plagioclase-phyric basalt (microdolerite), massive. Phenocrysts (2%–3%): tabular grains (0.5–0.8 mm) of plagioclase. Groundmass with intersertal-microdoleritic texture; laths (0.1–0.3 mm) of plagioclase (40%). Interstices: xenomorphic grains (0.1–0.3 mm) of clinopyroxene or their segregates, opaque minerals (5%), and altered glass (15%).

Alteration: slight (15%); clay mineral replaces interstitial glass.

Sample 115-713A-15R-4, 103–105 cm (Piece 4), Unit 4 [Z-1329]

Clinopyroxene-plagioclase-phyric basalt, vesicular. Phenocrysts (20%) are represent by glomerophyric segregates of xenomorphic grains of clinopyroxene and prismatic grains (0.2–0.5 mm) of plagioclase (labradorite [$An_{65–68}$]). Groundmass with vitrophyric texture; black glass (50%). Vesicles (30%, 0.1–0.3 mm up to 0.8–1.5 mm) completely or partly infilled with brownish green clay mineral. Veinlets (0.1–0.2 mm in thickness) infilled with clay mineral.

Alteration: slight to moderate (15%–20%).

Sample 115-713A-15R-5, 85–87 cm (Piece 5), Unit 5 [Z-52]

Sparsely plagioclase-phyric basalt, incompletely crystallized, sparsely vesicular (up to 0.2–0.3 mm, <1%). Phenocrysts: plagioclase (up to 1–1.5 mm, 10%). Groundmass; laths of plagioclase, various crystals of clinopyroxene, single crystals of olivine, opaque minerals, and interstitial glass (5%–7%).

Alteration: slight (10%); smectites replace interstitial glass and olivine.

XRD: smectite with ~40% mica layers; trace hydromica.

Sample 115-713A-18R-1, 93–95 cm (Piece 9), Unit 6 [Z-48]

Micro-clinopyroxene-plagioclase-phyric basalt, poorly crystallized, massive. Microphenocrysts of plagioclase (5%) and clinopyroxene (5%–7%). Groundmass is hyalopilitic texture; needle-shaped laths of plagioclase, various crystals of clinopyroxene, single crystals of olivine, opaque dust, and devitrified volcanic glass.

Alteration: scarce (<1%); smectites replace interstitial glass and olivine; opaque dust is oxidized through patches.

XRD: smectites with various content of interlayer cations: Na-K and Mg-Ca.

Sample 115-713A-19R-1, 132–134 cm (Piece 13), Unit 10 [Z-56]

Clinopyroxene-plagioclase-phyric hyalobasalt, poorly crystallized, massive. Phenocrysts of plagioclase (1.5–2.5 mm, 15%) and clinopyroxene (0.3–0.7 mm, 3%–5%). Groundmass is hyalopilitic texture; laths of plagioclase, clinopyroxene, single crystals of olivine, opaque dust, and devitrified volcanic glass.

Alteration: slight (1%–3%); smectites replace interstitial glass and olivine; opaque dust is oxidized through patches.

XRD: smectite.

Sample 115-713A-19R-2, 49–53 cm (Piece 3F), Unit 10 [Z-617]

Clinopyroxene-plagioclase-phyric basalt, vesicular. Phenocrysts (25%) are represented by idiomorphic and partly xenomorphic grains (0.3–0.5 mm) of clinopyroxene (10%). Plagioclase forms glomerophyric segregates of prismatic and xenomorphic grains (0.2–0.5 mm). Large grains of plagioclase: labradorite [$An_{59–60}$], small grains: labradorite [An_{52-54}]. Groundmass with vitrophyric texture; brownish black glass with sparse of needle-shaped microlites of plagioclase. Vesicles (2%–3%, 0.4–0.8 mm) infilled with black and altered green glass.

Alteration: slight; clay mineral replaces glass.

Sample 115-713A-19R-3, 9–12 cm (Piece 2A), Unit 11 [Z-618]

Olivine-plagioclase-clinopyroxene-phyric basalt, vesicular. Phenocrysts (15%–20%): idiomorphic (0.5–0.8 mm) grains of olivine; segregates of elongated-prismatic grains of plagioclase (andesine [An_{48}] and andesine-labradorite [An_{50}]) and clinopyroxene crystals. Groundmass with vitrophyric texture; brownish black glass which contains sparse microlites of plagioclase. Vesicles (2%, 0.2–0.5 mm) are present.

Alteration: slight; vesicles infilled with clay mineral.

Sample 115-713A-20R-1, 70–72 cm (Piece 5A), Unit 12 [Z-40]

Plagioclase-phyric basalt, almost completely crystallized, massive. Phenocrysts: plagioclase grains (1–4 mm, 15%). Groundmass is intersertal texture; laths and small tabular crystals of plagioclase, various crystals of clinopyroxene, single crystals of olivine, opaque minerals, and interstitial devitrified volcanic glass (5%–10%) with opaque dust.

Alteration: slight (10%); smectites replace interstitial glass and olivine.

XRD: smectite.

Sample 115-713A-20R-2, 104–108 cm (Piece 6B), Unit 13 [Z-619]

Clinopyroxene-plagioclase-phyric basalt, vesicular. Phenocrysts (20%–25%): idiomorphic grains (0.2–0.5 mm) and xenomorphic grains of clinopyroxene. Plagioclase forms sparse tabular and prismatic grains (up to 1 mm, labradorite [An_{60}]) which contain small inclusions of glass and laths of plagioclase (labradorite [An_{52}]). Groundmass with vitrophyric texture; black glass with sparse microlites of plagioclase. Vesicles (2%, 0.1–0.2 mm) infilled with clay mineral.

Alteration: slight.

Sample 115-713A 20R-3, 40–42 cm (Piece 2A), Unit 14 [Z-37]

Clinopyroxene-plagioclase-phyric hyalobasalt, poorly crystallized, sparsely vesicular (0.5–1.5 mm, <1%). Phenocrysts of plagioclase (0.8–2.5 mm, 15%–20%) occasionally form glomerophyric segregates. Microphenocrysts of clinopyroxene (0.5–1 mm, 5%) and single microphenocrysts of olivine are present. Groundmass is hyalopilitic texture; black volcanic glass with needle-shaped microlaths of plagioclase, crystals of clinopyroxene, and opaque minerals (opaque dust and small grains).

Alteration: scarce (1%); smectites replace olivine and interstitial glass; vesicles are filled with smectites and carbonate; opaque dust is slightly oxidized.

XRD: smectites with various content of interlayer cations: Na-K and Mg-Ca; smectites with ~10% mica layers.

Sample 115-713A-20R-4, 57–62 cm (Piece 1), Unit 18 [Z-620]

Plagioclase-phyric basalt, vesicular. Phenocrysts (20%): large (up to 5 mm) glomerophyric segregates of prismatic xenomorphic grains (0.3–0.8 mm) of plagioclase. Groundmass with poikilophitic-microlitic texture; poikilophitic segregates of xenomorphic grains (0.2–0.3 mm) of clinopyroxene and plagioclase. Single rounded vesicle (0.3 mm) infilled with carbonate.

Alteration: rock is fresh.

Sample 115-713A-20R-5, 65–67 cm (Piece 5B), Unit 20 [Z-65]

Clinopyroxene-plagioclase-phyric hyalobasalt, poorly crystallized, massive. Phenocrysts of plagioclase (15%), clinopyroxene (5%), and single microphenocrysts of olivine. Groundmass is hyalopilitic texture; devitrified volcanic glass with needle-shaped microlaths of plagioclase, fine grained segregate of clinopyroxene and opaque minerals.

Alteration: scarce (<1%); smectites replace olivine and interstitial glass.

XRD: smectite with ~10% mica layers.

Sample 115-713A-20R-6, 103–108 cm (Piece 1C), Unit 23 [Z-621]

Clinopyroxene-plagioclase-phyric basalt, vesicular. Phenocrysts (20%): glomerophyric segregates of grains (0.3–0.8 mm) of clinopyroxene and laths of plagioclase (labradorite [An_{56}]). Groundmass with pilotaxitic texture; microlites of plagioclase, pyroxene, small grains of opaque minerals, and glass. Sparse vesicles (2%–3%, 0.1–0.3 mm) infilled with chlorite.

Alteration: slight.

Sample 115-713A-21R-1, 73–75 cm (Piece 4B), Unit 27 [Z-71]

Sparsely clinopyroxene-plagioclase-phyric hyalobasalt, poorly crystallized, sparsely vesicular (5%). Phenocrysts of tabular plagioclase (0.5–2.5 mm, 1%–3%) and xenomorphic clinopyroxene (0.3–1 mm, 5%–7%). Groundmass is hyalopilitic texture; black devitrified volcanic glass with needle-shaped microlaths of plagioclase, fine grained segregate of clinopyroxene, and small grains of opaque minerals.

Alteration: scarce (~1%); smectites replace interstitial glass, vesicles infilled with clay mineral or carbonate.

XRD: smectites with various content of interlayer cations: Na-K and Ca-Mg.

Sample 115-713A-21R-2, 61–63 cm (Piece 4B), Unit 31 [Z-75]

Sparsely clinopyroxene-plagioclase-phyric hyalobasalt, poorly crystallized, sparsely vesicular. Phenocrysts of plagioclase (0.5–2.5 mm, 5%–7%) and xenomorphic clinopyroxene (0.2–0.6 mm, 3%). Groundmass is hyalopilitic texture; brown-black devitrified volcanic glass with needle-shaped microlaths of plagioclase, crystals of clinopyroxene, and small grains of opaque minerals.

Alteration: slight (1%–3%); smectites replace interstitial glass.

XRD: smectites with various content of interlayer cations: Na-K and Ca-Mg.

Sample 115-713A-21R-3, 83–85 cm (Piece 4A), Unit 33 [Z-73]

Plagioclase-phyric basalt, almost completely crystallized, massive. Phenocrysts: plagioclase (1.5–5 mm, 15%). Groundmass is intergranular texture; laths of plagioclase, xenomorphic crystals of clinopyroxene, single crystals of olivine (0.7–2 mm, 1%), opaque minerals, and interstitial glass (3%).

Alteration: slight (3%–5%); smectites replace interstitial glass and olivine; single vesicles (0.3 mm) are filled with smectites.

XRD: smectite; trace quartz (?).

Sample 115-713A-22R-1, 34–36 cm (Piece 5), Unit 35 [Z-66]

Sparsely plagioclase-phyric basalt, almost completely crystallized, vesicular (0.5–1.8 mm, 3%–5%). Phenocrysts of plagioclase (0.8–3.5 mm, 15%). Groundmass is intergranular texture; laths of plagioclase, xenomorphic crystals of clinopyroxene, single crystals of olivine (0.7–2 mm, 1%), opaque minerals, and interstitial glass.

Alteration: slight (5%–7%); smectites replace interstitial glass and olivine; vesicles are filled with smectites.

XRD: smectite; trace quartz(?).

Maldives Ridge (Hole 715A)

Sample 115-715A-23R-2, 28–31 cm (Piece 2A), Unit 4 [Z-622]

Sparsely plagioclase-phyric basalt, vesicular. Phenocrysts (5%): prismatic grains (0.5–1.7 mm) of plagioclase (labradorite [An_{56}]). Groundmass with hyalopilitic texture; microlites and laths of plagioclase (andesine-labradorite [An_{50}]) and black glass. Large (2–5 mm) vesicles (50%) are rounded in shape.

Alteration: rock is fresh; vesicles infilled with calcite.

Sample 115-715A-23R-3, 62–64 cm (Piece 11), Unit 7a [Z-79]

Aphyric basalt, fine grained, equigranular, almost completely crystallized, massive. Rock is intergranular texture; laths of plagioclase, small grains of clinopyroxene, opaque minerals, single crystals of olivine, rare xenomorphic accumulations of volcanic glass (~1%–3%). Single microphenocrysts of plagioclase (up to 1.5 mm) are present. Plagioclases content numerous inclusions of volcanic glass. Vesicles (0.1–1 mm, ~7%–10%) are oval and irregular in shape.

Alteration: slight (1%–3%); smectites replace olivine and interstitial glass.

XRD: smectite with various content of interlayer cations: Na-K and Ca-Mg.

Sample 115-715A-23R-3, 91–95 cm (Piece 14A), Unit 7a [Z-1333]

Sparsely plagioclase-phyric basalt (microdolerite). Phenocrysts (<1%): single glomerophyric segregates (0.7 mm) of plagioclase grains. Groundmass (99%) with intersertal-microdoleritic and microlitic texture; laths (0.1–0.4 mm) of plagioclase (65%, labradorite [An_{60}]), small xenomorphic grains (0.1–0.3 mm) of clinopyroxene (25%), opaque minerals (5%), and brown volcanic glass (5%).

Alteration: rock is fresh.

XRD: smectite with ~20% mica layers and mixed-layer chlorite-smectite mineral (~60% chlorite layers); minor hydromica with ~20% swelling interlayers.

Sample 115-715A-24R-1, 76–79 cm (Piece 11), Unit 7b [Z-623]

Aphyric basalt, massive. Rock with microlitic texture; microlaths (0.1–0.3 mm) of plagioclase (40%, labradorite [An_{52}]), segregate of clinopyroxene small grains (0.1–0.2 mm, 25%), altered volcanic glass (1%–2%), and opaque minerals (5%–8%).

Alteration: slight; clay mineral replaces glass.

Sample 115-715A-24R-2, 13–18 cm (Piece 2), Unit 7b [Z-624]

Sparsely plagioclase-phyric andesite-basalt (islandite), massive. Phenocrysts: single elongated-prismatic grain (1.2 mm) of plagioclase (andesine [An_{48}]). Groundmass with microlitic texture; microlaths (0.1–0.3 mm) of plagioclase (50%), segregate of xenomorphic grains of clinopyroxene (40%), abundant (10%–12%) pseudo-cubic and isometric grains (0.1–0.2 mm) of opaque minerals, and altered interstitial glass (1%).

Alteration: scarce (<1%); clay mineral replaces interstitial glass (<1%).

Sample 115-715A-24R-2, 30–38 cm (Piece 3), Unit 7b [Z-1334]

Aphyric basalt (microdolerite), massive. Rock: identical to Sample 115-715A-23R-3, 91–95 cm (Z-1333).

Alteration: slight; palagonite replaces glass.

Sample 115-715A-25R-2, 80–82 cm (Piece 3C), Unit 9 [Z-63]

Sparsely olivine-microphyric basalt, fine grained, equigranular, almost completely crystallized, massive. Microphenocrysts of olivine (0.7–1.5 mm, 3%–5%). Groundmass is intersertal texture; laths of plagioclase, clinopyroxene, opaque minerals, and interstitial glass (3%).

Alteration: slight (5%–7%); smectites replace interstitial glass and olivine.

XRD: smectite.

Sample 115-715A-25R-3, 0–4 cm (Piece 1A), Unit 9 [Z-625]

Aphyric basalt, vesicular. Rock with microlitic (microdoleritic) texture; unoriented laths (0.1–0.4 mm) of plagioclase (55%, labradorite [An_{51}]), xenomorphic grains (0.1–0.2 mm) of clinopyroxene (30%), opaque minerals (5%), and 10% of altered reddish brown olivine(?) with sizes 0.1–0.2 mm. Isometric vesicles (5%, up to 2.5 mm) are empty, occasionally they infilled with clay mineral.

Alteration: slight.

Sample 115-715A-25R-5, 108–112 cm (Piece 15), Unit 10 [Z-626]

Aphyric basalt, vesicular. Rock with microlitic (microdoleritic) texture; laths (0.1–0.3 mm) of plagioclase (andesine-labradorite [An_{50}], microlaths: andesine [An_{45}]). Clinopyroxene (30%) forms xenomorphic and idiomorphic grains (0.1–0.6 mm). Small (0.1–0.2 mm) rounded grains of completely altered olivine (10%) are present. Opaque minerals: 2%–3%. Altered interstitial glass: 2%–3%. Large vesicles (15%–20%, 3–4 mm) partly infilled with clay mineral.

Alteration: slight (10%–12%); clay mineral: iddingsite replace olivine, interstitial glass replaced by clay mineral, clay mineral from vesicles.

XRD: smectite with ~10% mica layers; white matter from veinlet: calcite.

Sample 115-715A-25R-6, 2–4 cm (Piece 1), Unit 10 [Z-1335]

Aphyric dolerite, fine grained. Rock with intersertal-poikilophitic texture; unoriented laths (0.1–0.7 mm) of plagioclase (60%, labradorite [An_{58}]), xenomorphic grains (0.3–0.7 mm) of clinopyroxene (25%) with laths of plagioclase (poikilophitic texture), xenomorphic grains (<0.1 mm) of opaque minerals (5%), and altered volcanic glass (10%).

Alteration: slight (10%).

XRD: smectite; gray-brown inclusion in rock: smectite; minor calcite; trace swelling chlorite(?).

Sample 115-715A-25R-6, 16–18 cm (Piece 1), Unit 10 [Z-57]

Olivine-phyric microdolerite, fine grained, equigranular, almost completely crystallized, massive. Microphenocrysts of olivine (0.7–1.5 mm, 3%–5%). Groundmass is microdoleritic texture; laths of plagioclase, hypidiomorphic crystals of clinopyroxene, opaque minerals, microphenocrysts of olivine (1%), and interstitial glass (3%).

Alteration: slight (1%–3%); smectites replace interstitial glass and olivine.

XRD: smectite with ~20% mica layers; trace mixed-layer chlorite-swelling chlorite mineral and chlorite(?).

Sample 115-715A-26R-2, 14–20 cm (Piece 1A), Unit 10 [Z-627]

Olivine-phyric basalt, vesicular. Phenocrysts (15%): sparse large (2.5–3 mm) idiomorphic crystals and microphenocrysts (0.2–0.4 mm) of altered olivine. Groundmass with microlitic (microdoleritic) texture; laths (0.2–0.5 mm) of plagioclase (40%, labradorite [An_{52}]), elongated-prismatic and xenomorphic grains of clinopyroxene (40%), opaque minerals (5%), and altered interstitial glass (5%). Vesicles (10%, 0.2–0.5 mm) are present.

Alteration: slight (15%); olivine almost completely replaced by clay mineral and iddingsite, clay minerals replace interstitial glass, vesicles infilled with clay minerals.

Sample 115-715A-26R-3, 17–19 cm (Piece 1B), Unit 10 [Z-62]

Olivine-phyric basalt, fine grained, incompletely crystallized, vesicular (0.5–5 mm). Groundmass is intersertal texture; laths and platy-laths crystals of plagioclase, small xenomorphic crystals of clinopyroxene, xenomorphic crystals of olivine (5%–7%), opaque minerals, and interstitial glass (3%).

Alteration: slight to moderate (20%); opaque minerals and rims around olivines are oxidized; smectites replace interstitial glass and olivine; vesicles are filled with smectites and carbonate.

XRD: smectite.

Sample 115-715A-29R-1, 38–42 cm (Piece 2A), Unit 12 [Z1336]

Olivine-phyric dolerite, medium grained, sparsely vesicular. Phenocrysts (5%): idiomorphic crystals (0.5–1.7 mm) of altered olivine, small grains form glomerophyric segregates. Groundmass with intersertal-doleritic texture; prismatic grains and laths (0.1–0.7 mm) of plagioclase (35%, labradorite [An_{60}] and andesine [An_{44}]), xenomorphic grains of clinopyroxene (25%), small rounded grains of olivine (10%), altered interstitial glass (10%), and opaque minerals (2%–3%). Sparse vesicles (0.5–2.4 mm) are present.

Alteration: moderate (35%); olivine completely replaced by iddingsite, clay minerals replace interstitial glass, vesicles infilled with clay minerals.

XRD: smectite.

Sample 115-715A-29R-1, 64–66 cm (Piece 2B), Unit 12 [Z-42]

Olivine-phyric basalt, medium grained, almost completely crystallized, massive. Groundmass is intergranular texture; laths of plagioclase (45%), xenomorphic crystals of clinopyroxene (40%), olivine (7%–10%), opaque minerals (2%–3%), and interstitial glass (5%).

Alteration: slight (15%); smectites replace interstitial glass and olivine.

XRD: smectite contain ~10% of mica layers; trace chlorite.

Sample 115-715A-29R-1, 95–97 cm (Piece 3A), Unit 13 [Z-51]

Olivine-phyric basalt, medium grained, almost completely crystallized, massive. Groundmass is intergranular texture; laths and small plates of plagioclase (50%), xenomorphic crystals of clinopyroxene (35%–40%), olivine (2%–3%), opaque minerals (5%), and interstitial devitrified glass (5%).

Alteration: slight (~10%); smectites replace interstitial glass and olivine.

XRD: smectite.

Sample 115-715A-29R-2, 80–82 cm (Piece 1F), Unit 13 [Z-67]

Olivine-phyric basalt, medium grained, almost completely crystallized, massive. Groundmass is intergranular texture; laths and small plates of plagioclase, xenomorphic crystals of clinopyroxene, olivine (3%–5%), opaque minerals (1%–3%), and interstitial devitrified glass (5%).

Alteration: slight (7%–10%); smectites replace interstitial glass and olivine.

XRD: smectite; trace chlorite.

Sample 115-715A-30R-2, 1–5 cm (Piece 1), Unit 15 [Z-628]

Aphyric dolerite, sparsely vesicular. Rock with doleritic texture; laths (0.2–0.8 mm) of plagioclase (40%, labradorite [$An_{51–52}$]), xenomorphic grains (0.2–0.7 mm) of clinopyroxene (40%), partly oriented small grains (0.2–0.4 mm) of altered olivine (10%), and opaque minerals (2%–3%). Large vesicles (5%–10%, 2–5 mm) are present.

Alteration: slight to moderate (20%); olivine completely replaced by iddingsite, vesicles completely infilled with clay minerals.

Sample 115-715A-30R-3, 28–30 cm (Piece 1), Unit 16 [Z-41]

Olivine-phyric basalt, medium grained, almost completely crystallized, sparsely vesicular. Groundmass is intergranular texture; laths and rare plates of plagioclase, xenomorphic crystals of clinopyroxene, olivine (5%–7%), opaque minerals, and interstitial devitrified glass. Vesicles (1%–3%) rounded and irregular in shape.

Alteration: slight (10%); smectites replace interstitial glass and olivine.

XRD: smectites with ~10% mica layers; trace mixed-layer chlorite-smectite mineral(?) and chlorite.

Sample 115-715A-30R-5, 30–32 cm (Piece 3), Unit 19 [Z-72]

Aphyric hyalobasalt, poorly crystallized, highly vesicular (0.5–5 mm, 50%). Rock is hyalopilitic texture; black volcanic glass with laths of plagioclase (15%–20%), xenomorphic crystals of clinopyroxene (5%), and opaque dust.

Alteration: strong (50%); vesicles are filled with carbonate; clay minerals replace interstitial glass.

XRD: smectite and chlorite.

Sample 115-715A-30R-5, 39–41 cm (Piece 4), Unit 19 [Z-43]

Sparsely plagioclase-phyric hyalobasalt, poorly crystallized, vesicular (up to 3–5 mm, 30%). Phenocrysts of plagioclase (1–1.5 mm, <1%). Rock is hyalopilitic texture; black volcanic glass with laths and small plates of plagioclase, small xenomorphic crystals of clinopyroxene, and opaque dust.

Alteration: moderate (25%); Fe hydroxides replace opaque minerals; vesicles are filled with carbonate.

XRD: calcite.

Sample 115-715A-30R-5, 98–100 cm (Piece 9), Unit 20 [Z-46]

Olivine-phyric basalt, medium grained, almost completely crystallized, massive. Rock is intergranular texture; laths and plates of plagioclase, xenomorphic crystals of clinopyroxene, hypidiomorphic crystals of olivine (10%), and interstitial glass (3%).

Alteration: slight (15%); smectites replace interstitial glass and olivine.

XRD: smectite; trace chlorite and calcite.

Sample 115-715A-31R-1, 103–105 cm (Piece 8B), Unit 21 [Z-45]

Sparsely olivine-plagioclase-phyric basalt, almost completely crystallized, vesicular (1–6 mm, 10%). Phenocrysts of plagioclase (1–1.5 mm, 1%) and olivine (0.7–1.5 mm, 1%). Groundmass is intergranular texture; laths and tabular crystals of plagioclase, xenomorphic crystals of clinopyroxene, opaque minerals, and interstitial volcanic glass.

Alteration: slight (15%); smectites replace interstitial glass and olivine; vesicles are filled with smectites or carbonate.

XRD: smectite.

Sample 115-715A-31R-2, 98–100 cm (Piece 6A), Unit 21 [Z-76]

Aphyric basalt, medium grained, almost completely crystallized, vesicular (1–2 mm, 3%–5%). Rock is intergranular texture; laths of plagioclase, xenomorphic clinopyroxene, hypidiomorphic olivine, interstitial glass, and opaque minerals.

Alteration: slight (10%–15%); rock is nonoxidized; smectites replace olivine and interstitial glass. Vesicles are filled with smectites.

XRD: smectites with various content of interlayers cations (Na-K and Ca-Mg) and contain ~20% of mica layers; trace chlorite.

Walvis Ridge (Leg 74)

Hole 525A

Sample 74-525A-53R-2, 87–90 cm (Piece 5B), Unit 1 [Z-398]

Aphyric andesite-basalt, medium grained, incompletely crystallized, vesicular. Rock is intersertal texture; chaotically located laths of plagioclase (55%), xenomorphic crystals of clinopyroxene (20%), interstitial volcanic glass (15%), and opaque minerals (magnetite + pyrite) 5%. Single crystals of K-feldspar occur sporadically. Glass contains of leizite(?) and analcime(?). Vesicles (0.3–2 mm, 10%) are rounded in shape.

Alteration: moderate (~30%); interstitial glass and glass from vesicles are replaced with smectites, zeolite occurs sporadically.

XRD: smectite.

Sample 74-525A-53R-3, 36–39 cm (Piece 3), Unit 1 [Z-397]

Aphyric andesite-basalt (basalt?), medium grained, incompletely crystallized, vesicular (0.2–2.5 mm, 2%–3%). Rock is intersertal texture; laths of plagioclase (50%), clinopyroxene (30%), interstitial volcanic glass (10%), and opaque minerals (3%). Single tabular crystals of K-feldspar are present. Glass contains of leizite(?) and analcime(?).

Alteration: moderate (~25%); interstitial glass is replaced with smectites, occasionally with admixture of calcite; vesicles are filled with smectites, calcite occurs occasionally.

XRD: smectite.

Sample 74-525A-55R-1, 107–110 cm (Piece) [Z-399]

Sediment.

XRD: hydromica and opal-CT; the preparation contains mainly amorphic in X-rays matter.

Sample 74-525A-56R-1, 43–46 cm (Piece 1G), Unit 3 [Z-400]

Aphyric basalt, fine grained, incompletely crystallized, highly vesicular (cavernous). Rock is intersertal texture; various laths of plagioclase (50%–55%), small grains of clinopyroxene (25%), interstitial volcanic glass (5%–7%), and opaque minerals (1%–3%). Vesicles have size 0.3–0.5 mm (20%).

Alteration: moderate (~30%); interstitial glass is replaced with smectites; vesicles are filled with calcite and thin pellicle of smectites on the walls of vesicles.

XRD: smectite; trace calcite.

Sample 74-525A-56R-2, 121–124 cm (Piece 1W), Unit 3 [Z-401]

Aphyric basalt, medium grained, inequigranular, almost completely crystallized, vesicular (1.5.–2.5 mm, ~15%). Rock is intergranular to subophitic texture; various laths of plagioclase (45%), clinopyroxene (40%), interstitial volcanic glass (<5%), and opaque minerals (1%–3%).

Alteration: slight to moderate (15%–20%); interstitial glass is replaced with smectites; vesicles are filled with smectites.

XRD: smectite; trace calcite.

Sample 74-525A-56R-3, 108–111 cm (Piece 1R), Unit 3 [Z-402]

Aphyric basalt, medium grained, inequigranular, almost completely crystallized, vesicular (0.3–3 mm, 15%). Rock is intergranular to subophitic texture; various laths of plagioclase (50%), clinopyroxene (25%), interstitial glass (5%), and opaque minerals (5%).

Alteration: moderate (~20%–25%); interstitial glass is replaced with smectites; vesicles are filled with secondary minerals in the folslighting succession: smectites on the walls of vesicles, oxidized opaque minerals and calcite (90% of the volume) in the centers of vesicles.

XRD: smectite; trace hydromica.

Sample 74-525A-56R-6, 81–84 cm (Piece 10), Unit 3 [Z-403]

Aphyric basalt, fine grained, inequigranular, almost completely crystallized, vesicular (0.3.–1.5 mm, 5%–7%). Rock; various laths of plagioclase (45%), clinopyroxene (40%), interstitial glass (1%–3%), and opaque minerals (5%–7%). Single hypidiomorphic tabular crystals of K-feldspar occur sporadically.

Alteration: slight (10%–15%); interstitial glass is replaced with smectites; vesicles are filled with smectites or calcite or both.

XRD: smectite; trace hydromica.

Sample 74-525A-58R-1, 106–109 cm (Piece 4D), Unit 3 [Z-404]

Aphyric basalt, fine grained, poorly crystallized, massive. Rock is hyalopilic texture; black volcanic glass (60%) filled with opaque dust, crystals of clinopyroxene and needle-shaped laths of plagioclase (40%).

Alteration: slight.

XRD: smectite and hydromica.

Sample 74-525A-58R-4, 82–85 cm (Piece 4C), Unit 4 [Z-405]

Aphyric basalt, fine grained, inequigranular, almost completely crystallized, vesicular (0.2–0.4 mm, 10%). Rock is intergranular texture; various (mostly thin) needle-shaped laths of plagioclase (30%), xenomorphic grains of clinopyroxene (50%), interstitial glass (5%), and needle-shaped crystals of opaque minerals (3%–5%).

Alteration: slight to moderate (~15%–20%); interstitial glass is replaced with smectites; vesicles are filled with smectites.

XRD: smectite.

Sample 74-525A-59R-3, 40–42 cm (Piece 1G), Unit 4 [Z-406]

Aphyric basalt, fine grained, inequigranular, incompletely crystallized, vesicular (0.2–0.6 mm, 10%). Rock is intersertal texture; various laths of plagioclase (40%), clinopyroxene (40%), interstitial glass (5%–7%), and opaque minerals (5%–7%).

Alteration: slight to moderate (~20%); interstitial glass is replaced with smectites; vesicles are filled with smectites or calcite.

XRD: smectite.

Sample 74-525A-60R-1, 41–44 cm (Piece 1ä), Unit 4 [Z-407]

Aphyric basalt, fine grained, inequigranular, incompletely crystallized, vesicular (0.2–0.5 mm, 5%–10%). Rock is intersertal texture; various laths of plagioclase (45%), clinopyroxene (35%), interstitial glass (5%–7%), and opaque minerals (3%–5%).

Alteration: slight to moderate (~20%); interstitial glass is replaced with smectites; vesicles are filled with smectites.

XRD: smectite.

Sample 74-525A-60R-3, 40–43 cm (Piece 1H), Unit 4 [Z-408]

Aphyric basalt, fine grained, incompletely crystallized, vesicular (1–4 mm, 10%). Rock is intersertal texture; small laths of plagioclase (40%), clinopyroxene (45%), interstitial glass (5%–7%), and both opaque minerals and dust (5%).

Alteration: slight (~15%); interstitial glass is replaced with smectites; vesicles are filled with calcite, smectites cover walls of vesicles; small laths and microlites of plagioclase (0.1–0.5 mm, 25%, andesine [An_{45}]), clinopyroxene

(up to 0.1 mm, 15%), interstitial glass (40%) with needles of opaque minerals (15%). Vesicles (0.1–0.4 mm, 5%) are filled with brownish green glass.

XRD: smectite and calcite.

Sample 74-525A-60R-4, 32–35 cm (Piece 1D), Unit 4 [Z-409]

Aphyric basalt, fine grained, poorly crystallized, microvesicular. Rock is hyalopilitic texture.

Alteration: rock is fresh.

XRD: smectite; trace hydromica.

Sample 74-525A-61R-2, 2–5 cm (Piece 1A), Unit 5 [Z-410]

Aphyric basalt, fine grained, poorly crystallized, vesicular (0.2–0.4 mm, 25%). Rock is intersertal to hyalopilitic texture; black volcanic glass filled with small laths of plagioclase and opaque dust.

Alteration: moderate (~25%–30%); small vesicles are filled with smectites, large ones: with calcite.

XRD: smectite; trace hydromica.

Sample 74-525A-63R-2, 104–107 cm (Piece 4A), Unit 5 [Z-411]

Aphyric basalt, fine grained, incompletely crystallized, massive. Rock is intersertal texture; laths of plagioclase and devitrified volcanic volcanic glass. The latter contains small xenomorphic crystals and crystallites of clinopyroxene and opaque dust. Needle-shaped crystals of opaque minerals and single vesicles (0.01 mm) are present.

Alteration: moderate (~25%); interstitial glass is replaced with smectites; vesicles are filled with calcite.

XRD: smectite; trace hydromica.

Hole 527

Sample 74-527-39R-2, 131–134 cm (Piece 1G), Unit 1 [Z-412]

Aphyric basalt, fine-medium grained, inequigranular, almost completely crystallized, massive. Rock is intergranular texture; laths of plagioclase (40%), various xenomorphic grains of clinopyroxene (40%), interstitial glass (10%), and opaque minerals (10%). Single microphenocrysts of plagioclase are present.

Alteration: slight (10%–15%).

XRD: smectite; trace hydromica.

Sample 74-527-39R-3, 64–67 cm (Piece 1G), Unit 1 [Z-413]

Plagioclase-phyric basalt, fine grained, inequigranular, incompletely crystallized, massive. Phenocrysts of plagioclase (1.5–8 mm, 25%). Groundmass is intersertal to intergranular texture; aggregate of laths of plagioclase (35%), clinopyroxene (40%), interstitial glass (15%), and opaque minerals (7%–8%).

Alteration: slight (~15%); interstitial glass is replaced with smectites.

XRD: smectite and hydromica; trace amphibole.

Sample 74-527-40R-1, 82–85 cm (Piece 3F), Unit 2 [Z-414]

Sparsely clinopyroxene-plagioclase-phyric basalt, medium grained, almost completely crystallized, massive. Phenocrysts of plagioclase (0.5–2 mm, 1%) and clinopyroxene (<1%). Groundmass is intergranular texture; aggregate of laths of plagioclase (40%), clinopyroxene (40%), interstitial glass (5%), opaque minerals (7%–10%), and single grains of olivine.

Alteration: slight (~5%–7%); interstitial glass and olivine are replaced with smectites.

XRD: smectite; trace hydromica and amphibole.

Sample 74-527-41R-3, 39–42 cm (Piece 1C), Unit 3 [Z-415]

Clinopyroxene-plagioclase-phyric basalt, medium grained, crystallized, massive. Phenocrysts of plagioclase (1–10 mm, 25%–30%) and clinopyroxene (1.5–2 mm, <1%). Groundmass; laths of plagioclase (45%), clinopyroxene (45%), opaque minerals (5%–7%), and olivine (1%–3%).

Alteration: slight (~5%).

XRD: smectite; trace hydromica and amphibole.

Sample 74-527-42R-2, 69–72 cm (Piece) [Z-416]

Sediment.

XRD: salcite and smectite; trace hydromica.

Sample 74-527-42R-4, 45–48 cm (Piece 1C), Unit 5 [Z-417]

Aphyric basalt, fine grained, equigranular, almost completely crystallized, massive. Rock is intergranular texture; laths of plagioclase (55%), clinopyroxene (35%–40%), interstitial glass (5%–7%), and opaque minerals (5%).

Alteration: slight (10%).

XRD: smectite; trace chlorite.

Sample 74-527-44R-3, 10–13 cm (Piece 1A), Unit 5 [Z-418]

Aphyric basalt, medium grained, equigranular, massive. Rock is intergranular texture; large laths of plagioclase (55%), various crystals of clinopyroxene (35%), interstitial glass (5%), olivine (<1%), and opaque minerals (5%–7%).

Alteration: slight (~5%–10%); interstitial glass and olivine are replaced with smectites.

XRD: two smectites with various composition of interlayers cations (Na-K and Ca-Mg); trace hydromica.

Hole 528

Sample 74-528-39R-2, 7–10 cm (Piece 1A), Unit 1 [Z-419]

Sparsely plagioclase-phyric basalt, medium grained, equigranular, almost completely crystallized, massive. Phenocrysts of plagioclase (0.7–2.5 mm, 1%–3%). Groundmass is intergranular to subophitic texture; laths of plagioclase (45%), clinopyroxene (45%), interstitial glass (5%), and opaque minerals (5%).

Alteration: slight (5%–10%).

XRD: smectite; trace hydromica and defective chlorite.

Sample 74-528-40R-2, 24–27 cm (Piece 1B), Unit 1 [Z-420]

Olivine-plagioclase-phyric basalt, medium grained, equigranular, incompletely crystallized, vesicular (1–1.5 mm, 5%). Phenocrysts of plagioclase (1–7 mm, 25%) and olivine (0.8–2 mm, 1%–3%). Groundmass is subophitic texture; laths of plagioclase (40%), clinopyroxene (45%), olivine (<1%), interstitial glass (5%), and opaque minerals (3%).

Alteration: slight (10%); interstitial glass and olivine is replaced with smectites; vesicles are filled with smectites.

XRD: smectite and mixed-layer smectite-chlorite mineral; hydromica, talc, and defective chlorite in trace amounts.

Sample 74-528-40R-5, 76–79 cm (Piece 1C), Unit 1 [Z-421]

Sparsely clinopyroxene-plagioclase-phyric basalt, medium grained, inequigranular, incompletely crystallized, massive. Phenocrysts of plagioclase (0.8–1 mm, 1%–3%) and clinopyroxene (0.8–1.5 mm, <1%). Groundmass is intergranular texture; laths of plagioclase (45%), clinopyroxene (40%), interstitial glass (5%–10%), and opaque minerals (5%–7%).

Alteration: slight (5%–10%).

XRD: two smectites with various cation composition of interlayers (Na-K and Ca-Mg); hydromica and defective chlorite in trace amounts.

Sample 74-528-42R-1, 32–35 cm (Piece 1C), Unit 2 [Z-422]

Aphyric basalt, fine grained, poorly crystallized, vesicular (0.3–0.8 mm, 15%–20%). Rock is hyalopilitic texture; devitrified volcanic glass which contains needle-shaped laths of plagioclase, crystals of clinopyroxene, and needle-shaped crystals of opaque minerals.

Alteration: moderate (30%–40%); walls of vesicles are lined with smectites.

XRD: smectite; trace hydromica.

Sample 74-528-43R-2, 85–88 cm (Piece 1F), Unit 4 [Z-423]

Aphyric basalt, fine grained, inequigranular, incompletely crystallized, vesicular (0.7–1.5 mm, 5%–10%). Rock is intersertal texture; laths of plagioclase (40%), clinopyroxene (40%), interstitial glass (5%–10%), and opaque minerals (3%).

Alteration: moderate (20%); vesicles are filled with calcite, walls of vesicles are lined with smectites; interstitial glass is replaced with smectites.

XRD: smectite; hydromica and chlorite in trace amounts.

Sample 74-528-44R-3, 94–97 cm (Piece 1E), Unit 5 [Z-424]

Plagioclase-phyric basalt, fine grained, incompletely crystallized, massive. Phenocrysts of plagioclase (1–5 mm, 5%–10%) are distributed in rock chaotically. Groundmass is intergranular to intersertal texture; laths of plagioclase (50%), clinopyroxene (40%), interstitial glass (5%–10%), and opaque minerals (5%).

Alteration: slight to moderate (~15%–20%).

XRD: smectite; hydromica and chlorite in trace amounts.

Sample 74-528-46R-1, 130–133 cm (Piece) [Z-425]

Sediment.

XRD: calcite and smectite with admixture of 10% of mica-like interlayers; hydromica and chlorite in trace amounts.

Sample 74-528-46R-3, 68–70 cm (Piece) [Z-426]

Sediment.

XRD: smectite; calcite and heulandite(?) in trace amounts.

Sample 74-528-46R-5, 70–74 cm (Piece) [Z-427]

Sediment.

XRD: calcite; trace quartz, smectite, heulandite/clinoptilolite(?), and hydromica.

Sample 74-528-47R-3, 67–70 cm (Piece 3B), Unit 8 [Z-428]

Sparsely micro-clinopyroxene-plagioclase-phyric basalt, fine grained, equigranular, incompletely crystallized, sparsely vesicular (0.2–0.3 mm, <1%). Microphenocrysts of plagioclase (up to 1 mm, <1%) and clinopyroxene (up to 0.8 mm, <1%). Groundmass is intergranular to intersertal texture; laths of plagioclase (50%), small grains of clinopyroxene (40%), interstitial glass (10%), and opaque minerals (7%–10%).

Alteration: moderate (~20%); interstitial glass is replaced with smectites; vesicles are filled with smectites.

XRD: smectite; trace hydromica.

Rio-Grande Ridge (Leg 72)

Hole 516F

Sample 72-516F-126R-1, 70–73 cm (Piece 2I), Unit 1 [Z-392]

Sparsely plagioclase-phyric basalt, fine grained, incompletely crystallized, vesicular (0.3–0.8 mm up to 2–5 mm, 35%). Phenocrysts of plagioclase (0.6–0.8 mm, 5%), groundmass: 60%, and vesicles: 35%. Groundmass is intersertal texture; various laths of plagioclase (up to 0.3–0.4 mm, 45%, andesine [An_{45}]), clinopyroxene (0.05 mm, 25%), interstitial glass, and opaque minerals.

Alteration: strong (40%–60%); plagioclase is carbonitized; vesicles are zonally filled with secondary minerals: smectites, zeolites, and calcite. The latter fills 80% of the total volume in vesicles.

XRD: smectite; trace hydromica.

Sample 72-516F-126R-2, 53–56 cm (Piece 1E), Unit 1 [Z-393]

Plagioclase-phyric basalt, fine grained, inequigranular, incompletely crystallized, vesicular. Phenocrysts of plagioclase (0.5–2 mm, 5%–7%). Groundmass is intersertal texture; various laths of plagioclase (45%), small and xenomorphic clinopyroxene (35%), interstitial glass (10%–15%), and opaque minerals (5%–7%). Single tabular crystals of K-feldspar. Vesicles have sizes of 0.3–0.8 mm (35%).

Alteration: moderate (~25%–30%); intersertal glass is replaced with smectites and partly carbonate.

XRD: smectite.

Sample 72-516F-127R-1, 55–58 cm (Piece 18), Unit 1 [Z-394]

Aphyric basalt, fine grained, inequigranular, incompletely crystallized, vesicular. Rock is intersertal texture; various laths of plagioclase (40%), xenomorphic clinopyroxene (35%), interstitial glass (10%), and opaque minerals (5%–7%). Elongated vesicles (1–3 mm, 5%–10%) tend to occur on lines.

Alteration: slight to moderate (~20%); vesicles filled with bluish green smectites and zeolites; intersertal glass is replaced with smectites and partly with carbonate.

XRD: smectite; trace hydromica.

Sample 72-516F-127R-3, 64–67 cm (Piece 1G), Unit 1 [Z-395]

Sparsely plagioclase-phyric basalt, fine grained, inequigranular, incompletely crystallized, vesicular. Phenocrysts of plagioclase (0.4–2 mm, 1%–5%). Groundmass is intersertal texture; various laths of plagioclase (45%), clinopyroxene (40%), interstitial glass (5%), and opaque minerals (5%). Single crystals of olivine are present.

Alteration: slight to moderate (~20%); intersertal glass and olivine are replaced with smectites and, partly, with carbonate.

XRD: smectite.

Sample 72-516F-128R-2, 126–129 cm (Piece 4B), Unit 2 [Z-396]

Aphyric basalt, fine grained, inequigranular, incompletely crystallized, sparsely vesicular. Rock is intergranular to intersertal texture; an aggregate of various laths of plagioclase (45%), xenomorphic clinopyroxene (45%), interstitial glass (5%), and opaque minerals (5%). Single phenocrysts of plagioclase and olivine are present. Elongated vesicles (1–3 mm, 5%–10%) tend to occur in lines.

Alteration: slight (10%); intersertal glass and olivine is replaced with smectites and, partly, with carbonate.

XRD: smectite.

Sulu Basin and Celebes Basin (Leg 124)

Sulu Basin (Hole 768C)

Sample 124-768C-74R-1, 100–104 cm (Piece 10B), Unit 1 [Z-660]

Aphyric basalt, vesicular. Rocks with intersertal texture; panicle like segregates of microlites and laths of plagioclase and clinopyroxene. Composition of plagioclase: approximately labradorite [An_{55}]. Interstices infilled by black glass. Vesicles (30%–35%) are rounded-isometric in shape.

Alteration: moderate (35%–40%); laths of plagioclase in central parts replaced by clay mineral and carbonate(?), vesicles completely infilled with clay mineral.

XRD: smectite; dark green matter from veinlet: smectite; trace quartz.

Sample 124-768C-75R-1, 142–146 cm (Piece 6), Unit 1 [Z-661]

Plagioclase-phyric basalt, vesicular. Phenocrysts (10%): prismatic and tabular grains of plagioclase. Groundmass with intersertal texture; panicle like and radial-radiant segregates of microlites and laths of plagioclase and clinopyroxene; idiomorphic grains (0.2–0.4 mm) of clinopyroxene. Composition of plagioclase: approximately labradorite [An_{54}]. Interstices infilled with black glass. Vesicles (50%, 0.1–0.3 mm up to 0.8 mm) are rounded and isometric in shape.

Alteration: strong (60%); laths of plagioclase in central parts of crystals replaced by clay mineral and smectites, phenocrysts of plagioclase replaced by carbonate; microcracks in plagioclase grains infilled with smectites; vesicles infilled with clay minerals.

XRD: smectite.

Sample 124-768C-77R-2, 26–30 cm (Piece 1D), Unit 1 [Z-662]

Olivine(?)-phyric basalt, highly vesicular. Phenocrysts: olivine(?) 5%. Groundmass with hyalopilitic texture; panicle like segregates of microlites of plagioclase; brown oxidized glass. Very small (up to 0.1–0.2 mm) vesicles are present.

Alteration: very strong (90%); olivine completely replaced by clay minerals; glass replaced by clay mineral; vesicles infilled with smectites.

XRD: smectite.

Sample 124-768C-80R-1, 90–92 cm (Piece 1L), Unit 1 [Z-124]

Sparsely olivine-phyric hyalobasalt, fine grained, poorly crystallized, vesicular (0.1–0.3 mm, <1%). Phenocrysts: olivine (0.2–0.8 mm, 5%) crystals are idiomorphic, tabular to diamond-like in shape. Small prismatic quench crystals of olivine are present. Groundmass is hyaline-subvariolitic texture; poorly crystallized volcanic glass with very small needle-shaped laths of plagioclase, hardly visible crystals of clinopyroxene, and opaque dust.

Alteration: strong (50%–60%); volcanic glass is replaced with green smectite and Fe hydroxides (through patches); olivine is replaced with green clay minerals and occasionally with calcite, olivine pseudomorphs are surrounded by a thin rim of opaque minerals, the latter fill veins in olivine.

XRD: smectite and swelling chlorite; trace hydromica.

Electron micrograph: b = 9.22 Å (trioctahedral smectite).

Sample 124-768C-80R-3, 65–71 cm (Piece 3B), Unit 1 [Z-1359]

Plagioclase-phyric basalt, highly vesicular. Phenocrysts (5%): prismatic grains (0.6–1 mm) of plagioclase. Groundmass (30%) with hyalopilitic texture; needle-shaped laths (0.4–1.5 mm) of plagioclase (10%) and interstitial glass (20%). Central parts of plagioclase contain inclusions of glass. Vesicles (65%, 0.1–0.6 mm) are isometric in shape.

Alteration: very strong (70%); plagioclase phenocrysts completely replaced by carbonate (30%) and clay mineral (70%); vesicles infilled with green clay mineral; calcite is present in central parts of several vesicles.

XRD: smectite; trace calcite and mixed-layer chlorite-smectite mineral.

Sample 124-768C-81R-1, 11–16 cm (Piece 2A), Unit X [Z-663]

Aphyric basalt, with intersertal texture, highly vesicular (60%). Rock: identical to Sample 124-768C-74R-1, 100–104 cm (Z-660).

Alteration: laths of plagioclase completely replaced by albite; central parts of case like laths of plagioclase almost completely replaced by smectites; vesicles completely infilled with smectites.

XRD: smectite; minor mixed-layer chlorite-smectite mineral.

Sample 124-768C-82R-1, 64–69 cm (Piece 6), Unit 1 [Z-1360]

Sparsely olivine-phyric basalt, highly vesicular. Phenocrysts (<5%): oxidized olivine (0.2–0.4 mm). Groundmass with hyalopilitic texture; radial-radiant segregates of needle-shaped case-like laths of plagioclase (5%–7%, labradorite [An_{60}]) and glass (30%) with crystals of dark color mineral and opaque dust. Vesicles demonstrate vary from 0.05 to 0.7 mm.

Alteration: strong (50%); olivine is oxidized; part of vesicles infilled with brownish green glass and other part of vesicles infilled with clay mineral; large vesicular or inclusion (8 mm in diameter) completely infilled with carbonate.

XRD: smectite; trace calcite and hydromica; white matter from veinlet: calcite; trace quartz; dark brown matter from veinlet: smectite with interlayer Ca cation; trace quartz.

Sample 124-768C-82R-2, 10–15 cm (Piece 2B), Unit 1 [Z-664]

Sparsely pyroxene(?)-phyric basalt, highly vesicular. Phenocrysts (5%): grains (0.3–1 mm) of completely altered pyroxene. Groundmass with intersertal texture; black glass and panicle like segregates of microlites and laths of case like altered plagioclase (labradorite [An_{50}]). Vesicles (50%) demonstrate vary from <0.1 to 0.7 mm.

Alteration: very strong (70%); pyroxene completely replaced by smectites, carbonate, and Fe hydroxides; plagioclase almost completely replaced by smectites; vesicles infilled with smectites.

XRD: smectite; trace mixed-layer smectite-swelling chlorite mineral(?).

Sample 124-768C-83R-3, 45–50 cm (Piece 4), Unit 1 [Z-1361]

Sparsely plagioclase-phyric basalt, highly vesicular. Phenocrysts (2%–3%): tabular grains (0.3–0.4 mm) of altered plagioclase. Groundmass (35%–40%) with hyalopilitic texture; dark brown glass with sparse crystallites of plagioclase. Vesicles (60%): small vesicles (90%, 0.05–0.4 mm) are isometric in shape and infilled with partly altered brownish green glass; vesicles with 0.4–0.6 mm (10%) are isometric in shape.

Alteration: moderate (~20%–25%); plagioclase phenocrysts completely replaced by greenish clay mineral; glass from vesicles partly (10%) replaced by clay mineral; vesicles with 0.4–0.6 mm completely infilled with clay mineral.

XRD: smectite; trace calcite and defective chlorite(?).

Sample 124-768C-84R-2, 84–87 cm (Piece 2A), Unit 1 [Z-665]

Rock completely replaced by smectites and chlorite.

XRD: smectite; trace mixed-layer smectite-swelling chlorite mineral.

Sample 124-768C-87R-1, 109–112 cm (Piece 5J), Unit 1 [Z-1362]

Aphyric basalt, vesicular. Rocks with pilotaxitic texture; microlites of plagioclase (25%, 0.2–0.4 mm, labradorite [An_{60}]) with glass in central parts. Interstices infilled with small grains (up to 0.1 mm) of clinopyroxene (15%) and brown glass (15%) with crystals of clinopyroxene and opaque minerals. Vesicles (45%) are isometric in shape.

Alteration: moderate (45%); vesicles are encrusted or completely infilled with clay mineral.

XRD: smectite with ~5% mica layers; trace mixed-layer smectite-swelling chlorite mineral.

Sample 124-768C-88R-1, 23–27 cm (Piece 1B), Unit 1 [Z-1363]

Aphyric basalt, vesicular. Rocks with vitrophyric texture; light greenish gray glass (40%) with sparse needle-shaped crystals of plagioclase. Vesicles (60%) are isometric in shape and demonstrate vary from 0.01 to 0.3 mm, vesicles infilled with green glass.

Alteration: slight (5%); glass from vesicles partly (5%) replaced by clay mineral.

XRD: smectite; trace calcite and chlorite.

Sample 124-768C-88R-2, 124–126 cm (Piece 7B), Unit 2 [Z-125]

Olivine-phyric basalt (dolerite?), fine grained, inequigranular, incompletely crystallized. Rock is subvariolitic (occasionally intersertal) texture; an segregate of radially oriented elongated (1:10 or 1:15) crystals of clinopyroxene (~30%) and laths of plagioclase (~45%). Isometric tabular crystals of pyroxene, angular through isometric grains of opaque minerals (8%–10%), and single idiomorphic crystals of olivine (up to 0.5 mm). Interstitial glass (10%–15%). Single vesicles (up to 0.7 mm).

Alteration: moderate (30%); Fe hydroxides partly replace of opaque minerals; volcanic glass, olivine, and partly plagioclase are replaced with green smectite; vesicles are filled by green smectites; xenomorphic grains of quartz and carbonate are present also.

XRD: smectite and swelling chlorite; trace chlorite.

Electron micrograph: b = 9.26 Å (trioctahedral smectite).

Sample 124-768C-89R-1, 69–70 cm (Piece 3B), Unit 2 [Z-1364]

Aphyric dolerite, fine grained. Rocks with intersertal-ophitic texture; tabular and prismatic grains of plagioclase (55%, 0.2–1 mm, labradorite [An_{60}]). Interstices: xenomorphic clinopyroxene grains (25%) and greenish brown glass (15%). Occasionally, glass almost completely crystallized with formation of orthoclase, albite, tridymite, quartz, and single grains of carbonate (total of these minerals is ~1%–2%). Opaque minerals (5%) is present.

Alteration: slight (10%–12%).

XRD: smectite; trace chlorite (~10% swelling interlayers) and hydromica (~10% swelling interlayers); blue and yellow matter from vesicles: smectite, hydromica (~5%–10% swelling interlayers), swelling chlorite, mixed-layer swelling chlorite-smectite mineral, and lomontite.

Sample 124-768C-89R-2, 82–86 cm (Piece 4B), Unit 2 [Z-666]

Clinopyroxene-plagioclase-phyric basalt, massive. Phenocrysts (10%): rounded grains of plagioclase (0.7–0.8 mm) with undulatory extinction and single phenocryst (1 mm) of altered clinopyroxene. Groundmass with doleritic-intersertal texture; rounded and short- and elongated-prismatic grains (0.2–0.7 mm) of plagioclase (labradorite [An_{63}]). Large laths (0.5–0.7 mm) have small inclusions of altered glass. Interstices consist of segregate of clinopyroxene grains (up to 0.2 mm), opaque minerals (7%–8%), and secondary minerals.

Alteration: slight to moderate (~20%); plagioclase phenocryst completely replaced by clay mineral and opacite; inclusions of glass in plagioclase replaced by clay mineral; clay mineral and uralite replace interstitial clinopyroxene.

XRD: smectite, swelling chlorite(?).

Sample 124-768C-89R-3, 74–76 cm (Piece 4), Unit 2 [Z-667]

Aphyric dolerite, medium grained, massive. Rocks with intersertal-doleritic texture; prismatic grains of plagioclase (0.5–0.7 mm, labradorite [An_{55}]). Interstices consist of xenomorphic clinopyroxene grains (0.2–0.6 mm), opaque minerals (2%–3%), and brown glass (20%). Occasionally, glass almost completely crystallized with formation of orthoclase, albite, tridymite, quartz, and single grains of carbonate (total of these minerals is ~1%–2%). Opaque minerals (5%) is present.

Alteration: slight (5%); plagioclase partly replaced by albite and sosurite; interstitial glass partly replaced by clay mineral.

XRD: smectite; trace chlorite and amphibole.

Sample 124-768C-89R-4, 83–87 cm (Piece 3A), Unit 2 [Z-1365]

Aphyric dolerite is intersertal-ophitic texture. Rock: identical to Sample 124-768C-89R-1, 69–70 cm (Z-1364).

Alteration: slight (3%–4%); interstitial glass partly replaced by clay mineral.

XRD: smectite and corrensite-like mineral; trace amphibole(?); gray-yellow spots in rock: smectite with ~10% mica layers and mixed-layer chlorite-smectite mineral (~30%–40% chlorite layers); trace quartz.

Sample 124-768C-90R-1, 16–18 cm (Piece 1A), Unit 2 [Z-126]

Olivine dolerite, medium grained, inequigranular, almost completely crystallized. Rock is intersertal-ophitic texture; laths of plagioclase (50%), clinopyroxene (40%), olivine (up to 2–3 mm, 1%–3%), and opaque minerals (1%). Plagioclase; elongated tabular laths-like idiomorphic crystals as long as 0.8–1.5 mm (elongation is 1:3–1:5). Clinopyroxene; hypidiomorphic tabular and elongated-tabular crystals (0.3–0.7 mm). Interstitial glass (5%) is present.

Alteration: slight (~10%–15%); volcanic glass, olivine, and partly plagioclase are replaced with green smectite; single vesicles are filled with green smectites.

XRD: smectite and swelling chlorite; trace chlorite and corrensite-like mineral or corrensite(?).

Sample 124-768C-90R-6, 58–62 cm (Piece 1B), Unit 2 [Z-668]

Aphyric dolerite, medium grained, massive. Rock with intersertal-doleritic texture; prismatic (0.2–0.5 mm) and laths like grains of zonal plagioclase (0.2–2 mm, labradorite [An_{55}]). Plagioclases content inclusions of glass. Interstices: xenomorphic clinopyroxene grains (0.3–0.5 mm), opaque minerals (5%–6%), and chlorite (10%).

Alteration: slight.

Sample 124-768C-90R-7, 98–103 cm (Piece 5), Unit 2 [Z-1366]

Aphyric dolerite with intersertal-ophitic texture. Rock: identical to Samples 124-768C-89R-1, 69–70 cm (Z-1364), and 89R-4, 83–87 cm (Z-1365).

Alteration: slight (7%–8%); interstitial glass partly replaced by clay mineral.

Sample 124-768C-91R-1, 55–57 cm (Piece 1C), Unit 2 [Z-127]

Olivine dolerite, medium grained, equigranular, almost completely crystallized. Rock is intergranular-ophitic texture; plagioclase (55%), clinopyroxene (35%), olivine (~1%), opaque minerals (0.01–0.4 mm, 5%–7%), and interstitial glass (3%–5%). Plagioclase; tabular lath-like idiomorphic and hypidiomorphic, often zonal, crystals 0.05–1.5 mm in length (elongation 1:1–1:5). Clinopyroxene; hypidiomorphic diamond-like tabular crystals (0.03–1 mm).

Alteration: slight (~10%–15%); volcanic glass, olivine, and partly plagioclase are replaced with smectite and smectite-chlorite aggregate; actinolite is probably present.

XRD: smectite and swelling chlorite; trace chlorite and corrensite-like mineral or corrensite.

Electron micrograph: b = 9.30 Å (trioctahedral chlorite?).

Sample 124-768C-92R-1, 54–56 cm (Piece 4A), Unit 3 [Z-128]

Olivine dolerite (microgabbro?), medium grained, inequigranular, almost completely crystallized. Rock is hypidiomorphic-granular texture; plagioclase (0.03–1.5 mm, 45%), clinopyroxene (0.05–0.5 mm, 35%), olivine (0.5–1 mm, 15%), opaque minerals (1%), and interstitial glass (1%–5%). Biotite occurs in trace amounts. Plagioclase; hypidiomorphic elongated-tabular crystals, sparsely by laths. Clinopyroxene; rounded-tabular crystals. Olivine; hypidiomorphic rounded to diamond-shaped and rounded-tabular crystals.

Alteration: moderate (~25%); volcanic glass, olivine, and partly plagioclase are replaced with smectite and smectite-chlorite aggregate; biotite is replaced with chlorite.

XRD: smectite; trace chlorite, talc, and hydromica.

Electron micrograph: b = 9.23 Å (trioctahedral smectite).

Sample 124-768C-92R-2, 95–100 cm (Piece 1H), Unit 3 [Z-1367]

Olivine-clinopyroxene-plagioclase gabbro. Rock with gabbroid texture; rounded-partly idiomorphic grains (0.4–0.7 mm) of partly oxidized (3%) and carbonatized (7% of grain volume) olivine (5%–6%), xenomorphic grains (0.4–1.2 mm) of clinopyroxene (45%), short-prismatic and xenomorphic tabular grains of plagioclase (40%), opaque minerals (10%), and spotty areas of clay mineral which replaces interstitial glass.

Alteration: slight (10%–12%).

XRD: smectite and chlorite with ~10% swelling interlayers; trace talc.

Sample 124-768C-92R-3, 108–111 cm (Piece 1E), Unit 3 [Z-1368]

Olivine-pyroxene-plagioclase gabbro-dolerite, tectonized. Rock with gabbroid texture; idiomorphic grains of oxidized olivine (1%–2%), xenomorphic grains of clinopyroxene (30%), prismatic grains of plagioclase (40%), opaque minerals (10%), and clay mineral (10%). Rock consists of three fragments (2–2.5 mm) of partly oxidized and completely chloritized vesicular basalt.

Alteration: slight (10%).

XRD: smectite and chlorite with ~10% swelling interlayers; trace mixed-layer smectite-swelling chlorite(?), talc, and amphibole(?).

Sample 124-768C-92R-3, 111–115 cm (Piece 1E), Unit 3 [Z-669]

Aphyric dolerite, massive. Rock with doleritic-intersertal texture; prismatic (0.2–1 mm) grains of plagioclase (labradorite [An_{55}]) with undulatory extinction. Interstices consist of xenomorphic clinopyroxene grains (0.3–0.5 mm) and opaque minerals (7%–8%).

Alteration: moderate (~40%); rock is chloritized.

XRD: mixed-layer smectite-chlorite mineral (~10% swelling interlayers) and smectite.

Sample 124-768C-92R-4, 0–5 cm (Piece 1), Unit 3 [Z-1369]

Olivine-pyroxene-plagioclase gabbro. Rock with gabbroid texture; olivine (5%), clinopyroxene (35%), plagioclase (40%), opaque minerals (10%), and chlorite (10%). Biotite is present (2%–3%).

Alteration: slight (10%–15%); olivine almost completely is oxidized and partly (3%–5%) replaced by chlorite; chlorite partly replaces all minerals.

XRD: smectite and chlorite with ~10% swelling interlayers; trace talc; white veinlet: calcite.

Sample 124-768C-93R-1, 40–42 cm (Piece 2B), Unit 3 [Z-129]

Olivine twopyroxene microgabbro, medium grained, equigranular, tectonized, hypidiomorphic-granular texture. Rock; plagioclase (45%), clinopyroxene (30%), olivine (10%), orthopyroxene (3%–5%), basaltic (brownish) hornblende (<1%), opaque minerals (5%–7%), and trace biotite. All minerals are highly fissured and partly or completely (e.g. Olivine) are replaced with secondary minerals. Minerals vary from 0.05 through 1 mm.

Alteration: strong (50%); olivine and partly plagioclase and pyroxenes are replaced with clay minerals; hornblende and biotite are replaced with chlorite; opaque minerals are oxidized and replaced with Fe hydroxides.

XRD: swelling chlorite; trace chlorite and talc.

Electron micrograph: b = 9.26 Å (trioctahedral mineral).

Sample 124-768C-93R-2, 10–14 cm (Piece 2C), Unit 3 [Z-670]

Aphyric dolerite, medium grained, with ophitic-intersertal texture, massive. Rock: identical to Sample 124-768C-92R-3, 111–115 cm (Z-669).

Alteration: moderate (~40%).

XRD: smectite and swelling chlorite; trace chlorite and talc.

Sample 124-768C-93R-3, 113–117 cm (Piece 2F), Unit 3 [Z-671]

Aphyric dolerite, with ophitic-intersertal texture, massive. Rock: identical to Samples 124-768C-92R-3, 111–115 cm (Z-669), and 93R-2, 10–14 cm (Z-670).

Alteration: very strong (70%); rock is chloritized.

XRD: smectite and swelling chlorite; trace chlorite, talc, and calcite.

Sample 124-768C-93R-4, 27–29 cm (Piece 3C), Unit 3 [Z-130]

Olivine microgabbro, highly tectonized.

Alteration: very strong (80%–90%).

XRD: smectite; trace chlorite and talc.

Electron micrograph: b = 9.26 Å (trioctahedral smectite and chlorite).

Sample 124-768C-95R-1, 89–91 cm (Piece 8), Unit 4 [Z-131]

Olivine hyalobasalt, fine grained, highly vesicular (0.03–0.7 mm, ~50%). Rock; devitrified volcanic glass with rare microphenocrysts of olivine (0.07–0.2 mm, 1%–5%). Very small laths of plagioclase form poorly expressed subvariolitic texture. Glass contains crystallites of pyroxene and opaque dust.

Alteration: strong (50%); volcanic glass and olivine are replaced with green smectites; vesicles and hair-thin cracks are filled with green smectites.

XRD: smectite.

Electron micrograph: b = 9.27 Å (trioctahedral smectite).

Sample 124-768C-96R-1, 108–111 cm (Piece 9A), Unit 4 [Z-1370]

Olivine-plagioclase-phyric basalt, vesicular. Phenocrysts (25%): idiomorphic grains (0.2–0.6 mm) of fresh olivine (8%); prismatic grains (0.2–2 mm) of plagioclase and their glomerophyric segregates (17%). Composition of

plagioclase-labradorite spar [An_{62-64}]. Groundmass (35%); from light cream to brown glass. Vesicles (40%, 0.1–0.7 mm) are rounded and oval in shape. Small vesicles (10%) completely infilled with green glass, the rest of vesicles (30%) are encrusted by green glass.

Alteration: rock is fresh.

XRD: mixed-layer chlorite-smectite mineral.

Sample 124-768C-96R-2, 0–5 cm (Piece 1A), Unit 4 [Z-1371]

Sparsely olivine-phyric basalt, vesicular. Phenocrysts (3%–4%): idiomorphic grains (0.4–0.5 mm) of olivine. Groundmass (50%) with hyalopilitic texture; almost colorless glass (15%), needle-shaped laths (up to 1.5 mm) of plagioclase (15%, oligoclase [An_{21}]), and microlites of clinopyroxene (20%). Vesicles (45%, 0.1–1.2 mm) are isometric in shape.

Alteration: moderate (35%); olivine is oxidized and replaced by chalcedony; vesicles are empty (20%) or infilled with opal (15%) and tridymite (10%).

XRD: analcime and mixed-layer chlorite-smectite mineral.

Sample 124-768C-97R-2, 9–13 cm (Piece 1B), Unit 4 [Z-672]

Sparsely olivine-phyric basalt, vesicular. Phenocrysts (2%–3%): grains (0.5 mm) of completely altered dark color mineral (olivine). Groundmass with pilotaxitic texture; needle-shaped microlites and microlaths of plagioclase; segregate of small grains clinopyroxene; opaque minerals (~10%); black glass. Vesicles (50%, 0.2–0.5 mm) demonstrate isometric in shape.

Alteration: strong (50%); olivine completely replaced by clay mineral and carbonate; vesicles infilled with clay minerals; central parts in sparse vesicles are filled with carbonate.

XRD: smectite; trace analcime.

Sample 124-768C-97R-3, 9–13 cm (Piece 2), Unit 4 [Z-1372]

Glassy crust of sparsely olivine-phyric basalt. Phenocrysts (2%–3%): by idiomorphic grains (up to 0.5 mm) of olivine. Groundmass with vitrophyric texture; glass (from light brown to black in color).

Alteration: slight; olivine completely replaced by Fe hydroxides and partly replaced by opal; needle-shaped aggregate of secondary minerals is located along thin cracks in glassy crust.

XRD: analcime and amphibole; minor smectite.

Sample 124-768C-97R-3, 89–94 cm (Piece 7A), Unit 4 [Z-673]

Aphyric basalt (dolerite?), vesicular. Rocks with intersertal-doleritic texture; prismatic and laths (0.3–1.2 mm) of plagioclase (labradorite [An_{60}]). Often plagioclase grains content inclusions of glass. Interstices: radial-radiant and panicle like segregates of needle-shaped grains of clinopyroxene; glass. Vesicles (25%–30%, 0.2–0.5 mm) are isometric in shape.

Alteration: plagioclase replaced by sosurite; glass partly replaced by brownish green smectites and chlorite; vesicles completely infilled with smectites.

XRD: smectite; trace analcime(?).

Sample 124-768C-98R-2, 60–65 cm (Piece 2C), Unit 5 [Z-1373]

Aphyric basalt, spotty structure, highly vesicular. Rocks with hyalopilitic texture; needle-shaped microlites of plagioclase (10%, andesine [An_{33}] and oligoclase [An_{18}]), grains of clinopyroxene (20%), and glass (from light green to brown in color). Vesicles (50%, 0.1–0.7 mm) are isometric and oval in shape. Vesicles (10%, 0.1–0.2 mm) are encrusted by light green glass.

Alteration: slight; occasionally vesicles infilled with tridymite and quartz.

XRD: analcime and corrensite-like mineral; trace chlorite and calcite.

Sample 124-768C-98R-3, 77–79 cm (Piece 3B), Unit 5 [Z-132]

Olivine-microphyric basalt, fine grained, highly vesicular (35%), intergranular texture. Microphenocrysts of olivine (0.5 mm, ~1%). Laths of plagioclase (35%) form “honeycomb” texture of rock. Central parts of honeycomb are occupied by vesicles (0.2–0.4 mm), surrounded by segregates of xenomorphic clinopyroxene (25%) with small grains of opaque minerals. Hypidiomorphic crystals of olivine (up to 1–1.3 mm) are present.

Alteration: strong; secondary minerals replace olivine and interstitial glass; vesicles are filled with green clay mineral, occasionally with an admixture of zeolites; central parts of some vesicles are filled with chalcedony.

XRD: analcime and corrensite(?).

Electron micrograph: b = 9.22 Å (trioctahedral mineral).

Sample 124-768C-98R-4, 0–5 cm (Piece 1A), Unit 5 [Z-1374]

Aphyric basalt, highly vesicular. Rock with hyalopilitic texture; glass (5%), needle-shaped microlites of plagioclase (15%, oligoclase [An_{18}]), and grains of clinopyroxene (30%). Vesicles (50%, 0.1–2.5 mm) are isometric in shape. Small vesicles (0.1–0.3 mm, 25%) partly or completely infilled with light green glass. Vesicles with 0.4–0.7 mm are empty (10%) or infilled with zeolite (5%) or quartz (chalcedony?) 5%. Large vesicles (1.2–2.5 mm, 5%) completely infilled with carbonate.

Alteration: slight.

XRD: corrensite-like mineral; minor calcite and analcime.

Sample 124-768C-92R-2, 16–21 cm (Piece 1D), Unit 6 [Z-1375]

Sparsely olivine-phyric basalt, highly vesicular. Phenocrysts (1%–2%): grains of olivine. Groundmass (49%) with hyalopilitic texture; brown glass with needle-shaped microlites of plagioclase (10%, oligoclase [$An_{20–24}$]) and microlites of clinopyroxene (25%). Vesicles (50%, 0.1–0.4 mm) are isometric in shape and completely infilled with green glass.

Alteration: moderate (30%); 30% of vesicles glass replaced by smectites.

XRD: smectite; trace calcite, mixed-layer smectite-swelling chlorite mineral, and amphibole(?).

Sample 124-768C-99R-3, 106–109 cm (Piece 4C), Unit 6 [Z-1376]

Sparsely olivine-phyric basalt, highly vesicular. Phenocrysts (2%–3%): xenomorphic grains (0.3–0.5 mm) of olivine. Groundmass (49%) with hyalopilitic texture; radial-radiant needle-shaped microlites of plagioclase (5%) and brownish black glass (30%). Vesicles (65%, 0.05–0.8 mm) are isometric in shape. Several vesicles (20%) infilled with smectitized glass.

Alteration: moderate (30%); smectites replace glass from several vesicles.

XRD: smectite; trace calcite.

Sample 124-768C-99R-4, 46–52 cm (Piece 3), Unit 6 [Z-1377]

Sparsely olivine-phyric basalt, highly vesicular. Phenocrysts: single (<1%) grains of olivine. Groundmass with vitrophyric texture; glass (20%) with sparse panicle like crystals of plagioclase and grains of clinopyroxene. Vesicles (80%, 0.01–0.4 mm) infilled with green glass.

Alteration: moderate (30%); olivine is oxidized; vesicles with sizes >0.2 mm (15%) are filled with smectites.

XRD: smectite; trace calcite and hydromica with ~10%–15% swelling interlayers; white veinlet: calcite.

Sample 124-768C-100R-1, 32–36 cm (Piece 3B), Unit 7 [Z-1378]

Aphyric basalt, vesicular. Rock with vitrophyric texture; black glass (70%) with sparse panicle like crystals of plagioclase. Vesicles (30%) demonstrate vary from 0.01 to 1.7 mm.

Alteration: moderate (30%); vesicles are filled with smectites.

XRD: smectite; trace calcite, swelling chlorite, and mixed-layer smectite-swelling chlorite mineral.

Sample 124-768C-100R-2, 13–19 cm (Piece 2), Unit 7 [Z-1379]

Aphyric basalt, vesicular. Rocks with microlitic texture; microlites and microlaths of plagioclase (30%, oligoclase [An_{24}] and albite), small (0.1–0.4 mm) isometric grains of clinopyroxene (30%), black glass, and opaque minerals. Vesicles (30%, 0.1–0.6 mm) are isometric and rounded in shape.

Alteration: moderate (30%); vesicles completely infilled with smectites or encrusted by smectites.

XRD: smectite; trace corrensite-like mineral, swelling chlorite, hydromica, and calcite.

Celebes Basin (Hole 770C)

Sample 124-770C-2R-3, 23–25 cm (Piece 2), Unit 1 [Z-133]

Sparsely micro-plagioclase-phyric olivine hyalobasalt, fine grained, massive. Microphenocrysts of plagioclase (0.3–0.8 mm, <1%) and hypidiomorphic crystals of olivine (up to 0.3 mm) are present. Groundmass: subvariolitic segregate of radially oriented crystals of plagioclase; crystals of pyroxene with admixture of opaque dust.

Alteration: slight (~10%–15%); volcanic glass and olivine is replaced with green smectite; cracks are filled with oxidized opaque minerals.

XRD: smectite.

Electron micrograph: b = 9.21 Å (trioctahedral smectite).

Sample 124-770C-3R-3, 36–38 cm (Piece 4B), Unit 1 [Z-134]

Sparsely micro-plagioclase-phyric olivine basalt, fine grained, inequigranular, incompletely crystallized. Microphenocrysts of plagioclase (0.3–1 mm, <5%). Hypidiomorphic crystals of olivine (0.2–0.8 mm, <1%) are presented. Groundmass; laths of plagioclase (50%) and fine grained aggregate of clinopyroxene (40%) with opaque dust. Interstitial glass (5%–7%). Texture of rock is subvariolitic-honeycomb.

Alteration: slight (10%); volcanic glass and olivine is replaced with green smectites.

XRD: smectite with interlayer Na-K and Ca-Mg cations.

Sample 124-770C-3R-4, 55–60 cm (Piece 6), Unit 1 [Z-1380]

Plagioclase-phyric basalt. Phenocrysts (10%): tabular grains (0.7–1.8 mm) of plagioclase (labradorite [An_{58}]). Groundmass (90%) with hyalopilitic to pilotaxitic texture; needle-shaped microlites and laths (up to 2 mm) of plagioclase (40%, andesine [An_{44}] and [An_{32}]), black glass (50%) with sparse segregates of small idiomorphic grains (0.1–0.3 mm) of olivine (2%–3%). Opaque minerals (1%–2%) are present.

Alteration: slight (2%–3%); olivine completely replaced by iddingsite and boulingite.

Sample 124-770C-4R-1, 17–19 cm (Piece 3A), Unit 2 [Z-135]

Plagioclase-phyric olivine hyalobasalt, sparsely vesicular. Phenocrysts of plagioclase (0.5–3 mm, 20%) and olivine (0.2–1 mm, 1%). Groundmass is subvariolitic texture; devitrified brown-black volcanic glass with needle-shaped laths of plagioclase, crystals of pyroxene, and opaque dust.

Alteration: slight (~5%); volcanic glass and olivine is replaced with green smectite; single vesicles are filled with smectites; opaque dust is oxidized.

XRD: smectite; trace chlorite.

Electron micrograph: b = 9.34 Å.

Sample 124-770C-4R-2, 134–140 cm (Piece 12E), Unit 2 [Z-1381-1]

Breccia: single fragment (2 mm) of aphyric basalt with hyalopilitic texture and small (0.7–0.9 mm) angular fragments of green volcanic glass. Matrix consists of carbonate and clay. Breccia is covered with Fe-Mn crust.

Sample 124-770C-4R-2, 134–140 cm (Piece 12E), Unit 2 [Z-1381-2]

Plagioclase-phyric basalt, sparsely vesicular. Phenocrysts (10%): prismatic grains (0.2–1.5 mm) of plagioclase (andesine [An_{46}]). Plagioclase grains content inclusions of glass. Groundmass (90%) with vitrophyric texture; brownish black glass (85%–87%) with sparse needle-shaped crystals of plagioclase. Vesicles (2%–3%, 0.1–0.2 mm) are rounded in shape.

Alteration: slight (10%); glass from plagioclase grains replaced by smectites, vesicles infilled with smectites.

Sample 124-770C-4R-3, 23–27 cm (Piece 3), Unit 2 [Z-674]

Plagioclase-phyric basalt, sparsely vesicular. Phenocrysts (20%–25%): elongated-prismatic grains (0.3–1 mm, labradorite [An_{55}] and 1–2.5 mm, labradorite [An_{68}]) of plagioclase. Phenocrysts with 0.3–1 mm, often they content glass. Groundmass with hyalopilitic texture; needle-shaped microlites and microlaths of plagioclase (labradorite [An_{52}]) and brownish black glass with rudimentary panicle like crystals of clinopyroxene. Vesicles (2%–3%, 0.1 mm) are present.

Alteration: slight; vesicles are filled with clay mineral.

Sample 124-770C-4R-3, 86–88 cm (Piece 9A), Unit 2 [Z-136]

Plagioclase-phyric olivine basalt, sparsely vesicular. Phenocrysts of plagioclase (0.5–1.5 mm, 15%–20%) and olivine (0.5–3 mm, <1%). Groundmass is subvariolitic-intersertal texture; devitrified volcanic glass with laths of plagioclase (40%–50%), crystals of pyroxene, and opaque dust. Rare and small vesicles are filled with black volcanic glass or smectites.

Alteration: slight (~10%–15%); volcanic glass and olivine is replaced with smectites, besides, olivine is replaced with limonite(?); carbonate is present.

XRD: Fe smectite.

Electron micrograph: b = 9.15 Å (dioctahedral smectite).

Sample 124-770C-5R-2, 11–13 cm (Piece 1A), Unit 3 [Z-137]

Plagioclase-phyric olivine basalt, fine-medium grained, sparsely vesicular. Phenocrysts of plagioclase (0.5–0.8 mm, 15%–20%) and olivine (0.3–0.8 up to 1.5 mm, 1%–3%). Groundmass is intergranular texture; laths of plagioclase (50%), crystals of clinopyroxene (40%–50%), small amounts of olivine, and opaque minerals. Vesicles are sparsely (<1%).

Alteration: slight to moderate (15%–20%); olivine is replaced with smectites and Fe hydroxides; vesicles are filled with smectites and Fe hydroxides.

XRD: Fe smectite; trace chlorite and talc(?).

Electron micrograph: b = 9.14 Å (smectite).

Sample 124-770C-5R-3, 89–91 cm (Piece 3B), Unit 3 [Z-138]

Plagioclase-phyric olivine basalt, fine-medium grained, sparsely vesicular (3%–5%). Phenocrysts of plagioclase (1–3 mm, 0.5–0.8 mm, 15%) and olivine (0.3–1 mm, 1%–3%). Groundmass is intergranular texture; laths of plagioclase (50%), crystals of clinopyroxene (45%), small amounts of olivine (<1%), interstitial volcanic glass (<1%), and opaque minerals (1%–3%).

Alteration: slight (~10%); olivine and interstitial glass are replaced with smectites and Fe hydroxides; vesicles are filled with smectites.

XRD: smectite; trace chlorite.

Electron micrograph: b = 9.30 Å (trioctahedral mineral [chlorite?]).

Sample 124-770C-5R-5, 34–38 cm (Piece 2), Unit 3 [Z-675]

Plagioclase-phyric basalt, medium grained, vesicular. Phenocrysts (10%): prismatic grains (1.2–4 mm, labradorite [An_{60}]) of plagioclase. Occasionally, grains of plagioclase consist of glass. Groundmass s doleritic texture; unoriented laths (0.3–1.2 mm) plagioclase (labradorite [An_{58}]), segregate of grains (0.2–0.3 mm up to 0.8 mm) of clinopyroxene (often with laths of plagioclase), and opaque minerals (5%). Vesicles (8%–10%, 1–1.5 mm) are rounded in shape.

Alteration: slight; vesicles are filled with Fe hydroxides and carbonate.

Sample 124-770C-5R-6, 67–72 cm (Piece 4A), Unit 3 [Z-1383]

Aphyric basalt, fine grained, sparsely vesicular, brecciated. Rock with intersertal-doleritic texture; prismatic (up to 2 mm) and tabular (0.2–0.7 mm) grains of plagioclase (35%, labradorite [An_{55}]), segregate of grains of clinopyroxene (45%), segregate of small (0.2–0.4 mm) idiomorphic grains of olivine, and glass (5%) with microlites of opaque minerals. Vesicles (5%, 0.8–1.2 mm) are present.

Alteration: moderate (35%–40%); olivine is oxidized; part of plagioclase grains replaced by aggregate of smectites and quartz, vesicles are filled with carbonate and clay minerals, single vesicle is filled with tridymite and tremolite(?); cracks of brecciated basalt infilled with carbonate.

Sample 124-770C-5R-6, 106–108 cm (Piece 5), Unit 3 [Z-139]

Olivine-plagioclase-phyric basalt, vesicular (<2 mm, ~5%). Phenocrysts of plagioclase (0.8–2.5 mm, 10%–15%) and olivine (0.3–0.7 mm, 3%–5%). Groundmass is intergranular texture; segregate of plagioclase and clinopyroxene and admixture of olivine and opaque minerals.

Alteration: slight (~10%); olivine and interstitial glass are replaced with smectites; Fe hydroxides replace of opaque minerals.

XRD: smectite; trace chlorite.

Electron micrograph: b = 9.17 Å (trioctahedral? smectite).

Sample 124-770C-6R-1, 67–71 cm (Piece 1D), Unit 4 [Z-676]

Plagioclase-phyric basalt, sparsely vesicular. Phenocrysts (15%): glomerophyric segregates of prismatic and tabular grains (0.8–3 mm) of plagioclase (labradorite [An_{62}]). Groundmass with microlitic texture; unoriented laths (0.3–0.8 mm) of plagioclase (labradorite [An_{56}]), segregate of small grains of clinopyroxene, and brown glass. Single vesicles (1%–2%, 0.3–0.6 mm) are rounded in shape and infilled with glass.

Alteration: slight; glass replaced by palagonite; several vesicles are filled with palagonite.

Sample 124-770C-6R-1, 73–77 cm (Piece 1D), Unit 4 [Z-140]

Plagioclase-phyric basalt, vesicular. Phenocrysts of plagioclase (0.3–2 mm, 5%). Groundmass is intersertal-microlitic texture; black devitrified glass with laths of plagioclase and their quench crystals, crystals of clinopyroxene, and opaque dust. Vesicles (0.3–0.7 mm, 10%–15%) are partly or completely filled with devitrified volcanic glass, occasionally with carbonate.

Alteration: slight (~5%).

XRD: smectite.

Electron micrograph: b = 9.21 Å (trioctahedral smectite).

Sample 124-770C-6R-1, 79–85 cm (Piece 2A), Unit 4 [Z-1384]

Olivine-plagioclase-phyric basalt, vesicular. Phenocrysts (30%): large prismatic grains (up to 4 mm, labradorite [An_{60}]) of plagioclase and glomerophyric segregates of smaller prismatic grains (andesine [An_{43}]) and small (up to 0.6 mm) idiomorphic grains of olivine. Groundmass with hyalopilitic texture; needle-shaped microlites and laths of plagioclase (10%) and brown glass (40%–45%) with crystals of clinopyroxene. Vesicles (10%, 0.7–1.2 mm) are rounded in shape. Half of vesicles infilled with black color to brownish red glass.

Alteration: slight (~5%–10%); plagioclase partly (5%–10%) replaced by albite; olivine is oxidized (occasionally, olivine completely replaced by carbonate); half of vesicles infilled with carbonate and Fe hydroxides; crack (0.8 mm in thickness) infilled by Fe hydroxides, smectites, zeolite, and carbonate.

Sample 124-770C-6R-4, 96–98 cm (Piece 6A), Unit 4 [Z-141]

Plagioclase-phyric basalt, vesicular. Phenocrysts of plagioclase (1–2.5 mm, 5%–7%). Groundmass is intersertal-subvariolitic texture; fine grained aggregate of clinopyroxene, laths of plagioclase, opaque dust, and small single grains of olivine. Vesicles (0.2–1 mm, 1%–3%) are empty or filled with calcite and smectites.

Alteration: slight (~5%); olivine is replaced by smectites and carbonate.

XRD: smectite.

Electron micrograph: b = 9.25 Å (trioctahedral smectite).

Sample 124-770C-7R-1, 93–100 cm (Piece 9A), Unit 4 [Z-1385]

Olivine-plagioclase-phyric basalt, crystallized, vesicular. Phenocrysts (20%): prismatic grains (0.5–2.5 mm, labradorite [An_{62}] and andesine [An_{45}]) of plagioclase (18%) with inclusions of glass; glomerophyric segregates of smaller prismatic grains of plagioclase (andesine [An_{43}]) and small (up to 0.5 mm) grains of olivine. Groundmass (70%) with microlitic texture; microlites and laths of plagioclase (35%, andesine [An_{38}]), microlites of clinopyroxene (30%), and opaque minerals (5%). Vesicles (10%, 0.8–1 mm) are rounded in shape. Vesicles are encrusted with green to black glass. Occasionally, vesicles (2%) are empty.

Alteration: olivine is oxidized; there are vesicles (8%) infilled with carbonate.

Sample 124-770C-7R-1, 107–112 cm (Piece 9B), Unit 4 [Z-1386]

Olivine-plagioclase-phyric basalt, crystallized, groundmass with microlitic texture, vesicular. Rock: identical to Sample 124-770C-7R-1, 93–100 cm (Z-1385).

Sample 124-770C-7R-3, 61–63 cm (Piece 2A), Unit 5 [Z-142]

Aphyric basalt, medium grained, almost completely crystallized, vesicular (0.3–0.4 mm, 5%). Groundmass is intergranular (occasionally subvariolitic) texture; laths of plagioclase, clinopyroxene, olivine, devitrified volcanic glass, and opaque minerals.

Alteration: slight (~10%); olivine and interstitial glass are replaced with smectites; vesicles are filled with smectites or carbonate.

XRD: Fe smectite; trace chlorite and hydromica.

Sample 124-770C-9R-2, 53–55 cm (Piece 5B), Unit 6 [Z-143]

Sparsely olivine-plagioclase-phyric basalt, almost completely crystallized, inequigranular, massive. Phenocrysts of plagioclase (1–2 mm, 2%–3%) and olivine (up to 1 mm, <1%). Groundmass is intergranular texture; plagioclase and clinopyroxene, and opaque minerals.

Alteration: slight (~5%).

XRD: smectite; trace goethite(?) and hydromica.

Electron micrograph: b = 9.23 Å (trioctahedral smectite).

Sample 124-770C-10R-2, 110–112 cm (Piece 3D), Unit 7 [Z-144]

Aphyric dolerite, almost completely crystallized, massive.

Alteration: slight ~5%); rock is oxidized in patches.

XRD: Fe smectite with ~10% of mica layer; trace chlorite, hydromica and amphibole(?).

Sample 124-770C-11R-1, 98–100 cm (Piece 7F), Unit 7 [Z-145]

Aphyric basalt, incompletely crystallized, massive. Groundmass; laths of plagioclase, clinopyroxene, small amounts of olivine, interstitial glass (<1%), and opaque minerals.

Alteration: slight (~5%–7%); olivine and interstitial glass are replaced with smectites.

XRD: smectite; trace chlorite, hydromica and amphibole(?).

Electron micrograph: b = 9.20 Å (trioctahedral smectite).

Sample 124-770C-12R-1, 11–13 cm (Piece 1), Unit 8 [Z-146]

Sparsely plagioclase-phyric dolerite, massive. Phenocrysts of plagioclase (up to 1–1.5 mm, 1%–2%). Single phenocrysts of olivine are present. Groundmass is intergranular-subophitic texture; plagioclase, clinopyroxene, opaque minerals, olivine, and small amounts interstitial glass.

Alteration: slight (~3%–5%).

XRD: smectite with ~20% mica layers; trace chlorite, hydromica, and talc(?).

Electron micrograph: b = 9.20 Å (trioctahedral smectite).

Sample 124-770C-12R-2, 79–84 cm (Piece 3C), Unit 8 [Z-1387]

Olivine-plagioclase-phyric dolerite, fine grained. Phenocrysts (30%): grains (up to 1.2 mm) of olivine (5%) and glomerophyric segregates of grains of plagioclase (25%, up to 2.5 mm, labradorite [An_{69}] and [An_{60}] and andesine [An_{48}]). Groundmass (70%) with doleritic texture; laths of plagioclase (35%, andesine [An_{43}]). Interstices consist of glass (3%), opaque minerals (2%), and segregate of small grains of clinopyroxene (25%).

Alteration: olivine completely replaced by carbonate and Fe hydroxides.

Sample 124-770C-12R-3, 140–142 cm (Piece 13), Unit 9 [Z-147]

Plagioclase-phyric basalt, sparsely vesicular. Phenocrysts of plagioclase (0.5–2 mm, 15%–20%) and rare crystals of olivine. Groundmass is intersertal texture; laths of plagioclase, aggregate of clinopyroxene, small amounts of olivine and interstitial glass, and opaque minerals. Vesicles (0.2–0.8 mm, <3%) are empty or filled with smectites.

Alteration: slight (~10%).

XRD: smectite with ~20% mica layers.

Mariana and Izu-Bonin Regions (Leg 125)

Hole 779A

Sample 125-779A-9R-2, 39–41 cm (Piece 4A), Unit 2 [Z-191]

Dunite serpentinized, coarse grained, tectonized. Primary minerals are represented by hypidiomorphic crystals of olivine (2–5 mm, 40%–60%), hypidiomorphic elongated crystals of orthopyroxene (1–3 mm, 1%–3%), and spinel (picotite?) with size 0.05–0.7 mm. Olivine is dissected by cracks in small fragments (0.05–0.4 mm). Cracks in both olivine and orthopyroxene are filled with serpentine.

Alteration: strong (~50%–60%); secondary minerals: serpentine, amphiboles, and Fe hydroxides (hematite?); serpentine replaces most volume of olivine and pyroxene, that is accompanied by transformation of hypidiomorphic texture of dunite to a loop texture; serpentine is presented mostly by chrysotile; sparsely, veins are filled with aggregate of chrysotile and antigorite; amphibole (actinolite) replace serpentinized orthopyroxene; small xenomorphic crystals oxides (hematite?) occur mostly in vein serpentine.

Sample 125-779A-11R-1, 82–86 cm (Piece 11), Unit 2 [Z-677]

Harzburgite serpentinized. Rock; olivine (80%), orthopyroxene (20%), and idiomorphic grains (0.5–1 mm) black spinel (1%).

Alteration: very strong (90%–95%); olivine completely is serpentinized (from lizardite to clinochrysotile), orthopyroxene partly (70%–80%) replaced by bastite (serpentine), spinel is oxidized.

Sample 125-779A-12R-1, 45–49 cm (Piece 7), Unit 2 [Z-678]

Harzburgite serpentinized; rock is completely altered. Orthopyroxene completely replaced by bastite. Cracks infilled with oxidized antigorite. Grains of hydrogarnet (0.05 mm) are present.

Sample 125-779A-14R-1, 20–22 cm (Piece 1B), Unit 2 [Z-192]

Harzburgite serpentinized, coarse grained, tectonized. Primary minerals are represented by hypidiomorphic crystals of olivine (2–4 mm, 60%–80%), hypidiomorphic elongated-tabular crystals of orthopyroxene (1–4 mm, 20%), and spinel (chrome-picotite?, 1%–3%) with size 0.1–1.1 mm. Olivine is dissected by cracks in small fragments (0.05–0.5 mm). Serpentine fill cracks in olivine and orthopyroxene. Orthopyroxene is distributed irregularly; often, it forms segregates. Some crystals of orthopyroxene contain rounded inclusions of olivine. Spinel is distributed irregularly and often is restricted to accumulations of orthopyroxene. Occasionally spinel contains inclusions of olivine and orthopyroxene. Rock is dissected by a series of cracks filled with serpentines. Texture of rock is hypidiomorphic; most intensively serpentinized areas demonstrate loop texture.

Alteration: slight to moderate (15%–20%); secondary minerals: serpentine, amphiboles, chlorite, and Fe hydroxides (hematite?); serpentine (chrysotile) replaces most volume of olivine and pyroxene and form loop texture; amphibole (actinolite) replaces serpentinized orthopyroxene; Fe oxides (hematite?) as small xenomorphic accumulation occur mostly in vein serpentine and partly in spinel.

XRD: serpentine (antigorite?); reflexes: 5.9C, 3.89C, 3.49C - undetermined mineral.

Electron micrograph: b = 9.30 Å (serpentine).

Electron microscopy: chrysotile is fibrous in shape; some fiber are empty along their axis; chrysotile occur sporadically; the next type of chrysotile is near to Povlen-chrysotile, but has high length/diameter ratio; the polytype of chrysotile is $2O_{rc}$; Povlen-chrysotile (D_c) with irregular structure is present; the length-slight fiber chrysotile is represented two polytypes: $2M_{c1}$ and D_c; morphological type is tube-in-tube; lizardite is represented as polycrystals with unclear complicated edges; antigorite forms pseudomorphs and resides in the degradation stage.

Sample 125-779A-16R-2, 109–111 cm (Piece 11), Unit 2 [Z-193]

Harzburgite serpentinized, coarse grained, tectonized. Primary minerals are represented by hypidiomorphic crystals of olivine (1–3 mm, 50%), hypidiomorphic tabular crystals of orthopyroxene (5–8 mm, 30%), and spinel (picotite?, <1% abundance; 0.05–0.3 mm). Olivine is dissected by cracks into fragments (0.01–0.05 mm). Cracks in both olivine and orthopyroxene are filled with serpentine. Some crystals of orthopyroxene contain small inclusions of olivine and spinel. Spinel is distributed irregularly; often, it is restricted to accumulations of orthopyroxene. Occasionally, spinel contains small inclusions of olivine. Rock is dissected by a series of cracks filled with serpentines.

Alteration: moderate (30%); serpentine (chrysotile, 20%–25%) replace most volume of olivine and pyroxene and fill cracks (up to 0.5 mm) in rock, and form loop texture; occasionally, amphibole (actinolite?) occur along cleavage faces, Fe oxides (hematite?, 0.03–0.07 mm) occur in vein serpentine; spinel is replaced along cracks and from the surface with opaque minerals.

XRD: serpentine; amphibole(?) and talc(?) in trace amounts; reflexes 5.9C, 3.89C, 3.49C -undetermined mineral.

Electron micrograph: b = 9.30 Å (serpentine).

Electron microscopy: chrysotile has length-slight fibrous in shape and occurs in small amount as polytype D_c; few particles of Povlen-chrysotile with polytype $2M_{c1}$ are determined; lizardite is the main serpentine mineral and usually demonstrates chaotically structure; antigorite occur in small amounts and demonstrate chaotically structure.

Sample 125-779A-17R-1, 106–110 cm (Piece 14), Unit 2 [Z-679]

Harzburgite serpentinized, medium grained, tectonized. Primary minerals are represented by isometric grains of olivine, crystals of orthopyroxene (10%), and idiomorphic cubic and xenomorphic grains (up to 1.5 mm) spinel.

Alteration: ~40%; olivine is lizardite (10%), orthopyroxene completely replaced by chlorite and very small grains of magnetite (relicts of bastite are located among aggregate of chlorite); spinel completely is oxidized; microcracks (0.1–1.5 mm) are filled with chrysotile, antigorite, and magnetite.

Sample 125-779A-17R-3, 70–72 cm (Piece 8B), Unit 2 [Z-194]

Harzburgite serpentinized, fine to medium grained, tectonized. Primary minerals are represented by xenomorphic crystals of olivine (up to 2–3 mm, 70%), isometrically rounded crystals of orthopyroxene (2–3 mm, 15%), and opaque minerals (chromite?, <1% abundance; 0.03–0.05 mm). Primary minerals are dissected by cracks in small fragments (0.01–0.03 mm). Cracks in both olivine and orthopyroxene are filled with serpentine. Primary texture of rock is hypidiomorphic, highly serpentinized areas demonstrate loop texture.

Alteration: serpentine (20%) fills cracks in olivine and orthopyroxene, and in cracks (up to 1.5–2 mm) in rock; serpentine; antigorite, in veins: by chrysotile; occasionally, amphibole (actinolite) occur along cleavage faces in orthopyroxene; some crystals of olivine are completely replaced with amphibole (actinolite) and contain small inclusions of opaque minerals (hematite?).

XRD: serpentine; talc(?) in trace amounts; reflexes 5.10C, 3.88C, 3.49C - mineral undetermined.

Electron micrograph: b = 9.28 Å (serpentine).

Electron microscopy: chrysotile demonstrate irregular structure and polytype D_c; single particles of disordered Povlen-chrysotile are registered; lizardite is of two morphological types: with curved layers and lath-like pseudomorphs; antigorite is irregular in structure; particles are quadrangle in shape.

Sample 125-779A-22R-3, 17–21 cm (Piece 2), Unit 2 [Z-680]

Apoharzburgite. Rock completely is serpentinized.

Sample 125-779A-22R-3, 17–21 cm (Piece 2), Unit 2 [Z-195]

Apodunitic serpentine, tectonized. Primary minerals almost completely replaced with serpentine. Rare relicts of olivine and orthopyroxene occur. Antigorite replaces olivine; antigorite with some admixture of amphibole (antigorite?)-chlorite aggregate replace orthopyroxene. Cracks are filled by chrysotile. Single xenomorphic crystals of spinel, almost completely replaced with Fe oxides (hematite?). Rock demonstrates loop (occasionally lattice) texture. Rock is presented by isometric grains (0.6–0.8 mm) of olivine, large (up to 6 mm) isometric grains of orthopyroxene (20%–25%), and grains (0.5–1 mm) of spinel (1%–2%).

Alteration: very strong (90%–95%).

XRD: serpentine.

Electron micrograph: b = 9.20 Å.

Electron microscopy: chrysotile is predominant mineral; there are many particles with length-slight fibber in shape; chrysotile has D_c, $2M_{c1}$, and $2O_{rc1}$ polytypes; the central empty of fibber is empty; lizardite is represented as crystals in small amount; antigorite has disordered structure and lath-like particles; the well ordered antigorite is represented as particles having big width and sharp edges.

Sample 125-779A-24R-1, 27–29 cm (Piece 5), Unit 2 [Z-681]

Harzburgite serpentinized, medium grained, tectonized. Rock is presented by isometric grains (0.6–0.8 mm) of olivine, large (up to 6 mm) isometric grains of orthopyroxene (20%–25%), and grains (0.5–1 mm) of spinel (1%–2%).

Alteration: strong (60%); olivine replaced by lizardite; orthopyroxene completely or partly (10%–100%) replaced by bastite and chlorite; spinel completely is oxidized, microcracks are filled with chrysotile and antigorite.

Sample 125-779A-26R-2, 53–55 cm (Piece 2A), Unit 2 [Z-196]

Harzburgite serpentinized, coarse grained, tectonized, hypidiomorphic (occasionally loop) texture. Primary minerals are represented by hypidiomorphic crystals of olivine (3–5 mm, 60%), hypidiomorphic elongated-tabular crystals of orthopyroxene (10%–15%), and picotite (0.08–1 mm, <1%) with size. Olivine is dissected by cracks in small fragments (0.01–0.05 mm). As a rule, orthopyroxene and spinel are fresh.

Alteration: moderate (~30%); serpentine (25%–30%) replace olivine; chrysotile fill interstitial space; cracks are filled with aggregate of chrysotile and antigorite; Fe oxides occur in cracks.

XRD: serpentine.

Sample 125-779A-29R-2, 0–5 cm (Piece 20), Unit 2 [Z-197]

Apodunitic serpentinite, tectonized. Primary minerals almost completely replaced with serpentine. Sparsely relicts of rounded-isometric crystals of olivine (3–5 mm, 3%–5%) and isometric diamond-shaped crystals of chromite (up to 0.8 mm, <1%).

Alteration: very strong (95%–99%); secondary minerals are represented by serpentines (90%–95%), which form chrysotile-antigorite aggregate; brown secondary mineral (iddingsite?) replace olivine; rock is brown color and probably saturated with Fe hydroxides.

XRD: serpentine; bifurcated reflex 3.63C and 3.60C - two varieties of a serpentine mineral are probably present.

Electron micrograph: b = 9.28 Å (serpentine).

Electron microscopy: chrysotile predominates and demonstrate well-ordered structure; there are many particles of chrysotile-asbestos with length/diameter ratio >5; Povlen-chrysotile was found in small amount with polytype $2O_{rc1}$; the small particles form aggregates; there are two polytypes $2M_{c1}$, and D_c; lizardite forms aggregates with chrysotile; antigorite demonstrates well-ordered structure with quadrangle in shape of crystal; this reflects enough space for crystallization during serpentinization; Fe oxide is represented as cubic crystals.

Sample 125-779A-31R-2, 87–89 cm (Piece 11A), Unit 2 [Z-198]

Apomicrogabbro cataclasite. Hardly visible pseudomorphs above plagioclase and possibly clinopyroxene are present. Primary texture of rock unrecognizable. Primary minerals are smashed to pieces, separated, and almost completely replaced with clay minerals. Oxidized opaque minerals occurs in minor (<1%) amounts. Judging from diamond-shaped pseudomorphs of iddingsite(?) rock contained olivine. It is probable that hydrogrossular(?) is present also.

Alteration: very strong (99%).

XRD: chlorite.

Sample 125-779A-31R-3, 30–34 cm (Piece 4), Unit 2 [Z-682]

Volcanic (basalt) breccia completely replaced by smectites.

XRD: chlorite.

Sample 125-779A-31R-CC, 10–12 cm (Piece 2), Unit 2 [Z-199]

Olivine-clinopyroxene-plagioclase-microphyric basalt, fine grained, incompletely crystallized, vesicular (0.5–2 mm, ~1%). Microphenocrysts; glomerophyric segregates diamond-shaped crystals of clinopyroxene with admixture of olivine. Rock contains elongated-tabular crystals of plagioclase. In total microphenocrysts are ~10%–20% abundance. Quantitatively they are about equal in amounts. Groundmass; small laths of plagioclase (40%–50%), crystals of pyroxene, oxidized opaque dust, and small areas (0.1–0.5 mm) interstitial volcanic glass. Hydrogrossular(?) tends to occur within the latter. Texture of rock is pilotaxic.

Alteration: strong (50%–60%); smectites, chlorite, carbonate, hydrogarnet, Fe oxides and Fe hydroxides replace both rock-forming minerals and interstitial glass, as well as occur in vesicles; single cracks are filled with calcite.

XRD: chlorite.

Sample 125-779A-34R-1, 63–65 cm (Piece 5A), Unit 2 [Z-200]

Apoharzburgite serpentinite, tectonized. Primary minerals almost completely replaced with serpentine. Sparsely relicts of orthopyroxene (2.5–4 mm, 1%–5%) and spinel (up to 1.5–2 mm, single grains).

Alteration: very strong (95%); secondary minerals are represented by serpentine (90%–95%), amphibole (actinolite), chlorite, and Fe hydroxides; serpentine forms chrysotile-antigorite aggregate in groundmass; amphibole and chlorite occur along cleavage faces in orthopyroxene; Fe hydroxides impregnate serpentine which replaces olivine.

XRD: serpentine.

Sample 125-779A-35R-1, 118–122 cm (Piece 10), Unit 2 [Z-201]

Apodunitic serpentinite. Primary minerals almost completely replaced with serpentine. Sparsely relicts of crystals of olivine (10%–15%), orthopyroxene (single smashed to pieces crystals up to 1.5–2 mm in length), spinel (up to 1.5 mm, <1%), and chromite (0.01–0.03 mm, single grains). Amphibole, most probably with chlorite, occur along cleavage faces of orthopyroxene.

Alteration: very strong (~90%); secondary minerals are represented by serpentines (80%–90%), amphibole(?) with admixture chlorite (1%–3%), and Fe oxides.

XRD: serpentine; bifurcated reflex 3.64C and 3.62C - two varieties of serpentine mineral are probably present.

Electron micrograph: b = 9.29 Å (serpentine).

Electron microscopy: chrysotile has length-slight fibber in shape and its total amount is ~10%–30%; there are two polytypes $2O_{rc1}$, and D_c; antigorite has well-ordered structure with sharp edges and quandrangle in shape; Fe oxide is represented as cubic crystals; lizardite is <chrysotile and morphologically it close to antigorite.

Hole 780C

Sample 125-780C-18R-1, 31–34 cm (Piece 2A), Unit 2 [Z-1388]

Verlite serpentinized (apoverlite serpentinite), tectonized. Rock; olivine (95%), clinopyroxene (5%), and spinel (<1%).

Alteration: very strong (75%); rock partly is oxidized (10%); olivine partly (70%) is serpentinized; clinopyroxene partly (30%–40%) replaced by calcite and Fe hydroxides; spinel is oxidized; microcracks are filled with small grains of magnetite.

Sample 125-780C-18R-1, 42–45 cm (Piece 2A), Unit 2 [Z-1389]

Lercolite serpentinized, tectonized. Rock; olivine (60%), orthopyroxene (25%), clinopyroxene (10%), and spinel (5%).

Alteration: moderate (40%–45%); rock partly is oxidized (2%–3%); olivine partly (40%) is serpentinized; pyroxenes are fresh (orthopyroxene is serpentinized ~5%), spinel is oxidized; microcracks are filled with serpentine.

Hole 786B

Sample 125-786B-4R-1, 142–144 cm (Piece 30), Unit 1 [Z-202]

Olivine-pyroxene-plagioclase-microphyric andesite-basalt (boninite?), fine grained, scarcely vesicular. Microphenocrysts of plagioclase (0.5–2 mm, 7%–10%), orthopyroxene (0.5–1.5 mm, 5%–7%), olivine (0.05–0.7 mm, 2%–5%), and single crystals of spinel (<1 mm). Groundmass is microlitic texture; poorly crystallized volcanic glass with small amounts of small laths of plagioclase, pyroxene, and opaque dust. Vesicles (~0.5 mm,

<1%) as a rule empty, occasionally filled with either devitrified volcanic glass which is impregnated with opaque dust or smectites. Within some vesicles rounded droplike aggregates of opaque matter (sulfides?).

Alteration: slight (<5%); olivine is replaced by smectites and Fe oxides, occasionally with calcite; orthopyroxene is replaced by smectites along margins and cleavage faces.

XRD: smectite with ~20% mica layers.

Sample 125-786B-5R-1, 25–27 cm (Piece 4A), Unit 1 [Z-203]

Twopyroxene-olivine-plagioclase-microphyric andesite (boninite), fine grained, sparsely vesicular. Microphenocrysts of plagioclase (0.5–2 mm, 5%–7%), orthopyroxene (up to 1.5–2 mm, 5%–7%), clinopyroxene (0.1–0.7 mm, 1%–4%), and olivine (0.3–1.2 mm, <1%). Groundmass is microlitic texture; volcanic glass with small amounts small laths of plagioclase, pyroxene, and opaque dust. Vesicles (0.5–2 mm, <1%) are filled with zeolite, occasionally walls of vesicles are lined with smectites. Thin cracks are filled with zeolite.

Alteration: slight (~10%); olivine is replaced with smectites and Fe oxides, occasionally with calcite; orthopyroxene is replaced with smectites along margins and cleavage faces.

Electron micrograph: b = 9.16 Å (smectite).

Sample 125-786B-6R-1, 100–104 cm (Piece 24), Unit 2 [Z-1390]

Hypersthene-plagioclase-phyric andesite (boninite), sparsely vesicular. Phenocrysts (5%–7%): idiomorphic grains (2%–3%, 0.6–0.8 mm) of hypersthene (orthopyroxene) and altered prismatic grains (0.5–0.7 mm) of plagioclase. Groundmass is pilotaxitic texture; microlites of plagioclase (20%), clino- and orthopyroxene (10%), light greenish cream volcanic glass (55%–60%), and opaque minerals (2%–3%).

Alteration: slight (~3%–4%); plagioclase completely replaced by opal(?), brownish green hydromica, and clay mineral.

Sample 125-786B-6R-2, 38–40 cm (Piece 8), Unit 2 [Z-204]

Olivine-microphyric basalt, fine grained almost aphanitic, sparsely vesicular. Microphenocrysts of olivine (0.2–2 mm, 3%–5%), plagioclase (up to 2 mm, single grains), and clinopyroxene (0.07–0.5 mm, <1%). Groundmass is pilotaxitic texture; small laths of plagioclase, crystals of pyroxene, and small grains of opaque minerals. Vesicles (0.1–0.3 mm, 2%–5%) as a rule empty. Walls of vesicles are lined with green smectites, occasionally they are filled with carbonate.

Alteration: slight (~10%); olivine is replaced with carbonate, Fe oxides, occasionally with admixture of zeolite.

XRD: smectite with ~20% of mica layers.

Electron micrograph: b = 9.26 Å (trioctahedral smectite).

Sample 125-786B-8R-1, 96–99 cm (Piece 17), Unit 3 [Z-1391]

Twopyroxene-plagioclase-phyric andesite. Phenocrysts (20%–25%): grains and glomerophyric segregates of plagioclase, orthopyroxene, and clinopyroxene. Groundmass is vitrophyric texture; prismatic grains (0.4–1.5 mm) of plagioclase (15%, andesine [$An_{47–49}$]), idiomorphic grains (0.5–1.2 mm) of orthopyroxene (2%–3%), idiomorphic grains of clinopyroxene (7%–8%), and brown glass (75%–80%).

Alteration: rock is fresh.

Sample 125-786B-9R-1, 0–7 cm (Piece 1), Unit 3 [Z-1392]

Twopyroxene-plagioclase-phyric andesite, vesicular. Phenocrysts (20%): hypersthene (2%), pigeonite (5%), and plagioclase (13%). Groundmass is vitrophyric texture; prismatic grains (0.3–0.5 mm) of pyroxenes, prismatic and elongated-prismatic grains (0.3–0.7 mm) of plagioclase (labradorite [An_{59}]), and cream glass (80%) with crystals of plagioclase and pyroxene.

Sample 125-786B-15R-1, 46–54 cm (Piece 7), Unit 3 [Z-1393-1]

Twopyroxene-plagioclase-phyric andesite. Phenocrysts (15%): prismatic grains (0.3–0.8 mm) of plagioclase (10%, labradorite [$An_{55–56}$]), orthopyroxene (1%), and clinopyroxene (4%). Groundmass is vitrophyric texture; glass (80%) with crystals of plagioclase and pyroxene, and opaque minerals (2%–3%). Vesicles (5%) are present.

Alteration: rock is fresh.

Sample 125-786B-15R-2, 126–130 cm (Piece 18), Unit 3 [Z-1394]

Lava breccia. Rock; angular fragments (1–5 mm) of andesite, matrix consists of small (up to 1 mm) angular fragments of andesite and angular fragments of light brown glass. Andesite: twopyroxene-plagioclase-phyric, vesicular. Phenocrysts (20%): hypersthene (2%–3%), pigeonite (2%–3%), and plagioclase (15%, labradorite [An_{56}]). Groundmass is vitrophyric texture; light cream glass (75%) with crystals of plagioclase and pyroxene.

Vesicles (2%–3%) are rounded (0.6 mm) and oval (1.5 mm) in shape, vesicles are empty. Microcracks are filled with opaque minerals.

Alteration: rock is fresh.

Sample 125-786B-16R-2, 8–12 cm (Piece 2), Unit 3 [Z-1395]

Twopyroxene-plagioclase-phyric andesite, vesicular. Phenocrysts (5%): hypersthene and pigeonite (1%, 0.2–0.4 mm), and prismatic grains (0.4–0.7 mm) of plagioclase (4%, labradorite [An_{60}]). Groundmass is vitrophyric texture; glass (80%) with crystals of plagioclase and pyroxene. Vesicles (15%, up to 2.5 mm) are rounded in shape, empty.

Alteration: rock is fresh.

Sample 125-786B-18R-1, 8–13 cm (Piece 2), Unit 4 [Z-1396]

Twopyroxene-plagioclase-phyric andesite, vesicular. Phenocrysts (25%): prismatic grains (0.4–0.6 mm) of hypersthene (1%), small grains (0.3–0.5 mm, single idiomorphic grain 1.7 mm) of pigeonite (4%), and prismatic and tabular grains (0.2–0.9 mm) of plagioclase (20%, labradorite [An_{60}]). Groundmass is vitrophyric texture; light cream glass (60%) with crystals of plagioclase and pyroxene. Vesicles (15%, 0.4–3.5 mm) are rounded and oval in shape, empty.

Alteration: rock is fresh.

Sample 125-786B-19R-1, 6–10 cm (Piece 2), Unit -4 [Z-1397]

Twopyroxene-plagioclase-phyric andesite, vesicular. Phenocrysts (15%): hypersthene (<1%), pigeonite (2%), and plagioclase (12%–13%, labradorite [$An_{58–60}$]). Phenocrysts are small (up to 0.5 mm) idiomorphic grains. Groundmass is vitrophyric texture; light cream glass (75%) with crystals of plagioclase and pyroxene. Vesicles (15%, 0.4–4.5 mm) are rounded and oval in shape, empty.

Alteration: rock is fresh.

Sample 125-786B-20R-1, 85–89 cm (Piece 14), Unit4 [Z-205]

Twopyroxene-olivine-microphyric andesite-basalt (boninite?), fine grained, sparsely vesicular. Microphenocrysts of orthopyroxene (0.3–0.5 mm, 1%–3%), clinopyroxene (0.1–0.5 mm, <1%), and olivine (0.5–1.5 mm, <1%). Groundmass is pilotaxitic texture; small laths of plagioclase, crystals of pyroxene, and small xenomorphic grains of opaque minerals. Occasionally, vesicles (0.5–2 mm, 1%–5%) are filled with zeolite or smectites with small grains of opaque minerals; walls vesicles are lined with smectites.

Alteration: slight (~10%–15%); olivine is replaced by smectite-chlorite aggregate with small grains of opaque minerals, occasionally with admixture of zeolite.

XRD: smectite with ~20% mica layers; trace chlorite(?).

Sample 125-786B-21R-2, 47–49 cm (Piece 3), Unit 7 [Z-206]

Twopyroxene-olivine-microphyric andesite-basalt (boninite?), fine grained, sparsely vesicular. Microphenocrysts of orthopyroxene (0.2–0.5 mm, 1%), clinopyroxene (0.2–0.5 mm, 1%–2%), and olivine (0.5–1 mm, 1%–3%). Groundmass is pilotaxitic texture; small laths of plagioclase, crystals of pyroxene, small xenomorphic grains of opaque minerals, and interstitial glass (10%–15%). Vesicles (0.5–2 mm, 5%–7%) are filled partly with black volcanic glass with opaque dust, center of vesicles present of carbonate. A crack 0.7–1.5 mm thick is filled with carbonate.

Alteration: moderate (~25%–30%); olivine is completely replaced with carbonate; thin opacite rim is built of Fe oxides; orthopyroxene is replaced with smectite–chlorite aggregate and amphibole along margins crystals and on cleavage faces; interstitial glass is replaced with green smectites.

XRD: smectite with ~20% mica layers.

Sample 125-786B-24R-1, 133–135 cm (Piece 12), Unit 9 [Z-207]

Twopyroxene-plagioclase-phyric andesite-dacite, glassy, vesicular. Phenocrysts of orthopyroxene (0.3–0.5 mm, 1%), clinopyroxene (0.2–0.7 mm, <1%), plagioclase (0.3–1.5 mm, 1%–2%), and magnetite (single grains). Groundmass is microlitic or hyalopilitic texture; volcanic glass with small laths of plagioclase. Vesicles (0.2–0.5 mm, 5%–7%) are partly or completely filled with zeolites, occasionally with black volcanic glass containing opaque dust. Hair-thin cracks are filled with smectites and zeolite.

Alteration: slight (~10%).

XRD: smectite with ~15% mica layers; trace chlorite(?).

Sample 125-786B-24R-1, 135–140 cm (Piece 22), Unit 9 [Z-1400]

Plagioclase-phyric andesite, vesicular. Phenocrysts (10%): prismatic grains (0.4–0.7 mm) of plagioclase (labradorite [An_{56}]). Groundmass is hyalopilitic texture; needle-shaped microlites (0.05–0.1 mm) of plagioclase and light cream glass (85%) with crystals of pyroxene. Vesicles (5%–7%, 0.2–0.5 mm) are rounded in shape, vesicles are empty and lined zeolite.

Alteration: rock is fresh.

XRD: phillipsite; trace smectite; white vein: phillipsite; trace smectite.

Sample 125-786B-25R-1, 82–86 cm (Piece 11), Unit 9 [Z-1401]

Clinopyroxene-plagioclase-phyric andesite-basalt, vesicular. Phenocrysts (5%): prismatic grains (0.3–0.6 mm) of plagioclase (4%, labradorite [An_{62}] and andesine [An_{38}]) and clinopyroxene grains (1%), 0.2–0.4 mm. Groundmass is vitrophyric texture; gray glass (75%) with crystals of plagioclase, pyroxene, and opaque dust. Vesicles (20%, 0.2–1.7 mm) are rounded and oval in shape, empty.

Alteration: slight.

Sample 125-786B-26R-1, 50–55 cm (Piece 7), Unit 9 [Z-1402]

Clinopyroxene-plagioclase-phyric andesite-basalt, vesicular. Phenocrysts (5%): prismatic and tabular grains (0.3–0.8 mm) of plagioclase (4%) and clinopyroxene grains (1%). Groundmass is vitrophyric texture; cream-gray glass (65%–70%) with crystals of plagioclase and pyroxene. Vesicles (30%–35%, 0.2–1.8 mm) are isometric in shape, empty.

Alteration: rock is fresh; needless of zeolite are lined of vesicle walls.

Sample 125-786B-27R-1, 58–62 cm (Piece 8), Unit 9 [Z-1403]

Lava breccia. Rock; angular fragments (2.5–10 mm) of andesite. Matrix consists of small (up to 1 mm) angular fragments of colorless glass with sparse grains of hypersthene, pigeonite, and plagioclase (2%–3% in total).

Alteration: rock is fresh.

Sample 125-786B-27R-2, 48–51 cm (Piece 6), Unit 11 [Z-208]

Twopyroxene-plagioclase-phyric andesite (boninite?), glassy, vesicular. Phenocrysts of orthopyroxene (1–2 mm, 5%), clinopyroxene (up to 1.5 mm, 2%), and plagioclase (0.5–2.5 mm, 7%). Groundmass is pilotaxitic texture; volcanic glass with small laths of plagioclase. Vesicles (0.2–0.5 mm, 3%–5%) are empty or occasionally party or completely filled with zeolite.

Alteration: moderate (~20%–30%); interstitial glass is replaced by smectites.

XRD: smectite with ~20% mica layers; trace chlorite(?).

Electron micrograph: b = 9.26 (trioctahedral smectite).

Sample 125-786B-30R-3, 31–33 cm (Piece 4), Unit 11 [Z-209]

Twopyroxene-plagioclase-phyric andesite (boninite), fine grained, sparsely vesicular. Phenocrysts of orthopyroxene (0.7–1.5 mm, 7%–10%), clinopyroxene (up to 2–2.5 mm, 3%–5%), plagioclase (up to 2–3 mm, 10%), and olivine (0.5–2 mm, <1%). Groundmass is hyalopilitic or pilotaxitic texture; volcanic glass with small laths of plagioclase, pyroxene, and opaque dust. Single small vesicles and hair-thin cracks are filled with smectites.

Alteration: slight (~10%–15%); orthopyroxene is replaced with smectites and serpentine(?) along cracks and crystal margins; olivine is completely replaced with smectites, carbonate, and opaque minerals; the latter form opacite rims around carbonate fragments in olivine; interstitial glass is replaced with green smectites.

XRD: smectite with ~20% mica layers, cristobalite(?).

Sample 125-786B-31R-2, 30–34 cm (Piece 3), Unit 11 [Z-683]

Olivine(?)-twopyroxene-plagioclase-phyric andesite-basalt (boninite?), massive. Phenocrysts (30%) of orthopyroxene (up to 0.9 mm), clinopyroxene (0.5–0.7 mm), plagioclase (0.3–2 mm, labradorite [An_{60}] and andesine-labradorite [An_{50}]), and completely altered grains (0.1–0.3 mm) of olivine (<1%). Groundmass is hyalopilitic texture; brownish green volcanic glass and microlites of plagioclase and clinopyroxene.

Alteration: olivine is completely replaced with carbonate and Fe hydroxides; cracks in orthopyroxene grains are filled with clay mineral.

Sample 125-786B-32R-1, 39–41 cm (Piece 8), Unit 11 [Z-210]

Twopyroxene-olivine-plagioclase-phyric andesite (boninite?), fine grained, sparsely vesicular. Phenocrysts of orthopyroxene (0.5–1.5 mm, 5%), clinopyroxene (0.3–2 mm, 1%–3%), olivine (0.2–1.5 mm, 1%), and plagioclase (0.1–2 mm, 10%). Groundmass is pilotaxitic texture; volcanic glass, small laths of plagioclase,

crystals of pyroxene, opaque dust, and small grains of opaque minerals. Single small vesicles are filled with green smectites.

Alteration: slight to moderate (~15%–30%); olivine is replaced with smectites, carbonate, and Fe oxides; orthopyroxene is replaced with smectites along margins and transversal cracks; interstitial glass partly is replaced with smectites; patches of Fe oxides are present.

XRD: smectite with ~20% mica layers, cristobalite(?); trace hydromica.

Electron micrograph: b = 9.19 Å (trioctahedral smectite).

Sample 125-786B-34R-2, 41–43 cm (Piece 4), Unit 15 [Z-211]

Twopyroxene-olivine-microphyric basalt, fine grained, vesicular. Microphenocrysts of orthopyroxene (0.7–2 mm, 1%), clinopyroxene (3%–5%), and olivine (0.3–1.5 mm, 3%–5%). Groundmass is intersertal (occasionally pilotaxitic) texture; incompletely crystallized volcanic glass with small laths of plagioclase, xenomorphic small crystals of pyroxene, and patches of opaque minerals. Vesicles (0.1–0.3 mm, 10%–15%) and cracks filled smectites, occasionally with zeolite or calcite.

Alteration: slight to moderate (~15%–30%); olivine is replaced completely with carbonate, often it is surrounded by Fe oxides with opacite rim; orthopyroxene is replaced with smectites along margins and transversal cracks; in central parts it is replaced with carbonate; interstitial glass is replaced with smectites.

XRD: smectite with ~20% mica layers; trace cristobalite(?) and calcite.

Electron micrograph: b = 9.19 Å (trioctahedral smectite).

Sample 125-786B-34R-4, 11–13 cm (Piece 1B), Unit 15 [Z-212]

Twopyroxene-olivine-microphyric basalt, fine grained. Microphenocrysts of orthopyroxene (0.3–1 mm, 5%), clinopyroxene (0.2–0.5 mm, 1%), and olivine (0.3–0.7 mm, 3%–5%). Groundmass is intersertal texture, partly pilotaxitic; laths of plagioclase, xenomorphic small crystals of pyroxene, and interstitial volcanic glass with rare and small crystals of opaque minerals (magnetite?). Cracks (up to 2 mm thick) are filled with carbonate. Chlorite occur along salbands.

Alteration: moderate to strong (~30%–50%); olivine is completely replaced with carbonate and chlorite (in central parts); iddingsite with inclusions of Fe oxides and opacite rim replace olivine along crystal margins; orthopyroxene is replaced with chlorite and amphibole(?) along cracks; interstitial glass is replaced with green smectites.

XRD: smectite with ~20% mica layers; trace cristobalite(?), hydromica, quartz(?), and calcite.

Sample 125-786B-35R-2, 29–31 cm (Piece 4), Unit 15 [Z-213]

Two pyroxene-plagioclase-phyric dacite, fine grained, highly vesicular. Phenocrysts of orthopyroxene (0.5–1.5 mm, 2%), clinopyroxene (0.3–0.7 mm, <1%), plagioclase (0.5–2 mm, 5%), and olivine (0.5–2 mm, <1%). Groundmass is hyalopilitic to variolitic texture; patchy volcanic glass (brownish gray and light green) with small laths of plagioclase, pyroxene, and opaque dust. Vesicles (0.2–2.5 mm, 15%–20%) as a rule are empty, walls are lined with smectites; zeolite and opaque minerals occur sporadically.

Alteration: clinopyroxene is replaced by smectites and zeolite(?); inclusions of glass in plagioclase are replaced with smectites.

XRD: smectite with ~20% mica layers, cristobalite(?); trace hydromica.

Sample 125-786B-37R-2, 97–99 cm (Piece 12A), Unit 15 [Z-214]

Sparsely pyroxene-plagioclase-phyric basalt (andesite-basalt?), glassy, vesicular. Groundmass is hyalopilitic texture; black devitrified volcanic glass with small laths of plagioclase, pyroxene, and opaque dust. Vesicles (0.5–5 mm, 10%–15%) and cracks are filled by carbonate.

Alteration: rock is fresh.

XRD: smectite with ~20% mica layers; trace cristobalite(?) and calcite.

Sample 125-786B-39R-1, 39–42 cm (Piece 10), Unit 15 [Z-1404]

Twopyroxene-plagioclase-phyric andesite, vesicular. Phenocrysts (25%): single idiomorphic grains (0.2–0.4 mm) of hypersthene and pigeonite (2% in total); glomerophyric segregates of prismatic grains (0.1–0.9 mm) of plagioclase (24%, labradorite [An_{58}] and andesine [An_{42}]). Phenocrysts are small (up to 0.5 mm) idiomorphic grains. Groundmass is vitrophyric texture; needle-shaped microlites of plagioclase (10%, andesine [An_{32}]), colorless glass (50%) with crystals of plagioclase and pyroxene, and opaque minerals (5%). Vesicles (25%, 0.1–0.2 mm) are isometric in shape, vesicles are empty.

Alteration: rock is fresh.

Sample 125-786B-39R-2, 13–17 cm (Piece 3), Unit 15 [Z-1405]

Lava (tuff?) breccia. Rock; angular fragments (0.5–4 mm) of pyroxene-plagioclase-phyric andesite. Phenocrysts (25%): single grains of clinopyroxene and glomerophyric segregates of prismatic grains (0.2–0.8 mm) of plagioclase (labradorite [An_{55}]). Groundmass is vitrophyric texture; cream glass (50%) with microlites of plagioclase, crystallites of pyroxene, and opaque dust.

Alteration: strong (50%); glass almost completely (80%) replaced by clay mineral; matrix (15%); zeolite.

Sample 125-786B-39R-2, 32–35 cm (Piece 4A), Unit 16 [Z-1406]

Twopyroxene-plagioclase-phyric andesite, vesicular. Phenocrysts (15%): hypersthene (4%), pigeonite (1%), and plagioclase (10%, labradorite [An_{55}] and andesine [An_{48}]). Groundmass is vitrophyric texture; glass with microlites and crystallites of plagioclase and pyroxene, and opaque minerals (5%). Vesicles (1–5 mm) are elongated oval in shape, empty. Walls of vesicles are lined with glass.

Alteration: rock is fresh.

Sample 125-786B-40R-1, 25–29 cm (Piece 6), Unit 16 [Z-1407]

Vitro-clastic tuff, moderate-fragmented, andesitic composition. Rock; angular fragments (0.1–7 mm) of volcanic glass with grains (1%) of pyroxene and plagioclase. Microvesicles (10%–30%) are empty.

Alteration: moderate to strong; brownish gray to light cream glass almost completely (80%) replaced by clay mineral; fragments of glass are oxidized; matrix; clay.

XRD: cristobalite; trace smectite, quartz, and amphibole.

Sample 125-786B-40R-2, 17–19 cm (Piece 15E), Unit 17 [Z-215]

Olivine-phyric basalt, fine grained, sparsely vesicular. Phenocrysts of olivine (0.3–2 mm, 10%–15%). Groundmass is intersertal texture; small laths of plagioclase, crystals of clinopyroxene, small grains of opaque minerals, and patches of interstitial glass. Sparsely vesicles (1.5–4 mm) are completely filled with calcite.

Alteration: moderate (~30%); olivine is replaced with smectites, carbonate, Fe oxides, and, occasionally, serpentine(?); interstitial glass is replaced with smectites with calcite and/or with calcite.

XRD: smectite with ~20% mica layers; trace cristobalite(?) and calcite.

Electron micrograph: b = 9.23 Å (trioctahedral smectite and mica).

Sample 125-786B-40R-3, 46–50 cm (Piece 1C), Unit 17 [Z-684]

Hypersthene(?)-olivine-phyric basalt, massive. Phenocrysts (1%): completely altered hypersthene (4%), pigeonite (1%), and plagioclase (10%, labradorite [An_{55}] and andesine [An_{48}]). Groundmass is pilotaxitic texture; needle-shaped microlites of plagioclase, panicle like grains of clinopyroxene, and altered glass. Isometric grains (0.1–0.2 mm) of orthoclase(?) are present (15%).

Alteration: phenocrysts completely replaced by clay mineral and carbonate; clay mineral replaces interstitial glass.

Sample 125-786B-42R-3, 116–120 cm (Piece 10C), Unit 19 [Z-685]

Twopyroxene-plagioclase-phyric andesite-basalt (boninite?), massive. Phenocrysts (40%–45%, from 0.1–0.2 mm to 0.3–1 mm): sparse grains of hypersthene (<1%) and clinopyroxene (augite) form idiomorphic grains and their segregates. Plagioclase (labradorite [An_{60}]) forms prismatic and tabular grains (0.5–1.5 mm). Plagioclases contain inclusions of glass. Groundmass is vitrophyric texture; black glass with opaque dust.

Alteration: slight (15%); hypersthene almost completely replaced by chlorite; rims of clinopyroxene grains replaced by clay mineral; interstitial glass partly (10%) is replaced with clay mineral.

Sample 125-786B-43R-2, 81–83 cm (Piece 7), Unit 19 [Z-258]

Pyroxene-plagioclase-phyric andesite (boninite?). Phenocrysts of orthopyroxene (0.05–0.7 mm, 1%–5%), clinopyroxene (0.07–1 mm, 1%), and plagioclase (0.1–1.5 mm, 5%–7%). Groundmass is hyaline texture; gray volcanic glass with crystals of pyroxene and opaque dust, and small isomorphic diamond-shaped crystals of olivine. Vesicles (0.5–2 mm, 5%–7%) are filled partly with black volcanic glass containing opaque dust, nuclear parts of vesicles are built of carbonate. A cracks 0.7–1.5 mm thick is filled with carbonate.

Alteration: slight (~10%–15%); olivine is completely filled with smectites.

XRD: smectite with ~20% mica layers; trace cristobalite(?) and hydromica (~20% swelling interlayers).

Sample 125-786B-44R-1, 21–25 cm (Piece 4), Unit 19 [Z-686]

Pyroxene-plagioclase-phyric basalt, massive. Phenocrysts (15%): idiomorphic prismatic and tabular grains (0.4–1.5 mm) of clinopyroxene and completely altered plagioclase grains. Groundmass is pilotaxitic intersertal texture; microlites of plagioclase and segregate of small grains of clinopyroxene. Intersticies consist of altered glass.

Alteration: moderate (30%–40%); phenocrysts completely replaced by clay mineral; clay mineral replaces glass.

Sample 125-786B-46R-2, 67–72 cm (Piece 8C), Unit 19 [Z-1408]

Crystal-vitric tuff (breccia). Large (up to 15 mm) isometric fragments are represented by twopyroxene-plagioclase-phyric andesite with vitrophyric texture, vesicular (vesicles are empty). Matrix (30%); small (0.1–0.5 mm) angular fragments of glass and crystals of pyroxene and plagioclase, they are cemented by brown clay.

Alteration: rock is fresh.

Sample 125-786B-48R-1, 98–102 cm (Piece 8), Unit 19 [Z-1409]

Breccia. Rock; rounded fragments (90%, 1–15 mm) of twopyroxene-plagioclase-phyric andesite with vary textures and matrix (10%). Matrix consists of small (0.1–0.4 mm) fragments of andesite and clay.

Alteration: fragments of andesite are fresh.

XRD: trace smectite, chlorite, quartz, and hydromica(?).

Sample 125-786B-48R-2, 85–88 cm (Piece 11), Unit 19 [Z-1410]

Lithoclastic breccia. Rock; fragments (90%, up to 20 mm) of twopyroxene-plagioclase-phyric andesite with vitrophyric textures, vesicular (they are empty), and matrix (10%). Groundmass: light cream glass.

Alteration: fragments of andesite are fresh.

Sample 125-786B-49R-2, 90–95 cm (Piece 4C), Unit 19 [Z-1411]

Lithoclastic breccia. Rock; fragments (99%, 4–10 mm) of twopyroxene-plagioclase-phyric andesite with vitrophyric textures, vesicular (they are empty), and matrix (1%). Groundmass: light cream glass (65%).

Alteration: breccia is replaced with clay mineral and oxidized (70%–80%); one fragment of andesite is completely oxidized; interstices glass from fragments of andesite replaced by clay mineral; matrix of breccia; clay mineral and zeolite.

XRD: smectite; trace phillipsite; gray-yellow matrix: phillipsite; trace smectite.

Sample 125-786B-50R-1, 27–30 cm (Piece 4A), Unit 19 [Z-1412]

Lava breccia. Rock; fragments (1–10 mm) of pyroxene-plagioclase-phyric andesite (phenocrysts: 20%, volcanic glass: 80%). Matrix (10%) consists of angular fragments of plagioclase and pyroxene, and cream glass.

Alteration: rock is fresh.

Sample 125-786B-51R-2, 0–5 cm (Piece 1), Unit 19 [Z-1413]

Twopyroxene-plagioclase-phyric andesite (boninite), vesicular. Phenocrysts (20%): idiomorphic grains (15%, 0.2–0.9 mm) of orthopyroxene (hypersthene-bronzite) (<1%), grains of augite (2%), and prismatic grains (0.5–1.5 mm) of plagioclase (labradorite [An_{55}]). Groundmass is vitrophyric texture; light cream glass (70%) with crystals of plagioclase and pyroxene. Vesicles (10%, 0.5–1.5 mm) are elongated-oval in shape. Vesicles are empty and encrusted by glass.

Alteration: one vesicle is filled with zeolite; microcrack (0.4 mm) infilled with zeolite and clay mineral.

Sample 125-786B-52R-1, 10–13 cm (Piece 2), Unit 19 [Z-1414]

Lava breccia. Rock; fragments (80%, 1–15 mm) of olivine-twopyroxene-phyric boninite (phenocrysts: 20%, colorless volcanic glass: 80%). Matrix (20%) consists of angular fragments of groundmass and phenocrysts from boninite. Phenocrysts cemented by cream glass or dark brown clay and carbonate.

Alteration: slight (5%); olivine completely replaced by iddingsite, opal(?), and carbonate.

Sample 125-786B-53R-1, 25–30 cm (Piece 1C), Unit 19 [Z-1415]

Olivine-twopyroxene-plagioclase-phyric andesite (boninite), vesicular. Phenocrysts (35%) are represented by olivine (1%), orthopyroxene (25%), clinopyroxene (4%), and plagioclase (5%). Groundmass is vitrophyric texture; small grains (0.2–0.6 mm) of completely altered olivine, xenomorphic grains (0.5–1.7 mm) of orthopyroxene, xenomorphic small grains (up to 0.9 mm) of augite, prismatic grains (0.4–1.2 mm) of plagioclase (0.3–2 mm, labradorite [An_{60}]), and glass. Vesicles (5%, 0.3–2.5 mm) are elongated-isometric and oval in shape. Vesicles are empty and encrusted by cream glass.

Alteration: olivine is completely replaced with iddingsite and opal(?); several vesicles (<1%) consist of carbonate.

Sample 125-786B-54R-1, 55–60 cm (Piece 6A), Unit 19 [Z-1416]

Lava breccia. Rock; fragments (85%, up to 12 mm) of olivine-twopyroxene-plagioclase-phyric boninite (phenocrysts: 25%, volcanic glass: 70%, and vesicles: 5%). Matrix (15%) consists of angular fragments (0.5–1.5 mm) of boninite. Fragments of boninite cemented by glass or dark brown clay and carbonate.

Alteration: slight (2%); olivine completely replaced by iddingsite; several (<1%) vesicles are filled with carbonate.

Sample 125-786B-54R-3, 67–71 cm (Piece 1J), Unit 19 [Z-1417]

Tuff. Rock; angular fragments (0.1–1.5 mm) of boninite and more small fragments of orthopyroxene and plagioclase crystals. Cement is absent.

Alteration: rock is fresh.

XRD: smectite.

Sample 125-786B-54R-4, 0–5 cm (Piece 1), Unit 19 [Z-1418]

Lava breccia. Rock; large (8–10 mm) fragments (80%) of boninite. Large fragments cemented by small (0.2–0.5 mm) fragments (15%) of boninite and glass (5%). Rock: identical to Sample 125-786B-54R-1, 55–60 cm (Z-1416).

XRD: trace smectite, chlorite, and quartz.

Sample 125-786B-55R-1, 132–138 cm (Piece 13C), Unit 19 [Z-1419]

Olivine-plagioclase-twopyroxene-phyric andesite (boninite), vesicular, brecciated. Phenocrysts (25%) are represented by olivine (2%), orthopyroxene (15%), clinopyroxene (3%), and plagioclase (5%). Groundmass (65%) is vitrophyric texture; idiomorphic grains (0.3–1.4 mm) of altered olivine, prismatic grains of orthopyroxene and clinopyroxene, prismatic grains (0.4–1.2 mm) of plagioclase (labradorite [An_{56}]) and their segregates (0.3–0.6 mm), and gray glass (1%–2%) with sparse microlites of pyroxene. Vesicles (10%, 0.2–2.5 mm) are elongated-isometric and oval in shape. Vesicles are empty and encrusted by glass.

Alteration: slight (2%); small grains of olivine are completely replaced with iddingsite and carbonate; crack (up to 2.5 mm in thickness) infilled with small (up to 0.6 mm) angular fragments of glass, mineral-phenocrysts from andesite (boninite), and carbonate.

Sample 125-786B-55R-3, 0–5 cm (Piece 1), Unit 19 [Z-1420]

Lava breccia. Rock; large (10–12 mm) fragments (80%) of olivine-twopyroxene-plagioclase-phyric boninite (phenocrysts: 25%, volcanic glass: 70%, and vesicles: 5%). Large fragments cemented by small (0.1–1.2 mm) fragments of boninite, glass, and clay.

Alteration: slight.

Sample 125-786B-56R-1, 20–25 cm (Piece 2B), Unit -19 [Z-1421]

Hypersthene-phyric andesite (boninite), vesicular. Phenocrysts (25%): idiomorphic grains (0.2–0.7 mm) of orthopyroxene (hypersthene-bronzite) and their glomerophyric segregates. Groundmass is vitrophyric texture; colorless glass (50%) with rudimentary crystals of pyroxene. Vesicles (25%, 0.2–0.5 mm) are rounded and oval in shape, they mainly (90%) are filled with greenish glass, other vesicles are empty.

Alteration: rock is fresh.

XRD: smectite; trace erionite; dark green clay from veinlet: smectite with ~20%–25% mica layers, erionite.

Sample 125-786B-56R-1, 97–102 cm (Piece 3), Unit 19 [Z-1422]

Lava breccia. Rock; fragments (0.5–5 mm) of andesite (80%) and light cream glass (20%). Rock: twopyroxene-olivine-plagioclase-phyric andesite (phenocrysts: 15%, volcanic glass: 40%, and vesicles: 30%). Cement: greenish brown glass.

Alteration: rock is fresh.

Sample 125-786B-56R-3, 50–55 cm (Piece 1C), Unit 19 [Z-1423]

Lava breccia. Rock; fragments (1–5 mm) of olivine-orthopyroxene boninite (85%) and colorless and light greenish cream glass (15%). Rock; phenocrysts: 25%, volcanic glass: 50%, and vesicles: 25%. Cement: greenish cream glass.

Alteration: slight.

Sample 125-786B-56R-5, 98–102 cm (Piece 1G), Unit 19 [Z-1424]

Lava breccia (fragments of boninite are cemented by glass). Rock: identical to Sample 125-786B-56R-3, 50–55 cm (Z-1423).

Sample 125-786B-57R-1, 41–43 cm (Piece 1B), Unit 20 [Z-257]

Pyroxene-olivine-phyric hyalobasalt, glassy, massive. Phenocrysts of clinopyroxene (0.08–0.9 mm, <1%), orthopyroxene (1%–5%), and olivine (7%–10%). Groundmass is hyaline intersertal texture; green volcanic glass with opaque dust and small crystals of undetermined mineral.

Alteration: moderate to high (30%–40%); olivine and probably orthopyroxene are completely replaced with smectites.

XRD: smectite with ~20% mica layers.

Electron micrograph: b = 9.18 Å (trioctahedral smectite).

Sample 125-786B-61R-4, 108–114 cm (Piece 6B), Unit 22 [Z-1425]

Plagioclase-phyric rhyolite, crystallized, vesicular. Rock; phenocrysts (15%), groundmass (75%), and vesicles (10%). Phenocrysts: prismatic grains of plagioclase and their segregates (0.5–2.5 mm, oligoclase [An_{29}]), small (0.1–0.3 mm) idiomorphic grains of dark-colored mineral (2%–3%), and idiomorphic grains (0.3 mm) of opaque minerals (1%). Groundmass is micropoikilitic texture; small (0.1 mm) rounded-isometric grains of quartz (1%) and grains of orthoclase with inclusions of microlites of albite (70%). Vesicles (0.1–2.5 mm) are filled with smectites or carbonate.

Alteration: very strong (90%); plagioclase partly replaced by sericite; dark-colored mineral completely replaced by green clay mineral; vesicles are filled with green clay mineral, carbonate and zeolite; microcrack (0.1 mm) completely infilled with carbonate.

XRD: quartz; trace chlorite and hydromica.

Sample 125-786B-61R-5, 37–39 cm (Piece 6), Unit 22 [Z-259]

Aphyric dazite (rhyolite?), poorly crystallized, sparsely vesicular. Rock is hyaline texture; devitrified volcanic glass with crystals of plagioclase, opaque dust, single xenomorphic crystals of K-feldspar. Vesicles filled with smectites or carbonate.

Alteration: moderate (~25%).

XRD: quartz; trace cristobalite(?) and chlorite.

Sample 125-786B-62R-1, 16–18 cm (Piece 2A), Unit 24 [Z-260]

Olivine(?)-pyroxene(?)-phyric hyaloandesite (boninite?), massive. Phenocrysts (15%–20%, sizes up to 2–3 mm) of orthopyroxene, clinopyroxene, and olivine. Groundmass is hyaline-hyolopilitic texture; green-gray volcanic glass with laths of plagioclase, crystals of clinopyroxene and opaque dust, and small xenomorphic crystals of olivine. Vesicles (0.5–2 mm, 5%–7%) filled partly with black volcanic glass with opaque dust, nuclear parts of vesicles are built of carbonate. A crack 0.7–1.5 mm thick is filled with carbonate.

Alteration: moderate (~25%); orthopyroxene, clinopyroxene, and olivine are completely replaced with smectites.

XRD: smectite with ~20% mica layers.

Sample 125-786B-63R-1, 118–121 cm (Piece 13), Unit 25 [Z-687]

Tuff, andesite-basaltic composition. Rock; angular fragments (0.1–5.5 mm) of volcanic glass, sparse fragments of grains of plagioclase (andesine [An_{47}]) and pyroxene. Cement; clay mineral.

Alteration: very strong (95%).

Sample 125-786B-64R-2, 88–92 cm (Piece 12), Unit 26 [Z-1426]

Plagioclase-phyric rhyolite, crystallized, vesicular. Rock; phenocrysts (8%–10%), groundmass (75%), and vesicles (15%). Phenocrysts: prismatic grains (0.6–1.5 mm) of plagioclase. Groundmass is micropoikilitic texture; small (<0.1 mm) rounded-isometric grains of quartz (2%–3%) and grains of orthoclase (60%–65%) with inclusions of plagioclase crystals, and opaque dust (<0.01 mm, 10%). Vesicles (0.2–1.5 mm) are rounded in shape. They are empty or lined by quartz.

Alteration: slight (10%–15%); plagioclase replaced by albite and undetermined mineral; orthoclase replaced by pelite; single vesicles infilled with carbonate.

Sample 125-786B-64R-3, 76–78 cm (Piece 8A), Unit 26 [Z-261]

Aphyric andesite-basalt, almost completely crystallized, sparsely vesicular. Microphenocrysts of plagioclase (0.5–2 mm, 7%–10%), orthopyroxene (0.5–1.5 mm, 5%–7%), olivine (0.05–0.7 mm, 2%–5%), and single crystals of spinel (<1 mm). Rock intersertal texture, partly taxitic; laths of plagioclase, pyroxene, opaque minerals, and interstitial glass (5%–7%), occasionally with hypidiomorphic grains of quartz. Vesicles (0.1–0.3 mm, ~5%) partly or completely filled smectites.

Alteration: moderate (25%–30%); interstitial glass and clinopyroxene (partly) is replaced with smectites.

XRD: smectite with ~20% mica layers.

Sample 125-786B-65R-1, 40–44 cm (Piece 3), Unit 26 [Z-688]

Sparsely pyroxene-phyric andesite-basalt (boninite?), massive. Phenocrysts: single glomerophyric segregate of three clinopyroxene grains (0.3 mm). Groundmass is pilotaxitic texture; microlites of plagioclase, very small grains of pyroxene, and interstitial glass with opaque dust.

Alteration: moderate (~30%); two grains of clinopyroxene replaced by clay mineral and carbonate; clay mineral replaces glass; carbonate replaces groundmass.

Sample 125-786B-65R-1, 102–107 cm (Piece 13), Unit 26 [Z-1427]

Plagioclase-phyric rhyolite, crystallized, vesicular. Rock; phenocrysts (10%), groundmass (70%), and vesicles (20%). Phenocrysts: prismatic grains (1.2–2.5 mm) of plagioclase. Groundmass is micropoikilitic texture; small (<0.1 mm) rounded-isometric grains of quartz (7%–8%), small isometric grains (0.1 mm) of orthoclase (60%) with inclusions of plagioclase crystals, and opaque dust. Vesicles (0.2–0.9 mm) are oval and isometric in shape. They are empty (5%) or lined by quartz.

Alteration: moderate (30%–40%); plagioclase replaced by undetermined mineral; occasionally single large (2.5 mm) phenocrysts of plagioclase completely replaced by carbonate (dominant) and clay mineral (trace); orthoclase replaced by pelite.

Sample 125-786B-65R-3, 39–41 cm (Piece 6), Unit 26 [Z-1428]

Plagioclase-phyric rhyolite with micropoikilitic texture, crystallized, vesicular. Rock: identical to Sample 125-786B-65R-1, 102–107 cm (Z-1427).

Sample 125-786B-65R-3, 48–52 cm (Piece 7), Unit 786B-26 [Z-689]

Tuff, andesite-basaltic (boninite?) composition. Rock; completely altered fragments of volcanic glass with microlites (crystallites) of plagioclase (andesine [An_{47}]), pyroxene (orthoclase?), and small (0.1 mm) rounded-isometric grains of quartz.

Alteration: rock is altered (completely).

Sample 125-786B-66R-1, 36–38 cm (Piece 5), Unit 26 [Z-690]

Plagioclase-phyric andesite (boninite?), massive. Phenocrysts (8%–10%): elongated-prismatic grains (0.3–0.8 mm) of plagioclase (5%). Plagioclase grains contain inclusions of glass. Groundmass is poikilititic texture; segregate of needle-shaped microlites (0.05–0.1 mm) of plagioclase, isometric grains (up to 0.1 mm) of feldspar, rounded-isometric grains of quartz, and idiomorphic grains (0.2–0.3 mm) of opaque minerals. Rock impregnated by opaque dust.

Alteration: slight (10%–15%); plagioclase phenocrysts partly replaced by pelite, occasionally they are carbonitized.

Sample 125-786B-66R-2, 0–5 cm (Piece 1A), Unit 26 [Z-1429]

Plagioclase-phyric rhyolite, crystallized. Rock; phenocrysts (10%) and groundmass (90%). Phenocrysts: tabular and prismatic grains (0.5–1 mm) of plagioclase. Groundmass is micropoikilitic texture; small (0.05–0.1 mm) grains of quartz (10%), small isometric grains of orthoclase with microlites of albite and opaque dust, and sparse skeletal grains (0.3 mm) of opaque minerals.

Alteration: very strong (70%–80%); plagioclase phenocrysts completely replaced by albite and microaggregates of sosurite; orthoclase replaced by pelite.

Sample 125-786B-66R-3, 51–56 cm (Piece 7), Unit 26 [Z-1430]

Orthoclase-plagioclase-phyric rhyolite, crystallized. Rock; phenocrysts (25%) and groundmass (75%). Phenocrysts: tabular and prismatic grains (0.5–1.5 mm) of plagioclase (15%) and tabular grains of orthoclase (10%). Groundmass is micropoikilitic texture; small (up to 0.1 mm) isometric grains of quartz (5%–7%%), orthoclase with opaque dust, and opaque minerals (2%–3%).

Alteration: strong to very strong (65%–70%); plagioclase phenocrysts replaced by albite; orthoclase replaced by pelite.

XRD: quartz; trace chlorite.

Sample 125-786B-67R-1, 77–79 cm (Piece 9), Unit 27 [Z-262]

Pyroxene-olivine-phyric basalt, fine grained, massive. Phenocrysts of orthopyroxene (up to 1–1.5 mm, 2%), clinopyroxene (<1%), and olivine (<1%). Groundmass is intersertal texture. It is by laths of plagioclase, clinopyroxene, olivine, and interstitial glass.

Alteration: moderate (~25%); olivine and interstitial glass are replaced with smectites.

XRD: smectites with ~20% mica layers contain various interlayer cations: Na-K and Mg-Ca; trace cristobalite(?) and quartz(?).

Electron micrograph: b = 9.18 Å (trioctahedral smectite).

Sample 125-786B-68R-1, 10–16 cm (Piece 1A), Unit 28 [Z-1431]

Breccia (tuff?), rhyolitic composition. Rock completely replaced by green-brown clay mineral.

Alteration: very strong (95%).

XRD: smectite; trace quartz and talc(?).

Sample 125-786B-69R-2, 79–81 cm (Piece 1F), Unit 28 [Z-263]

Hyaloandesite-dacite (boninite?), glassy, sparsely phyric. Phenocrysts of orthopyroxene(?) and olivine(?) with sizes up to 1–1.5 mm, 1%–3%. Crystals of quartz are present. Groundmass is hyaline texture, occasionally, taxitic; light green volcanic glass with laths-like microlites of plagioclase and opaque dust.

Alteration: moderate to high (~30–40%); olivine and orthopyroxene are completely replaced with smectites; carbonate occurs also.

XRD: smectites with ~20% mica layers; trace quartz(?).

Electron micrograph: b = 9.26 Å (trioctahedral smectite).

Sample 125-786B-69R-4, 107–110 cm (Piece 1D), Unit 28 [Z-1432]

Tuff, riolitic composition. Rock completely replaced by clay minerals.

Alteration: very strong (95%).

Sample 125-786B-70R-2, 46–48 cm (Piece 1F), Unit 28 [Z-264]

Hyaloandesite-basalt (boninite?), glassy, phyric, vesicular. Phenocrysts (up to 20%) of orthopyroxene(?) and olivine(?). Groundmass is taxitic texture; light green volcanic glass with laths of plagioclase and opaque dust. Crystals of quartz occur sporadically. Vesicles (up to 1.5 mm, ~5%) are filled with smectites and carbonate.

Alteration: strong (50%–60%); olivine and orthopyroxene are completely replaced with smectites.

XRD: smectites with ~20% mica layers contain various interlayer cations: Na-K and Mg-Ca.

Electron micrograph: b = 9.25 Å (trioctahedral smectite).

Sample 125-786B-70R-4, 0–5 cm (Piece 1), Unit 28 [Z-1433]

Orthopyroxene-phyric andesite(?), crystallized, fine grained. Rock with andesitic texture; phenocrysts (25%) and groundmass (75%).

Alteration: moderate (30%–35%).

XRD: smectite; trace quartz.

Sample 125-786B-71R-4, 32–36 cm (Piece 3), Unit 30 [Z-691]

Twopyroxene-plagioclase-phyric andesite-basalt (boninite?), massive. Rock: identical to Sample 125-786B-42R-3, 116–120 cm (Z-685).

Alteration: strong to very strong (60%–70%); orthopyroxene replaced by biotite and carbonate; clinopyroxene replaced by with andesitic texture and carbonate; carbonate, pelite and albite replace plagioclase; interstitial glass partly (10%–15%) replaced by clay mineral.

Sample 125-786B-72R-1, 15–17 cm (Piece 3), Unit 30 [Z-265]

Sparsely pyroxene-plagioclase-phyric andesite, poorly crystallized, vesicular. Phenocrysts of pyroxene, plagioclase, and olivine. Groundmass is hyaline texture, occasionally intersertal; green volcanic glass with laths of plagioclase and opaque dust. Crystals of quartz are present. Vesicles partly are filled with smectites.

Alteration: moderate to strong (40%–50%); olivine and orthopyroxene are completely replaced with smectites and carbonate.

XRD: smectite with ~20% mica layers; trace quartz(?).

Electron micrograph: b = 9.27 Å (trioctahedral smectite).

Sample 125-786B-72R-2, 50–55 cm (Piece 5), Unit 30 [Z-1434]

Lithoclastic tuff (breccia). Rock; fragments (80%, 3–12 mm) of andesite (boninite). Large fragments cemented by small (0.1–0.4 mm) fragments of andesite. Fragments of boninite are represented by altered ortho- and clinopyroxene, plagioclase (andesine [An_{37}]), altered glass, and opaque minerals (5%–7%).

Alteration: very strong (90%); pyroxenes completely replaced by clay mineral and partly by biotite; glass partly replaced by clay minerals; plagioclase partly replaced by albite or carbonate.

XRD: corrensite; trace chlorite and quartz.

Sample 126-792E-71R-1, 84–86 cm (Piece 8), Unit 1 [Z-219]

Plagioclase-phyric andesite-basalt, vesicular. Phenocrysts of plagioclase (0.3–3.5 mm, 35%). Groundmass is hyalopilitic texture; volcanic glass with small grains of clinopyroxene, laths of plagioclase, and opaque minerals. Vesicles (0.02–0.5 mm, 5%–7%) were filled with glass which later have been replaced with grassy-green smectites.

Alteration: slight (~5%–7%).

XRD: smectite with ~20% mica layers; trace cristobalite(?) and hydromica(?).

Electron micrograph: b = 9.23 Å (trioctahedral smectite).

Sample 126-792E-72R-1, 18–20 cm (Piece 2), Unit 1 [Z-220]

Plagioclase-phyric andesite-basalt, glassy, massive. Phenocrysts: plagioclase (0.03–2.5 mm, 25%). Single phenocrysts of clinopyroxene and olivine(?) are registered. Groundmass: hyaline texture; volcanic glass with small crystals of pyroxene and opaque minerals.

Alteration: moderate (~25%).

XRD: smectite; trace cristobalite(?).

Electron micrograph: b = 9.20 Å (trioctahedral smectite).

Sample 126-792E-73R-2, 76–78 cm (Piece 6B), Unit 1 [Z-221]

Clinopyroxene-plagioclase-phyric andesite-basalt, poorly crystallized, massive. Phenocrysts: plagioclase (0.3–2.5 mm, 20%), clinopyroxene (1–1.5 mm, <1%), orthopyroxene (?), and olivine(?). Groundmass: hyaline texture; light green volcanic glass with laths of plagioclase, small crystals of pyroxene, and opaque minerals.

Alteration: moderate (~30%).

XRD: smectite and cristobalite.

Electron micrograph: b = 9.20 Å (trioctahedral smectite).

Sample 126-792E-74R-1, 54–58 cm (Piece 5B), Unit 2 [Z-1450]

Plagioclase-phyric andesite, massive. Phenocrysts (35%): prismatic grains (0.3–1.7 mm) of plagioclase (labradorite [An_{55}] and andesine [An_{38}]). Sparse (<0.5%) small grains (up to 0.3 mm) of clinopyroxene are present. Groundmass: vitrophyric texture; volcanic glass and opaque minerals (3%–4%).

Alteration: rock is fresh.

Sample 126-792E-74R-2, 64–66 cm (Piece 6), Unit 3 [Z-222]

Clinopyroxene-plagioclase-phyric hyaloandesite-basalt, massive. Phenocrysts: plagioclase (0.5–2.5 mm, 25%) and clinopyroxene (0.2–0.5 mm, 1%–3%). Groundmass: hyaline texture; light green volcanic glass with tabular crystals of plagioclase, microlites of pyroxene, and opaque minerals.

Alteration: moderate (~30%).

XRD: smectite; trace cristobalite(?) and quartz.

Electron micrograph: b = 9.26 Å (trioctahedral smectite).

Sample 126-792E-75R-2, 62–64 cm (Piece 7), Unit 3 [Z-223]

Pyroxene-plagioclase-phyric hyaloandesite-dacite, massive. Phenocrysts: plagioclase (0.5–2.5 mm, 25%–30%) and clinopyroxene (0.2–1.5 mm, <1%). Highly altered crystals of hornblende(?) or orthopyroxene(?) are present. Groundmass: hyaline texture; by light greenish brown volcanic glass with laths of plagioclase and opaque minerals.

Alteration: moderate (~25%); hornblende(?) or orthopyroxene(?) is replaced by smectites, hydrotalcite(?), and tremolite-actinolite(?).

XRD: cristobalite(?); trace smectite and quartz.

Sample 126-792E-76R-1, 26–32 cm (Piece 3), Unit 4 [Z-1451]

Plagioclase-phyric andesite, massive. Phenocrysts (50%): tabular and prismatic grains (0.3–1.7 mm) of plagioclase (labradorite [An_{62}] and andesine [An_{48}]), occasionally they contain inclusions of glass. Groundmass: vitrophyric texture; represented by gray volcanic glass (50%). Rock: sparse (2%–3%) prismatic grains of dark-colored mineral (pyroxene?).

Alteration: slight (2%–3%); dark-colored mineral completely replaced by clay mineral.

Sample 126-792E-76R-1, 120–122 cm (Piece 11), Unit 5 [Z-224]

Pyroxene-plagioclase-phyric hyaloandesite-dacite, quartz-bearing, massive. Phenocrysts: plagioclase (0.5–2 mm, 25%) and clinopyroxene (0.2–1 mm, <1%). Highly altered crystals hornblende(?) or orthopyroxene(?). Rock: s crystals of quartz (0.1–0.5 mm, 1%–3%). Groundmass: hyaline texture; light green volcanic glass with laths of plagioclase and opaque minerals.

Alteration: moderate (~20%); hornblende(?) or orthopyroxene(?) is replaced by smectites, hydrotalcite(?), tremolite-actinolite(?).

XRD: smectite; trace cristobalite(?) and quartz.

Electron micrograph: b = 9.10 Å? (very slight).

Sample 126-792E-78R-1, 118–120 cm (Piece 14), Unit 5 [Z-225]

Plagioclase-phyric hyaloandesite, massive. Phenocrysts: plagioclase (0.2–2 mm, 30%) and single grains of clinopyroxene (0.2–1 mm, <1%). Highly altered crystals (~1%) of hornblende(?) or orthopyroxene(?) are registered. Groundmass: hyaline-hyalopilitic texture; light greenish gray volcanic glass with laths and small plates of plagioclase, opaque minerals, and single small rounded crystals of quartz.

Alteration: moderate (25%–30%); hornblende(?) or orthopyroxene(?) is completely replaced by smectites.

XRD: smectite; trace cristobalite(?).

Hole 793B

Sample 126-793B-1R-2, 82–84 cm (Piece 5A), Unit X [Z-226]

Sparsely clinopyroxene-olivine-phyric, fine grained, almost completely crystallized, massive. Phenocrysts: clinopyroxene (0.5–2 mm, <1%) and olivine (0.3–1.5 mm, 3%–5%). Groundmass: intergranular texture; laths of plagioclase (45%–50%), clinopyroxene (45%), interstitial glass (5%), and opaque minerals (1%–3%).

Alteration: slight (~10%); olivine is completely replaced with smectite-chlorite aggregate, occasionally with admixtures of carbonate; interstitial glass is replaced by smectite-chlorite aggregate.

Sample 126-793B-86R-1, 35–40 cm, Unit 1 [Z-1452]

Bronzite-plagioclase-clinopyroxene-phyric andesite, vesicular. Rock: phenocrysts (20%), glass (60%), and vesicles (20%). Phenocrysts: idiomorphic grains (0.2–1.7 mm) of orthopyroxene (bronzite?) 5%–7%, plagioclase (20%, labradorite [An_{58}] and andesine [An_{40}]), and clinopyroxene (25%–30%). Groundmass: vitrophyric texture; colorless volcanic glass with crystals of plagioclase and pyroxene.

Alteration: rock is fresh.

Sample 126-793B-88R-1, 62–67 cm, Unit 1 [Z-1453]

Twopyroxene-plagioclase-phyric andesite, vesicular. Rock: phenocrysts (20%), glass (60%), and vesicles (20%). Phenocrysts: prismatic grains of bronzite (3%), clinopyroxene (2%), and glomerophyric segregates of prismatic grains of plagioclase (15%, labradorite [An_{60}] and andesine [An_{43}]). Groundmass: hyalopilitic-trachydoid texture; light cream volcanic glass with microlites of plagioclase (andesine [An_{40}]) and needle-shaped crystallites of plagioclase and pyroxene grains. Vesicles (0.7–5 mm): elongated-oval in shape, usually empty. Small (0.3–0.6 mm) vesicles are empty or walls of vesicles are lined with glass.

Alteration: rock is fresh.

Sample 126-793B-92R-1, 0–5 cm, Unit 1 [Z-1454]

Twopyroxene-plagioclase-phyric andesite, sparsely vesicular. Rock consists of phenocrysts (30%), glass (65%–70%), and vesicles (3%–5%). Phenocrysts: idiomorphic grains (0.3–5 mm) of bronzite (20%), small grains (0.3–0.5 mm) of clinopyroxene (2%–3%), and prismatic grains (0.1–0.7 mm) of plagioclase (5%–7%, labradorite [An_{60}]). Groundmass is vitrophyric texture; cream volcanic glass with sparse microlites and crystallites of plagioclase. Vesicles (0.1–0.6 mm) are rounded in shape, usually empty or completely infilled with light green glass.

Alteration: rock is fresh.

Sample 126-793B-95R-2, 28–32 cm (Piece 1), Unit 3 [Z-227]

Hyalobasaltic autobreccia; fragments of clinopyroxene-olivine-phyric glassy vesicular basalt and fragments of altered volcanic glass. Within fragments vesicles (0.05–0.1 mm) are filled by smectites.

Alteration: moderate (35%).

Sample 126-793B-03R-1, 37–42 cm, Unit 9 [Z-1455]

Lithoclastic tuff (breccia). Rock; angular fragments (2–5 mm) of highly vesicular twopyroxene-plagioclase-phyric andesite (90%), vitrophyric texture. Fragments of basalt and andesite-basalt are present. Cement: radial-radiand aggregates of zeolites.

Sample 126-793B-104R-1, 96–98 cm (Piece 6B), Unit 10 [Z-228]

Clinopyroxene-plagioclase-phyric (phenocrysts 0.1–0.5 mm, 1%) basalt, fine grained, poorly crystallized, vesicular. Single tabular crystals of orthopyroxene(?) and olivine(?) are present. Groundmass is hyalopilitic texture; volcanic glass with crystals of pyroxene, plagioclase, olivine, and opaque dust. Vesicles (0.05–0.2 mm, 5%–7%) are filled with smectites.

Alteration: slight (~10%–15%); smectites completely replace orthopyroxene(?) and olivine(?).

XRD: smectites with various composition of interlayer cations: Na-K and Mg-Ca.

Electron micrograph: b = 9.20 Å (trioctahedral smectite).

Sample 126-793B-110R-2, 57–59 cm (Piece 1C), Unit 13 [Z-229]

Olivine-pyroxene-phyric basalt, fine grained, poorly crystallized, vesicular. Phenocrysts of clinopyroxene (up to 3–4 mm, 1%–2%), orthopyroxene (up to 2 mm, <1%), and olivine (less then 1%). Groundmass is hyalopilitic texture; devitrified glass with laths of plagioclase, small grains of clinopyroxene, olivine, and opaque minerals.

Alteration: slight (~10%–15%); olivine is completely replaced with smectites; orthopyroxene is partly replaced with smectites.

XRD: smectite; trace hydromica.

Electron micrograph: b = 9.20 Å (trioctahedral smectite).

Sample 126-793B-110R-4, 38–40 cm (Piece 1C), Unit 13 [Z-230]

Olivine-pyroxene-phyric basalt, fine grained, poorly crystallized, vesicular (<1%). Phenocrysts of clinopyroxene (0.9–3 mm, 3%–5%), orthopyroxene (single grains), olivine (less then 1%), and plagioclase (single grains). Groundmass is hyalopilitic texture; laths of plagioclase, small grains of clinopyroxene, opaque minerals, and interstitial glass (5%–7%).

Alteration: slight (~10%); olivine and interstitial glass are replaced with smectites.

Sample 126-793B-111R-1, 102–104 cm (Piece 9A), Unit 14 [Z-231]

Olivine-pyroxene-phyric basalt, fine grained, poorly crystallized, vesicular. Phenocrysts of clinopyroxene (5%–7%), orthopyroxene (5%), and olivine (less then 1%). Groundmass is hyalopilitic texture; devitrified volcanic glass with laths of plagioclase, small grains of clinopyroxene, and opaque minerals. Small angular to rounded crystals of quartz are known. Vesicles (5%–7%) are partly filled by smectites.

Alteration: slight (~10%); olivine, orthopyroxene, and interstitial glass are replaced with smectites.

Sample 126-793B-112R-1, 100–102 cm (Piece 3C), Unit 14 [Z-232]

Olivine-pyroxene-phyric basalt, fine grained, poorly crystallized, vesicular. Phenocrysts of clinopyroxene (3%), orthopyroxene (5%–7%), and olivine (less then 1%). Groundmass is taxitic texture; laths of plagioclase, small grains of clinopyroxene, interstitial glass, and opaque minerals. Small rounded-xenomorphic crystals of quartz are present. Small rounded vesicles (3%–5%) are filled with smectites.

Alteration: moderate to high (~30%–40%); olivine, orthopyroxene, and interstitial glass are replaced by smectites.

XRD: smectite; trace hydromica.

Electron micrograph: b = 9.26 Å (trioctahedral smectite) and 9.11 Å (mica).

Sample 126-793B-113R-3, 27–31 cm (Piece 1C), Unit 15 [Z-1456]

Olivine-twopyroxene-plagioclase-phyric andesite (boninite), vesicular. Rock: phenocrysts (20%), glass (70%), and vesicles (10%). Phenocrysts: altered olivine, idiomorphic grains (0.3–1 mm) of pyroxenes, glomerophyric segregates of small prismatic grains (0.3–0.7 mm) of plagioclase (labradorite [$An_{60–62}$]). Groundmass: vitrophyric texture; light cream volcanic glass with crystallites of plagioclase and pyroxene (90%). Vesicles (0.2–0.7 mm): rounded in shape, usually empty (2%–3%) or completely infilled with light green glass (7%–8%).

Sample 126-793B-114R-1, 69–71 cm (Piece 1D), Unit 17 [Z-233]

Olivine-clinopyroxene-plagioclase-phyric basalt, fine grained, poorly crystallized, vesicular. Phenocrysts: plagioclase (0.5–2.5 mm, 15%–20%), clinopyroxene (0.5–0.7 mm, 1%), and orthopyroxene (single grains). Groundmass: hyaline/hyalopilitic texture; black devitrified volcanic glass with laths of plagioclase, small grains of clinopyroxene, and opaque minerals. Vesicles (0.05–0.7 mm, ~7%–10%): filled with smectites.

Alteration: moderate (~20%–25%); olivine, orthopyroxene, and interstitial glass are replaced with smectites.

XRD: smectite; trace hydromica, heulandite(?), and chlorite(?).

Electron micrograph: b = 9.26 Å (trioctahedral smectite).

Hole 791B

Sample 126-791B-57R-1, 0–5 cm (Piece 1B), Unit 4 [Z-1435]

Sparsely plagioclase-phyric basalt, crystallized, vesicular. Phenocrysts (<1%): single prismatic grains of plagioclase (andesine [An_{45}]). Plagioclases contain fine inclusions of glass. Groundmass (75%): intersertal-microdoleritic texture; microlites (0.1–0.4 mm) of plagioclase (labradorite [An_{55}] and andesine [An_{48}]). Interstices: segregates of small (<0.1 mm) grains of clinopyroxene (15%), glass (5%), and opaque minerals (5%). Vesicles (25%, 0.1–0.4 mm and 0.7–1.1 mm): isometric and oval in shape, usually empty; walls of vesicles are lined with smectites.

Alteration: rock is fresh.

Sample 126-791B-57R-1, 52–56 cm (Piece 6), Unit 5 [Z-692]

Sparsely olivine-phyric basalt (microdolerite), vesicular. Phenocrysts: two large (2–2.5 mm) phenocrysts of olivine. Groundmass: intersertal texture; unoriented laths (0.1–0.5 mm) of plagioclase (andesine [An_{42}]). Interstices: segregates of small grains of augite, brownish green glass (5%), with opaque dust. Vesicles (30%–35%, 0.2–2.5 mm): rounded and isometric in shape.

Alteration: phenocrysts of plagioclase are partly replaced by carbonate; vesicles are partly or completely filled with clay minerals and zeolite.

Sample 126-791B-59R-1, 21–25 cm (Piece 1), Unit 6 [Z-1436]

Lava breccia. Rock: oval fragments (80%, 3–5 mm) of pyroxene-phyric basalt and cement (20%). Cement: small (<0.1 mm) fragments of basalt and green glass. Small vesicles in basalt are rounded in shape, usually empty; walls of vesicles are lined with green glass.

Alteration: rock is fresh.

Sample 126-791B-61R-1, 42–50 cm (Piece 9), Unit 8 [Z-143]

Plagioclase-phyric basalt, crystallized. Phenocrysts (15%): prismatic and tabular grains (0.5–1.7 mm) of plagioclase (labradorite [$An_{60–65}$]). Groundmass (85%): microlitic texture; microlites and microlaths (0.1–0.6 mm) of plagioclase (andesine [$An_{38–45}$] and occasionally labradorite [An_{55}]). Interstices: segregate of small (0.1 mm) grains of clinopyroxene (25%), brownish green glass (25%), and opaque minerals (5%–7%).

Alteration: moderate (25%); interstitial glass is replaced by clay minerals.

Sample 126-791B-63R-1, 65–70 cm (Piece 9), Unit 11 [Z-1438]

Aphyric hyalobasalt, glassy, vesicular. Rock: hyalopilitic texture; needle-shaped microlites and laths (up to 2 mm) of plagioclase (andesine [An_{32}]), microlites of clinopyroxene, and black to brownish green volcanic glass with crystals of clinopyroxene. Vesicles (0.01–0.5 mm, ~40%): usually empty; walls of vesicles are lined with green glass, very small vesicles are completely filled with glass. Single large (1.6 mm) vesicle is empty.

Alteration: rock is fresh.

Sample 126-791B-63R-1, 88–93 cm (Piece 12), Unit 11 [Z-1439]

Olivine-plagioclase-phyric basalt, noncrystallized, vesicular. Phenocrysts (20%): idiomorphic grains (0.6–1 mm) of olivine (10%) and glomerophyric segregates (up to 3.5 mm) of prismatic and tabular grains (0.5–2.5 mm) of plagioclase (10%, labradorite [An_{58}]). Groundmass (40%): vitrophyric texture; brownish green and black glass (25%). Vesicles (<0.3–0.6 mm, 40%): rounded and oval in shape; walls (>0.3 mm, 25%) are lined with glass and infilled with chalcedony in central parts. Small vesicles (75%) are completely filled with greenish glass.

Alteration: slight (10%–15%); olivine completely replaced by iddingsite; glass in vesicles is partly replaced by clay minerals; chalcedony in vesicles.

Sample 126-791B-64R-1, 48–52 cm (Piece 6), Unit 11 [Z-216]

Pyroxene-plagioclase-phyric hyalobasalt, glassy, vesicular. Phenocrysts (up to 20%): orthopyroxene(?) and olivine(?). The microphyric scoriaceous rock is hyaline texture, noncrystallized volcanic glass with tabular crystals of plagioclase (0.4–0.6 mm, 5%–7%), rounded crystals of orthopyroxene (0.2–0.3 mm, 1%–3%), and opaque minerals. Vesicles (0.01–0.5 mm, ~50%): usually empty; walls of vesicles are lined with smectites.

Alteration: slight to moderate (~20%).

XRD: smectite with ~20% mica layers.

Sample 126-791B-66R-2, 0–5 cm (Piece 1A), Unit 11 [Z-693]

Olivine-plagioclase-phyric basalt, highly vesicular. Phenocrysts (30%): idiomorphic grains (0.3–0.5 mm) of olivine (10%) and glomerophyric segregates of prismatic grains (0.1–0.8 mm up to 1.2 mm) of plagioclase (20%, andesine-labradorite [An_{50}]). Groundmass (40%): vitrophyric texture; light green glass. Vesicles (0.1–0.5 mm, 50%): oval in shape; walls (0.2–0.5 mm) are lined with glass. Small vesicles are completely filled with glass.

Alteration: slight; plagioclase grains with sizes >0.8 mm (up to 1.2 mm) are replaced by pelite; glass from vesicles is partly replaced by palagonite.

Sample 126-791B-67R-2, 123–125 cm (Piece 16), Unit 11 [Z-217]

Hyalobasaltic autobreccia is composed of various sizes of xenomorphic fragments of two types. The first type (90% of rock volume) is represented by light green devitrified glass with fragments of plagioclase, orthopyroxene, and small amounts of opaque minerals. Groundmass: hyaline texture. Vesicles (0.1–2 mm, 7%–10%): filled with palagonitized glass and smectites. The second type cements the first one. It is composed of black plagioclase-phyric glass with opaque dust and single crystals of orthopyroxene.

Alteration: moderate (~30%).

Electron micrograph: b = 9.20 Å (trioctahedral smectite).

Sample 126-791B-72R-2, 50–55 cm (Piece 6A), Unit 11 [Z-1440]

Plagioclase-phyric basalt, poorly crystallized, vesicular. Phenocrysts (15%): glomerophyric segregates of prismatic grains (0.4–1.5 mm) of plagioclase (labradorite [An_{58}]). Groundmass (45%): vitrophyric texture; light green to brownish black glass. Vesicles (0.1–0.7 mm, 40%): rounded in shape; walls (0.3–0.7 mm, 15%) are lined with glass, in central parts: chalcedony. Small vesicles (25%) usually are lined or completely infilled with glass.

Alteration: slight.

Sample 126-791B-73R-2, 73–75 cm (Piece 4B), Unit 11 [Z-694]

Lithoclastic tuff (breccia). Rock: large angular fragments (5–6 mm) of highly vesicular plagioclase-phyric basalt (glomerophyric segregates of plagioclase, 0.1–0.9 mm, andesine-labradorite [An_{50}], and black glass). Vesicles (60%, 0.3–0.8 mm): rounded in shape; walls are lined with green glass, central parts are infilled with zeolite. Cement: small fragments (0.1–0.3 mm) of hyalobasalt and green glass.

Alteration: rock is fresh.

Sample 126-791B-73R-2, 73–75 cm (Piece 4B), Unit 11 [Z-218]

Hyalobasaltic autobreccia: large (10–25 mm) fragments of plagioclase-phyric vesicular (30%–40%) basalt. Fragments are composed of light green devitrified glass with hyaline texture. These fragments are cemented with black aphyric vesicular hyalobasalt. Within fragments vesicles are filled with palagonitized glass; vesicles within matrix are empty or filled with smectites.

Alteration: slight (~10%).

XRD: smectite with ~20% mica layers; trace chlorite(?).

Electron micrograph: b = 9.20 Å (trioctahedral smectite).

Sample 126-791B-73R-2, 80–84 cm (Piece 4B), Unit 11 [Z-1441]

Orthopyroxene-phyric andesite (boninite), poorly crystallized, vesicular. Phenocrysts (20%): idiomorphic grains (0.2–0.8 mm) of orthopyroxene (bronzite). Groundmass: vitrophyric texture; pyroxene and colorless glass (55%) with very small crystals of plagioclase. Vesicles (25%, 0.1–0.6 mm): rounded in shape; walls are lined with greenish glass, occasionally completely infilled with glass.

Alteration: rock is fresh.

Sample 126-791B-75R-1, 97–105 cm (Piece 14), Unit 14 [Z-1442]

Sparsely plagioclase-phyric andesite, poorly crystallized, highly vesicular. Phenocrysts (5%): two tabular grains (0.4 mm) of andesine. Groundmass: vitrophyric texture; colorless to light brown glass (15%) with sparse microlites of plagioclase. Vesicles (80%, 0.1–0.4 mm): rounded in shape; partly or completely filled with light greenish glass.

Alteration: moderate (40%); plagioclase is replaced by pelite; 40% of vesicles are infilled with clay minerals.

Sample 126-791B-76R-2, 48–52 cm (Piece 6A), Unit 14 [Z-1443]

Lithoclastic tuff (breccia). Rock: angular fragments (1.5–5 mm) of highly vesicular plagioclase-phyric andesite. Andesite is poorly crystallized, plagioclase-phyric. Phenocrysts (25%): prismatic grains (0.5–0.7 mm) of plagioclase (labradorite [An_{68}]). Groundmass (60%): light green glass with microlites of plagioclase (andesine

[An_{42}]). Vesicles (15%, 0.1–0.4 mm): isometric in shape; walls are lined with reddish brown Fe hydroxides, central parts are infilled with green glass. Cement: small angular fragments (0.1–0.7 mm) of andesite.

Alteration: rock is fresh; single vesicles are filled with carbonate; carbonate is present in cement (5%–7% of total volume of breccia).

Sample 126-791B-76R-3, 40–45 cm (Piece 4B), Unit 15 [Z-1444]

Plagioclase-phyric dolerite, fine grained. Phenocrysts (5%): prismatic grains (0.8–1.2 mm) of plagioclase (labradorite [An_{64}]). Groundmass: intersertal-poikilophitic texture; isometric grains (0.3–1.5 mm) of clinopyroxene (30%), laths and prismatic grains of plagioclase (45%, 0.2–0.6 mm, andesine [An_{43}]), greenish brown glass (10%), and grains (0.1–0.3 mm) of opaque minerals (5%–7%).

Alteration: slight (5%–7%); glass is replaced by clay minerals.

Sample 126-791B-77R-2, 0–5 cm (Piece 1A), Unit 18 [Z-1445]

Litho-vitroclastic tuff. Rock: large fragments (up to 5 mm) of andesite and andesite-basalt (10%), small fragments (0.2–0.6 mm) of rocks (10%), altered plagioclase, and fragments of light green glass.

Alteration: very strong (80% or more); plagioclase is almost completely replaced by albite; chalcedony almost completely replaces rock.

Sample 126-791B-77R-2, 132–137 cm (Piece 6A), Unit 20 [Z-1446]

Litho-crystallo-vitroclastic tuff. Rock: angular fragments (0.1–0.6 mm) of different minerals (10%): grains of quartz (2%), plagioclase (6%), and orthoclase (2%). Fragments (up to 2.5 mm) of andesite and basalt (20%); fragments of glass (40%). Cement (30%): clay minerals.

Alteration: moderate (30%–40%); glass replaced by muscovite-phlogopite-like minerals; this mica-mineral (30%) cements fragments of rocks and minerals.

Sample 126-791B-77R-3, 18–23 cm (Piece 1B), Unit 20 [Z-1447]

Litho-crystallo-vitroclastic tuff. Rock is identical to Sample 126-791B-77R-2, 132–137 cm (Z-1446).

Alteration: moderate (30%–40%); mica (30%) replaces cement and fragments of glass.

Sample 126-791B-78R-1, 24–30 cm (Piece 4), Unit 24 [Z-1448]

Lava breccia. Rock: fragments (0.3–1.5 mm) of aphyric andesite and small fragments (0.1–0.3 mm) of plagioclase with inclusions of chloritized glass. Cement: colorless glass and very small fragments of rocks and minerals.

Alteration: slight (10%–15%); glass replaced by clay mineral.

Sample 126-791B-78R-1, 72–77 cm (Piece 8), Unit 24 [Z-1616]

Lava breccia of hyalobasalt with vitrophyric texture.

Alteration: very strong (80%); glass is replaced by clay minerals; albite and clay minerals replace plagioclase.

Sample 126-791B-79R-1, 5–8 cm (Piece 1), Unit 26 [Z-695]

Olivine-clinopyroxene-phyric trachybasalt, massive. Phenocrysts (15%): plagioclase and clinopyroxene (0.1–0.5 mm). Groundmass: intersertal texture; reddish brown laths (0.1–0.3 mm) of orthoclase(?) (80%), grains (up to 0.2 mm) of opaque minerals (15%), and green interstitial glass (5%).

Alteration: strong (50%); orthoclase is completely replaced by pelite; clay minerals replace glass; microcrack (0.3 mm) is infilled with opaque minerals, clay minerals, carbonate, and zoisite(?).

Sample 126-791B-79R-1, 45–50 cm (Piece 5A), Unit 28 [Z-1449]

Litho-vitroclastic tuff. Rock: sparse fragments (0.8 mm) of andesite (1%) and fragments of light green volcanic glass (50%–55%).

Alteration: moderate (35%–40%); rock replaced by orthoclase (adularia?).

West Philippine Basin, Palau-Kyushu Ridge, and Parece Vela Basin (Leg 59)

West Philippine Basin (Hole 447A)

Sample 59-447A-14R-1, 140–144 cm (Piece 4L), Unit 6a [Z-314]

Sparsely plagioclase-phyric basalt. Phenocrysts: plagioclase (0.4–1.6 mm, 5%, andesine [An_{46}]). Groundmass (95%): microlitic texture; laths and microlites (0.1–0.4 mm) of plagioclase (35%, andesine [An_{45}]). Interstices: segregates of clinopyroxene microlites (45%), opaque minerals (5%), small (0.1 mm) oxidized grains of olivine (5%), and volcanic glass. Vesicles are empty.

Alteration: slight (~5%–10%); plagioclase in central parts are occasionally completely replaced by zeolite; glass replaced by clay minerals; veinlets (0.7 mm thick) in rocks contain clay minerals and sparse fragments of altered glass.

XRD: smectite; trace quartz(?) and chlorite(?).

Sample 59-447A-14R-3, 53–58 cm (Piece 3D), Unit 6b [Z-315]

Sparsely plagioclase-phyric basalt, sparsely vesicular (1%–3%). Phenocrysts: plagioclase (1–1.5 mm, 3%). Single phenocrysts of olivine (up to 1 mm) are recognized. Groundmass: intersertal to subvariolitic texture; volcanic glass, small grains of clinopyroxene, and laths of plagioclase.

Alteration: moderate (~20%); smectites-chlorite aggregate replaces olivine and fills vesicles.

XRD: smectite and swelling chlorite(?); trace chlorite(?).

Sample 59-447A-15R-2, 116–121 cm (Piece 5D), Unit 6c [Z-316]

Sparsely plagioclase-phyric basalt, sparsely vesicular (5%). Phenocrysts: plagioclase and glomerophyric segregates (1–2 mm, 5%). Single phenocrysts of olivine (0.5–0.8 mm) are present. Groundmass: subvariolitic texture; volcanic glass, small grains of clinopyroxene, and laths of plagioclase.

Alteration: moderate (~20%–25%); smectites replace olivine and fill vesicles.

XRD: smectite.

Sample 59-447A-16R-2, 19–21 cm (Piece 3A), Unit 7 [Z-317]

Aphyric basalt, fine grained, almost completely crystallized, massive. Rock: intergranular texture (some areas subophitic); xenomorphic clinopyroxene (45%), laths of plagioclase (50%), olivine (1%–3%), and opaque minerals (1%–3%). Single vesicles are registered.

Alteration: moderate (~20%); smectites, chlorite, and carbonate replace olivine; vesicles are filled with carbonate.

XRD: smectite, chlorite(?), and hydromica(?) in trace amounts.

Sample 59-447A-16R-2, 87–89 cm (Piece 10), Unit 7 [Z-1144]

Aphyric dolerite, fine grained, massive. Rock: intersertal-ophitic texture; plagioclase (35%), clinopyroxene (40%), opaque minerals (5%), and glass (20%). Plagioclase forms laths (0.4–1.2 mm) with composition labradorite [An_{56}] and andesine [An_{45}]. Pyroxene forms xenomorphic grains (0.1–0.7 mm). Interstitial glass is black and altered.

Alteration: slight (~15%–18%); glass is almost completely replaced by brown secondary minerals.

Sample 59-447A-17R-3, 49–53 cm (Piece 5A), Unit 8a [Z-1145]

Plagioclase phyric andesite-basalt, fine grained, vesicular. Phenocrysts: plagioclase (0.3–0.6 mm, 5%–7%, andesine [An_{48}]). Groundmass (90%–93%): vitrophyric texture; black glass and needle-shaped microlites of plagioclase (2%–3%, 0.1–0.3 mm, andesine [An_{37}]). Vesicles (1%, 0.1–0.3 mm): rounded, empty.

Alteration: rock is fresh.

Sample 59-447A-19R-3, 115–120 cm (Piece 8G), Unit 8b [Z-318]

Olivine-pyroxene-plagioclase-phyric basalt, poorly crystallized, glassy, massive. Phenocrysts: plagioclase (3%), olivine (<1%), and orthopyroxene (single crystals are present). Groundmass: hyalopilitic texture; black volcanic glass and needle-shaped laths of plagioclase.

Alteration: slight (~10%–15%).

XRD: smectite.

Sample 59-447A-23R-1, 39–42 cm (Piece 2B), Unit 8d [Z-1146]

Pyroxene-plagioclase-phyric basalt, poorly crystallized, massive. Phenocrysts (10%): pyroxene (2%) forms xenomorphic grains (0.8–1 mm); glomerophyric segregates of prismatic grains of plagioclase (8%, 0.5–0.8 mm, labradorite [An_{68}], and several prisms: labradorite [An_{58}]). Groundmass: microlitic (microdoleritic) texture; laths of plagioclase (35%, 0.2–0.6 mm, labradorite [An_{52}] and andesine [An_{45}]). Interstices: segregates of small (0.1–0.3 mm) rounded and isometric grains of clinopyroxene (40%), brownish black glass (10%), and opaque minerals (5%).

Alteration: rock is fresh.

Sample 59-447A-23R-1, 51–58 cm (Piece 5D), Unit 8d [Z-1147]

Plagioclase-phyric basalt, fine grained, massive. Phenocrysts (5%): glomerophyric segregates of prismatic grains of plagioclase (0.7–1 mm). Groundmass: microlitic texture; laths of plagioclase (35%, 0.2–0.9 mm, labradorite

[An_{64}] and [An_{55}], and andesine [An_{40}]). Interstices: xenomorphic grains of clinopyroxene (40%, 0.1–0.6 mm), greenish brown glass (15%), and opaque minerals (5%).

Alteration: slight (10%–15%).

Sample 59-447A-24R-2, 25–39 cm (Piece 1B), Unit 9 [Z-1148]

Aphyric dolerite, fine grained, massive. Rock: doleritic texture; laths of plagioclase (40%, 0.3–1.5 mm, labradorite [An_{65}] and [An_{55}], and andesine [An_{40}]). Interstices: xenomorphic grains of clinopyroxene (45%, 0.2–0.5 mm), brownish green glass (10%), and opaque minerals (5%).

Alteration: slight (~15%); interstitial glass is replaced by hydrobiotite(?).

Sample 59-447A-24R-2, 99–102 cm (Piece 2D), Unit 9 [Z-1149]

Aphyric dolerite, fine grained, massive. Rock: ophitic texture; laths of plagioclase (45%, 0.4–1.5 mm, labradorite [An_{55}] and andesine [An_{40}]). Interstices: xenomorphic grains of clinopyroxene (40%, 0.2–0.6 mm), altered glass (6%–7%), and opaque minerals (3%–4%, 0.1 mm). Olivine forms small (0.2–0.3 mm) idiomorphic grains.

Alteration: slight (~10%); interstitial glass is replaced by clay minerals; chlorite(?) replaces olivine.

Sample 59-447A-25R-1, 40–42 cm (Piece 1C), Unit 9 [Z-319]

Aphyric dolerite, fine grained, inequigranular, massive. Rock: subophitic texture; laths of plagioclase (50%–55%), clinopyroxene (40%–45%), orthopyroxene (1%–5%), and opaque minerals (1%–3%). Interstitial glass is <1% abundance.

Alteration: slight (~10%); smectites and clay minerals replace interstitial glass.

XRD: smectite; chlorite and quartz(?) in trace amounts.

Sample 59-447A-27R-1, 21–25 cm (Piece 2B), Unit 10b [Z-1150]

Sparsely plagioclase-phyric basalt. Phenocrysts: single glomerophyric segregate (1%) of prismatic grains (0.5–0.8 mm) of plagioclase. Groundmass: microlitic texture; microlites of plagioclase (35%, 0.1–0.4 mm, labradorite [An_{68}] and [An_{50}]) and segregates of very small grains (45%, 0.05–0.1 mm) of plagioclase, brownish orange oxidized glass (15%), and opaque minerals (5%).

Alteration: slight (~15%); segregates of plagioclase grains are completely replaced by zeolite; microcracks (3%–4%, 0.1–0.2 thick) in rock are infilled with carbonate and zeolite.

Sample 59-447A-28R-1, 65–70 cm (Piece 4C), Unit 11a [Z-320]

Sparsely plagioclase-phyric basalt, poorly crystallized. Phenocrysts: elongated-platy crystals of plagioclase (5%–7%), partly replaced by K-feldspar. Groundmass: hyalopilitic texture; black volcanic glass containing needle-shaped laths of plagioclase.

Alteration: slight (~15%).

XRD: smectite.

Sample 59-447A-29R-4, 137–142 cm (Piece 3B), Unit 11b [Z-321]

Sparsely plagioclase-phyric basalt, poorly crystallized, sparsely vesicular (<1%). Phenocrysts: platy and elongated-platy crystals of plagioclase (5%). Single microphenocrysts of olivine are registered. Groundmass: hyalopilitic texture.

Alteration: slight to moderate (15%–20%); olivine is replaced by smectites.

XRD: smectite.

Sample 59-447A-30R-3, 89–94 cm (Piece 3C), Unit 11c [Z-322]

Sparsely plagioclase-phyric basalt, poorly crystallized, sparsely vesicular (<1%). Phenocrysts: platy and elongated-platy crystals of plagioclase (1%). Single microphenocrysts of olivine are present. Groundmass: hyalopilitic texture.

Alteration: slight to moderate (15%–20%); olivine is replaced by smectites; vesicles are filled with smectites, occasionally with carbonate.

XRD: smectite; trace quartz(?).

Sample 59-447A-32R-1, 99–105 cm (Piece 3K), Unit 11e [Z-323]

Sparsely plagioclase-phyric basalt, fine grained, crystallized, sparsely vesicular. Phenocrysts (5%): platy and prism crystals of plagioclase (0.4–0.6 mm, labradorite [An_{59}]). Vesicles (2%–3%): small (0.1–0.2 mm) and rounded in shape; infilled with glass or empty. Groundmass: microlitic texture; laths and microlites of plagioclase (30%, andesine [An_{43}] and [An_{48}]), clinopyroxene (50%, glass (5%), and opaque minerals (5%).

Alteration: slight (5%); several grains of plagioclase are replaced by zeolite (2%–3%); olivine is replaced by smectites and carbonate; vesicles are filled with smectites; some crystals of plagioclase are partly replaced by K-feldspar, occasionally with carbonate.

XRD: smectite; trace quartz(?).

Sample 59-447A-35R-3, 45–50 cm (Piece 2C), Unit 11e [Z-324]

Sparsely plagioclase-phyric basalt, poorly crystallized, sparsely vesicular. Phenocrysts: platy and elongated-platy crystals of plagioclase (10%–15%). Vesicles (<1%): small and rounded in shape. Groundmass: hyalopilitic texture; black volcanic glass with opaque dust and laths of plagioclase and single microphenocrysts of olivine.

Alteration: moderate (20%); olivine is replaced by smectites and carbonate; vesicles are filled with smectites; some crystals of plagioclase are partly replaced by K-feldspar, occasionally by carbonate.

XRD: smectite.

Sample 59-447A-36R-4, 31–36 cm (Piece 3A), Unit 11f [Z-325]

Oligoclase-plagioclase-phyric basalt, poorly crystallized, massive. Phenocrysts (10%): platy crystals of oligoclase(?) and elongated-platy crystals of plagioclase. The latter predominate in amounts. Single microphenocrysts of olivine occur also. Groundmass: pilotaxitic or (in some areas) subvariolitic texture; black volcanic glass with opaque dust and laths of plagioclase.

Alteration: moderate (~20%–25%); olivine(?) is replaced by smectites and carbonate.

XRD: smectite.

Palau-Kyushu Ridge (Hole 448)

Sample 59-448-37R-1, 32–37 cm (Piece 3C), Unit 6 [Z-1152]

Plagioclase-phyric basalt, vesicular. Phenocrysts (2%): two prism crystals of plagioclase (0.6 and 1.5 mm). Groundmass: pilotaxitic-microlitic texture; various grains microlites and laths of plagioclase (25%, 0.1–0.6 mm, labradorite [An_{60}] and andesine [An_{42}]), xenomorphic grains and segregates of pyroxene (20%, 0.1 mm), and black glass (5%). Vesicles (50%): large (1–2.5 mm) rounded empty vesicles (20%) and small (0.1–0.5 mm) isometric vesicles (30%). The latter are mainly empty (90%); 10% of small vesicles are encrusted with clay minerals.

Alteration: walls of several small vesicles are lined with smectites; veins and two large vesicles are infilled with carbonate.

Sample 59-448-38R-1, 45–50 cm (Piece 1H), Unit 6 [Z-1153]

Sparsely plagioclase-phyric basalt, incompletely crystallized, vesicular. Phenocrysts (2%): two glomerophyric segregates of plagioclase prismatic grains (0.3–0.5 mm). Vesicles (60%): large (1–2.5 mm) isometric empty vesicles (50%), and small (0.1–0.5 mm) isometric vesicles (30%). Groundmass: vitrophyric texture; black glass (35%), microlites of plagioclase (5%, labradorite [An_{52}]), and microlites of pyroxene (<1%).

Alteration: rock is fresh.

Sample 59-448-38R-1, 123–128 cm (Piece 5B), Unit 6 [Z-1154]

Sparsely plagioclase-phyric basalt, incompletely crystallized, vesicular. Phenocrysts (2%–3%): glomerophyric segregates of plagioclase prismatic grains (0.2–0.5 mm, labradorite [An_{55-56}]). Groundmass: hyalopilitic-vitrophyric texture; black glass, microlites of plagioclase (10%, andesine [An_{42}]), and grains of pyroxene (2%–3%). Vesicles (60%–65%): large (1–3 mm) rounded or isometric (30%–35%); empty, occasionally these large vesicles are completely infilled with carbonate; second type: small (0.1–0.3 mm) isometric (30%); also empty or infilled with carbonate.

Alteration: rock is fresh.

Sample 59-448-39R-1, 117–12 cm (Piece 10B), Unit 6 [Z-1155]

Sparsely plagioclase-pyroxene-phyric basalt, vesicular. Phenocrysts (2%–3%): single glomerophyric segregate of plagioclase prismatic grains (<1%) and several idiomorphic grains (0.3–0.5 mm) of pyroxene. Groundmass: hyalopilitic-vitrophyric texture; microlites of plagioclase (10%, andesine [An_{42-44}]), grains of pyroxene (2%–3%), and black glass (20%–25%). Vesicles (60%–65%): large (1.5–5 mm) isometric (35%) and small (0.05–0.3 mm) isometric (30%); all are empty.

Alteration: rock is fresh.

Sample 59-448-39R-2, 60–63 cm (Piece 2F), Unit 6 [Z-530]

Plagioclase-phyric andesite-basalt, vesicular. Phenocrysts (10%): glomerophyric segregates of plagioclase tabular and prismatic grains (0.5–0.9 mm, labradorite [An_{53}]) and a single grain of olivine (0.5 mm). Groundmass: doleritic-intersertal texture; microlites and laths of plagioclase (50%, labradorite [An_{52}] and andesine [An_{45}]). Interstices: segregates of small grains of clinopyroxene and black glass with opaque minerals. Vesicles (10%, 0.1–0.3 mm): rounded or rounded-isometric in shape; several are lined with palagonitized glass.

Alteration: rock is fresh.

Sample 59-448-43R-2, 45–50 cm (Piece 5), Unit 8 [Z-1156]

Aphyric basalt, crystallized, vesicular. Rock: microlitic texture; microlites of plagioclase (25%, 0.05–0.3 mm, andesine [An_{44}]), segregates of clinopyroxene grains (40%), brownish oxidized glass (10%), and opaque minerals (5%). Vesicles (20%): large, rounded (up to 1.5 mm) and small (18%, 0.1–0.5 mm); almost all (99%) are empty. Several vesicles are lined with crystals of zeolite.

Alteration: rock is fresh.

Sample 59-448-48R-1, 120–125 cm (Piece 11A), Unit 9 [Z-1157]

Aphyric basalt, crystallized, vesicular. Rock: microlitic texture; microlites of plagioclase (25%, andesine [$An_{46–48}$]), microlites of clinopyroxene (25%), and black glass (10%). Vesicles (40%, 0.05–0.9 mm, one vesicle: 1.7 mm) are empty. Several vesicles (1%–2%) are completely or partly infilled with zeolite.

Alteration: rock is fresh.

Sample 59-448-53R-2, 50–53 cm (Piece 1H), Unit 11 [Z-1158]

Aphyric basalt, crystallized, vesicular. Rock: microlitic texture; microlites of plagioclase (25%, 0.05–0.3 mm, andesine-labradorite [An_{50}] and andesine [An_{42}]), segregate of clinopyroxene very small grains (25%), and black glass (10%). Large rounded vesicles (10%, 1.5–5 mm) and small isometric vesicles (30%, 0.05–0.3 mm) are present. Large vesicles are empty or infilled with glass. Occasionally walls of vesicles are lined with chalcedony and zeolite.

Alteration: rock is fresh.

Sample 59-448-59R-2, 50–55 cm (Piece 2G), Unit 13 [Z-1159]

Plagioclase-phyric basalt, crystallized, vesicular. Phenocrysts (15%): glomerophyric segregates of plagioclase prismatic grains (0.5–2 mm, labradorite [$An_{60–62}$]). Groundmass: microlitic texture; microlites of plagioclase (25%, andesine [An_{46}]), microlites of clinopyroxene (20%), brownish glass (10%), and opaque minerals (3%–5%). Vesicles (25%): single rounded (up to 2.5 mm) vesicles and small (0.1–0.3 mm) isometric vesicles; all are empty.

Alteration: rock is fresh.

Sample 59-448-61R-3, 35–38 cm (Piece 1D), Unit 13 [Z-532]

Plagioclase-phyric andesite-basalt, massive. Phenocrysts (15%): tabular grains (0.9–2 mm, labradorite [An_{56}], zonal). Groundmass: pilotaxitic texture; laths of plagioclase (50%, 0.2–0.4 mm, andesine [An_{42}]), small isometric grains of clinopyroxene, green glass, and opaque minerals (10%).

Alteration: rock is fresh.

Hole 448A

Sample 59-448A-10R-4, 61–65 cm (Piece 4A), Unit 5 [Z-533]

Sparsely clinopyroxene-plagioclase-phyric andesite-basalt, vesicular. Phenocrysts: single glomerophyric segregates of plagioclase prismatic grains (2%–3%, 0.3–0.6 mm, labradorite [An_{55}]) and single grain of clinopyroxene (0.7 mm). Groundmass: pilotaxitic texture; laths of plagioclase (andesine [$An_{42–45}$]), small isometric grains of clinopyroxene, and brownish glass (15%). Isometric vesicles (5%, 0.1–0.6 mm) are empty or completely infilled with carbonate.

Alteration: rock is fresh.

Sample 59-448A-12R-4, 27–31 cm (Piece 2C), Unit 5 [Z-534]

Plagioclase-phyric basalt, massive. Phenocrysts (15%): glomerophyric segregates of plagioclase prismatic grains (0.5–1.5 mm, labradorite [An_{55}]). Groundmass (85%): vitrophyric-variolitic texture; brownish variolitic glass. Rock is glassy crust from the top of the flow.

Alteration: rock is fresh.

Sample 59-448A-13R-2, 70–75 cm (Piece 6A), Unit 6 [Z-1160]

Andesite tuff (volcanic ash). Rock: small (0.1 mm) angular or isometric fragments of light green glass.

Alteration: rock is fresh.

Sample 59-448A-14R-2, 58–64 cm (Piece 4B), Unit 11 [Z-1161]

Volcanic breccia with tuff. Rock: fragments (90%–95%) of basalt, andesite, andesite-dacite(?) (1–6 mm). Matrix (5%–10%): zeolite with small (0.1–0.5 mm) fragments of light green glass and black glass.

Alteration: matrix is zeolitized.

XRD: trace smectite with ~30%–40% mica layers; yellow fragments of rock: smectite and phillipsite.

Sample 59-448A-14R-2, 114–118 cm (Piece 4G), Unit 11 [Z-535]

Sparsely plagioclase-phyric andesite-basalt, vesicular. Phenocrysts: single prismatic phenocryst of zonal plagioclase (0.8 mm). Groundmass: hyalopilitic (intersertal?) texture; microlites and laths of plagioclase (0.2–0.5 mm, andesine [An_{42-48}]), small isometric grains of clinopyroxene, and glass (30%). Vesicles (20%, 0.2–0.3 mm): empty or infilled with glass.

Alteration: plagioclase phenocrysts are almost completely replaced by carbonate.

Sample 59-448A-15R-1, 14–19 cm (Piece 1B), Unit 13 [Z-326]

Plagioclase-phyric basalt, fine grained, vesicular. Phenocrysts: platy crystals of plagioclase (20%); occasionally, they form glomerophyric segregates. Single rounded crystals of K-feldspar are present. Vesicles (25%–30%): irregularly rounded in shape. Groundmass: intergranular texture; various grains of pyroxene, laths of plagioclase, and opaque minerals. Interstitial brownish black volcanic glass is present.

Alteration: slight to moderate (~15%–20%); walls of vesicles are lined with smectites.

XRD: smectite; chlorite(?) in trace amounts.

Sample 59-448A-16R-1, 47–52 cm (Piece 4B), Unit 13 [Z-327]

Plagioclase-phyric basalt, fine grained, almost completely crystallized, vesicular. Phenocrysts: platy crystals of plagioclase (15%). Single phenocrysts of pyroxene and K-feldspar are present. Groundmass: intergranular texture; various grains of pyroxene, laths of plagioclase, and opaque minerals. Interstitial brownish black volcanic glass is present. Vesicles: various sizes and irregular shapes.

Alteration: slight (~15%); vesicles are empty or partly filled with smectites, occasionally with admixtures of carbonate.

XRD: smectite is heterogeneous; trace hydromica(?).

Sample 59-448A-20R-1, 142–147cm (Piece 3B), Unit 14 [Z-328]

Aphyric basalt, poorly crystallized, highly vesicular. Single phenocrysts of plagioclase are present. Groundmass: hyalopilitic texture; black volcanic glass with opaque dust and laths of plagioclase. Vesicles (20%–25%): rounded in shape; filled with black volcanic glass and smectites.

Alteration: moderate (~25%); vesicles are partly filled with smectites.

XRD: smectite.

Sample 59-448A-22R-1, 11–14 cm (Piece 1C), Unit 15 [Z-536]

Aphyric andesite-basalt, sparsely vesicular. Rock: pilotaxitic texture; microlites and microlaths of plagioclase (0.1–0.4 mm, andesine [An_{38-42}]), small grains (0.1 mm) of pyroxene, greenish brown volcanic glass with opaque crystals, and opaque minerals (5%–7%).

Alteration: rock is fresh.

Sample 59-448A-26R-2, 134–137 cm (Piece 3A), Unit 17 [Z-1160]

Crystallo-vitroclastic tuff. Rock: very small (0.01–0.2 mm) angular fragments of plagioclase crystals, colorless and black volcanic glass, fragments of carbonate (80%), and clay minerals with foraminifers.

Sample 59-448A-26R-3, 72–75 cm (Piece 1H), Unit 17 [Z-538]

Litho-vitroclastic tuff. Rock: fragments of green volcanic glass (0.2–0.4 mm) and angular fragments of andesite-basalt with oxidized glass, and microlites of plagioclase.

XRD: mixed-layer smectite-illite minerals (~50%–60% mica layers).

Sample 59-448A-30R-1, 95–99 cm (Piece 4B), Unit 19 [Z-539]

Vitroclastic tuff. Rock: angular fragments of green volcanic glass (0.1–0.3 mm).

Sample 59-448A-32R-1, 67–69 cm (Piece 1G), Unit 20A [Z-540]

Aphyric andesite-basaltic microdolerite, massive. Rock: intersertal-microdoleritic texture; microlites and microlaths (0.1–0.4 mm) of plagioclase (60%, andesine [An_{42-44}]), small grains or segregates of clinopyroxene (20%), and glass (20%).

Alteration: interstitial glass is replaced by green clay minerals.

Sample 59-448A-33R-2, 10–15 cm (Piece 1A), Unit 20 [Z-329]

Aphyric basalt, incompletely crystallized, massive. Rock: intersertal texture; laths of plagioclase (50%), xenomorphic pyroxene (40%), opaque minerals (1%–3%), and interstitial glass (7%).

Alteration: moderate (~25%); interstitial glass is replaced by smectites.

XRD: smectite; trace hydromica (~20% swelling layers).

Sample 59-448A-38R-2, 88–90 cm (Piece 3A), Unit 23 [Z-330]

Aphyric basalt, fine grained, inequigranular, vesicular. Rock: pilotaxitic texture; laths of plagioclase, xenomorphic and elongated-prismatic crystals of clinopyroxene, and brownish green volcanic glass (~25%–30% each). Vesicles (20%) are small.

Alteration: moderate (~25%–30%).

XRD: smectite with ~10% mica layers.

Sample 59-448A-41R-2, 81–85 cm (Piece 5A), Unit 27 [Z-541]

Aphyric andesite-basalt, crystallized, vesicular. Rock: intersertal-microdoleritic texture; microlites and laths of plagioclase (60%, andesine [An_{47}]), small xenomorphic grains of clinopyroxene (15%), and gray-green volcanic glass (5%). Vesicles (20%, 0.1–0.9 mm): empty or completely infilled with glass or carbonate.

Sample 59-448A-45R-1, 69–71 cm (Piece 1D), Unit 31 [Z-331]

Aphyric basalt, fine grained, incompletely crystallized, vesicular (5%–10%). Rock: intersertal texture; laths of plagioclase (40%), xenomorphic clinopyroxene (40%), glass (10%), and opaque minerals (3%–5%).

Alteration: moderate (~20%); vesicles are filled with smectites.

XRD: smectite with ~10% mica layers.

Sample 59-448A-47R-1, 90–95 cm (Piece 1E), Unit 33 [Z-332]

Aphyric basalt, fine grained, incompletely crystallized, massive. Rock: intersertal texture; laths of plagioclase (50%), xenomorphic clinopyroxene (35%–40%), interstitial glass (5%), and opaque minerals (5%).

Alteration: moderate (~25%).

XRD: smectite and cristobalite(?).

Sample 59-448A-50R-3, 116–121 cm (Piece 8), Unit 36 [Z-542]

Crystallo-vitroclastic tuff. Fragments of volcanic glass (0.1–0.2 mm) cemented by ash. Fragments of plagioclase grains are present. Ash is partly replaced by clay minerals.

XRD: smectite with ~10% mica layers; trace amphibole.

Sample 59-448A-51R-1, 98–102 cm (Piece 9D), Unit 37 [Z-333]

Aphyric basalt, fine grained, incompletely crystallized, vesicular. Rock: intersertal texture; laths of plagioclase (45%), xenomorphic grains of clinopyroxene (40%), interstitial glass (10%), and opaque minerals (1%–3%). Small vesicles (2%–5%) are rounded in shape.

Alteration: moderate (~20%); vesicles are filled with smectites.

XRD: smectite; trace cristobalite(?).

Sample 59-448A-51R-3, 49–52 cm (Piece 3A), Unit 37 [Z-543]

Sparsely plagioclase-phyric andesite-basalt, massive. Phenocrysts: plagioclase (2%–3%) represented by prismatic grains (0.5–0.8 mm, labradorite [An_{53}]). Groundmass: intersertal-microlitic texture; microlites and microlaths of plagioclase (50%, 0.1–0.3 mm), small (up to 0.1 mm) grains of clinopyroxene (30%), brownish interstitial glass (15%), and opaque minerals (5%).

Alteration: palagonitized glass.

Sample 59-448A-53R-3, 0–5 cm (Piece 1A), Unit 40 [Z-1164]

Crystallo-vitroclastic breccia. Single large (2.5 mm) fragment of plagioclase and fragments (2–5 mm) of greenish brown volcanic glass with perlitic texture (andesite, andesite-dacite?). Matrix: small angular fragments of glass and zeolite.

Sample 59-448A-54R-3, 124–128 cm (Piece 8C), Unit 41 [Z-544]

Sparsely plagioclase-phyric andesite-basalt, massive. Phenocrysts: plagioclase (2%–3%); prismatic grains (0.4–0.5 mm). Groundmass: microlitic texture; microlites and microlaths of plagioclase (0.05–0.2 mm, andesine [An_{44}]), grains of clinopyroxene, greenish brown interstitial glass, and opaque minerals (5%–7%).

Alteration: plagioclase phenocrysts are partly replaced by pelite.

Sample 59-448A-57R-1, 33–36 cm (Piece 1D), Unit 43 [Z-545]

Aphyric andesite-basalt, vesicular. Rock: microlitic texture; laths of plagioclase (40%, 01–0.7 mm, andesine [An_{42-44}]), very small grains of clinopyroxene (45%), dark brown interstitial glass (10%), and opaque minerals (5%–7%). Vesicles (2%–3%) are empty or infilled with glass.

Alteration: interstitial glass is replaced by clay minerals.

XRD: smectite and cristobalite; trace mixed-layer smectite-chlorite mineral(?).

Sample 59-448A-62R-1, 98–102 cm (Piece 2), Unit 49 [Z-334]

Plagioclase-phyric basalt, fine grained, incompletely crystallized, massive. Phenocrysts: plagioclase (25%–30%); platy crystals that also form segregates. Groundmass: intersertal texture; plagioclase, clinopyroxene, interstitial glass, and opaque minerals.

Alteration: moderate (~20%); interstitial glass is filled with smectites.

XRD: smectite; trace cristobalite(?).

Sample 59-448A-65R-2, 10–15 cm (Piece 1B), Unit 51 [Z-335]

Aphyric basalt, fine grained, incompletely crystallized, vesicular. Rock: intersertal texture; laths of plagioclase (40%–45%), clinopyroxene (40%), interstitial glass (10%–15%), and opaque minerals (5%). Vesicles (1%–3%) are small and rounded in shape.

Alteration: moderate (~20%–25%); vesicles are filled with smectites.

XRD: smectites with various composition of interlayer cations (Na-K and Mg-Ca); trace cristobalite(?).

Sample 59-448A-66R-2, 78–83 cm (Piece 1D), Unit 51 [Z-546]

Aphyric andesite-basalt, vesicular. Rock: microlitic texture; microlaths of plagioclase (50%, 01–0.4 mm, andesine [An_{45}] and [An_{38}]), brown grains of clinopyroxene (30%, up to 0.1 mm), light brown interstitial glass (15%), and opaque minerals (5%, up to 0.1 mm). Vesicles (2%–3%) are present.

XRD: smectite; trace cristobalite.

Parece Vela Basin (Hole 449)

Sample 59-449-15R-2, 17–20 cm (Piece 1B), Unit 6a [Z-336]

Aphyric basalt, fine grained, poorly crystallized, vesicular. Rock: pilotaxitic texture; black volcanic glass with opaque dust and needle-shaped laths of plagioclase. Vesicles (0.1–0.2 mm) are rounded in shape.

Alteration: moderate (30%); vesicles are filled with green smectites; clayey-carbonate vein 3–5 mm thick is registered.

XRD: smectite with ~30%–40% mica layers; trace calcite, chlorite and talc(?).

Sample 59-449-17R-2, 2–6 cm (Piece 1A), Unit 6b [Z-337]

Aphyric basalt, fine grained, incompletely crystallized, vesicular. Rock: intergranular texture; laths of plagioclase, xenomorphic clinopyroxene, glass, and opaque minerals. Small vesicles (<1%) are rounded in shape.

Alteration: slight (15%); vesicles are filled with smectites and opaque minerals; interstitial glass is replaced by smectites.

XRD: smectites with ~30% mica layers; trace calcite and chlorite(?).

Mariana Trough and Mariana Forearc Region (Leg 60)

Hole 453

Sample 60-453-50R-2, 45–50 cm (Piece 6), Upper Polymict Breccia [Z-338]

Gabbro, large-crystalline, massive. Rock: hypidiomorphic-granular texture; clinopyroxene (up to 3 mm, 80%), plagioclase (up to 2.5 mm, 15%), olivine (1 mm, <5%), and opaque minerals (0.3–1 mm).

Alteration: slight (5%); secondary minerals are represented by smectite-chlorite aggregates, carbonate, and opal; clinopyroxenes are dissected by numerous cracks filled with ferrugineous chlorite-smectite aggregates; carbonate and opal occur in clinopyroxene as spots.

XRD: chlorite, smectite, and amphibole; trace talc(?).

Sample 60-453-51R-1, 8–12 cm (Piece 1), Upper Polymict Breccia [Z-339]

Gabbro, large-crystalline, massive, cataclastic. Rock: hypidiomorphic-granular texture; plagioclase (0.8–2.0 mm, 80%, labradorite [An_{62}]), clinopyroxene (0.5–2.5 mm, 15%), orthopyroxene (5%), and single grains of chrome spinel (0.5 mm).

Alteration: slight to moderate (15%–20%); pyroxenes suffered cataclasis, cracks are filled with chlorite, serpentine, and opaque minerals.

XRD: chlorite, smectite, and amphibole; trace talc(?) and hydromica(?).

Electron micrograph: b = 9.22 Å.

Sample 60-453-51R-3, 54–58 cm (Piece 4B), Upper Polymict Breccia [Z-340]

Gabbro, large-crystalline, massive, cataclastic, serpentinized. Rock: hypidiomorphic-granular texture; clinopyroxene (up to 6 mm, 70%), plagioclase (0.4–5 mm, 20%), individual crystals of amphibole, and isometric segregates of opaque minerals.

Alteration: moderate (30%); pyroxenes suffered cataclasis, cracks are filled with chlorite, serpentine, and opaque minerals; some grains of clinopyroxene are almost completely replaced by serpentines; clinopyroxene is replaced by amphibole along grain margins; cleavage faces in plagioclase are filled with clay minerals.

XRD: serpentine and chlorite; trace amphibole and talc(?).

Electron microscopy: lizardite; shape is close to quadrangle.

Sample 60-453-52R-2, 113–118 cm (Piece 10), Upper Polymict Breccia [Z-341]

Gabbro, large-crystalline, massive, cataclastic, amphibolitized. Rock: granoblastic texture; clinopyroxene (up to 6 mm, 80%), plagioclase (up to 6 mm, 20%), single crystals of chrome spinel (0.2–0.5 mm, 2%), and nonoxidized opaque minerals (0.3–0.5 mm, 0.5%). Chrome spinel tends to occur as inclusions along margins of plagioclase and pyroxene crystals.

Alteration: moderate (30%); pyroxenes suffered cataclasis; cracks are filled with serpentine and opaque minerals; amphibole and clay minerals occur in marginal and brecciated areas of clinopyroxene.

XRD: chlorite, serpentine, and amphibole; trace smectite and talc(?).

Electron micrograph: b = 9.21 Å (trioctahedral mineral).

Electron microscopy: lizardite is represented by flat crystals with various orientation, sizes, and shapes.

Sample 60-453-53R-3, 19–24 cm (Piece 3D), Upper Polymict Breccia [Z-342]

Olivine gabbro, large-crystalline, massive. Rock: granoblastic texture; plagioclase (0.25–5 mm, 80%), clinopyroxene (up to 5 mm, 15%), olivine (1.5–2.5 mm, <5%), and opaque minerals: magnetite (~20%). Chrome spinel tends to occur as inclusions along margins of plagioclase and pyroxene crystals.

Alteration: slight (15%); crystals of plagioclase and clinopyroxene are dissected by numerous cracks filled with clay minerals and carbonate; olivine is replaced by chlorite; cracks are filled with opaque minerals.

XRD: chlorite, serpentine, and amphibole; trace hydromica(?).

Electron microscopy: lizardite.

Electron micrograph: b = 9.25 Å (trioctahedral mineral).

Sample 60-453-53R-5, 88–91 cm (Piece 9B), Upper Polymict Breccia [Z-343]

Olivine gabbro, large-crystalline, massive. Rock: hypidiomorphic-granular texture; plagioclase (1–2.5 mm, 60%, labradorite [An_{56}]), olivine (0.8–2.5 mm, 25%), clinopyroxene (up to 1.5 mm, 15%), and opaque minerals:

magnetite (~20%). Chrome spinel tends to occur as inclusions along margins of plagioclase and pyroxene crystals.

Alteration: slight (15%).

XRD: chlorite and serpentine; trace amphibole.

Electron micrograph: b = 9.29 Å (trioctahedral mineral).

Electron microscopy: lizardite in small amounts relative to nonserpentine minerals.

Sample 60-453-55R-3, 50–55 cm (Piece 3I), Upper Polymict Breccia [Z-344]

Troctolite. Rock: olivine (40%), plagioclase (55%, 0.4–2.5 mm, labradorite [An_{56}]), clinopyroxene (up to 1.5 mm, 15%), and xenomorphic grains of black oxidized chrome spinel (5%).

Alteration: moderate (35%); olivine is almost completely replaced by serpentine and magnetite; limonite (goethite?) replaces magnetite; rock is oxidized (10%–15%).

XRD: serpentine and chlorite; trace smectite, mixed-layer chlorite-smectite mineral, amphibole and talc.

Electron micrograph: b = 9.26 Å (chrysotile).

Electron microscopy: lizardite is present as the flat crystals; trace of chrysotile of $2M_{c1}$ polytype.

Sample 60-453-55R-3, 142–147 cm (Piece 10B), Upper Polymict Breccia [Z-1165]

Basite-ultrabasite breccia. Rock: fragments (0.1–8 mm) of serpentinites, orthopyroxenes, clinopyroxenes, and plagioclases.

Alteration: serpentinite is replaced by brownish black aggregates of clay minerals, Fe hydroxides, carbonate, and hydromica; fragments of gabbro are replaced by chlorite and serpentine; zeolite replaces large (up to 2.5 mm) tabular grains of plagioclase.

XRD: chlorite; minor amphibole and hydromica; trace smectite, mixed-layer smectite-chlorite minerals, natrolite(?), and prenite(?).

Sample 60-453-55R-4, 82–84 cm (Piece 9A), Upper Polymict Breccia [Z-1166]

Basite-ultrabasite breccia is the same breccia of Sample 60-453-55R-4, 82–84 cm (Z-1165).

Alteration: slight (~10%).

XRD: chlorite, hydromica, and quartz; minor analcime; trace smectite.

Sample 60-453-55R-4, 127–131 cm (Piece 12C), Upper Polymict Breccia [Z-1167]

Gabbro, large-crystalline. Rock: plagioclase (70%, 0.7–5 mm, labradorite [An_{68}]), tremolite (25%, 0.1–0.7 mm), and dark green (hercynite) spinel (5%).

Alteration: moderate (25%); tremolite replaces pyroxene; single grains of plagioclase are partly replaced by aggregates of mica (1%).

Sample 60-453-56R-1, 40–45 cm (Piece 4C), Upper Polymict Breccia [Z-1168]

Basite breccia. Rock: large (up to 5 mm) fragments of sosuritized plagioclase (50%), more small (40%, up to 1 mm) angular fragments of plagioclase, clinopyroxene and orthopyroxene, and chloritized fragments of clinopyroxene(?). Matrix consists of dark brown clay minerals.

XRD: chlorite and smectite with ~20%–30% mica layers; minor hydromica; trace amphibole, talc, and analcime.

Sample 60-453-56R-2, 33–35 cm (Piece 6A), Upper Polymict Breccia [Z-1169]

Gabbro, large-crystalline. Rock: large (2.5–6 mm, labradorite [An_{60}]) isometric grains of plagioclase and segregates of small xenomorphic grains (0.5–2 mm) of plagioclase. Plagioclase is ~80% of rock volume.

Alteration: moderate (20%–25%); cracks (0.1–1.7 mm thick) are infilled with chlorite, tremolite, and granoblastic aggregates of quartz.

Sample 60-453-56R-2, 85–87 cm (Piece 12A), Upper Polymict Breccia [Z-1170]

Gabbro, medium grained. Rock: isometric grains of plagioclase (80%, 0.5–4 mm) and grains of pyroxene (20%).

Alteration: moderate (25%–30%); cracks (0.2–0.4 mm thick) infilled with chlorite; plagioclase is replaced by hydromica; pyroxene is completely replaced by chlorite and tremolite.

Sample 60-453-57R-4, 2–7 cm (Piece 1), Upper Polymict Breccia [Z-345]

Olivine gabbro, medium grained. Rock: granoblastic texture; plagioclase (0.5–3 mm, 80%, labradorite [An_{68}]), olivine and pyroxenes (up to 2.5 mm, 20%), opaque minerals (up to 0.5 mm), and chrome spinel.

Alteration: slight (10%); olivine and pyroxenes are strongly altered, they are replaced by serpentine and chlorite-smectite aggregate; cracks in olivine are filled with opaque minerals; chlorite-smectite aggregate fills cracks along cleavage faces in plagioclase.

XRD: serpentine and chlorite; trace smectite, amphibole and talc.

Electron micrograph: b = 9.28 Å (trioctahedral mineral).

Electron microscopy: lizardite is the predominant mineral with various in shape.

Sample 60-453-61R-1, 30–35 cm (Piece 5), Upper Polymict Breccia [Z-1171]

Breccia of tuff. Rock: fragments of andesite(?) and glass (15%) with perlitic texture.

Alteration: plagioclase is pelletized, chlorite replaces glass; matrix is replaced by carbonate.

XRD: mixed-layer smectite-chlorite minerals (~10%–20% swelling interlayers).

Sample 60-453-63R-1, 80–83 cm (Piece 4A), Upper Polymict Breccia [Z-1172]

Gabbro; granoblastic texture. Rock: plagioclase (45%, 0.5–2.5 mm, labradorite [$An_{58–62}$]), clinopyroxene (50%, 0.3–5 mm), opaque minerals (5%), and biotite (1%).

Alteration: rock is fresh.

Sample 60-453-63R-1, 130–135 cm (Piece 5I), Upper Polymict Breccia [Z-1173]

Gabbro, medium grained. Rock: xenomorphic grains of plagioclase (70%–75%, 0.7–2.5 mm, labradorite [An_{60}]), xenomorphic rounded grains of pyroxene (20%, 0.1–0.7 mm), and titanomagnetite (7%–8%, 0.4–0.9 mm).

Alteration: rock is fresh.

XRD: smectite with ~10% mica layers; trace chlorite.

Hole 454A

Sample 60-454A-5R-1, 3–7 cm (Piece 1), Unit 1 [Z-1174]

Aphyric basalt (microdolerite), crystallized, vesicular. Rock: microdoleritic texture; plagioclase (50%), clinopyroxene (30%), and vesicles (20%). Plagioclase is replaced by laths (0.2–0.8 mm, labradorite-bitovnite [An_{70}] and labradorite [An_{55}]) and xenomorphic grains, possibly more acid in composition. Pyroxene forms xenomorphic grains (0.1–0.5 mm). Vesicles (0.5–1.6 mm): empty, single vesicle is infilled with carbonate.

Alteration: rock is fresh.

Sample 60-454A-5R-1, 128–132 cm (Piece 17A), Unit 1 [Z-346]

Sparsely plagioclase-phyric, almost completely crystallized; sparsely vesicular (0.1–0.38 mm, 5%). Phenocrysts: large grains of plagioclase (0.4–1 mm, 15%). Groundmass: intergranular, subvariolitic, texture; laths of plagioclase, clinopyroxene, and opaque dust.

Alteration: slight (5%); walls of vesicles are lined with smectites and carbonate; interstitial glass is replaced by smectites and carbonate.

XRD: smectite with ~20% mica layer; trace talc(?).

Electron micrograph: b = 9.22 and 9.12–9.22 Å (serpentine).

Sample 60-454A-5R-2, 50–55 cm (Piece 4), Unit 1 [Z-1175]

Aphyric basalt, almost completely crystallized; sparsely vesicular. Rock: microlitic (microdoleritic) texture; needle-shaped laths (0.3–1.2 mm) of plagioclase (30%, labradorite [An_{55}] and andesine [An_{44}]), clinopyroxene (35%), volcanic glass (5%), and vesicles (30%). Vesicles (0.3–0.8 mm, 5%) are empty.

Alteration: rock is fresh.

Sample 60-454A-5R-3, 115–118 cm (Piece 6A), Unit 1 [Z-347]

Aphyric basalt, medium grained, almost completely crystallized, sparsely vesicular. Rock: intergranular texture; laths of plagioclase, clinopyroxene, devitrified volcanic glass (5%), olivine, and opaque dust. Vesicles (0.3–0.8 mm, 5%) are empty.

Alteration: slight (5%); several vesicles are lined with smectite; carbonate and clay mineral replace interstitial glass.

XRD: smectite with ~30% mica layer; talc and hydromica with swelling interlayers (~10%) occur in trace amounts.

Sample 60-454A-5R-4, 10–15 cm (Piece 2), Unit 1 [Z-1176]

Aphyric dolerite, medium grained, vesicular. Rock: intersertal-doleritic texture; prismatic and tabular grains of plagioclase (35%, 0.2–2 mm, labradorite [An_{60}] and andesine [An_{46}]), xenomorphic (0.3–0.7 mm) or prismatic

(1.5–1.7 mm) grains of clinopyroxene, olivine (10%, 0.2–0.5 mm), greenish brown volcanic glass (20%), and opaque minerals (1%–2%). Vesicles (15%, 0.2–0.8 mm) are lined with glass.

Alteration: slight (5%–10%); clay minerals replace interstitial glass.

Sample 60-454A-8R-1, 100–106 cm [Z-348]

Tuff.

XRD: smectite.

Electron micrograph: b = 9.20 Å (trioctahedral smectite).

Sample 60-454A-10R-1, 45–49 cm (Piece 2), Unit 3 [Z-349]

Aphyric basalt, medium grained, high vesicular (0.2–0.4 mm, 40%). Rock: hyalopilitic texture; laths of plagioclase (50%), clinopyroxene, devitrified volcanic glass, and opaque dust.

Alteration: slight (~10%); walls of vesicles are lined with smectites and carbonate; interstitial glass is replaced by smectites and carbonate.

XRD: smectite; hydromica, chlorite, amphibole, and talc(?).

Electron micrograph: b = 9.22 Å (trioctahedral smectite).

Sample 60-456A-11R-1, 58–62 cm (Piece 9) [Z-350]

Mudstone.

XRD: chlorite and quartz; trace smectite.

Sample 60-454A-11R-1, 102–109 cm (Piece 11), Unit 4 [Z-351]

Sparsely plagioclase-phyric basalt, incompletely crystallized, vesicular. Phenocrysts: plagioclase (0.3–0.6 mm, 10%), clinopyroxene (0.4–0.8 mm, 8%), and single grains of olivine (up to 0.3 mm). Groundmass: intersertal texture; laths of plagioclase, clinopyroxene, devitrified volcanic glass, and opaque dust. Vesicles (0.1–2 mm, 30%): vary from rounded to isometric and elongated in shape.

Alteration: moderate (20%); walls of vesicles are lined with smectites; interstitial glass and olivine are replaced with smectites.

XRD: smectite.

Electron micrograph: b = 9.22 Å (trioctahedral smectite).

Sample 60-454A-11R-2, 125–128 cm (Piece 7A), Unit 4 [Z-1177]

Aphyric basalt, incompletely crystallized, vesicular (65%). Rock: vitrophyric-microdoleritic texture; microlites (0.1–0.4 mm) of plagioclase (prismatic grains: labradorite [An_{55}], and microlites: andesine [An_{40}]), very small grains of clinopyroxene, black-brown volcanic glass (15%), and opaque dust. Vesicles (0.1–0.6 mm) are empty.

Alteration: slight; veinlets consist of clay minerals; several vesicles (<1%) are infilled with clay minerals.

Sample 60-454A-11R-4, 92–97 cm (Piece 5), Unit 4 [Z-352]

Sparsely olivine-clinopyroxene-plagioclase-phyric basalt, incompletely crystallized, vesicular. Microphenocrysts: plagioclase (0.2–0.4 mm, 5%), clinopyroxene (0.1–0.3 mm, 2%), and single grains of olivine (0.1–0.4 mm). Groundmass: intersertal, partly subvariolitic, texture; laths of plagioclase, clinopyroxene, devitrified volcanic glass, and opaque dust.

Alteration: slight (15%); walls of vesicles are lined with smectites; interstitial glass and olivine are replaced with smectites.

XRD: smectite with ~30% mica layers; trace hydromica.

Electron micrograph: b = 9.21 Å (trioctahedral smectite).

Sample 60-454A-12R-1, 116–120 cm (Piece 13), Unit 4 [Z-353]

Aphyric basalt, incompletely crystallized, vesicular (0.1–2 mm, 10%). Occasionally, microphenocrysts of plagioclase (0.3–0.5 mm, 5%) form glomerophyric segregates. Clinopyroxene (0.2–0.4 mm, <1%) and single grains of olivine are present. Groundmass: hyaline, occasionally subvariolitic, texture; laths of plagioclase, clinopyroxene, devitrified volcanic glass, olivine, and opaque dust.

Alteration: slight (15%); walls of vesicles are lined with smectites; interstitial glass and olivine are replaced with smectites.

XRD: smectite with ~40% mica layers; trace hydromica (with 10% swelling interlayers).

Electron micrograph: b = 9.23 Å (trioctahedral smectite).

Sample 60-454A-12R-2, 30–34 cm (Piece 3B), Unit 4 [Z-1178]

Sparsely plagioclase-phyric basalt, crystallized, vesicular. Single glomerophyric segregate of plagioclase (<1%). Groundmass: microlitic texture; needle-shaped laths of plagioclase (25%, 0.1–0.7 mm, laths, 0.7 mm: labradorite [An_{60}] and microlites: andesine [An_{42}]), segregates of clinopyroxene microlites (25%), black and green volcanic glass (10%), and opaque dust (~5%). Vesicles (40%, 0.1–0.8 mm, 30%) are present. Large vesicles (2%–3%, 0.8 mm) are empty; part of small vesicles (10%) are completely replaced by green glass, other parts of small vesicles (27%–28%) are empty.

Alteration: rock is fresh.

Sample 60-454A-13R-1, 11–15 cm [Z-354]

Sediment.

XRD: smectite.

Sample 60-454A-16R-1, 25–30 cm (Piece 5), Unit 5 [Z-355]

Aphyric basalt, incompletely crystallized, fine grained, highly vesicular. Sparse microphenocrysts of clinopyroxene (0.3 mm) are present. Groundmass: variolitic texture; laths of plagioclase, clinopyroxene, devitrified volcanic glass, and opaque dust. Vesicles (0.1–1.5 mm, 50%): rounded in shape.

Alteration: slight (10%); walls of vesicles are lined with smectites and microdruses of chlorite(?); interstitial glass is replaced by smectites.

Electron micrograph: b = 9.23 Å.

Hole 458

Sample 60-458-28R-1, 106–110 cm (Piece 14), Unit 1-1 [Z-356]

Aphyric basalt, medium grained, almost completely crystallized, highly vesicular (0.2–1 mm, 40%). Single microphenocrysts of clinopyroxene (0.1–0.3 mm). Groundmass: intergranular, occasionally subvariolitic, texture; laths of plagioclase, clinopyroxene, devitrified volcanic glass, olivine, and opaque dust. Single large vesicles are filled with volcanic glass and opaque dust.

Alteration: slight (3%); walls of vesicles are lined with smectites.

XRD: smectite; amphibole and chlorite in trace amounts.

Sample 60-458-29R-1, 103–108 cm (Piece 17), Unit 1-1 [Z-357]

Aphyric basalt, incompletely crystallized, vesicular (5%). Groundmass: hyalopilitic texture; laths of plagioclase, clinopyroxene, devitrified volcanic glass, and olivine.

Alteration: slight (15%); walls of vesicles are lined with smectites; interstitial glass is replaced by smectites.

XRD: smectite.

Electron micrograph: b = 9.26 Å (trioctahedral smectite).

Sample 60-458-30R-1, 111–113 cm (Piece 17), Unit 1-1 [Z-358]

Aphyric basalt, fine grained, incompletely crystallized, vesicular. Groundmass: hyalopilitic texture; laths of plagioclase, clinopyroxene, devitrified volcanic glass, olivine, and opaque dust. Vesicles (0.2–0.4 mm, 5%): rounded and elongated in shape.

Alteration: slight (10%); walls of vesicles are lined with smectites; interstitial glass and olivine are replaced by smectites.

XRD: smectite.

Electron micrograph: b = 9.24 Å.

Sample 60-458-31R-1, 116–120 cm (Piece 18), Unit 2-1 [Z-359]

Aphyric basalt, fine grained, almost completely crystallized, vesicular (0.2–1 mm, 15%). Groundmass: intergranular texture; laths of plagioclase, clinopyroxene, devitrified volcanic glass, and opaque dust.

Alteration: slight (~7%); walls of vesicles are lined with smectites; interstitial glass is replaced by smectites.

XRD: smectite with ~20%–25% mica layers and cristobalite; trace hydromica and amphibole.

Sample 60-458-32R-3, 90–95 cm (Piece 12A), Unit 2-1 [Z-360]

Aphyric andesite, almost completely crystallized, sparsely vesicular (0.2–0.5 mm, 3%). Groundmass: intergranular texture; laths of plagioclase, clinopyroxene, single grains of olivine, and devitrified volcanic glass with opaque dust.

Alteration: slight (5%); walls of vesicles are lined with smectites; interstitial glass and olivine are replaced by smectites.

XRD: cristobalite(?); smectite with ~30% mica layers; hydromica and amphibole in trace amounts.

Electron micrograph: b = 9.21 (very slight) and 9.10 Å.

Sample 60-458-33R-1, 32–37 cm (Piece 4), Unit 2-2 [Z-1179]

Aphyric andesite-basalt (boninite), crystallized, vesicular. Rock: microlitic texture; microlites and laths of plagioclase (30%, labradorite [An_{60}] and andesine [An_{43}]), segregate of clinopyroxene microlites (25%), and light greenish brown glass (5%). Vesicles (60%, 0.1–1.5 mm): isometric and empty.

Alteration: rock is fresh.

XRD: smectite; minor hydromica; trace quartz; veinlet: mixed-layer vermiculite-hydromica mineral; minor smectite with ~50% mica layers.

Sample 60-458-33R-2, 129–131 cm (Piece 14), Unit 2-3 [Z-361]

Aphyric andesite-basalt (boninite?), medium grained, incompletely crystallized, sparsely vesicular (0.2–0.4 mm, 2%). Groundmass: intergranular texture; laths of plagioclase, clinopyroxene, single grains of olivine, and devitrified volcanic glass with opaque dust.

Alteration: slight (~5%); walls of vesicles are lined with smectites; interstitial glass and olivine are replaced by smectites.

XRD: smectite; minor cristobalite(?); trace hydromica (~5% swelling interlayers).

Electron micrograph: b = 9.10 Å.

Sample 60-458-34R-2, 14–19 cm (Piece 1B), Unit 2-3 [Z-362]

Aphyric andesite-basalt, medium grained, almost completely crystallized, sparsely vesicular. Groundmass: intergranular texture; laths of plagioclase, clinopyroxene, single grains of olivine, and devitrified volcanic glass with opaque dust. Single vesicles have sizes of 0.2–0.8 mm.

Alteration: slight (~5%); interstitial glass and olivine are replaced by smectites.

XRD: smectite with ~10%–30% mica layers, cristobalite(?); minor hydromica.

Electron micrograph: b = 9.12 Å.

Sample 60-458-35R-2, 12–18 cm (Piece 2), Unit 2-4 [Z-363]

Aphyric basalt, fine grained, almost completely crystallized, vesicular (0.2–3 mm, 15%). Groundmass: subvariolitic texture; laths of plagioclase, clinopyroxene, single grains of olivine, and devitrified volcanic glass with opaque dust.

Alteration: slight (10%); walls of small vesicles are lined with smectites; large vesicles are filled with carbonate; interstitial glass is replaced by smectites.

XRD: smectite with ~10% mica layers and cristobalite; minor hydromica.

Sample 60-458-36R-1, 125–128 cm (Piece 18), Unit 2-4 [Z-1180]

Aphyric andesite-basalt (boninite), vesicular (10%, 0.1 mm). Rock: hyalopilitic texture; needle-shaped (0.1–0.2 mm) microlites of plagioclase (15%, labradorite [$An_{50–52}$] and andesine [An_{38}]), microlites of clinopyroxene (20%, 0.1–0.2 mm), hornblende(?) (2%–3%), and glass (50%).

Alteration: rock is fresh.

XRD: smectite.

Sample 60-458-37R-2, 70–75 cm (Piece 8C), Unit 2-6 [Z-364]

Aphyric olivine basalt, medium grained, incompletely crystallized, vesicular (0.2–0.5 mm, 10%). Phenocrysts: olivine (0.1–0.2 mm, 7%). Groundmass: intersertal, occasionally subvariolitic, texture; laths of plagioclase, clinopyroxene, olivine, devitrified volcanic glass with microlites of plagioclase and with opaque dust.

Alteration: slight (~5%); walls of vesicles are lined with smectites; interstitial glass and olivine are replaced by smectites.

XRD: smectite with ~10% mica layers; trace cristobalite, hydromica (~10% swelling interlayers), and amphibole.

Sample 60-458-39R-1, 100–102 cm (Piece 12A), Unit 3-1 [Z-365]

Aphyric basalt, fine grained, poorly crystallized, vesicular (0.2–0.5 mm, 5%). Groundmass: hyalopilitic texture; laths of plagioclase, clinopyroxene, olivine, devitrified volcanic glass, and opaque dust.

Alteration: slight (~15%); walls of vesicles are lined with smectites; interstitial glass, olivine, and partly clinopyroxene are replaced by smectites.

XRD: smectite with interlayer Na-K and Mg-Ca cations; trace hydromica (~20% swelling interlayers).

Sample 60-458-39R-2, 60–65 cm (Piece 6), Unit 3-1 [Z-1181]

Aphyric andesite-basalt (boninite), poorly crystallized. Rock: hyalopilitic texture; needle-shaped microlites (0.05–0.2 mm) of plagioclase (10%, andesine [An_{40}]), microlites of pyroxene (15%), and brown glass.

Alteration: rock is fresh.

Sample 60-458-40R-1, 143–147 cm (Piece 1Q), Unit 3-1 [Z-1182]

Aphyric andesite-basalt (boninite), vesicular. Rock: hyalopilitic texture; microlites (0.05–0.1 mm) of plagioclase (10%, andesine [An_{40}]), pyroxene (15%), brownish green grains (0.03–0.05 mm) of hornblende(?) (5%–7%), and brownish green glass (60%). Vesicles (10%, 0.1–0.4 mm) are empty.

Alteration: rock is fresh; single vesicle (0.8 mm) and microcrack (0.3 mm in thickness) are infilled with zeolite.

XRD: smectite with ~10% mica layers; veinlet: smectite with ~10% mica layers; trace analcime and phillipsite(?).

Sample 60-458-41R-1, 2–7 cm (Piece 1), Unit 4A-1 [Z-1183]

Plagioclase-phyric basalt, vesicular. Phenocrysts (2%–3%): prismatic grains (0.5–0.6 mm) of plagioclase. Groundmass: pilotaxitic texture; needle-shaped microlites (0.1–0.3 mm) of plagioclase (30%, andesine [An_{42}]), very small (<0.1 mm) grains of opaque minerals (7%–8%), and brown glass (35%). Vesicles (15%, 0.5–1 mm) mainly are empty.

Alteration: slight (10%–15%); interstitial glass (10%) replaced by clay minerals.

XRD: smectite with ~10% mica layers; trace cristobalite, hydromica, amphibole, and chlorite.

Sample 60-458-41R-1, 102–107 cm (Piece 1), Unit 4A-1 [Z-1184]

Sparsely clinopyroxene-phyric basalt, vesicular. Single (<1%) prismatic (2 mm) phenocryst of clinopyroxene. Microphenocryst (0.5 mm) of opaque minerals is present. Groundmass: pilotaxitic texture; microlites (0.05–0.1 mm) of plagioclase (30%, andesine [An_{44}]), very small (<0.1 mm) grains of opaque minerals (5%), and brown glass (55%). Vesicles (10%, 0.3–0.8 mm) are empty.

Alteration: rock is fresh.

Sample 60-458-41R-2, 40–45 cm (Piece 1), Unit 4A-1 [Z-1185]

Aphyric basalt, poorly crystallized. Rock: hyalopilitic texture; needle-shaped microlites (0.05–0.1 mm) of plagioclase (10%, andesine [An_{42}]) and brownish black glass.

Alteration: rock is fresh.

XRD: smectite with ~20% mica layers and cristobalite; trace hydromica.

Sample 60-458-42R-1, 60–65 cm (Piece 6), Unit 4B-1 [Z-1186]

Aphyric basalt, poorly crystallized, vesicular. Rock: hyalopilitic texture; needle-shaped microlites (0.1–0.4 mm) of pyroxene (25%) and light cream glass. Vesicles (5%, 0.2–0.5 mm) are empty.

Alteration: moderate (35%); pyroxene is partly (5%) or completely replaced by tremolite; clay minerals replace interstitial glass (50%).

Sample 60-458-43R-2, 45–50 cm (Piece 7), Unit 4B-1 [Z-1187]

Aphyric andesite-basalt (boninite). Rock: hyalopilitic texture; microlites (0.05–0.2 mm) of pyroxene (10%) and light cream glass.

Alteration: rock is fresh.

Sample 60-458-44R-1, 140–145 cm (Piece 11), Unit 4B-1 [Z-1188]

Aphyric andesite-basalt (boninite), poorly crystallized, vesicular. Rock: pilotaxitic texture; microlites (25%, 0.1–0.5 mm) of plagioclase, microlites of pyroxene (20%, 0.05–0.2 mm), dark green grains of amphibole (5%, 0.2–0.4 mm), and glass (50%). Vesicles (20%, 0.1–0.5 mm) are empty.

Alteration: slight (15%); clay minerals replace glass (15%).

XRD: veinlet: smectite.

Sample 60-458-45R-1, 130–135 cm (Piece 15A), Unit 4B-3 [Z-366]

Aphyric basalt, fine grained, poorly crystallized, vesicular (0.3–0.5 mm, 5%). Groundmass: subvariolitic texture; laths of plagioclase, clinopyroxene, olivine, devitrified volcanic glass, and opaque dust. Vesicles are filled with devitrified glass with opaque dust.

Alteration: slight (~15%); walls of vesicles are lined with smectites; interstitial glass, olivine, and partly clinopyroxene are replaced by smectites.

XRD: smectite.

Sample 60-458-46R-1, 89–91 cm (Piece 8), Unit4C-1 [Z-367]

Aphyric basalt, fine graine1d, poorly crystallized, sparsely vesicular (0.2–0.4 mm). Groundmass: hyalopilitic texture; laths of plagioclase, clinopyroxene, olivine, devitrified volcanic glass, and opaque minerals.

Alteration: slight (~10%); walls of vesicles are lined with smectites; interstitial glass is replaced by smectites.

XRD: smectite.

Sample 60-458-47R-1, 133–136 cm (Piece 17), Unit 5-1 [Z-368]

Aphyric basalt, fine grained, massive. Groundmass: trachytic texture; laths of plagioclase, clinopyroxene, devitrified volcanic glass, and opaque minerals. Vesicles have sizes of 0.1–0.3 mm (10%). Veins are as thick as 0.2–0.5 up to 1–1.5 mm.

Alteration: slight (~10%); walls of vesicles are lined with smectites; interstitial glass is replaced by smectites; microveins contain needle-shaped crystals of smectites.

XRD: smectite; trace amphibole.

Sample 60-458-48R-1, 42–47 cm (Piece 1), Unit 5-2 [Z-1189]

Sparsely clinopyroxene-phyric basalt, poorly crystallized, vesicular. Three prismatic phenocrysts of augite (2%, 0.8 mm). Groundmass: hyalopilitic texture; microlites (0.05–0.2 mm) of plagioclase (10%, andesine [An_{42}]) and dark brown glass (80%–85%). Vesicles (5%, 0.4–0.8 mm): rounded and lined black glass with zeolite.

Alteration: moderate (25%); clay mineral replaces glass (25%).

XRD: smectite.

Hole 459B

Sample 60-459B-59R-2, 50–55 cm [Z-369]

Sediment.

XRD: smectite with ~20% mica layers; trace hydromica (~20% swelling interlayers), chlorite, heulandite(?), and amphibole(?).

Sample 60-459B-60R-1, 125–127 cm (Piece 11), Unit 1 [Z-370]

Aphyric olivine basalt, medium grained, almost completely crystallized, vesicular (0.3–0.5 mm, 10%). Groundmass: intergranular texture; laths of plagioclase, clinopyroxene, olivine, devitrified volcanic glass, and opaque minerals.

Alteration: slight (~10%); walls of vesicles are lined with smectites; interstitial glass is replaced by smectites.

XRD: smectite; minor cristobalite; trace hydromica (~5% swelling interlayers).

Sample 60-459B-60R-2, 90–95 cm (Piece 8), Unit 1 [Z-371]

Aphyric olivine basalt, almost completely crystallized, vesicular (up to 0.5 mm, 10%). Groundmass: intergranular, occasionally intersertal, texture; laths of plagioclase, clinopyroxene, olivine, devitrified volcanic glass, and opaque minerals.

Alteration: slight (~15%); walls of vesicles are lined with smectites; interstitial glass is replaced by smectites and carbonate.

XRD: smectite with ~10% mica layers, cristobalite; trace hydromica (~10% swelling interlayers).

Sample 60-459B-61R-1, 19–22 cm (Piece 2), Unit 1 [Z-373]

Aphyric olivine basalt, incompletely crystallized, medium grained, vesicular. Groundmass: intersertal texture; laths of plagioclase, clinopyroxene, olivine, devitrified volcanic glass, and opaque minerals.

Alteration: slight (~15%); walls of vesicles are lined with smectites; interstitial glass is replaced by smectites.

XRD: smectite with ~20%–25% mica layers; minor cristobalite; trace hydromica (~20% swelling interlayers) and amphibole.

Sample 60-459B-61R-1, 141–145 cm (Piece 14), Unit 1 [Z-372]

Aphyric dolerite, vesicular. Rock: intersertal texture; laths of plagioclase (40%, 0.3–0.9 mm, labradorite [An_{55}] and andesine [An_{42}]), clinopyroxene (40%), and greenish gray glass with skeletal crystals of opaque minerals. Vesicles (0.6 mm) are empty.

Alteration: rock is fresh.

XRD: smectite with ~30% mica layers; minor cristobalite; trace hydromica (~10% swelling interlayers).

Sample 60-459B-62R-1, 44–46 cm (Piece 4), Unit 1 [Z-1190]

Aphyric dolerite, fine grained. Rock: intersertal-doleritic texture; laths (0.3–0.9 mm) of plagioclase (40%, 0.3–0.9 mm, labradorite [An_{58}] and andesine [An_{42}]), xenomorphic grains (0.1–0.4 mm) of clinopyroxene and their segregates (35%), black glass (20%), and opaque minerals (5%).

Alteration: rock is fresh.

Sample 60-459B-63R-1, 25–28 cm (Piece 3A), Unit 2 [Z-1191]

Aphyric andesite-basalt, poorly crystallized, vesicular. Rock: hyalopilitic texture; microlites of plagioclase (10%, 0.1–0.3 mm, andesine [An_{47}]), microlites (0.1–0.3 mm) of clinopyroxene (5%), and light gray-cream glass (70%). Vesicles (15%, 0.1–0.4 mm) are empty.

Alteration: rock is fresh.

Sample 60-459B-64R-1, 24–28 cm (Piece 2B), Unit 2 [Z-374]

Aphyric basalt, fine grained, vesicular (0.1–0.1 mm, 10%). Groundmass: hyalopilitic texture; laths of plagioclase, clinopyroxene, devitrified volcanic glass, and opaque minerals.

Alteration: slight (~25%–30%); walls of vesicles are lined with smectites; interstitial glass is replaced by smectites.

XRD: smectite; trace hydromica.

Sample 60-459B-65R-1, 82–85 cm (Piece 9), Unit 2 [Z-375]

Aphyric basalt, fine grained, vesicular. Groundmass: hyalopilitic (partly trachytic) texture; laths of plagioclase, clinopyroxene, devitrified volcanic glass, and opaque minerals. Vesicles have sizes of 0.1–2 mm (20%).

Alteration: moderate (~20%); walls of vesicles are lined with smectites; interstitial glass is replaced with smectites.

XRD: smectite; trace hydromica (~10% swelling interlayers) and quartz.

Sample 60-459B-66R-1, 40–45 cm (Piece 4B), Unit 3 [Z-376]

Aphyric andesite-basalt, medium grained, almost completely crystallized, massive. Rock: laths of plagioclase and K-feldspar(?) (0.4–0.5 mm, 65%), clinopyroxene (5%), quartz (0.2–0.4 mm, up to 5%), and single grains of amphibole. Groundmass: poikiloblastic texture; devitrified volcanic glass with microlites of clinopyroxene.

Alteration: slight (~3%); interstitial glass is replaced by smectites.

XRD: smectite with ~10% mica layers; trace hydromica (~10% swelling interlayers) and chlorite.

Sample 60-459B-67R-1, 107–112 cm (Piece 8B), Unit 3 [Z-377]

Aphyric andesite-basalt, coarse grained, incompletely crystallized, massive. Rock: ophitic texture; large laths of plagioclase (0.8–1.5 mm, 60%), clinopyroxene (0.2–0.4 mm, 5%), olivine (0.2–0.3 mm, ~5%), devitrified volcanic glass, and opaque minerals (up to 0.2 mm).

Alteration: slight (~10%); interstitial glass and olivine are replaced by smectites.

XRD: smectite with ~40% mica layers; minor cristobalite and hydromica.

Sample 60-459B-68R-1, 38–42 cm (Piece 3), Unit 3 [Z-378]

Aphyric andesite-basalt, fine grained, highly vesicular (0.3–1 mm, 50%). Groundmass: intersertal texture; laths of plagioclase, clinopyroxene, single grains of olivine, devitrified volcanic glass, and opaque minerals.

Alteration: moderate (~40%); vesicles are filled with smectites.

XRD: hydromica and smectite contains ~20% of mica layers; minor cristobalite.

Sample 60-459B-69R-1, 84–87 cm (Piece 12), Unit 4 [Z-379]

Aphyric andesite-basalt, fine grained, incompletely crystallized, vesicular (0.2–2 mm, 15%). Rock: intersertal texture; laths of plagioclase, clinopyroxene, olivine, devitrified volcanic glass, and opaque minerals.

Alteration: slight (10%); interstitial glass is replaced by smectites; walls of vesicles are lined with smectites.

XRD: smectite and cristobalite (?); trace hydromica.

Sample 60-459B-70R-1, 85–90 cm (Piece 6), Unit 4 [Z-1192]

Sparsely plagioclase-clinopyroxene-phyric andesite-basalt, vesicular. Phenocrysts (1%–2%): represented by tabular and prismatic grains (0.5–0.7 mm) of plagioclase and glomerophyric segregates of clinopyroxene xenomorphic grains (0.2–0.4 mm). Groundmass: hyalopilitic texture; needle-shaped microlites (0.1–0.3 mm) of plagioclase (15%, andesine [An_{45}]), opaque minerals (5%), and brown glass (70%). Vesicles (10%, 0.1–0.4 mm) are empty.

Alteration: rock is fresh.

Sample 60-459B-70R-1, 105–110 cm (Piece 7), Unit 4 [Z-1193]

Aphyric basalt, poorly crystallized, vesicular. Rock: pilotaxitic texture; microlites (0.1–0.2 mm) of plagioclase (30%, andesine [An_{47}]) and brownish black glass (50%). Vesicles (20%, 0.1–0.6 mm) are empty.

Alteration: rock is fresh.

Sample 60-459B-70R-2, 30–35 cm (Piece 2), Unit 4 [Z-1194]

Aphyric basalt, poorly crystallized, vesicular. Rock: hyalopilitic texture; microlites (0.1–0.4 mm) of plagioclase (25%, andesine [An_{43}]) and brownish black glass (70%). Vesicles (5%, 0.1–0.6 mm) are empty.

Alteration: rock is fresh.

Sample 60-459B-71R-1, 138–141 cm (Piece 8), Unit 4 [Z-380]

Aphyric basalt, fine grained, incompletely crystallized, vesicular. Rock: intersertal, occasionally hyalopilitic, texture; laths of plagioclase, clinopyroxene, devitrified volcanic glass, and opaque minerals. Vesicles have sizes of 0.2–0.5 mm (10%).

Alteration: moderate (~20%); interstitial glass is replaced by smectites; walls of vesicles are lined with smectites.

XRD: smectite; trace cristobalite and hydromica.

Sample 60-459B-72R-1, 124–128 cm (Piece 1), Unit 4 [Z-381]

Aphyric basalt, fine grained, incompletely crystallized, highly vesicular. Rock: intersertal texture; laths of plagioclase, clinopyroxene, devitrified volcanic glass, and opaque minerals. Vesicles: 0.05 mm and 0.3–0.6 mm (20%); are empty or lined by chlorite.

Alteration: moderate (~25%); interstitial glass is replaced with clay mineral; vesicles are lined with clay mineral.

XRD: smectite and cristobalite; trace hydromica (~5% swelling interlayers).

Sample 60-459B-73R-1, 0–5 cm, Unit 4 [Z-1195]

Aphyric andesite-basalt, crystallized, vesicular. Rock: pilotaxitic texture; microlites and microlaths (0.1–0.4 mm) of plagioclase (40%, andesine [An_{43}]), small grains (0.1 mm) of clinopyroxene (15%), glass (40%), and opaque minerals (1%–2%).

Alteration: slight to moderate (~20%); interstitial glass is replaced by clay minerals.

Sample 60-459B-73R-1, 120–125 cm, Unit 4 [Z-1196]

Sparsely pyroxene-plagioclase-phyric andesite-basalt, poorly crystallized, vesicular. Phenocrysts: single (<1%) prismatic grains (0.6–0.8 mm) of pyroxene and plagioclase. Groundmass: hyalopilitic texture; needle-shaped microlites of plagioclase (10%, andesine [An_{47}]), volcanic glass (85%), and opaque minerals (2%–3%). Vesicles (2%–3%, 0.6–0.7 mm): partly or completely infilled with brown and green glass.

Alteration: moderate to strong (~55%); glass is replaced by clay minerals.

XRD: smectite with ~20% mica layers; trace chlorite.

Sample 60-459B-73R-2, 75–80 cm, Unit 4 [Z-1197]

Sparsely plagioclase-phyric andesite-basalt. Phenocrysts (2%–3%): prismatic grains (0.3–0.8 mm, labradorite [An_{55}]) of plagioclase. Groundmass: hyalopilitic texture; needle-shaped microlites (0.1–0.2 mm) of plagioclase (15%, andesine [An_{48}]) and gray-cream volcanic glass (80%) with crystals of pyroxene and opaque minerals.

Alteration: rock is fresh.

Sample 60-459B-73R-3, 84–88 cm, Unit 4 [Z-382]

Aphyric basalt, fine grained, incompletely crystallized, vesicular. Rock: intersertal (partly hyalopilitic) texture; laths of plagioclase, clinopyroxene, devitrified volcanic glass, and opaque minerals. Vesicles have sizes of 0.2–1.5 mm (10%).

Alteration: slight (~10%); interstitial glass is replaced with smectites; walls of vesicles are lined with smectites.

XRD: smectite; trace hydromica and amphibole(?).

Japan Sea (Legs 127 and 128)

Hole 794C

Sample 127-794C-1R-1, 48–50 cm (Piece 7), Unit 2 [Z-1457]

Plagioclase-phyric dolerite, massive. Phenocrysts: prismatic grains (0.5–2.5 mm) of plagioclase (15%, labradorite [An_{60}]). Groundmass: intersertal-doleritic texture; unoriented prismatic grains (0.1–0.4 mm) of plagioclase (55%, labradorite [An_{60}]). Interstitial spaces are filled with altered volcanic glass (20%), grains of quartz (2%–3%), and skeletal grains of opaque minerals (10%).

Alteration: moderate (20%–25%); clay minerals completely replace interstitial glass.

Sample 127-794C-1R-1, 111–113 cm (Piece 9), Unit 2 [Z-234]

Plagioclase-phyric basalt (dolerite?), coarse grained, almost completely crystallized, vesicular. Phenocrysts: plagioclase (0.5–2.5 mm, 60%). Interstitial spaces are filled with devitrified volcanic glass. Groundmass: intergranular texture. Vesicles (0.2–0.5 mm, 10%): empty; walls are lined with smectites.

Alteration: moderate to high (~40%); smectites replace interstitial glass and femic minerals.

XRD: smectite; trace chlorite and defective chlorite.

Sample 127-794C-1R-1, 138–139 cm (Piece 11A), Unit 2 [Z-1458]

Plagioclase-phyric dolerite, fine grained, massive. Phenocrysts: prismatic grains (2–4 mm) of plagioclase (30%, labradorite [An_{68}]). Groundmass: intersertal-doleritic texture; prismatic grains (0.2–0.7 mm) of plagioclase (35%, labradorite [An_{55}]). Interstitial spaces are filled with greenish black volcanic glass (20%), segregates of very small (<0.1 mm) grains of clinopyroxene (5%), and opaque minerals (8%–10%).

Alteration: slight (~5%); clay minerals partly replace interstitial glass.

Sample 127-794C-4R-2, 82–84 cm (Piece 7G), Unit 2 [Z-235]

Plagioclase-phyric basalt (dolerite?), coarse grained, almost completely crystallized, vesicular. Phenocrysts: plagioclase (0.5–3 mm, 60%), clinopyroxene (0.3–0.8 mm, 8%), and olivine (0.2–0.5 mm, 5%). Groundmass: doleritic texture; devitrified volcanic glass, microlites of clinopyroxene, and opaque minerals. Vesicles (0.2–1 mm): filled with chlorite-smectite aggregates.

Alteration: moderate (~30%–35%); interstitial glass is filled with smectites.

XRD: smectite; trace chlorite and hydromica.

Sample 127-794C-7R-1, 56–61 cm (Piece 5A), Unit 3 [Z-1459]

Plagioclase-phyric dolerite, fine grained, massive.

Sample 127-794C-7R-1, 120–122 cm (Piece 6D), Unit 3 [Z-236]

Plagioclase-phyric basalt (dolerite?), medium grained, vesicular. Phenocrysts (0.4–0.8 mm, 60%): plagioclase. Groundmass: ophitic texture; devitrified volcanic glass, microlites of clinopyroxene, olivine, and opaque minerals. Vesicles (0.3–1 mm): filled with chlorite-smectite aggregate.

Alteration: strong (50%); interstitial glass and femic minerals are filled with clay minerals.

XRD: smectite with ~10% mica layers; trace defective chlorite and hydromica.

Sample 127-794C-10R-1, 85–87 cm (Piece 7E), Unit 4 [Z-237]

Sparsely plagioclase-phyric basalt, medium grained, vesicular. Phenocrysts (0.5–0.8 mm, 50%): plagioclase. Microphenocrysts (0.2–2 mm, 3%): clinopyroxene. Single grains of olivine occur sporadically. Groundmass: intersertal texture; devitrified volcanic glass, microlites of clinopyroxene, and opaque minerals. Vesicles (0.3–2.5 mm, 20%–25%): filled with chlorite-smectite aggregates.

Alteration: strong (50%); interstitial glass is filled with clay minerals.

XRD: smectite; trace hydromica.

Sample 127-794C-12R-1, 46–48 cm (Piece 1A), Unit 5 [Z-238]

Sparsely plagioclase-phyric basalt, medium grained, vesicular. Phenocrysts (0.4–1 mm, 40%): plagioclase. Groundmass: intersertal texture; devitrified volcanic glass, microlites of clinopyroxene, olivine(?), and opaque minerals. Vesicles (0.5–2.5 mm, 20%): filled with smectites.

Alteration: moderate (~25%); interstitial glass is filled with clay minerals.

XRD: smectite; trace hydromica (~20% swelling layers) and quartz.

Sample 127-794C-12R-6, 91–93 cm (Piece 1I), Unit 5 [Z-239]

Olivine-phyric basalt, fine grained, vesicular. Microphenocrysts (0.3 mm, 3%): plagioclase. Groundmass: intergranular texture devitrified volcanic glass, plagioclase, microlites of clinopyroxene, olivine, and opaque minerals. Vesicles (0.1–0.5 mm, 20%): empty; walls are lined with opaque dust and chlorite-smectite aggregate.

Alteration: scarce (~1%).

XRD: smectites with interlayer Na-K and Mg-Ca cations; trace defective chlorite, chlorite, and hydromica.

Hole 794D

Sample 128-794D-10R-2, 25–28 cm (Piece 1B), Unit 6 [Z-768]

Aphyric andesite-basalt, vesicular. Rock: pilotaxitic texture; microlaths and microlites (0.3–2 mm) of plagioclase (30%–35%; albite-oligoclase), interstitial glass, and opaque dust. Vesicles (50%; 0.1–0.5 mm): oval and oval-isometric in shape.

Alteration: very strong (70%); phenocrysts of plagioclase partly replaced by pelite; interstitial glass replaced by clay mineral; vesicles are filled with clay mineral.

XRD: mixed-layer smectite-chlorite mineral (~60% swelling interlayers); trace chlorite.

Sample 128-794D-11R-1, 39–43 cm (Piece 3E), Unit 6 [Z-769]

Sparsely plagioclase-phyric andesite-basalt, vesicular. Phenocrysts: single prismatic grain (2 mm) of plagioclase. Groundmass: microdoleritic-intersertal texture; microlaths (0.1–0.7 mm) of zonal plagioclase (from andesine [An_{32}] to andesine [An_{45}]) containing inclusions of glass. Interstices: segregates of very small grains (<0.1 mm) of clinopyroxene (30%), glass with opaque dust, and opaque minerals (~5%).

Alteration: moderate (40%); glass from plagioclase and interstitial glass are replaced by clay minerals.

Sample 128-794D-11R-1, 89–95 cm (Piece 3J), Unit 6 [Z-1483]

Aphyric dolerite, vesicular. Rock: doleritic texture; laths (0.3–0.6 mm) of plagioclase (30%, andesine [$An_{40–42}$]). Interstices: isometric small (0.1–0.2 mm) grains of clinopyroxene (30%), opaque minerals (10%), and greenish brown glass (5%). Vesicles (25%; 0.2–0.7 mm): isometric in shape.

Alteration: moderate (30%); interstitial glass is replaced by clay minerals; vesicles are filled with clay minerals (central parts of vesicles have more light color: celadonite?).

XRD: smectite; trace mixed-layer smectite-chlorite minerals(?) and chlorite.

Sample 128-794D-11R-2, 26–29 cm (Piece 1B), Unit 6 [Z-770]

Sparsely plagioclase-phyric andesite-basalt with microlitic-intersertal texture, vesicular. Rock is identical to Sample 128-794D-11R-1, 89–95 cm (Z-1483).

Sample 128-794D-11R-3, 108–112 cm (Piece 4), Unit 6 [Z-771]

Sparsely plagioclase-phyric andesite-basalt (microdolerite), vesicular. Phenocrysts: single grains (0.5–0.7 mm) of plagioclase (labradorite [An_{50}]). Groundmass: microdoleritic-intersertal texture; laths (0.2–0.7 mm) of plagioclase (andesine [An_{38}] and andesine [An_{42}]) with inclusions of glass. Interstices: segregates of small grains (up to 0.3 mm) of clinopyroxene, glass with opaque dust, and opaque minerals (~5%–7%). Vesicles (20%; 0.1–1.5 mm): present.

Alteration: moderate (30%); interstitial glass replaced by clay mineral; vesicles are filled with clay mineral.

XRD: smectite; trace chlorite and mixed-layer smectite-chlorite mineral.

Sample 128-794D-12R-1, 24–26 cm (Piece 2A), Unit 7 [Z-772]

Aphyric dolerite (andesite-basalt), medium grained. Rock: doleritic texture; laths (0.2–2 mm) of plagioclase (30%, from andesine [An_{43}] to andesine [An_{32}]). Interstices: segregates of small (up to 0.5 mm) grains of augite, rounded grains (0.2–0.4 mm) of olivine, and glass.

Alteration: slight; olivine partly replaced by clay minerals; clay minerals replace interstitial glass.

Sample 128-794D-12R-3, 107–111 cm (Piece 4C), Unit 7 [Z-773]

Aphyric dolerite (andesite-basalt), medium grained, massive. Rock: poikilophitic-intersertal texture; elongated-prismatic or isometric grains (0.2–2 mm) of plagioclase (andesine [$An_{32–35}$]), grains of augite with inclusions of plagioclase grains, opaque minerals (5%–7%), and glass (~20%).

Alteration: slight to moderate (20%); clay minerals replace interstitial glass.

Sample 128-794D-13R-1, 73–76 cm (Piece 3G), Unit 7 [Z-774]

Aphyric dolerite (andesite-basalt), medium grained, massive. Rock: doleritic-intersertal texture; prismatic and tabular grains (0.8–2 mm) of plagioclase (from andesine [An_{38}] to andesine [An_{43}]), small (0.2–0.4 mm up to 0.8 mm) isometric grains of augite with inclusions of plagioclase grains, opaque minerals (5%), and interstitial glass (~15%).

Alteration: slight (15%); clay minerals replace interstitial glass.

Sample 128-794D-14R-1, 72–76 cm (Piece 6A), Unit 7 [Z-775]

Aphyric dolerite (andesite-basalt), medium grained, massive. Rock: intersertal-doleritic texture; elongated-prismatic and tabular grains (0.5–2.5 mm) of plagioclase (andesine [$An_{42–45}$]) with inclusions of glass, isometric (0.3–0.8 mm up to 0.8 mm) grains of augite, Ti augite which contains inclusions of plagioclase grains, and skeletal micrograins of opaque minerals in interstitial glass.

Alteration: strong (60%); plagioclase is partly replaced by pelite; glass from plagioclase replaced by clay minerals; interstices consist of albite, hydrobiotite, needles of apatite, and pelletized orthoclase; clinopyroxene partly replaced by clay minerals.

XRD: smectite.

Sample 128-794D-15R-1, 79–85 cm (Piece 10A), Unit 7 [Z-1617]

Aphyric dolerite, medium grained, massive. Rock: intersertal-ophitic texture; prismatic and tabular grains (0.4–0.8 mm) of plagioclase (50%, labradorite [An_{55}] and andesine [An_{42}]), xenomorphic (0.1–0.7 mm) grains of clinopyroxene (30%), opaque minerals (5%), and brownish green interstitial glass (15%).

Alteration: slight (15%); interstitial glass replaced by clay minerals.

XRD: smectite; trace mixed-layer smectite-chlorite minerals and calcite.

Sample 128-794D-16R-1, 110–117 cm (Piece 12), Unit 8 [Z-1484]

Aphyric basalt, vesicular. Rock: intersertal-microlitic texture; microlites and large laths (0.7–1.4 mm) of plagioclase (50%, andesine [$An_{40–42}$]), very small segregates of clinopyroxene microlites (20%), and interstitial glass (20%). Vesicles (5%; 0.5–0.6 mm): sparse, isometric in shape; walls are lined with brownish green and black glass.

Alteration: slight to moderate (~20%); interstitial glass replaced by clay mineral.

Sample 128-794D-17R-1, 87–93 cm (Piece 8), Unit 8 [Z-1485]

Aphyric dolerite, medium grained. Rock: intersertal-ophitic texture; elongated-prismatic laths (0.5–1 mm) of plagioclase (45%, labradorite [An_{55}] and andesine [An_{44}]), xenomorphic grains (0.3–0.6 mm) of clinopyroxene (30%), opaque minerals (5%), and interstitial glass (20%).

Alteration: slight to moderate (~20%); interstitial glass replaced by clay minerals.

XRD: mixed-layer smectite-chlorite minerals; minor smectite; trace swelling chlorite.

Sample 128-794D-18R-1, 40–47 cm (Piece 6), Unit 8 [Z-1486]

Aphyric dolerite, medium grained. Rock: doleritic texture; prismatic and elongated-prismatic laths (0.5–1.5 mm) of plagioclase (40%, mainly andesine [$An_{42–44}$]), isometric grains and segregates of clinopyroxene (45%), opaque minerals (5%), and interstitial glass (10%).

Alteration: slight (10%); interstitial glass replaced by clay minerals.

XRD: smectite; trace swelling chlorite, mixed-layer smectite-chlorite minerals, and chlorite; dark brown veinlet: smectite; trace mixed-layer smectite-chlorite minerals.

Hole 795B

Sample 127-795B-35R-1, 60–62 cm (Piece 4), Unit 1 [Z-240]

Aphyric basalt, fine grained, vesicular. Groundmass: intergranular, trachytoid texture; volcanic glass with opaque dust, laths of plagioclase, microlites of clinopyroxene, and sparse olivine. Vesicles (0.2–1 mm, 10%): rounded and irregular in shape, filled with clay minerals. A crack (thickness 0.3–0.4 mm) is filled with clay minerals and opaque minerals.

Alteration: slight (~10%); interstitial glass is replaced with smectites.

XRD: smectites with Na-K and Mg-Ca interlayer cations.

Sample 127-795B-37R-1, 33–35 cm (Piece 3), Unit 3A [Z-696]

Clinopyroxene-plagioclase-phyric andesite-basalt (boninite?), vesicular. Phenocrysts (15%): prismatic grains (0.5–0.8 mm) of plagioclase (several grains are zonal) with inclusions of glass; segregates of partly idiomorphic grains (0.2–0.5 mm) of clinopyroxene. Groundmass: pilotaxitic texture; microlaths of plagioclase (andesine [$An_{38–42}$]) and oxidized black glass (nonoxidized parts of glass have greenish brown color). Vesicles (10%–15%; 0.3–1.5 mm): rounded and oval in shape.

Alteration: moderate; phenocrysts of plagioclase replaced by pelite and albite; glass in plagioclase replaced by clay mineral; interstitial glass is oxidized (partly); walls of vesicles are lined green glass, central parts of vesicles are filled with clay mineral.

Sample 127-795B-38R-1, 6–8 cm (Piece 1B), Unit 3A [Z-241]

XRD: smectite.

Sample 127-795B-38R-2, 87–92 cm (Piece 3B), Unit 3A [Z-1461]

Clinopyroxene-plagioclase-phyric andesite-basalt, vesicular. Phenocrysts (10%): prismatic grains (0.2–0.7 mm) of plagioclase (5%) with numerous (90%) inclusions of glass. Clinopyroxene (5%) forms xenomorphic grains and their segregates. Groundmass (80%): pilotaxitic texture; microlaths and microlites (0.1–0.5 mm) of plagioclase (50%, andesine [An_{45}]) and glass (25%). Vesicles (10%; 0.1–0.6 mm): rounded and oval in shape.

Alteration: moderate; glass in plagioclase partly replaced by clay mineral; small vesicles (8%) almost completely are filled with glass; walls of large vesicles (2%) are lined with glass (central parts of vesicles are filled with clay mineral).

Sample 127-795B-38R-4, 28–30 cm (Piece 2A), Unit 3A [Z-242]

Aphyric basalt, fine grained, vesicular. Groundmass: intersertal texture; volcanic glass with opaque dust, laths of plagioclase, microlites of clinopyroxene, and sparse olivine. Vesicles (0.3–1.2 mm, 30%): rounded and irregular in shape; some join to form microveins. A vein (0.8–1.5 mm thick) is filled with devitrified glass with microlites of clinopyroxene.

Alteration: moderate (~40%); interstitial glass is replaced by smectites; veins consist of smectites and probably zeolites.

XRD: smectite; trace hydromica and heulandite(?).

Sample 127-795B-39R-2, 22–24 cm (Piece 1B), Unit 3A [Z-1462]

Clinopyroxene-plagioclase-phyric andesite-basalt, vesicular. Phenocrysts (20%): prismatic grains (0.4–1.2 mm) of plagioclase (12%, labradorite [An_{62}]) with numerous inclusions of greenish brown glass. Clinopyroxene (8%) forms prismatic (0.6–0.7 mm) or xenomorphic (0.3–0.4 mm) grains and their segregates. Groundmass (40%): pilotaxitic texture; microlites of plagioclase (20%, andesine [An_{45}]), pyroxene (5%), and glass (15%). Vesicles (40%; 0.2–1.2 mm): oval in shape.

Alteration: moderate (40%); glass from plagioclase partly replaced by clay mineral; vesicles are lined with brown glass (central parts of vesicles are filled with clay mineral).

Sample 127-795B-40R-1, 27–29 cm (Piece 3B), Unit 3B [Z-243]

Aphyric basalt, medium grained, highly vesicular. Groundmass: intergranular texture; volcanic glass with opaque dust, laths of plagioclase, microlites of clinopyroxene, and sparse olivine. Vesicles (0.3–0.5 to 2.5 mm, 40%): filled with smectites, some vesicles are filled with zeolite, occasionally with devitrified glass.

Alteration: moderate (45%); interstitial glass, olivine, and plagioclase are replaced with smectites.

XRD: smectite; trace heulandite(?).

Sample 127-795B-40R-2, 123–125 cm (Piece 13), Unit 3B [Z-244]

Aphyric basalt, fine grained, highly vesicular. Groundmass: intergranular texture; volcanic glass with opaque dust, laths of plagioclase, and microlites of clinopyroxene. Vesicles (0.2–1.5 mm, 40%): filled with smectites, some filled with zeolite.

Alteration: strong (50%); interstitial glass and plagioclase are replaced by smectites.

XRD: smectite.

Hole 797C

Sample 127-797C-9R-1, 43–53 cm (Piece 9), Unit 1 [Z-1477]

Plagioclase-phyric basalt, crystallized, massive. Phenocrysts: prismatic grains (0.5–1.2 mm) of plagioclase. Groundmass: microlitic texture; microlites (0.1–0.3 mm) and microlaths (0.5–0.8 mm) of plagioclase (60%, mainly andesine [An_{38}] and [An_{43}]), segregate of very small (<0.1 mm) grains of clinopyroxene (15%), altered volcanic glass (in small amounts), and opaque minerals (5%).

Alteration: slight (15%–20%); interstitial glass is replaced with clay mineral.

Sample 127-797C-10R-1, 90–92 cm (Piece 2J), Unit 2 [Z-1478]

Sparsely plagioclase-phyric basalt, crystallized, massive. Phenocrysts: prismatic grains of plagioclase (5%, labradorite [An_{55}]). Groundmass (95%): microlitic texture; microlites and laths (0.1–0.6 mm) of plagioclase (65%, andesine [An_{48}]), very small (<0.1 mm) grains of clinopyroxene (10%), brown volcanic glass (20%) with crystals of opaque minerals.

Alteration: rock is fresh.

Sample 127-797C-10R-2, 125–127 cm (Piece 8E), Unit 2 [Z-245]

Aphyric basalt, fine grained, massive. Groundmass: intergranular, occasionally subvariolitic, texture; volcanic glass with opaque dust, laths of plagioclase, microlites of clinopyroxene, and olivine.

Alteration: slight (~10%); interstitial glass, olivine, and sparsely plagioclase are replaced with chlorite-smectite aggregate.

XRD: smectite with ~20% mica layers; trace chlorite.

Sample 127-797C-12R-2, 91–93 cm (Piece 1F), Unit 3 [Z-246]

Olivine-plagioclase-phyric basalt, coarse grained, massive. Rock: doleritic texture; laths of plagioclase (0.2–0.4 mm, 60%), devitrified volcanic glass (in small amounts), microlites of clinopyroxene (0.2–0.4 mm, 10%), opaque minerals, and olivine.

Alteration: slight (~15%); interstitial glass and olivine are replaced with chlorite-smectite aggregate.

XRD: smectites with ~20% mica layers and contain various interlayer cations (Na-K and Mg-Ca); trace chlorite and amphibole(?).

Sample 127-797C-12R-4, 85–89 cm (Piece 4D), Unit 3 [Z-756]

Sparsely plagioclase-phyric dolerite, fine grained, massive. Phenocrysts (3%–5%): prismatic grains (up to 1.5 mm, labradorite [An_{55}]) of plagioclase. Groundmass: doleritic-intersertal texture; laths (0.3–0.8 mm) of plagioclase (andesine [$An_{42–43}$]). Interstices: segregate of small grains of augite (~45%–47%), glass (~45%–47%), and opaque minerals (3%–5%).

Alteration: slight (10%–15%); interstitial glass replaced by clay mineral.

Sample 127-797C-13R-2, 99–102 cm (Piece 6C), Unit 3 [Z-757]

Sparsely plagioclase-phyric dolerite, fine grained, massive. Rock is identical to Sample 127-797C-12R-4, 85–89 cm (Z-756).

Sample 127-797C-14R-1, 88–94 cm (Piece 12A), Unit 4 [Z-1479]

Aphyric basalt, massive, brecciated. Rock: fragments of basalt and glassy crust. Basalt: microlites and laths of plagioclase (80%) and glass (20%).

Alteration: very strong (90%–95%); glassy crust completely replaced by clay minerals; rock replaced by aggregate of secondary minerals: albite, orthoclase, sericite, smectite, and chlorite.

XRD: smectite; trace chlorite (~10% swelling interlayers); clay matter from veinlet: smectite; trace swelling chlorite(?), and talc(?).

Sample 127-797C-16R-1, 53–55 cm (Piece 5B), Unit 5C [Z-247]

Olivine-plagioclase-phyric basalt (dolerite?), coarse grained, massive. Rock: ophitic texture; laths of plagioclase (0.5–1.5 mm, 60%), olivine (0.3–0.5 mm, 15%), clinopyroxene (0.2–0.4 mm, 10%), opaque minerals (0.1–0.3 mm, 5%), and devitrified volcanic glass (in small amounts).

Alteration: slight to moderate (~20%); interstitial glass and olivine are replaced by chlorite-smectite aggregate.

XRD: smectite; trace chlorite.

Sample 127-797C-16R-2, 64–68 cm (Piece 2C), Unit 5C [Z-758]

Sparsely plagioclase-phyric dolerite, fine grained with doleritic-intersertal groundmass texture, massive. Rock is identical to Samples 127-797C-12R-4, 85–89 cm (Z-756), and 13R-2, 99–102 cm (Z-757).

Sample 127-797C-19R-2, 51–53 cm (Piece 3B), Unit7 [Z-248]

Sparsely olivine-clinopyroxene-plagioclase-phyric basalt (dolerite?), coarse grained, massive, doleritic texture.

Alteration: slight (~15%); interstitial glass and olivine are replaced with chlorite-smectite aggregate.

XRD: smectite; trace chlorite and amphibole.

Sample 127-797C-19R-4, 2–5 cm (Piece 5B), Unit 7 [Z-759]

Plagioclase-phyric dolerite, medium grained, massive. Phenocrysts (15%): glomerophyric segregates of tabular grains (0.8–2 mm, labradorite [An_{50}]) of plagioclase. Plagioclase consists of inclusions of glass. Groundmass: doleritic texture; by laths (0.3–0.8 mm) of plagioclase (andesine [$An_{42–44}$]). Interstices: small (0.1–0.2 mm) rounded grains of olivine (2%–3%) and segregates of xenomorphic grains of augite with grains of opaque minerals (5%).

Alteration: slight (5%–7%); olivine partly replaced by clay mineral.

Sample 127-797C-19R-4, 51–56 cm (Piece 7A), Unit 7 [Z-1480]

Sparsely plagioclase-phyric basalt, massive. Phenocrysts (2%–3%): prismatic grains of plagioclase. Groundmass: pilotaxitic texture; microlites and laths of plagioclase (andesine [An_{49}] and labradorite [An_{52}]). Interstices: small (<0.1 mm) grains of clinopyroxene (20%), brown glass (10%), and opaque minerals (7%–8%).

Alteration: slight (2%–3%); glass partly replaced by clay minerals.

Sample 127-797C-20R-2, 104–108 cm (Piece 1D), Unit 8 [Z-1481]

Aphyric basalt, massive. Rock: pilotaxitic texture completely replaced by secondary minerals (albite, sericite, smectite, chlorite, and orthoclase?).

Alteration: very strong (95%).

XRD: smectite with ~10% mica layers and mixed-layer smectite-chlorite minerals (~10% swelling interlayers); minor corrensite; trace chlorite; veinlet: smectite and corrensite-like mineral; trace chlorite.

Sample 127-797C-21R-1, 55–57 cm (Piece 10), Unit 8 [Z-249]

Sparsely clinopyroxene-plagioclase-phyric basalt (dolerite?), coarse grained, massive, poikilophitic texture.

Alteration: slight (~10%); interstitial glass and olivine are replaced by chlorite-smectite aggregate.

XRD: smectite; trace chlorite, hydromica, and amphibole(?).

Sample 127-797C-21R-1, 76–80 cm (Piece 10), Unit 8 [Z-1482]

Aphyric dolerite, medium grained, massive. Rock: ophitic texture; prismatic grains (0.4–1.6 mm) of plagioclase (45%; labradorite [An_{55}] and andesine [An_{42}]), xenomorphic grains (0.2–1.7 mm) of clinopyroxene (35%), small (0.2–0.5 mm) grains of olivine (10%), glass (5%), and opaque minerals (5%).

Alteration: slight (15%); olivine completely replaced by green iddingsite; clay minerals replace interstitial glass.

XRD: mixed-layer smectite-chlorite minerals; minor smectite.

Sample 127-797C-21R-4, 110–112 cm (Piece 2B), Unit 8 [Z-760]

Aphyric dolerite, medium grained, massive. Rock: intersertal-doleritic texture; laths (0.2–2 mm) of plagioclase (andesine [An_{45}]), xenomorphic grains (0.3–0.7 mm) of augite, glass, and opaque minerals (3%–4%).

Alteration: slight to moderate (15%–20%); clay minerals replace interstitial glass.

XRD: smectite and mixed-layer smectite-chlorite minerals (~10% swelling interlayers); trace amphibole(?).

Sample 127-797C-21R-6, 10–14 cm (Piece 2), Unit 8 [Z-761]

Aphyric dolerite, medium grained, massive. Rock: intersertal-doleritic (occasionally, intersertal-ophitic) texture; by laths (0.3–2 mm) of plagioclase (80%, andesine [$An_{40–42}$]), xenomorphic grains of clinopyroxene (25%), glass (20%), and opaque minerals (5%). Single grains of clinopyroxene (up to 0.8 mm) with inclusions of plagioclase are present.

Alteration: slight to moderate (20%); clay minerals replace interstitial glass.

XRD: swelling chlorite and mixed-layer smectite-chlorite minerals; trace talc.

Sample 127-797C-24R-1, 95–97 cm (Piece 5D), Unit 9 [Z-250]

Plagioclase-phyric basalt (dolerite?), coarse grained, vesicular (0.2–0.8 mm, 10%), poikilophitic texture.

Alteration: slight (~15%); interstitial glass and olivine are replaced by chlorite-smectite aggregate; the latter fills vesicles.

XRD: smectites with interlayer Na-K and Mg-Ca cations; minor chlorite; trace talc.

Sample 127-797C-24R-4, 130–132 cm (Piece 7A), Unit 9 [Z-762]

Aphyric basalt (andesite-basalt: boninite?), massive. Rock: intersertal texture; laths (0.3–1.2 mm) of plagioclase, skeletal and needle-shaped grains of opaque minerals (25%) with hydrobiotite, completely altered clinopyroxene, and glass.

Alteration: strong to very strong (70%–75%); plagioclase replaced by clay minerals and albite; clinopyroxene completely replaced by brown secondary minerals; clay minerals replace interstitial glass.

XRD: smectite; minor mixed-layer smectite-chlorite minerals; trace chlorite; dark green veinlet: smectite and mixed-layer smectite-chlorite minerals; trace chlorite.

Sample 127-797C-24R-6, 64–66 cm (Piece 4), Unit 9 [Z-251]

Clinopyroxene-plagioclase-phyric basalt (dolerite?), coarse grained, vesicular (0.2–0.8 mm, 10%). Groundmass: poikilophitic texture.

Alteration: slight (~10%); interstitial glass and olivine are replaced by chlorite-smectite aggregate; the latter fills vesicles.

XRD: smectite; minor chlorite; trace amphibole(?).

Sample 127-797C-26R-1, 115–118 cm (Piece 17), Unit 10 [Z-763]

Aphyric basalt (andesite-basalt: boninite?), sparsely vesicular. Rock: microintersertal (pilotaxitic) texture; microlaths (0.1–0.5 mm) of plagioclase (35%–40%, oligoclase [An_{28}]), glass impregnated by dustlike magnetite, and small skeletal and needle-shaped grains (up to 0.1 mm) of opaque minerals (15%). Vesicles (0.4–0.6 mm): sparse; rounded in shape.

Alteration: strong (70%); plagioclase replaced by pelite and clay minerals; clay minerals replace interstitial glass; vesicles are filled with clay minerals.

XRD: corrensite-like mineral.

Sample 127-797C-27R-1, 68–70 cm (Piece 4G), Unit 11 [Z-252]

Aphyric basalt, fine grained, vesicular (0.2–0.8 mm, 15%). Groundmass: intergranular texture.

Alteration: slight to moderate (~20%); interstitial glass and olivine are replaced by clay minerals; vesicles are filled with clay minerals.

XRD: smectites with interlayer Na-K and Mg-Ca cations; trace hydromica.

Sample 127-797C-29R-1, 80–83 cm (Piece 2H), Unit 12 [Z-764]

Sparsely clinopyroxene-plagioclase-phyric basalt (andesite-basalt: boninite?), massive. Phenocrysts: single prismatic grains (up to 2 mm) of plagioclase (2%–3%, andesine [An_{42}]). Groundmass: microdoleritic-intersertal texture; laths (0.2–0.8 mm) of plagioclase (andesine [An_{38}]) with undulatory extinction, segregate small grains (<0.1 mm) of clinopyroxene (30%), greenish brown glass, and opaque minerals (7%–8%).

Alteration: slight.

XRD: smectite.

Sample 127-797C-31R-3, 114–116 cm (Piece 1E), Unit 13 [Z-253]

Aphyric basalt, vesicular (0.2–0.5 mm, 10%), intergranular texture.

Alteration: slight (~10%); interstitial glass and olivine are replaced by chlorite-smectite aggregate; the latter fills vesicles.

XRD: smectites with ~10% mica layers and with interlayer Na-K and Mg-Ca cations; trace hydromica.

Sample 127-797C-33R-1, 10–13 cm (Piece 2B), Unit 14 [Z-765]

Aphyric basalt (andesite-basalt). Rock: intersertal texture; laths (0.1–0.3 mm) of plagioclase, green glass, opaque dust, and small (0.1 mm) skeletal grains of opaque minerals (5%). Vesicles: (0.4–0.6 mm) sparse; rounded in shape.

Alteration: moderate (20%–25%); plagioclase is replaced by pelite and albite; clay minerals replace interstitial glass.

XRD: corrensite-like mineral.

Sample 127-797C-34R-1, 49–51 cm (Piece 3C), Unit 15 [Z-254]

Aphyric basalt, fine grained, vesicular (0.2–0.4 mm, 7%), intergranular texture.

Alteration: slight (~10%); interstitial glass and olivine are replaced by chlorite-smectite aggregate and carbonate; the latter fills vesicles.

XRD: smectites with interlayer Na-K and Mg-Ca cations; trace chlorite.

Sample 127-797C-41R-1, 42–44 cm (Piece 1A), Unit 19 [Z-255]

Sparsely plagioclase-phyric basalt, vesicular (0.2–0.5 mm, 20%), intersertal texture.

Alteration: moderate (~25%); interstitial glass and olivine are replaced by chlorite-smectite aggregate; the latter fills vesicles.

XRD: smectite; minor corrensite-like mineral; trace chlorite.

Sample 127-797C-44R-3, 47–49 cm (Piece 4A), Unit 20 [Z-256]

Andesite-basalt, coarse grained, vesicular (0.3–1 mm), intersertal texture.

Alteration: moderate (~25%); interstitial glass and olivine are replaced by chlorite-smectite aggregate; the latter fills vesicles.

XRD: corrensite-like mineral; minor chlorite.

Sample 127-797C-45R-1, 1–5 cm (Piece 1A), Unit 21 [Z-766]

Aphyric andesite-basalt, massive. Rock: intersertal texture; laths (0.3–0.8 mm, up to 2 mm) of plagioclase (from oligoclase [An_{28}] to andesine [An_{32}]), small (<0.1 mm) grains of clinopyroxene, green glass, and opaque minerals (7%–8%).

Alteration: moderate (40%–50%); plagioclase replaced by pelite and albite; clay minerals replace interstitial glass.

XRD: smectite; minor mixed-layer smectite-chlorite mineral.

Sample 127-797C-45R-4, 8–11 cm (Piece 1), Unit 21 [Z-767]

Aphyric dolerite (andesite-basalt), massive. Rock: intersertal-doleritic texture; laths and tabular grains (0.3–2 mm) of plagioclase (50%, from labradorite [An_{50}] to andesine [$An_{32–8}$]), small (0.2–0.5 mm) xenomorphic grains of augite, brownish green glass, and opaque minerals (5%–7%).

Alteration: moderate (20%); clay minerals replace interstitial glass.

XRD: smectite and swelling chlorite.

Lau Basin (Leg 135)

Hole 834B

Sample 135-834B-8R-2, 7–10 cm (Piece 1A), Unit 2 [Z-801]

Aphyric andesite-basalt, crystallized, vesicular. Rock: microdoleritic texture; microlites and microlaths (0.05–0.3 mm) of plagioclase (andesine [An_{45}]), segregates of small (up to 0.2 mm) isometric grains of clinopyroxene, and glass (<1%). Vesicles (20%; 0.2–1.2 mm): isometric in shape, empty, walls are lined with glass.

Alteration: slight; interstitial glass and glass from vesicles replaced by clay minerals.

Sample 135-834B-8R-2, 12–18 cm (Piece 1B), Unit 2 [Z-1487]

Aphyric andesite-basalt, crystallized, vesicular. Rock: microlitic (microdoleritic) texture; microlites and microlaths (up to 0.7 mm) of plagioclase (35%, andesine [$An_{40–42}$]), small (0.1–0.2 mm) isometric grains of clinopyroxene (30%), opaque minerals (7%), and brownish green volcanic glass (8%). Vesicles (20%; 0.2–0.7 mm): lined with clay minerals.

Alteration: slight (3%–5%); interstitial glass and glass from vesicles replaced by clay mineral.

Sample 135-834B-11R-2, 79–82 cm (Piece 3A), Unit 5 [Z-802]

Plagioclase-phyric andesite-basalt (dolerite), massive. Phenocrysts (20%): prismatic grains (1.2–2.5 mm) of plagioclase (labradorite [An_{50}]) and their segregates. Groundmass: ophitic texture; laths (0.3–1 mm) of plagioclase (andesine [$An_{43–45}$]). Interstices: xenomorphic grains (0.2–0.5 mm) of clinopyroxene and opaque minerals (~2%–3%).

Alteration: moderate (25%); plagioclase phenocrysts partly replaced by albite; clinopyroxene partly or completely replaced by hornblende (uralite).

Sample 135-834B-11R-3, 86–89 cm (Piece 3A), Unit 5 [Z-1488]

Aphyric dolerite, fine grained, vesicular. Rock: intersertal-poikilophitic texture; large (1.2–5 mm) grains of clinopyroxene (40%) with abundant laths of plagioclase, unoriented laths (0.2–0.7 mm) of plagioclase (25%, from andesine [An_{48}] to andesine [An_{42}]), small (0.1–0.2 mm) skeletal grains of opaque minerals (5%–7%), and volcanic glass (~10%). Vesicles (20%, 0.5–1.5 mm): isometric in shape.

Alteration: slight (10%–12%); interstitial glass replaced by clay minerals; walls of vesicles are lined with greenish brown radial-radiant clay minerals.

XRD: smectite; trace mixed-layer smectite-swelling chlorite mineral and cristobalite(?).

Sample 135-834B-12R-4, 130–134 cm (Piece 2), Unit 5 [Z-803]

Sparsely plagioclase-phyric basalt (dolerite), massive. Phenocrysts: single phenocryst of plagioclase (segregate of two oval-prismatic grains, up to 2 mm each). Groundmass: poikilophitic-intersertal texture; large (1.5–2.5 mm) isometric grains of clinopyroxene with inclusions of plagioclase microlaths. Interstices: microlaths (0.2–0.5 mm) of plagioclase (labradorite [An_{54}]), sparse small grains of pyroxene, green glass, and opaque minerals (~3%–4%).

Alteration: slight (15%); interstitial glass replaced by clay mineral.

Sample 135-834B-13R-1, 134–139 cm (Piece 4), Unit 5 [Z-1489]

Plagioclase-phyric dolerite, fine grained, vesicular. Phenocrysts (15%): glomerophyric segregates of tabular and prismatic grains (0.5–1.7 mm) of plagioclase (labradorite [$An_{60–62}$]). Groundmass: intersertal-poikilophitic texture; isometric grains (0.5–1.7 mm) of clinopyroxene (30%) with abundant inclusions of plagioclase laths (0.2–0.7 mm, andesine [An_{42}]). Interstices: opaque minerals (~5%–7%) and glass (10%). Vesicles (15%; 0.5–0.7 mm): isometric in shape.

Alteration: slight (10%–15%); interstitial glass replaced by clay mineral; walls of vesicles are lined clay mineral.

Sample 135-834B-13R-1, 139–142 cm (Piece 4), Unit 5 [Z-804]

Sparse plagioclase-phyric dolerite (basaltic composition) with intersertal-poikilophitic texture groundmass, sparsely vesicular. Rock is identical to Sample 135-834B-13R-1, 134–139 cm (Z-1489).

Alteration: slight (15%); interstitial glass replaced by clay mineral.

XRD: smectite; trace mixed-layer smectite-swelling chlorite mineral and cristobalite(?).

Sample 135-834B-22R-1, 87–90 cm (Piece 14A), Unit 7 [Z-805]

Plagioclase-phyric dolerite, massive. Phenocrysts (20%): tabular grains (0.5–1 mm) of plagioclase (labradorite [An_{58}]) and their segregates. Groundmass: doleritic texture; laths (0.3–0.5 mm) of plagioclase (andesine-labradorite [An_{50}] and andesine [$An_{46–48}$]). Interstices: segregates of small (<0.1–0.4 mm) grains of clinopyroxene, glass (1%–2%).

Alteration: slight; clay minerals replace glass; microcracks (5–6 mm) filled with pelite.

Sample 135-834B-28R-2, 76–78 cm (Piece 4B), Unit 7 [Z-806]

Plagioclase-phyric dolerite, fine grained, massive. Phenocrysts (20%): tabular and zonal elongated-prismatic grains (0.5–2 mm) of plagioclase (labradorite [An_{56}]) and their segregates. Small grains (0.2–0.4 mm) of olivine are present. Plagioclase grains contain inclusions of glass. Groundmass: doleritic texture; laths (0.2–1 mm) of plagioclase (labradorite [$An_{50–52}$]). Interstices: segregates of small grains of clinopyroxene, opaque minerals (7%–8%).

Alteration: rock is fresh.

XRD: smectite; trace mixed-layer smectite-swelling chlorite minerals and cristobalite.

Sample 135-834B-33R-2, 103–105 cm (Piece 5I), Unit 7 [Z-807]

Plagioclase-phyric dolerite, medium grained, massive. Phenocrysts (20%–25%): tabular and prismatic grains (0.8–2.2 mm) of plagioclase (labradorite [An_{60}]). Groundmass: doleritic texture; laths (0.2–0.8 mm) of plagioclase (labradorite [$An_{56–58}$]). Interstices: small isometric grains of clinopyroxene (90%), small (0.2–0.4 mm) rounded grains of olivine (6%), and glass (4%).

Alteration: slight; glass replaced by clay minerals.

Sample 135-834B-34R-2, 10–14 cm (Piece 1A), Unit 7 [Z-808]

Plagioclase-phyric dolerite, medium grained, with doleritic groundmass texture, massive. Rock is identical to Sample 135-834B-33R-2, 103–105 cm (Z-807).

Alteration: slight.

Sample 135-834B-47R-1, 71–74 cm (Piece 10), Unit 12 [Z-809]

Aphyric basalt, vesicular. Rock: pilotaxitic texture; microlites and laths (up to 0.8 mm) of plagioclase (labradorite [An_{50}]) and isometric grains of clinopyroxene (0.1–0.4 mm, up to 0.7 mm), often with grains of plagioclase. Isometric grains (0.3 mm) of olivine are present. Glass is black with abundant opaque dust. Opaque minerals (5%–7%) are present. Vesicles (20%–25%; 0.05–3 mm): rounded and isometric in shape. Small vesicles are partly or completely filled with green palagonitized glass; large vesicles are empty.

Alteration: slight.

XRD: trace cristobalite(?).

Sample 135-834B-49R-1, 97–100 cm (Piece 14B), Unit 12 [Z-810]

Sparsely plagioclase-phyric andesite-basalt, vesicular. Phenocrysts: single elongated-prismatic crystal (0.8 mm) of plagioclase. Groundmass: microdoleritic-intersertal texture; microlites and laths (0.3–1 mm) of plagioclase (60%, from andesine [An_{38}] to andesine [$An_{42–43}$]); large laths of plagioclase labradorite [An_{52}]. Interstices: segregate or small (up to 0.2 mm) grains of clinopyroxene. Greenish brown glass is present (<10%). Vesicles (10%; 0.2–0.5 mm) are empty or lined with glass.

Alteration: rock is fresh.

Sample 135-834B-49R-1, 131–135 cm (Piece 16), Unit 12 [Z-1490]

Aphyric basalt, vesicular. Rock: pilotaxitic texture; laths (0.1–0.8 mm) of plagioclase (35%, andesine [$An_{42–46}$]). Interstices: small (0.1–0.3 mm) rounded grains of clinopyroxene (25%), opaque minerals (5%), and greenish black glass. Vesicles (15%; 0.3–0.5 mm) are present. Walls of vesicles are lined with greenish black glass.

Alteration: rock is fresh.

Sample 135-834B-53R-1, 60–62 cm (Piece 5B), Unit 12 [Z-811]

Aphyric andesite-basalt, vesicular. Rock: pilotaxitic texture; microlites and laths (0.1–0.8 mm) of plagioclase (35%, from andesine [An_{38}] to andesine [An_{42}]). Interstices: small (0.1–0.3 mm) rounded-isometric grains of clinopyroxene (often with plagioclase) and black glass. Vesicles (30%–35%; 0.3–0.5 mm) are empty. Walls of vesicles are lined with glass.

Alteration: rock is fresh.

Bering Sea (Leg 19)

Hole 191

Sample 19-191-16R-1, 25–31 cm [Z-1101]

Olivine-plagioclase-phyric basalt, vesicular. Phenocrysts: idiomorphic grains (0.5–0.7 mm) of olivine (2%–3%) and glomerophyric segregates of tabular and prismatic grains (0.4–2 mm) of plagioclase (10%, labradorite [An_{52}]). Groundmass: hyalopilitic texture; skeletal caselike microlites and laths of plagioclase (15%) and black glass with crystals of plagioclase and pyroxene. Vesicles (5%, 0.5–0.7 mm) are rounded in shape and filled with black glass.

Alteration: slight; olivine is oxidized.

XRD: smectite.

Sample 19-191-16R-1, 78–83 cm [Z-1102]

Plagioclase-phyric basalt, vesicular. Phenocrysts: glomerophyric segregates of tabular grains (0.5–0.9 mm) of plagioclase (5%–7%, labradorite [An_{60}]). Groundmass: pilotaxitic texture; microlites and laths of plagioclase (40%, andesine [$An_{40–42}$]) and glass with crystals of clinopyroxene. Two brownish red grains (0.3 mm) of olivine(?) are present. Vesicles (5%, 0.2–0.5 mm) are rounded in shape and filled with black glass.

Alteration: slight (2%–3%); olivine(?) is oxidized; several vesicles consist of clay mineral.

XRD: smectite with ~15% mica layers; trace chlorite.

Sample 19-191-16R-1, 110–113 cm [Z-1103]

Plagioclase-phyric basalt, vesicular. Phenocrysts: glomerophyric segregates of small (0.1–0.6 mm) tabular and short-prismatic grains of plagioclase (5%, labradorite [An_{60}]). Groundmass: hyalopilitic texture; microlites and laths of plagioclase (20%, andesine [An_{46}]) and black glass. Vesicles (10%, 0.2–0.6 mm) are rounded in shape and filled with brown glass.

Alteration: fresh.

XRD: smectite with ~10% mica layers.

Southwest Indian Ridge (Leg 118)

Hole 735B

Sample 118-735B-7R-1, 41–43 cm (Piece 5), Unit 1 [Z-173]

Apogabbroic cataclasite, coarse grained, inequigranular, highly tectonized, dissected into fragments, which are cemented with medium-grained aplitic rock composed of quartz and feldspar. Relics of gabbro are represented by pseudoamorphic aggregate composed of amphibole, muscovite, and chlorite. Chlorite replaces a femic minerals (olivine or pyroxene). Texture is allotriomorphic-granular.

Alteration: very strong (80%); secondary minerals are quartz, chlorite, and amphibole.

XRD: paragonite(?), amphibole, and chlorite.

Sample 118-735B-12R-3, 99–101 cm (Piece 2I), Unit 2 [Z-174]

XRD: amphibole and chlorite; trace talc(?).

Sample 118-735B-19R-3, 19–21 cm (Piece 2A), Unit 2 [Z-175]

XRD: amphibole.

Sample 118-735B-20R-1, 73–75 cm (Piece 2E), Unit 2 [Z-176]

Gabbro, coarse grained, massive, tectonized, allotriomorphic-granular texture; plagioclase, amphibole replacing pyroxene, and olivine. Chlorite occurs sporadically in endocontact zones of amphibole. Olivine is replaced with chlorite along cracks. Mosaic quartz occurs sporadically, resulting in the formation of trondhjemite. Chlorite is localized in the interstitial space between crystals.

Alteration: strong (60%).

XRD: amphibole.

Sample 118-735B-24R-1, 17–19 cm (Piece 1B), Unit 2 [Z-177]

Gabbro, medium–coarse grained, tectonized, allotriomorphic-granular texture; plagioclase, clinopyroxene, amphibole, and olivine. Chlorite occurs at the contacts between rock-forming minerals. Olivine is replaced with chlorite along cracks. Often, olivine is surrounded by a rim composed of amphibole-chlorite aggregate with opaque dust and minerals resembling talc.

Alteration: moderate (~40%).

XRD: amphibole; trace chlorite and talc(?).

Sample 118-735B-32R-4, 4–6 cm (Piece 1A), Unit 2 [Z-178]

Gabbro, coarse grained, tectonized, allotriomorphic-granular texture; plagioclase, clinopyroxene, amphibole replacing pyroxene(?), and olivine. Amphibole (actinolite-tremolite) and chlorite occur at contacts of rock-forming minerals as grown celiphytic rims.

Alteration: moderate (~40%).

XRD: amphibole; trace chlorite and talc(?).

Sample 118-735B-41R-1, 36–38 cm (Piece 2A), Unit 3 [Z-179]

Gabbro, coarse grained, tectonized, allotriomorphic-granular texture; feldspar, clinopyroxene, amphibole, olivine, and quartz. Chlorite occurs in contacts of rock-forming minerals as grown celiphytic rims.

Alteration: moderate (30%).

XRD: amphibole; trace chlorite and talc(?).

Sample 118-735B-44R-2, 87–89 cm (Piece 1F), Unit 3 [Z-180]

Gabbro, coarse grained, tectonized, allotriomorphic-granular texture; feldspar, clinopyroxene, amphibole replacing clinopyroxene, and olivine. Feldspar predominates. Chlorite occurs in contacts of rock-forming minerals.

Alteration: slight to moderate (20%).

XRD: amphibole; trace chlorite and talc(?).

Sample 118-735B-49R-1, 57–59 cm (Piece 3C), Unit 4 [Z-181]

Gabbro, coarse grained, tectonized, allotriomorphic-granular texture; feldspar, clinopyroxene, amphibole, opaque minerals, and some admixture of quartz. Opaque minerals (~20% abundance) are located between rock-forming minerals. Chlorite-amphibole aggregate occurs at contacts of rock-forming minerals as celiphytic rims.

Alteration: moderate (25%).

XRD: amphibole and chlorite; trace talc(?).

Sample 118-735B-55R-3, 103–105 cm (Piece 4C), Unit 4 [Z-182]

Gabbro, medium grained, tectonized, granoblastic texture; large (0.9–3 mm) blastophyric grains of clinopyroxene (35%) and granoblastic aggregate of isometric grains (0.1–0.8 mm), plagioclase (30%), orthoclase (5%), and quartz. Opaque minerals (~20% abundance) cemented several areas of granoblastic aggregate.

Alteration: rock is fresh.

XRD: amphibole and chlorite; trace talc(?).

Sample 118-735B-58R-3, 26–28 cm (Piece 1B), Unit 5 [Z-183]

Gabbro, giant grained, fissured; feldspar, clinopyroxene, and amphibole. Cracks are filled with chlorite and quartz-feldspar aggregate.

Alteration: slight (10%).

XRD: amphibole and chlorite; trace talc(?).

Sample 118-735B-62R-1, 75–77 cm (Piece 2D), Unit 5 [Z-184]

Gabbro, coarse grained, tectonized, allotriomorphic-granular texture; feldspar, clinopyroxene, amphibole replacing pyroxene and olivine. Chlorite is scarce at the contacts between rock-forming minerals.

Alteration: scarce.

XRD: trace chlorite.

Sample 118-735B-73R-5, 63–65 cm (Piece 3), Unit 5 [Z-185]

Gabbro, coarse grained, tectonized, allotriomorphic-granular texture; plagioclase, clinopyroxene, amphibole, and single crystals of olivine. Chlorite occurs at the contacts between rock-forming minerals as thin celiphytic rims.

Alteration: slight (15%).

XRD: trace amphibole, chlorite, and talc.

Sample 118-735B-79R-5, 87–89 cm (Piece 6A), Unit 6 [Z-186]

Gabbro, coarse grained, tectonized, allotriomorphic-granular texture; plagioclase, clinopyroxene, and amphibole. Plagioclase sharply predominates. Chlorite occurs at the contacts between rock-forming minerals as thin celyphytic rims.

Alteration: slight (5%).

XRD: trace amphibole, chlorite, and talc.

Sample 118-735B-82R-6, 22–24 cm (Piece 3), Unit 6 [Z-187]

Gabbro leucocratic, coarse grained, tectonized, allotriomorphic-granular texture; plagioclase, clinopyroxene, amphibole, olivine(?), and opaque minerals. Chlorite-amphibole aggregate occurs at the contacts between rock-forming minerals as thin celyphytic rims and pockets.

Alteration: moderate (30%).

XRD: trace amphibole, chlorite, and talc(?).

Sample 118-735B-85R-7, 95–97 cm (Piece 6), Unit 6 [Z-188]

Gabbro, coarse grained, fissured, allotriomorphic-granular texture; plagioclase (labradorite [An_{55}], 1.2–3 mm, 60%). Interstices infilled with microcline (40%). Chlorite occurs at the contacts between rock-forming minerals as thin celyphytic rims.

Alteration: slight (7%).

XRD: amphibole and chlorite; trace talc(?).

Sample 118-735B-86R-3, 51–53 cm (Piece 1F), Unit 6 [Z-189]

Gabbro, coarse grained, tectonized, allotriomorphic-granular texture; plagioclase, clinopyroxene, and olivine(?). Rock is cut by a microvein filled with amphibole-chlorite-serpentine aggregate which contains hydrotalcite. Olivine is highly altered and chloritized. Chlorite occurs at the contacts between rock-forming minerals. Often, amphibole replaces clinopyroxene.

Alteration: moderate (~30%).

XRD: amphibole and chlorite; trace talc(?).

Sample 118-735B-88N-1, 60–62 cm (Piece 2C), Unit 6 [Z-190]

Gabbro, coarse grained, tectonized, allotriomorphic-granular texture; plagioclase, clinopyroxene, amphibole, and olivine. Chlorite-serpentine aggregate occurs at the contacts between rock-forming minerals as celyphytic rims and pockets (up to 2 mm).

Alteration: moderate (20%).

XRD: chlorite, serpentine(?), and amphibole.

Galicia Margin (Leg 103)

Hole 637A

Sample 103-637A-24R-1, 64–67 cm (Piece 4C) [Z-148]

XRD: calcite and serpentine.

Electron micrograph: b = 9.30 Å (serpentine).

Electron microscopy: chrysotile has length-slight fiber in shape with the clear central empty of fiber; structure type is tube-in-tube; there are the next polytypes of chrysotile: $2O_{rc1}$, $2M_{c1}$, and D_c; lizardite: in small amounts relative to chrysotile and represented as isometric particles; small amounts of aligned particles.

Sample 103-637A-25R-1, 66–69 cm (Piece 8B) [Z-149]

Apoperidotitic serpentinite. Rock: serpentine with small individual relics of olivine, orthopyroxene, and clinopyroxene. Relics of primary minerals are <1% abundance. Single crystals of picotite smashed into pieces are registered.

Alteration: very strong (90%); highly oxidized. Secondary minerals: serpentine and carbonate.

XRD: serpentine and calcite; trace talc(?).

Electron micrograph: b = 9.30 Å (serpentine).

Electron microscopy: chrysotile has length-slight fiber in shape; length/width usually close to 10–15, rarely ~1–2; most crystals have uncured layers with defects; the particles have the central empty of fiber; such chrysotile is named as “large fiber diameter chrysotile” or “Povlen-type chrysotile” because selected area electron diffraction pattern; there are aggregates with small particles of chrysotile and lizardite that correspond to initial stage of serpentinization; polytypes of chrysotile: $2O_{rc1}$, $2M_{c1}$, and D_c; a typical shape of chrysotile is tube-in-tube; lizardite: in small amount and crystals has structural defect.

Sample 103-637A-26R-2, 53–56 cm (Piece 1E) [Z-150]

Apoperidotitic serpentinite, tectonized. Rock: serpentine with small single relics of olivine, orthopyroxene, and clinopyroxene. Relics of primary minerals are <1% abundance. Single grains of picotite are registered.

Alteration: very strong (~90%); highly oxidized. Secondary minerals: serpentine of various generations and carbonate; it is probable that serpentinite is formed upon lherzolite.

XRD: serpentine and calcite; trace Fe smectite(?).

Electron micrograph: b = 9.26 Å (serpentine).

Electron microscopy: chrysotile is represented as subordinate minerals; it has length-slight fiber with the central empty of fiber; there is chrysotile-asbestos also; more common is chrysotile D_c polytype and rare disordered polytype $2M_{c1}$; Povlen-chrysotile has two polytypes: D_c and $2O_{rc1}$; the central empty of fiber is unclear; very often we can see joints of two crystals along their long axis; lizardite is represented as polycrystal aggregate having complicated shape with rough edges and curved layers; there are pseudomorphs of lizardite on host minerals; Fe oxide as cubic crystals.

Sample 103-637A-27R-1, 112–115 cm (Piece 15C) [Z-151]

Apoperidotitic serpentinite, tectonized. Rock: serpentine with small single relics of olivine and orthopyroxene. Picotite is <1% abundance.

Alteration: very strong (~90%–95%); highly oxidized; secondary minerals: serpentine and carbonate.

XRD: serpentine and calcite; smectite(?) and talc(?) in trace amounts.

Electron microscopy: chrysotile has length-slight fiber in shape with the central empty of fiber; some morphological defects of crystals; common polytype is D_c; Povlen-chrysotile has two polytypes: D_c and $2O_{rc1}$; the central empty of fiber is absent; lizardite has small particles; well-ordered crystals with sharp edges.

Sample 103-637A-28R-3, 103–106 cm (Piece 14) [Z-152]

Apoperidotitic serpentinite, tectonized. Rock: by serpentine with small single relics of olivine and orthopyroxene. Picotite is <1% abundance.

Alteration: very strong (~90%–95%); highly oxidized. Secondary minerals: serpentine and carbonate.

XRD: serpentine and calcite; trace amphibole and goethite.

Electron micrograph: b = 9.30 Å (serpentine).

Electron microscopy: chrysotile is length-slight fiber in shape with the clear center empty of fiber; cone in shape of chrysotile; some aggregates of parallel-oriented crystals were found with uncured layers; chrysotile probably transforms into lizardite or antigorite; morphological type is tube-in-tube; the polytypes are $2M_{c1}$ and D_c; lizardite is represented as monocrystals with sharp edges; antigorite was found as crystals with sharp edges.

APPENDIX B

See tables AT1–AT73 for data on abundance of major and trace elements in igneous rock samples referenced in this *Report*.

Table AT1. Abundance of major and trace elements (g/1000 cm^3) in igneous rocks, Hole 504B, Legs 69, 70, 83, 111, 137, 140, and 148 (Costa Rica Rift). (Continued on next twenty three pages.)

Leg	69	69	69	69	69	69	69
Hole	504B	504B	504B	504B	504B	504B	504B
Core, section	2R-1	4R-1	4R-3	4R-4	5R-2	6R-1	7R-2
Interval (cm)	108-110	62-64	108-111	42-45	142-146	65-69	64-68
Piece	233	274	322	330	387	404	459
Lab number	Z-883	Z-884	Z-885	Z-886	Z-887	Z-888	Z-889
Depth (mbsf)	275.58	280.62	282.08	284.92	292.42	299.15	309.64
Major elements (g/1000 cm^3):							
Si	650.1	474.9	510.9	612.1	636.1	498.3	428.7
Ti	11.83	10.11	10.57	12.18	12.81	11.37	8.75
Al	224.1	208.0	209.2	252.0	219.4	174.4	187.0
Fe^{+++}	125.7	43.9	82.1	56.3	128.4	95.6	39.5
Fe^{++}	114.0	85.8	58.4	99.5	94.5	76.3	75.6
Fe (Sum)	239.7	129.7	140.5	155.8	222.9	171.9	115.1
Mn	3.76	3.26	3.05	3.73	3.31	3.11	1.93
Mg	124.5	123.4	148.7	123.8	149.9	104.8	100.6
Ca	231.9	117.1	171.4	237.4	231.0	195.8	147.7
Na	51.34	30.77	33.22	46.03	43.11	30.29	41.18
K	6.17	6.44	1.73	4.88	3.78	1.30	2.55
P	1.25	0.58	0.51	1.05	0.99	0.78	0.75
Minor elements (g/1000 cm^3 x 10^{-3}):							
La	4.79	1.94	2.26	2.94	3.91	2.62	2.30
Ce	18.33	5.75	6.24	7.21	12.00	7.63	6.91
Nd	17.77	8.18	8.32	10.15	14.23	9.37	8.45
Sm	7.33	4.20	4.39	5.61	6.70	4.58	4.22
Eu	2.48	1.79	1.62	2.00	2.09	1.46	1.79
Tb	2.31	1.64	1.50	1.90	1.95	1.22	1.42
Yb	9.02	6.85	6.01	7.48	8.09	5.23	5.38
Lu	1.49	0.97	0.95	1.20	1.23	0.85	0.83
Sc		61.88	73.92	90.78			61.44
Cr	662.7	906.1	704.6	707.6	1143.9	872.0	614.4
Ni	200.2	176.8	177.9	189.6	301.3	305.2	132.5
Co	135.4	90.6	90.1	96.1	122.8	95.9	78.7
V	1099.8	729.3	559.0	614.1	758.9	534.1	649.0
Cu	186.1	108.3	113.2	157.5	189.7	102.5	86.4
Zn	276.4	141.4	140.9	168.2	200.9	161.3	119.0
Sn	5.92	5.97	5.54	6.41	4.19	3.27	4.80
Zr	160.7	97.2	97.0	117.5	125.6	109.0	78.7
Y	73.3	55.3	50.8	58.7	64.2	45.8	46.1
Nb			3.23	3.74	2.79		3.46
Rb	12.41	9.72	3.00	9.08	8.65	2.62	3.07
Sr	200.2	243.1	159.4	181.6	186.9	139.5	145.9
Ba	25.38	121.55	78.54	77.43	0.00	6.54	74.88
B		77.35	46.20	106.80			30.72
H_2O^+ (wt%)	0.89	6.92	2.68	1.33	0.53	0.65	1.95
Density (g/cm^3)	2.82	2.21	2.31	2.67	2.79	2.18	1.92
Fe_2O_3/FeO	1.23	0.57	1.56	0.63	1.51	1.39	0.58

Table AT1 (continued).

Leg	69	69	69	69	69	69	69
Hole	504B	504B	504B	504B	504B	504B	504B
Core, section	7R-3	8R-3	9R-1	10R-3	11R-1	12R-1	13R-4
Interval (cm)	61-65	61-66	142-147	17-20	61-64	39-43	40-42
Piece	481	538	583	643	667	714	806
Lab number	Z-890	Z-891	Z-892	Z-893	Z-894	Z-895	Z-896
Depth (mbsf)	311.11	320.11	326.92	337.67	344.11	352.89	366.40
Major elements (g/1000 cm^3):							
Si	559.2	424.5	575.7	597.5	621.7	677.8	641.1
Ti	8.51	5.59	11.41	13.47	15.59	12.15	13.50
Al	207.6	145.4	199.5	210.3	225.8	235.8	240.7
Fe^{+++}	128.8	92.0	166.0	129.3	124.2	109.0	51.7
Fe^{++}	39.0	59.4	37.5	65.0	65.3	94.5	123.1
Fe (Sum)	167.8	151.4	203.4	194.3	189.4	203.5	174.8
Mn	2.16	2.31	1.66	2.73	2.97	3.87	4.30
Mg	131.0	85.5	168.1	154.6	127.4	139.6	152.7
Ca	144.3	166.7	109.2	180.0	215.3	263.3	238.7
Na	44.75	28.64	47.52	46.61	49.95	49.26	40.21
K	8.84	1.86	10.23	3.37	4.54	4.15	2.77
P	0.77	0.73	0.94	1.18	1.19	1.03	1.09
Minor elements (g/1000 cm^3 x 10^{-3}):							
La	3.40	2.39	3.28	4.68	4.01	3.77	3.06
Ce	12.39	9.02	12.35	20.28	11.75	17.40	10.01
Nd	11.66	9.02	12.10	19.50	13.62	15.95	11.95
Sm	4.62	3.68	5.29	7.80	6.68	6.67	5.84
Eu	1.60	1.23	1.94	2.55	2.27	2.49	2.25
Tb	1.19	1.12	1.44	2.50	1.76	1.77	1.92
Yb	5.10	4.60	6.30	7.28	7.21	7.83	7.23
Lu	0.78	0.75	1.06	1.12	1.09	1.16	1.22
Sc							100.08
Cr	1263.6	772.8	793.8	1066.0	1068.0	1131.0	714.5
Ni	228.4	187.7	239.4	231.4	208.3	272.6	191.8
Co	102.1	92.0	126.0	127.4	114.8	145.0	119.5
V	940.4	574.1	1121.4	785.2	846.4	832.3	700.6
Cu	119.1	86.5	151.2	130.0	181.6	179.8	164.0
Zn	140.9	139.8	181.4	202.8	232.3	261.0	177.9
Sn	5.59	1.84	3.78	5.20	5.34	5.51	6.12
Zr	106.9	82.8	123.5	140.4	133.5	133.4	130.7
Y	46.2	38.6	55.4	75.4	72.1	69.6	66.7
Nb					3.20		3.34
Rb	7.53	22.08	11.59	6.50	12.82	8.99	5.84
Sr	211.4	121.4	204.1	221.0	235.0	214.6	202.9
Ba	9.72	0.00	20.16	7.80	16.02	0.00	66.72
B							97.30
H_2O^+ (wt%)	3.85	0.33	2.37	1.25	0.68	0.24	1.30
Density (g/cm^3)	2.43	1.84	2.52	2.60	2.67	2.90	2.78
Fe_2O_3/FeO	3.67	1.72	4.92	2.21	2.11	1.28	0.47

Table AT1 (continued).

Leg	69	69	69	69	69	69	69
Hole	504B	504B	504B	504B	504B	504B	504B
Core, section	15R-1	16R-1	16R-4	17R-1	18R-1	19R-1	20R-1
Interval (cm)	24-28	45-49	22-26	30-34	45-49	84-87	110-113
Piece	872	961	1005	1036	1087	1124	1173
Lab number	Z-901	Z-897	Z-898	Z-899	Z-900	Z-902	Z-903
Depth (mbsf)	375.24	384.45	388.72	393.30	398.45	403.84	413.10
Major elements (g/1000 cm^3):							
Si	602.7	616.9	644.3	610.6	619.0	601.1	654.7
Ti	15.29	11.95	16.46	15.77	20.56	17.84	16.11
Al	267.1	222.6	223.2	232.4	228.2	224.3	232.9
Fe^{+++}	84.0	112.6	95.6	117.2	125.9	129.4	72.3
Fe^{++}	84.6	83.2	103.3	68.8	91.4	73.1	116.4
Fe (Sum)	168.5	195.9	198.9	186.0	217.3	202.4	188.7
Mn	3.40	3.22	3.77	2.12	2.37	3.26	3.76
Mg	130.3	146.6	168.5	147.1	117.8	152.9	133.2
Ca	193.4	220.8	220.8	181.7	241.2	188.2	265.4
Na	50.86	44.98	43.29	50.01	48.19	45.83	46.66
K	6.15	4.14	1.90	3.64	4.17	3.73	0.71
P	1.20	0.97	1.37	1.32	1.95	1.96	1.00
Minor elements (g/1000 cm^3 x 10^{-3}):							
La	3.29	2.96	4.46	4.51	19.18	19.44	5.36
Ce	12.60	11.84	16.18	12.99	49.32	51.30	19.18
Nd	15.07	12.11	16.18	13.52	30.14	29.70	16.92
Sm	6.85	5.38	6.42	6.10	7.95	7.56	6.20
Eu	2.74	1.91	2.15	2.33	2.74	2.70	2.43
Tb	2.30	1.53	1.59	1.62	1.86	1.81	1.41
Yb	8.77	6.46	6.70	6.10	6.30	6.48	6.49
Lu	1.37	1.05	1.09	0.93	1.01	1.03	0.99
Sc	128.78						
Cr	822.0	753.2	1185.8	1219.0	1054.9	999.0	1071.6
Ni	194.5	231.3	446.4	437.3	263.0	378.0	304.6
Co	117.8	113.0	133.9	140.5	117.8	140.4	157.9
V	896.0	793.6	744.9	808.3	731.6	756.0	775.5
Cu	186.3	91.5	217.6	116.6	186.3	162.0	248.2
Zn	221.9	199.1	206.5	190.8	191.8	172.8	217.1
Sn	4.93	5.38	6.98	3.98	7.67	5.40	6.49
Zr	134.3	126.4	142.3	145.8	243.9	243.0	152.3
Y	79.5	59.2	72.5	66.3	71.2	64.8	62.0
Nb	3.29	4.57		3.45	25.76	26.19	
Rb	13.43	9.68	5.30	3.98	9.59	4.32	
Sr	230.2	180.2	228.8	254.4	411.0	405.0	262.3
Ba	84.94	8.07		10.60	19.18	18.90	22.56
B	147.96						
H_2O^+ (wt%)	4.11	0.86	0.61	1.52	0.62	2.02	0.50
Density (g/cm^3)	2.74	2.69	2.79	2.65	2.74	2.70	2.82
Fe_2O_3/FeO	1.10	1.50	1.03	1.89	1.53	1.97	0.69

Table AT1 (continued).

Leg	69	69	69	69	69	69	69
Hole	504B	504B	504B	504B	504B	504B	504B
Core, section	21R-2	21R-4	21R-5	22R-1	23R-1	24R-1	24R-3
Interval (cm)	126-130	116-120	63-66	108-109	32-35	125-128	128-129
Piece	1215	1253	1267	1280	1314	1349	1393
Lab number	Z-904	Z-905	Z-906	Z-907	Z-908	Z-909	Z-910
Depth (mbsf)	423.76	426.66	427.63	431.08	439.32	449.25	452.28
Major elements (g/1000 cm^3):							
Si	682.5	582.0	585.3	638.6	674.5	585.7	676.2
Ti	11.11	8.91	10.27	13.01	14.37	12.12	11.69
Al	258.7	220.3	266.2	238.8	252.1	249.5	240.8
Fe^{+++}	127.4	69.7	73.5	68.3	80.3	81.3	83.4
Fe^{++}	84.9	86.0	87.3	99.4	102.5	99.6	135.7
Fe (Sum)	212.3	155.7	160.8	167.7	182.8	180.9	219.1
Mn	3.29	1.98	3.52	5.45	3.44	3.30	1.83
Mg	154.0	135.5	142.5	151.2	140.4	148.7	142.5
Ca	263.0	225.6	222.0	248.2	272.8	185.6	259.7
Na	45.06	36.11	37.72	45.15	43.25	37.71	48.45
K	2.27	1.91	2.89	2.11	5.16	5.96	1.72
P	0.80	0.67	0.58	0.98	0.90	0.81	0.90
Minor elements (g/1000 cm^3 x 10^{-3}):							
La	2.79	2.19	2.16	5.54	2.92	2.37	3.78
Ce	10.20	7.06	8.28	16.90	9.93	9.04	13.39
Nd	11.40	9.32	9.61	18.01	12.56	10.11	14.84
Sm	5.10	4.28	4.54	7.48	5.55	4.52	6.98
Eu	1.92	1.61	1.71	2.19	2.07	1.94	2.30
Tb	1.68	1.29	1.68	1.91	1.58	1.57	1.95
Yb	6.30	5.54	5.87	8.31	6.42	6.38	8.15
Lu	1.02	0.83	0.80	1.25	1.11	0.93	1.31
Sc			72.09			87.78	
Cr	1380.0	957.6	987.9	1135.7	817.6	1103.9	1164.0
Ni	450.0	390.6	400.5	265.9	227.8	417.6	270.6
Co	180.0	133.6	138.8	133.0	128.5	146.3	154.2
V	960.0	705.6	712.9	698.0	846.8	843.2	1126.2
Cu	165.0	166.3	192.2	152.4	160.6	180.9	192.1
Zn	228.0	194.0	178.9	216.1	248.2	170.2	212.4
Sn	4.50	5.29	4.54	4.71	4.96	5.32	5.53
Zr	111.0	83.2	74.8	166.2	125.6	114.4	163.0
Y	57.0	47.9	56.1	72.0	61.3	50.5	78.6
Nb			3.47		3.21	4.52	
Rb		3.02	3.74		14.60	9.04	
Sr	162.0	131.0	149.5	213.3	169.4	154.3	183.3
Ba	12.00	15.12	93.45	24.93	20.44	71.82	23.28
B			42.72			74.48	
H_2O^+ (wt%)	0.78	0.75	2.16	0.90	0.55	3.34	0.40
Density (g/cm^3)	3.00	2.52	2.67	2.77	2.92	2.66	2.91
Fe_2O_3/FeO	1.67	0.90	0.94	0.76	0.87	0.91	0.68

Table AT1 (continued).

Leg	69	69	69	69	69	70	70
Hole	504B	504B	504B	504B	504B	504B	504B
Core, section	25R-2	26R-1	27R-2	28R-3	29R-1	32R-2	33R-1
Interval (cm)	62-66	15-18	55-58	69-73	31-34	137-140	70-72
Piece	1429	1449	1484	1530	1562	177	191
Lab number	Z-911	Z-912	Z-913	Z-914	Z-915	Z-919	Z-916
Depth (mbsf)	459.12	463.15	468.05	478.69	484.31	510.37	517.2
Major elements (g/1000 cm^3):							
Si	655.0	674.9	587.9	639.3	675.2	648.9	627.3
Ti	11.93	12.79	12.49	12.52	11.49	15.04	11.89
Al	218.3	237.6	242.8	231.6	226.1	249.8	261.2
Fe^{+++}	75.9	68.2	46.3	68.1	149.8	103.5	88.0
Fe^{++}	136.5	133.5	123.0	96.9	57.3	130.8	99.4
Fe (Sum)	212.4	201.7	169.3	165.0	207.1	234.4	187.4
Mn	4.84	2.04	4.55	1.97	4.72	4.62	4.45
Mg	153.0	144.9	160.6	142.9	146.0	160.4	130.0
Ca	255.5	265.0	209.4	234.3	261.0	231.1	263.6
Na	44.91	47.05	39.23	46.27	46.96	39.21	45.43
K	1.65	3.15	3.77	3.51	1.69	4.46	3.58
P	0.87	1.02	1.28	0.74	1.01	1.04	1.51
Minor elements (g/1000 cm^3 x 10^{-3}):							
La	3.38	4.05	2.66	3.30	4.32	3.20	2.79
Ce	12.97	12.43	8.51	11.55	15.55	10.19	9.87
Nd	14.66	17.63	10.37	13.48	17.28	12.51	10.72
Sm	6.20	7.80	5.05	5.78	7.20	5.24	4.51
Eu	2.28	2.66	2.15	2.31	2.51	1.95	1.75
Tb	1.83	2.31	1.65	1.65	2.13	1.78	1.38
Yb	7.90	9.83	6.38	7.15	8.93	6.98	5.64
Lu	1.18	1.53	1.04	1.07	1.38	1.19	0.90
Sc			79.80				
Cr	1198.5	910.4	683.6	962.5	864.0	960.3	958.8
Ni	251.0	268.8	282.0	255.8	253.4	299.7	479.4
Co	152.3	144.5	106.4	148.5	138.2	157.1	149.5
V	1071.6	930.6	670.3	1036.8	927.4	1105.8	738.8
Cu	191.8	190.7	156.9	165.0	239.0	203.7	231.2
Zn	225.6	239.9	183.5	198.0	239.0	232.8	197.4
Sn	5.92	6.36	4.52	5.78	6.05	5.24	5.08
Zr	157.9	153.2	103.7	137.5	158.4	131.0	135.4
Y	67.7	69.4	66.5	63.3	72.0	69.8	53.6
Nb			3.46	3.30			
Rb		7.23	5.85			4.66	7.33
Sr	180.5	182.1	162.3	165.0	181.4	125.1	214.3
Ba	14.10	17.34	82.46	19.25	23.04	11.64	19.74
B			58.52				
H_2O^+ (wt%)	0.35	0.31	2.11	1.77	0.23	1.72	1.64
Density (g/cm^3)	2.82	2.89	2.66	2.75	2.88	2.91	2.82
Fe_2O_3/FeO	0.62	0.57	0.42	0.78	2.91	0.88	0.98

Table AT1 (continued).

Leg	70	70	70	70	70	70	70
Hole	504B	504B	504B	504B	504B	504B	504B
Core, section	33R-1	33R-2	34R-1	34R-1	34R-2	35R-1	35R-2
Interval (cm)	86-88	14-16	19-24	140-142	18-21	110-112	14-16
Piece	193	202	220	235	240	274	283
Lab number	Z-917	Z-918	Z-550	Z-920	Z-921	Z-922	Z-923
Depth (mbsf)	517.36	518.14	525.69	526.9	527.18	535.6	536.14
Major elements (g/1000 cm^3):							
Si	602.7	663.6	653.2	627.0	544.7	594.7	378.3
Ti	12.92	15.00	16.29	13.98	11.49	10.93	7.75
Al	219.1	240.9	236.7	243.7	224.1	262.4	159.9
Fe^{+++}	65.2	57.6	65.9	92.1	84.1	101.3	45.2
Fe^{++}	116.2	125.7	124.0	96.5	92.8	78.4	67.8
Fe (Sum)	181.3	183.2	189.9	188.6	176.9	179.8	113.0
Mn	4.80	4.51	3.51	1.96	4.29	3.79	4.73
Mg	159.4	152.5	161.3	134.2	126.3	132.0	99.8
Ca	222.6	254.1	233.6	270.1	203.2	228.8	153.5
Na	39.58	42.31	45.35	42.95	40.96	39.35	24.91
K	2.91	3.86	3.48	1.87	8.16	3.61	2.09
P	1.29	1.52	0.94	0.49	0.99	0.59	0.39
Minor elements (g/1000 cm^3 x 10^{-3}):							
La	4.24	4.29	6.06	3.06	2.45	2.12	1.58
Ce	12.99	10.58	19.46	9.73	8.40	8.43	5.01
Nd	13.25	12.01		11.40	10.37	10.06	6.44
Sm	5.04	5.15	5.30	5.00	4.45	4.62	3.04
Eu	2.01	2.06	2.40	1.95	1.73	2.04	1.43
Tb	1.51	1.69	1.11	1.39	1.51	1.80	0.98
Yb	6.10	6.01	3.72	6.12	5.43	6.26	4.12
Lu	1.01	0.97	0.71	1.08	0.94	0.98	0.66
Sc			95.88			54.40	48.33
Cr	821.5	972.4	893.9	1173.2	1025.1	1006.4	474.4
Ni	424.0	543.4		500.4	382.9	413.4	175.4
Co	124.6	145.9	90.2	161.2	116.1	190.4	87.7
V	728.8	829.4		973.0	852.2	685.4	331.2
Cu	185.5	205.9		361.4	197.6	233.9	153.9
Zn	220.0	237.4	115.6	214.1	160.6	165.9	259.6
Sn	7.42	6.86		6.12	5.43	5.44	3.58
Zr	135.2	151.6		125.1	106.2	117.0	77.0
Y	55.7	62.9		61.2	54.3	54.4	34.0
Nb	2.92	4.00		3.89		3.54	
Rb	10.34	7.44			6.92	6.26	3.58
Sr	182.9	205.9		180.7	192.7	223.0	125.3
Ba	13.25	8.58		38.92	12.35	43.52	34.01
B						146.88	96.66
H_2O^+ (wt%)	0.75	0.78	0.97	1.11	1.89	2.91	4.46
Density (g/cm^3)	2.65	2.86	2.82	2.78	2.47	2.72	1.79
Fe_2O_3/FeO	0.62	0.51	0.59	1.06	1.01	1.44	0.74

Table AT1 (continued).

Leg	70	70	70	70	70	70	70
Hole	504B	504B	504B	504B	504B	504B	504B
Core, section	36R-1	36R-2	37R-1	37R-1	37R-2	37R-3	39R-2
Interval (cm)	91-110	25-27	15-20	55-60	75-78	14-17	97-102
Piece	301A	305	344	349	373	391	492
Lab number	Z-551	Z-924	Z-925	Z-926	Z-927	Z-928	Z-930
Depth (mbsf)	544.41	545.25	552.65	553.05	554.75	555.64	572.97
Major elements (g/1000 cm^3):							
Si	672.6	670.0	663.1	700.4	678.3	644.3	687.3
Ti	17.12	13.87	16.22	16.61	11.38	13.76	14.05
Al	235.1	232.3	230.9	247.6	223.1	224.4	247.9
Fe^{+++}	52.3	12.0	69.1	62.0	58.3	77.0	41.1
Fe^{++}	162.9	164.5	122.7	166.5	174.9	139.8	143.8
Fe (Sum)	215.2	176.5	191.9	228.5	233.2	216.8	184.9
Mn	3.10	4.87	3.15	1.91	5.05	4.61	4.31
Mg	142.3	165.9	157.9	155.2	157.8	142.5	145.0
Ca	265.1	229.5	251.7	263.0	239.1	243.3	265.6
Na	42.59	61.68	44.46	53.23	68.44	49.81	44.76
K	0.95	3.08	1.45	5.37	3.94	6.82	0.49
P	0.97	1.00	0.51	0.67	1.42	1.11	1.15
Minor elements (g/1000 cm^3 x 10^{-3}):							
La	3.48	2.69	4.56	17.33	3.23	2.67	2.64
Ce	19.14	5.72	12.83	36.48	10.58	11.24	9.86
Nd		10.87	12.26	22.80	12.64	11.80	11.60
Sm	6.64	5.72	4.85	5.78	5.88	5.62	5.22
Eu	2.81	2.46	1.91	2.10	2.38	2.08	1.91
Tb	1.97	1.72	1.77	1.92	1.79	1.71	1.71
Yb	8.03	7.72	6.84	8.21	8.53	7.31	6.38
Lu	1.42	1.17	1.08	1.34	1.35	1.26	1.04
Sc	133.40	80.08					
Cr	1006.3	643.5	997.5	1328.5	1029.0	829.0	826.5
Ni		237.4	273.6	267.5	258.7	222.0	281.3
Co	113.1	151.6	134.0	161.1	141.1	115.2	139.2
V	986.0	735.0	798.0	1231.2	946.7	744.7	812.0
Cu	252.3	205.9	250.8	316.2	211.7	165.8	223.3
Zn	229.1	214.5	239.4	261.4	238.1	196.7	197.2
Sn		5.72	6.84	9.42	5.88	4.78	4.93
Zr		114.4	119.7	133.8	135.2	120.8	130.5
Y		65.8	68.4	76.0	79.4	64.6	63.8
Nb		2.86	4.28	3.34		3.09	
Rb				7.60	6.76	14.33	
Sr		165.9	153.9	176.3	132.3	174.2	153.7
Ba			19.95	12.16	14.70	8.43	11.60
B		28.60					
H_2O^+ (wt%)	0.76	1.15	0.78	1.00	1.15	0.93	0.28
Density (g/cm^3)	2.90	2.86	2.85	3.04	2.94	2.81	2.90
Fe_2O_3/FeO	0.36	0.08	0.63	0.41	0.37	0.61	0.32

Table AT1 (continued).

Leg	70	70	70	70	70	70	70
Hole	504B	504B	504B	504B	504B	504B	504B
Core, section	40R-1	40R-2	41R-3	43R-1	44R-1	47R-1	47R-2
Interval (cm)	55-60	84-86	146-148	80-82	125-130	46-48	130-140
Piece	510	532	628	680	716	808	835
Lab number	Z-552	Z-553	Z-554	Z-555	Z-931	Z-556	Z-932
Depth (mbsf)	580.05	581.84	588.46	602.8	612.25	638.46	640.80
Major elements (g/1000 cm^3):							
Si	621.7	654.9	671.7	668.1	652.9	684.6	647.6
Ti	13.74	14.56	16.27	16.00	17.51	18.20	14.85
Al	233.9	255.7	254.5	240.3	231.7	228.7	234.4
Fe^{+++}	53.5	42.6	45.2	79.1	59.6	61.6	48.4
Fe^{++}	129.2	148.9	153.6	133.9	140.6	166.0	145.0
Fe (Sum)	182.8	191.6	198.8	212.9	200.2	227.6	193.4
Mn	3.46	2.84	3.35	3.59	4.66	3.84	4.14
Mg	189.3	144.9	140.8	147.1	136.0	155.9	156.7
Ca	243.7	248.8	264.9	264.9	264.3	257.6	229.3
Na	38.58	39.59	47.12	48.20	44.18	46.78	38.22
K	1.69	0.70	1.56	1.85	0.71	1.58	1.64
P	0.61	0.84	0.73	0.63	1.00	0.82	1.11
Minor elements (g/1000 cm^3 x 10^{-3}):							
La	4.83	2.97	5.80		2.71	4.69	2.45
Ce	22.76	22.07	29.00		11.28	32.23	9.87
Nd	16.30		23.49		12.69	24.61	11.56
Sm	5.54	6.40	9.18		5.36	8.67	5.36
Eu	2.71	2.75	4.13		2.14	3.24	2.51
Tb	1.66	1.80	2.36		1.69	1.97	1.97
Yb	6.53	6.71	7.66		7.33	7.26	8.18
Lu	0.79	0.93	0.77		1.16	1.03	1.35
Sc	120.83	118.86	113.10			125.99	121.26
Cr	1028.5	1154.6	817.8		1071.6	471.7	245.3
Ni					290.5		180.5
Co	95.5	101.9	104.4		135.4	111.3	143.8
V		594.3			803.7		809.3
Cu		614.1			236.9		183.3
Zn	193.9	203.8	168.2		225.6	257.8	211.5
Sn					11.00		7.05
Zr					126.9		121.3
Y					70.5		70.5
Nb					6.77		
Rb							
Sr					143.8		141.0
Ba					8.46		33.84
B							45.12
H_2O^+ (wt%)	2.03	0.71	0.57	0.47	0.40	0.25	1.92
Density (g/cm^3)	2.81	2.83	2.90	2.90	2.82	2.93	2.82
Fe_2O_3/FeO	0.46	0.32	0.33	0.66	0.47	0.41	0.37

Table AT1 (continued).

Leg	70	70	70	70	70	70	70
Hole	504B	504B	504B	504B	504B	504B	504B
Core, section	48R-1	49R-1	49R-1	49R-2	54R-1	56R-2	61R-1
Interval (cm)	113-115	122-126	140-147	7-10	35-38	92-95	55-60
Piece	871	932	933	936	1062	1121	1287
Lab number	Z-933	Z-934	Z-559	Z-560	Z-935	Z-936	Z-937
Depth (mbsf)	648.13	657.22	657.40	657.57	692.35	707.92	751.05
Major elements (g/1000 cm^3):							
Si	654.5	630.3	681.8	621.3	650.1	637.1	672.9
Ti	14.73	13.19	15.40	14.32	23.91	19.61	16.32
Al	247.1	234.1	251.9	222.0	227.3	215.2	257.5
Fe^{+++}	54.8	58.0	44.1	79.9	76.5	71.3	16.6
Fe^{++}	161.2	142.6	163.0	129.9	104.1	127.9	161.2
Fe (Sum)	216.0	200.7	207.1	209.7	180.6	199.2	177.8
Mn	4.13	3.86	3.84	2.94	2.41	4.76	4.08
Mg	172.1	180.6	143.3	156.1	141.9	149.7	142.6
Ca	191.6	183.4	271.8	207.1	243.1	218.5	251.4
Na	39.09	42.43	46.77	39.06	53.50	53.09	38.65
K	2.21	4.14	2.33	4.53	1.64	1.39	1.70
P	1.16	0.90	0.69	0.54	1.60	1.95	1.15
Minor elements (g/1000 cm^3 x 10^{-3}):							
La	2.77	1.84	4.70	4.35	9.73	8.22	3.50
Ce	9.44	5.26	22.93	22.30	27.80	23.02	11.68
Nd	11.80	7.88			23.35	20.00	13.72
Sm	5.61	4.38	7.14	6.66	8.34	6.85	6.42
Eu	2.54	1.87	3.23	2.39	3.06	3.29	2.54
Tb	2.24	2.07	2.30	2.14	2.78	2.38	2.51
Yb	8.85	7.59	8.72	6.98	9.17	7.12	9.64
Lu	1.45	1.17	1.25	1.09	1.42	1.18	1.20
Sc	138.65	140.16	123.48	114.24			108.04
Cr	501.5	730.0	984.9	606.6	750.6	630.2	934.4
Ni	227.2	257.0			228.0	200.0	309.5
Co	203.6	274.5	126.4	97.9	136.2	120.6	210.2
V	1141.7	969.4			1042.5	794.6	969.4
Cu	162.3	210.2			278.0	164.4	216.1
Zn	180.0	186.9		163.2	228.0	219.2	204.4
Sn	5.61	5.84			6.67	4.38	7.30
Zr	121.0	108.0			275.2	274.0	143.1
Y	67.9	61.3			83.4	82.2	78.8
Nb	3.54	4.09			7.23		
Rb	5.90	7.59			3.61		3.80
Sr	150.5	143.1			278.0	263.0	146.0
Ba	70.80	99.28			19.46	21.92	96.36
B	79.65	96.36					26.28
H_2O^+ (wt%)	4.65	6.70	0.55	1.98	0.46	0.69	2.48
Density (g/cm^3)	2.95	2.92	2.94	2.72	2.78	2.74	2.92
Fe_2O_3/FeO	0.38	0.45	0.30	0.68	0.82	0.62	0.11

Table AT1 (continued).

Leg	70	70	70	70	70	70	70
Hole	504B	504B	504B	504B	504B	504B	504B
Core, section	61R-2	61R-2	64R-1	64R-2	66R-2	67R-1	68R-1
Interval (cm)	145-149	145-149	65-68	32-35	0-5	45-49	83-87
Piece	1314	1314	1411	1424	1506	1527	1537
Lab number	Z-561	Z-938	Z-939	Z-562	Z-940	Z-941	Z-942
Depth (mbsf)	753.45	753.45	773.65	774.82	792.5	800.45	809.83
Major elements (g/1000 cm^3):							
Si	634.0	619.1	654.4	686.5	707.7	672.0	682.4
Ti	13.99	13.41	16.62	21.67	17.73	17.30	18.64
Al	205.5	226.4	189.2	218.6	243.8	231.4	241.8
Fe^{+++}	64.7	111.5	75.0	85.9	50.9	72.8	112.3
Fe^{++}	113.0	98.8	134.6	164.8	162.1	156.0	133.9
Fe (Sum)	177.6	210.3	209.6	250.7	213.0	228.8	246.2
Mn	3.92	3.95	4.08	4.55	2.60	5.30	5.72
Mg	153.0	166.7	150.6	152.9	150.1	161.4	156.3
Ca	221.1	205.8	214.8	252.9	273.1	260.0	276.0
Na	40.48	34.88	40.32	49.06	45.02	46.13	46.59
K	2.33	2.12	0.69	1.90	0.76	0.49	0.51
P	1.10	1.36	1.09	1.03	0.80	1.43	1.61
Minor elements (g/1000 cm^3 x 10^{-3}):							
La	3.24	2.80	2.98	5.02	5.45	3.22	3.64
Ce	11.07	12.74	12.20	22.45	12.73	10.84	10.61
Nd	7.02	12.74	12.47		14.24	13.48	13.64
Sm	5.40	5.09	5.42	8.61	5.76	6.45	6.36
Eu	2.00	2.04	1.87	3.01	2.15	1.99	2.24
Tb	1.97	1.70	1.73	2.30	2.03	2.23	2.21
Yb	7.29	7.08	6.23	9.91	7.58	7.91	8.48
Lu	1.16	1.05	1.06	1.83	1.21	1.32	1.27
Sc		121.69		135.70			
Cr	769.5	707.5	840.1	896.8	1081.7	615.3	666.6
Ni	245.7	237.7	238.5		296.9	237.3	260.6
Co	132.3	116.0	122.0	121.0	163.6	158.2	151.5
V	950.4	783.9	813.0		1227.2	996.2	1006.0
Cu	143.1	178.3	162.6		251.5	211.0	190.9
Zn	191.7	181.1	200.5	141.6	248.5	272.5	257.6
Sn	6.48	5.09	5.96		7.58	5.27	5.76
Zr	132.3	118.9	130.1			140.6	151.5
Y	64.8	67.9	65.0			73.3	78.8
Nb							
Rb							
Sr	116.1	130.2	157.2			152.4	154.5
Ba		138.67	13.55			14.65	18.18
B		42.45					
H_2O^+ (wt%)	1.57	4.62	0.85	0.42		0.50	0.43
Density (g/cm^3)	2.70	2.83	2.71	2.95	3.03	2.93	3.03
Fe_2O_3/FeO	0.64	1.25	0.62	0.58	0.35	0.52	0.93

Table AT1 (continued).

Leg	70	70	70	70	70	70	70
Hole	504B	504B	504B	504B	504B	504B	504B
Core, section	68R-1	69R-1	69R-1	69R-1	70R-1	70R-1	70R-1
Interval (cm)	107-111	14-17	74-77	77-81	17-20	79-82	127-130
Piece	1538	1540	1545	1545	1550	1556	1561
Lab number	Z-563	Z-564	Z-565	Z-943	Z-944	Z-567	Z-568
Depth (mbsf)	810.07	818.14	818.74	818.77	827.17	827.79	828.27
Major elements (g/1000 cm^3):							
Si	667.7	666.1	671.5	655.9	599.8	597.3	695.6
Ti	18.63	20.29	17.89	13.34	12.02	14.06	17.96
Al	225.3	221.7	216.3	216.7	205.1	199.9	244.2
Fe^{+++}	71.3	78.8	91.4	100.6	55.9	87.7	72.7
Fe^{++}	158.2	147.5	139.6	129.8	111.5	92.5	131.5
Fe (Sum)	229.5	226.4	230.9	230.4	167.3	180.3	204.2
Mn	4.95	5.33	4.26	5.15	2.65	2.59	4.18
Mg	155.7	149.1	157.1	153.2	156.8	148.0	161.1
Ca	262.8	249.3	246.8	237.9	207.3	204.6	276.2
Na	45.69	47.68	42.57	43.53	34.83	44.56	44.23
K	1.33	1.38	1.20	0.48	1.31	2.05	1.79
P	0.94	0.93	0.89	1.26	0.92	6.08	0.65
Minor elements (g/1000 cm^3 x 10^{-3}):							
La	4.07	5.17	3.76	3.40	2.16	2.32	3.00
Ce	24.44	22.96	19.94	11.32	8.15	19.87	24.00
Nd		16.93		13.30	9.21	20.38	18.60
Sm	7.45	6.37	8.03	6.23	4.21	7.59	6.60
Eu	3.26	2.58	2.74	2.29	1.95	2.86	2.56
Tb	1.96	1.46	2.19	2.07	1.53	1.74	1.76
Yb	9.65	7.09	7.21	8.21	6.05	7.38	4.88
Lu	1.57	1.07	1.57	1.30	1.03	1.35	1.09
Sc	139.68	129.15	127.16			108.36	90.00
Cr	765.3	574.0	734.1	537.7	565.5	884.9	885.0
Ni				215.1	231.4		
Co	133.9	143.5	141.6	147.2	128.9	90.3	102.0
V				967.9	723.3		
Cu				155.7	226.2		
Zn	439.4	315.7	329.5	268.9	186.7	209.0	75.0
Sn				5.66	5.00		
Zr				147.2	102.6		
Y				79.2	57.9		
Nb					5.00		
Rb							
Sr				133.0	118.4		
Ba				8.49	86.79		
B					26.30		
H_2O^+ (wt%)	0.72	0.61	1.09	0.74	4.09	1.71	0.81
Density (g/cm^3)	2.91	2.87	2.89	2.83	2.63	2.58	3.00
Fe_2O_3/FeO	0.50	0.59	0.73	0.86	0.56	1.05	0.61

Table AT1 (continued).

Leg	70	83	83	83	83	83	83
Hole	504B	504B	504B	504B	504B	504B	504B
Core, section	70R-2	72R-2	73R-2	77R-1	78R-1	79R-3	80R-1
Interval (cm)	20-23	60-64	56-59	78-81	60-64	50-54	5-10
Piece	1564	5	4	4	3D	4A	1
Lab number	Z-569	Z-570	Z-571	Z-572	Z-573	Z-574	Z-1301
Depth (mbsf)	828.7	845.5	854.56	889.28	898.1	908.00	910.05
Major elements (g/1000 cm^3):							
Si	669.4	666.5	673.2	665.3	663.4	652.3	570.7
Ti	17.08	13.87	13.88	16.39	18.34	17.13	14.69
Al	234.6	229.7	232.1	235.1	222.5	235.0	231.0
Fe^{+++}	71.8	80.7	83.8	51.1	65.5	41.9	79.9
Fe^{++}	119.4	115.8	120.2	136.2	129.3	134.7	114.0
Fe (Sum)	191.2	196.5	204.0	187.3	194.8	176.6	194.0
Mn	4.01	4.99	4.77	4.23	4.65	3.98	4.49
Mg	153.9	149.8	144.8	143.6	133.6	139.7	126.0
Ca	266.7	268.1	271.7	238.8	249.8	272.7	206.4
Na	45.68	42.38	39.14	63.43	57.69	45.14	50.24
K	1.67				1.19	0.00	0.88
P	0.63	0.51	0.51	0.50	0.62	0.50	0.46
Minor elements (g/1000 cm^3 x 10^{-3}):							
La	3.74	3.17	3.77	3.44	3.69	3.40	2.26
Ce	22.46	8.93	6.67	11.77	8.24	10.75	8.58
Nd		10.66	10.15	12.34	11.36	12.17	10.92
Sm	6.25	4.90	4.93	5.74	5.40	5.38	5.72
Eu	2.87	1.84	2.00	2.01	2.27	2.09	1.98
Tb	1.75	1.50	1.54	1.81	1.70	1.47	1.90
Yb	7.56	6.05	6.09	7.46	7.67	6.23	6.50
Lu	0.99	0.92	0.99	1.06	1.19	0.99	0.99
Sc	77.76						
Cr	754.6	1080.0	928.0	861.0	624.8	792.4	793.0
Ni		547.2	493.0	278.4	215.8	452.8	403.0
Co	97.9	158.4	142.1	117.7	116.4	124.5	176.8
V		1051.2	696.0	631.4	653.2	566.0	629.2
Cu		345.6	255.2	195.2	275.5	367.9	52.0
Zn	172.8	241.9	220.4	189.4	221.5	189.6	434.2
Sn			10.15	8.61	7.67	9.06	
Zr		118.1	116.0	137.8	133.5	138.7	117.0
Y		54.7	60.9	66.0	73.8	62.3	62.4
Nb		3.74	3.19		3.69	4.81	3.64
Rb		4.61	2.90				3.12
Sr		181.4	179.8	206.6	170.4	209.4	145.6
Ba		155.52	153.70	183.68	133.48	133.01	122.20
B							
H_2O^+ (wt%)	0.72	1.03	0.84	1.49	1.08	1.45	2.61
Density (g/cm^3)	2.88	2.88	2.90	2.87	2.84	2.83	2.60
Fe_2O_3/FeO	0.67	0.77	0.77	0.42	0.56	0.35	0.78

Table AT1 (continued).

Leg	83	83	83	83	83	83	83
Hole	504B	504B	504B	504B	504B	504B	504B
Core, section	80R-4	83R-2	84R-2	85R-1	88R-1	89R-2	90R-4
Interval (cm)	3-8	92-96	48-50	58-62	68-71	74-78	112-114
Piece	1A	6F	7	6B	4A	9	10A
Lab number	Z-1303	Z-1305	Z-1306	Z-1307	Z-575	Z-1309	Z-1310
Depth (mbsf)	914.33	930.87	948.48	956.08	977.18	987.74	1000.12
Major elements (g/1000 cm^3):							
Si	639.6	680.3	630.2	639.9	651.3	655.7	650.8
Ti	14.46	16.06	16.66	13.96	19.97	17.10	16.43
Al	201.9	234.0	202.9	175.3	220.7	208.9	224.2
Fe^{+++}	78.8	31.5	56.5	62.5	28.1	47.8	39.5
Fe^{++}	114.1	157.1	143.6	147.8	177.8	213.0	175.0
Fe (Sum)	192.9	188.5	200.1	210.4	205.9	260.8	214.5
Mn	1.89	4.33	2.80	5.74	6.89	2.48	2.65
Mg	113.9	165.6	147.6	131.8	144.4	149.5	150.6
Ca	236.3	257.6	212.9	141.8	258.7	226.7	217.1
Na	57.31	38.65	37.11	64.79	40.90	46.42	40.46
K	0.45	0.73	0.92	0.66	0.00	0.48	0.47
P	0.47	0.77	0.73	0.58	1.13	0.76	0.75
Minor elements (g/1000 cm^3 x 10^{-3}):							
La	2.36	3.21	3.00	2.09	8.27	2.85	3.96
Ce	8.04	9.93	10.10	6.79	18.81	9.50	14.15
Nd	10.99	12.26	13.10	10.18	17.10	12.10	15.28
Sm	5.90	6.42	6.55	4.96	6.27	6.34	6.79
Eu	2.01	2.19	2.16	1.51	2.22	2.10	2.24
Tb	1.80	1.96	2.05	1.59	1.68	2.10	2.32
Yb	6.70	7.30	8.19	6.53	7.13	7.78	7.64
Lu	0.99	1.11	1.26	0.97	1.00	1.21	1.22
Sc							
Cr	790.6	911.0	813.5	553.3	741.0	486.7	622.6
Ni	369.8	403.0	376.7	172.3	270.8	227.5	243.4
Co	123.3	157.7	169.3	151.4	114.0	135.4	130.2
V	576.2	738.8	739.8	579.4	627.0	682.6	600.0
Cu	176.9	353.3	122.9	143.6	168.2	1100.2	509.4
Zn	201.0	245.3	308.5	613.4	313.5	334.1	342.4
Sn					8.55		
Zr	117.9	125.6	136.5	117.5	182.4	126.7	144.3
Y	64.3	70.1	68.3	57.4	71.3	77.8	67.9
Nb	4.02		2.73		13.40	4.61	3.96
Rb	4.82	3.80	2.73			2.88	3.11
Sr	182.2	146.0	120.1	208.8	199.5	149.8	172.6
Ba	13.40	14.60		13.05	139.65	216.00	33.96
B							
H_2O^+ (wt%)	1.37	1.46	3.65	3.27	1.95	2.32	2.89
Density (g/cm^3)	2.68	2.92	2.73	2.61	2.85	2.88	2.83
Fe_2O_3/FeO	0.77	0.22	0.44	0.47	0.18	0.25	0.25

Table AT1 (continued).

Leg	83	83	83	83	83	83	83
Hole	504B	504B	504B	504B	504B	504B	504B
Core, section	91R-1	92R-3	94R-3	97R-1	97R-2	98R-1	99R-2
Interval (cm)	115-118	38-42	91-94	88-90	108-111	80-85	93-96
Piece	15	4	10	7	10	11	11
Lab number	Z-576	Z-577	Z-578	Z-1311	Z-579	Z-1312	Z-580
Depth (mbsf)	1004.65	1015.88	1034.41	1058.38	1060.08	1062.80	1073.93
Major elements (g/1000 cm^3):							
Si	638.7	701.5	654.1	551.9	708.5	609.3	655.7
Ti	16.01	15.15	14.73	14.53	17.93	14.84	21.51
Al	209.9	211.5	222.6	150.2	221.7	239.4	207.2
Fe^{+++}	27.5	27.1	32.6	52.2	43.5	46.7	72.6
Fe^{++}	167.8	182.3	157.3	139.1	169.7	158.5	146.5
Fe (Sum)	195.3	209.4	189.9	191.3	213.2	205.2	219.1
Mn	6.97	6.06	4.15	4.21	4.91	3.79	5.33
Mg	145.5	145.1	151.7	149.7	156.1	177.2	144.7
Ca	248.8	276.4	254.7	202.7	274.4	232.2	259.0
Na	47.98	40.84	38.13	24.04	46.84	31.60	43.01
K	0.00	0.00	0.00	0.62	0.00	0.72	0.00
P	0.49	0.66	0.49	0.65	0.53	0.88	0.75
Minor elements (g/1000 cm^3 x 10^{-3}):							
La	2.46	4.47	3.36	2.42	3.90	3.41	4.85
Ce	6.14	12.22	11.48	8.05	9.60	11.08	11.97
Nd	66.40	13.41	12.88	10.25	11.70	12.78	14.54
Sm	3.91	5.36	5.04	5.37	5.40	5.40	6.84
Eu	1.37	2.12	1.74	1.71	2.25	1.96	2.25
Tb	1.28	1.73	1.43	1.81	1.53	1.93	1.94
Yb	5.58	7.45	6.72	6.34	7.20	6.53	9.12
Lu	0.92	1.19	1.01	0.93	1.17	0.97	1.45
Sc							
Cr	725.4	506.6	896.0	712.5	780.0	752.6	541.5
Ni	265.1	220.5	392.0	231.8	249.0	491.3	216.6
Co	106.0	101.3	123.2	187.9	126.0	156.2	114.0
V	502.2	625.8	644.0	866.2	720.0	570.8	627.0
Cu	259.5	834.4	277.2	409.9	360.0	127.8	182.4
Zn	253.9	277.1	190.4	331.8	234.0	420.3	222.3
Sn	8.93	8.05	8.40		9.00		9.12
Zr	92.1	140.1	126.0	114.7	147.0	136.3	171.0
Y	61.4	74.5	58.8	63.4	72.0	59.6	88.4
Nb	3.35	3.87	3.08		4.80	3.41	3.99
Rb				2.44		3.41	
Sr	125.6	143.0	162.4	87.8	189.0	156.2	151.1
Ba	114.39	56.62	134.40	9.76	60.00	14.20	71.25
B							
H_2O^+ (wt%)	2.30	2.05	0.89	4.89	0.83	3.76	2.00
Density (g/cm^3)	2.79	2.98	2.80	2.44	3.00	2.84	2.85
Fe_2O_3/FeO	0.18	0.17	0.23	0.42	0.28	0.33	0.55

Table AT1 (continued).

Leg	83	83	83	83	83	83	83
Hole	504B	504B	504B	504B	504B	504B	504B
Core, section	100R-1	100R-1	104R-3	109R-1	111R-1	113R-1	116R-1
Interval (cm)	19-20	83-87	30-33	50-54	86-89	7-10	56-60
Piece	2A	10	5A	7	9	1	9
Lab number	Z-581	Z-1313	Z-582	Z-583	Z-1314	Z-584	Z-1315
Depth (mbsf)	1080.69	1081.33	1119.8	1154.00	1162.36	1171.07	1185.56
Major elements (g/1000 cm^3):							
Si	684.1	627.7	634.4	663.7	591.4	657.2	673.9
Ti	18.63	18.21	15.68	16.46	17.06	13.78	17.71
Al	207.1	168.8	239.0	231.9	252.3	249.8	231.3
Fe^{+++}	59.8	29.4	92.2	102.5	67.7	89.1	52.7
Fe^{++}	183.6	210.5	104.7	106.6	137.7	105.3	173.7
Fe (Sum)	243.4	239.9	196.9	209.2	205.3	194.4	226.4
Mn	5.90	5.04	3.70	3.10	2.59	2.48	3.89
Mg	142.0	141.8	151.1	151.2	152.3	160.8	148.6
Ca	262.3	159.3	251.7	254.4	239.3	261.1	253.7
Na	40.02	58.95	46.12	37.76	39.33	38.85	54.57
K	0.00	0.90	0.00	0.00	0.93	0.00	0.74
P	0.90	0.83	0.74	0.62	0.73	0.51	0.77
Minor elements (g/1000 cm^3 x 10^{-3}):							
La	4.07	3.50	3.95	3.43	4.14	2.72	2.94
Ce	12.80	13.99	11.28	8.58	16.01	9.25	11.17
Nd	14.84	14.53	13.54	12.30	14.08	10.40	13.23
Sm	6.69	6.73	5.64	4.86	6.07	4.34	7.06
Eu	1.80	2.26	2.06	1.83	2.18	1.71	2.32
Tb	2.04	2.37	1.52	1.69	1.82	1.24	2.47
Yb	8.73	7.53	7.05	6.86	6.62	5.78	8.82
Lu	1.40	1.26	1.07	1.06	0.99	0.90	1.35
Sc							
Cr	611.1	408.9	987.0	715.0	993.6	838.1	764.4
Ni	227.0	185.6	234.1	246.0	690.0	317.9	223.4
Co	128.0	123.7	129.7	131.6	165.6	135.8	158.8
V	698.4	551.5	733.2	743.6	662.4	606.9	711.5
Cu	256.1	53.8	245.3	314.6	386.4	317.9	226.4
Zn	232.8	269.0	236.9	214.5	226.3	228.3	194.0
Sn	10.19		8.46	7.72		9.25	
Zr	163.0	150.6	126.9	123.0	160.1	104.0	126.4
Y	81.5	72.6	67.7	68.6	63.5	57.8	76.4
Nb	5.24	4.30	3.67	3.72	2.76	5.20	
Rb		3.50			3.59		3.82
Sr	151.3	118.4	177.7	140.1	240.1	159.0	149.9
Ba	87.30	21.52	112.80	111.54	13.80	115.60	79.38
B							
H_2O^+ (wt%)	0.90	5.03	1.65	0.87	2.21	1.01	1.67
Density (g/cm^3)	2.91	2.69	2.82	2.86	2.76	2.89	2.94
Fe_2O_3/FeO	0.36	0.16	0.98	1.07	0.55	0.94	0.34

Table AT1 (continued).

Leg	83	83	83	83	83	83	83
Hole	504B	504B	504B	504B	504B	504B	504B
Core, section	117R-1	118R-1	121R-1	127R-1	130R-1	130R-3	132R-1
Interval (cm)	109-113	62-66	32-38	97-101	88-91	78-81	76-80
Piece	15	5	5	12	8	9A	10
Lab number	Z-1316	Z-585	Z-586	Z-587	Z-588	Z-1317	Z-589
Depth (mbsf)	1190.59	1194.62	1207.82	1254.47	1279.88	1282.78	1295.76
Major elements (g/1000 cm^3):							
Si	702.1	700.4	698.7	622.3	672.0	663.9	639.9
Ti	15.55	18.70	17.66	13.25	14.19	12.20	15.28
Al	243.8	240.1	233.7	233.8	255.9	260.8	248.9
Fe^{+++}	44.7	97.1	114.8	90.3	52.2	31.3	72.6
Fe^{++}	182.1	123.0	118.6	124.5	144.8	145.3	136.4
Fe (Sum)	226.8	220.1	233.4	214.8	196.9	176.7	209.0
Mn	4.20	1.63	2.53	3.47	3.94	3.43	3.55
Mg	138.2	159.2	146.1	155.0	161.2	175.6	142.8
Ca	254.6	256.6	257.3	260.6	288.4	262.7	279.3
Na	53.71	42.06	35.77	29.47	33.35	33.05	34.62
K	0.75	0.00	0.00	0.00	0.00	0.49	0.00
P	0.66	0.65	0.78	0.37	0.52	0.52	0.50
Minor elements (g/1000 cm^3 x 10^{-3}):							
La	2.49	3.29	2.58	2.77	2.97	2.45	2.75
Ce	9.90	11.36	7.40	7.28	7.13	10.22	8.87
Nd	11.70	14.35	14.21	9.80	9.21	10.80	9.44
Sm	5.40	6.28	6.22	4.20	4.16	4.67	4.00
Eu	2.07	2.33	2.49	1.71	1.66	1.61	1.72
Tb	1.83	1.91	2.10	1.32	1.40	1.46	1.37
Yb	5.40	8.37	8.88	5.60	5.35	5.26	5.72
Lu	0.84	1.32	1.39	0.81	0.83	0.82	0.92
Sc							
Cr	900.0	867.1	710.4	952.0	1069.2	1220.6	829.4
Ni	273.0	296.0	266.4	448.0	475.2	730.0	400.4
Co	189.0	143.5	145.0	137.2	142.6	213.2	128.7
V	828.0	926.9	888.0	588.0	683.1	671.6	600.6
Cu	231.0	290.0	275.3	308.0	326.7	414.6	314.6
Zn	414.0	278.1	266.4	204.4	219.8	224.8	223.1
Sn		9.87	9.47	8.40	10.99		9.15
Zr	114.0	134.6	136.2	106.4	109.9	99.3	117.3
Y	60.0	77.7	79.9	53.2	56.4	49.6	54.3
Nb		5.38	3.85	3.64			3.43
Rb	3.60					3.50	
Sr	159.0	146.5	127.3	165.2	178.2	157.7	168.7
Ba	27.00	98.67	130.24	84.00	95.04	29.20	145.86
B							
H_2O^+ (wt%)	1.55	0.72	0.71	1.24	1.05	1.28	1.01
Density (g/cm^3)	3.00	2.99	2.96	2.80	2.97	2.92	2.86
Fe_2O_3/FeO	0.27	0.88	1.08	0.81	0.40	0.24	0.59

Table AT1 (continued).

Leg	83	83	111	111	111	111	111
Hole	504B	504B	504B	504B	504B	504B	504B
Core, section	133R-1	134R-1	142R-1	142R-2	143R-1	145R-1	145R-2
Interval (cm)	46-50	147-150	129-132	40-44	124-127	103-105	74-76
Piece	7	19	17B	6	19	13A	7F
Lab number	Z-590	Z-1318	Z-597	Z-114	Z-598	Z-115	Z-116
Depth (mbsf)	1304.46	1314.47	1354.09	1354.70	1360.54	1379.33	1380.54
Major elements (g/1000 cm^3):							
Si	643.2	642.9	585.7	688.8	694.9	695.2	682.9
Ti	15.97	15.56	19.55	20.24	14.51	17.35	17.31
Al	223.8	208.6	194.4	252.2	256.7	254.2	253.0
Fe^{+++}	46.6	43.6	48.4	52.5	26.8	43.8	59.3
Fe^{++}	175.3	162.0	163.3	163.5	165.4	153.9	146.0
Fe (Sum)	222.0	205.5	211.7	216.0	192.1	197.7	205.3
Mn	4.88	4.02	4.31	4.20	2.61	4.20	3.96
Mg	143.7	124.1	127.6	145.6	160.1	156.3	153.6
Ca	265.7	238.1	209.5	279.6	280.2	286.5	289.5
Na	39.73	43.19	36.00	43.61	40.45	42.94	41.95
K	0.00	0.45	0.00	1.25	0.00	1.25	1.25
P	0.63	0.72	0.69	0.92	0.40	0.79	0.92
Minor elements (g/1000 cm^3 x 10^{-3}):							
La	3.12	2.42	2.61	4.20	3.02	4.21	3.59
Ce	5.40	9.52	10.44	12.60	10.27	12.64	6.28
Nd	9.37	10.61	11.22		11.17		
Sm	5.40	4.90	5.22	6.30	4.53	6.32	5.98
Eu	2.10	1.96	2.06	2.49	2.08	2.35	2.15
Tb	1.87	1.82	1.80	1.74	1.60	1.69	1.55
Yb	7.10	6.26	6.79	8.70	6.64	7.83	6.88
Lu	1.19	1.01	1.04	1.50	1.18	1.32	1.08
Sc				147.00		138.46	146.51
Cr	766.8	571.2	456.8	510.0	1047.9	1324.4	1285.7
Ni	235.7	204.0	193.1	360.0	440.9	481.6	403.7
Co	119.3	149.6	117.5	165.0	145.0	165.6	164.5
V	624.8	674.6	749.1	810.0	694.6	842.8	747.5
Cu	340.8	457.0	52.2	405.0	311.1	391.3	403.7
Zn	232.9	258.4	245.3	285.0	407.7	225.8	209.3
Sn	8.52		8.87		9.36		
Zr	122.1	111.5	112.2	114.0	111.7	102.3	80.7
Y	71.0	65.3	65.3	81.0	69.5	72.2	74.8
Nb		5.71	4.70		3.62		3.29
Rb		2.72					
Sr	125.0	141.4	130.5	147.0	175.2	168.6	125.6
Ba	110.76	29.92	73.08		93.62		
B							
H_2O^+ (wt%)	1.40	1.78	4.21	0.98	1.63	0.84	0.78
Density (g/cm^3)	2.84	2.72	2.61	3.00	3.02	3.01	2.99
Fe_2O_3/FeO	0.30	0.30	0.33	0.36	0.18	0.32	0.45

Table AT1 (continued).

Leg	111	111	111	111	111	111	111
Hole	504B	504B	504B	504B	504B	504B	504B
Core, section	145R-3	147R-1	147R-2	147R-2	148R-1	149R-1	152R-1
Interval (cm)	66-68	11-13	15-20	26-28	53-55	122-124	11-13
Piece	6A	3	1C	1D	8	16C	2
Lab number	Z-117	Z-118	Z-599	Z-119	Z-120	Z-121	Z-600
Depth (mbsf)	1381.96	1397.51	1399.05	1399.16	1407.33	1418.12	1436.01
Major elements (g/1000 cm^3):							
Si	681.9	690.3	690.9	649.2	698.0	692.9	577.2
Ti	17.29	17.20	16.48	17.74	22.98	22.90	15.23
Al	253.9	249.3	247.9	231.5	226.4	226.7	222.3
Fe^{+++}	53.1	54.5	45.0	57.5	53.2	53.8	68.9
Fe^{++}	151.5	142.1	146.5	143.2	187.3	185.2	214.3
Fe (Sum)	204.6	196.6	191.4	200.7	240.5	239.0	283.2
Mn	3.95	3.93	4.68	3.97	4.64	4.85	6.27
Mg	168.7	161.6	158.5	150.8	151.2	151.7	152.9
Ca	278.3	282.1	285.2	268.6	270.8	264.0	157.2
Na	41.91	46.56	40.57	46.02	48.44	48.26	52.83
K	1.25	1.24	0.00	1.18	1.99	1.24	0.00
P	0.79	0.78	0.66	0.75	1.05	1.04	0.49
Minor elements (g/1000 cm^3 x 10^{-3}):							
La	3.60	3.30	2.99	3.42	4.20	4.19	4.13
Ce	9.60	6.00	13.46	7.98	12.30	13.46	11.55
Nd			13.75				12.38
Sm	6.00	5.40	5.38	6.27	7.20	7.18	5.50
Eu	1.95	1.50	2.39	2.17	2.25	2.06	1.73
Tb	1.92	1.92	1.73	1.65	2.31	1.88	1.98
Yb	7.20	6.00	6.58	6.84	8.40	7.77	7.70
Lu	1.08	0.96	1.17	1.11	1.26	1.26	1.21
Sc	141.00	141.00		136.80	156.00	15.55	
Cr	1125.0	1440.0	1136.2	1211.3	360.0	388.7	852.5
Ni	510.0	495.0	269.1	413.3	285.0	299.0	261.3
Co	150.0	150.0	146.5	156.8	120.0	134.6	156.8
V	630.0	780.0	771.4	769.5	720.0	897.0	605.0
Cu	480.0	300.0	269.1	199.5	210.0	239.2	57.8
Zn	240.0	255.0	257.1	242.3	285.0	284.1	214.5
Sn			8.97				9.63
Zr	84.0	72.0	125.6	128.3	132.0	143.5	104.5
Y	69.0	63.0	62.8	68.4	84.0	83.7	57.8
Nb	3.30						4.13
Rb							
Sr	111.0	126.0	182.4	162.5	168.0	188.4	126.5
Ba			125.58				71.50
B							
H_2O^+ (wt%)	0.90	0.94	0.90	1.08	0.57	0.97	4.81
Density (g/cm^3)	3.00	3.00	2.99	2.85	3.00	2.99	2.75
Fe_2O_3/FeO	0.39	0.43	0.34	0.45	0.32	0.32	0.36

Table AT1 (continued).

Leg	111	111	111	111	111	111	111
Hole	504B	504B	504B	504B	504B	504B	504B
Core, section	154R-1	156R-1	158R-1	162M-1	163R-1	163R-1	169R-1
Interval (cm)	30-32	64-67	16-19	45-47	36-41	120-123	66-69
Piece	2C	13	3A	5	8	24	14
Lab number	Z-122	Z-601	Z-602	Z-123	Z-603	Z-1319	Z-604
Depth (mbsf)	1454.60	1464.44	1482.66	1511.95	1511.96	1512.80	1548.26
Major elements (g/1000 cm^3):							
Si	688.5	630.3	678.7	657.3	674.7	677.9	649.3
Ti	20.40	16.11	16.00	16.53	19.56	16.99	15.60
Al	230.2	200.1	219.9	240.6	237.6	261.9	221.0
Fe^{+++}	78.5	54.0	63.6	70.7	73.4	34.7	66.0
Fe^{++}	149.9	161.4	166.8	132.8	148.4	172.2	149.8
Fe (Sum)	228.5	215.5	230.4	203.4	221.8	206.9	215.9
Mn	3.96	3.00	3.21	4.00	2.76	3.43	2.63
Mg	151.4	141.0	152.2	142.4	143.1	126.2	144.9
Ca	278.4	234.8	268.9	269.7	259.6	260.1	255.8
Na	46.91	53.45	46.86	44.75	42.91	52.35	35.67
K	2.00	0.00	0.00	3.10	0.00	0.49	0.00
P	0.79	0.60	0.65	0.75	0.91	0.77	0.74
Minor elements (g/1000 cm^3 x 10^{-3}):							
La	3.59	3.85	3.82	3.43	3.82	2.46	3.65
Ce	10.47	10.73	11.17	9.44	10.88	8.50	9.27
Nd		13.75	13.23		13.52	12.31	11.80
Sm	6.28	6.33	6.47	5.72	6.76	5.86	6.18
Eu	2.51	2.31	2.03	1.94	2.82	1.99	2.50
Tb	1.97	2.20	2.06	1.54	2.15	1.96	1.74
Yb	7.18	8.53	8.53	6.58	8.82	7.33	7.59
Lu	1.14	1.38	1.41	1.00	1.29	1.11	1.24
Sc	143.52			137.28			
Cr	897.0	522.5	1005.5	1101.1	711.5	688.6	947.0
Ni	358.8	184.3	205.8	514.8	205.8	222.7	252.9
Co	149.5	118.3	129.4	157.3	129.4	149.4	146.1
V	867.1	649.0	758.5	686.4	808.5	741.3	1059.4
Cu	239.2	57.8	76.4	228.8	105.8	263.7	303.5
Zn	269.1	225.5	217.6	257.4	229.3	219.8	247.3
Sn		6.88	7.35		7.94		9.27
Zr	89.7	123.8	117.6	151.6	152.9	137.7	115.2
Y	74.8	71.5	73.5	62.9	79.4	67.4	67.4
Nb			3.82				3.37
Rb						5.27	
Sr	152.5	162.3	149.9	254.5	132.3	190.5	132.1
Ba		137.50	85.26		82.32	20.51	98.35
B							
H_2O^+ (wt%)	0.96	2.11	1.35	0.51	1.53	1.15	1.17
Density (g/cm^3)	2.99	2.75	2.94	2.86	2.94	2.93	2.81
Fe_2O_3/FeO	0.58	0.37	0.42	0.59	0.55	0.22	0.49

Table AT1 (continued).

Leg	137	137	140	140	140	140	140
Hole	504B	504B	504B	504B	504B	504B	504B
Core, section	177R-1	181M-1	186R-2	187R-1	189R-1	189R-2	190R-1
Interval (cm)	48-49	6-8	30-31	59-60	85-86	15-17	10-14
Piece	13	1	8	14	19	3	2
Lab number	Z-812	Z-813	Z-838	Z-839	Z-840	Z-841	Z-842
Depth (mbsf)	1604.98	1620.46	1628.10	1632.59	1651.85	1652.61	1655.20
Major elements (g/1000 cm^3):							
Si	692.0	657.8	638.7	672.0	698.0	638.2	650.0
Ti	17.93	17.02	17.75	16.43	17.56	10.70	9.52
Al	227.6	219.4	248.9	231.2	236.5	224.8	208.8
Fe^{+++}	57.0	54.0	43.4	48.1	55.4	31.6	26.4
Fe^{++}	172.4	166.3	161.4	157.4	168.0	140.6	159.4
Fe (Sum)	229.4	220.2	204.9	205.5	223.4	172.2	185.8
Mn	4.05	3.96	3.82	3.98	4.12	3.35	3.39
Mg	152.5	140.9	160.7	148.2	147.0	140.9	133.9
Ca	263.6	263.7	273.8	265.1	268.5	245.5	223.1
Na	37.28	35.38	34.88	41.71	37.97	36.12	23.37
K	0.00	0.00	0.00	0.00	0.00	0.00	0.00
P	1.01	0.87	1.14	1.00	1.03	0.59	0.60
Minor elements (g/1000 cm^3 x 10^{-3}):							
La	3.11	2.93	4.82	2.58	3.16	1.76	1.56
Ce	12.34	10.91	16.70	10.38	11.98	6.63	6.17
Nd	15.66	14.63	18.98	13.69	14.96	8.28	7.65
Sm	6.54	5.96	6.92	5.92	6.35	3.52	3.31
Eu	2.49	2.13	2.42	2.32	2.35	1.60	1.86
Tb	2.01	1.73	1.81	1.83	1.91	1.16	1.08
Yb	8.79	8.41	8.32	8.24	8.79	5.20	5.03
Lu	1.33	1.31	1.28	1.25	1.31	0.83	0.72
Sc							
Cr	500.2	661.7	1124.2	806.2	759.9	954.3	834.0
Ni	251.6	244.2	403.0	255.2	271.2	321.8	272.4
Co	133.2	125.0	131.4	118.9	134.1	107.3	100.1
V							
Cu	192.4	218.7	32.1	139.2	751.0	280.5	36.1
Zn	213.1	196.0	140.2	153.7	211.6	162.3	166.8
Sn							
Zr	148.0	139.2	189.8	139.2	149.0	88.0	80.6
Y	76.7	69.6	71.8	68.4	72.4	43.2	40.9
Nb	0.86	0.74	2.28	0.87	0.83	0.52	0.50
Rb		0.28	0.38		0.33	0.44	0.61
Sr	136.2	125.0	192.7	145.0	140.1	148.5	89.0
Ba							
B							
H_2O^+ (wt%)	1.24	1.43	2.73	1.60	1.22	3.09	5.98
Density (g/cm^3)	2.96	2.84	2.92	2.90	2.98	2.75	2.78
Fe_2O_3/FeO	0.37	0.36	0.30	0.34	0.37	0.25	0.18

Table AT1 (continued).

Leg	140	140	140	140	140	140	140
Hole	504B	504B	504B	504B	504B	504B	504B
Core, section	193R-1	194R-1	197R-1	198R-1	199R-1	200R-2	202R-1
Interval (cm)	49-51	42-44	31-33	52-54	54-57	50-52	23-25
Piece	13A	8	7	14	13	7B	7
Lab number	Z-844	Z-845	Z-846	Z-847	Z-848	Z-849	Z-850
Depth (mbsf)	1674.99	1680.82	1703.11	1712.72	1719.94	1730.60	1747.43
Major elements (g/1000 cm^3):							
Si	656.4	674.9	674.7	682.5	647.4	682.8	671.5
Ti	15.77	8.57	15.21	14.75	13.28	13.48	14.56
Al	228.2	224.1	232.0	247.9	243.5	258.4	240.4
Fe^{+++}	47.5	26.8	47.1	54.1	43.1	49.0	33.8
Fe^{++}	146.1	169.1	176.5	155.2	137.3	137.2	168.5
Fe (Sum)	193.7	195.9	223.6	209.2	180.4	186.2	202.3
Mn	4.12	3.54	3.79	3.90	3.48	3.44	4.48
Mg	136.4	145.2	145.8	169.9	162.4	172.1	152.9
Ca	260.0	235.1	241.0	271.1	260.6	276.9	270.7
Na	40.08	42.23	48.33	36.71	35.59	36.87	36.05
K	0.00	0.00	0.00	0.00	0.00	0.00	0.00
P	1.22	0.50	0.88	0.78	0.73	0.77	0.76
Minor elements (g/1000 cm^3 x 10^{-3}):							
La	3.45	1.32	2.04	2.72	2.83	2.89	2.76
Ce	13.16	5.10	8.56	10.52	10.44	10.79	10.10
Nd	15.68	6.80	11.33	13.10	12.03	12.19	12.75
Sm	6.68	3.02	4.91	5.50	4.90	4.98	5.44
Eu	2.46	1.50	2.01	2.15	1.98	2.03	2.12
Tb	1.81	0.95	1.46	1.67	1.42	1.43	1.60
Yb	7.92	4.29	6.80	7.39	6.03	6.20	8.00
Lu	1.16	0.60	1.02	1.14	0.91	1.01	1.11
Sc							
Cr	786.7	901.4	741.7	1097.3	1117.9	1290.3	986.5
Ni	274.5	319.7	257.0	430.6	438.7	476.8	346.3
Co	152.8	121.0	128.5	137.5	118.9	125.2	131.0
V							
Cu	288.7	14.4	38.0	305.0	249.0	262.2	1519.0
Zn	184.0	204.5	169.4	194.4	184.0	187.7	165.9
Sn							
Zr	130.2	72.0	113.9	128.6	121.7	125.2	128.0
Y	66.5	36.6	58.4	60.1	52.1		
Nb	0.85	0.40	0.61	0.72	1.02	0.86	0.79
Rb	0.45	0.35			0.28		
Sr	144.3	135.4	157.7	149.5	178.3	199.7	151.3
Ba							
B							
H_2O^+ (wt%)	2.12	3.82	2.31	1.41	1.27	1.09	1.40
Density (g/cm^3)	2.83	2.88	2.92	2.99	2.83	2.98	2.91
Fe_2O_3/FeO	0.36	0.18	0.30	0.39	0.35	0.40	0.22

Table AT1 (continued).

Leg	140	140	140	140	140	140	140
Hole	504B	504B	504B	504B	504B	504B	504B
Core, section	204R-1	208R-3	209R-1	209R-2	211R-1	213R-1	214R-1
Interval (cm)	15-19	3-5	102-103	66-68	70-72	66-68	30-32
Piece	4	1	14	10	16	19	5A
Lab number	Z-851	Z-852	Z-853	Z-854	Z-855	Z-856	Z-857
Depth (mbsf)	1756.65	1781.03	1788.52	1789.60	1799.20	1813.16	1818.90
Major elements (g/1000 cm^3):							
Si	665.3	661.0	633.4	638.5	659.1	666.4	651.8
Ti	16.65	9.50	6.92	12.35	14.10	13.58	9.03
Al	236.8	245.7	231.5	259.4	245.9	249.2	239.2
Fe^{+++}	49.7	41.3	39.8	47.7	48.1	44.9	43.7
Fe^{++}	144.5	156.5	175.6	119.6	144.3	148.1	153.0
Fe (Sum)	194.1	197.8	215.4	167.3	192.4	192.9	196.7
Mn	3.40	3.51	3.41	3.23	3.33	3.37	2.86
Mg	157.3	148.3	153.0	142.8	158.9	163.4	165.7
Ca	290.4	240.6	224.0	268.5	284.8	272.0	245.7
Na	38.40	38.41	32.85	34.90	36.38	38.15	36.47
K	0.00	0.00	0.00	0.00	0.00	0.00	0.00
P	1.15	0.37	0.36	0.73	0.88	0.76	1.24
Minor elements (g/1000 cm^3 x 10^{-3}):							
La	3.70	2.43	1.31	2.30	2.45	2.26	2.01
Ce	14.64	7.98	4.60	8.85	9.55	8.76	6.92
Nd	16.91	9.10	6.72	10.92	12.18	11.11	8.93
Sm	6.44	3.15	2.99	4.48	4.99	4.70	3.70
Eu	2.79	1.62	1.95	1.68	2.01	1.97	1.78
Tb	1.82	1.01	0.81	1.29	1.55	1.44	1.09
Yb	7.91	4.42	3.71	5.66	7.39	6.50	5.25
Lu	1.21	0.55	0.50	0.84	1.02	1.00	0.77
Sc							
Cr	1087.8	1052.0	1090.9	1226.4	1127.1	1073.1	786.4
Ni	373.4	358.4	379.4	358.4	400.0	399.8	476.4
Co	129.4	170.5	186.9	131.6	140.2	135.2	166.5
V							
Cu	17.6	14.5	16.7	271.6	324.1	235.2	14.4
Zn	120.5	156.1	178.6	148.4	137.2	129.4	132.0
Sn							
Zr	176.4	89.6	69.8	112.0	125.6	114.7	74.6
Y	70.0	39.6	31.8	49.8	60.7	57.3	45.3
Nb	2.15	0.52	1.06	0.84	0.85	0.76	0.57
Rb	0.41	0.43	0.36				0.32
Sr	211.7	179.2	159.0	173.6	151.8	149.9	157.9
Ba							
B							
H_2O^+ (wt%)	1.98	3.36	3.12	1.26	1.72	1.94	2.62
Density (g/cm^3)	2.94	2.89	2.79	2.80	2.92	2.94	2.87
Fe_2O_3/FeO	0.38	0.29	0.25	0.44	0.37	0.34	0.32

Table AT1 (continued).

Leg	140	140	140	140	140	148	148
Hole	504B	504B	504B	504B	504B	504B	504B
Core, section	214R-1	222R-1	225R-2	230R-1	238R-1	234R-1	240R-1
Interval (cm)	76-77	73-74	30-32	11-14	4-7	46-50	82-88
Piece	8	12A	5	3	2	14	21
Lab number	Z-858	Z-859	Z-860	Z-861	Z-862	Z-1586	Z-1587
Depth (mbsf)	1819.36	1885.33	1914.00	1953.11	1992.14	2000.86	2007.72
Major elements (g/1000 cm^3):							
Si	644.3	599.2	664.8	654.4	718.4	671.7	650.5
Ti	6.95	15.61	14.10	17.63	16.56	15.70	15.00
Al	208.0	240.9	243.0	214.4	248.6	244.0	263.2
Fe^{+++}	40.9	38.5	44.5	50.2	62.2	35.6	39.2
Fe^{++}	148.9	147.3	154.0	165.1	152.4	174.7	152.1
Fe (Sum)	189.7	185.8	198.5	215.3	214.6	210.3	191.3
Mn	2.63	3.40	3.78	3.65	4.04	3.38	3.15
Mg	153.2	165.4	158.1	138.5	169.2	135.1	144.0
Ca	250.4	248.7	266.5	247.8	289.5	273.6	269.4
Na	36.06	32.74	37.88	42.80	41.44	43.17	41.00
K	0.00	0.00	0.00	0.00	0.00	0.48	0.48
P	0.49	1.08	0.88	0.97	0.94	0.76	0.63
Minor elements (g/1000 cm^3 x 10^{-3}):							
La	1.85	3.66	2.44	2.93	3.04	2.90	2.60
Ce	5.91	13.52	9.60	10.91	11.63	12.76	10.12
Nd	6.92	15.24	12.33	13.95	14.45	13.92	13.01
Sm	2.94	5.93	5.25	6.08	5.89	5.51	5.49
Eu	1.96	2.08	2.09	2.34	2.29	1.83	1.85
Tb	0.87	1.69	1.57	1.87	1.77	1.91	1.91
Yb	4.14	7.40	7.19	8.37	7.60	6.38	7.23
Lu	0.59	1.14	1.07	1.26	1.12	1.02	1.07
Sc							
Cr	921.2	944.6	1078.8	421.3	1196.6	841.0	1150.2
Ni	366.8	498.6	379.9	245.5	359.6	269.7	549.1
Co	109.2	135.7	142.1	122.8	145.7	159.5	202.3
V						658.3	997.1
Cu	5.6	55.4	272.6	159.0	350.3	174.0	144.5
Zn	98.0	121.9	197.2	106.0	176.7	214.6	205.2
Sn							
Zr	64.4	160.7	121.8	145.1	148.8	121.8	106.9
Y	33.6	62.9	59.7	71.4	63.9	60.9	66.5
Nb	0.48	1.83	0.84	0.92	0.93	3.19	3.76
Rb	0.53						
Sr	137.2	171.7	162.4	139.5	189.1	162.4	159.0
Ba						14.50	80.92
B							
H_2O^+ (wt%)	3.85	3.22	1.38	1.07	1.01	0.79	1.09
Density (g/cm^3)	2.80	2.77	2.90	2.79	3.10	2.90	2.89
Fe_2O_3/FeO	0.31	0.29	0.32	0.34	0.45	0.23	0.29

Table AT1 (continued).

Leg	148	148	148
Hole	504B	504B	504B
Core, section	246R-1	249R-1	251R-1
Interval (cm)	87-90	85-89	35-40
Piece	25	27	6A
Lab number	Z-1588	Z-1589	Z-1590
Depth (mbsf)	2053.07	2072.05	2090.25
Major elements (g/1000 cm^3):			
Si	684.2	661.1	664.9
Ti	15.86	14.79	15.60
Al	256.8	270.4	256.9
Fe^{+++}	49.4	24.6	32.7
Fe^{++}	162.1	163.4	169.5
Fe (Sum)	211.4	188.1	202.2
Mn	3.72	3.41	3.43
Mg	155.7	145.4	158.3
Ca	272.4	264.7	263.5
Na	41.03	42.72	39.05
K	0.75	0.49	0.49
P	0.79	0.64	0.77
Minor elements (g/1000 cm^3 x 10^{-3}):			
La	2.99	2.93	2.60
Ce	11.06	8.79	11.80
Nd	13.75	13.19	13.28
Sm	5.98	5.57	5.90
Eu	2.03	1.88	1.80
Tb	2.21	2.29	2.30
Yb	7.18	6.45	7.67
Lu	1.05	0.97	1.12
Sc			
Cr	1202.0	928.8	885.0
Ni	508.3	430.7	486.8
Co	206.3	169.9	191.8
V	1037.5	741.3	722.8
Cu	448.5	161.2	271.4
Zn	209.3	234.4	212.4
Sn			
Zr	122.6	114.3	118.0
Y	62.8	58.6	62.0
Nb	4.49	4.10	4.13
Rb	5.08	4.40	4.13
Sr	167.4	172.9	156.4
Ba	29.90	20.51	50.15
B			
H_2O^+ (wt%)	0.60	1.98	1.33
Density (g/cm^3)	2.99	2.93	2.95
Fe_2O_3/FeO	0.34	0.17	0.21

Table AT2. Abundance of major and trace elements (g/1000 cm^3) in igneous rocks, Holes 855A and 855D, Leg 139 (Middle Valley, Juan de Fuca Ridge).

Leg	139	139	139
Hole	855A	855A	855D
Core, section	8R-1	9R-1	6R-1
Interval (cm)	36-39	10-14	55-58
Piece	5	2	8
Lab number	Z-814	Z-815	Z-816
Depth (mbsf)	65.16	74.40	114.45
Major elements (g/1000 cm^3):			
Si	672	669	670
Ti	38.7	27.4	28.9
Al	231	221	229
Fe^{+++}	86	83	60
Fe^{++}	191	165	165
Fe (Sum)	277	247	225
Mn	4.8	4.3	4.5
Mg	106	128	126
Ca	246	248	244
Na	57.8	56.9	53.1
K	4.9	3.1	3.6
P	2.9	1.7	1.8
Minor elements (g/1000 cm^3 x 10^{-3}):			
La	13.52	12.51	9.76
Ce	44.10	37.83	34.44
Nd	41.16	34.92	31.57
Sm	16.17	11.93	11.19
Eu	4.70	3.78	3.73
Tb	4.12	3.20	3.16
Yb	14.41	10.19	11.77
Lu	2.38	1.69	1.84
Cr	506	669	703
Ni	194	224	207
V	1005	858	907
Cu	185	218	189
Co	123	131	132
Zn	382	265	281
Sn	8.82	8.73	8.90
Zr	441	268	276
Y	138	90.2	97.6
Nb	10.0	13.4	8.3
Rb	9.11	3.78	8.32
Sr	323	349	316
Ba	91.1	113	149
H_2O^+ (wt%)	0.28	0.55	0.32
Density (g/cm^3)	2.94	2.91	2.87
Fe_2O_3/FeO	0.50	0.56	0.41

Table AT3. Abundance of major and trace elements (g/1000 cm^3) in igneous rocks, Holes 856A and 856B, Leg 139 (Bent Hill, Middle Valley, Juan de Fuca Rdge).

Leg	139	139	139	139
Hole	856A	856A	856A	856B
Core, section	13X-CC	14X-1	14X-CC	8H-CC
Interval (cm)	22-24	61-64	14-18	0-5
Piece	2A	4	2B	1
Lab number	Z-817	Z-818	Z-819	Z-820
Depth (mbsf)	113.39	115.11	115.92	63.66
Major elements (g/1000 cm^3):				
Si	680	639	631	651
Ti	16.0	15.4	15.2	15.2
Al	256	269	244	248
Fe^{+++}	37	35	62	61
Fe^{++}	155	154	122	120
Fe (Sum)	192	189	183	182
Mn	3.8	3.6	3.4	2.3
Mg	195	195	207	209
Ca	273	243	218	224
Na	45.5	42.6	40.7	45.4
K	1.5	1.7	1.5	1.2
P	0.7	0.9	0.6	0.6
Minor elements (g/1000 cm^3 x 10^{-3}):				
La	2.61	2.71	2.68	2.28
Ce	9.39	11.64	10.08	6.13
Nd	13.33	13.97	13.54	9.93
Sm	6.67	5.53	5.47	5.55
Eu	2.42	2.27	2.16	2.04
Tb	1.76	1.92	1.81	1.78
Yb	6.97	6.11	5.76	5.84
Lu	1.15	0.93	0.92	0.91
Cr	1682	1571	1656	1635
Ni	612	762	749	803
V	582	591	596	721
Cu	218	210	210	210
Co	152	154	150	193
Zn	291	224	213	219
Sn	6.97	6.69	6.62	7.01
Zr	106	98.9	97.9	108
Y	63.6	61.1	54.7	55.5
Nb	4.24	2.33	3.46	3.50
Rb	3.94		2.88	
Sr	176	166	156	161
Ba	197	178	121	14.6
H_2O^+ (wt%)	0.85	1.03	2.35	1.87
Density (g/cm^3)	3.03	2.91	2.88	2.92
Fe_2O_3/FeO	0.26	0.25	0.56	0.57

Table AT4. Abundance of major and trace elements (g/1000 cm^3) in igneous rocks, Hole 856H, Leg 169 (Bent Hill, Middle Valley, Juan de Fuca Ridge). (Continued on next page.)

Leg	169	169	169	169	169	169	169
Hole	856H	856H	856H	856H	856H	856H	856H
Core, section	55R-1	56R-1	56R-1	59R-1	60R-1	60R-2	61R-1
Interval (cm)	28-33	10-14	28-32	90-93	65-70	15-20	52-57
Piece	5A	3	5	13	11	3	5E
Lab number	Z-1591	Z-1592	Z-1593	Z-1594	Z-1595	Z-1596	Z-1597
Depth (mbsf)	431.98	434.40	434.58	461.60	466.35	467.35	468.72
Major elements (g/1000 cm^3):							
Si	554	557	476	378	598	653	547
Ti	32.9	34.1	32.9	38.0	35.0	35.1	33.5
Al	204	208	196	223	204	211	205
Fe^{+++}	115	69	102	63	61	61	49
Fe^{++}	319	340	348	387	204	160	353
Fe (Sum)	434	408	450	450	265	221	402
Mn	4.7	4.3	4.8	3.9	5.8	5.0	6.7
Mg	165	147	131	130	138	124	192
Ca	48	16	10	31	134	234	56
Na	1.6	1.6	2.0	2.1	22.6	32.1	2.5
K	0.2	0.2	0.2	0.4	0.4	0.5	0.2
P	2.3	2.3	2.3	2.3	2.3	2.3	2.2
S (total)	0.3		0.9			0.3	
Minor elements (g/1000 cm^3 x 10^{-3}):							
La	14.40	12.19	8.22	9.91	12.50	13.49	12.42
Ce	47.09	37.10	22.41	23.60	39.90	42.15	35.88
Nd	41.55	31.80	22.41	25.96	37.24	36.53	35.88
Sm	14.96	11.13	8.72	10.62	13.57	14.61	13.25
Eu	4.43	1.46	1.12	1.98	3.46	3.93	3.86
Tb	4.43	3.71	5.23	5.66	4.26	4.22	4.42
Yb	12.47	10.87	12.95	18.41	12.24	12.65	11.04
Lu	1.97	1.70	2.12	2.83	1.92	1.85	1.68
Cr	734	657	573	538	612	503	546
Ni	263	241	197	189	202	244	450
Co	233	225	234	208	173	141	179
V	1150	1026	959	1031	1091	764	687
Cu	55	80	82	42	359	3358	130
Zn	216	254	177	158	226	247	312
Zr	360	345	324	354	372	365	331
Y	111	109	134	177	120	115	105
Nb	10.0	10.3	7.5	10.9	12.2	13.5	5.8
Rb					2.93	2.81	
Sr	6.37	5.30	5.48		202	236	12.4
Ba	141	151	149	109	114	89.9	141
H_2O^+ (wt%)	7.48	7.08	7.89	8.37	4.49	2.11	7.33
Density (g/cm^3)	2.77	2.65	2.49	2.36	2.66	2.81	2.76
Fe_2O_3/FeO	0.40	0.23	0.33	0.18	0.34	0.43	0.16

Table AT4 (continued).

Leg	169	169	169	169	169	169	169
Hole	856H	856H	856H	856H	856H	856H	856H
Core, section	62R-1	63R-1	64R-1	64R-1	64R-2	65R-1	65R-2
Interval (cm)	89-90	30-35	10-14	75-80	132-136	0-5	54-59
Piece	15A	6A	3	13	20	1A	7
Lab number	Z-1598	Z-1599	Z-1600	Z-1601	Z-1602	Z-1603	Z-1604
Depth (mbsf)	471.19	480.20	489.60	490.25	492.32	494.20	496.12
Major elements (g/1000 cm^3):							
Si	442	496	541	479	503	580	642
Ti	33.4	33.4	33.9	33.5	29.8	28.3	31.4
Al	229	223	229	209	186	212	224
Fe^{+++}	98	85	53	70	61	59	35
Fe^{++}	399	216	195	238	299	173	165
Fe (Sum)	497	301	248	309	359	232	200
Mn	5.2	5.1	4.9	5.4	7.7	5.3	4.9
Mg	151	150	127	153	211	166	136
Ca	18	85	112	75	57	163	251
Na	1.5	22.3	28.4	16.5	5.1	27.0	42.3
K	0.2	0.4	0.6	0.4	0.4	0.4	0.5
P	2.2	2.1	2.2	2.2	2.0	1.9	2.1
S (total)	1.5	3.5	0.7	0.6			0.6
Minor elements (g/1000 cm^3 x 10^{-3}):							
La	7.34	11.99	14.93	8.12	9.88	10.87	12.45
Ce	20.44	40.80	45.54	27.06	33.80	29.15	39.62
Nd	15.72	35.70	37.95	29.52	31.20	26.50	36.79
Sm	5.24	13.52	12.65	11.81	11.44	10.60	12.17
Eu	1.23	3.32	3.54	2.31	2.86	2.92	3.40
Tb	1.81	4.08	4.05	3.44	3.38	3.18	3.40
Yb	7.34	10.97	10.88	11.56	10.14	9.54	11.04
Lu	1.26	1.68	1.62	1.80	1.61	1.46	1.53
Cr	487	490	519	462	471	477	521
Ni	215	212	240	204	138	167	218
Co	176	158	109	118	109	90	130
V	697	867	855	627	582	549	637
Cu	66	>25500	6970	5080	754	822	920
Zn	162	324	306	248	507	254	215
Zr	341	332	354	344	312	292	340
Y	50	112	116	108	101	90	113
Nb	11.0	12.2	9.4	11.6	9.9	11.1	13.0
Rb			3.54	2.71			
Sr	3.14	217	253	194	44.2	292	311
Ba	165	96.9	114	39.4	20.8	148	45.3
H_2O^+ (wt%)	8.56	5.71	4.64	6.69	7.25	3.55	1.93
Density (g/cm^3)	2.62	2.55	2.53	2.46	2.60	2.65	2.83
Fe_2O_3/FeO	0.27	0.44	0.30	0.33	0.23	0.37	0.23

Table AT5. Abundance of major and trace elements (g/1000 cm^3) in igneous rocks, Holes 857C and 857D, Leg 139 (Middle Valley, Juan de Fuca Ridge). (Continued on next five pages.)

Leg	139	139	139	139	139	139	139
Hole	857C	857C	857C	857C	857C	857C	857C
Core, section	59R-1	59R-1	59R-3	59R-4	60R-1	60R-1	61R-1
Interval (cm)	20-22	84-87	80-83	88-90	53-56	130-132	81-83
Piece	1	7	4	7	3	8	6
Lab number	Z-946	Z-821	Z-822	Z-823	Z-824	Z-948	Z-950
Depth (mbsf)	471.3	471.94	474.90	476.48	481.33	482.10	491.31
Major elements (g/1000 cm^3):							
Si	586	620	641	640	643	632	628
Ti	27.2	26.6	28.4	28.2	28.1	33.9	28.5
Al	222	212	230	220	226	228	235
Fe^{+++}	28	33	29	42	72	38	45
Fe^{++}	102	130	162	122	118	138	105
Fe (Sum)	130	163	191	164	189	176	150
Mn	4.2	4.3	4.0	4.3	4.8	5.6	4.3
Mg	140	118	124	133	128	135	155
Ca	198	242	276	247	257	261	231
Na	44.8	45.9	47.3	59.7	45.0	48.0	52.8
K	1.1	1.1	1.2	1.6	1.2	1.2	1.2
P	2.3	2.1	2.3	2.2	2.2	2.2	2.1
Minor elements (g/1000 cm^3 x 10^{-3}):							
La	16.07	15.78	21.66	16.28	17.73	15.68	13.57
Ce	43.35	42.08	57.00	49.68	54.34	44.80	38.78
Nd	33.15	34.19	37.05	35.88	40.04	33.60	30.47
Sm	10.97	11.57	11.40	12.14	11.73	10.92	9.42
Eu	3.06	4.21	3.42	3.86	3.72	3.92	3.05
Tb	2.55	2.60	2.45	2.76	2.77	2.63	2.60
Yb	8.93	8.68	7.98	8.28	8.87	8.96	7.20
Lu	1.38	1.37	1.17	1.35	1.34	1.37	1.08
Cr	689	689	698	704	678	476	767
Ni	153	163	234	221	215	193	205
V	566	634	707	651	635	588	748
Cu	135	145	242	265	200	258	116
Co	66.3	86.8	137	108	146	81.2	102
Zn	222	205	274	215	217	182	224
Sn	7.65	6.58	8.84	7.18	7.44	7.00	6.93
Zr	383	342	342	359	343	336	357
Y	89.3	81.5	88.4	88.3	94.4	84.0	88.6
Nb	11.7	13.9	12.3	11.9	13.4	12.3	12.7
Rb	3.32				5.15	2.80	
Sr	510	500	542	331	543	504	499
Ba	112	124	79.8	116	100	101	127
H_2O^+ (wt%)	2.82	1.27	1.99	1.48	1.53	1.36	1.99
Density (g/cm^3)	2.55	2.63	2.85	2.76	2.86	2.80	2.77
Fe_2O_3/FeO	0.30	0.29	0.20	0.38	0.68	0.31	0.48

Table AT5 (continued).

Leg	139	139	139	139	139	139	139
Hole	857C	857C	857C	857C	857C	857C	857C
Core, section	61R-2	62R-1	63R-1	64R-1	64R-1	64R-2	68R-1
Interval (cm)	8-10	70-72	50-52	18-20	41-44	46-49	97-100
Piece	1	5	4	2	3	5	16
Lab number	Z-951	Z-952	Z-954	Z-955	Z-825	Z-826	Z-827
Depth (mbsf)	492.08	500.7	510.2	519.58	519.81	521.36	558.97
Major elements (g/1000 cm^3):							
Si	539	518	600	583	601	597	596
Ti	23.4	22.0	23.0	23.2	23.3	25.0	26.5
Al	201	180	215	232	240	235	232
Fe^{+++}	51	58	39	31	31	53	67
Fe^{++}	105	102	147	138	158	142	131
Fe (Sum)	156	160	186	169	189	196	197
Mn	5.3	5.4	5.7	5.9	6.0	5.5	7.3
Mg	152	117	123	121	151	138	135
Ca	170	205	231	228	214	235	226
Na	41.7	28.6	38.6	42.7	39.2	39.2	33.6
K	1.0	1.0	0.9	1.1	1.1	0.9	1.1
P	1.6	1.3	1.6	1.5	1.6	1.9	1.7
Minor elements (g/1000 cm^3 x 10^{-3}):							
La	8.82	8.82	10.44	10.62	10.65	12.51	14.63
Ce	29.40	25.52	28.71	28.49	30.03	35.36	43.36
Nd	24.50	25.52	25.32	25.90	27.30	29.92	32.52
Sm	8.58	8.12	8.61	8.55	9.28	9.79	10.03
Eu	2.70	3.25	2.87	2.85	2.57	2.99	3.25
Tb	2.03	2.09	2.01	2.23	2.46	2.67	2.71
Yb	7.35	6.96	7.31	7.51	7.37	7.34	8.40
Lu	1.15	1.07	1.12	1.14	1.15	1.14	1.33
Cr	637	429	653	907	710	707	745
Ni	164	162	211	233	246	223	271
V	495	415	574	596	562	560	710
Cu	49	60	172	202	177	220	466
Co	108	92.8	115	122	106	95.2	133
Zn	306	209	339	264	273	275	268
Sn	6.37	6.03	6.53	5.96	7.64	7.07	8.13
Zr	294	255	240	233	254	272	298
Y	68.6	67.3	67.9	64.8	71.0	78.9	86.7
Nb	4.90	6.26	6.79	7.51	9.01	12.2	18.4
Rb	3.19	3.02					
Sr	343	534	339	337	328	354	325
Ba	71.1	48.7	73.1	57.0	161.1	155.0	100.3
H_2O^+ (wt%)	2.59	3.76	1.30	1.87	2.74	2.01	2.33
Density (g/cm^3)	2.45	2.32	2.61	2.59	2.73	2.72	2.71
Fe_2O_3/FeO	0.54	0.64	0.29	0.25	0.22	0.42	0.57

Table AT5 (continued).

Leg	139	139	139	139	139	139	139
Hole	857C	857C	857D	857D	857D	857D	857D
Core, section	68R-2	68R-3	1R-1	2R-1	3R-1	3R-2	8R-1
Interval (cm)	69-71	20-23	35-39	10-13	43-46	86-88	5-7
Piece	7	2	5A	3	4	10B	1
Lab number	Z-957	Z-828	Z-829	Z-831	Z-832	Z-959	Z-962
Depth (mbsf)	560.19	561.2	581.85	589.7	599.73	601.66	647.35
Major elements (g/1000 cm^3):							
Si	489	594	505	586	602	602	528
Ti	23.6	25.8	32.3	26.8	26.1	19.7	17.2
Al	236	238	227	216	244	261	209
Fe^{+++}	37	33	20	28	77	68	79
Fe^{++}	207	163	170	145	126	115	127
Fe (Sum)	245	195	190	173	203	183	206
Mn	10.4	7.0	11.1	4.2	4.9	4.7	2.4
Mg	142	145	173	125	122	128	157
Ca	154	218	105	223	233	228	82
Na	24.0	33.5	26.2	42.2	45.4	42.1	9.9
K	1.0	0.9	0.8	0.9	0.9	0.9	0.4
P	2.1	1.7	2.1	1.6	1.4	1.7	1.0
Minor elements (g/1000 cm^3 x 10^{-3}):							
La	14.69	13.50	13.94	11.40	8.74	10.15	8.99
Ce	42.33	29.70	44.82	36.26	30.03	33.84	23.09
Nd	32.37	25.92	37.35	28.49	26.21	31.02	20.66
Sm	9.71	9.45	13.20	9.84	9.56	10.15	6.80
Eu	2.49	2.65	3.74	2.85	3.00	3.10	1.70
Tb	2.49	2.38	3.24	2.59	2.54	2.68	1.90
Yb	8.96	8.10	11.70	8.03	8.19	9.31	6.80
Lu	1.39	1.24	1.79	1.32	1.34	1.47	1.14
Cr	398	702	672	596	551	649	904
Ni	251	262	224	212	207	220	340
V	640	670	931	534	513	649	948
Cu	535	262	491	381	524	197	102
Co	120	111	107	111	106	133	143
Zn	374	327	354	236	396	276	425
Sn	7.22	7.02	7.72	6.22	6.01	14.95	9.96
Zr	274	267	324	259	268	265	156
Y	79.7	75.6	107	80.3	84.6	90.2	58.3
Nb	15.7	18.6	12.0	12.7	9.28	5.36	3.89
Rb							
Sr	219	297	184	311	328	310	60.8
Ba	139.4	75.6	134	135	92.8	133	14.6
H_2O^+ (wt%)	3.95	2.62	6.28	2.04	2.16	1.10	6.91
Density (g/cm^3)	2.49	2.70	2.49	2.59	2.73	2.82	2.43
Fe_2O_3/FeO	0.20	0.22	0.13	0.22	0.68	0.65	0.69

Table AT5 (continued).

Leg	139	139	139	139	139	139	139
Hole	857D	857D	857D	857D	857D	857D	857D
Core, section	9R-1	12R-1	12R-1	12R-2	17R-3	18R-2	20R-1
Interval (cm)	23-25	25-27	106-108	17-19	72-74	84-85	64-66
Piece	4	5	14	3	11	9	8
Lab number	Z-833	Z-834	Z-963	Z-964	Z-967	Z-968	Z-969
Depth (mbsf)	657.13	686.15	686.96	687.57	737.62	745.94	763.14
Major elements (g/1000 cm^3):							
Si	563	488	411	636	604	665	589
Ti	40.5	23.2	19.9	23.9	33.2	31.7	18.0
Al	189	255	215	212	184	235	185
Fe^{+++}	94	26	50	67	123	116	113
Fe^{++}	240	150	157	172	102	111	125
Fe (Sum)	334	175	208	240	225	227	238
Mn	9.0	4.0	5.0	5.2	5.5	5.4	3.8
Mg	154	187	218	130	144	150	179
Ca	164	105	62	230	149	251	206
Na	25.4	13.2	6.3	44.5	46.6	45.5	31.2
K	0.9	0.4	0.6	1.2	0.9	1.0	0.9
P	2.6	1.6	1.1	1.8	1.8	1.7	1.3
Minor elements (g/1000 cm^3 x 10^{-3}):							
La	17.24	8.82	9.04	10.40	12.36	14.43	8.86
Ce	55.60	26.95	24.86	30.91	36.82	36.84	25.76
Nd	44.48	23.77	22.60	26.98	31.56	30.70	23.27
Sm	15.01	8.58	9.04	11.24	10.78	10.44	7.76
Eu	6.12	2.33	3.84	3.93	3.68	3.68	2.27
Tb	3.89	2.45	2.26	3.37	2.89	2.58	2.16
Yb	13.07	8.82	7.91	10.96	10.52	10.13	7.76
Lu	1.95	1.42	1.22	1.74	1.71	1.63	1.19
Cr	145	992	1006	225	237	236	817
Ni	139	434	418	152	139	144	457
V	767	799	848	745	481	381	532
Cu	70	47	66	185	79	89	83
Co	125	9.07	102	132	65.8	61.4	271
Zn	639	412	136	281	381	298	258
Sn	11.12	6.37	11.98	5.62	4.73	7.37	6.65
Zr	417	218	197	281	316	295	197
Y	128	78.4	76.8	95.5	99.9	101	60.9
Nb	16.7	7.60	5.88	5.34	10.5	12.6	7.76
Rb					4.21		
Sr	306	78.4	40.7	259	368	368	238
Ba	114	135	0.00	138	124	70.6	111
H_2O^+ (wt%)	4.22	6.60	8.45	2.00	3.70	1.86	3.24
Density (g/cm^3)	2.78	2.45	2.26	2.81	2.63	3.07	2.77
Fe_2O_3/FeO	0.43	0.19	0.36	0.44	1.34	1.16	1.00

Table AT5 (continued).

Leg	139	139	139	139	139	139	139
Hole	857D	857D	857D	857D	857D	857D	857D
Core, section	21R-1	23R-1	24R-2	26R-1	29R-2	33R-1	35R-1
Interval (cm)	59-61	57-59	4-7	58-60	36-39	81-83	29-31
Piece	6	10	1	6	4	13	5
Lab number	Z-835	Z-970	Z-836	Z-972	Z-973	Z-974	Z-975
Depth (mbsf)	772.79	792.07	802.74	820.88	850.26	888.61	907.49
Major elements (g/1000 cm^3):							
Si	669	641	623	638	631	630	611
Ti	27.2	23.8	25.4	20.1	29.3	35.0	41.0
Al	217	228	235	230	215	200	201
Fe^{+++}	42	100	38	90	73	106	150
Fe^{++}	186	127	140	97	134	131	123
Fe (Sum)	228	226	178	187	207	236	274
Mn	5.1	3.9	2.2	4.3	4.3	5.0	5.1
Mg	123	127	125	134	128	137	120
Ca	263	251	267	229	237	208	248
Na	47.1	43.9	49.4	53.3	49.2	45.2	54.3
K	1.2	0.9	1.2	1.4	1.2	0.7	0.7
P	1.9	1.7	1.8	1.8	2.2	1.9	2.6
Minor elements (g/1000 cm^3 x 10^{-3}):							
La	11.23	12.17	15.85	14.95	14.79	11.68	13.97
Ce	34.56	33.96	44.48	36.66	41.85	36.14	43.65
Nd	27.65	28.30	33.36	28.20	33.48	30.58	37.83
Sm	9.50	9.06	10.01	8.74	10.88	10.84	13.39
Eu	3.17	2.83	3.06	3.10	3.63	4.17	4.07
Tb	2.71	2.46	2.45	2.34	3.07	3.06	4.07
Yb	8.35	8.77	8.34	7.33	10.04	10.84	13.39
Lu	1.35	1.42	1.22	1.21	1.56	1.64	2.07
Cr	553	509	575	578	229	431	524
Ni	207	195	195	161	145	200	244
V	726	608	603	584	586	631	844
Cu	294	178	534	262	215	222	175
Co	132	136	91.7	124	92.1	91.7	163
Zn	259	306	278	209	243	353	314
Sn	7.20	6.79	7.51	7.61	4.74	4.73	6.98
Zr	274	258	272	271	335	306	378
Y	86.4	76.4	69.5	76.1	92.1	103	113
Nb	10.7	13.3	17.0	12.1	13.7	13.6	9.31
Rb		2.83	3.61		3.07		
Sr	346	340	500	451	391	361	407
Ba	132	153	122	158	167	147	61.1
H_2O^+ (wt%)	1.32	1.42	1.79	2.39	2.02	2.81	2.24
Density (g/cm^3)	2.88	2.83	2.78	2.82	2.79	2.78	2.91
Fe_2O_3/FeO	0.25	0.87	0.30	1.04	0.61	0.90	1.35

Table AT5 (continued).

Leg	139	139
Hole	857D	857D
Core, section	35R-1	36R-1
Interval (cm)	103-106	3-5
Piece	14A	1
Lab number	Z-837	Z-976
Depth (mbsf)	908.23	916.93
Major elements (g/1000 cm^3):		
Si	651	624
Ti	32.3	40.9
Al	202	200
Fe^{+++}	60	94
Fe^{++}	228	190
Fe (Sum)	289	284
Mn	7.7	5.1
Mg	122	127
Ca	246	227
Na	43.2	42.6
K	0.7	0.7
P	2.3	2.5
Minor elements (g/1000 cm^3 x 10^{-3}):		
La	13.01	13.68
Ce	37.57	39.90
Nd	34.68	37.05
Sm	12.14	12.83
Eu	4.34	3.99
Tb	3.18	3.42
Yb	12.43	12.54
Lu	2.05	1.94
Cr	491	470
Ni	260	205
V	844	755
Cu	191	205
Co	145	143
Zn	448	362
Sn	9.54	6.56
Zr	376	342
Y	124	120
Nb	15.6	9.98
Rb		
Sr	251	251
Ba	101	68.4
H_2O^+ (wt%)	2.02	2.03
Density (g/cm^3)	2.89	2.85
Fe_2O_3/FeO	0.29	0.55

Table AT6. Abundance of major and trace elements (g/1000 cm^3) in igneous rocks, Holes 858F and 858G, Leg 139 (Middle Valley, Juan de Fuca Ridge).

Leg	139	139	139	139	139	139	139	139
Hole	858F	858F	858F	858F	858G	858G	858G	858G
Core, section	26R-1	27R-1	28R-1	29R-1	1R-1	4R-1	7R-1	14R-1
Interval (cm)	93-95	25-27	43-45	39-41	14-16	35-37	32-34	10-12
Piece	11	6	8	8	2	9	6	2
Lab number	Z-977	Z-978	Z-979	Z-980	Z-981	Z-982	Z-983	Z-984
Depth (mbsf)	259.53	268.05	277.93	287.59	276.94	306.15	335.12	403.7
Major elements (g/1000 cm^3):								
Si	422	442	630	659	613	608	594	597
Ti	21.0	21.4	27.7	24.6	27.7	25.8	28.4	25.2
Al	148	163	235	236	225	240	223	209
Fe^{+++}	53	64	85	63	4	45	56	35
Fe^{++}	68	52	93	133	145	142	118	132
Fe (Sum)	120	115	178	195	149	187	174	167
Mn	1.2	1.7	1.8	2.3	3.5	3.4	5.0	4.7
Mg	90	88	134	153	134	119	120	147
Ca	159	166	247	243	197	259	253	206
Na	37.8	41.1	61.5	65.5	76.3	56.9	54.9	70.2
K	1.2	0.8	1.4	1.5	0.9	1.1	1.1	1.7
P	1.4	1.5	1.9	2.2	2.1	2.3	2.1	2.1
Minor elements (g/1000 cm^3 x 10^{-3}):								
La	10.18	10.67	16.86	16.06	14.15	16.23	15.39	12.62
Ce	29.60	32.98	47.77	46.72	42.72	49.50	45.90	42.08
Nd	20.35	23.28	33.72	35.04	32.04	35.75	35.10	34.19
Sm	6.85	7.18	10.40	10.51	10.41	11.28	11.34	10.78
Eu	2.59	2.52	3.65	3.50	3.47	4.13	3.51	3.42
Tb	1.61	1.88	2.61	2.72	2.51	2.75	2.70	2.89
Yb	5.55	5.82	7.87	8.47	8.01	8.53	8.37	8.68
Lu	0.85	0.85	1.21	1.34	1.23	1.29	1.27	1.29
Cr	416	446	604	613	694	688	540	618
Ni	118	126	177	158	176	193	167	168
Co	53.7	54.3	89.9	84.7	101.5	129.3	91.8	84.2
V	315	351	497	537	633	564	464	513
Cu	130	128	197	146	206	182	194	447
Zn	135	144	208	152	195	206	235	213
Sn	3.15	4.07	4.50	5.26	4.54	5.78	4.05	4.21
Zr	222	252	365	350	347	330	324	342
Y	53.7	54.3	75.9	84.7	77.4	79.8	75.6	78.9
Nb	8.70	8.34	12.65	13.43	12.02	11.55	10.80	11.57
Rb	2.04	2.33	3.65					
Sr	352	369	562	584	534	550	486	473
Ba	113	73.7	143	152	139	96.3	127	126
H_2O^+ (wt%)	1.98	2.66	2.26	2.21	2.89	1.50	2.33	2.17
Density (g/cm^3)	1.85	1.94	2.81	2.92	2.67	2.75	2.70	2.63
Fe_2O_3/FeO	0.86	1.37	1.01	0.52	0.03	0.36	0.53	0.30

Table AT7. Abundance of major and trace elements (g/1000 cm^3) in igneous rocks, Hole 1037B, Leg 169 (Escanaba Trough, Gorda Ridge). (Continued on next page.)

Leg	169	169	169	169	169	169	169
Hole	1037B	1037B	1037B	1037B	1037B	1037B	1037B
Core, section	57R-1	58R-1	58R-2	59R-1	60R-1	60R-1	61R-1
Interval (cm)	32-37	100-104	0-5	65-68	90-95	120-124	7-10
Piece	8A	7C	1	10	11A	11C	1A
Lab number	Z-1605	Z-1606	Z-1607	Z-1608	Z-1609	Z-1610	Z-1611
Depth (mbsf)	508.12	518.30	518.70	527.45	530.30	530.60	533.97
Major elements (g/1000 cm^3):							
Si	661	643	665	680	651	654	663
Ti	34.1	28.2	35.9	39.4	33.5	34.8	34.8
Al	212	222	211	207	219	222	229
Fe^{+++}	91	85	97	111	94	69	92
Fe^{++}	182	162	165	175	158	166	159
Fe (Sum)	273	247	262	286	252	235	251
Mn	4.3	3.4	4.3	4.6	4.5	4.5	4.4
Mg	142	169	143	125	140	144	135
Ca	215	193	204	221	213	219	219
Na	59.8	61.2	73.6	72.1	62.7	59.9	63.0
K	5.8	22.4	14.2	5.2	6.2	7.3	4.2
P	2.6	2.0	2.6	2.9	2.4	2.5	2.3
Minor elements (g/1000 cm^3 x 10^{-3}):							
La	19.50	14.69	18.10	19.77	17.39	18.30	18.33
Ce	49.47	43.20	55.48	61.95	54.15	51.48	58.20
Nd	40.74	34.56	43.80	50.15	45.60	42.90	46.56
Sm	13.68	11.23	14.31	16.23	15.11	15.16	15.42
Eu	4.66	3.46	4.38	4.43	4.56	4.58	4.66
Tb	4.07	3.17	4.09	5.02	4.28	4.00	4.07
Yb	12.80	10.37	12.85	14.75	13.11	12.58	12.80
Lu	1.75	1.41	1.84	1.92	1.91	1.80	1.78
Cr	597	599	666	714	690	609	631
Ni	300	469	269	212	257	269	242
Co	128	135	117	136	134	143	137
V	777	732	803	1062	969	972	786
Cu	125	58	158	207	123	235	137
Zn	271	190	222	207	245	246	244
Zr	407	317	409	443	371	400	407
Y	116	98	126	133	117	126	122
Nb	17.2	14.1	19.0	19.8	15.1	17.2	16.0
Rb	20.4	77.8	52.6	13.0	18.2	19.7	10.5
Sr	320	346	350	354	342	343	349
Ba	64.0	317	274	124	59.9	100	186
H_2O^+ (wt%)	0.91	1.00	0.75	0.23	0.30	0.38	0.56
Density (g/cm^3)	2.91	2.88	2.92	2.95	2.85	2.86	2.91
Fe_2O_3/FeO	0.56	0.58	0.65	0.71	0.66	0.46	0.65

Table AT7 (continued).

Leg	169	169
Hole	1037B	1037B
Core, section	62R-1	62R-3
Interval (cm)	13-17	52-56
Piece	2	4
Lab number	Z-1612	Z-1613
Depth (mbsf)	538.13	541.24
Major elements (g/1000 cm^3):		
Si	674	677
Ti	38.5	36.9
Al	221	205
Fe^{+++}	71	99
Fe^{++}	176	162
Fe (Sum)	247	261
Mn	4.8	4.3
Mg	148	119
Ca	227	243
Na	62.8	59.5
K	5.4	4.6
P	2.7	2.3
Minor elements (g/1000 cm^3 x 10^{-3}):		
La	18.29	17.46
Ce	59.00	64.02
Nd	47.20	46.56
Sm	15.05	15.13
Eu	4.72	4.66
Tb	4.43	4.37
Yb	12.98	13.39
Lu	1.89	1.92
Cr	714	780
Ni	189	183
Co	142	140
V	1068	1120
Cu	186	230
Zn	351	262
Zr	413	349
Y	133	119
Nb	15.3	16.3
Rb	12.4	17.8
Sr	354	349
Ba	112	105
H_2O^+ (wt%)	0.50	0.18
Density (g/cm^3)	2.95	2.91
Fe_2O_3/FeO	0.45	0.68

Table AT8. Abundance of major and minor elements (g/1000 cm^3) in igneous rocks, Hole 1038I, Leg 169 (Central Hill, Escanaba Trough).

Leg	169
Hole	1038I
Core, section	43X-3
Interval (cm)	3-7
Piece	2
Lab number	Z-1614
Depth (mbsf)	403.23
Major elements (g/1000 cm^3):	
Si	664
Ti	24.4
Al	244
Fe^{+++}	58
Fe^{++}	22
Fe (Sum)	81
Mn	3.2
Mg	138
Ca	246
Na	55.2
K	2.9
P	1.9
Minor elements (g/1000 cm^3 x 10^{-3}):	
La	16.18
Ce	49.13
Nd	31.79
Sm	9.83
Eu	3.47
Tb	2.31
Yb	8.09
Lu	1.16
Cr	867
Ni	249
Co	127
V	708
Cu	191
Zn	223
Zr	283
Y	80.9
Nb	18.8
Rb	6.36
Sr	491
Ba	462
H_2O^+ (wt%)	0.67
Density (g/cm^3)	2.89
Fe_2O_3/FeO	0.45

Table AT9. Abundance of major and trace elements (g/1000 cm^3) in basalts, Hole 477, Leg 64 (Gulf of California, Guaymas Basin). (Continued on next page.)

Leg	64	64	64	64	64	64	64
Hole	477	477	477	477	477	477	477
Core, section	9R-1	11R-2	12R-1	12R-2	12R-3	12R-4	12R-4
Interval (cm)	57-59	61-63	49-52	70-73	39-42	6-9	76-80
Piece	10	5	4	3C	3C	1A	1E
Lab number	Z-1254	Z-1255	Z-1256	Z-1257	Z-1258	Z-1259	Z-1260
Depth (mbsf)	60.57	79.11	86.99	88.7	89.69	90.86	91.56
Major elements (g/1000 cm^3):							
Si	569.2	598.6	589.7	620.9	606.6	644.0	601.9
Ti	30.2	22.8	22.7	24.8	23.3	26.5	24.2
Al	201.2	250.3	236.4	250.5	242.3	248.0	237.2
Fe^{+++}	58.4	64.4	73.9	82.2	68.5	91.8	61.6
Fe^{++}	134.8	114.5	108.5	115.7	119.9	119.2	126.3
Fe (Sum)	193.2	178.9	182.4	197.9	188.4	211.0	187.9
Mn	3.3	2.9	3.1	3.3	3.0	3.6	3.4
Mg	101.8	143.4	135.9	142.1	153.1	155.0	163.4
Ca	204.4	209.8	213.1	228.5	209.5	224.5	203.3
Na	60.0	53.7	53.7	59.2	57.1	62.1	55.7
K	3.5	2.7	3.1	3.3	3.2	3.6	3.4
P	2.1	1.4	1.5	1.7	1.8	1.9	1.8
Minor elements (g/1000 cm^3 x 10^{-3}):							
La	17.5	14.1	10.1				13.7
Ce	57.8	40.6	29.6				30.5
Nd	47.2	33.4					
Sm	0.0	10.7					
Eu	5.4	3.8	2.5				3.6
Tb	2.9	2.2	1.6				1.8
Yb	10.6	7.1					
Lu	1.6	1.1					
Cr	597.7	646.1	707.4	714.7	756.0	774.9	672.3
Ni	143.3	365.8	358.9	379.5	405.0	398.9	369.9
Co	123.5	133.5	136.2	144.0	151.2	163.6	151.2
V	644.7	507.3	550.2	595.6	580.5	645.8	545.4
Cu	195.1	186.9	172.9	182.8	164.7	189.4	189.0
Zn	237.1	256.3	246.3	252.1	213.3	226.7	243.0
Zr	345.8	256.3	251.5	304.7	270.0	315.7	297.0
Y	84.0	56.1	62.9	69.3	62.1	68.9	72.9
Nb	11.9	8.3	8.1	11.4	9.5	12.1	11.9
Rb		3.5	2.6	5.0	5.7	3.2	3.2
Sr	568.1	614.1	576.4	637.1	594.0	631.4	567.0
Ba	271.7	98.8	220.1	144.0	67.5	63.1	159.3
H_2O^+ (wt%)	0.13	0.61	0.20	0.43	0.33	0.42	0.62
Density (g/cm^3)	2.47	2.67	2.62	2.77	2.70	2.87	2.70
Fe_2O_3/FeO	0.48	0.63	0.76	0.79	0.64	0.86	0.54

Table AT9 (continued).

Leg	64	64	64	64
Hole	477	477	477	477
Core, section	12R-5	13R-1	13R-2	13R-2
Interval (cm)	46-50	53-62	13-17	146-150
Piece	1H	3H	3	8
Lab number	Z-1261	Z-1262	Z-1263	Z-1264
Depth (mbsf)	92.76	96.53	97.48	98.81
Major elements (g/1000 cm^3):				
Si	606.1	655.2	650.0	659.1
Ti	25.2	29.6	28.0	28.5
Al	252.6	248.9	262.6	253.2
Fe^{+++}	56.3	93.3	86.7	108.9
Fe^{++}	117.9	147.5	140.9	124.7
Fe (Sum)	174.2	240.9	227.6	233.6
Mn	3.2	3.6	3.4	3.4
Mg	122.0	143.0	141.5	148.2
Ca	221.6	234.9	237.1	236.1
Na	58.1	62.7	63.1	64.8
K	3.4	4.1	4.4	3.9
P	1.9	1.9	2.0	2.1
Minor elements (g/1000 cm^3 x 10^{-3}):				
La				13.6
Ce				36.9
Nd				
Sm				
Eu				2.9
Tb				2.2
Yb				
Lu				
Cr	645.6	832.2	773.8	797.0
Ni	220.6	262.8	242.4	225.6
Co	134.5	146.0	151.8	137.7
V	583.7	686.2	619.0	694.4
Cu	196.4	230.7	224.8	225.6
Zn	215.2	245.3	245.3	231.5
Zr	322.8	350.4	350.4	351.6
Y	72.6	81.8	75.9	73.3
Nb	11.8	13.7	13.7	14.7
Rb	3.5		3.8	5.6
Sr	645.6	671.6	671.6	673.9
Ba	201.8	131.4	186.9	252.0
H_2O^+ (wt%)	0.79	0.10	0.10	0.10
Density (g/cm^3)	2.69	2.92	2.92	2.93
Fe_2O_3/FeO	0.53	0.7	0.68	0.97

Table AT10. Abundance of major and trace elements (g/1000 cm^3) in basalts, Hole 483B, Leg 65 (Gulf of California).

Leg	65	65	65	65	65	65	65	65
Hole	483B	483B	483B	483B	483B	483B	483B	483B
Core, section	32R-1	32R-1	32R-1	32R-1	32R-1	32R-2	32R-2	32R-2
Interval (cm)	1-6	27-31	44-50	70-74	90-94	95-100	116-123	135-141
Piece	1	2B	2D	2F	3	4A	4C	6A
Lab number	Z-1275	Z-1276	Z-1277	Z-1278	Z-1279	Z-1280	Z-1281	Z-1282
Depth (mbsf)	262.51	262.77	262.94	263.2	263.4	264.95	265.16	265.35
Major elements (g/1000 cm^3):								
Si	668.0	676.8	674.9	690.8	662.1	704.7	662.6	681.9
Ti	29.3	29.2	30.0	30.4	29.5	31.0	29.4	30.1
Al	214.7	229.5	219.4	225.8	218.7	232.5	217.1	218.9
Fe^{+++}	140.7	129.8	132.1	118.2	131.2	131.6	184.6	130.6
Fe^{++}	128.8	115.2	147.3	146.0	124.2	133.8	114.4	142.6
Fe (Sum)	269.5	245.0	279.3	264.2	255.4	265.4	299.0	273.2
Mn	4.8	3.9	4.2	5.5	4.8	5.0	4.4	4.7
Mg	155.1	142.1	145.4	166.3	149.0	157.4	148.2	159.9
Ca	236.3	245.3	253.2	251.8	227.9	240.6	231.3	247.9
Na	57.1	56.8	57.5	57.3	58.9	60.1	57.6	57.0
K	4.2	1.2	1.3	2.0	2.7	3.9	7.2	1.3
P	1.7	1.6	1.6	1.7	1.8	1.9	1.7	1.6
Minor elements (g/1000 cm^3 x 10^{-3}):								
La				11.0				
Ce				33.6				
Nd				30.5				
Sm				11.6				
Eu				4.0				
Tb				3.4				
Yb				10.7				
Lu				1.8				
Cr	946.7	944.0	1043.0	1000.4	899.0	881.3	908.8	744.0
Ni	411.6	271.4	280.1	302.0	406.0	260.1	288.1	435.0
Co	167.6	171.1	181.8	164.7	162.4	149.9	151.5	183.0
V	1167.2	1150.5	1227.8	1143.8	1116.5	1132.2	1158.3	1245.0
Cu	255.8	227.2	208.6	201.3	229.1	241.7	234.6	219.0
Zn	296.9	330.4	256.3	305.0	304.5	275.4	285.1	270.0
Zr	288.1	292.1	289.1	305.0	290.0	306.0	288.1	288.0
Y	102.9	100.3	92.4	97.6	101.5	107.1	92.1	99.0
Nb	9.1	10.0	8.3	10.1	9.6	11.6	5.6	6.9
Rb	8.5			3.4	3.8	8.3	18.1	
Sr	323.4	324.5	327.8	335.5	348.0	367.2	326.7	330.0
Ba	147.0	123.9	137.1	67.1	81.2	198.9	187.1	27.0
H_2O^+ (wt%)	0.30	0.45	0.30	0.29	0.28	<0.1	0.48	0.20
Density (g/cm^3)	2.94	2.95	2.98	3.05	2.90	3.06	2.97	3.00
Fe_2O_3/FeO	1.21	1.25	1.00	0.90	1.17	1.09	1.79	1.02

Table AT11. Abundance of major and trace elements (g/1000 cm^3) in basalts, Hole 485A, Leg 65 (Gulf of California). (Continued on next two pages.)

Leg	65	65	65	65	65	65	65
Hole	485A	485A	485A	485A	485A	485A	485A
Core, section	11R-3	11R-3	12R-1	14R-1	17R-1	17R-1	23R-1
Interval (cm)	56-58	82-84	62-64	56-60	80-83	114-115	55-56
Piece	1A	1B	4A	1F	5	6C	4A
Lab number	Z-1283	Z-1284	Z-1285	Z-1286	Z-1287	Z-1288	Z-1289
Depth (mbsf)	149.01	149.27	155.62	160.06	181.30	181.64	212.05
Major elements (g/1000 cm^3):							
Si	623.0	657.3	716.4	727.6	685.7	685.5	702.9
Ti	27.6	23.1	41.8	37.7	37.6	45.2	40.4
Al	246.4	244.9	227.0	227.1	226.4	220.1	220.7
Fe^{+++}	102.1	44.3	69.1	48.3	96.5	86.6	91.1
Fe^{++}	84.5	165.8	241.9	227.1	150.2	179.1	170.2
Fe (Sum)	186.5	210.1	311.0	275.4	246.7	265.6	261.3
Mn	2.4	3.4	5.3	5.1	3.6	4.0	4.2
Mg	104.7	173.6	153.0	151.9	142.0	131.7	136.3
Ca	232.8	235.6	237.3	236.5	209.3	232.3	239.3
Na	47.9	51.6	41.3	45.7	47.8	39.3	52.1
K	2.3	2.7	1.3	1.3	1.7	2.5	3.0
P	3.9	3.4	5.7	6.1	4.4	5.3	4.8
Minor elements (g/1000 cm^3 x 10^{-3}):							
La							
Ce							
Nd							
Sm							
Eu							
Tb							
Yb							
Lu							
Sc	118.0	148.4	209.0	102.0	132.3	137.5	120.4
Cr	1461.2	552.9	421.2	302.8	270.5	200.3	481.6
Ni	786.8	436.5	262.1	309.0	470.4	227.2	331.1
Co	143.3	107.7	143.5	154.5	138.2	89.7	141.5
V	730.6	669.3	1092.0	988.8	1029.0	627.9	1053.5
Cu	255.7	305.6	365.0	324.5	352.8	164.5	316.1
Pb		61.1	71.8	68.0			24.1
Zn		349.2	655.2	741.6	646.8	508.3	511.7
Sn	8.4	7.3	9.4	9.3	8.8	6.0	9.0
Zr	264.1	261.9	405.6	401.7	441.0	418.6	421.4
Y	89.9	87.3	140.4	139.1	144.1	137.5	138.5
Nb	8.1	4.1	6.9	5.6	7.6	9.6	7.8
Rb							
Sr	449.6	378.3	255.8	299.7	294.0	293.0	331.1
Ba	168.6	203.7	249.6	228.7	191.1	143.5	210.7
H_2O^+ (wt%)	1.56	0.78	0.47	0.42	1.39	1.20	0.68
Density (g/cm^3)	2.81	2.91	3.12	3.09	2.94	2.99	3.01
Fe_2O_3/FeO	1.34	0.30	0.32	0.24	0.71	0.54	0.6

Table AT11 (continued).

Leg	65	65	65	65	65	65	65
Hole	485A	485A	485A	485A	485A	485A	485A
Core, section	24R-1	24R-1	26R-1	29R-2	30R-3	31R-2	31R-2
Interval (cm)	71-73	86-88	16-18	120-122	139-140	36-37	85-88
Piece	1D	1E	1B	3G	1P	1P	1G
Lab number	Z-1290	Z-1291	Z-1292	Z-1293	Z-1294	Z-1295	Z-1296
Depth (mbsf)	216.71	216.86	226.16	242.20	253.89	256.29	256.78
Major elements (g/1000 cm^3):							
Si	657.5	688.3	694.2	631.0	686.3	644.8	698.0
Ti	37.7	37.6	40.2	40.2	40.5	41.3	28.7
Al	225.6	246.8	226.6	233.0	254.4	225.5	230.9
Fe^{+++}	109.7	109.7	108.6	123.4	87.0	155.5	87.6
Fe^{++}	151.0	115.4	175.3	155.4	148.3	145.4	205.9
Fe (Sum)	260.7	225.1	283.9	278.8	235.3	300.9	293.6
Mn	4.3	3.9	4.7	4.5	3.7	4.9	4.5
Mg	143.1	150.5	142.5	160.7	134.0	124.4	165.2
Ca	218.2	213.4	234.2	212.7	211.3	186.4	208.6
Na	56.2	44.1	39.1	37.3	44.2	44.7	38.9
K	2.2	1.2	2.5	3.1	1.2	4.8	2.3
P	2.4	3.6	5.2	4.4	5.1	4.4	5.3
Minor elements (g/1000 cm^3 x 10^{-3}):							
La							
Ce							
Nd							
Sm							
Eu							
Tb							
Yb							
Lu							
Sc		118.4	151.0	145.0	62.4		197.6
Cr	638.0	355.2	362.4	359.6	302.9	717.5	608.0
Ni	278.4	355.2	332.2	234.9	261.4	252.6	349.6
Co	133.4	168.7	141.9	116.0	139.6	132.0	130.7
V	1189.0	947.2	1147.6	638.0	980.1	1090.6	1216.0
Cu		219.0	362.4	304.5	169.3		380.0
Pb		23.7	24.2	26.1	101.0		
Zn		550.6	694.6	420.5	504.9		
Sn		11.8	12.1	5.8	14.9		
Zr	406.0	384.8	422.8	406.0	297.0	315.7	456.0
Y	124.7	121.4	141.9	133.4	106.9	111.9	152.0
Nb	9.6	7.7	9.7	6.7	8.6	4.6	9.4
Rb				7.3	5.3	8.9	9.1
Sr	319.0	325.6	302.0	272.6	270.3	275.5	285.8
Ba	139.2	216.1	302.0	226.2	285.1	344.4	121.6
H_2O^+ (wt%)	0.68	1.00	0.67	1.08	1.42	1.27	1.06
Density (g/cm^3)	2.90	2.96	3.02	2.90	2.97	2.87	3.04
Fe_2O_3/FeO	0.81	1.06	0.69	0.88	0.65	1.19	0.47

Table AT11 (continued).

Leg	65	65	65	65
Hole	485A	485A	485A	485A
Core, section	33R-1	33R-2	38R-2	39R-5
Interval (cm)	135-136	85-87	36-37	2-6
Piece	1K	1I	6A	1
Lab number	Z-1297	Z-1298	Z-1299	Z-1300
Depth (mbsf)	269.35	270.35	314.76	328.02
Major elements (g/1000 cm^3):				
Si	675.4	689.1	614.8	651.1
Ti	27.0	37.7	33.8	29.6
Al	218.4	225.3	228.3	221.0
Fe^{+++}	110.6	88.1	87.6	77.5
Fe^{++}	130.1	203.6	105.5	153.5
Fe (Sum)	240.7	291.7	193.1	231.0
Mn	3.7	4.5	2.3	3.3
Mg	156.7	166.0	125.4	151.3
Ca	253.4	227.6	171.6	236.0
Na	38.5	43.9	43.4	37.9
K	3.2	5.1	2.2	1.7
P	5.6	7.1	4.2	5.4
Minor elements (g/1000 cm^3 x 10^{-3}):				
La			9.3	
Ce			31.9	
Nd			29.3	
Sm			11.2	
Eu			3.5	
Tb			2.7	
Yb			10.1	
Lu			1.6	
Sc		98.6	117.0	
Cr	594.0	523.6	585.2	629.2
Ni	231.7	523.6	345.8	237.4
Co	136.6	178.6	151.6	128.7
V	1128.6	1016.4	1250.2	972.4
Cu		308.0	282.0	
Pb		117.0	21.3	
Zn		646.8	393.7	
Sn		12.3		
Zr	415.8	431.2	319.2	314.6
Y	142.6	135.5	90.4	108.7
Nb	6.2	8.0	5.9	7.2
Rb	12.5	10.8	8.2	
Sr	279.2	277.2	319.2	286.0
Ba	112.9	191.0	226.1	257.4
H_2O^+ (wt%)	1.79	1.71	2.75	1.40
Density (g/cm^3)	2.97	3.08	2.66	2.86
Fe_2O_3/FeO	0.95	0.48	0.92	0.56

Table AT12. Abundance of major and trace elements (g/1000 cm^3) in basalts, Hole 473, Leg 63 (Gulf of California and Baja California).

Leg	63	63	63	63	63	63
Hole	473	473	473	473	473	473
Core, section	29R-1	30R-2	32R-2	32R-3	34R-1	34R-3
Interval (cm)	85-90	126-134	133-140	51-57	0-6	0-6
Piece	6D	3A	5L	1F	1A	1A
Lab number	Z-1245	Z-1246	Z-1247	Z-1248	Z-1730	Z-1731
Depth (mbsf)	248.35	254.76	268.83	269.51	284.00	287.00
Major elements (g/1000 cm^3):						
Si	644.0	669.6	608.5	695.4	683.6	684.0
Ti	27.3	27.8	28.9	33.7	34.8	34.8
Al	235.2	240.8	200.1	227.8	217.5	220.5
Fe^{+++}	73.4	77.1	102.0	79.8	65.7	70.7
Fe^{++}	109.5	114.4	126.7	181.4	206.6	204.3
Fe (Sum)	182.9	191.6	228.7	261.2	272.4	275.0
Mn	2.3	2.4	2.7	3.5	4.1	4.1
Mg	111.5	124.1	148.8	133.7	139.9	123.1
Ca	215.6	235.5	147.8	241.4	236.6	237.8
Na	67.1	63.8	57.0	57.5	56.9	59.3
K	3.0	3.1	4.5	5.0	4.9	4.9
P	1.1	1.4	0.6	2.0	2.2	3.0
Minor elements (g/1000 cm^3 x 10^{-3}):						
Cr	679.3	675.9	632.6	675.7		
Ni	184.8	193.1	184.5	203.3		
Co	157.6	150.5	152.9	161.5		
V	1010.7	994.0	962.1	1046.5		
Cu	198.3	215.8	158.2	173.4		
Zn	244.5	244.2	213.5	278.1		
Zr	271.7	267.0	290.0	328.9		
Y	78.8	79.5	94.9	113.6		
Nb	9.0	10.5	12.1	14.4		
Rb			2.9	3.9		
Sr	407.6	397.6	276.8	314.0		
Ba		36.9	68.5	98.7		
H_2O^+ (wt%)	0.61	0.58	2.14	0.50	0.42	0.36
Density (g/cm^3)	2.717	2.84	2.636	2.99	2.961	2.948
Fe_2O_3/FeO	0.75	0.75	0.89	0.49	0.53	0.39

Table AT13. Abundance of major and trace elements (g/1000 cm^3) in basalts, Hole 469, Leg 63 (Gulf of California and Baja California). (Continued on next page.)

Leg	63	63	63	63	63	63	63
Hole	469	469	469	469	469	469	469
Core, section	40R-1	41R-1	42R-1	42R-5	44R-1	46R-1	47R-3
Interval (cm)	30-32	7-10	117-120	112-115	3-8	134-138	86-92
Piece	1A	1A	1D	1C	1B	11	4
Lab number	Z-1229	Z-1723	Z-1230	Z-1231	Z-1232	Z-1233	Z-1724
Depth (mbsf)	368.80	371.57	379.17	385.12	396.03	411.34	417.86
Major elements (g/1000 cm^3):							
Si	583.2	608.7	661.5	569.4	599.0	573.7	628.9
Ti	18.2	19.0	21.1	17.2	30.8	34.2	35.5
Al	206.9	217.2	230.5	207.5	201.5	202.8	201.8
Fe^{+++}	90.1	84.1	109.8	85.7	174.2	230.9	196.9
Fe^{++}	54.1	75.4	55.9	84.9	99.3	64.0	110.6
Fe (Sum)	144.2	159.5	165.6	170.6	273.5	294.9	307.5
Mn	4.0	1.9	2.5	2.2	4.4	2.8	4.8
Mg	111.2	104.8	108.0	105.6	121.1	89.3	110.0
Ca	102.7	144.7	165.0	117.8	190.6	125.0	190.8
Na	61.9	69.4	77.5	66.1	58.3	61.9	56.5
K	64.6	11.5	8.0	20.9	8.4	20.8	11.5
P	1.2	12.5	2.1	1.8	2.1	3.0	1.7
Minor elements (g/1000 cm^3 x 10^{-3}):							
La			24.2				
Ce			61.2				
Nd			39.9				
Sm			10.9				
Eu			3.7				
Tb			2.2				
Yb			6.1				
Lu			1.1				
Cr	188.5		172.9	155.9	275.7	363.5	
Ni	79.8		87.8	80.3	143.3	143.4	
Co	111.2		106.4	108.7	124.3	153.6	
V	592.2		590.5	519.6	1302.8	1400.3	
Cu	70.1		55.9	87.4	178.4	169.0	
Zn	193.4		226.1	290.5	364.9	297.0	
Zr	314.2		345.8	307.1	297.3	358.4	
Y	65.3		71.8	59.1	116.2	99.8	
Nb	10.9		12.5	10.6	8.9	8.4	
Rb	62.8		19.4	42.5	20.3	35.8	
Sr	410.9		611.8	519.6	297.3	281.6	
Ba	797.6		718.2	661.4	297.3	235.5	
H_2O^+ (wt%)	1.04	1.06	0.47	1.24	0.54	1.43	0.74
Density (g/cm^3)	2.417	2.504	2.66	2.362	2.703	2.56	2.781
Fe_2O_3/FeO	1.85	1.24	2.18	1.12	1.96	4.01	1.98

Table AT13 (continued).

Leg	63	63	63	63
Hole	469	469	469	469
Core, section	48R-1	49R-1	50R-2	51R-1
Interval (cm)	49-53	84-88	27-32	34-40
Piece	Glass 5A	8A	3A	3
Lab number	Z-1235	Z-1236	Z-1237	Z-1238
Depth (mbsf)	423.49	432.84	441.77	450.34
Major elements (g/1000 cm^3):				
Si	649.2	663.8	619.1	506.2
Ti	31.0	33.8	29.8	19.4
Al	215.4	242.9	202.0	155.8
Fe^{+++}	217.6	156.8	124.8	125.2
Fe^{++}	76.7	92.0	156.4	79.5
Fe (Sum)	294.3	248.8	281.3	204.8
Mn	1.7	4.6	4.6	2.8
Mg	172.8	133.5	134.6	146.7
Ca	29.2	193.2	189.3	78.0
Na	54.8	66.3	48.7	53.3
K	22.5	9.0	9.5	10.2
P	1.1	2.1	2.0	1.8
Minor elements (g/1000 cm^3 x 10^{-3}):				
La				
Ce				
Nd				
Sm				
Eu				
Tb				
Yb				
Lu				
Cr		410.4	142.5	121.5
Ni		156.1	137.0	112.8
Co		138.7	139.7	115.0
V		1089.5	1000.1	802.9
Cu		179.2	145.2	97.7
Zn		323.7	331.5	171.4
Zr		317.9	287.7	180.1
Y		121.4	123.3	102.0
Nb		7.5	4.7	4.1
Rb		5.5	16.2	3.9
Sr		283.2	274.0	197.5
Ba		101.2	194.5	21.7
H_2O^+ (wt%)	4.13	0.29	1.00	1.59
Density (g/cm^3)	2.82	2.89	2.74	2.17
Fe_2O_3/FeO	3.15	1.89	0.89	1.75

Table AT14. Abundance of major and trace elements (g/1000 cm^3) in basalts, Hole 471, Leg 63 (Gulf of California and Baja California). (Continued on next page.)

Leg	63	63	63	63	63	63	63
Hole	471	471	471	471	471	471	471
Core, section	80R-1	80R-1	80R-2	81R-3	82R-1	82R-2	84R-1
Interval (cm)	78-84	135-140	98-102	59-65	127-132	15-18	9-16
Piece	6B	9A	6G	5	9	1B	2A
Lab number	Z-1725	Z-1239	Z-1726	Z-1727	Z-1240	Z-1241	Z-1242
Depth (mbsf)	751.28	751.85	752.98	763.59	770.27	770.65	787.09
Major elements (g/1000 cm^3):							
Si	580.7	576.8	491.3	567.6	603.8	592.6	600.2
Ti	37.2	31.3	30.1	26.7	20.0	19.7	27.6
Al	200.1	185.0	170.0	185.4	195.8	191.4	193.8
Fe^{+++}	104.0	97.3	89.7	63.0	63.6	58.7	94.4
Fe^{++}	115.8	75.7	117.1	99.5	146.4	146.8	112.3
Fe (Sum)	219.7	173.1	206.8	162.5	210.0	205.6	206.7
Mn	9.0	7.4	7.9	4.1	4.7	4.2	2.3
Mg	163.6	127.9	178.8	87.8	138.8	134.7	151.3
Ca	138.1	104.3	52.9	106.3	112.4	96.8	159.8
Na	60.8	48.8	44.5	81.7	66.9	59.9	68.7
K	11.0	12.9	34.5	48.2	53.1	51.9	12.1
P	1.1	3.0	1.1	2.3	1.7	1.5	1.8
Minor elements (g/1000 cm^3 x 10^{-3}):							
La						17.8	
Ce						45.7	
Nd						27.9	
Sm						7.6	
Eu						2.4	
Tb						1.8	
Yb						6.4	
Lu						1.1	
Cr		427.0			641.7	495.3	589.5
Ni		146.4			220.0	180.3	193.9
Co		102.5			154.5	101.6	165.1
V		590.5			699.3	579.1	948.4
Cu		168.4			180.7	198.1	199.1
Zn		207.4			230.5	210.8	214.8
Zr		366.0			199.0	188.0	366.8
Y		85.4			60.2	58.4	94.3
Nb		39.0			25.4	23.6	36.7
Rb		18.1			49.8	58.4	6.3
Sr		610.0			550.0	508.0	628.8
Ba		475.8			5133.2	5588.0	576.4
H_2O^+ (wt%)	2.43	2.68	5.48	2.82	3.53	3.65	2.04
Density (g/cm^3)	2.62	2.44	2.316	2.368	2.619	2.54	2.62
Fe_2O_3/FeO	1.0	1.43	0.85	0.7	0.48	0.44	0.94

Table AT14 (continued).

Leg	63	63	63	63
Hole	471	471	471	471
Core, section	84R-1	86R-1	87R-2	88R-2
Interval (cm)	107-114	63-69	19-26	0-6
Piece	6G	6D	1B	1A
Lab number	Z-1243	Z-1728	Z-1244	Z-1729
Depth (mbsf)	788.07	805.63	808.69	815.5
Major elements (g/1000 cm^3):				
Si	600.0	619.0	613.3	544.1
Ti	29.0	21.3	20.5	16.6
Al	191.7	240.9	229.7	172.2
Fe^{+++}	97.4	63.3	66.8	91.6
Fe^{++}	129.5	125.7	128.2	137.2
Fe (Sum)	227.0	189.1	195.0	228.8
Mn	4.2	3.9	3.7	4.4
Mg	141.2	135.9	149.9	247.2
Ca	169.8	219.0	215.6	161.9
Na	57.4	53.0	50.7	24.6
K	13.7	7.1	7.2	8.6
P	3.3	1.0	0.4	1.3
Minor elements (g/1000 cm^3 x 10^{-3}):				
La				
Ce				
Nd				
Sm				
Eu				
Tb				
Yb				
Lu				
Cr	543.3		649.4	
Ni	169.6		405.5	
Co	132.5		139.7	
V	927.5		635.7	
Cu	169.6		134.3	
Zn	204.1		150.7	
Zr	371.0		232.9	
Y	84.8		65.8	
Nb	34.5		24.4	
Rb	14.3		6.3	
Sr	583.0		520.6	
Ba	371.0		383.6	
H_2O^+ (wt%)	2.60	2.02	2.36	4.96
Density (g/cm^3)	2.65	2.743	2.74	2.648
Fe_2O_3/FeO	0.84	0.56	0.58	0.74

Table AT15. Abundance of major and trace elements (g/1000 cm^3) in basalts, Hole 332B, Leg 37 (Deep Drill Valley, Mid-Atlantic Ridge). (Continued on next two pages.)

Leg	37	37	37	37	37	37	37
Hole	332B	332B	332B	332B	332B	332B	332B
Core, section	1-5	6-1	11-1	16-2	17-1	21-1	22-1
Interval (cm)	121-124	94-96	58-60	37-40	97-103	12-15	105-108
Piece	11	10	3D	5	13	1A	9
Lab number	Z-280	Z-281	Z-282	Z-283	Z-284	Z-285	Z-286
Depth (mbsf)	149.21	285.44	361.08	409.87	418.47	455.62	466.05
Major elements (g/1000 cm^3):							
Si	623	670	651	623	638	636	621
Ti	12	22	20	16	16	15	16
Al	284	203	206	212	211	213	246
Fe^{+++}	77	95	76	86	80	48	53
Fe^{++}	67	141	137	130	149	156	148
Fe (Sum)	144	236	213	216	229	204	201
Mn	1.3	3.4	0.9	1.6	2.7	2.5	2.6
Mg	115	132	127	154	184	230	161
Ca	325	258	258	280	249	286	240
Na	35	48	46	45	45	41	50
K	3.7	11.0	8.8	4.7	6.5	4.5	4.2
P	0.2	1.3	1.0	0.6	0.2	0.1	0.2
Minor elements (g/1000 cm^3 x 10^{-3}):							
La	4.7	18.3	16.6	10.6	9.4	5.9	6.7
Ce	10.3	40.0	35.9	22.3	21.9	14.4	18.1
Nd					16.5	13.8	13.9
Sm	3.1	8.6	7.7	5.6	4.8	4.7	4.5
Eu	1.4	2.9	2.7	1.9	1.8	1.5	1.7
Tb	1.0	1.8	1.7	1.3	1.2	1.1	1.2
Yb	3.9	7.4	6.9	5.9	5.1	4.7	5.0
Lu	0.6	1.2	1.0	1.0	0.8	0.8	0.8
Cr	712	151	400	1215	1594	1222	779
Ni	433	194	276	726	783	1236	543
Co	115	100	110	151	157	156	125
V	433	357	566	614	655	339	529
Cu	293	171	133	168	256	147	139
Zn	154	257	276	195	213	132	195
Zr	47	160	144		91	68	95
Y	26.0	68.5	52.5	50.3	45.5	35.3	44.5
Nb	7.8	22.0	22.1	3.6	13.7	6.2	10.0
Rb	3.1	18.8	10.2	3.1	5.1	5.3	4.2
Sr	207	314	276		239	183	234
Ba		108	135				
H_2O^+ (wt%)	0.33	0.67	0.52	0.86	0.82	1.25	0.63
Density (g/cm^3)	2.79	2.85	2.76	2.79	2.85	2.90	2.78
Fe_2O_3/FeO	1.27	0.75	0.62	0.74	0.59	0.34	0.40

Table AT15 (continued).

Leg	37	37	37	37	37	37	37
Hole	332B	332B	332B	332B	332B	332B	332B
Core, section	24-1	29-1	33-2	37-3	41-1	42-2	43-1
Interval (cm)	71-75	94-98	30-33	17-20	65-69	22-25	132-136
Piece	8	5D	2	2	6A	1C	8C
Lab number	Z-287	Z-288	Z-289	Z-290	Z-291	Z-292	Z-293
Depth (mbsf)	484.71	532.44	571.3	610.67	646.15	656.72	665.82
Major elements (g/1000 cm^3):							
Si	638	620	651	669	662	647	617
Ti	16	15	15	16	15	15	19
Al	246	225	216	238	221	220	246
Fe^{+++}	52	66	79	82	55	91	77
Fe^{++}	150	125	141	127	168	127	120
Fe (Sum)	202	191	220	209	223	218	197
Mn	2.7	2.7	1.8	2.6	2.8	0.9	2.4
Mg	119	209	182	201	228	189	111
Ca	303	246	276	250	242	259	276
Na	51	42	46	48	44	43	44
K	4.3	5.6	5.0	6.8	3.3	3.7	4.2
P	0.2	0.5	0.3	0.3	0.4	0.1	0.6
Minor elements (g/1000 cm^3 x 10^{-3}):							
La	8.2	5.7	5.6	6.0	5.3	5.8	12.1
Ce	19.9	14.9	13.9	15.0	13.3	13.0	27.5
Nd	17.0	10.6	11.5	12.6	10.4	10.4	19.8
Sm	5.4	3.4	3.8	4.2	3.3	3.5	5.8
Eu	1.9	1.4	1.5	1.6	1.4	1.5	2.0
Tb	1.6	1.1	1.2	1.3	0.9	1.3	1.5
Yb	6.0	4.6	4.7	5.4	3.9	4.6	6.0
Lu	0.9	0.7	0.8	0.8	0.7	0.7	1.0
Cr	795	2121	2347	2505	2341	1346	467
Ni	454	917	945	825	1170	695	220
Co	119	155	156	159	199	145	115
V	540	444	369	555	444	391	495
Cu	159	244	207	270	252	217	165
Zn	227	172	177	195	163	145	192
Zr	99	60	71	57	59	72	102
Y	54.0	48.7	47.2	51.0	44.4	40.5	60.5
Nb	11.9	8.3	8.9	9.9	8.0	8.1	17.0
Rb	4.3	7.2	8.6	3.9		1.7	2.5
Sr	239	221	354	177	199	347	275
Ba	71		65	90			85
H_2O^+ (wt%)	0.55	1.58	0.85	1.72	0.78	1.28	1.00
Density (g/cm^3)	2.84	2.87	2.95	2.84	2.91	2.90	2.75
Fe_2O_3/FeO	0.39	0.58	0.62	0.72	0.36	0.79	0.71

Table AT15 (continued).

Leg	37	37	37
Hole	332B	332B	332B
Core, section	43-2	46-2	48-1
Interval (cm)	28-31	60-63	73-76
Piece	1C	3B	6
Lab number	Z-294	Z-295	Z-296
Depth (mbsf)	666.28	695.1	712.73
Major elements (g/1000 cm^3):			
Si	615	668	543
Ti	18	22	14
Al	259	206	175
Fe^{+++}	57	95	81
Fe^{++}	121	160	100
Fe (Sum)	178	255	181
Mn	2.4	3.2	2.7
Mg	120	134	139
Ca	260	236	206
Na	44	46	35
K	4.6	7.5	7.2
P	0.4	0.4	0.5
Minor elements (g/1000 cm^3 x 10^{-3}):			
La	11.7	17.7	14.3
Ce	26.2	39.9	31.1
Nd	19.1	31.4	21.5
Sm	5.7	8.6	5.7
Eu	2.0	2.9	2.0
Tb	1.6	2.1	1.4
Yb	6.3	7.4	5.0
Lu	0.9	1.2	0.7
Cr	424	185	801
Ni	273	185	359
Co	128	131	91
V	628	713	550
Cu	191	200	134
Zn	150	257	179
Zr	115	171	112
Y	57.4	77.0	45.4
Nb	16.7	20.8	17.9
Rb	1.9	6.0	3.6
Sr	301	314	225
Ba	96	168	96
H_2O^+ (wt%)	1.01	0.80	2.05
Density (g/cm^3)	2.73	2.85	2.39
Fe_2O_3/FeO	0.53	0.66	0.90

Table AT16. Abundance of major and trace elements (g/1000 cm^3) in basalts, Hole 648E, Leg 106 (Serocki Volcano, Mid-Atlantic Ridge Rift Valley).

Leg	106	106	106	106	106	106	106	106
Hole	648B	648B	648B	648B	648B	648B	648B	648B
Core, section	1R-1	1R-2	1R-3	3R-1	4R-1	4R-1	5R-1	6R-1
Interval (cm)	67-70	85-88	60-65	85-87	15-18	61-64	15-22	1-3
Piece	12	15	12	14	4	12	4	1
Lab number	Z-106	Z-107	Z-108	Z-109	Z-110	Z-111	Z-112	Z-113
Depth (mbsf)	7.27	8.95	10.20	15.15	21.25	21.71	14.75	25.71
Major elements (g/1000 cm^3):								
Si	663	663	647	654	651	663	646	647
Ti	33	33	32	35	32	31	37	37
Al	211	233	205	195	208	210	192	229
Fe^{+++}	81	45	90	86	63	48	84	82
Fe^{++}	188	184	189	185	190	208	182	162
Fe (Sum)	269	229	279	271	253	256	266	244
Mn	3.8	1.1	1.1	2.5	1.1	1.8	1.3	3.9
Mg	145	145	154	162	160	152	159	152
Ca	240	254	232	233	237	252	242	257
Na	70	65	69	64	64	66	67	70
K	9.9	7.5	8.2	5.8	7.4	5.3	3.1	7.8
P	1.1	1.0	1.9	0.6	1.5	1.3	1.8	2.1
Minor elements (g/1000 cm^3 x 10^{-3}):								
La	12.6	14.6	13.9	12.7	13.2	14.3	16.4	14.4
Ce	38.1	43.8	37.7	40.5	37.4	43.8	40.2	38.2
Sm	11.1	13.1	12.8	11.8	12.1	13.4	14.1	12.3
Eu	4.1	4.7	4.1	4.3	4.3	4.4	4.6	4.4
Tb	2.5	2.8	2.5	3.2	3.2	2.6	2.7	2.6
Yb	9.7	11.1	10.7	10.1	10.4	11.1	11.5	10.9
Lu	1.6	1.8	1.7	1.7	1.6	1.8	1.8	1.8
Sc	126	120	119	121	121	123	123	123
Cr	850	803	827	853	835	818	918	911
Ni	366	350	348	347	360	423	387	412
Co	147	117	131	116	115	161	129	162
V	938	847	986	1012	922	934	976	911
Cu	176	161	189	159	173	219	230	221
Zn	278	263	261	275	274	350	287	368
Zr	217	254	238	318	317	321	316	353
Y	108.4	108.0	101.5	101.2	103.7	111.0	109.1	111.7
Nb	10.5	9.1	8.7	9.2	8.9	9.1	10.0	7.6
Rb	3.5	3.2		2.9				3.5
Sr	246	321	287	405	403	409	344	412
H_2O^+ (wt%)	0.31	0.25	0.53	0.32	0.32	0.36	0.27	0.32
Density (g/cm^3)	2.93	2.92	2.90	2.89	2.88	2.92	2.89	2.94
Fe_2O_3/FeO	0.48	0.27	0.53	0.52	0.37	0.25	0.51	0.56

Table AT17. Abundance of major and trace elements (g/1000 cm^3) in igneous rocks, Holes 462 and 462A, Leg 61 (Nauru Basin, Pacific Ocean). (Continued on next four pages.)

Leg	61	61	61	61	61	61	61
Hole	462	462	462	462	462	462	462A
Core, section	60R-1	60R-2	61R-1	62R-2	63R-2	64R-1	17R-2
Interval (cm)	65-69	135-138	48-51	135-137	18-22	12-14	84-86
Piece	1A	9	3B	9	1	2	4B
Lab number	Z-1721	Z-1198	Z-1199	Z-1200	Z-1201	Z-1202	Z-1203
Depth (mbsf)	559.15	561.35	567.98	579.35	581.03	585.62	576.19
Major elements (g/1000 cm^3):							
Si	627.6	605.6	632.3	595.9	619.1	582.1	653.0
Ti	21.8	21.4	21.5	26.3	27.3	26.0	24.3
Al	237.7	209.7	233.1	217.3	211.6	215.1	228.0
Fe^{+++}	86.8	203.1	50.8	72.4	85.4	82.0	77.1
Fe^{++}	95.9	0.0	159.0	165.8	146.5	130.9	180.4
Fe (Sum)	182.7	203.1	209.8	238.3	232.0	212.9	257.5
Mn	3.4	4.6	5.2	5.0	4.4	4.8	5.6
Mg	126.4	129.7	128.5	128.6	127.8	118.7	129.0
Ca	220.0	216.7	249.7	204.7	194.2	191.1	245.4
Na	50.2	46.8	44.6	51.7	49.1	50.0	49.1
K	15.9	11.6	1.9	2.3	4.0	1.7	1.2
P	1.5		1.2	1.7	3.3	1.6	1.9
Minor elements (g/1000 cm^3 x 10^{-3}):							
La		10.2			11.4	12.0	10.2
Ce		32.3			35.2	36.4	26.6
Nd		25.3			29.8	28.6	
Sm		8.3			9.2	9.4	8.3
Eu		3.0			3.3	3.1	3.0
Tb		2.3			2.6	2.4	2.1
Yb		6.2			7.0	9.1	7.9
Lu		0.9			1.1	1.5	1.1
Cr	607.2	610.6	652.4	529.2	517.6	533.0	506.9
Ni	414.0	193.7	243.6	243.0	243.9	236.6	224.6
Co	276.0	118.4	179.2	164.7	197.8	169.0	178.6
V	910.8	928.1	1055.6	1152.9	1260.2	1170.0	1172.2
Cu	143.5	820.5	324.8	513.0	542.0	538.2	279.4
Zn	828.0	328.2	268.8	337.5	319.8	325.0	265.0
Zr	262.2	223.3	212.8	259.2	252.0	247.0	224.6
Y		99.5	70.0	64.8	75.9	70.2	74.9
Nb		12.6	14.3	15.9	13.3	14.0	15.0
Rb		23.4		3.5			
Sr		430.4	420.0	351.0	365.9	364.0	374.4
Ba		16.1	44.8	270.0	352.3	223.6	149.8
H_2O^+ (wt%)	2.19	2.09	1.79	1.85	2.24	2.25	1.09
Density (g/cm^3)	2.76	2.69	2.80	2.70	2.71	2.60	2.88
Fe_2O_3/FeO	1.01		0.36	0.49	0.65	0.48	0.48

Table AT17 (continued).

Leg	61	61	61	61	61	61	61
Hole	462A	462A	462A	462A	462A	462A	462A
Core, section	24R-1	27R-2	28R-1	29R-2	30R-3	32R-1	44R-2
Interval (cm)	12-14	71-76	92-94	105-108	14-17	10-14	12-14
Piece	2B	6	4	1G		2A	2
Lab number	Z-1204	Z-1205	Z-1206	Z-1207	Z-1208	Z-1209	Z-1210
Depth (mbsf)	606.12	628.03	630.92	638.3	648.14	655.6	730.62
Major elements (g/1000 cm^3):							
Si	605.7	696.1	701.7	693.6	700.1	634.6	692.5
Ti	24.3	26.8	27.6	26.4	26.3	25.4	15.5
Al	230.4	214.5	220.7	212.1	219.5	215.0	234.0
Fe^{+++}	82.8	73.4	86.1	65.3	69.2	61.0	42.5
Fe^{++}	175.5	207.1	195.7	207.9	208.3	215.6	205.7
Fe (Sum)	258.3	280.4	281.8	273.2	277.5	276.6	248.2
Mn	4.7	5.3	5.4	4.8	4.8	5.3	5.5
Mg	127.6	131.6	128.3	133.4	135.2	128.0	151.4
Ca	215.9	226.7	236.2	220.4	217.2	213.2	259.9
Na	51.0	45.7	52.2	51.0	51.3	55.6	46.7
K	4.4	4.2	2.7	5.2	18.6	18.0	4.9
P	1.9	3.2	1.7	3.2	3.3	1.7	1.6
Minor elements (g/1000 cm^3 x 10^{-3}):							
La	13.6					14.9	
Ce	38.9					40.0	
Nd	30.6					31.5	
Sm	10.6					10.0	
Eu	3.6					3.1	
Tb	2.6					2.4	
Yb	9.2					7.4	
Lu	1.4					1.2	
Cr	569.9	604.8	550.8	612.7	620.7	614.9	1045.4
Ni	255.8	247.8	249.8	260.5	261.4	251.7	406.9
Co	180.7	180.0	171.6	186.5	157.4	157.3	166.3
V	1251.0	1200.7	1143.8	1198.8	1277.1	1278.4	1104.8
Cu	556.0	545.8	556.9	518.0	564.3	514.8	430.7
Zn	314.1	342.2	340.1	337.4	401.0	211.6	335.6
Zr	258.5	253.7	264.9	242.7	237.6	251.7	151.5
Y	91.7	88.5	93.3	88.8	89.1	85.8	62.4
Nb	14.7	15.6	16.0	14.5	14.3	16.0	9.8
Rb					8.9	10.6	5.3
Sr	361.4	354.0	361.2	325.6	326.7	246.0	264.3
Ba	200.2	268.5	252.8	225.0	204.9	208.8	44.6
H_2O^+ (wt%)	1.94	0.75	1.11	1.73	0.42	2.00	Trace
Density (g/cm^3)	2.78	2.95	3.01	2.96	2.97	2.86	2.97
Fe_2O_3/FeO	0.53	0.39	0.48	0.35	0.37	0.31	0.23

Table AT17 (continued).

Leg	61	61	61	61	61	61	61
Hole	462A	462A	462A	462A	462A	462A	462A
Core, section	47R-1	50R-3	51R-4	52R-4	53R-1	55R-2	57R-1
Interval (cm)	95-96	130-134	27-30	33-36	143-146	50-52	145-147
Piece	9	1E	1F	1	7B	4	13
Lab number	Z-1211	Z-1212	Z-1213	Z-1214	Z-1215	Z-1216	Z-1217
Depth (mbsf)	747.95	777.75	783.17	792.43	793.43	803.00	816.95
Major elements (g/1000 cm^3):							
Si	655.5	653.1	652.0	665.7	695.8	660.8	660.7
Ti	16.0	15.6	18.7	17.1	15.8	14.0	15.8
Al	234.7	230.7	214.4	229.4	231.5	227.8	225.0
Fe^{+++}	35.3	72.8	92.2	66.3	62.2	50.0	89.2
Fe^{++}	201.0	152.6	158.8	172.9	151.6	192.0	132.5
Fe (Sum)	236.3	225.4	250.9	239.2	213.8	242.0	221.7
Mn	5.4	4.2	3.8	4.8	4.8	3.0	4.9
Mg	151.8	145.1	118.2	152.1	165.2	169.2	148.4
Ca	252.7	246.3	207.4	258.9	243.0	257.4	250.5
Na	42.4	41.3	45.5	51.8	42.5	41.6	49.0
K	2.7	1.0	7.4	4.6	3.0	1.5	6.0
P	1.0	1.5	0.9	1.0	1.9	1.3	2.3
Minor elements (g/1000 cm^3 x 10^{-3}):							
La			7.6				
Ce		20.1	22.1				
Nd			18.2				
Sm		6.0	6.2				
Eu		2.3	2.2				
Tb		1.5	1.9				
Yb			5.3				
Lu		1.0	0.8				
Cr	1363.0	426.0	1162.0	944.0	949.9	944.0	884.2
Ni	551.0	227.2	392.0	404.2	404.2	386.5	377.3
Co	182.7	161.9	184.8	159.3	153.4	153.4	158.4
V	870.0	1184.3	1307.6	1032.5	1067.9	1017.8	1002.2
Cu	667.0	335.1	504.0	398.3	442.5	413.0	432.0
Zn	484.3	244.2	252.0	277.3	259.6	274.4	265.0
Zr	205.9	161.9	159.6	159.3	159.3	159.3	161.3
Y		62.5	56.0	62.0	62.0	56.1	57.6
Nb		7.4	8.1	8.3	9.7	10.3	7.2
Rb		4.8	14.0				3.2
Sr		258.4	246.4	250.8	259.6	259.6	256.3
Ba		22.7	131.6	17.7	91.5	32.5	23.0
H_2O^+ (wt%)	1.05	1.00	2.28	1.20	0.92	1.36	1.20
Density (g/cm^3)	2.90	2.84	2.80	2.95	2.95	2.95	2.88
Fe_2O_3/FeO	0.20	0.53	0.65	0.43	0.46	0.29	0.75

Table AT17 (continued).

Leg	61	61	61	61	61	61	61
Hole	462A	462A	462A	462A	462A	462A	462A
Core, section	62R-2	65R-1	74R-4	79R-5	80R-2	88R-3	89R-2
Interval (cm)	148-150	59-61	25-31	140-146	122-124	9-11	15-16
Piece	2F	3	1A	1J	3	1A	1
Lab number	Z-1218	Z-1219	Z-1220	Z-1221	Z-1222	Z-1223	Z-1224
Depth (mbsf)	863.46	877.09	950.41	992.35	996.49	1035.49	1038.1
Major elements (g/1000 cm^3):							
Si	673.2	677.9	671.3	645.8	673.1	657.7	669.5
Ti	16.3	17.6	20.3	18.7	19.7	20.8	20.1
Al	232.6	244.9	239.3	229.1	218.4	211.9	214.5
Fe^{+++}	71.1	68.3	80.0	86.5	59.1	96.9	107.1
Fe^{++}	149.9	177.6	172.8	146.7	197.2	141.8	157.6
Fe (Sum)	220.9	245.9	252.8	233.2	256.3	238.6	264.7
Mn	4.5	4.4	4.3	5.1	5.9	3.9	5.0
Mg	158.1	140.2	134.7	139.8	143.3	119.4	140.6
Ca	231.8	243.4	232.4	252.9	232.0	224.8	232.4
Na	42.1	43.2	44.8	47.4	41.8	46.4	49.2
K	2.9	0.7	15.4	2.4	5.6	2.1	6.1
P	2.7	1.4	1.5	1.3	2.9	1.2	2.4
Minor elements (g/1000 cm^3 x 10^{-3}):							
La		7.6	8.6			5.8	
Ce		17.8	18.5			15.5	
Nd							
Sm		6.5	6.6			4.3	
Eu		2.2	2.5			1.6	
Tb		1.6	1.8			1.2	
Yb		6.3	7.2			4.9	
Lu		1.0	1.1			0.7	
Cr	823.7	911.4	249.1	792.0	540.2	540.2	567.5
Ni	280.3	279.3	222.7	279.4	251.1	218.8	235.7
Co	138.7	152.9	164.1	155.5	163.5	160.7	163.0
V	968.2	1023.1	1148.6	1042.6	1138.8	1127.4	1155.3
Cu	433.5	441.0	468.8	432.0	496.4	484.8	523.8
Zn	326.6	270.5	293.0	282.2	388.4	326.9	352.1
Zr	164.7	164.6	190.5	169.9	201.5	188.4	197.9
Y	63.6	61.7	70.3	63.4	70.1	72.0	72.8
Nb	7.8	7.9	7.9	8.6	10.2	7.5	10.5
Rb			7.6			3.3	
Sr	260.1	279.3	281.3	279.4	277.4	268.7	282.3
Ba	20.2	17.6	337.0	46.1	134.3	138.5	90.2
H_2O^+ (wt%)	1.01	1.00	1.15	1.47	1.89	0.25	1.31
Density (g/cm^3)	2.89	2.94	2.93	2.88	2.92	2.77	2.91
Fe_2O_3/FeO	0.53	0.43	0.52	0.66	0.33	0.76	0.76

Table AT17 (continued).

Leg	61
Hole	462A
Core, section	90R-3
Interval (cm)	88-90
Piece	1H
Lab number	Z-1225
Depth (mbsf)	1045.38
Major elements (g/1000 cm^3):	
Si	641.6
Ti	20.5
Al	219.5
Fe^{+++}	94.0
Fe^{++}	181.4
Fe (Sum)	275.4
Mn	5.4
Mg	137.1
Ca	252.4
Na	43.2
K	1.7
P	1.4
Minor elements (g/1000 cm^3 x 10^{-3}):	
La	
Ce	
Nd	
Sm	
Eu	
Tb	
Yb	
Lu	
Cr	566.4
Ni	228.3
Co	159.0
V	1127.1
Cu	505.8
Zn	332.4
Zr	208.1
Y	75.1
Nb	13.3
Rb	
Sr	274.6
Ba	20.2
H_2O^+ (wt%)	1.35
Density (g/cm^3)	2.89
Fe_2O_3/FeO	0.58

Table AT18. Abundance of major and trace elements (g/1000 cm^3) in basalts, Hole 595B, Leg 91 (South Pacific). (Continued on next page.)

Leg	91	91	91	91	91	91	91
Hole	595B	595B	595B	595B	595B	595B	595B
Core, section	2-1	3-1	3-2	4-1	4-2	4-3	5-1
Interval (cm)	30-35	119-124	68-72	17-22	8-13	145-147	90-95
Piece	3	5B	3B	1B	1A	4C	6
Lab number	Z-429	Z-430	Z-431	Z-432	Z-433	Z-434	Z-435
Depth (mbsf)	73.3	82.69	83.68	87.57	88.98	91.85	97.4
Major elements (g/1000 cm^3):							
Si	631	582	569	598	587	563	572
Ti	53	50	49	45	52	47	49
Al	225	205	216	204	215	218	210
Fe^{+++}	93	146	179	151	134	130	162
Fe^{++}	105	70	54	88	77	72	70
Fe (Sum)	198	216	233	239	211	202	232
Mn	3.0	2.9	2.9	3.7	3.5	3.4	3.7
Mg	99	103	89	93	99	90	89
Ca	192	148	130	167	149	140	152
Na	66	71	72	68	72	83	70
K	18.0	20.0	30.0	17.0	19.0	25.0	23.0
P	2.7	3.6	3.6	2.6	3.0	2.7	4.0
Minor elements (g/1000 cm^3 x 10^{-3}):							
La	16.9	17.2	16.7	14.7	15.5	15.9	16.9
Ce	54.6	51.3	48.7	49.8	49.1	50.4	46.2
Nd	51.9	43.6	46.2	47.2	43.9	47.9	38.5
Sm	18.0	16.2	16.9	15.5	16.3	16.1	16.2
Eu	5.7	5.4	5.4	5.5	5.4	5.5	5.4
Tb	4.6	4.4	4.1	4.2	4.4	4.0	4.1
Yb	17.7	15.4	15.6	15.2	15.2	14.9	15.4
Lu	2.7	2.4	2.4	2.3	2.4	2.2	2.4
Cr	120	113	97	115	124	96	115
Ni	164	133	133	147	163	141	139
Co	158	123	85	110	134	121	118
V	1133	1005	923	1179	1550	1450	1104
Cu	164	154	121	262	139	197	118
Zn	382	321	282	341	297	290	321
Zr	437	385	436	446	439	429	436
Y	155.6	146.2	148.8	141.5	131.7	143.8	146.3
Nb	14.2	14.4	11.3	10.2	10.6	12.4	10.0
Rb	43.7	30.8	25.7	28.8	31.0	23.0	35.9
Sr	300	282	308	315	310	303	334
Ba	46		49				
H_2O^+ (wt%)	1.55	1.50	2.18	1.46	1.42	1.91	1.70
Density (g/cm^3)	2.61	2.56	2.57	2.62	2.58	2.52	2.57
Fe_2O_3/FeO	0.98	2.34	3.67	1.91	1.94	1.99	2.56

Table AT18 (continued).

Leg	91	91	91	91
Hole	595B	595B	595B	595B
Core, section	5-2	6-1	6-2	7-3
Interval (cm)	87-91	136-142	129-131	18-22
Piece	7A	14	15	4
Lab number	Z-436	Z-437	Z-438	Z-439
Depth (mbsf)	98.87	106.96	108.39	117.88
Major elements (g/1000 cm^3):				
Si	592	528	564	647
Ti	48	46	50	39
Al	212	259	221	231
Fe^{+++}	161	86	111	101
Fe^{++}	83	68	81	103
Fe (Sum)	244	154	192	204
Mn	4.4	4.1	4.1	4.4
Mg	92	73	76	114
Ca	151	137	153	219
Na	71	64	62	79
K	23.3	33.0	28.0	16.2
P	3.3	4.2	3.2	1.6
Minor elements (g/1000 cm^3 x 10^{-3}):				
La	16.9	16.6	16.2	11.0
Ce	50.0	50.5	49.7	33.9
Nd	44.8	45.7	47.3	31.1
Sm	15.8	15.9	16.4	11.9
Eu	5.5	5.3	5.5	3.7
Tb	4.2	4.1	4.5	3.1
Yb	15.8	15.9	15.4	11.9
Lu	2.4	2.3	2.4	1.8
Cr	124	106	99	378
Ni	147	139	124	237
Co	153	115	107	121
V	1106	830	970	819
Cu	132	111	149	178
Zn	290	277	286	212
Zr	448	361	423	268
Y	144.8	151.5	146.7	107.3
Nb	14.2	10.1	10.7	7.9
Rb	26.3	33.7	21.9	22.0
Sr	290	265	298	311
Ba				
H_2O^+ (wt%)	1.70	1.83	1.76	1.04
Density (g/cm^3)	2.63	2.40	2.49	2.82
Fe_2O_3/FeO	2.17	1.41	1.53	1.09

Table AT19. Abundance of major and trace elements (g/1000 cm^3) in basalts, Hole 765D, Leg 123 (Argo Abyssal Plain, Indian Ocean).

Leg	123	123	123	123	123	123	123	123
Hole	765D	765D	765D	765D	765D	765D	765D	765D
Core, section	5R-5	7R-2	9R-1	17R-2	18R-1	22R-1	27R-2	27R-3
Inteval (cm)	143-145	135-137	17-21	49-52	82-84	2-4	31-33	4-6
Piece	3B	6B	1A	6	1E	1A	1C	1
Lab number	Z-89	Z-80	Z-81	Z-83	Z-90	Z-88	Z-85	Z-84
Depth (mbsf)	990.63	1004.85	1021.07	1093.69	1101.92	1138.62	1187.21	1188.44
Major elements (g/1000 cm^3):								
Si	644	655	649	655	676	654	668	604
Ti	23	30	28	30	28	26	31	29
Al	228	227	233	218	237	237	216	199
Fe^{+++}	85	66	84	67	141	87	102	148
Fe^{++}	122	113	123	143	121	158	127	146
Fe (Sum)	207	179	207	210	262	245	229	294
Mn	1.8	3.5	3.6	4.2	3.0	6.7	3.8	5.1
Mg	135	116	133	125	122	110	111	92.4
Ca	253	248	256	250	259	297	233	230
Na	56	61	58	58	63	49	66	59
K	2.4	19.0	3.4	7.4	20.2	10.2	18.3	19.7
P	1.0	1.1	1.3	1.6	1.0	1.3	1.6	1.6
Minor elements (g/1000 cm^3 x 10^{-3}):								
La	4.8	5.6	5.4	7.3	6.0	5.0	7.4	8.0
Ce	18.6	17.6	16.2	24.8	20.7	15.4	23.7	19.8
Sm	7.6	9.2	8.5	11.9	8.7	8.0	10.6	11.0
Eu	3.1	3.4	3.1	3.7	3.3	3.0	3.7	3.6
Tb	2.2	2.5	2.3	3.4	2.2	2.3	2.9	3.0
Yb	8.5	10.1	10.5	13.3	9.6	9.8	12.0	12.7
Lu	1.2	1.5	1.7	2.0	1.5	1.5	1.9	2.0
Sc	144	148	145	147	144	148	152	116
Cr	522	770	626	565	795	504	386	427
Ni	211	252	313	215	300	267	166	182
Co	113	140	137	141	165	157	117	105
V	677	812	896	776	960	844	864	846
Cu	169	90	230	130	225	252	72	105
Zn	226	224	273	246	270	255	343	251
Zr	195	182	219	240	300	154	249	209
Y	84.6	86.8	91.1	115.7	93.0	83.0	111.6	101.9
Nb	5.6	3.1	4.0	4.5	8.4	3.9	4.3	4.4
Rb		30.8		11.6	51.0	26.0	51.5	55.1
Sr	276	227	285	229	267	222	217	218
Ba		176	120	113	30	30		
H_2O^+ (wt%)	1.16	0.47	0.35	0.60	0.78	0.42	0.59	0.93
Density (g/cm^3)	2.82	2.80	2.85	2.82	3.00	2.96	2.86	2.75
Fe_2O_3/FeO	0.77	0.65	0.76	0.52	1.30	0.62	0.89	1.12

Table AT20. Abundance of major and trace elements (g/1000 cm^3) in basalts, Holes 801B and 801C, Leg 129 (Pigafetta Basin, Pacific Ocean). (Continued on next three pages.)

Leg	129	129	129	129	129	129	129
Hole	801B	801B	801B	801B	801B	801B	801B
Core, section	40R-1	41R-1	41R-1	42R-1	43R-2	43R-3	43R-4
Interval (cm)	29-33	26-31	130-136	87-91	10-15	126-129	32-40
Piece	5	3	3	5B	1B	17	4A
Lab number	Z-776	Z-777	Z-778	Z-779	Z-780	Z-781	Z-782
Depth (mbsf)	477.19	483.26	484.30	488.47	493.67	496.24	496.80
Major elements (g/1000 cm^3):							
Si	614.7	561.2	573.5	579.4	546.0	485.9	530.6
Ti	53.1	52.1	51.7	48.1	41.8	41.5	50.9
Al	248.3	222.7	222.8	243.3	199.4	198.0	230.3
Fe^{+++}	95.8	87.3	79.7	94.0	88.5	54.3	91.3
Fe^{++}	14.8	96.2	119.8	89.3	125.4	72.5	101.5
Fe (Sum)	110.6	183.5	199.5	183.3	213.9	126.8	192.8
Mn	1.5	2.8	3.1	2.9	3.2	9.2	3.9
Mg	42.8	82.3	78.1	100.7	141.5	48.5	61.9
Ca	33.2	154.7	145.4	157.4	125.4	156.4	112.0
Na	50.6	74.2	73.3	69.1	64.7	52.1	85.9
K	119.9	46.6	57.7	43.6	38.7	91.7	48.8
P	7.2	7.1	7.1	6.5	5.7	5.5	7.5
Minor elements (g/1000 cm^3 x 10^{-3}):							
La	89.3	79.9	96.2		75.4		90.7
Ce	183.5	167.2	196.5		124.8		181.4
Nd	89.3	81.2	94.0		70.2		95.8
Sm	19.6	19.1	19.6		17.2		22.2
Eu	5.7	6.1	6.5		4.9		5.8
Tb	3.0	2.7			2.4		3.0
Yb	5.0	6.1	6.9		5.5		7.6
Lu	0.7	0.8	1.2		0.9		1.2
Cr	220.7	191.3	161.7	357.8	634.4	191.1	257.0
Ni	163.7	120.5	119.3	192.2	626.6	156.8	168.8
Co							
V	491.0	699.5	728.8	614.1	525.2	519.4	650.2
Cu	49.6	115.3	116.6	112.1	85.8	88.2	100.8
Pb	2.5	7.9	26.5	5.3	20.8	22.1	12.6
Zn	183.5	235.8	238.5	210.9	241.8	176.4	367.9
Zr	515.8	712.6	755.3	656.8	590.2	534.1	619.9
Y	67.0	83.8	84.8	77.4	70.2	76.0	80.6
Nb	126.5	125.8	129.9	117.5	104.0	98.0	100.8
Rb	218.2	102.2	137.8	106.8	101.4	142.1	110.9
Sr	332.3	1357.2	1356.8	1463.2	1073.8	595.4	1018.1
Ba	1006.9	1084.7	1118.3	974.6	1255.8	1011.9	1378.4
H_2O^+ (wt%)	3.77	2.00	1.55	2.32	2.91	2.30	3.26
Density (g/cm^3)	2.48	2.62	2.65	2.67	2.60	2.45	2.52
Fe_2O_3/FeO	7.19	1.01	0.74	1.17	0.78	0.83	1.00

Table AT20 (continued).

Leg	129	129	129	129	129	129	129
Hole	801B	801B	801B	801C	801C	801C	801C
Core, section	44R-1	44R-2	44R-3	1R-1	1R-2	2R-1	2R-5
Interval (cm)	107-113	27-32	28-33	109-114	11-17	1-6	101-106
Piece	2E	4A	2	2G	1A	1A	2
Lab number	Z-783	Z-784	Z-785	Z-786	Z-787	Z-788	Z-789
Depth (mbsf)	502.77	503.42	504.91	494.79	495.06	503.01	509.5
Major elements (g/1000 cm^3):							
Si	560.7	615.4	544.0	530.2	563.1	594.4	562.3
Ti	48.7	50.2	46.3	42.4	44.9	49.0	49.1
Al	233.9	240.0	222.8	196.9	210.0	232.4	232.9
Fe^{+++}	75.3	67.2	71.4	63.9	76.5	62.1	73.0
Fe^{++}	62.4	65.1	95.7	125.6	130.6	57.2	123.6
Fe (Sum)	137.7	132.2	167.1	189.5	207.1	119.3	196.6
Mn	3.5	2.6	2.6	2.9	3.1	2.5	3.2
Mg	45.9	46.8	62.0	145.9	150.3	38.7	97.2
Ca	77.5	65.2	126.4	116.6	120.9	41.1	126.8
Na	57.7	60.8	74.0	64.7	71.9	45.9	71.2
K	94.6	120.6	46.9	36.7	40.3	130.0	47.8
P	6.2	6.2	6.1	6.6	6.2	6.4	6.1
Minor elements (g/1000 cm^3 x 10^{-3}):							
La	67.0	81.5	70.2	69.0	88.1	72.9	73.4
Ce	140.4	170.2	147.3	144.9	170.9	223.6	201.7
Nd	62.0	82.9	80.2	75.6	90.8	102.1	107.4
Sm	15.3	17.8	17.2	16.1	19.8	17.0	17.8
Eu	5.1	5.9	5.7	5.2	5.6	4.9	5.0
Tb	2.2		2.6	2.3	3.2	2.7	2.6
Yb		6.5	6.3	5.2	5.9	5.3	6.8
Lu		1.0	0.9	0.8	1.0	0.6	0.9
Cr	305.0	332.8	223.6	388.1	427.2	318.3	220.1
Ni	265.4	238.1	143.4	496.4	566.0	289.2	146.7
Co							
V	704.3	647.7	590.5	607.3	547.4	617.2	631.4
Cu	86.8	107.5	87.5	100.8	106.8	89.9	115.3
Pb	2.5	20.5	24.3	2.5	8.0	4.9	2.6
Zn	215.8	176.6	201.7	216.7	227.0	131.2	204.4
Zr	530.7	650.2	651.2	609.8	638.1	626.9	668.1
Y	67.0	79.4	80.2	68.0	74.8	85.1	81.2
Nb	104.2	112.6	106.9	103.3	112.1	109.4	104.8
Rb	156.2	171.5	111.8	100.8	109.5	160.4	110.0
Sr	620.0	796.2	1283.0	914.8	961.2	388.8	1307.4
Ba	1083.8	1359.4	962.3	1076.0	1316.3	1215.0	1079.4
H_2O^+ (wt%)	3.34	2.06	1.40	3.77	3.44	2.92	1.77
Density (g/cm^3)	2.48	2.56	2.43	2.52	2.67	2.43	2.62
Fe_2O_3/FeO	1.34	1.34	0.83	0.57	0.65	1.21	0.66

Table AT20 (continued).

Leg	129	129	129	129	129	129	129
Hole	801C	801C	801C	801C	801C	801C	801C
Core, section	3R-1	4R-1	4R-2	5R-1	5R-2	5R-3	5R-5
Interval (cm)	42-48	18-21	111-114	45-52	12-17	98-100	55-58
Piece	2C	4	13	2C	1A	4B	3C
Lab number	Z-790	Z-791	Z-792	Z-793	Z-794	Z-795	Z-796
Depth (mbsf)	512.63	521.88	524.18	531.65	532.58	534.75	537.24
Major elements (g/1000 cm^3):							
Si	505.1	970.3	1002.9	528.4	561.8	582.1	654.0
Ti	43.3	0.4	0.3	18.6	15.3	18.2	14.1
Al	203.3	1.7	8.6	286.6	208.4	270.0	239.3
Fe^{+++}	72.8	152.6	163.2	42.0	113.4	74.7	45.1
Fe^{++}	15.9	5.3	4.2	21.6	25.1	17.5	146.5
Fe (Sum)	88.7	158.0	167.4	63.7	138.5	92.2	191.6
Mn	0.8	0.4	0.4	2.1	3.5	0.8	3.9
Mg	41.0	5.7	3.6	52.9	52.0	32.5	176.9
Ca	28.4		1.9	300.3	166.3	167.7	244.2
Na	34.6	1.9	1.1	60.7	36.9	49.0	45.9
K	96.5	2.0	0.8	19.6	91.1	16.3	1.0
P	5.5	0.2	0.2	0.2	0.1	1.3	0.6
Minor elements (g/1000 cm^3 x 10^{-3}):							
La	67.3	1.1	1.5	4.6		4.8	3.5
Ce	153.0	2.1	2.2	18.0		16.0	12.5
Nd	73.4			21.2		18.9	14.0
Sm	15.1	0.2	0.2	6.7		8.0	5.8
Eu	4.7	0.1	0.1	2.7		3.1	2.4
Tb	2.2			1.6		2.1	2.0
Yb	5.3	0.1	0.1	5.9		4.8	6.4
Lu	0.9			0.9		0.8	0.9
Cr	316.2	44.8	49.2	885.1	722.9	742.9	1484.1
Ni	202.0	56.6	61.5	254.4	183.2	118.6	494.7
Co		33.0	34.4			48.4	171.7
V	579.4	153.4	135.3	731.4	364.0	609.8	611.1
Cu	112.2	61.4	64.0	214.7	218.4	326.7	238.6
Pb	2.0			2.7	5.0		
Zn	173.4	167.6	127.9	137.8	160.6	159.7	227.0
Zr	505.9	8.7	13.3	196.1	160.6	174.2	139.7
Y	65.3	2.4	3.7	71.6	47.7	58.1	61.1
Nb	93.8			5.3	10.0	5.1	
Rb	144.8	4.0	4.9	34.5	193.3	17.7	3.5
Sr	228.5	8.3	8.4	424.0	308.7	508.2	291.0
Ba	871.1	11.8	9.8	58.3	118.0	7.3	37.8
H_2O^+ (wt%)	4.00	1.24	1.58	2.02	2.53	2.32	0.59
Density (g/cm^3)	2.04	2.36	2.46	2.65	2.51	2.42	2.91
Fe_2O_3/FeO	5.09	31.93	43.18	2.16	5.03	4.73	0.34

Table AT20 (continued).

Leg	129	129	129	129
Hole	801C	801C	801C	801C
Core, section	7R-1	7R-3	8R-1	10R-1
Interval (cm)	53-58	38-41	9-12	55-60
Piece	4C	1E	2C	1G
Lab number	Z-797	Z-798	Z-799	Z-800
Depth (mbsf)	550.63	553.36	559.59	569.55
Major elements (g/1000 cm^3):				
Si	634.5	601.3	607.9	677.6
Ti	32.6	33.4	33.6	28.5
Al	197.1	204.1	198.7	217.7
Fe^{+++}	68.8	84.9	43.6	78.3
Fe^{++}	199.4	131.8	166.0	185.7
Fe (Sum)	268.2	216.7	209.6	264.1
Mn	4.4	3.2	4.8	4.1
Mg	118.1	108.0	91.3	128.8
Ca	224.4	224.6	248.7	250.5
Na	55.9	58.5	59.1	55.7
K	1.9	1.4	4.5	1.5
P	2.0	1.8	2.2	0.8
Minor elements (g/1000 cm^3 x 10^{-3}):				
La	15.1			10.2
Ce	42.5			31.7
Nd	37.5			31.3
Sm	11.9			10.1
Eu	4.2			3.9
Tb				
Yb	12.3			10.8
Lu	2.1			1.8
Cr	393.4	460.7	476.0	514.5
Ni	199.5	178.9	173.6	205.8
Co		154.5	140.0	
V	1169.0	1409.2	1237.6	1073.1
Cu	227.6	178.9	131.6	220.5
Pb	14.1			17.6
Zn	275.4	325.2	420.0	249.9
Zr	334.4	298.1	308.0	285.2
Y	123.6	103.0	114.8	111.7
Nb	14.1	10.3	6.4	14.7
Rb	2.8		8.7	2.9
Sr	320.3	352.3	336.0	332.2
Ba	89.9	35.2		41.2
H_2O^+ (wt%)	0.59	0.76	1.61	0.55
Density (g/cm^3)	2.81	2.71	2.80	2.94
Fe_2O_3/FeO	0.38	0.72	0.29	0.47

Table AT21. Abundance of major and trace elements (g/1000 cm^3) in hawaiites, Hole 430A, Leg 55 (Ojin seamount, Emperor Seamount chain).

Leg	55	55	55	55	55	55	55
Hole	430A	430A	430A	430A	430A	430A	430A
Core, section	5R-4	5R-5	5R-5	6R-1	6R-1	6R-2	6R-3
Interval (cm)	105-108	33-37	96-101	6-11	98-103	24-30	19-24
Piece	12	5	10	1	7B	4	2
Lab number	Z-1110	Z-1111	Z-1619	Z-1620	Z-1622	Z-1112	Z-1623
Depth (mbsf)	72.05	72.83	73.76	76.06	76.98	77.74	79.19
Major elements (g/1000 cm^3):							
Si	457.3	439.1	583.4	623.8	618.1	494.7	605.1
Ti	40.8	36.1	48.8	50.8	52.6	39.5	46.4
Al	172.7	156.6	215.2	224.6	233.5	177.9	227.7
Fe^{+++}	177.2	134.9	146.1	173.9	108.7	126.2	153.9
Fe^{++}	34.8	48.9	84.7	63.7	161.2	83.7	100.7
Fe (Sum)	212.0	183.8	230.9	237.6	269.9	209.9	254.6
Mn	3.9	1.5	1.8	1.7	2.9	2.3	3.0
Mg	24.4	42.1	64.8	56.5	85.1	72.2	78.5
Ca	141.6	93.4	122.1	133.2	169.9	98.5	119.4
Na	66.8	63.8	82.1	87.4	76.5	71.7	89.2
K	45.0	27.2	33.6	36.1	24.2	31.6	35.2
P	14.8	13.2	17.2	18.5	6.7	16.0	15.0
Minor elements (g/1000 cm^3 x 10^{-3}):							
La	95.5	84.9		110.3			113.8
Ce	238.7	212.3		295.9			298.1
Nd	143.2	125.5		174.9			178.9
Sm	36.9	32.8		45.7			46.1
Eu	11.1	9.7		15.3			15.2
Tb	4.8	4.1		7.0			7.0
Yb	7.8	6.8		10.2			10.0
Lu	1.2	0.8		1.6			1.6
Cr				53.8	252.0		230.4
Ni	45.6	54.0	61.4	75.3	148.4	46.6	135.5
Co	65.1	69.5	81.9	96.8	126.0	66.6	89.4
V	394.9	362.8	455.7	473.4	604.8	277.5	517.6
Cu	58.6	90.7	125.4	75.3	156.8	59.9	170.7
Zn	225.7	310.7	363.5	320.1	313.6	355.2	406.5
Zr	1009.1	887.8	1177.6	1264.3	518.0	1043.4	1273.7
Y	115.0	100.4	140.8	134.5	72.8	113.2	149.1
Nb	82.5	73.3	97.3	99.5	81.2	86.6	32.5
Rb	52.1	38.6	58.9	61.9	42.0	37.7	40.7
Sr	1388.8	1312.4	1510.4	1721.6	1358.0	1287.6	1653.1
Ba	651.0	540.4	512.0	672.5	616.0	499.5	840.1
H_2O^+ (wt%)	0.45	1.38	0.95	0.54	0.94	1.43	1.96
Density (g/cm^3)	2.17	1.93	2.56	2.69	2.80	2.22	2.71
Fe_2O_3/FeO	5.66	3.07	1.92	3.03	0.75	1.68	1.70

Table AT22. Abundance of major and trace elements (g/1000 cm^3) in basalts of alkalic series, Hole 432A, Leg 55 (Nintoku seamount, Emperor Seamount chain).

Leg	55	55	55	55	55	55	55	55
Hole	432A	432A	432A	432A	432A	432A	432A	432A
Core, section	2R-1	2R-2	2R-3	3R-1	3R-2	4R-3	4R-4	5R-1
Interval (cm)	99-104	102-107	43-48	9-12	15-20	140-145	80-83	100-105
Piece	8E	11E	1E	1	2	14	6B	2B
Lab number	Z-1624	Z-1627	Z-1629	Z-1113	Z-1631	Z-1633	Z-1114	Z-1635
Depth (mbsf)	42.49	43.52	44.93	55.09	55.15	68.90	69.70	72.00
Major elements (g/1000 cm^3):								
Si	601.6	592.8	545.2	461.1	648.9	582.2	560.0	628.6
Ti	44.6	42.2	32.7	46.5	54.4	52.7	54.1	51.9
Al	241.5	261.5	269.5	223.5	239.8	242.8	222.9	228.7
Fe^{+++}	100.2	153.6	173.7	232.5	111.0	194.4	199.0	100.5
Fe^{++}	132.5	71.3	28.6	21.5	141.1	99.1	80.3	119.6
Fe (Sum)	232.7	224.9	202.3	253.9	252.0	293.5	279.3	220.0
Mn	2.0	2.1	1.0	3.6	3.6	5.0	5.1	2.6
Mg	97.6	53.1	32.6	21.9	86.8	57.3	56.6	74.6
Ca	182.6	184.6	167.6	47.3	192.5	116.4	102.1	158.5
Na	62.7	72.5	68.8	44.7	78.7	68.8	69.6	83.8
K	19.3	25.3	25.5	42.2	31.5	33.8	28.7	40.2
P	7.2	7.9	5.1	6.5	7.3	6.4	7.3	8.3
Minor elements (g/1000 cm^3 x 10^{-3}):								
La				63.0	71.5	67.9		
Ce				138.6	151.6	135.7		
Nd				71.4	85.8	78.3		
Sm				16.2	19.2	17.5		
Eu				4.8	4.3	4.2		
Tb				2.5	2.6	2.2		
Yb				4.6	5.7	4.7		
Lu				0.7	0.9	0.8		
Cr	269.5	212.5	185.0	178.5	214.5	229.7	231.3	53.8
Ni	203.5	172.2	165.0	105.0	137.3	161.8	138.8	64.6
Co	165.0	118.4	97.5	69.3	105.8	114.8	123.4	86.1
V	682.0	583.7	550.0	401.1	600.6	569.0	586.0	451.9
Cu	242.0	172.2	125.0	132.3	171.6	146.2	161.9	80.7
Zn	316.3	247.5	230.0	315.0	343.2	323.6	380.4	328.2
Zr	440.0	457.3	350.0	483.0	572.0	522.0	514.0	1237.4
Y	57.8	56.5	47.5	54.6	77.2	65.3	72.0	137.2
Nb	71.5	75.3	57.5	79.8	91.5	83.5	82.2	102.2
Rb	35.8	45.7	45.0	58.8	54.3	52.2	51.4	53.8
Sr	1523.5	1802.3	1850.0	546.0	1401.4	1096.2	1053.7	1614.0
Ba	687.5	753.2	562.5	191.1	543.4	430.7	462.6	591.8
H_2O^+ (wt%)	1.51	0.98	0.93	4.50	1.27	3.10	2.71	1.42
Density (g/cm^3)	2.75	2.69	2.50	2.10	2.86	2.61	2.57	2.69
Fe_2O_3/FeO	0.84	2.39	6.75	12.05	0.87	2.18	2.76	0.93

Table AT23. Abundance of major and trace elements (g/1000 cm^3) in basalts of tholeiitic series, Hole 433C, Leg 55 (Suiko seamount, Emperor Seamount chain). (Continued on next seven pages.)

Leg	55	55	55	55	55	55	55
Hole	433C	433C	433C	433C	433C	433C	433C
Core, section	10R-4	12R-1	12R-2	12R-3	13R-2	14R-4	14R-4
Interval (cm)	118-121	75-80	136-141	54-57	69-72	26-31	47-52
Piece	8B	8A	3C	1D	1J	2A	2B
Lab number	Z-1115	Z-1116	Z-1645	Z-1117	Z-518	Z-1648	Z-1649
Depth (mbsf)	210.21	224.25	226.36	227.04	232.19	237.76	237.97
Major elements (g/1000 cm^3):							
Si	451.5	339.9	563.1	564.1	640.0	590.0	625.1
Ti	14.5	23.2	39.0	36.7	40.2	41.7	39.6
Al	98.1	120.7	201.8	189.1	198.0	191.1	208.1
Fe^{+++}	207.3	151.3	109.5	86.5	123.1	148.2	98.4
Fe^{++}		40.4	145.3	141.9	144.5	125.8	157.5
Fe (Sum)	207.3	191.8	254.8	228.4	267.6	274.0	255.9
Mn	3.2	0.9	1.4	2.4	4.9	2.9	2.9
Mg	258.6	84.3	151.8	116.4	134.9	120.9	105.6
Ca	100.7	50.2	170.6	174.3	219.5	174.9	185.9
Na	21.9	30.9	50.8	51.9	52.0	62.5	49.0
K	5.0	23.1	6.6	6.8	11.1	5.2	6.1
P	1.6	1.9	3.1	2.8	3.4	3.1	3.7
Minor elements (g/1000 cm^3 x 10^{-3}):							
La	12.1	22.7	26.2		34.2		
Ce	30.9	61.6	68.1		79.8		
Nd	19.3	38.9	44.5		51.3		
Sm	5.2	10.7	13.4		13.7		
Eu	1.1	3.2	3.4		4.6		
Tb	0.8	2.6	2.1		2.9		
Yb	2.1	4.7	5.0		5.7		
Lu	0.4	0.8	1.0		0.8		
Cr	2058.7	413.1	707.4	615.0	427.5	169.0	223.3
Ni	1808.8	228.4	364.2	361.4	219.5	139.9	153.3
Co	273.7	82.6	162.4	138.1	136.8	142.6	204.4
V	478.4	405.0	948.4	898.6	783.8	908.2	1143.3
Cu	135.7	209.0	243.7	286.1	208.1	245.5	244.8
Zn	238.0	149.0	251.5	258.5	256.5	258.7	269.0
Zr	152.3	226.8	366.8	326.3	399.0	396.0	376.6
Y	26.2	56.7	65.5	67.8	77.0	73.9	72.6
Nb	12.4	17.8	31.4	27.6	37.1	29.0	29.6
Rb	10.7	38.9	2.6	9.3	10.3	3.7	
Sr	211.8	291.6	707.4	690.3	769.5	739.2	753.2
Ba	97.6	56.7	165.1	276.1	202.4	147.8	322.8
H_2O^+ (wt%)	5.52	4.26	1.80	1.22	1.60	0.49	1.06
Density (g/cm^3)	2.38	1.62	2.62	2.51	2.85	2.64	2.69
Fe_2O_3/FeO		4.16	0.84	0.68	0.95	1.31	0.69

Table AT23 (continued).

Leg	55	55	55	55	55	55	55
Hole	433C	433C	433C	433C	433C	433C	433C
Core, section	15R-5	15R-5	15R-6	17R-1	19R-1	21R-3	23R-1
Interval (cm)	82-87	88-92	31-32	64-69	48-54	20-23	100-104
Piece	4B	4B	1C	5A	4C	2	5D
Lab number	Z-1118	Z-519	Z-1119	Z-1120	Z-1655	Z-520	Z-1121
Depth (mbsf)	249.32	249.38	250.06	256.14	261.98	282.20	299.00
Major elements (g/1000 cm^3):							
Si	559.0	600.9	655.7	698.3	552.6	591.8	471.8
Ti	44.1	45.2	45.2	47.0	42.8	35.5	28.9
Al	206.0	195.5	215.1	214.2	185.7	211.0	146.5
Fe^{+++}	181.5	203.0	297.1	47.0	138.8	134.6	233.3
Fe^{++}	96.1	86.3		241.8	94.4	113.6	
Fe (Sum)	277.6	289.3	297.1	288.8	233.2	248.2	233.3
Mn	2.4	2.5	4.1	4.4	2.9	1.1	1.2
Mg	104.5	111.5	115.0	110.9	111.6	129.3	120.7
Ca	146.5	180.0	225.4	242.4	153.1	173.3	74.6
Na	62.7	58.2	54.4	55.3	53.4	54.3	40.2
K	19.4	14.0	5.9	11.0	20.6	7.7	18.6
P	3.5	3.7	3.6	3.2	3.4	3.6	0.6
Minor elements (g/1000 cm^3 x 10^{-3}):							
La		32.3		32.9	20.3	32.3	22.3
Ce		75.3		86.7	54.6	80.7	58.0
Nd		56.5		62.8	37.2	53.8	37.9
Sm		16.9		18.8	11.2	15.3	10.5
Eu		5.9		6.3	3.0	5.4	3.1
Tb		3.2		4.2	2.2	3.2	1.9
Yb		7.3		6.9	5.0	5.9	3.6
Lu		1.0		1.1	0.8	0.8	0.5
Cr	148.5	215.2	180.0	224.3	193.4	529.9	586.5
Ni	133.1	148.0	150.5	158.5	156.2	290.5	501.8
Co	97.3	123.7	123.9	137.5	148.8	129.1	133.8
V	696.3	812.4	643.1	753.5	845.7	672.5	593.2
Cu	212.5	209.8	206.5	173.4	218.2	142.6	173.9
Zn	322.6	363.2	368.8	391.7	218.2	287.8	218.5
Zr	409.6	430.4	442.5	478.4	322.4	403.5	289.9
Y	69.1	86.1	88.5	89.7	59.5	78.0	31.2
Nb	25.6	35.0	32.5	32.9	27.3	32.3	21.4
Rb	12.0	6.2	3.8	9.3	14.6	3.0	40.1
Sr	716.8	780.1	870.3	837.2	570.4	780.1	446.0
Ba	94.7	193.7	241.9	314.0	195.9	191.0	116.0
H_2O^+ (wt%)	0.56	0.50	0.42	0.33	1.86	2.67	3.28
Density (g/cm^3)	2.56	2.69	2.95	2.99	2.48	2.69	2.23
Fe_2O_3/FeO	2.10	2.61		0.22	1.63	1.32	

Table AT23 (continued).

Leg	55	55	55	55	55	55	55
Hole	433C	433C	433C	433C	433C	433C	433C
Core, section	24R-1	24R-7	24R-7	24R-7	24R-7	27R-2	27R-6
Interval (cm)	12-15	104-108	108-114	133-139	141-144	131-134	38-43
Piece	2	3B	3C	3F	3G	6B	1H
Lab number	Z-1122	Z-522	Z-1662	Z-1123	Z-1124	Z-1125	Z-1126
Depth (mbsf)	307.62	317.24	317.28	317.53	317.61	338.81	343.88
Major elements (g/1000 cm^3):							
Si	570.2	606.7	592.2	597.3	589.4	544.2	
Ti	21.1	14.9	23.3	21.8	21.0	17.1	
Al	136.7	132.2	118.7	140.7	132.6	112.6	
Fe^{+++}	263.4	113.2	35.7	69.3	276.8	271.4	
Fe^{++}		165.8	214.8	200.9			
Fe (Sum)	263.4	279.0	250.5	270.3	276.8	271.4	
Mn	3.7	1.8	3.2	3.7	3.7	3.7	
Mg	312.8	372.7	424.7	377.6	374.1	415.2	
Ca	118.3	91.9	107.9	105.5	107.6	81.1	
Na	23.6	33.6	36.3	27.2	33.4	19.6	
K	2.8	24.1	30.4	5.1	25.4	3.0	
P	1.5	1.3	1.4	1.4	1.7	1.2	
Minor elements (g/1000 cm^3 x 10^{-3}):							
La		10.6		12.8			
Ce		24.1		34.8			
Nd		18.7		37.7			
Sm		6.3		7.8			
Eu		2.4		2.4			
Tb		1.3		1.4			
Yb		2.9		3.5			
Lu		0.4		0.6			
Cr	1987.7	1808.1	2044.5	2465.0	2423.6	2678.4	321
Ni	1779.2	2353.4	1972.0	1653.0	1722.8	1925.1	373
Co	266.9	258.3	240.7	295.8	262.8	334.8	99
V	628.3	490.8	371.2	643.8	601.5	574.7	624
Cu	166.8	89.0	153.7	205.9	154.8	203.7	222
Zn	328.0	246.8	234.9	342.2	338.7	340.4	202
Zr	194.6	149.2	179.8	194.3	198.6	186.9	
Y	44.5	40.2	40.6	40.6	40.9	33.5	
Nb	12.0	9.5	11.9	11.6	13.7	13.7	
Rb	5.8	34.4	40.6	9.0	43.8	10.0	
Sr	305.8	861.0	319.0	263.9	350.4	198.1	
Ba	214.1	221.0	243.6	156.6	169.4	97.7	
H_2O^+ (wt%)	4.89	2.64	3.17	4.59	3.36	4.46	5.68
Density (g/cm^3)	2.78	2.87	2.90	2.90	2.92	2.79	1.71
Fe_2O_3/FeO		0.76		0.38			6.20

Table AT23 (continued).

Leg	55	55	55	55	55	55	55
Hole	433C	433C	433C	433C	433C	433C	433C
Core, section	28R-1	28R-2	28R-2	28R-4	28R-4	28R-5	28R-5
Interval (cm)	42-47	19-21	66-73	30-37	57-65	77-81	107-109
Piece	2E	1D	4B	2C	5A	7B	6E
Lab number	Z-1668	Z-1127	Z-1128	Z-1129	Z-1672	Z-524	Z-1130
Depth (mbsf)	345.92	347.19	347.66	350.30	350.57	352.27	352.57
Major elements (g/1000 cm^3):							
Si	598.7	624.0	627.3	611.5	547.8	671.1	643.2
Ti	43.6	42.0	41.3	38.5	34.5	46.8	46.5
Al	200.6	201.5	207.4	203.6	182.3	220.8	208.4
Fe^{+++}	144.4	252.2	96.4	108.9	97.6	99.4	267.4
Fe^{++}	110.7		163.6	119.2	106.7	171.4	
Fe (Sum)	255.1	252.2	260.0	228.1	204.3	270.8	267.4
Mn	3.0	3.4	3.2	3.1	2.8	4.1	3.5
Mg	131.0	113.2	118.7	143.6	128.7	101.5	109.7
Ca	184.0	200.3	191.7	152.4	136.5	215.2	211.5
Na	59.1	50.7	53.8	52.9	47.4	55.6	53.7
K	8.4	4.3	6.6	26.1	23.4	9.2	4.9
P	3.2	3.0	3.1	3.2	2.9	4.2	4.1
Minor elements (g/1000 cm^3 x 10^{-3}):							
La						40.5	
Ce						101.2	
Nd						69.4	
Sm						20.5	
Eu						6.4	
Tb						4.0	
Yb						8.1	
Lu						1.2	
Cr	446.5	409.5	425.9	471.5	401.5	309.2	475.4
Ni	188.3	169.3	172.0	195.1	160.1	170.5	200.9
Co	150.6	125.6	120.1	135.5	95.6	124.3	147.2
V	914.6	627.9	636.1	953.9	831.7	728.3	962.2
Cu	204.4	240.2	226.6	170.7	217.5	225.4	240.6
Zn	282.5	368.6	354.9	365.9	229.4	375.7	350.9
Zr	430.4	409.5	409.5	406.5	382.4	520.2	481.1
Y	83.4	73.7	76.4	75.9	98.0	89.6	93.4
Nb	32.3	30.0	30.0	29.8	26.3	37.6	36.8
Rb	7.0	5.2	3.5	37.9	93.2	25.7	4.2
Sr	753.2	737.1	737.1	704.6	525.8	867.0	820.7
Ba	118.4	196.6	286.7	219.5	160.1	237.0	339.6
H_2O^+ (wt%)	0.52	0.59	0.77	1.32		0.52	0.59
Density (g/cm^3)	2.69	2.73	2.73	2.71	2.39	2.89	2.83
Fe_2O_3/FeO	1.45		0.65	1.02		0.64	

Table AT23 (continued).

Leg	55	55	55	55	55	55	55
Hole	433C	433C	433C	433C	433C	433C	433C
Core, section	31R-1	32R-1	34R-2	34R-3	34R-7	35R-6	36R-3
Interval (cm)	86-90	82-88	41-46	60-64	103-109	59-64	90-95
Piece	1L	3C	1K	1F	3L	1E	1K
Lab number	Z-525	Z-1674	Z-1131	Z-526	Z-1681	Z-1682	Z-1683
Depth (mbsf)	374.86	384.32	404.41	406.00	412.53	420.09	425.40
Major elements (g/1000 cm^3):							
Si	611.5	549.4	531.7	592.1	600.1	647.3	573.4
Ti	43.8	16.7	32.6	31.0	37.5	42.0	35.5
Al	219.2	94.1	198.2	179.2	184.3	200.6	156.5
Fe^{+++}	117.7	165.6	172.6	121.3	144.6	153.2	176.5
Fe^{++}	172.3	137.2	60.1	130.8	109.1	130.3	115.7
Fe (Sum)	290.0	302.8	232.7	252.1	253.7	283.5	292.2
Mn	1.8	3.7	3.0	4.4	4.3	4.1	3.6
Mg	133.0	517.1	181.5	243.9	166.4	161.1	191.4
Ca	198.7	59.6	143.2	159.8	187.3	196.2	150.7
Na	55.7	12.9	45.1	36.9	52.1	55.2	46.7
K	9.4	2.0	5.1	2.8	5.3	9.1	7.2
P	3.6	1.2	2.5	2.0	3.2	3.7	2.7
Minor elements (g/1000 cm^3 x 10^{-3}):							
La	33.8			18.0			
Ce	90.2			45.1			
Nd	59.2			31.0			
Sm	18.0			9.6			
Eu	5.9			3.1			
Tb	3.4			2.0			
Yb	7.1			4.2			
Lu	0.9			0.6			
Cr	578.1	2234.4	1313.3	1297.2	952.0	1027.2	1179.2
Ni	423.0	2469.6	841.5	1452.3	598.4	567.5	884.4
Co	126.9	352.8	153.0	177.7	182.2	180.4	214.4
V	634.5	535.1	841.5	569.6	707.2	762.4	860.3
Cu	352.5	144.1	237.2	197.4	206.7	337.6	257.3
Zn	304.6	241.1	293.3	287.6	261.1	296.8	246.6
Zr	479.4	164.6	280.5	273.5	408.0	465.6	348.4
Y	87.4	32.3	56.1	53.6	76.2	81.5	64.3
Nb	36.7	11.2	22.2	19.7	29.9	34.9	26.8
Rb	13.0	4.1		5.4	3.5	8.4	5.9
Sr	902.4	155.8	561.0	564.0	680.0	727.5	536.0
Ba	253.8	58.8	206.6	186.1	193.1	273.5	268.0
H_2O^+ (wt%)	1.24	5.06	3.18	3.97	1.07	0.80	1.99
Density (g/cm^3)	2.82	2.94	2.55	2.82	2.72	2.91	2.68
Fe_2O_3/FeO	0.76	1.34	3.19	1.03	1.47	1.31	1.70

Table AT23 (continued).

Leg	55	55	55	55	55	55	55
Hole	433C	433C	433C	433C	433C	433C	433C
Core, section	38R-5	39R-1	39R-2	39R-3	39R-5	39R-5	39R-6
Interval (cm)	90-94	119-122	35-40	88-93	2-8	87-94	38-43
Piece	1M	39	1H	1F	1A	1D	1B
Lab number	Z-527	Z-1132	Z-1133	Z-1134	Z-1135	Z-1136	Z-1137
Depth (mbsf)	447.40	451.19	451.85	453.88	456.02	456.87	457.88
Major elements (g/1000 cm^3):							
Si	594.3	344.5	463.3	575.0	613.9	645.0	622.1
Ti	33.3	19.8	31.3	34.2	36.6	38.1	36.0
Al	213.1	113.4	183.1	187.5	205.4	200.4	202.8
Fe^{+++}	106.6	121.5	138.9	88.7	85.2	263.6	75.1
Fe^{++}	157.7	54.0	69.4	165.1	181.7		187.9
Fe (Sum)	264.4	175.5	208.3	253.9	266.9	263.6	263.0
Mn	3.9	1.7	2.6	3.4	4.9	3.6	4.6
Mg	140.0	134.6	152.2	202.6	203.3	181.6	194.6
Ca	187.0	22.4	60.5	139.9	173.9	199.1	179.2
Na	48.5	30.4	43.6	44.2	40.8	44.8	40.9
K	4.0	18.4	13.7	5.9	9.1	5.4	7.4
P	2.9	1.2	1.6	2.5	2.9	3.2	2.6
Minor elements (g/1000 cm^3 x 10^{-3}):							
La	30.1	14.6	15.6			26.6	
Ce	63.0	38.9	41.2			73.0	
Nd	49.3	27.5	28.2			49.6	
Sm	14.8	8.1	8.2			14.9	
Eu	4.7	2.4	2.8			4.7	
Tb	3.3	1.4	1.6			2.6	
Yb	6.3	2.6	3.5			5.5	
Lu	0.8	0.3	0.6			0.8	
Cr	726.1	704.7	1052.5	1272.0	1156.2	1241.0	1008.2
Ni	411.0	437.4	683.6	795.0	699.4	773.8	710.0
Co	145.2	95.6	130.2	159.0	155.1	181.0	153.4
V	690.5	440.6	776.9	895.7	637.3	735.8	619.1
Cu	200.0	85.9	130.2	193.5	205.9	227.8	261.3
Zn	293.2	134.5	271.3	323.3	332.8	353.3	352.2
Zr	383.6	194.4	303.8	344.5	338.4	350.4	340.8
Y	74.0	37.3	32.6	61.0	64.9	67.2	68.2
Nb	30.1	15.7	21.7	25.2	26.8	27.2	27.3
Rb		19.4	23.9	3.2	3.1	4.1	6.2
Sr	739.8	210.6	412.3	583.0	634.5	700.8	653.2
Ba	161.7	100.4	106.3	265.0	157.9	224.8	178.9
H_2O^+ (wt%)	2.08	4.04	3.22	2.21	1.46	1.58	2.34
Density (g/cm^3)	2.74	1.62	2.17	2.65	2.82	2.92	2.84
Fe_2O_3/FeO	0.75	2.50	2.22	0.60	0.52		0.44

Table AT23 (continued).

Leg	55	55	55	55	55	55	55
Hole	433C	433C	433C	433C	433C	433C	433C
Core, section	41R-1	42R-1	45R-3	45R-4	45R-5	45R-5	45R-6
Interval (cm)	20-23	2-6	119-124	109-114	39-44	119-122	24-31
Piece	1C	1G	4D	4J	1C	3D	1A
Lab number	Z-528	Z-1138	Z-1140	Z-1704	Z-1141	Z-529	Z-1142
Depth (mbsf)	469.20	478.52	511.19	512.59	513.29	514.09	514.74
Major elements (g/1000 cm^3):							
Si	645.6	599.5	486.0	608.6	646.7	657.8	637.5
Ti	39.2	37.0	31.8	37.2	41.0	40.6	37.2
Al	220.0	191.6	177.5	216.7	227.6	200.0	214.5
Fe^{+++}	100.0	235.2	142.2	146.6	84.4	96.5	86.4
Fe^{++}	151.2		75.9	129.7	179.6	163.5	146.9
Fe (Sum)	251.2	235.2	218.1	276.2	264.0	260.0	233.3
Mn	1.3	2.7	2.1	3.2	4.2	2.2	4.1
Mg	117.7	120.8	101.4	103.1	110.5	151.7	113.7
Ca	193.5	188.9	135.2	195.8	226.9	215.4	200.9
Na	55.2	52.1	45.5	51.2	53.3	53.5	56.0
K	6.0	5.3	8.0	22.0	10.3	8.9	3.9
P	3.0	2.9	2.4	3.0	2.8	3.0	2.4
Minor elements (g/1000 cm^3 x 10^{-3}):							
La	27.5			19.3		24.4	20.3
Ce	61.8			52.3		51.7	54.8
Nd	45.0			41.3		43.1	38.4
Sm	14.3			12.1		13.2	12.9
Eu	4.8			3.3		4.6	3.8
Tb	3.4			2.0		2.9	2.6
Yb	7.0			6.1		6.6	5.5
Lu	1.0			1.0		1.0	0.8
Cr	632.3	640.8	422.4	569.3	686.4	588.4	597.3
Ni	230.4	221.6	162.8	231.0	246.0	186.6	219.2
Co	134.9	157.5	125.4	192.5	180.2	126.3	150.7
V	800.9	1041.3	853.6	1031.3	1072.5	760.6	926.1
Cu	219.2	227.0	116.6	255.8	357.5	358.8	326.1
Zn	303.5	336.4	272.8	244.8	348.9	358.8	378.1
Zr	365.3	347.1	286.0	330.0	343.2	344.4	328.8
Y	84.3	66.8	57.2	68.8	71.5	80.4	74.0
Nb	27.0	24.8	18.7	23.1	24.0	25.0	22.5
Rb	3.4	4.3	7.7	30.3	11.2	16.6	
Sr	730.6	667.5	550.0	687.5	743.6	774.9	726.1
Ba	207.9	213.6	118.8	203.5	248.8	212.4	148.0
H_2O^+ (wt%)	0.42	1.02	1.51	1.73	1.00	0.78	0.51
Density (g/cm^3)	2.81	2.67	2.20	2.75	2.86	2.87	2.74
Fe_2O_3/FeO	0.74		2.08	1.26	0.52	0.66	0.65

Table AT23 (continued).

Leg	55	55	55	55
Hole	433C	433C	433C	433C
Core, section	45R-6	46R-3	47R-1	49R-2
Interval (cm)	97-102	78-83	8-13	62-68
Piece	1G	2D	2A	1J
Lab number	Z-1707	Z-1709	Z-1710	Z-1712
Depth (mbsf)	515.47	520.28	526.08	547.12
Major elements (g/1000 cm^3):				
Si	600.8	588.0	627.0	573.7
Ti	35.4	36.6	39.7	46.2
Al	221.6	197.5	190.0	200.6
Fe^{+++}	93.1	176.3	153.0	184.2
Fe^{++}	128.0	105.8	140.6	112.9
Fe (Sum)	221.1	282.1	293.6	297.2
Mn	4.0	2.8	3.3	4.1
Mg	123.4	127.9	119.2	123.0
Ca	186.9	176.5	194.6	177.6
Na	52.2	58.5	59.2	60.7
K	10.7	11.4	7.0	8.3
P	2.5	2.9	3.5	3.8
Minor elements (g/1000 cm^3 x 10^{-3}):				
La				
Ce				
Nd				
Sm				
Eu				
Tb				
Yb				
Lu				
Cr	582.5	535.3	501.4	435.2
Ni	215.5	204.4	196.7	263.8
Co	204.8	182.9	166.2	119.7
V	696.9	957.6	747.9	511.4
Cu	212.8	258.2	232.7	340.0
Zn	308.6	263.6	321.3	266.6
Zr	319.2	376.6	415.5	462.4
Y	63.8	78.0	85.9	81.6
Nb	23.9	25.6	27.7	35.4
Rb	17.6	10.0	5.0	5.7
Sr	665.0	645.6	692.5	734.4
Ba	218.1	228.7	210.5	228.5
H_2O^+ (wt%)	1.42	0.56	0.41	1.82
Density (g/cm^3)	2.66	2.69	2.77	2.72
Fe_2O_3/FeO	0.81	1.85	1.21	1.81

Table AT24. Abundance of major and trace elements (g/1000 cm^3) in alkaline basalts, Hole 865A, Leg 143 (Allison Guyot, West Pacific Guyots). (Continued on next page.)

Leg	143	143	143	143	143	143	143
Hole	865A	865A	865A	865A	865A	865A	865A
Core, section	90R-5	90R-5	90R-6	91R-1	91R-2	91R-3	92R-3
Interval (cm)	52-58	52-58	45-50	112-118	20-25	22-28	80-86
Piece	5B	5B	2	13B	2	2	1
Lab number	Z-1492-1	Z-1492-2	Z-1493	Z-1494	Z-1495	Z-1496	Z-1497
Depth (mbsf)	837.24	837.24	838.58	842.22	842.64	844.03	850.27
Major elements (g/1000 cm^3):							
Si	398.0	198.2	547.3	486.5	463.2	462.8	373.4
Ti	47.2	10.6	53.8	52.3	54.3	53.7	61.0
Al	180.0	90.3	206.2	201.5	218.0	221.3	215.6
Fe^{+++}	176.1	122.0	127.7	116.0	111.6	94.3	114.0
Fe^{++}	38.3	101.1	108.1	86.4	69.8	72.4	11.0
Fe (Sum)	214.4	223.1	235.8	202.4	181.5	166.7	124.9
Mn	1.2	3.0	1.9	3.2	2.6	2.8	1.0
Mg	46.1	44.0	139.5	131.8	141.3	156.8	34.3
Ca	89.5	397.5	142.5	123.4	102.2	85.2	13.2
Na	22.2	10.8	41.9	38.1	37.4	31.9	18.5
K	72.0	16.6	44.8	16.6	15.7	27.9	20.5
P	5.8	4.9	9.1	8.1	7.9	9.2	2.1
Minor elements (g/1000 cm^3 x 10^{-3}):							
La	106.6	58.2					
Ce	229.9	112.0					
Nd	125.4	62.7					
Sm	27.2	14.6					
Eu	7.1	3.6					
Tb	4.0	1.7					
Yb	5.9	4.3					
Lu	0.9	0.7					
Cr	564.3	134.4	697.0	633.4	703.7	611.0	548.7
Ni	211.1	123.2	491.8	399.1	424.1	376.0	127.4
V	856.9	293.4	1123.0	1190.2	1258.2	1085.7	959.3
Cu	127.5	206.1	160.4	141.0	170.1	155.1	72.6
Co	62.7	67.2	173.6	160.1	158.4	105.8	63.7
Zn	198.6		207.8	196.0	198.1	213.9	92.0
Zr	710.6	219.5	815.3	812.6	838.8	822.5	920.4
Y	73.2	53.8	68.4	71.7	72.2	68.2	62.0
Nb	150.5	35.8	176.2	169.7	179.4	178.6	177.0
Rb	110.8	44.8	102.6	18.9	16.8	25.9	67.3
Sr	418.0	336.0	1499.1	1720.8	1234.9	1457.0	584.1
Ba	679.3	537.6	1446.5	1386.2		1316.0	1150.5
H_2O^+ (wt%)	4.41	4.14	2.93	3.85	4.21	5.04	7.20
Density (g/cm^3)	2.09	2.24	2.63	2.39	2.33	2.35	1.77
Fe_2O_3/FeO	5.11	1.34	1.32	1.49	1.78	1.45	11.53

Table AT24 (continued).

Leg	143	143	143	143	143	143	143
Hole	865A	865A	865A	865A	865A	865A	865A
Core, section	92R-4	93R-1	93R-2	93R-3	94R-1	94R-2	94R-4
Interval (cm)	45-47	30-36	0-8	47-49	97-102	102-105	133-143
Piece		4	1	2B	17D	16	9
Lab number	Z-1498	Z-1499	Z-1500	Z-1716	Z-1501	Z-1502	Z-1503
Depth (mbsf)	850.90	853.70	854.9	856.87	864.07	865.59	868.73
Major elements (g/1000 cm^3):							
Si	358.7	390.2	484.0	516.8	574.2	414.2	592.2
Ti	58.4	50.3	60.5	70.3	61.7	54.8	57.0
Al	190.6	196.4	207.8	219.9	221.8	175.9	235.5
Fe^{+++}	124.4	177.0	182.8	135.6	96.8	107.3	83.5
Fe^{++}	17.8	28.8	45.5	89.8	122.2	44.7	125.0
Fe (Sum)	142.2	205.8	228.3	225.4	219.0	152.0	208.5
Mn	2.2	1.9	0.9	4.5	3.4	2.4	2.6
Mg	24.6	27.8	97.2	173.6	133.6	108.3	120.6
Ca	4.9	26.3	45.7	145.7	201.2	86.9	170.8
Na	16.5	25.6	29.8	41.9	47.8	17.5	50.0
K	48.9	58.0	68.7	33.6	25.2	70.0	48.3
P	1.6	8.7	10.7	2.6	11.3	9.2	9.8
Minor elements (g/1000 cm^3 x 10^{-3}):							
La	107.1	103.1		113.0		75.3	140.3
Ce	221.0	229.2		263.6		206.4	242.0
Nd	107.1	103.1		113.0		103.2	123.8
Sm	18.7	19.1		22.9		20.0	26.7
Eu	5.8	6.3		7.5		6.0	6.1
Tb	2.2	2.5		3.0		2.6	3.0
Yb	2.7	4.6		5.1		4.1	7.2
Lu	0.3	0.7		0.7		0.6	1.0
Cr	149.6	439.3	519.2	495.0	602.8	554.7	258.5
Ni	119.0	248.3	238.4	255.6	402.8	193.5	220.0
V	629.0	502.3	962.9	712.9	1074.1	1042.8	530.8
Cu	100.3	76.4	103.8	137.2	161.7	157.0	129.3
Co	59.5	95.5	132.2	107.6	156.2	129.0	96.3
Zn	98.6	187.2	193.5	212.5	219.2	391.3	239.3
Zr	867.0	821.3	849.6	874.3	959.0	817.0	1017.5
Y	59.5	70.7	68.4	75.3	76.7	73.1	74.3
Nb	170.0	154.7	172.3	166.8	180.8	163.4	187.0
Rb	68.0	80.2	134.5	53.8	38.4	64.5	107.3
Sr	663.0	534.8	991.2	1533.3	2219.4	440.8	1952.5
Ba	578.0	725.8	873.2	1264.3	1589.2	1225.5	2200.0
H_2O^+ (wt%)	7.59	5.38	4.45	4.62	1.94	5.59	1.52
Density (g/cm^3)	1.70	1.91	2.36	2.69	2.74	2.15	2.75
Fe_2O_3/FeO	7.77	6.82	4.47	1.68	0.88	2.67	0.74

Table AT25. Abundance of major and trace elements (g/1000 cm^3) in alkaline basalts, Hole 866A, Leg 143 (Resolution Guyot, West Pacific Guyots). (Continued on next two pages.)

Leg	143	143	143	143	143	143	143	143
Hole	866A	866A	866A	866A	866A	866A	866A	866A
Core, section	171R-2	171R-4	178W-1	178W-1	179R-5	180R-1	180R-3	180R-4
Interval (cm)	109-111	131-134	37-38	79-81	40-45	27-32	67-72	12-17
Piece	3					3A	1D	1B
Lab number	Z-1504	Z-1505	Z-1506	Z-1507	Z-1508	Z-1509	Z-1510	Z-1511
Depth (mbsf)	1620.8	1623.86	1659.77	1660.19	1664.36	1667.67	1670.65	1671.6
Major elements (g/1000 cm^3):								
Si	426.6	440.3	561.0	398.7	594.0	627.3	623.8	626.9
Ti	45.1	50.4	62.4	43.5	45.5	47.4	46.4	46.2
Al	237.2	228.1	255.3	228.0	246.5	247.5	246.2	249.3
Fe^{+++}	226.5	258.0	388.4	336.8	160.7	107.0	95.6	108.6
Fe^{++}	15.2	11.2	2.8	2.9	76.7	142.8	162.3	150.2
Fe (Sum)	241.7	269.2	391.2	339.7	237.4	249.8	257.9	258.9
Mn	0.5	1.9	0.7	1.1	4.1	2.7	3.2	3.2
Mg	20.7	34.8	51.5	39.8	99.3	134.5	136.9	141.1
Ca	22.7	29.4	43.7	24.7	182.2	191.0	194.4	197.9
Na	18.8	22.9	31.1	20.6	64.4	62.3	60.0	63.7
K	83.1	79.2	32.6	14.9	12.7	9.5	8.7	9.2
P	0.7	1.3	2.6	0.4	2.8	3.2	3.0	2.9
Minor elements (g/1000 cm^3 x 10^{-3}):								
La	25.8	35.2	60.5	46.0				
Ce	47.3	79.2	170.5	63.5				
Nd	36.6	50.6	85.3	52.6				
Sm	9.7	12.3	20.6	12.7				
Eu	3.7	4.0	6.3	4.2				
Tb	1.5	1.7	3.6	2.6				
Yb	3.7	3.3	5.8	5.9				
Lu	0.6	0.5	0.9	0.9				
Cr	1204.0		866.3	1620.6	471.3	576.0	561.6	551.0
Ni	709.5		456.5	608.8	230.2	299.5	417.6	435.0
V	548.3		591.3	1594.3	597.3	979.2	705.6	690.2
Cu	109.7		112.8	102.9	180.8	210.2	216.0	214.6
Co	116.1		121.0	116.1	95.9	144.0	178.6	162.4
Zn	253.7		269.5	146.7	246.6	273.6	265.0	258.1
Zr	365.5		770.0	306.6	383.6	374.4	374.4	377.0
Nb	45.2		110.0	35.0	41.1	43.2	43.2	43.5
Y	32.3		77.0	48.2	68.5	69.1	69.1	66.7
Rb	77.4		55.0	32.9	18.9	17.0	14.4	17.7
Sr	83.9		275.0	212.4	1287.8	1267.2	1238.4	1305.0
Ba	101.1		112.8	13.1	131.5	460.8	1238.4	435.0
H_2O^+ (wt%)	7.1	5.43	5.63	6.23	1.29	1.41	1.67	1.22
Density (g/cm^3)	2.15	2.20	2.25	2.19	2.74	2.88	2.88	2.90
Fe_2O_3/FeO	16.55	25.60	154.42	129.12	2.33	0.83	0.66	0.80

Table AT25 (continued).

Leg	143	143	143	143	143	143	143	143
Hole	866A	866A	866A	866A	866A	866A	866A	866A
Core, section	182R-1	182R-2	182R-4	183R-1	184R-1	184R-2	185R-3	185R-4
Interval (cm)	3-8	58-63	72-74	125-131	23-28	23-26	41-46	26-32
Piece	2	3C	8	18B	4	3	1D	6B
Lab number	Z-1512	Z-1513	Z-1515	Z-1516	Z-1517	Z-1519	Z-1520	Z-1521
Depth (mbsf)	1682.83	1684.85	1687.63	1688.55	1692.53	1694.03	1700.07	1701.11
Major elements (g/1000 cm^3):								
Si	643.4	652.3	415.7	547.4	589.7	468.0	602.2	494.8
Ti	40.4	40.6	44.5	51.0	55.5	26.8	46.8	41.8
Al	235.9	254.1	170.2	198.5	218.8	167.3	214.0	183.6
Fe^{+++}	106.7	130.4	226.3	202.1	149.1	206.8	139.8	164.4
Fe^{++}	147.3	91.0	27.8	65.9	117.5	7.7	117.2	41.4
Fe (Sum)	254.0	221.4	254.1	267.9	266.6	214.5	257.0	205.9
Mn	3.0	3.0	1.0	3.4	5.3	0.9	3.2	1.8
Mg	153.5	110.0	40.5	113.1	106.5	70.8	131.7	125.0
Ca	185.9	215.4	69.2	106.2	152.8	68.4	172.4	68.7
Na	64.8	66.8	43.9	69.6	71.1	36.8	65.8	59.1
K	12.0	11.5	29.4	16.0	14.0	27.0	12.0	25.8
P	3.9	4.0	0.4	4.4	4.3	2.6	4.5	4.0
Minor elements (g/1000 cm^3 x 10^{-3}):								
La			65.3	63.0	70.2	75.6		
Ce			150.5	126.0	135.0	147.0		
Nd			83.2	68.0	72.9	88.2		
Sm			19.2	16.4	15.4	19.5		
Eu			6.5	4.8	4.9	5.9		
Tb			3.2	2.0	2.3	3.6		
Yb			5.9	5.8	5.7	8.2		
Lu			0.9	0.8	0.9	1.3		
Cr	675.1	884.5	336.6	428.4	448.2	457.8	489.5	476.9
Ni	465.6	498.8	263.3	342.7	229.5	270.9	357.5	221.5
V	547.1	638.0	475.2	902.2	923.4	415.8	572.0	583.1
Cu	215.3	240.7	132.7	224.3	135.0	121.8	203.5	176.3
Co	139.7	145.0	97.0	126.0	132.3	105.0	121.0	104.0
Zn	261.9	272.6	178.2	302.4	270.0	163.8	324.5	282.5
Zr	465.6	478.5	465.3	554.4	567.0	441.0	550.0	542.4
Nb	81.5	81.2	83.2	90.7	105.3	67.2	82.5	97.2
Y	78.6	75.4	53.5	78.1	86.4	88.2	74.3	65.5
Rb	37.8	31.9	41.6	19.9	32.4	31.5	23.9	27.1
Sr	960.3	1102.0	356.4	1008.0	1053.0	640.5	1045.0	836.2
Ba	1018.5	1189.0	336.6	604.8	324.0	525.0	412.5	904.0
H_2O^+ (wt%)	1.19	1.07	2.85	1.00	1.00	4.54	1.45	1.89
Density (g/cm^3)	2.91	2.90	1.98	2.52	2.70	2.10	2.75	2.26
Fe_2O_3/FeO	0.81	1.59	9.05	3.41	1.41	30.00	1.33	4.41

Table AT25 (continued).

Leg	143	143	143	143	143	143
Hole	866A	866A	866A	866A	866A	866A
Core, section	186R-1	186R-2	187R-1	188R-1	189R-1	189R-2
Interval (cm)	39-41	20-24	99-104	82-89	65-69	115-120
Piece	6	5	17	16A	5C	7C
Lab number	Z-1522	Z-1523	Z-1524	Z-1525	Z-1526	Z-1527
Depth (mbsf)	1707.39	1708.70	1716.79	1727.12	1735.55	1737.48
Major elements (g/1000 cm^3):						
Si	451.6	508.2	517.2	500.7	615.0	468.5
Ti	32.8	47.7	49.3	41.2	36.9	24.5
Al	124.3	207.8	221.0	178.7	190.8	140.8
Fe^{+++}	134.8	201.7	180.7	185.7	131.0	129.2
Fe^{++}	46.0	46.0	52.4	45.6	172.0	60.5
Fe (Sum)	180.8	247.7	233.1	231.3	302.9	189.7
Mn	0.7	1.5	2.1	1.7	4.1	3.0
Mg	158.6	120.3	102.7	143.6	217.3	219.7
Ca	42.1	84.0	101.1	63.9	171.4	39.1
Na	42.7	56.2	63.7	48.2	46.5	39.9
K	50.2	32.4	23.0	45.8	8.0	20.4
P	1.2	4.4	4.8	4.1	3.2	1.7
Minor elements (g/1000 cm^3 x 10^{-3}):						
La	40.4	72.3				
Ce	80.8	154.2				
Nd	42.4	86.8				
Sm	9.5	17.6				
Eu	2.8	3.9				
Tb	1.6	1.8				
Yb	2.8	5.3				
Lu	0.5	0.9				
Cr	377.7	535.0	445.3	593.9	1165.8	752.1
Ni	268.7	313.3	229.9	336.4	672.8	512.3
V	482.8	833.9	597.7	587.0	640.9	584.2
Cu	139.4	200.0	200.9	171.7	194.3	161.3
Co	92.9	125.3	92.0	118.3	185.6	141.7
Zn	149.5	192.8	217.8	194.9	266.8	187.5
Zr	404.0	602.5	641.3	556.8	391.5	250.7
Nb	70.7	98.8	118.6	106.7	60.9	39.2
Y	50.5	60.3	70.2	60.3	66.7	39.2
Rb	26.3	13.0	16.0	25.5	19.4	12.4
Sr	404.0	988.1	1161.6	765.6	754.0	392.4
Ba	505.0	698.9	1064.8	672.8	551.0	457.8
H_2O^+ (wt%)	3.20	1.34	1.34	1.33	2.11	3.43
Density (g/cm^3)	2.02	2.41	2.42	2.32	2.90	2.18
Fe_2O_3/FeO	3.26	4.87	3.83	4.52	0.85	2.37

Table AT26. Abundance of major and trace elements (g/1000 cm^3) in basanites, Hole 871C, Leg 144 (Limalok Guyot, West Pacific Guyots). (Continued on next page.)

Leg	144	144	144	144	144	144	144
Hole	871C	871C	871C	871C	871C	871C	871C
Core, section	35R-3	35R-3	36R-1	36R-2	36R-3	38R-1	38R-3
Interval (cm)	76-78	143-145	2-5	107-109	32-35	117-120	83-87
Piece	3C	5B	7B	11	3	10	4
Lab number	Z-1528	Z-863	Z-1530	Z-864	Z-865	Z-866	Z-867
Depth (mbsf)	455.07	455.80	461.89	463.58	464.26	472.97	475.49
Major elements (g/1000 cm^3):							
Si	402.0	459.4	437.8	480.7	515.6	546.9	554.2
Ti	47.3	55.0	57.4	44.0	48.3	44.1	45.7
Al	153.6	173.0	168.3	167.1	167.5	177.3	176.2
Fe^{+++}	217.8	182.0	230.8	101.5	132.2	124.3	133.9
Fe^{++}	28.2	54.2	64.4	81.1	111.6	130.8	140.1
Fe (Sum)	246.0	236.2	295.1	182.6	243.7	255.1	274.0
Mn	3.1	9.8	5.8	2.2	2.3	4.2	4.8
Mg	194.1	171.2	214.2	189.4	228.7	272.3	263.6
Ca	47.6	156.5	54.6	204.3	198.2	192.9	206.4
Na	28.6	22.2	24.9	21.3	19.8	45.0	42.2
K	11.7	10.5	11.3	5.7	5.0	13.7	12.3
P	5.1	7.0	7.3	6.6	7.2	7.2	6.9
Minor elements (g/1000 cm^3 x 10^{-3}):							
La	78.8	128.4	97.6				
Ce	78.8	296.4	87.8				
Nd	78.8	126.0	85.4				
Sm	14.9	24.7	15.1				
Eu	4.8	7.4	4.9				
Tb	2.2	2.7	2.3				
Yb	3.5	5.7	3.2				
Lu	0.5	0.8	0.4				
Cr	1073.1	1333.8	1268.8	1148.6	1291.2	1472.9	1470.0
Ni	525.6	617.5	646.6	716.3	887.7	972.4	999.6
Co	175.2	140.8	205.0	168.0	182.9	174.5	182.3
V	514.7	857.1	678.3	573.0	691.3	692.1	661.5
Cu	170.8	111.2	141.5	177.8	193.7	185.9	182.3
Zn	197.1	244.5	297.7	242.1	282.5	254.5	270.5
Zr	503.7	617.5	610.0	568.1	591.8	600.6	646.8
Nb	140.2	158.1	178.1	150.7	153.3	154.4	167.6
Y	46.0	76.6	70.8	66.7	67.3	65.8	79.4
Rb	48.2	32.1	43.9	12.6	19.1	24.6	32.3
Sr	503.7	889.2	658.8	1370.9	1358.5	2230.8	1734.6
Ba	635.1	988.0	1366.4	988.0	914.6	3003.0	2851.8
H_2O^+ (wt%)	4.57	4.91	6.13	3.22	4.29	2.95	3.53
Density (g/cm^3)	2.19	2.47	2.44	2.47	2.69	2.86	2.94
Fe_2O_3/FeO	8.59	3.73	3.99	1.39	1.32	1.06	1.06

Table AT26 (continued).

Leg	144	144	144	144	144	144
Hole	871C	871C	871C	871C	871C	871C
Core, section	38R-7	39R-1	39R-4	39R-5	40R-1	40R-4
Interval (cm)	0-5	6-10	0-5	120-124	126-130	98-101
Piece	1A	2	1	10C	10A	3D
Lab number	Z-1531	Z-868	Z-1532	Z-1533	Z-1534	Z-869
Depth (mbsf)	479.75	480.46	484.48	487.18	490.96	495.18
Major elements (g/1000 cm^3):						
Si	473.6	539.5	404.7	511.8	573.3	520.7
Ti	52.8	56.4	42.8	54.8	54.5	56.3
Al	147.0	184.4	122.7	152.8	160.2	158.1
Fe^{+++}	197.3	133.1	247.1	224.3	170.1	155.1
Fe^{++}	116.5	133.3	44.5	113.8	161.4	117.7
Fe (Sum)	313.8	266.3	291.5	338.1	331.5	272.8
Mn	3.7	4.5	3.4	4.7	4.9	4.7
Mg	233.0	229.0	275.3	278.2	312.7	259.5
Ca	168.4	245.8	21.2	196.0	195.6	233.3
Na	13.5	26.2	23.1	16.0	43.8	17.5
K	5.3	10.0	6.8	9.7	9.3	4.1
P	7.3	7.9	4.5	6.2	6.6	6.7
Minor elements (g/1000 cm^3 x 10^{-3}):						
La			77.5		97.0	
Ce			209.8		187.9	
Nd			95.8		97.0	
Sm			15.7		22.1	
Eu			5.5		6.7	
Tb			2.3		2.9	
Yb			3.2		4.5	
Lu			0.5		0.6	
Cr	1239.8	1310.4	1390.8	1887.6	1660.4	1698.0
Ni	704.7	878.4	957.6	1221.2	975.7	1584.8
Co	219.2	195.8	216.6	243.1	233.3	263.2
V	939.6	820.8	549.5	809.4	684.8	721.7
Cu	164.4	187.2	143.6	180.2	209.1	184.0
Zn	245.3	282.2	212.0	343.2	309.1	263.2
Zr	469.8	547.2	387.6	486.2	500.0	566.0
Nb	138.3	149.8	104.9	128.7	136.4	138.7
Y	73.1	60.5	47.9	68.6	75.8	76.4
Rb	19.1	40.3	27.4	28.6	45.5	27.7
Sr	548.1	1555.2	228.0	829.4	1363.5	905.6
Ba	809.1	921.6	273.6	600.6	848.4	721.7
H_2O^+ (wt%)	4.08	3.16	5.47	3.68	2.10	3.86
Density (g/cm^3)	2.61	2.88	2.28	2.86	3.03	2.83
Fe_2O_3/FeO	1.88	1.11	6.18	2.19	1.17	1.46

Table AT27. Abundance of major and trace elements (g/1000 cm^3) in alkali basalts and hawaiites, Hole 872B, Leg 144 (Lo-En Guyot, West Pacific Guyots). (Continued on next page.)

Leg	144	144	144	144	144	144	144	144
Hole	872B	872B	872B	872B	872B	872B	872B	872B
Core, section	5R-1	5R-3	5R-4	7R-1	7R-3	7R-4	7R-6	8R-1
Interval (cm)	56-58	104-108	65-68	8-12	32-37	102-107	10-15	50-54
Piece	6	10	10	1	1	3	3	7
Lab number	Z-870	Z-1536	Z-1537	Z-1538	Z-1539	Z-1540	Z-1541	Z-1542
Depth (mbsf)	145.36	148.66	149.77	164.08	166.24	168.44	170.30	173.60
Major elements (g/1000 cm^3):								
Si	621.8	589.9	516.1	473.4	485.0	550.8	618.6	458.8
Ti	40.6	35.2	32.6	33.3	31.8	35.5	39.9	32.7
Al	241.1	199.3	205.0	178.7	162.8	209.7	236.9	173.1
Fe^{+++}	93.6	144.2	167.7	211.1	186.4	162.3	101.0	212.1
Fe^{++}	101.4	106.2	49.8	4.0	12.9	44.3	100.9	14.9
Fe (Sum)	195.0	250.5	217.5	215.1	199.3	206.5	201.9	227.0
Mn	2.6	2.9	2.5	2.3	2.5	2.6	2.8	2.1
Mg	126.7	140.3	109.0	105.3	102.1	115.5	149.6	67.6
Ca	193.0	159.3	110.7	79.7	99.8	133.2	188.2	74.0
Na	64.8	58.3	81.0	53.3	57.6	62.2	61.6	45.8
K	28.6	23.5	17.7	32.4	61.2	27.8	23.0	37.8
P	4.7	3.4	2.4	3.5	3.6	3.7	4.7	3.2
Minor elements (g/1000 cm^3 x 10^{-3}):								
La								61.0
Ce								124.3
Nd								56.7
Sm								11.6
Eu								4.1
Tb								2.0
Yb								3.7
Lu								0.5
Cr	181.4	440.6	483.1	457.0	467.8	520.0	488.3	401.1
Ni	125.6	237.6	197.6	181.4	151.4	167.5	175.8	159.1
Co	103.2	141.5	102.5	80.6	79.1	105.0	103.2	115.5
V	585.9	587.4	505.1	513.0	402.3	487.5	477.1	503.6
Cu	133.9	168.2	153.7	141.1	126.6	150.0	161.8	126.4
Zn	273.4	256.3	217.2	273.3	180.8	200.0	248.3	167.9
Zr	530.1	400.5	341.6	380.8	339.0	400.0	446.4	359.7
Nb	100.4	80.1	73.2	76.2	74.6	82.5	94.9	71.9
Y	58.6	48.1	53.7	40.3	49.7	47.5	58.6	39.2
Rb	61.4	58.7	23.2	56.0	54.2	55.0	55.8	39.2
Sr	892.8	934.5	927.2	604.8	429.4	1075.0	1199.7	414.2
Ba	781.2	961.2	512.4	627.2	904.0	700.0	1032.3	436.0
H_2O^+ (wt%)	1.49	1.88	4.35	3.74	3.02	1.17	1.45	4.17
Density (g/cm^3)	2.79	2.67	2.44	2.24	2.26	2.50	2.79	2.18
Fe_2O_3/FeO	1.03	1.51	3.74	59.09	16.07	4.08	1.11	15.81

Table AT27 (continued).

Leg	144	144	144	144	144	144	144
Hole	872B	872B	872B	872B	872B	872B	872B
Core, section	8R-1	8R-2	8R-2	8R-4	9R-2	9R-3	9R-5
Interval (cm)	63-68	9-12	91-94	24-29	19-21	28-33	38-40
Piece	7	1	3	2	1	3	1A
Lab number	Z-1543	Z-1720	Z-1717	Z-871	Z-872	Z-1544	Z-1546
Depth (mbsf)	173.73	174.69	175.51	177.66	184.17	185.76	188.36
Major elements (g/1000 cm^3):							
Si	468.3	469.5	581.1	595.3	498.8	632.5	536.5
Ti	32.5	29.0	40.7	37.9	39.5	41.6	23.6
Al	161.0	189.6	202.0	247.3	209.5	218.6	143.4
Fe^{+++}	168.5	184.2	148.2	138.3	146.2	130.4	105.8
Fe^{++}	14.3	11.0	82.9	103.5	33.7	85.9	56.7
Fe (Sum)	182.8	195.2	231.1	241.8	180.0	216.4	162.4
Mn	2.9	0.6	1.5	0.9	2.5	2.8	1.6
Mg	95.4	72.2	102.0	117.5	29.3	107.8	133.1
Ca	124.2	107.6	204.2	213.4	111.3	174.8	98.2
Na	57.8	50.9	69.2	66.8	62.2	67.3	56.0
K	38.9	47.8	30.1	20.9	28.7	25.3	8.6
P	2.7	5.7	3.6	3.5	3.7	4.1	0.9
Minor elements (g/1000 cm^3 x 10^{-3}):							
La		55.0	72.9				
Ce		103.1	137.7				
Nd		43.5	64.8				
Sm		9.6	13.0				
Eu		3.4	4.9				
Tb		1.6	2.1				
Yb		2.7	4.1				
Lu		0.4	0.6				
Cr	405.8	366.4	245.7	653.2	229.5	128.3	1372.5
Ni	155.0	142.0	159.3	232.9	123.8	131.0	612.0
Co	107.2	103.1	105.3	133.5	90.0	92.8	117.0
V	513.0	380.1	561.6	602.1	803.3	491.4	528.8
Cu	123.1	114.5	151.2	156.2	146.3	152.9	141.8
Zn	168.7	164.9	224.1	275.5	177.8	240.2	157.5
Zr	364.8	320.6	513.0	482.8	450.0	436.8	218.3
Nb	68.4	64.1	97.2	82.4	81.0	90.1	33.8
Y	50.2	38.9	59.4	59.6	51.8	65.5	33.8
Rb	38.8	43.5	62.1	39.8	51.8	65.5	18.0
Sr	433.2	824.4	1026.0	1448.4	967.5	1078.4	148.5
Ba	433.2	595.4	783.0	568.0	562.5	1037.4	270.0
H_2O^+ (wt%)	3.37	6.15	2.02	2.07	3.32	1.08	4.25
Density (g/cm^3)	2.28	2.29	2.70	2.84	2.25	2.73	2.25
Fe_2O_3/FeO	13.05	18.63	1.99	1.48	4.82	1.69	2.07

Table AT28. Abundance of major and trace elements (g/1000 cm^3) in ankaramites, Hole 874B, Leg 144 (Wodejebato Guyot, West Pacific Guyots). (Continued on next page.)

Leg	144	144	144	144	144	144	144
Hole	874B	874B	874B	874B	874B	874B	874B
Core, section	22R-4	23R-1	23R-2	24R-1	24R-1	24R-1	24R-2
Interval (cm)	48-53	100-105	112-117	30-35	100-105	120-127	70-76
Piece	1	13	23	2	7	8	9
Lab.number	Z-1547	Z-1548	Z-1549	Z-1550	Z-1551	Z-1552	Z-1553
Depth (mbsf)	177.15	178.70	180.31	184.30	185.00	185.20	186.14
Major elements (g/1000 cm^3):							
Si	363.0	463.5	463.9	594.9	527.9	389.3	438.4
Ti	20.1	19.6	18.7	24.3	23.0	16.5	20.1
Al	93.6	99.7	95.2	109.0	101.4	66.5	74.5
Fe^{+++}	174.7	194.0	182.7	130.2	163.8	154.0	179.2
Fe^{++}	13.0	15.1	8.0	119.2	54.7	49.0	31.8
Fe (Sum)	187.8	209.1	190.7	249.3	218.5	203.0	211.0
Mn	3.4	3.4	3.2	3.9	3.2	1.5	1.3
Mg	203.9	304.8	329.5	390.1	304.1	325.9	315.6
Ca	95.4	69.0	66.1	148.2	96.9	250.6	124.4
Na	24.4	23.2	23.5	23.7	24.6	29.4	28.6
K	6.0	4.3	2.9	16.1	15.4	3.4	4.3
P	2.0	1.4	1.5	1.9	2.0	1.0	1.5
Minor elements (g/1000 cm^3 x 10^{-3}):							
La	39.2	42.1	35.0	40.3	43.0	24.5	28.1
Ce	56.8	74.9	69.9	100.8	73.4	44.7	42.1
Nd	35.3	39.8	35.0	51.8	45.5	25.0	25.7
Sm	8.6	9.1	8.2	10.4	10.1	6.3	7.0
Eu	2.4	3.0	3.0	2.9	3.3	2.0	2.2
Tb	1.2	1.5	1.5	1.5	1.6	1.0	1.1
Yb	2.2	2.3	2.3	2.9	3.0	1.8	1.9
Lu	0.3	0.4	0.3	0.5	0.4	0.3	0.3
Cr	1773.8	2199.6	1561.1	2880.0	2327.6	2314.4	1755.0
Ni	793.8	989.8	894.7	1123.2	1057.5	920.5	760.5
Co	307.7	264.4	226.0	233.3	222.6	186.7	187.2
V	341.0	402.5	321.5	532.8	521.2	536.5	337.0
Cu	56.8	81.9	90.9	89.3	83.5	65.8	30.4
Zn	301.8	276.1	247.0	311.0	273.2	139.4	65.5
Zr	215.6	231.7	202.7	288.0	253.0	121.0	175.5
Nb	37.2	39.8	32.6	43.2	43.0	22.1	28.1
Y	29.4	28.1	23.3	40.3	40.5	18.9	25.7
Rb	7.8	6.3	3.7	21.3	27.8	4.2	7.5
Sr	68.6	81.9	62.9	518.4	683.1	105.2	65.5
Ba	62.7	103.0	76.9	460.8	146.7	184.1	18.7
H_2O^+ (wt%)	5.05	5.78	4.47	2.69	5.3	6.02	6.14
Density (g/cm^3)	1.96	2.34	2.33	2.88	2.53	2.63	2.34
Fe_2O_3/FeO	14.91	14.27	25.36	1.21	3.33	3.33	6.51

Table AT28 (continued).

Leg	144	144	144
Hole	874B	874B	874B
Core, section	24R-2	24R-3	24R-4
Interval (cm)	120-124	125-130	54-72
Piece	18	18	3
Lab.number	Z-1554	Z-1555	Z-1718
Depth (mbsf)	186.64	188.19	189.04
Major elements (g/1000 cm^3):			
Si	471.9	538.9	568.6
Ti	24.0	24.8	35.1
Al	122.8	153.8	161.3
Fe^{+++}	178.8	89.4	170.1
Fe^{++}	11.2	46.3	95.3
Fe (Sum)	190.0	135.7	265.4
Mn	3.2	2.1	1.5
Mg	276.4	204.6	197.4
Ca	85.3	132.9	209.8
Na	25.0	37.2	48.0
K	21.7	19.8	19.8
P	2.2	2.1	2.4
Minor elements (g/1000 cm^3 x 10^{-3}):			
La	46.6	45.4	52.8
Ce	109.5	100.4	105.6
Nd	51.3	47.8	50.0
Sm	10.7	10.0	11.7
Eu	3.5	3.1	3.9
Tb	1.9	1.8	1.9
Yb	3.5	2.9	3.9
Lu	0.5	0.4	0.6
Cr	1339.8	1649.1	1598.5
Ni	717.6	764.8	597.7
Co	184.1	172.1	166.8
V	284.3	626.2	561.6
Cu	107.2	109.9	105.6
Zn	247.0	262.9	311.4
Zr	268.0	286.8	347.5
Nb	44.3	45.4	61.2
Y	37.3	40.6	58.4
Rb	25.6	50.2	41.7
Sr	86.2	812.6	764.5
Ba	205.0	334.6	889.6
H_2O^+ (wt%)	4.01	3.42	3.61
Density (g/cm^3)	2.33	2.39	2.78
Fe_2O_3/FeO	17.76	2.15	1.98

Table AT29. Abundance of major and trace elements (g/1000 cm^3) in hawaiites, basanites, and alkaline olivine basalts, Hole 878A, Leg 144 (MIT Guyot, West Pacific Guyots). (Continued on next five pages.)

Leg	144	144	144	144	144	144	144
Hole	878A	878A	878A	878A	878A	878A	878A
Core, section	78R-2	79R-2	79R-4	80R-5	80R-5	81R-2	81R-4
Interval (cm)	64-70	9-12	24-27	20-24	106-109	10-15	120-124
Piece	3B	1	1	1G	4B	1	12
Lab number	Z-1556	Z-873	Z-874	Z-1557	Z-876	Z-1558	Z-1559
Depth (mbsf)	724.12	733.22	736.07	747.16	748.02	752.55	756.35
Major elements (g/1000 cm^3):							
Si	597.6	575.9	614.9	556.2	544.7	553.0	562.6
Ti	53.4	50.2	50.4	64.0	57.3	64.6	64.9
Al	252.5	235.8	258.1	191.7	177.4	196.1	220.7
Fe^{+++}	160.1	196.9	132.0	148.2	152.5	221.1	199.3
Fe^{++}	82.2	51.7	48.1	126.2	111.5	70.2	76.6
Fe (Sum)	242.3	248.6	180.2	274.3	264.1	291.3	275.9
Mn	2.8	3.6	7.4	4.7	2.9	2.9	3.7
Mg	69.1	55.3	42.5	184.6	186.5	181.9	112.1
Ca	156.2	109.7	89.0	255.2	233.4	225.3	203.7
Na	71.4	63.4	64.4	33.5	34.7	33.5	42.9
K	43.8	82.6	105.8	13.8	15.1	17.8	35.3
P	9.5	8.4	9.7	8.5	7.7	8.3	9.3
Minor elements (g/1000 cm^3 x 10^{-3}):							
La	128.3			126.3			
Ce	382.2			278.4			
Nd	163.8			137.8			
Sm	27.3			31.6			
Eu	9.3			7.7			
Tb	4.4			3.7			
Yb	6.6			5.5			
Lu	0.9			0.7			
Cr	87.4	82.2	89.8	1435.0	1223.2	1125.8	611.6
Ni	106.5	106.0	232.3	588.4	722.8	527.3	422.6
Co	92.8	98.1	169.0	195.2	180.7	159.6	147.3
V	344.0	508.8	580.8	990.2	672.8	624.2	672.8
Cu	98.3	87.5	409.2	149.2	180.7	142.5	119.5
Zn	365.8	259.7	332.6	307.1	258.5	290.7	322.5
Zr	764.4	742.0	844.8	832.3	861.8	826.5	889.6
Nb	161.1	143.1	161.0	160.7	147.3	153.9	152.9
Y	79.2	74.2	84.5	74.6	83.4	68.4	86.2
Rb	103.7	132.5	129.4	19.5	139.0	22.8	80.6
Sr	1911.0	980.5	1293.6	1607.2	1417.8	1567.5	1723.6
Ba	464.1	954.0	1927.2	1320.2	708.9	239.4	333.6
H_2O^+ (wt%)	1.06	2.08	1.86	2.48	3.08	2.01	1.51
Density (g/cm^3)	2.73	2.65	2.64	2.87	2.78	2.85	2.78
Fe_2O_3/FeO	2.16	4.24	3.05	1.31	1.52	3.50	2.89

Table AT29 (continued).

Leg	144	144	144	144	144	144	144
Hole	878A	878A	878A	878A	878A	878A	878A
Core, section	81r-5	83R-3	84R-2	84R-3	84R-3	84R-5	85R-2
Interval (cm)	42-45	84-87	119-123	18-22	116-120	114-118	110-114
Piece	3A	4	6C	2A	8C	9B	8
Lab number	Z-1560	Z-877	Z-878	Z-1561	Z-1562	Z-879	Z-1563
Depth (mbsf)	756.94	774.00	782.55	783.04	784.02	786.95	791.90
Major elements (g/1000 cm^3):							
Si	554.4	436.7	547.4	542.1	544.5	555.0	564.8
Ti	64.4	52.3	47.9	55.9	54.4	48.2	58.4
Al	215.6	207.7	193.7	195.0	201.6	194.5	211.7
Fe^{+++}	176.1	248.0	156.6	164.6	128.3	109.6	156.2
Fe^{++}	106.1	16.3	78.6	101.5	140.3	136.4	126.1
Fe (Sum)	282.2	264.3	235.1	266.1	268.6	246.0	282.3
Mn	7.0	3.2	4.1	3.7	3.8	3.0	6.5
Mg	148.2	85.1	153.8	165.3	219.5	194.2	153.0
Ca	183.3	59.9	194.1	217.1	174.2	202.7	226.6
Na	40.9	31.6	32.9	29.4	22.6	35.5	38.1
K	32.6	33.2	29.5	24.6	24.1	25.8	28.2
P	9.0	10.0	7.1	7.5	8.3	6.8	8.8
Minor elements (g/1000 cm^3 x 10^{-3}):							
La					121.3		
Ce					245.3		
Nd					121.3		
Sm					25.7		
Eu					7.9		
Tb					3.7		
Yb					5.6		
Lu					0.7		
Cr	600.5	618.3	877.8	1012.9	978.5	538.2	707.5
Ni	411.4	206.1	625.1	601.7	597.8	281.5	495.3
Co	139.0	151.1	146.3	176.6	217.1	121.4	161.3
V	617.2	584.0	571.9	695.5	693.7	565.8	645.2
Cu	139.0	107.6	146.3	143.5	132.5	124.2	161.3
Zn	375.3	309.2	247.4	347.8	363.8	276.0	350.9
Zr	861.8	1122.1	851.2	772.8	817.8	828.0	877.3
Nb	152.9	185.5	149.0	151.8	160.7	143.5	181.1
Y	86.2	61.8	87.8	74.5	79.0	77.3	82.1
Rb	77.8	16.5	74.5	63.5	62.0	69.0	73.6
Sr	1695.8	1351.1	824.6	1656.0	1212.6	1559.4	1867.8
Ba	236.3	320.6	691.6	910.8	279.2	883.2	268.9
H_2O^+ (wt%)	2.26	5.47	2.65	3.71	4.17	2.54	1.84
Density (g/cm^3)	2.78	2.29	2.66	2.76	2.82	2.76	2.83
Fe_2O_3/FeO	1.85	16.93	2.22	1.80	1.02	0.89	1.38

Table AT29 (continued).

Leg	144	144	144	144	144	144	144
Hole	878A	878A	878A	878A	878A	878A	878A
Core, section	88R-3	89R-2	89R-4	90R-1	90R-2	90R-4	90R-6
Interval (cm)	88-92	0-5	31-35	90-95	32-36	115-120	0-5
Piece	7	1A	3	6C	1B	8	1
Lab number	Z-1564	Z-1565	Z-1566	Z-1567	Z-1568	Z-1569	Z-1570
Depth (mbsf)	821.59	828.82	831.83	838.10	838.78	842.61	844.36
Major elements (g/1000 cm^3):							
Si	505.6	576.0	634.1	626.9	515.4	525.2	612.2
Ti	53.9	58.5	55.8	51.3	44.7	57.5	56.0
Al	208.5	207.0	227.9	189.2	172.2	198.4	189.9
Fe^{+++}	209.5	198.9	134.5	171.8	205.1	221.9	170.8
Fe^{++}	27.7	87.1	128.4	86.0	16.8	14.2	105.7
Fe (Sum)	237.2	286.0	262.9	257.8	221.8	236.1	276.5
Mn	4.1	3.1	3.9	6.9	4.4	4.2	3.9
Mg	57.8	123.2	125.4	113.7	63.6	85.4	113.6
Ca	89.4	171.7	176.9	161.9	66.1	60.4	141.3
Na	55.6	57.0	68.6	74.6	57.4	58.5	66.3
K	46.7	29.2	36.0	41.1	40.1	45.9	36.9
P	7.8	7.8	9.0	9.5	8.3	9.5	9.2
Minor elements (g/1000 cm^3 x 10^{-3}):							
La		91.4	114.3	119.1		105.2	
Ce		235.5	266.6	271.5		231.8	
Nd		119.1	140.6	135.7		119.5	
Sm		26.0	32.2	30.5		31.1	
Eu		8.9	9.1	7.8		5.7	
Tb		3.6	4.4	3.3		2.9	
Yb		5.3	7.0	7.5		7.4	
Lu		0.7	1.0	1.2		1.1	
Cr	559.2	711.9	536.2	443.2	447.8	449.3	445.5
Ni	396.1	526.3	392.6	241.0	333.0	219.9	222.8
Co	107.2	133.0	99.6	83.1	85.5	105.2	107.3
V	480.0	598.3	357.5	476.4	423.0	831.7	577.5
Cu	102.5	105.3	108.4	108.0	101.3	102.8	99.0
Zn	314.6	374.0	445.4	440.4	326.3	370.5	412.5
Zr	699.0	651.0	849.7	941.8	787.5	979.9	962.5
Nb	130.5	116.3	146.5	155.1	130.5	126.7	121.0
Y	67.6	77.6	87.9	91.4	72.0	88.4	93.5
Rb	81.6	66.5	102.6	110.8	101.3	95.6	90.8
Sr	1351.4	1440.4	1816.6	1855.9	967.5	1027.7	1430.0
Ba	233.0	249.3	1963.1	1717.4	540.0	1147.2	660.0
H_2O^+ (wt%)	2.23	2.04	2.28	0.72	2.77	2.82	1.60
Density (g/cm^3)	2.33	2.77	2.93	2.77	2.25	2.39	2.75
Fe_2O_3/FeO	8.41	2.54	1.16	2.22	13.61	17.37	1.80

Table AT29 (continued).

Leg	144	144	144	144	144	144	144
Hole	878A	878A	878A	878A	878A	878A	878A
Core, section	91R-2	91R-4	92R-4	93R-1	93R-2	93R-3	94R-1
Interval (cm)	80-84	120-125	50-54	7-11	118-122	120-124	0-4
Piece	4B	13A	1C	3A	22	14	1A
Lab number	Z-1571	Z-1572	Z-1573	Z-1574	Z-1575	Z-1576	Z-880
Depth (mbsf)	848.80	852.14	860.62	865.77	868.37	869.83	875.40
Major elements (g/1000 cm^3):							
Si	641.1	630.6	596.8	528.4	584.6	563.1	594.8
Ti	60.1	62.0	56.7	49.5	54.4	52.9	48.8
Al	215.8	205.7	216.3	174.7	195.7	196.5	211.7
Fe^{+++}	114.6	109.3	158.9	168.3	170.6	197.4	134.9
Fe^{++}	128.1	166.2	93.1	47.4	75.2	40.1	84.2
Fe (Sum)	242.7	275.5	252.0	215.8	245.7	237.4	219.0
Mn	3.7	4.3	4.4	4.2	9.0	2.7	5.0
Mg	96.0	145.7	113.7	105.7	101.8	92.8	118.5
Ca	163.4	167.7	167.9	107.8	165.1	127.3	148.7
Na	71.0	66.3	64.5	56.7	70.8	62.0	61.7
K	38.5	33.4	31.5	29.8	32.1	31.4	32.8
P	9.6	9.7	7.6	7.0	8.4	7.7	7.5
Minor elements (g/1000 cm^3 x 10^{-3}):							
La		109.4		86.0	101.1		
Ce		265.0		188.8	234.1		
Nd		138.2		98.0	125.0		
Sm		34.6		23.2	29.3		
Eu		10.1		6.7	8.5		
Tb		4.3		3.3	4.0		
Yb		8.1		5.7	7.2		
Lu		1.0		0.8	1.0		
Cr	483.3	512.6	596.2	466.1	462.8	435.2	1008.8
Ni	219.2	230.4	483.0	382.4	244.7	253.4	686.0
Co	106.8	115.2	132.5	124.3	93.1	105.0	158.7
V	584.5	604.8	629.3	573.6	532.0	550.4	583.7
Cu	146.1	123.8	179.4	124.3	138.3	115.2	182.9
Zn	477.7	380.2	248.4	227.1	255.4	235.5	266.3
Zr	997.6	964.8	772.8	717.0	798.0	742.4	780.1
Nb	132.1	123.8	110.4	102.8	117.0	112.6	107.6
Y	106.8	100.8	85.6	76.5	93.1	94.7	83.4
Rb	92.7	83.5	85.6	74.1	82.5	81.9	56.5
Sr	1742.2	1728.0	1435.2	932.1	1529.5	1126.4	1640.9
Ba	674.4	1728.0	496.8	549.7	611.8	537.6	820.5
H_2O^+ (wt%)	1.14	1.16	1.91	2.66	1.23	2.04	2.50
Density (g/cm^3)	2.81	2.88	2.76	2.39	2.66	2.56	2.69
Fe_2O_3/FeO	1.00	0.73	1.90	3.94	2.52	5.48	1.78

Table AT29 (continued).

Leg	144	144	144	144	144	144	144
Hole	878A	878A	878A	878A	878A	878A	878A
Core, section	94R-2	94R-3	94R-5	94R-7	95R-3	95R-5	97R-1
Interval (cm)	0-5	124-129	102-107	70-74	125-128	0-5	20-24
Piece	1A	1	1	1	9	1	7B
Lab number	Z-1577	Z-1578	Z-1579	Z-1580	Z-1582	Z-1583	Z-1584
Depth (mbsf)	876.89	879.32	881.64	883.82	888.75	890.22	894.60
Major elements (g/1000 cm^3):							
Si	425.0	452.4	393.3	367.5	387.5	371.6	647.45
Ti	38.0	41.1	47.1	38.5	35.8	34.5	60.67
Al	142.0	145.6	131.2	144.2	140.0	130.5	214.47
Fe^{+++}	170.3	187.6	216.6	164.6	161.4	154.5	119.35
Fe^{++}							183.46
Fe (Sum)	170.3	187.6	216.6	164.6	161.4	154.5	302.82
Mn	1.1	3.3	4.1	4.3	2.7	1.1	3.67
Mg	74.4	64.8	64.3	59.1	58.7	60.7	117.59
Ca	29.1	38.4	40.1	28.5	45.6	42.9	183.55
Na	23.6	25.7	22.7	21.2	22.4	21.5	70.25
K	6.7	7.6	4.2	4.4	29.4	30.2	31.94
P	3.4	3.5	7.0	1.2	8.5	8.5	8.40
Minor elements (g/1000 cm^3 x 10^{-3}):							
La	68.1			58.6			99.96
Ce	156.4			145.0			220.50
Nd	77.3			89.2			123.48
Sm	17.7			22.3			32.34
Eu	3.3			5.3			6.76
Tb	2.0			3.3			3.53
Yb	4.4			5.9			7.64
Lu	0.7			1.0			1.32
Cr	309.1	330.0	353.1	513.2	292.4	278.8	270.48
Ni	182.2	256.7	276.6	264.9	152.2	134.5	229.32
Co	97.5	98.4	132.9	228.7	90.0	78.7	105.84
V	147.2	202.7	336.7	139.4	302.8	314.9	558.60
Cu	73.6	77.2	111.0	97.6	95.2	80.4	144.06
Zn	136.2	139.0	234.8	217.5	159.2	144.3	364.56
Zr	423.2	482.5	546.0	725.1	449.8	426.4	882.00
Nb	58.9	69.5	72.8	97.6	62.3	60.7	111.72
Y	69.9	73.3	63.7	61.4	57.1	55.8	105.84
Rb	27.6	29.0	6.6	15.6	50.2	39.4	79.38
Sr	239.2	250.9	273.0	418.3	328.7	328.0	1646.40
Ba	570.4	250.9	172.9	460.2	778.5	623.2	1323.00
H_2O^+ (wt%)	6.09	5.95	5.61	6.02	4.21	3.47	0.79
Density (g/cm^3)	1.84	1.93	1.82	1.67	1.73	1.64	2.94
Fe_2O_3/FeO							0.72

Table AT29 (continued).

Leg	144	144	144
Hole	878A	878A	878A
Core, section	97R-2	98R-2	98R-3
Interval (cm)	28-31	93-96	8-12
Piece	3D	5D	1B
Lab number	Z-881	Z-882	Z-1585
Depth (mbsf)	896.18	906.28	906.87
Major elements (g/1000 cm^3):			
Si	574.6	623.1	632.7
Ti	48.7	51.2	59.3
Al	209.1	209.9	210.4
Fe^{+++}	94.8	115.3	121.8
Fe^{++}	137.4	151.8	158.4
Fe (Sum)	232.2	267.0	280.3
Mn	2.8	3.8	3.7
Mg	98.2	154.6	153.3
Ca	155.9	185.7	184.6
Na	61.7	61.6	59.1
K	28.5	33.3	30.7
P	6.9	6.8	7.9
Minor elements (g/1000 cm^3 x 10^{-3}):			
La			
Ce			
Nd			
Sm			
Eu			
Tb			
Yb			
Lu			
Cr	425.7	748.8	586.0
Ni	232.2	748.8	571.4
Co	100.6	135.4	111.3
V	585.7	625.0	515.7
Cu	160.0	388.8	334.0
Zn	361.2	374.4	334.0
Zr	799.8	835.2	761.8
Nb	98.0	109.4	123.1
Y	90.3	89.3	82.0
Rb	80.0	72.0	79.1
Sr	1006.2	1612.8	1611.5
Ba	722.4	777.6	556.7
H_2O^+ (wt%)	1.47	1.26	1.38
Density (g/cm^3)	2.58	2.88	2.93
Fe_2O_3/FeO	0.77	0.84	0.86

Table AT30. Abundance of major and trace elements (g/1000 cm^3) in trachy-andesites, Hole 465A, Leg 62 (Southern Hess Rise, Pacific Ocean). (Continued on next page.)

Leg	62	62	62	62	62	62	62
Hole	465A	465A	465A	465A	465A	465A	465A
Core, section	41-2	42-1	42-3	43-2	44-1	44-3	45-1
Interval (cm)	90-93	128-132	98-103	130-135	112-116	118-123	81-85
Piece	11A	8A	9	14A	13B	7A	5D
Lab number	Z-383	Z-384	Z-385	Z-386	Z-387	Z-388	Z-389
Depth (mbsf)	421.4	429.78	432.48	440.8	448.62	457.68	457.81
Major elements (g/1000 cm^3):							
Si	546	532	549	599	597	598	606
Ti	16	15	16	18	16	16	14
Al	189	173	181	218	194	199	197
Fe^{+++}	54	60	66	36	61	52	69
Fe^{++}	6	13	5	9	9	16	20
Fe (Sum)	60	73	71	45	70	68	89
Mn	0.2	0.2	0.2	0.2	0.2	0.2	0.5
Mg	26	18	20	13	12	8	7
Ca	40	41	42	45	41	52	40
Na	84	84	75	85	91	79	83
K	69.0	83.0	79.0	77.0	91.0	116.0	117.0
P	2.6	2.2	1.8	2.1	1.5	1.1	1.0
Minor elements (g/1000 cm^3 x 10^{-3}):							
La	191.9	162.1	181.1	193.9	191.6	190.2	189.5
Ce	336.3	289.5	334.7	358.4	337.0	345.9	348.5
Nd	156.3	139.0	141.7	149.7	158.0	157.8	159.0
Sm	23.7	21.2	21.7	23.2	23.2	23.8	24.0
Eu	6.5	5.4	5.9	6.5	6.5	6.5	6.3
Tb	3.4	2.7	3.1	3.2	3.4	3.2	3.5
Yb	8.9	6.0	6.1	6.5	7.2	8.2	7.8
Lu	1.4	0.9	0.9	0.9	1.0	1.3	1.2
Ni	10		10		11		
Co	20	12	14	13	11	11	11
V	99	96	89	95	105	97	98
Cu		10	10			11	11
Zn	59	68	39	137	369	238	272
Zr	1128	1447	1201	1434	1622	1751	1546
Y	110.8	75.3	66.9	84.3	92.7	112.4	91.5
Nb	174.1	167.9	165.4	210.8	174.8	192.4	215.6
Rb	31.7	46.3	45.3	52.7	65.3	125.4	130.7
Sr	475	405	413	590	548	411	392
Ba	1286	1139	1201	1455	1432	1319	1372
H_2O^+ (wt%)	2.07	1.53	1.49	1.06	0.99	0.77	0.80
Density (g/cm^3)	1.98	1.93	1.97	2.11	2.11	2.16	2.18
Fe_2O_3/FeO	10.03	5.18	13.76	4.72	7.44	3.56	3.90

Table AT30 (continued).

Leg	62	62
Hole	465A	465A
Core, section	46-1	46-3
Interval (cm)	82-86	57-61
Piece	6G	8
Lab number	Z-390	Z-391
Depth (mbsf)	467.32	470.07
Major elements (g/1000 cm^3):		
Si	594	588
Ti	15	15
Al	196	203
Fe^{+++}	41	51
Fe^{++}	22	13
Fe (Sum)	63	64
Mn	0.7	0.5
Mg	4	16
Ca	78	97
Na	80	92
K	123.0	75.0
P	1.1	2.7
Minor elements (g/1000 cm^3 x 10^{-3}):		
La	186.5	191.8
Ce	329.0	356.9
Nd	155.7	160.6
Sm	21.9	24.5
Eu	6.4	6.9
Tb	3.3	3.1
Yb	7.5	5.6
Lu	1.1	0.8
Ni		11
Co	11	11
V	99	100
Cu	15	
Zn	318	145
Zr	1533	1517
Y	89.9	75.8
Nb	120.6	180.7
Rb	131.4	49.1
Sr	416	691
Ba	1228	1427
H_2O^+ (wt%)	1.12	1.21
Density (g/cm^3)	2.19	2.23
Fe_2O_3/FeO	2.07	4.24

Table AT31. Abundance of major and trace elements (g/1000 cm^3) in basalts, Hole 642E, Leg 104 (Vøring Plateau, Norwegian Sea). (Continued in next two pages).

Leg	104	104	104	104	104	104	104
Hole	642E	642E	642E	642E	642E	642E	642E
Core, section	9R-1	10R-2	15R-3	18R-4	22R-5	30R-2	40R-1
Interval (cm)	59-62	87-90	77-80	13-16	32-35	76-79	33-36
Piece	4E	12	14	1A	2	2A	2D
Lab number	Z-153	Z-154	Z-156	Z-157	Z-159	Z-160	Z-161
Depth (mbsf)	366.49	375.87	409.07	437.33	476.82	541.76	631.43
Major elements (g/1000 cm^3):							
Si	617	587	608	672	602	661	613
Ti	29	32	33	28	27	44	31
Al	232	232	215	234	229	210	214
Fe^{+++}	99	120	120	93	86	109	108
Fe^{++}	141	92	128	157	120	179	118
Fe (Sum)	240	212	248	250	206	288	226
Mn	3.8	2.8	4.0	3.5	3.2	3.7	3.1
Mg	133	105	128	154	115	129	136
Ca	255	199	235	268	250	249	239
Na	48	49	51	50	50	57	50
K	3.6	9.8	3.1	3.80	2.3	5.0	3.0
P	1.9	1.9	1.60	1.70	1.2	1.6	1.4
Minor elements (g/1000 cm^3 x 10^{-3}):							
La	14.7	13.4	10.7	12.9	11.0	20.9	16.8
Ce	36.8	31.6	30.3	30.0	26.9	53.1	38.6
Nd	31.1	26.3	26.4	27.0		41.3	33.1
Sm	10.2	9.2	9.1	9.0	8.1	13.0	10.7
Eu	3.7	3.4	3.6	3.6	3.5	4.7	3.9
Gd	12.7	11.1	12.9	12.9	11.8	16.8	12.1
Tb	2.4	2.1	2.3	2.3	2.1	3.2	2.1
Tm	1.3	0.9	1.1	1.2		1.7	1.0
Yb	7.9	5.3	6.6	6.9	6.2	8.8	7.4
Lu	1.2	0.8	1.0	1.1	0.9	1.4	1.1
Sc	127	134	118	135	124	139	
Cr	622	882	716	900	443	678	868
Ni	410	434	399	375	242	265	303
Co	161	211	168	168	150	150	154
V	693	816	551	645	564	825	716
Cu	334	242	330	300	510	295	154
Zn	226	187	248	204	201	230	207
Zr	158	226	190	168	118	292	223
Y	70.7	71.1	63.3	63.0	56.4	94.3	63.3
Nb	13.6	12.1	12.4	12.3	11.8	18.0	14.6
Rb		14.2	3.3	3.9		2.9	
Sr	368	368	413	450	349	531	468
Ba	57	58	72	81	51	121	83
H_2O^+ (wt%)	1.36	1.85	0.98	0.89	0.88	0.67	1.41
Density (g/cm^3)	2.83	2.63	2.75	3.00	2.69	2.90	2.75
Fe_2O_3/FeO	0.78	1.45	1.04	0.66	0.79	0.68	1.02

Table AT31 (continued).

Leg	104	104	104	104	104	104	104
Hole	642E	642E	642E	642E	642E	642E	642E
Core, section	46R-3	60R-1	60R-2	69R-2	78R-2	88R-2	91R-1
Interval (cm)	40-43	68-71	25-27	59-61	46-48	70-72	18-20
Piece	1C	14	1C	1D	5A	7B	3
Lab number	Z-162	Z-163	Z-164	Z-165	Z-166	Z-167	Z-168
Depth (mbsf)	691.5	785.58	786.65	865.29	942.36	1037	1063.48
Major elements (g/1000 cm^3):							
Si	661	527	576	613	618	632	544
Ti	42	39	41	30	38	26	21
Al	207	175	179	225	208	214	188
Fe^{+++}	109	171	154	118	131	137	143
Fe^{++}	189	82	106	119	135	107	56
Fe (Sum)	298	253	260	237	266	244	199
Mn	4.6	3.6	3.8	1.3	3.7	4.0	1.9
Mg	128	138	147	123	118	128	107
Ca	251	132	170	227	236	249	167
Na	53	47	48	52	52	47	40
K	3.7	15.7	7.5	4.2	3.1	10.0	21.4
P	2.1	1.8	1.8	1.6	1.9	1.4	1.6
Minor elements (g/1000 cm^3 x 10^{-3}):							
La	18.8	17.9	19.0	14.0	20.8	13.2	12.1
Ce	50.0	43.5	44.2	38.4	49.8	25.8	23.6
Nd	41.2	36.3	41.6	32.9	41.5	28.1	23.6
Sm	13.2	12.1	13.5	10.7	14.1	9.8	7.8
Eu	4.7	4.4	4.4	4.1	5.0	3.6	2.6
Gd	16.5	14.3	14.3	14.0	0.0	12.9	10.9
Tb	2.7	2.7	2.6	2.5	2.7	2.3	1.9
Tm		1.3				1.5	1.1
Yb	9.1	7.5	8.1	8.2	9.4	8.7	7.3
Lu	1.4	1.0	1.2	1.2	1.4	1.3	1.1
Sc	135	109	112	121	133	135	125
Cr	412	701	766	809	526	1067	603
Ni	294	278	325	302	222	351	201
Co	165	152	161	164	158	174	113
V	1000	1088	1169	850	803	814	1064
Cu	294	725	286	208	277	309	87
Zn	229	189	234	236	258	196	161
Zr	276	242	286	211	266	174	128
Y	85.3	72.5	72.7	68.5	80.3	70.2	70.9
Nb	16.2	14.0	16.1	10.7	15.2	10.4	7.3
Rb		7.0	3.4			53.3	96.9
Sr	470	363	416	411	498	393	236
Ba	103	58	75	52	94	84	
H_2O^+ (wt%)	0.45	1.63	1.35	0.91	0.52	0.84	1.33
Density (g/cm^3)	2.94	2.42	2.60	2.70	2.77	2.67	2.36
Fe_2O_3/FeO	0.64	2.30	1.61	1.10	1.08	1.42	2.84

Table AT31 (continued).

Leg	104	104	104	104
Hole	642E	642E	642E	642E
Core, section	94R-1	102R-2	105R-1	110R-1
Interval (cm)	32-34	45-47	64-66	39-41
Piece	1B	6	7A	5B
Lab number	Z-169	Z-170	Z-171	Z-172
Depth (mbsf)	1085.32	1155.45	1173.14	1220.29
Major elements (g/1000 cm^3):				
Si	656	506	692	561
Ti	23	17	23	19
Al	232	165	190	173
Fe^{+++}	68	36	122	197
Fe^{++}	166	6	208	22
Fe (Sum)	234	42	330	219
Mn	5.1	0.7	4.9	3.6
Mg	157	18	137	52
Ca	266	57	222	153
Na	43	32	55	68
K	3.2	126	5.0	24.0
P	1.4	2.2	1.3	1.4
Minor elements (g/1000 cm^3 x 10^{-3}):				
La	12.9	96.5	13.1	37.5
Ce	26.5	218.5	29.8	82.0
Nd	28.2	123.8	25.0	42.2
Sm	8.8	21.8	7.7	10.1
Eu	2.9	3.8	2.5	2.6
Gd	11.8	27.3	12.5	13.6
Tb	2.0	4.2	2.3	1.1
Tm		2.5	1.7	1.3
Yb	7.3	16.9	11.3	7.3
Lu	1.1	2.7	1.7	1.1
Sc	144	58	179	127
Cr	970	140	566	387
Ni	426	46	417	40
Co	159	25	208	129
V	661	300	1012	633
Cu	353	49	196	52
Zn	170	237	387	211
Zr	162	528	146	234
Y	64.7	147.5	98.2	82.0
Nb	5.6	41.9	5.1	17.1
Rb	6.5	309.5	17.9	86.7
Sr	323	273	193	281
Ba	1323	273	167	422
H_2O^+ (wt%)	1.33	1.36	0.86	1.64
Density (g/cm^3)	2.86	1.75	2.88	2.34
Fe_2O_3/FeO	0.45	6.69	0.65	10.09

Table AT32. Abundance of major and trace elements (g/1000 cm^3) in basalts, Hole 417A, Leg 51 (Bermuda Rise, Atlantic Ocean).

Leg	51	51	51
Hole	417A	417A	417A
Core, section	29-5	32-2	44-3
Interval (cm)	58-61	5-8	31-34
Piece	5	1	1A
Lab number	Z-511	Z-512	Z-513
Depth (mbsf)	271.58	295.05	397.81
Major elements (g/1000 cm^3):			
Si	597.9	564.2	679.4
Ti	26.1	23.5	26.1
Al	242.0	254.1	261.1
Fe^{+++}	137.7	157.8	86.2
Fe^{**}	72.5	54.5	140.0
Fe (Sum)	210.2	212.3	226.2
Mn	1.3	0.6	1.4
Mg	102.2	72.9	110.6
Ca	208.4	209.0	246.5
Na	45.2	40.7	49.2
K	17.5	32.6	2.2
P	1.8	2.9	1.7
Minor elements (g/1000 cm^3 x 10^{-3}):			
La	7.0	6.4	7.0
Ce	21.6	20.9	22.2
Nd	23.0	22.3	24.5
Sm	9.7	8.7	9.3
Eu	3.2	2.9	3.2
Tb	2.6	2.2	2.6
Yb	9.5	8.2	9.3
Lu	1.5	1.3	1.4
Cr	783.0	681.1	890.6
Ni	191.7	124.6	257.0
Co	110.7	95.4	146.0
V	958.5	720.8	963.6
Cu	221.4	209.4	271.6
Zn	297.0	217.3	254.0
Sn	4.9	6.4	7.0
Zr	243.0	227.9	245.3
Y	86.4	76.9	87.6
Nb	5.1	6.1	6.1
Rb	32.4	47.7	4.7
Sr	270.0	291.5	283.2
Ba	202.5	148.4	61.3
H_2O^* (wt%)	2.09	2.38	0.38
Density (g/cm^3)	2.70	2.65	2.92
Fe_2O_3/FeO	2.81	2.97	2.80

Table AT33. Abundance of major and trace elements (g/1000 cm^3) in basalts, Hole 418A, Legs 52 and 53 (Bermuda Rise, Atlantic Ocean). (Continued on next two pages.)

Leg	52	52	52	52	52	52	52
Hole	418A	418A	418A	418A	418A	418A	418A
Core, section	15-1	15-3	18-1	19-4	19-7	20-5	27-1
Interval (cm)	98-101	129-132	81-84	86-89	6-9	10-13	33-35
Piece	1I	4D	2F	1I	1A	1B	1D
Lab number	Z-297	Z-298	Z-299	Z-300	Z-301	Z-302	Z-303
Depth (mbsf)	320.98	324.29	339.81	353.36	357.06	363.10	393.83
Major elements (g/1000 cm^3):							
Si	623	612	653	685	612	706	643
Ti	20	21	20	22	23	26	27
Al	214	239	230	241	215	268	246
Fe^{+++}	88	89	73	66	64	58	96
Fe^{++}	124	97	157	162	135	156	106
Fe (Sum)	212	186	230	228	199	214	202
Mn	2.6	2.1	2.7	3.5	3.1	3.6	4.7
Mg	124	123	127	132	115	139	125
Ca	273	226	268	281	248	278	260
Na	52	55	52	55	54	58	58
K	3.7	5.0	3.8	4.0	3.8	4.4	2.9
P	0.9	1.1	0.1	0.7	2.2	2.2	2.8
Minor elements (g/1000 cm^3 x 10^{-3}):							
La	5.0	4.8	5.4	5.1	5.3	5.5	5.7
Ce	16.3	16.9	16.9	18.7	17.8	16.8	18.3
Nd	16.6	17.7	17.1	18.2	17.5	18.1	20.0
Sm	6.6	7.0	7.1	7.1	7.4	7.0	8.6
Eu	2.4	2.6	2.5	2.7	2.6	2.8	2.9
Tb	1.9	2.0	1.9	2.1	2.0	2.2	2.4
Yb	7.5	7.2	7.4	8.0	7.7	8.0	9.4
Lu	1.2	1.1	1.2	1.2	1.1	1.2	1.4
Cr	526	524	514	580	478	551	620
Ni	241	199	229	298	205	236	329
Co	102	97	106	110	104	119	137
V	553	618	657	774	611	627	771
Cu	291	201	171	268	279	367	357
Zn	166	193	171	250	292	220	271
Zr	127	140	137	152	149	168	
Y	69.2	72.5	68.6	77.4	66.4	82.6	82.9
Nb	6.4	7.0	6.9	7.4	5.3	7.0	3.7
Rb		2.4	2.0		2.4	3.7	1.4
Sr	277	322	286	327	292	337	
Ba							
H_2O^+ (wt%)	0.81	1.06	0.69	0.61	0.51	0.13	1.08
Density (g/cm^3)	2.77	2.68	2.86	2.98	2.91	2.92	2.86
Fe_2O_3/FeO	0.78	1.02	0.52	0.46	0.53	0.41	1.01

Table AT33 (continued).

Leg	52	52	52	53	53	53	53
Hole	418A	418A	418A	418A	418A	418A	418A
Core, section	27-2	38-1	38-3	52-1	52-4	77-2	77-3
Interval (cm)	91-93	41-44	10-13	61-64	29-32	57-60	33-36
Piece	5B	2C	1A	6B	2	4A	2B
Lab number	Z-304	Z-305	Z-306	Z-307	Z-308	Z-310	Z-311
Depth (mbsf)	395.91	479.91	482.60	592.81	596.99	795.17	796.43
Major elements (g/1000 cm^3):							
Si	557	596	626	645	651	634	779
Ti	24	22	26	22	22	27	32
Al	256	255	264	263	257	254	294
Fe^{+++}	171	87	82	67	66	43	54
Fe^{++}	73	73	105	128	132	129	178
Fe (Sum)	244	160	187	195	198	172	232
Mn	2.9	2.7	4.2	4.5	4.1	4.4	5.3
Mg	94	113	99	117	127	127	139
Ca	216	203	279	278	275	313	330
Na	46	50	52	56	48	53	59
K	2.5	23.3	10.2	3.6	1.5	3.0	3.4
P	1.8	2.0	2.5	2.4	2.2	2.7	2.1
Minor elements (g/1000 cm^3 x 10^{-3}):							
La	5.5	4.5	5.1	4.9	5.5	6.4	8.5
Ce	16.5	16.0	16.6	14.6	16.4	18.4	23.9
Nd	17.8	15.8	18.0	15.8	19.3	19.3	27.4
Sm	7.6	7.6	7.9	6.6	7.5	7.9	10.6
Eu	2.6	2.6	2.7	2.5	2.6	2.7	3.8
Tb	2.1	2.0	2.2	1.9	2.2	2.0	2.9
Yb	7.9	6.8	8.5	8.3	8.6	8.8	11.3
Lu	1.1	0.9	1.3	1.2	1.3	1.3	1.6
Cr	615	618	499	645	647	357	537
Ni	288	355	208	444	474	257	393
Co	107	158	79	115	103	111	140
V	733	697	592	602	632	672	974
Cu	314	250	310	315	244	263	359
Zn	275	302	254	258	279	284	376
Zr	168	150	175	140	132	155	150
Y	68.1	65.7	73.2	83.1	57.5	81.8	102.6
Nb	6.3	5.0	5.1	6.0	6.3	9.1	9.6
Rb	3.9	9.5	23.1			2.6	5.1
Sr	314	289	310	252	282	322	287
Ba		81					
H_2O^+ (wt%)	1.33	1.43	1.24	0.55	0.66	0.47	0.42
Density (g/cm^3)	2.62	2.63	2.82	2.86	2.87	2.92	2.80
Fe_2O_3/FeO	2.59	1.32	0.87	0.58	0.56	0.37	0.33

Table AT33 (continued).

Leg	53	53
Hole	418A	418A
Core, section	84-2	85-2
Interval (cm)	51-54	48-51
Piece	1D	3
Lab number	Z-312	Z-313
Depth (mbsf)	847.51	851.98
Major elements (g/1000 cm^3):		
Si	660	679
Ti	21	23
Al	267	251
Fe^{+++}	38	42
Fe^{++}	150	166
Fe (Sum)	188	208
Mn	4.4	4.7
Mg	142	152
Ca	265	274
Na	54	48
K	2.7	3.0
P	1.7	1.7
Minor elements (g/1000 cm^3 x 10^{-3}):		
La	5.3	5.1
Ce	15.8	16.4
Nd	16.1	17.6
Sm	7.0	7.2
Eu	2.4	2.7
Tb	1.9	1.9
Yb	7.9	8.1
Lu	1.2	1.3
Cr	482	657
Ni	453	508
Co	123	131
V	526	628
Cu	277	448
Zn	286	344
Zr	114	164
Y	75.9	77.7
Nb	7.3	5.1
Rb	1.8	2.7
Sr	202	290
Ba		
H_2O^+ (wt%)	0.50	1.20
Density (g/cm^3)	2.92	2.99
Fe_2O_3/FeO	0.29	0.28

Table AT34. Abundance of major and trace elements (g/1000 cm^3) in basalts, Hole 317A, Leg 33 (Manihiki Plateau, Pacific Ocean). (Continued on next page.)

Leg	33	33	33	33	33	33	33
Hole	317A	317A	317A	317A	317A	317A	317A
Core, section	31-3	31-4	32-1	32-2	32-3	32-4	32-5
Interval (cm)	20-23	91-94	93-95	120-124	60-65	112-117	58-63
Piece	4B	6D	2D	2I	2F	1G	1B
Lab number	Z-267	Z-268	Z-269	Z-270	Z-271	Z-272	Z-273
Depth (mbsf)	908.70	910.31	915.93	917.70	918.60	920.62	921.58
Major elements (g/1000 cm^3):							
Si	587	598	620	613	631	611	632
Ti	20	19	19	18	20	19	19
Al	209	196	218	212	213	210	215
Fe^{+++}	116	130	118	132	110	139	102
Fe^{++}	80	83	99	87	116	75	87
Fe (Sum)	196	213	217	219	226	214	189
Mn	6.2	2.4	1.9	2.4	2.6	2.5	1.5
Mg	149	141	137	116	137	160	157
Ca	211	205	233	230	244	240	262
Na	31	30	28	29	31	26	29
K	4.1	4.1	4.0	3.9	4.1	4.0	4.1
P	0.6	1.0	0.6	0.8	0.8	0.7	0.6
Minor elements (g/1000 cm^3 x 10^{-3}):							
La	10.4	9.3	8.9	10.3	10.2	7.6	6.9
Ce	23.4	22.7	22.2	24.0	22.9	19.0	18.2
Sm	6.8	6.5	6.2	7.4	7.2	5.7	5.2
Eu	2.6	2.3	2.3	2.6	2.5	2.1	1.9
Tb	1.5	1.4	1.4	1.6	1.7	1.6	1.4
Yb	6.5	6.2	6.2	7.4	7.4	5.7	5.5
Lu	1.0	0.9	1.0	1.1	1.1	0.9	0.9
Cr	663	671	502	414	358	840	1568
Ni	429	374	380	343	345	461	523
Co	166	170	163	158	138	146	165
V	988	904	786	791	717	718	729
Cu	689	697	339	316	262	325	413
Zn	325	374	339	316	303	258	267
Zr	120	124	103	103	113	68	77
Y	44.2	51.6	54.2	52.7	57.9	40.7	44.0
Nb	7.0	7.5	5.7	8.4	7.2	9.2	5.5
Rb	2.1	2.1	2.2	2.6	3.0	2.7	2.5
Sr	286	284	255	243	265	220	184
Ba		49	54	45	55	60	58
H_2O^+ (wt%)	0.95	0.58	0.78	0.23	0.64	0.45	0.28
Density (g/cm^3)	2.60	2.58	2.71	2.64	2.76	2.71	2.75
Fe_2O_3/FeO	1.62	1.74	1.32	1.68	1.05	2.07	1.31

Table AT34 (continued).

Leg	33	33	33	33	33	33
Hole	317A	317A	317A	317A	317A	317A
Core, section	32-6	33-2	33-3	34-1	34-2	34-4
Interval (cm)	64-66	20-25	46-51	32-34	136-141	136-140
Piece	1C	1B	1B	1B	5C	2T
Lab number	Z-274	Z-275	Z-276	Z-277	Z-278	Z-279
Depth (mbsf)	923.14	926.20	927.96	934.32	936.86	939.86
Major elements (g/1000 cm^3):						
Si	610	640	627	616	612	620
Ti	19	19	20	21	19	21
Al	196	205	223	210	217	216
Fe^{+++}	120	99	104	113	79	107
Fe^{++}	85	127	112	96	93	100
Fe (Sum)	205	226	216	209	172	207
Mn	2.5	3.9	2.6	5.4	3.0	2.3
Mg	169	165	162	135	127	128
Ca	240	252	242	221	217	234
Na	24	27	30	30	30	30
K	4.0	5.3	5.3	4.0	8.6	5.3
P	0.6	0.8	1.0	1.0	1.1	0.8
Minor elements (g/1000 cm^3 x 10^{-3}):						
La	8.0	9.2	10.0	15.7	14.8	11.8
Ce	17.7	22.4	25.0	37.3	36.3	29.5
Sm	5.9	6.7	7.2	8.5	8.6	8.0
Eu	2.0	2.1	2.4	2.9	2.9	2.7
Tb	1.4	1.6	1.7	2.2	1.9	1.7
Yb	5.9	6.4	6.9	7.2	7.0	7.0
Lu	0.9	1.0	1.1	1.1	1.1	1.1
Cr	1287	1090	574	613	752	777
Ni	496	405	333	333	350	402
Co	161	140	128	123	109	134
V	751	587	444	666	778	750
Cu	322	503	155	706	467	80
Zn	295	266	291	320	454	295
Zr	40	109	114	163	150	145
Y	42.9	47.5	49.9	53.3	54.4	48.2
Nb	4.8	7.3	5.8	9.1	10.6	8.8
Rb		2.5		2.4	11.4	3.7
Sr	161	268	272	293	285	295
Ba			53	51	70	59
H_2O^+ (wt%)	0.60	0.14	0.10	0.71	0.54	0.49
Density (g/cm^3)	2.68	2.80	2.77	2.67	2.59	2.68
Fe_2O_3/FeO	1.57	0.86	1.02	1.30	0.95	1.19

Table AT35. Abundance of major and trace elements (g/1000 cm^3) in basalts, Hole 254, Leg 26 (Ninetyeast Ridge, Indian Ocean).

Leg	26	26	26	26	26	26
Hole	254	254	254	254	254	254
Core, section	35-1	35-2	35-3	36-1	36-2	36-2
Interval (cm)	123-125	105-107	72-75	140-143	2-4	114-118
Piece	11	14	9	20	1	20
Lab number	Z-100	Z-101	Z-102	Z-103	Z-104	Z-105
Depth (mbsf)	311.23	312.55	313.72	316.40	316.52	317.64
Major elements (g/1000 cm^3):						
Si	557	582	558	541	529	480
Ti	39	42	40	45	42	39
Al	170	154	177	194	179	168
Fe^{+++}	137	186	146	150	190	251
Fe^{++}	166	156	140	109	104	41
Fe (Sum)	303	342	286	259	294	292
Mn	3.4	1.1	3.1	3.4	5.1	0.9
Mg	184	155	164	133	130	97
Ca	176	187	183	156	145	93
Na	46	52	54	57	48	51
K	7.2	6.4	7.7	11.1	9.1	10.3
P	1.8	2.6	1.4	1.5	2.4	1.7
Minor elements (g/1000 cm^3 x 10^{-3}):						
La	30.0	27.5	26.6	33.4	30.6	32.2
Ce	62.8	60.5	63.8	74.5	58.7	64.4
Sm	14.5	13.8	14.1	15.9	13.8	14.5
Eu	4.9	4.7	4.8	4.9	4.8	5.1
Tb	3.0	2.6	2.9	3.3	3.1	2.3
Yb	9.8	9.6	9.6	10.8	10.2	8.1
Lu	1.6	1.5	1.5	1.7	1.5	1.2
Sc	112	110	106	111	105	104
Cr	1324	1238	958	861	893	805
Ni	737	688	665	424	536	460
Co	191	179	160	141	179	161
V	737	770	665	1002	995	1035
Cu	273	440	266	154	574	426
Zn	328	330	293	321	306	276
Zr	213	261	266	231	383	253
Y	90.1	99.0	90.4	105.4	86.7	80.5
Nb	25.4	26.4	24.5	30.8	25.0	27.6
Rb	4.1	4.4	4.3	11.3	4.8	6.0
Sr	221	358	372	308	408	276
Ba	180	239	223	283	209	175
H_2O^+ (wt%0	3.93	2.55	2.21	2.99	3.61	4.08
Density (g/cm^3)	2.73	2.75	2.66	2.57	2.55	2.30
Fe_2O_3/FeO	0.92	1.32	1.16	1.71	2.03	6.79

Table AT36. Abundance of major and trace elements (g/1000 cm^3) in basalts, Hole 756D, Leg 121 (Ninetyeast Ridge, Indian Ocean). (Continued on next page.)

Leg	121	121	121	121	121	121	121
Hole	756D	756D	756D	756D	756D	756D	756D
Core, section	6R-1	6R-2	6R-2	7R-1	7R-2	7R-3	8R-1
Interval (cm)	23-25	32-35	91-95	136-138	26-28	59-63	16-19
Piece	4	1B	1C	12C	1C	2C	2
Lab number	Z-639	Z-640	Z-29	Z-22	Z-25	Z-641	Z-1337
Depth (mbsf)	158.53	160.12	160.71	169.36	169.76	171.56	177.86
Major elements (g/1000 cm^3):							
Si	653.6	616.7	627.0	605.5	644.0	626.8	604.7
Ti	32.1	30.1	32.8	43.4	40.4	35.3	34.1
Al	227.4	216.3	201.4	235.1	234.6	208.5	218.4
Fe^{+++}	148.6	74.2	183.8	145.8	126.5	133.8	178.1
Fe^{++}	105.2	161.1	127.5	80.5	105.5	119.9	74.7
Fe (Sum)	253.8	235.3	311.2	226.4	232.0	253.7	252.8
Mn	3.8	4.1	2.7	2.6	1.6	4.6	2.6
Mg	101.7	117.6	118.0	119.3	113.3	121.5	113.3
Ca	226.2	227.5	221.3	210.8	230.3	202.6	184.1
Na	57.7	54.3	62.3	61.6	72.3	56.0	48.2
K	13.1	5.1	19.4	11.6	12.2	16.9	10.6
P	2.2	1.8	2.2	2.4	2.4	2.1	2.5
Minor elements (g/1000 cm^3 x 10^{-3}):							
La	24.5	23.5		30.0	37.3	25.9	25.7
Ce	66.2	60.7		60.1	66.0	63.9	70.5
Nd	43.2	41.4				41.7	40.7
Sm	13.0	12.1		14.7	15.5	12.5	9.8
Eu	4.6	4.1		4.1	4.6	4.2	3.5
Tb	2.7	1.9		2.3	2.9	2.8	1.8
Yb	8.1	7.2		6.8	9.5	8.1	6.5
Lu	1.2	1.2		1.0	1.4	1.2	1.1
Sc				128.3	134.9		
Cr	662.4	483.0		655.2	602.7	569.9	487.8
Ni	221.8	168.4		251.2	264.0	194.6	176.2
Co	135.4	118.7		136.5	137.8	125.1	92.1
V	878.4	750.7		1092.0	961.5	742.3	555.6
Cu	210.2	256.7		450.5	889.7	202.9	243.9
Zn	308.2	240.1		234.8	258.3	264.1	192.4
Zr	345.6	303.6		354.9	344.4	333.6	325.2
Y	89.3	82.8		79.2	86.1	86.2	70.5
Nb	23.3	26.5		27.3	31.6	22.5	113.8
Rb	51.8	4.4		8.2	20.7	233.5	37.9
Sr	489.6	496.8		546.0	516.6	444.8	406.5
Ba	178.6	237.4		133.8	137.8	125.1	59.6
H_2O^+ (wt%)	0.82	0.79	1.40	0.24	0.75	1.14	1.89
Density (g/cm^3)	2.88	2.76	2.88	2.73	2.87	2.78	2.71
Fe_2O_3/FeO	1.57	0.51	1.60	2.01	1.33	1.24	2.65

Table AT36 (continued).

Leg	121	121	121	121	121	121
Hole	756D	756D	756D	756D	756D	756D
Core, section	8R-1	9R-1	9R-3	11R-1	11R-2	12R-2
Interval (cm)	72-75	36-38	119-121	115-118	95-99	69-72
Piece	14	5	4E	17	11D	1C
Lab number	Z-642	Z-5	Z-36	Z-643	Z-4	Z-16
Depth (mbsf)	178.42	187.76	191.59	207.75	209.05	218.39
Major elements (g/1000 cm^3):						
Si	615.7	618.5	651.1	622.1	600.1	628.9
Ti	30.1	43.2	30.4	33.8	43.2	42.4
Al	200.2	207.0	206.2	207.9	211.1	226.1
Fe^{+++}	118.0	142.3	126.7	136.6	169.7	97.1
Fe^{++}	110.0	113.8	161.0	92.6	110.0	120.2
Fe (Sum)	228.0	256.1	287.7	229.2	279.7	217.3
Mn	3.8	2.8	3.2	3.2	3.5	3.3
Mg	115.5	111.9	122.3	117.5	108.5	108.3
Ca	219.0	229.8	241.2	216.0	217.7	263.6
Na	51.5	56.4	59.1	49.7	55.2	59.5
K	9.6	14.3	7.6	9.3	16.1	9.3
P	1.7	2.2	2.1	1.6	2.2	1.3
Minor elements (g/1000 cm^3 x 10^{-3}):						
La	21.6	25.8	24.1	20.3	17.9	23.3
Ce	59.4	47.1	55.1	54.8	41.4	50.6
Nd	40.5			35.6		
Sm	11.3	12.7	13.1	11.0	9.7	11.5
Eu	3.5	3.9	3.8	3.8	3.3	3.9
Tb	2.4	2.3	2.3	2.7	1.9	2.1
Yb	6.5	5.8	7.3	6.9	5.5	6.7
Lu	0.9	1.1	1.2	1.1	0.9	1.0
Sc		135.7	130.5		129.7	134.9
Cr	594.0	747.9	638.0	589.1	538.2	528.3
Ni	197.1	235.5	237.8	186.3	259.4	247.3
Co	124.2	138.5	139.2	128.8	165.6	132.1
V	756.0	941.8	913.5	759.0	938.4	871.1
Cu	126.9	277.0	246.5	172.6	358.8	210.8
Zn	253.8	221.6	214.6	246.6	204.2	196.7
Zr	297.0	277.0	272.6	274.0	303.6	309.1
Y	54.0	74.8	87.0	68.5	74.5	75.9
Nb	21.3	26.3	27.3	20.0	24.6	22.8
Rb	148.5	30.5	7.8	35.6	49.7	14.3
Sr	432.0	443.2	464.0	411.0	441.6	505.8
Ba	132.3	102.5	118.9	158.9	96.6	84.3
H_2O^+ (wt%)	1.32	0.68	1.13	1.37	1.15	0.89
Density (g/cm^3)	2.70	2.77	2.90	2.74	2.76	2.81
Fe_2O_3/FeO	1.19	1.39	0.88	1.64	1.71	0.90

Table AT37. Abundance of major and trace elements (g/1000 cm^3) in basalts, Hole 757C, Leg 121 (Ninetyeast Ridge, Indian Ocean). (Continued on next two pages.)

Leg	121	121	121	121	121	121	121
Hole	757C	757C	757C	757C	757C	757C	757C
Core, section	8R-1	8R-2	9R-1	9R-2	9R-3	9R-4	9R-5
Interval (cm)	127-129	119-121	59-61	24-26	35-37	38-42	70-73
Piece	5A	3I	3	1A	1A	1A	2
Lab number	Z-9	Z-6	Z-1	Z-17	Z-18	Z-1338	Z-1339
Depth (mbsf)	373.67	375.09	382.59	383.74	385.35	385.82	387.47
Major elements (g/1000 cm^3):							
Si	479	585	570	600	581	527.5	483.8
Ti	20	16	16	19	16	10.2	16.6
Al	214	306	289	328	338	276.4	215.3
Fe^{+++}	109	82	99	55	51	82.1	171.2
Fe^{++}	29	38	52	56	46	23.1	0.0
Fe (Sum)	138	120	151	111	97	105.2	171.2
Mn	2.5	0.6	1.6	0.4	0.6	2.2	1.5
Mg	106	114	95	60	82	72.6	83.0
Ca	122	229	259	312	259	273.3	128.6
Na	62	44	41	42	39	51.3	80.4
K	38	21	22	5.7	7.4	16.2	32.1
P	1.0	0.8	0.7	0.6	0.4	0.6	1.3
Minor elements (g/1000 cm^3 x 10^{-3}):							
La	14.1	9.7	10.9	9.8	11.1		
Ce	31.8	18.6	22.9	23.5	23.0		
Nd							
Sm	6.1	5.1	4.8	4.9	4.5		
Eu	2.2	1.8	1.8	1.7	1.6		
Tb	1.2	1.4	1.0	0.9	0.9		
Yb	3.4	3.0	3.2	3.3	2.6		
Lu	0.5	0.4	0.5	0.5	0.4		
Sc	95	84	85	93	82		
Cr	568	446	559	355	502	448.9	522.7
Ni	213	208	279	191	248	157.4	153.4
Co	84	81	98	66	106	85.1	90.7
V	636	392	399	341	713	433.4	486.0
Cu	284	170	138	98	198	160.0	190.1
Zn	102	108	149	115	121	149.6	142.6
Zr	132	113	96	98	103	105.8	151.2
Y	43.1	32.4	31.9	38.2	26.1	28.4	41.0
Nb	10.9	10.3	10.6	9.3	8.4	7.7	10.4
Rb	40.9	32.4	63.8	4.4	5.8	21.4	34.6
Sr	250	513	452	519	554	980.4	993.6
Ba	86	78	45	49	63		280.8
H_2O^+ (wt%)	5.49	2.60	1.49	1.33	1.11	3.28	7.25
Density (g/cm^3)	2.27	2.70	2.66	2.73	2.64	2.58	2.16
Fe_2O_3/FeO	4.21	2.41	2.10	1.09	1.24	3.96	3.75

Table AT37 (continued).

Leg	121	121	121	121	121	121	121
Hole	757C	757C	757C	757C	757C	757C	757C
Core, section	9R-8	9R-7	10R-2	10R-3	11R-1	11R-1	12R-1
Interval (cm)	57-60	71-73	66-70	79-81	54-58	135-137	5-9
Piece	4A	1B	5A	2C	8B	9E	1
Lab number	Z-644	Z-30	Z-1340	Z-1341	Z-645	Z-34	Z-1342
Depth (mbsf)	390.67	391.71	393.74	395.33	401.94	402.75	411.15
Major elements (g/1000 cm^3):							
Si	599.3	657	454.6	491.6	521.1	480.8	612.9
Ti	10.7	15	9.4	10.9	10.9	16.2	16.4
Al	310.3	310	253.0	264.8	215.8	217.6	254.3
Fe^{+++}	76.3	69	79.6	101.7	154.0	127.0	113.3
Fe^{++}	52.4	79	12.6	27.6	25.5	41.8	57.0
Fe (Sum)	128.7	148	92.2	129.3	179.5	168.8	170.2
Mn	1.9	1.8	0.7	1.3	1.5	1.3	1.7
Mg	105.3	92	79.0	88.0	101.9	85.9	101.6
Ca	226.1	298	134.7	197.3	105.4	139.8	172.6
Na	36.6	57	68.7	43.5	59.5	59.7	51.4
K	23.0	14	27.1	20.1	40.8	39.1	35.0
P	0.8	0.3	0.7	0.7	0.8	0.7	0.8
Minor elements (g/1000 cm^3 x 10^{-3}):							
La	10.0	12.6	7.4		12.9	15.1	26.4
Ce	25.7	23.7	19.2		26.3	35.0	58.1
Nd	16.2		12.3		17.9		34.3
Sm	4.6	4.7	3.3		5.3	6.5	9.0
Eu	1.8	1.9	1.2		2.0	2.3	2.6
Tb	0.9	1.0	0.8		1.0	1.2	1.9
Yb	3.0	2.9	1.8		4.1	4.2	6.1
Lu	0.5	0.4	0.3		0.7	0.6	1.0
Sc		100				88.5	
Cr	499.5	454	452.7	398.4	341.8	256.3	245.5
Ni	178.2	258	120.4	144.0	126.7	128.2	142.6
Co	99.9	97	69.1	79.2	71.7	69.9	100.3
V	499.5	469	403.6	475.2	633.4	605.8	887.0
Cu	178.2	252	104.8	127.2	136.2	188.7	116.2
Zn	172.8	82	127.1	139.2	160.1	102.5	208.6
Zr	124.2	108	89.2	103.2	143.4	111.8	343.2
Y	32.4	28.4	22.3	26.4	45.4	37.3	58.1
Nb	7.6	9.4	7.1	6.5	9.8	10.5	20.1
Rb	70.2	7.9	31.2	36.0	47.8	44.3	47.5
Sr	459.0	498	981.2	780.0	334.6	885.4	475.2
Ba	132.3	82	15.6		64.5	79.2	171.6
H_2O^+ (wt%)	1.49	1.14	6.66	3.90	4.50	6.21	1.49
Density (g/cm^3)	2.70	2.93	2.23	2.40	2.39	2.33	2.64
Fe_2O_3/FeO	1.62	0.98	7.03	4.10	6.71	3.37	2.21

Table AT37 (continued).

Leg	121	121	121
Hole	757C	757C	757C
Core, section	12R-1	12R-2	12R-1
Interval (cm)	84-86	8-10	75-79
Piece	2	1	4
Lab number	Z-21	Z-13	Z-1343
Depth (mbsf)	411.94	412.68	413.20
Major elements (g/1000 cm^3):			
Si	656.2	630	480.4
Ti	20.1	20	13.0
Al	280.2	255	184.8
Fe^{+++}	60.3	119	134.0
Fe^{++}	91.3	75	18.9
Fe (Sum)	151.6	194	152.9
Mn	1.1	2.5	1.4
Mg	93.0	94	83.9
Ca	247.8	208	71.1
Na	51.0	54	89.3
K	24.0	34	35.6
P	0.8	0.6	1.0
Minor elements (g/1000 cm^3 x 10^{-3}):			
La	39.5	30.0	28.2
Ce	67.7	65.5	67.3
Nd			39.1
Sm	12.4	9.6	9.5
Eu	2.8	3.0	2.8
Tb	2.2	2.1	2.4
Yb	8.7	7.4	7.8
Lu	1.4	1.1	1.3
Sc	95.9	98	
Cr	259.4	251	312.5
Ni	155.1	158	108.5
Co	84.6	90	69.4
V	676.8	710	512.1
Cu	141.0	66	143.2
Zn	174.8	177	193.1
Zr	366.6	355	390.6
Y	76.1	79.2	76.0
Nb	24.0	23.8	23.9
Rb	33.8	57.3	36.9
Sr	451.2	410	130.2
Ba	149.5	205	
H_2O^+ (wt%)	1.39	0.89	5.12
Density (g/cm^3)	2.82	2.73	2.17
Fe_2O_3/FeO	0.73	1.77	7.88

Table AT38. Abundance of major and trace elements (g/1000 cm^3) in basalts, Hole 758A, Leg 121 (Ninetyeast Ridge, Indian Ocean). (Continued on next six pages.)

Leg	121	121	121	121	121	121	121
Hole	758A	758A	758A	758A	758A	758A	758A
Core, section	56R-1	57R-2	57R-3	57R-3	58R-1	58R-5	59R-7
Interval (cm)	21-23	110-114	7-9	37-41	41-43	55-57	52-56
Piece	2A	2	1	4	3	2A	1A
Lab number	Z-26	Z-647	Z-32	Z-648	Z-33	Z-8	Z-1344
Depth (mbsf)	508.61	520.5	520.97	520.98	527.51	533.65	544.84
Major elements (g/1000 cm^3):							
Si	631	551.7	514	535.9	584	576	599.8
Ti	20	27.2	19	26.4	20	25	20.6
Al	221	204.4	160	173.3	182	209	194.9
Fe^{+++}	113	142.2	174	157.1	137	132	132.8
Fe^{++}	121	81.2	112	88.5	116	101	94.1
Fe (Sum)	234	223.4	286	245.6	253	233	226.9
Mn	2.2	3.3	2.0	6.0	3.8	2.6	3.3
Mg	138	120.4	136	155.0	126	121	151.3
Ca	245	119.9	99	111.1	193	223	180.7
Na	55	50.1	56	46.2	60	43	45.1
K	2.6	12.2	14.3	1.7	3.9	3.3	3.3
P	0.7	2.0	0.4	1.9	0.9	0.6	1.2
Minor elements (g/1000 cm^3 x 10^{-3}):							
La	11.5	20.7	15.8	16.1	17.0	7.9	
Ce	20.7	53.5	28.3	43.4	31.0	21.0	
Nd		36.5		31.3			
Sm	5.6	10.9	7.1	10.1	7.7	6.0	
Eu	2.0	3.9	2.3	3.6	2.8	2.4	
Tb	1.3	2.4	1.7	2.7	1.8	1.7	
Yb	5.3	5.6	4.0	6.3	4.6	5.8	
Lu	0.8	0.9	0.6	1.0	0.7	0.9	
Sc	132		116		132	131	
Cr	672	619.7	212	149.4	217	215	243.7
Ni	280	167.7	189	135.0	206	246	191.3
Co	118	119.1	163	110.9	183	191	186.0
V	910	1324.4	909	1217.1	955	1624	1165.9
Cu	546	340.2	366	301.3	542	721	345.8
Zn	157	388.8	194	289.2	160	170	220.1
Zr	101	216.3	139	226.5	163	136	183.4
Y	50.4	72.9	49.6	67.5	67.1	49.8	60.3
Nb	7.6	16.5	10.6	16.9	12.6	10.2	7.9
Rb	3.6	5.3	4.5		4.1		6.0
Sr	280	364.5	283	337.4	310	314	220.1
Ba	45	94.8	52	53.0	88	60	175.5
H_2O^+ (wt%)	0.88	2.02	2.69	1.94	1.13	1.91	1.43
Density (g/cm^3)	2.80	2.43	2.36	2.41	2.58	2.62	2.62
Fe_2O_3/FeO	1.04	1.95	1.73	1.97	1.31	1.45	1.57

Table AT38 (continued).

Leg	121	121	121	121	121	121	121
Hole	758A	758A	758A	758A	758A	758A	758A
Core, section	60R-1	60R-2	60R-6	61R-2	61R-4	61R-7	62R-1
Interval (cm)	11-13	80-82	82-84	62-67	60-64	0-5	17-21
Piece	1B	2	1C	1A	1B	1A	2
Lab number	Z-31	Z-3	Z-27	Z-1345	Z-1346	Z-1347	Z-1348
Depth (mbsf)	546.01	548.20	554.22	556.53	559.43	562.91	564.47
Major elements (g/1000 cm^3):							
Si	576.6	568	652	613.5	610.7	573.2	498.2
Ti	22.5	28	26	24.4	23.3	22.8	20.9
Al	169.7	187	197	185.0	177.1	168.8	191.9
Fe^{+++}	146.4	147	138	135.1	140.8	134.3	121.4
Fe^{++}	127.9	105	143	111.4	99.2	84.9	79.9
Fe (Sum)	274.4	252	281	246.5	240.0	219.2	201.3
Mn	2.9	3.6	2.3	3.2	2.9	3.2	3.6
Mg	146.4	141	150	145.9	147.8	147.8	127.3
Ca	177.3	167	243	199.1	196.0	172.2	113.9
Na	54.1	47	58	46.0	41.1	45.4	47.0
K	3.8	4.0	3.4	3.4	2.5	3.0	3.5
P	1.2	1.3	1.0	1.3	1.2	1.2	1.3
Minor elements (g/1000 cm^3 x 10^{-3}):							
La	12.7	14.5	17.2				11.8
Ce	31.1	33.2	35.0				31.6
Nd							21.5
Sm	7.5	7.7	8.5				6.3
Eu	2.6	2.6	2.9				2.5
Tb	1.9	1.6	2.0				1.7
Yb	7.0	5.9	7.0				5.0
Lu	1.0	1.0	1.0				0.7
Sc	129.5	125	140				
Cr	194.3	574	511	532.6	530.0	559.7	565.0
Ni	199.4	281	274	217.9	222.6	198.3	194.4
Co	129.5	176	175	207.1	188.2	203.3	183.1
V	854.7	1313	1110	1264.3	1277.3	1330.3	1344.7
Cu	505.1	472	569	398.1	392.2	406.6	330.0
Zn	170.9	204	207	255.6	233.2	205.8	257.6
Zr	160.6	179	161	207.1	201.4	198.3	194.4
Y	69.9	58.7	67.2	69.9	58.3	57.7	42.9
Nb	12.4	13.3	12.8	12.1	11.4	10.3	11.3
Rb	6.0			5.6	4.5	4.3	0.0
Sr	310.8	332	350	349.7	344.5	338.9	316.4
Ba	72.5	54	58	263.6	169.6	160.6	339.0
H_2O^+ (wt%)	1.81	1.15	1.47	1.17	1.76	1.19	2.27
Density (g/cm^3)	2.59	2.55	2.92	2.69	2.65	2.51	2.26
Fe_2O_3/FeO	1.27	1.56	1.08	1.35	1.58	1.76	1.69

Table AT38 (continued).

Leg	121	121	121	121	121	121	121
Hole	758A	758A	758A	758A	758A	758A	758A
Core, section	62R-1	62R-3	62R-3	63R-1	63R-2	63R-5	64R-1
Interval (cm)	57-59	27-29	88-92	3-5	46-50	48-50	76-80
Piece	4A	2	8A	1	1B	1A	1A
Lab number	Z-23	Z-24	Z-649	Z-19	Z-1349	Z-7	Z-650
Depth (mbsf)	564.87	567.57	568.09	573.83	575.58	580.28	583.96
Major elements (g/1000 cm^3):							
Si	521.8	554	516.9	511	542.1	578	604.5
Ti	17.1	19	23.4	32	23.4	26	23.0
Al	236.4	270	171.7	176	190.5	202	194.4
Fe^{+++}	75.8	65	138.7	149	132.7	110	125.3
Fe^{++}	73.6	71	67.0	95	96.1	102	100.7
Fe (Sum)	149.5	136	205.7	244	228.7	212	226.0
Mn	1.4	2.2	4.0	3.5	3.2	3.2	3.3
Mg	145.1	112	131.0	148	142.3	148	133.3
Ca	158.5	230	119.5	101	150.1	210	195.3
Na	35.4	45	43.0	49	44.7	44	42.1
K	6.5	3.8	3.2	4.2	3.0	4.1	2.7
P	0.4	0.6	1.5	1.7	1.3	0.6	1.5
Minor elements (g/1000 cm^3 x 10^{-3}):							
La	9.8	9.9	12.9	20.2		12.5	14.6
Ce	20.3	20.1	34.1	42.8		28.6	36.5
Nd			25.0				26.1
Sm	4.8	4.8	7.7	10.0		7.3	8.6
Eu	1.6	1.6	2.7	2.9		2.6	2.9
Tb	1.0	1.1	2.0	2.1		1.7	2.1
Yb	3.3	3.6	5.0	7.4		5.7	7.3
Lu	0.5	0.5	0.8	1.1		0.9	1.2
Sc	98.0	107		112		130	
Cr	1278.7	918	556.2	43	536.3	507	443.7
Ni	322.7	306	172.5	138	196.8	239	169.7
Co	138.6	130	138.5	138	164.8	179	148.8
V	764.8	612	1180.4	857	1377.6	1144	913.5
Cu	270.1	207	240.6	512	324.7	429	339.3
Zn	86.0	117	238.4	181	243.5	161	271.4
Zr	95.6	89	183.9	236	201.7	153	232.3
Y	28.7	35.7	56.8	71.4	61.5	59.8	73.1
Nb	7.9	7.7	12.0	15.5	12.1	13.3	13.1
Rb	4.8		2.3		3.2		4.4
Sr	310.7	332	317.8	309	319.8	312	365.4
Ba	45.4	48	34.1	45	157.4	44	67.9
H_2O^+ (wt%)	2.74	2.08	2.25	3.61	1.39	1.25	1.35
Density (g/cm^3)	2.39	2.55	2.27	2.38	2.46	2.60	2.61
Fe_2O_3/FeO	1.14	1.01	2.30	1.74	1.54	1.21	1.38

Table AT38 (continued).

Leg	121	121	121	121	121	121	121
Hole	758A	758A	758A	758A	758A	758A	758A
Core, section	64R-2	65R-2	65R-4	65R-5	65R-6	66R-1	66R-3
Interval (cm)	130-135	10-15	58-62	1-6	25-27	31-35	44-46
Piece	1B	1A	1B	1A	1A	5A	1B
Lab number	Z-1350	Z-1351	Z-1352	Z-651	Z-28	Z-1353	Z-14
Depth (mbsf)	585.78	594.09	597.26	598.03	600.45	602.41	605.54
Major elements (g/1000 cm^3):							
Si	528.5	521.1	587.7	604.4	586	567.1	593
Ti	25.7	21.3	20.8	24.7	25	20.9	24
Al	193.6	197.8	203.2	194.7	170	192.9	210
Fe^{+++}	123.9	119.1	105.3	109.0	152	118.7	101
Fe^{++}	94.7	76.4	100.1	88.1	113	101.5	97
Fe (Sum)	218.6	195.5	205.4	197.1	265	220.2	198
Mn	3.9	3.6	3.3	4.0	3.0	3.0	2.0
Mg	134.2	130.2	138.6	133.4	135	139.6	138
Ca	147.2	157.8	206.0	230.4	220	186.6	222
Na	44.6	43.9	41.0	40.9	49	40.9	43
K	2.9	2.0	1.8	1.6	2.2	2.2	2.2
P	1.7	1.2	1.2	1.0	0.9	1.2	0.8
Minor elements (g/1000 cm^3 x 10^{-3}):							
La				13.3	12.6		10.3
Ce				34.6	26.2		25.0
Nd				26.1			
Sm				8.0	7.3		6.8
Eu				2.9	2.6		2.5
Tb				1.9	1.9		1.5
Yb				5.9	5.8		5.3
Lu				0.9	0.8		0.8
Sc					139		134
Cr	523.2	814.2	802.9	678.3	773	756.0	986
Ni	187.2	203.0	238.3	204.8	267	239.4	276
Co	189.6	181.7	186.5	154.3	144	196.6	153
V	1372.8	1293.3	1217.3	891.1	865	1209.6	947
Cu	355.2	344.6	383.3	271.3	485	337.7	395
Zn	271.2	200.6	217.6	242.1	173	239.4	153
Zr	213.6	184.1	176.1	162.3	162	184.0	124
Y	52.8	54.3	57.0	58.5	57.6	50.4	55.2
Nb	12.0	9.2	11.4	8.5	11.0	7.8	9.7
Rb	3.6	2.6	3.4				2.6
Sr	336.0	306.8	336.7	345.8	314	327.6	289
Ba	213.6	113.3	15.5	45.2	55	15.1	
H_2O^+ (wt%)	1.01	1.55	1.30	1.45	1.16	1.33	1.64
Density (g/cm^3)	2.40	2.36	2.59	2.66	2.62	2.52	2.63
Fe_2O_3/FeO	1.45	1.73	1.17	1.38	1.50	1.30	1.15

Table AT38 (continued).

Leg	121	121	121	121	121	121	121
Hole	758A	758A	758A	758A	758A	758A	758A
Core, section	66R-5	66R-5	67R-4	67R-4	67R-6	68R-3	69R-2
Interval (cm)	2-7	50-55	79-83	78-80	28-30	106-108	45-47
Piece	1A	1E	3	3	1	8	1
Lab number	Z-652	Z-1354	Z-653	Z-12	Z-35	Z-20	Z-10
Depth (mbsf)	607.61	608.09	616.73	616.78	619.28	624.86	632.15
Major elements (g/1000 cm^3):							
Si	531.7	519.0	567.9	488	567	509	610
Ti	20.3	21.5	25.6	27	19	21	24
Al	188.8	201.5	200.6	165	208	198	195
Fe^{+++}	131.2	118.4	137.4	107	103	107	153
Fe^{++}	80.5	81.9	83.0	75	94	60	108
Fe (Sum)	211.6	200.3	220.4	182	197	167	261
Mn	1.9	3.1	4.3	1.9	2.9	0.9	3.2
Mg	142.9	143.4	140.2	157	133	127	135
Ca	148.1	132.6	142.6	111	205	165	263
Na	41.7	46.1	48.2	41	45	41	44
K	1.7	2.7	2.2	3.8	1.7	4.2	3.4
P	1.2	1.7	1.6	1.1	0.8	0.7	0.8
Minor elements (g/1000 cm^3 x 10^{-3}):							
La	10.1		14.6	11.5	11.1	9.5	9.1
Ce	23.8		40.2	22.1	27.7	20.6	23.5
Nd	19.0		30.1				
Sm	6.0		9.5	6.0	6.8	5.3	6.6
Eu	1.9		3.3	2.2	2.1	1.8	2.5
Tb	1.6		2.4	1.7	1.3	1.0	1.5
Yb	4.8		6.0	4.0	4.5	3.7	5.8
Lu	0.7		0.9	0.6	0.8	0.6	0.9
Sc				106	126	113	136
Cr	816.0	722.9	426.7	248	743	531	665
Ni	199.2	222.8	145.6	181	257	203	277
Co	129.6	163.5	110.4	104	134	118	152
V	996.0	1185.0	1267.6	950	832	785	776
Cu	312.0	327.1	451.8	431	383	381	388
Zn	211.2	286.8	351.4	155	149	116	161
Zr	158.4	184.9	218.4	148	106	127	136
Y	48.0	61.6	62.8	42.0	42.8	34.7	58.2
Nb	10.8	8.5	13.1	11.3	9.1	6.9	10.5
Rb							
Sr	336.0	331.8	376.5	287	302	300	305
Ba	26.4		80.3	40	50	42	42
H_2O^+ (wt%)	2.00	1.74	2.05	2.97	1.35	2.90	1.27
Density (g/cm^3)	2.40	2.37	2.51	2.21	2.52	2.31	2.77
Fe_2O_3/FeO	1.81	1.61	1.61	1.58	1.22	1.98	1.58

Table AT38 (continued).

Leg	121	121	121	121	121	121	121
Hole	758A	758A	758A	758A	758A	758A	758A
Core, section	69R-5	69R-5	70R-2	71R-2	71R-3	72R-3	72R-4
Interval (cm)	18-21	120-123	47-50	104-107	87-89	0-5	90-95
Piece	1A	1C	4	8B	3B	1A	3
Lab number	Z-654	Z-1355	Z-655	Z-656	Z-2	Z-657	Z-658
Depth (mbsf)	635.77	636.79	641.37	651.14	652.47	660.92	663.15
Major elements (g/1000 cm^3):							
Si	625.0	522.3	556.9	542.5	585	666.4	564.6
Ti	18.6	19.7	21.6	15.3	27	18.2	17.2
Al	198.5	190.1	185.0	182.6	192	224.5	206.0
Fe^{+++}	118.0	134.8	125.1	132.8	112	131.9	110.4
Fe^{++}	108.5	87.7	75.4	66.1	105	110.4	66.4
Fe (Sum)	226.5	222.5	200.5	198.9	217	242.3	176.9
Mn	4.4	3.1	2.0	3.3	6.6	4.2	4.6
Mg	163.1	153.1	159.0	145.5	142	161.5	144.0
Ca	226.1	124.9	129.8	151.9	240	217.9	177.5
Na	38.2	43.0	43.5	40.3	45	44.7	40.4
K	1.4	7.6	3.4	2.5	3.1	3.0	1.1
P	1.2	1.3	2.0	1.4	1.4	2.0	1.5
Minor elements (g/1000 cm^3 x 10^{-3}):							
La	10.4		13.5	12.0	13.1	12.6	8.9
Ce	23.8		34.4	31.1	29.4	29.2	24.6
Nd	20.0		27.1	22.7		23.1	17.4
Sm	6.9		7.9	7.4	6.9	7.9	5.5
Eu	2.4		2.4	2.4	2.3	2.7	1.9
Tb	1.8		1.9	1.7	1.5	1.9	1.5
Yb	6.3		5.4	6.0	6.4	7.9	5.0
Lu	1.0		0.8	0.9	1.0	1.2	0.8
Sc					131		
Cr	589.1	539.8	622.4	607.1	641	657.0	607.6
Ni	246.6	216.9	189.4	176.9	312	207.3	188.5
Co	164.4	212.1	159.9	109.9	174	154.8	133.9
V	808.3	1132.7	1099.6	956.0	1228	992.8	1108.6
Cu	328.8	298.8	250.9	217.5	494	309.5	297.6
Zn	295.9	390.4	307.5	234.2	171	268.6	223.2
Zr	153.4	171.1	155.0	148.2	144	175.2	146.3
Y	54.8	53.0	61.5	52.6	58.7	61.3	47.1
Nb	8.8	8.4	10.8	11.0	14.7	11.7	10.4
Rb		6.0	5.4	5.7		8.8	
Sr	301.4	301.3	295.2	286.8	294	350.4	322.4
Ba	0.0	130.1	39.4	35.9		55.5	29.8
H_2O^+ (wt%)	0.52	2.27	2.41	1.91	1.28	1.48	1.51
Density (g/cm^3)	2.74	2.41	2.46	2.39	2.67	2.92	2.48
Fe_2O_3/FeO	1.21	1.71	1.84	2.23	1.19	1.33	1.85

Table AT38 (continued).

Leg	121	121	121	121
Hole	758A	758A	758A	758A
Core, section	73R-2	73R-3	73R-3	73R-4
Interval (cm)	71-74	85-87	136-140	105-110
Piece	1C	4F	5	8
Lab number	Z-659	Z-15	Z-1356	Z-1357
Depth (mbsf)	669.79	671.45	671.89	673.08
Major elements (g/1000 cm^3):				
Si	591.0	501	511.8	562.6
Ti	19.0	20	17.1	19.2
Al	201.8	179	169.7	197.6
Fe^{+++}	118.1	122	127.9	122.0
Fe^{++}	89.1	63	82.8	95.3
Fe (Sum)	207.2	185	210.8	217.3
Mn	1.9	2.6	3.3	3.8
Mg	148.2	139	150.6	136.6
Ca	186.9	141	124.1	179.8
Na	40.0	38	36.7	38.6
K	1.8	2.8	1.2	2.1
P	1.3	1.2	1.2	1.1
Minor elements (g/1000 cm^3 x 10^{-3}):				
La	10.8	10.6		
Ce	24.3	22.6		
Nd	20.4			
Sm	6.7	5.7		
Eu	2.2	2.0		
Tb	1.7	1.2		
Yb	6.2	4.1		
Lu	0.9	0.7		
Sc		104		
Cr	464.4	244	381.8	532.5
Ni	198.7	181	174.8	192.5
Co	147.1	104	163.3	162.5
V	1070.7	972	1196.0	1150.0
Cu	348.3	418	326.6	370.0
Zn	221.9	131	188.6	237.5
Zr	154.8	113	154.1	167.5
Y	54.2	42.9	41.4	62.5
Nb	12.6	10.2	8.3	7.5
Rb				4.0
Sr	283.8	226	230.0	275.0
Ba	38.7		11.5	185.0
H_2O^+ (wt%)	1.19	1.28	1.87	1.33
Density (g/cm^3)	2.58	2.67	2.30	2.50
Fe_2O_3/FeO	1.47	1.19	1.72	1.42

Table AT39. Abundance of major and trace elements (g/1000 cm3) in igneous rocks, Hole 747C, Leg 120 (Kerguelen Plateau). (Continued on next two pages.)

Leg	120	120	120	120	120	120	120
Hole	747C	747C	747C	747C	747C	747C	747C
Core, section	12R-1	12-2	12R-2	12-3	12R-3	13-1	13-1
Interval (cm)	53-56	6-9	85-87	18-22	146-148	6-10	98-102
Piece	7A	1	10	3A	12	1A	2D
Lab number	Z-91	Z-630	Z-92	Z-631	Z-93	Z-632	Z-633
Depth (mbsf)	303.53	304.56	305.35	306.18	307.46	312.56	313.48
Major elements (g/1000 cm^3):							
Si	444	542.4	555	600.3	626	640.8	583.4
Ti	27	25.4	26	23.8	30	25.7	24.8
Al	204	194.2	206	204.5	232	219.9	215.3
Fe^{+++}	127	103.3	147	119.0	83	97.2	165.4
Fe^{++}	19	71.1	100	104.1	108	122.5	49.9
Fe (Sum)	146	174.4	247	223.0	191	219.7	215.3
Mn	3.2	4.7	0.4	2.9	1.1	3.9	2.6
Mg	56	100.9	139	113.9	122	112.1	97.1
Ca	70	173.0	171	186.8	235	229.1	153.1
Na	46	38.2	52	48.3	68	49.9	50.4
K	29	20.6	15	12.4	17	7.7	17.3
P	1.6	2.1	2.0	2.0	1.9	2.4	1.8
Minor elements (g/1000 cm^3 x 10^{-3}):							
La	27.4	29.3	28.5	33.8	35.9	35.9	33.0
Ce	56.8	63.4	62.2	75.4	69.0	80.0	76.2
Nd		39.0		46.8		49.7	48.3
Sm	8.8	9.5	9.8	11.4	11.6	11.9	11.7
Eu	3.1	3.2	3.6	3.6	4.1	3.6	4.1
Tb	1.5	1.9	1.8	2.4	2.2	2.8	2.5
Yb	4.1	4.9	5.7	6.5	6.1	6.9	7.4
Lu	0.5	0.7	0.9	1.0	1.0	1.0	1.0
Sc	112		119		132		
Cr	784	695.4	699	637.0	662	676.2	647.7
Ni	186	183.0	207	166.4	235	179.4	157.5
Co	108	126.9	130	135.2	138	132.5	124.5
V	1058	871.1	829	811.2	690	861.1	932.2
Cu	108	219.6	259	278.2	276	345.0	355.6
Zn	186	209.8	246	244.4	262	237.4	218.4
Sn		6.6		6.5		6.6	6.4
Zr	372	292.8	246	312.0	359	303.6	304.8
Y	52.9	63.4	77.7	65.0	74.5	71.8	73.7
Nb	21.6	19.3	23.3	17.9	24.0	25.1	20.1
Rb	56.8	51.2	16.3	15.9	7.5	9.9	23.4
Sr	372	390.4	596	754.0	773	662.4	558.8
Ba	235	268.4	363	312.0	359	331.2	279.4
H_2O^+ (wt%)	3.56	2.81	2.30	1.35	0.69	0.57	1.57
Density (g/cm^3)	1.96	2.44	2.59	2.60	2.76	2.76	2.54
Fe_2O_3/FeO	7.37	1.61	1.63	1.27	0.85	0.88	3.68

Table AT39 (continued).

Leg	120	120	120	120	120	120	120
Hole	747C	747C	747C	747C	747C	747C	747C
Core, section	13R-3	14R-1	15R-1	15R-2	16R-2	16-2	16R-4
Interval (cm)	97-99	49-51	22-24	97-99	51-53	101-105	14-16
Piece	10B	3C	3A	13	1D	1G	1A
Lab number	Z-94	Z-95	Z-96	Z-97	Z-98	Z-635	Z-99
Depth (mbsf)	316.47	322.49	331.72	333.97	343.01	343.51	345.64
Major elements (g/1000 cm^3):							
Si	544	569	561	539	579	578.5	574
Ti	36	30	20	24	20	16.7	22
Al	233	216	223	176	201	220.3	192
Fe^{+++}	152	144	129	157	140	122.0	117
Fe^{++}	63	80	62	70	64	65.7	95
Fe (Sum)	215	224	191	227	204	187.7	212
Mn	0.4	3.0	1.6	1.6	1.0	3.5	3.5
Mg	106	124	128	156	124	119.7	170
Ca	143	191	164	166	189	175.0	208
Na	58	56	50	40	40	42.0	45
K	26	19	27	19	46	32.8	31
P	2.5	2.0	1.7	1.4	1.1	1.7	1.2
Minor elements (g/1000 cm^3 x 10^{-3}):							
La	47.5	44.2	33.2	25.5	36.3	33.4	37.4
Ce	87.5	85.8	68.9	56.1	77.7	72.0	64.1
Nd						41.1	
Sm	14.5	12.7	9.4	8.9	10.1	9.8	9.9
Eu	4.8	3.9	3.1	2.8	3.1	3.1	3.2
Tb	2.5	2.3	1.6	1.6	1.7	2.2	1.8
Yb	8.5	7.3	5.4	4.6	5.2	5.1	5.3
Lu	1.3	1.1	0.8	0.7	0.8	0.7	0.8
Sc	115	120	99	102	93		101
Cr	150	247	1033	1084	1114	873.8	774
Ni	225	260	344	344	298	269.9	307
Co	150	143	140	140	104	131.1	107
V	600	702	446	561	427	660.5	414
Cu	113	156	102	115	91	133.6	214
Zn	288	299	230	230	207	205.6	214
Sn						6.7	
Zr	375	237	222	224	135	257.0	246
Y	72.5	67.6	51.0	56.1	54.4	56.5	53.4
Nb	32.5	26.0	19.4	20.9	18.1	17.2	19.5
Rb	32.5	16.6	30.6	28.1	44.0	33.4	25.6
Sr	625	494	536	485	414	616.8	668
Ba	725	546	383	281	544	334.1	320
H_2O^+ (wt%)	1.65	1.23	2.93	5.14	2.56	2.61	2.66
Density (g/cm^3)	2.50	2.60	2.55	2.55	2.59	2.57	2.67
Fe_2O_3/FeO	2.67	2.00	2.30	2.51	2.44	2.07	1.38

Table AT39 (continued).

Leg	120	120
Hole	747C	747C
Core, section	16-5	16-5
Interval (cm)	0-3	105-108
Piece	1A	3C
Lab number	Z-637	Z-638
Depth (mbsf)	347.00	348.05
Major elements (g/1000 cm^3):		
Si	611.3	589.8
Ti	19.4	17.3
Al	230.1	224.8
Fe^{+++}	74.4	126.1
Fe^{++}	107.6	69.8
Fe (Sum)	182.0	195.9
Mn	2.1	2.7
Mg	130.9	110.3
Ca	212.6	172.3
Na	47.1	37.7
K	10.0	41.8
P	2.0	1.6
Minor elements (g/1000 cm^3 x 10^{-3}):		
La	34.7	31.2
Ce	77.4	72.8
Nd	42.7	39.0
Sm	10.4	9.4
Eu	2.9	3.1
Tb	2.1	2.0
Yb	5.9	5.2
Lu	0.9	0.7
Sc		
Cr	854.4	936.0
Ni	248.3	192.4
Co	136.2	119.6
V	587.4	572.0
Cu	213.6	135.2
Zn	205.6	176.8
Sn	6.7	6.0
Zr	264.3	254.8
Y	50.7	57.2
Nb	23.0	19.5
Rb	4.5	39.0
Sr	694.2	572.0
Ba	347.1	520.0
H_2O^+ (wt%)	1.38	2.59
Density (g/cm^3)	2.67	2.60
Fe_2O_3/FeO	0.77	2.01

Table AT40. Abundance of major and trace elements (g/1000 cm^3) in igneous rocks, Hole 1136A, Leg 183 (Kerguelen Plateau, Indian Ocean).

Leg	183	183	183	183	183
Hole	1136A	1136A	1136A	1136A	1136A
Core, section	15R-2	16R-1	17R-2	18R-2	19R-1
Interval (cm)	30-36	113-118	84-90	62-67	27-31
Piece	1B	5A	7	4B	4
Lab number	Z-1001	Z-1002	Z-1003	Z-1004	Z-1005
Depth (mbsf)	128.50	138.73	146.22	149.30	157.17
Major elements (g/1000 cm^3):					
Si	475	586	614	616	650
Ti	24.1	30.8	29.1	30.9	31.0
Al	175	200	207	201	209
Fe^{+++}	145	146	113	113	89.0
Fe^{++}	45.9	78.7	102	111	161
Fe (Sum)	191	225	215	224	250
Mn	0.3	0.6	2.1	3.6	3.7
Mg	59.9	98.1	101	101	107
Ca	112	145	152	156	191
Na	55.0	63.9	64.9	64.2	61.8
K	21.6	7.5	11.7	5.0	5.7
P	1.6	1.6	2.3	2.3	2.1
Minor elements (g/1000 cm^3 x 10^{-3}):					
La	16.0	21.2	28.5	25.9	23.9
Ce	35.4	47.9	57.0	54.4	52.3
Nd	25.0	32.8	41.4	38.9	38.5
Sm	8.1	10.3	13.2	11.7	12.1
Eu	2.9	3.5	4.4	4.1	4.1
Tb	1.9	2.5	3.4	2.8	2.7
Yb	4.4	5.8	7.5	7.5	7.4
Lu	0.7	1.0	1.3	1.2	1.3
Cr	572	542	518	479	509
Ni	129	186	158	166	154
V	1034	806	821	899	776
Cu	62.4	340	233	311	366
Co	81.1	118	104	109	96.3
Pb	12.5	12.6	15.5	15.5	13.8
Zn	183	209	220	241	256
Sn	7.9	9.6	8.5	9.1	8.3
Zr	200	219	280	269	275
Nb	11.4	14.6	17.6	18.4	17.3
Y	52.0	70.6	88.1	75.1	79.8
Rb	64.5	12.3	12.2	9.8	7.2
Sr	499	554	622	622	605
Ba	129	171	223	218	135
H_2O^+ (wt%)	1.58	1.28	1.25	1.19	0.90
Density (g/cm^3)	2.08	2.52	2.59	2.59	2.75
Fe_2O_3/FeO	3.51	2.07	1.24	1.13	0.62

Table AT41. Abundance of major and trace elements (g/1000 cm^3) in igneous rocks, Hole 1137A, Leg 183 (Kerguelen Plateau, Indian Ocean). (Continued on next page.)

Leg	183	183	183	183	183	183	183
Hole	1137A	1137A	1137A	1137A	1137A	1137A	1137A
Core, section	27R-1	29R-1	29R-3	32R-3	32R-7	34R-3	39R-2
Interval (cm)	100-105	38-43	5-9	71-76	46-50	18-23	114-119
Piece	15	1B	1B	1C	1C	1	9
Lab number	Z-1007	Z-1008	Z-1009	Z-1010	Z-1011	Z-1012	Z-1014
Depth (mbsf)	248.60	258.46	259.95	278.77	284.18	297.07	334.64
Major elements (g/1000 cm^3):							
Si	493	659	545	626	626	566	578
Ti	35.7	48.6	31.4	33.3	41.2	68.9	25.0
Al	163	219	177	226	211	177	178
Fe^{+++}	132	102	129	83.2	114	205	108
Fe^{++}	41.2	111	43.3	105	118	74.3	59.9
Fe (Sum)	173	214	172	188	233	279	168
Mn	1.9	2.2	1.5	2.3	2.6	3.2	4.8
Mg	84.7	95.7	109	94.8	95.5	53.2	71.2
Ca	61.0	168	78.3	169.3	172.5	75.8	43.7
Na	52.5	62.4	54.3	62.6	55.9	47.9	57.0
K	55.1	18.1	51.8	10.4	11.2	105	105
P	3.5	4.4	3.0	3.3	4.0	8.2	3.3
Minor elements (g/1000 cm^3 x 10^{-3}):							
La	57.0	68.8	41.9	47.3	61.0	274	57.0
Ce	124	151	86.2	105	133	448	114
Nd	67.5	85.3	51.3	57.9	71.6	194	61.6
Sm	16.5	20.1	13.3	15.0	18.8	39.8	14.4
Eu	5.1	6.3	4.2	4.7	5.8	9.0	4.6
Tb	2.5	3.0	2.2	2.6	2.9	5.5	2.5
Yb	5.1	6.3	4.7	5.0	6.1	10.7	5.0
Lu	0.8	1.0	0.7	0.8	0.9	1.7	0.8
Cr	154	231	373	421	398	548	223
Ni	67.5	110	105	132	125	167	68.4
V	612	853	536	710	814	535	689
Cu	90.7	143	93.2	124	175	139	91.2
Co	71.7	110	86.2	92.1	98.1	57.3	52.4
Pb	14.8	22.0	14.0	18.4	18.6	52.3	18.2
Zn	198	344	228	218	257	207	198
Sn	7.0	9.9	7.7	8.9	8.7	11.0	6.2
Zr	506	633	396	447	530	1419	410
Nb	38.0	41.3	28.0	34.2	37.1	122.0	27.4
Y	76.0	90.8	55.9	65.8	79.5	129	79.8
Rb	73.9	17.1	69.9	20.3	8.7	227	171
Sr	928	1513	1188	1420	1458	1643	570
Ba	612	660	722	579	504	896	570
H_2O^+ (wt%)	2.03	0.79	3.03	1.20	0.19	0.72	0.99
Density (g/cm^3)	2.11	2.75	2.33	2.63	2.65	2.49	2.28
Fe_2O_3/FeO	3.57	1.02	3.31	0.88	1.07	3.07	2

Table AT41 (continued).

Leg	183	183	183
Hole	1137A	1137A	1137A
Core, section	39R-3	43R-2	45R-1
Interval (cm)	6-14	84-92	121-126
Piece	2		1
Lab number	Z-1015	Z-1016	Z-1017
Depth (mbsf)	335.06	353.89	362.91
Major elements (g/1000 cm^3):			
Si	614	561	541
Ti	30.9	4.6	26.4
Al	219	135	179
Fe^{+++}	112	77.5	97.1
Fe^{++}	90.0	8.5	50.2
Fe (Sum)	202	86.0	147
Mn	5.0	0.9	5.2
Mg	96.9	8.8	55.4
Ca	108	7.7	86.1
Na	62.2	11.1	0.0
K	44.3	63.4	163
P	3.6	0.6	2.4
Minor elements (g/1000 cm^3 x 10^{-3}):			
La	63.8	344	34.8
Ce	128	742	71.9
Nd	71.4	290	41.8
Sm	18.1	52.5	10.4
Eu	5.4	3.8	3.2
Tb	2.8	6.5	1.9
Yb	6.6	11.6	3.9
Lu	1.0	1.7	0.6
Cr	247	54.3	394
Ni	94.4	39.8	99.8
V	745	177	499
Cu	140	72.4	137
Co	71.4	23.5	55.7
Pb	17.9	59.7	16.2
Zn	235	235	179
Sn	7.7	9.2	5.8
Zr	510	1122	383
Nb	33.2	123.1	25.5
Y	79.1	125	58.0
Rb	61.2	150	278
Sr	1046	143	1346
Ba	536	43.4	742
H_2O^+ (wt%)	0.76	2.19	2.03
Density (g/cm^3)	2.55	1.81	2.32
Fe_2O_3/FeO	1.39	10.14	2.15

Table AT42. Abundance of major and trace elements (g/1000 cm^3) in igneous rocks, Hole 1138A, Leg 183 (Kerguelen Plateau, Indian Ocean). (Continued on next page.)

Leg	183	183	183	183	183	183	183
Hole	1138A	1138A	1138A	1138A	1138A	1138A	1138A
Core, section	78R-1	80R-4	81R-1	81R-2	82R-2	82R-5	83R-4
Interval (cm)	60-64	35-40	34-39	51-57	76-81	19-23	19-24
Piece		2A	4A	2A	9	4	1
Lab number	Z-1018	Z-1019	Z-1020	Z-1021	Z-1022	Z-1023	Z-1024
Depth (mbsf)	727.6	751.05	756.24	757.82	767.86	771.73	779.7
Major elements (g/1000 cm^3):							
Si	431	565	549	571	625	554	599
Ti	8.4	31.2	27.9	33.1	31.9	35.0	35.5
Al	105	201	173	196	152	170	186
Fe^{+++}	81.6	181	133	101	135	91.4	73.4
Fe^{++}	3.5	66.7	81.4	136	88.1	167	202
Fe (Sum)	85.1	248	215	237	223	258	276
Mn	0.6	3.9	2.5	5.3	2.4	4.9	5.0
Mg	17.5	101	92.2	94.4	81.2	95.4	95.1
Ca	29.3	171	152	200	142	186	200
Na	26.0	51.7	46.6	51.4	43.1	52.1	57.3
K	13.5	5.0	17.2	8.5	33.4	4.0	4.7
P	1.0	2.4	2.2	2.3	1.8	2.7	3.2
Minor elements (g/1000 cm^3 x 10^{-3}):							
La	68.6	25.0	28.1	30.4	34.6	31.7	39.3
Ce	146	60.0	53.8	68.3	69.2	73.2	83.8
Nd	74.5	37.5	35.1	40.5	39.5	43.9	49.8
Sm	16.1	9.3	9.1	11.4	10.9	11.7	13.9
Eu	2.9	3.5	3.3	4.0	3.5	3.9	4.2
Tb	3.4	2.1	1.9	2.4	2.5	2.4	2.6
Yb	10.1	5.8	6.1	8.1	7.2	8.1	10.0
Lu	1.6	1.0	1.0	1.3	1.1	1.3	1.6
Cr	43.8	245	187	248	156	178	231
Ni	43.8	145	145	167	93.9	137	139
V	258	925	948	1341	709	1074	1035
Cu	86.1	400	339	342	346	415	445
Co	29.2	103	93.6	121	61.8	117	115
Pb	14.6		14.0	15.2	12.4	17.1	15.7
Zn	128	198	206	271	205	264	320
Sn	7.3	9.5	7.0	9.6	4.7	9.5	11.0
Zr	438	300	257	304	321	366	419
Nb	58.4	23.5	22.2	25.3	27.2	29.3	31.4
Y	78.8	60.0	70.2	75.9	79.0	87.8	105
Rb	58.4	10.5	23.4	11.1	56.8	4.6	3.7
Sr	788	525	1100	519	914	537	524
Ba	146	205	208	195	217	107	91.7
H_2O^+ (wt%)	3.95	0.36	1.30	0.95	1.52	0.64	0.52
Density (g/cm^3)	1.46	2.50	2.34	2.53	2.47	2.44	2.62
Fe_2O_3/FeO	25.64	3.01	1.82	0.83	1.71	0.61	0.40

Table AT42 (continued).

Leg	183	183	183	183	183	183
Hole	1138A	1138A	1138A	1138A	1138A	1138A
Core, section	83R-5	84R-5	86R-3	87R-2	88R-2	88R-2
Interval (cm)	106-109	20-25	72-74	76-81	47-53	91-96
Piece	9	1C	8	13	2A	4
Lab number	Z-1025	Z-1026	Z-1029	Z-1031	Z-1032	Z-1033
Depth (mbsf)	781.99	790.03	807.82	815.92	825.28	825.72
Major elements (g/1000 cm^3):						
Si	508	598	553	539	434	496
Ti	26.9	31.0	34.0	38.0	31.6	38.8
Al	168	198	170	169	118	152
Fe^{+++}	86.1	124	116	126	136	158
Fe^{++}	117	154	183	185	73.4	144
Fe (Sum)	203	278	299	310	209	302
Mn	2.1	6.6	6.7	9.1	4.0	6.0
Mg	86.3	98.1	84.9	87.4	67.8	83.5
Ca	157	198	135	154	118	136
Na	48.3	57.0	76.6	53.9	41.8	51.2
K	7.9	6.4	7.8	11.4	21.1	11.6
P	2.7	3.2	3.6	4.2	2.1	3.8
Minor elements (g/1000 cm^3 x 10^{-3}):						
La	35.2	42.1	44.8	63.7	56.8	80.2
Ce	83.6	108	115	132	135	185
Nd	52.8	63.1	67.2	83.3	78.4	112
Sm	14.3	15.8	18.9	23.8	21.6	29.8
Eu	4.2	5.3	6.0	6.9	5.1	7.3
Tb	2.6	2.9	3.5	3.7	3.3	4.4
Yb	7.5	8.4	10.2	12.3	11.8	14.0
Lu	1.2	1.3	1.6	1.9	1.8	2.1
Cr	198	168	127	85.8	58.8	68.7
Ni	123	129	92	93.1	70.6	87.0
V	1071	1091	884	1193	843	1138
Cu	297	395	610	466	510	561
Co	110	116	102	123	66.6	103
Pb	15.4	15.8	17.4	14.7	13.7	18.3
Zn	238	323	304	355	251	389
Sn	9.7	8.9	6.7	8.6	5.9	11.7
Zr	374	447	573	564	510	573
Nb	30.8	34.2	44.8	49.0	43.1	43.5
Y	90.2	103	112	123	112	133
Rb	11.4	2.9	11.2	13.2	41.2	17.9
Sr	572	552	473	564	1196	435
Ba	123	216	115	85.8	314	140
H_2O^+ (wt%)	1.29	0.30	2.33	1.06	4.96	1.54
Density (g/cm^3)	2.20	2.63	2.49	2.45	1.96	2.29
Fe_2O_3/FeO	0.82	0.90	0.70	0.75	2.06	1.23

Table AT43. Abundance of major and trace elements (g/1000 cm^3) in igneous rocks, Hole 1140A, Leg 183 (Kerguelen Plateau, Indian Ocean). (Continued on next page.)

Leg	183	183	183	183	183	183	183
Hole	1140A	1140A	1140A	1140A	1140A	1140A	1140A
Core, section	27R-1	27R-1	27R-2	31R-1	31R-1	32R-3	32R-4
Interval (cm)	17-27	63-67	78-83	9-13	76-79	5-10	17-20
Piece	1A	4	3B	1	5	2	2
Lab number	Z-1034	Z-1035	Z-1036	Z-1037	Z-1038	Z-1039	Z-1040
Depth (mbsf)	239.47	239.93	241.49	270.59	271.26	278.25	279.83
Major elements (g/1000 cm^3):							
Si	657	647	637	598	632	589	644
Ti	21.5	19.5	19.6	33.0	37.2	49.2	19.2
Al	231	224	223	221	220	187	235
Fe^{+++}	100	131	125	105	76.4	80.7	159
Fe^{++}	165	136	137	112	154	169	73.5
Fe (Sum)	265	267	262	217	230	249	232
Mn	1.1	4.1	3.6	3.7	3.7	2.6	2.3
Mg	116	127	144	88.3	97.9	85.51	115
Ca	250	248	233	213	215	177	220
Na	55.9	57.0	56.4	55.4	61.9	59.7	57.0
K	3.2	10.8	2.7	12.9	8.3	11.3	19.6
P	1.6	1.4	7.5	3.4	2.8	3.9	1.7
Minor elements (g/1000 cm^3 x 10^{-3}):							
La	11.0	11.8	10.7	34.1	38.2	130.1	32.0
Ce	23.8	31.8	28.8	83.8	90.1	318.6	88.1
Nd	24.7	28.9	25.9	55.0	57.3	195.1	67.3
Sm	10.4	11.0	10.1	15.5	14.7	54.6	22.4
Eu	3.8	3.8	3.7	5.2	5.5	16.9	9.6
Tb	2.4	2.8	2.5	2.6	3.3	9.1	6.7
Yb	8.1	8.1	7.2	7.3	7.9	22.8	19.2
Lu	1.2	1.1	1.1	1.0	1.1	3.0	3.0
Cr	769	795	850	270	410	436	2162
Ni	267	243	294	128	199	299	833
V	885	858	893	917	1016	2581	2819
Cu	493	405	461	354	396	943	1682
Co	145	107	170	94.32	128	273	400
Pb	17	14	14	16	16	39	40.0
Zn	270	254	268	267	437	891	737
Sn	9.86	9.83	7.20	8.91	8.19	24.71	20.0
Zr	234.9	225	225	199	437	1105	1842
Nb	10.4	7.8	10.4	7.9	30.0	84.5	160.2
Y	84.1	92.5	83.5	83.8	90.1	280	208
Rb		26.6	4.3	20.7	6.8	37.1	96.1
Sr	377	376	346	655	710	1626	881
Ba	157	83.8	138	244	328	975	88.1
H_2O^+ (wt%)	1.36	1.02	1.39	0.91	0.87	0.93	1.65
Density (g/cm^3)	2.90	2.89	2.88	2.62	2.73	2.55	2.83
Fe_2O_3/FeO	0.67	1.07	1.02	1.04	0.55	0.53	2.41

Table AT43 (continued).

Leg	183	183	183	183	183	183	183
Hole	1140A	1140A	1140A	1140A	1140A	1140A	1140A
Core, section	34R-1	34R-3	35R-1	35R-1	36R-4	37R-1	37R-2
Interval (cm)	117-121	100-105	35-42	83-87	61-67	93-99	55-60
Piece	4D	3	2A	4	2D	1D	2A
Lab number	Z-1041	Z-1042	Z-1043	Z-1044	Z-1045	Z-1046	Z-1047
Depth (mbsf)	295.27	297.78	303.85	304.33	317.52	318.23	318.97
Major elements (g/1000 cm^3):							
Si	585	580	656	665	678	657	660
Ti	18.2	17.6	23.9	22.8	21.3	21.1	18.8
Al	216	222	231	222	225	227	43.91
Fe^{+++}	84.1	125	132	97.1	89.2	88.0	116
Fe^{++}	136	60.1	145	148	158	136	141
Fe (Sum)	220	185	279	245	247	224	257
Mn	3.3	1.8	3.2	3.2	3.0	3.1	3.9
Mg	115	132	120	107	139	109	115
Ca	199	192	250	256	251	247	258
Na	51.0	51.5	59.8	61.2	61.8	60.0	60.6
K	1.8	7.9	11.0	12.4	2.8	2.6	3.9
P	1.3	1.3	1.5	1.5	1.6	1.5	1.7
Minor elements (g/1000 cm^3 x 10^{-3}):							
La	10.0	9.3	11.7	12.3	11.5	12.9	12.7
Ce	24.2	28.3	32.2	37.3	35.4	39.2	37.4
Nd	21.1	21.6	28.1	28.7	26.6	30.8	31.7
Sm	7.7	7.7	10.5	10.0	9.1	9.5	9.8
Eu	2.8	2.8	3.8	4.0	3.8	3.6	3.7
Tb	1.9	2.1	2.8	2.4	2.5	2.4	2.4
Yb	6.2	5.9	7.9	7.5	6.5	7.0	7.5
Lu	1.0	1.0	1.3	1.3	1.0	1.1	1.2
Cr	707	822	498	517	590	504	576
Ni	216	247	190	132	189	185	236
V	969	900	929	1010	994	1014	1071
Cu	411	398	498	474	502	518	533
Co	159	139	144	112	159	154	184
Pb	12.9	15.4	17.6	14.4	17.7	16.8	14.4
Zn	239	234	226	287	274	272	288
Sn	9.25	9.00	9.7	9.5	10.6	10.6	8.6
Zr	185	164	226	221	221	218	219
Nb	10.0	5.4	10.5	11.2	7.4	12.0	11.2
Y	66.8	64.3	85.0	89.0	82.6	78.4	80.6
Rb		12.6	26.4	26.7			3.2
Sr	283	283	352	344	384	336	346
Ba	123	69.4	82.0	106	133	81.2	89.3
H_2O^+ (wt%)	1.40	1.99	0.74	0.68	1.00	0.42	0.55
Density (g/cm^3)	2.57	2.57	2.93	2.87	2.95	2.80	2.88
Fe_2O_3/FeO	0.69	2.31	1.01	0.73	0.63	0.72	0.91

Table AT44. Abundance of major and trace elements (g/1000 cm^3) in basalts, Hole 706C, Leg 115 (Mascarene Plateau, West Indian Ocean).

Leg	115	115	115	115	115	115	115	115
Hole	706C	706C	706C	706C	706C	706C	706C	706C
Core, section	3R-2	4R-2	5R-1	5R-1	5R-3	6R-1	8R-2	9R-1
Interval (cm)	21-23	111-113	38-40	113-115	69-71	38-40	26-28	72-74
Piece	3	15	2C	10	9	2	1C	8
Lab number	Z-60	Z-64	Z-38	Z-59	Z-50	Z-54	Z-39	Z-47
Depth (mbsf)	55.61	66.21	73.58	74.33	76.89	83.28	104.06	112.72
Major elements (g/1000 cm^3):								
Si	496	505	566	471	546	521	577	591
Ti	48	54	47	43	53	56	40	20
Al	144	144	173	146	146	144	190	233
Fe^{+++}	147	128	164	88	152	143	138	101
Fe^{++}	132	148	159	130	175	135	136	117
Fe (Sum)	279	276	323	218	327	278	274	218
Mn	3.2	3.5	3.1	3.1	3.6	3.0	2.1	2.5
Mg	69	70	87	94	75	75	76	82
Ca	158	174	188	162	162	158	208	221
Na	52	51	59	50	53	55	68	51
K	22.6	8.0	22.7	10.2	23.6	25.0	27.8	15.9
P	3.9	3.9	4.0	3.4	3.6	4.3	4.2	1.0
Minor elements (g/1000 cm^3 x 10^{-3}):								
La	52.3	48.4	41.9	43.0	47.4	52.4	54.9	14.4
Ce	120.4	112.9	102.2	86.0	112.2	107.2	115.0	26.3
Sm	17.7	18.4	19.4	15.7	19.2	19.1	21.7	7.1
Eu	5.7	6.2	5.2	5.4	6.2	6.2	5.5	2.5
Tb	2.7	3.5	2.9	3.2	4.0	3.6	3.1	1.5
Yb	5.5	8.1	7.9	7.3	8.0	8.6	10.5	5.5
Lu	0.9	1.1	1.1	1.0	1.0	1.2	1.5	0.8
Sc	82	85	97	86	122	9	99	102
Cr	66	60	107	75	72	62	214	81
Ni	132	154	165	138	142	114	193	158
Co	95	131	144	129	167	114	120	92
V	932	784	878	645	1110	898	915	643
Cu	239	304	238	269	279	298	225	347
Zn	364	293	246	269	399	286	246	131
Zr	523	392	498	473	524	524	523	116
Y	100.0	99.1	94.3	88.2	99.8	104.9	112.4	52.5
Nb	43.2	48.4	47.2	23.7	49.9	47.7	49.7	13.7
Rb	68.2	5.1	60.2	4.3	49.9	69.1	91.5	31.5
Sr	591	369	681	581	474	572	654	394
Ba	136	161	189	148	160	191	222	92
H_2O^+ (wt%)	1.36	1.29	0.85	0.78	2.12	1.90	0.65	1.50
Density (g/cm^3)	2.27	2.30	2.59	2.27	2.49	2.47	2.61	2.63
Fe_2O_3/FeO	1.23	0.96	1.15	0.75	0.97	1.17	1.13	0.96

Table AT45. Abundance of major and trace elements (g/1000 cm^3) in basalts, Hole 707C, Leg 115 (Mascarene Plateau, West Indian Ocean). (Continued on next two pages.)

Leg	115	115	115	115	115	115	115
Hole	707C	707C	707C	707C	707C	707C	707C
Core, section	22R-1	22R-2	23R-1	23R-1	23R-4	24R-1	25R-1
Interval (cm)	94-98	49-51	32-36	98-100	0-3	138-140	108-110
Piece	11A	3A	1C	1N	1A	6	1H
Lab number	Z-1323	Z-78	Z-1325	Z-69	Z-605	Z-606	Z-70
Depth (mbsf)	376.54	377.59	385.62	386.28	389.62	396.28	405.58
Major elements (g/1000 cm^3):							
Si	524.3	515.8	584.7	651.8	623.1	487.4	603.2
Ti	11.9	14.8	9.8	14.1	10.4	17.5	28.4
Al	171.5	177.4	220.2	214.3	209.9	171.7	198.7
Fe^{+++}	112.6	111.2	103.7	116.6	103.2	88.7	110.0
Fe^{++}	104.1	98.6	87.1	119.4	108.6	76.0	135.3
Fe (Sum)	216.7	209.9	190.8	236.0	211.8	164.6	245.3
Mn	5.6	1.3	2.4	2.3	2.4	1.1	2.9
Mg	130.4	131.5	141.0	153.6	142.8	72.7	108.8
Ca	144.6	140.5	206.8	229.0	233.7	159.0	210.5
Na	44.6	45.0	28.1	49.0	53.8	33.2	49.8
K	3.0	5.5	1.5	4.9	9.7	1.4	3.8
P	0.4	0.4	0.3	0.1	0.4	1.2	1.3
Minor elements (g/1000 cm^3 x 10^{-3}):							
La		2.2		2.0			12.4
Ce		7.8		5.1			26.4
Sm		3.6		3.7			9.5
Eu		1.4		1.5			3.4
Tb		1.1		1.3			2.3
Yb		3.9		6.3			9.2
Lu		0.6		1.0			1.4
Sc		125.4		153.9			145.2
Cr	389.8	148.2	716.8	584.3	510.5	212.2	200.6
Ni	227.4	209.8	376.3	333.5	289.4	131.8	211.2
Co	174.0	118.6	192.0	136.8	144.7	96.8	110.9
V	1160.0	816.2	1049.6	712.5	810.8	1102.1	950.4
Cu	429.2	524.4	384.0	441.8	423.2	166.9	580.8
Zn	255.2	177.8	235.5	185.3	218.4	185.4	200.6
Sn					7.4	5.6	
Zr	78.9	57.0	66.6	48.5	71.0	164.8	142.6
Y	41.8	50.2	35.8	45.6	49.1	72.1	76.6
Nb	4.6		3.6			9.3	11.4
Rb		2.3			2.7	9.9	
Sr	132.2	107.2	174.1	145.4	133.8	189.5	192.7
Ba					13.7	20.6	
H_2O^+ (wt%)	1.04	1.16	1.20	1.46	1.19	1.60	1.15
Density (g/cm^3)	2.32	2.28	2.56	2.85	2.73	2.06	2.64
Fe_2O_3/FeO	1.20	1.25	1.32	1.09	1.06	1.30	0.90

Table AT45 (continued).

Leg	115	115	115	115	115	115	115
Hole	707C	707C	707C	707C	707C	707C	707C
Core, section	25R-2	25R-3	25R-4	25R-5	26R-1	26R-2	26R-3
Interval (cm)	38-42	108-111	42-45	110-114	81-86	123-125	71-73
Piece	1C	1M	1G	1P	1N	10	1H
Lab number	Z-607	Z-608	Z-609	Z-610	Z-611	Z-1326	Z-49
Depth (mbsf)	406.33	408.43	409.27	411.45	415.11	416.91	418.01
Major elements (g/1000 cm^3):							
Si	625.4	574.5	662.5	611.5	646.0	620.9	604.7
Ti	22.1	20.5	24.0	21.4	21.5	24.2	28.1
Al	214.4	192.9	228.7	211.7	216.0	221.3	188.5
Fe^{+++}	131.2	122.8	129.4	120.5	108.0	89.6	83.4
Fe^{++}	122.5	117.3	140.1	128.3	153.9	141.6	169.3
Fe (Sum)	253.7	240.1	269.5	248.8	262.0	231.2	252.7
Mn	4.1	2.0	1.6	2.1	2.4	3.2	3.3
Mg	102.0	117.0	130.6	122.0	117.4	120.7	105.8
Ca	223.6	203.3	217.4	201.1	223.1	202.4	207.7
Na	50.6	47.2	54.0	49.6	49.9	51.4	48.0
K	4.4	2.6	2.5	2.1	1.9	2.5	3.5
P	1.3	1.2	1.3	1.6	1.6	1.3	1.3
Minor elements (g/1000 cm^3 x 10^{-3}):							
La							11.2
Ce							26.1
Sm							8.4
Eu							2.9
Tb							2.1
Yb							8.6
Lu							1.3
Sc							135.7
Cr	253.0	264.2	261.0	289.4	240.8	440.1	224.5
Ni	204.0	182.9	188.5	193.0	190.4	216.0	221.9
Co	136.0	129.5	142.1	144.7	131.6	189.0	138.3
V	1128.8	1193.8	1276.0	1211.4	1148.0	1404.0	1278.9
Cu	326.4	271.8	414.7	482.4	532.0	688.5	861.3
Zn	272.0	241.3	272.6	241.2	263.2	340.2	224.5
Sn	8.2	7.9	7.8	7.2	7.6		
Zr	204.0	193.0	220.4	198.3	207.2	202.5	182.7
Y	89.8	81.3	110.2	88.4	89.6	81.0	83.5
Nb	10.9	7.1	12.2	10.2	9.0	11.3	11.5
Rb	11.4	2.5				2.7	
Sr	247.5	248.9	287.1	249.2	263.2	270.0	242.7
Ba		15.2	220.4		19.6	205.2	44.4
H_2O^+ (wt%)	0.92	0.80	1.09	1.18	0.93	0.57	0.90
Density (g/cm^3)	2.72	2.54	2.90	2.68	2.80	2.70	2.61
Fe_2O_3/FeO	1.19	1.16	1.03	1.04	0.78	0.70	0.55

Table AT45 (continued).

Leg	115	115	115	115	115	115	115
Hole	707C	707C	707C	707C	707C	707C	707C
Core, section	26R-5	26R-7	27R-4	27R-5	27R-6	28R-2	28R-3
Interval (cm)	62-65	46-48	46-49	32-36	29-31	53-55	133-135
Piece	1L	1E	2B	5	2A	6A	12
Lab number	Z-612	Z-61	Z-613	Z-614	Z-77	Z-44	Z-58
Depth (mbsf)	420.64	423.76	428.67	429.98	431.69	435.63	437.93
Major elements (g/1000 cm^3):							
Si	670.5	649.8	681.8	656.1	664.0	557.2	633.7
Ti	24.2	29.2	25.2	22.6	28.6	25.3	29.6
Al	231.7	202.3	231.5	225.2	233.2	175.5	190.4
Fe^{+++}	112.1	120.7	105.2	104.5	88.4	91.2	139.1
Fe^{++}	159.3	211.3	193.8	159.6	201.0	215.7	160.7
Fe (Sum)	271.3	332.0	299.0	264.1	289.4	306.9	299.8
Mn	4.7	4.5	4.9	1.8	4.6	2.9	3.5
Mg	141.2	120.3	114.5	105.7	116.1	94.2	121.4
Ca	240.4	219.3	249.0	238.9	251.2	227.4	207.5
Na	55.6	52.5	52.8	50.3	55.4	54.1	52.3
K	2.3	4.8	2.0	2.4	4.4	4.9	5.9
P	1.3	1.4	1.5	1.4	1.6	1.3	1.6
Minor elements (g/1000 cm^3 x 10^{-3}):							
La		12.7			12.9	12.0	13.6
Ce		28.8			29.4	32.0	33.2
Sm		8.9			9.4	9.1	9.1
Eu		3.2			3.5	2.9	3.0
Tb		2.4			2.7	2.1	2.0
Yb		9.8			10.6	8.3	6.6
Lu		1.5			1.6	1.0	0.9
Sc		146.9			152.9	128.2	141.3
Cr	255.4	256.3	268.2	284.0	217.6	138.8	155.1
Ni	207.9	239.0	202.6	204.5	229.3	218.9	221.6
Co	148.5	144.0	143.0	142.0	132.3	157.5	138.5
V	1351.4	1172.2	1049.0	1028.1	961.4	907.8	817.2
Cu	564.3	864.0	536.4	559.5	823.2	961.2	775.6
Zn	267.3	302.4	268.2	267.0	255.8	229.6	221.6
Sn	9.5		7.5	8.2			
Zr	228.7	184.3	226.5	224.4	199.9	165.5	182.8
Y	95.0	89.3	92.4	93.7	97.0	90.8	83.1
Nb	7.4	12.7	11.9	11.4	13.8	11.2	5.3
Rb		3.5		2.8		5.1	3.3
Sr	282.2	256.3	268.2	275.5	282.2	293.7	271.5
Ba		66.2	26.8	17.0	61.7	37.4	44.3
H_2O^+ (wt%)	1.00	0.75	0.56	0.84	0.39	0.82	0.76
Density (g/cm^3)	2.97	2.88	2.98	2.84	2.94	2.67	2.77
Fe_2O_3/FeO	0.78	0.63	0.60	0.73	0.49	0.47	0.96

Table AT46. Abundance of major and trace elements (g/1000 cm^3) in basalts, Hole 713A, Leg 115 (Chagos Bank, West Indian Ocean). (Continued on next two pages.)

Leg	115	115	115	115	115	115	115	115
Hole	713A	713A	713A	713A	713A	713A	713A	713A
Core, section	13R-1	13R-3	14R-3	15R-1	15R-3	15R-4	15R-4	15R-5
Interval (cm)	97-99	16-20	99-101	77-79	52-57	64-69	103-105	85-87
Piece	10C	3	5	4B	2B	1	4	5
Lab number	Z-53	Z-1328	Z-74	Z-55	Z-615	Z-616	Z-1329	Z-52
Depth (mbsf)	108.67	110.78	121.19	127.47	130.17	131.57	131.96	133.55
Major elements (g/1000 cm^3):								
Si	556	627.4	610	633	630.3	627.1	586.8	625
Ti	24	22.8	29	24	18.3	23.1	25.1	29
Al	179	223.8	215	193	204.9	193.6	187.5	195
Fe^{+++}	62	83.7	110	112	74.2	105.8	169.2	100
Fe^{++}	170	138.5	129	167	147.3	157.9	147.8	190
Fe (Sum)	232	222.1	239	279	221.6	263.7	317.0	290
Mn	4.1	1.7	4.3	4.6	4.5	3.7	1.9	5.0
Mg	121	126.7	125	144	137.3	131.1	105.2	113
Ca	217	224.1	241	229	228.5	211.7	189.7	223
Na	46	52.9	60	50	48.3	49.6	54.2	53
K	5.2	3.7	10.8	7.8	3.7	4.1	8.7	5.1
P	1.2	1.2	1.7	1.2	1.6	1.6	1.9	1.6
Minor elements (g/1000 cm^3 x 10^{-3}):								
La	10.3		15.1	10.5				13.0
Ce	25.0		33.0	27.2				33.3
Sm	7.5		11.5	7.9				9.1
Eu	3.0		3.6	3.1				3.3
Tb	1.9		2.7	2.2				2.2
Yb	8.0		11.5	8.8				9.7
Lu	1.2		1.8	1.3				1.4
Sc	123		140	145				147
Cr	458	712.4	412	780	639.2	462.4	462.0	471
Ni	225	197.3	275	284	201.3	171.4	190.1	249
Co	143	200.0	190	150	144.2	133.3	142.6	177
V	768	1260.4	962	681	748.0	943.8	1240.8	1289
Cu	588	485.0	714	667	516.8	652.8	950.4	818
Zn	238	493.2	264	244	263.8	266.6	340.6	291
Zr	180	221.9	214	162	185.0	214.9	250.8	213
Y	85.0	79.5	96.2	85.1	68.0	78.9	108.2	105.3
Nb	11.0	14.0	12.4	10.8	7.9	9.8	14.3	14.1
Rb	2.5	6.0	27.5	8.2	9.0	9.8	20.6	3.3
Sr	238	274.0	250	238	247.5	258.4	240.2	241
Ba	45	180.8	80	54	19.0	65.3	145.2	80
H_2O^+ (wt%)	0.99	0.39	0.32	1.69	0.66	0.58	0.45	1.06
Density (g/cm^3)	2.50	2.74	2.75	2.84	2.72	2.72	2.64	2.77
Fe_2O_3/FeO	0.40	0.67	0.96	0.74	0.56	0.74	1.27	0.58

Table AT46 (continued).

Leg	115	115	115	115	115	115	115	115
Hole	713A	713A	713A	713A	713A	713A	713A	713A
Core, section	18R-1	19R-1	19R-2	19R-3	20R-1	20R-2	20R-3	20R-4
Interval (cm)	93-95	132-134	49-53	9-12	70-72	104-108	40-42	57-62
Piece	9	13	3F	2A	5A	6B	2A	1
Lab number	Z-48	Z-56	Z-617	Z-618	Z-40	Z-619	Z-37	Z-620
Depth (mbsf)	156.13	165.72	166.28	167.38	174.60	176.39	177.30	178.92
Major elements (g/1000 cm^3):								
Si	659	662	661.7	689.5	646	643.3	641	628.0
Ti	21	20	16.8	16.0	19	16.4	19	14.7
Al	223	224	207.2	240.5	228	211.4	224	220.4
Fe^{+++}	96	90	91.3	76.7	86	77.1	91	69.1
Fe^{++}	155	171	153.5	154.0	122	150.8	145	131.1
Fe (Sum)	251	261	244.8	230.7	208	227.9	236	200.2
Mn	3.0	3.9	3.8	3.8	3.2	3.7	3.3	3.2
Mg	130	126	131.5	140.2	131	130.5	115	127.4
Ca	273	264	258.8	260.3	284	240.9	272	254.1
Na	53	43	49.9	54.4	62	48.0	58	47.3
K	13.5	8.0	10.6	9.3	5.1	7.5	4.1	1.8
P	0.8	0.8	1.0	1.1	0.5	1.0	0.6	1.1
Minor elements (g/1000 cm^3 x 10^{-3}):								
La	7.0	7.6			7.4		6.8	
Ce	18.5	18.6			18.5		18.1	
Sm	7.0	6.4			6.8		7.1	
Eu	2.5	2.7			2.3		2.4	
Tb	1.9	1.8			1.8		1.9	
Yb	7.0	7.6			6.8		7.9	
Lu	1.1	1.2			1.1		1.3	
Sc	153	148			148		147	
Cr	288	335	441.8	461.9	300	290.9	292	290.0
Ni	217	241	159.6	166.9	357	146.8	272	170.7
Co	123	134	125.4	134.1	200	121.9	136	130.1
V	939	873	798.0	834.4	856	761.8	948	818.4
Cu	352	305	399.0	566.2	556	332.4	495	433.6
Zn	176	244	210.9	214.6	183	257.6	170	238.5
Zr	114	108	142.5	157.9	103	141.3	102	138.2
Y	70.4	69.8	65.6	65.6	65.6	69.3	79.3	62.3
Nb	7.0	6.4	8.0	6.6	6.6	6.1	9.6	6.0
Rb	18.5	17.5	31.4	19.7	4.9	19.9		
Sr	279	273	273.6	289.1	285	263.2	258	271.0
Ba	44	44	71.3	29.8		41.6	42	
H_2O^+ (wt%)	0.76	0.76	0.28	0.41	0.60	0.79	0.58	0.34
Density (g/cm^3)	2.93	2.91	2.85	2.98	2.85	2.77	2.83	2.71
Fe_2O_3/FeO	0.69	0.59	0.66	0.55	0.78	0.57	0.70	0.59

Table AT46 (continued).

Leg	115	115	115	115	115	115
Hole	713A	713A	713A	713A	713A	713A
Core, section	20R-5	20R-6	21R-1	21R-2	21R-3	22R-1
Interval (cm)	65-67	103-108	73-75	61-63	83-85	34-36
Piece	5B	1C	4B	4B	4A	5
Lab number	Z-65	Z-621	Z-71	Z-75	Z-73	Z-66
Depth (mbsf)	180.55	182.38	184.03	185.41	187.13	190.54
Major elements (g/1000 cm^3):						
Si	674	681.9	577	672	655	663
Ti	20	17.8	18	20	20	21
Al	226	231.8	213	230	234	224
Fe^{+++}	65	78.0	75	100	87	83
Fe^{++}	174	150.8	122	168	155	162
Fe (Sum)	239	228.8	197	268	242	245
Mn	3.9	4.2	3.6	4.9	4.8	4.1
Mg	140	143.5	118	138	139	126
Ca	238	277.7	238	288	286	272
Na	55	50.5	49	58	52	46
K	8.9	2.0	1.5	7.0	1.7	3.4
P	0.8	1.0	0.7	1.2	0.8	0.8
Minor elements (g/1000 cm^3 x 10^{-3}):						
La	8.2		6.9	8.1	7.9	6.9
Ce	19.6		15.5	18.6	15.5	18.2
Sm	7.0		6.4	7.8	7.6	5.8
Eu	2.7		2.4	2.7	2.6	2.6
Tb	1.8		1.8	2.0	2.0	1.6
Yb	7.6		7.1	9.3	8.8	6.9
Lu	1.2		1.1	1.5	1.3	1.1
Sc	114		145	159	161	150
Cr	316	316.7	265	237	307	300
Ni	202	189.4	204	216	249	257
Co	117	153.9	122	120	149	153
V	702	879.1	781	660	722	809
Cu	410	577.2	471	360	512	506
Zn	176	257.5	214	195	228	231
Zr	111	151.0	104	105	108	116
Y	70.2	71.0	58.5	72.0	70.2	66.4
Nb	7.6	8.6	6.9	8.4	7.9	6.4
Rb	18.1			14.4		
Sr	269	287.1	234	270	249	269
Ba	50	44.4		66		43
H_2O^+ (wt%)	1.25	0.40	0.37	0.15	0.36	0.76
Density (g/cm^3)	2.66	2.96	2.86	3.00	2.92	2.82
Fe_2O_3/FeO	0.42	0.57	0.69	0.66	0.57	0.57

Table AT47. Abundance of major and trace elements (g/1000 cm^3) in basalts, Hole 715A, Leg 115 (Maldives Ridges, West Indian Ocean). (Continued on next three pages.)

Leg	115	115	115	115	115	115	115
Hole	715A	715A	715A	715A	715A	715A	715A
Core, section	23R-2	23R-3	23R-3	24R-1	24R-2	24R-2	25R-2
Interval (cm)	28-31	62-64	91-95	76-79	13-18	30-38	80-82
Piece	2A	11	14A	11	2	3	3C
Lab number	Z-622	Z-79	Z-1333	Z-623	Z-624	Z-1334	Z-63
Depth (mbsf)	212.54	214.42	214.67	221.26	222.03	222.20	232.30
Major elements (g/1000 cm^3):							
Si	465.2	598	606.3	632.0	644.1	629.4	625
Ti	43.6	41	35.5	36.3	31.9	37.3	21
Al	167.5	228	197.3	200.4	199.5	206.0	215
Fe^{+++}	125.9	186	239.3	199.4	183.9	138.2	86
Fe^{++}	103.4	108	96.6	137.9	183.5	182.1	153
Fe (Sum)	229.3	294	335.9	337.3	367.4	320.3	239
Mn	3.3	3.7	3.5	3.6	4.8	4.0	4.0
Mg	55.1	111	110.4	105.8	109.6	113.0	178
Ca	209.9	199	183.9	202.4	189.7	199.7	213
Na	50.2	61	55.5	54.2	53.7	55.6	40
K	13.8	24.9	18.8	21.8	17.4	6.2	6.7
P	5.8	3.6	3.0	3.3	3.0	3.0	1.4
Minor elements (g/1000 cm^3 x 10^{-3}):							
La		28.0					12.8
Ce		58.7					27.9
Sm		14.5					6.3
Eu		4.8					2.2
Tb		3.4					1.5
Yb		12.0					6.0
Lu		1.9					1.0
Sc		140					120
Cr	91.6	193	390.6	208.1	240.7	399.0	1651
Ni	84.7	224	223.2	173.9	162.4	244.5	697
Co	98.5	120	195.3	128.3	124.7	185.5	157
V	748.8	964	1367.1	960.5	803.3	1382.5	655
Cu	215.3	207	390.6	698.3	406.0	370.9	242
Zn	389.3	335	418.5	370.5	295.8	368.1	179
Zr		335	334.8	356.3	319.0	337.2	142
Y		117.4	108.8	114.0	101.5	106.8	56.9
Nb		36.3	33.5	37.1	31.9	33.7	19.1
Rb		120.2	173.0	185.3	46.4	6.5	4.8
Sr		307	334.8	342.0	319.0	337.2	213
Ba		226	253.9	139.7	133.4	309.1	122
H_2O^+ (wt%)	1.48	0.79	0.99	0.79	1.09	0.25	2.89
Density (g/cm^3)	2.29	2.80	2.79	2.85	2.90	2.81	2.85
Fe_2O_3/FeO	1.35	1.92	2.75	1.61	1.11	0.84	0.62

Table AT47 (continued).

Leg	115	115	115	115	115	115	115
Hole	715A	715A	715A	715A	715A	715A	715A
Core, section	25R-3	25R-5	25R-6	25R-6	26R-2	26R-3	29R-1
Interval (cm)	0-4	108-112	2-4	16-18	14-20	17-19	38-42
Piece	1A	15	1	1	1A	1B	2A
Lab number	Z-625	Z-626	Z-1335	Z-57	Z-627	Z-62	Z-1336
Depth (mbsf)	232.39	236.36	236.60	237.66	240.76	242.67	268.08
Major elements (g/1000 cm^3):							
Si	579.6	575.5	582.4	618	619.7	406	612.3
Ti	15.7	14.6	16.5	20	15.9	17	23.9
Al	211.4	192.2	206.2	192	216.0	180	221.9
Fe^{+++}	103.1	112.1	75.6	94	50.0	186	113.3
Fe^{++}	96.2	91.4	144.6	179	181.4	19	118.4
Fe (Sum)	199.3	203.5	220.2	273	231.4	205	231.7
Mn	4.0	3.1	3.6	4.0	4.6	3.9	3.5
Mg	153.9	165.4	176.1	191	183.8	40	151.3
Ca	202.4	187.5	196.8	211	209.3	251	213.1
Na	40.5	40.4	37.5	40	38.0	40	45.1
K	7.2	11.0	5.2	7.9	5.9	20.8	5.1
P	1.6	1.6	1.4	1.6	1.7	2.3	2.0
Minor elements (g/1000 cm^3 x 10^{-3}):							
La				13.4		11.6	
Ce				28.3		28.4	
Sm				6.6		5.7	
Eu				2.3		2.0	
Tb				1.5		1.3	
Yb				6.3		5.2	
Lu				1.0		0.8	
Sc				117		96	
Cr	969.4	1032.0	984.2	1687	1078.0	1214	943.9
Ni	589.5	614.0	571.9	1001	658.0	437	460.9
Co	146.7	147.1	186.2	192	159.6	120	187.7
V	634.0	624.4	704.9	629	630.0	634	930.1
Cu	204.4	258.0	210.1	629	263.2	262	331.2
Zn	241.0	224.5	255.4	234	221.2	147	270.5
Zr	149.3	147.1	159.6	114	168.0	98	229.1
Y	49.8	56.8	53.2	60.0	58.8	48.1	74.5
Nb	14.4	14.4	18.9	19.4	18.5	16.2	26.5
Rb	13.4	43.9	10.1	10.9	13.2	15.7	6.1
Sr	225.3	201.2	220.8	254	238.0	241	386.4
Ba	49.8	67.1	258.0	140	173.6	147	303.6
H_2O^+ (wt%)	2.32	2.10	2.50	2.82	2.16	1.88	1.52
Density (g/cm^3)	2.62	2.58	2.66	2.86	2.80	2.19	2.76
Fe_2O_3/FeO	1.19	1.36	0.58	0.58	0.31	11.16	1.06

Table AT47 (continued).

Leg	115	115	115	115	115	115	115
Hole	715A	715A	715A	715A	715A	715A	715A
Core, section	29R-1	29R-1	29R-2	30R-2	30R-3	30R-5	30R-5
Interval (cm)	64-66	95-97	80-82	1-5	28-30	30-32	39-41
Piece	2B	3A	1F	1	1	3	4
Lab number	Z-42	Z-51	Z-67	Z-628	Z-41	Z-72	Z-43
Depth (mbsf)	268.34	268.65	270.00	271.48	273.98	277.00	277.09
Major elements (g/1000 cm^3):							
Si	596	585	614	641.2	613	304	394
Ti	21	46	25	21.5	20	17	21
Al	206	173	202	229.7	177	143	170
Fe^{+++}	90	88	108	78.1	110	123	165
Fe^{++}	155	181	153	162.6	158	22	51
Fe (Sum)	245	269	261	240.7	268	145	216
Mn	3.3	4.0	3.3	4.8	2.4	3.1	2.7
Mg	150	77	148	171.0	159	36	36
Ca	235	189	2152	220.1	230	519	237
Na	46	64	41	41.4	50	45	43
K	4.7	18.3	7.7	7.3	10.4	15.0	13.5
P	1.6	4.2	1.6	1.9	1.5	2.3	2.0
Minor elements (g/1000 cm^3 x 10^{-3}):							
La	19.7	38.4	16.9		15.9	15.9	17.8
Ce	35.7	84.5	36.1		36.3	27.3	35.3
Sm	9.1	16.6	8.0		8.4	7.9	8.5
Eu	3.0	5.9	2.8		2.7	2.3	2.7
Tb	1.8	3.8	1.7		1.6	1.6	1.7
Yb	6.0	10.8	6.1		6.1	5.9	6.2
Lu	1.1	1.7	0.9		0.9	0.9	0.9
Sc	112	128	117		106	87	93
Cr	1207	95	1157	1011.5	851	486	851
Ni	532	174	546	520.2	711	188	332
Co	156	146	150	161.8	148	52	95
V	713	1345	610	684.9	516	372	685
Cu	250	218	291	202.3	176	248	685
Zn	170	525	241	260.1	139	67	141
Zr	162	410	161	216.8	131	136	162
Y	60.3	128.1	63.8	63.6	61.4	52.0	60.0
Nb	21.4	53.8	23.0	22.5	20.9	18.1	20.7
Rb	5.2	30.7	9.7	12.1	10.6	14.4	11.6
Sr	384	461	361	375.7	363	396	394
Ba	129	384	150	57.8	240	119	139
H_2O^+ (wt%)	2.12	0.79	2.28	1.74	2.35	1.18	0.89
Density (g/cm^3)	2.74	2.56	2.77	2.89	2.79	2.48	2.07
Fe_2O_3/FeO	0.65	0.54	0.78	0.53	0.78	6.22	3.60

Table AT47 (continued).

Leg	115	115	115
Hole	715A	715A	715A
Core, section	30R-5	31R-1	31R-2
Interval (cm)	98-100	103-105	98-100
Piece	9	8B	6A
Lab number	Z-46	Z-45	Z-76
Depth (mbsf)	277.68	279.23	280.68
Major elements (g/1000 cm^3):			
Si	574	535	630
Ti	25	22	23
Al	209	192	247
Fe^{+++}	142	157	161
Fe^{++}	111	71	84
Fe (Sum)	253	228	245
Mn	4.0	2.0	3.7
Mg	128	132	173
Ca	271	197	210
Na	47	46	51
K	11.2	10.7	11.0
P	1.4	2.0	2.1
Minor elements (g/1000 cm^3 x 10^{-3}):			
La	15.0	16.7	20.9
Ce	36.9	32.4	41.3
Sm	8.8	9.0	9.4
Eu	2.4	2.5	3.0
Tb	1.7	1.6	1.8
Yb	6.0	6.0	7.1
Lu	0.9	0.9	1.0
Sc	114	37	115
Cr	837	1060	1047
Ni	667	674	856
Co	167	132	150
V	667	786	655
Cu	341	250	310
Zn	165	190	233
Zr	142	172	204
Y	59.6	57.4	59.0
Nb	21.9	24.7	28.0
Rb	13.6	14.0	17.7
Sr	426	324	413
Ba	150	92	177
H_2O^+ (wt%)	2.20	2.25	2.48
Density (g/cm^3)	2.77	2.50	2.66
Fe_2O_3/FeO	1.42	2.46	2.12

Table AT48. Abundance of major and trace elements (g/1000 cm^3) in basalts, Hole 525A, Leg 74 (Walvis Ridge, Atlantic Ocean). (Continued on next page.)

Leg	74	74	74	74	74	74	74
Hole	525A	525A	525A	525A	525A	525A	525A
Core, section	53-2	53-3	56-1	56-2	56-3	56-6	58-1
Interval (cm)	87-90	36-39	43-46	121-124	108-111	81-84	106-109
Piece	5B	3	1G	1W	1R	10	4D
Lab number	Z-398	Z-397	Z-400	Z-401	Z-402	Z-403	Z-404
Depth (mbsf)	575.97	576.96	602.53	604.81	606.18	610.41	622.16
Major elements (g/1000 cm^3):							
Si	459	464	458	584	573	584	515
Ti	29	28	37	19	20	20	19
Al	202	200	152	207	196	214	154
Fe^{+++}	55	69	116	79	110	109	145
Fe^{++}	12	50	130	99	99	94	101
Fe (Sum)	67	119	246	178	209	203	246
Mn	0.1	0.6	1.3	0.4	0.6	0.8	2.7
Mg	16.6	15	56.5	74	68	69	27
Ca	106	136	227	176	166	167	235
Na	60	61	54	61	62	70	61
K	22.3	19.7	12.5	15.9	24.7	27.2	25.3
P	2.5	1.0	2.2	3.4	3.3	2.8	3.0
Minor elements (g/1000 cm^3 x 10^{-3}):							
La	41.8	39.8	57.9	59.0	66.8	73.1	61.9
Ce	81.8	81.5	120.7	118.0	133.5	148.8	126.3
Nd	49.1	47.7	70.0	68.9	69.2	75.7	66.9
Sm	11.6	11.3	14.7	15.5	16.1	17.4	14.9
Eu	3.6	3.8	5.1	5.2	4.9	6.1	4.7
Tb	2.0	2.2	2.7	3.0	2.7	3.3	2.7
Yb	4.9	5.4	6.0	5.9	6.4	7.3	6.2
Lu	0.7	0.8	0.9	0.9	1.0	1.1	1.0
Cr	645	636	60	86	37	88	111
Ni	82	149	60	74	49	76	124
Co	82	239	84	86	62	88	124
V	945	855	555	639	297	630	718
Cu	418	239	97	135	37	88	111
Zn	636	368	157	246	136	265	223
Zr	363	358	459	443	470	504	446
Y	54.5	57.7	72.4	66.4	71.7	75.7	71.8
Nb	32.7	29.8	45.9	46.7	49.5	50.4	44.6
Rb	36.3	27.8	7.0	12.8	37.1	27.7	32.2
Sr	709	716	966	1008	940	908	1040
Ba	600	537	555	320	346	731	570
H_2O^+ (wt%)	1.12	1.12	1.92	2.73	1.98	1.45	1.11
Density (g/cm^3)	1.82	1.99	2.41	2.46	2.47	2.52	2.48
Fe_2O_3/FeO	4.88	1.53	0.99	0.89	1.23	1.30	1.60

Table AT48 (continued).

Leg	74	74	74	74	74	74	74
Hole	525A	525A	525A	525A	525A	525A	525A
Core, section	58-4	59-3	60-1	60-3	60-4	61-2	63-2
Interval (cm)	82-85	40-42	41-44	40-43	32-35	2-5	104-107
Piece	4C	1G	1D	1H	1D	1A	4A
Lab number	Z-405	Z-406	Z-407	Z-408	Z-409	Z-410	Z-411
Depth (mbsf)	626.42	634	640.51	643.5	644.92	651.12	671.14
Major elements (g/1000 cm^3):							
Si	572	560	552	453	548	494	552
Ti	18	21	18	19	19	34	34
Al	220	210	210	150	205	177	212
Fe^{+++}	76	82	111	113	111	110	72
Fe^{++}	81	82	43	60	82	61	69
Fe (Sum)	157	164	154	173	193	171	141
Mn	1.7	0.6	0.4	2.5	0.2	3.4	2.0
Mg	67	64	57	33	63	56	52
Ca	142	140	141	264	138	158	120
Na	63	62	61	54	62	62	73
K	15.5	15.2	15.0	13.8	16.4	31.0	42.6
P	3.0	3.0	2.6	2.1	7.0	4.3	4.3
Minor elements (g/1000 cm^3 x 10^{-3}):							
La	73.1	79.3	66.4	63.7	79.9	97.7	105.6
Ce	148.6	158.5	141.9	129.6	164.4	199.9	227.3
Nd	96.7	76.9	73.2	70.5	84.6	95.4	110.2
Sm	18.6	18.2	17.4	16.1	19.3	20.9	23.0
Eu	5.9	5.6	5.5	4.8	5.9	6.1	6.9
Tb	3.3	2.8	2.7	2.5	2.8	3.2	3.9
Yb	7.3	8.6	7.3	6.6	7.8	8.4	9.6
Lu	1.1	1.1	1.0	1.0	1.1	1.1	1.4
Cr	71	23	80	68	82	80	103
Ni	94	93	126	91	211	45	69
Co	83	82	114	80	164	68	92
V	920	816	893	614	916	636	803
Cu	153	140	137	102	164	68	69
Zn	330	245	252	148	235	227	253
Zr	519	490	504	432	564	659	712
Y	84.9	97.9	82.4	79.6	94.0	90.9	112.5
Nb	49.5	51.3	48.1	38.7	51.7	61.3	64.3
Rb	8.7	10.5	11.4	8.0	10.3	38.6	29.8
Sr	1014	979	1030	955	1010	909	987
Ba	637	629	526	523	775	863	1148
H_2O^+ (wt%)	2.18	2.10	2.14	1.64	2.44	5.48	1.30
Density (g/cm^3)	2.36	2.33	2.29	2.27	2.35	2.27	2.30
Fe_2O_3/FeO	1.04	1.11	2.87	2.11	1.51	2.01	1.16

Table AT49. Abundance of major and trace elements (g/1000 cm^3) in igneous rocks, Hole 527, Leg 74 (Walvis Ridge, Atlantic Ocean).

Leg	74	74	74	74	74	74
Hole	527	527	527	527	527	527
Core, section	39-2	39-3	40-1	41-3	42-4	44-3
Interval (cm)	131-134	64-67	82-85	39-42	45-48	10-13
Piece	1G	1G	3F	1C	1C	1A
Lab number	Z-412	Z-413	Z-414	Z-415	Z-417	Z-418
Depth (mbsf)	344.31	345.14	347.32	353.89	364.45	380.6
Major elements (g/1000 cm^3):						
Si	631	640	659	672	591	607
Ti	22	30	31	23	41	31
Al	206	204	201	260	185	187
Fe^{+++}	217	122	126	81	152	151
Fe^{++}	82	159	181	156	142	135
Fe (Sum)	299	281	307	237	294	286
Mn	3.3	3.1	3.9	1.8	2.3	2.1
Mg	103	109	114	105	100	85
Ca	190	214	230	275	134	176
Na	63	64	66	62	90	80
K	15.4	16.8	13.2	6.4	29.2	25.3
P	0.2	0.9	1.5	0.5	3.4	2.0
Minor elements (g/1000 cm^3 x 10^{-3}):						
La	36.1	36.4	34.8	19.8	74.0	74.1
Ce	72.1	72.8	69.5	41.4	142.7	137.7
Nd	49.9	50.4	49.2	29.6	71.3	71.5
Sm	13.0	13.4	12.5	8.0	16.6	15.4
Eu	4.2	4.2	4.1	3.0	5.3	4.8
Tb	3.1	3.1	2.9	1.8	2.9	2.9
Yb	11.6	11.8	11.3	7.1	9.0	10.3
Lu	1.7	1.7	1.7	1.2	1.3	1.4
Cr	166	196	188	236	53	40
Ni	153	154	174	192	92	93
Co	139	126	145	133	132	119
V	832	980	898	739	766	609
Cu	555	560	666	532	185	318
Zn	374	322	333	251	225	371
Zr	269	272	246	157	291	371
Y	110.9	109.3	107.2	73.9	92.5	92.7
Nb	33.3	33.6	31.9	18.9	66.0	66.2
Rb	16.4	23.8	13.6	7.4	47.6	39.7
Sr	388	420	406	414	581	636
Ba	416	392	348	201	845	847
H_2O^+ (wt%)	1.21	0.76	0.56	0.55	1.41	0.83
Density (g/cm^3)	2.77	2.80	2.90	2.96	2.64	2.65
Fe_2O_3/FeO	2.94	0.85	0.77	0.58	1.19	1.25

Table AT50. Abundance of major and trace elements (g/1000 cm^3) in igneous rocks, Hole 528, Leg 74 (Walvis Ridge, Atlantic Ocean).

Leg	74	74	74	74	74	74	74
Hole	528	528	528	528	528	528	528
Core, section	39-2	40-2	40-5	42-1	43-2	44-3	47-3
Interval (cm)	7-10	24-27	76-79	32-35	85-88	94-97	67-70
Piece	1A	1B	1C	1C	1F	1E	
Lab number	Z-419	Z-420	Z-421	Z-422	Z-423	Z-424	Z-428
Depth (mbsf)	475.07	484.74	489.76	501.32	512.35	522.94	549.67
Major elements (g/1000 cm^3):							
Si	624	629	638	581	622	611	571
Ti	24	22	25	36	27	28	36
Al	224	258	236	175	226	214	206
Fe^{+++}	84	88	83	143	110	124	114
Fe^{++}	129	119	130	99	120	112	91
Fe (Sum)	213	207	213	242	230	236	205
Mn	1.5	1.3	2.4	3.5	2.2	3.0	4.2
Mg	130	114	109	77	99	94	85
Ca	220	256	261	98	243	197	151
Na	73	57	59	93	61	72	78
K	14.6	11.4	11.4	57.8	13.4	22.2	26.8
P	1.1	1.1	1.0	3.3	1.1	1.1	4.4
Minor elements (g/1000 cm^3 x 10^{-3}):							
La	33.1	28.0	31.0	126.5	38.5	58.9	72.5
Ce	63.5	59.3	62.0	272.7	79.8	117.8	152.5
Nd	33.1	33.9	33.8	119.0	41.3	58.9	75.0
Sm	9.1	8.5	8.7	21.8	9.9	14.2	16.8
Eu	3.3	2.7	3.1	6.7	3.3	4.6	5.5
Tb	2.2	2.0	2.0	3.2	2.1	2.4	3.0
Yb	7.5	6.2	6.8	10.2	6.6	8.0	10.0
Lu	1.1	1.0	1.0	1.4	1.0	1.2	1.5
Cr	122	107	194	12	157	230	85
Ni	155	178	217	35	212	161	113
Co	133	122	155	97	143	129	128
V	746	396	775	662	811	870	888
Cu	566	565	437	64	550	348	195
Zn	276	189	225	298	261	281	275
Zr	224	192	225	545	223	321	425
Y	69.0	53.7	64.8	116.5	66.0	83.0	97.5
Nb	27.1	25.2	26.5	133.9	38.5	58.9	67.5
Rb	30.4	31.1	23.9	74.4	13.8	26.8	40.0
Sr	718	763	676	422	688	616	750
Ba	442	339	394	1612	468	884	1050
H_2O^+ (wt%)	1.14	1.22	1.22	1.61	0.97	1.31	1.72
Density (g/cm^3)	2.76	2.83	2.82	2.48	2.75	2.68	2.50
Fe_2O_3/FeO	0.72	0.82	0.71	1.60	1.02	1.23	1.39

Table AT51. Abundance of major and trace elements (g/1000 cm^3) in basalts, Hole 516F, Leg 72 (Rio Grande Rise, Atlantic Ocean).

Leg	72	72	72	72	72
Hole	516F	516F	516F	516F	516F
Core, section	126-1	126-2	127-1	127-3	128-2
Interval (cm)	70-73	53-56	55-58	64-67	126-129
Piece	2I	1E	18	1G	4B
Lab number	Z-392	Z-393	Z-394	Z-395	Z-396
Depth (mbsf)	1253.30	1254.63	1258.15	1261.24	1269.36
Major elements (g/1000 cm^3):					
Si	455	472	509	515	579
Ti	34	36	38	42	43
Al	165	179	194	190	190
Fe^{+++}	68	73	96	71	98
Fe^{++}	108	128	112	179	232
Fe (Sum)	176	201	208	250	330
Mn	3.2	1.9	2.5	2.0	1.6
Mg	50	78	55	88	94
Ca	181	187	139	168	191
Na	59	58	54	59	61
K	19.3	8.6	22.9	8.7	8.2
P	1.0	0.4	1.3	2.3	3.3
Minor elements (g/1000 cm^3 x 10^{-3}):					
La	43.2	43.9	50.3	36.3	42.5
Ce	90.8	87.8	103.1	80.3	93.6
Nd	68.1	65.9	71.9	51.8	62.4
Sm	16.8	15.6	18.9	14.5	16.4
Eu	5.0	4.9	5.5	4.9	5.7
Tb	3.9	3.4	3.8	2.8	3.4
Yb	9.1	8.5	7.7	7.3	8.2
Lu	1.3	1.3	1.2	1.1	1.3
Cr	79	110	72	78	113
Ni	91	110	132	155	128
Co	91	98	108	168	128
V	727	927	959	907	879
Cu	659	464	1007	544	652
Zn	250	256	264	233	298
Zr	341	439	360	440	425
Y	111.3	90.3	86.3	75.1	85.1
Nb	25.0	29.3	31.2	31.1	31.2
Rb	34.1	9.5	33.6	10.6	10.5
Sr	636	708	671	829	709
Ba	152	366	221	311	369
H_2O^+(wt%)	1.40	1.13	2.46	2.10	1.54
Density (g/cm^3)	2.27	2.44	2.40	2.59	2.84
Fe_2O_3/FeO	0.70	0.63	0.95	0.44	0.47

Table AT52. Abundance of major and trace elements (g/1000 cm^3) in igneous rocks, Hole 768C, Leg 124 (Sulu Sea, Pacific Ocean). (Continued on next five pages.)

Leg	124	124	124	124	124	124	124	124
Hole	768C	768C	768C	768C	768C	768C	768C	768C
Core, section	74R-1	75R-1	77R-2	80R-1	80R-3	81R-1	82R-1	82R-2
Interval (cm)	100-104	142-146	26-30	90-92	65-71	11-16	64-69	10-15
Piece	10B	6	1D	1L	3B	2A	6	2B
Lab number	Z-660	Z-661	Z-662	Z-124	Z-1359	Z-663	Z-1360	Z-664
Depth (mbsf)	1057.30	1067.32	1082.30	1096.50	1099.10	1100.71	1106.24	1107.15
Major elements (g/1000 cm^3):								
Si	500.8	441.3	431.2	457.0	446.1	433.8	440.1	502.9
Ti	11.7	9.6	11.6	14.7	11.3	12.9	12.6	14.5
Al	183.5	147.2	157.0	178.3	169.0	156.9	174.4	192.8
Fe^{+++}	120.2	115.9	110.9	108.9	115.6	90.9	121.4	117.7
Fe^{++}	30.7	36.5	22.5	27.3	29.8	42.8	36.4	36.8
Fe (Sum)	150.9	152.4	133.4	136.2	145.4	133.7	157.8	154.6
Mn	2.9	3.2	2.5	2.2	3.5	4.4	3.0	4.6
Mg	118.5	130.2	122.1	125.7	134.5	137.3	126.8	138.9
Ca	155.9	141.7	95.8	105.2	106.3	104.7	113.0	122.3
Na	37.4	30.9	35.6	38.9	34.1	35.7	37.5	38.0
K	18.9	15.0	18.8	26.1	27.0	21.6	25.7	30.8
P	1.5	1.4	1.5	1.7	1.5	1.3	1.5	2.1
Minor elements (g/1000 cm^3 x 10^{-3}):								
La				9.6	6.4		7.2	
Ce				22.6	18.1		20.7	
Nd					14.2		14.9	
Sm				5.1	4.7		5.2	
Eu				2.1	1.5		1.8	
Tb				1.4	1.4		1.5	
Yb				5.7	2.9		4.1	
Lu				0.8	0.4		0.6	
Sc				80.0	0.0			
Cr	1282.5	1414.5	1022.9	922.5	1040.3	1326.6	869.4	1157.7
Ni	528.8	604.8	405.3	471.5	432.6	564.3	320.9	442.7
Co	132.8	137.4	96.5	82.0	115.4	120.8	97.3	106.7
V	877.5	690.9	781.7	615.0	824.0	796.0	852.8	821.7
Cu	110.3	112.8	86.9	112.8	144.2	162.4	115.9	111.2
Zn	153.0	131.2	135.1	164.0	152.4	148.5	176.0	168.0
Sn	4.7	4.9	3.9			4.4		4.3
Zr	117.0	104.6	111.9	112.8	117.4	132.7	124.2	143.0
Y	47.3	30.8	56.0	49.2	39.1	29.7	39.3	59.0
Nb	4.5	4.3	5.2	4.5	4.5	5.3	3.9	5.4
Rb	22.5	22.6	21.2	30.8	33.0	19.4	37.3	34.1
Sr	360.0	287.0	231.6	246.0	226.6	198.0	248.4	249.7
Ba	11.3	12.3	13.5		20.6	13.9	51.8	13.6
H_2O^+ (wt%)	1.94	2.64	3.08	3.36	3.10	2.46	2.36	2.70
Density (g/cm^3)	2.25	2.05	1.93	2.05	2.06	1.98	2.07	2.27
Fe_2O_3/FeO	4.35	3.53	5.48	4.43	4.32	2.36	3.71	3.56

Table AT52 (continued).

Leg	124	124	124	124	124	124	124	124
Hole	768C	768C	768C	768C	768C	768C	768C	768C
Core, section	83R-3	84R-2	87R-1	88R-1	88R-2	89R-1	89R-2	89R-3
Interval (cm)	45-50	84-87	109-112	23-27	124-126	69-70	82-86	74-76
Piece	4	2A	5J	1B	7B	3B	4B	4
Lab number	Z-1361	Z-665	Z-1362	Z-1363	Z-125	Z-1364	Z-666	Z-667
Depth (mbsf)	1113.98	1117.94	1137.39	1146.23	1148.74	1156.39	1158.02	1159.24
Major elements (g/1000 cm^3):								
Si	466.3	456.1	468.1	486.9	560.3	609.2	582.7	617.3
Ti	12.7	11.4	14.1	14.4	16.5	13.8	19.8	18.0
Al	187.3	166.1	189.3	181.4	209.3	210.9	194.9	226.8
Fe^{+++}	104.4	100.5	140.9	104.1	99.5	64.9	111.6	87.0
Fe^{++}	33.9	46.3	53.4	42.5	56.2	52.2	59.2	65.1
Fe (Sum)	138.4	146.8	194.4	146.5	155.7	117.0	170.7	152.0
Mn	2.6	3.9	3.7	2.9	3.0	3.6	4.5	4.6
Mg	137.0	133.8	151.8	149.8	104.8	120.0	137.1	108.1
Ca	112.7	107.0	158.4	105.4	160.2	203.6	134.1	195.2
Na	39.9	33.7	37.0	31.2	68.8	71.0	54.6	63.1
K	12.3	24.3	9.4	10.0	17.8	14.8	27.6	20.9
P	0.8	1.3	2.4	1.0	1.5	1.2	1.8	1.9
Minor elements (g/1000 cm^3 x 10^{-3}):								
La	5.4		8.3	5.0	9.4	7.7		
Ce	16.1		25.3	14.0	20.9	23.5		
Nd	12.8		18.6	13.1		19.6		
Sm	4.7		6.2	5.7	6.0	6.4		
Eu	1.5		2.3	1.9	1.5	2.1		
Tb	1.1		1.7	1.7	1.5	1.9		
Yb	3.4		5.8	4.4	6.0	5.6		
Lu	0.5		1.0	0.7	0.9	0.9		
Sc					96.0			
Cr	1219.8	1277.2	1023.5	1270.2	492.0	497.3	191.7	746.7
Ni	550.0	426.4	501.4	433.6	264.0	181.1	164.3	256.8
Co	145.5	115.4	144.9	135.8	96.0	91.8	112.1	115.3
V	941.6	848.7	1028.1	996.5	480.0	594.2	921.3	778.1
Cu	126.3	100.9	177.1	138.0	144.0	81.6	169.3	144.1
Zn	181.9	140.1	195.5	190.5	204.0	173.4	216.6	180.8
Sn		4.3					5.2	5.2
Zr	137.0	129.8	147.2	151.1	141.6	147.9	191.7	199.1
Y	27.8	33.0	43.7	39.4	50.4	53.6	62.3	55.0
Nb	4.1	4.5	6.2	6.1	5.3	6.1	7.0	6.8
Rb	23.5	28.8	20.9	21.9	33.6	66.3	47.3	28.8
Sr	278.2	206.0	299.0	240.9	288.0	357.0	298.8	366.8
Ba	115.6	18.5	78.2	72.3		135.2	19.9	21.0
H_2O^+ (wt%)	2.86	2.42	2.73	3.30	1.77	1.12	2.59	1.82
Density (g/cm^3)	2.14	2.06	2.30	2.19	2.40	2.55	2.49	2.62
Fe_2O_3/FeO	3.42	2.41	2.93	2.72	1.97	1.38	2.10	1.49

Table AT52 (continued).

Leg	124	124	124	124	124	124	124	124
Hole	768C	768C	768C	768C	768C	768C	768C	768C
Core, section	89R-4	90R-1	90R-6	90R-7	91R-1	92R-1	92R-2	92R-3
Interval (cm)	83-87	16-18	58-62	98-103	55-57	54-56	95-100	108-111
Piece	3A	1A	1B	5	1C	4A	1H	1E
Lab number	Z-1365	Z-126	Z-668	Z-1366	Z-127	Z-128	Z-1367	Z-1368
Depth (mbsf)	1160.45	1165.46	1172.85	1174.06	1175.45	1185.04	1186.90	1188.28
Major elements (g/1000 cm^3):								
Si	596.4	596.1	634.8	634.9	633.8	590.9	550.6	551.9
Ti	22.9	19.9	18.4	14.6	18.8	15.8	11.6	11.3
Al	209.8	213.4	227.8	233.5	237.9	208.1	166.0	149.1
Fe^{+++}	132.2	86.6	98.0	82.3	94.3	74.4	129.7	143.4
Fe^{++}	55.2	77.5	71.0	66.5	75.8	97.4	66.9	86.7
Fe (Sum)	187.4	164.1	169.1	148.8	170.1	171.8	196.7	230.1
Mn	5.8	4.0	2.7	4.8	4.3	3.0	4.0	4.5
Mg	94.1	100.8	106.3	110.8	123.2	233.2	286.4	311.3
Ca	155.7	180.0	183.8	192.1	235.2	173.1	125.3	128.9
Na	66.3	70.8	53.5	55.0	56.0	33.9	21.4	22.1
K	16.9	15.3	20.7	27.1	10.4	2.5	2.0	2.5
P	2.4	1.8	2.1	1.6	1.8	1.0	0.9	1.2
Minor elements (g/1000 cm^3 x 10^{-3}):								
La		8.9			11.3	8.1		
Ce		21.8			27.5	19.4		
Nd								
Sm		6.6			8.0	5.4		
Eu		2.5			2.8	1.7		
Tb		1.5			1.9	1.4		
Yb		6.1			6.9	5.4		
Lu		0.8			1.0	0.8		
Sc		116.8			123.8	91.5		
Cr	151.8	127.0	218.1	235.9	357.5	2152.0	2751.0	2918.7
Ni	134.1	152.4	154.3	174.9	233.8	1479.5	1336.2	1312.7
Co	75.9	88.9	103.7	84.8	82.5	174.9	209.6	196.4
V	860.2	711.2	704.9	675.8	577.5	403.5	503.0	529.9
Cu	134.1	76.2	146.3	148.4	110.0	188.3	125.8	134.5
Zn	194.8	152.4	183.5	214.7	178.8	215.2	209.6	247.5
Sn			5.3					
Zr	247.9	165.1	196.8	201.4	162.3	113.0	96.9	110.3
Y	75.9	61.0	58.5	61.0	60.5	40.4	36.7	45.7
Nb	9.9	6.1	6.1	8.5	6.1	3.8	3.9	4.3
Rb	21.8	20.1	21.3	31.8	10.5	3.2	6.8	6.5
Sr	354.2	304.8	345.8	344.5	385.0	322.8	188.6	182.9
Ba	10.1		21.3	167.0			76.0	139.9
H_2O^+ (wt%)	2.04	2.39	2.00	1.61	1.76	3.25	3.87	4.19
Density (g/cm^3)	2.53	2.54	2.66	2.65	2.75	2.69	2.62	2.69
Fe_2O_3/FeO	2.66	1.24	1.53	1.38	1.38	0.85	2.16	1.84

Table AT52 (continued).

Leg	124	124	124	124	124	124	124	124
Hole	768C	768C	768C	768C	768C	768C	768C	768C
Core, section	92R-3	92R-4	93R-1	93R-2	93R-3	93R-4	95R-1	96R-1
Interval (cm)	111-115	0-5	40-42	10-14	113-117	27-29	89-91	108-111
Piece	1E	1	2B	2C	2F	3C	8	9A
Lab number	Z-669	Z-1369	Z-129	Z-670	Z-671	Z-130	Z-131	Z-1370
Depth (mbsf)	1188.31	1188.63	1191.90	1193.10	1195.58	1196.27	1211.29	1221.08
Major elements (g/1000 cm^3):								
Si	544.3	544.1	488.6	567.9	467.1	489.2	475.5	467.5
Ti	11.2	10.2	13.9	11.4	8.3	15.1	15.3	13.1
Al	168.5	162.1	147.2	162.3	119.5	141.1	188.9	145.1
Fe^{+++}	99.0	116.3	110.4	81.1	103.1	116.9	91.9	75.8
Fe^{++}	89.8	89.6	57.6	124.0	64.5	62.3	43.9	51.7
Fe (Sum)	188.8	205.9	167.9	205.1	167.6	179.2	135.7	127.5
Mn	4.8	4.3	2.8	1.5	3.4	2.2	4.8	3.1
Mg	305.3	303.7	254.0	258.5	277.3	252.4	137.1	94.0
Ca	128.3	135.4	144.7	138.5	141.4	173.9	122.9	86.2
Na	22.9	18.9	24.2	22.8	13.9	21.8	40.6	65.1
K	2.7	2.7	3.4	2.3	2.4	2.8	16.6	29.2
P	1.2	1.0	1.1	1.4	1.0	1.0	1.7	1.2
Minor elements (g/1000 cm^3 x 10^{-3}):								
La			5.8			5.4	10.6	
Ce			13.7			13.8	23.8	
Nd								
Sm			3.8			3.7	7.1	
Eu			1.6			1.6	2.4	
Tb			1.0			1.0	1.7	
Yb			4.1			4.2	5.6	
Lu			0.6			0.6	0.8	
Sc			72.0			81.2	84.2	
Cr	2182.9	3258.5	2760.0	2393.3	1762.5	2091.0	702.0	436.5
Ni	1420.2	1510.9	1920.0	1683.2	1316.0	1599.0	432.0	163.0
Co	202.5	218.1	204.0	273.5	181.0	184.5	86.4	75.7
V	539.2	532.0	372.0	557.6	446.5	332.1	518.4	426.8
Cu	155.2	404.3	84.0	257.7	63.5	73.8	86.4	170.7
Zn	228.8	212.8	192.0	178.8	159.8	196.8	151.2	161.0
Sn	7.4			6.6	6.1			
Zr	118.4	101.1	69.6		79.9	78.7	140.4	141.6
Y	36.8	37.2	33.6		28.2	34.4	43.2	42.7
Nb	4.2	5.3	2.9		3.3	2.7	5.2	4.9
Rb	5.5	8.2	6.5		6.8	5.9	28.1	29.1
Sr	181.5	186.2	189.6		126.9	228.8	280.8	291.0
Ba	13.2	101.1			7.1			232.8
H_2O^+ (wt%)	4.74	3.69	5.22	4.03	6.06	4.57	3.86	2.15
Density (g/cm^3)	2.63	2.66	2.40	2.63	2.35	2.46	2.16	1.94
Fe_2O_3/FeO	1.23	1.44	2.13	0.73	1.78	2.08	2.33	1.63

Table AT52 (continued).

Leg	124	124	124	124	124	124	124	124
Hole	768C	768C	768C	768C	768C	768C	768C	768C
Core, section	96R-2	97R-2	97R-3	98R-2	98R-3	98R-4	99R-2	99R-3
Interval (cm)	0-5	9-13	89-94	60-65	77-79	0-5	16-21	106-110
Piece	1A	1B	7A	2C	3B	1A	1D	4C
Lab number	Z-1371	Z-672	Z-673	Z-1373	Z-132	Z-1374	Z-1375	Z-1376
Depth (mbsf)	1221.42	1231.11	1233.35	1241.50	1243.17	1243.51	1250.70	1250.00
Major elements (g/1000 cm^3):								
Si	446.2	478.5	572.5	503.3	465.0	446.5	498.0	502.0
Ti	14.1	14.4	14.7	14.7	14.5	14.3	14.8	14.4
Al	148.3	151.5	184.7	175.7	192.2	169.5	190.2	206.7
Fe^{+++}	84.0	93.0	98.3	75.2	81.9	86.6	127.1	114.6
Fe^{++}	51.0	64.0	53.9	60.5	52.4	61.4	30.6	33.8
Fe (Sum)	135.0	157.0	152.2	135.6	134.3	147.9	157.7	148.4
Mn	2.9	1.8	3.2	3.5	2.8	3.3	2.4	2.8
Mg	89.3	124.6	131.1	110.7	79.8	103.0	88.5	102.2
Ca	89.4	149.2	193.8	113.7	111.3	125.5	120.9	130.1
Na	63.4	51.2	50.3	75.1	93.0	65.1	61.8	55.6
K	28.4	12.4	17.2	23.5	17.2	15.7	14.0	12.2
P	1.3	1.6	1.5	1.2	1.6	1.5	1.5	1.4
Minor elements (g/1000 cm^3 x 10^{-3}):								
La					8.5			
Ce					21.3			
Nd								
Sm					6.0			
Eu					2.1			
Tb					1.4			
Yb					5.5			
Lu					0.8			
Sc					85.2			
Cr	415.0	1034.0	1190.4	433.2	340.8	430.5	540.6	581.6
Ni	131.2	506.0	644.8	179.0	149.1	168.0	209.3	297.5
Co	65.6	116.6	136.4	70.7	42.6	75.6	67.6	75.5
V	496.0	697.4	595.2	479.6	394.1	478.8	741.2	777.0
Cu	137.0	77.0	71.9	161.3	53.3	67.2	137.3	146.5
Zn	150.5	147.4	166.2	163.5	127.8	157.5	163.5	170.9
Sn		4.8	4.7					
Zr	150.5	136.4	153.8	154.7	138.5	147.0	152.6	151.0
Y	48.3	44.0	49.6	55.3	46.9	50.4	69.8	64.4
Nb	4.1	5.7	4.7	4.2	4.5	5.9	3.5	5.3
Rb	29.0	15.4	10.7	30.9	16.4	29.4	32.7	24.4
Sr	231.6	220.0	372.0	353.6	383.4	273.0	370.6	333.0
Ba	56.0	15.4	12.4	210.0		48.3	8.7	15.5
H_2O^+ (wt%)	3.19	4.01	2.64	3.34	5.62	4.32	2.70	2.29
Density (g/cm^3)	1.93	2.20	2.48	2.21	2.13	2.10	2.18	2.22
Fe_2O_3/FeO	1.83	1.61	2.03	1.38	1.74	1.57	4.62	3.76

Table AT52 (continued).

Leg	124	124	124
Hole	768C	768C	768C
Core, section	99R-4	100R-1	100R-2
Interval (cm)	46-52	32-36	13-19
Piece	3	3B	2
Lab number	Z-1377	Z-1378	Z-1379
Depth (mbsf)	1253.79	1259.12	1260.43
Major elements (g/1000 cm^3):			
Si	532.0	533.0	557.0
Ti	15.0	13.7	16.1
Al	213.9	200.0	206.9
Fe^{+++}	123.0	100.8	83.5
Fe^{++}	37.2	56.4	59.3
Fe (Sum)	160.2	157.3	142.8
Mn	2.9	2.8	3.8
Mg	129.8	128.0	120.7
Ca	136.8	144.8	164.4
Na	51.9	55.1	56.1
K	14.8	8.9	13.9
P	1.6	1.5	1.4
Minor elements (g/1000 cm^3 x 10^{-3}):			
La			8.2
Ce			26.4
Nd			21.6
Sm			7.2
Eu			2.9
Tb			2.0
Yb			6.0
Lu			1.0
Sc			
Cr	737.8	596.7	648.0
Ni	338.0	362.7	355.2
Co	104.7	103.0	124.8
V	975.8	800.3	892.8
Cu	173.7	105.3	64.8
Zn	211.8	173.2	220.8
Sn			
Zr	154.7	145.1	172.8
Y	52.4	49.1	57.6
Nb	3.3	7.3	2.9
Rb	30.9	20.8	23.8
Sr	309.4	351.0	408.0
Ba	19.0	18.7	19.2
H_2O^+ (wt%)	2.88	2.32	1.58
Density (g/cm^3)	2.38	2.34	2.40
Fe_2O_3/FeO	3.67	1.99	1.57

Table AT53. Abundance of major and trace elements (g/1000 cm^3) in igneous rocks, Hole 770C, Leg 124 (Celebes Sea, Pacific Ocean). (Continued on next three pages.)

Leg	124	124	124	124	124	124	124
Hole	770C	770C	770C	770C	770C	770C	770C
Core, section	2R-3	3R-3	3R-4	4R-1	4R-2	4R-3	4R-3
Interval (cm)	23-25	36-38	55-60	17-19	134-140	23-27	86-88
Piece	2	4B	6	3A	12E	3	9A
Lab number	Z-133	Z-134	Z-1380	Z-135	Z-1381	Z-674	Z-136
Depth (mbsf)	426.43	436.26	437.95	442.77	445.44	445.83	446.46
Major elements (g/1000 cm^3):							
Si	612	604	621.2	638	605.7	627.6	630
Ti	38	38	36.8	26	21.2	19.6	26
Al	234	217	235.6	253	252.1	261.6	252
Fe^{+++}	137	103	109.1	100	105.9	117.2	102
Fe^{++}	91	98	102.4	89	67.9	43.8	77
Fe (Sum)	228	201	211.5	189	173.8	160.9	179
Mn	7.2	4.4	4.7	3.1	2.9	3.0	2.4
Mg	90	90	99.3	107	93.6	100.6	98
Ca	236	219	223.0	258	223.1	245.9	261
Na	72	69	66.8	57	55.2	50.3	55
K	8.2	6.5	3.2	5.4	8.5	7.2	11.2
P	3.1	3.5	3.0	2.2	1.3	1.2	2.0
Minor elements (g/1000 cm^3 x 10^{-3}):							
La	25.1	25.3		9.5			7.5
Ce	63.5	61.2		26.0			19.6
Nd							
Sm	22.6	16.2		9.0			7.7
Eu	5.2	5.1		3.4			2.8
Tb	3.6	3.7		2.4			2.1
Yb	12.1	11.7		8.7			7.5
Lu	1.6	1.6		1.1			1.0
Sc	110	117		112			113
Cr	552	559	668.9	938	962.0	707.2	911
Ni	276	293	368.6	392	508.8	195.8	317
Co	110	120	144.7	112	201.4	130.6	110
V	745	745	1051.1	616	954.0	535.8	566
Cu	124	133	199.3	140	180.2	125.1	124
Zn	262	279	330.3	224	238.5	198.6	221
Zr	469	399	464.1	171	182.9	193.1	116
Y	113.2	109.1	114.7	75.6	76.9	65.3	66.2
Nb	16.6	15.4	15.3	5.3	6.4	4.9	4.1
Rb	9.7			9.5	7.2	8.4	11.6
Sr	580	532	491.4	308	291.5	272.0	204
Ba		122	16.4		15.9	27.2	
H_2O^+ (wt%)	0.95	1.86	0.46	0.81	0.73	0.54	0.85
Density (g/cm^3)	2.76	2.66	2.73	2.80	2.65	2.72	2.76
Fe_2O_3/FeO	1.67	1.18	1.18	1.25	1.73	2.98	1.47

Table AT53 (continued).

Leg	124	124	124	124	124	124	124
Hole	770C	770C	770C	770C	770C	770C	770C
Core, section	5R-2	5R-3	5R-5	5R-6	6R-1	6R-1	6R-4
Interval (cm)	11-13	89-91	34-38	106-108	67-71	73-77	96-98
Piece	1A	3B	2	5	1D	1D	6A
Lab number	Z-137	Z-138	Z-675	Z-139	Z-676	Z-140	Z-141
Depth (mbsf)	453.81	456.09	457.42	460.76	462.57	462.63	467.36
Major elements (g/1000 cm^3):							
Si	632	625	592.8	597	612.1	619	631
Ti	27	24	22.6	26	26.0	26	26
Al	270	242	221.9	222	247.5	235	269
Fe^{+++}	101	119	117.0	96	156.2	99	69
Fe^{++}	59	67	53.1	84	16.3	73	74
Fe (Sum)	160	186	170.1	180	172.5	172	143
Mn	2.4	2.4	3.3	3.0	3.2	3.0	2.4
Mg	118	131	113.4	117	105.3	103	93
Ca	246	239	233.2	263	239.2	250	260
Na	58	57	48.1	58	54.7	64	62
K	11.3	9.6	8.0	11.1	8.7	11.1	9.6
P	2.1	2.6	1.5	3.0	1.8	2.6	2.4
Minor elements (g/1000 cm^3 x 10^{-3}):							
La	9.8	9.2		12.4		12.3	11.8
Ce	21.8	24.5		30.3		30.0	30.3
Nd							
Sm	8.7	8.3		10.7		10.1	10.2
Eu	2.8	3.1		3.6		3.5	3.6
Tb	2.2	2.2		2.5		2.4	2.7
Yb	7.8	8.1		8.8		9.0	9.4
Lu	1.1	1.1		1.3		1.3	1.4
Sc	115	111		118		112	113
Cr	840	792	694.3	701	623.3	642	770
Ni	504	334	406.1	371	276.4	259	289
Co	168	125	146.7	124	135.5	96	138
V	546	487	602.6	495	598.9	464	536
Cu	182	181	212.2	179	216.8	150	165
Zn	266	222	209.6	206	211.4	218	220
Zr	204	245	207.0	217	241.2	221	256
Y	72.8	72.3	73.4	77.0	81.3	84.6	82.5
Nb	9.0	8.3	6.6	9.1	7.9	9.6	9.6
Rb	15.4	12.0	21.7	13.2	21.7	14.2	16.0
Sr	364	389	314.4	303	406.5	410	468
Ba			26.2		27.1		
H_2O^+ (wt%)	1.19	1.34	1.25	2.14	0.95	1.93	1.05
Density (g/cm^3)	2.80	2.78	2.62	2.75	2.71	2.73	2.75
Fe_2O_3/FeO	1.92	1.97	2.45	1.26	10.66	1.52	1.04

Table AT53 (continued).

Leg	124	124	124	124	124	124	124
Hole	770C	770C	770C	770C	770C	770C	770C
Core, section	7R-1	7R-1	7R-3	9R-2	10R-2	11R-1	12R-1
Interval (cm)	93-100	107-112	61-63	53-55	110-112	98-100	11-13
Piece	9A	9B	2A	5B	3D	7F	1
Lab number	Z-1385	Z-1386	Z-142	Z-143	Z-144	Z-145	Z-146
Depth (mbsf)	472.43	472.57	475.11	492.83	503.10	511.18	520.01
Major elements (g/1000 cm^3):							
Si	563.8	595.1	613	632	645	638	631
Ti	24.6	25.4	26	31	32	36	30
Al	207.9	216.7	237	221	223	217	212
Fe^{+++}	152.8	144.7	96	114	112	82	160
Fe^{++}	62.6	69.2	70	80	86	98	94
Fe (Sum)	215.4	214.0	166	194	198	180	254
Mn	3.1	2.7	2.3	4.6	4.6	2.8	2.9
Mg	81.1	98.7	94	98	115	105	130
Ca	253.8	224.8	251	236	240	238	241
Na	53.3	56.1	58	68	69	70	58
K	13.8	10.8	11.6	10.8	9.6	7.6	10.3
P	2.1	1.5	2.9	1.2	3.1	2.2	1.4
Minor elements (g/1000 cm^3 x 10^{-3}):							
La			9.9	19.6	19.0	18.0	12.1
Ce			26.4	44.2	47.4	46.2	31.6
Nd							
Sm			9.3	13.5	12.6	12.0	9.5
Eu			3.2	3.6	4.5	4.4	3.2
Tb			2.2	2.8	3.1	2.7	2.3
Yb			8.5	11.0	11.7	10.9	8.6
Lu			1.3	1.7	1.7	1.7	1.3
Sc			115	119	123	128	123
Cr	830.5	834.8	828	621	530	503	890
Ni	324.9	323.3	254	345	335	326	474
Co	117.9	143.1	147	138	167	163	144
V	938.0	954.0	668	635	586	762	631
Cu	102.2	103.4	160	97	70	150	129
Zn	225.3	302.1	227	262	265	245	244
Zr	243.7	251.8	267	442	391	435	247
Y	83.8	82.2	80.1	99.4	108.8	97.9	91.8
Nb	8.6	8.2	10.4	11.9	14.2	12.8	10.0
Rb	24.1	21.2	13.6	12.4	10.0	3.3	27.6
Sr	314.4	344.5	401	580	502	517	316
Ba	15.7	18.6					
H_2O^+ (wt%)	1.54	1.05	1.11	1.04	0.64	0.80	1.90
Density (g/cm^3)	2.62	2.65	2.67	2.76	2.79	2.72	2.87
Fe_2O_3/FeO	2.71	2.32	1.54	1.59	1.44	0.94	1.89

Table AT53 (continued).

Leg	124	124
Hole	770C	770C
Core, section	12R-2	12R-3
Interval (cm)	79-84	140-142
Piece	3C	13
Lab number	Z-1387	Z-147
Depth (mbsf)	522.02	524.30
Major elements (g/1000 cm^3):		
Si	630.0	625.9
Ti	23.6	25.8
Al	218.0	235.8
Fe^{+++}	148.7	94.8
Fe^{++}	92.3	87.8
Fe (Sum)	241.0	182.6
Mn	1.8	2.4
Mg	130.3	118.9
Ca	225.2	243.8
Na	51.9	57.3
K	6.2	10.0
P	1.5	0.7
Minor elements (g/1000 cm^3 x 10^{-3}):		
La	9.6	10.2
Ce	26.9	27.3
Nd	24.3	
Sm	9.3	8.3
Eu	3.1	2.8
Tb	2.6	2.1
Yb	8.2	8.0
Lu	1.4	1.3
Sc		115.9
Cr	1109.4	869.4
Ni	481.1	331.2
Co	169.8	151.8
V	883.0	552.0
Cu	249.0	151.8
Zn	217.9	248.4
Zr	220.7	204.2
Y	79.2	77.3
Nb	5.9	7.7
Rb	12.5	16.3
Sr	277.3	303.6
Ba	19.8	
H_2O^+ (wt%)	1.54	1.02
Density (g/cm^3)	2.83	2.76
Fe_2O_3/FeO	1.79	1.20

Table AT54. Abundance of major and trace elements (g/1000 cm^3) in igneous rocks, Hole 779A, Leg 125 (Conical Seamount, Mariana Trench Region). (Continued on next two pages.)

Leg	125	125	125	125	125	125	125
Hole	779A	779A	779A	779A	779A	779A	779A
Core, section	9R-2	11R-1	12R-1	14R-1	16R-2	17R-1	17R-3
Interval (cm)	39-41	82-86	45-49	20-22	109-111	106-110	70-72
Piece	4A	11	7	1B	11	14	8B
Lab number	Z-191	Z-677	Z-678	Z-192	Z-193	Z-679	Z-194
Depth (mbsf)	69.99	88.12	97.35	116.40	138.09	146.26	148.90
Major elements (g/1000 cm^3):							
Si	450	443.1	425.2	578	504	523.0	524
Ti	1.6			3.1	2.7		1.8
Al	3.7	9.9	12.4	8.6	4.3	15.1	3.1
Fe^{+++}	116	112.4	114.9	122	153	104.6	130
Fe^{++}	34	31.3	13.8	59	23	46.9	33
Fe (Sum)	150	143.7	128.7	181	176	151.5	163
Mn	3.3	3.2	3.4	4.2	3.5	4.4	3.6
Mg	681	574.5	593.4	790	692	727.9	749
Ca	12	25.7	16.4	15	13	20.0	12
Na	1.8	2.1	2.1	2.0	3.6	1.9	2.0
K	0.7	0.6	0.4	1.2	1.9	0.7	1.2
P	0.1			0.1	0.1		0.1
Minor elements (g/1000 cm^3 x 10^{-3}):							
La	0.08			0.06	0.08		0.15
Ce							
Nd							
Sm	0.02			0.02	0.04		0.01
Eu							
Tb							
Yb	0.05			0.15	0.08		0.06
Lu				0.02	0.01		
Sc	18			28	28		20
Cr	4806	2217.6	2510.0	6171	6417	2830.0	6132
Ni	4940	2066.4	2158.6	5418	5580	2603.6	6716
Co	235	327.6	313.8	265	265	362.2	350
V	59	236.9	233.4	75	70	254.7	85
Cu		40.3	37.7	60	31	53.8	
Zn	69	136.1	138.1	90	61	167.0	73
Sn		6.6	6.0			7.1	
Zr							
Y		3.0					
Nb							
Rb		3.8				4.5	
Sr	27	20.2	47.7		28		
Ba			7.5				
H_2O^+ (wt%)	12.19	13.43	13.71	5.05	9.63	7.28	9.60
Density (g/cm^3)	2.67	2.52	2.51	2.94	2.71	2.83	2.76
Fe_2O_3/FeO	3.79	3.99	9.25	2.30	7.25	2.48	4.40

Table AT54 (continued).

Leg	125	125	125	125	125	125	125
Hole	779A	779A	779A	779A	779A	779A	779A
Core, section	22R-3	24R-1	26R-2	29R-2	31R-2	31R-3	31R-CC
Interval (cm)	17-21	27-29	53-55	0-5	87-89	30-33	10-12
Piece	2	5	2A	20	11A	4	2
Lab number	Z-680	Z-681	Z-196	Z-197	Z-198	Z-682	Z-199
Depth (mbsf)	173.27	187.47	208.53	237.00	257.07	257.93	262.30
Major elements (g/1000 cm^3):							
Si	294.4	443.7	523	359	542	490.0	529
Ti			2.7	0.7	33	28.8	34
Al	13.3	18.5	6.3	6.0	229	199.9	206
Fe^{+++}	161.0	105.1	114	113	114	63.3	96
Fe^{++}	4.0	18.3	51	8	209	227.5	174
Fe (Sum)	165.0	123.4	165	121	323	290.8	270
Mn	4.6	4.4	3.5	2.7	5.1	3.5	4.6
Mg	607.6	601.6	710	544	130	139.3	127
Ca	7.7	13.0	16	9	471	386.0	464
Na	2.6	2.5	1.9	1.5	6	2.9	19.8
K	0.4	0.6	1.2	1.0	1.3	0.2	3.0
P			0.1	0.1	0.3	1.7	0.4
Minor elements (g/1000 cm^3 x 10^{-3}):							
La			0.06	0.09	7.2	9.4	8.3
Ce					20.9	27.7	23.2
Nd					22.2	24.7	26.1
Sm			0.01	0.01	9.4	10.0	10.7
Eu					2.7	3.0	3.3
Tb					2.3	2.8	2.8
Yb			0.08	0.02	9.0	11.4	11.0
Lu			0.01		1.4	1.7	1.6
Sc			17	15	140		140
Cr	2400.0	2530.0	5620	3885	515	664.8	505
Ni	1716.0	2201.1	6323	4662	281	265.9	267
Co	280.8	303.6	281	233	686	177.3	653
V	196.8	227.7	81	49	140	739.6	89
Cu	36.0	38.0	31		156	243.8	134
Zn	220.8	136.6	84	73	437	470.9	327
Sn	6.2	6.3				9.7	
Zr					212	263.2	217
Y					90.5	97.0	86.1
Nb					5.9	5.3	5.6
Rb		3.0					
Sr	8.2	35.4		22	184	108.0	143
Ba	7.2	10.1			119	49.9	98
H_2O^+ (wt%)	17.97	12.49	8.17	14.31	4.79	4.46	4.53
Density (g/cm^3)	2.40	2.53	2.72	2.22	2.95	2.77	2.97
Fe_2O_3/FeO	44.67	6.37	2.46	16.40	0.60	0.31	0.62

Table AT54 (continued).

Leg	125	125
Hole	779A	779A
Core, section	34R-1	35R-1
Interval (cm)	63-65	118-122
Piece	5A	10
Lab number	Z-200	Z-201
Depth (mbsf)	293.93	294.48
Major elements (g/1000 cm^3):		
Si	388	431
Ti	2.8	2.0
Al	10.4	1.9
Fe^{+++}	102	151
Fe^{++}	23	6
Fe (Sum)	125	157
Mn	3.5	3.5
Mg	583	638
Ca	13	12
Na	4.1	2.9
K	1.0	0.4
P	0.1	0.1
Minor elements (g/1000 cm^3 x 10^{-3}):		
La	0.14	0.08
Ce	0.48	0.52
Nd		
Sm	0.07	0.05
Eu	0.01	0.01
Tb	0.02	0.03
Yb	0.07	0.05
Lu	0.01	0.01
Sc	20	18
Cr	4800	5698
Ni	3600	4144
Co	60	78
V	36	39
Cu	300	311
Zn	156	130
Sn		
Zr		
Y		
Nb		
Rb		
Sr	41	34
Ba		
H_2O^+ (wt%)	13.90	13.45
Density (g/cm^3)	2.40	2.59
Fe_2O_3/FeO	4.95	30.48

Table AT55. Abundance of major and trace elements (g/1000 cm^3) in igneous rocks, Hole 780C, Leg 125 (Conical Seamount, Mariana Trench Region).

Leg	125	125
Hole	780C	780C
Core, section	18R-1	18R-1
Interval (cm)	31-34	42-45
Piece	2A	2A
Lab number	Z-1388	Z-1389
Depth (mbsf)	154.31	154.42
Major elements (g/1000 cm^3):		
Si	419.4	474.7
Ti	0.6	0.8
Al	12.4	7.2
Fe+++	96.0	134.1
Fe++	52.5	41.6
Fe (Sum)	148.5	175.7
Mn	2.2	2.6
Mg	657.8	664.8
Ca	2.0	11.0
Na	0.8	1.0
K	0.4	0.5
Minor elements (g/1000 cm^3 x 10^{-3}):		
La	0.2	0.6
Sm	0.1	0.1
Eu	0.0	0.0
Yb	0.2	0.2
Lu	0.0	0.0
Cr	1581	4216
Ni	1696	1958.4
Co	321.3	353.6
V	133.6	185.0
Cu	15.4	65.3
Zn	154.2	174.1
Zr	3.9	4.9
Rb	2.6	0.0
Sr	8.7	8.2
Ba	12.9	13.6
H_2O^+ (wt%)	12.23	10.71
Density (g/cm^3)	2.57	2.72
Fe_2O_3/FeO	2.04	3.58

Table AT56. Abundance of major and trace elements (g/1000 cm^3) in igneous rocks, Hole 786B, Leg 125 (Izu-Bonin Forearc Basin). (Continued on next eight pages.)

Leg	125	125	125	125	125	125	125
Hole	786B	786B	786B	786B	786B	786B	786B
Core, section	4R-1	5R-1	6R-1	6R-2	8R-1	9R-1	15R-1
Interval (cm)	142-144	25-27	100-105	38-40	96-99	0-7	46-54
Piece	30	4A	24	8	17	1	7
Lab number	Z-202	Z-203	Z-1390	Z-204	Z-1391	Z-1392	Z-1393-2
Depth (mbsf)	190.42	198.85	209.20	210.08	228.56	237.10	295.46
Major elements (g/1000 cm^3):							
Si	528	527	488.5	583	633.3	619.5	613.0
Ti	8.0	7.6	4.9	9.8	4.8	4.8	5.1
Al	174	155	164.8	181	203.9	208.2	204.1
Fe^{+++}	51	77	102.7	110	78.1	66.3	124.1
Fe^{++}	55	35	41.0	38	73.9	67.7	19.6
Fe (Sum)	106	112	143.7	148	152.0	134.1	143.8
Mn	1.4	1.5	1.9	2.1	2.1	2.0	1.2
Mg	57	70	90.3	99	58.1	60.8	38.7
Ca	119	100	139.1	193	130.1	134.6	84.8
Na	71	49	41.2	57	58.8	58.3	68.6
K	18	24	5.0	10	11.2	10.4	47.2
P	0.3	0.1	0.4	0.1	0.6	0.6	
Minor elements (g/1000 cm^3 x 10^{-3}):							
La	7.7	1.0		6.7			
Ce	13.5	2.4		8.8			
Nd	12.3	1.9		9.6			
Sm	3.6	0.7		3.3			
Eu	1.0	0.4		0.9			
Gd	4.2	1.0		4.5			
Tb	0.8	0.2		0.8			
Tm	0.4			0.5			
Yb	2.2	0.7		3.1			
Lu	0.3	0.1		0.5			
Sc	65	58		88			
Cr	768	786	909.0	1076	54.5	53.8	85.0
Ni	162	299	404.0	621	118.5	105.3	99.1
Co	40	70	99.0	120	56.9	51.5	47.2
V	505	378	464.6	645	497.7	456.3	488.5
Cu	101	199	115.1	65	284.4	205.9	226.6
Zn	131	139	163.6	167	199.1	173.2	158.1
Zr	81	82	70.7	57	132.7	124.0	136.9
Y	24.2	7.4	20.2	35.9	26.1	37.4	5.2
Nb					2.4	4.4	4.0
Rb	20.2	33.8	153.5	16.0	17.5	15.9	80.2
Sr	424	318	303.0	311	284.4	514.8	377.6
Ba	73	40	12.1	43	16.6	14.0	49.6
H_2O^+ (wt%)	1.06	2.21	1.11	1.02	1.15	1.33	4.03
Density (g/cm^3)	2.02	1.99	2.02	2.39	2.37	2.34	2.36
Fe_2O_3/FeO	1.04	2.45	2.79	3.22	1.18	1.09	7.03

Table AT56 (continued).

Leg	125	125	125	125	125	125	125
Hole	786B	786B	786B	786B	786B	786B	786B
Core, section	15R-2	16R-2	18R-1	19R-1	20R-1	21R-2	24R-1
Interval (cm)	126-130	8-12	8-13	6-10	85-89	47-49	133-135
Piece	18	2	2	2	14	3	12
Lab number	Z-1394	Z-1395	Z-1396	Z-1397	Z-205	Z-206	Z-207
Depth (mbsf)	297.73	306.15	323.98	333.66	344.15	354.97	383.23
Major elements (g/1000 cm^3):							
Si	399.4	531.0	429.0	570.9			496
Ti	3.1	4.1	3.6	4.0			6.3
Al	131.0	160.2	149.7	168.1			144
Fe^{+++}	70.5	71.7	78.3	68.9			57
Fe^{++}	21.1	68.1	51.7	74.9			36
Fe (Sum)	91.6	139.8	129.9	143.8			93
Mn	0.9	1.7	1.6	2.0			1.5
Mg	33.4	44.7	44.3	51.3			26
Ca	39.2	79.1	94.9	101.5			64
Na	46.3	50.9	42.9	49.9			58
K	30.4	11.8	11.7	11.7			19
P		0.4	0.2	0.3			0.3
Minor elements (g/1000 cm^3 x 10^{-3}):							
La					2.2	4.4	6.7
Ce					4.5	7.8	12.6
Nd					3.2	5.4	9.3
Sm					0.7	1.7	2.8
Eu					0.5	0.6	0.8
Gd					1.3	2.2	4.2
Tb					0.3	0.4	0.6
Tm					0.8	0.3	0.3
Yb					1.4	2.0	1.9
Lu					0.2	0.3	0.3
Sc					75	70	39
Cr	39.3	51.2	109.4	84.0	1675	2189	61
Ni	60.4	53.2	73.5	92.4	463	378	53
Co	30.2	51.2	37.6	52.5	148	90	35
V	279.4	457.0	319.8	487.2	532	398	438
Cu	219.0	145.8	126.5	163.8	89	60	228
Zn	96.6	163.5	153.9	178.5	158	129	149
Zr	99.7	120.2	95.8	107.1	55	48	107
Y	4.7	15.8	13.7	15.1	10.2	16.5	19.3
Nb	2.1	3.9	2.9	3.6			
Rb	51.3	17.9	16.2	16.8	7.5	17.7	26.3
Sr	241.6	433.4	393.3	441.0	256	279	350
Ba		78.8	54.7	37.8	10	50	96
H_2O^+ (wt%)	3.66	2.32	1.68	1.82	1.37	1.02	2.10
Density (g/cm^3)	1.51	1.97	1.71	2.10	1.97	1.99	1.75
Fe_2O_3/FeO	3.71	1.17	1.68	1.02	1.17	1.92	1.74

Table AT56 (continued).

Leg	125	125	125	125	125	125	125
Hole	786B	786B	786B	786B	786B	786B	786B
Core, section	21R-2	24R-1	25R-1	27R-2	30R-3	31R-2	32R-1
Interval (cm)	47-49	135-140	82-86	48-51	31-33	30-34	39-41
Piece	3	22	11	6	4	3	8
Lab number	Z-1399	Z-1400	Z-1401	Z-208	Z-209	Z-683	Z-210
Depth (mbsf)	354.91	383.25	392.32	412.78	443.01	451.14	459.39
Major elements (g/1000 cm^3):							
Si	457.8	460.7	667.9	437	697	721.6	714
Ti	3.0	4.0	4.3	6.2	8.9	3.1	9.0
Al	127.6	148.8	150.8	120	188	180.7	175
Fe^{+++}	78.4	52.2	64.5	78	94	88.5	92
Fe^{++}	51.0	40.5	42.1	26	16	30.2	38
Fe (Sum)	129.4	92.8	106.7	104	110	118.7	130
Mn	2.1	1.5	1.1	1.6	1.8	1.0	1.4
Mg	58.3	33.1	21.5	82	81	96.7	79
Ca	135.4	57.4	59.9	73	157	134.7	145
Na	37.9	57.8	71.5	32	58	57.4	60
K	8.1	19.0	14.8	19	15	12.6	19
P	0.7	0.7	0.9	0.08	0.3	0.5	0.2
Minor elements (g/1000 cm^3 x 10^{-3}):							
La				7.6	4.3		5.6
Ce				15.0	8.8		11.1
Nd				9.5	4.8		8.9
Sm				2.7	1.7		2.5
Eu				0.7	0.6		0.7
Gd				2.0	1.8		3.3
Tb				0.4	0.3		0.5
Tm				0.2	0.2		0.3
Yb				1.2	1.5		1.9
Lu				0.2	0.3		0.3
Sc				51	80		73
Cr		43.9	50.6	473	1355	1155.7	1113
Ni		65.9	46.4	262	364	393.7	354
Co		47.3	38.0	34	63	86.4	51
V		434.3	390.4	161	427	467.4	392
Cu		120.0	143.5	237	113	177.8	127
Zn		145.3	139.3	144	151	154.9	152
Zr		142.0	154.0	42	73	124.5	83
Y		20.3	25.3	9.0	18.1	18.5	19.2
Nb		1.9	4.6			3.8	
Rb		28.7	177.2	28.7	22.1	24.1	30.4
Sr		388.7	422.0	203	402	431.8	430
Ba		62.5	128.7	220	105	22.9	121
H_2O^+ (wt%)	1.01	2.07	0.20	3.23	0.43	0.37	1.22
Density (g/cm^3)	1.83	1.69	2.11	1.69	2.51	2.54	2.53
Fe_2O_3/FeO	1.71	1.43	1.70	3.40	6.63	3.25	2.70

Table AT56 (continued).

Leg	125	125	125	125	125	125	125
Hole	786B	786B	786B	786B	786B	786B	786B
Core, section	34R-2	34R-4	35R-2	37R-2	39R-1	39R-2	40R-1
Interval (cm)	41-43	11-13	29-31	97-99	39-42	32-35	25-29
Piece	4	1B	4	12A	10	4A	6
Lab number	Z-211	Z-212	Z-213	Z-214	Z-1404	Z-1406	Z-1407
Depth (mbsf)	480.21	482.91	489.79	509.87	527.19	528.62	536.55
Major elements (g/1000 cm^3):							
Si	579	667	586	616	538.6	469.6	513.7
Ti	4.9	4.8	5.5	5.2	3.7	3.8	3.8
Al	157	166	164	187	170.8	163.6	159.1
Fe^{+++}	67	86	53	94	79.2	61.2	58.6
Fe^{++}	54	65	27	45	28.1	66.7	60.6
Fe (Sum)	121	151	80	139	107.3	127.8	119.2
Mn	2.0	2.7	0.9	2.2	0.6	1.7	1.9
Mg	120	142	34	103	35.0	50.7	42.8
Ca	193	169	84	193	89.3	85.0	72.0
Na	52	58	69	74	57.1	45.9	55.5
K	9	16	11	11	7.9	8.0	20.7
P	0.3	0.2	0.5	0.4	0.9	0.4	1.1
Minor elements (g/1000 cm^3 x 10^{-3}):							
La	4.2	3.9	6.4	3.8			
Ce	8.3	8.1	13.6	8.3			
Nd			10.2	5.5			
Sm	1.9	1.9	2.6	2.0			
Eu	0.7	0.6	0.8	0.7			
Gd			3.8	2.5			
Tb	0.5	0.4	0.6	0.5			
Tm			0.4	0.4			
Yb	2.1	2.0	2.2	2.2			
Lu	0.3	0.3	0.3	0.4			
Sc							
Cr	2714	1827	108	1368	40.7	36.4	35.7
Ni	708	679	50	477	71.8	69.2	79.0
Co	130	91	16	100	58.2	54.6	45.1
V	519	378	240	427	514.1	709.8	398.6
Cu	54	70	80	38	91.2	156.5	347.8
Zn	153	144	120	163	141.6	169.3	186.1
Zr	54	57	100	68	106.7	101.9	92.1
Y	22.4	20.6	22.0	21.6	27.2	18.0	22.6
Nb			2.2		2.9	2.4	
Rb	17.2	39.2	13.6	27.6	13.2	18.0	28.2
Sr	330	339	360	377	485.0	418.6	319.6
Ba	35	37	92	48	147.4		
H_2O^+ (wt%)	1.37	2.29	1.55	1.22	0.81	2.42	1.57
Density (g/cm^3)	2.32	2.61	2.00	2.51	1.94	1.82	1.88
Fe_2O_3/FeO	1.38	1.47	2.16	2.35	3.14	1.02	1.08

Table AT56 (continued).

Leg	125	125	125	125	125	125	125
Hole	786B	786B	786B	786B	786B	786B	786B
Core, section	40R-2	40R-3	42R-3	43R-2	44R-1	49R-2	51R-2
Interval (cm)	17-19	46-50	116-120	81-83	21-25	90-95	0-5
Piece	15E	1C	10C	7	4	4C	1
Lab number	Z-215	Z-684	Z-685	Z-258	Z-686	Z-1411	Z-1413
Depth (mbsf)	537.97	539.20	559.70	567.31	574.81	624.85	643.70
Major elements (g/1000 cm^3):							
Si	570	552.7	669.2	593	591.9	479.0	524.2
Ti	5.2	3.7	3.2	4.0	5.2	3.6	3.1
Al	173	156.2	165.7	167	158.6	136.3	140.2
Fe^{+++}	90	131.7	99.4	73	138.3	76.1	54.8
Fe^{++}	60	27.6	21.6	31	41.9	50.7	92.4
Fe (Sum)	150	159.3	121.0	104	180.1	126.9	147.2
Mn	3.0	1.4	1.3	1.9	3.0	2.5	2.7
Mg	153	150.1	83.7	74	176.0	69.6	139.6
Ca	202	290.3	119.0	132	146.1	77.6	109.3
Na	47	36.7	58.3	61	41.1	40.9	39.7
K	8	5.5	14.9	17	7.6	15.1	9.3
P	0.3	0.5	0.5	0.3	0.4	0.4	1.6
Minor elements (g/1000 cm^3 x 10^{-3}):							
La	3.7			3.7			15.3
Ce	9.7			9.3			37.6
Nd				6.6			23.0
Sm	2.1			2.0			5.9
Eu	0.8			0.7			1.6
Gd							
Tb	0.6			0.4			1.2
Tm							
Yb	2.2			1.4			5.2
Lu	0.4			0.2			0.9
Sc							
Cr	1544	1196.7	755.2	760	1303.8	283.7	1525.7
Ni	1145	815.3	195.9	242	836.4	151.9	372.0
Co	162	131.5	73.2	59	142.7	58.6	87.8
V	548	518.1	441.3	375	615.0	488.6	564.3
Cu	75	65.8	63.7	33	81.2	283.7	
Zn	149	149.9	153.4	110	162.4	129.9	171.4
Zr	52	76.3	113.3	71	76.3	78.7	79.4
Y	22.7	20.0	18.9	11.2	22.9	15.9	54.3
Nb			2.4		3.7	3.5	4.0
Rb	14.7	15.5	23.6	22.0	19.2	29.3	14.4
Sr	299	368.2	424.8	375	295.2	366.0	334.4
Ba		10.5	21.2	86	12.3	51.2	
H_2O^+ (wt%)	1.47	0.92	0.57	2.06	1.88	2.74	1.29
Density (g/cm^3)	2.49	2.63	2.36	2.20	2.46	1.83	2.09
Fe_2O_3/FeO	1.67	5.30	5.11	2.59	3.67	1.67	0.66

Table AT56 (continued).

Leg	125	125	125	125	125	125	125
Hole	786B	786B	786B	786B	786B	786B	786B
Core, section	52R-1	54R-1	55R-1	56R-1	56R-1	57R-1	61R-4
Interval (cm)	10-13	55-60	132-138	20-25	97-102	41-43	108-114
Piece	2	6A	13C	2B	3	1B	6B
Lab number	Z-1414	Z-1416	Z-1419	Z-1421	Z-1422	Z-257	Z-1425
Depth (mbsf)	652.00	671.75	682.12	690.30	691.07	700.21	734.09
Major elements (g/1000 cm^3):							
Si	646.8	546.0	606.8	602.8	632.6	609	732.5
Ti	3.4	3.2	3.9	4.0	4.1	3.8	4.8
Al	168.8	135.7	151.1	144.3	158.4	134	142.2
Fe^{+++}	47.9	43.3	57.1	80.7	64.0	111	26.8
Fe^{++}	106.2	70.1	75.5	45.8	67.8	32	41.6
Fe (Sum)	154.1	113.4	132.6	126.5	131.9	143	68.4
Mn	2.9	1.9	3.0	2.2	2.1	3.5	0.9
Mg	146.3	131.5	106.9	165.2	166.5	178	5.2
Ca	115.1	130.0	113.3	57.0	73.8	44	49.3
Na	45.7	32.7	38.5	47.3	50.9	52	70.8
K	9.3	7.1	11.5	24.9	29.5	24	26.3
P	1.0	0.2	0.3	0.3	0.4	0.2	0.9
Minor elements (g/1000 cm^3 x 10^{-3}):							
La	9.8	3.5	4.1	3.2	4.4	3.3	7.4
Ce	23.5	8.3	9.5	8.1	10.6	7.2	18.8
Nd	13.5	5.2	6.1	5.1	7.0	4.9	11.4
Sm	3.7	1.5	1.8	1.4	2.1	1.7	3.1
Eu	1.2	0.6	0.8	0.6	0.9	0.5	1.0
Gd						1.1	
Tb	0.8	0.3	0.5	0.3	0.5	0.4	0.7
Tm						0.2	
Yb	3.2	1.4	1.6	1.5	1.8	1.4	2.4
Lu	0.5	0.2	0.3	0.3	0.3	0.2	0.4
Sc							
Cr	1359.8	1242.6	1288.2	1817.0	1694.0	2684	46.0
Ni	399.4	475.2	488.2	437.0	469.5	467	41.6
Co	78.4	82.8	92.7	92.0	96.8	77	37.2
V	539.0	457.8	497.2	483.0	537.2	537	157.7
Cu	127.4	119.9	395.5	96.6	101.6	198	70.1
Zn	200.9	143.9	153.7	165.6	169.4	128	164.3
Zr	90.7	69.8	81.4	75.9	94.4	49	170.8
Y	31.9	11.8	14.7	12.4	17.7	12.6	28.5
Nb	4.7	2.8		3.2	3.1		4.6
Rb	19.4	17.4	27.1	36.8	38.7	25.7	52.6
Sr	367.5	414.2	339.0	230.0	290.4	490	284.7
Ba				13.8	12.1	63	89.8
H_2O^+ (wt%)	1.63	2.62	2.52	3.15	3.00	4.44	0.96
Density (g/cm^3)	2.45	2.18	2.26	2.30	2.42	2.33	2.19
Fe_2O_3/FeO	0.50	0.69	0.84	1.96	1.05	3.84	0.72

Table AT56 (continued).

Leg	125	125	125	125	125	125	125
Hole	786B	786B	786B	786B	786B	786B	786B
Core, section	61R-5	61R-5	62R-1	63R-1	64R-2	64R-3	65R-1
Interval (cm)	37-39	35-40	16-18	118-121	88-92	76-78	40-44
Piece	6	6	2A	13	12	8A	3
Lab number	Z-259	Z-1615	Z-260	Z-687	Z-1426	Z-261	Z-688
Depth (mbsf)	735.07	735.05	738.56	749.18	760.02	761.46	767.80
Major elements (g/1000 cm^3):							
Si	699	651.5	621	468.1	737.7	651	614.0
Ti	4.7	5.0	4.3	2.6	3.8	9.0	5.6
Al	143	147.3	137	138.5	150.1	229	229.5
Fe^{+++}	41	25.6	68	73.1	28.3	80	72.8
Fe^{++}	12	33.5	64	4.5	25.3	54	63.5
Fe (Sum)	53	59.1	132	77.5	53.6	134	136.3
Mn	1.2	0.9	2.0	0.3	0.9	3.0	1.4
Mg	2.9	8.7	152	58.5	11.1	77	91.1
Ca	61	37.3	82	46.4	22.3	136	129.7
Na	84	81.2	53	37.3	54.8	67	53.1
K	30	27.4	27	33.8	76.1	10	23.0
P	1.0	0.8	0.2	0.3	0.7	0.4	0.7
Minor elements (g/1000 cm^3 x 10^{-3}):							
La	9.6		4.1	4.2		4.5	
Ce	17.4		8.5	10.6		12.7	
Nd	14.5		6.9	6.9		10.2	
Sm	4.0		2.1	2.0		3.5	
Eu	1.0		0.6	0.6		1.2	
Gd	5.1		2.3				
Tb	0.9		0.5	0.4		0.7	
Tm	0.6						
Yb	3.2		2.1	1.6		3.2	
Lu	0.5		0.3	0.3		0.5	
Sc							
Cr	21	40.2	3331	8.5	56.7	70	85.0
Ni	38	36.2	758	54.1	61.0		85.0
Co	11	32.2	110	40.6	37.1	57	65.0
V	128	144.7	436	349.8	150.4	647	537.5
Cu	138	64.3	230	109.9	69.8	249	192.5
Zn	149	144.7	149	108.2	198.4	174	235.0
Zr	125	186.9	48	118.3	167.9	80	125.0
Y	27.6	28.1	18.4	11.3	24.0	24.4	30.0
Nb	2.3	6.0		2.2	5.5		3.8
Rb	40.4	50.3	32.2	50.7	93.7	9.2	22.0
Sr	194	221.1	186	287.3	174.4	373	350.0
Ba	234	152.8	103	130.1	1722.2	72	275.0
H_2O^+ (wt%)	0.89	0.67	1.90	2.79	0.38	1.14	2.60
Density (g/cm^3)	2.13	2.01	2.30	1.69	2.18	2.49	2.50
Fe_2O_3/FeO	3.83	0.85	1.19	18.22	1.24	1.63	1.27

Table AT56 (continued).

Leg	125	125	125	125	125	125	125
Hole	786B	786B	786B	786B	786B	786B	786B
Core, section	65R-1	65R-3	65R-3	66R-2	66R-3	67R-1	68R-1
Interval (cm)	102-107	39-44	48-52	0-5	51-56	77-79	10-16
Piece	13	6	7	1A	7	9	1A
Lab number	Z-1427	Z-1428	Z-689	Z-1429	Z-1430	Z-262	Z-1431
Depth (mbsf)	768.42	770.76	770.85	778.54	780.55	787.47	796.40
Major elements (g/1000 cm^3):							
Si	766.6	684.0	723.3	707.8	717.2	654	663.5
Ti	3.7	3.8	3.2	3.8	3.8	5.1	4.2
Al	141.1	148.7	133.7	146.2	145.6	203	161.4
Fe^{+++}	34.3	18.4	63.6	14.7	29.4	40	40.3
Fe^{++}	20.7	37.6	14.9	34.2	31.8	72	55.3
Fe (Sum)	55.0	56.0	78.5	48.9	61.2	112	95.6
Mn	0.5	1.1	0.9	1.0	1.0	4.1	1.5
Mg	15.4	18.9	20.5	18.3	16.8	172	122.0
Ca	25.2	21.2	33.7	13.9	16.6	151	58.2
Na	63.7	50.3	50.7	49.7	53.6	55	67.1
K	52.9	64.8	72.8	76.5	62.7	6	2.2
P	0.6	0.6	0.6	0.6	0.7	0.2	0.5
Minor elements (g/1000 cm^3 x 10^{-3}):							
La	8.6	7.7		7.4		2.8	5.5
Ce	22.0	19.8		20.0		6.7	15.2
Nd	13.2	12.7		12.6		4.9	8.7
Sm	3.3	3.3		3.4		1.5	2.3
Eu	1.1	1.1		0.9		0.7	0.9
Gd							
Tb	0.7	0.7		0.6		0.4	0.5
Tm	0.0	0.0					
Yb	3.3	2.7		2.3		1.9	2.1
Lu	0.5	0.4		0.4		0.3	0.3
Sc							
Cr	57.2	54.1	74.8	48.3	63.6	2192	1702.0
Ni	57.2	47.8	55.0	42.0	46.6	877	471.5
Co	35.2	35.4	39.6	35.7	38.2	116	105.8
V	151.8	143.5	231.0	140.7	148.4	516	469.2
Cu	59.4	164.3	182.6	165.9	144.2	142	213.9
Zn	213.4	268.3	270.6	354.9	233.2	168	179.4
Zr	162.8	160.2	171.6	163.8	173.8	67	115.0
Y	24.2	22.9	28.6	27.3	23.3	12.4	18.4
Nb	5.5	5.4	3.3	4.2	5.5		4.4
Rb	57.2	79.0	85.8	84.0	76.3	11.3	3.9
Sr	202.4	185.1	189.2	172.2	203.5	309	310.5
Ba	1386.0	894.4	858.0	1407.0	1272.0	49	20.7
H_2O^+ (wt%)	0.29	0.94	1.04	0.74	0.71	2.07	1.32
Density (g/cm^3)	2.20	2.08	2.20	2.10	2.12	2.58	2.30
Fe_2O_3/FeO	1.84	0.54	4.75	0.48	1.03	0.61	0.81

Table AT56 (continued).

Leg	125	125	125	125	125	125	125
Hole	786B	786B	786B	786B	786B	786B	786B
Core, section	69R-2	69R-4	70R-2	70R-4	71R-4	72R-1	72R-2
Interval (cm)	79-81	107-110	46-48	0-5	32-36	15-17	50-55
Piece	1F	1D	1F	1	3	3	5
Lab number	Z-263	Z-1432	Z-264	Z-1433	Z-691	Z-265	Z-1434
Depth (mbsf)	799.59	802.37	808.86	811.19	820.26	823.75	825.6
Major elements (g/1000 cm^3):							
Si	626	616.0	603.2	612.2	621.6	656	675.1
Ti	4.0	2.3	4.3	2.7	3.1	4.8	2.5
Al	127	139.7	137.4	161.3	153.7	194	174.1
Fe^{+++}	81	81.3	68.0	70.3	95.4	73	50.7
Fe^{++}	38	54.8	43.4	56.7	20.2	48	71.5
Fe (Sum)	119	136.1	111.5	127.1	115.6	121	122.2
Mn	1.9	2.0	3.3	1.5	1.8	2.0	2.1
Mg	95	123.4	120.4	139.6	110.1	100	98.5
Ca	68	62.7	102.6	78.4	66.4	124	85.2
Na	69	71.1	57.5	53.6	46.6	64	48.9
K	4	2.2	5.3	1.6	8.5	4	10.3
P	0.4	0.5	0.5	0.4	0.4	0.3	0.4
Minor elements (g/1000 cm^3 x 10^{-3}):							
La	5.7	4.5	5.0	4.1	5.2	6.1	4.3
Ce	12.8	11.9	10.4	10.5	13.4	12.0	11.3
Nd	8.9	7.4	6.3	6.9	7.8	8.8	7.2
Sm	2.0	2.0	1.7	1.9	1.9	2.7	2.0
Eu	0.8	0.7	0.7	0.7	0.6	0.8	0.7
Gd							
Tb	0.5	0.5	0.6	0.4	0.4	0.5	0.4
Tm							
Yb	1.9	2.0	2.0	1.8	1.7	2.3	1.9
Lu	0.3	0.3	0.3	0.3	0.3	0.4	0.3
Sc							
Cr	2130	1462.5	2260.0	1751.9	1187.2	1954	903.8
Ni	652	495.0	598.9	584.0	739.2	342	330.2
Co	98	123.8	108.5	167.2	116.5	98	94.0
V	348	463.5	384.2	842.7	537.6	611	445.9
Cu	217	303.8	113.0	169.5	280.0	159	190.4
Zn	261	141.8	203.4	213.0	358.4	171	161.5
Zr	74	105.8	67.8	82.4	100.8	83	91.6
Y	17.4	18.5	19.4	19.9	18.1	24.4	19.3
Nb	3.5	3.2	2.9	2.3	3.8	4.2	3.4
Rb	2.4		5.0		7.8	2.2	8.0
Sr	217	270.0	248.6	297.7	313.6	391	301.3
Ba	72	24.8	83.6		53.8	61	
H_2O^+ (wt%)	2.20	0.93	3.32	1.37	3.55	2.22	2.53
Density (g/cm^3)	2.17	2.25	2.26	2.29	2.24	2.44	2.41
Fe_2O_3/FeO		1.65	1.74	1.38	5.25	1.66	0.79

Table AT57. Abundance of major and trace elements (g/1000 cm^3) in igneous rocks, Hole 792E, Leg 126 (Izu-Bonin Forearc Basin). (Continued on next page.)

Leg	126	126	126	126	126	126	126
Hole	792E	792E	792E	792E	792E	792E	792E
Core, section	71R-1	72R-1	73R-2	74R-1	74R-2	75R-2	76R-1
Interval (cm)	84-86	18-20	76-78	54-58	64-66	62-64	26-32
Piece	8	2	6B	5B	6	7	3
Lab number	Z-219	Z-220	Z-221	Z-1450	Z-222	Z-223	Z-1451
Depth (mbsf)	810.74	819.68	831.46	839.34	840.94	850.32	857.96
Major elements (g/1000 cm^3):							
Si	586	582	605	469.2	564	680	755.3
Ti	9	10	14	6.1	13	14	6.1
Al	220	214	207	192.9	182	189	189.8
Fe^{+++}	98	97	102	111.7	94	88	89.1
Fe^{++}	38	34	37	30.3	36	29	20.8
Fe (Sum)	136	131	139	142.0	130	117	109.8
Mn	2.4	1.9	1.2	1.6	0.5	0.2	0.8
Mg	54	50	65	57.5	58	34	56.3
Ca	158	143	165	126.1	140	144	90.2
Na	43	51	44	30.9	46	50	48.3
K	4.5	5.7	4.4	2.7	4.5	5.3	16.3
P	1.0	2.3	2.4	0.2	0.5	0.8	0.7
Minor elements (g/1000 cm^3 x 10^{-3}):							
La	3.0	6.9	9.8		3.6	6.6	
Ce	9.2	18.4	30.4		10.1	17.9	
Nd	10.8	14.6	23.4		9.4	17.2	
Sm	3.7	5.8	9.4		4.3	7.1	
Eu	1.2	1.5	1.9		1.2	1.8	
Gd		7.4	11.0		5.4	9.6	
Tb	1.0	1.5	2.1		1.0	1.9	
Tm		1.0	1.0		0.8	0.8	
Yb	4.1	6.9	7.3		4.7	5.4	
Lu	0.6	1.1	1.1		0.7	0.8	
Cr	37	36	59	62.1	21	14	52.1
Ni	34	34	35	52.4	28	26	49.6
Co	46	56	37	66.0	34	82	62.0
V	412	627	749	514.1	514	494	466.2
Cu	62	157	70	219.2	96	106	136.4
Zn	172	168	187	163.0	161	153	248.0
Zr	62	74	73	83.4	66	68	116.6
Y	36.6	40.3	79.6	17.7	81.3	51.7	109.1
Nb		2.5		3.5	4.3	2.4	5.2
Rb	6.6	5.6	5.9	7.8	6.2	6.3	47.1
Sr	344	358	374	329.8	321	329	322.4
Ba	48	40	47	13.6	178	42	14.9
H_2O^+ (wt%)	1.49	1.01	1.12	1.53	1.14	0.83	0.95
Density (g/cm^3)	2.35	2.24	2.34	1.94	2.14	2.35	2.48
Fe_2O_3/FeO	2.87	3.16	3.07	4.10	2.94	3.41	4.76

Table AT57 (continued).

Leg	126	126
Hole	792E	792E
Core, section	76R-1	78R-1
Interval (cm)	120-122	118-120
Piece	11	14
Lab number	Z-224	Z-225
Depth (mbsf)	858.90	877.78
Major elements (g/1000 cm^3):		
Si	617	648
Ti	11	13
Al	183	215
Fe^{+++}	76	102
Fe^{++}	25	38
Fe (Sum)	101	140
Mn	0.5	1.1
Mg	35	57
Ca	133	151
Na	49	49
K	4.0	5.1
P	0.5	0.5
Minor elements (g/1000 cm^3 x 10^{-3}):		
La	3.7	5.1
Ce	10.8	14.0
Nd	11.7	15.9
Sm	4.3	5.5
Eu	1.4	1.4
Gd	5.2	7.2
Tb	1.0	1.3
Tm	0.6	0.8
Yb	3.7	5.3
Lu	0.6	0.8
Cr	13	24
Ni	22	29
Co	60	34
V	313	386
Cu	194	108
Zn	140	169
Zr	86	67
Y	49.7	55.4
Nb	2.2	2.7
Rb	4.1	5.8
Sr	324	362
Ba	60	48
H_2O^+ (wt%)	0.67	0.78
Density (g/cm^3)	2.16	2.42
Fe_2O_3/FeO	3.36	3.02

Table AT58. Abundance of major and trace elements (g/1000 cm^3) in igneous rocks, Hole 793B, Leg 126 (Izu-Bonin Forearc Basin). (Continued on next page.)

Leg	126	126	126	126	126	126	126
Hole	793B	793B	793B	793B	793B	793B	793B
Core, section	1R-2	86R-1	88R-1	92R-1	95R-2	103R-1	104R-1
Interval (cm)	82-84	35-40	62-67	0-5	28-32	37-42	96-98
Piece	5A				1		6B
Lab number	Z-226	Z-1452	Z-1453	Z-1454	Z-227	Z-1455	Z-228
Depth (mbsf)	588.82	1404.25	1423.52	1460.10	1490.78	1566.67	1576.86
Major elements (g/1000 cm^3):							
Si	636	534.1	531.1	625.1	542	499.3	570
Ti	16	3.3	4.1	3.3	10	3.7	11
Al	191	165.9	209.1	158.1	121	162.8	173
Fe^{+++}	97	105.2	66.3	58.1	96	84.6	76
Fe^{++}	103	16.8	56.0	98.6	38	22.7	82
Fe (Sum)	200	122.0	122.2	156.7	134	107.3	158
Mn	2.9	3.1	2.1	2.7	2.3	1.5	1.9
Mg	157	67.3	72.8	173.8	147	81.8	132
Ca	202	95.9	146.5	142.9	141	67.3	177
Na	41	39.3	34.1	32.5	32	34.9	34
K	8.9	26.1	13.7	9.6	21.1	10.9	9.6
P	0.5		0.5	0.2	0.2	0.3	0.1
Minor elements (g/1000 cm^3 x 10^{-3}):							
La	3.7				1.9		3.5
Ce	11.4				4.4		9.0
Nd	11.7				5.0		7.1
Sm	4.5				1.7		2.6
Eu	1.5				0.5		0.8
Gd	6.4				1.0		3.3
Tb	1.2				0.4		0.6
Tm	0.7				0.3		
Yb	4.5				1.6		2.0
Lu	0.7				0.2		0.3
Cr	811	461.6	333.3	784.0	2398	138.5	330
Ni	319	184.2	103.2	213.2	251	89.7	83
Co	106	105.6	68.8	102.9	76	72.2	71
V	692	165.6	473.0	502.3	436	676.7	543
Cu	319	894.2	107.5	122.5	120	152.1	177
Zn	200	209.1	163.4	174.0	142	117.0	153
Zr	69	124.2	96.8	68.6	31	72.2	57
Y	39.9	9.9	30.1	22.3	14.8	14.2	13.7
Nb	4.3	4.1	2.6	4.2	2.4	2.5	
Rb	8.8	47.6	23.7	14.5	37.1	17.4	7.8
Sr	263	186.3	365.5	281.8	349	175.5	307
Ba	117	99.4	12.9	17.2		13.7	
H_2O^+ (wt%)	1.01	3.28	1.57	1.73	3.26	3.73	2.18
Density (g/cm^3)	2.66	2.07	2.15	2.45	2.18	1.95	2.36
Fe_2O_3/FeO	1.04	6.98	1.32	0.66	2.77	4.15	1.04

Table 58 (continued).

Leg	126	126	126	126	126	126
Hole	793B	793B	793B	793B	793B	793B
Core, section	110R-2	110R-4	111R-1	112R-1	113R-3	114R-1
Interval (cm)	57-59	38-40	102-104	100-102	27-31	69-71
Piece	1C	1C	9A	3C	1C	1D
Lab number	Z-229	Z-230	Z-231	Z-232	Z-1456	Z-233
Depth (mbsf)	1635.87	1638.68	1644.42	1654.10	1665.82	1673.09
Major elements (g/1000 cm^3):						
Si	583	592	569	594	542.6	496
Ti	11	11	9	10	3.7	9
Al	136	143	149	146	179.4	169
Fe^{+++}	86	102	117	97	64.1	83
Fe^{++}	73	77	65	69	90.9	55
Fe (Sum)	159	179	182	166	155.0	138
Mn	1.1	1.1	1.1	0.8	2.9	1.6
Mg	151	159	150	143	132.5	90
Ca	187	170	163	166	138.0	143
Na	43	45	48	51	33.5	44
K	17.3	20.1	19.6	23.0	3.7	14.2
P	0.3	0.5	0.6	0.8	0.2	0.2
Minor elements (g/1000 cm^3 x 10^{-3}):						
La	4.7	4.6	3.8	3.8		3.5
Ce	8.5	9.2	6.6	6.7		7.0
Nd		0.0	7.1	6.7		7.4
Sm	2.4	2.7	2.6	2.4		3.1
Eu	1.0	1.0	0.9	0.8		1.0
Gd			3.6	4.1		
Tb	0.6	0.8	0.6	0.7		0.6
Tm			0.3	0.4		
Yb	2.6	2.7	2.3	2.6		2.1
Lu	0.5	0.4	0.4	0.4		0.3
Cr	2133	1446	1493	1793	578.3	536
Ni	320	325	356	370	184.5	227
Co	142	133	119	131	117.0	103
V	640	554	545	645	517.5	721
Cu	64	108	64	120	112.5	82
Zn	166	157	166	167	186.8	155
Zr	33	46	31	48	81.0	52
Y	23.7	23.6	22.0	23.9	15.1	19.6
Nb	3.6				2.5	
Rb	30.8	33.7	35.6	52.6	6.8	26.8
Sr	284	289	332	311	382.5	494
Ba	36	55	40	69	18.0	58
H_2O^+ (wt%)	1.45	0.95	1.51	1.25	1.01	2.25
Density (g/cm^3)	2.37	2.41	2.37	2.39	2.25	2.06
Fe_2O_3/FeO	1.31	1.48	2.00	1.56	0.78	1.69

Table AT59. Abundance of major and trace elements (g/1000 cm^3) in igneous rocks, Hole 791B, Leg 126 (Sumisu Rift, Izu-Bonin Arc-Trench System). (Continued on next two pages.)

Leg	126	126	126	126	126	126	126
Hole	791B	791B	791B	791B	791B	791B	791B
Core, section	57R-1	57R-1	59R-1	61R-1	63R-1	63R-1	64R-1
Interval (cm)	0-5	52-56	21-25	42-50	65-70	88-93	48-52
Piece	1B	6	1	9	9	12	6
Lab number	Z-1435	Z-692	Z-1436	Z-1437	Z-1438	Z-1439	Z-216
Depth (mbsf)	925.90	926.42	945.41	964.92	984.35	984.58	993.48
Major elements (g/1000 cm^3):							
Si	588.4	545.9	495.8	591.0	384.2	350.5	385.3
Ti	23.5	14.9	12.7	17.1	9.8	8.7	11.2
Al	214.3	214.1	208.5	236.9	162.0	144.5	158.1
Fe^{+++}	80.3	115.4	84.0	74.5	62.8	46.3	64.2
Fe^{++}	144.0	92.3	84.1	105.9	79.9	83.8	81.0
Fe (Sum)	224.3	207.7	168.1	180.4	142.7	130.1	145.2
Mn	3.7	4.2	2.5	3.0	2.3	2.2	2.4
Mg	137.6	131.9	121.3	118.9	96.4	94.7	93.7
Ca	82.9	182.3	157.7	213.4	109.4	99.2	115.2
Na	65.6	46.3	44.2	50.8	31.8	27.5	36.7
K	5.2	9.4	4.4	3.0	6.7	5.7	9.3
P	2.9	1.8	1.6	1.9	0.6	0.6	0.6
Minor elements (g/1000 cm^3 x 10^{-3}):							
La							3.9
Ce							10.6
Nd							
Sm							3.2
Eu							1.3
Gd							
Tb							0.8
Yb							2.7
Lu							0.4
Cr		615.0	463.7	448.9	374.5	360.9	318.6
Ni	49.4	389.1	181.4	183.2	131.3	122.4	97.4
Co	79.0	128.0	89.6	103.2	87.5	87.5	67.3
V	906.5	632.5	436.8	650.2	371.0	588.3	477.9
Cu	103.7	107.9	94.1	193.5	126.0	124.0	115.1
Zn	281.6	160.6	174.7	227.0	141.8	135.2	123.9
Zr	212.4	170.7	152.3	193.5	89.3	77.9	62.0
Y	59.3	45.2	42.6	54.2	21.0	19.1	23.0
Nb	6.2	3.3	5.8	4.6	3.0	2.4	0.0
Rb	6.9	20.3	8.1	3.9	11.0	10.8	9.2
Sr	666.9	627.5	492.8	619.2	332.5	278.3	283.2
Ba	69.2	17.6	107.5	100.6	45.5	41.3	26.6
H_2O^+ (wt%)	0.10	1.76	0.90	0.11	1.38	1.39	2.73
Density (g/cm^3)	2.47	2.51	2.24	2.58	1.75	1.59	1.77
Fe_2O_3/FeO	0.62	1.39	1.11	0.78	0.87	0.62	0.88

Table AT59 (continued).

Leg	126	126	126	126	126	126	126
Hole	791B	791B	791B	791B	791B	791B	791B
Core, section	66R-2	67R-2	72R-2	73R-2	75R-1	76R-2	76R-3
Interval (cm)	0-5	123-125	50-55	80-84	97-105	48-52	40-45
Piece	1A	16	6A	4B	14	6A	4B
Lab number	Z-693	Z-217	Z-1440	Z-1441	Z-1442	Z-1443	Z-1444
Depth (mbsf)	1013.78	1024.83	1072.40	1081.90	1100.27	1110.98	1112.40
Major elements (g/1000 cm^3):							
Si	396.5	386.3	395.6	388.3	442.1	437.7	565.6
Ti	10.2	11.6	11.0	11.6	12.2	12.3	16.2
Al	163.3	153.3	170.5	177.3	162.6	171.6	244.6
Fe^{+++}	54.0	67.6	112.0	110.3	125.5	168.0	106.3
Fe^{++}	75.4	74.5	50.5	56.9	54.7	30.0	87.3
Fe (Sum)	129.4	142.1	162.5	167.2	180.1	198.0	193.6
Mn	3.2	2.8	2.8	2.7	2.3	2.7	3.7
Mg	92.5	86.4	116.1	117.4	130.8	151.5	131.9
Ca	105.2	124.1	62.1	63.8	89.7	69.9	164.5
Na	33.3	35.0	47.1	42.2	37.8	27.3	50.4
K	7.8	6.9	15.0	13.6	5.6	19.4	2.4
P	0.6	2.5	0.6	0.7	1.8	0.6	1.4
Minor elements (g/1000 cm^3 x 10^{-3}):							
La		9.0					
Ce		22.9					
Nd		17.6					
Sm		5.6					
Eu		1.8					
Gd		6.3					
Tb		1.0					
Yb		3.7					
Lu		0.6					
Cr	380.6	299.2	464.1	445.0	398.0	404.2	578.9
Ni	99.1	96.8	135.6	118.4	116.6	124.7	242.3
Co	83.2	66.9	95.5	95.5	104.5	101.1	132.6
V	685.0	704.0	720.1	744.9	848.2	741.8	1020.0
Cu	97.4	114.4	137.5	120.3	126.6	96.8	140.3
Zn	113.3	123.2	133.7	139.4	136.7	133.3	232.1
Zr	86.7	56.3	97.4	101.2	96.5	101.1	132.6
Y	24.8	49.3	26.7	26.7	42.2	23.7	40.8
Nb	1.9	0.0	4.4	3.2	3.6	3.9	4.6
Rb	7.6	6.2	11.5	12.2	6.6	25.8	
Sr	283.2	299.2	286.5	286.5	301.5	236.5	586.5
Ba	8.9	28.2		36.3	40.2	120.4	96.9
H_2O^+ (wt%)	2.97	2.74	5.61	5.00	1.92	5.12	0.89
Density (g/cm^3)	1.77	1.76	1.91	1.91	2.01	2.15	2.55
Fe_2O_3/FeO	0.8	1.01	2.47	2.15	2.55	6.22	1.35

Table AT59 (continued).

Leg	126	126	126	126	126	126
Hole	791B	791B	791B	791B	791B	791B
Core, section	77R-2	77R-2	77R-3	78R-1	79R-1	79R-1
Interval (cm)	0-5	132-137	18-23	24-30	5-8	45-50
Piece	1A	6A	1B	4	1	5A
Lab number	Z-1445	Z-1446	Z-1447	Z-1448	Z-695	Z-1449
Depth (mbsf)	1119.61	1120.93	1121.29	1128.54	1137.65	1138.05
Major elements (g/1000 cm^3):						
Si	537.3	600.0	577.4	646.7	625.0	572.2
Ti	5.7	13.5	13.2	14.3	22.7	10.3
Al	89.1	191.6	191.6	211.8	246.2	247.5
Fe^{+++}	68.8	52.7	59.4	74.8	138.2	59.7
Fe^{++}	22.5	83.4	95.4	80.2	152.7	131.1
Fe (Sum)	91.3	136.1	154.7	155.0	290.9	190.8
Mn	1.1	2.2	2.7	3.2	8.3	4.0
Mg	49.2	84.3	104.4	117.0	87.6	131.4
Ca	446.3	42.8	59.0	70.4	115.3	34.2
Na	41.4	32.7	31.9	56.6	107.5	78.0
K	1.5	55.5	42.4	18.7	15.0	54.4
P	0.9	2.4	2.4	3.0	2.2	0.8
Minor elements (g/1000 cm^3 x 10^{-3}):						
La						
Ce						
Nd						
Sm						
Eu						
Gd						
Tb						
Yb						
Lu						
Cr	56.4	47.9	46.6	446.8	28.0	129.5
Ni	46.6	41.0	41.9	123.0	28.0	91.4
Co	44.1	45.6	46.6	75.3	78.4	91.4
V	139.7	250.8	265.6	607.4	708.4	901.7
Cu	61.3	107.2	109.5	183.2	81.2	124.5
Zn	563.5	392.2	284.3	278.6	288.4	223.5
Zr	61.3	216.6	221.4	163.2	190.4	68.6
Y	23.3	98.0	109.5	42.7	58.8	30.5
Nb	4.2	6.2	5.8	6.0	4.2	3.8
Rb	2.9	155.0	132.8	15.6	27.7	58.4
Sr	188.7	171.0	202.7	476.9	924.0	1016.0
Ba		177.8	149.1	20.1	140.0	482.6
H_2O^+ (wt%)	0.99	3.28	3.84	2.56	2.02	4.47
Density (g/cm^3)	2.45	2.28	2.33	2.51	2.80	2.54
Fe_2O_3/FeO	3.40	0.70	0.69	1.04	1.01	0.51

Table AT60. Abundance of major and trace elements (g/1000 cm^3) in basalts, Holes 447A, Leg 59 (West Philippine Basin, Philippine Sea). (Continued on next two pages.)

Leg	59	59	59	59	59	59	59
Hole	447A	447A	447A	447A	447A	447A	447A
Core, section	14-1	14-3	15-2	16-2	16R-2	17R-3	19-3
Interval (cm)	140-144	53-58	116-121	19-21	87-89	49-53	115-120
Piece	4L	3D	5D	3A	10	5A	8G
Lab number	Z-314	Z-315	Z-316	Z-317	Z-1144	Z-1145	Z-318
Depth (mbsf)	114.40	116.53	124.66	132.69	133.22	143.49	156.15
Major elements (g/1000 cm^3):							
Si	573	602	599	576	624.9	643.1	436
Ti	21	21	20	18	17.7	22.0	16
Al	260	251	260	244	253.9	248.4	169
Fe^{+++}	130	121	104	102	113.3	122.1	61
Fe^{++}	81	69	74	78	80.2	98.5	74
Fe (Sum)	211	190	178	180	193.5	220.6	135
Mn	3.8	4.5	4.2	3.2	3.5	3.5	2.7
Mg	100	104	102	91	120.6	113.3	80
Ca	243	235	242	284	238.5	209.1	175
Na	55	60	54	58	53.1	53.0	35
K	9.8	16.4	11.1	21.2	6.8	13.9	8.9
P	1.9	1.3	2.0	1.8	1.0	1.2	1.1
Minor elements (g/1000 cm^3 x 10^{-3}):							
La	7.0	7.1	6.5	8.8			4.6
Ce	19.9	18.0	20.0	23.2			12.0
Nd	17.5	15.6	16.2	18.5			12.5
Sm	7.0	6.6	6.5	6.9			5.2
Eu	2.6	2.2	2.3	2.5			1.9
Tb	2.0	1.7	1.6	1.8			1.6
Yb	7.5	7.1	6.8	7.7			6.4
Lu	1.1	1.0	1.1	1.2			1.0
Cr	713	655	595	965	637.9	481.6	598
Ni	377	410	298	441	281.0	184.8	251
Co	110	120	97	102	129.3	106.4	87
V	592	423	365	744	354.1	994.0	502
Cu	296	287	284	229	365.3	246.4	174
Zn	323	355	352	248	230.4	316.4	222
Zr	164	150	143	149	188.3	198.8	100
Y	67.3	62.8	65.0	74.4	61.8	84.0	57.9
Nb	7.8	5.2	6.2	6.6	5.6	6.7	3.9
Rb	11.0	16.1	9.7	82.8	18.5	42.0	12.5
Sr	323	300	325	331	365.3	229.6	129
Ba					19.7	131.6	
H_2O^+ (wt%)	1.74	2.12	1.85	1.87	1.35	0.80	1.41
Density (g/cm^3)	2.69	2.73	2.71	2.76	2.81	2.80	2.77
Fe_2O_3/FeO	1.79	1.95	1.56	1.46	1.57	1.38	0.91

Table AT60 (continued).

Leg	59	59	59	59	59	59	59
Hole	447A	447A	447A	447A	447A	447A	447A
Core, section	23R-1	23R-1	24R-2	24R-2	25-1	27R-1	28-1
Interval (cm)	39-42	51-58	25-39	99-102	40-42	21-25	65-70
Piece	2Â	5D	1B	2D	1C	2B	4C
Lab number	Z-1146	Z-1147	Z-1148	Z-1149	Z-319	Z-1150	Z-320
Depth (mbsf)	180.39	180.51	186.75	187.49	191.40	207.71	217.15
Major elements (g/1000 cm^3):							
Si	684.6	592.0	600.6	626.8	659	584.9	530
Ti	19.7	16.6	14.5	14.8	22	14.5	12
Al	236.0	205.5	255.4	264.3	283	264.7	233
Fe^{+++}	79.3	59.1	52.6	48.8	90	106.0	96
Fe^{++}	126.5	128.7	109.2	131.2	128	72.2	69
Fe (Sum)	205.8	187.8	161.8	179.9	218	178.2	165
Mn	4.1	3.4	3.3	3.4	4.1	3.6	2.8
Mg	160.4	129.4	161.1	178.9	93	122.8	148
Ca	233.1	206.1	232.1	232.2	266	218.5	221
Na	47.5	41.0	46.9	48.1	51	49.4	43
K	1.5	1.5	1.2	1.2	2.0	8.3	27.8
P	1.0	0.9	0.5	0.6	1.0	0.6	2.3
Minor elements (g/1000 cm^3 x 10^{-3}):							
La					5.3		8.8
Ce					15.8		24.2
Nd					15.8		19.7
Sm					6.2		6.3
Eu					2.3		2.5
Tb					1.8		1.9
Yb					6.7		7.6
Lu					1.0		1.3
Cr	817.6	632.5	817.2	881.1	1188	951.4	1172
Ni	397.1	344.1	651.0	674.5	880	469.0	328
Co	186.9	144.2	174.5	183.7	173	147.4	88
V	1115.4	898.2	581.7	660.1	543	723.6	668
Cu	262.8	220.1	360.1	252.6	243	321.6	176
Zn	327.0	242.9	241.0	232.5	220	241.2	290
Zr	163.5	139.2	146.8	157.9	123	155.4	139
Y	73.0	63.3	58.2	60.3	52.8	53.6	47.9
Nb	3.5				5.3		11.1
Rb			3.6	2.9	1.5	13.7	30.2
Sr	195.6	172.0	304.7	315.7	293	294.8	237
Ba	14.6	22.8					
H_2O^+ (wt%)	0.65	0.28	1.79	1.57	1.72	1.78	1.67
Density (g/cm^3)	2.92	2.53	2.77	2.87	2.89	2.68	2.59
Fe_2O_3/FeO	0.70	0.51	0.54	0.41	0.78	1.63	1.55

Table AT60 (continued).

Leg	59	59	59	59	59
Hole	447A	447A	447A	447A	447A
Core, section	29-4	30-3	32-1	35-3	36-4
Interval (cm)	137-142	89-94	99-105	45-50	31-36
Piece	3B	3C	3K	2C	3A
Lab number	Z-321	Z-322	Z-323	Z-324	Z-325
Depth (mbsf)	231.37	238.39	253.49	278.45	288.81
Major elements (g/1000 cm^3):					
Si	641	624	619	566	570
Ti	19	16	16	17	15
Al	236	234	257	259	257
Fe^{+++}	94	94	99	132	133
Fe^{++}	99	94	96	83	59
Fe (Sum)	193	188	195	215	192
Mn	3.5	3.0	3.5	3.7	3.3
Mg	130	138	121	121	79
Ca	263	254	277	266	244
Na	47	46	45	69	62
K	11.5	10.7	12.3	15.7	23.3
P	0.2	0.2	0.2	0.5	0.4
Minor elements (g/1000 cm^3 x 10^{-3}):					
La	5.3	5.5	3.9	3.8	4.0
Ce	15.1	15.7	10.7	12.1	12.4
Nd	14.0	13.2	11.2	11.8	11.3
Sm	5.3	5.5	4.8	4.9	4.7
Eu	2.0	2.0	1.7	2.0	1.9
Tb	1.5	1.5	1.3	1.4	1.4
Yb	6.2	6.1	5.6	6.0	5.8
Lu	1.0	0.9	0.9	0.9	1.0
Cr	1122	1061	1277	1045	1134
Ni	449	413	393	357	448
Co	132	121	115	110	116
V	617	551	618	522	699
Cu	280	204	393	247	195
Zn	266	165	267	193	224
Zr	93	96		85	95
Y	67.3	60.6	4.5	66.0	65.9
Nb	9.0	7.4	14.6	4.9	5.5
Rb	10.7	9.6	9.3	17.9	17.1
Sr	202	212		203	219
Ba					
H_2O^+ (wt%)	0.94	1.16	1.23	1.14	1.95
Density (g/cm^3)	2.80	2.76	2.81	2.75	2.64
Fe_2O_3/FeO	1.05	1.11	1.13	1.76	2.50

Table AT61. Abundance of major and trace elements (g/1000 cm^3) in igneous rocks, Hole 448 and 448A, Leg 59 (Palau-Kyushy Ridge, Philippine Sea). (Continued on next four pages.)

Leg	59	59	59	59	59	59	59
Hole	448	448	448	448	448	448	448
Core, section	37R-1	38R-1	38R-1	39R-1	39R-2	43R-2	48R-1
Interval (cm)	32-37	45-50	123-128	117-122	60-63	45-50	120-125
Piece	3C	1H	5B	10B	2F	5	11A
Lab number	Z-1152	Z-1153	Z-1154	Z-1155	Z-530	Z-1156	Z-1157
Depth (mbsf)	337.82	347.45	348.23	353.17	354.10	377.45	424.20
Major elements (g/1000 cm^3):							
Si	411.1	431.8	382.8	453.6	532.9	409.5	461.1
Ti	16.1	16.7	14.8	17.6	20.9	16.0	18.1
Al	137.8	149.1	130.1	155.9	191.8	161.8	182.2
Fe^{+++}	107.4	104.1	90.9	108.1	81.0	112.2	121.7
Fe^{++}	123.2	122.8	102.5	132.0	152.0	109.0	136.4
Fe (Sum)	230.6	226.9	193.5	240.1	233.0	221.3	258.1
Mn	3.5	3.6	3.0	3.5	5.1	3.5	3.3
Mg	53.3	61.4	49.9	66.1	77.4	42.6	43.1
Ca	129.2	202.2	107.5	132.5	174.6	117.0	134.7
Na	35.9	37.2	33.7	38.3	44.5	39.2	46.6
K	9.0	10.7	12.2	10.6	10.3	10.2	8.3
P	2.1	1.8	1.8	1.8	2.2	3.6	3.2
Minor elements (g/1000 cm^3 x 10^{-3}):							
La							
Ce							
Nd							
Sm							
Eu							
Tb							
Yb							
Lu							
Cr	58.9	57.0	45.1	60.3	83.5	37.0	39.5
Ni	64.4	67.5	53.4	62.3	78.9	59.2	62.4
Co	73.6	76.0	63.5	80.4	120.6	59.2	66.6
V	868.5	865.1	763.2	964.8	1194.8	758.5	1023.4
Cu	294.4	284.9	190.4	271.4	348.0	231.3	301.6
Zn	237.4	310.2	193.7	271.4	313.2	288.6	384.8
Sn					7.2		
Zr	92.0	99.2	83.5	104.5	123.0	101.8	126.9
Y	53.4	57.0	100.2	76.4	78.9	62.9	83.2
Nb					2.8		
Rb	18.4	19.4	25.1	16.9	18.3	18.3	12.7
Sr	276.0	316.5	250.5	301.5	348.0	314.5	353.6
Ba	47.8	21.1	130.3	144.7	18.6	44.4	178.9
H_2O^+ (wt%)	0.89	1.19	0.66	0.86	0.44	1.47	0.89
Density (g/cm^3)	1.84	2.11	1.67	2.01	2.32	1.85	2.08
Fe_2O_3/FeO	0.97	0.94	0.99	0.91	0.59	1.14	0.99

Table AT61 (continued).

Leg	59	59	59	59	59	59	59
Hole	448	448	448	448A	448A	448A	448A
Core, section	53R-2	59R-2	61R-3	10R-4	12R-1	13R-2	14R-2
Interval (cm)	50-53	50-55	35-38	61-65	27-31	70-75	114-118
Piece	1H	2G	1D	4A	2C	6A	4G
Lab number	Z-1158	Z-1159	Z-532	Z-533	Z-534	Z-1160	Z-535
Depth (mbsf)	472.50	529.50	549.70	295.11	309.27	346.15	487.14
Major elements (g/1000 cm^3):							
Si	528.8	519.5	550.0	514.4	541.2	373.6	520.1
Ti	14.2	13.2	15.3	18.6	18.5	8.0	14.3
Al	189.0	181.1	195.2	186.0	188.1	127.7	187.1
Fe^{+++}	87.9	93.3	93.5	128.1	126.5	128.2	169.6
Fe^{++}	145.7	121.4	117.4	144.0	160.5	3.4	98.9
Fe (Sum)	233.5	214.7	210.8	272.0	287.0	131.6	268.5
Mn	3.6	3.1	3.2	4.3	4.2	1.6	3.5
Mg	79.7	65.1	66.4	78.5	83.6	41.0	86.3
Ca	157.7	144.4	172.6	185.4	176.3	48.0	172.4
Na	43.3	41.8	49.4	44.7	44.9	31.1	46.0
K	9.8	9.0	22.0	9.9	9.6	40.3	9.5
P	1.2	1.6	1.2	1.9	1.7	0.1	2.5
Minor elements (g/1000 cm^3 x 10^{-3}):							
La							
Ce							
Nd							
Sm							
Eu							
Tb							
Yb							
Lu							
Cr	45.4	85.0	90.4	89.7	87.1	95.8	162.8
Ni	77.2	74.1	90.4	77.9	79.9	65.9	89.7
Co	86.3	76.3	107.1	99.1	96.8	48.7	101.5
V	969.3	876.4	856.8	1262.6	1161.6	293.6	1593.0
Cu	408.6	549.4	392.7	424.8	435.6	235.5	306.8
Zn	304.2	305.2	238.0	306.8	338.8	136.6	354.0
Sn			6.0	6.1	6.5		6.6
Zr	118.0		164.2	120.4	121.0	51.8	132.2
Y	54.5	154.8	64.3	61.4	62.9	8.8	68.4
Nb		58.9	3.8	2.4			
Rb	12.5	12.4	33.3	22.2	18.4	65.9	15.1
Sr	385.9	348.8	380.8	330.4	338.8	150.7	377.6
Ba	27.2	21.8	38.1	33.0	14.5	7.9	21.2
H_2O^+ (wt%)	0.60	0.92	0.45	0.33	0.45	4.95	0.93
Density (g/cm^3)	2.27	2.18	2.38	2.36	2.42	1.57	2.36
Fe_2O_3/FeO	0.67	0.86	0.88	0.99	0.88	41.58	1.91

Table AT61 (continued).

Leg	59	59	59	59	59	59	59
Hole	448A	448A	448A	448A	448A	448A	448A
Core, section	15-1	16-1	20-1	22R-1	26R-2	26R-3	32R-1
Interval (cm)	14-19	47-52	142-147	11-14	134-137	72-75	67-69
Piece	1B	4B	3B	1C	3A	1H	1G
Lab number	Z-326	Z-327	Z-328	Z-536	Z-1162	Z-538	Z-540
Depth (mbsf)	527.64	537.47	566.92	584.61	615.84	616.72	661.17
Major elements (g/1000 cm^3):							
Si	503.3	527.5	455.2	469.6	433.6	426.3	537.3
Ti	12.7	15.4	13.7	13.5	9.2	11.2	20.8
Al	205.0	208.7	179.6	192.6	128.6	135.4	186.7
Fe^{+++}	88.0	81.3	101.7	119.0	180.2	166.9	169.3
Fe^{++}	96.6	118.3	92.8	56.1	4.4	5.3	90.8
Fe (Sum)	184.5	199.5	194.5	175.1	184.7	172.3	260.1
Mn	2.9	3.0	2.5	2.1	3.5	3.4	3.3
Mg	58.5	58.2	47.6	51.0	64.2	64.7	60.0
Ca	157.1	172.7	137.8	123.1	30.4	34.6	139.2
Na	46.9	47.2	44.2	53.7	39.4	39.7	50.7
K	23.7	17.9	23.5	20.4	46.1	51.8	32.0
P	0.4	0.3	0.5	1.9	0.1	0.9	1.7
Minor elements (g/1000 cm^3 x 10^{-3}):							
La	7.6	8.4	8.0				
Ce	20.1	19.0	17.0				
Nd	17.0	19.0	16.6				
Sm	5.7	6.3	6.2				
Eu	1.9	2.0	2.0				
Tb	1.5	1.6	1.7				
Yb	6.1	6.3	6.6				
Lu	1.0	1.0	1.1				
Cr	50.1	67.8	36.0	44.4	100.4	96.5	53.8
Ni	74.1	76.8	58.0	54.5	59.5	54.6	65.5
Co	50.1	70.1	50.0	62.6	74.4	60.1	86.6
V	479.6	610.2	540.0	1212.0	643.6	555.1	1099.8
Cu	392.4	565.0	320.0	70.7	119.0	491.4	67.9
Zn	185.3	226.0	240.0	198.0	152.5	112.8	327.6
Sn				4.8		4.4	5.9
Zr	113.4	140.1	128.0	149.5	59.5	60.1	117.0
Y	56.7	58.8	74.0	74.7	16.2	29.1	58.5
Nb	4.8	3.2	4.2	2.2		2.0	
Rb	24.0	15.6	24.0	34.3	87.4	87.4	58.5
Sr	305.2	384.2	300.0	404.0	132.1	120.1	327.6
Ba	109.0	128.8	56.0	58.6	50.2	25.5	21.1
H_2O^+ (wt%)	1.34	0.64	1.70	0.81	6.54	5.16	1.13
Density (g/cm^3)	2.18	2.26	2.00	2.02	1.86	1.82	2.34
Fe_2O_3/FeO	1.01	0.76	1.22	2.36	45.39	34.69	2.07

Table AT61 (continued).

Leg	59	59	59	59	59	59	59
Hole	448A	448A	448A	448A	448A	448A	448A
Core, section	33-2	38-2	41R-2	45-1	47-1	50R-3	51-1
Interval (cm)	10-15	88-90	81-85	69-71	90-95	116-121	98-102
Piece	1A	3A	5A	1D	1E	8	9D
Lab number	Z-329	Z-330	Z-541	Z-331	Z-332	Z-542	Z-333
Depth (mbsf)	665.10	710.38	729.31	765.69	775.40	796.56	802.48
Major elements (g/1000 cm^3):							
Si	605.4	514.0	545.3	624.5	672.5	354.2	617.3
Ti	19.8	13.4	13.3	17.9	19.8	12.8	19.6
Al	195.1	179.0	202.5	208.3	211.4	116.9	191.1
Fe^{+++}	140.4	125.0	145.7	138.1	118.1	151.1	160.1
Fe^{++}	135.1	68.6	89.3	99.2	152.9	34.5	84.2
Fe (Sum)	275.5	193.6	235.0	237.2	271.0	185.5	244.2
Mn	3.4	4.3	3.8	3.3	3.6	2.0	2.6
Mg	72.8	105.3	89.9	92.1	70.5	73.9	76.1
Ca	155.5	144.7	157.6	161.1	170.9	60.4	122.8
Na	54.8	41.1	49.5	49.6	55.1	42.5	49.9
K	21.0	12.2	5.3	5.5	9.4	6.3	8.9
P	0.3	0.2	1.4	0.2	0.4	1.3	0.6
Minor elements (g/1000 cm^3 x 10^{-3}):							
La	5.1	3.3		4.1	7.6		5.2
Ce	17.5	8.9		11.3	20.1		14.1
Nd	15.2	8.7		10.8	17.1		14.1
Sm	6.1	3.6		4.6	6.5		6.2
Eu	2.2	1.4		2.0	2.6		2.2
Tb	1.6	1.1		1.2	1.9		1.6
Yb	7.4	4.5		5.1	8.4		6.9
Lu	1.2	0.7		0.9	1.2		1.1
Cr	20.3	814.0	100.0	72.0	27.1	98.6	22.2
Ni	55.9	234.2	78.5	82.2	70.5	55.7	66.7
Co	81.3	89.2	111.9	100.2	92.1	68.4	113.6
V	736.6	758.2	1273.3	796.7	867.2	1097.1	765.7
Cu	109.2	579.8	678.3	539.7	325.2	429.3	395.2
Zn	317.5	189.6	219.0	257.0	257.5	206.7	284.1
Sn			6.7			3.8	
Zr	81.3	66.9	95.2	61.7	108.4	76.3	93.9
Y	71.1	37.9	47.6	43.7	62.3	36.6	66.7
Nb	3.3	5.4		6.4	8.9	1.6	2.5
Rb	30.5	13.4	7.4	3.3	8.7	4.9	6.4
Sr	330.2	289.9	380.8	359.8	325.2	270.3	321.1
Ba	86.4	33.5	40.5	74.5	113.8	23.9	108.7
H_2O^+ (wt%)	0.97	2.11	1.07	1.06	0.92	2.81	1.45
Density (g/cm^3)	2.54	2.23	2.38	2.57	2.71	1.59	2.47
Fe_2O_3/FeO	1.15	2.02	1.81	1.55	0.86	4.87	2.11

Table AT61 (continued).

Leg	59	59	59	59	59	59
Hole	448A	448A	448A	448A	448A	448A
Core, section	51R-3	54R-3	57R-1	62-1	65-2	66R-2
Interval (cm)	49-52	124-128	33-36	98-102	10-15	78-83
Piece	3A	8C	1D	2	1B	1D
Lab number	Z-543	Z-544	Z-545	Z-334	Z-335	Z-546
Depth (mbsf)	804.94	832.74	846.83	887.98	906.6	912.78
Major elements (g/1000 cm^3):						
Si	636.5	572.6	616.3	624.1	586.9	595.8
Ti	24.0	19.2	20.2	16.8	19.7	18.8
Al	192.6	206.6	202.6	256.6	194.0	190.6
Fe^{+++}	155.5	156.1	158.9	109.1	144.9	164.4
Fe^{++}	111.5	71.0	84.2	107.1	105.3	77.6
Fe (Sum)	267.0	227.1	243.2	216.2	250.2	242.0
Mn	4.3	3.3	3.2	2.9	2.8	2.5
Mg	65.3	74.5	63.5	70.5	90.2	65.4
Ca	147.3	139.4	141.3	210.9	159.7	123.3
Na	50.9	50.6	54.8	50.1	50.4	50.9
K	5.5	4.7	5.5	6.3	4.5	6.0
P	1.7	1.7	2.0	0.2	0.3	1.7
Minor elements (g/1000 cm^3 x 10^{-3}):						
La				8.0	5.2	
Ce				17.5	12.6	
Nd				15.9	13.4	
Sm				5.6	5.5	
Eu				1.9	2.0	
Tb				1.3	1.5	
Yb				5.3	6.2	
Lu				0.9	1.0	
Cr	25.6	62.4	49.8	55.7	39.7	24.0
Ni	66.6	69.6	57.3	98.1	64.5	67.2
Co	115.2	103.2	87.2	79.5	67.0	96.0
V	939.5	984.0	1025.9	768.5	669.6	1096.8
Cu	396.8	360.0	535.4	371.0	496.0	336.0
Zn	371.2	304.8	311.3	238.5	198.4	302.4
Sn	7.2	4.6	5.5			6.2
Zr	138.2	132.0	139.4	95.4	81.8	127.2
Y	76.8	60.0	69.7	45.1	59.5	67.2
Nb	3.1	3.4	2.5	3.7		4.1
Rb	8.2	5.5	9.2	1.6	1.5	10.1
Sr	332.8	360.0	398.4	503.5	347.2	336.0
Ba	35.8	12.0	17.4	103.4	79.4	14.4
H_2O^+ (wt%)	0.90	1.19	0.94	0.60	1.20	1.13
Density (g/cm^3)	2.56	2.40	2.49	2.65	2.48	2.40
Fe_2O_3/FeO	1.55	2.44	2.10	1.13	1.53	2.35

Table AT62. Abundance of major and trace elements (g/1000 cm^3), Hole 449, Leg 59 (Parece Vela Basin, Philippine Sea).

Leg	59	59
Hole	449	449
Core, section	15-2	17-2
Interval (cm)	17-20	2-6
Piece	1B	1A
Lab number	Z-336	Z-337
Depth (mbsf)	115.67	134.52
Mjor elements (g/1000 cm^3):		
Si	539	539
Ti	17	17
Al	227	227
Fe^{+++}	113	113
Fe^{++}	67	67
Fe (Sum)	180	180
Mn	2.7	2.7
Mg	78	78
Ca	243	243
Na	49	49
K	9.3	9.3
P	0.2	0.2
Minor elements (g/1000 cm^3 x 10^{-3}):		
La	8.8	8.0
Ce	22.6	18.8
Nd	16.2	16.6
Sm	5.4	5.5
Eu	2.3	2.0
Tb	1.6	1.5
Yb	6.9	6.3
Lu	1.1	1.0
Cr	515	691
Ni	282	364
Co	93	126
V	393	465
Cu	282	226
Zn	167	201
Zr	110	108
Y	54.0	65.3
Nb	11.3	7.8
Rb	15.2	16.1
Sr	368	327
Ba	56	55
H_2O^+ (wt%)	1.74	1.06
Density (g/cm^3)	2.45	2.51
Fe_2O_3/FeO	1.88	1.68

Table AT63. Abundance of major and trace elements (g/1000 cm^3) in igneous rocks, Hole 453, Leg 60 (West Side of the Mariana Trough). (Continued on next page.)

Leg	60	60	60	60	60	60	60
Hole	453	453	453	453	453	453	453
Core, section	51-1	51-3	52-2	53-3	53-5	55-3	55-4
Interval (cm)	8-12	54-58	113-118	19-24	88-91	50-53	127-131
Piece	1	4B	10	3D	9B	3I	12C
Lab number	Z-339	Z-340	Z-341	Z-342	Z-343	Z-344	Z-1167
Depth (mbsf)	474.58	478.04	486.63	496.69	500.38	516.00	518.27
Major elements (g/1000 cm^3):							
Si	570	589	521	666	561	493	558.9
Ti	5.6	6.3	4.1	12.4	3.3	9.2	0.5
Al	330	282	325	246	371	325	414.9
Fe^{+++}	84	69	104	80	61	145	72.9
Fe^{++}	73	69	106	114	79	87	113.8
Fe (Sum)	157	138	210	194	140	232	186.8
Mn	2.2	2.5	2.4	3.2	1.3	1.7	2.8
Mg	183	200	199	232	147	186	183.4
Ca	299	356	254	398	319	230	244.5
Na	13	17	16	15	14	11	16.6
K	6.6	6.1	7.6	7.2	3.1	2.8	10.2
P	0.1						0.3
Minor element (g/1000 cm^3 x 10^{-3}):							
La	0.61	0.70	0.42	0.80	0.28	0.18	
Ce	1.30	1.54	0.93	2.15	0.54	0.26	
Nd							
Sm	0.38	0.73	0.19	1.54	0.25	0.06	
Eu	0.27	0.35	0.23	0.64	0.21	0.15	
Tb	0.08	0.22	0.03	0.42	0.07		
Yb	0.27	0.61	0.16	1.41	0.19	0.05	
Lu	0.04	0.09	0.03	0.22	0.03	0.01	
Cr	188	588	25	514	129	436	29.8
Ni	188	183	198	193	158	264	178.8
Co	174	116	207	173	126	222	214.6
V	101	224	159	385	77	319	149.0
Cu	81	50	57	90	60	44	134.1
Zn	145	73	176	80	46	150	470.8
Zr							7.5
Y				13.8	3.4	3.6	3.9
Nb	3.8	4.4			4.3		
Rb	9.3	6.7	12.2	11.9	5.7	3.1	12.2
Sr	985	728	906	642	1032	861	953.6
Ba	130	64	311	109			804.6
H_2O^+ (wt%)	2.71	2.05	3.10	1.97	2.01	4.33	1.56
Density (g/cm^3):	2.90	2.91	2.83	3.06	2.87	2.78	2.98
Fe_2O_3/FeO	1.28	1.11	1.08	0.78	0.85	1.85	0.71

Table AT63 (continued).

Leg	60	60	60	60	60
Hole	453	453	453	453	453
Core, section	56-2	56-2	57-4	63-1	63-1
Interval (cm)	33-35	85-87	2-7	80-83	130-135
Piece	6A	12A	1	4A	5I
Lab number	Z-1169	Z-1170	Z-345	Z-1172	Z-1173
Depth (mbsf)	523.83	524.35	536.02	589.30	589.80
Major elements (g/1000 cm^3):					
Si	542.7	622.8	529	657.3	666.8
Ti	1.1	1.2	2.7	10.3	11.2
Al	430.4	381.6	345	166.9	173.3
Fe^{+++}	8.2	10.3	101	148.9	117.7
Fe^{++}	84.6	72.4	78	180.5	217.4
Fe (Sum)	92.7	82.7	179	329.5	335.2
Mn	2.1	1.7	1.5	5.1	5.7
Mg	83.0	70.9	169	185.9	180.6
Ca	264.3	179.2	257	198.6	213.0
Na	21.2	57.4	11	39.8	32.3
K	13.3	33.4	5.9	4.0	5.2
P	0.1	0.1		0.1	0.6
Minor element (g/1000 cm^3 x 10^{-3}):					
La			0.42	3.2	3.8
Ce			0.65	9.6	11.1
Nd				9.6	9.9
Sm			0.12	3.5	3.8
Eu			0.17	1.3	1.1
Tb				0.9	1.0
Yb			0.05	4.1	4.4
Lu			0.01	0.7	0.7
Cr	0.0	27.4	51	122.2	125.1
Ni	81.6	76.7	264	93.1	96.0
Co	114.2	60.3	230	189.2	180.4
V	141.4	134.3	39	1053.4	1038.9
Cu	57.1	54.8	53	238.6	157.1
Zn	185.0	156.2	107	293.9	273.5
Zr	10.6	15.3		40.7	43.7
Y	4.4	6.6		32.0	37.8
Nb					
Rb	14.4	49.3	4.2		
Sr	1332.8	1233.0	983	523.8	611.1
Ba	1060.8	1616.6	152	241.5	270.6
H_2O^+ (wt%)	2.26	2.56	3.87	1.55	0.84
Density (g/cm^3):	2.72	2.74	2.81	2.91	2.91
Fe_2O_3/FeO	0.11	0.16	1.44	0.92	0.60

Table AT64. Abundance of major and trace elements (g/1000 cm^3) in igneous rocks, Hole 454A, Leg 60 (West Side of the Mariana Trough, Philippine Sea). (Continued on next page.)

Leg	60	60	60	60	60	60	60
Hole	454A	454A	454A	454A	454A	454A	454A
Core, section	5-1	5-1	5-2	5-3	5-4	10-1	11-1
Interval (cm)	3-7	128-132	50-55	115-118	10-15	45-49	102-109
Piece	1	17A	4	6A	2	2	11
Lab number	Z-1174	Z-346	Z-1175	Z-347	Z-1176	Z-349	Z-351
Depth (mbsf)	67.03	68.28	69.00	71.15	71.60	113.45	123.02
Major elements (g/1000 cm^3):							
Si	538.1	560	499.7	534	571.1	462	508
Ti	14.0	16	12.7	15	13.0	12	15
Al	214.1	203	198.8	194	220.5	175	188
Fe^{+++}	60.2	95	35.5	70	51.7	77	45
Fe^{++}	69.7	62	84.3	83	93.9	62	90
Fe (Sum)	130.0	157	119.8	153	145.6	139	135
Mn	2.6	1.8	2.0	1.6	2.5	0.8	1.9
Mg	90.4	117	91.5	114	151.2	76	100
Ca	226.9	224	197.8	209	206.7	180	182
Na	43.4	61	40.8	56	51.2	48	45
K	4.6	7.1	2.9	5.3	3.3	6.5	6.7
P	0.4	1.0	0.9	1.0	0.9	1.3	1.0
Minor elements (g/1000 cm^3 x 10^{-3}):							
La		8.6		8.2		7.6	9.1
Ce		18.4		20.6		19.2	23.8
Nd		17.2		15.9		14.0	16.9
Sm		5.2		5.2		4.2	5.6
Eu		2.0		2.0		1.6	1.9
Tb		1.3		1.3		1.0	1.3
Yb		4.9		4.7		4.0	5.0
Lu		0.8		0.7		0.6	0.8
Cr	441.8	725	526.8	656	680.0	475	405
Ni	166.9	467	204.3	293	387.5	221	228
Co	70.5	106	90.3	89	100.0	64	72
V	277.3	418	423.6	422	322.5	401	347
Cu	143.4	172	197.8	269	165.0	120	130
Zn	171.6	155	174.2	148	187.5	116	108
Zr	141.0	103	129.0	108	135.0	102	111
Y	51.7	51.6	47.3	46.8	47.5	40.1	45.5
Nb	4.9	4.7	5.2	4.7	4.3	4.6	6.1
Rb	9.2	6.9	4.7	5.4	5.0	11.8	9.1
Sr	399.5	369	344.0	422	375.0	441	412
Ba	63.5	54	98.9	84	35.0	158	54
H_2O^+ (wt%)	1.18	1.27	0.74	1.42	0.68	1.07	1.22
Density (g/cm^3)	2.35	2.35	2.15	2.34	2.50	2.00	2.17
Fe_2O_3/FeO	1.00	1.68	0.47	0.94	0.61	1.39	0.56

Table AT64 (continued).

Leg	60	60	60	60	60
Hole	454A	454A	454A	454A	454A
Core, section	11-2	11-4	12-1	12-2	16-1
Interval (cm)	125-128	92-97	116-120	30-34	25-30
Piece	7A	5	13	3B	5
Lab number	Z-1177	Z-352	Z-353	Z-1178	Z-355
Depth (mbsf)	124.75	127.42	132.16	132.80	162.25
Major elements (g/1000 cm^3):					
Si	478.4	532	492	472.0	518
Ti	11.5	14	13	11.3	17
Al	189.1	200	183	171.8	181
Fe^{+++}	38.7	55	60	36.9	75
Fe^{++}	77.9	84	67	72.6	85
Fe (Sum)	116.6	139	127	109.5	160
Mn	1.9	1.3	1.6	1.6	2.4
Mg	90.5	132	102	96.4	102
Ca	165.4	179	177	167.7	177
Na	39.9	47	44	32.7	50
K	1.9	4.7	3.5	2.2	12.3
P	0.9	1.0	0.9	1.0	1.3
Minor elements (g/1000 cm^3 x 10^{-3}):					
La		8.1	8.3		10.2
Ce		18.9	19.3		24.5
Nd		15.2	17.2		22.3
Sm		4.8	4.9		6.7
Eu		1.8	1.8		2.2
Tb		1.1	1.1		1.5
Yb		4.4	4.2		5.6
Lu		0.7	0.7		0.8
Cr	526.3	553	508	500.0	623
Ni	275.4	392	307	270.0	289
Co	81.6	85	76	74.0	69
V	469.2	299	328	464.0	434
Cu	134.6	175	195	64.0	111
Zn	163.2	138	127	128.0	156
Zr	130.6	104	119	132.0	147
Y	42.8	43.8	46.6	38.0	60.1
Nb	2.9	5.1	4.9	3.2	5.6
Rb		5.5	3.4		19.4
Sr	428.4	415	424	580.0	378
Ba	87.7	76	91	80.0	87
H_2O^+ (wt%)	1.00	1.50	1.02	0.65	1.14
Density (g/cm^3)	2.04	2.30	2.12	2.00	2.23
Fe_2O_3/FeO	0.55	0.74	1.00	0.57	0.98

Table AT65. Abundance of major and trace elements (g/1000 cm^3) in igneous rocks, Hole 458, Leg 60 (Mariana Fore-arc Basin). (Continued on next three pages.)

Leg	60	60	60	60	60	60	60
Hole	458	458	458	458	458	458	458
Core, section	28-1	29-1	30-1	31-1	32-3	33-1	33-2
Interval (cm)	106-110	103-109	111-113	116-120	90-95	32-37	127-131
Piece	14	17	17	18	12A	4	14
Lab number	Z-356	Z-357	Z-358	Z-359	Z-360	Z-1179-2	Z-361
Depth (mbsf)	257.56	267.03	276.61	286.16	298.40	304.32	306.77
Major elements (g/1000 cm^3):							
Si	454	461	474	541	628	452.1	601
Ti	7	6.7	6.3	6.6	7.4	2.9	8.0
Al	151	156	157	178	188	122.6	192
Fe^{+++}	47	77	80	96	65	70.5	83
Fe^{++}	80	44	44	61	81	35.6	61
Fe (Sum)	127	121	124	157	146	106.1	144
Mn	2.2	1.1	1.3	1.7	1.7	4.5	2.6
Mg	101	102	101	83	79	94.6	164
Ca	155	133	135	179	189	111.5	107
Na	34	37	38	45	44	28.5	44
K	6.6	14.8	18.3	14.1	19.5	13.6	19.4
P			0.09	0.3	0.3	0.3	0.3
Minor elements (g/1000 cm^3 x 10^{-3}):							
La	0.9	1.7	1.7	2.4	2.3	1.2	1.9
Ce	2.3	3.5	3.0	5.3	5.3	3.5	4.0
Nd	1.9	3.3	3.2	4.6	4.3	2.9	4.3
Sm	0.7	1.0	1.0	1.5	1.5	1.0	1.6
Eu	0.3	0.4	0.4	0.6	0.6	0.3	0.6
Tb	0.3	0.3	0.2	0.4	0.5	0.3	0.5
Yb	1.1	0.9	0.8	2.1	1.9	1.3	2.3
Lu	0.2	0.1	0.1	0.4	0.3	0.2	0.4
Cr	286	580	601	255	342	401.1	433
Ni	152	180	183	139	140	138.0	166
Co	74	81	77	73	72	73.6	81
V	381	503	384	420	313	419.5	404
Cu	86	58	69	89	108	524.4	76
Zn	133	155	144	166	108	110.4	147
Zr	44	43	47	49	43	42.3	45
Y	19.0	10.4	7.7	22.1	20.2	9.9	18.8
Nb	5.7						
Rb	6.5	19.3	23.6	123.9	154.2	55.2	35.7
Sr	156	174	169	215	212	141.7	216
Ba				58	48	12.9	59
H_2O^+ (wt%)	1.23	2.31	2.19	1.03	0.79	3.65	0.40
Density (g/cm^3)	1.90	1.99	1.97	2.21	2.41	1.84	2.38
Fe_2O_3/FeO	0.66	1.93	2.03	1.76	0.90	2.20	1.50

Table AT65 (continued).

Leg	60	60	60	60	60	60	60
Hole	458	458	458	458	458	458	458
Core, section	34-2	35-2	36-1	37-2	39-1	39-2	40-1
Interval (cm)	14-19	12-18	125-128	70-75	100-102	60-65	143-147
Piece	1B	2	18	8C	12A	6	1Q
Lab number	Z-362	Z-363	Z-1180	Z-364	Z-365	Z-1181	Z-1182
Depth (mbsf)	315.14	324.62	333.75	344.20	362.00	363.10	371.93
Major elements (g/1000 cm^3):							
Si	617	454	440.5	517	440	509.1	441.1
Ti	8.3	7.5	3.6	8.4	7.4	4.4	3.9
Al	198	180	158.2	185	166	194.7	174.4
Fe^{+++}	88	72	76.7	83	63	63.1	82.3
Fe^{++}	64	61	44.2	59	51	65.2	36.9
Fe (Sum)	152	133	120.9	142	114	128.3	119.1
Mn	2.5	1.7	2.1	1.9	1.8	2.4	1.4
Mg	90	63	89.4	81	75	92.6	73.2
Ca	197	162	102.3	180	128	141.9	101.0
Na	47	41	31.5	41	37	33.0	34.3
K	20.0	19.9	9.5	22.1	13.4	9.1	15.1
P	0.3	0.4	0.1	0.4	0.2	0.1	0.2
Minor elements (g/1000 cm^3 x 10^{-3}):							
La	2.0	2.1	0.9	2.4	1.0	1.2	1.1
Ce	5.1	4.5	2.7	4.5	2.8	3.6	3.3
Nd	4.4	3.9	2.5	4.5	2.8	3.0	2.8
Sm	1.7	1.7	0.9	1.8	1.2	1.0	0.9
Eu	0.6	0.6	0.3	0.7	0.5	0.4	0.5
Tb	0.5	0.5	0.3	0.5	0.4	0.3	0.3
Yb	2.4	2.1	1.2	2.6	1.6	1.7	1.2
Lu	0.4	0.3	0.2	0.5	0.3	0.3	0.2
Cr	611	285	627.9	561	918	702.6	607.2
Ni	203	136	180.2	190	248	189.9	154.6
Co	95	70	114.7	84	94	109.7	77.3
V	464	417	700.7	582	487	822.9	610.9
Cu	78	68	646.1	86	83	118.2	90.2
Zn	151	126	163.8	136	147	156.1	158.2
Zr	56	52	58.2	43	37	67.5	60.7
Y	17.6	17.3	12.2	19.2	14.3	12.9	8.5
Nb		2.1					2.2
Rb	46.4	56.2	8.7	79.8	14.5	11.0	27.6
Sr	227	213	172.9	183	165	211.0	180.3
Ba	66	58	20.0	67		16.9	202.4
H_2O^+ (wt%)	0.40	1.01	1.34	0.83	2.12	1.73	2.84
Density (g/cm^3)	2.44	1.94	1.82	2.16	1.84	2.11	1.84
Fe_2O_3/FeO	1.54	1.30	1.93	1.56	1.38	1.08	2.48

Table AT65 (continued).

Leg	60	60	60	60	60	60	60
Hole	458	458	458	458	458	458	458
Core, section	41-1	41-1	41-1	42-1	43-2	44-1	45-1
Interval (cm)	2-7	102-107	40-45	60-65	45-50	140-145	130-135
Piece	1	1	1	6	7	11	15A
Lab number	Z-1183	Z-1184	Z-1185	Z-1186	Z-1187	Z-1188	Z-366
Depth (mbsf)	380.02	381.02	381.90	390.10	400.95	409.90	419.30
Major elements (g/1000 cm^3):							
Si	406.4	470.3	421.9	444.0	459.1	439.1	463
Ti	9.8	11.7	10.1	6.0	6.2	6.0	8.7
Al	152.4	175.5	156.7	160.6	164.1	159.7	162
Fe^{+++}	99.1	102.2	102.8	124.2	116.2	99.2	97
Fe^{++}	20.9	24.2	19.5	25.2	27.0	38.3	42
Fe (Sum)	120.0	126.4	122.3	149.4	143.3	137.5	139
Mn	1.1	1.0	1.2	1.2	1.3	1.4	1.6
Mg	27.8	23.4	29.5	70.1	75.9	78.6	82
Ca	76.1	93.6	73.9	111.9	118.2	111.9	135
Na	71.2	66.8	55.8	38.7	40.1	36.4	38
K	17.0	19.8	17.7	10.3	8.8	5.4	7.0
P	2.7	1.5	1.7	0.5	0.4	0.3	0.2
Minor elements (g/1000 cm^3 x 10^{-3}):							
La				4.9	4.2	2.2	2.1
Ce				13.2	12.0	6.5	4.8
Nd				9.6	8.7	5.6	4.6
Sm				3.0	2.7	2.0	1.9
Eu				1.1	0.9	0.7	0.8
Tb				0.7	0.7	0.5	0.6
Yb				3.2	2.9	2.2	2.5
Lu				0.6	0.5	0.4	0.4
Cr		18.5		441.8	478.6	405.5	704
Ni	49.8	44.4	47.0	127.8	131.2	152.5	241
Co	38.2	40.7	37.0	63.9	61.8	85.6	83
V	444.9	453.3	403.2	680.6	671.6	725.4	637
Cu	102.9	103.6	697.2	105.3	117.7	167.4	66
Zn	159.4	161.0	154.6	165.4	169.8	182.3	203
Zr	142.8	168.4	142.8	82.7	83.0	83.7	60
Y	83.0	50.0	53.8	33.8	30.9	16.7	23.2
Nb	3.5	4.3	4.2		1.9		
Rb	44.8	48.1	48.7	30.1	27.0	14.7	12.4
Sr	265.6	296.0	252.0	225.6	250.9	223.2	193
Ba	71.4	90.7	109.2	11.3	9.7	48.4	
H_2O^+ (wt%)	1.87	0.98	1.56	2.20	1.75	2.26	1.90
Density (g/cm^3)	1.66	1.85	1.68	1.88	1.93	1.86	1.93
Fe_2O_3/FeO	5.27	4.70	5.87	5.47	4.78	2.88	2.55

Table AT65 (continued).

Leg	60	60	60
Hole	458	458	458
Core, section	46-1	47-1	48-1
Interval (cm)	89-91	133-136	42-47
Piece	8	17	1
Lab number	Z-367	Z-368	Z-1189
Depth (mbsf)	428.39	438.33	446.92
Major elements (g/1000 cm^3):			
Si	469	494	465.0
Ti	13.8	14.8	11.5
Al	175	182	173.1
Fe^{+++}	125	135	148.6
Fe^{++}	41	60	39.1
Fe (Sum)	166	195	187.7
Mn	1.4	1.7	1.3
Mg	56	64	74.6
Ca	92	111	90.2
Na	58	61	49.5
K	10.7	11.5	8.3
P	0.6	0.9	0.7
Minor elements (g/1000 cm^3 x 10^{-3}):			
La	4.1	4.2	
Ce	10.9	11.9	
Nd	10.5	12.1	
Sm	4.3	4.6	
Eu	1.6	1.9	
Tb	1.2	1.3	
Yb	4.7	6.1	
Lu	0.7	0.9	
Cr	16	10	40.2
Ni	121	94	94.5
Co	90	84	84.4
V	721	1151	1202.0
Cu	68	178	197.0
Zn	205	377	233.2
Zr	95	132	116.6
Y	39.0	48.2	50.3
Nb	2.7	2.1	2.4
Rb	14.2	13.4	20.1
Sr	253	335	261.3
Ba			108.5
H_2O^+ (wt%)	1.93	1.61	2.52
Density (g/cm^3)	1.95	2.09	2.01
Fe_2O_3/FeO	3.36	2.51	4.22

Table AT66. Abundance of major and trace elements (g/1000 cm^3) in igneous rocks, Hole 459B, Leg 60 (Mariana Fore-arc Basin). (Continued on next two pages.)

Leg	60	60	60	60	60	60	60
Hole	459B	459B	459B	459B	459B	459B	459B
Core, section	60-1	60-2	61-1	61-1	62-1	63-1	64-1
Interval (cm)	125-127	90-95	19-22	141-145	44-46	25-28	24-28
Piece	11	8	2	14	4	3A	2B
Lab number	Z-370	Z-371	Z-373	Z-372	Z-1190	Z-1191	Z-374
Depth (mbsf)	559.75	560.90	568.19	569.41	577.94	587.25	596.74
Major elements (g/1000 cm^3):							
Si	577	740	582	598	599.0	407.9	483
Ti	14	18	14	14	9.4	7.6	12
Al	188	247	199	189	198.6	166.0	185
Fe^{+++}	97	131	89	81	107.2	85.7	103
Fe^{++}	66	87	77	87	76.3	46.6	50
Fe (Sum)	163	218	166	168	183.5	132.4	153
Mn	2.2	3.1	2.6	2.7	2.7	1.7	2.0
Mg	83	126	94	94	113.4	56.7	80
Ca	176	246	192	199	184.3	106.0	135
Na	52	64	54	53	46.6	41.9	56
K	7.4	9.7	9.3	8.6	7.8	11.4	16.6
P	0.6	0.8	0.6	0.5	0.6	0.5	0.9
Minor elements (g/1000 cm^3 x 10^{-3}):							
La	3.2	4.3	2.9	2.9			3.3
Ce	7.9	11.0	7.9	8.5			8.2
Nd	9.5	13.7	8.6	8.7			8.8
Sm	3.5	4.9	3.4	3.4			3.5
Eu	1.3	1.8	1.3	1.4			1.3
Tb	1.0	1.3	1.0	0.9			0.9
Yb	3.7	5.8	3.8	3.6			4.3
Lu	0.6	0.9	0.6	0.6			0.7
Cr	104	198	371	303	399.3	94.0	154
Ni	139	183	144	170	148.8	99.2	123
Co	93	137	96	121	94.2	73.1	103
V	672	823	742	728	488.6	826.5	740
Cu	185	259	646	170	136.4	208.8	72
Zn	232	305	275	243	210.8	201.8	226
Zr	76	91	65	75	99.2	81.8	70
Y	34.8	45.7	38.3	36.4	37.2	31.3	41.1
Nb		3.4			2.5	2.4	3.1
Rb	19.7	79.2	38.3	38.8	24.8	22.6	26.7
Sr	255	366	287	267	272.8	208.8	226
Ba					19.8	10.4	
H_2O^+ (wt%)	0.62	0.43	0.37	0.76	0.70	1.95	0.86
Density (g/cm^3)	2.32	2.50	2.43	2.43	2.48	1.74	2.06
Fe_2O_3/FeO	1.64	1.68	1.29	1.03	1.56	2.05	2.32

Table AT66 (continued).

Leg	60	60	60	60	60	60	60
Hole	459B	459B	459B	459B	459B	459B	459B
Core, section	65-1	66-1	67-1	68-1	69-1	70-1	70-1
Interval (cm)	82-85	40-45	107-112	38-42	84-87	85-90	105-110
Piece		4B	8B	3	12	6	7
Lab number	Z-375	Z-376	Z-377	Z-378	Z-379	Z-1192	Z-1193
Depth (mbsf)	606.82	615.90	626.07	634.88	644.84	654.35	654.55
Major elements (g/1000 cm^3):							
Si	420	617	626	587	535	484.3	512.8
Ti	14	14	16	13	12	13.3	14.0
Al	176	181	200	175	185	172.2	184.1
Fe^{+++}	112	150	130	127	80	137.6	122.2
Fe^{++}	49	69	77	61	62	66.4	71.5
Fe (Sum)	161	219	207	188	142	204.0	193.7
Mn	1.8	2.7	2.5	2.2	1.2	2.0	2.2
Mg	27	57	55	51	53	63.2	48.7
Ca	106	142	147	124	148	105.4	112.9
Na	65	60	59	53	56	55.7	61.5
K	16.2	15.5	25.4	33.0	11.2	9.4	13.9
P	1.5	0.9	1.6	0.7	0.4	1.3	1.5
Minor elements (g/1000 cm^3 x 10^{-3}):							
La	7.7	3.6	3.9	2.7	5.3		
Ce	18.0	10.1	12.6	9.1	13.5		
Nd	17.6	12.5	11.3	9.1	10.6		
Sm	6.6	4.6	4.4	3.4	4.0		
Eu	2.3	1.7	1.9	1.3	1.5		
Tb	2.2	1.3	1.5	1.0	1.2		
Yb	9.0	5.8	5.7	4.1	5.1		
Lu	1.5	1.0	0.9	0.7	0.8		
Cr	9	12	12	23	74	41.2	46.6
Ni	45	96	74	91	74	65.9	67.8
Co	27	120	99	91	74	72.1	78.4
V	898	891	911	640	634	737.5	954.0
Cu	81	84	74	23	63	100.9	118.7
Zn	206	253	394	194	211	208.1	201.4
Zr	106	99	111	94	95	131.8	154.8
Y	84.4	53.0	27.1	36.6	44.4	74.2	70.0
Nb	3.2				2.1		
Rb	26.9	77.0	54.2	54.9	12.9	22.7	57.2
Sr	251	226	246	219	317	247.2	254.4
Ba	43	53	44		53	43.3	17.0
H_2O^+ (wt%)	0.72	0.85	0.75	1.86	0.82	1.32	1.01
Density (g/cm^3)	1.84	2.41	2.42	2.29	2.11	2.06	2.12
Fe_2O_3/FeO	2.53	2.42	1.86	2.31	1.43	2.30	1.90

Table AT66 (continued).

Leg	60	60	60	60	60	60	60
Hole	459B	459B	459B	459B	459B	459B	459B
Core, section	70-2	71-1	72-1	73-1	73-1	73-2	73-3
Interval (cm)	30-35	138-141	124-128	0-5	120-125	75-80	84-88
Piece	2	8					
Lab number	Z-1194	Z-380	Z-381	Z-1195	Z-1196	Z-1197	Z-382
Depth (mbsf)	655.30	664.38	673.74	682.00	683.20	684.25	685.84
Major elements (g/1000 cm^3):							
Si	491.3	546	486	476.2	464.3	498.4	477
Ti	16.2	16	17	13.4	11.8	12.7	15
Al	194.6	175	151	174.3	171.2	192.9	182
Fe^{+++}	151.0	106	125	105.8	142.7	178.5	102
Fe^{++}	60.0	80	79	73.9	37.0	27.2	69
Fe (Sum)	211.0	186	204	179.8	179.7	205.7	171
Mn	3.2	1.7	2.2	2.4	2.5	2.7	1.1
Mg	83.5	58	39	53.0	46.4	73.9	67
Ca	119.1	124	133	128.8	100.6	112.3	121
Na	53.9	61	60	53.7	55.6	58.7	60
K	7.4	13.1	16.3	19.5	8.3	12.0	10.5
P	1.0	0.2	0.1	1.0	1.1	0.6	0.5
Minor elements (g/1000 cm^3 x 10^{-3}):							
La		5.9	5.8			4.6	7.5
Ce		17.8	15.3			12.6	17.2
Nd		15.7	12.1			10.4	15.8
Sm		5.9	5.2			3.5	5.9
Eu		1.9	1.7			1.3	1.8
Tb		1.8	1.6			0.9	1.7
Yb		7.4	7.2			5.7	7.1
Lu		1.1	1.2			1.0	1.1
Cr	70.4			65.0	48.5	48.6	10
Ni	105.6	43	60	75.1	69.8	86.2	61
Co	92.4	65	70	87.3	71.8	90.6	71
V	1051.6	718	866	964.3	779.9	917.2	729
Cu	160.6	65	70	81.2	122.2	145.9	61
Zn	217.8	228	191	231.4	217.3	289.5	274
Zr	132.0	113	101	127.9	139.7	145.9	120
Y	61.6	39.1	58.4	46.7	64.0	39.8	62.8
Nb		2.2	2.2	2.4		0.0	2.6
Rb	16.7	19.7	20.1	38.6	17.3	21.9	14.2
Sr	264.0	261	221	243.6	291.0	265.2	284
Ba	39.6	57	42	101.5	67.9	97.2	
H_2O^+ (wt%)	1.73	1.02	1.08	1.03	2.01	2.50	1.10
Density (g/cm^3)	2.20	2.17	2.01	2.03	1.94	2.21	2.03
Fe_2O_3/FeO	2.80	1.46	1.77	1.59	4.29	7.29	1.65

Table AT67. Abundance of major and trace elements (g/1000 cm^3) in igneous rocks, Holes 794C and 794D, Legs 127 and 128 (Yamato Basin, Japan Sea). (Continued on next two pages.)

Leg	127	127	127	127	127	127	127	127
Hole	794C	794C	794C	794C	794C	794C	794C	794C
Core, section	1R-1	1R-1	1R-1	4R-2	7R-1	7R-1	10R-1	12R-1
Interval (cm)	48-50	111-113	138-139	82-84	56-61	120-122	85-87	46-48
Piece	7	9	11A	7G	5A	6D	7E	1A
Lab number	Z-1457	Z-234	Z-1458	Z-235	Z-1459	Z-236	Z-237	Z-238
Depth (mbsf)	560.28	560.91	561.18	583.82	601.46	602.10	623.65	634.76
Major elements (g/1000 cm^3):								
Si	579.9	584.0	560.8	587.3	519.3	500.5	548.4	523.0
Ti	20.3	22.7	24.4	21.1	15.7	18.0	22.3	20.1
Al	260.9	242.3	221.0	231.5	201.7	203.7	216.7	191.9
Fe^{+++}	93.5	100.9	127.3	113.5	105.2	99.1	92.3	94.1
Fe^{++}	78.7	90.6	62.7	77.0	47.7	53.2	65.3	63.2
Fe (Sum)	172.2	191.5	190.0	190.5	152.9	152.3	157.7	157.3
Mn	2.8	2.9	3.2	1.4	2.0	1.8	0.9	1.3
Mg	97.2	113.2	105.8	118.5	133.7	130.3	122.8	154.4
Ca	123.7	140.0	126.3	187.2	84.1	107.8	141.7	95.5
Na	58.1	65.4	61.2	61.5	57.9	55.6	52.2	55.2
K	28.5	28.9	18.4	15.6	14.6	10.4	15.5	21.3
P	2.5	3.0	2.1	2.5	1.7	2.3	1.8	2.1
Minor elements (g/1000 cm^3 x 10^{-3}):								
La		23.2		18.1		21.5	26.1	22.8
Ce		51.6		46.6		49.7	61.6	50.2
Nd		36.1		28.5		31.6	33.2	29.6
Sm		10.3		8.0		8.1	8.3	7.5
Eu		3.6		2.8		2.9	2.8	2.5
Gd		11.6		9.6				
Tb		2.0		1.7		1.6	1.6	1.5
Tm				0.8				
Yb		5.7		4.7		6.3	5.5	5.9
Lu		0.8		0.7		1.0	0.8	0.9
Cr	161.9	154.8	178.9	207.2	631.7	689.3	616.2	820.8
Ni	65.8	43.9	68.6	69.9	190.4	293.8	308.1	193.8
Co	108.8	85.1	102.9	116.6	80.6	158.2	94.8	75.2
V	910.8	799.8	1053.5	699.3	900.5	700.6	948.0	969.0
Cu	169.5	167.7	164.2	129.5	114.2	158.2	130.4	136.8
Zn	599.6	516.0	458.2	233.1	174.7	180.8	201.5	205.2
Zr	235.3	227.0	220.5	183.9	208.3	203.4	199.1	196.1
Y	48.1	56.8	44.1	46.6	47.0	52.0	47.4	47.9
Nb	19.2	20.1	15.4	17.6	11.6	12.4	23.7	16.0
Rb	48.1	31.0	24.0	18.4	24.6	5.9	10.4	16.4
Sr	910.8	774.0	869.8	906.5	537.6	565.0	568.8	524.4
Ba	556.6	387.0	441.0	310.8	459.2	293.8	284.4	319.2
H_2O^+ (wt%)	2.34	2.14	1.33	1.17	0.91	4.39	1.51	2.20
Density (g/cm^3)	2.53	2.58	2.45	2.59	2.24	2.26	2.37	2.28
Fe_2O_3/FeO	1.32	1.24	2.26	1.64	2.45	2.07	1.57	1.65

Table AT67 (continued).

Leg	127	128	128	128	128	128	128	128
Hole	794C	794D	794D	794D	794D	794D	794D	794D
Core, section	12R-3	10R-2	11R-1	11R-1	11R-2	11R-3	12R-1	12R-3
Interval (cm)	71-73	25-28	39-43	89-95	26-29	108-112	24-26	107-111
Piece	11C	1B	3E	3J	1B	4	2A	4C
Lab number	Z-1460	Z-768	Z-769	Z-1483	Z-770	Z-771	Z-772	Z-773
Depth (mbsf)	637.89	643.95	651.79	652.29	653.08	655.20	660.94	664.75
Major elements (g/1000 cm^3):								
Si	513.4	455.9	560.6	537.0	513.3	537.8	637.2	572.5
Ti	16.6	12.7	17.3	16.3	14.9	15.2	27.0	25.8
Al	203.2	169.8	201.8	191.3	195.5	203.0	234.8	211.5
Fe^{+++}	112.7	75.2	141.8	85.4	115.6	88.9	76.2	107.4
Fe^{++}	34.8	53.8	45.6	84.9	56.3	79.0	148.9	89.9
Fe (Sum)	147.5	129.0	187.5	170.3	171.9	167.9	225.0	197.2
Mn	2.0	1.8	6.4	2.3	2.6	3.1	4.6	4.0
Mg	137.6	138.0	162.3	162.8	167.3	179.0	127.0	108.3
Ca	129.5	15.1	170.9	112.3	118.2	135.9	212.4	191.7
Na	46.0	10.8	45.6	46.2	39.9	39.6	60.3	57.1
K	3.8	104.1	9.1	6.5	5.7	7.3	4.9	3.8
P	2.0	1.9	1.9	1.8	1.7	1.7	1.9	1.9
Minor elements (g/1000 cm^3 x 10^{-3}):								
La								
Ce								
Nd								
Sm								
Eu								
Gd								
Tb								
Tm								
Yb								
Lu								
Cr	483.4	679.0	787.2	704.5	734.0	656.1	734.1	627.5
Ni	166.4	300.7	349.3	333.2	372.8	401.0	257.6	225.9
Co	116.3	89.2	93.5	152.3	107.2	114.2	130.2	128.0
V	786.6	659.6	627.3	963.9	675.7	631.8	637.1	652.6
Cu	123.1	104.8	98.4	128.5	116.5	104.5	180.1	135.5
Zn	161.9	186.2	157.4	166.6	158.4	179.8	260.4	220.9
Zr	214.3	77.6	105.8	116.6	109.5	102.1	254.8	243.5
Y	45.6	29.1	29.5	33.3	32.6	29.2	83.1	75.3
Nb	16.2	5.4	6.4	6.0	6.3	5.8	6.6	6.0
Rb	3.0	52.4	5.9	3.1	3.7	4.9	4.7	3.8
Sr	615.6	50.4	688.8	642.6	582.5	583.2	526.3	502.0
Ba	319.2	228.9	78.7	78.5	165.4	121.5	66.5	128.0
H_2O^+ (wt%)	0.97	4.97	1.91	2.61	1.79	3.03	1.06	0.80
Density (g/cm^3)	2.28	1.94	2.46	2.38	2.33	2.43	2.77	2.51
Fe_2O_3/FeO	3.60	1.55	3.45	1.12	2.28	1.25	0.57	1.33

Table AT67 (continued).

Leg	128	128	128	128	128	128
Hole	794D	794D	794D	794D	794D	794D
Core, section	13R-1	14R-1	15R-1	16R-1	17R-1	18R-1
Interval (cm)	73-76	72-76	79-85	110-117	87-93	40-47
Piece	3G	6A	10A	12	8	6
Lab number	Z-774	Z-775	Z-1617	Z-1484	Z-1485	Z-1486
Depth (mbsf)	666.73	671.22	680.69	690.40	699.47	708.3
Major elements (g/1000 cm^3):						
Si	582.9	644.2	624.0	565.9	633.8	618.2
Ti	26.2	27.6	29.2	23.0	26.4	27.6
Al	231.0	237.9	264.4	254.0	255.9	235.4
Fe^{+++}	84.4	83.1	74.2	78.5	78.2	87.2
Fe^{++}	98.1	151.2	104.1	69.6	126.9	83.3
Fe (Sum)	182.6	234.2	178.3	148.1	205.1	170.6
Mn	2.2	4.7	4.1	2.2	2.9	3.0
Mg	115.7	142.8	105.4	111.6	127.5	125.4
Ca	186.7	214.1	204.7	145.5	207.3	189.7
Na	58.3	60.7	64.9	63.3	62.5	66.5
K	4.8	5.0	2.3	5.5	3.8	4.1
P	1.7	1.8	2.2	2.3	2.0	2.2
Minor elements (g/1000 cm^3 x 10^{-3}):						
La						
Ce						
Nd						
Sm						
Eu						
Gd						
Tb						
Tm						
Yb						
Lu						
Cr	629.7	726.8	775.2	771.8	764.3	801.0
Ni	385.5	248.0	247.5	213.2	275.4	261.7
Co	143.9	125.4	190.4	134.8	171.4	178.9
V	552.6	641.3	1074.4	992.3	1006.0	1019.9
Cu	154.2	185.3	223.0	142.1	207.9	240.3
Zn	215.9	94.1	258.4	235.2	238.9	253.7
Zr	239.0	253.7	272.0	294.0	261.3	267.0
Y	74.5	85.5	84.3	68.6	81.5	88.1
Nb	8.5	6.6	9.0	11.8	9.3	9.1
Rb	2.8	5.7		4.4	4.8	3.2
Sr	514.0	513.0	707.2	612.5	533.9	534.0
Ba	79.7	82.7	19.0	115.2	196.7	333.8
H_2O^+ (wt%)	1.57	0.92	0.85	0.87	1.67	0.91
Density (g/cm^3)	2.57	2.85	2.72	2.45	2.81	2.67
Fe_2O_3/FeO	0.96	0.61	0.79	1.25	0.69	1.16

Table AT68. Abundance of major and trace elements (g/1000 cm^3) in igneous rocks, Hole 797C, Legs 127 (Yamato Basin, Japan Sea). (Continued on next four pages.)

Leg	127	127	127	127	127	127	127
Hole	797C	797C	797C	797C	797C	797C	797C
Core, section	9R-1	10R-1	10R-2	12R-2	12R-4	13R-2	14R-1
Interval (cm)	43-53	90-92	125-127	91-93	85-89	99-102	88-94
Piece	9	2J	8E	1F	4D	6C	12A
Lab number	Z-1477	Z-1478	Z-245	Z-246	Z-756	Z-757	Z-1479
Depth (mbsf)	561.03	570.90	572.75	591.71	594.42	601.29	609.18
Major elements (g/1000 cm^3):							
Si	566.6	605.5	625	596	611.2	604.0	465.1
Ti	19.9	19.5	22	20	18.8	17.5	13.4
Al	246.5	261.6	267	275	264.0	273.1	190.8
Fe^{+++}	101.8	69.9	18	44	61.9	47.4	68.9
Fe^{++}	61.7	88.0	112	77	116.0	92.6	66.4
Fe (Sum)	163.5	157.9	130	121	177.9	140.0	135.2
Mn	3.1	3.1	7.8	5.0	5.7	5.9	2.4
Mg	77.2	105.7	167	110	130.1	123.8	148.0
Ca	165.4	198.5	216	220	242.7	184.4	61.4
Na	72.9	66.4	70	71	58.8	60.8	41.5
K	5.7	2.2	4.3	3.6	1.9	1.4	6.2
P	1.4	1.4	0.2	0.9	1.1	1.2	1.0
Minor elements (g/1000 cm^3 x 10^{-3}):							
La			9.9	8.0			
Ce			24.4	26.6			
Nd			22.1	21.0			
Sm			7.7	6.9			
Eu			2.8	2.9			
Tb			1.8	1.8			
Yb			5.7	5.9			
Lu			0.9	0.9			
Cr	759.5	702.3	723	931	599.9	678.3	592.8
Ni	367.5	389.6	453	479	432.5	420.3	193.4
Co	129.9	135.2	156	133	125.6	138.3	99.8
V	813.4	604.2	397	532	463.1	558.6	540.8
Cu	269.5	246.5	241	199	223.2	244.7	160.2
Zn	188.7	204.1	198	186	175.8	202.2	151.8
Sn					6.7	6.7	
Zr	245.0	259.7	181	178	214.8	204.8	158.1
Y	51.5	58.3	45.3	45.2	55.8	42.6	37.4
Nb	4.4	5.6		4.8	3.6		
Rb	5.1		3.1				8.3
Sr	759.5	768.5	680	638	669.6	611.8	322.4
Ba	19.6	37.1	65	48	22.3	16.0	16.6
H_2O^+ (wt%)	1.50	1.75	3.30	2.22	1.10	1.66	4.91
Density (g/cm^3)	2.45	2.65	2.76	2.66	2.79	2.66	2.08
Fe_2O_3/FeO	1.83	0.88	0.18	0.64	0.59	0.57	1.15

Table AT68 (continued).

Leg	127	127	127	127	127	127	127
Hole	797C	797C	797C	797C	797C	797C	797C
Core, section	16R-1	16R-2	19R-2	19R-4	19R-4	20R-2	21R-1
Interval (cm)	53-55	64-68	51-53	2-5	51-56	104-108	55-57
Piece	5B	2C	3B	5B	7A	1D	10
Lab number	Z-247	Z-758	Z-248	Z-759	Z-1480	Z-1481	Z-249
Depth (mbsf)	627.83	629.34	658.11	660.41	660.90	668.44	676.15
Major elements (g/1000 cm^3):							
Si	628	575.6	665	634.1	560.2	469.7	612
Ti	25	20.1	22	16.2	16.9	15.6	13
Al	274	269.2	280	263.0	261.0	234.8	238
Fe^{+++}	67	49.4	46	35.4	61.7	70.7	80
Fe^{++}	93	83.2	113	135.8	71.7	110.5	110
Fe (Sum)	160	132.6	159	171.2	133.4	181.2	190
Mn	7.5	8.7	4.8	3.5	2.2	1.4	2.8
Mg	125	111.8	128	140.4	88.3	162.4	161
Ca	216	197.6	252	231.4	228.4	77.5	197
Na	71	57.7	74	57.1	66.7	42.1	66
K	2.6	1.7	3.9	1.9	1.8	9.2	4.2
P	1.1	1.3	0.5	1.0	0.9	1.0	0.8
Minor elements (g/1000 cm^3 x 10^{-3}):							
La	7.9				8.0	8.2	7.2
Ce	25.2				24.0	21.6	18.4
Nd	21.9				20.1	19.2	16.5
Sm	7.6				7.0	6.5	6.6
Eu	3.1				2.6	2.4	2.5
Tb	2.0				1.7	1.6	1.5
Yb	6.7				5.4	4.1	5.8
Lu	1.0				0.8	0.6	0.8
Cr	968	691.2	936	683.6	768.8	787.2	688
Ni	589	460.8	409	228.8	234.8	360.0	509
Co	182	138.2	175	125.6	157.4	177.6	151
V	561	558.1	453	491.0	598.6	859.2	440
Cu	210	215.0	205	226.0	239.9	160.8	206
Zn	224	225.3	243	189.7	211.6	163.2	206
Sn		6.4		6.7			
Zr	174	202.2	132	161.8	165.1	165.6	138
Y	58.9	46.1		55.8	46.4	40.8	55.0
Nb	7.9	2.6		4.7	2.6	5.3	4.1
Rb	4.2					26.4	4.4
Sr	617	588.8	468	474.3	541.8	288.0	468
Ba		25.6		14.0		100.8	63
H_2O^+ (wt%)	2.24	1.44	1.64	0.96	1.73	6.40	2.63
Density (g/cm^3)	2.80	2.56	2.92	2.79	2.58	2.40	2.75
Fe_2O_3/FeO	0.8	0.66	0.45	0.29	0.96	0.71	0.81

Table AT68 (continued).

Leg	127	127	127	127	127	127	127
Hole	797C	797C	797C	797C	797C	797C	797C
Core, section	21R-1	21R-4	21R-6	24R-1	24R-4	24R-6	26R-1
Interval (cm)	76-80	110-112	10-14	95-97	130-132	64-66	115-118
Piece	10	2B	2	5D	7A	4	17
Lab number	Z-1482	Z-760	Z-761	Z-250	Z-762	Z-251	Z-763
Depth (mbsf)	676.36	680.94	682.80	705.05	709.54	712.24	724.35
Major elements (g/1000 cm^3):							
Si	609.8	630.6	614.0	657	626.2	663	482.9
Ti	16.5	14.5	14.8	13	17.9	23	43.1
Al	263.2	271.1	260.1	225	265.8	252	196.7
Fe^{+++}	48.6	47.5	59.1	97	40.9	40	96.1
Fe^{++}	115.2	105.3	114.2	126	111.0	143	130.6
Fe (Sum)	163.8	152.8	173.3	223	151.9	183	226.7
Mn	1.7	4.6	5.6	8.0	4.8	2.3	9.7
Mg	134.0	129.8	122.9	158	127.2	152	102.5
Ca	191.4	229.8	224.1	242	228.8	256	47.7
Na	65.9	56.0	54.9	70	53.8	70	67.2
K	3.0	2.8	2.8	4.9	3.0	4.4	29.5
P	1.0	1.1	1.0	0.9	1.2	1.2	4.5
Minor elements (g/1000 cm^3 x 10^{-3}):							
La				8.2		8.0	45.2
Ce				21.7		22.8	108.5
Nd				17.6		16.9	67.8
Sm				7.3		7.1	18.3
Eu				2.8		2.8	5.2
Tb				1.8		1.7	3.6
Yb				6.2		5.9	11.1
Lu				0.9		0.9	1.7
Cr	631.0	609.4	671.8	674	673.8	681	90.4
Ni	359.0	437.7	429.8	293	255.8	296	40.7
Co	146.9	138.5	146.9	132	134.8	133	115.3
V	535.8	459.8	462.4	410	492.3	385	784.2
Cu	174.1	232.7	195.8	161	231.0	148	65.5
Zn	299.2	191.1	206.7	220	200.8	237	305.1
Sn		6.1	6.5		6.6		7.5
Zr	176.8	180.1	185.0	188	214.5	172	632.8
Y	59.8	47.1	51.7	64.5	52.3	59.3	117.5
Nb	5.4	4.2	3.8	7.0	4.1	4.1	24.9
Rb	3.0	4.2	2.7	4.7		7.4	31.6
Sr	489.6	554.0	489.6	528	605.0	593	429.4
Ba	16.3	13.9	27.2	65	27.5	53	194.4
H_2O^+ (wt%)	2.46	1.54	1.62	2.12	1.31	1.79	3.06
Density (g/cm^3)	2.72	2.77	2.72	2.93	2.75	2.86	2.26
Fe_2O_3/FeO	0.47	0.47	0.47	0.86	0.41	0.31	0.82

Table AT68 (continued).

Leg	127	127	127	127	127	127	127
Hole	797C	797C	797C	797C	797C	797C	797C
Core, section	27R-1	29R-1	31R-3	33R-1	34R-1	41R-1	44R-3
Interval (cm)	68-70	80-83	114-116	10-13	49-51	42-44	47-49
Piece	4G	2H	1E	2B	3C	1A	4A
Lab number	Z-252	Z-764	Z-253	Z-765	Z-254	Z-255	Z-256
Depth (mbsf)	733.58	745.40	767.14	781.70	791.49	852.82	884.77
Major elements (g/1000 cm^3):							
Si	572	619.7	592	516.7	546	600	607
Ti	35	31.4	33	30.7	39	35	32
Al	189	205.1	196	222.7	197	201	170
Fe^{+++}	147	112.5	101	101.1	113	93	89
Fe^{++}	79	89.9	83	118.3	94	145	131
Fe (Sum)	226	202.4	184	219.4	207	238	220
Mn	3.8	3.5	7.2	8.2	12.2	9.1	2.0
Mg	124	95.8	114	130.8	103	129	99
Ca	119	128.2	186	57.1	168	162	59
Na	80	70.4	77	65.8	71	64	96
K	17.7	21.9	18.0	25.8	18.8	8.4	2.6
P	2.6	3.3	2.8	3.8	3.0	2.9	3.7
Minor elements (g/1000 cm^3 x 10^{-3}):							
La	27.6		36.3		36.2	30.4	40.4
Ce	70.1		83.0		82.7	71.8	98.4
Nd	45.1		51.9		46.5	52.5	58.1
Sm	13.3		14.3		13.2	15.7	16.7
Eu	4.5		4.7		4.7	5.2	4.5
Tb	2.8		3.1		2.5	3.3	3.3
Yb	8.8		9.1		9.3	11.9	10.1
Lu	1.4		1.4		1.4	1.7	1.6
Cr	476	127.0	285	264.0	530	442	88
Ni	138	73.7	143	79.2	194	138	63
Co	93	94.0	104	72.0	103	124	81
V	927	863.6	752	816.0	1085	911	858
Cu	138	96.5	143	91.2	129	166	101
Zn	313	236.2	285	230.4	401	318	290
Sn		9.4		8.9			
Zr	376	482.6	363	576.0	388	387	505
Y	100.2	99.1	106.4	96.0	85.3	102.2	108.5
Nb	17.3	18.8	14.5	22.6	20.4	14.9	23.0
Rb	16.5	21.1	17.4	24.0	24.3	9.9	35.3
Sr	676	685.8	675	600.0	672	525	278
Ba	276	584.2	311	576.0	253	105	303
H_2O^+ (wt%)	1.57	0.80	0.98	3.13	2.08	3.57	3.84
Density (g/cm^3)	2.51	2.54	2.59	2.40	2.58	2.62	2.52
Fe_2O_3/FeO	2.07	1.39	1.35	0.95	1.33	0.71	0.76

Table AT68 (continued).

Leg	127	127
Hole	797C	797C
Core, section	45R-1	45R-4
Interval (cm)	1-5	8-11
Piece	1A	1
Lab number	Z-766	Z-767
Depth (mbsf)	890.91	894.95
Major elements (g/1000 cm^3):		
Si	564.5	658.7
Ti	32.1	24.7
Al	207.6	229.8
Fe^{+++}	60.3	99.9
Fe^{++}	143.9	130.3
Fe (Sum)	204.1	230.2
Mn	4.0	4.1
Mg	135.6	115.4
Ca	111.0	198.7
Na	50.3	60.0
K	35.6	9.2
P	2.8	2.9
Minor elements (g/1000 cm^3 x 10^{-3}):		
La	27.8	
Ce	75.9	
Nd	45.5	
Sm	13.4	
Eu	4.0	
Tb	3.0	
Yb	9.9	
Lu	1.5	
Cr	480.7	433.0
Ni	106.3	138.7
Co	108.8	127.4
V	834.9	693.4
Cu	136.6	141.5
Zn	222.6	257.5
Sn	8.1	8.5
Zr	404.8	424.5
Y	96.1	96.2
Nb	11.4	15.0
Rb	63.3	8.8
Sr	455.4	707.5
Ba	354.2	311.3
H_2O^+ (wt%)	3.34	1.03
Density (g/cm^3)	2.53	2.83
Fe_2O_3/FeO	0.95	0.85

Table AT69. Abundance of major and trace elements (g/1000 cm^3) in igneous rocks, Hole 795B, Legs 127 (Japan Basin, Japan Sea).

Leg	127	127	127	127	127	127	127	127
Hole	795B	795B	795B	795B	795B	795B	795B	795B
Core, section	35R-1	37R-1	38R-1	38R-2	38R-4	39R-2	40R-1	40R-2
Interval (cm)	60-62	33-35	6-8	87-92	28-30	22-24	27-29	123-125
Piece	4	3	1B	3B	2A	1B	3B	13
Lab number	Z-240	Z-696	Z-241	Z-1461	Z-242	Z-1462	Z-243	Z-244
Depth (mbsf)	693.80	712.93	722.26	724.17	726.98	733.62	741.87	744.33
Major elements (g/1000 cm^3):								
Si	481	466.8	535	501.0	486	528.9	462	498
Ti	15	13.8	18	13.5	20	11.6	15	13
Al	204	206.3	237	227.1	221	183.6	177	171
Fe^{+++}	76	73.9	67	92.1	88	83.3	74	95
Fe^{++}	28	49.5	52	25.7	47	46.1	28	42
Fe (Sum)	104	123.4	119	117.8	135	129.4	102	137
Mn	0.8	3.7	3.9	3.3	1.9	2.4	2.0	2.3
Mg	56	68.5	84	71.4	78	72.3	80	88
Ca	109	150.3	159	151.1	163	122.8	130	128
Na	52	45.4	56	54.0	49	49.4	39	51
K	11.5	8.9	10.6	8.5	9.9	5.8	4.5	6.5
P	3.0	2.3	1.9	2.3	1.5	3.0	0.6	2.3
Minor elements (g/1000 cm^3 x 10^{-3}):								
La	21.7		13.1		11.7		7.5	16.6
Ce	57.1		32.2		28.1		21.2	37.4
Nd	35.5		20.7		18.1		14.1	24.9
Sm	9.7		5.5		5.4		4.2	6.2
Eu	3.2		2.1		1.9		1.8	2.5
Tb	1.8		1.0		0.9		1.0	1.3
Yb	7.3		4.4		3.7		3.7	5.2
Lu	1.1		0.6		0.5		0.6	0.8
Cr	16	101.5	81	131.8	76	115.0	91	89
Ni	26	85.3	92	79.9	86	87.8	97	125
Co	33	75.1	76	86.4	65	83.6	71	77
V	197	822.2	1036	1019.5	971	836.0	869	706
Cu	30	109.6	150	138.2	151	146.3	106	135
Zn	236	162.4	207	187.9	194	238.3	174	208
Zr	236	136.0	115	164.2	112	140.0	104	89
Y	63.0	42.6	39.1	49.7	34.5	100.3	30.9	51.9
Nb	13.8	7.1	9.2	8.6	11.2	7.5	5.0	11.4
Rb	13.6	17.7	16.6	19.0	13.8	15.7	3.7	10.4
Sr	552	466.9	483	518.4	475	647.9	328	374
Ba	160	26.4	131	237.6	114	156.8	48	85
H_2O^+ (wt%)	2.20	0.91	2.40	0.47	1.65	1.13	3.01	3.00
Density (g/cm^3)	1.97	2.03	2.30	2.16	2.16	2.09	1.95	2.08
Fe_2O_3/FeO	3.05	1.66	1.44	3.99	2.08	2.01	2.91	2.51

Table AT70. Abundance of major and trace elements (g/1000 cm^3) in basalts, Hole 834B, Leg 135 (Lau Basin, Pacific Ocean). (Continued on next page.)

Leg	135	135	135	135	135	135	135	135
Hole	834B	834B	834B	834B	834B	834B	834B	834B
Core, section	8R-2	8R-2	11R-2	11R-3	12R-4	13R-1	13R-1	22R-1
Interval (cm)	7-10	12-18	79-82	86-89	130-134	134-139	139-142	87-90
Piece	1A	1B	3A	3A	2	4	4	14A
Lab number	Z-801	Z-1487	Z-802	Z-1488	Z-803	Z-1489	Z-804	Z-805
Depth (mbsf)	127.46	127.51	152.07	153.64	160.51	162.34	162.39	224.07
Major elements (g/1000 cm^3):								
Si	558.9	560.9	612.9	558.3	566.6	572.7	570.2	623.8
Ti	17.7	20.3	17.6	16.5	16.5	17.7	14.5	18.7
Al	206.0	223.8	234.7	208.4	226.9	213.2	223.9	255.8
Fe^{+++}	72.7	59.9	74.6	78.0	50.5	71.1	60.1	83.6
Fe^{++}	99.0	94.8	101.0	84.9	100.0	99.1	89.3	88.4
Fe (Sum)	171.8	154.7	175.6	162.9	150.5	170.2	149.4	172.0
Mn	2.3	7.3	2.5	2.5	2.4	8.9	2.2	2.6
Mg	102.8	111.9	124.9	124.9	123.6	119.1	131.4	107.8
Ca	193.9	179.0	221.6	180.4	208.7	176.3	207.6	244.7
Na	54.9	59.7	57.2	53.9	49.2	55.6	49.1	57.9
K	4.3	3.7	3.4	2.7	2.8	3.0	3.0	3.7
P	1.4	1.4	1.5	1.1	1.2	1.2	1.1	1.6
Minor elements (g/1000 cm^3 x 10^{-3}):								
La								
Ce								
Nd								
Sm								
Eu								
Tb								
Yb								
Lu								
Cr	168.0	176.7	614.1	612.4	684.8	617.5	702.8	832.7
Ni	139.2	123.4	261.7	212.3	254.0	239.6	281.1	327.6
Co	112.8	118.6	125.5	134.2	117.0	153.1	128.0	142.0
V	616.8	890.6	547.4	634.4	602.6	827.5	544.7	614.3
Cu	192.0	198.4	224.3	219.6	201.7	279.1	195.8	196.6
Zn	177.6	198.4	197.6	331.8	159.4	217.4	160.6	202.0
Zr	201.6	210.5	218.9	187.9	166.8	200.1	168.2	234.8
Y	55.2	58.1	61.4	51.2	52.3	51.9	47.7	71.0
Nb	5.5	6.3	4.8	4.1		4.2		4.6
Rb	3.1	2.7	4.8	2.4	5.2	3.5	5.3	6.6
Sr	432.0	435.6	427.2	414.8	398.4	444.6	401.6	409.5
Ba	21.6	79.9	26.7	70.8	12.5	79.0	15.1	13.7
H_2O^+ (wt%)	0.99	0.75	1.40	1.74	1.22	1.24	1.79	0.90
Density (g/cm^3)	2.40	2.42	2.67	2.44	2.49	2.47	2.51	2.73
Fe_2O_3/FeO	0.82	0.70	0.82	1.02	0.56	0.80	0.75	1.05

Table AT70 (continued).

Leg	135	135	135	135	135	135	135
Hole	834B	834B	834B	834B	834B	834B	834B
Core, section	28R-2	33R-2	34R-2	47R-1	49R-1	49R-1	53R-1
Interval (cm)	76-78	103-105	10-14	71-74	97-100	131-135	60-62
Piece	4B	5I	1A	10	14B	16	5B
Lab number	Z-806	Z-807	Z-808	Z-809	Z-810	Z-1490	Z-811
Depth (mbsf)	254.56	283.07	287.77	364.21	374.17	374.51	393.10
Major elements (g/1000 cm^3):							
Si	589.3	593.9	632.5	553.7	601.7	598.7	546.0
Ti	18.9	20.5	21.4	31.7	34.6	30.2	31.8
Al	243.4	253.0	270.3	177.4	206.9	203.7	181.7
Fe^{+++}	50.1	66.7	61.5	116.8	112.2	93.0	120.5
Fe^{++}	112.2	113.4	116.1	116.9	87.0	137.2	95.2
Fe (Sum)	162.2	180.1	177.6	233.7	199.2	230.2	215.7
Mn	2.3	2.9	2.7	3.9	2.9	6.8	3.3
Mg	118.0	115.7	133.1	51.6	59.1	66.9	58.4
Ca	223.9	229.6	242.8	147.2	147.6	131.4	136.2
Na	54.3	56.1	58.7	69.0	81.8	79.0	67.6
K	1.5	2.4	2.4	13.4	5.5	2.5	9.4
P	1.4	1.4	1.6	2.3	2.8	2.1	2.2
Minor elements (g/1000 cm^3 x 10^{-3}):							
La				9.7			
Ce				28.3			
Nd				28.3			
Sm				10.9			
Eu				3.3			
Tb				2.4			
Yb				8.7			
Lu				1.3			
Cr	832.0	851.2	990.5			56.6	
Ni	260.0	274.0	441.5	68.4	67.0	49.2	64.4
Co	132.6	122.4	133.0	80.2	101.7	123.0	94.3
V	585.0	585.2	636.8	826.0	880.4	1087.3	793.5
Cu	187.2	223.4	237.7	118.0	136.4	157.4	115.0
Zn	171.6	170.2	203.8	295.0	240.6	285.4	253.0
Zr	241.8	231.4	243.4	306.8	322.4	332.1	299.0
Y	65.0	63.8	67.9	89.7	94.2	93.5	92.0
Nb	3.4	3.7	5.4	2.6	4.0	5.7	4.4
Rb		2.9	3.7	37.8	5.5	3.9	18.9
Sr	416.0	425.6	452.8	472.0	471.2	442.8	414.0
Ba	7.8	16.0	11.3	191.2	213.3	236.2	13.8
H_2O^+ (wt%)	1.36	1.32	0.99	2.38	1.47	0.38	1.55
Density (g/cm^3)	2.60	2.66	2.83	2.36	2.48	2.46	2.30
Fe_2O_3/FeO	0.5	0.65	0.59	1.11	1.43	0.75	1.41

Table AT71. Abundance of major and trace elements (g/1000 cm^3) in basalts, Hole 191, Leg 19 (Kamchatka Basin, Bering Sea).

Leg	19	19	19
Hole	191	191	191
Core, section	16R-1	16R-1	16R-1
Interval (cm)	25-31	78-83	110-113
Lab number	Z-1101	Z-1102	Z-1103
Depth (mbsf)	910.25	910.78	911.1
Major elements (g/1000 cm^3):			
Si	618.2	625.49	610.73
Ti	29.3	30.07	29.38
Al	224.8	217.61	217.15
Fe^{+++}	113.6	123.00	118.09
Fe^{++}	84.7	98.18	98.28
Fe (Sum)	198.3	221.18	216.37
Mn	5.3	5.42	5.09
Mg	103.5	103.91	101.54
Ca	195.6	208.64	216.61
Na	63.3	67.98	63.18
K	8.9	5.12	2.27
P	2.4	2.32	2.39
Minor elements (g/1000 cm^3 x 10^{-3}):			
La	16.0	15.02	14.15
Ce	56.1	49.14	45.39
Nd	42.7	38.22	34.71
Sm	15.0	13.65	13.08
Eu	4.5	4.10	4.01
Tb	4.0	3.55	3.20
Yb	11.7	10.92	9.88
Lu	1.8	1.67	1.44
Cr	582.1	567.84	582.06
Ni	184.2	174.72	165.54
Co	128.2	122.85	125.49
V	726.2	709.80	694.20
Cu	259.0	245.70	232.29
Zn	309.7	240.24	229.62
Zr	373.8	382.20	373.80
Y	106.8	109.20	101.46
Nb	9.3	10.10	11.21
Rb	23.8	14.74	0.00
Sr	427.2	436.80	427.20
Ba	235.0	248.43	202.92
H_2O^+ (wt%)	1.64	1.81	1.17
Density (g/cm^3)	2.67	2.73	2.67
Fe_2O_3/FeO	1.49	1.39	1.34

Table AT72. Abundance of major and trace elements (g/1000 cm^3) in basalts, Hole 735B, Leg 118 (Southwest Indian Ridge). (Continued on next page.)

Leg	118	118	118	118	118	118	118
Hole	735B	735B	735B	735B	735B	735B	735B
Core, section	7D-1	20R-1	24R-1	32R-4	41R-1	49R-1	55R-3
Interval (cm)	41-43	73-75	17-19	4-6	36-38	57-59	103-105
Piece	5	2E	1B	1A	2A	3C	4C
Lab number	Z-173	Z-176	Z-177	Z-178	Z-179	Z-181	Z-182
Depth (mbsf)	26.41	84.93	105.67	153.04	196.36	236.57	269.03
Major elements (g/1000 cm^3):							
Si	646	713	672	706	731	652	636
Ti	5	10	15	11	17	133	142
Al	301	255	230	298	237	178	190
Fe^{+++}	62	60	67	40	49	174	136
Fe^{++}	85	91	123	64	121	334	424
Fe (Sum)	147	151	190	104	170	508	560
Mn	2.9	3.1	1.8	2.1	3.9	6.4	7.6
Mg	174	188	182	144	134	135	131
Ca	228	304	252	307	256	225	230
Na	71	62	66	66	89	77	68
K	7.8	2.6	3.2	2.5	3.2	4	3.6
P	0.1	0.1	0.3	0.1	0.3	0	0.4
Minor elements (g/1000 cm^3 x 10^{-3}):							
La	4.4	3.7	3.5	2.6	2.2	2.1	3.2
Ce	11.7	9.2	10.0	7.5	7.8	7.3	12.2
Nd	8.5	7.1	8.8		12.3	13.3	21.6
Sm	2.9	2.9	4.1	3.3	4.2	5.3	8.4
Eu	1.8	1.6	2.2	2.4	2.6	3.0	5.1
Gd	3.5	4.6	6.7	6.0	6.0	8.6	10.5
Tb	0.6	0.8	1.1	1.0	1.3	1.8	2.3
Tm			0.6			0.9	1.5
Yb	2.3	2.9	4.1	3.0	5.1	6.0	9.8
Lu	0.3	0.4	0.6	0.5	0.8	0.9	1.6
Sc	38	132	126	114		179	216
Cr	335	1524	424	481	36	20	27
Ni	612	552	380	331	99	113	111
Co	111	95	149	51	84	256	270
V	73	267	366	114	359	2326	1233
Cu		104	140	81	57	186	257
Zn		92	88		90	366	456
Zr	47		56	39	39	106	216
Y	20.4	27.3	43.9	29.1	44.9	59.8	91.2
Nb						5.3	8.1
Rb	8.5			3.0			
Sr	467	429	439	481	449	498	405
H_2O^+ (wt%)	1.27	0.33	0.82	0.23	0.43	0.66	0.91
Density (g/cm^3)	2.92	3.01	2.93	3.00	2.99	3.32	3.38
Fe_2O_3/FeO	0.82	0.73	0.61	0.70	0.45	0.58	0.35

Table AT72 (continued).

Leg	118	118	118	118	118	118	118
Hole	735B	735B	735B	735B	735B	735B	735B
Core, section	58R-3	73R-5	79R-5	82R-6	85R-7	86R-3	88N-1
Interval (cm)	26-28	63-65	87-89	22-24	95-97	51-53	60-62
Piece	1B	3	6A	3	6	1F	2C
Lab number	Z-183	Z-185	Z-186	Z-187	Z-188	Z-189	Z-190
Depth (mbsf)	283.76	372.13	421.37	450.72	481.45	484.51	500.60
Major elements (g/1000 cm^3):							
Si	718	749	634	695	694	724	648
Ti	13	10	9	10	10	11	8
Al	212	299	324	267	285	203	328
Fe^{+++}	67	51	39	53	36	58	40
Fe^{++}	128	57	94	99	97	96	97
Fe (Sum)	195	108	133	152	133	154	137
Mn	2.1	1.0	1.1	0.7	2.1	2.4	1.6
Mg	172	129	166	168	214	182	242
Ca	287	337	234	288	291	304	225
Na	64	66	56	55	52	65	51
K	3.2	2.6	1.2	2.5	3.3	1.3	1.2
P	0.3	0.3	0.2	0.3	0.1	0.1	0.1
Minor elements (g/1000 cm^3 x 10^{-3}):							
La	6.3	1.4	1.8	1.2	1.2	5.1	0.9
Ce	20.8	4.7	5.1	4.2	3.1	15.4	2.2
Nd	25.9	6.6	4.3	4.5	4.0	15.1	2.0
Sm	10.2	2.6	1.7	1.9	1.7	4.8	0.6
Eu	2.6	1.5	1.2	1.3	1.2	1.6	0.8
Gd	12.4	3.7	2.5	3.0	2.8	6.3	0.6
Tb	2.7	0.7	0.4	0.5	0.5	1.2	0.1
Tm	1.8						
Yb	11.5	2.6	1.2	1.8	1.7	5.4	0.5
Lu	1.6	0.4	0.2	0.3	0.3	1.0	0.1
Sc	157	147	37	107	104	133	21
Cr	543	953	799	2148	4830	1176	271
Ni	317	222	656	537	675	437	902
Co	84	37	114	125	98	90	126
V	301	187	86	215	169	277	60
Cu	93	84	106	75	95	42	186
Zn	84		63	84	61		30
Zr	60	31	40	33		54	
Y	87.4	40.6	13.1	18.2	17.2	42.2	6.6
Nb							
Rb							
Sr	392	500	371	328	399	452	481
H_2O^+ (wt%)	0.43	0.29	0.24	0.26	0.42	0.87	0.42
Density (g/cm^3)	3.01	3.12	2.85	2.98	3.07	2.96	3.01
Fe_2O_3/FeO	0.58	0.99	0.46	0.59	0.41	0.67	0.46

Table AT73. Abundance of major and trace elements (g/1000 cm^3) in serpentinized harzburgites, Hole 637A, Leg 103 (Galicia Margin, eastern Atlantic Ocean).

Leg	103	103	103	103
Hole	637A	637A	637A	637A
Core, section	25R-1	26R-2	27R-1	28R-3
Interval (cm)	66-69	53-56	112-115	103-106
Piece	8B	1E	15C	14
Lab number	Z-149	Z-150	Z-151	Z-152
Depth (mbsf)	228.66	239.23	248.02	260.63
Major elements (g/1000 cm^3):				
Si	283	360	376	172
Ti	2.6	2.8	3.1	1.5
Al	4.8	16.2	20.2	12.7
Fe^{+++}	80	107	102	79
Fe^{++}	4.4	4.0	9.4	2.0
Fe (Sum)	84	111	111	81
Mn	2.0	2.1	2.4	1.3
Mg	350	432	446	144
Ca	188	102	120	573
Na	22	4.4	6.5	11
K	2.3	1.5	1.6	1.9
P	0.2	0.3	0.2	0.3
Minor elements (g/1000 cm^3 x 10^{-3}):				
La	0.49	0.44	0.46	0.46
Ce	1.21	1.42	1.23	1.24
Sm	0.30	0.37	0.35	0.32
Eu	0.09	0.07	0.03	0.06
Tb	0.06	0.07	0.08	0.06
Yb	0.19	0.39	0.23	0.18
Lu	0.03	0.07	0.06	0.03
Sc	22.3	21.9		17.7
Cr	3138	3388	3359	2043
Ni	3037	5028	3822	3214
Co	170	171	134	44
V	77	77	63	87
Cu	38	55	32	
Zn	28	37	46	28
Sr	61	33	51	99
Ba				30
H_2O^+ (wt%)	10.39	11.70	10.73	3.17
Density (g/cm^3)	2.02	2.19	2.32	2.30
Fe_2O_3/FeO	20.11	29.48	12.18	44.18